Pan Stanford Series on Nanomedicine Vol. 1

Handbook of Clinical Nanomedicine

Nanoparticles, Imaging, Therapy, and Clinical Applications

edited by
Raj Bawa
Gerald F. Audette
Israel Rubinstein

Handbook of

Clinical Nanomedicine

Vol. 1

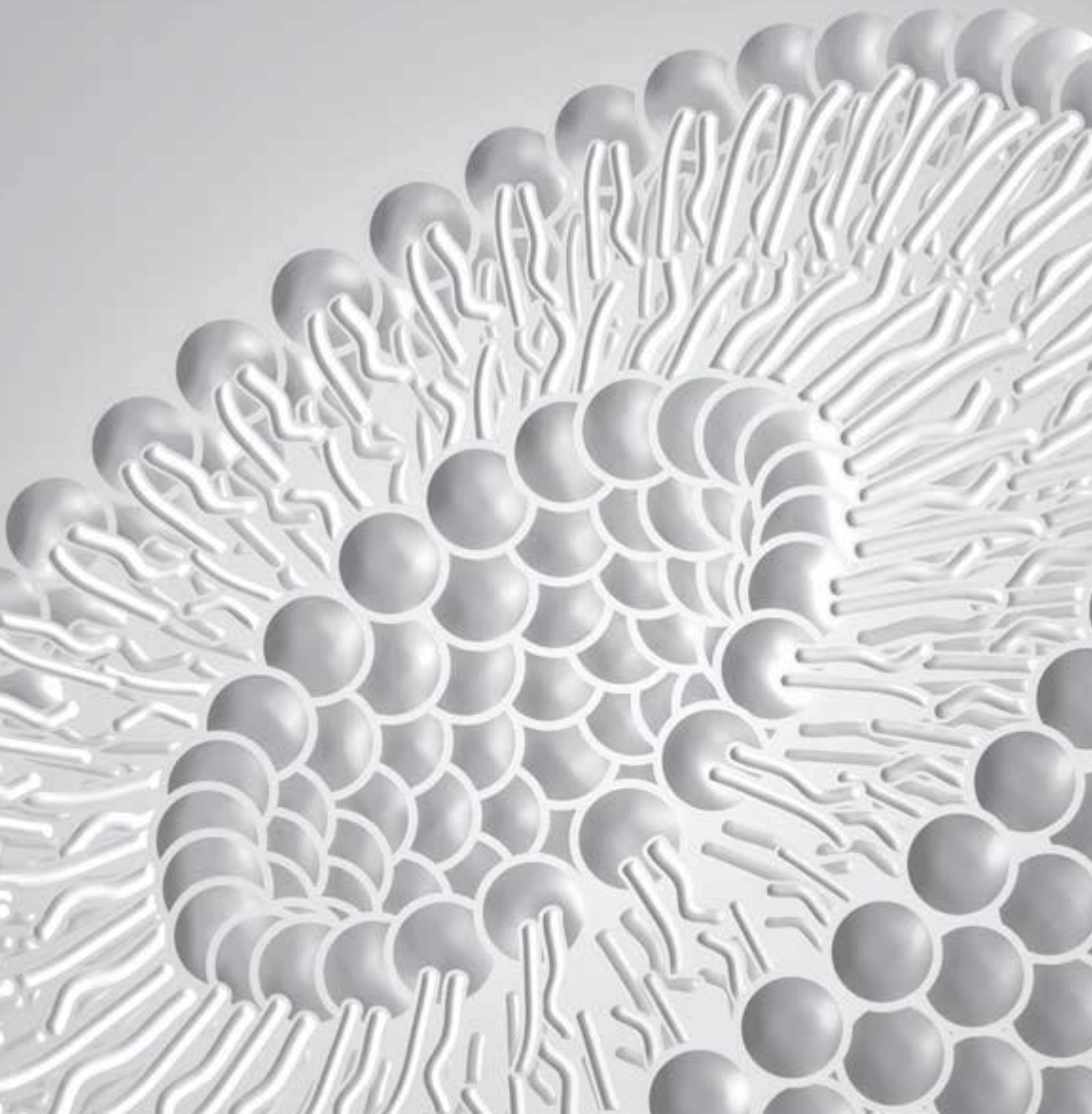

Pan Stanford Series on Nanomedicine

Series Editor
Raj Bawa

Titles in the Series

Published

Vol. 1
Handbook of Clinical Nanomedicine: Nanoparticles, Imaging, Therapy, and Clinical Applications
Raj Bawa, Gerald F. Audette, and Israel Rubinstein, eds.
2016
978-981-4669-20-7 (Hardcover)
978-981-4669-21-4 (eBook)

Vol. 2
Handbook of Clinical Nanomedicine: Law, Business, Regulation, Safety, and Risk
Raj Bawa, ed., Gerald F. Audette and Brian E. Reese, asst. eds.
2016
978-981-4669-22-1 (Hardcover)
978-981-4669-23-8 (eBook)

Forthcoming

Vol. 3
Immune Effects of Biopharmaceuticals and Nanomedicines
Raj Bawa, János Szebeni, Thomas J. Webster, and Gerald F. Audette, eds.
2017

Vol. 4
Impact of Nanobiotechnology on the Future of Medicine and Personalized Medicine
Shaker A. Mousa and Raj Bawa, eds.
2017

Pan Stanford Series on Nanomedicine Vol. 1

Handbook of
Clinical Nanomedicine
Nanoparticles, Imaging, Therapy, and Clinical Applications

edited by

Raj Bawa, MS, PhD
Patent Agent, Bawa Biotech LLC, Ashburn, Virginia, USA
Adjunct Professor, Department of Biological Sciences
Rensselaer Polytechnic Institute, Troy, New York, USA
Scientific Advisor, Teva Pharmaceutical Industries, Ltd., Israel

Gerald F. Audette, PhD
Associate Professor, Department of Chemistry
Acting Director, Centre for Research on Biomolecular Interactions
York University, Toronto, Canada

Israel Rubinstein, MD
Professor, Department of Medicine
University of Illinois at Chicago, College of Medicine, Chicago, Illinois, USA
Associate Chief of Staff for Research and Development
Jesse Brown VA Medical Center, Chicago, Illinois, USA

PAN STANFORD PUBLISHING

Published by

Pan Stanford Publishing Pte. Ltd.
Penthouse Level, Suntec Tower 3
8 Temasek Boulevard
Singapore 038988

Email: editorial@panstanford.com
Web: www.panstanford.com

Note from the Series Editor and Publisher

It should be noted that knowledge and best practices in the various fields represented in this handbook (such as medicine, pharmacology, biotechnology, toxicology, pharmaceutical sciences, materials science, etc.) are constantly changing. As new research and experience broaden our knowledge base, changes in research methods, legal and business practices or medical treatments may become necessary. Therefore, the reader is advised to consult the most current information regarding: (i) various products, companies or procedures featured; (ii) recommended doses, methods, duration of administration and contraindications; and (iii) legal, business or commercial information provided. It is imperative that researchers, physicians, lawyers, policymakers and business professionals always rely on their own experience and knowledge in evaluating and using any information, procedures, formulations or experiments described herein. To the fullest extent of the law, neither the publisher nor the authors or editors, make any representations or warranties, express or implied, with respect to information presented in this book. They assume no liability for any injury and/or damage to persons or property as a matter of products liability, negligence or otherwise, or from any use or operation of any methods, products, drugs, medical procedures, instructions, legal opinions or ideas presented in this handbook.

A catalogue record for this book is available from the Library of Congress and the British Library.

Handbook of Clinical Nanomedicine: Nanoparticles, Imaging, Therapy, and Clinical Applications

ISBN 978-981-4669-20-7 (Hardcover)
ISBN 978-981-4669-21-4 (eBook)
ISBN 978-981-4316-17-0 (Set, Hardcover)
ISBN 978-981-4411-66-0 (Set, eBook)

Printed in the USA

This book is dedicated with love to my father,

Dr. S. R. Bawa,

on his 85th birthday,
dad, grandfather, inspiration, anatomist,
electron microscopist, department founder,
professor and head, university dean
—the best teacher I ever had.
–R.B.

About the Editors

Raj Bawa, MS, PhD, is president of Bawa Biotech LLC, a biotech/pharma consultancy and patent law firm based in Ashburn, VA, USA that he founded in 2002. He is an inventor, entrepreneur, professor and registered patent agent licensed to practice before the U.S. Patent & Trademark Office. Trained as a biochemist and microbiologist, he has been an active researcher for over two decades. He has extensive expertise in pharmaceutical sciences, biotechnology, nanomedicine, drug delivery and biodefense, FDA regulatory issues, and patent law. Since 1999, he has held various adjunct faculty positions at Rensselaer Polytechnic Institute in Troy, NY, where he is currently an adjunct professor of biological sciences and where he received his doctoral degree in three years (biophysics/biochemistry). Since 2004, he has been an adjunct professor of natural and applied sciences at NVCC in Annandale, VA. He is a scientific advisor to Teva Pharmaceutical Industries, Ltd., Israel. He has served as a principal investigator of National Cancer Institute SBIRs and reviewer for both the National Institutes of Health and the National Science Foundation. In the 1990s, Dr. Bawa held various positions at the US Patent & Trademark Office, including primary examiner for 6 years. He is a life member of Sigma Xi, co-chair of the Nanotech Committee of the American Bar Association and serves on the global advisory council of the World Future Society. He has authored over 100 publications, co-edited four texts and serves on the editorial boards of 17 peer-reviewed journals, including serving as a special associate editor of *Nanomedicine* (Elsevier) and an editor-in-chief of the *Journal of Interdisciplinary Nanomedicine* (Wiley). Some of Dr. Bawa's awards include the Innovations Prize from the Institution of Mechanical Engineers, London, UK (2008); Appreciation Award from the Undersecretary of Commerce, Washington, DC (2001); the Key Award from Rensselaer's Office of Alumni Relations (2005); and Lifetime Achievement Award from the American Society for Nanomedicine (2014).

Gerald F. Audette, PhD, has been a faculty member at York University in Toronto, Canada, since 2006. Currently, he is an associate professor in the Department of Chemistry and acting director of the Centre for Research on Biomolecular Interactions at York University. He received his doctorate in 2002 from the Department of Biochemistry at the University of Saskatchewan in Saskatoon, Canada. Working with Drs. Louis T. J. Delbaere and J. Wilson Quail (1995–2001), Dr. Audette's research focused on the elucidation of the protein–carbohydrate interactions that occur during blood-group recognition (in particular during the recognition of O blood type) using high-resolution X-ray crystallography. Dr. Audette conducted his postdoctoral research at the University of Alberta (2001–2006) in Edmonton, Canada. Working with Drs. Bart Hazes and Laura Frost; his research again utilized high-resolution protein crystallography to examine the correlation between protein structure and biological activity of type IV pilins that are assembled into pili used by bacteria for multiple purposes, including cellular adhesion during infection. It was during these studies that Dr. Audette identified the generation of protein nanotubes from engineered pilin monomers. Dr. Audette also studied the process of bacterial conjugation (or lateral gene transfer) using the F-plasmid conjugative system of *Escherichia coli*. Current research directions include: structure/function studies of proteins involved in bacterial conjugation systems, the structural and functional characterization of several type IV pilins (the monomeric subunit of the pilus), their assembly systems, and adapting these unique protein systems for applications in bionanotechnology. Dr. Audette has previously served as co-editor-in-chief of the *Journal of Bionanoscience* (2007–2010).

Israel Rubinstein, MD, is professor of medicine at the College of Medicine, University of Illinois at Chicago, USA. He is member of the section of pulmonary, critical care, allergy and sleep medicine in the Department of Medicine, University of Illinois at Chicago. He is an attending physician at the University of Illinois Hospital and Health Sciences System and Jesse Brown VA Medical Center in Chicago. Dr. Rubinstein

is also the associate chief of staff for research and development at the Jesse Brown Veterans Administration Medical Center. Prior to his appointment at the University of Illinois at Chicago, he was associate professor of medicine at the University of Nebraska Medical Center in Omaha, Nebraska, USA. Dr. Rubinstein received his medical degree from the Hebrew University-Hadassah School of Medicine in Jerusalem, Israel. He was a medical resident in Israel, fellow in respirology at the University of Toronto and a research fellow at the Cardiovascular Research Institute, University of California at San Francisco. Dr. Rubinstein holds 18 issued and pending patents and has authored close to 200 peer-reviewed papers in scientific journals. Dr. Rubinstein's funded research endeavors center around nanomedicine and targeted drug delivery with specific focus on lipid-based products and repurposing. Currently, he serves as editor-in-chief of *Nanotechnology, Science and Applications*, associate editor of the *International Journal of Nanomedicine*, and editorial board member of several scientific journals. Dr. Rubinstein is member of the scientific advisory board of the International Academy of Cardiology. He is a fellow of the American Heart Association as well as the American College of Physicians and the American College of Chest Physicians. In addition, he is a member of the American Thoracic Society, American Physiological Society, American Society for Pharmacology and Experimental Therapeutics, and American Microbiology Society. Dr. Rubinstein is a board member and director of Advanced Life Sciences, a publicly traded biopharmaceutical company based in Woodridge, Illinois, USA. He is a co-founder of ResQ Pharma, an emerging clinical stage pharmaceutical company focusing on repurposing FDA-approved drugs for cardiopulmonary resuscitation and drug overdoses.

Contents

Section III: Therapy and Clinical Applications

List of Corresponding Authors

Fritz Allhoff Department of Philosophy, 3004 Moore Hall, Western Michigan University, 1903 W. Michigan Avenue, Kalamazoo, MI 49008, USA, Email: fritz.allhoff@wmich.edu

Gerald F. Audette Department of Chemistry and the Centre for Research on Biomolecular Interactions, York University, Life Sciences Building 327C, 4700 Keele Street, Toronto, Ontario M3J 1P3, Canada, Email: audette@yorku.ca

Yechezkel Barenholz Laboratory of Membrane and Liposome Research, Department of Biochemistry and Molecular Biology, Institute of Medical Research Israel-Canada, The Hebrew University-Hadassah Medical School, POB 12272, Jerusalem 9112102, Israel, Email: chezyb@ekmd.huji.ac.il

Randall Barton NanoViricides, Inc., One Controls Drive, Shelton, CT 06484, USA, Email: rwbbarton@nanoviricides.com

Raj Bawa Bawa Biotech LLC, 21005 Starflower Way, Ashburn, VA 20147, USA, Email: bawa@bawabiotech.com

Frank J. Boehm NanoApps Medical, Inc., 141 Empress Avenue South, Thunder Bay, ON, Canada P7B 4N6, Email: cellrepair777@hotmail.com

Michelle S. Bradbury Department of Radiology, Memorial Sloan Kettering Cancer Center, 1275 York Avenue, New York, NY 10065, USA, Email: bradburm@mskcc.org

Jill B. Conner Teva Pharmaceutical Industries, Ltd., Specialty Life Cycle Initiatives, 11100 Nall Avenue, Overland Park, KS 66211, USA, Email: Jill.Conner@tevapharm.com

José das Neves INEB-Instituto de Engenharia Biomédica, University of Porto, Rua do Campo Alegre, 823, 4150-180, Porto, Portugal, Email: j.dasneves@ineb.up.pt

Jason L. J. Dearling Division of Nuclear Medicine and Molecular Imaging, Department of Radiology, Boston Children's Hospital and Harvard Medical School, 300 Longwood Avenue, Boston, MA 02115, USA, Email: jason.dearling@childrens.harvard.edu

Angelika Domschke Angelika Domschke Consulting LLC, 3379 Ennfield Way, Duluth, GA 30096, USA, Email: angeldomschke@aol.com

Rutledge Ellis-Behnke Department of Brain and Cognitive Sciences, Massachusetts Institute of Technology, Cambridge, MA 02139, USA, Email: rutledg@mit.edu

Marianna Foldvari School of Pharmacy, University of Waterloo, 200 University Avenue West, Waterloo, ON, Canada N2L 3G1, Email: foldvari@uwaterloo.ca

Mario Ganau Department of Surgical Science, Asse Didattico di Medicina, Cittadella Universitaria, S.S. 554. 09042 Monserrato (CA), Italy, Email: mario.ganau@singularityu.org

Howard E. Gendelman Department of Pharmacology and Experimental Neuroscience, College of Medicine, University of Nebraska Medical Center, Omaha, NE 68198, USA, Email: hegendel@unmc.edu

Levi A. Gheber Department of Biotechnology Engineering, Ben-Gurion University of the Negev, PO Box 653, Beer-Sheva 84105, Israel, Email: glevi@bgu.ac.il

James K. Gimzewski Department of Chemistry and Biochemistry, University of California, 607 Charles E. Young Drive East, Los Angeles, CA 90095-1569, USA, Email: gimzewski@cnsi.ucla.edu

Todd Giorgio Department of Biomedical Engineering, Vanderbilt University, VU Station B 351620, Nashville, TN 37235-1620, USA, Email: todd.d.giorgio@vanderbilt.edu

D. W. Green Department of Oral Biosciences, Faculty of Dentistry, University of Hong Kong, The Prince Philip Dental Hospital, 34 Hospital Road, Sai Ying Pun, Hong Kong, Email: dwgreen@hku.hk

Frank X. Gu Department of Chemical Engineering, University of Waterloo, 200 University Avenue West, Waterloo, Ontario, N2L 3G1, Canada, Email: frank.gu@uwaterloo.ca

G. S. Gupta Department of Biophysics, Panjab University, Chandigarh 160014, India, Email: drgsgupta53@rediffmail.com

Lesley M. Hamming Winston & Strawn LLP, 35 W. Wacker Drive, Chicago, IL 60601-9703, USA, Email: LHamming@winston.com

Karolina Jurczyk University of Medical Sciences, Conservative Dentistry and Periodontology Department, Bukowska 70 Str., 60-812 Poznan, Poland, Email: karolajur@gmail.com

Manzoor Koyakutty Cancer Nanomedicine, Amrita Centre for Nanosciences and Molecular Medicine, Amrita Institute of Medical Sciences and Research Centre, Amrita Vishwa Vidyapeetham University, Ponekkara PO, Kochi, Kerala 682041, India, Email: manzoork@aims.amrita.edu

Alexey Krasnoslobodtsev Department of Physics, University of Nebraska at Omaha, 6001 Dodge Street, Omaha, NE 68182, USA, Email: akrasnos@unomaha.edu

Harold W. Kroto Department of Chemistry & Biochemistry, Florida State University, 95 Chieftan Way, Tallahassee, FL 32306-4390, USA, Email: kroto@chem.fsu.edu

Alf Lamprecht Laboratory of Pharmaceutical Engineering, Faculty of Medicine and Pharmacy, University of Franche-Comté Besançon, France, Email: alf.lamprecht@univ-fcomte.fr

Ki-Bum Lee Department of Chemistry and Chemical Biology, Rutgers New Brunswick-Busch Campus, Rutgers, 610 Taylor Road, Piscataway, NJ 08854, USA, Email: kblee@chem.rutgers.edu

Claus-Michael Lehr Helmholtz-Institute for Pharmaceutical Research Saarland, Department of Drug Delivery, Saarland University, 66123 Saarbrücken, Universitätscampus E8 1, Germany, Email: Claus-Michael.Lehr@helmholtz-hzi.de

Didier Letourneur INSERM U1148, LVTS, Cardiovascular Bio-Engineering, X. Bichat Hospital, Paris, France, Email: didier.letourneur@inserm.fr

Julianna Lisziewicz eMMUNITY Inc., 4400 East West Hwy, Bethesda, MD 20814, USA, Email: julianna.lisziewicz@emmunityinc.com

Catherine M. Lockhart Department of Pharmaceutics, University of Washington, Box 357610, H272 Health Science Building, 1959 NE Pacific Street, Seattle, WA 98195 USA, Email: cmo4@uw.edu

Yuri Lyubchenko Department of Pharmaceutical Sciences, University of Nebraska Medical Center, 601 S. Saddle Creek Road, Omaha, NE 68106, USA, Email: ylyubchenko@unmc.edu

Supriya Mahajan Department of Medicine, Division of Allergy, Immunology, and Rheumatology, State University of New York at Buffalo, 6074 UB's Clinical and Translational Research Center, 875 Ellicott Street, Buffalo, NY 14203, USA, Email: smahajan@buffalo.edu

Yashwant R. Mahajan Centre for Knowledge Management of Nanoscience and Technology, 12-5-32/8, Vijaypuri Colony, Tarnaka, Secunderabad 500017, Telangana, India, Email: mahajanyrm@gmail.com

Heidi M. Mansour The University of Arizona, College of Pharmacy, 1703 E. Mabel Street, Tucson, AZ 85721-0207, USA, Email: mansour@pharmacy.arizona.edu

Cécilia Ménard-Moyon CNRS, Institut de Biologie Moléculaire et Cellulaire, Laboratoire d'Immunopathologie et Chimie Thérapeutique (UPR 3572), 15 Rue René Descartes, 67084 Strasbourg, Cedex, France, E-mail: c.menard@ibmc-cnrs.unistra.fr

Andrew Owen Department of Molecular and Clinical Pharmacology, Institute of Translational Medicine, University of Liverpool, 70 Pembroke Place, Liverpool L69 3GF, UK, Email: aowen@liverpool.ac.uk

Dan Peer Laboratory of NanoMedicine, Britannia Building, 2nd Floor Room 226, Tel Aviv University, Tel Aviv 69978, Israel, Email: peer@tauex.tau.ac.il

Adriele Prina-Mello School of Medicine and Centre for Research on Adaptive, Nanostructures and Nanodevices, Institute of Molecular Medicine, Trinity College, Dublin D8, Ireland, Email: prinamea@tcd.ie

Víctor F. Puntes Inorganic Nanoparticles Group, Catalan Institute of Nanotechnology (ICN-2), 08193 Bellaterra, Barcelona, Spain, Email: victor.puntes.icn@gmail.com

Steve Rannard Department of Chemistry, University of Liverpool, Liverpool L697ZD, United Kingdom, Email: srannard@liv.ac.uk

Ruxana T. Sadikot Emory University School of Medicine, Section of Pulmonary and Critical Care Medicine, 201 Dowman Drive, Atlanta, GA 30322, USA, Email: ruxana.sadikot@emory.edu

Georgette B. Salieb-Beugelaar Nanomedicine Research Group, Clinic for Intensive Care Medicine, University Hospital Basel, Petersgraben 4, CH-4031 Basel, Switzerland, Email: beugelaar@swissnano.org

Krutika K. Sawant Pharmacy Department, Faculty of Technology and Engineering, The Maharaja Sayajirao University of Baroda, Kalabhavan, Vadodara 390001, Gujarat, India, Email: dr_krutikasawant@rediffmail.com

Marc Schneider Department of Pharmacy, Biopharmaceutics and Pharmaceutical Technology, Saarland University, Campus A4 1, D-66123 Saarbrucken, Germany, Email: marc.schneider@mx.uni-saarland.de

Ariel Sobarzo Department of Microbiology, Immunology and Genetics, Faculty of Health Sciences, Ben-Gurion University of the Negev, POB 653, Beer-Sheva 84105, Israel, Email: tautau.ariel@gmail.com

Srinivas Sridhar Department of Physics, Northeastern University, 435 Egan Research Center, 120 Forsyth Street, Boston, MA 02115, USA, Email: s.sridhar@neu.edu

Nicole F. Steinmetz Biomedical Engineering, Case Western Reserve University, School of Medicine, 10900 Euclid Avenue, Cleveland, OH 44106 USA, Email: nicole.steinmetz@case.edu

Melanie Swan MS Futures Group, PO Box 61258, Palo Alto, CA 94306, USA, Email: m@melanieswan.com

Takuya Tsuzuki Research School of Engineering, College of Engineering and Computer Science, Australian National University, Ian Ross Building 31, North Road, Canberra, ACT 0200, Australia, Email: takuya.tsuzuki@anu.edu.au

Melike Üner Istanbul University, Faculty of Pharmacy, Department of Pharmaceutical Technology, Beyazit 34116, Istanbul, Turkey, Email: unerm@istanbul.edu.tr

Suresh P. Vyas Drug Delivery Research Laboratory, Department of Pharmaceutical Sciences, Dr. H. S. Gour University, Sagar, MP 470003, India, Email: vyas_sp@rediffmail.com

Shu Wang Department of Nutritional Sciences, Texas Tech University, 1301 Akron Avenue, Lubbock, TX 79409-1270, USA, Email: shu.wang@ttu.edu

Andrew T. S. Wee Department of Physics, National University of Singapore, 2 Science Drive 3, Singapore 117542, Email: phyweets@nus.edu.sg

Miguel Weil Cell Screening Facility for Personalized Medicine, Laboratory for Neurodegenerative Diseases and Personalized Medicine, The George S. Wise Faculty of Life Sciences, Tel Aviv University, 69978 Ramat Aviv, Tel Aviv, Israel, Email: miguelw@tauex.tau.ac.il

Ulrich Wiesner Department of Materials Science and Engineering, Cornell University, 330 Bard Hall, Ithaca, NY 21047, USA, Email: ubw1@cornell.edu

Lijie Grace Zhang Department of Mechanical and Aerospace Engineering, The George Washington University, 800 22nd Street NW, 3590 Science and Engineering Hall, Washington, DC 20052, USA, Email: lgzhang@gwu.edu

Foreword

Major medical advances that emerged during the nineteenth and early twentieth century were based on either “bottom-up” or “top-down” type particle dimensions. In this regard, the importance of early pico/sub-nanoscale (i.e., 0.001–1 nm) elemental/small molecule “bottom-up” therapies is well known. Examples include therapies based on elemental mercury or arsenic compounds (i.e., treatment of syphilis), radium (i.e., cancer therapy) or nineteenth century pharma (i.e., antipyrine, quinine, aspirin, etc.). On the other hand, significant medical insights emerged concurrently with Louis Pasteur’s germ theory of disease (1862) that emphasized “top-down” type particle dimensions. Specifically, this theory emphasized that microbes such as bacteria possessed macro-/micron scale (i.e., micron to mm) dimensions and caused diseases. Additionally, in 1928, Alexander Fleming was the first to report the therapeutic benefits of controlling infection by the use of antibiotic molds (i.e., small-molecule penicillin). Until recent times however, very little attention has been devoted to the role of nano-sized (i.e., 1–1000 nm) particles and phenomena residing between these two upper and lower hierarchical extremes. Progress toward this new perspective first required critical insights into life sustaining nanoparticles (proteins, DNA, RNA) developed by Linus Pauling, Max Perutz et al. and Francis Crick/James Watson, respectively. Pioneering structural characterization, vaccines and insights developed by Alex Klug, Jonas Salk and others concerning life-threatening nanoparticles such as viruses clearly demonstrated the important role that “good and bad nanoparticles” could play in defining the human conditions of either *health* or *disease*. These pioneering scientists laid the groundwork for understanding life processes and, more importantly, the critical role that *nanometric* dimensions might play in future medical advancements. In fact, it was Linus Pauling’s deep insights into the nanoscale dimensions and dynamics of proteins (i.e., Hemoglobin) that undoubtedly allowed him to diagnose and propose the first rational therapies for sickle cell anemia as early as 1949. Pauling’s seminal work on sickle cell anemia may represent the very first example of nanomedicine in practice. That withstanding,

it was Richard Feynman's famous California Institute of Technology lecture in 1959 titled *"There is Plenty of Room at the Bottom"* that officially launched the present nanotechnology explosion/revolution. Since that time, the recognized impact of nanoscale complexity on biology and traditional medicine has grown dramatically as witnessed by an exponential increase in publications/patents, establishment of national/global scientific societies and the emergence of several mainstream journals/publishers—all focusing on the new emerging frontier of *nanomedicine* and *bionanotechnology.*

My earliest connections to nanomedicine began with industrial/academic activities (1990–2005) which focused on the use of abiotic, nanoscale particles called dendrimers for a variety of biological/medical applications. It was found that, by properly modifying these synthetic nanoparticles as a function of size, shape, surface chemistry, flexibility, architecture or composition, it was possible to selectively mimic, intervene, complex or control the *in vivo* inter/intracellular dynamics of many important biological nanoparticles such as proteins, DNA, and RNA with minimal cytotoxicity. These strategies provided some of the early working examples of rational *in vivo* protein mimicry, gene/viral complexation, immuno-diagnostics and targeted drug-delivery by design. Not only did these lead to many successful gene transfection, cardio-diagnostic, antiviral/bacterial and pending targeted drug-delivery products, but they also provided an unbridled personal optimism for the unlimited future possibilities expected in the field of nanomedicine.

It is from this broad perspective, that I have had the pleasure to review the *Handbook of Clinical Nanomedicine: Nanoparticles, Imaging, Therapy, and Clinical Applications*, which is the first in the series on clinical nanomedicine texts edited by Dr. Raj Bawa. The distinguished editors (Raj Bawa, PhD, Gerald F. Audette, PhD, and Israel Rubinstein, MD) have successfully organized critical contributions from an international team of experts into three important sections that constitute this handbook. Throughout all three sections, the editors and authors remain loyal to the handbook theme. They provide a systematic and rational coverage of major issues and challenges encountered in the progression of nanomedical concepts to working prototypes, clinical applications, nanodevices and imaging tools. More specifically, **Section I** provides a general introduction to nanomedicine, along with historical/

background information and ten, recent significant nanomedical advancements. The important chapter on nanotechnology nomenclature and definitional issues of nanotherapeutics highlights the fact that nanomedicines cannot be pigeonholed into any specific numerical range or dimension, especially in the context of drug delivery. **Section II** consists of a balanced discussion of several nanosystems, nanodevices and imaging tools including magnetic resonance imaging, atomic force microscopy, multi-modal imaging/diagnostics, *in vivo* imaging techniques, image-based analysis related to stem cells, and bacterial/viral nanomachines as tools for biomedicine. Of particular interest is the chapter on the first-in-human molecular targeting and cancer imaging via ultrasmall dual-modality C-dots. The inspirational story of C_{60} Buckminsterfullerene by Nobel Laureate Dr. Kroto reveals the unique perspectives of many scientists who made major contributions to its discovery. **Section III** overviews important clinical applications of nanotherapeutics for topical/transdermal delivery; targeted cancer and antiviral therapies; and inflammatory, cardiovascular, respiratory and neuronal diseases. Applications of bionanomaterials for orthopedics and dentistry are reflected in two excellent chapters. This section also provides suitable attention to more specialized topics such as nanolithography and biochips for viral detection, 3D nano/microfabrication techniques for tissue and organ regeneration, solutions to combat emerging superbugs, diagnostics of Ebola, HIV-specific immunotherapy, and nanoneurosurgery. A superb chapter on the first FDA-approved nanodrug product (Doxil®) by its inventor, Dr. Yechezkel (Chezy) Barenholz, is a fascinating read. The important chapter on the blockbuster MS drug, Copaxone®, by experts from Teva Pharmaceutical Industries, highlights the new era of biosimilars, nanosimilars and NBDCs.

The *Handbook* provides a well-edited, reader-friendly, multidisciplinary roadmap that clearly communicates essential nanomedical information in a style that is attractive to both the novice and expert. It offers the appropriate advice required to advance nanomedical innovations from the concept stage to working prototypes, clinical applications and, finally, to commercial reality. The diversity and expertise of the authors has produced a well-balanced, comprehensive reference resource which successfully bridges communication and terminology gaps often encountered in such multi-disciplinary efforts. As a result, the *Handbook* should be of interest to individuals from academia, industry and

government in fields ranging from medicine, biotechnology, drug development, pharmaceutical sciences, engineering, policy, FDA law and commercialization. This authoritative and comprehensive reference bridges the gap between basic biomedical research, engineering, medicine and law while providing a thorough understanding of nano's potential to address (i) medical problems from both the patient and health provider's perspective, and (ii) current applications and their potential in a healthcare setting. I view the *Handbook of Clinical Nanomedicine: Nanoparticles, Imaging, Therapy, and Clinical Applications* as an essential reference asset that should be invaluable to all who are interested in the explosive growth and future promise of this new emerging area.

Donald A. Tomalia, PhD
December 2015

Dr. Donald Tomalia received his Bachelor of Arts degree in chemistry from the University of Michigan and his PhD in physical organic chemistry from Michigan State University in 1968 while working at The Dow Chemical Company. In 1990, he moved to Michigan Molecular Institute as professor and director of Nanoscale Chemistry and Architecture. He has subsequently founded three dendrimer-based nanotechnology companies: Dendritech, Inc.; Dendritic Nanotechnologies, Inc.; and NanoSynthons LLC. Dr. Tomalia is currently director of the National Dendrimer & Nanotechnology Center, CEO/founder of NanoSynthons LLC, distinguished visiting professor at Columbia University, adjunct professor in the department of chemistry at the University of Pennsylvania and affiliate professor in the department of physics at Virginia Commonwealth University. He is famous for his discovery of dendrimers and has received several awards for his accomplishments and contributions to science, including the 2012 Wallace H. Carothers Award. He has authored over 250 publications and is the inventor or coinventor of 128 patents. He currently serves as an associate editor of the *Journal of Nanoparticle Research* (Springer); as member of the Executive Advisory Board of the European Foundation for Clinical Nanomedicine; and as a faculty member of Faculty 1000 Biology. In 2011, Dr. Tomalia was inducted into the Thomas Reuters Hall of Citation Laureates in Chemistry, a listing of the 40 most highly cited international scientists in the field of chemistry.

Small Is Beautiful
Preface by the Series Editor

Back in 2002, I presented on nanomedicine at the Canadian Space Agency, a few hours' drive from Montreal. The audience was primarily composed of materials scientists and engineers. After a few excellent questions from the audience, I realized that physical scientists and pharmaceutical scientists view the nanoworld quite differently and that there is tension between the two camps. This was back then, but the state of affairs is the same today, maybe even more profound. Since then, *nano* has become more sectorized, with nanomedicine[1] at the forefront along with nanoelectronics.[2]

[1]Nanomedicine, an offshoot of nanotechnology, may be defined as the science and technology of diagnosing, treating and preventing disease and improving human health via nano. This exciting and interdisciplinary *arena* is driven by collaborative research, patenting, commercialization, business development and technology transfer within diverse areas such as biomedical sciences, chemical engineering, biotechnology, physical sciences, and information technology. Optimists see nano as an enabling technology, a sort of next industrial revolution that could enhance the wealth and health of nations. They promise that at least within the medical sector of nano, nanodrugs will be a healthcare game-changer by offering patients access to personalized medicine. Pessimists, on the other hand, take a cautionary position, preaching instead a "go-slow" approach, pointing to a lack of sufficient scientific information on health risks and general failure on the part of regulatory agencies and patent offices. As usual, the reality is somewhere between such extremes. Whatever your stance, nano has already permeated virtually every sector of the global economy, with potential applications consistently inching their way into the marketplace. Nano continues to evolve and play a pivotal role in various industry segments, spurring new directions in research and development and translational efforts.

[2]The prefix "nano" in the SI measurement system denotes 10^{-9} or one-billionth. There is no firm consensus over whether the prefix "nano" is Greek or Latin. While the term "nano" is often linked to the Greek word for "dwarf," the ancient Greek word for "dwarf" is actually spelled "nanno" (with a double "n") while the Latin word for dwarf is "nanus" (with a single "n"). While a nanometer refers to one-billionth of a meter in size (10^{-9} m = 1 nm), a nanosecond refers to one billionth of a second (10^{-9} s = 1 ns), a nanoliter refers to one billionth of a liter (10^{-9} l = 1 nl) and a nanogram refers to one billionth of a gram (10^{-9} g = 1 ng). The diameter of an atom ranges from about 0.1 to 0.5 nm. Some other interesting comparisons: fingernails grow around a nanometer/second; in the time it takes to pick a razor up and bring it to your face, the beard will have grown a nanometer; a single nanometer is how much the Himalayas rise in every 6.3 seconds; a sheet of newspaper is about 100,000 nanometers thick; it takes 20,000,000 nanoseconds (50 times per second) for a hummingbird to flap its wings once; a single drop of water is ~50,000 nanoliters; a grain of table salt weighs ~50,000 nanograms.

However, there is still a clear need for "true" interdisciplinarity because of the different approaches of physical scientists versus pharmaceutical scientists with respect to generation, examination, analysis and discussion of nanomedicine data. I have been extremely cognizant of this fact as I have developed this book series so that *everyone* finds it relevant and useful.

Each stand-alone volume in this series is focused broadly on nanomedicine, pharma and various branches of medicine. It is essential reading for both the novice and the expert in fields ranging from medicine, pharmaceutical sciences, biotechnology, immunology, engineering, FDA law, intellectual property, policy, future studies, ethics, licensing, commercialization, risk analysis and toxicology. Each volume is intended to serve as a useful reference resource for professionals but also to provide supplementary readings for advanced courses for graduate students and medical fellows. Diversity within the broad and evolving arena of nanomedicine is reflected in the expertise of the distinguished contributing authors. All chapters contain key words, figures in full-color and an extensive list of references. As compared to other books on the market, each volume in the series is comprehensive, truly multidisciplinary and intended to be a stand-alone reference resource—all presented in an easily accessible, user-friendly format. The editors have skillfully curated each chapter to reflect the most relevant and current information possible. The range of topics covered in each volume as well as the interdisciplinary approach of the volumes will attract a global audience and serve as a definitive resource, reference and teaching supplement. My purpose in *constructing* each volume is to provide chapters that give the reader a better understanding of the subject matter presented therein but also to provoke reflection, discussion and catalyze collaborations between the diverse stakeholders. Each volume is essentially a guided tour of critical topics and issues that should arouse the reader's curiosity so that they will engage more profoundly with the broader theme reflected.

Since 2002, I have been involved in almost all aspects of nanoscience, nanomedicine and nanotechnology—patent prosecution, teaching, research, FDA regulatory filings, conference organizer and speaker. I have intimately seen the evolution of nanomedicine. I have cheered on the cutting-edge discoveries and inventions but also stood up to criticize inept governmental regulatory policies, spotty patent examination at patent offices, hyped-up press

releases from eminent university labs and inaccurate depiction of nano by the press and politicians.[3]

While the nano die was cast long ago, it is well entrenched now and there is no turning back. Although the air may be thick with news of nano-breakthroughs and a hot topic for discussion in industry, pharma, patent offices and regulatory agencies, the average citizen on the street knows very little about what constitutes a nanoproduct, a nanomaterial or a nanodrug. This was apparent to me early on when the CBS station in Albany, NY, while interviewing me for a story on nanotechnology, approached people on the street and asked them to define nano. To my amazement, not a single person could come up with a description of the term. At the time, I was well aware that there were close to two thousand marketed products that incorporated nano in some fashion. This issue persists. Mind you, these interviews were taking place a few blocks from the massive, world-class education and research complex comprising Albany Nanotech (now SUNY Polytechnic Institute's Colleges of Nanoscale Science and Engineering), where billions have been invested each year since the early 1990s. Recognizing that the so-called "nanorevolution" will have limited impact unless all stakeholders, especially the public, are fully on board, I immediately initiated an annual nano-conference that continues to this day. The conference is free to all attendees and for the first dozen years was held at Rensselaer Polytechnic Institute in Troy, NY, while the most recent one was held this fall at Albany College of Pharmacy and Health Sciences in Albany, NY.

Louis Pasteur famously said: *"Science knows no country, because knowledge belongs to humanity, and is the torch which illuminates the world. Science is the highest personification of the nation because that nation will remain the first which carries the furthest the works of thought and intelligence."* Perhaps, nothing is truer in this regard than nanoscience, nanotechnology and nanomedicine. However, we are in a rapidly changing, globalized world—politically, economically, societally, environmentally and technologically. At the present time in our history, national boundaries are rendered artificial or eroding,

[3]Too often though, start-ups, academia and companies exaggerate basic research developments as potentially revolutionary advances and claim these early-stage discoveries as confirmation of downstream novel products and applications to come. Nanotechnology's potential benefits are frequently overstated or inferred to be very close to application when clear bottlenecks to commercial translation exist. Many have desperately tagged or thrown around the "nano" prefix to suit their purpose, whether it is for federal research funding, patent approval of the supposedly novel technologies, raising venture capital funds, running for office or seeking publication of a journal article.

there are few true leaders on the global stage, the world power dynamics are shifting and the outdated bureaucratic structures firmly in place are unable to deal effectively with the emerging knowledge economy. These changes are also causing a certain degree of chaos in the world of *nano*. From my perspective, there is a combination of excitement, potential, confusion, hype, and misinformation in this regard—all of this seen more than in other fields when they were evolving. It is true that in the heady days of any new, emerging technology, definitions tend to abound and are only gradually documented via reports, journals, books and dictionaries. Ultimately, standard-setting organizations like the International Organization for Standardization (ISO) and American Society for Testing and Materials (ASTM) International produce technical specifications. This evolution is typical and essential as the development of terminology is a prerequisite for creating a common language needed for effective communication in any field. Clearly, a similar need for an internationally agreed definition for key terms like nanotechnology, nanoscience, nanomedicine, nanobiotechnology, nanodrug, nanotherapeutic, nanopharmaceutical and nanomaterial, has gained urgency.[4] Nomenclature, technical specifications, standards, guidelines and best practices are critically needed to advance nanotechnologies in a safe and responsible manner. Contrary to some commentators, terminology does matter because it prevents misinterpretation and confusion. It is essential for research activities, harmonized regulatory governance, accurate patent searching and prosecution, standardization of procedures, manufacturing and quality control, assay protocols, decisions by granting agencies, effective review by policymakers, ethical analysis, public dialogue, safety assessment, and more. Also, nomenclature is critical to any translational and commercialization efforts. All definitions of nanotechnology based on size or dimensions must be dismissed, especially in the context of medicine and pharmaceutical science, for the reasons elaborated in chapter 6 of this volume.[5]

[4]Similar disagreements over terminology and nomenclature are seen in other fields as well. For example, the term "super resolution microscopy," the subject of the 2014 Nobel Prize, is considered an inaccurate description of the technique.

[5]Nanoscale therapeutics may have unique properties (nanocharacter) that can be beneficial for drug delivery but there is no specific size or dimensional limit where superior properties reside. Hence, a size limitation below 100 nm cannot be touted as the basis of novel properties of nanotherapeutics. In fact, properties other than size can also have a dramatic effect on the nanocharacter of nanodrugs: shape/geometry, zeta potential, specific nanomaterial class employed, composition, delivery route, crystallinity, aspect ratio, surface charge, etc. See: Bawa, R. (2016). What's in

Viable *sui generis* definition of nano having a bright-line size range as applied to nanodrugs blurs with respect to what is truly nanoscale; it is unnecessary, misleading, and in fact, may never be feasible. Since the 100 nm boundary has no solid scientific or legal basis, this series will avoid using the inaccurate and random sub-100 nm definition of nano.[6]

The volumes in this series will extensively cover advances in drug delivery[7] as this is leading all developments in nanomedicine. The following points serve to highlight the major impact of nanoscale drug delivery systems:

- Novel nanodrugs and nanocarriers are being developed that address fundamental problems of traditional drugs because of the ability of these compounds to overcome poor water solubility issues, alter unacceptable toxicity profiles, enhance bioavailability, and improve physical/chemical stability. Additionally, via tagging with targeting ligands, these nanodrug formulations can serve as innovative drug delivery systems for enhanced cellular uptake or localization of therapeutics into tissues of interest (i.e., site-specific targeted delivery).

---

a name? Defining "nano" in the context of drug delivery. In: Bawa, R., Audette, G. and Rubinstein, I. eds. *Handbook of Clinical Nanomedicine: Nanoparticles, Imaging, Therapy, and Clinical Applications*, Chapter 6, Pan Stanford Publishing, Singapore.

[6]Definitions along these lines will instead be employed in this book series: *The design, characterization, production, and application of structures, devices, and systems by controlled manipulation of size and shape at the nanometer scale (atomic, molecular, and macromolecular scale) that produces structures, devices, and systems with at least one novel/superior characteristic or property."* See: Bawa, R. (2007). Patents and nanomedicine. *Nanomedicine (London),* **2**(3), 351–374.

[7]Although numerous nanodrugs have been routinely used in medicinal products for decades without any focus or even awareness of their nanocharacter, it is only within the past two decades that they have been highlighted due to their potential of revolutionizing drug delivery. Obviously, the Holy Grail of any drug delivery system is to deliver the correct dose of a particular active agent to a specific disease or tissue site within the body while simultaneously minimizing toxic side effects and optimizing therapeutic benefit. This is often not achievable via conventional drugs. However, the potential to do so may be greater now via engineered nanodrugs. Often, nanodrugs transport active agents to their target binding sites (ligands, receptors, active sites, etc.) to impart maximum therapeutic activity with maximum safety (i.e., protect the body from adverse reactions) while preventing the degradation/denaturation/inactivation of the active agent during delivery/transit. Targeting can be achieved or enhanced by (i) linking specific ligands or molecules (e.g., antibodies, glycoproteins, etc.) to the carrier, or (ii) by altering the surface characteristics of the carrier. Furthermore, therapeutics that have side effects due to triggering an immune response (e.g., complement activation) or cleared by the reticuloendothelial (RES) system can be entrapped, encapsulated or embedded within a nanoparticle coat or matrix.

Various FDA-approved liposomal, solid nanoparticle-based, antibody-drug conjugate (ADC) and polymer-drug conjugate delivery platforms overcome associated issues such as (i) low solubility (Abraxane), (ii) extremely high drug toxicity (Brentuximab vedotin and Trastuzumab emtansine), and (iii) side effects related to high doses of free drug (Doxil, Marqibo, DaunoXome).

- Reformulation of old, shelved therapeutics into nanosized dosage forms could offer the possibility of adding new life to old therapeutic compounds. Classic examples include drugs developed as nanocrystalline products (Rapamune, Emend, Triglide).
- Coupled with advances in pharmacogenomics, smart nanomachines, information technology and personalized medicine, upcoming innovations in nanomedicine may even generate multifunctional entities enabling simultaneous diagnosis, delivery and monitoring of APIs.

Emerging technologies are particularly problematic for governmental regulatory agencies, given their independent nature, slow response rate, significant inertia and a general mistrust of industry. Major global regulatory systems, bodies and regimes regarding nanomedicines are not fully mature, hampered in part by a lack of specific protocols for preclinical development and characterization. Additionally, in spite of numerous harmonization talks and meetings, there is a lack of consensus on the different procedures, assays and protocols to be employed during pre-clinical development and characterization of nanomedicines. On the other hand, there is a rise of diverse nanospecific regulatory arrangements and systems, contributing to a dense global regulatory landscape, full of gaps and devoid of central coordination. It is often observed that governmental regulatory bodies lack technical and scientific knowledge to support risk-based regulation, thereby leaving a significant regulatory void. In fact, the “baby steps” undertaken by the FDA over the past decade have led to regulatory uncertainty. There are potentially serious and inhibitory consequences if nanomedicine is overregulated. A balanced approach is required here, at least on a case-by-case basis, which addresses the needs of commercialization against mitigation of inadvertent harm to patients or the environment. Obviously, not everything “nanomedical” needs to be regulated. However, more is clearly needed from regulatory agencies like the FDA and EMA

than a stream of guidance documents that are generally in draft format, position papers that lack any legal implication, presentations that fail to identify key regulatory issues and policy papers that are often short on specifics. There is a very real need for regulatory guidelines that follow a science-based approach (not policy-based) that are responsive to the associated shifts in knowledge and risks. Other critically important and interrelated regulatory law themes that will permeate this series include transnational regulatory harmonization, FDA law, generic biowaivers, nanosimilars, combination products (nanotheranostics) and non-biologic complex drugs (NBCDs).

Let me highlight the translational issues and efforts pertaining to nanomedical products by using the classic example of drug R&D. Creating drugs today is time-consuming, expensive and enormously challenging. *De novo* drug discovery and development is a 10-17 year process from idea to marketed drug. It may take up to a decade for a drug candidate to enter clinical trials with less than 10% of the tested candidates in trials reaching the market. In fact, more drugs come off patent each year than approved by the FDA. According to a 2014 study by the Tufts Center for the Study of Drug Development, developing a new prescription medicine that gains marketing approval is estimated to cost nearly $2.6 billion. It is clear to everyone that in the past decade, great strides have been made in basic science and research. This is obviously critical to any advanced society. However, the enormous medical advances that should have come from the large public investment in biomedical research are largely absent from a translation point-of-view. All stakeholders—pharma, patients, academia, NIH—have suffered and are to blame for the valley of death. Each needs to re-examine their role and become an active, full partner in the drug development ecosystem so that translation is more robust. Similarly, although great strides have been made in nanomedicine generally at the "science" level, especially with respect to drug delivery and imaging, it continues to be dogged by challenges and bottlenecks at the "translational" level. In pharma, translational research involves the many elements that contribute to the successful conversion of an idea into a drug. Translation of drug products is a challenge faced by pharma at various levels. Bridging the chasm between *drug discovery research activities* and the *successful translation of a drug to the market* is a daunting task that requires varying degree of participation from key stakeholders—

pharma, academia, nonprofit and for-profit institutions, federal agencies and regulatory bodies, diseases foundations and patients. So far, the process of converting basic research in nanomedicine into commercially viable products has been difficult. Securing valid, defensible patent protection from the patent offices along with clearer regulatory/safety guidelines from regulatory agencies is critical to commercialization. This has been a mixed bag at best and much more is warranted. If translation of nanomedicine is to be a stellar success, it is important that some order, central coordination and uniformity be introduced at the transnational level. It is true that this decade has witnessed relatively more advances and product development in nanomedicine than the previous. In this context, many point to the influence of nanomedicine on the pharmaceutical, device and biotechnology industries. One can now say that R&D is in full swing and novel nanomedical products are starting to arrive in the marketplace. It is hoped that nanomedicine will eventually blossom into a robust industry. We will have to see whether there will be giant technological leaps (that can leave giant scientific, ethical and regulatory gaps) or paradigm-shifting advances (that necessitate extraordinary proof and verification). In the meantime, tempered expectations are in order.

Key players must come together on a global platform to address some of these crucial issues impacting effective translational efforts. It is important that the public's desire for novel nanomedical products, venture community's modest investment, federal infusion of funds and big pharma's lingering interest in nanomedicine continues. In the end, the long-term prognosis and development of nanomedicine will hinge on effective nanogovernance, issuance of valid patents, clearer safety guidelines, public transparency and full commitment of all the key stakeholders involved—big pharma, academia, governmental regulatory agencies, policy-makers, the venture community and the consumer-patient. Together, these stakeholders can help drive progress and make the future happen faster. Science fiction may become science fact. Not only is this possible, but it *will* happen. *The Times They Are a-Changin*'.

Raj Bawa, MS, PhD
Ashburn, Virginia, USA
December 22, 2015

Acknowledgements

Richard J. Apley, Litman Law Offices/Becker & Poliakoff, Washington, DC, USA

Lajos P. Balogh, AA Nanomedicine & Nanotechnology Consulting, North Andover, MA, USA

Yechezkel (Chezy) Barenholz, Hebrew University-Hadassah Medical School, Israel

S. R. Bawa, Bawa Biotech LLC, Schenectady, New York, USA

Sangita Bawa, Novo Nordisk Inc., Princeton, New Jersey, USA

Nancy A. Blair-DeLeon, Institute of Electrical and Electronics Engineers, New York, New York, USA

Sara Brenner, SUNY Polytechnic Institute, Albany, New York, USA

Stanford Chong, Pan Stanford Publishing Pte. Ltd., Singapore

Jill B. Conner, Teva Pharmaceutical Industries, Ltd., Overland Park, Kansas, USA

Jay K. Doshi, Family Dental Care, Spring, Texas, USA

Kamal C. Doshi, Shared Towers VA LLC, McLean, Virginia, USA

Eileen S. Ewing, American Bar Association, Chicago, USA

Howard E. Gendelman, University of Nebraska Medical Center, Omaha, Nebraska, USA

Harvinder Ghumman, Inova Health System, Reston, Virginia, USA

Susan P. Gilbert, Rensselaer Polytechnic Institute, Troy, New York, USA

Paulette Goldweber, John Wiley & Sons, Inc., Hoboken, New Jersey, USA

Neil Gordon, Guanine Inc., Montreal, Quebec, Canada

Drew Harris, Nanotechnology Law & Business, Austin, Texas, USA

Jim Hurd, NanoScience Exchange, San Francisco, California, USA

Meghana Kamath Hemphill, John Wiley & Sons, Inc., Hoboken, New Jersey, USA

Arvind Kanswal, Pan Stanford Publishing Pte. Ltd., Singapore

Francesca Lake, Future Medicine Ltd., London, UK

Gregory Lanza, Washington University Medical School, Saint Louis, Missouri, USA

Gregory N. Mandel, Temple University Beasley School of Law, Philadelphia, Pennsylvania, USA

Rajesh Mehra, Chantilly Family Practice Center, Chantilly, Virginia, USA

Lucinda Miller, Northern Virginia Community College, Annandale, Virginia, USA

Shaker A. Mousa, Albany College of Pharmacy and Health Sciences, Albany, New York, USA

Stefan Muhlenbach, Vifor Pharma, Ltd. and University of Basel, Switzerland

J. Michael Nicholas, Teva Pharmaceutical Industries, Ltd., Overland Park, Kansas, USA

Thurman K. Page, (formerly of) US Patent & Trademark Office, Alexandria, Virginia, USA

Michael Slaughter, CRC Press/Taylor & Francis Group, Boca Raton, Florida, USA

Gert Storm, Utrecht University, Utrecht, Netherlands

Robin Taylor, University of Nebraska Medical Center, Omaha, Nebraska, USA

Mary A. Vander Maten, Northern Virginia Community College, Annandale, Virginia, USA

Thomas J. Webster, Northeastern University, Boston, Massachusetts, USA

Vera Weinstein, Teva Pharmaceutical Industries, Ltd., Netanya, Israel

Tracy Wold, Morton Publishing, Englewood, Colorado, USA

Section I

General Introduction and Beginnings

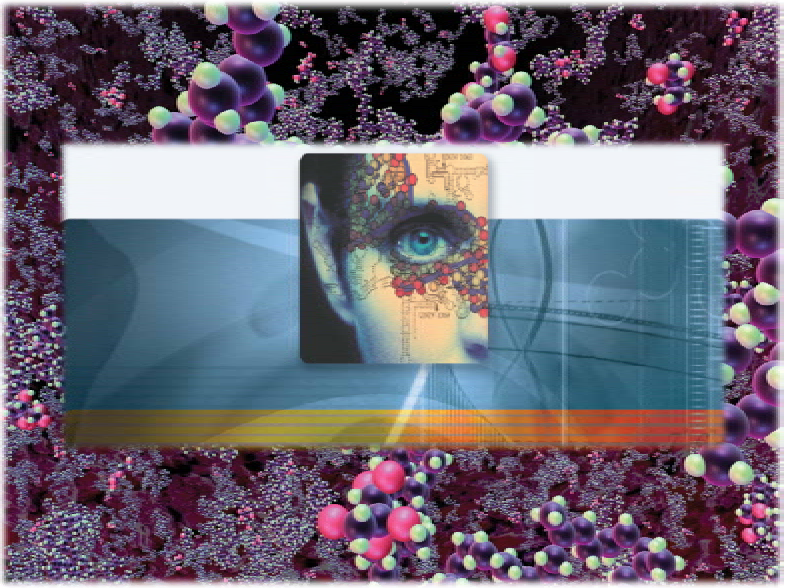

Chapter 1

Science at the Nanoscale: Introduction and Historical Perspective

Chin Wee Shong, PhD,[a] Sow Chorng Haur, PhD,[b] and Andrew T. S. Wee, PhD[b]

[a]*Department of Chemistry, National University of Singapore, Singapore*
[b]*Department of Physics, National University of Singapore, Singapore*

Keywords: nanoscale, carbon nanotubes, bionanotechnology, lithography, molecular electronics, miniaturisation, atomic force microscope, scanning probe microscope, scanning tunnelling microscopy, fullerenes, spintronics

1.1 The Development of Nanoscale Science

The prefix *nano* comes from the Greek word for *dwarf,* and hence *nanoscience* (the commonly used term nowadays for nanoscale science) deals with the study of atoms, molecules and nanoscale particles, in a world that is measured in nanometres (billionths of a metre or 10^{-9}, see Section 1.2). The development of nanoscience can be traced to the time of the Greeks and Democritus in 5th century B.C., when people thought that matter could be broken down to an indestructible basic component of matter, which scientists now call *atoms.* Scientists have since discovered the

Handbook of Clinical Nanomedicine: Nanoparticles, Imaging, Therapy, and Clinical Applications
Edited by Raj Bawa, Gerald F. Audette, and Israel Rubinstein

ISBN 978-981-4669-20-7 (Hardcover), 978-981-4669-21-4 (eBook)
www.panstanford.com

whole periodic table of different atoms (elements) along with their many *isotopes.* The 20th century A.D. saw the birth of nuclear and particle physics that brought the discoveries of *sub-atomic particles,* entities that are even smaller than atoms, including *quarks, leptons,* etc. But these are well below the nanometre length scale and therefore not included in the history of nanoscale science and technology.

The beginnings and developments of *nanotechnology,* the application of nanoscience, are unclear. The first nanotechnologists may have been medieval glass workers using medieval forges, although the glaziers naturally did not understand why what they did to gold made so many different colours. The process of nanofabrication, specifically in the production of gold nanodots, was used by Victorian and medieval churches which are famed for their beautiful stained glass windows. The same process is used for various glazes found on ancient, antique glazes. The colour in these antiques depends on their nanoscale characteristics that are quite unlike microscale characteristics.

The modern origins of nanotechnology are commonly attributed to Nobelist Dr. Richard Feynman, who on December 29, 1959, at the annual meeting of the American Physical Society at Caltech, delivered his now classic talk *"There's Plenty of Room at the Bottom"* [1]. He described the possibility of putting a tiny "mechanical surgeon" inside the blood vessel that could locate and do corrective localized surgery. He also highlighted a number of interesting problems that arise due to miniaturisation since "all things do not simply scale down in proportion". Nanoscale materials stick together by molecular van der Waals attractions. Atoms also do not behave like classical objects, for they satisfy the laws of quantum mechanics. He said, "... as we go down and fiddle around with the atoms down there, we are working with different laws, and we can expect to do different things." Feynman said he was inspired by biological phenomena in which "chemical forces are used in repetitious fashion to produce all kinds of weird effects (one of which is the author)". He predicted that the principles of physics should allow the possibility of manoeuvring things atom by atom.

Feynman described such atomic scale fabrication as a *bottom-up* approach, as opposed to the *top-down* approach that is

commonly used in manufacturing, for example in silicon integrated circuit (IC) fabrication whereby tiny transistors are built up and connected in complex circuits starting from a bare silicon wafer. Such top-down methods in wafer fabrication involve processes such as thin film deposition, lithography (patterning by light using masks), etching, and so on. Using such methods, we have been able to fabricate a remarkable variety of electronics devices and machinery. However, even though we can fabricate feature sizes below 100 nanometres using this approach, the ultimate sizes at which we can make these devices are severely limited by the physical laws governing these techniques, such as the wavelength of light and etch reaction chemistry.

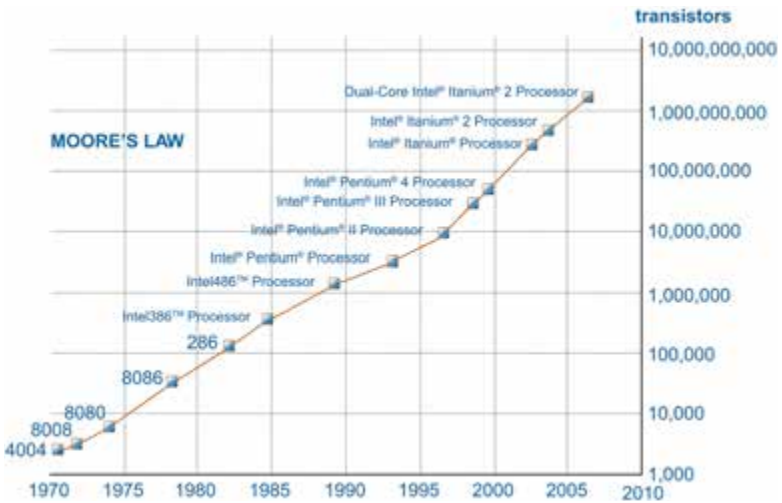

Figure 1.1 Moore's law predicts rapid miniaturization of ICs. Reprinted with permission from Intel Corporation © Copyright Intel Corporation.

Figure 1.1 shows that the trend in miniaturisation of ICs will ultimately be limited by quantum mechanics, certainly at scales larger than atoms and molecules. Gordon Moore, co-founder of Intel, made the observation in 1965 (now known as "Moore's law") that the number of transistors per square inch on integrated circuits had doubled every year since the integrated circuit was invented. Whilst this trend in IC miniaturisation has more or less been obeyed until now, the current CMOS technology will hit a

"wall" soon as quantum and ballistic electron effects become dominant. The most optimistic proponents of ICs believe that major innovations will be required to reach the ultimate operating limit of the silicon transistor: a length for functional features around 10 nm, or about 30 atoms long.

Bottom-up manufacturing, on the other hand, could provide components made of single molecules, which are held together by covalent forces that are far stronger than the forces that hold together macro-scale components. Furthermore, the amount of information that could be stored in devices built from the bottom-up would be enormous.

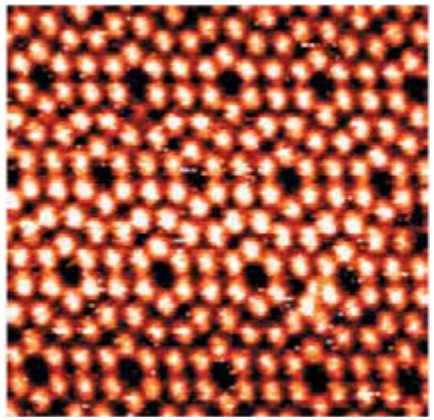

Figure 1.2 STM image of the Si(111)-7×7 reconstructed surface showing atomic scale resolution of the top-most layer of silicon atoms.

Since Feynman's early visionary ideas on nanotechnology, there was little progress until in 1981 when a new type of microscope, the scanning tunnelling microscope (STM), was invented by a group at IBM Zurich Research Laboratory [2]. The STM uses a sharp tip that moves so close to a conductive surface that the electron wavefunctions of the atoms in the tip overlap with the surface atom wavefunctions. When a voltage is applied, electrons "tunnel" through the vacuum gap from the foremost atom of the tip into the surface (or *vice versa*). In 1983, the group published the first STM image of the Si(111)-7×7 reconstructed surface, which nowadays can be routinely imaged as shown in Fig. 1.2 [3]. In 1986, Gerd Binnig and Heinrich Rohrer shared the Nobel Prize in Physics "for their design of the scanning tunneling microscope".

This invention led to the development of the atomic force microscope (AFM) and a whole range of related scanning probe microscopes (SPM), which are the instruments of choice for nanotechnology researchers today.

At around the same time in 1985, Dr. Robert Curl, Dr. Harold Kroto and Dr. Richard Smalley made the completely unexpected discovery that carbon can also exist in the form of very stable spheres, which they named fullerenes (or *buckyballs*) [4]. The carbon balls with chemical formulae C_{60} or C_{70} are formed when graphite is evaporated in an inert atmosphere (Fig. 1.3). A new carbon chemistry has developed from this discovery, and it is now possible to enclose metal atoms in them, and to create new organic compounds. Not long after in 1991, Iijima et al. reported Transmission Electron Microscopy (TEM) observations of hollow graphitic tubes or carbon nanotubes (Fig. 1.3), which form another member of the fullerene structural family [5]. The strength and flexibility of carbon nanotubes makes them potentially useful in many nanotechnology applications. Carbon nanotubes are now used as composite fibres in polymers and concrete to improve the mechanical, thermal and electrical properties of the bulk product. They also have potential applications as field emitters, energy storage materials, molecular electronics components, and so on. Some important events in the historical development of nanoscience and nanotechnology are summarised in Table 1.1.

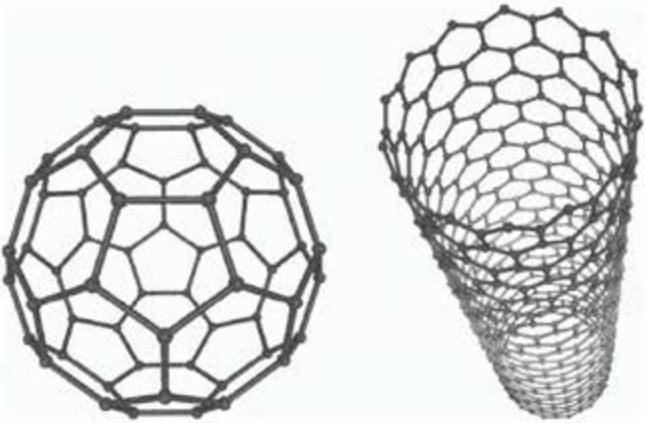

Figure 1.3 Schematic of a C_{60} buckyball (left) and carbon nanotube (right).

Table 1.1 Some important events in the historical development of nanoscience and nanotechnology

5th Century B.C.	Democritus and Leucippus, determined that matter was made up of tiny, indivisible particles in constant motion.
1803	English chemist and physicist, John Dalton (1766–1844), developed the first useful atomic theory of matter.
1897	Cambridge physicist J. J. Thomson (1856–1940), proposed that the mysterious cathode rays were streams of particles (later became known as electrons) much smaller than atoms.
1911	Thomson's student, Ernest Rutherford, determined there was a centre of the atom, now known as the nucleus, and electrons revolved around the nucleus.
1914	Swedish physicist Niels Bohr, advanced atomic theory further in discovering that electrons travelled around the nucleus in fixed energy levels.
1959	Feynman gives after-dinner talk describing molecular machines building with atomic precision.
1974	Taniguchi uses term "nano-technology" in paper on ion-sputter machining.
1977	Drexler originates molecular nanotechnology concepts at MIT.
1981	Scanning tunnelling microscopy (STM) invented by Gerd Binnig and Heinrich Rohrer at IBM Zurich.
1985	Buckyball discovered by Robert Curl, Harold Kroto and Richard Smalley.
1986	Atomic Force Microscopy (AFM) invented by Binnig, Quate and Gerber.
1989	IBM logo spelled in individual atoms by Don Eigler at IBM Almaden.
1990	*Nanotechnology:* First nanotechnology journal by Institute of Physics UK.
1991	Carbon nanotube discovered by Iijima at NEC, Japan.
1993	First Feynman Prize in Nanotechnology awarded.
1997	First nanotechnology company founded: Zyvex.
2000	President Clinton announces US National Nanotechnology Initiative.

In summary, the key events in the short history of modern nanotechnology may be described as follows: The vision of nanotechnology was first popularised by Feynman in 1959, when he outlined the prospects for atomic-scale engineering. In 1981, Binnig and Rohrer invented the *scanning tunnelling microscopy*, which enabled scientists to "see" and manipulate atoms for the first time. Corresponding advancements in *supramolecular chemistry,* particularly the discovery of the buckminsterfullerenes (or buckyballs) by Curl, Kroto and Smalley gave scientists a whole class of nanoscale building blocks with which to construct a whole range of nanostructures.

1.2 The Nanoscale

To start off our discussion on the nanoscale, we first refer to the metric system. The following table gives a summary of the metric system.

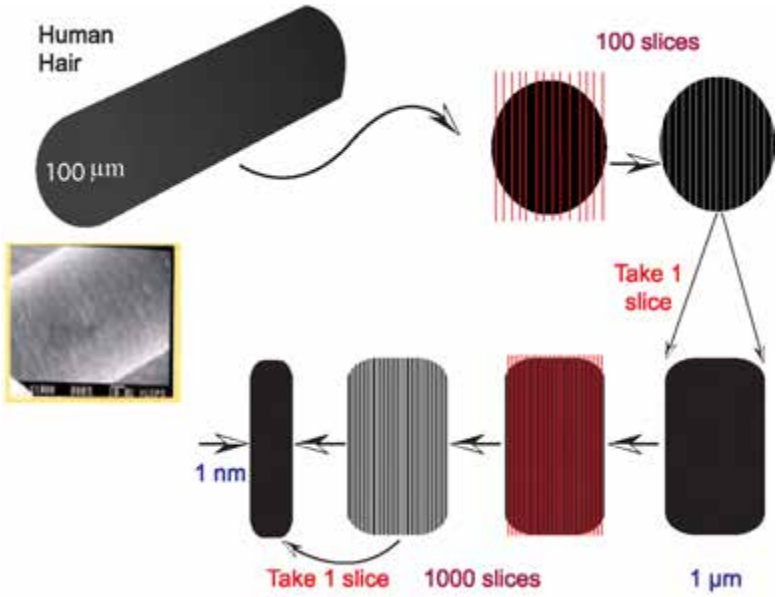

Figure 1.4 Schematic showing systematic cutting down of the cross section of a human hair.

Sometimes it is difficult to appreciate the smallness of the nanoscale. It is thus useful to relate the size scale to items that we commonly find in our home. For example, imagine you take a single strand of human hair. The cross section of a human hair is circular in shape (let us assume to be 100 μm in diameter), and imagine you have a very sharp knife. Use the knife to slice the cross section of the human hair into 100 slices with equal width. After which take out one of the 100 slices and use yet another sharp knife to cut the cross section of that single slice into 1000 slices, again with uniform width. If one takes out one of the 1000 slices, the width of the single strip is equal to 1 nanometre!!! The above hypothetical process is illustrated in Fig. 1.4. This is an extremely small size scale and yet there are a lot of fascinating phenomena for us to discover.

Table 1.2 shows the metric system units, symbols and prefixes relevant to the nanoscale, as well as representative objects at each size scale. Figure 1.5 shows images representing different size scales from one nanometre to one metre.

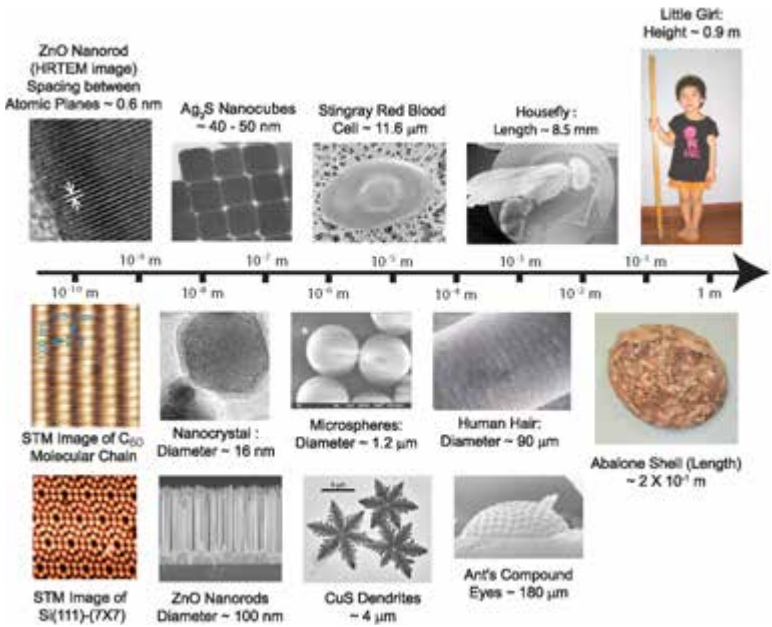

Figure 1.5 Scale of things.

Table 1.2 Metric system units, symbols and prefix

Yotta-	Ym	10^{24}	1,000,000,000,000,000,000,000,000	The Great Wall, a network of galaxies has a length of 4.7 Ym and a width of 1.8 Ym.
Zetta-	Zm	10^{21}	1,000,000,000,000,000,000,000	Mean diameter of the Andromeda Galaxy is 200,000 light years. That is about 2 × 2 Zm.
Exa-	Em	10^{18}	1,000,000,000,000,000,000	The distance from the Sun to the galactic centre is now estimated at 26,000 light-years ~ 246 Em.
Peta-	Pm	10^{15}	1,000,000,000,000,000	Distance to our nearest star is about 4.3 light years ~40 Pm.
Tera-	Tm	10^{12}	1,000,000,000,000	The size of our solar system is about 12×10^{12} m.
Giga-	Gm	10^{9}	1,000,000,000	Diameter of Sun is about 1.4×10^{9} m.
Mega-	Mm	10^{6}	1,000,000	The total length of The Great Wall of China is about 5×10^{6} m.
kilo	km	10^{3}	1,000	Size of Singapore is about 42 km × 23 km.
hecto	hm	10^{2}	100	Height of the Great Pyramid of Giza is about 140 m.
deka	dam	10^{1}	10	Length of a type of dinosaur (Apatosorus) ~20 m.
metre	m	10^{0}	1	Height of a 7-year-old child.
deci	dm	10^{-1}	1/10	Size of our palm.
centi	cm	10^{-2}	1/100	Length of a bee.
milli	mm	10^{-3}	1/1,000	Thickness of ordinary paperclip.
micro	μm	10^{-6}	1/1,000,000	Size of typical dust particles.
nano	nm	10^{-9}	1/1,000,000,000	The diameter of a C_{60} molecule is about 1 nm.
pico	pm	10^{-12}	1/1,000,000,000,000	Atomic radius of a Hydrogen Atom is about 23 pm.

Table 1.2 (*Continued*)

femto	fm	10^{-15}	1/1,000,000,000,000,000	Size of a typical nucleus of an atom is 10 femtometres.
atto	am	10^{-18}	1/1,000,000,000,000,000,000	Estimated size of an electron.
zepto	zm	10^{-21}	1/1,000,000,000,000,000,000,000	Really small.
yocto	ym	10^{-24}	1/1,000,000,000,000,000,000,000,000	Really really small.

If one poses a question, how small is a nanometre? Here are some interesting answers:

(1) the diameter of the C_{60} buckyball molecule
(2) half as wide as a DNA molecule
(3) 2 times the diameter of a rubidium atom
(4) 10 times the diameter of a hydrogen atom
(5) The de Broglie wavelength of an electron with an energy of 1.5 eV
(6) how much your fingernails grow each second
(7) how much the Himalayas rise in every 6.3 seconds
(8) the thickness of a drop of water spread over a square metre

1.3 Examples of Interesting Nanoscience Applications

(a) Bionanotechnology One of the most exciting areas of applications of nanotechnology must be in the field of biomedical healthcare and disease treatment. The story of tiny "nanobots" acting as *miniaturised doctors* entering our body to repair damaged cells and to kill foreign bacteria alike is certainly not unheard of to many people. While this remains science fiction in many aspects till today, nobody can say for sure that it will never come to pass in the future.

A more promising application of bionanotechnology that has attracted much interest from researchers and industries is the development of nano-drug delivery systems. In our modern busy lifestyle, administration of drugs has progressed from the teaspoon to time-release capsules or implants. Nanotechnology promises delivery mechanisms that can administer drugs at desired rates and at the exact location in the body. This requires the fabrication of precise nanostructures for drug-eluting coatings, membranes,

or even implants. For example, researchers at the University of California, San Francisco have demonstrated how they can use nanotubes made from biocompatible metal oxides to hold therapeutic drugs and deliver these agents in a highly-controlled manner [6]. On the other hand, the dendrimer, a highly branched polymer, has also been investigated by many as a natural form of nanoparticle carrying myriad sites for drug loading. All these developments not only translate to time-saving and better treatments, they also help avoid side effects caused by large doses taken orally or by injection. There are also the potential benefits of extension of the bioavailability and economic life-span of proprietary drugs. In 2005, the industry consulting firm NanoMarkets predicted that nanotechnology-enabled drug delivery systems would to generate over US $1.7 billion in 2009 and over $4.8 billion in 2012.

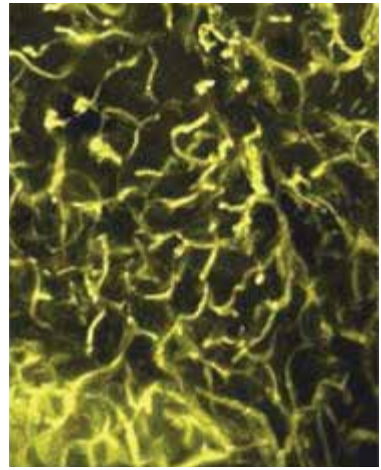

Figure 1.6 The branched capillary structure, feeding adipose tissue in a living mouse, is revealed with multiphoton fluorescence microscopy as nanocrystal quantum dots circulate through the bloodstream. From Larson D. T. et al., *Science* **300,** 1434–1436 (2003). Reprinted with permission from AAAS.

Another development in nanoscience that has excited many biomedical researchers is the use of quantum dots (abbreviated QDs) in bio-imaging. These are tiny crystals that give strong fluorescence signals and, when injected into cells,

allow unprecedented details inside the cells to be imaged. A nice 3D imaging example was demonstrated by Cornell researchers (Fig. 1.6) whereby tiny blood vessels beneath a mouse's skin were viewed with CdSe/ZnS QDs circulating through the bloodstream. The images appear so bright and vivid in high-resolution that researchers can see the vessel walls ripple at 640 times per minute.

(b) Spintronics For many years, scientists and engineers have created a host of electrical devices that rely on electrons in the materials. Such devices include the ubiquitous transistor and the powerful microprocessor. These devices exploit the charge carried by the electrons for their normal function, and they communicate with each other through the flow of electric charges. However, there is another important intrinsic property of electrons that has been neglected in these devices—the spin of the electron. Spin is a purely quantum mechanical property. We normally think of the spin of an electron using the analogy of a spinning top. The spin can be clockwise or counterclockwise in direction. In the case of electrons, the spin could be pointing in the "up" direction or in the "down" direction. The spin in the electron is easily influenced by an externally applied magnetic field. Spin electronics, or *spintronics,* refers to electrical devices that utilise the spin properties of the electrons in addition to their electrical charge in creating useful devices. Scientists and engineers hope to control the spin of electrons within a spintronics device to produce useful devices. As the spintronics device can be influenced by the presence of an electric field, magnetic field or light, the device represents a single device that integrates the multiple functionalities with optoelectronics and magnetoelectronics.

There are a number of spintronics devices that have been realised. The most widely used spintronics device is the Giant Magnetoresistive (GMR) device commonly used in magnetic hard-disk drives. Typically, a simple GMR device consists of two layers of ferromagnetic materials separated by a very thin spacer layer which is nonmagnetic. A simple illustration of such a spin valve device is shown in Fig. 1.7. One of the layers is referred to as the "pinned" layer where its magnetisation direction remains in a fixed direction. The other ferromagnetic layer is known as the "free" layer where its magnetisation direction depends on the externally applied magnetic field. When the two magnetisation

vectors of the ferromagnetic layers are oriented in the same direction, an electrical current will flow freely. On the other hand, if the magnetisation vectors are oriented in the opposite direction, there is a high resistance to the flow of electrons due to spin dependent scattering. The magnitude of the change in the resistance at these two different states is called the Giant Magnetoresistance Ratio. Hence this GMR device is highly sensitive to the external magnetic field which is capable of switching the relative magnetic orientation of the ferromagnetic layers. Thus it is widely used as the read head for magnetic hard disk drives.

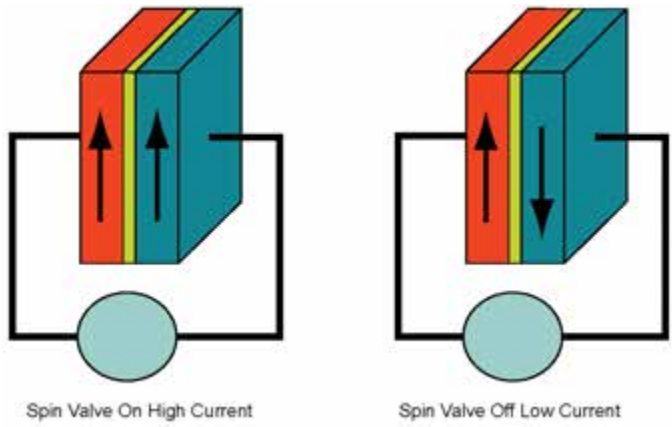

Figure 1.7 Schematic diagram of a simple spin valve.

There are many other spintronics devices that scientists and engineers are working on. These include the spin-based transistor, spin-polarizer, spintronics solar cell, magnetic tunnel junction, and spin-based quantum computer where the spin of a single electron trapped in a quantum dot is used as a *qubit.*

(c) Molecular electronics The emerging field of molecular electronics is now becoming a popular alternative paradigm to current silicon microelectronics. In 1974, Drs. Ari Aviram and Mark Ratner, then at New York University, published a paper in *Chemical Physics Letters* proposing that individual molecules might exhibit the behaviour of basic electronic devices [7]. Their hypothesis, formulated long before anyone was able to test it, was so radical that it was not pursued for another 15 years. The story continued in

December 1991, when Drs. James Tour and Mark Reed discovered they had a common interest at a small gathering of "moletronics" researchers in the Virgin Islands. The meeting was hosted by Ari Aviram, who was then working at IBM's Thomas J. Watson Research Center in New York. They started collaborating, but it was not until 1997 when they successfully used the so-called "break-junction" technique to measure the conductance of a single molecule [8]. In their work, benzene-1,4-dithiol molecules were self-assembled onto two facing gold electrodes of a mechanically controllable break junction to form a stable gold-sulphur-aryl-sulphur-gold system (Fig. 1.8). This allowed the direct observation of charge transport through the molecules for the first time. Their study provided a quantitative measure of the conductance of a junction containing a single molecule, which is a fundamental step towards the realization of the new field of molecular electronics.

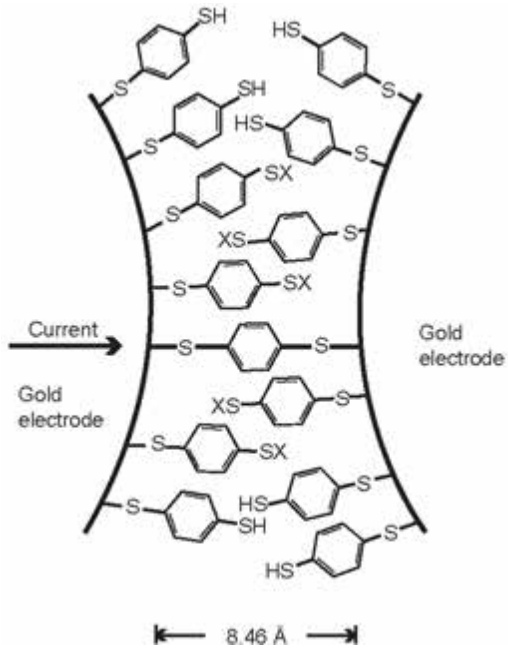

Figure 1.8 Schematic of the gold-sulphur-aryl-sulphur-gold system. From Reed et al., *Science,* **278,** 252 (1997). Reprinted with permission from AAAS.

Many papers have since followed demonstrating conductance measurements on single molecules and simple single molecule devices. A useful review of the early days of the field has been written by Drs. Carroll and Gorman [9]. Nanogaps were formed using electromigration whereby a high electric field causes gold atoms to move along the current direction, eventually causing a nanogap. A research team at Hewlett-Packard (HP) Laboratories has proposed the crossbar architecture as the most likely path forward for molecular electronics [10]. A crossbar consists of one set of parallel nanowires less than 100 atoms wide that cross over a second set (Fig. 1.9). A molecule or material that can be stimulated electrically to conduct either more electricity or less is sandwiched between the two sets of wires. The resulting interwire junctions form a switch at each intersection between crossing wires that can hold its "on" or "off" status over time. Such switches may be able to scale down to nearly single-atom dimensions, and this approach suggests how far the future miniaturisation of ICs might someday go.

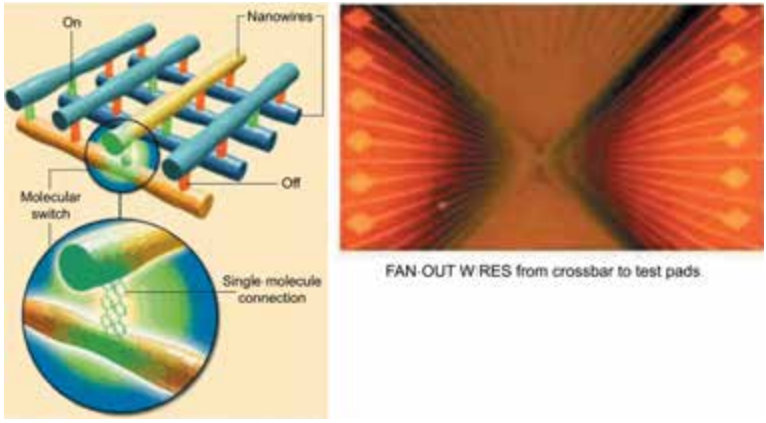

Figure 1.9 Left: Schematic showing how the switch is formed at the junction between two crossing nanowires that are separated by a single monolayer of molecules. Right: Picture of fan-out wires that connect the nanoscale circuits to the microscale. Reprinted with permission from P. J. Kuekes, G. S. Snider, R. S. Williams, Crossbar nanocomputers. *Sci. Am.,* 72–80 (2005). Copyright © 2005 by Scientific American, Inc. All rights reserved.

Disclosures and Conflict of Interest

This chapter is a revised version of the author's chapter that originally appeared in 2010 in *Science at the Nanoscale: An Introductory Textbook*, Pan Stanford Publishing Pte Ltd., Singapore. The authors declare that no writing assistance was utilized in the production of this manuscript and the authors have received no payment for its preparation. The findings and conclusions here reflect the current views of the authors.

Corresponding Author

Dr. Andrew T. S. Wee
Department of Physics, National University of Singapore
2 Science Drive 3, Singapore 117542
Email: phyweets@nus.edu.sg

About the Authors

Chin Wee Shong is associate professor in the Department of Chemistry at the National University of Singapore. Her research explores the fundamental properties of materials with physical dimension in between individual molecules and the bulk. Currently, her research focuses on the synthesis and characterization of several types of nanomaterials including: (i) semiconducting sulfide and oxide nanocrystals (ii) core/shell and doped functional nanomaterials, (iii) hybridized nanoparticles/polymer composites, (iv) nanomagnets, and (v) surface-derivatized metallic nanoparticles. Dr. Chin and her group aim to optimize the properties of these nanomaterials via chemical preparation and improve their desired functions with various characteristics. Most of their projects involve multidisciplinary collaborative efforts.

Sow Chorng Haur is professor in the Department of Physics and group leader of the Nanomaterials Research Lab at the National University of Singapore. His research focuses on the study of a wide variety of nanostructured materials, aiming to understand the physical properties

of these nanomaterials and how these properties are influenced by the morphology, stoichiometry and structures and these nanomaterials. His current research focuses on the understanding of the structural assembly and growth mechanism of the nanostructures, in order to achieve greater control in the material composition, physical structure, physical properties and functionality. He is also interested in the synthesis of new classes of nanomaterials and exploring different methods to incorporate two or more different nanostructures together with controlled architecture.

Andrew T. S. Wee is professor in the Department of Physics and vice president (University and Global Relations) at the National University of Singapore. His research interests are in the field of surface and interface science and include scanning tunneling microscopy (STM) and synchrotron radiation studies of the molecule–substrate interface, organic–organic heterojunctions, and graphene and related nanomaterials.

References

1. Feynman, R. P. (1960). There's plenty of room at the bottom. *Eng. Sci.*, **23(5)**, 22–36.
2. Binnig, G., Rohrer, H., Gerber, C., Weibel, E. (1982). Tunneling through a controllable vacuum gap. *App. Phys. Lett.,* **40**, 178–180.
3. Binnig, G., Rohrer, H., Gerber, C., Weibel, E. (1983). 7 × 7 reconstruction on Si(111) resolved in real space. *Phys. Rev. Lett.,* **50**, 120–123.
4. Kroto, H. W., Heath, J. R., O'Brien, S. C., Curl, R. E., Smalley, R. E. (1985). C_{60}: Buckminsterfullerene. *Nature,* **318**, 162–163.
5. Iijima, S. (1991). Helical microtubules of graphitic carbon. *Nature,* **354**, 56–58.
6. Lee, C. C., Gillies, E. R., Fox, M. E., Guillaudeu, S. J., Fréchet, J. M., Dy, E. E., Szoka, F. C. (2006). A single dose of doxorubicin-functionalized bow-tie dendrimer cures mice bearing C-26 colon carcinomas. *Proc. Natl. Acad. Sci. U. S. A.*, **103**(9450), 16649–16654.
7. Aviram, A., Ratner, M. A. (1974). Molecular rectifiers. *Chem. Phys. Lett.,* **29**(2), 277–283.

8. Reed, M. A., Zhou, C., Muller, C. J., Burgin, T. P., Tour, J. M. (1997). Conductance of a molecular junction. *Science,* **278**, 252–254.
9. Carroll, R. L., Gorman, C. B. (2002). The genesis of molecular electronics. *Angew. Chem. Int. Ed.,* **41**, 4378–4400.
10. Kuekes, P. J., Snider, G. S., Williams, R. S. (2005). Crossbar nanocomputers. *Sci. Am.,* **293**, 72–80.

Chapter 2

Nanomedicine: Dynamic Integration of Nanotechnology with Biomedical Science

Ki-Bum Lee, PhD,[a] Aniruddh Solanki, PhD,[b] John Dongun Kim, PhD,[c] and Jongjin Jung, PhD[d]

[a]*Department of Chemistry and Chemical Biology, Rutgers, The State University of New Jersey, New Jersey, USA*
[b]*Brigham and Women's Hospital, Harvard Medical School, Cambridge, Massachusetts, USA*
[c]*Department of Biological Sciences, Korea Advanced Institute of Science and Technology, Korea*
[d]*Hannam University, Korea*

Keywords: nanopatterning, nanomaterial design, nanocarriers, drug delivery, nanoarrays, microfluidics, biomolecules, molecular imaging

2.1 Introduction

The recent emergence of nanotechnology is setting high expectations in biological science and medicine, and many scientists now predict that nanotechnology will solve many key questions of biological systems that transpire at the nanoscale. Nanomedicine, broadly defined as the approach of science and engineering at the nanometer scale toward biomedical applications, has been drawing considerable attention in the area of nanotechnology. Given that the sizes of functional elements in biology are at the nanometer

Handbook of Clinical Nanomedicine: Nanoparticles, Imaging, Therapy, and Clinical Applications
Edited by Raj Bawa, Gerald F. Audette, and Israel Rubinstein

ISBN 978-981-4669-20-7 (Hardcover), 978-981-4669-21-4 (eBook)
www.panstanford.com

scale range, it is not surprising for nanomaterials to interact with biological systems at the molecular level. In addition, nanomaterials have novel electronic, optical, magnetic, and structural properties that cannot be obtained from either individual molecules or bulk materials. These unique features can be precisely tuned in order for scientists to explore biological phenomena in many ways. For instance, extensive studies have been done with chip-based or solution-based bio-assays, drug delivery, molecular imaging, disease diagnosis, and pharmaceutical screening [1–4]. In order to realize these applications, it is crucial to develop methods that investigate and control the binding properties of individual biomolecules at the fundamental nanometer level. This will require enormous time, effort, and interdisciplinary expertise of physical sciences associated with both biology and engineering. The overall goal of nanomedicine is to develop safer and more effective therapeutics as well as novel diagnostic tools. To date, nanotechnology has revolutionized biomedical science step by step not only by improving efficiency and accuracy of current diagnostic techniques, but also by extending scopes for the better understanding of diseases at the molecular level [5–8]. In this chapter, nanomaterials and their applications in biomedical research will be discussed.

2.2 Designing Nanomaterials for Biology and Medicine

One of the important technological aspects in nanomedicine lies in the ability to tune materials in a way that their spatial and temporal scales are compatible with biomolecules. That said, materials and devices fabricated at the nanometer scale can investigate and control the interactions between biomolecules and their counterparts at almost the single molecule level. This, in turn, indicates that nanomaterials and nanodevices can be fabricated to show high sensitivity, selectivity, and control properties, which usually cannot be achieved in bulk materials. The wide range of the scale of biointeractions is described in Fig. 2.1.

Given that one of the major goals of biology is to address the spatial-temporal interactions of biomolecules at the cellular or integrated systems level, the integration of nanotechnology

in biomedicine would bring a breakthrough in current biomedical research efforts. In order to apply nanotechnology to biology and medicine, several conditions must be considered: (i) nanomaterials should be designed to interact with proteins and cells without perturbing their biological activities, (ii) nanomaterials should maintain their physical properties after the surface conjugation chemistry, and (iii) nanomaterials should be biocompatible and non-toxic.

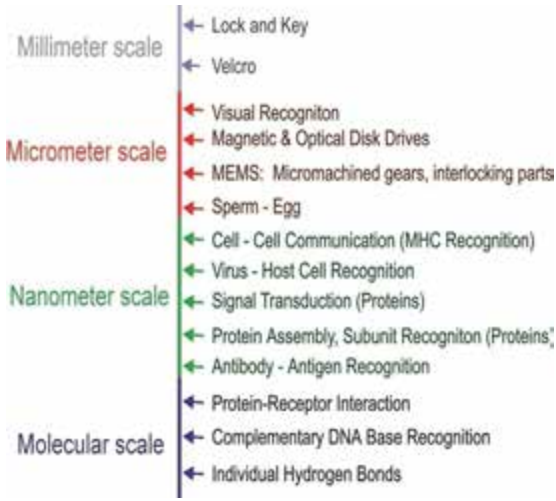

Figure 2.1 Scale of biomolecular interactions.

In general, there are two approaches to build nanostructures or nanomaterials: "top-down" and "bottom-up" methods. Typically, the bottom-up approach utilizes self-assembly of one or more defined molecular building blocks to create higher-ordered functional entities. For the bottom-up approach, the physical and chemical criterion, such as pH, concentration, temperature, and intrinsic properties of building blocks, must be fulfilled. On the other hand, the top-down approach usually involves processes such as lithography, etching, and lift-off techniques to fabricate micro- and nanoscopic structured materials from bulk materials. In many cases, nanomedicine strategies have been derived from what was originally a conventional biomedical application, with a certain degree of modification to address some scientific questions or technical limitations. As far as the applications of nanostructures

are concerned, we will examine two examples, nanoparticles and nanoarrays/biochips, which are heavily used in biomedical applications.

2.2.1 Inorganic Nanoparticles

Deoxyribonucleic acid (DNA), ribonucleic acid (RNA), peptides, and proteins are nanometer scale components that are the best examples of nanomaterials found in nature [9, 10]. For example, DNA has a double-stranded helical structure with a diameter of 2 nm, RNA has a single strand structure with a diameter of 1 nm, and most of protein sizes are less than 15 nm. Likewise, the sizes of functional elements in biology are at the nanoscale level, which inevitably generate significant interests at the intersection between nanotechnology and biological science. Even though much progress in the life sciences has been achieved over the last few decades, biological and physiological phenomena still remain beyond our understanding, because the interactions between elementary biomolecules and other higher components, such as viruses, bacteria, and cells, are complex and delicate. Moreover, the interactions of two biocomponents start from the single molecule level, where the recognition sites lie in a nanoscale domain. Thus, studies of these biological components require not only an ability to handle the biological properties, but also to develop highly advanced tools or techniques to analyze the biological systems [11–14].

Bioconjugated nanomaterials have recently been used as cellular labeling agents to study the biological phenomena at the nanometer level. With significant advancements in synthetic and modification methodologies, nanomaterials can be tuned to desired sizes, shapes, compositions, and properties [15]. Inorganic nanoparticles are one of the most promising examples, since they can be synthesized easily in large quantities from various materials using relatively simple methods. Also, the dimensions of the nanoparticles can be tuned from one to a few hundred nanometers with monodispersed size distribution. Moreover, they can be made up of different metals, metal oxides, and semiconducting materials, whose compositions and sizes are listed in Table 2.1. Given many distinct properties, nanoparticles can be readily tailored

with biomolecules via combined methodologies from bioorganic, bioinorganic, and surface chemistry.

Table 2.1 Selection of available nanoparticle compositions, sizes, and shapes

Particle composition	Particle size (nm)
Metals	
Au	2–250
Ag	1–80
Pt	1–20
Cu	1–50
Semiconductors	
CdX (X = S, Se, Te)	1–20
ZnX (X = S, Se, Te)	1–20
TiO_2	2–18
PbS	3–50
ZnO	1–30
GaAs, InP	1–15
Ge	6–30
Magnetic	
Fe_3O_4	6–40
Various polymer compositions	20 nm to 500 μm

Despite many significant advances in synthetic and surface modification methods, the fundamental development of bioconjugation methods must first be achieved in order for the nanoparticles to be fully utilized. The bioconjugation strategies involve procedures for coupling biomolecules to nanomaterials, enabling the nanoparticles not only to be applied for clinical applications but also to ask and answer fundamental questions in cell biology. For the past few years, many methods have been developed for bio-labeled nanocomposites in various applications in cell biology: cell labeling [19–22], cell tracking, and *in vivo* imaging [23, 24].

2.2.2 Coupling of Nanoparticles with Biomolecules

Interdisciplinary knowledge from molecular biology, bioorganic chemistry, bioinorganic chemistry, and surface chemistry must

be employed to functionalize nanostructures with biomolecules. Although nanostructures can be synthesized from various materials using several methods, the coupling and functionalization of nanostructures with biomolecules should be carried out in controlled manners such as a specific salt concentration or pH [9]. Three common methods of functionalizing nanoparticles with biomolecules are: (i) direct interaction between nanoparticles and biomolecules via electrostatic interactions or physical adsorptions, (ii) typical conjugation chemistry using organic linker molecules, and (iii) streptavidin-biotin affinity between functionalized nanoparticles.

Typically, solution phase synthesis of nanostructures is carried out in the presence of surfactants such as citrate, phosphates, and alkanethiols. The surfactants not only interact with the atoms of nanostructures by either chemisorption or physisorption at the surface of nanostructures, but also stabilize nanostructures and prevent interparticle aggregation. Using the exchange reactions, surfactant molecules attached on the nanoparticles can be replaced by biomolecules, making direct biomolecule-nanoparticle covalent bonds. For example, gold nanoparticles can be modified with proteins consisting of cysteine residues or with thiol functionalized DNA molecules.

There are different types of coupling methods, where the electrostatic forces between proteins and citrate stabilized nanoparticles are used for the coupling. For the nanoparticles that are relatively unstable, the core-shell strategies can be applied to stabilize the nanoparticles [25, 26]. For example, silver core-shell nanoparticles coated by thin layer of gold can be successfully functionalized with thiol-functionalized DNA [25]. Many semiconductor nanoparticles can also be linked with proteins or DNA by adding a hydrophobic silica shell [16, 27, 28]. Silica surfaces can be tailored with biomolecules, utilizing well known cross-linking methodologies, such as silanization chemisty and self-assembly monolayer (SAM) chemistry [29–32].

2.2.3 Fabrication of Nanoarrays and Biochips

The search for novel ways to explore and understand biomolecular interactions has been sought in many ways, since interactions between biomolecules are fundamentally intriguing. For example,

how proteins such as fibrinogen, fibronectin, and retronectin influence the adhesion of cells and control their morphology and physiology has been a central question of cell biology [33, 34]. Several approaches have been examined over the past few years to comprehend these phenomena, and one of these approaches is the assembly of interfacial proteins constructed on micro- or nanoscale [35]. The biomolecular patterned surfaces are not only useful for probing biochemical interactions within whole cells but also crucial for biosensing. However, the realization of these applications is challenging, since the control of the interactions between proteins and surfaces with respect to a binding direction and biomolecular density is technically and biologically not easy to achieve [36]. Therefore, patterning techniques capable of high resolution—molecular to submicron scale—and compatible with biomolecules will be required. Typically, current chip-based biodetection strategies pattern molecules with an analyte-capturing ability on the chip surfaces in the micro-/nano scale. This application of chip-based biosensing will allow scientists to detect various analytes at concentrations as low as picomolar in massively parallel ways. The aforementioned features are invaluable for the advancement in genomics and proteomics via generating DNA and protein arrays [15]. Yet, the key challenge lies in the fabrication of miniaturized surface structures in the form of nanoarrays that would allow for multi-magnitude orders of complex detection in the same chip and for improved detection sensitivity. There are many techniques available for patterning surfaces in terms of resolution and compatibility with soft materials (Table 2.2). Among different techniques, one primary distinction is whether the method uses a resist-based process or deposition of materials onto a surface directly. Although the indirect, resist-based patterning methods, such as photolithography, are multi-step processes that require specialized resists and etching protocols, they are currently by far the most widely used methods in industrial applications.

By contrast, direct-printing methods are typically useful for patterning soft materials such as small organic or biological molecules with ease. Microcontact printing, developed by Whitesides and coworkers [37–44], is a good example of a direct-printing method using elastomer stamps which can be “inked” with molecules and then used to transfer the inking molecules in a form

of desired patterns to various substrates. This technique has been used to generate large area patterns of soft materials on surfaces with pattern resolutions approaching 100 nm. However, the technique is limited in its capability to generate multiple, chemically diverse, high-resolution patterns in alignment on a surface. Therefore, in terms of resolution to sub-100 nm, there is a high demand to develop methods of high-resolution lithographic techniques. Since the invention of scanning probe microscopes (SPMs), many scientists have realized that it might be possible to manipulate matter, atom-by-atom or molecule-by-molecule [45, 46]. The early attempts to develop patterning methodologies from SPMs were able to demonstrate the high-resolution capabilities of these instruments.

Table 2.2 Features of selected lithography techniques

Technique	Resolution limit	Mode	Comments
Photolithography	Currently ~100nm	Parallel only	Resist based, indirect
Electron beam lithography	5–10 nm	Serial only	Resist based, indirect
Indirect SPM methods	AFM 5–10 nm STM atomic	Serial only	Resist based, indirect
Microcontact printing	~100 nm	Parallel only	Direct write or indirect
Ink-jet printing	6 μm	Serial	Direct write
Dip-pen nanolithography	5–10 nm	Parallel or serial	Direct write

The majority of SPM surface patterning methods have focused on either impressive but inherently slow scanning tunneling microscope (STM) based methods for moving individual atoms around on a surface in ultra high vacuum (UHV), or on indirect methods using atomic force microscope (AFM) and STM for stepwise etching of organic monolayers on a surface and backfilling with the molecule of interest [37, 47–50]. However, resist-based approaches are inherently restricted to serial processes, and can only be used for a few molecule-substrate combinations. In 1999, Mirkin and his coworkers developed dip-pen nanolithography

(DPN). DPN uses an AFM tip to transfer "ink" molecules onto a substrate through a water meniscus (Fig. 2.2) [3, 51, 52]. DPN is simple, and its resolution is comparable to electron-beam lithography.

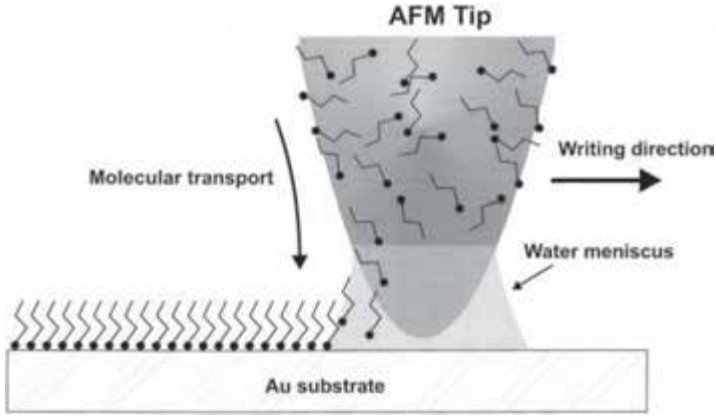

Figure 2.2 Schematic representation of Dip-Pen Nanolithography. "Ink" molecules coated on the AFM tip are transferred to the Au substrate through a water meniscus. Reprinted from Ref. 52 with permission from AAAS.

2.3 Application of Nanomaterials in Biomedical Research

Biomedical scientists have seen a great potential in the nanotechnology application. As a result, they have tried to incorporate the intrinsic properties of nanomaterials with conventional techniques in an attempt to improve detection methods and treatments for greater results [53, 54]. Recently, many studies have reported that innovative nanotechnology has improved biomolecular detection sensitivity, diagnostic accuracy, and treatment efficiency [55–59].

2.3.1 Molecular Imaging for Diagnosis and Detection

Optical imaging methods, such as fluorescence microscopy, differential interference contrast microscopy (DICM), and UV-Vis spectroscopy, are one of the most widely used methods for studying

biological systems. These methods are simple and highly sensitive, yet tend to have high background noise that is mainly caused by cellular autofluorescence from labeled molecules [60]. Also the lack of quantitative data, requirement for the long observation time, and the loss of signals due to photobleaching in biological systems have initiated a need for new imaging agents. In order to complement conventional optical imaging methods, the approach using nanoprobes is one of the major research efforts in nanomedicine mainly due to their ability to recognize and characterize pre-symptomatic diseases [61]. Typically, the nanoprobes comprise of hybrid organic materials such as nanoliposomes and polymeric nanosystems, or inorganic nanoparticles such as quantum dots and magnetic nanomaterials. Depending on the composition and properties of nanomaterials, they can be further utilized *in vitro*, *ex vivo*, and *in vivo* imaging applications. Typical examples include vast arrays of functions such as cell or DNA labeling, molecular imaging, and angiogenesis as an imaging agent, particularly in tumor tissues [15].

Quantum dots (QDs) are fluorescent semiconducting nanocrystals that can be used to overcome limitations associated with the more commonly used organic fluorophores. QDs offer many advantages such as high quantum yields, high molar extinction coefficients, wide range of absorption spectra from UV to near IR, narrow emission spectra, resistance to photobleaching and chemical degradation, and long fluorescence lifetimes (>10 ns). Their unique photophysical properties allow time-gated detection for separating their signal from that of the background noise resulting from cell autofluorescence [62–65]. Quantum dots are typically 2–8 nm in diameter and their shapes and sizes can be customized by modifying the variables—temperature, duration, and ligand molecules—used in their synthesis. Thus by changing their size and composition, it is possible to precisely tune the absorption and emission spectra to increase or decrease the band gap energy. Due to their narrow emission spectra, they can be used effectively in multiplexing experiments where multiple biological units can be labeled simultaneously. One such study was demonstrated by Jain and coworkers [66]. The QDs were applied *in vivo* to spectrally distinguish multiple species within the tumor tissue [66]. More specifically, they demonstrated that QDs can be customized to concurrently image and differentiate the tumor vessels. The group

also examined the accessibility to tumor cells depending on the size of QDs. Sizes and compositions of QDs have been extensively studied by many groups [59, 67–70]. Wright and coworkers [71] studied QDs with CdSe core with ZnS shell (CdSe/ZnS) and found that they have potent brightness which is advantageous for optical imaging. The group further studied the core/shell QDs conjugated with an antibody against the respiratory syncytial virus (RSV), a virus which is responsible for causing infections in the lower respiratory tract. It was shown that the use of QDs reduced the detection time from over four days to one hour. In fact, the results were very valuable from a therapeutic point of view as the available antiviral agent against the RSV is effective only when administered in the initial stages of the infection. Moreover, QDs enable scientists to study live cells and to track down the mechanism of biological processes in a real-time manner due to their resistance to photo-bleaching over long periods of time. The ability to track cells *in vivo* without having to sacrifice animals signifies a great improvement over the current techniques. Figures 2.3 and 2.4 show two examples of QD imaging: one is the high sensitivity and multicolor capability of QD imaging in live animals and the other is the detection of cancer marker Her2 with QD-streptavidin [21].

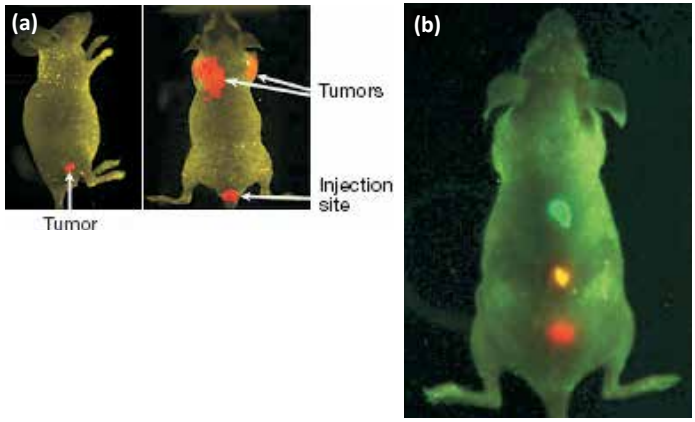

Figure 2.3 Imaging in live animals using quantum dots (QDs). (a) Molecular targeting and *in vivo* imaging using antibody-(QD) conjugate. (b) *In vivo* imaging of multicolored QD-encoded microbeads. Reprinted from Ref. 62 with permission from Nature Publishing Group.

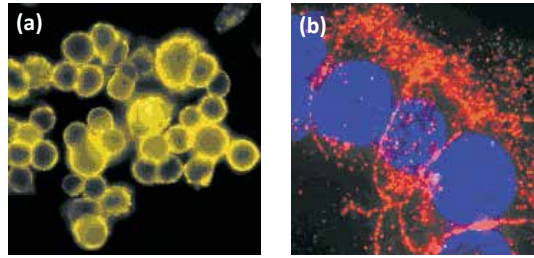

Figure 2.4 Detection of cancer marker Her2 *in vitro* with QD-streptavidin. (a) Her2 detected on surface of free cells using QD 560-streptavidin (yellow). (b) Her2 detected on a section of mouse mammary tumor tissue using QD 630-streptavidin (red). Reprinted from Ref. 21 with permission from Nature Publishing Group.

Cytotoxicity is a primary issue in QD applications [72], because the release of Cd^{2+} and Se^{2-} ions from QDs could interfere with cell viability or function [73, 74]. While the toxicity may not be critical at low concentrations optimized for labeling, it could be detrimental for the embryo development at higher concentrations. Yet, the problem can be solved by coating the QDs and making them biologically inert or by maintaining a safe concentration range. Several studies have reported that QDs can effectively accomplish their task without adversely affecting cellular processes [75, 76].

Other noble metal nanoparticles, such as Au, Ag, and Cu nanoparticles, are receiving as much attention as QDs, because they exhibit other unique and modifiable optical properties [77]. Typically, when spherical nanoparticles are exposed to electromagnetic field at a certain frequency, the free electrons on a metal surface, known as plasmons, undergo coherent oscillation, resulting in a strong enhancement of absorption and scattering of electromagnetic radiation. In case of noble metal nanoparticles, the surface plasmon resonance (SPR) of a metal surface especially yields intense colors and unique optical properties [78]. These noble metals have a greater potential for applications than other materials, because the resonance for Au, Ag, and Cu lie at visible frequencies and they have a high stability [77]. Furthermore, Au nanoparticles are insusceptible to photobleaching and can be easily synthesized in a wide range of sizes (4–80 nm) for tunable size-dependent optical properties. They are biocompatible and

devoid of cytotoxicity, which are big advantages over QDs where cytotoxicity can be a limiting factor. The use of biocompatible, nontoxic capping material is critical for medical applications of Au nanoparticles [79] Another reason that makes gold nanoparticles more attractive for optical imaging in biology is the well-defined chemistry between biomolecules with a gold surface. By modifying the surface of Au nanoparticles with an amine or thiol moiety [80], for instance, the nanoparticles can mount antibodies and specifically target tumor cells and biomolecules, such as folic acid [81, 82] and transferrin [83, 84], for imaging and drug/gene delivery. This was well demonstrated in a study by Richards-Kortum and coworkers [85], where the group used 12 nm Au nanoparticles conjugated with anti-EGFR (epithelial growth factor receptor) monoclonal antibodies to image cervical epithelial cancer cell which exhibited an over expression of EGFR as compared to healthy cells. In their study, the conjugation was due to the electrostatic adsorption of the antibody molecules onto the citrate-capped and negatively charged Au nanoparticles.

The use of nanowires and nanotubes in the electrical detection method of analytes at extremely low concentration is one of the hot topics in nanomedicine. Their usage has two major advantages—high sensitivity and fast responses without tedious labeling steps. However, these nanostructures are not as readily functionalized as aforementioned quantum dots or nanoparticles. The unique advantages of these nanomaterials come from their one-dimensional morphological structures, and many researchers are trying to utilize them as a highly sensitive and selective signal transduction medium. For example, Lieber and coworkers [86] synthesized silicon nanowires with peptide nucleic acid (PNA) functionalization, and demonstrated how the synthetic material could detect DNA without labeling. A subsequent study modified silicon nanowires with biotin to detect picomolar concentrations of streptavidin and demonstrated high sensitivity to change in conductivity of the nanowires upon the biotin-streptavidin binding. Similar studies have also been carried out by Dai and coworkers [87], where they focused on the application of carbon nanotubes as a material for the sensitive detection. The scheme (Fig. 2.5) [86] illustrates a basic structure of electrical detection of biomolecules with nanowire sensor.

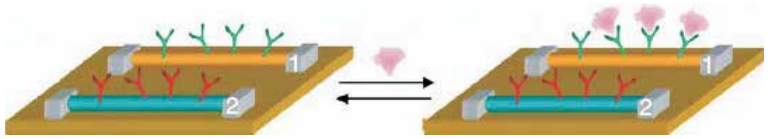

Figure 2.5 Schematic showing two nanowire devices, 1 and 2, within an array, where nanowires were modified with different (1, green; 2, red) antibody receptors. Reprinted from Ref. 86 with permission from Nature Publishing Group.

Magnetic nanoparticles are emerging as novel contrast reagents for magnetic resonance imaging (MRI) [88–95], revolutionizing current diagnostic tools. Since their unique properties allow precise control of size and composition, magnetic nanocrystals offer great potential for highly specific MRI for biological systems [96–99]. The nanocrystals tend to behave as a single magnetic domain in which all nuclear spins couple to create a single large magnetic domain. At certain temperatures and crystal sizes, these moments wander randomly (superparamagnetic), or become locked in one direction, making the material ferromagnetic [88, 94]. Magnetic nanocrystals of differing compositions and sizes can be synthesized to generate ultra-sensitive molecular images. Cheon and coworkers [98] developed iron oxide magnetic nanoparticles which were doped with +2 cations such as Fe, Co, Ni, or Mn. It was observed that Mn-doped iron oxide nanoparticles were highly sensitive for detecting cancer cells. The nanoparticles even made it possible to image small tumors *in vivo*. In the same study, it was noted that 12 nm Mn-doped nanoparticles were bioconjugated with herceptin to have specificity towards the cancer cells. This approach is expected to improve the early diagnosis of diseases, which is critical for increasing survival rates.

2.3.2 Treatment of Diseases

The motivation to develop nanomedicine stemmed from the limitations of current treatments, such as surgery, radiation, or chemotherapy, which often damage healthy cells as well as tumor cells. To address the problem, novel therapeutics which could passively or actively target cancerous cells were developed. To date many nanomedicines are being administered to treat patients. For instance, nanomedicines such as liposomes (DaunoXome)

[100–102], polymer coated liposomes (Doxil) [100, 103, 104], polymer-protein conjugates (Oncaspar) [105, 106] antibodies (Herceptin) [107–109], and nanoparticles (Abraxane) [110] are already bringing clinical benefits to patients around the world. Most of the nanotherapeutics take two main paths to achieve their goals—passive targeting and active targeting [111].

Rapid vascularization takes place within tumor tissues in order to supply nutrients for fast tumor growth. This inevitably causes the development of a defective, leaky architecture along with damaged lymphatic drainage. This leads to the enhanced permeation and retention (EPR) effect, which helps the injected nanoparticles to preferentially permeate and accumulate in the tumor tissue [111, 112]. In order for the passive mechanism to be efficient, the size and surface properties of the nanoparticles should be well controlled. The nanoparticle size should be less than 100 nm, and the surface should be hydrophilic to prevent the uptake by the macrophages of the reticuloendothelial system (RES), which would significantly improve the circulation half-life of the nanoparticles. This is achieved by coating their surfaces with hydrophilic polymers such as polyethylene glycol (PEG), poloxamers, poloxamines, and polysaccharides [113] since a hydrophilic nanoparticle surface avoids the adsorption of plasma proteins.

Another passive targeting method utilizes the unique environment around the tumor, such as cancer-specific enzymes, high or low pH of the tumor tissue, to release the drug/biomolecules within the tumor tissue [114]. Otherwise inactive nanoparticle-drug conjugate molecules can specifically be activated by the tumor-specific environment when they reach the tumor site. The release takes place within the tumor tissue, considerably increasing the drug efficiency. Yet another method to passively target the tumor is by using direct local delivery of anticancer agents into the tumors. This is an effective technique, but can be highly invasive and the access to certain tumors such as lung cancers may be impossible [114].

Active targeting is usually achieved by conjugation of targeting moieties such as proteins, peptides, antibodies, and carbohydrates with nanoparticles. These ligands act as guided missiles which deliver the nanoparticles to the specific cancer tissue and cells. For example, when Doxil (liposomal doxorubicin)

is attached to an antibody against a growth factor overexpressed in breast cancer (ErbB2), it shows faster and greater tumor regression compared to unmodified Doxil [115]. Similarly, several targeting ligands are available for nanocarriers to deliver drugs at specified locations [116].

2.3.3 Nanocarriers for Drug Delivery

Nanocarriers, 2 to 100 nm in diameter, are designed to deliver multiple drugs and/or imaging agents [117]. They have high surface to volume ratios which allow high density functionalization of their surfaces with targeting moieties. Promising nanocarriers summarized in Fig. 2.6 include liposomes, polymeric micelles, dendrimers, carbon nanotubes, and inorganic nanoparticles [111].

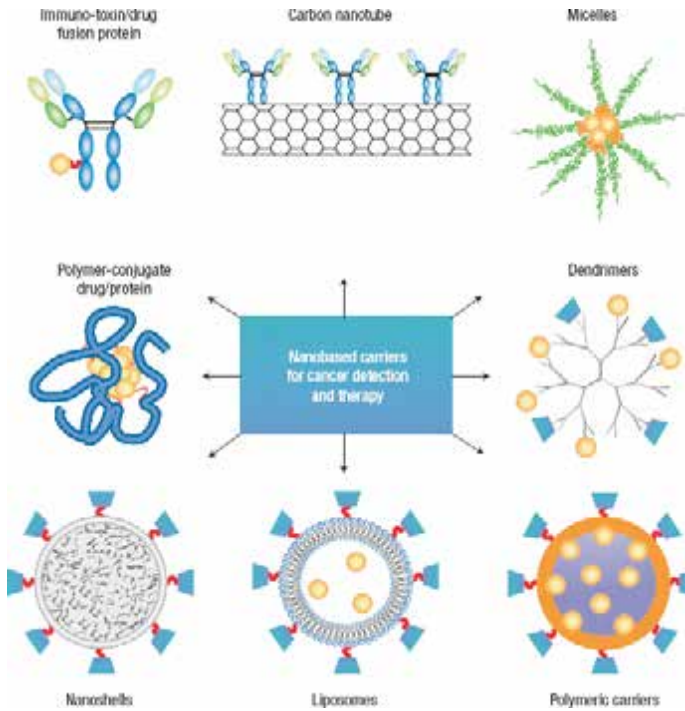

Figure 2.6 Examples of various drug delivery agents which typically include three components: a nanocarrier, a targeting moiety conjugated to the nanocarrier, and a therapeutic agent. Reprinted from Ref. 111 with permission from the Nature Publishing Group.

Polymers such as poly lactic acid (PLA) and poly lactic co-glycolic acid are the most extensively studied and commonly used materials for nanoparticle-based delivery systems [57, 118–122]. Additionally, natural polymers such as chitosan and collagen have already been vigorously studied for encapsulation of drugs with their intrinsic biocompatibility [123–126]. The use of polymers has significant advantages because the drugs or biomolecules can be encapsulated easily without chemical modification processes, while maintaining a high cost efficiency and yield. Release of the encapsulated cargo of the polymeric nanoparticles takes place via diffusion through the polymer matrix, or swelling of the nanoparticles [127–132] due to changes in a local environment such as pH or specific enzyme. Efficiency can be further improved by attaching targeting moieties, and also by passivating the surfaces for longer circulation half-lives. For example, using PEG, Huang and coworkers formulated carbohydrate conjugated chitosan nanoparticles which effectively targeted the liver cancer cells (HepG2). In the study, the carbohydrate used for targeting was galactose, which specifically bound to the asialoglycoprotein (ASGP) receptors overexpressed in the HepG2 cells [133].

Lipid-based carriers are attractive due to several properties such as biocompatibility, biodegradability, and ability to protect drugs from harsh environments. These properties came from the unique amphiphilic structure of liposomes, where the spherical amphiphiles consist of closed structures that contain one or more concentric lipid bilayers with an inner aqueous phase. Due to the amphiphilic nature, lipid-based carriers can be easily modified to entrap both hydrophobic and hydrophilic drugs [134–136]. However, Liposomes are rapidly cleared from circulation by the Kupffer cells in the liver. Thus, coating them with PEG could increase their circulation half-life [137, 138]. Overall, liposomes have shown reduced toxicity and preferential accumulation in the tumor tissue by EPR effect [127]. They could also be actively targeted by attaching antibodies to their surface.

Dendrimers are well defined molecules which are built at a nanoscale with monodispersed systems with sizes ranging from 3 to 10 nm. They have unique molecular architectures and properties, both of which result in easy conjugation chemistry with targeting molecules, making them attractive for the development of nanomedicines [127, 139–142]. Several studies have confirmed that conjugated dendrimers can be found concentrated in the tumor and

liver tissue in contrast to non-targeted polymer folates. Increased therapeutic activity and marked reduction in toxicity was also observed [143].

The synthesis of colloidal gold was first reported in 1857 [144]. However, it was about 100 years later when scientists found out that the gold particles could bind proteins without altering their activity, paving a way for their application in biological systems. Several studies confirm that gold nanoparticles are easily taken up by cells [83, 145–147]. The biocompatibility of gold nanoparticles can be further enhanced by PEG coating that prevents uptake by RES. For example, PEG-coated gold nanoparticle formulation, developed by CytImmune Sciences [78], which carries the tumor necrosis factor (TNF), is currently under human trials. These gold nanoparticles showed preferential accumulation in MC-38 colon carcinoma tumors and no uptake by liver or spleen. It was further reported that this system is less toxic and more effective in reducing tumor burden than native TNF [148]. Gold nanoparticles are also very useful for delivering nucleic acids. As seen previously, their surface allows for easy functionalization with thiols which makes attachment of oligonucleotides on the surface relatively easy. In a recent study by Mirkin and coworkers, it was reported that the cellular uptake of gold nanoparticles increased with the increase in density of the oligonucleotides on the particle surface [149].

Magnetic nanoparticles are extremely promising as novel drug delivery agents [150]. They show several advantages which are not seen in most nanoparticle-based systems. They can resolve problems related to polydispersity and irregular branching, both of which are common in polymeric nanocarriers. Magnetic nanoparticles, for example, can act as contrasting agents for MRI application [151]. Also, drug loaded magnetic nanoparticles can be guided or held in place with applied external magnetic field using their superb magnetic susceptibility. The magnetic nanoparticles can also be heated to induce hyperthermia of the tissue upon exposure to the external magnetic field. The magnetic nanoparticles can be further functionalized with targeting ligands to improve their uptake efficiency, minimize their toxicity, and prevent them from aggregating [152, 153]. This is typically done by coating them with hydrophilic to neutral compounds such a PEG, dextran, or HSA, which not only stabilizes the particles but also increases their half-life in blood.

With photothermal cancer therapy, which uses optical heating for tumor ablation, doctors can deal with tumors in a non-invasive manner [154–159]. It could be a method of choice for tumors which are inaccessible for surgery or radiotherapy, both of which kill healthy cells along with tumor cells. For this specific application, gold nanoparticles are most widely used, because the gold nanoparticles have ability to effectively convert strongly absorbed NIR light to localized heat, and hence are useful in selective photothermal therapy. Using active and passive targeting, these nanoparticles can be localized into the tumor tissue, increasing the effectiveness of the heat produced and at the same time minimizing the non-specificity of treatment. In a recent study, Li and coworkers developed gold nanocages (<45 nm) which were specifically designed to strongly absorb in the NIR region for photothermal therapy [160]. These nanocages were conjugated to anti-HER2 monoclonal antibodies against the epidermal growth factor receptor (EGFR), overexpressed on the surface of breast cancer cells [160, 161]. They concluded that the death of cancer cells increased linearly with increase in irradiation power density, thus making the immunogold nanocages effective photothermal therapeutics agents.

2.4 Nanosystematic Approach for Cell Biology

Cells are single living units of organisms which first receive the input perturbation signals from disease and injury, and then return the output signals to their microenvironments. Conventional experimental studies on particular cellular responses are typically conducted on a large cell population, which inevitably produces data measured from inhomogeneous distribution of cellular responses. Unless cellular behaviors and processes are isolated from inhomogeneous signals at the level of single cell, it would be extremely difficult to elucidate the intricate cellular systems and analyze the complex dynamic signaling transductions. In order to better study and control the responses of cells towards outer stimuli, scientists need to characterize the full range of cell behaviors, such as self-renewal, differentiation, migration, and apoptosis, from the single cell level or even the single molecule level. In particular, understanding how a genotypic aspect affects a cell phenotype

is a complicated process, which can barely be revealed by conventional biomedical approaches. In order to understand these processes, the two distinct approaches—bottom-up and top-down—can be applied in a combinatorial way.

2.4.1 Microfluidics and Micropatterns

Microfluidic devices offer a robust analytical approach, allowing rapid analysis of cell assays in a parallel way to investigate complex cell behaviors (Fig. 2.7) [162–165]. Microfluidic devices have advantages over the macroscopic setting, such as reduced sample/reagent volume, high surface-to-volume ratios, an improved control of the physical/chemical microenvironments, and high throughput/automatic capabilities [166, 167]. These characteristics would be beneficial for understanding new aspects of complex cell dynamics (e.g. stem cell differentiation and cancer cell apoptosis) and tissue engineering. Although there have been a few examples of microfluidic systems used to culture and assay stem cells [166–169], the stem cell assays in microfluidic gradients have not been fully explored. Generation of microfluidic gradients have been demonstrated by Whiteside and coworkers [170], and further studies have been done to study cell behaviors in gradients (Fig. 2.8).

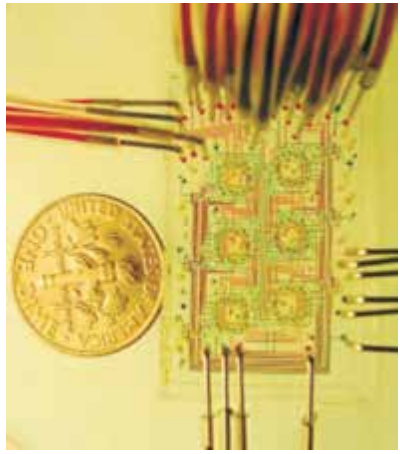

Figure 2.7 An optical micrograph of a microfluidic device. The coin is 18 mm in diameter. Reprinted from Ref. 171 with permission from AAAS.

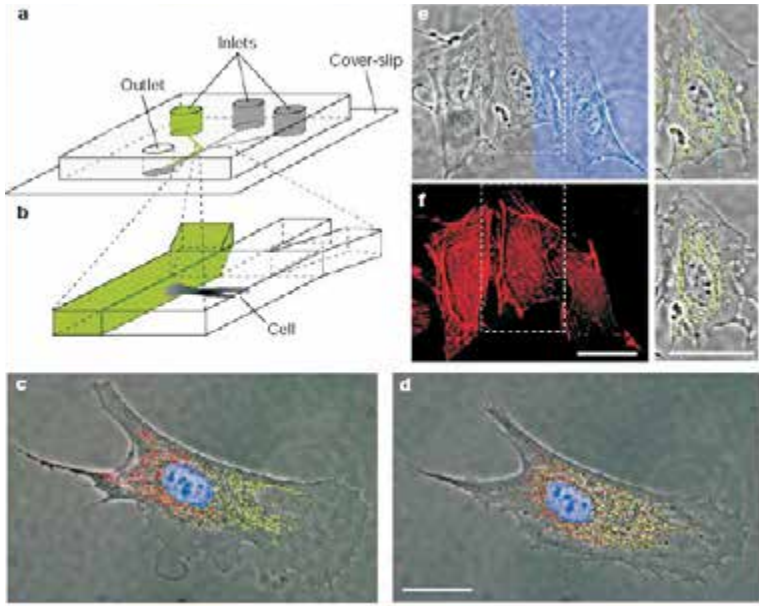

Figure 2.8 Microfluidics to study a single bovine endothelial cell using multiple laminar streams which deliver membrane permeable molecules to selected subcellular domains. Reprinted from Ref. 170 with permission from Nature Publishing Group.

The use of micro- or nanometer scale patterned surfaces is also one of the useful approaches to study individual cells at the single cell level. Typically, the patterns are generated by microcontact printing, where a soft-lithographed material transfers molecules through conformal contact on substrates with planar or non-planar topographies to form SAMs. The key advantage of microcontact printing is that a variety of features can be generated simultaneously on a surface in a single step, thus making patterning easier and faster as compared to scanning probe techniques which require longer time and effort to generate patterns.

2.4.2 Nanopatterning for Stem Cell Research

Although stem cells hold great potential for the treatment of a number of devastating injuries and damages caused by degenerative diseases [172, 173], a better control of microenvironment that

closely interacts with stem cells should be achieved before therapeutic applications can be fully realized. It is because stem cell fate is controlled by two prime factors; the intrinsic regulators, such as growth factors and signaling molecules, and the extracellular microenvironments, such as extracellular matrix (ECM). To date, there are few conventional methods available to study regulatory and extracellular microenvironmental cues that control stem cell fate at the single cellular level as well as in a combinatorial way. Stem cells normally reside within specific extracellular microenvironments [174, 175], known as "stem cell niches", comprising a complex mixture of soluble and insoluble ECM signals. The signals regulate stem cell behavior, such as self-renewal, migration, and differentiation [176–178]. For example, cell adhesion and ECM play important roles in early stem cell development. Cell adhesion process, which keeps the inner cell mass intact, is mediated by cadherins and integrins, which are further regulated post-translationally via protein kinase C and other signaling molecules (Fig. 2.9). The process determines

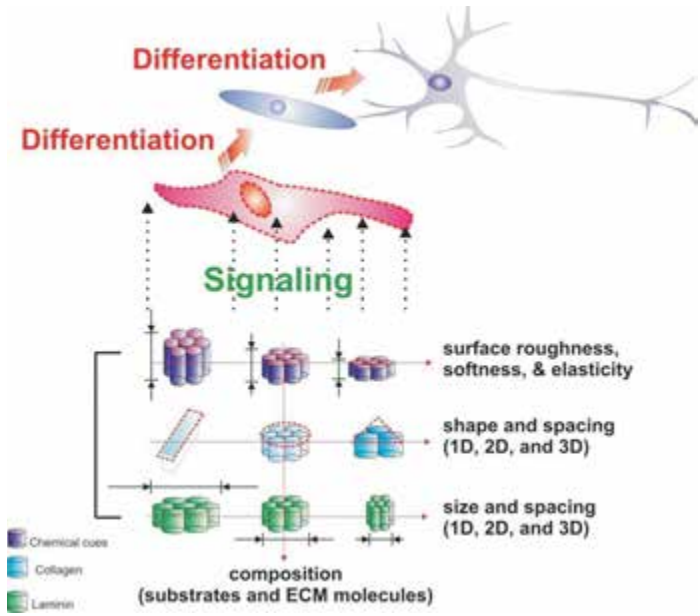

Figure 2.9 Application of micro-/nanoscale surface engineering in stem cells. Micro- and nanostructures that interact with stem cells at the molecular level can be utilized to control stem cell fate.

cellular allocation and spatial organization of the inner cell mass (ICM) in the blastocyst [179]. Likewise, *in vivo* stem cells come in contact with various soluble and insoluble ECM components that affect their differentiation. *In vitro* studies also have shown how ECM components and growth factors regulate the differentiation of stem cells [180]. Several combinatorial high-throughput screening approaches on the function of soluble signal molecules on stem cell differentiations have been reported [181].

However, similar approaches for screening the function of insoluble cues are limited due to the technical difficulty of identifying, isolating, and modulating individual stem cells from their surroundings. For instance, an extracellular matrix array format fabricated by conventional macro/micro patterning techniques has been used to probe cellular differentiation and migration [182, 183]. Very recently, a combinatorial ECM microarray was used to investigate the role of the ECM components in the differentiation of mouse embryonic stem cells (mESCs) towards an early hepatic fate [182]. This technology required 1000 times less protein than a conventional method. There still is plenty of room for improvement in this approach in terms of pattern density, recognition sensitivity, and small sample requirement. In addition, relatively little is known about the subcellular interaction mechanisms between stem cells and ECM molecules and how such events eventually influence stem cell differentiation and migration. Moreover, it is still unknown how insoluble or soluble extrinsic signaling molecules identify their molecular target proteins and receptors at the single molecule level. The application of nanotechnology in stem cell biology will help to address those challenges.

2.5 Conclusion

Nanomedicine is where traditional biomedical science meets nanotechnology. The synergetic effect offers new possibilities in diagnosis and treatment of many malicious human diseases. Moreover, the advancement in nanomedicine allows scientists in cell biology and physiology to investigate targeted bio-interactions at the fundamental molecular level. However, for the potential of nanomedicine to be fully realized, multimodal technologies for

cell recognition and molecular imaging, and targeted delivery should be developed. This challenge requires an interdisciplinary approach from a high level of expertise in each field of science. In the near future nanomedicine may bring revolutionary breakthroughs in not only the entire field of medicine, but also in fundamental biology.

Disclosures and Conflict of Interest

The authors gratefully acknowledge helpful comments on the manuscript from David Wang, Birju Shah, and Staci C. Brown. The authors declare that no writing assistance was utilized in the production of this chapter and they have received no payment for its preparation. This chapter is a revised and reformatted version of the authors' original chapter that appeared in *Nanomedicine: A Systems Engineering Approach*, Pan Stanford Publishing, Singapore.

Corresponding Author

Dr. Ki-Bum Lee
Department of Chemistry and Chemical Biology
Rutgers New Brunswick-Busch Campus
Rutgers, 610 Taylor Road, Piscataway, NJ 08854, USA
Email: kblee@chem.rutgers.edu

About the Authors

Ki-Bum Lee is associate professor in the Department of Chemistry and Chemical Biology at Rutgers University, USA. He received his PhD in 2004 from Northwestern University (Evanston, IL) and was a postdoctoral research fellow from 2004 to 2007 at the Scrrips Research Institute. Dr. Lee's primary research interest is developing and integrating nanotechnology and chemical biology to modulate signaling pathways in cancer and stem cells. Specifically, his research focuses on identifying the various microenvironmental cues (e.g., soluble signals, cell–cell interactions, and insoluble/physical signals) affecting stem cell and cancer cell fate and thereafter utilizing these cues for the neuro-differentiation of stem cells and apoptosis of brain tumor cells. He and his group

are also developing novel platforms to deliver biomolecules and to control the signaling elements inside cells in a spatiotemporally controlled manner. Taken together, his research program works to lay the groundwork for the rational step-by-step emulation of cellular microenvironments using nanomaterials.

Aniruddh Solanki received his PhD in 2013 and is currently a postdoctoral research fellow at Harvard Medical School, Brigham and Women's Hospital, Boston, MA, USA.

John Dongun Kim is a postdoctoral research fellow at Korea Advanced Institute of Science and Technology (KAIST) and recipient of Cheong-Am (TJ Park) science fellowship. He received his PhD at Rutgers University in chemistry in 2013, after which he moved to South Korea to join a structural biology group. His current research interests include RNA biochemistry and bacterial infection.

Jongjin Jung earned his BS degree in biochemistry at Yonsei University, Korea, in 2001. After one year of research work at Yonsei University, he proceeded to Rutgers University, USA, where he received his PhD degree in chemistry and chemical biology in 2010. His doctoral work was on single-molecule fluorescence spectroscopy for fast-protein folding and nanobiotechnology and was conducted under the research guidance of both Dr. David S. Talaga and Dr. Ki-Bum Lee. He joined the faculty of the Department of Chemistry at Hannam University, Korea, in 2015, following three-and-a-half-year postdoctoral research with Dr. Joung Kyu Park at Korea Research Institute of Chemical Technology. Currently, his research is focused on the synthesis and surface modifications of fluorescence and magnetic nanoparticles for bio-applications and the development of bio-electronic materials for stem cell engineering.

References

1. Alivisatos, P. (2004). The use of nanocrystals in biological detection. *Nat*. *Biotechnol*., **22**, 47–52.
2. Chan, W. C. W., Nie, S. M. (1998). Quantum dot bioconjugates for ultra sensitive nonisotopic detection. *Science*, **281**, 2016–2018.
3. Ginger, D. S., Zhang, H., Mirkin, C. A. (2004). The evolution of dip-pen nanolithography. *Angew*. *Chem*. *Intl*. *Ed*., **43**, 30–45.
4. Penn, S. G., He, L., Natan, M. J. (2003). Nanoparticles for bioanalysis. *Curr*. *Opin*. *Chem*. *Biol*., **7**, 609–615.
5. Alivisatos, P., Barbara, P. F., Castleman, A. W., Chang, J., Dixon, D. A., Klein, M. L., McLendon, G. L., Miller, J. S., Ratner, M. A., Rossky, P. J., Stupp, S. I., Thompson, M. E. (1998). From molecules to materials: Current trends and future directions. *Adv*. *Mater*., **10**, 1297–1336.
6. Elghanian, R., Storhoff, J. J., Mucic, R. C., Letsinger, R. L., Mirkin, C. A. (1997). Selective colorimetric detection of polynucleotides based on the distance-dependent optical properties of gold nanoparticles. *Science*, **277**, 1078–1081.
7. Mirkin, C. A., Letsinger, R. L., Mucic, R. C., Storhoff, J. J. (1996). A DNA-based method for rationally assembling nanoparticles into macroscopic materials. *Nature*, **382**, 607–609.
8. Storhoff, J. J., Mirkin, C. A. (1999). Programmed materials synthesis with DNA. *Chem*. *Rev*., **99**, 1849–1862.
9. Niemeyer, C. M. (2001). Nanoparticles, proteins, and nucleic acids: Biotechnology meets materials science. *Angew*. *Chem*. *Intl*. *Ed*., **40**, 4128–4158.
10. Niemeyer, C. M. (2002). Nanotechnology: Tools for the biomolecular engineer. *Science*, **297**, 62–63.
11. Weizmann, Y., Patolsky, F., Lioubashevski, O., Willner, I. (2004). Magneto- mechanical detection of nucleic acids and telomerase activity in cancer cells. *J*. *Am*. *Chem*. *Soc*., **126**, 1073–1080.
12. Willner, I. (1997). Photoswitchable biomaterials: En route to optobioelectronic systems. *Acc*. *Chem*. *Res*., **30**, 347–356.
13. Willner, I. (2001). Protein hinges for bioelectronics—Changes in protein conformation have been exploited to create chemoresponsive bio-electronic sensors. *Nature Biotechnol*., **19**, 1023–1024.
14. Willner, I. (2002). Biomaterials for sensors, fuel cells, and circuitry. *Science*, **298**, 2407–2408.

15. Rosi, N. L., Mirkin, C. A. (2005). Nanostructures in biodiagnostics. *Chem*. *Rev*., **105**, 1547–1562.
16. Bruchez, M., Moronne, M., Gin, P., Weiss, S., Alivisatos, A. P. (1998). Semi-conductor nanocrystals as fluorescent biological labels. *Science*, **281**, 2013–2016.
17. S. Clarke, J., Hollmann, C. A., Zhang, Z. J., Suffern, D., Bradforth, S. E., Dimitrijevic, N. M., Minarik, W. G., Nadeau, J. L. (2006). Photophysics of dopamine-modified quantum dots and effects on biological systems. *Nat*. *Mater*., **5**, 409–417.
18. Ahrens, E. T., Flores, R., Xu, H. Y., Morel, P. A. (2005). *In vivo* imaging platform for tracking immunotherapeutic cells. *Nat*. *Biotechnol*., **23**, 983–987.
19. Byassee, T. A., Chan, W. C. W., Nie, S. M. (2000). Probing single molecules in single living cells. *Anal*. *Chem*., **72**, 5606–5611.
20. Jaiswal, J. K., Mattoussi, H., Mauro, J. M., Simon, S. M. (2003). Long-term multiple color imaging of live cells using quantum dot bioconjugates. *Nat*. *Biotechnol*., **21**, 47–51.
21. Wu, X. Y., Liu, H. J., Liu, J. Q., Haley, K. N., Treadway, J. A., Larson, J. P., Ge, N. F., Peale, F., Bruchez, M. P. (2003). Immunofluorescent labeling of cancer marker Her2 and other cellular targets with semiconductor quantum dots. *Nat*. *Biotechnol*., **21**, 41–46.
22. Bulte, J. W. M., Douglas, T., Witwer, B., Zhang, S. C., Strable, E., Lewis, B. K., Zywicke, H., Miller, B., van Gelderen, P., Moskowitz, B. M., Duncan, I. D., Frank, J. A. (2001). Magnetodendrimers allow endosomal magnetic labeling and *in vivo* tracking of stem cells. *Nat*. *Biotechnol*., **19**, 1141–1147.
23. Chan, W. C. W., Maxwell, D. J., Gao, X. H., Bailey, R. E., Han, M. Y., Nie, S. M. (2002). Luminescent quantum dots for multiplexed biological detection and imaging. *Curr*. *Opin*. *Biotechnol*., **13**, 40–46.
24. Lewin, M., Carlesso, N., Tung, C. H., Tang, X. W., Cory, D., Scadden, D. T., Weissleder, R. (2000). Tat peptide-derivatized magnetic nanoparticles allow *in vivo* tracking and recovery of progenitor cells. *Nat*. *Biotechnol*., **18**, 410–414.
25. Bailly, M., Yan, L., Whitesides, G. M., Condeelis, J. S., Segall, J. E. (1998). Regulation of protrusion shape and adhesion to the substratum during chemotactic responses of mammalian carcinoma cells. *Exp*. *Cell Res*., **241**, 285–299.
26. Cao, Y. W., Jin, R., Mirkin, C. A. (2001). DNA-modified core-shell Ag/Au nanoparticles. *J*. *Am*. *Chem*. *Soc*., **123**, 7961–7962.

27. Gao, X. H., Chan, W. C. W., Nie, S. M. (2002). Quantum-dot nanocrystals for ultrasensitive biological labeling and multicolor optical encoding. *J. Biomed. Opt.*, **7**, 532–537.

28. Hu, J. T., Odom, T. W., Lieber, C. M. (1999). Chemistry and physics in one dimension: Synthesis and properties of nanowires and nanotubes. *Acc. Chem. Res.*, **32**, 435–445.

29. MacBeath, G. (2002). Protein microarrays and proteomics. *Nat. Gen.*, **32**, 526–532.

30. MacBeath, G. (2001). Proteomics comes to the surface—Microarrays of purified proteins, representing most of the yeast genome, prove useful for studying protein function on a genome-wide scale. *Nat. Biotechnol.*, **19**, 828–829.

31. MacBeath, G., Schreiber, S. L. (2000). Printing proteins as microarrays for high-throughput function determination. *Science*, **289**, 1760–1763.

32. MacBeath, G., Koehler, A. N., Schreiber, S. L. (1999). Printing small molecules as microarrays and detecting protein-ligand interactions en masse. *J. Am. Chem. Soc.*, **121**, 7967–7968.

33. Chen, C. S., Mrksich, M., Huang, S., Whitesides, G. M., Ingber, D. E. (1997). Geometric control of cell life and death. *Science*, **276**, 1425–1428.

34. Mrksich, M. (1998). Tailored substrates for studies of attached cell culture. *Cell. Mol. Life Sci.*, **54**, 653–662.

35. Sniadecki, N., Desai, R. A., Ruiz, S. A., Chen, C. S. (2006). Nanotechnology for cell-substrate interactions. *Ann. Biomed. Eng.*, **34**, 59–74.

36. Lee, Y. S., Mrksich, M. (2002). Protein chips: From concept to practice. *Trends Biotechnol.*, **20**, S14–S18.

37. Gates, B. D., Xu, Q. B., Love, J. C., Wolfe, D. B., Whitesides, G. M. (2004). Unconventional nanofabrication. *Ann. Rev. Mater. Res.*, **34**, 339–372.

38. Gates, B. D., Xu, Q. B., Stewart, M., Ryan, D., Willson, C. G., Whitesides, G. M. (2005). New approaches to nanofabrication: Molding, printing, and other techniques. *Chem. Rev.*, **105**, 1171–1196.

39. Mrksich, M., Whitesides, G. M. (1996). Using self-assembled monolayers to understand the interactions of man-made surfaces with proteins and cells. *Ann. Rev. Biophys. Biomol. Struct.*, **25**, 55–78.

40. Qin, D., Xia, Y. N., Rogers, J. A., Jackman, R. J., Zhao, X. M., Whitesides, G. M. (1998). Microfabrication, microstructures and microsystems, *Microsyst. Technol. Chem. Life Sci.*, **194**, 1–20.

41. Weibel, D. B., Garstecki, P., Whitesides, G. M. (2005). Combining microscience and neurobiology. *Curr*. *Opin*. *Neurobiol*., **15**, 560–567.

42. Whitesides, G. M., Ostuni, E., Takayama, S., Jiang, X. Y., Ingber, D. E. (2001). Soft lithography in biology and biochemistry. *Ann*. *Rev*. *Biomed*. *Eng*., **3**, 335–373.

43. Xia, Y. N., Rogers, J. A., Paul, K. E., Whitesides, G. M. (1999). Unconventional methods for fabricating and patterning nanostructures. *Chem*. *Rev*., **99**, 1823–1848.

44. Xia, Y. N., Whitesides, G. M. (1998). Soft lithography. *Angew*. *Chem*. *Intl*. *Ed*., **37**, 551–575.

45. Liu, G. Y., Xu, S., Qian, Y. L. (2000). Nanofabrication of self-assembled monolayers using scanning probe lithography. *Acc*. *Chem*. *Res*., **33**, 457–466.

46. Wouters, D., Schubert, U. S. (2004). Nanolithography and nanochemistry: Probe-related patterning techniques and chemical modification for nanometer-sized devices. *Angew*. *Chem*. *Intl*. *Ed*., **43**, 2480–2495.

47. Salaita, K., Wang, Y. H., Mirkin, C. A. (2007). Applications of dip-pen nanolithography, *Nat*. *Nanotechnol*., **2**,145–155.

48. Loos, J. (2005). The art of SPM: Scanning probe microscopy in materials science. *Adv*. *Mater*., **17**, 1821–1833.

49. Tang, Q., Shi, S. Q., Zhou, L. M. (2004). Nanofabrication with atomic force microscopy. *J*. *Nanosci*. *Nanotechnol*., **4**, 948–963.

50. Wouters, D., Schubert, U. S. (2004). Nanolithography and nanochemistry: Probe-related patterning techniques and chemical modification for nanometer-sized devices. *Angew*. *Chem*. *Intl*. *Ed*., **43**, 2480–2495.

51. Hong, S. H., Zhu, J., Mirkin, C. A. (1999). Multiple ink nanolithography: Toward a multiple-pen nano-plotter. *Science*, **286**, 523–525.

52. Piner, R. D., Zhu, J., Xu, F., Hong, S. H., Mirkin, C. A. (1999). Dip-pen nano-lithography. *Science*, **283**, 661–663.

53. Katz, E., Willner, I. (2004). Integrated nanoparticle-biomolecule hybrid systems: Synthesis, properties, and applications. *Angew*. *Chem*. *Intl*. *Ed*., **43**, 6042–6108.

54. Liao, H. W., Nehl, C. L., Hafner, J. H. (2006). Biomedical applications of plasmon resonant metal nanoparticles. *Nanomedicine*, **1**, 201–208.

55. Hyafil, F., Cornily, J. C., Feig, J. E., Gordon, R., Vucic, E., Amirbekian, V., Fisher, E. A., Fuster, V., Feldman, L. J., Fayad, Z. A. (2007). Noninvasive

detection of macrophages using a nanoparticulate contrast agent for computed tomography. *Nat. Med.*, **13**, 636–641.

56. Karp, J. M., Langer, R. (2007). Development and therapeutic applications of advanced biomaterials. *Curr. Opin. Biotechnol.*, **18**, 454–459.
57. Langer, R., Tirrell, D. A. (2004). Designing materials for biology and medicine. *Nature*, **428**, 487–492.
58. LaVan, D. A., McGuire, T., Langer, R. (2003). Small-scale systems for *in vivo* drug delivery. *Nat. Biotechnol.*, **21**, 1184–1191.
59. Son, S. J., Bai, X., Lee, S. (2007). Inorganic hollow nanoparticles and nano-tubes in nanomedicine. Part 2: Imaging, diagnostic, and therapeutic applications. *Drug Discov. Today*, **12**, 657–663.
60. Wu, W. W., Li, A. D. (2007). Optically switchable nanoparticles for biological imaging. *Nanomedicine*, **2**, 523–531.
61. de Chermont, Q. L., Chaneac, C., Seguin, J., Pelle, F., Maitrejean, S., Jolivet, J. P., Gourier, D., Bessodes, M., Scherman, D. (2007). Nanoprobes with near-infrared persistent luminescence for *in vivo* imaging. *Proc. Natl. Acad. Sci. U. S. A.*, **104**, 9266–9271.
62. Gao, X. H., Yang, L. L., Petros, J. A., Marshal, F. F., Simons, J. W., Nie, S. M. (2005). *In vivo* molecular and cellular imaging with quantum dots. *Curr. Opin. Biotechnol.*, **16**, 63–72.
63. Michalet, X., Pinaud, F. F., Bentolila, L. A., Tsay, J. M., Doose, S., Li, J. J., Sundaresan, G., Wu, A. M., Gambhir, S. S., Weiss, S. (2005). Quantum dots for live cells, *in vivo* imaging, and diagnostics. *Science*, **307**, 538–544.
64. Nie, S. M., Xing, Y., Kim, G. J., Simons, J. W. (2007). Nanotechnology applications in cancer. *Ann. Rev. Biomed. Eng.*, **9**, 257–288.
65. Rhyner, M. N., Smith, A. M., Gao, X. H., Mao, H., Yang, L. L., Nie, S. M. (2006). Quantum dots and multifunctional nanoparticles: New contrast agents for tumor imaging. *Nanomedicine*, **1**, 209–217.
66. Stroh, M., Zimmer, J. P., Duda, D. G., Levchenko, T. S., Cohen, K. S., Brown, E. B., Scadden, D. T., Torchilin, V. P., Bawendi, M. G., Fukumura, D., Jain, R. K. (2005). Quantum dots spectrally distinguish multiple species within the tumor milieu *in vivo*. *Nat. Med.*, **11**, 678–682.
67. Bailey, R. E., Nie, S. M. (2003). Alloyed semiconductor quantum dots: Tuning the optical properties without changing the particle size. *J. Am. Chem. Soc.*, **125**, 7100–7106.
68. Rosenthal, S. J., McBride, J., Pennycook, S. J., Feldman, L. C. (2007). Synthesis, surface studies, composition and structural characterization

of CdSe, core/shell and biologically active nanocrystals. *Surf. Sci. Rep.*, **62**, 111–157.

69. Wang, D. S., He, J. B., Rosenzweig, N., Rosenzweig, Z. (2004). Superparamagnetic Fe_2O_3 Beads-CdSe/ZnS quantum dots core-shell nanocomposite particles for cell separation. *Nano Lett.*, **4**, 409–413.
70. Yin, Y., Alivisatos, A. P. (2005). Colloidal nanocrystal synthesis and the organic-inorganic interface. *Nature*, **437**, 664–670.
71. Bentzen, E. L., House, F., Utley, T. J., Crowe, J. E., Wright, D. W. (2005). Progression of respiratory syncytial virus infection monitored by fluorescent quantum dot probes. *Nano Lett.*, **5**, 591–595.
72. Jamieson, T., Bakhshi, R., Petrova, D., Pocock, R., Imani, M., Seifalian, A. M. (2007). Biological applications of quantum dots. *Biomaterials*, **28**, 4717–4732.
73. Ipe, B. I., Lehnig, M., Niemeyer, C. M. (2005). On the generation of free radical species from quantum dots. *Small*, **1**, 706–709.
74. Kirchner, C., Liedl, T., Kudera, S., Pellegrino, T., Javier, A. M., Gaub, H. E., Stolzle, S., Fertig, N., Parak, W. J. (2005). Cytotoxicity of colloidal CdSe and CdSe/ZnS nanoparticles. *Nano Lett.*, **5**, 331–338.
75. Derfus, A. M., Chan, W. C. W., Bhatia, S. N. (2004). Probing the cytotoxicity of semiconductor quantum dots. *Nano Lett.*, **4**, 11–18.
76. Hoshino, A., Fujioka, K., Oku, T., Suga, M., Sasaki, Y. F., Ohta, T., Yasuhara, M., Suzuki, K., Yamamoto, K. (2004). Physicochemical properties and cellular toxicity of nanocrystal quantum dots depend on their surface modification. *Nano Lett.*, **4**, 2163–2169.
77. Link, S., El-Sayed, M. A. (2003). Optical properties and ultrafast dynamics of metallic nanocrystals. *Ann. Rev. Phys. Chem.*, **54**, 331–366.
78. Jain, P. K., El-Sayed, I. H., El-Sayed, M. A. (2007). Au nanoparticles target cancer. *Nano Today*, **2**, 18–29.
79. Connor, E. E., Mwamuka, J., Gole, A., Murphy, C. J., Wyatt, M. D. (2005). Gold nanoparticles are taken up by human cells but do not cause acute cytotoxicity. *Small*, **1**, 325–327.
80. Niemeyer, C. M., Ceyhan, B. (2001). DNA-directed functionalization of colloidal gold with proteins. *Angew. Chem. Intl. Ed.*, **40**, 3685–3688.
81. Bhattacharya, R., Patra, C. R., Earl, A., Wang, S. F., Katarya, A., Lu, L. C., Kizhakkedathu, J. N., Yaszemski, M. J., Greipp, P. R., Mukhopadhyay, D., Mukherjee, P. (2007). Attaching folic acid on gold nanoparticles using

noncovalent interaction via different polyethylene glycol back bones and targeting of cancer cells. *Nanomedicine*, **3**, 224–238.

82. Dixit, V., Van den Bossche, J., Sherman, D. M., Thompson, D. H., Andres, R. P. (2006). Synthesis and grafting of thioctic acid-PEG-folate conjugates onto Au nanoparticles for selective targeting of folate receptor- positive tumor cells. *Bioconjug. Chem*., **17**, 603–609.
83. Chithrani, B. D., Chan, W. C. W. (2007). Elucidating the mechanism of cellular uptake and removal of protein-coated gold nanoparticles of different sizes and shapes, *Nano Lett*., **7**, 1542–1550.
84. Yang, P. H., Sun, X. S., Chiu, J. F., Sun, H. Z., He, Q. Y. (2005). Transferrin-mediated gold nanoparticle cellular uptake. *Bioconjug. Chem*., **16**, 494–496.
85. Sokolov, K., Nida, D., Descour, M., Lacy, A., Levy, M., Hall, B., Dharmawardhane, S., Ellington, A., Korgel, B., Richards-Kortum, R. (2007). Molecular optical imaging of therapeutic targets of cancer. *Adv*. *Cancer Res*., **96**, 299–344.
86. Zheng, G. F., Patolsky, F., Cui, Y., Wang, W. U., Lieber, C. M. (2005). Multiplexed electrical detection of cancer markers with nanowire sensor arrays. *Nat*. *Biotechnol*., **23**, 1294–1301.
87. Chen, R. J., Bangsaruntip, S., Drouvalakis, K. A., Kam, N. W. S., Shim, M., Li, Y. M., Kim, W., Utz, P. J., Dai, H. J. (2003). Noncovalent functionalization of carbon nanotubes for highly specific electronic biosensors. *Proc*. *Natl*. *Acad*. *Sci*. *U*. *S*. *A*., **100**, 4984–4989.
88. Caruthers, S. D., Wickline, S. A., Lanza, G. M. (2007). Nanotechnological applications in medicine, *Curr*. *Opin*. *Biotechnol*., **18**, 26–30.
89. Corot, C., Robert, P., Idee, J. M., Port, M. (2006). Recent advances in iron oxide nanocrystal technology for medical imaging. *Adv*. *Drug Deliv*. *Rev*., **58**, 1471–1504.
90. Gupta, A. K., Gupta, M. (2005). Synthesis and surface engineering of iron oxide nanoparticles for biomedical applications. *Biomaterials*, **26**, 3995–4021.
91. Koo, Y. E. L., Reddy, G. R., Bhojani, M., Schneider, R., Philbert, M. A., Rehemtulla, A., Ross, B. D., Kopelman, R. (2006). Brain cancer diagnosis and therapy with nanoplatforms. *Adv*. *Drug Delivery Rev*., **58**, 1556–1577.
92. Raty, J. K., Liimatainen, T., Kaikkonen, M. U., Grahn, O., Airenne, K. J., Yla-Herttuala, S. (2007). Non-invasive Imaging in gene therapy. *Mol*. *Ther*., **15**, 1579–1586.

93. Rogers, W. J., Meyer, C. H., Kramer, C. M. (2006). Technology insight: *In vivo* cell tracking by use of MRI. *Nat. Clin. Pract. Cardiovasc. Med.*, **3**, 554–562.

94. Thorek, L. J., Chen, A., Czupryna, J., Tsourkas, A. (2006). Superparamagnetic iron oxide nanoparticle probes for molecular imaging. *Ann. Biomed. Eng.*, **34**, 23–38.

95. Weber, W. A., Czernin, J., Phelps, M. E., Herschman, H. R. (2008). Technology Insight: Novel imaging of molecular targets is an emerging area crucial to the development of targeted drugs. *Nat. Clin. Pract. Oncol.*, **5**, 44–54.

96. Huh, Y. M., Jun, Y. W., Song, H. T., Kim, S., Choi, J. S., Lee, J. H., Yoon, S., Kim, K. S., Shin, J. S., Suh, J. S., Cheon, J. (2005). *In vivo* magnetic resonance detection of cancer by using multifunctional magnetic nanocrystals. *J. Am. Chem. Soc.*, **127**, 12387–12391.

97. Jun, Y. W., Huh, Y. M., Choi, J. S., Lee, J. H., Song, H. T., Kim, S., Yoon, S., Kim, K. S., Shin, J. S., Suh, J. S., Cheon, J. (2005). Nanoscale size effect of magnetic nanocrystals and their utilization for cancer diagnosis via magnetic resonance imaging. *J. Am. Chem. Soc.*, **127**, 5732–5733.

98. Lee, J. H., Huh, Y. M., Jun, Y., Seo, J., Jang, J., Song, H. T., Kim, S., Cho, E. J., Yoon, H. G., Suh, J. S., Cheon, J. (2007). Artificially engineered magnetic nanoparticles for ultra-sensitive molecular imaging. *Nat. Med.*, **13**, 95–99.

99. Song, H. T., Choi, J. S., Huh, Y. M., Kim, S., Jun, Y. W., Suh, J. S., Cheon, J. (2005). Surface modulation of magnetic nanocrystals in the development of highly efficient magnetic resonance probes for intracellular labeling. *J. Am. Chem. Soc.*, **127**, 9992–9993.

100. Allen, T. M., Martin, F. J. (2004). Advantages of liposomal delivery systems for anthracyclines. *Semin. Oncol.*, **31**, 5–15.

101. Cattel, L., Ceruti, M., Dosio, F. (2003). From conventional to stealth liposomes a new frontier in cancer chemotherapy. *Tumori*, **89**, 237–249.

102. Sparano, J. A., Winer, E. P. (2001). Liposomal anthracyclines for breast cancer. *Semin. Oncol.*, **28**, 32–40.

103. Gabizon, A., Shmeeda, H., Barenholz, Y. (2003). Pharmacokinetics of pegylated liposomal doxorubicin—Review of animal and human studies. *Clin. Pharmacokinet.*, **42**, 419–436.

104. Hynes, N. E., Lane, H. A. (2005). ERBB receptors and cancer: The complexity of targeted inhibitors. *Nat. Rev. Cancer*, **5**, 341–354.

105. Duncan, R., Vicent, M. J., Greco, F., Nicholson, R. I. (2005). Polymer-drug conjugates: Towards a novel approach for the treatment of endrocine-related cancer. *Endocr. Relat. Cancer*, **12**, S189–S199.

106. Senter, P. D., Springer, C. J. (2001). Selective activation of anticancer prodrugs by monoclonal antibody-enzyme conjugates. *Adv. Drug Deliv. Rev.*, **53**, 247–264.

107. Dancey, J. E., Chen, H. X. (2006). Strategies for optimizing combinations of molecularly targeted anticancer agents, *Nat. Rev. Drug Discov.*, **5**, 649–659.

108. Imai, K., Takaoka, A. (2006). Comparing antibody and small-molecule therapies for cancer. *Nat. Rev. Cancer*, **6**, 714–727.

109. Marshall, S. A., Lazar, G. A., Chirino, A. J., Desjarlais, J. R. (2003). Rational design and engineering of therapeutic proteins. *Drug Discov. Today*, **8**, 212–221.

110. Brannon-Peppas, L., Blanchette, J. O. (2004). Nanoparticle and targeted systems for cancer therapy. *Adv. Drug Deliv. Rev.*, **56**, 1649–1659.

111. Peer, D., Karp, J. M., Hong, S., FaroKhzad, O. C., Margalit, R., Langer, R. (2007). Nanocarriers as an emerging platform for cancer therapy. *Nat. Nanotechnol.*, **2**, 751–760.

112. Brigger, I., Dubernet, C., Couvreur, P. (2002). Nanoparticles in cancer therapy and diagnosis. *Adv. Drug Deliv. Rev.*, **54**, 631–651.

113. Allen, T. M. (1994). The use of glycolipids and hydrophilic polymers in avoiding rapid uptake of liposomes by the mononuclear phagocyte system. *Adv. Drug Deliv. Rev.*, **13**, 285–309.

114. Kim, G. J., Nie, A. S. (2005). Targeted cancer nanotherapy. *Nanotoday*, **8**, 28–33.

115. Park, J. W., Kirpotin, D. B., Hong, K., Shalaby, R., Shao, Y., Nielsen, U. B., Marks, J. D., Papahadjopoulos, D., Benz, C. C. (2001). Tumor targeting using anti-her2 immunoliposomes. *J. Control. Release*, **74**, 95–113.

116. Torchilin, V. P. (2006). Multifunctional nanocarriers. *Adv. Drug Deliv. Rev.*, **58**, 1532–1555.

117. Moghimi, S. M., Hunter, A. C., Murray, J. C. (2005). Nanomedicine: Current status and future prospects. *FASEB J.*, **19**, 311–330.

118. Betancourt, T., Brown, B., Brannon-Peppas, L. (2007). Doxorubicin-loaded PLGA nanoparticles by nanoprecipitation: Preparation, characterization and *in vitro* evaluation. *Nanomedicine*, **2**, 219–232.

119. Duncanson, W. J., Figa, M. A., Hallock, K., Zalipsky, S., Hamilton, J. A., Wong, J. Y. (2007). Targeted binding of PLA microparticles with lipid-PEG- tethered ligands. *Biomaterials*, **28**, 4991–4999.

120. Panyam, J., Labhasetwar, V. (2003). Biodegradable nanoparticles for drug and gene delivery to cells and tissue. *Adv*. *Drug Deliv. Rev*., **55**, 329–347.

121. Soppimath, K. S., Aminabhavi, T. M., Kulkarni, A. R., Rudzinski, W. E. (2001). Biodegradable polymeric nanoparticles as drug delivery devices. *J. Control. Release*, **70**, 1–20.

122. Vasir, J. K., Labhasetwar, V. (2007). Biodegradable nanoparticles for cytosolic delivery of therapeutics. *Adv*. *Drug Deliv. Rev*., **59**, 718–728.

123. Dang, J. M., Leong, K. W. (2006). Natural polymers for gene delivery and tissue engineering. *Adv*. *Drug Deliv. Rev*., **58**, 487–499.

124. des Rieux, A., Fievez, V., Garinot, M., Schneider, Y. J., Preat, V. (2006). Nanoparticles as potential oral delivery systems of proteins and vaccines: A mechanistic approach. *J. Control. Release*, **116**, 1–27.

125. Liu, Y. J., Li, Y. L., Liu, S. C., Li, J., Yao, S. Z. (2004). Monitoring the self-assembly of chitosan/glutaraldehyde/cysteamine/Au-colloid and the binding of human serum albumin with hesperidin. *Biomaterials*, **25**, 5725–5733.

126. Peppas, N. A., Hilt, J. Z., Khademhosseini, A., Langer, R. (2006). Hydrogels in biology and medicine: From molecular principles to bionanotechnology, *Adv*. *Mater*., **18**, 1345–1360.

127. G. Gaucher, M. H. Dufresne, V. P. Sant, N. Kang, D. Maysinger, and J. C. Leroux, Block copolymer micelles: Preparation, characterization and application in drug delivery, *J. Control. Release*, **109**, 169–188 (2005).

128. Jones, M. C., Ranger, M., Leroux, J. C. (2003). pH-sensitive unimolecular polymeric micelles: Synthesis of a novel drug carrier. *Bioconjug. Chem*., **14**, 774–781.

129. Lee, E. S., Oh, K. T., Kim, D., Youn, Y. S., Bae, Y. H. (2007). Tumor pH-responsive flower-like micelles of poly(L-lactic acid)-b-poly (ethylene glycol)-b-poly (L-histidine). *J. Control. Release*, **123**, 19–26.

130. Lin, W. J., Juang, L. W., Lin, C. C. (2003). Stability and release performance of a series of pegylated copolymeric micelles. *Pharm*. *Res*., **20**, 668–673.

131. Seow, W. Y., Xue, J. M., Yang, Y. Y. (2007). Targeted and intracellular delivery of paclitaxel using multi-functional polymeric micelles. *Biomaterials*, **28**, 1730–1740.

132. Wang, X. L., Jensen, R., Lu, Z. R. (2007). A novel environment-sensitive biodegradable polydisulfide with protonatable pendants for nucleic acid delivery. *J*. *Control. Release*, **120**, 250–258.

133. Mi, F. L., Wu, Y. Y., Chiu, Y. L., Chen, M. C., Sung, H. W., Yu, S. H., Shyu, S. S., Huang, M. F. (2007). Synthesis of a novel glycol conjugated chitosan and preparation of its derived nanoparticles for targeting HepG2 cells. *Biomacromolecules*, **8**, 892–898.

134. Elbayoumi, T. A., Pabba, S., Roby, A., Torchilin, V. P. (2007). Antinucleosome antibody-modified liposomes and lipid-core micelles for tumor-targeted delivery of therapeutic and diagnostic agents. *J. Liposome Res.*, **17**, 1–14.

135. Lacoeuille, F., Hindre, F., Moal, F., Roux, J., Passirani, C., Couturier, O., Cales, P., Le Jeune, J. J., Lamprecht, A., Benoit, J. P. (2007). *In vivo* evaluation of lipid nanocapsules as a promising colloidal carrier for paclitaxel. *Intl. J. Pharm.*, **344**, 143–149.

136. Leroux, J. C. (2007). Injectable nanocarriers for biodetoxification. *Nat. Nanotechnol.*, **2**, 679–684.

137. Lian, T., Ho, R. J. Y. (2001). Trends and developments in liposome drug delivery systems. *J. Pharm. Sci.*, **90**, 667–680.

138. Moghimi, S. M., Davis, S. S. (1994). Innovations in avoiding particle clearance from blood by Kupffer cells—cause for reflection. *Crit. Rev. Ther. Drug Carrier Syst.*, **11**, 31–59.

139. Cho, S. Y., Allcock, H. R. (2007). Dendrimers derived from poly-phosphazene-poly(propyleneimine) systems: Encapsulation and triggered release of hydrophobic guest molecules. *Macromolecules*, **40**, 3115–3121.

140. Paleos, C. M., Tsiourvas, D., Sideratou, Z. (2007). Molecular engineering of dendritic polymers and their application as drug and gene delivery systems. *Mol. Pharm.*, **4**, 169–188.

141. Seib, F. P., Jones, A. T., Duncan, R. (2007). Comparison of the endocytic properties of linear and branched PEIs, and cationic PAMAM den drimers in B16f10 melanoma cells. *J. Control. Release*, **117**, 291–300.

142. Shi, X. G., Wang, S. H., Meshinchi, S., Van Antwerp, M. E., Bi, X. D., Lee, I. H., Baker, J. R. (2007). Dendrimer-entrapped gold nanoparticles as a platform for cancer-cell targeting and Imaging. *Small*, **3**, 1245–1252.

143. Kukowska-Latallo, J. F., Candido, K. A., Cao, Z. Y., Nigavekar, S. S., Majoros, I. J., Thomas, T. P., Balogh, L. P., Khan, M. K., Baker, J. R. (2005). Nanoparticle targeting of anticancer drug improves thera peutic response in animal model of human epithelial cancer. *Cancer Res.*, **65**, 5317–5324.

144. Crumbliss, A. L., Perine, S. C., Stonehuerner, J., Tubergen, K. R., Zhao, J., Henkens, R. W., O'Daly, J. P. (2004). Colloidal gold as a biocompatible immobilization matrix suitable for the fabrication of enzyme electrodes by electrodeposition. *Biotechnol. Bioeng.*, **40**, 483–490.

145. Huff, T. B., Hansen, M. N., Zhao, Y., Cheng, J. X., Wei, A. (2007). Controlling the cellular uptake of gold nanorods. *Langmuir*, **23**, 1596–1599.

146. Kneipp, J., Kneipp, H., McLaughlin, M., Brown, D., Kneipp, K. (2006). *In vivo* molecular probing of cellular compartments with gold nanoparticles and nanoaggregates. *Nano Lett.*, **6**, 2225–2231.

147. Shukla, R., Bansal, V., Chaudhary, M., Basu, A., Bhonde, R. R., Sastry, M. (2005). Biocompatibility of gold nanoparticles and their endocytotic fate inside the cellular compartment: A microscopic overview. *Langmuir*, **21**, 10644–10654.

148. Paciotti, G. F., Meyer, L., Weinreich, D., Goia, D., Pavel, N., McLaughlin, R. E., Tamarkin, L. (2004). Colloidal gold: A novel nanoparticle vector for tumor directed drug delivery. *Drug Deliv.*, **11**, 169–183.

149. Rosi, N. L., Giljohann, D. A., Thaxton, C. S., Lytton-Jean, A. K. R., Han, M. S., Mirkin, C. A. (2006). Oligonucleotide-modified gold nanoparticles for intracellular gene regulation. *Science*, **312**, 1027–1030.

150. Neuberger, T., Schopf, B., Hofmann, H., Hofmann, M., von Rechenberg, B. (2005). Super paramagnetic nanoparticles for biomedical applications: Possibilities and limitations of a new drug delivery system. *J. Magn. Magn. Mater.*, **293**, 483–496.

151. Sosnovik, D. E., Weissleder, R. (2007). Emerging concepts in molecular MRI. *Curr. Opin. Biotechnol.*, **18**, 4–10.

152. Garcia, I., Zafeiropoulos, N. E., Janke, A., Tercjak, A., Eceiza, A., Stamm, M., Mondragon, I. (2007). Functionalization of iron oxide magnetic nanoparticles with poly(methyl methacrylate) brushes via grafting-from atom transfer radical polymerization. *J. Polym. Sci. Part A Polym. Chem.*, **45**, 925–932.

153. Lattuada, M., Hatton, T. A. (2007). Functionalization of monodisperse magnetic nanoparticles. *Langmuir*, **23**, 2158–2168.

154. El-Sayed, H., Huang, X. H., El-Sayed, M. A. (2006). Selective laser photo-thermal therapy of epithelial carcinoma using anti-EGFR anti body conjugated gold nanoparticles. *Cancer Lett.*, **239**, 129–135.

155. Everts, M., Saini, V., Leddon, J. L., Kok, R. J., Stoff-Khalili, M., Preuss, M. A., Millican, C. L., Perkins, G., Brown, J. M., Bagaria, H., Nikles, D. E., Johnson, D. T., Zharov, V. P., Curiel, D. T. (2006). Covalently linked au

nanoparticles to a viral vector: Potential for combined photothermal and gene cancer therapy. *Nano Lett*., **6**, 587–591.

156. Huang, X. H., El-Sayed, I. H., Qian, W., El-Sayed, M. A. (2006). Cancer cell imaging and photothermal therapy in the near-infrared region by using gold nanorods. *J*. *Am*. *Chem*. *Soc*., **128**, 2115–2120.
157. Seo, W. S., Lee, J. H., Sun, X. M., Suzuki, Y., Mann, D., Liu, Z., Terashima, M., Yang, P. C., McConnell, M. V., Nishimura, D. G., Dai, H. J. (2006). FeCo/graphitic- shell nanocrystals as advanced magnetic-resonance-imaging and near-infrared agents. *Nat*. *Mater*., **5**, 971–976.
158. Zharov, V. P., Mercer, K. E., Galitovskaya, E. N., Smeltzer, M. S. (2006). Photothermal nanotherapeutics and nanodiagnostics for selective killing of bacteria targeted with gold nanoparticles. *Biophys*. *J*., **90**, 619–627.
159. Barham, C. P., Jones, R. L., Biddlestone, L. R., Hardwick, R. H., Shepherd, N. A., Barr, H. (1997). Photothermal laser ablation of Barrett's oesophagus: Endoscopic and histological evidence of squamous re-epithelialisation. *Gut*, **41**, 281–284.
160. Chen, Y., Wang, D. L., Xi, J. F., Au, L., Siekkinen, A., Warsen, A., Li, Z. Y., Zhang, H., Xia, Y. N., Li, X. D. (2007). Immuno gold nanocages with tailored optical properties for targeted photothermal destruction of cancer cells. *Nano Lett*., **7**, 1318–1322.
161. Loo, C., Lowery, A., Halas, N., West, J., Drezek, R. (2005). Immunotargeted nanoshells for integrated cancer imaging and therapy. *Nano Lett*., **5**, 709–711.
162. Ismagilov, R. F., Maharbiz, M. M. (2007). Can we build synthetic, multicellullar systems by controlling developmental signalling in space and time?. *Curr*. *Opin*. *Chem*. *Biol*., **11**, 604–611.
163. Dittrich, P. S., Manz, A. (2006). Lab-on-a-chip: Microfluidics in drug discovery. *Nat*. *Rev*. *Drug Discv*., **5**, 210–218.
164. Dittrich, P. S., Tachikawa, K., Manz, A. (2006). Micro total analysis systems. Latest advancements and trends. *Anal*. *Chem*., **78**, 3887–3907.
165. El-Ali, J., Sorger, P. K., Jensen, K. F. (2006). Cells on chips. *Nature*, **442**, 403–411.
166. Falconnet, D., Csucs, G., Grandin, H. M., Textor, M. (2006). Surface engineering approaches to micropattern surfaces for cell-based assays. *Biomaterials*, **27**, 3044–3063.
167. Khademhosseini, A., Langer, R., Borenstein, J., Vacanti, J. P. (2006). Microscale technologies for tissue engineering and biology. *Proc*. *Natl*. *Acad*. *Sci*. *U*. *S*. *A*., **103**, 2480–2487.

168. Nagrath, S., Sequist, L. V. Maheswaran, S., Bell, D. W., Irimia, D., Ulkus, L., Smith, M. R., Kwak, E. L., Digumarthy, S., Muzikansky, A., Ryan, P., Balis, U. J., Tompkins, R. G., Haber, D. A., Toner, M. (2007). Isolation of rare circulating tumour cells in cancer patients by microchip technology. *Nature*, **450**, 1235–U10.

169. Moore, P. (2005). Cell biology: Ion channels and stem cells. *Nature*, **438**, 699–704.

170. Dertinger, S. K. W., Jiang, X. Y., Li, Z. Y., Murthy, V. N., Whitesides, G. M. (2002). Gradients of substrate-bound laminin orient axonal specification of neurons. *Proc*. *Natl*. *Acad*. *Sci*. *U*. *S*. *A*., **99**, 12542–12547.

171. Balagadde, F. K., You, L. C., Hansen, C. L., Arnold, F. H., Quake, S. R. (2005). Long-term monitoring of bacteria undergoing programmed population control in a microchemostat. *Science*, **309**, 137–140.

172. Martino, G., Pluchino, S. (2006). The therapeutic potential of neural stem cells. *Nat*. *Rev*. *Neurosci*., **7**, 395–406.

173. Temple, S. (2001). The development of neural stem cells. *Nature*, **414**, 112–117.

174. Fuchs, E., Tumbar, T., Guasch, G. (2004). Socializing with the neighbors: Stem cells and their niche. *Cell*, **116**, 769–778.

175. Moore, K. A., Lemischka, I. R. (2006). Stem cells and their niches. *Science*, **311**, 1880–1885.

176. Kratchmarova, I., Blagoev, B., Haack-Sorensen, M., Kassem, M., Mann, M. (2005). Mechanism of divergent growth factor effects in mesenchymal stem cell differentiation. *Science*, **308**, 1472–1477.

177. Lutolf, M. P., Hubbell, J. A. (2005). Synthetic biomaterials as instructive extracellular microenvironments for morphogenesis in tissue engineering. *Nat*. *Biotechnol*., **23**, 47–55.

178. Watt, F. M., Hogan, B. L. M. (2000). Out of eden: Stem cells and their niches. *Science*, **287**, 1427–1430.

179. Fleming, T. P., Sheth, B., Fesenko, I. (2001). Cell adhesion in the preim- plantation mammalian embryo and its role in trophectoderm differentiation and blastocyst morphogenesis. *Front*. *Biosci*., **6**, D1000–D1007.

180. Yoder, M. C., Williams, D. A. (1995). Matrix molecule interactions with hematopoietic stem-cells. *Exp*. *Hematol*., **23**, 961–967.

181. Ding, S., Schultz, P. G. (2004). A role for chemistry in stem cell biology. *Nat*. *Biotech*., **22**, 833–840.

182. Flaim, C. J., Chien, S., Bhatia, S. N. (2005). An extracellular matrix microarray for probing cellular differentiation. *Nat*. *Methods*, **2**, 119–125.

183. Soen, Y., Mori, A., Palmer, T. D., Brown, P. O. (2006). Exploring the regulation of human neural precursor cell differentiation using arrays of signaling microenvironments. *Mol*. *Syst*. *Biol*., **2**, 37.

Chapter 3

A Small Introduction to the World of Nanomedicine

Rutledge Ellis-Behnke, PhD

Department of Ophthalmology, Medical Faculty Mannheim of the Ruprecht-Karls-University of Heidelberg, Germany; Department of Brain and Cognitive Sciences, Massachusetts Institute of Technology, Cambridge, Massachusetts, USA; Center of Excellence for Aging and Brain Repair, University of South Florida Morsani College of Medicine, Tampa, Florida, USA

Keywords: nanomedicine, traditional Chinese medicine, nanomarkers, quantum dots, flow cytometry, TessArae® chip, US Food and Drug Administration

3.1 Introduction

Although presently there is no universally accepted definition or nomenclature for nanotechnology and nanomedicine, these broad areas of research and development are not new [1, 2]. However, understanding how the *effects* of the nanoscale change the way therapeutics are measured and delivered is new. Nanomedicine, or the use of nanotechnology in medicine, now fundamentally changes how we think not only about therapeutics, but also about newly emerging molecular medical devices [3, 4].

Handbook of Clinical Nanomedicine: Nanoparticles, Imaging, Therapy, and Clinical Applications
Edited by Raj Bawa, Gerald F. Audette, and Israel Rubinstein

ISBN 978-981-4669-20-7 (Hardcover), 978-981-4669-21-4 (eBook)
www.panstanford.com

Traditional Chinese medicine (TCM) [5] doctors have long known that you cannot cure a problem with one compound. Some 2000 years ago, the Chinese invented the first pills, a collection of herbs coated with honey that acted as a binder that helped deliver the medicine directly to the patient's stomach without degradation. This was also one of the first targeted therapeutic delivery systems. Nanotechnology is the new "TCM honey" of the pharmaceutical world. It can help bind the therapeutics together without changing their activity and helps target them to the correct location. By allowing for specific targeting, nanotechnology can also help decrease the amount needed and can provide structure to an otherwise unstructured environment, so that everything stays where it is needed.

3.2 Size Medicine

Nanomedicine, or *size* medicine, sounds like a silly concept. There was no *micro*medicine revolution, so why now is there a need to name this the *nano*medicine revolution? Each time in history that there has been an increase in resolution by a power of ten, science and technology have leapt ahead with new discoveries with the full impact felt several decades later. Why is this any different from any other power of ten increases in resolution? Because in this particular stage of increase in resolution lies the fundamental change in many properties of interaction, where we can now measure and understand the interaction at the molecular scale. You may be thinking that this does not seem correct, that we have been making small molecules in the pharmaceutical industry for years. So, what are the implications of this particular change? Nanotechnology not only changes how we calculate the dose, but also how we manufacture the materials. But let me put forth three of the most important differences, demonstrating how nanomedicine will fundamentally change how we discover, produce and deliver these new, sometimes revolutionary, therapeutics and devices.

3.2.1 The Myth of Small Molecules

It is true that a drug formulation is compounded initially as small molecules floating around in a large vat to very specific standards.

However, once the material is dried, it is no longer individual molecules but an aggregate of 100,000 to 1 million molecules in a large complex matrix. Moreover, the amount of drug that is delivered, after going through the gut, is very small compared to the original dose. *We know that when the size of a nanoparticle or molecule is less than 10 nanometers, permeability goes to almost infinity, while solubility does not change.* So now, picture the delivery of a large aggregate of molecules versus dispersion at the nanoscale where single molecules can be separated. This seemingly simple change allows for drugs that have solubility problems to be delivered with very high efficiency at a 100 nanogram dose while the original 500 milligram dose may not be capable of delivering the same effect.

3.2.2 Nanomedicine Drug Delivery Has Implications That Go Beyond Medicine

Nanomedicine drug delivery has implications that go way beyond medicine; it will also make a tremendous impact on the environment. Individual molecules can be delivered to specific targets, without breakdown, until the therapeutic effect is achieved and the material then breaks down and is eliminated. The therapeutics release only when the correct target is reached. With this type of formulation and construction, the quantity delivered can be decreased 10 to 50 fold. Imagine spraying an analgesic on a piece of paper: slip the entire paper into your mouth and the drug is absorbed. Now compare that with the traditional analgesic pill that must travel through your entire system before starting to work. Think about how that reduction in dose will reduce the amount of waste generated during the manufacturing process, and the resultant changes in how the supply chain is managed. With just the reduction of an analgesic from 500 *milli*grams down to 100 *nano*grams, the amount of weight to be transported will decrease by a very large percentage.

The implications of these changes also create new hurdles to measure the amount of therapeutic delivered and the possibility of increased toxicity. The converse is true, where the therapeutic is delivered to the target, and only the target. In cancer, the MTD (maximum tolerable dose) is the limit that everyone wants to reach to kill the tumor and cancer cells while keeping the patient

alive. In nanotechnology there is a new type of MTD, maximum *targeted* dose, which completely changes the treatment paradigm. This is so important because it demonstrates the possibility of treating people without side effects. Some of these treatments are already being used in the clinic today and many more are on the way [1, 2].

3.2.3 Form Leads to Function

This increase in resolution has also enabled the production of new shapes of materials that better target specific cell types or penetrate new barriers without creating damage. We have also learned that the three dimensional orientation of the targeting ligand is important to the endocytosis of the carrier. So, by changing the shapes of these carriers it is possible to target a specific stage in one cell group while leaving alone the remaining cells of the same cell group that are at a different stage. This form of targeting can also be extended to the coatings on medical devices, such as creating a catheter that reduces the ability of bacteria to adhere to it. The change in structure would prevent bacteria from adhering to it, stopping or reducing the incidence of urinary tract infections. In these cases, the shape is the key to their functionality. The forms are already in the nanorealm and are very well defined.

3.3 Newer Areas of Emerging Therapeutics

Several exciting areas of emerging therapeutics include (1) the creation of steric interference to effect the binding of a therapeutic, (2) the use of nanomarkers to identify diseased cells, and (3) the use of a chip to diagnose up to 100 viruses and every strain of these viruses that currently does not exist [6, 7].

Steric interference can block or facilitate the binding of a therapeutic by changing the charge of the molecule and thus the ability of a therapeutic to bind. In leukemia, increased efficacy has been shown in binding studies that use the crystal structure to find the correct molecular adaptor and ligand to target the specific type of leukemia [8, 12]. This is currently also being used to treat viruses such as HIV, along with the understanding of how to block infection with HIV where different pathways along the

replication cycle and release cycle are also being attacked. This could only be done with the understanding of the molecular interactions that the nanoscale has enabled us to understand [10–12].

Nanomarkers show great promise in identifying very sparse populations of cells that represent a disease state. One of the greatest revolutions that I believe advanced medicine even more than anesthetics was the pathology revolution. This runs the gamut from the discovery of stains that identified pathogens on slides by Paul Ehrlich and his cousin Karl Weigert, to the Golgi silver nano stain. However, increased resolution allows for increased fidelity of treatment. With conventional dyes, such resolution is generally only achievable in perfect conditions with fresh dye [13].

Quantum dots are used as markers as many of them do not fade and allow re-measurement again and again, which is impossible with many of the current fluorescent dyes. Although many quantum dots are toxic and will never be used inside a human, they are still extremely useful to diagnose disease [14].

Today the next revolution in markers is in flow cytometry. A new generation of highly visible nanomarkers allow for finer separation of diseased cells in order to better target the therapy to either control or cure the disease, as opposed to just prescribing a pill. Both of these nanotools will arguably have as great an impact on nanomedicine as the therapies themselves [15–17].

How do you reconcile the advances of technology with the ability to regulate them, based on old technology? The TessArae® chip, which is currently used in Hong Kong hospitals, can diagnose up to 100 viruses and every strain of these viruses that currently does not exist. This leads to the issue of regulating the diagnosis of something that does not exist, which is in direct conflict with current US regulations where every variation of the test must be performed, even for a diagnostic. Obviously, there is a problem if the virus does not currently exist. This scenario highlights the fact that adapting such new technologies in the clinic, when the technology is beyond the ability of the regulators to understand and approve, is a challenge. This challenge is even greater given that the current regulatory regimes like the US Food and Drug Administration are inadequately prepared to handle the emerging field of nanomedicine [18].

3.4 Safety

No discussion on nanomedicine would be complete unless it dealt with safety, in not only the body but also how materials move through the body to treat cancer with a targeted therapy or to restore a malfunctioning gene in a particular system.

3.4.1 Toxicity

Applying nanotechnology for targeted drug delivery has led to increased efficacy, while decreasing the side effects. Normally, toxicity and persistence is handled at the end of a successful treatment strategy; however, there are ways to minimize toxicity in advance by choosing materials that are known to be inert or by making them below the immunological recognition threshold [19]. Not all nanomaterials cause problems, such as materials that are sequestered in a location that will not cause secondary inflammation. Understanding how the materials are cleared, and doing some simple tests of these materials with cells, provides a good indication of toxicity [19]. In addition, the toxicity of not just the target cells but that of the blood brain barrier (BBB) must be taken into account including how these new materials affect the integrity of that system and its ability to repair itself [20]. In some cases a very toxic substance is necessary to penetrate the BBB and target cancer. On the other hand, in the case of specific cancers with short survival times, there is less concern with the side effects and clearance, because there are no complete cures.

3.4.2 Nanomaterials and the Environment

This also extends to how the materials influence the environment after they are excreted and their persistence over time. What happens when they are in the water supply? How are they broken down in the environment, or not? What are the implications of these materials on the life cycle of aquatic life? In some parts of the world, there are large concentrations of antibiotics in river sediment. This can create problems for long-term resistance and drive evolutionary pressures of new bacteria to emerge. Will nanomaterials do the same thing? There is some indication that

many will not drive evolutionary pressures because nanomaterials have been made by fires for centuries (soot is a form of carbon nanotube) and there do not appear to be major side effects from these; however, this has to be monitored closely [21]. It is necessary here to mention the controversy surrounding the toxicity of carbon nanotubes (CNT) and provide a brief indication of how they affect the CNS. There are two sides to the CNT story, with the final outcome as to the usefulness of CNTs in the CNS still to be decided. The ongoing issues of immunogenicity and toxicity surrounding the use of CNTs will only be clarified after heavy metals and other seeds can be reduced in the manufacturing process, and the careful characterization of the physical properties become standardized [22–25].

3.5 Fad, Promises, or Reality?

Is nanomedicine a fad or is there real change? Objective measurements are the goal of every clinician. Measuring blood pressure was one of the first followed by measuring eye pressure for glaucoma. Now, imaging agents have the ability to stage cancer, diagnose a neurological disease and its progression, as in MS, or measure growing or dying neurons and tissue in the brain. This is where nanotechnology and many new contrast agents, such as gold and other nanoparticles, coupled with Fe or even rods that have a dipole movement, are making great strides [26]. There are new classes of imaging agents that use photo-acoustic signals from polymers for both imaging and delivery of therapeutics to the brain [27]. This sensitivity increase, along with the use of MR to look at metabolic levels in brain cells, will elevate imaging well beyond just contrast secondary signals to actual direct measurement of what is happening in the cell [28, 29]. Although most of these measurements are noninvasive, it is important not to neglect the measurement of tissue that has been removed, or is growing in a dish, in order to look at the distribution of receptors on the surface of a cell and how that value may impact the dose required to get therapeutically relevant level to the site of action [30]. Nanomedicine could have a greater impact in medicine than the introductions of anesthetics and antibiotics *combined*.

Disclosures and Conflict of Interest

The author declares that he has no conflict of interest and has no affiliations or financial involvement with any organization or entity discussed in this chapter. The opinions and conclusions here reflect the current views of the author. They should not be attributed, in whole or in part, to the organizations with which he is affiliated, nor should they be considered as expressing an opinion with regard to the merits of any particular company or product discussed herein. Nothing contained herein is to be considered as the rendering of legal advice.

Corresponding Author

Dr. Rutledge Ellis-Behnke
Department of Brain and Cognitive Sciences
Massachusetts Institute of Technology
Cambridge, Massachusetts 02139, USA
Email: rutledg@mit.edu

About the Author

Rutledge Ellis-Behnke is director of the Nanomedicine Translational Think Tank at the Medical Faculty Mannheim of the University of Heidelberg, Germany. In addition, he holds affiliate positions in the department of brain and cognitive sciences at the MIT; the Center of Excellence for Aging and Brain Repair at the University of South Florida Morsani College of Medicine; the Institute for Regenerative Medicine at Wake Forest University School of Medicine; and the School of Systems Biology at George Mason University. Previously, he was an associate professor in the faculty of medicine at the University of Hong Kong as well as associate director of the Technology Transfer Office.

Dr. Ellis-Behnke is redefining tissue engineering for nanomedicine. His research is focused on reconnecting the disconnected parts of the brain—with the goal of being able to provide a prescription to restore quality of life after brain or spinal

cord trauma, or stroke. In animals, he was the first to repair the brain showing reversal of blindness; to stop bleeding in less than 15 seconds without clotting; to preserve stem cells; and to immobilize prostate cancer stem cells. He has more than 100 worldwide patents and pending patent applications and his "Nano Neuro Knitting" and "Immediate Hemostasis" technologies have each been licensed to companies for translation to humans. *MIT Technology Review* named his "Nanohealing" discoveries one of the "Top 10 Emerging Technologies." Dr. Ellis-Behnke received a PhD from MIT in Neuroscience, a Bachelor of Science from Rutgers University and graduated from Harvard Business School's Advanced Manager's Program. Prior to returning to school to pursue his PhD, Dr. Ellis-Behnke held various management positions including senior vice president of Huntingdon, a public company for pharmaceutical testing and consulting services. In 1995, he was co-founder/CEO of one of the first Internet companies in the world to do online commerce. Dr. Ellis-Behnke is an associate editor for the journal *Nanomedicine: NBM* and serves on the editorial board of *Nanomedicine & Biotherapeutic Discovery*. He is a member of the scientific advisory board of the Glaucoma Foundation.

References

1. Bagchi, D., Bagchi, M., Moriyama, H., Shahidi, F., eds. (2013). *Bionanotechnology: A Revolution in Biomedical Sciences and Human Health.* Wiley Blackwell, UK.
2. Bawa, R. (2008). Nanoparticle-based therapeutics in humans: A survey. *Nanotechnol. Law Bus.,* **5**(2), 135–155.
3. Reisner, D. E., Brauer, S., Zheng, W., Bawa, R., Alvelo, J., Gericke, M., Vulpe, C. (2012). Bionanotechnology. In: Abu-Faraj, Z. O. (ed.). *Handbook of Research on Biomedical Engineering Education and Advanced Bioengineering Learning: Interdisciplinary Concepts, Medical Information Science Reference*, Hershey PA, USA, pp. 436–489.
4. Hornyak, G. L., Dutta, J., Tibbals, H., Rao, A. (2008). *Introduction to Nanoscience*. CRC Press, Boca Raton, FL, USA.
5. O'Brien, K. A., Xue, C. C. (2003). The theoretical framework of Chinese medicine. In: Leung, P. C., Xue, C. C., Cheng, Y. C., eds. *A Comprehensive Guide to Chinese Medicine*. River Edge, NJ: World Scientific Publishing Co.

6. Woo, P. C. Y., Lau, S. K. P., Choi, G. K. Y., Fung, H. T., Shek, K. C., Miao, J., Chan, B. Y. L., Ng, K. H. L., Ngan, A. H. Y., Ellis-Behnke, R. G., Que, T. L., Kam, C. W., Yuen, K. Y. (2010). Resequencing microarray for detection of human adenoviruses in patients with conjunctivitis. *J. Clin. Virol*., **47**, 282–285.
7. Woo, P. C. Y., Lau, S. K. P., Choi, G. K. Y., Fung, H. T., Shek, K. C., Miao, J., Chan, B. Y. L., Ng, K. H. L., Ngan, A. H. Y., Ellis-Behnke, R. G., Que, T. L., Kam, C. W., Yuen, K. Y. (2010). Resequencing microarray for detection of human adenoviruses in patients with community-acquired gastroenteritis: A proof-of-concept study. *J. Med. Microbiol*., **59**, 1387–1390.
8. Kitchen, D. B., Decornez, H., Furr, J. R., Bajorath, J. (2004). Docking and scoring in virtual screening for drug discovery: Methods and applications. *Nat. Rev. Drug Discov.,* **3**, 935–949.
9. Blundell, T. L., Jhoti, H., Abell, C. (2002). High-throughput crystallography for lead discovery in drug design. *Nat. Rev. Drug Discov.*, **1**, 45–54.
10. Kreutzberg, G. W. (1996). Microglia: A sensor for pathological events in the CNS. *Trends Neurosci.*, **19**, 312–318.
11. Mamo, T., Moseman, E. A., Kolishetti, N., Salvador-Morales, C., Shi, J., Kuritzkes, D. R., Langer, R., Von Andrian, U., Farokhzad, O. C. (2010). Emerging nanotechnology approaches for HIV/AIDS treatment and prevention. *Nanomedicine* (*Lond*), **5**, 269–285.
12. Moghimi, S. M., Hunter, A. C., Murray, J. C. (2005). Nanomedicine: Current status and future prospects. *FASEB J.*, **19**, 311–330.
13. Dyar, M. T. (1947). A cell wall stain employing a cationic surface-active agent as a mordant. *J. Bacteriol.,* **53**, 498.
14. Zhang, C., Ji, X., Zhang, Y., Zhou, G., Ke, X., Wang, H., Tinnefeld, P., He, Z. (2013). One-pot synthesized aptamer-functionalized CdTe:Zn^{2+} quantum dots for tumor-targeted fluorescence imaging *in vitro* and *in vivo*. *Anal. Chem.* May 31 (Epub ahead of print).
15. Kim, S.-J., Blumling, III J., Davidson, M. C., Saad, H., Eun, S.-Y., Silva, G. A. (2012). Calcium and EDTA induced folding and unfolding of calmodulin on functionalized quantum dot surfaces. *J. Nanoneurosci*., **2**, 75–81.
16. Buibas, M., Silva, G. A. (2013). A framework for simulating and estimating the state and functional topology of complex dynamic geometric networks. *Neural. Comput.,* **23**, 183–214.
17. Boll, H., Nittka, S., Doyon, F., Neumaier, M., Marx, A., Kramer, M., Groden, C., Brockmann, M. A. (2011). Micro-CT based experimental liver imaging using a nanoparticulate contrast agent: A longitudinal study in mice. *PLoS One*, **6**, e25692.

18. Bawa, R. (2013). FDA and nanotech: Baby steps lead to regulatory uncertainty. In: Bagchi, D., et al. (ed.). *Bionanotechnology: A Revolution in Biomedical Sciences and Human Health*. Wiley Blackwell, UK, pp. 720–732.
19. Linkov, I., Satterstrom, F. K., Corey, L. M. (2008). Nanotoxicology and nanomedicine: making hard decisions. *Nanomedicine*, **4(2)**, 167–71.
20. Kim, Y., Kong, S. D., Chen, L.-H., Pisanic, T. R., Jin, S., Shubayev, V. I. (2013). *In vivo* nanoneurotoxicity screening using oxidative stress and neuroinflammation paradigms. *Nanomedicine*, **7(9)**, 1057–1066.
21. Oberdörster, G., Oberdörster, E., Oberdörster, J. (2005). Nanotoxicology: An emerging discipline evolving from studies of ultrafine particles. *Environ. Health Perspect.*, **113**, 823–839.
22. Bardi, G., Tognini, P., Ciofani, G., Raffa, V., Costa, M., Pizzorusso, T. (2009). Pluronic-coated carbon nanotubes do not induce degeneration of cortical neurons *in vivo* and *in vitro*. *Nanomedicine*, **5(1)**, 96–104.
23. Foldvari, M., Bagonluri, M. (2008). Carbon nanotubes as functional excipients for nanomedicines: II. Drug delivery and biocompatibility issues. *Nanomedicine*, **4(3)**, 183–200.
24. Foldvari, M., Bagonluri, M. (2008). Carbon nanotubes as functional excipients for nanomedicines: I. pharmaceutical properties. *Nanomedicine*, **4(3)**, 173–182.
25. Vittorio, O., Raffa, V., Cuschieri, A. (2009). Influence of purity and surface oxidation on cytotoxicity of multiwalled carbon nanotubes with human neuroblastoma cells. *Nanomedicine*, **5(4)**, 424–431.
26. Liang, Y.-X., Cheung, S. W. H., Chan, K. C. W., Wu, E. X., Tay, D. K. C., Ellis-Behnke, R. G. (2011). CNS regeneration after chronic injury using a self-assembled nanomaterial and MEMRI for real-time *in vivo* monitoring. *Nanomedicine*, **7(3)**, 351–359.
27. Kohl, Y., Kaiser, C., Bost, W., Stracke, F., Fournelle, M., Wischke, C., et al. (2011). Preparation and biological evaluation of multifunctional PLGA-nanoparticles designed for photoacoustic imaging. *Nanomedicine*, **7(2)**, 228–237.
28. Steinmetz, N. F. (2010). Viral nanoparticles as platforms for next-generation therapeutics and imaging devices. *Nanomedicine*, **6(5)**, 634–641.
29. Yu, Z., McKnight, T. E., Ericson, M. N., Melechko, A. V., Simpson, M. L., Morrison, B. (2012). Vertically aligned carbon nanofiber as nano-neuron interface for monitoring neural function. *Nanomedicine*, **8(4)**, 419–423.

30. Kawas, L. H., Benoist, C. C., Harding, J. W., Wayman, G. A., Abu-Lail, N. I. (2013). Nanoscale mapping of the Met receptor on hippocampal neurons by AFM and confocal microscopy. *Nanomedicine*, **9(3)**, 428–438.

Chapter 4

Top Ten Recent Nanomedical Research Advances

Melanie Swan, MBA
Research Fellow, MS Futures Group, Palo Alto, California, USA

Keywords: nanomedicine, bio-nanomaterials, nanodevices, future studies, drug delivery, regenerative medicine, stem cells, DNA nanotechnology, synthetic biology, optogenetics, transcranial magnetic stimulation, stapled peptides, nanoparticles, microneedle arrays, neural stem cells

4.1 Introduction

This chapter provides a summary of recent research advances as of 2011 in the top 10 areas of nanomedicine, bio-nanomaterials, and nanodevices from a future studies perspective. A summary of the advances is provided in Table 4.1, which organizes the 10 areas into categories and highlighting the key findings in each area. The first category, Drug Delivery, includes nanoparticles, stapled peptides, and microneedle arrays. Next, Organ Repair subsumes regenerative medicine and stem cell research. The category Fundamental Nanomedical Technologies includes the integration of organic and inorganic matter and DNA nanotechnology. Engineering

Handbook of Clinical Nanomedicine: Nanoparticles, Imaging, Therapy, and Clinical Applications
Edited by Raj Bawa, Gerald F. Audette, and Israel Rubinstein

ISBN 978-981-4669-20-7 (Hardcover), 978-981-4669-21-4 (eBook)
www.panstanford.com

of biology includes synthetic biology and biomimetic synthesis. Working with the Brain includes a review of contemporary neural research findings. Results from approximately fifty different research projects are discussed in this chapter.

Table 4.1 Summary of key research results by nanomedicine category

A. Drug delivery
1. Nanoparticles: cytosolic drug delivery, cell therapies, and peptoids • Cytosolic drug delivery with light activation and peptide conjugates • Improved cell therapy viability using integrated nanoparticles • Drug development via synthesis of alkylated antimicrobial peptoids
2. New class of drugs: stapled peptides • Stapled peptide formation through hydrocarbon bonds and chemical reactions • Stapled peptide-generated oncogene MCL-1 inhibitor (BCL-2 family protein) in clinical trials
3. Drug delivery and biomonitoring: microneedle array • Transdermal delivery and controlled material release via thin films • Silicon pancreas system mimics normal insulin function
B. Organ repair
4. Regenerative medicine: conduits, augments, blood-vessel and skin printing • Hollow organs: lab-generated bladders
• Solid organs: conduits and augments • Solid organs: vascularization • Skin regeneration: portable skin printing system
5. Stem cells: heart, spinal cord, adipose-derived, neural • Heart: cardioprotection via DRRSAb (sodium potassium ATPase antibody), improved stem cell viability by seeding microthread sutures with human mesenchymal stem cells (hMSCs) • Adipose-derived stem cells: easily harvestable alternative for heart and kidney injury treatment and breast reconstruction • Spinal cord injury: human embryonic stem cell (hESC)-derived oligodendrocyte progenitor cell, GRNOPC1, in clinical trials • Neural stem cells: tested for stroke recovery in a UK-based clinical trial • Process innovation: bio-mimicking soft substrates superior to conventional rigid substrates in culturing and direct conversion of skin cells to functional neurons

C. Fundamental nanomedical technologies

6. Integration of organic and inorganic materials
   - Biomolecular interface: genetically engineered peptides (GEPIs) used to improve surface chemistry between implants and human tissue
   - Organic-inorganic hybrids: engineered fusion proteins, graphene sheets sandwiched in phospholipid bilayers, catenanes and rotaxanes

7. DNA nanotechnology
   - Structures: molecular calipers, 11-state nanomachine, tensegrity nanostructures, improved control circuitry via compiled chemical equations, microfluidic channel control through torque and temperature
   - Transport systems: DNA walkers in the form of molecular spiders and light-driven motors, demonstration of a molecular assembly line

D. The engineering of biology

8. Synthetic biology: genetic engineering and assembly
   - DNA assembly: synthetic chromosome, improved throughout via DNA microchips and robotic sequencing
   - Parts Registry: *in vivo* reference standards, restriction enzyme-constructed protein fusions, BioScaffolds for rapid circuit generation
   - Nanomedical applications: tunable extracellular matrices and DNA damage sensors

9. Bio-nanomaterials characterization and biomimetic synthesis
   - Metabolic engineering: RNA scaffolds organize *in vivo* enzymatic pathways to amp hydrogen production, cyanobacteria as a feedstock alternative for biochemicals production
   - Biomineralization: crystal nucleation and bifacially differentiated interstitial composites
   - Systems-level cooperation: multi-organism signaling networks

E. Working with the Brain

10. Intelligence: brain coprocessors, brain-computer interfaces, transcranial magnetic stimulation
    - Optogenetics: activating and silencing specific neurons, distributed neural targeting via multi-waveguide probe, brain coprocessor
    - Brain-computer interfaces (BCIs): improved control through fatigue reduction and motor imagery training
    - Transcranial magnetic stimulation (TMS): clinical treatment of depression, motor learning enhancement, visual system elucidation

A future studies methodology was employed to select the advances on the basis of three criteria. First, findings were identified from research published in the last one to two years (i.e., from mid-2009 to mid-2011) from established leaders in different nanomedical fields, in some cases follow-on work in areas of previous achievement. Second, research advances were selected based on their stage of maturity such that they could possibly have a bench to bedside translational impact within the next decade, ideally within the next five years. Advances in regenerative medicine are particularly exemplary of meeting this requirement. Third, research results were selected on the basis of being fundamental technologies that could address whole new classes of problems in nanomedicine and beyond. Strong examples of these fundamental technologies are achievements in molecular programming, synthetic biology, and the integration of organic and inorganic matter. The scope of this analysis was necessarily limited and certain key research may have been unintentionally omitted.

4.2 Top 10 Areas of Recent Advance in Nanomedicine, Bio-Nanomaterials, and Nanodevices

4.2.1 Nanoparticles: Cytosolic Drug Delivery, Cell Therapies, and Peptoids

- Cytosolic drug delivery with light activation and peptide conjugates
- Improved cell therapy viability using integrated nanoparticles
- Drug development via synthesis of alkylated antimicrobial peptoids

One of the most established applications in nanomedicine is using nanoparticles for drug delivery. A contemporary challenge is conveying drug molecules through the cell wall to the interior of the cell. Two recent advances in intracellular drug delivery pass nanoparticles into cells and then burst their membranes to disgorge the cargo. The membrane-bursting, or endosomal breakage, is conducted using light activation and peptide conjugation. In light-mediated endosomal breakage (Fig. 4.1), nanoparticles have been developed that can be loaded with a variety of compounds, targeted

to specific cells (e.g., cancer cells), and released into the cytosol [1]. These nanoparticles are highly monodispersed mesoporous silica nanoparticles that are size-tunable in the range of 30–200 nm. Endosomal breakage for intracellular drug delivery has also been achieved through peptide conjugates. A peptide that mimics viral fusion protein sequences, GALA (repeating Glu-Ala-Leu-Alaamino acid sequences), is attached to nanoparticles. GALA helps nanoparticle cargo to escape by imitating the process of virus gene release from endosomes into the cell [2].

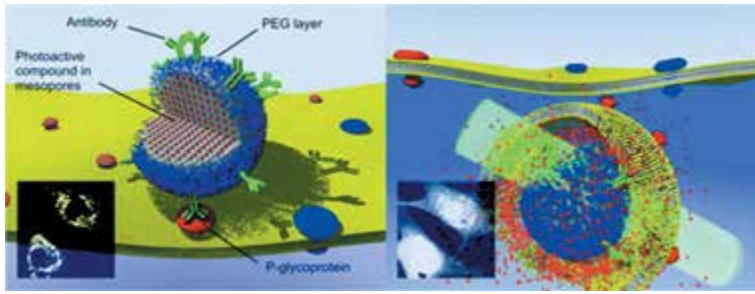

Figure 4.1 Nanoparticle cargo discharge through light activation [1]. Reprinted (adapted) with permission from Febvay, S., Marini, D. M., Belcher, A. M., Clapham, D. M. (2010). Targeted cytosolic delivery of cell-impermeable compounds by nanoparticle-mediated, light-triggered endosome disruption. *Nano Lett.*, **10**(6), 2211–2219. Copyright (2010) American Chemical Society.

Nanoparticles are also being used in cellular therapies (introducing new cells into tissues for therapeutic purposes), where a limitation is the rapid decline of the viability and function of transplanted cells. One solution conjugates drug-loaded nanoparticles onto the surface of therapeutic cells to provide ongoing pseudoautocrine stimulation until the cells are established in their new environment. This method could be used to improve targeted drug delivery, cancer treatment, and stem cell grafts [3].

Another advance in the use of nanoparticles is developing drugs that avoid the natural resistance systems of the body. One technique created alkylated antimicrobial peptoids with improved protease resistance as mimics to naturally occurring antimicrobial peptides (AMPs). AMPs are important as the first line of defense against pathogens. Unlike conventional antibiotics, AMPs kill

bacteria via nonspecific membrane interactions, a mechanism which reduces the probability of resistance development. Synthesized antimicrobial peptoids could be used in drug development and immune system characterization [4].

4.2.2 New Class of Drugs: Stapled Peptides

- Stapled peptide formation through hydrocarbon bonds and chemical reactions
- Stapled peptide-generated oncogene MCL-1 inhibitor (BCL-2 family protein) in clinical trials

The two current classes of drugs in industry-wide use, small molecules and biologics, are limited in that they can only target about 20% of all proteins [5]. Stapled peptides might possibly lead to the creation of a new class of drugs that could target a much wider range of proteins and intracellular substances. This is a technique that makes proteins more rigid in order to penetrate cell walls. The stronger structure also gives stapled peptides a longer life by making them more resistant to protease degradation. One method for making stapled peptides is synthetically enhancing 3-D alpha-helix protein segments with hydrocarbon bonds. This visually resembles a staple that is holding parts of the peptide together (Fig. 4.2), hence the name. This method is currently in clinical trials for the inhibition of a BCL-2 family protein, oncogene MCL-1,

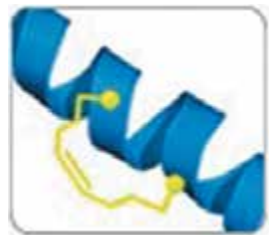

Figure 4.2 Stapled peptide: Synthetic enhancement rigidifies peptide side chains for entry into the cytosol. Reprinted with permission from Gregory L. Verdine per Schafmeister, C. E., Po, J., Verdine, G. L. (2000). An all-hydrocarbon cross-linking system for enhancing the helicity and metabolic stability of peptides. *J. Am. Chem. Soc*., **122**(24), 5891–5892, and Verdine, G. L., Walensky, L. D. (2007). The challenge of drugging undruggable targets in cancer: Lessons learned from targeting BCL-2 family members. *Clin. Cancer Res*., **13**(24), 7264–7270.

using an exclusive inhibitor, the MCL-1 BH3 helix, which could reinstate the normal apoptosis process in cancer cells [6]. Other methods of making stapled peptides use chemical reactions, combining molecules with light [7], and catalyzing chemical side chains of peptides into helical structures that can enter cells more easily [8].

4.2.3 Drug Delivery and Biomonitoring: Microneedle Array

- Transdermal delivery and controlled material release via thin films
- Silicon pancreas system mimics normal insulin function

Microneedle arrays are small rectangles with, in the example in Fig. 4.3, 400 needles, each thinner than the diameter of a human hair. These arrays could have a wide range of potential applications in supplementing and replacing the traditional needle-based delivery of vaccines and drugs. In addition, they may have novel applications in continuous health monitoring and the delivery of vitamins, nutrients, and other substances for fine-tuned physical and mental performance management. Transdermal drug delivery, where the stratum corneum barrier layer of the skin is penetrated, is already conducted without the use of traditional needles. Earlier-stage transdermal delivery systems are in clinical use for small, lipophilic, low-dose drugs, and drugs needing enhanced targeting and time release. Targeting is conducted through chemical enhancers, non-cavitational ultrasound, and iontophoresis [9].

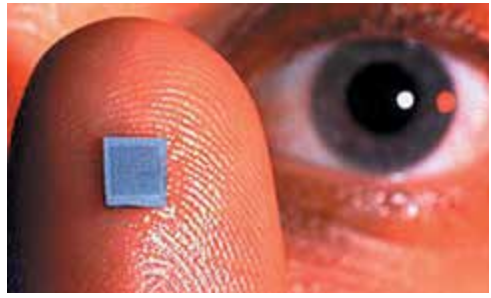

Figure 4.3 Example of microneedle array (400 needles, each thinner than a human hair). Photo courtesy of Georgia Institute of Technology.

Microneedle arrays are the leading technique in the next generation of transdermal delivery. Simple coatings used in early microneedle arrays are being replaced by thin films that allow more robust control over substance release and the solid-state stabilization of environmentally sensitive encapsulated materials [10]. Microneedle arrays are also being explored for ongoing condition management, for example in diabetes with the 'silicon pancreas' system. The silicon pancreas consists of a continuous glucose monitor embedded in the skin and a pair of insulin and glucagon pumps. The pumps control alpha and beta cells to mimic insulin activity which gives diabetics an approximately normal response to blood sugar levels [11].

4.2.4 Regenerative Medicine: Conduits and Augments, Blood-Vessel, and Skin Printing

- Hollow organs: lab-generated bladders
- Solid organs: conduits, augments, and vascularization
- Skin regeneration: portable skin printing system

Regenerative medicine, also known as tissue engineering, bioprinting, and biofabrication, is an example of a nanomedical field which was perceived as revolutionary even a few years ago, but now seems almost commonplace, at least conceptually. Replacement organs grown from one's own stem cells (i.e., autologous), like the urethra shown in Fig. 4.4 are desirable since this would avoid immune system rejection and a lifetime of immunosuppressive drugs and their side effects. Progress has been made in the organ regeneration of bladders, urethras, and tracheas, and additional work is underway in the liver, kidney, pancreas, intestine, and other organs. Some of the key challenges in tissue engineering are cell sources, vascularization, optimal biomaterials, and scaffolding.

Hollow organs like the bladder are easier to create than solid organs like the liver and kidney. The current status is that a few dozen lab-generated bladders have been implanted in humans. There are also examples of human trachea implants, and the creation of a bioengineered human larynx [12]. An early stage of solid organ regenerative medicine is developing conduits and augments. Conduits provide linkage, for example the urinary conduit

is linked to the outside of the body for waste removal and augments provide a supplemental internal path for normal operations in organs like the kidney. Vascularization is an important contemporary focus for being able to generate a wider range of complex organs. Some recent vascularization research successes include 3-D bioscaffolds developed with decellularization [13], alginate gels [14], and blood vessel printing [15]. Regenerative medicine is not just for internal organs; work is being conducted in skin generation. For example, a portable skin printing system has been developed for potential battlefield use, covering burn wounds with living skin grafts comprised of fibroblasts and keratinocytes [16].

Figure 4.4 Regenerative medicine: replacement urethra grown from a patient's own stem cells. Photo courtesy of Wake Forest Institute for Regenerative Medicine.

4.2.5 Stem Cells: Heart, Spinal Cord, Adipose-Derived, and Neural Advances

- Heart: increased cardioprotection via DRRSAb (sodium potassium ATPase antibody), improved stem cell viability by seeding microthread sutures with hMSCs
- Adipose-derived stem cells: easily harvestable alternative for heart and kidney injury treatment and breast reconstruction
- Spinal cord injury: human embryonic stem cell (hESC)-derived oligodendrocyte progenitor cell, GRNOPC1, in clinical trials
- Neural stem cells: tested for stroke recovery in a UK-based clinical trial
- Process innovation: bio-mimicking soft substrates superior to conventional rigid substrates in culturing and direct conversion of skin cells to functional neurons

In addition to regenerative medicine, stem cell research is another area of potential significant near-term impact. Research is being carried out in a variety of types of stem cells. The heart is one of the least regenerative muscle tissues, so producing contractile cells is a key focus of stem cell therapies. Progress continues in improving the delivery, attachment, proliferation, and survival of cardiomyocytes (heart muscle cells). Techniques such as growth factor cocktails, hydrogels, patches, and natural cell-signaling mechanisms are used to promote cardioprotection (cell survival) [17]. One approach found increased cardioprotection by administering DRRSAb, an antibody that can transmit extracellular signals to intracellular compartments. The normal cellular activity of sodium potassium ATPase in moving materials across the cell membrane was thereby stimulated, and this promoted cell survival. DRRSAb is contemplated as a potential drug for treating heart failure [18]. Another cardiac stem cell advance increased stem cell proliferation and the efficiency and localization of cell delivery by seeding fibrin microthreads with 50,000 human mesenchymal stem cells (hMSCs). Once populated, the threads (Fig. 4.5) would be sutured into live tissue [19].

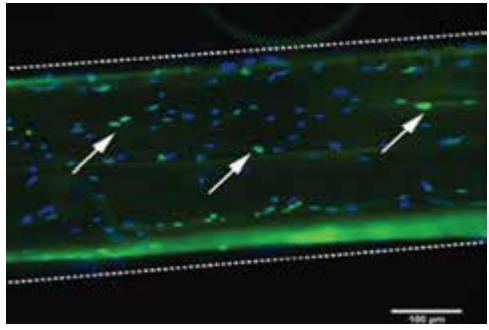

Figure 4.5 Stem cell example: fibrin microthread seeded with human mesenchymal stem cells (hMSCs). Image courtesy of Glenn Gaudette, PhD.

Another cardiac advance uses adipose cells as an alternative to bone marrow cells since they have a 200× denser concentration of stem cells and are much easier to harvest. The adipose-derived stem cells are injected directly into injury sites such as the heart [20, 21] and kidney [22] to help repair injury and replace dying

cells. Adipose-derived stem cells may be appropriate for other uses too such as breast reconstruction, if it can be confirmed that no active disease is present [23]. Other kinds of stem cells are being investigated for *in vivo* uses. The first human stem cell clinical trials for spinal injury are underway with two enrolled patients as of June 2011 [24] to investigate the use of hESC-derived oligodendrocyte progenitor cells, GRNOPC1, in the treatment of paralysis [25]. Neural stem cell research is underway in stroke recovery in a U.K.-based clinical trial in patients sustaining neural deficit over time [26]. Process innovations are also forthcoming, mouse embryonic stem cells were found to have greater self-renewal and pluripotency when maintained on soft substrates that matched the intrinsic stiffness of their natural environment versus the rigid substrates of conventional culturing [27]. Another technique bypasses stem cells by converting skin cells directly into functional neurons; this could be used in Parkinson's disease and Alzheimer's disease replacement cell therapies and other disease treatment [28].

4.2.6 Organic-Inorganic Integration: Biomolecular Interface and Organic-Inorganic Hybrids

- Biomolecular interface: genetically engineered peptides (GEPIs) used to improve surface chemistry between implants and human tissue
- Organic-inorganic hybrids: engineered fusion proteins, graphene sheets sandwiched in phospholipid bilayers, catenanes and rotaxanes

The integration of organic and inorganic materials is critical next-generation functionality in nanomedicine. An immediate practical application is having an effective biomolecular interface for prosthetics and implants since uncontrolled interactions can occur between synthetic materials and human tissues and infection is an ongoing problem. So far, surface chemistry has been altered with molecular immobilization techniques using anti-fouling polymers and cell growth factors but this has limited the range of usable materials. A recent advance employed peptide motifs that were selected to bind to gold, platinum, glass, and titanium to modify surfaces with a polyethylene glycol anti-fouling polymer and the integrin ligand RGD. This allowed the cell-surface chemistry

to be modified in a more manageable manner, reducing infection and extending the range of usable materials [29].

A fundamental research focus is the deliberate creation of organic-inorganic hybrids, which are nanomaterials that have the properties of both organic and inorganic matter. One example is engineered fusion proteins where inorganic-binding peptides are conjugated with bioluminescence proteins. The fusion proteins can be used as bioimaging molecular probes both targeting minerals (through fluorescent labeling) and monitoring the rate of biomineralization (through induced reactions) [30]. Another example is graphene sheets sandwiched in the hydrophobic interior of a phospholipid (Fig. 4.6). The phospholipid layers of the membrane electrically isolate the embedded graphene from the external solution, which means that the composite system could be used in biosensors and bioelectronic materials [31].

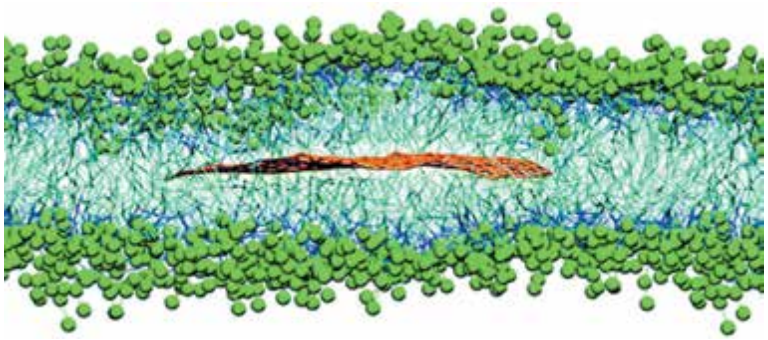

Figure 4.6 Integrating organic and inorganic materials: graphene sheet sandwiched in the hydrophobic interior of a phospholipid. Reprinted with permission from Titov, A. V., Král, P., Pearson, R. (2010). Sandwiched graphene–membrane superstructures. *Am. Chem. Soc. Nano*, **4**(1), 229–234. Copyright (2010) American Chemical Society.

A third example in the creation of hybrid material is catenanes and rotaxanes. These are mechanically interlocked molecular structures built from two components, one organic, such as an amine, and one inorganic, such as a metal [32]. Current research includes the investigation of manufacturing these materials at scale. So far, a dozen different kinds of rotaxanes have been produced in batches. Distinct types of hydrogen bonds with different dynamics have been demonstrated in the organic and in-

organic portions of the structures that could be manipulated in the construction of large molecules for use in nanomedicine. In an advanced rotaxane formation, inorganic ring components were formed of heterometallic octa-nuclear cages with fluoride and pivalate anions bridging the metal centers. Organic dialkylammonium threads were added to form the interlocked structures [33]. The complexity of the components and the intricate management of their interactions suggest that an important fundamental nanotechnology has been developed.

4.2.7 DNA Nanotechnology

- Structures: molecular calipers, 11-state nanomachine, tensegrity nanostructures, improved control circuitry via compiled chemical equations, microfluidic channel control through torque and temperature
- Transport systems: DNA walkers in the form of molecular spiders and light-driven motors, demonstration of a molecular assembly line

DNA nanotechnology seeks to build precise structures, devices, and systems from the molecular level up to the macro level. In contrast to DNA's traditional use as an information carrier, it is employed in the DNA nanotechnology field as a structural building material. DNA nanotechnology is concerned with the construction of nanostructures (i.e., hollow polyhedrons and solid geometrically precise crystal lattices), nanomechanical transport systems (i.e., molecular motors and walkers that can change shape and move along DNA pathways), and molecular computing (i.e., switches for DNA computation and molecular programming) [34, 35].

A number of sophisticated innovations in DNA nanotechnology structures have occurred. Nanoscale molecular calipers were developed with a flexible hinge for measuring small distances and forces [36]. The calipers were formed using DNA orgami (the nanoscale folding of DNA to create two and three dimensional shapes) which is an important method in the directed self-assembly of molecules. Another advance was the creation of an 11-state machine, an actuator where a strand of DNA binds to lock the device in any one state to the exclusion of the others. The actuator

can be fine-tuned to distances between components at a resolution of less than 1 nm which is important in nanomedical device control, for example in threading a 6 nm streptavidin molecule through a 2 nm DNA hole [37]. Another advance was the development of tensegrity (tensional integrity) nanostructures, structures that remain stable through compression and tension, and have high strength-to-weight ratios and resilience. They have long been used in macroscale architecture, engineering, and robotics, and are now being implemented at the nanoscale [38], which could be important for nanomedical devices in withstanding the high pressures that occur in the body.

Control circuitry for chemical reaction networks is an important focus in the next generation of DNA nanotechnology. Compiling systems of chemical equations into real-life chemical systems has been achieved via groups of DNA molecules that closely approximate the expected dynamics [39]. Microfluidic nanodevices (nanoscale-sized manufactured devices) are important in the sorting of nanomaterials, where the fine-tuned control of channel openings is a challenge. Mechanically controllable molecular pores formed by carbon nanotubes and nanocones have been developed that allow different rates of liquid to flow through the pores as rotational torque is applied [40]. In another case, a temperature-sensitive triblock copolymer brush was used to create a switchable nanofluidic device that opens with the increase of temperature [41].

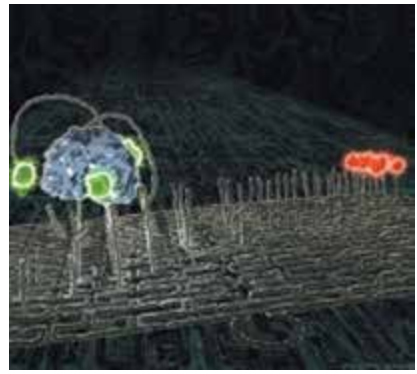

Figure 4.7 DNA walker example: molecular "spiders" can be directed to move across flat surfaces made of DNA to deliver cargo. Image courtesy of Paul Michelotti.

There are also advances in DNA nanotechnology transport systems, moving cargo in nanoscale environments. In DNA walkers, sophistication was increased with the development of a molecular spider (Fig. 4.7) that acted autonomously (i.e., started, followed, turned, and stopped) by sensing its environment [42]. The spider was comprised of a streptavidin molecule as an inert body and three deoxyribozymes as catalytic legs. In another example, a walker moved bi-directionally along a four-foothold molecular track, depending on the application of external stimuli (i.e., acid, base, UV light, and visible light). Directionality was achieved by the isomerization of a stilbene moiety through a Brownian ratchet mechanism in the molecular track [43]. One potential use of DNA walkers is to mimic and augment cellular transport systems. One extension of this is molecular assembly lines modeled on the ribosome, such as a controlled motion system that has been developed with a track, a motor, and fuel all made from DNA [44].

4.2.8 Synthetic Biology: Genetic Engineering and DNA Assembly

- DNA assembly: synthetic chromosome, improved throughput via DNA microchips and robotic sequencing
- Parts registry: *in vivo* reference standards, restriction enzyme-constructed protein fusions, BioScaffolds for rapid circuit generation
- Nanomedical applications: tunable extracellular matrices and DNA damage sensors

Synthetic biology is the design, engineering, and construction of biological systems, either de novo systems or the redesign of existing systems such as enzymes, genetic circuits, and cells. Despite being a relatively new field, it is already heralded by some that the biology revolution may be to the 21st century what the computer revolution was to the 20th century. One fundamental challenge is the synthetic printing of long strands of DNA and assembling shorter sequences into longer chromosomes and genomes. A landmark achievement occurred in May 2010 with the first booting to life of a synthetically created chromosome, the 1.08 million base pair bacterium *Mycoplasma mycoides* [45].

Recent advances have improved DNA sequencing throughput and cost by an order of magnitude [46], for example by using DNA microchips to genotype more variants simultaneously [47] and a robotic next-generation sequencing system for picking sequences directly off a high-throughput platform [48].

The Registry of Standard Biological Parts is a core resource for synthetic biology, a freely accessible online catalog that contained over 5000 available parts (i.e., components for biological design) as of December 2010 [49]. Advances have focused on improving ways to work with the standardized parts and speeding up design-build-test iterations. For example, *in vivo* reference standards were developed to decrease performance variance across experimental conditions and measurement instruments. One case demonstrated a 50% decrease in gene transcription promoter variance [50]. The construction of protein fusions is another improvement. Protein fusions (i.e., fusing proteins together into more complex molecules) are not feasible in the current parts assembly standard due to an automatically included scar sequence, which encodes a stop codon. Restriction enzymes BglII and BamHI were employed in a new assembly standard that replaces the scar sequence with an innocuous sequence, a glycine-serine peptide linker [51]. Another advance was the creation of a new part, a BioScaffold, for use in the rapid generation of synthetic biological circuits. The BioScaffold is inserted into cloning vectors and excised from them later during the process to leave a gap into which other DNA elements may be placed as shown in Fig. 4.8 [49].

Practical applications of synthetic biology are arising in nanomedicine. One is *ex vivo* cellular scaffolding, which is important in regenerative medicine, for example in the construction of heart valves. Single-sided DNA strands were used to make a structurally tunable DNA-based extracellular matrix where properties such as growth and scaffold stiffness could be directed [52]. Another nanomedical application is the development of DNA damage sensors using genetically fragmented firefly luciferase to detect the products of DNA damage: UV-modified DNA and 8-oxoguanine lesioned DNA (a lesion in DNA caused by reactive oxygen species (ROS)). DNA damage monitoring, and eventually repair, could be important in improving genetic instability and deterring cancer [53] and other pathologies such as aging.

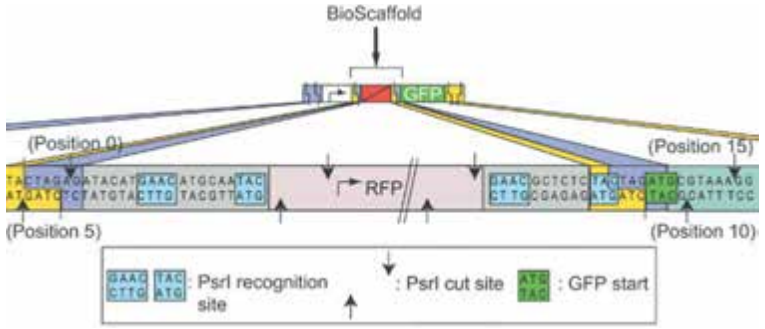

Figure 4.8 Example of a BioScaffold embedded into a biological test circuit to manage the scarring that occurs in the process of synthetic DNA assembly. Reproduced from Norville, J. E., Derda, R., Gupta, S., Drinkwater, K. A., Belcher, A. M., et al. (2010). Introduction of customized inserts for streamlined assembly and optimization of BioBrick synthetic genetic circuits. *J. Biol. Eng*., **4**, 17. © 2010 Norville et al; licensee BioMed Central Ltd.

4.2.9 Biomimetic Synthesis: Feedstock, Biomineralization, and Cooperative Phenotypes

- Metabolic engineering: RNA scaffolds increase hydrogen production, cyanobacteria as a feedstock alternative for biochemical production
- Biomineralization: crystal nucleation and bifacially differentiated interstitial composites
- Systems-level cooperation: multi-organism signaling networks

Biomimetic synthesis, the understanding and mimicking of biological systems in the creation of bio-nanomaterials, is an important research area for nanomedicine. A key application of biomimetics (and synthetic biology) is metabolic engineering. Metabolic engineering is the optimization of genetic and regulatory processes within cells to increase the cells' production of certain substances, for example biofuels and bioindustrial chemicals. One advance in increasing cell productivity was achieved using programmable RNA scaffolds. RNA was assembled into scaffolds with protein docking sites specifically co-localizing two proteins used to generate hydrogen from water and energy. Hydrogen production was increased roughly 24-fold [54]. A second advance investigated cyanobacteria as an alternative feedstock for use

in bioindustrial chemical generation. Cyanobacteria (Fig. 4.9) and other organisms that obtain energy through *photosynthesis* could be an attractive alternative to currently used carbohydrate feedstocks due to lower cost, simpler input requirements, higher environmental tolerance, and carbon-neutrality [55].

Nature excels in generating biomaterials (matter that interacts with biological systems), many of which have sought-after properties in nanomedicine. Biomineralization, the methods living organisms use to produce minerals to harden tissues, is an important and much-studied materials generation process. In a recent example, the complexity of the molluscan shell mineral assembly process in red abalone (*Haliotis rufescens*) was detailed. A number of layered sheets of shell interact in several steps through bifacially differentiated interstitial composites, with one of the surfaces acting as a crystal nucleator. This kind of technique might possibly be applied in the synthetic manufacture of biomaterials for nanomedicine and other uses [56].

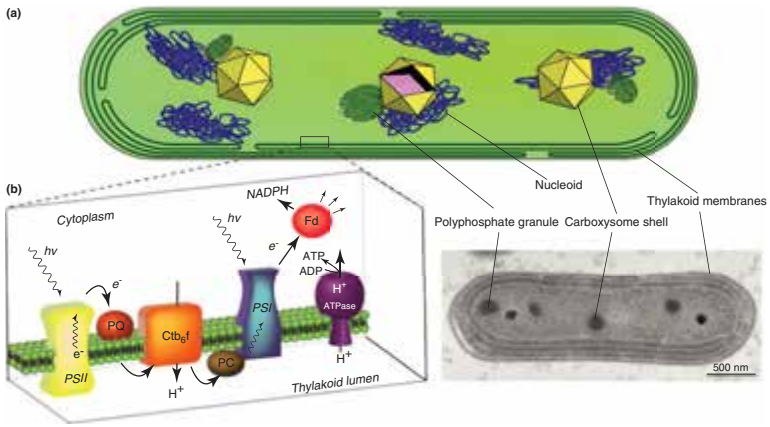

Figure 4.9 The straightforward organization of Cyanobacteria suggests its potential use as a feedstock. Reprinted from *Trends Biotechnol*., **29**(2), Ducat, D. C., Way, J. C., Silver, P. A., Engineering cyanobacteria to generate high-value products, 95–103, Copyright (2011), with permission from Elsevier.

The systemic nature of biological signaling networks is also being applied to nanomedicine. For example, metabolic synergy was found in *Escherichia coli* colonies as cooperative phenotypes showed more growth on average, aiding the proliferation of their

conjugate partners by cross-feeding essential metabolites, and thereby expanding the source of their own metabolites [57]. These kinds of methods might be useful in facilitating tissue growth in regenerative medicine as a diversity of signaling occurs between cell types.

4.2.10 Intelligence: Optogenetics, Brain-Computer Interfaces, and Transcranial Magnetic Stimulation

- Optogenetics: activating and silencing specific neurons, distributed neural targeting via multi-waveguide probe, brain coprocessor
- Brain-computer interfaces (BCIs): improved control through fatigue reduction and motor imagery training
- Transcranial magnetic stimulation (TMS): clinical treatment of depression, motor learning enhancement, visual system elucidation

Working with the brain is one of the final and most interesting frontiers in the application of nanomedicine. It is contemplated that current and future technologies used for the treatment of neural conditions and rehabilitation might eventually also be used for neural enhancement. Optogenetics is one such example. This technology uses light to control gene expression and is an important fundamental technique that greatly extends the ability to perturb cells *in vivo*. It works by modifying *in vivo* protein modules to contain photoisomerizable chromophores that then undergo observable conformational changes when activated by specific wavelengths of light [58]. One application of optogenetics is the activating and silencing of specific neurons. This is accomplished by getting the neurons of interest to express photosensitive proteins that are then stimulated by light. A recent advance, shown in Fig. 4.10, extends the range of action for this process from a single target via one optical fiber to multiple targets via a multi-waveguide probe [59].

Other research is extending first generation optogenetic technologies such as genetically encoded calcium reporters, fluorescent proteins, and neural activators with second-generation technologies such as voltage reporters, neural silencers, and

functionally extended fluorescent proteins [60]. Over time, optogenetic advances could possibly lead to tools like a brain coprocessor which would read out activity from a brain circuit, compute an instantaneous response for influencing the circuit, and send stimulus back into the brain to achieve this control strategy [61].

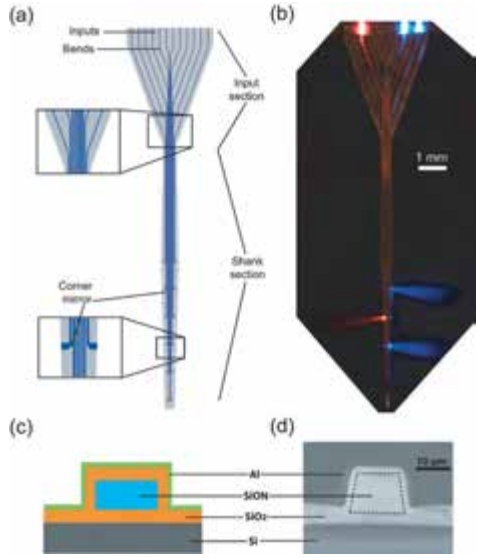

Figure 4.10 New optogenetic tool: a multi-waveguide implantable probe for light delivery to sets of distributed brain targets. Reproduced with permission from Zorzos, A. N., Boyden, E. S., Fonstad, C. G. (2010). Multiwaveguide implantable probe for light delivery to sets of distributed brain targets. *Optics Lett.*, **35**(24), 4133–4135.

Brain-computer interfaces are devices that translate signals from the cortical surface of the brain into computer control inputs, for example, helping paralyzed individuals to communicate with the environment. An advance was achieved in reducing BCI control fatigue through better alignment of natural motor response with machine operations [62]. It was also found that motor imagery training may improve BCI control [63]. Another technique for working with the brain is transcranial magnetic stimulation (TMS), non-invasively stimulating the brain via an electromagnetic coil placed on the scalp that delivers short bursts of energy to

neural cells. TMS is possibly useful in treating depression [64], Parkinson's disease, stroke, and other conditions. TMS may also enhance motor learning [65] and has helped to elucidate vision system processing, specifically how the brain synthesizes the ventral (object vision) and dorsal (spatial and motion vision) datastreams [66].

4.3 Conclusion

This review provided an analysis of the top 10 areas of contemporary research advances in nanomedicine, bio-nanomaterials, and nanodevices. Approximately 50 individual findings were organized into 5 categories: Drug Delivery, Organ Repair, Fundamental Nanomedical Technologies, the Engineering of Biology, and Working with the Brain. The advances were selected from a future studies perspective such that they are fundamental enabling technologies developed by leaders in their fields that could have a broad impact beyond their initial application area in the next five to ten years. A summary of the advances follows.

4.3.1 Summary

Drug delivery, particularly with nanoparticles, has long been an important application in nanomedicine. Cytosolic drug delivery is a contemporary focus with advances in endosomal breakage via light activation and peptide conjugates. Nanoparticles are also being conjugated to live cells to improve survivability in cell therapies. A further use of nanoparticles is in drug development via synthesized peptoids, which avoid the natural resistance systems of the body. A new technique, stapled peptides, is employed to make proteins more durable and might greatly extend the current range of biological targets for drugs. Microneedle arrays are in development for enhanced transdermal drug delivery with thin-film coatings that facilitate material release and continuous condition management.

Organ repair through regenerative medicine and stem cell therapies could have an extensive near-term impact. Human implantation of hollow organs such as the bladder and trachea has already been demonstrated. Progress is being made in underlying

technologies like vascularization that are required for the generation of solid organs like the heart and liver. Conduits and augments have been developed to extend the *in vivo* functionality of existing organs and other techniques have focused on skin regeneration through printed living skin grafts. Stem cell therapies are in research for a number of cell types including cardiac, adipose, spinal cord, and neural stem cells. Some advances focus on improving stem cell survival and proliferation including cardiomyocyte antibodies and stem cell-seeded microthreads. Other advances present alternatives to earlier methods, finding adipose-derived stem cells to be superior to bone marrow-derived stem cells, converting skin cells directly into functional neurons, and improving culturing techniques through nature-mimicking soft substrates. Clinical trials using stem cell therapies are underway for spinal cord injury and stroke rehabilitation.

Fundamental nanotechnologies such as the integration of organic and inorganic matter enable macroscale nanomedical applications. Genetically engineered peptides were used to alter the surface chemistry of implants to reduce infection. Organic-inorganic hybrids were developed such as engineered fusion proteins that could be used as bioimaging probes, graphene sheets sandwiched in phospholipid bilayers that could be used as biosensors, and catenanes and rotaxanes, which can be produced at scale and used in nanomedical devices. Advances in DNA nanotechnology structures included the development of molecular calipers and an 11-state nanomachine for conducting small-scale measurements. Resilient tensegrity structures for withstanding the pressures in the body were developed, along with digital control circuitry implemented in real-life systems. Fine-tuned channel control was achieved in microfluidic devices through torque and temperature. Advances in DNA transport systems included two DNA walkers, a spider that acted autonomously, and a walker that moved in response to external stimuli such as light. A molecular assembly line based on the ribosome was demonstrated in a controlled motion system built with DNA-based parts.

The engineering of biology is a potential high-impact field for the 21st century, in nanomedicine and beyond. The current status of synthetic biology is improving tools and techniques for reading (sequencing) and writing (synthesizing) DNA. The

first synthetically created chromosome was booted to life and DNA sequencing throughput and cost improvements have been made through DNA microchips and automation. Methods have been developed for faster design-build-test iteration in biological circuits such as reducing performance variation, generating protein fusions, inserting new sequences, and reusing existing circuits. Practical applications in nanomedicine include DNA damage sensors and tunable extracellular scaffolds for use in regenerative medicine. In biomimetic synthesis and metabolic engineering, programmable RNA scaffolds were used to increase intracellular hydrogen production and cyanobacteria was proposed as a viable feedstock for biochemical production. In materials characterization, the biomineralization process of a molluscan shell was determined to involve multiple differentiated sheets and crystal nucleation. In biological signaling networks, *Escherichia coli* colonies were found to engage in the cross-feeding of essential metabolites as a means of proliferation.

Working with the brain continues to be an exciting frontier. A fundamental enabling technology, optogenetics, uses light to control gene expression. Specific neurons can be activated or silenced, either as a single target or now with multiple targets via a multi-wave guide probe. In brain-computer interfaces (BCIs), improved control has been realized through fatigue reduction and improved motor imagery training. Another technique, Transcranial Magnetic Stimulation (TMS) is being used in the clinical treatment of depression and to elucidate the processes of motor learning and perception.

4.3.2 Conclusions and Future Implications

Ultimately, nanomedicine, bio-nanomaterials, and nanodevices could be instrumental in continuing the medical tradition of eradicating whole classes of problems over time. Some of the immediate prospects for nanomedical technologies could include a more extensive proliferation of nanoparticle-based pharmaceutical remedies, autologous regenerated tissue as a standard therapy experienced by thousands, and the design and programming of synthetic biological tools to facilitate both wellness maintenance and the repair of pathologies. In the short-term, a much wider

variety of conditions might be targeted including tissue, organ, and limb repair, infectious disease, common disease conditions such as heart disease, diabetes, metabolic disease, and cancer, all manner of neurological disorders and suboptimal characterizations, and complex systems phenomena like aging. Longer-term prospects include realizing that these nanomedical technologies are not just the latest problem-solving mechanism for bench to bedside translational medicine, but rather usher in a completely new era of medicine. The conceptualization of health and medicine could grow beyond cure as the desired endpoint, extending outcomes to improvement, normalization, prevention, and enhancement. The larger context for nanomedicine, bio-nanomaterials, and nanodevices is in contributing to the eventual ability to characterize, understand, and proactively manage all biological processes, human and otherwise.

Disclosures and Conflict of Interest

The author declares that she has no conflict of interest and has no affiliations or financial involvement with any organization or entity discussed in this chapter. This includes employment, consultancies, honoraria, grants, stock ownership or options, expert testimony, patents (received or pending) or royalties. No writing assistance was utilized in the production of this manuscript and the author has received no payment for preparation of this chapter. The findings and conclusions here reflect the current views of the author. They should not be attributed, in whole or in part, to the organizations with which they are affiliated, nor should they be considered as expressing an opinion with regard to the merits of any particular company or product discussed herein. Nothing contained herein is to be considered as the rendering of legal advice.

Corresponding Author

Melanie Swan
MS Futures Group
PO Box 61258, Palo Alto, CA 94306, USA
Email: m@melanieswan.com

About the Author

Melanie Swan is a research generalist in science, technology, and applied genomics. She is the principal of the MS Futures Group and the founder of DIYgenomics, a personalized medicine non-profit organization, based in California, USA. Ms. Swan's educational background includes an MBA in finance and accounting from the Wharton School of the University of Pennsylvania, a BA in French and economics from Georgetown University, and recent coursework in bioscience, nanotechnology, physics, and computer science. She is a faculty member at Singularity University and an affiliate scholar at the Institute for Ethics and Emerging Technologies. Ms. Swan's career has focused on research, finance, and entrepreneurship, including founding a technology startup company, GroupPurchase. She was Director of Research at Telecoms Consultancy Ovum RHK and previously held management and finance positions at iPass in Silicon Valley, J.P. Morgan in New York, Fidelity in Boston, and Arthur Andersen in Los Angeles. Ms. Swan serves as an advisor to research foundations, government agencies, corporations, and startups. She is an Advisory Board member of the Foundational Questions Institute, Lifeboat Foundation, and Accelerating Studies Foundation, and speaks French, Spanish, and Portuguese.

References

1. Febvay, S., Marini, D. M., Belcher, A. M., Clapham, D. M. (2010). Targeted cytosolic delivery of cell-impermeable compounds by nanoparticle-mediated, light-triggered endosome disruption. *Nano Lett.,* **10**(6), 2211–2219.
2. Nakase, I., Kogure, K., Harashima, H., Futaki, S. (2011). Application of a fusiogenic peptide GALA for intracellular delivery. *Methods Mol. Biol.,* **683**, 525–533.
3. Stephan, M. T., Moon, J. J., Um, S. H., Bershteyn, A., Irvine, D. J. (2010). Therapeutic cell engineering with surface-conjugated synthetic nanoparticles. *Nature Med.,* **16**(9), 1035–1041.
4. Chongsiriwatana, N. P., Miller, T. M., Wetzler, M., Vakulenko, S., Karlsson, A. J., et al. (2011). Short alkylated peptoid mimics of antimicrobial lipopeptides. *Antimicrob. Agents Chemother.,* **55**(1), 417–420.

5. Wolfson, W. (2009). Aileron staples peptides. *Chem. Biol.,* **16**(9), 910–912.
6. Stewart, M. L., Fire, E., Keating, A. E., Walensky, L. D. (2010). The MCL-1 BH3 helix is an exclusive MCL-1 inhibitor and apoptosis sensitizer. *Nat. Chem. Biol.,* **6**(8), 595–601.
7. Madden, M. M., Muppidi, A., Li, Z., Li, X., Chen, J., Lin, Q. (2011). Synthesis of cell-permeable stapled peptide dual inhibitors of the p53-Mdm2/Mdmx interactions via photoinduced cycloaddition. *Bioorg. Med. Chem. Lett.,* **21**(5), 1472–1475.
8. Schafer-N ApSLersö Parkalle (2011). New techniques for stapling peptides could spur development of drugs for cancer, other diseases. Available at: http://www.physorg.com/news/2011-02-techniques-stapling-peptides-spur-drugs.html (accessed on August 7, 2014).
9. Prausnitz, M. R., Langer, R. (2008). Transdermal drug delivery. *Nat. Biotechnol.,* **26**(11), 1261–1268.
10. DeMuth, P. C., Su, X., Samuel, R. E., Hammond, P. T., Irvine, D. J. (2010). Nano-layered microneedles for transcutaneous delivery of polymer nanoparticles and plasmid DNA. *Adv. Mater.,* **22**(43), 4851–4856.
11. Upson, S. (2011). Bionic Pancreas: Artificial organ could improve control over diabetes. Available at: http://spectrum.ieee.org/biomedical/devices/bionic-pancreas/?utm_source=techalert&utm_medium=email&utm_campaign=103012 (accessed on August 7, 2014).
12. Baiguera, S., Gonfiotti, A., Jaus, M., Comin, C. E., Paglierani, M., et al. (2011). Development of bioengineered human larynx. *Biomaterials,* **32**(19), 4433–4442.
13. Baptista, P. M., Siddiqui, M. M., Lozier, G., Rodriguez, S. R., Atala, A., et al. (2011). The use of whole organ decellularization for the generation of a vascularized liver organoid. *Hepatology,* **53**(2), 604–617.
14. Kerdjoudj, H., Boulmedais, F., Berthelemy, N., Mjahed, H., Louis, H., et al. (2011). Cellularized alginate sheets for blood vessel reconstruction. *Soft Matter,* **7**, 3621–3626.
15. Anonymous. (2010). First fully bioprinted blood vessels. Available at: http://www.organovo.com/news/press/42 (accessed on August 7, 2014).
16. Stomp, W. (2010). *In situ* skin bioprinting for burn wounds. Available at: http://medgadget.com/archives/2010/11/in_situ_skin_bioprinting_for_burn_wounds.html (accessed on August 7, 2014).

17. Scudellari1, M. (2009). The delivery dilemma. *Nat. Rep. Stem Cells,* **104,** doi:10.1038/stemcells.2009.104.

18. Zheng, J., Koh, X., Hua, F., Li, G., Larrick, J. W., Bian, J. S. (2011). Cardioprotection induced by Na(+)/K(+)-ATPase activation involves extracellular signal-regulated kinase 1/2 and phosphoinositide 3-kinase/Akt pathway. *Cardiovasc. Res.,* **89**(1), 51–59.

19. Proulx, M. K., Carey, S. P., Ditroia, L. M., Jones, C. M., Fakharzadeh, M., et al. (2011). Fibrin microthreads support mesenchymal stem cell growth while maintaining differentiation potential. *J. Biomed. Mater. Res. Part A,* **96**(2), 301–312.

20. Shah, S. (2010). Adipose-derived stem cells show promise in treatment of chronic ischemia. Available at: http://medgadget.com/archives/2010/05/adiposederived_stem_cells_show_promise_in_treatment_of_chronic_ischemia.html (accessed on August 7, 2014).

21. Gravitz, L. (2011). Fat cells for broken hearts. Available at: http://www.technologyreview.com/biomedicine/32229/?mod=related (accessed on August 7, 2014).

22. Feng, Z., Ting, J., Alfonso, Z., Strem, B. M., Fraser, J. K., et al. (2010). Fresh and cryopreserved, uncultured adipose tissue-derived stem and regenerative cells ameliorate ischemia-reperfusion-induced acute kidney injury. *Nephrol. Dial. Transplant.,* **25**(12), 3874–3884.

23. Zimmerlin, L., Donnenberg, A. D., Rubin, J. P., Basse, P., Landreneau, R. J., et al. (2011). Regenerative therapy and cancer: *In vitro* and *in vivo* studies of the interaction between adipose-derived stem cells and breast cancer cells from clinical isolates. *Tissue Eng. Part A,* **17**(1–2), 93–106.

24. Krassowska, A. (2011). Geron presents data from GRNOPC1 trial at international conferences on spinal cord medicine and rehabilitation. Available at: http://www.businesswire.com/news/home/20110607005736/en/Geron-Presents-Data-GRNOPC1-Trial-International-Conferences (accessed on August 7, 2014).

25. Keirstead, H. S., Nistor, G., Bernal, G., Totoiu, M., Cloutier, F., et al. (2005). Human embryonic stem cell-derived oligodendrocyte progenitor cell transplants remyelinate and restore locomotion after spinal cord injury. *J. Neurosci.,* **25**(19), 4694–4705.

26. Ghosh, P. (2010). Stem cells used in stroke trial. Available at: http://www.bbc.co.uk/news/health-11763681 (accessed on August 7, 2014).

27. Chowdhury, F., Li, Y., Poh, Y. C., Yokohama-Tamaki, T., Wang, N., et al. (2010). Soft substrates promote homogeneous self-renewal of

embryonic stem cells via downregulating cell-matrix tractions. *Public Library Sci. One,* **5**(12), e15655.

28. Qiang, L., Fujita, R., Yamashita, T., Angulo, S., Rhinn, H., et al. (2011). Directed conversion of Alzheimer's disease patient skin fibroblasts into functional neurons. *Cell,* **146**(3), 359–371.
29. Khatayevich, D., Gungormus, M., Yazici, H., So, C., Cetinel, S., et al. (2010). Biofunctionalization of materials for implants using engineered peptides. *Acta Biomater.,* **6**(12), 4634–4641.
30. Yuca, E., Karatas, A. Y., Seker, U. O., Gungormus, M., Dinler-Doganay, G., et al. (2011). *In vitro* labeling of hydroxyapatite minerals by an engineered protein. *Biotechnol. Bioeng.,* **108**(5), 1021–1030.
31. Titov, A. V., Král, P., Pearson, R. (2010). Sandwiched graphene–membrane superstructures. *Am. Chem. Soc. Nano,* **4**(1), 229–234.
32. Swan, M. (2010). Engineering life into technology: The application of complexity theory to a potential phase transition in intelligence. *Symmetry,* **2**, 150–183.
33. Ballesteros, B., Faust, T. B., Lee, C. F., Leigh, D. A., Muryn, C. A., et al. (2010). Synthesis, structure, and dynamic properties of hybrid organic-inorganic rotaxanes. *J. Am. Chem. Soc.,* **132**(43), 15435–15444.
34. Seeman, N. C. (2010). Nanomaterials based on DNA. *Ann. Rev. Biochem.,* **79**, 65–87.
35. Krishnan, Y., Simmel, F. C. (2011). Nucleic acid based molecular devices. *Angew. Chem.* (*International edition in English*), **50**(14), 3124–3156.
36. Castro, C. E., Kilchherr, F., Kim, D. N., Shiao, E. L., Wauer, T., et al. (2011). A primer to scaffolded DNA origami. *Nat. Methods,* **8**(3), 221–229.
37. Zhang, Z., Olsen, E. M., Kryger, M., Voigt, N. V., Torring, T., et al. (2011). A DNA tile actuator with eleven discrete states. *Angew. Chem.* (*International edition in English*), **50**(17), 3983–3987.
38. Liedl, T., Högberg, B., Tytell, J., Ingber, D. E., Shih, W. M. (2010). Self-assembly of three-dimensional prestressed tensegrity structures from DNA. *Nat. Nanotechnol.,* **5**(7), 520–524.
39. Soloveichik, D., Seelig, G., Winfree, E. (2010). DNA as a universal substrate for chemical kinetics. *Proc. Natl. Acad. Sci. U. S. A.,* **107**(12), 5393–5398.
40. Titov, A. V., Wang, B., Sint, K., Král, P. (2010). Controllable synthetic molecular channels: Biomimetic ammonia switch. *J. Phys. Chem. B,* **114**(2), 1174–1179.
41. Cheng, L., Cao, D. (2011). Designing a thermo-switchable channel for nanofluidic controllable transportation. *Am. Chem. Soc. Nano,* **5**(2), 1102–1108.

42. Lund, K., Manzo, A. J., Dabby, N., Michelotti, N., Johnson-Buck, A., et al. (2010). Molecular robots guided by prescriptive landscapes. *Nature,* **465**(7295), 206–210.
43. Barrell, M. J., Campaña, A. G., von Delius, M., Geertsema, E. M., Leigh, D. A. (2011). Light-driven transport of a molecular walker in either direction along a molecular track. *Angew. Chem.* (*International edition in English*), **50**(1), 285–290.
44. Wickham, S. F., Endo, M., Katsuda, Y., Hidaka, K., Bath, J., et al. (2011). Direct observation of stepwise movement of a synthetic molecular transporter. *Nat. Nanotechnol.,* **6**(3), 166–169.
45. Gibson, D. G., Glass, J. I., Lartigue, C., Noskov, V. N., Chuang, R. Y., et al. (2010). Creation of a bacterial cell controlled by a chemically synthesized genome. *Science,* **329**(5987), 52–56.
46. Algire, M., Krishnakumar, R., Merryman, C. (2010). Megabases for kilodollars. *Nat. Biotechnol.,* **28**(12), 1272–1273.
47. Kosuri, S., Eroshenko, N., Leproust, E. M., Super, M., Way, J., et al. (2010). Scalable gene synthesis by selective amplification of DNA pools from high-fidelity microchips. *Nat. Biotechnol.,* **28**(12), 1295–1299.
48. Matzas, M., Stähler, P. F., Kefer, N., Siebelt, N., Boisguérin, V., et al. (2010). High-fidelity gene synthesis by retrieval of sequence-verified DNA identified using high-throughput pyrosequencing. *Nat. Biotechnol.,* **28**(12), 1291–1294.
49. Norville, J. E., Derda, R., Gupta, S., Drinkwater, K. A., Belcher, A. M., et al. (2010). Introduction of customized inserts for streamlined assembly and optimization of BioBrick synthetic genetic circuits. *J. Biol. Eng.,* **4**, 17.
50. Kelly, J. R., Rubin, A. J., Davis, J. H., Ajo-Franklin, C. M., Cumbers, J., et al. (2009). Measuring the activity of BioBrick promoters using an *in vivo* reference standard. *J. Biol. Eng.,* **3**, 4.
51. Anderson, J. C., Dueber, J. E., Leguia, M., Wu, G. C., Goler, J. A., et al. (2010). BglBricks: A flexible standard for biological part assembly. *J. Biol. Eng.,* **4**(1), 1.
52. Aldaye, F. A., Senapedis, W. T., Silver, P. A., Way, J. C. (2010). A structurally tunable DNA-based extracellular matrix. *J. Am. Chem. Soc.,* **132**(42), 14727–14729.
53. Furman, J. L., Mok, P. W., Badran, A. H., Ghosh, I. (2011). Turn-on DNA damage sensors for the direct detection of 8-oxoguanine and photoproducts in native DNA. *J. Am. Chem. Soc.,* **133**(32), 12518–12527.
54. Delebecque, C. J., Lindner, A. B., Silver, P. A., Aldaye, F. A. (2011). Organization of intracellular reactions with rationally designed RNA assemblies. *Science,* **333**(6041), 470–474.

55. Ducat, D. C., Way, J. C., Silver, P. A. (2011). Engineering cyanobacteria to generate high-value products. *Trends Biotechnol.,* **29**(2), 95–103.

56. Falini, G., Sartor, G., Fabbri, D., Vergni, P., Fermani, S., et al. (2011). The interstitial crystal-nucleating sheet in molluscan Haliotis rufescens shell: A bio-polymeric composite. *J. Struct. Biol.,* **173**(1), 128–137.

57. Wintermute, E. H., Silver, P. A. (2010). Emergent cooperation in microbial metabolism. *Mol. Syst. Biol.,* **6**, 407.

58. Toettcher, J. E., Voigt, C. A., Weiner, O. D., Lim, W. A. (2011). The promise of optogenetics in cell biology: Interrogating molecular circuits in space and time. *Nat. Methods,* **8**(1), 35–38.

59. Zorzos, A. N., Boyden, E. S., Fonstad, C. G. (2010). Multiwave guide implantable probe for light delivery to sets of distributed brain targets. *Opt. Lett.,* **35**(24), 4133–4135.

60. Knöpfel, T., Lin, M. Z., Levskaya, A., Tian, L., Lin, J. Y., et al. (2010). Toward the second generation of optogenetic tools. *J. Neurosci.,* **30**(45), 14998–15004.

61. Boyden, E., Allen, B., Fritz, D. (2010). Brain coprocessors: The need for operating systems to help brains and machines work together. Available at: http://www.technologyreview.com/computing/26329/?a=f (Accessed on August 7, 2014).

62. Bai, O., Lin, P., Huang, D., Fei, D. Y., Floeter, M. K. (2010). Towards a user-friendly brain-computer interface: Initial tests in ALS and PLS patients. *Clin. Neurophysiol.,* **121**(8), 1293–1303.

63. Halder, S., Agorastos, D., Veit, R., Hammer, E. M., Lee, S., et al. (2011). Neural mechanisms of brain-computer interface control. *Neuroimage,* **55**(4), 1779–1790.

64. Duckworth, K. (2009). Transcranial magnetic stimulation (TMS or rTMS). Available at: http://www.nami.org/Content/ContentGroups/Helpline1/Transcranial_Magnetic_Stimulation_%28rTMS%29.htm (accessed on August 7, 2014).

65. Jayaram, G., Galea, J. M., Bastian, A. J., Celnik, P. (2011). Human locomotor adaptive learning is proportional to depression of cerebellar excitability. *Cereb. Cortex,* **8**, 1901–1909.

66. Prime, S. L., Vesia, M., Crawford, J. D. (2011). Cortical mechanisms for trans-saccadic memory and integration of multiple object features. *Philos. Trans. R. Soc. Lond. Series B Biol. Sci.,* **366**(1564), 540–553.

Chapter 5

The Coming Era of Nanomedicine[1]

Fritz Allhoff, JD, PhD

Department of Philosophy,
Western Michigan University, Kalamazoo, Michigan, USA

Keywords: nanomedicine, nanoethics, nanomaterials, nanoparticles, nanotechnology, patents, FDA, ethical and social issues, FDA regulatory governance, toxicity

5.1 Introduction

In this chapter, the author presents some general background on nanomedicine, particularly focusing on some of the investment that is being made in this emerging field (Section 5.2). The bulk of this chapter, though, explores two areas in which the impact of nanomedicine is likely to be most significant: diagnostics and medical records (Section 5.3) and treatment (Section 5.4), including surgery and drug delivery. Under each discussion, the author surveys some of the ethical and social issues that are likely to arise in these applications.

[1]This chapter is a revised and updated version that was originally published in the *American Journal of Bioethics* (2009) **9**(10), 3–11. See also, Allhoff, F., Lin, P., Moore, D. (2010). *What Is Nanotechnology and Why Does It Matter? From Science to Ethics*. Wiley-Blackwell, Oxford, Chapter 11.

Handbook of Clinical Nanomedicine: Nanoparticles, Imaging, Therapy, and Clinical Applications
Edited by Raj Bawa, Gerald F. Audette, and Israel Rubinstein

ISBN 978-981-4669-20-7 (Hardcover), 978-981-4669-21-4 (eBook)
www.panstanford.com

Nanotechnology has been hailed as the "next Industrial Revolution"[2] and promises to have substantial impacts into many areas of our lives. Such impacts will be manifest through many of the applications that nanotechnology will enable; these applications will take advantage of features that are only realized through nanoscale manipulations. And, through these technological advances, many ethical and social issues have been raised.[3]

What, though, is nanotechnology? Various definitions of "nano" have sprung up over the years and there is no universally accepted nomenclature for terms such as "nanomaterials," nanomedicine," and even "nanotechnology."[4] Recently, the FDA stretched the upper limit of nanotechnology to 1000 nm (from 100 nm), albeit unofficially.[5] Various experts have highlighted the flaws in having a sub-100 nm definition of nanotechnology, especially concerning nanomedicine. Clearly, this highlights the importance of establishing a uniform "nano" terminology for harmonized FDA regulatory governance, manufacturing and quality control, safety assessment, and patent review. I adopt the following practical definition of nanotechnology from 2007, one that is unconstrained by an arbitrary size limitation[6]:

> "The design, characterization, production, and application of structures, devices, and systems by controlled manipulation of size and shape at the nanometer scale (atomic, molecular, and macromolecular scale) that produces structures, devices, and systems with at least one novel/superior characteristic or property."

This above definition suggests two necessary (and jointly sufficient) conditions for nanotechnology. The first is an issue of *scale*: nanotechnology is concerned with things of a nanometer

[2]National Nanotechnology Initiative: Leading to the Next Industrial Revolution, National Science and Technology Council's Committee on Technology, February 2000. Available at: http://clinton4.nara.gov/media/pdf/nni.pdf (accessed August 2, 2014).

[3]For discussion of several different areas in which these concerns are manifest, see Allhoff et al. (2007). See also Allhoff and Lin (2008). See also Allhoff et al. (2010), especially Part III.

[4]Bawa, R. (2013). See also Tinkle et al. (2014).

[5]Conner et al. (2015).

[6]Bawa (2007).

size range. "Nano" (from the Greek *nannos*, "very short man") means one billionth, and in nanotechnology, the relevant billionth is that of a meter. Nanometers are the relevant scales for the size of atoms; for example, a hydrogen atom is 7.874×10^{-10} ft. in diameter, which is an unwieldy scale to use since we could rather describe the same dimension as about a quarter of a nanometer. The second issue has to do with that of *novelty*: nanotechnology does not *just* deal with small things, but rather must deal with them in a way that takes advantage of or results in superior or novel structures/devices/systems due to some properties that are manifest *because* of the nanoscale.[7]

Applications of nanotechnology to medicine are already under way and offer tremendous promise; these applications often go under the moniker of "nanomedicine" or, sometimes, "bionanotechnology."[8] In this chapter, I will present some general background on nanomedicine, particularly focusing on some of the investment that is being made in this emerging field (Section 5.2). The bulk of the chapter, though, will consist in explorations of two areas in which the impacts of nanomedicine are likely to be most significant: diagnostics and medical records (Section 5.3) and treatment (Section 5.4), including surgery and drug delivery.[9] In each of these sections, I will survey some of the ethical and social issues that are likely to arise in these applications.

5.2 The Rise of Nanomedicine

Before moving forward with more substantive discussion, let us start with a simple conceptual worry, which is how to properly delimit the scope of nanomedicine. Other applications of nanotechnology raise ethical issues, but the status of nanomedicine is somewhat different, in at least a couple of ways. First, as we will see in subsequent sections, nanomedicine is not always about specific products, as have been considered in some of these other

[7]For further discussion of this and other definitions of nanotechnology, see Allhoff (2007); also see Conner et al. (2015) and Bawa (2007).

[8]See, for example, Vo-Dinh (2007). See also Niemeyer and Mirkin (2004). Finally, see Niemeyer and Mirkin (2007).

[9]Some of that discussion will be adapted from Allhoff (2007).

applications. Rather, nanomedicine can be about techniques in ways that have largely not been considered elsewhere. This challenges some of the classifications in the sense that there is not always some specific *thing* that can be looked at and assessed as nanotechnology (or not). This point will become clearer in the remainder of the chapter.

Second, at the time of writing, the non-scientific literature on nanomedicine is still somewhat undeveloped. In doing the research for this chapter, I was only able to find a handful of papers that even countenanced nanomedicine's ethical and social dimensions.[10] This is in stark contrast to some of the topics that have received more attention elsewhere: in a nanotechnology context, the developing world, environment, privacy, enhancement and the military have all received more scholarly attention than nanomedicine.[11,12] This is peculiar, especially in the cases of enhancement and the military, which are far more speculative and, to some extent, futuristic than nanomedicine. One suggestion as to why this could be the case is that nanomedicine, unlike some of the other applications of nanotechnology, simply does not raise any ethical or social concerns that have not already appeared in other guises. But my view is closer to the claim that *none* of these applications raises any substantively new concerns; they only change the context in which those concerns are realized.[13] This sort of skepticism is not to cast aspersions on the present project, which can be about elucidating those contexts instead of trying to motivate some new theoretical approach altogether. Nevertheless, the asymmetry between ethical discussion of nanomedicine and other applications of nanotechnology bears notice.

[10]A preliminary database searching (e.g., JSTOR and Philosophers' Index) of the scientific literature on nanomedicine indicates that it is more substantial while the *non-scientific* literature is quite anemic.

[11]Allhoff et al. (2007); Allhoff and Lin (2008).

[12]Toxicity is an issue related to nanomedicine that has been present in many of these other areas; questions of how to deal with toxic risk, for example, have ethical dimensions. Toxicity will figure into the below discussions of diagnostics and treatment, though that particular focus has not been adequately explored elsewhere.

[13]See, for example, Allhoff (2007).

One of the few significant contributions to discussion of the ethical issues in medicine comes from Drs. Raj Bawa and Summer Johnson.[14] Bawa and Johnson, before moving to particular discussions about nanomedicine, offer some general comments about the pharmaceutical industry that warrant attention, particularly as is relevant for much of the investment that is being made in nanomedicine. Drug companies are always striving to increase the success rate of their products, as well as to decrease research and development (R&D) costs, including time to development. Getting a new drug to market is an extremely daunting task: the economic cost can be as high as $800M[15]; the time to market is usually 10–15 years; and only one of every 8000 compounds initially screened for drug development ultimately makes it to final clinical use.[16] Annual R&D investment by drug companies has climbed from $1B in 1975 to $40B in 2003, though the number of new drugs approved per year has not increased at all; it has stayed at relatively constant 20–30 approvals per year.[17] (New drugs account for only approximately 25% of the approvals, with the other 75% coming from reformulations or combinations of already-approved drugs.) And, due to these high costs, only about 30% of new drugs are recovering their R&D costs. Although all these numbers and statistics are not the most current, these trends continue. International pressures are mounting on US pharmaceutical companies as well, especially with production being increased in low-cost countries such as India and China, coupled with the expiration of some American patents.[18]

None of this is to lament the plights of pharmaceutical companies. The biggest ones—e.g., Johnson and Johnson, Pfizer, Bayer, and GlaxoSmithKline—have annual revenues at or close to $50B, and all have under $10B/year investments in R&D. Even factoring in total expenses, these biggest companies have annual

[14]Bawa and Johnson (2008). Also see Bawa and Johnson (2007).

[15]DiMasi et al. (2003). Also see Adams and Brantner (2006).

[16]Bawa and Johnson (2007), p. 211.

[17]Sussman, N. L., and Kelly, J. H. (2003). Saving time and money in drug discovery: A preemptive approach. In: *Business Briefings: Future Drug Discovery 2003*, Business Briefings, Ltd., London.

[18]Bawa and Johnson (2008), p. 212.

profits of over $10B each.[19] But of course, those companies always want to become more profitable, and nanotechnology offers promise in this regard. It is worth quoting Bawa and Johnson at length:

> Nanotechnology not only offers potential to address [the above] challenging issues but it can also provide significant value to pharma portfolios. Nanotechnology can enhance the drug discovery process via miniaturization, automation, speed and the reliability of assays. It will also result in reducing the cost of drug discovery, design and development and will result in the faster introduction of new cost-effective products to the market. For example, nanotechnology can be applied to current micro-array technologies, exponentially increasing the hit rate for promising compounds that can be screened for each target in the pipeline. Inexpensive and higher throughput DNA sequencers based on nanotechnology can rescue the time for both drug discovery and diagnostics. It is clear that nanotechnology-related advances represent a great opportunity for the drug industry as a whole.[20]

As expected, pharmaceutical companies are already investing in nanotechnology. Analysts have predicted that, by 2014 the market for pharmaceutical applications of nanotechnology will be close to $18B annually;[21] another report indicates that the U.S. demand for medical products incorporating nanotechnology will increase over 17% per year to $53B in 2011 and $110B in 2016.[22,23] Globally, hundreds of nanotherapeutics and nanodevices either are in the clinical testing pipeline or already approved.[24] There are various market predictions and forecasts for nano-medicines. For examples, one report[25] predicts that the global nanomedicine market will hit US$130.9 billion by 2016 while another report[26] expects it to reach a value of US$177.60 billion within the next five years.

[19] *MedAdNews* (2007).
[20] Bawa and Johnson (2008), p. 212.
[21] Hunt (2004).
[22] The Freedonia Group, Inc. (2007)
[23] Bawa and Johnson (2008), p. 212.
[24] Mansour et al. (2015). Also see, Bawa (2008).
[25] Fischer (2014).
[26] Transparency Market Research (2014).

The worry is that all of this investment and interest in nanotechnology, particularly as is motivated by a race to secure profitable patents, will lead to a neglect of important ethical issues that should be explored. Bawa and Johnson point out, correctly, that the time for such reflection is not once these technologies come to market, but before R&D even begins.[27] Insofar as the investments are large and growing and, as mentioned above, insofar as the ethical literature on nanomedicine is almost nonexistent, this imperative has already been violated. The principal ethical issues will have to do with safety, especially toxicity: some of these issues have to do with the nanomaterials involved in nanomedicine, which have been poorly studied thus far, particularly as they interact with complex biological organisms. It is quite likely that some of these applications will have unwelcome results in their hosts, at least some of which might not be predicted ahead of time.

5.3 Diagnostics and Medical Records

Consider the trajectory of some particular health remediation. Effectively, there are two central steps: first, health care professionals have to assess the health of their patients—through both diagnostics and using pre-existing medical records—and, second, they have to choose some treatment plan to address the patients' health issues. This is surely an oversimplified view of medicine, particularly as it fails to include any of medicine's social aspects (e.g., interaction with patients). But, for our purposes, it will work just fine: figure out what is wrong with the patient, and then fix it. There are all sorts of diagnostic tools available to the medical community, ranging from simple patient interviews and examinations up to more sophisticated imaging tools like computerized tomography (CT), magnetic resonance imaging (MRI), and positron emission tomography (PET). Other diagnostic tools include blood work, DNA analysis, urine analysis, x-rays, and so on. Moreover, there are all sorts of ways to gain access to patients' medical histories. Again, simple patient interviews, while limited, can be effective, and medical records, prepared by other

[27] Bawa and Johnson (2008), pp. 212–213.

health care professionals, can offer a wealth of salient information. Once the diagnosis has been made, treatment can proceed whether through, for example, surgery or drugs, to which we will return in Section 5.4.

Starting with diagnostics and deferring medical records for below, many diagnostic techniques are limited, particularly given certain maladies that health care professionals would like to be able to effectively diagnose. Cancer, for example, is one arena in which nanotechnology is likely to have the biggest impact, and this impact will come both in terms of improved diagnostics and improved treatment.[28] Many cancer cells have a protein, epidermal growth factor receptor (EGFR), distributed on the outside of their membranes; non-cancer cells have much less of this protein. By attaching gold nanoparticles to an antibody for EGFR (anti-EGFR), researchers have been able to bind the nanoparticles to the cancer cells.[29] Once bound, the cancer cells manifest different light scattering and absorption spectra than benign cells.[30] Pathologists can thereafter use these results to identify malignant cells in biopsy samples.

This is just one example, but it has three noteworthy features: cost, speed, and effectiveness. Given some other traditional diagnostics that have been available, this one offers an improvement in all three regards. And while cancer is a critical health problem that must be addressed, the general approach that this diagnostic uses can be generalized beyond just cancer. To wit, if nanoparticles can differentially bind to something—by which I mean that they bind more readily to that thing than to everything else—then it will be easier to identify. And improved diagnostics lead to improved treatments, which lead to better health outcomes.

Diagnostically, the concerns with these sorts of applications center around toxicity, particularly when the applications are utilized *in vivo* (as opposed to *in vitro*). Conventional diagnostic mechanisms, however, manifest the same structural features as nano-diagnostics (i.e., applications of nanotechnology to diagnostics); there do not seem to be any substantially new issues raised in this regard. Consider, for example, x-rays, which use electromagnetic radiation to generate images that can be used for

[28]National Cancer Institute (2005).

[29]El-Sayed et al. (2006).

[30]El-Sayed et al. (2005).

medical diagnostics. But radiation, absorbed in large dosages, is carcinogenic, so health care professionals have to be judicious in their application thereof.[31] The radiation outputs for x-rays are reasonably well understood, as are their toxicities in regards to human biology.[32] As when considering treatment options, health care professionals must consider these toxicities, as well as the benefits of this diagnostic mechanism (perhaps as contrasted with other options). Nano-diagnostics admit of a similar deliberative model, even if some of the risks are, at present, less well understood.

Another possibility is "lab-on-a-chip" technologies, which could detect "cells, fluids or even molecules that predict or indicate disease states."[33] These devices could also provide real-time monitoring of various biometric indicators, such as blood glucose levels, as might be useful to a diabetic.[34] Again, the issues could have to do with toxicity, depending on how these chips are deployed. They might be kept inside the body indefinitely or permanently, which could be different from some of the binding diagnostics that, if administered *in vivo*, would ideally leave the body soon thereafter (e.g., if the cancer cells to which they bound were destroyed; see Section 5.4). Certainly clinical trials will be important, but it could be hard to get the sort of data that would be relevant for long-term effects. For example, perhaps the diagnostics only manifest toxicity some distant years in the future and only after they have been degraded; this information might not even be available for decades.

Depending on how this information is stored and shared, it could give rise to privacy issues: nano-sized chips could be implanted into individuals and serve as repositories for

[31]Note that one of the pioneers of radioactivity, Marie Curie, died from aplastic anemia, which was almost certainly caused by exposure to radiation. Rosalind Franklin, whose work on x-ray crystallography was critical to the discovery of the double helical structure of DNA, contracted ovarian cancer at a relatively young age; again, her work was almost certainly responsible.

[32]There have been numerous studies of the effects of the use x-ray technology in diagnostic procedures. For a recent overview of data relating to risk of cancer, see Berrington de Gonzalez and Darby (2004). Also, see Kereiakes and Rosenstein (1980) and National Research Council (1990).

[33]Bawa and Johnson (2008), p. 218. See also Craighead (2006).

[34]Bawa and Johnson (2008), p. 218.

medical information, thus enabling quick access by health care professionals.[35] Strictly speaking, this does not seem to be a diagnostic function, but one of medical record keeping. In other words, these chips are "passive" in the sense that they are merely storing information. In the previous paragraph, though, I characterized chips that, in some sense, are "active": they could actually determine what is going on in the body and then make that informational available. This distinction is irrelevant ethically insofar as there are privacy issues regardless, but the passive applications are likely to have more information. In terms of diagnostics then, the focus should probably be on the active applications, but the passive ones, in virtue of their greater informational potential, give rise to greater privacy concerns. However, I think some skepticism is warranted regarding the privacy issue since, in all likelihood, the chips would merely contain some identification number that would allow access to patients' records through some medical database; the chip itself would not actually contain any medical information, so there is no privacy worry. (Even the identification number could require authentication or decryption as further protections and to prevent the possibility of tracking and surveillance).

However, what are these databases and how are they supposed to work? First, we do not presently have the infrastructure to support this sort of databasing. The ideal is supposed to be something like the following: imagine that someone from California happens to be traveling to New York on business, when she falls seriously ill and is rushed, unconscious, to the emergency room. Maybe even, in the rush to get her to the emergency room, her identification is lost. The emergency room staff can simply scan her triceps, plug her identification number into the database and learn who she is, what previous conditions she has, what drugs she is allergic to, and so on. Treatment can then ensue given this access to her history and records. But, of course, no such database exists.[36] And several issues exist for its implementation.

[35]For more discussion, see Allhoff, Lin and Moore (2010), Chapter 10.

[36]Interestingly, I have not been able to find anything written on this issue, despite the fact that the media has often characterized these applications of nanotechnology to be revolutionary for medicine. The following discussion will therefore be inherently speculative.

First, it would be a huge endeavor and, presumably, very expensive. We would have to think about whether such a project would be worthwhile particularly given that, at least in many cases, there are fairly straightforward ways of getting access to the relevant medical information (e.g., by asking the patient or by using identification to contact a relative). To be sure, this will not always work (e.g., with patients who are unconscious and lack relatives and/or identification), but we would have to think about how many cases could not be handled by more conventional means and whether it would be a worthwhile investment of resources to develop this new system. Second, even if the chips themselves did not pose any substantial privacy worries, the database itself might. If all the medical information really went on some sort of national server, then it could be hacked. If it were retained locally, but allowed for remote access (as it would have to), the same worries would apply. Third, even if the privacy issues were mitigated and gave rise to improved outcomes, there could be ethical issues insofar as those outcomes would only be available to citizens of wealthier countries as with other disparities, questions of distributive justice arise.[37]

There are some other aspects of nanomedicine that are promising and probably without any significant ethical worries. For example, "quantum dots have been used as an alternative to conventional dyes as contrast agents due to their high excitability and ability to emit light more brightly and over long periods of time."[38] If we can use quantum dots, especially *in vitro*, to allow for more sensitive detection, then this is a useful application. As mentioned above, *in vivo* uses raise issues about toxicity, but there are certainly benign applications of nanomedicine that should be pursued if they increase our diagnostic abilities. These other issues mentioned above, regarding toxicity and privacy, are quite likely superable, though ethical attention needs to be paid to how we move forward. (And, as discussed in Section 5.2, it is unlikely that this imperative has yet been recognized.) Having now offered discussion of how nanomedicine could affect diagnostics and medical record keeping, let us now move on to treatment.

[37]See, for example, Allhoff, Lin, and Moore (2010), Section 7.2.

[38]Bawa and Johnson (2008), p. 218. See also Alivisatos (2001).

5.4 Treatment

In this section, I will consider how nanomedicine can be used to improve treatment options, and I propose to draw a distinction between two different kinds of treatment: surgery and drugs. "Surgery" comes from the Greek χειρουργική and through the Latin *chirurgiae* that is often translated as "hand work." Many cardiac techniques, for example, have to be done manually (literally, by hand) in the sense that a surgeon has to physically intervene on the heart of a patient. Some of these techniques can now be performed remotely, automatically, and so on, but the basic unifier is direct intervention on a physical system by a physician or proxy. Surgery can be contrasted with drug treatment, by which I mean the administration of some pharmacological substance that is prescribed for remediation of some physical ailment; this latter part of the definition is to distinguish drug *treatment* from other uses of drugs (e.g., recreational). Drugs are often less direct than surgery in the sense that their introduction is not (always) localized. For example, a patient may swallow some pills that have downstream physiological effects in his body, but those effects are mediated by more other processes than the effects of surgery would be. However, nothing substantial hangs on this distinction, it is useful for mode of presentation.[39]

Nano-surgery—by which I mean surgical applications of nanotechnology—enables techniques that are more precise and less damaging than traditional ones; let me offer a few examples.[40] First, a Japanese group has performed surgery on living cells using atomic force microscopy with a nanoneedle (6–8 μm in length and 200–300 nm in diameter).[41] This needle was able to penetrate both cellular and nuclear membranes, and the thinness of the needle prevented fatal damage to those cells. In addition to ultra-precise and safe surgical needles, laser surgery at the nanoscale is

[39]It is worth noting that there are probably non-surgical treatments that do not involve drugs. I do not mean to set up a false dichotomy between surgery and drugs. For example, rest might be a treatment for soreness, but it is neither surgical nor drug-related. Nor, though, is it relevant to nanomedicine; for our purposes, the distinction between surgical and drug-related treatments will suffice, without implying that they are exhaustive.

[40]See also Ebbesen and Jensen, (2006).

[41]Obataya et al. (2005). Quoted in Ebbesen and Jensen (2006), p. 2.

also possible: femtosecond near-infrared (NIR) laser pulses can be used to perform surgery on nanoscale structures inside living cells and tissues without damaging them.[42] Because the energy for these pulses is so high, they do not destroy the tissue by heat—as conventional lasers would—but rather vaporize the tissue, preventing necrosis of adjacent tissue.[43] I already discussed in Section 5.3 that gold nanoparticles can be used for cancer diagnostics insofar as they can be attached to anti-EGFR which would then bind to EGFR;[44] once bound, cancer cells manifest different light scattering and absorption spectra than benign cells, thus leading to diagnostic possibilities. But this technology can be used for cancer treatment as well as diagnostics: since the gold nanoparticles differentially absorb light, laser ablation can then be used to destroy the attached cancer cells without harming adjacent cells.[45]

What these applications have in common is that they allow for direct intervention at the cellular level. While some traditional laser technologies, for example, have allowed for precision, the precision offered by surgery at the nanoscale is unprecedented. It is not just the promise of being able to act on individual cells, but even being able to act *within* cells without damaging them. Contrast some of this precision offered by nano-surgery with some more traditional surgical techniques. Just to take an extreme example, consider lobotomies, especially as were practiced in the first half of the 20th century: these procedures were effectively carried out by inserting ice picks through the patient's eye socket, and the objective was to sever connections to and from the prefrontal cortex in the hopes of treating a wide range of mental disorders. Independently of whatever other ethical concerns attached to lobotomies—that have fallen out of practice since the introduction of anti-psychotics such as chlorpromazine—these procedures could hardly have any degree of precision.

[42]Tirlapur and König (2003).

[43]Ebbesen and Jenson (2006), p. 2.

[44]Recall that EGFR is a protein that is usually more often prevalent on cancer cells than on non-cancer cells; anti-EGFR is an antibody.

[45]Some commentators talk about those applications for cancer treatment under the aegis of drug delivery but, for us, this does not sound quite right: it is not the *drug* that is being bound to the cancer cells, but rather a nanoparticle that is thereafter used to absorb light, heat the cancer cell, and destroy it. For this reason, this author classifies it as a surgical tool.

Even given the dark history of lobotomies, one of its highlights was the invention of more precise surgical devices; for example, António Egas Moniz's introduction of the leucotome, for which he won the Nobel Prize in 1949. However surgeries are practiced, precision is always important, by which I mean roughly that surgeons want to be able to access the damaged area of the patient's body without simultaneously compromising anything not damaged. The gains in precision from ice picks to nano-surgery are multiple orders of magnitude, and even the gains in precision from recent surgical advances to nano-surgery could be a full order of magnitude.

So what are the worries? As was alluded to in Section 5.2 and will be discussed more in Section 5.5, the principal one is that these surgical techniques carry risks, and that, in the excitement to rush them to market, those risks will not be adequately explored or assessed. For now, though, it is worth noticing that there is nothing special about nano-surgery in this regard: whatever stance we otherwise adopt toward risk are equally transferrable to this context. That said, it is not obvious what the risks could be for nano-surgery, though dismissal of potential risks could certainly be one of them. Some of the applications with drug delivery do seem more risky than using high-precision surgical techniques, though I will argue below that those are not endemic to nanomedicine either. Of course there are the generic worries about distributive justice and health care such that only a few might have access to nano-surgical technologies, but those again have nothing in particular to do with nano-surgery.

But let me say something about the use of nanoparticles; as discussed above, these might play a role in various cancer treatments. Of particular concern is the toxicity from nanoparticles that might be used, as well as other safety concerns. Whatever is to be said about these risks, though, it hardly follows that similar concerns do not attach to more traditional approaches. Consider, for example, chemotherapy, which uses cytotoxic drugs to treat cancer. The downside of chemotherapy is that these drugs are toxic to benign cells as well as to malignant ones, and there are side effects such as immunosuppression, nausea, vomiting, and so on. When physicians are prescribing chemotherapy, they therefore have to think about these risks and whether the risks are justified. But whether the treatment option involves nanoparticles or not,

this basic calculus is unchanged: physicians must choose the treatment option that offers the best prognosis. Toxicity or side effects count against these outcomes, and improved health counts in favor of them. Obviously, there are epistemic obstacles to such forecasting, and physicians must be apprised of the relevant toxicity and side effect data, but there is nothing unique to nanomedicine in this regard.[46]

The point that I want to make is that there are *already* risks in treatments and there is no good reason to think that the risks of nano-surgery are any higher than the risks characteristic to conventional medicine. In fact, there are good reasons to think that the risks of nano-surgery are actually lower and that the benefits are higher. For example, compare laser ablation of malignant cells to chemotherapy. Chemotherapy, as mentioned above, is a hard process and one with enormous costs to the patient (including physical and psychological). If nanomedicine allows us, unlike chemotherapy, to destroy the malignant cells without harming the rest of the organism, it is a definite improvement. Are the nanoparticles that would be utilized toxic? Do they pass out of the body after the treatment? Even supposing that the answers are yes and no, respectively, it is quite probable that these new treatments would be improvements over the old. That is not to say that due diligence is not required, but I suspect that, in the end, there will not be that much to fear, at least at the appropriate comparative level.

Turning now to drug delivery, there are myriad advantages that nanomedicine will be able to confer. Per the discussion in Section 5.2, there is already a tremendous interest from the pharmaceutical companies in terms of incorporating nanotechnology into their product lines, and that interest is the primary driving force in the rise of nanomedicine; this is not to say that the above-discussed nano-surgical techniques are not impressive, just that they are probably not as profitable. Let me go through three traditional challenges in drug delivery, and explain how nanotechnology can mitigate them.

First, consider absorption of drugs: when drugs are released into the body, they need to be absorbed as opposed to pass through.

[46]As mentioned above, a lack of information about risks is more of an issue in nanomedicine than in some more traditional forms of medicine, though this does not affect general, formal deliberative models.

Nanotechnology can facilitate a reduction in the size of drugs (or at least their delivery mechanisms) and therefore, an increase in their surface-to-volume ratios. The basic idea here is that it is the surfaces of materials that are most reactive and that, by increasing surface-to-volume ratios, greater reactivity is achieved. As the body absorbs drugs, it has to act on the surfaces of those drugs and, by having more surface area per unit volume, the drugs can be dissolved faster, or even be rendered soluble at all. Speed of absorption is of critical importance to the success of drugs, and nanotechnology will make a difference in this regard. Also, it is worth noting that nanomedicine may obviate the need for oral (or other) administrations of drugs in some cases and allow for topical administration: because the drugs will be smaller, they will be more readily absorbed transdermally. Insofar as some patients would prefer this method of administration, it offers another advantage.

Second, it is not always the case that fast absorption is ideal since, in some cases, it would be better if the drug were released slowly over time. Consider, for example, time-release vitamins: because vitamins B and C are water soluble, they quickly flush from the body if not administered in some time-release manner. If the options were taking a vitamin every couple of hours or else taking one that is slowly released over a longer period of time, there are obvious advantages to the latter. Nanotechnology could be used to create better time-release capacities insofar as it could allow for smaller apertures through which the pharmacological molecules would dissipate. In other words, nanotechnology could help to create lattices with openings through which, for example, single molecules would pass. If only single molecules could pass at any given time from the delivery system (e.g., the capsule), then it would take a longer time to disperse the drug supply and, depending on the application, this could lead to more effective treatment.

Third, because nanotechnology will be able to engineer smaller drugs, the associative drugs might be able to traverse various membranes or other biological barriers that had previously restricted their usefulness. For example, consider the blood-brain barrier, which is a membrane that restricts the passage of various chemical substances (and other microscopic entities, like bacteria) from the bloodstream into the neural tissue. Nanoparticles are

able to pass this barrier, thus opening up new possibilities for treatment of psychiatric disorders, brain injuries, or even the administration of neural anesthetic.[47] In this case, nanomedicine is not just improving existing treatment options, but perhaps even creating new ones.

Again tabling issues of distributive justice, the principal concern with bringing nanotechnology to bear on drug delivery has to do with toxicity and other risks: we simply do not know how these technologies will interact with the body, and there could be negative consequences. As with the discussion of nano-surgery, I am inclined to think that the benefits conferred by the application of nanotechnology to drug delivery outweigh the risks, though the risks in drug delivery are probably greater than the risks with nano-surgery. It is worth reiterating, though, that risks pertaining to delivery are not unique to nanomedicine. Consider, for example, the celebrated case of Jesse Gelsinger, who died in a gene therapy trial.[48] Gelsinger had ornithine transcarbamylase deficiency: he lacked a gene that would allow him to break down ammonia (a natural byproduct of protein metabolism). An attempt to deliver this gene through adenoviruses was made, and Gelsinger suffered an immunoreaction that led to multiple organ failure and brain death. Whether talking about vectors for genetic interventions or nanoparticles, we surely have to think carefully about toxicity, immunoreactions, and other safety concerns; the point is merely that these issues are not unique to nanomedicine.

5.5 Moving Forward

In this last section, let me try to tie together various themes that have been developed in the preceding three and, in particular, make some comments about the future of nanomedicine. Throughout, I have indicated skepticism about whether nanomedicine raises any new ethical or social issues, or at least ones that have not already been manifest with existing technologies. This skepticism applies to various other areas of nanoethics as well, though perhaps more so to medicine. Issues in privacy might, for example, be transformed by the proliferation of radio frequency identification

[47]Bawa, R. (2010). The blood-brain barrier. *In*: D. H. Guston (editor). *Encyclopedia of Nanoscience and Society*, SAGE Publications, Inc., Thousand Oaks, CA, pp. 54–55.

[48]Philipkowski (1999).

(RFID), though I doubt it.[49] But the issues with nanomedicine seem to be, at most, risks (e.g., toxicity and safety) and distributive justice, and in fairly standard ways. Of course these considerations ought to be taken into account, but they should always be taken into account and nothing inherent to nanomedicine makes us think differently about them.

What does make nanomedicine interesting, at least from an ethical perspective, is its extreme profitability. As mentioned in Section 5.2, pharmaceutical companies make tens of billions a dollar on year in profits, and this leads to a different motivational scheme than exists in other applications of nanotechnology. For example, consider nanotechnology and the developing world. The developing world, practically by definition, simply does not have tremendous amounts of money. Staying with pharmaceuticals, a primary ethical concern is that drugs critical for health in the developing world just are not developed because they would not be profitable; consider, for example, the billions of dollars spent in the US on erectile dysfunction drugs as against the lack of investment for lifesaving anti-malarial medication. This is not to say that the developing world cannot be made profitable,[50] but it has a long way to go to rival domestic profitability.

Applications of nanotechnology to RFID tags raise privacy worries, particularly given the profitability of the RFID industry and the expected proliferation of its products. Wal-Mart, for example, has mandated that its principal suppliers use RFID tags on their deliveries in order to facilitate more effective inventorying.[51] Under a reasonable estimate of a billion tags a year, the revenues would be $50M annually at $0.05/tag. If Wal-Mart only used 1% of the produced tags, the annual *revenue* for the

[49] See Allhoff, Lin, and Moore (2010), Chapter 10. An RFID tag communicates a unique identification number to an electronic reader by radio waves, thus abrogating the need for either physical contact with the tag (e.g., such as would be necessary to read a bar code), or even a direct line of sight to the tag. These tags have a small microchip, as well as a radio antenna which can transmit data from the chip to the reader. This reader also contains an antenna, as well as a demodulator which can transform the analog radio signal into digital data that can then be used by a computer. Privacy advocates worry that these signals and data can be used for tracking and surveillance.

[50] The Health Impact Fund, for example, seeks to incentivize private pharmaceutical companies to invest in global public health. See Hollis and Pogge (2008).

[51] RFID-enabled inventory allows that line of sight would not be required (cf., scannable bar codes) and furthermore, that inventory could be done remotely.

entire RFID industry (on tags) would be $5B, which is about half the annual *profit* of single, large pharmaceutical company. There are other economic impacts of RFID technology, including scanners, manufacturing, training, and so on, but, even aggregated, these have to fall well short of the economic impacts of nanomedicine.

Other oft-discussed applications of nanotechnology are probably even less profitable still: consider the environment, human enhancement,[52] and the military.[53] It is always hard to make the environment profitable, particularly since it is more often governments than consumers or industry that have to produce the capital outlay. There will be profit in repairing or protecting the environment, but it will be of a far lesser scale than that available to pharmaceutical companies through investment in nanomedicine. Enhancement will only be available to some people, and some of the widespread availability that the nanomedia has prognosticated warrants serious skepticism. At least in the US, nearly everyone will take some pharmacological product at some stage of their lives, and many (or most) of those will be transformed by nanomedicine. Therefore, the scope and, again, profitability are very high for nanomedicine. Finally, consider the military, which is a little more tricky. The Department of Defense, for example, had budget requests in the order of $ 500 plus in recent years. However, it is still hard to get a sense for what implications these and upcoming wars will have for sellers of nanotechnology.[54] Obviously the wars in Iraq and Afghanistan played a large role in this expenditure, as do overall personnel. Will government military contractors be as motivated to pursue nanotechnology as pharmaceutical companies? Or to put it a different way, will nanotechnology have a bigger economic impact on the military than on medicine? I suspect not, but will not pursue that suspicion here.

Regardless, the point is merely that nanomedicine is likely to be one of the most—if not *the* most—profitable application of nanotechnology and, furthermore, one that is going to be primarily pursued by pharmaceutical companies committed to making profits. These features give rise to ethical concerns insofar as they

[52]For more discussion, see Allhoff, Lin and Moore (2010).

[53]Altman (2006). See also Moore (2007).

[54]Department of Defense, Office of Management and Budget. Available online at http://www.whitehouse.gov/omb/factsheet_department_defense (accessed on January 16, 2015).

are harbingers for market-first, ethics-last mantras. Imagine that Johnson and Johnson is competing with Pfizer to bring out the next greatest drug; a multi-year patent and billions of dollars hang in the balance. There is a lot of pressure to be first. And, potentially, a lot to be gained by cutting corners along the way, whether during pharmacological development, clinical trials, complete disclosure, or whatever. Organizations like the FDA will have to be extremely vigilant but, of course, they always have to be vigilant. The profits are there to be had whether the drugs incorporate nanotechnology or not so, in that sense, this is nothing new. The only point is that these pressures are likely to be more significant in nanomedicine than many or all other applications of nanotechnology.

Moving forward, we must develop an engagement between nanomedicine's promise and its ethical and social implications. In Section 5.2, I pointed out that there has been very little academic or public work done on these issues; at the time of writing, not more than a couple of papers.[55] Surely this needs to be remedied. To have the pharmaceutical companies developing products without an existing forum to discuss the potential effects of those products—including toxicity and other risks—is not good. Again, some of those effects might not be manifest for many years, as we simply do not have long-term research about how nanotechnology interacts with the body. The promise is certainly high, but it should be negotiated clearly and carefully with attention to ethical and social implications and an accompanying discourse.

Disclosures and Conflict of Interest

The author declares that he has no conflict of interest and has no affiliations or financial involvement with any organization or entity discussed in this chapter. No writing assistance was utilized in the production of this manuscript and the author has received no payment for preparation of this chapter. Nothing contained herein is to be considered as the rendering of legal advice.

[55]A notable exception to this, particularly in terms of public engagement, is The European Working Group on Ethics in Science and new Technologies to the European Commission (2007). An abridged version is published as "Ethical Aspects of Nanomedicine: A Condensed Version of the EGE Opinion 21" in Allhoff and Lin (2008), pp. 187–206.

Corresponding Author

Dr. Fritz Allhoff
Department of Philosophy
3004 Moore Hall, Western Michigan University
1903 W. Michigan Ave., Kalamazoo, MI 49008, USA
Email: fritz.allhoff@wmich.edu

About the Author

Fritz Allhoff is an associate professor in the department of philosophy and school of medicine at Western Michigan University. Dr. Allhoff completed his PhD in philosophy at the University of California, Santa Barabara and his JD at the University of Michigan, where he graduated *magna cum laude*. He has held visiting posts at the American Medical Association, University of Michigan, University of Oxford, and the University of Pittsburgh. His primary fields of research are applied ethics, ethical theory, and philosophy of law. His latest books include *What Is Nanotechnology and Why Does It Matter?—From Science to Ethics* (Wiley-Blackwell, 2010; with Patrick Lin and Daniel Moore) and *Terrorism, Ticking Time-Bombs, and Torture* (University of Chicago, 2012), and his popular work has been featured in *Slate, The Atlantic, and The Huffington Post*. He co-founded the International Intelligence Ethics Association and serves on the editorial board for the International Committee of Military Medicine (Switzerland). Dr. Allhoff is currently working on a grant pertaining to ethical issues in cyberwarfare, funded by the National Science Foundation.

References

Adams, C. P., Brantner, V. V. (2006). Estimating the cost of new drug development: Is it really $802M?. *Health Aff.,* **25**(2), 420–428.

Alivisatos, A. P. (2001). Less is more in medicine. *Sci. Am.,* **285**(3), 66–73.

Allhoff, F. (2007). On the autonomy and justification of nanoethics. *Nanoethics*, **1**(3), 185–210.

Allhoff, F. (2009). The coming era of nanomedicine. *Am. J. Bioeth*., **9**(10), 3–11.

Allhoff, F., et al. (2007). *Nanoethics: The Ethical and Social Dimension of Nanotechnology*, John Wiley & Sons, Hoboken, NJ.

Allhoff, F., Lin, P., eds. (2008). *Nanotechnology & Society: Current and Emerging Ethical Issues*, Springer, Dordrect.

Allhoff, F., Lin, P., and Moore, D. (2010). *What Is Nanotechnology and Why Does It Matter?: From Science to Ethics*. Wiley-Blackwell, Oxford.

Altman, J. (2006). *Military Nanotechnology: New Technology and Arms Control*. Routledge, London.

Bawa, R. (2007). Special report: Patents and nanomedicine. *Nanomedicine* **2**(3), 351–374.

Bawa, R. (2008). Nanoparticle-based therapeutics in humans: A survey. *Nanotechnol. Law Bus.,* **5**(2), 135–155.

Bawa, R. (2013). FDA and nanotech: Baby steps lead to regulatory uncertainty. In: Bagchi, D., et al. eds. *Bionanotechnology: A Revolution in Biomedical Sciences and Human Health*. Wiley Blackwell, UK, pp. 720–732.

Bawa, R., Johnson, S. (2007). The ethical dimensions of nanomedicine. *Med. Clin. North Am.,* **91**(5), 881–887.

Bawa, R., Johnson, S. (2008). Emerging issues in nanomedicine and ethics. In: Allhoff, F., Lin, P., eds., *Nanotechnology & Society: Current and Emerging Ethical Issues*. Springer, Dordrecht, pp. 207–223.

Bawa, R. (2010). The blood-brain barrier. *In*: D. H. Guston (editor). *Encyclopedia of Nanoscience and Society*, SAGE Publications, Inc., Thousand Oaks, CA, pp. 54–55.

Berrington de Gonzalez, A., Darby, S. (2004). Risk of cancer from diagnostic X-rays: Estimates for the UK and 14 other countries. *Lancet*, **363**(9406), 345–351.

Conner, J. B., Bawa, R., Nicholas, J. M., Weinstein, V. (2015). Copaxone® in the era of biosimilars and nanosimilars. In: Bawa, R., Audette, G., and Rubinstein, I. eds. *Handbook of Clinical Nanomedicine: Nanoparticles, Imaging, Therapy, and Clinical Applications,* Chapter 28*,* Pan Stanford Publishing, Singapore (in press).

Craighead, H. G. (2006). Future lab-on-a-chip technologies for interrogating individual molecules. *Nature*, **442**, 387–393.

Department of Defense, Office of Management and Budget. Available online at: http://www.whitehouse.gov/omb/factsheet_department_defense (on January 16, 2015).

DiMasi, J. A., Hansen, R. W., Grabowski, H. G. (2003). The price of innovation: New estimates of drug development costs. *J. Health Econ.,* **22**, 151–185.

Ebbesen, M., Thomas G. J. (2006). Nanomedicine: Techniques, potentials, and ethical implications. *J. Biomed. Biotechnol.,* **2006**, 1–11.

El-Sayed, I., Huang, X., El-Sayed, M. A. (2005). Surface plasmon resonance scattering and absorption of anti-EGFR antibody conjugated gold nanoparticles in cancer diagnostics: Applications in oral cancer. *Nano Lett.,* **5**(5), 829–834.

El-Sayed, I., Huang, X., El-Sayed, M. A. (2006). Selective laser photo-thermal therapy of epithelial carcinoma using anti-EGFR antibody conjugated gold nanoparticles. *Cancer Lett.,* **239**(1), 129–135.

European Group on Ethics. (2008). Ethical aspects of nanomedicine: A condensed version of the EGE opinion 21. In: Allhoff, F., Lin, P. eds., *Nanotechnology & Society: Current and Emerging Ethical Issues*. Springer, Dordrecht, pp. 187–206.

European Working Group on Ethics in Science and New Technologies to the European Commission, The. (2007). Opinion on the Ethical Aspects of Nanomedicine. Opinion No. 21. European Commission, Brussels, January 17.

Fischer, S. (2014). Regulating nanomedicine. IEEE Pulse, Available at: http://pulse.embs.org/march-2014/regulating-nanomedicine/ (accessed on May 10, 2014).

Freedonia Group, Inc., The (2007). Nanotechnology in Healthcare, Freedonia, Cleveland, OH. Available at: http://www.freedoniagroup.com/brochure/21xx/2168smwe.pdf (accessed on August 26, 2014).

Freitas, Jr., R. A. (2007). Personal choice in the coming era of nanomedicine. In: Allhoff F., et al., eds. *Nanoethics: The Ethical Implications of Nanotechnology*. John Wiley & Sons, (Hoboken, NJ, pp. 161–172.

Hollis, A., Pogge. T. (2008) The Health Impact Fund: Making new medicines accessible for all (Incentives for Global Health, 2008). Available at: http://healthimpactfund.org/ (accessed on August 28, 2014).

Hunt, W. H. (2004). Nanomaterials: Nomenclature, novelty, and necessity. *J. Mater.,* **56**, 13–19.

Kereiakes, J. G., Rosenstein, M. (1980). *Handbook of Radiation Doses in Nuclear Medicine and Diagnostic X-Ray*. CRC Press, Boca Raton, FL.

Lin, P., Allhoff, F. (2008). Nanotechnology and Human Enhancement: A Symposium. In: *Nanoethics: The Ethics of Technologies that Converge at the Nanoscale,* **2**(3), 251–327.

Mansour, H. M., Park, C.-W., Bawa, R. (2015). Design and development of approved nanopharmaceutical products. In: Bawa, R., Audette, G., Rubinstein, I. eds. *Handbook of Clinical Nanomedicine: Nanoparticles,*

Imaging, Therapy, and Clinical Applications, Chapter 9, Pan Stanford Publishing, Singapore (in press).

MedAdNews (2007). The Top 50 Pharmaceutical Companies Charts & Lists. *MedAdNews,* **13**(9).

Moor, J., Allhoff, F., Lin, P., Weckert, J., (2007). *Nanoethics: The Social & Ethical Implications of Nanotechnology*, John Wiley & Sons, Hoboken, NJ, pp. 267–275.

National Cancer Institute (2005). Targeted gold nanoparticles detect oral cancer cells. *Nanotech News*, April 25.

National Nanotechnology Initiative: Leading to the Next Industrial Revolution, National Science and Technology Council's Committee on Technology, February 2000. Available at: http://clinton4.nara.gov/media/pdf/nni.pdf (accessed on August 2, 2014).

National Research Council (1990). *Health Effects of Exposure to Low Levels of Ionizing Radiation*. National Academies Press, Washington, DC.

Niemeyer, C. M., Mirkin, C. A. (2004). *Nanobiotechnology: Concepts, Applications, and Perspectives*. Wiley-VCH, Weinheim, Germany.

Niemeyer, C. M., Mirkin, C. A. (2007). *Nanobiotechnology II: More Concepts and Applications*. Wiley-VCH, Weinheim, Germany.

Obataya, I., et al. (2005). Nanoscale operation of a living cell using an atomic force microscope with a nanoneedle. *Nano Lett.,* **5**(1), 27–30.

Philipkowski, K. (1999). Another change for gene therapy. *Wired*, October 1. Available at: http://archive.wired.com/science/discoveries/news/1999/10/31613 (accessed on January 16, 2015).

Sussman, N. L., Kelly, J. H. (2003). Saving time and money in drug discovery: A pre-emptive approach. In *Business Briefings: Future Drug Discovery 2003*. Business Briefings, Ltd., London.

Tinkle, S., McNeil, S. E., Mühlebach, S., Bawa, R., Borchard, G., Barenholz, Y., Tamarkin, L., Desai, N. (2014). Nanomedicines: Addressing the scientific and regulatory gap. *Ann. N. Y. Acad. Sci.,* **1313**, 35–56.

Tirlapur, U. K., König, K. (2003). Femptosecond near-infrared laser pulses as a versatile non-invasive tool for intra-tissue nanoprocessing in plants without compromising viability. *Plant J.,* **31**(2), 365–374.

Transparency Market Research, Nanomedicine Market (Neurology, Cardiovascular, Anti-inflammatory, Antiinfective and Oncology Applications)—Global Industry Analysis, Size, Share, Growth, Trends and Forecast, 2013–2019. Available at: www.transparencymarketresearch.com/nanomedicine-market.html (accessed May 27, 2014).

Vo-Dinh, T. (2007). *Nanotechnology in Biology and Medicine: Methods, Devices, and Applications*. CRC Press, Boca Raton, FL.

Chapter 6

What's in a Name? Defining "Nano" in the Context of Drug Delivery[1]

Raj Bawa, MS, PhD

Patent Law Department, Bawa Biotech LLC, Ashburn, Virginia, USA
Department of Biological Sciences, Rensselaer Polytechnic Institute, Troy, New York, USA

Keywords: nanotechnology, nanoscience, nanomedicine, nanobiotechnology, nanopharmaceutical, nanodrug, nanomaterial, Abbreviated New Drug Application (ANDA), patents, commercialization, technology transfer, research and development (R&D), US Food and Drug Administration (FDA), the European Medicines Agency (EMA), Environmental Protection Agency (EPA), Centers for Disease Control and Prevention (CDC), National Institute for Occupational Safety and Health (NIOSH), World Intellectual Property Organization (WIPO), US Patent and Trademark Office (PTO), International Organization for Standardization (ISO), American Society for Testing and Materials (ASTM) International, Organization for Economic Co-operation and Development (OECD), patent proliferation, nomenclature, regulatory definition, drug delivery, engineered nanotherapeutics, drug delivery systems (DDS), site-specific delivery, nanopotential, nanoscale, nanocharacter, nanodimensions, specific surface area (SSA), controlled manipulation, nanoparticles (NPs)

[1] *What's in a name?* is a mystery short story by Isaac Asimov that appeared in the June 1956 issue of *The Saint Detective Magazine* under the title *Death of a Honey-Blonde*. Also see, Shakespeare's *Romeo and Juliet* (Act 2, Scene 2): *"What's in a name? That which we call a rose by any other name would smell as sweet."*

Handbook of Clinical Nanomedicine: Nanoparticles, Imaging, Therapy, and Clinical Applications
Edited by Raj Bawa, Gerald F. Audette, and Israel Rubinstein

ISBN 978-981-4669-20-7 (Hardcover), 978-981-4669-21-4 (eBook)
www.panstanford.com

6.1 Introduction

"*Small is beautiful.*"

—Leopold Kohr, Economist (1909–1994)

The air is thick with news of nano-breakthroughs. Although "nano" is a hot topic for discussion in industry, pharma, patent offices and regulatory agencies, the average citizen knows very little about what constitutes a nanoproduct, a nanomaterial or a nanodrug. Still, there is no shortage of excitement and hype when it comes to anything "nano." Optimists see nanotechnology as an enabling technology, a sort of next industrial revolution that could enhance the wealth and health of nations. They promise that at least within the medical sector of nano, nanodrugs will be a healthcare game-changer by offering patients access to personalized medicine. Pessimists, on the other hand, take a cautionary position, preaching instead a "go-slow" approach, pointing to a lack of sufficient scientific information on health risks and general failure on the part of regulatory agencies and patent offices. Whatever your stance, nanotechnology has already permeated virtually every sector of the global economy, with potential applications consistently inching their way into the marketplace.[2] But, is

[2]The late Nobelist Dr. Richard E. Smalley, a champion of nanotechnology, made a bullish predication to the US Congress in 1999: "*The impact of nanotechnology on the health, wealth, and lives of people will be at least the equivalent of the combined influences of microelectronics, medical imaging, computer-aided engineering and manmade polymers.*" See: Kumar, C. S. S. R., Hormes, J., Leuschner, C. (2005). *Nanofabrication Towards Biomedical Applications: Techniques, Tools, Applications, and Impact*, Wiley, page 376.

President Bill Clinton in 2000 declared: "*Imagine the possibilities: materials with ten times the strength of steel and only a small fraction of the weight—shrinking all the information housed at the Library of Congress into a device the size of a sugar cube—detecting cancerous tumors when they are only a few cells in size. Some of our research goals may take 20 or more years to achieve, but that is precisely why there is an important role for the federal government.*" White House Report (2000). *National Nanotechnology Initiative: Leading to the Next Industrial Revolution*.

A US Undersecretary of Commerce in 2003 made a grand predication that appears more hype in hindsight: "*On a human level, nano's potential rises to near Biblical proportions. It is not inconceivable that these technologies could eventually achieve the truly miraculous: enabling the blind to see, the lame to walk, and the deaf to hear; curing AIDS, cancer, diabetes and other afflictions; ending hunger; and even supplementing the power of our minds, enabling us to think great thoughts, create new knowledge, and gain new insights*." Philip J. Bond's remarks at the World Nano-Economic Congress, Washington, DC on Sept. 9, 2003, quoted in the Center for Responsible Nanotechnology, Hype Part I, Responsible Nanotechnology. Available

nano the driving force behind a new industrial revolution in the making or simply a repacking of old scientific ideas? For most stakeholders, dissecting hope from hype is difficult.

In reality, nanotechnology is the natural continuation of the miniaturization of materials and medical products that have been steadily arriving in the marketplace. It continues to evolve and play a pivotal role in various industry segments, spurring new directions in research, patents, commercialization and technology transfer. Too often though, start-ups, academia and companies exaggerate basic research developments as potentially revolutionary advances and claim these early-stage discoveries as confirmation of downstream novel products and applications to come. Nanotechnology's potential benefits are frequently overstated or inferred to be very close to application when clear bottlenecks to commercial translation exist. Many have desperately tagged or thrown around the "nano" prefix to suit their purpose, whether it is for federal research funding, patent approval of the supposedly novel technologies, raising venture capital funds, running for office or seeking publication of a journal article.[3] All

at: http://crnano.typepad.com/crnblog/2005/06/bond_sept_9_200.html (accessed on September 20, 2015).

[3]Some business leaders and scientists view nanotechnology and nanomedicine as the next industrial revolution, but widespread business and public support is still lacking. Although the increased media attention and hype has generally led to confusion, caution and even suspicion, there is also ample awareness, interest and even excitement. The popular press, government and ill-informed politicians have fueled this interest. For example, contributing to this are references to nanotechnology in popular culture, with mentions in movies (*The Hulk, The Tuxedo*), books (Michael Crichton's *Prey,* Neal Stephenson's *The Diamond Age,* Greg Bear's *Slant,* William Gibson's *Idoru*, Robin Cook's *Nano*), video games (*Metal Gear Solid* series), and on TV (most notably, in various incarnations of *Star Trek*). Even Prince Charles has weighed in on the topic. See: Favi, P. M., Webster, T. J. (2016). Is nanotechnology toxic? Was Prince Charles correct? In: Bawa, R., et al., eds. *Handbook of Clinical Nanomedicine: Law, Business, Regulation, Safety, and Risk,* Chapter 46, Pan Stanford Publishing, Singapore. Also see: Sherriff, L. (2004). Prince Charles gives forth on nanotech. *The Register* (July 12, 2004). Available at: www.theregister.co.uk/2004/07/12/nano_prince/ (accessed on May 21, 2015). In part, because of this prevalent misinformation and hype, it is critical to educate all key players (the public, entrepreneurs, lawyers, policy makers, investors, the venture community, scientists, educators, etc.) involved in nano regarding its potential impacts, benefits, safety issues and challenges. In a world of increasing scientific misconduct, it is imperative that the integrity and authoritativeness of information provided in any text, news story or journal article on nanotechnology can be guaranteed. Clearly, accuracy of information that is disseminated as well as the transparency of the disseminating entity (industry,

of this is happening while thousands of over-the-counter products containing silver nanoparticles, nanoscale titanium dioxide and carbon nanoparticles continue to stream into the marketplace without adequate safety testing, labeling or regulatory review. Silver nanoparticles are effective antimicrobial agents but their potential toxicity remains a major concern. Similarity, nanoscale titanium dioxide, present in powdered Dunkin doughnuts and Hostess Donettes, has been classified as a potential carcinogen by NIOSH while the World Health Organization (WHO) has linked it in powder form to cancers.

While the widespread use of nanomaterials and nanoparticles in consumer products over the years has become pervasive and exposure inescapable, the 1980s and 1990s saw limited applications of these rather than the transformative applications envisioned. Even so, governments across the globe, impressed by "nano-potential," continued to stake their claims by doling out billions for research and development (R&D).[4] Universities have jumped into

academia, government, news outlets) will be crucial to the future course of nanomedicine and nanotechnology (success, failure or partial acceptance).

[4]Nano-developments are often driven by what some of us refer to as "nanopotential." This is obviously true more for certain sectors of nanotech than others. In this regard, one of the most widely cited predictions was in 2001. A National Science Foundation (NSF) report that forecasted the creation of a trillion dollar industry for nanotech by 2015. This report, now proven false, was often quoted in articles, business plans, conference presentations and grant applications. National Science Foundation (2001). *Societal Implications of Nanoscience and Nanotechnology*. Available at: http://www.wtec.org/loyola/nano/NSET.Societal. Implications/nanosi.pdf (accessed on April 10, 2015). Given such flawed projections, Michael Berger of Nanowerk accurately pointed out: *"These trillion-dollar forecasts for an artificially constructed "market" are an irritating, sensationalist and unfortunate way of saying that sooner or later nanotechnologies will have a deeply transformative impact on more or less all aspects of our lives."* See: Nanowerk Spotlight. (2007). Debunking the trillion dollar nanotechnology market size hype. Available at: http://www.nanowerk.com/spotlight/spotid=1792.php (accessed on September 21, 2015).

There are also various technical reports highlighting the potential market for nanotech. Again, one must take all such predictions with caution and not draw too many conclusions therefrom ("*A good decision is based on knowledge and not on numbers*." – Plato). For example, a 2012 report by the RNCOS Industry Research Solutions stated that the US leads the nanotechnology market and accounts for an estimated share of around 35% of the global nanotechnology market while the global nanotechnology market was projected to reach US $26 billion by the end of 2014, growing at a compound annual growth rate (CAGR) of around 20% since 2011. See: *RNCOS US Nanotechnology Market Leading Globally from Nanotechnology Forecast to 2014*. Available at: http://www.rncos.com/Report/IM376.htm (accessed on September 20, 2015). On the other hand, BCC

the fray with the clear indication of patenting as much "nano" as they can grab. Academia, start-ups and companies still exaggerate basic research or project potential downstream applications based on early-stage discoveries. Boundaries between science, government and industry continue to be blurred. Venture has mostly shied away in recent years, though industry-university alliances have continued to develop. Stakeholders, especially investors and consumer-patients, get nervous about the "known unknown" novel applications, uncertain health risks, industry motives and governmental transparency. Wall Street's early interest in nano has been somewhat tempered over the years, from cautionary involvement to generally shying away, partly due to the definitional issue.[5] In spite of anemic product development, patent filings and patent grants have continued unabated [1–3]. It is no secret that nanopatents of dubious scope and breath, especially on foundational nanomaterials and upstream nanotechnologies, have been granted by patent offices around the world. In fact, "patent prospectors" have been on a global quest for "nanopatent land grabs" since the early 1980s. As a result, patent thickets in certain sectors of nanotechnology have arisen that could have a chilling impact on commercialization activities. This author believes that issues such as effective patent reform, adaptive regulatory guidance, commercialization efforts and consumer health are all intertwined and need special attention while addressing nanotechnology. In this regard, science-based governance that promotes commercialization on one hand and balances consumer health on the other is critically needed. Such a regulatory framework must be based on ethical norms that promote (i) information gathering, (ii) collective participation of stakeholders, (iii) transparency, (iv) consensus and (v) accountability.

Research reported that the global nanomedicine market was valued at $214.2 billion in 2013 and $248.3 billion in 2014 and the total market is projected to grow at a compound annual growth rate (CAGR) of 16.3% from 2014 through 2019 and reach $528 billion by 2019. See: *Nanotechnology in Medical Applications: The Global Market*. Available at: http://www.bccresearch.com/market-research/healthcare/nanotechnology-medical-applications-market-hlc069c.html (accessed on December 2, 2015).

[5]In this regard, an early story is still applicable today: *"...nanotechnology remains difficult to define, causing additional uncertainties for investors... Some companies have used the nano-technology label to hype unrelated products, while many real advances are occurring inside big companies such as Intel, where the developments have only a modest impact on stock prices."* See: Regalado, A., Hennessey, R. (2004). Nanosys pulls IPO putting nanotech revolution on hold. *Wall Street Journal*, August issue.

Nanomedicine, an offshoot of nanotechnology, may be defined as the science and technology of diagnosing, treating and preventing disease and improving human health via nano. Nanomedicine is driven by collaborative research, patenting, commercialization, business development and technology transfer within diverse areas such as biomedical sciences, chemical engineering, biotechnology, physical sciences, and information technology. This decade has witnessed relatively more advances and product development in nanomedicine. In this context, many point to the influence of nanomedicine on the pharmaceutical, device and biotechnology industries. One can now say that R&D is in full swing and novel nanomedical products are starting to arrive in the marketplace. Still, revolutionary nanotech breakthroughs are just promises at this stage. They are likely to be reflected in real products downstream; they will arrive down the road. It is hoped that nanomedicine will eventually blossom into a robust industry. In the meantime, tempered expectations are in order. Giant technological leaps can leave giant scientific, ethical and regulatory gaps. Extraordinary claims and paradigm-shifting advances necessitate extraordinary proof and verification.

A balanced view of nanotech is elegantly reflected in a recent book [4a]:

> *Nanotechnology has been hyped by techies who cannot wait to order a wristwatch with the entire Library of Congress stored inside; while others bespeak the hysteria of rapidly self-replicating gray goo. Much that is nano is burdened with over-expectations and misunderstanding. As usual, the reality lives somewhere between such extremes. Nanotechnology is like all technological development: inevitable. It is not so much a matter of what remains to be seen; the fun question is, who will see it? Will we? Will our children? Their children? Turns out, we will all get to see some. Nanotechnology is already changing the way we live, and it is just getting started.*

The following excerpt pertaining to nanomedicine and nanopharmaceuticals accurately traces the evolution of terminology while highlighting the issue that "nano" is a relabeling of earlier terms [4b]:

> *The new concept of nanomedicine arose from merging nanoscience and nanotechnology with medicine. Pharmaceutical scientists quickly adopted nanoscience terminology, thus "creating" "nanopharmaceuticals". Moreover, just using the term "nano"*

intuitively implied state-of-the-art research and became very fashionable within the pharmaceutical science community. Colloidal systems reemerged as nanosystems. Colloidal gold, a traditional alchemical preparation, was turned into a suspension of gold nanoparticles, and colloidal drug-delivery systems became nanodrug delivery systems. The exploration of colloidal systems, i.e., systems containing nanometer sized components, for biomedical research was, however, launched already more than 50 years ago and efforts to explore colloidal (nano) particles for drug delivery date back about 40 years. For example, efforts to reduce the cardiotoxicity of anthracyclines via encapsulation into nanosized phospholipid vesicles (liposomes) began at the end of the 1970s. During the 1980s, three liposome-dedicated US start-up companies (Vestar in Pasadena, CA, USA, The Liposome Company in Princeton, NJ, USA, and Liposome Technology Inc., in Menlo Park, CA, USA) were competing with each other in developing three different liposomal anthracycline formulations. Liposome technology research culminated in 1995 in the US Food and Drug Administration (FDA) approval of Doxil®, "the first FDA-approved nanodrug". Notwithstanding, it should be noted that in the liposome literature the term "nano" was essentially absent until the year 2000. (Citations omitted)

6.2 Brief Historical Background

"There's plenty of room at the bottom."

—Richard Feynman, Physicist (1918–1988)

The concept of nanotechnology,[6] before the word itself, harks back to Nobel Laureate Dr. Richard Feynman, the charismatic physics professor from Caltech. He is credited with inspiring the development of nanotechnology through his provocative and prophetic lecture on December 29, 1959 at an American Physical Society meeting held at Caltech [5]:

Now the name of the talk is 'There's Plenty of Room at the Bottom'—not just 'There's Room at the Bottom' ... . I will not discuss how we are going to do it, but only that it is possible in principle—in other words, what is possible according to the laws of physics. I am not inventing anti-gravity, which is possible someday only if the laws are not what we think. I am telling you what could be done if the laws are what we think; we are not doing it simply because we haven't gotten around

[6]This author questions the traditional assumption that the nanotechnology pedigree descended from this lecture, given that "nanotechnology" is not a modern invention, discovery or science but has been around for a millennia.

> *to it … . I am not afraid to consider the final question as to whether, ultimately — in the great future — we can arrange atoms the way we want; the very atoms, all the way down!*[7]

In this famous talk, he focused on the ability to manipulate individual atoms and molecules by discussing the storage of information on a very small scale; writing and reading in atoms; about miniaturization of the computer; and building tiny machines, factories and electronic circuits with atoms. Dr. Feynman also suggested the idea to shrink computing devices down their physical limits (miniaturization of the computer), where "wires should be 10 or 100 atoms in diameter;" this was realized in 2009 by Samsung, which produced devices built with 30 nm technology. Additionally, he proposed that focused electron beams could write nanoscale features on a substrate (writing and reading in atoms); this was realized via e-beam lithography. He also envisioned superior microscopes, ideas that are now reflected in the form of the scanning tunneling microscope (STM), transmission electron microscope (TEM), atomic force microscope (AFM), and other examples of probe microscopy.

It appears that the term "nano" was first used in a biological context in 1908 by H. Lohmann to describe a small organism [6a]. The concept of precision manufacturing of materials with nanometer tolerances at will from the very basic building blocks was christened "nanotechnology" in 1974 by Dr. Norio Taniguchi of Tokyo Science University. He coined the term via his seminal paper [6b] titled "*On the Basic Concept of Nano-Technology,*" (with a hyphen) that he presented in Tokyo, Japan at the International Conference on Production Engineering. He wrote:

> *In the processing of materials, the smallest bit size of stock removal, accretion or flow of materials is probably of one atom or one molecule, namely 0.1–0.2 nm in length. Therefore, the expected limit*

[7]At this talk, Dr. Feynman offered a prize of $1,000 to anyone to solve two challenges. The first challenge involving the construction of a tiny motor. This was achieved in 1960 by William McLellan, who constructed the first tiny electrical motor (less than 1/64th of an inch) using conventional tools. The second challenge involving fitting the entire *Encyclopedia Britannica* on the head of a pin by writing the information from a book page on a surface 1/25,000 smaller in linear scale. This was accomplished in 1985 by Tom Newman, who successfully reduced the first paragraph of *A Tale of Two Cities* by 1/25,000. See also, Hess, K. (2012). Room at the bottom, plenty of tyranny at the top. In: Goddard, W. A., et al., eds. *Handbook of Nanoscience, Engineering, and Technology,* 3rd ed., Chapter 2, CRC Press, Boca Raton, Florida.

size of fineness would be of the order of 1 nm … ."Nano-technology" mainly consists of the processing … separation, consolidation and deformation of materials by one atom or one molecule.

In the 1980s, major breakthroughs propelled the growth of nanotech further. The invention of the scanning tunneling microscope (STM) in 1981 by Drs. Gerd Binnig and Heinrich Rohrer at IBM's Zurich Research Laboratory provided visualization of atom clusters and bonds for the first time [6c]. The discovery of fullerenes (C_{60}) in 1985 by Drs. Harry Kroto, Richard Smalley and Robert Curl was another major advance [6d]. Both groups won the Nobel prize.

The technological significance of nanoscale phenomena and devices was explored by Dr. K. Eric Drexler in the mid-1980s. He built upon Dr. Feynman's concept of a billion tiny factories by theorizing that these factories could be replicated via computer-control instead of human-operator control and highlighted the potential of "molecular nanotechnology" (MNT). He popularized this idea in his 1986 book titled *Engines of Creation: The Coming Era of Nanotechnology* [7]. However, I consider MNT an entertaining academic diversion. Although serious work should continue on MNT, I do not believe in its near-term feasibility because fabrication of efficient devices on a molecular/atomic scale that can conduct MNT currently does not exist.[8]

In 1991, Drs. Donald M. Eigler and Erhard K. Schweizer of the IBM Almaden Research Center in San Jose, California, demonstrated the ability to manipulate atoms via the STM by forming the acronym "IBM" on a substrate of chilled crystal of nickel using 35 individual atoms of xenon. This technology demonstrated how the STM, which until then had been used to image surfaces or atoms/molecules on surfaces with atomic precision (nanoscale topography),

[8]In this regard, the reader is directed to a 2006 report from the National Research Council (NRC) titled *A Matter of Size: Triennial Review of the National Nanotechnology Initiative*, The National Academies Press, Washington, DC: *"Although theoretical calculations can be made today, the eventually attainable range of chemical reaction cycles, error rates, speed of operation, and thermodynamic efficiencies of such bottom-up manufacturing systems cannot be reliably predicted at this time. Thus, the eventually attainable perfection and complexity of manufactured products, while they can be calculated in theory, cannot be predicted with confidence. Finally, the optimum research paths that might lead to systems which greatly exceed the thermodynamic efficiencies and other capabilities of biological systems cannot be reliably predicted at this time. Research funding that is based on the ability of investigators to produce experimental demonstrations that link to abstract models and guide long-term vision is most appropriate to achieve this goal."*

could now be used to manipulate matter at the nanoscale. In my opinion, this concept of "controlled manipulation" is the foundation of nanotechnology and a key component of my definition of the term (Section 6.3).

The historical origins and development of nanotechnology can be summarized as follows [8]:

> *Although nanotechnology is a relatively recent development in scientific research, the development of its central concepts happened over a longer period of time. The emergence of nanotechnology in the 1980s was caused by the convergence of experimental advances such as the invention of the scanning tunneling microscope in 1981 and the discovery of fullerenes in 1985, with the elucidation and popularization of a conceptual framework for the goals of nanotechnology beginning with the 1986 publication of the book Engines of Creation. The field was subject to growing public awareness and controversy in the early 2000s, with prominent debates about both its potential implications as well as the feasibility of the applications envisioned by advocates of molecular nanotechnology, and with governments moving to promote and fund research into nanotechnology.*

6.3 What is "Nano"?

"*What's the use of their having names*," *the Gnat said, "if they won't answer to them?"*
"No use to them," *said Alice; "but it's useful to the people that name them, I suppose. If not, why do things have names at all?" "I can't say," the Gnat replied.*
Through the Looking Glass and What Alice Found There, Chapter 3
—Lewis Carroll (1832–1898), Writer and Mathematician

As discussed earlier, the term nanotechnology is very much in vogue. Yet there is still no international scientifically-accepted nomenclature or uniform regulatory definition associated with it [9–15]. This definitional issue, or lack thereof, continues to be one of the most significant problems shared by regulators,[9] policy-

[9]It is worth quoting a recent publication [31] that highlights some of the challenges confronting regulatory agencies like the FDA and EMA regarding nanotech, partly due to this nano-nomenclature issue:
"There are potentially serious and inhibitory consequences if nanodrugs are overregulated, and a balanced approach is required, at least on a case-by-case basis, that addresses the needs of commercialization against mitigation of inadvertent

makers, researchers and legal professionals [9–15]. In particular, regulatory agencies and entities such as the US Food and Drug Administration (FDA), the European Medicines Agency (EMA), Environmental Protection Agency (EPA), the Centers for Disease Control and Prevention (CDC), National Institute for Occupational Safety and Health (NIOSH), World Intellectual Property Organization (WIPO), the US Patent and Trademark Office (PTO), International Organization for Standardization (ISO) Technical Committee on Nanotechnology (ISO/TC229), American Society for Testing and Materials (ASTM) International and the Organization for Economic Co-operation and Development Working Party on Manufactured Nanomaterials (OECD WPMN) continue to grapple with this critical issue.[10] Clearly, the need for an internationally agreed definition for key terms like nanotechnology, nanoscience, nanomedicine, nanobiotechnology, nanodrug, nanotherapeutic, nanopharmaceutical and nanomaterial, has gained urgency.[11] It is critical for harmonized regulatory governance, accurate patent searching and prosecution, standardization of procedures, assays and manufacturing, quality control, safety assessment, and more.

In this chapter, the following terms are used interchangeably as they all pertain to a "drug or therapeutic": nanomedicines, nanodrugs, nanotherapeutics and nanopharmaceuticals. Similarly, these "technology" terms are used interchangeably: nano, nanotech and nanotechnology.

So, what does the prefix "nano" refer to?[12] Any term with

harm to patients or the environment. Obviously, not every nanotherapeutic or nano-enabled product needs to be regulated. However, more is clearly needed from regulatory agencies like the FDA and EMA than a stream of guidance documents that are in draft format, position papers that lack any legal implication, presentations that fail to identify key regulatory issues and policy papers that are often short on specifics. There is a very real need for regulatory guidelines that follow a science-based approach that are responsive to the associated shifts in knowledge and risks."

[10]For example, see: Kica, E., Bowman, D. M. (2012). Regulation by means of standardization: Key legitimacy issues of health and safety nanotechnology standards. *Jurimetrics Journal*, **53**, 11–56: *"Despite the often provocative nature of many of the nanotechnology-related initiatives and activities, the undertakings of the ISO/TC229 and the OECD WPMN have remained a quiet and uncontroversial affair… The work of TC229 and the WPMN to date is still embryonic in nature, with only limited outputs and impacts*."

[11]Similar disagreements over terminology and nomenclature are seen in other fields as well. For example, the term "super resolution microscopy," the subject of the 2014 Nobel Prize, is considered an inaccurate description of the technique.

[12]The prefix "nano" in the SI measurement system denotes 10^{-9} or one-billionth. There is not even a consensus over whether the prefix "nano" is Greek or Latin.

this prefix is broad in scope. Consider the widely used terms, nanotechnology, nanomedicine and nanopharmaceutical, all of which are a bit misleading since they do not refer to a single technology or entity. The terms nanotechnology and nanomedicine refer to interdisciplinary areas that draw from the interplay among numerous materials, products and applications from several technical and scientific fields. This includes materials science, engineering, biochemistry, protein science, biotechnology, medicine, colloid science, physics, supramolecular chemistry, physical chemistry, surface science, etc. [9–18]. Nanotechnology results from a combined extension of such diverse fields into the nanoscale. In other words, nanotech is an umbrella term encompassing several technical/scientific fields, processes and properties at the nano/micro scale [9–18]. In a sense, it has brought various players with divergent scientific and engineering backgrounds together to create a novel common language.

There is confusion over the definition of nanotechnology and, partly because of a lack of any standard nomenclature, various inconsistent definitions have sprung up over the years [19].[13] For

While the term "nano" is often linked to the Greek word for "dwarf," the ancient Greek word for "dwarf" is actually spelled "nanno" (with a double "n") while the Latin word for dwarf is "nanus" (with a single "n").

A nanometer refers to one-billionth of a meter in size (10^{-9} m = 1 nm), a nanosecond refers to one billionth of a second (10^{-9} s = 1 ns), a nanoliter refers to one billionth of a liter (10^{-9} l = 1 nl) and a nanogram refers to one billionth of a gram (10^{-9} g = 1 ng). The diameter of an atom ranges from about 0.1 to 0.5 nm. Some other interesting comparisons: fingernails grow around a nanometer/second; in the time it takes to pick a razor up and bring it to your face, the beard will have grown a nanometer; a single nanometer is how much the Himalayas rise in every 6.3 seconds; a sheet of newspaper is about 100,000 nanometers thick; it takes 20,000,000 nanoseconds (50 times per second) for a hummingbird to flap its wings once; a single drop of water is ~50,000 nanoliters; a grain of table salt weighs ~50,000 nanograms.

[13]Add to this confusion is the fact that nanotechnology is nothing new and has been around for hundreds, possibly thousands, of years. Damascus sword blades, encountered by Crusaders in the 5th century, have shown now to sometimes contain nanowires and carbon nanotubes. Another early example of nanomaterials in products dates back to the 4th century (Roman times) in stained glass where gold nanoparticles were incorporated therein to exhibit a range of colors. The most prominent example of this is the Lycurgus Cup on display at the British Museum. This cup, depicting King Lycurgus being dragged into the underworld by Ambrosia, contains a decorative pigment that is a suspension of gold and silver nanoparticles of about 70 nm whereby reflected light appears green but transmitted light appears red. Later on in the 7th century, a colloidal suspension of tin oxide and gold nanoparticles (Purple of Cassius) was used to color glass. Another early example of technology far outpacing science is in the 9th century

instance, nanotechnology has been *inaccurately* defined by the NNI[14] since the 1990s as "the understanding and control of matter at the nanoscale, at dimensions between approximately 1 and 100 nanometers, where unique phenomena enable novel applications…" (this often-cited definition is flawed for various reasons as discussed ahead). Others label it as the manipulation, precision placement, measurement, modeling or manufacture of matter in the sub-100 nm range. Some definitions increase the upper limit to 200 nm or 300 nm or even 1000 nm. Some definitions omit a lower range, others refer to sizes in one, two or three dimensions while others require a size plus special/unique property or *vice versa* [19]. None of these definitions is scientifically

when Arab potters used nanoparticles in their glazes so that objects would change color depending on the viewing angle (the so-called "polychrome lustre"). Nanoscale carbon black particles ("high-tech soot nanoparticles") have been in use as reinforcing additives in tires for over a century. The accidental discovery of precipitation hardening in 1906 by Wilm in Duralumin alloys is considered a landmark development for metallurgists; this is now attributed to nanometer-sized precipitates. Modern nanotechnology may be considered to start in the 1930s when chemists generated silver coatings for photographic film. In 1947, Bell Labs discovered that the semiconductor transistor had components that operated on the nanoscale. A large number of nanomaterials and nanoparticles have been synthesized over the last two decades, yet the EPA and the FDA do not seem to know how to regulate most of them. Obviously, consumers should be cautious about potential exposure but industry workers should be more concerned. For example, see: Bradley, R. (2015). The great big question about nanomaterials. *Fortune* **171**(4), 192–202. Available at: http://fortune.com/2015/03/06/nanomaterials/ (accessed on November 10, 2015).

Many molecules in nature squarely fall within the definition of nanotechnology as they are in the nanoscale range, similar in size to commercialized nanotherapeutics. However, these "non-engineered" nanoscale structures encompass nanoscience, and I exclude them from the nanotechnology umbrella. Examples of non-engineered nanoscale particles or biological structures include a: virus particle (~20–450 nm); protein (~5–50 nm); gene (~2 nm wide and 10–100 nm long); red blood cell (~7,000 nm wide); single hair from the head (50,000–100,000 nm wide); and DNA (the diameter of a coil is ~1 nm). In other words, most of molecular medicine and biotechnology could easily be classified as nano. Technically speaking, biologists were studying all these nanoscale biomolecules long before the term was even coined. In this regard, even though the National Institutes of Health (NIH) concurs that while much of biology is grounded in nanoscale phenomena, it has not reclassified most of its basic research portfolio as nano.

[14]National Nanotechnology Initiative (NNI) is the US government's inter-agency program for coordinating, planning and managing R&D in nanoscale science, engineering, technology, and related efforts across 25+ agencies and programs. The NNI has been regularly reviewed by the President's Council of Advisors on Science and Technology (PCAST) since the council was designated in 2004.

or legally plausible from a pharma perspective; they also exclude many applications with significant consequence to medicine. This cut-off fails to encompass the unique physiological behavior that can occur at the nanoscale. For instance, consider the case of gold and silver nanoparticles that naturally exhibit fundamentally different properties than at the macroscale. A definition like the one from the NNI based purely on size (or dimension) does not distinguish between (i) naturally occurring versus engineered nanoscale properties; or (ii) spherical nanoparticles versus the newer generation of nanoparticles having high aspect ratios.

In fact, the ambiguousness of this definitional issue is apparent whenever the "nano" prefix is used [20]:

> *Nanofiltration is frequently associated with nanotechnology — obviously because of its name. However, the term "nano" in nanofiltration refers — according to the definition of the International Union of Pure and Applied Chemistry (IUPAC) — to the size of the particles rejected and not to a nanostructure as defined by the International Organisation of Standardisation (ISO) in the membrane. Evidently, the approach to standardisation of materials differs significantly between membrane technology and nanotechnology which leads to considerable confusion and inconsistent use of the terminology. There are membranes that can be unambiguously attributed to both membrane technology and nanotechnology such as those that are functionalized with nanoparticles, while the classification of hitherto considered to be conventional membranes as nanostructured material is questionable.*

All definitions of nanotechnology based on size or dimensions should be dismissed. Furthermore, one should avoid puncturing every sentence with the prefix "nano." There is simply no scientific basis or logic to limiting all nanotechnology to a sub-100 nm limitation; it is illogical, random and foolish. Moreover, "nano" is not simply a metric of length, and nanoscale research does not accept such rigid limitations on dimensionality (Table 6.1). The arbitrary sub-nano cutoff from the NNI has been correctly criticized over the years [21]:

> *The 100 nm size boundary used in these definitions, however, only loosely refers to the nano-scale around which the properties of materials are likely to change significantly from conventional*

equivalents. ***In reality, there is no clear size cut-off for this phenomenon, and the 100 nm boundary appears to have no solid scientific basis****. A change in properties of particulate materials in relation to particle size is essentially a continuum, which although more likely to happen below 100nm size range, does not preclude this happening for some materials at sizes above 100 nm… [emphasis added]*

Given this backdrop, I propose the following definition of nanotechnology, one that is unconstrained by an arbitrary size limitation or dimensionality [22]:

> *The design, characterization, production, and application of structures, devices, and systems by controlled manipulation of size and shape at the nanometer scale (atomic, molecular, and macromolecular scale) that produces structures, devices, and systems with at least one novel/superior characteristic or property.*

This definition above has four key features:

- First, it recognizes that the properties and performance of the synthetic, engineered "*structures, devices, and systems*" are inherently rooted in their nanoscale dimensions. The definition focuses on the unique physiological behavior of these "*structures, devices, and systems*" that is occurring "*at the nanometer scale*;" it does not focus on any shape, aspect ratio, specific size or dimensionality.
- Second, the focus of this flexible definition is on "technology" that has commercial potential from a consumer perspective, not "nanoscience" or basic R&D conducted in a lab setting that may lack commercial implication.
- Third, the "*structures*, *devices*, *and systems*" that result must be "*novel/superior*" compared to their bulk, conventional counterparts in some fashion.
- Fourth, the concept of "*controlled manipulation*" (as compared to "self-assembly") is critical, as emphasized by others [23]:

A main theme in nanotechnology is ***controlled*** *self-assembly, with the goal being to generate functional materials with a high degree of precision… [emphasis added]*

Table 6.1 Basic nomenclature for various "nano" terms that correctly exclude any reference to a dimension or size

• The Royal Academy of Engineering: "*Nanoscience is the study of phenomena and manipulation of materials at atomic, molecular and macromolecular scales, where the properties differ significantly from those at a larger scale*;" "*Nanotechnologies are the design, characterization, production and application of structures, devices and systems by controlling shape and size at nanometer scale*." Available at: http://www.nanotec.org.uk/report/chapter2.pdf (accessed on October 20, 2015); also see: Yang, W., Peters, J. I., Williams, R. O. (2008). Inhaled nanoparticles: A current review. *Int. J. Pharm*., **356**, 239–247.
• The National Institutes of Health Roadmap for Medical Research in Nanomedicine: *"An offshoot of nanotechnology, nanomedicine refers to highly specific medical intervention at the molecular level for curing disease or repairing damaged tissues, such as bone, muscle, or nerve*." Available at: http://pubs.niaaa.nih.gov/publications/arh311/12-13.pdf (accessed on October 20, 2015).
• Dr. Richard Smalley: "*Nanotechnology is the art and science of building stuff that does stuff at the nanometer scale*." Quoted from: http://facilityexecutive.com/2006/12/scientists-say-nano-is-here-but-so-are-the-risks-2/ (accessed on October 20, 2015).
• Springer Handbook of Nanotechnology, 1st ed.: "*Nanotechnology literally means any technology on a nanoscale that has applications in the real world. Nanotechnology encompasses the production and application of physical, chemical, and biological systems at scales ranging from individual atoms or molecules to submicron dimensions, as well as the integration of the resulting nanostructures into larger systems.*" Available at: http://www.springer.com/978-3-642-02524-2 (accessed on July 16, 2015).
• The European Science Foundation: "*The field of 'Nanomedicine' is the science and technology of diagnosing, treating and preventing disease and traumatic injury, of relieving pain, and of preserving and improving human health, using molecular tools and molecular knowledge of the human body*." Nanomedicine: An ESF_European Medical Research Councils Forward Look Report (2005). Available at: http://www.esf.org/fileadmin/Public_documents/Publications/Nanomedicine.pdf (accessed on October 20, 2015).
• Merriam-Webster Dictionary: *"...the science of manipulating materials on an atomic or molecular scale especially to build microscopic devices..."* Available at: http://www.merriam-webster.com/dictionary/nanotechnology (accessed on October 2, 2015).

- The Smalley Institute at Rice University: *"…nanotechnology is quite simply the application of knowledge at the nanoscale."* Available at: http://smalley.rice.edu/content.aspx?id=42 (accessed on February 20, 2015).
- The Center for Responsible Nanotechnology: *"Nanotechnology is the engineering of functional systems at the molecular scale. This covers both current work and concepts that are more advanced. In its original sense, 'nanotechnology' refers to the projected ability to construct items from the bottom up, using techniques and tools being developed today to make complete, high performance products."* Available at: http://www.crnano.org/whatis.htm (accessed on September 16, 2015).
- HowStuffWorks: *"Nanotechnology is a multidisciplinary science that looks at how we can manipulate matter at the molecular and atomic level."* Available at: http://science.howstuffworks.com/what-is-nanotechnology.htm (accessed on October 20, 2015).
- Scientific American: *"The field is a vast grab bag of stuff that has to do with creating tiny things that sometimes just happen to be useful. It borrows liberally from condensed-matter physics, engineering, molecular biology and large swaths of chemistry."* Stix, G. (2001). Little big science. *Scientific American*, September issue.

It is best not to blindly use any specific size range or dimension while discussing anything "nano." If a size-limitation *must* be associated with or tagged onto the definition of nanotechnology while discussing nanotherapeutics or nanodrug delivery, the term may be loosely considered ranging in size from 1–1,000 nm (up to a micron, μ) for reasons elaborated ahead (see Sections 6.4 and 6.5). Such labeling would make nanoparticle drug delivery systems (nanoproducts or nanoformulations) consistent with wet science where colloidal solutions (in contrast to solutions or suspensions) contain particles that have at least one dimension ranging from 1–1,000 nm (see footnote 21). In this regard, it is worth mentioning an important report from the UK House of Lords Science and Technology Committee that recommended that the term "nanoscale" should have an upper boundary of 1,000 nm (at least for the purpose of food regulations), contrary to the ISO and ASTM International determinations that scientific usage be restricted to no greater than 100 nm [24]:

> *We recommend … that any regulatory definition of nanomaterials … not include a size limit of 100 nm but instead refer to 'the nanoscale' to ensure that all materials with a dimension under 1000 nm are considered…*

In fact, many experts propose definitions along these similar lines, especially in the context of nanodrugs or pharmaceutical applications [8, 25a, 25b, 25c, 25d, 25e, 25f]:

> *Nanotechnology means putting to use the unique physical properties of atoms, molecules, and other things measuring roughly 0.1–1000 nm.* [8]

> *Nanoparticles are defined as being submicronic* (*<1 μm*) *colloidal systems generally made of polymers* (*biodegradable or not*). *They were first developed in the mid 1970s by Birrenbach and Speiser* (*1976*). *Nanoparticles generally vary in size from 10 to 1000 nm. The drug is dissolved, entrapped, encapsulated, or attached to a nanoparticle matrix.* [25a]

> *In drug delivery and clinical applications the technology to nanonize (ie, to reduce in size to below 1000 nm) is one of the key factors for modern drug therapy, now and in the years to come… Based on the size unit, in the pharmaceutical area nanoparticles should be defined as having a size between a few nanometers and 1000 nm (=1 μm); microparticles therefore possess a size of 1–1000 μm.* [25b]

> *[f]or most pharmaceutical applications, nanoparticles are defined as having a size up to 1,000 nm…* [25c]

> *The limitation of sizes to the 1–100 nm range, however, is not meaningful as new and highly valuable interactions of materials with complex biological systems have been observed at sizes considerably above the 100-nm upper limit…Within industry, a general agreement has been voiced at many conferences that the size range is not the focus but rather the improvement and optimization of material properties to deliver patient benefits is the key. As such, a broader range of dimensions, from 1 to 1000 nm is typically considered the nanomedicine range…* [25d]

> *Nanotherapeutics apply the physical and chemical properties of nanomaterials (1–1000 nm in size) for the prevention and treatment of diseases.* [25e]

> *In its application form for investigational medicinal products (IMPs), Swissmedic, the authority regulating medical products in*

> *Switzerland, requires investigators to elaborate and specify whether the IMP contains nanoparticles with at least one dimension in the nanoscale (1–1000 nm) and whether the IMP has a function and/or mode of action based on nanotechnology characteristics either in the active substance or adjuvant.* [25f]

Michael Berger, the Founder of Nanowerk LLC and editor of the company's popular nanotechnology website (nanowerk.com), succinctly explains the criticality of establishing functional standards and nomenclature in nanotechnology [26]:

> *The lack of a unified standard, or the existence of different standards, can have dire consequences. A few years ago, the Mars Climate Orbiter spacecraft was destroyed because a navigation error caused the spacecraft to fly too deep into the atmosphere of Mars. This error arose because a NASA subcontractor used Imperial units (pound-seconds) instead of the metric units (newton-seconds) as specified by NASA. But even in the U.S., economic and scientific needs assure the continued creeping adoption of the metric standard in various areas. Nanotechnology is such a case, were the metric system is the undisputed only standard — used even by U.S. researchers — and sparing us conversion tables for nanometer to nanoinch and nanofoot, and nanoliter to nanogallon… Standards have a much larger role in our society than just agreeing measurements. As the British Standards Institution (BSI) explains it, put at its simplest, a standard is an agreed, repeatable way of doing something. It is a published document that contains a technical specification or other precise criteria designed to be used consistently as a rule, guideline, or definition. Standards help to make life simpler and to increase the reliability and the effectiveness of many goods and services we use… The need for standardization also exists in various fields of nanotechnology in order to support commercialization and market development, provide a basis for procurement, and support appropriate legislation/regulation. The lack of nanotechnology standards poses several major challenges because right now there are no internationally agreed terminology/definitions for nanotechnology, no internationally agreed protocols for toxicity testing of nanoparticles, no standardized protocols for evaluating environmental impact of nanoparticles, no standardized measurement techniques and instruments, no standardized calibration procedures and certified references materials... Standards create comparability and any standard is a collective work. Committees of manufacturers, users, research organizations, government departments and consumers work together to draw*

up standards that evolve to meet the demands of society and technology.

A similar concern is echoed by other commentators [25f]:

The definition of nanomedicine has implications for many aspects of translational research including fund allocation, patents, drug regulatory review processes and approvals, ethical review processes, clinical trials and public acceptance. Given the interdisciplinary nature of the field and common interest in developing effective clinical applications, it is important to have honest and transparent communication about nanomedicine, its benefits and potential harm. A clear and consistent definition of nanomedicine would significantly facilitate trust among various stakeholders including the general public while minimizing the risk of miscommunication and undue fear of nanotechnology and nanomedicine.

Some global standard-setting organizations that are active in defining nano-standards and nano-nomenclature are:

- ANSI-Nanotechnology Standards Panel in the US
- ASTM Committee E56 on Nanotechnology
- BSI British Standards Committee for Nanotechnologies (NTI/1)
- European Committee for Standardization (CEN)
- IEC group for nanotechnology standardization for electrical and electronic products and systems (TC 113)
- IEEE Nanotechnology Standards Working Group
- ISO Technical Committee on Nanotechnologies (TC 229)

6.4 Physical Scientists versus Pharmaceutical Scientists: Different Views of the Nanoworld

"It has been my experience that I am always true from my point of view, but am often wrong from the point of view of my honest critics. I know that we are both right from our respective points of view…"

—Mahatma Gandhi (1869–1948), Apostle of Nonviolence

Interdisciplinarity is the hallmark of nanotechnology and nanomedicine. Nevertheless, physical scientists and pharmaceutical scientists view the nanoworld quite differently; clearly, there is

tension between the two camps [27, 28]. Let me illustrate this with the example of nanoparticles. The physical scientist, may for example, look at the *intrinsic* novel properties like the specific wavelength of light emitted from a quantum dot due to variations in the quantum dot's size. Other examples of properties of particular significance to a physical scientist, but of little interest to a pharmaceutical scientist, include the increased wear resistance of a nanograined ceramic due to the Hall-Petch effect [29] or quantum confinement where one photon can excite two or more excitons (electron-hole pairs) in semiconductor nanoparticles [30]. The arbitrary upper size limit of 100 nm proposed by the NNI may be relevant to a physical scientist since this is sometimes the size range at which there is a transition between bulk and nonbulk properties of metals and metal compounds. On the other hand, the pharmaceutical scientist is more interested in the *extrinsic* novel properties of nanoparticles that arise because of their interaction with biological systems or nanodrug formulation/efficacy properties that improve bioavailability, reduce toxicity, lower required dose or enhance solubility.

Materials can be scaled down (miniaturized, micronized, nanonized, etc.) many orders of magnitude from macroscopic to microscopic via conventional techniques, with specific change or no change in properties. As materials are scaled down further to nanodimensions (say, from around 100 nm down to the size of atoms (~0.2 nm)), changes in optical,[15] electrical, mechanical and conductive properties, often profound, *may* be observed. In other words, this size variation of materials *may* result in unexpected properties not found in their larger bulk counterparts that make for novel application opportunities. *It is important to note, however, that there is no certainty that there will be a change in characteristics at this size range: a nanomaterial in the size range of 1–100 nm does not automatically possess unique "nanocharacteristics" distinct from its bulk counterpart*. In this context, when there is a change in

[15]A century after artisans used metallic particles as colorants, Michael Faraday in 1857 studied the interaction of light (photons) with gold particles and established that both the type of material and particle size were important factors in determining the specific color of emitted light. The area of research we now refer to as photonics was born. Nanometer-scale particles from the same block of gold (yellow) can have a range of colors (emitted light) like orange, red or purple.

properties or behavior of materials, the reasons are twofold: (i) an increase in relative surface area, i.e., a large surface-to-volume ratio (producing increased chemical reactivity, which can make nanomaterials more useful for biomedical applications but can also increase the risk of potential health/environmental hazards); and (ii) an enhanced dominance of quantum effects (which impact the material's optical, physical, surface, magnetic, or electrical properties).

However, the quantum mechanical nature of materials at the nanoscale, where classical macroscopic laws of physics do not operate, are irrelevant when it comes to pharmaceutical science, especially drug delivery, drug formulation and most nano-assays (refer to Section 6.5 for further details). The sub-100 nm size range *may* be significant to a nanophotonic company where the quantum dot's size dictates the color of light emitted therefrom. But, this arbitrary size limitation is *not* critical to a pharmaceutical scientist from a formulation, delivery or efficacy perspective because the desired property (such as V_{max}, pharmacokinetics or PK, area under the curve or AUC, ζ-potential, etc.) may be achieved with a particle size range greater than 100 nm. Moreover, as stated previously, pharmaceutical scientists prefer a labeling consistent with colloidal solutions while discussing nanoformulations where particles have at least one dimension ranging from 1–1,000 nm (see footnote 21).

A timely, new journal from Wiley, the *Journal of Interdisciplinary Nanomedicine*, highlights the clear need for "true" interdisciplinarity because of the different approaches of physical scientists versus pharmaceutical scientists with respect to not only generation of data but also during the examination, analysis and discussion of these data [31]:

> *Nanomedicine by nature is interdisciplinary, with benefits being realized at the interface of science and engineering, physical science and engineering, chemical science and engineering, cellular and molecular biology, pharmacology and pharmaceutics, medical sciences and technology and combinations thereof. The difference in perspective between disciplines may be partly responsible for the lack of nomenclature or universally accepted definition for various "nano" terminologies, which causes issues with publication consistency, regulatory agencies, patent offices, industry and the business community… . Ultimately, for a clinical scientist or physician the true value of a particular material lies in*

its clinical utility balanced against any potential adverse effects. Therefore, effective translation of nanomedicine candidates requires a "technological push" coupled to a "clinical pull", which is bridged by logical intermediary data that mechanistically demonstrate the efficacy and safety in biological systems... . Given this backdrop, there is a clear need for "true" interdisciplinarity during the generation of robust nanomedicine data but also during examining, discussing or analyzing these data because interpretation by physical scientists is often different than by biological scientists.

6.5 Is Drug Delivery at the Nanoscale Special? Does Size Matter?

"Tomorrow's science is today's science fiction."

—Stephen W. Hawking (1942–), Physicist

Nanomedicine has blossomed into a robust industry. Nanomedicine may be defined as the science and technology of diagnosing, treating and preventing disease and improving human health via nano. Rapid advances and product development in nanomedicine are in full swing as it continues to influence the pharmaceutical, device and biotechnology industries. Nanomedicine is driven by collaborative research, patenting, commercialization, business development and technology transfer within diverse areas such as biomedical sciences, chemical engineering, biotechnology, physical sciences, and information technology.

The major impact of nanomedicine today is in the context of drug delivery:

- Novel nanodrugs and nanocarriers are being developed that address fundamental problems of traditional drugs because of the ability of these compounds to overcome poor water solubility issues,[16] alter unacceptable toxicity profiles, enhance bioavailability,[17] and improve physical/chemical

[16]Approximately 40% of the new drug candidates emerging from drug discovery have poor water profiles, a critical issue that continues to plague drug research programs. See: Stegemann, S., Leveiller, F., Franchi, D., de Jong, H., Linden, H. (2007). When poor solubility becomes an issue: From early stage to proof of concept. *European Journal of Pharmaceutical Sciences*, **31**, 249–251.

[17]Bioavailability refers to the extent and rate (how much and how quickly) a drug enters blood circulation or reaches its intended target (site of action). Ninety five percent (95%) of all new potential therapeutics demonstrate poor PK and bioavailability; "nano" may be able to address some of these issues. See: Brayden, D.

stability. Additionally, via tagging with targeting ligands,[18] these nanodrug formulations can serve as innovative drug delivery systems (DDS) for enhanced cellular uptake or localization of therapeutics into tissues or organelles of interest (i.e., site-specific targeted delivery). Various FDA-approved liposomal, solid nanoparticle-based, antibody-drug conjugate (ADC) and polymer-drug conjugate delivery platforms overcome associated issues such as (i) low solubility (Abraxane), (ii) extremely high drug toxicity (Brentuximab vedotin and Trastuzumab emtansine), and (iii) side effects related to high doses of free drug (Doxil, Marqibo, DaunoXome).

- Reformulation of old, shelved therapeutics into nanosized dosage forms could offer the possibility of adding new life to old therapeutic compounds. Classic examples include drugs developed as nanocrystalline products (Rapamune, Emend, Triglide).
- Coupled with advances in pharmacogenomics, smart nanomachines, information technology and personalized medicine, upcoming innovations in nanomedicine may even generate multifunctional entities enabling simultaneous diagnosis, delivery and monitoring of therapies [32].

As a result, nanodrugs are being developed to allow delivery of active agents more efficaciously to the patient while minimizing side effects, improving drug stability *in vivo* and increasing blood circulation time.[19] Apart from these pharmacological benefits, nanodrug formulations also offer real economic value to a drug company—the opportunity to reduce time-to-market, extend the

J. (2003). Controlled release technologies for drug delivery. *Drug Discovery Today*, **8**, 976–978.

[18]In biochemistry, a ligand is defined as an antibody, hormone or drug that binds to a receptor and may have applications in diagnosing or treating disease. In chemistry, the term often refers to a molecule, ion or atom that is bonded to the central metal atom of a coordination compound.

[19]Although numerous nanodrugs have been routinely used in medicinal products for decades without any focus or even awareness of their nanocharacter, it is only within the past two decades that they have been highlighted due to their potential of revolutionizing drug delivery. Obviously, the Holy Grail of any drug delivery system is to deliver the correct dose of a particular active agent to a specific disease or tissue site within the body while simultaneously minimizing toxic side effects and optimizing therapeutic benefit. This is often not achievable via conventional drugs. However, the potential to do so may be greater via engineered nanodrugs.

economic life of proprietary drugs, and create additional revenue streams. Nanodrugs are starting to influence the commercial drug landscape now and are likely to impact medical practice and healthcare delivery in the future. In the meantime, the FDA-approved nanodrugs that are arriving in the marketplace span both intravenous as well as non-intravenous products. Some are completely novel while others are redesigned variations of earlier versions (Fig. 6.1). The first generation of nanodrugs mainly address single challenges like targeted delivery, while the second and third generations in development can offer two or more functions together (delivery and imaging) or overcome multiple physiological barriers to deliver their drug payloads. However, most nanodrug products are still in their infancy, being at the pre-clinical development stage or in clinical trials. As these products continue to move out of the laboratory and into the clinic, governmental agencies such as the FDA, EMA, WIPO, and the PTO[20] continue to struggle to encourage their development while imposing some sort of order in light of regulatory, safety and patent concerns. But, is this really possible without a coherent, manageable nomenclature or appropriate regulatory terminology?

There is no formal definition for a nanotherapeutic formulation (or nanodrug product). I define a nanotherapeutic formulation

[20]For over a decade, the PTO continues to classify US nanopatents into Class 977 where, according to its own recent data, they currently number 5,000+. But, it is immediately apparent that there is something wrong with this statistic since there are more than 15,000 issued US patents on nanoparticles alone. In fact, this classification system is imprecise because of the simple fact that the PTO's definition of "nano" is incorrectly based on the flawed NNI definition that limits all nanostructures and nanoproducts to a sub-100 nanometer size range. For example, see *U.S. Patent and Trademark Office (USPTO)*; Available at: http://www.nano.gov/node/599 (accessed on October 20, 2015): "*Notably, the USPTO adopted the NNI definition of nanotechnology in its development of the first detailed, patent-related nanotechnology classification hierarchy of any major intellectual property office in the world*." As a result, the PTO numbers are a gross underestimate and miss the majority of nanotech-related patents (out of ~9 million US patents issued). Therefore, PTO statistics on nanopatents should be considered as indicative of the overall trend, not actual number of nanonotech-related patents. Also, see *Top countries in field of nanotechnology patents in 2013*; Available at: http://statnano.com/news/45648 (accessed on October 20, 2015): "*According to the statistics released by Statnano based on nanotechnology patents and nanotechnology published patent applications, a sum total of 21,379 patents related to nanotechnology have been granted in USPTO in 2013, and about 31,350 nanotechnology patents have been published. A growth of more than 60% is observed in the number of nanotechnology patents in USPTO in comparison with 2012*…."

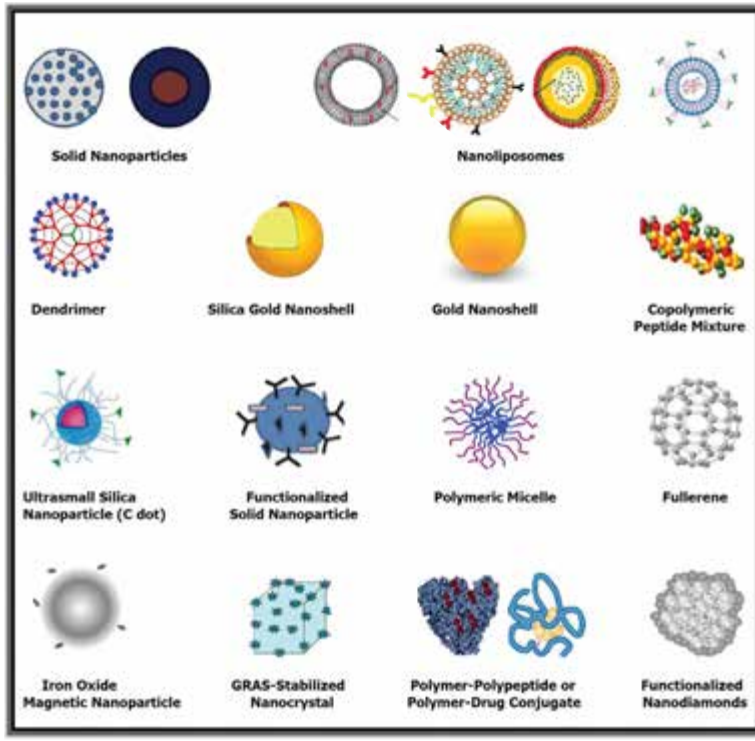

Figure 6.1 Schematic Illustrations of Nanoscale Drug Delivery System Platforms (Nanotherapeutics or Nanodrug Products). Shown are nanoparticles (NPs) used in drug delivery that are either approved, are in preclinical development or are in clinical trials. They are generally considered as first or second generation multifunctional engineered NPs, generally ranging in diameters from a few nanometers to a micron. Active biotargeting is frequently achieved by conjugating ligands (antibodies, peptides, aptamers, folate, hyaluronic acid) tagged to the NP surface via spacers or linkers like PEG. NPs such as carbon nanotubes and quantum dots, although extensively advertised for drug delivery, are specifically excluded from the list as this author considers them commercially unfeasible for drug delivery. Non-engineered antibodies and naturally occurring NPs are also excluded. Antibody-drug conjugates (ADCs) are encompassed by the cartoon labelled "Polymer-Polypeptide or Polymer-Drug Conjugate." This list of NPs is not meant to be exhaustive, the illustrations are not meant to reflect three dimensional shape or configuration and the NPs are not drawn to scale. Abbreviations: NPs: nanoparticles; PEG: polyethylene glycol; GRAS: Generally Recognized As Safe; C dot: Cornell dot; ADCs: Antibody-drug conjugates.

(or nanodrug product) as: (1) a formulation, often colloidal, containing therapeutic particles (nanoparticles) ranging in size from 1–1,000 nm; *and* (2) either (a) the carrier(s) is/are the therapeutic (i.e., a conventional therapeutic agent is absent) or (b) the therapeutic is directly coupled (functionalized, solubilized, entrapped, coated, etc.) to a carrier.[21] This definition parallels that proposed by experts [8, 25a, 25b, 25c, 25d, 25e, 25f] and disregards that offered by US federal agencies, most notably the NNI.

As is shown in Fig. 6.1, the various nanodrug product platforms are diverse in size, shape, structural design, charge, rigidity, and composition. Their physicochemical properties or "nanocharacter" *often* provides an advantage as compared to their "bulk" or larger counterparts primarily because of their reduced size, which is significantly smaller than the typical 10–100 μm size of most eukaryotic cells. These properties are critical in determining not only their overall biodistribution and tissue binding/persistence/clearance, but also their toxicity potential given that inert bulk materials can become toxic when formulated as nanomaterials. Often, nanodrugs transport active agents to their target binding sites (ligands, receptors, active sites, etc.) to impart maximum therapeutic activity with maximum safety (i.e., protect the body from adverse reactions) while preventing the degradation/denaturation/inactivation of the active agent during delivery/transit. As mentioned above, targeting can be achieved or enhanced by (i) linking specific ligands or molecules (e.g., antibodies, glycoproteins, etc.) to the carrier, or (ii) by altering the surface characteristics of the carrier. Furthermore, therapeutics that have side effects due to triggering an immune response (e.g., complement activation) or cleared by the reticuloendothelial (RES) system may be entrapped, encapsulated or embedded within a nanoparticle coat or matrix.

In a clinical setting, some or all of the features of nanodrugs below could correlate to an enhanced *in vivo* bioperformance:

[21]A "colloid" is a chemical system composed of a continuous medium (continuous phase) throughout which are distributed small particles (dispersed phase), typically ranging from 1–1,000 nm in size (disperse phase), that do not settle out under the influence of gravity and; the particles may be in emulsion or in suspension. In general, colloidal particles are aggregates of numerous atoms or molecules, but are too small to be seen with an ordinary optical microscope. They pass through most filter papers, but can be detected via light scattering and sedimentation. See: Atkins, P., de Paula, J. (2006). *Physical Chemistry*, 8th ed., Freeman and Co., New York, p. 682; Also see: Colloids. Available at: http://chemwiki.ucdavis.edu/Physical_Chemistry/Physical_Properties_of_Matter/Solutions_and_Mixtures/Colloid (accessed on October 21, 2015).

- In general, as a particle's size decreases to nanoscale dimensions, a greater proportion of its atoms are located on the surface relative to its core (Fig. 6.2), *often* rendering the particle more chemically reactive or endowing the particle with size-dependent melting properties. However, depending on the intended use, such enhanced activities could either be advantageous (antioxidation, carrier capacity for drugs, enhanced uptake and interaction with tissues) or disadvantageous (toxicity issues, instability and induction of oxidative stress) [33].[22]
- It is also a scientific fact that, as we granulate a particle into smaller particles, the total surface area of the smaller particles becomes much greater relative to its volume (i.e., an enormously increased surface area-to-volume ratio[23]) (Table 6.2; Figs. 6.3a and 6.3b). As materials are scaled down from macroscopic to nanoscopic, the interfacial and surface properties dominate particle interactions instead of gravity. However, from a drug delivery perspective, smaller particles have a higher dissolution rate, water solubility and saturation solubility compared to their larger counterparts. This change in properties *may* result in superior bioavailability, as a higher percentage of active agents are available at the site of action (tissue or disease site).[24] This *may* translate into a reduced drug dosage needed by the patient, which in turn *may* reduce the potential side effects and offer superior drug compliance.

[22]A classic example of this is nanosilver (previously known as "colloidal silver"), a highly reactive and antimicrobial form of silver, whose side effects on humans and the environment have been well documented for over a century.

[23]One of the most utilized properties of nanoparticles is their high specific surface area (SSA). Specific surface area is defined as the surface area per unit weight as expressed in the following equation:

$$S = \frac{6000}{d \cdot \rho},$$

where S denotes the specific surface area in m^2/g, d represents the particle diameter in nm and ρ is the density of the material in g/cm^3. As the particle size decreases, relatively more atoms become exposed on the particle surface (Fig. 6.2). In other words, as the particle size is reduced, the specific surface area increases.

[24]A classic example of improving drug bioavailability is Élan Corporation's (since 2013, Perrigo Company PLC) NanoCrystal® technology, where nanodrug particles are produced by a proprietary attrition-based wet-milling technique that reduces their size to less than one micron (μ). This technology has generated 6+ marketed drugs. For a discussion of nanocrystal technology and drug delivery, see [25b].

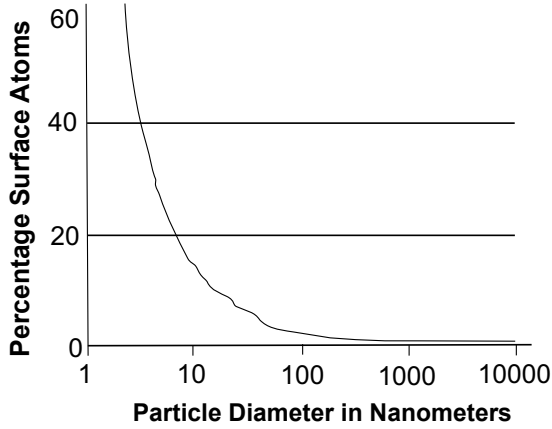

Figure 6.2 Particle Size Versus Percentage Surface Atoms. As the particle size decreases, the percentage of atoms displayed on the surface of the particle relative to the total atoms in the particle increases exponentially. In other words, the fewer the number of atoms in a particle, a greater percentage of atoms are found on the surface of the particle. In this hypothetical graph, a particle with a 10 nm diameter has ~10–15% atoms displayed on the surface whereas a 50 nm particle has about ~6–8% surface atoms. (Copyright © 2016 Raj Bawa. All rights reserved.)

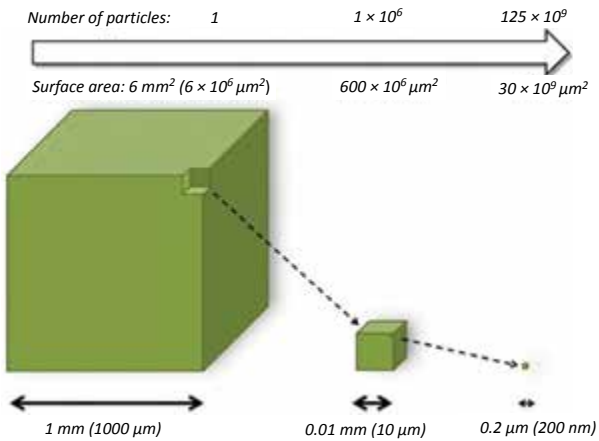

Figure 6.3a Comparison of size, number of particles formed and available surface area when taking a single cubic structure of 1 mm^3 and reduce its dimensions systematically to 10 μm^3 and then 200 nm^3. (courtesy of Dr. Andrew Owen and Dr. Steve P. Rannard, University of Liverpool, UK).

Particle	A	B	C
Diameter	d	0.1d	0.01d
Particles per mass unit	n	1,000n	1,000,000n
Surface area per mass unit	A	10A	100A

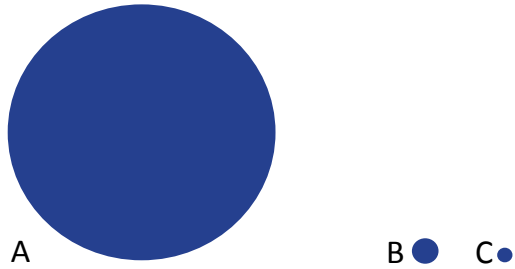

Figure 6.3b Spheres of decreasing size and the relationship between their diameters and surface areas. The surface of a spherical particle scales with its radius^2 while its volume scales with radius^3. Hence, the surface-to-volume is inversely proportional to the size. In other words, as the particle size decreases, the number of particles per mass unit increases by the cube of the size difference factor (i.e., a 1,000-fold increase for a 10-fold decrease in size). In addition, the surface area per mass unit, along with the percentage of atoms in the material being present on the particle surface, increases by the size difference (i.e., a 10-fold increase for a 10-fold decrease in size). Adapted with kind permission of Pan Stanford Publishing, Singapore.

Table 6.2 Surface-to-volume Atomic Ratio of Spherical Gold Particles

Particle Diameter (nm)	Total Atom Count	Surface Atoms (%)	Specific Surface Area (m^2/g)
1000	~30,000,000,000	~0.2	0.3
100	~30,000,000	~1.6	~3
10	~30,000	~15	~31
1	~30	~90	~310

Note: As the particle size is reduced, the specific surface area increases. As shown in this table, when the diameter of gold particles is reduced to 1 nm, 1 g of nanoparticles has a surface area of as large as ~300 m^2. On the other hand, if the gold particles have a diameter of 0.1 mm, then 1 g of the powder has only ~0.003 m^2 of surface area. This means that as much as 100 kg of ~0.1 mm-sized gold particles are required to provide the same surface area as 1 g of ~1 nm-sized gold nanoparticles (courtesy of Dr. Takuya Tsuzuki, Australian National University and Pan Stanford Publishing, Singapore).

- Finally, nanoparticle therapeutics have a greater potential for interaction with biological tissues, i.e., an increase in adhesiveness onto biosurfaces.[25] This can be a tricky, double-edged issue. On one side, the multiple binding sites of nanodrugs ("multivalence"[26]) allow for superior binding to tissue receptors, but on the other side, intrinsic toxicity of any given mass of nanoparticles is often greater than that of the same mass of larger particles. Nanoparticle therapeutics (e.g., liposomes) can also contribute to "signal enhancement" (10^5–10^6) over that of a single drug molecule because of the enormous payload (500,000–1,000,000) of encapsulated active molecules.

In the pharmaceutical sciences, "nano" offers several *potential* advantages in the context of drug delivery that pharma is interested in. Some of these advantages include [34]:

- increased bioavailability due to enhanced water solubility of hydrophobic drugs because of the large specific surface area;
- ability to protect biologically unstable drugs from the hostile bioenvironment of use/delivery/release (e.g., against potential enzymatic or hydrolytic degradation);
- extended drug residence time at a particular site of action or within specific targeted tissue and/or extended systemic circulation time;
- controlled drug release at a specific desired site of delivery;
- endocytosis-mediated transport of drugs through the epithelial membrane;
- bypassing or inhibition of efflux pumps such as P glycoprotein;
- targeting of specific carriers for receptor-mediated transport of drugs;
- enhanced drug accumulation at the target site so as to reduce systemic toxicity;

[25]For example, nanoparticles like dendrimers work more effectively than small molecule therapeutics. Small molecules have the ability to interact with only a select few cell surface receptors while dendrimers can potentially interact with multiple receptors simultaneously, thereby potentiating the biological effect.

[26]In the context of drug delivery, multivalency is the chemical interaction of ligands with several identical binding sites (receptors) on a multi-presented cell. In biological systems, multivalent interactions are widely used (e.g., in cellular recognition and signal transduction) and are generally stronger than the individual bonding of a corresponding number of monovalent ligands to a multivalent receptor.

- biocompatibility and biodegradability;
- high drug-loading capacity;
- long-term physical and chemical stability of drugs; and
- improved patient compliance.

Therefore, in general terms, it can be concluded that nanoscale therapeutics may have unique properties (nanocharacter) that can be beneficial for drug delivery but there is no bright-line size or dimensional limit where superior properties are found. Hence, the size limitation below 100 nm cannot be touted as the basis of novel properties of nanotherapeutics. In fact, properties other than size can also have a dramatic effect on the nanocharacter of nanodrugs: shape/geometry, zeta potential, specific nanomaterial class employed, composition, delivery route, crystallinity, aspect ratio, surface charge, etc. Clearly, numerous nanomaterials and their corresponding nanodrugs such as liposomes (80–200 nm), block copolymer micelles (50–200 nm), nanoparticles (20–200 nm), and nanosize drug crystals (100–1000 nm) fall outside the sub-100 nm size range (Fig. 6.1). In addition, there are no clear scientific boundaries to distinguish the nano from the non-nano space, especially with respect to drug products. Moreover, as stated earlier, a sub-100 nm range is not critical to a drug company from a formulation, delivery, or efficacy perspective because the desired or novel physicochemical properties (e.g., improved bioavailability, reduced toxicities, lower dose, or enhanced solubility) may be achieved in a size outside this arbitrary range. For example, the surface plasmon-resonance (SPR)[27] in gold or silver nanoshells or nanoprisms that imparts their unique property as anticancer thermal drug delivery agents also operates at sizes greater than 100 nm. Similarly, at the tissue level, the enhanced permeability and retention (EPR)[28] effect that

[27]A variety of light-triggered delivery systems are currently under development. Near infrared light (NIR) is a promising source of radiation that is absorbed by nanosilver and nanogold particles but not biological tissue. This property can be exploited if these particles (alone or with incorporated active agents) are targeted to tumors and irradiated via NIR, thereby causing thermolysis of tumors without damage to the surrounding tissue.

[28]There are two major concepts in drug delivery systems (DDS) in oncology: (i) active targeting that involves tumor targeting via the specific binding ability between an antibody and antigen or between the ligand and its receptor; and (ii) passive targeting achieved via the EPR effect. Although not a generalization, if the nanoparticle is too small (<10 nm?), it is generally rapidly excreted via renal filtration while particles too large (>~150 nm?) may not penetrate deep inside tumor tissue. It should be pointed out that these are general statements as there

makes nanoparticle drug delivery an attractive option operates in a wide range, with nanoparticles of 100–1000 nm diffusing selectively (extravasation and accumulation) into the tumor [35]. At the cellular level, size range for optimal nanoparticle uptake and processing depends on many factors but is often beyond 100 nm. Liposomes in a size range (diameter) of about 150–200 nm have been shown to have a greater blood residence time than those with a size below 70 nm. Furthermore, there are numerous FDA-approved and/or marketed nanodrug products where the particle size doesnot fit the sub-100 nanometer profile: Abraxane (~130 nm), Myocet (~190 nm), Amphotec (~130 nm), Epaxal (~150 nm), Inflexal (~150 nm), Lipo-Dox (180 nm), Oncaspar (50–200 nm), Copaxone (1.5 to 550 nm), etc.

This does not imply that any size will do for nanodrug delivery. For example, submicron sizes are generally considered essential for biological distribution of biopharmaceuticals for safety reasons [36]. Particles greater than 5 μm can often cause pulmonary embolism following intravenous injection [37]. Therefore, submicron particle size is preferred for all parenteral formulations. In ophthalmic applications, the optimal particle size is less than 1 μm because microparticles around 5 μm can cause a scratchy feeling in the eyes [38].

If a size limit *must* be tagged onto nanodrugs, then an upper limit of 1000 nm may be most appropriate (refer to pages 143–144). The FDA, which was involved in the formulation of the inaccurate sub-100 nm NNI definition, has not adopted any "official" regulatory definition for nanotechnology or nanoscale. However, since 2011, following the publication of a "draft" guidance document,[29] it uses an awkward, loose and "unofficial" size-based

is a wide variability in nanoparticles types and sizes employed to achieve the desired result or therapeutic outcome. For example, sterically-stabilized liposomes of 400 nm diameter were shown to penetrate into tumor interstitium. One has to examine the specific nanoparticle on a case-by-case basis to see whether it is scavenged by RES (e.g., Kupffer cells in liver) or internalized by target cells through endocytosis. Size obviously is important while engineering nanoparticles for tumor applications but it needs to be fine-tuned depending upon the nanomaterial used, route of delivery, application sought, toxicity issues, etc.

[29]The FDA's use of "unofficial" definitions and "draft" guidance documents is legendary and the subject of concern, ridicule and criticism. Such FDA recommendations are nonbinding and come with a standard disclaimer: "*This draft guidance, when finalized, will represent the Food and Drug Administration's (FDA's) current thinking on this topic. It does not create or confer any rights for or on any person and does not operate to bind FDA or the public. You can use an*

definition for engineered nanoproducts or products that employ nanotechnology that either: (i) have at least one dimension in the 1–100 nm range; or (ii) are of a size range of up to 1000 nm (i.e., 1 μm), provided the novel/unique properties or phenomenon (including physical/chemical properties or biological effects) exhibited are attributable to these dimensions greater than 100 nm [39].

As stated previously, various other governmental agencies also continue to use the vague NNI definition based on a sub-100 nm size. Clearly, as elaborated in this chapter, such definitions based on size or dimensions alone fall short on both scientific and legal grounds. In this context, consider the following sample questions and the limitation of this impractical definition becomes amply clear vis-à-vis nanomedicine products:

- What if, the primary nanostructures (below 100 nm) are in an agglomerated or aggregated form that is above 100 nm?
- What if, the unique "nanocharacter" is lost if the nanomaterial, nanoproduct or nanoparticles are not in an agglomerated or aggregated form?
- What if, the size of these agglomerates or aggregates lies outside of the NNI definition but they nervelessness possess or display novel nanocharacteristics identical to their nanoscale counterparts from which they arose?
- What if, unique or novel nanoproperties exist at various size ranges, some even above 100 nm?
- What if, only a certain fraction of nanomaterial, nanoproduct or nanoparticles (1%, 10%, 50%, 90%, etc.) are in the sub-100 nm nanoscale while the rest are not?
- What if, macroscale agglomerates give off primary nanoparticles in the presence of surfactants, enzymes or by action of certain biochemicals?
- What if, there is a wide batch-to-batch variability in size or dimensions (above and below 100 nm) dependent upon unique manufacturing protocols, yet the batches retain their unique nanoscale properties?

alternative approach if the approach satisfies the requirements of the applicable statutes and regulations ..." For example, see: Watson, E. (2014). Senators to FDA: Stop using draft guidance to make substantive policy changes. Available at: http://www.foodnavigator-usa.com/Regulation/Senators-to-FDA-Stop-using-draft-guidance-to-make-big-policy-changes (accessed on October 1, 2015).

- What if, different assays or characterization protocols of the same nanomaterial, nanoproduct or nanoparticles provided disparate data on size (range, fraction, etc.)?
- What if, the unique nanocharacter or novel toxicity profile is only manifested when exposed to certain biological environments?
- What if, the unique nanocharacter is lost in certain biological environments or as a result of interaction with certain tissue?

6.6 Summary and Future Prospects

"You see things; and you say 'Why?' But I dream things that never were; and I say 'Why not?'"

—George Bernard Shaw, Playwright (1856–1950)

Nomenclature, technical specifications, standards, guidelines and best practices are critically needed to advance nanotechnologies in a safe and responsible manner. Contrary to a few commentators, terminology does matter because it prevents misinterpretation and confusion. However, defining nanotechnology, from any perspective (scientific, regulatory, patent law, ethics, policy), is no easy task. So far, no real consensus has been reached on basic "nano" terms such as nanotechnology, nanodrug, nanomedicine, nanomaterial, nanotherapeutic, nanoparticle, nanoscale, etc. In fact, finding a consensus on nanonomenclature is a challenge, especially with the diversity and scope of scientific disciplines, voices and technologies encompassed by the nanotechnology umbrella. An official, scientifically credible and legally workable definition of nanotechnology as applied to nanoparticle drug delivery systems or nanoformulations does not currently exist. It is clear that nanotechnology as applied to drug delivery does not need to have any unique size cut-off for the simple fact that such artificial boundaries are completely irrelevant from an efficacy or formulation perspective.

Pharmaceutical companies do not need to be told by a government agency that unless their formulation or product is in a particular size range, they cannot refer to it as a nanodrug product or nanoformulation. There is no law that governs this and, more

importantly, it makes no sense to do so for the simple fact that it is scientifically and legally irrelevant for the reasons enumerated in this chapter. The key point is this: *viable sui generis definition of nano having a bright-line size range as applied to nanodrugs blurs with respect to what is truly nanoscale; it is unnecessary, misleading, and in fact, may never be feasible.*

It is important that some order, central coordination and uniformity be introduced at the transnational level to address the rise of diverse nano terms seen in the patent literature, journal articles and the press. This is also critical to prevent a significant scientific, legal and regulatory void from developing. It is apparent to this author that this has contributed to the evolving patent thicket[30] in certain sectors along with a lack of specific protocols for preclinical development, slower nano-characterization and confusion in the scientific literature. In the near future, stakeholders ranging from patent professionals, scientists, drug regulatory community, pharmaceutical companies, policy-makers and governmental agencies must come together on a global platform to address, define and formulate formal definitions and nomenclature for various "nano" terms. In the meantime, this chapter should provide guidance to these stakeholders. It is important that the public's desire for novel nanoproducts, venture community's investment and big pharma's interest in nanomedicine is not quenched.

Disclosures and Conflict of Interest

This work was supported by Bawa Biotech LLC, Ashburn, VA, USA. The author is a scientific advisor to Teva Pharmaceutical Industries, Ltd., Israel, and declares that he has no conflict of interest and has no affiliations or financial involvement with any organization or entity discussed in this chapter. No writing

[30]The lack of universal terminology is creating patent thickets in certain areas of nanomedicine. For example, the carbon nanotube (CNT) patent landscape is a tangled mess, partly due to a lack of nano-nomenclature because of which inventors and scientists have employed distinct terms to refer to CNTs. As a result, contrary to the foundation of US patent law, various US patents on CNTs have been granted with legally identical claims. See: Harris, D., Bawa, R. (2007). The carbon nanotube patent landscape in nanomedicine: an expert opinion. *Expert Opinion on Therapeutic Patents*, **17**(9), 1165–1174.

assistance was utilized in the production of this chapter and no payment was received for its preparation. The findings and conclusions here reflect the current views of the author and should not be attributed, in whole or in part, to the organizations with which he is affiliated.

Corresponding Author

Dr. Raj Bawa
Bawa Biotech LLC
21005 Starflower Way
Ashburn, VA 20147, USA
Email: bawa@bawabiotech.com

About the Author

Raj Bawa, is president of Bawa Biotech LLC, a biotech/pharma consultancy and patent law firm based in Ashburn, VA, USA that he founded in 2002. He is an inventor, entrepreneur, professor and registered patent agent licensed to practice before the U.S. Patent & Trademark Office. Trained as a biochemist and microbiologist, he has been an active researcher for over two decades. He has extensive expertise in pharmaceutical sciences, biotechnology, nanomedicine, drug delivery and biodefense, FDA regulatory issues, and patent law. Since 1999, he has held various positions at Rensselaer Polytechnic Institute in Troy, NY, where he is currently an adjunct professor of biological sciences and where he received his doctoral degree in three years (biophysics/biochemistry). Since 2004, he has been an adjunct professor of natural and applied sciences at NVCC in Annandale, VA. He is a scientific advisor to Teva Pharmaceutical Industries, Ltd., Israel. He has served as a principal investigator of National Cancer Institute SBIRs and reviewer for both the NIH and NSF. In the 1990s, Dr. Bawa held various positions at the US Patent & Trademark Office, including primary examiner for 6 years. He is a life member of Sigma Xi, co-chair of the Nanotech Committee of the American Bar Association and serves on the global advisory council of the World Future Society. He has authored

over 100 publications, co-edited four texts and serves on the editorial boards of 17 peer-reviewed journals, including serving as a special associate editor of *Nanomedicine* (Elsevier) and an editor-in-chief of the *Journal of Interdisciplinary Nanomedicine* (Wiley). Some of Dr. Bawa's awards include the Innovations Prize from the Institution of Mechanical Engineers, London, UK (2008); Appreciation Award from the Undersecretary of Commerce, Washington, DC (2001); the Key Award from Rensselaer's Office of Alumni Relations (2005); and Lifetime Achievement Award from the American Society for Nanomedicine (2014).

References

1. Bawa, R. (2007). Nanotechnology patent proliferation and the crisis at the US Patent Office. *Albany Law J. Sci. Technol.,* **17**(3), 699–735.
2. Bawa, R. (2009). Patenting inventions in bionanotechnology: A primer for scientists and lawyers. In: Reisner, D. E., ed. *Bionanotechnology: Global Prospects,* CRC Press, Boca Raton, FL, pages 309–337.
3. Bawa, R. (2016). Emerging issues in nanodrugs and nanomedicine. In: Wellons, H. B., Ewing, E. S., eds. *Biotechnology and the Law*, 2nd ed., American Bar Association, Chicago, IL.
4. (a) Rogers, B., Pennathur, S., Adams, J. (2011). *Nanotechnology: Understanding Small Systems*, 2nd ed., CRC/Taylor & Francis, Boca Raton, FL, chapter 1.

   (b) Weissig, V., Pettinger, T. K., Murdock, N. (2014). Nanopharmaceuticals (part 1): products on the market. *Int. J. Nanomed.*, **9**, 4357–4373.
5. Feynman, R. P. (1991). There's plenty of room at the bottom. *Science*, **254**, 1300–1301. Available at: http://www.zyvex.com/nanotech/feynman.html (accessed on September 9, 2015).
6. (a) Lohmann, H. (1908). Untersuchungen zur feststellund des vollstandigen gehaltes desMeeres an plankton. *Wiss. Meeresunters. Kiel, N.F.*, **10**, 129–370.

   (b) Taniguchi, N. (1974). On the basic concept of nano-technology, *Proc. Intl. Conf. Prod. Eng., Tokyo, Part II*, Japan Society of Precision Engineering, pages 18–23.

   (c) Binnig, G., Rohrer, H. (1986). Scanning tunneling microscopy. *IBM J. Res. Dev.*, **30**, 4.

   (d) Kroto, H. W., Heath, J. R., O'Brien, S. C., Curl, R. F., Smalley, R. E. (1985). C_{60}: Buckminsterfullerene. *Nature*, **318**(6042), 162–163;

Kroto, H. W., ed. (2015). C_{60} *Buckminsterfullerene: Some Inside Stories*, Pan Stanford Publishing, Singapore.

7. Drexler, E. (1986). *Engines of Creation: The Coming Era of Nanotechnology*, Anchor Books, New York. Available at: http://e-drexler.com/p/06/00/EOC_Cover.html (accessed on November 3, 2015).
8. History of nanotechnology. Available at: http://en.wikipedia.org/wiki/History_of_nanotechnology (accessed on November 3, 2015).
9. Bawa, R. (2010). Nanopharmaceuticals. *Eur. J. Nanomed.*, **3**(1), 34–39.
10. Bawa, R. (2016). FDA and Nano: Baby steps, regulatory uncertainty and the bumpy road ahead. In: Bawa, R., Audette, G., Reese, B., eds. *Handbook of Clinical Nanomedicine: Law, Business, Regulation, Safety, and Risk*, Pan Stanford Publishing, Singapore, chapter 17.
11. Mansour, H. M., Park, C.-W., Bawa, R. (2016). Design and development of approved nanopharmaceutical products. In: Bawa, R., Audette, G., Rubinstein, I., eds. *Handbook of Clinical Nanomedicine: Nanoparticles, Imaging, Therapy, and Clinical Applications,* Pan Stanford Publishing, Singapore, chapter 9.
12. Tinkle, S., McNeil, S. E., Mühlebach, S., Bawa, R., Borchard, G., Barenholz, Y., Tamarkin, L., Desai, N. (2014). Nanomedicines: Addressing the scientific and regulatory gap. *Ann. New York Acad. Sci.*, **1313**, 35–56.
13. Stein, R. A. (2014). Nanotechnology: Is the magic bullet becoming reality? *Genetic Engineering & Biotechnology News,* Available at: http://www.genengnews.com/insight-and-intelligence/nanotechnology-is39the-magic-bullet-becoming-reality/77900016/ (accessed on October 10, 2015).
14. Fischer, S. (2014). Regulating nanomedicine. *IEEE Pulse*, **5**(2), 21–24. Available at: http://pulse.embs.org/march-2014/regulating-nanomedicine/(accessed on October 10, 2015).
15. Johnson, D. (2014). Nanomedicines will be big once they emerge from regulatory troubles. *IEEE Spectrum*. Available at: http://spectrum.ieee.org/nanoclast/at-work/innovation/nanomedicines-will-be-big-once-they-emerge-from-regulatory-troubles (accessed on October 10, 2015).
16. Bawa, R., Bawa, S. R., Mehra, R. (2016). The translational challenge in medicine at the nanoscale. In: Bawa, R., Audette, G., Reese, B., eds. *Handbook of Clinical Nanomedicine: Law, Business, Regulation, Safety, and Risk*, Pan Stanford Publishing, Singapore, chapter 58.
17. Siew, A. (2014). Current issues with nanomedicines. *PharmTech Europe*. Available at: http://www.pharmtech.com/current-issues-nanomedicines (accessed on November 3, 2015).

18. Davenport, M. (2014). Closing the gap for generic nanomedicines. *Chem. Eng. News*, **92**(45), 10–13. Available at: http://cen.acs.org/articles/92/i45/Closing-Gap-Generic-Nanomedicines.html (accessed on October 10, 2015).

19. Lövestam, G., et al. (2010). Considerations on a definition of nanomaterial for regulatory purposes. European Commission. Available at: https://ec.europa.eu/jrc/sites/default/files/jrc_reference_report_201007_nanomaterials.pdf (accessed on October 10, 2015).

20. Mueller, N. C., et al. (2012). Nanofiltration and nanostructured membranes: Should they be considered nanotechnology or not? *J. Hazardous Mater.*, **211–212**, 275–280.

21. Kreyling, W. G., Semmler-Behnke, M., Chaudhry, Q. (2010). A complementary definition of nanomaterial. *Nano Today*, **5**, 165–168.

22. Bawa, R. (2007). Patents and nanomedicine. *Nanomedicine (Lond.)*, **2**(3), 351–374.

23. Steinmetz, N. F., Manchester, M. (2016). Viral nanoparticles: Tools for materials science and biomedicine. In: Bawa, R., Audette, G., Rubinstein, I., eds. *Handbook of Clinical Nanomedicine: Nanoparticles, Imaging, Therapy, and Clinical Applications*, Pan Stanford Publishing, Singapore, chapter 28.

24. House of Lords Science and Technology Committee: Nanotechnologies and Food, vol. I and II. Available at: http://www.publications.parliament.uk/pa/ld200910/ldselect/ldsctech/22/22i.pdf (accessed on October 10, 2015); also see: Klaessig, F., Marrapese, M., Abe, S. (2011). Current perspectives in nanotechnology terminology and nomenclature. In: Murashov, V., Howard, J., eds. *Nanostructure Science and Technology*, Springer Science+Business Media, New York, pp. 21–52.

25. (a) Bogunia-Kubik, K., Sugisaka, M. (2002). From molecular biology to nanotechnology and nanomedicine. *BioSystems*, **65**, 123–138.

    (b) Junghanns, J.-U. A. H., Müller, R. H. (2008). Nanocrystal technology, drug delivery and clinical applications. *Int. J. Nanomed.*, **3**(3), 295–310.

    (c) Ledet, G., Mandal, T. K. (2012). Nanomedicine: Emerging therapeutics for the 21st century. *U.S. Pharm.*, **37**(3), 7–11.

    (d) McDonald, T. O., Siccardi, M., Moss, D., Liptrott, N., Giardiello, M., Rannard, S., Owen, A. (2015). The application of nanotechnology to drug delivery in medicine. In: Dolez, P., ed. *Nanoengineering: Global Approaches to Health and Safety Issues*, Elsevier, pages 173–223.

(e) Wong, J. (2015). Nanotherapeutics. In: Escoffier, L. Ganau, M. and Wong, J., eds. *Commercializing Nanomedicine: Industrial Applications, Patents, and Ethics*, Pan Stanford Publishing, Singapore, chapter 4; Tibbals, H. F. (2011). *Medical Nanotechnology and Nanomedicine*, CRC Press, Boca Raton, FL.

(f) Satalkar, P., Elger, B. S., Shaw, D. (2015). Defining nano, nanotechnology and nanomedicine: Why should it matter? *Science and Engineering Ethics*, September Issue, pages 1–22.

26. Nanotechnology standards. Available at: http://www.nanowerk.com/spotlight/spotid=5736.php (accessed on November 3, 2015).
27. Silva, G. (2006). Neuroscience nanotechnology: Progress, opportunities, challenges. *Nat. Rev. Neurosci.*, **7**(1), 65–74.
28. Khushf, G. (2011). The ethics of nano-neuro convergence. In: *Oxford Handbook of Neuroethics*, Oxford University Press, UK, pages 467–492.
29. Schiøtz, J., Jacobsen, K. W. (2003). A maximum in the strength of nanocrystalline copper. *Science*, **301**(5638), 1357–1359.
30. Ellingson, R. J., Beard, M. C., Johnson, J. C., Yu, P., Micic, O. I., Nozik, A. J., Shabaev, A., Efros, A. L. (2005). Highly efficient multiple exciton generation in colloidal PbSe and PbS quantum dots. *Nano Lett.*, **5**, 865–871.
31. Owen, A., Rannard, S., Bawa, R., Feng, S.-S. (2015). Editorial: Interdisciplinary nanomedicine publications through interdisciplinary peer-review. *J. Interdisciplinary Nanomed.,* **1**(1), 1–5.
32. Bawarski, W. E., Chidlowsky, E., Bharali, D. J., Mousa, S. A. (2008). Emerging nanopharmaceuticals. *Nanomedicine: NBM*, **4**, 273–282.
33. Yang, W., Peters, J. I., Williams, R. O. (2008). Inhaled nanoparticles: A current review. *Int. J. Pharm.*, **356**, 239–247.
34. Conner, J. B., Bawa, R., Nicholas, J. M., Weinstein, V. (2016). Copaxone® in the era of biosimilars and nanosimilars. In: Bawa, R., Audette, G., Rubinstein, I., eds. *Handbook of Clinical Nanomedicine: Nanoparticles, Imaging, Therapy, and Clinical Applications,* Pan Stanford Publishing, Singapore, chapter 28.
35. Hughes, G. A. (2005). Nanostructure-mediated drug delivery. *Nanomedicine: NBM*, **1**, 22–30.
36. Mansour, H. M., Rhee, Y. S., Wu, X. (2009). Nanomedicine in pulmonary delivery. *Int. J. Nanomed.,* **4**, 299–319.
37. Wissing, S., Kayser, O., Muller, R. (2004). Solid lipid nanoparticles for parenteral drug delivery. *Adv. Drug Deliv. Rev.,* **56**(9), 1257–1272.

38. De Campos, A. M., Diebold, Y., Carvalho, E. L. S., Sanchez, A., Jose Alonso, M. (2004). Chitosan nanoparticles as new ocular drug delivery systems: *In vitro* stability, *in vivo* fate, and cellular toxicity. *Pharm. Res.,* **21**(5), 803–810.

39. McCarty, M. (2011). FDA's new nanoscale materials guidance sets bar at 1,000 nm. *Med. Device Daily*, **15**(110), 1–9.

Section II

Nanoparticles, Nanodevices, and Imaging

Chapter 7

Properties of Nanoparticulate Materials

Takuya Tsuzuki, PhD

Research School of Engineering, College of Engineering and Computer Science, Australian National University, Ian Ross Building 31, North Road, Canberra, ACT 0200, Australia

Keywords: nanoparticles, nanocomposites, high surface area, solubility enhancements, particle dispersion, light scattering, luminescence, electrical properties, optical properties, rheology, magnetic properties, plasmonics, physical properties, semiconductors

7.1 Introduction

Nanomaterials are a new class of industrial materials. Owing to their unique properties and the recent developments in synthesis methods, current and potential applications of nanomaterials are rapidly expanding into many industries and markets. For the successful development of nano-enabled commercial products, it is critical to understand the unique properties of nanoparticles and how the desired properties can be manifested in the end products. This chapter gives an overview of the unique properties and characteristics of nanoparticulate materials.

Handbook of Clinical Nanomedicine: Nanoparticles, Imaging, Therapy, and Clinical Applications
Edited by Raj Bawa, Gerald F. Audette, and Israel Rubinstein

ISBN 978-981-4669-20-7 (Hardcover), 978-981-4669-21-4 (eBook)
www.panstanford.com

The word "*nano*" originated from the Greek word *νᾶνος* (nanos), meaning "dwarf". Scientifically, "nano" means one billionth of a unit. One nanometre (nm) is a length scale equivalent to the one billionth of a metre. Thus, "nano"-materials are materials that possess "miniscule" dimensions. Although there is no universally accepted definition for nanomaterials, nanomedicine or nanotechnology, according to ISO TS 27687, nanomaterials are defined as the materials that have a characteristic scale of 1–100 nm. To put this in perspective, the size ratio between a nanoparticle of 1 nm in diameter and a soccer ball is equivalent to the size ratio between a soccer ball and the Earth.

The term nanotechnology is a bit misleading given that it is not a single technology but an umbrella term encompassing several technical/scientific fields and processes and properties at the nano/micro scale [74–76]. Various definitions of nanotechnology have sprung up over the years. Recently, the FDA correctly stretched the upper limit of nanotechnology to 1000 nm, albeit unofficially [76]. Clearly, this highlights the importance of establishing a uniform "nano" terminology for harmonized FDA regulatory governance and patent review [74–76]. Given this backdrop, the following practical definition of nanotechnology has been previously proposed, one that is unconstrained by an arbitrary size limitation [77]:

"The design, characterization, production, and application of structures, devices, and systems by controlled manipulation of size and shape at the nanometer scale (atomic, molecular, and macromolecular scale) that produces structures, devices, and systems with at least one novel/superior characteristic or property."

The association of humans with nanomaterials is not new. In fact, colloid chemistry has been dealing with the synthesis and characterisation of nanoparticles for centuries. Nevertheless, nanomaterial science is regarded as a relatively young research field. In fact, it is only since the 1980s that we have seen the progressive development of the knowledge, techniques and instruments for imaging, measuring, manipulating and fabricating nanoscale objects [69].

For example, in 1981, a new instrument, the scanning tunnelling microscope, was invented. The instrument enabled scientists to see and manipulate individual atoms for the first time in human history. In addition, since 1980, many new discoveries

were made regarding the unique properties of nanomaterials that differ from the properties of their bulk counterparts [11, 12, 21, 64]. Many new types of nanomaterials have also been found. Buckminsterfullerenes, spherical molecules consisting of only 60 carbon atoms (Fig. 7.1a), were discovered in 1985 [29]. Carbon nanotubes (CNTs), another type of nanomaterial consisting only of carbon atoms (Fig. 7.1b) were re-discovered in 1991 [24]. Graphene, yet another carbon-based nanomaterial, comprising a single-atom-thick layer (Fig. 7.1c), was isolated for the first time in 2004 [6]. These new types of carbon-based nanomaterials exhibit unique properties unobtainable from the conventional carbon-based materials. For example, CNTs show tensile strength 300 times higher than steel and can carry an electric current density 1,000 times higher than metals [5].

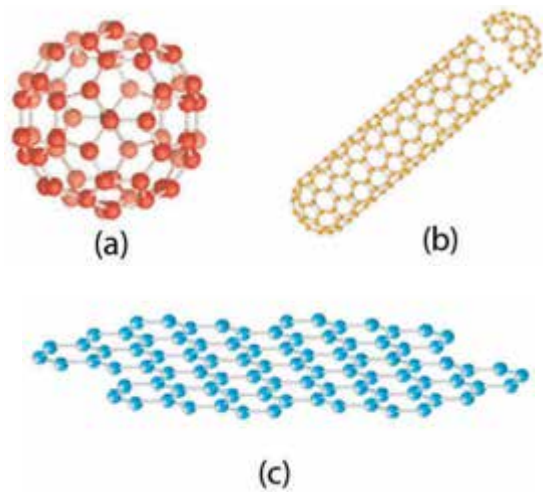

Figure 7.1 Carbon-based new nanomaterials; (a) C60 fullerene, (b) carbon nanotube and (c) graphene. Reproduced from Ref. [26] with permission from Elsevier.

These developments of new instruments and techniques as well as the discoveries of new properties and materials have given rise to a new wave of materials science and technology in nanoscale dimensions. During its development, nanotechnology has promoted the convergence of many fields of science and has ignited an explosion of multidisciplinary research and development

activities in the areas of physics, chemistry, biology, electronics, medical, pharmaceutical, textile, food and so on [56, 57].

The development of nanotechnology has also provided tools to analyse the natural materials around us at a nanoscale dimension. For example, it was found that small-scale hairy structures, such as the ones on lotus leaves, create water-repellent (super-hydrophobic) surfaces [10]. It was also found that bone is a natural nanocomposite consisting of ceramic nanoparticles and protein molecules [70]. The mixture of hard-but-brittle ceramic nano-particles and soft-but-flexible protein gives bones special mechanical properties. Mimicking this structure enables the production of lightweight and high-strength materials, which in turn enables the reduction of energy consumption in vehicles and aircraft.

The development of the knowledge, techniques and instruments for imaging, measuring, manipulating and fabricating nanoscale objects has given us not only an insights into Mother Nature but also the opportunities to improve our life in many ways [22, 38, 49, 51, 55].

7.2 Nanoparticulate Materials

Nanoparticulate materials consist of nanoscale particles [66]. They do not necessarily have to be spherical in shape. Particles with many different shapes including a hollow-shell, rods, belt, needle, wire, tube, disk or plate, can also be regarded as nanoparticulate materials, as long as one of the dimensions, for instance, the thickness of the plates, is less than 100 nm (Fig. 7.2) [68].

Nanoparticulate materials are of significant interest in many fields of science because their sizes are similar to the characteristic length scale of key physical and biological parameters. For example, the electron mean free path in metals is typically <100 nm, exciton-Bohr diameters in semiconductors are 1–100 nm, magnetic domain wall thicknesses are 10–100 nm and the wavelength of ultraviolet light is <350 nm. In biological materials, the diameter of a DNA helix is ~5 nm, the size of a typical virus is 20–300 nm and many other biomolecules fall into the nanoscale range. Because of these similarities in size, many new properties are manifested in nanoscale materials and many new applications in physical, chemical and biological science are

realised. The unique properties of nanoparticles are discussed in detail in the sections that follow:

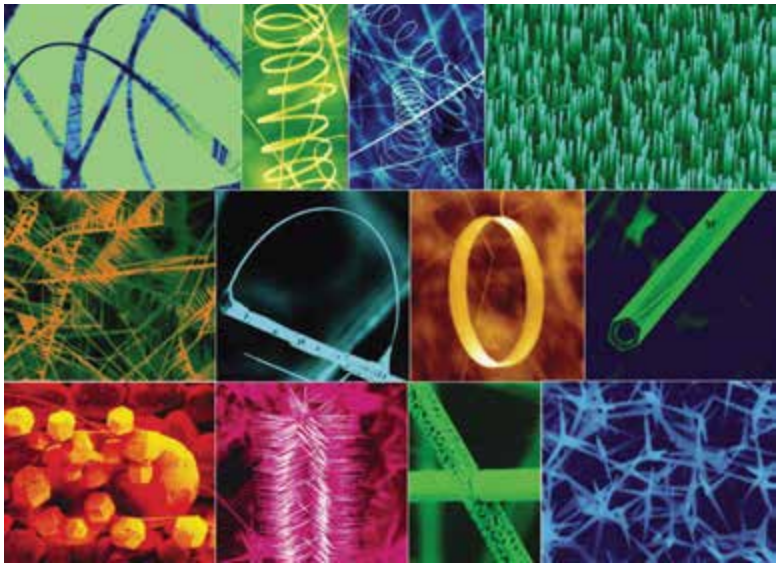

Figure 7.2 A collection of nanostructures of ZnO synthesized under controlled conditions by thermal evaporation of solid powders. Reprinted from Ref. [68] with permission from Elsevier.

7.3 Common Characteristics of All Types of Nanoparticulate Materials

Because of their extremely small size, nanomaterials exhibit new or enhanced properties compared with the same materials of larger dimensions [4]. The unique properties are influenced by the size, shape, crystallinity and other structures of nanoparticles. Since the 1980s, the methods used to control the size and structure of nanoparticles have been considerably improved. As a result, nanoparticles can now be designed to exhibit the desired properties by careful control of their structures. The ability to tailor the unique properties of nanoparticles has caused rapid progress in the commercialisation of nanomaterial-related products. This section discusses the characteristics and unique properties of nanoparticles that are common to all material types including metals, semiconductors and insulators.

7.3.1 High Surface Area

7.3.1.1 Specific surface area

One of the most utilized properties of nanoparticles is their high specific surface area. Specific surface area is defined as the surface area per unit weight as expressed in Eq. 7.1:

$$S = \frac{6000}{d \cdot \rho}, \tag{7.1}$$

where S is the specific surface area in m^2/g, d is the particle diameter in nanometres and ρ is the density of the material in g/cm^3. As the particle size decreases, more atoms become exposed on the particle surface. In other words, the number of atoms on the surface increases relative to the total number of atoms. As such, as the particle size is reduced, the specific surface area increases. For example, when the diameter of gold particles is reduced to 1 nm, 1 g of nanoparticles has a surface area of as large as ~300 m^2. On the other hand, if the gold particles have a diameter of 0.1 mm, 1 g of the powder has only ~0.003 m^2 of surface area (Table 7.1). This means that as much as 100 kg of ~0.1 mm-sized gold particles are required to provide the same surface area as 1 g of ~1 nm-sized gold nanoparticles.

Table 7.1 Surface-to-volume atomic ratio of spherical gold particles (approx. only)

Particle diameter (nm)	Total atom count	Surface atoms (%)	Specific surface area (m^2/g)
1000	~30,000,000,000	~0.2	0.3
100	~30,000,000	~1.6	~3
10	~30,000	~15	~31
1	~30	~90	~310

The high surface area of nanoparticulate materials is useful for many applications that utilize surface-related functionality, including catalytic and photocatalytic activities, gas sensing abilities and solubility.

7.3.1.2 Melting point depression

Nanomaterials melt at lower temperatures than bulk materials. Melting point depression is important in applications that involve high temperatures such as three-way automotive catalysts and ceramic forging.

Melting temperature is associated with the so-called cohesive energy of materials. Cohesive energy is defined as the energy difference between the atoms in the solid and the atoms in a free state. Hence, cohesive energy is related to the thermal energy required to free the atoms from the solid. In general, solids with a higher cohesive energy require a higher temperature to melt.

Chemical bonds between atoms provide positive cohesive energy. Since the atoms on the surface have fewer neighbouring atoms than the atoms inside of the particles, the increase of surface-to-volume atomic ratio in nanoparticles leads to reduced cohesive energy as in Eq. 7.2 [41]:

$$E_{\text{cohesive}} = E_{\text{bulk}}\left(1 - \frac{a}{d}\right), \tag{7.2}$$

where E_{cohesive} is the cohesive energy of a nanoparticle, E_{bulk} is the cohesive energy of bulk, d is the nanoparticle diameter and a is the atomic diameter. Figure 7.3 shows the example of melting point depression in gold nanoparticles [8].

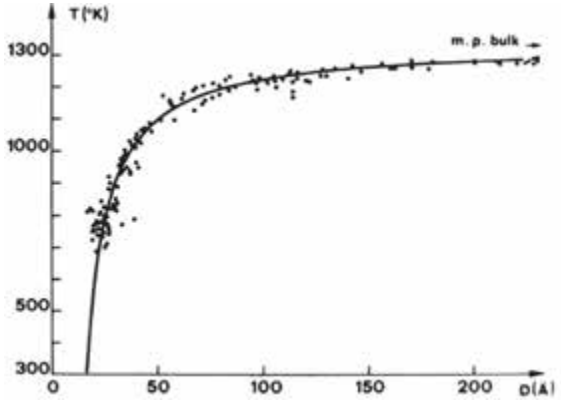

Figure 7.3 Melting point of fold nanoparticles as a function of particle size. Reprinted with permission of the American Physical Society from Ref. [8].

7.3.1.3 Solubility enhancement

At the atomic scale, the dissolution of materials by solvents occurs at the surface of materials. As a consequence, smaller particles with a higher specific surface area have higher solubility. The high solubility of nanoparticulate materials is useful for many applications in the food, pharmaceutical, medical as well as agricultural sectors to enhance bioavailability and nutrient delivery.

When the particles have a wide size distribution, the particles in the solution tend to experience the so-called "Ostwald ripening", where smaller particles dissolve and re-deposit onto larger particles, as a result of their size-dependent solubility. This "ripening" results in a narrower particle size distribution with a larger mean particle size than those of the original particle size distribution.

Semiconductor nanoparticles exhibit photo-induced dissolution effects. When semiconductor nanoparticles are irradiated with the light having a high enough energy, electrons and holes are generated via the photo-excitation of valence band electrons to the conduction bands. The photo-generated electrons and holes facilitate redox reactions and ultimately induce dissolution of nanoparticles that are normally thermodynamically hindered. This light-enhanced dissolution, sometimes called photo-corrosion, is more prominent in smaller nanoparticles due to their high surface areas. It may cause problems in the product integrity of particle-suspension systems or in the environmental safety of accidentally released nanoparticles.

7.3.1.4 Reduced sintering temperature

As the particle size is reduced, metal and ceramic powders start sintering at significantly lower temperatures [61]. Some examples of size-dependent sintering onset-temperatures are listed in Table 7.2 [20, 61]. The possible reasons for the reduced sintering temperature in nanoparticles are (i) enhanced diffusibility of surface atoms and (ii) shorter distances (=particle diameter) for the grain boundaries to move. The reduction of particle size into nanoscale also reduces the time required to form a fully dense sintered body [16].

Table 7.2 Size-dependent sintering onset-temperatures, T

Material	Particle diameter (nm)	Sintering onset-temperature, $T(K)$	T/T_m
TiO_2	13	823	0.40
	40	950	0.46
Fe	30	393	0.21
	2,000	900	0.50

Note: T_m is the melting point of bulk material [20, 61].

A fine grain size and full densification are two most important factors for obtaining reproducible and improved properties of consolidated ceramics. The unique sintering charac-teristics of nanoparticles can be utilized to decrease process cost in the production of ceramics in solid oxide fuel cells, bioceramic implants and dental applications. The reduced sintering temp-erature helps to cast/consolidate the powder without the addition of sintering aids, undesired crystal structure transformation and thermal decomposition.

7.3.1.5 Thermodynamically metastable crystal structures

Surface energy is a product of surface area, A, and free surface energy per unit surface area, γ:

$$\Delta G = \gamma \cdot A, \tag{7.3}$$

where the surface energy, ΔG, is expressed in the form of excess free energy created by the formation of a new surface. In nano-particles, the thermodynamics of crystal structures are altered by the large surface energy derived from the high surface area [35, 42]. The crystal structure is determined so as to minimize the total energy of the system including both bulk and surface energies.

Different crystals have different bulk and surface energies. Even if the chemical compositions are the same, different polymorphs (crystal structures) have different bulk and surface energies. In some cases, a polymorph that is most thermodynamically stable at room temperature under atmospheric pressure has a surface energy higher than that of the other metastable polymorphs.

When particle size is reduced to nanoscale, the high surface area gives rise to high net surface energies and, as a result, structural transitions occur.

For example, rutile, a polymorph of TiO_2, has a surface energy (when anhydrous) of 2.2 J/m^2, whereas anatase, another polymorph of TiO_2, has an anhydrous surface energy of 0.74 J/m^2, much lower than that of rutile [42]. In a bulk form, rutile is thermodynamically more stable than anatase. However, when the size of TiO_2 particles is reduced to nanoscale, the anatase structure becomes more favourable than the rutile structure, in order to reduce the total energy of the system. This transition occurs around 50 nm.

This size effect on the crystal structure is depicted in Fig. 7.4 for ZrO_2 as a function of specific surface area. In the bulk form, the monoclinic crystal structure is the thermodynamically most stable structure of ZrO_2. However, ZrO_2 nanoparticles tend to have a tetragonal or amorphous structure rather than the monoclinic structure. This is because the tetragonal and amorphous structures have surface energies lower than that of the monoclinic structure. The preferential formation of metastable crystal structures in TiO_2 and ZrO_2 was experimentally demonstrated [42].

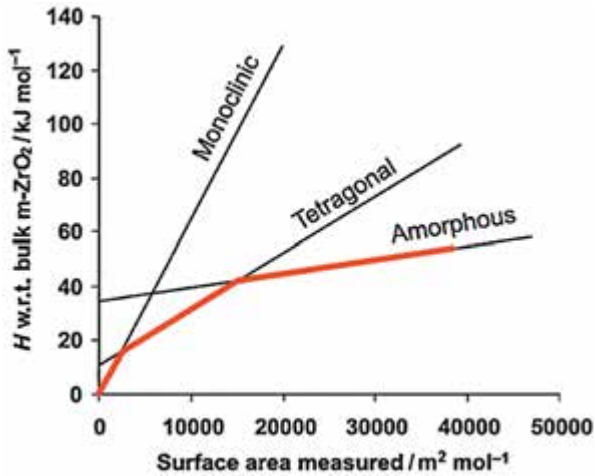

Figure 7.4 Phase stability crossover of nanocrystalline ZrO_2. The thick red line segments indicate the energetically stable phases. Reprinted with permission of John Wiley and Sons, Inc. from Ref. [54].

Table 7.3 lists materials that show preferential formation of metastable phases in nanoscale. Since the surface energy depends on the crystal facets, the critical size to cause phase transition also depends on particle morphology [3]. It is reported that the critical pressure to cause crystal phase transition in nanoparticles is also influenced by particle size in many materials [60].

Table 7.3 Metastable crystal phase formation in nanoparticles

Material	Particle diameter	Observed crystal structure in nanoparticles	Thermodynamically stable structure in a bulk form	Ref.
TiO_2	13 nm	Anatase	Rutile	[30]
ZrO_2	40 nm	Tetragonal	Monoclinic	[50]
Al_2O_3	30 nm	Cubic (γ-)	Hexagonal (α-)	[35]
Y_2O_3	10 nm	Monoclinic	Cubic	[18, 19]
Fe_2O_3	<30 nm	Cubic (γ-)	Hexagonal (α-)	[43]
Cu_2O	<25 nm	Cubic	Monoclinic	[48]
Ce_2S_3	10–80 nm	Cubic	Orthorhombic	[65]
ZnS	2.8 nm		Hexagonal	[53]
$BaTiO_3$	<30 nm	Cubic	Tetragonal	[23]

Note: References listed are examples only.

The size dependence of crystal structures has a significant implication in many applications of nanoparticles. One example is the production of dense ZrO_2 ceramics for dental or biomedical implants. The sintering of ZrO_2 requires temperatures over 1000°C. At such high temperatures, the tetragonal phase is more stable than the monoclinic phase. Hence, sintering of micron-sized ZrO_2 powder leads to crystal phase transformation from monoclinic to tetragonal. This often results in crack formation in the sintered body because of the volume change associated with the crystal phase transition. The use of ZrO_2 nanoparticles with the tetragonal crystal structure will overcome this problem.

Another example is the production of TiO_2 nanoparticles for UV screening applications. Visible transparency is essential to many of UV screening applications. This can be achieved by using nanoparticles as a UV screening agent, owing to their low light-scattering powder. However, the synthesis of nanoscale TiO_2 often

results in the anatase phase that has much higher photoactivity than rutile, resulting in unfavourable side effects in UV screening applications.

It is also reported that the luminescence characteristics of rare earth doped Y_2O_3 nano-phosphors depend on the crystal structures of the Y_2O_3 host and thus can show size dependency [13].

7.3.1.6 Luminescent quenching

Luminescence is the phenomenon in which external energy input causes the emission of light from materials. Nanoparticles with luminescence properties have various uses in electronics and biomedical applications. The major drawback of nanoscale phosphors and luminescent materials is their low quantum efficiency (the ratio between input energy and output emission energy) compared to that of larger particles or bulk crystals. This luminescence quenching is mainly due to the surface defects acting as non-radiative recombination sites for the photo-excited electrons and holes, wherein excited charges are trapped by defects and combined to generate heat instead of light. As the particle sizes are reduced, the specific surface area increases, and hence the number of surface defects increases. Thus, a reduction of particle size normally results in reduced luminescence intensity.

In some cases, surface defects give rise to additional luminescence frequency, especially in semiconductor nanoparticles. In metal oxide nanoparticles, surface defects such as oxygen vacancies and cation (metal ion) vacancies can create additional electron energy levels in the bandgap. When the electrons are transferred from a defect energy level to the lower valence band energy level, the energy difference is emitted as light [1]. As the particle size is reduced to gain larger surface areas, this defect luminescence dominates over the bulk luminescence. The surface defect luminescence has been extensively investigated for ZnO and SiO_2 nanoparticles [15]. Surface defect luminescence is sensitive to the environment surrounding the nanoparticles and chemical species on the surfaces, so that it can be used for the detection of gas or biological molecules. For the applications of luminescent nanoparticles in electronic devices, it is critical to suppress the surface-defect-derived luminescence.

7.3.1.7 Surface treatments

The surface chemistry of nanoparticles is extremely sensitive to the following factors:

- synthesis routes
- crystallinity
- crystal structure
- the crystal facet exposed on the particle surface
- molecules attached on the surface (particle growth limiting agents, dispersants, etc.)

These factors affect the surface-related unique characteristics of nanoparticles including solubility, melting and sintering temperatures, luminescence intensity and crystal structure. This fact implies that even if the mean particle size, size distribution and specific surface area are the same, nanoparticles prepared using different techniques may exhibit very different properties. In this regard, it is difficult to predict the properties of commercial nanoparticle products from the material safety data sheet (MSDS) or even from product specification sheets, as these documents rarely contain sufficient information on the surface chemistry of the products. By the same token, tailoring surface chemistry by applying ligands, impurities and other foreign materials enables the control of the unique surface-related properties of nanoparticles without changing the particle size and shape [15].

7.3.2 Small Light-Scattering Power

Another widely used property of nanoparticles is the high optical transmission of particle suspension systems. The turbidity of particle dispersion systems results from light scattering by the suspended particles. When the diameter of particles becomes smaller than the optical wavelength, the scattering of light by the particles becomes negligible. As a result, the turbidity of the system decreases and transparency increases.

This effect is described by the Rayleigh approximation of Mie scattering theory as expressed in Eq. 7.4 [7]:

$$I_{\text{scat}} = I_0 \frac{8\pi^4 d^6}{r^2 \lambda^4} \left(\frac{m^2 - 1}{m^2 + 2} \right)^2 (1 + \cos^2 \theta), \tag{7.4}$$

where I_0 is the intensity of incident light, I_{scat} is the intensity of scattered light by a particle, d is the particle diameter, λ is the wavelength of incident light, r is the radial distance, θ is the scattering angle and m is the relative refractive index defined as

$$m = \frac{n_{particle}}{n_{media}}, \tag{7.5}$$

where $n_{particle}$ and n_{media} are the refractive index of the particle and its surrounding medium, respectively. This approximation is valid when the particle diameter and the optical wavelength fulfil the following condition:

$$\frac{2\pi d}{\lambda} << 1. \tag{7.6}$$

As can be seen in Eq. 7.4, the light scattering efficiency of a particle decreases proportionally to the 6th power of the particle diameter. As such, a slight decrease in particle size leads to drastic change in the turbidity and in turn the transparency of nanoparticle dispersion systems. For instance, when the particle diameter is halved from 100 nm to 50 nm, the light scattering intensity is reduced to 3% of the original value.

Normally, nanoparticles smaller than 100 nm meet the condition in Eq. 7.6 for the scattering of visible light (λ: 400–750 nm). Hence, when nanoparticles of this size range are well dispersed in a transparent medium, the particle suspension system will appear highly transparent. This effect is useful in many applications of nanoparticles, including phosphorescent panels, UV screening coatings and sunscreens, transparent polymer nanocomposites and diesel fuel additives, where transparency has high commercial value.

7.3.3 Phonon Confinement Effects

Rare earth oxides and oxysulfides make excellent nano-phosphors by the doping with rare earth ions such as Eu^{3+}. The localized electronic states of the doped rare earth ions are influenced by the nanoscale dimension of particles through electron–phonon interactions.

In a small particle, phonons (= sound, the vibration of atoms and molecules) have to form standing waves, or they will be cancelled out by self-interference while moving back and forth within a confine space. The standing waves can have only certain wavelengths or frequencies in a small box. This fact has two important implications:

(i) Since energy is directly related to wavelength, confined phonons can only have certain discrete energy values.

(ii) As the size of the box decreases, the longest wavelength that the standing wave can take, becomes shorter (Fig. 7.5). Hence, the lowest energy associated with the confined phonons increases as the particle size decreases.

To put this in technical terms, phonon confinement in nanoscale particles modifies the phonon density of states from continuous to discrete, resulting in a lack of low-frequency phonon modes [44]. Since low-frequency phonons largely contribute to the non-radiative relaxation between the closely spaced crystal-field energy levels, the phonon-confinement effect gives rise to a significant change in the luminescence dynamics [32]. For example, the fluorescence lifetime of nano-phosphors can be significantly longer than that of bulk materials due to the phonon-confinement effect [31].

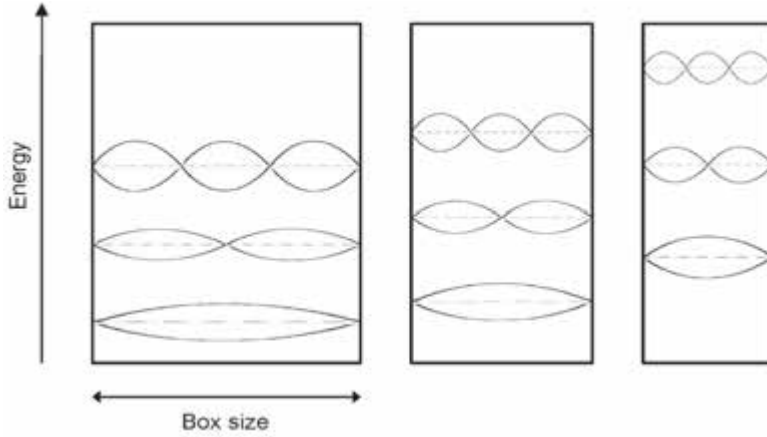

Figure 7.5 Schematic diagram of standing waves in a confined space. It can be noted that the longest allowed wavelength is reduced as the box size decreases.

7.3.4 Nanoparticle Suspension Systems

7.3.4.1 Distance between particles

In many of the applications, nanoparticles are used either in a solid matrix as part of a nanocomposite or in a liquid medium as a nanoparticle dispersion system. When the particle size is reduced to nanoscale, the environment around the nanoparticles in those nanocomposites and nanosuspension systems needs to be considered "nano-scopically".

Of particular importance is the distance between nanoparticles. Assuming that spherical nanoparticles form a uniform spatial distribution in a nanocomposite, the surface-to-surface distance between particles can be given as

$$\frac{D}{d} = \left(\frac{A}{f_V}\right)^{1/3} - 1 \tag{7.7}$$

where D is the mean surface-to-surface distance between spherical particles, d is the particle diameter and f_V is the volume fraction of particles in the media [58]. The A value is the maximum achievable volume fraction of nanoparticles in the system.

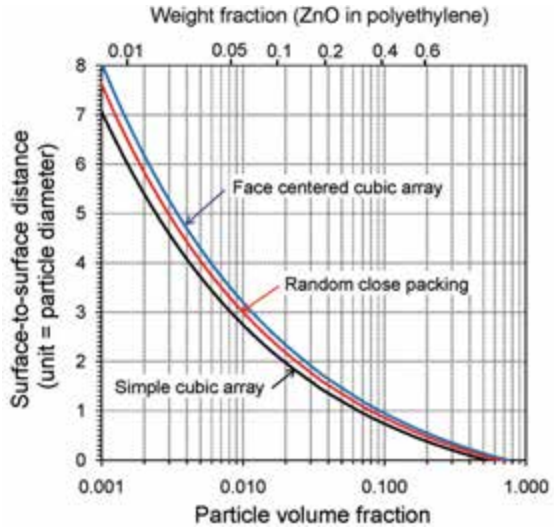

Figure 7.6 Mean gap distance between particles (D/d) as a function of particle volume fraction.

Equation 7.7 is plotted in Fig. 7.6 for three hypothetical particle configurations, namely, random close packing (A = 0.64), face-centred cubic packing (hexagonal close packing, A = 0.74), and simple cubic packing (A = 0.52). Note that the y-axis is the distance between particle surfaces (*n.b.*, not a core-to-core distance), D/d, with the particle diameter as a length unit. It is evident that, as the particle's volume fraction increases, the mean surface-to-surface distance between particles quickly becomes comparable to the particle diameter. Even if the particle concentration is as low as 1 vol% (f_V = 0.01), the mean gap distance is only ~3 times larger than the particle diameter. For micron-sized particles, this gap is still large, in micron scale. However, for nanoparticles such as commercial silver colloids of ~10 nm in diameter, the gap between particles is only ~30 nm at this relatively low particle concentration.

Also presented in Fig. 7.6 as a practical example, is the surface-to-surface particle distance as a function of weight fraction for ZnO nanoparticles dispersed in polyethylene. Some sunscreens or plastic products contain up to 20 wt% (0.2 weight fraction) of ZnO in organic matrices as a UV screening agent. As can be seen in Fig. 7.6, when ZnO nanoparticles of 30 nm in diameter are dispersed in polyethylene at 20 wt% particle concentration, the mean gap distance between particles is only ~45 nm.

This close proximity between nanoparticles in particle suspension systems and nanocomposites can cause serious practical problems in the handling of nanoparticles. Some examples of the implications of short particle-to-particle distances will be discussed below.

7.3.4.2 Particle dispersion

In order to take advantage of the unique properties of nanoparticles, it is critical to assure that particles are well separated from each other. This means that a uniform distribution of the host matrix material between particles is required in nanocomposites and particle-suspension systems. However, when the gap between particles is as small as the nanoparticles themselves, there is a high risk of particle agglomeration. The high surface reactivity and enhanced van der Waals forces of nanoscale particles aggravates the problem. To ensure the high degree of particle dispersion, it

is common to introduce polymeric surfactants or dispersants into the system. However, the concentration and molecular weight of those polymeric additives have to be carefully selected. When the particle concentration is too high, a long-chain surfactant with a high molecular weight may bridge particles and cause particle flocculation. In addition, if the host matrix material is a polymer with a high molecular weight, the uniform distribution of the polymer molecules in the nanoscale gap between particles may be challenging to achieve.

7.3.4.3 Rheology

When manufacturers replace conventional micron-sized powder with nanoparticles, they tend to simply swap the raw powder ingredient in the production line, with no change in the process equipment or process parameters. However, this simple-substitution approach often causes serious problems. Even if the same powder concentration is used, nanoparticles give significantly higher viscosity than micron-sized particles, due to the extremely short surface-to-surface distance between particles and a higher number of particles in the unit volume. By reducing the particle size, a normally "watery" particle suspension becomes a thick gel. Hence, a new production facility or processing equipment may be required for the handling of nanoparticles.

Another consideration in handling nanoparticles is that by increasing the concentration of nanoscale particles, the flow behaviour of a particle suspension system changes from Newtonian to shear-thin and finally to shear-thick. The transition of the flow behaviour occurs at much lower particle concentrations than the conventional large particles.

7.3.4.4 Light scattering

Particle sizing: The dynamic light scattering technique is a common method to measure the size distribution of nanoscale particles. However, at high particle concentration, the technique faces a severe limitation. This technique assumes that the Brownian motion of nanoparticles causes the Doppler shift in the frequency of scattered light. Since the speed of particle diffusion depends on particle size, the detected spectrum of Doppler shift gives the information about the particle size distribution. This measurement

principle works well assuming that the light is scattered by a particle only once (single light scattering). However, when the particle concentration becomes high, multiple light scattering effects become non-negligible, which reduces apparent particle size.

Transparency: When both particle size and the distance between particles become much smaller than the wavelength of light, the nanocomposite or nanoparticle suspension system appears as a uniform material to the probe light. As a result, light scattering by particles becomes negligible. In addition, multiple light scattering effects increase the coherent forward light scattering [63]. As such, high particle concentration results in unexpectedly high optical transmittance. This phenomenon is useful in the applications of nanoparticles for transparent functional nanocomposite films, where a large quantity of nanoparticles is required to gain high functionality while retaining high transparency of the composites. Figure 7.7 shows such an example of a refractive-index-engineered nanocomposites film. In the particle concentration range between f_V = 0.08 and 0.2, the refractive index of the nanocomposites was continuously modified as the particle concentration increased, while optical transmittance was hardly altered, [63].

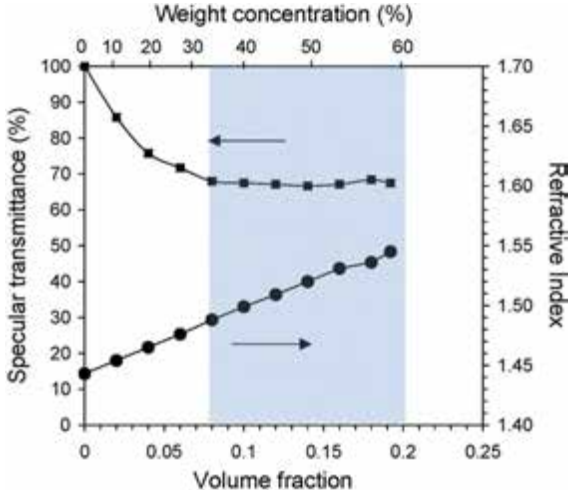

Figure 7.7 Refractive indices and specular transmittance of ZnO/caprylic capric triglyceride hybrid films at 550 nm. Reproduced with permission of Wiley-VCH from Ref. [63].

7.4 Characteristics of Specific Types of Nanoparticulate Materials

In Section 7.3, the characteristics and unique properties of nanoparticles that are common to all material types including metals, semiconductors and insulators were discussed. This section reviews the unique properties of nanoparticles specific to the material types.

7.4.1 Semiconductor Nanoparticles

Quantum size effects that can be observed in semiconductor nanoparticles are one of the most striking properties of nanoparticles. Quantum size effects, sometimes referred to as quantum confinement effects, are commonly described as the effects arising from electrons and holes confined in a small space. In quantum mechanics, electrons and holes are treated as "matter waves". Owing to the requirement for matter waves to form standing waves in a confined space, the electrons and holes can have only discrete energy levels, in the same way as confined phonons (see Section 7.3.3). Like the situation with phonons, the lowest energy that the confined electrons can take (ground state energy level) increases as the particle size decreases. Nanoparticles that exhibit quantum size effects are called quantum dots [28].

In semiconductor materials, the energy gap between the valence band (the highest energy band occupied by electrons) and the conduction band (lowest unoccupied energy band) is relatively small so that electrons in the valence band can be readily excited to the conduction band by heat or UV-light. The energy gap between these two bands is called bandgap energy. Any light having energy larger than the bandgap energy can be absorbed by semiconductors and its energy used for the excitation of electrons. The excited electron leaves a hole in the valence band. Since electrons and holes have opposite electric charges, they are bound together via an electrostatic attractive force and form a pair known as an exciton. When the hole and the electron recombine, a photon (light) is emitted, which results in a phenomenon called luminescence. In bulk semiconductors, the lowest energy

required to create an exciton is roughly the same as the bandgap energy, and the light energy emitted upon the collapse of an exciton is also nearly the same as the bandgap energy.

When the size of semiconductor nanoparticles becomes smaller than the critical size for exciton, called the exciton-Bohr diameter, the exciton shows quantum confinement effects. In such quantum dots, the minimum energy to create excitons is the sum of the bulk bandgap energy and the ground state energy level of a confined exciton (Fig. 7.8). This minimum energy determines the wavelength of light to be absorbed and emitted. The minimum energy can be increased by reducing the size of the quantum dots. In this way, the excitation energy and, in turn, emission energy of light can be controlled by changing the size of nanoparticles. Hence, the colour of emitted light can be tailored using the same semiconductor materials, by changing the particle size of the quantum dots. Figure 7.9 shows the example of CdSe quantum dots [11]. As the size of the CdSe quantum dots increases, the colour of the luminescence changes in a continuous manner from blue through green, yellow, orange, to red. This size-dependent emission can be used in many applications from quantum lasers to biomarkers [9].

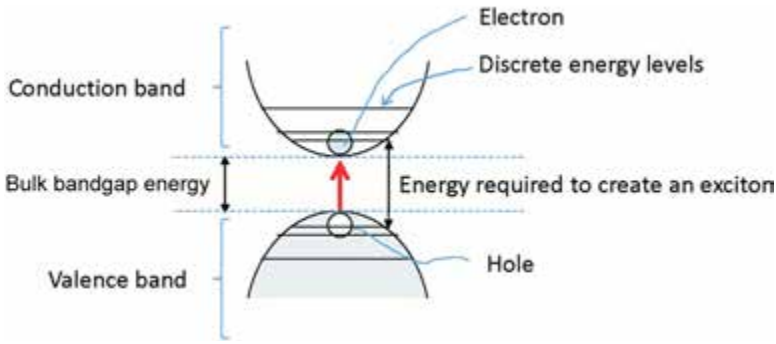

Figure 7.8 Schematic diagram of excitation energy in semiconductor quantum dots.

Different semiconductor materials have different exciton Bohr diameters and bandgap energies. As such, by using different semiconductor materials in different particle sizes, a wide range of luminescence spectra can be obtained [37].

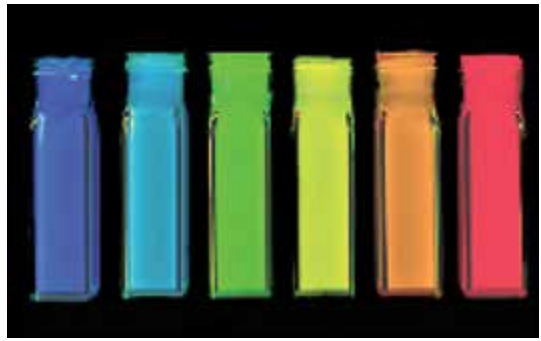

Figure 7.9 Colour photograph demonstrating the wide spectral range of bright fluorescence from different size samples of (CdSe) ZnS ranging from 2.3 to 5.5 nm in diameter. Their photoluminescence peaks occur at (going from left to right) 470, 480, 520, 560, 594 and 620 nm. Reprinted with permission of the American Chemical Society from Ref. [11].

7.4.2 Metal Nanoparticles

Plasmonics in metal nanoparticles is another often-quoted example of the unique properties of nanoparticles [34, 39]. The size reduction of metal particles results in drastic changes in the electronic properties, as the motion of the electrons is restricted in the finite dimension of particles. As a result, metal nanoparticles absorb and scatter light much more strongly than bulk materials. The enhanced optical response of metal nanoparticles is due to the collective oscillation of electrons known as plasmons that are excited on the particle surface by external light. The surface plasmon on nanoparticles has a characteristic resonance frequency. When incoming light has the same frequency as the plasmon resonance frequency, the light is strongly absorbed by metal nanoparticles and then re-emitted in the same frequency.

The frequency of the surface plasmon is influenced by the type of metal, particle size, particle shape, the dielectric environment on the surface and inter-particle spacing [27, 45]. For example, spherical silver and gold nanoparticles appear yellow and red, respectively, very different to their bulk colours. The colour of silver nanoparticles can be further tailored by controlling the particle shape (Fig. 7.10) [59]. The colour of gold nanorods changes with

the aspect ratio (Fig. 7.11) [40]. The colour of gold nano-shells depends on the shell-thickness [47].

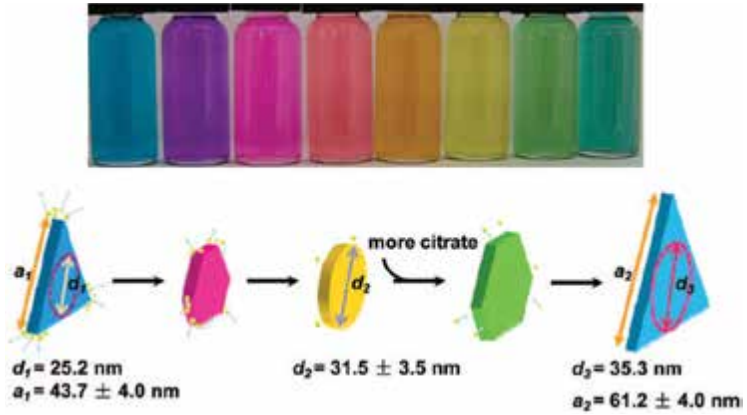

Figure 7.10 Colour of silver nanoparticles with different shapes and sizes. The lower illustration describes the photoconversion of nano-prism to nanodisk and reconstruction of silver nanoprism during the modification of a synthesis parameter. Reprinted with permission of the American Chemical Society from Ref. [59].

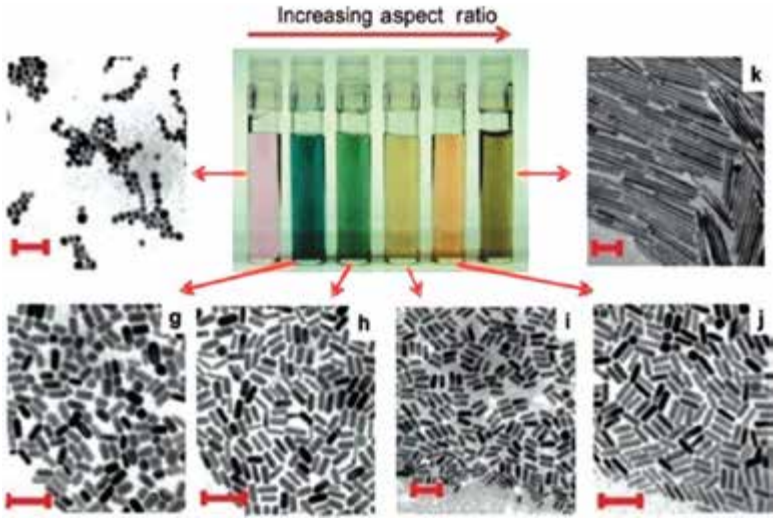

Figure 7.11 Photographs of aqueous solutions of gold nanorods as a function of aspect ratio. Reprinted with permission of the American Chemical Society from Ref. [40].

The strong coupling between light and plasmons in nanoparticles gives rise to new phenomena including optical force enhancement and the light-controlled anisotropic growth of nanoparticles [27]. The surface plasmonics of nanoparticles find many applications in optics, opto-electronics, magneto-optics, chemical and biological sensing and tagging, solar cells, diagnostic medical imaging, carriers of quantum bits and so on [25].

7.4.3 Carbon-Based Nanomaterials

7.4.3.1 Fullerenes

Fullerenes are molecules consisting of carbon atoms with a hollow cage-like structure (Fig. 7.1). Sometimes carbon nanotubes and graphenes are included in fullerene families. In this section, only spherical fullerenes also known as Bucky balls or buckminster-fullerenes are discussed. They are named after Richard Buckminster Fuller, as the atomic arrangement in fullerenes resembles the structure of Fuller's famous geodesic dome.

Table 7.4 Key attributes of spherical fullerenes [36]

Properties/ characteristics	Descriptions and applications
n-Type semiconductors	An active component in *pn*-junctions in organic photovoltaic cells and organic electronic devices such as transistors, light emitting diodes and photo-detectors. C60 inks for solar cell applications are currently on the market.
Anti-oxidant	Estimated to be 100 times more effective than current leading antioxidants such as Vitamin E. Health and personal care applications are considered and skin care product are already commercialised.
Free radical scavenging	Controlling the radical-related neurological damage of diseases as Alzheimer's disease.
Super-conductors	Doped C60 shows superconductivity but only at extremely low temperatures (38K for Cs-doped C60) and hence the commercial application of this property has not been explored.

There are many "magic numbers" of carbon atoms that can form stable hollow cage structures. However, the majority of commercially used spherical fullerenes is C60 (buck minster fullerene), in which a single layer of 60 carbon atoms forms a closed-cage structure in icosahedral-symmetry. The layer contains 20 hexagonal and 12 pentagonal rings and has the same appearance as a soccer ball.

Fullerenes have properties useful to many applications as listed in Table 7.4. Their small size (diameter ~1 nm) is useful for potential medical applications, such as targeted gene or drug delivery and imaging contrast agents [2]. Some commercial products containing C60 have already appeared, especially in the cosmetic, solar cell and polymer composite sectors.

7.4.3.2 Carbon nanotubes

Carbon nanotubes are cylindrical-shaped molecules consisting of only carbon atoms. The structure is made of single or multiple graphene sheets rolled up into a tube form. Carbon nanotubes can have many structures in terms of diameter, the number of wall layers, length and straightness. Single-wall carbon nanotubes (SWCNTs) have a typical diameter of ~1 nm and multi-wall carbon nanotubes (MWCNTs) can be as large as ~50 nm in diameter. A tube length can be 100,000,000 times of the diameter [67].

The electrical characteristics of SWCNTs depend on the chirality, i.e. the way the graphene sheet is rolled [71]. As shown in Fig. 7.12, there are three types of structures. The "armchair" structures have a metallic nature. The "zigzag" structures can be either semi-metallic or semiconducting, depending on the diameter. The tubes with a chiral angle between 0° and 30° are either semi-metals or semiconductors. Metallic SWCNTs have high electrical conductivity similar to copper. In addition, SWCNTs possess excellent mechanical properties, as listed in Table 7.5 along with other unique attributes. For many electronic applications, the selectivity of chirality is critical [72]. MWCNTs share excellent mechanical and thermal properties with SWCNTs. Their electrical properties are more complex than SWCNTs but are reported to be always electrically conductive.

Table 7.5 Key attributes of single-wall carbon nanotubes [73]

Properties/ characteristics	Descriptions and applications
High stiffness	Young's moduli of SWCNTs or MWCNTs are ~5 times higher than steel.
High strength	Tensile strength of CNTs are 10–40 times higher than steel.
High hardness	The bulk modulus of CNTs can be ~500 GPa, comparable or slightly higher than diamond.
High elasticity	~18% elongation to failure.
High electrical conductivity	Room temperature resistivity is similar to or lower than the in-plane resistivity of graphite. The electric current density can be 1,000 times higher than copper.
High thermal conductivity	CNTs have high thermal conductivity, ~10 times higher than copper, along the tube axis, but significantly low thermal conductivity perpendicular to the tube axis.

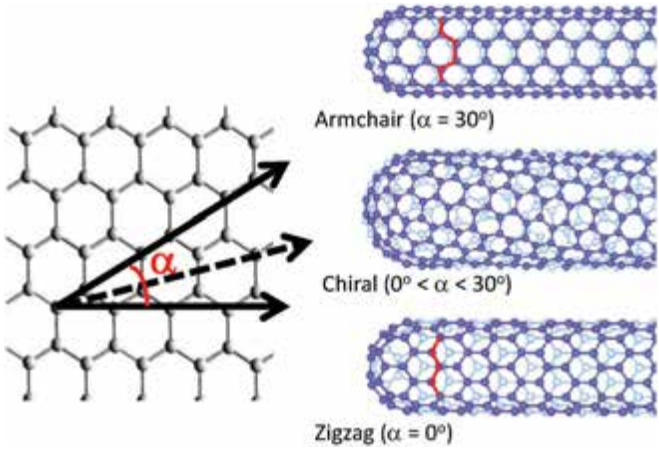

Figure 7.12 Chirality of SWCNTs, with different wrapping angles, α.

Although CNTs are depicted as straight tubes in many illustrations, in reality, CNTs have different degrees of entanglement and bends. As expected, different structures (diameter, wall thickness, chirality, branching, etc.) result in different properties and toxicity [52]. The degree of agglomeration and the impurity levels stemming from the growth catalysts also largely affect these properties. In many applications where CNTs are embedded in

host matrices, surface modification is applied on the tubes, which again alters some of the properties. Owing to the diverse range of unique properties, the applications of CNTs cover many industries, including electronics, automotive, medical, energy and construction.

7.4.3.3 Graphenes

Graphene is a one-atom-thick planar sheet of carbon atoms packed in a honeycomb crystal lattice (Fig. 7.1) [14]. For a long time, it was believed that freestanding graphene was too unstable to exist. However, in 2004, freestanding graphene was successfully prepared in a laboratory [6, 46]. The research on the properties, as well as the synthesis methods, of graphene is still in the early stages. Some properties of graphenes are listed in Table 7.6. Investigations on the applications of graphene in conductive polymer nanocom-posites for electronics, drug delivery systems and organic pollutant absorption materials have been steadily progressing.

Table 7.6 Key attributes of graphene [14]

Properties/characteristics	Descriptions and applications
High electron mobility	The electron mobility is independent of temperature between 10 K and 100 K. The theoretical electrical resistivity is lower than silver, the lowest resistivity material known at room temperature.
High strength	The tensile strength of graphene is 130 GPa, higher than CNTs. The fracture strength is 100 times higher than that of steel.
High thermal conduction	At near room temperature, the measured thermal conductivity of graphene exceeds that of CNTs.

7.4.4 Magnetic Nanomaterials

Magnetic nanoparticles exhibit unusual properties compared to the bulk magnetic materials [17, 33]. The magnetic characteristics of nanoparticles are strongly influenced by finite-size and surface effects.

7.4.4.1 Magnetic materials

Magnetism in materials stems from the spin magnetic moment of electrons. The overall magnetic moment of the material is determined by the distribution of the orientation of spin magnetic moments across the material. Every material has electrons and, hence, can respond to an external magnetic field in one way or another. However, the phrase "magnetic materials" is commonly applied to ferromagnetic, ferrimagnetic and paramagnetic material. Those special materials can be magnetised along the same direction as the external magnetic field (i.e., positive magnetic susceptibility). As a result, they are attracted to external magnetic fields.

Paramagnetic materials have randomly oriented spins. When an external magnetic field is applied, the spins align with the magnetic field to exhibit magnetisation. However, when the external field is removed, the spin orientation becomes random again and paramagnetic materials cease to be "magnets".

On the other hand, ferromagnetic and ferrimagnetic materials can form permanent magnets. In those materials, the spin magnetic moments tend to align spontaneously along easy-magnetisation axes that are dictated by the crystal structure. This parallel alignment of spins occurs in microscopic regions called magnetic domains. Normally many magnetic domains exist in bulk materials. The spins are aligned within each domain, but the spins in separate domains point in different directions. When a ferromagnetic material is magnetized by an external magnetic field, the domains that have the spin direction parallel with the external field, increase their volume at the expense of the volume of other domains (Fig. 7.13). This gives raise to the overall magnetisation in the same direction as the external magnetic field. In ferromagnetic and ferrimagnetic materials, the change in the domain volume requires a certain amount of energy and is somehow restricted. In a technical term, this phenomenon is called domain wall pinning. When the external field is turned off, each domain does not regain the original volume and the overall magnetisation stays in the same direction as the external magnetic field.

The response of overall magnetisation to the external field is often described using a hysteresis curve (Fig. 7.13). The area that is enclosed in the hysteresis loop represents the quantity

of energy that is lost during a cycle in which the domain volume or spin directions in the domains are changed. The lost energy is normally converted to heat. This effect is used for the hyperthermic treatment of cancer cells with nanoscale permanent magnets. In this treatment, magnetic nanoparticles are targeted to cancer cells and an alternating external magnetic field is applied to them. This makes the nano-magnet generate heat in the localised area around the cancer cells, resulting in the death of the cancer cells by overheating. The magnetic field required to cancel the overall magnetisation is called coercivity. The highest magnetisation achievable is called the saturation magnetisation. The higher the coercivity and saturation magnetisations, the more energy loss occurs during the hysteresis cycle.

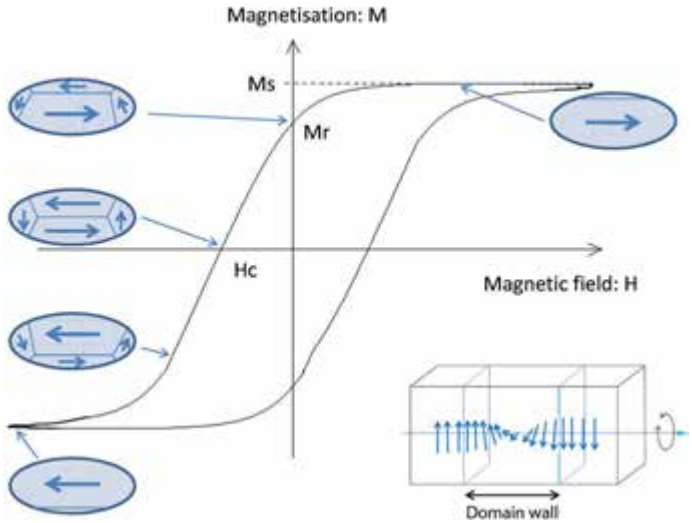

Figure 7.13 Magnetic hysteresis loop of ferromagnetic materials and associated domain structures. Hc: coercivity, Mr: remnant magnetisation, and Ms: saturation magnetisation. The inset shows the spin orientation within a domain wall.

7.4.4.2 Finite size effect: single domain

A domain wall is a region between two magnetic domains. In a domain wall, the direction of spin changes gradually across the wall thickness (Fig. 7.13). Since the spins are forces to have slightly off-aligned direction to each other, certain energy is required

to create domain walls. The thickness of domain walls varies depending on the magnetic materials, but is typically in the range of ~100 nm.

When the size of a magnetic nanoparticle is reduced to the dimension similar to the thickness of domain walls, only one magnetic domain can be formed in the particle, because there is no sufficient room in the particle to create domain walls. The reversal of the magnetisation in a single domain nanoparticle requires higher energy than the multi-domain bulk material, as the reversal needs to rely on the coherent spin-rotation within the domain instead of domain-wall movement. Consequently, as the particle size is reduced to a single domain size, the coercivity of magnetic particles becomes higher (Fig. 7.14). The size range where a ferromagnetic material forms a single domain is normally between 10 and 100 nm.

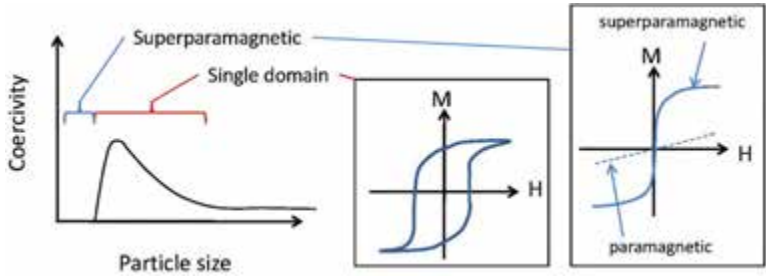

Figure 7.14 Particle size effect on the coercivity of magnetic nanoparticles.

Single domain magnetic nanoparticles offer the possibility of effective targeted cancer treatment through hyperthermia. Because of their small size, magnetic nanoparticles can be administered directly into the blood stream to circulate around the body. Surface treatment with a certain protein enables targeted accumulation of the magnetic nanoparticles only in pathological areas or organs. The single domain nature of the magnetic nanoparticles ensures that effective heat generation can be induced by the alternating external magnetic field, only in the targeted region, which, in turn, resulting in the death of tumour cells by localised heat. Other important applications include high-density magnetic recording media.

7.4.4.3 Finite size effect: superparamagnetism

When the size of magnetic nanoparticles is reduced further from the single domain size, thermal energy exceeds the energy required to align spins. As a result, the direction of magnetisation in the nanoparticles fluctuates between two orientations anti-parallel to each other along an easy-magnetisation axis. This causes the magnetic nanoparticles to behave like a paramagnetic material and their coercivity becomes zero (Fig. 7.14). However, their magnetic susceptibility is significantly higher than that of the conventional paramagnetic materials. This means that superparamagnetic materials respond to an external magnetic field much more strongly than normal paramagnetic materials.

Superparamagnetic materials have a combination of strong responsivity to magnetic fields and the ability to become non-magnetic in the absence of an external magnetic field. This unique characteristic offers many applications including ferro-fluid, magnetic separators, magnetic resonance imaging contrast agents and other biomedical applications.

7.4.4.4 Surface effect

When the size of magnetic nanoparticles is further reduced, saturation magnetisation decreases. This effect is caused by the fact that the surface of magnetic materials often has a random spin orientation (spin glass) that does not contribute to magnetisation. When the particle size is reduced, the relative volume of the spin glass layer on the surface increases compared to the total volume of the particle. Hence, the saturation magnetisation varies with particle size, according to Eq. 7.8 [62]:

$$\frac{M_S}{M_{S0}} = \frac{(d - 2t)^3}{d^3}, \tag{7.8}$$

where d is the particle diameter, t is the thickness of the surface layer, M_S is the particle's saturation magnetisation and M_{S0} is the bulk saturation magnetisation. The thickness of the spin glass is nearly independent (~1 nm) of the particle diameter. Figure 7.15 shows the effect of particle size on the saturation magnetisation

of $MnFe_2O_4$ and γ-Fe_2O_3 nanoparticles. This effect determines the lower size limit of superparamagnetic nanoparticles usable in many applications.

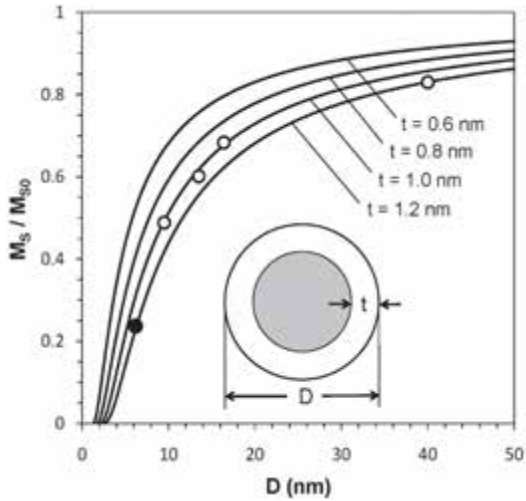

Figure 7.15 Solid curves: particle-size (D) dependence of normalised saturation magnetisation (M_S/M_{S0}) for various values of shell thickness (t), calculated on the basis of Eq. (7.8); M_{S0} denotes the saturation magnetisation for bulk material. Filled circle: data point for γ-Fe_2O_3 nanoparticles. Open circles: data points for $MnFe_2O_4$ nanoparticles. Inset: schematic picture of a particle, consisting of a ferrimagnetic core (shaded region) and a spin-glass shell. Reprinted from Ref. [62] with permission from Elsevier.

7.5 Summary

Nanoparticulate materials exhibit unique properties that are unobtainable from their bulk counterparts. For example, they have very high specific surface areas that give rise to enhanced reactivity and solubility, reduced melting and sintering temperatures, as well as altered crystal structures. Their small physical size induces quantum confinement effects in phonons and electrons to create many new optical and electronic properties. Magnetic nanoparticles exhibit unusual properties resulting from their high surface areas and small diameters. An understanding of these unique properties of nanomaterials is not only critical to

the successful development of nano-enabled commercial products but also essential to the standardisation, regulation and safety assessment of nanomaterials.

Disclosures and Conflict of Interest

The opinions and perspectives here reflect the current views of the author. The author declares that he has no conflict of interest and has no affiliations or financial involvement with any organization or entity discussed in this chapter. No writing assistance was utilized in the production of this manuscript and the author has received no payment for its preparation. This chapter is a revised version of the chapter that originally appeared in *Nanotechnology Commercialization* (2013), T. Tsuzuki (Editor), Chapter 1, Pan Stanford Publishing, Singapore.

Corresponding Author

Dr. Takuya Tsuzuki
Research School of Engineering
College of Engineering and Computer Science
Australian National University, Ian Ross Building 31, North Road
Canberra, ACT 0200, Australia
Email: takuya.tsuzuki@anu.edu.au

About the Author

Takuya Tsuzuki is an associate professor in the Australian National University College of Engineering and Computer Science. He received a PhD in condensed matter physics from Kyoto University, Japan and a graduate certificate in technology management from La Trobe University. He was chief technology officer of one of the first nanotechnology companies in Australia, where he contributed to the successful commercialization of the university patents he co-developed. Dr. Tsuzuki played a key role in the large-scale production and product development of commercial nanoenabled products. The commercialization effort was internationally recognized

as Frost & Sullivan's 2005 Excellence in Technology of the Year Award. He was nominated as a Certified Materials Professional by the Institute of Materials Engineering Australasia, Ltd. and served as Chair of Materials Australia Nanotechnology Special Interest Group at Materials Australia. He serves as a member of Standards Australia Committees and Joint Standards Australia/Standards New Zealand Committees for ISO TC 229 (Nanotechnologies) standards. He is also a participant in the Roundtable Discussions on National Enabling Technologies Strategy consultation by the Australian Government's Department of Industry, Innovation, Science, Research and Tertiary Education.

References

1. Allan, G., Delerue, C., Lannoo, M. (2006). Nature of luminescent surface starts of semiconductor nanocrystallites, *Phys. Rev. Lett.*, **76**, 2961–2964.
2. Bakry, R., Vallant, R. M., Najam-ul-Haq, M., Rainer, M., Szabo, Z., Huck, C. W., Bonn, G. K. (2007). Medical applications of fullerenes, *Int. J. Nanomed.*, **2**, 639–649.
3. Barnard, A. S., Zapol, P. (2004). A model for the phase stability of arbitrary nanoparticles as a function of size and shape, *J. Chem. Phys.*, **121**, 1775770.
4. Batsanov, S. S. (2011). Size effect in the structure and properties of condensed matter, *J. Struct. Chem.*, **52**, 602–615.
5. Bellucci, S. (2005). Carbon nanotubes: physics and applications, *Phys. Status Solidi (c)*, **2**, 34–47.
6. Berger, C., Song, Z., Li, T., Li, X., Ogbazghi, A. Y., Feng, R., Dai, Z., Marchenkov, A. N., Conrad, E. H., First, P. N., de Heer, W. A. (2004). Ultrathin epitaxial graphene: 2D electron gas properties and a route toward graphene-based nanoelectronics, *J. Phys. Chem. B*, **108**, 19912–19916.
7. Bohren, C. F., Huffman, D. R. (1998). *Absorption and Scattering of Light by Small Particles* (Wiley-VCH, Weinheim).
8. Buffat, P., Borel, J. P. (1976). Size effect on the melting temperature of gold particles, *Phys. Rev. A*, **13**, 2287–2298.
9. Chan, W. C. W., Maxwell, D. J., Gao, X., Bailey, R. E., Han, M., Nie, S. (2002). Luminescent quantum dots for multiplexed biological detection and imaging. *Curr. Opin. Biotechnol.*, **13**, 40–46.

10. Cheng, Y. T., Rodak, D. E., Wong, C. A., Hayden, C. A. (2006). Effects of micro- and nano-structures on the self-cleaning behaviour of lotus leaves, *Nanotechnology*, **17**, 1359–1362.
11. Dabbousi, B. O., Rodriguez-Viejo, J., Mikulec, F. V., Heine, J. R., Mattoussi, H., Ober, R., Jensen, K. F., Bawendi, M. G. (1997). (CdSe) ZnS core–shell quantum dots: synthesis and characterization of a size series of highly luminescent nanocrystallites, *J. Phys. Chem. B*, **101**, 9463–9475.
12. Daniel, M. C., Astruc, D. (2004). Gold nanoparticles: assembly, supramolecular chemistry, quantum-size-related properties, and applications toward biology, catalysis, and nanotechnology, *Chem. Rev.*, **104**, 293–346.
13. Dosev, D., Guo, B., Kennedy, I. M. (2006). Photoluminescence of Eu^{3+}:Y_2O_3 as an indication of crystal structure and particle size in nanoparticles synthesized by flame spray pyrolysis, *Aerosol. Sci.*, **37**, 402–421.
14. Geim, A. K., Novoselov, K. S. (2007). The rise of graphene, *Nat. Mater.*, **6**, 183–191.
15. Gong, Y., Andelman, T., Neumark, G. F., O'Brien, S., Kuskovsky, I. L. (2002). Origin of defect-related green emission from ZnO nano- particles: effect of surface modification, *Nanoscale Res. Lett.*, **2**, 297–302.
16. Groza, J. R. (2007). Nanocrystalline powder consolidation methods. In: Koch, C. C. ed. *Nanostructured Materials, Processing, Properties and Applications*, William Andrew Publishing, Norwich, New York, 2nd ed., Chapter 5, pp. 173–234.
17. Gubin, S. P. (2009). *Magnetic Nanoparticles* (Wiley-VCH, Weinheim).
18. Guo, B., Harvey, A. S., Neil, J., Kennedy, I. M., Navrotsky, A., Risbud, S. H. (2007). Atmospheric pressure synthesis of heavy rare earth sesquioxides nanoparticles of the uncommon monoclinic phase, *J. Am. Ceram. Soc.*, **90**, 3683–3686.
19. Guo, B., Harvey, A., Risbud, S. H., Kennedy, I. M. (2006). The formation of cubic and monoclinic Y_2O_3 nanoparticles in a gas-phase flame process, *Philos. Mag. Lett.*, **86**, 457–467.
20. Hahn, H., Logas, J., Averhack, R. S. (1990). Sintering characteristics of nanocrystalline TiO_2, *J. Mater. Res.*, **5**, 609–614.
21. Hayashi, T., Tanaka, K., Haruta M. (1987). Selective vapour phase epoxidation of propylene over Au/TiO_2 catalysts in the presence of oxygen and hydrogen, *J. Catal.*, **178**, 566–575.
22. Holister, P., Weener, J. W., Román-Vas, C., Harper, T. (2003). *Nanoparticles: Technology White Paper Nr 3* (Cientifica, UK).

23. Hoshina, T., Kakemoto, H., Tsurumi, T., Wada, S., Yashima, M. (2006). Size and temperature induced phase transition behaviors of barium titanate nanoparticles, *J. Appl. Phys.*, **99**, article number 054311.

24. Iijima, S. (1991). Helical microtubules of graphitic carbon, *Nature*, **354,** 56–58.

25. Jain, P. K., Lee, K. S., El-Sayed, I. H., El-Sayed, M. A. (2006). Calculated absorption and scattering properties of gold nanoparticles of different size, shape, and composition: applications in biological imaging and biomedicine. *J. Phys. Chem. B*, **110**, 7238–7248.

26. Katsnelson, M. I. (2007). Graphene: carbon in two dimensions, *Mater. Today*, **10**, 20–27.

27. Kelly, K. L., Coronado, E., Zhao, L. L., Schatz, G. C. (2002). The optical properties of metal nanoparticles: the influence of size, shape, and dielectric environment, *J. Phys. Chem. B*, **107**, 668–677.

28. Klimov, V. I. (2010). *Nanocrystal Quantum Dots*, 2nd ed. (CRC Press, Boca Raton, USA).

29. Kroto, H. W., Heath, J. R., O'Brien, S. C., Curl, R. F., Smalley, R. E. (1985). C60: Buckminsterfullerene, *Nature*, **318,** 162–163.

30. Levchenko, A. A., Li, G., Boerio-Goates, J., Woodfield, B. F., Navrotsky, A. (2006). TiO_2 stability landscape: polymorphism, surface energy, and bound water energetic, *Chem. Mater.*, **18**, 6324–6332.

31. Liu, L., Ma, E., Li, R., Liu, G., Chen, X. (2007). Effects of phonon confinement on the luminescence dynamics of Eu_{3+} doped Gd_2O_3 nanotubes, *Nanotechnology*, **18**, article number 015403.

32. Liu, G. K., Chen, X. Y., Zhuang, H. Z., Li S., Niedbala, R. S. (2003). Confinement of electron–phonon interaction on luminescence dynamics in nanophosphors of Er^{3+}: Y_2O_2S, *J. Solid State Chem.*, **171**, 123–132.

33. Lu, A. H., Salabas, E. L., Schüth, F. (2007). Magnetic nanoparticles: synthesis, protection, functionalization and applications, *Angew. Chem. Int. Ed.*, **46**, 1222–1244.

34. Lu, X., Rycenga, M., Skrabalak, S. E., Wiley, B., Xia, Y. (2009). Chemical synthesis of novel plasmonic nanoparticles, *Ann. Rev. Phys. Chem.*, **60**, 167–192.

35. McHale, J. M., Auroux, A., Perrotta, A. J., Navrotsky, A. (1997). Surface energies and thermodynamic phase stability in nanocrystalline aluminas, *Science*, **277**, 788–791.

36. Mélinon, P., Masenelli, B. (2011). *From Small Fullerenes to Superlattices—Science and Applications* (Pan Stanford, Singapore).

37. Michalet, X., Pinaud, F. F., Bentolila, L. A., Tsay, J. M., Doose, S., Li, J. J., Sundaresan, G., Wu, A. M., Gambhir, S. S., Weiss, S. (2005). Quantum dots for live cells, *in vivo* imaging and diagnostics, *Science*, **307**, 538–544.

38. Mirkin, C. A. (2005). The beginning of a small revolution, *Small*, **1**, 14–16.

39. Mody, V. V., Siwale, R., Singh, A., Mody, H. R. (2010). Introduction to metallic nanoparticles, *J. Pharm. Bioall. Sci.*, **2**, 282–289.

40. Murphy, C. J., Gole, A. M., Stone, J. W., Sisco, P. N., Alkilany, A. M., Goldsmith, E. C., Baxter, S. C. (2008). Gold nanoparticles in biology: beyond toxicity to cellular imaging, *Acc. Chem. Res.*, **41**, 1721–1730.

41. Nanda, K. K., Sahu S. N., Behera, S. N. (2002). Liquid-drop model for the size-dependent melting of low-dimensional systems, *Phys. Rev. A*, **66,** article number 013208.

42. Navrotsky, A. (2011). Nanoscale effects on thermodynamics and phase equilibria in oxide systems, *Chem. Phs. Chem.*, **12**, 2207–2215.

43. Navrotsky, A., Mazeina, L., Majzlan, J. (2008). Size-driven structural and thermodynamic complexity in iron oxides, *Science*, **319**, 1635–1638.

44. Nirmal, M., Brus, L. (1998). Luminescence photophysics in semiconductor nanocrystals, *Acc. Chem. Res.*, **32**, 407–414.

45. Noguez, C. (2007). Surface plasmons on metal nanoparticles: the influence of shape and physical environment, *J. Phys. Chem. C*, **111**, 3806–3819.

46. Novoselov, K. S., Geim, A. K., Morozov, S. V., Jiang, D., Zhang, Y., Dubonos, S. V., Grigorieva, I. V., Firsov, A. A. (2004). Electric field effect in atomically thin carbon films. *Science*, **306,** 666–669.

47. Oldenburg, S. J., Averitt, R. D., Westcott, S. L., Halas, N. J. (1998). Nanoengineering of optical resonances, *Chem. Phys. Lett.*, **288**, 243–247.

48. Palkar, V. R., Ayyub, P., Chattopadhyay, S., Multani, M. (1996). Size-induced structural transitions in the Cu-O and Ce-O systems, *Phys. Rev. B*, **53**, 2167–2170.

49. Pérez, J., Bax, L., Escolano, C. (2005). *Roadmap Report on Nanoparticles* (Willems & van den Wildenberg).

50. Pitcher, M. W., Ushakov, S. V., Navrotsky, A., Woodfield, B. F., Li, G., Boerio-Goates, J., and Tissue, B. M. (2005). Energy crossovers in nanocrystalline zirconia, *J. Am. Ceram. Soc.*, **88**, 160–167.

51. Pitkethly, M. J. (2004). Nanomaterials—the driving force, *Mater. Today*, **7,** Suppl. 1, 20–29.

52. Poland, C. A., Duffin, R., Kinloch, I., Maynard, A., Wallace, W. A. H., Seaton, A., Stone, V., Brown, S., MacNee, W., Donaldson, K. (2008).

Carbon nanotubes introduced into the abdominal cavity of mice show asbestos-like pathogenicity in a pilot study, *Nat. Nanotechnol.*, **3**, 423–428.

53. Qadri, S. B., Skelton, E. F., Dinsmore, A. D., Hu, J. Z., Kim, W. J., Nelson, C., Ratna, B. R. (2001). The effect of particle size on the structural transition in zinc sulfide, *J. Appl. Phys.*, **89**, 1328066.
54. Ranade, M. R., Navrotsky, A., Zhang, H. Z., Banfield, J. F., Elder, S. H., Zaban, A., Borse, P. H., Kulkarni, S. K., Doran, G. S., Whitfield, H. J. (2002). Energetics of nanocrystalline TiO_2, *Proc. Natl. Acad. Sci.*, **99**, 6476–6481.
55. Roco, M. C. (1999). Nanoparticles and nanotechnology research, *J. Nanopart. Res.*, **1**, 1–6.
56. Rotello, V. M. (2004). *Nanoparticles: Building Block for Nanotechnology* (Springer, New York).
57. Schmid, G. (2004). *Nanoparticles: From Theory to Application* (Wiley-VCH Verlag, Weinheim).
58. Wolfgang M., Sigmund, W. M., Bell, N. S., Bergström, L. (2000). Novel powder-processing methods for advanced ceramics, *J. Am. Ceram. Soc.*, **83**, 1557–1574.
59. Tang, B., Xu, S., An, J., Zhao, B., Xu, W. (2009). Photoinduced shape conversion and reconstruction of silver nanoprisms, *J. Phys. Chem. C*, **113**, 7025–7030.
60. Tolbert, S. H., Alivisatos, A. P. (1994). Size dependence of a first order solid-solid phase transition: wurtzite to rock salt transformation in CdSe nanocrystals. *Science*, **265**, 373–376.
61. Trusov, L. I., Lapovok, V. N., Novikov, V. I. (1989). *Science of Sintering*, eds. Uskokovic, D. P., Plamour III, H., Spriggs, R. M., "Problems of sintering in ultrafine powders" (Plenum Press, New York). 185–192.
62. Tsuzuki, T., Schäffel, F., Muroi, M., McCormick, P. G. (2011). Magnetic properties of mechanochemically synthesised γ-Fe_2O_3 nanoparticles, *J. Alloy. Compd.*, **509**, 5420–5425.
63. Tsuzuki, T. (2008). Abnormal transmittance of refractive-index modified ZnO-organic hybrid films, *Macromol. Mater. Eng.*, **293**, 109–113.
64. Tsuzuki**,** T., Robinson, J. S., McCormick, P. G. (2002). UV-shielding ceramic nanoparticles synthesised by mechanochemical processing, *J. Aus. Ceram. Soc.*, **38**, 15–19.
65. Tsuzuki, T., McCormick, P. G. (1999). Synthesis of ultrafine Ce_2S_3 powder by mechanochemical processing, *Mater. Sci. Forum*, **315–317**, 586–591.

66. Yokoyama, T., Naito, M., Nogi, K., Hosokawa M. (2007). *Nanoparticle Technology Handbook* (Elsevier, UK).

67. Wang, X., Li, Q., Xie, J., Jin, Z., Wang, J., Li, Y., Jiang, K., Fan, S. (2009). Fabrication of ultralong and electrically uniform single-walled carbon nanotubes on clean substrates, *Nano Lett.*, **9**, 3137–3141.

68. Wang, Z. L. (2004). Nanostructures of zinc oxide, *Mater*. *Today*, **7**, 26–33.

69. Shong, C.W., Haur, S. C., and Wee, A. T. S. (2015). Science at the nanoscale: introduction and historical perspective. In: Bawa, R., Audette, G., and Rubinstein, I. eds. *Handbook of Clinical Nanomedicine: Nanoparticles, Imaging, Therapy, and Clinical Applications*, Pan Stanford Publishing, Singapore.

70. Weiner, S., Wagner, H. D. (1998). The material bone: structure–mechanical function relations, *Ann*. *Rev*. *Mater*. *Sci*., **28**, 271–298.

71. Weisman, R. B. (2004). Simplifying carbon nanotube identification, *Ind*. *Phys*., February/March 2004, 24–27.

72. Wilder, J. W. G., Venema, L. C., Rinzler, A. G., Smalley, R. E., Dekker, C. (1998). Electronic structure of atomically resolved carbon nanotubes, *Nature*, **391,** 59–62.

73. Zhang, Q. (2011). *Carbon Nanotubes and Their Applications* (Pan Stanford Publishing, Singapore).

74. Bawa, R. (2013). FDA and nanotech: Baby steps lead to regulatory uncertainty. In: D. Bagchi, et al., eds. *Bionanotechnology: A Revolution in Biomedical Sciences and Human Health*. Wiley Blackwell, UK, pp. 720–732.

75. Tinkle, S., McNeil, S. E., Mühlebach, S., Bawa, R., Borchard, G., Barenholz, Y., Tamarkin, L., Desai, N. (2014). Nanomedicines: addressing the scientific and regulatory gap. *Ann*. *N*. *Y*. *Acad*. *Sci*.,**1313,** 35–56.

76. Conner, J. B., Bawa, R., Nicholas, J. M., Weinstein, V.. (2015). Copaxone® in the era of biosimilars and nanosimilars. In: Bawa, R., Audette, G., and Rubinstein, I., eds. *Handbook of Clinical Nanomedicine: Nanoparticles, Imaging, Therapy, and Clinical Applications*, Pan Stanford Publishing, Singapore.

77. Bawa, R. (2007). Special report—patents and nanomedicine. *Nanomedicine*, **2**(3), 351–374.

Chapter 8

Solid Drug Nanoparticles: Methods for Production and Pharmacokinetic Benefits

Andrew Owen, PhD,[a] and Steve P. Rannard, DPhil[b]

[a]*Department of Molecular and Clinical Pharmacology, University of Liverpool, United Kingdom*
[b]*Department of Chemistry, University of Liverpool, United Kingdom*

Keywords: nanomedicine, nanomilling, intestinal absorption, emulsion-templated freeze-drying, spray drying, depot, solid drug nanoparticles, homogenization, pharmacokinetics, oral dose, long acting formulations

8.1 Introduction

The formation of nanoparticles for drug delivery applications has been approached using several strategies. These are divided into two general approaches, namely, forming a nanocarrier for the drug [1, 2] or making a nanoparticle directly from the active pharmaceutical ingredient (API). Solid drug nanoparticles (SDNs) [3] are predominantly used for oral dosed therapies containing poorly soluble compounds and, recently, the production of long acting (LA) injected depot formulations. The issue of poor water-

Handbook of Clinical Nanomedicine: Nanoparticles, Imaging, Therapy, and Clinical Applications
Edited by Raj Bawa, Gerald F. Audette, and Israel Rubinstein

ISBN 978-981-4669-20-7 (Hardcover), 978-981-4669-21-4 (eBook)
www.panstanford.com

solubility of current and future APIs is considerable within the pharmaceutical industry and estimates vary from 40–90% of potential new API candidates having poor or limited solubility. This has the impact of reducing the success rate within the development pipeline and also impeding the effectiveness of many medicines in current clinical use. The impact of solubility on drug delivery is often interpreted using the biopharmaceutical classification system (BCS) and nanocarrier and SDN strategies are being discussed to overcome such solubility issues [4, 5]. Poor water-solubility may also lead to difficulties in formulating compounds into viable dosage forms (for example tablets, capsules, syrups, gels or depots) and SDNs have been used to overcome manufacturing problems, allowing products to reach patients. The purpose of this chapter is to provide an overview of current methodologies for manufacture of SDNs and to use specific examples that highlight the pharmacokinetic benefits that they confer.

8.2 Physical Properties of Solid Drug Nanoparticles

SDNs, frequently referred to as nanosuspensions or nano-dispersions, typically consist of drug particles with an average diameter of less than 1 μm (1000 nm) that are suspended within a liquid and stabilized by soluble polymers and surfactants. A poorly water-soluble API that is within this size range will have a considerably increased surface area when compared to the same mass of API with particles in the multi-micron size range. As a comparison, a single 1 mm (1000 μm) cube of poor water-soluble API will have a surface area of 6×10^6 μm^2 ($6 \times 1000 \times 1000$ μm). If this cube of API is broken into identical 10 μm (10,000 nm) cubes, each new API particle would only have a surface area of 600 μm^2. However, 1×10^6 particles of this size would have been generated from the larger particle that collectively would present a surface area of 600×10^6 μm^2. A reduction in particle size from 10 μm to 200 nm (0.2 μm) would create 125×10^9 cubic API nanoparticles, each with a surface area of just 0.24 μm^2, but a collective surface area of 30×10^9 μm^2; a 5000-fold increase in surface area over the single 1 mm API particle (Fig. 8.1). The

consideration of particle surface area is important due to the Noyes–Whitney (Eq. 8.1) and Kelvin (Eq. 8.2) equations [6].

$$\frac{dC}{dt} = \left[\frac{DA}{hV}\right]\left[C_s - C\right] \tag{8.1}$$

$$\ln\frac{S_{app}}{S_0} = \frac{2\gamma V_m}{rRT} \tag{8.2}$$

The Noyes–Whitney equation relates the dissolution rate (dC/dt) directly to the surface area of the material that is dissolving (A) and a significant increase in surface area, as demonstrated above, will have a considerable increase in the observed dissolution rate. The Kelvin equation demonstrates an unexpected effect of decreasing size into the nanoscale regime; the ratio of the apparent solubility (S_{app}) and equilibrium solubility (S_0) is inversely proportional to the particle radius (r), again leading to an improvement in the apparent solubility of a compound with decreasing particle size.

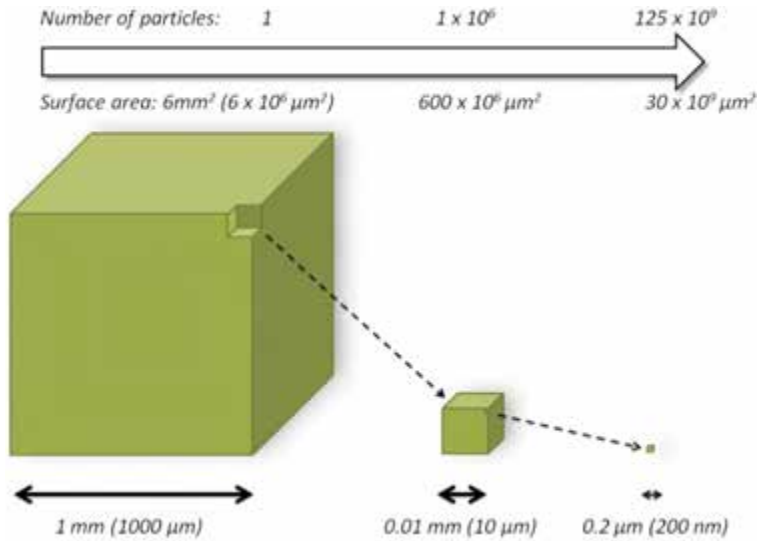

Figure 8.1 Comparison of size, number of particles formed and available surface area when taking a single cubic structure of 1 mm^3 and reduce its dimensions systematically to 10 μm^3 and then 200 nm^3.

Solubility is a thermodynamically controlled property and it is important to understand that the actual solubility of a compound is determined by a range of different parameters including temperature, pH and ionic strength. As such, the actual solubility of a compound under fixed conditions has a fixed value. However, the rate at which a material attains an equilibrium concentration can be affected, and particle size is a crucial parameter that offers opportunities within the pharmaceutical industry.

8.3 Approaches for Solid Drug Nanoparticle Manufacture

SDNs are produced using a range of different approaches that can be generally classified as either attrition or liquid manipulation methods (Fig. 8.2). It is also common to characterize these approaches as either "top-down" or "bottom-up" strategies, respectively.

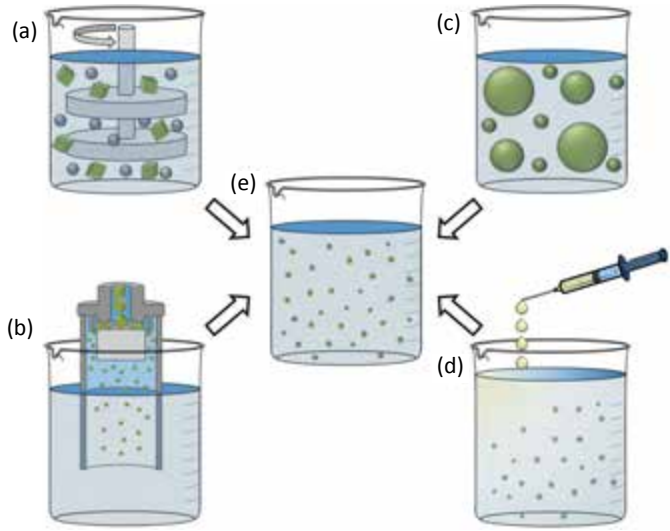

Figure 8.2 Schematic comparison of different solid and liquid processing steps to form solid drug nanoparticles. (a) "top-down" media milling of particles, (b) "top-down" high pressure homogenization, (c) "bottom-up" processing of emulsions, and (d) "bottom-up" nanoprecipitation from a good solvent into an antisolvent.

8.3.1 Attrition Approaches

Attrition techniques involve the physical fracturing of large particles of API to form smaller populations of drug particles. This can be achieved through a direct milling approach (Fig. 8.2a) that grinds the API, usually within a liquid environment and in the presence of a milling medium (hard solid spheres that contact the drug particles and impart a direct physical force) [7]. Milling has been achieved within the dry state and in aqueous and non-aqueous liquids. However, water is the favoured nano-milling liquid. As an industrial approach, nano-milling is most effective for solid, high melting point (>80°C), highly crystalline APIs but has limitations for semi-solid, low melting point, solvent-sensitive, amorphous or temperature-sensitive compounds. As an attrition process that aims to grind large insoluble API particles into sub-micron particles, significant damage to milling equipment and contamination from the milling/grinding medium or walls of the vessel has also been reported [3]. Despite these limitations, nano-milling has been very effective and a large range of therapies have been successfully developed and are currently prescribed in clinics globally [8, 9].

Another major attrition approach is high-pressure homogenization (Fig. 8.2b). Drawing similarities from nano-milling, relatively large particles of API are mixed with a liquid and forced at high pressure (up to 4000 bar) through a valve with a very small aperture [6]. The liquid medium may be aqueous or non-aqueous [10]. The aperture is adjusted by the movement of a piston within the valve and the process of forcing the liquid through such a small space leads to a simultaneous increase in dynamic pressure (the kinetic energy per unit volume) and decrease in static pressure within the liquid. The decrease in static pressure to values below the vapour pressure of the liquid leads to boiling within the valve and the formation of gas bubbles which undergo cavitation and break the API particles into ever decreasing sizes [11]. Considerable heat may be generated during high-pressure homogenization and cooling of the equipment used is important. As such, aqueous homogenization is not recommended for temperature or hydrolysis sensitive drug compounds; non-aqueous homogenization has been developed that may operate at temperatures below the freezing point of water. Milling is often used to prepare the initial suspension of larger particles for homogenization, leading to additional processing steps.

8.3.2 Liquid Manipulation Approaches

Two liquid manipulation techniques that have maintained popularity for SDN formation are emulsion processing (Fig. 8.2c) and nanoprecipitation (Fig. 8.2d). Emulsions can be utilized in various ways to produce SDNs. However, in all cases the poorly water-soluble drug compound is dissolved into a water immiscible solvent, or mixture of solvents, and mixed with aqueous solutions to generate solvent droplets dispersed within an aqueous continuous phase. The removal of the solvent can be achieved by various techniques including diffusion or evaporation [12] and, more recently, by freeze-drying which generates a porous solid containing SDNs that can be redispersed into water (emulsion templated freeze/spray drying; ETFSD) [13, 14]. The approach achieves high drug loading (up to 85 weight% in the dry state), is rapidly translatable to spray dry manufacture, if warranted to simplify achievement of scale, and may have a number of advantages over attrition approaches such as nanomilling (Table 8.1). These "bottom-up" processes utilize solutions of APIs to allow nanoparticles to be formed in water, but the solubility of the drug compound within a water-immiscible solvent environment may also lead to challenges, in addition to the handling of volatile solvents. Nanoprecipitation (Fig. 8.2d) utilizes water miscible organic solvents to prepare solutions that are mixed, often vigorously, with water as the precipitant liquid to form particles of the water-insoluble API in a water/solvent mixture; the organic solvent is often later removed by evaporation. Nanoprecipitation may be achieved using supercritical fluids [15], evaporative precipitation [16] and microfluidics [17].

Table 8.1 Nanomilling versus emulsion-templated freeze/spray drying

Factor	Nanomilling	ETFSD
API form	Crystalline API only	Crystalline or amorphous API (Liquids and waxes)
API melting point	High melting point API only	Melting point not relevant
Access to approved excipients	Narrow	Wide

Factor	Nanomilling	ETFSD
Formation of combination SDNs	Only possible if APIs are co-crystallized but mixing possible	Readily achievable (with multiple APIs per particle or by mixing)
Impurities in final product	Some reports of impurities from milling agents (and mill)	Low risk of impurities
Compatibility with HTS for research and development	More compatible with generation of large amounts of single dispersion	**Freeze-drying** rapidly generates small amounts (>300 options/week with 1 mg API per formulation)
Scalability	Correlation between processing time/energy input and particle size	**Spray-drying** rapidly translatable to Kg scale once optimum properties defined
Stability	Produces liquid formulations with inherent stability issues (can subsequently be spray-dried)	One-step formation of a solid (demonstrated capsule/tablet compatible) or storable as a solid for liquid redispersion before dosing
Scaled cost	Process-dependent	Process-dependent but as low as $4–$16 per Kg demonstrated

8.4 Pharmacokinetic Advantages

Several compounds have been shown to benefit from pharmacokinetic features observed when formulated into SDNs. An abridged list of current medicines that have SDN formulations is presented in Table 8.1. SDN formulations have proven to overcome a number of issues in drug delivery and have found application for both oral and intramuscular administration formats. Irrespective of the route of delivery, SDNs are assumed to dissolve after delivery and release dissolved molecules of the active drug into the systemic circulation. Recent data have shown that SDNs are able to cross-intestinal cell monolayers

as intact nanoparticles [18] but it is likely that the majority of API present within the body is free from the nanoparticles. This feature simplifies regulatory approval of such nanomedicines since the API is distributed and cleared from the body in a similar way to their non-nanoformulation equivalents. However, this also means that benefits for passive targeting of certain cell and tissue types that have been observed with nanocarrier-based medicines [19] are unlikely to be achievable from for SDNs from oral or intramuscular delivery. However, recent preclinical data have emerged for intravenously administered SDNs [20]. A diagrammatical representation of the pharmacokinetic benefits that have been achieved clinically using SDNs is given in Fig. 8.3.

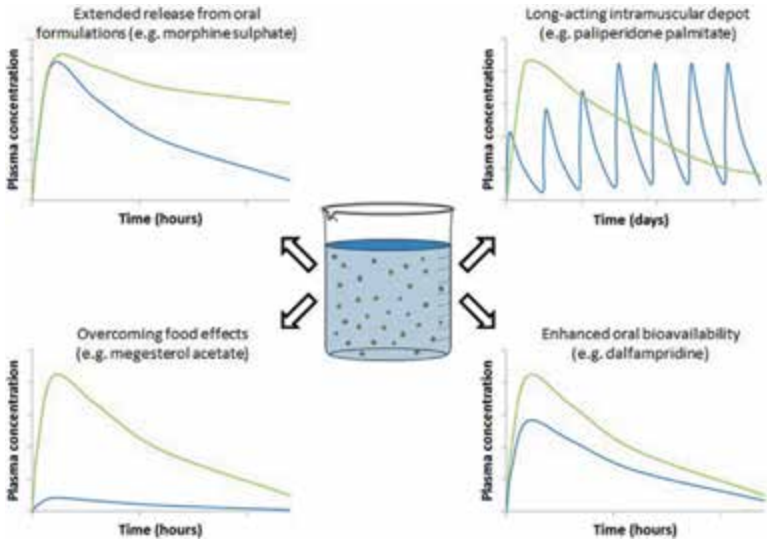

Figure 8.3 Pharmacokinetic benefits have been achieved through formulation of solid drug nanoparticles across a number of agents used in the treatment of multiple diseases. Benefits for oral administration formats have included extended release (turning twice daily into once daily oral regimens), enhanced oral bioavailability (enabling delivery of "difficult" molecules or sometimes enabling bioequivalence from a lower dose), and overcoming food interactions that negatively impact pharmacokinetics. For parenteral delivery, a number of long-acting agents enabling up to once quarterly administration have recently been developed.

Table 8.2 Selected marketed products using SDNs [6, 8, 9]

Brand Name	Generic/Other Name	Indication
Rapamune®	Sirolimus	Immunosuppression
Emend®	Aprepitant	Antiemetic
Tricor®	Fenofibrate	Hypercholesterolemia
Megace® ES	Megestrol Acetate	Antianorexia
Triglide®	Fenofibrate	Hypercholesterolemia
Avinza®	Morphine sulphate	Acute pain
Focalin® XR	Dexmethylphenidate	ADHD
Ritalin® LA	Methylphenidate	ADHD
Naprelan®	Naproxen	Arthritis
Theodur®	Theophylline	Bronchodilation
Invega® Sustenna®	Paliperidone palmitate	Antipsychotic
Ampyra®	Dalfampridine	Multiple sclerosis
Verelan®	Verapamil	Hypertension
Rilpivirine LA	Rilpivirine	HIV
S/GSK1265744	GSK744	HIV

8.4.1 Benefits for Oral Delivery

A number of benefits have been explicitly shown for the pharmacokinetics of APIs formulated as SDNs and subsequently delivered orally by ingestion. A number of specific examples of improved oral bioavailability are evident, which have either enabled oral delivery of insoluble APIs, which were otherwise difficult to formulate, or have enabled therapeutic pharmacokinetics from lower doses of API. Dalfampridine (4-aminopyridine) is a voltage-dependent potassium channel blocker and an extended release (ER) formulation of this API (Ampyra®; dalfampridine ER) was developed using the Elan Drug Technologies Matrix Drug Absorption System (MXDAS®), receiving FDA approval in January 2010 with subsequent launch in March 2010 [21]. Dalfampridine ER has been shown to improve walking speed, walking endurance, and community participation in patients with late multiple sclerosis [22]. Pharmacokinetic benefits of dalfampridine ER compared to the immediate release formulation were recently exemplified

by a review of the published and unpublished pharmacokinetic data [23]. To summarize, dalfampridine ER exhibited longer time to maximum plasma concentration (T_{max} = 3.2 h), a longer apparent plasma half-life ($T_{1/2}$ = 6.4 h) and higher area under the plasma concentration–time curve (AUC = 284.8 ng·h/mL) compared to the immediate release formulation (1.2 h, 3.7 h and 184.6 ng·h/mL, respectively) despite a lower maximum concentration (C_{max} = 21.6 versus 46.4 ng/mL). The change in ratio of C_{max} to minimum plasma concentration (C_{min}) is extremely interesting and may be particularly important for APIs which exhibit concentration-dependent adverse drug reactions (ADRs) but that require maintenance of a high C_{min} (e.g. risk of resistance).

Improved oral bioavailability has also been shown for other APIs such as megesterol acetate [24, 25]. The SDN formulation of megesterol acetate was approved by the FDA for treatment of anorexia, cachexia or significant unexplained weight loss in patients with AIDS in July 2005 [25]. The SDN formulation has been shown to only subtle differences to a micronized formulation in terms of C_{max} (1,618 versus 1,364 ng/mL), T_{max} (2.91 versus 3.85 h), $T_{1/2}$ (39.75 versus 32.84 h) and AUC (15,287 versus 16,757 ng · h/mL) in the fed state, despite a lower dose (625 mg in 5 mL versus 800 mg in 20 mL) [24]. Importantly, megesterol acetate represents an excellent paradigm for the ability to overcome food effects with the SDN formulation having higher C_{max} (1,133 versus 187 ng/mL), shorter T_{max} (1.72 versus 5.89 h), longer $T_{1/2}$ (33.68 versus 31.38 h) and higher AUC (11,301 versus 7,011 ng · h/mL) in the fed state, despite the lower dose and volume.

The specific advantage of ER has also been explicitly shown for other APIs when SDNs are combined with other formulation strategies for oral formulations. A good example of this is illustrated by the reformulation of methylphenidate (Ritalin®). Methylphenidate is a CNS stimulant that works by inhibiting noradrenaline and dopamine reuptake into presynaptic neurons [26]. The drug was first approved by the FDA for treatment of attention deficit/hyperactivity disorder (ADHD) in the 1950s [27] but was subsequently reformulated to overcome pharmacokinetic inadequacies. The ER formulation was approved in June 2002. This formulation was created using Elan Drug Technologies SODAS® (Spheroidal Oral Drug Absorption System), which

creates beads (1 to 2 mm in diameter) with drug at their core and subsequently coated with layers of different polymers and excipients that control drug release [28]. The formulation exhibits a bimodal release that mimics the pharmacokinetics of a twice-daily regimen even though it is only administered once daily [29, 30]. The pharmacokinetic properties have been determined in a number of studies that showed an initial C_{max} of 7 ng/mL at T_{max} 2.1 h followed by a second C_{max} of 9.3 ng/mL at T_{max} 5.6 h [30] and advantages were again observed compared to another formulation in terms of food effects [31].

Another example of an ER oral formulation is represented by the reformulation of morphine, also using SODAS® technology (Avinza®) [32, 33], approved for the treatment of chronic pain in March 2002. The 24 h steady-state pharmacokinetics of morphine along with its 6-glucuronide (active) and 3-glucuronide (non-active as opioid agonist) metabolites were compared between Avinza® and a twice-daily formulation in patients with chronic pain [34]. A comparable AUC (323 versus 312 ng·h/mL), C_{max} (21.2 versus 26.1 ng/mL) and C_{min} (8.88 versus 5.36 ng/mL) was observed between the two formulations but 30 min plasma concentrations (C_{30}) were higher for Avinza® indicating a more rapid attainment of therapeutic concentrations (17.1 versus 11.0 ng/mL). The last plasma concentration (C_{last}) was also comparable despite the difference in dosing frequency (11.9 versus 8.14 ng/mL). Importantly, as for dalfampridine ER, a more favourable C_{max} to C_{min} ratio was also observed (44% lower for Avinza®).

8.4.2 Benefits for Parenteral Delivery

A number of recent SDN formulations have been developed for long-acting (LA) intramuscular depot formulations with the potential for once monthly (e.g. paliperidone palmitate [35] and rilpivirine [36, 37]) or even longer (e.g. S/GSK1265744 [38]). The oral once-daily formulation of paliperidone was first approved for the treatment of schizophrenia December 2006 [39]. Subsequently, an SDN formulation of the paliperidone palmitate pro-drug was approved in July 2009 for once-monthly administration of an intramuscular (deltoid or gluteal) LA depot injection. Although paliperidone concentrations in the first week have been shown

to be higher after administration to the deltoid muscle than the gluteal muscle, similar concentrations have been reported at steady-state [40]. In 2009, Samtani et al. conducted a population pharmacokinetic analysis of paliperidone intramuscular depot in pooled data from 1795 patients (18,530 plasma samples) from 11 trials [35]. Interestingly, the model best described the pharmacokinetics when entry into the systemic circulation was via a combination of zero-order followed by first-order kinetics, and while the AUC appeared to be dose-proportional, C_{max} was not proportional at higher doses. The steady-state pharmacokinetics of paliperidone palmitate were subsequently further characterized in a multicenter study involving 30 sites in 10 countries [41]. The AUC was shown to increase from 2nd, 8th through 14th administration of the depot reaching 31,970 ng.h/mL by the 14th administration. At this point, C_{max}, C_{min}, T_{max} and average plasma concentration across the dosing interval (C_{avg}) were 56.5 ng/mL, 35.1 ng/mL, 7 days and 47.8 ng/mL, respectively.

LA depot formulations are of specific relevance to the treatment of chronic diseases and are especially important when there are severe consequences of low patient adherence to therapy. Of particular interest in this regard are antiretroviral SDN formulations, which are currently in late stage development for therapy as well as prevention of infection in high risk populations [42–45]. Patient non-adherence to oral antiretroviral therapies is a major driver for virological failure and associated with the emergence of drug resistance due to sub-therapeutic plasma concentrations when doses are missed [46]. Importantly, resistance in HIV is transmissible between individuals and cross resistance within classes of antiretrovirals [47] make LA regimens an attractive option to tackle adherence issues. Pill fatigue is another factor driving LA drug development and a recent survey of the interests and attitudes of HIV patients indicated 84% would definitely or probably try monthly injectable nanoformulated antiretroviral therapy [48]. Two LA antiretroviral drugs are currently in late stage development by Janssen and ViiV Healthcare [36–38] and studies are underway to determine their utility for co-administration as a therapy option [38, 49]. The pharmacokinetics of an early SDN LA formulation of rilpivirine have been extensively studied across species and according to subcutaneous versus intramuscular administration formats, which indicated similar

pharmacokinetics irrespective of route of administration [36]. However, it should be noted that formulation development is still ongoing and currently published data may not represent the most recent formulations nor those that are eventually finally approved.

8.5 Conclusions

There are a number of available options for creation of SDN-based formulations but, to date, nanomilling has proven to be the most successful in terms of the number of products approved by the FDA for clinical use. Achievable benefits that have been empirically shown in humans include ER oral formulations, improved bioavailability, dose reduction, overcoming food effects and LA depot formulations enabling 1 month (or longer) administration formats. There is currently a lack of information regarding whether intact nanoparticles enter the systemic circulation after administration of an SDN formulation, which is driven predominantly by the absence of bioanalytical assays that are able to discriminate SDNs from dissolved drug. Some investigators have explored surface functionalization of SDNs in order to achieve targeted delivery of SDNs and there are exciting preclinical data indicating that there may be benefits to this approach [50]. Conversely, the presence of particulates within the body may warrant additional regulation since certain nanomedicines introduced directly into the body intravenously confer altered distribution to the API and certain other nanomaterials are known to elicit off-target effects, for example on the immune system [51, 52] and liver [53]. We have recently developed a flow cytometric assay capable of discriminating intact SDNs from plasma debris [54] but are yet to apply this protocol in samples from patients receiving an SDN formulation. Our own work utilising ETFSD to create antiretretroviral formulations has shown that generating SDNs from an API does not guarantee a beneficial effect on pharmacological behaviour and it is possible to tune SDN performance using different excipients, z-average diameter or zeta potential [14]. Therefore, early integration of pharmacology with materials synthesis is required to select lead candidate formulations for further development.

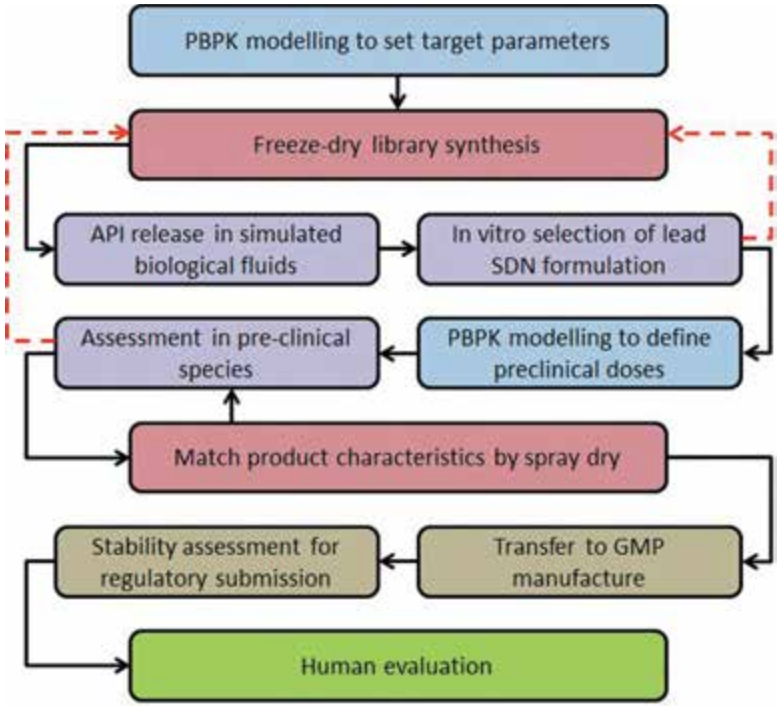

Figure 8.4 Proposed scheme for development of SDN formulations using emulsion-templated freeze/spray drying (ETFSD). PBPK modelling may be useful to initially define target characteristics for formulations (e.g., API release rate). Freeze-drying is useful to synthesize large numbers of candidate formulations from low amounts of API that can then be assessed *in vitro* to select leads matching target properties. PBPK models may then be utilized to predict doses and sampling design prior to evaluation in pre-clinical doses. Following lead selection, physical properties can be matched using spray-dry manufacture for oral formulations (to facilitate achievement of scale) but may not be preferred for parenteral administration due to issues with sterility. For an existing licensed API it may then be possible to rapidly translate a product by transferring to GMP manufacture, conducting stability assessments for regulatory submissions and bridging through human bioequivalence studies. Red dotted lines represent areas where careful iteration between manufacture and pharmacological evaluation may help optimize formulation.

To this end, physiologically based pharmacokinetic (PBPK) modelling may be useful for defining target characteristics for SDNs and predicting pre-clinical and clinical doses to streamline development [14, 55, 56] in a similar way to that of new API development [57, 58]. A proposed scheme for developing SDN formulations using the ETFSD technology is provided in Fig. 8.4. Formation of SDNs has proven to be successful for conferring pharmacological benefits to numerous APIs with poor aqueous solubility and may also have application in targeting of diseased cells/or tissues if they can be successfully delivered as intact nanoparticles into the systemic circulation.

Abbreviations

A: Surface area

ADHD: Attention deficit/hyperactivity disorder

AIDS: Acquired immunodeficiency syndrome

API: active pharmaceutical ingredient

AUC: area under the plasma concentration–time curve

C_{30}: Plasma concentration at 30 min

C_{avg}: Average plasma concentration across the dosing interval

C_{last}: Last plasma concentration

C_{max}: Maximum plasma concentration

C_{min}: Minimum plasma concentration

CNS: Central nervous system

dC/dt: Dissolution rate

ER: Extended release

FDA: Food and Drug Administration

GMP: Good manufacturing practice

GSK: Glaxo Smith Kline

HIV: Human immunodeficiency virus

LA: Long acting

MXDAS®: Matrix Drug Absorption System

PBPK: Physiologically based pharmacokinetic modelling

r: Particle radius

S_0: Equilibrium solubility

S_{app}: Apparent solubility

SDN: Solid drug nanoparticle

SODAS®: Spheroidal Oral Drug Absorption System

$T_{1/2}$: Plasma half-life

T_{max}: time to maximum plasma concentration

Disclosures and Conflict of Interest

The authors declare that no writing assistance was utilized and no payment received in the production of this chapter. This work was supported by grants from the Engineering and Physical Sciences Research Council (UK), and National Institutes of Health (US). The authors are co-inventors of patents relating to solid drug nanoparticle formulations and have recently been involved in the start-up, Tandem Nano, Ltd (UK) to commercialize these formulations. Prof. Andrew Owen has received research funding from Merck, Astra Zeneca, Pfizer and Janssen and consultancy from Merck and Norgine. Prof. Steve Rannard has received funding from IOTA NanoSolutions Ltd and Unilever, and consultancy from Bayer CropScience.

Corresponding Authors

Professor Andrew Owen
Department of Molecular and Clinical Pharmacology
Institute of Translational Medicine, University of Liverpool
70 Pembroke Place, Liverpool L69 3GF, UK
Email: aowen@liverpool.ac.uk

Professor Steve Rannard
Department of Chemistry, University of Liverpool
Liverpool L697ZD, United Kingdom
Email: srannard@liv.ac.uk

About the Authors

Andrew Owen, PhD, FSB, holds a personal chair in the Department of Molecular and Clinical Pharmacology at the University of Liverpool, UK. He is also affiliated to the MRC Centre for Drug Safety Science and the Wolfson Centre for Personalised Medicine. Prof. Owen has contributed to over 110 original research and review publications, book chapters and patent applications. In recent years, research funding has been secured from the Medical Research Council, Engineering and Physical Sciences Research Council, US National Institutes of Health and the British Society for Antimicrobial Chemotherapy. He is chair of the British Society for Nanomedicine (www.BritishSocietyNanomedicine.org), a fellow of the Society of Biology and a member of the Nanomed Focus Group Steering Committee and British Pharmacological Society. Prof. Owen is also a member of the editorial board for *Nanomedicine: Nanotechnology, Biology and Medicine*.

Steve Rannard, DPhil, FRSC, holds a personal chair at the University of Liverpool in the Department of Chemistry. He is also the academic lead in the School of Physical Sciences for Nanomedicine and the Director of the Liverpool Radiomaterials Chemistry Laboratory. Prior to his academic career, Prof. Rannard worked for 16 years in the chemical industry in companies such as Cookson, Courtaulds and Unilever. He has cofounded three start-up companies and is co-inventor of more than 50 patent families. His academic research has been supported by the Royal Society (Industry Fellowship), Research Councils (UK), Engineering and Physical Sciences Research Council (UK), the National Institutes of Health (US) and charitable funding from Fight for Sight and the British Society for Antimicrobial Chemotherapy. He is co-founder and Vice-Chair of the British Society for Nanomedicine and a Fellow of the Royal Society for Chemistry.

References

1. Nishiyama, N. (2007). Nanomedicine: Nanocarriers shape up for long life. *Nat. Nanotechnol.,* **2**(4), 203–204.
2. Peer, D., Karp, J. M., Hong, S., Farokhzad, O. C., Margalit, R., et al. (2007). Nanocarriers as an emerging platform for cancer therapy. *Nat. Nanotechnol.,* **2**(12), 751–760.
3. Rabinow, B. E. (2004). Nanosuspensions in drug delivery. *Nat. Rev. Drug Discov.,* **3**(9), 785–796.
4. Brough, C., Williams, R. O., 3rd. (2013). Amorphous solid dispersions and nano-crystal technologies for poorly water-soluble drug delivery. *Int. J. Pharm.,* **453**(1), 157–166.
5. Kumar, S., Bhargava, D., Thakkar, A., Arora, S. (2013). Drug carrier systems for solubility enhancement of BCS class II drugs: a critical review. *Crit. Rev. Ther. Drug Carrier Syst.,* **30**(3), 217–256.
6. Junghanns, J. U. A. H., Muller, R. H. (2008). Nanocrystal technology, drug delivery and clinical applications. *Int. J. Nanomed.,* **3**(3), 295–309.
7. Peltonen, L., Hirvonen, J. (2010). Pharmaceutical nanocrystals by nanomilling: Critical process parameters, particle fracturing and stabilization methods. *J. Pharm. Pharmacol.,* **62**(11), 1569–1579.
8. Schutz, C. A., Juillerat-Jeanneret, L., Mueller, H., Lynch, I., Riediker, M., et al. (2013). Therapeutic nanoparticles in clinics and under clinical evaluation. *Nanomedicine*, **8**(3), 449–467.
9. Bawa, R. (2008). Nanoparticle-based therapeutics in humans: A survey. *Nanotechnol. Law Bus.,* **5**(2), 135–155.
10. Paun, J. S., Tank, H. M. (2012). Nanosuspension: An emerging trend for bioavailability enhancement of poorly soluble drugs. *Asian J. Pharm. Technol.,* **2**(4), 157–168.
11. Keck, C. M., Muller, R. H. (2006). Drug nanocrystals of poorly soluble drugs produced by high pressure homogenisation. *Eur. J. Pharm. Biopharm.,* **62**(1), 3–16.
12. Horn, D., Rieger, J. (2001). Organic nanoparticles in the aqueous phase: Theory, experiment, and use. *Angew. Chemie Int. Ed.,* **40**(23), 4331–4361.
13. Zhang, H. F., Wang, D., Butler, R., Campbell, N. L., Long, J., et al. (2008). Formation and enhanced biocidal activity of water-dispersable organic nanoparticles. *Nat. Nanotechnol.,* **3**(8), 506–511.
14. McDonald, T. O., Giardiello, M., Martin, P., Siccardi, M., Liptrott, N. J., et al. (2013). Antiretroviral solid drug nanoparticles with enhanced

oral bioavailability: Production, characterization, and *in vitro–in vivo* correlation. *Adv. Healthc. Mater.*, **3**(3), 400–411.

15. Rogers, T. L., Hu, J. H., Yu, Z. S., Johnston, K. P., Williams, R. O. (2002). A novel particle engineering technology: Spray-freezing into liquid. *Int. J. Pharm.,* **242**(1–2), 93–100.
16. Li, X. S., Wang, J. X., Shen, Z. G., Zhang, P. Y., Chen, J. F., et al. (2007). Preparation of uniform prednisolone microcrystals by a controlled microprecipitation method. *Int. J. Pharm.,* **342**(1–2), 26–32.
17. Ali, H. S. M., York, P., Blagden, N. (2009). Preparation of hydrocortisone nanosuspension through a bottom-up nanoprecipitation technique using microfluidic reactors. *Int. J. Pharm.,* **375**(1–2), 107–113.
18. McDonald, T. O., Martin, P., Patterson, J. P., Smith, D., Giardiello, M., et al. (2012). Multicomponent organic nanoparticles for fluorescence studies in biological systems. *Adv. Funct. Mater.,* **22**(12), 2469–2478.
19. Lehner, R., Wang, X. Y., Marsch, S., Hunziker, P. (2013). Intelligent nanomaterials for medicine: Carrier platforms and targeting strategies in the context of clinical application. *Nanomed. Nanotechnol. Biol. Med.,* **9**(6), 742–757.
20. Zhang, H., Wang, X., Dai, W., Gemeinhart, R. A., Zhang, Q., et al. (2014). Pharmacokinetics and treatment efficacy of camptothecin nanocrystals on lung metastasis. *Mol. Pharm.*, **11**(1), 226–233.
21. Jara, M., Barker, G., Henney, H. R. (2013). Dalfampridine extended release tablets: 1 year of postmarketing safety experience in the US. *J. Neuropsychiatr. Dis. Treat.,* **9,** 365–370.
22. Cameron, M. H., Fitzpatrick, M., Overs, S., Murchison, C., Manning, J., et al. (2014). Dalfampridine improves walking speed, walking endurance, and community participation in veterans with multiple sclerosis: A longitudinal cohort study. *Mult. Scler.*, **20**(6), 733–738.
23. Weir, S., Torkin, R., Henney, H. R. (2013). Pharmacokinetic profile of dalfampridine extended release: Clinical relevance in patients with multiple sclerosis. *Curr. Med. Res. Opin.,* **29**(12), 1627–1636.
24. Deschamps, B., Musaji, N., Gillespie, J. A. (2009). Food effect on the bioavailability of two distinct formulations of megestrol acetate oral suspension. *Int. J. Nanomed.,* **4**, 185–192.
25. Par Pharmaceutical. (2007). Megestrol acetate nanocrystal dispersion oral suspension, PAR 100.2, PAR-100.2. *Drugs R&D*, **8**(4), 251–254.
26. Del Campo, N., Chamberlain, S. R., Sahakian, B. J., Robbins, T. W. (2011). The roles of dopamine and noradrenaline in the pathophysiology and treatment of attention-deficit/hyperactivity disorder. *Biol. Psychiatr.,* **69**(12), e145–157.

27. Morris, S. M., Petibone, D. M., Lin, W. J., Chen, J. J., Vitiello, B., et al. (2012). The genetic toxicity of methylphenidate: A review of the current literature. *J. Appl. Toxicol.,* **32**(10), 756–764.

28. Verma, R. K., Garg, S. (2001). Current status of drug deliver technologies and future directions. *Pharm. Technol. On-Line,* **25**(2), 1–14.

29. Lyseng-Williamson, K. A., Keating, G. M. (2002). Extended-release methylphenidate (Ritalin((R)) LA). *Drugs*, **62**(15), 2251–2259.

30. Markowitz, J. S., Straughn, A. B., Patrick, K. S., DeVane, C. L., Pestreich, L., et al. (2003). Pharmacokinetics of methylphenidate after oral administration of two modified-release formulations in healthy adults. *Clin. Pharmacokinet.,* **42**(4), 393–401.

31. Haessler, F., Tracik, F., Dietrich, H., Stammer, H., Klatt, J. (2008). A pharmacokinetic study of two modified-release methylphenidate formulations under different food conditions in healthy volunteers. *Int. J. Clin. Pharmacol. Ther.,* **46**(9), 466–476.

32. Semenchuk, M. R. (2002). Avinza Elan. *Curr. Op. Investig. Drugs.,* **3**(9), 1369–1372.

33. Elan Corporation. (2002). Morphine oral. Avinza. *Drugs R&D*, **3**(3), 208–209.

34. Portenoy, R. K., Sciberras, A., Eliot, L., Loewen, G., Butler, J., et al. (2002). Steady-state pharmacokinetic comparison of a new, extended-release, once-daily morphine formulation, Avinza, and a twice-daily controlled-release morphine formulation in patients with chronic moderate-to-severe pain. *J. Pain Symptom Manage.,* **23**(4), 292–300.

35. Samtani, M. N., Vermeulen, A., Stuyckens, K. (2009). Population pharmacokinetics of intramuscular paliperidone palmitate in patients with schizophrenia: A novel once-monthly, long-acting formulation of an atypical antipsychotic. *Clin. Pharmacokinet.,* **48**(9), 585–600.

36. van't Klooster, G., Hoeben, E., Borghys, H., Looszova, A., Bouche, M. P., et al. (2010). Pharmacokinetics and disposition of rilpivirine (TMC278) nanosuspension as a long-acting injectable antiretroviral formulation. *Antimicrob. Agents Chemother.,* **54**(5), 2042–2050.

37. Baert, L., van't, Klooster, G., Dries, W., Francois, M., Wouters, A., et al. (2009). Development of a long-acting injectable formulation with nanoparticles of rilpivirine (TMC278) for HIV treatment. *Eur. J. Pharm. Biopharm.,* **72**(3), 502–508.

38. Spreen, W. R., Margolis, D. A., Pottage, J. C., Jr. (2013). Long-acting injectable antiretrovirals for HIV treatment and prevention. *Curr. Opin. HIV AIDS,* **8**(6), 565–571.

39. ALZA Corp. for Janssen. (2007). New drug for schizophrenia. *FDA Consum.*, **41**(2), 6.

40. Hough, D., Lindenmayer, J. P., Gopal, S., Melkote, R., Lim, P., et al. (2009). Safety and tolerability of deltoid and gluteal injections of paliperidone palmitate in schizophrenia. *Prog. Neuro-Psychopharmacol. Biol. Psychiatry*, **33**(6), 1022–1031.

41. Coppola, D., Liu, Y., Gopal, S., Remmerie, B., Samtani, M. N., et al. (2012). A one-year prospective study of the safety, tolerability and pharmacokinetics of the highest available dose of paliperidone palmitate in patients with schizophrenia. *BMC Psychiatry*, **12**, 26.

42. Taha, H., Morgan, J., Das, A., Das, S. (2014). Parenteral Patent Drug S/GSK1265744 has the potential to be an effective agent in pre-exposure prophylaxis against HIV infection. *Recent Patents Anti-Infect. Drug Discov.*, **8**(3), 213–218.

43. Spreen, W., Min, S., Ford, S. L., Chen, S., Lou, Y., et al. (2013). Pharmacokinetics, safety, and monotherapy antiviral activity of GSK1265744, an HIV integrase strand transfer inhibitor. *HIV Clin. Trials.,* **14**(5), 192–203.

44. Friend, D. R., Clark, J. T., Kiser, P. F., Clark, M. R. (2013). Multipurpose prevention technologies: Products in development. *Antivir. Res.,* **100** Suppl, S39–S47.

45. Abraham, B. K., Gulick, R. (2012). Next-generation oral preexposure prophylaxis: Beyond tenofovir. *Curr. Opin. HIV AIDS,* **7**(6), 600–606.

46. Li, J. Z., Paredes, R., Ribaudo, H. J., Svarovskaia, E. S., Kozal, M. J., et al. (2012). Relationship between minority nonnucleoside reverse transcriptase inhibitor resistance mutations, adherence, and the risk of virologic failure. *AIDS*, **26**(2), 185–192.

47. Tang, M. W., Shafer, R. W. (2012). HIV-1 Antiretroviral resistance: Scientific principles and clinical applications. *Drugs,* **72**(9), E1–E25.

48. Williams, J., Sayles, H. R., Meza, J. L., Sayre, P., Sandkovsky, U., et al. (2013). Long-acting parenteral nanoformulated antiretroviral therapy: Interest and attitudes of HIV-infected patients. *Nanomedicine,* **8**(11), 1807–1813.

49. Ford, S. L., Gould, E., Chen, S., Margolis, D., Spreen, W., et al. (2013). Lack of pharmacokinetic interaction between rilpivirine and integrase inhibitors dolutegravir and GSK1265744. *Antimicrob. Agents Chemother.,* **57**(11), 5472–5477.

50. Puligujja, P., McMillan, J., Kendrick, L., Li, T., Balkundi, S., et al. (2013). Macrophage folate receptor-targeted antiretroviral therapy facilitates drug entry, retention, antiretroviral activities and

biodistribution for reduction of human immunodeficiency virus infections. *Nanomedicine,* **9**(8), 1263–1273.

51. Dobrovolskaia, M. A., McNeil, S. E. (2007). Immunological properties of engineered nanomaterials. *Nat. Nanotechnol.,* **2**(8), 469–478.
52. Zolnik, B. S., Gonzalez-Fernandez, A., Sadrieh, N., Dobrovolskaia, M. A. (2010). Nanoparticles and the immune system. *Endocrinology,* **151**(2), 458–465.
53. Kermanizadeh, A., Gaiser, B. K., Johnston, H., Brown, D. M., Stone, V. (2013). Toxicological impact of engineered nanomaterials on the liver: A review. *Br. J. Pharmacol*., **171**(17), 3980–3987.
54. Liptrott, N., Giardiello, M., Hunter, J., Tatham, L., Tidbury, L., et al. (2014). Flow cytometric analysis of the physical and protein-binding characteristics of antiretroviral based solid drug nanoparticle suspensions. *Nanomedicine*, (in press).
55. Moss, D. M., Siccardi, M. (2014). Optimising nanomedicine pharmacokinetics using PBPK modelling. *Br. J. Pharmacol*., **171**(17), 3963–3979.
56. Siccardi, M., Martin, P., McDonald, T. O., Liptrott, N. J., Giardiello, M., et al. (2013). Nanomedicines for HIV therapy. *Ther. Deliv.,* **4**(2), 153–156.
57. Shiran, M. R., Proctor, N. J., Howgate, E. M., Rowland-Yeo, K., Tucker, G. T., et al. (2006). Prediction of metabolic drug clearance in humans: *In vitro*-in vivo extrapolation vs allometric scaling. *Xenobiotica,* **36**(7), 567–580.
58. Kostewicz, E. S., Aarons, L., Bergstrand, M., Bolger, M. B., Galetin, A., et al. (2014). PBPK models for the prediction of in vivo performance of oral dosage forms. *Eur. J. Pharm. Sci.,* **57C**, 300–321.

Chapter 9

Design and Development of Approved Nanopharmaceutical Products

Heidi M. Mansour, PhD, RPh,[a] Chun-Woong Park, PhD,[b] and Raj Bawa, MS, PhD[c,d]

[a]*The University of Arizona, College of Pharmacy, Tucson, Arizona, USA*
[b]*College of Pharmacy, Chungbuk National University, Cheongju, Republic of Korea*
[c]*Patent Law Department, Bawa Biotech LLC, Ashburn, Virginia, USA*
[d]*Department of Biological Sciences, Rensselaer Polytechnic Institute, Troy, New York, USA*

Keywords: nanotechnology, nanopharmaceutical, nanomedicine, parenteral delivery, oral delivery, dermal and transdermal delivery, pulmonary delivery, US Food and Drug Administration, patent, liposomes, microemulsions, polymeric micelles, theragnostics, NanoCrystal® technology, Abbreviated New Drug Application, US Patent & Trademark Office, commercialization, PEGylation, colloid, nanoparticles, bioequivalent

9.1 Introduction

9.1.1 Nanotechnology and Nanomedicine

Nanotechnology and nanomedicine, the high-risk, high-payoff global phenomenon, is in full swing. Advances in these areas are driven by collaborative research, patenting, commercialization, business

Handbook of Clinical Nanomedicine: Nanoparticles, Imaging, Therapy, and Clinical Applications
Edited by Raj Bawa, Gerald F. Audette, and Israel Rubinstein

ISBN 978-981-4669-20-7 (Hardcover), 978-981-4669-21-4 (eBook)
www.panstanford.com

development, and technology transfer within diverse areas such as chemical engineering, biomedicine, physical sciences, and information technology [1–3].

The confusion and ambiguity surrounding the definition of nanotechnology continues to be one of the most significant problems shared by regulators, policy-makers, researchers, and legal professionals alike. Various companies, universities and individuals have thrown around the "nano" prefix to suit their limited purpose, whether it is for research funding, patent approval, raising venture capital or seeking publication in a journal.

Different definitions of nanotechnology have sprung up over the years. Nanotechnology has been described as the manipulation, precision placement, measurement, modeling or manufacture of matter in the sub-100 nm range [4], or in the 1 to 200 nm range [5, 6]. However, there are a number of reports in the scientific literature that mention a size ranging from 1 to 1000 nm in both nanotechnology and pharmaceutical science [7–10].

Although the term "nanotechnology" is widely used, there is no internationally accepted definition or nomenclature associated with it [3]. In fact, the term nanotechnology is a bit misleading since it is not one technology but encompasses several technical and scientific fields such as medicine, materials science, chemistry, physics, engineering and biology. One can view it as an umbrella term used to define the products, processes and properties at the nano/micro scale [3]. To reduce ambiguity, the following practical definition of nanotechnology has been proposed by Dr. Raj Bawa, which is unconstrained by an arbitrary size limitation [3]:

> *The design, characterization, production, and application of structures, devices, and systems by controlled manipulation of size and shape at the nanometer scale (atomic, molecular, and macromolecular scale) that produces structures, devices, and systems with at least one novel/superior characteristic or property.*

Submicron materials are essential for biological distribution of biopharmaceuticals for safety reasons [11]. Particles larger than 5 μm can cause pulmonary embolism following intravenous injection with fatal results [12–15]. Therefore, submicron particle size is required for all parenteral formulations. In ophthalmic applications, the optimal particle size is less than 1000 nm

because microparticles around 5 μm can cause a scratchy feeling in the eyes [16, 17].

In the pharmaceutical sciences, "nano" offers several advantages in the context of drug delivery that pharma is interested in [3, 18]:

- increase in the apparent solubility and dissolution rate of a drug in relation to *in vivo* bioavailability enhancement due to the large specific surface area (i.e., high surface area per unit weight) of drug particles;
- protection of encapsulated or absorbed therapeutic agents from the hostile bioenvironment of use/delivery/release (e.g., against potential enzymatic or hydrolytic degradation);
- extended drug residence time at a particular site of action or within specific targeted tissue and/or extended systemic circulation time;
- controlled drug release at a specific desired site of delivery;
- enhanced drug accumulation at the target site so as to reduce systemic toxicity;
- offering a high drug-loading capacity;
- improved patient compliance; and
- ability to act as adjuvants in vaccine delivery.

Just like nanotechnology, there is no universally accepted definition of nanomedicine. The European Science Foundation [19] defines nanomedicine as follows:

> *[T]he science and technology of diagnosing, treating, and preventing disease and traumatic injury, of relieving pain, and of preserving and improving human health, using molecular tools and molecular knowledge of the human body.*

In addition, according to Dr. Thomas Webster, nanomedicine may be divided into five main disciplines [20]:

- analytical tools;
- nanoimaging;
- nanomaterials and nanodevices;
- novel therapeutics and drug delivery systems; and
- clinical, regulator, and toxicological issues.

The National Institutes of Health (NIH) Roadmap for Medical Research in Nanomedicine [21] defines nanomedicine as follows:

> *[A]n offshoot of nanotechnology, refers to highly specific medical interventions at the molecular scale for curing disease or repairing damaged tissues, such as bone, muscle, or nerve.*

Accordingly, nanomedicine could be summarized as *"emerged medicinal approaches from nanotechnology at the level of molecules and atoms"* [20]. In other words, the treatment, diagnosis, monitoring and control of biological systems may be referred to as nanomedicine [22]. In this regard, diagnostic trials and drug delivery devices are receiving the most intensive focus [23]. There also has been extensive research on the development of nanomedicines such as solid nanoparticles, liposomes, nanoemulsions and dendrimers for the specific delivery of drugs to target tissues [3, 24].

9.1.2 Nanopharmaceuticals: Nanomedicine Delivery Systems

Nanopharmaceuticals (Fig. 9.1) have received a lot of attention due to their potential to revolutionize drug delivery systems [25]. The most critical aspect in drug delivery systems is to deliver the correct dose of a particular active agent to a specific disease site in order to reduce toxic side effects as well as to optimize the therapeutic effect of the active agent as compared to the classic drawbacks of traditional therapeutics [25–27]. In other words, nanopharmaceuticals can be used for targeted drug delivery to the site of diseased tissue or lesion to improve the uptake of poorly soluble drugs and/or the improvement of drug bioavailability [28–30].

Colloidal drug delivery carriers such as liposomes, micelles, and solid nanoparticles, have been intensively investigated for their use in the pharmaceutical field. Nanopharmaceuticals are often described as colloidal drug delivery carriers of 10 to 1000 nm [31]. Nanopharmaceuticals are synthesized by various methods (self-assembly, vapor or electrostatic deposition, aggregation, nanomanipulation, imprinting, etc.) where the protocol is dictated by factors such as the specific therapeutic used and the desired delivery route [32].

From a material science perspective, nanopharmaceuticals can be divided into two types—"hard" and "soft"—although there are obvious intermediate versions (Table 9.1) [33]. Hard-type nanopharmaceuticals, such as polymeric nanoparticles [34–37] and lipid nanoparticles [15, 38–40], have less flexibility and are less

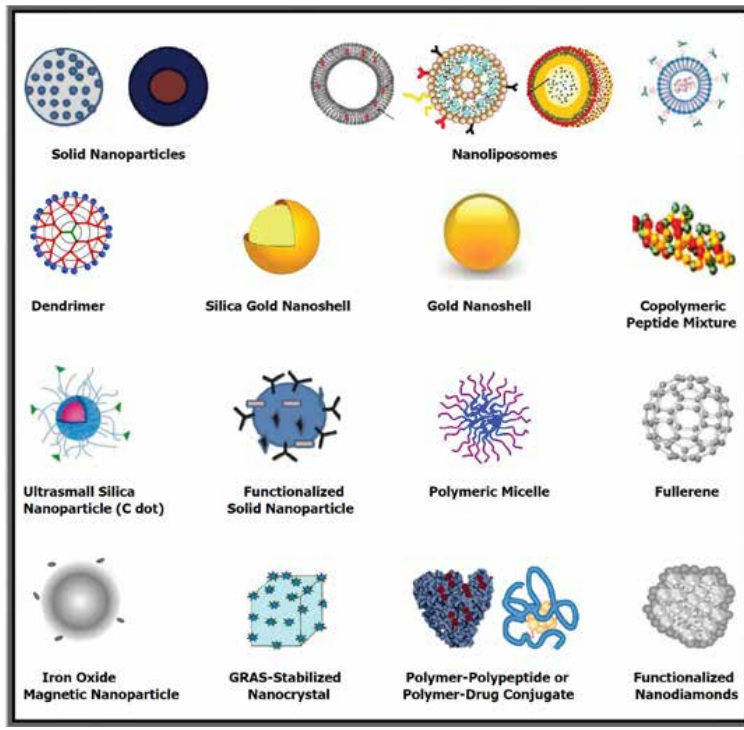

Figure 9.1 Schematic Illustrations of Nanoscale Drug Delivery System Platforms (Nanotherapeutics or Nanodrug Products). Shown are nanoparticles (NPs) used in drug delivery that are either approved, are in preclinical development or are in clinical trials. They are generally considered as first or second generation multifunctional engineered NPs, generally ranging in diameters from a few nanometers to a micron. Active biotargeting is frequently achieved by conjugating ligands (antibodies, peptides, aptamers, folate, hyaluronic acid) tagged to the NP surface via spacers or linkers like PEG. NPs such as carbon nanotubes and quantum dots, although extensively advertised for drug delivery, are specifically excluded from the list as this author considers them commercially unfeasible for drug delivery. Non-engineered antibodies and naturally occurring NPs are also excluded. Antibody-drug conjugates (ADCs) are encompassed by the cartoon labelled "Polymer-Polypeptide or Polymer-Drug Conjugate." This list of NPs is not meant to be exhaustive, the illustrations are not meant to reflect three dimensional shape or configuration and the NPs are not drawn to scale. Abbreviations: NPs: nanoparticles; PEG: polyethylene glycol; GRAS: Generally Recognized As Safe; C dot: Cornell dot; ADCs: Antibody-drug conjugates.

elastic. In contrast, soft type systems, including liposomes [41–45], nanoemulsions [46–48], submicron lipid emulsions [49–54], nanogels [55–57], and polymeric micelles [58–60], can be deformed and reformed to varying degrees by external or internal stress [24]. Hard systems can block capillaries and fenestrae that have dimensions similar to the particles, but soft systems are better able to navigate capillary beds and tissue extracellular spaces [33].

Table 9.1 Various types of nanopharmaceutical delivery systems based on hard and soft nanomaterials

Category		Nanopharmaceutical delivery systems	Reference
Hard types	Polymer-base	Polymeric nanoparticles	[34–37]
	Lipid-base	Lipid nanoparticles	[15, 38–40]
Soft types	Lipid-base	Liposomes	[41–45]
	Lipid-base	Lipid emulsions	[49–54]
	Lipid-base	Microemulsions	[46–48]
	Polymer-base	Polymeric micelles	[58–60]
	Polymer-base	Nanogels	[55–57]

Liposomes were initially reported to serve as a model for cell membranes in biophysical studies [61]. Liposomes are phospholipid vesicles of varying sizes, ranging from 50 to above 1000 nm, formed by one or several lipid bilayers with an aqueous phase both inside and between the bilayers [62]. Liposome formulations have the potential (due to targeting) to reduce toxicity and increase accumulation at the target site with or without expression of target recognition molecules on lipid membranes [42]. Liposomes have advantages such as [63, 64]:

- drug encapsulation versatility in their aqueous compartments (hydrophilic drugs), in their bilayers (lipophilic drugs) or both (amphiphilic drugs); and
- potential to offer a high level of safety due to their inherent nontoxic, non-immunogenic and biodegradable property.

Polymeric nanoparticles are defined as solid colloidal particles composed of polymeric materials ranging in size from 1 to 1000 nm. They are classified as nanocapsules, which are vesicular systems with a polymeric shell plus an inner core and nanospheres, which are a polymeric matrix [8]. Polymeric micelles are defined as self-assembled nanomaterials of amphiphilic block copolymers con-

taining hydrophobic and hydrophilic blocks. Polymeric micelles are nanoscopic therapeutic systems that incorporate therapeutic agents, molecular targeting and diagnostic imaging capabilities that are emerging as the next generation of multifunctional nanomedicine intended to improve the therapeutic outcome of drug therapy [59].

For lipid nanoparticles, three different types of lipid nanoparticles exist [15, 65–67]:

- Solid Lipid Nanoparticles (SLN): colloidal particles of a lipid matrix that is solid at body temperature;
- Nanostructured Lipid Carriers (NLC): composition of solid lipid and a spatially different liquid lipid as the carrier; and
- Lipid Drug Conjugates (LDC): salt formation or covalent linkage of insoluble drug–lipid conjugate bulk with a solid matrix.

Nanogels are aqueous dispersions of hydrogel particles formed by physically or chemically cross-linked polymer networks of nanoscale size. They can be prepared by different methods such as self-assembly of polymers, polymerization of monomers, cross-linking of preformed polymers, or template-assisted nanofabrication. They can be stored in a dried form at ambient temperature to easily be re-suspended in aqueous media, forming particulate dispersions with a nano-sized hydrodynamic diameter [55, 56, 68].

The application potential of nanopharmaceuticals is related to some of their unique features and properties that make ideal for drug delivery relative to traditional drug formulations. Some of these include [3, 69]:

- nanoscale dimensions/small size (high surface area-to-volume ratio);
- reduced systemic toxicity due to a reduced required dose;
- controlled drug release profile;
- modified drug pharmacokinetics;
- enhanced drug accumulation at/in the target site;
- ability to protect the active agents against potential enzymatic or hydrolytic degradation (long-term physical and chemical drug stability);
- high drug-loading capacity;
- extended systemic circulation or residence time;

- efficient delivery of poorly water-soluble active agents;
- enormous compositional range and variety of active agents and carriers that can be formulated/packaged in the drug formulation;
- superior biological distribution and targeting capabilities due to site-specific targeting moieties or ligands attached thereto; and
- potential for various delivery routes (oral, topical, intravenous, etc.).

Because the above-mentioned features can be engineered into a delivery system along with effective delivery to target various biological sites; hence, this area is gaining traction [70]. There are a number of FDA-approved, marketed nano-pharmaceuticals [3] that can be administered by various routes as listed in Table 9.2. Table 9.3 lists examples of commercialized biomedical, vaccine and diagnostic imaging products that incorporate nanotechnology. Table 9.4 lists examples of FDA-approved nanopharmaceutical products used as therapeutics. However, numerous nanopharmaceuticals are still at the development or clinical trial phase due to the complex nature of human medicinal applications. This chapter will discuss approved nanopharmaceutical products for drug delivery (from a design and development perspective) via various administration routes including parenteral, oral, transdermal and pulmonary. In this chapter, the following equivalent terms are used interchangeably: nanodrugs, nanomedicines, and nanopharmaceuticals.

Table 9.2 Routes of Administration used for marketed nanopharmaceutical products.

Route of Administration
Oral
Injectible
Intravenous (IV)
Intramuscular (IM)
Subcutaneous (SQ)
Intrathecal (IT)
Intravitreal/Intraocular
Topical
Ocular
Transdermal
Pulmonary

Table 9.3 Select list of marketed biomedical products that incorporate nanotechnology for diagnostic imaging, dental restoration, tissue engineering and vaccination.

Nanotechnology	Commercial product name	Use
Carboxydextran-coated superparamagnetic iron oxide nanoparticles	Resovist®	MRI contrast agent for diagnostic imaging
superparamagnetic iron oxide nanoparticles	Feridex I.V.®	MRI contrast agent for diagnostic imaging
Nanofiller	ESPE Filtek®	Dental restoration
Nanostructured crystals	NanOss® Bioactive 3D	Advanced bone graft of synthetic human bone (tissue engineering)
Virosomes	Epaxal®	Vaccination (Hepatitis A)

Table 9.4 Select list of marketed nanopharmaceutical products.

Nanotechnology	Drug	Commercial product name	Use
PEGylated liposomes	Doxorubicin	Doxil®	Cancer
PEGylatedbiologic	hGH (human growth hormone)	Somavert®	Acromegaly
Liposomes	Amphotericin B	AmBisome®	Fungal infections (antifungal)
NanoCrystal®	Sirolimus	Rapamune®	Transplant rejection prevention
SMEDDS (self-microemulsifying drug delivery systems)	Saquinavir	Forovase®	Viral infections (antiviral)
PEGylatedbiologic	anti-VEGF (vascular endothelial growth factor) aptamer	Macugen®	Macular degeneration
Albumin-bound nanoparticles	Paclitaxel	Abraxane®	Cancer

9.2 Approved Nanopharmaceutical Products: Parenteral Drug Delivery

The parenteral administration route can directly access systemic circulation with a rapid onset of drug action, achieving an advanced molecular targeting to specific organs and tissue sites [71]. However, there are certain classic disadvantages with this approach, namely, (i) insufficient drug accumulation at target sites while large amounts are dissipated and/or (ii) undesirable drug localization at normal tissue sites [72]. Given these drawbacks, there is extensive research focused on increasing efficiency and bioavailability of nanomedicines delivered parenterally. Current strategies under investigation include the following:

- *Creating a protective barrier around the nanomedicines*: This can be accomplished by creating steric hindrance, hydrodynamic volume effects and/or charge repulsions around the nanomedicines. For example, polyethylene glycol (PEG), an FDA-approved polymeric excipient, provides both steric hindrance and hydrodynamic volume effects for the protection of nanomedicines with an extended period of time resulting in enhanced circulation activity [45].
- *Conjugation of targeting ligands to the surface of nanocarriers*: Various target receptors such as human epidermal receptor-2, transferrin receptor, folate receptor, and vascular endothelial growth factor receptor are examples for this strategy [73–75].
- *Stimuli-triggered systems*: Examples include ultrasonic, magnetic, electric and light from external-regulated stimuli as well as thermo-sensitive, pH-sensitive and enzyme-substrate reactions following as self-regulated stimuli [76].
- *Theragnostics*: Therapeutic and diagnostic agents are merged into a single carrier to monitor real-time bio-distribution and target accumulation of nanocarriers while enhancing the pharmacological efficacy of drugs [77, 78]. For the parenteral drug delivery of nanomedicines, intravenous injection can be used for certain drugs having long half-lives. Additionally, long-acting parenteral injections are also administered through intramuscular and subcutaneous routes [79].

There have been numerous approved marketed liposome-based nanopharmaceutical products over the past several years, which establishes liposomal delivery as a viable option for drug delivery. Currently marketed liposomal products are based on passive targeting such as accumulation of carriers at disease sites via extravasation through a leaky vasculature [80]. Other research is based on active targeting via conjugation of site-directing ligands [80], triggered-release systems [81], cationic delivery systems [82], and multifunctional liposome systems [76, 83]. Polymeric nanoparticles and micelles are able to increase their potentials with the PEGylation or PEG coating of these particles to prolong the circulation time of polymeric nanoparticles [60, 84, 85]. The surface of polymeric nanoparticles can be conjugated via targeting ligands, such as antibodies, engineered antibody fragments, proteins and peptides. Polymeric micelles can incorporate hydrophobic drugs by chemical conjugation or physical entrapment. On the other hand, the hydrophilic shell of these polymeric micelles can consist of PEG moieties (i.e., PEGylated liposomal nanocarrier systems), imparting prolonged circulation time through a combination of steric hindrance and hydrodynamic volume effects, as discussed earlier [86–88].

DOXIL® (Schering-Plough Corp., Kenilworth, NJ, USA; ALZA, Mountain View, CA, USA), is a pegylated liposomal doxorubicin (PLD) formulation, known as CAELYX® outside the US. Doxorubicin is a cytotoxic anthracycline antibiotic isolated from *Streptomyces peucetius,* var. *caesius*. The molecular formula of the drug is $C_{27}H_{29}NO_{11}\cdot HCl$ with a molecular weight of 579.99 g/mol [89]. DOXIL® is doxorubicin confined in liposomes that have been sterically stabilized by grafting polyethylene glycol onto the surface (STEALTH® Liposome) [90, 91]. Its circulation half-life is reported around 73.9 h, whereas doxorubicin has a half-life of <10 min [92, 93]. Prolonged circulation facilitates greater uptake of PLD liposomes by tumor tissue. PLD accumulates selectively in metastatic breast carcinoma tissue, resulting in a 10-fold higher intracellular drug concentration compared with adjacent normal tissue [94]. DOXIL® is provided as a sterile, translucent, red liposomal dispersion in 10-mL glass, single-use vials. Each vial contains 20 mg doxorubicin HCl at a concentration of 2 mg/mL and a pH of 6.5 [95]. The STEALTH® liposome carriers are composed of *N*-(carbonyl-methoxypolyethylene glycol 2000)-1,2-

distearoyl-*sn*glycero-3-phosphoethanolamine sodium salt (MPEG-DSPE), 3.19 mg/mL; fully hydrogenated soy phosphatidylcholine (HSPC), 9.58 mg/mL; and cholesterol, 3.19 mg/mL. Each mL also contains ammonium sulfate, approximately 2 mg; histidine as a buffer; hydrochloric acid and/or sodium hydroxide for pH control; and sucrose to maintain isotonicity [95]. Greater than 90% of the drug is encapsulated in the STEALTH® liposomes, and it is indicated for (1) ovarian cancer after failure of platinum-based chemotherapy, (2) AIDS-related Kaposi's sarcoma after failure of prior systemic chemotherapy or intolerance to such therapy, and (3) multiple myeloma in combination with bortezomib in patients who have not previously received it [95].

Taxanes are an important drug class of antitumor agents for the treatment of advanced and early-stage breast cancer. FDA-approved marketed taxane products include paclitaxel (TAXOL®; Bristol-Myers Squibb Co, Princeton, NJ, USA) and Docetaxel (TAXOTERE®; Aventis Pharmaceuticals Inc., Bridgewater, NJ, USA) [96]. Furthermore, these drug formulations have shown remarkable anti-tumor activity against malignancies including non-small-cell lung cancer and ovarian cancer [97, 98]. Due to their high hydrophobicity, taxanes have a disadvantage in that they cannot be easily compounded into pharmaceutical formulations. Hence, to overcome poor water solubility of these drugs, paclitaxel lipid-based formulations are used with a mixture of 50:50 Cremophor EL® (a non-ionic surfactant polyoxyethylated castor oil; BASF, Florham Park, NJ, USA) and ethanol [99]. Similarly, docetaxel is formulated in polysorbate 80 and ethanol diluents [100]. However, it should be emphasized that these conventional solvent-based formulations can cause serious and dose-limiting toxicities [97, 101–103].

Novel albumin-based formulations have been recently developed for paclitaxel. These formulations are highly soluble, Cremophor-free and increase the circulation time of the drug. Albumin is well known as a natural carrier of endogenous hydrophobic molecules that are bound via a reversible non-covalent interaction [104]. Albumin-bound paclitaxel (ABRAXANE®; Celgene Corporation, Summit, NJ, USA) is a strategy for the solvent-related problems of paclitaxel and it has been recently approved by the FDA for pretreated, metastatic breast cancer patients [105]. ABRAXANE® is an albumin-bound colloidal suspension of

paclitaxel with a mean particle size of around 130 nm. It is also free from any kind of solvent. This product is supplied as a white to yellow, sterile, lyophilized powder for reconstitution with 20 mL of 0.9% sodium chloride injection, USP prior to intravenous infusion. Each single-use vial contains 100 mg of paclitaxel and approximately 900 mg of human albumin. Each milliliter of reconstituted suspension contains 5 mg paclitaxel [105]. Furthermore, in preclinical studies of athymic mice with human breast cancer, ABRAXANE® has a higher penetration into tumor cells with an increased antitumor activity compared to an equal dose of standard paclitaxel [106].

Although the incidence is decreasing, cryptococcal meningitis is still the most common manifestation of systemic fungal infection in HIV-infected patients and it remains associated with significant morbidity and mortality [107]. Amphotericin B deoxycholate has been considered for the initial treatment of cryptococcal meningitis in patients with HIV infection because initial treatment with the triazoles, fluconazole, and itraconazole is probably less effective [108]. Unfortunately, despite therapeutic advantages, amphotericin B deoxycholate may be associated with significant nephrotoxicity and acute infusion-related adverse effects. In order to reduce the risk of nephrotoxicity, AmBisome® (NeXstar Pharmaceuticals, Inc., San Dimas, CA, USA), a liposomal nanopharmaceutical product has been launched. This nanopharmaceutical product has received FDA approval for the treatment of patients with (1) cryptococcal meningitis-HIV infection; (2) mycosis as an empiric therapy for a presumed fungal infection in patients with febrile neutropenia; (3) systemic mycosis due to *aspergillus, candida, and cryptococcus* in patients refractory to amphotericin B deoxycholate or where renal impairment or unacceptable toxicity precludes the use of amphotericin B deoxycholate; and (4) visceral leishmaniasis [109, 110].

Infection with hepatitis C virus is the most common blood-borne infection in the US, eclipsing even HIV infection [111]. Interferon-α acts mainly as an immunomodulator and enhances the host cell-mediated immune response in clearing the virus [112]. In the case of protein drugs, such as interferon-α, there have been enzymatic degradation and rapid clearance, which can lead to wide fluctuations in blood levels due to frequent administration.

PEGylation is a process with the attachment of PEG to prolong *in vivo* half-life of the protein. Two kinds of nanopharmaceutical products of PEGylated interferon-α have been marketed [113]. PEGylated interferon-α2b (PEGASYS®; Hoffmann–La Roche Ltd., Basel, Switzerland) contains covalently linked recombinant interferon-α2b and a straight chain molecule of 12 kDa PEG. PEGylated interferon-α2a (PEGINTRON®; Schering-Plough, Kenilworth, NJ, USA) is made up of interferon-α2a and a 40 kDa branched PEG [112, 114].

Nanopharmaceutical products based on submicron lipid emulsions were launched for the purpose of parenteral nutrition (INTRALIPID®) in the 1960s [115], and lipid emulsion formulations have been approved for marketed products such as diazepam (DIAZUMULS®; Pfizer, USA), etomidate (ETOMIDATE® Lipuro; Braun Melsungen, Germany) and propofol (DIPRIVAN®; AstraZeneca, USA) [51].

One very exciting area in nanomedicine is the use of magnetic (Fe_3O_4) nanoparticles as diagnostics [116, 117]. The magnetic properties of nanoparticles can be leveraged in diagnostics for disease states such as tumors, atherosclerosis, sclerosis, rheumatoid arthritis, and gliomas [118, 119]. Magnetic resonance imaging is working with the superparamagnetic function of iron oxide nanoparticles for biopharmaceutical imaging [120]. Moreover, Fe_3O_4 particles also have superior biocompatibility, excellent chemical stability and low toxicity. Resovist® (Bayer-Schering Pharma, Germany) is a liver-specific magnetic resonance (MR) contrast agent and its active agents are carboxydextran-coated superparamagnetic iron oxide (SPIO) particles (ferucarbotran). The coating prevents the iron-oxide particles from aggregating and makes the compound highly hydrophilic. Resovist® exhibits low viscosity, is isotonic to blood plasma, and the hydrodynamic diameters of the coated particles range between 45 and 60 nm [121, 122].

9.3 Approved Nanopharmaceutical Products: Oral Drug Delivery

Oral delivery is the most common administration route. This is mainly because of its high level of patient compliance due to its

non-invasive nature, simplicity and convenience. Nanomedicines based on oral drug delivery have been extensively investigated and have resulted in various approved, marketed products. However, the oral delivery of liposomes has been somewhat limited due to their unpredictable absorption profiles and the rapid degradation of liposomes in the GI tract via interaction with bile salts [123, 124]. As a result, surface-modified liposomal systems were prepared for the biological instability of liposomes, which showed some success in intestinal absorption of protein drugs [125, 126]. Proliposomes were alternatively introduced and are defined as dry, free-flowing particles that have the ability to form liposomal dispersion when dispersed in an aqueous phase [127–129].

Some advantages of polymer-based nanomedicines include the following [3, 24, 130–133]:

- increasing bioavailability with enhanced water solubility of hydrophobic drugs due to a large specific surface area;
- ability to protect biologically unstable drugs from the hostile environment of the gastrointestinal tract;
- extending drug residence time through strong mucoadhesive properties;
- controlled drug release;
- facilitating transport of the drug through the epithelial membrane via endocytosis;
- bypassing or inhibiting efflux pumps such as P-glycoprotein; and
- targeting specific carriers for receptor-mediated transport.

NanoCrystal® technology (ELAN Corporation, Ireland) [3] is (1) an enabling technology for evaluating NCEs that exhibit poor water solubility and (2) a valuable tool for optimizing the performance of current drugs. NanoCrystal® technology can be applied to both parenteral and oral dosage forms and can reduce particle size to less than 1 μm by proprietary attrition-based wet-milling techniques [134]. This nano-sized formulation can increase the surface area resulting in an increase in solubility and surface stabilization by the surface adsorption of selected GRAS (Generally Regarded As Safe) stabilizers [135]. This technology has resulted in various solid oral nanomedicines on the market.

Examples include RAPAMUNE® (sirolimus), TRICOR® (fenofibrate), EMEND® (aprepitant), and MEGACE® ES (megestrol acetate). RAPAMUNE® is an immunosuppressive agent indicated for the prophylaxis of organ rejection in patients aged ≥13 years receiving renal transplants. The pills should not be crushed, chewed, or split. Patients unable to take the tablets should be prescribed the solution form and instructed on its proper use [136]. TRICOR® is a lipid-regulating agent available in tablet form for oral administration. Each tablet mainly contains GRAS additives such as hypromellose 2910 (3 cps), docusate sodium, sucrose, sodium lauryl sulfate, lactose monohydrate, silicified microcrystalline cellulose, crospovidone, and magnesium stearate. TRICOR® is indicated as adjunctive therapy to diet to reduce elevated LDL-C, Total-C, Triglycerides and Apo B, and to increase HDL-C in adult patients with primary hypercholesterolemia or mixed dyslipidemia [137]. EMEND® is a substance P/neurokinin 1 (NK1) receptor antagonist. It is indicated (in combination with other antiemetic agents) for the prevention of acute and delayed nausea and vomiting associated with initial and repeat courses of highly emetogenic cancer chemotherapy (HEC) including high-dose cisplatin, and the prevention of nausea and vomiting associated with initial and repeat courses of moderately emetogenic cancer chemotherapy (MEC) for the prevention of postoperative nausea and vomiting (PONV) [138]. Each capsule contains a GRAS additive such as sucrose, microcrystalline cellulose, hydroxypropyl cellulose, and sodium lauryl sulfate [138]. MEGACE® ES oral suspension is a progestin indicated for the treatment of anorexia, cachexia, or an unexplained, significant weight loss in patients with a diagnosis of acquired immunodeficiency syndrome (AIDS). MEGACE® ES also contains the following GRAS inactive ingredients: alcohol, artificial lime flavor, citric acid monohydrate, docusate sodium, hypromellose, natural and artificial lemon flavor, purified water, sodium benzoate, sodium citrate dihydrate, and sucrose [139].

The Self-Emulsifying Drug Delivery System (SEDDS) has been intensively studied to enhance the bioavailability of poor water-soluble drugs. SEDDS is an anhydrous pre-concentrated system of microemulsion, which is composed of oil, surfactant, and co-surfactant, and SMEDDS is capable of self-microemulsification after coming in contact with the physiological fluids on

ingestion under gentle agitation. The agitation required for self-emulsification comes from native stomach and intestinal motility [140–142]. There are several products (NEORAL® and NORVIR®) that are commercially available as SMEDDS formulations in the US [143]. In spite of the various advantages of SEDDS, the large amount of surfactant and co-surfactant in these systems is associated with high levels of biological toxicity [143].

9.4 Approved Nanopharmaceutical Products: Dermal and Transdermal Drug Delivery

For dermal and transdermal drug delivery, liposomal nanomedicines have been shown to enhance drug permeation into the epidermis and dermis following localization of active agents at the targeted site of action as well as reduce the loss of these active agents due to percutaneous absorption [62, 144]. Liposomal nanomedicines can greatly enhance the penetration of macromolecule drugs as well as small molecule drugs. Enhancement of skin permeation via liposomal nanomedicines has been mainly due to the presence of specific types and ratios of phospholipids and cholesterol [145]. The formulation factors of liposomal nanomedicines are likely due to the thermodynamic lamellar phase of the liposome bilayer such as liquid crystalline state, gel state, crystalline state, size, charge, and lamellar structure such as multilamellar, unilamellar, and non-lamellar hexagonal [44].

Lipid nanoparticles are attractive carriers for topical pharmaceutical (and cosmetics) products because of their occlusive properties, ability to increase skin hydration, ability to tailor drug release, protection of the drug against degradation, increase of skin penetration associated with targeting, and avoidance of systemic uptake [65, 146]. Although there are only cosmetic products on the market containing lipid nanoparticles at the present time, the market launch of pharmaceutical topical products is expected in the near future [65].

One of the most intensively researched areas for topical/transdermal drug delivery is that of submicron emulsions. This is due to the their higher solubilization capacity for both lipophilic and hydrophilic drugs, ease of formulation, thermodynamic

stability, and ability to enhance skin permeation [147]. Despite these advantages, microemulsion systems present safety issues in long-term applications due to skin irritation by the presence of large amounts of surfactants and co-surfactants [148, 149].

Micelle nanoparticles (MNPs) have been developed for transdermal delivery of active agents. ESTRASORB® (Novavax Inc., USA) is the first nanoengineered topical dosage form that is approved by the FDA for hormone replacement therapy, thereby representing commercial validation of the MNP technology [150]. The *in vitro* Franz cell diffusion study was conducted using human cadaver skin, and three formulations of ESTRASORB® were evaluated [150]: (1) one containing about 9% w/w ethanol; (2) a commercial estradiol gel containing about 40% w/w ethanol; and (3) a 100% ethanolic solution of estradiol. ESTRASORB® is commercially manufactured on a kiloton scale and GRAS additives are used [151]. MNP drug delivery offers a potentially fast and inexpensive pharmaceutical development model by using drugs already proven safe and effective to create new proprietary formulations [150].

9.5 Approved Nanopharmaceutical Products: Pulmonary Drug Delivery

The lung is an attractive target for drug delivery because it offers a noninvasive means to provide not only local lung effects but also possible high systemic bioavailability, avoidance of first-pass metabolism, faster onset of therapeutic action, and the availability of a large surface area [5, 152]. Nanomedicines for pulmonary drug delivery have many advantages [5, 153], such as the ability to:

- achieve a relatively uniform drug distribution;
- enhance the solubility of the drug beyond its own aqueous solubility;
- achieve a sustained-release effect of the inhaled nanodrug;
- deliver macromolecules;
- reduce toxic side effects;
- improve patient compliance; and
- increase drug internalization by cells.

The inhalation devices for pulmonary drug delivery can be divided into three different categories: (1) nebulizers, (2) pressurized Metered Dose Inhalers (pMDIs), and (3) dry powder inhalers (DPIs) [152]. In most cases, nanomedicines can be delivered to the lungs by nebulization of colloidal dispersions or by using pMDIs and DPIs in solid form [5]. Because of the small size and strong particle-to-particle interaction of nanomedicines, particle agglomeration and settlement can easily occur in colloidal dispersions. Also, chemical instability of colloidal dispersions is an issue due to carrier hydrolysis and drug degradation [11]. To overcome these physical and chemical instabilities, there have been several research approaches such as freeze-drying, spray-drying, spray freeze-drying, or supercritical fluid preparation of nanocarriers to provide a storage form [154]. The delivery of nanomedicines to the lungs is limited as individual nanocarriers do not deposit efficiently in the lungs via diffusion, sedimentation or impaction, resulting in the exhalation of a majority of the inhaled dose [11, 152]. Therefore, micron-sized powder carriers containing nanoparticles or agglomerated nanoparticles can be designed to improve the inhalation aerosol delivery of nanoparticles for deep lung delivery by DPIs [155].

The field of nanopharmaceuticals for pulmonary delivery is in its infancy as basic research is conducted in this critically important area. For liposomal drug delivery, the marketed pharmaceutical phospholipid-based product for the treatment of infant respiratory distress syndrome is SURFAXIN® (lucinactant) Intratracheal Suspension, which is a synthetic lung surfactant in combination with the recombinant surface-active polypeptide, KL_4 [156]. In lung cancer nanomedicine pulmonary delivery research, the liposomal combination of paclitaxel and cyclosporin A was evaluated in mice animal models for pulmonary metastases of renal-cell carcinoma [157]. Pulmonary metastases were also achieved in a murine renal carcinoma model with nanoliposomal 9-Nitrocamptothecin inhalation aerosols [158]. The proof-of-concept of proliposome formulations of liposomal nanomedicines has been demonstrated using spray-dried DPI powders [159–162].

Solid lipid nanoparticles (SLNs) can be investigated for non-invasive pulmonary delivery of therapeutic drugs [163–165]. SLNs could deliver insulin via the pulmonary administration

route with both *in vitro* and *in vivo* stability as well as prolonging hypoglycemic effect [163]. The thymopentin-loaded SLNs could enhance drug absorption and offer a sustained drug-release effect [165]. Epirubicin-loaded SLNs have been prepared as an inhalable formulation for treatment of lung cancer [164]. In animal models, these SLNs resulted in higher drug concentrations in the lungs and in plasma following inhalation of epirubicin-SLNs as compared to those following administration of an epirubicin solution [164].

9.6 Conclusions and Future Prospects

One of the major impacts of nanomedicine is taking place in the context of drug delivery. Active agents that failed as conventional formulations due to unacceptable toxicity profiles, poor bioavailability, solubility issues, or physical/chemical instability may be "reconfigured" as nanoformulations. Additionally, with targeting ligands, these formulations can be innovative therapeutic agents for the enhancement of cellular uptake into tissues of interest. As a result, nanomedicines are being developed to allow delivery of active agents more efficaciously to the patient while minimizing side effects, improving drug stability *in vivo* and increase blood circulation time. Apart from these pharmacological benefits, they also offer real economic value to a drug company—the ability to reduce time-to-market, extend the economic life of proprietary drugs and create additional revenue streams, thereby significantly affecting the drug commercialization landscape [3].

There has been a classic lifecycle management option practiced by drug companies in case of reformulation with nanotechnology. Nanopharmaceuticals are usually not bioequivalent to their parent versions and, hence, cannot apply for FDA approval via an Abbreviated New Drug Application (ANDA) under section 505(b)(j) of the Federal Food, Drug, and Cosmetic Act [3a, 168, 169]. In other words, a nanodrug is generally not bioequivalent to a microcrystalline or solubilized form of the same drug (i.e., nano is not always bioequivalent to its bulk or larger counterpart). Hence, a New Drug Application (NDA) under the 505 (b)(1) route may need to be filed at the FDA. Obviously, if a nanopharmaceutical is bioequivalent to its parent version, an ANDA can be filed to seek regulatory

approval. Therefore, when warranted, the FDA should treat nanoversions of active ingredients as NCEs. This will ensure that drugs, biologics, etc. that have been previously approved by the FDA but later presented to the agency as modified nanoversions will undergo a new and rigorous round of safety testing in order to obtain premarket approval [3, 169].

Nanomedical advances and the FDA system for governing it are inevitably intertwined. However, the "baby steps" the FAD has undertaken over the past decade have led to regulatory uncertainty [166–169]. Whether the FDA eventually creates new regulations, tweaks existing ones, for the time being it should at least look at nanomedical products on a case-by-case basis [168, 169]. It is imperative that flexible and science-based regulation of nanopharmaceutical development must balance innovation and R&D with the principle of ensuring maximum public health protection. Regulatory oversight must evolve in concert with newer generations of these drugs and not lag, as is the case currently [3, 168, 169].

The toxicity of many nanoscale materials will not be fully apparent until they are widely distributed and their exposure is felt by a diverse population [169]. Therefore, postmarket tracking or a surveillance system must be adopted to assist in nanomedical product recalls [169]. Although toxicological testing for health risks of such products is not currently a complete science [170], nevertheless, it is crucial to monitor their unique properties (if any) that may lead to serious adverse effects and toxicity. Because it is well established that premarket testing of nanodrugs will not detect all adverse reactions [171], it is essential that long-term testing of nanoscale materials be in place to allow safety testing. In this regard, toxicity data specific to nanomaterials needs to be collected and an effective risk research strategy devised [169]. Currently, there are few reliable means to identify marketed "nano-containing" products, and consumers are unable to judge for themselves which ones may be toxic. Hence, the FDA should seriously contemplate nano ingredient labeling on a case-by-case basis.

So far, the process of converting basic research in nanomedicine into commercially viable products has been difficult. Securing valid, defensible patent protection from the US Patent & Trademark

Office [172, 173] along with clearer regulatory and safety guidelines from the FDA [168, 169] are critical to any commercialization effort pertaining to nanopharmaceuticals.

In the future, novel "multifunctional" nanopharmaceuticals will be designed as new generations of drug delivery systems to target specific organs or specific tissues. Currently, nanodrug delivery systems are being developed to target even individual cells or organelles. As we rapidly enter the age of "nanotheranostics", it is likely that nanopharmaceuticals will become prime tools in treating numerous diseases [174, 175]. However, even though the use of nanotechnology for drug delivery is promising and a highly attractive application area, additional funding, basic research and translational research from "bench-to-bedside" is needed. In the end, the long-term prognosis and development of nanopharmaceuticals will hinge on effective nanogovernance, issuance of valid patents, clearer safety guidelines and transparency with the consumer on all issues "nano" [3]. Naturally, this will require the full commitment of all the key players' involved—big pharma, academia, governmental regulatory agencies, the venture community and the public [3].

Disclosures and Conflict of Interest

The authors declare that they have no conflict of interest with any organization or entity discussed in this chapter. Dr. Bawa is scientific advisor to Teva Pharmaceutical Industries, Ltd. (Israel). No writing assistance was utilized in the production of this chapter and the authors have received no payment for its preparation. The findings and conclusions here reflect the current views of the authors. Nothing contained herein is to be considered as the rendering of legal advice.

Corresponding Authors

Dr. Heidi M. Mansour
The University of Arizona, College of Pharmacy
1703 E. Mabel St., Tucson, Arizona 85721-0207, USA
Email: mansour@pharmacy.arizona.edu

Dr. Raj Bawa
Bawa Biotech LLC
21005 Starflower Way
Ashburn, VA 20147, USA
Email: bawa@bawabiotech.com

About the Authors

Heidi M. Mansour is a faculty member at the College of Pharmacy at the University of Arizona (UA) in Tucson, Arizona (USA) with faculty member affiliations in the UA BIO5 Research Institute, the UA Institute of the Environment, and the UA Comprehensive Cancer Center. She has published more than 55 peer-reviewed scientific journal papers, 8 book chapters, and 70 scientific conference abstracts and is co-editor of a book on nanomedicine drug delivery published in 2013 by CRC Press/Taylor & Francis. Her research program has enjoyed funding from federal sources and the pharmaceutical industry. Dr. Mansour leads a multidisciplinary group of postdoctoral scholars, visiting scholars, visiting professors, graduate students, and physician-scientist (MD/PhD) fellows. Dr. Mansour is an active, long-time member of numerous professional organizations and elected member to honor societies, including the Sigma Xi Scientific Research Honor Society, Rho Chi Pharmaceutical Honor Society, and Golden Key International Honor Society. She serves on the editorial advisory boards of several journals. She has a BS in pharmacy with honors and distinction (School of Pharmacy), a PhD minor in advanced physical and interfacial chemistry (Department of Chemistry), and a PhD major in drug delivery/pharmaceutics (School of Pharmacy) from the University of Wisconsin-Madison. She completed postdoctoral fellowships at the U.W.-Madison and at the University of North Carolina-Chapel Hill in the Division of Molecular Pharmaceutics receiving the UNC-Chapel Hill Postdoctoral Award for Research Excellence from the Office of the Vice-Chancellor, AAPS (American Association of Pharmaceutical Scientists) Postdoctoral Fellow Award in Research Excellence, and the PhRMA (Pharmaceutical Researchers & Manufacturers of America) Foundation Postdoctoral Fellowship award in Pharmaceutics.

She has served on the Graduate Faculty at UNC-Chapel Hill for several years. She is an expert member of NIH NICHD U.S. Pediatric Formulations Initiative (PFI) New Drug Delivery Systems (NDDS) Aerosols Working Group. She regularly serves as an expert reviewer for scientific journals and grant funding agencies.

Raj Bawa is president of Bawa Biotech LLC, a biotech/pharma consultancy and patent law firm he founded in 2002 and based in Ashburn, Virginia, USA.. He is an inventor, entrepreneur, professor, and a registered patent agent licensed to practice before the U.S. Patent & Trademark Office. Trained as a biochemist and microbiologist, he has been an active researcher for over two decades. He has extensive expertise in pharmaceutical sciences, biotechnology, nanomedicine, drug delivery and biodefense-related scientific, FDA regulatory, and patent law issues. Since 1999, he has held various adjunct faculty positions at Rensselaer Polytechnic Institute in Troy, NY, where he is currently an adjunct professor of biological sciences and where he received his PhD (biophysics/biochemistry; 1987–1990). Since 2004, he has been an adjunct associate professor of natural and applied sciences at NVCC in Annandale, VA. Since 2012, he has been a scientific advisor to Teva Pharmaceutical Industries, Ltd., Israel. He previously served as patent legal advisor at Sequoia Pharmaceuticals, Gaithersburg, MD, and as senior scientist at SynerGene Therapeutics, Inc., Potomac, MD. He recently served as the principal investigator of two National Cancer Institute/SBIR contracts titled "Targeted nanocomplexed iron oxide for early detection with concurrent hyperthermia treatment of cancer" and "A targeted nanocomplex for early detection of lung cancer." In the 1990s, Dr. Bawa held various positions at the US Patent & Trademark Office, including primary examiner (6 years) and instructor at the US Patent Academy. He is a life member of Sigma Xi, founding director of the American Society for Nanomedicine, and co-chair of the Nanotech Committee of the American Bar Association. He has authored over 100 publications, co-edited two books, and presented or chaired at over 200 conferences worldwide. He serves on the editorial boards of 16 peer-reviewed journals. Some of Dr. Bawa's awards include the Innovations Prize from the Institution of Mechanical Engineers, London, UK (2008);

Appreciation Award from the Undersecretary of Commerce, Washington, DC (2001); a Research Fellowship from Rensselaer (1989–1990); the Key Award from Rensselaer's Office of Alumni Relations (2005); and Lifetime Achievement Award from the American Society for Nanomedicine (2014).

Chun-Woong Park received an MS in 2005 in pharmaceutics and a PhD in physical pharmacy in 2008 from Sungkyunkwan University, Republic of Korea. From 2010 to 2011, he was a postdoctoral visiting scholar at the University Of Kentucky College of Pharmacy, USA. Currently, he is an assistant professor at the College of Pharmacy at Chungbuk National University, Republic of Korea. His current research focuses on advanced particle engineering design for dry powder inhalation aerosols and gastroretentive drug delivery system using a PUMICETM matrix system.

References

1. Han, J. (2009). Bimedical nanoengineering for nanomedicine. In: Reisner, D. E., ed. *Bionanotechnology: Global Prospects*. CRC, Boca Raton, FL; pp. 269–289.
2. Hornyak, G. L., Dutta, J., Tibbals, H., Rao, A. (2008). Nanoscience and nanotechnology—the distinction. In: Hornyak, G. L. (ed.), Introduction to nanoscience. CRC Press, Boca Raton, FL; pp. 1–20.
3. (a) Bawa, R. (2010). Nanopharmaceuticals. *Eur. J. Nanomed.,* **3**(1), 34–39.

   (b) Bawa, R. (2015). Emerging issues in nanodrugs and nanomedicine. *In*: H. B. Wellons and E. S. Ewing (Editors): *Biotechnology and the Law*, 2nd edition, American Bar Association, Chicago, IL (in press).

   (c) Bawa, R. (2015). What's in a Name? Defining "nano" in the context of drug delivery. *In*: Bawa, R., Audette, G. and Rubinstein, I. (Editors): *Handbook of Clinical Nanomedicine: Nanoparticles, Imaging, Therapy, and Clinical Applications*, Chapter 6. Pan Stanford Publishing, Singapore.

   (d) Bawa, R., Szebeni, J., Bawa S. R., Mehra, R. (2015). Nanoscale therapeutics: Introductory overview of key issues. *In*: Bawa, R., Audette, G. and Rubinstein, I. (Editors): *Handbook of Clinical Nanomedicine: Nanoparticles, Imaging, Therapy, and Clinical Applications*, Chapter 27. Pan Stanford Publishing, Singapore.

4. Shekunov, B. (2005). Nanoparticle technology for drug delivery: From nanoparticles to cutting-edge delivery strategies-part I. *Drugs Invest. Drugs J.,* **8**(5), 399.
5. Sung, J. C., Pulliam, B. L., Edwards, D. A. (2007). Nanoparticles for drug delivery to the lungs. *Trends Biotechnol.,* **25**(12), 563–570.
6. Cho, K., Wang, X., Nie, S., Chen, Z. G., Shin, D. M. (2008). Therapeutic nanoparticles for drug delivery in cancer. *Clin. Cancer Res.,* **14**(5), 1310.
7. Brigger, I., Dubernet, C., Couvreur, P. (2002). Nanoparticles in cancer therapy and diagnosis. *Adv. Drug Deliv. Rev.,* **54**(5), 631–651.
8. Tiwari, S. B., Amiji, M. M. (2006). A review of nanocarrier-based CNS delivery systems. *Curr. Drug Deliv.,* **3**(2), 219–232.
9. Kaur, I. P., Bhandari, R., Bhandari, S., Kakkar, V. (2008). Potential of solid lipid nanoparticles in brain targeting. *J. Control. Release,* **127**(2), 97–109.
10. Davis, M. E. (2008). Nanoparticle therapeutics: An emerging treatment modality for cancer. *Nat. Rev. Drug Discov.,* **7**(9), 771–782.
11. Mansour, H. M., Rhee, Y. S., Wu, X. (2009). Nanomedicine in pulmonary delivery. *Int. J. Nanomed.,* **4**, 299–319.
12. Driscoll, D. F., Bhargava, H. N., Li, L., Zaim, R. H., Babayan, V. K., et al. (1995). Physicochemical stability of total nutrient admixtures. *Am. J. Health-Syst. Pharm.,* **52**(6), 623.
13. Koster, V., Kuks, P., Lange, R., Talsma, H. (1996). Particle size in parenteral fat emulsions, what are the true limitations? *Int. J. Pharm.,* **134**(1–2), 235–238.
14. Park, J. W., Park, E. S., Chi, S. C., Kil, H. Y., Lee, K. H. (2003). The effect of lidocaine on the globule size distribution of propofol emulsions. *Anesth. Analg.,* **97**(3), 769.
15. Wissing, S., Kayser, O., Muller, R. (2004). Solid lipid nanoparticles for parenteral drug delivery. *Adv. Drug Deliv. Rev.,* **56**(9), 1257–1272.
16. Zimmer, A., Kreuter, J. (1995). Microspheres and nanoparticles used in ocular delivery systems. *Adv. Drug Deliv. Rev.,* **16**(1), 61–73.
17. De Campos, A. M., Diebold, Y., Carvalho, E. L. S., Sanchez, A., Jose Alonso, M. (2004). Chitosan nanoparticles as new ocular drug delivery systems: *In vitro* stability, *in vivo* fate, and cellular toxicity. *Pharm. Res.,* **21**(5), 803–810.
18. Wu, X., Mansour, H. M. (2011). Nanopharmaceuticals II: Application of nanoparticles and nanocarrier systems in pharmaceutics and nanomedicine. *Int. J. Nanotechnol.,* **8**(1), 115–145.

19. *Nanomedicine—an ESF–european medical research councils (EMRC) forward look report. Strasbourg cedex*. (2004). France.
20. Webster, T. J. (2006). Nanomedicine: What's in a definition? *Int. J. Nanomed.,* **1**(2), 115.
21. *National Institute of Health Roadmap for Medical Research: Nanomedicine* (2006). USA: National Institutes of Health NIH.
22. Park, J. H., Lee, S., Kim, J. H., Park, K., Kim, K., et al. (2008). Polymeric nanomedicine for cancer therapy. *Prog. Polymer Sci.,* **33**(1), 113–137.
23. Resnik, D. B., Tinkle, S. S. (2007). Ethical issues in clinical trials involving nanomedicine. *Contempor. Clin. Trials,* **28**(4), 433–441.
24. Rhee, Y. S., Mansour, H. M. (2011). Nanopharmaceuticals I: Nanocarrier systems in drug delivery. *Int. J. Nanotechnol.,* **8**(1), 84–114.
25. Park, K. (2007). Nanotechnology: What it can do for drug delivery. *J. Control. Release,* **120**(1–2), 1.
26. Koo, O. M., Rubinstein, I., Onyuksel, H. (2005). Role of nanotechnology in targeted drug delivery and imaging: A concise review. *Nanomed. Nanotechnol. Biol. Med.,* **1**(3), 193–212.
27. Jain, K. (2005). Nanotechnology-based drug delivery for cancer. *Technol. Cancer Res. Treat.,* **4**(4), 407.
28. Ould-Ouali, L., Noppe, M., Langlois, X., Willems, B., Te Riele, P., et al. (2005). Self-assembling peg-p (cl-co-tmc) copolymers for oral delivery of poorly water-soluble drugs: A case study with risperidone. *J. Control. Release,* **102**(3), 657–668.
29. Kipp, J. (2004). The role of solid nanoparticle technology in the parenteral delivery of poorly water-soluble drugs. *Int. J. Pharm.,* **284**(1–2), 109–122.
30. Suri, S. S., Fenniri, H., Singh, B. (2007). Nanotechnology-based drug delivery systems. *J. Occup. Med. Toxicol.,* **2**(1), 16.
31. Bawa, R. (2011). Regulating nanomedicine—can the FDA handle it? *Curr. Drug Deliv.,* **8**(3), 227–234.
32. Bawa, R. (2008). Nanoparticle-based therapeutics in humans: A survey. *Nanotechnol. Law Bus.,* **5**(2), 135–155.
33. Florence, A. T. (2009). Pharmaceutical aspects of nanotechnology. In: Florence, A. T., Siepmann, J. (ed.), *Modern pharmaceutics. Informa Healthcare*, London, UK; pp. 453–492.
34. Von Werne, T., Patten, T. E. (1999). Preparation of structurally well-defined polymer-nanoparticle hybrids with controlled/living radical polymerizations. *J. Am. Chem. Soc.,* **121**(32), 7409–7410.

35. Pridgen, E. M., Langer, R., Farokhzad, O. C. (2007). Biodegradable, polymeric nanoparticle delivery systems for cancer therapy. *Nanomedicine,* **2**(5), 669–680.

36. Hussain, F., Hojjati, M., Okamoto, M., Gorga, R. E. (2006). Review article: Polymer-matrix nanocomposites, processing, manufacturing, and application: An overview. *J. Composite Mater.,* **40**(17), 1511.

37. Van Vlerken, L. E., Amiji, M. M. (2006). Multi-functional polymeric nanoparticles for tumour-targeted drug delivery. *Exp. Opin. Drug Deliv.,* **3**(2), 205–216.

38. Mueller, R. H., Maeder, K., Gohla, S. (2000). Solid lipid nanoparticles (sln) for controlled drug delivery-a review of the state of the art. *Eur. J. Pharm. Biopharm.,* **50**(1), 161–177.

39. Muller, R., Radtke, M., Wissing, S. (2002). Nanostructured lipid matrices for improved microencapsulation of drugs. *Int. J.Pharm.,* **242**(1–2), 121–128.

40. Almeida, A. J., Souto, E. (2007). Solid lipid nanoparticles as a drug delivery system for peptides and proteins. *Adv. Drug Deliv. Rev.,* **59**(6), 478–490.

41. Lian, T., Ho, R. J. Y. (2001). Trends and developments in liposome drug delivery systems. *J. Pharm. Sci.,* **90**(6), 667–680.

42. Samad, A., Sultana, Y., Aqil, M. (2007). Liposomal drug delivery systems: An update review. *Curr. Drug Deliv.,* **4**(4), 297–305.

43. Malam, Y., Loizidou, M., Seifalian, A. M. (2009). Liposomes and nanoparticles: Nanosized vehicles for drug delivery in cancer. *Trends Pharm. Sci.,* **30**(11), 592–599.

44. El Maghraby, G., Barry, B., Williams, A. (2008). Liposomes and skin: From drug delivery to model membranes. *Eur. J. Pharm. Sci.,* **34**(4–5), 203–222.

45. Allen, T. M. (1994). Long-circulating (sterically stabilized) liposomes for targeted drug delivery. *Trends Pharmacol. Sci.,* **15**(7), 215–220.

46. Lawrence, M. J., Rees, G. D. (2000). Microemulsion-based media as novel drug delivery systems. *Adv. Drug Deliv. Rev.,* **45**(1), 89–121.

47. Wu, W., Wang, Y., Que, L. (2006). Enhanced bioavailability of silymarin by self-microemulsifying drug delivery system. *Eur. J. Pharm. Biopharm.,* **63**(3), 288–294.

48. Jadhav, K., Shaikh, I., Ambade, K., Kadam, V. (2006). Applications of microemulsion based drug delivery system. *Curr. Drug Deliv.,* **3**(3), 267–273.

49. Hashida, M., Kawakami, S., Yamashita, F. (2005). Lipid carrier systems for targeted drug and gene delivery. *Chem. Pharm. Bull.,* **53**(8), 871–880.
50. Davis, S. S., Washington, C., West, P., Illum, L., Liversidge, G., et al. (1987). Lipid emulsions as drug delivery systems. *Ann. N Y Acad. Sci.,* **507**(1), 75–88.
51. Collins-Gold, L., Lyons, R., Bartholow, L. (1990). Parenteral emulsions for drug delivery. *Adv. Drug Deliv. Rev.,* **5**(3), 189–208.
52. Charman, W. N. (2000). Lipids, lipophilic drugs, and oral drug delivery: Some emerging concepts. *J. Pharm. Sci.,* **89**(8), 967–978.
53. Jamaty, C., Bailey, B., Larocque, A., Notebaert, E., Sanogo, K., et al. (2010). Lipid emulsions in the treatment of acute poisoning: A systematic review of human and animal studies. *Clin. Toxicol.,* **48**(1), 1–27.
54. Pouton, C. W. (2000). Lipid formulations for oral administration of drugs: Non-emulsifying, self-emulsifying and "self-microemulsifying" drug delivery systems. *Eur. J. Pharm. Sci.,* **11**, S93–S98.
55. Vinogradov, S. V. (2006). Colloidal microgels in drug delivery applications. *Curr. Pharm. Des.,* **12**(36), 4703.
56. Vinogradov, S. V., Zeman, A. D., Batrakova, E. V., Kabanov, A. V. (2005). Polyplex nanogel formulations for drug delivery of cytotoxic nucleoside analogs. *J. Control. Release,* **107**(1), 143–157.
57. Raemdonck, K., Demeester, J., De Smedt, S. (2008). Advanced nanogel engineering for drug delivery. *Soft Matter,* **5**(4), 707–715.
58. Kataoka, K., Harada, A., Nagasaki, Y. (2001). Block copolymer micelles for drug delivery: Design, characterization and biological significance. *Adv. Drug Deliv. Rev.,* **47**(1), 113–131.
59. Nasongkla, N., Bey, E., Ren, J., Ai, H., Khemtong, C., et al. (2006). Multifunctional polymeric micelles as cancer-targeted, mri-ultrasensitive drug delivery systems. *Nano Lett.,* **6**(11), 2427–2430.
60. Maeda, H., Bharate, G., Daruwalla, J. (2009). Polymeric drugs for efficient tumor-targeted drug delivery based on epr-effect. *Eur. J. Pharm. Biopharm.,* **71**(3), 409–419.
61. Bangham, A., Standish, M., Watkins, J. (1965). Diffusion of univalent ions across the lamellae of swollen phospholipids. *J. Mol. Biol.,* **13**(1), 238–252, IN226–IN227.
62. Gershkovich, P., Wasan, K. M., Barta, C. A. (2008). A review of the application of lipid-based systems in systemic, dermal/transdermal, and ocular drug delivery. *Crit. Rev. Ther. Drug Carrier Syst.,* **25**(6), 545.

63. Mansour, H. M., Rhee, Y. S., Park, C. W., Deluca, P. P. (2011). Lipid nanoparticulate drug delivery and nanomedicine. In: Ahmad, M. U. (ed.), *Lipids in Nanotechnology*. AOCS Press, Chicago, Illinois; pp. 221–268.

64. Antimisiaris, S. G., Kallinteri, P., Fatouros, D. G. (2007). Liposomes and drug delivery. In: Gad, S. C., ed., *Pharmaceutical Manufacturing Handbook: Production and Processes.* John Wiley & Sons, Inc., Hoboken, NJ, pp. 443–535.

65. Pardeike, J., Hommoss, A., Muller, R. H. (2009). Lipid nanoparticles (SLN, NLC) in cosmetic and pharmaceutical dermal products. *Int. J. Pharm.,* **366**(1–2), 170–184.

66. Joshi, M. D., Muller, R. H. (2009). Lipid nanoparticles for parenteral delivery of actives. *Eur. J. Pharm. Biopharm.,* **71**(2), 161–172.

67. Muchow, M., Maincent, P., Muller, R. H. (2008). Lipid nanoparticles with a solid matrix (sln, nlc, ldc) for oral drug delivery. *Drug Dev. Ind. Pharm.,* **34**(12), 1394–1405.

68. Kabanov, A. V., Vinogradov, S. V. (2009). Nanogels as pharmaceutical carriers: Finite networks of infinite capabilities. *Angew. Chem. Int. Ed.,* **48**(30), 5418–5429.

69. Torchilin, V. P. (2005). Lipid-core micelles for targeted drug delivery. *Curr. Drug Deliv.,* **2**(4), 319–327.

70. Marcato, P. D., Duran, N. (2008). New aspects of nanopharmaceutical delivery systems. *J. Nanosci. Nanotechnol.,* **8**(5), 2216–2229.

71. Constantinides, P. P., Chaubal, M. V., Shorr, R. (2008). Advances in lipid nanodispersions for parenteral drug delivery and targeting. *Adv. Drug Deliv. Rev.,* **60**(6), 757–767.

72. Metselaar, J. M., Mastrobattista, E., Storm, G. (2002). Liposomes for intravenous drug targeting: Design and applications. *Mini Rev. Med. Chem.,* **2**(4), 319–329.

73. Rosenthal, S. J., Tomlinson, I., Adkins, E. M., Schroeter, S., Adams, S., et al. (2002). Targeting cell surface receptors with ligand-conjugated nanocrystals. *J. Am. Chem. Soc.,* **124**(17), 4586–4594.

74. Cambi, A., Lidke, D. S., Arndt-Jovin, D. J., Figdor, C. G., Jovin, T. M. (2007). Ligand-conjugated quantum dots monitor antigen uptake and processing by dendritic cells. *Nano Lett.,* **7**(4), 970–977.

75. Byrne, J. D., Betancourt, T., Brannon-Peppas, L. (2008). Active targeting schemes for nanoparticle systems in cancer therapeutics. *Adv. Drug Deliv. Rev.,* **60**(15), 1615–1626.

76. Torchilin, V. (2009). Multifunctional and stimuli-sensitive pharmaceutical nanocarriers. *Eur. J. Pharm.Biopharm.,* **71**(3), 431–444.

77. Bentzen, S. M. (2005). Theragnostic imaging for radiation oncology: Dose-painting by numbers. *Lancet Oncol.,* **6**(2), 112–117.

78. Majumdar, D., Peng, X. H., Shin, M. (2010). The medicinal chemistry of theragnostics, multimodality imaging and applications of nanotechnology in cancer. *Curr. Top. Med. Chem.,* **10**(12), 1211–1226.

79. Rhee, Y. S., Park, C. W., Deluca, P. P., Mansour, H. M. (2010). Sustained-release injectable drug delivery. *Pharm. Technol.,* s6–s13.

80. Webb, M. S., Rebstein, P., Lamson, W., Bally, M. B. (2007). Liposomal drug delivery: Recent patents and emerging opportunities. *Recent Patents Drug Deliv. Formulation*, **1**(3), 185–194.

81. Wu, G., Mikhailovsky, A., Khant, H. A., Fu, C., Chiu, W., et al. (2008). Remotely triggered liposome release by near-infrared light absorption via hollow gold nanoshells. *J. Am. Chem. Soc.,* **130**(26), 8175–8177.

82. Watanabe, Y., Nomoto, H., Takezawa, R., Miyoshi, N., Akaike, T. (1994). Highly efficient transfection into primary cultured mouse hepatocytes by use of cation-liposomes: An application for immunization. *J. Biochem.,* **116**(6), 1220.

83. Torchilin, V. P. (2006). Multifunctional nanocarriers. *Adv. Drug Deliv. Rev.,* **58**(14), 1532–1555.

84. Kumari, A., Yadav, S. K., Yadav, S. C. (2010). Biodegradable polymeric nanoparticles based drug delivery systems. *Colloids Surf. B Biointerfaces* **75**(1), 1–18.

85. Mansour, H. M., Sohn, M. J., Al-Ghananeem, A., Deluca, P. P. (2010). Materials for pharmaceutical dosage forms: Molecular pharmaceutics and controlled release drug delivery aspects. *Int. J. Mol. Sci.,* **11**(9), 3298–3322.

86. Matsumura, Y. (2008). Poly (amino acid) micelle nanocarriers in preclinical and clinical studies. *Adv. Drug Deliv. Rev.,* **60**(8), 899–914.

87. Matsumura, Y. (2008). Polymeric micellar delivery systems in oncology. *Japanese J. Clin. Oncol.,* **38**(12), 793.

88. Bae, Y., Kataoka, K. (2009). Intelligent polymeric micelles from functional poly (ethylene glycol)-poly (amino acid) block copolymers. *Adv. Drug Deliv. Rev.,* **61**(10), 768–784.

89. Arcamone, F. (1981). Molecular interactions. In: Arcamone, F. (ed.), *Doxorubicin: Anticancer Antibiotics*. Academic Press, UK; pp. 93–99.

90. Andreopoulou, E., Gaiotti, D., Kim, E., Downey, A., Mirchandani, D., et al. (2007). Pegylated liposomal doxorubicin HCl: Experience with

long-term maintenance in responding patients with recurrent epithelial ovarian cancer. *Ann. Oncol.,* **18**(4), 716.

91. Lyass, O., Uziely, B., Ben Yosef, R., Tzemach, D., Heshing, N. I., et al. (2000). Correlation of toxicity with pharmacokinetics of pegylated liposomal doxorubicin (doxil) in metastatic breast carcinoma. *Cancer,* **89**(5), 1037–1047.
92. O'brien, M., Wigler, N., Inbar, M., Rosso, R., Grischke, E., et al. (2004). Reduced cardiotoxicity and comparable efficacy in a phase iii trial of pegylated liposomal doxorubicin HCl (Caelyx/Doxil) versus conventional doxorubicin for first-line treatment of metastatic breast cancer. *Ann. Oncol.,* **15**(3), 440.
93. Gabizon, A., Shmeeda, H., Barenholz, Y. (2003). Pharmacokinetics of pegylated liposomal doxorubicin: Review of animal and human studies. *Clin. Pharm.,* **42**(5), 419–436.
94. Symon, Z., Peyser, A., Tzemach, D., Lyass, O., Sucher, E., et al. (1999). Selective delivery of doxorubicin to patients with breast carcinoma metastases by stealth liposomes. *Cancer,* **86**(1), 72–78.
95. Doxil® (doxorubicin hcl liposome injection) for intravenous infusion. Available at: http://www.accessdata.fda.gov/drugsatfda_docs/label/2012/050718s043lbl.pdf (accessed on January 16, 2015).
96. Miele, E., Spinelli, G. P., Tomao, F., Tomao, S. (2009). Albumin-bound formulation of paclitaxel (abraxane, abi-007) in the treatment of breast cancer. *Int. J. Nanomed.,* **4**, 99.
97. Choy, H. (2001). Taxanes in combined modality therapy for solid tumors. *Crit. Rev. Oncol./Hematol.,* **37**(3), 237–247.
98. Hainsworth, J. D. (2004). Practical aspects of weekly docetaxel administration schedules. *Oncol.,* **9**(5), 538.
99. Rowinsky, E. K., Cazenave, L. A., Donehower, R. C. (1990). Taxol: A novel investigational antimicrotubule agent. *J. Natl. Cancer Inst.,* **82**(15), 1247.
100. Bissery, M. C., Nohynek, G., Sanderink, G. J., Lavelie, F. (1995). Docetaxel (taxotere (r)) a review of preclinical and clinical experience. Part I: Preclinical experience. *Anti Cancer Drugs,* **6**(3), 339.
101. Rowinsky, E. K., Donehower, R. C. (1995). Paclitaxel (taxol). *N. Eng. J. Med.,* **332**(15), 1004.
102. Gianni, L., Kearns, C. M., Giani, A., Capri, G., Vigano, L., et al. (1995). Nonlinear pharmacokinetics and metabolism of paclitaxel and its pharmacokinetic/pharmacodynamic relationships in humans. *J. Clin. Oncol.,* **13**(1), 180.

103. Weiss, R. B., Donehower, R., Wiernik, P., Ohnuma, T., Gralla, R., et al. (1990). Hypersensitivity reactions from taxol. *J. Clin. Oncol.,* **8**(7), 1263.

104. Purcell, M., Neault, J., Tajmir-Riahi, H. (2000). Interaction of taxol with human serum albumin. *Biochim. Biophys. Acta (BBA)–Protein Struct. Mol. Enzymol.,* **1478**(1), 61–68.

105. Abraxane® for injectable suspension (paclitaxel protein-bound particles for injectable suspension). Available at: http://www.accessdata.fda.gov/drugsatfda_docs/label/2012/021660s031lbl.pdf (accessed on January 16, 2015).

106. Desai, N., Trieu, V., Yao, Z., Louie, L., Ci, S., et al. (2006). Increased antitumor activity, intratumor paclitaxel concentrations, and endothelial cell transport of cremophor-free, albumin-bound paclitaxel, ABI-007, compared with cremophor-based paclitaxel. *Clin. Cancer Res.,* **12**(4), 1317.

107. Dismukes, W. E. (1988). Cryptococcal meningitis in patients with aids. *J. Infect. Dis.,* **157**(4), 624.

108. Saag, M. S., Powderly, W. G., Cloud, G. A., Robinson, P., Grieco, M. H., et al. (1992). Comparison of amphotericin b with fluconazole in the treatment of acute AIDs-associated cryptococcal meningitis. The niaid mycoses study group and the aids clinical trials group. *N. Eng. J. Med.,* **326**(2), 83.

109. Jeon, G. W., Koo, S. H., Lee, J. H., Hwang, J. H., Kim, S. S., et al. (2007). A comparison of ambisome¢ç to amphotericin b for treatment of systemic candidiasis in very low birth weight infants. *Yonsei Med. J.,* **48**(4), 619.

110. Dismukes, W. E. (2000). Introduction to antifungal drugs. *Clinical Infectious Diseases*, **30**(4), 653.

111. Rajender Reddy, K., Modi, M. W., Pedder, S. (2002). Use of peginterferon alfa-2a (40 kd)(pegasys) for the treatment of hepatitis c. *Adv. Drug Deliv. Rev.,* **54**(4), 571–586.

112. Hui, A., Chan, H. L. Y., Cheung, A. Y. K., Cooksley, G., Sung, J. J. Y. (2005). Systematic review: Treatment of chronic hepatitis b virus infection by pegylated interferon. *Aliment. Pharmacol. Ther.,* **22**(6), 519–528.

113. Cooksley, W. G. (2004). Treatment with interferons (including pegylated interferons) in patients with hepatitis B. *Semin. Liver Dis.,* **24 Suppl 1**, 45–53.

114. Bukowski, R. M., Tendler, C., Cutler, D., Rose, E., Laughlin, M. M., et al. (2002). Treating cancer with peg intron. *Cancer,* **95**(2), 389–396.

115. Wretlind, A. (1981). Development of fat emulsions. *J. Parenter. Enteral Nutr.,* **5**(3), 230.
116. Mornet, S., Vasseur, S., Grasset, F., Duguet, E. (2004). Magnetic nanoparticle design for medical diagnosis and therapy. *J. Mater. Chem.,* **14**(14), 2161–2175.
117. Thorek, D. L. J., Chen, A. K., Czupryna, J., Tsourkas, A. (2006). Superparamagnetic iron oxide nanoparticle probes for molecular imaging. *Ann. Biomed. Eng.,* **34**(1), 23–38.
118. Shubayev, V. I., Pisanic, I., Thomas, R., Jin, S. (2009). Magnetic nanoparticles for theragnostics. *Adv. Drug Deliv. Rev.,* **61**(6), 467–477.
119. Duguet, E., Vasseur, S., Mornet, S., Devoisselle, J. M. (2006). Magnetic nanoparticles and their applications in medicine. *Nanomedicine* **1**(2), 157–168.
120. Mccarthy, J. R., Kelly, K. A., Sun, E. Y., Weissleder, R. (2007). Targeted delivery of multifunctional magnetic nanoparticles. *Nanomedicine,* **2**(2), 153–167.
121. Vogl, T. J., Schwarz, W., Blume, S., Pietsch, M., Shamsi, K., et al. (2003). Preoperative evaluation of malignant liver tumors: Comparison of unenhanced and spio (Resovist)-enhanced mr imaging with biphasic ctap and intraoperative us. *Eur. Radiol.,* **13**(2), 262–272.
122. Reimer, P., Rummeny, E. J., Daldrup, H. E., Balzer, T., Tombach, B., et al. (1995). Clinical results with resovist: A phase 2 clinical trial. *Radiology,* **195**(2), 489.
123. Singh, R., Singh, S., Lillard, J. W. (2008). Past, present, and future technologies for oral delivery of therapeutic proteins. *J. Pharm. Sci.,* **97**(7), 2497–2523.
124. Arien, A., Goigoux, C., Baquey, C., Dupuy, B. (1993). Study of *in vitro* and *in vivo* stability of liposomes loaded with calcitonin or indium in the gastrointestinal tract. *Life Sci.,* **53**(16), 1279–1290.
125. Chen, H., Torchilin, V., Langer, R. (1996). Polymerized liposomes as potential oral vaccine carriers: Stability and bioavailability. *J. Control. Release,* **42**(3), 263–272.
126. Xing, L., Dawei, C., Liping, X., Rongqing, Z. (2003). Oral colon-specific drug delivery for bee venom peptide: Development of a coated calcium alginate gel beads-entrapped liposome. *J. Control. Release,* **93**(3), 293–300.
127. Payne, N. I., Timmins, P., Ambrose, C. V., Ward, M. D., Ridgway, F. (1986). Proliposomes: A novel solution to an old problem. *J. Pharm. Sci.,* **75**(4), 325–329.

128. Song, K. H., Chung, S. J., Shim, C. K. (2002). Preparation and evaluation of proliposomes containing salmon calcitonin. *J. Control. Release,* **84**(1–2), 27–37.

129. Yan-Yu, X., Yun-Mei, S., Zhi-Peng, C., Qi-Neng, P. (2006). Preparation of silymarin proliposome: A new way to increase oral bioavailability of silymarin in beagle dogs. *Int. J. Pharm.,* **319**(1–2), 162–168.

130. Yoncheva, K., Guembe, L., Campanero, M., Irache, J. (2007). Evaluation of bioadhesive potential and intestinal transport of pegylated poly (anhydride) nanoparticles. *Int. J. Pharm.,* **334**(1–2), 156–165.

131. Desai, M. P., Labhasetwar, V., Amidon, G. L., Levy, R. J. (1996). Gastrointestinal uptake of biodegradable microparticles: Effect of particle size. *Pharm. Res.,* **13**(12), 1838–1845.

132. Foger, F., Hoyer, H., Kafedjiiski, K., Thaurer, M., Bernkop-Schnurch, A. (2006). *In vivo* comparison of various polymeric and low molecular mass inhibitors of intestinal p-glycoprotein. *Biomaterials,* **27**(34), 5855–5860.

133. Francis, M. F., Cristea, M., Winnik, F. M. (2005). Exploiting the vitamin b12 pathway to enhance oral drug delivery via polymeric micelles. *Biomacromolecules,* **6**(5), 2462–2467.

134. Merisko-Liversidge, E., Liversidge, G. G., Cooper, E. R. (2003). Nanosizing: A formulation approach for poorly-water-soluble compounds. *Eur. J. Pharm. Sci.,* **18**(2), 113–120.

135. Junghanns, J. U. A. H., Muller, R. H. (2008). Nanocrystal technology, drug delivery and clinical applications. *Int. J. Nanomed.,* **3**(3), 295.

136. Rapamune® (sirolimus) oral solution and tablets. Available at: Http://Www.Accessdata.Fda.Gov/Drugsatfda_Docs/Label/2010/021110s055lbl.Pdf (accessed on January 6, 2015).

137. Tricor-fenofibrate tablet. Available at: http://www.accessdata.fda.gov/drugsatfda_docs/label/2010/021656s019lbl.pdf (accessed on January 6, 2015).

138. Emend® (aprepitant) capsules. Available at: http://www.Accessdata.Fda.Gov/Drugsatfda_Docs/Label/2010/021549s017lbl.Pdf (Accessed on January 6, 2015).

139. Megace® ES (megestrol acetate) oral suspension. Available at: http://Www.Accessdata.Fda.Gov/Drugsatfda_Docs/Label/2010/021778s008lbl.Pdf (accessed on January 6, 2015).

140. Cui, J., Yu, B., Zhao, Y., Zhu, W., Li, H., et al. (2009). Enhancement of oral absorption of curcumin by self-microemulsifying drug delivery systems. *Int. J. Pharm.,* **371**(1–2), 148–155.

141. Chen, Y., Li, G., Wu, X., Chen, Z., Hang, J., et al. (2008). Self-microemulsifying drug delivery system (SMEDDS) of vinpocetine: Formulation development and *in vivo* assessment. *Biol. Pharm. Bull.,* **31**(1), 118–125.

142. Ali, H., Siddiqui, A., Nazzal, S. (2010). The effect of media composition, pH, and formulation excipients on the *in vitro* lipolysis of self-emulsifying drug delivery systems (sedds). *J. Dispersion Sci. Technol.,* **31**(2), 226–232.

143. Talegaonkar, S., Azeem, A., Ahmad, F. J., Khar, R. K., Pathan, S. A., et al. (2008). Microemulsions: A novel approach to enhanced drug delivery. *Recent Patents Drug Deliv. Form.,* **2**(3), 238–257.

144. Scheindlin, S. (2004). Transdermal drug delivery: Past, present, future. *Mol. Int.,* **4**(6), 308.

145. Perez-Cullell, N., Coderch, L., De La Maza, A., Parra, J. L., Estelrich, J. (2000). Influence of the fluidity of liposome compositions on percutaneous absorption. *Drug Deliv.,* **7**(1), 7–13.

146. Schafer-Korting, M., Mehnert, W., Korting, H. C. (2007). Lipid nanoparticles for improved topical application of drugs for skin diseases. *Adv. Drug Deliv. Rev.,* **59**(6), 427–443.

147. Santos, P., Watkinson, A., Hadgraft, J., Lane, M. (2008). Application of microemulsions in dermal and transdermal drug delivery. *Skin Pharm. Physiol.,* **21**(5), 246–259.

148. Lopez, A., Llinares, F., Cortell, C., Herraez, M. (2000). Comparative enhancer effects of span 20 with tween 20 and azone on the *in vitro* percutaneous penetration of compounds with different lipophilicities. *Int. J. Pharm.,* **202**(1–2), 133–140.

149. Zhang, P., Gao, W., Zhang, L., Chen, L., Shen, Q., et al. (2008). *In vitro* evaluation of topical microemulsion of apsaicin free of surfactant. *Biol. Pharm. Bull.,* **31**(12), 2316–2320.

150. Lee, R. W., Shenoy, D. B., Sheel, R. (2010). Micellar nanoparticles: Applications for topical and passive transdermal drug delivery. In: Kulkarni, V. S. (ed.), *Handbook of Non-Invasive Drug Delivery Systems*. Elsevier, Oxford, UK; pp. 37–58.

151. Estrasorb™ (estradiol topical emulsion). Available at: Http://Www.Accessdata.Fda.Gov/Drugsatfda_Docs/Label/2003/21371_Estrasorb_Lbl.Pdf (accessed on January 16, 2015).

152. Hickey, A. J., Mansour, H. M. (2009). Delivery of drugs by the pulmonary route. In: Florence, A. T., Siepmann, J. (ed.), *Modern Pharmaceutics*. Informa Healthcare, London, UK; pp. 191–219.

153. Bailey, M. M., Berkland, C. J. (2009). Nanoparticle formulations in pulmonary drug delivery. *Med. Res. Rev.,* **29**(1), 196–212.

154. Hickey, A. J., Mansour, H. M. (2008). Formulation challenges of powders for the delivery of small molecular weight molecules as aerosols. In: Florence, A., Siepmann, J. (ed.), *Modified-Release Drug Delivery Technology*. Informa Healthcare, London, UK; pp. 573–602.

155. Park, C. W., Hayes, D. J., Mansour, H. M. (2011). Pulmonary inhalation aerosols for targeted antibiotics delivery. *Eur. Pharm. Rev.,* **16**(1), 32–36.

156. Mansour, H. M., Damodaran, S., Zografi, G. (2008). Characterization of the *in situ* structural and interfacial properties of the cationic hydrophobic heteropolypeptide, kl4, in lung surfactant bilayer and monolayer models at the air-water interface: Implications for pulmonary surfactant delivery. *Mol. Pharm.,* **5**(5), 681–695.

157. Koshkina, N. V., Golunski, E., Roberts, L. E., Gilbert, B. E., Knight, V. (2004). Cyclosporin a aerosol improves the anticancer effect of paclitaxel aerosol in mice. *J. Aerosol Med.,* **17**(1), 7–14.

158. Koshkina, N. V., Kleinerman, E. S., Waldrep, C., Jia, S. F., Worth, L. L., et al. (2000). 9-nitrocamptothecin liposome aerosol treatment of melanoma and osteosarcoma lung metastases in mice. *Clin. Cancer Res.,* **6**(7), 2876.

159. Lo, Y., Tsai, J., Kuo, J. (2004). Liposomes and disaccharides as carriers in spray-dried powder formulations of superoxide dismutase. *J. Control. Release,* **94**(2–3), 259–272.

160. Chougule, M., Padhi, B., Misra, A. (2007). Nano-liposomal dry powder inhaler of tacrolimus: Preparation, characterization, and pulmonary pharmacokinetics. *Int. J. Nanomed.,* **2**(4), 675.

161. Bi, R., Shao, W., Wang, Q., Zhang, N. (2008). Spray-freeze-dried dry powder inhalation of insulin-loaded liposomes for enhanced pulmonary delivery. *J. Drug Target.,* **16**(9), 639–648.

162. Changsan, N., Chan, H. K., Separovic, F., Srichana, T. (2009). Physico-chemical characterization and stability of rifampicin liposome dry powder formulations for inhalation. *J. Pharm. Sci.,* **98**(2), 628–639.

163. Liu, J., Gong, T., Fu, H., Wang, C., Wang, X., et al. (2008). Solid lipid nanoparticles for pulmonary delivery of insulin. *Int. J. Pharm.,* **356**(1–2), 333–344.

164. Hu, L., Jia, Y., Wending. (2010). Preparation and characterization of solid lipid nanoparticles loaded with epirubicin for pulmonary delivery. *Pharmazie,* **65**(8), 585–587.

165. Li, Y. Z., Sun, X., Gong, T., Liu, J., Zuo, J., et al. (2010). Inhalable microparticles as carriers for pulmonary delivery of thymopentin-loaded solid lipid nanoparticles. *Pharm. Res.,* **27**(9), 1977–1986.

166. Bawa, R., Melethil, S., Simmons, W. J., Harris, D. (2008). Nanopharmaceuticals–patenting issues and FDA regulatory challenges. *Sci. Tech. Lawyer,* **5**(2), 10–15.

167. Paradise, J., Diliberto, G., Tisdale A., Kokkoli, E. (2008). Exploring emerging nanobiotechnology drugs and medical devices. *Food Drug Law J.,* **63**, 407–411.

168. Bawa, R. (2011). Regulating nanomedicine: can the FDA handle it? *Curr. Drug Deliv.,* **8**, 227–234.

169. Bawa, R. (2013). FDA and nanotech: Baby steps lead to regulatory uncertainty. In: Bagchi, D., et al. (ed.), *Bionanotechnology: A Revolution in Biomedical Sciences and Human Health,* Wiley Blackwell, UK, pp. 720–732.

170. Nel, A., Xia, T., Mädler, L., Li, N. (2006). Toxic potential of materials at the nanolevel. *Science,* **311**(5761), 622–627.

171. Reed, S. D., Anstrom, K. J., Seils, D. M., Califf, R. M., Schulman, K. A. (2008). Use of larger versus smaller drug-safety databases before regulatory approval: The trade-offs. *Health Aff.,* **27**(5), 360–370.

172. Bawa, R. (2007). Nanotechnology patent proliferation and the crisis at the US Patent Office. *Albany Law J. Sci. Technol.,* **17**(3), 699–735.

173. Bawa, R. (2009). Patenting inventions in bionanotechnology–A primer for scientists and lawyers. In: Reisner, D. E. (ed.), *Bionanotechnology: Global Prospects,* CRC Press, Boca Raton, FL, 309–337.

174. Kievit, F. M., Zhang, M. (2011). Cancer nanotheranostics: Improving imaging and therapy by targeted delivery across biological barriers. *Adv. Mater.,* **23**(36), H217–H247.

175. Terreno, E., Uggeri, F., Aime, S. (2012). Image guided therapy: The advent of theranostic agents. *J. Control. Release,* **161,** 328–337.

Further Readings

1. Bagchi, D., Bagchi, M., Moriyama, H., Shahidi., F., eds. (2013). *Bionanotechnology: A Revolution in Biomedical Sciences and Human Health.* Wiley Blackwell, UK.

2. Prasad, P. N. (2012). *Introduction to Nanomedicine and Nanobioengineering.* John Wiley & Sons, Inc., Hoboken, New Jersey.

3. Stein, R. A. (2014). Nanotechnology: Is the magic bullet becoming reality? *Genetic Engineering & Biotechnology News,* Available at: http://www.genengnews.com/insight-and-intelligence/nanotechnology-is-the-magic-bullet-becoming-reality/77900016/ (accessed on January 18, 2015).
4. Fischer, S. (2014). Regulating nanomedicine. *IEEE Pulse*, Available at: http://pulse.embs.org/march-2014/regulating-nanomedicine/ (accessed on January 18, 2015).
5. Johnson, D. (2014). Nanomedicines will be big once they emerge from regulatory troubles. Available at: http://spectrum.ieee.org/nanoclast/at-work/innovation/nanomedicines-will-be-big-once-they-emerge-from-regulatory-troubles (accessed on January 18, 2015).
6. US Food and Drug Administration. Fact Sheet Nanotechnology. (2012). Available at: http://www.fda.gov/food/guidanceregulation/guidancedocumentsregulatoryinformation/ingredientsadditivesgraspackaging/ucm300914.htm (accessed on January 18, 2015).
7. Nicholas, J. M. (2012). Complex drugs and biologics: Scientific and regulatory challenges for follow-on products. *Drug Information J.,* **46(2)**, 197–206.
8. Mühlebach, S. A. Vulto, de Vlieger, J. S. B., V. Weinstein, B. Flühmann, V. P. Shah. (2013). The authorization of non-biological complex drugs (NBCDs) follow-on versions: Specific regulatory and interchangeability rules ahead? *Gen. Biosimilars Initiat. J.,* **2(4)**, 204–207.
9. Schellekens, H., Klinger, E, Muhlebach, S., et al. (2011). The therapeutic equivalence of complex drugs. *Regul. Toxicol. Pharm.,* **59**, 176–183.
10. Schellekens, H., Stegemann, S., Weinstein, V., et al. (2013). How to regulate nonbiological complex drugs (NBCD) and their follow-on versions: Points to consider. *AAPS J.,* **16(1)**, 15–21.
11. Desai, N. (2012). Challenges in development of nanoparticle-based therapeutics. *AAPS J.,* **14(2)**, 282–295.
12. Ehmann, F., Sakai-Kato, K., Duncan, R., Hernán Pérez de la Ossa D., Pita R, et al. (2013). Next-generation nanomedicines and nanosimilars: EU regulators' initiatives relating to the development and evaluation of nanosimilars. *Nanomedicine,* **8(5)**, 849–856.
13. Holloway, C., Mueller-Berghaus, J., Lima, B. S., Lee, S. L., Wyatt, J. S., et al. (2012). Scientific considerations for complex drugs in light of established and emerging regulatory guidance. *Ann. N Y Acad. Sci.,* **1276**, 26–36.

14. Tinkle, S., McNeil, S. E., Mühlebach, S., Bawa, R., Borchard. G., et al. (2014). Nanomedicines: addressing the scientific and regulatory gap. *Ann. N Y Acad. Sci.,* **1313,** 35–56.

15. Duncan, R., Gaspar, R. (2011). Nanomedicine(s) under the microscope. *Mol. Pharm.,* **8(6)**, 2101–2104.

17. Conner, J. B., Bawa, R., Nicholas, J. M., Weinstein, V. (2015). Copaxone® in the era of biosimilars and nanosimilars. In: Bawa, R., Audette, G., Rubinstein, I. (ed.), *Handbook of Clinical Nanomedicine: Nanoparticles, Imaging, Therapy, and Clinical Applications,* Chapter 28*.* Pan Stanford Publishing, Singapore.

36. Marchant, G. E., Atkinson, B., Banko, D., Bromley, J., Cseke, E., et al. (2012). Big issues for small stuff: Nanotechnology regulation and risk management. *Jurimetrics J.,* **52**, 243–277.

37. Duvall, M. N., Wyatt, A. M., Yeung, F. S. (2012). Navigating FDA's approach to approval of nanoparticle-based drugs and devices. *Nanotechnol., Law Bus.,* **8**, 226–244.

38. Falkner, R., Jaspers, N. (2012). Regulating nanotechnologies: Risk, uncertainty and the global governance gap. *Global Environ. Politics,* **12(1)**, 30–55.

39. Theodore, L., Stander, L. (2013). Regulatory concerns and health/hazard risks associated with nanotechnology. *Pace Environ. Law Rev.,* **30(2)**, 469–485.

40. Siew, A. (2014). Current issues with nanomedicines. *PharmTech Europe* Available at: http://www.pharmtech.com/pharmtech/Drug+Delivery/Current-issues-with-nanomedicines/ArticleStandard/Article/detail/837368 (accessed on January 18, 2015).

41. Davenport, M. (2014). Closing the gap for generic nanomedicines. *Chemical & Engineering News*, **92**(45), 10–13. Available at: http://cen.acs.org/articles/92/i45/Closing-Gap-Generic-Nanomedicines.html (accessed on January 20, 2015).

42. Torchilin, V. (ed.) (2014). *Handbook of Nanobiomedical Research: Fundamentals, Applications and Recent Developments*. World Scientific Publishing Co., Hackensack, NJ.

Chapter 10

Nanosizing Approaches in Drug Delivery

Sandip Chavhan, PhD, Kailash Petkar, PhD, and Krutika Sawant, PhD

Drug Delivery Research Laboratory, Pharmacy Department, The Maharaja Sayajirao University of Baroda, Vadodara, Gujarat, India

Keywords: particle size engineering, colloidal delivery systems, solubility enhancement, bioavailability, hydrophobic drugs, top-down approach, bottom-up approach, applications

10.1 Introduction

Almost 40% of the new drug candidates emerging from drug discovery programs have poor water solubility and this trend is not expected to change in the future [1]. Nowadays, a large portion of new molecules come from combinatorial chemistry that focuses on target-receptor geometry, target identification and lead candidate generation. However, candidates emerging from these screens invariably have high molecular mass and high Log P, which contribute to insolubility. Moreover, the high affinity and highly specific binding to molecular targets generally entails some degree of hydrophobic interactions, which lead to solubility

Handbook of Clinical Nanomedicine: Nanoparticles, Imaging, Therapy, and Clinical Applications
Edited by Raj Bawa, Gerald F. Audette, and Israel Rubinstein

ISBN 978-981-4669-20-7 (Hardcover), 978-981-4669-21-4 (eBook)
www.panstanford.com

constraints. Hence, development of suitable formulations for poorly water-soluble drugs is the major challenge for formulation scientists. Recent research on drug delivery for drugs with poor water solubility mainly focuses on nanotechnology-based strategies aimed at improving their therapeutic performance.

Available strategies for poorly water-soluble drugs include use of aqueous mixtures with an organic solvent (e.g., water-ethanol) [2], solubilization [3], formation of complexes (e.g., using β-cyclodextrins) [4], solid dispersions [5], co-crystallization [6], exploiting the effects of pH or preparing salt forms [7]. However, these approaches have certain limitations that include safety issues associated with co-solvents, the requirement of sufficient ionizing groups for salt formation, the necessity of possessing sufficient solubility in oils or other hydrophobic media, restriction of having a suitable molecular size and shape for incorporation in the cyclodextrin ring, etc. Hence, identification of a universal formulation approach for drugs having poor water solubility is the mainstay of drug delivery research throughout the world.

Nanoparticulate technology has been investigated for numerous drugs for a large number of applications. The nanoparticulate delivery systems have proven their potential toward fulfilling the need for improved health care and better patient compliance due to their versatility, flexibility and adaptability. Nanoparticulate delivery systems include polymeric nanoparticles, solid lipid nanoparticles, nanoemulsions, liposomes, nanostructured lipid carriers, nanogels, and drug nanoparticles. Pure drug nanoparticles are nowadays considered a viable formulation route for the oral administration of drugs having poor dissolution rate and/or aqueous solubility [8]. The ability to formulate poorly water-soluble compounds as nanometer-sized particles can have a dramatic effect on their performance, such as enhancing bioavailability, eliminating food effects, allowing for dose escalation; thereby improving their efficacy and safety. The potential of nanosized particles to alter tissue distribution after intravenous dosing should always be a consideration. For pure drug nanoparticles, tissue distribution by intravenous dosing depends upon the particle size and surface properties. However, solubility of a compound in blood is the primary attribute that determines its tissue distribution. If the compound is soluble in blood, the pure drug nanoparticles will show a pharmacokinetic profile similar to its solution and if

the compound has poor solubility in blood, the nanosized drug will behave similarly as other nanoparticulate formulations [9]. Nanosizing technology (nanonization) has also been applied to reduce variability in pharmacokinetic behavior of oral dosage forms [10]. Nanosizing a drug or formulating it as a nanoparticulate system results in its better dissolution and solubilization due to increase in surface area and saturation solubility. Pure drug nanoparticles have an edge over liposomes, microemulsions and polymeric nanoparticles in terms of commercialization, drug loading capacity, site-specific delivery, cost effectiveness, carrier associated side effects, local delivery and delivery of poorly water soluble and highly lipid soluble drugs [11]. Since this approach has been adapted to handle milligram quantities of drug substance, it provides an avenue for the research scientist to improve screening efforts without having to deal with solubility-related performance issues. The utility of this technology has been proven from the number of marketed/available products based on these techniques. Moreover, for marketed products that have performance issues related to poor solubility of the active, reformulation into nanosized dosage forms could offer the possibility of adding new life to old compounds while improving their efficacy and patient compliance.

10.1.1 Mechanism of Solubility Enhancement by Nanonization

Nanonization of drug particles leads to an increase in the surface area, resulting in increased dissolution rate, according to Noyes–Whitney equation (Eq. 10.1).

$$\frac{dX}{dt} = \frac{D \cdot S}{h\left(C_s - \frac{X_d}{V}\right)}, \tag{10.1}$$

where, dX/dt is the dissolution rate, X_d is the amount dissolved, D is the diffusion coefficient, S is the particle surface area, V is the volume of fluid available for dissolution, C_s is the saturation solubility, and h is the effective boundary layer thickness.

The equation shows that the dissolution rate of a drug is proportional to the surface area available for dissolution. This

principle has been extensively used in micronization of drugs for improving their oral bioavailability. Obviously, a decrease in particle size to nanometer range will further increase the dissolution rate due to the significant increase in effective particle surface area. As per Prandtl equation (Eq. 10.2), nanonization results in decreased diffusion layer thickness surrounding the particles and increased concentration gradient between the surface of the particle and bulk solution, which facilitates particle dissolution by increasing dissolution velocity.

$$h_{\mathrm{H}} = k \cdot \left(\frac{L^{1/2}}{V^{1/3}} \right), \tag{10.2}$$

where h_{H} is the hydrodynamic boundary layer thickness, k is a constant, V is the relative velocity of the flowing liquid against a flat surface, and L is the length of the surface in the direction of flow.

It is clear from Eqs. 10.1 and 10.2 that nanosizing is a suitable approach for increasing bioavailability of poorly soluble drugs, where dissolution is the rate-limiting step in systemic absorption [12].

Another important aspect of nanonization is an increase in saturation solubility, which can be explained by the Kelvin–Gibbs (Eq. 10.3) and the Ostwald–Freundlich (Eq. 10.4) equations. As per the Kelvin equation, the vapor pressure increases with increasing curvature of the droplet of a liquid in gas. If this is extended to a solid, it implies that the dissolution pressure increases with decrease in particle size. According to Ostwald–Freundlich equation, the increased saturation solubility is due to the creation of high-energy surfaces when disrupting the more or less ideal drug microcrystal to a nanoparticle [13].

$$\ln \frac{P_{\mathrm{r}}}{P_{\infty}} = \frac{2\gamma M}{rRT\rho} \tag{10.3}$$

$$S = S_{\infty} \exp\left(\frac{2\gamma M}{r\rho RT} \right), \tag{10.4}$$

where, P_{r} is the dissolution pressure of a particle with radius r, P_{∞} is the dissolution pressure of infinitely large particle, S is the

saturation solubility of the nanosized drug, S_∞ is the saturation solubility of an infinitely large drug crystal, γ is the crystal medium interfacial tension, M is the compound molecular weight, r is the particle radius, ρ is the density, R is the gas constant, and T is the temperature.

The theoretical backgrounds of Kelvin, Ostwald–Freundlich, and Prandtl equations support the fact that below a size of approximately 1–2 μm, the saturation solubility is a function of the particle size.

Nanosized particles also possess increased adhesiveness due to increased contact area of these particles as compared to microparticles. Moreover, they have stronger curvature leading to enhanced dissolution pressure, and reduction in diffusional distance as compared to microparticles, which in turn causes increase in dissolution velocity and consequent improvement in saturation solubility of the drug [14].

10.2 Current Nanonization Strategies

The two main approaches used for nanosizing drugs or formulating drug nanoparticles are top-down and bottom-up approaches. The top-down approach is widely used and generally referred to as nanosizing. This approach is based on use of mechanical force to convert large crystalline particles to nanosized drug particles. The bottom-up approach involves controlled precipitation (i.e., the drug is dissolved in one solvent and it is then precipitated by addition of an antisolvent in a controlled manner). Some of the widely employed technologies are briefly described here.

10.2.1 Media Milling

This is a widely used top-down approach for nanonization of drugs. Among all methods reported for nanosizing drug particles in pharmaceutical industry, the media milling technique is considered the leader with highest commercial applicability. In this technique, the drug particles are subjected to media milling wherein the high-energy shear forces generated because of impaction of the milling media with the drug provide energy to

disintegrate the drug microparticles to nanosized drug particles. In this method, the milling chamber is charged with milling pearls, dispersion medium (e.g., water), drug powder and a stabilizer. The pearls are rotated at a very high speed to generate strong shear forces that disintegrate the drug powder into nanoparticles [15]. The schematic diagram of the nanosizing process using media milling technology is shown in Fig. 10.1.

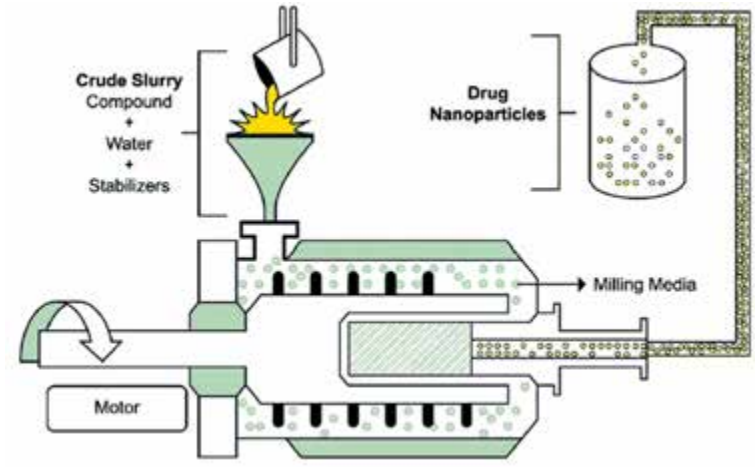

Figure 10.1 Schematic diagram of nanosizing process using media milling. Reproduced with permission from [9].

Physical characteristics of the resulting nanoparticles depend on the number of milling pearls, milling time, speed, temperature and the amount of drug and stabilizer. The milling time usually varies from few hours to days based on properties of the compound and extent of particle size reduction needed to achieve the desired product performance. Generally used milling media include glass, zirconium oxide or highly cross-linked polystyrene resin. Salt assisted milling was recently used for nanosizing of fenofibrate [16].

The media milling technique has been utilized from the laboratory to small-scale operations and finally on a large scale (i.e., the processing of drug from few milligrams to 500–1000 kg of active per batch in a reproducible manner is possible). One important aspect to be considered with such a particle size reduction method is the increase in surface energy due to which

the nanoparticles tend to aggregate. Therefore, surface stabilization is essential to prevent aggregation of nanoparticles. Stabilization of drug nanoparticles is generally achieved by steric, electrostatic or a combination of both types of interactions. Surfactants are generally used to stabilize the particles and selection of the stabilizer is a crucial parameter. In addition to stabilizing the drug nanoparticles against aggregation, care must be taken to avoid or control Ostwald ripening. Ostwald ripening is a result of enhanced solubility of small nanosized particles, which may solubilize or re-crystallize onto larger particles in the formulation. The most effective means of detecting Ostwald ripening is by particle size analysis wherein particle size growth while processing and during storage is observed with time. Performing basic solubility testing on the drug compound at various pH conditions and in stabilizer solutions can help to detect Ostwald ripening. In addition to its shelf stability, it is also important to ensure compatibility of nanosized formulation in the appropriate biological fluid. Recently M. Liversidge and E. Liversidge have detailed the applications of wet media milling technology for nanosizing of poorly water-soluble compounds [9].

The advantages of the media milling method include applicability for drugs having poor solubility in water as well as in organic solvents, capacity to handle very dilute to highly concentrated suspensions, flexibility to handle large quantity of drugs, easy scale up, reproducibility and narrow size distribution. Some limitations include contamination of the final product by the milling media due to erosion occurring during milling and greater time and energy consumed during the process. The problem of microbial contamination may occur if the processing time is too high and the scale up may get affected if the quantity of milling media required is too high.

10.2.2 High-Pressure Homogenization

The second approach for production of drug nanoparticles via the top-down disintegration mechanism is high-pressure homogenization (HPH). As an advanced nanonization strategy, HPH offers an excellent choice for producing high-quality drug nanoparticles on an industrial scale. Two homogenization principles are applied; Piston gap fluidization and microfluidization.

In the first method, a suspension of the drug and surfactant is forced under pressure through a nanosized aperture valve of a high-pressure homogenizer and particle size reduction occurs based on the cavitation principle. Particle size is also reduced due to high shear forces and the collision of the particles against each other. In this method, the major concern is the need for drug particles to be in a micronized state before loading and the high number of homogenization cycles required [17]. The size of the drug nanocrystals that can be achieved mainly depends on the intensity of the homogenizer, number of homogenization cycles and temperature. The particles/crystals break during nanonization preferentially at weak points, (i.e., imperfections) and the number of imperfections reduces with decreasing particle size. Thus, the force required to break the crystals increases with decreasing particle size.

The second method, microfluidization, is based on a jet stream principle. In this method, the drug suspension is accelerated and passes with a high velocity in a specially designed homogenization chamber (either Z or Y shaped), leading to reduction in particle size of the drug due to collisions between particles and shear forces generated.

HPH is carried out in either water or a non-aqueous medium. For water sensitive drugs, non-aqueous media are suitable. Nanopure® is a new homogenization technique in which homogenization of drug particles is carried out in non-aqueous media (e.g., propylene glycol) or mixtures of water with water miscible liquids (e.g. PEG, glycerol). Nanoedge® technique uses combination of homogenization and precipitation techniques to avoid the growth of drug nanoparticles during precipitation.

The advantages of the HPH method include applicability for drugs having poor solubility in water as well as in organic solvents, capacity to handle very dilute to highly concentrated suspensions, feasibility of industrial scale up, permits aseptic production, low risk of product contamination, etc. The limitations of this method include a prerequisite for the drug to be in a micronized state before homogenization, high cost of equipment, need of high number of homogenization cycles and possible contamination by metal ions from homogenizer.

10.2.3 Precipitation

Although the precipitation method has been applied to prepare small particles for many years, it has been used for preparation of nanoparticles for drug delivery since the 1980s [18]. In this method, the formation of crystalline or semi crystalline drug nanoparticles occurs by nucleation and growth of drug crystals. This process takes advantage of difference in solubility of the drug in two miscible solvents. Here, the drug is dissolved in a solvent (generally an organic solvent), and this solution is then added into a miscible antisolvent (generally aqueous phase). Due to this addition, high super saturation occurs suddenly and results in rapid nucleation and precipitation. The mixing step is very crucial because supersaturation of the solution is the driving force for nanoprecipitation. The nanoparticles formed after precipitation have a tendency to agglomerate, as there is a drastic increase in the free energy of the system. Hence, stabilizers are added to the aqueous phase to modify the surface of the precipitated nanoparticles and lower the interfacial tension, thereby inhibiting crystal growth. The drug nanoparticles can be processed further to remove the solvent, and dried drug nanoparticles can be obtained by a suitable technique. The choice of solvents and stabilizers and the mixing process are key factors to control the size and stability of the drug nanocrystals. The parameters that affect the process performance include, volume ratio of antisolvent to solvent, stirring rate, drug content and temperature. The challenge in the liquid precipitation process is that most small-molecule drugs tend to form relatively large crystals within the range of 10–100 μm [19].

Recently, a sonoprecipitation approach has been reported claiming to avoid the problem of formation of aggregates because of poor mixing during nanosizing. Here, ultrasound mixing provides uniform conditions throughout the vessel during the anti-solvent process. Ultrasound intensifies the mass transfer when it propagates through a liquid medium and initiates cavitation. Cavitational bubbles are formed during the negative-pressure period of the sound wave and when it implodes, a localized hot spot with a high temperature and pressure is formed, releasing a powerful shock wave. Seconds after ultrasound is applied, the solvent

and anti-solvent are mixed homogeneously, reaching maximum supersaturation so that primary nucleation and crystal growth are implemented rapidly [20]. These effects bring considerable benefits to the crystallization process, such as induction of primary nucleation, reduction of crystal size, inhibition of agglomeration and manipulation of crystal size distribution [21].

Another innovative method that has been reported for the generation of nanoparticles by precipitation is high gravity reactive precipitation or Highee technology. The method generates nanomaterials by employing high gravity mixing of reactants on the molecular level with the help of a rotating packed bed (RPB). The high gravity micromixing helps in enhancing the mass transfer and heat transfer between the reactants by several magnitudes, thus inducing rapid nucleation of the final product while suppressing the crystal growth. As the reactants enter the rotating packed bed, they are spread or split into very thin films or nanodroplets under the high shear created by the high gravity. An intense micromixing and centrifugal force together help in enhanced mass transfer resulting in the production of nanoparticles [22].

The advantages of the precipitation process include simplicity, low cost of equipment, easy scale up, avoids use of high energy such as disintegration, which prevents denaturation of drug [23], and possible formation of amorphous state enabling increase in solubility [24]. Its limitations are necessity of drug to be soluble in one of the solvents, the need for the solvent to be miscible with the antisolvent and removal of the residual solvent at the end of the process.

10.2.4 Supercritical Methods

The application of supercritical fluid (SCF) technology in preparation of microparticles and microparticulate drug delivery systems is well established and the current focus is on nanomaterials. SCF technologies have demonstrated great potential in particle engineering and have emerged as an alternative to most of the existing techniques. SCF technology has been used to manufacture fine particles of medicinal substances by a build-up process (i.e., in contrast to conventional bottom-up technique, this involves growing of the particles in a controlled fashion to attain desired

morphology). A SCF is defined as a substance that is at a pressure and temperature greater than its critical point [25]. Supercritical fluids are gases or liquids at temperatures and pressures above their critical points (T_c, critical temperature; P_c, critical pressure). Above these points, the SCF exists as a single phase with several advantageous properties of both liquids and gases. The properties that make supercritical fluids particularly attractive to produce nanomaterials are gas-like diffusivities, continuously tunable solvent power/selectivity and possibility of complete elimination at the end of the process [26].

The most widely used SCF for pharmaceutical applications is carbon dioxide due to its low critical temperature (31.18°C), attractiveness for heat sensitive materials including products sourced from biologicals, non-flammability, non-toxicity, GRAS (generally regarded as safe) status and low cost. Supercritical carbon dioxide (CO_2) creates very rapid, uniform, and extremely high supersaturation in the solution due to its excellent thermodynamic and transport properties, which lead to formation of nanoparticles/microparticles with narrow particle size distribution.

Various SCF particle design processes using supercritical CO_2 have been investigated for production of micro/nanoparticles. Two SCF technologies are generally used for particle size reduction of neat drug particles, Rapid Expansion of Supercritical Solutions (RESS) and Supercritical Anti Solvent (SAS) process (Fig. 10.2). The first process uses supercritical fluid as a solvent while the latter uses supercritical fluid as an antisolvent. Other SCF techniques are based on slight modification to these systems. In the case of RESS, the supercritical fluid is used to dissolve the solid material (drug) under high pressure and temperature, thus forming a homogeneous supercritical phase. Thereafter, the solution is expanded through a nozzle and drug nanoparticles are formed. At the rapid expansion point right at the opening of the nozzle, there is a sudden pressure drop that forces the dissolved material to precipitate out of the solution.

In the SAS method, the solid material (drug) is dissolved in an organic solvent and a supercritical fluid is then forced by means of pressure to dissolve in it. In this way, the volume of the system is expanded, thus lowering the density, and therefore the solubility of the material of interest is also decreased. As a result, the material precipitates out of the solution as a solid with a

very small particle diameter. The factors that affect the particle properties include solubility of material, pre-expansion conditions, spray device, solvent extraction and mass transfer.

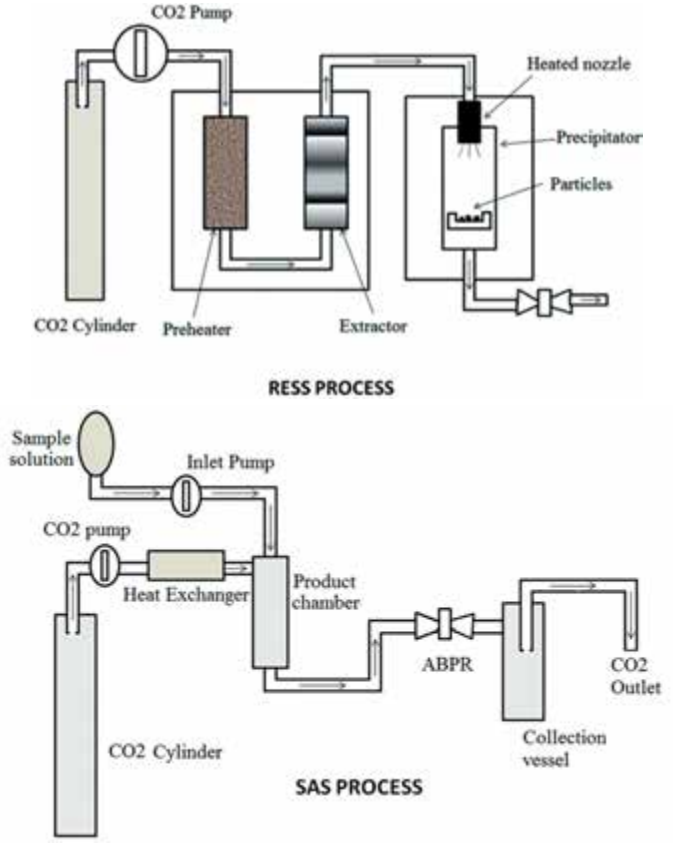

Figure 10.2 Schematic of RESS and SAS process.

A new technique called the supercritical antisolvent with enhanced mass transfer (SAS-EM) is a modification of the SAS and was introduced for improving the mass transfer between the solution and the antisolvent. This process generates an ultrasound field that enhances mass transfer and thus leads to formation of particles smaller than those from SAS [27]. Recently, an improved technique using both supercritical antisolvent precipitation and rapid expansion from supercritical to aqueous solution (RESAS) was used for production of drug nanoparticles [28].

The advantages of the supercritical method include better control over the process, mild operating conditions, and production of solvent free particles. The supercritical methods are also single step processes, suitable for a variety of compounds and are considered green alternatives (i.e., they have the potential of being GMP compliant) [29]. Moreover, the product need not be subjected to any further post-treatment. The major limitation of the supercritical methods is the high equipment cost and the poor understanding of the particle formation phenomenon.

10.2.5 Aerosol Flow Reactor Method

The aerosol flow reactor method is a simple and efficient one-step continuous process for engineering drug nanoparticles with narrow particle size distribution. In this method, the drug is dissolved in a suitable biocompatible volatile solvent and atomized with the help of a pressurized inert carrier gas into nanodroplets by means of an atomizer. The nanodroplets suspended in the inert carrier gas are then passed through a heated tubular laminar flow reactor maintained at a temperature sufficient to evaporate the solvent. The drug nanoparticles are formed due to instantaneous evaporation of the solvent that induces supersaturation of the drug in the inert gas. The parameters that affect the process performance include temperature, drug solubility, solution concentration, type of atomizer and atomizing efficiency. The advantages of this method include formation of dried nanoparticles with unimodal size distribution and better control over size and morphology of the particles.

10.2.6 Microemulsion Template Technology

The use of partially water-miscible, biocompatible organic solvents through microemulsion as a template has been described for engineering drug nanoparticles [30]. These systems are applicable for drugs that are soluble in either volatile organic solvents or partially water miscible solvents. In this technique, an organic solvent or mixture of solvents loaded with the drug is added slowly to an aqueous medium with stirring at a high speed that leads to formation of small droplets (containing the drug dissolved in the organic solvent) emulsified in the aqueous vehicle. As

the stirring progresses at high speed, the droplet size is further reduced. The process is also accompanied by slow evaporation of the organic solvent from the droplets. Once the organic solvent is evaporated completely, pure drug particles stabilized by surfactant are left behind, suspended in the aqueous vehicle. The advantages of this technique are enhanced drug solubilization, long shelf life, ease of production, possibility to control the product size by controlling the emulsion droplet size and easy scale-up. The limitations are use of hazardous solvents and high amount of surfactants.

10.3 Conversion to Solid Dosage Forms

During the last decade, interest in nanonization of drugs has rapidly grown as witnessed from the vast literature on the subject and the number of marketed products manufactured using this approach. Generally, the final formulation obtained using nanonization methods is in a liquid form. However, solid dosage forms are considered more attractive due to their convenience (marketing aspects) and possible stability issues associated with nanoparticles in their suspended state. The main advantage of conversion to solid state includes avoidance of stability issues that are associated with liquid dosage forms. The instability can be physical (Ostwald ripening and agglomeration) or chemical (Hydrolysis). Therefore, conversion of nanosized formulations to solid dosage form should be considered as an almost essential step in the production of a final nanoparticulate dosage form intended for oral delivery. Technically, transformation of nanosized formulation into solid products can be achieved using established unit-operations such as freeze-drying, spray-drying, pelletization and granulation [31]. The selection of the method usually depends upon the simplicity of the method and its cost effectiveness. Out of the various processes reported, freeze drying and spray drying are the most commonly used techniques for conversion of nanosized liquid formulation to solid state. The product obtained after conversion to solid state can be used as such (e.g., as a powder for reconstitution or as rapidly disintegrating freeze-dried single dosage forms). Alternatively, further processing steps such as capsule filling or compression into tablets can be performed. Only

a few studies are reported on further processing of solid nanosized powder [32, 33].

It should be kept in mind that even though conversion to solid state definitely adds some advantages to a nanosized formulation, it should not affect the primary objective of nanosized formulations (i.e., rapid disintegration of the solid form and redispersion of the individual nanoparticles), and should not impose a barrier on the overall dissolution process. The wetting and disintegration characteristics of the nanosized products upon addition of the solid form to water should be able to maintain these dissolution characteristics. Thus, various matrix formers are added to the nanosized formulation before conversion to solid dosage form in order to achieve redispersion in water. Typical matrix formers reported in literature are sugars (e.g., sucrose/ saccharose, lactose), sugar alcohols (e.g., mannitol, sorbitol) and water-soluble polymers (e.g., PVP, polyvinyl alcohol, long chain PEG). Although these matrix formers are valuable for redispersion of the formulation, their ability to preserve high dissolution rate might be different. Thus, selection of the matrix former should be based on proper evaluation. A recent study evaluated the dissolution performance of nine model drug compounds after freeze-drying and spray-drying. This study confirmed that de-agglomeration upon redispersion can indeed become a rate-limiting step in the overall dissolution process. Furthermore, the results showed that the decrease in dissolution rate was correlated with the surface hydrophobicity of the nanoparticles [32]. There are a limited number of studies that emphasize the maintenance of rapid dissolution after conversion to solid dosage forms. Thus, it is most important to systematically evaluate the effects of the drying process and the matrix former used after using any method for conversion to solid state. In addition to the drug properties, these parameters are equally important and should be carefully considered during nanosizing.

10.4 Pharmaceutical Applications and Commercialization Aspects

Nanosizing technology can play a critical role as an enabling technology for poorly water-soluble and/or poorly permeable

Table 10.1 Nanosized formulations: marketed, FDA approved, and under development (compiled August 2014) [34–40]

Drug	Category/ indication	Drug delivery company	Pharma company	Route	Status (FDA approval)
Sirolimus	Immunosuppressant	Elan Nanosystems	Wyeth	Oral	Marketed (Aug 2000)
Aprepitant	Antiemetic	Elan Nanosystems	Merck	Oral	Marketed (March 2003)
Fenofibrate	Hypercholestrrolemic	Elan Nanosystems	Abbott Laboratories	Oral	Marketed (Nov 2004)
Fenofibrate	Hypercholesterolemic	Elan Nanosystems	SkyePharma	Oral	Marketed (May 2005)
Megestrol Acetate	Antianorexic	Elan Nanosystems	Par Pharmaceuticals	Oral	Marketed (July 2005)
Morphine sulfate	Psychostimulant	Elan Nanosystems	King Pharmaceuticals	Oral	Marketed (March 2002)
Dexmethyl-phenidate HCl	Attention Deficit Hyperactivity	Elan Nanosystems	Novartis	Oral	Marketed (May 2005)
Methylphenidate HCl	Attention Deficit Hyperactivity	Elan Nanosystems	Novartis	Oral	Marketed (June 2002)
Naproxen sodium	Anti-inflammatory	Elan Nanosystems	Victory Pharma	Oral	Marketed (May 2007)

(*Continued*)

Table 10.1 (*Continued*)

Drug	Category/ indication	Drug delivery company	Pharma company	Route	Status (FDA approval)
Diltiazem HCl	Antihypertensive	Elan Nanosystems	Tanabe	Oral	Marketed (July 2001)
Verapamil HCl	Antihypertensive	Elan Nanosystems	Schwarz	Oral	Marketed (Jan 1999)
Tizanidine HCl	Muscle relaxant	Elan Nanosystems	Acorda	Oral	Marketed (Aug 2002)
Paliperidone Plmitate	Antipsychotic	Elan Nanosystems	Janssen	Parenteral	Marketed (July 2009)
Cytokine Inhibitor	Crohn's disease	Elan Nanosystems	Cytokine Pharma-Sciences	Oral	Phase II
Calcium phosphate	Mucosal vaccine adjuvant	BioSante	Self-developed	Oral	Phase I
Insulin	Antidiabetic	BioSante	Self-developed	Oral	Phase I
2-methoxy estradiol	Anticancer	Elan Nanocrystal	EntreMed	Oral	Phase II
2-methoxy estradiol	Recurrant glioblastoma	Elan Nanocrystal	EntreMed	Oral	Phase II
2-methoxy estradiol and Tamozolomide	Anticancer	Elan Nanocrystal	EntreMed	Oral	Phase II

(*Continued*)

Table 10.1 (*Continued*)

Drug	Category/ indication	Drug delivery company	Pharma company	Route	Status (FDA approval)
2-methoxy estradiol and Bevacizumab	Carcinoid tumor	Elan Nanocrystal	EntreMed	Oral	Phase II
2-methoxy estradiol & Sanitinib Malate	Renal cell carcinoma	Elan Nanocrystal	EntreMed	Oral	Phase II
2-methoxy estradiol	Prostate cancer	Elan Nanocrystal	EntreMed	Oral	Phase II
Paclitaxel	Anticancer	American Bioscience	American Pharmaceutical Partners	Intravenous	Phase III
Undisclosed multiple	Anti-infective	Baxter Nanoedge	Undisclosed	Oral/ intravenous	Preclinical to Phase II
Undisclosed	Anticancer	Baxter Nanoedge	Undisclosed	Intravenous/oral	Preclinical to Phase I
Diagnostic Agent	Imaging agent	Elan Nanosystems	Photogen	Intravenous	Phase I/II
Thymectacin	Anticancer	Elan Nanosystems	NewBiotics/Ilex Oncology	Intravenous	Phase I/II
Busulfan	Anticancer	SkyePharma	Superguns	Intrathecal	Phase I
Budesonide	Antiasthmatic	Elan Nanosystems	Sheffield Pharmaceuticals	Pulmonary	Phase I
Silver	Antieczematic	Nucryst	Self-developed	Topical	Phase II

molecules having significant *in vitro* activity. The particles obtained are in the range of 1–1000 nm and have shown their application by various routes of administration like oral, parenteral/intravenous, dermal, mucosal and pulmonary and also as targeted drug delivery system. The nanosizing approach can also provide a solution for new drug development activities of drugs having solubility issues and can be useful in preclinical as well as clinical studies. Their small size and increased surface area lead to increased dissolution rate and increased bioavailability. Due to their nanoparticulate nature, they have potential for targeting of Mononuclear phagocytic system (MPS), with unusual pharmacokinetic consequences. As the major focus is on newer systems that will have more chances of getting into market within a short period of time, nanosizing technology has gained attention of formulation scientists and manufacturers. Currently, most abundant number of nanosized pure drug products are in the market as compared to other nanoparticulate systems, proving the commercialization capability of nanonization approaches.

The list of nanosized products in the market and under clinical trials is given in Table 10.1. It can be observed that while most marketed products and formulations undergoing clinical studies are based on oral route, drug delivery by other routes is also being explored. Recent scientific reports have also proved the potential of nanosized products by various routes of administrations such as intravenous, ocular, transdermal, pulmonary, and for targeted delivery.

10.5 Conclusions

Nanosizing of poorly soluble actives using different nanosizing technologies is a popular approach for overcoming their solubility and bioavailability problems. The main attractive features of this technology include increased dissolution velocity, increased saturation solubility, improved bioadhesion, ease of production, and versatile nature of the system for modification as a drug delivery system. The number of products currently in market and under clinical trials, coupled with the large number of patents and research papers indicate the growing importance of this technology. The main advantage of this system is that it does

not require a carrier and hence its performance solely depends on the impact of the particle size-engineering tool on the drug properties. Therefore, safety and toxicity issues and approval procedures may be least complicated for products based on this approach as compared to other nanoparticulate systems. However, major concerns that remain for all nanotechnology based products such as the issues of exposure hazards, stringent manufacturing conditions and possibility of unforeseen effects, adverse effects and toxicity apply to this system. Once these concerns are sorted out, plain drug nanosized particles will become a very effective approach for formulation of drugs with poor water solubility as nanosizing is being preferred among currently available nanotechnology based approaches due to its simplicity and 'stand alone' characteristics. Moreover, its current market status clearly indicates that the value of this new platform is going to increase in near future. Significant amount of research focused on this area and applications of these findings to drug delivery platform are likely to increase in coming years.

Abbreviations

GRAS: Generally regarded as safe
HPH: High pressure homogenization
MPS: Mononuclear phagocytic system
PEG: Polyethylene glycol
PVP: Polyvinyl pyrrolidone
RESAS: Rapid expansion from supercritical to aqueous solution
RESS: Rapid expansion of supercritical solutions
SAS-EM: Supercritical antisolvent with enhanced mass transfer
SAS: Supercritical anti solvent
SCF: Supercritical fluid

Disclosures and Conflict of Interest

The authors declare that they have no conflict of interest and have no affiliations or financial involvement with any organization or entity discussed in this chapter. This includes employment, consultancies, honoraria, grants, stock ownership or options, expert testimony, patents (received or pending) or royalties. No

writing assistance was utilized in the production of this chapter and the authors have received no payment for its preparation. The findings and conclusions here reflect the current views of the authors. They should not be attributed, in whole or in part, to the organizations with which they are affiliated, nor should they be considered as expressing an opinion with regard to the merits of any particular company or product discussed herein. Nothing contained herein is to be considered as the rendering of legal advice.

Corresponding Author

Dr. Krutika K. Sawant
Pharmacy Department
Faculty of Technology and Engineering
The Maharaja Sayajirao University of Baroda
Kalabhavan, Vadodara 390001, Gujarat, India
Email: dr_krutikasawant@rediffmail.com

About the Authors

Sandip S. Chavhan has completed PhD in Pharmacy from the Drug Delivery Research Laboratory in the Department of Pharmacy, The Maharaja Sayajirao University of Baroda, India. He did Bachelor of Pharmacy from Amravati University and Master of Pharmacy (Pharmaceutics) from Pune University, India. Dr. Chavhan's research interest is focused on nanosizing approaches for drugs with low bioavailability. He has eight research publications, two abstracts and one book chapter.

Kailash C. Petkar completed his PhD in Pharmacy from the Drug Delivery Research Laboratory in the Department of Pharmacy, The Maharaja Sayajirao University of Baroda, India. He received Bachelor of Pharmacy from Nagpur University and Master of Pharmacy (Biopharmaceutics) from Shivaji University. He is currently involved in the research pertaining to polymer modification, biomaterial development,

nanoparticulate approaches for drug and vaccine delivery. Dr. Petkar has published 12 research articles and 1 book chapter. He is a recipient of prestigious Commonwealth Fellowship, UK. Presently he is a faculty at National Institute of Pharmaceutical Education and Research (NIPER), Raebareli, India.

Krutika K. Sawant is a Professor of Pharmaceutics at the Pharmacy Department of The Maharaja Sayajirao University of Baroda, Vadodara, India. She received her BPharm, MPharm, and PhD from The Maharaja Sayajirao University of Baroda in the year 1984, 1987, and 1993, respectively. Dr. Sawant has been involved in teaching and research in the field of Pharmaceutical Technology and Formulation Development since 1990. Her area of specialization includes Formulation Development of Controlled, Novel and Targeted drug delivery systems. Dr. Sawant has over 70 original research publications and 3 book chapters to her credit. She is a reviewer of many international journals. She has guided more than 60 MPharm and 15 PhD students.

References

1. Stegemann, S., Leveiller, F., Franchi, D., de Jong, H., Linden, H. (2007). When poor solubility becomes an issue: From early stage to proof of concept. *Eur. J. Pharm. Sci.,* **31**, 249–251.
2. Jouyban, A. (2007). In silico prediction of drug solubility in water-dioxane mixtures using the Jouyban-Acree model. *Pharmazie*, **62**, 46–50.
3. Dulfer, W. J., Bakker, M. W., Govers, H. A. (1995). Micellar solubility and micelle/water partitioning of polychlorinated biphenyls in solutions of sodium dodecyl sulfate. *Environ. Sci. Technol.,* **29**, 985–992.
4. Tokumura, T., Muraoka, A., Machida, Y. (2009). Improvement of oral bioavailability of flurbiprofen from flurbiprofen/b-cyclodextrin inclusion complex by action of cinnarizine. *Eur. J. Pharm. Biopharm.,* **73**, 202–204.
5. Nepal, P. R., Han, H., Choi, H. (2010). Enhancement of solubility and dissolution of Coenzyme Q10 using solid dispersion formulation. *Int. J. Pharm.,* **383**, 147–153.

6. Shiraki, K., Takata, N., Takano, R., Hayashi, Y., Terada, K. (2008). Dissolution improvement and the mechanism of the improvement from cocrystallization of poorly water-soluble compounds. *Pharm. Res.,* **25**, 2581–2592.
7. Gwak, H., Choi, J., Choi, H. (2005). Enhanced bioavailability of piroxicam via salt formation with ethanolamines. *Int. J. Pharm.,* **297**, 156–161.
8. Kesisoglou, F., Panmai, S., Wu, Y. (2007). Nanosizing-oral formulation development and biopharmaceutical evaluation. *Adv. Drug Deliv. Rev.,* **59**, 631–644.
9. Mersiko-Liversidge, E., Liversidge, G. G. (2011). Nanosizing for oral and parenteral drug delivery: A perspective on formulating poorly-water soluble compounds using wet media milling technology. *Adv. Drug Deliv. Rev.,* **63(6)**, 427–440.
10. Shono, Y., Jantratid, E., Kesisoglou, F., Reppas, C., Dressman, J. B. (2010). Forecasting *in vivo* oral absorption and food effect of micronized and nanosized aprepitant formulations in humans. *Eur. J. Pharm. Biopharm.,* **76**, 95–104.
11. Date, A. A., Patravale, V. B. (2004). Current strategies for engineering drug nanoparticles. *Curr. Opin. Colloid Interface Sci.,* **9**, 222–235.
12. Sharma, P., Garg, S. (2010). Pure drug and polymer based nano-technologies for the improved solubility, stability, bioavailability and targeting of anti-HIV drugs. *Adv. Drug Deliv. Rev.,* **62**, 491–502.
13. Muller, R. H., Peters, K. (1998). Nanosuspensions for the formulation of poorly soluble drugs I. Preparation by a size-reduction technique. *Int. J. Pharm.,* **160**, 229–237.
14. Müller, R. H. and Möschwitzer, J. (2000) Nanosuspensions for the formulation of poorly soluble drugs, In: Nielloud, F., Marti-Mestres, G., edss. *Pharmaceutical Emulsions and Suspensions*, 2nd edition, Marcel Dekker, New York, USA, pp. 386–390.
15. Merisko-Liversidge, E., Liversidge, G. G., Cooper, E. R. (2003). Nanosizing: A formulation approach for poorly water-soluble compounds. *Eur. J. Pharm. Sci.,* **18**, 113–120.
16. Mochalin, V. N., Sagar, A., Gour, S., Gogotsi, Y. (2009). Manufacturing nanosized fenofibrate by salt assisted milling. *Pharm. Res.,* **26**, 1365–1370.
17. Chingunpituk, J. (2007). Nanosuspension technology for drug delivery. *Walailak J. Sci. Technol.,* **4**, 139–153.
18. Siostrom, B., Kronberg, B., Carlfors, J. (1993). A method for the preparation of submicron particles of sparingly water soluble drugs by

precipitation in oil-in-water emulsions. 1. Influence of emulsification and surfactant concentration. *J. Pharm. Sci.,* **82**, 579–583.

19. Kashchiev, D. (2000). *Nucleation: Basic Theory with Applications.* Butterworth-Heinemann, Oxford, pp. 30–33.
20. Dhumal, R. S., Biradar, S. V., Yamamura, S., Paradkar, A. R. (2008). Preparation of amorphous cefuroxime axetil nanoparticles by sonoprecipitation for enhancement of bioavailability. *Eur. J. Pharm. Biopharm.,* **70**, 109–115.
21. Louhi-Kultanen, M., Karjalainen, M., Rantanen, J., Huhtanen, M., Kallas, J. (2006). Crystallization of glycine with ultrasound. *Int. J. Pharm.,* **320**, 23–29.
22. Chen, J. F., Zhou, M. Y., Shao, L., Wang, Y. Y., Yun, J., Chew, N., Chan, H. K. (2004). Feasibility of preparing nanodrugs by high gravity reactive precipitation. *Int. J. Pharm.,* **269**, 267–274.
23. Zhong, J., Shen, Z., Yang, Y., Chen, J. (2005). Preparation and characterization of uniform nanosized cephradine by combination of reactive precipitation and liquid anti-solvent precipitation under high gravity environment. *Int. J. Pharm.,* **301**, 286–293.
24. Kipp, J. E. (2004). The role of solid nanoparticle technology in the parenteral delivery of poorly water-soluble drugs. *Int. J. Pharm.,* **284**, 109–122.
25. Subramaniam, B., Rajewski, R. A., Snavely, K. (1997). Pharmaceutical processing with supercritical carbon dioxide. *J. Pharm. Sci.,* **86**, 885–890.
26. Reverchon, E., Adami, R. (2006). Nanomaterials and supercritical fluids. *J. Supercrit. Fluids*, **37**, 1–22.
27. Chattopadhyay, P., Gupta, R. B. (2001). Production of griseofulvin nanoparticles using supercritical CO_2 antisolvent with enhanced mass transfer. *Int. J. Pharm.,* **228**, 19–31.
28. Tozuka, Y., Miyazaki, Y., Takeuchi, H. (2010). A combinational supercritical CO_2 system for nanoparticle preparation of indomethacin. *Int. J. Pharm.,* **386**, 243–248.
29. York, P. (1999). Strategies for particle design using supercritical fluid technologies. *PSTT*, **2**, 430–440.
30. Trotta, M., Gallarate, M., Carlotti, M. E., Morel, S. (2003). Preparation of griseofulvin nanoparticles from water-dilutable microemulsions. *Int. J. Pharm.,.* **254**, 235–242.
31. Muller, R. H., Moschwitzer, J., Bushrab, F. N. (2006). Manufacturing of nanoparticles by milling and homogenization techniques. In: Gupta,

R. B., Kompella, U. B., eds. *Nanoparticle Technology for Drug Delivery, Drugs and the Pharmaceutical Sciences*, vol. 159. Taylor & Francis Group LLC, New York, USA, pp. 21–51.

32. Van Eerdenbrugh, B., Froyen, L., Van Humbeeck, J., Martens, J. A., Augustijns, P., Van den Mooter, G. (2008). Drying of crystalline drug nanosuspensions pharm—the importance of surface hydrophobicity on dissolution behavior upon redispersion. *Eur. J. Pharm. Sci.*, **35**, 127–135.
33. Dolenc, A., Kristl, J., Baumgartner, S., Planinsek, O. (2009). Advantages of celecoxib nanosuspension formulation and transformation into tablets. *Int. J. Pharm.,* **376**, 204–212.
34. Nekkanti, V., Pillai, R., enkateshwarlu, V., Harisudhan, T. (2009). Development and characterization of solid oral dosage form incorporating candesartan nanoparticles. *Pharm. Dev. Technol.,* **14**, 290–298.
35. Rainbow, B. E. (2004). Nanosuspensions in drug delivery. *Nat. Rev. Drug Discov.,* **3**, 785–796.
36. Bawa, R. (2010). Nanopharmaceuticals. *Eur. J. Med.,* **3**, 34–40.
37. Shegokar, R., Muller, R. H. (2010). Nanocrystals: Industrially feasible multifunctional formulation technology for poorly soluble actives. *Int. J. Pharm.,* **399**, 129–139.
38. Eerdenbrugh, B. V., Mooter, G. V., Augustijns, P. (2008). Top-down production of drug nanocrystals: Nanosuspension stabilization, miniaturization and transformation into solid products. *Int. J. Pharm.,* **64**, 64–75.
39. Tinkle, S., McNeil, S., Muhlebach, S., Bawa, R., Borchard, G., Barenholz, Y., Tamarkin, L., Desai, N. (2014). Nanomedicines: Addressing the scientific and regulatory gap. *Ann. N. Y. Acad., Sci.,* **1313**, 35–56.
40. Moschwitzer, J. P. (2013). Drug nnocrystals in the commertial pharmaceutical develpiment process. *Int. J. Pharm.,* **453**, 142–153.

Chapter 11

Multilayered Nanoparticles for Personalized Medicine: Translation into Clinical Markets

Dania Movia, PhD,[a] Craig Poland, PhD,[b] Lang Tran, PhD,[b] Yuri Volkov, PhD,[a] and Adriele Prina-Mello, PhD[a]

[a]*School of Medicine and Centre for Research on Adaptive Nanostructures and Nanodevices, Institute of Molecular Medicine, Trinity College, Dublin, Ireland*
[b]*Institute of Occupational Medicine, Research Avenue North, Riccarton, Edinburgh, UK*

Keywords: engineered nanoparticles, personalized medicine, risk assessment, modeling, structure–activity relationship, quantitative nanostructure–toxicity relationship, multilayered theranostic ENP, high throughput screening, high content screening translational medicine, nanomedicine

11.1 Introduction

Multilayered, theranostic engineered nanoparticles (ENP) are one of the major emerging materials in nanoscale science and technology programs [1]. Breakthroughs derived from the clinical effectiveness of ad hoc designed ENP are enabling in fact the development of

Handbook of Clinical Nanomedicine: Nanoparticles, Imaging, Therapy, and Clinical Applications
Edited by Raj Bawa, Gerald F. Audette, and Israel Rubinstein

ISBN 978-981-4669-20-7 (Hardcover), 978-981-4669-21-4 (eBook)
www.panstanford.com

a new generation of personalized medicine tools and leading to the next innovation revolution.

Personalized medicine denotes treatments tailored to individual patients. This approach originates from a growing understanding that diseases and patients are heterogeneous, and therefore treatments need to be individualized. Indeed millions of patients respond differently in terms of efficacy or safety to drugs (such as (i) β-blockers, a common treatment for cardiovascular disease and (ii) anti-depressants) commonly employed in clinics [2]. A recent study showed for example that an average of 10 deaths per 1000 hospitalized patients can be directly attributed to adverse side reactions to commercially available drugs [3], a data that demands the urgent improvement of drug delivery practices.

The efficacy of personalized treatment approaches is based on the ability to formulate the precise drug and dosage that every patient needs, and therefore it offers the great opportunity to decrease the amount of unnecessary treatment and cost, focusing the efforts on the at-risk tissue/organ target. Several pharmacogenomics biomarkers have been approved by regulatory agencies (such as the European Medicines Agency (EMA) and the U.S. Food and Drug Administration (FDA)) to predict and evaluate drug responses, thus moving toward the application of personalized medicine in drug prescription. Unfortunately, personalized medicine has had only a partial impact on routine patient care. This is due mainly to the limited number of convenient pharmaceutical tools available to make this approach broadly accessible for all clinicians and patients [4]. As a solution, undertaking an interdisciplinary approach could better enable the successful translation of personalized medicine into an efficiently established clinical option [5].

11.2 Multilayered Engineered Nanoparticles

The use of ENP in the medical/clinical field is well established [6], through the use, for example, of superparamagnetic iron oxide nanoparticles (SPIONs) as magnetic resonance imaging (MRI) contrast agents. According to the report published by BCC Research, “the market value of the nanomedicine industry was

$63.8 billion and $72.8 billion in 2010 and 2011, respectively" [7]. The same report estimates that the nanomedicine market will reach $130.9 billion by 2016, covering various therapeutic categories such as cardiovascular, infections, central nervous system (CNS) diseases and cancer [7, 8]. Many nanotheranostics are currently commercialized (even though they are not directly available to the consumer) and they are employed by researchers and physicians to treat specific diseases, including cancer (e.g., NanoXray nanoparticles from Nanobiotix and Abraxane®).

In the near future, ad hoc modified ENP are expected to improve disease treatment through a more adaptive and personalized approach to medicine [9]. Ideally, ENP will accumulate in the site of interest (targeting component) allowing the diagnosis of diseases and the evaluation of the treatment efficacy (imaging/diagnosis component) while tracking the drug delivery and release to the targeted tissue/cell (personalized therapy component) [9]. ENP surface modifications can be achieved by "layering," a common protocol used in basic research and able to produce multilayered theranostic ENP with personalized medicine application. "Layering" of iron oxide nanoparticles generates, for example, functional SPIONs formed by three main components: (1) an iron oxide core functioning as MRI contrast agent, (2) a biocompatible coating and (3) a therapeutic coating targeted with a pharmacogenomics biomarker [10, 11] (Fig. 11.1).

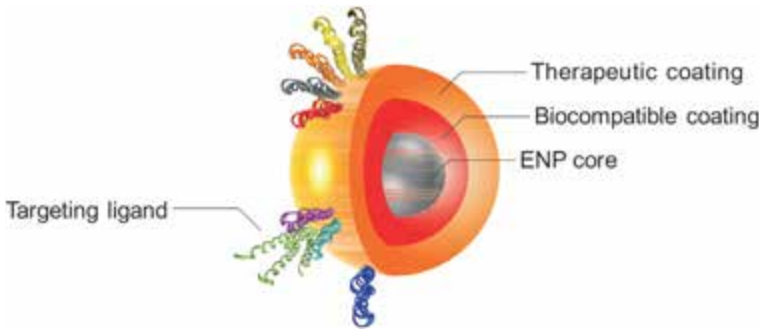

Figure 11.1 Schematic of a multilayered SPION with personalized medicine application. The figure depicts the three main components formed by "layering" an iron oxide nanoparticle: (1) ENP core, (2) biocompatible coating, and (3) therapeutic coating/targeting ligand.

11.2.1 Advantages of the Use of Multilayered ENP in Personalized Medicine

Compared to conventional pharmaceutical products, nanometric drug delivery systems can often lead to higher drug bioavailability with lower dose (thus decreasing the adverse side effects). In addition, targeting moieties decorating the ENP surface can direct efficiently the clinical treatment to the affected tissue/cell with optimal selectivity [12]. The combination of a personalized medicine approach with theranostic ENP has therefore the potential to make drug delivery safer and with better pharmacotherapeutic outcomes [13].

11.2.2 Disadvantages of the Use of Multilayered ENP in Personalized Medicine

Although the interest in multilayered ENP as personalized medicine tools is widespread, the clinical application of these materials implies the development of a cost-effective validation of their clinical effectiveness and safety. ENP need to demonstrate their advantages in comparison with current clinical practice in terms of efficacy, without raising the costs associated with their risk assessment.

Stakeholders and society consider cost-effectiveness as an essential requirement for novel clinical products. This stems from data showing that many expensive new clinical/pharmaceutical products have not always delivered significantly better results in terms of efficacy and/or safety than their more affordable predecessors. A similar case could rise for ENP with personalized medicine application: risk assessment research becomes therefore an essential part of the innovation of multilayered ENP [14] and it has to take place during the innovation process, in a cost-effective manner, similarly to the clinical/pharmaceutical model where hazards and risks of new drugs are addressed at an early stage in research.

11.3 The Risk Assessment of Multilayered ENP

As stated by Eaton in a recently published perspective on nanopharmaceuticals: “Many authors argue that nanoparticles

(NPs) (as drugs) have unusual properties but this assertion promotes the false idea to the public that there is something unusual or uncontrolled in this size range" [14]. Across a recent series of conferences, meetings, and global initiatives, the nanomedicine and nano- and toxicology communities have identified the fundamental need of a joint dialogue to overcome the hurdle of the insufficient data available on the risk associated to ENP. This has been reported to be mainly linked to the incomplete and/or contrasting information on the properties that determine the ENP impact on human health [15, 16]. Indeed, as compared to the safety of other pharmaceutical products, ENP risk assessment has the added complications of the ENP "nano" size (which can influence their properties and activity, as depicted in Table 11.1) and of the lack of standardized experimental approaches and models. As a consequence, over the past five years there has been an on-going debate on the most appropriate test strategies to use for assessing the ENP hazard.

Table 11.1 ENP properties that define key challenges in the assessment of the adverse and unintended behavior of ENP-related materials

ENP properties	Risk assessment key challenges
Shape	Influences toxic responses.
Size	• Affects penetration into cells and organs • Accumulation and retention effects (long-term toxic effects)
High surface area	• Enhanced contact area with surroundings • Catalytic or reactive sites exposed on the ENP surface • Formation of reactive oxygen species
Solubility	• With decreasing size and increasing surface area, the solubility of ENP may be increased • Contributes to the release of cytotoxic or inflammogenic components
Thousands of possible variants (different synthetic methods, impurities, coatings)	Ability to handle large number of ENP (High-throughput assay development)

Within this debate, there are two main issues that can be associated with the conventional, OECD-approved procedures used for assessing the risk of ENP. The first issue concerns the prevalence of non-harmful chemicals [17]. Using OECD-approved procedures, more than 87% of chemicals registered as new chemicals over the last 25 years were in fact not acutely toxic [17] and 93% of them did not show any hazard for human health [18]. Transposing this trend to the ENP field, it would seem that toxicological studies are looking for a rare hazard among thousands of variants of ENP [17] of which, the majority may not be a hazard for human health. It is this great variety of ENP that need to be tested which is the second important issue. Clearly, not all can be evaluated in *in vivo* studies for ethical and economic reasons [17]: indeed a single *in vivo* study can cost $50,000 [19] (approximately €37,000) and require an average of 3200 animals for a two-generation test on a single compound [20]. Conventional *in vivo* studies conducted on even those ENP currently in commerce could total a billion and half dollars (approximately €1 billion) and it could take 30–50 years to be completed.

International efforts have geared toward establishing consistent risk assessment approaches for ENP [21–24]. Currently, nanotechnology policies and regulation are encouraging the development and validation of new test models, the implementation of *in vitro* high-throughput screening tools [17, 19, 25, 26] and the assessment of the physico-chemical properties of the tested ENP within the experimental test systems used for the ENP risk assess-ment [27–29]. In recent years, a number of paradigms have emerged in nanotoxicology: (1) the bio-nano interface/protein corona paradigm [30], (2) the oxidative stress paradigm [24] and (3) the pathogenic fiber paradigm [31], to name a few. Such theoretical paradigms are helpful as platforms from which to interpret a large range of *in vitro* data, thus accelerating the rate of gathering toxicological data on ENP. However, a standardized strategy for assessing, modeling and potentially tuning the impact on human health of theranostic ENP as personalized medicine tools is still lacking.

11.4 The Translation of Multilayered ENP in Clinical Markets

One of the main milestones toward the successful translation of multilayered ENP into a safe, clinical personalized medicine technology is the integration of decision preferences for assessing and tuning the toxicity and behavior of ENP. Such decision preferences are to be determined by the perspectives of the different stake-holders groups, who give different weights to various decision criteria, such as cost, efficacy and risks to human health (although such decision preferences may change when/if new information becomes available).

The novel strategy should exploit optimized "decision-making tools" that drive the product-development decisions and that meet the goals of the recent REACH and OECD directives and policies, decreasing development costs and failures, and leading to targeted animal testing only if necessary. This will reduce ultimately the product development costs and it will allow the translation of major research investments and advances on ENP into clinical products that benefit patients [32, 33].

The toxicity of an ENP is driven by one or more components of its physico-chemical make-up and the interaction of these components with a biological system and as such, the physico-chemical properties of ENP are keys in defining the toxicological outputs of a specific ENP [16]. Once identified and understood the biologically effect dose (BED), this driving component, can be tuned to the advantage of the ENP's intended purpose or avoided to create a product that is "safe-by-design". Examples of physico-chemical properties of ENP that have been linked to their biological activity include geometry (i.e., size and shape), crystal structure, agglomeration and aggregation state of ENP (including potential toxicity of dispersants) as well as issues such as the concentration of impurities (e.g., transition metals). Examples such as these are also recognized as major issues in the evaluation of the ENP impact on human health [34]. Indeed the interaction with and distribution of ENP in the body can depend not only on the physico-chemical characteristics of the isolated ENP, but also on exogenous

factors such as differences in the specific protein content and make-up of the environment dependent on route of exposure or translocation (blood, skin, lungs) [29, 35]. Nevertheless, the toxicological consequences of the modification of each of these parameters are only incompletely understood.

For accelerating the translation of these materials into clinical markets, the impact of multilayered ENP on human health should be modeled systematically on the relationship between surface properties and ENP toxicity behavior (quantitative nanostructure-toxicity relationship (QNTR)). Indeed the usefulness of quantitative relationships has been extensively proved in the pharmaceutical industry over several decades. The development of such QNTR model should be based on the alteration of the toxic behavior of well-characterized ENP (identified with the term "core") by the process of "layering," thus obtaining a "safe-by-layer" tuning of the ENP properties (Fig. 11.2).

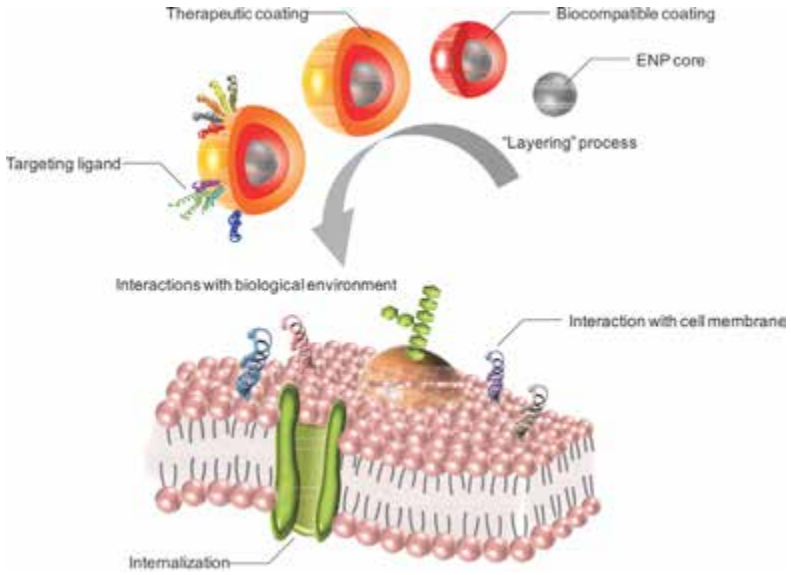

Figure 11.2 Schematic of the "safe-by-layer" assessment of the ENP impact on human health. Two are the main stages of this approach: the in-house "layering" of an ENP core and the evaluation of the ENP interactions with a biological environment (e.g., interaction with cell membrane, cell internalization).

Efforts to decrease costs and failures in drug discovery have been made since the 1990s, when the major cause of clinical failures was unacceptable ADME/pharmacokinetics of new drug candidates [36]. Implementation of *in vitro* ADME models significantly reduced this problem [36]. Following the pharmaceutical industry example, the currently available *in vitro* models should be implemented with various techniques and technologies (described in detail in the following) with the aim of building an assessment and modeling tool for predicting and tuning the impact on human health of multilayered ENP.

Studies start ideally from an inert, non-harmful ENP (e.g., a FDA-approved ENP) and move toward the assessment of the changes in toxicity behavior of the ENP when modified by a "layering" approach with well-characterized chemical moieties. This process involves the selection of well-characterized (FDA-approved) ENP obtained from commercial sources. The use of a commercially available material as starting point overcomes the lack of standardized nanomaterials that makes it difficult to compare results published from different research groups and organizations.

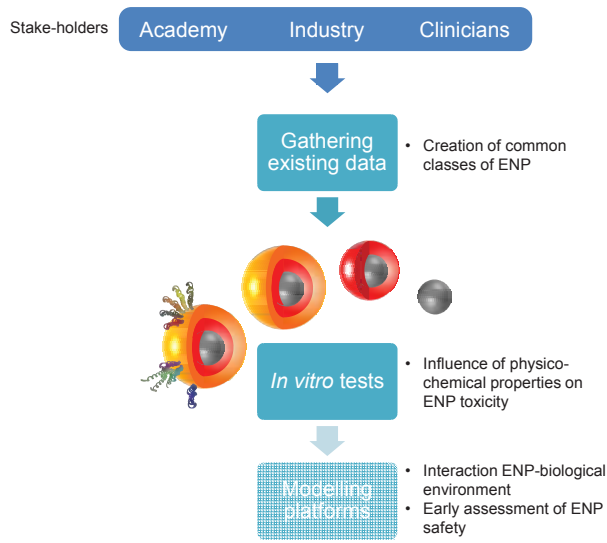

Figure 11.3 Flow-chart describing the backbone of the assessment and modeling tool proposed for predicting and tuning the safety of multilayered ENP with personalized medicine application.

The backbone of this assessment and modeling tool is formed by (1) prioritization of existing information on the ENP core; (2) *in vitro* testing of the ENP core engineered by "layering"; and finally (3) categorization and modeling of how surface modifications can or cannot influence the toxicity behavior of ENP by *in silico* technologies (Fig. 11.3).

11.4.1 Desk Assessment: Gathering Existing Data

As strongly encouraged by the recent literature and EU publications, ENP risks need to be prioritized by gathering information from existing academic, industry and clinical studies before carrying out *in vitro*/*in vivo* experiments. Common classes of ENP with shared toxicity behavior can be defined through this step. An expert curation of literature and of risk-assessment documentation using industrial standards (ISO Norms) for quality assurance is needed at this stage. The data extraction should also be combined with controlled vocabularies and toxicological ontologies. The combination of such data extraction methods with ISO Norms sets the basis for a standardized operating protocol (SOP) for reviewing nanotoxicology literature, thus affecting positively the entire research community [37]. Unified platforms must be developed to permit compatibility in handling different data gathered from unrelated sources, similarly to drug databases and clinical trials reports. Thus, the scientific knowledge of specific effects of ENP in the human body would be greatly enhanced.

11.4.2 *In vitro* tests

In this phase, systematic *in vitro* tests identify how the changes of ENP physico-chemical properties (associated with the "layering" processes) influence the cellular responses. In line with the pharma-sector development strategy, the new REACH guidelines and various expert opinions [17, 20], *in vitro* tests should include decision points (that depend on interim results) and should take into great consideration negative results (avoiding publication bias, i.e., non-publishing of negative results [38]) and the perspective of the stake-holders groups [2], who may have divergent views on the importance of the decision criteria selected (efficacy, selectivity and/or safety of the theranostic ENP). The use of high-

throughput techniques is highly recommended as powerful, efficient, reliable and reproducible tool so as to link the *in vitro* toxicity outcomes with pathological effects *in vivo* (such as membrane damage and production of reactive oxygen species (ROS)). The preponderance of *in vitro* methods aligns with the recent European Union regulations seeking to minimize research in animals. Whilst the transition of experimental results gained from animals across to humans is well understood based on various physical parameters, the translation from *in vitro* findings to real human health effects and especially conversion of dose remains challenging. Indeed a major issue is the potential for false positive/negative results, which may hinder confidence within *in vitro* results as to their predictive power. The provision for complex *in vitro* (co-cultures [39], 3D cell models [40], *in vitro* ADME models) and *in vivo* studies should be in place therefore when necessary to extract relevant information associated to the toxicity triggered by different pharmacokinetic (ADME), efficacy and rate with which ENP can be distributed and accumulated in the human body. *In vitro* cell-free experiments need also to be integrated to identify the molecular moieties (e.g., proteins) adsorbing onto the ENP surface [41] and to quantify the ENP oxidative potential (i.e., their ability to generate ROS, consume antioxidant and/or cause oxidative degradation of organic molecules) to build a complete mechanistic picture.

11.4.3 Modeling Platforms: *in silico* Technologies

These technologies provide categorization of the common features that various ENP may share when modified by "layering" with specific compounds that influence their toxicity behavior [42–46]. This allows deducing patterns that are common to a class of "layering" compounds.

In silico technologies can be helpful at various levels. First, *in silico* technologies can be used to generate computerized models (based on computational chemistry calculations) of the interaction of ENP with different biological environments, thus integrating and maximizing the information gathered from the *in vitro* cell-free experiments. Second, an *in silico* model for the early assessment of ENP safety can be developed. Such models generate knowledge of the surface properties that lead to

biological injury and it can produce a database that can be useful to the fast optimization of lead theranostic ENP. The compositional assessment platform developed should benefit from all levels of the risk assessment process, i.e., gathering of existing data (level 1), physico-chemical characterization (level 2), cell-free experiments (level 3), computational modeling of the interactions ENP-biological environment (level 4) and *in vitro* tests (level 5), as depicted in Fig. 11.4. Selected ENP can be further tested *in vivo* at a later stage (level 7), validating the results obtained from *in vitro* screening (and feeding back as part of a continuous validation loop), elucidating specific pathways and biomarkers, and leading to clinically approved theranostic ENP for Personalized Medicine.

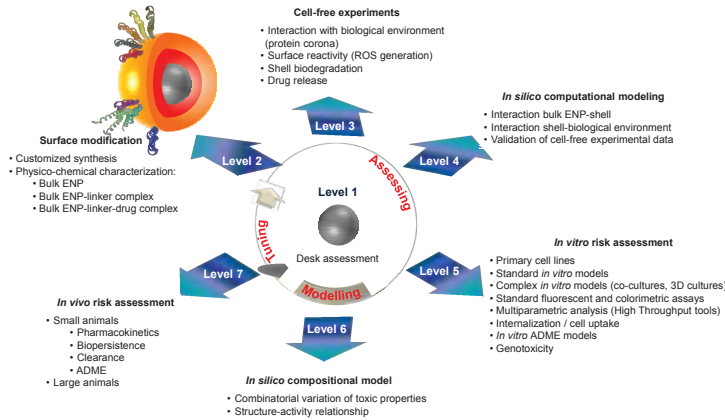

Figure 11.4 Assessing, modeling, and tuning the ENP impact on human health. This process is depicted in various phases. The first phase involves the selection of non-harmful ENP obtained from commercial sources, used as reference, and the evaluation of existing information (level 1). The surface of the ENP is then modified by "layering" approaches (level 2). The engineered ENP produced are subjected to physico-chemical characterization (level 2), cell-free experiments (level 3) and *in vitro* safety screening and assessment (level 5). Computational chemistry calculations are also carried out to study the interactions of ENP with the biological environment (level 4). The identified toxic and non-toxic ENP are used to develop a compositional tool that contains variations of the toxic outcomes of the modified FDA-approved ENP as defined by the various "layers" used (level 6). Selected ENP are then tested *in vivo* (level 7).

11.5 Conclusions

Risk assessment research is an essential part of the open-innovation of ENP as a personalized medicine technology and has to take place during the development process itself, similarly to the pharmaceutical model where hazards and risks of new products are addressed at an early stage in research.

Adoption of an ad hoc testing strategy for the evaluation of multilayered ENP products conveys toward a quicker translation process of emerging and promising ENP into pre-clinically and then clinically approved personalized medicine tools. Defining the relationship between surface structure and ENP health impact (QNTR) as generated by the risk assessment creates the basis for a SOP for the robust tuning of ENP impact on human health, reducing screening costs and animal experiments. Animals should be used only where alternative methods do not exist, enforcing and adhering to the "3R" principle (i.e., *reduction* in the number of animals used, *refinement* of the techniques in which animals are used, and *replacement* with non-animal procedures). Successful safety labeling and information dissemination is also expectable: the quick generation of a list of potential safe market products based on ENP will in fact accelerate the innovation process, allowing the smart design and optimization of novel/lead, non-harmful ENP. Many important pharmaceutical products now on the market (e.g., sulfamethoxazole, cefalotin and analogs, captopril) were discovered and optimized in the past following this very approach, commonly known as QSAR (quantitative structure–activity relationship) or QSPR (quantitative structure–property relationship). In addition, reducing the costs and increasing dissemination will attract smaller companies into the market which further pushes ENP development and diversity.

In conclusion, a standardized testing strategy will deliver a commercially viable tool with direct potential on the patenting/licensing phase that permits categorization and labeling of potential ENP-based nanomedical products with reduced impact on human health toward the consolidation of a "helping-without-harm" personalized medicine.

Abbreviations

BED: Biologically effect dose
ENP: Engineered nanoparticles
QNTR: Quantitative nanostructure-toxicity relationship
QSAR: Quantitative structure–activity relationship
SOP: Standardized operating protocol
SPIONs: Superparamagnetic iron oxide nanoparticles
ROS: reactive oxygen species
QSPR: quantitative structure–property relationship
FDA: food and drug administration
ADME: absorption, distribution, metabolism, and excretion
SOP: standardized operating protocol
REACH: Regulation for Registration, Evaluation, Authorisation and Restriction of Chemicals
ISO: International Organization for Standardization

Disclosures and Conflict of Interest

This work was partially supported by the EU FP7 NAMDIATREAM project (NMP-2009-LARGE-3-246479), MULTIFUN project (NMP-2010-LARGE-4-262943) and Science Foundation Ireland CRANN-CSET (Pathfinder project).

The authors declare that they have no conflict of interest and have no affiliations or financial involvement with any organization or entity discussed in this chapter. This includes employment, consultancies, honoraria, grants, stock ownership or options, expert testimony, patents (received or pending) or royalties. No writing assistance was utilized in the production of this chapter and the authors have received no payment for its preparation.

Corresponding Author

Dr. Adriele Prina-Mello
School of Medicine and Centre for Research on Adaptive Nanostructures and Nanodevices
Institute of Molecular Medicine
Trinity College, Dublin D8, Ireland
Email: prinamea@tcd.ie

About the Authors

Dania Movia is a post-doctoral researcher at the Centre for Research on Advanced and Adaptive Nanostructures (CRANN) of Trinity College Dublin (Ireland). In 2007, she was awarded a BSc in Medicinal Chemistry at University of Trieste (Italy). In 2011, she completed her PhD in Chemistry at Trinity College Dublin. Currently she is involved in a Flaghip FP7 project focused at the development of a common European approach to the regulatory testing of Manufactured Nanomaterials (NANoREG). Dr. Movia has published international peer-reviewed papers and book chapter focusing on the toxicology and application of smart nanomaterials.

Craig Poland is a research toxicologist within the SAFENANO section at the Institute of Occupational Medicine in Edinburgh. Dr. Poland's work at the IOM focuses on the provision of experimental toxicology into the potential hazards of nanomaterials to inform risk assessment of these novel materials. His research interests lie understanding how nanomaterials and particulates in general interact with biological systems, how this can lead to the development of disease and how such negative interactions can be avoided or exploited. Dr. Poland has published many international peer-reviewed papers and book chapters focusing on the toxicology of nanomaterials.

Lang Tran is currently the principal toxicologist at the Institute of Occupational Medicine. He has been working in field of particle toxicology for over 20 years. His early work was in the toxicity of manmade mineral fibers and low-toxicity poorly soluble particles. Recently, Lang has become involved extensively in nanotoxicology. He is one of the founders of the *Nanotoxicology Journal* and has published extensively in this field. He is currently the coordinator of FP7 MARINA and ENPRA.

Yuri Volkov received his MD from the Moscow Medical University and subsequently a PhD in biomedical sciences from the Institute of Immunology, Moscow. He is currently in the Department of Clinical Medicine, Trinity College Dublin (TCD). His research interests are focused in nanomedicine and biomedical applications of nanotechnologies, molecular mechanisms of immune system functioning in health and disease, cell adhesion and migration in inflammation and cancer, intracellular signalling and cytoskeletal dynamics, and advanced cell and molecular imaging. Prof. Volkov coordinates a large-scale EU FP-7 funded Consortium "NAMDIATREAM" (www.namdiatream.eu), which unites the expertise of 22 European academic, research, clinical, and industrial partners toward the development of nanotechnological toolkits for early diagnostics and treatment monitoring of major types of malignant diseases. He is also a lead TCD partner for EU FP-7 LSP "MULTIFUN" and "Celtic Alliance for Nanohealth" Ireland-Wales INTERREG Consortium.

Adriele Prina-Mello is a CRANN Investigator, a senior research fellow of the School of Medicine, a part-time lecture at Trinity College Dublin, the vice-chair of the Nanodiagnostic working group of the European Technology Platform of Nanomedicine, a Nanosafety Cluster member, and recently national coordinator of the NANoREG project on regulatory testing of nanomaterials. He has extensively published his work in biomedicine, nanotechnology, nanotoxicology, and nanomedicine research. Dr. Prina-Mello's main research interest is in the development of future applications of nanoparticles and nanomaterials in the biomedical and bioengineering field. He has also established active collaborative projects with the School of Bioengineering, Pharmacy at Trinity College. He is involved in developing and advancing several multidisciplinary research projects between the University, Research Hospital, and Industry partners for future applications in medicine and nanotechnology industry. Dr. Prina-Mello is involved in several EU FP7 funded projects: Deputy Coordinator of NAMDIATREAM (NMP), dissemination coordinator of MULTIFUN (NMP), and TCD partner

of Celtic Alliance for NanoHealth (INTERREG) and Science Foundation Ireland CRANN Pathfinder project.

References

1. Chen, X., Gambhir, S. S., Cheon, J. (2011). Theranostic nanomedicine. *Acc. Chem. Res.*, **44**(10), 841–841.
2. Linkov, I., Bates, M. E., Canis, L. J., Seager, T. P., Keisler, J. M. (2011). A decision-directed approach for prioritizing research into the impact of nanomaterials on the environment and human health *Nat. Nanotechnol.*, **6,** 784–787.
3. Ebbesen, J., Buajordet, I., Erikssen, J., Brors, O., Hilberg, T., et al. (2001). Drug-related deaths in a department of internal medicine. *Arch. Intern. Med.,* **161**(19), 2317–2323.
4. Vizirianakis, I. S. (2011). Nanomedicine and personalized medicine toward the application of pharmacotyping in clinical practice to improve drug-delivery outcomes. *Nanomedicine*, **7**(1), 11–17.
5. Vizirianakis, I. S. (2005). Improving pharmacotherapy outcomes by pharmacogenomics: From expectation to reality? *Pharmacogenomics*, **6**(7), 701–711.
6. Yildirimer, L., Thanh, N. T. K., Loizidou, M., Seifalian, A. M. (2011). Toxicological considerations of clinically applicable nanoparticles. *Nano Today*, **6**, 585–607.
7. Chai, C. Global Nanomedicine Market to Reach $130.9 Billion by 2016, Available at: http://www.azonano.com/news.aspx?newsID=24136 (accessed on October 18, 2014).
8. Global Industry Analyst, I. Nanotechnology in Medical Applications: The Global Market, Available at: http://www.bccresearch.com/report/nanotechnology-medical-applications-global-market-hlc069b.html (Accessed on October 18, 2014).
9. Lammers, T., Aime, S., Hennink, W. E., Storm, G., Kiessling, F. (2011). Theranostic nanomedicine. *Acc. Chem. Res.*, **44**(10), 1029–1038.
10. Kievit, F. M., Zhang, M. (2011). Surface engineering of iron oxide nanoparticles for target cancer therapy. *Acc. Chem. Res.,* **44**(10), 853–862.
11. Yigit, M. V., Moore, A., Medarova, Z. (2012). Magnetic nanoparticles for cancer diagnosis and therapy. *Pharm. Res.,* **29**(5), 1180–1188.
12. Ventola, C. L. (2012). The nanomedicine revolution: Part 1: Emerging concepts. *P T*, **37**(9), 512–525.

13. Doane, T. L., Burda, C. (2012). The unique role of nanoparticles in nanomedicine: Imaging, drug delivery and therapy. *Chem. Soc. Rev.,* **41**(7), 2885–2911.
14. Eaton, M. A. W. (2011). How do we develop nanopharmaceuticals under open innovation? *Nanomed. Nanotechnol. Biol. Med.*, **7**(4), 371–375.
15. The Editors (2012). Join the dialogue. *Nat. Nanotechnol.*, **7**(9), 545.
16. Schrurs, F., Lison, D. (2012). Focusing the research efforts. *Nat. Nanotechnol.*, **7**(9), 546–548.
17. Hartung, T. (2009). Toxicology for the twenty-first century. *Nature*, **460**(7252), 208–212.
18. Hoffmann, S., Cole, T., Hartung, T. (2005). Skin irritation: Prevalence, variability, and regulatory classification of existing *in vivo* data from industrial chemicals. *Regul. Toxicol. Pharm.*, **41**(3), 159–166.
19. Service, R. F. (2008). Nanotechnology: Can high-speed tests sort out which nanomaterials are safe? *Science*, **321**(5892), 1036–1037.
20. Höfer, T., Gerner, I., Gundert-Remy, U., Liebsch, M., Schulte, A., et al. (2004). Animal testing and alternative approaches for the human health risk assessment under the proposed new European chemicals regulation. *Arch. Toxicol.*, **78**(10), 549–564.
21. Stone, V., Johnston, H., Schins, R. P. F. (2009). Development of *in vitro* systems for nanotoxicology: Methodological considerations. *Crit. Rev. Toxicol.*, **39**(7), 613–626.
22. Jones, C. F., Grainger, D. W. (2009). *In vitro* assessments of nanomaterial toxicity. *Adv. Drug Deliv. Rev.,* **61**(6), 438–456.
23. Meng, H., Xia, T., George, S., Nel, A. E. (2009). A predictive toxicological paradigm for the safety assessment of nanomaterials. *ACS Nano*, **3**(7), 1620–1627.
24. Nel, A., Xia, T., Madler, L., Li, N. (2006). Toxic potential of materials at the nanolevel. *Science*, **311**(5761), 622–627.
25. Walker, N. J., Bucher, J. R. (2009). A 21st century paradigm for evaluating the health hazards of nanoscale materials? *Toxicol. Sci.*, **110**(2), 251–254.
26. Byrne, F., Prina-Mello, A., Whelan, A., Mohamed, B. M., Davies, A., et al. (2009). High content analysis of the biocompatibility of nickel nanowires. *J. Magn. Magn. Mater.*, **321**(10), 1341–1345.
27. Rivera Gil, P., Oberdorster, G., Elder, A., Puntes, V., Parak, W. J. (2010). Correlating physico-chemical with toxicological properties of nanoparticles: The present and the future. *ACS Nano*, **4**(10), 5527–5531.

28. Oberdorster, G., Maynard, A., Donaldson, K., Castranova, V., Fitzpatrick, J., et al. (2005). Principles for characterizing the potential human health effects from exposure to nanomaterials: Elements of a screening strategy. *Particle Fibre Toxicol.*, **2**(1), 1–8.

29. Nel, A. E., Madler, L., Velegol, D., Xia, T., Hoek, E. M., et al. (2009). Understanding biophysicochemical interactions at the nano-bio interface. *Nat. Mater.,* **8**(7), 543–557.

30. Lynch, I., Cedervall, T., Lundqvist, M., Cabaleiro-Lago, C., Linse, S., et al. (2007). The nanoparticle–protein complex as a biological entity: a complex fluids and surface science challenge for the 21st century. *Adv. Colloid Interface Sci.*, **134–35**, 167–174.

31. Donaldson, K., Murphy, F. A., Duffin, R., Poland, C. A. (2010). Asbestos, carbon nanotubes and the pleural mesothelium: A review of the hypothesis regarding the role of long fibre retention in the parietal pleura, inflammation and mesothelioma. *Particle Fibre Toxicol*., **7**(5), 1–7.

32. Weinshilboum, R. (2003). Inheritance and drug response. *N. Engl. J. Med.,* **348**(6), 529–537.

33. Advancing Regulatory Science for Public Health, Available at: http://www.fda.gov/ScienceResearch/SpecialTopics/RegulatoryScience/ucm228131.htm (accessed on October 18, 2014).

34. Aitken, R., Stone, V., Hankin, S., Aschberger, K., Baun, A., Christensen, F., Fernandes, T., Hansen, S. F., Hartmann, N. B., Hutchinson, G., et al. (2010). *Engineered Nanoparticles: Review of Health and Environmental Safety (ENRHES)*, Project Final Report, European Commission: Brussels, Belgium, pp. 350–365.

35. Walczyk, D., Bombelli, F. B., Monopoli, M. P., Lynch, I., Dawson, K. A. (2010). What the Cell "sees" in bionanoscience. *J. Am. Chem. Soc.,* **132**(16), 5761–5768.

36. Cottens, S., Eaton, M., Fuhr, J., Geary, S., Johnson, D. S., Li G., Raveglia, L., Robertson, G. M., Westwell, A. (2011). Ask the experts: Future of the pharmaceutical industry. Interview by Future Medicinal Chemistry. *Future Med. Chem*., **3**(15), 1863–72.

37. Reich, E. S. (2011). Nano rules fall foul of data gap. *Nature*, **480**, 160–161.

38. Hankin, S., Boraschi, D., Duschl, A., Lehr, C. M., Lichtenbeld, H. (2011). Towards nanotechnology regulation: Publish the unpublishable. *Nano Today*, **6**(3), 228–231.

39. Muller, L., Riediker, M., Wick, P., Mohr, M., Gehr, P., et al. (2010). Oxidative stress and inflammation response after nanoparticle exposure:

Differences between human lung cell monocultures and an advanced three-dimensional model of the human epithelial airways. *J. R. Soc. Interface*, **7**, S27–S40.

40 Movia, D., Prina-Mello, A., Bazou, D., Del Canto, E., Volkov, Y., et al. (2011). Screening the cytotoxicity of single-walled carbon nanotubes using novel 3D tissue-mimetic models. *ACS Nano*, **5**(11), 9278–9290.

41. Lynch, I., Salvati, A., Dawson, K. A. (2009). Protein-nanoparticle interactions: What does the cell see? *Nat. Nanotechnol.*, **4**(9), 546–547.

42. Romoser, A., Ritter, D., Majitha, R., Meissner, K. E., McShane, M., et al. (2011). Mitigation of quantum dot cytotoxicity by microencapsulation. *PloS One*, **6**(7).

43. Berg, J. M., Romoser, A., Banerjee, N., Zebda, R., Sayes, C. M. (2009). The relationship between pH and zeta potential of similar to 30 nm metal oxide nanoparticle suspensions relevant to *in vitro* toxicological evaluations. *Nanotoxicology*, **3**(4), 276–283.

44. Sayes, C. M., Warheit, D. B. (2009). Characterization of nanomaterials for toxicity assessment. *Wiley Interdiscip. Rev. Nanomed. Nanobiotechnol.*, **1**(6), 660–670.

45. Warheit, D. B., Reed, K. L., Sayes, C. M. (2010). Assessing the role of surface characteristics in nanoparticle-related pulmonary toxicity and inflammation. *Int. J. Toxicol.*, **29**(1), 133–134.

46. Fubini, B., Ghiazza, M., Fenoglio, I. (2010). Physico-chemical features of engineered nanoparticles relevant to their toxicity. *Nanotoxicology*, **4**(4), 347–363.

Chapter 12

Nanomaterials for Pharmaceutical Applications

Brigitta Loretz, PhD,[a] Ratnesh Jain, PhD,[b] Prajakta Dandekar, PhD,[c] Carolin Thiele, PhD,[d] Yamada Hiroe, PhD,[a] Babak Mostaghaci, PhD,[e] Lian Qiong, MSc,[f] and Claus-Michael Lehr, PhD[a,f]

[a]*Helmholtz Institute for Pharmaceutical Research Saarland, Helmholtz Centre for Infection Research, Saarbrücken, Germany*
[b]*Department of Chemical Engineering, Institute of Chemical Technology, Mumbai, India*
[c]*Department of Pharmaceutical Sciences and Technology, Institute of Chemical Technology, Mumbai, India*
[d]*CureVac GmbH, Tübingen, Germany*
[e]*Physical Intelligence Department, Max-Planck Institute for Intelligent Systems, Stuttgart, Germany*
[f]*Department of Biopharmaceutics and Pharmaceutical Technology, Saarland University, Saarbrücken, Germany*

Keywords: drug carriers, small molecules, biopharmaceuticals, translation, technical and regulatory challenges

12.1 Introduction

Since several years we witness nanotechnology as an extremely active research and development topic. One particular area with high expectations is the application in health care, which is referred

Handbook of Clinical Nanomedicine: Nanoparticles, Imaging, Therapy, and Clinical Applications
Edited by Raj Bawa, Gerald F. Audette, and Israel Rubinstein

ISBN 978-981-4669-20-7 (Hardcover), 978-981-4669-21-4 (eBook)
www.panstanford.com

to as nanomedicine. Nanomedicine comprises all applications of nanotechnology in diagnosis, prevention and treatment of diseases, including also technical approaches or nano-machines such as pacemakers, biochips, hearing aids, and medical flow sensors. To be more specific we have chosen the word nano-pharmaceuticals for the purpose of this chapter. Herein we discuss the potential of carriers in the sub-micron dimension for advanced drug delivery.

Physical and chemical properties, in particular solubility, permeability and chemical/biological stability are factors that may limit the bioavailability of a drug and consequently also the use in medicine/clinics. Highly potent actives can be discarded or delayed for such reasons. In general drugs can be classified in two groups, which also distinguish them in their degree of dependency on delivery systems. On the one hand there are chemically manufactured small molecules and on the other hand the so called biopharmaceuticals, which are macromolecules generated by means of biotechnological methods. Biopharmaceuticals comprise mainly protein and peptide drugs as well as nucleotide drugs. In case of small molecules, medicinal chemistry approaches sometimes can improve properties such as solubility, stability toward metabolic degradation or reduced toxicity in order to create more efficient agents. In cases where this is not possible formulations are needed to achieve efficient and safe pharmaceuticals. The term “drug delivery” implies a rather complicated process where the right concentration in time has to be achieved at the target location, ideally even with high specificity. In particular anti cancer drugs may benefit from targeted carriers to minimize the adverse effects in healthy tissue and maximize toxicity for cancer cells. In contrast, for biopharmaceuticals a delivery system is always required since their shared properties are large molecule size, structural complexity and fast metabolism. All these features hinder the achievement of sufficing bioavailability of the “naked” molecule. Biopharmaceuticals with their huge diversity however, are believed to realize personalized medicine to treat complex diseases with variable origin. But these new and highly promising drug candidates, originating from the enormous progress in genetics and biotechnology, are absolutely reliant on adequate delivery systems and technologies to exploit their therapeutic

potential. In this regard medicine and pharmaceutical industry's hopes are pinned on the emerging science of nanotechnology.

This chapter provides an overview on currently investigated or unmet therapeutic needs, which could be opportunities for nanoscale delivery systems, summarize in brief the current arsenal of nanocarrier technologies and their ongoing translation into the clinics. Finally we discuss the challenges for developing future nanopharmaceuticals.

12.2 Therapeutic Needs and Opportunities for Nanopharmaceuticals

12.2.1 Delivery of Small-Molecule Drugs

A well-designed drug delivery system may be of advantage even for established drugs (i.e., small molecules) because it can improve the therapeutic index, for example, by altering the pharmacokinetic and the body distribution [1]. For other actives a safe and efficient application without delivery system may even be impossible. The delivery systems used cover a wide range of materials and structural complexity. Within this chapter we mainly discuss nanoparticulate approaches. The optimal delivery system varies with the physicochemical and pharmacological properties of the active.

Pharmaceutical industry prefers oral administration, but this route is limited for actives with sufficient water solubility, a reasonable up-take rate through the intestinal epithelium and limited degradation in the intestinal milieu. A very frequent problem is the poor water solubility. This problem can be overcome by comparatively simple approaches. NanoCrystal® technology developed by Elan Drug Technologies, for example, refers to nanoparticles made from pure active by a proprietary process for size reduction and stabilization. The solubility is increased due to the enormously enlarged surface. Another approach also referred to as nanomedicine is to add a polymeric tag to the active (polymer-prodrugs) to improve the solubility or disposition in the body [2]. Estimations on drug development state that 70% of new molecular entities in industrial candidate pipelines suffer from low water solubility [3].

Low permeability through intestinal epithelium is a result of high molecular weight, low lipophilicity and limited solubility at intestinal pH. For several classes of drugs a low permeability is more or less intrinsic. In order to overcome their limitation to intravenous application covalent modification may help to increase lipophilicity or solubility. Alternatively the unfavorable properties may be masked by some carrier system. Nanoparticle formulations can enable new application routes, e.g., by facilitating transport over epithelial barriers, or by protection against hurtful pH environment or enzymatic degradation. Replacing intravenous injection by oral, pulmonary, nasal or transdermal application is of course favored by patients. The opportunity to control the release of the active, for example, by diffusion or degradation of the particle matrix is a further big advantage.

Several potent drugs are afflicted with severe adverse effects when they are systemically applied. Local application is not always possible because the target side might be difficult to access or distributed. In these cases we aim for a system that can use body-own signals to navigate to the site of action. Carriers in the right size distribution can play an important role here. On the one hand they have to be transportable via the circulation to reach their target. In order to achieve longer residence times in circulation particles have to be shielded from reticuloendothelial system (RES), which can, for example, be managed by surface PEGylation [4]. On the other hand accumulation at the preferred target side can be managed by two concepts: “passive” targeting via the so-called enhanced permeation and retention effect [5, 6] or “active” targeting via coupling of specific homing signals for receptor-recognition. Targeted drug delivery systems are a field of active research today producing essential know-how. Paul Ehrlich’s vision of the “magic bullet” in the ending 19th century has gained a new dimension since selectivity that cannot be provided from the active itself can be achieved with a smart delivery system. Several recent reviews provide more detailed information on this topic [7–9].

An important current trend is to use carriers for more than simple delivery containers. Rather they are supposed to act as platforms with multiple functions [10]. To fulfill diagnostic functions they are equipped with molecular recognition tools. Various labels and dyes are incorporated for imaging via magnet

resonance imaging (MRI) or positron emission tomography (PET). These imaging techniques are important for diagnosis as well as for tracing the success of (targeted) therapy. With growing know-how and techniques in nanotechnology particles can be engineered that act as multifunctional platform for early diagnosis, therapy and disease/therapy monitoring ("Theranostics") [11, 12]. Such nanomedicines could deliver more than one active, in near future probably even in a well-controlled sequence, and offer the possibility to be modified or equipped with a distinct set of specific targeting molecules or contrast agents for multimodal imaging. Figure 12.1 summarizes in a scheme the main functions of nanocarriers for (1) small-molecule drugs and (2) for biopharmaceuticals and further depicts how surface modifications and co-encapsulation can advance the carrier into a multifunctional platform.

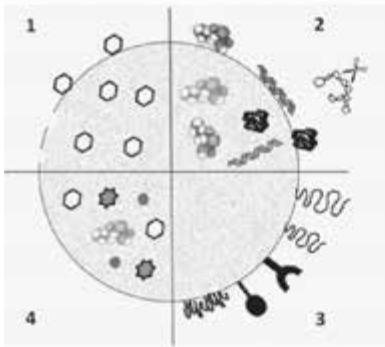

1. **Small molecule active**
   - Improved solubility
   - Controlled release
   - Reduced off-target effects
2. **Biopharmaceuticals**
   - Protection
   - Size reduction, charge neutralization
   - Cellular uptake
3. **Surface modification**
   - Long circulation
   - Targeting
   - Cell penetration
   - Coating
4. **Multifunctional platform**
   - Magnetic imaging and targeting
   - "Drug cocktail" i.e., multiple actives

Figure 12.1 Functions of carrier particles for (1) Small molecular drugs and (2) Biopharmaceuticals. (3) Possible surface modifications for improvement of pharmacokinetic performance. (4) Possible combinations of various payloads for multiple tasks within one carrier.

12.2.2 Macromolecular Biopharmaceuticals

Advances in biotechnology and molecular biology has brought up many drug candidates belonging to the group of

macromolecular biopharmaceuticals, including proteins and peptides, plus nucleotide actives such as plasmids and various oligonucleotides. "Clinical development of these types of pharmaceuticals may not be possible without some type of carrier system that allows these new entities to access target tissues and cells" [1]. Primarily these type of molecules need protection against degradation by enzymes or environmental conditions and they need shuttles to enable the delivery across the biological barriers, e.g., like absorptive epithelia but also cell membranes.

12.2.2.1 Proteins, peptides

With increasing knowledge of complex interrelations in molecular biology we get to know more and more proteins and peptides that can be used as therapeutic agents. Proteins and peptides with various functions nowadays are considered drugs, including enzymes, hormones, inhibitors of angiogenesis, inhibitors of amyloidogenesis, antibodies, vaccines, and antimicrobial or immunomodulatory peptides. Protein drugs are a growing part in the market of pharmaceuticals. They promise to make such diseases treatable that were untreatable with small-molecule drugs. A further advantage is the high similarity or even identity with body own molecules and therefore reduced adverse effects. Their speed in further growth is however limited by the high price, resulting from complicated production, and from difficulties in achieving sufficient bioavailability *in vivo*. Preservation of the fragile secondary and tertiary structure during production, in storage and after application in the circulation until the target is reached is the main obstacle. For the production biotechnology is asked for solutions. For the delivery problem nanotechnology is an often proposed strategy. Issues such as shelf life stability (preventing denaturation or/and aggregation), short circulation time due to elimination by renal clearance, reticuloendothelial system (RES) uptake or enzymatic degradation, can be reduced by packing proteins into suitable carriers. Additional positive impacts carriers can cause include a controlled release and active or passive targeting to the site of action. Proteins with intracellular targets have to face the entry beyond plasma membrane and the escape from the lysosome as added hurdles [9]. Current

challenges in protein delivery using nanotechnology is to develop methods for particle generation in very gentle conditions, since shear forces, heat, interfaces of water and organic phase are causing conformational changes in proteins [13]. Altered conformation may lead to lose of function but also to immunogenicity.

Predominant route of application for protein drugs is currently still parenteral injection. Other routes such as nasal, pulmonary, and oral application would raise the patients compliance and are the field of active research [14]. Suitable carriers are mandatory to make use of these routes. A prominent example is the delivery of insulin. The huge number of people suffering diabetes and being dependent on insulin injection is the driver of continued research for alternative, more convenient delivery strategies [15, 16]. An innovative strategy Liu et al. recently published the delivery of a transcription factor protein with a supramolecular nanoparticle system, which self-assembles upon addition of the modular components in non-covalent complexes [17]. By delivery of a transcription factor the expression level of multiple genes can be altered.

12.2.2.2 Nucleic acids

The therapeutic possibilities of nucleotide drugs in the last two decades expanded notably. Genes can be introduced but also silenced. The discoveries of siRNA and miRNA and their functions was a mile stone in understanding mechanisms of gene expression and opened new therapeutic approaches. At the same time gene introduction tools advanced with inducible or cell type specific promoters, smaller plasmid sizes, or adjustable stability of the transgene protein to mention just few achievements. At present a pool of nucleotide drug candidates is already there and still growing. A view on gene therapy trials conducted so far show a majority of viral vectors. However, in research a shift toward non-viral delivery is apparent and numerous polymeric or lipid carriers have been developed for this purpose. The report “Drug Delivery Technologies: Players, Products & Prospects to 2018” [18] sees significant opportunities for future commercial development, in particular the development of new polymers and biopolymers as carriers, the development of targeting strategies and the identification and delivery of polygenic genes in order to allow

therapies of multi-gene-based diseases. The RNAi nucleic acid drug delivery market is currently growing at high compound annual growth rate [19]. Success of siRNA is dependent of drug delivery platforms, which assist the active in more than simple shielding from enzymatic degradation. The key is an effective transport inside target cells and a controlled release in cytoplasm.

Nucleotides as drugs have some advantages in comparison to peptides/proteins. They are comparably easy to produce. From the delivery point of view they are all quite similar molecules. This allows at least to some extent transferring the know-how and knowledge from one delivery system for a special siRNA or pDNA to others or even a mixture of several sequences [20]. In consequence a rather universal delivery platform for nucleotides should be easier feasible, while proteins differ in size and properties to an extent that favors tailored carrier synthesis.

The history of gene delivery research evidences the high complexity factor of this task. Advancements in technical analytics, in chemical synthesis, in molecular cell biology and several other fields give starting points for directed improvements. Using selected endocytosis mechanisms or signals for intracellular transport, using smart carriers capable of sensing and changing in response to their environment are approaches to realize the use of genes as medicine.

Most non-viral delivery systems for nucleic acids concentrate currently on siRNA delivery, which does not need access to the nucleus, or aim for applications where a moderate transfection efficacy is sufficient, like in the case of vaccination. In a recent publication thioketal nanoparticles were demonstrated to deliver functional siRNA even on the oral route [21]**.** In another study cationic solid lipid nanoparticles were used to formulate three pDNAs coding for the isotypes of a *Leishmania* enzyme. This formulation strategy resulted in higher protection levels in vaccinated mice [20]**.**

12.2.3 Drugs that Need Efficient Targeting

12.2.3.1 “Nano-oncology”

Cancer persists to be one of the main challenges to the scientific community despite the multi-dimensional efforts being conducted for providing an efficient treatment. This may be attributed to the

limitations posed by the inherent physicochemical properties of the currently available anti-cancer agents. The hydrophilicity, surface charge and polarity of most of these drugs are unsuitable for their effective transport to the tumor tissues. Other barriers that hamper the effectiveness of anti-cancer agents include the altered apoptotic mechanisms of cancerous cells, altered transportation, the efflux systems responsible for multi-drug resistant effect (MDR), etc. [22]. This results in non-specific toxicity. Pharmaceutical nanomaterials offer the potential to overcome these drawbacks and hence are being actively explored by pharmaceutical scientists, for instance, the US national cancer institute (NCI) has founded an Alliance for Nanotechnology in Cancer (ANC).

Nanocarriers may gain access to the cancer tissues by active as well as passive targeting approaches. Provided that nanoparticles avoid their rapid elimination by the reticuloendothelial (RES) system, for instance, by polyethylene glycol (PEG) coating, which can provide longer circulation times, they can permeabilize through the defective tumor vasculature [22]. Tumor tissue has leaky vasculature and defective angiogenesis. Once inside the tumor, the defective lymphatic drainage retains the nanoparticles for prolonged time periods, where they can then release the associated drug in a controlled manner. This mechanism, which forms the basis of passive targeting, is referred to as the enhanced permeability and retention (EPR) effect. The reported size-dependency of this phenomenon ranges in particle sizes <400 nm sometimes even <200 nm [23]. Despite its practicability for clinical applications, passive targeting may sometimes be rendered ineffective owing to the MDR effect of cancer cells caused by overexpression of their natural efflux systems (e.g., P-glycoprotein efflux). Such difficulties may be overcome by active targeting, in which the nanoparticle surface is modified with suitable ligands or molecules capable of recognizing specific receptors, overexpressed selectively on tumor cells [24, 25]. Active targeting is a versatile option due to the availability of a wide range of targeting moieties, including proteins (antibodies), nucleic acids (aptamers), peptides, vitamins, and carbohydrates [23]. Although the extent of internalization of nanoparticles by this approach is directly proportional to their binding affinity to the receptor, excessively strong bond may reduce the internalization, which calls for the employment of alternative strategies such as

multivalent binding [26, 27]. Targeting nanoparticles may also be accomplished by stimuli responsive nanocarriers, composed of materials sensitive to the acidic intra-tumor environment [25].

These advantages of nanocarriers for cancer therapy are being extensively exploited through investigations concerning a variety of nanocarriers such as inorganic nanoparticles, polymer conjugates, polymeric and lipidic nanoparticles, micelles, dendrimers, and liposomes, which are being explored for numerous applications, including drug delivery, imaging, photothermal therapies, radiation therapies, sentinel lymph node mapping, etc. [23]. Nano-oncology is the field with most formulations already used in the clinics or involved in the process of translation. Therefore we discuss these examples in Section 12.4 and present promising upcoming techniques.

12.2.3.2 Drug delivery over the blood–brain barrier

Lots of serious social and economic problems are accompanied with neurological diseases such as cancers, inborn errors of metabolism, infectious diseases and aging [28]. Blood–brain barrier (BBB) is a protective impermeable system, which mainly consists of endothelial cells that controls and limits the transport of molecules to the brain using various strategies [29]. Drugs that are intended to reach the brain could be administrated systematically only if they have the capability to cross BBB or some undesirable invasive methods should be used to introduce the drugs directly to the brain tissue [30].

Among all of the promising biopharmaceutical agent that have been developed for central nervous system (CNS) disorders, only very few of them (<5%) can be used because the other ones are not able to reach to the desired site of action in sufficient therapeutic quantity [31]. Nanoparticles have shown the ability to transport various types of drugs, including low molecular drugs, macromolecules, and new biological entities to the brain using non-invasive administration, and sometimes they could reduce the side effects related to toxicity of the drugs due to limitation of drug leaching [30, 32]. Applications of various nanoparticles for usage in drug delivery to brain have been investigated. Nanoparticles coated with polysorbate 80 or polyoxamer 188 have been used for the delivery of drugs such as loperamide, dalargin, kyotorphin, tubocurarine, and doxorubicin [33]. It has been shown

that poly(butylcyanoacrylate) nanoparticles are able to deliver hexapeptide dalargin, doxorubicin and other agents into brain [32]. Some efforts also have been done to deliver imaging contrast agents to brain. One example is pegylated fluorescein-doped magnetic silica nanoparticles. It was shown that these nanoparticles could penetrate BBB via transcytosis of vascular endothelial cells [34]. Plenty of researches have been done on application of nanoparticles for brain drug delivery. The key point in this field is to reach a balance between BBB crossing capability, biodegradability and excellent biocompatibility of desired nanoparticles [30, 31].

12.2.3.3 Autoimmune diseases

Autoimmune diseases are a group of more than 70 different disorders in which the immune system recognizes and antagonize normal cells or components. Some common diseases within this group are rheumatoid arthritis, multiple sclerosis and Lupus erythematosus. Unlike other medical issues the incidence of autoimmune diseases is rising. Current therapies treat the symptoms but are not able to cure these chronic diseases. Efficient and safe treatments are of highest medical interest. Identification of disease origins as well as therapeutic targets is ongoing and has already led to several biopharmaceuticals such as siRNAs and interleukins as novel candidates [21, 35, 36]. For example, Tak-1 reduction mediated with siRNA was shown to decrease IFN-γ producing T cells and thus may be a target molecule for the treatment for autoimmune disease [37].

Delivery techniques will play an important role in realization of these new approaches. Immunomodulators need a targeted delivery because otherwise their systemic administration causes severe adverse effects. Small particulates have an advantage here because they accumulate in inflammation/disease caused lesions [38]. This effect can be harnessed for early diagnosis as well as for treatment [38, 39]. A selective accumulation of particles of specific size in inflamed GI-mucosa could be demonstrated *in vitro* and *in vivo* [40–42]. On top of such passive targeting, selectins and cellular adhesion molecules can be used for active targeting of inflammations modeling the leukocyte homing. Even more sophisticated approaches use pathophysiological changes in the tissue environment, such as lowered pH value

for triggered drug release of smart systems [43]. In particular macrophages are an attractive target. Their regulatory function in inflammation provides opportunities for therapeutic interventions while their natural function to take up particles by phagocytosis simultaneously facilitates specific delivery. For example, in a rat model of collagen-induced arthritis a poly(amidoamine) dendrimer carrier with folic acid targeting loaded with the anti-inflammatory active methotrexate could reduce arthritic disease effects [44]. Aouadi et al. used siRNA to successfully down regulate the proinflammatory cytokine TNF-α delivered by β-1,3-D-glucan particles via the oral route [45].

12.2.3.4 Vaccination

Disease prevention via vaccination is a story of success. With continuously growing understanding of immunological mechanisms it might eventually expand to currently not yet realizable vaccinations against diseases such as HIV or cancer. Specialized cells of the immune system are responsible for collecting and reporting particulate matter invading our body. While macrophages are phagocytizing rather large particles, dendritic cells are more in the focus of recent approaches to effectively carrying antigens into lymph nodes [46]. Particles (e.g., alum) are a known and used adjuvant since many years. Optimized carriers in regard of effective uptake and recognition by dendritic cells (DCs) and other cells, controlled release of intact antigen for effective antibody response, but also the selection of the right material for carrier and adjuvants will advance vaccination. A recent promising system was published by Pulendran and coworkers [47]. They used PLGA nanoparticles to deliver antigen together with the adjuvants MPLA and R837, which recognize the important Toll-like receptor (TLR) 4 and 7, respectively. The delivery allowed combining the two adjuvants in a controlled release system, which resulted in robust immunity against influenza.

12.3 Current Arsenal of Nanocarriers

Materials used for nanocarriers are inorganic, natural or synthetic lipids or polymers or mixtures thereof. The main groups of

Table 12.1 Main groups of nanoparticles developed for drug delivery

Nanoparticulate material	Size (nm)	Chemical materials	Therapeutic agent(s) carried	Advantages	Limitations
(Biodegradable) Polymers 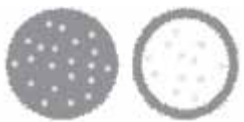	10–250	*Natural*: chitosan, alginate, carbohydrates, starch, cellulose, … *Synthetic*: poly(lactic-*co*-glycolic acid) = PLGA, polyvinylpyrrolidon, poly(caprolacton), poly(anhydride), Polystyrene, ...	pDNA, proteins, peptides, low-MW organic compounds	Sustained localized drug delivery for weeks	Exocytosis of undissolved nanoparticles. Fixed functionality after synthesis may require new synthetic pathways for alternate surface functionalities
Ceramics 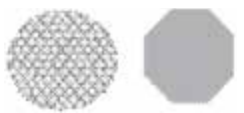	<100	Silica, hydroxya-patite, zirconium dioxide, titanium dioxide, zinc oxide, iron oxide ...	Proteins, DNA, chemotherapeutic agents, high-MW organic compounds	Easily prepared, water dispersible, stable in biological environments	Exocytosis of undissolved nanoparticles, surface decoration instead of encapsulation
Metals 	<50	Gold, silver, platinum, ...	Proteins, DNA, chemotherapeutic agents	Small particles present a large surface area for surface decoration delivery	Toxicity of materials, exocytosis of undissolved nanoparticles, time-consuming synthesis, surface decoration instead of encapsulation

(*Continued*)

Table 12.1 (*Continued*)

Nanoparticulate material	Size (nm)	Chemical materials	Therapeutic agent(s) carried	Advantages	Limitations
Polymeric Micelles 	<100	amphiphilic block copolymers using PLA, PCL, PEG, PEO ...	Proteins, DNA, chemotherapeutic agents	Suitable for water-insoluble drugs due to hydrophobic core	Toxicity of materials, fixed functionality after synthesis
Dendrimers 	<10	Polyamidoamine, poly(propyleneimine)	Chemotherapeutic agents, antibacterial, antiviral agents, DNA, high-MW organic compounds	Suitable for hydrophobic or hydrophilic drugs	May use toxic materials, time-consuming synthesis, fixed functionality after synthesis may require new synthetic pathways for alternate surface functionalities
Liposomes 	50–100	Phospholipids such as DOTAP, DDAB, DOTMA, DOPE, ...	Chemotherapeutic agents, proteins, DNA	Reduced systemic toxicity, increased circulation time	Fixed functionality after synthesis, some leakage of encapsulated agent, lack of colloidal stability

Source: Adopted from [48] with some modifications.
Note: A schematic example for the particle architecture is provided as well as some major pro and cons of the carrier type.

nanoparticles developed for drug delivery applications are mentioned in Table 12.1. Polymeric NPs are either solid matrix particles or core–shell systems (nanospheres) with liquid cores. In their simplest form, drug nanocrystals the particles are pure active (formulated by milling or high pressure homogenization) and dispersed in liquid media called nanosuspension. Ceramic NPs are nanocrystals or porous particles consisting of non-metals, which can be synthesized by wet precipitation or milling processes. As drug carriers crystals from metal ions are used for their uniform small size, which provides large surfaces for decoration with functionalities. Polymeric micelles are core–shell nanostructures formed via self-assembly of amphiphiles (polymers or lipids) in aqueous medium. Dendrimers are polymers with a three-dimensional branched structure and possibility of multiple functionalizations. Liposomes are composed of one or several concentric lipid bi-layers interspaced by aqueous or buffer filled spaces. From Table 12.1 summarizing also limitations it is easy to see that today no ideal carrier exists. A wide range is given for the technological level of particle generation starting from simple random complexes reaching until complicated multiple material containing organized structures. Nevertheless, few nanocarriers are now in clinical use mainly for very serious diseases with strictly limited therapeutic indication as selected examples (Table 12.3) show. While the approved systems are belonging to a first rather simple generation of carriers the R&D pipeline is full of more sophisticated carriers. Some of these highly organized nanostructures generated in multiple step processes are described as examples for upcoming technologies (see Section 12.4.3).

12.4 Translation of Nanopharmaceuticals into Clinics

12.4.1 Approved Nanopharmaceuticals

First clinical approved nanocarriers, even not recognized as “nano” in the beginning, were polymer-protein and polymer-drug conjugates. In 1990, SMANCS produced by Yamanouchi and named

Zinostatin stimalamer® was the first polymer–protein conjugate to be applied in market [49]. Also PEG-L-asparaginase (Oncaspar®), the Enzon trademark for pegaspargase, belongs to this carrier type being a conjugate of modified enzyme L-asparaginase linked to multiple PEG chains. It is an oncolytic agent used in combination chemotherapy for the treatment of patients with acute lymphoblastic leukemia (ALL) [2].

Next liposomes, able to better shield the actives due to the encapsulation into lipids, entered the field of clinical therapies. In 1995, liposomal daunorubicin (DaunoXome®) is the first-line therapy of choice for advanced AIDS-related Kaposi's sarcoma. The liposome carrier allows daunorubicin to prolong retention time in the body resulting in enhanced drug amount delivered to the cancer cells, while having fewer side effects on healthy tissue [50, 51]. A few years later Doxil, a PEGylated liposome with longer circulation time was approved by the US Food and Drug Administration (FDA). The success of Doxil® gave an important impulse in the development of carrier technologies. A further step stone was the approval of Abraxane®, consisting of albumin nanoparticles for the improved delivery of paclitaxel compared to previous standard Taxol®. Further there are several antibody conjugates and nanocrystals in clinical use.

12.4.2 Nanopharmaceuticals Currently in Clinical Trials

Opaxio® (poly-L-glutamic acid [PGA]–paclitaxel conjugate, formerly known as Xyotax® from Cell Therapeutics Inc.) is an example for a drug conjugate that demonstrates quite well how long it may take to get a medicine approved. While research of PGA-paclitaxel started approximately 20 years ago [52] recently reported phase III trials show that Opaxio® is expected to reach the market in the near future as a potential treatment for ovarian, non-small cell lung and esophageal cancers [53, 54].

In this respect it is not surprising that no more complex, constructed nanocarriers could get approval until now, but first targeted carriers and platform technologies are in clinical phase I or II testing. Table 12.3 highlights some nano-enabled carriers that are currently in clinical testing.

Table 12.2 Selected approved pharmaceuticals using nanotechnology

Pharmaceutical trade name	Active	Therapeutic indication	Delivery system	Company	Approval
SMANCS Zinostatin Stimalamer	Neocarzinostatin (NCS) protein	Hepatocellular carcinoma	SMA-polymer-protein conjugate	Yamanouchi (now Astellas)	1990
Oncaspar	L-Asparaginase	Acute lymphoblastic leukemia (ALL)	PEG-protein conjugate	Enzon	1994
DaunoXome	Doxorubicin citrate	Advanced HIV-associated Kaposi's sarcoma	Liposome injection	Gilead Siences	1995
Zoladex	Goserelin acetate	Prostate or breast cancer, endometriosis	Polymer rods	AstraZeneca	1998
Doxil/Caelyx	Doxorubicin HC1	Ovarian cancer	Stealth liposome preparation for injection	Ortho Biotech	1999
Rapamune	Sirolimus	Immunosuppresant	NanoCrystals	Pfizer	2000
Mylotarg	Anti CD33-antibody	Recurrent AML	Monoclonal antibody	Wyeth	2000 2010 withdrawn
Abraxane	Paclitaxel	Metastatic breast cancer	Albumin particles	Abraxis Biosciences	2005
Invega sustenna	Paliperidone palmitate	Schizophrenia	NanoCrystals	Janssen	2009

Table 12.3 Pharmaceuticals using nanotechnology in various phases of clinical trials (status 2011)

Name	Active	Therapeutic indication	Delivery system	Company/inventor	Clinical phase
OPAXIO™ formerly XYOTAX™	Paclitaxel prodrug	Non-small cell lung cancer	Polyglutamate polymer	Cell therapeutics	III
EZN-2208	Irinotecan	Metastatic Breast cancer	PEG-conjugate	Enzon Pharmaceuticals	II
IT-101	Camptothecin	Solid tumors	Cyclosert™ cyclodextrin NP	Calando pharmaceuticals	I
AP5346/ ProLindac™	Oxiplatin	Ovarian cancer	HPMA conjugate	Access Pharmaceuticals	II
MBP-426	Oxiplatin	Advanced or Metastatic Solid tumors	Transferrin-targeted liposome	Mebiopharm	II
NK105	Paclitaxel	Solid tumors	Micelle	Nippon kayaku	II
CALAA01	siRNA	Solid tumors	RONDEL™ polymer NP	Calando pharmaceuticals	I
Cornell Dots	Radioactive iodine as PET label	Imaging tumors	PEG coated silica spheres	Hybrid silica Technologies	I
DermaVir	Plasmid DNA	Topical immunization against HIV/AIDS	mPEI particles	Genetic immunity	II

CALAA-01 is Calando's lead RNAi therapeutics program based on Rondel™ delivery. CALAA-01 nanoparticles consist of a cyclodextrin-based polymer, transferrin protein targeting ligand, polyethylene glycol (PEG) for stability, and a siRNA duplex targeting the M2 of ribonucleotide reductase (RRM2), a well-established cancer target. An interim analysis of Phase I data from 15 solid tumor patients treated with the drug showed that it was well tolerated, including at the highest dose tested so far [55].

12.4.3 Upcoming Technologies

The applications of nanomaterials in pharmaceutical arena are infinite. Although only a few of these products are currently available in the market, the R&D pipeline is flooded with numerous promising technologies and systems based on these. Here we will just highlight some of them that—with contributions from the industry, academia, and regulatory authorities—may hopefully someday transform into viable therapies.

12.4.3.1 Nanoparticle-based technologies

Calando Pharmaceuticals, USA, has developed Cyclosert™, a platform technology comprising of nanoparticles formulated using cyclodextrin conjugated to therapeutic agents. These nanoparticles, varying between 30 and 60 nm in size, exhibit site specific drug targeting accompanied by controlled drug release, which is claimed to lower the toxicity of the therapeutic agent. Cerulean Pharma Inc., USA, has successfully completed Phase I trials of the product, CRLX101, based on this technology in various cases of relapsed or refractory solid tumors and the product has now progressed to Phase II trials of non-small cell lung cancer [56–59]. Another interesting technology for targeted drug delivery to cancers are the polymersomes. This technology is composed of bi-layers of biodegradable synthetic polymers, with properties similar to phospholipids. This allows their simultaneous loading with both hydrophilic and hydrophobic anti-cancer actives (paclitaxel and doxorubicin), resulting in an additive effect of both the drugs [60]. Marillion Pharmaceuticals, USA, is developing lipoprotein-based nanoparticle technology with the possibility of multivalent attachment of single or numerous tumor targeting

moieties to the same nanoparticle. Thus the technology has been claimed to have a wider application range. NOF Corporation, Japan, has developed PUREBRIGHT® technology in which cholesterol pullulan-based hydrogel nanoparticles are used to formulate cancer vaccines [61]. Self-assembling nanoparticles of poloxamer CRL1005 form the basis of vaccine delivery technology of Vical Incorporated USA. The product TransVax™ targeting Cytomegalovirus, based on this technology, is presently undergoing clinical trials [62]. Nanoparticles formulated using porin proteins form the basis of the Proteosomes™ technology being employed by GlaxoSmithKline, UK for developing nasal vaccines for respiratory syncytial virus, influenza, allergy etc. Here, the porins have been stated to interact with dendritic cells that elicit the immune response [61]. Apart from developing technologies based on advantages derived from matrix material of nanoparticles, researchers have also attempted to exploit the benefits provided by various shapes of nanoparticles for an enhanced drug delivery. Dependence of nanoparticle shape on improving nanoparticle uptake and hence efficacy has been proven by scientists through various investigations [63]. Mitragotri and coworkers have developed technology based on formation and stretching of films of materials, using routine laboratory chemicals and equipment, to result in nanoparticles with more than 20 discrete shapes. The researchers have claimed a precise and repetitive control over particle size and shape, with this technology, even when producing larger batches of particles [64]. Likewise, Caruso's research group has employed emulsion templating technology to produce nanocapsules of controlled size and thickness [65]. An interesting development is the lithographic approach developed by DeSimone and coworkers named PRINT® (**P**article **R**eplication **I**n **N**on-wetting **T**emplates), which allows to produce size and shape controlled particles [66–68].

12.4.3.2 Nanoemulsion-based technologies

A nanoemulsion-based platform technology (NanoStat™) has been developed by NanoBio® Corporation, USA for topical delivery of drugs effective against bacteria, fungi, spores and viruses (even HIV), with several products based on this technology being already in Phase I and II of clinical trials [61]. The same technology is also being employed for delivery of nasal vaccines against

respiratory syncytial virus, hepatitis B, etc., while the product for seasonal influenza has already progressed to clinical trials. The success of these formulations has been attributed to enhanced permeability of the nanoemulsion across nasal mucosa to deliver the antigen to immune cells of the body [69].

12.4.3.3 Micelle-based technologies

Cisplatin containing and PEG-poly (glutamic acid) block copolymer-based micellar technology has been introduced by NanoCarrier Ltd., Japan. Pre-clinical studies established the improved tumor retention and increased circulation times of these carriers and further clinical studies are presently in progress. The company has also developed the Medicelle™ technology comprising platin containing PEG-poly (glutamic acid)-based micelles in collaboration with Debiopharm, Switzerland, to improve the effectiveness of the anti-cancer agent due to EPR effect [61, 70]. Another polymer micelle-based platform, NanoViricide™, had been developed by NanoViricides Inc, USA, which acts by binding to multiple sites of the virus particle and ultimately results in its disassembly. The technology has been employed by the company to develop products effective against AIDS, herpes, influenza, eye infections, bird-flu, etc., which are currently in pre-clinical evaluations [71].

12.4.3.4 Liposome-based technologies

Aphios Corporation, USA, has employed supercritical fluid technology (SuperFluids™) to formulate liposomes containing paclitaxel and camptothecin [72]. Another liposome-based technology encapsulating anti-cancer therapeutics is the Protein Stabilized Nanoparticle (PSN™) technology, which is being used for targeted delivery of Docetaxel and Irinotecan [73].

12.4.3.5 Dendrimer-based technologies

Starpharma Ltd., Australia, has developed an aqueous vaginal gel (VivaGel®), based on their dendrimer technology, for avoiding or curtailing the transmission of sexually transmitted diseases, including HIV. This product, which acts by preventing the attachment of pathogens to body cells, is currently in Phase II trials [74]. An auxiliary firm of this corporation plans to employ their dendrimer-

based platforms, Priostar™ and STARBURST, for targeted drug delivery in diseases such as cancer [75].

12.4.3.6 Cationic nanoparticles for nucleic acid delivery

Cationic nanoparticles find special utility for delivery of nucleic acids (pDNA, oligonucloetides, siRNA) due to their ability to condense polynucleotides that assists in stabilization and transport of such actives. They are known to facilitate cellular adhesion and internalization as well as escape from the endo-lysosomal compartment. The principle of ionic interaction works with inorganic particles such as amine-functionalized silica [76] and with cationic polymers [77].

These benefits of nanocarriers were exploited by Tekmira while developing their SNALP (stable nucleic acid-lipid particles) technology, which is now being used by Alnylam Pharmaceuticals, USA, for developing various siRNA-based therapeutics. One of the projected applications of this technology is in cancer therapy, where the nanoparticles have been hypothesized to be retained in tumor vasculature due to EPR effect and then fuse with the cancer cells to release the nucleic acids into the cellular cytoplasm. Products of this technology directed against dyslipidemia/hypercholesterolemia, amyloidosis and solid tumors are in Phase I trials [78, 79]. Similarly, Calando Pharmaceuticals Inc, Canada, has developed the cyclodextrin-based RONDEL™ technology, which is now majority-owned and further developed under Arrowhead [79, 80].

If all these technologies are further pursued, simultaneously addressing the challenges posed by the existing therapeutic nanoparticles, the nanotechnology-based products are sure to play a significant role the pharmaceutical market in the next decade.

12.4.4 Requirements/Needed Support

While nanomedicine has demonstrated great promises in various drug delivery and imaging applications, these applications present a great demand of acceptability from the pharmaceutical industries, regulatory agencies, scientific societies and public at large.

12.4.4.1 Social and ethical requirements

Exploring social and ethical issues of nanomedicine is a primary requirement to increase the adaptability of these technologies. It is expected that a developed understanding and interdependence of science, technology and society can lead to creation of important legislations and policies. The social acceptability is particularly important to avoid the obstacles encountered by the scientific community during the development of genetic engineering and biotechnology. Various public surveys indicate that the public attitude toward nanomedicine is generally positive due to the potential health benefits [81]. However in recent years there have been growing concerns regarding the toxicological implications of nanoparticles to the human health and environment. To circumvent the mass confusion arising out of such contradictory views regarding the potential outcomes of nanomedicines, the present scenario calls for initiation of awareness campaigns and information distribution procedures to spread the correct knowledge about drug delivery carriers. Such initiatives can also influence the political agenda, resulting in establishment of more rational policies based on more facts than confusion [82, 83]. Thus, a more conscious and vigilant behavior from society can be helpful for the availability of nanomedicines of practical use to the public.

12.4.4.2 Regulatory requirements

European Union (EU) and the United States Food and Drug Administration (US FDA) have already introduced various task forces to review the potential of nanomedicines and to setup appropriate guidance for the development of nanomedicine. Although numerous reports have been already made by these agencies regarding this issue, it requires a systematic and rational approach to arrive at well-accepted regulatory solutions. Various reports published by EU and US FDA have indicated that creating regulatory guidelines require expertise and support from the diverse disciplines such as medicine, biology, chemistry, physics, material science, and engineering [83–85].

While product development in the field of nanomedicine is rapidly growing, the knowledge on the related effects is still in

nascent stages. The current understanding to generate the risk profile of nanomaterials and nanopharmaceuticals, hazard identification and risk assessment needs to be carried out on a case-to-case basis [84, 85]. However, the need of the hour is to correlate all the data accessed by different national and international regulatory agencies. There is a need to harmonize these guidelines and develop a broad understanding to initiate adoption of rational regulatory policies. This will ultimately allow rapid introduction of nanopharmaceutical products into the society.

12.4.4.3 Technological and industrial requirements

Nanoparticulate formulations have seen significant progress in pharmaceutical industry during the last decade. Pharmaceutical companies specifically focused their R&D expenditure on these "new dosage forms" due to the patent expiry of existing drugs, drug discovery of lipophilic molecules and to attain better targeting. Various nanotechnology-based pharmaceutical products have already been approved for therapeutic use [86, 87]. Although there are multiple products in the market, pharmaceutical industry has not achieved the anticipated success with these due to several reasons. Most of the nanopharmaceuticals belong to the category of nanocrystals while the number of products where drugs are encapsulated in polymeric/lipidic carriers is relatively limited. The technical reasons for this limitation is the unavailability of suitable biodegradable polymers, large scale processes of nanoparticle manufacturing, lack of toxicity data and difficulty of setting up *in vitro*/*in vivo* correlation [87, 88]. These factors are serious obstacles to the further expansion of nanopharmaceutical products.

There is an immediate need for new biodegradable polymers to be synthesized. Pharmaceutical industry had to look beyond the poly-lactic acid class of polymers for large-scale use [9]. Manufacturing nanoparticles at larger scale is also limited and scaling up the laboratory processes in industries has not really materialized in all the cases. A focused research and machinery needs to be investigated and validated for the large scale processing of nanoparticles. Effective methods for the large scale generation of monodisperse nanoparticles made of pharmaceutically

acceptable materials are urgently needed and just about to emerge (e.g., PRINT technology [68]). Rapid generation of toxicity data is restricted by the lack of suitable guidelines [84, 86, 88] and existing data are sometimes not publicly accessible. Apart from that, the safety evaluation of nanomaterials may require different protocols both *in vitro* and *in vivo* compared to conventional ("non-nano") materials.

To summarize, for materializing the market success of nanopharmaceutical products, a multifaceted research approach is needed to address the gaps in toxicological and regulatory issues.

12.5 Challenges for Developing Future Nanopharmaceuticals

12.5.1 New Materials

12.5.1.1 Biodegradability

An important potential for improvement of drug carriers is the need for further raw material. Polymers are of high interest due to the good stability polymeric carriers provide and their potential for further modifications. In particular, for nanocarriers that might reach and enter many tissues and cells throughout the body, biodegradability is an invaluable advantage. The current choice of biodegradable polymers is limited. Polylactide (PLA), biodegradable polyester, is one of the most common polymers used in the field of drug delivery. PLA itself is hydrophobic and the hydrolysis in the human body very slow. To speed up the degradation process hydrophilic parts can be included into the polymer chain. The resulting amphiphilic block-copolymers are widely used in pharmaceutical applications because of their faster degradation compared to pure PLA and their ability to self-assemble into nanoscaled particles. Poly(lactid-*co*-glycolid) (PLGA) is known to form nanoparticles in high quality using various production methods and encapsulate drugs. A further application in the field of gene delivery is possible when coating with a cationic polymer such as chitosan is carried out [89]. Although being currently the gold standard of biodegradable polymeric

nanoparticles, PLGA NPs are slow in degradation and create an acidic milieu during disintegration [90, 91].

As many drugs need repeated dosing within days carriers with shorter degradation time and intracellular degradation are needed. Degradation can occur via hydrolysis or by enzymatic degradation. Several research teams are working on the enlargement of the pool of biodegradable polymers by using cleavable ketal- [92, 93], acetal [94] or ester bonds [95].

A new amphiphilic biodegradable methoxypolyethylene glycol/poly(D,L-lactide)/poly(ethyl ethylene phosphate) (MPEG-*b*-PEAb-PEEP) block copolymer was synthesized in the group of Zhang [96] by ring-opening polymerization of ethyl ethylene phosphate (EEP) with methoxypolyethylene glycol/poly(D,L-lactide) (MPEG-b-PEA) as a macroinitiator. The biodegradability together with the self-assembling capability into nanomicelles in aqueous systems suggests a use in drug delivery.

Biodegradable Polymers are often adopted from nature making use of existing degrading enzymes. Starch, for example, can be chemically modified to make it better suitable as nanoscaled drug delivery system. Propylated starch was shown to be a suitable carrier for various model drugs but needed a rather high degree of substitution [97]. Another example for nanoparticles based on starch is a nanoplexes consisting of anionic starch and cationic cyclodextrin (CD) derivatives. A hydrophobic compound can be included in the CD cavity and the resulting complex is then used for the formation of particles [98].

In order to prevent an initial burst in the drug release but enable efficient release at acidic pH a polymer with two distinct pH responsive linkages (β-aminoester and ketal) was synthesized and demonstrated to provide good stability in neutral pH but rapid degradation in pH 5 [99].

12.5.1.2 Multifunctional, smart polymers

In order to create intelligent systems sensing environmental factors and reacting on special triggers to advance pharmaceuticals several smart polymers were developed. Stimuli responsive polymers have been studied intensively in these decades. There are many stimuli possibilities in chemical (pH and solvent), physical

(temperature, light, magnetic and ultra sound) and biological milieu (enzymes, receptors). Many systems aim to use differences in the natural milieu at the target side. pH changes or intracellular reductive potential are harnessed for triggering drug release. Chaturbedy et al. made pH-responsive organic-inorganic hybrid spheres by coating the colloidal polystyrene spheres with polyelectrolyte-protected aminoclay and Mg phyllo(organo)silicate, which can change sphere size depends on the pH and release ibuprofen and eosin [100].

Kono et al. [101] designed liposomes based on a block copolymer with temperature-responsive drug release and magnetic imaging functions. The liposomes provided high resolution magnetic resonance (MR) images. They are stable at physiological temperatures and exhibited release of doxorubicin after mild heating [101].

Wang et al. [102] synthesized multi-stimuli responsive graft polymer. This amphiphilic graft polymer exhibit sharp response to temperature, pH and ionic strength. It can self-assemble into stable micro/nano micelles in aqueous solution, which can encapsulate hydrophobic guest molecules [102].

In recent years, researchers are interested in water-soluble stimuli responsive polymeric systems that show a phase transition in response to environmental stimulus such as temperature, pH, specific ions and electric field. Several research groups have reported the preparation of pH and temperature sensitive polymers based on poly(*N*-isopropylacrylamide) for biomedical applications [103].

A nanoformulation of curcumin loaded biodegradable thermoresponsive chitosan-*g*-poly(*N*-isopropylacrylamide) (chitosan-*g*-NIPAAM)-*co*-polymeric nanoparticles (TRC-NPs) was prepared by ionic cross-linking method. The lower critical solution temperature was dependent on the amount of NIPAAM and rose from pure PNIPAAM at 32–44°C in the copolymer. Flow cytometric analysis of curcumin loaded TRC-NPs showed increased apoptosis on PC3 cells [104].

A different strategy is to apply particles that accumulate at the target side and then start the drug release by a local external pulse such as NIR light irradiation, ultra sound or magnetic treatment. One such system was designed when a hollow, porous

gold cage was loaded with various model drugs and covered with a temperature sensitive polymer. These nanosystems were capable for NIR photothermal effect and triggerable drug release [105].

12.5.1.3 Mimicing biological structures

The development of the new materials using clinically approved polymers that can mimic biological structures would be advantageous for the further application as nanopharmaceuticals. Polyvinyl alcohol (PVA) is, for example, a well-known, clinically approved synthetic analog of hyaluronic acid.

Hartwell et al. described the preparation of an injectable collagen–glycosaminoglycan scaffold containing PVA networks, and evaluated its efficacy for use in tissue engineering for the application of skin cells. The PVA-borate networks improved the architecture and mechanical properties [106].

For vaccination mimicking microorganism structures is a viable approach. In a recent investigation glucan shells originating for *Saccharomyces* cell walls were purified and efficiently used as antigen carriers [107].

The engineering of most successful biological materials is also a promising strategy. Silk-elastin-like protein polymers could be synthesized by genetic engineering, enabeling a precise control over the polymer structure and therefore allowed the formation of very uniform carrier particles [108].

12.5.2 In silico Approaches and Databases

Interdisciplinary cooperation between technology, pharmacy/biology, material scientists and mathematics or computer scientists should advance development of optimized carriers. Many parameters impact carrier performance, including size, charge, surface area, hydrophobicity, functional groups, shape and flexibility. As first step data sets with comparable experimental results have to be created. Then mathematical models and computer simulations could assist rational particle design. Biochemical properties or particle interactions within physiological fluids, nanotoxicology in humans and the environment could become predictable. First models on distinctive properties are already known [109–112].

12.5.3 Ensuring Quality of Nanopharmaceuticals

The FDA's current Good Manufacturing Practices (cGMPs) for pharmaceutical industry are designed to ensure that the final product is manufactured according to specific guidelines of manufacturing, processing, and handling to ensure that the final products is safe and effective for its intended use. Although there are no standard guidelines for nanopharmaceuticals, manufacturing of nanopharmaceuticals must follow the cGMP guidelines of manufacturing and control. To manufacture safe and effective nanopharmaceuticals there are some challenges that need to be overcome by the researchers and pharmaceutical industry in near future [113].

The following sections of this chapter focus on some of the currently faced, major challenges that restrict a smooth transition of the nanopharmaceuticals from laboratories to the market.

12.5.3.1 Characterization techniques

Challenges of nanopharmaceuticals characterization are one major factor for their difficult transition to the market. Many nanopharmaceuticals meant for therapeutic and clinical use comprise of a variety of materials that have unique optical, electronic and structural properties on nanoscale, properties totally absent in bulk materials. These properties can negatively affect the development of reproducible and valid assays such as colorimetric and enzymatic assays that rely on measurement of inherent material characteristics such as absorbance, surface characteristics. Characterization also influences the fine tuning of nanoparticle structure, scale up, performance and safety. Suitable characterization method development is also mandatory for compliance of nanopharmaceutical products with the guidelines of FDA and other regulatory agencies [113–116].

12.5.3.2 Reproducibility and scale-up

Another important aspect is scalability. Cost effective and parameter controlled manufacturing of nanoparticles is still a major challenge for the pharmaceutical industry. Appropriate standards to manufacture nanoparticles and nanomaterials are still in development and large scale manufacturing is still in nascent stages. One of the major reasons behind this challenge is engineering

the machinery and instrumentation for production. Most of the available machinery is limited to laboratory scale and amount of research for engineering, to adapt it to large scale manufacture, is less understood [115–117].

12.5.3.3 Sterilization methods

Most of the nanopharmaceuticals developed at present are being utilized for parenteral administration. These nanopharmaceuticals require suitable sterilization methods and control, which at the same time must not hamper the inherent characteristics of the formulations. Nanopharmaceuticals may be manufactured with lipidic or polymeric matrices and may further be surface modified with ligands or antibodies. Additionally, recent development in biopharmaceutical research has allowed inclusion of genetic material within the nanopharmaceutical carriers. In large, nanopharmaceuticals comprise complex molecules and structures with various limitations (temperature or irradiation sensitivity, size exciding sterile filtration limit, etc.). Selection of suitable sterilization methods poses a great challenge to the pharmaceutical industry.

12.5.3.4 Quality control and quality assurance

Pharmaceutical industry is well acquainted with quality control (QC) and quality assurance (QA) of pharmaceutical products. However, nanopharrnaceuticals exhibit new characteristics and hence newer or modified methodologies to guarantee reproducibility of these aspects. Hence, the existing parameters and methodologies must be revised to suit the novel properties of nanopharmaceuticals. This includes methods to assess them at various stages of production, right from the raw materials to the finished products. Most of the developed nanopharmaceuticals consist of novel materials and hence the pharmaceutical industry needs to adopt a new methodologies to control the afore-mentioned parameters [118]. Appropriate analytical methods are the most important keys to control and regulate the quality and quantity of therapeutic molecule inside the dosage forms. Nanopharmaceuticals specifically exhibit a great challenge with reference to the design of suitable analytical methods and their validation [119]. Development of accurate and precise chromatography methods,

methods to determine *in vitro* release profiles, methods to determine the amount of encapsulated actives, and validation of these are some of the tasks that the pharmaceutical industry needs to seriously look into.

12.6 Conclusions and Future Perspectives

Nanotechnology has definitely brought up new perspectives also for the field of medicine and pharmaceutics. Targeted delivery to specific cells or organs, individual variable biomarkers and intracellular delivery as well as combinations with diagnostic and imaging tools seem to become feasible. Today however, the fraction of approved nanotherapeutics is still insignificant in comparison with the investigatorial efforts of the scientific community. This may be attributed partly to safety concerns and fears for unknown risks these novel materials may cause. Nanotechnology scientists should inform about risks without creating hysteria. A clear separation of environmental pollution and industrial nanoparticles in contrast to carrier particles engineered for the application in humans or animals is important. Pharmaceutical scientists have to take safety constrains serious and must evaluate from the beginning not only perspectives but also drawbacks and limitations. The various interaction possibilities of nanomaterials with biological materials are challenging and need appropriate attention. Usage and development of suitable materials and in depth evaluation of carrier effects is mandatory. Many investigations addressing these issues are already in progress. The simultaneous development of nanosafety along with nanotechnology is important. This may delay the quick transition into daily life and also prevent hasty usage and hazard. Therefore it might take a little while, indeed, before we will find more complicated nanoscaled drug delivery systems in the clinics. Easier systems with simple and robust fabrication methods using few components should meanwhile not be neglected since their realization might be less complicated. Moreover the cost-effective production should make nanomedicines affordable especially for developing countries with their high needs. Many sophisticated multi component carriers currently in development seem difficult to be controlled at the high quality

level needed for pharmaceuticals with present instruments. The necessary development of machinery and methods will delay the clinical use of these systems. The enormous capabilities of such platform delivery systems, which we aimed to highlight in various examples within this chapter, will make up for the immense efforts to realize them.

Disclosures and Conflict of Interest

The authors declare that they have no conflict of interest and have no affiliations or financial involvement with any organization or entity discussed in this chapter. This includes employment, consultancies, honoraria, grants, stock ownership or options, expert testimony, patents (received or pending) or royalties. No writing assistance was utilized in the production of this chapter and the authors have received no payment for its preparation. This is a revised version of the author's chapter that originally appeared in *Safety Aspects of Engineered Nanomaterials*, (W. Luther and A. Zweck, eds.), 2013, Pan Stanford Publishing Pte. Ltd., Singapore.

Corresponding Author

Dr. Claus-Michael Lehr
Helmholtz Institute for Pharmaceutical Research Saarland
Department of Drug Delivery, Saarland University
66123 Saarbrücken, Universitätscampus E8 1, Germany
Email: Claus-Michael.Lehr@helmholtz-hzi.de

About the Authors

Brigitta Loretz studied microbiology at the University of Innsbruck. During her master thesis, she characterized the promoter of the murine chemokine CXCL-11. In April 2007, she received her PhD from the Department of Pharmaceutical Technology, University of Innsbruck, for her work on novel strategies for oral gene delivery. For her first postdoc, she joined the Biopharmaceutics and Pharmaceutical Technology group at Saarland University in June

2007. After the foundation of the Helmholtz-Institute for Pharmaceutical Research Saarland, she changed to the Helmholtz Institute at the very beginning and is working there as senior scientist. Her research interests are nanoparticulate carriers for intracellular delivery of biopharmaceutics, with special focus on biodegradable polymers.

Ratnesh Jain received his PhD from the Department of Pharmaceutical Sciences and Technology, Institute of Chemical Technology, Mumbai. During this tenure, he received a fellowship from the Department of Atomic Energy, Government of India. His doctoral work was focused on the development and evaluation of various polymeric nanocarriers such as micelles and nanoparticles. Subsequently, he joined the Department of Biopharmaceutics and Pharmaceutical Technology, Saarland University, Saarbrucken, as a postdoctoral fellow, where he was engaged in formulating polymeric nanoparticles of hydrophobic anti-cancer agents. He was awarded the prestigious Alexander von Humboldt Postdoctoral Fellowship by the AvH Foundation, Germany, and completed the associated research in the Department of Drug Delivery, Helmholtz Institute for Pharmaceutical Research Saarland, Saarbrucken, Germany. He is currently UGC Assistant Professor in Engineering Sciences and Ramalingaswami Fellow in the Department of Chemical Engineering at the Institute of Chemical Technology, Mumbai. His research group focuses on the formulation of polymeric nanocarriers such as nanoparticles, micelles, and nanoplexes for improving the solubility and bioavailability of poorly soluble drug moieties.

Prajakta Dandekar received her PhD from the Department of Pharmaceutical Sciences and Technology, Institute of Chemical Technology, Mumbai. Her doctoral research involved the development of polymeric nanoparticles for natural therapeutic agents. Later, she joined the Department of Macromolecular Organic Chemistry, University of Saarland, Saarbrucken, as a post-doctoral researcher and was involved in formulating nanoparticles of

new hydrophobic starch polymers for encapsulating hydrophobic anti-cancer actives. She was the first woman scientist from India to be awarded the European Respiratory Society-Marie Curie Joint Postdoctoral Fellowship (long-term) and conducted the associated research involving formulation of nanoparticles for intracellular siRNA delivery at the Department of Drug Delivery, Helmholtz Institute for Pharmaceutical Research Saarland, Saarbrucken, Germany. From January 2012 until October 2014, she worked as Dr. John Kapoor Assistant Professor in Pharmaceutical Technology at the Department of Pharmaceutical Sciences and Technology, Institute of Chemical Technology, Matunga, Mumbai. Currently, she is UGC Assistant Professor in Engineering Sciences and Ramanujan Fellow in the same department. Her research interests involve design of siRNA-polymer nanocarriers, pulmonary disorders, development of *in vitro* cellular models, and tissue engineering for preclinical research.

Carolin Thiele studied chemistry at Saarland University. In July 2010, she received her PhD from the department of Organic and Macromolecular Chemistry for her work on the synthesis of cyclodextrin and starch derivatives for improved drug delivery. After her PhD, she changed the field from chemistry to pharmacy and joined as a post-doctoral research scientist the group of Prof. Lehr (Drug Delivery) at the Helmholtz-Institute for Pharmaceutical Research Saarland. Her research was focused on the synthesis, characterization, and *in vitro* testing of cationic starch derivatives for gene delivery applications. Since August 2013, Dr. Thiele is working at CureVac GmbH as scientist in the Product Design and Formulation department with research focus on the development and evaluation of different delivery technologies for mRNA.

Yamada Hiroe studied polymer chemistry at the Tokyo Institute of Technology, Japan, earning an MSc in 2007. From April 2007 until September 2010, when she joined the Lehr group at the Helmholtz Centre for Infection Research, she spent several years working as a chemist in the chemical industry in Germany. Hiroe's PhD research

topic was the design of starch-based polymers for gene delivery applications. She defended her PhD in August 2014 and is since then working as postdoc at the Helmholtz-Institute for Pharmaceutical research Saarland.

Babak Mostaghaci studied bachelor and master of materials science and engineering at Isfahan University of Technology, Iran. For master thesis, he worked on "bacterial synthesis of nano-crystalline hydroxyapatite using Serratia marcesence PTCC 1187." He earned his PhD from Helmholtz-Institute for Pharmaceutical Research, Saarland in 2015 after working on "synthesis of amino-modified calcium phosphate nanoparticles used for gene delivery application." He is now a postdoctoral fellow in Max-Planck-Institute for Intelligent system, Stuttgart, studying on intelligent systems for drug delivery.

Lian Qiong studied at the Department of Chemistry of Shanghai Normal University. In June 2008, she got her master's degree for her work on functionalized multi-walled carbon nanotubes for antisense oligodeoxynucleotides delivery. She joined the Department of Biopharmaceutics and Pharmaceutical Technology at Saarland University as a PhD student in 2009. Her area of research is the use of nanoparticles based on biodegradable polymers as anticancer drug carries for intracellular delivery.

Claus-Michael Lehr is professor at Saarland University as well as cofounder and head of the department "Drug Delivery" of the recently established Helmholtz-Institute for Pharmaceutical Research Saarland (HIPS). The HIPS is the first permanently installed institution explicitly dedicated to pharmaceutical research and is a branch of the Helmholtz Centre for Infection Research (HZI) in Braunschweig. Additionally, Prof. Lehr is cofounder of Across Barriers GmbH and PharmBioTec GmbH. The main focus of Prof. Lehr's research is exploring the biological barriers, in particular the gastrointestinal tract, the skin, and the lungs and, on the other hand, developing the appropriate carriers capable of cross-

ing these epithelial barriers and deliver the active molecule to the target. Prof. Lehr is (co)author of more than 250 papers, which have been cited ~4500 times (h-index 38). He was the recipient of the CRS Young Investigator Award (2001), the APV Research Award 2006 for outstanding achievements in the Pharmaceutical Sciences and the biannual International Price 2008 of the Belgian Society for Pharmaceutical Sciences. In 2011, his team was awarded the German national research award on alternatives to animal testing. Prof. Lehr is fellow of the American Association of Pharmaceutical Scientists (AAPS, 2010) and corresponding honorary member of the French Academy of Pharmaceutical Sciences (2012). He serves on different national and international scientific and editorial committees and is co-editor of the *European Journal of Pharmaceutics and Biopharmaceutics*. He is regularly involved in the organization of international conferences.

References

1. Allen, T. M., Cullis, P. R. (2004). Drug delivery systems: Entering the mainstream. *Science*, **303**(5665), 1818–1822.
2. Duncan, R. (2003). The dawning era of polymer therapeutics. *Nat. Rev. Drug Discov.*, **2**(5), 347–360.
3. Benet, L. Z., Broccatelli, F., Oprea, T. I. (2011). BDDCS applied to over 900 drugs. *AAPS J.*, **13**(4), 519–547.
4. Jokerst, J. V., et al. (2011). Nanoparticle PEGylation for imaging and therapy. *Nanomedicine*, **6**(4), 715–728.
5. Maeda, H., Bharate, G. Y., Daruwalla, J. (2009). Polymeric drugs for efficient tumor-targeted drug delivery based on EPR-effect. *Eur. J. Pharm. Biopharm.*, **71**(3), 409–419.
6. Noguchi, Y., et al. (1998). Early phase tumor accumulation of macromolecules: A great difference in clearance rate between tumor and normal tissues. *Cancer Sci.*, **89**(3), 307–314.
7. Danhier, F., Feron, O., Préat, V. (2010). To exploit the tumor microenvironment: Passive and active tumor targeting of nanocarriers for anticancer drug delivery. *J. Control. Release*, **148**(2), 135–146.
8. Huynh, N. T., et al. (2010). The rise and rise of stealth nanocarriers for cancer therapy: Passive versus active targeting. *Nanomedicine*, **5**(9), 1415–1433.

9. Torchilin, V. P. (2010). Passive and active drug targeting: Drug delivery to tumors as an example. In: Schäfer-Korting, M., ed. *Drug Delivery: Handbook of Experimental Pharmacology*, vol. 197, pp. 3–53.
10. Chacko, A. M., et al. (2011). Targeted nanocarriers for imaging and therapy of vascular inflammation. *Curr. Opin. Colloid Interface Sci.*, **16**(3), 215–227.
11. Torchilin, V. (2009). Multifunctional and stimuli-sensitive pharmaceutical nanocarriers. *Eur. J. Pharm. Biopharm.*, **71**(3), 431–444.
12. Sanvicens, N., Marco, M. P. (2008). Multifunctional nanoparticles—properties and prospects for their use in human medicine. *Trends Biotechnol.*, **26**(8), 425–433.
13. Brown, L. R. (2005). Commercial challenges of protein drug delivery. *Expert. Opin. Drug Deliv.*, **2**(1), 29–42.
14. Moeller, E. H., Jorgensen, L. (2009). Alternative routes of administration for systemic delivery of protein pharmaceuticals. *Drug Discov. Today Technol.*, **5**(2–3), e89–e94.
15. Díaz, A., et al. (2010). Nanoencapsulation of insulin into zirconium phosphate for oral delivery applications. *Biomacromolecules*, **11**(9), 2465–2470.
16. Zhang, X. G., et al. (2008). PEG-grafted chitosan nanoparticles as an injectable carrier for sustained protein release. *J. Mater. Sci. Mater. Med.*, **19**(12), 3525–3533.
17. Liu, Y., et al. (2011). Delivery of intact transcription factor by using self-assembled supramolecular nanoparticles. *Angew. Chem. Int. Ed.*, **50**(13), 3058–3062.
18. Barton C. (2009). *Nucleic Acid Drug Delivery Technologies: Players, products & prospects to 2018* (Volume III), Espicom, New York, NY, USA.
19. RNAi Drug Delivery: Technologies and Global Markets. Available at: http://www.bccresearch.com/market-research/biotechnology/rnai-drug-delivery-bio076b.html (accessed on February 2, 2015).
20. Doroud, D., et al. (2011). Delivery of a cocktail DNA vaccine encoding cysteine proteinases type I, II and III with solid lipid nanoparticles potentiate protective immunity against *Leishmania* major infection. *J. Control. Release*, **153**(2), 154–162.
21. Wilson, D. S., et al. (2010). Orally delivered thioketal nanoparticles loaded with TNF-α-siRNA target inflammation and inhibit gene expression in the intestines. *Nat. Mater.*, **9**(11), 923–928.

22. Pellequer, Y., Lamprecht, A. (2009). In: Lamprecht, A., ed. *Nanoscale Cancer Therapeutics in Nanotherapeutics Drug Delivery Concepts in Nanoscience*, Pan Stanford Publishing Pte. Ltd., Singapore. pp. 93–124.
23. Peer, D., et al. (2007). Nanocarriers as an emerging platform for cancer therapy. *Nat. Nanotechnol.*, **2**(12), 751–760.
24. Torchilin, V. P. (2005). Recent advances with liposomes as pharmaceutical carriers. *Nat*. *Rev*. *Drug Discov*., **4**(2), 145–160.
25. Torchilin, V. P. (2007). Targeted pharmaceutical nanocarriers for cancer therapy and imaging. *AAPS J.*, **9**(2), E128–E147.
26. Adams, G. P., et al. (2001). High affinity restricts the localization and tumor penetration of single-chain Fv antibody molecules. *Cancer Res.*, **61**(12), 4750–4755.
27. Hong, S., et al. (2007). The binding avidity of a nanoparticle-based multivalent targeted drug delivery platform. *Chem. Biol.*, **14**(1), 107–115.
28. Karkan, D., et al. (2008). A unique carrier for delivery of therapeutic compounds beyond the blood-brain barrier. *PLOS One*, **3**(6), 1.
29. Juillerat-Jeanneret, L. (2008). The targeted delivery of cancer drugs across the blood-brain barrier: Chemical modifications of drugs or drug-nanoparticles? *Drug Discov. Today* **13**(23–24), 1099–1106.
30. Wohlfart, S., Gelperina, S., Kreuter, J. (2011). Transport of drugs across the blood-brain barrier by nanoparticles. *J. Control. Release*, **161**(2), 264–273.
31. Barbu, E., et al. (2009). The potential for nanoparticle-based drug delivery to the brain: Overcoming the blood-brain barrier. *Expert Opin. Drug Deliv.*, **6**(6), 553–565.
32. Shieh, P. C., et al. (2009). Future prospects of nanoparticles on brain targeted drug delivery. *J. Neuro-Oncol.*, **93**(2), 285–286.
33. Kreuter, J., et al. (2009). Transferrin- and transferrin-receptor-antibody-modified nanoparticles enable drug delivery across the blood-brain barrier (BBB). *Eur. J. Pharm. Biopharm.*, **71**(2), 251–256.
34. Ku, S., et al. (2010). The blood-brain barrier penetration and distribution of PEGylated fluorescein-doped magnetic silica nanoparticles in rat brain. *Biochem. Biophys. Res. Commun.*, **394**(4), 871–876.
35. Carvalho, V., et al. (2011). Self-assembled dextrin nanogel as protein carrier: Controlled release and biological activity of IL-10. *Biotechnol. Bioeng.*, **108**(8), 1977–1986.

36. Hallaj-Nezhadi, S., Lotfipour, F., Dass, C. R. (2010). Nanoparticle-mediated interleukin-12 cancer gene therapy. *J. Pharm. Pharm. Sci.*, **13**(3), 472–485.

37. Courties, G., et al. (2010). *In vivo* RNAi-mediated silencing of TAK1 decreases inflammatory Th1 and Th17 cells through targeting of myeloid cells. *Blood*, **116**(18), 3505–3516.

38. Ulbrich, W., Lamprecht, A. (2010). Targeted drug-delivery approaches by nanoparticulate carriers in the therapy of inflammatory diseases. *J. R. Soc. Interface*, **7**(Suppl. 1), S55–S66.

39. Tu, C., et al. (2011). Receptor-targeted iron oxide nanoparticles for molecular MR imaging of inflamed atherosclerotic plaques. *Biomaterials*, **32**(29), 7209–7216.

40. Laroui, H., et al. (2010). Drug-Loaded nanoparticles targeted to the colon with polysaccharide hydrogel reduce colitis in a mouse model. *Gastroenterology*, **138**(3), 843–853.

41. Moulari, B., et al. (2008). The targeting of surface modified silica nanoparticles to inflamed tissue in experimental colitis. *Biomaterials*, **29**(34), 4554–4560.

42. Lamprecht, A., Schäfer, U., Lehr, C. M. (2001). Size-dependent bioadhesion of micro- and nanoparticulate carriers to the inflamed colonic mucosa. *Pharm. Res.*, **18**(6), 788–793.

43. Mahmoud, E. A., et al. (2011). Inflammation responsive logic gate nanoparticles for the delivery of proteins. *Bioconjug. Chem.*, **22**(7), 1416–1421.

44. Thomas, T. P., et al. (2011). Folate-targeted nanoparticles show efficacy in the treatment of inflammatory arthritis. *Arthritis Rheum.*, **63**(9), 2671–2680.

45. Aouadi, M., et al. (2009). Orally delivered siRNA targeting macrophage Map4k4 suppresses systemic inflammation. *Nature*, **458**(7242), 1180–1184.

46. Akagi, T., et al. (2007). Protein direct delivery to dendritic cells using nanoparticles based on amphiphilic poly(amino acid) derivatives. *Biomaterials*, **28**(23), 3427–3436.

47. Kasturi, S. P., et al. (2011). Programming the magnitude and persistence of antibody responses with innate immunity. *Nature*, **470**(7335), 543–550.

48. Adair, J. H., et al. (2010). Nanoparticulate alternatives for drug delivery. *ACS Nano*, **4**(9), 4967–4970.

49. Vicent, M. J., Duncan, R. (2006). Polymer conjugates: Nanosized medicines for treating cancer. *Trends Biotechnol.*, **24**(1), 39–47.
50. Anonymous (2003). Drugs of choice for cancer. *Treat. Guidel. Med. Lett.*, **1**(7), 41–52.
51. Eric A. F. (1997). The design and development of DaunoXome® for solid tumor targeting *in vivo*. *Adv. Drug Deliv. Rev.*, **24**(2–3), 133–150.
52. Li, C., et al. (1999). Antitumor activity of poly(L-glutamic acid)-paclitaxel on syngeneic and xenografted tumors. *Clin. Cancer Res.*, **5**(4), 891–897.
53. Li, C., Wallace, S. (2008). Polymer-drug conjugates: Recent development in clinical oncology. *Adv. Drug Deliv. Rev.*, **60**(8), 886–898.
54. Chipman, S. D., et al. (2006). Biological and clinical characterization of paclitaxel poliglumex (PPX, CT-2103), a macromolecular polymer–drug conjugate. *In. J. Nanomed.*, **1**(4), 375–383.
55. Ribas, A., et al. (2010). Systemic delivery of siRNA via targeted nanoparticles in patients with cancer: Results from a first-in-class phase I clinical trial. *J. Clin. Oncol.*, **28**(15s), 3022.
56. Jain, K. K. (2010). Advances in the field of nanooncology. *BMC Med.*, **8**, 83.
57. Svenson, S., et al. (2011). Preclinical to clinical development of the novel camptothecin nanopharmaceutical CRLX101. *J. Control. Release*, **153**(1), 49–55.
58. Study of CRLX101 (Formerly Named IT-101) in the Treatment of Advanced Solid Tumors. Available at: http://clinicaltrials.gov/show/NCT00333502 (accessed on February 2, 2015).
59. A Phase 2 Study of CRLX101 in Patients With Advanced Non-Small Cell Lung Cancer. Available at: http://clinicaltrials.gov/show/NCT01380769 (accessed on February 2, 2015).
60. Ahmed, F., et al. (2006). Biodegradable polymersomes loaded with both paclitaxel and doxorubicin permeate and shrink tumors, inducing apoptosis in proportion to accumulated drug. *J. Control. Release*, **116**(2 SPEC. ISS.), 150–158.
61. Jain, K. (2008). Nanopharmaceuticals. In: *The Handbook of Nanomedicine*, Humana/Springer: Totowa, Chapter 4, pp. 119–160.
62. Infectious Disease Vaccines. Available at: http://www.vical.com/products/infectious-disease-vaccines/asp0113/default.aspx (accessed on February 2, 2015).

63. Decuzzi, P., Ferrari, M. (2008). The receptor-mediated endocytosis of nonspherical particles. *Biophys. J.*, **94**(10), 3790–3797.

64. Champion, J. A., Katare, Y. K., Mitragotri, S. (2007). Making polymeric micro-and nanoparticles of complex shapes. *Proc. Nat. Acad. Sci. U. S. A.*, **104**(29), 11901–11904.

65. Cui, J., et al. (2010). Monodisperse polymer capsules: Tailoring size, shell thickness, and hydrophobic cargo loading via emulsion templating. *Adv. Funct. Mater.*, **20**(10), 1625–1631.

66. Rolland, J. P., et al. (2005). Direct fabrication and harvesting of monodisperse, shape-specific nanobiomaterials. *J. Am. Chem. Soc.*, **127**(28), 10096–10100.

67. Euliss, L. E., et al. (2006). Imparting size, shape, and composition control of materials for nanomedicine. *Chem. Soc. Rev.*, **35**(11), 1095–1104.

68. Gratton, S. E. A., et al. (2007). Nanofabricated particles for engineered drug therapies: A preliminary biodistribution study of PRINT™ nanoparticles. *J. Control. Release*, **121**(1–2), 10–18.

69. NanoBio Corporation. Available at: http://www.nanobio.com/Vaccines/Mucosal-Vaccines.html (accessed on December 7, 2014).

70. Matsumura, Y. (2008). Poly(amino acid) micelle nanocarriers in preclinical and clinical studies. *Adv. Drug Deliv. Rev.*, **60**(8), 899–914.

71. *A New Era in Targeted Anti-Viral Therapeutics*. Available at: http://www.nanoviricides.com (accessed on February 2, 2015).

72. Aphios Granted US Patent for Drug Delivery Technique Reduces Toxicity and Improves Efficacy of Taxol. Available at: http://www.aphios.com/news-and-current-events/press-releases-and-news/press-releases-archive/1999-press-releases/185-aphios-granted-us-patent-for-drug-delivery-technique-reduces-toxicity-and-improves-efficacy-of-taxol.html (accessed on December 7, 2014).

73. Azaya Therapeutics. Available at: http://www.azayatherapeutics.com/index.php/news/20-azaya-therapeutics-presents-phase-i-data-at-asco-and-completes-offering (accessed on December 7, 2014).

74. Rupp, R., Rosenthal, S. L., Stanberry, L. R. (2007). VivaGel (SPL7013 Gel): A candidate dendrimer—microbicide for the prevention of HIV and HSV infection. *Int. J. Nanomed.*, **2**(4), 561–566.

75. Kumar, P., et al. (2010). eds. Dendrimer: A novel polymer for drug delivery. *J. Innovative Trends Pharm. Sci*., **1**, 252–269.

76. Kneuer, C., et al. (2000). A nonviral DNA delivery system based on surface modified silica-nanoparticles can efficiently transfect cells *in vitro*. *Bioconjug. Chem.*, **11**(6), 926–932.

77. Ravi Kumar, M. N. V., Bakowsky, U., Lehr, C. M. (2004). Preparation and characterization of cationic PLGA nanospheres as DNA carriers. *Biomaterials*, **25**(10), 1771–1777.

78. Schmidt, C. (2011). RNAi momentum fizzles as pharma shifts priorities. *Nat. Biotechnol.*, **29**(2), 93–94.

79. Xu, L., Anchordoquy, T. (2011). Drug delivery trends in clinical trials and translational medicine: Challenges and opportunities in the delivery of nucleic acid-based therapeutics. *J. Pharm. Sci.*, **100**(1), 38–52.

80. RONDEL™. Available at: http://www.arrowheadresearch.com/technology/rondel (accessed on December 7, 2014).

81. Ethical and social aspects of biotechnology. Available at: http://ubiquity.acm.org/article.cfm?id=964683 (accessed on December 7, 2014).

82. Hammond, M., Kompella, U. (2006). Nanotechnology and nanoparticles: Clinical, ethical, and regulatory issues. In: Gupta, R., Kompella, U., eds. *Nanoparticle Technology for Drug Delivery*, Taylor & Francis Group: New York. pp. 381–395.

83. NANOMED Roundtable Report Summary. Available at: http://cordis.europa.eu/result/rcn/46272_en.html (accessed on December 7, 2014).

84. Hodge, G., Bowman, D., Maynard, A. (2010). Introduction: The regulatory challenges for nanotechnologies. In: Hodge, G., Bowman, D., Maynard, A., eds. *International Handbook on Regulating Nanotechnologies,* Edward Elgar Publishing Limited, Cheltenham. pp. 3–24.

85. European Commission. Available at: http://ec.europa.eu/ (accessed on December 7, 2014).

86. (a) Bawa, R., Johnson, S. (2010). The ethical implications of nanomedicine must be considered. In: Langwith, J., ed. *Nanotechnology*, Greenhaven Press, Farmington Hills. pp. 187–197.

    (b) Bawa, R. and S. Johnson. (2008). Emerging issues in nanomedicine and ethics In: Allhoff, F., and Lin P., (editors), *Nanotechnology & Society: Current and Emerging Ethical Issues*, Springer, Dordrecht, 207–223.

    (c) Bawa, R. and S. Johnson. (2007). The ethical dimensions of nanomedicine. *The Medical Clinics of North America*, **91**(5), 881–887.

87. (a) Bawa, R. (2009). Nanopharmaceuticals for drug delivery—a review. *Touch Brief*, **6**, 122–127.

    (b) Bawa, R. (2015). Emerging issues in nanodrugs and nanomedicine. In: Wellons, H. B., and Ewing, E. S., (Editors): *Biotechnology and the Law*, 2nd edition, American Bar Association, Chicago, IL (*in press*).

88. Wagner, V., et al. (2006). The emerging nanomedicine landscape. *Nat. Biotech.*, **24**(10), 1211–1217.

89. Kumar, M., et al. (2004). Cationic poly(lactide-*co*-glycolide) nanoparticles as efficient *in vivo* gene transfection agents. *J. Nanosci. Nanotechnol.*, **4**(8), 990–994.

90. Weiss, B., et al. (2006). Nanoparticles made of fluorescence-labelled poly(L-lactide-*co*-glycolide): Preparation, stability, and biocompatibility. *J. Nanosci. Nanotechnol.*, **6**(9–10), 3048–3056.

91. Panyam, J., et al. (2003). Polymer degradation and *in vitro* release of a model protein from poly(D,L-lactide-*co*-glycolide) nano- and microparticles. *J. Control. Release*, **92**(1–2), 173–187.

92. Knorr, V., Ogris, M., Wagner, E. (2008). An acid sensitive ketal-based polyethylene glycol-oligoethylenimine copolymer mediates improved transfection efficiency at reduced toxicity. *Pharm. Res.*, **25**(12), 2937–2945.

93. Kwon, Y. J., Shim, M. S. (2010). Acid-transforming polypeptide micelles for targeted nonviral gene delivery. *Biomaterials*, **31**(12), 3404–3413.

94. Knorr, V., et al. (2008). Acetal linked oligoethylenimines for use as pH-sensitive gene carriers. *Bioconjug. Chem.*, **19**(8), 1625–1634.

95. Kim, S. W., et al. (2000). Biodegradable polyester, poly[alpha-(4 aminobutyl)-L-glycolic acid], as a non-toxic gene carrier. *Pharm. Res.*, **17**(7), 811–816.

96. Wu, Q., et al. (2011). Synthesis and micellization of amphiphilic biodegradable methoxypolyethylene glycol/poly(D,L-lactide)/polyphosphate block copolymer. *Reactive Funct. Polym.*, **71**(9), 980–984.

97. Santander-Ortega, M. J., et al. (2010). Nanoparticles made from novel starch derivatives for transversal drug delivery. *J. Control. Release*, **141**(1), 85–92.

98. Thiele, C., et al. (2011). Nanoparticles of anionic starch and cationic cyclodextrin derivatives for the targeted delivery of drugs. *Polym. Chem*, **2**(1), 209–215.

99. Sankaranarayanan, J., et al. (2010). Multiresponse strategies to modulate burst degradation and release from nanoparticles. *ACS Nano*, **4**(10), 5930–5936.

100. Chaturbedy, P., Jagadeesan, D., Eswaramoorthy, M. (2010). pH-sensitive breathing of clay within the polyelectrolyte matrix. *ACS Nano*, **4**(10), 5921–5929.

101. Kono, K., et al. (2011). Multi-functional liposomes having temperature-triggered release and magnetic resonance imaging for tumor-specific chemotherapy. *Biomaterials*, **32**(5), 1387–1395.

102. Wang, R., et al. (2011). Well-defined multi-stimuli responsive fluorinated graft poly(ether amine)s (fgPEAs). *Polymer*, **52**(2), 368–375.

103. Prabaharan, M., et al. (2008). Stimuli-responsive chitosan-graft-poly(*N*-vinylcaprolactam) as a promising material for controlled hydrophobic drug delivery. *Macromol. Biosci.*, **8**(9), 843–851.

104. Rejinold, N. S., et al. (2011). Biocompatible, biodegradable and thermo-sensitive chitosan-*g*-poly (*N*-isopropylacrylamide) nanocarrier for curcumin drug delivery. *Int. J. Biol. Macromol.*, **49**(2), 161–172.

105. Yavuz, M. S., et al. (2009). Gold nanocages covered by smart polymers for controlled release with near-infrared light. *Nat. Mater.*, **8**(12), 935–939.

106. Hartwell, R., et al. (2011). A novel hydrogel-collagen composite improves functionality of an injectable extracellular matrix. *Acta Biomater.*, **7**(8), 3060–3069.

107. Huang, H., et al. (2010). Robust stimulation of humoral and cellular immune responses following vaccination with antigen-loaded β-Glucan particles. *MBio*, **1**(3), e00164-10.

108. Anumolu, R., et al. (2011). Fabrication of highly uniform nanoparticles from recombinant silk-elastin-like protein polymers for therapeutic agent delivery. *ACS Nano*, **5**(7), 5374–5382.

109. Ferrari, M. (2008). The mathematical engines of nanomedicine. *Small*, **4**(1), 20–25.

110. Ziemys, A., Ferrari, M., Cavasotto, C. N. (2009). Molecular modeling of glucose diffusivity in silica nanochannels. *J. Nanosci. Nanotechnol.*, **9**(11), 6349–6359.

111. Liu, J., et al. (2010). Computational model for nanocarrier binding to endothelium validated using *in vivo*, *in vitro*, and atomic force microscopy experiments. *Proc. Nat. Acad. Sci. U. S. A.*, **107**(38), 16530–16535.

112. Dell'Orco, D., et al. (2010). Modeling the time evolution of the nanoparticle-protein corona in a body fluid. *PLoS One*, **5**(6), e10949.

113. McNeil, S. (2010). Challenges for nanoparticle characterization. In: McNeil, S., ed. *Characterization of Nanoparticles Intended for Drug Delivery*, Humana Press. pp. 9–15.

114. Rao, A., et al. (2007). Characterization of nanoparticles using atomic force microscopy. *J. Phys. Conf. Ser.*, **61**(1), 971–976.

115. Hall, J. B., et al. (2007). Characterization of nanoparticles for therapeutics. *Nanomedicine*, **2**(6), 789–803.

116. Haskell, R. (2006). Physical characterization of nanoparticles. In: Gupta, R., Kompella, U. B., eds. *Nanoparticle Technology for Drug Delivery*, Taylor & Francis Group, New York. pp. 103–132.
117. Bellucci, S., et al. (2010). Micro-Raman study of the role of sterilization on carbon nanotubes for biomedical applications. *Nanomedicine*, **5**(2), 209–215.
118. The National Archives. Available at: http://www.nationalarchives.gov.uk/ (accessed on December 7, 2014).
119. Marchant, G., et al. (2009). International Harmonization of Regulation of Nanomedicine. *Studies in Ethics, Law & Technology*. Available at: http://works.bepress.com/gary_marchant/3 (accessed on January 7, 2015).

Chapter 13

Polysaccharides as Nanomaterials for Therapeutics

Shoshy Mizrahy, MSc,[a,b] and Dan Peer, PhD[a,b]

[a]*Laboratory of Nanomedicine*, *Department of Cell Research and Immunology*, *George S. Wise Faculty of Life Science*, *Tel Aviv University*, *Tel Aviv*, *Israel*
[b]*Center for Nanoscience and Nanotechnology Tel Aviv University*, *Tel Aviv*, *Israel*

Keywords: polysaccharides, glycosaminoglycans, hyaluronan, nanoparticles, liposomes

13.1 Introduction

The use of polysaccharides as building blocks in the development of nano-size drug delivery systems is rapidly growing. This can be attributed to the outstanding virtues of polysaccharides such as biocompatibility, biodegradability low toxicity, and low cost. In addition, the variety of physicochemical properties and the ease of chemical modifications enable the preparation of a wide array of nanoparticles. This chapter describes the properties of common polysaccharides and the main mechanisms for polysaccharide-based nanoparticle preparation and provides examples from the

Handbook of Clinical Nanomedicine: Nanoparticles, Imaging, Therapy, and Clinical Applications
Edited by Raj Bawa, Gerald F. Audette, and Israel Rubinstein

ISBN 978-981-4669-20-7 (Hardcover), 978-981-4669-21-4 (eBook)
www.panstanford.com

conceptual design toward pre-clinical and clinical applications. Over the past two decades, nanoparticle-based therapeutics have been introduced for the treatment of cancer, diabetes, allergy, inflammation, and infections [1, 2]. The growing interest in nanoparticles derives from the outstanding advantages they offer, which include protection of the drug from premature degradation, lower therapeutic toxicity, ability to deliver poorly-water-soluble drugs, controlled drug release mechanisms, and improved intracellular penetration [2].

The size and surface characteristics of a nanoparticle are crucial for the control of its biodistribution *in vivo*. The small size, which enables nanoparticles to pass through the smallest capillaries also promotes passive tumor targeting due to the enhanced permeability and retention (EPR) effect of the tumor vasculature. The passive targeting is achieved by extravasation of nanoparticles through increased permeability of the tumor vasculature and ineffective lymphatic drainage [2]. In addition, it has been shown that a combination of nanometric size and hydrophilic surface delays particle uptake by the mononuclear phagocyte system (MPS) and therefore promotes long circulation [3].

As the requirements from the nanoparticle are becoming clear, so are the requirements from the materials used for their preparation. These materials should be biocompatible and preferably biodegradable, well characterized, and easily functionalized [2]. Polysaccharides successfully fulfill all of these requirements and are therefore widely used for the preparation of nanoparticles for drug delivery.

13.2 Polysaccharides

Polysaccharides are polymers of monosaccharides joined by glycosidic bonds. These highly abundant molecules are from various origins, including algal origin (e.g., alginate and carrageenan), plant origin (e.g., cellulose, pectin and guar gum), microbial origin (e.g., dextran and xanthan gum), and animal origin (e.g., chitosan, hyaluronan, chondroitin and heparin) [4]. Naturally occurring polysaccharides are diverse in their physiochemical properties; there are multiple chemical structures (Fig. 13.1), the chemical composition greatly varies and so do the molecular

weight (Mw) and ionic nature. This versatility also contributes to a wide range of biological activities. From a pharmaceutical standpoint, polysaccharides possess many favorable characteristics such as lack of toxicity, good biocompatibility stability, low cost, hydrophilic nature, and availability of reactive sites for chemical modification. In addition, many polysaccharides possess bioadhesive properties, especially for mucosal surfaces, which have been used for both targeting and prolonging drug residence time. All of these qualities have led to the growing use of polysaccharides in drug delivery systems.

The properties of common polysaccharides used for the preparation of drug delivery systems are detailed below.

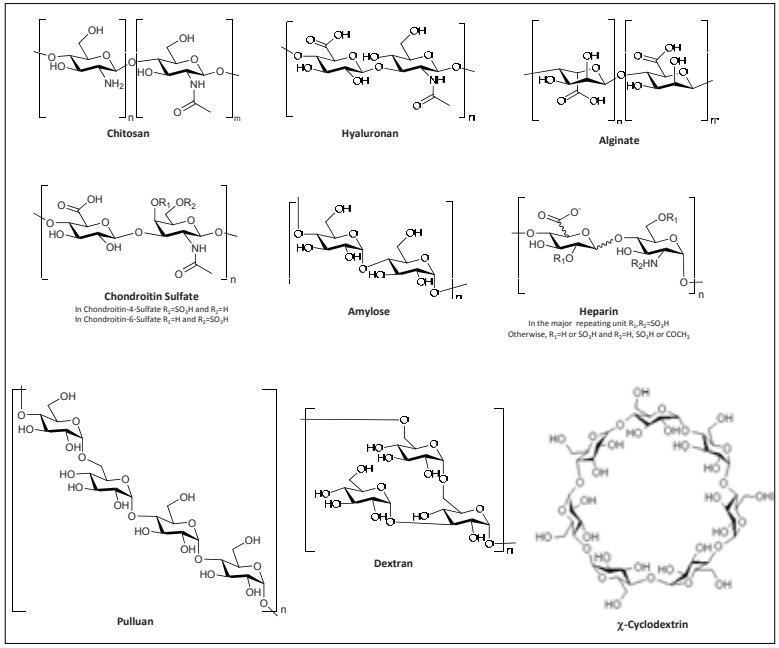

Figure 13.1 Chemical structures of polysaccharides. (i-Cyclo dextrin structure obtained with permission from http://www.chemblink.com.

13.2.1 Chitosan

Chitosan is a linear polysaccharide composed of β-(1,4)-linked D-glucosamine and iV-acetyl-D-glucomasine (Fig. 13.1). Chitosan

is obtained by deacetylation from chitin, a highly abundant polysaccharide, which is the main component of crustaceans exoskeleton [5]. Chitosan and its derivates are currently the most widely used polysaccharides in newly developed drug delivery systems. Chitosan-based delivery systems have been described for nasal, ocular, oral, parenternal, and transdermal drug delivery [6–9]. Among the many advantages of chitosan are its low cytotoxicity and biocompatibility [10, 11]. In addition, chitosan is positively charged and therefore can interact with negatively charged molecules such as negatively charged polysaccharides, polyanions, nucleic acid and negatively charged proteins. Its positive charge also facilitates adherence to mucosal surfaces, which are mostly negatively charged [12, 13]. In addition, the ability of chitosan to open tight junctions between epithelial cells and therefore increase the permeation of macromolecular drugs across the mucosal epithelia has been demonstrated [14, 15]. In spite of these advantages, chitosan is inherently insoluble in aqueous solutions above pH 6.5 [16, 17]. High degree of deacetylation, low molecular weight, and chemical modification can facilitate water solubility of chitosan. These factors also affect particle properties such as size, surface charge, drug entrapment efficiency, and stability [18].

13.2.2 Alginate

Alginate is a linear anionic polysaccharide composed of alternating blocks of 1,4-linked (β-D-mannuronic acid) (M) and a-1-guluronic acid (G) residues (Fig. 13.1). The monomer composition of alginate is variable and can consist of homopolymeric blocks and alternating M and G residues [19]. The composition, sequence, and molecular weight determine the physical properties of alginate [20]. Alginates are extracted mainly from brown algae and acetylated forms of alginate can be isolated from the bacteria *Pseudomonas* and *Azotobacter* [20].

As a polymer for drug delivery purposes, alginate possesses several attractive properties: It is biocompatible, non-toxic, and water soluble and has the highest mucoadhesive strength compared with other natural polysaccharides such as chitosan and carboxymethylcellulose [21, 22].

13.2.3 Hyaluronan

Hyaluronan (HA) is a linear high-Mw glycosaminoglycan (GAG) composed of alternating disaccharide units of D-glucuronic acid and iV-acetyl-D-glucosamine with β-(1,4) interglycosidic linkage [23] (Fig. 13.1). Hyaluronan possesses remarkable hydrodynamic properties, especially related to its viscosity and ability to retain water [24]. It was previously regarded important mostly for joint lubrication or organ structural stability [24]. However, HA was found to be essential for proper cell growth, embryonic development, healing processes, inflammation, and tumor development [24, 25]. As opposed to other GAGs, HA is not sulfated, not linked to a protein and naturally produced by bacteria as a capsule [23]. Commercially available HA is either produced through bacterial fermentation of *Streptococcus* species or extracted from rooster combs, umbilical cords, synovial fluids, or vitreous humor [26]. However, HA obtained from these production methods is usually very polydispersed; therefore, a method to produce HA of a defined size has also been developed [27, 28].

There are several advantages of HA that make it suitable for drug delivery: It is water soluble, biodegradable, biocompatible, non-toxic, and non-immunogenic and can be easily chemically modified [29, 30]. In addition, it is the major ligand for CD44 and RHAMM (CD168) and therefore is suitable for targeting CD44 and RHAMM-expressing cells [25, 31]. CD44 and CD168 are overexpressed by various tumors, for example, squamous cell carcinoma, ovarian, colon, stomach, glioma, and many types of leukemia, lymphoma, and myeloma [32–34], which makes the use of HA as a targeting agent even more attractive.

13.2.4 Dextran

Dextran is a high-Mw branched polysaccharide composed of a-(1,6)-linked glucan with side chains attached to the three positions of the backbone glucose units (Fig. 13.1). Dextran is obtained from bacterial cultures of the lactic-acid bacteria such as *Leuconostoc mesenteroides* NRRL B-512 [4]. Dextran is water soluble and is also soluble in a wide range of solvents, among

them methyl sulphoxide, ethylene glycol, glycerol, and 4-methylmorpholine-4-oxide. Low-Mw dextran and not the native dextran is usually used for both clinical purposes (mainly due to its antithrombotic effect) and nanoparticle preparation. Low-Mw dextran is usually achieved by acid hydrolysis of the native dextran [35]. The polyanion dextran sulfate is derivate of dextran, which contains approximately two to three sulfate groups per glucosyl residue [36]. Dextran sulfate is a biodegradable polymer that has been widely used in pharmaceutical applications [36]. However, dextran sulfate is not completely inert material. It has inhibitory and stimulatory effects on several enzymes [37], and it possesses the ability to stimulate B-cell proliferation [38] and to increase permeability of lymphocytes [39].

13.2.5 Cyclodextrins

Cyclodextrins are cyclic oligomers of a-(1,4)-linked-glucopyranosyl that are produced from starch by enzymatic conversion (Fig. 13.1). There are three main members of the cyclodextrin family, composed of six, seven, and eight glucose units and known as a-, (B-, and y-CD), respectively. Cyclodextrins have a hydrophilic exterior and a hydrophobic cavity that enables them to act as hosts to hydrophobic molecules [40]. This ability to form inclusion complexes has been widely studied since its discovery. It is utilized in many industrial products, analytical methods, and technologies [41], including the production of cyclodextrin-based nanoparticles [42]. Cyclodextrins are biocompatible, do not elicit immune responses, and have low toxicities in animals and humans [43]. Therefore, they are used in pharmaceutical applications for numerous purposes, including improving the bioavailability of drugs [43]. Cyclodextrin-based therapeutics have been reviewed elsewhere [43].

13.2.6 Arabinogatactan

Arabinogalactan is a long, highly branched natural polysaccharide composed mostly of galactose and arabinose. Arabinogalactan is extracted mainly from the Larix tree and is available at 99.9% purity with reproducible Mw and physicochemical properties

[44]. The unusual water solubility (70% w/w in water), biocompatibility, biodegradability, and ease of drug conjugation in an aqueous medium make arabinogalactan attractive as a potential drug carrier [44].

13.2.7 Pullulan

Pullulan is neutral, homopolysaccharide consisting of a-(1,6)-linked maltotriose residues (Fig. 13.1). It is produced from starch primarily by strains of the fungus *Aureobasidium pullulans* [45]. Pullulan's structure unique linkage pattern contributes to exceptional physiochemical properties such as adhesiveness, water solubility, and relatively low viscosity upon dissolving in water. Therefore, pullulan and its derivatives have been used industrially in foods and pharmaceuticals [45].

13.2.8 Heparin

Heparin is a linear glycosaminoglycan (GAG) composed of repeating disaccharide units of 1,4-linked uronic acid D-glucuronic (GlcAor 1-iduronic acid (IdoA) and D-glucosamine (GlcN)) (Fig. 13.1). The uronic acid usually comprises 90 percent 1-idopyranosyluronic acid (1-iduronic acid, IdoA) and 10 percent D-glucopyranosyluronic acid (D-glucuronic acid, GlcA). In addition, there are structural variations at the disaccharide level [46]. Due to high content of sulfo and carboxyl groups, heparin has the highest negative charge density of any known biological molecule [46]. The Mw of heparin varies between 5–40 kDa and it is extracted mainly from mucosal tissues of porcine and bovine [46]. Clinically, heparin has been used as an anticoagulant since the 1930s [46]. The anticoagulant activity of heparin requires direct interaction with the serine protease inhibitor antithrombin III, which causes a conformational change that allows antithrombin III to inhibit thrombin and other serine proteases within the coagulation cascade [47]. Heparin is produced exclusively by mast cells (as opposed to the structurally related GAG heparan sulphate) [23]. Beyond its anticoagulant activity, heparin has been shown to have antiviral activity and ability to inhibit complement activation, tumor growth and angiogenesis [47].

13.3 Main Mechanisms of Nanoparticle Preparation from Polysaccharides

13.3.1 Cross-Linking

In cross-linked nanoparticles, the polymeric chains are inter connected by cross-linkers, leading to the formation of a 3D network (Figs. 13.2a,b) [48]. The main factor that determines the properties of a cross-linked nanoparticle such as drug release and mechanical strength is the cross-linking density, which is determined by the molar ratio between the cross-linker and the polymer repeating units [48]. There are two types of cross-linked nanoparticles determined by the nature of the cross-linking agents: covalently cross-linked nanoparticles and ionically cross-linked nanoparticles.

13.3.1.1 Covalent cross-linking

In a covalently cross-linking nanoparticle, the network structure is permanent since irreversible chemical links are formed (Fig. 13.2a) [48]. The rigid network allows absorptions of water and bioactive compounds without the dissolution of the nanoparticle even when the pH drastically changes [48]. A covalently cross-linked nanoparticle can contain more than one type of polysaccharide. The covalent bonds are the main interactions that form the 3D network although secondary interactions such as hydrogen bonds and hydrophobic interactions also exist [48]. Covalent cross-linkers are molecules with at least two reactive functional groups that allow the formation of bridges between the polymeric chains [49]. The most common covalent cross-linkers used with polysaccharides are dialdehydes such as glutaraldehyde [50, 51]. However, dialdehydes are highly toxic, and therefore biocompatible alternatives have been tested. For example, natural di- and tricarboxilic acids have been used for intramolecular cross-linking of chitosan, which was facilitated by the condensation agent 1-ethyl-3-[3-dimethylaminopropyl] carbodiimide hydrochloride (EDC) [52]. Genipin, a natural biocompatible cross-linker isolated from the fruits of *Gardenia jasminoides* Ellis, is another option [53].

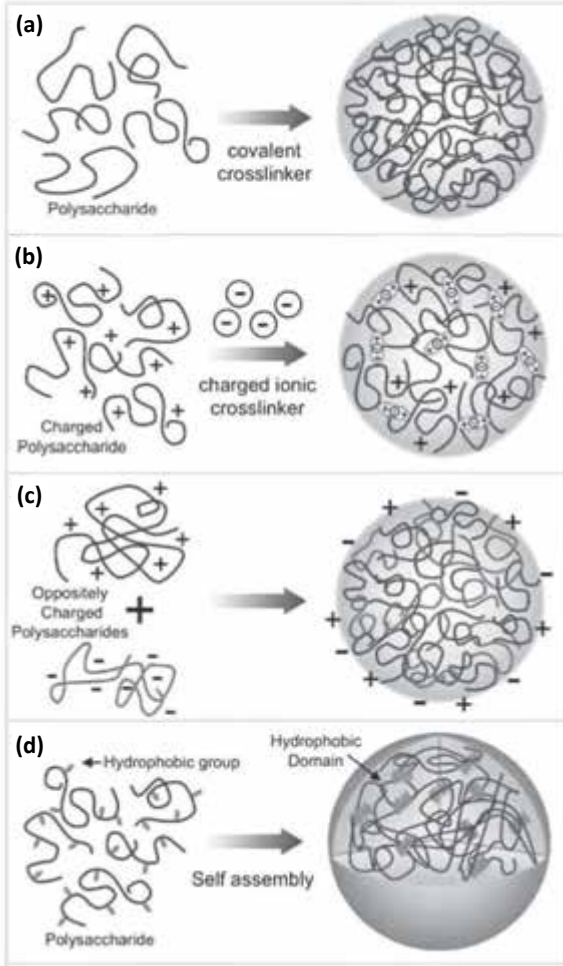

Figure 13.2 Common mechanism for polysaccharide based nanoparticle preparation. (a) Covalent cross-linking. (b) Ionic cross-linking. (c) Polyelectrolyte complexation (PEC). (d) Self-assembly of hydrophobically modified polysaccharides.

13.3.1.2 Ionic cross-linking

Ionic cross-linking represents a simple alternative to covalent cross-linking for charged polysaccharides. This method enables the preparation of nanoparticles by the formation of reversible ionic

cross-linking and since no harsh preparation or toxic cross-linkers are used these nanoparticles are generally considered biocompatible [48]. Charged polysaccharide can form ionic cross-linked nanoparticles with oppositely charged ions or small ionic molecules (Fig. 13.2b). For example, the polyanion tripolyphosphate (TPP) has been widely used to cross-link the chitosan, and divalent cations such as Ca^{2+} have been used to cross-link alginate [54, 55]. The mechanism of nanoparticle formation is based on electrostatic interactions between the polysaccharide and oppositely charged ionic cross-linker [56]. The ionic bonds form bridges between the polysaccharide chains and are the main interactions inside the network, although as with covalent cross-linking, additional interaction such as hydrogen bonds are also present [48]. Several factors influence the cross linking reaction, most crucial are the size of the cross-linker and the global charge of the cross-linker and the polysaccharide [48, 57]. Unlike covalently cross-linked nanoparticles, ionic cross-linked nanoparticles are generally pH sensitive, a welcome trait for drug delivery purposes. However, this pH sensitivity also contributes to instability of the ionic cross-linked network [48, 58, 59].

13.3.2 Polyelectrolyte Complexation (PEC)

Polyelectrolyte complexes (PEC) are formed by direct electrostatic interactions of oppositely charged polyelectrolytes in solution (Fig. 13.2c). PEC represents another biocompatible option for drug delivery since no toxic covalent cross-linkers are used. These complexes resemble ionic cross-linking since non-permanent networks are formed that are more sensitive to changes in environmental conditions [26]. However, unlike ionic cross-linking, in which ions or ionic molecules react with the polyelectrolyte, in PEC the interaction is between the polyelecrolyte and larger molecules with a broad MW range [60]. The formation and stability of PEC is determined mainly by the degree of interaction between the polyelectrolytes [49]. The later is a factor of the charge density and distribution of each of the oppositely charged polyelectrolyte. The chemical environment is also crucial: The pH of the solution, the ionic strength, the temperature, and the duration and mixing order. Secondary factors are the Mw of the

polyelectrolytes and their flexibility [26, 49, 60, 61]. The formed interaction can be reinforced by ionic cross-linking [49, 62]. For example, TPP and magnesium sulfate were used to stabilize PEC of chitosan with gamma poly(glutamic acid) [63]. Positively charged polysaccharides, namely chitosan, can form PEC with variety negatively charged polymers such as the polysaccharides alginate, dextran sulfate, chondroitin sulfate, hyaluronan, carboxymethyl cellulose, carrageenan and heparin, peptides such as poly-*g*-glutamic acid,nucleic acid and synthetic polymers [49, 61, 64–66].

13.3.3 Self-Assembly

Upon grafting hydrophobic moieties onto a hydrophilic polysaccharide an amphiphilic copolymer is created. In aqueous solutions, amphiphilic copolymers tend to self-assemble into nanoparticles in which the inner core is hydrophobic and the shell is hydrophilic. The hydrophilic shell serves as a stabilizing interface between the hydrophobic core and the external aqueous environment (Fig. 13.2d) [67]. This self-assembly is via hydrophobic interactions, mainly in order to minimize interfacial free energy [61, 64]. The formed nanoparticles are characterized by prolonged circulation and thermodynamic stability [68]. In addition, since the core is hydrophobic, these nanoparticles have been used for the delivery of hydrophobic drugs. Several properties such as size, surface charge, loading efficiency, stability, and biodistribution can be altered for a particular application. For example, the size of the nanoparticles can be controlled by adjusting the length of the hydrophobic moiety and the length of the polymer [67]. Scaling relations for this purpose have been developed [67]. In addition, the surface charge, which affects particle serum stability and cellular uptake, can be altered by controlling the degree of substitution, the length of the hydrophobic moiety or the nature of the hydrophobic moiety [61, 69]. For example, a cationic derivatization of the hydrophobic moiety has been used to promote cellular uptake [70]: amine bearing cholesterol but not cholesterol without an amine, demonstrated protein cellular delivery when grafted onto pullulan to create self-assembled nanoparticles [70].

Polysaccharides can be modified with a wide range of hydrophobic moieties among them bile acids (e.g., 5(B-cholanic acid, cholic acid and deoxycholic acid), fatty acids (e.g., palmitoyl acid, stearic acid, oleic acid) [61], cholesterol, and hydrophobic drugs.

13.4 Polysaccharide-Based Nanoparticles

13.4.1 Chitosan-Based Nanoparticles

Chitosan's nature and the ease of chemical modifications enable multiple nanoparticle preparation schemes among them: covalent cross-linking, ionic cross-linking, polyelectrolyte complexation, desolvation, and self-assembly [71].

Early works describing chitosan nanoparticles for drug delivery were based on covalently crossing chitosan with glutaraldehyde [50]. However, since glutaraldehyde is highly toxic, biocompatible alternatives for covalent cross-linking have been developed, such as condensation reactions with 1-ethyl-3-[3-dimethylaminopropyl]carbodiimide hydrochloride, which was used to facilitate intramolecular cross-linking of chitosan by natural di- and tricarboxylic acids [52]. This method allows the formation of polycations, polyanions, and polyampholyte nanoparticles.

Since chitosan is positively charged, ionic cross-linked nanoparticles can be prepared using polyanions; among them the most widely used is tripolyphosphate (TPP). The wide use of TPP in the preparation of chitosan nanoparticles is a result of both being non-toxic and of the ability to modulate particle size, morphological properties and surface charge mainly by controlling the chitosan to TPP weight ratio [72]. The first TPP cross-linked chitosan nanoparticles for drug delivery were developed by Alonso's group [73]. The method was based on a principle reported previously by Bodmeier et al. [56]. Alonso's group later reported the use of these particles for protein [74, 75], oligonucleotide, and plasmid DNA delivery [76, 77]. The resulting chitosan/TPP nanoparticles for DNA delivery were in the range of 100–300 nm depending on the Mw of the chitosan and showed high physical stability and encapsulation efficiencies both for plasmid DNA and dsDNA oligomers (20-mers), independent of chitosan's Mw. The

low-Mw chitosan/TPP nanoparticles gave high gene expression levels in HEK 293 cells and mediated a strong beta-galactosidase expression *in vivo* after intratracheal administration. Chitosan/TPP nanoparticles were also developed for the delivery of double-stranded small interfering RNA (siRNA) [78]. In this study, particle size was shown to be affected by chitosan's Mw, concentration, chitosan-to-TPP weight ratio, and pH. *In vitro* studies of these particles in two types of cells lines, CHO Kl and HEK 293, revealed that chitosan/TPP nanoparticles with entrapped siRNA enhanced gene silencing in comparison with chitosan-siRNA complexes. This was possibly due to their high binding capacity and loading efficiency.

As mentioned, the positive charge of chitosan enables the formation of polyelectrolyte complexes (PEC) with negatively charged polymers such as negatively charged polysaccharides, nucleic acids, negatively charged peptides and poly(acrylic acid). Polyelectrolyte complexation is one of the most frequently used methods to prepare chitosan nanoparticles. PEC of chitosan with gamma-poly-(glutamic acid), a natural, non-toxic, and biodegradable negatively charged polymer have been prepared for oral administration of insulin [63]. These nanoparticles, which were stabilized with TPP and magnesium sulfate were pH sensitive and had an average size of 218 nm in diameter. The particles were shown to be safe, adhere to mucosal surfaces and to induce a significant hypoglycemic action for at least 10 h in diabetic rats when administered orally. The bioavailability of insulin, which was determined from plasma insulin concentration, was of 15%. The same group previously reported transdermal delivery of DNA containing chitosan-gamma-poly-(glutamic acid) nanoparticles [79]. These nanoparticles shown improved skin penetration and enhanced gene expression in comparison with nanoparticles solely comprised of chitosan and DNA. This can be attributed to a greater density of the gamma-poly-(glutamic acid) containing nanoparticles, which contributed to a larger penetration momentum into the skin barrier. In a following study [80] the gamma-poly-(glutamic acid) containing nanoparticles showed a significant increase in cellular uptake and transfection efficiency of HT1080 (human fibrosarcoma) cells in comparison with DNA-chitosan nanoparticles. Another study describing PEC of chitosan and DNA have reported by Krishnendu et al. [81] who

have shown that theses PEC can generate immunologic protection in a murine model of peanut allergy. The mice who received nanoparticles containing a dominant peanut allergen gene produced secretory IgA and serum IgG2a and showed a substantial reduction in allergen-induced anaphylaxis associated with reduced levels of IgE, plasma histamine and vascular leakage. More recently plasmid-chitosan PEC was applied in the delivery of FGF-2 and PDGF-BB [82]. Plasmid-chitosan PEC containing FGF-2/PDGF-BB genes were injected into BALB/C mice. Several formulations were tested, which differed in the degree of chitosan deacetylation and Mw ELISA assays performed on mice sera showed FGF-2 and PDGF-BB expression. In addition, induction of specific antibodies against these proteins has been shown. PEC containing highly deacetylated low-Mw chitosan, were found to efficiently induce protein expression with minimal production of neutralizing antibodies, which was also confirmed by histological analyses.

Recently, PEC of ultrapure chitosan monomers was used for ocular gene delivery [83]. The nanoparticle preparation which was based on a method developed by Koping-Hoggard et al. [84] had an average size of ~100 nm in diameter and a strong positive charge. This formulation demonstrated effective transfection of COS-7 cells *in vitro* and luciferase gene expression 5.4 times greater than polyethylenimine-DNA nanoparticles upon injection to rat corneas. The preparation method of PEC of chitosan and DNA was further improved by Artursson, who optimized the balance between stability and unpacking of PEC containing chitosan oligomers of different sizes [85]. PEC of chitosan oligomers and pDNA have several advantages over PEC of high-Mw chitosan and pDNA: High-Mw chitosan form extremely stable PEC with DNA, which delays the release of DNA and therefore results in a slow onset of action. In addition, these PEC are of aggregated shapes, their viscosity at concentration used for *in vivo* delivery is very high and their solubility at a physiological pH is low [84].

Chemical modification, usually by utilizing the primary amino groups of chitosan, is another way to improve its physiochemical properties. For example, conjugation of hydrophobic moieties such as deoxycholic acid and cholesterol to chitosan allows solvent induced self-assembly into nanoparticles [86, 87]. This principle was used for preparation of 5(B-cholanic acid) (HGC)-modified

glycol chitosan nanoparticles for the delivery of the antiangiogenic peptide RGD [88]. The RGD (Arg-Gly-Asp) peptides can specifically target $\alpha_v\beta_3$ integrins on angiogenic endothelial cells and therefore inhibit angiogenesis and tumor growth [89]; however, these peptides have short half-life *in vivo*, and thus a delivery system is required. The self-assembled polymeric nanoparticles of glycol chitosan nanoparticles modified with hydrophobic bile acid analogs have hydrophilic shells of glycol chitosan and hydrophobic cores of bile acid derivatives. The hydrophobically modified glycol chitosan was prepared by covalently attaching 5(B-cholanic acid) through amide formation. The nanoparticles have a diameter of 230 nm and loading efficiency >85%. The nanoparticles demonstrated prolonged and sustained release and inhibition of HUVEC adhesion *in vitro*. In the *in vivo* study, the RGD containing nanoparticles inhibited bFGF-induced angiogenesis and significantly decreased tumor growth and microvessel density in comparison with native RGD peptide. These particles were previously used by the same group for gene delivery and for the chemotherapeutic agents doxorubicin and paclitaxel [90, 91]. Other modifications of chitosan such as addition of thiol groups and trimethylation can improve the mucoadhesive and permeation-enhancing properties of chitosan [92]. Trimethylated chitosan (TMC) is also characterized by increased solubility in neutral pH [93]. Finally, targeted delivery of chitosan nanoparticles has been achieved simply by conjugation of targeting ligand to chitosan for example; nanoparticles containing galactosylated chitosan were used for hepatic gene delivery [94]. In addition, folate-conjugated chitosan nanoparticles were used for the delivery of interleukin-1 receptor antagonist (IL-IRa) gene in rats with adjuvant induced arthritis [95]. IL-IRa is a natural blocker of the inflammatory cytokine IL-1. When administered *in vivo*, the folate modified chitosan-DNA nanoparticles offered improved protection against inflammation and abnormal bone metabolism in comparison with naked DNA and chitosan-DNA complexes.

13.4.2 Alginate-Based Nanoparticles

The early preparations of alginate-based nanoparticles were based on the ability of alginate to form 3D network upon ionic inter- and intramolecular cross-linking with divalent ions [56]. Ever since,

several preparation mechanisms have been utilized and alginate-based nanoparticles have been developed for the delivery of proteins, genes, antitubercular and antifungal drugs [96].

Calcium cross-linked alginate nanoparticles containing econazole and antitubercular drugs were utilized for the treatment of murine tuberculosis [54]. The encapsulated drugs were detectable above minimum inhibitory concentration for 15 days after administration in lung, liver and spleen of the treated mice in comparison with 12–24 h of the free drugs. In addition, the alginate nanoparticles managed to reduce bacterial burden in the lung and spleen of mice infected with *Mycobacterium tuberculosis* by more than 90% at 15 fold lower dosages in comparison with free drugs.

Chitosan alginate nanoparticles were used for the transmucosal delivery of insulin [97]. The nanoparticles were prepared by ionic cross-linking of chitosan and TPP, which was followed by complexation with alginate. Insulin was associated to the CS-TPPAL nanoparticles with loading efficiency of 41–52%. The CS-TPP-AL nanoparticles were administered nasally and exhibited a capacity to enhance systemic absorption of insulin. The duration of the hypoglycemic response was dependent on the Mw of alginate.

Recently, surfactant-alginate hybrid nanoparticles have been employed for dual chemotherapy and photodynamic therapy on a murine drug-resistant tumor model [98]. The obtained nanoparticles had an average size of 73 nm measured by dynamic light scattering (DLS) and contained doxorubicin and methylene blue with encapsulation efficiencies of 78% and 82%, respectively. Following administration to Balb/c mice bearing syngeneic JC tumors (mammary adenocarcinoma), the dual therapy managed to significantly inhibit tumor growth and improved animal survival. The treatment resulted in enhanced tumor accumulation of both doxorubicin and methylene blue, significant inhibition of tumor cell proliferation, and increased induction of apoptosis.

Chemically modified alginate has also been used for the preparation of nanoparticles. As with chitosan, chemical modifications improve the physiochemical characteristics of alginate. For example, thiolated alginate achieved by covalent attachment of cysteine improves the mucoadhesive properties of alginate

and provides improved stability of the drug delivery system [99]. Hydrophobically modified alginate have also been produced [100].

13.4.3 Hyaluronan-Based Nanoparticles

HA-based nanocarriers were developed using several approaches such as HA-drug conjugates, which restore their cytotoxicity upon cell internalization by receptor-mediated endocytosis [32], PEC with polycations and ionically cross-linked nanoparticles. Chemically modified HA have also been widely used for the delivery of proteins, peptides, and nucleotides [101]. Chemical modifications assist in prolonging HA half-life; however, beyond a certain level of modification, HA loses the ability to bind its receptors [101].

HA-drug conjugates utilize several chemical groups on hyaluronan: the carboxylate on the glucuronic acid, the iV-acetylglucosaminehydroxyl, the reducing end, and the acetyl group, which can be enzymatically removed from the iV-acetylglucosamine [25]. In addition to targeting, HA conjugation has been used to increase drug solubility. This quality was used for the delivery of the hydrophobic antimitotic chemotherapeutic agent paclitaxel [102–104]. HA-paclitaxel conjugates exhibited greater cytotoxicity to CD44 overexpressing cells (HCT-116 and MCF-7) and reduced cytotoxicity to CD44-deficient cells (NIH-3T3) in comparison with free paclitaxel [103]. HA-drug conjugates are internalized via CD44 receptor-mediated endocytosis and drug is released mainly by intracellular enzymatic hydrolysis [25]. Recently, HA conjugation was used for the delivery and improved serum stability of exendin 4 [105]. Exendin 4 (exenatide) is a 39-amino acid peptide incretin mimetic that exhibits gluco-regulatory activities [106]. Exendin 4 has been shown to induce glucose-dependent enhancement of insulin secretion, glucose-dependent suppression of inappropriately high glucagon secretion, slowing of gastric emptying, reduction of food intake and body weight, and an increase in (3-cell mass) [105]. However, exendin 4 has a significantly short half-life, which limits its clinical applications [105]. Conjugation to vinyl sulfone-modified HA resulted in 20 times improved *in vitro* serum stability without loss of bioactivity. The size of these HA-exendin 4 conjugates was not reported. HA-exendin 4 conjugates lowered glucose levels in type 2 db/

db mice and the hypoglycemic effect lasted up to 3 days after injection. In addition, insulin immunohistochemical analysis of islets in db/db mice confirmed the improved insulinotropic activity of the HA-exendin 4 conjugates. HA conjugates have also been suggested for the treatment of acute pro myelocytic leukemia (APL) [107]. APL patients often relapse due to resistance to the therapy, all-trans retinoic acid. Because of the molecular basis of APL alteration and previous success with treating tumors with HA conjugated to the histone deacetylase inhibitor butyric acid [108, 109], conjugation of HA to both all-trans retinoic acid and butyric acid has been tested. The size of these HA conjugates was not reported. *In vitro*, the HA conjugates induced growth arrest and terminal differentiation in retinoic acid sensitive cells and apoptosis in retinoic acid resistant cells. *In vivo*, HA conjugates led to a significant increase in survival time of a retinoic acid sensitive APL murine model in comparison with that induced by a maximum tolerated dose of retinoic acid alone. In addition, in a retinoic acid resistant murine model, the HA conjugates were active in contrast to retinoic acid that was completely ineffective [107].

As described above, PEC have been used to prepare HA-based nanoparticles. HA-chitosan nanoparticles have demonstrated the ability to transport genes across the ocular mucosa and transfect ocular tissue [110]. The nanoparticles were prepared by ionically cross-linking of chitosan with TPP, which was followed by PEC with HA. The HA-low-Mw chitosan nanoparticles led to high expression levels of the transfected alkaline phosphatase in a human corneal epithelium model. Upon topical administration to rabbits, the nanoparticles managed to overcome cellular barriers and were located inside the corneal and conjunctival cells, suggesting that they penetrate the epithelia by a transcellular pathway. In addition, the *in vivo* transfection levels reached were significant.

As with other polysaccharides, self-assembly of hydrophobically modified HA has been used for nanoparticle preparation. Poly(lactic-*co*-(glycolic acid)) (PLGA)-modified HA copolymers were shown to self-assemble in aqueous solution into micelle nanoparticles [111]. The sizes of doxorubicin loaded HA micelle nanoparticles were ranging from 120–285 nm in diameter depending on the Mw of HA and the percent of grafted PLGA.

In vitro, the micelles exhibited higher cellular uptake and greater cytotoxicity in comparison with free doxorubicin for CD44 over-expressing cells (HCT-116) suggesting that they were taken up by the cells via HA receptor-mediated endocytosis [111]. The same group has recently prepared self-assembled HA nanoparticles for the delivery of paclitaxel by grafting an amine-terminated hydrotropic oligomer onto HA [112]. Active tumor targeting by self-assembled HA-5(B-cholanic acid) nanoparticles has also been shown [113]. Particle size could be controlled in the range of 240–430 nm by varying the degree of substitution of the hydrophobic moiety. *In vitro*, fluorescently labeled Cy5.5-HA-nanoparticles were detected in the cytosol of CD44 overexpressing cells (SCC7) to a much greater extent than cells with low CD44 expression (CV-1). When administered systemically to tumor-bearing mice, the nanoparticles were shown to selectively accumulate in tumor sites. Smaller HA-NPs were able to reach the tumor site more effectively than larger HA-NPs. In addition, the concentration of the nanoparticles in the tumor site was dramatically reduced when mice were pretreated with free HA. This suggests an additional active targeting mechanism, beyond the passive targeting of the EPR effect.

13.4.4 Dextran-Based Nanoparticles

Several strategies have been reported ford extran-based nanoparticles among them dextran-drug conjugates and self-assembly of hydrophobically modified dextran [114, 115]. The cardiotoxicity of doxorubicin can be significantly reduced by conjugation to dextran and followed by encapsulation in chitosan nanoparticle [116]. Upon conjugation of poorly water-soluble drugs to dextran, hydrophobic derivatives that self-assemble into nanoparticles are formed [117]. The self-assembled nanoparticles were shown to have high loading efficiency. Particle size was strongly influenced by the degree of dextran modification and preparation technique.

Dextran sulfate-based nanoparticles have been mostly prepared by PEC, exploiting the anionic nature of dextran sulfate for electrostatic interaction with positively charged polycations (for example, chitosan and polyethylenimine.) Huang et al. [118] prepared chitosan-dextran sulfate PEC for the controlled release of vascular endothelial growth factor (VEGF). VEGF, a growth factor

that stimulates angiogenesis and therefore desired as a therapeutic approach for ischemic conditions was shown to generate new blood vessels *in vivo*. However, intravenously injected VEGF was not clinically successful and implantable controlled release devices have shown that localized and sustained release of VEGF is required for its favorable action. Nanoparticles of ~250 nm were prepared in which the heparin-binding domain of VEGF was utilized to bind the polyanion dextran sulfate. The encapsulation efficiency of VEGF was high (85%) and controlled release (near linear) of active VEGF was persisted was persistent for more than 10 days. The activity of VEGF was determined by ELISA and by the ability to stimulate endothelial cell proliferation (mitogenic assay). PEC containing different polycations (polyethylenimine and poly-L-lysine) were also tested; however, chitosan-dextran sulfate complexes were preferred because of their biodegradability, desirable particle size, higher entrapment efficiency, controlled release, and mitogenic activity. In a following study by the same group [119], Repifermin®-containing nanoparticles were prepared in the same manner. Repifermin® is a truncated form of fibroblast growth factor-10 that exhibits promise in wound-healing applications. The challenge of the delivery lies in the instability of this protein. The resulting 250 nm nanoparticles showed high encapsulation efficiency and the release of active Repifermin® was controlled for more than 10 days. In addition, the mitogenic activity of Repifermin® on human umbilical cord vascular endothelial cells was only demonstrated for encapsulated and not free Repifermin®.

Zinc-stabilized complexes of dextran sulfate and polyethylenimine have been used for the delivery of proteins [62], DNA, and the poorly water-soluble antifungal agent amphotericin B [120]. The preparation method of these nanoparticles was complex coacervation, a method that was usually used for microencapsulation [120]. The effects of preparation conditions and composition on the physicochemical properties of the particles have been determined [120]. The sizes of the amphotericin B-containing nanoparticles were 100–600 nm, a zeta potential of 30 mV and drug recovery efficiency of up to 85%. Particle size was shown to be controlled by processing parameters such as the pH of the PEI solutions, the ratio of the two polymers and the concentrations of dextran sulfate and zinc sulfate. The

amphotericin B-containing nanoparticles displayed no toxicity in tissue culture in contrast to free drug and were almost as efficacious as free drug in killing *Candida albicans*.

13.4.5 Cyclodextrin-Based Nanoparticles

Amphiphilic cyclodextrins have been widely used for the preparation of nanoparticles for drug delivery. This can be attributed to the outstanding drug-loading efficiencies of amphiphilic cyclodextrin-based nanoparticles that do not require the presence of surfactant in the preparation [121]. In addition, nanoparticles can be prepared directly from pre-formed inclusion complexes of drug with amphiphilic cyclodextrins, which ensures both high drug loading and delayed burst effect [121]. Interestingly, the first experimental therapeutic to provide targeted delivery of siRNA in humans utilized a cyclodextrin-based nanoparticle [122].

Choisnard et al. prepared self-assembled nanoparticles of decanoate (B-cyclodextrin esters) and hexanoate (B-cyclodextrin esters) [123]. The mean size and polydispersity were significantly affected by the nature of solvent used in the nano-precipitation technique. In addition, the globular shape of nanoparticle was determined by the hydrophobic moiety used for modification [123].

Cyclodextrin-containing polymers have demonstrated unique capabilities for nucleic acid delivery: They have demonstrated low *in vitro* and *in vivo* toxicities when compared with other non-cyclodextrin-containing polycations such as poly-L-lysine and polyethylenimine. In addition, these polycations form self-assembled nanoparticles with oligonucleotides [124]. These advantages have been utilized for the preparation of the first clinically tested nanoparticle for siRNA delivery, which is composed of cyclodextrin-containing polycation, a polythethylene glycol (PEG) steric stabilization agent, and human transferrin as a targeting ligand [122]. Structurally, the cyclodextrin-containing polycation assembles with the siRNA primarily via electrostatic interactions. It condenses siRNA and protects it from nuclease degradation. The cyclodextrins within the polymer chains that reside on the surface of the nanoparticles are used for assembling PEG, which is conjugated to adamantine. The assembly of PEG-adamantine is due to inclusion complex formation between the

adamantine and cyclodextrin. The same principle is applied for the assembly of the targeting ligand transferrin, which was chosen since its receptor is upregulated on cancer cells. Primary results from phase I clinical trials using RRM2 siRNA-containing nanoparticles have been recently published [125]. Following systemic administration to patients with solid cancers, tumor biopsies revealed intracellular and dose dependent localization of the nanoparticles. In addition, specific reductions of both RRM2 mRNA and protein levels were observed. 5-RLMRACE analyses have shown that this reduction was mediated by an RNAi mechanism [125]. The paper describing results from the clinical studies did not contain data regarding the effects on human metabolism and immune response. However, following long-term administration to mice, no abnormalities in interleukin-12 and IFN-alpha, liver and kidney function tests, complete blood counts, or pathology of major organs were observed [42]. The administered nanoparticles used for delivery of *EWS-FLll* siRNA, demonstrated a significant and ligand specific inhibition of tumor growth in a murine model of metastatic Ewing's sarcoma [42].

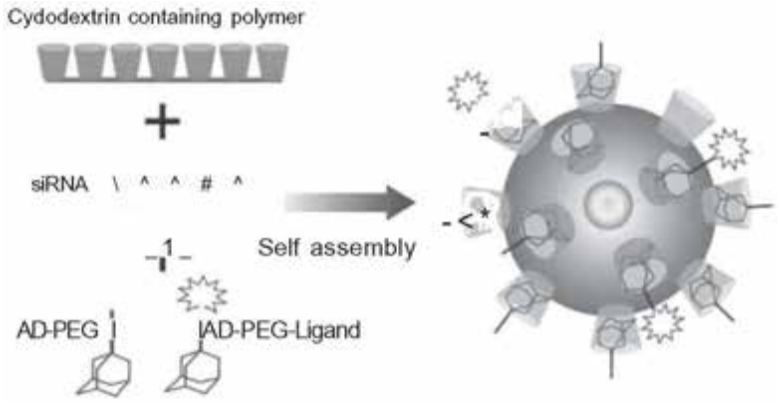

Figure 13.3 Self-assembly of cyclodestrin-based nanoparticle. The delivery components are a water-soluble, linear cyclodextrin-containing polymer (CDP), siRNA, an adamantane (AD-PEG) conjugate (AD-PEG), and the targeting component that is an adamantane conjugate of PEG that has a ligand conjugated at the end opposite to the adamantane (AD-PEG-Ligand). Modified from Ref. 122.

13.4.6 Arabinogalactan-Based Nanoparticles

Arabinogalactan has been used as a carrier for drug conjugates [44, 126]. Recently, Arabinogalactan-folic acid-drug conjugates for targeted delivery and activated drug release were prepared [127]. The targeted nanovehicle was formed by conjugation of folic acid and the anticancer drug methotrexate to arabinogalactan. The use of folic acid as a targeting ligand derives from fact that cancer cells overexpress receptors for nutrients in order to maintain their fast-growing metabolism [2] one of these receptor is folate receptor, which is overexpressed in malignant cells including ovary, brain, kidney, breast, colon, and lung [127]. Another advantage of using nutrient receptors as targets is that they enable internalization of the nanocarrier via receptor-mediated endocytosis. The activated drug release was achieved by linking methotrexate to arabinogalactan by an endosomally cleavable peptide Gly-Phe-Leu-Gly (GFLG). The nanocarrier displayed significant cytotoxic activity to folate receptor over expressing cells in comparison with folate receptor-deficient cells.

13.4.7 Pullulan-Based Nanoparticles

Pullulan has been demonstrated to self-assemble into nanoparticles after modification by hydrophobic molecules, such as cholesterol and stearic acid [128, 129]. In addition, pullulan drug conjugated and covalently cross-linked pullulan nanoparticles have been reported [130, 131]. Overall, pullulan-based nanoparticles have been used for the delivery of proteins, anticancer drugs, imaging agents, and nucleotides [69, 129, 130, 131].

Akiyoshi has been studying self-assembled nanoparticles of cholesterol modified pullulan for more than a decade [69, 70, 129, 132–135]. The hydrophobized pullulan was shown to form relatively monodisperse and colloidally stable nanoparticles (20–30 nm) in water upon self-aggregation [132]. The self-assembled nanoparticles demonstrated the ability to complex various hydrophobic substances, including soluble proteins such as Insulin. The complex between the nanoparticle and protein solution was easily formed by simply mixing the two components [129]. The particle size did not change after complexation with proteins [136]. The complexation with insulin occurred faster

than with larger proteins such as a-chymotrypsin or BSA. The nanoparticles showed high colloidal stability and no dissociation of insulin or precipitation were observed. The complexation contributed greatly to the thermal stability of insulin (even after heating for 6 h at 90°C) and protected insulin from enzymatic degradation. *In vivo* experiments demonstrated preservation insulin's bioavailability [129]. The ability of these nanoparticles to thermally stabilize proteins was investigated further [133]. The molecular chaperon-like activity was demonstrated on proteins using a system consisting of the cholesterol-pullulan nanoparticles and (B-cyclodextrin). Capture of heat-denatured unfolded protein and the release of the refolded form were achieved and the irreversible protein aggregation upon heating was completely prevented, recovering almost 100% of protein activity. Intracellular protein delivery by self-assembled nanoparticles of cationic cholesteryl group-bearing pullulans was also demonstrated [69]. While particle size did not change significantly upon replacing the cholesterol with the cationic cholesteryl group, the zeta potential became positive (+7.7 ±0.1 mV in comparison with—1.3 ± 0.4). In addition, the binding constant to the model protein, BSA, significantly grew. The cholesteryl-pullulan nanoparticles demonstrated a more effective internalization of protein to into HeLa cells in comparison with cationic liposomes and a protein transduction domain (PTD)-based carrier. Upon cell internalization, the protein-containing nanoparticle dissociated and the protein was released. Recently, cholesteryl-pullulan nanoparticles were used as an antigenic protein delivery system for adjuvant-free intranasal vaccines [70]. Intranasal delivery of a nontoxic subunit fragment of Clostridium botulinum type-A neurotoxin using these nanoparticles induced vigorous botulinum-neurotoxin A-neutralizing serum IgG and secretory IgA antibody responses. In addition, intranasally immunization of tetanus toxoid with the nanoparticles induced strong tetanus-toxoid-specific systemic and mucosal immune responses.

13.5 Polysaccharide-Coated Nanoparticles

Surface modification of nanoparticles with polysaccharides, an outcome of the cell surface polysaccharide discovery, has remarkable advantages for drug delivery systems: It endows the nanoparticle

with long-term circulation and increased stability. In addition, it provides targeting abilities: pullulan coating have been used for hepatic delivery [137], alginate and chitosan coating have been used for mucosal delivery [138], mannan coating facilitated uptake by macrophages [139] and HA-coated nanoparticles have been used to target CD44 overexpressing cells [3, 140, 141]. Another advantage is cryoprotection, which has been reported for several polysaccharides [18, 142]. Polysaccharide-decorated liposomes demonstrated reduced permeability to water-soluble encapsulated materials and protection from degradation by lipases [143].

Coating nanoparticles with polysaccharide can be achieved by adsorption, incorporation, copolymerization, or covalent grafting [144] and has been reported for many polysaccharides, including pectin, pullulan, mannan, HA, heparin, chitosan, and dextran [144, 145].

13.5.1 Chitosan-Coated Nanoparticles

The cationic nature of chitosan enables its adherence to mucosal surfaces. In addition, the ability of chitosan to open tight junctions between epithelial cells has also been demonstrated [14]. These characteristics make chitosan appealing as a coating agent of nanocarriers designed for mucosal delivery. For example, chitosan-coated poly-£-caprolactone (PECL) nanoparticles allowed the bioavailability of the anti-inflammatory drug indomethacin in the cornea and aqueous humor following topical ocular instillation [144]. In addition, chitosan coating of liposomes enhanced mucosal adhesion in rat intestine [146]. The degree of adhesion showed strong correlation to the amount of chitosan on the surface of the liposomes. When the chitosan-coated liposomes were used for the delivery of insulin, the effect determined by blood glucose levels was more significant and longer lasting in comparison with uncoated liposomes possibly due to mucoadhesion facilitated by the chitosan coat.

Chitosan coating can be used to replace the cationic polymers and lipids currently used for nucleic acid delivery thus overcoming the toxicity, which is the major obstacle in using these compounds. Chitosan-coated nanoparticles can interact with nucleic acids, improving the nanoparticle loading efficiency and transfection properties [144].

Structural benefits of coating nanoparticles with chitosan have also been demonstrated: Chitosan-coated liposomes were more stable in stimulated gastric fluids in comparison with uncoated liposomes [147]. Chitosan-coated PECL nanoparticles also demonstrated enhanced physical stability [18]. In addition, the chitosan coating also facilitated the redispersion of lyophilized PECL nanoparticles.

13.5.2 Hyaluronan-Coated Nanoparticles

The HA capsule of group A streptococci enables it to escape the host immune response [148] and therefore provides long-term circulation. This trait has been successfully adopted for the delivery of mitomycin C using HA-coated liposomes (tHA-LIP) (Fig. 13.4a) [141]. tHA-LIP were 7-fold and 70-fold longer circulating in comparison with uncoated liposomes and free mitomycin C in three murine tumor models: BALB/c-bearing C-26 solid tumors; C57BL/6-bearing B16F10.9, or D122 lung metastasis [141]. The HA on the tHA-LIP was covalently attached using EDC via the glucuronic carboxylate to phosphatidylethanolamine in the pre-formed liposomes. The tHA-LIP demonstrated slower drug efflux and higher encapsulation efficiency. In addition, since the effect of tHA-LIP is CD44 dependent, these nanoparticles demonstrated significantly higher cytotoxicity *in vitro* on CD44 overexpressing cells and increased drug accumulation in tumors *in vivo*. The later resulted in decreased metastasis, inhibition of tumor growth, and prolonged survival. These effects were later demonstrated with doxorubicin-loaded tHA-LIP [3]. This study also compared tHA-LIP with poly(ethylenglycol) (PEG)-coated liposomes ("stealth" liposomes). This was done since PEGylation, a common hydrophilic surface modification of drug delivery systems, has demonstrated prevention of recognition by the immune system. The tHA-LIP were long circulating more than all tested controls, including uncoated and PEGylated liposomes in healthy and tumor-bearing mice.

Recently, HA-coated paclitaxel-clusters (PTX-GAGs) have been prepared for selective tumor targeting (Fig. 13.4b) [149]. The aqueous insolubility of PTX was utilized in this preparation by mixing it with lipids that self-assembled into nano-size clusters. The clusters were then coated with HA to facilitate targeting of

CD44. When tested *in vivo*, these nanoparticles managed to induce tumor arrest in a murine model of colon adenocarcinoma and were significantly more potent than free PTX.

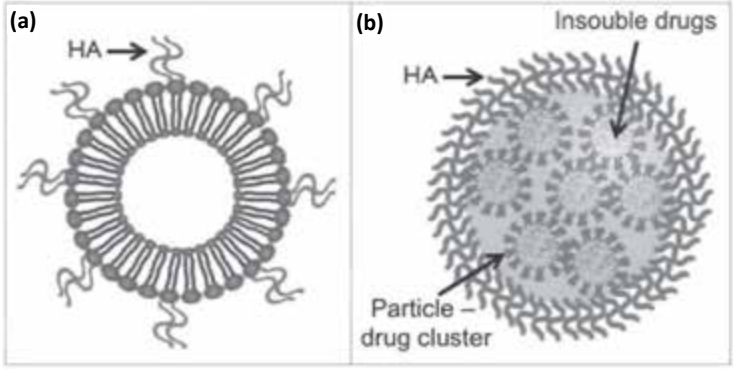

Figure 13.4 Hyaluronan-coated nanoparticles: (a) Hyaluronan-coated liposome (tHA-LIP). (b) Paclitaxel-clusters coated with hyaluronan (PTX-GACs).

Targeting of CD44 was also demonstrated for liposomes decorated with HA oligomers [140, 150]. Unlike in the preparation of the previously described tHA-LIP, the HA oligosaccharides were conjugated by reductive amination to phosphatidylethanolamine prior to liposome preparation. The oligosaccharide-decorated liposomes demonstrated CD44-dependent uptake, that could be blocked by both free HA and anti-CD44 antibodies. Liposome uptake was dependent on ligand density; however, as little as 0.1 HA molar percent managed to facilitate targeting. In addition, doxorubicin encapsulated in the oligosaccharide-decorated liposomes was significantly more cytotoxic to CD44 overexpression cells in comparison with free drug.

Another clinically relevant advantage of the liposomal HA coat is cryoprotection [142]. Cryoprotection provides the liposomes with a longer shelf life since it prevents the reversion of lyophilized unilamellar liposomes to multilamellar liposomes upon rehydration. The tested lyophilized tHA-LIP demonstrated the ability to retain the same dimensions, zeta potentials, encapsulation efficiencies and half-life of drug release of the original systems upon redispersion. HA cryoprotects possibly by providing substitute structure-stabilizing H-bonds.

13.5.3 Heparin- and Dextran-Coated Nanoparticles

Heparin has been shown to inhibit complement activation at different stages by increasing the activity of protein H [151]. Since the activation of the complement system plays an important role in opsonization and uptake of particles by the mononuclear phagocyte system (MPS), surface modification of nanoparticles with heparin seemed promising [151]. And indeed, a heparin coat significantly promoted long-term circulation of nanoparticle [151]. The heparin-modified poly(methyl methacrylate) (PMMA) nanoparticles elongated the *in vivo* half-life from only a few minutes to 5 h [151]. Dextran-coated nanoparticles also demonstrated longer *in vivo* half-life but to a lesser extent in comparison with heparin, probably since dextran has been shown to activate the complement system [152]. *In vitro*, the heparin- or dextran-coated nanoparticles were also demonstrated to be less taken up by a macrophagic cell line in comparison with uncoated nanoparticles [151]. The steric barrier formed by dense brush-like arrangement of the attached polysaccharide chains could contribute to the long-circulating properties of the heparin (or dextran)-coated PMMA nanoparticles.

Recently an artificial oxygen carrier based on a polysaccharide-decorated nanoparticle was demonstrated [153]. The core-shell nanoparticles, developed as red blood cell substitutes, were covered with a long brush of polysaccharides (heparin, dextran, or dextran sulfate) and demonstrated very low complement activation. The nanoparticles were obtained by using a redox radical polymerization mechanism in aqueous medium, which was followed by adsorption or coupling of hemoglobin. Interestingly, a former heparin-coated oxygen carrier developed by the same group demonstrated a highly improved cell line tolerance in the presence of hemoglobin [154]. In addition, the anticoagulant properties of heparin were preserved upon coating the nanoparticles with heparin. When benzene tetracarboxylic acid (BTCA) was used as a coupling agent for hemoglobin to dextran-coated nanoparticles, the loading capacity showed a 9.3-fold increase. The modification of nanoparticles by BTCA slightly increased complement activation; however, this activation was

reverted by the further addition of hemoglobin. The bound hemoglobin preserved its ability for exchanging oxygen [153].

13.6 Summary

The variety of naturally occurring polysaccharide properties has been successfully utilized to create multiple nano-size drug delivery systems. The advantages of polysaccharides enable the preparation of nanocarriers for the delivery of proteins, peptides, antibiotics and nucleic acids using several administration routes. In addition, preliminary results from the first phase I clinical trial using a polysaccharide nanocarrier for siRNA delivery have been presented.

Further understanding of the mechanisms involved in drug delivery will result in improved drug delivery systems tailor-made for a particular application.

Disclosures and Conflict of Interest

The authors wish to thank Dr. Micha Fridman from the TAU School of Chemistry for his help in the presentation of the polysaccharide chemical structures.

The authors declare that they have no conflict of interest and have no affiliations or financial involvement with any organization or entity discussed in this chapter. This includes employment, consultancies, honoraria, grants, stock ownership or options, expert testimony, patents (received or pending), or royalties. No writing assistance was utilized in the production of this chapter and the authors have received no payment for its preparation. The findings and conclusions here reflect the current views of the authors. They should not be attributed, in whole or in part, to the organizations with which they are affiliated, nor should they be considered as expressing an opinion with regard to the merits of any particular company or product discussed herein. Nothing contained herein is to be considered as the rendering of legal advice. This is a revised version of the author's chapter that originally appeared in *Handbook of Harnessing Biomaterials in Nanomedicine: Preparation, Toxicity, and Applications* (Dan Peer, editor), 2012, Pan Stanford Publishing Pte. Ltd., Singapore.

Corresponding Author

Prof. Dan Peer
Laboratory of NanoMedicine
Britannia Building, 2nd floor room 226
Tel Aviv University, Tel Aviv 69978, Israel
Email: peer@tauex.tau.ac.il

About the Authors

Shoshy Mizrahy received her BSc in Biotechnology and Food Engineering from the Technion, Israel Institute of Technology in 2002. From 2002–2003 she worked as a research assistant at Bio-Technology General (Israel) Ltd. She then obtained her MSc in Pathology from Tel Aviv University school of Medicine (2006). From 2006–2009 she worked as a researcher in Procognia Ltd. focusing on glycobiology and glycochemistry. From 2009 she is a PhD graduate student in the Laboratory of nanomedicine at Tel Aviv University focusing on novel nano-sized delivery systems made from polysaccharides for the delivery of therapeutic payloads to hematological malignancies.

Dan Peer received his PhD in biophysics and biochemistry from Tel Aviv University. From 2005–2008 he did his postdoctoral studies at Harvard Medical School. During his time at Harvard he developed several novel strategies to deliver siRNAs and other therapeutic payloads to immune cells using targeted nanoparticles. In 2008 he established the laboratory of NanoMedicine at Tel Aviv University. His current research includes developing novel strategies for targeted nanomedicines based on polysaccharides, probing and manipulating the immune system with nanomaterials, harnessing RNAi as a tool for drug discovery and for therapeutic applications, and developing tools to study immuno-nanotoxicity. He is also the director of the FTA: Nanomedicine for personalized theranostics and the Leona M. and Harry B. Helmsley Nanotechnology Research fund.

He is the President of the Israeli Chapter of the Controlled Release Society and an elected member of the Israel young academy of Science.

References

1. Petros, R. A., DeSimone, J. M. (2010). Strategies in the design of nanoparticles for therapeutic applications. *Nat. Rev. Drug Discov.*, **9**, 615–627.
2. Peer, D., Karp, J. M., Hong, S., Farokhzad, O. C., Margalit, R., et al. (2007). Nanocarriers as an emerging platform for cancer therapy. *Nat. Nanotechnol.*, **2**, 751–760.
3. Peer, D., Margalit, R. (2004). Tumor-targeted hyaluronan nanoliposomes increase the antitumor activity of liposomal doxorubicin in syngeneic and human xenograft mouse tumor models. *Neoplasia*, **6**, 343–353.
4. Sinha, V. R., Kumria, R. (2001). Polysaccharides in colon-specific drug delivery. *Int. J. Pharm.*, **224**,19–38.
5. Muzzarelli, R. (1973). Chitosan. In: R. Muzzarelli, ed. *Natural Chelating Polymers*, Pergamon Press, Oxford, pp. 144–176.
6. Alpar, H. O., Somavarapu, S., Atuah, K. N., Bramwell, V. W. (2005). Biodegradable mucoadhesive particulates for nasal and pulmonary antigen and DNA delivery. *Adv. Drug Deliv. Rev.*, **57**, 411–430.
7. Paolicelli, P., de la Fuente, M., Sanchez, A., Seijo, B., Alonso, M. J. (2009). Chitosan nanoparticles for drug delivery to the eye. *Expert Opin. Drug Deliv.*, **6**, 239–253.
8. Takeuchi, H., Yamamoto, H., Kawashima, Y. (2001). Mucoadhesive nanoparticulate systems for peptide drug delivery. *Adv. Drug Deliv. Rev.*, **47**, 39–54.
9. Valenta, C., Auner, B. G. (2004). The use of polymers for dermal and transdermal delivery. *Eur. J. Pharm. Biopharm.*, **58**, 279–289.
10. Sashiwa, H., Saimoto, H., Shigemasa, Y., Ogawa, R., Tokura, S. (1990). Lysozyme susceptibility of partially deacetylated chitin. *Int. J. Biol. Macromol.*, **12**, 295–296.
11. Muzzarelli, R., Baldassarre, V., Conti, F., Ferrara, R., Biagini. G., et al. (1988). Biological activity of chitosan: Ultrastructural study. *Biomaterials*, **9**, 247–252.
12. Ilium, L., Farraj, N. F., Davis, S. S. (1994). Chitosan as a novel nasal delivery system for peptide drugs. *Pharm. Res.*, **11**, 1186–1189.

13. Lehr, C. M., Bouwstra, J. A., Schacht, E. H., Junginger, H. E. (1992). *In vitro* evaluation of mucoadhesive properties of chitosan and some other natural polymers. *Int. J. Pharm*., **78**, 43–48.
14. Artursson, R., Lindmark, T., Davis, S. S., Ilium, L. (1994). Effect of chitosan on the permeability of monolayers of intestinal epithelial cells (Caco-2). *Pharm. Res*., **11**, 1358–1361.
15. Thanou, M., Verhoef, J. C., Marbach, R., Junginger, H. E. (2000). Intestinal absorption of octreotide: W-trimethyl chitosan chloride (TMC) ameliorates the permeability and absorption properties of the somatostatin analogue *in vitro* and *in vivo*. *J. Pharm. Sci*., **89**, 951–957.
16. Kubota, N., Eguchi, Y. (1997). Facile preparation of water-soluble W-acetylated chitosan and molecular weight dependence of its water-solubility. *Polym. J*., **29**, 123–127.
17. Varum, K. M., Ottoy, M. H., Smidsrod, O. (1994). Water-solubility of partially W-acetylated chitosans as a function of Ph—effect of chemical composition and depolymerization. *Carbohydr. Polym*., **25**, 65–70.
18. Calvo, R., Remunan-Lopez, C., Vilajato, J. L., Alonso, M. J. (1997). Development of positively charged colloidal drug carriers: Chitosan coated polyester nanocapsules and submicron-emulsions. *Colloid Polym. Sci*., **275**, 46–53.
19. Bhattarai, N., Zhang, M. Q. (2007). Controlled synthesis and structural stability of alginate-based nanofibers. *Nanotechnology*, **18**, 455601.
20. George, M., Abraham, T. E. (2006). Polyionichydrocolloids for the intestinal delivery of protein drugs: Alginate and chitosan—a review. *J. Control. Release*, **114**, 1–14.
21. Shilpa, A., Agrawal, S. S., Ray, A. R. (2003). Controlled delivery of drugs from alginate matrix. *J. Macromol. Sci. Polym. Rev*., **C43**, 187–221.
22. Ch'ng, H. S., Park, H., Kelly, R., Robinson, J. R. (1985). Bioadhesive polymers as platforms for oral controlled drug delivery II: Synthesis and evaluation of some swelling, water-insoluble bioadhesive polymers. *J. Pharm. Sci*., **74**, 399–405.
23. Varki, A. (2009). *Essentials of Glycobiology*. Cold Spring Harbor Laboratory Press, Cold Spring Harbor, NY; xxix, 784 p.
24. Toole, B. P. (2004). Hyaluronan: From extracellular glue to pericellular cue. *Nat. Rev. Cancer*, **4**, 528–539.
25. Piatt, V. M., Szoka, F. C., Jr. (2008). Anticancer therapeutics: Targeting macromolecules and nanocarriers to hyaluronan or CD44, a hyaluronan receptor. *Mol. Pharm*., **5**, 474–486.

26. Hamman, J. H. (2010). Chitosan based polyelectrolyte complexes as potential carrier materials in drug delivery systems. *Marine Drugs*, **8**, 1305–1322.

27. Jing, W., DeAngelis, P. L. (2004). Synchronized chemoenzymatic synthesis of monodisperse hyaluronan polymers. *J. Biol. Chem.*, **279**, 42345–42349.

28. DeAngelis, P. L., Oatman, L. C., Gay, D. F. (2003). Rapid chemoenzymatic synthesis of monodisperse hyaluronan oligosaccharides with immobilized enzyme reactors. *J. Biol. Chem.*, **278**, 35199–35203.

29. Pouyani, T., Prestwich, G. D. (1994). Functionalized derivatives of hyaluronic acid oligosaccharides: Drug carriers and novel biomaterials. *Bioconjug. Chem.*, **5**, 339–347.

30. Prestwich, G. D., Marecak, D. M., Marecek, J. F., Vercruysse, K. R., Ziebell, M. R. (1998). Controlled chemical modification of hyaluronic acid: Synthesis, applications, and biodegradation of hydrazide derivatives. *J. Control. Release*, **53**, 93–103.

31. Mohapatra, S., Yang, X., Wright, J. A., Turley, E. A., Greenberg, A. H. (1996). Soluble hyaluronan receptor RHAMM induces mitotic arrest by suppressing Cdc2 and cyclin B1 expression. *J. Exp. Med.*, **183**, 1663–1668.

32. Day, A. J., Prestwich, G. D. (2002). Hyaluronan-binding proteins: Tying up the giant. *J. Biol. Chem.*, **277**, 4585–4588.

33. Shigeishi, H., Fujimoto, S., Hiraoka, M., Ono, S., Taki, M., et al. (2009). Overexpression of the receptor for hyaluronan-mediated motility, correlates with expression of microtubule-associated protein in human oral squamous cell carcinomas. *Int. J. Oncol.*, **34**, 1565–1571.

34. Krause, D. S., Spitzer, T. R., Stowell, C. P. (2010). The concentration of CD44 is increased in hematopoietic stem cell grafts of patients with acute myeloid leukemia, plasma cell myeloma, and non-Hodgkin lymphoma. *Arch. Pathol. Lab. Med.*, **134**, 1033–1038.

35. Borgstrom, S., Gelin, L. E., Zederfeldt, B. (1959). The formation of vein thrombi following tissue injury: An experimental study in rabbits. *Acta Chirurgica Scandinavica Supplementum*, **247**, 1–36.

36. Nimesh, S., Kumar, R., Chandra, R. (2006). Novel polyallylamine-dextran sulfate-DNA nanoplexes: Highly efficient non-viral vector for gene delivery. *Int. J. Pharm.*, **320**, 143–149.

37. Zimmermann, K., Preinl, G., Ludwig, H., Greulich, K. O. (1983). Inhibition of hyaluronidase by dextran sulfate and its possible application in anticancer treatment. *J. Cancer Res. Clin. Oncol.*, **105**, 189–190.

38. Wetzel, G. D., Kettman, J. R. (1981). Activation of murine B cells. II. Dextran sulfate removes the requirement for cellular interaction during lipopolysaccharide-induced mitogenesis. *Cell*. *Immunol*., **61**, 176–189.

39. Ataullakhanov, R. I., Ataullakhanov, F. I., Abdullaev, D. M. (1984). Increase in the permeability of the lymphocyte plasma membrane for uni- and bivalent cations and low-molecular metabolites following exposure to mitogenic polyanions. *Biull Eksp Biol Med*., **98**, 81–84.

40. Sallas, F., Darcy, R. (2008). Amphiphilic cyclodextrins—advances in synthesis and supramolecular chemistry. *Eur*. *J*. *Org*. *Chem*., **6**, 957–969.

41. Szejtli, J. (1998). Introduction and general overview of cyclodextrin chemistry. *Chem*. *Rev*., **98**, 1743–1754.

42. Hu-Lieskovan, S., Heidel, J. D., Bartlett, D. W., Davis, M. E., Triche, T. J. (2005). Sequence-specific knockdown of EWS-FLI1 by targeted, nonviral delivery of small interfering RNA inhibits tumor growth in a murine model of metastatic Ewing's sarcoma. *Cancer Res*., **65**, 8984–8992.

43. Davis, M. E., Brewster, M. E. (2004). Cyclodextrin-based pharmaceutics: Past, present and future. *Nat*. *Rev*. *Drug Discov*., **3**, 1023–1035.

44. Falk, R., Domb, A. J., Polacheck, I. (1999). A novel injectable water-soluble amphotericin B-arabinogalactan conjugate. *Antimicrob*. *Agents Chemother*., **43**, 1975–1981.

45. Leathers, T. D. (2003). Biotechnological production and applications of pullulan. *Appl*. *Microbiol*. *Biotechnol*., **62**, 468–473.

46. Linhardt, R. J. (2003). 2003 Claude S. Hudson Award address in carbohydrate chemistry. Heparin: Structure and activity. *J*. *Med*. *Chem*., **46**, 2551–2564.

47. Kemp, M. M., Linhardt, R. J. (2010). Heparin-based nanoparticles. *WIREs Nanomed*. *Nanobiotechnol*., **2**, 77–87.

48. Berger, J., Reist, M., Mayer, J. M., Felt, O., Peppas, N. A. et al. (2004). Structure and interactions in covalently and ionically cross-linked chitosan hydrogels for biomedical applications. *Eur*. *J*. *Pharm*. *Biopharm*., **57**, 19–34.

49. Berger, J., Reist, M., Mayer, J. M., Felt, O., Gurny, R. (2004). Structure and interactions in chitosan hydrogels formed by complexation or aggregation for biomedical applications. *Eur*. *J*. *Pharm*. *Biopharm*., **57**, 35–52.

50. Ohya, Y., Shiratani, M., Kobayashi, H., Ouchi, T. (1994). Release behavior of 5-fluorouracil from chitosan-gel nanospheres immobilizing 5-fluorouracil coated with polysaccharides and their cell-specific cytotoxicity. *J. Macromol. Sci.: Pure Appl. Chem.*, **A31**, 629–642.

51. Banerjee, T., Mitra, S., Kumar Singh, A., Kumar Sharma, R., Maitra, A. (2002). Preparation, characterization and biodistribution of ultrafine chitosan nanoparticles. *Int. J. Pharm.*, **243**, 93–105.

52. Bodnar, M., Hartmann, J. F., Borbely, J. (2005). Preparation and characterization of chitosan-based nanoparticles. *Biomacromolecules*, **6**, 2521–2527.

53. Chen, K. Y., Liao, W. J., Kuo, S. M., Tsai, F. J., Chen, Y. S., et al. (2009). Asymmetric chitosan membrane containing collagen I nanospheres for skin tissue engineering. *Biomacromolecules*, **10**, 1642–1649.

54. Ahmad, Z., Sharma, S., Khuller, G. K. (2007). Chemotherapeutic evaluation of alginate nanoparticle-encapsulated azole antifungal and antitubercular drugs against murine tuberculosis. *Nanomedicine*, **3**, 239–243.

55. Ahmad, Z., Sharma, S., Khuller, G. K. (2005). Inhalable alginate nanoparticles as antitubercular drug carriers against experimental tuberculosis. *Int. J. Antimicrob. Agents*, **26**, 298–303.

56. Bodmeier, R., Chen, H. G., Paeratakul, O. (1989). A novel approach to the oral delivery of micro- or nanoparticles. *Pharm. Res.*, **6**, 413–417.

57. Mi, F. L., Shyu, S. S., Lee, S. T., Wong, T. B. (1999). Kinetic study of chitosan-tripolyphosphate complex reaction and acid-resistive properties of the chitosan-tripolyphosphate gel beads prepared by in-liquid curing method. *J. Polym. Sci. B: Polym. Phys.*, **37**, 1551–1564.

58. Draget, K. I., Varum, K. M., Moen, E., Gynnild, H., Smidsrod, O. (1992). Chitosan cross-linked with Mo(VI) polyoxyanions: A new gelling system. *Biomaterials*, **13**, 635–638.

59. Mi, F. L., Chen, C. T., Tseng, Y. C., Kuan, C. Y., Shyu, S. S. (1997). Iron(III)-carboxymethylchitin microsphere for the pH-sensitive release of 6-mercaptopurine. *J. Control. Release*, **44**, 19–32.

60. Bhattarai, N., Gunn, J., Zhang, M. (2010). Chitosan-based hydrogels for controlled, localized drug delivery. *Adv. Drug Deliv. Rev.*, **62**, 83–99.

61. Park, J. H., Saravanakumar, G., Kim, K., Kwon, I. C. (2010). Targeted delivery of low molecular drugs using chitosan and its derivatives. *Adv. Drug Deliv. Rev.*, **62**, 28–41.

62. Tiyaboonchai, W., Woiszwillo, J., Sims, R. C., Middaugh, C. R. (2003). Insulin containing polyethylenimine-dextran sulfate nanoparticles. *Int. J. Pharm*., **255**, 139–151.

63. Sonaje, K., Lin, Y. H., Juang, J. H., Wey SR Chen CT, et al. (2009). *In vivo* evaluation of safety and efficacy of self-assembled nanoparticles for oral insulin delivery. *Biomaterials*, **30**, 2329–2339.

64. Liu, Z., Jiao, Y., Wang, Y., Zhou, C., Zhang, Z. (2008). Polysaccharides-based nanoparticles as drug delivery systems. *Adv. Drug Deliv. Rev*., **60**, 1650–1662.

65. Howard, K. A., Paludan, S. R., Behlke, M. A., Besenbacher, F., Deleuran, B., et al. (2009). Chitosan/siRNA nanoparticle-mediated TNF-alpha knockdown in peritoneal macrophages for anti-inflammatory treatment in a murine arthritis model. *Mol. Ther*., **17**, 162–168.

66. Oyarzun-Ampuero, F. A., Brea, J., Loza, M. I., Torres, D., Alonso, M. J. (2009). Chitosan-hyaluronic acid nanoparticles loaded with heparin for the treatment of asthma. *Int. J. Pharm*., **381**, 122–129.

67. Allen, C., Maysinger, D., Eisenberg, A. (1999). Nano-engineering block copolymer aggregates for drug delivery. *Colloids Surf. B: Biointerfaces*, **16**, 3–27.

68. Letchford, K., Burt, H. (2007). A review of the formation and classification of amphiphilic block copolymer nanoparticulate structures: Micelles, nanospheres, nanocapsules and polymersomes. *Eur. J. Pharm. Biopharm*., **65**, 259–269.

69. Ayame, H., Morimoto, N., Akiyoshi, K. (2008). Self-assembled cationic nanogels for intracellular protein delivery. *Bioconjug. Chem*., **19**, 882–890.

70. Nochi, T., Yuki, Y., Takahashi, H., Sawada, S., Mejima, M., et al. (2010). Nanogel antigenic protein-delivery system for adjuvant-free intranasal vaccines. *Nat. Mater*., **9**, 572–578.

71. Janes, K. A., Calvo, P., Alonso, M. J. (2001). Polysaccharide colloidal particles as delivery systems for macromolecules. *Adv. Drug Deliv. Rev*., **47**, 83–97.

72. Gan, Q., Wang, T., Cochrane, C., McCarron, P. (2005). Modulation of surface charge, particle size and morphological properties of chitosan-TPP nanoparticles intended for gene delivery. *Colloids Surf. B: Biointerfaces*, **44**, 65–73.

73. Calvo, P., Remunan-Lopez, C., Vilajato, J. L., Alonso, M. J. (1997). Novel hydrophilic chitosan-polyethylene oxide nanoparticles as protein carriers. *J. Appl. Polym. Sci*., **63**, 125–132.

74. Fernandez-Urrusuno, R., Calvo, R., Remunan-Lopez, C., Vila-Jato, J. L., Alonso, M. J. (1999). Enhancement of nasal absorption of insulin using chitosan nanoparticles. *Pharm. Res.*, **16**, 1576–1581.

75. De Campos, A. M., Sanchez, A., Alonso, M. J. (2001). Chitosan nanoparticles: A new vehicle for the improvement of the delivery of drugs to the ocular surface. Application to cyclosporin A. *Int. J. Pharm.*, **224**, 159–168.

76. Csaba, N., Koping-Hoggard, M., Alonso, M. J. (2009). Ionically cross-linked chitosan/tripolyphosphate nanoparticles for oligonucleotide and plasmid DNA delivery. *Int. J. Pharm.*, **382**, 205–214.

77. Csaba, N., Koping-Hoggard, M., Fernandez-Megia, E., Novoa-Carballal, R., Riguera, R., et al. (2009). Ionically cross-linked chitosan nanoparticles as gene delivery systems: Effect of PEGylation degree on *in vitro* and *in vivo* gene transfer. *J. Biomed. Nanotechnol.*, **5**, 162–171.

78. Katas, H., Alpar, H. O. (2006). Development and characterisation of chitosan nanoparticles for siRNA delivery. *J. Control. Release*, **115**, 216–225.

79. Lee, P. W., Peng, S. F., Su, C. J., Mi, F. L., Chen, H. L., et al. (2008). The use of biodegradable polymeric nanoparticles in combination with a low pressure gene gun for transdermal DNA delivery. *Biomaterials*, **29**, 742–751.

80. Peng, S. F., Yang, M. J., Su, C. J., Chen, H. L., Lee, P. W., et al. (2009). Effects of incorporation of poly(gamma-glutamic acid) in chitosan/DNA complex nanoparticles on cellular uptake and transfection efficiency. *Biomaterials*, **30**, 1797–1808.

81. Roy, K., Mao, H. Q., Huang, S. K., Leong, K. W. (1999). Oral gene delivery with chitosan-DNA nanoparticles generates immunologic protection in a murine model of peanut allergy. *Nat. Med.*, **5**, 387–391.

82. Jean, M., Smaoui, F., Lavertu, M., Methot, S., Bouhdoud, L., et al. (2009). Chitosan-plasmid nanoparticle formulations for IM and SC delivery of recombinant FGF-2 and PDGF-BB or generation of antibodies. *Gene Ther.*, **16**, 1097–1110.

83. Klausner, E. A., Zhang, Z., Chapman, R. L., Multack, R. F., Volin, M. V. (2010). Ultrapure chitosan oligomers as carriers for corneal gene transfer. *Biomaterials*, **31**, 1814–1820.

84. Koping-Hoggard, M., Varum, K. M., Issa, M., Danielsen, S., Christensen, B. E., et al. (2004). Improved chitosan-mediated gene delivery based on easily dissociated chitosan polyplexes of highly defined chitosan oligomers. *Gene Ther.*, **11**, 1441–1452.

85. Strand, S. P., Lelu, S., Reitan, N. K., de Lange Davies, C., Artursson, P., et al. (2010). Molecular design of chitosan gene delivery systems with an optimized balance between polyplex stability and polyplex unpacking. *Biomaterials*, **31**, 975–987.

86. Zahr, A. S., Davis, C. A., Pishko, M. V. (2006). Macrophage uptake of core–shell nanoparticles surface modified with poly(ethylene glycol). *Langmuir*, **22**, 8178–8185.

87. Zhang, J., Chen, X. G., Li, Y. Y., Liu, C. S. (2007). Self-assembled nanoparticles based on hydrophobically modified chitosan as carriers for doxorubicin. *Nanomedicine*, **3**, 258–265.

88. Kim, J. H., Kim, Y. S., Park, K., Kang, E., Lee, S., et al. (2008). Self-assembled glycol chitosan nanoparticles for the sustained and prolonged delivery of antiangiogenic small peptide drugs in cancer therapy. *Biomaterials*, **29**, 1920–1930.

89. Pasqualini, R., Koivunen, E., Ruoslahti, E. (1997). Alpha v integrins as receptors for tumor targeting by circulating ligands. *Nat. Biotechnol.*, **15**, 542–546.

90. Son, Y. J., Jang, J. S., Cho, Y. W., Chung, H., Park, R. W., et al. (2003). Biodistribution and anti-tumor efficacy of doxorubicin loaded glycol-chitosan nanoaggregates by EPR effect. *J. Control. Release*, **91**, 135–145.

91. Kim, J. H., Kim, Y. S., Kim, S., Park, J. H., Kim, K., et al. (2006). Hydrophobically modified glycol chitosan nanoparticles as carriers for paclitaxel. *J. Control. Release*, **111**, 228–234.

92. Kast, C. E., Bernkop-Schnurch, A. (2001). Thiolated polymers-thiomers: Development and *in vitro* evaluation of chitosan-thioglycolic acid conjugates. *Biomaterials*, **22**, 2345–2352.

93. Florea, B. I., Thanou, M., Junginger, H. E., Borchard, G. (2006). Enhancement of bronchial octreotide absorption by chitosan and W-trimethyl chitosan shows linear *in vitro/in vivo* correlation. *J. Control. Release*, **110**, 353–361.

94. Jiang, H. L., Kwon, J. T., Kim, Y. K., Kim, E. M., Arote, R., et al. (2007). Galactosylated chitosan-graft-polyethylenimine as a gene carrier for hepatocyte targeting. *Gene Ther.*, **14**, 1389–1398.

95. Fernandes, J. C., Wang, H., Jreyssaty, C., Benderdour, M., Lavigne, R., et al. (2008). Bone-protective effects of nonviral gene therapy with folate-chitosan DNA nanoparticle containing interleukin-1 receptor antagonist gene in rats with adjuvant-induced arthritis. *Mol. Ther.*, **16**, 1243–1251.

96. Hamidi, M., Azadi, A., Rafiei, P. (2008). Hydrogel nanoparticles in drug delivery. *Adv*. *Drug Deliv*. *Rev*., **60**, 1638–1649.
97. Goycoolea, F. M., Lollo, G., Remunan-Lopez, C., Quaglia, F., Alonso, M. J. (2009). Chitosan-alginate blended nanoparticles as carriers for the transmucosal delivery of macromolecules. *Biomacromolecules*, **10(7)**, 1736–1743.
98. Khdair, A., Chen, D., Patil, Y., Ma, L., Dou, Q. P., et al. (2010). Nanoparticle mediated combination chemotherapy and photodynamic therapy overcomes tumor drug resistance. *J*. *Control*. *Release*, **141**, 137–144.
99. Bernkop-Schnurch, A., Kast, C. E., Richter, M. F. (2001). Improvement in the mucoadhesive properties of alginate by the covalent attachment of cysteine. *J*. *Control*. *Release*, **71**, 277–285.
100. Leonard, M., De Boisseson, M. R., Hubert, R., Dalencon, F., Dellacherie, E. (2004). Hydrophobically modified alginate hydrogels as protein carriers with specific controlled release properties. *J*. *Control*. *Release*, **98**, 395–405.
101. Oh, E. J., Park, K., Kim, K. S., Kim, J., Yang, J. A., et al. (2010). Target specific and long-acting delivery of protein, peptide, and nucleotide therapeutics using hyaluronic acid derivatives. *J*. *Control*. *Release*, **141**, 2–12.
102. Luo, Y., Prestwich, G. D. (1999). Synthesis and selective cytotoxicity of a hyaluronic acid-antitumor bioconjugate. *Bioconjug*. *Chem*., **10**, 755–763.
103. Lee, H., Lee, K., Park, T. G. (2008). Hyaluronic acid-paclitaxel conjugate micelles: Synthesis, characterization, and antitumor activity. *Bioconjug*. *Chem*., **19**, 1319–1325.
104. Xin, D., Wang, Y., Xiang, J. (2010). The use of amino acid linkers in the conjugation of paclitaxel with hyaluronic acid as drug delivery system: Synthesis, self-assembled property, drug release, and *in vitro* efficiency. *Pharm*. *Res*., **27**, 380–389.
105. Kong, J. H., Oh, E. J., Chae, S. Y., Lee, K. C., Hahn, S. K. (2010). Long acting hyaluronate-exendin 4 conjugate for the treatment of type 2 diabetes. *Biomaterials*, **31**, 4121–4128.
106. Buse, J. B., Henry, R. R., Han, J., Kim, D. D., Fineman, M. S., et al. (2004). Effects of exenatide (exendin-4) on glycemic control over 30 weeks in sulfonylurea-treated patients with type 2 diabetes. *Diab*. *Care*, **27**, 2628–2635.
107. Coradini, D., Pellizzaro, C., Scarlata, I., Zorzet, S., Garrovo, C., et al. (2006). A novel retinoic/butyric hyaluronan ester for the treatment of acute promyelocytic leukemia: Preliminary preclinical results. *Leukemia*, **20**, 785–792.

108. Coradini, D., Pellizzaro, C., Miglierini, G., Daidone, M. G., Perbellini, A. (1999). Hyaluronic acid as drug delivery for sodium butyrate: Improvement of the anti-proliferative activity on a breast-cancer cell line. *International Journal of Cancer*, **81**, 411–416.

109. Coradini, D., Zorzet, S., Rossin, R., Scarlata, I., Pellizzaro, C., et al. (2004). Inhibition of hepatocellular carcinomas *in vitro* and hepatic metastases *in vivo* in mice by the histone deacetylase inhibitor HA-But. *Clin*. *Cancer Res*., **10**, 4822–4830.

110. de la Fuente, M., Seijo, B., Alonso, M. J. (2008). Bioadhesive hyaluronan-chitosan nanoparticles can transport genes across the ocular mucosa and transfect ocular tissue. *Gene Ther*., **15**, 668–676.

111. Lee, H., Ahn, C. H., Park, T. G. (2009). Poly[lactic-co-(glycolic acid)]-grafted hyaluronic acid copolymer micelle nanoparticles for target-specific delivery of doxorubicin. *Macromolecular Biosciences*, **9**, 336–342.

112. Saravanakumar, G., Choi, K. Y., Yoon, H. Y., Kim, K., Park, J. H., et al. (2010). Hydrotropic hyaluronic acid conjugates: Synthesis, characterization, and implications as a carrier of paclitaxel. *Intrenational Journal of Pharmaceutics*, **394**, 154–161.

113. Choi, K. Y., Chung, H., Min, K. H., Yoon, H. Y., Kim, K., et al. (2010). Self-assembled hyaluronic acid nanoparticles for active tumor targeting. *Biomaterials*, **31**, 106–114.

114. Lemarchand, C., Couvreur, R., Besnard. M., Costantini, D., Gref, R. (2003). Novel polyester-polysaccharide nanoparticles. *Pharm*. *Res*., **20**, 1284–1292.

115. Choi, K. C., Bang, J. Y., Kim, C., Kim, P. I., Lee, S. R., et al. (2009). Antitumor effect of adriamycin-encapsulated nanoparticles of poly(D-L-lactide-*co*-glycolide)-grafted dextran. *J*. *Pharm*. *Sci*., **98**, 2104–2112.

116. Bisht, S., Maitra, A. (2009). Dextran-doxorubicin/chitosan nanoparticles for solid tumor therapy. *WIREs Nanomed Nanobiotechnol*, **1**, 415–425.

117. Hornig, S,, Bunjes, H., Heinze, T. (2009). Preparation and characterization of nanoparticles based on dextran–drug conjugates. *Journal of Colloid and Interface Science*, **338**, 56–62.

118. Huang, M., Vitharana, S. N., Peek, L. J., Coop, T., Berkland, C. (2007). Polyelectrolyte complexes stabilize and controllably release vascular endothelial growth factor. *Biomacromolecules*, **8**, 1607–1614.

119. Huang, M., Berkland, C. (2009). Controlled release of repifermin from polyelectrolyte complexes stimulates endothelial cell proliferation. *J*. *Pharm*. *Sci*., **98**, 268–280.

120. Tiyaboonchai, W., Woiszwillo, J., Middaugh, C. R. (2001). Formulation and characterization of amphotericin B-polyethylenimine-dextran sulfate nanoparticles. *J. Pharm. Sci.*, **90**, 902–914.
121. Memisoglu-Bilensoy, E., Vural, I., Bochot, A., Renoir, J. M., Duchene, D., et al. (2005). Tamoxifen citrate loaded amphiphilic beta-cyclodextrin nanoparticles: *In vitro* characterization and cytotoxicity. *J. Control. Release*, **104**, 489–496.
122. Davis, M. E. (2009). The first targeted delivery of siRNA in humans via a self-assembling, cyclodextrin polymer-based nanoparticle: From concept to clinic. *Mol. Pharm.*, **6**, 659–668.
123. Choisnard, L., Geze, A., Putaux, J. L., Wong, Y. S., Wouessidjewe, D. (2006). Nanoparticles of beta-cyclodextrin esters obtained by self-assembling of biotransesterified beta-cyclodextrins. *Biomacromolecules*, **7**, 515–520.
124. Spinner, N. B., Gibas, Z., Kline, R., Berger, B., Jackson, L. (1992). Placental mosaicism in a case of 46,XY,-22,+t(22;22)(pll;qll) or i(22q) diagnosed at amniocentesis. *Prenatal Diagnosis*, **12**, 47–51.
125. Davis, M. E., Zuckerman, J. E., Choi, C. H., Seligson, D., Tolcher, A., et al. (2010). Evidence of RNAi in humans from systemically administered siRNA via targeted nanoparticles. *Nature*, **464**, 1067–1070.
126. Elgart, A., Farber, S., Domb, A. J., Polacheck, I., Hoffman, A. (2010). Polysaccharide pharmacokinetics: Amphotericin B arabinogalactan conjugate—a drug delivery system or a new pharmaceutical entity? *Biomacromolecules*, **11**, 1972–1977.
127. Pinhassi, R. I., Assaraf, Y. G., Farber, S., Stark, M., Ickowicz, D., et al. (2010). Arabinogalactan-folic acid–drug conjugate for targeted delivery and target-activated release of anticancer drugs to folate receptor overexpressing cells. *Biomacromolecules*, **11**, 294–303.
128. Akiyama, E., Morimoto, N., Kujawa, R., Ozawa, Y., Winnik, F. M., et al. (2007). Self-assembled nanogels of cholesteryl-modified polysaccharides: Effect of the polysaccharide structure on their association characteristics in the dilute and semidilute regimes. *Biomacromolecules*, **8**, 2366–2373.
129. Akiyoshi, K., Kobayashi, S., Shichibe, S., Mix, D., Baudys, M., et al. (1998). Self-assembled hydrogel nanoparticle of cholesterol-bearing pullulan as a carrier of protein drugs: Complexation and stabilization of insulin. *J. Control. Release*, **54**, 313–320.
130. Lu, D., Wen, X., Liang, J., Gu, Z., Zhang, X., et al. (2009). A pH-sensitive nano drug delivery system derived from pullulan/doxorubicin conjugate. *Journal of Biomedical Materials Research Part B: Applied Biomaterials*, **89**, 177–183.

131. Gupta, M., Gupta, A. K. (2004). Hydrogel pullulan nanoparticles encapsulating pBUDLacZ plasmid as an efficient gene delivery carrier. *J. Control. Release*, **99**, 157–166.

132. Akiyoshi, K., Deguchi, S., Moriguchi, N., Yamaguchi, S., Sunamoto, J. (1993). Self-aggregates of hydrophobized polysaccharides in water—formation and characteristics of nanoparticles. *Macromolecules*, **26**, 3062–3068.

133. Akiyoshi, K., Sasaki, Y., Sunamoto, J. (1999). Molecular chaperone-like activity of hydrogel nanoparticles of hydrophobized pullulan: Thermal stabilization with refolding of carbonic anhydrase B. *Bioconjug. Chem.*, **10**, 321–324.

134. Hasegawa, U., Sawada, S., Shimizu, X., Kishida, X., Otsuji, E., et al. (2009). Raspberry-like assembly of cross-linked nanogels for protein delivery. *J. Control. Release*, **140**, 312–317.

135. Sawada, S., Akiyoshi, K. (2010). Nano-encapsulation of lipase by self-assembled nanogels: Induction of high enzyme activity and thermal stabilization. *Macromolecular Biosciences*, **10**, 353–358.

136. Nishikawa, X., Akiyoshi, K., Sunamoto, J. (1994). Supramolecular assembly between nanoparticles of hydrophobized polysaccharide and soluble protein complexation between the self-aggregate of cholesterol bearing pullulan and alpha-chymotrypsin. *Macromolecules*, **27**, 7654–7659.

137. Cui, Z., Mumper, R. J. (2002). Plasmid DNA-entrapped nanoparticles engineered from microemulsion precursors: *In vitro* and *in vivo* evaluation. *Bioconjug. Chem.*, **13**, 1319–1327.

138. Borges, O., Cordeiro-da-Silva, A., Romeijn, S. G., Amidi, M., de Sousa, A., et al. (2006). Uptake studies in rat Peyer's patches, cytotoxicity and release studies of alginate coated chitosan nanoparticles for mucosal vaccination. *J. Control. Release*, **114**, 348–358.

139. Cui, Z., Hsu, C. H., Mumper, R. J. (2003). Physical characterization and macrophage cell uptake of mannan-coated nanoparticles. *Drug Development and Industrial Pharmacy*, **29**, 689–700.

140. Eliaz, R. E., Szoka, F. C., Jr. (2001). Liposome-encapsulated doxorubicin targeted to CD44: A strategy to kill CD44-overexpressing tumor cells. *Cancer Res.*, **61**, 2592–2601.

141. Peer, D., Margalit, R. (2004). Loading mitomycin C inside long circulating hyaluronan targeted nano-liposomes increases its antitumor activity in three mice tumor models. *Int. J. Cancer*, **108**, 780–789.

142. Peer, D., Florentin, A., Margalit, R. (2003). Hyaluronan is a key component in cryoprotection and formulation of targeted unilamellar liposomes. *Biochim*. *Biophys*. *Acta*, **1612**, 76–82.

143. Sunamoto, J., Iwamoto, K. (1986). Protein-coated and polysaccharide-coated liposomes as drug carriers. *Crit*. *Rev*. *Ther*. *Drug*. *Carrier Syst*., **2**, 117–136.

144. Lemarchand, C., Gref, R., Couvreur, P. (2004). Polysaccharide-decorated nanoparticles. *Eur*. *J*. *Pharm*. *Biopharm*., **58**, 327–341.

145. Jones, M. N. (1994). Carbohydrate-mediated liposomal targeting and drug-delivery. *Adv*. *Drug Deliv*. *Rev*., **13**, 215–249.

146. Takeuchi, H., Yamamoto, H., Niwa, T., Hino, T., Kawashima, Y. (1996). Enteral absorption of insulin in rats from mucoadhesive chitosan-coated liposomes. *Pharm*. *Res*., **13**, 896–901.

147. Filipovic-Grcic, J., Skalko-Basnet, N., Jalsenjak, I. (2001). Mucoadhesive chitosan-coated liposomes: Characteristics and stability. *J*. *Micro-encapsul*., **18**, 3–12.

148. Ouskova, G., Spellerberg, B., Prehm, P. (2004). Hyaluronan release from *Streptococcus* pyogenes: Export by an ABC transporter. *Glycobiology*, **14**, 931–938.

149. Rivkin, I., Cohen, K., Koffler, J., Melikhov, D., Peer, D., et al. (2010). Paclitaxel clusters coated with hyaluronan as selective tumor-targeted nanovectors. *Biomaterials*, **31**, 7106–7114.

150. Eliaz, R. E., Nir, S., Szoka, F. C., Jr. (2004). Interactions of hyaluronan-targeted liposomes with cultured cells: Modeling of binding and endocytosis. *Methods Enzymol*., **387**, 16–33.

151. Passirani, C., Barratt, G., Devissaguet, J. R., Labarre, D. (1998). Long circulating nanoparticles bearing heparin or dextran covalently bound to poly(methyl methacrylate). *Pharm*. *Res*., **15**, 1046–1050.

152. Passirani, C., Barratt, G., Devissaguet, J. R., Labarre, D. (1998). Interactions of nanoparticles bearing heparin or dextran covalently bound to poly(methyl methacrylate) with the complement system. *Life Sci*., **62**, 775–785.

153. Chauvierre, C., Manchanda, R., Labarre, D., Vauthier, C., Marden, M. C., et al. (2010). Artificial oxygen carrier based on polysaccharidespoly (alkylcyanoacrylates) nanoparticle templates. *Biomaterials*, **31**, 6069–6074.

154. Chauvierre, C., Leclerc, L., Labarre, D., Appel, M., Marden, M. C., et al. (2007). Enhancing the tolerance of poly(isobutylcyanoacrylate) nanoparticles with a modular surface design. *Int*. *J*. *Pharm*., **338**, 327–332.

Chapter 14

The Story of C_{60} Buckminsterfullerene

Harold W. Kroto, PhD

Department of Chemistry & Biochemistry, Florida State University, Florida, USA

Keywords: fullerenes, self-assembly, nanotechnology, C_{60}, carbon, microwave spectroscopy, photodissociation, mass spectrometry, Buckyball, Buckminsterfullerene, icosahedral, arc-discharged carbon, carbon soot, Isolated Pentagon Rule (IPR), Isolated Multiplet Pentagon Rule (IMPR), diffuse interstellar bands (DIBs)

The story of discovery of C_{60} buckminsterfullerene is not only multifaceted but also convoluted, and this makes the assembly of a coherent, straightforward account very difficult, if not impossible. The bare bones are to be found in three key papers: (a) An experiment, in 1985, designed to re-create the conditions in cool carbon stars serendipitously uncovered the existence an all-carbon species which was conjectured to be a molecule consisting of 60 equivalent C atoms located at the corners of a truncated icosahedral closed cage [1a]. (b) In 1990 the molecule was extracted by sublimation from the deposit of a carbon arc and the spheroidal shape proven by X-ray analysis [2]. (c) Simultaneously, in 1990,

Handbook of Clinical Nanomedicine: Nanoparticles, Imaging, Therapy, and Clinical Applications
Edited by Raj Bawa, Gerald F. Audette, and Israel Rubinstein

ISBN 978-981-4669-20-7 (Hardcover), 978-981-4669-21-4 (eBook)
www.panstanford.com

Sir Harry Kroto with giant fullerene structures. Photograph by Anne-Katrin Purkiss.

the molecule was created independently, solvent-extracted and the truncated icosahedral pattern confirmed by the detection of a single NMR line and the chromatographic method of isolating fullerenes developed [3]. Furthermore in this study the ultimate unequivocal confirmation that a whole family of fullerenes existed was obtained by the detection of the 5-line NMR spectrum for C_{70}. Then the field exploded and today, on average, about a thousand papers are published each year describing research advances involving fullerenes. An essentially complete review [4] surveyed the status of the fullerene field up to December 31, 1990. It is arguable, and I would argue it, that the main aspect of the discovery was not the fact that C_{60} could be created, but that it self-assembled spontaneously, because this resulted in a reassessment of our perspective on the general dynamic factors which control structure assembly processes at nanoscale dimensions. In so doing it kick-started nanoscience and nanotechnology and became an iconic character of the field.

By themselves the published research papers present a rather arid account, yielding little insight into how and why the breakthrough actually occurred. This is almost always the case in science where personal accounts are rarely available. However, in this case many were genuinely interested in the breakthrough and several personal accounts, and general articles were written by some members of the groups primarily involved in the discovery and extraction [5–16] Numerous articles were published by journalists such as that by Taubes [17] in general science magazines as well as two books [18, 19] and a collection of rather intimate interviews by Hargittai [20].

The origins of the name "buckminsterfullerene" and the family name "fullerene" are discussed by Applewhite [21] and Nickon and Silversmith [22]. There was also a film produced by the BBC, some excerpts of which may occasionally be viewed on YouTube [23]. There are numerous indirect accounts often propagating inaccuracies, to be found littering the literature; for instance, several accounts claim, erroneously, that C_{60} was first detected in space! Having perused the plethora of material available, I still feel that many interesting aspects are missing and the recent compendium [1b] attempts to fill some of the interesting gaps and help to create a more satisfying and intimate picture of how the discovery actually came about. The articles and reprints collected in

the compendium [1b] should be considered more as a supplement to previous accounts offering a more detailed perspective on the breakthrough and the way advances in general often arise by the confluence of ideas and factors from widely differing sources.

When a convoluted event occurs, "Rashomon" factors occasionally apply in that some contributions do not appear to fit well together. The film *Rashomon* by director Akira Kurosawa, which is based on two short stories, "In the Grove" and "Rashomon" by Ryűnosuke Akutagawa, deals with this sort of situation. The determination of what actually happened was not Kurosawa's aim in this film as all the accounts are completely incompatible and embellished by each individual's personal ego. However, in a real situation something definite actually happens and the lesson I *personally* draw from *Rashomon* is that *in a real case* individuals tend to present their personal "realities" and these can offer deeper and more complete insights into multifaceted events. Basically Objectivity with a capital O is to be found in the Totality of the Subjectivity with capitals T and S, respectively. An interesting corollary of Kurosawa's thesis is that individuals, not directly involved who seek to present the definitive story, can also not be relied upon to evince disinterested accounts as they present their own personal "biased" views! The conclusion is that there is no such thing as a single "objective" story containing no conflicting elements!

The recent compendium [1b] contains copies of most of the papers detailing advances that I personally (!) feel were crucial steps on the way to the discovery of the fullerenes and their extraction. Because existing accounts in my opinion [5–16] paint an incomplete picture, I asked some key researchers who laid the foundations for the discovery or were involved with key aspects of the story to contribute to an introductory section of the compendium [1b]. Fortunately almost all kindly agreed to pen their recollections and their new accounts provide fascinating new insights into how the breakthrough occurred and highlight the fact that scientific research is an intrinsically human and totally unpredictable activity. With hindsight I think one can recognize at least three major trails leading inexorably to the revelation that, like Orson Welles who lurked in the shadowy backstreets of Vienna in the famous film *The Third Man*, a third well-defined allotropic form of carbon has, since time immemorial, been

Table 14.1 Diagrammatic representation of the various disparate pathways which led up to the discovery of C_{60} in the laboratory and space

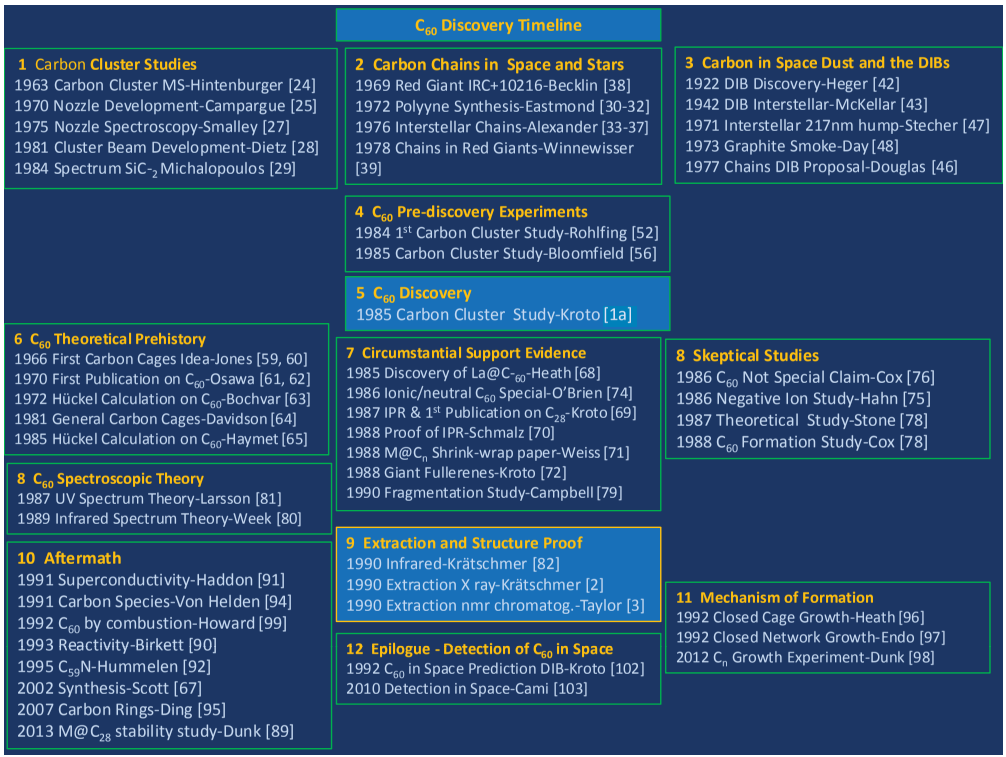

lurking in the dark recesses of the universe. It is hard to credit the fact that the discovery of a molecular allotrope of carbon did not occur until nearly the end of the 20th century when the element involved is the most multitalented and by far the most well-studied in the Periodic Table. The breakthrough involved the amalgamation of a kaleidoscope of disparate research studies and the diagram in Table 14.1 has been devised to provide a semblance of rational order. Discoveries that appear to arrive from "left field" litter the sciences and serve as a ubiquitously unheeded warning to those who think they know how science should be done and what science should be funded.

14.1 Carbon Cluster Studies

The Carbon Cluster Pathway involved the development of techniques to study the mass spectra of molecules and clusters of refractory materials, in particular carbon. Between 1958 and 1963 Hintenberger and colleagues published a series of fascinating papers which contain what I consider to be landmark mass spectrometric observations on pure carbon species which they found in the products of arc-discharged graphite [24]. They observed species with as many 33 carbon atoms! It is interesting to conjecture how different the history of the fullerenes might have been had their study extended to twice as many atoms! Another key event was the development of the supersonic nozzle by Roger Campargue which produced cold ensembles of molecules in the gas phase [25]. A review article outlining his personal perspective is reproduced here [26]. The next step on this trail was the combination of the supersonic nozzle with a tunable laser in a landmark advance by Rick Smalley, Lennard Wharton and Donald Levy which enabled them to produce molecules in the gas phase at sufficiently low internal temperatures which facilitated the analysis of extremely complex electronic spectra, such as that of NO_2 [27]. Lennard Wharton has written an account of his personal recollections [1b], which reveals just how much careful background work was involved in developing this major breakthrough. During the research on this introductory chapter, quite fortuitously, Sydney Leach, a long-time friend and occasional coworker, mentioned his involvement with the start of Roger's nozzle studies

and Sydney has sent a short (already published) anecdote [1b] about the way in which Roger's original gas phase dynamics research programme came into being. This is a further fascinating insight into the seemingly haphazard and totally unpredictable way that important scientific breakthroughs occur.

The next crucial step and certainly the most technically crucial step was the creation of the laser vapourisation supersonic cluster beam instrument by Rick Smalley's group at Rice University in 1981 [28]. This advance enabled the mass spectra of large clusters created from refractory precursor materials to be detected for the first time and in some case the measurement of their spectra, such as SiC_2 [29]. This elegant technique, more than any other, has revolutionised the study of refractory clusters, and Michael Duncan, who was a PhD student on this development, has also contributed a detailed and quite fascinating personal account [1b] which shows how this major breakthrough came about. In particular Michael describes how the machine, affectionately named "Ap2" which uncovered the existence of C_{60}, came to be constructed in the first place. It is my view that the discovery of C_{60} was the raison d'être of this brilliant technical advance.

14.2 Carbon Chains in Space and Stars

The Carbon Chain Pathway started in a totally different field with the development of organic synthetic techniques by David Walton at Sussex who created extended linear carbon chain structures called polyynes with alternating single and triple bonds [30–32] and the study of the molecular dynamics of these chains by molecular spectroscopy (microwave rotational spectroscopy) in a collaboration between David and my spectroscopy group. In fact the key catalyst was a unique Chemistry by Thesis course, initiated by the then dean of the School of Molecular Sciences, Colin Eaborn. In this course chemistry undergraduates at the University of Sussex were able to obtain BSc degrees by carrying out research more or less full-time for two years. The student involved in the study of the first cyanopolyyne HC_5N, Anthony Alexander, did an outstanding job [33]. When the rotational frequencies had been measured they were used in a collaboration

between our Sussex group and Takeshi Oka, Lorne Avery, Norm Broten and John Macleod at the National Research Council (NRC) in Canada, and this resulted in the discovery by radioastronomy of the unexpectedly high abundance of HC_5N in the interstellar medium [34]. Then Colin Kirby, at the time a grad student, achieved the difficult synthesis of HC_7N devised by David and measured its spectrum [35] which enabled us to detect it in space [36]. Then using the frequencies Takeshi imaginatively predicted the frequency of HC_9N and we detected it as well [37]. It was this series of Sussex/NRC laboratory and radioastronomy studies which uncovered the, at the time amazing, abundance of the long carbon chain molecules in space. The next step in the story was the detection by Eric Becklin, Gerry Neugebauer and their coworkers of an amazing object emitting infrared radiation an order of magnitude greater than any previously observed IR source and the identification of the object as the cool red giant carbon star IRC+10216 [38].

Eric has also provided a personal account in the compendium [1b] which nicely captures the euphoria that often accompanies a moment when an important discovery is made, in this case of an exceptional new source of infrared radiation. A subsequent radioastronomy study focused on this star resulted in the exciting (certainly to me) observation by Gisbert Winnewisser and Malcolm Walmsley [39] that our long carbon chain cyanopolyynes molecules were being ejected from IRC+10216 into the interstellar medium. These results catalysed preliminary conjectures about the importance of carbon in the interstellar medium and stars [40, 41] which were later to stimulate the experiments which resulted in the discovery of C_{60}.

14.3 Carbon in Space Dust and the Diffuse Interstellar Bands (DIBs)

A third primary pathway involves a couple of “Interstellar Mysteries” which are arguably two of the most intriguing in the whole of the sciences. One involves a discovery, made originally in 1922 by Heger, of some curious absorption features in the spectra of stars [42] which came to be known as the diffuse interstellar

bands (DIBs). The interstellar nature of these features was unequivocally confirmed during the 1930s and their properties summarised by McKellar in 1940 [43]. The DIB field has been extensively and carefully reviewed by Herbig [44, 45]. The tantalising puzzle of the nature of the carrier is still today, almost a century later, unsolved, although scores of spectroscopists and astrophysicists have ruminated long and hard over the identity, observationally, experimentally and theoretically. The observing sessions which revealed the abundance of the carbon chains in space were carried out at the National Research Council Telescope in Algonquin Park Canada, and I went there a few times to participate in our observations. During one of these visits Alec Douglas discussed his thoughts with me on the carriers of the DIBs and in particular he suggested the possibility that extended carbon chain species related to those we had discovered might be involved [46]. A second important interstellar feature is also involved in the story. This is a strong absorption band at 217 nm which Stecher conjectured might be due to carbonaceous dust particles [47].

Subsequently Day and Donald Huffman carried out a very important laboratory study on the UV spectrum of carbon smoke and showed that this conjecture was quite convincing [48].

14.4 C_{60} Pre-discovery Experiments

The specific aim of the discovery experiment was actually very simple: To simulate the supposed chemistry in the atmosphere of a star such as IRC+10216 and show that the polyynes HC_nN (n = 5, 7, 9), which we had detected in the ISM, could be created when carbon atoms nucleate in an atmosphere containing nitrogen and hydrogen (e.g. NH_3) and so support my hypothesis that the chains originated in stars [40, 41]. At the time, *in situ* ion molecule reactions [49, 50] and/or grain surface catalysis [51] were the two strongest candidates able to account for most other interstellar molecules. In my mind neither theory could account for the chains we had observed as there appeared to be too many “heavy” carbon atoms to be created by the very slow processes in the very tenuous interstellar gas and they also were surely just too heavy to be

sufficiently easily vapourised from a solid surface. Bob Curl had invited me to visit Rice after a conference organised by Jim Boggs at Austin, and during this visit in Easter 1984 Bob showed me a manuscript detailing a resonant 2-photon ionisation (R2PI) spectrum obtained by Rick Smalley's group which indicated that SiC_2 had, unexpectedly, a triangular structure [29]. This was extremely interesting to me as my group had focused over the previous decade on the creation of whole families of new molecules involving multiple bonds to second and third row elements (i.e. containing >C = S, >C = Se, —B = S, >C = P — and — C ≡ P moieties) [41] and I had been ruminating for quite a while over how we might tackle the problem of creating molecules containing the >C = Si< moiety, which I knew would be quite difficult. Bob encouraged me to go over to see Rick in his laboratory and while Rick was describing Ap2, which was his pride and joy at the time, the basic experiment described above formed in my mind. Furthermore, the possibility of a second experiment also formed: This was to measure the R2PI spectra of various carbon chain species and confirm or otherwise the contention of Alec Douglas's that carbon chains might be the carriers of the DIBs [46]. That evening in the Curl household, I discussed these ideas with Bob, and over the following 17 months the technical issues, mainly pertaining to the difficulties involved in carrying out the more complex R2PI/DIB experiment, were the subject of letters sent to and fro between us (these were pre-email days!).

Two or three months after my Easter 1984 visit to Rice, I was sitting in the Sussex University Chemistry Laboratory coffee room when my colleague Tony Stace handed me a copy of a fascinating paper [52] by a group at Exxon which to my amazement, and "slight" irritation, presented details of essentially the basic experiment I had proposed three months previously to the Rice group. This paper contained the most fascinating new observation that the overall carbon mass spectrum pattern was actually bimodal and that in addition to the set detected by Hintenberger's group [24], which seemed to peter out around C_{30} or so, a second set of only even numbered species began to appear above ca. C_{30} rising to a maximum in the C_{50} to C_{70} region and tailing off around C_{100}. The Exxon group suggested these new features were due to "carbyne" [53], a mythical creature whose existence has been the

subject of controversy for getting on for half a century [54]. In 1982 Smith and Buseck had shown essentially conclusively that the "carbyne" proposal had been based on an experimental artifact [55]. One thing about which I was pretty certain was that this hypothetical material made no more sense from a chemical point of view than the Loch Ness Monster makes from an evidence-based logical viewpoint. Polyynes explode with great violence if any attempt is made to isolate and condense them, and in our Sussex microwave spectroscopy work we took great precautions to ensure they remained in the vapour phase at low pressures. After the discovery experiment in September 1985 [1a] we realised that the mass spectrometric peak of C_{60} in this Exxon paper was actually somewhat stronger than other adjacent peaks but the significance of this strength had gone unrecognised. A second paper by Bloomfield *et al.*, also carried out prior to our experiment, had probed the photodissociation characteristics of C_{60} [56]. As far as I can tell, neither of these two groups varied the clustering conditions with a view to probing the creation process itself. Had this been done I suspect that both groups would have realized that the C_{60} signal could be made dominant and this would have alerted them to the fact that something exceptional was involved and worthy of further careful examination. Thus we realised that C_{60} had been in the literature for some 18 months prior to our discovery in September 1985. Although scores of researchers must have seen the peak (I also)—it was even labelled C_{60}—no one appears to have considered it seriously! When I first saw the Exxon paper my first reaction was that the new family of only even-numbered carbon species might be planar graphene flakes of various shapes and sizes. That even-numbered graphene flakes might be more stable than odd-numbered ones did not seem that implausible at the time.

14.5 The Discovery of C_{60}

In September 1985, about 17 months after my first visit, Curl and Smalley finally agreed that we should carry out the basic experiment which I had proposed. The carrot for the Rice group was that the basic experiment, to simply simulate a stellar carbon atmosphere,

was, to all intents and purposes, a necessary preliminary to the much more complicated and seemingly "more important (!)" DIB study. The actual discovery experiments were carried out by the students Jim Heath, Sean O'Brien, Yuan Liu and me in the space of less than two weeks. A fourth student, Qing-Ling Zhang, who had only just started was also involved in some of these experiments. The students threw themselves wholeheartedly into the project, especially Jim Heath. We also had an improved weapon at our disposal, in the shape of a refined nozzle assembly, which Sean had designed. At the start of the experiments we had a rather irritating problem in that we were unable to print out our data, but fortunately Yuan worked hard to resolve this problem and within a couple of days, on 4 September 1985, we had a paper copy showing a dominant mass spectrometric peak at 720 amu which indicated that a species with 60 carbon atoms was very special indeed (Fig. 14.1).

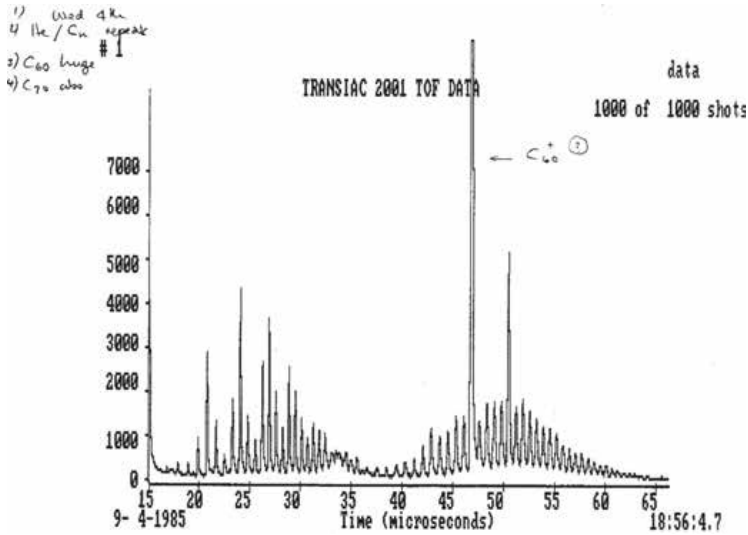

Figure 14.1 Birthday "card" printout on 4 September 1985, the day on which C_{60} was recognised as very special. On that day Yuan also noted that C_{60} and C_{70} are very strong in the Ap2 lab book. Reproduced with permission from Ref. 8. Copyright Wiley-VCH Verlag GmbH & Co. KGaA.

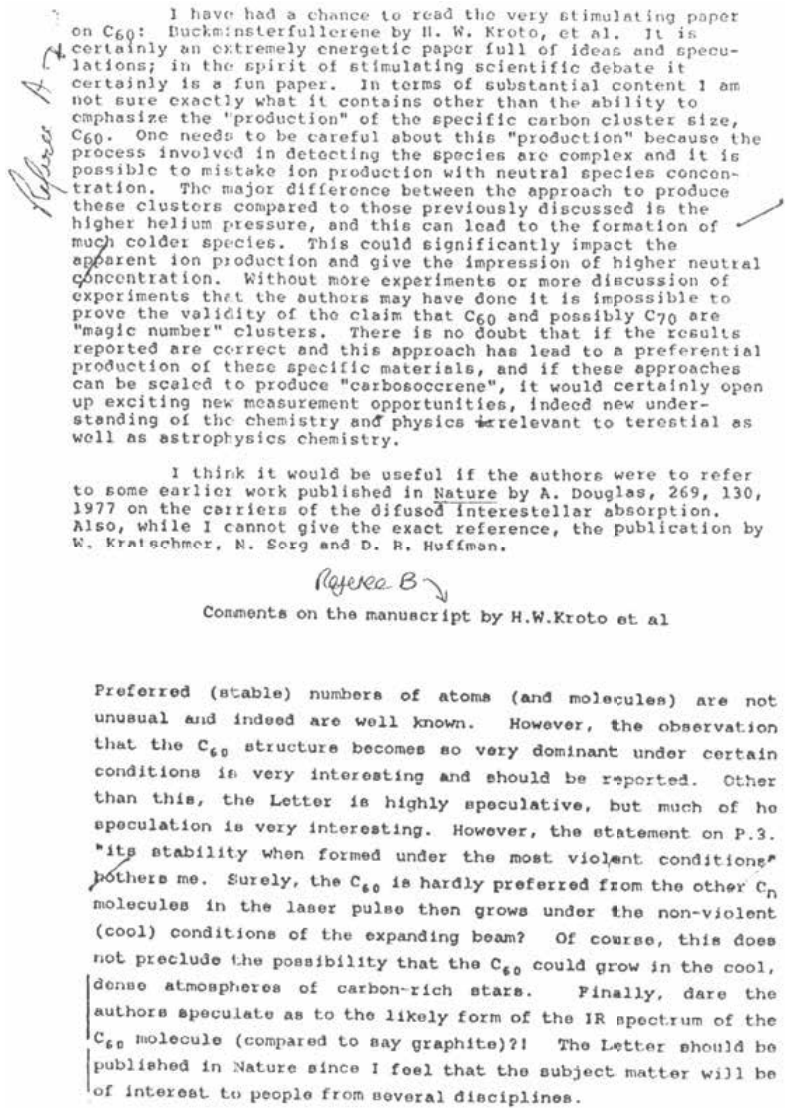

Referee A

I have had a chance to read the very stimulating paper on C_{60}: Buckminsterfullerene by H. W. Kroto, et al. It is certainly an extremely energetic paper full of ideas and speculations; in the spirit of stimulating scientific debate it certainly is a fun paper. In terms of substantial content I am not sure exactly what it contains other than the ability to emphasize the "production" of the specific carbon cluster size, C_{60}. One needs to be careful about this "production" because the process involved in detecting the species are complex and it is possible to mistake ion production with neutral species concentration. The major difference between the approach to produce these clusters compared to those previously discussed is the higher helium pressure, and this can lead to the formation of much colder species. This could significantly impact the apparent ion production and give the impression of higher neutral concentration. Without more experiments or more discussion of experiments that the authors may have done it is impossible to prove the validity of the claim that C_{60} and possibly C_{70} are "magic number" clusters. There is no doubt that if the results reported are correct and this approach has lead to a preferential production of these specific materials, and if these approaches can be scaled to produce "carbosoccrene", it would certainly open up exciting new measurement opportunities, indeed new understanding of the chemistry and physics ~~is~~ relevant to terestial as well as astrophysics chemistry.

I think it would be useful if the authors were to refer to some earlier work published in Nature by A. Douglas, 269, 130, 1977 on the carriers of the difused interestellar absorption. Also, while I cannot give the exact reference, the publication by W. Kratschmer, N. Sorg and D. R. Huffman.

Referee B

Comments on the manuscript by H.W.Kroto et al

Preferred (stable) numbers of atoms (and molecules) are not unusual and indeed are well known. However, the observation that the C_{60} structure becomes so very dominant under certain conditions is very interesting and should be reported. Other than this, the Letter is highly speculative, but much of he speculation is very interesting. However, the statement on P.3. "its stability when formed under the most violent conditions" bothers me. Surely, the C_{60} is hardly preferred from the other C_n molecules in the laser pulse then grows under the non-violent (cool) conditions of the expanding beam? Of course, this does not preclude the possibility that the C_{60} could grow in the cool, dense atmospheres of carbon-rich stars. Finally, dare the authors speculate as to the likely form of the IR spectrum of the C_{60} molecule (compared to say graphite)?! The Letter should be published in Nature since I feel that the subject matter will be of interest to people from several disciplines.

Figure 14.2 Comments of the referees on the paper accepted by *Nature* on 18 October 1985.

Although several personal perspectives on the discovery experiments are to be found in the accounts written by Bob Curl [5, 7, 9], Rick Smalley [5, 7, 11] and me [6, 8, 10] the personal

account that Sean has written for the recent book [1b] presents a valuable new perspective. It gives an intimate insight into the hectic discovery period in a way that only a young student (as Sean was at the time) can see it. Among other things, Sean describes how some key technical refinements that he made to the nozzle of Ap2 facilitated variation of the clustering conditions and enabled us to find a way of making the C_{60} peak a dominant character among a veritable myriad of lesser ones. On 13 September, some nine days after the Buckyball's birthday on 4 September 1985 (Fig. 14.2), the paper was received by *Nature*! The paper was accepted on 18 October, and it is interesting to peruse the comments of the referees (Fig. 14.2).

The experiments which were the original aim, to use the cluster beam apparatus to simulate circumstellar shell chemistry, were actually carried out [57, 58] and confirmed beautifully the conjecture that long cyanopolyyne chains may be readily created in the hot, chaotic, carbonaceous gas of red giant stars. Understandably, however, these studies were somewhat sidelined due to the antics of the newly discovered all-carbon prima donna.

14.6 C_{60} Theoretical Prehistory

After news of our observations became known we quickly discovered that there had also been another fascinating road, travelled in a parallel abstract universe by a small, disparate band of imaginative theoreticians, all seemingly unaware of each others' efforts. I went to a spectroscopy conference in Riccione, Italy, scarcely a week after the discovery and excitedly announced, in a very short special three-minute presentation, that we had observed a strong signal for a species with 60 carbon atoms and had proposed the truncated icosahedral closed cage structure for the species. A former student of mine, Julie August, who was present at the conference returned to Nottingham University with the news and her then supervisor, Martyn Polliakoff, wrote to tell me that his friend David Jones had, in a highly imaginative 1966 New Scientist article under the pseudonym Daedalus [59, 60], already described how an extended graphene sheet consisting of hexagonal network would close if 12 pentagonal disclinations can somehow be introduced among the hexagons intrinsic to

graphite. For me there was a crucial revelation in David's article; this was the fact, which is a consequence of Euler's law, that the insertion of 12 pentagons among any number of hexagons is necessary and sufficient to close a network. I immediately realised that a minimum of 60 carbon atoms was needed to close a cage if abutting pentagons are to be avoided. This requirement together with the fact that pentalene C_8H_6 (which consists of two fused pentagons) is unstable, indeed antiaromatic as generally discussed in undergraduate Quantum Chemistry courses, was the first piece of circumstantial evidence supporting our structural proposal. It was for me the sort of convincing evidence I needed to convince myself that our structure proposal must be correct, and I would not have to commit suicide! David has also kindly penned a few notes describing how he came upon this highly original conjecture [1b]. Within a few more days we discovered that David's paper was not the only one discussing pure carbon cages. My friend and colleague Nenad Trnajstic at the Institut Rudjer Boskovic in Zagreb informed me that there were some more papers: Eiji Osawa had in 1970 published the idea of C_{60} itself [61] in Japanese. The following year the idea was further elaborated on in his book *Aromaticity*, written with Zenichi Yoshida [62]. This appears to be the very first publication ever on C_{60}. Eiji has kindly also contributed a personal account detailing how he came to his highly imaginative conclusion that C_{60} might be stable and possibly aromatic [1b] and has translated the section of his book [62] dealing with C_{60} [1b]. Nenad also informed me that in 1972, two years after Eiji's publication, Bochvar and Gal'pern had published the Hückel calculation for C_{60} [63]. Then we discovered that Davidson in 1980 [64] had also published a Hückel analysis. Just after news of our discovery became known, Fritz Shaeffer at Berkeley informed us that Tony Haymet had just a few months previously, given a presentation on C_{60}. Haymet published his study a few months later [65]. As well as this set of highly imaginative quantum chemists who had been ruminating over the C_{60} molecule, there was at least one experimental synthetic research project, that by Orville Chapman at UCLA, which had focused on devising a traditional synthetic strategy to create C_{60} [66]. This daunting task was finally successfully accomplished by Larry Scott *et al.* in 2002 [67]. Larry has also written a fascinating account of his journey which gives a valuable insight

into the way this beautiful molecule can stimulate new science [1b]. Sean [1b] describes how the Rice group was apprised of some previous work and argues, with some reason, that we should have been more careful before submitting the manuscript for publication and made some effort to check whether there was any previous literature on C_{60}! Of course, that is far easier today with the Internet than it was in 1985.

Thus in retrospect, in chronological order, the key advances and/or observations which underpinned the basic discovery experiment were (a) the detection of the mass spectra of large carbon species with up to 33 atoms in the product of a carbon arc discharge by Hintenberger and coworkers, (b) the synthesis and microwave study of cyanopolyynes at Sussex and their subsequent detection in the interstellar medium by the Sussex/NRC Canada radioastronomy collaboration, (c) the development of the laser vaporisation supersonic cluster beam mass spectrometric technique by Smalley's Rice University group which revolutionised the study of refractory clusters, and (d) the discovery of the carbon star IRC+10216 by Becklin, Neugebauer and colleagues and the subsequent discovery that our cyanopolyynes were being ejected from IRC+10216 into the interstellar medium by Winnewisser and Walmsley.

14.7 The Circumstantial Supporting Evidence

After the discovery, numerous projects were devised to prove, either by extraction or otherwise, our contention that C_{60} was indeed the buckminsterfullerene structure we had proposed. Joint Rice/Sussex studies were carried out as well as studies by the Rice and Sussex groups independently, and in time an overwhelming body of circumstantial evidence was assembled. Jim Heath was particularly heavily involved in the follow-up work at Rice as well as the first experiments. Some of the key observations, made during the period after discovery and prior to the Krätschmer *et al.* paper [2] in 1990, which gave the strongest supporting evidence for the buckminsterfullerene structure were:

(i) The creation of the lanthanum complex La@C_{60} from which it was shown that it was impossible to dislodge the

La atom, so providing good evidence that the La atom was not on the outside but possibly trapped inside the putative cage [68]. In addition, in this paper a rather neat structure for C_{70} was proposed in which a ring of 10 carbon atoms was inserted between two C_{30} half-domes, fitting in nicely with the fact that C_{70} was clearly the second favoured entity experimentally.

(ii) The Isolated Pentagon Rule (IPR) to rationalise the strengths of C_{60} and C_{70} as well as the Isolated Multiplet Pentagon Rule (IMPR) to rationalise the prominence of other features such as C_{28} and C_{50} were proposed [69]. These rules had been derived on the basis of simple molecular-model construction together with knowledge of aromatic and anti-aromatic reactivity. Tom Schmalz, William Seitz, Doug Klein and Gerald Hite in their very nice simultaneous much more detailed theoretical study [70] proved the IPR and IMPR conjectures theoretically. In fact this advance was, at least for me, absolutely conclusive, as it indicated that *if C_{60} were actually a cage, then C_{70} had to be the second favoured species because no IPR structure existed between C_{60} and C_{70}*. I remembered thinking that although another solution might exist for a 60-atom species, there was no way that another solution would cough up both C_{60} and C_{70}.

(iii) An important result of the generalised IMPR rule [69, 70] was the proposal that a C_{28} species should be a tetravalent "superatom" with a tetrahedral structure (Fig. 14.3a) which has special stability [69]. This result was corroborated by mass spectroscopic data such as that shown in Fig. 14.3b, where C_{28} can be shown under certain clustering conditions to be special.

(iv) The so-called "Shrink-Rap" experiment [71] showed that on laser photodissociation $M@C_{60}$ lost C_2 fragments sequentially until the $M@C_n$ species of a given minimum n fragmented completely into small carbon species when the cage became too small to encase the enclosed metal atom completely. The size of the endohedral complex prior to complete fragmentation increased commensurate with the known size of the encapsulated atom.

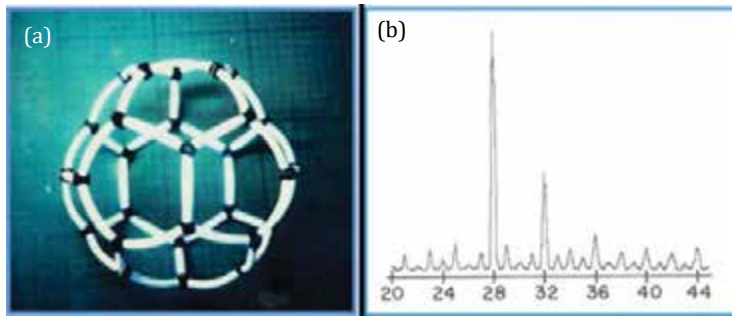

Figure 14.3 (a) Polaroid image of the first molecular model of C_{28} photographed where it was constructed, on our coffee table [69] at home in Sussex. (b) Carbon cluster mass spectrum under certain conditions in the C_{20}–C_{44} range (Rice/Sussex unpublished data, 1985).

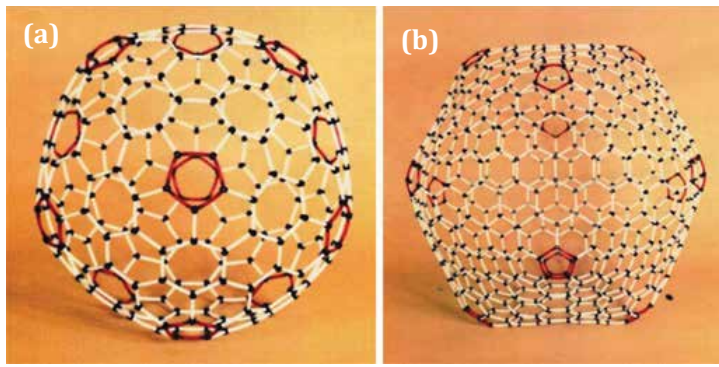

Figure 14.4 (a, b) Photographs of the beautiful molecular models C_{240} and C_{540}, in the first study of giant fullerenes; constructions by Ken McKay at Sussex [72]. Note how the curvature is focused in the regions of the pentagonal (red) disclinations and the overall shape becomes more closely icosahedral as the number of atoms in the cage increases.

(v) In the first study of giant fullerenes it was deduced on the basis of simple model building that they exhibited quasi-icosahedral shapes (Fig. 14.4a, b) and this result explained the structures of previously puzzling electron microscope images of certain macroscopic carbon particles as consisting of concentric fullerene cages in onion-like or Russian Doll configurations [72, 73].

(vi) In an important paper [74] it was shown that the C_{60} species we had detected was special whether positively or negatively charged or indeed neutral, contrary to one claim [75].

During this period, I developed my "**4/5 Rule of Scientific Reliability**":

If one has a hypothesis one should carry out at least five different studies to ascertain whether the hypothesis is correct or not: If 4 out of 5 studies fit the hypothesis, it is almost certainly correct (with the emphasis on the word almost); if on the other hand only 1 out of 5 fits, the hypothesis is almost certainly wrong (again with the accent on the word almost!). As a corollary, if only 1 out of 5 did not fit, it will usually be found that that study had been subject to some error and subsequently found to fit under more careful scrutiny.

14.8 Skeptical Studies

It is probably hard for young chemistry students today, for whom the buckminsterfullerene has ever been an elegant iconic star, embedded in the rich tapestry of the Chemical Universe rather like Halley's comet in the famous Bayeux Tapestry or the painting by Giotto, to realise that for some the buckminsterfullerene structure was, at the time it was proposed, somewhat bewildering and highly unconvincing. The fact that it happened at roughly the same time as the "Cold Fusion" saga did not help either. Indeed the proposal appeared to be so revolutionary that several papers were published which were strongly critical not only of our structural conjecture but also our experimental observations. A footnote in the first skeptical paper titled "$C_{60}La$: a Deflated Soccerball?" [76] indicated that a detailed study, which was to be published later, would show that the strength of the C_{60} signal which we had detected was not an indication of special character but rather an artefact which depended on a complex "interplay" of various experimental parameters involved in our measurement. These claims were totally at variance with the observations which we had by then made and when the paper, mentioned in the footnote, was subsequently published [77], it did not support the negative claims made. A claim, made in another skeptical paper, that the negative carbon ion distribution did not support the special nature of C_{60} [75] was refuted unequivocally by a careful exhaustive

study which we carried out in response [74]. Paradoxically, a mechanistic transformation published in skeptical theoretical paper [78] which poured even more doubt on our buckminsterfullerene structural proposal is now used frequently to explain mechanistic aspects of fullerene dynamics! A few more skeptical papers were published but by and large, as time passed, the onslaught was repulsed and gradually the increasing weight of supportive studies by us, together with those of numerous other groups such as the fragmentation study by Eleanor Campbell, Ingolf Hertel and coworkers [79], indicated overwhelmingly that C_{60} was indeed a stable entity and that the structure was almost certainly a truncated icosahedron. The set of skeptical papers represents yet another typical example of the fact that some breakthroughs, which appear to conflict with received wisdom, can encounter significant negative criticism before becoming accepted. They also serve as an object lesson on how extremely careful one should be when criticising the work of others!

14.9 Spectroscopic Theory

Many researchers, in particular theoreticians, embraced the new proposal enthusiastically and were stimulated to examine some important likely properties of C_{60}. Of the many early studies discussed in the review paper [4], two papers which appear to have been influential in the extraction breakthrough by the Heidelberg/Arizona team serve to summarise two key theoretical results:

(a) Theoretical studies such as that by Weeks and Harter [80] indicated that only 4 vibrational modes should be infrared active and provided approximate and fairly accurate associated infrared frequencies.

(b) Some studies such as that of Larsson *et al.* [81] predicted roughly that the UV spectrum of C_{60} should lie fairly close to the 217 nm feature described above.

14.10 Extraction and Structure Proof

As indicated above, theoreticians found the fullerene conjecture fascinating and produced the key predictions (a) and (b) in the

above paragraph on the vibrational and electronic spectra which proved to be important in the work of Wolfgang Krätschmer, Lowell Lamb, Kostas Fostiropoulos and Donald Huffman, who announced in 1990 that they had extracted macroscopic amounts of C_{60} [2]. I do not think there is any more elegant story in the whole of chemistry in the latter half of the 20th century than the detective story which led on from the early Day/Huffman 1977 study of carbon dust [48] via the proposed infrared spectrum of C_{60} to success in extraction. I also think that this must be the most historically important example of the use of infrared finger-printing in an important chemical advance. This experiment vanquished all criticism by producing as evidence images of crystals extracted from the deposit of arc-discharged carbon which X-ray analysis indicated consisted of arrays spheroidal carbon molecules almost exactly as expected, 1 nm apart, centre to centre.

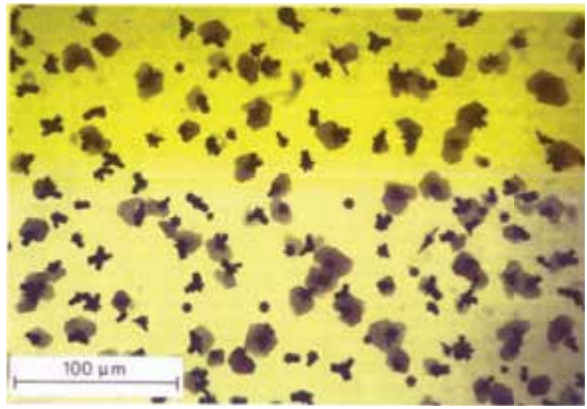

Figure 14.5 The amazing (at the time) photograph of crystalline carbon produced by Krätschmer and coworkers [2]. Photograph courtesy of Wolfgang Krätschmer. One of the most important images in the whole of science.

Simultaneously, in an independent study the 720 amu mass spectrum of C_{60} was measured at the University of Sussex by Ala'a Abdul Sada from a deposit of arc-discharged carbon. A red solution was extracted a few weeks later by Jonathan Hare and five days prior to the submission of the Krätschmer *et al.* paper [2] for publication! The one-line NMR spectrum was also measured by Tony Avent, thus proving conclusively, once and for all, that

all the carbon atoms were identical and the truncated icosahedral structure was the only possible solution [3].

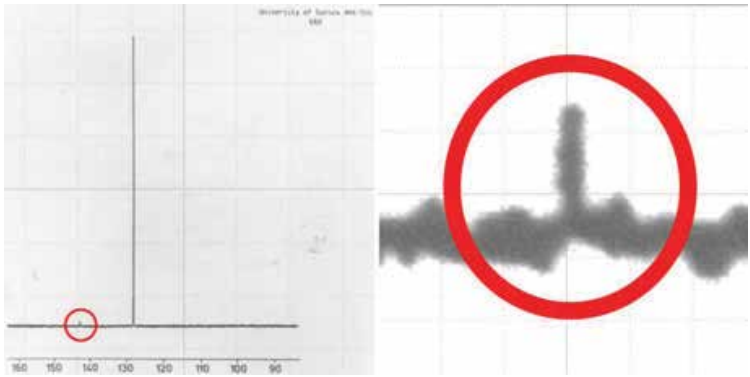

Figure 14.6 The first detection of the NMR line of C_{60} is the tiny blip at ca δ = 143. Reproduced from Ref. [3] with permission from The Royal Society of Chemistry. Small is, as they say, beautiful!

The chromatographic method of separating various members of the fullerene family was developed at Sussex by my late colleague Roger Taylor with advice from another our colleagues, Jim Hanson. The final absolute and unequivocally definitive proof was provided by the detection of a five-line NMR spectrum of the chromatographically isolated sample of C_{70} [3].

In the case of the Sussex group an earlier electron microscope study of arc-discharged carbon had indicated that the morphology of the resulting carbon deposit changed dramatically from an even, flat, very thin layer deposit to a floccular one as the pressure of argon gas under which it was formed increased. Further work on this project, which had suggested perhaps that roundish carbon structures like C_{60} might be involved, was thwarted by the lack of financial support. It was resurrected when Michael Jura, an astrophysicist friend and colleague at UCLA, sent me some very interesting preliminary results that Krätschmer *et al.* had reported at an astrophysical conference in Capri [82]. As recounted above, a red solution of a C_{60}/C_{70} extract was produced from arc-discharged graphite rods five days before the Krätschmer *et al.* manuscript arrived at Sussex from *Nature* for review detailing their brilliant results [2]. Lowell Lamb and Jonathan Hare were

research students in the Krätschmer *et al.* group and our Sussex group respectively and their personal accounts published in the recent compendium [1b] give a delightfully intimate insight into the excitement that they experienced as young researchers during those heady days.

Figure 14.7 The first pure samples of C_{60} and C_{70} in benzene solution separated by chromatography at the University of Sussex. Reproduced from Ref. [3] with permission from The Royal Society of Chemistry. In benzene solution C_{60} is magenta and C_{70} on the right red.

In retrospect we can see that the original work on carbon smoke by Day and Huffman [48] and the later detection of the UV and infrared spectra [2, 10, 82] together with the post-discovery theoretical work on the electronic and vibrational spectra of C_{60} [80, 81] were crucial factors in the brilliant detective story surrounding the extraction of C_{60} by the Heidelberg/Arizona group.

14.11 Aftermath Studies

At least one organic chemist, Orville Chapman at UCLA, had initiated a serious effort to create C_{60} by a traditional synthetic route [66] This non-trivial feat was finally accomplished by Larry Scott and his group [67]. First Larry developed an elegant alternative route to the bowl-shaped molecule corannulene $C_{20}H_{12}$, which is a pentagonal ring surrounded by five hexagonal rings

[83]. Larry's new strategy was simpler than that in the seminal early work of Barth and Lawton [84]. In doing so Larry has started to map out the strategy for the engineering of extended carbon nanostructure which I think will be necessary if carbon-based nanotechnology is to fulfil the fantastic promise that electrical and tensile strength studies imply are possible. Such advances are only going to be achieved if absolutely perfect carbon nanostructures can be realised on a consistent bulk scale—for instance, bundles of perfect hexagonally packed single-walled nanotubes all of the same diameter and preferably same chirality. Larry has also kindly agreed to pen an article which highlights the thinking and strategy development behind this beautiful advance [1b].

The result of all the above studies has been an explosion of research into the chemistry and physics of the fullerenes which now runs at approximately a thousand papers per year. Further study of the material produced by the Krätschmer/Huffman technique resulted in the discovery by Sumio Iijima [85] that nanotubes could also be produced and the realisation that they had in fact been observed some years before by Morinobu Endo and co-workers [86]. In fact the discovery of C_{60} re-awakened intense interest in fundamental aspects of carbon chemistry and carbon materials science. In particular it ignited the field of carbon nanoscience and nanotechnology and may even have created the new tsunami of interest in carbon science which led to the most recent explosion of research into grapheme [87].

A paper in 1993 on U@C_{28} [88] presented interesting support for the prediction I made five years earlier in 1987 [69], that the small fullerene C_{28} (Fig. 14.3) should be (a) special, (b) tetrahedral and (c) tetravalent. Recent highly detailed experiments utilising the remarkable resolution of the FT-ICR-MS developed by Alan Marshall at FSU have shown that the species M@C_{28} (M = Ti, Zr and U) are indeed very special [89], providing unequivocal empirical evidence for the predicted special nature of C_{28}. Paul Birkett at Sussex, working with my colleagues Roger Taylor and David Walton, discovered that C_{60} could add six Cl atoms in a fascinating symmetric pattern [90]. This result can be considered to be basically a fullerene addition reactivity pattern analogous to the ortho-, meta- and para-directivity observed in the reactivity of benzene upon substitution. Robert Haddon, then at

Bell labs, and colleagues discovered that K intercalated in crystalline C_{60} was superconducting at the relatively high temperature of 18 K[91] and this led to a flurry of interest in organic superconductivity. Work at UCLA by Fred Wudl's group led to the discovery of the fact that nitrogen could replace a carbon atom to form a $C_{59}N$ analogue which forms the stable dimer $(C_{59}N)_2$ [92]. At FSU we have used the FT-ICR-MS to study the way that B can displace a C atom in C_{60} to form the species $C_{59}B$[93] which has so far not been isolated. Perhaps one of the most interesting results was obtained by Mike Bowers and his coworkers, who showed, using an ion drift tube technique, that in the range C_n (n = 1–60) there are at least five different families of pure carbon species [94] in carbon vapour! One family is the linear chains and another set monocyclic rings which have been reliably identified by John Maier's group in Basel [95]. We of course identified the third the closed-cage fullerenes but two other families in the drift tube study still have to be identified with a significant degree of certainty.

14.12 Mechanism

As far as post-1990 fullerene research is concerned, it is hard to pick out all the key breakthroughs among some 20,000 or more papers but from a personal perspective there are a few. There have been numerous papers ruminating over various possible mechanisms for the formation of fullerenes and their elongated analogues the nanotubes, and the situation is certainly complicated. Two papers which suggested that closed-cage growth might be involved in the case of C_{60} and the nanotubes were published in 1992 by Jim Heath [96] and by Morinobu Endo and me [97], respectively. A closed-cage mechanism has now been unequivocally confirmed experimentally [98] as operating under the same conditions as those under which C_{60} was discovered in the original experiment [1a]. The experiments were carried out at the National High Field Magnet Laboratory (NHFML) at Florida State University (FSU) using the exquisite state-of-the-art resolution afforded by the Fourier transform ion cyclotron resonance mass spectrometer (FT-ICR-MS) developed by Alan Marshall.

These experiments showed that carbon cages can indeed "ingest" small carbon species such as C, C_2, etc., to form larger and larger fullerenes [98]. Paul Dunk has written his personal account of cluster experiments [89, 98] showing again how important youthful exuberance and imagination are to the propagation of fundamental research [1b]. A study published in 1992 by Jack Howard's group indicated that C_{60} can be readily extracted from hydrocarbon flames [99].

It might be noted that in 1986, some six years earlier, we published a paper [100] in which it was suggested that C_{60} might be involved in some way in combustion processes during the soot formation phase. This conjecture was severely criticised at the time by Frenklach and Ebert [101]. In this context it may be worthy of some careful thought that (a) hydrocarbon flames have been studied assiduously since at least the time of Michael Faraday, and as far as we know, no single combustion scientist either discovered fullerenes in their flames or predicted their presence theoretically prior to our discovery [1a], and (b) the Mitsubishi Chemical Company extracts C_{60} in kilogram quantities from the soot produced by the combustion of (I understand) methane! One obvious conclusion one might draw from these observations is that, even after all the decades of research into soot formation, the hydrocarbon combustion process which creates the soot from which fullerenes are extracted in commercial quantities is not understood at all and needs to be explained!

14.13 Epilogue: Detection of C_{60} in Space

Finally, as described above, the quest for an understanding of the existence of our long carbon chain molecules in space was the catalyst of the experiment using Rick Smalley's cluster beam apparatus which revealed that C_{60} self-assembled spontaneously under conditions which simulated the conditions in red giant carbon stars such as IRC+10216. This led, at least in my mind, to the conviction that C_{60} must be lurking in space [23, 40, 41]. Furthermore, the probability that the molecule existed in space and the possibility that it might be involved in some way with the diffuse interstellar bands were proposed in a paper with Michael

Jura [102]. In this paper we suggested that some C_{60} molecules in space were highly likely to have attached atoms and if these atoms were relatively abundant such as Na, Mg, Ca, etc., this should give rise to relatively strong charge-transfer bands which might account for some of the DIBs. In 2010 the conjecture that C_{60} must be in space was beautifully, indeed amazingly, confirmed by Jan Cami, Jeronimo Bernard-Salas, Els Peeters and Sarah Elizabeth Malek [103], who were able to assign all the detected features in a Spitzer Telescope IR spectrum of a young planetary nebula to C_{60} and C_{70}. Thus the story has turned full circle twice: from the synthesis in the laboratory of carbon molecules ca. 1 nm in length to the detection of these molecules in various regions of the interstellar medium and then back to a terrestrial laboratory to uncover the existence of a 1 nm diameter soccerball-shaped all-carbon object and now back into space yet again. It has been a tremendously exciting roller coaster research ride for almost everyone involved, and what is more, the ride is not yet over and if anyone thinks it might be, a casual skim through the pages of *An Atlas of Fullerenes*, by Patrick Fowler and David Manalopoulos [104], might just change their mind!

Disclosures and Conflict of Interest

The author declares that he has no conflict of interest. No writing assistance was utilized by the author in the production of this chapter. This chapter is reprinted from the 2015 book *C_{60} Buckminsterfullerene: Some Inside Stories,* edited by Harry Kroto, Pan Stanford Publishing, Singapore, and appears here with kind permission of the publisher.

Corresponding Author

Dr. Harold W. Kroto
Department of Chemistry & Biochemistry
Florida State University
95 Chieftan Way
Tallahassee, FL 32306-4390, USA
Email: kroto@chem.fsu.edu

About the Author

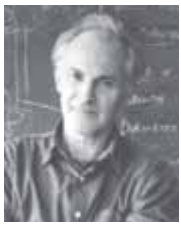

Sir Harold (Harry) Walter Kroto is the British chemist who shared the 1996 Nobel Prize in Chemistry with Robert Curl and Richard Smalley. Dr. Kroto is the Francis Eppes Professor of Chemistry at the Florida State University, USA, which he joined in 2004. Prior to that, he spent a large part of his career at the University of Sussex, UK, where he now holds an emeritus professorship. He is a fellow of the Royal Society. Dr. Kroto was educated at Sheffield University, UK, where he obtained a first class honors BSc degree in chemistry (1961) and a PhD in molecular spectroscopy (1964).

References

1. (a) Kroto, H. W., Heath, J. R., O'Brien, S. C., Curl, R. F., Smalley, R. E. (1985). *Nature*, **318**, 162–163.

   (b) Kroto, H. W., ed. (2015). *C_{60} Buckminsterfullerene: Some Inside Stories*, Pan Stanford Publishing, Singapore.
2. Krätschmer, W., Lamb, L., Fostiropoulos, K., Huffman, D. R. (1990). *Nature*, **347**, 354–358.
3. Taylor, R., Hare, J. P., Abdul–Sada, A. K., Kroto, H. W. (1990). *J. Chem. Soc. Chem. Commun.*, 1423–1425.
4. Kroto, H. W., Allaf, A. W., Balm, S. P. (1991). *Chem. Rev.*, **91**, 1213–1235.
5. Curl, R. F., Smalley, R. E. (1988). *Science*, **242**, 1017–1022.
6. Kroto, H. W. (1988). *Science*, **242**, 1139–1145.
7. Curl, R. F., Smalley, R. E. (Oct 1991). *Sci. Am.*, **32**.
8. Kroto, H. W. *Angew. Chem. Int. Edit.*, **31**, 111–129.
9. Curl, R. F. (1992). *Rev. Mod. Phys.*, 69, 691–702 (1997), from Nobel Lecture, **187–231** (1996).
10. Kroto, H. W. (1997). *Rev. Mod. Phys.*, **69**, 703–722, from *Les Prix Nobel 1997*, Nobel Lecture, **187–231** (1996).
11. Smalley, R. E. (1997). *Rev. Mod. Phys.*, **69**, 723–730, from *Les Prix Nobel 1997*, Nobel Lecture, **187–231** (1996).
12. Krätschmer, W. (2000). In: W. Andreoni, ed. *The Physics of Fullerene-Based and Fullerene Related Materials*, Kluwer.

13. Campbell, E. E. B., Hertel, I. V. (1996). The physics of fullerenes in the gas phase. In: Krätschmer, W., Schuster, H., ed. *Von Fuller bis zu Fullerenen*, Vieweg Verl., Heidelberg, pp. 143–160.
14. Krätschmer, W. (2003). In: Prashant, V. K., Guldi, D. M., Souza, F. D., ed. *The Building Blocks of Next Generation Nanodevices*, The Electrochemical Society.
15. Fostiropoulos, K. (1992). *Int. J. Mod. Phys. B*, **06**, 3791–3800.
16. Huffman, D. R. (1991). *Phys. Today,* **44**, 22–29.
17. Taubes, G. (1991). *Science*, **253**, 1476–1479.
18. Baggott, J. (1994). *Perfect Symmetry*: *Accidental Discovery of Buckminsterfullerene*, Oxford University Press.
19. Aldersey Williams, H. (1997). *The Most Beautiful Molecule: The Discovery of the Buckyball*, Wiley.
20. Hargittai, I. (2000). *Candid Science*: *Conversations with Famous Chemists*, Imperial College Press.
21. Applewhite, E. J. (July 1995). *The Chemical Intelligence*, vol 1 No. 3, Springer. Available at: http://www.4dsolutions.net/synergetica/eja1.html (accessed on October 26, 2015).
22. Nickon, A., Silversmith, E. F. (1987). *Organic Chemistry*, *The Name Game: Modern Coined Terms and Their Origins*, Pergamon, New York.
23. BBC Horizon UK TV film (1993). *Molecules with Sunglasses* (also Nova US). Available at: http://www.youtube.com/watch?v=xVZRGcg-BXI (accessed on October 26, 2015).
24. Hintenberger, H., Franzen, J., Schuy, K. D. (1963). *Z Naturforsch,* **18a**, 1236–1237.
25. Campargue, R. (1970). *J. Chem. Phys.*, **52**, 1795–1802.
26. Campargue, R. (2004). 24th International Symposium on Rarefied Gas Dynamics, *AIP Conf. Proc.,* **762**, 32–46.
27. Smalley, R. E., Wharton, L., Levy, D. H. (1975). *J. Chem. Phys.*, **63**, 4977– 4989.
28. Dietz, T. G., Duncan, M. A., Powers, D. E., Smalley, R. E. (1981). *J. Chem. Phys.*, **74**, 6511–6512.
29. Michalopoulos, L., Geusic, M. E., Langridge-Smith, P. R. R., Smalley, R. E. (1984). *J. Chem. Phys.*, **80**, 3556–3560.
30. Eastmond, R., Walton, D. R. M. (1968). *Chem Comm*, 204–205.
31. Eastmond, R., Walton, D. R. M. (1972). *Tetrahedron*, **28**, 4601–4616.
32. Johnson, T. R., Walton, D. R. M. (1972). *Tetrahedron,* **28**, 5221–5236.

33. Alexander, A. J., Kroto, H. W., Walton, D. R. M. (1976). *J. Mol. Spectrosc.*, **62**, 175–180.
34. Avery, L. W., Broten, N. W., MacLeod, J. M., Oka, T., Kroto, H. W. (1976). *Astrophys. J.*, **205**, L173–L175.
35. Kirby, C., Kroto, H. W., Walton, D. R. M. (1980). *J. Mol. Spectrosc.*, **83**, 261.
36. Kroto, H. W., Kirby, C., Walton, D. R. M., Avery, L. W., Broten, N. W., MacLeod, J. M., Oka, T. (1978). *Astrophysics. J.*, **219**, L133–L137.
37. Broten, N. W., Oka, T., Avery, L. W., MacLeod, J. M., Kroto, H. W. (1978). *Astrophys. J.*, **223**, L105–L107.
38. Becklin, E. E., Frogel, J. A., Hyland, A. R., Kristian, J., Neugebauer, G. (1969). *Astrophys. J.,* **158**, L133–L137.
39. Winnewisser, G., Walmsley, C. M. (1978). *Astrophys. J.*, **70**, L37–L39.
40. Kroto, H. W. (1981). *Int. Rev. Phys. Chem.*, **1**, 309–376.
41. Kroto, H. W. (1982). *Chem. Soc. Rev.*, **11**, 435–491.
42. Heger, M. L. (1922). *Lick Observatory Bull.*, **337**, 141–145.
43. McKellar, A. (1942). *Pub. Dom. Ap. Obs.*, **7**, 251.
44. Herbig, G. H. (1975). *Astrophys. J.*, **196**, 129–160.
45. Herbig, G. H. (1995). *Annu. Rev. Astron. Astrophys.*, **33**, 19–74.
46. Douglas, A. E. (1977). *Nature*, **269**, 130–132.
47. Stecher, T. P. (1969). *Astrophys. J.*, **157**, L125.
48. Day, K. L., Huffman, D. R. (1973). *Nature*, **243**, 50.
49. Solomon, P. M., Klemperer, W. (1972). *Astrophys. J.*, **178**, 389.
50. Herbst, E., Klemperer, W. (1973). *Astrophys. J.*, **185**, 505–533.
51. Greenberg, J. M. (2002). *Surf. Sci.*, **500**, 793–822.
52. Rohlfing, E. A., Cox, D. M., Kaldor, A. (1984). *J. Chem. Phys.*, **81**, 3322–3330.
53. Whittaker, A. G. (1978). *Science*, **200**, 763.
54. Kroto, H. W. (Nov. 2010). *Chemistry World*. Available at: http://www.rsc.org/chemistryworld/Issues/2010/November/CarbyneOtherMythsAboutCarbon.asp (accessed on October 26, 2015).
55. Smith, P. P. K., Buseck, P. R. (1982). *Science*, **216**, 984–986.
56. Bloomfield, L. A., Geusic, M. E., Freeman, R. R., Brown, W. (1985). *Chem. Phys. Lett.*, **121**, 33–37.
57. Heath, J. R., Zhang, Q., O'Brien, S. C., Curl, R. F., Kroto, H. W., Smalley, R. E. (1987). *J. Am. Chem. Soc.*, **109**, 359–363.

58. Kroto, H. W., Heath, J. R., O'Brien, S. C., Curl, R. F., Smalley, R. E. (1987). *Astrophys. J.*, **314**, 352–355.
59. Jones, D. E. H. (1966). *N. Sci.*, **245**, 118–119.
60. Jones, D. E. H. (1982). *The Inventions of Daedalus*, Freeman, Oxford.
61. Osawa, E. (1970). *Kagaku*, **25**, 854–863 [in Japanese].
62. Yoshida, Z., Osawa, E. (1971). *Aromaticity*, Kagakudojin [in Japanese].
63. Bochvar, D. A., Gal'pern, E. G. (1973). *Dokl. Akad. Nauk. USSR*, **209**, 610– 612; *Proc. Acad. Sci. USSR*, **209**, 239–241. [in English].
64. Davidson, R. A. (1981). *Theor. Chim. Acta*, **58**, 193–195.
65. Haymet, A. D. J. (1985). *Chem. Phys. Lett.*, **122**, 421–424.
66. Chapman, O. [cf. ref. 18 book by Baggott and ref. 23 BBC Horizon film].
67. Scott, L. T., Boorum, M. M., McMahon, B. J., Hagen, S., Mack, J., Blank, J., Wegner, H., de Meijere, S. (2002). *Science*, **295**, 1500–1503.
68. Heath, J. R., O'Brien, S. C., Zhang, Q., Liu, Y., Curl, R. F., Kroto, H. W., Tittel, F. K., Smalley, R. E. (1985). *J. Am. Chem. Soc.*, **107**, 7779–7780.
69. Kroto, H. W. (1987). *Nature*, **329**, 529–531.
70. Schmalz, T. G., Seitz, W. A., Klein, D. J., Hite, G. E. (1988). *J. Am. Chem. Soc.*, **110**, 1113–1127.
71. Weiss, F. D., Elkind, J. L., O'Brien, S. C., Curl, R. F., Smalley, R. E. (1988). *J. Am. Chem. Soc.*, **110**, 4464–4465.
72. Kroto, H. W., McKay, K. G. (1988). *Nature*, **331**, 328–331.
73. McKay, K. G., Kroto, H. W., Wales, D. J. (1992). *J. Chem. Soc. Faraday Trans.*, **88**, 2815–2821.
74. O'Brien, S. C., Heath, J. R., Kroto, H. W., Curl, R. F., Smalley, R. E. (1986). *Chem. Phys. Lett.*, **132**, 99–102.
75. Hahn, M. Y., Honea, E. C., Paguia, A. J., Schriver, K. E., Camarena, A. M., Whetten, R. L. (1986). *Chem. Phys. Lett.*, **130**, 12–16.
76. Cox, D. M., Trevor, D. J., Reichmann, K. C., Kaldor, A. (1986). *J. Am. Chem. Soc.*, **108**, 2457–2458.
77. Cox, D. M., Reichmann, K. C., Kaldor, A. (1988). *J. Chem. Phys.*, **88**, 1588–1597.
78. Stone, A. J., Wales, D. J. (1986). *Chem. Phys. Lett.*, **128**, 501–503.
79. Campbell, E. E. B., Ulmer, G., Busmann, H.–G., Hertel, I. V. (1990). *Chem. Phys. Lett.*, **175**, 505–510.
80. Weeks, D. E., Harter, W. G. (1989). *J. Chem. Phys.*, **90**, 4744–4771.

81. Larsson, S., Volosov, A., Rosen, A. (1987). *Chem. Phys. Lett.*, **137**, 501.
82. Krätschmer, W., Fostiropoulos, K., Huffman, D. R. (1989). In: ed. Bussoletti, E., Vittone, A. A., *Dusty Objects in the Universe*, Kluwer, pp. 89–93.
83. Scott, L. T., Hashemi, M. M., Meyer, D. T., Warren, H. B. (1991). *J. Am. Chem. Soc.*, **113**, 7082–7084.
84. Barth, W. E., Lawton, R. G. (1966). *J. Am. Chem. Soc.*, **88**, 380–381.
85. Iijima, S. (1980). *J. Cryst. Growth*, **50**, 675–683.
86. Oberlin, A., Endo, M., Koyama, T. (1976). *J. Cryst. Growth*, **32**, 335–349.
87. Geim, A. K., Novoselov, K. S. (2007). *Nat. Mater.*, **6**, 183–191.
88. Guo, T., Diener, M. D., Chai, Y., Alford, M. J., Haufler, R. E., McClure, S. M., Ohno, T. R., Weaver, J. H., Scuseria, G. E., Smalley, R. E. (1992). *Science*, **257**, 1661–1664.
89. Dunk, P. W., Kaiser, N. K., Mulet–Gas, M., Rodríguez–Fortea, A., Poblet, J. M., Shinohara, H., Hendrickson, C. L., Marshall, A. G., Kroto, H. W. (2012). *J. Am. Chem. Soc.*, **134**, 9380–9389.
90. Birkett, P. R., Avent, A. G., Darwish, A. D., Kroto, H. W., Taylor, R., Walton, D. R. M. (1993). *J. Chem. Soc. Chem. Commun.*, 1230.
91. Haddon, R. C., Hebard, A. F., Rosseinsky, M. J., Murphy, D. W., Duclos, S. J., Lyons, K. B., Miller, B., Rosamilia, J. M., Fleming, R. M., Kortan, A., Glarum, S. H., Makhija, A. V., Muller, A. J., Eick, R. H., Zahurak, S. M., Tycko, R., Dabbagh, G., Thiel, F. A. (1991). *Nature*, **350**, 320–322.
92. Hummelen, J. C., Knight, B., Pavlovich, J., González, R., Wudl, F. (1995). *Science*, **269**, 1554–1556.
93. Dunk, P. W., Rodríguez-Fortea, A., Kaiser, N. K., Shinohara, H., Poblet, J. M., Kroto, H. W. (2013). *Angew. Chem. Int. Ed.*, **52**, 315–319.
94. von Helden, G., Hsu, M.-T., Kemper, P. R., Bowers, M. T. (1991). *J. Chem. Phys.*, **95**, 3835–3837.
95. Ding, H., Maier, J. P. (2007). *J. Phys. Conf. Ser.*, **61**, 252.
96. Heath, J. R. (1992). In: Hammond, G. S., Kuck, V. J., ed. *Fullerenes: Synthesis, Properties and Chemistry of Large Carbon Clusters*, ACS Symposium Series No. 481, pp. 1–23.
97. Endo, M., Kroto, H. W. (1992). *J. Phys. Chem.*, **96**, 6941–6944.
98. Dunk, P. W., Kaiser, N. K., Hendrickson, C. L., Quinn, J. P., Ewels, C. P., Nakanishi, Y., Sasaki, Y., Shinohara, H., Marshall, A. G., Kroto, H. W. (2012). *Nat. Commun.*, **3**, 855.
99. Howard, J. B., McKinnon, J. T., Makarovsky, Y., Lafleur, A. L., Johnson, M. E. (1992). *Nature*, **352**, 6331.

100. Zhang, Q. L., O'Brien, S. C., Heath, J. R., Liu, Y., Curl, R. F., Kroto, H. W., Smalley, R. E. (1986). *J. Phys. Chem.*, **90**, 525–528.
101. Frenklach, M., Ebert, L. B. (1988). *J. Phys. Chem.*, **92**, 561–563.
102. Kroto, H. W., Jura, M. (1992). *Astron. Astrophys.*, **263**, 275–280.
103. Cami, J., Bernard-Salas, J., Peeters, E., Malek, S. E. (2010). *Science*, **329**, 1180.
104. Fowler, P. W., Manalopoulos, D. E. (1995). *An Atlas of Fullerenes*, Oxford.

Chapter 15

Applications of Nanoparticles in Medical Imaging

Jason L. J. Dearling, PhD, and Alan B. Packard, PhD

Division of Nuclear Medicine and Molecular Imaging,
Department of Radiology,
Boston Children's Hospital and Harvard Medical School,
Boston, Massachusetts, USA

Keywords: medical imaging, contrast agents, micelles, liposomes, dendrimers, radioopaque elements, radioopaque nanoparticles, ultrasound contrast agents, core–shell nanoparticles, tissue targeting

15.1 Introduction

Medical imaging offers a powerful tool for the detection and characterization of disease. In order to take full advantage of the possibilities offered, imaging agents with specific uptake in the target tissue are required. The development of these agents presents several challenges, as the agents must have sufficient absolute uptake at the target site to be detectable, must clear from

Handbook of Clinical Nanomedicine: Nanoparticles, Imaging, Therapy, and Clinical Applications
Edited by Raj Bawa, Gerald F. Audette, and Israel Rubinstein

ISBN 978-981-4669-20-7 (Hardcover), 978-981-4669-21-4 (eBook)
www.panstanford.com

other tissues to achieve contrast, and should be non-toxic and non-immunogenic.

In this chapter, we discuss how the use of biomaterials has advanced the development of novel nanoparticles as contrast agents for computed tomography (CT) and ultrasound (US).

An essential role of medical imaging is the ability to discriminate between normal and diseased tissue. This discrimination can be achieved by using contrast agents that selectively accumulate in the diseased tissue, increasing the signal from that tissue, thus distinguishing it from adjacent, normal, tissue. The increasing ability of therapies to address specific subtypes of disease as well as the associated increases in the cost of these therapies demands a corresponding improvement in the ability to define disease, preferably non-invasively and to assess response to therapy in near real time. Medical imaging has the ability to answer these demands through increasingly specific contrast agents.

In the spectrum of available molecular imaging technologies, nuclear medicine, using either single-photon or positron-emitting tracers, provides the greatest sensitivity, with the ability to detect targets that are present at the nanomolar level. The trade-off for this high sensitivity is relatively lower resolution (5–10 mm) than is available with magnetic resonance imaging (MRI), computed tomography (CT), or ultrasound (US), all of which can achieve anatomic resolution of 1 mm or less. However, MRI, CT, and US require a much greater mass of contrast agent at the imaging site to provide adequate differentiation between normal and diseased tissue. An obvious way to provide this increase in mass is through the use of targeted nanoparticles, which by their very nature deliver a large mass of material to the target, assuming that the technical challenges associated with delivering such a massive particle to an *in vivo* target can be overcome. These challenges include evading the body's defenses against particulate contaminants (including the reticuloendothelial system), developing a particle that is small enough not to be trapped in the capillary bed while still large enough to provide an adequate signal once it reaches the target, and overcoming the toxicological challenge inherent in administering a significant mass of material intravenously. The development of novel biomaterials offers a great opportunity to overcome

these challenges. The aim of this review is to discuss the role of biomaterials in development of contrast agents in two fields, CT and US, their similarities and differences, and how the novel properties of nanoparticles have facilitated this development.

Owing to the breadth of this subject and space limitations, this review is not intended to be comprehensive, but rather to provide an introduction to the requirements of the field, as well as an overview of how advances in nanotechnology have exploited the unique properties of biomaterials to address the challenges outlined above.

15.2 Contrast Media for Computed Tomography

Computed tomography (CT) is an imaging modality in which x-rays are projected through the subject at different angles and the resulting data are then reconstructed into three-dimensional images. X-rays are able to pass through the different types of tissue to varying degrees, with bone being relatively radiodense, air being essentially radiotransparent, and water lying between these two extremes. The attenuation of the x-rays is measured in Hounsfield Units (HU), with air and water arbitrarily set to 0 and 1000, respectively. As soft tissues tend to have very similar radiodensities, CT imaging can be significantly improved by injecting radioopaque compounds intravenously, improving the definition of vascular structures and providing some degree of soft tissue targeting and differentiation.

There is both a need and an opportunity for new CT contrast agents that target specific tissues or provide prolonged imaging times. Magnetic resonance imaging (MRI) can also provide high-resolution anatomic images as well as quantitative information on blood flow, but CT offers both technical and pragmatic advantages compared with MRI; there is a direct proportionality between x-ray absorption and contrast agent concentration, simplifying quantitative studies, and CT is less expensive and more widely available than MRI. The primary disadvantage of CT compared with MRI is that CT scans involve exposure to ionizing radiation, but the radiation dose can be minimized by only imaging the region of

interest and by careful selection of imaging parameters (i.e., power (kvp) and x-ray current).

CT contrast media must be very water soluble because of the large quantities that are injected. The solubility requirement results in rapid clearance from the blood, which in turn limits the available imaging time. Prolonging the clearance time, by means such as increasing the molecular weight of the agent, has, therefore, been an important research focus. A second research focus is the development of CT contrast agents that target specific tissues. This objective has proved difficult to achieve because a significant mass of the contrast agent must accumulate in the target tissue before the tissue density increases enough to improve the contrast of the image. This requirement, in turn, increases the risk of toxicity. While iodine is the primary element used in CT contrast agents, primarily because of its low cost and minimal toxicity, a third research focus is the evaluation of radiodense elements other than iodine (e.g., barium).

15.2.1 Macromolecular Contrast Agents

To address the problem of increasing the time available for imaging, the most straightforward approach is to increase the size of the contrast agent to the nanoparticle range (typically 1–100 nM), which slows its clearance from the blood (for more detailed discussion, see Hallouard et al. [1]). If one adopts this approach, the choices that must be made are: (1) What type of nanoparticle to use and how this choice affects the particle's *in vivo* behavior, (2) What radioopaque element will be used and how will it be attached to the nanoparticle, and (3) What other steps are required for *in vivo* use? In terms of which nanoparticle is optimal, there has been a progression in the field from use of the relatively simple micelles, to more complex but also more efficacious liposomes, to dendrimers, and finally to the use of microcrystalline or particulate forms of radioopaque elements. We will consider each of these in turn.

15.2.1.1 Micelles

Micelles are single-layer vesicles that form spontaneously in surfactant solutions when the surfactant concentration exceeds

the critical micelle concentration (CMC). The CMC varies with the surfactant, so the materials used in the manufacture of intravenously administered micellar drugs must be chosen so that the CMC is low enough that the micelle does not collapse when the drug is diluted upon injection, achieving the desired goal of remaining intact in the circulatory system for a prolonged period of time.

Micelles can be used as contrast agents in two ways: The micelle can be used as a carrier, with the radioopaque element transported in the hydrophobic core of the micelle, or the radioopaque element can be covalently attached to the polymer constituents of the micelle, to either the hydrophilic outer "head" or the hydrophobic inner "tail." Covalent attachment of the radioopaque element to the constituents of the micelle is ideal as it improves retention of the element by the micelle, increasing specificity, and also reducing toxicity.

For a micellar CT contrast agent to be effective, it must deliver sufficient mass of the radioopaque element to the tissue of interest to increase the tissue density versus that of adjacent tissue. Improved carrying capacity can be achieved through using larger hydrophobic molecules, but with the downside that this increases the CMC, which in turn means that a higher micelle concentration is required to achieve adequate *in vivo* stability. Therefore, the use of micelles in CT imaging is inherently limited.

In early studies of the use of micelles as CT contrast agents, micelles were used as carriers for iodinated molecules. However, a significant weakness of this approach was the loss of the iodinated molecules from the core of the micelle. In a more recent study of micelles as CT contrast agents, Torchilin et al. [2] used amphipathic block-polymers containing iodine. These compounds form micelles with an average diameter of 80 nm and an iodine content of 33.8%. Detectable organ opacification was observed from 5 min to 3 h post-injection in rats; attenuation increased from 85 HU to 253 HU in the aorta and from 92 HU to 156 HU in the liver post-micelle injection over this 3 h window. The authors note that while this was a significant achievement in the use of micelles as CT contrast agents, much more work must be carried out before these materials are ready for clinical use. For recent reviews, see Ref. [3].

15.2.1.2 Liposomes

As candidate nanoparticles, liposomes have several advantages over micelles: Their manufacture is more controllable, they are mechanically stronger, they are less susceptible to collapse on dilution, they can be used as carriers for hydrophilic and hydrophobic molecules, and they can be derivatized with targeting moieties more easily.

Liposomes, first described by Bangham in 1964 [4], consist of amphipathic phospholipids that form bilayered vesicles in aqueous solutions. In contrast to micelles, the core of liposomes is hydrophilic. They can, therefore, act as vehicles for either hydrophilic compounds (in the core) or hydrophobic compounds, for example iodinated polymers, in the lipidbilayer. Early liposomes comprised phosphatidyl choline (PC) from egg and cholesterol. These "conventional," or "C," liposomes have been superseded by sterically stabilized, or "S," liposomes (see Ref. [5] for further discussion). Improvements have also been made in the combinations of fatty acids and lipids used in the manufacture of liposomes and in surface modification of the particles so as to evade *in vivo* clearance mechanisms, thereby extending the circulation time and improving uptake at the site of interest.

The materials used in the preparation of liposomes must provide structural strength and stability while at the same time reducing interactions with proteins in order to extend the circulation time. The stability and mechanical strength of liposomes is based on a rigid bilayer that requires lipids with a high phase-transition temperature. The bilayer is typically comprised of a common lipid such as phosphatidyl choline and a mixture of the fatty acids stearate and oleate. Addition of a small amount of cholesterol increases the fluidity of the bilayer by modifying its crystalline nature. Keeping the formulation simple is also beneficial, as mixtures of lipids with different phase transition temperatures can lead to instability *in vivo*.

The rapid loss of liposomes from the blood in early studies was attributed to both their size and interaction with clearing mechanisms. Since larger liposomes (>100 nm) are cleared more quickly than smaller ones, maintaining diameters below this threshold during the manufacturing process is critical. On the other hand, larger liposomes can carry more payload, increasing

their potential efficacy as contrast agents. Reducing their interaction with clearing mechanisms has required several iterations. The primary clearance mechanism is the mononuclear phagocyte system (MPS), also known as the reticuloendothelial system (RES). One early attempt to evade this system was to replicate the outer coatings of red blood cells by incorporating molecules such as the monosialoganglioside GM1 into the liposome [6]. GM1 carries a negative charge, and it was found that inclusion of other negatively charged molecules, such as phosphatidylserine (PS) or phosphatidyl glycerol (PG), on the outer shell of the liposome also reduced RES clearance, though at high levels this advantage was offset by increased liver uptake, possibly through interaction with Kupffer cells [7]. An additional consideration is that directly accessible negative charges, such as those provided by PS and PG, can increase interaction with proteins whereas shielded negative charges, such as those on GM1, increase the zeta potential of the nanoparticle but are not accessible to direct interaction with proteins [8]. This proves to be a double advantage as increasing the zeta potential also reduces aggregation, improving the stability of the liposomes during manufacture, storage, and after injection. More recently, GM1 has been replaced by polyethylene glycol (PEG), which also reduces interactions with the RES and is chemically well defined, as well as being much less expensive than GM1. While PEG does reduce opsonization, there is evidence that PEG-coated liposomes still induce a complement-based immune response [9].

A range of sizes of PEG has been evaluated. With higher MW PEGs (e.g., 5 kDa) there is steric hindrance of the ability of ligands attached to the liposome to bind to their targets [10], while for lower MW PEGs (e.g., 750 Da) the circulation time is shorter [11], leading to use of PEGs in 2 kDa range. Alternatively, the targeting ligand, which could be an antibody, peptide, or other targeting molecule, can be attached to the PEG so that it is held outside the PEG coating, reducing steric hindrance while simultaneously increasing circulation time [12].

Current methods of encapsulating small-molecule, water-soluble, iodinated compounds in the liposome core still leave a significant amount of contrast agent in the bulk formulation medium resulting in uptake of the non-encapsulated material in the kidney shortly after injection. This can confound quantitative

studies as it suggests a triphasic clearance of the nanoparticle or a faster initial clearance phase than is actually the case. However, the presence of this excess material in the bulk formulation solution has the advantage of reducing the rate of loss of the contrast agent from the core of the nanoparticle *in vitro*, which results in a longer shelf life and more consistent imaging results [13]. This problem arises because the rate of loss of the iodinated contrast agent from the liposome core is related to the concentration difference across the lipid bilayer and also to the osmotic pressure difference. This can be avoided by using the iodinated-polymer method where the iodine is covalently bound to the lipid itself, effectively precluding loss of the iodine from the liposome. Another approach to avoiding this problem was discussed by Wei et al. [14] who developed a multilamellar (rather than unilamellar) liposomal construct. This had the advantage of entrapping high concentrations of iodohexol (50 mg/mL) within the liposomal core while reducing the loss of the iodine by diffusion through the bilayer. A further development of this approach was reported by Kweon et al. [15], who used a mixture of water-soluble and oil-based iodinated compounds. The water-soluble material is trapped in the hydrophilic core while the oil-based material is trapped in the hydrophobic bilayer, resulting in a significant increase in radioopacity in the target organ. Encapsulating iopamidol, a water-soluble iodine contrast agent, in liposomes (giving an iodine concentration of 13.8 mg/mL in the formulation) resulted in a relatively small improvement in contrast. However, loading the liposomes with both iopamidol and lipiodol, an iodinated oil, resulted in iodine concentrations as high as 49.2 mg/mL in the combined formulation, and the lipiodol did not disrupt the liposomal structure. A limitation of this approach is that increasing the amount of lipiodol in the liposome resulted in a mixture that was too viscous to produce a liposomal dispersion. This formulation included cholesterol in addition to 1,2-dimyristoyl-sn-glycero-3-phosphocholine (DMPC), which increased the rigidity of the liposomal structure, reducing leakage of entrapped iopamidol and increasing its concentration within the liposomes by 1.6-fold. The *in vivo* performance of these liposomes was encouraging, with an increase of 30 HU, and the material also showed delayed clearance from the circulation. For comparison, iopamidol, which is commonly used as a contrast agent

by itself, produces an increase of <7 HU when used at the same iodine concentration.

15.2.1.3 Dendrimers

Dendrimers are large, synthetic, branched molecules made from repeats of chemical units built around an inner core. The attraction of these materials as imaging agents is that the structure is highly defined and the size can be precisely controlled by controlling the number of repeats (generations). The outer face of these molecules can be chemically modified, so they can be targeted relatively simply. One of the drawbacks of the dendrimers is the synthesis, which can require up to several days depending on the formulation.

Fu et al. [16] reported the synthesis, characterization, and initial imaging studies with a dendrimer-based CT contrast agent. This compound was composed of a PEG core derivatized at each end with polylysine dendrimers. Different lengths of PEG and numbers of generations of polylysine were used to construct molecules of differing sizes with a large number of sites available for iodination. The resulting compounds had molecular weights ranging from 21.7 kDa to 66.4 kDa (compared with 0.82 kDa for iodohexol). An initial imaging study with PEG12000-carbamate-Gen4-IOB showed good contrast in the liver of a rat, including the visualization of the blood vessels. The 35 min blood half-life of this compound meant that contrast was still evident 30+ min after intravenous injection, much longer than is seen with conventional tracers which have blood half-lives of <5 min. This agent was used to measure the plasma volume and endothelial permeability of subcutaneous xenograft breast cancer xenograft tumors [17].

15.2.2 Other Radioopaque Elements

In addition to iodine, a number of other elements have desirable characteristics for CT contrast agents and are being developed for use. For example, in work by Rabin et al. [18], nanocrystals of Bi_2S_3 were coated with the polymer polyvinylpyrrolidone (PVP). (The uncoated crystals could not be used as imaging agents because of aggregation and rapid clearance.) When these nanoparticles were tested *in vivo*, sufficient increases in contrast

were achieved for clear imaging of vascular structures. The blood half-life was 140 ± 15 min, which is significantly longer than that of commercial iodinated agents (typically <10 min). At later time points, the enhancement of tissues involved in the RES was observed, leading to the suggestion that the agent could be used to image the liver and detect tumor metastases in that organ. The toxicity of these nanoparticles was tested *in vivo* and found to be much lower than the free bismuth ions (LD50s of 8 mM and 100 mM for bismuth ions and Bi_2S_3 nanoparticles, respectively).

Gold nanoparticles (AuNPs) also have potential application in this field, with gold's higher atomic number (79) than iodine (53) resulting in greater attenuation of x-rays. As with bismuth particles, AuNPs have to be coated, for example with gum Arabic, to reduce their hematological and renal toxicity [19]. They have been shown to be stable *in vivo* and to produce good contrast in CT applications [19, 20]. Another advantage of AuNPs is that they have a large surface-area-to-volume ratio, providing more opportunity for surface modification. For example, Aydogan et al. reported the modification of AuNPs with a structural analogue of glucose, 2-deoxy-D-glucose (2DG) [21]. This modification increased their uptake by tumor cells *in vitro* by a factor of 4 compared with unmodified AuNPs, although the exact mechanism of uptake has yet to be fully defined. In another example, targeting was achieved by entrapping AuNPs in dendrimers, then targeting the combined nanoparticle using folate attached to the outside of the dendrimer, resulting in improved binding to KB cells (human epithelial carcinoma cells) *in vitro* [22].

15.2.3 Targeting

These last examples introduce the topic of targeting contrast nanoparticles to tissues or diseases of interest. Some degree of tumor targeting by nanoparticles is achieved passively because of differences in tumor blood vessel structure compared with that of normal tissues, through what is known as the enhanced permeability and retention (EPR) effect [23]. More specific targeting can be achieved either by designing the materials so that they are sensitive to differences in environmental conditions, such as pH, or by attaching targeting molecules such as peptides or antibodies to the exterior of the macromolecule.

Optimal targets for nanoparticle targeting are on the luminal side of blood vessels, as extravasation of macromolecules can be slow. One case where this would be of great value is the detection and description of atherosclerosis. The two following examples demonstrate different methods of identifying atherosclerotic plaques with potential to rupture. Currently, atherosclerotic plaques can be imaged using intravascular ultrasound (IV-US) or by MRI. However, both of these methods have drawbacks, including the invasive nature of IV-US and the long time required for MRI, because tissue movement reduces the image quality. CT is faster and less expensive than both of these techniques and the resolution is high enough to detect the biological features of atherosclerosis. Danila et al. [24] encapsulated iohexol in liposomes and then attached anti-ICAM-1 antibodies to the liposomes to target them to inflamed vasculature. This resulted in immunoliposomes that bind specifically to activated human coronary artery endothelial cells *in vitro*. In another example, Wyss et al. [25] coated liposomes with a peptide that binds E-selectin with high affinity and measured their *in vitro* and *in vivo* selectivity. In an ischemia-reperfusion injury model, increased uptake by activated endothelial cells was observed compared with controls. In a tumor imaging study, targeting the liposomes did not affect their blood half-lives, but it did extend tumor residence of the particles.

15.2.4 CT Contrast Agent Summary

In this section, we considered the properties required of CT contrast agents and how appropriate biomaterials are being selected. A primary requirement for the development of targeted CT contrast agents is that sufficient mass of radiodense material must accumulate at the site of interest to cause a corresponding change in the attenuation of the incident x-ray beam. Sufficient mass is also necessary for ultrasound contrast agents, except that they must also possess echogenicity for detection, placing a further developmental constraint on these nanoparticles. It is also necessary that there be a change in the attenuation of the incident x-ray beam or that sufficient radiodense material accumulate at the site of interest. Neither (x-rays or radiodensity) is applicable to US. We will now consider how these imaging probes are being developed.

15.3 Ultrasound

Medical ultrasonography uses reflected sound waves with frequencies above 20 MHz to construct images. This technology has been used for several decades to visualize a range of anatomic features in the human body. Ultrasound can be used to evaluate cardiac abnormalities, such as blood vessel wall inflammation, as an early indicator of heart disease. It can also be used to detect blood clots, such as deep-vein thromboses. More intense US beams can also be used therapeutically. Thus, one of the more interesting features of ultrasound is that, in some cases, it can be used both to detect and to treat disease.

Ultrasound has a number of advantages over other imaging modalities: It is relatively inexpensive and portable and has a low risk profile, with no exposure to ionizing radiation and no inherent toxicity associated with the potential contrast agents (i.e., no iodine or gadolinium is required). The primary disadvantage is that imaging is confined to a relatively small area of interest. Advantages over MRI include high resolution (of the order of 10's of microns, enabling imaging of small blood vessels) and that repeat scans can be made immediately, which is difficult with MRI if repeated administration of contrast agents is required.

Until relatively recently, all US was carried out without the use of contrast agents. The past 10 years, however, have witnessed the introduction of the first US contrast agents. The agents enhance the US image by creating differences in the sound reflection, or echogenicity, between different anatomic compartments. For example, intravenous administration of encapsulated air bubbles (microbubbles) results in an increased difference in echogenicity between the lumen of the vessel and its surroundings. Ultrasound contrast agents (UCAs) have a number of desirable characteristics that they share with CT contrast agents, such as low toxicity and ease of formulation and administration. Additionally, as with CT contrast agents, the mass of imaging agent concentrating at the site of disease is important in achieving a good signal-to-noise ratio. However, the nature of the imaging modality adds additional constraints above those required for CT contrast agents. For example, large bubbles are required for good echogenicity, but if they are too large, they become trapped in

microvasculature, especially in the lung. Initially, the microbubbles that were used were of the order of 100 μm, while the current microbubbles are <5 μm in diameter. The microbubbles must flex to produce signal, but at the same time, they must be strong enough to withstand the pressures in the left side of the heart without rupturing if they are to have a long circulation time, a requirement for optimal concentration at the site of interest. As with all contrast agents, the optimal UCA will depend on the purpose of the imaging study. It must have adequate echogenicity to produce a high-contrast image and also strong enough to withstand the US beam used for detection, but if it is designed to be susceptible to rupture by more intense US radiation, then local signal can be artificially reduced to enable repeated studies. Another way in which the ability of microbubbles to be "fractured on demand" can be exploited is as targeted drug delivery vehicles. A drug can be encapsulated in the microbubbles, the bubbles are then administered intravenously, and an US beam can be used to fracture the bubbles at the target site, delivering the drug specifically to that site.

In the development of UCAs, three components must be optimized: the shell, the core, and the targeting moiety. We will discuss each of these in turn.

15.3.1 Shell

The composition of the UCAs shell determines its physical properties, most important, its mechanical elasticity. If it is too brittle, then it will fracture too easily, but if it is too elastic, then it will not produce an adequate signal (see McCulloch et al. [26]). The optimal UCA for each purpose varies—for example, a more brittle shell might be used as a drug delivery vehicle so that it can be ruptured more easily at the target site.

The shell can be made of protein, galactose, lipid, or polymers (see Ref. [27]). Following early studies with a range of water-based solutions, encouraging results were obtained with microbubbles consisting of air trapped in a denatured albumin shell made by sonication of an albumin solution. This was an important development because it provided the first useful US contrast agent, but the method of manufacture produced a wide range of particle sizes. This is a significant issue in UCA development because

different sized bubbles have different echogenicities. Also, as noted previously, larger bubbles are trapped in small blood vessels, especially in the lungs, hindering transition from the venous injection to arterial distribution, and reducing the circulation time of a significant fraction of the particles. On the other hand, smaller microbubbles also have poor persistence, because they can be damaged by ultrasound radiation.

Lipid-based shells have a number of desirable properties. They are smaller (<5 μm), it is easier to control their size, they are mechanically much more robust than microbubbles, and the composition of the shell can be altered to optimize their properties. Alkan-Onyuksel and colleagues [28] systematically investigated the echogenicity of liposomes produced from combinations of phosphatidylcholine (PC), phosphatidylglycerol (PG), phosphatidylethanolamine (PE) and cholesterol, selected because they are the main constituent of cell membranes (PC), confer a negative charge (PG), provide options for conjugation (PE), and increase rigidity (cholesterol). They found that high concentrations of PE (e.g., 4%), low concentrations of PG (1%), and constant cholesterol (30%) gave highest echogenicity. These findings were confirmed by *in vitro* and *in vivo* studies. It was also found that echogenicity was related to the structure of the liposomes. More echogenic liposomes tended to have multilamellar structures, while the less echogenic liposomes had thick, unseparated, unilamellar structures. It was suggested that the formulation of the liposomes caused these differences, with, for example, the negative charge of PG preventing aggregation and the small head of PE affecting the formation of the multiwalled structures. In later work by the same group [29], it was found that entrapment of air in the liposomes during the lyophilization step in their manufacture was a requirement for their echogenicity. The inclusion of mannitol in the formulation as a cryoprotectant resulted in the exposure of hydrophobic regions to air during lyophilization and then its subsequent retention in the rehydrated form.

15.3.2 Core

In addition to the above-described issues of size, etc., the nature of the fluid entrapped within the microbubble also influences

its imaging characteristics. Air is easily incorporated into microbubbles, but is soluble in blood, so it escapes from the bubble and shortens the potential imaging time. The rate of diffusion of air from microbubbles can be reduced by, for example, using biopolymer shells. Heavy gases have lower solubility in blood and so lead to the UCAs having longer persistence. Polyfluorinated carbon gases (PFCs) are also poorly soluble in water and are liquids at room temperature, and their non-toxicity, stability, and low acoustic impedance make them attractive fluids to use as the core of microbubble contrast agents.

Marsh et al. [30] systematically investigated the echogenicity of seven PFCs at a range of temperatures between 25°C and 45°C. Their conclusion was that perfluorohexane had the lowest acoustic impedance within this temperature range (the acoustic impedance of distilled water at 37°C is approximately 1.5 g/cm^2-s, while perfluorohexane is approximately 0.8 g/cm^2-s), and therefore would provide a good enhancement agent as it has a very different impedance compared with water, resulting in good contrast. The group then extended this work by investigating the suitability of various fluids as the core of targeted microbubbles *in vitro* [31]. This study investigated the observation that targeting the microbubbles to a surface improved their impedance. The authors suggested that this improvement was due to the development of a reflective interface between the targeted surface and the medium surrounding it.

The introduction of fluids into nanoparticles and then ensuring their entrapment, at least for the duration of scanning, presents a challenge that can be met in various ways. One interesting method of introducing the gas *in vivo* was reported by Kang et al. [32], who used polyesters with carbonate side-chains to produce nanoparticles, which, when injected intravenously, produce nanobubbles that coalesce into microbubbles. Water diffuses into the microbubbles and cleaves the carbonate side-chain forming carbon dioxide *in situ*. The viability of this approach was confirmed by ultrasound imaging *in vivo*. Another advantage of this technology is that the nanobubbles are themselves not visible at 100 μm US resolution, but once they arrive at the target tissue and coalesce into microbubbles, the size increases and the bubbles become visible by US.

The transition of UCAs from protein-based microbubbles to optimized liposomal particles containing gases that further enhance the US signal also provides a greatly improved platform for derivatization using specific ligands to facilitate targeting. The two main areas that have been investigated for UCA targeting are inflammation and cancer.

15.3.3 Targeting Inflammation

UCAs can be actively targeted to specific tissues in two ways, by inclusion of a targeting moiety on the one or more of the chemical constituents of the UCA or by chemical attachment of a targeting ligand, such as a peptide or antibody, to one of its constituents. The size and the composition of the shell, especially in the case of protein-based shells, will also affect the distribution *in vivo*, providing additional biological information. This "passive" targeting can provide information on blood flow, the lymphatic system, or the systems that interact with foreign agents in the body, such as phagocytic lymphocytes. It could be argued that microbubbles with a shell consisting of denatured albumin represent both passive and active targeting of inflammation because the microbubble itself provides a marker of increased vascular permeability while the albumin shell interacts with activated endothelial cells. It has also been noted that in some cases albumin-based microbubbles are retained in the myocardium, leading to an enhanced US signal. It was hypothesized that this was due to interaction between the microbubbles and the inflamed endothelial tissue. Villanueva et al. [33] tested this hypothesis in an *in vitro* study in which they found that albumin-based microbubbles adhered strongly to the exposed inflamed extracellular matrix of endothelial cells. In related work also targeting inflammation, Unger et al. [34] coupled a hexapeptide representing the minimum functional unit from fibrinogen (amino acid sequence KQAGDV) to a lipid, incorporated the functionalized lipid into a PFC-containing liposome, and observed increased binding of this UCA to blood clots *in vitro*. Similarly, Christiansen et al. [35] used phosphatidylserine (PS) containing lipid microbubbles to target leukocytes in order to quantify inflammation from myocardial reperfusion injury. Including PS in the lipid composition

increased complement-mediated microbubble attachment to the activated leukocytes involved in inflammation. The authors report both quantitative and qualitative agreement between the localization of microbubbles in infarcted inflamed tissue and reference methods used to detect and quantify inflammation: ^{99m}Tc-RP517 was used to detect neutrophils and TTC staining to describe viable tissue. This method has also been used to detect inflammation in renal ischemia/reperfusion injury [36].

15.3.4 Targeting Cancer

Ellegala et al. [37] used the peptide echistatin to target microbubbles to neovasculature expressing the integrin $a_v\beta_3$. The targeted microbubbles were retained preferentially within the microvasculature of intracerebrally implanted U87MG tumors (i.e., orthotopic) as detected by confocal microscopy of fluorescently labeled microbubbles. Ultrasound imaging was carried out 10 min after bolus injection of targeted microbubbles and increased contrast was observed between 14 and 28 days post tumor inoculation. Leong-Poi et al. [38] also reported targeting of angiogenesis for ultrasound detection using both echistatin and an anti-a_v integrin antibody to achieve significant increases in US contrast compared with controls. The animal model used by these investigators was based on the injection of the proangiogenic factor FGF into the cremaster muscle to stimulate vessel development. FGF can also be used to stimulate vessel development in infarcted myocardial muscle, presenting the opportunity to monitor the response of injured tissue to this therapeutic agents using ultrasound. In another example, Lui et al. [39] demonstrated *in vitro* targeting of polylactic-acid-based UCAs using the anti-HER2 antibody Herceptin as the targeting agent and observed an increase in echogenicity by HER2-antigen-positive cells.

15.4 Summary

The increasing personalization of medicine and its increasing ability to specifically target appropriate medicines to ever-smaller populations of patients demands a corresponding improvement in our ability to more precisely characterize and describe disease.

Medical imaging offers the opportunity to detect, describe, and, in some cases, treat disease, as well as the ability to monitor the response of diseased tissue to therapy. Here we have briefly considered some aspects of the development of contrast agents for both computed tomography and ultrasound imaging. Both modalities have advantages as well as limitations, depending on the specific application. Through the appropriate use of biomaterials within the field of nanotechnology, these challenges are gradually being addressed.

Disclosures and Conflict of Interest

The opinions and perspectives here reflect the current views of the authors. The authors declare that they have no conflict of interest and have no affiliations or financial involvement with any organization or entity discussed in this chapter. No writing assistance was utilized in the production of this chapter and the authors have received no payment for its preparation. This is a revised version of the author's chapter that originally appeared in *Handbook of Harnessing Biomaterials in Nanomedicine: Preparation, Toxicity, and Applications* (Dan Peer, editor), 2012, Pan Stanford Publishing Pte. Ltd., Singapore.

Corresponding Author

Jason L. J. Dearling
Division of Nuclear Medicine and Molecular Imaging
Department of Radiology,
Boston Children's Hospital and Harvard Medical School,
300 Longwood Avenue, Boston, MA 02115, USA
Email: jason.dearling@childrens.harvard.edu

About the Authors

Jason Dearling received his PhD from the University of Kent. He studied the structure-activity relationship between small molecules and their whole-body and intratumoral distribution, leading to the hypoxia tracer Cu-ATSM. He then studied tumor biology with Profs. R. Barbara Pedley and Richard Begent at University College

London with the specific aim of quantifying the effect of the tumor microenvironment on targeted radiation therapy of colorectal cancer. This work led to combination therapies that are now in clinical trials. Dr. Dearling then moved to Boston to work with Drs. Alan Packard and Stephan Voss at Harvard Medical School and Boston Children's Hospital on another highly therapy-resistant cancer, neuroblastoma, where his objective is to develop an individualized approach to treating these patients by preventing the growth of metastases that arise after initial therapy.

Alan Packard is the director of the Radiopharmaceutical Research Laboratory at Children's Hospital, Boston, Massachusetts; senior research associate of Nuclear Medicine and Molecular Imaging and Assistant Professor of Radiology at Harvard Medical School. He received his PhD in inorganic chemistry from Colorado State University and completed a postdoctoral fellowship in technetium chemistry at the University of Cincinnati. Dr. Packard is active in the leadership of the Society of Nuclear Medicine and Molecular Imaging where he currently serves as general program chair. The two primary goals of his research program are the development and preclinical evaluation of (1) radiometal-based PET (positron emission tomography) imaging agents and therapeutics and (2) ^{18}F-labeled compounds for the PET imaging of heart disease and neurological disorders.

References

1. Hallouard, R., et al. (2010). Iodinated blood pool contrast media for preclinical X-ray imaging applications—a review. *Biomaterials*, **31**(24), 6249–6268.
2. Torchilin, V. P., Frank-Kamenetsky, M. D., Wolf, G. L. (1999). CT visualization of blood pool in rats by using long-circulating, iodine-containing micelles. *Acad. Radiol.*, **6**(1), 61–65.
3. Torchilin, V. P. (2007). Micellar nanocarriers: Pharmaceutical perspectives. *Pharm. Res.*, **24**(1), 1–16.
4. Bangham, A. D., Home, R. W. (1964). Negative staining of phospholipids and their structural modification by surface-active agents as observed in the electron microscope. *J. Mol. Biol.*, **8**, 660–668.

5. Allen, T. M. (1994). Long-circulating (sterically stabilized) liposomes for targeted drug delivery. *Trends Pharmacol. Sci.*, **15**(7), 215–220.
6. Gabizon, A., Papahadjopoulos, D. (1988). Liposome formulations with prolonged circulation time in blood and enhanced uptake by tumors. *Proc. Natl. Acad. Sci. U. S. A.*, **85**(18), 6949–6953.
7. Dijkstra, J., et al. (1984). Interaction of liposomes with Kupffer cells *in vitro*. *Exp. Cell. Res.*, **150**(1), 161–176.
8. Lasic, D. D., et al. (1991). Sterically stabilized liposomes: A hypothesis on the molecular origin of the extended circulation times. *Biochim. Biophys. Acta*, **1070**(1), 187–192.
9. Moghimi, S. M., Szebeni, J. (2003). Stealth liposomes and long circulating nanoparticles: Critical issues in pharmacokinetics, opsonization and protein-binding properties. *Prog. Lipid Res.*, **42**(6), 463–478.
10. Mori, A., et al. (1991). Influence of the steric barrier activity of amphipathic poly(ethyleneglycol) and ganglioside GM1 on the circulation time of liposomes and on the target binding of immunoliposomes *in vivo*. *FEBS Lett.*, **284**(2), 263–266.
11. Woodle, M. C., et al. (1992). Versatility in lipid compositions showing prolonged circulation with sterically stabilized liposomes. *Biochim. Biophys. Acta*, **1105**(2), 193–200.
12. Koning, G. A., et al. (2003). Interaction of differently designed immunoliposomes with colon cancer cells and Kupffer cells. An *in vitro* comparison. *Pharm. Res.*, **20**(8), 1249–1257.
13. Leander, P., et al. (2001). A new liposomal liver-specific contrast agent for CT: First human phase-I clinical trial assessing efficacy and safety. *Eur. Radiol.*, **11**(4), 698–704.
14. Wei, X., et al. (2005). Liposomal contrast agent for CT imaging of the liver. *Conf. Proc. IEEE Eng. Med. Biol. Soc.*, **6**, 5702–5705.
15. Kweon, S., et al. (2010). Liposomes coloaded with iopamidol/lipiodol as a RES targeted contrast agent for computed tomography imaging. *Pharm. Res.*, **27**(7), 1408–1415.
16. Fu, Y., et al. (2006). Dendritic iodinated contrast agents with PEG-cores for CT imaging: Synthesis and preliminary characterization. *Bioconjug. Chem.*, **17**(4), 1043–1056.
17. Simon, G. H., et al. (2005). Initial computed tomography imaging experience using a new macromolecular iodinated contrast medium in experimental breast cancer. *Invest. Radiol.*, **40**(9), 614–620.
18. Rabin, O., et al. (2006). An X-ray computed tomography imaging agent based on long-circulating bismuth sulphide nanoparticles. *Nat. Mater.*, **5**(2), 118–122.

19. Kattumuri, V., et al. (2007). Gum arabic as a phytochemical construct for the stabilization of gold nanoparticles: *in vivo* pharmacokinetics and X-ray contrast imaging studies. *Small*, **3**(2), 333–341.
20. Boote, E., et al. (2011). Gold nanoparticle contrast in a phantom and juvenile swine: Models for molecular imaging of human organs using x-ray computed tomography. *Acad. Radiol.*, **17**(4), 410–417.
21. Aydogan, B., et al. (2010). AuNP-DG: deoxyglucose-labeled gold nanoparticles as X-ray computed tomography contrast agents for cancer imaging. *Mol. Imaging Biol.*, **12**(5), 463–467.
22. Shi, X., et al. (2007). Dendrimer-entrapped gold nanoparticles as a platform for cancer-cell targeting and imaging. *Small*, **3**(7), 1245–1252.
23. Matsumura, Y., Maeda, H. (1986). A new concept for macromolecular therapeutics in cancer chemotherapy: Mechanism of tumoritropic accumulation of proteins and the antitumor agent smancs. *Cancer Res.*, **46**(12 Pt 1), 6387–6392.
24. Danila, D., et al. (2009). Antibody-labeled liposomes for CT imaging of atherosclerotic plaques: *In vitro* investigation of an anti-ICAM antibody-labeled liposome containing iohexol for molecular imaging of atherosclerotic plaques via computed tomography. *Tex. Heart Inst. J.*, **36**(5), 393–403.
25. Wyss, C., et al. (2009). Molecular imaging by micro-CT: Specific E-selectin imaging. *Eur. Radiol.*, **19**(10), 2487–2494.
26. McCulloch, M., et al. (2000). Ultrasound contrast physics: A series on contrast echocardiography, article 3. *J. Am. Soc. Echocardiogr.*, **13**(10), 959–967.
27. Lindner, J. R. (2004). Microbubbles in medical imaging: Current applications and future directions. *Nat. Rev. Drug Discov.*, **3**(6), 527–532.
28. Alkan-Onyuksel, H., et al. (1996). Development of inherently echogenic liposomes as an ultrasonic contrast agent. *J. Pharm Sci.*, **85**(5), 486–490.
29. Huang, S. L., et al. (2002). Physical correlates of the ultrasonic reflectivity of lipid dispersions suitable as diagnostic contrast agents. *Ultrasound Med. Biol.*, **28**(3), 339–448.
30. Marsh, J. N., et al. (2002). Temperature dependence of acoustic impedance for specific fluorocarbon liquids. *J. Acoust. Soc. Am.*, **112**(6), 2858–2862.
31. Marsh, J. N., et al. (2002). Improvements in the ultrasonic contrast of targeted perfluorocarbon nanoparticles using an acoustic transmis-

sion line model. *IEEE Trans. Ultrason. Ferroelectr. Freq. Control.*, **49**(1), 29–38.

32. Kang, E., et al. (2010). Nanobubbles from gas-generating polymeric nanoparticles: Ultrasound imaging of living subjects. *Angew. Chem. Int. Ed. Engl.*, **49**(3), 524–528.
33. Villanueva, F. S., et al. (1997). Albumin microbubble adherence to human coronary endothelium: Implications for assessment of endothelial function using myocardial contrast echocardiography.™ *Coll. Cardiol.*, **30**(3), 689–693.
34. Unger, E. C., et al. (1998). *In vitro* studies of a new thrombus-specific ultrasound contrast agent. *Am. J. Cardiol.*, **81**(12A), 58G–61G.
35. Christiansen, J. R., et al. (2002). Noninvasive imaging of myocardial reperfusion injury using leukocyte-targeted contrast echocardiography. *Circulation*, **105**(15), 1764–1767.
36. Lindner, J. R., et al. (2000). Microbubble persistence in the microcirculation during ischemia/reperfusion and inflammation is caused by integrinand complement-mediated adherence to activated leukocytes. *Circulation*, **101**(6), 668–675.
37. Ellegala, D. B., et al. (2003). Imaging tumor angiogenesis with contrast ultrasound and microbubbles targeted to alpha(v)beta3. *Circulation*, **108**(3), 336–341.
38. Leong-Poi, H., et al. (2003). Noninvasive assessment of angiogenesis by ultrasound and microbubbles targeted to alpha(v)-integrins. *Circulation*, **107**(3), 455–460.
39. Liu, J., et al. (2007). Biodegradable nanoparticles for targeted ultrasound imaging of breast cancer cells *in vitro*. *Phys. Med. Biol.*, **52**(16), 4739–4747.

Chapter 16

Nanoimaging for Nanomedicine

Yuri L. Lyubchenko, PhD, DSc,[a] Yuliang Zhang,[a] Alexey V. Krasnoslobodtsev, PhD,[b] and Jean-Christophe Rochet, PhD[c]

[a]*Department of Pharmaceutical Sciences, University of Nebraska Medical Center, Omaha, Nebraska, USA*
[b]*Department of Physics, University of Nebraska at Omaha, Omaha, Nebraska, USA*
[c]*Department of MCMP, Purdue University, West Lafayette, Indiana, USA*

Keywords: nanomedicine, nanoimaging, atomic force microscopy, AFM, DNA imaging with AFM, force spectroscopy, intermolecular interactions, protein aggregation, amyloids, α-synuclein, amyloid-β, Alzheimer's disease, Parkinson's disease, protein misfolding

16.1 Introduction

Nanomedicine can be broadly defined as a branch of medicine focused on diagnosis and treatment of diseases via nanotechnology. Nanomedicine developments have advanced in two major directions. One is the development of nano-carriers for drugs to improve the pharmacokinetics of drug delivery and release processes with a focus on targeted delivery of drugs. The other is the development of novel approaches for diagnosis and treatment of diseases with the use of nanoimaging and nanomanipulation technologies. This chapter outlines a few examples of research primarily related to the

Handbook of Clinical Nanomedicine: Nanoparticles, Imaging, Therapy, and Clinical Applications
Edited by Raj Bawa, Gerald F. Audette, and Israel Rubinstein

ISBN 978-981-4669-20-7 (Hardcover), 978-981-4669-21-4 (eBook)
www.panstanford.com

second direction of nanomedicine utilizing atomic force microscopy (AFM), a fundamental technique of nanotechnology. AFM belongs to a family of scanning probe microscopy (SPM) techniques. The prototype scanning tunneling microscope instrument was conceived by Binnig and Rohrer [1], who were awarded the Nobel Prize in 1986 for this invention. AFM was invented in 1986 [2]. Its development by the Hansma group [3] resulted in the commercial production of the AFM, and as a result, the instrument has become available to the biological community.

16.2 Basic Principles of AFM

Figure 16.1 illustrates the basic principles of AFM operation. A sharp AFM tip (triangle) reads the profile of the sample (bumpy profile) by scanning over the sample surface [4].

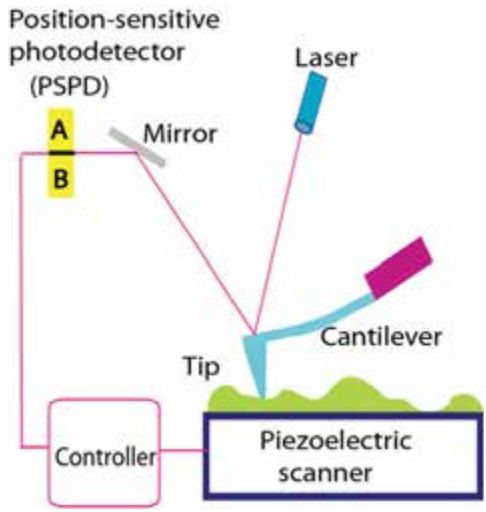

Figure 16.1 Schematic illustration explaining basic principles of AFM operation. Reproduced from ref. 4 with permission. Copyright (2011) Elsevier.

The tip is attached to a cantilever that works as a spring pressing the tip against the sample to reproduce the surface profile. The vertical position of the tip is measured by a laser light reflected from the cantilever to the position-sensitive photodetector (PSPD). In this particular scheme, the tip is stationary, but the

sample mounted on the piezoelectric scanner moves. There are a number of important features of the AFM instrument. First, the scanner controls the position of the sample relative to the tip, so *x*–*y* position of the tip can be controlled with accuracy better than 1 nm. Second, the tip can be atomically sharp. Third, the vertical displacement of the tip relative to the surface is determined with sub-nanometer accuracy. These three major factors lay the foundation for the capability of AFM to provide a topographic image with atomic accuracy. Indeed, the atomic resolution for AFM was achieved in early work [5] where the atomic-scale periodicities of calcite as well as the expected relative positions of the atoms within each unit cell were obtained. Importantly, attractive forces on the order of 10 pico Newton (pN) acting between single atomic sites on the sample and the front atoms of the tip were directly measured. Note the paper [6] in which both calcium and oxygen atoms at the cleavage plane of $CaSO_4$ surface were identified. A breakthrough in high-resolution AFM imaging occurred with implementation of the so-called non-contact mode (NC-AFM; see review [7]), offering a unique tool for real space atomic-scale studies of surfaces and nanoparticles, as well as thin films irrespective of the substrate being electrically conducting or non-conducting. AFM provides atomic resolution even for isolated organic molecules [8]; it does not require any coating or staining of the sample and importantly the scanning can be performed in any medium including water. These two characteristics make AFM superior to other nanoimaging techniques.

16.3 AFM: Imaging of Biological Samples

16.3.1 AFM Imaging of DNA and Protein–DNA Complexes

DNA was one of the first biological samples imaged with AFM (reviewed in [9]). Introduction of a gentle imaging mode (tip oscillating or Tapping Mode [10]) and the development of sample preparation methods made it possible to image DNA reliably and routinely (see reviews [9, 11, 12]), although the sample preparation issue should be taken into careful consideration to avoid potential artifacts.

Figure 16.2 shows images of two biological samples to illustrate the power of Tapping Mode for biological applications. An image of circular DNA with extruded cruciform structure (indicated with an arrow) [13] is shown in Figure 16.2a. The DNA appears as a filament with a uniform thickness. Note that transmission electron microscopy was not as efficient in the study of alternative DNA structures. Figure 16.2b shows an AFM image of reconstituted chromatin assembled on purified histone octamers [14]. Nucleosomal particles formed by the wrapping of DNA around histone octamers are unambiguously seen as bright globular features (blobs). In a majority of cases, the sizes of the blobs are almost identical and no damage to the nucleosomes is seen primarily due to the use of Tapping Mode for imaging.

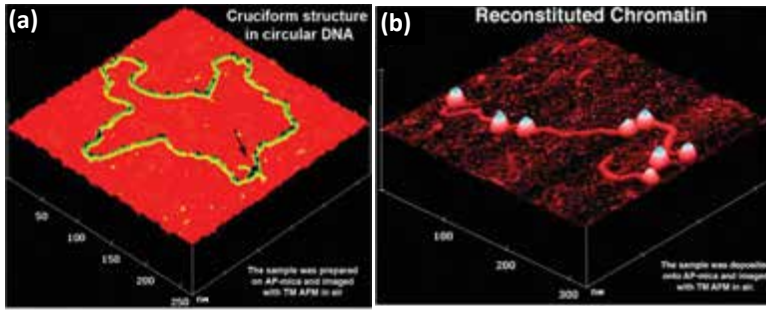

Figure 16.2 AFM images of (a) circular pUC8F14C plasmid DNA with a cruciform protrusion (indicated with an arrow) and (b) reconstituted chromatin. Reproduced from ref. 4 with permission. Copyright (2011) Elsevier.

16.3.2 AFM of Protein Amyloid Aggregates

AFM was instrumental in the study of the protein misfolding and aggregation process. Misfolding and aggregation of a protein is critically involved in the development of such devastating neurodegenerative disorders as Alzheimer's (AD) and Parkinson's (PD) diseases [15, 16] (see also chapter 21 in this book). The class of amyloid proteins may spontaneously form fibrils (Figs. 16.3a,c). The straight morphology indicates high stiffness of the fibrils in Fig. 16.3c [16]. The stiffness of the fibrils was analyzed in detail by Knowles et al. [17]. It was suggested that the major contribution to the fibril's rigidity is provided by the hydrogen-bonding network of

backbone-backbone interactions that is modulated by side-chain interactions.

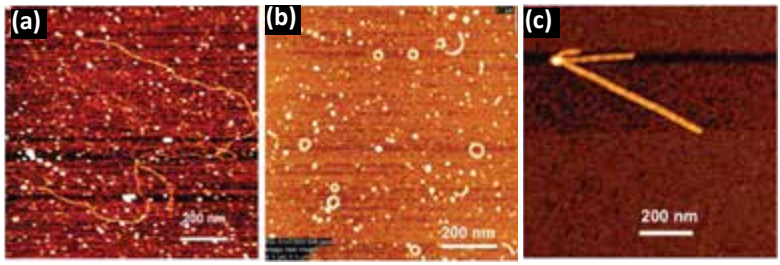

Figure 16.3 AFM images of A-beta peptide aggregated in different morphologies: protofilaments (a), toroids (pore-like structures, rings) (b), and fibrils (c). Reproduced from ref. 16 with permission. Copyright © 2006 Wiley-Liss, Inc.

This finding reinforces the hypothesis that the ability to form amyloid fibrils is a generic property of the polypeptide backbone and explains why so many unrelated proteins form fibrillar aggregates [18]. It has also been observed that many amyloids, for example amyloid-beta (Aβ) peptide, amylin, and alpha-synuclein (α-Syn) form annular particles that resemble membrane pores (Fig. 16.3b). Importantly, such pore-like structures are formed when reconstituted in membranes [19, 20]. Electrophysiological studies have confirmed typical channel-like activity, including signature single channel conductance [20–23]. The formation of such channels within the cell membrane has been proposed as a pathogenic mechanism for several neurodegenerative disorders (e.g., Alzheimer's and Parkinson's diseases) and systemic diseases (diabetes, cancer, and heart disease) [21, 24].

16.3.3 AFM of Membranes

Imaging of membrane proteins with AFM has been a research focus for several groups. Membrane-associated proteins such as ion channels and receptors are often targets for drugs [25]. AFM imaging with high spatial resolution allows one to observe single membrane proteins and reveal their structural peculiarities [26]. For example, AFM was used to monitor structures of bacteriorhodopsin—a light-driven proton pump found in Halobacteria. Apparently, in bacteriorhodopsin, one of the polypeptide loops

connecting transmembrane helices E and F exhibits high flexibility [27, 28]. Such flexibility was suggested to be important for the function of the protein as there is a conformational change of the protein during the photocycle.

16.3.4 AFM of Cells

AFM is widely used for imaging of single live cells, providing high-resolution images of cell wall structural details. Using such an approach, it is possible to directly visualize the effects of drugs on cell surfaces. AFM imaging was used to probe the surface of live *Mycobacterium tuberculosis* revealing the effect of its interactions with four antimycobacterial drugs: isoniazid, ethionamide, ethambutol, and streptomycin [29]. Treatment with these drugs induced major cell-surface alterations. Such ultrastructural alterations were observed in the form of layered structures, striations, and porous morphologies. These modifications were suggested to reflect the inhibition of the synthesis of major cell wall constituents [29, 30].

Significant differences in the surface topography and morphology of red blood cells (RBCs) from healthy humans and patients with systemic lupus erythematosus (SLE) were observed with atomic force microscopy [31]. AFM revealed characteristic circular-shaped holes on the surface of RBCs from SLE patients under physiological conditions. Such morphological changes were postulated to correlate with previously published changes in the SLE erythrocyte membrane [31].

16.4 Dynamic Biological Events: Time-lapse AFM

Imaging in aqueous solutions is the best way to preserve native structures of biological systems. In addition, time-lapse AFM imaging in aqueous solutions enables direct visualization of the dynamics of molecules and molecular systems at the nanoscale level due to the possibility to obtain high resolution. The potential of AFM for direct imaging of actual molecular processes was demonstrated by the group of P. Hansma in the very early stages of AFM development, in which the visualization of fibrin polymerization was observed

[32, 33]. However, progress in AFM imaging of biological processes required substantial improvements of AFM instrumentation. The introduction of tapping mode imaging [34] considerably eased the problem of sample movement by the tip. Note that imaging in aqueous solutions eliminates the resolution-limiting capillary effect, so images of DNA molecules with parameters very close to crystallographic ones can be obtained [35]. The advances in this technique are described (see Chapter 21). We would like to note in this regard recent advances in high-speed time lapse that enabled to jump from the minute-scale data acquisition rate for a conventional AFM instrument to the video-rate data acquisition. The progress in the development of the high-speed AFM (HS AFM) instrumentation was made primarily due to development of Ando's group [36–39]. These advances enabled Ando's group to visualize the dynamics of individual myosin molecules with a 100 millisecond temporal resolution [38, 39]. Note the application of this technology to study the dynamics of site-specific DNA binding proteins in the subsecond time scale [40] and dynamics of reconstituted chromatin [41]. The latter study revealed a sliding mechanism, which was characterized with fluctuation within approximately 50 nm along the DNA strand. In addition, histone dissociation was visualized, and two distinct modes of dissociation were identified. This emerging novel instrumentation has also been applied to study the process by which the site-specific EcoRII protein searches for specific binding sites on DNA [42].

The capability of HS AFM to identify and characterize intrinsically disordered regions (IDR) in proteins has been demonstrated in a series of publications from Ando's group [43–45]. IDR were identified in a number of proteins, and their structural plasticity can play an important role in the misfolding and aggregation of amyloid proteins associated with neurodegenerative diseases such as AD and PD [46]. Structural characterization of ID segments with X-ray crystallography cannot be performed due to their highly dynamic structure, and this feature also complicates the use of electron microscopy and traditional AFM imaging [45]. In their pioneering work, Miyagi et al. [45] was able to identify IDR segments in the histone chaperone that FAcilitates Chromatin Transcription (FACT) protein critically involved in regulation of chromatin transcription. The video rate data acquisition (up to 17

frames per second) made it possible to unambiguously identify two major IDR segments in the protein. Moreover, the mechanical properties of these segments were evaluated leading the authors to conclude that IDR segments are slightly more relaxed compared to random coil regions of the proteins. Recently the same group applied HS AFM to characterize the effect of phosphorylation on structural and dynamic properties of ID segments of FACT [43]. The AFM data demonstrated that the protein's phosphorylation leads to the formation of globular features within the flexible ID segment. These are rather dynamic features, and their stability is increased with the extent of phosphorylation. This relationship between phosphorylation and stability can explain the inhibitory effect of FACT phosphorylation on nucleosome binding. As mentioned above, the role of ID segments in the self-assembly of proteins in disease-prone aggregates has been widely discussed. However, the lack of experimental approaches capable of their characterization has significantly impeded progress in understanding molecular mechanisms underlying the aggregation process. HS AFM can fill the gap in our understanding of the protein self-assembly process. Note in this regard the ability of HS AFM to characterize protein dynamics at the nanoscale, as aggregation is a process accompanied by the formation of various transient states of the protein [47, 48].

16.5 AFM Force-Spectroscopy and Intermolecular Interactions

AFM is an instrument with dual capabilities. In addition to imaging as described above, AFM is capable of probing mechanical properties of systems at the nanoscale. Such capability is provided by the AFM probe, which can be positioned with sub-nanometer accuracy in all three dimensions, as well the AFM cantilever (Fig. 16.1), the stiffness of which can be varied over a broad range.

16.5.1 Mechanical Properties of Cells

AFM measurements of mechanical properties of various surfaces such as modulus of elasticity (reversible deformation of the sample), hardness (resistance to permanent shape change), yield

strength (the stress at which a predetermined amount of permanent deformation occurs), fracture toughness (resistance to fracture when a crack is present), scratch hardness (resistance to fracture due to friction) and wear properties (resistance to erosion by the action of another surface) are reviewed in [49]. The applications of this methodology for cell mechanics are very broad. One of the examples related to nanomedicine is the identification of cancer cells [50]. Several reports showed that the rigidity of cancer cells measured with AFM is quite different from that of normal cells [50–53]. Cancer cells from patients were reported to be 70% less stiff than normal cells [50].

AFM was also instrumental in understanding the mechanism of bone strength [54]. AFM force spectroscopy helped to identify the fracture-resisting protein-based "glue" that binds mineral plates of nacre together. This "glue" contains "sacrificial bonds" that both protect the polymer backbone and dissipate energy. The separation of mineralized collagen fibrils under loading is consistent with the findings of AFM studies that crack formation and bone fracture occur between the mineralized collagen fibrils. Based on this knowledge, novel diagnostic tools are being tested to diagnose bone diseases [55]. Another example of the advantageous use of AFM is early diagnosis of osteoporosis [56]. It has been shown that the cartilage of osteoarthritic animals is stiffer and collagen fibers become thicker. Nanoscale characterization of structural changes of the articular cartilage can detect progressing damage much earlier than routine methods.

16.5.2 AFM Force-spectroscopy

The ability of AFM to measure intermolecular and intarmolecular interaction is also linked to the cantilever's mechanical properties and this area of applications belongs to the force spectroscopy field. Figure 16.4 graphically describes this mode of AFM operation. This chapter also describes a number of AFM force spectroscopy applications. Here in the two subsections below we outline recent advances in the study of interactions of alpha-synuclein (α-Syn) and molecular mechanisms of protein misfolding and aggregation.

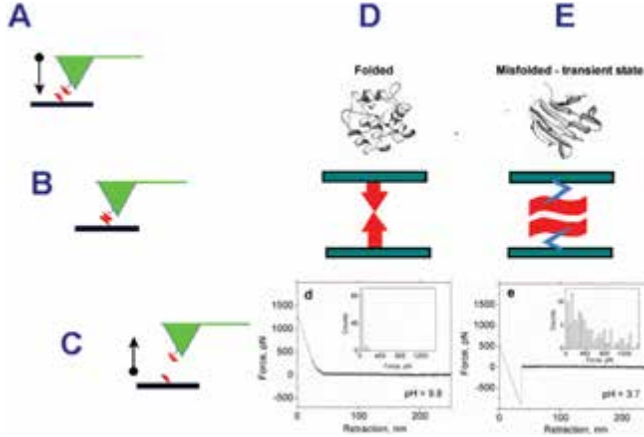

Figure 16.4 Scheme explaining the nanoprobing approach for detecting and analyzing misfolded states of the protein. Proteins anchored to the substrate surface and the AFM tip (A) are brought into contact (B) and then pulled apart (C). The rupture forces of the complexes depend on the protein conformation—low forces (force curve "d") for normally folded proteins (D) and large rupture forces (force curve "e") correspond to a misfolded state of the protein (E). Reproduced from ref. 16 with permission. Copyright © 2006 Wiley-Liss, Inc.

16.5.2.1 Nanoprobing of protein misfolding and interactions

Misfolding and aggregation of proteins are associated with a wide range of human pathologies termed *protein misfolding* (*deposition*) *neurodegenerative disorders* such as AD, PD, and Huntington's diseases, as well as systemic and localized amyloidoses, and transmissible encephalopathies [16, 57]. Understanding the mechanisms underlying the self-assembly of proteins and peptides into nano-aggregates of various sizes and morphologies would facilitate the development of efficient therapies and diagnostic tools for these devastating diseases. Although it is well known that the same protein can form fibrillar, pore-like, spherical, or amorphous aggregates (Fig. 16.3) with diverse biological consequences, the conditions leading to misfolding and the formation of various complexes are unclear. The lack of efficient methods to characterize the complex aggregation process is the major reason for our limited knowledge. A process that may appear simple by existing techniques may actually have many steps and a variety of important intermediate states—each with its own unique dynamics.

Intermediate states are stabilized by weak interactions that are typically transient and difficult to measure [47].

Single-molecule biophysics techniques can help to image molecular intermediates, follow molecular-scale events in real time, and measure a wide range of intermolecular interactions as has been demonstrated over the last few years [58]. For example, conformational dynamics of the prion protein [59] and alpha-synuclein (α-Syn) [60] were studied with single-molecule fluorescence, including Förster resonance energy transfer (FRET). Use of the AFM pulling approach to study conformational transitions in α-Syn showed that the disease-associated mutations in the protein facilitate its misfolding [61]. Interestingly, changes in environmental conditions such as high ionic strength and the presence of Cu^{2+}, which are known to increase the propensity of α-Syn to aggregate, shifted the conformational equilibrium toward beta-like structures that are directly related to the aggregation of α-Syn [62].

It has been shown that AFM is capable of directly probing aggregation-prone states of proteins and their interactions [16, 63–66]. In this approach, the proteins are anchored to the surfaces of the AFM substrate (mica) and the probe (Fig. 16.4A), and the interaction between such anchored molecules is measured in approach-retraction cycles (Figs. 16.4A–C). The forces stabilizing the complex are measured at the rupture event (Fig. 16.4C). The rupture force is low if the complex is weak (normal state of the protein; Fig. 16.4D; the force curve is shown as inset "d" in this scheme), but the forces increase if the protein adopts a misfolded conformation as illustrated in Fig. 16.4E and inset "e." Additionally, there is a broader range of forces for the misfolded conformation (Fig. 16.4E) as compared with the normal state of the protein (Fig. 16.4D). AFM experiments with different proteins confirmed this relationship, demonstrating a direct correlation between the propensity of a protein to aggregate and the strength of the interprotein interaction [16, 63, 64].

It is important to note that the described approach is entirely different from traditional ones. It allows unambiguous measurement of pair-wise protein–protein interactions (Fig. 16.5a), avoiding the effect of multiple interactions complicating quantitative analysis of the aggregation process. Moreover, this nanoprobing approach is capable of locating regions of the protein responsible for the pathology related conformational changes [66].

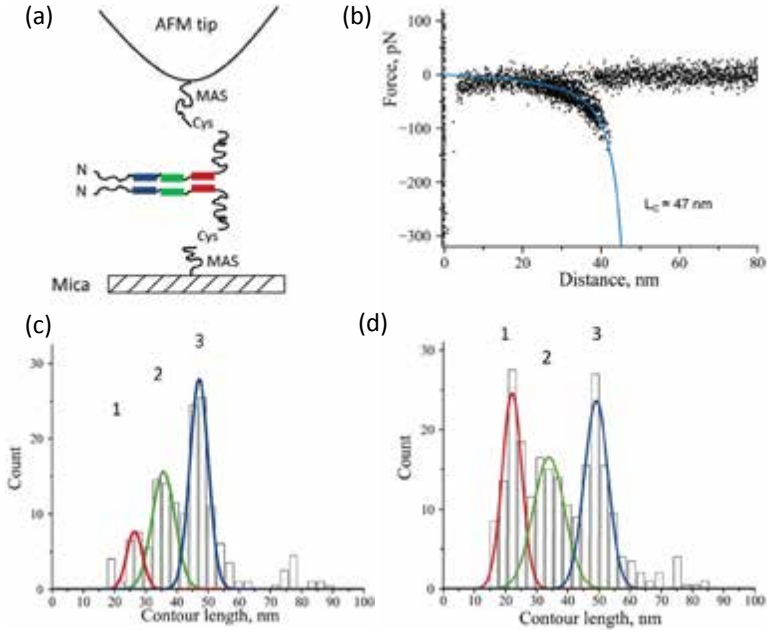

Figure 16.5 Schematic representation of experimental setup. (a) α-Synuclein molecules were covalently attached on MAS (maleimide silatrane)-functionalized mica and silicon nitride tips. (b) Superposition of representative force–distance curves illustrating the single molecule detection of the interaction between two wild type alpha-synuclein molecules in the presence of spermidine. (c and d) Histograms of contour lengths for wild type α-synuclein and A30P mutant, respectively, in the presence of spermidine. Reproduced from ref. 69.

Force–distance curves measured with force spectroscopy detect specific rupture events. These specific events are observed between aggregation-prone (misfolded) states of proteins. It has been demonstrated that force spectroscopy detects interactions between α-Syn molecules under conditions that induce conformational transitions associated with enhanced aggregation such as low pH [67], the presence of multivalent cations (Al^{3+}, Zn^{2+}) [68] or cellular polyamines [69]. Figure 16.5b shows the superposition of several force–distance curves detected in the presence of the cellular polyamine spermidine [69]. The appearance of rupture events suggests that spermidine promotes the misfolding process of α-Syn. The position of the rupture events reports on the distance

where the rupture is taking place. By fitting the force curves with a worm like chain model, we were able to measure contour lengths (Fig. 16.5b). The methodology described in [66] for the contour length analysis enables one to identify the segment of the protein that defines the interprotein interactions and is thus responsible for the misfolding process. This analysis performed for wild type (WT) α-Syn in the presence of spermidine led to the conclusion that several conformations of WT α-Syn are responsible for the formation of the dimer. As indicated in Fig. 16.5c, a statistical histogram of measured contour length values has three clear peaks. The Gaussian fit of the histogram resulted in maxima of distributions at 26, 36, and 47 nm defined as peaks 1, 2, and 3, respectively. The identification of the misfolding prone segment of the protein is in line with pathology related properties of α-Syn. Indeed, peaks 2 and 3 of pathological interactions for wild-type α-Syn correspond to the region known as the non-amyloid-beta component (NAC) found in amyloid plaques in Alzheimer's disease [70, 71]. NAC comprises amino acids 61–95 of α-Syn and was shown to readily aggregate *in vitro* [70, 72, 73]. The position of the shortest interaction (peak 1) is outside the NAC region suggesting that the interacting segments that are capable of forming dimers extend beyond this region into the C-terminal part. Interestingly, AFM data show that the A30P mutation alters interactions between α-Syn proteins (Fig. 16.5d). Similar analysis of contour lengths performed with the A30P mutant showed that the segments of the protein involved in the dimerization are the same as for WT. However, the ratio between the peaks is quite different with a greater contribution from the shortest peak (*peak 1*) for the A30P mutant. This mutation is linked to familial Parkinson's [74] and the AFM data provide a structural basis for the protein's role in disease development. The differences in the misfolding patterns observed between WT α-Syn and the A30P mutant may be responsible for the higher propensity of the mutant to aggregate and cause early-onset PD [69].

16.5.2.2 Molecular mechanisms of protein assembly into disease-prone aggregates

The ability to perform force spectroscopy analysis at the single-molecule level [15] enables the application of dynamic force spectroscopy (DFS), a quantitative approach introduced by Evans

and Ritchie (reviewed in [75]). In the DFS approach, pair-wise interactions are probed over a broad range of pulling rates. Rupture forces are determined for each force–distance curve, and distributions of forces are obtained and analyzed as described [15]. The results of DFS analysis for α-Syn are shown in Fig. 16.6. The plot of the most probable force versus the logarithm of the pulling rate is shown in Fig. 16.6a. The experimental data points are nicely approximated with a linear plot, which according to the DFS theory suggests that the dimer dissociation is characterized by a one-barrier energy profile (Fig. 16.6b), and the barrier height is 28 k_BT corresponding to an off-rate (dissociation rate) constant value of ~1 s [66]. This is one of the major findings from the DFS analysis suggesting that dimeric complexes formed by misfolded α-Syn protein are stable and dissociate in the range of seconds.

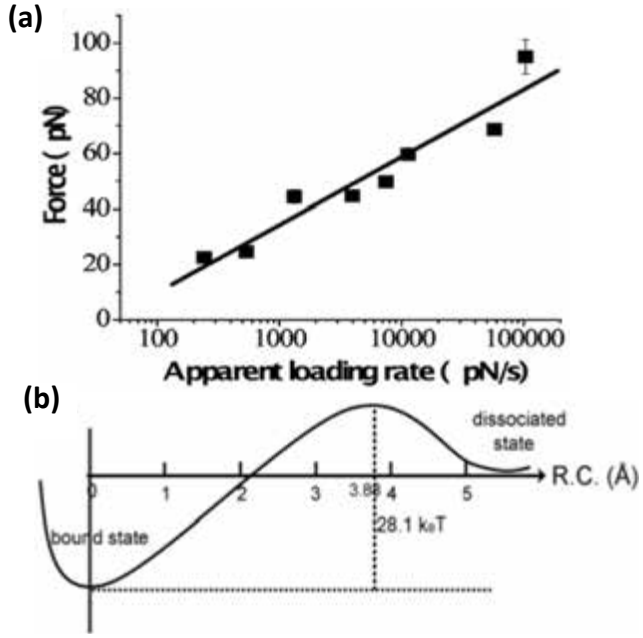

Figure 16.6 DFS analysis of α-Syn interactions. (a) DFS plot for AFM probing of α-Syn interaction measured at pH 5.1. The linear relationship indicates that the dissociation of an α-Syn dimer follows a one-barrier path shown in (b). The energy of the barrier is 28.1 k_BT; the complex lifetime is 0.27 ± 0.13 s. Reproduced from ref. 15 with permission. Copyright © 2010 John Wiley & Sons, Inc.

This differs markedly from the dynamics of monomers, which occurs on a microsecond-nanosecond time scale. Similar studies were performed on Aβ peptides of various sizes [76–78] and the Sup35 protein [79]. The common feature of these studies is that dimers, compared to monomers, are highly stable. Therefore, the dimerization of misfolded proteins is a mechanism by which the transient misfolded state of a protein (required for aggregation) is stabilized. Therefore, it was proposed that the formation of dimers is the key step for aggregation and that the long lifespans of dimeric complexes promote the selection of the misfolding-aggregation paths from non-pathologic pathways [15]. However, these studies left a number of unanswered questions: How does the misfolded dimer form? Do the monomers adopt misfolded states prior to their assembly into the dimer or does the conformational transition occur during the interaction of the monomers? How dynamic is the dimer? What is the structure of the dimer? How does the dimer structure relate to the protein conformation within stable assemblies such as fibrils?

These questions were answered in a paper by Lovas et al. [78], in which steered molecular dynamics (MD) simulation was applied to directly analyze the dimerization process of Aβ(14–23) peptide (HQKLVFFAED) terminated with cysteine at its N-terminus [80]. This particular segment contains the "central hydrophobic cluster" of Aβ, which is critically involved in Aβ aggregation [81]. Indeed, Aβ(14–23) forms amyloid fibrils after 24 h of incubation at room temperature at a concentration of 100 μM (Fig. 16.7a) and the single molecule force spectroscopy study showed that immobilized Aβ(14–23) monomers interact forming dimers with a lifetime of ~1 s (Figs. 16.7b,c).

MD simulations of the dynamics of this peptide in the monomeric form in an aqueous environment showed no formation of any extended β-sheet conformation. However, changes were observed when two monomers were brought into close proximity, allowing them to interact (Fig. 16.7d). During the initial 350 ns period, the distance fluctuates between monomers with no considerable change of the monomer secondary structure. After 350 ns, a rearrangement occurred that resulted in the formation of an antiparallel β-sheet conformation (red arrows in snapshot 6 in Fig. 16.7d). Thus, the inter-molecular interactions of the monomers triggered conformational changes within the individual pep-

tide chain, which led to the formation of the antiparallel β-sheet structure. The arrangement of monomers in an antiparallel orientation leads to the cooperative formation of a β-sheet conformer. Moreover, the dimer remains stable during entire 400 ns simulation period as it is evidenced from Fig. 16.7e in which a DSSP diagram is shown. The largest cluster of the trajectory contained 82.1% of the explored structures. A representative structure of the largest cluster is shown in the snapshot to the right of the diagram.

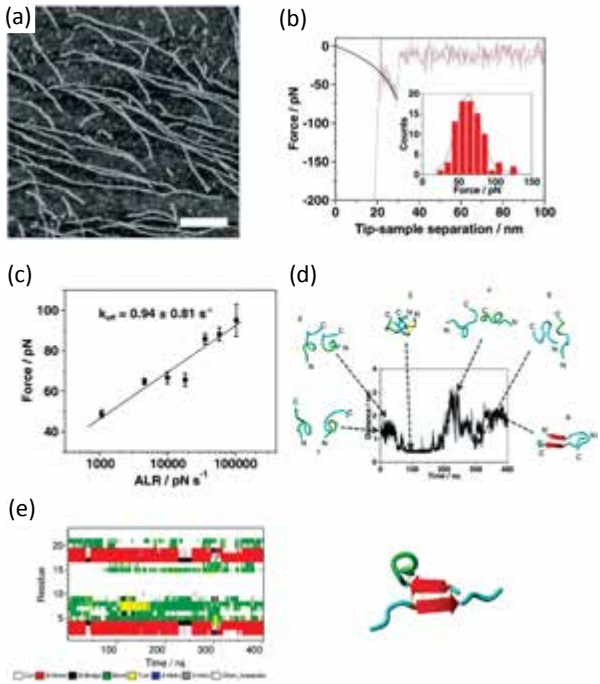

Figure 16.7 Experimental and computational studies of Aβ(14–23) interactions. (a) AFM images of aggregates, scale bar is 200 nm. (b) The results of the force spectroscopy: a typical force curve with insert showing the distribution of rupture forces fitted with Gaussian function. (c) Dynamic force spectroscopy data. (d) Time trajectory of the dimer dynamics simulated by MD. (e) The time-dependent secondary structure (DSSP diagram) for the next 400 ns simulations (left) and the central structure of the largest cluster of the MD simulation (right). Reproduced from ref. 78 with permission. Copyright © 2013 American Chemical Society.

Computational analysis of the rupture process suggests that the antiparallel β-sheet structure of the dimer is stabilized not only by hydrogen bonds, but also by salt bridges and weakly polar interactions of the side chains. These studies suggest that protein misfolding is a rare process, but the interprotein interaction can facilitate the protein conformational transition leading to the formation of dimers with enormously high lifetimes. Indirectly this hypothesis is supported by the results of an earlier paper [82] in which structural rearrangements of globular proteins during misfolding were analyzed. The authors proposed that the structural transition to aggregation prone states occurs at the protein–protein contacts formed by the normally assembled proteins.

A model for protein misfolding and the early stages of the self-assembly process in which the protein misfolded state is stabilized by dimer formation was proposed by Lyubchenko et al. [15]. The model shown in Fig. 16.8 amends that model by incorporating a second pathway in which misfolding occurs within dimers prior to their misfolding. This second aggregation pathway identified in computational analysis may be a preferable route for short peptides, although other findings [82] provide additional evidence in support of the critical role of interpeptide and interprotein interactions in protein conformational transitions triggering the amyloid-type aggregation process.

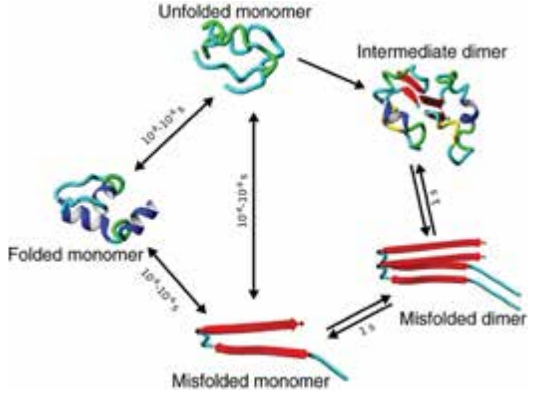

Figure 16.8 Schematic representation of the protein dynamics model. The transitions of the folded (native) state of a protein to unfolded and misfolded states are shown for simplicity only. Characteristic times for the transition between these states as well as the dimer lifetime are shown above the arrows.

16.6 Concluding Remarks

Studies over the past decade demonstrated that AFM imaging is a valuable tool for the recognition and visualization of objects at nanoscale. The capability of AFM to operate at ambient conditions was one of the major factors making it possible to use this instrumentation for biomedical studies. Moreover, AFM is capable of operating in aqueous solutions to perform topographic studies of fully hydrated samples. The advent of high-speed AFM operating in aqueous solutions with video rate data acquisition speed brought AFM studies to another level at which biological processes at the nanoscale can be visualized and quantitatively analyzed. This unique capability of high-speed AFM is illustrated by a few examples, but the technique is under development, so new applications of high-speed AFM to complex biological systems are on the horizon. In addition to topographic imaging, AFM is capable of measuring intermolecular interactions. Importantly, the same instrument can operate in both modes, which is a unique feature of AFM. The use of both AFM modalities will advance our understanding of important health related phenomena. The ability of AFM force spectroscopy to quantitatively measure interprotein interaction opens prospects for understanding molecular mechanisms of pathogenesis of such devastating diseases as Alzheimer's, Parkinson's and prion diseases. The technique at the current level of development is capable of quantitative characterization of small molecules as the most potent candidates for successful treatment of these neurological disorders. The combined use of both AFM modes on the same system, in addition to future technological advances, will be beneficial to the development of treatments targeting different stages of these diseases.

Abbreviations

AFM: atomic force microscopy
Aβ: amyloid-beta
α-Syn: alpha-synuclein
DFS: dynamic force spectroscopy
HS AFM: high-speed AFM

IDR: intrinsically disordered regions
FACT: The histone chaperone that FAcilitates Chromatin Transcription
MD: Molecular Dynamics
PSPD: position-sensitive photodetector
RBC: red blood cell
SLE: systemic lupus erythematosus
FRET: Förster resonance energy transfer
NAC: non-amyloid-beta component
WT: wild type
AD: Alzheimer's Disease
PD: Parkinson's Disease

Disclosures and Conflict of Interest

This work was supported by the following US grants: DOE (DE-FG02-08ER64579), NIH (1P01GM091743 and 1 R01 GM096039) and NSF (EPS-1004094).

The authors declare that they have no conflict of interest and have no affiliations or financial involvement with any organization or entity discussed in this chapter. This includes employment, consultancies, honoraria, grants, stock ownership or options, expert testimony, patents (received or pending) or royalties. No writing assistance was utilized in the production of this chapter and the authors have received no payment for its preparation.

Corresponding Authors

Dr. Yuri Lyubchenko
Department of Pharmaceutical Sciences
University of Nebraska Medical Center
601 S. Saddle Creek Road, Omaha, NE 68106, USA
Email: ylyubchenko@unmc.edu

Dr. Alexey Krasnoslobodtsev
Department of Physics
University of Nebraska at Omaha
6001 Dodge Street, Omaha, NE 68182, USA
Email: akrasnos@unomaha.edu

About the Authors

Yuri Lyubchenko is professor in the Department of Pharmaceutical Sciences, College of Pharmacy, at the University of Nebraska Medical Center, USA. He obtained his PhD from the Moscow Institute of Physics and Technology and his DSc degree from the Institute on Molecular Genetics, Moscow, Russia. His current interest is focused on understanding the molecular mechanisms of DNA replication, repair and recombination in conjunction with elucidating novel approaches for the treatment of cancer and HIV. The elucidation of molecular mechanisms of the development of Alzheimer's, Parkinson's, and prion diseases are other areas of interest. Dr. Lyubchenko serves on a number of journal editorial boards, including as an associate editor of *Nanomedicine: Nanotechnology, Biology and Medicine.*

Yuliang Zhang is a graduate student in the Department of Pharmaceutical Sciences, College of Pharmacy, at the University of Nebraska Medical Center, USA. He obtained his MS degree from Northeast Forestry University in China. His current interest is elucidating the molecular mechanisms of protein misfolding at the early stage and propelling the development of specific diagnostic, therapeutic, and potentially preventive treatments of protein misfolding diseases.

Alexey Krasnoslobodtsev completed his PhD in Physical Chemistry at the New Mexico State University. He is currently an assistant professor at the Department of Physics, University of Nebraska at Omaha. His research primarily focuses on biomedical applications of nanotechnology studying the mechanism of protein misfolding and protein–protein interactions; developing ultrasensitive biosensing nano-platforms; and combining nanoimaging tools with spectroscopic techniques. The major aim of his research is to facilitate therapeutic development, as well as advanced imaging and early diagnostics.

Jean-Christophe Rochet is an associate professor in the Department of Medicinal Chemistry and Molecular Pharmacology, College of Pharmacy, at Purdue University. He obtained his PhD from the University of Alberta, Canada, and pursued post-doctoral studies at Brigham and Women's Hospital, Harvard Medical School. His research group has a long-standing interest in understanding mechanisms of neurotoxicity and neuroprotection in neurodegenerative diseases such as Parkinson's disease (PD). Dr. Rochet's studies in cellular models that reproduce key aspects of PD pathogenesis have yielded new insights into genetic and chemical suppressors of neurodegeneration. He has served as Principal Investigator on a number of studies funded by NIH and other agencies such as the Michael J. Fox Foundation.

References

1. Binnig, G., Rohrer, H., Gerber, C., Weibel, E. (1982). Surface studies by scanning tunneling microscopy. *Phys. Rev. Lett.*, **49**(1), 57.
2. Binnig, G., Quate, C. F., Gerber, C. (1986). Atomic force microscope. *Phys. Rev. Lett.*, **56**(9), 930–933.
3. Hansma, P. K., Elings, V. B., Marti, O., Bracker, C. E. (1988). Scanning tunneling microscopy and atomic force microscopy: Application to biology and technology. *Science*, **242**(4876), 209–216.
4. Lyubchenko, Y. L. (2011). Preparation of DNA and nucleoprotein samples for AFM imaging. *Micron*, **42**(2), 196–206.
5. Ohnesorge, F., Binnig, G. (1993). True atomic resolution by atomic force microscopy through repulsive and attractive forces. *Science*, **260**(5113), 1451–1456.
6. Sokolov, I. Y., Henderson, G. S., Wicks, F. J. (1999). Theoretical and experimental evidence for "true" atomic resolution under non-vacuum conditions. *J. Appl. Phys.*, **86,** 5537–5540.
7. Lauritsen, J. V., Reichling, M. (2010). Atomic resolution non-contact atomic force microscopy of clean metal oxide surfaces. *J. Phys. Condensed Matter*, **22**(26), 263001.
8. Gross, L., Mohn, F., Moll, N., Meyer, G., Ebel, R., et al. (2010). Organic structure determination using atomic-resolution scanning probe microscopy. *Nat. Chem.*, **2**(10), 821–825.

9. Lyubchenko, Y. L. (2004). DNA structure and dynamics: An atomic force microscopy study. *Cell Biochem. Biophys.*, **41**(1), 75–98.
10. Zhong, Q., Inniss, D., Kjoller, K., Elings, V. B. (1993). Fractured polymer/silica fiber surface studied by tapping mode atomic force microscopy. *Surf. Sci.*, **290**(1–2), L688–L692.
11. Lyubchenko, Y. L., Shlyakhtenko, L. S., Gall, A. A. (2009). Atomic force microscopy imaging and probing of DNA, proteins, and protein DNA complexes: Silatrane surface chemistry. *Methods Mol. Biol.*, **543**, 337–351.
12. Lyubchenko, Y. L., Shlyakhtenko, L. S. (2009). AFM for analysis of structure and dynamics of DNA and protein–DNA complexes. *Methods*, **47**(3), 206–213.
13. Shlyakhtenko, L. S., Hsieh, P., Grigoriev, M., Potaman, V. N., Sinden, R. R., et al. (2000). A cruciform structural transition provides a molecular switch for chromosome structure and dynamics. *J. Mol. Biol.*, **296**(5), 1169–1173.
14. Yodh, J. G., Woodbury, N., Shlyakhtenko, L. S., Lyubchenko, Y. L., Lohr, D. (2002). Mapping nucleosome locations on the 208-12 by AFM provides clear evidence for cooperativity in array occupation. *Biochemistry*, **41**(11), 3565–3574.
15. Lyubchenko, Y., Kim, B.-H., Krasnoslobodtsev, A., Yu, J. (2010). Nanoimaging for protein misfolding diseases. *Wiley Interdisciplinary Reviews: Nanomedicine and Nanobiotechnology*, **2**(5), 526–543.
16. Lyubchenko, Y. L., Sherman, S., Shlyakhtenko, L. S., Uversky, V. N. (2006). Nanoimaging for protein misfolding and related diseases. *J. Cell. Biochem.*, **99**, 53–70.
17. Knowles, T. P., Fitzpatrick, A. W., Meehan, S., Mott, H. R., Vendruscolo, M., et al. (2007). Role of intermolecular forces in defining material properties of protein nanofibrils. *Science*, **318**(5858), 1900–1903.
18. Chiti, F., Dobson, C. M. (2006). Protein misfolding, functional amyloid, and human disease. *Ann. Rev. Biochem.*, **75**, 333–366.
19. Lin, H., Bhatia, R., Lal, R. (2001). Amyloid beta protein forms ion channels: Implications for Alzheimer's disease pathophysiology. *FASEB J.*, **15**(13), 2433–2444.
20. Quist, A., Doudevski, I., Lin, H., Azimova, R., Ng, D., et al. (2005). Amyloid ion channels: A common structural link for protein-misfolding disease. *Proc. Natl. Acad. Sci. U. S. A.*, **102**(30), 10427–10432.
21. Lal, R., Lin, H., Quist, A. P. (2007). Amyloid beta ion channel: 3D structure and relevance to amyloid channel paradigm. *Biochim. Biophys. Acta*, **1768**(8), 1966–1975.

22. Quist, A. P., Chand, A., Ramachandran, S., Daraio, C., Jin, S., et al. (2007). Atomic force microscopy imaging and electrical recording of lipid bilayers supported over microfabricated silicon chip nanopores: Lab-on-a-chip system for lipid membranes and ion channels. *Langmuir*, **23**(3), 1375–1380.
23. Zakharov, S. D., Hulleman, J. D., Dutseva, E. A., Antonenko, Y. N., Rochet, J. C., et al. (2007). Helical alpha-synuclein forms highly conductive ion channels. *Biochemistry*, **46**(50), 14369–14379.
24. Lal, R., Arnsdorf, M. F. (2010). Multidimensional atomic force microscopy for drug discovery: A versatile tool for defining targets, designing therapeutics and monitoring their efficacy. *Life Sci*., **86**(15–16), 545–562.
25. Muller, D. J. (2008). AFM: A nanotool in membrane biology. *Biochemistry*, **47**(31), 7986–7998.
26. Muller, D. J., Engel, A. (2007). Atomic force microscopy and spectroscopy of native membrane proteins. *Nat. Protoc.*, **2**(9), 2191–2197.
27. Muller, D. J., Sass, H. J., Muller, S. A., Buldt, G., Engel, A. (1999). Surface structures of native bacteriorhodopsin depend on the molecular packing arrangement in the membrane. *J. Mol. Biol.*, **285**(5), 1903–1909.
28. Engel, A., Muller, D. J. (2000). Observing single biomolecules at work with the atomic force microscope. *Nat. Struct. Biol.*, **7**(9), 715–718.
29. Alsteens, D., Verbelen, C., Dague, E., Raze, D., Baulard, A. R., et al. (2008). Organization of the mycobacterial cell wall: A nanoscale view. *Pflugers Arch*., **456**(1), 117–125.
30. Alsteens, D., Dague, E., Verbelen, C., Andre, G., Dupres, V., et al. (2009). Nanoscale imaging of microbial pathogens using atomic force microscopy. *Wiley Interdisciplinary Rev.: Nanomed. Nanobiotechnol*., **1**(2), 168–180.
31. Kamruzzahan, A. S., Kienberger, F., Stroh, C. M., Berg, J., Huss, R., et al. (2004). Imaging morphological details and pathological differences of red blood cells using tapping-mode AFM. *Biol. Chem*., **385**(10), 955–960.
32. Drake, B., Prater, C. B., Weisenhorn, A. L., Gould, S. A., Albrecht, T. R., et al. (1989). Imaging crystals, polymers, and processes in water with the atomic force microscope. *Science*, **243**(4898), 1586–1589.
33. Hansma, H. G., Weisenhorn, A. L., Edmundson, A. B., Gaub, H. E., Hansma, P. K. (1991). Atomic force microscopy: Seeing molecules of lipid and immunoglobulin. *Clin*. *Chem*., **37**(9), 1497–1501.

34. Hansma, H. G., Sinsheimer, R. L., Groppe, J., Bruice, T. C., Elings, V., et al. (1993). Recent advances in atomic force microscopy of DNA. *Scanning*, **15**(5), 296–299.

35. Lyubchenko, Y. L., Shlyakhtenko, L. S. (1997). Visualization of supercoiled DNA with atomic force microscopy *in situ*. *Proc. Natl. Acad. Sci. U. S. A.*, **94**(2), 496–501.

36. Ando, T., Kodera, N., Naito, Y., Kinoshita, T., Furuta, K., et al. (2003). A high-speed atomic force microscope for studying biological macromolecules in action. *Chemphyschem*, **4**(11), 1196–1202.

37. Ando, T., Kodera, N., Takai, E., Maruyama, D., Saito, K., et al. (2001). A high-speed atomic force microscope for studying biological macromolecules. *Proc. Natl. Acad. Sci. U. S. A.*, **98**(22), 12468–12472.

38. Ando, T., Uchihashi, T., Kodera, N., Yamamoto, D., Miyagi, A., et al. (2008). High-speed AFM and nano-visualization of biomolecular processes. *Pflugers Arch.*, **456**(1), 211–225.

39. Ando, T., Uchihashi, T., Kodera, N., Yamamoto, D., Taniguchi, M., et al. (2007). High-speed atomic force microscopy for observing dynamic biomolecular processes. *J. Mol. Recognit.*, **20**(6), 448–458.

40. Crampton, N., Yokokawa, M., Dryden, D. T., Edwardson, J. M., Rao, D. N., et al. (2007). Fast-scan atomic force microscopy reveals that the type III restriction enzyme EcoP15I is capable of DNA translocation and looping. *Proc. Natl. Acad. Sci. U. S. A.*, **104**(31), 12755–12760.

41. Suzuki, Y., Higuchi, Y., Hizume, K., Yokokawa, M., Yoshimura, S. H., et al. Molecular dynamics of DNA and nucleosomes in solution studied by fast-scanning atomic force microscopy. *Ultramicroscopy*, **110**(6), 682–688.

42. Gilmore, J. L., Suzuki, Y., Tamulaitis, G., Siksnys, V., Takeyasu, K., et al. (2009). Single-molecule dynamics of the DNA-EcoRII protein complexes revealed with high-speed atomic force microscopy. *Biochemistry*, **48**(44), 10492–10498.

43. Hashimoto, M., Kodera, N., Tsunaka, Y., Oda, M., Tanimoto, M., et al. (2013). Phosphorylation-coupled intramolecular dynamics of unstructured regions in chromatin remodeler FACT. *Biophys. J.*, **104**(10), 2222–2234.

44. Ando, T., Kodera, N. (2012). Visualization of mobility by atomic force microscopy. *Methods Mol. Biol.*, **896**, 57–69.

45. Miyagi, A., Tsunaka, Y., Uchihashi, T., Mayanagi, K., Hirose, S., et al. (2008). Visualization of intrinsically disordered regions of proteins

by high-speed atomic force microscopy. *Chemphyschem*, **9**(13), 1859–1866.

46. Uversky, V. N. (2009). Intrinsic disorder in proteins associated with neurodegenerative diseases. *Front. Biosci*., **14**, 5188–5238.
47. Bemporad, F., Chiti, F. (2012). Protein misfolded oligomers: Experimental approaches, mechanism of formation, and structure–toxicity relationships. *Chem. Biol*., **19**(3), 315–327.
48. Bemporad, F., De Simone, A., Chiti, F., Dobson, C. M. (2012). Characterizing intermolecular interactions that initiate native-like protein aggregation. *Biophys. J*., **102**(11), 2595–2604.
49. Sokolov, I. (2006). Atomic force microscopy in cancer cell research, In: Nalwa, H. S., Webster, T., eds. *Cancer Nanotechnology*, American Scientific Publishers' Inc., pp. 1–17.
50. Cross, S. E., Jin, Y. S., Rao, J., Gimzewski, J. K. (2007). Nanomechanical analysis of cells from cancer patients. *Nat. Nanotechnol*., **2**(12), 780–783.
51. Goldmann, W. H., Ezzell, R. M. (1996). Viscoelasticity in wild-type and vinculin-deficient (5.51) mouse F9 embryonic carcinoma cells examined by atomic force microscopy and rheology. *Exp. Cell Res.*, **226**(1), 234–237.
52. Goldmann, W. H., Galneder, R., Ludwig, M., Xu, W., Adamson, E. D., et al. (1998). Differences in elasticity of vinculin-deficient F9 cells measured by magnetometry and atomic force microscopy. *Exp. Cell Res.*, **239**(2), 235–242.
53. Lekka, M., Laidler, P., Gil, D., Lekki, J., Stachura, Z., et al. (1999). Elasticity of normal and cancerous human bladder cells studied by scanning force microscopy. *Eur. Biophys. J*., **28**(4), 312–316.
54. Thompson, J. B., Kindt, J. H., Drake, B., Hansma, H. G., Morse, D. E., et al. (2001). Bone indentation recovery time correlates with bond reforming time. *Nature*, **414**(6865), 773–776.
55. Diez-Perez, A., Guerri, R., Nogues, X., Caceres, E., Pena, M. J., et al. (2010). Microindentation for *in vivo* measurement of bone tissue mechanical properties in humans. *J. Bone Miner. Res*., **25**(8), 1877–1885.
56. Stolz, M., Gottardi, R., Raiteri, R., Miot, S., Martin, I., et al. (2009). Early detection of aging cartilage and osteoarthritis in mice and patient samples using atomic force microscopy. *Nat. Nanotechnol*., **4**(3), 186–192.
57. Chiti, F., Dobson, C. M. (2009). Amyloid formation by globular proteins under native conditions. *Nat. Chem. Biol*., **5**(1), 15–22.

58. Deniz, A. A., Mukhopadhyay, S., Lemke, E. A. (2008). Single-molecule biophysics: At the interface of biology, physics and chemistry. *J. R. Soc. Interface*, **5**(18), 15–45.

59. Wang, H., Duennwald, M. L., Roberts, B. E., Rozeboom, L. M., Zhang, Y. L., et al. (2008). Direct and selective elimination of specific prions and amyloids by 4,5-dianilinophthalimide and analogs. *Proc. Natl. Acad. Sci. U. S. A.*, **105**(20), 7159–7164.

60. Ferreon, A. C., Gambin, Y., Lemke, E. A., Deniz, A. A. (2009). Interplay of alpha-synuclein binding and conformational switching probed by single-molecule fluorescence. *Proc. Natl. Acad. Sci. U. S. A.*, **106**(14), 5645–5650.

61. Brucale, M., Sandal, M., Di Maio, S., Rampioni, A., Tessari, I., et al. (2009). Pathogenic mutations shift the equilibria of alpha-synuclein single molecules towards structured conformers. *Chembiochem*., **10**(1), 176–183.

62. Sandal, M., Valle, F., Tessari, I., Mammi, S., Bergantino, E., et al. (2008). Conformational equilibria in monomeric alpha-synuclein at the single-molecule level. *PLoS Biol.*, **6**(1), e6.

63. Kransnoslobodtsev, A. V., Shlyakhtenko, L. S., Ukraintsev, E., Zaikova, T. O., Keana, J. F., et al. (2005). Nanomedicine and protein misfolding diseases. *Nanomed.: Nanotechnol. Biol. Med*., **1**(4), 300–305.

64. McAllister, C., Karymov, M. A., Kawano, Y., Lushnikov, A. Y., Mikheikin, A., et al. (2005). Protein interactions and misfolding analyzed by AFM force spectroscopy. *J. Mol. Biol.*, **354**(5), 1028–1042.

65. Yu, J., Lyubchenko, Y. L. (2009). Early stages for Parkinson's development: Alpha-synuclein misfolding and aggregation. *J. Neuroimmune Pharmacol.*, **4**(1), 10–16.

66. Yu, J., Malkova, S., Lyubchenko, Y. L. (2008). alpha-Synuclein misfolding: Single molecule AFM force spectroscopy study. *J. Mol. Biol.*, **384**(4), 992–1001.

67. Krasnoslobodtsev, A. V., Volkov, I. L., Asiago, J. M., Hindupur, J., Rochet, J. C., et al. (2013). alpha-Synuclein misfolding assessed with single molecule AFM force spectroscopy: Effect of pathogenic mutations. *Biochemistry*, **52**(42), 7377–7386.

68. Yu, J., Warnke, J., Lyubchenko, Y. L. (2011). Nanoprobing of alpha-synuclein misfolding and aggregation with atomic force microscopy. *Nanomed.: Nanotechnol. Biol. Med*., **7**(2), 146–152.

69. Krasnoslobodtsev, A. V., Peng, J., Asiago, J. M., Hindupur, J., Rochet, J. C., et al. (2012). Effect of spermidine on misfolding and interactions of alpha-synuclein. *PLOS ONE*, **7**(5), e38099.

70. Han, H., Weinreb, P. H., Lansbury, P. T., Jr. (1995). The core Alzheimer's peptide NAC forms amyloid fibrils which seed and are seeded by beta-amyloid: Is NAC a common trigger or target in neurodegenerative disease? *Chem. Biol*., **2**(3), 163–169.

71. Ueda, K., Fukushima, H., Masliah, E., Xia, Y., Iwai, A., et al. (1993). Molecular cloning of cDNA encoding an unrecognized component of amyloid in Alzheimer disease. *Proc. Natl. Acad. Sci. U. S. A.*, **90**(23), 11282–11286.

72. El-Agnaf, O. M., Bodles, A. M., Guthrie, D. J., Harriott, P., Irvine, G. B. (1998). The N-terminal region of non-A beta component of Alzheimer's disease amyloid is responsible for its tendency to assume beta-sheet and aggregate to form fibrils. *Eur. J. Biochem*., **258**(1), 157–163.

73. El-Agnaf, O. M., Jakes, R., Curran, M. D., Middleton, D., Ingenito, R., et al. (1998). Aggregates from mutant and wild-type alpha-synuclein proteins and NAC peptide induce apoptotic cell death in human neuroblastoma cells by formation of beta-sheet and amyloid-like filaments. *FEBS Lett*., **440**(1–2), 71–75.

74. Kruger, R., Kuhn, W., Muller, T., Woitalla, D., Graeber, M., et al. (1998). Ala30Pro mutation in the gene encoding alpha-synuclein in Parkinson's disease. *Nat. Genet*., **18**(2), 106–108.

75. Evans, E. (2001). Probing the relation between force–lifetime–and chemistry in single molecular bonds. *Annu. Rev. Biophys. Biomol. Struct*., **30**, 105–128.

76. Kim, B. H., Lyubchenko, Y. L. (2014). Nanoprobing of misfolding and interactions of amyloid beta 42 protein. *Nanomed.: Nanotechnol. Biol. Med*., **10**, 871–878.

77. Kim, B. H., Palermo, N. Y., Lovas, S., Zaikova, T., Keana, J. F., et al. (2011). Single-molecule atomic force microscopy force spectroscopy study of Abeta-40 interactions. *Biochemistry*., **50**(23), 5154–5162.

78. Lovas, S., Zhang, Y., Yu, J., Lyubchenko, Y. L. (2013). Molecular mechanism of misfolding and aggregation of Abeta(13–23). *J. Phys. Chem. B*, **117**(20), 6175–6186.

79. Portillo, A. M., Krasnoslobodtsev, A. V., Lyubchenko, Y. L. (2012). Effect of electrostatics on aggregation of prion protein Sup35 peptide. *J. Phys. Condensed Matter*, **24**(16), 164205.

80. Lovas, S., Zhang, Y., Lyubchenko, Y. L. (2012). Insight into Aβ misfolding and aggregation, In: Kokotos, G., Copnstantinou-Kokotou, V., Matsoukas, J., eds. *Peptides 2012-Proceedings of the 32nd European Peptide Symposium*, European Peptide Society, University of Athens, Laboratory of Organic Chemistry, Athens, Greece, pp. 56–57.

81. Tjernberg, L. O., Tjernberg, A., Bark, N., Shi, Y., Ruzsicska, B. P., et al. (2002). Assembling amyloid fibrils from designed structures containing a significant amyloid beta-peptide fragment. *Biochem. J.*, **366**(Pt 1), 343–351.

82. Castillo, V., Ventura, S. (2009). Amyloidogenic regions and interaction surfaces overlap in globular proteins related to conformational diseases. *PLoS Comput. Biol.*, **5**(8), e1000476.

Chapter 17

Nanoparticles for Multi-Modality Diagnostic Imaging and Drug Delivery

Catherine M. Lockhart, PharmD, and Rodney J. Y. Ho, PhD

Department of Pharmaceutics, University of Washington, Seattle, USA

Keywords: diagnostic imaging, multi-modality, contrast, nanoparticles, positron emission tomography, magnetic resonance imaging, ultrasound, computed tomography, single photon emission computed tomography

17.1 Imaging

Radiological imaging is a major component in diagnosis and staging of cancer and other pathological processes *in vivo*, providing a more complete, non-invasive view of internal structural and functional biological processes. In most diseases, early detection of the pathological state is key to improving treatment outcomes, and advances in diagnostic technology are improving the ability to detect small abnormalities in tissue, such as early-stage tumors.

A variety of imaging modalities are available for clinical use, including magnetic resonance imaging (MRI), computed tomography

Handbook of Clinical Nanomedicine: Nanoparticles, Imaging, Therapy, and Clinical Applications
Edited by Raj Bawa, Gerald F. Audette, and Israel Rubinstein

ISBN 978-981-4669-20-7 (Hardcover), 978-981-4669-21-4 (eBook)
www.panstanford.com

(CT), positron emission tomography (PET), single photon emission computed tomography (SPECT), and ultrasound imaging (US). There are strengths and limitations associated with each imaging modality and each is used to capitalize on its characteristic capabilities. No single modality is perfect, and they differ in detection sensitivity, limits of spatial resolution, and depth of penetration or range of image generation. PET and SPECT are highly sensitive to functional information, and can detect biological activity generated by a small number of cells or molecules, but lack the ability to detect structural details. MRI and CT boast high spatial resolution and provide superb detail of biological structures. US images have relatively high sensitivity, but poorer resolution, often with inferior image quality; however, the devices are inexpensive, portable, and convenient to use while still providing valuable real-time functional information [1, 2].

All currently approved imaging modalities in use clinically are generally regarded as safe, although several carry the risk of exposure to ionizing radiation. Specifically, CT exposes the patient to external X-rays, while PET and SPECT rely on internally administered radioisotopes that necessarily result in exposure to ionizing radiation. The strength of a radioactive source is defined according to units of becquerels (Bq) or curies (Ci), which measures the rate of emission. A becquerel is a very small unit of measure, while a curie is a very large unit of measure, so multiples are typically used. Common multiples typically used for Bq are kilobecquerel (kBq = 1000 Bq) and megabecquerel (MBq = 1000 kBq); common multiples used for Ci are millicurie (1000 mCi = 1 Ci) and microcurie (1000 μCi = 1 mCi).

- 1 Bq = 1 radiation emission event per second
- 1 Ci = 37,000,000 kBq = 37,000 MBq

Measurements of radiation dose or exposure are defined in terms of absorbed dose expressed in units of gray (Gy) or equivalent dose expressed in units of sieverts (Sv) or millisieverts (1000 mSv = 1 Sv) and is a more practical measure of tissue exposure.

- 1 Gy = 1 joule of energy absorbed per kilogram of organ or tissue
- 1 Sv = absorbed dose in Gy x a radiation weighting factor

The radiation weighting-factor used in determining Sv depends upon the type of radiation exposure and the energy of that radioactive particle. Further description is beyond the scope of this chapter, but may be found in more detail elsewhere [3]. Old units are still encountered including rad (1 Gy = 100 rads) and rem (1 Sv = 100 rem). In this chapter, we will use the units of Gy and Sv.

We are routinely exposed to background radiation due to the sun and other natural and artificial sources at levels of approximately 2.8 mSv per year, but additional radiation exposure may lead to increased risk of cancer. There is still debate over the long-term impact of low-dose radiation from diagnostic imaging on cancer risk, but it is not without concern [4]. People who work in fields such as diagnostic imaging where the risk of ionizing exposure is high are monitored to limit total exposure to 100 mSv per five years (20 mSv per year), and no more than 50 mSv in any one year; however, patients who undergo diagnostic imaging are not monitored for exposure. For members of the public, the limits are set at 1 mSv per year on average over any five-year period [5]. Table 17.1 lists some examples of approximate exposure levels by modality compared to an average plain chest X-ray.

Table 17.1 Radiation exposure from common medical imaging procedures

Device	Radiation source	Exposure (mSv): average (range)	Equivalent chest X-rays
Chest X-ray	X-ray	0.34 (0.02–0.67)	1
CT—chest	X-ray	6.0 (4.1–8.0)	17
CT—abdominal	X-ray	11.8 (7.6–16.0)	35
PET—tumor	^{18}FDG (400 MBq dose)	7.6	22
PET—cardiac	^{15}O-water (1100 MBq dose)	1.2	3.5
SPECT—brain	^{99m}Tc (800 MBq dose)	7.4	22
SPECT—tumor	^{123}I (400 MBq dose)	5.2	15

Note: Adapted from references 4 and 6.

Table 17.2 Comparison of major characteristics of clinical imaging modalities

Imaging modality	Method of image generation	Clinical use	Advantages	Disadvantages
High resolution				
Magnetic resonance imaging (MRI)	• Magnetic and electromagnetic fields manipulate the atomic energy state of hydrogen atoms	• Superb for soft tissue • Musculoskeletal • Neurological • Cardiovascular • Tumor imaging	• High spatial resolution: 25–100 μm • Excellent soft-tissue resolution • No ionizing radiation	• Poor sensitivity: mM to μM • Long acquisition time (min/h)
Computed tomography (CT)	• X-ray	• Dense tissue • Bone • Calcified structures	• High spatial resolution: 50–200 μm • Excellent structural images • Short acquisition time (min)	• Ionizing radiation • Poor soft-tissue resolution
High sensitivity				
Positron emission	• Positron-emitting radioisotope administered intravenously	• Tumor imaging • Biological processes	• Quantitative and semi-quantitative information	• Ionizing radiation • Poor resolution: 1–3 mm

Imaging modality	Method of image generation	Clinical use	Advantages	Disadvantages
tomography (PET)	• Pairs of gamma rays detected by scintillation photodetectors	• Tissue distribution of molecules	• High sensitivity: pM	• Long acquisition time (minutes to hours)
Single photon emission computed tomography (SPECT)	• Gamma-emitting radioisotope is administered • Single gamma rays detected by scintillation photodetectors	• Tumor imaging • Biological processes • Tissue distribution of molecules	• Quantitative and semi-quantitative information • High sensitivity	• Ionizing radiation • Poor resolution: 1–3 mm • Long acquisition time (min/h)
Ultrasound imaging (US)	• Tissue acoustic impedance of sound waves generated by a transducer is detected	• Muscles • Tendons • Organs • Physiological processes • High Intensity Focused Ultrasound (HIFU) for tissue ablation and therapeutic treatment	• No ionizing radiation • Real-time visualization • Short acquisition time (min) • Portable • Inexpensive • High sensitivity	• Low resolution • Contrast agents are limited • Whole-body imaging is not possible • Limited tissue depth penetration (several cm)

Note: Adapted from references 2, 8, and 9.

Detailed descriptions of each imaging modality are beyond the scope of this chapter, but excellent texts and articles with in-depth discussions of imaging technology are available elsewhere [7]. It is important to understand the basic principles, strengths, and limitations of each modality to grasp the role and relevance of nanoparticles in molecular imaging. Table 17.2 summarizes characteristics of the major imaging devices available for clinical use.

17.2 Multi-Modality Imaging

Different imaging techniques have different strengths and weaknesses; so combining two complementary modalities for a single image offers synergistic advantages over using each modality alone. MRI has high spatial resolution and is superb for providing structural information and a detailed anatomical view. Contrast-enhanced CT is also considered high resolution with emphasis on dense tissue differentiation. Conversely, PET, SPECT, and US have high sensitivity and are capable of detecting very subtle functional activity at the expense of anatomical detail. Researchers are actively investigating the means of capturing the complementary strengths of high resolution and high sensitivity modalities in dual-modality devices to generate a more complete picture of biological structure and function [8].

Some dual-imaging modalities have become available both clinically and pre-clinically, and are proving to be essential tools in disease diagnosis and treatment by combining the benefits of complementary information while overcoming some of the limitations observed in single modality images. To date, the prominent dual-modality imaging devices in clinical practice include PET/CT, SPECT/CT, and MRI/US, which combine the high resolution of CT for anatomical information and attenuation correction, with sensitive functional information and the ability of direct quantification provided by PET, SPECT, and US in a powerful, non-invasive image modality. Combined CT and PET or SPECT scanners are available commercially and are favored over their single- modality counterparts for clinical cancer diagnosis, staging, and evaluation of therapeutic response. While each modality has excellent attributes on its own for certain applications, neither is

perfect in providing both structural and functional information, a limitation that is largely overcome by combining the two to produce a more complete, singular image. This is particularly useful in oncology, in which a lesion can be clearly detected using PET or SPECT with anatomical location pinpointed using CT [8, 10].

The multi-modality combination of PET and MRI is regarded as the next important contribution to cancer diagnosis, and preliminary devices are under development in several research laboratories [11]. MRI produces superb high-resolution images with detailed structural information, particularly in soft tissues, while PET is extremely sensitive in detecting functional processes. MRI also provides discrimination of a variety of parameters, including cell trafficking, functional MRI measurements, magnetic resonance spectroscopy (MRS), and contrast-enhanced images [8]. The depth of information that can potentially emerge from the combination of MRI and PET is likely to open many more avenues for early detection of pathological processes and sensitive analysis of treatment progress.

Most diagnostic imaging is optimized through use of modality-specific probes that enhance the ability to differentiate structural information and more clearly trace functional activity. For example, gas trapped in microbubbles improves vascular contrast in ultrasound imaging; manipulating tissue density with radiopaque contrast agents can generate more structural detail in CT images; MRI images can be enhanced by administration of paramagnetic probes to improve tissue relaxivity characteristics; a positron-emitting radiotracer is required for scintillation and photodetection for PET, and a gamma-emitting radiotracer is required for SPECT [2, 12].

Nanoparticles are perfectly suited to become dual-modality imaging probes. Nanoparticles have a high payload capacity and can be designed to carry contrast agents or molecular probes, along with therapeutic moieties in a single particle. They can also incorporate ligands, such as peptides or antibodies with affinity for a particular receptor or tissue type, conjugated to the nanoparticle surface to reduce non-specific tissue accumulation and reduce toxic side effects that often arise from agents such as gadolinium (Gd^{3+}) used in MRI. A single particle for multi-modality molecular imaging requires incorporation of each specific probe necessary for both modalities in the device. One major advantage

to introducing a single, multi-functional nanoparticle is that the pharmacokinetics of all moieties will necessarily be the same since kinetic behavior will be governed by the particle overall, rather than each compound individually [12, 13]. This is important in synchronizing images produced by two distinct modalities to reflect the same physical position spatially, but also the same physiological activity temporally. This cannot be achieved through separate administration of multiple imaging agents with varying pharmacokinetic properties. Table 17.3 lists some of the major probes associated with each imaging modality [1, 2]. Note that this list is not exhaustive.

Table 17.3 Commonly used contrast agents or probes for clinical imaging modalities

Imaging modality	Contrast agent or molecular probe
Magnetic resonance imaging (MRI)	• Gadolinium (Gd^{3+}) • Iron oxide particles (SPIO, USPIO) • Manganese oxide
Computed tomography (CT)	• Barium • Iodine • Krypton • Xenon
Positron emission tomography (PET)	• ^{11}C • ^{18}F • ^{64}Cu • ^{68}Ga • ^{124}I
Single photon emission computed tomography (SPECT)	• ^{99m}Tc • ^{123}I • ^{111}In • ^{117}Lu
Ultrasound imaging (US)	• Gas-filled microbubbles

Note: Adapted from references 1 and 2.

Theranostic nanoparticles are at the forefront of design in targeted drug therapy. Combining the functionality of molecular imaging probes with therapeutic compounds in a single nanoparticle allows for real-time visualization of biodistribution

and drug delivery. Several multi-modality nanoparticles are under development and show great promise for individualized medicine.

17.3 Nanoparticles

Nanoparticles come in many forms from a variety of materials, but all share the common feature of size on a nanometer scale. In medical diagnostic or therapeutic applications, the predominant nanoparticles are produced from lipids, polymers, or built around a solid core. Lipids are amphipathic molecules with a polar head group and a long, lipophilic tail. When placed in solution, lipids spontaneously aggregate into spherical vesicles with the lipophilic tails oriented together, protected from the aqueous environment by hydrophilic polar head-groups. The lipids can form either single layer micelles with a lipophilic core or liposomal vesicles with a bi-layer membrane containing an aqueous core, and a lipophilic space within the membrane [14]. Figure 17.1 illustrates the basic configuration of lipids in micelles and liposomes.

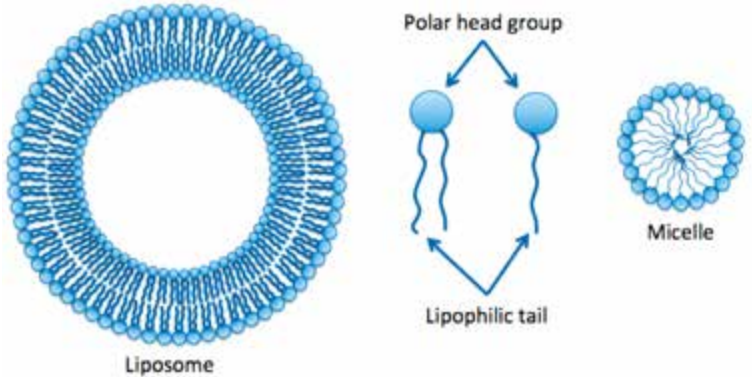

Figure 17.1 Lipid molecules with a polar head, and one or more lipophilic hydrocarbon tails aggregate to form bi-layer liposomes or monolayer micelle nanoparticles.

Therapeutic and diagnostic moieties can be incorporated in lipid nanoparticles in three main ways: (1) conjugated on the surface, (2) embedded in the lipophilic membrane (liposomes) or internal lipophilic space (micelles), and (3) encapsulated in the

core of liposomes (Fig. 17.2). Surface conjugation is useful for large molecules and targeting moieties for site-specific accumulation, although the payload capacity is limited by available surface area, and the lipid must be able to stably bind the molecule. The lipophilic intra-membrane space of liposomes and the lipophilic core of micelles are useful for carrying hydrophobic or poorly soluble molecules. Again, payload capacity is limited by finite space and the molecules must be sufficiently small to be contained within the lipophilic region. Core encapsulation in liposomes is the preferred method for incorporating a high payload of molecules that are stable in an aqueous environment. Capacity is limited only by the size of the liposome. This is useful for moieties that have unfavorable pharmacokinetics, have a severe toxicity profile, or are sensitive to the external biological environment. Targeted liposomes can extend the half-life of compounds, reduce non-specific tissue accumulation, and protect molecules from premature degradation.

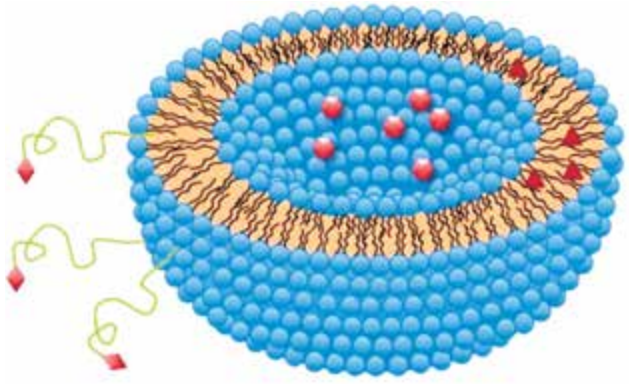

Figure 17.2 Molecules can be incorporated into liposomes by encapsulation in the aqueous core (hexagons), conjugation to the surface via ligands (diamonds), or embedding in the lipid membrane (triangles).

Nanoparticles have also been designed around a solid core of material that possesses desirable properties for applications in diagnostic imaging contrast. Gold, paramagnetic, or superparamagnetic nanoparticles can be used as a functional core upon which other moieties can be layered or conjugated for further functional activity. Figure 17.3 illustrates an example configuration of a solid

core nanoparticle with functional characteristics designed into the layers including targeting moieties, therapeutic agents, or other imaging probes [8]. The core of these nanoparticles provide contrast for either MRI or CT, but the surface layers can include probes for other diagnostic imaging or therapeutic agents either embedded within the layer or conjugated on the external surface. Table 17.4 compares major characteristics of each nanoparticle, including advantages and disadvantages of each, as well as examples of clinical applications.

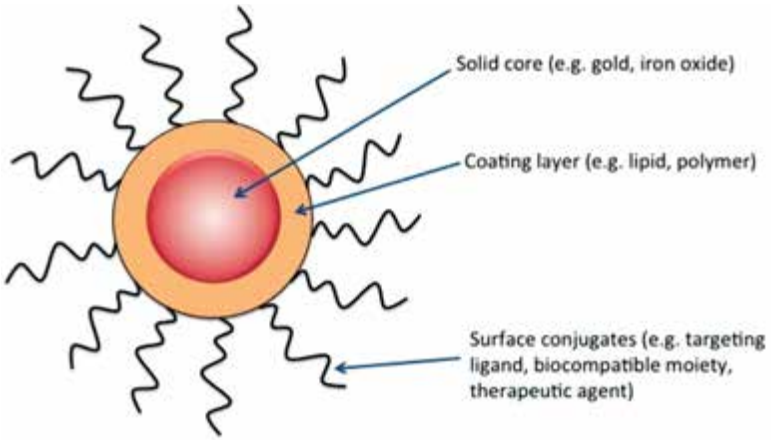

Figure 17.3 The basic concept of a solid core nanoparticle. A solid core, which may be magnetic for MRI contrast, or another highly proton-dense material for CT contrast, is surrounded by a layer of lipid or other compousnd to control biological behavior of the nanoparticle or add functionality, and surface ligands are added for targeting or therapeutic activity.

Successful nanoparticles in use clinically, or with the potential for clinical applications in diagnostic imaging and drug delivery, must possess certain characteristics to be compatible as biomedicine. First, they must be sized appropriately for predictable and reliable distribution. Typically, nanoparticles in biomedical applications are most versatile when they have diameters less than approximately 100 nm. This is small enough to penetrate into narrow vasculature and to avoid detection by the reticuloendothelial system (RES), and large enough to carry significant payload while avoiding glomerular filtration and excretion through the

Table 17.4 Comparison of major characteristics of nanoparticles in imaging and drug delivery

Nanoparticle	Example materials	Advantages	Disadvantages
Liposome	• Phosphatidyl choline (PC) • Phosphatidyl ethanolamine (PE)	• Improved pharmacokinetics • Targeted tissue delivery • High payload capacity • Biocompatible lipid membrane	• Poorly designed liposomes degrade rapidly due to biocompatibility • Can activate the reticuloendothelial system (RES) and accumulate in liver or spleen
Micelle	• poly(ethylene glycol)-b-poly(D,L-lactide) (PEG-PLA) • poly(ethylene glycol)-*co*-polycaprolactone (PEG-PCL) • poly(ethylene glycol)-b-poly(L-lysine) (PEG-P(Lys)) • Di-stearoyl-polyethylene glycol-phosphatidylethanolamine (DSPE)	• Very small size • Targeted tissue delivery	• Size limits payload capacity • Not useful for encapsulating hydrophilic compounds
Solid Core	• Superparamagnetic iron oxide (SPIO) • Iron oxide (IO) • Gold nanoparticles	• Small size • Size is easy to control • Targeted tissue delivery	• Payload capacity limited to external layers

Note: Adapted from reference 15.

kidney. Second, nanoparticles must be biocompatible such that systemic administration will not generate undue toxicity, and will provide the intended benefit in a biological environment. This includes application of surface treatments and targeting moieties to control distribution and disposition *in vivo*. Also, they must not be reactive or generate severe adverse reactions. Safety in humans must be proven before nanoparticles may be considered for clinical use. Nanoparticles must also accumulate in sufficient quantities systemically or at the targeted tissue site, and remain long enough to be detected by the imaging modalities. Further, nanoparticles must be stable under physiological conditions such as pH and temperature, and be unaffected by minor fluctuations in each. They must also be stable under storage conditions and not degrade or lose potency during the expected length of time between formulation and use. Finally, nanoparticles must be capable of carrying payload including molecular imaging probes and drug moieties that may or may not have similar chemical properties, and may or may not behave similarly under matching conditions [12].

The versatility of nanoparticles as delivery vehicles is showing promise in dual-modality diagnostic imaging, with the future goal of incorporating a therapeutic moiety into a theranostic particle. The expected advantages of combining multiple moieties in a single nanoparticle include (1) single IV administration to reduce patient discomfort and exposure to multiple injections, (2) potential for reduced toxicity and reduced dose, and (3) improved and synergistic pharmacokinetics both spatially and temporally.

17.4 Targeted Nanoparticles for Multi-Modality Molecular Imaging

17.4.1 SPECT or PET/CT

The combination of PET or SPECT with CT has proven indispensable in diagnostic imaging. PET and SPECT are extremely valuable in detecting disease *in vivo*, but they are limited by poor anatomical definition so precise lesion localization is very difficult. The introduction of nearly simultaneous CT imaging provided both attenuation correction for PET and SPECT images, but also

contributed anatomical detail, dramatically improving the power of these tools for characterization of pathogenic states. This valuable combination also allows for whole-body imaging in a single visit [16]. For PET and SPECT imaging, administration of positron- or gamma-emitting radiotracers is essential for image generation. For CT, administration of a radiopaque contrast agent with a high-Z number (number of protons in the atomic nucleus) greatly improves spatial resolution and structural anatomic information.

Currently in the clinic, these two agents must be administered independently, but there is interest in developing a single nanoparticle to simultaneously deliver both a radiopaque agent for CT contrast, and a radioisotope for PET or SPECT imaging. To date, research has been limited, but opportunities exist to combine nanoparticles containing a high-Z element (e.g., iodine or barium) to provide CT contrast, with surface conjugates to carry radioisotopes for PET or SPECT functional imaging. Combining contrast-enhanced CT with a standard PET/CT protocol shows some benefit in tumor localization and can provide valuable information particularly in the head and neck, or bowel and pelvic regions. Further, not all tumors demonstrate sufficient uptake of PET radiotracers such as (^{18}F) Fluorodeoxyglucose (^{18}F-FDG), which probes tumor metabolic activity, so contrast-enhanced CT may be of significant benefit in tumors that are not FDG-avid [17].

A major challenge in the combination of CT contrast and PET or SPECT radiotracers involves solving the issue of temporal compatibility. CT scans are very fast, taking only seconds to minutes, while PET and SPECT take minutes to hours to complete. Thus, a single nanoparticle must be retained in circulation long enough to accommodate image collection by both modalities. Also, specific targeting to diseased tissue is typically the goal in nanoparticle design for PET or SPECT imaging to enhance early detection of pathological processes. In CT, the target tissues for contrast may be more broadly dispersed or less specific, as the goal is differentiation of tissue types surrounding a lesion rather than enhancing the lesion itself. Also, there is question regarding whether or not contrast-enhanced CT is really necessary in PET/CT imaging since the radiotracer alone may provide sufficient lesion delineation [17]. Therefore, the benefit and feasibility of combining

CT contrast with PET radiotracers in a single nanoparticle remains to be explored.

17.4.2 MRI/CT

Little attention has been paid to combining MRI and CT since both modalities are considered high resolution, but some current reports have emerged detailing dual-modality contrast agents for MRI and CT [18]. The purported benefit of combining images from MRI and CT lies in the excellent soft-tissue visualization provided by MRI and bony or dense-tissue visualization provided by CT [19]. Furthermore, the inherently more straightforward quantitation ability of CT is complementary to the relative sensitivity of MRI to distribution of molecules in the body. This combination is useful for follow-up and post-treatment evaluation of diseases including cancer.

Dual-function nanoparticles were developed by Alric et al. that displayed effective contrast for both MRI and X-ray based CT [20]. These gold-core nanoparticles were coated with gadolinium chelated to diethylenetriaminepentaacetic acid (DTDTPA) bound by disulfide bonds and finished with a thiolated polyethylene glycol (PEG) shell for surface hydration and increased plasma circulation time. Gold was easily manipulated to control size, shape, and surface characteristics of the particles and exhibited superior contrast capability compared with commonly used iodinated compounds. CT contrast improvement of gold was similar to that of other substances such as bismuth sulfide, but it was easier to fabricate particles with deliberate characteristics. The gadolinium chelates layered on the gold core provided MRI contrast enhancement equivalent to commonly used gadolinium-based products available commercially [20].

Phantom studies showed 50.7 mM of the gold nanoparticle preparation gave equivalent quantified X-ray absorption as 280 mM of iodine, suggesting a dose reduction in administered contrast agent is possible. Studies in mice and rats were performed by administering 300 μL (mice) or 0.6 to 1.2 mL (rats) containing the equivalent of 10 mg/mL of gold with 5 mM Gd in 150 mM buffer at pH 7.4, confirmed that these low doses provided images with equivalent CT contrast enhancement compared to previous studies using 270 mg/mL gold content. Also, 5 mM of gadolinium

chelated to the surface of the gold significantly improved the contrast enhancement of MRI compared to commercial formulations. Furthermore, no overt toxicity or adverse effects were observed in the animals as long as 6 weeks after administration, and the particles circulated freely without undue accumulation in lungs, liver, kidney, or spleen. *In vivo* experiments in human subjects have not been reported. These particles were not used therapeutically, but the authors predict applicability in planning and treatment as a radiosensitizer prior to radiotherapy of tumor tissue [20].

Embolization therapy is commonly used to control abnormal bleeding, occlude angiogenic tumor vessels, repair malformed blood vessels, and treat aneurisms and other blood vessel pathologies. This therapy requires a radiopaque probe, commonly a spherical polymeric particle that must be visualized with X-ray angiography to monitor treatment progress. Hagit et al. recently developed a nanoparticle with radiopaque properties required for embolization therapy, but could be visualized with both X-ray and magnetic resonance. This nanoparticle, capable of combined CT and MRI contrast, was created with a radiopaque polymerized core of the vinylic monomer 20 methacryloyloxyethyl (2,3,5-triiodobenzoate) (MAOETIB), coated with layers of magnetic maghemite (γ-Fe_2O_3) nanoparticles. The radiopacity of the MAOETIB core was compatible with visualization requirements for embolization, and was visible using CT, while iron oxide particles embedded in the shell coating provided contrast enhancement for MRI. Animal studies confirmed visualization capability using both CT and MRI, and the particles were effective in embolization treatment in a rat kidney tumor embolization model. Compatibility with CT allowed for pre-and post-treatment quantitation of tumor and treatment progress with the potential to improve and optimize current embolization therapy [18].

Iodinated contrast compounds for CT commonly used for image enhancement are cleared very quickly by the kidney, which limits imaging time and capability in clinical use. Iron–platinum alloy (FePt) nanoparticles developed by Chou et al. have been shown to be very stable, maintain longer systemic presence, and have excellent superparamagnetic properties and high X-ray absorption suitable for both MRI and CT image enhancement. FePt is relatively simple to synthesize and the size and shape of the final

particles are easily controlled, providing a versatile platform for many applications. Surface conjugation is similar to that of gold and other metal nanoparticles, and is typically achieved through thiol–metal bonds, which allows modifications for clinical use. These FePt nanoparticles were synthesized and conjugated with antibodies to Her2 proteins for breast cancer-specific tumor targeting, suggesting a potential for not only specificity in diagnostic imaging, but also the potential for future therapeutic options [19].

17.4.3 MRI/US

Magnetic resonance and ultrasound imaging techniques were first integrated in the early 1990s as a therapeutic application. High-intensity focused ultrasound (HIFU) was used for tissue ablation and was performed under the visual guidance of MRI [21]. Prior to this time, focused ultrasound was used successfully in treating tumors in animal models, but the tissue ablation was guided either visually with the un-aided eye, or by using B-mode ultrasound to obtain an approximate focal location within a body plane [22]. B-mode ultrasound allows for non-invasive visualization, but the image quality lacks precision and detail of tissues structures. Using MRI to visualize anatomy at the site of ablation allowed researchers to take advantage of the high-resolution MRI to determine precise targets [23].

Combination of MRI and HIFU did not become clinically relevant until 2000 when the first commercial magnetic resonance guided focused ultrasound device for treating benign and malignant tumors emerged. Magnetic guided focused ultrasound was approved in 2004 by the Food and Drug Administration (FDA) in the United States for treatment of uterine fibroids [24]. Trials are ongoing to validate use of this technology for treating conditions such as benign prostatic hyperplasia (BPH) and for ablation of solid tumors in body organs including breast, liver, pancreas, and bone metastases.

Administration of paramagnetic contrast agents (e.g., gadolinium, superparamagnetic iron oxide particles (SPIO), and manganese), which reduce relaxation times of locally excited protons, enhances soft tissue differentiation in MRI images, and improves target visualization for ultrasound ablation [25]. Magnetic resonance

images not only improve therapeutic ultrasound targeting, but also allow for evaluation of HIFU-induced tissue damage in real-time to reduce adverse effects of therapy [26].

Contrast enhanced ultrasonography is gaining favor as gas-filled microbubbles injected intravenously circulate in the blood and greatly improve the image quality of vasculature by creating more visual variation between tissue regions. This is particularly valuable in echocardiography to enhance images of cardiac vasculature, including microvasculature, for earlier identification of myocardial pathology [27]. Furthermore, adding targeting ligands to the surface of lipid-encapsulated microbubbles is being investigated as a means to improve tissue-specific imaging [28]. Microbubbles are also under exploration as a means for drug delivery when blasted with HIFU. The focused sound waves cause cavitation in cell membranes making them "leaky" to allow drug molecules to enter the target cell more easily, quickly, and in greater concentration. Focused ultrasound also causes some microbubbles to burst, releasing their contents into the extracellular space near a cell disrupted by temporary cavitation. This allows specific, targeted drug delivery to a tissue region or cell, reducing systemic exposure and adverse effects [29].

Until very recently, there was limited exploration into a single contrast agent able to accommodate both MRI and US. A microbubble preparation containing embedded superparamagnetic iron-oxide (SPIO) nanoparticles was developed by Yang et al. and evaluated for capability as a simultaneous contrast agent for MRI and US. A microbubble was designed and fabricated with a core of N_2 gas surrounded by a poly-D-L-lactide (PLA) layer embedded with SPIO nanoparticles and coated in a polyvinyl alcohol (PVA) shell. The double layered polymer shell measured 50–70 nm in thickness, which allowed even distribution of the 12 nm SPIO particles within the polymer. Contrast enhancement was observed for US due to the gas core, and simultaneously for MRI due to inclusion of SPIO particles [30].

To date, dual-modality MRI/US contrast nanoparticles have not been used for therapeutic applications by focused US tissue ablation, microbubble cavitation, or delivery of drug moieties to a target site, but the possibility exists. MRI has been used successfully to visualize US-mediated drug delivery, but either no-contrast, or separate MRI contrast agents were administered [29].

These techniques have been explored with some success using nanoparticles and US independent of other modalities [31].

17.4.4 PET/MRI

The combination of PET and MRI is considered the next major frontier in dual-modality imaging technology. Integration of the high resolution and morphological capability of MRI with the superior sensitivity of PET would provide complimentary information and a more complete picture of pathological structure and function *in vivo*, particularly in the abdomen and other regions requiring detailed soft-tissue resolution. Several approaches have been explored to combine these two modalities, and currently small-animal scanners have been produced for pre-clinical investigation [11, 32]. The evolution of a single scanner with PET and MRI imaging capability invites development of dual-function nanoparticles to carry MRI contrast and PET radiotracers in a single injection.

Most nanoparticles under investigation as PET/MRI probes are based upon a solid core with magnetic properties and surface-treated with radiotracers and targeting moieties (Fig. 17.3). Paramagnetic compounds, such as gadolinium or manganese, provide contrast in MRI and result in enhanced bright regions of the image. Conversely, superparamagnetic iron oxide (SPIO) compounds result in enhanced dark regions of the image [12].

A bifunctional iron-oxide nanoparticle probe was developed by Lee et al. and targeted to specifically bind tumor-expressed integrin $\alpha_v\beta_3$ to enhance dark regions in MRI images. In this case, iron oxide (IO) nanoparticle cores, with an average diameter of 5 nm, were coated with polyaspartic acid (PASP) as a conjugation linker layer. They were then conjugated with cyclic arginine-glycineaspartic (RGD) peptides and the macrocyclic chelating agent DOTA for integrin $\alpha_v\beta_3$ recognition. The iron-oxide core provided contrast enhancement for MRI, and the nanoparticle was further labeled with a positron-emitting radiotracer, ^{64}Cu, to allow simultaneous PET imaging. *In vitro* studies proved the affinity of these particles to integrin $\alpha_v\beta_3$ and *in vivo* studies in mice showed that this particle provided MRI contrast as well as a functional radiotracer for PET. While this particle was not evaluated for treatment capabilities, a therapeutic moiety could be incorporated to allow for targeted drug delivery with simultaneous multi-modality imaging [33].

In a similar approach, a dual-modality imaging probe was developed around a superparamagnetic iron oxide core nanoparticle. The SPIO crystalline core was coated in a polyethylene glycol (PEG)-phospholipid micelle layer. This technique resulted in PEG exposed on the surface of the nanoparticles to form a hydrated layer, improving water solubility of the nanoparticle, and imparting protection from protein absorption and degradation by the reticuloendothelial system (RES). 1,4,7,10-Tetraazacyclododecane-1,4,7,10-tetraacetic acid mono(N-hydroxysuccinimide ester) (DOTA-NHS) was conjugated to the PEG-functionalized lipids to provide a site for labeling with the positron-emitting radioisotope ^{64}Cu. Preclinical *in vivo* studies showed the SPIO core enhanced dark regions MRI images, and the emission from the ^{64}Cu chelated to the surface of these nanoparticles was detectable by PET scanners [34].

Choi et al. designed a nanoparticle that begins with a core of manganese-doped magnetism-engineered iron oxide ($MnFe_2O_4$) that is combined with ^{124}I for PET detection. $MnFe_2O_4$ is an excellent MRI contrast agent that has been shown to enhance the MRI relaxation coefficient by two- to three-fold, compared with SPIO formulations. The core was conjugated to the tyrosine residue in serum albumin to provide a stable platform for efficient labeling of the PET radionuclide ^{124}I directly to the tyrosine. These probes had a hydrodynamic size of 32 nm for lymphatic imaging. Preclinical studies showed superior images and localization of lymph nodes due to fusion of sensitive PET images with soft-tissue contrast of MRI. This probe shows promise for clinical imaging of physiological and biological events, and there is also potential to include a therapeutic moiety [35].

Silica is non-toxic and biocompatible and well suited to nanoparticle design. Patel et al. developed an iron oxide-based nanoparticle consisting of an iron oxide core as an MRI probe, coated with a porous silica shell for biocompatibility. The surface was further modified with a ligand capable of coordinating with radioisotopes for PET imaging. Contrast enhancement for MRI requires water coming in close contact with the iron oxide. The porous silica shell allows water to penetrate the external layers of the nanoparticle to gain intimate contact with the core. Synthesis has been optimized such that single or multiple iron oxide

nanocrystals can be encapsulated in the silica matrix to control contrast effects. It has been reported that clusters of iron oxide may provide superior contrast characteristics compared to single particles, so the ability to control nanoparticle content is valuable in nanoparticle probe design. *In vitro* results are promising [36].

Beyond simple determination of the presence or absence of tumors, there is potential for garnering more complex physiological information through combined PET/MRI imaging using carefully designed multi-modality nanoprobes. For example, nanoparticle contrast agents targeted specifically to biomarkers such as vascular endothelial growth factor (VEGF) and VEGF receptor (VEGFR) are capable of imaging the presence and process of tumor angiogenesis, an identified target for therapeutic delivery. This enables simultaneous visualization and drug delivery [37]. It is reasonable to assume multi-functional nanoparticles could be readily designed to track other biomarkers and elucidate relevant pathological processes through combined PET/MRI imaging for more accurate diagnosis and localized drug delivery.

17.5 Conclusions and Future Prospects

There is great promise for the role of nanoparticles in diagnostic imaging and drug delivery. While there are many examples in research showing promise in preclinical applications, there have yet to be significant advances into clinical practice. One limitation is a matter of technology. Other than PET/CT, dual-modality imaging devices are sparse in the clinical realm. Prototype pre-clinical small animal devices are available for combined PET and MRI, for example, but the technology has yet to reach the clinic. Additionally, nanoparticles for diagnostic imaging are still expensive to produce in clinical quantities, relative to existing contrast and drug formulations. For nanoparticles to take hold commercially, they must have proven superior performance compared to the current standard of care to justify an initially increased cost. Improved pharmacokinetic behavior of nanoparticles targeted with peptides, and surface chelates to bind diagnostic and therapeutic moieties may provide sufficient tissue specificity, potency, and improved image quality to gain favor. Finally, there are many theoretical and early-stage examples of multi-functional

nanoparticles that can act as imaging probes and simultaneously deliver therapeutic moieties, but in general the research is not mature enough to fully understand the behavior and use of these particles on a clinical scale for human pathologies. This suggests a wide opportunity in the future of design and development of so-called theranostic nanoparticles, and there are examples that fulfill this promise.

Bui et al., for example, described a lipid nanoparticle platform with gadolinium embedded in the membrane. They demonstrated improved MRI contrast with a dramatically lower dose, approximately one-third of the typical clinical dose of gadolinium contrast. This particle showed improved pharmacokinetics, and avoided renal excretion and thus overexposure of toxic gadolinium in the kidneys and bladder, which can often obscure image results when those organs are not of interest diagnostically. To date, this nanoparticle is only designed for single modality imaging, but is likely to be sufficiently versatile to allow incorporation of a radiolabeled moiety for PET imaging, and can easily be formulated to encapsulate drug for targeted delivery [38].

Imaging and treatment for cancer will likely garner the most interest for development and application of nanoparticles in diagnostic imaging and drug delivery. It has been estimated that cancer-related expenditure in the United States exceeds $100 billion annually, so research in early detection and improved treatment is expected to grow [9]. There is great promise in nanoparticles to provide exciting and valuable advancements toward improving clinical outcomes through enhancing diagnostic capabilities, and controlling therapeutic delivery. Nanomedicine is perhaps the next great frontier in biomedical research and clinical application.

Disclosures and Conflict of Interest

The authors declare that they have no conflict of interest and have no affiliations or financial involvement with any organization or entity discussed in this chapter. This includes employment, consultancies, honoraria, grants, stock ownership or options, expert testimony, patents (received or pending), or royalties. No writing assistance was utilized in the production of this chapter and the authors have received no payment for its preparation. The

findings and conclusions here reflect the current views of the authors. They should not be attributed, in whole or in part, to the organizations with which they are affiliated, nor should they be considered as expressing an opinion with regard to the merits of any particular company or product discussed herein. Nothing contained herein is to be considered as the rendering of legal advice.

Corresponding Author

Catherine M. Lockhart
Department of Pharmaceutics, University of Washington
Box 357610, H272 Health Science Building
1959 NE Pacific Street, Seattle, WA 98195 USA
Email: cmo4@uw.edu

About the Authors

Catherine M. Lockhart received a doctor of pharmacy from the Department of Pharmaceutics at the University of Washington where she is currently a graduate student pursuing a PhD in pharmaceutical sciences. She has three undergraduate degrees, a bachelor of fine arts in theatre arts and a bachelor of science in visual communications from the University of Idaho and a bachelor of science in electrical engineering from the University of Washington. From 2006 through 2009, she was a research scientist at the Imaging Research Lab in the Department of Radiology at the University of Washington, where her work focused on positron emission tomography physics and computed tomography. She holds one patent and has 16 publications, including five manuscripts, nine abstracts, and two book chapters. She is currently pursuing a PhD in pharmaceutical sciences.

Rodney J. Y. Ho is a professor of pharmaceutics and director of the DNA Sequencing and Gene Analysis Center at University of Washington, Seattle. He also holds appointments at Clinical Pharmacology, Fred Hutchinson Cancer Research Center, the Center for AIDS and STD Research,

the Center for Human Development and Disability, the Center for Ecogenetics at University of Washington, and the Washington National Primate Research Center. He served as an Associate Dean for Research and New Initiatives from 2006 to 2009, and is an editor for the Journal of Pharmaceutical Sciences. He is an elected fellow of the American Association for the Advancement of Science and was an elected chair of the American Association for the Advancement of Sciences. He is also an elected fellow of the American Association of Pharmaceutical Scientists and is named as one of the top 25 entrepreneurs in the Pacific Northwest. Dr. Ho is a recipient of the prestigious Paul R. Dawson Biotechnology Award in 2009, cited for his teaching and scholarship in biotechnology. Dr. Ho received his undergraduate degree from the University of California, Davis, in 1983 and master's and PhD in 1985 and 1987, respectively, from the University of Tennessee, focusing on biochemistry and drug targeting. His post-doctoral fellowship focused on infectious diseases at the Division of Infectious Diseases, Stanford University School of Medicine, before joining the University of Washington, School of Pharmacy as an assistant professor in December 1990. Dr. Ho was promoted to associate professor with tenure in 1996 and full professor rank in 2002. In 2003, he founded the DNA Sequence and Gene Analysis Center and serves as the director for the Center. Dr. Ho's accomplishments include 6 patents and more than 12 patent disclosures, over 100 original research publications, 20 book chapters, and 2 edited books.

References

1. Jennings, L., Long, N. (2009). "Two is better than one"—probes for dual-modality molecular imaging. *Chem. Commun. (Cambridge, England)*, **24**, 3511–3524.
2. Pysz, M., Gambhir, S., Willmann, J. (2010). Molecular imaging: Current status and emerging strategies. *Clin. Radiol.*, **65**(7), 500–516.
3. United States Nuclear Regulatory Commission. NRC: 10 CFR 20.1004 Units of radiation dose. Available at: http://www.nrc.gov/reading-rm/doc-collections/cfr/part020/part020-1004.html (accessed on February 8, 2012).
4. Holmes, E. B., Taylor, C. R. Ionizing radiation exposure with medical imaging. Available at: http://emedicine.medscape.com/article/1464228-overview (accessed on February 10, 2012).

5. Wrixon, A. D. (2008). New ICRP recommendations. *J. Radiol. Prot.*, **28**, 161–168.
6. Mattsson, S., Söderberg, M. (2011). Radiation dose management in CT, SPECT/CT and PET/CT techniques. *Radiat. Prot. Dosimetry*, 1–9.
7. Adam, A., Dixon, A. K., (eds) (2008). *Adam: Grainger and Allison's Diagnostic Radiology*, 5th ed., Elsevier Churchill Livingstone, Philadelphia.
8. Cheon, J., Lee, J.-H. (2008). Synergistically integrated nanoparticles as multimodal probes for nanobiotechnology. *Acc. Chem. Res.*, **41**(12), 1630–1640.
9. Hahn, M. A., Singh, A. K., Sharma, P., Brown, S. C., Moudgil, B. M. (2011). Nanoparticles as contrast agents for *in vivo* bioimaging: Current status and future prospects. *Anal. Bioanal. Chem*., **399**, 3–27.
10. Lucignani, G. (2009). Nanoparticles for concurrent multimodality imaging and therapy: The dawn of new theragnostic synergies. *Eur. J. Nucl. Med. Mol. Imaging*, **36**(5), 869–874.
11. Catana, C., Wu, Y., Judenhofer, M., Qi, J., Pichler, B., et al. (2006). Simultaneous acquisition of multislice PET and MR images: Initial results with a MR-compatible PET scanner. *J. Nucl. Med.*, **47**(12), 1968–1976.
12. Tilcock, C. (1999). Delivery of contrast agents for magnetic resonance imaging, computed tomography, nuclear medicine and ultrasound. *Adv. Drug Deliv. Rev.*, **37**(1–3), 33–51.
13. Jarzyna, P., Gianella, A., Skajaa, T., Knudsen, G., Deddens, L., et al. (2010). Multifunctional imaging nanoprobes. *Wiley Interdisciplinary Rev. Nanomed. Nanobiotechnol.*, **2**(2), 138–150.
14. Cormode, D., Skajaa, T., Fayad, Z., Mulder, W. (2009). Nanotechnology in medical imaging: Probe design and applications. *Arterioscler. Thromb. Vasc. Biol.*, **29**(7), 992–1000.
15. Lian, T., Ho, R. J. Y. (2001). Trends and developments in liposome drug delivery systems. *J. Pharm. Sci.*, **90**(6), 667–680.
16. Lonsdale, M., Beyer, T. (2010). Dual-modality PET/CT instrumentation-today and tomorrow. *Eur. J. Radiol.*, **73**(3), 452–460.
17. Antoch, G., Freudenberg, L., Beyer, T., Bockisch, A., Debatin, J. (2004). To enhance or not to enhance? 18F-FDG and CT contrast agents in dual-modality 18F-FDG PET/CT. *J. Nucl. Med.*, **45**(Suppl 1), 56S–65S.
18. Hagit, A., Soenke, B., Johannes, B., Shlomo, M. (2010). Synthesis and characterization of dual modality (CT/MRI) core–shell microparticles for embolization purposes. *Biomacromolecules*, **11**(6), 1600–1607.

19. Chou, S.-W., Shau, Y.-H., Wu, P.-C., Yang, Y.-S., Shieh, D.-B., et al. (2010). *In vitro* and *in vivo* studies of FePt nanoparticles for dual modal CT/MRI molecular imaging. *J. Am. Chem. Soc.*, **132**(38), 13270–13278.
20. Alric, C., Taleb, J., Le Duc, G., Mandon, C., Billotey, C., et al. (2008). Gadolinium chelate coated gold nanoparticles as contrast agents for both X-ray computed tomography and magnetic resonance imaging. *J. Am. Chem. Soc.*, **130**(18), 5908–5915.
21. Cline, H., Schenck, J., Hynynen, K., Watkins, R., Souza, S., et al. (1992). MR-guided focused ultrasound surgery. *J. Comput. Assist. Tomogr.*, **16**(6), 956–965.
22. Adams, J., Moore, R., Anderson, J., Strandberg, J., Marshall, F., et al. (1996). High-intensity focused ultrasound ablation of rabbit kidney tumors. *J. Endourol.*, **10**(1), 71–75.
23. Rowland, I., Rivens, I., Chen, L., Lebozer, C., Collins, D., et al. (1997). MRI study of hepatic tumours following high intensity focused ultrasound surgery. *Br. J. Radiol.*, **70**, 144–153.
24. Exablate 2000 Premarket Approval. Food and Drug Administration. (2004).
25. Mei, J., Cheng, Y., Song, Y., Yang, Y., Wang, F., et al. (2009). Experimental study on targeted methotrexate delivery to the rabbit brain via magnetic resonance imaging-guided focused ultrasound. *J. Ultrasound Med.*, **28**(7), 871–880.
26. Chan, A. (2005). History of MR guided focused ultrasound: A literature review. *InSightec White Paper*, **1**(1), 1–8.
27. Modonesi, E., Balbi, M., Benzante, G.P. (2010). Limititation and potential clinical application on contrast echocardiography. *Curr. Cardiol. Rev.*, **6**, 24–30.
28. Morawski, A., Lanza, G., Wickline, S. (2005). Targeted contrast agents for magnetic resonance imaging and ultrasound. *Curr. Opin. Biotechnol.*, **16**(1), 89–92.
29. Deckers, R., Rome, C., Moonen, C. (2008). The role of ultrasound and magnetic resonance in local drug delivery. *J. Magn. Reson. Imaging*, **27**(2), 400–409.
30. Yang, F., Li, Y., Chen, Z., Zhang, Y., Wu, J., et al. (2009). Superparamagnetic iron oxide nanoparticle-embedded encapsulated microbubbles as dual contrast agents of magnetic resonance and ultrasound imaging. *Biomaterials*, **30**(23–24), 3882–3890.
31. Lentacker, I., Geers, B., Demeester, J., De Smedt, S., Sanders, N. (2010). Design and evaluation of doxorubicin-containing microbubbles

for ultrasound-triggered doxorubicin delivery: Cytotoxicity and mechanisms involved. *Mol. Ther.*, **18**(1), 101–108.

32. Judenhofer, M., Wehrl, H., Newport, D., Catana, C., Siegel, S., et al. (2008). Simultaneous PET-MRI: A new approach for functional and morphological imaging. *Nat. Med.*, **14**(4), 459–465.
33. Lee, H.-Y., Li, Z., Chen, K., Hsu, A., Xu, C., et al. (2008). PET/MRI dual-modality tumor imaging using arginine-glycine-aspartic (RGD)-conjugated radiolabeled iron oxide nanoparticles. *J. Nucl. Med.*, **49**(8), 1371–1379.
34. Glaus, C., Rossin, R., Welch, M., Bao, G. (2010). *In vivo* evaluation of Cu-64-labeled magnetic nanoparticles as a dual-modality PET/MR imaging agent. *Bioconjug. Chem.*, **21**, 715–722.
35. Choi, J.-S., Park, J., Nah, H., Woo, S., Oh, J., et al. (2008). A hybrid nanoparticle probe for dual-modality positron emission tomography and magnetic resonance imaging. *Angew. Chem. Int. Ed. Engl.*, **47**(33), 6259–6262.
36. Patel, D., Kell, A., Simard, B., Deng, J., Xiang, B., et al. (2010). Cu^{2+}-labeled, SPION loaded porous silica nanoparticles for cell labeling and multifunctional imaging probes. *Biomaterials*, **31**(10), 2866–2873.
37. Cai, W., Chen, X. (2008). Multimodality molecular imaging of tumor angiogenesis. *J. Nucl. Med.*, **49**(Suppl 2), 113S–28S.
38. Bui, T., Stevenson, J., Hoekman, J., Zhang, S., Maravilla, K., et al. (2010). Novel Gd nanoparticles enhance vascular contrast for high-resolution magnetic resonance imaging. *PloS One*, **5**(9), e13082.

Chapter 18

Magnetic Nanoparticles for Magnetic Resonance Imaging: A Translational Push toward Theranostics

Ryan A. Ortega,[a,b] Thomas E. Yankeelov, PhD,[c] and Todd D. Giorgio, PhD[a,b]

[a]*Department of Biomedical Engineering, Vanderbilt University, Nashville, Tennessee, USA*
[b]*Vanderbilt Institute of Nanoscale Science and Engineering, Vanderbilt University, Nashville, Tennessee, USA*
[c]*Vanderbilt University Institute of Imaging Science, Nashville, Tennessee, USA*

Keywords: nanotechnology, iron oxide nanoparticles, magnetic resonance imaging, superparamagnetism, magnetic contrast agents, theranostic nanomaterials

18.1 Introduction

Iron oxide nanoparticles have been utilized as tools for exploring magnetic phenomenon since the 1930s [1]. Based on the prediction and subsequent observation of enhanced magnetic properties of nanoscale iron oxide particles, these materials were increasingly utilized in the realm of biotechnology in the early 1980s for

Handbook of Clinical Nanomedicine: Nanoparticles, Imaging, Therapy, and Clinical Applications
Edited by Raj Bawa, Gerald F. Audette, and Israel Rubinstein

ISBN 978-981-4669-20-7 (Hardcover), 978-981-4669-21-4 (eBook)
www.panstanford.com

in vitro applications such as magnetic cell separations, protein purification, and immunoassays [2–4]. Shortly thereafter, it was shown that the same formulations of iron oxide–based materials used for cell separation were effective contrast agents for magnetic resonance imaging (MRI) [5–7]. Many of the particle formulations designed and developed in the late 1980s-early 1990s have been in continual clinical use and have undergone consistent improvements since their inception. Most clinically available materials are almost two decades old and, despite a substantial number of new, academically investigated iron oxide-based diagnostic and therapeutic tools, there has been no clinical translation of iron oxide nanoparticles that substantially deviate from the original formulas.

The original iron oxide nanoparticle–based contrast agents are fabricated by the coprecipitation of iron oxides from iron salts and consist of a crystalline iron oxide core ranging 5–10 nm in diameter and a dextran coating ranging approximately 50–150 nm in diameter [8–10]. It was discovered that these particles are both passively and preferentially taken up by the liver and spleen, and the first imaging efforts were aimed at providing contrast enhancement of these tissues [6, 7]. These materials were soon joined in clinical use by silica-coated particles made by a similar process [10, 11]. In the late 1990s, improved coating methods allowed for the industrial scale production of ultrasmall iron oxide nanoparticles, which, due to their smaller size, could be passively transported into the lymph system [12, 13]. Most of the clinically available iron oxide contrast agents share these characteristics: facile industrial fabrication by the coprecipitation method, dextran-based or silica-based surface coating, passive uptake by certain tissues due to their size, and a relatively wide size distribution.

In addition to these well-characterized materials, academia has produced many novel iron oxide-based nanostructures with potential as diagnostic and/or therapeutic tools. Many particle formulations have been developed with different physical, chemical, and biological properties [14]. Furthermore, active targeting mechanisms have been well established in the academic sector for over a decade and advanced materials employing both diagnostic and therapeutic techniques (theranostic nanomedicine) are

quickly approaching clinical feasibility [15]. These new materials must exhibit large magnetizations, narrow size distributions, colloidal stability, and biocompatibility that matches or exceeds that of existing materials to be clinically efficacious [8, 9, 16, 17]. In order to improve these nanomaterials for clinical translation, the quality of these parameters and others must be continually improved. The primary means for doing so are through improving the control of nanoparticle fabrication and/or by altering the surface presented by the particles to cells and tissues. In this review, we will examine the physical and biological properties of iron oxide–based nanomaterials for clinical uses and explore more novel materials poised for clinical translation. We will present multiple fabrication techniques and conclude with some basic recommendations aimed at facilitating the clinical translation of new magnetic nanomaterials.

18.2 Properties of Iron Oxide Nanoparticles

Although the metal component of magnetic nanoparticles is not intentionally presented to biological structures, the iron oxide core contributes greatly to the diagnostic or therapeutic efficacy of these materials and is responsible for their magnetic behavior. One of the most important parameters of these particles is particle diameter. The size of the iron oxide core will largely determine the magnetic properties of the particle and, therefore, will control the contrast produced in MR images. Core size also controls, in part, functional characteristics pertinent to other uses such as heat production in magnetically induced hyperthermia. The biocompatibility of these nanomaterials is also of the utmost importance for clinical translation. Particle surface coatings must be carefully chosen to preserve and enhance the biocompatibility of the metallic oxide core.

18.2.1 Geometric Properties

Most clinically available and investigational iron oxide nanomaterials consist of magnetite, Fe_3O_4, maghemite, γ-Fe_2O_3, or some combination of the two. Hematite, α-Fe_2O_3, has been investigated as well, but has not received the same degree of attention due

to smaller magnetization values and more arduous fabrication routes [18]. Due to its inverse spinal crystalline structure with no vacancies, magnetite generally has stronger magnetization than magnetite given an identical applied magnetic field. This behavior is observed because magnetite has a defect spinal structure with repeating iron atom vacancies making it essentially an iron-deficient form of magnetite [19]. However, magnetite is very sensitive to oxidation during fabrication. The result is that most particle formulations are either partly or entirely maghemite.

The diameter of an iron oxide nanoparticle greatly affects multiple magnetic parameters and the nanometer scale of these particles offers unique magnetic, thermal, and biological properties [20]. The saturation magnetization, spontaneous or resting magnetization, and the magnetic susceptibility are all controlled by particle size [21]. This results in a highly non-linear influence of size on particle magnetic behavior, though smaller particles tend to have smaller saturation magnetizations [22, 23]. This behavior is further complicated by the presence of a magnetically inert layer at the surface of the particle caused by a disordered crystalline structure, a result of the fabrication method [21, 23, 24]. The crystalline structure of the entire particle also plays a role in the magnetic properties, with highly crystalline particles exhibiting stronger magnetizations, making them more efficacious for clinical uses [8]. All of these effects are represented by a single phenomenon describing the enhanced magnetic properties of nanoscale iron oxide nanoparticles: superparamagnetism.

18.2.2 Superparamagnetism

Superparamagnetism is a size-dependent magnetic phenomenon that occurs in nanoscale crystals of many ferro-, ferri-, and antiferromagnetic materials. First predicted in 1930, superparamagnetism is a state of enhanced magnetic properties in a particle due to the presence of a single magnetic domain [1, 25]. In a bulk sample of these materials, the magnetic moments of multiple domains act unidirectionally to produce a stable spontaneous magnetization in ferromagnetic and ferromagnetic materials, or cancel out to produce a state of no magnetism as in antiferromagnetic materials. However, when the particle size is sufficiently small, the iron oxide crystal contains a single magnetic domain. Due to direc-

tionally randomizing thermal fluctuations, bulk solutions of these particles have no magnetization at room temperature in the absence of an externally applied magnetic field [26]. This behavior is similar to paramagnetic behavior and follows many of the same physical laws as paramagnetism; however, single domain particles exhibit stronger magnetization compared to multi-domain paramagnetic materials, giving rise to the term superparamagnetism or superparamagnetic iron oxides (SPIOs) [25].

Particle size plays an important role in the magnetic properties of SPIOs: above a particular diameter, an iron oxide particle forms multiple domains. For example, an iron oxide crystal 150 nm in diameter exhibits magnetization, susceptibility, and coercivity that are predictable using the bulk properties and relationships of that material [23]. As particle size decreases to approximately 30 nm for iron oxides, the crystal becomes single domain, loses its coercive behavior, deviates from bulk property characteristics and displays enhanced magnetization [5]. It is the enhanced magnetization and magnetic susceptibility that makes SPIOs effective as MRI contrast agents.

18.2.2.1 Superparamagnetic mechanisms for MRI contrast

One of the most well known applications for SPIOs is for enhancing contrast in MRI. SPIOs are a strong enhancers of transverse relaxation, resulting in dark negative contrast when they are employed for T_2- and T_2^*-weighted MRI [27]. They are also capable of producing positive contrast when employed at lower concentrations and smaller sizes in T_1-weighted MRI [28]. Negative contrast T_2 agents also undergo relaxation on the order of 1–100 ms, which is favorable for moving systems like the bowel, and act to reduce ghost artifacts [5].

18.2.3 Biocompatibility

One of the major advantages of SPIO contrast agents is that they are highly biocompatible. The gadolinium used in other contrast agents is toxic and must be delivered with a chelating agent to increase biocompatibility [29]. The high biocompatibility of SPIO agents are due to two factors: the natural metabolism of iron *in vivo* and the enhanced biocompatibility of the surface coating

[30]. A coating layer is necessary for clinical SPIO nanomaterials in order to prevent aggregation and impart hydrophilicity and colloidal stability in biological fluids [8]. The oldest clinically available SPIOs are coated in dextran and are cleared rapidly from circulation [31]. This is due primarily to the total size of the particles. In most cases, the ultimate fate of clinically available SPIOs is dependent on the total particle size derived from the iron oxide core and the thickness of the surface coat. The most common method of clearance for most of these particles, which are approximately 10–200 nm, is uptake by the cells of the reticuloendothelial system (RES). The majority of particles in this size range are endocytosed by Kupffer cells in the liver or into endothelial cells or RES cells of the spleen. The particles are then metabolized via the lysosomal pathway 1–2 days after internalization, and the iron is incorporated into hemoglobin over 28–40 days [31, 32]. Larger particles are quickly opsonized by plasma proteins and are cleared by phagocytic cells in the spleen [16]. Advanced fabrication methods have allowed for the repeatable production of ultrasmall superparamagnetic iron oxides (USPIOs) [13, 33]. These smaller particles, often smaller than 10 nm in diameter, are capable of evading RES clearance due to their size and can enter the lymph system, penetrate tissue, and are cleared by the renal system [10, 34]. The clinically available SPIO and USPIO materials, as well as newer investigational materials, have repeatedly been shown to be highly biocompatible.

18.3 Fabrication

The fabrication mechanism chosen for SPIOs and USPIOs plays a critical role in their efficacy as diagnostic and therapeutic agents. Particle magnetization and susceptibility depend largely on particle size, population size distribution, crystallinity, and surface coat [16]. These parameters are established during fabrication and different synthetic routes, though they produce particles of similar sizes, may produce dissimilar materials due to differences in size distribution, crystallinity, or other parameters [35, 36]. The fabrication route chosen to design novel materials for clinical applications is non-trivial and each method has advantages and disadvantages.

18.3.1 Coprecipitation from Iron Salts

The first method of SPIO fabrication developed was the coprecipitation of iron oxide from iron salt precursors [37]. For this technique, iron-containing salts such as ferric chloride and ferrous chloride hydrates are oxidized or aged in stoichiometric mixtures in aqueous media [2, 20, 38]. Particle formation begins by a burst of nucleation during which few iron atoms rapidly clump together. Slow growth of the particles then occurs as iron solutes diffuse to the particle surface, forming successive, regularly arranged layers on the growing surface [17]. This method of particle formation allows for large, industrial sized batches of SPIOs to be produced and allows for some degree of control over the oxidation of the resultant particles by altering solution pH and the molar ratio of reactants. Particle coating and stabilization can be done during the synthesis by adding the desired coating molecule to the coprecipitation solution [20]. Varied particle coatings have been investigated using this fabrication route, including proteins, lipids, natural carbohydrate polymers, and synthetic polymers [29, 39]. The first generation of coatings tended to be thick and irregular, reducing the effectiveness of the materials, but more recent techniques allow for thin and homogenous coatings that improve magnetic properties and prevent protein adsorption [40]. One major disadvantage of this fabrication method is that it allows for little control of particle size and size distribution relative to other techniques [41, 42]. This is largely due to the difficulty inherent in preventing further nucleation of new particles during the growth phase.

In order to improve control of size and size distribution, nucleation or growth arresting coating molecules can be added during particle synthesis. The addition of organic surfactants, polymers, or anionic monomers can narrow the particle size distribution by preventing nucleation during growth, forming larger particles, or preventing growth during nucleation, forming smaller particles [41]. However, this technique is very sensitive to the molar ratio of the stabilizing agent to the iron salt, making size control difficult, though it is possible to make USPIOs by adding a strong arresting molecule during the growth phase [43]. During coprecipitation, the Fe^{2+}/Fe^{3+} ratio is also important for size control: size increases with this ratio and only ratios between

0.4 and 0.6 produce clinically efficacious nanomaterials [30]. Increasing the mixing intensity also decreases particle size by mechanically preventing the settling of solutes on the particle surface [38]. Because materials made via the coprecipitation route contain both maghemite and magnetite, these particles possess more disordered crystallinity, which can be improved by performing the synthesis in an oxygen free environment [20, 42, 44].

18.3.2 Thermal Decomposition of Iron Precursors

Though all clinically approved SPIO and USPIO materials are made via the coprecipitation route, the thermal decomposition of iron-containing organic precursors has become a highly preferred (in academic settings) synthesis technique, and is a strong candidate for the synthetic route of the next generation of clinically translated iron oxide nanomaterials. To produce particles by thermal decomposition, a surfactant and an organic iron precursor such as iron acetylacetonate, iron carboxylate, iron cupferronates, or iron carbonyls are heated to high temperatures in a high boiling point solvent in an oxygen free environment [24]. The particles are then exposed to oxygen, allowing oxide formation and particle nucleation and growth. The resultant particle forms already coated in the surfactant used during synthesis; common surfactants are steric acid, oleylamine, and oleic acid [45].

Thermal decomposition has become a popular fabrication route due to a product that is highly crystalline, displays facile size control, and exhibits very small size distributions: standard deviations in particle diameter can be as small as ±5% of the mean size, whereas coprecipitation methods generally produce size distributions approximately ±10–20% of the mean size [46]. Particle shape and size can be precisely controlled by manipulating reaction time and temperature, the concentration of reactants, and the surfactant, precursor, or solvent used [17]. Particle geometries able to be fabricated by thermal decomposition include spheres, pyramids, diamonds, and cubes [47]. Generally, the addition of greater amounts of surfactant will increase particle size in a highly predictable fashion, though these surfactants must be removed or further functionalized prior to *in vitro* or *in vivo* use [24]. This process is also industrially scalable, though the high temperatures

necessary for the reaction are potentially hazardous at large scales, increasing the cost of safety precautions. Though the products of thermal decomposition are very pure and highly crystalline due to the high temperatures used for fabrication, they are not water soluble *in situ* [45]. Further functionalization for water solubility and biocompatibility is relatively facile by performing ligand exchange of the surfactant or by further modifying the surfactant itself [42].

18.3.3 Emulsion-Mediated Synthesis

Synthetic routes occurring in aqueous solutions can be modified to utilize the size-restricting capabilities of microemulsions to control particle size and size distribution. The mechanism for enhanced size control relies on the predictable sizes of polymer and lipid micelles and similar structures in the emulsion inside of which the iron oxide particles are forming [48]. The size-restricting environment physically prevents particle growth past a certain size determined by the geometric constraints of the structures in the emulsion. This fabrication mechanism can also be used to coat iron oxide particles *in situ* by controlling the components of the microemulsion. Emulsion-mediated synthetic routes have proven highly successful for silanization of iron oxide nanoparticles. By using silica containing micelles as nanoscale reactors for particle fabrication, the resultant materials have a coherent, well-organized silica coat and a very narrow size distribution [49]. One major downside to this mechanism is that the solvent used to create the microemulsion for synthesis must be removed prior to further functionalization or clinical use; this process is often difficult and only partially successful [50]. Also, due to the volume occupied by structures comprising the emulsion, particle yields from these methods are relatively low [16].

18.3.3.1 Polyol process

Due to the facile nature of *in situ* surface functionalization provided by emulsion-mediated fabrication, it is possible to fabricate water-soluble particles in a single reaction. The polyol process uses polyols such as ethylene glycol and polyethylene glycol as solvents for

iron-containing precursors in solution. The entire solution is boiled until the metal is solubilized and reduced to form nucleation sites [51]. The polyol forms micelle-like structures around the emerging particles, providing tunable size control, narrow size distribution, and water solubility. The high temperatures used also create highly crystalline products [52].

18.3.4 Gas Phase Synthesis

Gas phase methods of particle fabrication utilize macro-scale reactors to continuously produce iron oxide nanoparticles from iron-containing precursor gases. These methods produce materials with narrow size distributions and good crystallinity. For example, laser pyrolysis uses a high powered laser to heat iron precursor gases to high temperatures to create a sustained chemical reaction capable of producing highly stable particle populations as small as 2 nm [17]. The materials created are highly monodisperse, fabricated in a single step, and highly crystalline due to the high temperatures used [53]. Chemical vapor deposition of iron oxides from a high temperatures gas in a vacuum has also been used to fabricate SPIOs and USPIOs [54]. Though gas phase methods can have continuous production of particles, the yields are relatively low, and the equipment used can be expensive and difficult to scale up for industrial applications [19].

18.4 Clinically Available Diagnostic Materials

Current clinical uses for superparamagnetic iron oxides are limited almost exclusively to contrast enhancement in MRI. Commercially available iron oxide contrast agents have a wide range of hydrodynamic sizes, but are all fabricated by the coprecipitation method [46]. These materials have iron oxide cores ranging in diameter approximately 5–20 nm and surface coats of varying composition ranging approximately 5–300 nm in diameter. Clinically available materials display wide size ranges, moderate crystallinity, and are generally less characterized than current investigational materials [2, 55]. Delivery of these contrast agents to their target tissues is a passive, size-dependent phenomenon

[8, 9]. The total size of the contrast agents plays a primary role in deciding their ultimate fate [12, 56].

18.4.1 Dextran-Coated Materials

Some of the first SPIO materials investigated for medical use were particles coated with dextran 40,000 during fabrication [4]. Twenty years later, dextran-coated particles are still actively used in a clinical setting as a diagnostic tool. The first material developed was ferumoxide (AMI-25; Feridex®, Endorem®), an SPIO consisting of dextran-coated iron oxides. Ferumoxides have an iron oxide core 4–6 nm in diameter and a total diameter of 80–180 nm, which cause these particles to be sequestered 80% in the liver and 5–10% in the spleen with a blood residence time of approximately 6 min [31]. Investigations of these early particles showed that dextran coating provided increased colloidal stability and biocompatibility at pH ranges of 2–10 by increasing interparticle electrostatic repulsion and steric hindrance [29, 57].

Later dextran-coated materials were developed to improve particle size distributions and magnetic properties. Ferumoxtran (AMI-227; Sinerem®, Combidex®) is a dextran covered particle with a more uniform coat than ferumoxide and a much smaller particle size due to this more organized coat [13, 22]. These 15–30 nm particles were the first USPIOs and exhibited much longer blood retention times (>24 h) and are transported to different organs and tissues than larger materials [32, 58]. Ferumoxytol, a 30 nm carboxymethyl-dextran–coated USPIO, also shows narrower size distributions and similar transport capabilities [17]. Larger particles with narrower size distributions have also been fabricated using carboxydextran as a coating molecule. Ferucarbotran (SHU-555; Resovist®, Supravist®) has a narrow size distribution and a total particle size of approximately 60 nm, placing this material in an ambiguous size range between SPIO and USPIO, with characteristics of both [28].

18.4.2 Polymer and Small Molecule Coatings

Silica-coated SPIOs and USPIOs were developed to leverage the high biocompatibility and facile functionalization capacity of silane

molecules for use in contrast enhanced MRI [55, 59]. Ferumoxsil (AMI-121; Lumirem®, Gastromark®) is a 300 nm, silica-coated SPIO, which is used to provide gastrointestinal (GI) contrast via oral delivery due to its larger size. The size and silica coating of these particles allows them to have a longer residence time in the GI tract because they are not absorbed and do not irritate the intestinal mucosa [11]. Furthermore, because these particles are miscible in the bowel contents, it is not necessary that they replace the bowel contents to produce efficacious image contrast, allowing for a reduced dose of the contrast agent [5].

Other small molecule coatings formed during coprecipitation have also been successfully translated into clinical use. VSOP C184 is a monomeric citric acid-coated USPIO. By utilizing 4 nm iron oxide crystals for the particle, and the small citric acid molecule as the coat, developers of VSOP C184 have fabricated one of the smallest USPIOs to enter into clinical trials: 7 nm in total diameter [60]. The size arresting effect of adding the citrate during particle formation creates very narrow size distributions, but also decreases the crystallinity of the iron oxide [61].

Simple polymer coatings of coprecipitation formed iron oxide have also undergone clinical trials, but have seen limited success in full clinical translation. A polyethylene glycol (PEG) modified starch has been used to coat iron oxides to form USPIOs with long blood residence times [62]. This material, feruglose (NC100150; Clariscan®), has an average diameter of 20 nm and displays enhanced biocompatibility due to the PEG coating [44]. The PEG coating also acts to create “stealth” particles, which are able to evade blood clearance and degradation [63, 64]. Despite promising initial clinical trials, feruglose development has largely been abandoned.

Other polymers have also been investigated for use in modifying existing clinical contrast agents. Chitosan is a polysaccharide that is widely used in bioapplications. It has been used to impart enhanced hydrophilicity and biocompatibility to iron oxide nanoparticles [65]. Polyvinyl alcohol also adds these properties to iron oxides and can also prevent particle aggregation in biological solution, making particle populations highly monodisperse *in vivo* [39]. Polyacrylic acid also improves stability and can aid in bioadhesion [66].

18.4.3 Some Clinical Indications and Experimental Uses

The coating moiety of a specific SPIO or USPIO plays a role in determining the blood retention time of these materials *in vivo*; however, particle size is still the predominate determiner of particle delivery location. In general, long blood half-lives are preferable for biomedical applications, and neutral charge in combination with hydrophilic surfaces prevent protein adsorption [9]. There is no ideal particle size and composition for all clinical applications. Rather, each application requires a precise selection of iron oxide size, total particle size, and surface coating.

18.4.3.1 Organs and cells of the reticuloendothelial system

SPIOs were first used as liver contrast agents due to the rapid uptake of particles by the Kupffer cells, modified macrophages present in the liver [6]. Approximately 30 min after IV administration of dextran-coated SPIOs, 80% of the particles are taken up by the liver and are visible in contrast enhanced images up to 6 h after administration [14, 28]. Liver lesions do not take up the contrast agent and are visible on MRI scans as hyperintense regions, significantly increasing lesion-to-liver contrast by over an order of magnitude relative to native contrast and allowing for detection of lesions as small as 3 mm [67]. A significant percentage of these materials are also taken up by RES cells in the spleen and detection of lesions in this organ can be improved by an order of magnitude [7].

Cells of the liver and spleen are not the only RES cells that preferentially uptake SPIOs. Any location with active macrophages, such as sites of inflammation, will show increased uptake of moderate to large sized SPIOs [68]. SPIO and USPIO contrast enhanced MR images have been used to quantify bone marrow response to therapeutic irradiation due to the presence of active macrophages performing endothelial cell rearrangement of the irradiated tissue [69]. Iron oxide particles have also been used to measure renal graft rejection and kidney damage in a rat model [70]. Ferumoxide enhanced image data was compared favorably to histopathology and showed that it could be used to monitor graft rejection [71].

18.4.3.2 Blood and lymph

USPIOs show increased blood retention time and are also small enough to enter into the lymph system. These characteristics make them useful blood pool, lymph node, and vascular tumor contrast agents. Ferumoxsil has been used to measure blood volume changes in the brain as well as myocardial perfusion, providing results comparable to Gd-DTPA perfusion imaging at 3.5% of the dose [57, 72]. Ferumoxtran has been used in contrast enhanced magnetic resonance angiography to improve contrast in the renal artery, right coronary, vena cava, and portal vein despite not increasing signal noise [73, 74].

Measurement of lymph node size is a widely used method of determining lymph node involvement in cancer [75]. USPIOs are small enough to enter the lymph system and have been used to aid in lymph node tumor staging [33]. In a study of 80 prostate cancer patients with lymph node biopsy or resection, MRI of the nodes was performed before and 24 h after Ferumoxtran injection. Contrast enhanced imaging identified all patients with nodal metastases, detecting masses 5–10 mm in size [56]. Successful results have also been recorded in nodal staging for esophageal and bladder cancer [76, 77].

18.5 Potential Future Clinical Applications

Developing new uses for existing SPIO-based contrast agents enables the continued translation of these agents into different clinical settings. Novel diagnostic procedures using SPIOs will continue to drive academic research, the section of industry producing these agents, and, most importantly, will continue to save lives and increase quality of life. However, there has been little clinical translation of novel SPIO-based contrast agents in the past decade. The majority of the clinically available SPIO contrast agents are synthesized by the co-precipitation method, present similar surface modifications (either a form of dextran or a silane surface), and rely on passive delivery to the target tissue or cell type.

18.5.1 Active Targeting Agents

Unlike clinically available materials, active targeting agents rely on specific ligand-receptor interaction to provide greatly enhanced cellular or molecular specificity for contrast enhancement. Cellular and molecular imaging allows for non-invasive and repeatable *in vivo* imaging of specific cells, molecules, or biological process in a three-dimensional, time resolved fashion. The first active targeting was done with antibodies for tumor detection; it exhibited poor specificity, but was a revolutionary concept [78]. As antibodies became more sophisticated, antibody-based probes became more specific, but were quickly taken up by the RES due to their large size [79]. Small molecule ligands, such as folic acid or a cyclic arginine-glycine-aspartic acid (RGD) peptide, allow smaller particles to escape clearance and reach their intended target [80]. Furthermore, small molecule moieties allow for multiple ligands to be attached to the particle surface, allowing for the possibility of multivalent binding events [81].

Small molecule ligands have been used with iron oxide nanoparticles for many targeted imaging schemes. The folic acid receptor is upregulated in many cancer phenotypes and functionalizing particle surfaces with folic acid has shown to be an efficacious method of targeting and imaging these tumor cells [64]. Targeted apoptosis of tumor cells has also been quantified by conjugating synaptotagmin I to SPIOs, which binds to the membrane of apoptotic cells [82]. Conjugation of holo-transferrin allows for transgene expression monitoring over an extended period as an increase in cell surface receptors produces a significant MR signal change over time [83]. Small amounts of contrast agent can produce a large effect due to the persistence of particle binding, extended cytoplasmic presence after endocytosis, persistence of cellular labeling through multiple cell divisions, and a large change in MR signal per unit of metal, especially on T_2^* weighted images [84, 85].

18.5.2 Activatable Contrast Agents

Activatable contrast agents are being investigated as switchable contrast agents for MRI. An activatable iron oxide contrast agent

consists of aggregates of SPIOs or USPIOs bound together by a degradable linking moiety. The linking molecule is degradable by specific enzymatic activity, which is the target of the imaging diagnostic [86]. Clustered materials exhibit magnetic behavior as if the cluster were a single large particle. Upon cluster degradation and particle dispersal, the MR signal of the interrogated volume changes in T_2-, T_2^*-, and T_1-weighted scans because contrast enhancement is a function of spatial distribution of iron oxide, and because water can now diffuse around the particle more readily [87]. Quantitative enzymatic sensing has been demonstrated using single-stranded DNA-linked USPIO clusters sensitive to a specific DNA cleaving enzyme. Upon the addition of the enzyme, the clusters degrade, increasing the T_2 relaxation time of the sample in solution two-fold [88, 89]. The deaggregation and dispersion event has also been shown to be reversible via thermocycling, indication potential use for long-term diagnostic quantification of enzymatic activity.

18.5.3 Theranostic Iron Oxide Nanomaterials

Theranostics is a relatively new field in medical technology that combines some form of diagnostic tool with a closely related therapeutic technique, utilizing the same material for both. Iron oxide nanoparticles are well suited for clinical translation for theranostic uses due to their size, biocompatibility, multiple functions, and unique physical and biological properties.

18.5.3.1 Targeted drug delivery

Using drug-loaded iron oxide nanoparticles, it is possible to perform simultaneous imaging and drug delivery. Several studies have shown that SPIO-bound chemotherapeutics, such as methotrexate, can be efficaciously delivered to tumor tissue, and that these same materials can be used to image the tissue and monitor drug release [90]. At endosomal pH, the drug is cleaved from the particle and delivered to the cell. This method of drug delivery shows significant cytotoxicity and image contrast enhancement. The particles are able to maintain their viability as contrast agents for up to 144 h [91]. The same magnetic fields used to image the drug-loaded particles can also be used to guide delivery to the target

tissue. Strong, directed magnetic fields can be used to accumulate drug-loaded particles at a specific *in vivo* location [92]. The magnetic force on the particle must exceed the force of the blood flow; therefore this method of drug delivery favors small vessels due to the reduced flow rates [93]. The particles retained at the target site are taken up by local endothelial cells. Due to the targeted delivery, lower drug concentrations can be used, reducing adverse side effects [94].

18.5.3.2 Magnetically induced hyperthermia

Due to the high magnetic susceptibility of SPIOs and USPIOs, the energy deposited by a rapidly alternating magnetic field (greater than 500 kHz) is released as thermal energy [95]. This iron oxide–mediated mechanism of magnetic-to-thermal energy transduction is a highly effective method for generating local tissue hyperthermia, which is designed to have a direct cell killing effect and act as an adjuvant to other types of therapy [96, 97]. Tumor cells are more sensitive to temperature increases than normal cells, and are prime targets for targeted hyperthermia as an adjuvant therapy [98]. For example, localized hyperthermia has been shown to improve treatment of glioblastoma multiforme when used as an adjuvant to gamma therapy [99]. It has been shown in a hamster model that dextran-coated SPIOs accumulate in tumor stroma upon intratumoral injection and are capable of heating the surrounding tissue to 42–45°C with the application of a 500 kHz AC magnetic field [100]. Tumor cells disappeared from the area following heating, and the treatment group exhibited significantly better survival as compared to the control.

18.6 Conclusions

Current investigational fabrication methods show more advantageous size distributions, magnetic properties, and tuneability, but must be modified for industrial scale production to facilitate translation. Furthermore, functionalization techniques have also been greatly improved in the past decade and active targeting has been shown to be very feasible and has the potential to revolutionize image guided diagnostics if well implemented. The quality of these new materials could potentially revise many of the conclusions

drawn in this field that are based on older commercial iron oxide-based contrast agents.

In order to expedite clinical translation of new materials, it would be beneficial for researchers in academia and industry to develop a standardized vocabulary, methods, and safety criteria for active and reactive iron oxide diagnostics and theranostics. It is also important to investigate new materials in long-term safety trials, moving past proof-of-concept studies. Finally, it would be advantageous for researches in bionanotechnology to encourage government regulatory agencies to create a set of definitions and regulations specifically for nanoparticles designed for clinical use: materials that blur the line between drug and device.

Disclosures and Conflict of Interest

The authors would like to acknowledge the following grants: NCI R01 CA138599, CDMRP BCRP BC095472.

The authors declare that they have no conflict of interest and have no affiliations or financial involvement with any organization or entity discussed in this chapter. This includes employment, consultancies, honoraria, grants, stock ownership or options, expert testimony, patents (received or pending) or royalties. No writing assistance was utilized in the production of this chapter and the authors have received no payment for its preparation. The findings and conclusions here reflect the current views of the authors. They should not be attributed, in whole or in part, to the organizations with which they are affiliated, nor should they be considered as expressing an opinion with regard to the merits of any particular company or product discussed herein. Nothing contained herein is to be considered as the rendering of legal advice.

Corresponding Author

Dr. Todd Giorgio
Department of Biomedical Engineering, Vanderbilt University
VU Station B 351620, Nashville, TN37235-1620, USA
Email: todd.d.giorgio@vanderbilt.edu

About the Authors

Ryan Ortega is a PhD candidate in the Department of Biomedical Engineering at Vanderbilt University and is a member of the Vanderbilt Institute of Nanoscale Science and Engineering. He received a BE and an MS from Vanderbilt, both in biomedical engineering. His research is primarily focused on designing nanoparticles for diagnosis and therapy of cancer and other focal diseases. Previously, he has worked to develop polymeric nanoparticles for transdermal drug delivery and cardiovascular stent functionalization as well as created mathematical models of iron oxide nanoparticle magnetic behavior to inform particle design. Currently, he is working on a joint venture with Vanderbilt Cancer Biology to design nanoparticles to deliver cancer immunology-based therapeutics for breast cancer treatment.

Tom Yankeelov is an Ingram Associate Professor of cancer research and an associate professor of radiology and radiological sciences, physics, biomedical engineering, and cancer biology at Vanderbilt University. He received an MA in applied mathematics (1998) and an MS in physics (2000) from Indiana University. His doctorate in biomedical engineering is from SUNY at Stony Brook (2003), where he completed his dissertation at Brookhaven National Laboratory. His research program is focused on developing, validating, and applying quantitative imaging methods for the early prediction of the response of cancer to therapy. This program has resulted in 56 peer-reviewed publications, over 100 conference proceedings, and over 40 presentations at scientific meetings. Dr. Yankeelov is an active member of the editorial boards of *Medical Physics* and MRI. He is Director of Cancer Imaging Research in both the Vanderbilt University Institute of Imaging Science and the Vanderbilt-Ingram Cancer Center where he is currently expanding the use of quantitative MRI and PET (and their combination) in clinical trials.

Todd D. Giorgio is professor and chair of biomedical engineering and professor of chemical and biomolecular engineering at Vanderbilt University. He is a member of the Vanderbilt-Ingram Cancer Center in the Experimental Therapeutics program. Dr. Giorgio also holds an appointment in the Interdisciplinary Materials Science program and serves on the administrative committee of the Vanderbilt Institute of Nanoscale Science and Engineering. His research is primarily focused on the quantitative understanding of complex biological system interactions with gene and drug delivery materials. His work over the most recent period includes a strong focus on nanoscale materials and their applications to the solution of problems in biology and medicine, characterized as "nanomedicine." Prof. Giorgio is also active in educational research in nanobiotechnology, including leadership and participation in a NSF-supported ERC distributed among five academic institutions. He is an elected Fellow of the American Institute for Medical Biological Engineering and the Biomedical Engineering Society. He received his PhD from Rice University and his BS from Lehigh University, both in chemical engineering.

References

1. Frenkel, J., Dorfman, J. (1930). Spontaneous and induced magnetization in ferromagnetic bodies. *Nature,* **126**, 274–275.
2. Chatterjee, J., Haik, Y., Chen, C. J. (2003). Size dependent magnetic properties of iron oxide nanoparticles. *J. Magn. Magn. Mater.,* **257**, 113–118.
3. Kronick, P., Gilpin, R. W. (1986). Use of superparamagnetic particles for isolation of cells. *J. Biochem. Biophys. Methods,* **12**, 73–80.
4. Molday, R. S., Mackenzie D. (1982). Immunospecific ferromagnetic iron-dextran reagents for the labeling and magnetic separation of cells. *J. Immunol. Methods,* **52**, 353–367.
5. Hahn, P. F., Stark, D. D., Saini, S., Lewis, J. M., Wittenberg, J., et al. (1987). Ferrite particles for bowel contrast in MR imaging–design issues and feasibility studies. *Radiology,* **164**, 37–41.
6. Saini, S., Stark, D. D., Hahn, P. F., Bousquet, J. C., Introcasso, J., et al. (1987). Ferrite particles: A superparamagnetic MR contrast agent for enhanced detection of liver-carcinoma. *Radiology,* **162**, 217–222.

7. Weissleder, R., Hahn, P. F., Stark, D. D., Elizondo, G., Saini, S., et al. (1988). Superparamagnetic iron-oxide–enhanced detection of focal splenic tumors with MR imaging. *Radiology,* **169**, 399–403.
8. Corot, C., Robert, P., Idee, J. M., Port, M. (2006). Recent advances in iron oxide nanocrystal technology for medical imaging. *Adv. Drug Deliv. Rev.,* **58**, 1471–1504.
9. Qiao, R. R., Yang, C. H., Gao, M. Y. (2009). Superparamagnetic iron oxide nanoparticles: From preparations to *in vivo* MRI applications. *J. Mater. Chem.,* **19**, 6274–6293.
10. Wang, Y. X. J., Hussain, S. M., Krestin, G. P. (2001). Superparamagnetic iron oxide contrast agents: Physicochemical characteristics and applications in MR imaging. *Eur. Radiol.,* **11**, 2319–2331.
11. Hahn, P. F., Stark, D. D., Lewis, J. M., Saini, S., Elizondo, G., et al. (1990). 1st clinical-trial of a new superparamagnetic iron-oxide for use as an oral gastrointestinal contrast agent in MR imaging. *Radiology,* **175**, 695–700.
12. Mergo, P. J., Engelken, J. D., Helmberger, T., Ros, P. R. (1998). MRI in focal liver disease: A comparison of small and ultra-small superparamagnetic iron oxide as hepatic contrast agents. *J. Magn. Reson. Imaging,* **8**, 1073–1078.
13. Weissleder, R., Elizondo, G., Wittenberg, J., Rabito, C. A., Bengele, H. H., et al. (1990). Ultrasmall superparamagnetic iron-oxide: characterization of a new class of contrast agents for MR imaging. *Radiology,* **175**, 489–493.
14. Pouliquen, D., Lejeune, J. J., Perdrisot, R., Ermias, A., Jallet P. (1991). Iron-oxide nanoparticles for use as an MRI contrast agent–pharmacokinetics and metabolism. *Magn. Reson. Imaging.,* **9**, 275–283.
15. Weissleder, R., Lee, A. S., Fischman, A. J., Reimer, P., Shen, T., et al. (1991). Polyclonal human immunoglobulin-G labeled with polymeric iron-oxide–antibody MR imaging. *Radiology,* **181**, 245–249.
16. Gupta, A. K., Gupta, M. (2005). Synthesis and surface engineering of iron oxide nanoparticles for biomedical applications. *Biomaterials,* **26**, 3995–4021.
17. Laurent, S., Forge, D., Port, M., Roch, A., Robic, C., et al. (2008). Magnetic iron oxide nanoparticles: Synthesis, stabilization, vectorization, physicochemical characterizations, and biological applications. *Chem. Rev.,* **108**, 2064–2110.
18. Zelenakova, A., Kovac, J., Zelenak, V. (2010). Magnetic properties of Fe_2O_3 nanoparticles embedded in hollows of periodic nanoporous silica. *J. Appl. Phys.,* **108**, 034323.

19. Teja, A. S., Koh, P. Y. (2009). Synthesis, properties, and applications of magnetic iron oxide nanoparticles. *Prog. Cryst. Growth Charact. Mater.,* **55**, 22–45.
20. Kim, D. K., Zhang, Y., Voit, W., Rao, K. V., Muhammed M. (2001). Synthesis and characterization of surfactant-coated superparamagnetic monodispersed iron oxide nanoparticles. *J. Magn. Magn. Mater.,* **225**, 30–36.
21. Millan, A., Urtizberea, A., Silva, N. J. O., Palacio, F., Amaral, V. S., et al. (2007). Surface effects in maghemite nanoparticles. *J. Magn. Magn. Mater.,* **312**, L5–L9.
22. Gilbert, I., Millan, A., Palacio, F., Falqui, A., Snoeck, E., et al. (2003). Magnetic properties of maghemite nanoparticles in a polyvinylpyridine matrix. *Polyhedron,* **22**, 2457–2461.
23. Goya, G. F., Berquo, T. S., Fonseca, F. C., Morales, M. P. (2003). Static and dynamic magnetic properties of spherical magnetite nanoparticles, *J. Appl. Phys.,* **94**, 3520–3528.
24. Woo, K., Hong, J., Choi, S., Lee, H. W., Ahn, J. P., et al. (2004). Easy synthesis and magnetic properties of iron oxide nanoparticles. *Chem. Mater.,* **16**, 2814–2818.
25. Bean, C. P., Livingston, J. D. (1959). Superparamagnetism. *J. Appl. Phys.,* **30**, 120S.
26. Sjogren, C. E., Brileysaebo, K., Hanson, M., Johansson, C. (1994). Magnetic characterization of iron-oxides for magnetic-resonance-imaging. *Magn. Reson. Med.,* **31**, 268–272.
27. Webb, A. (2003). Introduction to Biomedical Imaging, *IEEE Press Series in Biomedical Engineering*.
28. Reimer, P., Tombach, B. (1998). Hepatic MRI with SPIO: Detection and characterization of focal liver lesions. *Eur. Radiol.,* **8**, 1198–1204.
29. Pouliquen, D., Perdrisot, R., Ermias, A., Akoka, S., Jallet, P., et al. (1989). Superparamagnetic iron-oxide nanoparticles as a liver MRI contrast agent–contribution of microencapsulation to improved biodistribution. *Magn. Reson. Imaging,* **7**, 619–627.
30. Babes, L., Denizot, B., Tanguy, G., Le Jeune, J. J., Jallet, P. (1999). Synthesis of iron oxide nanoparticles used as MRI contrast agents: A parametric study. *J. Colloid Interface Sci.,* **212**, 474–482.
31. Weissleder, R., Stark, D. D., Engelstad, B. L., Bacon, B. R., Compton, C. C., et al. (1989). Superparamagnetic iron-oxide–pharmacokinetics and toxicity. *Am. J. Roentgenol.,* **152**, 167–173.

32. Schulze, E., Ferrucci, J. T., Poss, K., Lapointe, L., Bogdanova, A., et al. (1995). Cellular uptake and trafficking of a prototypical magnetic iron-oxide label in-vitro. *Invest. Radiol.,* **30**, 604–610.

33. Weissleder, R., Elizondo, G., Wittenberg, J., Lee, A. S., Josephson, L., et al. (1990). Ultrasmall superparamagnetic iron-oxide–an intravenous contrast agent for assessing lymph-nodes with MR imaging. *Radiology,* **175**, 494–498.

34. Song, H. T., Choi, J. S., Huh, Y. M., Kim, S., Jun, Y. W., et al. (2005). Surface modulation of magnetic nanocrystals in the development of highly efficient magnetic resonance probes for intracellular labeling. *J. Am. Chem. Soc.,* **127**, 9992–9993.

35. Kim, D. K., Zhang, Y., Voit, W., Kao, K. V., Kehr, J., et al. (2001). Superparamagnetic iron oxide nanoparticles for bio-medical applications, *Scripta Mater.,* **44**, 1713–1717.

36. Taylor, A. P., Barry, J. C., Webb, R. I. (2001). Structural and morphological anomalies in magnetosomes: Possible biogenic origin for magnetite in ALH84001. *J. Microsc. Oxf.,* **201**, 84–106.

37. Ricketts, C. R., Cox, J. S. G., Fitzmaur, C., Moss, G. F. (1965). Iron dextran complex. *Nature,* **208**, 237.

38. Massart, R., Cabuil, V. (1987). Effect of some parameters on the formation of colloidal magnetite in alkaline-medium–yield and particle-size control. *J. Chim. Phys. Phys. Chim. Biol.,* **84**, 967–973.

39. Lee, J., Isobe, T., Senna, M. (1996). Preparation of ultrafine Fe_3O_4 particles by precipitation in the presence of PVA at high pH. *J. Colloid Interface Sci.,* **177**, 490–494.

40. Portet, D., Denizot, B., Rump, E., Lejeune, J. J., Jallet, P. (2001). Nonpolymeric coatings of iron oxide colloids for biological use as magnetic resonance imaging contrast agents. *J. Colloid Interface Sci.,* **238**, 37–42.

41. Bee, A., Massart, R., Neveu S. (1995). Synthesis of very fine maghemite particles. *J. Magn. Magn. Mater.,* **149**, 6–9.

42. Roca, A. G., Veintemillas-Verdaguer, S., Port, M., Robic, C., Serna, C. J., et al. (2009). Effect of nanoparticle and aggregate size on the relaxometric properties of MR contrast agents based on high quality magnetite nanoparticles. *J. Phys. Chem. B,* **113**, 7033–7039.

43. Li, Z., Tan, B., Allix, M., Cooper, A. I., Rosseinsky, M. J. (2008). Direct coprecipitation route to monodisperse dual-functionalized magnetic iron oxide nanocrystals without size selection. *Small,* **4**, 231–239.

44. Gupta, A. K., Wells, S. (2004). Surface-modified superparamagnetic nanoparticles for drug delivery: Preparation, characterization, and cytotoxicity studies. *IEEE Trans. Nanobiosci.,* **3**, 66–73.

45. Sun, S. H., Zeng, H., Robinson, D. B., Raoux, S., Rice, P. M., et al. (2004). Monodisperse MFe_2O_4 (M = Fe, Co, Mn) nanoparticles. *J. Am. Chem. Soc.,* **126**, 273–279.

46. Casula, M. F., Floris, P., Innocenti, C., Lascialfari, A., Marinone, M., et al. (2010). Magnetic resonance imaging contrast agents based on iron oxide superparamagnetic ferrofluids. *Chem. Mater.,* **22**, 1739–1748.

47. Cheon, J. W., Kang, N. J., Lee, S. M., Lee, J. H., Yoon, J. H., et al. (2004). Shape evolution of single-crystalline iron oxide nanocrystals. *J. Am. Chem. Soc.,* **126**, 1950–1951.

48. Strable, E., Bulte, J. W. M., Moskowitz, B., Vivekanandan, K., Allen, M., et al. (2001). Synthesis and characterization of soluble iron oxide-dendrimer composites. *Chem. Mater.,* **13**, 2201–2209.

49. Zhang, M., Cushing, B. L., O'Connor, C. J. (2008). Synthesis and characterization of monodisperse ultra-thin silica-coated magnetic nanoparticles. *Nanotechnology,* **19**, 085601 doi:10.1088/0957-4484/19/8/085601.

50. Yang, H. H., Zhang, S. Q., Chen, X. L., Zhuang, Z. X., Xu, J. G., et al. (2004). Magnetite-containing spherical silica nanoparticles for biocatalysis and bioseparations. *Anal. Chem.,* **76**, 1316–1321.

51. Cai, W., Wan, J. Q. (2007). Facile synthesis of superparamagnetic magnetite nanoparticles in liquid polyols. *J. Colloid Interface Sci.,* **305**, 366–370.

52. Merikhi, J., Jungk, H. O., Feldmann, C. (2000). Sub-micrometer CoAl2O4 pigment particles–synthesis and preparation of coatings. *J. Mater. Chem.,* **10**, 1311–1314.

53. Tartaj, P., Morales, M. D., Veintemillas-Verdaguer, S., Gonzalez-Carreno, T., Serna, C. J. (2003). The preparation of magnetic nanoparticles for applications in biomedicine. *J. Phys. D Appl. Phys.,* **36**, R182–R197.

54. Tavakoli, A., Sohrabi, M., Kargari, A. (2007). A review of methods for synthesis of nanostructured metals with emphasis on iron compounds. *Chem. Papers,* **61**, 151–170.

55. Jung, C. W., Jacobs, P. (1995). Physical and chemical-properties of superparamagnetic iron-oxide MR contrast agents–ferumoxides, ferumoxtran, ferumoxsil. *Magn. Reson. Imaging,* **13**, 661–674.

56. Harisinghani, M. G., Barentsz, J., Hahn, P. F., Deserno, W. M., Tabatabaei, S., et al. (2003). Noninvasive detection of clinically occult lymph-node metastases in prostate cancer. *N. Engl. J. Med.,* **348**, U2491–U2495.

57. Berry, I., Benderbous, S., Ranjeva, J. P., Gracia Meavilla, D., Manelfe, C., et al. (1996). Contribution of Sinerem (R) used as blood-pool contrast agent: Detection of cerebral blood volume changes during apnea in the rabbit. *Magn. Reson. Med.,* **36**, 415–419.

58. Mclachlan, S. J., Morris, M. R., Lucas, M. A., Fisco, R. A., Eakins, M. N., et al. (1994). Phase-I clinical-evaluation of a new iron-oxide MR contrast agent. *J. Magn. Reson. Imaging,* **4**, 301–307.

59. Aslam, M., Fu, L., Li, S., Dravid, V. P. (2005). Silica encapsulation and magnetic properties of FePt nanoparticles. *J. Colloid Interface Sci.,* **290**, 444–449.

60. Taupitz, M., Wagner, S., Schnorr, J. (2004). Phase I clinical evaluation of citrate-coated monocrystalline very small superparamagnetic iron oxide particles as a new contrast medium for magnetic resonance imaging. (vol 39, pg 394, 2004), *Investigative Radiology,* **39**, 625–625.

61. Liu, C., Huang, P. M. (1999). Atomic force microscopy and surface characteristics of iron oxides formed in citrate solutions. *Soil Sci. Soc. Am. J.,* **63**, 65–72.

62. Saeed, M., Wendland, M. F., Engelbrecht, M., Sakuma, H., Higgins, C. B. (1998). Value of blood pool contrast agents in magnetic resonance angiography of the pelvis and lower extremities. *Eur. Radiol.,* **8**, 1047–1053.

63. Paul, K. G., Frigo, T. B., Groman, J. Y., Groman, E. V. (2004). Synthesis of ultrasmall superparamagnetic iron oxides using reduced polysaccharides. *Bioconjug. Chem.,* **15**, 394–401.

64. Zhang, Y., Kohler, N., Zhang, M. Q. (2002). Surface modification of superparamagnetic magnetite nanoparticles and their intracellular uptake. *Biomaterials,* **23**, 1553–1561.

65. Kim, E. H., Lee, H. S., Kwak, B. K., Kim, B. K. (2005). Synthesis of ferrofluid with magnetic nanoparticles by sonochemical method for MRI contrast agent. *J. Magn. Magn. Mater.,* **289**, 328–330.

66. Iijima, M., Yonemochi, Y., Tsukada, M., Kamiya, H. (2006). Microstructure control of iron hydroxide nanoparticles using surfactants with different molecular structures. *J. Colloid Interface Sci.,* **298**, 202–208.

67. Stark, D. D., Weissleder, R., Elizondo, G., Hahn, P. F., Saini, S., et al. (1988). Superparamagnetic iron-oxide–clinical-application as a contrast agent for MR imaging of the liver. *Radiology,* **168**, 297–301.

68. Corot, C., Petry, K. G., Trivedi, R., Saleh, A., Jonkmanns, C., et al. (2004). Macrophage imaging in central nervous system and in carotid atherosclerotic plaque using ultrasmall superparamagnetic iron oxide in magnetic resonance imaging. *Invest. Radiol.,* **39**, 619–625.

69. Daldrup, H. E., Link, T. M., Blasius, S., Strozyk, A., Konemann, S., et al. (1999). Monitoring radiation-induced changes in bone marrow histopathology with ultra-small superparamagnetic iron oxide (USPIO)-enhanced MRI. *J. Magn. Reson. Imaging,* **9**, 643–652.

70. Beckmann, N., Cannet, C., Fringeli-Tanner, M., Baumann, D., Pally, C., et al. (2003). Macrophage labeling by SPIO as an early marker of allograft chronic rejection in a rat model of kidney transplantation. *Magn. Reson. Med.,* **49**, 459–467.

71. Yang, D. W., Ye, Q., Williams, M., Sun, Y., Hu, T. C. C., et al. (2001). USPIO-enhanced dynamic MRI: Evaluation of normal and transplanted rat kidneys. *Magn. Reson. Med.,* **46**, 1152–1163.

72. Simonsen, C. Z., Ostergaard, L., Vestergaard-Poulsen, P., Rohl, L., Bjornerud, A., et al. (1999). CBF and CBV measurements by USPIO bolus tracking: Reproducibility and comparison with Gd-based values. *J. Magn. Reson. Imaging,* **9**, 342–347.

73. MayoSmith, W. W., Saini, S., Slater, G., Kaufman, J. A., Sharma, P., et al. (1996). NIR contrast material for vascular enhancement: Value of superparamagnetic iron oxide. *Am. J. Roentgenol.,* **166**, 73–77.

74. Stillman, A. E., Wilke, N., Li, D. B., Haacke, E. M., McLachlan, S. (1996). Ultrasmall superparamagnetic iron oxide to enhance MRA of the renal and coronary arteries: Studies in human patients. *J. Comput. Assist. Tomogr.,* **20**, 51–55.

75. Koh, D., Cook, G. J. R., Husband, J. E. (2003). New horizons in oncologic imaging. *N. Engl. J. Med.,* **348**, 2487–2488.

76. Deserno, W. M. L. L. G., Harisinghani, M. G., Taupitz, M., Jager, G. J., Witjes, J. A., et al. (2004). Urinary bladder cancer: Preoperative nodal staging with ferumoxtran-10-enhanced MR imaging. *Radiology,* **233**, 449–456.

77. Nishimura, H., Tanigawa, N., Hiramatsu, M., Tatsumi, Y., Matsuki, M., et al. (2006). Preoperative esophageal cancer staging: Magnetic resonance imaging of lymph node with ferumoxtran-10, an ultrasmall superparamagnetic iron oxide. *J. Am. Coll. Surg.,* **202**, 604–611.

78. Cerdan, S., Lotscher, H. R., Kunnecke, B., Seelig, J. (1989). Monoclonal antibody-coated magnetite particles as contrast agents in magnetic-resonance imaging of tumors. *Magn. Reson. Med.,* **12**, 151–163.

79. Huh, Y. M., Jun, Y. W., Song, H. T., Kim, S., Choi, J. S., et al. (2005). *In vivo* magnetic resonance detection of cancer by using multifunctional magnetic nanocrystals. *J. Am. Chem. Soc.,* **127**, 12387–12391.

80. Sun, C., Sze, R., Zhang, M. Q. (2006). Folic acid-PEG conjugated superparamagnetic nanoparticles for targeted cellular uptake and detection by MRI. *J. Biomed. Mater. Res. Part A,* **78A**, 550–557.

81. Montet, X., Montet-Abou, K., Reynolds, F., Weissleder, R., Josephson, L. (2006). Nanoparticle imaging of integrins on tumor cells. *Neoplasia,* **8**, 214–222.

82. Zhao, M., Beauregard, D. A., Loizou, L., Davletov, B., Brindle, K. M. (2001). Non-invasive detection of apoptosis using magnetic resonance imaging and a targeted contrast agent. *Nat. Med.,* **7**, 1241–1244.

83. Weissleder, R., Moore, A., Mahmood, U., Bhorade, R., Benveniste, H., et al. (2000). *In vivo* magnetic resonance imaging of transgene expression. *Nat Med,* **6**, 351–355.

84. Arbab, A. S., Yocum, G. T., Kalish, H., Jordan, E. K., Anderson, S. A., et al. (2004). Efficient magnetic cell labeling with protamine sulfate complexed to ferumoxides for cellular MRI. *Blood,* **104**, 1217–1223.

85. Bulte, J. W. M., Douglas, T., Witwer, B., Zhang, S. C., Strable, E., et al. (2001). Magnetodendrimers allow endosomal magnetic labeling and *in vivo* tracking of stem cells. *Nat. Biotechnol.,* **19**, 1141–1147.

86. Josephson, L., Perez, J. M., Weissleder, R. (2001). Magnetic nanosensors for the detection of oligonucleotide sequences, *Angew. Chem. Int. Ed.,* **40**, 3204–3206.

87. Tanimoto, A., Oshio, K., Suematsu, M., Pouliquen, D., Stark, D. D. (2001). Relaxation effects of clustered particles. *J. Magn. Reson. Imaging,* **14**, 72–77.

88. Perez, J. M., O'Loughin, T., Simeone, F. J., Weissleder, R., Josephson, L. (2002). DNA-based magnetic nanoparticle assembly acts as a magnetic relaxation nanoswitch allowing screening of DNA-cleaving agents. *J. Am. Chem. Soc.,* **124**, 2856–2857.

89. Yu, S. S., Scherer, R. L., Ortega, R. A., Bell, C. S., O'Neil, C. P., et al. (2011). Enzymatic- and temperature-sensitive controlled release of ultrasmall superparamagnetic iron oxides (USPIOs), *J. Nanobiotechnol.,* **9**, doi: 10.1186/1477-3155-9-7.

90. Kohler, N., Sun, C., Wang, J., Zhang, M. Q. (2005). Methotrexate-modified superparamagnetic nanoparticles and their intracellular uptake into human cancer cells. *Langmuir,* **21**, 8858–8864.

91. Kohler, N., Sun, C., Fichtenholtz, A., Gunn, J., Fang, C., et al. (2006). Methotrexate-immobilized poly(ethylene glycol) magnetic nanoparticles for MR imaging and drug delivery. *Small,* **2**, 785–792.

92. Alexiou, C., Schmid, R. J., Jurgons, R., Kremer, M., Wanner, G., et al. (2006). Targeting cancer cells: Magnetic nanoparticles as drug carriers. *Eur. Biophys. J. Biophys. Lett.,* **35,** 446–450.

93. Joubert, J. C. (1997). Magnetic microcomposites as vectors for bioactive agents: The state of art. *An. Quim.,* **93**, S70–S76.

94. Lubbe, A. S., Bergemann, C., Riess, H., Schriever, F., Reichardt, P., et al. (1996). Clinical experiences with magnetic drug targeting: A phase I study with 4′-epidoxorubicin in 14 patients with advanced solid tumors. *Cancer Res.,* **56**, 4686–4693.

95. Hiergeist, R., Andra, W., Buske, N., Hergt, R., Hilger, I., et al. (1999). Application of magnetite ferrofluids for hyperthermia. *J. Magn. Magn. Mater.,* **201**, 420–422.

96. Andra, W., d'Ambly, C. G., Hergt, R., Hilger, I., Kaiser, W. A. (1999). Temperature distribution as function of time around a small spherical heat source of local magnetic hyperthermia. *J. Magn. Magn. Mater.,* **194**, 197–203.

97. Wust, P., Hildebrandt, B., Sreenivasa, G., Rau, B., Gellermann, J., et al. (2002). Hyperthermia in combined treatment of cancer. *Lancet Oncol.,* **3**, 487–497.

98. Moroz, P., Jones, S. K., Gray, B. N. (2002). The effect of tumour size on ferromagnetic embolization hyperthermia in a rabbit liver tumour model. *Int. J. Hyperthermia,* **18**, 129–140.

99. Sneed, P. K., Stauffer, P. R., McDermott, M. W., Diedrich, C. J., Lamborn, K. R., et al. (1998). Survival benefit of hyperthermia in a prospective randomized trial of brachytherapy boost +/- hyperthermia for glioblastoma multiforme. *Int. J. Radiat. Oncol. Biol. Phys.,* **40**, 287–295.

100. Wada, S., Tazawa, K., Furuta, I., Nagae, H. (2003). Antitumor effect of new local hyperthermia using dextran magnetite complex in hamster tongue carcinoma. *Oral Dis.,* **9**, 218–223.

Chapter 19

First-in-Human Molecular Targeting and Cancer Imaging Using Ultrasmall Dual-Modality C Dots

Michelle S. Bradbury, MD, PhD,[a] and Ulrich Wiesner, PhD[b]

[a]*Department of Radiology, Sloan Kettering Institute for Cancer Research, New York, New York, USA*
[b]*Department of Materials Science & Engineering, Cornell University, Ithaca, New York, USA*

Keywords: C dots, ultrasmall fluorescent silica nanoparticles, fluorescent nanomaterials, fluorescence or dual-modality imaging, inorganic-organic hybrid nanoparticles, nanomedicine, molecular targeting, cancer imaging, first-in-human clinical trials, human metastatic melanoma, PET imaging, integrins, cyclo-Arg-Gly-Asp-Tyr (cRGDY)

19.1 Introduction

Nanomedicine as a term first appeared in scientific articles in 2000 and employs nanoscale materials with unique medical effects [1]. A characteristic feature of nanotechnology based cancer medicines is that new functionality is added to existing products making them multifunctional, more potent via multivalency, and therefore

Handbook of Clinical Nanomedicine: Nanoparticles, Imaging, Therapy, and Clinical Applications
Edited by Raj Bawa, Gerald F. Audette, and Israel Rubinstein

ISBN 978-981-4669-20-7 (Hardcover), 978-981-4669-21-4 (eBook)
www.panstanford.com

more competitive [2, 3]. As an example, in cancer drug therapy liposomal formulations of existing drugs lower toxicity and increase targeting efficiency [4, 5]. Significant progress has been made in the past 15 years, and a number of nanomedicine products for cancer treatment are already on the market [6, 7]. But significant challenges lie ahead [8]. The chemistry of nanomaterials is not as well understood as that of molecules, and production of nanomedicines, e.g. based on dendrimers or pharmaceutical grade liposomes, is expensive [9]. Furthermore, while there is a tremendous pipeline of scientific projects on nanoscale materials for nanomedicine, only a vanishing small number actually gets into the clinic [10]. In order to safely translate laboratory innovation into the clinic, a workshop convened in 2008 by the FDA and the Alliance for Nano Health (ANH) identified seven priority areas to overcome top scientific hurdles for translation [11]. At the top of this list was the determination of biodistribution of nanoparticles as well as the development of imaging modalities for visualizing the biodistribution over time [11]. A more detailed discussion of these and other translational challenges that the field of nanomedicine faces, particularly as applied to cancer care settings, is provided elsewhere [12, 13]. Amongst the molecular imaging technologies perhaps the biggest growth area in oncology is occupied by optical/fluorescence imaging, and in particular by near infrared (NIR) fluorescence imaging [14, 15]. It is an inexpensive alternative to established imaging technologies (MRI, CT, PET), can be miniaturized (consider smart phones) for integration into minimally invasive surgical tools and promises to help visualize the expression and activity of particular molecules, cells and biological processes that influence the behavior of tumors and/or responsiveness to therapeutic drugs [16–18]. However, development and translation of NIRF nanoprobes have been slow as (i) fluorescent probes in water usually have low quantum yields, (ii) optical readouts are not quantitative, (iii) optical imaging is only relevant for tissue close to the skin surface, or tissue accessible by endoscopy and intraoperative visualization, (iv) there are considerable regulatory hurdles, and (v) there are lower profit margins for imaging than for therapeutic drugs [14, 15].

Figure 19.1a shows the schematic of a first-generation clinically translated particle platform—an inorganic-organic

hybrid core–shell silica nanoparticle encapsulating near infrared (NIR; 650–900 nm) fluorescent dye Cy5 (Abs./Em. ~650/670 nm), and coated with polyethylene glycol (PEG) chains that bind targeting peptides (cRGDY) and ^{124}I radiolabels to create functionalized, dual modality (optical/PET) fluorescent dye encapsulating and ^{124}I labeled colloids referred to as Cornell dots or simply C dots (^{124}I-cRGDY-PEG-C dots) [19, 20]. Absorbance-matched aqueous solutions of C dots and free dye reveal that covalently silica encapsulated fluorophores are brighter than free dye (see Fig. 19.1b), thereby increasing their optical detection sensitivity and signal to noise ratios (S/N). In previous studies, this brightness enhancement has been correlated to an increase in quantum yield due to a change in dielectric constant when moving from water to silica, as well as to the increased rigidity of the dye in the silica environment resulting in, respectively, increases in radiative rates and decreases in non-radiative rates of the encapsulated dyes [21, 22]. The particle coating with a neutral PEG layer minimizes interactions with the biological environment while simultaneously providing steric colloidal stability in high salt containing blood serum (~0.1 molar in NaCl). The targeting cRGDY peptide binds specifically and with high affinity to $\alpha_v\beta_3$ integrin receptors over-expressed on invasive melanoma [23] and is involved in metastasis and angiogenesis [24–37]. Finally, preparing dual-modality dots with radiolabels, yields both PET activity and optical readouts that permit quantitative pharmacokinetics (PK) and body clearance assessments over time, as well as real-time imaging and monitoring of patients during surgery, respectively.

Translation of such multifunctional nanoparticle platforms into the clinic for cancer diagnostics and therapy requires innovation at every level, from their synthesis and chemistry/surface chemistry, to their characterization, all the way to the development of protocols for biomedical experiments [38]. Silica as a particle platform already simplifies synthesis protocols of such multifunctional probes relative to, e.g. multistep organic dendrimer or other organic carrier synthesis approaches [39]. The silica nanoparticle described in Fig. 19.1 is one of only three fluorescent inorganic particle platforms that have been synthesized down to sizes below 10 nm, allowing for efficient renal clearance [40–42]. The other two platforms, quantum dots (Q dots) and carbon dots (CDs), are plagued with toxicity issues and suffer from low brightness in the red/NIR part

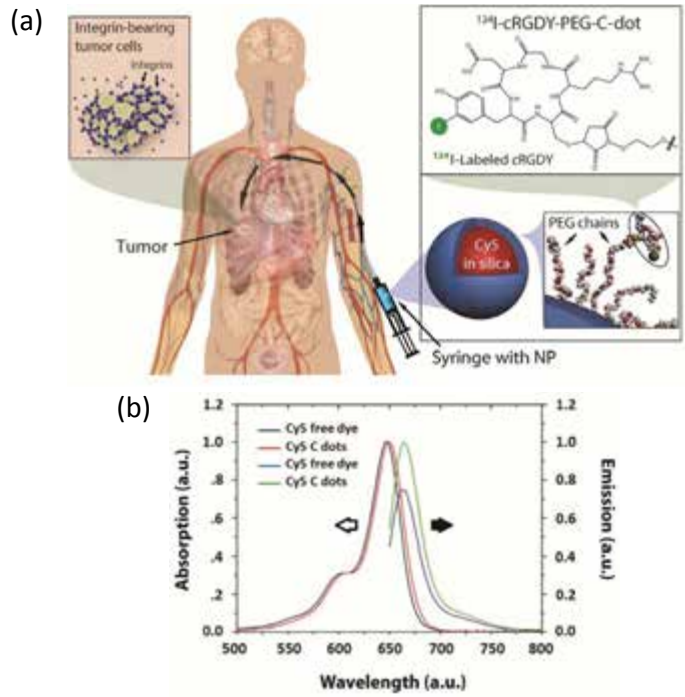

Figure 19.1 Core–shell inorganic-organic hybrid silica nanoparticles (^{124}I-cRGDY-PEG-C dots). (a) Schematic of the hybrid (PET-optical) imaging nanoparticle (NP) probe showing the core-containing Cy5 dye and surface-attached poly(ethylene glycol) (PEG) chains some of which bear cRGDY peptide ligands at their ends and ^{124}I radiolabels. cRGDY binds to human $\alpha_v\beta_3$ integrin–expressing tumors. (b) Absorption-matched spectra (left, open black arrow) and emission spectra (right, solid black arrow) for free and encapsulated dyes. Reprinted from reference [20] with kind permission of the American Association for the Advancement of Science.

of the optical spectrum [43, 44]. Respectively, making their use for clinical translation challenging. C dot characterization has made effective use of fluorescence correlation spectroscopy (FCS) [21, 22]. This technique shares a similar measurement mechanism with dynamic light scattering (DLS), which extracts particle diffusion information from the autocorrelation of signal intensity fluctuations resulting in hydrodynamic radius information [45, 46]. However, instead of scattered light, FCS uses fluorescence, and is thus more sensitive to the characterization of small particles or molecules

whose scattering is weak. Furthermore, the autocorrelation function, $G(\tau)$, at $\tau = 0$, $G(\tau = 0)$, provides information about particle concentration which in turn allows relative brightness evaluations at the single particle level. FCS thus provides a wealth of valuable information on these fluorescent nanoparticles from a single measurement, which can be used as feedback for the effective optimization of synthesis protocols.

19.2 Pre-Clinical Studies

In order to clinically translate this ultrasmall silica particle platform for molecular cancer imaging, serial PET and optical imaging studies were initially performed in human melanoma xenograft models [47] and in spontaneous melanoma miniswine models [48] to identify integrin-expressing lesions following systemic or local administration of the particle tracer, respectively. Tumor-targeted ^{124}I-cRGDY-PEG-C dots were found to exhibit hallmarks of an ideal diagnostic probe, selectively targeting disease (and metastases) while exhibiting bulk renal clearance. The ability to *"target or clear"* was achieved by tuning particle sizes below that of the effective renal glomerular filtration size cutoff of 10 nm [49, 50]. This maximized particle probe safety by reducing non-specific uptake in the reticuloendothelial system (RES), thereby abrogating potential off-target toxicities [47]. In melanoma miniswine models, targeted C dots demonstrated improved target-to-background ratios, as against free dyes, at sites of lymph node metastases using intraoperative optical imaging guidance. Higher sensitivity and specificity was also found relative to the standard-of-care radiotracer used to stage melanoma, ^{18}F-fluorodeoxyglucose (^{18}F-FDG) [48].

On the basis of the stability and reproducibility of its surface chemical designs, its favorable clearance and toxicity profiles, and its active targeting kinetics in melanoma models, ^{124}I-cRGDY-PEG-C dots received FDA IND approval as a PET-optical platform for molecular cancer imaging in human subjects, as well as an NIR fluorescent particle for intraoperative mapping of cancer-bearing sentinel lymph nodes (SLNs). These silica nanoparticles thus constitute the first fluorescent hybrid inorganic platform of its class and properties to be approved for clinical use as a drug for targeted molecular imaging of integrin-expressing cancers.

19.3 Clinical Trial Design

Prior to using C dots for intraoperative applications in humans, we conducted an initial microdosing clinical trial [20] using serial PET imaging to evaluate the pharmacokinetic (PK) and clearance profiles of the hybrid fluorescent silica particle tracer, ^{124}I-cRGDY-PEG-C dots, in five human subjects with metastatic melanoma (Fig. 19.2a). Radiation doses, as well as plasma and urine metabolic activity, were additionally estimated over a two-week interval for bio-stability and particle integrity using gamma counting and radio thin-layer chromatography (radioTLC).

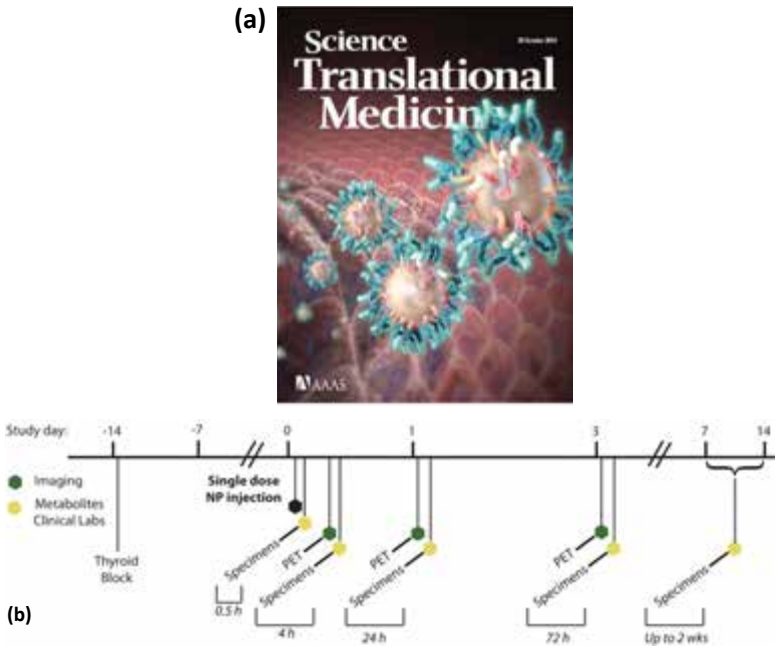

Figure 19.2 Overview of first-in-human study design. (a) Artistic rendering of the hybrid (PET-optical) imaging NP. (b) Clinical trial events after single-dose particle injection. Timeline denotes acquisition of serial PET-CT imaging studies and collection of blood and urine specimens. Reprinted from reference [20] with kind permission of the American Association for the Advancement of Science.

All five patients received single-dose intravenous (i.v.) injections of approximately 185 megabequerels (MBq) (~3.4–6.7

nmol) ^{124}I-cRGDY-PEG-C dots (specific activity range 27.8–57.4 GBq/μmol). Particle tracer doses were well tolerated over the study period based upon a safety evaluation, which included laboratory indications of particle (drug) toxicity, blood and urine specimen analyses. All subjects had whole-body PET-CT imaging evaluations at 2–4, 24, and 72 h post-injection (p.i.) to determine organ uptake and clearance profiles of this particle tracer (Fig. 19.2b).

19.4 Particle Tracer PK and Metabolic Analyses

Serial whole-body PET and PET-CT PK profiles are illustrated for a representative patient over a 72 h period (Fig. 19.3a); imaging findings were comparable for all human subjects over this time interval. Region-of-interest analyses performed on PET images for all 5 patients showed low tissue activity (i.e., values shown as 1/1000th of a percent of the injected dose per gram, %ID/g) in all major organs and tissues, as well as minimal retained activity values at the end of the study interval (Fig. 19.3b). Whole-body clearance half-times were estimated to range from 13–21 h. Interestingly, the RES demonstrated no notable accumulation, a finding that is not found for many larger-particle (>10 nm) platforms, proteins, and hydrophobic molecules [51]. For instance, ^{111}In-labeled liposomes ~90 nm i.d. have demonstrated median clearance half-time values ranging from 40 to 103 h in patients with locally advanced malignancies [52], as against C dot whole-body clearance half-time values. In the former case, the biodistribution pattern was consistent with RES uptake, as activity was found within the liver, spleen, and bone marrow. In another study recruiting colorectal carcinoma subjects and administering ^{131}I-labeled humanized monoclonal antibody A33, twice the C dot diameter, whole-body clearance half-time values were found to range from 120 to 176 h in [53]. These findings highlight the importance of utilizing such an ultrasmall platform (C dots) to achieve the foregoing results – one that in size is below the effective renal glomerular filtration size cutoff [47, 49]. Collectively, the above findings pointed to an inorganic-organic hybrid targeted particle tracer that was safe and exhibited a PK signature that is different from larger PET particle systems—one in which bulk renal clearance predominates without significant RES system uptake.

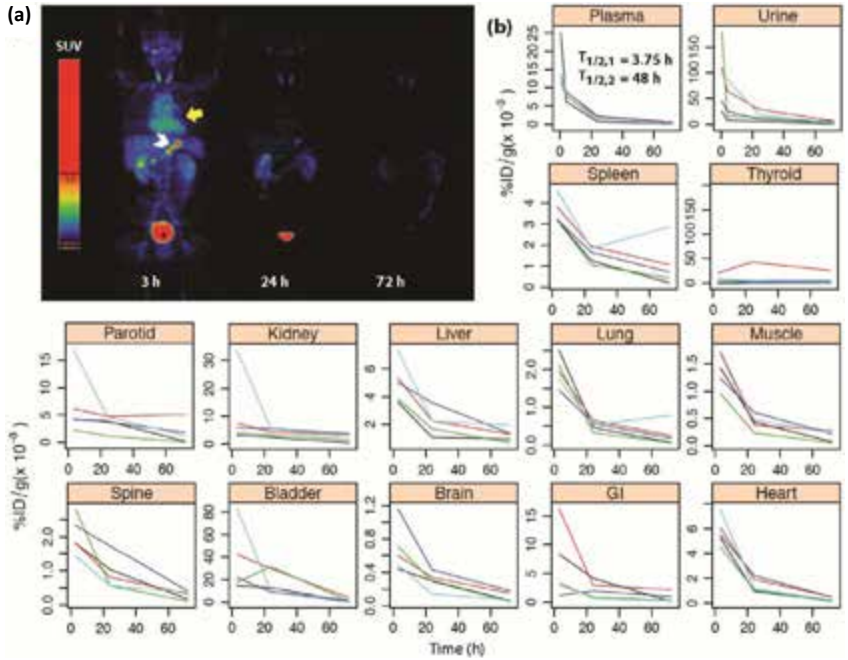

Figure 19.3 Whole-body distribution and pharmacokinetics of ^{124}I-cRGDY-PEG-C dots. (a) Maximum intensity projection PET images at 2, 24, and 72 h after intravenous injection of ^{124}I-cRGDY-PEG-C dots (Patient #3) reveal probe activity in bladder (*), heart (yellow arrow), and bowel (white arrowhead), displayed as SUV values. (b) Decay-corrected percent injected dose per gram (%ID/g) of urine and plasma collected at approximately 30 min, 4, 24, and 72 h following injection of the particles as determined by gamma-counting. ROIs were drawn on major organs for each patient's PET scans to derive standardized uptake values and %ID/g. Data for major organs and tissues are plotted individually for n = 5 patients. Plasma clearance half-times, $T_{1/2,1}$ and $T_{1/2,2}$, are attributed to renal and hepatobiliary clearance, respectively. Reprinted from reference [20] with kind permission of the American Association for the Advancement of Science.

Although PK signature is a function of the particle size, it can additionally be altered by other key physicochemical properties, including charge, shape, and surface chemistry. In an earlier study conducted using normal murine models, the majority of C dots (<10 nm) without a PEG coat demonstrated hepatic accumulation

[41], while, by contrast, ^{124}I-cRGDY-PEG-C dots demonstrated bulk renal clearance. Interestingly, although diameters of alternative probes reported in the literature, such as macromolecules (albumin) [54] or other particle types (gold nanoparticles) [55], are similar or smaller in size than the particles used here, different PK profiles were observed due to variations in other physicochemical properties. Further, the PK signature of ^{124}I-cRGDY-PEG-C dots differed from those of RES agents and antibodies, as no appreciable particle tracer accumulation was seen within the liver, spleen, lung, or bone marrow.

Importantly, human particle tracer distributions, clearance profiles, and dosimetry were similar to those found in our preclinical melanoma models [47, 50]. Biexponential clearance behavior was observed for gamma counted plasma samples (Fig. 19.3b); the more rapid initial half-time (i.e., $t_{1/2,1} \sim 3.75$ h) was attributed to renal excretion, whereas hepatobiliary clearance presumably accounted for the slower-clearing component [20]. A large fraction of the administered activity was eliminated via the urinary system (Fig. 19.3b); order of magnitude higher activity concentrations were found in the bladder relative to those seen in liver. These data were consistent with ~90% of the administered activity being excreted via the kidneys and ~10% via the hepatobiliary route. Importantly, the route of excretion is a key consideration in developing particle tracers; gut activity can potentially confound image interpretation or mask metastatic disease. For ^{124}I-cRGDY-PEG-C dots, gut activity was minimized. Finally, particle PK and estimated organ effective doses were comparable to those found for other commonly used diagnostic radiotracers (~1 mSv/MBq).

19.5 Clinical Multimodal Imaging with ^{124}I-cRGDY-PEG-C Dots in Melanoma Patients

Tumor uptake and localization were observed in several patients with melanoma using PET imaging after administration of ^{124}I-cRGDY-PEG-C dots [20]. In one such patient, a ~5 mm well-defined cystic lesion was seen in the right anterior lobe of the pituitary gland on axial and sagittal magnetic resonance (MR) images (Fig. 19.4a); the pituitary gland is known to lack a blood-brain

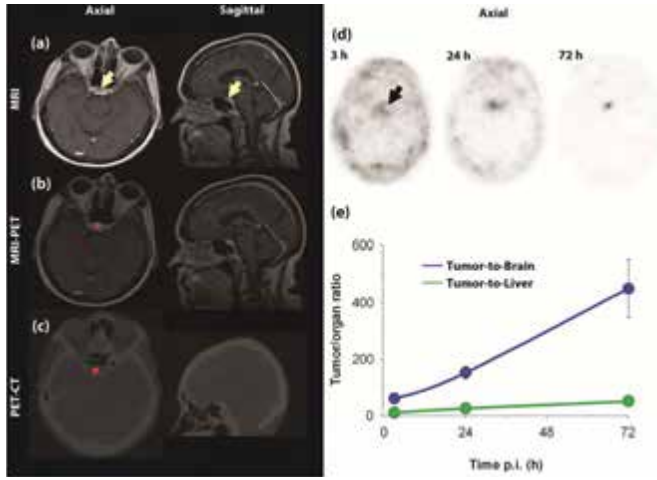

Figure 19.4 Multimodal imaging of particle uptake in a pituitary lesion. (a) Multiplanar contrast-enhanced MR axial and sagittal images of Patient #2 at 72 h p.i. demonstrate a subcentimeter cystic focus (arrows) within the right aspect of the anterior pituitary gland. (b) Co-registered axial and sagittal MRI-PET images reveal increased focal activity (red, ^{124}I-cRGDY-PEG-C dots) localized to the lesion site. (c) Axial and sagittal PET-CT images localize activity to the right aspect of the sella. (d) Axial PET images of ^{124}I-cRGDY-PEG-C dots in the brain at 3, 24, and 72 h p.i. demonstrate progressive accumulation of activity within the sellar region. (e) Tumor-to-brain and tumor-to-liver activity ratios as a function of p.i. time. Data are averages ± SD (n = 1 ROI measurement per time point) calculated from images in (d) Reprinted from reference [20] with kind permission of the American Association for the Advancement of Science.

barrier. This lesion was presumed to be a pituitary microadenoma—an intracranial neoplasm known to exhibit malignant properties, such as neoangiogenesis and invasion into adjacent peritumoral tissues. Precise co-registration of this PET-avid focus with multiplanar MRI (Fig. 19.4b) and CT (Fig. 19.4c) images localized this lesion to the anterior pituitary gland. Initially seen as a focus of intense particle tracer uptake, it continued to accumulate activity over a 72 h interval (arrow, Fig. 19.4d) while a corresponding decrease in surrounding background signal was observed, thus yielding overall high tumor-to-background (to-brain ~500; to-liver ~50) ratios (Fig. 19.4e). As the lesion diameter was slightly less

than the resolution [full width half maximum (FWHM) ~6 mm] of the clinical PET scanner, partial volume corrections [56] needed to be made to the computed ratios. This increase in signal reflects a net accumulation of particle activity within the lesion over time.

It is important to highlight the ability of PET to accurately estimate the fraction of the injected particle load that accumulates at tumor sites, in addition to monitoring time-varying particle uptake [20, 57]. For the presumed pituitary adenoma, PET imaging showed a progressive net accumulation of ^{124}I-cRGDY-PEG-C dot activity within this lesion (Fig. 19.4d), consistent with specific uptake, noting that the actual integrin receptor expression status was unknown. Altered integrin expression levels have, in fact, been found to be associated with adenomatous transformation [58], with prior studies showing enhanced $\alpha_v\beta_3$ integrin expression levels primarily involving adenomatous stromal cells, as well as the parenchyma of adenomas. The fraction of the injected particle load of 2×10^{15} that accumulated at the tumor site, roughly 1.78×10^{11} particles, or 0.01%, of the injected dose (Fig. 19.4d), was determined using the measured maximum SUV (SUV_{max}) of the lesion at 72 h p.i., the approximate mass of the lesion, and the patient's body mass.

19.6 Conclusions and Future Prospects

In summary, our clinical trial findings are consistent with a well-tolerated sub-10 nm inorganic-organic hybrid particle tracer exhibiting in vivo stability and distinct, reproducible pharmacokinetic signatures defined by renal excretion. No toxic or adverse events attributable to the particles were observed. Coupled with preferential uptake and localization of the probe at sites of disease, these first-in-human results suggest safe use of these particles in human cancer diagnostics. In several patients, melanoma-targeted C dots were found to preferentially accumulate at tumor target sites by PET imaging, offering the exciting possibility that this ultrasmall platform could improve melanoma staging efforts, select patients for targeted antiangiogenesis treatments, and detect residual disease at sites of surgical resection. In the future, it is expected that this particle will be further adapted as a cancer-targeted therapy, one that could enhance combinatorial treatment strategies by enabling highly localized therapeutic

delivery. Finally, the versatility of C dots highlights the potential of this platform to personalize clinical cancer care, as particles can be modified with different tumor-targeting moieties tailored to meet individual patient needs for a variety of applications.

Disclosures and Conflict of Interest

Prof. Wiesner and Dr. Bradbury are inventors of patents held by Cornell University and Memorial Sloan Kettering Cancer Center on C dots and related technology. They are co-founders of a startup company that has licensed the patents and is currently raising funds to commercialize C dot technology. The authors declare that their spouses, partners, or children have no financial relationships relevant to the submitted work. The authors declare that no writing assistance was utilized and no payment received in its production.

Corresponding Authors

Dr. Michelle S. Bradbury
Department of Radiology
Memorial Sloan Kettering Cancer Center
1275 York Avenue, New York, NY 10065, USA
Email: bradburm@mskcc.org

Prof. Ulrich Wiesner
Department of Materials Science and Engineering
Cornell University
330 Bard Hall, Ithaca, NY 21047, USA
Email: ubw1@cornell.edu

About the Authors

Michelle S. Bradbury is a clinician-scientist and the director of Intraoperative Imaging in the Department of Radiology at Memorial Sloan Kettering Cancer Center (MSKCC) in New York City, USA. In addition, she is an associate member and attending on the Neuroradiology and Molecular Imaging and Therapy Services in the

Department of Radiology at MSKCC, and holds a joint appointment in the Sloan Kettering Institute for Cancer Research in the Molecular Pharmacology and Chemistry Program. She works with a multidisciplinary team of clinicians and basic scientists focused on translational nanooncology and the diagnosis and treatment of human cancers. As a practicing neuroradiologist, Dr. Bradbury is currently leading a number of clinical trials in intraoperative and oncological settings using ultrasmall fluorescent inorganic-organic hybrid core–shell silica nanoparticles for molecular cancer imaging developed by her collaborator, Prof. Ulrich Wiesner; particles have been co-developed for applications requiring both optical and PET imaging. Her particular focus is on the use of these novel inorganic platforms to identify new biomarkers for imaging, staging, and/or for predicting response to targeted therapies in clinically relevant models that, in turn, can be validated in future clinical trial designs. Additional work in nanobiology identifies particle-driven alterations in biological responses, using baseline findings to guide next-stage therapeutic developments.

Ulrich Wiesner is the Spencer T. Olin Professor of Materials Science and Engineering at Cornell University, Ithaca, USA. In addition, he is a field member in Chemistry and Chemical Biology, Chemical and Biomolecular Engineering, and Biomedical Engineering at Cornell. For more than 15 years, he has worked to develop novel ultrasmall and bright fluorescence silica nanomaterials for interrogating biological systems. His recent work has focused on the use of water-based solvent systems to enable more economical particle synthesis as well as precise control of particle surface chemistry, thereby deriving clinically promising particle architectures, compositions, and sizes tuned for renal clearance and clinical translation. Prof. Wiesner has collaborated with Dr. Bradbury to translate such nanomaterials into the clinic for both intraoperative and oncological applications.

References

1. Wagner, V., Dullaart, A., Bock, A. K., Zweck, A. (2006). The emerging nanomedicine landscape. *Nat. Biotechnol.,* **24**, 1211–1217.

2. Duncan, R. (2006). Polymer conjugates as anticancer nanomedicines. *Nat. Rev. Cancer,* **6**, 688–701.
3. Ferrari, M. (2005). Cancer nanotechnology: Opportunities and challenges. *Nat. Rev. Cancer,* **5**, 161–171.
4. Hrkach, J., Von Hoff, D., Mukkaram Ali, M., Andrianova, E., Auer, J., et al. (2012). Preclinical development and clinical translation of a PSMA-targeted docetaxel nanoparticle with a differentiated pharmacological profile. *Sci. Trans. Med.,* **4**, 128ra139.
5. Gabizon, A. A. (2001). Stealth liposomes and tumor targeting: One step further in the quest for the magic bullet. *Clin. Cancer Res.,* **7**, 223–225.
6. Safra, T., Muggia, F., Jeffers, S., Tsao-Wei, D. D., Groshen, S., et al. (2000). Pegylated liposomal doxorubicin (Doxil): Reduced clinical cardiotoxicity in patients reaching or exceeding cumulative doses of 500 mg/m^2. *Ann. Oncol.,* **11**, 1029–1033.
7. Gabizon, A. A. (2001). Pegylated liposomal doxorubicin: Metamorphosis of an old drug into a new form of chemotherapy. *Cancer Invest.,* **19**, 424–436.
8. Scheinberg, D. A., Villa, C. H., Escorcia, F. E., McDevitt, M. R. (2010). Conscripts of the infinite armada: Systemic cancer therapy using nanomaterials. *Nat. Rev. Clin. Oncol.,* **7**, 266–276.
9. Gillies, E. R., Frechet, J. M. (2005). Dendrimers and dendritic polymers in drug delivery. *Drug Discov.Today,* **10**, 35–43.
10. Peer, D., Karp, J. M., Hong, S., Farokhzad, O. C., Margalit, R., et al. (2007). Nanocarriers as an emerging platform for cancer therapy. *Nat. Nanotechnol.,* **2**, 751–760.
11. Sanhai, W. R., Sakamoto, J. H., Canady, R., Ferrari, M. (2008). Seven challenges for nanomedicine. *Nat. Nanotechnol.,* **3**, 242–244.
12. Gabizon, A., Bradbury, M., Prabhakar, U., Zamboni, W., Libutti, S., et al. (2014). Cancer nanomedicines: Closing the translational gap. *Lancet,* **384**, 2175–2176.
13. Duncan, R., Gaspar, R. (2011). Nanomedicine(s) under the microscope. *Mol. Pharm.,* **8**, 2101–2141.
14. Weissleder, R., Pittet, M. J. (2008). Imaging in the era of molecular oncology. *Nature,* **452**, 580–589.
15. He, X., Gao, J., Gambhir, S. S., Cheng, Z. (2010). Near-infrared fluorescent nanoprobes for cancer molecular imaging: Status and challenges. *Trends Mol. Med.,* **16**, 574–583.

16. Kim, S., Lim, Y. T., Soltesz, E. G., De Grand, A. M., Lee, J., et al. (2004). Near-infrared fluorescent type II quantum dots for sentinel lymph node mapping. *Nat. Biotechnol.,* **22**, 93–97.
17. Tanaka, E., Choi, H. S., Fujii, H., Bawendi, M. G., Frangioni, J. V. (2006). Image-guided oncologic surgery using invisible light: Completed pre-clinical development for sentinel lymph node mapping. *Ann. Surg. Oncol.,* **13**, 1671–1681.
18. Kobayashi, H., Koyama, Y., Barrett, T., Hama, Y., Regino, C. A., et al. (2007). Multimodal nanoprobes for radionuclide and five-color near-infrared optical lymphatic imaging. *ACS Nano,* **1**, 258–264.
19. Benezra, M., Penate-Medina, O., Zanzonico, P. B., Schaer, D., Ow, H., et al. (2011). Multimodal silica nanoparticles are effective cancer-targeted probes in a model of human melanoma. *J. Clin. Invest.,* **121**, 2768–2780.
20. Phillips, E., Penate-Medina, O., Zanzonico, P. B., Carvajal, R. D., Mohan, P., et al. (2014). Clinical translation of an ultrasmall inorganic optical-PET imaging nanoparticle probe. *Sci. Trans. Med.,* **6**, 260ra149.
21. Larson, D. R., Ow, H., Vishwasrao, H. D., Heikal, A. A., Wiesner, U., Webb, W. W. (2008). Silica nanoparticle architecture determines radiative properties of encapsulated fluorophores. *Chem. Mater.,* **20**, 7.
22. Ow, H., Larson, D. R., Srivastava, M., Baird, B. A., Webb, W. W., et al. (2005). Bright and stable core-shell fluorescent silica nanoparticles. *Nano Lett.,* **5**, 113–117.
23. Albelda, S. M., Mette, S. A., Elder, D. E., Stewart, R., Damjanovich, L., et al. (1990). Integrin distribution in malignant melanoma: Association of the beta 3 subunit with tumor progression. *Cancer Res.,* **50**, 6757–6764.
24. Brooks, P. C., Montgomery, A. M., Rosenfeld, M., Reisfeld, R. A., Hu, T., et al. (1994). Integrin alpha v beta 3 antagonists promote tumor regression by inducing apoptosis of angiogenic blood vessels. *Cell,* **79**, 1157–1164.
25. Brooks, P. C., Clark, R. A., Cheresh, D. A. (1994). Requirement of vascular integrin alpha v beta 3 for angiogenesis. *Science,* **264**, 569–571.
26. Petitclerc, E., Stromblad, S., von Schalscha, T. L., Mitjans, F., Piulats, J., et al. (1999). Integrin alpha(v)beta3 promotes M21 melanoma growth in human skin by regulating tumor cell survival. *Cancer Res.,* **59**, 2724–2730.

27. Hood, J. D., Cheresh, D. A. (2002). Role of integrins in cell invasion and migration. *Nat. Rev. Cancer,* **2**, 91–100.

28. Cheresh, D. A., Spiro, R. C. (1987). Biosynthetic and functional properties of an Arg-Gly-Asp-directed receptor involved in human melanoma cell attachment to vitronectin, fibrinogen, and von Willebrand factor. *J. Biol. Chem.,* **262**, 17703–17711.

29. Cheresh, D. A., Harper, J. R. (1987). Arg-Gly-Asp recognition by a cell adhesion receptor requires its 130-kDa alpha subunit. *J. Biol. Chem.,* **262**, 1434–1437.

30. Haubner, R., Wester, H. J., Reuning, U., Senekowitsch-Schmidtke, R., Diefenbach, B., et al. (1999). Radiolabeled alpha(v)beta3 integrin antagonists: A new class of tracers for tumor targeting. *J. Nucl. Med.,* **40**, 1061–1071.

31. Poethko, T., Schottelius, M., Thumshirn, G., Hersel, U., Herz, M., et al. (2004). Two-step methodology for high-yield routine radiohalogenation of peptides: (18)F-labeled RGD and octreotide analogs. *J. Nucl. Med.,* **45**, 892–902.

32. Li, C., Wang, W., Wu, Q., Ke, S., Houston, J., et al. (2006). Dual optical and nuclear imaging in human melanoma xenografts using a single targeted imaging probe. *Nucl. Med. Biol.,* **33**, 349–358.

33. Decristoforo, C., Faintuch-Linkowski, B., Rey, A., von Guggenberg, E., Rupprich, M., et al. (2006). [99mTc]HYNIC-RGD for imaging integrin alphavbeta3 expression. *Nucl. Med. Biol.,* **33**, 945–952.

34. Alves, S., Correia, J. D., Gano, L., Rold, T. L., Prasanphanich, A., et al. (2007). In vitro and in vivo evaluation of a novel ^{99m}Tc(CO)3-pyrazolyl conjugate of cyclo-(Arg-Gly-Asp-d-Tyr-Lys). *Bioconjug. Chem.,* **18**, 530–537.

35. Decristoforo, C., Hernandez Gonzalez, I., Carlsen, J., Rupprich, M., Huisman, M., et al. (2008). ^{68}Ga- and ^{111}In-labelled DOTA-RGD peptides for imaging of alpha(v)beta3 integrin expression. *Eur. J. Nucl. Med. Mol. Imaging,* **35**, 1507–1515.

36. Hultsch, C., Schottelius, M., Auernheimer, J., Alke, A., Wester, H. J. (2009). (18)F-Fluoroglucosylation of peptides, exemplified on cyclo(RGDfK). *Eur. J. Nucl. Med. Mol. Imaging,* **36**, 1469–1474.

37. Wei, L., Ye, Y., Wadas, T. J., Lewis, J. S., Welch, M. J., et al. (2009). (64)Cu-labeled CB-TE2A and diamsar-conjugated RGD peptide analogs for targeting angiogenesis: Comparison of their biological activity. *Nucl. Med. Biol.,* **36**, 277–285.

38. Valtchev, V., Tosheva, L. (2013). Porous nanosized particles: Preparation, properties, and applications. *Chem. Rev.,* **113**, 6734–6760.

39. Burns, A., Ow, H., Wiesner, U. (2006). Fluorescent core-shell silica nanoparticles: Towards "Lab on a Particle" architectures for nanobiotechnology. *Chem. Soc. Rev.,* **35**, 1028–1042.

40. Choi, H. S., Liu, W., Misra, P., Tanaka, E., Zimmer, J. P., et al. (2007). Renal clearance of quantum dots. *Nat. Biotechnol.,* **25**, 1165–1170.

41. Burns, A. A., Vider, J., Ow, H., Herz, E., Penate-Medina, O., et al. (2009). Fluorescent silica nanoparticles with efficient urinary excretion for nanomedicine. *Nano Lett.,* **9**, 442–448.

42. Huang, X., Zhang, F., Zhu, L., Choi, K. Y., Guo, N., et al. (2013). Effect of injection routes on the biodistribution, clearance, and tumor uptake of carbon dots. *ACS Nano,* **7**, 5684–5693.

43. Li, L., Wu, G., Yang, G., Peng, J., Zhao, J., et al. (2013). Focusing on luminescent graphene quantum dots: Current status and future perspectives. *Nanoscale,* **5**, 4015–4039.

44. Hola K, Zhang, Y., Wang, Y., Giannelis, E. P., Zborila, R., Rogach, A. L. (2014). Carbon dots: Emerging light emitters for bioimaging, cancer therapy and optoelectronics. *Nano Today*, **9**(5), 590–603.

45. Hess, S. T., Huang, S., Heikal, A. A., Webb, W. W. (2002). Biological and chemical applications of fluorescence correlation spectroscopy: A review. *Biochemistry,* **41**, 697–705.

46. Bacia, K., Kim, S. A., Schwille, P. (2006). Fluorescence cross-correlation spectroscopy in living cells. *Nat. Methods,* **3**, 83–89.

47. Benezra, M., Penate-Medina, O., Zanzonico, P. B., Schaer, D., Ow, H., et al. (2011). Multimodal silica nanoparticles are effective cancer-targeted probes in a model of human melanoma. *J. Clin. Invest.,* **121**, 2768–2780.

48. Bradbury, M. S., Phillips, E., Montero, P. H., Cheal, S. M., Stambuk, H., et al. (2013). Clinically-translated silica nanoparticles as dual-modality cancer-targeted probes for image-guided surgery and interventions. *Integr. Biol.,* **5**, 74–86.

49. Choi, C. H., Zuckerman, J. E., Webster, P., Davis, M. E. (2011). Targeting kidney mesangium by nanoparticles of defined size. *Proc. Natl. Acad. Sci. U. S. A.,* **108**, 6656–6661.

50. Burns, A. A., Vider, J., Ow, H., Herz, E., Penate-Medina, O., et al. (2009). Fluorescent silica nanoparticles with efficient urinary excretion for nanomedicine. *Nano Lett.,* **9**, 442–448.

51. Prabhakar, U., Maeda, H., Jain, R. K., Sevick-Muraca, E. M., Zamboni, W., et al. (2013). Challenges and key considerations of the enhanced permeability and retention effect for nanomedicine drug delivery in oncology. *Cancer Res.,* **73**, 2412–2417.

52. S. Stewart, K. J. H. (1997). The biodistribution and pharmacokinetics of stealth liposomes in patients with solid tumors. *Oncology,* **11,** 5.

53. Scott, A. M., Lee, F. T., Jones, R., Hopkins, W., MacGregor, D., et al. (2005). A phase I trial of humanized monoclonal antibody A33 in patients with colorectal carcinoma: Biodistribution, pharmacokinetics, and quantitative tumor uptake. *Clin. Cancer Res.,* **11**, 4810–4817.

54. Stehle, G., Wunder, A., Schrenk, H. H., Hartung, G., Heene, D. L., et al. (1999). Albumin-based drug carriers: Comparison between serum albumins of different species on pharmacokinetics and tumor uptake of the conjugate. *Anti-Cancer Drugs,* **10**, 785–790.

55. Leifert, A., Pan-Bartnek, Y., Simon, U., Jahnen-Dechent, W. (2013). Molecularly stabilised ultrasmall gold nanoparticles: Synthesis, characterization and bioactivity. *Nanoscale,* **5**, 6224–6242.

56. Soret, M., Bacharach, S. L., Buvat, I. (2007). Partial-volume effect in PET tumor imaging. *J. Nucl. Med.,* **48**, 932–945.

57. Kelloff, G. J., Krohn, K. A., Larson, S. M., Weissleder, R., Mankoff, D. A., et al. (2005). The progress and promise of molecular imaging probes in oncologic drug development. *Clin. Cancer Res.,* **11**, 7967–7985.

58. Farnoud, M. R., Veirana, N., Derome, P., Peillon, F., Li, J. Y. (1996). Adenomatous transformation of the human anterior pituitary is associated with alterations in integrin expression. *Int. J. Cancer,* **67**, 45–53.

Chapter 20

Atomic Force Microscopy for Nanomedicine

Shivani Sharma, PhD,[a,b] and James K. Gimzewski, PhD[a,b,c]

[a]*Department of Chemistry and Biochemistry, University of California, Los Angeles, California, USA*
[b]*California NanoSystems Institute, University of California, Los Angeles, California, USA*
[c]*International Center for Materials Nanoarchitectonics Satellite, National Institute for Materials Science, Tsukuba, Japan*

Keywords: atomic force microscopy, nanomedicine, cancer diagnosis, cellular nanomechanics, exosomes, biomarker detection, ex vivo detection, real-time kinetics detection, single molecule detection, cell elasticity, cellular dynamics

20.1 Introduction

Because of increasing healthcare costs, changing demographics and rapid growth in chronic illnesses, it is very likely that many healthcare systems around the world will become unsustainable by 2015. Worldwide healthcare spending is expected to grow from 9% of worldwide Gross Domestic Product to 15% by 2015, and by 2050 the world's population older than 60 years will triple from 600 million to over 2 billion. Moreover, according

Handbook of Clinical Nanomedicine: Nanoparticles, Imaging, Therapy, and Clinical Applications
Edited by Raj Bawa, Gerald F. Audette, and Israel Rubinstein

ISBN 978-981-4669-20-7 (Hardcover), 978-981-4669-21-4 (eBook)
www.panstanford.com

to the World Health Organization, the number of people in US only with a chronic illness will grow from 118 million in 1995 to 157 million in 2020. Therefore, new technologies will be needed to overcome these challenges such as implementation of nanotechnology applications for healthcare. In particular, the development of a wide spectrum of emerging nano-enabled technologies may hold great promise for medicine and healthcare benefits by complementing and enhancing the current diagnostic and therapeutic capabilities of existing healthcare systems. Indeed, nanotechnology could be the crucial enabling technology that will turn the promise of theranostics [1] into reality, i.e., personalized therapy customized to serve patient needs based on their exact genetic and molecular diagnostics.

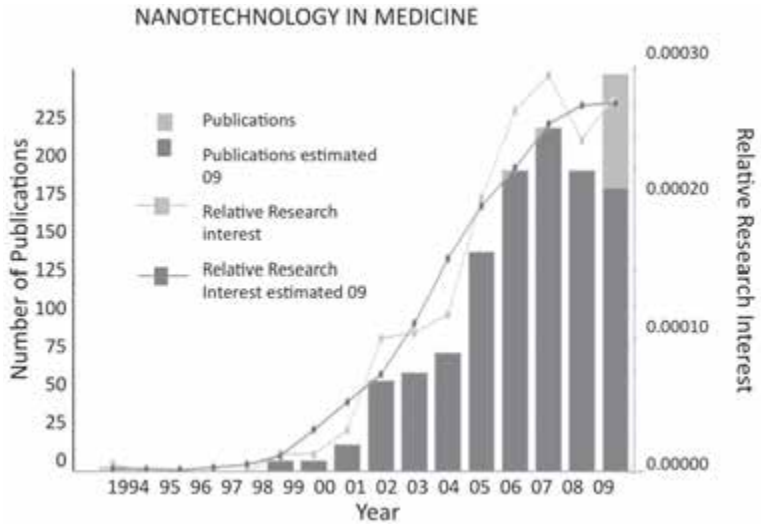

Figure 20.1 Trends in the number of research articles on nanotechnology and medicine published during the last 15 years (Pubmed Citation Index) and relative research interest in the field.

It is advantageous to use nanotechnology for medical applications since most biological processes, including those processes leading to cancer and other diseases, occur at the nanoscale (1–100 nm). Nanotechnology allows the understanding and manipulation of these biological processes at the cellular, sub-cellular and single-molecule level. Rapid interest in the medical applications has led to the emergence of a new field

called nanomedicine [2]. Nanomedicine refers to the specialized application of nanotechnology for diagnosing, treating and preventing disease and improving human health. A bibliographic analysis of research articles in the Pubmed Citation Index shows that nanomedicine has seen a surge in research activity over the past decade, with publication numbers rising from 25 in year 2000 by a factor of 10 up to 2009 (Fig. 20.1).

The overall goal of nanomedicine is to achieve accurate and early diagnosis, effective treatment with minimal or no side effects and rapid and non-invasive monitoring of treatment efficacy. Traditionally, medicine takes a generalized approach to treat diseases, though the response may vary dramatically among individuals. The development of nanotechnology-based theranostic tests involving cellular, proteomic and genomic level testing platforms such as microchips represents a paradigm shift in patient care. It provides unique, individualized medications for each patient, being more targeted and cost-effective. Based on unique capabilities, nanoscale science probes cells and biomolecules in their physiological states at forces, displacement resolutions and concentrations at the piconewton, nanometre and picomolar scales, respectively. Studying human diseases from a nanoscale perspective may lead to better understanding of the pathophysiology and pathogenesis of a variety of human diseases by correlating changes occurring at the molecular and cellular levels to changes in patient physiology. This will provide an alternative and better approach to assess the onset or progression of diseases as well as to identify targets for therapeutic interventions. Such measurements, previously not technically achievable, facilitate quantitative studies on the morphological, biophysical and biochemical nano and microscale properties of biological cells and their organization. Several recently developed nanotechnological tools and probe techniques that have influenced healthcare research and development include the following: nanoparticles for imaging and drug delivery, atomic force microscopy (AFM), molecular force spectroscopy, nanomaterials and microfluidics in management of major diseases such as cardiovascular diseases, cancer, diabetes and other diseases. Table 20.1 outlines some uses of molecules, molecular assemblies, materials and devices in the range of 1–100 nm, and the exploitation of the unique properties and processes at this dimensional scale.

Table 20.1 Nanotechnology-based medical tools for diagnostics and therapeutics

	Benefits	Examples
Drug delivery		
Nanoparticles liposomes, virosomes, polymerosomes, nanosuspensions	Greater affectivity, biocompatibility, low toxicity	*Abraxane*™ against advanced breast cancer; 130 nm albumin-bound paclitaxel particles† *Doxil*® for ovarian cancer and Kaposi's sarcoma; polyethylene glycol (PEG)-coated lipid nanoparticles evade the potential impact of the immune system†. *Emend*® Anti-nausea drug for chemotherapy patients containing aprepitant; colloidal suspension of surface stabilized NanoCrystal particles (<1000 nm)
Therapeutics		
Fullerenes, dendrimers, nanoshells	Low side effects, multiple drug therapy, targeted drug release to tumour cells reducing toxic side effects; thermal drug release	*BrachySil*™ 30 mm BioSilicon particles encapsulating radioactive 32P bonded within silicon microcrystalline shell, remain localized and deliver targeted dose of beta radiation *Aurimune* Recombinant human tumour necrosis factor alpha-coated pegylated colloidal Au nanoparticles *Gold Nanorods* *Nanobomb* Laser heating of hydrated carbon nanotubes kills tumour cells
Medical imaging Nanoparticles for MRI, ultrasound contrast	Detection of small tumours	*Magnetic Nanoclinic* is a thin silica bubble, the surface of which can be customized using a peptide carrier group

	Benefits	Examples
Supermagnetic iron oxide nanoparticles		to selectively target cancer cells. Inside the bubble are ferromagnetic nanoparticles that exhibit a strong inclination to align in the direction of a magnetic field
***In vitro* diagnostic devices/sensors**		
Nanotubes, nanowires, nanocantilevers, AFM	High sensitivity detection of analytes, infectious agents, pathophysiology of single cells, biomolecules	*Nanomix* Carbon nanotube-based sensors for monitoring respiratory functions *Bioforce* Uses AFM for detecting whole viruses *Cell Tracks* Ferrofluids for cancer cell detection *Nanochips* DNA/RNA microarray technology; Implantable Personal ID device†
Biomaterials		
Dental fillers, nano-hydroxyapatite implant coating	Self-assembling particles or nanomaterials with improved biocompatibility and mechanical properties	Nanoscale CAP dual acid etched surfaces improves bone healing Retina Implantat AG Bone replacement materials: Hydroxyapatite (HA) tricalcium phosphate-Ostim®, VITOSS® Nanostructured HA for hip, knee implant coating and dental prostheses
Bioimplants		
	Long-term detection and assessment	EKG monitor glucose sensors, implantable cardioverter defibrillator†

†FDA approved

20.2 AFM for Cancer Diagnosis

Cancer is a complex disease involving multiple molecular and cellular processes arising from a gradual accumulation of genetic changes in individual cells (Fig. 20.2). It continues to be the leading cause of death worldwide and is presently responsible for about 25% of all deaths [3]. It is estimated that there will be about 15 million new cases of cancer annually by 2010 [4]. National Cancer Institute committed $114 billion for nanotechnology research on cancer detection. Earlier diagnosis has been shown to be the most important factor in prognostic outcome [5] highlighting the critical need for developing novel approaches for early cancer detection. Additionally, quantification of cancer cell physiology

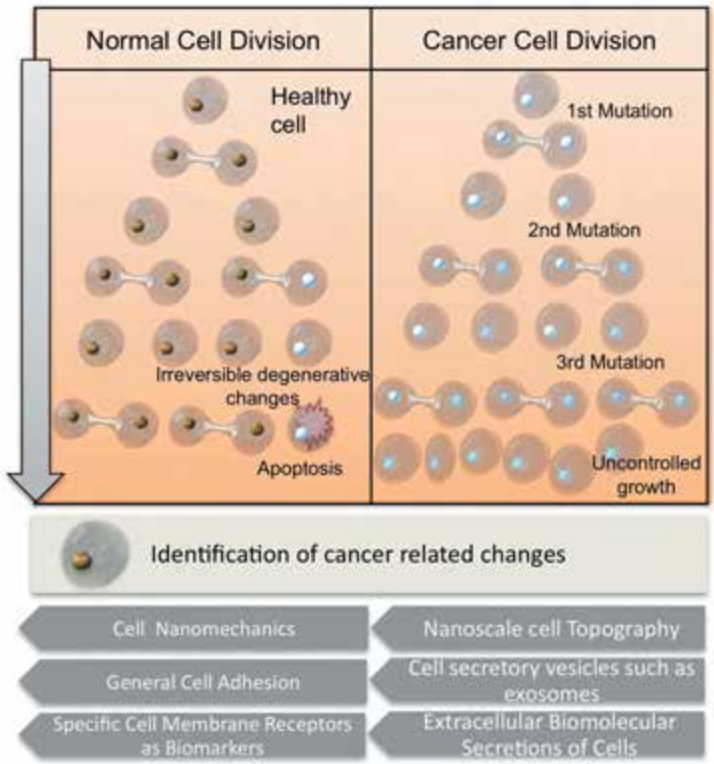

Figure 20.2 Schematics of normal (healthy) and abnormal cancer cell division showing genetic aberrations and novel techniques to identify cancer-related changes in cells.

is required for customization of drug therapies based on specific characteristics and extent of abnormality of cancer cell populations as well as the response of cancer cell populations to therapies. Cancer diagnosis has been widely and aggressively pursued by various nanotechnology research initiatives. In particular, this chapter will highlight some recent AFM techniques developed for cancer diagnostics based on unique nanoscale properties and/or structure of cancer cells or tumour-associated biomolecules.

20.2.1 Cellular Nanomechanics: Using AFM for Cancer Detection

Conventionally, detection of cancerous cells is based on morphological analysis though it is realized that diagnosis based on morphological examination can be difficult [6], with cyto-morphological analysis alone showing about a 50–70% accuracy for diagnosing cancer [7]. Despite using complementary techniques, including histochemical, immunohistochemical and ultrastructural techniques, to develop better diagnostic protocols, the ability to detect early-stage tumours, such as those of the breast, prostate, cervix or colon, has not significantly improved in the past 30 years [7]. The need for developing new technologies to overcome these limitations is thus evident. Cellular and molecular biomechanics of cancer cells is an exciting area, which characterizes the rheological properties of cancer cells and relates the measurable mechanical properties to their molecular basis. Changes in the rheological properties may provide useful information for cancer diagnosis and physical evidence to understand therapeutic mechanisms of various anti-cancer agents. Recent advances in experimental biomechanics have enabled direct and real-time mechanical probing and manipulation of single cells and molecules with nano and picoscale resolutions.

Several studies reported on differences in rigidity of cancer cells from normal cells [8]. Although the detailed physiological mechanisms and propagation of mechanical properties of normal versus tumour cells are still being investigated, AFM-based cytological analysis provides an entirely new technological platform for cancer diagnosis and evaluation by quantitatively measuring the Young's modulus of cells [9]. Low stiffness of cancer cells may

be caused by a partial loss of actin filaments and/or microtubules, and therefore lowers the density of the cellular scaffold [10]. In general, malignant cells respond either more elastically (softer) or less viscously to the applied stress since metastatic cells must squeeze to go through the surrounding tissue matrix when they make their way into the circulatory systems where they are directed to establish distant settlements [11].

AFM has emerged as an important instrument for the investigation of mechanical properties associated with live cells [12]. It is considered as a powerful tool for probing biological samples with sub-nanometre resolution thus providing tremendous insight regarding the surface features and cellular nanomechanics [13], or cellular processes based on the mechanical properties of living cells [14]. An AFM consists of a cantilever (with tip mounted to the soft cantilever spring), a sample stage and an optical beam deflection system which consists of a laser diode and a position-sensitive photodiode. A schematic diagram of an AFM tip interacting with an individual cell is shown in Fig. 20.3.

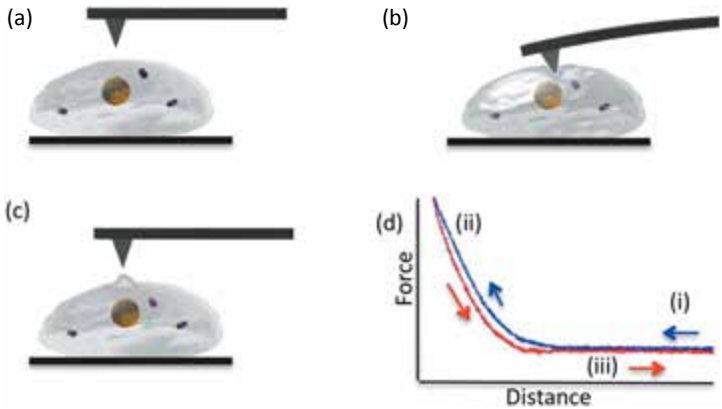

Figure 20.3 Schematic of an AFM probing a cell surface (a) AFM tip approaching cell surface, (b) indented into cell surface and (c) retracted from cell surface. (d) Typical force–displacement curve ((i–iii) correspond to the positions described earlier), recorded as the "approach" and "retract" curves of the cantilever as it moves towards and away from the surface. The force acting on the cantilever is recorded as a function of the piezoelectric crystal displacement. Mechanical properties, such as the Young's modulus (E) or cell stiffness, can be calculated from force curves using a Hertz model.

Mechanical measurements acquired using AFM rely on measuring the force as the tip is pushed towards (Fig. 20.3a), indented into (Fig. 20.3b) and retracted from the sample or cell surface in this case (Fig. 20.3c). The cantilever is mounted on the end of a piezoelectric tube scanner which is used to bring the tip into contact with the surface. The force is measured by recording the deflection (vertical bending) of the cantilever. As described earlier, the cantilever deflection is usually detected by a laser beam focused on the free end of the cantilever and reflected into a photodiode; this deflection is directly proportional to the force. Force–displacement curves are obtained by monitoring the deflection of the cantilever (Fig. 20.3d). The microcantilever-based system allows us to probe the local Young's modulus (E) or "stiffness" of living cells, performs force spectroscopy measurements with piconewton resolution and provides a sensor to record *in vivo* measurements of the cell wall at sub-nanometre resolution. In particular, AFM is a key tool in acquiring kinetic information, and real-time signals of living cells, and is capable of offering *in vivo* single-cell diagnostics. AFM measurements provide a greater understanding of structure, function and relationships of biological macromolecules, thus generating characteristics inherent to specific biological cells [15]. These emerging concepts aid in the development of new types of nanomechanical sensors, which may contribute significantly to the understanding of changes in cytoarchitecture, which are characteristic of cellular de-differentiation, malignant transformation, growth activation, cell motility and disease states.

Cross et al. [9] reported a novel approach to identify and diagnose cancerous cells based on cellular nanomechanical behaviour through the implementation of AFM. Quantitative measurements showed that the metastatic tumour cells obtained from human patients were about five times softer than normal mesothelial cells despite showing similar morphology. The use of AFM to probe and study single biological systems on the nanoscale can yield information about the integrity and local nanomechanical properties of these cells [16]. The AFM approach may help to understand the mechanics inherent to changes in cytoarchitecture and dynamics under *in vitro* conditions and elucidate the mechanisms and related biological alterations

associated with tumour phenotype. AFM-based cytological analysis can quantify the pathophysiology and potential aggressiveness of individual tumours. It could also be used for customization/ monitoring of drug therapies based on specific cancer cell characteristics in near future.

20.2.2 Sub-Cellular Vesicles for the Detection of Novel Cancer Markers from Biological Fluids

The development of nanotechnology-based methods for early cancer detection from easily assessable body fluids such as blood [17], urine [18], or saliva [19] can be highly beneficial for diagnostics and monitoring treatment response and remain of paramount importance. One such class of biomarkers that has gained renewed interest is a unique type of sub-100 nm membrane-bound secretory vesicles called "exosomes". Exosomes are secreted by a wide range of normal mammalian cell types [20] and released into body fluids such as epididymal fluid, seminal plasma, broncoalveolar fluid, pleural effusions, ascites, amniotic fluid, blood and urine via exocytosis [21]. Malignancy and other diseases cause elevated exosome secretion and tumour-antigen enrichment of exosomes associated with cancer cells [22, 23]. Their physiological functions are unclear; however, exosomes possess cell type-specific membrane and proteins enclosed in a lipid bilayer, and serve to signal the physiological state of various distant cells without direct access to the originating tissue or cells themselves. Previous studies have identified populations of various types of normal and tumour-derived exosomes. These vesicles hold tremendous promise as biomarkers for several types of cancers. Yet, because of their small size, sensitive and quantitative detection tools are needed for their individual characterization. Currently, exosomes characterization includes electron microscopy-based morphological analysis and semi-quantitative proteomic and transcriptional analysis of exosome populations [24]. Single vesicle structural and surface molecular details on human saliva exosomes considered as potential non-invasive biomarker resource for oral cancer [19] have been studied recently using AFM [25]. Single exosomes vesicle ultrastructure, quantitative surface molecular constitution and nanomechanical

characteristics of exosomes may be helpful for understanding the role of exosomes in intercellular communication and delivery of genetic components through the extracellular domain (Fig. 20.4a).

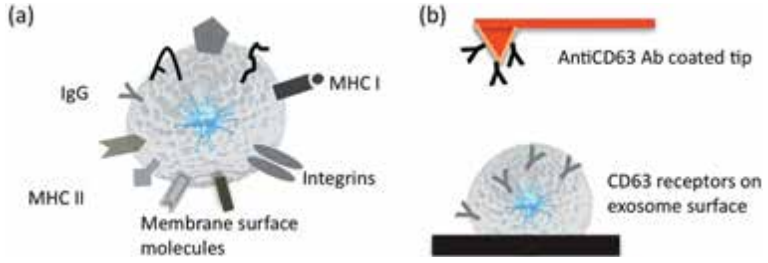

Figure 20.4 (a) Schematic showing exosome vesicle and surface receptors. (b) Schematic of receptor recognition spectroscopy via adhesion force measurements between AntiCD63 IgG-functionalized AFM tips and exosome surface.

AFM has developed as a useful single-molecule tool for sensing and mapping molecular recognition interactions on biological cell interfaces [26, 27]. Cell type-specific markers such as CD63 receptors on individual exosomes can be analysed using force spectroscopy. Force spectroscopy relies on measuring the interaction force with piconewton sensitivity as the tip is pushed towards the sample and retracts from it in the z direction. The force is monitored by measuring the deflection (vertical bending) of the cantilever. Measuring molecular receptors on the exosome surface requires recording force curves between the modified tips (antiCD63 antibody) and the exosomes surface. At large tip–sample separation distances, the force experienced by the tip is zero. As the tip approaches the surface, the cantilever may bend upwards owing to repulsive forces until the tip jumps into contact with the exosome surface (Fig. 20.4b). Upon retracting the tip from the surface, in the event of successful binding of the antiCD63 antibody to the complementary receptors on the vesicle surface, the curve shows an unbinding event calculated as the adhesion "pull-off" force. The rupture force represents the unbinding force between complementary antiCD63 IgG receptors and ligand molecules borne on the vesicle outer membrane. The recognition of single receptor molecules on biological fluid-derived

exosomes, such as saliva, can potentially detect surface tumour-antigen-enriched cancer exosomes, and thereby enable early cancer diagnosis where conventional methods may prove ineffective because of sensitivity limitations.

20.2.3 Ex vivo Molecular Recognition for Early Cancer Detection

Several emerging nanodevices can provide rapid and sensitive detection of cancer-related molecules by enabling detection of biomolecular changes in diseased states. It is increasingly evident that the single-molecule detection sensitivities of nanodevices hold tremendous advantages for early detection of cancer—a critical step in improving cancer treatment. Miniaturization of such diagnostic tools, as in the case of nanocantilevers and nanowires, also enables possible screening for multiple cancer markers on a single device, thereby allowing cancer screening being faster and more cost-efficient.

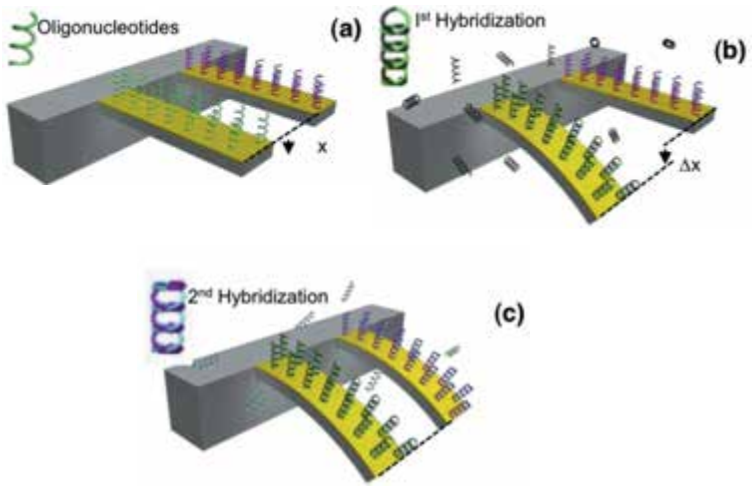

Figure 20.5 Scheme illustrating hybridization of different oligonucleotides functionalized over each cantilever. (a) Differential signal is set to zero. (b) Hybridization of first (black) complementary sequence resulting in increased differential signal, Δx. (c) Second oligonucleotide (cyan)-functionalized cantilever bent because of binding of second matching oligonucleotide (magenta).

Gimzewski et al. [28] pioneered the concept that biomolecular binding events yield forces and deformations that might be detected and recognized by appropriately selective sensing nanostructures, leading to new approaches to multiplexed molecular recognition (Fig. 20.5).

Primary examples of such devices are micro- or nanocantilevers, which deflect and change resonant frequencies as a result of affinity binding e.g., nucleic acid hybridization or proteomic binding events occurring on their free surfaces. A nanocantilever is a thin silicon nitride (typically 1 μm thick, 500 μm long, 100 μm wide) projection attached to a microchip. The cantilevers' surfaces are covered with a layer of receptor probes with a specific binding affinity to target sequence. Because of the extreme thinness of the probe, any adjacent bindings of probes to target molecules would cause the cantilever to locally bend at those binding sites through steric and charge interactions. The resulting bending could then be measured dynamically through the change in resonance frequency in response to the added mass, or statically through the deflection of a laser beam in response to bending. The biochemically induced surface stress was shown to directly and specifically transduce molecular recognition into nanomechanical responses in a cantilever array. Cantilevers in an array were functionalized with a selection of oligonucleotides of variable lengths. The differential deflection of the cantilevers was found to provide a true molecular recognition signal, despite large nonspecific responses of individual cantilevers. Hybridization of complementary oligonucleotides shows detection of a single-base mismatch between two 12-mer oligonucleotides (Fig. 20.5). The nanometre-sized cantilevers, being extremely sensitive and able to detect single molecules of DNA or proteins, also provide fast and sensitive detection for cancer-related molecules. Other applications include microcantilevers to detect single nucleopeptides in a 10-mer DNA target oligonucleotide without the use of extrinsic fluorescent or radioactive labeling [29, 30]. Quantitation of prostate serum albumin at clinically significant concentrations has also been demonstrated [29]. Nanocantilevers possess extraordinary multiplexing capability [31]. In future, fabrication of arrays of cantilevers may allow the simultaneous reading of proteomic profiles or the entire proteome.

Based on similar concept, silicon nanowires can be engineered to detect molecular markers of cancer cells in microfluidic channel devices. Because of their tiny size (20–100 nanometres wide), they exhibit special properties such as superconductivity, and extremely high sensitivity to outside electric fields. Nanowires can be coated with a probe such as an antibody that binds to a target protein. Proteins that bind to the antibody can change the nanowire's electrical conductance, and this can be measured by a detector [32]. Each nanowire may bear a different antibody or oligonucleotide, a short stretch of DNA that can be used to recognize specific RNA sequences or proteins secreted by cancer cells [33]. Self-assembled carbon nanotubes and probe DNA oligonucleotides are immobilized by covalent binding to the nanotubes [34]. When hybridization between the probe and the target DNA sequence occurs, the change is noted as a voltage peak [35]. The nano-based biosensors being developed are more efficient and more selective than current detectors and may be utilized as alternative and complementary cancer detection probes.

20.2.4 Cell Nanomechanical Motion

Cells are dynamic structures that display nanometre to micrometre scale motions at their cell membranes. The AFM can investigate the nanomechanical motion of the cell surface ranging from yeast [16] to cardiomyocytes [36]. If the AFM tip is held stationary over a cell surface that is vibrating or moving, the tip will bend and follow these motions. The AFM can thus be used as an ultra-sensitive, high-resolution motion detector. AFM may be used to probe the surface of cells under a variety of external and internal environmental conditions to obtain an oscillatory signal of nanomechanical origin. This oscillatory, periodic signal can be converted into sound and used as an indicator of cell health. The process termed as "sonocytology" enables cell damage detection; for example, when microtubule and actin dissociating agents used in chemotherapy are added, a change in cell elasticity is discernable much earlier than biochemical measurements of cell death [16]. Thus, by observing their motion, the healthy and cancerous cells can be distinguished. Sonocytology may thus be used as a diagnostic tool by analyzing variations in cell nanomechanical motions. In future, sonocytology may be incorporated as a complementary

tool into medical disciplines such as cancer research and make cancer detection possible before a tumour forms and significant cellular biophysical and biochemical changes manifest.

20.3 Summary and Conclusions

Nanomedicine is an emerging field with significant potential to yield new generation of scientific and technological approaches and advance clinical tools and devices. Diagnostics and biosensors are among the earliest applications of nanotechnology rapidly translating from research to clinical environments. They provide alternative and better approaches to assess the onset or progression of diseases. Diseases such as cancer can be quantified based on morphological, biophysical and biochemical nanoscale properties of cells and subcellular structures. In particular, AFM techniques developed for cancer diagnostics enable detection of nanoscale properties and/or structure of cancer cells or tumour-associated biomolecules. The next generation of AFMs can be integrated with complementary methodologies, including ionic conductance, total internal reflection fluorescence, fluorescence resonance energy transfer and fluorescence imaging, microfluidics, and physico-chemical measurements, thereby enabling a detailed structure–function studies of biological tissues [37]. Cancer-associated rapid quantitative changes in whole-cell morphology, motion and mechanical rigidity via live cell interferometry [38] can also be combined with the dynamic capability of AFM. The flexibility and high-resolution capability of these integrated tools will invariably provide new and exciting information from multiscale biological systems. An approximate 20-year generic gestation period exists between any science discovery and its implementation in the market [39]. However, rapid growth of nano-enabled products and devices in the healthcare market during the last five years suggests imminent emergence of nano-enabled technologies [2]. As the capability to detect and measure nano-dimensional changes in cells and their environment and using novel platforms to derive physiological information progresses, medical applications of nano-enabled and nano-enhanced products and technologies including AFM are bound to rise in the coming years.

Disclosures and Conflict of Interest

The authors declare that they have no conflict of interest and have no affiliations or financial involvement with any organization or entity discussed in this chapter. This includes employment, consultancies, honoraria, grants, stock ownership or options, expert testimony, patents (received or pending) or royalties. No writing assistance was utilized in the production of this chapter and the authors have received no payment for its preparation. The findings and conclusions here reflect the current views of the authors. They should not be attributed, in whole or in part, to the organizations with which they are affiliated, nor should they be considered as expressing an opinion with regard to the merits of any particular company or product discussed herein. Nothing contained herein is to be considered as the rendering of legal advice. This chapter is a reformatted and revised version of the author's chapter that appeared in *Life at the Nanoscale: Atomic Force Microscopy of Live Cells*, 2011 (Yves Dufrêne, editor), Pan Stanford Publishing Pte. Ltd., Singapore.

Corresponding Author

Dr. James K. Gimzewski
Department of Chemistry and Biochemistry
University of California, 607 Charles E. Young Drive East
Los Angeles, CA 90095-1569, USA
Email: gimzewski@cnsi.ucla.edu

About the Authors

Shivani Sharma received her PhD in biomedical engineering from the Indian Institute of Technology, Delhi, India. She is currently a project scientist at the California NanoSystems Institute at the University of California, Los Angeles, USA. Her research interests focus on AFM-based cellular mechanics and cancer diagnostics, exosomes as novel cancer biomarkers, molecular recognition spectroscopy to identify disease biomarkers and the role of mechanical force in cellular signaling using single cell force spectroscopy.

James Gimzewski is a distinguished professor of chemistry at the University of California, Los Angeles, USA; director of the Nano & Pico Characterization Core Facility of the California NanoSystems Institute; scientific director of the Art|Sci Center and principal investigator and satellites co-director of the WPI Center for Materials NanoArchitectonics in Japan. Prior to joining the UCLA faculty, he was a group leader at IBM Zurich Research Laboratory, where he conducted research in nanoscale science and technology for more than 18 years. Dr. Gimzewski pioneered research on mechanical and electrical contacts with single atoms and molecules using scanning tunneling microscopy and was one of the first persons to image molecules with STM. His accomplishments include the first STM-based fabrication of molecular suprastructures at room temperature using mechanical forces to push molecules across surfaces, the discovery of single molecule rotors and the development of new micromechanical sensors based on nanotechnology, which explore ultimate limits of sensitivity and measurement. This approach was recently used to convert biochemical recognition into Nanomechanics. His current interests are in the nanomechanics of cells and bacteria where he collaborates with the UCLA Medical and Dental Schools. He is involved in projects that include the operation of X-rays, ions and nuclear fusion using pyroelectric crystals, direct deposition of carbon nanotubes and single molecule DNA profiling. Dr. Gimzewski is also involved in numerous art-science collaborative projects that have been exhibited in museums throughout the world.

References

1. Warner, S. (2004). Diagnostics + therapy = theranostics. *The Scientist*, **18**, 38–39.
2. Wagner, V., Dullaart, A., Bock, A. K., Zweck, A. (2006). The emerging nanomedicine landscape. *Nat. Biotechnol.*, **24**, 1211–1217.
3. Jemal, A., Murray, T., Ward, E., Samuels, A., Tiwari, R. C., Ghafoor, A., Feuer, E. J., Thun, M. J. (2005). Cancer statistics. *CA. Cancer. J. Clin.*, **55**, 10–30.
4. Lee, G. Y. H., Lim, C. T. (2007). Biomechanics approaches to studying human diseases. *Trends Biotechnol.*, **25**, 111–118.

5. Christofori, G. (2006). New signals from the invasive front. *Nature*, **441**, 444–450.
6. Osterheld, M. C., Liette, C., Anca, M. (2005). Image cytometry: An aid for cytological diagnosis of pleural effusions. *Diagn. Cytopathol.*, **32**, 173–176.
7. Bedrossian, C. W. (1994). Cytopathology: In search of a new identity. *Diagn. Cytopathol.*, **10**, 1–2.
8. (a) Goldmann, W. H., Ezzell, R. M. (1996). Viscoelasticity in wild-type and vinculin-deficient (5.51) mouse F9 embryonic carcinoma cells examined by atomic force microscopy and rheology. *Exp. Cell Res.*, **226**, 234–237.

   (b) Lekka, M., Laidler, P., Gil, D., Lekki, J., Stachura, Z., and Hrynkiewicz, A. Z. (1999). Elasticity of normal and cancerous human bladder cells studied by scanning force microscopy. *Eur. Biophys. J.*, **28**, 312–316.

   (c) Weisenhorn, A. L., Khorsandi, M., Kasas, S., Gotzos, V., Butt, H. J. (1993). Deformation and height anomaly of soft surfaces studied with an AFM. *Nanotechnology*, **4**, 106–113.
9. Cross, S. E., Jin, Y.-S., Rao, J., Gimzewski, J. K. (2007). Nanomechanical analysis of cells from cancer patients, *Nat. Nanotechnol.*, **2**, 780–783.
10. Daisuke, Y., Shusaku, K., Tadaomi, T. (2005). Regulation of cancer cell motility through actin reorganization. *Cancer Sci.*, **96**, 379–386.
11. Farina, K. L., Wyckoff, J. B., Rivera, J., Lee, H., Segall, J. E., Condeelis, J. S., Jones, J. G. (1998). Cell motility of tumor cells visualized in living intact primary tumors using green fluorescent protein. *Cancer Res.*, **58**, 2528–2532.
12. (a) Rotsch, C., Jacobson, K., Radmacher, M. (1999). Dimensional and mechanical dynamics of active and stable edges in motile fibroblasts investigated by using atomic force microscopy, *Proc. Natl. Acad. Sci. USA*, **96**, 921–926.

    (b) Pelling, A. E., Li, Y., Shi, W., Gimzewski, J. K. (2005). Nanoscale visualization and characterization of *Myxococcus xanthus* cells with atomic force microscopy. *Proc. Natl. Acad. Sci. USA*, **102**, 6484–6489.
13. Sharma, S., Cross, S. E., French, S., Gonzalez, O., Petzold, O., Baker, W., Wanda, W., Yougsunthon, R., Baker, D., Gimzewski, J. (2009). Influence of substrates on hapatocyes: A nanomechanical study. *J. Scanning. Probe. Microsc.*, **4**, 7–16.
14. Suresh, S. (2007). Biomechanics and biophysics of cancer cells. *Acta. Biomater.*, **3**, 413–438.

15. Zullo, S. J., Srivastava, S., Looney, J. P., Barker, P. E. (2002). Nanotechnology: Emerging developments and early detection of cancer. A two-day workshop sponsored by the National Cancer Institute and the National Institute of Standards and Technology, August 30–31, 2001, on the National Institute of Standards and Technology Campus, Gaithersburg, MD, USA. *Dis. Markers*, **18**, 153–158.
16. Pelling, A. E., Sehati, S., Gralla, E. B., Valentine, J. S., Gimzewski, J. K. (2004). Local nanomechanical motion of the cell wall of *Saccharomyces cerevisiae*. *Science*, **305**, 1147–1150.
17. Skog, J., Wurdinger, T., van Rijn, S., Meijer, D. H., Gainche, L., Sena-Esteves, M., Curry, W. T., Jr., Carter, B. S., Krichevsky, A. M., Breakefield, X. O. (2008). Glioblastoma microvesicles transport RNA and proteins that promote tumour growth and provide diagnostic biomarkers. *Nat. Cell Biol.*, **10**, 1470–1476.
18. Pisitkun, T., Shen, R., Knepper, M. A. (2004). Identification and proteomic profiling of exosomes in human urine. *Proc. Natl. Acad. Sci. USA*, **101**, 13368–13373. Epub 23 August 2004.
19. Ogawa, Y., Kanai-Azuma, M., Akimoto, Y., Kawakami, H., Yanoshita, R. (2008). Exosome-like vesicles with dipeptidyl peptidase IV in human saliva. *Biol. Pharm. Bull.*, **31**, 1059–1062.
20. Keller, S., Sanderson, M., Stoeck, A., Altevogt, P. (2006). Exosomes: From biogenesis and secretion to biological function. *Immunol. Lett.*, **107**, 102–108.
21. Simpson, R. J., Jensen, S. S., Lim, J. W. (2008). Proteomic profiling of exosomes: Current perspectives. *Proteomics*, **8**, 4083–4099.
22. Andre, F., Schartz, N. E. C., Movassagh, M., Flament, C., Pautier, P., Morice, P., Pomel, C., Lhomme, C., Escudier, B., Le Chevalier, T., Tursz, T., Amigorena, S., Raposo, G., Angevin, E., Zitvogel, L. (2002). Malignant effusions and immunogenic tumour-derived exosomes. *Lancet*, **360**, 295–305.
23. Wolfers, J., Lozier, A., Raposo, G., Regnault, A., Thery, C., Masurier, C., Flament, C., Pouzieux, S., Faure, F., Tursz, T., Angevin, E., Amigorena, S., Zitvogel, L. (2001). Tumor-derived exosomes are a source of shared tumor rejection antigens for CTL cross-priming. *Nat. Med.*, **7**, 297–303.
24. Thery, C., Zitvogel, L., Amigorena, S. (2002). Exosomes: Composition, biogenesis and function. *Nat. Rev. Immunol.*, **2**, 569–579.

25. (a) Palanisamy, V., Sharma, S., Deshpande, A., Zhou, H., Gimzewski, J., Wong, D. (2010). Nanostructural and transcriptomic analyses of human saliva derived exosomes, *PLoS One*, **5**, e8577.

(b) Sharma, S., Rasool, H., Palanisamy, V., Wong, D. T. Gimzewski, J. K. (2010). Structural-mechanical characterization of nanoparticle exosomes in human saliva, using correlative AFM, FESEM, and force spectroscopy. *ACS Nano*, **4**, 1921–1926.

26. Moy, V. T., Florin, E. L., Gaub, H. E. (1994). Intermolecular forces and energies between ligands and receptors. *Science*, **266**, 257–259.

27. Hinterdorfer, P., Baumgartner, W., Gruber, H. J., Schilcher, K., and Schindler, H. (1996). Detection and localization of individual antibody-antigen recognition events by atomic force microscopy. *Proc. Natl. Acad. Sci. USA*, **93**, 3477–3481.

28. Fritz, J., Baller, M. K., Lang, H. P., Rothuizen, H., Vettiger, P., Meyer, E., Guntherodt, H., Gerber, C., Gimzewski, J. K. (2000). Translating biomolecular recognition into nanomechanics. *Science*, **288**(5464), 316–318.

29. Wu, G., Datar, R. H., Hansen, K. M., Thundat, T., Cote, R. J., Majumdar, A. (2001). Bioassay of prostate-specific antigen (PSA) using microcantilevers. *Nat. Biotechnol.*, **19**, 856–860.

30. Majumdar, A. (2002). Bioassays based on molecular nanomechanics. *Dis. Markers*, **18**, 167–174.

31. Yue, M., Stachowiak, J. C., Majumdar, A. (2004). Cantilever arrays for multiplexed mechanical analysis of biomolecular reactions. *Mech. Chem. Biosyst.*, **1**, 211–220.

32. McAlpine, M. C., Agnew, H. D., Rohde, R. D., Blanco, M., Ahmad, H., Stuparu, A. D., Goddard, W. A., III, Heath, J. R. (2008). Peptide-nanowire hybrid materials for selective sensing of small molecules. *J. Am. Chem. Soc.*, **130**, 9583–9589.

33. Bunimovich, Y. L., Shin, Y. S., Yeo, W. S., Amori, M., Kwong, G., Heath, J. R. (2006). Quantitative real-time measurements of DNA hybridization with alkylated nonoxidized silicon nanowires in electrolyte solution. *J. Am. Chem. Soc.*, **128**, 16323–16331.

34. Cai, H., Cao, X., Jiang, Y., He, P., Fang, Y. (2003). Carbon nanotube-enhanced electrochemical DNA biosensor for DNA hybridization detection. *Anal. Bioanal. Chem.*, **375**, 287–293.

35. Williams, K. A., Veenhuizen, P. T., de la Torre, B. G., Eritja, R., Dekker, C. (2002). Nanotechnology: Carbon nanotubes with DNA recognition. *Nature*, **420**, 761.

36. Domke, J., Parak, W. J., George, M., Gaub, H. E., Radmacher, M. (1999). Mapping the mechanical pulse of single cardiomyocytes with the atomic force microscope. *Eur. Biophys. J.*, **28**, 179–186.
37. Lal, R., Arnsdorf, M. F. (2010). Multidimensional atomic force microscopy for drug discovery: A versatile tool for defining targets, designing therapeutics and monitoring their efficacy. *Life Sci.*, **86**, 545–562.
38. Reed, J., Troke, J. J., Schmit, J., Han, S., Teitell, M. A., Gimzewski, J. K. (2008). Live cell interferometry reveals cellular dynamism during force propagation. *ACS Nano,* **2**, 841–846.
39. The 2006 Nanomedicine, Device & Diagnostics Report (2006). *Nanobiotech News*, National Health Information, Atlanta, USA.

Chapter 21

Atomic Force Microscopy Imaging and Probing of Amyloid Nanoaggregates

Yuri L. Lyubchenko, PhD, DSc, and Luda S. Shlyakhtenko, PhD

Department of Pharmaceutical Sciences,
University of Nebraska Medical Center, Omaha, Nebraska, USA

Keywords: nanomedicine, nanoimaging, atomic force microscopy, AFM, force spectroscopy, amyloids, Alzheimer's disease, Parkinson's disease, Huntington's disease

21.1 Introduction

Misfolding and aggregation of proteins are common threads linking a number of important human health problems. Misfolded and aggregated proteins induce cellular stress and activate immunity in neurodegenerative diseases. They may possess cytotoxic properties, resulting in the dysfunction and loss of cells in the affected organs. Despite the involvement of protein misfolding and abnormal interactions in the development of human pathologies, very little is currently known about the molecular mechanisms underlying these processes. Factors that lead to protein misfolding and aggregation *in vitro* are poorly understood, not to mention the

Handbook of Clinical Nanomedicine: Nanoparticles, Imaging, Therapy, and Clinical Applications
Edited by Raj Bawa, Gerald F. Audette, and Israel Rubinstein

ISBN 978-981-4669-20-7 (Hardcover), 978-981-4669-21-4 (eBook)
www.panstanford.com

complexities involved in the formation of protein nanoparticles with different morphologies (e.g., the nanopores) *in vivo*. A clear understanding of the molecular mechanisms of misfolding and aggregation might facilitate development of rational approaches to prevent pathologies mediated by protein misfolding. The conventional tools currently available to researchers can only provide a snapshot of a living system, whereas much of the subtle or short-lived information is unattainable. Existing and emerging nanotools may help solve these problems by opening entirely novel avenues for the development of early diagnostic and therapeutic approaches. This chapter focuses on the application of atomic force microscopy (AFM), a fundamental technique of nanotechnology that can address protein misfolding problems.

21.2 Protein Misfolding and Diseases

Misfolding and aggregation of proteins link a number of important human health problems associated with protein deposition diseases, including neurodegenerative disorders such as Parkinson's disease, Down's syndrome, Alzheimer's, Huntington's disease, systemic and localized amyloidoses, and transmissible encephalopathies [1]. The primary and perhaps most important causative elements in most neurodegenerative processes are misfolded and aggregated proteins. Misfolded or aggregated proteins induce cellular stress and activate immunity in neurodegenerative diseases, which result in neuronal dysfunction and cell death. The accumulation of abnormal protein aggregates exerts toxicity by disrupting intracellular transport, overwhelming protein degradation pathways, and/or disturbing vital cell functions. In addition, the formation of inclusion bodies is known to represent a primary problem associated with the recombinant production of therapeutic proteins [2]. Formulation of these therapeutic proteins into delivery systems and their *in vivo* delivery are often complicated by protein association [3]. Finally, since protein refolding is frequently accompanied by transient association of partially folded intermediates, the propensity to aggregate is considered a general characteristic of the majority of partially folded proteins [1, 4, 5]. Thus, protein folding abnormalities and subsequent events underlie a multitude of pathologies and

difficulties associated with protein therapeutic applications. Current demographic trends indicate the need for age-related and other degenerative disorder therapeutics; and macromolecular therapeutics will be at the forefront of future medical developments. The field of medicine therefore can be dramatically advanced by establishing a fundamental understanding of key factors leading to the misfolding and self-aggregation of proteins involved in various protein folding pathologies.

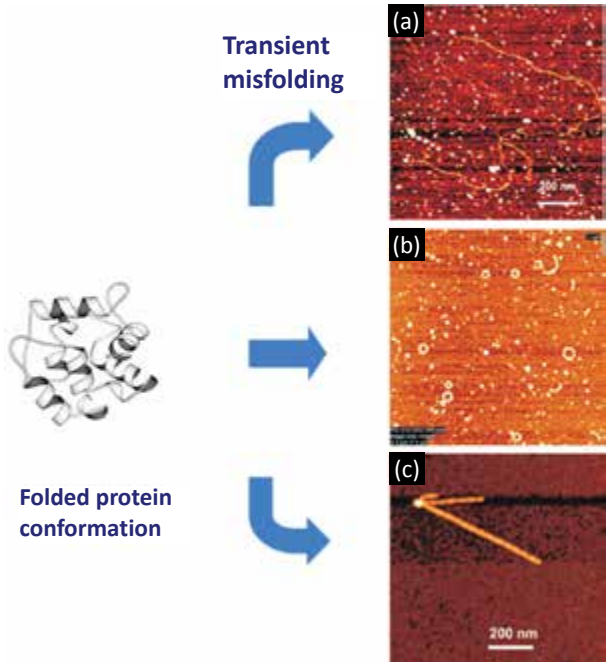

Figure 21.1 Schematic of protein misfolding and aggregation. A normally folded protein can undergo conformational transitions into various misfolded states that may aggregate into different morphologies. AFM images of Aβ peptide aggregated into protofilaments, toroids (rings), and fibrils are shown in plates (a), (b), and (c), respectively. Reproduced with permission from [7]. Copyright © 2012, John Wiley and Sons.

Figure 21.1 illustrates that protein misfolding leads to the formation of aggregates of different morphologies—protofilaments (a); annular aggregates (b) and fibrils (c). These morphologies are typically analyzed by electron microscopy (EM) or atomic

force microscopy (AFM). The AFM images obtained in our lab are shown in the figure. Despite the involvement of protein misfolding and abnormal interactions in the development of disease, very little is currently known about the molecular mechanisms underlying these processes.

For example, Figs. 21.1a–c show that different misfolded states lead to the formation of different aggregates; however, this is currently a purely hypothetical view with very little support. Although it is well known that the same protein under pathological conditions can lead to the formation of fibrillar, pore-like, spherical, or amorphous aggregates with diverse biological consequences [6], the conditions leading to misfolding and the formation of such abnormal complexes are unclear, let alone the means to prevent their formation. The mechanisms underlying aggregation in biological systems *in vivo* are even less clearly understood due to the experimental difficulties associated with monitoring aggregates in their natural environment. Without a clear understanding of the protein misfolding and aggregation phenomena, there is little hope for the development of appropriate early diagnostic tools and efficient therapeutics capable of preventing the development of protein deposition diseases.

21.3 AFM Characterization of the Nanoscale Structure of Amyloid Aggregates

Amyloid fibrillogenesis can be studied using a wide arsenal of modern biophysical approaches developed for the analysis of protein structure, conformational transitions and folding (reviewed in [8]). Nanoimaging techniques such as transmission EM and AFM are excellent tools for distinguishing various morphologies of self-assembled aggregates. These techniques allowed for the classification of several protein aggregate families: protofilaments (subfibrils), oligomers and fibrils, as illustrated in Figs. 21.1a–c. AFM studies were instrumental in further characterization of amyloid fibrils.

Figure 21.2 shows AFM images of fibrils formed by spontaneous aggregation of α-synuclein protein in an acidic (pH 3) aqueous solution. The sample contains short, thin fibrils (indicated with 1) and thicker, longer fibrils (indicated with 2a and 2b).

Thin fibrils are protofibrils of the protein, which associate to form mature thick fibrils. The association is evidenced by images of fibrils, 2a, that have a clear twisted morphology with frayed ends. At the same time, fibrils indicated by 2b do not have a similar clear twisted morphology. The smooth and twisted morphologies of the fibrils suggest that different assembly pathways exist for fibril formation, and/or it indicates differences in the structure of the protofibrils themselves.

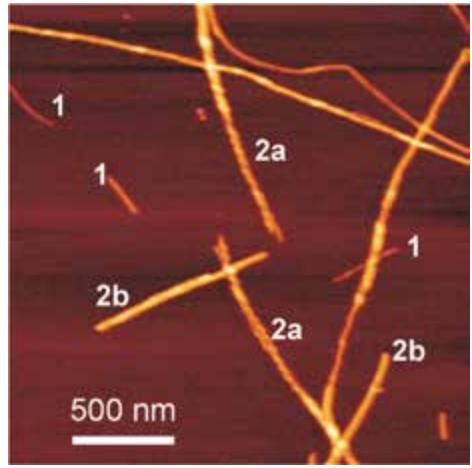

Figure 21.2 AFM images of fibrils formed by α-synuclein protein. The fibrils were assembled spontaneously during the incubation of the protein solution (100 nM) in an acidic solution (pH 3). The sample was deposited on APS-mica [9], rinsed dried and imaged in air with MultiMode AFM (Veeco) operating in Tapping Mode.

Numerous results show that environmental conditions are critical for self-assembly kinetics. AFM imaging was instrumental in the clarification of the effect of pH on self-assembly, as illustrated by the effect of pH on the aggregation of lysozyme [7]. The protein solution (10 μg/mL) was incubated at 57°C in glycine buffer (0.15 M) at pH 2.0, pH 2.7, and pH 3.7. The image of the sample prepared at pH 2.0 is shown in Fig. 21.3a. Fibrils are clearly seen, although the sample prepared at these conditions is characterized by the appearance of short fibrils and small globular aggregates. The sample prepared at pH 2.7 has a predominately fibrillar morphology (Fig. 21.3b) with fibrils as long as several

microns. The incubation of lysozyme at pH 3.7 did not lead to the formation of fibrils or large aggregates (Fig. 21.3c). Similar results were obtained for other proteins, suggesting that the interaction potential between all of the proteins increases sharply with a decrease in pH. Results obtained by AFM imaging concurred with results from force spectroscopy probing (see Section 21.5) and demonstrated that the rate of protein aggregation increases dramatically at pH values corresponding to maximum interprotein interactions.

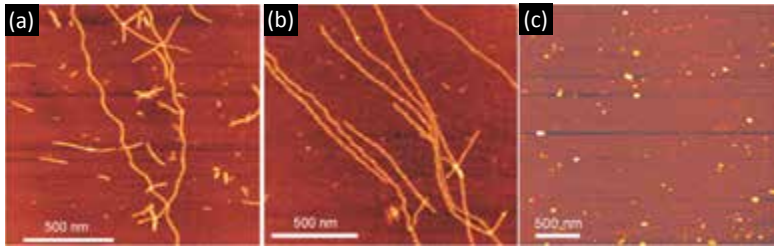

Figure 21.3 AFM images of fibrils formed by lysozyme at different pH values: (a) pH 2, (b) pH 2.7 and (c) pH 3.7. The samples were deposited onto an APS mica surface [9]. Images were acquired in air with MultiMode AFM (Veeco) operating in Tapping Mode. Reproduced with permission from [7]. Copyright © 2012, Elsevier.

Although a rather straight shape is a common feature of amyloid fibrils, the aggregates formed by Htt Exon 1 (Q67) have an alternate morphology with extensive branching [10]. This is a segment of the huntingtin protein that contains multiple repeats of glutamines that are responsible for the development of Huntington's disease [11]. A gallery of AFM images of four different assemblies is shown in Fig. 21.4. This protein forms fibrils, but instead of being isolated, they are stuck to one another. Branched morphology is a distinct feature of Htt fibrils that distinguish them dramatically from other filamentous aggregates, such as those formed by amyloid β peptide and α-synuclein.

The majority of models for fibril formation include in-register, parallel intermolecular alignment of monomers—when strands form two or more parallel β-sheets through intermolecular hydrogen bonding (see, for example, [12–14]). These models predict the amyloid-type fibril structure to be long and straight with an

un-branched morphology (see Fig. 21.4), but they do not explain the branched morphology and thickness variations observed for huntingtin fibrils. The explanation provided in [10, 15] suggests that Htt fibrils can grow in two directions—perpendicular and parallel to the fibril structure proposed in [16]. The parallel orientation of flat β-sheet structures allows for greater variations in the number of stacked sheets, thereby explaining the irregularity of the fiber thickness. The bulges, which are formed by the parallel orientation of the fibril axis, function as buds for growing new fibrils. In the majority of amyloids, such as fibrils formed by amyloid β peptides and α-synuclein, the lateral interaction between β-sheets is relatively weak, therefore the stacked arrangement of the planes is most likely the predominant conformation of the fibril. The formation of branched structures suggests that in the case of Htt protein, both lateral and stacked interactions are comparable; therefore, lateral interactions lead to the arrangement of the planes along the fibril's axis, in parallel with the stacking arrangement of the planes, which leads to branching.

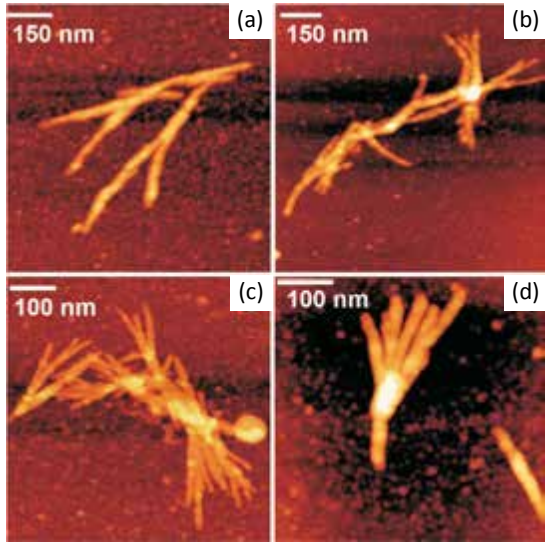

Figure 21.4 AFM images of Htt (Q7) aggregates. Images were taken in air with the Nanoscope IIIa AFM operating in Tapping mode [10]. Reproduced with permission from [10]. Copyright © 2012, Elsevier.

21.4 AFM Visualization of Dynamic Biological Events

One of the most distinct features of AFM is its ability to operate in aqueous solutions, thereby providing structural resolution at the nanoscale level. Imaging in aqueous solutions is the most effective way to preserve native structures of biological systems. In addition, the ability to obtain high-resolution images combined with time-lapse AFM imaging in aqueous solutions enables direct visualization of molecular dynamics and systems at the nanoscale level. The earliest demonstration of the potential of AFM to directly image actual molecular processes was performed by the group of P. Hansma, in which they visualized fibrin polymerization [17, 18]. However, AFM imaging of biological processes required substantial improvements of the AFM instrumentation. The introduction of Tapping Mode imaging [19] considerably alleviated the problem of sample movement by the tip. Note that imaging in aqueous solutions eliminates the resolution limiting capillary effect, therefore images of DNA molecules can be obtained with parameters very close to those of crystallographic images [20].

21.4.1 Time-Lapse Imaging of Protein–DNA Complexes

The time-lapse AFM technique was successfully applied by a number of groups actively working with DNA. Early joint efforts of the Hansma and Bustamante groups demonstrated the ability to image the assembly process of RNA polymerase-DNA complexes in a series of time-lapse images [21]. Sliding of the polymerase along DNA was visualized [22], thereby leading to the conclusion that diffusion of RNA polymerase along DNA constitutes a mechanism for accelerated promoter localization. Later studies [23] showed that during transcription initiation, the promoter DNA wraps nearly 300 degrees around the polymerase. Time-lapse AFM observations of interactions of DNA with photolyase [24] showed association, dissociation, and movement of photolyase over the DNA. The latter result suggests a sliding mechanism by which photolyase can scan DNA for damaged sites. Time-lapse AFM was recently used to image the human Rad50/Mre11/Nbs1 complex [25]. High-resolution AFM imaging revealed the

unusual morphology of the protein complex, and the dynamic and structural changes occurring upon binding to DNA. The Mg-assisted immobilization technique was used in these studies.

Recent papers [26, 27] illustrate the application of time-lapse AFM in the visualization of the unwrapping process of nucleosomes. Nucleosome dynamics are a key property of chromatin, providing access to DNA wrapped around the histone core. Recent single molecule studies using fluorescence and time resolved techniques detected local dissociation of DNA from nucleosomes in the absence of remodeling proteins (e.g., [28–31]); however, the spatial range of these dynamics was unanswered. Time-lapse AFM enabled the direct observation of nucleosome dynamics assembled on a 353 bp DNA substrate containing a 147 bp nucleosome positioning sequence.

Figure 21.5 shows a nucleosome starting as a complex with 2 turns of the DNA wrapped around the histone octamer (frame 1); the nucleosome unwraps during frame 2, losing one DNA turn; and finally undergoes full dissociation in frame 3. APS-mica methodology was used in these studies.

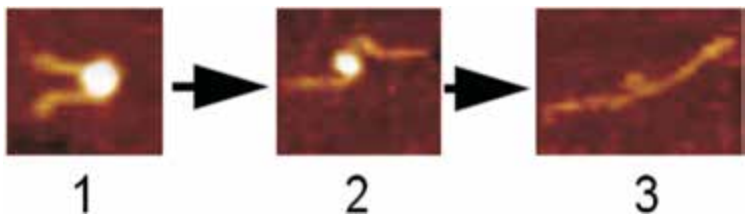

Figure 21.5 Time-lapse AFM images of reconstituted mononucleosome particles taken in aqueous solution. See [27] for details. Reproduced with permission from [27]. Copyright © 2009, American Chemical Society.

21.4.2 Dynamics of Protein–DNA Complexes with High-Speed AFM

The primary drawback of the AFM time-lapse studies described above is the slow (minute-scale) data acquisition rate of a conventional AFM instrument; therefore, most biological system dynamics remain undetectable. Ando's group has developed a high speed-AFM (HS-AFM) instrument operating almost 1000 times faster and capable of acquiring data with a sub-second rate

[32–35]. The development of this instrument enabled Ando's group to visualize the dynamics of individual myosin molecules with a 100 ms temporal resolution [34, 35]. This instrumentation was used to study the dynamics of site-specific DNA binding proteins in the sub-second time scale [36] and the dynamics of reconstituted chromatin [37]. The latter study revealed the sliding mechanism, which was characterized within approximately 50 nm along the DNA strand. In addition, two distinct mechanisms of histone dissociation were visualized. This emerging novel instrumentation has also recently been used to study the dynamics of various protein–DNA systems [37–43].

21.4.3 Dynamics of Protein Assembly in Nanofibrils with AFM Nanoimaging

Time-lapse AFM was successfully applied to monitor the self-assembly of several amyloidogenic proteins [44, 45], including amylin and amyloid β peptide [46, 47]. A single fiber growth assay was used to examine the heterogeneity of amyloid fibrils formed by the yeast Sup35 prion protein [48]. This assay used two variants of Sup35, one of which was modified to bind specific antibodies. Antibody binding increased the thickness of the fiber 3-fold, thus providing a means of identification of one type of the protein by AFM. This study found that Sup35 spontaneously forms multiple and distinct fibril types. These types differ by their degree of polarity and overall growth rate. The diversity in properties of the fibrils may account for the wide range of prion strain phenotypes [48].

An assembly of individual fibrils formed by amyloid β 25–35 was studied by a modified application of AFM, scanning force kymography [49]. In this modification of AFM, the tip is scanned repeatedly along the fibril axis only and the end of the fibril is detected by the sudden change in topographical height. The scan angle was adjusted parallel with the fibril orientation while the scan along the direction perpendicular to the fibril axis was disabled and consecutive line scans were assembled into a distance versus time image. By scanning fibrils only, this method eliminated the need to scan the whole image. This modification significantly increased the temporal resolution, allowing the measurement of the single fibril elongation process. Using

this method, fibril assembly was shown to be polarized and discontinuous. The growth phases were followed by pauses in a stepwise manner, suggesting a fluctuation of amyloid states in which growth may be either permitted or inhibited [49].

21.5 AFM Force Spectroscopy and Intermolecular Interactions

AFM instrument has dual capabilities. In addition to the imaging described above, AFM is capable of measuring intermolecular interactions and probing mechanical properties of biological systems at the nanoscale level. This capability is due to the AFM probe that can be positioned with sub-nanometer accuracy in all three dimensions, and the ability to vary the stiffness of the AFM cantilever.

21.5.1 AFM Force Spectroscopy

AFM force spectroscopy is defined as the methodology of probing intermolecular and intramolecular interactions. In a typical experiment, the interactions are probed between the molecules immobilized on the tip and the surface, as schematically shown in Fig. 21.6. Upon approaching the tip to the surface (Fig. 21.6a) the molecules interact and form a complex (Fig. 21.6b). The strength of this complex is probed by retracting the tip away from the surface. Initially the tethers are stretched (Figs. 21.6c,d) followed by the rupture of the complex (Fig. 21.6e). The cantilever deflection detects all of these steps in a force–distance curve, shown schematically in Fig. 21.6f.

The range of AFM force spectroscopy applications is very broad, varying from interactions of isolated molecules to interactions of a tip-immobilized ligand with receptors on a cell surface (many of these examples are reviewed in [50]). The feasibility of this approach to study complex biological systems has been proven by two back-to-back early publications in which different systems have been analyzed. In one study [51], interactions between complementary DNA regions immobilized on the AFM tip and on the surface were probed. The DNA sequences were repeats of four nucleotides enabling the formation of duplexes of different

lengths. The AFM pulling approach was capable of detecting the heterogeneity of duplexes and characterizing the strength of the duplexes of different lengths. In another publication [52], biotin–avidin interactions were studied enabling the analysis of structural information of the biotin–avidin complex.

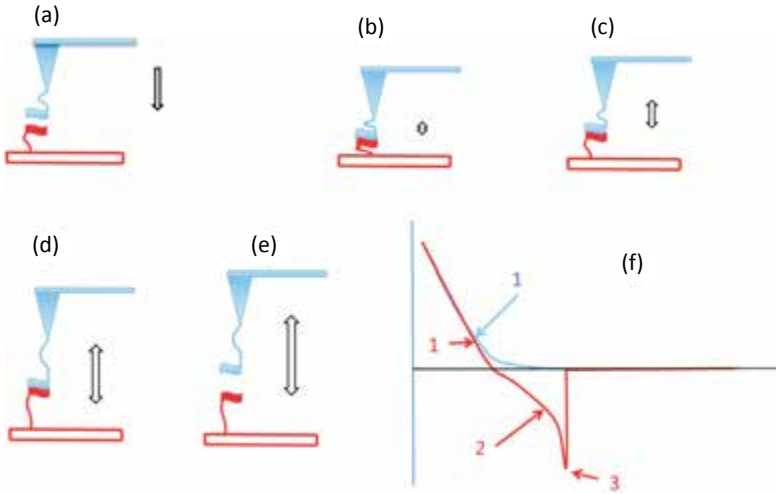

Figure 21.6 AFM to measure the interaction of the molecules immobilized on the AFM tip and surface. (a–e) Schematic for the approaching the tip (a), formation of the complex (b), extension of the tethers (c), rupture event (d) followed by the dissociation of the complex and (e) the loss of contact with the surface. The force–distance curve corresponding to this event is shown in f.

Measurements of intermolecular interactions with force spectroscopy were shown to delineate between normal and abnormal protein folding [53]. The interactions of Cx43 hemichannels reconstituted in supported lipid bilayers with individual antibodies and with connexin mimetic peptides were measured using single molecule force spectroscopy [53]. Distinct signatures of the extracellular and cytoplasmic sides of hemichannels reconstituted in bilayers allowed the observation of specific recognition of the extracellular side by mimetic peptides, whereas the anti-CT antibodies recognized only the cytoplasmic side of the hemichannel [53]. In a recent publication [54], AFM force spectroscopy revealed the coupling between the intercellular

adhesion molecule-1 (ICAM-1) to the monocytic cell line THP-1, as well as cell adhesion and cell stiffness.

21.5.2 AFM Probing of Protein Misfolding

As we mentioned above, protein misfolding and aggregation are considered the main causative agents for the development of neurodegenerative diseases such as Alzheimer's, Parkinson's, and Huntington's diseases, as well as systemic and localized amyloidoses, and transmissible encephalopathies [55, 56]. However, our knowledge of the molecular mechanisms of the protein self-assembly process into disease-prone aggregates is very limited. Understanding the mechanisms underlying these processes would facilitate the development of efficient therapeutic and diagnostic tools for these devastating diseases. Although it is well known that the same protein can form fibrillar, pore-like, spherical, or amorphous aggregates with diverse biological consequences, the conditions leading to misfolding and the formation of various complexes are unclear. The lack of efficient methods to characterize the complex aggregation process is the primary reason for our limited knowledge. A process that may appear simple by existing techniques may actually have many steps and a variety of important intermediate states—each with its own unique dynamics. Intermediate states are stabilized by weak interactions that are typically transient and difficult to measure.

Single-molecule biophysics techniques can help to image molecular intermediates, follow molecular-scale events in real time, and measure a wide range of intermolecular interactions [57]. For example, conformational dynamics of prion protein [58] and α-synuclein [59] were studied with single-molecule fluorescence, including fluorescence energy transfer (FRET) spectroscopy.

The AFM pulling approach was used to study conformational transitions of α-synuclein, demonstrating that the disease-associated mutations in the protein facilitate its misfolding [61]. Beta-like conformations are directly related to aggregation of α-synuclein [62]. Interestingly, changes in environmental conditions such as high ionic strength and the presence of Cu^{2+}, which are also known to increase the propensity of α-synuclein to aggregate, shifted the conformational equilibrium towards β-like structures.

It has recently been shown that AFM is capable of directly probing aggregation-prone states of proteins and their interactions [7, 55, 60, 63, 64]. This approach is schematically shown in Fig. 21.7 for probing interactions between amyloid-β peptides [65, 66]. The peptides are anchored to the surfaces of the AFM substrate (mica) and the probe, and the interaction between the anchored molecules is measured in the approach-retraction cycles. The forces stabilizing the complex are measured at the rupture event. The rupture force is low if the complex is weak (normal state of the protein), but the forces increase if the protein adopts a misfolded conformation. It is important to note that the described approach is entirely different from traditional approaches. It allows unambiguous measurement of pair-wise protein–protein interactions, avoiding the effect of multiple interactions complicating quantitative analysis of the aggregation process.

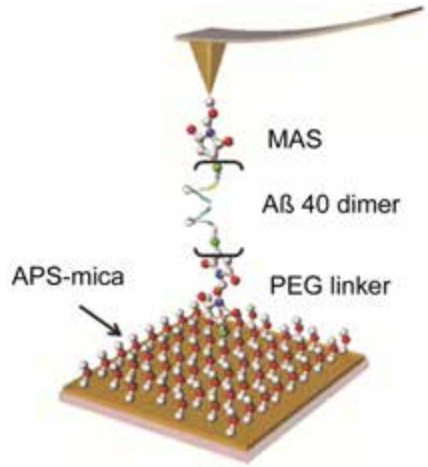

Figure 21.7 Schematic for single molecule probing of interactions between amyloid β peptide (Aβ40). The peptide is immobilized on an APS-functionalized mica surface via a flexible PEG tether. The same peptide is immobilized to the AFM tip using the MAS tethering method [60].

Further improvements of the immobilization and surface chemistry techniques made it possible to perform force spectroscopy analysis at the single-molecule level [60, 63–65, 67, 68]. This approach enabled the development of quantitative approaches

such as dynamic force spectroscopy (DFS), introduced by Evans and Ritchie (reviewed in [69]).

In the DFS approach, pair-wise interactions are probed over a broad range of pulling rates. Rupture forces are determined for each force–distance curve, and force distributions are obtained, as shown in Fig. 21.8a. The DFS analysis required the system to pull with different rates. Therefore, the probing experiments were performed in a broad range of loading rates (0.1~100 nN/s). To generate the DFS spectrum, more than 25,000 force curves were collected.

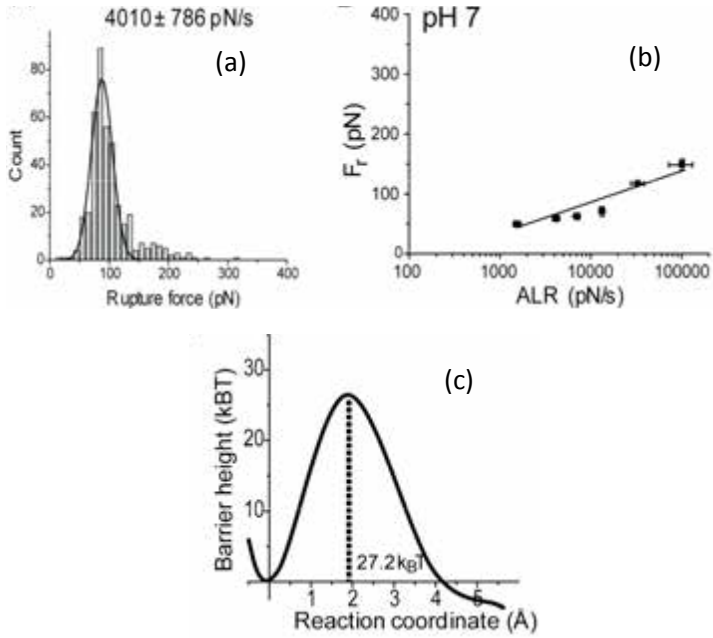

Figure 21.8 Results of the dynamic force spectroscopy (DFS) analysis for pH 7. (a) The histograms of the rupture force distribution measured at pH 7 at the apparent loading rate of 4010 pN/s. The most probable rupture force (F_r) was calculated by Gaussian fitting and the values obtained for a series of loading rates were plotted as shown in (b). The solid lines represent the best fit for the data points in two regimes according to Bell's model. (c) Profile of the energy landscape calculated from the DFS plot above. See [66] for details. Reproduced with permission from [66]. Copyright © 2012 American Chemical Society.

The most probable force is plotted on the DFS graph against the logarithm of the pulling rate (Fig. 21.8b). The DFS plot is approximated by one line, and its intercept and slope were used to reconstruct the energy landscape profile for the dissociation of the dimer, as shown in Fig. 21.8c. One of the major findings from the DFS analysis for Aβ40 peptide is that dimeric complexes formed by misfolded peptides are relatively very stable and dissociate in the range of seconds. This differs markedly from the dynamics of monomers, which dissociate on a microsecond-nanosecond time scale. Similar data were obtained for α-synuclein (α-Syn) [63, 64] and Sup 35 peptide [70], suggesting that elevated lifetimes are a common phenomenon for misfolded dimers [65].

Combined, these studies led to the conclusion that dimerization is the mechanism by which the misfolded state is stabilized [65]. It was also hypothesized that dimer formation is the key step of the entire aggregation process and that the dimers are the primary building blocks for protein aggregation.

Importantly, the same nanoprobing approach is capable of locating regions of the protein responsible for pathology-related conformational changes [64]. Force–distance curves measured with force spectroscopy detect specific rupture events (Fig. 21.9a). The position of the rupture event determines the distance where the rupture takes place. By fitting the force curves with the worm-like chain model we were able to measure contour lengths, L_c, that comprise the length of the flexible linker and the N-terminal segment of the peptide not involved in dimer formation. Therefore, subtracting the lengths of the linkers from the experimentally measured contour length yields the length of the N-terminal segment of the peptide preceding the structured segment of Aβ40 involved in the interpeptide interaction. We tested and applied this approach in our recent work on the localization of interacting segments in misfolded α-synuclein [63, 71].

The application of this approach to Aβ40 peptide and a thorough statistical analysis of the contour lengths showed that not only one contour length value, but a set of contour lengths is characteristic for Aβ40 dimer rupture. This characteristic is demonstrated in Fig. 21.9b in which four force curves with different contour lengths are assembled. These findings suggest that the peptide can form dimers in different ways, as schematically shown in Fig. 21.9b [66]. The peptides can interact via β-hairpins,

corresponding to the shorter contour length, L_{c1}. The interaction between the hairpin and C-terminal segment of the peptide is represented by the longer contour length, L_{c2}, and the longest contour length value, L_{c3}, corresponds to the peptides' interactions via C-terminal ends. The appearance of rupture events with the shortest contour length, L_{c0}, suggests that N-terminal regions of the peptide are involved in peptide folding in the dimer, thereby shortening the non-structural N-terminal segment. This assumption is in agreement with molecular dynamic simulation analysis [72].

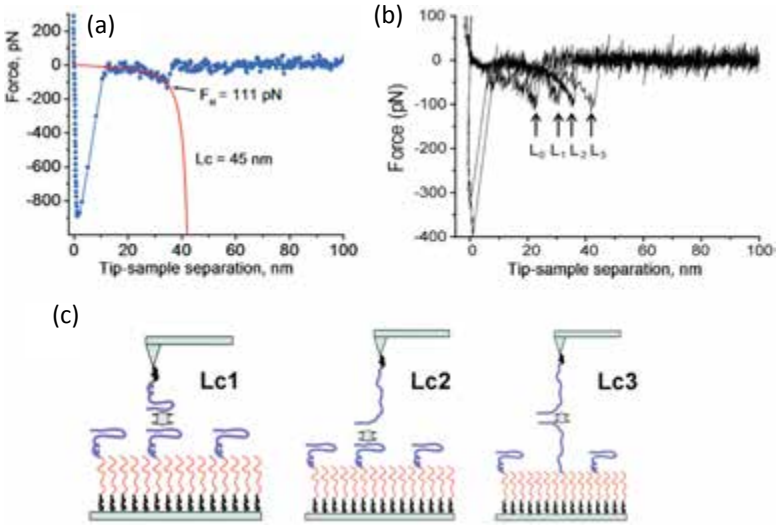

Figure 21.9 Contour length analysis of rupture events for Aβ40 dimers. (a) The individual force curve (blue) approximated with the worm-like chain model (WLC, red line). The values for the rupture force (F_R = 111 pN) and contour length (L_c = 45 nm) are indicated. (b) A set of four force curves with different rupture lengths. The rupture positions are indicated with arrows. (c) The model for the formation of misfolded Aβ40 dimers with different conformations corresponding to different contour lengths, L_{c1}, L_{c2}, and L_{c3}, as measured in the force probing experiments. See [66] for details. Reproduced with permission from [66]. Copyright © 2012 American Chemical Society.

A similar approach was used to analyze the effect of spermidine on the misfolding of α-Syn [73]. These studies showed that the

conformations of misfolded dimers vary, suggesting that these different dimer conformations can lead to different aggregation self-assembly pathways and to the formation of aggregates with different morphologies. Another finding of the α-Syn study is that increased levels of spermidine and potentially other polyamines can initiate the disease-related process of α-Syn aggregation [73].

21.5.3 Nanomanipulation

The ability of AFM to scan a sample with different forces enabled the analysis of the inner structure of biological surfaces *in situ* in aqueous solution. The force applied during scanning can be varied from virtually zero to highly destructive ones. By using destructive forces, it is possible to dissect soft biological samples, thereby resembling surgical intervention. Using the AFM tip as a "nanosurgical" tool, a bacterial cell wall was dissected to reveal its inner structure [74]. After peeling back the outer cell wall, an inner wall structure was imaged with AFM revealing a new structure—striations of peptidoglycans with 26 nm-thick twisted strands [74]. Another example of successful "surgical operation" with AFM on a cell was performed with the use of a modified AFM tip. The AFM tip was made into a long, sharp needle using focused ion beam etching. By using this needle and AFM it was possible for the researchers to penetrate the cell to a depth of 1–2 μm, passing through both the cellular and nuclear membranes and reaching the nucleus [75].

Recently, AFM tips have been used for the nanomechanical manipulation of biological objects. Fabricated tips, termed nanoscalpels, have the shape of a thin blade with a thickness of 20–30 nm and a width of 100–200 nm [76]. These "nanoscalpels" were used on mammalian cells to make narrow incisions and measure local elastic and inelastic characteristics of cells. Since AFM allows for the simultaneous control of the applied cutting force and the depth of the incision, "nanoscalpels" are potentially useful for the "nanodissection" of biological objects to expose their internal structures for *in situ* imaging and investigation [76].

Manipulation of the sample using the AFM tip and AFM nanolithography can be performed accurately and reproducibly as demonstrated recently with α-Syn aggregates [77]. In this approach, the image is acquired and the nanolithography tool is used, in

which a high force is applied to a selected area. The procedure is illustrated in Fig. 21.10a in which a sinusoidal trace in the middle of the long α-Syn fibril is indicated with a blue sinusoidal line. Nanolithography was performed on the blue trace, followed by rescanning of the same area, demonstrating the result of nanomanipulation. Rescanning shows that the selected fibril was broken into three parts (Fig. 21.10b) that were displaced from the original positions by the tip. The broken sections of the fibril perfectly overlap with the selected nanolithography path (Fig. 21.10c). The width of the fibril (~10 nm) in the overlaid image (Fig. 21.10c) clearly shows that nanometer accuracy can be readily obtained by positioning the tip over a selected area.

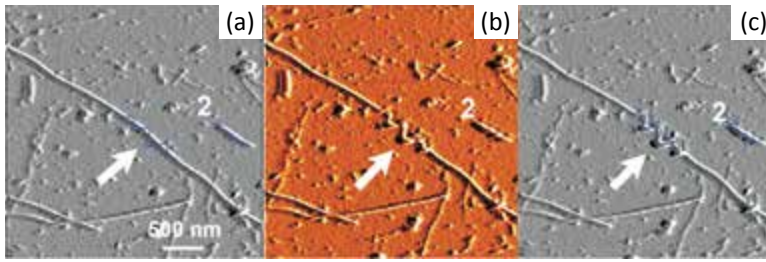

Figure 21.10 AFM images of α-synuclein fibrils before (a) and after (b,c) performing the nanolithography procedure over the longest fibril using a wavy path drawn in (a) with a blue line. A broken fibril is clearly seen in (b). Image c is the overlay of (a) and (b), demonstrating how the projected path coincides with the nanolithography results. The short fibril indicated with 2 was probed along the fibril with a low loading force. See [77] for details. Reproduced with permission from [77]. Copyright © 2012, Elsevier.

This capability was critical in the development of a novel nanotweezers technology in which the AFM tip was used to select antibodies specifically bound to a defined type of protein aggregate [77]. Tagged antibodies (bacteriophage display antibodies) were mixed with the protein sample containing aggregates of different morphologies. Complexes of tagged antibody molecules with a specific protein aggregate morphology were identified by scanning. The AFM was then switched to the nanolithography mode of operation in an attempt to remove a single specifically targeted aggregate-antibody complex from the surface. The selected antibody

gene was recovered from the AFM tip, amplified by single molecule PCR and used for further characterization.

21.6 Conclusions

AFM has become a valuable tool for nanomedical applications at the nanoscale level. Traditional topographic imaging is complemented by AFM force spectroscopy, which is capable of quantitative characterization of intermolecular interactions. This technique has significant potential in a broad field of biomedicine and pharmaceutics, specifically for the design and development of novel drugs. The interaction of the molecule of interest with the target (e.g., receptor) can be characterized quantitatively, enabling the identification of a drug candidate with the strongest inhibitory activity towards this interaction. One of the methods for developing novel therapeutics for neurodegenerative disorders such as Alzheimer's, Parkinson's and Huntington's is to generate antibodies that can be used to prevent accumulation of toxic forms of proteins associated with the development of disease. These antibodies can be used in conjunction with other therapeutics to develop a non-invasive long-term successful therapeutic treatment for these neurological disorders associated with protein aggregation. Development of the nanotweezer technology, which is capable of generating antibodies with distinct aggregate-specificity, is the first step in this therapeutic approach. We believe that further development of nanoimaging approaches will provide new important insights into the mechanism of many diseases. The use of these methods will advance our understanding of important health-related phenomena, facilitating the development of effective novel treatments, early diagnostic means, and preventions for AD, PD, and many other diseases.

Abbreviations

Aβ: Amyloid beta peptide
AFM: Atomic force microscopy
AD: Alzheimer's disease
DFS: Dynamic force spectroscopy
EM: Electron microscopy

FRET: Fluorescence energy transfer
Htt: Huntingtin protein
MAS: Maleimide silatrane
PD: Parkinson's disease
PEG: Polyethylene glycol

Disclosures and Conflict of Interest

This work was supported by the following US grants: DOE (DE-FG02-08ER64579), NIH (1P01GM091743 and 1 R01 GM096039) and NSF (EPS—1004094).

The authors declare that they have no conflict of interest and have no affiliations or financial involvement with any organization or entity discussed in this chapter. This includes employment, consultancies, honoraria, grants, stock ownership or options, expert testimony, patents (received or pending) or royalties. No writing assistance was utilized in the production of this chapter and the authors have received no payment for its preparation.

Corresponding Author

Dr. Yuri L. Lyubchenko
Department of Pharmaceutical Sciences
University of Nebraska Medical Center
601 S. Saddle Creek Road, Omaha, NE 68106, USA
Email: ylyubchenko@unmc.edu

About the Authors

Yuri Lyubchenko is professor in the Department of Pharmaceutical Sciences, College of Pharmacy, at the University of Nebraska Medical Center, USA. He obtained his PhD degree from the Moscow Institute of Physics and Technology and his DSc degree from the Institute on Molecular Genetics, Moscow, Russia. His current interest is focused on understanding the molecular mechanisms of DNA replication, repair, and recombination in conjunction with elucidating novel approaches for the treatment of cancer and HIV. The elucidation

of molecular mechanisms of the development of Alzheimer's, Parkinson's and prion diseases are other areas of interest. Dr. Lyubchenko serves on a number of journal editorial boards, including as an associate editor of *Nanomedicine: Nanotechnology, Biology, and Medicine.*

Luda Shlyakhtenko is a research associate professor in the Department of Pharmaceutical Sciences, College of Pharmacy at the University of Nebraska Medical Center, USA. She obtained her PhD from the Moscow Institute of Physics and Technology, Moscow, Russia. Her primary current research interest is elucidating the molecular mechanisms of interactions of natural anti-HIV defense APOBEC proteins with DNA, and her future goal is to develop an efficient treatment for AIDS. She utilizes AFM as a primary tool and is interested in developing novel AFM approaches for various biomedical applications.

References

1. Dobson, C. M. (2004). Principles of protein folding, misfolding and aggregation. *Semin. Cell Dev. Biol.*, **15**, 3–16.
2. Fink, A. L. (1998). Protein aggregation: Folding aggregates, inclusion bodies and amyloid. *Folding Des.*, **3**, R9–R23.
3. Demidov, V. V. (2004). Nanobiosensors and molecular diagnostics: A promising partnership. *Expert Rev. Mol. Diagn.*, **4**, 267–268.
4. Ptitsyn, O. B. (1995). How the molten globule became. *Trends Biochem. Sci.*, **20**, 376–379.
5. Uversky, V. N. (2002). What does it mean to be natively unfolded? *Eur. J. Biochem.*, **269**, 2–12.
6. Uversky, V. N. (2003). A protein-chameleon: Conformational plasticity of alpha-synuclein, a disordered protein involved in neurodegenerative disorders. *J. Biomol. Struct. Dyn.*, **21**, 211–234.
7. McAllister, C., Karymov, M. A., Kawano, Y., Lushnikov, A. Y., Mikheikin, A., Uversky, V. N., Lyubchenko, Y. L. (2005). Protein interactions and misfolding analyzed by AFM force spectroscopy. *J. Mol. Biol.*, **354**, 1028–1042.

8. Lazo, N. D., Grant, M. A., Condron, M. C., Rigby, A. C., Teplow, D. B. (2005). On the nucleation of amyloid beta-protein monomer folding. *Protein Sci.*, **14**, 1581–1596.
9. Lyubchenko, Y. L., Shlyakhtenko, L. S., Gall, A. A. (2009). Atomic force microscopy imaging and probing of DNA, proteins, and protein DNA complexes: Silatrane surface chemistry. *Methods Mol. Biol.*, **543**, 337–351.
10. Dahlgren, P. R., Karymov, M. A., Bankston, J., Holden, T., Thumfort, P., Ingram, V. M., Lyubchenko, Y. L. (2005). Atomic force microscopy analysis of the Huntington protein nanofibril formation. *Nanomed. Nanotechnol. Biol. Med.*, **1**, 52–57.
11. Snell, R. G., MacMillan, J. C., Cheadle, J. P., Fenton, I., Lazarou, L. P., Davies, P., MacDonald, M. E., Gusella, J. F., Harper, P. S., Shaw, D. J. (1993). Relationship between trinucleotide repeat expansion and phenotypic variation in Huntington's disease. *Nat. Genet.*, **4**, 393–397.
12. Ma, B., Nussinov, R. (2002). Stabilities and conformations of Alzheimer's beta-amyloid peptide oligomers (Abeta 16-22, Abeta 16-35, and Abeta 10-35): Sequence effects. *Proc. Natl. Acad. Sci. U. S. A.*, **99**, 14126–14131.
13. Petkova, A. T., Ishii, Y., Balbach, J. J., Antzutkin, O. N., Leapman, R. D., Delaglio, F., Tycko, R. (2002). A structural model for Alzheimer's beta-amyloid fibrils based on experimental constraints from solid state NMR. *Proc. Natl. Acad. Sci. U. S. A.*, **99**, 16742–16747.
14. Tycko, R. (2003). Insights into the amyloid folding problem from solid-state NMR. *Biochemistry*, **42**, 3151–3159.
15. Dahlgren, P. R., Karymov, M. A., Bankston, J., Holden, T., Thumfort, P., Ingram, V. M., Lyubchenko, Y. L. (2005). Atomic force microscopy analysis of the Huntington protein nanofibril formation. *Dis. Mon.*, **51**, 374–385.
16. Der-Sarkissian, A., Jao, C. C., Chen, J., Langen, R. (2003). Structural organization of alpha-synuclein fibrils studied by site-directed spin labeling. *J. Biol. Chem.*, **278**, 37530–37535.
17. Drake, B., Prater, C. B., Weisenhorn, A. L., Gould, S. A., Albrecht, T. R., Quate, C. F., Cannell, D. S., Hansma, H. G., Hansma, P. K. (1989). Imaging crystals, polymers, and processes in water with the atomic force microscope. *Science*, **243**, 1586–1589.
18. Hansma, H. G., Weisenhorn, A. L., Edmundson, A. B., Gaub, H. E., Hansma, P. K. (1991). Atomic force microscopy: Seeing molecules of lipid and immunoglobulin. *Clin. Chem.*, **37**, 1497–1501.

19. Hansma, H. G., Sinsheimer, R. L., Groppe, J., Bruice, T. C., Elings, V., Gurley, G., Bezanilla, M., Mastrangelo, I. A., Hough, P. V., Hansma, P. K. (1993). Recent advances in atomic force microscopy of DNA. *Scanning*, **15**, 296–299.
20. Lyubchenko, Y. L., Shlyakhtenko, L. S. (1997). Visualization of supercoiled DNA with atomic force microscopy *in situ*. *Proc. Natl. Acad. Sci. U. S. A.*, **94**, 496–501.
21. Guthold, M., Bezanilla, M., Erie, D. A., Jenkins, B., Hansma, H. G., Bustamante, C. (1994). Following the assembly of RNA polymerase-DNA complexes in aqueous solutions with the scanning force microscope. *Proc. Natl. Acad. Sci. U. S. A.*, **91**, 12927–12931.
22. Kasas, S., Thomson, N. H., Smith, B. L., Hansma, H. G., Zhu, X., Guthold, M., Bustamante, C., Kool, E. T., Kashlev, M., Hansma, P. K. (1997). Escherichia coli RNA polymerase activity observed using atomic force microscopy. *Biochemistry*, **36**, 461–468.
23. Rivetti, C., Guthold, M., Bustamante, C. (1999). Wrapping of DNA around the E. coli RNA polymerase open promoter complex. *EMBO J.*, **18**, 4464–4475.
24. van Noort, S. J., van der Werf, K. O., Eker, A. P., Wyman, C., de Grooth, B. G., van Hulst, N. F., Greve, J. (1998). Direct visualization of dynamic protein–DNA interactions with a dedicated atomic force microscope. *Biophys. J.*, **74**, 2840–2849.
25. Moreno-Herrero, F., de Jager, M., Dekker, N. H., Kanaar, R., Wyman, C., Dekker, C. (2005). Mesoscale conformational changes in the DNA-repair complex Rad50/Mre11/Nbs1 upon binding DNA. *Nature*, **437**, 440–443.
26. Lyubchenko, Y. L., Shlyakhtenko, L. S. (2009). AFM for analysis of structure and dynamics of DNA and protein–DNA complexes. *Methods*, **47**, 206–213.
27. Shlyakhtenko, L. S., Lushnikov, A. Y., Lyubchenko, Y. L. (2009). Dynamics of nucleosomes revealed by time-lapse atomic force microscopy. *Biochemistry*, **48**, 7842–7848.
28. Bucceri, A., Kapitza, K., Thoma, F. (2006). Rapid accessibility of nucleosomal DNA in yeast on a second time scale. *EMBO J.*, **25**, 3123–3132.
29. Koopmans, W. J., Brehm, A., Logie, C., Schmidt, T., van Noort, J. (2007). Single-pair FRET microscopy reveals mononucleosome dynamics. *J. Fluoresc.*, **17**, 785–795.

30. Tims, H. S., Widom, J. (2007). Stopped-flow fluorescence resonance energy transfer for analysis of nucleosome dynamics. *Methods*, **41**, 296–303.

31. Li, G., Levitus, M., Bustamante, C., Widom, J. (2005). Rapid spontaneous accessibility of nucleosomal DNA. *Nat. Struct. Mol. Biol.*, **12**, 46–53.

32. Ando, T., Kodera, N., Naito, Y., Kinoshita, T., Furuta, K., Toyoshima, Y. Y. (2003). A high-speed atomic force microscope for studying biological macromolecules in action. *ChemPhysChem*, **4**, 1196–1202.

33. Ando, T., Kodera, N., Takai, E., Maruyama, D., Saito, K., Toda, A. (2001). A high-speed atomic force microscope for studying biological macromolecules. *Proc. Natl. Acad. Sci. U. S. A.*, **98**, 12468–12472.

34. Ando, T., Uchihashi, T., Kodera, N., Yamamoto, D., Miyagi, A., Taniguchi, M., Yamashita, H. (2008). High-speed AFM and nano-visualization of biomolecular processes. *Pflugers Arch.*, **456**, 211–225.

35. Ando, T., Uchihashi, T., Kodera, N., Yamamoto, D., Taniguchi, M., Miyagi, A., Yamashita, H. (2007). High-speed atomic force microscopy for observing dynamic biomolecular processes. *J. Mol. Recog.*, **20**, 448–458.

36. Crampton, N., Yokokawa, M., Dryden, D. T., Edwardson, J. M., Rao, D. N., Takeyasu, K., Yoshimura, S. H., Henderson, R. M. (2007). Fast-scan atomic force microscopy reveals that the type III restriction enzyme EcoP15I is capable of DNA translocation and looping. *Proc. Natil. Acad. Sci. U. S. A.*, **104**, 12755–12760.

37. Gilmore, J. L., Suzuki, Y., Tamulaitis, G., Siksnys, V., Takeyasu, K., Lyubchenko, Y. L. (2009). Single-molecule dynamics of the DNA-EcoRII protein complexes revealed with high-speed atomic force microscopy. *Biochemistry*, **48**, 10492–10498.

38. Suzuki, Y., Higuchi, Y., Hizume, K., Yokokawa, M., Yoshimura, S. H., Yoshikawa, K., Takeyasu, K. (2010). Molecular dynamics of DNA and nucleosomes in solution studied by fast-scanning atomic force microscopy. *Ultramicroscopy*, **110**, 682–688.

39. Lyubchenko, Y. L., Shlyakhtenko, L. S., Ando, T. (2011). Imaging of nucleic acids with atomic force microscopy. *Methods*, **54**, 274–283.

40. Miyagi, A., Ando, T., Lyubchenko, Y. L. (2011). Dynamics of nucleosomes assessed with time-lapse high-speed atomic force microscopy. *Biochemistry*, **50**, 7901–7908.

41. Suzuki, Y., Gilmore, J. L., Yoshimura, S. H., Henderson, R. M., Lyubchenko, Y. L., Takeyasu, K. (2011). Visual analysis of concerted cleavage by type

IIF restriction enzyme sfii in subsecond time region. *Biophys. J.*, **101**, 2992–2998.

42. Shlyakhtenko, L. S., Lushnikov, A. Y., Miyagi, A., Li, M., Harris, R. S., Lyubchenko, Y. L. (2012). Nanoscale structure and dynamics of ABOBEC3G complexes with single-stranded DNA. *Biochemistry*, **51**, 6432–6440.
43. Shlyakhtenko, L. S., Lushnikov, A. Y., Miyagi, A., Lyubchenko, Y. L. (2012). Specificity of binding of single-stranded DNA-binding protein to its target. *Biochemistry*, **51**, 1500–1509.
44. Hoyer, W., Cherny, D., Subramaniam, V., Jovin, T. M. (2004). Rapid self-assembly of alpha-synuclein observed by in situ atomic force microscopy. *J. Mol. Biol.*, **340**, 127–139.
45. Kowalewski, T., Holtzman, D. M. (1999). *In situ* atomic force microscopy study of Alzheimer's beta-amyloid peptide on different substrates: New insights into mechanism of beta-sheet formation. *Proc. Natil. Acad. Sci. U. S. A.*, **96**, 3688–3693.
46. Goldsbury, C., Green, J. (2005). Time-lapse atomic force microscopy in the characterization of amyloid-like fibril assembly and oligomeric intermediates. *Methods Mol. Biol.*, **299**, 103–128.
47. Goldsbury, C., Kistler, J., Aebi, U., Arvinte, T., Cooper, G. J. (1999). Watching amyloid fibrils grow by time-lapse atomic force microscopy. *J. Mol. Biol.*, **285**, 33–39.
48. DePace, A. H., Weissman, J. S. (2002). Origins and kinetic consequences of diversity in Sup35 yeast prion fibers. *Nat. Struct. Biol.*, **9**, 389–396.
49. Kellermayer, M. S., Karsai, A., Benke, M., Soos, K., Penke, B. (2008). Stepwise dynamics of epitaxially growing single amyloid fibrils. *Proc. Natil. Acad. Sci. U. S. A.*, **105**, 141–144.
50. Eibl, R. H., Moy, V. T. (2005). Atomic force microscopy measurements of protein-ligand interactions on living cells. *Methods Mol. Biol.*, **305**, 439–450.
51. Lee, G. U., Chrisey, L. A., Colton, R. J. (1994). Direct measurement of the forces between complementary strands of DNA. *Science*, **266**, 771–773.
52. Florin, E. L., Moy, V. T., Gaub, H. E. (1994). Adhesion forces between individual ligand-receptor pairs. *Science*, **264**, 415–417.
53. Liu, F., Arce, F. T., Ramachandran, S., Lal, R. (2006). Nanomechanics of hemichannel conformations: Connexin flexibility underlying channel opening and closing. *J. Biol. Chem.*, **281**, 23207–23217.

54. Rico, F., Chu, C., Abdulreda, M. H., Qin, Y., Moy, V. T. (2010). Temperature modulation of integrin-mediated cell adhesion. *Biophys. J.*, **99**, 1387–1396.

55. Lyubchenko, Y. L., Sherman, S., Shlyakhtenko, L. S., Uversky, V. N. (2006). Nanoimaging for protein misfolding and related diseases. *J. Cell. Biochem.*, **99**, 53–70.

56. Chiti, F., Dobson, C. M. (2009). Amyloid formation by globular proteins under native conditions. *Nat. Chem. Biol.*, **5**, 15–22.

57. Deniz, A. A., Mukhopadhyay, S., Lemke, E. A. (2008). Single-molecule biophysics: At the interface of biology, physics and chemistry. *J. R. Soc. Interface*, **5**, 15–45.

58. Wang, H., Duennwald, M. L., Roberts, B. E., Rozeboom, L. M., Zhang, Y. L., Steele, A. D., Krishnan, R., Su, L. J., Griffin, D., Mukhopadhyay, S., Hennessy, E. J., Weigele, P., Blanchard, B. J., King, J., Deniz, A. A., Buchwald, S. L., Ingram, V. M., Lindquist, S., Shorter, J. (2008). Direct and selective elimination of specific prions and amyloids by 4,5-dianilinophthalimide and analogs. *Proc. Natil. Acad. Sci. U. S. A.*, **105**, 7159–7164.

59. Ferreon, A. C., Gambin, Y., Lemke, E. A., Deniz, A. A. (2009). Interplay of alpha-synuclein binding and conformational switching probed by single-molecule fluorescence. *Proc. Natil. Acad. Sci. U. S. A.*, **106**, 5645–5650.

60. Kransnoslobodtsev, A. V., Shlyakhtenko, L. S., Ukraintsev, E., Zaikova, T. O., Keana, J. F., Lyubchenko, Y. L. (2005). Nanomedicine and protein misfolding diseases. *Nanomedicine*, **1**, 300–305.

61. Brucale, M., Sandal, M., Di Maio, S., Rampioni, A., Tessari, I., Tosatto, L., Bisaglia, M., Bubacco, L., Samori, B. (2009). Pathogenic mutations shift the equilibria of alpha-synuclein single molecules towards structured conformers. *ChemBioChem*, **10**, 176–183.

62. Sandal, M., Valle, F., Tessari, I., Mammi, S., Bergantino, E., Musiani, F., Brucale, M., Bubacco, L., Samori, B. (2008). Conformational equilibria in monomeric alpha-synuclein at the single-molecule level. *PLoS Biol.*, **6**, e6.

63. Yu, J., Lyubchenko, Y. L. (2009). Early stages for Parkinson's development: Alpha-synuclein misfolding and aggregation. *J. Neuroimmune Pharmacol.*, **4**, 10–16.

64. Yu, J., Malkova, S., Lyubchenko, Y. L. (2008). alpha-Synuclein misfolding: Single molecule AFM force spectroscopy study. *J. Mol. Biol.*, **384**, 992–1001.

65. Lyubchenko, Y., Kim B.-H., Krasnoslobodtsev, A., Yu, J. (2010). Nanoimaging for protein misfolding diseases. *Wiley Interdisciplinary Rev. Nanomed. Nanobiotechnol.*, **2**, 5154–5162.

66. Kim, B. H., Palermo, N. Y., Lovas, S., Zaikova, T., Keana, J. F., Lyubchenko, Y. L. (2011). Single-molecule atomic force microscopy force spectroscopy study of abeta-40 interactions. *Biochemistry*, **50**, 526–543.

67. Krasnoslobodtsev, A. V., Shlyakhtenko, L. S., Lyubchenko, Y. L. (2007). Probing Interactions within the synaptic DNA-SfiI complex by AFM force spectroscopy. *J. Mol. Biol.*, **365**, 1407–1416.

68. Krasnoslobodtsev, A. V., Portillo, A. M., Deckert-Gaudig, T., Deckert, V., Lyubchenko, Y. L. (2010). Nanoimaging for prion related diseases. *Prion*, **4**, 265–274.

69. Evans, E. (2001). Probing the relation between force-lifetime- and chemistry in single molecular bonds. *Ann. Rev. Biophys. Biomol. Struct.*, **30**, 105–128.

70. Portillo, A. M., Krasnoslobodtsev, A. V., Lyubchenko, Y. L. (2012). Effect of electrostatics on aggregation of prion protein Sup35 peptide. *J. Phys. Condensed Matter.*, **24**, 164205.

71. Yu, J., Warnke, J., Lyubchenko, Y. L. (2011). Nanoprobing of alpha-synuclein misfolding and aggregation with atomic force microscopy. *Nanomed. Nanotechnol. Biol. Med.*, **7**, 146–152.

72. Urbanc, B., Betnel, M., Cruz, L., Bitan, G., Teplow, D. B. (2010). Elucidation of amyloid beta-protein oligomerization mechanisms: Discrete molecular dynamics study. *J. Am. Chem. Soc.*, **132**, 4266–4280.

73. Krasnoslobodtsev, A. V., Peng, J., Asiago, J. M., Hindupur, J., Rochet, J. C., Lyubchenko, Y. L. (2012). Effect of spermidine on misfolding and interactions of alpha-synuclein. *PloS One*, **7**, e38099.

74. Firtel, M., Henderson, G., Sokolov, I. (2004). Nanosurgery: Observation of peptidoglycan strands in Lactobacillus helveticus cell walls. *Ultramicroscopy*, **101**, 105–109.

75. Obataya, I., Nakamura, C., Han, S., Nakamura, N., Miyake, J. (2005). Nanoscale operation of a living cell using an atomic force microscope with a nanoneedle. *Nano Lett.*, **5**, 27–30.

76. Beard, J. D., Burbridge, D. J., Moskalenko, A. V., Dudko, O., Yarova, P. L., Smirnov, S. V., Gordeev, S. N. (2009). An atomic force microscope nanoscalpel for nanolithography and biological applications. *Nanotechnology*, **20**, 445302.

77. Shlyakhtenko, L. S., Yuan, B., Emadi, S., Lyubchenko, Y. L., Sierks, M. R. (2007). Single-molecule selection and recovery of structure-specific antibodies using atomic force microscopy. *Nanomedicine*, **3**, 192–197.

Chapter 22

Image-Based High-Content Analysis, Stem Cells and Nanomedicines: A Novel Strategy for Drug Discovery

Leonardo J. Solmesky, PhD, Yonatan Adalist, MSc, and Miguel Weil, PhD

Laboratory for Personalized Medicine and Neurodegenerative Diseases, Department of Cell Research and Immunology, The George S. Wise Faculty of Life Sciences, Tel Aviv University, Ramat Aviv, Israel

Keywords: high content analysis, high content screening, drug discovery, stem cells, nanomedicines, personalized medicine, cell imaging, drug efficacy, drug toxicity, nanocarriers, pharmacological activity

22.1 Introduction

Image-based high content screening (HCS) is rapidly gaining recognition as the future of drug discovery. The ability to screen vast amounts of possible therapeutic agents in a relatively short time, while obtaining various levels of information about each target cell's biology, has an immense potential. Moreover, since

Handbook of Clinical Nanomedicine: Nanoparticles, Imaging, Therapy, and Clinical Applications
Edited by Raj Bawa, Gerald F. Audette, and Israel Rubinstein

ISBN 978-981-4669-20-7 (Hardcover), 978-981-4669-21-4 (eBook)
www.panstanford.com

the screening is done using cells, it is possible to look for a broader phenotype than, for example, when focusing on the activity of an isolated enzyme. This allows the search for new drugs for diseases with unknown molecular hallmarks or with multifactorial causes. The recently achieved advances in human stem cell research have opened the way to a new horizon in medical technology. Our ability to manipulate these cells will allow us to change the focus of drug development from generic to personal. Consequently, it will be possible to characterize the effect of a repertoire of available therapies for a certain disease using the cells obtained from a certain individual. This would offer an unparalleled achievement, and its contribution to the success rate of treatments could prove truly astronomical. Similarly to the way high-content screening is revolutionizing the process of drug discovery, the application of these methods using human stem cells together with nanotechnology for improving targeted drug delivery, is expected to produce the next major breakthrough for personalized medicine in the pharmaceutical industry.

Drug discovery and development is an extremely dynamic process and the challenges it involves are constantly changing. As in most commercial industries, there are numerous external aspects that affect the pharmaceutical industry. Thus, the process of constructing a successful research and development strategy that is cost-effective includes components such as focus on diseases with the highest potential return on investment, increased R&D productivity, and the achievement of unquestionable benefit versus risk.

During recent years, the pharmaceutical industry has been struggling with dwindling R&D productivity. A few of the causes of this lower productivity are the prolonged R&D cycles, immensely prolonged approval times, and staggering rates of drug attrition. For example, over 90% of the drugs entered into clinical trials fail to gain FDA approval [1]. Whereas due to the regulatory authorities it would appear difficult to speed up the approval times, the long R&D cycles and high attrition rates are factors that could be addressed by the pharmaceutical companies through using novel or improved technologies for drug discovery. Technological improvements that would allow a more cost-efficient R&D process would also open the way for development of drugs that would treat those diseases that, under the current

conditions, may not receive the funding and attention necessary for significant progress to be made. It is quite clear that by improving the screening technologies used in this industry, it will be possible to revolutionize an industry that has been falling short of fulfilling its true potential for quite some time.

22.2 Image-Based High-Content Screening

Image-based HCS is rapidly gaining recognition as the future of drug discovery. The ability to screen vast amounts of possible therapeutic agents in a relatively short time, while obtaining various levels of information about the biology of each cell under the influence of each tested compound, seems to offer immense potential [2].

In addition, the high content of this technology facilitates increased robustness of the employed assays. In screening, the most commonly used parameter for monitoring assay quality is the Z′ factor, which is based on one selected readout. However, biological assays are able to monitor multiple readouts when using image-based HCS. It has been suggested that an extension of the Z′ factor, which integrates multiple readouts for assay quality assessment, will enable increased robustness of the assay [3].

Furthermore, since the screening is performed with cells rather than using a specific target, such as a protein, it allows the filtering of those compounds that are most likely to pass the pharmacokinetic tests during the process of drug testing (i.e., only compounds that have suitable solubility, permeability and stability for the target cells will be able to produce a hit in the screening). This technology thereby optimizes the process of drug discovery, allowing the discarding of those molecules that, while possibly optimal for effective influence of the protein involved in the disease, would not be suitable for therapy in a cellular context due to pharmacokinetic barriers [4].

Moreover, screening employing cells makes it possible to look for a broader phenotype in the process (i.e., rescue from induced apoptosis by a compound) than, for example, when focusing on the activity of an isolated enzyme; thus, it allows the process of drug discovery to be applied to diseases with unknown molecular

hallmarks or multifactorial causes [5]. Such diseases have until recently been very far from being curable. Now, however, image-based HCS brings hope for a change in this situation.

The introduction of advances in microscopy, like *z*-autofocus and *x*–*y* axes sample positioning has allowed the use of image-based analysis for high-throughput screenings. Until the introduction of such advances, these screenings were generally carried out by end-point reactions, showing only a global outcome from any well (i.e., change in fluorescence intensity). The introduction of these new features has allowed the automation of microscopy and its incorporation into the field of high-throughput screening [6].

In addition, developments in liquid handling automation now enable the preparation of samples in a high-throughput approach, allowing easy screening of collections of thousands of compounds [7]. Furthermore, the software tools for analyzing the output of the screening have been further developed to optimize object segmentation [8] in the images and to allow the extraction of information at all the cellular and intracellular levels [9]. Moreover, many of the applications for biological analysis are even already preset in the software of the HCS systems, in increasingly friendly program interfaces for the operator. Some of these typically used biological software applications are listed in Table 22.1.

Table 22.1 Typical applications for biological analysis using image based HCS technology

Some pre-set biological applications in HCS systems
Cell count
Nuclear size
Cell size
Cell cycle
Cell perimeter
Neurite analysis (number, length, branching)
Protein expression or reporter expression (intensity, localization)
Organelles (number, size, morphology, distance to nuclei, etc.)
Texture

The possibility to obtain an almost unlimited quantity of biological parameters from a large number of cell images taken from multi-well plates poses a challenge for informatics and data management, which needs to be addressed by every HCS core facility. Some of these use their own homemade programs for solving all their customary needs, while others use commercially available software able to deal with the chemistry of the compounds, hit identification, library management, and visualization of the results [10, 11].

Table 22.2 Current commercially available instruments for image based HCS and their optics

Company	HCS system	Optics	Website
Amnis	ImageStream	Wide field	lwww.amnis.com
BD biosciences	BD pathway 855	Wide field/ confocal	www.bdbiosciences.com
BD biosciences	BD pathway 435	Wide field/ confocal	www.bdbiosciences.com
GE healthcare	IN cell analyzer 2000	Wide field	www.biacore.com
Intelligent Imaging Innovations	3I marianas	Wide field	www.intelligentimaging.com
Leica microsystems	TCS SP5	Confocal	www.leicamicrosystems.com
Molecular devices	ImageXpress ULTRA	Confocal	www.moleculardevices.com
Molecular devices	ImageXpress MICRO	Wide field	www.moleculardevices. com
Olympus	Scan^{R}	Wide field	www.olympus.com
Perkin elmer	Opera	Confocal	www.perkinelmer.com
Perkin elmer	Operetta	Wide field/ confocal	www.perkinelmer.com
Thermo scientific	Cellomics ArrayScan VTI	Wide field/ confocal	www.cellomics.com

Since the field first began to evolve and continues to do so, several companies have inundated the market with instruments

suitable for HCS analysis. Table 22.2 lists the most representative instruments currently available for image-based HCS and their type of optics. Their characteristics differ regarding light source, the feasibility of carrying out kinetic assays, autofocus technology, resolution, dynamic range of the camera, and software for analysis, among several other features. Moreover, almost every brand offers its own proprietary algorithms for cell analysis and there are even companies that also offer kits for developing the assays [4].

High-throughput screening technologies are widely used in the early stages of drug discovery in order to rapidly evaluate the properties of thousands of compounds. In most cases, pre-existing libraries of compounds are used, although in some cases customized libraries are employed [12]. In addition, before large naive libraries are tested, many companies will use a library that consists of compounds that have already been approved as drugs. If a compound that has already been FDA approved shows potential for a particular target, R&D departments will save enormous amounts of both time and money [13]. Altogether, high-throughput screening technologies are paving the way to the development of novel strategies that will enable the discovery of drugs at affordable commercial risks for as yet incurable and rare diseases.

22.3 Stem Cells Used for Lead Discovery

Unmet medical needs are essentially the stimulus behind the development of new therapies. Drug discovery is driven by the need to add medical value while concomitantly limiting the costs for the pharmaceutical industry. Understanding and treatment of the pathology, rather than symptomatic relief, is the cardinal factor in drug discovery. This approach necessitates model systems that will emulate the pathological conditions as faithfully as possible. An excellent way to achieve this is to rely on human-derived cells rather than animal-derived cell lines that express specific proteins to mimic a human disease or condition. The use of animal-derived cells or tissues to develop selective drugs is problematic, since their success in treatment of animals or animal models does not always translate into efficacy in humans. There

are vast differences in the biological background between the animal model and humans. These differences are believed to be major factors in the difficulty of matching treatment success in these models to the actual beneficial use of such drugs for human clinical trials [14]. Another approach taken is to use immortalized or cancerous human cells to obtain unlimited number of cells for drug-testing trials compared with primary cells directly isolated from human tissue. These are in many cases better models than the animal equivalent, but they still do not necessarily provide an accurate indication of the effects of compounds on normal human cells. This is due to the fact that any immortalized or cancerous cell could have vast differences in its gene expression pattern and, in turn, in its biochemistry, when compared with its non-immortalized counterpart. Recent advances in stem cell (SC) technology have the potential to allow production of a virtually limitless supply of normal human cells that can be differentiated into any specific cell type, except those cell types that make up the extra-embryonic tissues such as the placenta [15]. If this potential is realized, we may witness a leap in our ability to screen for new cell type specific drugs.

SC can differentiate into clinically relevant cell types with uniform physiological characteristics that allow improved target validation decisions [16]. Additionally, SC may allow inclusion of previously unavailable cell types to be used to screen the libraries of therapeutic candidates [17].

These reasons make the use of SC for image-based high-content screening a very valuable option for novel drug discovery.

22.3.1 Stem Cells

During the first stages of life for multi-cellular organisms, a fertilized oocyte is the progenitor for an entire organism. This single cell creates all the different tissues and cell types with all their various characteristics and functions needed to perform as a multicellular organism. During embryogenesis, cells both proliferate and differentiate, thus enabling the growth of tissues and organs.

In an adult organism, most tissues and organs maintain a homeostasis wherein cells continually die and are continually replenished. The extent of this ability varies considerably among

organisms and among different types of tissues. Some flatworms are capable of regenerating most of their bodies and even use this as a method of reproduction by splitting into two parts, with each half subsequently repairing itself into a whole [18–21]. While mammals in general and humans specifically do have regenerative capabilities, they do not enjoy anything similar to this spectacular level of plasticity. The liver, epidermis, small intestine and hematopoietic system are a few examples of relatively replenishable cells in mammals [22–25]. We owe this fantastic and necessary capability to SC.

SC are capable of undergoing both self-renewal and differentiation into specific specialized cell types. Embryonic stem cells (ESC) are pluripotent; hence, they bear the potential to produce all the cell types of an embryo [26], while the slightly more specialized multipotent cells that reside in the tissues and organs of multi-cellular organisms are much more restricted in their "choice" of cellular fate. Recently, it has been shown that some adult stem cells, under certain culture conditions, are able to differentiate into other cell types unusual to their tissue of origin [27].

22.3.2 Human Embryonic Stem Cells

Exploiting the great potential that lies in human ESC (hESC) would be an immense advantage in our attempt to improve the drug discovery process.

The ESC research started with seminal studies in murine embryos obtained by *in vitro* fertilization in the 1970s and 1980s [26, 28]. This conduced to the current ability to generate and maintain human ESC in culture by the late 1990s [29]. Since hESCs are the progenitors of all the cells in the human body, we can deduce that they have the capability, under the correct conditions, to be "guided" to form the cells needed for any potential drug screening.

This unlimited potential is in fact both a blessing and a curse for our purposes. Clearly it is a blessing in the sense that ESCs can eventually be used to differentiate into virtually any cell type that, in turn, can be employed as a screening tool for almost any disease. As a result of their pluripotency, however, it is also an immensely complex task to direct such cells homogenously to a

specific desired fate [30]. Difficult as this may be, in recent years great leaps have, nonetheless, been made in this area and more and more protocols are being developed [31–34]. Other problems that arise when considering wide-scale use of hESCs are the ethical concerns of some financing and federal bodies in funding research using these types of cells [35]. However, the way in which hESC are currently being obtained is slowly producing a gain in the number of supporters, or at least is allowing the possibility to obtain these cells from *in vitro* fertilized embryos with serious genetic diseases, since it is based on the use of embryos discarded following pre-implantation genetic diagnosis (PGD) procedures. In such procedures, the embryos selected for research (at the early blastocyst stage) were found positive for a genetic disorder and would never be implanted into the mother's uterus [36, 37]. These offer good platform tools by which to study basic cellular and molecular mechanisms of inheritable diseases such as Huntington's disease [38], Fragile X syndrome [39], cystic fibrosis, and numerous other diseases [38, 40]. Obviously, these hESC lines will be of great importance for drug-screening purposes for such incurable diseases.

These difficulties aside, there is a general consensus that given the time and funding to develop the proper protocols, hESCs will constitute the basis for countless innovations on a long list of various medical fields. Drug discovery is one of the top issues on that list.

22.3.3 Adult Mesenchymal Stem Cells

Any adult tissue that harbors regenerative or self-repairing capabilities on some level is highly likely to contain stem cells that, despite their slightly more differentiated state, retain the aptitude to reproduce the variety of cells that form that tissue.

Mesenchymal stem cells (MSCs) are one of the several types of adult stem cells. This specific type of adult stem cell has received great attention due to its potential in regenerative medicine [41].

In the early 1970s, the first adult MSCs were isolated and were shown to retain the capability to create bone and reproduce an hematopoietic microenvironment [42]. These cells have shown the capability to differentiate into osteoblasts, chondrocytes,

adipocytes, myoblasts, and other mesenchymal cell types [43–46] and thus are prime candidates as screening tools for a variety of conditions that involve such cell types. A unique advantage of hMSC that makes them highly useful for HCS methodologies resides in the fact that they are able to survive for prolonged periods of time under serum-free culture conditions without altering their stem cell properties described above. Properties like the pattern of surface markers and the ability to differentiate to either osteoblasts or adipocytes are retained under these conditions [47].

The serum-free conditions allow direct identification of the biological effects of compounds on these cells with out possible serum interference [48]. This fact will certainly present hMSC from bone marrow as a valuable platform for drug screenings and personalized medicine.

22.3.4 Induced Pluriputent Stem Cells

Another prospect by which to circumvent the problems embodied in the use of hESCs is the use of a new and extremely promising technology that is capable of returning somatic cells to a nearly embryonic state of pluripotency.

Induced pluripotent stem cells (iPSC) are derived from somatic cells and have the ability to differentiate to almost every type of tissue (like ESC) by the co-overexpression of specific transcription factors (Oct3/4, Sox2, Klf4, and c-Myc) using retroviral vectors [49]. Researchers have found that iPSC share similar characteristics to those of ES cells, such as cell morphology, self-renewal, surface marker antigens, pattern of gene expression, telomerase activity, and the epigenetic status of pluripotent cell-specific genes [50].

Clearly, the principal advantage of iPSC is that they can be derived from a patient with a certain disease, constituting a platform from which to produce any required cell type in order to study the etiology of the disease [51]. Most interestingly, this approach can be used as a model of the disease that has the identical genetic traits of the individual that donated the tissue sample. Today iPSC can also be generated from readily available tissues such as blood [52], skin, or even hair [53]. This advantage makes iPSC ideal candidates to produce neurons and glia from living

individuals suffering from neurodegenerative diseases, constituting a remarkable platform for translational research and personalized medicine [54].

22.4 Personalized Medicine Platforms

Personalized medicine refers to the tailoring of strategies to detect, treat, and prevent disease based on an individual's molecular characteristics [55].

Over the past century, medical care has been based on epidemiological studies of large cohorts. However, this type of medicine does not consider the genetic variability of individuals within a population. Consequently, failure in the treatment or unwanted side effects may arise in certain individuals. The incorporation of pharmacogenomics into clinical drug development offers the opportunity for pharmaceutical companies to evaluate drugs with a better understanding of the effects that specific genetic variants will have on drug response [56]. The goal of personalized medicine is to provide consideration to such individual differences in order to optimize the treatment.

Traditionally, this approach has been limited to the consideration of a patient's family history, environment, behaviors, and clinical parameters (such as cholesterol levels and blood pressure) for tailoring individual care [57, 58].

Several advances in a number of molecular profiling technologies, such as proteomics, metabolomics, or genomics, now allow the personalization of the treatment of a given individual. In addition, HCS of drugs using the cells derived from an individual as target may allow for a greater degree of personalized medicine than is currently available.

The advances achieved with hMSCs and iPSCs have opened the way to a new horizon in medical technology. These stem cells, and more specifically our ability to manipulate them, will allow us to change the focus of drug development from generic to personal. Thus, it will be possible to characterize the effect of a repertoire of therapies available for a certain disease in the cells obtained from a certain individual. This can be an unparalleled achievement and its contribution to the success rate of treatments may be truly astronomical. For example, effective treatment for

cancer is far from a certainty. Large numbers of chemo-therapeutic drugs are available, but many patients are unresponsive to a large portion of the various treatments. If the stem cell technique is used, it may be possible to improve the effectivity of the treatments by individual selection of treatment choices using the autologous stem cell based approach.

22.5 Stem Cells as Tools for Improvement of Safety and Toxicology

While lack of efficacy is the main cause of failure in clinical testing, toxicity accounts for approximately 30% of the attrition rate [59]. Traditional safety studies in animals are resource- and time consuming. As a consequence, in order to predict adverse clinical effects at a lower cost, cell-based assays have been introduced at earlier stages of the drug discovery process [60]. These assays allow monitoring of the known mechanisms of drug toxicity, such as apoptosis, oxidative stress, mitochondrial dysfunction, micronuclei, phospholipidosis [61], and steatosis [62].

Micronuclei are small, stainable bodies outside the nucleus that form when a chromosome or its fragment is not incorporated into one of the daughter nuclei during cell division, constituting a hallmark of genetic toxicity. Therefore, it is widely used as an assay for risk assessment of the cancer-inducing potential of a new drug, which is required by regulatory agencies for drug approval. The image-based high-content analysis of micronuclei has been shown to have good correlation with *in vivo* micronucleus assays [63].

Since hepatotoxicity is one of the major reasons for drug non-approval, the development of an assay predictive of drug-induced liver toxicity has been considered imperative. Individual conventional assays in animals have not been reliable in predicting human hepatotoxicity. However, when cellular assays are used in combination, as it is possible using the HCS approach, the level of hepatotoxicity prediction is improved for these assays (e.g., mitochondrial activity, glutathione and cell proliferation). Furthermore, the predictive value can be dramatically increased in HCS assays that use human hepatocyte cell lines. Thus,

the assessment of multiple pre-lethal hepatotoxic effects of a potential drug on individual live cells, including mitochondrial toxicity, oxidative stress, deregulation of calcium homeostasis, phospholipidosis, apoptosis, and antiproliferative effects, can be well predicted [64].

Despite these achievements, considerable challenges remain with regard to the design of the toxicity assays and the cell source used. The low proliferation rate of primary human hepatocytes makes them less suitable for cytotoxic assessment. Furthermore, primary human hepatocytes are phenotypically unstable under current cell culture conditions, and de-differentiate rapidly. Therefore, stem cells could be used for deriving hepatocyte cells in order to provide the cell numbers required for toxicity screenings.

22.6 Advances in Nanomedicine for Drug Discovery Using HCS

Nanotechnologies employ materials that have a functional organization in at least one dimension on the nanometer scale [65]. Many of these engineered polymeric devices are capable of interacting with biological systems on a molecular level [66].

Great potential for their use arises from the fact that nanotechnological applications exhibit bulk macro-scale chemical properties that are unique to the engineered material, while not necessarily possessed by the molecules if not arranged in a specific fashion [67, 68]. By utilizing this trait, it is possible to develop entities capable of multiple specific functions either concomitantly or even in a predefined order [69]. A prevalent example of this lies in the emerging field of drug targeting.

Drug targeting is defined as selective drug delivery to specific physiological sites, organs, tissues, or cells where a drug's pharmacological activities are required. In principle, a drug distributes uniformly throughout the whole body when it is injected into the bloodstream, and when it arrives at sites other than the therapeutic sites, this may cause toxic side effects. By increasing delivery to the targeted therapeutic sites, and reducing delivery to the untargeted sites, an improved therapeutic index

can be obtained with enhanced and reduced drug action at the desired and the undesired sites, respectively. The essence of this concept lies in a separation of functions for the selective pharmacological action: The carrier plays a role in delivery to the designated sites; while the drug plays a role in the pharmacological activity [70, 71].

There are multiple carriers used as drug delivery systems (e.g., liposomes, micelles, microspheres, nanoparticles, nanogels, and bionanocapsules) [72–76]. These are generally colloidal molecules that vary in size from 1 to 1000 nm, which are utilized to direct drugs to a specific tissue or organ due to their possessing a molecular structure to which therapeutic drugs can be attached, entrapped or adsorbed [72, 77, 78,78a].

While nanomedicines are rising in popularity, the area of neurodegenerative diseases is seizing center stage. This is a result of nanomedicine's ability to improve delivery of drugs to the central nervous system (CNS) [79–81]. One of the main difficulties in administering drugs to the CNS is that of infiltrating the blood-brain barrier (BBB). The BBB is essentially a physical barrier that regulates the passage of substances between the bloodstream and the brain. It does this by inhibiting unsupervised molecule entry to the CNS via both paracellular and via transcellular pathways [82].

The endothelial membrane has a large surface area that creates an effective transcellular passive diffusion pathway for small gaseous molecules and lipid-soluble agents. On the other hand, hydrophilic molecules are generally not let through. Owing to extremely tight junctions between the cells that constitute the endothelium, passive paracellular diffusion of soluble molecules through the BBB is also inhibited. Additionally, there are specific transporters that allow the entry of many nutrients, such as amino acids, nucleosides, and glucose [83–85].

Nano-carriers can facilitate passage beyond the BBB in various ways. Some nanoparticles have a local toxic effect at the brain vasculature, which leads to a partial permeability of the endothelial cells [86]. Some nanoparticles can open the tight junctions between endothelial cells and allow the drug to penetrate either in free form or together with the carrier [87]. There are also

nanoparticles that mediate transcytosis through the endothelial cell layer [88].

Not only are there high numbers of possible carriers, but each carrier type can usually be constructed by a variety of molecules as long as these molecules have similar characteristics. For example, a liposome can be constructed from a huge variety of naturally occurring or modified phospholipids, or even a combination of different phospholipids in a single liposome. To add an additional level of complexity, each carrier is capable of transporting a huge variety of therapeutic agents.

Because of the immense combinatory options in this promising field, we suggest a novel approach by which to hasten the much-needed progress in this area. In a similar fashion to how high-throughput and high-content screening have revolutionized the way in which we search for standard drugs, the application of these methods using human stem cells to the developing field of nanomedicines has the potential to lead to the next big breakthrough in the pharmaceutical industry.

22.7 Conclusions

The common denominator in most *in vitro* drug discovery applications is the biological component whose functionalities and responses to a battery of compounds are being assayed. There is a substantial need for physiological cell models and, in particular, for efficacy and safety studies. The properties of stem cells that make them so attractive for use for these studies too lie in their ability to produce a variety of specific cell types that can be used for cell-specific assays.

Concomitantly, the introduction of nanomolecules may conduce to improving therapies by allowing, for example, the delivery of drugs directly to the desired target. The combination of both technologies, image-based HCS and nanomolecules, using stem cells as target for the study, is expected to contribute to improve current therapy efficacies, finding new drugs for currently incurable diseases and also to the designing of personalized medicine platforms.

Disclosures and Conflict of Interest

The authors declare that they have no conflict of interest and have no affiliations or financial involvement with any organization or entity discussed in this chapter. This includes employment, consultancies, honoraria, grants, stock ownership or options, expert testimony, patents (received or pending) or royalties. No writing assistance was utilized in the production of this chapter and the authors have received no payment for its preparation. The findings and conclusions here reflect the current views of the authors. They should not be attributed, in whole or in part, to the organizations with which they are affiliated, nor should they be considered as expressing an opinion with regard to the merits of any particular company or product discussed herein. Nothing contained herein is to be considered as the rendering of legal advice. This is a revised version of the author's chapter that originally appeared in *Handbook of Harnessing Biomaterials in Nanomedicine: Preparation, Toxicity, and Applications* (Dan Peer, editor), 2012, Pan Stanford Publishing Pte. Ltd., Singapore.

Corresponding Author

Prof. Miguel Weil
Cell Screening Facility for Personalized Medicine
Laboratory for Neurodegenerative Diseases and Personalized Medicine, The George S. Wise Faculty of Life Sciences
Tel Aviv University, 69978 Ramat Aviv, Tel Aviv, Israel
Email: miguelw@tauex.tau.ac.il

About the Authors

Leonardo J. Solmesky is the manager of the Cell Screening Facility for Personalized Medicine (CSFPM) at Tel Aviv University, Israel. This facility has performed high content screening, specially for drug discovery for orphan diseases and also for nanoparticles characterization. He holds a PhD and a MSc from Tel Aviv University. In addition, he previously graduated as pharmacist and biochemist from Universidad de Buenos Aires, Argentina. Dr. Solmesky is the author of several publications.

Yonatan Adalist currently works as Director of Business Development in the Freemind group. This group is a consulting firm specializing in assisting life sciences organizations. Mr. Adalist holds a MSc from Tel Aviv University.

Miguel Weil is the head of the CSFPM and group leader at the Laboratory of Neurodegenerative Diseases and Personalized Medicine. Prof. Weil is the author of several publications in the field of developmental cell biology, apoptosis and neurodegenerative diseases. Recently with the creation of the CSFPM, he is directing several cell-based drug screening projects on rare neurodegenerative diseases.

References

1. Kola, I., Landis, J. (2004). Can the pharmaceutical industry reduce attrition rates? *Nat. Rev. Drug Discov.,* **3**(8), 711–715.
2. Zock, J. (2009). Applications of high content screening in life science research. *Comb. Chem. High. Throughput Screen.,* **12**(9), 870–876.
3. Kiimmel, A., Gubler, H., Gehin, P., Beibel, M., Gabriel, D., Parker, C. (2010). Integration of multiple readouts into the Z′ factor for assay quality assessment. *J. Biomol. Screen.,* **15**(1), 95–101.
4. Zanella, F., Lorens, J., Link, W. (2010). High content screening: Seeing is believing. *Trends Biotechnol.,* **28**(5), 237–245.
5. Tarnok, A., Pierzchalski, A., Valet, G. (2010). Potential of a cytomics top-down strategy for drug discovery. *Curr. Med. Chem.,* **17**(16), 1719–1729.
6. Conrad, C., Gerlich, D. (2010). Automated microscopy for high-content RNAi screening. *J. Cell Biol.,* **188**(4), 453–461.
7. Pepperkok, R., Ellenberg, J. (2006). High-throughput fluorescence microscopy for systems biology. *Nat. Rev. Mol. Cell. Biol.*, **7**(9), 690–696.
8. Fenistein, D., Lenseigne, B., Christophe, T., Brodin, P., Genovesio, A. (2008). A fast, fully automated cell segmentation algorithm for high-throughput and high-content screening. *Cytometry A.,* **73**(10), 958–964.

9. Rabal, O., Link, W., Serelde, B., Bischoff, J., Oyarzabal, J. (2010). An integrated one-step system to extract, analyze and annotate all relevant information from image-based cell screening of chemical libraries. *Mol. Biosyst.,* **6**(4), 711–720.
10. Jackson, D., Lenard, M., Zelensky, A., Shaikh, M., Scharpf, J., Shaginaw, R., et al. (2010). HCS road: An enterprise system for integrated HCS data management and analysis. *J. Biomol. Screen.,* **15**(7), 882–891.
11. Kozak, K., Bakos, G., Hoff, A., Bennett, E., Dunican, D., Davies, A., et al. (2010). Workflow-based software environment for large-scale biological experiments. *J. Biomol. Screen.,* **15**(7), 892–899.
12. Korn, K., Krausz, E. (2007). Cell-based high-content screening of small-molecule libraries. *Curr. Opin. Chem. Biol.,* **11**(5), 503–510.
13. Ou, H., Cunningham, L., Francis, S., Brandon, C., Simon, J., Raible, D., et al. (2009). Identification of FDA-approved drugs and bioactives that protect hair cells in the zebrafish (Danio rerio) lateral line and mouse (Mus musculus) utricle. *J. Assoc. Res. Otolaryngol.*, **10**(2), 191–203.
14. Wendler, A., Wehling, M. (2010). The translatability of animal models for clinical development: Biomarkers and disease models. *Curr. Opin. Pharmacol.,* **10**(5), 601–606.
15. Li, W., Ding, S. (2010). Small molecules that modulate embryonic stem cell fate and somatic cell reprogramming. *Trends Pharmacol. Set.*, **31**(1), 36–45.
16. McNeish, J., Roach, M., Hambor, J., Mather, R., Weibley, L., Lazzaro, J., et al. (2010). High-throughput screening in embryonic stem cell-derived neurons identifies potentiators of alpha-amino-3-hydroxyl-5-methyl-4-isoxazolepropionate-type glutamate receptors. *J. Biol. Chem.*, **285**(22), 17209–17217.
17. Zweigerdt, R. (2009). Large scale production of stem cells and their derivatives. *Adv. Biochem. Eng. Biotechnol.,* **114**, 201–235.
18. Salo, E., Baguna, J. (2002). Regeneration in planarians and other worms: New findings, new tools, and new perspectives. *J. Exp. Zool.*, **292**(6), 528–539.
19. Reddien, P., Sánchez Alvarado, A. (2004). Fundamentals of planarian regeneration. *Annu. Rev. Cell. Dev. Biol.*, **20**, 725–757.
20. Saló, E. (2006). The power of regeneration and the stem-cell kingdom: Freshwater planarians (Platyhelminthes). *Bioessays.*, **28**(5), 546–559.
21. Sánchez Alvarado, A. (2006). Planarian regeneration: Its end is its beginning. *Cell*, **124**(2), 241–245.

22. Schwartz, R., Verfaillie, C. (2010). Hepatic stem cells. *Methods Mol. Biol*., **640**, 167–179.

23. Schreder, A., Pierard, G., Paquet, P., Reginster, M., Pierard-Franchimont, C., Quatresooz, P. (2010). Facing towards epidermal stem cells (Review). *Int. J. Mol. Med.,* **26**(2), 171–174.

24. Garrison, A., Helmrath, M., Dekaney, C. (2009). Intestinal stem cells *Pediatr. Gastroenterol. Nutr.*, **49**(1), 2–7.

25. Loutit, J. (1968). Versatile haemopoietic stem cells. *Br. J. Haematol.,* **15**(4), 333–336.

26. Martin, G. (1998). Isolation of a pluripotent cell line from early mouse embryos cultured in medium conditioned by teratocarcinoma stem cells. *Proc. Natl. Acad. Sci. USA,* **78**(12), 7634–7638.

27. Wu, X., Wang, S., Chen, B., An, X. (2010). Muscle-derived stem cells: Isolation, characterization, differentiation, and application in cell and gene therapy. *Cell Tissue Res.*, **340**(3), 549–567.

28. Evans, M., Kaufman, M. (1981). Establishment in culture of pluripotential cells from mouse embryos. *Nature,* **292**(5819), 154–156.

29. Thomson, J., Itskovitz-Eldor, J., Shapiro, S., Waknitz, M., Swiergiel, J., Marshall, V., et al. (1998). Embryonic stem cell lines derived from human blastocysts. *Science,* **282**(5391), 1145–1147.

30. Keller, G. (1995). *In vitro* differentiation of embryonic stem cells. *Curr. Opin. Cell Biol.,* **7**(6), 862–869.

31. Kleger, A., Seufferlein, T., Malan, D., Tischendorf, M., Storch, A., Wolheim, A., et al. (2010). Modulation of calcium-activated potassium channels induces cardiogenesis of pluripotent stem cells and enrichment of pacemakerlike cells. *Circulation,* **122**(18), 1823–1836.

32. Roelandt, P., Pauwelyn, K., Sancho-Bru, P., Subramanian, K., Ordovas, L., Vanuytsel, K., et al. (2010). Human embryonic and rat adult stem cells with primitive endoderm-like pheno type can be fated to definitive endoderm, and finally hepatocyte-like cells. *PLoS One*, **5**(8), el2101.

33. Rezania, A., Riedel, M., Wideman, R., Karanu, F., Ao, Z., Warnock, G., et al. (2011). Production of functional glucagon-secreting alpha cells from human embryonic stem cells. *Diabetes,* **60**(1), 239–247. Epub 2010 Oct 22.

34. Valensi-Kurtz, M., Lefler, S., Cohen, M., Aharonowiz, M., Cohen-Kupiec, R., Sheinin, A., et al. (2010). Enriched population of PNS neurons derived from human embryonic stem cells as a platform for studying peripheral neuropathies. *PLoS One,* **5**(2), e9290.

35. Cash, G. (2010). Embryonic stem cells: Court decision a threat to science itself. *Nature,* **467**(7313), 271.

36. Tuffs, A. (2010). German MPs are to vote on allowing preimplantation genetic diagnosis. *BMJ*, 341×6017.

37. Adiga, S., Kalthur, G., Kumar, R., Girisha, K. (2010). Preimplantation diagnosis of genetic diseases. *J. Postgrad Med.,* **56**(4), 317–320.

38. Ben-Yosef, D., Malcov, M., Eiges, R. (2008). PGD-derived human embryonic stem cell lines as a powerful tool for the study of human genetic disorders. *Mol. Cell Endocrinol.,* **282**(1–2), 153–158.

39. Eiges, R., Urbach, A., Malcov, M., Frumkin, T., Schwartz, T., Amit, A., et al. (2007). Developmental study of fragile X syndrome using human embryonic stem cells derived from preimplantation genetically diagnosed embryos. *Cell Stem Cell.,* **1**(5), 568–577.

40. Löser, P., Schirm, J., Guhr, A., Wobus, A., Kurtz, A. (2010). Human embryonic stem cell lines and their use in international research. *Stem Cells,* **28**(2), 240–246.

41. Parekkadan, B., Milwid, J. (2010). Mesenchymal stem cells as therapeutics. *Annu. Rev. Biomed. Eng.*, **12**, 87–117.

42. Friedenstein, A., Chailakhjan, R., Lalykina, K. (1970). The development of fibroblast colonies in monolayer cultures of guinea-pig bone marrow and spleen cells. *Cell Tissue Kinet.*, **3**(4), 393–403.

43. Bianco, P., Robey, P., Simmons, P. (2008). Mesenchymal stem cells: Revisiting history, concepts, and assays. *Cell Stem Cell.,* **2**(4), 313–319.

44. Caplan, A. (2007). Adult mesenchymal stem cells for tissue engineering versus regenerative medicine. *J. Cell. Physiol.*, **213**(2), 341–347.

45. Kolf, C., Cho, E., Tuan, R. (2007). Mesenchymal stromal cells. Biology of adult mesenchymal stem cells: Regulation of niche, self-renewal and differentiation. *Arthritis Res. Ther.*, **9**(1), 204.

46. Prockop, D. (1997). Marrow stromal cells as stem cells for nonhematopoietic tissues. *Science,* **276**(5309), 71–74.

47. Solmesky, L., Abekasis, M., Bulvik, S., Weil, M. (2009). Bone morphogenetic protein signaling is involved in human mesenchymal stem cell survival in serum-free medium. *Stem Cells Dev.,* **18**(9), 1283–1292.

48. Solmesky, L., Lefler, S., Jacob-Hirsch, J., Bulvik, S., Rechavi, G., Weil, M. (2010). Serum free cultured bone marrow mesenchymal stem cells as a platform to characterize the effects of specific molecules. *PLoS One*, **5**(9).

49. Takahashi, K., Yamanaka, S. (2006). Induction of pluripotent stem cells from mouse embryonic and adult fibroblast cultures by defined factors. *Cell,* **126**(4), 663–676.
50. Liu, S., Fu, R., Huang, Y., Chen, S., Chien, Y., Hsu, C., et al. (2011). Induced pluripotent stem (iPS) cell research overview. *Cell Transplant.,* **20**(1), 15–19. Epub 2010 Sep 30.
51. Dimos, J., Rodolfa, K., Niakan, K., Weisenthal, L., Mitsumoto, H., Chung, W., et al. (2008). Induced pluripotent stem cells generated from patients with ALS can be differentiated into motor neurons. *Science,* **321**(5893), 1218–1221.
52. Ye, Z., Cheng, L. (2010). Potential of human induced pluripotent stem cells derived from blood and other postnatal cell types. *Regen. Med.,* **5**(4), 521–530.
53. Aasen, T., Belmonte, J. (2010). Isolation and cultivation of human keratinocytes from skin or plucked hair for the generation of induced pluripotent stem cells. *Nat. Protoc.,* **5**(2), 371–382.
54. Chakraborty, C., Shah, K., Cao, W., Hsu, C., Wen, Z., Lin, C. (2010). Potentialities of induced pluripotent stem (iPS) cells for treatment of diseases. *Curr. Mol. Med.*, **10**(8), 756–762.
55. Committee on State of the Science of Nuclear Medicine, Council NR. *Advancing Nuclear Medicine Through Innovation.* National Academy Press, Washington, DC; 2007.
56. Murphy, M. (2000). Current pharmacogenomic approaches to clinical drug development. *Pharmacogenomics,* **1**(2), 115–123.
57. Foster, M., Sharp, R., Mulvihill, J. (2001). Pharmacogenetics, race, and ethnicity: Social identities and individualized medical care. *Ther. Drug Monit.,* **23**(3), 232–238.
58. Kernan, W., Launer, L., Goldstein, L. (2010). What is the future of stroke prevention? Debate: Polypill versus personalized risk factor modification. *Stroke,* **41**(10 Suppl), S35–S38.
59. Whitebread, S., Hamon, J., Bojanic, D., Urban, L. (2005). Keynote review: *In vitro* safety pharmacology profiling: An essential tool for successful drug development. *Drug Discov. Today*, **10**(21), 1421–1433.
60. Schoonen, W., Westerink, W., Horbach, G. (2009). High-throughput screening for analysis of *in vitro* toxicity. *EXS.,* **99**, 401–452.
61. Gum, R., Hickman, D., Fagerland, J., Heindel, M., Gagne, G., Schmidt, J., et al. (2001). Analysis of two matrix metalloproteinase inhibitors and their metabolites for induction of phospholipidosis in rat and human hepatocytes(l). *Biochem. Pharmacol.,* **62**(12), 1661–1673.

62. McMillian, M., Grant, E., Zhong, Z., Parker, J., Li, L., Zivin, R., et al. (2001). Nile Red binding to HepG2 cells: An improved assay for *in vitro* studies of hepatosteatosis. *In vitro Mol. Toxicol.,* **14**(3), 177–190.

63. Fenech, M. (2005). *In vitro* micronucleus technique to predict chemosensitivity. *Methods Mol. Med.,* **111**, 3–32.

64. Diaz, D., Scott, A., Carmichael, P., Shi, W., Costales, C. (2007). Evaluation of an automated *in vitro* micronucleus assay in CHO-K1 cells. *Mutat. Res.,* **630**(1–2), 1–13.

65. Kreuter, J., Nanoparticles, J., Swarbrick, J. C., Boylan, eds. (1994). *Encyclopedia of Pharmaceutical Technology,* New York (1994).

66. Singh, R., Lillard, J. J. (2009). Nanoparticle-based targeted drug delivery. *Exp. Mol. Pathol.*, **86**(3), 215–223.

67. Iijima, S. (1991). Helical microtubules of graphitic carbon. *Nature,* **354**(6348), 56–58.

68. Adler-Abramovich, L., Aronov, D., Beker, R., Yevnin, M., Stempler, S., Buzhansky, L., et al. (2009). Self-assembled arrays of peptide nanotubes by vapour deposition. *Nat. Nanotechnol.,* **4**(12), 849–854.

69. Wagner, E. (2007). Programmed drug delivery: Nanosystems for tumor targeting. *Expert. Opin. Biol. Ther.,* **7**(5), 587–593.

70. Barratt, G. (2000). Therapeutic applications of colloidal drug carriers. *Pharm. Sci. Technol. Today*, **3**(5), 163–171.

71. Gregoriadis, G. (1997). Targeting of drugs. *Nature*, **265**(5593), 407–411.

72. Juliano, R., McCullough, H. (1980). Controlled delivery of an antitumor drug: Localized action of liposome encapsulated cytosine arabinoside administered via the respiratory system. *J. Pharmacol. Exp. Ther.*, **214**(2), 381–387.

73. Takada, K., Yoshimura, H., Shibata, N., Masuda, Y., Yoshikawa, H., Muranishi, S., et al. (1986). Effect of administration route on the selective lymphatic delivery of cyclosporin A by lipid-surfactant mixed micelles. *J. Pharmacobiodyn.,* **9**(2), 156–160.

74. Widder, K., Senyel, A., Scarpelli, G. (1978). Magnetic microspheres: A model system of site specific drug delivery *in vivo*. *Proc. Soc. Exp. Biol. Med.,* **158**(2), 141–146.

75. Vinogradov, S., Bronich, T., Kabanov, A. (2002). Nanosized cationic hydrogels for drug delivery: Preparation, properties and interactions with cells. *Adv. Drug Deliv. Rev*., **54**(1), 135–147.

76. Burger, K., Staffhorst, R., de Vijlder, H., Velinova, M., Bomans, P., Frederik, R., et al. (2002). Nanocapsules: Lipid-coated aggregates of cisplatin with high cytotoxicity. *Nat. Med.*, **8**(1), 81–84.

77. Weckenmann, H., Matzku, S., Strieker, H. (1988). Optimisation of the covalent binding of monoclonal antibodies to liposomes. *Arzneimittelforschung.,* **38**(11), 1556–1563.

78. Hagiwara, A., Takahashi, T. (1987). A new drug-delivery-system of anticancer agents: Activated carbon particles adsorbing anticancer agents. *In vivo.* **1**(4), 241–252.

78a. Bawa, R. (2013). FDA and nanotech: Baby steps lead to regulatory uncertainty. In: D. Bagchi, et al. eds. *Bionanotechnology: A Revolution in Biomedical Sciences and Human Health*. John Wiley & Sons, Ltd., UK, pp. 720–732.

79. Begley, D. (2004). Delivery of therapeutic agents to the central nervous system: The problems and the possibilities. *Pharmacol. Ther.,* **104**(1), 29–45.

80. Pignatello, R., Panto, V., Salmaso, S., Bersani, S., Pistara, V., Kepe, V., et al. (2008). Flurbiprofen derivatives in Alzheimer's disease: Synthesis, pharmacokinetic and biological assessment of lipoamino acid prodrugs. *Bioconjug. Chem.,* **19**(1), 349–357.

81. Deguchi, Y., Hayashi, H., Fujii, S., Naito, T., Yokoyama, Y., Yamada, S., et al. (2000). Improved brain delivery of a nonsteroidal anti-inflammatory drug with a synthetic glyceride ester: A preliminary attempt at a CNS drug delivery system for the therapy of Alzheimer's disease. *J. Drug Target.,* **8**(6), 371–381.

82. Reese, T., Karnovsky, M. (1967). Fine structural localization of a blood-brain barrier to exogenous peroxidase. *J. Cell Biol.,* **34**(1), 207–217.

83. Ermisch, A. (1992). Peptide receptors of the blood-brain barrier and substrate transport into the brain. *Prog. Brain Res.*, **91**, 155–161.

84. Chishty, M., Begley, D., Abbott, N., Reichel, A. (2003). Functional characterisation of nucleoside transport in rat brain endothelial cells. *Neuroreport,* **14**(7), 1087–1090.

85. Pardridge, W. (1993). Transport of insulin-related peptides and glucose across the blood-brain barrier. *Proc. Natl. Acad. Sci.,* **692**, 126–137.

86. Olivier, J., Fenart, L., Chauvet, R., Pariat, C., Cecchelli, R., Couet, W. (1999). Indirect evidence that drug brain targeting using polysorbate 80-coated polybutylcyanoacrylate nanoparticles is related to toxicity. *Pharm. Res.,* **16**(12), 1836–1842.

87. Gummerloch MKaN, E. A. (1992). *Drug Entry into the Brain and Its Pharma-cologic Manipulation.* Springer, Berlin.

88. Wang, Y., Lui, P., Li, J. (2009). Receptor-mediated therapeutic transport across the blood-brain barrier. *Immunotherapy,* **1**(6), 983–993.

Chapter 23

Viral Nanoparticles: Tools for Materials Science and Biomedicine

Nicole F. Steinmetz, PhD,[a] and Marianne Manchester, PhD[b]

[a]*Department of Biomedical Engineering, Case Western Reserve University, Cleveland, Ohio, USA*
[b]*Translational Technologies and Bioinformatics, Pharmaceutical Sciences, Pharma Research and Early Development, F. Hoffmann-La Roche, Ltd., Basel, Switzerland*

Keywords: viral nanoparticles, nanoobjects, biological nanomaterials, virus-like particles, viral nanotechnology, icosahedral viruses, rod-shaped viruses, functionalization, particle stability, structural symmetry, polyvalency

Viruses have long been studied as pathogens, with the goal of understanding viral infection and disease. More recently viruses have begun to be regarded as building blocks and tools for nanotechnology. Viruses are exploited as *platforms*; that is, they are used as templates or scaffolds for the design of novel nanomaterials. A wide variety of viral platforms have been studied and utilized for applications ranging from materials to medicine. This chapter will provide an introduction to the role of viral nanoparticles (VNPs) in nanotechnology.

Handbook of Clinical Nanomedicine: Nanoparticles, Imaging, Therapy, and Clinical Applications
Edited by Raj Bawa, Gerald F. Audette, and Israel Rubinstein

ISBN 978-981-4669-20-7 (Hardcover), 978-981-4669-21-4 (eBook)
www.panstanford.com

23.1 What Is Nano?

Nanotechnology is a highly interdisciplinary field that brings together researchers from different scientific backgrounds and has created a novel common language. It is a collective term for a broad range of novel topics concerned with matter on the nanometer scale. Nanotechnology sits at the interface of biology, chemistry, physics, material science, and medicine. Nanotechnology is found and applied in nearly every scientific area.

Nano is a somewhat fashionable term; in common speech, it is used as a prefix to denote something that is smaller than usual. As of this writing, the term "*Apple iPod nano*" is the first hit on a *Google* search of the term "nano." The word nano is derived from the ancient Greek word for dwarf. In a scientific context the prefix nano is used to describe "a billionth of something." A nanometer is a billionth of a meter (10^{-9} m = 1 nm), and a nanosecond is a billionth of a second (10^{-9} s = 1 ns).

Figure 23.1 illustrates how tiny nano is. An aphid insect (Fig. 23.1, panel a) is about 1 mm in size. The aphid is about 1,000,000 times bigger than a nanometer. Human hairs (Fig. 23.1, panel b) have an average diameter of 100 μm and are thus 10 times smaller than the aphid and still 100,000 times bigger than a nanoparticle. Panel C shows a plant cell, which is about 10 μm in size and thus 10,000 bigger than a nanometer. Particles formed by the plant virus *Cowpea mosaic virus* (CPMV; Fig. 23.1, panel d) are about 30 nm in diameter and thus nanoparticles. One would need around 50,000,000 VNPs to fill up the interior of a cell.

A single atom is a fraction of a nanometer in size; molecules, including biological molecules, are typically nanometers in size and can thus be regarded as nanoobjects. In recent years a range of biological molecules have been exploited for nanosciences and nanotechnology. Nucleic acids, for example, are used as construction materials to generate highly ordered 2D and 3D structures and assemblies such as nanotubes and nanocages. A main theme in nanotechnology is controlled self-assembly, with the goal being to generate functional materials with a high degree of precision. Nanotechnology, then, requires chemical and physical control at the molecular level. Nucleic acids, proteins, and viruses are essentially naturally occurring nanomaterials

capable of self-assembly with a high degree of precision. This property, coupled to the relative ease of experimentally controlling and producing biological nanomaterials, has led to tremendous interest in their nanotechnology applications. Viruses, and VNPs in particular, possess a number of traits that make them exceptionally outstanding candidates.

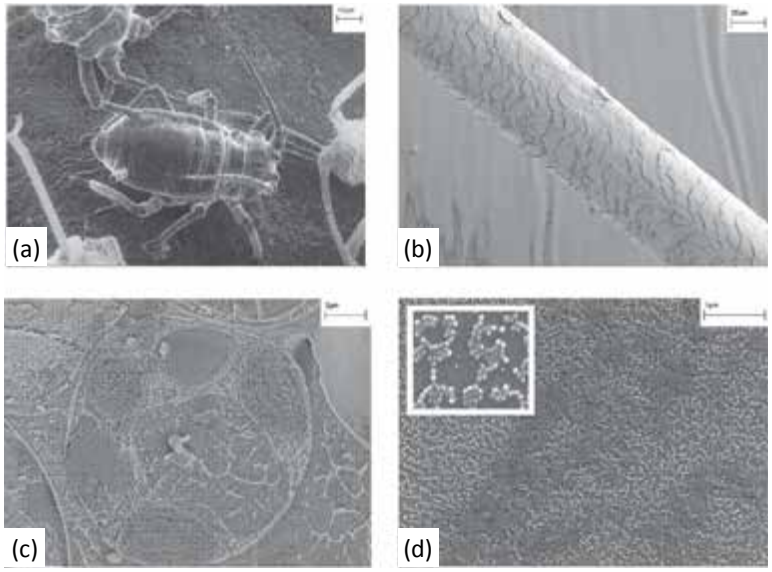

Figure 23.1 Scanning electron micrographs of aphids on leaf (a), human hair (b), fractured plant cell (c), and *Cowpea mosaic virus* particles (d). Panel a–c provided by courtesy of Kim C. Findlay, John Innes Centre, Norwich (UK). Panel d from Steinmetz, N. F., et al., unpublished.

23.2 Where Did it all Begin? A History of VNPs: From Pathogens to Building Blocks

The word *virus* is Latin and means "poison." Viruses are infectious agents, and generally pathogens. It was not, however, until the end of the 19th century that viruses were discovered as infectious agents. The first virus to be recognized as an infectious agent distinct from bacteria was the plant pathogen *Tobacco mosaic virus* (TMV) [1]. Today more than 5,000 viruses have been discovered

and described, although this likely represents a fraction of those found in nature. Viruses cause many human diseases, from the common cold and chicken pox to more serious infections such as AIDS (acquired immune deficiency syndrome, which is caused by the *Human immunodeficiency virus* [HIV]) and SARS (severe acute respiratory syndrome, which is caused by SARS coronavirus). Virology—the science of studying viruses—is thus a highly important discipline in regard to human health.

Viruses infect all forms of life. Generally, animal viruses infect animals, including humans; plant viruses infect plants; and bacteriophages infect bacteria. Archaeal viruses are those that infect Archaea. Archaea show similarities with bacteria as well as with eukaryotes, and although they are prokaryotes, it has been suggested that they are more closely related to the eukaryotes [2].

In their simplest form, viral particles consist of a nucleic acid genome and a protective protein coat termed the capsid. Some viruses have additional structural features such as a lipid envelope, or they may consist of separate head and tail structures. In brief, the nucleic acid genome encodes the genetic information that is needed to produce viral progeny. In addition to cellular attachment, an important function of the capsid of non-enveloped viruses is the protection of the nucleic acid genome. This tends to make non-enveloped viral particles extremely robust. With a few exceptions, nearly all viruses utilized in nanotechnology are non-enveloped particles. The envelope for enveloped viruses also plays a role in the initial stages of the infection process, including binding to surface receptors and internalization into the host cell.

Viruses have now been studied for more than 100 years, and detailed knowledge about the structure and function of many viruses has been gathered. For many years the emphasis has been on the understanding of viral infection and disease, and it still is. Being able to control or treat viral infections is an important goal in human medicine (as well as veterinary medicine and agriculture). Every year novel viruses or virus strains evolve with the potential to cause disease and death worldwide. For instance, at the time of writing this book, the *Influenza* virus strain H1N1 (also referred to as “swine flu”) has emerged and quickly spread all over the world. The science of fundamental virology will always play an important role in medicine.

By the 1950s, researchers had begun thinking of viruses as tools in addition to pathogens. Bacteriophages, for example, played a key role in the development of molecular biotechnology. Bacteriophage genomes and components of the protein expression machinery have been widely utilized as tools for understanding fundamental cellular processes such as nucleic acid replication, transcription, and translation. Virus genomes are small and the genetic elements that control expression of the genome are highly efficient and multifunctional. On the basis of these properties, several viruses have been exploited as expression systems in biotechnology. Several cloning vectors are derivatives of bacteriophages, and typical examples include the *Escherichia coli* phages λ and M13. Various phage-encoded promoters (DNA sequences that facilitate transcription of DNA into RNA) have been utilized to regulate gene expression. An overview of tools used for molecular biology can be found in *Molecular Cloning: A Laboratory Manual*, by Sambrook and Russell [3]. The use of viruses as cloning and expression vectors is not restricted to phages; plant viruses, insect viruses, and mammalian systems have also been engineered for these purposes.

Another early application evaluated was *bacteriophage therapy*, the use of bacteriophages to combat bacterial infections. With the development of antibiotics (compounds that kill bacteria), which have proven to be more efficient and comprehensive compared with bacteriophage therapy, few efforts were made toward its further development. Other applications include *bacteriophage-mediated microbial control* (applied in the food industry) and *phage display technologies* that allow screening for biological protein-binding partners. More recent developments include the use of bacteriophages for *vaccine* production and *gene delivery* approaches. Developments in using bacteriophages for biotechnological applications were reviewed by Clark and March [4] and Marks and Sharp [5].

In the 1970s many efforts focused on the production of virus-like particles (VLPs) for use in anti-viral vaccines (reviewed in [6–8]). A VLP is a particle consisting of the capsid but lacking the genome. A VLP is the replication-deficient and thus non-infectious counterpart of a VNP. Chimeric VLPs and VNPs have also been designed. A chimera is a genetically modified version of a naturally occurring particle or cell. In vaccine development,

chimeras are used as carriers or platforms for the presentation of antigenic sequences (sequences that induce an immune response) of other pathogens (reviewed in [6–8]).

In the 1980s researchers began exploiting plant viruses as expression vectors (a DNA-based plasmid that promotes the expression of foreign genes) to produce pharmaceutical proteins in plants. Advantages of protein production in plants are the absence of contamination with animal products, low production costs, and—when using viral expression vectors—achievement of high expression levels. A range of pharmaceutically relevant proteins including therapeutic antibodies have been successfully produced using viral vectors such as TMV, CPMV, and *Potato virus X* (PVX) [9–13].

Viruses Became VNPs. Beginning about 20 years ago, the focus on exploiting viruses and their capsids for biotechnology began to shift toward using them for nanotechnology applications. Douglas and Young (Montana State University, Bozeman, MT, USA) were the first to consider the utility of a virus capsid as a nanomaterial [14]. The virus of interest in their studies was the plant virus *Cowpea chlorotic mottle virus* (CCMV). CCMV is a highly dynamic platform with pH- and metal ion-dependent structural transitions. Douglas and Young made use of these capsid dynamics and exchanged the natural cargo (nucleic acid) with a synthetic material, in this case encapsulating the organic polymer polyanetholesulfonic acid. Since then many materials have been encapsulated into CCMV and other VNPs. The system was further engineered to allow not only the entrapment of materials but also the size-constrained and spatially controlled synthesis of materials within both the capsid and other protein cages. A protein cage is a hollow, generally spherical protein structure that is typically assembled by multiple copies of protein monomers and thus has similarities to a viral capsid.

At about the same time, the research team led by Mann (University of Bristol, UK) pioneered a new area using the rod-shaped particles of TMV. The particles were used as templates for the fabrication of a range of metallized nanotube structures using mineralization techniques [15]. These techniques have received great attention during recent years. In particular the contributions of Belcher and colleagues at the Massachusetts Institute of Technology (MIT, Cambridge, MA, USA) led to the

development of a new technology that allowed for the generation of a large range of mineralized nanotubes and nanowires for use in batteries and data storage devices [16–18].

A third direction began a few years later. In 2002, the first study was reported in which bioconjugation chemistries had been applied to a VNP. The research teams led by Johnson and Finn (The Scripps Research Institute, La Jolla, CA, USA) showed, in a proof-of-concept study, that small chemical modifiers such as organic dyes and nanogold particles could be covalently attached to the surface of CPMV. Attachment and display was achieved with atomic precision [19]. Since then, various chemistries ranging from standard techniques utilizing commercially available reagents to complex and advanced reactions have been developed. The establishment of a wide variety of bioconjugation protocols for VNPs was an important development and can be regarded as fundamental to viral nanotechnology. Functional molecules such as therapeutic or imaging molecules for drug delivery and imaging applications, for example, can be covalently attached and displayed on the VNPs, and this has opened the door for developing "smart" devices for medical applications.

The field of viral nanotechnology is still a young discipline that is rapidly evolving. A broad range of VNP platforms have been exploited or show promise in applications ranging from the development of battery electrodes to medical imaging and drug delivery.

23.3 Why VNPs? Materials Properties of VNPs

When a virologist looks at a virus, he or she might see a pathogen, an infectious agent that is causing a disease. What does a chemist or a materials scientist see in VNPs? Working at the interface of chemistry and medicine, we see tiny building blocks, platforms that can be tuned with functionalities. A VNP can be regarded as a platform that is used as a template or scaffold for the generation of functional materials. The regular surface properties of VNPs allow one to covalently attach functional molecules (termed *functionalizing*). VNPs are *programmable* and *tunable*, as they can be *functionalized* with a broad range of molecules used for manifold applications. The covalent modification can also lead to a *tuning*

of the materials properties; for example, the charge properties can be altered by attaching neutral groups to charged surface groups on the viral capsid.

VNPs occur in two basic shapes, icosahedral and rod (Fig. 23.3); an icosahedron is a polyhedron with 20 triangular faces. More complex structures such as head–tail bacteriophages, enveloped viruses, and even spindle- and bottle-shaped particles can also be found. For example, the particles of *Acidianus* bottle-shaped virus (ABV) indeed look like a bottle (Fig. 23.2). ABV is an archaeal virus of the family *Ampulliviridae* with particles about 230 nm long and 4–75 nm wide [20].

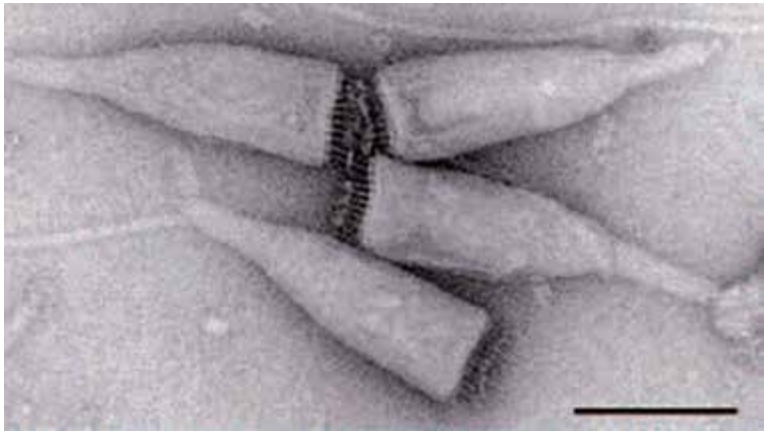

Figure 23.2 Transmission electron micrograph of *Acidianus* bottle-shaped virus. The scale bar represents 100 nm. Reproduced with permission from Prangishvili, D., Forterre, P., Garrett, R. A. (2006) Viruses of the Archaea: a unifying view, *Nat. Rev. Microbiol.*, **4**(11), 837–848 [20].

Icosahedral particles range in their size from 18 nm to 500 nm. Rod-shaped or filamentous VNPs can reach up to 2 μm in length. The structure of many viruses has been solved to atomic or near-atomic resolution, and many of these structures and accompanying structural information can be found at the Virus Particle ExploreR database (VIPER; at www.viperdb.scripps.edu). Structures of VNPs currently under investigation and use for potential applications in nanotechnology are shown in Fig. 23.3.

A whole library of VNPs has become available, offering a large variety of building blocks with varying structural and chemical properties. Each VNP can be selected for its most suitable applications. For example, the reversible permeability of CCMV has led to its use as a constrained chemical reaction vessel [14, 21, 22]. Filamentous or rod-shaped VNPs such as the bacteriophage M13 and TMV have been metal-coated and used as nanowires and nanotubes in the fabrication of lithium–ion battery electrodes and data storage devices [16–18, 23]. The development of VNPs for nanotechnology applications has fueled the search for novel VNPs possessing exotic structural or chemical features, and these are often found as infectious agents of extremophile hosts. For example, the hyperthermophile organism *Sulfolobus islandicus* thrives at 80°C and pH < 3.0. The associated filamentous archaeal virus *Sulfolobus islandicus* rod-shaped virus 2 (SIRV2) is both extremely stable owing to its host natural habitat, and uniquely exploitable as a template for site-selective and spatially controlled bioconjugation. Functionalities can be attached and displayed at either the virus body or its ends [24].

From a materials science point of view, VNPs are exceptionally robust; as mentioned earlier, a primary function of the capsid is the protection of the encapsidated nucleic acid. As a result temperature- and pH-stability is increased. Several VNPs sustain temperatures as high as 60°C for several hours. In terms of pH stability, various particles remain intact over a pH range of 2–10. These characteristics make them feasible building blocks for the generation of novel materials. Chemists have also found that many VNPs are stable in a range of solvent–buffer mixtures, which is essential for chemical modification procedures.

VNPs can be produced on a large scale at low costs and in short time frames. The particles have a high degree of symmetry and polyvalency, and they are monodisperse, meaning that every single particle looks virtually identical in size and shape to all other particles formed by that species. In addition to the ability to self-assemble into discrete particles, VNPs also show a propensity for self-organization. Straightforward crystallization procedures lead to self-organization, and 2D and 3D crystals can be readily obtained [19, 25]. In addition self-supporting crystalline thin films in the centimeter range, especially of rod-shaped VNPs, can be fabricated [26, 27].

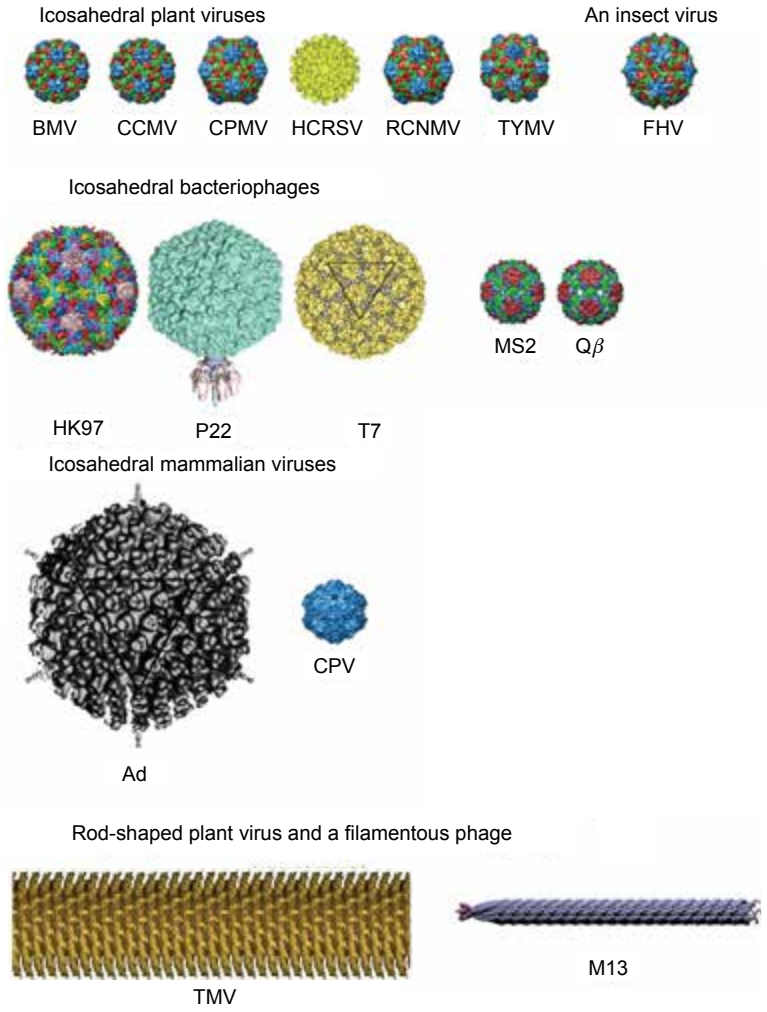

Figure 23.3 A snapshot of the viral nanoparticles (VNPs) that are currently exploited and developed for materials science and medicine. The list is continuously growing; these are the VNPs in use as of May 2009. Icosahedral plant viruses: *Brome mosaic virus* (BMV), *Cowpea chlorotic mottle virus* (CCMV), *Cowpea mosaic virus* (CPMV), *Hibiscus chlorotic ringspot virus* (HCRSV), *Red clover necrotic mottle virus* (RCNMV), *Turnip yellow mosaic virus* (TYMV). Icosahedral insect virus: *Flock house virus* (FHV). Icosahedral bacteriophages: HK97, P22,

T7, MS2, and Qβ. Note P22 and T7 are head-tail phages. The tail is shown for P22, not for T7. Icosahedral mammalian viruses: *Adenovirus* and *Canine parvovirus* (CPV). Rod-shaped and filamentous viruses: *Tobacco mosaic virus* (TMV), a plant virus, and M13, a bacteriophage. Images of the following VNPs were reproduced from the VIPER database (www.viperdb.scripps.edu): BMV, CCMV, CPMV, RCNMV, TYMV, FHV, HK97, MS2, Qβ, and CPV. The structure of HCRSV was reproduced from Doan, D. N., et al. (2003) *J. Struct. Biol.*, **144**(3), 253–261 [28]. The cryo-electron microscopy structure of P22 was reproduced with permission from Chang, J., et al. (2006) *Structure*, **14**(6), 1073–1082 [29]. The T7 structure was taken with permission from Agirrezabala, X., et al. (2007) *Structure*, **15**, 461–472 [30]. *Adenovirus* cryo-electron microscopy reconstruction was reproduced with permission from Johnson, J. E., Speir, J. A. (1997) *J. Mol. Biol.*, **269**(5), 665–675 [31]. The cryo-reconstruction of TMV was provided by Bridget Carragher and Clint Potter; data were collected and processed at the National Resource for Automated Molecular Microscopy at the Scripps Research Institute. M13 was taken with permission from Khalil, A. S., et al. (2007) *PNAS*, **104**(12), 4892–4897 [32].

23.4 Summary

A large variety of nanobuilding blocks are available and have commanded the attention of chemists and materials scientists. Initial proof-of-concept studies focused on developing chemical modification strategies. Bioconjugation chemistries that allow for site-selective covalent modification have been adapted to VNPs. Further selective entrapment and encapsulation techniques have been developed. A broad range of mineralization and metal deposition techniques have also been applied. With all these modification protocols in hand, research has moved toward the development of functional devices. Today VNPs are utilized for manifold applications that range from materials to biomedicine.

Viral nanotechnology is a young discipline just emerging from its infancy. It is an intriguing field with wide-ranging opportunities. It is an exciting time to be working at the virus–chemistry interface!

Disclosures and Conflict of Interest

The opinions and perspectives here reflect the current views of the authors. The authors declares that they have no conflict of interest and has no affiliations or financial involvement with any organization or entity discussed in this chapter. No writing assistance was utilized in the production of this chapter and the authors have received no payment for its preparation. This chapter is a revised version of the author's chapter that originally appeared in *Viral Nanoparticles: Tools for Materials Science and Biomedicine*, 2011, Pan Stanford Publishing, Singapore.

Corresponding Author

Dr. Nicole F. Steinmetz
Biomedical Engineering
Case Western Reserve University
School of Medicine
10900 Euclid Avenue, Cleveland OH 44106 USA
Email: nicole.steinmetz@case.edu

About the Authors

Nicole F. Steinmetz is assistant professor of biomedical engineering at Case Western Reserve University School of Medicine, Cleveland, OH, where she is leading a research laboratory interfacing of bio-inspired, molecular engineering approaches with medical research, technology development, and materials science. Recognizing the inter-disciplinary nature of the research, Dr. Steinmetz holds secondary appointments and is a trainer in Radiology, Materials Science and Engineering, and Macromolecular Science and Engineering, Pathology, Pharmacology, Molecular Virology. Dr. Steinmetz trained at The Scripps Research Institute, La Jolla, CA, John Innes Centre, Norwich, UK (PhD in Bionanotechnology), and RWTH-Aachen University in Germany (Masters in Molecular Biotechnology). Dr. Steinmetz was named a Crain's Cleveland Business 40 under 40 honoree (2014); in 2011, Dr. Steinmetz was named Mt. Sinai Scholar, she is a 2009 recipient of the NIH/NIBIB Pathway to

Independence Grant (K99/R00), a previous American Heart Association Post-doctoral Fellow, (2008–2009) and former Marie Curie Early Stage Training Fellow (2004–2007). Dr. Steinmetz serves on the Editorial Board of Wiley Interdisciplinary Reviews (WIREs) on Nanomedicine and Nanobiotechnology; she serves on the Advisory Editorial Board for the ACS journal Molecular Pharmaceutics. Dr. Steinmetz has chaired symposia at ACS and MRS; she is the Session Chair for the Protein and Viral Nanoparticle Track at FNANO and the Co-Chair of the Gordon Conference of Physical Virology (2015). Dr. Steinmetz has authored more than 60 peer-reviewed journal articles, reviews, and book chapters; she has authored and edited books on Virus-based nanotechnology. Research in the Steinmetz Lab is funded through grants from federal agencies, National Institute of Health, National Science Foundation, Department of Energy, and private foundations, including Susan G. Komen Foundation and American Heart Association.

Marianne Manchester is the head of Immunoassay and Metabolomics technologies at F. Hoffmann-La Roche in Basel, Switzerland. For much of her career, Dr. Manchester has studied novel virus based nanotechnologies for tumor targeting and vaccine development, and the underlying mechanisms of formulation targeting and pharmacodynamics. She served on the faculty first at The Scripps Research Institute in La Jolla, California, USA (1998–2009), and then at the Skaggs School of Pharmacy and Pharmaceutical Sciences at the University of California, San Diego, California, USA (2009–2014). She has developed tissue directed nanoparticles that show specificity for tumors *in vivo*, and was the first to demonstrate the utility of viral nanoparticles as a tool for intravital vascular imaging. She has been instrumental in developing virus-based structural scaffolds for antigen presentation that demonstrate the positive effects of whole antigen display and antigen multivalency on protective immunity. From 2002–2014, she led NIH-sponsored programs in tumor nanotechnology, and multivalent nanotechnologies for vaccine development. She has also developed novel mass spectrometry-based approaches for

identifying new therapeutic targets for human disease. Since 2014, she is at Roche Pharmaceuticals, Pharma Research and Early Development (pRED), in the Translational Technologies and Bioinformatics (TTB) Division of Pharmaceutical Sciences.

References

1. Zaitlin, M. (1898). The discovery of the causal agent of the tobacco mosaic disease. In: Kung, S. D., Yang, S. F., eds. *Discoveries in Plant Biology*, World Publishing, Hong Kong, pp. 105–110.
2. Woese, C. R., Fox, G. E. (1977). Phylogenetic structure of the prokaryotic domain: The primary kingdoms. *Proc. Natl. Acad. Sci. U. S. A.,* **74**(11), 5088–5090.
3. Russell, D. W., Sambrook, J., (2001). *Molecular Cloning: A Laboratory Manual*. Cold Spring Harbor Laboratory Press, USA.
4. Clark, J. R., March, J. B. (2006). Bacteriophages and biotechnology: Vaccines, gene therapy and antibacterials. *Trends Biotechnol*., **24**(5), 212–218.
5. Marks, T., Sharp, R. (2000). Bacteriophages and biotechnology: A review. *J. Chem.Technol. Biotechnol*., **75**, 6–17.
6. Garcea, R. L., Gissmann, L. (2004). Virus-like particles as vaccines and vessels for the delivery of small molecules. *Curr. Opin. Biotechnol.,* **15**(6), 513–517.
7. Grgacic, E. V., Anderson, D. A. (2006). Virus-like particles: Passport to immune recognition. *Methods,* **40**(1), 60–65.
8. Ludwig, C., Wagner, R. (2007). Virus-like particles-universal molecular toolboxes. *Curr. Opin. Biotechnol*., **18**(6), 537–545.
9. Awram, P., Gardner, R. C., Forster, R. L., Bellamy, A. R. (2002). The potential of plant viral vectors and transgenic plants for subunit vaccine production. *Adv. Virus Res*., **58**, 81–124.
10. Canizares, M. C., Nicholson, L., Lomonossoff, G. P. (2005). Use of viral vectors for vaccine production in plants. *Immunol*. *Cell Biol*., **83**(3), 263–270.
11. Johnson, J., Lin, T., Lomonossoff, G. (1997). Presentation of heterologous peptides on plant viruses: Genetics, structure, and function. *Annu. Rev. Phytopathol*., **35**, 67–86.
12. Porta, C., Lomonossoff, G. P. (1998). Scope for using plant viruses to present epitopes from animal pathogens. *Rev. Med. Vir*., **8**(1), 25–41.

13. Scholthof, H. B., Scholthof, B. G., Jackson, A. O. (1996). Plant virus vectors for transient expression of foreign proteins in plants. *Annu. Rev. Phytopathol*., **34**, 229–323.
14. Douglas, T., Young, M. (1998). Host-guest encapsulation of materials by assembled virus protein cages. *Nature*, **393**, 152–155.
15. Shenton, W., Douglas, T., Young, M., Stubbs, G., Mann, S. (1999). Inorganic-organic nanotube composites from template mineralization of Tobacco mosaic virus. *Adv. Mater*., **11**, 253–256.
16. Lee, Y. J., Yi, H., Kim, W. J., Kang, K., Yun, D. S., et al. (2009). Fabricating genetically engineered high-power lithium-ion batteries using multiple virus gene. *Science*, **324**(5930), 1051–1055.
17. Nam, K. T., Kim, D. W., Yoo, P. J., Chiang, C. Y., Meethong, N., et al. (2006). Virus-enabled synthesis and assembly of nanowires for lithium ion battery electrodes. *Science*, **312**(5775), 885–888.
18. Nam, K. T., Wartena, R., Yoo, P. J., Liau, F. W., Lee, Y. J. et al. (2008). Stamped microbattery electrodes based on self-assembled M13 viruses. *Proc. Natl. Acad. Sci. U. S. A.*, **105**(45), 17227–17231.
19. Wang, Q., Lin, T., Tang, L., Johnson, J. E., Finn, M. G. (2002). Icosahedral virus particles as addressable nanoscale building blocks. *Angew. Chem. Int. Ed*., **41**(3), 459–462.
20. Prangishvili, D., Forterre, P., Garrett, R. A. (2006). Viruses of the Archaea: A unifying view. *Nat. Rev. Microbiol*., **4**(11), 837–848.
21. Douglas, T., Young, M. (1999). Virus particles as templates for material synthesis. *Adv. Mater*., **11**, 679–681.
22. Douglas, T., Strable, E., Willits, D. (2002). Protein engineering of a viral cage for constrained material synthesis. *Adv. Mater*., **14**, 415–418.
23. Tseng, R. J., Tsai, C., Ma, L., Ouyang, J., Ozkan, C. S., Yang, Y. (2006). Digital memory device based on Tobacco mosaic virus conjugated with nanoparticles. *Nat. Nanotechnol*., **1**, 72–77.
24. Steinmetz, N. F., Bize, A., Findlay, K. C., Lomonossoff, G. P., Manchester, M., et al. (2008). Site-specific and spatially controlled addressability of a new viral nanobuilding block: Sulfolobus islandicus rod-shaped virus 2. *Adv. Funct. Mater*., **18**, 3478–3486.
25. Sun, J., DuFort, C., Daniel, M. C., Murali, A., Chen, C., et al. (2007). Core-controlled polymorphism in virus-like particles. *Proc. Natl. Acad. Sci. U. S. A.,* **104**(4), 1354–1359.
26. Kuncicky, D. M., Naik, R. R., Velev, O. D. (2006) Rapid deposition and long-range alignment of nanocoatings and arrays of electrically conductive wires from tobacco mosaic virus. *Small,* **2**(12), 1462–1466.

27. Lee, S. W., Woods, B. W., Belcher, A. M. (2003). Chiral smectic C structures of virus-based film. *Langmuir*, **19**, 1592–1598.

28. Doan, D. N., Lee, K. C., Laurinmaki, P., Butcher, S., Wong, S. M., Dokland, T. (2003). Three-dimensional reconstruction of hibiscus chlorotic ringspot virus. *J. Struct. Biol.*, **144**(3), 253–261.

29. Chang, J., Weigele, P., King, J., Chiu, W., Jiang, W. (2006). Cryo-EM Asymmetric Reconstruction of Bacteriophage P22 Reveals Organization of its DNA Packaging and Infecting Machinery. *Structure,* **14**(6), 1073–1082.

30. Agirvezabala, X., Velazquez-Muriel, J. A., Gomez-Puerta, P., Scheres, S. H. W., Carazo, J. M., Carrascosa, J. L. (2007). Quasi-atomic model of bacteriophage T7 procapsid shell: Insights into the structure and evolution of a basic fold. *Structure*, **15**(4), 461–472.

31. Johnson, J. E., Speir, J. A. (1997). Quasi-equivalent viruses: A paradigm for protein assemblies. *J. Mol. Biol.*, **269**(5), 665–675.

32. Khalil, A. S., Ferrer, J. M., Brau, R. R., Kottmann, S. T., Noren, C. J., et al. (2007). Single M13 bacteriophage tethering and stretching. *Proc. Natl. Acad. Sci. U. S. A.*, **104**(12), 4892–4897.

Chapter 24

Bacterial Secretion Systems: Nanomachines for Infection and Genetic Diversity

Agnesa Shala, PhD, Michele Ferraro, MSc, and Gerald F. Audette, PhD
Department of Chemistry and the Centre for Research on Biomolecular Interactions, York University, Canada

Keywords: biological nanomachines, multi-drug resistance, bacterial infection, bacterial evolution, conjugation, secretion systems, membrane transport, protein interactions

24.1 Introduction

Current nanoscale approaches dealing with infection and disease focus on the "nanoization" of therapeutics as well as developing and tracking the nano-drug interactions with cellular targets. These approaches are either top-down, making current drugs nanosized by a variety of methods, or bottom-up, providing nanoscale control of compound crystallization and methodologies for drug formulations. An alternative viewpoint to understanding how to deal with infection is to examine the means by which viruses and

Handbook of Clinical Nanomedicine: Nanoparticles, Imaging, Therapy, and Clinical Applications
Edited by Raj Bawa, Gerald F. Audette, and Israel Rubinstein

ISBN 978-981-4669-20-7 (Hardcover), 978-981-4669-21-4 (eBook)
www.panstanford.com

microorganisms infect host cells and evade therapeutic strategies. In effect, microorganisms utilize sophisticated nanomachines purpose-built for the transfer of genetic material and effector molecules. A detailed understanding of how these nanosystems are assembled from their component proteins, as well as their effects on infection and the development of resistance strategies, is critical to the development of more streamlined approaches to dealing with infection and drug resistance in pathogenic organisms.

The diversity of environments in which bacteria live imposes many challenges, requiring substantial plasticity and adaptability in the genome of the organism. The interactions between bacteria, their environment and other species is an intricate interplay of diversity and adaptation in a mélange of chemical, biological and physical pressures [1]. It has been shown that in *Escherichia coli* sexual recombination increases rates of adaptation ~3-fold under conditions of environmental stress [2, 3]. This adaptability, while advantageous for the organism living under adverse conditions [4, 5] poses significant challenges to human health and infectious diseases, which make up ~25% of all annual deaths worldwide [6, 7]. Indeed, the recent outbreak of hemolytic uremic syndrome (HUS) linked to enterohemorrhagic *Escherichia coli* (EHEC) in Germany resulted in over 3500 infections leading to 50 deaths [8]. Furthermore, an outbreak of *Clostridium difficile* in southern Ontario, Canada, in the spring of 2011 resulted in the death of 16 patients within 6 weeks of the reported outbreak [9]. Addressing these outbreaks is becoming increasingly challenging due to the innate and acquired drug resistances that these organisms possess.

It has been over 80 years since Sir Alexander Fleming gave the world its first antibiotic, penicillin [10]. During the 20 years following the introduction of penicillin, roughly half of the antibacterial drugs used today would be supplied to modern medicine [11]. In addition, between the launch of quinolones in 1962 and the US FDA approval of oxazolidnones in 2000, no new antibiotics made their way to the clinic [12]; this is truly a significant innovation gap. Overall, the rate of traditional antibiotic discovery is in decline [13], and as such, more targeted, structure-based methods have emerged to develop novel antibiotics [14–17]. However, it is becoming a trend that antibiotics, given enough time, will fail to provide the necessary means of combating microbes.

This is not so much a result of the properties of antibiotics themselves but rather the ability of microbes to become resistant to them.

To a bacterium, development of antibiotic resistance is merely a particular adaptation for a given environment. The imposition of such selective pressures (i.e., antibiotics) impart the need to find adaptive mutations to provide growth advantages through natural [18–20] and adaptive [4, 5, 19, 21–23] means. It is sobering to consider the arsenal that bacteria have developed for multi-drug resistance [23–25] and the increasing occurrence of multi-drug resistant (Mdr) Gram-positive [26] and Gram-negative [24, 27, 28] pathogens. A detailed understanding of the adaptive process is essential to develop better therapeutic strategies targeting Mdr pathogens, for example through disarming virulence-associated factors rather than direct killing [29].

24.2 Bacterial Secretion Systems

Bacteria have evolved specialized secretion systems to support the transfer of macromolecules across cellular membranes; these secretion systems are numbered types I through VIII [22, 30–36]. Types I and V secretion systems are relatively simplistic, containing 1 to 3 component proteins, while Types II, III and IV are more complex [21, 37]. The type IV secretion system (T4SS) is the most complex, containing between 8 and 20 core proteins; bioinformatics has shown that T4SSs are ancestrally related to bacterial conjugation systems [38]. Below is a brief overview of secretion systems I, II, III, V, VI, VII and VIII (Sections 24.2.1 through 24.2.7); the type IV secretion system is discussed in greater detail in Section 24.3. As the current discussion of these multiple secretion systems is by necessity brief, the reader is directed to the many excellent and substantive reviews highlighted herein for greater insight into the particular aspects of the secretion systems and their roles in infection, virulence, and adaptation.

24.2.1 The Type I Secretion System

One of the most streamlined bacterial secretion systems is the type I secretion system (T1SS). The T1SS is a Sec-independent pathway that involves the transport of substrates with an

uncleaved carboxy-terminal signal sequence [39], for example the *E. coli* α-hemolysin HlyA [40]. In Mdr bacteria, one means of resistance is the efflux of antibiotics from the cell through this T1SS, a rather straightforward example of resistance through removal of the drug [23–25].

T1SSs contain three proteins: an outer membrane (OM) pore, an inner membrane (IM) bound ATP-binding cassette (ABC) used to power protein secretion, and an adapter protein that connects these two components [41 ,42]. The prototypical T1SS in *E. coli* is composed of the HlyB (ABC), TolC (OM pore) and HlyD (adapter) proteins [43–45]. Crystallographic analysis of TolC [46] has shown that a TolC trimer forms a 12-stranded antiparallel β-barrel that spans the OM, while the periplasm-spanning domain of the protein is composed of α-helices (Fig. 24.1). TolC forms a 140 Å (14 nm) long tunnel 3.5 nm in diameter through which effector molecules can travel [46]. In addition, HlyD has been shown to be trimeric, enabling its interaction with TolC; the resultant complex is a structure that spans both inner and OMs thereby bridging the periplasmic space [41, 42, 46].

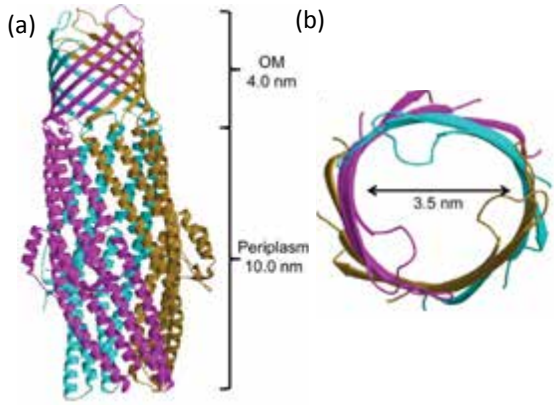

Figure 24.1 The T1SS protein TolC. (a) The full length TolC trimer (PDB ID 1EK9) [45] is composed of a 4 nm outer membrane-spanning β-barrel connected to a 10 nm α-helical periplasmic domain that interacts with the inner membrane protein HlyD enabling effector efflux from the cell. (b) End-on view of the outer membrane-spanning domain highlighting the 3.5 nm diameter opening of the TolC tunnel. Figures 24.1, 24.3b–e, 24.4a, and 24.5b,c were produced using Molscript [144] and Raster3D [145].

24.2.2 The Type II Secretion System

The type 2 secretion system (T2SS), first described in *Klebsiella oxytoca* [47] is one of the more complex secretion systems in addition to being one of the more versatile. For instance, *Vibrio cholera* employs a T2SS in the secretion of its cholera toxin [48–53] as does secretion of the Shiga toxin by enteropathogenic *E. coli* [51, 54–56]. In addition, a T2SS is utilized in the assembly of the type IV pilus (T4P), a fiber-like structure that serves multiple roles in the interaction of a bacteria and its environment, in *Pseudomonas aeruginosa* [37, 57–62]. Interestingly, T2SS proteins have been shown to have homologies to other secretion systems, including the type III secretion system (T3SS) [63, 64] and T4SS [37, 41, 65].

The T2SS is typically referred to as the main terminal branch (MTB) of the Sec-dependent pathway, also known as the general secretory pathway (GSP). The T2SS is utilized to secrete a range of effectors including proteases, cellulases, lipases, and toxins that destroy various tissues and contribute to disease [51]. Depending on the particular T2SS, the system is encoded by 12–16 genes generally localized to a single operon [49, 50]. Secretion through a T2SS is a two-step Sec-dependent process [66, 67]. The first step involves the ATP-dependant transport of a protein substrate containing an N-terminal signal sequence via the Sec pathway across the IM into the periplasm [41, 49–51, 65]. Once the protein has reached the periplasmic space, the signal peptide is cleaved, thereby enabling translocation across the OM through the OM secretion complex. This OM complex is a ring-like assembly of an integral membrane protein (for example PulD and PilQ in *V. cholera* and *P. aeruginosa* T2SS, respectively) that forms a 5–10 nm pore through which the toxin or T4P emerges [37, 51, 63].

24.2.3 The Type III Secretion System

Numerous Gram-negative pathogens, including *Salmonella typhimurium* [68] and *Burkholderia pseudomallei* [69], use a T3SS to deliver effector molecules to target cells. However, the prototypical T3SS is the *Yersina pestis* system, which delivers the Yop proteins [70]. Often termed the injectisome, T3SSs produce a flagella-like filament that is utilized by these pathogens during the infection process [41, 71]. With approximately 30 proteins, the T3SS is one

of the more complex secretion systems [41, 68, 69, 71]. Similar to T1SS, the T3SS is a Sec-independent secretion system; proteins secreted through a T3SS do not contain a cleavable signal peptide, a hallmark of proteins secreted via Sec-dependent pathways [72].

A defining feature of the T3SS is the needle complex, a 120 nm structure that spans both inner and OMs of the bacterium [69, 71, 72]. The 8 nm-wide injectisome needle extends out toward the target cell approximately 60–80 nm and is analogous to the flagellar hook [72–74]. It is through this needle complex that the contact dependent secretion of effector proteins into the target cell occurs. Effector proteins secreted by T3SSs have the capacity to manipulate the host cell in several ways. For example, some bacteria secrete effector proteins that generate a signal for the host cell to engulf the bacterium allowing for quick and efficient access into the host cell machinery and infection of the entire tissue, while others modify the host's cell cycle or induce apoptosis [75]. The T3SS is indeed a versatile weapon in the bacterial arsenal for infection.

24.2.4 The Type V Secretion System

The simplest protein secretion system is the type V secretion system (T5SS). All subclasses of the T5SS (Va, Vb, and Vc) share a common mechanism of secretion whereby transport through the IM is in a Sec- or SRP-mediated fashion, followed by effector self-translocation through the OM [41, 76, 77]. Both the Va and Vc subclass effector molecules contain a C-terminal β-domain connected to the effector domain that assembles into a transmembrane β-barrel, enabling the effector domain to cross the OM. Two such examples of the Va and Vc subclass proteins are the monomeric NaIP autotransporter of *Neisseria meningitides* [78] and the trimeric Hia adhesin of *Haemophilus influenzae* [79–81]. The Vb subclass is a two-partner system (Tps) that generates two polypeptides, the effector (TpsA) and translocator (TpsB). Both TpsA and TpsB contain their own signal sequence for translocation across the IM. In the periplasm TpsB, which recognizes a specific TpsA protein, forms a membrane-spanning β-barrel that is capable of exporting very large proteins (100 kDa) across the OM. An example of the Vb T5SS subclass is the SphB1 autotransporter of *Bordetella pertusis*, shown to be involved in the maturation and release of the filamentous hemagglutinin FhaB [41, 82].

24.2.5 The Type VI Secretion System

The Type VI secretion system (T6SS) is a relatively recently identified system that is utilized by both pathogenic and non-pathogenic Gram-negative bacteria including *V. cholerae*, *Y. pestis*, *S. typhimurium*, and *E. coli* [83]. As of 2009, T6SSs have been identified within 92 sequenced bacterial genomes, each containing approximately 15 to 25 genes [84]. T6SSs are tightly regulated with other virulence determinants, including T3SS, quorum sensing and flagellar synthesis through the crosstalk of multiple regulators [83–85]. This crosstalk of multiple regulators is likely a key component in bacterial pathogenesis mediated through T6SS effector secretion, and is an area of significant on-going research [85].

Structurally, T6SSs span both inner and OMs across the periplasm through a protein complex whose components have not entirely been elucidated [85], although most proteins identified thus far are employed in the formation of the protein channel that facilitates the translocation of substrates across the peptidoglycan (PG) layer [84]. Recent electron microscopy (EM) and X-ray crystallogrpahic studies indicate that the T6SS is analagous to the T4 phage baseplate assembly [86], suggesting a syringe-like mode of effector translocation. Bacteria with a functional T6SS will secrete both the hemolysin co-regulated protein (Hcp) and the valine-glycine repeat protein G (VgrG). Hcp forms a hexameric ring structure that polymerizes to form tubes that are 100 nm long, with outer and inner diameters of 9.0 and 4.0 nm, respectively [87]. The Hcp tube is capped by VgrG, which forms a trimer containing a C-terminal triple-stranded β-helix [86]; it is the VgrG trimer that forms a needle shaped structure used to breach the cell membrane [82, 86] and enable effector molecule delivery.

24.2.6 The Type VII Secretion System

The type VII secretion system (T7SS) is another recently identified secretion system, initially identified in the Gram-positive *Mycobacterium tuberculosis* [35]. A unique feature of *Mycobacterium* is the presence of a mycomembrane, which is formed through covalent cross-linking of mycolic acids (hydroxylated branch-chain fatty acids) to the cell wall forming a hydrophobic barrier [88]; the T7SS is required for protein secretion across the mycomembrane. Interestingly, the mycobacterial genome can encode up to five

of these transport systems, termed ESX-1 to ESX-5, and that two of these systems, ESX-1 and ESX-5, are involved in virulence [36].

Although there is limited structural data of the ESX-1 components, it is assumed that they form a multi-subunit cell envelope-spanning complex similar to that in type I–IV secretion systems [35]. It has, however, been shown through protein–protein interaction studies that the 6 kDa early secreted antigenic target (ESAT-6) and the 10 kDa culture filtrate protein (CFP-10) are functionally dependent on one another as each protein forms a 2-helix hairpin held together by hydrophobic interactions [89]. Both proteins have been shown to be important for the virulence of *M. tuberculosis*, as they are T-cell antigenic targets. Specifically, the disruption of genes Rv3860, Rv3871, and Rv3877 have been shown to prevent ESAT-6 and CFP-10 secretion thereby abolishing virulence [35]. Further research in the field will continue to shed light into this unique secretion system in which all of the secreted proteins are co-dependent on each other for secretion.

24.2.7 The Type VIII Secretion System

The type VIII secretion system (T8SS) is recognized in *E. coli* as being responsible for the formation of aggregative fibers, also known as curli [90]. These fibers are primarily involved in bacterial biofilm formation and attachment to nonbiotic surfaces [91]. The key component of these systems is the formation of the oligomeric secretion channel, formed by lipoprotein CsgG, in the OM similar to T2SS and T5SS. Curli are extracellular fibers of 4 to 7 nm in diameter, involved in cell-to-cell contacts in Gram-negative bacteria [92]. The expression of the curli subunits, CsgA and CsgB, are highly regulated by environmental signals and the two-component systems [93–95]. The formation of the curli is restricted to the cell surface, where the secretion of the soluble unstructured curli subunits [96–97] occurs via the T8SS transport system [98]. The curli fibers share biochemical and structural characteristics with amyloid fibers, formed of fibrous protein aggregates, causing Alzheimer's and Parkinson's diseases [36]. Unlike the misfolded protein amyloids, curli result from dedicated biosynthetic pathways by the T8SS and are considered important amyloids for bacterial survival [99].

24.3 The Type IV Secretion System

The type IV secretion system (T4SS) is the most complex of the secretion systems, containing between 8 and 20 core proteins; bioinformatics has shown that T4SSs are ancestrally related to bacterial conjugation systems [37, 38, 100–104]. The T4SS is also the most versatile secretion system, playing multiple roles in the cell (Fig. 24.2). In addition to conjugative DNA transport, T4SSs are utilized in DNA uptake/release [101–105] and can mediate the transport of virulence factors, such as the CagA oncoprotein of *Helicobacter pylori* [104, 105], the pertussis toxin of *Bordetella spp.* [106] and the oncogenic Ti plasmid of *Agrobacterium tumefaciens* [102] into target cells. Due to subtleties in genetic organization, shared homologies and evolutionary relationships, T4SSs have been differentially classified depending upon their roles in virulence or conjugation [37, 102, 104]. These systems are highlighted below.

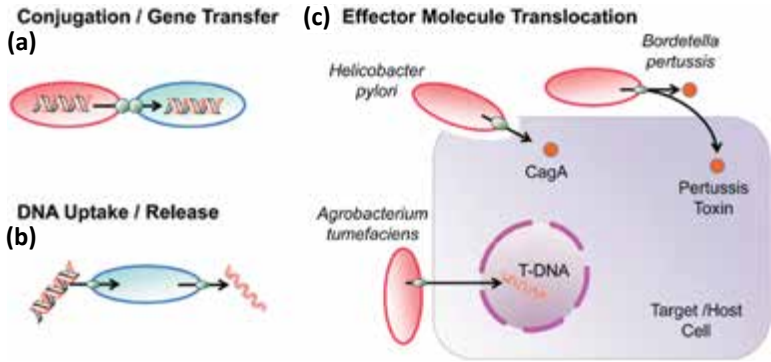

Figure 24.2 The versatile T4SS. Gram-negative bacteria utilize T4SSs for a range of functions including: (a) conjugation/gene transfer, for example in the F plasmid of *E. coli* [37, 38]; (b) DNA uptake and/or release as seen in *C. jejuni*, *H. pylori* and *N. gonorrhoeae* [102–105]; and (c) translocation of effector molecules, such as the tumor-inducing (Ti) plasmid of *A. tumefaciens* (T-DNA) [102], the pertussis toxin of *B. pertussis* [106] or the CagA oncoprotein of *H. pylori* [104, 105] (Adapted with permission from Cascales and Christie (2003). *Nat. Rev. Microbiol.*, **1**, 137–149 [104]).

24.3.1 Secretion of Effector Molecules: CagA and the Ti Plasmid

The T4SS plays a major role in the infection process of many Gram-negative species. The archetype for T4SSs is the tumor-inducing (Ti) plasmid from *A. tumefaciens*, the main function of which is the secretion of effector T-DNA into cells resulting in crown gall disease in plants [102, 104, 107, 108]. As such, a significant body of functional biochemical and genetic research has been conducted on this system [100, 102–105, 108–111]. Based on the evolutionarily similarities/homologies of the core proteins, nomenclature of T4SS components can be related to the virulence (Vir) proteins of the Ti system (Table 24.1).

A prime example of an effector protein secreted by a T4SS is the CagA oncoprotein of *H. pylori*, the causative agent of chronic active gastritis (Cag), peptic ulcer disease, the formation of gastric mucosa-associated lymphoma and gastric cancer [112]. There are three T4SS subtypes recognized in *H. pylori*; the most conserved and well studied is the ComB system, which mediates the transport of environmental DNA into the bacteria genome. The second subtype is less conserved and is associated with genetic exchange. The third T4SS subtype is present in virulent strains and is responsible for the production and secretion of the oncogenic CagA (homologies to the Ti system proteins are shown in Table 24.1). During the infection process, the bacterium secretes CagA into the cellular cytosol through a T4SS whose genes are localized within the Cag pathogenicity island. Upon injection of CagA into a host cell, the protein is phosphorylated and can interact with more than 20 signal transduction proteins. These interactions are detrimental to host epithelial cells, which result in loss of function in cell–cell adhesion, signaling, adherence, and proliferation [113–115]. In addition to CagA, the T4SS delivers a portion of the bacterial PG into the cell. The PG is recognized by Nod1 resulting in induction of NFκB-activated transcription of proinflammatory response regulators by the cell to the *H. pylori* infection [113].

The architecture of the *H. pylori* Cag T4SS is shown in Fig. 24.3. Cagβ (a VirD4 homolog) is a hexameric coupling protein that recruits substrates to the T4SS apparatus (Fig. 24.3b) [116]. These proteins include CagE (VirB3), CagW (VirB6), and CagV (VirB8) (Fig. 24.3d) [117], which assist in nucleation of the T4SS channel

and substrate secretion [110, 114, 115]. Cagα (VirB11) is an ATPase and forms a hexameric ring 10–12 nm in diameter at the cytoplasmic base of the T4SS (Fig. 24.3e) [118]; this is a dynamic structure, opening and closing depending ATP binding and hydrolysis [107, 119]. CagA is funneled through these structures into the core T4SS pore complex of CagT-X-Y (VirB7-9-10) for transfer/secretion. The T4SS pore complex spans both inner and OMs, breaching the PG through the hydrolase activity of Cagγ (VirB1) [110, 120].

Table 24.1 Homologies/similarities between several type IV secretion systems

	T4SS system				
(Proposed)	**Effector transport**		**Conjugation**		
function/homology	**Ti**	**Cag**	**F**	**R27**	**pKM101**
Pilin	VirB2	CagC	TraA	TrhA	TraM
Cyclase				TrhP	
Acetylase			TraX		
Lysozyme	VirB1	Cagγ	Orf169	Orf130	TraL
Pore	VirB3	CagE	TraL	TrhL	TraA
Secretion	VirB4	CagE	TraC	TrhC	TraB
Pore	VirB5	CagL	TraE	TrhE	TraC
Pore	VirB6	CagW	TraG	TrhG	TraD
Lipoprotein	VirB7	CagT	TraV	TrhV	TraN
Pore	VirB8	CagV			TraE
Secretion/pore	VirB9	CagX	TraK	TrhK	TraO
Pore	VirB10	CagY	TraB	TrhB	TraF
Secretion	VirB11	Cagα			TraG
Pore			TraF	TrhF	
Pore			TraH	TrhH	
Pore			TraW	TrhW	
Pore			TrbC	TrhW	
Pore			TraU	TrhU	
Adhesin			TraN	TrhN	
Relaxase			TraI	TraI	TraI
Transport			TraD	TraG	TraJ

Note: Adapted from references [109–111] and references therein, with permission.

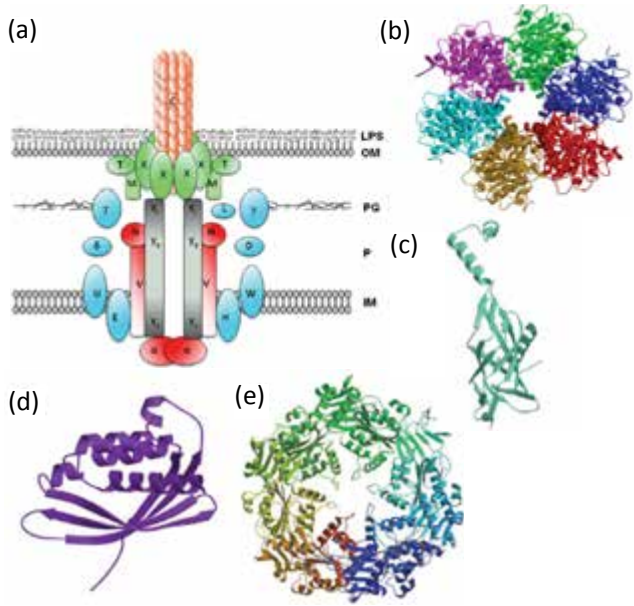

Figure 24.3 The *H. pylori* Cag T4SS. (a) A model of the Cag T4SS spanning the inner membrane (IM), periplasm (P), peptidoglycan (PG), outer membrane (OM) and lipopolysaccharide (LPS). The CagA oncoprotein is transferred through this complex into target cells. T4SS component proteins are labeled, and homologies to other T4SSs are shown in Table 24.1. (b) Structure of the hexameric coupling protein Cagβ (VirD4) homolog TrwB from the R388 conjugative plasmid (PDB ID 1EQS) [105]. (c) The periplasmic domain of the CagY (VirB10) homolog ComB10 from *H. pylori* (PDB ID 2BHV) [117], a component of the T4SS pore complex at the outer membrane. (d) The *A. tumefaciens* VirB8 (CagV) protein (PDB ID 2CC3) [119], which assists in nucleation of the T4SS channel and substrate secretion. (e) The hexamierc VirB11 (Cagα) (PDB ID 1NLZ) [118], an ATPase that localizes to the cytoplasmic base of the T4SS complex.

24.3.2 Bacterial Conjugation: The F Plasmid

Bacterial conjugation is the transfer of DNA from a donor to a recipient cell thereby distributing new genetic elements for survival in unique environments [4, 5], including genes responsible for Mdr [23, 32]. Conjugation is a plasmid-driven process [32, 33, 121], and is initiated by the interaction of the conjugative pilus of a donor

cell with the cell surface of a recipient [122]. The extension and retraction of the conjugative pilus is a dynamic process [123] aimed at actively identifying potential recipient cells. After attaching to a recipient, the conjugative pilus is retracted by the conjugative T4SS, resulting in the intimate association between donor and recipient cell, known as a mating pair [124–126]. Plasmid DNA is transferred through a membrane-associated supramolecular structure known as the mating pair formation (Mpf) complex, composed of T4SS proteins. The Mpf complex stabilizes the mating pair to shear forces [127, 128]; however, it is not required for DNA transfer. Indeed, F plasmid transfer can occur over large distances in liquid media without a stable mating pair via the F pilus itself [129]. Following the ATP-dependent transfer of the plasmid ssDNA, the recipient cell is released, the complementary strand of plasmid DNA is synthesized and the recipient cell is now a potential donor.

Initially identified by Lederberg & Tatum [130], the F plasmid of *E. coli* remains a paradigm for studying bacterial conjugation. All genes necessary for F-mediated conjugation are located in the 33.3 kb transfer (*tra*) region of the 100 kb F plasmid [131]. Sequence and bioinformatics analysis indicate that the F plasmid shares 8 of the 10 essential T4SS proteins, including the pilin (*traA*) itself, of other conjugative T4SS (Table 24.1) [37, 38, 131]. During F-mediated conjugation, recipient cell binding is likely mediated by the F pilus itself; unlike other cellular-binding pili (i.e., Pap pili [132]), the F pilus does not appear to have a tip-associated adhesin. The mating pair is stabilized through the interactions of $TraN_F$ and $TraG_F$, and F plasmid DNA is transferred from donor to recipient cell through a $TraB_F$-$TraK_F$-$TraV_F$ core complex [133] by the ATP-dependent coupling protein $TraD_F$.

Despite the accumulation of a wealth of biochemical data for several T4SSs [37, 38, 102–105, 107–109], detailed structural studies of conjugative T4SSs are only more recently becoming available. Recently, cryo-electron microscopic [134] and crystallographic [135] studies of the T4SS core complex from the conjugative pKM101 plasmid, an IncN homolog of the F plasmid, have been reported (Fig. 24.4). In the core complex of the pKM101 T4SS, $TraF_{KM101}$, a homolog of $TraB_F$/VirB10, co-purifies with $TraN_{KM101}$ ($TraV_F$/VirB7) and $TraO_{KM101}$ ($TraK_F$/VirB9) as a 1.1 MDa complex [134]. The TraF-N-O trimer form a membrane bound tetradecameric complex forming a T4SS pore enabling substrate passage [134, 135].

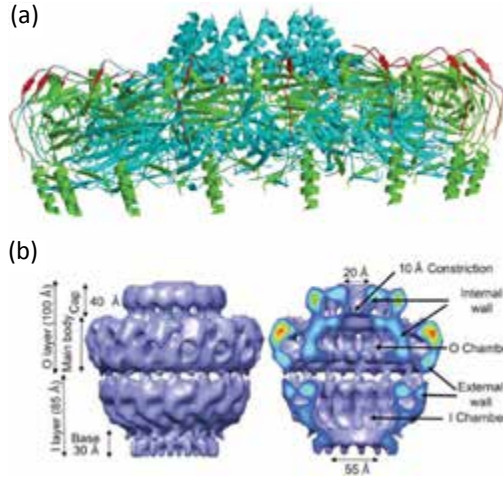

Figure 24.4 A T4SS pore complex. (a) The structure of the TraF-N-O tetradecamer from the pKM101 conjugative plasmid (PDB ID 3JQO) (Adapted with permission from Chandran et al. (2009). *Nature*, **462**, 1011–1016 [135]). This tetradecamer, composed of $TraF_{KM101}$ (cyan), $TraN_{KM101}$ (red) and $TraO_{KM101}$ (green), forms the cap region of the pore located at the outer membrane. (b) Cryo-EM reconstruction of the T4SS pore, which contains an outer (O) and inner (I) layer (Adapted with permission from Fronzes et al. (2009). *Science*, **323**, 266–268 [135]). The left image is a full reconstruction of the pore, while the right image is a cut-away and highlights transverse nature of the complex itself and dimensions of the inner and outer membrane openings.

Overall, the core complex (Fig. 24.4b) is approximately 19 nm in height with an overall diameter of 17.2 nm and is composed of an inner (I) and outer (O) layer [134]. The O layer has two sections: the cap formed by the α2 and α3 helices of $TraF_{KM101}$ (Fig. 24.4a) has an outer diameter of 11.0 nm and is 4.0 nm high; the main body itself is 18.5 nm in diameter and 6.0 nm high (Fig. 24.4b) [134, 135]. The cap region contains a 2.0 nm diameter opening at the surface that tapers off to 1.0 nm as it moves inward to the main body of the pore. The 3 nm internal chamber of the complex is 11 nm wide and is formed at the interface between the I and O layers (Fig. 24.4b). The I layer can be described as a cup with a chamber similar to that of the O layer 6.0 nm high. The chamber tapers off as it approaches the IM, and has a 5.5 nm opening at the base

(Fig. 24.4b) [135], thereby allowing the assembly of the conjugative pilus and DNA transfer from donor to recipient cell.

Structural characterization of T4SS-mediated conjugation to date has focused primarily on the F pilus itself and the initiation of conjugative DNA transfer. The F pilus is a long, flexible polymer of the pilin protein (TraA) with an outer diameter of 8–9 nm [38, 136]. In addition, while no structure of TraA (the pilin) is available, the structure of the pilus itself was recently determined using cryo-EM methods (Fig. 24.5a) [136]. The F pilus is unique in that it adopts an entirely different symmetry from other pili, for example the T2SS-assembled T4P of *P. aeruginosa* [59, 60]. The F pilus has two distinct subunit packing schemes that both result in a central lumen of ~3.0 nm, large enough for the passage of ssDNA through

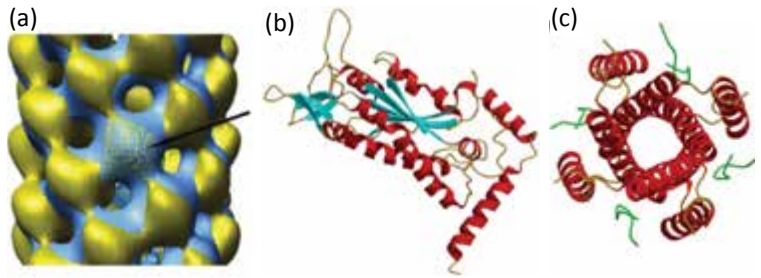

Figure 24.5 Structural characterization of F plasmid-mediated conjugative transfer. (a) Cryo-EM reconstruction of the conjugative F-pilus [136]. Assembly of the F-pilus from TraA pilin monomer (highlighted by a black arrow and yellow mesh) is different than other pili [59, 60]. Shown is a superposition of reconstructions with either 4-start right handed (yellow) or 1-start left-handed (blue) helical symmetry, that appear to coexist in the F pilus and result in an ~3.0 nm central lumen [136]. (Adapted with permission from Wang et al. (2009). *J. Mol. Biol.*, **385**, 22–29 [136]). (b) Crystal structure of the N-terminal relaxase domain of TraI (PDB ID 1P4D) [138]. TraI interacts with the F plasmid at origin of transfer (*oriT*) through via a beta-sheet binding cleft (cyan), resulting in the nicking of the F plasmid DNA. (c) The crystal structure of the interaction of a C-terminal peptide of TraD (green) with the core eight-helix bundle (red) of TraM (PDB ID 3D8A) [144]. TraM binds the nicked DNA near the oriT and transports it to the base of the F T4SS where it interacts with TraD. The interaction of TraM and TraD results in the ATP-dependent transfer of the conjugative ssDNA from donor to recipient cell through the central lumen of the F pilus.

the central core of the pilus [136]. DNA transfer is initiated through the interaction of the relaxase TraI with the F plasmid at the origin of transfer (*oriT*) (Fig. 24.5b) [137, 138] through a binding cleft bounded by a 5-stranded β-sheet and flexible α-helical domain [139–141]. Following interaction with TraI and the nicking of plasmid DNA, TraM, which binds near the *oriT*, is recruited. TraM contains a core eight helical bundle [142], which interacts with the C-terminal domain of TraD (Fig. 24.5c) [143] for ATP-dependent transfer of the ssDNA through the core T4SS complex.

24.4 Conclusions

Similar to human delivery machines such as planes, trains, and automobiles, bacteria have developed nanoscale machines, the types I-VIII secretion systems, to aid in their delivery services. Bacterial secretion systems provide routes of virulence and the transport of resistance markers, providing significant challenges to human health. Secretion systems, from the simple three protein T1SS to the complex multi-protein T4SS, provide bacteria a range of means by which they can affect resistance, infection, virulence and genetic diversity via the transfer of DNA, effector molecules and/or toxins from one cell to another. As this brief review highlights, there is significant understanding into the functions of these complex bacterial nanomachines. However, much remains unclear. Moving forward, the structural characterization of the protein components of these systems will lead to a more comprehensive view of the secretion systems, and reveal potential novel nano-drug interactions with these cellular nanomachines. A more comprehensive understanding of the transfer processes used by microorganisms for the delivery of molecules into and out of cells can also lead to more tailored nanobiopharmaceutics, improving drug bioavailability and efficacy.

Abbreviations

ABC : ATP-Binding Cassette
Cag : Chronic atrophic gastritis, also used form Cag protein nomenclature (i.e., CagA)

CFP-10 : Culture filtrate protein 10
CM : Cellular membrane
EHEC : Enterohemorrhagic *Escherichia coli*
ESAT-6 : Early secretory antigenic target 6
ESX : Early secretory antigenic target 6 system
GSP : General secretory pathway
Hcp : Hemolysin co-regulated protein
HUS : Hemolytic uremic syndrome
IncN : Incompatibility group N
Mdr : Multi-drug resistance
Mpf : Mating pair formation
MTB : Main terminal branch
NFκB : Nuclear factor κB
OM : Outer membrane
oriT : Origin of transfer
PG : Peptidoglycan
T1SS : Type I secretion system
T2SS : Type II secretion system
T3SS : Type III secretion system
T4SS : Type IV secretion system
T5SS : Type V secretion system
T6SS : Type VI secretion system
T7SS : Type VII secretion system
T8SS : Type VIII secretion system
Ti : Tumor inducing
T-DNA : Tumor-inducing (Ti) plasmid from *Agrobacterium tumefaciens*
tra : Transfer region(and genes/proteins) of the *E. coli* F plasmid
Tps : Two-partner system
Va : The T5aSS subclass
Vb : The T5bSS subclass
Vc : The T5cSS subclass
VgrG : Valine-glycine repeat protein
Vir : Virulence genes/proteins of the Ti plasmid

Disclosures and Conflict of Interest

This work was supported by grants from the Natural Sciences & Engineering Council of Canada (NSERC), the Canadian Foundation for Innovation, and York University.

The authors declare that they have no conflict of interest and have no affiliations or financial involvement with any organization or entity discussed in this chapter. This includes employment, consultancies, honoraria, grants, stock ownership or options, expert testimony, patents (received or pending) or royalties. No writing assistance was utilized in the production of this chapter and the authors have received no payment for its preparation.

Corresponding Author

Dr. Gerald F. Audette
Department of Chemistry and the Centre for Research on Biomolecular Interactions, York University
Life Sciences Building 327C, 4700 Keele Street
Toronto, Ontario M3J 1P3, Canada
Email: audette@yorku.ca

About the Authors

Agnesa Shala was born in Kosovo and moved to Canada in 1999. She received her BSc (Hons.) in chemistry in 2007 and PhD in 2014. Dr. Shala's current research interests focus on protein–protein interactions in type IV secretion systems, in particular the pore-forming proteins TraW and TrbC of the conjugative F-plasmid of *E. coli* and the structural consequences of protein phosphorylation in sensing two component systems in *Staphylococcus aureus*.

Michele Ferraro received her BSc (Hons.) in 2011 from the Department of Biology at York University. Ms. Ferraro's MSc research focused on the structural and functional characterization of the thioredoxin-motif containing protein TraF of the type IV secretion system from the conjugative F-plasmid of *E. coli*., and she received her MSc in 2013.

Gerald F. Audette is an associate professor in the Department of Chemistry at York University in Toronto, Canada. Current research directions in his lab include structure/function studies of proteins involved in bacterial conjugation (lateral gene transfer) systems, the structural and functional characterization of several type IV pilins (the monomeric subunit of the pilus), their assembly systems, and adapting these unique protein systems for applications in bionanotechnology. Prior to joining the faculty at York University, Dr. Audette conducted his doctoral research in the laboratory of Profs. Louis Delbaere and J. Wilson Quail at the University of Saskatchewan and postdoctoral fellowships in the laboratories of Profs. Bart Hazes and Laura Frost at the University of Alberta. Dr. Audette serves on the editorial board of *Current Biomedical Engineering* and was co-editor-in-chief of the *Journal of Bionanoscience* from 2008 to 2010. He is a founding member of the Centre for Research on Biomolecular Interactions at York University and is currently its acting director.

References

1. Little, A. E. F., Robinson, C. J., Peterson, S. B., Raffa, K. F., Handelsman, J. (2008). Rules of engagement: Interspecies interactions that regulate microbial communities. *Ann. Rev. Microbiol.*, **62**, 375–401.
2. Davies, J. (1994). Inactivation of antibiotics and the dissemination of resistance genes. *Science*, **264**(5157), 375–382.
3. Cooper, T. F. (2007). Recombination speeds adaptation by reducing competition between beneficial mutations in populations of *Escherichia coli*. *PLoS Biol.*, **5**, e225.
4. Ochman, H., Lawrence, J. G., Groisman, E. A. (2000). Lateral gene transfer and the nature of bacterial innovation. *Nature*, **405**, 299–304.
5. Wilkins, B. M., Frost, L. S. (2001). Mechanisms of gene exchange between bacteria. In: M. Sussman, ed. *Molecular Medical Microbiology*, Academic Press, London, pp. 355–400.
6. Morens, D. M., Folkers, G. K., Fauci, A. S. (2004). The challenge of emerging and re-emerging infectious diseases. *Nature*, **430**, 242–249.
7. Morens, D. M., Folkers, G. K., Fauci, A. S. (2008). Emerging infections: A perpetual challenge. *Lancet Infect. Dis.*, **8**, 710–719.
8. World Health Organization. Outbreaks of *E. coli* O104:H4 infection. Available at: http://www.euro.who.int/en/health-topics/emergencies/

international-health-regulations/outbreaks-of-e.-coli-o104h4-infection (accessed on April 25, 2014).

9. CTV News, Canadian Press. Ontario calls in federal help in *C. difficile* outbreak.Availableat:http://www.ctv.ca/CTVNews/Health/20110707/clostridium-difficile-outbreak-help-110707 (accessed on April 25, 2012).
10. Fleming, A. (1929). On the antibacterial action of cultures of a penicillium, with special reference to their use in the isolation of *B. influenzae*. *Br. J. Exp. Pathol.*, **10**, 226–236.
11. Davies, J. (1994). Inactivation of antibiotics and the dissemination of resistance genes. *Science*, **264**(5157), 375–382.
12. Walsh, C. (2003). Where will new antibiotics come from? *Nat. Rev. Microbiol.*, **1**, 65–70.
13. Nathan, C. (2004). Antibiotics at the crossroads. *Nature*, **431**(7011), 899–902.
14. Kuhn, P., Wilson, K., Pach, M. G., Stevens, R. C. (2002). The genesis of high-throughput structure-based drug discovery using protein crystallography. *Curr. Opin. Chem. Biol.*, **6**, 704–710.
15. Kan, C.-C., Hambly, K., Debe, D. A. (2005). Structure-based drug discovery. In: Rapley, R., Harborn, S., eds. *Molecular Analysis and Genome Discovery*. John Wiley & Sons, Ltd, Chichester, UK, pp. 295–322.
16. Erhardt, P. (2009). Drug discovery. In: Hacker, M., Messer, W., Bachman, K., eds. *Pharmacology*. Academic Press, San Diego, USA; pp. 475–500.
17. Lanter, J., Zhang, X., Sui, Z. (2011). Medicinal chemistry inspired fragment-based drug discovery. *Methods Enzymol.*, **493**, 421–445.
18. Barrick, J. E., Yu, D. S., Yoon, S. H., Jeong, H., Oh, T. K., Schneider, D., Lenski, R. E., Kim, J. F. (2009). Genome evolution and adaptation in a long-term experiment with *Escherichia coli*. *Nature*, **461**(7268), 1243–1247.
19. Cooper, T. F., Rozen, D. E., Lenski, R. E. (2003). Parallel changes in gene expression after 20,000 generations of evolution in *Escherichia coli*. *Proc. Natl. Acad. Sci. U. S. A.*, **100**, 1072–1077.
20. Sniegowski, P. D., Gerrish, P. J., Lenski, R. E. (1997). Evolution of high mutation rates in experimental populations of *E. coli*. *Nature*, **387**(6634), 703–705.
21. Remaut, H., Waksman, G. (2004). Structural biology of bacterial pathogenesis. *Curr. Opin. Struct. Biol.*, **14**, 161–170.

22. Juhas, M., Crook, D. M., Hood, D. W. (2008). Type IV secretion systems: Tools of bacterial horizontal gene transfer and virulence. *Cell. Microbiol.*, **10**, 2377–2386.

23. Alekshun, M. N., Levy, S. B. (2007). Molecular mechanisms of antibacterial multidrug resistance. *Cell*, **128**, 1037–1050.

24. Poole, K. (2001). Multidrug resistance in Gram-negative bacteria. *Curr. Opin. Microbiol.*, **4**, 500–508.

25. Levy, S. B., Marshall, B. (2004). Antibacterial resistance worldwide: Causes, challenges and responses. *Nat. Med.*, **10**, S122–S129.

26. Witte, W., Cuny, C., Klare, I., Nubel, U., Strommenger, B., Werner, G. (2008). Emergence and spread of antibiotic-resistant Gram-positive bacterial pathogens. *Int. J. Med. Microbiol.*, **298**, 365–377.

27. Schubert, S., Darlu, P., Clermont, O., Wieser, A., Magistro, G., Hoffman, C., Weinert, K., Tenaillon, O., Matic, I., Denamur, E. (2008). Role of intraspecies recombination in the spread of pathogenicity islands within the *Escherichia coli* species. *PLoS Pathog.*, **5**, e1000257.

28. Ota, K. V., Jamieson, F., Fisman, D. N., Jones, K. E., Tamari, I. E., Ng, L.-K., Towns, L., Rawte, P., Di Prima, A., Wong, T., Richardson, S. (2009). Prevalence of and risk factors of quinoline-resistant *Neisseria gonorrhoeae* infection in Ontario. *Can. Med. Assoc. J.*, **180**, 287–290.

29. Baron, C., Coombes, B. (2007). Targeting bacterial secretion systems: Benefits of disarmament in the microcosm. *Infect. Disord. Drug Targets*, **7**, 19–27.

30. Thanassi, D. G., Hultgren, S. J. (2000). Multiple pathways allows for protein secretion across the bacterial outer membrane. *Curr. Opin. Cell Biol.*, **12**, 420–430.

31. Chen, I., Christie, P. J., Dubnau, D. (2005). The ins and outs of DNA transfer in bacteria. *Science*, **310**, 1456–1460.

32. Frost, L. S., Leplae, R., Summers, A. O., Toussaint, A. (2005). Mobile genetic elements: The agents of open source evolution. *Nat. Rev. Microbiol.*, **3**, 722–732.

33. Thomas, C. M., Nielsen, K. M. (2005). Mechanisms of, and barriers to, horizontal gene transfer between bacteria. *Nat. Rev. Microbiol.*, **3**, 711–721.

34. Saier, M. H., Jr. (2006). Protein secretion and membrane insertion systems in Gram-negative bacteria. *J. Membr. Biol.*, **214**, 75–90.

35. Abdallah, A. M., Gey van Pittius, N. C., DiGiuseppe Champion, P. A., Cox, J., Luirink, J., Vandenbrouke-Grauls, C. M. J. E., Appelmelk, B. J., Bitter, W.

(2007). Type VII secretion—mycobacteria show the way. *Nat. Rev. Microbiol.*, **5**, 883–891.

36. Chapman, M. R., Robinson, L. S., Pinker, J. S., Roth, R., Heuser, J., Hammar, M., Normak, S., Hultgren, S. J. (2002). Role of *Escherichia coli* curli operons in directing amyloid fiber formation. *Science*, **295**, 851–855.
37. Hazes, B., Frost, L. S. (2008). Towards a systems biology approach to study type II/IV secretion systems. *Biochim. Biophys. Acta*, **1778**, 1389–1850.
38. Lawley, T. D., Klimke, W. A., Gubbins, M. J., Frost, L. S. (2003). F factor is a true type IV secretion system. *FEMS Microbiol. Lett.*, **224**, 1–15.
39. Duong, F., Lazdunski, A., Murgier, M. (1996). Protein secretion by heterologous bacterial ABC-transporters: The C-terminus secretion signal of the secreted protein confers high recognition specificity. *Mol. Microbiol.*, **21**, 459–470.
40. Hueck, C. J. (1998). Type III protein secretion systems in bacterial pathogens of animals and plants—cellular and molecular impact of type III secretion in bacteria. *Microbiol. Mol. Biol. Rev.*, **62**, 379–433.
41. Henderson, I. R., Navarro-Garcia, F., Desvaux, M., Fernandez, R. C., Aldeen, D. A. (2004). Type V protein secretion pathway: The autotransporter story. *Microbiol. Mol. Biol. Rev.*, **68**(4), 692–744.
42. Bleves, S., Viarre, V., Salacha, R., Michel, G. P. F., Filloux, A., Voulhous, R. (2010). Protein secretion systems in *Pseudomonas aeruginosa*: A wealth of pathogenic weapons. *Int. J. Med. Microbiol.*, **300**, 534–543.
43. Binet, R., Letoffe, S., Ghigo, J. M., Delepelaire, P., Wandersman, C. (1997). Protein secretion by Gram-negative bacterial ABC exporters—a review. *Gene*, **192**, 7–11.
44. Gentschev, I., Dietrich, G., Goebel, W. (2002). The *E. coli* α-hemolysin secretion system and its use in vaccine development. *Trends Microbiol.*, **10**, 39–45.
45. Holland, I. B., Schmitt, L., Young, J. (2005). Type 1 protein secretion in bacteria, the ABC-Transporter dependent pathway. *Mol. Membr. Biol.*, **22**, 29–39.
46. Koronakis, V., Sharff, A., Koronakis, E., Luisi, B., Hughes, C. (2000). Crystal structure of the bacterial membrane protein TolC central to multidrug efflux and protein export. *Nature*, **405**, 914–919.
47. d'Enfert, C., Ryter, A., Pugsley, A. P. (1987). Cloning and expression in *Escherichia coli* of the *Klebsiella pneumonia*e genes for production, surface localization and secretion of the lipoprotein pullulanase. *EMBO J.*, **6**, 3531–3538.

48. Zhang, R., Scott, D. L., Westbrook, M. L., Nance, S., Spangler, B. D., Shipley, G. G., Westbook, E. M. (1995). The Three-dimensional crystal structure of Cholera Toxin. *J. Mol. Biol.*, **251**, 563–573.

49. Sandkvist, M. (2001). Biology of type II secretion. *Mol. Microbiol.*, **40**, 271–283.

50. Sandkvist, M. (2001). Type II secretion and pathogenesis. *Infect. Immun.*, **69**, 3523–3535.

51. Johnson, T. L., Abendroth, J., Hol, W. G. J., Sandkvist, M. (2006). Type II secretion: From structure to function. *FEMS Microbiol. Lett.*, **255**(2), 175–186.

52. Sanchez, J., Holmgren, J. (2008). Cholera toxin structure, gene regulation and pathophysiological and immunological aspects. *Cell. Mol. Life Sci.*, **65**, 1347–1360.

53. Locht, C., Coutte, L., Mielcarek, N. (2011). The ins and outs of pertussis toxin. *FEBS J.*, **278**, 1–15.

54. Karmali, M. A., Ptetric, M., Lim, C., Fleming, P. C., Arbus, G. S., Lior, H. (1985). The association between idiopathic haemolytic uremic syndrome and infection by verotoxin-producing *Escherichia coli*. *J. Infect. Dis.*, **151**, 775–782.

55. Karmali, M. (2004). Infection by shiga toxin–producing *Escherichia coli*. *Mol. Biotechnol.*, **26**, 117–122.

56. Gyles, C. L. (2007). Shiga toxin–producing *Escherichia coli*: An overview. *J. Anim. Sci.*, **85**, E45–E62.

57. Mattick, J. S. (2002). Type IV pili and twitching motility. *Ann. Rev. Microbiol.*, **56**, 289–314.

58. Peabody, C. R., Chung, Y. J., Yen, M.-R., Vidal-Ingigliardi, D., Pugsley, A.P., Saier, M. H., Jr. (2003). Type II protein secretion and its relationship to bacterial type IV pili and archaeal flagella. *Microbiology*, **149**, 3051–3072.

59. Craig, L., Pique, M. E., Tainer, J. A. (2004). Type IV pilus structure and bacterial pathogenicity. *Nat. Rev. Microbiol.*, **2**, 363–378.

60. Craig, L., Li, J. (2008). Type IV pili: Paradoxes in form and function. *Curr. Opin. Struct. Biol.*, **18**, 267–277.

61. Burrows, L. L. (2005). Weapons of mass retraction. *Mol. Microbiol.*, **57**, 878–888.

62. Audette, G. F., Hazes, B. (2007). Development of protein nanotubes from a multi-purpose biological structure. *J. Nanosci. Nanotechnol.*, **7**, 2222–2229.

63. Bitter, W., Koster, M., Latijnhouwers, M., de Cock, H., Tommassen, J. (1998). Formation of oligomeric rings by XcpQ and PilQ, which

are involved in protein transport across the outer membrane of *Pseudomonas aeruginosa*. *Mol. Microbiol.*, **27**, 209–219.

64. Koebnik, R., Locher, K. P., van Gelder, P. (2000). Structure and function of bacterial outer membrane proteins: Barrels in a nutshell. *Mol. Microbiol.*, **37**, 239–253.
65. Filloux, A. (2004). The underlying mechanisms of type II protein secretion. *Biochim. Biophys. Acta*, **1694**, 163–179.
66. vanWely, K. H., Swaving, J., Freundl, R., Driessen, A. J. (2001). Translocation of proteins across the cell envelope of Gram-positive bacteria. *FEMS Microbiol. Rev.*, **25**, 437–454.
67. Economou, A. (2002). Bacterial secretome: The assembly manual and operating instructions. *Mol. Membr. Biol.*, **19**, 159–169.
68. Valdez, Y., Ferreira, R. B., Finlay, B. B. (2009). Molecular mechanisms of *Salmonella* virulence and host resistance. *Curr. Top. Microbiol. Immunol.*, **337**, 93–127.
69. Sun, G. W., Gan, Y.-H. (2010). Unraveling type III secretion systems in the highly versatile *Burkholderia pseudomallei*. *Trends Microbiol.*, **18**, 561–568.
70. Michiels, T., Wattiau, P., Brasseur, R., Ruysschaert, J.-M., Cornelis, G. (1990). Secretion of Yop Proteins by Yersiniae. *Infect. Immun.*, **58**, 2840–2849.
71. Hayes, C. S., Aoki, S. K., Low, D. A. (2010). Bacterial contact-dependent delivery systems. *Ann. Rev. Genet.*, **44**, 71–90.
72. Galán, J. E., Collmer, A. (1999). Type III secretion machines: Bacterial devices for protein delivery into host cells. *Science*, **284**, 1322–1328.
73. Aizawa, S. I. (2001). Bacterial flagella and type III secretion systems. *FEMS Microbiol. Lett.*, **202**, 157–164.
74. Blocker, A., Komoriya, K., Aizawa, S. I. (2003). Type III secretion systems and bacterial flagella: Insights into their function from structural studies. *Proc. Natl. Acad. Sci. U. S. A.*, **100**, 3027–3030.
75. Gophna, U., Ron, E. Z., Graur, D. (2003). Bacterial type III secretion systems are ancient and evolved by multiple horizontal-transfer events. *Gene*, **312**, 151–163.
76. Henderson, I. R., Navarro-Garcia, F., Nataro, J. P. (1998). The great escape: Structure and function of the autotransporter proteins. *Trends Microbiol.*, **6**, 370–378.
77. Henderson, I. R., Cappello, R., Nataro, J. P. (2000). Autotransporter proteins, evolution and redefining protein secretion. *Trends Microbiol.*, **8**, 529–532.

78. Oomen, C. J., van Ulsen, P., Van Gelder, P., Feijen, M., Tommassen, J., Gros, P. (2004). Structure of the translocator domain of a bacterial autotransporter. *EMBO J.*, **23**, 1257–1266.

79. St Geme, J. W. III, and Cutter, D. (2000). The *Haemophilus influenzae* Hia adhesin is an autotransporter protein that remains uncleaved at the C terminus and fully cell associated. *J. Bacteriol.*, **182**, 6005–6013.

80. Surana, N. K., Cutter, D., Barenkamp, S. J., St Geme, J. W. (2004). The *Haemophilus influenza*e Hia Autotransporter contains an unusually short trimeric translocator domain. *J. Biol. Chem.*, **279**, 14679–14685.

81. Yeo, H.-J., Cotter, S. E., Laarman, S., Juehne, T., St. Geme, J. W. III, and Waksman, G. (2004). Structural basis for host recognition by the *Haemophilus influenzae* Hia autotransporter. *EMBO J.*, **23**, 1245–1256.

82. Coutte, L., Antoine, R., Drobecq, H., Locht, C., Jacob-Dubuisson, F. (2001). Subtilisin-like autotransporter serves as maturation protease in a bacterial secretion pathway. *EMBO J.*, **20**, 5040–5048.

83. Bingle, L. E., Bailey, C. M., Pallen, M. J. (2008). Type VI secretion: A beginner's guide. *Curr. Opin. Microbiol.*, **11**, 3–8.

84. Pukatzki, S., McAuley, S. B., Miyata, S. T. (2009). The type VI secretion system: Translocation of effectors and effector-domains. *Curr. Opin. Microbiol.*, **12**, 11–17.

85. Leung, K. Y., Siame, B., Snowball, H., Mok, Y.-K. (2011). Type VI secretion regulation: Crosstalk and intracellular communication. *Curr. Opin. Microbiol.*, **14**, 9–15.

86. Leiman, P. G., Basler, M., Ramagopal, U. A., Bonanno, J. B., Sauder, J. M., Pukatzki, S., Burley, S. K., Almo, S. C., Mekalanos, J. J. (2009). Type VI secretion apparatus and phage tail-associated protein complexes share a common evolutionary origin. *Proc. Natl. Acad. Sci. U. S. A.*, **106**, 4154–4159.

87. Ballister, E. R., Lai, A. H., Zuckermann, R. N., Cheng, Y., Mougous, J. D. (2008). *In vitro* self-assembly of tailorable nanotubes from a simple protein building block. *Proc. Natl. Acad. Sci. U. S. A.*, **105**, 3733–3738.

88. Minnikin, D. E., Kremer, L., Dover, L. G., Besra, G. S. (2002). The methyl-branched fortifications of *Mycobacterium tuberculosis*. *Chem. Biol.*, **9**, 545–553.

89. Renshaw, P. S., Lightbody, K. L., Veverka, V., Muskett, F. W., Kelly, G., Frenkiel, T. A., Gordon, S. V., Hewinson, R. G., Burke, B., Norma, J., Williamson, R. A., Carr, M. D. (2005). Structure and function of the complex formed by the tuberculosis factors CFP-10 and ESAT-6. *EMBO J.*, **24**, 2491–2498.

90. Evans, L. E., Chapman, M. R. (2014). Curli biogenesis: Order out of disorder. *Biochim. Biophys. Acta*, **1843**, 1551–1558.

91. Goyal, P., Van Gerve, N., Jonckheere, W., Remaut, H. (2013). Crystallization and preliminary X-ray crystallographic analysis of the curli transporter CsgG. *Acta Crystallogr.*, **F69**, 1349–1353.

92. Collinson, S. K., Emody, L., Muller, K. H., Trust, T. J., Kay, W. W. (1991). Purification and characterization of thin, aggregative fimbriae from *Sallmonella enteritidis*. *J. Bacteriol.*, **173**, 4773–4781.

93. Gerstel, U., Romling, U. (2001). Oxygen tension and nutrient starvation are major signals that regulate agfD promoter activity and expression of the multicellular morphotype in *Salmonella typhimurium*. *Environ. Microbiol.*, **3**, 638–648.

94. Olsen, A., Anrqvist, A., Hammar, M., Normak, S. (1993). Environmental regulation of curli production in *Escherichia coli*. *Infect. Agents Discuss.*, **2**, 272–274.

95. Prigent-Combaret, C., Vidal, O., Dorel, C., Lejeune, P. (1999). Abiotic surface sensing and biofilm-dependent regulation of gene expression in *Escherichia coli*. *J. Bacteriol.*, **181**, 5993–6002.

96. Hammar, M., Brian, Z., Normak, S. (1996). Nucleator-dependent intercellular assembly of adhesive curli organelles in *Escherichia coli*. *Proc. Natl. Acad. Sci. U. S. A.*, **93**, 6562–6566.

97. Hammer, N. D., Schmidt, J. C., Chapman, M. R. (2007). The curli nucleator protein, CsgB, contains an amyloidogenic domain that directs CsgA polymerization. *Proc. Natl. Acad. Sci. U. S. A.*, **104**, 12494–12499.

98. Soto, G. E., Hultgren, S. J. (1999). Bacterial adhesins: Common themes and variations in architecture and assembly. *J. Bacteriol.*, **181**, 1059–1071.

99. Desvaux, M., Hebraud, M., Talon, R., Henderson, I. R. (2009). Secretion and subcellular localization of bacterial proteins: A semantic awareness issue. *Trends Microbiol.*, **17**, 139–145.

100. Christie, P. J. (2001). Type IV secretion: Intercellular transfer of macromolecules by systems ancestrally related to conjugation machines. *Mol. Microbiol.*, **40**, 294–305.

101. Yeo, H.-J., Waksman, G. (2004). Unveiling molecular scaffolds of the type IV secretion system. *J. Bacteriol.*, **186**, 1919–1926.

102. Christie, P. J., Atmakuri, K., Krishnamoorthy, V., Jakubowski, S., Cascales, E. (2005). Biogenesis, architecture, and function of bacterial type IV secretion systems. *Ann. Rev. Microbiol.*, **59**, 451–485.

103. Alvarez-Martinez, C. E., Christie, P. J. (2009). Biological diversity of prokaryotic type IV secretion systems. *Microbiol. Mol. Biol. Rev.*, **73**, 775–808.

104. Cascales, E., Christie, P. J. (2003). The versatile bacterial type IV secretion systems. *Nat. Rev. Microbiol.*, **1**, 137–149.

105. Backert, S., Selbach, M. (2008). Role of type IV secretion in *Helicobacter pylori* pathogenesis. *Cell. Microbiol.*, **10**, 1573–1581.

106. Shrivastava, R., Miller, J. F. (2009). Virulence factor secretion and translocation by *Bordetella* species. *Curr. Opin. Microbiol.*, **12**, 88–93.

107. Fronzes, R., Christie, P. J., Waksman, G. (2009). The structural biology of type IV secretion systems. *Nat. Rev. Microbiol.*, **7**, 703–714.

108. Lessl, M., Lanka, E. (1994). Common mechanisms in bacterial conjugation and Ti-mediated T-DNA transfer to plant cells. *Cell*, **77**, 321–324.

109. Christie, P. J. (2004). Type IV secretion: The *Agrobacterium* VirB/D4 and related conjugation systems. *Biochim. Biopys. Acta*, **1694**, 219–234.

110. Fischer, W. (2011). Assembly and molecular mode of action of the *Helicobacter pylori* Cag type IV secretion apparatus. *FEBS Journal*, **278**, 1203–1212.

111. Lawley, T., Wilkins, B. M., Frost, L. S. (2004). Bacterial conjugation in Gram-negative bacteria. In: Phillips, G. J., Funnell, B. E., eds. *Plasmid Biology*, ASM Press, Washington DC, USA, pp. 203–226.

112. Kutter, S., Buhrdorf, R., Haas, J., Schneider-Brachert, W., Haas, R., Fischer, W. (2008). Protein subassemblies of the *Helicobacter pylori* Cag Type IV Secretion System revealed by localization and interaction studies. *J. Bacteriol.*, **190**, 2161–2171.

113. Viala, J., Chaput, C., Boneca, I. G., Cardona, A., Girardin, S. E., Moran, A. P., Athman, R., Memet, S., Huerre, M. R., Coyle, A. J., DiStefano, P. S., Sansonetti, P. J., Labigna, A., Bertin, J., Pholpott, D. J., Ferrero, R. L. (2004). Nod1 responds to peptidoglycan delivered by *Helicobacter pylori cag* pathogenicity island. *Nature Immunology*, **5**, 1166–1174.

114. Backert, S., Meyer, T. F. (2006). Type IV secretion systems and their effectors in bacterial pathogenesis. *Curr. Opin. Microbiol.*, **9**, 207–217.

115. Terradot, L., Waksman, G. (2011). Architecture of the *Helicobacter pylori* Cag-type IV secretion system. *FEBS J.*, **278**, 1213–1222.

116. Gomis- Ruth, F. X., Moncallan, G., Perez-Luque, R., Gonzalez, A., Cabezon, E., de la Cruz, F., Coll, M. (2011). The bacterial conjugation protein TrwB resembles ring helicases and F_1-ATPase. *Nature*, **409**, 637–641.

117. Terradot, L., Bayliss, R., Oomen, C., Leonard, G. A., Baron, C., Waksman, G. (2005). Structures of two core subunits of the bacterial type IV secretion system, VirB8 from *Brucella suis* and ComB10 from *Helicobacter pylori*. *Proc. Natl. Acad. Sci. U. S. A.*, **102**, 4596–4601.

118. Savvides, S. N., Yeo, H.-J., Beck, M. R., Blaesing, F., Lurz, E., Lanka, E., Buhrdorf, R., Fischer, W., Haas, R., Waksmann, G. (2003). VirB11 ATPases are dynamic hexameric assemblies: New insights into bacterial type IV secretion. *EMBO J.*, **9**, 1969–1980.

119. Bailey, S., Ward, D., Middleton, R., Grossmann, J. G., Zambryski, P. C. (2006). *Agrobacterium tumefaciens* VirB8 structure reveals potential protein–protein interaction sites. *Proc. Natl. Acad. Sci. U. S. A.*, **103**, 2582–2587.

120. Christie, P., Vogel, J. P. (2000). Bacterial type IV secretion: Conjugation systems adapted to deliver effector molecules to host cells. *Trends Microbiol.*, **8**, 354–360.

121. Juhas, M., Crook, D. M., Hood, D. W. (2008). Type IV secretion systems: Tools of bacterial horizontal gene transfer and virulence. *Cell. Microbiol.*, **10**, 2377–2386.

122. Anthony, K. G., Sherburne, C., Sherburne, R., Frost, L. S. (1994). The role of the pilus in recipient cell recognition during bacterial conjugation meditated by F-like plasmids. *Mol. Microbiol.*, **13**, 939–953.

123. Clarke, M., Maddera, L., Harris, R. L., Silverman, P. M. (2008). F-pili dynamics by live-cell imaging. *Proc. Natl. Acad. Sci. U. S. A.*, **105**, 17978–17981.

124. Lederberg, J. (1956). Conjugal pairing in *Escherichia coli*. *J. Bacteriol.*, **71**, 497–498.

125. Achtman, M. (1975). Mating aggregates in *Escherichia coli* conjugation. *J. Bacteriol.*, **123**, 505–515.

126. Durrenberger, M. B., Villiger, W., Bachi, Th. (1991). Conjugational junctions: Morphology of specific contacts in conjugating *Escherichia coli* bacteria. *J. Struct. Biol.*, **107**, 146–156.

127. Bradley, D. E., Taylor, D. E., Cohen, D. R. (1980). Specification of surface mating systems among conjugative drug resistance plasmids in *Escherichia coli* K-12. *J. Bacteriol.*, **143**, 1466–1470.

128. Manning, P. A., Morelli, G., Achtman, M. (1981). TraG protein of the F sex factor of *Escherichia coli* K-12 and its role in conjugation. *Proc. Natl. Acad. Sci. U. S. A.*, **78**, 7487–7491.

129. Babic, A., Lindner, A. B., Vulic, M., Stewart, E. J., Radman, M. (2008). Direct visualization of horizontal gene transfer. *Science*, **319**, 1533–1536.

130. Lederberg, J., Tatum, E. L. (1946). Gene recombination in *Escherichia coli*. *Nature*, **158**, 558.

131. Frost, L. S., Ippen-Ihler, K., Skurray, R. A. (1994). Analysis of the sequence and gene products of the transfer region of the F sex factor. *Microbiol. Rev.*, **58**, 162–210.

132. Lindberg, F., Lund, B., Johansson, L., Normark, S. (1987). Localization of the receptor-binding protein adhesin at the tip of the bacterial pilus. *Nature*, **328**, 84–87.

133. Harris, R. L., Hombs, V., Silverman, P. (2001). Evidence that F-plasmid proteins TraV, TraK and TraB assemble into an envelope-spanning structure in *Escherichia coli*. *Mol. Microbiol.*, **42**, 757–766.

134. Fronzes, R., Schäfer, E., Wang, L., Saibil, H. R., Orlova, E. V., Waksman, G. (2009). Structure of a type IV secretion system core complex. *Science*, **323**, 266–268.

135. Chandran, V., Fronzes, R., Duquerroy, S., Cronin, Navaza, J., Waksman, G. (2009). Structure of the outer membrane complex of a type IV secretion system. *Nature*, **462**, 1011–1016.

136. Wang, Y. A., Yu, X., Silverman, P. M., Harris, R. L., Egelman, E. H. (2009). The Structure of F-Pili. *J. Mol. Biol.*, **385**, 22–29.

137. Reeves, P., Willets, N. (1974). Plasmid specificity of the origin of transfer of sex factor F. *J. Bacteriol.*, **120**, 125–130.

138. Stern, J. C., Schildbach, J. F. (2001). DNA Recognition by F factor TraI36: Highly sequence-specific binding of single stranded DNA. *Biochemistry*, **40**, 11586–11595.

139. Datta, S., Larkin, C., Schildbach, J. F. (2003). Structural insights into single-stranded DNA binding and cleavage by F factor TraI. *Structure*, **11**, 1369–1379.

140. Street, L. M., Harley, M. J., Stern, J. C., Larkin, C., Williams, S. L., Miller, D. L., Dohm, J. A, Rodgers, M. E., Schildbach, J. F. (2003). Subdomain organization and catalytic residues of the F factor TraI relaxase domain. *Biochim. Biophys. Acta*, **1646**, 86–99.

141. Larkin, C., Datta, S., Harley, M. J., Anderson, B. J., Ebie, A., Hargreaves, V., Schildbach, J. F. (2005). Inter- and intramolecular determinants of the specificity of single-stranded DNA binding and cleavage by the F factor relaxase. *Structure*, **13**, 1533–1544.

142. Lu, J., Edwards, R. A., Wong, J. J. W., Manchak, J., Scott, P. G., Frost, L. S., Glover, J. N. M. (2006). Protonation-mediated structural flexibility in the F conjugation regulatory protein, TraM. *EMBO J.*, **25**, 2930–2939.

143. Lu, J., Wong, J. J. W., Edwards, R. A., Manchak, J., Frost, L. S., Glover, J. N. M. (2008). Structural basis of specific TraD-TraM recognition during F plasmid-mediated bacterial conjugation. *Mol. Microbiol.*, **70**, 89–99.

144. Kraulis., J. (1991). MOLSCRIPT: A program to produce both detailed and schematic plots of protein structures. *J. Appl. Crystallogr.*, **24**, 946–950.

145. Merritt, E. A., Bacon, D. J. (1997). Raster3D: Photorealistic molecular graphics. *Methods Enzymol.*, **277**, 505–524.

Chapter 25

The Vascular Cartographic Scanning Nanodevice

Frank J. Boehm

NanoApps Medical, Inc.,
Lakehead University, Thunder Bay, Ontario, Canada

Keywords: nanomanufacturing, nanomedical, self-assembly, bottom-up, top-down, autonomous, medical imaging, nanodevice, Vascular Cartographic Scanning Nanodevice (VCSN), Gastrointestinal Micro Scanning Device (GMSD), spatial data acquisition

25.1 Introduction

Envisioners and designers of nanomedical devices may draw their inspiration from a number of sources. These might include the myriad mechanisms and processes that operate at both macroscale and nanoscale domains in the natural world, which may be interpreted and transformed into functional synthetic analogs

Handbook of Clinical Nanomedicine: Nanoparticles, Imaging, Therapy, and Clinical Applications
Edited by Raj Bawa, Gerald F. Audette, and Israel Rubinstein

ISBN 978-981-4669-20-7 (Hardcover), 978-981-4669-21-4 (eBook)
www.panstanford.com

via biomimetics. Other inspirational sparks may emanate from purely anthropogenic dreamscapes, which reside within the realms of fantasy and science fiction. There is always the chance that completely unexpected serendipitous discovery might arrive from "nowhere" to the utter joy of long toiling recipients who might have been looking for answers for many years in one area, only to have a pivotal insight surprisingly light up when triggered by a completely unrelated event, as if a gift from some parallel universe that has "crossed over." Incremental inspirational glimmers, and much more rarely, dramatic brilliant bursts thereof may indeed be gleaned through voluminous thoughtful, disciplined, and deliberate experimentation.

From whatever quarter such inspiration may appear, it may be suggested that a certain "cognitive stance" might serve as a useful prerequisite to facilitate and breed the flames of inspiration, creativity, and innovation, which may likely percolate into reality. This attitude might encompass in varying degrees, a blend of excitement and prospective adventure, an insatiable childlike curiosity, open mindedness and playfulness, enthusiasm and positiveness, combined with responsibility, integrity; and importantly, persistence, interspersed with a modicum of naivety, and humbleness in the recognition that one can clearly never "know it all." Hence, the vibrant collaboration of individuals who encompass diverse areas of expertise will be indispensible toward the development of advanced, safe, and efficacious nanomedical devices and systems.

In actual terms, the development of innovative nanomedical concepts and designs may consist of the heterogeneous fusion of many of the above elements in combination with, from an engineering perspective, what may be perceived to be practically achieved in a manner that is not cost prohibitive. These considerations may encompass the selection of appropriate materials, as well as the development of optimized techniques that are to be employed for the synthesis of nanoscale components and devices from the "bottom–up" (e.g., utilizing advanced chemistries [1, 2], or via still conceptual, albeit steadily advancing nanomanufacturing technologies [3–5]), or "top–down" strategies that include microelectromechancial systems (MEMs) [6, 7] and nanoelectromechanical systems (NEMs) [8, 9], lithographic

patterning techniques [10, 11] that may achieve features with resolutions from 10 to 100 nm, and nanoscale/molecular imprinting [12–15], stamping [16, 17], and molding [18, 19], which can provide 20–40 nm features.

25.2 Vascular Cartographic Scanning Nanodevice

The vascular cartographic scanning nanodevice (VCSN) (Fig. 25.1) will be manifest as an advanced autonomous ~1 μm in diameter nanomedical device for *in vivo* imaging applications, and comprised of integrated modular components that work in conjunction with external "outbody" control infrastructures. A far less complex, albeit still nanocomponent-driven precursor to the VCSN device would be manifest as a much physically larger (~3 mm in diameter) *in vivo* nanomedical imaging instrument, called the gastrointestinal micro scanning device (GMSD).

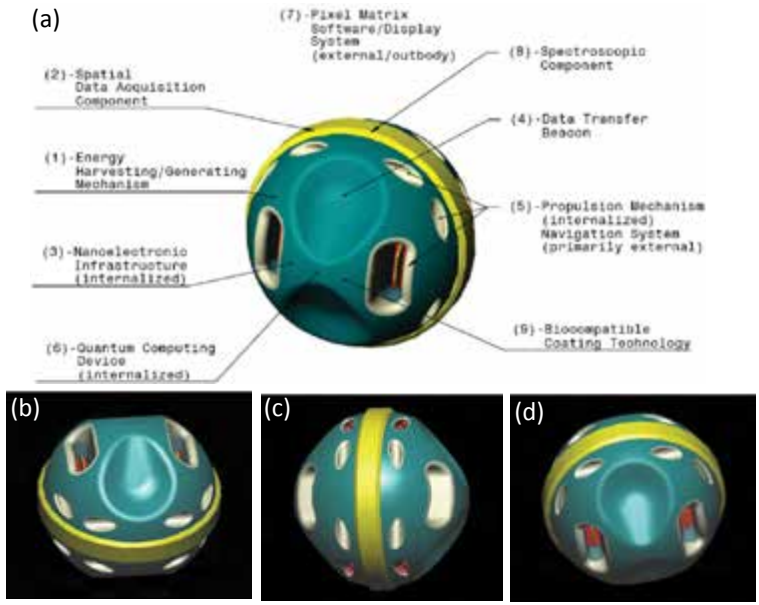

Figure 25.1 Artistic representation of: (a) Anatomy of conceptual vascular cartographic scanning nanodevice (VCSN). (b–d) various VCSN orientations.

It is hoped that the brief descriptions conveyed here of these conceptual nanomedical device exemplars, may serve as preliminary templates to perhaps illustrate how conceptualists and designers of future sophisticated nanomedical components, devices, and systems might approach the tremendous challenges that will confront them. Far more intensive and demanding tasks will be allotted to nanomedical engineers who are charged with the daunting task of devising real-world strategies as relates to the actual fabrication and functionalization of these nanoscale "medical dream machines." A few examples of the many tasks involved may include, as described earlier, the selection of appropriate nanomaterials; the design and development of robust, dependable, and scalable self-assembly (nanomanufacturing) capabilities; self-quality control verification and test strategies; the development of pragmatic component designs that will operate effectively under myriad constraints imposed by human physiology *in vivo*; novel approaches for modular nanocomponent/nanoelectronics integration; and the interfacing of multiple nanometric components with outbody computers and a conceptual "NanoNav" dedicated nanomedical device navigation system.

The conceptual VCSN constitutes a fully autonomous nanoscale *in vivo* medical imaging device and system. Many thousands of identical such nanodevices would likely operate in parallel to scan/image the entire human vasculature down to the level of the smallest capillary lumen (e.g., ~3 μm diameter) in high-resolution three-dimensional (3D) digitized format.

25.3 Overview of Envisaged VCSN Capabilities

(1) Capacity for the generation of a very high-resolution (less than ~1 μm) 3D rendering of the complete human vasculature down to the capillary level. It may also be applied to the imaging of the lymphatic system, the glymphatic system (exclusive to the brain), and in a simplified form (e.g., GMSD) the gastrointestinal tract (GIT).

(2) Ability to distinguish and superimpose vascular and neurological plaque deposits and lesions with high accuracy against the topographically rendered backdrop of healthy endothelial wall surfaces.

(3) Quantification of vascular wall thicknesses along with the identification and highlighting of "hot spots" at any site within the vasculature or glymphatic system, such as imminent blockages or aneurysms that are at risk of rupturing. This capacity will be of particular value when enabling the clear elucidation of such risk sites for subsequent mitigation *in situ* within the brain.

(4) Capacity for physicians to "fly-through" all scanned areas via a joystick and computer display for the highly detailed inspection of any desired site within the system. The acquired spatial data may also enable holographic rendering and virtual travel through all imaged systems.

(5) Ability to facilitate the targeting of tumors by revealing instances of nascent angiogenesis in close proximity to tumor growth sites. The VCSN will comprise multiple modularly integrated nanoscale components, subsystems, and primary systems that are connected via a dynamic nanoelectronic/nanophotonic infrastructure. These entities will be organized and assembled in a prioritized and sequentially hierarchical manner. An intrinsic developmental process that may drive the conceptualization and evolution of individual functional modules, such as the propulsion system, may initially encompass several potential candidate technologies. The most promising of these candidates might be selected on the basis of their demonstration of superior performance when applied to specific tasks and when challenged with a variety of dedicated trials.

A preliminary research and discovery phase would serve to thoroughly define the perceived scope and developmental timeline of the VCSN. This might consist of a strategy that involves the preliminary identification and description, in as much detail as is possible, of every primary and secondary nanometric component, mechanism, and system. It will be a necessary and prudent step toward realistically discerning exactly which potential elements of each system might be feasible insofar as manufacturability and functionality when scaled down to the nanometer range. This exercise may manifest itself as a process of elimination, or may result in a superior hybrid design whereby several of the most desirable elements that are extracted from a number of options

may ultimately prove to be the most favorable solution. The fundamental physics, chemistry, electronics, thermodynamics, and mechanics behind each of the selected component attributes will be systematically tested, theoretically, through the implementation of task-specific computer modeling, in conjunction with hands-on experimentation against predetermined parameters and a protocol checklist. This organization may assist in the determination and generation of proof-of-principal guidelines, while also serving to verifiably refute the feasibility of the use of certain components in particular applications, or negating the combination of specific elements.

25.4 Summary of VCSN Components

Each envisaged nanoscale element and system comprising the VCSN will embody its own specific set of investigative, conceptualization, design pathways, and associated tasks. These components, in order of perceived importance, are as follows:

(1) *Energy-harvesting/generating components*
Constitute the primary and auxiliary power harvesting/generating sources for all primary, secondary, and multiple redundant VCSN systems. These mechanisms might harvest and catalyze readily available molecular biofuels (e.g., glucose, hydrogen) from the *in vivo* environment, and convert them into electron flow. There are many additional potential nanoscale energy harvesting and generating technologies (e.g., thermopiles, piezoelectronics, hydrostatics, and biomimetic entities and processes) that will be worthy of exploration.

(2) *Spatial data acquisition component*
Functions as the spatial data acquisition signal emitter and receiver that will constitute the scanning mechanism. With this component as well, several potential technologies exist, or might be extrapolated (e.g., capacitive ultrasound, nanoscale time-of-flight LIDAR), which will warrant serious investigation.

(3) *Nanoelectronic/nanophotonic infrastructure*
Conveys and modulates the electrical current and photonic streams that enable myriad critical VCSN functions (e.g.,

propulsion, onboard navigation controls, computing, and communications) including the emission and reception of scanning pulses from the spatial data acquisition array, and to facilitate the transfer of acquired spatial information to a data transfer beacon for transmission to outbody computers for final processing, image reconstruction, and display. Various nanoelectronic/nanophotonic components and conveyance conduits such as highly conductive carbon nanotubes, organic/inorganic nanowires or conductive polymeric nanofibers, and nanoscale chalcogenide (photoconductive glass) derived optical nanofibers might electronically and photonically interconnect and interface all nanodevice elements.

(4) *Data transfer beacon*

Transmits collected spatial data to an "outbody" receiver, which is interfaced with the Pixel Matrix (PM) image reconstruction system. It is also utilized as the primary communications node for receiving external commands as well as for inter-nanodevice coordination. In addition, it would serve to lock onto an external homing signal upon completion of the scanning procedure, or for emergency egress from the patient.

(5) *Propulsion and navigational systems*

Endows the nanodevice with autonomy *in vivo* and enables travel in any orientation and direction while within this environment. Movement is initiated and guided by transmitted command signals under external computer control via a dedicated "NanoNav" navigation system, perhaps akin to a miniaturized GPS system. An onboard computer (quantum or possibly DNA based) will assist in this regard by emanating positional coordinate feedback data.

(6) *Nanoscale computation*

Enables the capacity for command data storage, working protocols, and spatial data backup at a high level of redundancy for fail-safe nanodevice operation, propulsion, and navigation, including internal, interdevice, and external communications. This component might be manifest as a solid-state quantum computer or an organized biomolecular device comprising restriction nuclease and ligase hardware working in conjunction with software-encoded DNA duplex

arrays. Alternatively, all optical nanoscale computing may be implemented to reduce the cumulative thermal footprint that may conceivably be generated by possibly millions of *in vivo* nanodevices.

(7) *Pixel Matrix (PM) display system*

Translates acquired spatial data into digitized display format with ultrahigh image resolution. Each endothelial wall target "hit" that is initiated and measured by onboard ultrasonic transducer arrays (or other selected spatial data acquisition mechanisms) would be represented by a pixel that is assigned to a calculated position in 3D space on a display. This software might also have the capacity for discerning vascular wall thicknesses so as to facilitate aneurysm detection via the isolation of secondary echo signatures from the spatial data set.

(8) *Spectroscopic component*

Elucidates the chemical composition of scanned entities so as to accurately differentiate plaque deposits and lesions from healthy (background) vascular endothelial or lymphatic constituents by utilizing mass spectroscopic analysis. This capability may assist in the whole-body mapping and compositional analysis of pathogenic aggregates, regardless of their makeup (e.g., vascular plaques, neurological beta-amyloid plaques, lipofuscin, cholesterol, and oxysterols).

(9) *Biocompatible coating technology*

Endows nanodevices with reliable stealth qualities so that they may circumvent any level of immune response while they operate *in vivo*, through the utilization of inert and biocompatible materials (e.g., diamondoid, sapphire materials) as the main building materials of nanodevices, or via the use of bioinert diamondoid or polymeric thin-film coatings.

25.5 Discussion

As a critical part of their development, each individual component of the VCSN will be subjected to stringent testing for safety, reliable

functionality, and robustness. Further rigorous testing will ensue as subsequent entities are developed and integrated with various other dedicated components to eventually comprise a complete and fully functional autonomous nanomedical scanning/imaging. Thus, contributing to the eventual establishment of a worldwide "health care equilibrium", where every individual has equal access to the same high quality medical/nanomedical care, no matter where they happen to reside, or under what conditions they live.

A practical deficiency that might be addressed in global healthcare through the proposed development of the conceptual VCSN would be the potential alleviation of the very limited or non-availability of advanced medical imaging technologies in remote and impoverished regions of the world. The envisaged sophisticated nature of this innovative medical imaging technology combined with its inherent miniaturization might cost effectively facilitate access to important and medical diagnostic tools for virtually any individual on the globe.

As an autonomous nanodevice with a finite energy storage capacity, due to extreme physical constraints on available real estate, the VCSN will incorporate several strata of operational redundancy. This will be particularly critical where the harvesting and conversion of energy are concerned, toward ensuring the uninterrupted operation and capability for *in vivo*/outbody communications. The VCSN might harvest power via the chemical catalysis of glucose, hydrogen, other appropriate biomolecules or ions within the *in vivo* environment of patients, thereby having the advantageous attribute of self-sustainability while in operation. Alternately, the VCSN may be induced to generate onboard power through activation by external sources. It may be possible that a hybrid, three-tiered energy capability might also evolve, whereby primary power is generated via external activation; onboard energy harvesting serves as a secondary supplementary source, and stored battery power provides a sufficient backup, should the very rare instance occur where both higher echelon systems go offline, or are otherwise disrupted or incapacitated.

The bulk of conventional power required for sustaining the VCSN infrastructure would be for the operation of the external computer that houses the PM image reconstruction software, along with additional compact/modular hardware (e.g., NanoNav guidance beacons, and communications infrastructure). These

power requirements might be met via a dedicated, hybrid power-harvesting/generating "kit" that integrates solar, wind, fuel cell, mechanical crank, or other practicable, robust, and efficient power generating sources. Thus, the entire setup for VCSN scanning procedures may achieve full functionality in remote, and if necessary, physically confined areas.

The implementation of the scanning procedure would be quite straightforward as a prescribed dose of thousands of identical VCSN units may be injected, diffused through an adhered patch or topical gel, swallowed as a pill, or administered as oral thin-film wafers or drops. Once the nanodevices ingress to the bloodstream, they will self-organize, orient themselves, and report their positions using micron resolution X-, Y-, Z-coordinates relative to an established external reference point. This "confluence fiducial" may be established via the intersection of several propagating electromagnetic beams, which emanate from dedicated beacons, utilized to demarcate the patient scanning volume in 3D space. When the scanning procedure has been completed (e.g., ~5 min), an externally activated homing signal would direct all nanodevices to a predetermined "outbody" egress site where they would be collected and stored for subsequent molecular disassembly and recycling.

An imperative infrastructural element inherent to the VCSN developmental strategy will be manifest as an optimized and highly efficient nanomanufacturing capability, to ensure that VCSN units may be produced cost effectively via massively parallel fabrication (e.g., DNA mediated self-assembly) techniques [2, 20–26], such that they can be economically administered as single-use entities, and recyclable for reuse in non-medical applications. This strategy would negate a range of cumulative expenditures and time-consuming procedures involved with nanodevice sterilization and storage for eventual redeployment. The latter prospect, however, will likely elicit an understandably strong psychological resistance, even if there should be a qualified assurance of safety provided. This is, no doubt, firmly grounded on innate concerns regarding undesirable and indeed, unacceptable pathogenic biotransmission.

As the VCSN units will comprise biocompatible elements in accordance with established nanomedical protocols, they might be disposed of under similarly stringent procedures, as exists for

standardized medical refuse, though due to their small physical size they will likely undergo separate processing, or ideally, recycling for benign integration into bulk products. As an option to a targeted egress strategy, once a scanning procedure has been completed, the nanodevices may be allowed to diffuse naturally from the patient via various bodily fluids, though they would be tagged for tracking to ensure that their removal from the patient is complete.

25.6 VCSN Advantages

The envisaged practical advantages offered by the VCSN and its associated infrastructure will include the following:

(1) Compactness and portability, as its operation will require a relatively small footprint. This would enable simple and quick setup and power-up procedures in developing countries and remote terrestrial environments. In the aerospace domain, it may be utilized as an element of an onboard medical diagnostics suite on military and medical aircraft, and for space travel if reconfigured for integration into spacesuits and spacecraft, and to provide a compact yet powerful medical imaging capability for future Moon and Mars habitats.
(2) Frugal energy consumption.
(3) Relatively inexpensive to administer and operate.
(4) Rapid scanning time (e.g., ~5 min).
(5) Ultrahigh resolution digital spatial data. Inherent flexibility for display in several different formats, and ease of file transmission to medical personnel internationally, via secure telecommunications networks.
(6) Potential for enabling the drastic reduction or elimination of long waiting queues for critical medical imaging technologies.

Conventional medical imaging technologies such as magnetic resonance imaging (MRI) and computed tomography (CT) are very expensive and, hence, out of reach for developing countries. They are also physically unwieldy, power hungry, and have long waiting times for their use. Although current ultrasound imaging technology is improving, it is still relatively crude in resolution and

administration, and the resulting imagery is segmental in nature, in contrast to whole-body scanning. The VCSN is envisioned as having the capability for rendering complete systems (e.g., vascular, lymphatic, glymphatic, or gastrointestinal) in ultrafine detail, displaying all luminal surfaces and wall thicknesses with the possibility of also distinguishing their chemical compositions.

Since there is an increasingly strong demand for smaller and more compact medical technologies that are endowed with enhanced and more complex capabilities, the VCSN would constitute an exponential step in this direction. The investigation and eventual development of initial and subsequent generations of components aimed at implementation for VCSN technology may conceivably be directly applied, or adapted for any future nanomedical device and system. These components might be designed in such a way that they can be fabricated in modular form and, to some extent, adhere to a predetermined standardized format to assist in enabling future specialized nanomedical diagnostic and therapeutic capabilities and devices (e.g., ultrafine *in vivo* spectroscopic biopsy, cell-targeted drug delivery, vascular/neurological plaque removal devices, lysosome lipofuscin dissolution or removal, chromosome repair or replacement, bone mineral delivery and repair devices for the remediation of osteoporosis, and prospective cell repair devices).

25.7 The Gastrointestinal Micro Scanning Device

The Gastrointestinal Micro Scanning Device (GMSD) (Fig. 25.2) will serve as a formative and far less complex precursor to the VCSN in that it will not have the capacity for propulsion or navigation. It will, however, utilize nascent forms of the quantum computing, nanoelectronics, spatial data acquisition, and PM technologies that are envisaged for the VCSN. Hence, the GMSD, in addition to serving as spatial data acquisition device, may also have utility as a test bed of sorts that is employed to identify and resolve technical, integrative, and functional issues toward the further evolution of the VCSN.

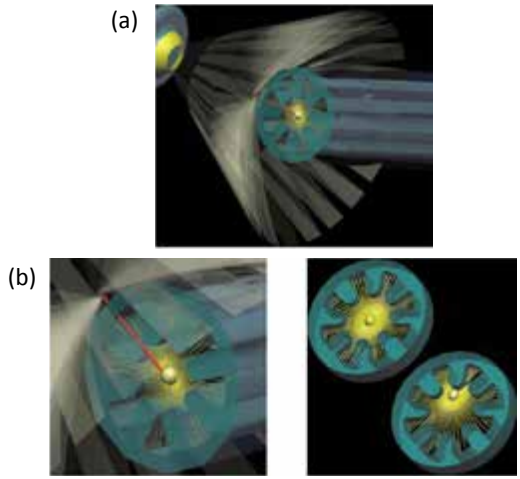

Figure 25.2 (a) Artistic representation of conceptual Gastrointestinal Micro Scanning Device (GMSD) depicting communications link between the Pulse Generator/Data Transfer unit (PGDT) and the Bright Ball (BB) internal scanning device. (b) Auto adjustment of BB acquisition interrogating signals in response to a shift from central position within lumen of GIT.

The GMSD system will consist of three distinct components working in unison to generate a very high-resolution 3D topography of the entire internal surface of the GIT. The GMSD would accomplish this task by employing

(1) An internalized (via ingestion) scanning device.
(2) An external signal generation and data transfer unit.
(3) A PM display element.

(1) *Bright Ball (BB) Scanning Device*

The BB scanning device would have a spherical morphology of ~3 mm in diameter. (A thorough assessment would be conducted using computer modeling and *in vitro* testing to ascertain the optimal physical parameters for the device to eliminate the possibility of the BB getting physically "snagged" en route through the GIT.) Most of the outer surface of the device, save the area required for acoustic communications beacons, will consist of a continuous tessellated array of ~1 μm in diameter emitter/receiver (ER) units, which may take

the form of micron-scale capacitive ultrasonic transducers, each of which would constitute a standalone measuring instrument. Individual units might be positioned and bonded to their neighbors with a polymeric adhesive that is both biocompatible and biodegradable (e.g., 3,4-dihydroxybenzoic acid combined with chitosan). This bonding material would encapsulate all of the ER units to comprise a solid sphere, which might be finished with a translucent thin film of gold to impart a highly polished and reflective surface. The ER units would be calibrated beforehand, and distance measurements of the internal topography of the GIT would be performed using time-of-flight calculations. The resulting imagery could be reconstructed via the quantification of variances in relation to an initial reference calibration.

(2) *Pulse Generator/Data Transfer Unit (PGDT)*

The pulse generator/data transfer unit is the component that would trigger the activity of the internalized BB device with an appropriate, specifically encrypted signal. The BB would be activated to scan subsequent to receiving this specific signal only. Once active, the BB would transmit a constant data stream to the PGDT. The PGDT would serve as the data transfer device when linked to a computer and the PM software. It would be affixed to an appropriate area of the patient's abdominal surface and would stay in place for the duration of the scan.

(3) *PM Display*

The PM display would process the data supplied to it by the PGDT to reconstruct a very high resolution "pixel per hit" 3D rendering of the total scanned area that has been traversed by the BB. The software would enable "fly-through" and cross-sectional capabilities, allowing physicians (using a joystick, computer mouse, or touch screen display) to inspect the entire GIT to elucidate any potential problem areas in great detail. One may envision that the acquired digitized information might be translated to holographic and virtual reality formats as well. The physician would thus recognize any anomalous topography consistent with tumor growth, lesions, and other abnormal features that may exist in the GIT using this procedure.

25.8 Description of Scanning Procedure

The setup for the GMSD operational procedure would be relatively simple to implement.

Initially, the BB would be administered orally to the patient in the same manner as a pill.

Next, an adhesive and waterproof PGDT thin-film patch would be affixed to the skin of patient's abdomen. At this juncture, a system calibration would be performed to assure that the communication link between the BB and the PGDT is functioning properly. A test scan would also be performed to configure the image resolution. Following these procedures, the patient would be allowed to leave the physician's office, clinic, or hospital to go about his/her normal routine.

The internalized BB would now progress along with the natural peristaltic rhythms of the GIT and be naturally eliminated at the conclusion of the transit timeline. The patient would subsequently return to the appropriate facility in two or three days time (contingent on the assessed GIT transit time) to have the PGDT patch removed. The PGDT will have continually accumulated all of the data acquired by the BB during the designated scanning period. This device would then be interfaced with a computer via a USB port to stream all of the acquired data to the PM software housed within the computer. The data would now be translated into high-resolution 3D imagery on a display.

The interrogating signals emitted by the BB would have the capacity for passing through the contents of the small and large intestines as if transparent, through the utilization of a selective signal filtering algorithm. The scanning signals would have no harmful effect on any cell or tissue, even with prolonged exposure. The PGDT would emit a unique pulsed signal (e.g., ultrasonic, near-infrared), which when received by sensors embedded within the surface of the BB would trigger all of the ERs embedded to fire and emit their scanning beams simultaneously in every direction. The PM software would calculate the precise BB location and orientation and would correlate the hits obtained within predetermined parameters to construct a cross section of the GIT representing its internal topography. These digitized segments would be sequentially pieced together to form a seamless and spatially accurate rendering of the system.

25.9 Additional Issues

The BB device would be stored in a sterilized environment until it is ready for use to negate any risk of infection. Additionally, due to the fairly rapid transit time (~two days) from ingestion to elimination, the chances of eliciting an immune response should be very low. Following elimination, the BB will cease to function, as it requires the specialized PGDT-generated pulsed signals for activation and operation. The shell of the BB, as described earlier, might include a biodegradable and environment/ecosystem-compatible polymeric binding compound that may be formulated to break down following a predetermined duration of exposure to an aqueous environment, releasing the physical support of all ER units. The ER units would subsequently separate, becoming in essence, nonfunctional micron-sized particulates that may break down further into harmless elements.

The GMSD would serve as a beneficial, minimally invasive, biocompatible diagnostic system for generating high-resolution 3D imagery of the GIT. It would be relatively simple to implement, minimize any chance of infection or discomfort, and the scanning would not be disruptive to the patient, who could carry on with his/her normal affairs. In addition, the GMSD would be biodegradable and environmentally compatible. This novel nanomedical imaging system would serve as a boon to physicians by providing of a new and more precise method for imaging the GIT. It would aid them by offering more detailed information as to the health status of the GIT in order to prescribe the appropriate preventative or therapeutic care, and would assist by acting as an accurate diagnostic tool, thereby increasing the efficacy of their treatments.

Disclosures and Conflict of Interest

The author declares that he has no conflict of interest and has no affiliations or financial involvement with any organization or entity discussed in this chapter. No writing assistance was utilized in the production of this chapter and the author has received no payment for its preparation.

Corresponding Author

Frank J. Boehm
NanoApps Medical, Inc.
141 Empress Avenue South
Thunder Bay, ON, Canada P7B 4N6
Email: cellrepair777@hotmail.com

About the Author

Frank J. Boehm has been involved with nanotechnology and especially nanomedicine since 1996 and has been evolving numerous concepts and designs for advanced nanomedical diagnostic and therapeutic components, devices and systems to address myriad disease states. His aim is to develop and transform these concepts into real world applications for global benefit. He serendipitously encountered the concept of nanotechnology on the Internet in 1996 and immediately become fascinated with its virtually limitless potential, particularly as relates to the field of medicine. He passionately proceeded to evolve and textually articulate a number of advanced concepts and designs toward near-term and longer-term nanomedical components, devices, and systems. Concomitantly, he initiated relationships with numerous research scientists and thought leaders in the disciplines of nanotechnology and nanomedicine across the globe.

In recognizing the immense potential of nanomedicine to impart positive paradigm shifts across the medical domain (e.g., precisely targeted drug delivery, vascular/neurological/cellular plaque removal, completely non-invasive surgical procedures, physiological systems and longevity enhancement) he was deeply motivated to write more extensively on the topic. In 2013 he published a book entitled: *Nanomedical Device and Systems Design: Challenges, Possibilities, Visions*, by CRC Press. In parallel, he managed to engage the interest of several researchers in the US and Canada in his nanomedical concepts, and in 2009 formed the startup, NanoApps Medical, Inc. The aim of this company is to investigate and develop advanced, efficacious, and economical nanomedical diagnostic and

therapeutic devices and systems for the benefit of individuals in both the developing and developed worlds.

References

1. Gu, H., Chao, J., Xiao, S. J., Seeman, N. C. (2010). A proximity-based programmable DNA nanoscale assembly line. *Nature*, **465**(7295), 202–205.
2. Boehm, F. J. (2004). An investigation of nucleic acid/DNA-based manufacturing, Thirty Essential Nanotechnology Studies: #10. Center for Responsible Nanotechnology, Menlo Park, CA. Available at: http://wise-nano.org/w/Boehm_DNA_Study (last accessed on May 21, 2014).
3. Freitas, R. A. Jr. (2011). Diamondoid mechanosynthesis for tip-based nanofabrication. In: Tseng, A., ed. *Tip-Based Nanofabrication: Fundamentals and Applications*, Springer, New York, Chapter 11, pp. 387–400.
4. Tarasov, D., Akberova, N., Izotova, E., Alisheva, D., Astafiev, M., Freitas, R. A. Jr. (2010). Optimal tool tip trajectories in a hydrogen abstraction tool recharge reaction sequence for positionally controlled diamond mechanosynthesis. *J. Comput. Theor. Nanosci.*, **7**, 325–353.
5. Chen, Y., Xu, Z., Gartia, M. R., Whitlock, D., Lian, Y., Liu, G. L. (2011). Ultrahigh throughput silicon nanomanufacturing by simultaneous reactive ion synthesis and etching. *ACS Nano,* **5**(10), 8002–8012.
6. Butler, E. J., Folk, C., Cohen, A., Vasilyev, N. V., Chen, R., Del Nido, P. J., Dupont, P. E. (2011). Metal MEMS tools for beating-heart tissue approximation. *IEEE Int. Conf. Robot. Autom.*, 411–416.
7. Wheeler, J. W., Dabling, J. G., Chinn, D., Turner, T., Filatov, A., Anderson, L., Rohrer, B. (2011). MEMS-based bubble pressure sensor for prosthetic socket interface pressure measurement. *Conf. Proc. IEEE Eng. Med. Biol. Soc*., 2925–2928.
8. Basarir, O., Bramhavar, S., Ekinci, K. L. (2012). Motion transduction in nanoelectromechanical systems (NEMS) arrays using near-field optomechanical coupling. *Nano Lett.*, **12**(2), 534–539.
9. Khaleque, T., Abu-Salih, S., Saunders, J. R., Moussa, W. (2011). Experimental methods of actuation, characterization and prototyping of hydrogels for bioMEMS/NEMS applications. *J. Nanosci. Nanotechnol.*, **11**(3), 2470–2479.
10. Basnar, B., Willner, I. (2009). Dip-pen-nanolithographic patterning of metallic, semiconductor, and metal oxide nanostructures on surfaces. *Small*, **5**(1), 28–44.

11. Zhou, X., Boey, F., Huo, F., Huang, L., Zhang, H. (2011). Chemically functionalized surface patterning. *Small*, **7**(16), 2273–2289.
12. Shi, G., Lu, N., Xu, H., Wang, Y., Shi, S., Li, H., Li, Y., Chi, L. (2012). Fabrication of hierarchical structures by unconventional two-step imprinting. *J. Colloid. Interface Sci.*, **368**(1), 655–659.
13. Villegas, J. E., Swiecicki, I., Bernard, R., Crassous, A., Briatico, J., Wolf, T., Bergeal, N., et al. (2011). Imprinting nanoporous alumina patterns into the magneto-transport of oxide superconductors. *Nanotechnology*, **22**(7), 075302.
14. Hien Nguyen, T., Ansell, R. J. (2012). N-Isopropylacrylamide as a functional monomer for noncovalent molecular imprinting. *J. Mol. Recognit.*, **25**(1), 1–10.
15. Xu, H., Schönhoff, M., Zhang, X. (2011). Unconventional layer-by-layer assembly: Surface molecular imprinting and its applications. *Small,* **8**(4), 517–523.
16. Taylor, C., Marega, E., Stach, E. A., Salamo, G., Hussey, L., Muñoz, M., Malshe, A. (2008). Directed self-assembly of quantum structures by nanomechanical stamping using probe tips. *Nanotechnology*, **19**(1), 015301.
17. Zeira, A., Berson, J., Feldman, I., Maoz, R., Sagiv, J. (2011). A bipolar electrochemical approach to constructive lithography: Metal/monolayer patterns via consecutive site-defined oxidation and reduction. *Langmuir*, **27**(13), 8562–8575.
18. Bass, J. D., Schaper, C. D., Rettner, C. T., Arellano, N., Alharbi, F. H., Miller, R. D., Kim, H. C. (2011). Transfer molding of nanoscale oxides using water-soluble templates. *ACS Nano.*, **5**(5), 4065–4072.
19. De Marco, C., Eaton, S. M., Levi, M., Cerullo, G., Turri, S., Osellame, R., High-fidelity solvent-resistant replica molding of hydrophobic polymer surfaces produced by femtosecond laser nanofabrication. *Langmuir*, **27**(13), 8391–8395, 2011.
20. Hadorn, M., Eggenberger Hotz, P. (2010). DNA-mediated self-assembly of artificial vesicles. *PLoS One*, **5**(3), e9886.
21. Maune, H. T., Han, S. P., Barish, R. D., Bockrath, M., III, W. A. Rothemund, P. W., Winfree, E. (2010). Self-assembly of carbon nanotubes into two-dimensional geometries using DNA origami templates. *Nat. Nanotechnol.*, **5**(1), 61–66.
22. Sun, X., Hyeon Ko, S., Zhang, C., Ribbe, A. E., Mao, C. (2009). Surface-mediated DNA self assembly. *J. Am. Chem. Soc.*, **131**(37), 13248–13249.
23. Cheng, W., Campolongo, M. J., Cha, J. J., Tan, S. J., Umbach, C. C., Muller, D. A., Luo, D. (2009). Freestanding nanoparticle superlattice sheets controlled by DNA. *Nat Mater.*, **8**(6), 519–525.

24. Ofir, Y., Samanta, B., Rotello, V. M. (2008). Polymer and biopolymer mediated self-assembly of gold nanoparticles. *Chem. Soc. Rev.*, **37**(9), 1814–1825.
25. Samanta, D., Shanmugaraju, S., Joshi, S. A., Patil, Y. P., Nethaji, M., Mukherjee, P. S. (2012). Pillar height dependent formation of unprecedented Pd(8) molecular swing and Pd(6) molecular boat via multicomponent self-assembly. *Chem. Commun. (Camb.)*, **48**, 2298–2300.
26. Breen, J. M., Clérac, R., Zhang, L., Cloonan, S. M., Kennedy, E., Feeney, M., McCabe, T., Williams, D. C., Schmitt, W. (2012). Self-assembly of hybrid organic–inorganic polyoxovanadates: Functionalised mixed-valent clusters and molecular cages. *Dalton Trans.*, **41**(10), 2918–2926.

Chapter 26

Advancements in Ophthalmic Glucose Nanosensors for Diabetes Management

Angelika Domschke, PhD

Angelika Domschke Consulting LLC, Duluth, Georgia, USA

Keywords: diabetes management, continuous glucose monitoring, minimally invasive glucose monitoring, ophthalmic glucose sensor, contact lens glucose sensor, tear glucose measurements, ophthalmic non-invasive glucose measurement

26.1 Introduction: Importance of Diabetes Management

Diabetes represents one of the primary health concerns of the twenty-first century. However, the most common method of glucose level monitoring (finger-stick method) can be as problematic as the disease itself, as diabetics are required to obtain blood

Handbook of Clinical Nanomedicine: Nanoparticles, Imaging, Therapy, and Clinical Applications
Edited by Raj Bawa, Gerald F. Audette, and Israel Rubinstein

ISBN 978-981-4669-20-7 (Hardcover), 978-981-4669-21-4 (eBook)
www.panstanford.com

samples up to five times per day. This procedure is painful and inconvenient, and as a result, patients tend to test themselves less frequently, which translates to less effective glycemic control. This situation has been described by experts in the field as comparable to a "glycemic" roller coaster ride that diabetes patients must endure on a daily basis, blindfolded. Each finger stick provides only an isolated snapshot of the blood glucose value in real time, devoid of any information in regard to how low or high the level will fall or rise over the next moments (Fig. 26.1). This constitutes a frightening situation indeed, albeit one that has bolstered the many research efforts currently underway, in an attempt to assist with remedying this situation. Noninvasive and continuous glucose monitoring (CGM) comprises one of the most highly investigated areas, which may have great potential to increase patient usage. This strategy may significantly improve the lives and health of diabetes patients [1–3].

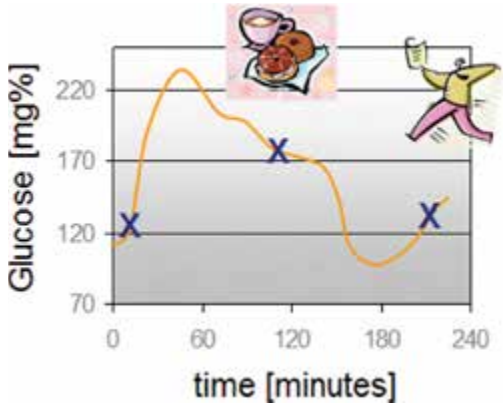

Figure 26.1 Exemplary time course of blood glucose levels, depicting high and low glucose values that may go undetected using regular finger-stick glucose measurement.

26.2 Current Continuous Glucose Monitoring Devices

Several CGM devices are currently available: Guardian® REAL-Time (Medtronic), Dexcom G4™ (DexCom), Paradigm® REAL-Time Revel™ and insulin pump (Mini-Med), FreeStyle Navigator® (Abbott), GlucoDay® S (Menarini Diagnostics microdialysis system

for clinical use, not released in the United States). These monitors consist of a disposable needle sensor wire, a transmitter, and a receiver. The sensor wire is inserted by the patient or is injected clinically under the skin with replacement times from 2 to 7 days. A detailed description of three types of sensor devices has been reported by Brett Ives et al. [4].

The availability of a complete glucose profile, enabled by these methods, was proven beneficial for glycemic control [5]. However, for a variety of reasons, large-scale implementation of these monitoring devices in diabetic care still awaits a breakthrough. For example, the method of sensor insertion is painful; frequent replacement increases the risk of inflammation; they are often noticeable, and in some cases have limited water resistance. They are also very expensive (over $5000 per year) [6], and insurance coverage is approved on a case-by-case basis only. Another point of concern is a relatively low accuracy. As evidenced in several studies, the median relative absolute difference (RAD), a measure of sensor accuracy comparing sensor readings to reference glucose levels, ranges from 12% to 20% [6–10]. The newest generation of CGM systems is purported to be within a 20% RAD, yet still does not approach the accuracy of current home glucose monitors. However, it is important to note that sensor accuracy has improved over time and will continue to progress with technological advancements, offering a means to enhance the efficacy of current diabetes care.

26.3 Noninvasive Continuous Glucose Monitoring Devices

In recent years, numerous efforts have been focused on the development of noninvasive or minimally invasive sensors that would allow convenient, pain-free and CGM for diabetic patients. Noninvasive detection may be achieved by the use of sensing elements that are placed on the skin, combined with a detection device that can sense tissue glucose without piercing the skin. Some examples include iontophoretic extraction of glucose through the epidermis, visible (or near-IR absorption) spectrometry, and polarimetry. A comprehensive evaluation of noninvasive glucose monitoring, spanning 14 technologies and 16 devices has been reported by Tura et al. [11].

26.4 Advantages of Noninvasive and Continuous Ophthalmic/Contact Lens Glucose Sensors

An alternative approach to noninvasive or minimally invasive CGM would be to extract measurements from saliva, urine, or tear fluid. A major disadvantage of this method is that almost all of these fluids have the requirement of being collected prior to measurement and, therefore, truly continuous sensing has not yet been a possibility. Among several available body fluids, tear fluid has a number of distinct advantages insofar as glucose sensing. It is directly assessable *in situ* from the eye; it possesses a direct correlation to glucose levels in blood [12]; and the fluid is confined to a small area, which is relatively free from interfering compounds that are unrelated to internal metabolism (e.g., saliva may be contaminated with food residues). Contact lenses have been verified as safe for use in diabetic patients [13]. The use of a contact lens that is in direct and continuous contact with ocular tear fluid may provide a unique opportunity for noninvasive and CGM in the eye. Recently, several contact lens sensor designs have emerged that might allow for continuous monitoring and interrogation of the tear fluid. Some of the most advanced designs among those that have succeeded in the exploration of *in vivo* measurements [14, 15] are based on fluorescence and spectrophotometric methods. Other very promising designs make use of micro/nanoelectronic technologies. This chapter will focus on the most advanced methods, with a brief excursion to investigate microelectronic contact lens glucose sensors.

26.5 Requirements for Ophthalmic/Contact Lens Glucose Sensors

Ophthalmic glucose sensors, and in particular, contact lens–based glucose sensors, operate in a unique physiological environment, which creates a set of equally unique requirements for such sensing devices. One of these is the prerequisite of very high sensitivity to enable the accurate tracking of tear fluid glucose levels, which are substantially lower than those of blood or interstitial fluid. Nondiabetic and diabetic blood glucose values range from ~80

to ~400 mg/dL. Mean values for diabetic and nondiabetic tear glucose, as reported by Morris et al., are 6.3 ± 0.7 mg/dL (0.35 ± 0.04 mmol/L) and 2.9 ± 0.5 mg/dL (0.16 ± 0.03 mmol/L), respectively [16].

Tear fluid glucose concentrations depend strongly on the tear collection methodology. Significantly higher values have been reported for collection methods that mechanically irritate the ocular surface in comparison to nonirritating methods, indicating that disruptive collection methods can trigger the release of glucose from damaged cells and its subsequent diffusion into the tear fluid. A detailed study that relates the historical results of tear glucose levels and tear collection methods for glucose measurement was published by Asher et al. [17]. The mean values reported by Morris et al. were derived from a study that compared the dynamic differences of tear glucose between 121 diabetic and non-diabetic subjects following the administration of a carbohydrate load. A quantitative chromatographic analysis of tear glucose was utilized. These values are representative of the nonirritating values evaluated by Asher, and serve as a good reference point.

A second key requirement is the establishment of a stable, fully reversible, accurate, and sufficiently rapid response over the tear glucose value range. Changes in sensor sensitivity and signal may occur over time due to the degradation of sensing molecules (e.g., conformational changes of protein glucose receptors; photobleaching of organic dye molecules, which may be used for fluorescence sensor devices; or leaching of sensing units from the device). Some of these alterations may be compensated for to a certain degree via recalibration. However, frequent recalibration using blood samples would defeat the purpose and aim of a minimally invasive measurement technique. The response time of the sensor must be on the order of several minutes to be able to track accurately and in a timely fashion, increasing and decreasing blood glucose levels. Sensing units as well as the surrounding matrix play a significant role in the response rate.

Many sensing units consist of glucose-binding assays. A key to the success of these sensors resides in optimal binding kinetics under physiological conditions to allow rapid and reversible binding and release. For other enzyme-based tests, the minimal or zero consumption of analytes is important so as to avoid an

imbalance in the local levels of glucose, which may impede tracking accuracy.

Some sensor techniques require the encapsulation of sensing molecules prior to embedding the sensor within the contact lens matrix to avoid leaching and/or to stabilize the sensor molecules. In these cases, the morphology of the capsule must be optimized not only to avoid the leaching of the sensor molecules but also to maintain sufficient permeability so as to facilitate the free flow of glucose into and out of the capsule. The leaching of sensing molecules from synthetic sensors may be avoided relatively easily by chemically binding or physically trapping the sensor molecules within the surrounding matrix. Binding or entrapment within protein-based sensors, however, represents a significant hurdle due to the potential loss of sensor activity.

Many reported techniques employ hydrogel contact lens matrices (e.g., polymers and copolymers based on poly(hydroxyethyl methacrylates), poly(vinylalcohols), poly(acrylamides)). The high percentage of water contained within these materials (~50% to 70%) allows for the free flow of glucose through the hydrogel matrix. Over the last decade, hydrogel contact lens materials have been gradually replaced by more advanced silicone hydrogels, which offer superior health benefits due to their high oxygen permeability [18]. These materials have a significantly lower water content (less than ~40%), which greatly reduces or inhibits the glucose flow throughout the matrix. To use these state-of-the art materials, sensor systems must be attached to the surface of the silicone hydrogel contact lenses.

A third requirement is selectivity, which is one of the primary motivations behind the great attention that has been given to the development of enzymatic sensor assays with high specificity for glucose over synthetic glucose-binding ligands, such as boronic acids. Synthetic sensors require optimization in order to obtain higher selectivity for glucose over interfering tear fluid components such as glycosylated proteins and lactate. Synthetic sensors, however, remain attractive due to their high stability and relatively easy immobilization to avoid leaching, which can be a key factor in the production process and shelf-life requirements for contact lens sensors (e.g., today's contact lens production relies on highly efficient sterilization processes such as autoclaving). Heat and pressure ranges applied in this process will degenerate

protein-based sensors, but leave boronic acid–based sensors unharmed.

Most contact lens sensors require a handheld readout device that is used in combination with the glucose sensor contact lens to allow for the convenient monitoring of glucose levels by the patient. The development of such a handheld device, however, involves an equivalent level of complexity as the contact lens sensor unit itself.

26.6 Fluorescence-Based Glucose Sensing

One of the most intensely researched glucose-sensing methods is based on fluorescence measurements. Fluorescence is a form of luminescence, whereby an excitable molecule (a fluorophore) absorbs light of a specific wavelength and subsequently releases a lower energy photon. Fluorescence is a rapid (sub-microsecond) emission process that accompanies transitions from singlet-excited states to ground states. The emitted light is thereby shifted to a longer wavelength relative to that of the activating light, which enables highly sensitive measurements due to the zero background, as excitation irradiation may be conveniently filtered. Excitation and emission wavelengths, in conjunction with inherent fluorescence kinetics, are dependent on the chemical composition and attributes of the particular fluorophore involved. The chemical environment within which a fluorophore is immersed imparts an influence as well, due to the interactions with the surrounding molecules, once it is raised to an excited state.

These characteristics impart a number of distinct advantages for the utilization of fluorescence measurements in biological environments. An extensive overview is provided by Pickup et al. [19]. The following advantages are of particular interest for tear fluid–based glucose analysis:

- Very high sensitivity, allowing for even single-molecule detection methods [20].
- Versatility of readout options, including not only fluorescence intensity measurements, but also fluorescence decay times: The advantages of time-resolved fluorescence measurements for *in vivo* sensing [21] are that they may be obtained independent of the effects of tissue resident light scattering

and of fluorophore concentration, which become critical in systems that are subject to photobleaching or fluorophore loss via diffusion or degradation.

- Sensitivity to surrounding molecules, as described by Pickup et al. [19] (e.g., the structure and distribution of biomolecules may also be probed by the phenomenon of fluorescence (or Forster) resonance energy transfer (FRET) [22, 23]. This involves the nonradiative energy transfer from a fluorescent donor molecule to an acceptor molecule in close proximity (which need not be fluorescent), and is typically brought about by dipole–dipole interactions. In this dynamic, the rate of energy transfer is inversely proportional to R6 (1/R6 is the long-range van der Waals interaction/attraction that governs the behavior of all atoms and molecules), where R is the distance between the donor and the acceptor. Thus, FRET is an exceptionally sensitive Angstrom-level measure of the subtle changes in molecular distances (e.g., within a molecule, as the tertiary structure undergoes alterations on binding with a ligand, or between molecules, as a ligand displaces a labeled analog from a labeled receptor).

Glucose sensors based on FRET are well known, and numerous devices have been reported and patented worldwide. Detailed reviews of fluorescence-based glucose assays, such as glucose-binding lectins, apoenzymes, and synthetic boronic acid receptors, are conveyed by Cote and McShane and Ballerstadt et al. [24, 25]. While fluorescence-based glucose sensing has gained immense academic attention, the implementation of such a technology currently presents significant hurdles, and hence, only a few groups have reported significant advancements that encompass extensive in vitro testing or *in vivo* proofs of concept. Some of the most promising and advanced technologies toward the realization of ophthalmic fluorescence-based glucose sensors are introduced in the following section.

March and Herbrechtsmeier et al. ALCON (formerly CIBA VISION) have investigated and developed fluorescence-based contact lens sensors and reported on the initial clinical trials that implemented this technology [14, 26]. The team also pioneered the first handheld photofluorometer (Fig. 26.2) to track alterations in fluorescence intensity in response to changes in glucose concentration. The sensing units comprise hydrogel-encapsulated

nanospheres that contain competitive glucose-binding assay components (tetramethylrhodamine isothiocyanate concanavalin A [TRITC-Con A] and fluorescein isothiocyanate dextran [FITC-dextran]), which operate on the basis of FRET. As glucose levels rise, FITC-labeled dextran molecules are displaced by glucose molecules, which results in decreased FRET and increased fluorescence intensity in alignment with elevated glucose levels. In contrast, as glucose levels fall, higher concentrations of FITC-dextran molecules bind to the TRITCCon A, and hence, fluorescence intensity is reduced [27] (Figs. 26.3 and 26.5). The nanospheres are embedded within a polyvinyl alcohol-based (Nelfilcon A) hydrogel contact lens matrix. The team succeeded in preparing clinical grade contact lenses by UV light polymerization utilizing CIBA VISION's patented Light Stream Technology TM (Fig. 26.4).

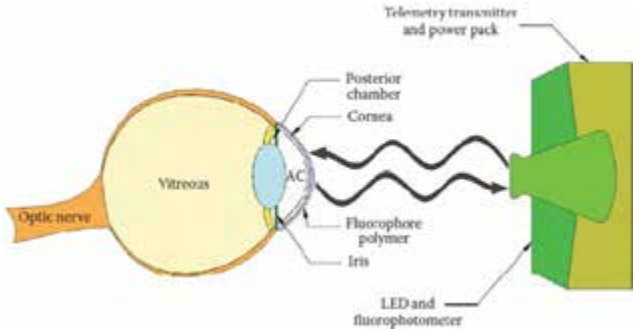

Figure 26.2 Depiction of interrogation of a contact lens glucose sensor via a handheld photofluorometer device. (Derived and redrawn from March, W., et al. (2006). *Diab. Technol. Ther*., **8**(3), 312. With permission.)

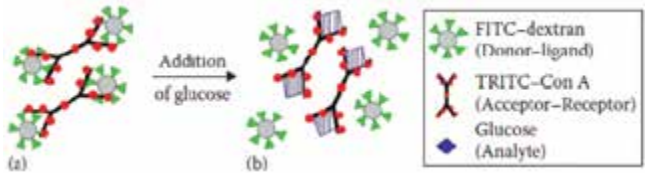

Figure 26.3 (a, b) Schematic of hydrogel-encapsulated nanospheres containing competitive glucose-binding FITC-dextran/TRITC-Con A complexes. (Reproduced with permission from Chinnayelka, S., Microcapsule biosensors based on competitive binding and fluorescence resonance energy transfer assays, PhD dissertation, Louisiana Tech University, Ruston, LA, 2005.)

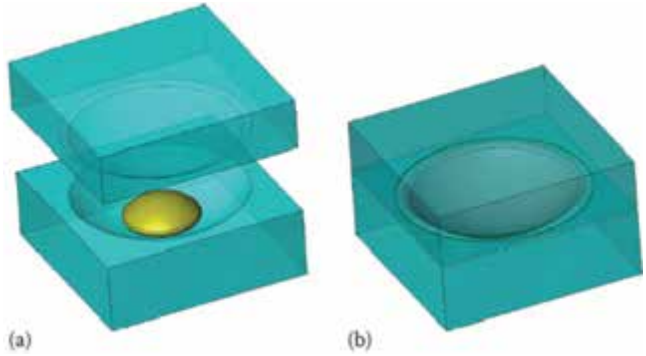

Figure 26.4 (a) Nanosphere-infused hydrogel is deposited in a quartz mold having patient-appropriate curvature. (b) Contact lens is shaped and cured via exposure to UV light. (Derived and redrawn from March, W., et al. (2006). *Diab. Technol. Ther.*, **8**(3), 312. With permission.)

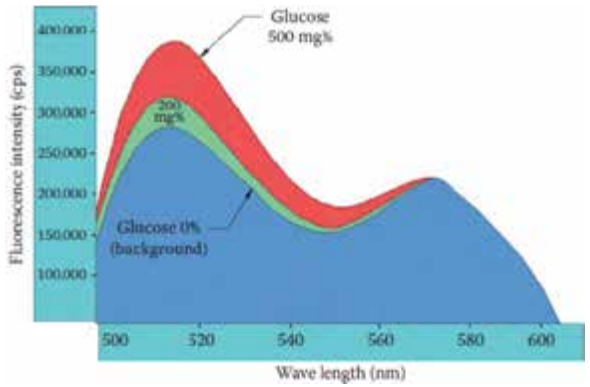

Figure 26.5 Fluorescence spectra of contact lens depicting one peak (514 nm) from fluorescein (rises with increases in glucose concentration) and another (574 nm) from rhodamine (remains static with increases in glucose concentration). (Redrawn representation from March, W., et al. (2006). *Diab. Technol. Ther.*, **8**(3), 312. With permission.)

The contact lens sensor appeared to track blood glucose concentrations of five diabetic subjects who wore these sensors and one normal (control) nondiabetic subject. Responses had to be individually scaled for each subject in order for the fluorescence signal to fit the blood glucose concentration profile. Nevertheless, these early *in situ* results clearly demonstrated that there is indeed

a correlation between glucose level changes in tears and blood (Figs. 26.5 and 26.6). These pioneering results have strongly encouraged further research efforts in the ophthalmic sensor domain.

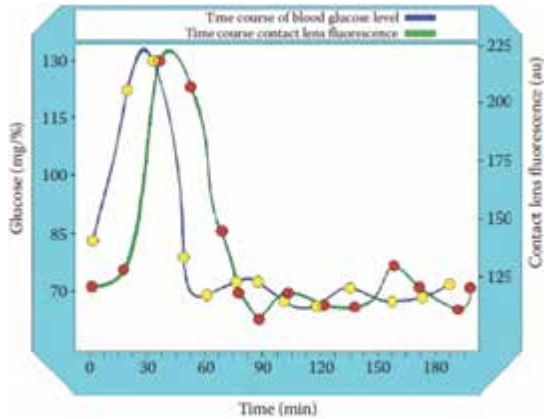

Figure 26.6 Depiction of correlation between blood glucose concentration and contact lens fluorescence. (Redrawn representation from March, W., et al. (2006). *Diab. Technol. Ther.*, **8**(3), 312. With permission.)

This sensor technology platform was further technologically advanced by Eyesense GmbH (a diagnostic device company spun out from Novartis and CIBA VISION) in the form of an ophthalmic glucose sensor implant. The diminutive ophthalmic implant sensor is inserted beneath the conjunctiva, which is a delicate transparent membrane that lines the inner eyelids and is continuous across the anterior portion of the eye ball, covering the white of the eye (sclera). The implanted subconjunctival sensor may be inserted at the outer zone of the eye in a simple, sutureless, and painless procedure that can be performed by an ophthalmologist within only three minutes. This sensor monitors glucose concentrations in the interstitial fluid, which are in the same range as those of the blood, and therefore far easier to monitor than the much lower tear glucose concentrations.

Eyesense reports via its website [28] that the dimensions, morphology, and composition of its "mini-sensor" are designed and adapted such that no foreign body sensation is elicited. In addition, the sensor is invisible to other individuals and may

reside within the eye of the patient for up to 1 year, after which it is replaced by an ophthalmologist. While carrying the insert, the patient requires only an unobtrusive measuring device to quantify blood glucose in a completely noninvasive manner. The device analyzes fluorescence signals, and following a single and simple calibration, displays blood glucose levels in typical units. The biggest advantage of this innovative technology is that the patient may measure glucose levels as often as he or she wishes by simply placing the small photometer in front of the eye. The very rapid (~20 s) and easy measurements incur no extra costs with their frequency of use.

A subconjunctival implant has significant technical advantages over skin-implantable glucose sensors due to the high transparency of the conjunctiva, which contains minimal vascularization and pigmentation. The concept of subconjunctival implants has been reported previously by Abreu as a suitable system for the noninvasive measurement of chemical substances such as glucose [29].

Zhang et al., at the University of Western Ontario, recently developed a fluorescence contact lens sensor based on nanocomposites [30, 31]. The sensor units comprise fluorescent mesoporous silica nanoparticles (FMSNs) (0~55 nm) (Fig. 26.7), which physically entrap and stabilize glucose assay components such as FITC-dextran and TRITC-Con A, via ionic interaction.

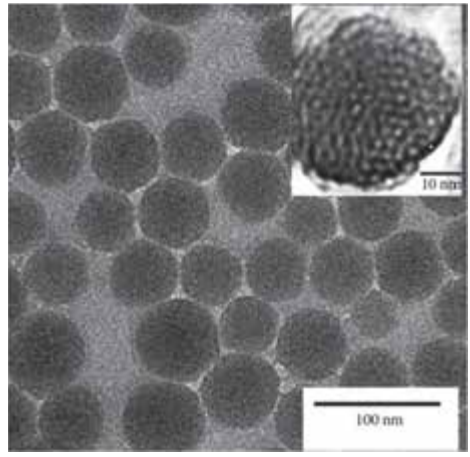

Figure 26.7 Transmission electron microscopy (TEM) micrograph of FMSNs. (Reproduced from Zhang, J., et al., *J. Diab. Sci. Technol*., **5**(1), 166, Copyright 2011. With permission.)

The group applied a two-step photopolymerization process in the casting of optical nanoparticles (NPs) into soft hydrogel lens materials. Initially, fluorescent NPs were assembled on a pretreated poly(dimethylsiloxane) slice through spin-coating. Subsequently, the optical probe was embedded within a hydrophilic hydrogel lens material (2-hydroxyethyl methacrylate) through UV polymerization of the monomeric formulation. The device was able to detect glucose concentrations in the range from 0.04 to 4 mM, which is well within tear glucose monitoring parameters. The response times reported for detection in a 0.1 mM glucose solution were less than five minutes, and the sensor response capability remained stable for five days. The stabilizing effect of the porous silica NPs against the photobleaching of FITC (Fig. 26.8) (constituting a major concern with this technology) was tested, and significant improvements in the functionality of FMSNs were demonstrated [30, 31].

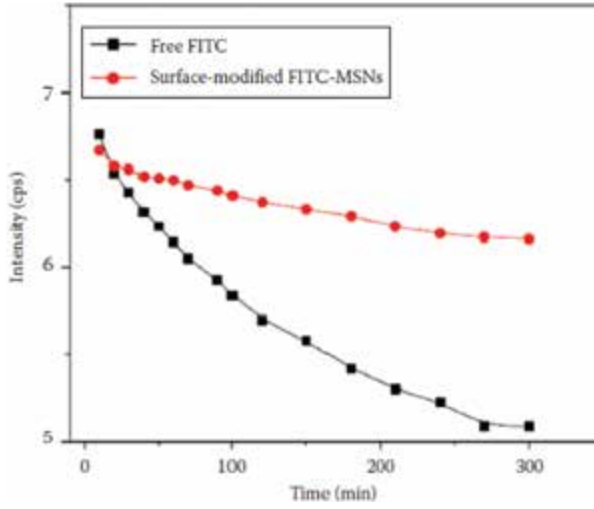

Figure 26.8 Photobleaching activity of free and surface-modified FITC. (Reproduced from Zhang, J., et al., *J. Diab. Sci. Technol.,* **5**(1), 166, Copyright 2011. With permission.)

Badugu, Lakowicz, and Geddes (Medical Biotechnology Center, University of Maryland) developed and studied the *in vitro* response of glucose-sensing contact lenses with fluorescent sensor probes that were based on fluorophore-containing boronic acids. This sensor technique exploits modifications in the electronic properties

and geometries of boron atoms, which induce fluorescence spectral changes in the probes when glucose binds to the boronic acid moiety. The boronic acid group is an electron-deficient Lewis acid having a sp2-hybridized boron atom with a trigonal planar conformation. The anionic form of boronic acid, created in the presence of glucose, is characterized by a more electron-rich sp3-hybridized boron atom having a tetrahedral geometry.

Modifications in the electronic properties and geometries at the boron atom induces fluorescence spectral changes in the probes. Upon addition of glucose, the electron density of the boron atom is increased, facilitating partial neutralization of the positively charged quaternary nitrogen of the quinolinium moiety. This interaction has been termed a "charge neutralization–stabilization mechanism" [32–34] (Fig. 26.9). The lenses detect glucose changes of up to several millimolar in the tear glucose concentration range for diabetics with a 90% response time of ~10 min (i.e., time required for the fluorescence signal to deviate by 90% from its original state) [32] (Fig. 26.10).

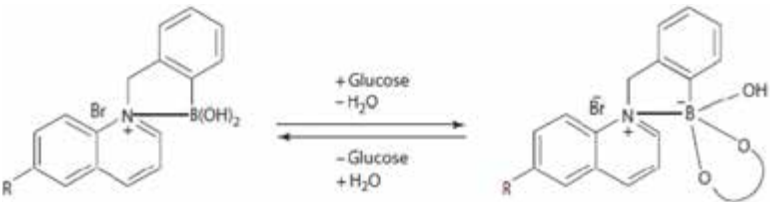

Figure 26.9 Schematic representation of the charge neutralization–stabilization mechanism as relates to glucose sensing. The bold line shown between the N+ and boron atom in the structure shown at right indicates an increased interaction between them, and is not intended to show covalent bond formation between the two atoms. (Reproduced from Badugu, R., et al. (2005). *Curr. Opin. Biotechnol*., **16**(1), 100. With permission.)

Since the sensor probes of this platform were not chemically bound to the contact lens matrix, the stability of the sensor was investigated by the group, who reported on shelf-life testing over several months, utilizing both wet and dry lens storage. The results revealed identical sugar-sensing capacities, indicating that no lens polymer–fluorophore interactions or probe degradation took

place over this time period. While this initial shelf-life testing is encouraging, the leaching of noncovalently bonded molecules from the contact lens matrix may still pose a concern in view of stringent FDA regulations in regard to medical sensing device safety and efficacy. Other aspects of this technology to be addressed in the future will likely include boronic acid selectivity over interfering tear fluid components such as lactate and glycoproteins, and the design of a robust and highly accurate handheld readout device.

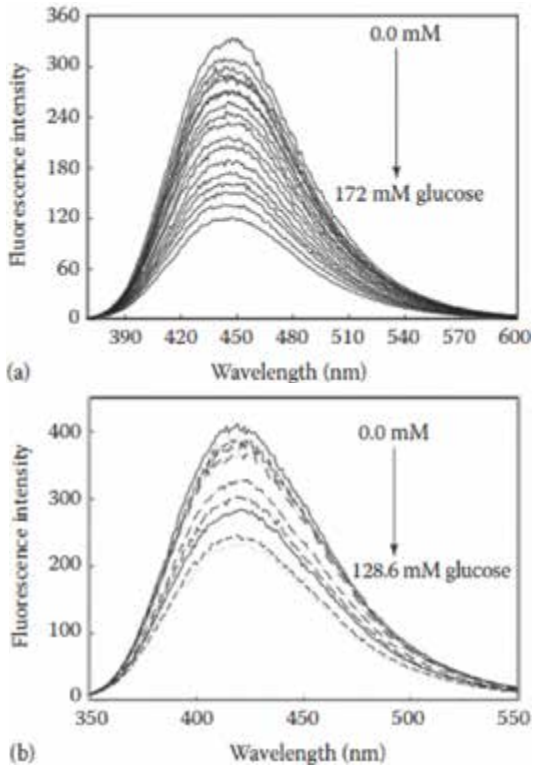

Figure 26.10 Illustration of response of contact lens sensors to low concentrations (<2 mM) of glucose. Emission spectra of (a) an N-(boronobenzyl)-6-methoxyquinolinium bromide (o-BMOQBA)- and (b) an N-(boronobenzyl)-6-ethylquinolinium bromide (o-BMQBA)-doped contact lens under escalating glucose concentrations. (Adapted from Badugu, R., et al. (2005). *Curr. Opin. Biotechnol.,* **16**(1), 100; Badugu, R., et al. (2004). *J. Fluoresc.*, **14**(5), 617. With permission.)

26.7 Colorimetric Sensors Based on Periodic Optical Nanostructures

A unique and different class of glucose sensors incorporates periodic optical nanostructures that are designed to affect the motion of photons. The interaction of light with these nanostructures results in distinct color phenomena that may also be observed in nature, where it is termed "structural" color. A well-known example of structural color operates in the mineral opal. The distinct brilliance of opal colors is caused by a lattice of high-refractive-index material (silica spheres), which are embedded within a low-refractive-index matrix. Other well-researched natural examples are the colors of butterfly wings such as those of the *Lycaenidae* species [36–38] (Fig. 26.11). The scales of these butterfly wings contain three-dimensional (3D) photonic structures which are typically composed of a matrix of chitin (high-refractive-index material) containing regularly arranged spherical air spaces (low-refractive-index material) known as an inverse opal structure. Another example is the brilliant coloration found in the feathers of the peacock. Stacked melanin rods, interspersed with air pockets, make up periodic optical nanostructures. Differences in color are achieved by changing the lattice spacing of the rods [39] (Fig. 26.12).

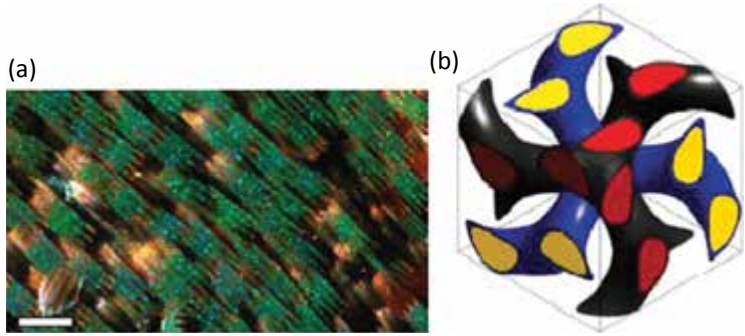

Figure 26.11 (a) Light micrograph depicting randomly oriented opalescent crystallite domains in the ventral wing cover scales of *Callophrys gryneus* (*Lycaenidae*). (Scale bar: 100 μm.) (b) 3D core–shell double gyroid model of a photonic butterfly wing scale cell. (Reproduced from Saranathan, V., et al. (2010). *Proc. Natl. Acad. Sci. U. S. A.*, **107**(26), 11676. Copyright 2003. National Academy of Sciences, U.S.A. With permission.)

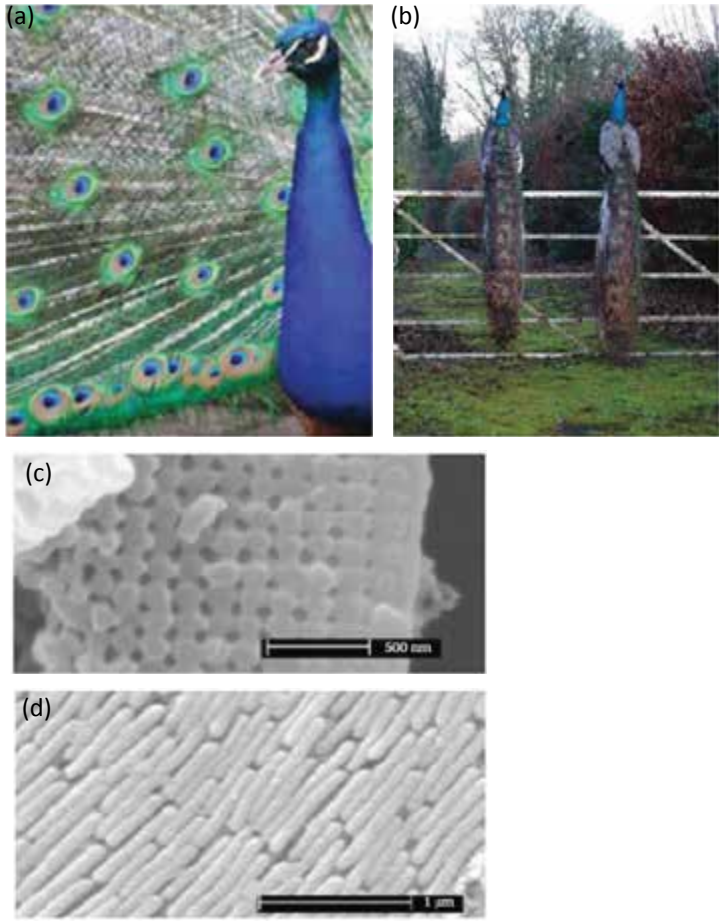

Figure 26.12 (a, b) Examples of iridescent peacock plumage. (Copyright Ian Paterson, and licensed for reuse under Creative Commons License.) (c, d) Scanning electron microscope images of peacock barbule structures. Melanin rods coupled via keratin and interspersed with air pockets comprise periodic optical nanostructures. Differences in color are achieved by alterations in the lattice spacing of the rods. (Reproduced from Zi, J., et al. (2003). *Proc. Natl. Acad. Sci. U. S. A.*, **100**(22), 12576. Copyright 2003. National Academy of Sciences, U.S.A. With permission.)

Lattices composed of points, spheres, or other structures have found widespread use in the form of thin film optics, with applications ranging from low and high reflective coatings on lenses

and mirrors to color-changing inks. Under white light illumination, such lattices diffract light and produce a characteristic spectral peak with a wavelength that is governed in approximation to the Bragg equation: $m\lambda = 2nd\sin\lambda$, where m is the diffraction order; λ is the wavelength of light; n is the average refractive index; θ is the angle of illumination to the normal; and d is the spacing of the lattice (Fig. 26.13). The most subtle variations in the spacing of the nanolattices initiate color shifts that may easily be detected by a spectrophotometer. Ease of fabrication, high sensitivity, and their status as a known technology for integration into readout devices, make optical nanostructures particularly suitable as ophthalmic sensors.

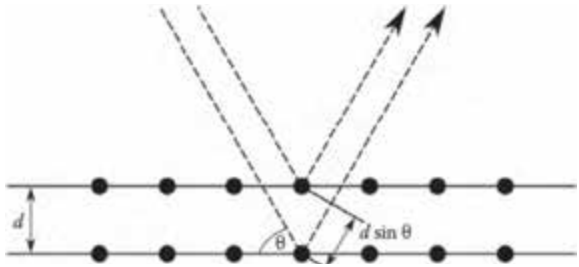

Figure 26.13 Schematic of Bragg diffraction. (From Wikimedia Commons.)

26.8 Holographic Glucose Sensors

A collaborative team led by Domschke ALCON (formerly CIBA VISION) and Lowe (Institute for Biotechnology at the University of Cambridge, United Kingdom) developed a unique holographic platform based on periodic optical nanostructures that are suitable for contact lens applications. The platform combines a simple reflection hologram [40] recorded within a hydrogel matrix with covalently bonded 3-acrylamidophenylboronic acid (3-APB) as the glucose-binding ligand. The construction of such a holographic reflection grating is depicted in Fig. 26.14.

When holographic reflection gratings are illuminated by white light, they act as sensitive wavelength filters in the same manner as crystalline colloidal arrays and reflect only a specific narrow wavelength band that is governed by the Bragg equation [42]. Changes in the swelling state of the hydrogel within which the grating is recorded will alter the fringe distance and hence the reflected

color that may be detected by a hand-held spectrophotometer. The hydrogels were synthesized using 3-APB, which has the capacity for forming reversible covalent bonds (Fig. 26.15) with glucose [43].

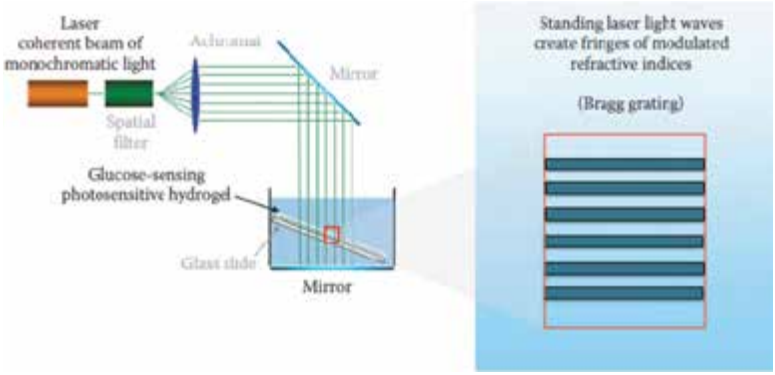

Figure 26.14 Schematic drawing of the hologram fabrication process: The hologram is produced by passing a single collimated laser beam through the photosensitive hydrogel, backed by a mirror. Interference between the incident and reflected beams creates a permanent modulated refractive index in the form of fringes. (From Domschke, A., Oral presentation at the *International Conference on Nanoscience and Technology* (*ICN+T*), Keystone, CO, 2008.)

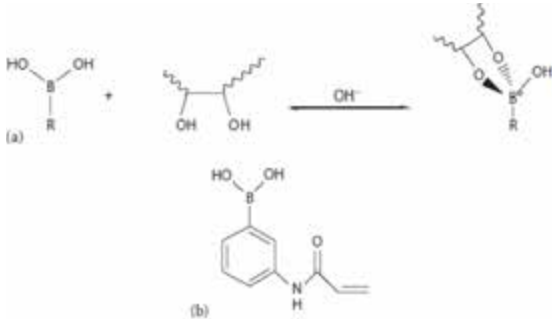

Figure 26.15 (a) The reversible binding that occurs between boronic acids and cis-diols in aqueous media. (b) Structure of 3-APB. (Reproduced from Kabilan, S., et al. (2005). *Biosens. Bioelectron.*, **20**(8), 1602. Copyright 2005. Elsevier. With permission.)

The binding of glucose to 3-APB moieties causes the hydrogel to swell, which in turn alters the fringe distances that may be employed to quantify the glucose concentration [43, 44]. The team

demonstrated the capability of 3-APB (and other derivative)-based holographic glucose sensors to reversibly and continuously function in complex biological media at physiological pH, ionic strength, and physiological glucose levels [43, 45]. Boronic acids are known to bind cis-diols, including a variety of sugars [46–48] and hydroxy acids [49]. However, other than glucose, sugars are typically not found in a free state within physiological solutions at high concentrations. Many sugars are present in the form of macromolecular carbohydrate structures and as glycoproteins, but these do not affect the hologram as they cannot diffuse into the hydrogel matrix and bind to the pendant phenylboronic acid groups. On the other hand, α-hydroxy acid and lactic acid are present at millimolar concentrations within the blood and other physiological fluids and might therefore interfere with glucose detectors that incorporate boronate-based sensing systems. The team also developed various sensor systems with an enhanced selectivity for glucose versus interfering lactic acid [44] (Fig. 26.16).

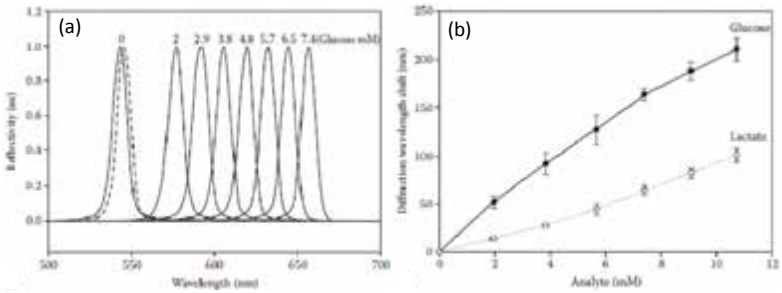

Figure 26.16 (a) The resulting diffraction spectra of a 25 mol% 3-APB hologram immersed in PBS (pH 7.4) solutions of varying glucose concentrations at 30°C. The dashed line indicates the diffraction peak observed after exposure to 7.4 mM glucose and subsequently rinsing the hologram with PBS. (b) Response of a 20 mol% 3-APB hologram to variations in glucose and lactate concentrations in PBS (pH 7.4) at 30°C. (From Kabilan, S., et al. (2005). *Biosens. Bioelectron.,* **20**(8), 1602. Copyright 2005. Elsevier. With permission.)

The holographic sensor units were embedded in a Nelfilcon A, polyvinylalcohol contact lens matrix, and contact lenses were fabricated by UV light polymerization, utilizing CIBA VISION's patented Light Stream Technology TM. The contact lens glucose sensors were subsequently extracted and autoclaved to render the

contact lens sterile and biocompatible. Promising initial clinical studies were performed that indicated the capacity for tracking glucose response for ~30 min [45].

Figure 26.17 shows the actual holographic contact lens in a normal patient's eye (subject A), a plot of blood glucose concentration against time after glucose administration in subject A, and the response of the holographic sensor for the same period in the same subject [15]. There appears to be a slight time delay between increased blood glucose and the contact lens sensor response. A polynomial may be derived for each individual patient that can partially correct for this delay, as previously described [50]. While further long-term testing is required to fully develop such a sensor, the method shows considerable promise over the current continuous monitoring systems, as it is less invasive and may be cost-effectively mass produced.

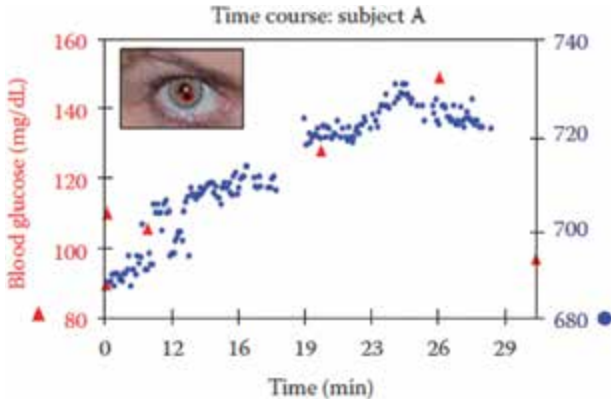

Figure 26.17 Photograph of a normal patient (subject A) wearing a holographic contact lens; a plot of response of the holographic sensor for the same period in the same subject. (From Domschke, A. M., *Chimia* (*Aarau*), **64**(1–2), 43, 2010.)

26.9 Photonic Crystal Glucose Sensors

Photonic crystal contact lens glucose sensors have been investigated by Asher, Department of Chemistry, University of Pittsburgh [51], that consist of a crystalline colloidal array embedded within a polymer network. The network contains pendent phenylboronic acid groups that diffract light in the visible spectral region. The

pendent boronic acid groups bind glucose in a "sandwich-like" complex, forming additional cross-links within the hydrogel. As these additional cross-links form, the hydrogel shrinks (Fig. 26.18). This alters the lattice spacing of the colloidal array, which results in a blueshift of the diffracted light in proportion to the glucose in solution. Diabetic patients employ a mirror to examine the color of the photonic crystal sensor in the contact lens in comparison to the color depicted on a calibrated reference color wheel (Fig. 26.19). Alternatively, a handheld spectrophotometer might be developed to discern the color shift.

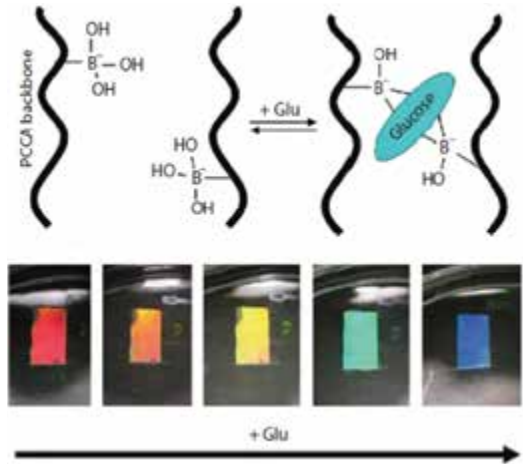

Figure 26.18 Schematic of a polymerized crystalline colloidal array (PCCA) with attached glucose binding phenylboronic acid ligands. With increased glucose concentration, the hydrogel shrinks resulting in a blueshift of the diffracted light in proportion to the glucose in solution. (Reproduced from Asher Research Group, Department of Chemistry, University of Pittsburgh, http://www.pitt.edu/~asher/homepage/colgrp.html, accessed on December 2, 2014. With permission.)

Photonic crystals under investigation for their application in prototype contact lens sensors were fabricated via the self-assembly of highly charged monodispersed polystyrene nanospheres (Ø ~100 nm) within a crystalline colloidal suspension, which formed photonic crystal templates [51]. The crystal arrays were embedded within a polyacrylamide-based hydrogel matrix that was functionalized with boronic acid groups. Sensitivity and

response times were optimized, which resulted in changes in glucose concentrations at rates comparable to the expected rates of glucose concentration changes in blood (~five minute response time in a 0.2 mM D-glucose solution) [53] (Fig. 26.20).

Figure 26.19 Conceptual drawing of photonic tear glucose sensing utilizing a mirror to examine the color of the photonic crystal sensor in the contact lens and compare the color to that of a calibrated reference color wheel. (Reproduced from Asher Research Group, Department of Chemistry, University of Pittsburgh, Colloid Group, http://www.pitt.edu/~asher/homepage/colgrp.html#pcca, accessed March 12, 2012. With permission.)

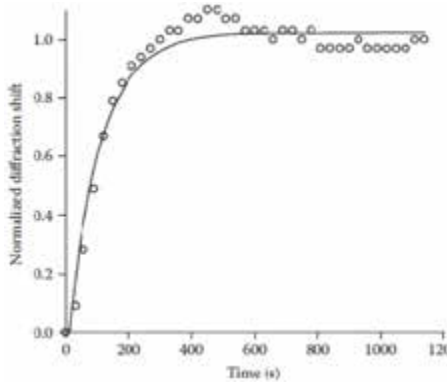

Figure 26.20 Response kinetics of *n*-hexylacrylate PCCA glucose sensors in artificial tear fluid when challenged with freshly prepared 0.15 mM D glucose solutions at pH 7.4 at 37°C. A rapid blueshift of the diffraction (~11 nm) is observed saturating within ~300 s. (Reproduced from Ben-Moshe, M., et al. (2006). *Anal. Chem*., **78**(14), 5149. Copyright 2006. American Chemical Society. With permission.)

Some remaining challenges include the successful demonstration of glucose determination *in situ*, where factors such as sensor specificity, reproducibility, and robustness will play a significant role. This technology has been licensed for development by Glucose Sensing Technologies, LLC, which is exploring advanced photonic crystal-based platforms such as high-diffraction efficiency two-dimensional (2D) photonic crystals for applications in molecular recognition and chemical sensing [54].

26.10 Microelectromechanical-Based Sensors

Techniques for the fabrication of microelectromechanical (MEMS) and nanoelectromechanical (NEMS) systems have advanced greatly over the last decade. The implementation of miniaturized sensors interfaced with wireless power delivery systems and sensing readout circuitry is now a reality, which has opened up the new field of small-scale sensor research, including microscale and nanoscale glucose sensors [55]. Microfabrication techniques have been developed to integrate structures into polymeric matrices that are compatible for use in contact lenses. Based on these advancements, MEMS-based contact lens glucose sensors have been developed that bear great promise.

Parviz and his team at the University of Washington have developed a microfabricated (3 μW) wirelessly powered amperometric contact lens glucose sensor. The sensor electrode suite (e.g., working, counter, and reference electrodes) was generated via photoresist and thin metal film deposition techniques, utilizing a poly(ethylene terephthalate) film substrate. The film was then heat-modeled into a lens-like shape and functionalized with a glucose oxidase enzyme/titania sol/gel membrane covered by a layer of Nafion®, a sulfonated tetrafluoroethylene-based fluoropolymer-copolymer. The team also developed an interface chip for contact lens borne electronic circuits for wireless readout, including a wireless power delivery system and sensing readout circuitry (adopting a 2.4 GHz carrier frequency), signal processing and communication subsystems. The sensor system consumes 3 W and may be powered over a distance of 15 cm [56, 57].

The sensor exhibited promising sensitivity, repeatability (linear correlation coefficient of 0.9968 over 25 samples), and rapid response times (e.g., response to the subsequent addition

of 0.1 mM glucose solution reached 90% of the maximum value in less than 20 s) for low glucose concentrations (0.1–0.6 mM), which are relevant for tear glucose measurements. The sensor can attain a minimum detection of less than 0.01 mM glucose. The team also reported interference rejection for ascorbic acid, urea, and lactate. Future investigations will focus on enhanced stability, the attainment of more efficient interference rejection, and the transfer of the technology into biocompatible contact lens materials [56–58]. This nascent prototype design is intriguing by virtue of its low detection limit, which is of particular interest for diabetes management, as it allows more accurate detection of hypoglycemic glucose levels. Hypoglycemia can ensue following insulin administration and may induce serious complications for patients, including seizures, unconsciousness, and (rarely) permanent brain damage or death.

A very promising soft MEMS contact lens biosensor (SCL-biosensor) for the novel noninvasive biomonitoring of tear fluids was fabricated and tested in an *in vivo* animal model by Mitsubayashi and coworkers at the Tokyo Medical and Dental University (Fig. 26.21). Flexible microelectrode systems with sensor and reference electrodes were fabricated on a 70 μm thin polydimethylsiloxane (PDMS) film. The electrode system was attached to the PDMS lens surface using a PDMS binder. A mixture of glucose oxidase and a copolymer (consisting of 2-methacryloyloxyethyl phosphorcholine and 2-ethylhexylmethacrylate) was applied to the active region of the sensor and cured. Subsequently, an overcoat of the copolymer was applied so as to avoid enzyme leakage. The electrode terminal was connected to a potentiostat to facilitate *in vitro* and *in vivo* measurements [59].

The *in vitro* measurements demonstrated a quick and sensitive response in an appropriate tear glucose concentration range between 0.03 and 5.0 mM. The team successfully conducted an *in vivo* measurement in a rabbit model, obtaining a stable output current for the basal tear glucose concentration. The estimated basal concentration was 0.11 mM which falls within the range of human nondiabetic levels. The contact lens sensor was able to track the changes in tear glucose levels induced by changes in blood glucose via the oral administration of glucose. The tear glucose levels followed the blood glucose with a delay of about 10 min.

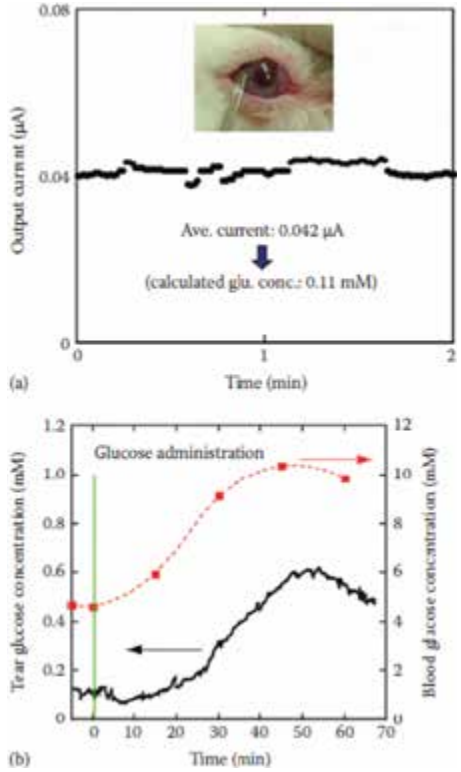

Figure 26.21 (a) SCL-biosensor on ocular site of rabbit model generated a stable (0.042 μA) output current, and basal tear glucose concentration was estimated to be 0.11 mM. (b) Plot of chronological alteration in tear and blood glucose concentrations. The registration of changes in tear glucose values lagged ~15 to 20 min behind those of blood glucose values. (Reproduced from Chu, M. X., et al. (2011). *Talanta*, **83**(3), 960. With permission.)

A 3D enzyme-based glucose contact lens sensor was developed by Patel et al. at Simon Fraser University (Burnaby, BC) (Figs. 26.22 and 26.23). In this approach, working and reference electrodes with pillar-like geometries were prepared to realize a 3D topography with an enhanced surface area (up to 300% over 2D analogs) contained on a small footprint (1 × 2 mm^2). The electrode was fabricated on a flexible PDMS film by employing standard MEMS techniques. Glucose oxidase was immobilized on the gold electrode surface, and glucose responses to selected 3D topographies were

tested, which resulted in the achievement of a high sensitivity, utilizing a 200 μm-high square pillar pattern. Sensitivities to glucose concentrations as low as 0.04 mM were reported [60].

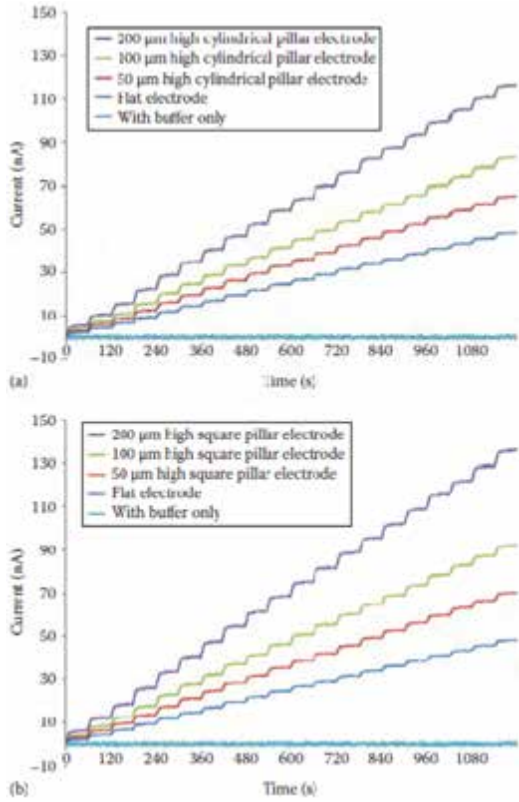

Figure 26.22 Measured amperometric responses for different 3D electrode geometries. The response is measured at 0.5 V with respect to the Ag/AgCl (reference) electrode. (a) Amperometric response for different designs with the cylindrical pillars along with the flat electrode response. The amperometric response in phosphate buffer is also shown for comparison of the noise. The amperometric current increases with improvement in the electrode surface area. (b) Amperometric response for different designs with the square pillars along with the flat electrode response. Similar to the cylindrical pillars, the amperometric current increases with improvement in the surface area of the electrode. (Reproduced from Patel, J. N., et al. (2011). *J. Diabetes Sci. Technol.*, **5**(5), 1036. Copyright 2011. *J. Diab. Sci. Technol*. With permission.)

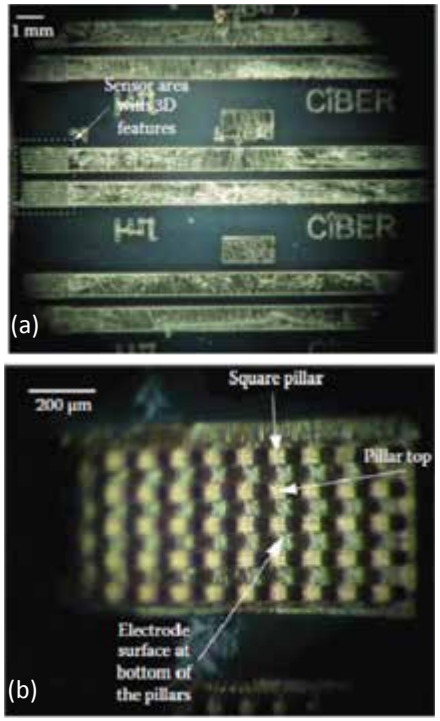

Figure 26.23 Microscopic image of electrodes immediately following PDMS-based sensor removal from the glass-backing plate. (a) Three consecutive sensors with pillar electrodes are shown along with connecting conductors for testing. The actual sensor area is highlighted in the image. (b) Magnified view of the pillar electrodes with square pillars. Ordered array of square pillars on working electrode are uniformly covered with Cr/Au metal layer. The square pillar feature along with the top and bottom of the metal-covered pillar is indicated in the image. (Reproduced from Patel, J. N., et al. (2011). *J. Diab. Sci. Technol*., **5**(5), 1036. Copyright 2011. *J. Diab. Sci. Technol*. With permission.)

Amperometric enzyme-based MEMS systems were further developed and culminated in an interesting alternative ophthalmic sensor. A team led by Wang at Arizona State University and the University of California fabricated a miniaturized flexible film electrochemical biosensor that operated within the lacrimal canaliculus. The lacrimal canaliculi (lacrimal ducts) are the small channels in each eyelid that begin at tiny orifices, termed punta

lacrimalia, which are seen on the margins of the lids (Fig. 26.24). *In vitro* testing of the new sensor that employed laterally rolled screen-printed band electrodes and glucose-oxidase containing ink exhibited rapid response when challenged with glucose concentrations in the range between 0.02 and 20 mM (Fig. 26.25). The enzyme electrode was covered with electropolymerized polytyramine to minimize contributions from typical electroactive interferant species such as ascorbic and uric acids [61].

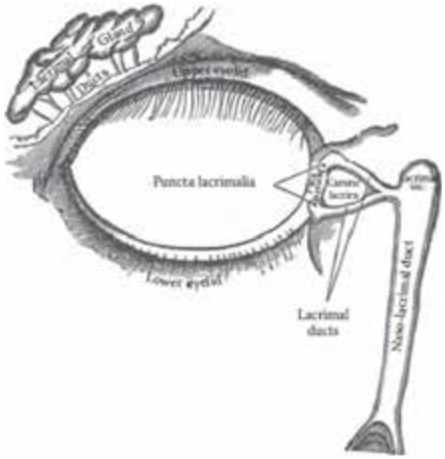

Figure 26.24 Schematic depicting the location of lacrimal ducts. (From Gray, H., *Anatomy of the Human Body,* Lea & Febiger, Philadelphia, PA, 1918, Bartleby.com, 2000.)

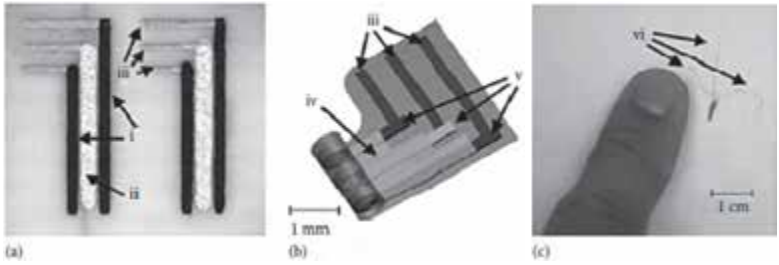

Figure 26.25 (a) Screen-printed tri-electrode microflow electrochemical biosensor: (i) carbon-based working/counter electrodes; (ii) Ag/AgCl reference electrodes; (iii) copper contacts. (b) Rendering of partially rolled sensor: (iii) copper contacts; (iv) insulator; (v) screen-printed inks. (c) Rolled silicone-coated electrode: (vi) electrical contacts. (Reproduced from Kagie, A., et al. (2008). *Electroanalysis*, **20**(14), 1610. With permission.)

26.11 Progress and Remaining Challenges toward the Development of Ophthalmic Glucose Sensors

In recent years, the development of noninvasive and continuous ophthalmic glucose monitoring devices for the progressive management of diabetes has been greatly advanced. Progress toward meeting the challenging requirements for the implementation of such sensing devices has been reported for a large variety of both established and emerging sensor platforms. Very high sensitivity is one example of requisite criteria that has been the centerpiece of enduring efforts over many years. Sensitivity levels have been reported to not only encompass diabetic or normal tear glucose levels, but also hypoglycemic levels. Microelectromechanical-based sensor techniques have been reported with outstanding sensitivities that are up to 10 times lower than normal tear glucose levels. The accurate monitoring of glucose concentrations that may fall to hypoglycemic levels is critical, in that if these levels remain unnoticed, they may culminate in severe health implications, including coma and death.

The development of stable sensing units represents an additional major challenge. A creative solution in this area, however, has been successfully demonstrated via the encapsulation of very sensitive protein-based sensor moieties. Here, one of the most promising advances was realized through the use of a stable fluorescence-based ocular sensing subconjunctival insert that makes possible an annual replacement schedule. A convenient handheld readout device was developed in conjunction with the implanted sensor that enables patients to self-monitor their glucose levels.

Systems based on synthetic sensing units (e.g., boronic acid derivatives) exhibited remarkably short-term stability when subjected to the typical thermal and pressure demands inherent to autoclaving, which is employed as a sterilization method in the process of manufacturing contact lenses. A perceived drawback of boronic acid-based sensors is selectivity for glucose over other interfering tear analytes, specifically lactic acid. Nevertheless, in this area as well, advances have been reported that demonstrate very encouraging selectivity, which significantly increases the importance of boronic acid platforms.

Sufficiently rapid response times, accuracy, and repeatability are the crucial requirements for contact lens integrated sensing devices that have been optimized for many sensors *in vitro*. A number of well-advanced contact lens sensor platforms have demonstrated the achievement of these requirements *in vivo*, indicating that measured tear glucose levels can track blood glucose levels well. Variable lag times between tear glucose results and blood glucose levels have been reported that range from ~0 to 20 min. Considerable work has been done toward the elucidation and understanding of correlations between blood and tear resident glucose levels. Interestingly, further complex physiological aspects of this relationship have been discovered, such as the variation of lag times and magnitude of response between individuals; single subjects from day to day; and even between the left and right eyes of single subjects. Lag and response times are, to a certain degree, also dependent on the type of sensor and the matrix that surrounds the sensing unit, which adds another layer of complexity. The multifaceted physiological aspects of tear glucose monitoring, and in particular the variations in lag times, remain the most significant challenges.

Accuracy and reliability are absolute necessities for meeting sanctioned safety and efficacy standards, as the long-term well-being of diabetic patients, and in certain cases of hypoglycemia, the lives of the patients are completely dependent on these requirements. Therefore, calibrations of non-invasive glucose sensors are necessary to accurately account for any possible variations in the correlation between the blood and tear glucose levels. Numerous required calibrations, however, greatly reduce the appeal of noninvasive sensors. Consequently, a considerable segment of the overall sensor development must include a very costly clinical evaluation that establishes the need for calibration, which ultimately verifies the value of new noninvasive sensor techniques. This represents a very demanding hurdle for all ophthalmic sensor platforms.

It remains to be seen if the development of contact lens integrated glucose monitoring devices is sufficiently rapid to keep pace with the introduction of alternative approaches such as stem cell treatments [63] and nascent nanomedical therapeutics [64], which may efficiently help fight or even cure diabetes in the future.

26.12 Outlook

Many technologies introduced in this chapter bear the potential for much broader applications, which are yet to be realized. Tear fluid contains a variety of physiological analytes, such as Na^+, K^+, Ca^{2+}, Mg^{2+}, histamine, urea, lactate, and cholesterol, as well as a multitude of biomarkers that could be monitored in the near future through similar contact lens–based sensing platforms.

Aside from tear fluid analytes, a different type of contact lens sensor that assists in the management of diabetes-related eye diseases, recently obtained much scientific attention. A common complication of diabetes is open-angle glaucoma, which is associated with elevated eye pressure in conjunction with typical glaucomatous nerve damage. Most treatments are aimed at lowering the eye pressure to avoid such nerve damage. For efficient glaucoma management, the monitoring of the interocular pressure is very important [65]. To the extent that contact lens sensors that measure interocular pressure have been evolving, some very advanced devices have been developed by companies that anticipate commercial release in the near future. Some of these sophisticated devices include MEMS-based systems that have been developed by companies such as STMicroelectronics to accurately measure very subtle shape changes of the eye [66]. These wireless MEMS sensors act as both a transducer and an antenna within a smart contact lens named "Sensimed Triggerfish" [66], which is an embedded sensor system that incorporates a strain gauge in a smart lens platform, which is designed to monitor the curvature of the eye (Fig. 26.26).

Other contact lens–based pressure-sensing devices remain in various stages of development [67] with some positive results reported subsequent to comparative studies with a conventional dynamic contour tonometer. Of these, slit-lamp mounted (DCT) and handheld (HH) technologies look promising [68].

Another diabetes-related eye disease is the so-called "dry eye syndrome," also known as keratoconjunctivitis sicca [69]. Dry eye symptoms are conventionally treated with lubricating eye drops. The challenge for an effectual treatment based on eye drops remains a controlled rate of delivery of the eye drop over time, which actually reaches the ocular surface. This is not a trivial matter given the speed at which the administered eye drop drains

through the puncta or spills over the lids, and the compliance of the patient with regard to the frequency and dosage. Therefore, the regulated time release of an appropriate lubricant over extended periods by way of a smart contact lens would be advantageous.

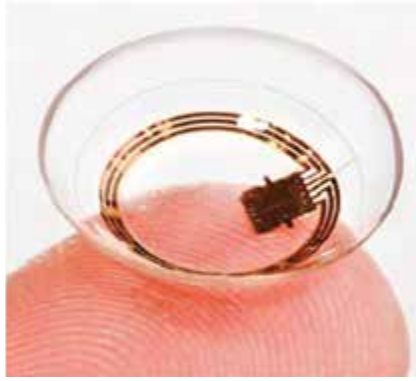

Figure 26.26 Sensimed smart lens measures interocular pressure. (Copyright 2012. Sensimed AG, Lausanne, Switzerland. With permission.)

Several institutions are working on strategies for smart drug-releasing contact lenses. One such device developed by a team from the Children's Hospital Boston; the Massachusetts Eye and Ear Infirmary's ophthalmology department; Schepens Eye Research Institute in Boston; and the Massachusetts Institute of Technology's chemical engineering department, sandwiches pharmaceuticals between two layers of polymeric film [70]. In laboratory tests, these multilayered lenses demonstrated the ability to release ciprofloxacin for up to 100 days. Research in the development of drug-releasing contact lenses has been attempted by a number of other research groups, who have reported significant progress [71]. These innovations are raising hopes that such devices might be available in the relatively near future.

Taking into account the many emerging advanced smart contact lens technologies, the future appears to hold great promise for the implementation of state-of-the-art devices for the management of diabetes in the form of multifunctional contact lenses. These lenses might not only monitor multiple diabetes-related analytes and symptoms, but may also be endowed with the capacity for treating ocular discomfort in an all-in-one approach.

Disclosures and Conflict of Interest

The author declares that she has no conflict of interest and has no affiliations or financial involvement with any organization or entity discussed in this chapter. No writing assistance was utilized nor any compensation received in the production of this chapter.

Corresponding Author

Dr. Angelika Domschke
Angelika Domschke Consulting LLC
3379 Ennfield Way, Duluth GA 30096, USA
Email: angeldomschke@aol.com

About the Author

Angelika Domschke is a visionary and scientist with 20 years of experience, at the forefront of innovation in biomedical devices for large medical device companies and startups. She holds a PhD in polymer chemistry and has extensive expertise in program management, from concept to product launch. She has been awarded 26 patents, which generated significant revenue encompassing medical devices, nanosensors, implants, and materials test methods. Her vocation is the discovery of unique emerging technologies spanning nanomedical devices to integrated complimentary medicine.

References

1. Hirsch, I. B. (2009). Clinical review: Realistic expectations and practical use of continuous glucose monitoring for the endocrinologist. *J. Clin. Endocrinol. Metab.,* **94**(7), 2232–2238.
2. Garg, S. K., Smith, J., Beatson, C., Lopez-Baca, B., Voelmle, M., Gottlieb, P. A. (2009). Comparison of accuracy and safety of the SEVEN and the Navigator continuous glucose monitoring systems. *Diab. Technol. Ther.,* **11**(2), 65–72.
3. Scaramuzza, A. E., Iafusco, D., Rabbone, I., Bonfanti, R., Lombardo, F., Schiaffini, R., Buono, P., Toni, S., Cherubini, V., Zuccotti, G. V. (2011). Use of integrated real-time continuous glucose monitoring/insulin

pump system in children and adolescents with type 1 diabetes: A 3-year follow-up study. Diabetes Study Group of the Italian Society of Paediatric Endocrinology and Diabetology. *Diab. Technol. Ther.,* **13**(2), 99–103.

4. Ives, B., Sikes, K., Urban, A., Stephenson, K., Tamborlane, W. V. (2010). Practical aspects of realtime continuous glucose monitors: The experience of the Yale children's diabetes program. *Diab. Edu.* **36**(1), 53–62.
5. Edelman, S. V., Bailey, T. S. (2009). Continuous glucose monitoring health outcomes. *Diab. Technol. Ther.,* **11**(1), S68–S74.
6. Walsh, J., Roberts, R., Continuous Glucose Monitors, Diabetes Mall, Available at: http://www.diabetesnet.com/diabetes-technology/meters-monitors/continuous-monitors/compare-current-monitors (accessed on May 21, 2014).
7. Diabetes Research in Children Network (DirecNet) Study Group, The accuracy of the guardian RT continuous glucose monitor in children with type 1 diabetes. *Diab. Technol. Ther.,* **10**(4), 266–272, 2008.
8. Wilson, D. M., Beck, R. W., Tamborlane, W. V., Dontchev, M. J., Kollman, C., Chase, P., Fox, L. A., Ruedy, K. J., Tsalikian, E., Weinzimer, S. A. (2007). DirecNet Study Group, The accuracy of the FreeStyle Navigator continuous glucose monitoring system in children with type 1 diabetes. *Diab. Care,* **30**(1), 59–64.
9. Garg, S. K., Schwartz, S., Edelman, S. V. (2004). Improved glucose excursions using an implantable real-time continuous glucose sensor in adults with type 1 diabetes. *Diab. Care*, **27**,734–738.
10. The Diabetes Research in Children Network (DirecNet) Study Group, Accuracy of the modified continuous glucose monitoring system (CGMS®) sensor in an outpatient setting: Results from a Diabetes Research in Children Network (DirecNet) study. *Diab. Technol. Ther.,* **7**(1), 109–113, 2005.
11. Tura, A., Maran, A., Pacini, G. (2007). Non-invasive glucose monitoring: Assessment of technologies and devices according to quantitative criteria. *Diab. Res. Clin. Pract.,* **77**(1), 16–40.
12. Baca, J. T., Taormina, C. R., Feingold, E., Finegold, D. N., Grabowsk, J. J., Asher, S. A. (2007). Mass spectral determination of fasting tear glucose concentrations in nondiabetic volunteers. *Clin. Chem.,* **53**(7), 1370–1372.
13. March, W., Long, B., Hofmann, W., Keys, D., McKenney, C. (2004). Safety of contact lenses in patients with diabetes. *Diab. Technol. Ther.,* **6**(1), 49–52.

14. March, W., Lazzaro, D., Rastogi, S. (2006). Fluorescent measurement in the non-invasive contact lens glucose sensor. *Diab. Technol. Ther.,* **8**(3), 312–317.
15. Domschke, A. M. (2010). Continuous non-invasive ophthalmic glucose sensor for diabetics. *Chimia (Aarau),* **64**(1–2), 43–44.
16. Lane, J. D., Krumholz, D. M., Sack, R. A., Morris, C. (2006). Tear glucose dynamics in diabetes mellitus. *Curr. Eye Res.,* **31**(11), 895–901.
17. Alexeev, V. L., Das, S., Finegold, D. N., Asher, S. A. (2004). Photonic crystal glucose-sensing material for non-invasive monitoring of glucose in tear fluid. *Clin. Chem.,* **50**(12), 2353–2360.
18. Sweeney, D., du Toit, R., Keay, L., Jalbert, I., Sankaridurg, P. R., Stern, J., Skotnitsky, C., Stephensen, A., Covey, M., Holden, B. A., Rao, G. N. (2004). Clinical performance of silicone hydrogel lenses. In: Sweeney D, ed. *Silicone Hydrogels: Continuous-Wear Contact Lenses*. Butterworth Heinemann, British Contact Lens Association, Edinburgh, 164–216.
19. Pickup, J. C., Hussain, F., Evans, N. D., Rolinski, O. J., Birch, D. J. (2005). Fluorescence-based glucose sensors. *Biosens. Bioelectron.,* **20**(12), 2555–2565.
20. Yim, S. W., Kim, T., Laurence, T. A., Partono, S., Kim, D., Kim, Y., Weiss, S., Reitmair, A. (2012). Four-color alternating-laser excitation single-molecule fluorescence spectroscopy for next-generation biodetection assays. *Clin. Chem.,* **58**(4), 707–716.
21. Lakowicz, J. R. (1994). Emerging biomedical applications of time-resolved fluorescence spectroscopy. In: Lakowicz, J. R., ed. *Topics in Fluorescence Spectroscopy*, vol. 4, Plenum Press, New York, pp. 1–19.
22. Selvin, P. R. (1995). Fluorescence resonance energy transfer. *Methods Enzymol.,* **246**, 300–334.
23. Lakowicz, J. R. (1999). *Principles of Fluorescence Spectroscopy*, 2nd ed. Kluwer Academic/Plenum Publishers, New York.
24. Coté, G. L., McShane, M., Pishko, M. (2009). Fluorescence-based glucose biosensors, Glucose optical sensing and impact, edited by Valery Tuchin, Taylor & Francis Group, Boca Raton, FL, Chapter 11, pp. 319–352.
25. Ballerstadt, R., Gowda, A., McNichols, R. (2004). Fluorescence resonance energy transfer-based near-infrared fluorescence sensor for glucose monitoring. *Diab. Technol. Ther.,* **6**(2), 191–200.
26. March, W. F., Mueller, A., Herbrechtsmeier, P. (2004). Clinical trial of a noninvasive contact lens glucose sensor. *Diab. Technol. Ther.,* **6**(6), 782–789.

27. Chinnayelka, S. (2005). Microcapsule biosensors based on competitive binding and fluorescence resonance energy transfer assays, PhD dissertation, Louisiana Tech University, Ruston, LA.
28. Painless blood glucose measurement for diabetics without blood tests. Eyesense AG. Available at: http://www.eyesense.com/(accessed on May 21, 2014).
29. Abreu, M. M., U.S. Patent No. 6,544,193, April 8, 2003.
30. Zhang, J., Hodge, W., Hutnick, C., Wang, X. (2011). Noninvasive diagnostic devices for diabetes through measuring tear glucose. *J. Diab. Sci. Technol.,* **5**(1), 166–172.
31. Zhang, J., Hodge, W. G. (2010). US20100113901.
32. Badugu, R., Lakowicz, J. R., Geddes, C. D. (2005). A glucose-sensing contact lens: From bench top to patient. *Curr. Opin. Biotechnol.,* **16**(1), 100–107.
33. Badugu, R., Lakowicz, J. R., Geddes, C. D. (2005). Fluorescence sensors for monosaccharides based on the 6-methylquinolinium nucleus and boronic acid moiety: Potential application to ophthalmic diagnostics. *Talanta,* **65**(3), 762–768.
34. Badugu, R., Lakowicz, J. R., Geddes, C. D. (2005). Boronic acid fluorescent sensors for monosaccharide signaling based on the 6-methoxyquinolinium heterocyclic nucleus: Progress toward noninvasive and continuous glucose monitoring. *Bioorg. Med. Chem.,* **13**(1), 113–119.
35. Badugu, R., Lakowicz, J. R., Geddes, C. D. (2004). Ophthalmic glucose monitoring using disposable contact lenses: A review. *J. Fluoresc.,* **14**(5), 617–633.
36. Kumar, C. S. S. R. (2010). *Biomimetic and Bioinspired Nanomaterials.* Wiley, New York.
37. Saranathan, V., Osuji, C. O., Mochrie, S. G., Noh, H., Narayanan, S., Sandy, A., Dufresne, E. R., Prum, R. O. (2010). Structure, function, self-assembly of single network gyroid (I4132) photonic crystals in butterfly wing scales. *Proc. Natl. Acad. Sci. U. S. A.,* **107**(26), 11676–11681.
38. Vértesy, Z., Bálint, Z., Kertész, K., Vigneron, J. P., Lousse, V., Biró, L. P. (2006). Wing scale microstructures and nanostructures in butterflies: Natural photonic crystals. *J. Microsc.,* **224**(Pt 1), 108–110.
39. Zi, J., Yu, X., Li, Y., Hu, X., Xu, C., Wang, X., Liu, X., Fu, R. (2003). Coloration strategies in peacock feathers. *Proc. Natl. Acad. Sci. U. S. A.,* **100**(22), 12576–12578.

40. Denisyuk, Y. N. (1965). On the reproduction of the optical properties of an object by the wave field of its scattered radiation. *Opt. Spectrosc.,* **18**, 152–157.
41. Domschke, A. (2008). Ophthalmic glucose nano-sensor. Oral presentation at the International Conference on Nanoscience and Technology (ICN+T), Keystone, CO.
42. Nave, R., Bragg's law. HyperPhysics, Section 6.1, Georgia State University. Available at: http://hyperphysics.phy-astr.gsu.edu/hbase/quantum/bragg.html (accessed on May 21, 2014).
43. Kabilan, S., Blyth, J., Lee, M. C., Marshall, A. J., Hussain, A., Yang, X. P., Lowe, C. R. (2004). Glucosesensitive holographic sensors. *J. Mol. Recogn.,* **17**(3), 162–166.
44. Kabilan, S., Marshall, A. J., Sartain, F. K., Lee, M. C., Hussain, A., Yang, X., Blyth, J., Karangu, N., James, K., Zeng, J., Smith, D., Domschke, A., Lowe, C. R. (2005). Holographic glucose sensors. *Biosens. Bioelectron.,* **20**(8), 1602–1610.
45. Domschke, A., March, W. F., Kabilan, S., Lowe, C. (2006). Initial clinical testing of a holographic non-invasive contact lens glucose sensor. *Diab. Technol. Ther.,* **8**(1), 89–93.
46. Lorand, J. P., Edwards, J. O. (1959). Polyol complexes and structure of the benzeneboronate ion. *J. Org. Chem.,* **24**, 769–774.
47. Yang, W. Q., Yan, J., Springsteen, G., Deeter, S., Wang, B. H. (2003). A novel type of fluorescent boronic acid that shows large fluorescence intensity changes upon binding with a carbohydrate in aqueous solution at physiological pH. *Bioorg. Med. Chem. Lett.,* **13**(6), 1019–1022.
48. Lavigne, J. J., Anslyn, E. V. (1999). Teaching old indicators new tricks: A colorimetric chemosensing ensemble for tartrate/malate in beverages. *Angew. Chem. Int. Ed. Engl.,* **38**(24), 3666–3669.
49. Gray, C. W., Jr. Houston, T. A. (2002). Boronic acid receptors for alpha-hydroxycarboxylates: High affinity of Shinkai's glucose receptor for tartrate. *J. Org. Chem.,* **67**(15), 5426–5428.
50. March, W. F. (2002). Dealing with the delay. *Diab. Technol. Ther.,* **4**(1), 49–50.
51. Reese, C. E., Guerrero, C. D., Weissman, J. M., Lee, K., Asher, S. A. (2000). Synthesis of highly charged, monodisperse polystyrene colloidal particles for the fabrication of photonic crystals. *Colloid Interf. Sci.,* **232**(1), 76–80.

52. Asher Research Group, Department of Chemistry, University of Pittsburgh, Colloid Group, Available at: http://www. pitt.edu/~asher/homepage/colgrp.html#pcca (accessed on May 21, 2014).

53. Ben-Moshe, M., Alexeev, V. L., Asher, S. A. (2006). Fast responsive crystalline colloidal array photonic crystal glucose sensors. *Anal. Chem.,* **78**(14), 5149–5157.

54. Zhang, J. T., Wang, L., Luo, J., Tikhonov, A., Kornienko, N., Asher, S. A. (2011). 2D array photonic crystal sensing motif. *J. Am. Chem. Soc.,* **133**(24), 9152–9155.

55. Deshpande, D. C., Yoon, H., Khaing, A. M., Varadan, V. K. (2008). Development of a nanoscale heterostructured glucose sensor using modified microfabrication processes. *J. Micro/Nanolith. MEMS MOEMS,* **7**, 023005.

56. Liao, Y. T., Yao, H., Parviz, B. A., Otis, B. (2011). A 3μW wirelessly powered CMOS glucose sensor for an active contact lens, *Solid-State Circuits Conference Digest of Technical Papers (ISSCC), 2011 IEEE International*, San Francisco, CA, pp. 38–40.

57. Yao, H., Shum, A. J., Cowan, M., Lähdesmäki, I., Parviz, B. A. (2011). A contact lens with embedded sensor for monitoring tear glucose level. *Biosens. Bioelectron.,* **26**(7), 3290–3296.

58. Yao, H., Afanasiev, A., Lahdesmaki, I., Parviz, B. A. (2011). A dual microscale glucose sensor on a contact lens, tested in conditions mimicking the eye, 5734353 abstract, *Micro Electro Mechanical Systems (MEMS), 2011 IEEE 24th International Conference*, Cancun, Mexico, pp. 25–28.

59. Chu, M. X., Miyajima, K., Takahashi, D., Arakawa, T., Sano, K., Sawada, S., Kudo, H., Iwasaki, Y., Akiyoshi, K., Mochizuki, M., Mitsubayashi, K. (2011). Soft contact lens biosensor for *in situ* monitoring of tear glucose as non-invasive blood sugar assessment. *Talanta,* **83**(3), 960–965.

60. Patel, J. N., Gray, B. L., Kaminska, B., Gates, B. D. (2011). Flexible three-dimensional electrochemical glucose sensor with improved sensitivity realized in hybrid polymer microelectromechanical systems technique. *J. Diab. Sci. Technol.,* **5**(5), 1036–1043.

61. Kagie, A., Bishop, D. K., Burdick, J., La Belle, J. T., Dymond, R., Felder, R., Wang, J. (2008). Flexible rolled thick-film miniaturized flow-cell for minimally invasive amperometric sensing. *Electroanalysis,* **20**(14), 1610–1614.

62. Gray, H. (2000). *Anatomy of the Human Body*. Lea & Febiger, Philadelphia, PA, 1918, Bartleby.com.

63. Larijani, B., Nasli Esfahani, E., Amini, P., Nikbin, B., Alimoghaddam, K., Amiri, S., Malekzadeh, R., Mojahed Yazdi, N., Ghodsi, M., Dowlati, Y., Sahraian, M. A., Ghavamzadeh, A. (2012). Stem cell therapy in treatment of different diseases. *Acta Med. Iran,* **50**(2), 79–96.

64. Krol, S., Ellis-Behnke, R., Marchetti, P. (2012). Nanomedicine for treatment of diabetes in an aging population: State-of-the-art and future developments. *Maturitas,* **73**(1), 61–67.

65. Alvarado, J., Diabetes and Your Eyesight, Glaucoma Research Foundation, Available at: http://www.glaucoma.org/glaucoma/diabetes-and-youreyesight.php (accessed on May 21, 2014).

66. Wilson, R., Contact lens has MEMS devise to measure glaucoma. *Electronics Weekly.* 2010. Available at: www.electronicsweekly.com/Articles/2010/03/24/48276/contact-lens-has-mems-device-tomeasure-glaucoma.htm (accessed on May 21, 2014).

67. Leonardi, M., Pitchon, E. M., Bertsch, A., Renaud, P., Mermoud, A. (2009). Wireless contact lens sensor for intraocular pressure monitoring: Assessment on enucleated pig eyes. *Acta Ophthalmol.,* **87**(4), 433–437.

68. Twa, M. D., Roberts, C. J., Karol, H. J., Mahmoud, A. M., Weber, P. A., Small, R. H. (2010). Evaluation of a contact lens-embedded sensor for intraocular pressure measurement. *J. Glaucoma.,* **19**(6), 382–390.

69. Chous, P. (2012). Dry Eyes and Diabetes Often Go Hand In Hand, High risk of disorder calls for tight control of glucose levels, dLife, LifeMed Media, Inc. Available at: http://www.dlife.com/diabetes/complications/eyecare/chous_sept2006 (accessed on May 21, 2014).

70. Ciolino, J. B., Hoare, T. R., Iwata, N. G., Behlau, I., Dohlman, C. H., Langer, R., Kohane, D. S. (2009). A drug-eluting contact lens. *Invest. Ophthalmol. Vis. Sci.,* **50**(7), 3346–3352.

71. Singh, K., Nair, A. B., Kumar, A., Kumria, R. (2011). Novel approaches in formulation and drug delivery using contact lenses. *J. Basic Clin. Pharm.,* **2**(2), 87–101.

Section III

Therapy and Clinical Applications

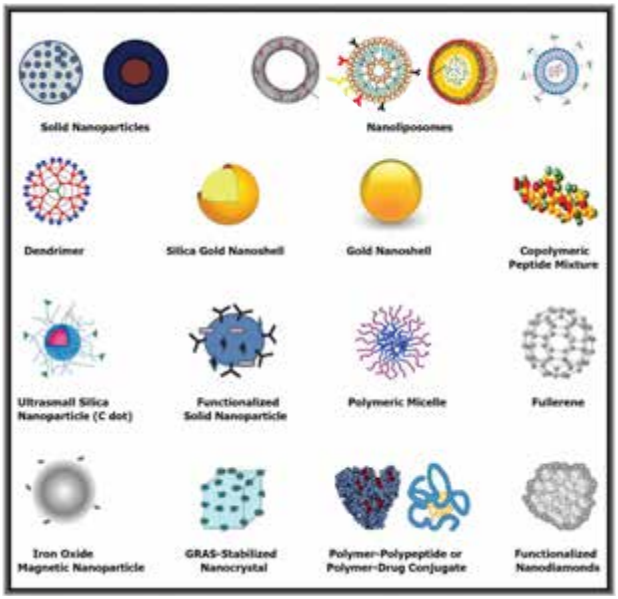

Chapter 27

Towards Nanodiagnostics for Bacterial Infections

Georgette B. Salieb-Beugelaar, PhD,[a,b] and Patrick R. Hunziker, MD[a,b]

[a]*Nanomedicine Research Group, Clinic for Intensive Care Medicine, University Hospital Basel, Basel, Switzerland*
[b]*The European Foundation for Clinical Nanomedicine (CLINAM), Basel, Switzerland*

Keywords: *E. coli*, *S. typhi*, *S. pneumonia*, lateral flow devices, microfluidics, lab-on-a-chip, nanodiagnostics, nanoparticles, nanotechnology, point-of-care, nanofluidics, computer models, nucleic acids, polymerase chain reaction

27.1 Introduction

The era of nanoscience and nanotechnology has brought along a broad spectrum of new technologies and devices that can handle, analyze, and visualize tiny samples of matter. The relevance of these technologies for diagnosis of infectious disease in general has been reviewed recently [1]. This critical review extends the cited work by examining in-depth the emerging use of nanotechnologies including micro/nanofluidics for diagnosing bacterial infections. Because of their clinical relevance in developed

Handbook of Clinical Nanomedicine: Nanoparticles, Imaging, Therapy, and Clinical Applications
Edited by Raj Bawa, Gerald F. Audette, and Israel Rubinstein

ISBN 978-981-4669-20-7 (Hardcover), 978-981-4669-21-4 (eBook)
www.panstanford.com

and in developing countries, an emphasis is laid on the diagnosis of typhoid fever, *E. coli* infections, and pneumococcal infections.

A bacterial infection can be identified in several ways such as (1) detection of microbial antigens or metabolites in patients' blood, urine, stool, or other samples, (2) detection of specific nucleic acids (mRNA, DNA), (3) presence of whole bacteria, (4) detection of bacterial growth in a suited culture medium, and (5) detection of a specific serologic response to an infection. Method selection for diagnosis depends on the bacterial type, the clinical manifestation or the location of the infection, the epidemiologic setting, the available health care budget, and many other factors. In diseases like typhoid fever due to *S. typhi*, as few as 1 bacterium per microliter of blood may be present but may hide intracellularly in >50% [2], explaining false negative blood cultures even in manifest infection.

E. coli might be detected in stool of patients; however, specific serotypes responsible for the post-diarrheal hemolytic uremic syndrome may not be detectable anymore in the late stage of the infection, resulting in false negative culture results [3]. In addition, *E. coli*, including the opportunistic serotypes, may also be present in the stool of healthy individuals ($\sim 10^7$ colony forming units (CFU)/g stool) [4].

Antigenic similarities among all *E. coli* serotypes and common features shared with other bacterial strains (such as the lipopolysaccharides), renders the detection of a specific pathogen even more challenging.

Each of the selected bacterial infections discussed will be introduced, followed by a presentation of (1) current diagnostics (where possible with a focus on rapid tests that can be used at the point of care (POC)), (2) developed/commercial microfluidic devices or Lab-on-a-Chip (LOC) devices, and (3) nanotechnology-based diagnostics (nanodiagnostics). In this context, POC is defined as the testing for the presence of an infection using a device that can be used outside the central laboratory near the bedside of the patient. LOC is defined as a miniaturized (typically a microfluidic) device that is also known as a micro-total-analytical system on which specific laboratory functions are miniaturized and integrated on a single chip. In the final part of the review, the remaining challenges are discussed ending with a conclusion.

As a comprehensive review of the huge body of work that is being performed is out of scope of this chapter, we aim to provide an update of the latest achievements in the field. The cited articles were collected by cross-referencing online keyword searches (e.g., "*S. pneumoniae* diagnostics," "typhoid fever," and "EHEC") in citation and database searching (e.g., Scopus, Sciencedirect, and Pubmed) from January 2000 to December 2014. The works perceived as most important are exemplarily presented in this review. The emphasis of the literature citations is on the evolution of lateral flow and micro/nanofluidic tests for point-of-care applications.

27.2 Diagnostics for Bacterial Infections: From the State of the Art to Nanodiagnostics

27.2.1 *Streptococcus pneumoniae*

27.2.1.1 General

Streptococcus pneumoniae (pneumococcus) is a spherical, Gram-positive bacterium colonizing the nasal area and capable of causing life-threatening disease such as pneumonia, meningitis, bronchitis, sinusitis and otitis media in both developing countries and industrialized countries.

To date, 93 different serotypes are identified that all differ in chemical structure and immunogenicity, posing a challenge for diagnostics [5]. Pneumococcal disease causes over 1.6 millions of deaths annually, mostly among children, older people, and patients with immunodeficiencies [6–8]. Pneumococcal infection is frequently an indication of a defect in the defense of the host, an overwhelming inoculum, an exposure to a particularly virulent microorganism, a hematogenous spread from a distant infected site or pulmonary aspiration. Virulent factors of *S. pneumoniae* include the capsular polysaccharides, the pneumococcal surface protein A (PspA) and protein C (PspC), the pneumococcal surface adhesin A (PsaA) or Hic (see Fig. 27.1). PspA is expressed in all strains of *S. pneumoniae* [9]. The N-terminus is exposed on the bacterial surface and is classified into three families based on sequence homologies in the DNA. Ninety-five percent of all

S. pneumoniae carry PspA of family 1 and 2 (PsapA1 and PsapA2, respectively). PspC has a structure related to PspA; however, the N-terminus is different. This protein is present in about 75% of all pneumococci types and interferes with the complement system by binding of factor H in human plasma, resulting in protection against both complement attach and phagocytosis. PspC exists also in another variant, the factor H-binding inhibitor of complement (Hic), which is mainly found in serotype 3 [10–12].

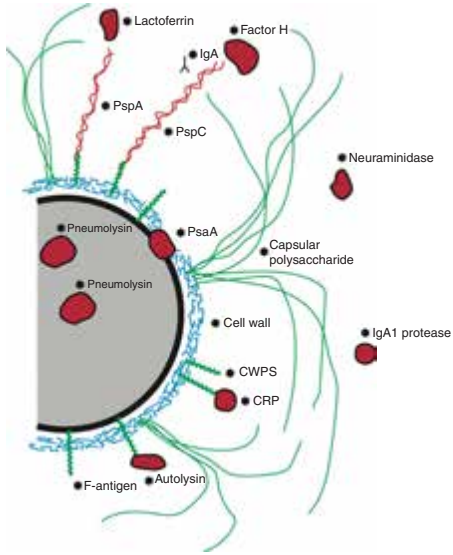

Figure 27.1 The virulent factors of *S. pneumoniae* (Streptococcus pneumonia: *Textbook in Diagnosis, Serotyping, Virulence Factors and Enzyme-Linked Immunosorbent Assay* (*ELISA*) *for Measuring Pneumococcal Antibodies*, 2nd version, Statens Serum Institut, Denmark).

Linder and coworkers [8] investigated the human antibody response towards PspA, PspC, and Hic of 41 patients during an invasive infection and found that a strong immune response against PspA usually develops during recovery. The high degree of cross-reactivity between the PspA and PspC antibodies renders them less suitable for diagnostics [8]. Wright and coworkers [13] showed that persistent antigen exposure from *S. pneumonia* colonization can induce protective defenses of the immune system against carriage and disease. The immunoglobin responses were

directed towards various protein targets except the capsular polysaccharides [13].

27.2.1.2 Diagnostics

The diagnosis of pneumococcal disease requires the isolation of the organism from a sterile site of the human body such as blood, ascites, pleural fluid, or cerebrospinal fluid [14]. The current reference methods for diagnosis are culture, ELISA and polymerase chain reaction (PCR). When using rapid tests of respiratory secretions for diagnosis, an additional confirmation method is usually required to exclude the possibility of carriage in the nasopharynx area. In young children (<10 years) such carrier state is found in 30–60%, whereas in adults the prevalence is 1–10% [14]. The conventional Neufeld "Quellung" reaction may also be used for diagnosis but is expensive, labor-intensive and prone to errors. Its developer, the German bacteriologist Friedrich Neufeld discovered that antibodies against specific capsular antigens of *S. pneumonaie* can be produced and used to distinguish between pneumococcal serotypes. After antibody binding and methylene Blue staining, the bacteria look swollen (German "Quellung") when visualized under the microscope.

The genotypic and serotypic variability of pneumococci is a challenge [15, 16] that requires particular attention when developing new diagnostics. Leung and coworkers [17] presented the "sequetyping" method, a single PCR sequencing strategy for the serotyping of pneumococci by using a single primer pair. The capsulation locus (*cps*) of 23 different vaccine serotypes was investigated by using the alignment software ClustalX. Two well-conserved primer-binding sites were selected by the Primer–Finder algorithm covering the regulatory gene *cpsB*. This selected region at the end of the *cps* region is specific for *S. pneumoniae*. *In silico* predictions revealed that from the current know 92 serotypes, 84 serotypes will deliver a PCR product. The nucleotide order was determined by cycle sequencing and using the same primers. The sequences were compared with the GenBank database and a BLAST score of >98% was considered as the correct serotype. According to the *in silico* predictions, 46 serotypes could be identified by the selected region. The primers were used to analyze 138 pneumococcal strains that included 48 serotypes. Reproducibility was proven by the correct identification of

different strains of a serotype. The 23 vaccine serotypes were identified correctly for 86%. This method is promising for diagnosis and the identification of new serotypes but not suitable for use in resource-poor environments. Tuerlinckx and coworkers [18] evaluated a serotype-specific ELISA for the etiologic diagnosis in children with pneumonia acquired in community (CAP).

All children (<15 years) had a CAP confirmed by a radiogram (n = 163). Pneumococcal infection was confirmed by positive blood and/or pleural fluid culture (n = 35) and the non-proven pneumococcal patients (n = 128) were also evaluated. The Quellung reaction was used to define the serotype and ELISA was used to diagnose the IgG and IgA antibodies specific for nine serotypes. The serological response rate with the ELISA was 82.8% and the serotyping results agreed well with the results of the Quellung reaction. With this ELISA it was possible to demonstrate the presence of pneumococcal CAP in 55% of the children with a negative culture result.

Pereira et al. [19] measured the levels of C-reactive protein (CRP), lactate, leucocytes, procalcitonin (PCT), D-dimer, cortisol, and brain natriuretic peptide (BNP) in patients with severe CAP within 12 h after receiving the first antibiotic dose. The patients (n = 64) were admitted to the intensive care unit and 33 had a confirmed pneumococcal infection, 13 had other bacterial causes (including *E. coli*, *S. aureus*, and *L. pneumophila*) and 18 patients had viral infection only in particular H1N1 and H3N2. In patients with pneumococcal disease, significantly higher levels of lactate, BNP, CRP and PCT were found. PCT at a level of >17 ng/mL could identify the patients with severe pneumococcal CAP that may profit from antibiotics, while at lower PCT levels pneumococcal CAP was unlikely. Thus, multiparameter testing for pneumococcal disease is often desirable (see, Salieb-Beugelaar and Hunziker [1]).

27.2.1.3 Microfluidics for *S. pneumoniae*

Van Heirstraeten [20] and coworkers presented a microfluidic device for analysis of community acquired lower respiratory tract infections that is capable of performing automated sample preparation, including lysis, nucleic acid purification, and concentration. After isolation of the nucleic acids, reverse transcription PCR or a fluoremetric assay was performed to measure nucleic acid concentration. Sample preparation in

this microdevice resulted in higher or similar concentration of bacterial DNA or viral RNA compared to the conventional benchtop experiments. The device was tested with swabs as well as cultured microorganisms and represents a step forward to the application in a point-of-care test for rapid diagnosis of community acquired lower respiratory tract infections. Dhoubhadel et al. [21, 22] developed a nanofluidic real time PCR system capable to identify 50 serotypes. One hundred ninety-four patients (age <5 years, culture positive, lytA PCR positive) and 140 healthy children (age <5 years, culture and lytA PCR positive) were investigated with this method. The lytA PCR of nasopharyngeal samples was included to confirm pneumococcus. They showed that a higher bacterial load of a serotype in the nasopharynx suggests higher transmission of this serotype. In addition, the co-colonization of multiple serotypes was associated with acute respiratory infections. Figure 27.2 presents the bacterial load of specific serotypes of *S. pneumoniae* in patients and healthy children.

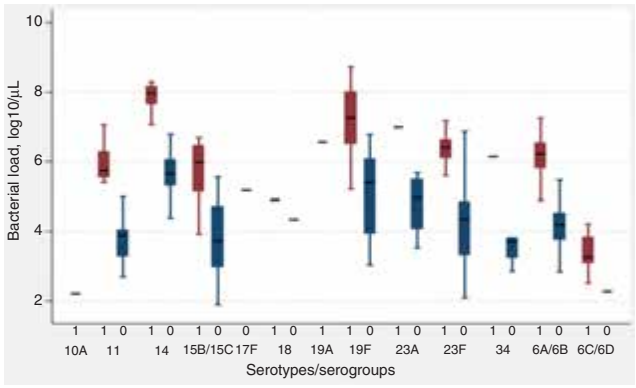

Figure 27.2 The bacterial loads of specific serotypes in patients (red) and healthy children (blue). Reproduced with permission from Dhoubhadel, B. G., et al. (2014). *PLoS One*, **9**, e110777, doi:10.1371/journal.pone.0110777 [22].

An alternative to PCR, which requires a protocol cycling through of different temperatures, loop mediated isothermal amplification of nucleic acids (LAMP) can be used. Luo et al. [23] developed an operationally simple and cost-time effective microfluidic device for LAMP. Its capabilities were documented

with the detection of *K. pneumonia*, *M. tuberculosis*, and *H. influenza*, while *S. pneumoniae* lacking from the panel, its inclusion is not expected to pose major challenges). The amplification of the target was measured by the electrochemical signal of methylene blue at eight etched indium tin oxide electrochemical reactors. The potential of this approach was highlighted with the analysis of multiple genes both qualitatively and quantitatively with a limit of detection of 16, 17, and 28 copies/μL for *H. influenza*, *K. pneumoniae*, and *M. tuberculosis*, respectively.

27.2.1.4 Nanodiagnostics for *S. pneumoniae*

Shi et al. [24] presented a rolling cycle amplification of DNA using gold nanoparticles as surface plasmon resonance sensors. The probes included long oligonucleotides, whereby boundary sequences were complementary to the adjacent sequences (also called padlock probes). These probes were coupled to the gold nanoparticles and were specific for bacterial pathogen sequences in 16S rDNA. Hybridization of the target with the probes brings the two ends in contact, resulting in circularization. The advantage of these probes is the flexibility for test development and the potential for targeting a variety of organisms (for further reading, see Szemes et al. [25]). Six different pathogens were investigated: *E. coli*, *S. dysenteriae*, *S. epidermidis*, *A. aureus*, *E. faecalis*, and *S. pneumonia*. The device identified the six pathogens with 0.5 pM probe quantities and a limit of detection of 0.5 pg/μL genomic DNA in clinical samples.

An electronic nose to detect the complex metabolites that are produced by microorganisms during an infection was presented by Tang et al. [26] following prior work by Schmid [27]. The miniaturized gas sensing and battery powered device has eight sensors incorporated (manufactured of polymer-carbon nanocomposites) and includes a learning kernel. The capability to identify ventilator-associated pneumonia (VAP) was verified in clinical trial where 74 infected samples with confirmed *Klebsiella* (n = 35) and *Pseudomonas aeruginosa* (n = 39) including 43 controls were analyzed. Upon usage of the learning kernel, the accuracy was for the infected patients improved from 91.89% to 100%. Even though not all presented examples include the detection of *S. pneumoniae*, it is clear that the detection of microbiological pathogens is moving into the field of nanodiagnostics.

27.2.2 *Salmonella typhi*

27.2.2.1 General

Waterborne diseases are affecting thousands of lives. Poor sanitation and limited access to clean water are the main causes. *Salmonella enterica* serotype Typhi is a Gram-negative rod-shaped and flagellated bacterium responsible for typhoid fever, an infection restricted to humans. Globally, 22 million individuals are infected annually of which ~200,000 die [28]. *S. typhi* and the related bacterium *S. paratyphi* A, which leads to a similar clinical syndrome, belong to the large family of Salmonella bacteria. Over 2000 serotypes are known, which are classified by their differential surface "H" (flagella) and "O" (lipopolysaccharides, LPS) antigens. Types with a common "O" antigen are grouped together. *S. typhi* belongs to serogroup D that has O9 and O12 in common [29]. Infection with *S. typhi* begins with the ingestion of contaminated food, followed by invasion of the gastrointestinal mucosa by the bacteria and translocation to the lymphoid follicles (Fig. 27.3) where the bacteria can survive and even replicate

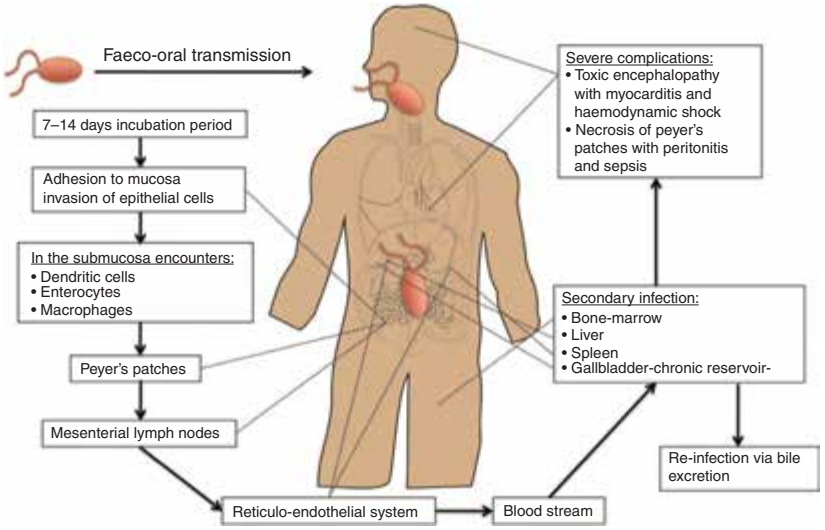

Figure 27.3 Dissemination of *S. typhi* in the host during a systemic infection. Reproduced with permission from de Jong, H. K., Parry, C. M., van der Poll, T., Wiersinga, W. J. (2012). *PLoS Pathog*., **8**, e1002933. doi:10.1371/journal.ppat.1002933.

inside macrophages. Subsequently, they are spread via the bloodstream to the spleen, liver and intestinal lymph nodes [30]. The typical incubation period is between 8 and 14 days [31]. Symptoms include fever, weakness, anorexia, and abdominal pain, and potential complications are gastrointestinal bleeding, intestinal perforation, and encephalopathy [32].

Immune cells and antibody-mediated immune responses play a role in controlling and clearing *S. typhi* infection [33]. Vaccines are available, but not very effective, although with the emergence of multidrug-resistant bacteria, the development of new vaccines would be very urgent [34].

27.2.2.2 Diagnostics

The diagnosis of a *S. typhi* infection can be done by the cultivation of blood, stool, urine, or duodenal contents. The specificity of a culture is considered as 100%. The reported sensitivities in literature vary. Gotuzzo and coworkers [35] showed that the organism could be isolated from 98% of bone marrow cultures of patients, while only 70% were blood culture positive. Even after five days of antibiotic therapy, such bone marrow cultures can remain positive [36]. Within the first week of onset, cultures from blood, stool, and intestinal secretion are positive in ~85–90% of the cases. In a later stage of the infection, this is 20–30% lower. The use of stool cultures alone yielded a sensitivity of <50% and for urine this is even less [37]. Another method to diagnose is detection of target bacterial DNA in samples by PCR. However, the number of bacteria circulating in blood of patients with bacteremia is <1 CFU/mL blood [2]. Thus, the human DNA is dominating, which may result in false negative results due to reduced sensitivity or false positive results due to nonspecific binding of the primers. Zhou et al. [38] developed a method to enrich the target bacterial *fliC-d* gene. Human DNA is removed from the blood samples. Ox bile is used to lyse the human blood cells, while *S. typhi* is resistant. The released Human DNA is subsequently degraded by Micrococcal nuclease. Experiments with spiked blood samples showed that this method enhanced the PCR sensitivity by 1000 fold. Urine may also be used to diagnose typhoid fever by PCR as developed by Kumar et al. [39]. This two-step PCR yielded a sensitivity and specificity of 90.9% and 100%, respectively, for blood samples, 95.5% and 100%, respectively,

for urine samples and 68.1% and 85% for stool samples. Blood cultures had a sensitivity of 31.8% and a specificity of 100%. An intriguing observation was reported by Ahirwar et al. [40]. They exposed urine, blood and stool samples of acute typhoid fever patients (n = 90) and chronic typhoid carriers (n = 36) to acidic pH. Isolation after the acidic exposure yielded 77.7% of the acute patients to be positive for *S. typhi*, compared to 8.8% provided with the conventional method. In chronic carriers provided 42% positive samples for *S. typhi* that was 5.5% when the conventional method was applied. The acid shock enhances the multiplication of the bacteria and as a consequence increases the isolation rates from samples.

The application of serological tests for *S. typhi* is limited as a result of false positives due to prior infections or cross-reaction with non-Salmonella bacteria. Therefore, a positive result always requires an additional confirmation method as a positive culture or PCR. A common method is the agglutination test introduced in the late nineteenth century by Widal and Secard, where specific antibodies in patient serum result in the aggregation of a cell suspension. In case of a *S. typhi* infection, these antibodies (the agglutinins) are directed against the H (flagellar) and the O (somatic) bacterial antigens. Bakr and coworkers [41] compared the sensitivity, specificity and accuracy of 4 different brands of Widal tests for the anti-H and O antibodies. One hundred fifty clinically suspected patients and a negative control group (n = 25) were investigated. As reference test an IgM anti-LPS ELISA was used (91/150). Serum samples were diluted (1/80, 1/160, and 1/320). They concluded that a four-fold rise of the antibody titer was not demonstrable (clinical diagnosed patients) and H agglutinins were less specific and sensitive when comparing to O agglutinins. Even though the Widal tests cannot be used to confirm an infection due to the low sensitivity and specificity, in the absence of other methods in resource-poor areas, this test is a possible alternative. In addition, a negative test is a good indication for the absence of the disease as concluded by Andualem et al. [42]. They investigated a Widal test and found a sensitivity of 71.4%, a specificity of 68.4%, a positive predictive value of 5.7% and a negative predictive value of 98.9%. For further reading, see Olopoenia et al. [43], who reviewed this test since its introduction in 1896.

Another rapid test is the Tubex method, to detect IgM specific for the O9 LPS in patient sera. Ley and coworkers [44] investigated the use of Tubex among hospitalized children (n = 139) in Tanzania with blood culture as reference method (n = 33), culture confirmed non-typhi infections (n = 49) and other non-salmonella infections (n = 57). The non-typhi samples were used as control, resulting in a sensitivity of 79% and a specificity of 89%. They concluded that apart from a shorter time to obtain results, results of the Tubex test are comparable to the Widal test.

Keddy et al. [45] investigated the performance of various rapid antibody diagnostic tests with blood culture as the reference method in sub-Saharan African sites. They concluded that the single-tube Widal test and semiquantitative slide agglutination test performed poorly. The included Tubex and Typhidot tests performed better but still not comparable to the blood culture. The Tubex had a sensitivity and specificity of 73% and 69%, respectively, Typhidot IgM 75% and 60.7%, respectively, and Typhidot IgG 69.2% and 70.4%, respectively. It is thus evident that the available tests for diagnosis of salmonella infection leave a large unmet need for simple, inexpensive, reliable, and fast point-of-care use. The search for new salmonella biomarkers is ongoing; Liang and coworkers [46] performed a protein microarray with 2724 *S. typhi* antigens (~63% of all predicted proteins) and identified IgM antibodies against 77 and IgG antibodies against 16 novel antigen targets in the serum of acute typhoid patients and healthy controls. The antigens specific for IgMs produced a 97% and 91% sensitivity and specificity, respectively, whereas the antigens specific for IgGs produced a 97% and 80% sensitivity and specificity, respectively. This type of investigation contributes to both the understanding of the immune responses of the human body during infection and may lead to the development for novel rapid tests for diagnosis of typhoid fever.

27.2.2.3 Microfluidics for *S. typhi*

Limited work has been done on the application of microfluidic devices for the detection of antigens or antibodies specific for *S. typhi*. Lafleur and coworkers [47] developed a multilayered microfluidic immunoassay card for the detection of IgM antibodies against *S. typhi* LPS and *P. falciparum* HRPII antigen in blood discussed in Salieb-Beugelaar and Hunziker [1]. The available

samples were limited (n = 9) and included positive and negative clinical samples. The detection of *S. typhi* IgM on the card was compared by laboratory ELISA and bench-top rapid flow-through membrane immunoassay. The volume of each sample was not enough to perform the tests in duplicate. The ELISA was done in duplicate. The intensity response of the card was comparable to both the bench-top assay and the ELISA. The clinical utility of the cards could not be evaluated as a result of the limited number of samples.

27.2.2.4 Nanodiagnostics for *S. typhi*

Das et al. [48] recently published an electrochemical DNA sensor for the detection of the *S. typhi* Vi gene. A self-assembled layer of organosilane 3-mercaptopropyltrimethoxysilane (MPTS) on top of a screen-printed electrode was used to electrochemically deposit gold nanoparticles. On the surfaces of the nanoparticles, thiol-modified DNA probes were immobilized to detect target nucleic acid of *S. typhi*. After the characterization of the sensor by atomic force microscopy, cyclic voltammetry and electrochemical impedance spectroscopy, the performance of the sensor was measured by differential pulse voltammograms, using methylene blue as a hybridization indicator. In more than 98% of the isolates of patients, this gene was expressed. Linearity was from 1.0×10^{-11} to 0.5×10^{-8} M. The limit of detection was ~50 pM. Typhi detection in real samples appears to be an ongoing project of this promising early work.

27.2.3 *Escherichia coli*

27.2.3.1 General

The Gram-negative, rod-shaped, and facultative anaerobic bacterium *E. coli* is responsible for outbreaks of both waterborne and foodborne diseases. Physiologically, this bacterium is present in huge numbers in the intestinal lumen of human and warm-blooded animals. While usually innocuous, a breakup of the gastrointestinal barriers even otherwise non-pathogenic *E. coli* strains can cause an infection. The bacterium is used as an indicator of fecal contamination in water quality assessment [49]. Clinical syndromes associated with diarrheagenic *E. coli* include (1) watery diarrhea caused by enterotoxic *E. coli* (ETEC), (2) infantile

diarrhea caused by enteropathogenic *E. coli* (EPEC), (3) hemorrhagic colitis and hemolytic uremic syndrome caused by enterohemorrhagic *E. coli* (EHEC), (4) dysentery caused enteroinvasive *E. coli* (EIEC), and (5) persistent diarrhea in children and patients infected with HIV caused by enteroaggregative *E. coli* (EAEC) [50, 51]. EHEC is responsible for isolated outbreaks of diarrhea, bloody diarrhea and a cause of postdiarrheal hemolytic uremic syndrome (HUS) [52] where the O157:H7 serotype is the globally dominating cause [53]. The diagnosis of EHEC is based on the detection of the Shiga toxin in feces and the isolation and characterization of the strain, but the causative *E. coli* often is no longer detectable at the time of onset of HUS, rendering diagnosis difficult. In addition, HUS may also be caused by other Shiga toxin producing serotypes including the *S. dysenteriae* serotype 1 [54]. According to the WHO, ETEC is the leading bacterial cause of diarrhea in the developing world and is the most common cause of traveler's diarrhea. It is estimated that approximately 210 million cases per year with around 380,000 deaths are caused by ETEC [55, 56]. The strain is known to produce colonization factors that enhance adherence to the intestinal mucosa [57], in addition, the bacteria produce two types of toxins, the heat stable (ST) and/or the heat labile (LT) enterotoxin. The latter leads to an immune response in humans [58]. For further reading, we recommend the review of Isidean and coworkers [59]. Vaccines are available, but their protection is limited in potency and usually abates with a few months. Steinsland et al. [60] reported that natural infections provide also protection as reflected by the decreasing rates of diarrhea with age and/or the lower ratios of symptomatic infections with increasing age. This suggests the hypothesis that immunization in early life might represent an effective preventive strategy.

27.2.3.2 Diagnostics

For the diagnosis of these infections, stool cultures or PCR tests are the gold reference methods. There is ongoing PCR tests development as shown by the recently published multiplex PCR of Andrade and coworkers [61] for the detection of both typical and atypical EAEC. Typical EAEC expressing the AggR regulon is a

global cause of childhood diarrhea [62], whereas atypical forms of EAEC do not express this regulon.

Andrade et al. [61] designed four amplicons of four different genes; aggR (346 bp), aaiA (476 pb), aatA (630 bp) and aaiG (782 bp). A multiplex PCR was performed with 406 *E. coli* isolates that were collected in an earlier study [63]. The final collection included 199 non-pathenogenic *E. coli*, 3 EHEC, 17 ETEC, 16 EIEC, 81 DAEC, 32 EPEC (18 atypical, 14 typical) and 58 EAEC (20 atypical, 38 typical). From all strains, 75 were detected by the PCR with at least one PCR product, of which 55 belonged to the EAEC pathotype (17 atypical, 38 typical). A sensitivity of 94.8% and a specificity 94.3% were found with a detection limit of 125 ng of purified genomic DNA.

Rapid tests are used mostly for toxin detection in food samples or bacterial cultures. The Duopath Verotoxin rapid test was developed for the detection of Shiga toxin 1 and 2 (Stx1 and Stx2, respectively) of EHEC in human stool samples and was evaluated by Grif et al. [64]. Compared with a commercial ELISA and PCR, the rapid test showed a lower sensitivity and specificity. For Stx1 the sensitivity and specificity for the rapid test was 46.15% and 79.8%, respectively, while the PCR was reported to be 100%. For Stx2 the sensitivity and specificity for the rapid test was 75% and 99.1%, respectively, while also here the PCR was declared to be perfect in sensitivity and specificity. The EHEC-ELISA was not able to distinguish between the two toxins and provided a sensitivity of 94.6% and specificity of 96.3% compared to the PCR.

Specific antibodies against the lipopolysaccharides (LPS) of the bacteria can also be detected; however, there is a chance of false positive due to the presence of cross-reactive antibodies against epitopes of LPS of different bacteria (including other *E. coli* strains) [65].

Recently, bacterial glycoengineering technology was used to generate recombinant glycoproteins that were composed of a polysaccharide (O121, O145, or O157) coupled to a carrier protein [66]. They demonstrated that these glycoproteins could be used as antigen in ELISA to discriminate between confirmed infected patients (O157, O145, or O121) and healthy children (total $n = 71$).

Of all positive samples, the infection was confirmed by positive isolation of the bacteria from stools, detection of fecal Stx on Vero cells by using antibodies (Stx1 and Stx2) and/or PCR specific for the stx 1/2 genes by using a sample from the MacConky Sorbitol agar plate. Three different groups were composed and analyzed with the new glyco-ELISA. The first group included patients that were diagnosed for another infectious disease (n = 14).

All obtained samples were serologically negative for the three glycoprotein-antigens and hereby confirming their high specificity. The second group included patients with a diagnosis of HUS or bloody diarrhea (n = 13). Of the analyzed samples, 92.3% were serologically positive for the glycoprotein-antigens (7.7% O121, 30.8% O145 and 53.8% O157). The third group included patients with a clinical diagnosis of HUS or bloody diarrhea without a confirmation of the infection by stool culture of a specific PCR (n = 44). Of these samples, 79.5% were serologically positive (2.3% O121, 15.9% O145 and 56.8% O157). They also identified a specific IgM response in almost all samples indicating that it might be possible to diagnose an infection in the early stages.

27.2.3.3 Microfluidics for *E. coli*

Agrawal and coworkers [67] developed a PDMS multiplexed microfluidic device for the quantitative or the multiplexed detection of waterborne pathogens. The capability of the device was shown with the detection of *E. coli* and *S. typhimurium*. In Fig. 27.4, a schematic representation of the immuno assay is presented. Each microfluidic channel contains three different zones: the pre-capture zone, the capture zone and the detection zone, respectively. In each zone, a magnet is embedded. In the (pre)capture zones, the immunomagnetic separation of the target bacteria from the sample was achieved through the specific binding of the antibody conjugated magnetic nanoparticles with the bacteria. Subsequently, the bacteria-magnetic beads complexes are moved towards the detection zone where specific antibody labeled Quantum Dots are used to visualize the presence of the target bacteria. The working range for both types of bacteria was

10^3 to 10^7 CFU/mL. The capabilities of the device might be further investigated by the detection of *E. coli* in diluted stool samples.

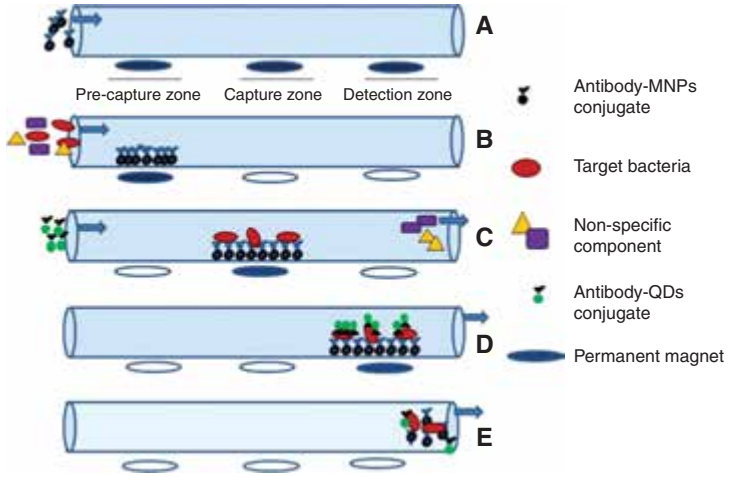

Figure 27.4 (A) The microfluidic channels contain three different zones. The antibody conjugated magnetic nanoparticles are entrapped with a permanent magnet. In B and C, the target bacteria are captured, and in D, the quantum dot-labeled antibody is used to visualize the presence of the target bacteria. Reproduced with permission from Agrawal, S., Morarka, A., Bodas, D., Paknikar, K. M. (2012). *Appl. Biochem. Biotechnol.*, **167**, 1668–1677 [67].

Jian et al. [68] developed a high throughput microfluidic device for the detection of airborne bacteria including *E. coli*. Bioaerosols (made by using an aerosol generator) with numbers of *E. coli* ranging from 10^4 to 10^6 CFU/mL where used to determine the sensitivity of the microfluidic chip. *E. coli*, *C. koseri*, *S. aureus*, *K. pneumoniae*, *E. faecalis*, and *P. aeruginosa* were used to validate the system. For each organism an amplicon was designed such that the difference in between was ~40 bp in order to differentiate between the PCR product by gel electrophoresis. The bacteria were first captured and then enriched by using microfluidic chip containing a staggered herringbone mixer structure, and consecutively they were amplified by the use of a high-throughput continuous-flow PCR chip. Amplified products were analyzed

by 1.5% agarose gel electrophoresis. No cross-contamination between different channels was found, and proof of concept for efficient mixing of reagents and sample and finally precise control of fluids through microvalves (loading and mixing) was achieved.

27.2.3.4 Nanodiagnostics for *E. coli*

Pandey and coworkers [69] presented 3D cystine flowers and palm like structures that are used to develop high performance electrochemical immunosensors. The capabilities of these sensors were investigated by the detection of *E. coli* bacterium (O157:H7). A linear range from 10 to 3×10^9 CFU/mL with a LOD of 4.7 CFU/mL was determined for the 3D flower, and for the palm leaves the linear range was 10^3 to 3×10^9 CFU/mL and the LOD 9.64×10^2 CFU/mL.

This difference could be explained by the nanostructured surface of the 3D flowers (confirmed by the increased surface roughness), leading to an increased surface area and consequently a larger available surface for the immobilization of antibodies. The shelf life of the sensors was 35 days at 4°C in PBS.

Cheng et al. [70] presented a novel amperometric immunosensor based on functionalized four-layer magnetic nanoparticles for the detection for *E. coli* (O157:H7). The core is magnetic Fe_3O_4, the second layer is Prussian blue, the third layer is *N*-(2-aminoethyl)-3-aminopropyltrimethoxylsilane and the final layer is the gold (Au) nanoparticle shell. Antibodies specific for O157:H7 were bound on the nanoparticle surface by using Au-SH bonds. (Turning of the electricity can regenerate the sensor). Heat killed *E. coli* was detected with a linear range of 3.6×10^3 to 3.6×10^6 CFU/mL. The investigators published the development of another novel sensor for the amperometric detection of *E. coli* (O157:H7) [71]. Here, graphene oxide was used as a nanocarrier for the electrostatic adsorption of SiO_2 nanoparticles (Au coated) and immobilization of thionine (see Fig. 27.5).

On this surface, large amounts of G-quadruplex DNA and signal DNA were immobilized. After addition of hemin, a hemin/G-quadruplex is formed and acts as a signal tag for the detection of the eaeA gene of *E. coli* (O157:H7). The developed sensor is capable to detect the eaeA gene with a linear range of 0.02 to

50 nM and with a limit of detection of 0.01 nM. The latest discussed work opens the door to the development of nanodiagnostics for the detection of any pathogen.

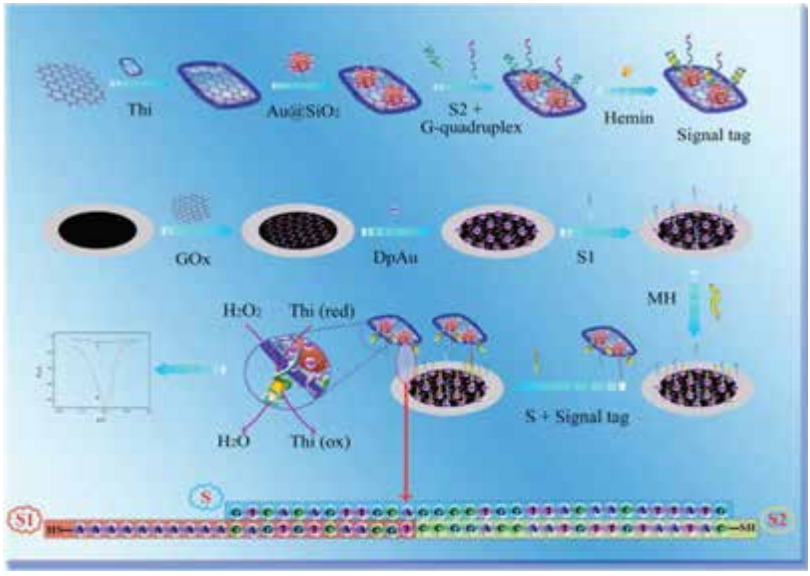

Figure 27.5 The fabrication of the nanocomposite DNA biosensor and the detection of the sample. Reproduced with permission from Li, Y., Deng, J., Fang, L., Yu, K., Huang, H., Jiang, L., et al. (2015). *Biosens. Bioelec.*, **63**, 1–6 [71].

27.3 Future Challenges for *in vitro* Diagnostics Suited for Infectious Diseases

In this review, we selected three pressing bacterial infections and used a short description of the clinical relevance and the pathogenesis as basis to concisely discuss the current diagnostic approach with an emphasis on rapid diagnostics. Then, we progressed to new developments for these infections based on microfluidic and nanodiagnostic technologies. In general, the number of available microfluidic devices for POC diagnosis in general has increased dramatically including the increased use of nanotechnology for part of these devices, but the pace of progress

is variable for the infections considered in this work. Reasons for faster or slower progress include the genetic, immunologic, and clinical complexity of some disease, the different commercial potential or the attention of the media for given disease. In our view, the development opportunities for "new" diagnostic devices include the following:

(A) Improving and miniaturizing current clinical standard methods to simplify diagnosis in resource pour environment.

(B) Expanding the targets of successfully introduced devices that were designed for a specific disease. An example is the existing low-cost, single-use, rapid, and accurate POC device for the detection of influenza A [72]. Solid phase extraction and RNA amplification (RT-PCR) are integrated on this chip. This device might be applicable for the design of RT-PCRs of other infections.

(C) Multiparameter testing in a single assay of various targets of a given bacterium or including other strains and biomarkers, which are not strain-specific but predictive of severity or outcome. This will contribute to a rapid and specific differential diagnosis; lead to a better treatment and as a result decreases the risk of development of resistant bacteria. An example is the discussed work of Shi et al. [24], who developed a rolling cycle amplification for the detection of six different bacteria. Another example is concurrent measurement of PCT levels in serum of patients with severe CAP [19], where levels below 17 ng/mL could identify patients with an infection unlikely to be caused by pneumococci. The development of microfluidic total analysis systems including several parameters and organisms in one design may thus enhance rapid and specific diagnostics.

(D) Mobile phone-based diagnostics. Resource-poor environments often do have the access to mobile phones and their networks. These might be used as an operating medical device in the field as presented by Stemple et al. [73]. In this work, the LED light of the mobile phone was used as the light source and the camera as detector. *P. falciparum* HRPII was successfully detected in 10% blood with a LOD of 1 pg/mL.

(E) Novel design concepts. An example is the laminated card concept of Lafleur and coworkers [47], which is capable

of detecting Typhi-specific antibodies (IgM) and the *P. falciparum* HRP2 antigen. All the reagents were stored in a dry form on the card and to run the test, only the buffer and the sample were required.

Another important and rapid developing field is the use of computer models. Computer performance enables the prediction of the performance and the optimization of novel devices before they are built as illustrated by the work of Zimmermann and coworkers [74]. This will enhance the basic scientific understanding of molecular behavior in nanofluidics and/or nanoconfinements and practically lead to improved point-of-care devices. In addition, software might also be used for the identification of new molecular targets. Soni et al. [75] presented the "Genome to hits" strategy, which is a novel strategy that incorporates steps such as the prediction of a gene, the determination of the tertiary protein structure and the identification of an active protein site. This pathway provides a novel approach to identify new molecules from genomic information that might be relevant for diagnostics or vaccines.

Progress in terms of sensitivity is bounded by the fact that less than a single biomolecule is in the given sample volume. The goals to attain by the improvement in fabrication techniques will therefore consist of parallelization to multiple targets and in the incorporation of more complex sample handling on-chip, and therefore reduced complexity for the end user. Energy autonomous systems, improved electronics, optimized software, and wireless (mobile phone) technologies will contribute significantly to the microfluidic and nano aspects of upcoming and inexpensive POC devices for use in resource-poor areas. Maximal simplicity of the end user will be a *sine qua non* for the success of such devices.

27.4 Conclusion

Nanodiagnostics is a rapidly evolving field. Key issue is the clever use of new technologies for the development and improvement of LOC and/or POC devices and to enable such devices for multiparameter testing. A rewarding goal is the development

of multiparameter tests for diseases with common symptoms, e.g., "acute febrile syndromes" as for example in the DiscoGnosis project (www.discognosis.eu). Here, one single POC device is developed for the detection of malaria (*P. falciparum*), *S. typhi*, dengue, and pneumococcal infection concurrently, with inclusion of nucleic acid testing and protein detection on the same disk.

Disclosures and Conflict of Interest

The authors would like to thank Prof. Rutledge Ellis-Behnke of the Department of Brain and Cognitive Sciences, Massachusetts Institute of Technology, Cambridge, USA, for his support in knowledge. This review has been written to contribute to the DiscoGnosis project, which has the core objective to develop a platform that would allow the detection of malaria and similar pathogenic diseases in a rapid, multiplexed, and non-invasive way (www.discognosis.eu). This project is supported by the European Commission through the 7th Framework Programme on Research and Technological Development within the Objective FP7 ICT-2011.3.2 and under Grant Agreement No. 318408. The authors have no other relevant affiliations or financial involvement with any organization or entity discussed in this chapter. No writing assistance was utilized in the production of this chapter and the authors have received no payment for its preparation. This chapter was originally published as Salieb-Beugelaar, G., Hunziker, P. (2015). Towards nano-diagnostics for bacterial infections. *Eur. J. Nanomed.*, **7**(1), 37–50 (DOI 10.1515/ejnm-2015-0010) and appears here, with edits, by kind permission of the publisher, Walter de Gruyter GmbH, Berlin, Germany.

Corresponding Author

Dr. Georgette B. Salieb-Beugelaar
Nanomedicine Research Group
Clinic for Intensive Care Medicine
University Hospital Basel
Petersgraben 4, CH-4031 Basel, Switzerland
Email: beugelaar@swissnano.org

About the Authors

Georgette Salieb-Beugelaar's professional life started in the fields of clinical genetics, DNA research, and diagnostics at the Academic Medical Centre in Amsterdam (the Netherlands) in 1996. She studied in parallel chemistry at the University of Utrecht (the Netherlands) between 2000 and 2003. In 2005, her professional field transitioned to the microfluidic and nanofluidic world at the University of Twente in Enschede (the Netherlands) and she investigated single DNA molecules in nanoconfined environments on chips, which resulted in PhD degree in 2009. In the following two years, she worked at the Korean Institute of Science and Technology (Saarbrücken, Germany) on nanodroplet pseudocrystals in microfluidic chips. Since November 2012, she has been a member of the multidisciplinary NanoMedicine Group of Prof. Patrick Hunziker, working for the DiscoGnosis project. Dr. Salieb-Beugelaar currently serves as scientific managing editor of the *European Journal of Nanomedicine* and managing editor of *Progress in Materials Science* (Elsevier).

Patrick Hunziker studied medicine at the University of Zurich, Switzerland. He received a doctoral degree based on thesis work in experimental immunology from the University of Zurich and did further research in experimental hematology at University Hospital in Zurich, Switzerland. He earned specialist degrees in internal medicine, cardiology, and intensive care medicine. As a fellow of the Massachusetts General Hospital, Harvard Medical School, he worked on cardiac imaging in a joint project with the Massachusetts Institute of Technology, Cambridge. His professional activities in Europe, the US, Africa, and China gave him a broad insight into the needs for the medicine of the future in a variety of settings. Dr. Hunziker became involved in medical applications of nanoscience in the late 1990s and has been a pioneer-physician in nanomedicine in Switzerland since then. With improved prevention, diagnosis, and cure of cardiovascular disease as his

main research topic, he worked in the nanoscience fields of atomic force microscopy, nano-optics, micro/nanofluidics, nanomechanical sensors and polymer nanocarriers for targeting. He is the founding president of the European Society of Nanomedicine, cofounder of the European Foundation for Clinical Nanomedicine, coinitiator of the European Conference for Clinical Nanomedicine and is clinically active as deputy head of the clinic for intensive care medicine at the University Hospital Basel, Switzerland. In November 2008, Dr. Hunziker became professor for cardiology and intensive care medicine at the University of Basel.

CLINAM
European Foundation for Clinical Nanomedicine

The European Foundation for Clinical Nanomedicine is a non-profit institution based in Basel, Switzerland. This institution was set up in 2007 and aimed at advancing medicine to the benefit of individuals and society through the application of nanoscience and targeted medicine. Aiming at prevention, diagnosis, and therapy through nanomedicine, the foundation supports clinically focused research and the interaction and information flow between clinicians, researchers, the public, and all stakeholders in the field of nanomedicine. Recognition of the major future impact of nanoscience on medicine and the rapid advances seen in the medical applications of nanoscience were a comprehensive catalogue of projects that the foundation would pursue, including:

- for clinical nanomedicine and targeted medicine, which also included clinicians;
- the establishment of a research lab dedicated to nanomedicine and targeted medicine;
- the creation of the *European Journal of Nanomedicine*;
- the creation of a European and International Society for Nanomedicine;
- involvement in national research projects and European framework calls;
- the realization of a worldwide network for all stakeholders in nanomedicine and targeted medicine as the main elements of cutting-edge medicine;

- the inclusion of the implications of nanomedicine for patient and mankind.

The status in 2015

CLINAM's major goal is to support the development and application of nanomedicine and targeted medicine off to a good start:

- The CLINAM Summit has emerged as a valuable place of interaction for launching collaboration, gathering new ideas, and learning about novel methodologies and technologies as well as novel projects, including numerous EU-wide efforts, in nanomedicine and targeted medicine (www.clinam.org).
- The annual *European Summit for Clinical Nanomedicine and Targeted Medicine*, held anually in Basel, continues to grow and has become a worldwide interdisciplinary nanomedicine platform attracting hundreds of participants from around the globe.
- CLINAM founded the *European Journal of Nanomedicine* (de Gruyter, Berlin) with Patrick Hunziker and Jan Mollenhauer as the editors-in-chief and Beat Löffler and Georgette B. Salieb-Beugelaar as the scientific and managing editors. The *European Journal of Nanomedicine* (http://www.degruyter.com/view/j/ejnm) focuses on fields ranging from nano(bio)technological engineering and characterization to clinically translatable innovative prevention, diagnostics, and therapies for major and neglected human diseases. The readership is multidisciplinary, including scientists in chemistry, physics, engineering, pharmacology, molecular biology, biomedicine, and clinicians. The journal is aimed at people in academic, industrial, and regulatory environments, as well as the informed public and policymakers. The main topics covered are experimental, analytical, (pre-) clinical, preventive and therapeutic nanomedicine, nanomaterials, nanobiotechnology, nanodiagnostics, nontoxicity, nanoimaging technologies, vanguard nanotechnologies, implementation and implications of nanomedicine, and personalized nanomedicine.
- CLINAM founded the European Society for Nanomedicine, (ESNAM), which has more than 700 members today.

- CLINAM was one of the driving forces for the formation of the International Society for Nanomedicine, (ISNM) which brings together Japan, Korea, USA, Canada, Europe, South America, India, and Australia in cooperation. For 2016, the First ISNM Summer School is planned to be in Korea. Dr. Hunziker is President of the ISNM.
- The CLINAM Nanomedicine Research Lab, associated with the University Hospital of Basel, is led by Dr. Hunziker.
- CLINAM is involved in several large international research projects and is currently participating in two Framework Projects of Europe in Research and Dissemination (DiscoGnosis and NanoAthero). Furthermore, CLINAM is involved in applications within the EU project, Horizon 2020.
- 
Beat Löffler is CEO of CLINAM and is responsible for the management, dissemination projects and organizing the annual conference program. He has an MA in humanities (FU Berlin, Germany) and honorary MD (University of Basel, Switzerland). Dr. Löffler has initiated or delivered, with his company *Löffler Associates Concept Engineering*, key contributions to a number of important activities in Basel and the trinational upper-Rhine valley that have evolved into international prominence.

Assisting in translation from research to practical applications

The pathway from the innovative idea to the application, development, regulatory approval, and commercialization of nanomedical drugs is complex and requires a detailed understanding of the cause of the disease in question. The nature of nanodrugs and their use require a high level of knowledge in disciplines, including physics, chemistry, pharmacology, biology, engineering, and nanotechnology. Dialogue and exchange between all these disciplines are essential. The translation from research findings to applications in nanomedicine and targeted medicine has been developing well and is now on the agenda of global players in the pharmaceutical industry. The decision makers in

pharmaceutical companies are starting to appreciate the quality and potential of nanomedicine and targeted medicine for significantly increasing the output of diagnostics and therapeutic products that are less invasive and have fewer side effects. By bringing the relevant stakeholders together, CLINAM has achieved an actively promoting role in the translation process.

CLINAM is moving toward personalized medicine

In the coming decades, medicine will experience a transformation in the direction of personalized diagnosis and treatment, taking into consideration the individual aspects of the patient and their disease. A key role is played by high-resolution molecular profiling techniques, which have often been made less expensive by nanomedicine. CLINAM offers excellent opportunities for organizations that are engaged in worldwide efforts aimed at achieving this goal, exchanging expertise, and launching joint ventures for acceleration of this process.

Collaboration with organizations

The board of the CLINAM Foundation cooperates with many organizations that are willing and able to bring skilled expertise to nanomedicine. The goal of all members is to continue to use this neutral platform European and Global summit for nanomedicine as an international melting pot for cutting-edge medicine.

Outlook

As a non-profit organization, CLINAM has an opportunity to assist industry as well. The CLINAM Summit has emerged as an outstanding forum for the translation of research from bench to bedside, for European and international networking, offering an ideal setting to establish and nurture collaboration between industries and academia and serving as a point of contact with customers.

References

1. Salieb-Beugelaar, G. B., Hunziker, P. R. (2014). Towards nano-diagnostics for rapid diagnosis of infectious diseases: Current technological state. *Eur. J. Nanomed*., **6**, 11–28.

2. Wain, J., Diep, T. S., Ho, V. A., Walsh, A. M., Hoa, N. T., Parry, C. M., et al. (1998). Quantitation of bacteria in blood of typhoid fever patients and relationship between counts and clinical features, transmissibility, and antibiotic resistance. *J. Clin. Microbiol.*, **36**, 1683–1687.
3. Mody, R. K., Luna-Gierke, R. E., Jones, T. F., Comstock, N., Hurd, S., Scheftel, J., et al. (2012). Infections in pediatric postdiarrheal hemolytic uremic syndrome: Factors associated with identifying shiga toxin-producing *Escherichia coli*. *Arch. Pediatr. Adolesc. Med.*, **166**, 902–909.
4. Kurakawa, T., Kubota, H., Tsuji, H., Matsuda, K., Takahashi, T., Ramamurthy, T., et al. (2013). Intestinal Enterobacteriaceae and *Escherichia coli* populations in Japanese adults demonstrated by the reverse transcription-quantitative PCR and the clone library analyses. *J. Microbiol. Meth.*, **92**, 213–219.
5. Calix, J. J., Dagan, R., Pelton, S. I., Porat, N., Nahm, M. H. (2012). Differential occurrence of *Streptococcus pneumoniae* serotype 11e between asymptomatic carriage and invasive pneumococcal disease isolates reflects a unique model of pathogen microevolution. *Clin. Infect. Dis.*, **54**, 794–799.
6. Weekly epidemiological record Relevé épidémiologique hebdomadaire. 23 March 2007, 82nd Year/23 Mars 2007, 82e Année, No. 12, 2007, 82, 93–104. Available at: http://www.who.int/wer (accessed on August 27, 2015).
7. Hausdorff, W. P., Bryant, J., Paradiso, P. R., Siber, G. R. (2000). Which pneumococcal serogroups cause the most invasive disease: Implications for conjugate vaccine formulation and use, part I. *Clin. Infect. Dis.*, **30**(1), 100–121.
8. Linder, A., Hollingshead, S., Janulczyk, R., Christensson, B., Akesson, P. (2007). Human antibody response towards the pneumococcal surface proteins PspA and PspC during invasive pneumococcal infection. *Vaccine*, **25**, 341–345.
9. Hollingshead, S. K., Becker, R., Briles, D. E. (2000). Diversity of PspA: Mosaic genes and evidence for past recombination in Streptococcus pneumoniae. *Infect. Immun.*, **68**, 5889–5900.
10. Brooks-Walter, A., Briles, D. E., Hollingshead, S. K. (1999). The pspC gene of Streptococcus pneumoniae encodes a polymorphic protein, PspC, which elicits cross-reactive antibodies to PspA and provides immunity to pneumococcal bacteremia. *Infect. Immun.*, **67**, 6533–6542.

11. Janulczyk, R., Iannelli, F., Sjoholm, A. G., Pozzi, G., Bjorck, L. (2000). Hic, a novel surface protein of Streptococcus pneumonia that interferes with complement function. *J. Biol. Chem.*, **275**, 37257–37263.

12. Iannelli, F., Chiavolini, D., Ricci, S., Oggioni, M. R., Pozzi, G. (2004). Pneumococcal surface protein C contributes to sepsis caused by Streptococcus pneumoniae in mice. *Infect. Immun.*, **72**, 3077–3080.

13. Wright, A. K., Ferreira, D. M., Gritzfeld, J. F., Wright, A. D., Armitage, K., Jambo, K. C., et al. (2012). Human nasal challenge with Streptococcus pneumoniae is immunising in the absence of carriage. *PLoS Pathog.*, **8**, e1002622.

14. Song, J. Y., Nahm, M. H., Moseley, M. A. (2013). Clinical implications of pneumococcal serotypes: Invasive disease potential, clinical presentations, and antibiotic resistance. *J. Korean. Med. Sci.*, **28**, 4–15.

15. Bentley, S. D., Aanensen, D. M., Mavroidi, A., Saunders, D., Rabbinowitsch, E., Collins, M., et al. (2006). Genetic analysis of the capsular biosynthetic locus from all 90 pneumococcal serotypes. *PLoS Genet.*, **2**, e31.

16. McEllistrem, M. C., Noller, A. C., Visweswaran, S., Adams, J. M., Harrison, L. H. (2004). Serotype 14 variants of the France 9V–3 clone from Baltimore, Maryland, can be differentiated by the cpsB gene. *J. Clin. Microbiol.*, **42**, 250–256.

17. Leung, M. H., Bryson, K., Freystatter, K., Pichon, B., Edwards, G., Charalambous, B. M., et al. (2012). Sequetyping: Serotyping Streptococcus pneumoniae by a single PCR sequencing strategy. *J. Clin. Microbiol.*, **50**, 2419–2427.

18. Tuerlinckx, D., Smet, J., De Schutter, I., Jamart, J., Vergison, A., Raes, M., et al. (2013). Evaluation of a WHO-validated serotype-specific serological assay for the diagnosis of pneumococcal etiology in children with community-acquired pneumonia. *Pediatr. Infect. Dis. J.*, **32**, e277–e284.

19. Pereira, J. M., Teixeira-Pinto, A., Basílio, C., Sousa-Dias, C., Mergulhão, P., Paiva, J. A. (2013). Can we predict pneumococcal bacteremia in patients with severe community-acquired pneumonia? *J. Crit. Care.*, **28**, 970–974.

20. Van Heirstraeten, L., Spang, P., Schwind, C., Drese, K. S., Ritzi- Lehnert, M., Nieto, B., et al. (2014). Integrated DNA and RNA extraction and purification on an automated microfluidic cassette from bacterial and viral pathogens causing community-acquired lower respiratory tract infections. *Lab Chip*, **14**, 1519–1126.

21. Dhoubhadel, B. G., Yasunami, M., Yoshida, L. M., Thi, H. A., Thi, T. H., Thi, T. A., et al. (2014). A novel high-throughput method for molecular

serotyping and serotype-specific quantification of Streptococcus pneumoniae using a nanofluidic real-time PCR system. *J. Med. Microbiol.*, **63**(Pt 4), 528–539.

22. Dhoubhadel, B. G., Yasunami, M., Nguyen, H. A., Suzuki, M., Vu, T. H., Thi Thuy Nguyen, A., et al. (2014). Bacterial load of pneumococcal serotypes correlates with their prevalence and multiple serotypes is associated with acute respiratory infections among children less than 5 years of age. *PLoS One*, **9**, e110777.
23. Luo, J., Fang, X., Ye, D., Li, H., Chen, H., Zhang, S., et al. (2014). A real-time microfluidic multiplex electrochemical loop-mediated isothermal amplification chip for differentiating bacteria. *Biosens. Bioelectron*., **60**, 84–91.
24. Shi, D., Huang, J., Chuai, Z., Chen, D., Zhu, X., Wang, H., et al. (2014). Isothermal and rapid detection of pathogenic microorganisms using a nano-rolling circle amplification-surface plasmon resonance biosensor. *Biosens. Bioelectron*., **62**, 280–287.
25. Szemes, M., Bonants, P., de Weerdt, M., Baner, J., Landegren, U., Schoen, C. D. (2005). Diagnostic application of padlock probes—multiplex detection of plant pathogens using universal microarrays. *Nucleic Acids Res.*, **33**, e70.
26. Tang, K. T., Chiu, S. W., Shih, C. H., Chang, C. L., Yang, C. M., Yao, D. J., et al. (2014). 24.5 A 0.5 V 1.27 mW nose-on-a-chip for rapid diagnosis of ventilator-associated pneumonia (Conference Paper). *IEEE International Solid-State Circuits Conference 2014*, **57**, article number 6757496, pp. 420–421.
27. Schmid, D., Lang, H., Marsch, S., Gerber, C., Hunziker, P. (2008). Diagnosing disease by nanomechanical olfactory sensors—system design and clinical validation. *Eur. J. Nanomed*., **1**, 44–47.
28. Centers for Disease Control and Prevention. Typhoid fever. Available at: http://wwwnc.cdc.gov/travel/diseases/typhoid (accessed August 27, 2015).
29. Grimont, P. A., Weill, F. X. (2007). WHO collaboration centre for reference and research on salmonella. Antigenic formulae of the Salmonella serovars. 9th ed. Available at: https://www.pasteur.fr/ip/portal/action/WebdriveActionEvent/oid/01s-000036-089 (accessed on August 27, 2015).
30. Jones, B. D. (1997). Host responses to pathogenic Salmonella infection. *Genes Dev.*, **11**, 679–687.
31. Levine, M. M., Tacket, C. O., Sztein, M. B. (2001). Host–Salmonella interaction: Human trials. *Microbes Infect.*, **3**, 1271–1279.

32. Parry, C. M., Hien, T. T., Dougan, G., White, N. J., Farrar, J. J. (2002). Typhoid fever. *N. Engl. J. Med.*, **347**, 1770–1782.

33. Ravindran, R., McSorley, S. J. (2005). Tracking the dynamics of T-cell activation in response to Salmonella infection. *Immunology*, **114**, 450–458.

34. Marathe, S. A., Lahiri, A., Negi, V. D., Chakravortty, D. (2012). Typhoid fever & vaccine development: A partially answered question. *Indian J. Med. Res.*, **135**, 161–169.

35. Gotuzzo, E., Echevarría, J., Carrillo, C., Sánchez, J., Grados, P., Maguiña, C., et al. (1994). Randomized comparison of aztreonam and chloramphenicol in treatment of typhoid fever. *Antimicrob. Agents Chemother*., **38**, 558–562.

36. Gasem, M. H., Dolmans, W. M., Isbandrio, B. B., Wahyono, H., Keuter, M., Djokomoeljanto, R. (1995). Culture of Salmonella typhi and Salmonella paratyphi from blood and bone marrow in suspected typhoid fever. *Trop. Geogr. Med.*, **47**, 164–167.

37. Brusch, J. L., Garvey, T., Corales, R., Schmitt, S. K. (2014). Typhoid fever. Medscape; Emedicine; updated April 2014. Available at: http://emedicine.medscape.com/article/231135-workup (accessed on September 25, 2015).

38. Zhou, L., Pollard, A. J. (2012). A novel method of selective removal of human DNA improves PCR sensitivity for detection of Salmonella Typhi in blood samples. *BMC Infect. Dis.*, **12**, 164.

39. Kumar, G., Pratap, C. B., Mishra, O. P., Kumar, K., Nath, G. (2012). Use of urine with nested PCR targeting the flagellin gene (fliC) for diagnosis of typhoid fever. *J. Clin. Microbiol*., **50**, 1964–1967.

40. Ahirwar, S. K., Pratap, C. B., Patel, S. K., Shukla, V. K., Singh, I. G., Mishra, O. P., et al. (2014). Acid exposure induces multiplication of Salmonella enterica serovar Typhi. *J. Clin. Microbiol*., **52**, 4330–4333.

41. Bakr, W. M., El Attar, L. A., Ashour, M. S., El Toukhy, A. M. (2011). The dilemma of Widal test—which brand to use a study of four different Widal brands: A cross sectional comparative study. *Ann. Clin. Microbiol. Antimicrob.*, **10**, 7.

42. Andualem, G., Abebe, T., Kebede, N., Gebre-Selassie, S., Mihret, A., Alemayehu, H., et al. (2014). A comparative study of Widal test with blood culture in the diagnosis of typhoid fever in febrile patients. *BMC Res. Notes*, **7**, 653.

43. Olopoenia, L. A., King, A. L. (2000). Widal agglutination test—100 years later: Still plagued by controversy. *Postgrad. Med. J.*, **76**, 80–84.

44. Ley, B., Thriemer, K., Ame, S. M., Mtove, G. M., von Seidlein, L., Amos, B., et al. (2011). Assessment and comparative analysis of a rapid diagnostic test (Tubex®) for the diagnosis of typhoid fever among hospitalized children in rural Tanzania. *BMC Infect. Dis.*, **11**, 147.

45. Keddy, K. H., Sooka, A., Letsoalo, M. E., Hoyland, G., Chaignat, C. L., Morrissey, A. B., et al. (2011). Sensitivity and specificity of typhoid fever rapid antibody tests for laboratory diagnosis at two sub-Saharan African sites. *Bull. World Health Organ.,* **89**, 640–647.

46. Liang, L., Juarez, S., Nga, T. V., Dunstan, S., Nakajima-Sasaki, R., Davies, D. H., et al. (2013). Immune profiling with a Salmonella Typhi antigen microarray identifies new diagnostic biomarkers of human typhoid. *Sci. Rep.*, **3**, 1043.

47. Lafleur, L., Stevens, D., McKenzie, K., Ramachandran, S., Spicar-Mihalic, P., Singhal, M., et al. (2012). Progress toward multiplexed sample-to-result detection in low resource settings using microfluidic immunoassay cards. *Lab Chip*, **12**, 1119–1127.

48. Das, R., Sharma, M. K., Rao, V. K., Bhattacharya, B. K., Garg, I., Venkatesh, V., et al. (2014). An electrochemical genosensor for Salmonella typhi on gold nanoparticles-mercaptosilane modified screen printed electrode. *J. Biotechnol.*, **188C**, 9–16.

49. Heijnen, L., Medema, G. (2009). Method for rapid detection of viable *Escherichia coli* in water using real-time NASBA. *Water Res.*, **43**, 3124–3132.

50. Nataro, J., Kaper, J. B. (1998). Diarrheagenic *Escherichia coli*. *Clin. Microbiol. Rev.*, **11**, 142–201.

51. Mayer, H. B., Wanke, C. A. (1995). Enteroaggregative *Escherichia coli* as a possible cause of diarrhea in an HIV-infected patient. *N. Engl. J. Med.*, **332**, 273–274.

52. Gianantonio, C., Vitacco, M., Mendilaharzu, F., Rutty, A., Mendilaharzu, J. (1964). The hemolytic-uremic syndrome. *J. Pediatr.*, **64**, 478–491.

53. Tarr, P. I., Gordon, C. A., Chandler, W. L. (2005). Shiga-toxin-producing *Escherichia coli* and haemolytic uraemic syndrome. *Lancet*, **365**, 1073–1086.

54. Salvadori, M., Bertoni, E. (2013). Update on hemolytic uremic syndrome: Diagnostic and therapeutic recommendations. *World J. Nephrol.*, **2**, 56–76.

55. Gupta, S. K., Keck, J., Ram, P. K., Crump, J. A., Miller, M. A., Mintz, E. D. (2008). Part III. Analysis of data gaps pertaining to enterotoxigenic

Escherichia coli infections in low and medium human development index countries, 1984–2005. *Epidemiol. Infect.*, **136**, 721–738.

56. Wennerås, C., Erling, V. (2004). Prevalence of enterotoxigenic *Escherichia coli*-associated diarrhoea and carrier state in the developing world. *J. Health. Popul. Nutr.*, **22**, 370–382.
57. Qadri, F., Svennerholm, A. M., Faruque, A. S., Sack, R. B. (2005). Enterotoxigenic *Escherichia coli* in developing countries: Epidemiology, microbiology, clinical features, treatment, and prevention. *Clin. Microbiol. Rev.*, **18**, 465–483.
58. Stoll, B. J., Svennerholm, A. M., Gothefors, L., Barua, D., Huda, S., Holmgren, J. (1986). Local and systemic antibody responses to naturally acquired enterotoxigenic *Escherichia coli* diarrhea in an endemic area. *J. Infect. Dis.*, **153**, 527–534.
59. Isidean, S. D., Riddle, M. S., Savarino, S. J., Porter, C. K. (2011). A systematic review of ETEC epidemiology focusing on colonization factor and toxin expression. *Vaccine*, **29**, 6167–6178.
60. Steinsland, H., Valentiner-Branth, P., Gjessing, H. K., Aaby, P., Mølbak, K., Sommerfelt, H. (2003). Protection from natural infections with enterotoxigenic *Escherichia coli*: Longitudinal study. *Lancet*, **362**, 286–291.
61. Andrade, F. B., Gomes, T. A., Elias, W. P. (2014). A sensitive and specific molecular tool for detection of both typical and atypical enteroaggregative *Escherichia coli*. *J. Microbiol. Meth.*, **106**, 16–18.
62. Tokuda, K., Nishi, J., Imuta, N., Fujiyama, R., Kamenosono, A., Manago, K., et al. (2010). Characterization of typical and atypical enteroaggregative *Escherichia coli* in Kagoshima, Japan: Biofilm formation and acid resistance. *Microbiol. Immunol.*, **54**, 320–329.
63. Gomes, T. A., Vieira, M. A., Abe, C. M., Rodrigues, D., Griffin, P. M., Ramos, S. R. (1998). Adherence patterns and adherence-related DNA sequences in *Escherichia coli* isolates from children with and without diarrhea in Säo Paulo city, Brazil. *J. Clin. Microbiol.*, **36**, 3609–3613.
64. Grif, K., Orth, D., Dierich, M. P., Würzner, R. (2007). Comparison of an immunochromatographic rapid test with enzyme-linked immunosorbent assay and polymerase chain reaction for the detection of Shiga toxins from human stool samples. *Diagn. Microbiol. Infect. Dis.*, **59**, 97–99.
65. Chart, H., Cheasty, T. (2008). Human infections with verocytotoxin-producing *Escherichia coli* O157—10 years of *E. coli* O157 serodiagnosis. *J. Med. Microbiol.*, **57**(Pt 11), 1389–1393.

66. Melli, L. J., Ciocchini, A. E., Caillava, A. J., Vozza, N., Chinen, I., Rivas, M., et al. (2015). Serogroup-specific bacterial engineered glycoproteins as novel antigenic targets for diagnosis of Shiga toxin-producing-*Escherichia coli*-associated hemolytic-uremic syndrome. *J. Clin. Microbiol.*, **53**, 528–538.

67. Agrawal, S., Morarka, A., Bodas, D., Paknikar, K. M. (2012). Multiplexed detection of waterborne pathogens in circular microfluidics. *Appl. Biochem. Biotechnol.*, **167**, 1668–1677.

68. Jiang, X., Jing, W., Zheng, L., Liu, S., Wu, W., Sui, G. A. (2014). Continuous-flow high-throughput microfluidic device for airborne bacteria PCR detection. *Lab Chip*, **14**, 671–676.

69. Pandey, C. M., Sumana, G., Tiwari, I. (2014). Nanostructuring of hierarchical 3D cystine flowers for high-performance electrochemical immunosensor. *Biosens. Bioelectron.*, **61**, 328–335.

70. Cheng, P., Huang, Z. G., Zhuang, Y., Fang, L. C., Huang, H., Deng, J., et al. (2014). A novel regeneration-free *E. coli* O157:H7 amperometric immunosensor based on functionalised four-layer magnetic nanoparticles. *Sens. Actuators B*, **204**, 561–556.

71. Li, Y., Deng, J., Fang, L., Yu, K., Huang, H., Jiang, L., et al. (2015). A novel electrochemical DNA biosensor based on HRP-mimicking hemin/G-quadruplex wrapped GOx nanocomposites as tag for detection of *Escherichia coli* O157:H7. *Biosens. Bioelectron.*, **63**, 1–6.

72. Cao, Q., Mahalanabis, M., Chang, J., Carey, B., Hsieh, C., Stanley, A., et al. (2012). Microfluidic chip for molecular amplification of influenza A RNA in human respiratory specimens. *PLoS One*, **7**, e33176.

73. Stemple, C. C., Angus, S. V., Park, T. S., Yoon, J. Y. (2014). Smartphone-based optofluidic lab-on-a-chip for detecting pathogens from blood. *J. Lab. Autom.*, **19**, 35–41.

74. Zimmermann, M., Delamarche, E., Wolf, M., Hunziker, P. (2005). Modeling and optimization of high-sensitivity, low-volume microfluidic-based surface immunoassays. *Biomed Microdevices*, **7**, 99–110.

75. Soni, A., Pandey, K. M., Ray, P., Jayaram, B. (2013). Genomes to hits in silico—a country path today, a highway tomorrow: A case study of chikungunya. *Curr. Pharm. Des.*, **19**, 4687–4700.

Chapter 28

Copaxone® in the Era of Biosimilars and Nanosimilars

Jill B. Conner, MS, PhD,[a] Raj Bawa, MS, PhD,[b,c] J. Michael Nicholas, PhD,[a] and Vera Weinstein, PhD[d]

[a]*Teva Pharmaceutical Industries, Ltd., Specialty Life Cycle Initiatives, Global Specialty Medicines, Overland Park, Kansas, USA*
[b]*Bawa Biotech LLC, Ashburn, Virginia, USA*
[c]*Department of Biological Sciences, Rensselaer Polytechnic Institute, Troy, New York, USA*
[d]*Teva Pharmaceutical Industries, Ltd., Discovery and Product Development, Global Research and Development, Netanya, Israel*

Keywords: copaxone®, glatiramer acetate, relapsing-remitting multiple sclerosis (RRMS), nanotechnology, nanopharmaceutical, nanomedicine, nanodrug, subcutaneous delivery, non-biologic complex drug (NBCD), colloidal solution, follow-on biologics, biosimilar, nanosimilar, Abbreviated New Drug Application (ANDA), bioequivalence, biowaivers, immunogenicity, pharmacokinetics (PK), pharmacodynamics (PD), Food and Drug Administration (FDA), European Medicines Agency (EMA), patent, US Patent and Trademark Office (PTO), reference listed drug (RLD), surface plasmon-resonance (SPR), enhanced permeability and retention (EPR), dynamic light scattering (DLS), atomic force microscopy (AFM), cryogenic temperature transmission electron microscopy (Cryo-TEM), zeta potential, size exclusion chromatography, ion mobility mass spectrometry (IMMS), heat maps, immunomodulator, altered peptide ligand (APL), myelin basic protein (MBP), auto-reactive antibodies, anti-glatiramer acetate antibodies, hypersensitivity reactions

Handbook of Clinical Nanomedicine: Nanoparticles, Imaging, Therapy, and Clinical Applications
Edited by Raj Bawa, Gerald F. Audette, and Israel Rubinstein

ISBN 978-981-4669-20-7 (Hardcover), 978-981-4669-21-4 (eBook)
www.panstanford.com

28.1 Introduction

28.1.1 Nanoterminology and the Issue of Size in Drug Delivery

Rapid advances and product development in nanomedicine are in full swing as it continues to influence the pharmaceutical, device and biotechnology industries [1a, 1b, 2]. Nanomedicine is driven by collaborative research, patenting, commercialization, business development and technology transfer within diverse areas such as biomedical sciences, chemical engineering, biotechnology, physical sciences, and information technology.

Although various "nano" terms, including "nanotechnology," "nanopharmaceutical," "nanodrug," "nanotherapeutic," "nanomaterial," and "nanomedicine," are widely used, there is confusion, disagreement and ambiguity regarding their definitions. In fact, there is no precise definition of nanotechnology as applied to pharmaceuticals or in reference to drug delivery. This haunts regulators, patent offices, policy-makers, drug formulation scientists, pharma executives, and legal professionals [3–9]. In particular, regulatory agencies and governmental entities such as US Food and Drug Administration (FDA), the European Medicines Agency (EMA), Environmental Protection Agency (EPA), Centers for Disease Control and Prevention (CDC), National Institute for Occupational Safety and Health (NIOSH), International Organization for Standardization (ISO) Technical Committee on Nanotechnology (ISO/TC229), ASTM International, the Organization for Economic Co-operation and Development (OECD) Working Party on Manufactured Nanomaterials (OECD WPMN) and the US Patent and Trademark Office (PTO) continue to grapple with this critical issue [3].

The term nanotechnology is a bit misleading given that it is not one technology, but an umbrella term encompassing several technical/scientific fields, processes and properties at the nano/micro scale [3, 6–9]. Various definitions of nanotechnology have sprung up over the years [3]. Some label it as the manipulation, precision placement, measurement, modeling or manufacture of matter in the sub-100 nm range [10], or in the 1–200 nm range [11, 12]. Some definitions omit a lower range, others refer to sizes in one, two or three dimensions while others require a size plus

special/unique property or *vice versa*. Others point to a size ranging from 1 to 1000 nm in both nanotechnology and pharmaceutical science [13–16]. This latter definition may be the most appropriate from a drug delivery perspective. The FDA, which has not adopted any "official" regulatory definition in this regard, now uses a loose definition for products that involve/employ nanotechnology and stretched the upper limit to 1000 nm. This underscores the urgency of establishing a uniform "nano" terminology. The need for an internationally agreed definition for key terms like nanotechnology, nanoscience, nanomedicine, nanobiotechnology, nanodrug, nanotherapeutic, nanopharmaceutical and nanomaterial is critical [3]. This is important for harmonized regulatory governance, accurate patent searching and prosecution, standardization of procedures, assays and manufacturing, quality control, safety assessment, and more.

Given this backdrop, and the fact that there is no international scientifically accepted nomenclature or uniform regulatory definition pertaining to nanotechnology [6–9], the following widely-accepted definition unconstrained by an arbitrary size limitation has been previously proposed [3, 9]:

> *The design, characterization, production, and application of structures, devices, and systems by controlled manipulation of size and shape at the nanometer scale (atomic, molecular, and macromolecular scale) that produces structures, devices, and systems with at least one novel/superior characteristic or property.*

This definition above has four key features [3]:

- First, it recognizes that the properties and performance of the synthetic, engineered "*structures, devices, and systems*" are inherently rooted in their nanoscale dimensions. The definition focusses on the unique physiological behavior of the "*structures, devices, and systems*" that is occurring at the nanoscale; it does *not* focus on any shape, aspect ratio, specific size or dimensionality.
- Second, the focus of this flexible definition is on "technology" that has commercial potential from a consumer perspective, not "nanoscience" or basic R&D conducted in a lab-setting that almost certainly lacks commercial implications.
- Third, the "*structures, devices, and systems*" that result must be "*novel/superior*" compared to their bulk, conventional counterparts.

- Fourth, the concept of "*controlled manipulation*" as compared to "self-assembly" is critical to the definition.

Size limitation below 100 nm is frequently touted as the basis of novel properties of nanopharmaceuticals. However, this is simply not true or critical to a drug company from a formulation, delivery, or efficacy perspective because the desired or novel physicochemical properties (e.g., improved bioavailability, reduced toxicities, lower dose or enhanced solubility) may be achieved in a size outside this arbitrary range. For example, the surface plasmon-resonance (SPR) in gold or silver nanoshells/nanoprisms that imparts their unique property as anticancer thermal drug delivery agents also generally operates at sizes greater than 100 nm. Similarly, at the tissue level, the enhanced permeability and retention (EPR) effect that makes passive nanoparticle drug delivery an attractive option operates in a wide range, with nanoparticles of 100–1000 nm diffusing selectively (extravasation and accumulation) into the tumor. At the cellular level, the size range for optimal nanoparticle uptake and processing depends on many factors but is often beyond 100 nm. Liposomes in a size range (diameter) of about 150–200 nm have been shown to have a greater blood residence time than those with a size below 70 nm. In fact, there are numerous FDA-approved and marketed nanonanodrug products where the particle size does not fit the sub-100 nanometer profile: Abraxane (~120 nm), Myocet (~190 nm), DepoCyt (10–20 micometer), Amphotec (~130 nm), Epaxal (~150 nm), DepoDur (10–20 μm), Inflexal (~150 nm), Lipo-Dox (180 nm), Oncaspar (50–200 nm), etc.

This does not imply that any size will do for delivering nanopharmaceuticals. For example, submicron sizes are generally considered essential for biological distribution of biopharmaceuticals for safety reasons [17]. Particles greater than 5 μm can often cause pulmonary embolism following intravenous injection [18]. Therefore, submicron particle size is preferred for all parenteral formulations. In ophthalmic applications, the optimal particle size is less than 1 μm because microparticles around 5 μm can cause a scratchy feeling in the eyes [19].

Just like nanotechnology, there is no universally accepted definition of nanomedicine. The European Science Foundation [20] correctly defines nanomedicine as:

> *[T]he science and technology of diagnosing, treating, and preventing disease and traumatic injury, of relieving pain, and of preserving and improving human health, using molecular tools and molecular knowledge of the human body.*

The National Institutes of Health (NIH) Roadmap for Medical Research in Nanomedicine [21] defines nanomedicine as:

> *[A]n offshoot of nanotechnology, refers to highly specific medical interventions at the molecular scale for curing disease or repairing damaged tissues, such as bone, muscle, or nerve.*

Although numerous nanodrugs have been routinely used in medicinal products for decades without any focus or even awareness of their nano-character, it is only within the past two decades that they have been highlighted due to their potential of revolutionizing drug delivery [3, 22]. Obviously, the "Holy-Grail" of any drug delivery system is to deliver the correct dose of a particular active agent to a specific disease site while minimizing toxic side effects and optimizing therapeutic benefit. This is often not achievable via traditional drugs [22–26]. However, the potential now exists via engineered nanopharmaceuticals.

Many liquid nanopharmaceuticals are colloidal drug delivery systems of 1–1000 nm [3, 26]. Their nano-character—functional complexity and application potential—is related to one or more of the following properties [25–26]:

- nano-scale dimensions/small size (high surface area-to-volume ratio)
- reduced toxicity
- controlled-release property
- altered/modified pharmacokinetics
- enormous compositional range and variety of therapeutics and carriers that can be formulated/packaged
- superior biological distribution and targeting capabilities due to the ability to attach specific targeting moieties
- various delivery route potential (oral, topical, intravenous, subcutaneous, etc.)
- variety of shapes/geometries (Fig. 28.1)
- crystallinity
- aspect ratio
- surface charge

There are numerous potential advantages of nanopharmaceuticals, and harnessing them depends on various factors such as

their mode of delivery and specific class employed [25–29]. Some of these advantages include:

- increased bioavailability due to enhanced water solubility of hydrophobic drugs because of the large specific surface area;
- ability to protect biologically unstable drugs from the hostile bioenvironment of use/delivery/release (e.g., against potential enzymatic or hydrolytic degradation);
- extended drug residence time at a particular site of action or within specific targeted tissue and/or extended systemic circulation time;
- controlled drug release at a specific desired site of delivery;
- endocytosis-mediated transport of drugs through the epithelial membrane;
- bypassing or inhibition of efflux pumps such as P-glycoprotein;
- targeting of specific carriers for receptor-mediated transport of drugs;
- enhanced drug accumulation at the target site so as to reduce systemic toxicity;
- providing biocompatibility and biodegradability;
- offering a high drug-loading capacity;
- providing long-term physical and chemical stability of drugs; and
- improved patient compliance.

In this chapter, the following equivalent terms are used interchangeably: nanodrug, nanotherapeutic, nanomedicine and nanopharmaceutical. Again, there is no formal definition for a nanotherapeutic. In this chapter, we will employ Dr. Bawa's definition [3] for a nanotherapeutic formulation (or nanodrug product) as being*: (1) a formulation, often colloidal, containing therapeutic

*This definition parallels that proposed by numerous experts and disregards that presented by US federal agencies like the NNI. See also:

Bogunia-Kubik, K., Sugisaka, M. (2002). From molecular biology to nanotechnology and nanomedicine. *BioSystems*, **65**, 123–138.

Junghanns, J.-U. A. H., Müller, R. H. (2008). Nanocrystal technology, drug delivery and clinical applications. *Int. J. Nanomed*., **3**(3), 295–310.

Ledet, G., Mandal, T. K. (2012). Nanomedicine: Emerging therapeutics for the 21st century. *U.S. Pharm*., **37**(3), 7–11.

McDonald, T. O., Siccardi, M., Moss, D., Liptrott, N., Giardiello, M., Rannard, S., Owen, A. (2015). The application of nanotechnology to drug delivery in medicine. In: P. Dolez, ed. *Nanoengineering: Global Approaches to Health and Safety Issues*, Elsevier, pp. 173–223.

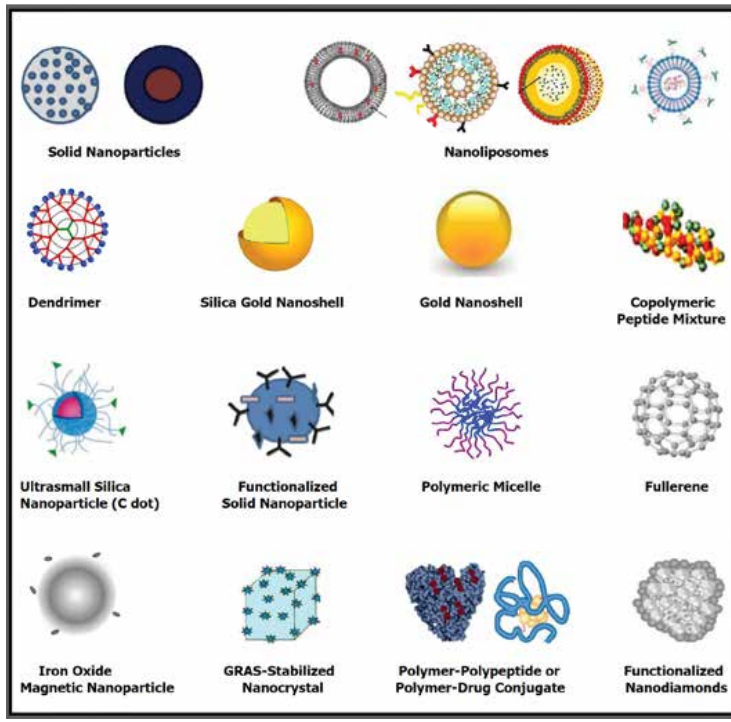

Figure 28.1 Schematic Illustrations of Nanoscale Drug Delivery System Platforms (Nanotherapeutics or Nanodrug Products). Shown are nanoparticles (NPs) used in drug delivery that are either approved, are in preclinical development or are in clinical trials. They are generally considered as first or second generation multifunctional engineered NPs, generally ranging in diameters from a few nanometers to a micron. Active biotargeting is frequently achieved by conjugating ligands (antibodies, peptides, aptamers, folate, hyaluronic acid) tagged to the NP surface via spacers or linkers like PEG. NPs such as carbon nanotubes and quantum dots, although extensively advertised for drug delivery, are specifically excluded from the list as this author considers them commercially unfeasible for drug delivery. Non-engineered antibodies and naturally occurring NPs are also excluded. Antibody-drug conjugates (ADCs) are encompassed by the cartoon labelled "Polymer-Polypeptide or Polymer-Drug Conjugate." This list of NPs is not meant to be exhaustive, the illustrations are not meant to reflect three dimensional shape or configuration and the NPs are not drawn to scale. Abbreviations: NPs: nanoparticles; PEG: polyethylene glycol; GRAS: Generally Recognized As Safe; C dot: Cornell dot; ADCs: Antibody-drug conjugates.

particles (nanoparticles) ranging in size from 1–1,000 nm; *and* (2) either (a) the carrier(s) is/are the therapeutic (i.e., a conventional therapeutic agent is absent), or (b) the therapeutic is directly coupled (functionalized, solubilized, entrapped, coated, etc.) to a carrier. There are a number of FDA-approved, commercialized nanopharmaceuticals [7, 8, 25–27] (Fig. 28.1) for intravenous use as well as for non-intravenous delivery. However, numerous nanopharmaceuticals are still at the development or clinical trial phase. This chapter focuses on Copaxone®, a drug developed and marketed by Teva Pharmaceutical Industries, Ltd., Israel (NYSE: TEVA) and indicated for the treatment of patients with relapsing forms of multiple sclerosis (MS) [30].

28.1.2 Copaxone® (Glatiramer Acetate) and Multiple Sclerosis

Copaxone® is a non-biologic (synthetic) complex drug ("NBCD") and first-generation nanomedicine composed of an uncharacterized mixture of immunogenic polypeptides in a colloidal solution. The active ingredient in Copaxone®—glatiramer acetate—is a heterogeneous synthetic mixture of polypeptides comprising four amino acids (L-glutamic acid, L-alanine, L-lysine, and L-tyrosine) in a defined molar ratio [37]. Glatiramer acetate has immunomodulatory effects on innate and acquired immunity and is indicated for the treatment of patients with relapsing forms of multiple sclerosis (MS) [30]. Copaxone® is currently available as a daily 20 mg subcutaneous injection (approved in the United States in 1996). A 40 mg subcutaneous injection, administered three times a week was approved in 2014 in the United States and Europe.

MS is a chronic degenerative autoimmune disease in which inflammatory infiltrates damage the myelin sheath and central axons, impeding neuronal conduction [60]. MS affects an estimated 2.3 million people worldwide, a majority of whom are women [61]. MS typically strikes young adults; most patients are diagnosed between ages 20–50 [61]. Symptoms of MS include visual disturbances, ataxia, weakness, fatigue, cognitive impairment, depression, sexual dysfunction, lack of bladder control and spasticity [60, 62]. The cause of MS is unknown; however, a combination of several factors are implicated [63]. It is generally

accepted that MS involves an immune-mediated process directed against the myelin in the central nervous system [63].

Until the development of disease-modifying therapies (DMTs) such as Copaxone®, only symptomatic therapy was available to MS patients. Currently there are several DMTs approved in the EU, Canada, and US for the treatment of RRMS. However, Copaxone® is unique in several ways. Copaxone® is the first drug to show proven therapeutic efficacy in MS and the first product to have a copolymer of amino acids as its active ingredient [64]. Copaxone® is not a single molecular entity, rather a it is heterogeneous mixture of potentially millions of distinct, synthetic polypeptides of varying lengths, some containing up to 200 amino acids with structural complexity comparable to that of proteins, or even more complex than proteins [37]. It is presently impossible to isolate and identify its pure components even via the most technologically sophisticated multidimensional separation techniques [37]. The complexity of glatiramer acetate is amplified by several aspects [37, 46, 65]: (1) the active moieties in glatiramer acetate are unknown; (2) the mechanisms of action are not completely elucidated; (3) pharmacokinetic testing is not indicative of glatiramer acetate bioavailability; (4) pharmacodynamic testing is not indicative of therapeutic activity and there are no biomarkers available as surrogate measures of efficacy; and (5) small changes in the glatiramer acetate mixture can change its immunogenicity profile. Therefore, analogous to biological products, synthetic glatiramer acetate is defined, in large part, by its well-controlled manufacturing process that has been used by Teva for more than 20 years.

28.2 Non-Biologic Complex Drugs and Regulatory Pathway for Follow-On Products

Medicinal products can be broadly divided into three classes: (1) small-molecule drugs, (2) biologic drugs, and (3) non-biological (synthetic) complex drugs or NBCDs. NBCDs have been defined as medicinal products that are not biological medicines. In NBCDs, the active agent or therapeutic moiety is not a homo-

molecular structure but consists of different yet closely related and often nanoparticulate structures that cannot be isolated, fully quantitated, and/or characterized via standard analytical or physicochemical techniques [66] (Fig. 28.2). It is also unknown which structural elements might affect their therapeutic performance [66]. As stated earlier, Copaxone® is a NBCD. In addition to Copaxone®, other NBCDs include certain liposomes and iron-carbohydrate drugs. NBCDs typically use multiple starting components and the final product(s) represents the result of a complex and often proprietary manufacturing process. In this regard, if one of the starting components or final products exhibit nano-dimensions or nano-characteristics, the term nanomedicine is often employed.

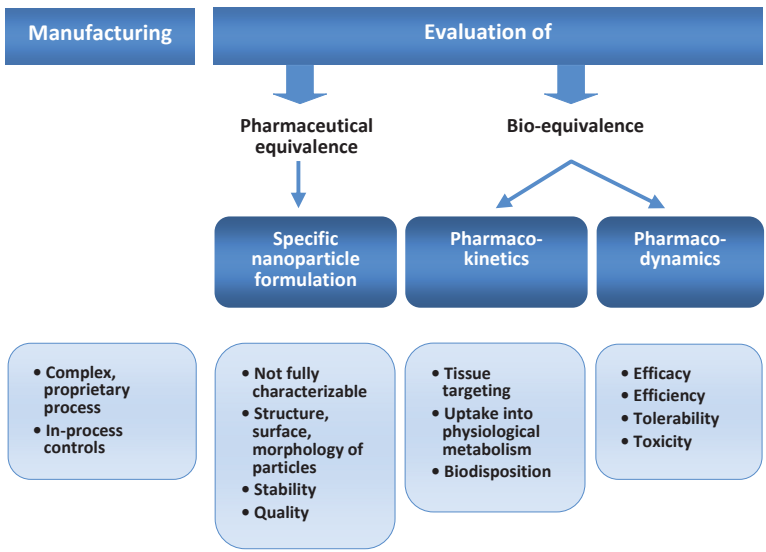

Figure 28.2 NBCDs therapeutic equivalence from manufacturing to safety and efficacy. Reproduced with permission from [66].

Both the FDA and the EMA regulate new drugs and biologics for approval and licensure. In the US, small-molecule drugs are regulated under the Food, Drug and Cosmetics Act ("FDCA" or "FD&C Act"). However, biologics are currently regulated under both the Public Health Service Act ("PHSA") and FDCA because some products also fall within the older FDCA approval route of "drugs."

Although the PHSA uses the term "biologics" when referring to biological products, there are other interchangeably equivalent terms in this regard: "biopharmaceuticals," "biomolecular drugs," "biologic drugs," and "protein products." Branded biologics are referred to as "pioneer," "branded" or "reference" biologics. Small molecule drugs approved by the FDA are known as New Chemical Entities (NCEs) while approved biologics are referred to as New Biological Entities (NBEs). As a result, a new drug application for an NCE is known as a New Drug Application (NDA), whereas a new drug application for an NBE is called a Biologic License Application (BLA). Note that prior to the 1980s there were very few marketed biologics, so the very term "pharmaceutical" or "drug" implied a small molecule drug.

The classic generic pathway for a small molecule drug relies on the therapeutic equivalence to the innovator or reference listed drug (RLD). This entails that it be pharmaceutically equivalent (i.e., identical active substance) and bioequivalent (i.e., comparable pharmacokinetics) as established in a small volunteer study that does not require formal clinical efficacy or safety studies. The acceptance intervals must show that for bioequivalence the logarithm transformed AUC and C_{max} ratios must lie within an acceptance range of 0.80 to 1.25 for the 90% confidence intervals [68]. This classic generic approval approach has been successful for many well-defined, small, low-molecular weight drugs where the analytical testing fully characterized the product.

The pathway to a biosimilar product is different. The concept of similarity was introduced in the general biosimilar guidelines published by the EMA in 2005 [68, 69a]. They were revised in 2014 [69b]. To become authorized as a biosimilar in the European Union (EU) the applicant needs to show similarity in quality, safety and efficacy [69a]. A biosimilar needs a full quality dossier comparable with that of an original biological product. The application should also contain a comparison in physicochemical and other *in vitro* characteristics showing no clinically relevant differences between the biosimilar and innovator. Full toxicity programs need not be repeated and animal pharmacokinetic (PK) and pharmacodynamic (PD) studies may be used to demonstrate similarity with the original. To show clinical similarity, it is not necessary to present equivalent efficacy in all clinical endpoints for every indication for which the

original product is registered. Using a biological endpoint that is sensitive to show possible differences in clinical activity between products is allowed.

In 2010, the Biosimilars Act was enacted into law that established an approval route for biosimilars in the US.† The FDA published draft guidances for biosimilars (also known as follow-on biologics or subsequent entry biologics) in 2012 which state that biosimilar applicants should include analytical studies that (i) demonstrate the biological product as being highly similar to the reference product notwithstanding minor differences in clinically inactive components; (ii) include animal studies including the assessment of toxicity; and (iii) provide a clinical study or studies (including the assessment of immunogenicity and PK/PD) that are sufficient to demonstrate safety, purity, and potency in one or more appropriate conditions of use for the reference product is licensed and intended to be used and for which licensure is sought for the biological product [70a]. The agency also stated that it has

†*See*: Biosimilars, Available at: http://www.fda.gov/Drugs/DevelopmentApprovalProcess/HowDrugsareDevelopedandApproved/ApprovalApplications/TherapeuticBiologicApplications/Biosimilars/default.htm (accessed on October 6, 2015):

The Patient Protection and Affordable Care Act (Affordable Care Act), signed into law by President Obama on March 23, 2010, amends the Public Health Service Act (PHS Act) to create an abbreviated licensure pathway for biological products that are demonstrated to be "biosimilar" to or "interchangeable" with an FDA-licensed biological product. This pathway is provided in the part of the law known as the *Biologics Price Competition and Innovation Act* (BPCI Act). Under the BPCI Act, a biological product may be demonstrated to be "biosimilar" if data show that, among other things, the product is "highly similar" to an already-approved biological product.

A biosimilar product is a biological product that is approved based on a showing that it is highly similar to an FDA-approved biological product, known as a reference product, and has no clinically meaningful differences in terms of safety and effectiveness from the reference product. Only minor differences in clinically inactive components are allowable in biosimilar products.

An *interchangeable* biological product is biosimilar to an FDA-approved reference product and meets additional standards for interchangeability. An interchangeable biological product may be substituted for the reference product by a pharmacist without the intervention of the health care provider who prescribed the reference product.

FDA requires licensed biosimilar and interchangeable biological products to meet the Agency's rigorous standards of safety and efficacy. That means patients and health care professionals will be able to rely upon the safety and effectiveness of the biosimilar or interchangeable product, just as they would the reference product.

the discretion to determine that an element described above is unnecessary [70a]. An updated version of this guidance was published in 2015 [70b]. The FDA approved the first biosimilar in March 2015. The product developed by Sandoz and called Zarxio (filgrastim-sndz) is the less expensive alternative to Amgen's Neupogen® (filgrastim), a biologic that boosts leucocytes in cancer patients. In addition, a generic version of Remicade® is poised to receive FDA approval later in 2015. The FDA currently has four applications under regulatory review.

The therapeutic equivalence for the third class of follow-on synthetic complex drugs, or NBCDs, has been a hot topic of conversation for the last few years. A workshop on NBCDs was held in Leiden, Netherlands in 2009. The goal of this workshop was to collaborate with various stakeholders, including manufacturers of original products as well as generics and biosimilars, to produce a consensus paper about the scientific issues involved in showing therapeutic equivalence of NBCDs to support the development of harmonized regulatory pathways for NBCD follow-on products [67]. Additional critical discussions on this topic have been held at various workshops and conferences:

- the FIP Centennial Congress held in Amsterdam, Netherlands in 2012;
- the New York Academy of Sciences conference held in New York City in 2012 [73];
- the EUFEPS Regulatory Science Network Workshop held in Ankara, Turkey in 2012;
- the AAPS Meeting held in San Antonio, Texas, USA in 2013;
- the New York Academy of Sciences conference held in New York City in 2013 [74];
- the FDA Public Hearing in 2014 on "Challenges for Non-Biological Complex Drugs" held in Silver Spring, Maryland, USA; and
- the International Symposium on Scientific and Regulatory Advances in Complex Drugs held in Budapest, Hungary in 2014.

The consensus of these meetings is similar: (i) NBCDs are a diverse group of products that cannot be fully characterized because they are extremely complex; (ii) NBCDs cannot be evaluated by any of the existing regulatory pathways developed by EMA and

FDA, i.e., regulatory guidelines for small molecules and biologics (generic drugs and biosimilars respectively) cannot be extrapolated to NBCDs; and (iii) no dedicated regulatory pathways for NBCD follow-on versions exist [68]. Due to heterogeneity and complexity, although NBCDs may share certain features with biologicals, they are much more complex. This is especially true for Copaxone® which contains many "biological-like" constituents; however, it cannot be copied (on the other hand, the sequences of biologicals and biosimilars are identical). NBCD mixtures cannot be fully defined via physico-chemical analysis, and their biological and clinical characteristics are highly dependent upon the specific manufacturing process [68] (Fig. 28.2). In contrast, biosimilars are better understood and the pharmaceutical ingredients in those products are better characterized than the NBCD mixtures. Even then, at least the same basic regulatory guidelines/principles that are used for biosimilars should be used for NBCDs, such as the need for animal and/or clinical data and the need to show similarity in quality, safety, and efficacy. The requirements for follow-on NBCDs should be based on the biosimilar approach with specific requirements based on the science of the individual product. In summary, the new regulatory pathways developed for biologics may serve as the basis for regulating (with case-by-case adjustments) follow-on NBCD products [68]. The reader is directed to an outstanding recent text that discusses various scientific aspects and the regulatory landscape of NBCDs [76].

28.3 Nanomedicines and Regulatory Pathway for Nanosimilars

Glatiramoids are NBCDs [77]. Copaxone® (glatiramer acetate), the first and most studied glatiramoid, is a first-generation nanomedicine that comprises a nano-sized polypeptide mixture with molecules and molecular structures ranging from 1.5 to 550 nm in size. The data demonstrating the colloidal properties of Copaxone® and the nanomedicine attributes are discussed in detail in Section 28.4.

Currently the FDA, EMA, and other regulatory agencies examine each new nanomedicine product on a product-by-product basis [71]. There generally is a lack of recognition that nanomedicine products need their own therapeutic category or regulatory

pathway [71]. However, as the first generation nanomedicine products are coming off patent, regulatory agencies will need to determine what the requirements are for a follow-on nanomedicine product or a nanosimilar product. As many of the NBCDs are also nanomedicines, the requirements for follow-on NBCDs are facing the same lack of regulatory clarity.

The EMA in 2013 published a paper on next-generation nanomedicines and nanosimilars [72]. This paper notes that in order to demonstrate similarity, there is a need for stepwise comparability studies to generate evidence substantiating the similar nature, in terms of quality, safety, and efficacy of the nanosimilar and the originator/innovator nanomedicine [72]. As nanomedicines differ significantly in their complexity, a case-by-case or product/class specific approach for their evaluation may be necessary [72]. This paper [72] also stresses that any drug developed for comparison to the innovator product must demonstrate equivalence in terms of quality, safety and efficacy prior to grant of market authorization. In addition, given the degree of complexity of many nanomedicine products, special scientific considerations may be required to ensure this equivalence of performance [72]. The EMA has also published reflection papers on intravenous liposomal products developed with reference to an innovator product and nano-sized colloidal iron-based preparations developed with reference to an innovator product. To date, there is no reflection paper from the EMA or guidance document from the FDA for glatiramer acetate.

The FDA, on the other hand, continues to state that it will regulate nanomedicine products under its current regulatory regime and that this framework is sufficiently robust and flexible [42], a view not shared by most experts [7, 8, 26].

28.4 Colloidal and Nanomedicine Properties of Copaxone®

Copaxone® is produced using well-established solution polymerization techniques [52]. The nanoscale size of glatiramer acetate molecules is an intrinsic process-related property associated with its chemical nature. The consistent manufacturing process employed by Teva Pharmaceutical Industries, Inc. creates a mixture of glatiramer acetate polypeptides with an average

molecular weight (MW) ranging from 5000–9000 Daltons (the MW distribution of the glatiramer acetate components spans a range of 2500–20,000 Daltons) [37]. The polypeptides in glatiramer acetate appear to range from approximately 20 to 200 amino acids in length, with an average polypeptide length of about 60 amino acids [53]. The theoretical length of glatiramer acetate molecules ranges from 3 to 30 nm, with an average of about 8 nm for the peptide of 7000Da MW. However, as described further below, the molecules and molecular associations in glatiramer acetate appear to reach up to 550 nm.

The FDA has defined the term "colloid" for regulatory purposes as "a chemical system composed of a continuous medium (continuous phase) throughout which are distributed small particles, 1 to 1000 nm in size (disperse phase), that do not settle out under the influence of gravity; the particles may be in emulsion or in solution." [54]. While this definition, which appears to be derived from Dorland's Medical Dictionary for Health Consumers [55], is generally considered accurate, a more precise, scientific definition is as follows [56]:

> *A colloid, or disperse phase, is a dispersion of small particles of one material in another. In this context, "small" means something less than about 500 nm in diameter (about the wavelength of visible light). In general, colloidal particles are aggregates of numerous atoms or molecules, but are too small to be seen with an ordinary optical microscope. They pass through most filter papers, but can be detected by light scattering and sedimentation.*

Regardless of the definition applied, Copaxone® unquestionably is a colloidal solution. Glatiramer acetate nanoparticles are within the typical colloidal size range of 1 to 1000 nm (1 μm) (denoted as radius (*r*) in Stoke's law) and are uniformly suspended in a continuous medium (mannitol solution). The mannitol solution is a "true" solution, i.e. it is a homogenous solution in which the ratio of solute to solvent remains constant and in which all of the solute particles have diameters less than 10^{-7} centimeters (<10 nm), and the mannitol in solution cannot be centrifuged or filtered from the solution. As such, the aqueous mannitol solution constitutes a continuous medium. The glatiramer acetate nanoparticles dispersed in the mannitol solution do not precipitate under the influence of normal gravitational forces, even when stored at 2–8°C for up to 2 years; thus, Copaxone® is stable under these conditions.

The results of traditional colloidal assessments capable of distinguishing compositional features of Copaxone® at the molecular level further confirm the colloidal nature of Copaxone® [57]. These experiments, which included ultracentrifugation, DLS, AFM, cryogenic temperature, transmission electron microscopy, and zeta potential testing, demonstrate the following:

- Copaxone® is composed of two, distinct populations of polypeptides, both of which are within the size range for colloids (i.e. 1 to 1000 nm).
- The glatiramer acetate polypeptides are stable and distributed uniformly throughout the aqueous mannitol medium.
- Copaxone® constituents can be separated into layers by ultracentrifugation and then easily reconstituted, indicating that Copaxone® is a lyophilic colloidal solution in which the dispersed particles are well-solvated and stabilized rather than a true solution in which the dispersed particles are dissolved.
- Copaxone® has a high zeta potential, suggesting that it is highly stable and resists flocculation and settling under normal gravitational forces.

The results of this testing are discussed in more detail below:

Separation by Ultracentrifugation and Resuspension

Stable colloids do not "settle out under the influence of" normal gravitational forces. However, they will potentially exhibit separation of the disperse phase under increased gravitational forces, such as ultracentrifugation. The stability of colloidal solutions is characterized by, among other things, Stoke's law ($dx/dt = 2r^2 (d_c - d_p)g/9h$). By increasing gravity (g) through ultracentrifugation where ($d_c - d_p$) is negative, dx/dt can be increased sufficiently to separate the suspended particles in the stable colloidal solutions.

To show that Copaxone® is not a "true" solution, a Copaxone® sample was ultracentrifuged for 24 h at 4°C under 530,000g ("treated sample"). The sample was segregated into a concentrated layer of higher MW polypeptide moieties (a whitish, dispersed phase in the lower layer of the centrifuged sample) and a layer of lower MW polypeptide moieties (a more translucent upper layer). The upper and the lower layers of the treated sample were tested

for glatiramer acetate concentrations, which were measured using size exclusion chromatography and compared with the untreated Copaxone® sample (Fig. 28.3). The concentration of glatiramer acetate in the upper layer of the treated sample was about 1/10 of the concentration in the lower layer.

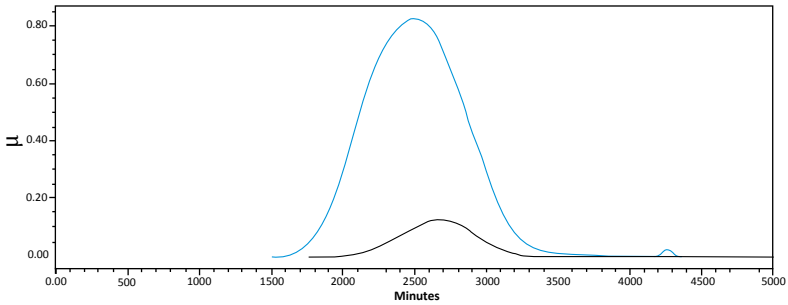

Figure 28.3 Size exclusion chromatography. Relative concentrations and molecular weight distribution profiles of the upper layer (shown in black), and lower layer (shown in blue) of the Copaxone® sample after ultracentrifugation.

The treated sample layers were then re-mixed by vortexing, and the concentration of glatiramer acetate in the reconstituted solution was measured again. The concentration of the reconstituted sample was equivalent to that of the original untreated sample (Fig. 28.4).

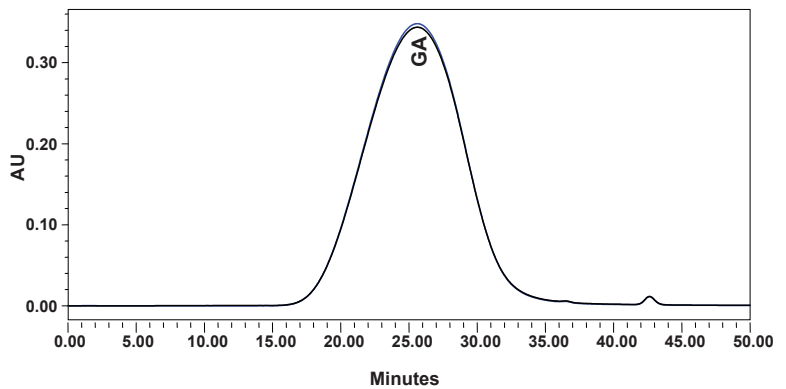

Figure 28.4 Size exclusion chromatography overlaid profiles of the untreated (shown in black) and reconstituted (shown in blue) Copaxone® samples.

This testing demonstrates that Copaxone® constituents can be concentrated under strong centrifugal force, and the resulting concentrate can be easily reconstituted to its original composition. In other words, Copaxone® can be reversibly re-suspended, a property expected only of a colloidal solution, not that of a true solution.

Dynamic Light Scattering (DLS)

DLS determines particle size in solution by measuring their diffusion rate (Brownian motion). Small molecules diffuse more quickly than large molecules. Molecules of different sizes scatter light at different intensities. DLS measures intensity as a function of particle sizes; however, it is important to note that DLS results are qualitative and not quantitative. The capacity of a large molecule to scatter light is significantly higher than that of a small molecule; therefore, a single large molecule can scatter light more intensely than a large population of small particles. Thus, the results of DLS should be evaluated accordingly: the area under the peak does not correlate with the number of particles (population size) represented by that peak.

Scientists at Teva developed and optimized operational DLS conditions for the glatiramoid class of compounds. Measurements were sensitive to particle sizes in the nm range (1–1000 nm). Robust manufacturing process was demonstrated by the reproducibility of results of multiple measurements on many different Copaxone® batches manufactured at varying time periods. DLS measurements were performed on Copaxone® diluted with a 20 mM NaCl solution and filtered through a 1.2 μm disc filter prior to analysis, and on samples obtained by ultracentrifugation at different G-forces (the upper layers and the constituents concentrated at the bottom).

DLS analysis shows that the untreated Copaxone® mixture consists of two main polypeptide populations. The first population is characterized by a distribution of particle sizes in the range of 1.5 to 15 nm, with the most abundant size being approximately 5.6 nm. The second population contains particles in the range of 20 to 550 nm, with the most abundant size being approximately 111 nm (Fig. 28.5). The first population likely represents “mono-particles,” or separated molecules, which comprise the most abundant

fraction; whereas the second population can be attributed to larger entities (e.g., labile intermolecular associates) that may be formed by interactions between amino acid sequences on the polypeptide chains.

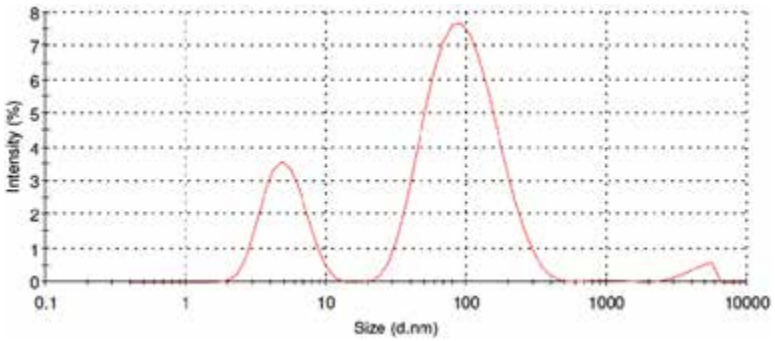

Figure 28.5 A typical (untreated) Copaxone® DLS scan.

The dispersed Copaxone® solution was exposed to ultracentrifugation at different G-forces. As mentioned above, ultracentrifugation resulted in a clear upper layer and a viscous whitish fraction. The upper layer and the material concentrated at the bottom were then tested by DLS (after reconstitution in water). At 290,000*g*, the upper layer still contained both "light" and "heavy" peaks (Fig. 28.6a), whereas the lower fraction contained the "heavy" peak only (Fig. 28.6b), Ultracentrifugation at higher G-force (650,000*g*) resulted in a more effective concentration of the heavy peak (Fig. 28.6c,d).

Thus, after ultracentrifugation, there was a change in the profile of the suspended glatiramer acetate nanoparticles with regard to their size distribution, i.e. the larger molecularly associated nanoparticles segregated at the bottom, whereas the smaller nanoparticle associates remained in the upper layer. The extent of concentration of the larger associates at the bottom was proportional to the applied G-force value. This separation would not have been observed if Copaxone® was a true, homogenous solution.

In summary, the Copaxone® solution was successfully separated by ultracentrifugation into several populations of constituents according to their sizes, as determined by DLS.

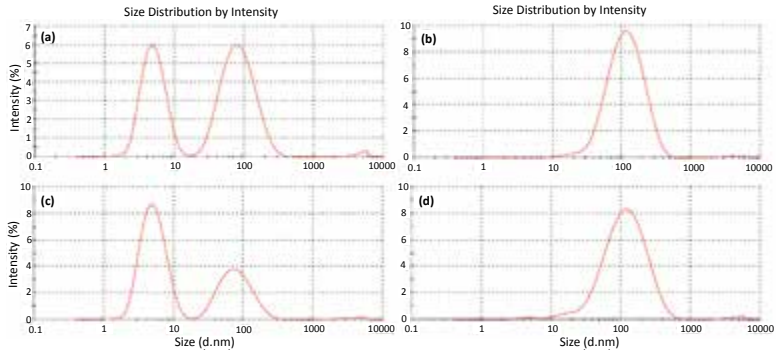

Figure 28.6 DLS results of the Copaxone® sample after ultracentrifugation at different G-forces. The Copaxone® sample was subjected to ultracentrifugation at the conditions described in panels a–d. (a) Upper layer after 2 h ultracentrifugation at 290,000*g*: two populations are observed; the relative amount of smaller particles is increased compared with non-treated Copaxone®. (b) Bottom fraction after 2 h ultracentrifugation at 290,000*g* re-suspended in water: only the larger size components are observed. (c) Upper layer after 2 h ultracentrifugation at 650,000*g*: the relative amount of larger particles is even more reduced due to further separation under higher G-force. (d) Bottom fraction after 2 h ultracentrifugation at 650,000*g* re-suspended in water: only the higher size constituents are observed.

It is noteworthy that re-solution in water of the larger molecularly-associated nanoparticles from the material obtained at the bottom of the tube resulted in the observation of only the larger particles. This indicates that the larger particles are labile intermolecular associates of several nano-sized "mono"-molecules arranged in a thermodynamically preferable disposition and thus are relatively stable. The observation of the two distinct populations of particles in the original analysis further supports this conclusion. If the solution were merely a mix of agglomerates, one would have expected a continuum of particle size distribution over the range. The appearance of two distinct populations of particles shows that Copaxone® is a colloidal system that is more complex than a mere solution of agglomerated particles and actually comprises a unique microstructure of two particulate populations. In other words, this DLS testing demonstrates that Copaxone® comprises thermodynamically stable, nano-sized association complexes.

Atomic Force Microscopy (AFM)

AFM is a type of scanning tunneling microscopy. AFM produces images of the surface ultrastructure of a substance with molecular resolution under physiological conditions. The samples are dried with nitrogen prior to scanning. The resolution of this technique varies from about 0.1 nm to the sub-micron range. Via AFM, the size (length, width, and height) of individual particles can be measured and the results can be visualized in three dimensions.

A typical topographic image of a Copaxone® dried sample is shown in Fig. 28.7. A Copaxone® aliquot from a syringe and a placebo sample from an identical syringe were dried with nitrogen on a flat support, and then scanned to produce the surface ultrastructure with molecular resolution. AFM analysis of Copaxone® samples revealed dispersed "dot-like" and "string-like" components. In the placebo syringes, no such entities were apparent, indicating that the particles observed in the Copaxone® samples did not originate from mannitol or from any part of the syringes (i.e., they are characteristic of glatiramer acetate).

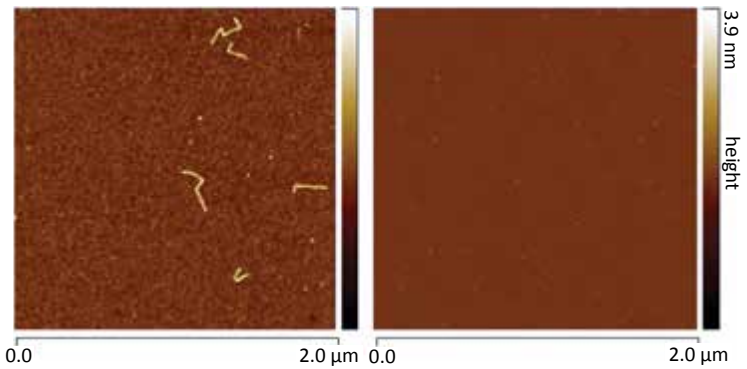

Figure 28.7 Typical topographic image of Copaxone® and placebo bulk solutions. AFM analysis of Copaxone® samples (left) from a bulk solution in a syringe revealed dispersed "dots" and "strings" particles. In the placebo syringes (right), no such entities were visible, indicating that the particles observed in the Copaxone® samples (left) did not originate from mannitol or from any part of the syringes (they are characteristic of glatiramer acetate).

The DLS study above indicated that the population of larger sized particles under the peak on the right (Fig. 28.3) (about 110 nm

average size distribution) can be concentrated at the bottom of a tube by ultracentrifugation. In order to characterize the strings detected by the AFM technique in the Copaxone® sample and to investigate correlations between the results of the DLS scans and the AFM images, samples described in the DLS study above (the bottom fractions) were diluted with water, dried with nitrogen and analyzed.

AFM images for those fractions from a Copaxone® batch (at a higher resolution) are shown in Fig. 28.8. The concentrated "heavy" material appeared to contain the same string-like entities as seen in the untreated Copaxone® samples (Fig. 28.7, left), although, as expected, at a higher concentration. No round shaped particles were detected in the lower layer. By contrast, analysis of the upper layer revealed none of the string-like particles present in the lower fraction. This, correlates with data obtained via DLS testing indicating two subpopulations of particles with different average sizes, and supports the assumption that the strings are the larger sized particles in the Copaxone® sample.

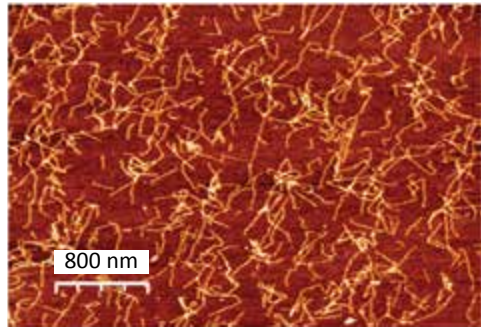

Figure 28.8 Topographic image for "heavy" fraction from Copaxone®, separated by ultracentrifugation. Results shown in this figure complement results of the DLS study, in that AFM established that the heavier population of Copaxone® polypeptides consists of string-like entities of variable sizes.

The DLS and AFM data above taken together confirms the colloidal characteristics of Copaxone®, namely, that it maintains a homogenous appearance throughout its 2-year shelf life (i.e., it contains polypeptide particles of different sizes that do not precipitate under gravity) but it can be separated into subpopulations under ultracentrifugation. These techniques also demonstrate

the presence of stable polypeptide particles within the colloidal size distribution range (1–1000 nm).

Cryogenic Temperature Transmission Electron Microscopy (Cryo-TEM)

Cryo-TEM is a method of obtaining high-resolution, direct images of molecules or molecular assemblies in their native environment. Thus, it can elucidate the nature of the basic building blocks that make up a sample, covering a wide range of length scales from a few nm to several microns. Rapid freezing of the sample prevents alterations in the sample and eliminates potential structural changes, redistribution of elements, and/or the washing away or evaporation of substances originally present in the sample [58]. This technique was used to confirm results of DLS and AFM testing, and to eliminate the impact (if any) of sample preparation on the size, shape, and type of Copaxone® molecular assemblies.

A drop of Copaxone® was placed onto a TEM copper grid (to prevent the formation of ice crystals) and analyzed at –170°C. Samples were analyzed in different locations on the grid, using variable magnification, in an attempt to detect the potential existence of both larger and smaller structures. A placebo (mannitol solution) was used as control (Fig. 28.9).

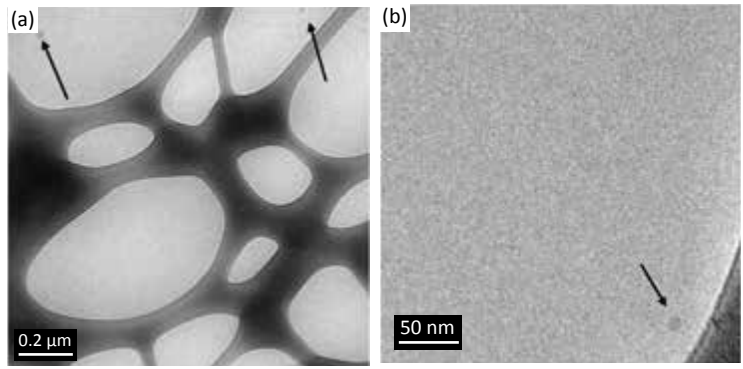

Figure 28.9 Typical Cryo-TEM results for a placebo (mannitol solution) sample: (a) Moderate magnification, (b) high magnification. The sample contained globule particles, with varying sizes of 30 ± 5 nm, as indicated by the black arrows. These globules most likely originated from the silicon oil droplets present in the syringe.

Copaxone® samples tested under the same conditions appear quite different (Fig. 28.10). They largely contain three populations of particles dispersed in the continuous mannitol solution: fibers (or strings) of 60–300 nm length, spherical particles of ~4 nm, and globules of ~30 nm; the latter are consistent with the globules in the placebo sample.

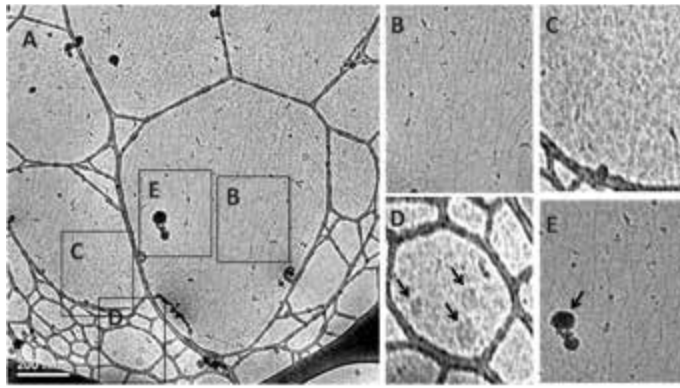

Figure 28.10 (A) Cryo-TEM image of typical structures present in Copaxone® samples. Images B through E are enlarged areas of image A. (B) Fibers of 60–300 nm length and width of 6 ± 1 nm. (C) Spherical particles of ~4 nm in diameter. (D) Globules of ~30 nm in diameter (also detected in placebo samples, see Fig. 28.5 above); (E) Black frost particles (not related to the sample).

Results of Cryo-TEM analysis support results of DLS and AFM testing. Examination of native structural features of the Copaxone® sample, as in the DLS and AFM experiments, revealed two populations of glatiramer acetate nanoparticles dispersed in the aqueous mannitol phase:

- One population of Copaxone® nanoparticles were spherical with sizes being 4 ± 2 nm (Fig. 28.10C), which correspond to the smaller polypeptide moieties shown on the DLS scans (Fig. 28.5, peak on left), and with the "dot-like" structures on topographic AFM images (Fig. 28.7, left).
- The second population of polypeptides appeared as "strings" with lengths of ~60 to 300 nm (Fig. 28.10B), which correspond with the DLS peak indicating larger moieties (Fig. 28.5, peak on right) and the topographic images from

the AFM analysis showing elongated fibers (Figs. 28.7, left and 28.8).

The polypeptide's particle size distribution and their dispersion in the continuous mannitol aqueous phase shown in the Cryo-TEM study provide additional evidence of the colloidal nature of Copaxone®.

Zeta Potential

The stability of colloidal solutions "is determined by the balance of attractive and repulsive forces between individual particles. The repulsive force prevents two particles from approaching one another and adhering together" [57]. If the repulsive force is sufficiently high, the colloidal solution "will resist flocculation and the colloidal system will be stable" [57].

Zeta potential is a measure of the electrokinetic potential in colloidal systems. The magnitude of the zeta potential gives an indication of the stability of a colloidal system. If all the particles have a large negative or positive zeta potential then they will tend to repel each other and, as noted above, there is no tendency to flocculate. However, if the particles have low zeta potential values then there is no force to prevent the particles from coming together and flocculating. The dividing line between stable and unstable is generally taken at either +30 mV or –30 mV. Particles with zeta potentials more positive than +30 mV or more negative than –30 mV are normally considered stable [59].

Representative zeta potential results for three Copaxone® batches are shown in Fig. 28.11 and results are summarized in Table 28.1. Placebo (mannitol solution) exhibited a zeta potential that was about 5 mV.

Table 28.1 Summary of Zeta potential results.

		Zeta potential (mV)	
Sample	**Batch**	**Average**	**STDV**
Copaxone®	1	36.5	2.3
	2	37.4	2.0
	3	34.5	1.0
Placebo	—	5.5	

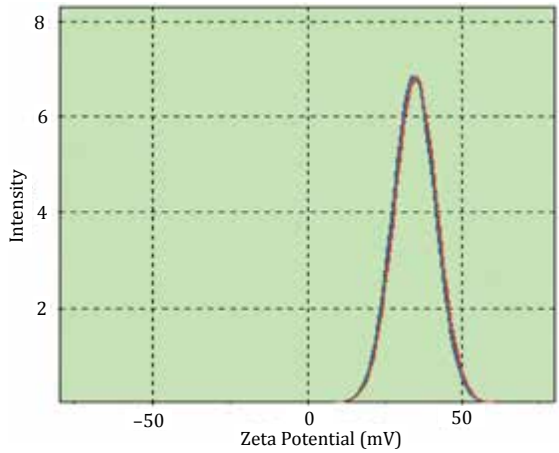

Figure 28.11 Zeta potential of three batches of Copaxone®.

As shown in Table 28.1, the zeta potentials are approximately 34–37 mV, indicating the stability of the colloidal solution through strong electrostatic repulsion of Copaxone® moieties, which prevents their flocculation. Zeta potential results confirm the physical stability of the Copaxone® colloidal solution.

Summary of Test Results

The results of these studies—ultracentrifugation and reconstitution, DLS, AFM, Cryo-TEM, and zeta potential—complement each other and, taken together, confirm that Copaxone® is a stable, lyophilic colloidal solution. These studies show that under adequate centrifugal force, Copaxone® can be separated into layers exhibiting different concentrations that are easily re-dispersed back to the original concentration upon vortexing. They demonstrate the presence of solvated, stable, nano-sized molecules and associations dispersed homogenously within the aqueous mannitol solution. The sufficiently high zeta potential values attest to the stability of the colloidal solution caused by electrostatic forces in the product. The dual population of small and large nanoparticles observed in the analysis is supportive of the unique and distinct microstructure of the Copaxone® product.

28.5 Immunogenicity

There is one aspect of Copaxone® that raises special safety and effectiveness concerns that merit heightened vigilance with respect to the approval of any potentially interchangeable follow-on glatiramer acetate product. *In particular, glatiramer acetate is an immunomodulator*. In other words, Copaxone® is intended to achieve its therapeutic effects by interacting with and modulating a patient's immune system over an extended period of time. For this reason, Copaxone®'s package insert warns that chronic use has the potential to alter healthy immune function as well as induce pathogenic immune mechanisms, although no such effects have been observed with Copaxone® [30].

As discussed above, due to the complexity and inexorable link between the manufacturing process and quality, any follow-on product almost certainly will differ from Copaxone®'s structure and composition of active ingredients because it will be made using a different manufacturing process than that used by Teva. Although it is not possible to fully characterize and compare these complex mixtures, differences are revealed via sophisticated analytical techniques. Purported generic glatiramer acetate so-called generic products have been approved in India, Argentina, and Mexico. A variety of physicochemical tests have been done on these products and they have been proven to be similar to Copaxone® in some basic features. However, they are different in the bulk composition of constituents when analyzed via methods for analysis of complex closely related molecules. In this regard, a widely used analytical tool for characterization of complex mixtures of biologics in the context of biosimilars is the ion mobility mass spectrometry (IMMS) [75]. The ion mobility method applies multidimensional separation techniques based on size, shape, charge and mass of the molecules in the sample mixture and is capable of separating isomeric peptides that chromatographic techniques cannot. The analysis produces a three-dimensional heat map to highlight intensity differences of peptides at various mass/charge and drift times. The difference between the intensities of heat maps for the generics as compared to Copaxone® (result of subtraction of generic heat map from that of Copaxone®) show highlighted areas indicating different polypeptide populations compared to those of Copaxone® lots tested (Fig. 28.12).

A quantitative assessment of these differences in heat maps was used that integrates the intensity values within these highlighted areas to produce a total intensity value (TIV). If the composition of a sample was exactly the same as the reference Copaxone®, the heat map would theoretically have no highlighted areas and a TIV = 0. Conversely, heat maps with more highlighted areas signify greater difference to the reference Copaxone® and will have a higher TIV. As shown in Fig. 28.13, the TIVs of Copaxone® batches are within a narrow range of its inherent batch-to-batch variability, whereas the generics were 8–13 fold higher (Fig. 28.13). Clearly, these results indicate a profound difference in size, shape and charge of the constituent polypeptides in Copaxone® as compared to the purported generic products.

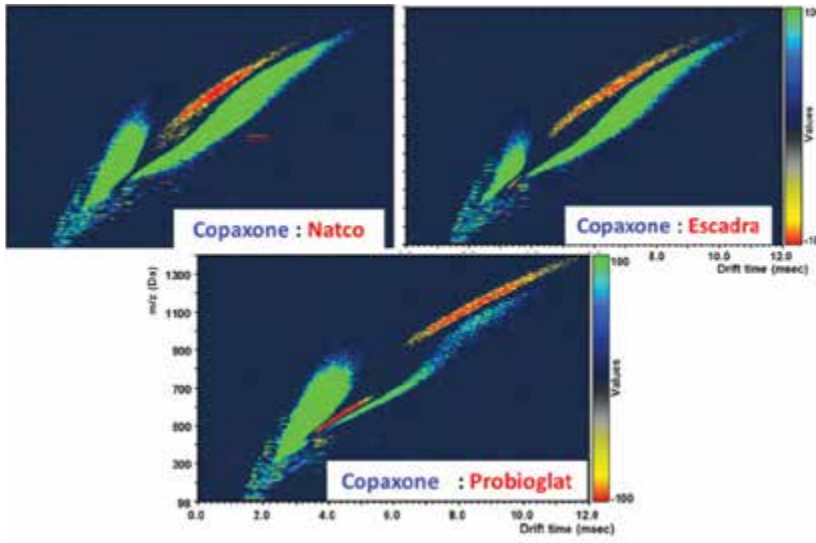

Figure 28.12 IMMS heat map: Copaxone® versus generics.

Because Copaxone® is an immunomodulator, a follow-on product characterized by different constituent population could have significant and unpredictable differences from Copaxone® in its immunological mechanisms, raising major safety and efficacy concerns. The potential risks associated with such follow-on products include increased immunogenicity, immunotoxicity, induction of additional autoimmune disorders, lack of efficacy,

and exacerbation of the MS disease processes. Moreover, because of the nature of both RRMS and Copaxone®, these risks may not develop for months or years and, once apparent, may be irreversible. *It is thus critical to ensure that any proposed follow-on product has a long-term immunogenicity profile that is comparable to Copaxone®'s before approval. This can only be done based upon data from appropriate clinical testing*.

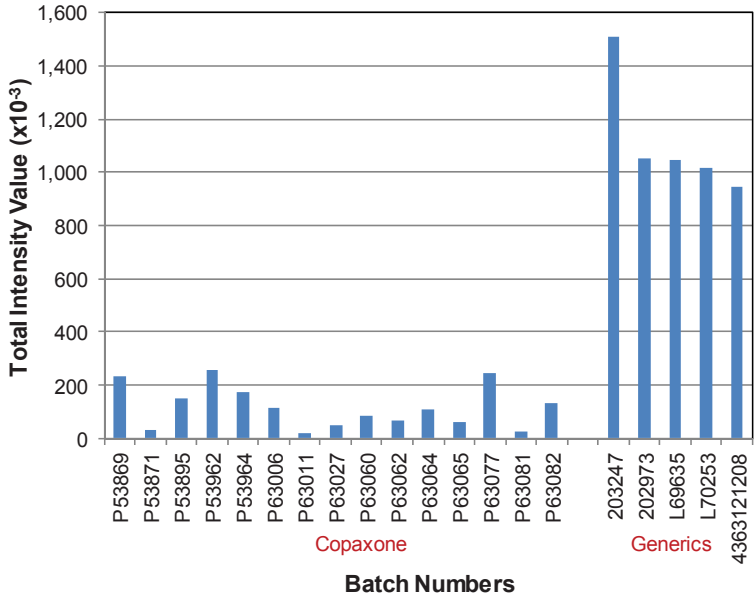

Figure 28.13 Total intensity values (TIV) obtained from comparison of heat maps of various Copaxone® batches and generics.

Glatiramer acetate is a highly immunogenic antigen-based therapy, and anti-glatiramer acetate antibodies are detected in all treated patients and animals [31]. These antibodies, however, do not neutralize biological activity or clinical efficacy and are not associated with local or systemic adverse effects in RRMS patients receiving chronic treatment [32–34]. In fact, some evidence suggests that anti-glatiramer acetate antibodies may enhance the biological activity of Copaxone® [35].

The anti-glatiramer acetate antibody profile (titers and isotypes) changes with repeated glatiramer acetate administration, resulting in a unique response profile over time. In RRMS patients,

anti-glatiramer acetate antibody levels peak between 3 and 6 months of treatment initiation, and then gradually decline [30]. Anti-glatiramer acetate antibodies are mainly of the IgG class. Studies conducted by various groups report that, initially, anti-glatiramer acetate IgG-2 antibodies predominate but with continued treatment, antibodies gradually shift to the IgG-1 isotype, which is consistent with the glatiramer acetate-reactive T cell shift from a Th1 to a Th2 phenotype [31]. After months of treatment, anti-glatiramer acetate IgG-4 antibodies become evident [34].

Evidence of anti-glatiramer acetate IgE antibodies is equivocal. Investigations by Teva had indicated that anti-glatiramer acetate IgE antibodies were infrequent and at low levels, not dose-related, and their detection was not associated with clinical adverse events or hypersensitivity reactions [36].

For proposed follow-on glatiramer acetate products, the risk of unwanted immunogenicity is significant. Even if a follow-on glatiramer acetate product has very similar properties to Copaxone® and is produced by a method that is basically similar to the Teva process, the efficacy, safety, and the immunogenicity of the follow-on product can still differ markedly from those of Copaxone® [37]. Several product-related factors can influence its immunogenicity profile. Potential immunogenic risks associated with antibodies to a proposed follow-on glatiramer acetate product include: (1) formation of immune-complexes; (2) development of drug neutralizing antibodies; (3) hypersensitivity reactions; and (4) induction of additional autoimmune disorders.

Anti-glatiramoid antibodies with a different repertoire than that of anti-glatiramer acetate antibodies could lead to formation of immune complexes. Immune-complex deposition in the glomeruli can cause kidney damage over time, becoming clinically evident only after long-term use of the drug [38–39]. In preclinical studies of chronic glatiramer acetate administration to rats and monkeys, there was marginal and only equivocal signs of glatiramer acetate and complement localization in the glomeruli [30]. Localization of immune complexes in the kidney was not found in a longer, 2-year bioassay [36]. Immune-complex disease, presenting as glomerulonephritis, was not seen in clinical studies of glatiramer acetate and was reported only once during extensive post-marketing experience with Copaxone® [36]. In contrast, in a toxicity study of chronic administration of the higher molecular weight

glatiramoid TV-5010 to rats, dose-dependent glomerulonephritis attributed to immune-complex deposition was observed at all tested TV-5010 dose levels [40]. This finding reinforces the importance of conducting chronic toxicity studies of proposed follow-on glatiramer acetate products, as longer-term adverse effects such as glomerulonephritis may not be apparent in short-term studies.

While anti-glatiramer acetate antibodies do not inhibit (but may enhance) the therapeutic activity of Copaxone® [31], slight variations in the primary, secondary, and tertiary structure of the active ingredient in a proposed follow-on product may result in the induction of anti-drug antibodies with neutralizing activity. Experience with different recombinant tumor necrosis factor alpha (TNF-α) antagonist drugs demonstrates the variety of antibody profiles possible for individual agents within the same drug class. Anti-infliximab antibody level is associated with decreased therapeutic response, whereas, anti-etanercept antibody level does not appear to influence drug effectiveness or adverse events [40]. The influence of anti-adalimumab antibodies on drug efficacy and adverse events is controversial; serum adalimumab concentrations can be dramatically lower in patients with anti-adalimumab antibodies, possibly because of increased drug clearance due to immune-complex formation [40].

Antibodies to many therapeutic peptides have been reported to induce hypersensitivity. NBI 5788, like glatiramer acetate, is an altered peptide ligand (APL) of myelin basic protein (MBP). NBI 5788 caused a relatively high rate (9%) of hypersensitivity reactions in MS patients in a phase II clinical trial, leading to early discontinuation of the study [41]. Hypersensitivity reactions can be immediate and are usually mediated by specific IgE antibodies, which trigger clinical signs and symptoms of variable severity, from benign urticaria to life-threatening bronchospasm, angioedema, or anaphylactic shock. Importantly, long-term follow-up of patients who received NBI 5788 showed that even short-term therapy with an APL can induce long-term persistence of altered responses to both the APL and the native protein/peptide [45].

Pathogenic antibodies and T cells can induce autoimmune reactions. When an epitope on an exogenous peptide or protein bears similarities to amino acid sequences on an endogenous protein in body constituents (molecular mimicry), anti-exogenous-

protein antibodies can neutralize the biological activity of the endogenous protein, leading to severe adverse events [43–44]. Glatiramer acetate originally was designed to mimic/resemble the encephalitogen, MBP [46] and preclinical and *in vitro* studies show that glatiramer acetate is cross-reactive with MBP at the cellular and humoral levels [31]. Despite this cross-reactivity, glatiramer acetate is not encephalitogenic (the encephalitogenic potential of Copaxone® batches is routinely tested by Teva). Rather than induce MBP-specific T cells, *in vitro* and *ex vivo* studies have shown the opposite: glatiramer acetate inhibits expansion and induces anergy of MBP-specific T cells [47–49]. Similarly, although monoclonal anti-glatiramer acetate antibodies can cross-react with MBP, polyclonal anti-glatiramer acetate antibodies from treated patients do not, and glatiramer acetate does not induce auto-reactive antibodies [31].

Since the active amino acid sequences in the glatiramer acetate mixture responsible for its efficacy are unknown, it is impossible to predict whether follow-on products will have the same efficacy as Copaxone®. They could have a weaker anti-inflammatory effect and/or enhance a pro-inflammatory environment, further exacerbating MS pathogenic processes. A reduced anti-inflammatory effect may provide less effective control of MS relapses, which would be difficult to detect in the post-marketing environment because MS relapses and progression of disability are not completely abolished by any MS therapy. On the other hand, creation or amplification of a pro-inflammatory environment would likely increase relapse rate and progression of disability or worse (e.g. have a profound encephalitogenic effect). Clinical trials of non-glatiramoid APLs of MBP in MS patients have shown that very strong responses to the APL can augment disease-related immune responses to the native antigen or produce intolerable immune-mediated secondary effects, including hypersensitivity reactions [41, 45].

Clinical experience with CGP77116, which, like Copaxone®, is an APL of MBP, exemplifies this risk. CGP77116 was associated with unexpected pro-inflammatory encephalitogenic effects, inducing brain inflammation that necessitated early termination of a study in RRMS patients [50]. In contrast to results of *in vitro* studies, CGP77116 *in vivo* caused substantial expansion of CGP77116-specific T cells that were cross-reactive with native MBP—a

necessary prerequisite for "bystander suppression." However, rather than stimulating an anti-inflammatory T-cell phenotype, the majority of activated CGP77116-specific T cells were of a pro-inflammatory (Th0/Th1) phenotype. Moreover, in some patients, worsening disease could be linked to CGP77116-induced expansion of MBP-specific T cells, which likely exacerbated pathogenic demyelination [50].

Finally, the potential for the development of cross-reactive neutralizing antibodies must be assessed before any regulatory authority approves any follow-on glatiramer acetate product intended to be used interchangeably with Copaxone®. Switching between two complex polypeptide products with subtle differences in structure and/or composition may increase the chance of cross-reactivity, a phenomenon that has been observed with interferon beta products [51]. Upon switching from Copaxone® to a follow-on product or using them interchangeably, antibodies formed against Copaxone® may neutralize the activity of the proposed generic product and *vice versa*. If this were the case, patients would be left without any effective treatment. Again, there is no evidence that progression of neurologic disability associated with untreated MS can ever be reversed.

Although Copaxone® is not currently regulated as a "biological product" in the US or Europe, it nevertheless shares many of the same characteristics as biological products, including a large and complex molecular structure and concomitantly complex interactions with the immune system. Consequently, the same scientific justifications for requiring data on the risks of switching "interchangeable" biological products, on a product-by-product basis, should apply equally to proposed generic glatiramer acetate products that are intended to be used interchangeably with Copaxone®. Indeed, because Copaxone® is intended to be used chronically, and because its effects on the immune system appear to evolve over time, there is no way to predict the effect of a "switch" or for that matter, multiple switches, on safety or effectiveness without conducting adequate and well-controlled clinical trials.

28.6 Conclusions and Future Prospects

The complexity of Copaxone® raises safety and effectiveness concerns that merit heightened vigilance with respect to the

approval of potentially interchangeable follow-on glatiramer acetate versions. Currently there is no defined mechanism for follow-on versions of NBCDs such as certain liposomal drugs, glatiramoids like Copaxone® and iron-sugar complexes. As discussed earlier, this is because the classical paradigm for abbreviated authorizations of conventional small molecules is not appropriate or valid because NBCDs lack a homo-molecular structure that cannot be fully quantitated or characterized via conventional physicochemical analytical tools and their composition and quality generally depends upon the manufacturing process and controls. As a result, originator NBCDs are not fully characterizable, some are not amenable to therapeutic bioequivalence testing, and comprehensive regulatory evaluation and guidelines for follow-on versions of NBCDs or nanosimilars are currently not developed. Consequently, they present a challenge to regulatory bodies like the FDA and EMA, manufacturers, physicians, and pharmacists.

Disclosures and Conflict of Interest

The authors declare that no writing assistance was utilized in the production of this chapter and the authors have received no payment for its preparation. Nothing contained herein is to be considered as the rendering of legal advice. Dr. Bawa is a scientific advisor to Teva Pharmaceutical Industries, Ltd. (Israel).

Corresponding Authors

Dr. Jill B. Conner
Teva Pharmaceutical Industries, Ltd.
Specialty Life Cycle Initiatives
11100 Nall Avenue
Overland Park, KS 66211, USA
Email: Jill.Conner@tevapharm.com

Dr. Raj Bawa
Bawa Biotech LLC
21005 Starflower Way
Ashburn, VA 20147, USA
Email: bawa@bawabiotech.com

About the Authors

Jill B. Conner joined Teva Pharmaceutical Industries, Ltd. in 2006 in the Medical Affairs department, where she was Senior Director of Medical Operations, before she took her current position as Director of Specialty Life Cycle Initiatives, Overland Park, Kansas, USA. She currently is responsible for the life cycle management for innovative products. Prior to working at Teva, she spent several years as a medical technologist before she focused her work in drug approval research with management positions in CRL-Medinet followed by director positions in Clinical Operations/ Project Management at United BioSource Corporation. Over the years, Dr. Conner has been involved with all aspects of clinical research including design and conduct of Phase I–IV clinical trials, retrospective database analyses, chart reviews, and investigator-initiated trials. Dr. Conner received her PhD in international health from TUI University, an MS in management from Baker University, and a BS in medical technology from the University of Missouri-Kansas City, USA.

Raj Bawa is president of Bawa Biotech LLC, a biotech/pharma consultancy and patent law firm based in Ashburn, VA, USA that he founded in 2002. He is an inventor, entrepreneur, professor and registered patent agent licensed to practice before the U.S. Patent & Trademark Office. Trained as a biochemist and microbiologist, he has been an active researcher for over two decades. Since 1999, he has held various positions at Rensselaer Polytechnic Institute in Troy, NY, where he is currently an adjunct professor of biological sciences and where he received his doctoral degree in three years (biophysics/biochemistry). Since 2004, he has been an adjunct professor of natural and applied sciences at NVCC in Annandale, VA. He is a scientific advisor to Teva Pharmaceutical Industries, Ltd., Israel. He has served as a principal investigator of National Cancer Institute SBIRs and reviewer for both the NIH and NSF. In the 1990s, Dr. Bawa held various positions at the US Patent & Trademark Office, including primary examiner for 6 years. He is a life member of Sigma Xi, co-chair of the Nanotech Committee of

the American Bar Association and serves on the global advisory council of the World Future Society. He has authored over 100 publications, co-edited four texts and serves on the editorial boards of 17 peer-reviewed journals, including serving as a Special Associate Editor of *Nanomedicine* (Elsevier) and an Editor-in-Chief of the *Journal of Interdisciplinary Nanomedicine* (Wiley).

J. Michael Nicholas received his PhD in pharmacology from the University of Tennessee Center for Health Sciences. After postdoctoral work at the University of Mississippi in Jackson he joined Mylan Pharmaceuticals in Morgantown, WV, as Director of Scientific Affairs. While at Mylan, he later served as Director of Scientific and Regulatory Affairs and was involved with the development and approval of both generic and branded products. Following Mylan, he accepted a position with Marion Laboratories in Kansas City in the Regulatory Affairs department. Over the years, Dr. Nicholas has been involved with all aspects of regulatory matters including product development and approval. While at Marion Laboratories, Marion Merrell Dow and Hoechst Marion Roussel, Dr. Nicholas served as the Director of Product Approval within the Regulatory Affairs Department and directed the submission of INDs, NDAs, and their subsequent approval. Prior to his current position, he was vice president, US Regulatory Affairs and Compliance, Marketed Products for Aventis Pharmaceuticals and was responsible for regulatory matters for approved products. Currently, Dr. Nicholas is vice-president of Specialty Life Cycle Initiatives for Teva Brand Pharmaceuticals, Overland Park, Kansas, USA and is responsible for product life cycle planning.

Vera Weinstein received her PhD in synthetic organic chemistry from the Hebrew University of Jerusalem, Israel (HUJI). After several years at HUJI as a senior lecturer, she joined Portman Pharmaceutical Industries as chief research chemist and was involved with the development of branded products. In 1996, Dr. Weinstein accepted a position with Teva as an Analytical Team Leader, and later as CMC Program Leader in Innovative R&D. At her present position,

Dr. Weinstein is Senior Director, Scientific Affairs, Discovery and Product Development, Global R&D, Teva Pharmaceutical Industries, Ltd., Israel.

References

1 (a) Bawa, R., Audette, G., Rubinstein, I., eds. (2016). *Handbook of Clinical Nanomedicine: Nanoparticles, Imaging, Therapy, and Clinical Applications,* Pan Stanford Publishing, Singapore.

(b) Bawa, R., ed.; Audette, G. F., Reese, B. E., astt. eds. (2016). *Handbook of Clinical Nanomedicine: Law, Business, Regulation, Safety, and Risk*, Pan Stanford Publishing, Singapore.

2. Torchilin, V., ed. (2014). *Handbook of Nanobiomedical Research: Fundamentals, Applications and Recent Developments,* World Scientific Publishing Co., Hackensack, New Jersey.
3. Bawa, R. (2016). What's in a name? Defining "nano" in the context of drug delivery. In: Bawa, R., Audette, G. and Rubinstein, I. eds. *Handbook of Clinical Nanomedicine: Nanoparticles, Imaging, Therapy, and Clinical Applications*, Chapter 6, Pan Stanford Publishing, Singapore.
4. Stein, R. A. (2014). Nanotechnology: Is the magic bullet becoming reality? *Genetic Engineering & Biotechnology News.* Available at: http://www.genengnews.com/insight-and-intelligence/nanotechnology-is-the-magic-bullet-becoming-reality/77900016/ (accessed on October 1, 2015).
5. Fischer, S. (2014). Regulating nanomedicine. *IEEE Pulse*. Available at: http://pulse.embs.org/march-2014/regulating-nanomedicine/ (accessed on October 2, 2015).
6. Davenport, M. (2014). Closing the gap for generic nanomedicines. *Chemical & Engineering News*, **92**(45), 10–13. Available at: http://cen.acs.org/articles/92/i45/Closing-Gap-Generic-Nanomedicines.html (accessed on October 1, 2015).
7. Bawa, R., Melethil, S., Simmons, W. J., Harris, D. (2008). Nanopharmaceuticals: Patenting issues and FDA regulatory challenges. *SciTech Lawyer,* **5**(2), 10–15.
8. Bawa, R. (2013). FDA and nanotech: Baby steps lead to regulatory uncertainty. In: Bagchi, D., et al., eds. *Bionanotechnology: A Revolution in Biomedical Sciences and Human Health.* Wiley Blackwell, UK, pp. 720–732.

9. Bawa, R. (2007). Nanotechnology patent proliferation and the crisis at the US Patent Office. *Albany Law J. Sci. Technol*., **17**(3), 699–735.
10. Shekunov, B. (2005). Nanoparticle technology for drug delivery: From nanoparticles to cutting-edge delivery strategies. *I. Drugs*, **8**(5), 399.
11. Sung, J. C., Pulliam, B. L., Edwards, D. A. (2007). Nanoparticles for drug delivery to the lungs. *Trends Biotechnol.,* **25**(12), 563–570.
12. Cho, K., Wang, X., Nie, S., Chen, Z. G., Shin, D. M. (2008). Therapeutic nanoparticles for drug delivery in cancer. *Clin. Cancer Res.,* **14**(5), 1310.
13. Brigger, I., Dubernet, C., Couvreur, P. (2002). Nanoparticles in cancer therapy and diagnosis. *Adv. Drug Deliv. Rev.,* **54**(5), 631–651.
14. Tiwari, S. B., Amiji, M. M. (2006). A review of nanocarrier-based CNS delivery systems. *Curr. Drug Deliv.,* **3**(2), 219–232.
15. Kaur, I. P., Bhandari, R., Bhandari, S., Kakkar, V. (2008). Potential of solid lipid nanoparticles in brain targeting. *J. Control. Release,* **127**(2), 97–109.
16. Davis, M. E. (2008). Nanoparticle therapeutics: An emerging treatment modality for cancer. *Nat. Rev. Drug Discov.,* **7**(9), 771–782.
17. Mansour, H. M., Rhee, Y. S., Wu, X. (2009). Nanomedicine in pulmonary delivery. *Int. J. Nanomed.,* **4**, 299–319.
18. Wissing, S., Kayser, O., Muller, R. (2004). Solid lipid nanoparticles for parenteral drug delivery. *Adv. Drug Deliv. Rev.,* **56**(9), 1257–1272.
19. De Campos, A. M., Diebold, Y., Carvalho, E. L. S., Sanchez, A., Jose Alonso, M. (2004). Chitosan nanoparticles as new ocular drug delivery systems: *In vitro* stability, *in vivo* fate, and cellular toxicity. *Pharm. Res.,* **21**(5), 803–810.
20. Nanomedicine. ESF–European Medical Research Councils forward look report. Available at: http://www.esf.org/fileadmin/Public_documents/Publications/Nanomedicine.pdf (accessed on October 2, 2015).
21. NIH roadmap for medical research. National Institutes of Health. Available at: http://pubs.niaaa.nih.gov/publications/arh311/12-13.pdf (accessed on October 2, 2015).
22. Park, K. (2007). Nanotechnology: What it can do for drug delivery. *J. Control. Release,* **120**(1–2), 1.
23. Koo, O. M., Rubinstein, I., Onyuksel, H. (2005). Role of nanotechnology in targeted drug delivery and imaging: A concise review. *Nanomedicine,* **1**(3), 193–212.

24. Jain, K. (2005). Nanotechnology-based drug delivery for cancer. *Technol. Cancer Res. Treat.,* **4**(4), 407.
25. Bawa, R. (2008). Nanoparticle-based therapeutics in humans: A survey. *Nanotechnol. Law Bus.,* **5**(2), 135–155.
26. Mansour, H. M., Park, C-W., Bawa, R. (2016). Design and development of approved nanopharmaceutical products. In: Bawa, R., Audette, G., Rubinstein, I., eds. *Handbook of Clinical Nanomedicine: Nanoparticles, Imaging, Therapy, and Clinical Applications,* Chapter 9, Pan Stanford Publishing, Singapore.
27. Bawa, R. (2010). Nanopharmaceuticals. *Eur. J. Nanomed.,* **3**(1), 34–39.
28. Yoncheva, K., Guembe, L., Campanero, M., Irache, J. (2007). Evaluation of bioadhesive potential and intestinal transport of pegylated poly (anhydride) nanoparticles. *Int. J. Pharm.,* **334**(1–2), 156–165.
29. Desai, M. P., Labhasetwar, V., Amidon, G. L., Levy, R. J. (1996). Gastrointestinal uptake of biodegradable microparticles: Effect of particle size. *Pharm. Res.,* **13**(12), 1838–1845.
30. Copaxone® prescribing information. Available at: https://www.copaxone.com/Resources/pdfs/PrescribingInformation.pdf (accessed on October 2, 2015).
31. Brenner, T., Arnon, R., Sela M., et al. (2001). Humoral and cellular immune responses to copolymer 1 in multiple sclerosis patients treated with Copaxone®. *J. Neuroimmunol.,* **115**, 152–160.
32. Teitelbaum, D., Brenner, T., Abramsky, O., et al. (2003). Antibodies to glatiramer acetate do not interfere with its biological functions and therapeutic efficacy. *Mult. Scler.,* **9**, 592–599.
33. Karussis, D., Teitelbaum, D., Sicsic, C., et al. (2010). Long-term treatment of multiple sclerosis with glatiramer acetate: Natural history of the subtypes of anti-glatiramer acetate antibodies and their correlation with clinical efficacy. *J. Neuroimmunol.,* **220**, 125–130.
34. Farina, C., Vargas, V., Heydari, N., et al. (2002). Treatment with glatiramer acetate induces specific IgG4 antibodies in multiple sclerosis patients. *J. Neuroimmunol.,* **123**, 188–192.
35. Ure, D. R., Rodriguez, M. (2002). Polyreactive antibodies to glatiramer acetate promote myelin repair in murine model of demyelinating disease. *FASEB,* **16**, 1260–1262.
36. Data on File. Teva Pharmaceutical Industries, Ltd., 2012.
37. Varkony, H., Weinstein, V., Klinger, E., et al. (2009). The glatiramoid class of immunomodulator drugs. *Expert Opin. Pharmacother.,* **10**(4), 657–668.

38. Chen, M., Daha, M. R., Kallenberg, C. G. (2010). The complement system in systemic autoimmune disease. *J. Autoimmun.,* **34**, J276–J286.

39. Nangaku, M., Couser, W. G. (2005). Mechanisms of immune-deposit formation and the mediation of immune renal injury. *Clin. Exp. Nephrol.,* **9**, 183–191.

40. Aikawa, N. E., de Carvalho, J. F., Almeida Silva, C. A., et al. (2010). Immunogenicity of anti-TNF-alpha agents in autoimmune diseases. *Clin. Rev. Allergy Immunol.,* **38**, 82–89.

41. Kappos, L., Comi, G., Panitch, H., et al. (2000). Induction of a non-encephalitogenic type 2 T helper-cell autoimmune response in multiple sclerosis after administration of an altered peptide ligand in a placebo-controlled, randomized phase II trial. *Nat. Med.,* **6**, 1176–1182.

42. US Food and Drug Administration. Fact Sheet Nanotechnology. Available at: http://www.fda.gov/ScienceResearch/SpecialTopics/Nanotechnology/ucm402230.htm (accessed on October 4, 2015).

43. Kromminga, A., Schellekens, H. (2005). Antibodies against erythropoietin and other protein-based therapeutics: An overview. *Ann. N. Y. Acad. Sci.,* **1050**, 257–265.

44. Li, J., Yang, C., Xia, Y., et al. (2001). Thrombocytopenia caused by the development of antibodies to thrombopoietin. *Blood,* **98**, 3241–3248.

45. Kim, H. J., Antel, J. P., Duquette, P., et al. (2002). Persistence of immune responses to altered and native myelin antigens in patients with multiple sclerosis treated with altered peptide ligand. *Clin. Immunol.,* **104**, 105–114.

46. Johnson, K. P. (2010). Glatiramer acetate and the glatiramoid class of immunomodulator drugs in multiple sclerosis: An update. *Expert Opin. Drug Metab. Toxicol.,* **6**, 643–660.

47. Neuhaus, O., Farina, C., Yassouridis, A., et al. (2000). Multiple sclerosis: Comparison of copolymer-1-reactive T cell lines from treated and untreated subjects reveals cytokine shift from T helper 1 to T helper 2 cells. *Proc. Natl. Acad. Sci.,* **97**, 7452–7457.

48. Dabbert, D., Rosner, S., Kramer, M., et al. (2000). Glatiramer acetate (copolymer-1)-specific, human 5T cell lines: Cytokine profile and suppression of T cell lines reactive against myelin basic protein. *Neurosc. Lett.,* **289**, 205–208.

49. Teitelbaum, D., Aharoni, R., Arnon, R., et al. (1988). Specific inhibition of the T-cell response to myelin basic protein by the synthetic copolymer Cop 1. *Proc. Natl. Acad. Sci.,* **85**, 9724–9728.

50. Bielekova, B., Goodwin, B., Richert, N., et al. (2000). Encephalitogenic potential of the myelin basic protein peptide (amino acids 83–99) in multiple sclerosis: Results of a phase II clinical trial with an altered peptide ligand. *Nat. Med.,* **6**, 1167–1175.
51. Bertolotto, A., Malucchi, S., Milano E., et al. (2000). Interferon beta neutralizing antibodies in multiple sclerosis: Neutralizing activity and cross-reactivity with three different preparations. *Immunopharmacology,* **48**, 95–100.
52. Duncan, R., Gaspar, R. (2011). Nanomedicine(s) under the microscope. *Mol. Pharmacol.,* **8**(6), 2101–2104.
53. Krull, I., Cohen, S. (2009). The complexity of glatiramer acetate and the limits of current multidimensional analytical methodologies in the attempt to characterize the product. Letter in reference to Citizen Petition FDA-2008-P-0529 to the Dockets Management Brand, FDA, January 16, 2009.
54. Letter to David Zuchero, et al. FDA-2004-P-0494, p. 4, no. 13 (March 31, 2011).
55. Dorland's Medical Dictionary for Health Consumers. Definition of colloid. Available at: http://medical-dictionary.thefreedictionary.com/colloid (accessed on June 4, 2015).
56. Atkins, P., De Paula, J. (2006). *Physical Chemistry*, 8th ed. Freeman, W. H., and Company, New York, pp. 682.
57. Yang, Y., Shah, R. B., Gaustino, P. J., Raw, A., et al. (2010). Thermodynamic stability assessment of a colloidal iron drug product: Sodium ferric gluconate. *J. Pharm. Sci.,* **99**(1), 142–153.
58. Danino, D., Talmon, Y. (2005). In: Weiss, R. G., Terech, P., eds. *Molecular Gels: Materials with Self-Assembled Fibrillar Networks*, Springer, The Netherlands, pp. 251–272.
59. Jayaraman, M. S., Bharali, D. J., Sudha, T., Mousa, S. A. (2012). Nano chitosan peptide as a potential therapeutic carrier for retinal delivery to treat age-related macular degeneration. *Mol. Vis.,* **18**, 2300–2308.
60. Noseworthy, J. H., Lucchinetti, C., Rodriguez, M., et al. (2000). Multiple sclerosis. *N. Engl. J. Med.,* **343**, 938–952.
61. National Multiple Sclerosis Society. Who gets MS. Available at: http://www.nationalmssociety.org/What-is-MS/Who-Gets-MS (accessed on June 8, 2015).
62. National Multiple Sclerosis Society. MS Symptoms. Available at: http://www.nationalmssociety.org/Symptoms-Diagnosis/MS-Symptoms (accessed on June 8, 2015).

63. National Multiple Sclerosis Society. What causes MS? Available at: http://www.nationalmssociety.org/What-is-MS/What-Causes-MS (accessed on June 8, 2015).

64. Sela, M. (1998). Poly(alpha-amino acids)–From a better understanding of immune phenomena to a drug against multiple sclerosis. *Acta Polymer.,* **49**, 523.

65. Nicholas, J. M. (2012). Complex drugs and biologics: Scientific and regulatory challenges for follow-on products. *Drug Inf. J.,* **46**(2), 197–206.

66. Mühlebach, S., Vulto, A., de Vlieger, J. S. B., Weinstein, V., Flühmann, B., Shah, V. P. (2013). The authorization of non-biological complex drugs (NBCDs) follow-on versions: Specific regulatory and inter change ability rules ahead? *Gen. Biosimilars Init. J.,* **2**(4), 204–207.

67. Schellekens, H., Klinger, E., Muhlebach, S., et al. (2011). The therapeutic equivalence of complex drugs. *Regul. Toxicol. Pharmacol.,* **59**, 176–183.

68. Schellekens, H., Stegemann, S., Weinstein, V., et al. (2013). How to regulate nonbiological complex drugs (NBCD) and their follow-on versions: Points to consider. *AAPS J.,* **16**(1), 15–21.

69. (a) European Medicines Agency. Guideline on similar biological medicinal products. London, UK. Available at: http://www.ema.europa.eu/docs/en_GB/document_library/Scientific_guideline/2013/05/WC500142978.pdf (accessed on June 4, 2015).

    (b) European Medicines Agency. Guideline on similar biological medicinal products. London, UK. Available at: http://www.ema.europa.eu/docs/en_GB/document_library/Scientific_guideline/2014/10/WC500176768.pdf (accessed on June 4, 2015).

70. (a) US Food and Drug Administration. (2012). Guidelines for industry. Scientific considerations for demonstrating biosimilarity to a reference product. Available at: http://www.fda.gov/downloads/Drugs/GuidanceComplianceRegulatoryInformation/Guidances/UCM291128.pdf (accessed on June 8, 2015).

    (b) US Food and Drug Administration. (2012). Guidelines for industry. Scientific considerations for demonstrating biosimilarity to a reference product. Available at: http://www.fda.gov/downloads/drugs/guidancecomplianceregulatoryinformation/guidances/ucm291128.pdf (accessed on June 8, 2015).

71. Desai, N. (2012). Challenges in development of nanoparticle-based therapeutics. *AAPS J.,* **14**(2), 282–295.

72. Ehmann, F., Sakai-Kato, K., Duncan, R., et al. (2013). Next-generation nanomedicines and nanosimilars: EU regulators' initiatives relating to the development and evaluation of nanosimilars. *Nanomedicine,* **8**(5), 849–856.

73. Holloway, C., Mueller-Berghaus, J., Lima, B. S., Lee, S. L., Wyatt, J. S., et al. (2012). Scientific considerations for complex drugs in light of established and emerging regulatory guidance. *Ann. N. Y. Acad. Sci.,* **1276**, 26–36.

74. Tinkle, S., McNeil, S. E., Mühlebach, S., Bawa, R., Borchard. G., et al. (2014). Nanomedicines: Addressing the scientific and regulatory gap. *Ann. N. Y. Acad. Sci.,* **1313**, 35–56.

75. Berkowitz, S. A., Engen, J. R., Mazzeo, J. R., Jones, G. B. (2012). Analytical tools for characterizing biopharmaceuticals and the implications for biosimilars. *Nat. Rev. Drug Discov.,* **11**, 527–540.

76. Crommelin, D. J. A., de Vlieger, J. S. B. (2015). *Non-Biologic Complex Drugs: The Science and the Regulatory Landscape*, Springer, Switzerland.

77. Weinstein, V., Schwartz, R., Grossman, I., Zeskind, B., and Nicholas, J. M. (2015). Glatiramoids. In: Crommelin, D. J. A., de Vlieger, J. S. B., eds. *Non-Biologic Complex Drugs: The Science and the Regulatory Landscape*, Springer, Switzerland, pages 107–148.

Chapter 29

Doxil®: The First FDA-Approved Nanodrug—From an Idea to a Product (January 2015 Update)

Yechezkel Barenholz, PhD

Laboratory of Membrane and Liposome Research,
Department of Biochemistry and Molecular Biology,
Institute of Medical Research Israel-Canada,
The Hebrew University-Hadassah Medical School, Jerusalem, Israel

Keywords: Doxil®, liposomes, doxorubicin, delivery, anticancer, biodistribution, therapeutic efficacy, pegylated nano-liposomes, drug release rate, pharmacokinetics, tumor targeting, clinical trials, drug development

Doxil® Understanding Is Still Ongoing

Research on Doxil® development was started in 1987. The first provisional patents were filed in 1987/1988 and the FDA approved it in 1995. Doxil has been in clinical use since 1996. Despite the long time (~28 years) that has passed and the extensive experience with its use, new information on its physicochemical and biological features is coming out. It seems that Doxil still keeps some secrets to be revealed. The new data obtained in recent years already enable a better understanding of Doxil's mechanism

Handbook of Clinical Nanomedicine: Nanoparticles, Imaging, Therapy, and Clinical Applications
Edited by Raj Bawa, Gerald F. Audette, and Israel Rubinstein

ISBN 978-981-4669-20-7 (Hardcover), 978-981-4669-21-4 (eBook)
www.panstanford.com

of action (MoA) and suggest combinations of Doxil with other drugs and/or biologicals, as well as use of other means that may improve its therapeutic index by improving its efficacy and/or reducing its side effects.

29.1 Historical Perspective

I want to start this review with my recollection of a very early and cool morning in November 1995 that I will never forget. Most of the Liposome Technology Inc. (LTI) employees and I were in the big noisy storage area of LTI at 1050 Hamilton Court, Menlo Park, CA, with a lot of food, drinks, and many discussions, waiting nervously to see online the FDA's Oncologic Drug Advisory Committee (ODAC) meeting in Washington, DC, at which a recommendation to the FDA to approve or disapprove **Doxil®** for Kaposi's sarcoma indication should be given. ODAC's session started at 08.00 AM Eastern time (05.00 AM California time). The happy end of that morning was that Doxil's approval was recommended. Doxil is actually an abbreviation of the words "**DOX**orubicin **I**n **L**iposomes." Doxil® is sold in Europe as Caelyx®.

Doxil vials (Fig. 29.1) were distributed for clinical use by Sequus Pharmaceuticals (previously LTI) as early as 1996. A cryo-transmission electron micrograph (cryo-TEM) of a Doxil/Caelyx dispersion is described in Fig. 29.2.

Direct work on Doxil development was initiated in Israel and the USA 7.5 years earlier; however, the history of Doxil goes back to 1979 when Alberto Gabizon and I started collaborating on the development of liposomes as a drug delivery system of cytotoxic drugs for the treatment of cancer. This idea stems from Paul Ehrlich's (1906) classical "magic bullet" working hypothesis that by targeting the desired drug to the diseased tissue the "therapeutic index" (ratio) and "the protective ratio" of the drug (for definitions see Wikipedia) should be significantly increased by either improving therapeutic efficacy or lowering toxicity, and preferably by a combination of both. The overall effect is improvement of drug therapeutic effects.

Liposomes were proposed as a good option for a drug delivery system (DDS) by Alec Bangham already in the late 1960s, soon

after he described liposomes as an excellent model system for biological membranes in 1964 (for historical perspectives see Barenholz, 1992; Bangham, 1993; Lasic, 1996).

Figure 29.1 Doxil vial as sold by Sequus Pharmaceuticals (1996).

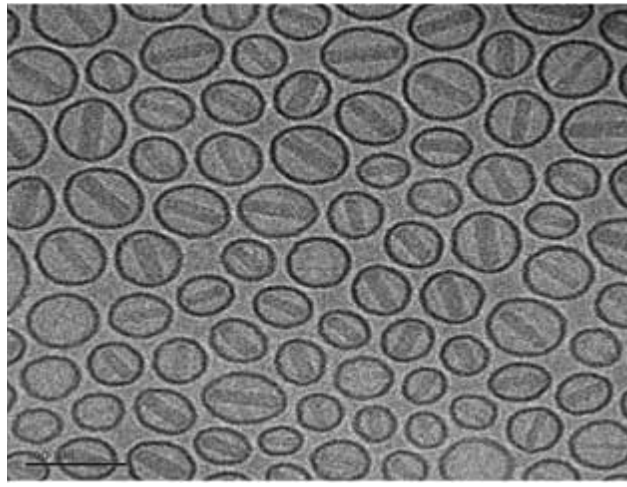

Figure 29.2 Cryo-TEM of Caelyx batch 101371803. Scale bar: 100 nm.

However, in 1979, 15 years after liposomes' first description by Bangham (rev. in Bangham, 1993), the use of liposomes as a drug delivery system was still in its infancy. When, on January 4,

2011, I searched in Delphion, which covers all patents and patent applications (granted and pending), I found that until January 1979 liposomes were mentioned anywhere in the text of patents (including background) only 170 times, while in the claims (protected), liposomes were referred to even less, only 33 times. In April 2011, when I wrote the original review, the situation was much different. Anywhere in the patents' text (including background), liposomes were mentioned 224,836 times and in the patents' claims (protected) liposomes were referred to 19,210 times. These numbers kept increasing and on December 14, 2014, these numbers further reached the level of 281,256 referrals in patent body and 27,980 in patent claims. In the last 5 years, the rate of increase was much reduced as the liposome patent arena became very crowded and therefore it became very difficult to get liposome patent applications approved in the USA, Europe, and elsewhere.

Similar differences exist regarding scientific publications: Fewer than 1200 publications that involved liposomes appeared in January 1979, while today more than 0.1% of all scientific papers published in life and health sciences involve liposomes. On April 4, 2011, Doxil had more than 171,000 Google citations, while on December 14, 2014, it had more than 296,000 citations.

Despite the poor and minimal information available on liposomes as a DDS in 1979, Gabizon and I selected liposomes as our preferred DDS. Our decision was based on the common knowledge at that time, which can be summarized as follows:

- Liposomes can encapsulate both hydrophilic and amphipathic low- and high-molecular-weight active pharmaceutical ingredients (APIs) as well as biologicals (which include peptides, proteins, and nucleic acids;
- The API is "encapsulated" in, and/or associated with, the liposome as is, namely, in its native form without the need of covalent binding or other chemical modification;
- For hydrophilic and amphipathic active pharmaceutical ingredients, encapsulation is "passive" in nature, which means it is done during the process of liposome fabrication. For amphipathic/hydrophobic drugs/agents, encapsulation is determined mainly by the interaction of the drug/agent with the liposomal membrane, which can be described

in terms of liposome membrane to medium partition coefficients (Barenholz and Cohen, 1995; Barenholz, 2001, 2003; Kedar et al., 1994a, 1994b; Grant et al., 2001; Joseph et al., 2006; Even-Or et al., 2010). For water-soluble drugs, the encapsulation is determined by two main parameters: drug/agent degree of solubility in the lipid hydration medium and the liposome trapped aqueous volume (Barenholz, 2001, 2003; Grant et al., 2001). This means that for most applications of water-soluble drugs that require nano-liposomes [in the 1970s and the 1980s these were referred to as small unilamellar vesicles (SUV)], the passive loading approaches are a poor option, as the product will have a drug-to-lipid ratio that is too low for achieving the therapeutic drug concentration required for human use. This is even more so for drugs/agents having poor aqueous solubility. For example, the therapeutic dose of doxorubicin is ~50 mg/m^2 (~100 mg per each administration). The latter was a major obstacle for the development of drugs based on nano-liposomes, which today we know are the preferred ones for systemic application of liposome-based drugs;

- The pharmacokinetics (PK) and biodistribution (BD) of the drug/agent encapsulated is modified to a large extent by being encapsulated in liposomes, especially to achieve high accumulation in the RES and to avoid many other tissues (e.g., heart). This can be controlled to some extent by the physicochemical properties of the liposomes [size distribution, electrical charge, and level of rigidity (fluidity)];
- The physicochemical properties can be controlled by liposome lipid composition and method of liposome preparation;
- Phospholipids, glycolipids, and sterols, which are the main building blocks of liposomes, are of natural sources, or are semi-synthetic or fully synthetic, having natural stereochemistry, and therefore believed to be biocompatible.

In the 1980s the overall expectation of liposomes as a broad spectrum drug delivery system was low. This was summarized in an almost "lethal" (to the medical application of liposomes) *Cancer Research* paper by Poste et al. (1982). This 1982 important paper claimed the following:

> *"Functional and ultrastructural studies of liposomes injected i.v. into inbred C57BL/6N mice were performed to determine whether free liposomes can traverse capillaries. In the liver and spleen, organs with discontinuous (sinusoidal) capillaries, ultrastructural and cell fractionation studies revealed that small (300 to 800 Å diameter), sonicated, unilamellar liposomes were more efficient in penetrating liver sinusoids to interact with hepatocytes than were large (0.5 to 10 μm) multilamellar liposomes. Ultrastructural studies of the behavior of liposomes in the continuous capillaries of the lungs revealed that circulating phagocytic cells engulf the liposomes in the capillaries. Transcapillary migration of free liposomes was not observed. We conclude that free liposomes are unable to extravasate to reach the alveoli for subsequent engulfment by alveolar macrophages. Instead, liposomes in the lung capillaries are engulfed by circulating blood phagocytes which subsequently migrate to the alveoli to become alveolar macrophages. Experiments on the recruitment of blood monocytes into the lungs subjected to whole- or partial-body X-radiation confirmed that transfer of i.v.-injected liposomes to the alveolar compartment was mediated by blood monocytes. The inability of liposomes to escape from continuous capillaries and their rapid uptake by circulating and fixed phagocytic cells calls into question the feasibility of using liposomes to "target" drugs to cells in extravascular tissues."*

This and Poste's 1983 publication were "catastrophic" to the medical application of liposomes as it led the scientific community as well as the major grant agencies, the Pharma industry, and the venture capital community to lose interest in this field. It took 10 more years for the field to recover and gain back some trust that enabled the development of more than 12 FDA-approved liposomal drugs from 1995 to the present.

Poste's papers were published when we were in the middle of the development of our liposomal doxorubicin formulation and set the conditions for our selection of liver tumors as the preferred tumor choice. Only very little information and help from very few relevant published papers were available to us in 1979, as exemplified by Gregoriadis et al. (1974) and Richardson et al. (1979). A few other groups all over the world that were "fed" by the same available scientific information were working in parallel to us on the development of similar systems (see below).

As described above, the 1980s were problematic for the field of liposome medical applications. Nevertheless, it was an exciting time for the development of liposomal drugs as three startup companies were founded in the US alone: Vestar at Pasadena, California; The Liposome Company (TLC) at Princeton, New Jersey; and Liposome Technology Inc. (LTI) at Menlo Park, California. None of them survived. Although support money was short, these companies succeeded to initiate, and later in the 1990s, when money became more available, to develop most of the FDA-approved liposomal drugs. Interestingly, all three companies selected and had different intellectual property (I.P.) on liposomal anthracyclines as one of their leading products [Doxil® of LTI (now sold by Johnson & Johnson, DaunoXome of Vestar (now sold by Diatos), and Myocet of TLC (now sold by Zenous Pharma Sopherion Therapeutics)]. This clearly demonstrates that these three startup companies worked along similar lines of thought.

29.2 First-Generation Liposomal Doxorubicin: Liver-Directed Liposomal Doxorubicin

29.2.1 Background

The common knowledge available in 1980 on liposomes as drug carriers (see above) suggests that liposomes should be mainly useful to treat diseases that are localized at RES organs, which are enriched with MPS activities. Therefore, we selected liver hepatocellular carcinoma (HCC) as the tumor target of choice. This tumor type, although not a major disease in the Western world, is the most abundant tumor in the Far East, especially Japan and in China.

Our idea was that the liposomes loaded with the drug will be cleared fast from the circulation by the RES system and will be taken up efficiently by the phagocytic cells, mainly in the liver. There the liposomes were expected to reach and be processed at the phagosomes and endosomes followed by drug release to the cytoplasm. From there it can be further released in the liver and to the circulation and become available to kill cancer cells that reside in the liver in proximity to the RES cells. The optimal chemical stability of doxorubicin at low endosome/lysosome pH and the

fact that the doxorubicin is an amphipathic weak base are supportive of the MPS cells acting as a doxorubicin depot. In effect, the proposed MoA is that the liposomes loaded with the anticancer drug will deliver the drug to the MPS cells that serve as a drug depot for liver tumor treatment.

A high dose of doxorubicin (50 mg/m^2) is needed to achieve therapeutic efficacy. The physicochemical properties and especially the low doxorubicin solubility are unfavorable to achieve sufficient passive loading into a 100 nm liposome's intra-liposome aqueous phase. Therefore, larger liposomes have to be used and drug encapsulation has to be improved by getting the drug to be membrane associated.

At that time, we (Gabizon and Barenholz) were not the only group that selected doxorubicin (or anthracyclines) as the anticancer drug of choice for development of liposome-based cancer treatment. Other scientists in academia worked along similar considerations, which were based on the same common knowledge (Rahman et al., 1980, 1985, 1986a, 1986b; Forssen and Tokes, 1979, 1981, 1983; Olson et al., 1982; Van Hoesel et al., 1984; Mayhew et al., 1983, 1987; Mayhew and Rustum, 1985; Storm et al., 1987, and others).

Most liposomal doxorubicin formulations that were developed during the 1980s took advantage of doxorubicin's being an amphipathic weak base that can associate efficiently with negatively charged membrane lipids. Doxorubicin's mannose primary amine-derived positive charge enables doxorubicin association with negatively charged phospholipids (such as PS, PA, PG, DPG, and gangliosides), while its hydrophobic rings support doxorubicin partition into the liposome lipid bilayer (Forssen and Tokes, 1979, 1981; Mayhew et al., 1983; Rahman et al., 1985; Storm et al., 1987). The working hypothesis behind all these studies called for the use of liposomes that are larger than the nano-scale of Doxil, as these larger negatively charged liposomes can better and faster be taken up by the RES system, and be processed there to release the active drug. Not less important is that liposomes of such size may carry high enough drug to reach therapeutic levels for human treatment.

We selected doxorubicin as our drug of choice based on medical, scientific, and practical considerations. Doxorubicin, like many other anthracyclines, is produced by one of the *Streptomyces*

bacteria, (*Streptomyces peucetius* var. caesius). It was discovered in the 1960s near the Adriatic Sea, which explains the source of the brand name Adriamycin. It showed significant anticancer activity (Blum and Carter, 1974; McKelvey et al., 1976; Gundersen et al., 1986). Doxorubicin acts on the nucleic acids of dividing cells by two main mechanisms of action. First, it inhibits DNA and RNA synthesis by intercalating between base pairs of the DNA/RNA strands, thus preventing the replication of rapidly growing cancer cells. This mechanism is based on the chemistry and physics of the doxorubicin molecule (its positively charged mannose amine, which binds efficiently to negatively charged nucleic acid phosphate di-ester groups, and the excellent fit of the drug's anthroquinone planar ring structure for intercalation into the double-stranded DNA. Altogether, these structural features lead to high affinity of the drug to double-stranded nucleic acids in a way that is not metabolism dependent. Second, doxorubicin inhibits topoisomerase-II enzyme, preventing the relaxing of super-coiled DNA and thus blocking DNA transcription and replication. Its third major biological effect is that it forms iron-mediated free radicals that cause oxidative damage to DNA, proteins, and cell membrane lipids. Especially sensitive are the mitochondrial membranes due to their high level of the negatively charged phospholipid cardiolipin, for which doxorubicin has a high affinity. This property was the basis of Rahman and coworkers' (1980, 1985, 1986a, 1986b) selection of cardiolipin as their formulation's negatively charged lipid. This oxidative damaging effect is now considered one of the main reasons for doxorubicin's toxicities and side effects, especially the cardio-toxicity, which determines the allowed cumulative dose to be <550 mg/m^2. The heart muscle is enriched in mitochondria (and therefore in cardiolipin). This explains in part the drug's cardio-toxicity. Routine treatment by doxorubicin is given intravenously using a relatively high drug dose, in the range of 10 to 50 mg/m^2 (rev. in Weiss, 1992; Skeel, 1999; Minotti et al., 2004; Takimoto and Calvo, 2008; Kenyon, 2008).

In spite of being more than 40 years in clinical use, doxorubicin is still considered one of the most efficacious anticancer drugs ever developed, and it became one of the main "first line" anticancer drugs almost from its discovery. It is effective against more types of cancer (including leukemias, lymphomas, and breast, uterine, ovarian, and lung cancers) than

any other class of chemotherapy agents (Skeel, 1999; Weiss, 1992; Minotti et al., 2004).

However, like most other chemotherapeutic drugs, doxorubicin has toxicities and side effects associated with its clinical use. Its most dangerous toxicity is the cumulative dose-dependent cardiotoxicity leading to irreversible congestive heart failure, which considerably limits its usefulness (upper accumulative dose of 550 mg/m^2). Its other side effects include severe myelosuppression, nausea and vomiting, mucocutaneous effects [(stomatitis, alopecia, severe local tissue damage, and hyperpigmentation of skin overlying veins used for drug injection) (Skeel et al., 1999; Peng et al., 2005; Takimoto and Calvo, 2005; Kenyon, 2008)].

It is the combination of doxorubicin's clinical use for such a broad spectrum of tumor types, and the very large number of patients treated with it, combined with its major deficiencies of dose limiting and accumulating dose limiting toxicities that made it a very appealing and attractive candidate to benefit from a delivery system. This was the major driving force for us selecting doxorubicin as the drug of choice. The scientific supportive reasons that were available in 1980 were that the drug's stability (Beijnen et al., 1985), its chemistry and physicochemical properties were well established, and its ADME (**a**bsorption, **d**istribution, **m**etabolism, and **e**xcretion) was common knowledge (Andrews et al., 1980).

Our practical reasons that supported and encouraged work with doxorubicin are its distinct spectral properties that allow easy quantification of doxorubicin level, its chemical degradation, and even state of aggregation, as well as changes in its local environment (pH and level of hydrophobicity). Doxorubicin's reasonably high molar extinction at 486 nm (12,500 OD/M at acidic pH) allows for its easy spectrophotometric quantification, especially when combined with HPLC, providing bioanalytical tools required for the development of doxorubicin based formulations.

Another major practical advantage of doxorubicin is its long wavelength (>550 nm), and high quantum yield fluorescence emission. The use of fluorescence detection increases the limit of detection compared to the absorbance determination by more than 100-fold. The fluorescence excitation and emission

spectra are distinguished from each other and both are sensitive to the environment. This enables one to study the interaction of doxorubicin with the environment. Doxorubicin's excitation and emission fluorescence spectra are both sensitive to the above described absorbance variables, but because the limits of detection and sensitivity are much higher compared to when absorbance is used, this enables one to follow doxorubicin PK and BD for long periods of time (Barenholz et al., 1993; Haran et al., 1993; Amselem et al., 1993a, 1993b; Bandak et al., 1999; Gabizon et al., 1994, 2003).

29.2.2 Liposomal Doxorubicin (First Generation) from Design to Formulation, Characterization, and Stability

Today there are many options of drug delivery systems to select from as doxorubicin delivery systems (Tinkle et al., 2014). However, in 1979 the options were much more limited and included mainly liposome- and polymer emulsion-based systems. Our selection of liposomes as the preferred delivery system was based on the following considerations related to liposomes being:

- biocompatible
- biodegradable
- non-immunogenic
- familiar to the scientific community
- have known pharmacokinetics and biodistribution
- have known metabolism

Therefore, from the toxicology point of view, they have advantages over most of the other drug delivery systems for medical/pharmaceutical applications. The same advantages are even stronger today.

However, the first step is to evaluate if the desired API matches delivery by liposomes. The approaches aim to study the level of such a match based on drug and liposome physicochemical properties. Highly relevant to drug loading and encapsulation is its liposome membrane/liposome medium partition coefficient. In most cases these data are not available and require experimental work that is not trivial (Amselem et al., 1993; Grant et al.,

2001). In many cases this parameter is related to two partition coefficients of the API: the first one is the partition coefficient between a very low dielectric medium and aqueous buffers at defined pHs, such as heptane/aqueous phase or oil/aqueous phase; the second is the partition coefficient between a medium of intermediate dielectric constant (such as octanol) and aqueous buffers. These two partition coefficients were used to determine API classification.

API classification

When we started to work on liposomes as drug carriers and searched for APIs that suited delivery by liposomes, for simplicity and convenience, we classified all APIs into three categories based on their oil/buffer and octanol/buffer partition coefficients (K_p). Molecules of very low values in both partition coefficients are by definition water soluble; molecules having low oil/buffer K_p and medium to high octanol/buffer K_p are amphipathic, while molecules having high oil/buffer K_p are lipophilic (Barenholz, 2003; Barenholz and Cohen, 1995, and references listed therein). It was found that the octanol/buffer partition coefficient is indicative of agent transmembrane diffusion and therefore it was relevant to loading stability and the drug release profile.

From principles to practice

The first stage was to evaluate drug suitability, which requires collecting all the available information on the chemical and physicochemical properties of the API, including parameters such as the above two partition coefficients. The common knowledge and our own experience teach us that agents having a high oil/buffer K_p such as lycopene are inappropriate for a liposomal carrier due to bilayer packing constraints. If a high level of such API-loading is required it will be better off in an emulsion carrier. As many of the APIs include ionizable moieties, it is recommended to obtain the partition coefficient values at three different pHs (below, above, and close to the pKa of the API). Knowing the electrostatic properties of the agent may help one to optimize selection of liposome lipid composition (improving drug loading and/or preventing liposome aggregation). Solubility and solubility product in the medium of liposome preparation and the intra-liposomal aqueous phase (if possible at the three pHs above)

are all important parameters for assessing API suitability. These partition coefficients determine if the API should be loaded into the liposome membrane or the intra-liposomal aqueous phase. Therefore, the ability to affect these partition coefficients through small chemical modifications of the API and/or through liposome membrane composition and/or aqueous medium composition are all important tools in determining liposome loading and release (Barenholz, 2001, 2003; Barenholz and Cohen, 1995; Amselem et al., 1993). Today we have much better tools to assess the level of match between API and delivery by liposomes and these novel approaches even help us to choose which approach of drug loading should be used (Zucker et al., 2009; Cern et al., 2012, 2014).

Based on the above considerations we designed, studied, and compared a few liposomal formulations, all having three lipid components: (1) a phosphatidylcholine (PC) as the "liposome-forming lipid"; (2) cholesterol, which is needed to eliminate phase transitions, and to reduce sensitivity to changes in temperatures as well as increasing physical stability upon storage and in biological fluids by transforming the liposome lipid bilayer to be in a liquid ordered (LO) phase (Mouristen, 2005; Barenholz and Cevc, 2000); (3) a negatively charged phospholipid as a source of the negative charge needed to increase and stabilize doxorubicin association (partition) to the liposomes' membranes.

During 8 years (1980 to 1988), we studied the fabrication and the physicochemical properties of many liposomal compositions loaded with doxorubicin. For these we compared small unilamellar, large unilamellar, large oligolamellar, and large multilamellar liposomes, referred to as SUV, LUV, OLV, and MLV, respectively. In all of the above, most doxorubicin was associated with the liposomes' bilayer(s). We also studied short- and long-term physical stability (defined by changes in size distribution and drug-to-lipid mole ratio), and chemical stability of the lipids and the doxorubicin of the formulation. In our *in vivo* studies in mice we studied pharmacokinetics (PK) and biodistribution (BD) in normal and tumor-bearing mice, as well as toxicity and tolerability in rodents, and finally their therapeutic efficacy in several models of tumor-bearing mice. The specific *in vitro* screening parameters included efficiency of drug capture (loading = encapsulation = association), preservation of *in vitro* cytotoxicity (on tumor cells in culture), and the stability of drug-liposome association in body

fluids (mainly plasma). The *in vivo* screening parameters included *in vivo* tissue distribution with special focus on levels in the heart (due to doxorubicin cardio-toxicity), and anticancer activity. As our main indication was hepatic tumors such as hepatocellular carcinoma (HCC), representative tumor models relevant to hepatic tumors were used. Toxicological evaluation included general toxicology and cardio-toxicity. The pharmaceutical screening included critical analysis of the factors involved in the pharmaceutical development and was done along the lines of Quality by Design (QbD), focused on measuring the effect of lipid composition, liposome lamellarity, size distribution, and doxorubicin to lipid mole ratio on shelf life, comparing "wet" versus lyophilized formulations, quality control tests, API release of the liposomal assembly (equivalent to dissolution test), and other parameters.

Our studies on this system are described in many publications (Gabizon et al., 1982; Gabizon et al., 1983; Gabizon et al., 1985; Gabizon et al., 1986a, 1986b; Gabizon et al., 1988a, 1988b; Gabizon et al., 1989a, 1989b; Druckmann et al., 1989; Goren et al., 1990; Goren, 1990; Amselem et al., 1990; Amselem et al., 1992; Amselem et al., 1993a,1993b; Barenholz and Amselem, 1993; Barenholz et al., 1993; Horowitz et al., 1992). Our studies clearly demonstrated that the negatively charged lipids (at physiological pH) in the formulation were essential to meet the needs of high efficiency of doxorubicin encapsulation. The fact that level of drug loading (capture) is >50-fold higher than what is expected from the trapped aqueous volume determined by ^{3}H-inulin (Amselem et al. 1990; Haran et al. 1993) indicated that most of the captured drug is not in the intraliposome aqueous phase but rather associated with the negatively charged liposomal membranes. Diphosphatidyl glycerol (cardiolipin, DPG), phosphatidyl glycerol (PG), and phosphatidylserine (PS) were all active in improving the encapsulation, with DPG encapsulation being the best in terms of drug association, in agreement with the highest association constant of DPG doxorubicin of 1.6×10^{-6}, compared with 1.8×10^{-4} for PS and ~0.0 for PC (Goormaghtigh and Ruysschaert, 1984). Exposure to serum (without large dilution!) did not cause significant doxorubicin release. For practical reasons such as DPG availability and cost (at that time) as well as potential immunogenicity, we excluded the DPG from our studies.

Another important aspect of this research was that unilamellar vesicles (either SUV < 100 nm or LUV ~100 nm in diameter) capture much less drug, and lose their drug content faster than vesicles of the same lipid composition in larger sizes and lamellarity (Goren et al. 1990; Goren, 1990) including either large (>100 nm) oligolamellar (OLV) or multilamellar large vesicles (MLV). Large and small are functional definitions that describe vesicles in which the external two leaflets of the external lipid bilayer have different (SUV) or almost the same (OLV and MLV) curvature (Lichtenberg and Barenholz, 1988). This was another warning signal that could predict a failure in humans, which we did not understand in the early 1980s.

Finally, we found that formulations composed of saturated lipids have significantly lower drug capture than formulations which are based on phospholipids of the identical headgroups but having unsaturated hydrocarbon chains. Namely, unsaturated phospholipids seemed to be superior to saturated phospholipids. This may be explained by the larger free volume in the membrane composed of unsaturated lipids, which leaves more space for the drug.

With both PS- and PG-containing OLV (as the negatively charged lipid), we achieved a similar drug-to-lipid ratio over the broad range of 0.05–0.26 (depending on fine tuning, Amselem et al. 1990, 1992), but as PS is less chemically stable and more expensive, PG became our negatively charged lipid of choice. The formulation was optimized for various variables, of which level of PG (demonstrated in Fig. 29.3) is one of the main ones.

Our optimal OLV-DOX formulation was 300–500 nm in diameter; it was composed of egg PC : egg PG : cholesterol (7: 3: 4 mole ratio) and was fabricated by extrusion (Amselem et al., 1989–1990, 1990, 1992). Due to the use of egg-derived unsaturated phospholipids (PC and PG) acyl chains were composed of ~50 mole% unsaturated fatty acids [C18:1 (30.2%) > C18:2 (16.3%) > C20:4 (3.5%) > C22: 5 (0.9%) > C22:6 (0.7%)] Barenholz et al., 1993; Barenholz and Amselem, 1993). We had to deal with two types of chemical stability issues: acyl ester hydrolysis, and lipid auto/peroxidation (Lichtenberg and Barenholz, 1988). Major efforts were dedicated to solve these stability issues. The best protection against oxidative damage was obtained by inclusion of 1.5 mole% D-α-tocopherol succinate (TCS) in the lipid mixture. This by itself

was not sufficient and therefore the fabrication and storage of the formulation was done in the presence of the highly efficient iron ion chelating agent Desferal (deferoxamine mesylate) using an aqueous medium of 0.15 M NaCl (saline) containing 200 μM Desferal, at pH range of pH 5.7–6.8 at 4°C (Barenholz and Gabizon, 1990, 1991; Amselem et al., 1990; Barenholz and Amselem, 1993; Barenholz et al., 1993). Under such conditions doxorubicin degradation was minimal (<5%), lipid hydrolysis was low (<5%), cholesterol degradation was below detection limit, and lipid oxidation was minimal even after 19 months storage at 4°C (Barenholz and Amselem, 1993). TCS acts as a pro-antioxidant slowly hydrolyzing and continuously supplying α-tocopherol as an active antioxidant, while Desferal, being a very potent iron chelating agent, effectively neutralizes iron ions that are highly potent inducers of lipid and doxorubicin auto/peroxidation (Lichtenberg and Barenholz, 1988; Barenholz and Amselem, 1993).

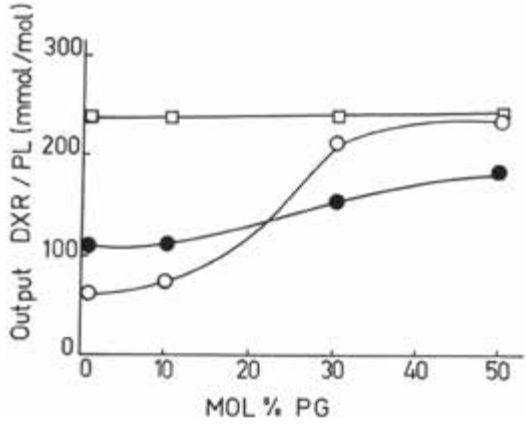

Figure 29.3 Optimization of OLV-DOX to the mole percent PG. Effect on doxorubicin association with the liposomes (Amselem et al., 1990). Key to symbols: □–□, DOX/PL mole/mole; ○–○, hydration of lyophilized lipids by DOX solution (Scheme I, Method I in Amselem et al., 1990); ●–●, mixing lipid and DOX ethanolic solutions followed by drying and hydration (Scheme I, Method II in Amselem et al., 1990).

The optimal doxorubicin-loaded egg (E)-derived phospholipids and cholesterol (EPC/EPG/Cholesterol/TCS 7:3:4:0.2) OLV-DOX formulation showed reasonable shelf life and good physical stability in plasma (<5% release in 1 h at 37°C). However, today

we know that this approach of testing stability in plasma was misleading, as the dilution of the OLV-DOX used was small and therefore the liposome membrane to aqueous medium doxorubicin partition coefficient can protect against a major drug leakage (Amselem et al., 1993a).

29.2.3 Cytotoxicity to Cells in Culture (*in vitro* Studies)

In vitro testing of this formulation (OLV-DOX) in tumor cells in culture using two cell lines, the J-6456 lymphoma and the P388 leukemia, indicated that encapsulation of the doxorubicin in the OLV has almost no effect on the IC_{50} [compare 1.1×10^{-8} M for the liposomal drug with 1.8×10^{-8} M for the free drug (Gabizon and Barenholz, 1988)]. At the time the experiment was performed, we did not understand that this should be a "red flag" suggesting unwanted relatively fast dilution-induced major drug leakage from the liposomes in the cell growth medium. At a later stage when we evaluated why this formulation failed in a human clinical trial (see below), we found that no growth inhibition of the cells (no cytotoxicity) was observed if the cation exchanger Dowex-50 was present in the cell medium. This cation exchanger selectively and efficiently binds the positively charged free doxorubicin, but not liposome-associated drug (Druckmann et al., 1989; Amselem et al., 1990). This strongly suggests the free drug released from the OLV-DOX in the cell medium is responsible for most of the cytotoxicity and not the liposome associated drug. The same elimination of drug cytotoxicity by the cation exchanger was also obtained for free doxorubicin (F-DOX).

29.2.4 Pharmacokinetics and Biodistribution Studies in Mice

Preclinical PK and BD studies of the above optimal OLV-DOX in normal and tumor-bearing mice met all our objectives and expectations. Biodistribution studies showed that the encapsulation of DOX into these OLV increased liver (the target organ) and spleen DOX uptake concomitantly while reducing DOX levels in the heart, kidneys, and small intestine) as well as reducing organ and plasma clearance of the drug (Gabizon et al., 1982, 1983). In mice bearing liver metastasis, the DOX level after i.v.

injection of OLV-DOX reached a level several-fold higher than after injection of an equal amount of F-DOX. This was paralleled by a large reduction in the viability of tumor cells isolated from the liver of tumor-bearing mice (by a Percoll density gradient) after injection of OLV-DOX, which was achieved only after administration of OLV-DOX and not of F-DOX.

29.2.5 Toxicity

We studied the toxicity of a few liposomal doxorubicin formulations of different lipid compositions in small rodents as a part of the selection process of the optimal formulation. Here we will summarize our comparison of the leading formulation of EPC/EPG/Cholesterol/TCS 7:3:4:0.2 OLV-DOX with free drug (F-DOX). The comparison included a few studies that included single-dose and multi-dose experiments (Gabizon et al., 1986a). We demonstrated that OLV-DOX is much less toxic than F-DOX; LD_{50} value of OLV-DOX is twofold higher than the LD_{50} value of F-DOX. The lower toxicity of OLV-DOX was also demonstrated by higher, close to normal, body weight and organ weights and almost no histopathological damage to kidney and myocardium. The low level of cardio-toxicity observed was fully reversible. It is also very important that, despite the fact that i.v. administration of OLV-DOX resulted in high accumulation of doxorubicin in the liver, hepatotoxicity was minimal and limited to some megalonucleosis, with slight changes in liver function observed at the end of a 6-month-long experiment in rodents. The much lower toxicity of OLV-DOX than of F-DOX is related first to the fact the encapsulation in the OLV affected dramatically the drug biodistribution with much less drug reaching the heart and the kidneys (Gabizon et al., 1982, 1983). However, this is not the only effect of the encapsulation. Not less important is the effect on subcellular distribution, which results in diminishing interaction of the intracellular doxorubicin with the mitochondria. The latter may explain part of the chronic free drug toxicity (related to the high affinity of the drug to the mitochondrial lipid cardiolipin (DPG). The bottom line of the toxicity studies is that our OLV-DOX is significantly less toxic and safer than F-DOX.

29.2.6 Therapeutic Efficacy

For the therapeutic efficacy, we studied two *in vivo* models of tumor-bearing mice with major involvement of RES organs, the J-6456 lymphoma with predominant dissemination to the liver (Gabizon et al., 1982, 1983, 1985), and the BCL1 leukemia, which infiltrates mainly the spleen and bone marrow (Gabizon et al., 1986b). In both models OLV–DOX was much superior to F-DOX at equal drug dose and, as higher doses of OLV-DOX can be administered due to its superior LD_{50}, the therapeutic efficacy of OLV-DOX is superior to that of F-DOX. Levels of the drug after administration of OLV-DOX i.v. in the J-6456 lymphoma cells isolated from the liver of tumor-bearing mice (by a Percoll density gradient) were more than 3-fold higher than after injection of an equal dose of F-DOX for at least the first 64 h post drug administration (i.e., compare 195 and 25 ng of drug per 10^7 isolated lymphoma cells for DOX-OLV and F-DOX, respectively, at 24 h post injection). Table 29.1 is one of many examples that clearly show that the therapeutic efficacy of OLV-DOX in mice bearing J-6456 metastatic lymphoma was also much superior to an equal dose of F-DOX.

Table 29.1 Superior anti-tumor activity of OLV-DOX over F-DOX based on survival time (days)[a]

Exp.	No. of Mice	Mean ± S.E.	Median (range)	$p^{a,b}$
Untreated	7	19.3 + 0.5	18.5 (18–21)	<0.01
F-DOX	8	40.5 + 2.3	40.0 (28–50)	<0.01
OLV-DOX (PG:PC:Chol)	8	71.1 + 12.9	53.0 (41–148)	

Note: For more details see Gabizon et al. (1985).

[a]BALB/c mice inoculated with 10^6 J-6456 cells and treated i.v. with 8 $mgkg^{-1}$ doxorubicin in either free or liposome-entrapped form.

[b]Wilcoxon test: F-DOX analyzed versus Untreated; OLV-DOX analyzed versus F-DOX.

One explanation for the fact that we did not get a cure or many long-term (>100 days) mice survivors is the presence of metastatic lymphoma cells in tissues other than liver and spleen, to which OLV-DOX does not deliver high drug levels.

This is an important lesson to learn about our OLV-DOX performance.

Overall, the above results suggested that our treatment modality with OLV-DOX may meet the expectation of being superior to F-DOX in treatment of liver tumors including liver metastasis in humans.

In 1985, based on the above formulation design and characterization, combined with our rodent studies that showed acceptable toxicology (significantly better than F-DOX), and being superior in small rodents to F-DOX in PK, BD, and therapeutic efficacy, we started to plan and apply for a Phase I clinical trial approval at the Hadassah University Hospital. IND application was submitted and was approved in 1985 by the Hadassah University Hospital Helsinki Committee and the Israel Ministry of Health (MOH).

29.2.7 Scale-Up

The preparation for the clinical trials required fabrication of the OLV-DOX in liter-scale batches, concomitantly with the development of quality control assays (Barenholz et al., 1989; Gabizon et al., 1989b; Amselem et al., 1989–90, 1990, 1992, 1993a, 1993b; Gabizon et al., 1991; Barenholz and Amselem, 1993; Barenholz and Crommelin, 1994).

29.3 OLV-DOX Clinical Trials

29.3.1 What Was Known in 1985 on "First in Man" Studies and the Clinical Use of Liposomes as Carriers of Drugs and Imaging Agents?

The first clinical use of liposomes dates back to 1974, when the fate of radiolabeled liposomes was examined in three cancer patients (Gregoriadis et al., 1974). This was followed by Gregoriadis and coworkers' use of liposomes as a carrier for the enzyme glucocerebrosidase (a beta-glucosidase) for enzyme replacement therapy for Gaucher's disease treatment (Belchetz et al., 1977). More extensive studies in humans with radiolabeled "fluid"-phase sonicated liposomes indicated that the major tissues of liposome uptake are the liver and spleen (Richardson et al., 1979). A similar study in which the distribution of technetium-99m-

labeled MLV in patients with Hodgkin's disease was performed by Perez-Soler et al. (1985). This, the earliest report in the literature on the therapeutic use of liposomes as drug carriers given systemically to a sizable group of patients, described the experience gained after administration of amphotericin-B in liposomes. It showed clear beneficial antifungal activity without apparent toxicity at doses in which serious toxic effects of the free drug occurs. A similar study with another liposomal amphotericin-B formulation down-sized by ultrasonic irradiation (sonication) that resulted in small mostly unilamellar vesicles, was performed later in cancer patients having fungal infections by Sculier and coworkers (1988). A pilot human study with the water-insoluble cytotoxic drug NSC 251635 was also performed (Sculier et al., 1986).

One early clinical "first in man" study was performed with a liposomal doxorubicin formulation by Kumai et al. (1985). They reported on a treatment of liver cancer by local (hepatic intra-arterial) injection of small doses of liposomal doxorubicin, up to 15 mg/m^2, in 10 cancer patients with liver metastasis. The main side effect Kumai et al. (1985) found was fever, which could be explained by a small contamination of the liposomal formulation with endotoxin. Our main take-home lesson from all the above "first in man" trials was that preparation of liposomal formulations for clinical use is feasible. These early experiments were very helpful in convincing the Hadassah Hospital ethical committee and Israel MOH to grant permission for our "first in man" and Phase I clinical trials of OLV-DOX.

29.3.2 Phase I Clinical Trials of Liposomal Doxorubicin (OLV-DOX)

EPC/EPG/Cholesterol/TCS (7:3:4:0.2) OLV DOX, having a doxorubicin (membrane-associated) to phospholipid mole ratio of 0.056 and a size distribution of 200–500 nm was used in our clinical trials. In our first study (Gabizon et al., 1989a, 1989b), 32 patients, most of them with a primary or a metastatic liver cancer refractory to conventional therapy were treated. A total of 69 courses of therapy was administered by intravenous infusion of a suspension of OLV-DOX (0.5–2.0 mg DOX/mL) in physiological saline containing 200 μM Desferal (pH 6.2) at an approximate

infusion rate of 2 mL/min given on a 3-week intermittent schedule.

OLV-DOX and phospholipid doses were escalated from 20 mg/m^2 and 0.3 g/m^2 to 120 mg/m^2 and 3.2 g/m^2 for DOX and phospholipids, respectively. Treatment was generally well tolerated, and acute toxic effects such as nausea and vomiting were mild and infrequent. Chills and fever (>38°C) were observed upon infusion. Median WBC nadir counts were 2700, 2300, and 700/μL at 85, 100, and 120 mg/m^2, respectively. All three patients receiving 120 mg/m^2 developed grade 4 leukopenia and fever requiring intravenous antibiotics, and, in two of them, severe stomatitis (grades 3 and 4) was observed. Significant hair loss was apparent in all patients receiving doses higher than 50 mg/m^2. This also should have been a warning signal (which we did not understand then) of the possibility of fast drug release from the OLV upon infusion. The maximal tolerated dose (MTD) of OLV-DOX appears to be 120 mg/m^2, with leukopenia and stomatitis being the dose-limiting factors. While the sub-acute toxicity of OLV-DOX appeared to be qualitatively similar to that of F-DOX, its tolerance was better, as it exceeded the recommended dose of free drug (75 instead of 60 mg/m^2) in the standard 3-weekly schedule.

This clinical study with OLV-DOX shows that administration of this formulation to humans is feasible even at higher than conventional dose levels of free drug (60–75 mg/m^2) and it appears to be well tolerated. Based on this Phase I study, the recommended starting dose for Phase II studies would be >75 mg/m^2. It should be noted that most of the patients entered in this study suffered from heavy neoplastic involvement of the liver, and most of them had been previously treated with various cytotoxic agents including free doxorubicin. There is suggestive evidence that doxorubicin-induced myelosuppression is more severe when the tumor shows a major liver involvement (McKelvey et al., 1976; Gundersen et al., 1986). This may lead to increase in liposome localization in the bone marrow (Perez-Soler et al., 1985). Therefore it seems that patient populations that have heavy neoplastic involvement of the liver are not suitable for being treated with a high dose of OLV-DOX. However, higher doses could be administered to other patient populations with acceptable

toxicity. Regarding acute toxicity, nausea and vomiting appear to be substantially attenuated when compared to the common clinical experience with free DOX at standard 3-weekly doses (Blum and Carter, 1974). Fever, a rather uncommon side effect of free DOX therapy, was observed in a relatively high percentage of cases. Although the immediate reaction may still be attributable to a low amount of endotoxin, undetectable in the rabbit test, the delayed reaction appears to be a specific feature of DOX-OLV. One possible explanation is that this treatment induces interleukin-l secretion by doxorubicin-activated macrophages (Mace et al., 1988) following DOX-OLV localization in tissue macrophages and breakdown of endocytosed liposomes. The sub-acute toxicity of OLV-DOX appears to be qualitatively similar to that of free DOX, with leucopenia and stomatitis being the most significant dose-limiting factors. These data should be another warning signal (that we ignored) that the drug is released relatively fast from the liposomes into the blood circulation. A similar finding has been obtained in a another clinical study (Treat et al., 1989), with DOX encapsulated in liposomes composed of cardiolipin, PC, stearylamine, and cholesterol, although the MTD and recommended dose for Phase II studies reported (90 and 75 mg/m^2, respectively) are lower than in our study. Drug causing myelosuppression may reach the bone marrow in several ways. The ability of liposomes to localize in the bone marrow, a tissue rich in sinusoidal capillaries, has been demonstrated in animals (Gregoriadis and Senior, 1986), and in humans (Perez Soler et al., 1985). Today our interpretation of these results is that all these formulations that share having the doxorubicin associated with the liposome membrane (and not in the liposome aqueous phase), also share a fast dilution-induced drug leakage from the liposomes into the blood circulation. This may explain the myelosuppressive effect of the liposomal formulations. Another possible explanation is that drug that was released from the liver and spleen macrophages reached the circulation after the liposomes were endocytosed and processed. Although human pharmacokinetic studies with liposomal doxorubicin have been previously reported (Gabizon et al., 1989; Rahman et al., 1989), they did not enable discrimination between the various explanations, as the measurements done at that time did not provide separation between free drug and liposome-associated

drug in the plasma. These two forms of doxorubicin can now be resolved by the methodology of using the cation exchanger Dowex-50, described by Druckmann et al. (1989) and Gabizon et al. (1994), or by other separation approaches.

The bottom line of our first in man clinical trial indicated that while the administration of DOX-OLV to humans is feasible and even up-shifted the MTD, the major side effects were similar to those of the free drug. This was disappointing and not in agreement with our expectations, which were based on our mice results. There the DOX-OLV was superior in all aspects [PK, BD, tolerability, and efficacy (see above)]. In order to benefit from the disappointing human trial results we decided to put major efforts into the understanding of the differences observed between the failed human study (Gabizon et al., 1989b) and the successful mice studies (rev. in Gabizon and Barenholz, 1988). For this we decided to study pharmacokinetics and liposome localization by imaging studies in patients.

29.3.3 OLV-DOX Pharmacokinetics, Biodistribution, and *in vivo* Imaging in Humans

The PK and BD study in humans (Gabizon et al., 1991) included 19 patients receiving OLV-DOX. It was carried out within the framework of a Phase I clinical trial (Gabizon et al., 1989a, 1989b; Barenholz et al., 1990). The formulation of DOX-OLV tested consisted of the DOX-OLV described above. Plasma clearance of total drug extracted from the plasma after DOX-OLV infusion followed a bi-exponential decay curve with a pattern and PK parameters similar to those reported (and confirmed by us) for free DOX. The plasma concentration of drug circulating in liposome-associated form was also determined using the method described by Druckmann et al. (1989), which is based on separation of free and liposome-associated drug by the cation exchanger Dowex-50 (which selectively binds the free drug but not the liposome-associated drug). These special studies were performed in seven patients. Liposome-associated drug was found to be rapidly cleared from plasma; its ratio to non-liposome-associated drug appeared to correlate with liver reserves, with highest ratios in patients with normal liver function. Liposomes' clearance was

measured after free drug and protein-associated drug were removed by Dowex-50 cation-exchange resin (Druckmann et al., 1989). The remaining plasma that contained the OLV-DOX was thereafter processed for HPLC drug analysis, as detailed elsewhere (Barenholz et al., 1990; Gabizon et al., 1991). Measurements of total and liposome-associated plasma doxorubicin were obtained. The level of free and protein-bound drug was inferred by subtracting the concentration of liposome-associated drug from that of total doxorubicin. In three of these patients we also measured the concentration of PG in plasma to follow the clearance of liposomes (Barenholz et al., 1990; Gabizon et al., 1991; Amselem et al., 1993). PG was selected as a liposome marker because of its negligible concentration in human plasma (<5 nmoles/mL) relative to the concentration of total phospholipids (2,000–4,000 nmoles/mL). Phosphatidylethanolamine (PE) was chosen as an internal standard due to its absence in the DOX-OLV formulation and its being in a concentration range of similar order of magnitude to the phospholipids infused as OLV-DOX. Plasma samples were extracted after a complete trinitrophenylation of the plasma aminolipids (PE and phosphatidylserine) and of DOX by trinitrobenzene sulfonate (TNBS). The step of trinitrophenylation was essential to optimize the chromatographic separation. The different phospholipids were quantified using low-phosphorus silica gel thin layer plates. The reduction in PG plasma concentration with time was used to calculate liposome plasma clearance, while the change of ratio of DOX to PG in the plasma was used to calculate rate of DOX release from DOX-OLV in the patients' plasma.

The results obtained in these three patients indicate that liposome-associated doxorubicin has a fast clearance (Fig. 29.4), which resembles that of F-DOX and was much faster than the liposome clearance. This explains the fast reduction of DOX/PG mole ratio (Fig. 29.4, inset) suggesting that liposomes lose most of their drug payload during the first 30 min of circulation.

To learn about the liposome organ distribution, imaging studies were carried out with doxorubicin-free ^{111}indium-deferoxamine-labeled liposomes of the same composition and size distribution as the OLV-DOX. In order to retain the remote-loaded ^{111}In in the intra-liposome aqueous phase the liposomes

were prepared by hydration of the lipids in a medium containing 200 μM of the chelating agent deferoxamine mesylate (DF) aimed to bind the ^{111}In. Un-encapsulated DF was removed from the extra-liposomal medium by passage through a Dowex-50 cation-exchange resin, then liposomes were remotely loaded with ^{111}In by incubation with an ^{111}In-oxine (Amersham) complex at room temperature for about 30 min. Free (unloaded) ^{111}In-oxine was removed by gel permeation chromatography. Approximately 90% of the label became liposome-associated. These liposomes are referred to as ^{111}In-OLV. Patients were imaged using a dose of ~700 μCi of ^{111}In and 300 mg phospholipid given by bolus i.v. administration. Whole body frontal and posterior images were obtained immediately after injection, 2 h, and 24 h later, using a Gamma camera (Apex 415 Elscint, Haifa, Israel). For details see Gabizon et al. (1991). The results show clearly that in seven out of nine patients the ^{111}In-OLV were cleared predominantly by liver and spleen and to a lesser extent by bone marrow. In two patients with active hepatitis and severe liver dysfunction, there was minimal liver uptake and increased spleen and bone marrow uptake. For all patients analyzed except one hepatoma patient, intrahepatic and extrahepatic tumors were not imaged by liposomes (Fig. 29.4 and Figs. 6–9 in Gabizon et al., 1991), suggesting that liposome uptake is restricted to cells of the reticuloendothelial system (RES). These observations indicate that a major fraction of this OLV-DOX formulation is rapidly cleared by the RES, and that the mechanism of drug delivery should probably be the combined result of slow release from the RES depot and drug leakage from circulating liposomes. However, the contribution of the RES is dependent on the level of drug remaining in the liposomes while being taken up by the RES, and the level of free drug should be dependent on the rate of drug release from the liposomes. The slower the release rate, the larger should be the benefits. If drug release in plasma is fast, no beneficial gain of delivery via the administrated liposomes (over administration of free drug) is expected. Unfortunately, in human subjects the latter occurred. As shown in Fig. 29.5, the OLV-DOX shows fast release of their doxorubicin payload in plasma, and therefore, the therapeutic benefits expected of these liposomes compared to free doxorubicin should be minimal, if any.

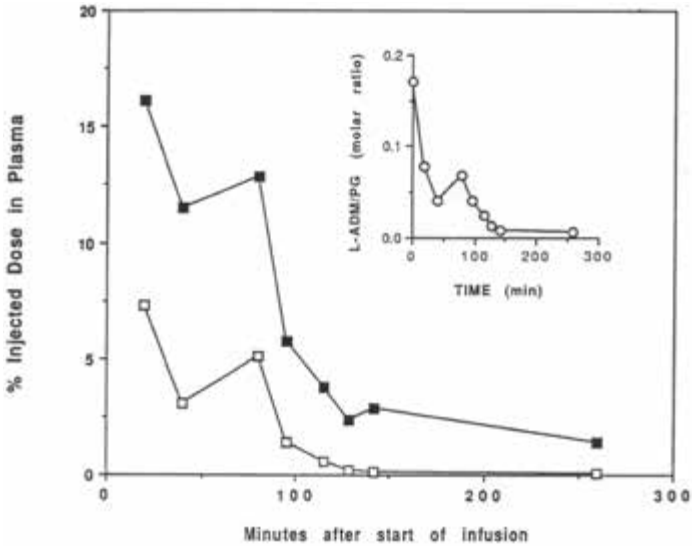

Figure 29.4 Plasma clearance of liposomal doxorubicin (white squares) and PG (black squares) (Gabizon et al., 1991; Amselem et al., 1993). Adriamycin (ADM) = doxorubicin (DOX).

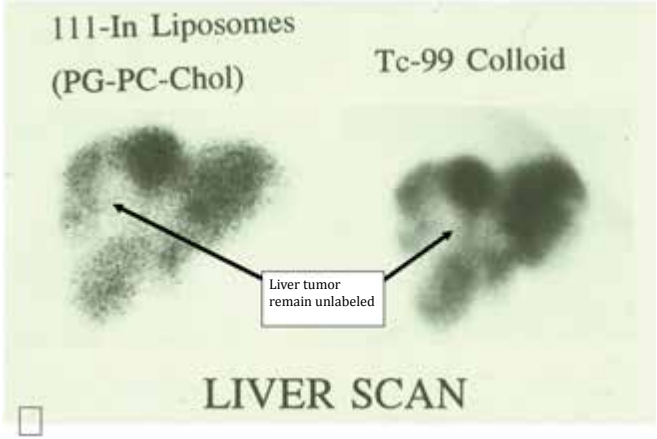

Figure 29.5 Liver scintigraphies 2 h after injection of patient with radiolabeled ^{111}In-OLV or ^{99}Tc- colloid (Gabizon et al., 1991). This figure clearly demonstrates that conventional liposomes (OLV-DOX) do not target liver tumor and behave similarly to ^{99}Tc- colloid.

The same OLV-DOX that failed in humans has been shown to have reduced toxicity and improved antitumor efficacy in experimental animal models (rev. in Gabizon and Barenholz, 1988). Namely, the beneficial effects in mice were not reproduced in our Phase I clinical study (Gabizon et al., 1989a, 1989b). Although the maximal tolerated dose (MTD) of DOX-OLV was increased in relation to the MTD of free drug administered at the conventional 3-weekly schedule; however, in humans the dose-limiting acute toxicity (the myelotoxicity) of OLV-DOX is very similar to that of free doxorubicin. Thus, although the toxicities of free DOX and OLV-DOX differ somewhat quantitatively, they are qualitatively very similar.

The "bottom line" conclusions of our human clinical trials are based on the PK and BD human study in which the results of clearance of drug and the liposomes (DOX and liposome PG) are combined with the results of the radiolabeled ^{111}In-OLV human imaging experiment. The latter clearly indicates that in humans who retain significant liver function the OLV accumulate in the liver and spleen RES, but without reaching the liver tumor. What is more problematic is that there is a fast dilution-induced drug release of the OLV-DOX in the blood already during the i.v. infusion. This means that in humans the liposomes reaching the liver are almost drug free, so our basic working hypothesis that the RES will act as a drug depot is not valid for human treatment. Another important conclusion is the confirmation that in humans severe liver dysfunction will have a large effect on RES-directed liposomes; then more liposomes will reach the spleen and the bone marrow and drug leakage of the circulating liposomes will become the main factor that determines drug fate.

29.3.4 Conclusions of Our Clinical Experience with OLV-DOX as the Basis for the Development of Novel Liposomal DOX for Treatment of Metastatic Tumors

Our study that reports on the PK and BD of OLV-DOX and on imaging of ^{111}In-OLV in humans (Gabizon et al., 1991) is the first study in which a complete pharmacokinetic and biodistribution analysis of a drug-liposome dosage form in human patients was described.

The clearance of DOX when delivered as OLV-DOX is a composite of two processes: (i) clearance of liposomes containing DOX by the RES, predominantly liver and spleen; and (ii) clearance of DOX released from liposomes in plasma. The analysis, which includes PK of total drug (DOX), liposome-associated DOX, and liposome markers (PG and ^{111}In-OLV), suggests that both processes operate in human patients and that factors such as the patient's liver function may affect their relative contribution.

Delivery of DOX in liposome-entrapped form (OLV-DOX) has been proposed as a means to reduce the toxicity of DOX and improve its therapeutic index based on a number of preclinical studies (rev. in Gabizon and Barenholz, 1988).

The PK, BD, and imaging data (Gabizon et al., 1991) suggest that the reduced clinical toxicity of OLV-DOX results from a somewhat lower peak level of free drug and possibly some changes in the tissue distribution of the liposomes, with possibly some drug accumulation in the RES at the expense of other tissues. The main limitations of our therapeutic strategy based on OLV-DOX, as revealed by this study, are the significant drug leakage and preferential RES uptake. These shortcomings are probably the result of the basic formulation physicochemical characteristics, such as the following:

(i) Drug entrapment in the liposome bilayer as opposed to encapsulation in liposome aqueous interior. Bilayer-associated drug may be more accessible to be released from the liposomes to the plasma upon dilution and to associate with plasma proteins (Goren et al., 1990, Goren, 1990). This process will be affected by the degree of dilution upon injection, which is also dependent on the mode of administration (greater dilution effect occurs for slow infusion than for bolus injection). The association of doxorubicin with liposomes is related to the drug-liposomes association constant [which determines the liposome/medium (liposome/plasma) partition coefficient (K_p)]. The question is how high K_p has to be in order to prevent a major drug leakage in plasma. This may be a key issue which may explain the difference between our success in rodents and failure in humans (Amselem et al., 1993a; Barenholz and Cohen, 1995; Barenholz, 2001, 2003). Plasma volume in mice

is ~1.0 mL compared with 3,500 mL in humans. Therefore, upon slow infusion, the liposomes undergo a very large dilution of 3500-fold for each mL that reaches the plasma, compared with only a 5-fold dilution occurring after the bolus injection of the same liposomes to mice. The fast free drug clearance keeps this huge dilution effect active throughout the time of infusion. The observation of a sudden burst of drug leakage shortly after injection (Fig. 4 in Gabizon et al., 1991) is compatible with the dilution effect.

(ii) The presence of a high mole fraction of PG in the liposome bilayer may accelerate uptake by the RES (Gabizon and Papahadjopoulos, 1988). It may also induce complement activation (Szebeni et al., 2007 and rev. in Szebeni and Barenholz, 2011; Szebeni et al., 2011).

(iii) In extra-hepatic tissues the liposome size is too large to allow for extravasation (Hwang, 1987). Therefore these liposomes cannot benefit from the enhanced permeability and retention (EPR) effect, which was first described by Matsumura and Maeda (1986) and more recently reviewed by Maeda et al. (2009). This effect may allow for selective accumulation of nanoparticles in tumors due to unique micro-anatomy of blood vessels there (but not in normal healthy tissue) being porous and permeable to 100-nm particles. In addition, the tumor tissue is poor in lymphatic drainage, which enables prolonged retention of the nanoparticles there, followed by local (tumor) drug release and/or for the liposomes to be taken up by the tumor cells.

Based on this analysis, the fact that the same dose-limiting bone marrow toxicity was observed with DOX-OLV and with F-DOX is not surprising and can be assigned, to a large extent, to the fast drug leakage from circulating liposomes.

In view of the OLV-DOX fast plasma drug release and changes in tissue distribution and bioavailability, it is uncertain whether the somewhat increased tolerated dosage of OLV-DOX (over F-DOX) will result in an enhanced antitumor activity. The liposomes used here are cleared quickly by the RES of liver and spleen and to a lesser extent by the bone marrow. Our studies suggest that the mechanism of antitumor activity of OLV-DOX is complex, and presumably results from exposure of tumor cells to drug leaking

from circulating liposomes and drug released from the RES. Obviously, drug leakage from circulating liposomes is undesirable since it increases toxicity. Regarding drug release from the RES, the clinical conditions most likely to benefit from this approach are limited. This approach should not work for treatment of solid tumors, as in most solid tumors drug exposure in relation to dosage may be suboptimal. The OLV-DOX will be highly sensitive to factors such as RES/liver function, site of tumor involvement, and proximity of tumor cells to RES cells.

The failure of our OLV-DOX approach in humans has some basic "take home massages" that if used right should lead us to the development of a liposomal doxorubicin formulation which should be less toxic and more efficacious than free DOX in humans. This failure served as the main driving force and as the basis for Doxil® development.

29.4 Doxil® Development

29.4.1 Turning DOX-OLV Failure into Doxil Success

We started our clinical trial of OLV-DOX in 1985. In summer of 1985 after we already had treated two patients, I started my sabbatical at Liposome Technology Inc. (LTI) at Menlo Park. That year, LTI also licensed from Yissum two pending patent applications of Barenholz and Gabizon on OLV-DOX (Barenholz and Gabizon, 1990, 1991). One year later LTI staff became involved in the OLV-DOX clinical trial and expanded it to include, in addition to Israel, also the UK. The UK studies were led locally by Roger New (Amselem et al., 1992). This trial expansion allowed us to increase patient number. By 1987 it became evident to us that this specific OLV-DOX formulation would not become a viable product and is not good enough for further development. We decided to exploit the results of this study to bring us closer to understand the requirements for a viable product that could overcome all (or at least most) of the deficiencies demonstrated by our OLV-DOX. These included the facts that in this failed formulation, doxorubicin is liposome-membrane-associated and that liposome membrane is composed of two fluid unsaturated phospholipids (having the

solid ordered to liquid disordered phase transition much below 37°C): (i) the zwitterionic "fluid" liposome-forming lipid EPC, and (ii), the negatively charged "fluid" liposome-forming lipid EPG, and cholesterol. These failed liposomes were oligolamellar, and of size distribution in the range of 200–500 nm. The combination of this size distribution range and lipid composition resulted in fast uptake of the liposomes by the RES; namely, there was no RES avoidance. Not less important are the facts that in the liver the liposomes were not taken up by tumors but by the liver macrophages (Gabizon et al., 1991). In addition, these liposomes reached the liver with a very low level of drug (Gabizon et al., 1991; Amselem et al., 1993a) due to the fact that most encapsulated drug was membrane-associated (electrostatically), and in the plasma of the infused patients it undergoes fast dilution-induced drug release. In addition, such large liposomes could not make use of extravasation typical of nano-particulates (having long circulation time) via the porous blood vessels of the tumor tissue. This unique nano-anatomy can be used as the Achilles' heel of the cancer tissue for selective accumulation of macromolecules and nanoparticles in the tumor tissue.

The microanatomy of tumor blood vessels and its relevance to tumor therapy was studied extensively by Jain and coworkers (Hashizume et al., 2000), while Bassermann (1986) described the changes in vascular pattern of tumors and surrounding tissues during different phases of metastatic growth. Jain and coworkers also point out the high pressure in tumors (but not in healthy tissues), which reduces drug diffusion from blood vessels into the tumors, thereby reducing the therapeutic efficacy and increasing toxicity of chemotherapy.

After our failed "first in man" clinical trial with OLV-DOX we were back at square one, but we were much more educated and more knowledgeable on both the scientific and technological levels of the issue and the needs to solve the major problems described above. We were also confident that development of liposomal doxorubicin is feasible. Therefore we decided to look for an alternative liposomal doxorubicin formulation which can overcome all the above deficiencies and will be able to reach most metastatic solid tumors and will not be limited to liver-residing tumors.

Table 29.2 The requirements to achieve therapeutically efficacious passively targeted drug loaded liposomes and means to fulfill them

	Main requirements to achieve therapeutically efficacious passive targeting of liposomes to cancer tissues	**Physicochemical and biophysical solutions used to meet the requirements**
	Requirements	**Solutions**
1.	Extended circulation time in intact form in the human plasma	Development of sterically stabilized liposomes (SSL) composed of high T_m lipids, cholesterol, and a lipopolymer such as ^{2000}PEG-DSPE
2.	Sufficient levels and stable loading of drug in order for long circulating nano-liposomes to reach disease site with liposomes loaded with drug at a level needed to achieve therapeutic efficacy [$t_{1/2}$ of drug release in blood should be longer than circulation $t_{1/2}$]	Use of pH or ammonium ion gradients for remote (active) loading of amphipathic weak bases or acids into long-circulating nano-liposomes
3.	Extravasation into diseased tissue (tumor)	Using small enough (<120 nm, preferably <100 nm) nano-liposomes in order to efficiently extravasate through the gaps in the tumor vasculature (taking advantage of the EPR effect)
4.	Getting active drug into target cells	Releasing drug from liposomes through selective drug leakage at site due to diseased tissue properties, or using: collapsible ion gradient, or liposomes sensitive to secretory phospholipases, or by applying physical means such as heat (thermosensitive nSSL) or ultrasound or by internalization after active targeting.

Note: For relevant references, see Table 1 in Barenholz (2007).

We decided that in order for the liposomes to become an approved anticancer drug the liposomes should be characterized by the following features:

- The drug PK and BD should be controlled by the liposomes, with the liposomal drug demonstrating a highly prolonged plasma circulation time to give it the time needed to achieve drug tumor accumulation.
- In order to be efficacious the liposomes should reach the tumors loaded with a therapeutically high enough drug level.
- Be at the nano scale (nano-liposomes) so they will be able to take advantage of the EPR effect and extravasate from the blood vessels at the tumor into the tumor tissue.
- Drug should be available to tumor cells either by drug release at the tumor site or by the drug loaded nano-liposomes being internalized by the tumor cells.

Table 29.2 describes the requirements we found necessary to achieve therapeutically efficacious passively targeted drug-loaded liposomes for tumor treatment.

29.4.2 Requirements to Achieve Therapeutically Efficacious Passively Targeted Drug Loaded Liposomes and Means to Fulfill Them

Table 29.2 summarizes the requirements to achieve therapeutically efficacious passively targeted drug loaded liposomes and means to fulfill them (based on Barenholz, 2007).

In order to save time, all four aspects described in Table 29.2 were investigated in parallel at four different locations: LTI labs at Menlo Park, CA, by LTI scientists; Papahadjopoulos' lab at University of California, San Francisco (UCSF), by Alberto Gabizon; Terry Allen's lab at the University of Alberta in Canada; and Barenholz's lab in Jerusalem.

LTI, Terry Allen, and Alberto Gabizon/Dimitri Papahadjopoulos worked on getting liposomes of extended circulation and RES avoidance, which due to being at the nano-range size can take advantage of the EPR effect (Matsumura and Maeda, 1986). The EPR effect was expected to result in selective nano-particulates extravasation from the tumor capillaries reaching the tumor tissue. The liposomes with prolonged circulation time and RES

avoidance were termed by Dr. Frank Martin of LTI "Stealth®" liposomes and this unique property of liposomes was referred to as "Stealthness," which means unseen or unrecognized as particulates by the RES.

At the same time I and my student Gilad Haran (now a professor at the Weizmann Institute) were working on the development of a remote and stable loading method for doxorubicin, which should enable the formulation to reach sufficient level of drug to achieve therapeutic efficacy in humans under conditions that the drug when reaching the tumor will be bioavailable to the tumor cells (Barenholz and Haran, 1993, 1994; Haran et al., 1993).

29.4.3 Liposomes Having Prolonged Blood Circulation

In 1987, when I came back to Jerusalem after 1½ years of sabbatical at LTI, Alberto Gabizon just started his sabbatical with Dimitri Papahadjopoulos at USCF. Each of us started to work on different aspects related to how to achieve an improved liposomal doxorubicin formulation. Alberto focused his studies on how to prolong blood circulation of liposomes while I focused on how to achieve stable and high drug loading into liposomes and nano-liposomes. Alberto during his sabbatical worked, with LTI's support and blessing, on liposome formulations with extended circulation time. Terry Allen at the University of Alberta was the first to describe such formulations (Allen and Chonn, 1987; Allen, 1989, US patent 4,837,028). In 1986 we at LTI decided to support her research on this issue. LTI scientists looked also for long-circulating liposomal formulations of various lipid compositions that differed from those studied by Allen and by Gabizon. The latter two scientists added known (but not frequently used) lipids to the liposome lipid composition in order to reach extended circulation time and selective tumor localization, with the focus on gangliosides (Allen) or hydrogenated phosphatidylinositol, HPI (Gabizon). LTI scientists tried and studied novel lipids that were not recognized as known natural lipid species (Woodle et al., 1990, 1991, rev. in Woodle and Lasic, 1992; Woodle, 1993). All three of these groups (associated with LTI) worked in parallel on different formulations and all were using small unilamellar liposomes with narrow unimodal size distribution having a mean size of ~100 nm. These nano-liposomes were prepared by medium pressure extrusion

using polycarbonate filters with defined pore size (Hunt and Papahadjopoulos, 1985, US patent 4,529,561 licensed by UCSF to LTI). All these three labs used different lipid compositions in order to achieve the same goal of extended circulation time, RES avoidance, and intra-tumor accumulation. Terry Allen achieved it by inclusion of sphingomyelin and GM1 ganglioside as liposome-membrane components. Alberto Gabizon was using hydrogenated phosphatidylinositol (HPI) that he included in small liposomes composed of "solid" (high-T_m) lipids and cholesterol (Gabizon and Papahadjopoulos, 1988), while LTI scientists started working with DSPE-PEG [(Annie Yau-Yang's idea combined with Carl Redmann's chemical synthesis (Woodle et al., 1991, US patent 5,013,556, Woodle et al., 1990, rev. in Woodle and Lasic, 1992, and in Woodle, 1993)]. LTI was not the only group to work with PEG-DSPE; at the same time Volodia Torchilin and Leaf Huang and their teams joined forces and worked on it too (Klivanov et al., 1990), as well as Gregor Cevc's lab in Munich (Blume and Cevc, 1990). A comprehensive review on pegylated liposomes is given in many of the chapters in *Stealth Liposomes*, edited by Dan Lasic and Frank Martin (Lasic and Martin, 1995).

29.4.4 The Lesson Learned from Pegylated Proteins

The inspiration and motivation to start working with pegylated lipids like PEG-DSPE came to Annie Yau-Yang and others at LTI from pioneering research in the 1970s by Frank Davis, Abraham Abuchowski, and colleagues who foresaw the potential of the conjugation of polyethylene glycol (PEG) to proteins (Abuchowski et al., 1977). Abuchowski founded Enzon Pharmaceuticals, Inc., which brought three pegylated protein-based drugs to the market. Various length (~350–50,000 Da) chains of PEG polymer are available. Low-molecular-weight drugs were also pegylated. However, the main pegylated products so far are a few proteins and one liposomal formulation—Doxil® (the topic of this review article). For peptides and proteins (including antibody fragments), mainly relatively large PEG polymers of >5000 Da were used. It was found that pegylation helps to improve safety and efficacy as well as to reduce the immunogenicity of many therapeutics (Veronese and Harries, 2002; Veronese and Pasut, 2005). The

suggested mechanism by which pegylation works is that it is a result of the alterations it produces in the physicochemical properties of the molecule to which the PEG residue is covalently attached. These may include changes in level of hydration, conformation, electrostatic binding, and hydrophobicity/ hydrophilicity balance. Level of hydration of the covalently attached highly flexible and highly hydrated PEG [3 to 4 molecules of water per 1 ethylene oxide oxygen (Tirosh et al., 1997, 1998)] induces changes in structure and leads to increase in size and bulkiness. This results in "steric stabilization" which reduces nonspecific protein-protein interaction and nonspecific protein-cell interactions. These physical and chemical changes increase systemic retention of the therapeutic agent. Also, it can influence the binding affinity of the therapeutic moiety to the cell receptors and can alter the absorption and distribution patterns. PEG polymer has two reactive OH groups (one at each end of the PEG); in order to prevent the PEG from inducing intra- and inter-cross linkages, one of these hydroxyl groups was methylated to form mPEG, which in this review is referred to as just PEG).

PEGylation increases the molecular weight and bulkiness of a molecule as well as its level of hydration (see Fig. 29.6), and can impart several significant pharmacological advantages over the native unmodified molecule, such as;

- improved agent solubility
- extended circulating life
- therefore reducing dosage frequency, without diminished efficacy with potentially reduced toxicity
- increased drug stability
- enhanced protection from proteolytic degradation
- reduced immunogenicity

In addition pegylated drugs may have the following commercial advantages:

- opportunities for new delivery formats and dosing regimens
- extended patent life of previously approved drugs

This resulted in the development of many pegylated protein and peptide drugs (only a few of which made it to the market). Now the clinical value of pegylation is well established. ADAGEN (PEG-bovine adenosine deaminase), manufactured by Enzon, was

the first pegylated protein (approved by the FDA in March 1990) to enter the market. It is used to treat X-chromosome-linked severe combined immunogenicity syndrome, as an alternative to bone marrow transplantation and enzyme replacement by gene therapy. Now a large number of pegylated protein and peptide pharmaceuticals are in clinical use. Following are the most successful examples:

- **PEGASYS:** Pegylated interferon alpha for use in the treatment of chronic hepatitis C and hepatitis B (Hoffmann-La Roche)
- **Pegintron:** Pegylated interferon alpha for use in the treatment of chronic hepatitis C and hepatitis B (Schering-Plough/Enzon)
- **Oncaspar:** Pegylated L-asparaginase for the treatment of acute lymphoblastic leukemia in patients who are hypersensitive to the native unmodified form of L-asparaginase (Enzon). This drug was recently approved as a first-line treatment.
- **Neulasta:** Pegylated recombinant methionyl human granulocyte colony-stimulating factor for severe cancer chemotherapy induced neutropenia (Amgen)

Many other pegylated peptides and proteins are now in clinical trials or under development.

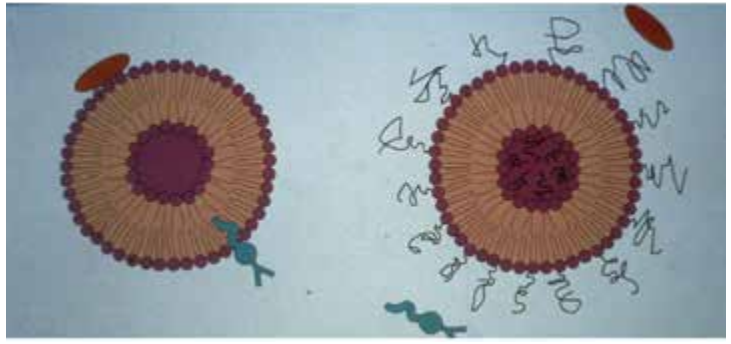

Figure 29.6 A cartoon showing a comparison between conventional and sterically stabilized (pegylated) liposomes (SSL, Stealth liposomes) (Courtesy of the late D. Lasic). The cartoon shows lack of insertion of opsonins into the membrane of Stealth liposomes.

The success of pegylated proteins was the driving force for the successful development of Doxil® as the first FDA-approved liposomal drug and nanodrug (November 17, 1995). In lipids, PEG chains of >350 to 15,000 were tried (equivalent to 8 to 334 ethylene oxide units) and various considerations such as the metabolism of the pegylated lipids and the rate of secretion via the kidneys were used in the decision for which PEG length to select for lipid pegylation.

29.4.5 Why, of All Long Circulating Nano-Liposomes Evaluated, the Pegylated Nano-Liposomes Were Selected as the Basis of Doxil

Each of the labs working on long circulating liposomes described above has its publications and patents on its unique liposome formulations. Having various scientific and practical features (availability, cost, species specificity, etc.), GM1-ganglioside-based formulation was excluded for various reasons described elsewhere (Woodle, 1993; Allen, 1995). At LTI, HPI and PEG-DSPE remained in the race. In order for LTI to decide which of the two lipids will be the one to use in evaluating the novel formulation in human, we performed in 1991 a critical comparative PK experiment in Beagle dogs (Gabizon et al., 1993). Dog is a preferred animal due to its much larger plasma volume (~500 mL), which resembles much better that of human beings in studying the effect of dilution-induced drug release (Gabizon et al., 1991; Amselem et al., 1993a). Therefore, dogs are superior for relevant PK studies to small rodents with their very small plasma volume (and therefore almost no dilution).

The Beagle dog doxorubicin PK study clearly demonstrated that although both liposomal formulations were much better than F-DOX, the PEG-DSPE formulation was superior, as it showed much slower plasma clearance than the HPI formulation.

Using mice peritoneal macrophages (obtained from the ascetic fluid of mice treated with thioglycolate), *in vitro* uptake of Doxil is 40% of the uptake of liposomes of similar size and lipid compositions but lacking 5 mole% PEG-DSPE (Emanuel et al., 1996a). This reduction in macrophage uptake is in direct correlation

with the increase in plasma circulation time. The increase in mole% of PEG-DSPE can further reduce macrophage uptake and probably the nSSL circulation time (Emanuel et al., 1996a, 1996b). For more details on the effect of PEG-DSPE on nano-liposomes, see Garbuzenko et al. (2005).

29.4.6 Remote Loading of Doxorubicin into nSSL to Form Doxil

29.4.6.1 The obligatory need for drug remote loading

For liposome formulation designed for metastatic tumor treatment, intravenous (i.v.) administration is the only option. This determines that only liposomes that can benefit from the EPR effect by being able to extravasate from the blood circulation into the tumor may enable therapeutic efficacy. Because these liposomes have to be small, in the nano-range, a very high level of stable (during storage and blood circulation) drug loading is a must. However, due to the combination of needs for the nano-liposome having the intra-liposomal trapped aqueous volume of only about 1×10^{19} L (calculated from Doxil's ellipsoid axial ratio (determined by cryo-TEM)) and considering the high doxorubicin dose of 50 mg/m^2 required for therapeutic activity, it is critical to achieve a high intra-liposome drug concentration, in the range of hundreds of mM, which is not an easy task, especially since solubility of doxorubicin in the aqueous phase is limited (Barenholz et al., 1993). When the loading is poor, so will be the drug/lipid ratio. This means that either therapeutic levels of drug cannot be reached or therapeutic use of such liposomes will require administering very large amounts of liposomes. In addition, when the loading is inefficient there is a great loss of the active agent during the loading and a need to remove unloaded drug. Therefore, the use of liposomes as a vehicle becomes inefficient as well as uneconomical. The major requirements of drug loading into nano-liposomes are (1) to achieve a high level of loading of active agent in the liposome and to make this loading stable during handling and storage, irrespective of the nature of the agent and (2) to fit the release rate of the loaded active agent to specific therapeutic aims of the liposome formulation.

A careful analysis of the currently available loading approaches reveals clearly that the remote loading approach is the best, and in many cases the only, way to achieve the desired intra-liposome drug concentration (usually defined as drug-to-lipid mole ratio) (Barenholz, 2003, 2007, 2012).

29.4.6.2 Active pharmaceutical ingredient (API) classification and its relevance for drug suitability for efficient remote loading

In 1985 we looked for a simple way to classify drugs by their physicochemical features in a way that will enable the formulator to predict which loading approach to use or, specifically if a drug is suited for a remote loading approach. At that time, with very little available information, we came up with an oversimplified approach and classified all agents into three categories based on their oil/buffer and octanol/buffer partition coefficients (K_p). Category I, molecules having high oil/buffer K_p, which are considered lipophilic; these molecules do not fit liposomes as their carrier and are suitable for delivery via various types of emulsions. Category II, molecules having low oil/buffer partition coefficient and medium to high octanol/buffer K_p; such molecules are amphipathic. Category III, molecules of very low values in both partition coefficients; these by definition are defined as being water-soluble. For some of the molecules, those which are amphipathic weak acids or bases, the classification to group II or III is related to the degree of ionization and therefore it is pH dependent (Barenholz and Cohen, 1995; Barenholz, 2001, 2003). Although the use of octanol/water partition coefficient to determine suitability of molecules to reside in a lipid bilayer is controversial, it is well established that it is indicative of agent transmembrane diffusion rate (Stein, 1986), and therefore it is relevant to loading efficiency, loading stability, and the drug release profile.

In the last five years, We have developed novel modeling approaches to predict the suitability of APIs for the desired remote loading. Here we describe the use of data-mining algorithms on a databank based on the Barenholz Lab's 15 years of liposome research experience with remote loading of nine different APIs. This enabled us to build a dataset of API remote loading drugs

from which to construct a model that relates drug physicochemical properties and remote loading conditions to remote loading efficiency. This modeling is based on more variables than only the partition coefficient (log*P* and/or log*D*) that we used previously (Barenholz and Cohen, 1995; Barenholz, 2003). It includes the details on apolar and polar surface areas of the desired molecule (and the ratio between the two surface areas), its pKa, and log*D* at different pHs. This enables us to better predict, analyze, and optimize the loading process. In order to have an efficient remote loading, pKa and log*D* have to be in a certain range, which defines the range of being amphipathic weak acid or base. This means that at least a certain fraction of the loaded molecule has to be uncharged, and in this range of log*D* we found the apolar and polar surface areas to be highly informative indicators. In addition, sufficient drug solubility in the remote loading medium is required (Zucker et al., 2009).

Later we extended our dataset to 60 remote loaded APIs in 366 loading experiments. This enabled us to further improve our modeling to achieve quantitative structure property relationship (QSPR) models of remote liposome loading. These models are based on both experimental conditions and computed chemical descriptors that were employed as independent variables to predict the initial drug/lipid ratio (D/L) required to achieve high loading efficiency. Both binary (to distinguish high vs. low initial D/L) and continuous (to predict real D/L values) models were generated using advanced machine learning approaches and 5-fold external validation. The external prediction accuracy for binary models was as high as 91–96%; for continuous models the mean coefficient R^2 for regression between predicted versus observed values was 0.76–0.79. It was concluded that QSPR models can be used to identify candidate drugs expected to have high remote loading capacity, while simultaneously optimizing the design of formulation experiments.

In addition, these modeling approaches are also expected to help in designing pro-drugs by transforming them to be amphipathic weak acids or bases suitable for remote loading, thereby enabling remote loading of desired APIs that by themselves cannot be remote loaded (Cern et al., 2012).

Finally, these modeling-dependent predictions were validated. First, they have been used to virtually screen a large API database

to identify candidate molecules for liposomal remote loading. Then candidate APIs were considered for experimental validation based on their predicted remote loading efficiency as well as additional considerations such as availability, recommended dose, and relevance to disease. Three compounds were selected for experimental testing, and all three APIs were confirmed to be correctly classified by previously built and reported QSPR models developed with iterative stochastic elimination (ISE) and k-nearest neighbors (kNN) approaches. In addition, 10 new molecules with known remote liposome loading efficiency that were not used in QSPR model development were identified in the published literature and employed as an additional model validation set. The overall external accuracy of the models was found to be 82–92%. This study presents the first successful attempt to employ QSPR models for the rational design of liposomal drugs, proving the models' utility as efficient and reliable computational tools for the selection of drug candidates suitable for remote loading of liposomes (Cern et al., 2014).

29.4.6.3 The basis of remote loading

As discussed above, only remote (active) drug loading may enable transforming pegylated nano-liposomes (nano-sterically stabilized liposomes, referred to as nSSL) into an approved efficacious drug. This drug loading approach is based on the strategy of fabricating nano-liposomes that exhibit a transmembrane intra-liposome high/external medium low) ion gradient, which acts as the driving force for the remote loading of amphipathic weak acid or base drugs into these liposomes. Historically, in the Barenholz Lab the remote loading approach began from the need to achieve a highly efficient and stable liposomal drug encapsulation that would be stable during storage and, after administration, during the long circulation time in the blood (up to 100 h half-life, Gabizon et al., 2003). This approach was recently discussed by us in detail for nine different drugs (Zucker et al., 2009). It was applied for remote loading of the amphipathic weak base anticancer drug doxorubicin and was the basis for the first FDA-approved pegylated nano-liposomal anticancer drug Doxil®. Since the approval of Doxil (1995), it was successfully employed for other drugs and agents in our and other laboratories (Barenholz and Haran, 1993,

1994; Haran et al., 1993; Lasic et al., 1992, 1995; Clerc and Barenholz, 1995, 1998; Bolotin et al., 1994; Barenholz, 2001, 2007, 2010; Grant et al., 2004; Wasserman et al., 2007; Avnir et al., 2008; Zucker et al., 2009; Cern et al., 2012, 2014).

Overall, from our own experience with nine different drugs (Zucker et al., 2009), we concluded that a transmembrane ammonium sulfate gradient is most suitable for stable encapsulation of amphipathic weak bases, while a transmembrane calcium acetate gradient is most suitable for loading amphipathic weak acids.

The basis of these nano-chemical loading engines is that liposomes are fabricated to exhibit the desired pH and/or ion gradient by using salts composed of either weak bases (e.g., ammonium) or weak acids (e.g., acetate). The degree of ionization of these compounds is pH dependent, their ionized species (i.e., ammonium and acetate) have a very low permeability coefficient and octanol-to-buffer partition coefficient, and therefore they do not, or only very slowly, permeate the liposome lipid bilayer, while their un-ionized species have high permeability as well as octanol-to-buffer partition coefficient (exemplified by ammonia gas and acetic acid) and therefore can diffuse relatively fast across the lipid bilayer and reach the intra-liposome aqueous phase (rev. in Barenholz, 2001, 2007, Zucker et al., 2009). The magnitude of the intra-liposome high/external medium low transmembrane gradient of such ions is the driving force for remote loading, as they can be exchanged with amphipathic drugs (weak acids with acetate and weak bases with ammonium). The counter ion of the gradient-forming ion (e.g., sulfate or calcium in the case of ammonium or acetate gradient, respectively) can be selected so that it will control the state of aggregation and precipitation/crystallization of the drug counter ion salt in the intra-liposome aqueous phase, thereby contributing to control the efficiency and stability of remote loading, as well as drug release rate at various temperatures (Clerc and Barenholz, 1998; Barenholz et al., 2001; Wasserman et al., 2007).

It is important to note that the successful application of this nano-chemical engine benefits from the very small trapped aqueous volume of nano-liposomes (i.e., $\sim 1 \times 10^{-19}$ L per a single Doxil liposome), which supports faster and higher accumulation, as well as intra-liposome precipitation of drug counter ion salt in crystalline or non-crystalline forms.

29.4.6.4 Ammonium sulfate transmembrane-gradient-driven doxorubicin loading into nSSL

For the remote loading of doxorubicin into nSSL, we applied the transmembrane ammonium sulfate gradient under conditions that $[(NH_4)_2SO_4]_{lip} >> [(NH_4)_2SO_4)]_{med}$ (lip is the nSSL and med is the extra-liposome medium). Figure 29.7 describes the overall mechanism of this loading process. The drug loading is actually a base exchange of the amphipathic weak base drug with the ammonium ions. For doxorubicin >90% drug encapsulation was obtained. Doxorubicin is accumulated in the intra-liposome aqueous phase, where it reaches a concentration >100-fold the drug level in the loading medium (this explains why we refer to it as active loading, as it goes against the drug concentration gradient). Based on various spectral analyses, including X-ray diffraction (Barenholz and Haran, 1993; Haran et al., 1993; Lasic et al., 1992, 1995), almost all the encapsulated doxorubicin is in the intra-liposome aqueous phase and most of it is in the form of aggregated (crystalline) $[doxorubicin]_2SO_4$ salt. The loading is dependent on the ammonium ion gradient, while the loading stability is dependent on the liposome lipid composition and on the level of $[doxorubicin]_2SO_4$ precipitation, as well as temperature. The ammonium sulfate transmembrane-gradient-driven drug loading differs from most other remote loading approaches since it neither requires fabrication of liposomes in acidic pH, nor alkalinization of the extra-liposome aqueous phase.

Doxil is a good example of remote loading by an ammonium sulfate gradient under conditions that $[(NH_4)_2SO_4]_{lip} >> [(NH_4)_2SO_4)]_{med}$. Figure 29.7 describes the overall mechanism of this loading process. (For more details see Barenholz and Haran, 1993, 1994; Haran et al., 1993; Bolotin et al., 1994; Lasic et al., 1992; Lasic et al., 1995; Clerc and Barenholz, 1998; Barenholz, 2001, 2007; Zucker et al., 2009.)

The efficiency of loading by this method and its stability are dependent on the following (Barenholz and Cohen, 1995; Barenholz, 1998):

(1) the large ($\sim 10^{12}$) difference in permeability coefficient of the neutral ammonia (10^{-1} cm/s) and the SO_4^{2-} anion ($<10^{-12}$ cm/s)
(2) the initial pH gradient having the $[H^+]_{lip} >> [H^+]_{med}$

(3) the low solubility of $(\text{doxorubicin})_2\text{–}SO_4$ (>2 mM), which also minimizes intra-liposomal osmotic pressure and therefore helps to keep liposome integrity
(4) the asymmetry in doxorubicin partition coefficient (K_p)
(K_p lip/external med > K_p lip/intra-lip med)
(K_p oct/external med > K_p oct/intra-lip med)

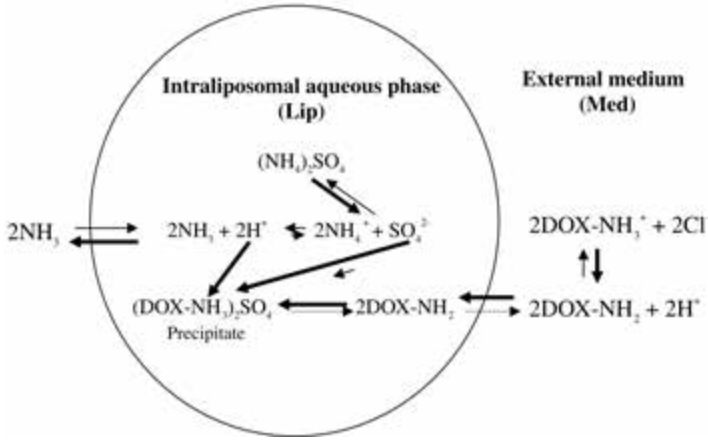

Figure 29.7 Doxorubicin remote loading into nSSL exhibiting a transmembrane ammonium ion gradient ⟶ represents processes occurring during drug loading, ⟶ represents processes occurring during drug release.

K_p is a partition coefficient between the two phases defined in the brackets. Lip = liposome membrane, med = aqueous medium either external or intraliposomal, oct = bulk octanol phase.

This asymmetry means that the K_p of doxorubicin (abbreviated as DOX) in the extra-liposomal medium supports influx in a direction opposite to the ammonium sulfate gradient (namely, into the liposomes), while the K_p of DOX in the intra-liposomal aqueous phase acts to reduce partition into the membrane, thereby reducing the desorption rate (k_{off}). The reduction in DOX K_p in the intra-liposomal aqueous phase is driven by the ammonium sulfate remaining inside the intra-liposomal aqueous phase after DOX remote loading. Therefore, it seems that ammonium sulfate plays a multifactorial role in the remote loading and retention of the loaded drug in the liposomes. For Doxil the interplay between

the above four points, when combined with Doxil membrane composition and liposome size, determines liposome performance.

Another issue, so far neglected, which is especially relevant to drugs such as doxorubicin, is their tendency to self-aggregate (rev. in Fülöp et al., 2013), forming oligomers of various mer number. This phenomenon results from the stacking of the planar aromatic rings of the anthracyclines due to interaction between the π electrons of the rings. This self-aggregation is facilitated by increasing ionic strength. DOX dimers appear already at 1 μM and larger aggregates at higher DOX concentrations. The effect of such oligomerization on therapeutic efficacy is not yet clear. However, based on simple geometric considerations, it is obvious that non-monomeric DOX cannot interact with DNA in the same way as monomeric DOX, and the exact location between the two DNA strands should differ (Fülöp et al., 2013). Therefore, the way by which the drug is internalized (monomers versus aggregated form) by the tumor cell may be an important factor in drug efficacy.

The breakthrough in using remote (active) loading driven by the transmembrane ammonium sulfate gradient for the doxorubicin is one of the main reasons that enabled successful clinical use of Doxil and its approval by the regulatory agencies worldwide.

29.4.7 The Role of Drug Release Rate (k_{off})

The results of liposome loading when combined with liposome structure, lipid composition, and site of injection will determine rate of drug release in plasma (Barenholz and Cohen, 1995). For example, for i.v.-administrated liposomal drug formulation, only when the drug release (determined by k_{off}) is slower than the liposome clearance (k_c) will the liposome determine drug pharmacokinetics and biodistribution. When $k_{off} > k_c$, then the ratio k_{off}/k_c is a measure of the rate of drug release *in vivo*. Controlling this ratio is obligatory to achieve controlled drug release in blood or in the tissues reached by the liposomes. Therefore, this ratio also affects therapeutic efficacy of the liposomal drug. For drugs of fast clearance, when $k_{off} >> k_c$ the benefits of use of liposomes for drug delivery will be minimal or none, as the performance of the

liposomal drug will be similar to that of the free drug. This is exemplified by our first generation failed OLV-DOX formulation (see above). An efficient and functional way to test the release rate is a cytotoxicity test measuring doxorubicin IC_{50} in cell culture. As described by Horowitz et al. (1992), Doxil has ~2 orders of magnitude higher IC_{50} (lower cytotoxic activity) than free doxorubicin, while as described in Section 29.2.3 above, our failed OLV-DOX has similar IC_{50} to free doxorubicin. These differences demonstrate nicely that the large dilution-induced release that basically "killed" the performance of OLV-DOX in humans does not occur in Doxil. To make sure that our interpretation is correct we studied the effect of nigericin on doxorubicin release and IC_{50}. Nigericin is an ionophore that collapses the pH and ammonium gradient by exchanging the intra-liposome protons with extra-liposome medium potassium ions. Exposure of Doxil to nigericin caused complete drug release (Barenholz, 2007), which was paralleled by reducing the IC_{50} to the low level of free doxorubicin, proving that Doxil's excellent drug retention is the reason for Doxil's better IC_{50} (Horowitz et al., 1992).

However, the opposite (very low k_{off}) is as bad. Namely, when k_{off} is too slow and there is no liposome uptake by the target cells, there will be no therapeutic efficacy even if the loaded liposomes will reach the target very efficiently, as the free drug concentration at the target tissue will be too low. The absolute necessity of drug release was demonstrated in the instance of Stealth cisplatin (Zamboni et al., 2004), which is identical to Doxil in lipid composition, size, circulation time, and accumulation at the tumor site. However, it lacks therapeutic activity due to insufficient drug release (Lasic et al., 1999; Peleg-Shulman et al., 2001; Zamboni, et al., 2004).

Recently the utility of the limitation and restriction of remote loading of hydrophobic/amphipathic APIs to include only APIs, which "as is" are amphipathic weak acids or bases, was reduced by two new concepts. First, direct chemical modification of the API to chemically convert it to a weak amphipathic acid or base prodrug, which will be remotely loaded, and then when release occurs or in the liposomes once in the body, the prodrug will be hydrolyzed to the active drug. This is exemplified by the use of hemisuccinate derivatives of steroids, prodrugs that are amphipathic weak acids (Avnir et al., 2008, 2011; Waknine et al., 2013). The

second approach, more general and not requiring any chemical modification, is described by Sure et al., 2014. These authors complexed the hydrophobic drugs into cyclodextrins designed to fit remote loading by binding them covalently to ionizable weak acidic or weak basic groups. These complexes present sufficient aqueous solubility concomitantly with behaving like amphipathic weak acids or bases so they can be remotely loaded by trans-membrane ion and/or proton gradient in the same way as APIs, which are amphipathic weak acids or bases that are remotely loaded (Barenholz, 2001, 2003; Zucker et al., 2009; Cern et al., 2012; Cern et al., 2014). This novel approach is increasing very much the repertoire of APIs that meet the requirements of remote loading.

29.4.8 Doxil: Each Part Matters

In Doxil each part matters and contributes to the optimized performance (Fig. 29.8). Doxil is an excellent example to demonstrate the obligatory role of lipid biophysics in the success of liposome-based drugs.

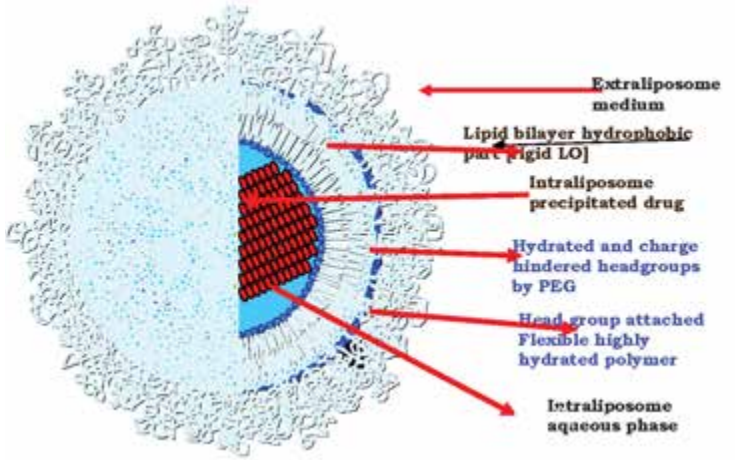

Figure 29.8 A cartoon of Doxil® = pegylated nano (<100 nm) unilamellar liposome. It is based on cryo-TEM, SAXS, WAXS, DLS, compressibility, and doxorubicin absorbance and fluorescence (Lasic et al., 1992, 1995; Haran et al., 1993, Tirosh et al., 1998).

A calculation based on the lipid molar concentration of the components and on liposome size reveals that 1 mL of the Doxil dispersion contains 2.3×10^{14} liposomes and each liposome contains ~10,000–20,000 molecules of doxorubicin, >95% of which is in the crystalline phase.

29.4.9 Doxil-Related I.P.

It is important to note that Doxil® is based on two families of patents. One family covers the effect of adding the lipopolymer PEG-DSPE as a liposome lipid component on liposome circulation time (Woodle et al., 1991; US patent 5,013,556).

The second patent family is on the transmembrane-driven remote loading of amphipathic weak bases such as doxorubicin (Barenholz and Haran, 1993 and 1994, US patents 5,192,549 and 5,316,771). Namely, there is no direct patent on Doxil!

It took 7.5 years from the submission of these two families of patent applications in 1988/1989 until Doxil approval in November 1995. As remote loading patents were extended until March 9, 2010, Doxil enjoyed 14 years of patent protection.

29.5 Doxil Performance in Humans

29.5.1 Pharmacokinetics and Passive Targeting to Tumors

The data presented in Fig. 29.9 are the first proof for passive targeting due the EPR effect in humans (Gabizon et al., 1994a).

Doxorubicin, when administered as Doxil, demonstrated high and selective tumor localization as was first demonstrated in our “first in man Doxil” study, in Jerusalem in 1991–1994 and published in *Cancer Research* in 1994 (Gabizon et al., 1994; Fig. 29.9).

This pilot study, which includes 53 courses of Doxil (average 3 per patient spaced 3 to 4 weeks apart) was aimed to characterize and compare in cancer patients the pharmacokinetics and accumulation of doxorubicin in malignant effusions after administration of Doxil or of free drug (DOX). It clearly demonstrated much higher levels of doxorubicin both in cells and

interstitial fluids of the tumor after Doxil administration than after DOX administration. Using the cationic ion exchanger Dowex-50 (Druckmann et al., 1989; Amselem et al., 1990), we found that more than 98% of the plasma doxorubicin after Doxil i.v. administration is liposome associated. Pharmacokinetics was determined for 25 and 50 mg/m^2. The plasma elimination time of Doxil followed a biexponential curve with half-lives of 2 and 45 h (median values), most of the dose being cleared from plasma under the longer half-life. A large difference in volume of distribution was also found (4 L for Doxil versus 254 L for free DOX. Similarly, doxorubicin derived from Doxil showed a much slower rate of clearance (compare 0.1 L/h for Doxil with 45 L/h for free DOX).

The types of Doxil-derived doxorubicin metabolites in patients' urine were identical to those of patients injected with free DOX; however, the overall urinary excretion in the Doxil group was significantly reduced. Most encouraging were the results on the level of drug at the malignant effusions, which were 4 to 16 times higher than after free DOX administration. In addition, doxorubicin level there peaked after Doxil administration between 3 to 7 days, which means the exposure of the tumor cell to the drug is much longer than after free DOX administration. HPLC analysis of the drug at the tumor site demonstrated that a large fraction of the doxorubicin was metabolized to the conventional metabolites of doxorubicin. The fact that doxorubicin is metabolized only intracellularly and not in the plasma, indicates internalization of the doxorubicin derived from Doxil by cells. Two different mechanisms may explain this: Doxorubicin can be released outside the tumor cell and be taken up by it, or Doxil can be taken up by the tumor cell and then doxorubicin is released. These data are in excellent agreement with our preclinical studies and indicate that stable remote loading of doxorubicin into long-circulating nano-liposomes serves well the objective of passive targeting of doxorubicin to tumors. Our 1994 *Cancer Research* paper is the first demonstration of the of EPR relevance in cancer patients to antitumor therapy by nanodrugs.

The localization of Doxil in humans' tumors was further supported by direct fluorescence microscopy of patient biopsies (Symon et al., 1999).

For extended information on the superiority of the pharmacokinetic (PK) performance of Doxil, see Gabizon et al.

(2003). That review summarizes the PK profile in humans at doses between 10 and 80 mg/m^2. The PK has one or two distribution phases: an initial phase, with a half-life of 1–3 h, and a second phase responsible for most of the clearance, with a half-life of 30–90 h. The AUC after a dose of 50 mg/m^2 is approximately 300-fold greater than that with free drug. Clearance and volume of distribution are drastically reduced (at least 250-fold and 60-fold, respectively). These studies indicate the importance of utilizing the distinct pharmacokinetic parameters of pegylated liposomal doxorubicin in dose scheduling.

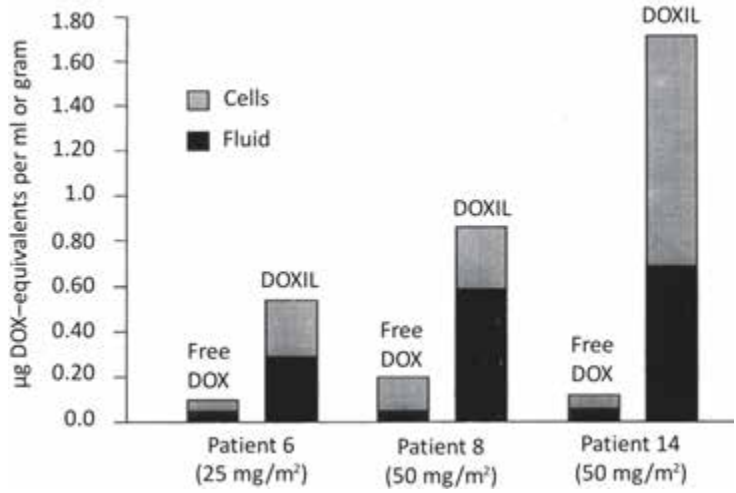

Figure 29.9 Doxorubicin levels in patients' tumor biopsies, comparing free doxorubicin and Doxil (from Gabizon et al., 1994a, 1995).

29.5.2 Doxil Tolerability

It was already demonstrated in our *Cancer Research* publication (Gabizon et al., 1994a) that overall Doxil is well tolerated and shows a distinct superiority over free DOX in most evaluated side effects. However, two side effects not typical of what is observed for conventional doxorubicin treatment were observed. The first of these shows up as flushing and shortness of breath; it is also referred to as acute infusion reaction or pseudo-allergy (Gabizon et al., 2008; Szebeni and Barenholz, 2011) and is reduced by reducing rate of infusion. This side effect was recently reviewed by

Szebeni and Barenholz, 2011 and Szebeni et al., 2011. The second effect that results is grade 2 or 3 of desquamating dermatitis and is referred to as Palmar Plantar Erythrodysthesia (PPE) or "foot and hand syndrome." The second effect increased with dose and was more pronounced for 3-week intervals than 4-week intervals between treatments (for more details see Solomon and Gabizon, 2008). For more details on Doxil tolerability and side effects see Doxil homepage (www.doxil.com) and drugs online (www.drugs.com/pro/doxil.html).

29.5.3 Doxil Therapeutic Indications

In this review I will not discuss in detail Doxil's clinical performance, which is covered in many scientific papers, reviews, and reports. On December 14, 2014, Doxil Google citations exceeded 296,000 citations, compared with 171,000 on April 4, 2011. Many of these citations are related to clinical aspects of Doxil.

A good starting point to review clinical aspects of Doxil use is covered in two reviews, one by Solomon and Gabizon (2008), the second by Ferrandina et al., 2010; also in Wikipedia and two highly relevant Web sites, Doxil homepage (www.doxil.com), and drugs online (www.drugs.com/pro/doxil.html). A summary of indications approved for Doxil by U.S. FDA and/or European Medicines Evaluation Agency (EMA) and approval year is given below.

- AIDS-related Kaposi's sarcoma: Superior efficacy over former conventional therapy (1995).
- Recurrent ovarian cancer: Superior efficacy and improved safety profile over comparator drug (topotecan) (1998), as demonstrated first by Gordon et al., 2001.
- Metastatic breast cancer: Equivalent efficacy and reduced cardiotoxicity compared to free doxorubicin (2003).
- Multiple myeloma: Equivalent efficacy and improved safety profile compared to free doxorubicin combo. Superior efficacy in combination with bortezomib over single agent bortezomib (2007).
- Many more drug combinations which involve Doxil are currently in various stages of clinical work including studies with other low-molecular-weight APIs and with antibodies.

If successful, they will further extend clinical use of Doxil and its generic, Lipodox. The combination with low-molecular-weight APIs is exemplified by the combination with Yondelis (trabectedin), a novel, multimodal, synthetically produced antitumor agent, originally derived from the sea squirt, *Ecteinascidia turbinata*. The anticancer medicine works by preventing the tumor cells from multiplying. It is approved in 77 countries within North America, Europe, South America, and Asia, for the treatment of advanced soft-tissue sarcomas as a single-agent, and in 70 countries for relapsed ovarian cancer in combination with Doxil/Caelyx (doxorubicin HCl liposome injection).

- In addition, regarding cardiac function, Doxil demonstrates major reduction of cardiotoxicity as compared to free doxorubicin in all settings (2000).

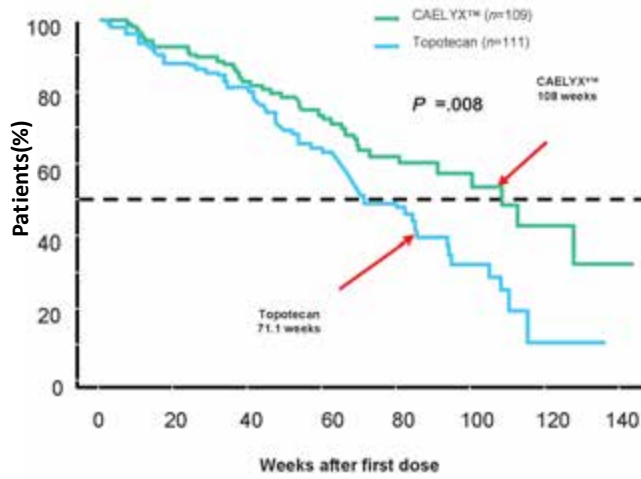

Figure 29.10 Caelyx™ (=Doxil) is superior to topotecan in ovarian cancer survival (from Gordon et al. 2001).

29.5.4 Relevance of Tumor Microenvironment to the Therapeutic Efficacy of Doxil

Doxil® shows much higher drug levels in the tumor tissue than does doxorubicin administered as free drug. This is explained by the enhanced permeability and retention (EPR) effect (Gabizon, et al.

1994; Barenholz, 2012). Many aspects related to the relationship between therapeutic efficacy and the EPR effect remain controversial despite extensive research. Recent studies by Song et al. (2015) and Chauhan et al. (2012) show a large variability in the EPR effect and in the microenvironments of two mouse tumor models representing breast tumor subtypes. These studies demonstrate that Doxil acts primarily by direct cytotoxic effect, and that differences in the extracellular collagen matrix can neither explain the differences in PLD tumor accumulation, nor in therapeutic efficacy. However, although getting enough nanodrug to the tumor site is essential, it is not sufficient. The API must enter the tumor cell in order to be efficacious. This review focuses on how the doxorubicin from Doxil reaches the tumor cells.

Based on pharmacokinetic (PK) and biodistribution (BD) studies, it has been established that with Doxil in both animal models (Song et al., 2014) and in humans (Gabizon et al., 1994; Barenholz, 2012) there is only minimal drug release in the blood; virtually all the drug circulating in plasma is encapsulated in liposomes. Tumor cell uptake of intact Doxil liposomes is not a major factor in delivering doxorubicin to tumor cells (Horowitz et al., 1992; Huang et al., 1992; Yuan et al., 1994; Jung et al., 2009). Achieving therapeutic efficacy is therefore dependent on sufficient levels of drug release. The absolute necessity of drug release was demonstrated in the instance of Stealth cisplatin, (Zamboni et al., 2004) which is identical to Doxil in lipid composition, size, circulation time, and accumulation at the tumor site. However, it lacks therapeutic activity due to insufficient drug release (Peleg-Shulman et al., 2001; Zamboni et al., 2004).

We (Silverman and Barenholz, unpublished results) propose that ammonia resulting from tumor cell metabolism, primarily glutaminolysis, enhances doxorubicin release from Doxil in tumor tissue at therapeutically effective levels. Indeed, drug release in tumor interstitial fluid is much faster than in plasma (Fig. 4 in Gabizon, 1995). We searched for a tumor micro-environment factor that relates to the unique metabolome of tumor cells. This search led us to glutaminolysis, a metabolic pathway predominant in tumor cells (Moreadith and Lehninger, 1984). Because of cancer cells' increased requirement for energy in comparison to healthy cells, the standard glycolytic pathway is supplemented or even

replaced by the glutaminolysis pathway (Wang et al., 2015). Glutaminolysis imaging was performed by Koglin et al. (2011), using (4S)-4-(3-18F-fluoropropyl)-L-glutamate (^{19}F-FSPG) as a PET tracer in tumor-bearing mice, where ^{19}F-FSPG makes it possible to discriminate between non-cancerous inflamed tissue, which lacks glutaminolysis, and tumors, which do use glutaminolysis (Fig. 29.5 in Koglin et al., 2011). The same ^{19}F-FSPG has been successfully used by Baek et al. (2012, 2013) in humans. This not only confirms the activity of glutaminolysis in tumors, but also potentially provides a method to predict the efficacy of Doxil treatment at the level of the individual patient.

A few words about glutaminolysis, a metabolic pathway unique to tumor metabolome, in which glutamine, the most abundant amino acid in plasma (Meister, 1956) together with glutamate, are the major respiratory substrates of cancer cells. In glutaminolysis, for each glutamine molecule that enters the metabolic pathway, two ammonia molecules are produced. In this respect, this metabolic pathway of tumor cells was shown to differ substantially from the metabolic pathways in the mitochondria of normal cells. (Moreadith and Lehninger, 1984). The glutaminolytic pathway and its connection to ammonia was just recently examined by Wang et al. (2015), who state that ammonia is not merely a byproduct of glutaminolysis, but is necessary for cancer cells to maintain their pH. A major role of glutaminolysis in tumor cell metabolism is to produce intermediates that in normal cells are produced by the Krebs cycle. In tumors, the Krebs cycle is much less effective than in normal tissue. Ammonia gas is both highly diffusible and highly membrane-permeable, and its permeability coefficient in cholesterol-containing lipid bilayers is very high, 0.13 cm/s (Deamer and Bramhall, 1986; de Gier, 1993). Therefore it should be internalized by liposomes very quickly.

In a way, this process is the “reverse” of the remote loading process (described in Fig. 29.7). Accordingly, Doxil, which reached the tumor by the EPR effect, internalizes neutral ammonia gas produced during tumor cell glutaminolysis. In the intraliposome aqueous phase this ammonia acquires protons from the doxorubicin and the resultant uncharged doxorubicin is released from the liposome to the tumor interstitial fluid.

29.6 What Is New about Doxil since 2011

This is an update of a 2011 review (Barenholz, 2011). Since then much more work related to Doxil has been done, which explains the additional 125,000 Google citations. Although most of these citations are related to clinical aspects, there are many that deal with preclinical and basic research. As Doxil's patents expired in 2009, major efforts by many players were dedicated to the development of a generic version of Doxil. However, this is not an easy task, as is obvious from the very long time passed between the patent expiration date and the date of the approval of the first generic, Lipodox, by Sun Pharma in February 2013.

The explanation of the difficulties is related to the requirements of the FDA, especially with regard to the CMC and *in vitro* equivalence requirements, as summarized below.

FDA CMC requirements of "Generic of Doxil" (http://www.fda.gov/downloads/Drugs/GuidanceComplianceRegulatoryInformation/Guidances/UCM199635.pdf)

This CMC is based on detailed chemical and physicochemical parameters and includes:

Equivalent composition and its relevance:

Chemical: drug-to-lipid ratios, amounts of free and encapsulated drug, percent drug encapsulation, lipid bilayer phase transitions, excipients

In depth liposome characterization including:

Liposome size distribution and morphology as demonstrated on multiple batches and samples of test and reference products (number of lamellae, lipid bilayer phase transition and X-ray diffraction pattern of lipid bilayers and intraliposome drug nanocrystal, also liposome entrapped volume)

Internal liposome environment:

Drug loading using an ammonium sulfate gradient, internal pH, magnitude of the pH gradient across the membrane, equivalence in the doxorubicin sulfate level, presence and structure by SAXS, WAXS and cryo-TEM of DOX-sulfate precipitate inside the liposomes

Surface properties:

Electrical surface and zeta potential, PEG layer thickness, equivalent concentrations and size of grafted PEG at the surface, equivalent PEG-lipid chemistry to prevent premature cleavage of the PEG from the liposome surface

Equivalent drug release rates in a variety of conditions that result in equivalent drug delivery to target (tumor) cells

Under different physiologically relevant solutions, e.g., human plasma, a range of pH values, a range of temperatures, under low frequency ultrasound.

These requirements will also be applied to other liposome based nanodrugs under development. In order to achieve all the above FDA requirements, we built a network of experts, and together we developed these methodologies (see acknowledgments below).

29.7 Conclusions, Take Home Lessons, and What Is Next?

To sum up, the anticancer nanodrug Doxil shows good clinical performance in a variety of neoplastic conditions due to its improved antitumor therapeutic efficacy and unique reduced safety profile, especially its impressive reduction in cardiac toxicity when compared with conventional doxorubicin. Of the more than 10 liposomal drugs approved (Zhang et al., 2001), Doxil has the most extensive clinical use.

Based on Doxil's success, various novel drug formulations, including modified Doxil, or those based on other drugs or drug combinations with a similar approach to that of Doxil, are now at different stages of development. These novel nanodrug formulations should have reduced (or no) side effects of acute infusion reactions, or of hand and foot syndrome. One approach to achieve the latter objective is to slightly reduce the half-life of the liposomal doxorubicin by replacing the sulfate-counterion of the ammonium used for the remote loading with the monovalent counterion methanesulfonate (MS). The use of MS, which has a permeability coefficient similar to sulfate, but does not induce intra-liposome drug precipitation, results in a somewhat faster drug release rate. But without loss of therapeutic efficacy in tumor-

bearing mice. bearing-mice. This relatively small but distinct effect on the release rate leads to significantly lower frequency and severity of hand and foot syndrome (Barenholz et al., 2013, US Patent application). hand and foot syndrome. Other ways to extend and improve nano-liposome-based anticancer therapy is to have a better control of drug release (rev. in Barenholz, 2007, 2012) using external means, such as hyperthermia (Needham et al., 2000, 2001; Andrianov et al., 2014); focused ultrasound (Schroeder et al., 2007, 2009a, 2009b); or use of a drug combination by remote loading of two drugs that act synergistically into one liposome (Zucker et al., 2010, 2012); or a combination of two different treatment modalities such as Doxil and interleukin 2 (IL-2) in liposome-based immunotherapy (Cabanas et al., 1999). The latter stems from the fact that doxorubicin when administered as Doxil is not toxic to the immune system and therefore IL-2 when delivered in liposomes is highly efficacious. The idea behind this chemo-immuno treatment combination is that the Doxil will take care of most of the tumor burden, while the immunotherapy elicited by the IL-2 will activate the intact immune system enabling it to kill the residual tumor cells (Cabanas et al., 1999). The use of liposomal IL-2 results in lower toxicity of the IL-2 and prolongation of IL-2 circulation time without loss of its potency (Kedar et al., 1994a, 1994b). A very promising approach is the one used recently by Jain and coworkers (Diop-Frimpong et al., 2011). Accordingly, losartan, which inhibits collagen I synthesis was used to modify the interstitial tumor environment, leading to increase in Doxil (and other nano-particulates) accumulation in tumors, thereby increasing Doxil therapeutic efficacy.

The story of Doxil development carries two important messages. The first one is that Doxil's successful development opens the way to major improvement in tumor therapy and especially it served as a gold standard in the new field referred to as nanomedicine. The second one is that development of such a complex drug system requires having a highly multidisciplinary team that can deal in an integrative way with all the expertise needed (Gabizon et al., 1995, 1999; Barenholz, 2003, 2007, 2012). Not less important is the recognition that the understanding and optimal utilization of physicochemical principles are crucial to the successful development of such a complex drug product.

29.8 Doxil Historical Perspectives

Pre-Doxil era (liver passively targeted by liposomal doxorubicin)
1979 Gabizon and Barenholz start their basic research on liposomal doxorubicin
1984 The first clinical trial with liposomal doxorubicin based on conventional non-pegylated large negatively charged oligolamellar liposomes (OLV-DOX)
1985 LTI licensed the OLV-DOX technology
1987 Clinical trial of OLV-DOX failed
1987/1988 Barenholz developed and Yissum, R & D Company of the Hebrew University of Jerusalem, Israel patented new concept of doxorubicin remote loading, driven by transmembrane gradient of ammonium sulfate. The first patent was filed in 1988. This technology was licensed to LTI and serves as one of the legs of Doxil (Barenholz and Haran, 1993, 1994).
1989 LTI patented the Stealth concept and registered Stealth®
1989 Gabizon and LTI started to develop sterically stabilized (Stealth) liposomes
1989 LTI, Gabizon, and Barenholz started Doxil® development
1991–1992 Doxil "First in man" clinical trial in Jerusalem
1994 Gabizon and Barenholz's major publication on Doxil clinical trial (*Cancer Research*)
1995 (November 17) FDA approved Doxil
1996 First Doxil sales in USA and (as Caelyx) Europe
2009 (March) US patent expired
2011 Ben Venue laboratories, Inc., the only site where Doxil/Caelyx was produced, was shut down
2013 (February) FDA approved Lipodox as the first Doxil generic

29.9 Personal Touch

The road to the development of Doxil® involved many people; most of them became my personal friends with whom I interacted for many years. This story started in 1984 when I met Dimitri Papahadjopoulos from UCSF, a long-time friend and colleague "liposomologist." We met at various conferences since 1974, when I was on an extended sabbatical (1973–1976) at the Department of Biochemistry of the University of Virginia (UVA) Medical School, in

Charlottesville, VA. The reason for me to come to UVA for sabbatical was that this department, headed by Thomas Thompson, was one of the world centers (and considered a Mecca) of membrane and liposome biophysical research. Thomas Thompson and other scientists of UVA, especially Chien Huang and Burt Litman, were leading membrane and liposome physical chemists. An important part of my PhD research was carried out in 1969 at the Animal Research Council Institute at Babraham, near Cambridge, UK, under the supervision of Rex Dawson and Peter Quinn, from whom I learned about lipid monolayers at the air/water interface, and Alec Bangham, who introduced me to liposomes.

I believed that lipid and membrane physical chemistry are crucial to membrane research, and that is why I decided to spend my first sabbatical at UVA. The UVA group was in tight competition with the UCSF group of Dimitri Papahadjopoulos, although the interests of the two groups were only partially overlapping, as the UVA focused on lipid biophysics and physical chemistry and the UCSF group focused more on biologically relevant topics such as fusion, interaction of liposomes with cells, etc. Every time Dimitri and I met, we talked extensively on science (mainly membrane and liposome research), as well as on culture, art, history, food, and wine. Dimitri kept telling me about Liposome Technology Inc. (LTI), a startup located at Menlo Park, CA, which focuses its R & D in the field of liposome-based diagnostic and medical applications. Dimitri, together with his previous student Frank Szoka, were the scientific founders and mentors of this company. Nick Arvanitidis was convinced by Dimitri to be LTI CEO, and Frank Martin, another student of Dimitri's was the first LTI employee. Nick brought with him Sally Davenport, Carl Grove, and Kathy, who had worked in Nick's previous R & D company, to deal with LTI administration.

Dimitri asked me if I would be interested to spend a sabbatical at LTI. He told me that it is a great challenge but also a large reward regarding satisfaction. He already knew about our efforts in the field of drug delivery and that we were close to the "first in man" experiment, but he was more interested in my knowledge and experience in lipid and liposome biophysics and physical chemistry, as he well understood that this is the heart of the matter of developing liposomal products. I hesitated as, so far, most of my research was academic in nature. Dimitri proposed that I come to his lab at UCSF, give a seminar there, and he would organize my visit at LTI so I would be able to judge for myself if spending a

sabbatical at LTI would be of any interest to me. I also got a formal invitation from Nick, LTI CEO, to visit LTI and spend a day there.

As things looked serious, I consulted with Hanna, my wife, who supported me and encouraged me to evaluate this interesting proposition. I knew this was not easy for her, as it meant that I may be away from home (in California) for long periods of time and she would have to take care, alone, of our four daughters, the dog, and our home, which is not easy. With her encouragement, I accepted Dimitri's and Nick's offers to visit. My visit at Dimitri's and at LTI was organized for December 1984. My seminar at Dimitri's lab was on glycosphingolipid biophysics, which was followed by discussion with Dimitri's lab people. The next day Dimitri drove me to LTI in Menlo Park, which at that time was a startup company of ~40 people, where I spent the whole day talking with many company employees. After dinner with Nick and some good wine, Nick and I had a long conversion in which Nick was trying to convince me to spend my sabbatical at LTI. Nick is Greek, and as such he understood well the Mediterranean mentality and way of thinking, so we understood each other very well. Without going into detail and possibly with the aid of the good wine served continuously by Nick, late at night I agreed to seriously consider his proposal. Nick drove me to my San Francisco hotel very late that night. The excitement, together with the 10 h jetlag, made it very difficult for me to sleep.

Returning to Israel, I discussed Nick's proposal with Hanna, and with her support and encouragement, I accepted it. I told Dimitri and Nick that I would not be able to come unless LTI would support our OLV-DOX program. It took a short time until the LTI board decided to accept my request. Frank Szoka, Dimitri, and Nick called me from the board meeting at 02:00 AM Israel time and woke me up, to tell me that LTI had accepted my request. But their condition was that I assure them of my continuous involvement in their relevant research, and R & D programs. LTI support meant what was considered a large grant at that time, which would allow us to continue our OLV-DOX research, and especially the "first in man" clinical trial. So, it seemed we had a deal, the small details of which still needed to be finalized.

At about that time, I was approached by another US company that proposed to license from us the OLV-DOX technology and product. Their proposal was tempting, as it involved what I considered then a large sum of money, up-front and reasonable

royalties. However, this company requested that Alberto and I would be used only as consultants and not be involved in the research and R & D of the product. I did not like this idea, as we looked upon the product as a baby we have to nurture to maturity. I preferred LTI to the other company as I believed that our day-to-day involvement in the product development is crucial to the program's success. The future would show that I was right. So I convinced Moshe Vigdor, the CEO of Yissum (the Research and Development Company of The Hebrew University of Jerusalem) to accept LTI's proposal. It did not take Nick long to come to Israel and finish the LTI–Yissum first license agreement, which was the basis for a master agreement that continued for 21 years. It started with LTI with Nick as CEO and went all the way to Johnson & Johnson.

After Doxil's approval by the FDA, there was a change of management at LTI, and Craig Henderson, a top-level oncologist from UCSF (who had been involved in Doxil's clinical development), became LTI CEO. Then, the company name was changed to Sequus. Craig and others sold Sequus to ALZA, Mountain View, CA (a major drug delivery company), with Doxil (due to its increasing sales) being one of the main reasons for the deal. It did not take a long time for ALZA to be bought by Johnson and Johnson, which until then was hardly involved in drug delivery systems. Again, Doxil was one of the main reasons for the deal. All the rest is history!

During this fantastic very long voyage of 50 wonderful years of active research, I met many fascinating people, with whom I interacted and/or collaborated, and many of them remain lifelong friends. The 36 years I worked on liposomal doxorubicin were a unique experience I will never forget. It enabled me to be involved in a very complicated and complex process of drug development and approval by FDA and EMA and to enjoy Doxil/Caelyx approval worldwide. This gained knowledge enabled me together with others to develop other liposome-based drugs. In terms of satisfaction, the reward from the development of Doxil is unmatched by any of my other achievements. Now I am trying hard to transfer my experience, part of which is summarized in this review, to many students and others worldwide.

Special Acknowledgments

This review is dedicated to my wife, Hanna. Without her encouragement, advice, patience, dedication, and support

throughout our 55 years of life together, I would not have been able to accomplish my part of Doxil development. I also want to thank my four daughters, Chagit, Ayelet, Tamar, and Avigail, who grew up during the years described in this review; their husbands, Uri, Perri, Ron, and Assaf; and last but not least our 12 grandchildren, Yael, Yuval, Amit, Omri, Inbar, Mika, Rotem, Guy, Eyal, Gal, Dror, and Kfir, who give us so much joy. Our daughters and grandchildren were my escape during periods of despair.

Professionally, I would like to thank a few of the many people who deserve my gratitude: Alberto Gabizon, a 35-year partner in exciting research, including Doxil development, and a friend (the many shared papers and patents with him are excellent evidence of our highly productive collaborative interaction); the late Demetrios (Dimitri) Papahadjopoulos, for his friendship and intellectual stimulus; and Nick Arvanidis, from whom I learned about priorities in applied research and for the many heated disputes we had. I also want to thank all my many lab people and my collaborators who have participated in these exciting Doxil-related studies.

Disclosures and Conflict of Interest

No writing assistance was utilized in the production of this chapter and the author has received no payment for its preparation. The findings and conclusions here reflect the current views of the author. This chapter is a completely updated and revised version of the author's 2011 chapter published in *Handbook of Harnessing Biomaterials in Nanomedicine: Preparation, Toxicity, and Applications,* edited by Peer, D., Pan Stanford Publishing, Singapore.

Corresponding Author

Yechezkel Barenholz, PhD
Laboratory of Membrane and Liposome Research
Department of Biochemistry and Molecular Biology
Institute of Medical Research Israel-Canada
The Hebrew University-Hadassah Medical School
POB 12272, Jerusalem 9112102, Israel
Email: chezyb@ekmd.huji.ac.il

About the Author

Professor Yechezkel (Chezy) Barenholz is head of the Liposome and Membrane Research Lab and is also the Daniel G. Miller Professor in Cancer Research at Hebrew University. He has been on the faculty at Hebrew University since 1968 and has been a professor there since 1981. He was a visiting professor at the University of Virginia School of Medicine, Charlottesville, VA (1973–2005) and was the F.C. Donders Chair Professor at the Faculty of Pharmacy, University of Utrecht, The Netherlands (1992). He was also a visiting professor at Kyoto University, Japan (1998); La Sapeinza University, Rome, Italy (2006); Jiaotong University, Shanghai, China (2006); King's College, London, UK, (2006); and the Technical University of Denmark, Copenhagen, Denmark (2010). His current research focuses on the development of drugs based on drug delivery systems (DDS) best exemplified by the anticancer Doxil®, the first nano liposomal drug and the first FDA-approved (1995) nano-drug used worldwide. Professor Barenholz is an author of more than 385 scientific publications totaling more than 17,000 citations. He is a co-inventor in more than 30 approved patent families. He was an executive editor of *Progress in Lipid Research*, an editor of four Special Issues, and is on the editorial board of five scientific journals.

Professor Barenholz is a founder of NasVax Ltd., Moebius Medical Ltd., LipoCure Ltd., and Ayana Ltd. All are in an advanced stage of the development of liposomal drugs based on Professor Barenholz's inventions and expertise. He has been awarded the F.C. Donders Chair at the University of Utrecht, the Kaye Award (1995 and 1997) from Hebrew University, the Alec D. Bangham Award (1998), Teva Founders Prize (2001), an Honorary Doctorate degree from the Technical University of Denmark (2012), the International Controlled Release Society's CRS Founders Award (2012), and the Israeli chapter of the International Controlled Release Society's Award (2014). In 2003, Professor Barenholz founded the Barenholz Prizes from Doxil® royalties to encourage excellence and innovation in the applied sciences of Israeli PhD students.

Professor Barenholz is married to Dr. Hanna Barenholz and they have 4 daughters and 12 grandchildren.

References

Abuchowski, A., McCoy, J. R., Palczuk, N. C., van Es, T., Davis, F. F. (1977). Effect of covalent attachment of polyethylene glycol on immunogenicity and circulating life of bovine liver catalase. *J. Biol. Chem.*, **252**(11), 3582–3586.

Allen, T. M. (1989). Liposomes with enhanced circulation time. U.S. Patent 4,837,028.

Allen, T. M. (1995). From fusion to magic bullets: The influence of Dimitri Papahadjopoulos. *J. Liposome Res.*, **5**, 657–667.

Allen, T. M., Chon, A. (1987). Large unilamellar liposomes with low uptake by reticuloendothelial system. *FEBS Lett.*, **223**, 42–46.

Amselem, S., Cohen, R., Barenholz, Y. (1993a). In vitro tests to predict in vivo performance of liposomal dosage forms. *Chem. Phys. Lipids*, **64**, 219–237.

Amselem, S., Cohen, R., Druckmann, S., Gabizon, A., Goren, D., Abra, R. M., Huang, A., New, R., Barenholz, Y. (1992). Preparation and characterization of liposomal doxorubicin for human use. *J. Liposome Res.*, **2**, 93–123.

Amselem, S., Gabizon, A., Barenholz, Y. (1989–90). Evaluation of a new extrusion device for the production of stable oligolamellar liposomes in a liter scale. *J. Liposome Res.*, **1**, 287–301.

Amselem, S., Gabizon, A., Barenholz, Y. (1990). Optimization and upscaling of doxorubicin-containing liposomes for clinical use. *J. Pharm. Sci.*, **79**, 1045–1052.

Amselem, S., Gabizon, A., Barenholz, Y. (1993b). A large-scale method for the preparation of sterile and non-pyrogenic liposomal formulations of defined size distributions for clinical use. In: Gregoriadis, G., ed. *Liposome Technology*, 2nd ed., vol. I, *Liposome Preparation and Related Techniques*, CRC Press, Boca Raton, FL, pp. 501–525.

Andrews, P. A., Brenner, D. E., Chou, F. T., Kubo, H., Bachur, N. R. (1980). Facile and definitive determination of human Adriamycin and Daunorubicin metabolites by high-pressure liquid chromatography. *Drug Metab. Dispos.*, **8**, 152–156.

Andriyanov A. V., Koren E., Barenholz Y., Goldberg S. N. (2014). Therapeutic efficacy of combining PEGylated liposomal doxorubicin and radiofrequency (RF) ablation: comparison between slow-drug-releasing, non-thermosensitive and fast-drug-releasing, thermosensitive nano-liposomes. *PLoS ONE*, **9**(5), 1–12, e92555.

Avnir, Y., Barhum-Turjeman, K., Tolchinski, D., Sigal, A., Kizelstein, P., Tzemach, D., Gabizon, A., Barenholz, Y. (2012). Fabrication principles and their contribution to the superior in vivo therapeutic efficacy of nano-liposomes remote loaded with glucocorticoids. *PLoS ONE*, **6**(10).

Avnir, Y., Ulmansky, R., Wasserman, V., Even-Chen, S., Broyer, M., Barenholz, Y., Naparstek, Y. (2008). Amphipathic weak acid glucocorticoid prodrugs remote loaded into nano-sterically stabilized liposomes: A novel approach to treat autoimmune arthritis. *Arthritis Rheum*., **58**(1), 119–129.

Baek, S., Choi, C. M., Ahn, S. H., Lee, J. W., Gong, G., Ryu, J. S., Oh, S. J., Bacher-Stier, C., Fels, L., Koglin, N., Hultsch, C., Schatz, C. A., Dinkelborg, L. M., Mittra, E. S., Gambhir, S. S., Moon, D. H. (2012). Exploratory clinical trial of (4S)-4-(3-[18F]fluoropropyl)-L-glutamate for imaging xC-transporter using positron emission tomography in patients with non-small cell lung or breast cancer. *Clin. Cancer Res.* **18**(19), 5427–5437.

Baek, S., Mueller, A., Lim, Y. S., Lee, H. C., Lee, Y. J., Gong, G., Kim, J. S., Ryu, J. S., Oh, S. J., Lee, S. J., Bacher-Stier, C., Fels, L., Koglin, N., Schatz, C. A., Dinkelborg, L. M., Moon, D. H. (2013). (4S)-4-(3-18F-fluoropropyl)-L-glutamate for imaging of xC transporter activity in hepatocellular carcinoma using PET: preclinical and exploratory clinical studies. *J. Nucl. Med.,* **54**(1), 117–123.

Bandak, S., Ramu, A., Barenholz, Y., Gabizon, A. (1999). Reduced UV-induced degradation of doxorubicin encapsulated in polyethylene glycol-coated liposomes. *Pharm*. *Res*., **16**, 841–846.

Bangham, A. D. (1993). Liposomes: The Babraham connection. *Chem*. *Phys*. *Lipids*, **64**, 275–285.

Barenholz, Y. (1992). Liposome production: Historic aspects. In: Braun-Falco, O., Korting, H. C., Maibach, H. I., eds. *Liposome Dermatics*, Springer Verlag, Berlin, pp. 69–81.

Barenholz, Y. (1998). Design of liposome-based drug carriers: From basic research to application as approved drugs. In: Lasic, D. D., Papahadjopoulos, D., eds. *Medical Applications of Liposomes*, Elsevier Science, Amsterdam, pp. 541–565.

Barenholz, Y. (2001). Liposome application: Problems and prospects. *Curr*. *Opin*. *Colloid. Interface Sci*., **6**, 66–77.

Barenholz, Y. (2003). Relevancy of drug loading to liposomal formulation therapeutic efficacy. *J. Liposome Res.*, **13**, 1–8.

Barenholz, Y. (2007). Amphipathic weak base loading into preformed liposomes having a transmembrane ammonium ion gradient: From the bench to approved Doxil®. In: Gregoriadis, G., ed. *Liposome Technology*, 3rd ed., vol. II, Informa Healthcare, New York, pp. 1–26.

Barenholz, Y. (2011). Doxil—The first FDA-approved nano-drug: From an idea to a product. In: Peer, D., ed. *Handbook of Harnessing Biomaterials in Nanomedicine: Preparation, Toxicity, and Applications,* Pan Stanford Publishing Pte Ltd, Singapore, Chapter 12, pp. 335–398.

Barenholz, Y. (2012). Doxil®—The first FDA-approved nano-drug: Lessons learned. *J. Con. Rel*., **160**, 117–134.

Barenholz, Y., Amselem, S. (1993b). Quality control assays in the development and clinical use of liposome-based formulations. In: Gregoriadis, G., ed. *Liposome Technology*, 2nd ed., vol. I, *Liposome Preparation and Related Techniques*, CRC Press, Boca Raton, FL, pp. 527–616.

Barenholz, Y., Amselem, S., Goren, D., Cohen, R., Gelvan, D., Samuni, A., Golden, E. B., Gabizon, A. (1993a). Stability of liposomal-doxorubicin formulation: Problems and prospects. *Med*. *Res*. *Rev*., **13**, 449–491.

Barenholz, Y., Berman, T., Friedman, D. (2013). Stable liposomes for drug delivery. U.S. patent application. WO/2013/114377 A1.

Barenholz, Y., Cevc, G. (2000). Structure and properties of membranes. In: Baszkin, A., Norde, W., eds. *Physical Chemistry of Biological Surfaces,* Marcel Dekker, New York, pp. 171–241.

Barenholz, Y., Cohen, R. (1995). Rational design of amphiphile-based drug carriers and sterically stabilized carriers. *J. Liposome Res*., **5**, 905–932.

Barenholz, Y., Crommelin, D. J. A. (1994). Liposomes as pharmaceutical dosage forms. In: Swarbrick, J., Boylan, J. C., eds. *Encyclopedia of Pharmaceutical Technology*, vol. 9, Marcel Dekker, New York, pp. 1–39.

Barenholz, Y., Druckmann, N. S., Cohen, R., Amselem, S., Sulkes, A., Gabizon, A. (1989). Complete pharmacokinetic analysis of liposome-associated doxorubicin in cancer patients. In: Rubinstein, E., Adam, D., eds. *Recent Advances in Chemotherapy: Antimicrobial Section 1: Proceedings of the 16th Int'l Congress of Chemotherapy,* E. Lewin-Epstein Ltd., Jerusalem, p. 303.1.

Barenholz, Y., Gabizon, A. (February 6, 1990). Liposome/doxorubicin composition and method. U.S. Patent 4,898,735.

Barenholz, Y., Gabizon, A. (August 27, 1991). Liposome/anthraquinone drug composition and method. U.S. Patent 5,043,166 (also see U.S. Patent 4,797,285).

Barenholz, Y., Haran, G. (March 9, 1993). Method of amphipathic drug loading in liposomes by pH gradient. U.S. Patent 5,192,549.

Barenholz, Y., Haran, G. (May 31, 1994). Liposomes: Efficient loading and controlled release of amphipathic molecules. U.S. Patent 5,316,771 (also Europe and Israel).

Barenholz, Y., Naparstek, Y., Avnir, Y., Ulmansky, R. (June 29, 2010). The use of liposomal glucocorticoids for treating inflammatory states. U.S. Patent 7,744,920, 2010.

Bassermann, R. (1986). Changes of vascular pattern of tumors and surrounding tissue during different phases of metastatic growth. *Recent Results Cancer Res*., **100**, 256–257.

Belchetz, P. E., Crawley, J. C., Braidman, I. P., Gregoriadis, G. (1997). Treatment of Gaucher's disease with liposome-entrapped glucocerebroside: Beta-glucosidase. *Lancet*, **8029**, 116–117.

Beijnen, J. H., Rosing, H., de Vries, P. A., Underberg, W. J. M. (1985). Stability of anthracycline antitumor agents in infusion fluids. *J. Parenter*. *Sci*. *Technol*., **39**, 220–222.

Blum, R. H., Carter, S. K. (1974). Adriamycin: A new anticancer drug with significant clinical activity. *Ann*. *Intern*. *Med*., **80**, 249–259.

Blume, G., Cevc, G. (1990). Liposomes for sustained drug release in vivo. *Biochim*. *Biophys*. *Acta*, **1029**, 91–97.

Bolotin, E. M., Cohen, R., Bar, L. K., Emanuel, N., Ninio, S., Lasic, D. D., Barenholz, Y. (1994). Ammonium sulfate gradients for efficient and stable remote loading of amphipathic weak bases into liposomes and ligandoliposomes. *J. Liposome Res*., **4**, 455–479.

Cabanes, A., Even-Chen, S., Zimberof, J., Barenholz, Y., Kedar, E., Gabizon, A. (1999). Enhancement of antitumor activity of polyethylene glycol-coated liposomal doxorubicin with soluble and liposomal interleukin-2. *Clin*. *Cancer Res*., **5**, 687–693.

Cern, A., Barenholz, Y., Tropsha, A., Goldblum, A. (2014). Computer-aided design of liposomal drugs: In silico prediction and experimental validation of drug candidates for liposomal remote loading, *J. Control. Release,* **173**, 125–131.

Cern, A., Golbraikh, A., Sedykh, A., Tropsha, A., Barenholz, Y., Goldblum, A. (2012). Quantitative structure—property relationship modeling of remote liposome loading of drugs. *J. Control. Release*, **160**, 147–157.

Chauhan, V. P., Stylianopoulos, T., Martin, J. D., Popovic, Z., Chen, O., Kamoun, W. S., Bawendi, M. G., Fukumura, D., Jain, R. K. (2012). Normalization of tumour blood vessels improves the delivery of nanomedicines in a size-dependent manner. *Nat. Nanotechnol.,* **7**(6), 383–388.

Clerc, S., Barenholz, Y. (1998). A quantitative model for using acridine orange as a trans-membrane pH gradient probe. *Anal*. *Biochem*., **259**, 104–111.

de Gier, J. (1993). Osmotic behaviour and permeability properties of liposomes. *Chem. Phys. Lipids*, **64**(1–3), 187–196.

Deamer, D. W., Bramhall, J. (1986). Permeability of lipid bilayers to water and ionic solutes. *Chem. Phys. Lipids,* **40**(2–4), 167–188.

Diop-Frimpong, B., Chauhan, V. R., Krane, S., Boucher, Y., Jain, R. K. (2011). Losartan inhibits collagen I synthesis and improves distribution and efficacy on nanotherapeutics in tumors. *Proc Natl Acad Sci USA*, **108**(7), 299–2914.

Druckmann, S., Gabizon, A., Barenholz, Y. (1989). Separation of liposome-associated doxorubicin from non-liposome-associated doxorubicin in human plasma, implications for pharmacokinetic studies. *Biochim*. *Biophys*. *Acta*, **980**, 381–384.

Emanuel, N., Kedar, E., Bolotin, E. M., Smorodinsky, N. I., Barenholz, Y. (1996a). Preparation and characterization of doxorubicin-loaded sterically stabilized immune-liposomes. *Pharm*. *Res*., **13**, 352–359.

Emanuel, N., Kedar, E., Bolotin, E. M., Smorodinsky, N. I., Barenholz, Y. (1996b). Targeted delivery of doxorubicin via sterically stabilized immunoliposomes: Pharmacokinetics and biodistribution in tumor-bearing mice. *Pharm*. *Res*., **13**, 861–868.

Even-Or (Flasterstein), O., Samira, S., Rochlin, E., Balasingam, S., Mann, A. J., Lambkin-Williams, R., Spira, J., Goldwaser, I., Ellis, R., Barenholz, Y. (2010). Immunogenecity, protective efficacy and mechanism of novel CCS adjuvanted influenza vaccine. *Vaccine*, **28**, 6527–6541.

Ferrandina, G., Corrado, G., Lorusso, D., Fuoco, G., Pisconti, S., Scambia, G. (2010). Pegylated liposomal doxorubicin in the management of ovarian cancer. *Ther. Clin. Risk Manag.*, **6**, 463–483.

Forssen, E. A., Tokes, Z. A. (1979). In vitro and in vivo studies with adriamycin liposomes. *Biochem*. *Biophys*. *Res*. *Commun*., **91**, 1295–1301.

Forssen, E. A., Tokes, Z. A. (1981). Use of anionic liposomes for the reduction of chronic doxorubicin induced cardiotoxicity. *Proc*. *Natl*. *Acad*. *Sci*. *U. S. A.*, **78**, 1873–1877.

Forssen, E. A., Tokes, Z. A. (1983). Improved therapeutic benefits of doxorubicin by entrapment in anionic liposomes. *Cancer Res*., **43**, 546–550.

Fülöp, Z., Gref, R., Loftsson, T. (2013). A permeation method for detection of self-aggregation of doxorubicin in aqueous environment. *Int. J. Pharmaceut*., **454**, 559–561.

Gabizon, A., Amselem, S., Goren, D., Cohen, R., Druckmann, S., Fromer, I., Chisin, R., Peretz, T., Sulkes, A., Barenholz, Y. (1991b). Preclinical and clinical experience with doxorubicin with a doxorubicin iposome preparation. *J. Liposome Res*., **1**, 491–502.

Gabizon, A. A., Barenholz, Y. (1988). Adriamycin-containing liposomes in cancer chemotherapy. In: Gregoriadis, G., ed. *Liposomes as Drug Carriers*, Wiley, New York, pp. 365–379.

Gabizon, A., Barenholz, Y. (1999). Liposomal anthracyclines—from basics to clinical approval of pegylated liposomal doxorubicin. In: Janoff, A. S., ed. *Liposomes: Rational Design*, Marcel Dekker, New York, pp. 343–362.

Gabizon, A., Barenholz, Y. (2005). A method for drug loading. WO 2005/046643 A2.

Gabizon, A. A., Barenholz, Y., Bialer, M. (1993). Prolongation of the circulation time of doxorubicin encapsulated in liposomes containing a polyethylene glycol-derivatized phospholipid: Pharmacokinetic studies in rodents and dogs. *Pharm*. *Res*., **10**, 703–708.

Gabizon, A., Chisin, R., Amselem, S., Druckmann, S., Cohen, R., Goren, D., Fromer, I., Peretz, T., Sulkes, A., Barenholz, Y. (1991a). Pharmacokinetic and imaging studies in patients receiving a formulation of liposome-associated Adriamycin. *Br*. *J*. *Cancer*, **64**, 1125–1132.

Gabizon, A., Catane, R., Uziely, B., Kaufman, B., Safra, T., Cohen, R., Martin, F., Huang, A., Barenholz, Y. (1994). Prolonged circulation time and enhanced accumulation in malignant exudates of doxorubicin encapsulated in polyethylene-glycol coated liposomes. *Cancer Res.*, **54**, 987–992.

Gabizon, A., Dagan, A., Goren, D., Barenholz, Y., Fuks, Z. (1982). Liposomes as in vivo carriers of Adriamycin: Reduced cardiac uptake and preserved antitumor activity. *Cancer Res*., **42**, 4734–4739.

Gabizon, A., Goren, D., Barenholz, Y. (1998). Investigation on the anti-tumor efficacy of liposome–associated doxorubicin in murine tumor models. *Isr*. *J*. *Med*. *Sci*., **24**, 512–517.

Gabizon, A., Goren, D., Fuks, Z., Barenholz, Y., Dagan, A., Meshorer, A. (1983). Enhancement of Adriamycin delivery to liver metastatic

cells with increased tumoricidal effect using liposomes as drug carriers. *Cancer Res.*, **43**, 4730–4735.

Gabizon, A., Goren, D., Fuks, Z., Meshorer, A., Barenholz, Y. (1985). Superior therapeutic activity of liposome-associated Adriamycin in a murine metastatic tumour model. *Br. J. Cancer*, **51**, 681–689.

Gabizon, A., Goren, D., Ramu, A., Barenholz, Y. (1996). Design, characterization and anti-tumor activity of Adriamycin-containing phospholipid vesicles. In: Gregoriadis, G., Senior, J., Poste, G., eds. *Targeting of Drugs with Synthetic Systems*, NATO ASI Series, Plenum, New York, pp. 229–238.

Gabizon, A., Huang, A., Martin, R., Barenholz, Y. (1995). Doxorubicin encapsulation in polyethylene glycol-coated liposomes: Initial clinical pharmacokinetic studies in solid tumors. In: Lasic, D. D., Martin, E., eds. *Stealth Liposomes*, CRC Press, Boca Raton, FL, Chapter 21, pp. 245–255.

Gabizon, A., Isacson, R., Rosengarten, O., Tzemach, D., Shmeeda, H., Sapir, R. (2008). An open-label study to evaluate dose and cycle dependence of the pharmacokinetics of pegylated liposomal doxorubicin. *Cancer Chemother. Pharmacol.* **1**(4), 695–702.

Gabizon, A., Meshorer, A., Barenholz, Y. (1986). Comparative long-term study of the toxicities of free and liposome-associated doxorubicin in mice after intravenous administration. *J. Natl. Cancer Inst.*, **77**, 459–469.

Gabizon, A., Papahadjoupoulos, D. (1988). Liposome formulations with prolonged circulation time in blood and enhanced uptake by tumors. *Proc. Natl. Acad. Sci. U. S. A.*, **85**, 6949–6953.

Gabizon, A., Peretz, T., Sulkes, A., Amselem, S., Ben-Yosef, R., Ben-Baruch, N., Catane, R., Biran, S., Barenholz, Y. (1989a). Systemic administration of doxorubicin-containing liposomes in cancer patients: Phase I study. *Eur. J. Cancer Clin. Oncol.*, **25**, 1795–1803.

Gabizon, A., Shmeeda, H., Barenholz, Y. (2003). Pharmacokinetics of pegylated liposomal doxorubicin: Review of animal and human studies. *Clin. Pharmacokinet.*, **42**, 419–436.

Gabizon, A. A., Sulkes, A., Peretz, T., Druckmann, S., Goren, D., Amselem, S., Barenholz, Y. (1989b). Liposome-associated doxorubicin: Preclinical pharmacology and exploratory clinical phase. In: Fidler, I. J., Lopez-Berestein, G., eds. *Liposomes in the Therapy of Infectious Diseases and Cancer*, A. R. L., New York, pp. 391–402.

Garbuzenko, O., Barenholz, Y., Priev, A. (2005). Effect of grafted PEG on liposome size and on compressibility and packing of lipid bilayer. *Chem. Phys. Lipids,* **135**, 117–129.

Goormaghtigh, E., Ruysschaert, J. M. (1984). Anthracycline glycoside membrane interaction. *Biochim*. *Biophys*. *Acta*, **779**, 271–188.

Gordon, A. N., Fleagle, J. T., Guthrie, D., Parkin, D. E., Gore, M. E., Lacave, A. J. (2001). Recurrent epithelial ovarian carcinoma: A randomized phase III study of pegylated liposomal doxorubicin versus topotecan. *J. Clin*. *Oncol.*, **19**(14), 3312–3322.

Gordon, A. N., Granai, C. O., Rose, P. G., Hainsworth, J., Lopez, A., Weissman, C, Rosales, R., Sharpington, T. (2000). Phase II study of liposomal doxorubicin in platinum-and paclitaxel-refractory epithelial ovarian cancer. *J. Clin*. *Oncol.*, **18**(17), 3093–3100.

Goren, D. (1990). Liposomes as doxorubicin carriers: A means to improve the therapeutic index of the drug. PhD thesis submitted and approved by the Hebrew University of Jerusalem.

Goren, D., Gabizon, A., Barenholz, Y. (1990). The influence of physical characteristics of liposomes containing doxorubicin on their pharmacological behavior. *Biochim*. *Biophys*. *Acta*, **1029**, 285–294.

Grant, G. J., Barenholz, Y., Bansinath, M., Davidson, E. M. (2004). A novel liposomal Bupivacaine formulation to produce ultralong-acting analgesia. *Anesthesiology*, **101,** 133–137.

Grant, G. J., Barenholz, Y., Piskoun, B., Bansinath, M., Turndorf, H., Bolotin, E. (2001). DRV liposomal bupivacaine: Preparation, characterization and in vivo evaluation in mice. *Pharm*. *Res.*, **18**, 336–343.

Gregoriadis, G., Senior, J. (1986). Liposomes in vivo: A relationship between stability and clearance? In: Gregoriadis, G., Senior, J., Poste, G., eds. *Targeting of Drugs with Synthetic Systems*, Plenum, London, pp. 183–192.

Gregoriadis, G., Swain, C. R., Wills, E. J., Tavill, A. S. (1974). Drug-carrier potential of liposomes in cancer chemotherapy. *Lancet*, **1**, 1313–1316.

Gundersen, S., Kvinnsland, S., Klepp, O., Kvaloy, S., Lund, E., Host, H. (1986). Weekly Adriamycin versus VAC in advanced breast cancer. A randomized trial. *Eur*. *J*. *Cancer Clin*. *Oncol*., **22**, 1431–1434.

Haran, G., Cohen, R., Bar, L. K., Barenholz, Y. (1993). Transmembrane ammonium sulfate gradients in liposomes produce efficient and stable entrapment of amphipathic weak bases. *Biochim*. *Biophys*. *Acta*, **1151**, 201–215.

Hashizume, H., Baluk, P., Morikawa, S., McLean, J. W., Thurston, G., Roberge, S., Jain, R. K., MacDonald, D. M. (2000). Openings between defective endothelial cells explain tumor vessel leakiness. *Am*. *J*. *Pathol.*, **156**, 1363–1380.

Horowitz, A. T., Barenholz, Y., Gabizon, A. A. (1992). In vitro cytotoxicity of liposome-encapsulated doxorubicin: Dependence on liposome composition and drug release. *Biochim*. *Biophys*. *Acta*, **1109**, 203–209.

Huang, S. K., Lee, K. D., Hong, K., Friend, D. S., Papahadjopoulos, D. (1992). Microscopic localization of sterically stabilized liposomes in colon carcinoma-bearing mice. *Cancer Res.*, **52**(19), 5135–5143.

Hunt, C. A., Papahadjopoulous, D. R. (July 16, 1985). Method for producing liposomes in selected size range, U.S. patent 4,529,561.

Hwang, K. J. (1987). Liposome pharmacokinetics. In: Ostro, M. J., ed., *Liposomes: From Biophysics to Therapeutics,* Marcel Dekker, New York, p. 109.

Joseph, A., Itskovitz Cooper, N., Samira, S., Flasterstein, O., Eliyahu, H., Simberg, D., Goldwaser, I., Barenholz, Y., Kedar, E. (2006). A new intranasal influenza vaccine based on a novel polycationic lipid ceramide carbamoyl spermine (CCS). I. Immunogenicity and efficacy studies in mice. *Vaccine*, **24**, 3990–4006.

Jung, S. H., Seong, H., Cho, S. H., Jeong, K. S., Shin, B. C. (2009). Polyethylene glycol-complexed cationic liposome for enhanced cellular uptake and anticancer activity. *Int. J Pharm.* **382**(1–2), 254–261.

Kedar, E., Braun, E., Rutkowski, Y., Emanuel, N., Barenholz, Y. (1994b). Delivery of cytokines by liposomes. II. Interleukin-2 encapsulated in long-circulating sterically stabilized liposomes: Immunomodulatory and anti-tumor activity in mice. *J. Immunother*., **16**, 115–124.

Kedar, E., Rutkowski, Y., Braun, E., Emanuel, N., Barenholz, Y. (1994a). Delivery of cytokines by liposomes. I. Preparation and characterization of interleukin-2 encapsulated in long-circulating sterically stabilized liposomes. *J. Immunother.*, **16**, 47–59.

Kenyon, J. (2008). Chemotherapy and cardiac toxicity—the lesser of two evils, Doctors Lounge Website, available at http://www.doctorslounge.com/index.php/blogs/page/14030.

Klivanov, A. L., Maruyama, K., Torchilin, V. R., Huang, L. (1990). Amphipathic polyethyleneglycols effectively prolong the circulation time of liposomes. *FEBS Lett*., **268**, 235–237.

Koglin, N., Mueller, A., Berndt, M., Schmitt-Willich, H., Toschi, L., Stephens, A. W., Gekeler, V., Friebe, M., Dinkelborg, L. M. (2011). Specific PET imaging of xC-transporter activity using a (1)(8)F-labeled glutamate derivative reveals a dominant pathway in tumor metabolism. *Clin. Cancer Res*., **17**(18), 6000–6011.

Kumai, K., Takahashi, T., Tsubouchi, K., Shino, K., Ishbiki, K. K., Abe, O. (1985). Selective hepatic arterial infusion of liposomes containing anti tumor agents. *Jpn. J. Cancer Chemother*., **12**, 1946–1948.

Lasic, D. D. (1996). On the history of liposomes. In: Lasic, D. D., Barenholz, Y., eds., *Handbook of Non-Medical Applications of Liposomes*, vol. 1, CRC Press, Boca Raton, FL, pp. 1–12.

Lasic, D. D., Ceh, B., Stuart, M. C. A., Guo, L., Frederik, P. M., Barenholz, Y. (1995). Transmembrane gradient driven phase transitions within vesicles: Lessons for drug delivery. *Biochim*. *Biophys*. *Acta*, **1239**, 145–156.

Lasic, D. D., Frederik, P. M., Stuart, M. C. A., Barenholz, Y., Mcintosh, T. J. (1992). Gelation of liposome interior. A novel method for drug encapsulation. *FEBS Lett.*, **312**, 255–258.

Lasic, D. D., Martin, F., eds., (1995). *Stealth Liposomes*, CRC Press, Boca Raton, FL.

Lasic, D. D., Vainer, J. J., Working, P. K. (1999). Sterically stabilized liposomes in cancer therapy and gene delivery. *Curr*. *Opin*. *Mol*. *Ther*., **1**, 177–185.

Lichtenberg, D., Barenholz, Y. (1988). Liposomes: Preparation, characterization, preservation. In: Glick, D., ed. *Methods of Biochemical Analysis*, Wiley, New York, **33**, 337–462.

Lopez-Berestein, G., Fainstein, V., Hopfer, R., et al. (1985). Liposomal amphotericin B for the treatment of systemic fungal infections in patients with cancer, a preliminary study. *J. Infect*. *Dis*., **151**, 704–710.

Maeda, H., Bharate, G. Y., Daruwalla, J. (2009). Polymeric drugs for efficient tumor-targeted drug delivery based on EPR-effect. *Eur*. *J*. *Pharm*. *Biopharm*., **71**, 409–419.

Mace, K., Mayhew, E., Mihich, E., Ehrke, M. J. (1988). Alterations in murine host defense functions by Adriamycin or liposome-encapsulated Adriamycin. *Cancer Res*., **48**, 130–136.

Martin, R., Caignard, A., Olson, O., Jeanin, J. R., Leclerc, A. (1982). Tumoricidal effect of macrophages exposed to Adriamycin in vivo and in vitro. *Cancer Res*., **42**, 3851–3855.

Matsumura, Y., Maeda, H. (1986). A new concept for macromolecular therapeutics in cancer chemotherapy: Mechanism of tumor tropic accumulation of proteins and antitumor agent SMANCS. *Cancer Res*., **46**, 6387–6392.

Mayhew, E. G., Goldrosen, M. H., Vaage, J., Rustum, Y. M. (1987). Effects of liposome-entrapped doxorubicin on liver metastases of mouse colon carcinomas 26 and 38. *J. Natl*. *Cancer Inst*., **78**, 707–713.

Mayhew, E., Rustum, Y. (1985). The use of liposomes as carriers of therapeutic agents. In: Rein, R., ed. *Molecular Basis of Cancer*. *Part B: Macromolecular Recognition*, *Chemotherapy and Immunology*, Alan R. Liss, New York, pp. 301–310.

Mayhew, E., Rustum, Y., Vail, W. J. (1983). Inhibition of liver metastases of M5076 tumor by liposome-entrapped Adriamycin. *Cancer Drug Deliv*., **1**, 43–58.

McKelvey, E. M., Gottlieb, J. A., Wilson, H. E., et al. (1976). Hydroxyldaunomycin (Adriamycin) combination chemotherapy in malignant lymphoma. *Cancer*, **38**, 1484–1493.

Minotti, G., Menna, P., Salvatorelli, E., Cairo, G., Gianni, L. (2004). Anthracyclines: Molecular advances and pharmacologic developments in antitumor activity and cardiotoxicity. *Pharmacol*. *Rev*., **56**(2), 185–229.

Moreadith, R. W., Lehninger, A. L. (1984). The pathways of glutamate and glutamine oxidation by tumor cell mitochondria; Role of mitochondrial NAD(P)+-dependent malic enzyme. *J. Biol. Chem.* **259**(10), 6215–6221.

Mouristen, O. G. (2005). *Life as a Matter of Fat*, Springer, Berlin, Chapter 14, pp. 149–157.

Needham, D., Anyarambhatia, G., Kong, G., Dewhirst, M. W. (2000). A new temperature-sensitive liposome for use with mild hyperthermia: Characterization and testing in human tumor xenograft model. *Cancer Res.*, **60**, 1197–1201.

Needham, D., Dewhirst, M. W. (2001). The development and testing of new temperature-sensitive drug delivery system for treatment of solid tumors. *Adv*. *Drug Deliv*. *Rev*., **53**, 285–305.

Olson, E., Mayhew, E., Maslow, D., Rustum, Y., Szoka, E. (1982). Characterization, toxicity, and therapeutic efficacy of Adriamycin encapsulated in liposomes. *Eur*. *J*. *Cancer Clin*. *Oncol*., **18**, 167–176.

Peleg-Shulman, T., Gibson, D., Cohen, R., Abra, R., Barenholz, Y. (2001). Characterization of sterically stabilized cisplatin liposomes by nuclear magnetic resonance. *Biochim*. *Biophys*. *Acta*, **1510**, 278–291.

Peng, X., Chen, B., Lim, C. C., Sawyer, D. B. (2005). The cardiotoxicology of anthracycline chemotherapeutics: Translating molecular mechanism into preventative medicine. *Mol*. *Intervent*., **5**(3), 163–171.

Perez-Soler, R., Lopez-Berestein, G., Kasi, L. R., et al. (1985). Distribution of technetium-99m labeled multilamellar liposomes in patients with Hodgkin's disease. *J. Nucl*. *Med*., **26**, 743–749.

Poste, G. (1983). Liposome targeting in vivo: Problems and opportunities. *Biol*. *Cells*, **47**, 19–38.

Poste, G., Bucana, C., Raz, A., Bugelski, P., Kirsh, R., Fidler, I. J. (1982). Analysis of the fate of systemically administered liposomes and implications for their use in drug delivery. *Cancer Res*., **42**, 1412–1422.

Rahman, A., Carmichael, D., Harris, M., Roh, J. K. (1986a). Comparative pharmacokinetics of free doxorubicin and doxorubicin entrapped in cardiolipin liposomes. *Cancer Res*., **46**, 2295–2299.

Rahman, A., Fumagalli, A., Barbieri, B., Schein, P. S., Casazza, A. M. (1986b). Antitumor and toxicity evaluation of free doxorubicin and doxorubicin entrapped in cardiolipin liposomes. *Cancer Chemother*. *Pharmacol*., **16**, 22–27.

Rahman, A., Kessler, A., More, N., et al. (1980). Liposomal protection of Adriamycin-induced cardiotoxicity in mice. *Cancer Res*., **40**, 1532–1537.

Rahman, A., More, N., Schein, P. S. (1982). Doxorubicin-induced chronic cardiotoxicity and its protection by liposomal administration. *Cancer Res*., **42**, 1817–1822.

Rahman, A., Roh, J. K., Treat, J. (1989). Preclinical and clinical pharmacology of doxorubicin entrapped in cardiolipin liposomes. In: Lopez-Berestein, G., Fidler, I. J., eds. *Liposomes in the Therapy of Infectious Diseases and Cancer*, Alan R. Liss, New York, pp. 367–389.

Rahman, A., White, G., More, N., Schein, P. S. (1985). Pharmacological, toxicological, and therapeutic evaluation in mice of doxorubicin entrapped in cardiolipin liposomes. *Cancer Res*., **45**(2), 796–803.

Richardson, V. J., Ryman, B. E., Jewkes, R. F., et al. (1979). Tissue distribution and tumor localization of technetium-99m labeled liposomes in cancer patients. *Br*. *Cancer J*., **40**, 35–43.

Schroeder, A., Avnir, Y., Weisman, S., Najajreh, Y., Gabizon, A., Talmon, Y., Kost, J., Barenholz, Y. (2007). Controlling liposomal drug release with low frequency ultrasound: Mechanism and feasibility. *Langmuir*, **23**(7), 4019–4025.

Schroeder, A., Honen, R., Turjeman, K., Gabizon, A., Kost, J., Barenholz, Y. (2009a). Ultrasound triggered release of cisplatin from liposomes in murine tumors. *J. Control*. *Release*, **137**, 63–68.

Schroeder, A., Kost, J., Barenholz, Y. (2009b). Ultrasound, liposomes, and drug delivery: Principles for using ultrasound to control the release of drugs from liposomes. *Chem*. *Phys*. *Lipids*, **162**, 1–16.

Sculier, J. R., Coune, A., Brassine, C., et al. (1986). Intravenous infusion of high doses of liposomes containing NSC 251635, a water-insoluble cytostatic agent. A pilot study with pharmacokinetic data. *J. Clin. Oncol.*, **4**, 789–797.

Sculier, J. R., Coune, A., Meunier, F., et al. (1988). Pilot study of amphotericin B entrapped in sonicated liposomes in cancer patients with fungal infections. *Eur. J. Cancer Clin. Oncol.*, **24**, 527–538.

Skeel, R. T. (1999). *Handbook of Cancer Chemotherapy*, 5th ed., Lippincott Williams & Wilkins, Philadelphia, pp. 100–101.

Solomon, R., Gabizon, A. A. (2008). Clinical pharmacology of liposomal anthracyclines: Focus on pegylated liposomal doxorubicin. *Clin. Lymphoma Myeloma*, **8**, 21–32.

Song, G., Darr, D. B., Santos, C. M., Ross, M., Valdivia, A., Jordan, J. L., Midkiff, B. R., Cohen, S., Nikolaishvili-Feinberg, N., Miller, C. R., Tarrant, T. K., Rogers, A. B., Dudley, A. C., Perou, C. M., Zamboni, W. C. (2014). Effects of tumor microenvironment heterogeneity on nanoparticle disposition and efficacy in breast cancer tumor models. *Clin. Cancer Res.,* **20**(23), 6083–6095.

Stein, W. D. (1986). *Transport and Diffusion Across Cell Membranes*, Academic Press, Orlando, FL, Chapter 2.

Storm, G., Roerdink, F. H., Steerenberg, P. A., de Jong, W. H., Crommelin, D. J. A. (1987). Influence of lipid composition on the antitumor activity exerted by doxorubicin-containing liposomes in a rat solid tumor model. *Cancer Res.*, **47**, 3366–3372.

Symon, Z., Peyser, A., Tzemach, D., Lyass, O., Sucher, E., Shezen, E., Gabizon, A. (1999). Selective delivery of doxorubicin to patients with breast carcinoma metastases by stealth liposomes. *Cancer*, **86**, 72–78.

Szebeni, J., Alving, C. R., Rosivall, L., Bunger, R., Baranyi, L., Bedocs, P., Toth, M., Barenholz, Y. (2007). Animal models of complement-mediated hypersensitivity reactions to liposomes and other lipid-based nanoparticles. *J. Liposome Res.*, **17**, 1–11.

Szebeni, J., Barenholz, Y. (2011). Complement activation, immunogenicity, and immune suppression as potential side effects of liposomes. In: Peer, D., ed. *Handbook of Harnessing Biomaterials in Nanomedicine: Preparation, Toxicity, and Applications*, Pan Stanford Publishing, Singapore Chapter 11.

Szebeni, J., Bedocs, P., Urbanics, R., Bunger, R., Rosivall, L., Toth, M., Barenholz, Y. (2012). Prevention of infusion reactions to PEGylated liposomal doxorubicin via tachyphylaxis induction by placebo vesicles: A porcine model. *JCR*, **160**, 382–387.

Szebeni, J., Muggia, F., Gabizon, A., Barenholz, Y. (2011). Activation of complement by therapeutic liposomes and other lipid excipient-based therapeutic products: Prediction and prevention. *Adv*. *Drug Deliv*. *Rev*., **63,** 1020–1030.

Takimoto, C. H., Calvo, E. (2008). Principles of oncologic pharmacotherapy. In: Pazdur, R., Wagman, L. D., Camphausen, K. A., Hoskins, W. J., eds. *Cancer Management: A Multidisciplinary Approach*, 11th ed., UBM Medica, Norwalk, CT.

Tinkle, S., McNeil, S. E., Mühlebach, S., Bawa, R., Borchard, G., Barenholz, Y., Tamarkin, L., Desai, N. (2014). Nanomedicines: addressing the scientific and regulatory gap. *Ann. N.Y. Acad. Sci*., **1313**, 35–56.

Tirosh, O., Barenholz, Y., Katzhendler, Y., Priev, A. (1998). Hydration of polyethylene glycol-grafted liposomes. *Biophys*. *J*., **74**, 1371–1379

Tirosh, O., Kohen, R., Katzhendler, J., Gorodetsky, R., Barenholz, Y. (1997). Novel synthetic phospholipid protects lipid bilayers against oxidative damage: Role of hydration layer and bound water. *J. Chem*. *Soc*. *Perkin Trans*., **2**, 383–389.

Treat, J., Greenspan, A. R., Rahman, A. (1989). Liposome encapsulated doxorubicin—preliminary results of phase I and phase II trials. In: Lopez-Berestein, G., Fidler, I. J., eds. *Liposomes in the Therapy of Infectious Diseases and Cancer*, Alan R. Liss, New York, pp. 353–365.

Van Hoesel, Q. G., Steerenberg, P. A., Crommelin, D. J., et al. (1984). Reduced cardiotoxicity and nephrotoxicity with preservation of antitumor activity of doxorubicin entrapped in stable liposomes in the LOU/M Wsl rat. *Cancer Res*., **44**, 3698–3705.

Veronese, F. M., Harris, J. M. (2002). Introduction and overview of peptide and protein pegylation. *Adv*. *Drug Deliv*. *Rev*., **54**(4), 453–456.

Veronese, F. M., Pasut, G. (2005). Pegylation, successful approach to drug delivery. *Drug Discov*. *Today*, **10**(21), 1451–1458.

Waknine-Grinberg, J., H., Even-Chen, S., Avichzer, J., Turjeman, K., Bentura-Marciano, A., Haynes, R. K., Weiss, L., Allon, N., Ovadia, H., Golenser, J., Barenholz, Y. (2013). Glucocorticosteroids in nano-sterically stabilized liposomes are efficacious for elimination of the acute symptoms of experimental cerebral malaria. *PLoS ONE*, **8**(8), 1–17, e72722.

Wang, L., Zhou, H., Wang, Y., Cui, G., Di, L. J. (2015). CtBP maintains cancer cell growth and metabolic homeostasis via regulating SIRT4. *Cell Death Dis.,* **6**, e1620.

Wasserman, V., Kizelsztein, P., Garbuzenko, O., Kohen, R., Ovadia, H., Tabakman, R., Barenholz, Y. (2007). The antioxidant tempamine:

In vitro antitumor and neuroprotective effects and optimization of liposomal encapsulation and release. *Langmuir*, **23**(4), 1937–1947.

Weiss, R. B. (1992). The anthracyclines: Will we ever find a better doxorubicin? *Semin. Oncol.*, **19**(6), 670–686.

Woodle, M. C. (1993). Surface-modified liposomes: Assessment and characterization for increased stability and prolonged blood circulation. *Chem. Phys. Lipids*, **64**, 249–262.

Woodle, M. C., Lasic, D. D. (1992). Sterically stabilized liposomes. *Biochim. Biophys. Acta*, **113**, 171–199.

Woodle, M. C., Martin, F. J., Yau-Yang, A., Redmann, C. T. (1991). Liposomes with enhanced circulation time. U.S. Patent 5,013,556.

Woodle, M. C., Newman, M., Collins, L., Redmann, C., Martin, F. (1990). Improved long circulating (Stealth) liposomes using synthetic lipids. *Symp. Control. Release Bioact. Mater.*, **17**, 77.

Yuan, F., Leunig, M., Huang, S. K., Berk, D. A., Papahadjopoulos, D. Jain, R. K. (1994). Microvascular permeability and interstitial penetration of sterically stabilized (Stealth) liposomes in a human tumor xenograft. *Cancer Res.*, **54**(13), 3352–3356.

Zamboni, W. C., Gervais, A. C., Egorin, M. J., Schellens, J. H., Zuhowski, E. G., Pluim, D., Joseph, E., Hamburger, D. R., Working, P. K., Colbern, G., Tonda, M. E., Potter, D. M., Eiseman, J. L., (2004). Systemic and tumor disposition of platinum after administration of cisplatin or STEALTH liposomal-cisplatin formulations (SPI-077 and SPI-077 B103) in a preclinical tumor model of melanoma. *Cancer Chemother. Pharmacol.* **53**(4), 329–336.

Zhang, Y. P., Ceh, B., Lasic, D. D. (2001). In: Damitziu, S., ed. *Liposomes in Drug Delivery in Polymeric Biomaterials*, 2nd ed., Marcel Dekker, New York, Chapter 29, pp. 783–821.

Zucker, D., Andriyanov, A., V., Steiner, A., Raviv, U., Barenholz, Y. (2012). Characterization of PEGylated nanoliposomes co-remotely loaded with topotecan and vincristine: relating structure and pharmacokinetics to therapy efficacy. *J. Control. Release*, **160**, 181–189.

Zucker, D., Barenholz, Y. (2010). Optimization of vincristine-topotecan combination—paving the way for improved chemotherapy regimens by nano-liposomes. *J. Control. Release*, **146**, 326–333.

Zucker, D., Marcus, D., Barenholz, Y., Goldblum, A. (2009). Liposome drug's loading efficiency: A working model based on loading conditions and drug's physicochemical properties. *J. Control. Release*, **139**, 73–80.

Chapter 30

Nanotechnology and the Skin Barrier: Topical and Transdermal Nanocarrier-Based Delivery

Hagar I. Labouta, PhD,[a,c] and Marc Schneider, PhD[b]

[a]*Department of Chemistry,*
Faculty of Science & Cellular and Molecular Bioengineering Research Lab,
Schulich School of Engineering, University of Calgary, Calgary, Canada
[b]*Department of Pharmacy, Biopharmaceutics and Pharmaceutical Technology,*
Saarland University, Saarbrucken, Germany
[c]*Pharmaceutics, Faculty of Pharmacy, Alexandria University, Alexandria, Egypt*

Keywords: topical drug delivery, transdermal drug delivery, skin penetration enhancement, skin nanocarrier-based drug delivery, skin nanoparticle penetration/permeation, skin penetration mechanism, polymeric nanoparticles, lipid-based nanoparticles, inorganic nanoparticles

30.1 Introduction

Topical and transdermal drug delivery is a therapeutic target of great potential advantages that is still limited by the barrier function of the skin. Skin penetration enhancement techniques have been explored to improve the local or the systemic bioavailability and

Handbook of Clinical Nanomedicine: Nanoparticles, Imaging, Therapy, and Clinical Applications
Edited by Raj Bawa, Gerald F. Audette, and Israel Rubinstein

ISBN 978-981-4669-20-7 (Hardcover), 978-981-4669-21-4 (eBook)
www.panstanford.com

increase the range of drugs for topical and transdermal delivery. One of these enhancement techniques is encapsulation of the active agent in nanoparticles. This chapter highlights the ongoing research on the use of nanocarriers in topical/transdermal delivery and the potential mechanism of facilitated skin transport. Basic understanding of the interaction of the nanoparticles with the skin barrier is considered crucial for designing optimal topical and transdermal nanocarriers. Therefore, more emphasis has been given to analyze the research outcomes of the behavior of the nanoparticles when coming in contact with the skin surface and their interaction with the skin. The current status and knowledge of skin penetration of nanoparticles and the potential mechanism(s) of penetration/permeation are reviewed. Factors of significance for enhanced or limited skin transport of nanoparticles and approaches adopted to breach the skin barrier for enhanced particle penetration are highlighted.

There is a considerable interest in the skin as a site of drug application for either local or systemic effect. However, the skin as a formidable barrier to penetrants represents the first challenge for the success of topical and transdermal drug delivery.

30.1.1 Skin Barrier

Skin is a unique biological barrier composed of several highly organized and heterogeneous layers. Skin is composed of three layers, epidermis, dermis, and hypodermis, from outside moving deeper inside. However, from a penetration perspective, only the epidermis and the dermis are important. Stratum corneum (SC) is the outermost epidermal layer, to which the main barrier function of the skin is attributed. SC is formed of a laminate of compressed keratin-filled corneocytes (keratinocytes) anchored in a lipophilic matrix, composed mainly of ceramides, free fatty acids and cholesterol. It is generally believed that the resistivity of the SC is attributed to the intercellular lipids in combination with the geometrical arrangement of the corneocytes. In addition to the complex skin composition and the different skin layers, there are a number of skin appendages present such as hair follicles, sweat and sebaceous glands [1].

Despite the excellent barrier function, the skin has been the target of topical and transdermal delivery of drugs, cosmetics and

even vaccine and gene delivery. This will be briefly discussed in the next section.

30.1.2 Topical and Transdermal Delivery

Topical delivery is confined to a situation in which the drug is intended for localized treatment of certain dermatological conditions, e.g., eczema, psoriasis, etc. In such case, the active agent should *penetrate* into the skin to reach the site of action but not reaching the systemic circulation, thus avoiding systemic side effects. In *transdermal delivery*, however, the active agent *permeates* through the whole skin thickness with the different skin layers reaching the systemic circulation to elicit a therapeutic response. Release of a therapeutic agent from the applied formulation to the skin surface and its transport across the skin layers to the systemic circulation is a multistep process which involves: (a) release from the formulation, (b) partitioning into the SC, (c) penetration through the SC, principally via the lipidic intercellular pathway (Other potential routes of transport across the SC include the intracellular pathway and transport through skin appendages, mainly the hair follicles and sebaceous glands) (d) partitioning from the SC into the viable epidermis, (e) diffusion through the viable epidermis into the upper dermis, and (f) uptake into the local capillary network eventually reaching the systemic circulation. Accordingly, an ideal permeant should have a sufficient lipophilicity to partition into the SC, but also sufficient hydrophilicity to enable further partitioning into the viable epidermis [2–4].

Transdermal drug delivery offers great advantages over the oral route. By delivering a steady flow of drugs into the bloodstream over an extended period of time, transdermal systems can avoid the "peak and valley" effect of the oral therapy and can enable a more controlled and effective treatment. Away from controlled delivery, other advantages include minimizing the first-pass metabolism, avoidance of drug degradation under the influence of the harsh acidity of the stomach, and prevention of possible erratic delivery due to food interactions. However, there are several factors that limit the success of transdermal technology. This includes the following:

- Local skin irritation associated with the application of certain drugs and formulations.

- Due to the excellent diffusional resistance offered by the skin barrier, the daily drug dose that could be transdermally delivered is limited. Thus, this route is usually confined for potent drugs. In addition, a lag time is usually associated with the delivery of the drug across the skin, resulting in a delay in onset of action.
- Not only for the dose, but also according to the partition coefficient, not all the drugs are suitable for transport across the skin.
- This is in addition to intra-individual variation in the absorption rate for different application sites and inter-individual variations among different patients of different skin types.

In response, significant effort has been devoted to developing strategies to overcome the impermeability of intact human skin. These strategies include chemical penetration enhancers, physical enhancement techniques, and, more recently, encapsulation of the active agent inside delivery systems, of which the nanoparticulate systems are of great potential [4–5]. This chapter will focus on the use of nanoparticles for topical and transdermal drug delivery.

30.2 Enhancement of Drug Penetration via Encapsulation in Nanocarriers

The development of nanocarriers for topical and transdermal drug delivery has become a field of major interest in dermatology. However, the mechanism of enhancement of drug penetration or even permeation is still unclear, with a lot of controversy regarding the fate of the nanocarrier itself, several research articles have shown enhanced skin penetration/permeation of active agents encapsulated in nanocarriers over traditional dermatological formulations, as will be discussed in this section. Moreover, the developed nanocarrier-based formulations offer other advantages: controlled release of the entrapped agent, which can be further, altered by modulating the properties of the nanocarrier and the matrix/shell composition. Controlling the delivery of pharmaceutical and cosmeceutical actives to the skin offer great potential over conventional dermatological vehicles. A fundamental shortcoming of the latter, standard approach is the availability of the applied

active agent in a relatively high concentration in the applied skin area, resulting in cycles of short-term overmedication and long-term under medication. This would further lead to adverse skin reactions as a result of excessive direct contact with the active agent. In contrast, nanocarrier-based formulations would allow for progressive delivery of the active agents into the skin along with a favorable tolerability profile, reducing the probability of occurrence of skin reactions while maintaining activity. Finally yet importantly, encapsulating the active agent in a delivery system would protect the encapsulant from external influences thus enhancing the physical and chemical stability of the encapsulated active ingredients. A summary of the research outcomes of some selected nanoparticulate delivery systems in topical/transdermal delivery and the potential mechanism of facilitated skin transport is discussed in the following paragraphs.

30.2.1 Liposomes and Vesicles

Liposomes are spherical structures formed of concentric lipid bilayers with an aqueous phase inside and between the lipid bilayers [6]. They are either unilamellar or multilamellar vesicles. Liposomes have attractive biological properties including biocompatibility and easy control of the size, charge and surface properties, etc. However, they suffer from poor stability [6].

Mezei and Gulasekharam [7–8] were the first to employ liposomes as a skin drug delivery system. Their goal was to provide a localized depot in the skin increasing drug deposition within the skin and minimizing systemic side effects. They reported four- to five-fold increased penetration of triamcinolone acetonide into the epidermis and dermis and reduced percutaneous absorption compared to a control ointment [7] or gel [8]. Later, a series of studies showed the localizing effects of liposomes and its dependency on the lipid composition, especially for liposomes made from SC lipids, and on the method of preparation [9]. Niosomes, vesicles prepared from non-ionic surfactants, were also formulated for localizing drugs, especially antifungal agents, within the skin at the site of action [10–12].

Several workers have also studied the potential of liposomes for targeting the skin appendages. For instance, carboxyfluorescein was found to localize in the hair follicles after application of

dye-loaded liposomes [13–14]. Liposomes were also reported as penetration enhancers increasing the penetration of co-administered hydrophilic molecules [15–16]. Though the majority of the current research studies have focused on the investigation and formulation of liposomes for topical skin drug delivery [17–18], yet some early research outcomes have also reported improved transdermal delivery from these vesicular systems [19–20]. Cevc and Blume [21] claimed that certain classes of lipid vesicles, ultradeformable vesicles (transferosomes), can squeeze between the corneocytes and penetrate intact to the deep layers of the skin and may progress far enough to reach the systemic circulation. Transdermal immunization with proteins by means of ultradeformable vesicles was even feasible as reported by Paul et al. [22].

Mechanism of action: Despite the intensive research, the mechanism by which vesicular systems deliver drugs into the intact skin is still unclear. However, it is generally postulated that their delivery mechanism is associated with accumulation of the liposomes and associated drug in the SC and the upper skin layers, with minimal drug penetrating into the deeper tissues and systemic circulation [4]. Nevertheless, several mechanisms have been suggested for liposomes as skin drug delivery systems. The proposed different mechanisms supported by positive findings in literature as well as counteracting results were extensively reviewed by El Maghraby et al. [23]. These include penetration enhancement effect, vesicle adsorption to or fusion with the SC, intact vesicular skin penetration and transappendageal penetration. Moreover, the transdermal hydration gradient was also reported by Cevc and Blume [21] as a driving force for the penetration of ultradeformable vesicles through the SC into the epidermis.

30.2.2 Solid Lipid Nanoparticles and Nanostructured Lipid Carriers

Since the beginning of the nineties, attention from various research groups has focused on formulation and applications of solid lipid nanoparticles (SLN), colloidal carrier systems prepared from solid lipids. SLN have shown great potential especially in the field of skin delivery, considered as being the next generation of topical

delivery systems after liposomes. They combine the advantages of liposomes and polymeric nanoparticles. The solid matrix of SLN provides the ability to protect chemically labile ingredients against chemical decomposition and the possibility to modulate drug release. Similar to liposomes they are composed of physiologically well-tolerated excipients and due to their small particle size, they possess similar adhesive properties leading to film formation on the skin [24–25]. Nanostructured lipid carriers (NLC) composed of a solid lipid matrix with a certain content of liquid lipid are a new generation of lipid nanoparticles. The incorporation of liquid lipids leads to great imperfections in the crystal lattice of the nanoparticles leading to improved drug loading capacity and reduced drug expulsion during storage [24, 26–27]. SLN and NLC have been used for skin delivery of various drugs such as vitamin A [28], econazole nitrate [29], penciclovir [30], isotretinoin [31], flurbiprofen [32], glucocorticoids [33], etc.

Mechanism of action: The mechanism of enhancement of skin penetration of the loaded active agents is still not fully understood. However, it is thought that the enhanced skin transport is primarily due to enhanced contact of the active agent with the skin resulting from the large particle surface area and an increase in skin hydration caused by the occlusive film formed on the skin surface by SLN and NLC [4, 34]. Wissing and Müller [35] reported a distinct increase in skin hydration following 4 weeks application of SLN-enriched cream compared to conventional cream.

30.2.3 Polymeric Nanoparticles

Not as extensively as lipid nanocarriers, polymeric nanoparticles have been also investigated for drug and vaccine delivery to the skin. Polymeric nanoparticles offer several advantages, such as established preparation methodology, relative stability compared to lipid carriers, and higher pharmacoeconomic value for systems based on cheap polymers. The release characteristics of entrapped agents can be altered by modulating the properties of nanoparticles and the polymers used, offering great diversity for potential biomedical applications.

Various polymers could be used for fabrication of nanoparticles offering great flexibility in designing a delivery

system with optimal properties. Minoxidil was entrapped in poly(ε-caprolactone)-block-polyethylene glycol nanoparticles for the aim of transdermal delivery [36]. The prepared nanoparticles were found more effective in transdermal delivery compared to ethanolic solution of the drug and to a physical mixture of the drug with blank nanoparticles. Efficiency of transdermal transport was dependent on the size of the nanoparticles and the shunt route was the main route of drug permeation, as shown in confocal images of fluorescently labeled nanoparticles in guinea pig skin. A multifunctional core-shell nanoparticle system, which can be delivered into the epidermis via a gene gun, was developed by Lee et al. [37] for transdermal DNA delivery and epidermal Langerhans cells tracking. The core of the nanoparticles was used to load fluorescent quantum dots for ultrasensitive detection of Langerhans cell migration following transdermal delivery, while a reporter gene was electrostatically adsorbed onto the positively-charged glycol chitosan shell. Results obtained by the authors indicate potential use of the developed system in immunotherapy and vaccine delivery. Concomitant techniques were also applied to enhance transdermal delivery from nanoparticles. For instance, electroporation [38] and microneedles [39] were employed to enhance transdermal delivery of insulin and plasmid DNA, respectively, from polymeric nanoparticles. Contrary to these results, loading of octyl methoxycinnamate, a highly lipophilic sunscreen, in poly(ε-caprolactone) nanoparticles did not result in enhancement of skin permeation with no drug detected in the receptor solution after 6 h, but higher availability in the SC was observed [40].

Mechanism of action: The mechanism by which polymeric nanoparticles facilitate skin transport remains ambiguous. Several studies were focused to investigate the potential mechanism of facilitated drug delivery into the skin from polymeric nanoparticles. The distribution of polystyrene nanoparticles across porcine skin was investigated by confocal laser scanning microscopy. Preferential accumulation of nanoparticles was observed in the hair follicles in a size dependent manner [41]. The role of the hair follicles as a depot for the nanocarriers and thus facilitated drug transport into the viable skin tissue was also demonstrated by Rancan et al. [42]. Potential skin penetration of nanoparticles

into the viable skin tissue will be discussed in detail in Section 30.3.

30.2.4 Inorganic Nanoparticles

Inorganic nanoparticles, titanium dioxide and zinc oxide nanoparticles, are currently present in many marketed sunscreen agents, having the advantage of being transparent thus aesthetically preferred by the consumer over bulk powders [43]. Silver nanoparticles are topically used for their higher antimicrobial efficiency compared to other silver salts due to their extremely large surface area with size diameters that are generally smaller than 100 nm providing better contact with microorganisms [44]. Besides, few studies investigated the potential role of inorganic nanoparticles for facilitated skin delivery. For instance, co-administration of protein drugs with gold nanoparticles was proved a simple yet effective method for overcoming the skin barrier for percutaneous vaccine delivery, where robust immune responses were elicited in the tested animals on employing such a non-invasive delivery strategy [45].

Mechanism of action: Many research groups are currently concerned with assessing the ability of inorganic nanoparticles to overcome the SC into the deeper viable skin layers (DSL), being easier to prepare with sizes less than 100 nm than polymeric nanoparticles. This is extensively discussed in the next section.

30.3 Skin Penetration/Permeation of Nanoparticles

Studying the behavior of the nanoparticles when coming in contact with the skin surface and their interaction with the skin is considered crucial for designing optimal topical and transdermal nanocarriers in terms of their physicochemical parameters, e.g., size, shape, surface chemistry. This is in addition to studying formulation and environmental factors influencing transport of nanoparticles across the skin. This section will give an overview of the current status and knowledge of skin penetration of nanoparticles, the potential mechanism(s) of penetration/ permeation. Finally, factors found of significance for enhanced or

limited skin transport of nanoparticles and approaches adopted to overcome the skin barrier are highlighted.

30.3.1 State of the Art

Investigating the ability of nanoparticles to traverse the SC into the DSL and even reaching the systemic circulation is considered a relatively recent area of research that currently attracts a lot of attention in the research community. However, due to the great diversity of the employed experimental setups, contradictory outcomes, particle penetration of the SC or the opposite, were reported by the different research laboratories. The primary difference among these experimental setups is the *in vitro* or *in vivo* skin model used for mimicking the barrier function of human skin. Though excised human skin is regarded as the "gold standard" for *in vitro* skin penetration studies [46], most of the particle penetration studies were conducted on animal skin (porcine, mouse and rat skin) either as an *in vitro* model, or *in vivo*. However, there are structural and morphological differences between human and animal skin especially in terms of the density of the hair follicles, SC and total skin thickness, the amount of skin lipids, in addition to variations among animal species. This would definitely result in different penetration behaviors [46–47]. This could be justified by the limited availability of human skin driving most of the research laboratories to depend mainly on animal skin for their studies. This is in addition to the different physicochemical parameters of the model particles, skin exposure time, the applied dose, the diffusion area, etc. All this makes it quite difficult to compare the data generated by different laboratories and reach to a conclusion regarding the current status of skin penetration of nanoparticles.

Table 30.1 lists the reported outcomes for studying the skin penetration of selected nanoparticles, classified according to the core material, showing the current controversy on the status of skin penetration among researchers. It should be noted here that the nanoparticles used as model particles, mostly inorganic nanoparticles, for these skin penetration experiments have also different surface coatings that should also have an impact on the behavior of the nanoparticles. For instance, quantum dots were either coated with carboxylic acids [48–51] or PEG and amine groups [51–52].

Table 30.1 Selected examples from the literature showing the current debate on the status of skin penetration of nanoparticles.

Mean size diameter of NP, nm	Skin type	Additional enhancement approach	Reported penetration	Ref.
I. Polymeric nanoparticles				
(a) Polystyrene anoparticles				
20 & 200	Pig	—	No	[41]
40 & 200	Mouse	Tape-stripping	Yes	[53]
100 – 150	Human	Microneedles	Yes/No (inconsistency in results)	[54]
(b) PLGA nanoparticles				
290	Human	—	No	[55]
160.1, 205.5, 288.2	Human	Microneedles	Yes*	[56]
200	Human	—	No	[57]
328.2	Human	—	No	[58]
(c) Fullerenes				
1	Rat	In organic solvents (chloroform, toluene, cyclohexane) & mineral oil	Yes (except for mineral oil)	[59]
3.5 (Fullerene-substituted phenylalanine derivative of a nuclear localization peptide sequence)	pig (dermatomed)	— 60–90 min flexion	No Yes**	[60]

(*Continued*)

Table 30.1 (*Continued*)

Mean size diameter of NP, nm	Skin type	Additional enhancement approach	Reported penetration	Ref.
(d) Polycaprolactone-block-PEG nanoparticles				
40–130	Hairy guinea pig-*in vitro* Mice-*in vivo*	—	Yes	[61]
II. Vesicles				
100–150	Human	—	No#	[62–63]
97.6(SL)/78.8 (EL)/57.7(SEL)	Human	—	No/No/Yes	[64]
III. Cell penetrating peptide engrafted lipid nanocrystals				
180	Rat skin	—	Yes*	[65]
IV. Inorganic nanoparticles				
(a) Quantum dots				
4	Human	Untreated Massage Tape-stripping Tape-stripping +Massage	No No No Yes	[48]
4.1	Mouse (*in vitro* & *in vivo*)	—	Yes	[49]

Mean size diameter of NP, nm	Skin type	Additional enhancement approach	Reported penetration	Ref.
6	Rat	— Flexion Tap-stripping Abrasion	No No Yes (only on VE surface) Yes	[50]
7	Reconstructed human	—	No	[52]
15 – 45	Porcine	—	Yes	[51]
(b) Magnetic nanoparticles				
4.9	Human	—	Yes	[66]
(c) Gold nanoparticles				
10	Human	— Dermaportation	Yes Yes	[67]
15, 102, 198	Rat	—	Yes	[68]
~6 thiol-coated in toluene/ lecithin-coated in water ~15 (cetrimide-coated in toluene)	Human	— —	Yes/Yes Yes No/Yes/Yes	[69–70]

(*Continued*)

Table 30.1 (*Continued*)

Mean size diameter of NP, nm	Skin type	Additional enhancement approach	Reported penetration	Ref.
~15 (citrate-stabilized in water)		–/$CHCl_3$ + methanol/Tape-stripping		
11.6	Mouse (in vivo)	—	Yes	[45]
(d) Silver nanoparticles				
25	Human	— Abrasion	Yes[##] Yes[##]	[71–72]
20, 50, 80	Porcine (*in vivo*)	—	No	[73]
(e) Zinc oxide nanoparticles				
15–40	Human	—	No	[74]
10	Mouse	— OA, EtOH & OA-EtOH	No Yes	[75]
30	Human	—	No	[76]
(f) Titanium dioxide nanoparticles				
207, 30 and fibrils of length 57 and width 15	Porcine (*in vivo*)	—	No	[77]
35 (uncoated & coated) & 10 × 100, 250[+]	Porcine	–/Tape-stripping/Hair removal	No/No/Penetration for 35 coated NP	[78]

Mean size diameter of NP, nm	Skin type	Additional enhancement approach	Reported penetration	Ref.
4,10,21,25,60,90	Porcine	—	No	[79]
4,60	(*in vitro*–1 day)	—	Yes	
10,21,25,60	Porcine	—	Yes	
	(*in vivo*–30 days)			
	Mouse			
	(*in vivo*–60 days)			
20–100	Pig, healthy human skin & human skin grafted on a severe combined immune-deficient mouse model	—	No	[80]

Note: Unless indicated, skin penetration/permeation experiment was carried out *in vitro*.

*The authors based their conclusion on tracking the fluorophore, which was encapsulated in the nanoparticles, but not covalently bound to them.The use of nanoparticles containing covalently bound dye ensures that the fluorescence detected subsequent to application of nanoparticles formulations, originates from the nanoparticles and not from the free fluorophores.

**The status of skin penetration was checked after 48 h of skin exposure, however the maximum exposure time should be 24 h, after which the skin integrity is deteriorated [81].

#Elastic vesicles could reach the deeper layers of the SC in comparison to rigid vesicles being trapped in the upper 2–5 μm of the SC.

##Low penetration was observed for both untreated skin and after abrasion with higher penetration for damaged skin.

+These are the primary sizes, however aggregation was reported for these nano-dispersions.

OA: oleic acid, EtOH: ethanol and SL, EL and SCL: surfactant containing-, ethanol containing- and surfactant and ethanol containing liposomes.

30.3.2 Mechanism of Skin Penetration of Nanoparticles

Similarly, the main route and the potential mechanism of skin penetration of nanoparticles are not fully clear. Several studies investigated the mechanism of skin penetration of nanoparticles. The intercellular lipidic route was shown to be the route of skin penetration of different types of quantum dots, as revealed by TEM examination [82–83]. Recently, we studied the effect of deteriorating the barrier function of human skin on penetration of 15 nm polar gold nanoparticles, with no passive penetration through intact human skin [70]. Removal of the epidermal lipids by chloroform/methanol mixture resulted in penetration of the tested AuNP indicating that the intercellular lipids are the main barrier for skin penetration of nanoparticles. Complete removal of the SC resulted however in significant increase in penetration into the DSL. This is a hint that the barrier function of the SC to particle penetration does not rely only on the intercellular lipids, but possibly through the intracellular pathways as well. Not only this but also the follicular pathway is regarded as a possible route for skin penetration of nanoparticles. This is despite the fact that the skin appendages occupy roughly about 1/1000 of the skin surface. Polystyrene nanoparticles were shown to preferentially accumulate in the follicular openings in a time-dependent manner. This localization appears to be dependent on particle size; 20 nm nanoparticles showed higher accumulation in the follicular regions rather than 200 nm [41]. Dependence of the diffusion depths of nanoparticles inside the hair follicles on their particle sizes, ranging from 122 to 1000 nm, was also reported by Patzelt et al. [84]. The results revealed that the particles of medium size (643 and 646 nm) diffused deeper into the porcine hair follicles than smaller or larger particles. On the contrary, Lekki et al. [85] have studied the possible role of the follicular pathway on the percutaneous uptake of TiO_2 nanoparticles of 20 nm width and 100 nm length. Though particles were observed as deep as about 400 nm inside the follicle, no particles were observed in the surrounding vital tissue undervaluing the role of the transfollicular pathway as a possible mechanism of penetration of particles falling in such size range.

It could be concluded so far that there is no general mechanism of skin penetration of nanoparticles. This again differs from one case to another depending on the physicochemistry of the model nanoparticles, the used skin model, as well as other environmental and formulation conditions.

30.3.3 Factors Playing a Role in Skin Penetration of Nanoparticles

Bringing topically applied materials to the nano-size range does not guarantee their ability to penetrate the skin or at least not behaving in a similar manner with the skin barrier. Similar to drug penetration, the physicochemical parameters of the nanoparticles are believed to play a key role in governing the skin penetration of nanoparticles.

The particle size is a major determinant of skin penetration of nanoparticles [70], in which the penetration of ~6 nm AuNP was higher than ~15 nm AuNP when applied on the skin in the same vehicle (toluene) for 24 h. Other studies have investigated the effect of size on the follicular penetration of nanoparticles. For instance, polymeric beads, 40 nm diameter, were shown to diffuse deep into the hair follicles and then penetrating into adjacent deep tissues, however the same phenomenon was not observed for both 750 and 1500 nm diameter particles [86]. Furthermore, knowing that the skin surface is negative under normal physiological conditions [87], nanoparticles with different surface charges would likely interact with the skin barrier in clearly distinctive manners. Wu et al. [88] studied the penetration of polymeric nanoparticles with different surface charge. Expectedly, cationic nanoparticles showed more affinity for the negatively charged skin surface in contrast to the anionic carriers and delivered a significantly greater amount of the encapsulant to the SC but all particles reached the same depth in the SC. In contrast to the permselectivity of the skin based on surface charge, Kohli et al. [89] reported that negatively charged latex nanoparticles, 50 and 500 nm diameter could permeate porcine skin but not neutral and positively-charged nanoparticles. The authors attributed the permeation to the repulsive forces between the negatively charged lipids within the skin and the applied particles. According to the authors, these

forces may result in temporary initiation of channels within the skin allowing for particle permeation. The authors also claimed that there might be threshold charge that has to be reached to allow adequate repulsion of lipids permitting particle permeation through the skin explaining why other examined negatively-charged nanoparticles, 100 and 200 nm, did not show permeation. Ryman-Rasmussen et al. [51] also showed a shape dependency for particle penetration, showing more favorable penetration for spherical over ellipsoid nanoparticles.

In addition to the size, shape and surface charge, we have recently shown that the hydrophobicity of the particle surface favors skin penetration of AuNP through human skin [70]. In this study, citrate-stabilized ~15 nm AuNP could not penetrate human skin after 24 h of skin exposure, while hydrophobic AuNP of the same size could penetrate into deeper layers. A similar pattern was observed for smaller ~6 nm AuNP, in which surface modification of hydrophobic thiol-coated AuNP using lecithin yielded relatively hydrophilic AuNP with lower skin penetration ability [70]. It should be mentioned here, however, that these particles were applied in different vehicles affecting particle penetration but not to a great extent, as was shown by our results.

Other factors that were shown to play a role in skin penetration of nanoparticles include the concentration of the applied nanodispersion and skin exposure to nanoparticles [70].

30.3.4 Approaches to Overcome the Skin Barrier: Application for Enhanced Particle Penetration

Several approaches have been adopted simultaneous to skin application of nanoparticles to either induce or enhance particle penetration. Most of these approaches are typically physical methods; however, chemical agents were also investigated for enhanced particle penetration. These approaches are listed in Table 30.2. However, it should be noted here that the use of these approaches did not always result in satisfactory results. Some of these approaches are shortly discussed below.

Partial or complete removal of the SC, to which the barrier function of the skin is attributed, by either tape-stripping [48, 50, 53, 90] or dermabrasion [50, 90] was explored by several researchers for induction of skin penetration of nanoparticles.

Table 30.2 Literature survey of the attempts employed to induce/enhance skin penetration of nanoparticles

Enhancement approach	References
Tape-stripping/cyanoacrylate stripping	[48, 50, 53, 90]/ [86]
Dermabrasion	[50, 60, 90]
Mechanical flexion	[50, 60]
Massage	[48, 91]
Microneedles	[54, 56]
Dermaporation by pulsed electromagnetic field	[67]
UV-exposure	[92–93]
Hyperthermia	[83]
Electrophoresis	[94]
Dermaportation	[67]
Sonophoresis	[95–96]
Chemical enhancers	[75, 90, 95–97]

Mechanical flexion, a method that simulates flexing movements such as repetitive wrist bending, was used by Rouse et al. [60] to induce skin penetration of 3.5 nm diameter fullerene particles. However, fixing an excised skin in an automated apparatus for mechanical flexion for some time does not mimic the clinical conditions. On the other hand, manual massaging, a more acceptable approach, for short time (5–10 min) was later explored by Gratieri et al. [48] to drive the quantum dots to penetrate into the DSL of human skin. However, no satisfactory results were obtained since quantum dots were observed in the DSL only after massaging of damaged skin (tape-stripped) for 10 min.

Another approach involves the use of minimally-invasive microneedle array technology to perforate the SC, forming microchannels that allow enhanced skin delivery. Each array consists of micron-sized needles, potentially fabricated from silicon, metal, glass or various polymers, projecting out from a patch-like support. This approach allowed the penetration of fluorescently labeled polystyrene nanoparticles, 100–150 nm in diameter through human skin, however there was no consistency in results as reported by the authors [54]. Other adopted approaches for enhanced particle penetration through the skin barrier are listed in Table 30.2.

30.4 Conclusion

The development of nanocarriers for topical and transdermal drug delivery is considered by several researchers a potential step forward in the field of dermatology, being proved to provide several advantages over traditional formulations. However, the current research status is characterized by many contradictions among the results reported by the different research laboratories, in addition to case-to-case variations. Unfortunately, the key factors in most of these studies were not yet identified and/or quantified in terms of size, lipophilicity, etc. Therefore, future research should focus more on the basic understanding of the mechanism of enhancement of the penetration/permeation of the encapsulated active agent as well as the fate of the nanocarrier itself. This would ultimately allow for more success on the praxis level for local treatment of several skin diseases in which controlling the carrier geometry and surface properties would have more control on the depth penetrated by the particles in the skin. On the other hand, clinical applications necessitating transdermal drug delivery are yet more challenging referring to the minimal percentage of applied particles permeating the whole barrier thickness for some investigated particles, or even no permeation for others. This is especially the case for healthy skin. Transdermal drug delivery would, however, benefit from the depot effect of nanoparticles penetrating into the upper layers of the SC or deeper inside the skin thus, they are not washed off easily.

Disclosures and Conflict of Interest

The authors declare that they have no conflict of interest and have no affiliations or financial involvement with any organization or entity discussed in this chapter. This includes employment, consultancies, honoraria, grants, stock ownership or options, expert testimony, patents (received or pending) or royalties. No writing assistance was utilized in the production of this chapter and have received no payment for its preparation. The findings and conclusions here reflect the current views of the authors. They should not be attributed, in whole or in part, to the organizations with which they are affiliated, nor should they be considered as expressing an opinion with regard to the merits

of any particular company or product discussed herein. Nothing contained herein is to be considered as the rendering of legal advice.

Corresponding Author

Dr. Marc Schneider
Department of Pharmacy
Biopharmaceutics and Pharmaceutical Technology
Saarland University, Campus A4 1, D-66123 Saarbrucken, Germany
Email: marc.schneider@mx.uni-saarland.de

About the Authors

Hagar I. Labouta is currently a postdoctoral fellow at Helmholtz Institute for Pharmaceutical Research-Saarland (HIPS), Helmholtz Centre for Infection Research (HZI) in Saarbrücken, Germany. She studied pharmacy at the University of Alexandria, Alexandria, Egypt, where she later joined the Department of Pharmaceutics and obtained her master's degree in drug delivery. She obtained her PhD Saarland University, Germany under the supervision of Dr. Marc Schneider. During her PhD, she investigated the interaction of gold nanoparticles with the skin barrier using multiphoton microscopy.

Marc Schneider is a professor of pharmaceutical nanotechnology at Saarland University in Saarbrücken, Germany. He was president and vice-president of the Controlled Release Society-Local Chapter, Germany, in 2011 and 2010, respectively. Currently, he serves as co-editor-in-chief for *Drug Delivery Letters*. Dr. Schneider is a trained physicist who did his undergraduate studies at the Technical University Kaiserslautern and at Ruprecht-Karls Heidelberg University, Germany. He received his diploma/master from the Free University, Berlin, Germany in 1998 focusing on medicinal physics. Following this, he worked as a scientist at the Max Delbrück Center for Molecular Medicine before joining the Max Plank Institute for Colloids and Interfaces for his PhD. He obtained

a PhD degree in 2002 from Potsdam University in experimental physics on polymers at interfaces. His post-doctoral training focused on imaging of fluorescent proteins with multiphoton microscopy together with Alberto Diaspro, Genoa, Italy. In 2005, Dr. Schneider joined Prof. Lehr's lab at Saarland University, Germany. In 2007, he was promoted to associate professor with tenure option that he is holding currently. Dr. Schneider's accomplishments include 2 patents and over 45 original research publications.

References

1. Andersen, I. E., Jaeger, B. (1999). Danish participatory models scenario workshops and consensus conferences: Towards more democratic decision-making. *Sci. Public Policy*, **26**, 331–340.
2. Appel, I. (1996). Stufen der Risikoabwehr. Zur Neuorientierung der umweltrechtlichen Sicherheitsdogmatik im Gentechnikrecht, *Natur und Recht*, 227–235.
3. Arkin, E. (1991). Evaluation for risk communicators. Evaluation and Effective Risk Communications Workshop Proceedings, Interagency Task Force on Environmental, Cancer and Heart and Lung Disease. Washington, DC, US Environmental Protection Agency.
4. Bainbridge, W. S. (2002). Public attitudes toward nanotechnology. *J. Nanoparticle Res.*, **4**, 561–570.
5. Berger, P. L., Luckmann, T. (1966). *The Social Construction of Reality: A Treatise in the Sociology of Knowledge*, Anchor Books, New York.
6. Besley, J. C., Kramer, V. L., Priest, S. H. (2008). Expert opinion on nanotechnology: Risks, benefits, and regulation. *J. Nanoparticle Res.*, **10**, 549–558.
7. Böl, G.-F., Epp, A., Hertel, R. (2010). Perception of nanotechnology in Internet-based discussions, *BfR-Wissenschaft 04/2010*, Bundesinstitut für Risikobewertung.
8. Brossard, D., Scheufele, D. A., Kim, E., Lewenstein, B. V. (2009). Religiosity as a perceptual filter: Examining processes of opinion formation about nanotechnology. *Public Understanding Sci.*, **18**, 546–558.
9. Carius, R., Renn, O. (2003). Partizipative Risikokommunikation. Wege zu einer risikomündigen Gesellschaft. *Bundesgesundheitsblatt* Gesundheitsforschung *Gesundheitsschutz*, **46**, 578–585.

10. Cobb, M. D. (2011). Creating informed public opinion: Citizen deliberation about nanotechnologies for human enhancements. *J. Nanoparticle Res.*, **13**, 1533–1548.
11. Cobb, M. D., MacOubrie, J. (2004). Public perceptions about nanotechnology: Risks, benefits and trust. *J. Nanoparticle Res.*, **6**, 395–405.
12. Commission of the European Communities (2000). Communication from the commission on the precautionary principle; COM (2000) 1.
13. Currall, S. C., King, E. B., Lane, N., Madera, J., Turner, S. (2006). What drives public acceptance of nanotechnology? *Nat. Nanotechnol.*, **1**, 153–155.
14. Epp, A., Hertel, R., Böl, G.-F. (2008). Formen und Folgen behördlicher Risikokommunikation. *BfR-Wissenschaft 01/2008*, Bundesinstitut für Risikobewertung.
15. Eurobarometer (2010). Special Eurobarometer Biotechnology. Report, European Commissions.
16. Fischhoff, B., Slovic, P., Lichtenstein, S., Read, S., Combs, B. (1978). How safe is safe enough? A psychometric study of attitudes towards technological risks and benefits. *Policy Sci.*, **9**, 127–152.
17. Friedman, S. M., Egolf, B. P. (2011). A longitudinal study of newspaper and wire service coverage of nanotechnology risks. *Risk Anal.*, **31**, 1701–1717.
18. Friedman, S. M., Egolf, B. P. (2005). Nanotechnology: Risks and the media. *IEEE Technol. Society Mag.*, **24**, 5–11.
19. FSA. (2011). *FSA Citizens Forums: Nanotechnology and food*.
20. Fujita, Y., Yokoyama, H., Abe, S. (2006). Perception of nanotechnology among the general public in Japan. *Asia Pacific Nanotech Weekly*, **4**, TNS-BMRB Report.
21. Gaskell, G., Ten Eyck, T., Jackson, J., Veltri, G. (2004). Public attitudes to nanotechnology in Europe and the United States. *Nat. Mater.*, **3**, 496.
22. Gaskell, G., Eyck, T. T., Jackson, J., Veltri, G. (2005). Imagining nanotechnology: Cultural support for technological innovation in Europe and the United States. *Public Understanding Sci.*, **14**, 81–90.
23. Göpfert, W. (2003). Wie gehen Journalisten mit Risiken um? Reflexionen über ein schwieriges Berichterstattungsfeld. *Bundesgesundheitsblatt—Gesundheitsforschung—Gesundheitsschutz*, **46**, 574–577.

24. Götte, S., Göbel, A. (2008). Zweitevaluation der Bekanntheit des Bundesinstitutes für Risikobewertung. Bundesinstitut für Risikobewertung. Available at: http://www.bfr.bund.de/cm/343/zweitevaluation_der_bekanntheit_des_bfr_abschlussbericht_2008.pdf (accessed on June 17, 2014).
25. Grobe, A., Eberhard, C., Hutterli, M. (2005). Nanotechnologie im Spiegel der Medien: Medienanalyse zur Berichterstattung über Chancen und Risiken der Nanotechnologie., St. Gallen, Stiftung Risiko-Dialog.
26. Groffman, P. M., Stylinski, C., Nisbet, M. C., Duarte, C. M., Jordan, R., Burgin, A., Andrea Previtali, M., Cary, J. C. (2010). Restarting the conversation: Challenges at the interface between ecology and society. *Front. Ecol. Environ.*, **8**, 284–291.
27. Hamlett, P., Cobb, M. D., Guston, D. (2008). National Citizen's Technology Forum Report, Nanotechnologies and Human Enhancement. Arizona State University, 2008.
28. Heidenescher, M. (1999). Die Beobachtung des Risikos: zur Konstruktion technisch-ökologischer Risiken in Gesellschaft und Politik. *Soziologische Schriften*, **68**, Berlin, Duncker & Humblot.
29. Hertel, R., Henseler, G. (2007). ERiK—Development of a multi-stage risk communication process. *BfR-Wissenschaft 04/2007* Bundesinstitut für Risikobewertung.
30. Ho, S. S., Scheufele, D. A., Corley, E. A. (2010). Making sense of policy choices: Understanding the roles of value predispositions, mass media, and cognitive processing in public attitudes toward nanotechnology. *J. Nanoparticle Res.*, **12**, 2703–2715.
31. Priest, S. H. (2012). *Nanotechnology and the Public. Risk Perception and Risk Communication*, CRC Press/Taylor and Francis Group, Boca Raton, Florida.
32. Joy, B. (2000). Why the future doesn't need us. *Wired Mag.*, April issue.
33. Jung, T. (2003). Der Risikobegriff in Wissenschaft und Gesellschaft. *Bundesgesundheitsblatt—Gesundheitsforschung—Gesundheitsschutz*, **46**, 542–548.
34. Kahan, D. M., Slovic, P., Braman, D. (2007). *Nanotechnology Risk Perceptions: The Influence of Affect and Values*, Woodrow Wilson International Center for Scholars.
35. Kanerva, M. (2009). Assessing risk discourses: Nano S&T in the Global South, *United Nations University Working Paper Series*.

36. Kasperson, R. E., Renn, O., Slovic, P., Brown, H. S., Emel, J., Goble, Kasperson, J. X., Ratick, S. (1988). The social amplification of risk: A conceptual framework. *Risk Anal.*, **8**, 177–187.

37. Kasperson, R. E., Kasperson, J. X. (1996). The social amplification and attenuation of risk. *Ann. Am. Acad. Polit. Soc. Sci.*, **545**, 95–104.

38. Kjærgaard, R. S. (2010). Making a small country count: Nanotechnology in Danish newspapers from 1996 to 2006. *Public Understanding Sci.*, **19**, 80–97.

39. Kjølberg, K. L. (2009). Representations of nanotechnology in Norwegian newspapers—Implications for public participation. *NanoEthics*, **3**, 61–72.

40. Klinke, A., Renn, O. (2002). A new approach to risk evaluation and management: Risk-based, precaution-based, and discourse-based strategies. *Risk Anal.*, **22**, 1071–1094.

41. Kohring, M., Marcinkowski, F., Donk, J., Metag, J. (2011). Das Bild der Nanotechnologie in deutschen Printmedien. Eine frameanalytische Langzeitstudie. *Publizistik*, **56,** 199–219.

42. Kurzenhäuser, S., Epp, A. (2009). Perception of health risks. Psychological and social factors. *Bundesgesundheitsblatt—Gesundheitsforschung—Gesundheitsschutz*, **52**, 1141–1146.

43. Kuzma, J. (2011). Audiences, stakeholders, cultures and nanotechnology risk. Nanotechnology and the public. In: Priest, S. H., ed. *Risk Perception and Risk Communication*, CRC Press, London.

44. Luhmann, N. (1996). Die Realität der Massenmedien. Westdeutscher Verlag, Opladen.

45. Luhmann, N. (1996). Gefahr Oder Risiko, Solidarität oder Konflikt. In: Königswieser, R., ed. *Risiko-Dialog: Zukunft ohne Harmonie-Formel*, Köln, pp. 38–46.

46. MacOubrie, J. (2006). Nanotechnology: Public concerns, reasoning and trust in government. *Public Understanding Sci.*, **15**, 221–241.

47. McComas, K. A., Besley, J. C. (2011). Fairness and nanotechnology concern. *Risk Anal.*, **31**, 1749–1761.

48. Nisbet, M. C., Scheufele, D. A. (2009). What's next for science communication? Promising directions and lingering distractions. *Am. J. Bot.*, **96**, 1767–1778.

49. OECD. (2002). OECD Guidance document on risk communication for chemical risk management. Report no. ENV/JM/MONO(2002) 18, Organization for Economic Co-Operation and Development (OECD), Environment Directorate, Paris.

50. Pidgeon, N, Kasperson, R. E., Slovic, P. (2003). *The Social Amplification of Risk*, Cambridge University Press.
51. Pidgeon, N., Rogers-Hayden, T. (2007). Opening up nanotechnology dialogue with the publics: Risk communication or "upstream engagement"? *Health Risk Soc.*, **9**, 191–210.
52. Powell, M. C., Colin, M. (2009). Participatory paradoxes: Facilitating citizen engagement in science and technology from the top-down? *Bull. Sci. Technol. Soc.*, **29**, 325–342.
53. Priest, S., Greenhalgh, T., Kramer, V. (2010). Risk perceptions starting to shift? U.S. citizens are forming opinions about nanotechnology. *J. Nanoparticle Res.*, **12**, 11–20.
54. Priest, S. (2011). In: Priest, S. H., ed. *Nanotechnology and the Public, Risk Perception and Risk Communication*, CRC Press, London.
55. Priest, S., Lane, T., Greenhalgh, T., Hand, L. J., Kramer, V. (2011). Envisioning emerging nanotechnologies: A three-year panel study of South Carolina citizens. *Risk Anal.*, **31**, 1718–1733.
56. Rayner, S. (2003). Democracy in the age of assessment: Reflections on the roles of expertise and democracy in public-sector decision making. *Sci. Public Pol.*, **30**, 163–170.
57. Regulation No. 178/2002, European Commission.
58. Reichl, F. Xaver, Schwenk, M. (2004). Regulatorische Toxikologie: Gesundheitsschutz. *Umweltschutz, Verbraucherschutz*/Franz-Xaver Reichl; Michael Schwenk. Berlin [u.a.]: Springer; ISBN 3-540009-85-X (German).
59. Renn, O. (1999). A model for an analytic—Deliberative process in risk management. *Environ. Sci. Technol.*, **33**, 3049–3055.
60. Renn, O. (2007). Risiko: Über Den Gesellschaftlichen Umgang Mit Unsicherheit/Ortwin Renn München, oekom-Verl.
61. Savadori, L., Savio, S., Nicotra, E., Rumiati, R., Finucane, M., Slovic, P. (2004). Expert and public perception of risk from biotechnology. *Risk Anal.*, **24**, 1289–1299.
62. Scheufele, D. A., Lewenstein, B. V. (2005). The public and nanotechnology: How citizens make sense of emerging technologies. *J. Nanopart. Res.*, **7**, 659–667.
63. Scheufele, D. A., Corley, E. A., Dunwoody, S., Shih, T. J., Hillback, E., Guston, D. H. (2007). Scientists worry about some risks more than the public. *Nat. Nanotechnol.*, **2**, 732–734.
64. Siegrist, M. (2010). Predicting the future: Review of public perception studies of nanotechnology. *Human Ecol. Risk Asses.*, **16**, 837–846.

65. Siegrist, M., Keller, C., Kiers, H. A. L. (2005). A new look at the psychometric paradigm of perception of hazards. *Risk Anal.*, **25**, 211–222.

66. Siegrist, M., Keller, C., Kastenholz, H., Frey, S., Wiek, A. (2007). Laypeople's and experts' perception of nanotechnology hazards. *Risk Anal.*, **27**, 59–69.

67. Siegrist, M., Cousin, M. E., Kastenholz, H., Wiek, A. (2007). Public acceptance of nanotechnology foods and food packaging: The influence of affect and trust. *Appetite*, **49**, 459–466.

68. Slovic, P. (1987). Perception of risk. *Science*, **236**, 280–285.

69. Slovic, P. (1992). Perception of risk: Reflections on the psychometric paradigm. *Soc. Theories Risk*, Westport, Praeger.

70. Slovic, P. (2000). *The Perception of Risk*, Earthscan Publications Ltd.

71. Slovic, P., Finucane, M. L., Peters, E., MacGregor, D. G. (2004). Risk as analysis and risk as feelings: Some thoughts about affect, reason, risk, and rationality. *Risk Anal.*, **24**, 311–322.

72. Te Kulve, H. (2006). Evolving repertoires: Nanotechnology in daily newspapers in the Netherlands. *Sci. Cul.*, **15**, 367–382.

73. Ulbig, E., Hertel, R., Böl, G.-F. (2010). Communication of risk and hazard from the angle of different stakeholders, Bundesinstitut für Risikobewertung.

74. Wilsdon J., et al. (2006). The technical and social complexity of nanotechnologies demands a genuine dialogue between scientists and the public.

75. Zimmer, R., Hertel, R., Böl, G.-F. (2009). BfR Consumer Conference Nanotechnology, Bundesinstitut für Risikobewertung.

76. Zimmer, R., Hertel, R., Böl, G.-F. (2009). Public perceptions about nanotechnology, Bundesinstitut für Risikobewertung.

77. Zimmer, R., Hertel, R., Böl, G.-F. (2010). BfR Delphi Study on Nanotechnology, Bundesinstitut für Risikobewertung.

78. Zimmer, R., Hertel, R., Böl, G.-F. (2010). Risk perception of nanotechnology—analysis of media coverage. Bundesinstitut für Risikobewertung.

79. Wu, J., Liu, W., Xue, C., Zhou, S., Lan, F., et al. (2009). Toxicity and penetration of TiO_2 nanoparticles in hairless mice and porcine skin after subchronic dermal exposure. *Toxicol. Lett.*, **191**(1), 1–8.

80. Gontier, E., Ynsa, M.-D., Biro, T., Hunyadi, J., Kiss, B., et al. (2008). Is there penetration of titania nanoparticles in sunscreens through skin?

A comparative electron and ion microscopy study. *Nanotoxicology*, **2**(4), 218–231.

81. OECD (23 November 2004) *Draft Guideline 428: Skin absorption: In vitro method*. OECD Guideline for the Testing of Chemicals (accessed).
82. Zhang, L. W., Yu, W. W., Colvin, V. L., Monteiro-Riviere, N. A. (2008). Biological interactions of quantum dot nanoparticles in skin and in human epidermal keratinocytes. *Toxicol. Appl. Pharmacol.*, **228**(2), 200–211.
83. Upadhyay, P. (2006). Enhanced transdermal-immunization with diptheria-toxoid using local hyperthermia. *Vaccine*, **24**(27–28), 5593–5598.
84. Patzelt, A., Richter, H., Knorr, F., Schafer, U., Lehr, C. M., et al. (2011). Selective follicular targeting by modification of the particle sizes. *J. Control. Release*, **150**(1), 45–48.
85. Lekki, J., Stachura, Z., Dabros, W., Stachura, J., Menzel, F., et al. (2007). On the follicular pathway of percutaneous uptake of nanoparticles: Ion microscopy and autoradiography studies. *Nuclear Instruments and Methods in Physics Research Section B: Beam Interactions with Materials and Atoms. Nuclear Microprobe Technology and Applications (ICNMTA2006) and Proton Beam Writing (PBW II)*, *10th International Conference on Nuclear Microprobe Technology and Applications and 2nd International Workshop on Proton Beam Writing*, **260**(1), 174–177.
86. Vogt, A., Combadiere, B., Hadam, S., Stieler, K. M., Lademann, J., et al. (2006). 40 nm, but not 750 or 1,500 nm, nanoparticles enter epidermal CD1a+ cells after transcutaneous application on human skin. *J. Invest. Dermatol.*, **126**(6), 1316–1322.
87. Marro, D., Guy, R. H., Begoña Delgado-Charro, M. (2001). Characterization of the iontophoretic permselectivity properties of human and pig skin. *J. Control. Release*, **70**(1–2), 213–217.
88. Wu, X., Landfester, K., Musyanovych, A., Guy, R. H. (2010). Disposition of charged nanoparticles after their topical application to the skin. *Skin Pharmacol. Physiol.*, **23**(3), 117–123.
89. Kohli, A. K., Alpar, H. O. (2004). Potential use of nanoparticles for transcutaneous vaccine delivery: Effect of particle size and charge. *Int. J. Pharm.*, **275**(1–2), 13–17.
90. Gopee, N. V., Roberts, D. W., Webb, P., Cozart, C. R., Siitonen, P. H., et al. (2009). Quantitative determination of skin penetration of PEG-coated CdSe quantum dots in dermabraded but not intact SKH-1 hairless mouse skin. *Toxicol. Sci.*, **111**(1), 37–48.

91. Ossadnik, M., Richter, H., Teichmann, A., Koch, S., Schäfer, U., et al. (2006). Investigation of differences in follicular penetration of particle-and nonparticle-containing emulsions by laser scanning microscopy. *Laser Phys.*, **16**(5), 747–750.
92. Mortensen, L., Zheng, H., Faulknor, R., De Benedetto, A., Beck, L., et al. (2009). Increased in vivo skin penetration of quantum dots with UVR and in vitro quantum dot cytotoxicity. In: *Colloidal Quantum Dots for Biomedical Applications IV*. SPIE, San Jose, CA, USA.
93. Mortensen, L. J., Oberdorster, G., Pentland, A. P., Delouise, L. A. (2008). In vivo skin penetration of quantum dot nanoparticles in the murine model: The effect of UVR. *Nano Lett.*, **8**(9), 2779–2787.
94. Chen, H.-Y., Zhao, Q., Su, K.-L., Lin, Y.-C. Development of transdermal delivery chip system: Deliver gold nanoparticles into human stratum corneum. in *3rd annual IEEE international conference on nano-micro engineered and molecular system*. 2008. Hainan island, China.
95. Paliwal, S., Menon, G. K., Mitragotri, S. (2006). Low-frequency sonophoresis: Ultrastructural basis for stratum corneum permeability assessed using quantum dots. *J. Invest. Dermatol.*, **126**(5), 1095–1101.
96. Seto, J. E., Polat, B. E., Lopez, R. F. V., Blankschtein, D., Langer, R. (2010). Effects of ultrasound and sodium lauryl sulfate on the transdermal delivery of hydrophilic permeants: Comparative in vitro studies with full-thickness and split-thickness pig and human skin. *J. Control. Release*, **145**(1), 26–32.
97. Labouta, H. I., El-Khordagui, L. K., Schneider, M. (in press). Could chemical enhancement of gold nanoparticle penetration be extrapolated from established approaches for drug permeation? *Skin Pharmacol. Physiol*.

Chapter 31

Application of Nanotechnology in Non-Invasive Topical Gene Therapy

Mahmoud Elsabahy, PhD,[a,b,c] Maria Jimena Loureiro, MSc,[a] and Marianna Foldvari, PhD, DPharmSci[a]

[a]*School of Pharmacy and Waterloo Institute of Nanotechnology, University of Waterloo, Waterloo, Ontario, Canada*
[b]*Department of Pharmaceutics, Faculty of Pharmacy, Assiut University, Assiut, Egypt*
[c]*Laboratory for Synthetic-Biologic Interactions, Department of Chemistry, Texas A&M University, College Station, Texas, USA*

Keywords: nanomedicine, topical delivery, dermal and transdermal delivery, gene therapy, non-viral vectors, gemini-lipid nanoparticles, biphasic vesicles, transfersomes, niosomes, plasmid, nucleic acid, skin, liposomes, pharmaceutics, nanocarrier, needle-free, non-invasive, administration route

31.1 Introduction

Human diseases associated with genetic mutations can be treated by the introduction of a vector encoding a healthy gene, by using a therapeutic DNA/RNA construct to enhance gene expression, or to inhibit production of deleterious proteins (e.g., oncoproteins). Thus, the delivery of intracellular nucleic acid-based drugs can be exploited for vaccination and for the treatment of several diseases

Handbook of Clinical Nanomedicine: Nanoparticles, Imaging, Therapy, and Clinical Applications
Edited by Raj Bawa, Gerald F. Audette, and Israel Rubinstein

ISBN 978-981-4669-20-7 (Hardcover), 978-981-4669-21-4 (eBook)
www.panstanford.com

such as cancer, viral infections and, dermatological diseases [1–4]. Many nucleic acid-based therapeutics (e.g., plasmid DNA (pDNA), antisense oligonucleotides (AON) and small interfering RNA (siRNA)) have either been approved or in different phases of clinical trials [5–8]. However, the clinical outcome of the different gene therapies is still unsatisfactory. Gene delivery is hindered by the rapid extra- and intracellular enzymatic degradation, thereby reducing the amount that is available in the host to elicit the response. The cellular uptake of these genetic products is usually very low due to their high molecular weights and anionic nature. After cellular entry, nucleic acids can be degraded in the endosomal/lysosomal compartments. The small fraction that may escape from the endosomes/lysosomes is exposed to cytoplasmic degradation. In addition, the nuclear membrane represents an additional barrier for gene transcription, when using pDNA. Moreover, an additional barrier exists for topical gene delivery; the limited penetration through the stratum corneum (SC), the outermost layer of the skin and the most recognized barrier for dermal and transdermal delivery of drugs, proteins and nucleic acids.

Many delivery systems have been developed to overcome the barriers associated with the use of genetic materials. However, most of these vectors (either viral or non-viral) are usually delivered parenterally, through different administration routes, such as, intravenous, intramuscular, subcutaneous, intradermal, and epidermal injections. These methods involve piercing the skin and most likely the underlying tissues. Due to the invasiveness of these methods, topical administration could be a very attractive and non-invasive gene therapy approach.

Liposomes were among the first vehicles that have been used for topical gene delivery. Although liposomes were considered as a promising approach, recent reports have shown that liposomes made solely from phospholipids may not be able to penetrate deep into the dermal skin layers [9, 10]. Hence, other liposomal compositions or nanoparticles (e.g., transfersomes, ethosomes, niosomes, nanoemulsions, gemini-lipid nanoparticles, and biphasic vesicles) have been developed to enhance penetration through the SC. This chapter focuses on the recent advances in engineering non-invasive (i.e., non-injectable), non-viral nanovectors for dermal/transdermal delivery of different genetic materials and on their future prospects.

31.2 Topical Delivery as an Alternative Route of Administration

Genetic materials are usually delivered parenterally, using different routes of administration including intravenous, intramuscular, subcutaneous, and intradermal, which is often traumatic and expensive in terms of administration and disposal. The most common method is the intravenous injection of the DNA/RNA aqueous solutions. Due to the invasiveness of these methods, dermal delivery appears to be promising, in that such delivery could be non-invasive and reduce the systemic exposure to the drug. Alternatively, a topical patch can be used for transdermal (systemic) delivery without encountering the first pass effect. In addition, topical administration is simple and allows repeated treatment and can be done by the patient. A topical approach could also lower the cost because the strict sterility requirement for parenteral preparations is unnecessary for topical administration. Furthermore, topical immunization is a very attractive approach because the skin is a very active immune surveillance site, rich in dendritic cells such as Langerhans cells in the epidermis and immature dendritic cells in the dermis [11, 12]. However, these advantages are contingent upon successful delivery of the DNA/RNA through the skin. There is still a great challenge to delivering nucleic acid molecules through the skin due to their large size, negative charge and other physicochemical properties. The SC is considered as the main permeability barrier to effective dermal/transdermal delivery of polynucleotides. Therefore, it is important to incorporate nucleic acids into nanocarriers, which may be also loaded or mixed with some chemicals (e.g., permeation enhancers), to enhance their penetration through the SC and subsequent uptake into the cells.

31.3 Biological Barriers toward Topical Gene Therapy

31.3.1 Skin Barrier

The skin is the outermost layer of the body. The thickness of human skin ranges from 1 to 2 mm. It is composed of four main

layers: the SC (10–20 μm), viable epidermis (50–200 μm), dermis and subcutaneous tissue (1–2 mm) [13]. The SC is the first barrier encountered in dermal/transdermal delivery. It is highly hydrophobic and contains 15–20 layers of terminally differentiated keratinocytes (corneocytes) embedded in an intercellular lipid-rich matrix. Corneocytes are polygonal, elongated, and flattened cells, which contain intracellular cross-linked macrofibrillar bundles of keratin giving corneocytes a rigid structure. Corneo-desmosomes connect corneocytes into the ordered superstructure of the SC [14]. Extracellular lipid accounts for ~10% of the dry weight of this layer while 90% is intracellular protein (mainly keratin) [15, 16]. The SC lacks phospholipids, but is enriched with ceramides and neutral lipids (cholesterol, fatty acids and cholesteryl esters) that are arranged in a multi-lamellar bilayers and form so called "lipid channels" [17]. Interdigitated long-chain-*v*-hydroxyceramides provide cohesion between corneocytes by forming tight lipid envelopes around the corneocyte protein component [18]. This highly structured and organized assembly makes SC the major permeability barrier to external materials. Hence, SC is regarded as the rate-limiting factor in the penetration of therapeutic agents through the skin. The ability of various agents to interact with the intercellular lipids of the SC therefore dictates the degree to which absorption is enhanced.

31.3.2 Cellular Barriers

Introducing nucleic acids into biological tissues encounters many physiological barriers that alter their cellular biodistribution and intracellular bioavailability. Following administration, unmodified DNA and RNA rapidly degrade by extra- and intracellular enzymes before they can reach the surface of the target cells. This definitely influences their activity and interaction with the cells, compromising the therapeutic outcomes of nucleic acids. In addition, nucleic acids have very limited cellular uptake because of their hydrophilic nature and high molecular weight. A small fraction that can be taken up by the cells is usually internalized into vesicles (i.e., endosomes), which convert later into lysosomes. Accumulation and subsequent digestion of nucleic acids inside the lysosomes preclude them from reaching their cytoplasmic or nuclear targets and is an important barrier to their efficacy.

In addition, translocation into the nucleus is very challenging especially in case of plasmid DNA.

31.4 Nanomedicines for Non-Invasive Topical Gene Delivery Applications

31.4.1 Engineering Non-Viral Vectors for Topical Gene Therapy

The delivery of genetic materials into cells requires the use of a vehicle. Despite the promising results that were expected and achieved with the use of viral vectors, induction of unwanted immune responses, high risk of insertional mutagenesis, limited size of the DNA that can be cloned into the viral vector and storage difficulties limit their safe and clinical applications [19–22]. It has been observed that even inactivated viruses can stimulate an immune response, which could potentially result in death [20]. Non-viral vectors offer many advantages including absence of viral components and lack of immunogenicity; they are less expensive, easily manufactured and can be readily altered to form different combinations depending on the desired treatment and are suitable for genes of various sizes. It is believed or hoped that non-viral delivery systems can overcome problems seen using viral delivery. In addition, certain polymers may not be immunogenic allowing repeated use of the polymer delivery system, unlike viral vectors, which can only be used once due to immune responses elicited to the vector.

An ideal topical gene delivery system should have the following characteristics (Fig. 31.1): (1) be as non-invasive as possible; (2) efficiently condense the nucleic acid into a size that is small enough to penetrate through the skin layers and enter cells; (3) enhance the permeation through the SC that covers the skin surfaces; (4) stabilize the nucleic acid in all environments experienced before and after administration (e.g., solution, skin layers and the cell); (5) form complexes with excess positive charge to provide higher complex stability with the negatively charged DNA/RNA as well as a better interaction with negatively charged cell membranes; (6) decorate with a targeting moiety to enhance specific binding and subsequent endocytosis into the target cells;

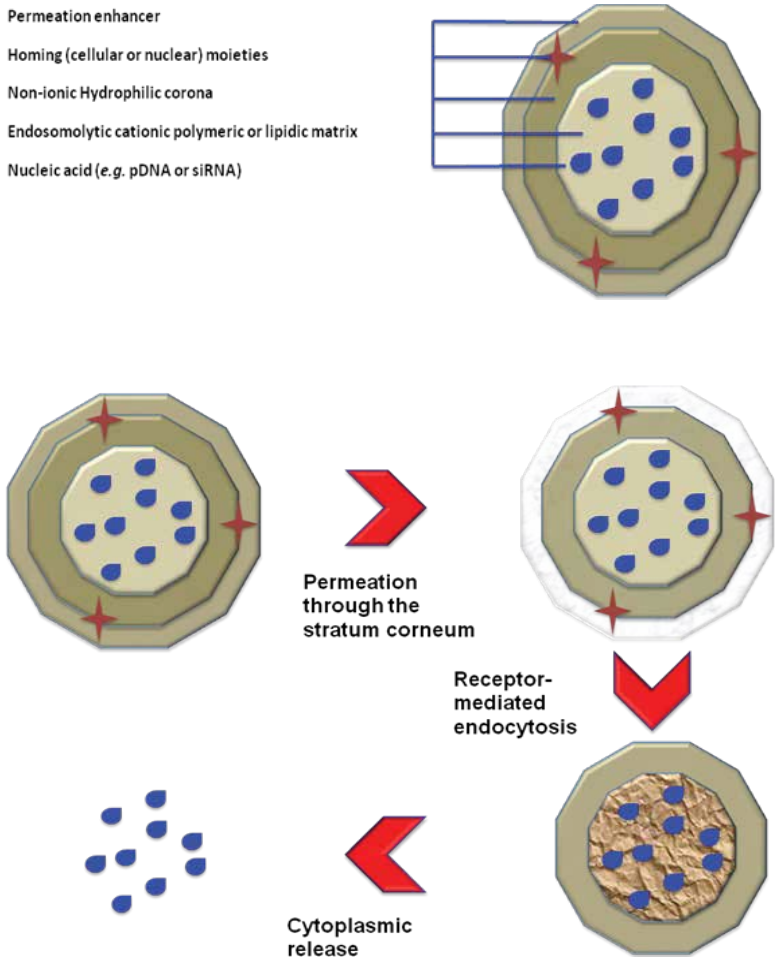

Figure 31.1 The ideal carrier for topical gene delivery should: (1) enhance the permeation through the SC that covers the skin surface; (2) be decorated with targeting moieties or has excess positive charges to bind to cells and be endocytosed; (3) contain a hydrophilic corona to avoid recognition by the immune system (unless it is desired); (4) contain a fusogenic lipid or membrane destabilizing polymers to allow escape from the endosomes/lysosomes into the cytoplasm; and (5) contain a nuclear homing sequence to increase expression efficiency, in case of using pDNA.

(7) include a fusogenic lipid or membrane destabilizing polymers to allow escape from the endosomes/lysosomes into the cytoplasm; (8) provide intermediate stability; be strong enough to carry the nucleic acids to the target site, but dissociate from them at their target cellular compartments; and (9) contain a nuclear homing sequence to increase expression efficiency, in case of using pDNA.

Examples of the most commonly employed non-viral vectors for gene delivery include polyplexes [23–26], lipoplexes [27, 28], PEGylated lipoplexes [29], polyion complex micelles [30–33], nanoparticles [1, 34, 35], and gels and mucoadhesives [36, 37]. However, in this chapter, we will focus on the design of some of the nanovectors that have been successfully used for topical gene delivery (e.g., liposomes, ethosomes, transfersomes, niosomes, emulsions, gemini-lipid nanoparticles, and biphasic vesicles). Hence, in the following sections, the use of these nanostructures to enhance the permeation of genetic materials though the skin (i.e., overcoming the skin barrier) will be highlighted. The use of other specific components (e.g., cell targeting moieties, nuclear homing sequences and endosomolytic agents) to enhance the efficiency of gene delivery and overcome the cellular barriers has been recently reviewed by our group [38].

31.4.2 Nanostructures as Potential Enhancers of Dermal and Transdermal Gene Delivery

Due to the macromolecular structures and large size of nucleic acids, transdermal delivery is problematic. Consequently, systems were investigated and developed in order to make nucleic acids more compact and enable their cutaneous delivery. Recently, advances in miniaturized technology have allowed researchers to shift their focus toward nanostructured permeation enhancers. Nanostructured vehicles could not only condense the nucleic acid to deliver but also disrupt and perturb lipids that are found in the skin layers. Liposomes, transfersomes, niosomes, ethosomes, emulsions, biphasic vesicles, and gemini-lipid nanoparticles are examples of these nanostructures that have different properties that contributed to their success as skin permeation enhancers (Table 31.1).

Table 31.1 Non-invasive nanomedicines exploited to enhance the topical gene delivery into the skin

Vehicle/composition	Nucleic acid	Disease/ animal model	Permeation-enhancing strategies	Remarks	Ref.
1. Non-ionic liposomes: Glyceryl dilaurate (GDL), cholesterol and polyoxyethylene-10 stearyl ether (POE-10) 2. Cationic liposomes: GDL, POE-10, cholesterol and DOTAP 3. PEGylated liposomes: DOPE- PEG2000, cholesterol and distearoylphosphatidylcholine (DSPC)	pDNA/ β-galactosidase and luciferase	Rat *in vivo* Formulations were applied on a hairless rat skin	1. Lipid vesicles 2. Cationic lipids 3. Endosomolytic lipids	Nonionic liposomes were the most efficient vehicles for transdermal delivery followed by cationic and PEGylated liposomes	[39]
Transfersomes: Egg PC and sodium cholate, sodium deoxycholate or Tween 80	pDNA/ GFP	Mice *in vivo* Hair was removed by shaving followed by hair-removing cream	1. Edge activator (Sodium cholate, sodium deoxycholate or Tween 80) 2. Lipid vesicles	1. Sodium cholate and sodium deoxycholate-based formulations showed substantial transdermal absorption, while Tween 80-based formulation did not show any transdermal absorption 2. Sodium cholate was found to be the most appropriate edge activator	[40]

Vehicle/composition	Nucleic acid	Disease/ animal model	Permeation-enhancing strategies	Remarks	Ref.
Cationic transfersomes: DOTMA and sodium deoxycholate	pDNA/HBsAg	Mice *in vivo*/ Genetic immunization Hair was shaved and formulations were applied with gentle rubbing	1. Sodium cholate 2. Cationic lipid (DOTMA)	Formulation elicited significantly higher anti-HBsAg antibody titer and cytokines levels as compared to naked DNA and a comparable efficiency to intramuscular HBsAg administration	[41]
Cationic transfersomes: DOTAP and sodium cholate	siRNA/Myosin Va exon F	Primary melanocytes *in vitro* No skin was used	1. Sodium cholate 2. Cationic lipid (DOTAP)	The best ratio was found to be 6 DOTAP: 1 sodium cholate (w:w)	[42]
Cationic transfersomes: DOTAP, DOPE and sodium deoxycholate	pDNA/murine IL-4	K14-VEGF transgenic mice *in vivo*/Psoriasis *In vitro*: Hair was removed by hair-removing cream and excess subcutaneous fat and connective tissues	1. Sodium cholate 2. Cationic lipid (DOTAP) 3. Endosomolytic lipids	1. The pDNA was transdermally delivered to vicinal sites of epidermis and hair follicles and the pDNA expression was detected in ear skin 2. Antipsoriatic effect was observed in the treated mice	[43]

(*Contiued*)

Table 31.1 (*Contiued*)

Vehicle/composition	Nucleic acid	Disease/ animal model	Permeation-enhancing strategies	Remarks	Ref.
		were removed *In vivo*: the formulations were applied to the ear skin			
Niosomes: Span 85 and cholesterol Liposomes: Soya PC and cholesterol	pDNA/HBsAg	Mice/Genetic immunization Hair was shaved and formulations were applied with gentle rubbing	1. Lipid vesicles 2. Surfactant	Topical niosomes elicited a comparable serum antibody titer and cytokines levels as compared to intramuscular recombinant HBsAg and topical liposomes	[44]
Elastic and non-elastic cationic niosomes: (Tween61/cholesterol/DDAB) in 25% ethanol or water	pDNA/tyrosinase	Melanocytes and rat skin *in vitro* Hair was removed by hair-removing cream and excess subcutaneous fat and connective tissues were removed	1. Surfactants 2. Cationic lipid 3. Lipid vesicles 4. Ethanol	The pDNA-loaded in elastic and non-elastic niosomes were found in viable epidermis and dermis. Transdermal delivery was only possible with the elastic cationic niosomes	[45]

Vehicle/composition	Nucleic acid	Disease/ animal model	Permeation-enhancing strategies	Remarks	Ref.
Water in oil nanoemulsions: Tween 80, Span 80 and olive oil	pDNA/ chloramphenicol acetyltransferase or human IFN-α2	Mice *in vivo* Both hairy and hairless mice were used. For hairy mice, hair was shaved before the topical treatment	1. Surfactant 2. Oil	1. More efficient than naked DNA or cationic liposomes 2. Deposition of pDNA was observed primarily in follicular keratinocytes 3. It was suggested that the formulations deliver pDNA through the hair follicles	[46]
Ethanol-in-perflubron microemulsion	pDNA/Luciferase or β-galactosidase	Mice/Genetic immunization (model antigen) Hair was shaved before the topical treatment	1. Ethanol 2. Surfactants	The emulsion led to 45-fold increase in the serum specific total antibody titer to β-galactosidase over naked pDNA	[47]
Ethanol-in-perflubron microemulsion	pDNA/anthrax protective antigen protein	Mice/Genetic immunization against anthrax Hair was shaved before the topical treatment	1. Ethanol 2. Surfactant	The formulation led to significant anthrax protective antigen-specific antibody responses	[48]

(*Contiued*)

Table 31.1 (*Contiued*)

Vehicle/composition	Nucleic acid	Disease/ animal model	Permeation-enhancing strategies	Remarks	Ref.
Biphasic lipid vesicles-Biphasix	pDNA/ bovine herpesvirus type-1 glycoprotein D	Mice/Genetic immunization Hair was shaved before the topical treatment (patches)	1. Lipid vesicles 2. Different permeation enhancers	pDNA-loaded in biphasic vesicles was delivered into the viable layers of human skin *in vitro*. *In vivo*, the formulations induced glycoprotein D-specific immune responses in mice	[49, 50]
Gemini-lipid nanoparticles (*in vitro*) Gemini surfactants based-liposomes and nanoemulsions and Dc-chol liposomes (*in vivo*)	Bicistronic pDNA/ GFP and IFN-γ	PAM212 *in vitro* Mice *in vivo* Hair was shaved before the topical treatment (patches)	1. Gemini surfactant 2. Lipid vesicles 3. Permeation enhancers (e.g., diethylene glycol monoethyl ether)	1. Gemini surfactants with C3 spacer showed the highest activity 2. Both gemini-based liposomes and nanoemulsions produced significantly higher level of IFN-γ in the skin than naked DNA or a liposomal Dc-chol control	[51]
Gemini-lipid nanoparticles	Bicistronic pDNA/ GFP and IFN-γ	IFN-γ-deficient mice *in vivo* Hair was shaved before the topical treatment (patches)	1. Gemini surfactant 2. Lipids	Treatment with Dc-chol liposomes (control) caused skin irritation and damage, whereas gemini nanoparticles showed no skin toxicity. Both formulations induced high gene expression	[52]

Vehicle/composition	Nucleic acid	Disease/ animal model	Permeation-enhancing strategies	Remarks	Ref.
Gemini-lipid nanoparticles	pDNA/Luciferase	COS-7 *in vitro* No skin was used	1. Gemini surfactant 2. Lipid vesicles 3. pH-sensitivity	Imparting pH-sensitivity by incorporating imino substituent within the surfactant spacer enhanced the transfection efficiency of the gemini nanoparticles (~9-fold) compared to unsubstituted surfactant	[35]
Gemini-lipid nanoparticles	Bicistronic pDNA/GFP and IFN-γ	COS-7, PAM212 and Sf 1Ep cell lines *in vitro* No skin was used	1. Gemini surfactant 2. Lipid vesicles 3. Amino acid substitution	Amino acid-substituted gemini surfactants showed higher transfection as compared to the unsubstituted ones	[53]
Lipid-modified octaarginine peptide envelope	pDNA/Luciferase or bone morphogenetic protein type IA receptor	Mice *in vivo* Hair was shaved before the topical treatment	1. Peptides targeting 2. Lipids	1. Comparable efficiency to adenovirus-mediated transfection, with lower toxicity 2. The formulation had a significant impact on hair growth *in vivo*	[54]

(*Contiued*)

Table 31.1 (*Contiued*)

Vehicle/composition	Nucleic acid	Disease/ animal model	Permeation-enhancing strategies	Remarks	Ref.
				3. The peptide mediates internalization via macropinocytosis, which avoids lysosomal degradation	
Cationic nanoliposomes: DOTAP, DOPE and distearoylphosphatidyl ethanolamine (DSPE)-PEG2000	siRNA/B-Raf and Akt3	Different cell lines (e.g., fibroblasts, keratinocytes, melanocytes) Reconstructed skin containing melanocytic lesions Mice/melanoma Mice were ultrasound-treated for 15 min followed by topical application of the formulations	1. Cationic lipid 2. Endosomolytic lipids 3. Lipid vesicles 4. Low-frequency ultrasound	1. Ultrasound application enhanced the penetration of nanoliposomal-siRNA complexes throughout the epidermal and dermal layers of the reconstructed skin and the animal skin 2. ~65% decrease in early or invasive cutaneous melanoma	[55]

Vehicle/composition	Nucleic acid	Disease/ animal model	Permeation-enhancing strategies	Remarks	Ref.
1. Cationic liposomes: (dipalmitoylphosphatidylcholine (DPPC)/cholesterol/DDAB) in water 2. Cationic niosomes: (Tween61/ cholesterol/DDAB) in water 3. Elastic cationic liposomes: (DPPC/ cholesterol/DDAB) in 25% ethanol 4. Elastic cationic niosomes: (Tween61/ cholesterol/DDAB) in 25% ethanol	pDNA/ Luciferase	Rat *in vitro* Hair was removed by hair-removing cream and excess subcutaneous fat and connective tissues were removed For the SC stripping, rat skin was pretreated with 10 sequential adhesive tape strips in order to eliminate all SC	1. Iontophoresis or SC stripping pre-treatment 2. Surfactants 3. Cationic lipids 4. Lipid vesicles 5. Ethanol	The ability of the vesicles to protect the DNA from degradation was ranked as elastic niosomes > elastic liposomes > niosomes > liposomes Transdermal absorption through rat skin was higher for niosomes versus liposomes and for elastic formulations versus the non-elastic formulations Pre-treatment with SC stripping or iontophoresis was very important to enhance the transdermal gene delivery (e.g., the DNA-loaded in the non-elastic formulations was not able to penetrate the SC without pre-treatment)	[56]

(*Contiued*)

Table 31.1 (*Contiued*)

Vehicle/composition	Nucleic acid	Disease/ animal model	Permeation-enhancing strategies	Remarks	Ref.
Fibrin hydrogel and lipoplexes	pDNA/ Luciferase or GFP and Luciferase	3T3 fibroblasts *in vitro* No skin was used	Fibrin hydrogel was exploited for controlled release topical gene delivery applications	1. Transgene expression persisted for at least 10 days (i.e., controlled release) 2. The limitation for this technique could be the possible interactions between fibrin and lipoplexes, which lower the nucleic acid amount available for cellular internalization	[57]
Fibrin and lipoplexes (Lipofectin)	pDNA/ GFP (*in vitro*) or β-galactosidase and luciferase (*in vivo*)	3T3 fibroblasts *in vitro* Rabbit *in vivo*/ Rabbit ear ulcer model Hair was removed from the rabbit ear by shaving	Fibrin scaffold was exploited for controlled release topical gene delivery applications	Significantly higher protein expressions for the two reporter genes at day 7 when compared to lipoplexes alone	[58]

Note: Composition of the nanocarriers, type of nucleic acid, and the strategies used to enhance the delivery through the skin are presented.

Liposomes: Because of their similar composition with cell membranes, liposomes or vesicles consisting of lipid bilayers of phospholipids mixed with other lipid chains or additives have the ability to disrupt lipid bilayers in the skin. A path created by this disruption would allow the delivery of nucleic acid through the skin layers. Several mechanisms were proposed to explain the bilayer disruption and consequent enhanced delivery by liposomal vesicles. The first concept suggests that intact liposomes permeate through the SC, protecting and delivering their preload, so that both the skin and liposomes remain intact during penetration [59]. Another mechanism suggests that liposomes do not penetrate the skin as whole vesicles, but rather the dissociated vesicle components act as a chemical permeation enhancer for the released drug [60, 61]. These lipids penetrate into the SC and fuse with the lipid matrix of the intercellular bilayers, destabilizing them through fluidization. Consequently, the driving force for permeation of free molecules is increased and therefore the permeation is enhanced. The same mechanisms were postulated for other lipid-based vehicles (e.g., transfersomes). However, the exact mechanism depends on the lipid composition of the carrier, size, net charge, skin/animal model, and the presence of additives [61–64]. For instance, the efficiency of liposomes in transdermal delivery of pDNA was found to be dependent on the structure, composition and charge of the vesicles [39]. Although a controversial matter—it is hypothesized that because of the lack of deformability, liposomes are not able to penetrate past the SC layers. If liposomes were more malleable, they would be able to deform (i.e., contract and expand) and thus find their way through different paths within the lipid bilayers.

Transfersomes: Further research to improve liposomal delivery systems led to the development of transfersomes. Transfersomes, first introduced by Cevc et al. [63], are a special type of liposomes, characterized by the presence of "edge activator", which destabilizes a liposome's lipid bilayers and thereby increases its deformability. Edge activator (e.g., sodium cholate and sodium deoxycholate) incorporated into the liposomal membrane is responsible for imparting the structural flexibility to transfersomes. Highly deformable and flexible characteristics of transfersomes allow them to squeeze through intercellular regions of the SC and thus delivering biomolecules across skin barrier. An interesting study was carried out to evaluate the importance of the edge activator

[40]. The authors have used sodium cholate, sodium deoxycholate, or Tween 80 to prepare the transfersomes. The Tween 80-based liposomes did not show any *in vivo* transdermal absorption in mice. On the contrary, both sodium cholate- and sodium deoxycholate-based transfersomes showed high levels of pDNA in the liver. Based on least cellular toxicity, sodium cholate was nominated as the most appropriate edge activator for transdermal delivery of pDNA. Cationic lipids have been also utilized to impart cationic characteristic to transfersomes, which allows them to have a tighter complexation with nucleic acids and increases their binding to cells [42]. In this case, the vesicles were composed of cationic lipid (e.g.,*N*-[1-(2,3-dioleyloxy)propyl]-*N*,*N*,*N*-trimethylammonium chloride (DOTMA), dimethyldioctadecyl ammonium bromide (DDAB) and 1,2-dioleoyl-3-(trimethylammonium) propane (DOTAP)) and sodium cholate or sodium deoxycholate as the edge activator. Transfersomes have been exploited for the delivery of pDNA carrying different genes [40, 41]. For instance, pDNA-encoding Hepatitis B surface antigen (HBsAg) was loaded into cationic transfersomes and applied topically to mice. The pDNA-loaded cationic transfersomes elicited significantly higher anti-HBsAg antibody titer and cytokines levels (interleukin (IL)-2 and interferon (IFN)-γ) than naked pDNA and a comparable effect to intramuscular recombinant HBsAg administration [41]. In addition, Li et al. [43] have used cationic transfersomes for transdermal delivery of pDNA expressing IL-4 in K14-VEGF transgenic mice skin for the treatment of psoriasis. In this formulation, 1,2-dioleoyl-sn-glycerol-3-phosphoethanolamine (DOPE) was incorporated into the transfersomes composition (i.e., DOTAP, DOPE, and sodium deoxycholate). DOPE lipid has been commonly used for the preparation of pH-sensitive liposomes because the lamellar-to-inverted hexagonal (H_{II}) phase transition occurring in DOPE-containing bilayers promotes release of endosome contents into the cytoplasm and is usually associated with high transfection efficiency [38, 65]. The pDNA loaded in this formulation was transdermally delivered to vicinal sites of epidermis and hair follicles and the pDNA expression was detected in ear skin and consequently antipsoriatic effect was observed in the treated mice. Furthermore, cationic transfersomes have been used for the delivery of other nucleic acids (e.g., siRNA) [42].

Ethosomes: Ethosomes are soft, malleable vesicles composed mainly of phospholipids, ethanol (relatively high concentration), and water. It has been shown that, for transdermal delivery, ethosomes have a higher penetration depth compared to liposomes and hydroethanolic solutions [66–71]. Incorporation of high concentration of alcohol is considered to be the main contributing factor to the enhanced skin permeation of ethosomes. This could be due to perturbing the bilayer organization in the SC. The perturbing effect can result from the interactions between the ethanol and intercellular lipids, which increase lipid fluidity and decrease the density of the lipid layers. In addition, the presence of ethanol allows for a softer and malleable nanostructure, which could fuse with the skin lipids and squeeze through small openings created in the disturbed SC lipids [72]. All these mechanisms explain that the drugs incorporated into ethosomes are delivered deeper and in larger quantities in the skin as compared to the conventional liposomes. Having said that, it is not simply the ethanol nor the liposomes that enhance skin penetration, but rather a synergistic mechanism between the different components. Although there has not been much research on using ethosomes in gene delivery, we are mentioning this type of vesicles because this aspect (i.e., the use of ethanol) has been used to enhance the elasticity and deformability of other lipid vesicles (e.g., niosomes) [45].

Niosomes: Investigation of nanostructured penetration enhancers led to promising but not optimal results. Hence, other modifications of the vesicles composition have been tested and led to the development of niosomes. Niosomes are surfactant-based liposomes that are usually composed of non-ionic surfactants and cholesterol. Cationic lipids can be also incorporated into the vesicles composition to form cationic niosomes. Furthermore, hydroethanolic solution can be used to hydrate the vesicles to form elastic niosomes [45]. Incorporation of ethanol, surfactant, and lipids into niosomes were found to enhance flexibility and elasticity of the vesicles, which is associated with enhanced penetration through the intercellular spaces of the SC. In addition, niosomes have shown improved performance, higher stability, and lower cost of production than liposomes [45, 56]. pDNA-encoding HBsAg was encapsulated into niosomes composed of Span 85 and cholesterol and liposomes composed of soya phosphatidylcholine

(PC) and cholesterol and applied topically to mice. Topical niosomes elicited a comparable serum antibody titer and endogenous cytokines levels to intramuscular recombinant HBsAg and topical liposomes. However, the proposed system was considered simpler, more stable and cost effective compared to liposomes [44]. The use of ethanol to hydrate niosomes has been also exploited to enhance the efficiency of the vesicles [45, 56]. For instance, a pDNA-encoding tyrosinase enzyme was loaded into cationic niosomes (Tween 61/cholesterol/DDAB) and rehydrated with 25% ethanol or water to form elastic and non-elastic niosomes, respectively. The pDNA loaded in both types of niosomes were found in viable epidermis and dermis. However, transdermal delivery of the pDNA was only possible with the elastic cationic noisome, as confirmed by the Franz-diffusion cell assay experiments. This formulation produced higher tyrosinase gene expression than the naked plasmid or the plasmid loaded into the other formulations [45].

Emulsions: Emulsions are thermodynamically stable colloidal dispersions composed of water, oil, surfactant and often a co-surfactant. Micro and nanoemulsions have been widely investigated for drug and gene delivery. To engineer emulsion that is appropriate and efficient for dermal/transdermal delivery, one must take into account each of the constituents: aqueous phase, oil phase and surfactants/co-surfactants. The aqueous phase is typically water, which can enhance skin permeation as a chemical enhancer. The oil phase can be made up of fatty acids, alcohols, medium chain triglycerides or vegetable oils (e.g., olive oil). Depending on the composition of the oil phase, the method of skin permeation differs. Saturated and unsaturated fatty acids, for example, can perturb the SC lipid bilayer by creating separate domains (phase separation), which would therefore induce a highly permeable pathway within the SC. The type of surfactant used for stabilizing the colloidal dispersions also has an impact on the permeation capabilities of the emulsion. In fact, surfactants play an important role in skin permeation enhancement due to many reasons. First, the absorption of surfactant on skin can increase tissue hydration, which in turn increases the emulsion permeation [73]. Second, they can facilitate the fusion of microemulsion particles through the bilayers [74, 75]. Finally, if micelles were to form during penetration, they would possess the potential to extract lipids from the SC, and thus increasing the permeation of hydrophilic

compounds [76]. Most nonionic surfactants (e.g., Tween and Span) are regarded as safe for human skin application because they are less irritating than their ionic counterparts. Finally, co-surfactants are often used in order to aid in the emulsion formation, promoting its thermodynamic stability and enhance the permeation efficiency of emulsions. In addition to the essential components of the emulsion, thickening agents, such as, gelatin or Carbopol, can be also added to prolong the absorption of the formulations form the skin [77, 78]. The difference in therapeutic responses observed between the different emulsions for dermal and transdermal delivery depends mainly on the type, composition (selection of oil phase, surfactants, co-surfactants, antioxidants, etc.), size and the route of administration. Emulsions, especially the water-in-oil (w/o) type, have shown promising potential in enhancing absorption and delivery of nucleic acids. In fact, Wu et al. [46] have used w/o nanoemulsions (Tween 80, Span 80 and olive oil) to formulate pDNA-encoding for chloramphenicol acetyltransferase or human IFN-α2 for topical application in mice. Significant deposition of the pDNA, primarily in follicular keratinocytes, was observed 24-h after the topical application. On the contrary, none of the control cationic liposome formulations mediated any transgenic protein expression. In addition, Cui et al. [47] have prepared ethanol-in-perflubron microemulsion from FSN-100 fluorosurfactant (commercially available inert non-ionic surfactant), ethanol and pDNA. The emulsion led to 45-fold increase in total antibody titer to β-galactosidase over naked pDNA. Consequently, the same emulsion was used for the delivery of pDNA-encoding anthrax protective antigen protein and used for genetic immunization in mice. The emulsion led to significant anthrax protective antigen-specific antibody responses [48].

Biphasic vesicles: Unlike conventional liposomes, biphasic vesicles are multi-compartmental lipid vesicles consisting of multiple, concentric mixed-lipid bilayers, oil droplets, micellar and aqueous subunit compartments. They are prepared by mixing a phospholipid phase with a submicrometer (nano) emulsion phase, creating multicompartmental lipid vesicles. The interesting features of the biphasic vesicles combined with the possibility of adding specific combination of permeation-enhancing excipients, have contributed to their successful use for topical delivery of different therapeutics. Biphasic vesicles have been used for topical

delivery of proteins (e.g., insulin) [79] and vaccine antigens [80–82] in animal models. In addition, they have been exploited for the delivery of IFNα in healthy human subjects and patients with human papillomavirus infection [83]. The mechanism of interaction between the biphasic vesicles and the skin has been recently investigated [84]. Surprisingly, and different from the previously suggested mechanisms for interactions between lipid vesicles and skin, it was suggested that the interaction of biphasic vesicles with SC lipids results in the formation of a three-dimensional cubic *Pn3m* polymorphic phase by the molecular rearrangement of intercellular lipids. The applications of biphasic vesicles have been extended to the topical delivery of genetic materials. Foldvari and coworkers have successfully delivered significant quantities of pDNA into the viable layers of human skin by using biphasic vesicles [49]. When these formulations were loaded with pDNA encoding bovine herpesvirus type-1 glycoprotein D and applied topically into mice, both cellular and humoral immunity were induced and significant gene expression was observed in the draining lymph nodes [50].

Gemini nanoparticles: Cationic gemini surfactants are a novel category of non-viral delivery vectors with potential applications in gene therapy. These surfactants are built from two ionic head groups, which are attached to their hydrocarbon tails and also connected to each other with a spacer or linker [85]. The two-alkyl chains of gemini surfactants lower their critical micelle concentration by one or two orders of magnitude and thus resulting in higher efficiency in reducing surface/interfacial tension and tendency to self-assemble at lower concentration [86]. In addition, gemini surfactants have lower cellular toxicity and greater structural variability than their classical monovalent counterparts [87].

Electrostatic interactions between gemini surfactants and nucleic acids (i.e., DNA/RNA) form positively charged nanoparticles (~100–200 nm) that are able to interact with cells and be endocytosed [88]. Addition of a helper lipid (e.g., DOPE) induces polymorphic phase behavior, which correlates with increased transfection efficiency [35, 38]. Worth mentioning is that for topical application to the skin, these nanoparticles are designed to include appropriate chemical enhancers. The presence of chemical

enhancers as part of the nanoparticles components facilitates the penetration of the nanoparticles through the SC and thus bringing the nanoparticles in contact with the underlying tissues.

Chemical modifications of the alkyl tails and spacer group of these compounds can modulate their physicochemical behavior in a way that can enhance their ability to complex genetic materials and transfect cells. Varying the length, degree of unsaturation and substitution of different functional groups in the spacer and alkyl tails can provide opportunities to tailor the chemical structures of gemini surfactants, which can greatly affect the transfection efficiency of the formed complexes. For example, the transfection efficiency of the 3-carbon spacer-based gemini-lipid nanoparticles was found to be the most efficient [51], while substitution of the alkyl spacer of 12-7NH-12 gemini surfactant with pH-sensitive imino-group resulted in a nine-fold higher transfection level compared to the unsubstituted surfactants [35]. Imparting pH-sensitivity to the nanoparticles aids in the endosomal destabilization and cytoplasmic release of the loaded nucleic acids. Foldvari research group has reported the feasibility of using different gemini-based nanoparticles for the topical delivery of different antigen-encoding plasmids. For instance, cationic gemini surfactant (16-3-16) and another cationic lipid cholesteryl 3b-(-N-[dimethylamin-oethyl]carbamate) [Dc-chol]-based DNA nanoparticles have been employed for the topical IFN-γ gene delivery in IFN-γ-deficient mice. The topically applied gemini nanoparticles induced higher gene expression as compared to the untreated control and naked DNA and showed no skin toxicity. Although treatment with Dc-chol-based formulations induced comparable gene expression to the gemini nanoparticles, skin irritation and damage were observed [52]. Foldvari and coworkers have demonstrated [51, 52, 89] that high levels of IFN-γ expression could be achieved in the skin of a mouse model of scleroderma (Tsk1/+) after non-invasive application of pDNA coding for IFN-γ, using a gemini surfactant-based nanoparticles. Higher level of IFN-γ expression in the skin was observed as compared with the naked pDNA-treated or untreated animals. Moreover, a 70–72% reduction of procollagen type I-α1 mRNA levels was observed, along with histological evidence of reduced skin thickness compared with that of the untreated animals. Recently, coupling amino acid moieties to the imino spacer

has been utilized to further increase and prolong gene expression due to the ability of these moieties to condense and deliver nucleic acids [53]. It was hypothesized that an additive effect can be achieved by coupling the highly efficient imino-substituted spacer of gemini surfactants with amino acid/dipeptide residues. Nanoparticles based on these modified gemini surfactants were utilized to encapsulate a bicistronic pDNA (i.e., green fluorescent protein (GFP) and IFN-γ). The nanoparticles have shown higher transfection than the unsubstituted ones in different cell lines (e.g., COS-7 and PAM212).

31.5 Toward Needle-Free Future Nanomedicines

Topical gene therapy is of great importance in the treatment of genetic and acquired diseases. The skin is an attractive target tissue for gene transfer because it is the largest organ in the body, easily accessible and can be targeted to treat skin disorders as well for systemic delivery. Topical delivery can improve safety and compliance and provide a patient-friendly non-invasive option instead of parenteral administration. Cutaneous gene therapy, although a promising approach for many dermatologic and autoimmune diseases, has not progressed to the stage of clinical trials, mainly due to the lack of an effective gene delivery system that can overcome the skin barrier. Safety and patient compliance will be the driving forces for further advancement in engineering novel delivery systems that can shift the parenteral use of many drugs toward the dermal/transdermal route of administration.

Future work should focus mainly on (1) the use of active targeting to allow site-specific delivery of the nucleic acids; (2) developing controlled release platforms; (3) combining the available delivery systems with minimally invasive techniques to enhance delivery efficiency; (4) comparative studies; and (5) further advancement toward the clinic.

Active targeting is usually achieved by decorating the nanovectors with targeting moieties (e.g., folic acid or targeting peptides) to enhance cellular uptake by promoting internalization, which could in turn improve transfection, while decreasing toxicity to normal (i.e., non-targeted) cells. It can be also exploited

to direct the delivery systems to specific disease sites or cellular types. Nanocarriers can be conjugated to peptides that, for example, specifically target the intercellular adhesion molecule-1 (ICAM-1) expressed by melanoma cells in the skin [90–92]. We have previously shown the feasibility of targeting M21 melanoma cells by using liposomes-decorated with proteins or peptide ligands [91, 92]. Lipid-modified octaarginine peptide envelope nanoparticles have been investigated to deliver pDNA-encoding for luciferase or bone morphogenetic protein type IA receptor in mice. The nanoparticles induced comparable efficiency to adenovirus-mediated transfection, with lower toxicity. In addition, the topical application of the formulations had a significant impact on hair growth *in vivo* [54]. These results were explained by the ability of peptide moieties to mediate the internalization via macropinocytosis, which avoids lysosomal degradation and thus increasing the intracellular bioavailability of the nucleic acids.

The release of nucleic acids and the absorption of the formulations themselves can be modified by loading them onto a natural scaffold (e.g., fibrin scaffold) [57, 58]. Topical gene delivery from these entities allows for sustained release of the nucleic acids. For instance, Kulkarni et al. [58] have reported that a fibrin-lipoplex system had significantly higher and more persistent transfection compared to lipoplexes alone (Lipofectin) in a rabbit ear ulcer model, suggesting that this fibrin-lipoplex system is suitable for controlled release topical gene delivery applications. The limitation for this technique could be the possible interactions between fibrin and the lipoplexes, which lower the cellular internalization of the lipoplexes.

Finally, combination with minimally invasive techniques to enhance the delivery efficiency has been also investigated. For example, Tran et al. [55] have developed nanoliposomal ultrasound-mediated approach for delivering ^{V600E}B-Raf and Akt3 targeting-siRNA into melanocytic tumors in the skin to retard melanoma development. The formulation showed high transfection efficiency in different cell lines (e.g., fibroblasts, keratinocytes, melanocytes), reconstructed skin containing melanocytic lesions and led to effective inhibition of early or invasive cutaneous melanomas in melanoma mouse models (~65% decrease in early or invasive cutaneous melanoma). Alternatively, the transdermal absorption of pDNA into rat skin from elastic cationic liposomes and niosomes

was enhanced by the application of iontophoresis or SC stripping [56].

31.6 Conclusions

Topical gene therapy is of great importance in the treatment of many genetic, autoimmune and dermatological diseases. Dermal and transdermal gene delivery can improve safety and compliance and provide a patient-friendly non-invasive option instead of parenteral administration. Many nanostructured delivery vehicles have been developed to overcome the barriers associated with the use of genetic materials. These nanomedicines have been successfully used for topical gene delivery due to their ability to disrupt and perturb lipids that are found in the skin layers and efficiently deliver their loaded nucleic acids to the targeted subcellular compartments. Integration of permeation enhancers, targeting moieties (e.g., cellular or nuclear), elasticity and deformability-enhancing chemicals (e.g., edge activators, ethanol), lipids (e.g., endosomolytic, fusogenic or cationic), surfactants and natural scaffold have been all contributed to the further advancement in engineering supramolecular assemblies for topical gene delivery applications, which can have potential applications for the treatment of dermatological disorders and other diseases. Future work should focus mainly on developing controlled release and site-specific gene delivery platforms and on moving these nanotechnology-based products toward the clinic.

Disclosures and Conflict of Interest

Grant support received from the Natural Sciences and Engineering Research Council of Canada (NSERC) and Canadian Institutes of Health Research (CIHR) is gratefully acknowledged.

The authors declare that they have no conflict of interest and have no affiliations or financial involvement with any organization or entity discussed in this chapter. This includes employment, consultancies, honoraria, grants, stock ownership or options, expert testimony, patents (received or pending) or royalties. No writing assistance was utilized in the production of this chapter and the authors have received no payment for its preparation.

The findings and conclusions here reflect the current views of the authors. They should not be attributed, in whole or in part, to the organizations with which they are affiliated, nor should they be considered as expressing an opinion with regard to the merits of any particular company or product discussed herein. Nothing contained herein is to be considered as the rendering of legal advice.

Corresponding Author

Dr. Marianna Foldvari
School of Pharmacy, University of Waterloo
200 University Avenue West, Waterloo, ON, Canada N2L 3G1
Email: foldvari@uwaterloo.ca

About the Authors

Mahmoud Elsabahy received his PhD in pharmaceutical sciences in 2010 from the Faculty of Pharmacy, University of Montreal, Canada, under supervision of Dr. Jean-Christophe Leroux. He was a postdoctoral fellow at the Drug Delivery and Pharmaceutical Nanotechnology Central Laboratory at the School of Pharmacy, University of Waterloo under the direction of Dr. M. Foldvari. His expertise includes drug delivery system design using polymeric, lipid and other soft materials for gene and cancer therapies. Currently he is a lecturer at the Faculty of Pharmacy, Assiut University, Egypt, and the assistant director of the Laboratory for Synthetic-Biologic Interactions at the Department of Chemistry, Texas A&M University, College Station, Texas, USA.

Maria Jimena Loureiro recently graduated from the Department of Chemical Engineering, University of Waterloo, Canada. She has conducted research as a co-op student for two consecutive terms in Dr. M. Foldvari's laboratory. She is currently a graduate student at the University of Toronto, Canada.

Marianna Foldvari is a professor of pharmaceutical sciences at the School of Pharmacy, University of Waterloo, Canada. She previously served as the Canada Research Chair in Bionanotechnology and Nanomedicine (2007–2014). Dr. Foldvari's expertise is in pharmaceutics, dosage form and drug delivery system design, nanotechnology, non-viral delivery methods, vaccine development, pharmaceutical nanotechnology. She has over 20 years of experience as an academic researcher and in research and development in the pharmaceutical industry through technology transfer activities. Her research program focuses on non-invasive drug delivery, gene therapy and pharmaceutical development of nanoenabled products. Dr. Foldvari is one of the founding members of the International Society of Nanomedicine (ISNM) and serves on the board of directors of the American Society for Nanomedicine (ASNM). She is an associate editor of *Nanomedicine: Nanotechnology*, *Biology and Medicine*, and an honorary editorial board member of *Research and Reports in Transdermal Drug Delivery*. She serves as an editorial board member of *Scientifica* (Pharmaceutics Division), *Journal of Nanomedicine and Biotherapeutic Discovery*, *Current Patents in Nanomedicine*, *Journal of Controlled Release*, *Current Drug Delivery*, and *International Journal of Pharmaceutical Compounding*.

References

1. Schiffelers, R. M., Ansari, A., Xu, J., Zhou, Q., Tang, Q., et al. (2004). Cancer siRNA therapy by tumor selective delivery with ligand-targeted sterically stabilized nanoparticle. *Nucl. Acids Res.*, **32**(19), e149.
2. Watanabe, T., Umehara, T., Kohara, M. (2007). Therapeutic application of RNA interference for hepatitis C virus. *Adv. Drug Deliv. Rev.*, **59**(12), 1263–1276.
3. Rice, J., Ottensmeier, C. H., Stevenson, F. K. (2008). DNA vaccines: Precision tools for activating effective immunity against cancer. *Nat. Rev. Cancer*, **8**(2), 108–120.
4. Meyer, M., Wagner, E. (2006). Recent developments in the application of plasmid DNA-based vectors and small interfering RNA therapeutics for cancer. *Human Gene Ther.*, **17**(11), 1062–1076.

5. de Fougerolles, A., Vornlocher, H. P., Maraganore, J., Lieberman, J. (2007). Interfering with disease: A progress report on siRNA-based therapeutics. *Nat. Rev. Drug Discov.*, **6**(6), 443–453.
6. Williams, J. A., Carnes, A. E., Hodgson, C. P. (2009). Plasmid DNA vaccine vector design: Impact on efficacy, safety and upstream production. *Biotechnol. Adv.*, **27**(4), 353–370.
7. Elsabahy, M., Nazarali, A., Foldvari, M. (2011). Non-viral nucleic acid delivery: Key challenges and future directions. *Curr. Drug Deliv.*, **8**(3), 235–244.
8. Orr, R. M. (2001). Technology evaluation: Fomivirsen, Isis Pharmaceuticals Inc/CIBA vision. *Curr. Opin. Mol. Ther.*, **3**(3), 288–294.
9. Lasch, J., Laub, R., Wohlrab, W. (1992). How deep do intact liposomes penetrate into human skin? *J. Control. Release*, **18**(1), 55–58.
10. El Maghraby, G. M., Williams, A. C., Barry, B. W. (2006). Can drug-bearing liposomes penetrate intact skin? *J. Pharm. Pharmacol.*, **58**(4), 415–429.
11. Banchereau, J., Steinman, R. M. (1998). Dendritic cells and the control of immunity. *Nature*, **392**(6673), 245–252.
12. Bodey, B., Bodey, B., Jr., Kaiser, H. E. (1997). Dendritic type, accessory cells within the mammalian thymic microenvironment. Antigen presentation in the dendritic neuro-endocrine-immune cellular network. *In vivo*, **11**(4), 351–370.
13. Foldvari, M. (2000). Non-invasive administration of drugs through the skin: Challenges in delivery system design. *Pharm. Sci. Technol. Today*, **3**(12), 417–425.
14. Chapman, S. J., Walsh, A. (1990). Desmosomes, corneosomes and desquamation. An ultrastructural study of adult pig epidermis. *Arch. Dermatolol. Res.*, **282**(5), 304–310.
15. Schurer, N. Y., Plewig, G., Elias, P. M. (1991). Stratum corneum lipid function. *Dermatologica*, **183**(2), 77–94.
16. Gray, G. M., Yardley, H. J. (1975). Lipid compositions of cells isolated from pig, human, and rat epidermis. *J. Lipid Res.*, **16**(6), 434–440.
17. Breathnach, A. S., Goodman, T., Stolinski, C., Gross, M. (1973). Freeze-fracture replication of cells of stratum corneum of human epidermis. *J. Anat.*, **114**(Pt 1), 65–81.
18. Wertz, P. W., Swartzendruber, D. C., Kitko, D. J., Madison, K. C., Downing, D. T. (1989). The role of the corneocyte lipid envelopes in cohesion of the stratum corneum. *J. Invest. Dermatol.*, **93**(1), 169–172.

19. Verma, I. M., Somia, N. (1997). Gene therapy-promises, problems and prospects. *Nature*, **389**(6648), 239–242.
20. Lehrman, S. (1999). Virus treatment questioned after gene therapy death. *Nature*, **401**(6753), 517–518.
21. Waehler, R., Russell, S. J., Curiel, D. T. (2007). Engineering targeted viral vectors for gene therapy. *Nat. Rev. Gen.*, **8**(8), 573–587.
22. Young, L. S., Searle, P. F., Onion, D., Mautner, V. (2006). Viral gene therapy strategies: From basic science to clinical application. *J. Pathol.*, **208**(2), 299–318.
23. Boeckle, S., von Gersdorff, K., van der Piepen, S., Culmsee, C., Wagner, E., et al. (2004). Purification of polyethylenimine polyplexes highlights the role of free polycations in gene transfer. *J. Gen. Med.*, **6**(10), 1102–1111.
24. Cho, Y. W., Kim, J. D., Park, K. (2003). Polycation gene delivery systems: Escape from endosomes to cytosol. *J. Pharm. Pharmacol.*, **55**(6), 721–734.
25. Choi, J. S., Nam, K., Park, J. Y., Kim, J. B., Lee, J. K., et al. (2004). Enhanced transfection efficiency of PAMAM dendrimer by surface modification with L-arginine. *J. Control. Release*, **99**(3), 445–456.
26. De Smedt, S. C., Demeester, J., Hennink, W. E. (2000). Cationic polymer based gene delivery systems. *Pharm. Res.*, **17**(2), 113–126.
27. Bettinger, T., Carlisle, R. C., Read, M. L., Ogris, M., Seymour, L. W. (2001). Peptide-mediated RNA delivery: A novel approach for enhanced transfection of primary and post-mitotic cells. *Nucl. Acids Res.*, **29**(18), 3882–3891.
28. Domashenko, A., Gupta, S., Cotsarelis, G. (2000). Efficient delivery of transgenes to human hair follicle progenitor cells using topical lipoplex. *Nat. Biotechnol.*, **18**(4), 420–423.
29. Hinrichs, W. L., Mancenido, F. A., Sanders, N. N., Braeckmans, K., De Smedt, S. C., et al. (2006). The choice of a suitable oligosaccharide to prevent aggregation of PEGylated nanoparticles during freeze thawing and freeze drying. *Int. J. Pharm.*, **311**(1–2), 237–244.
30. Oishi, M., Nagasaki, Y., Itaka, K., Nishiyama, N., Kataoka, K. (2005). Lactosylated poly(ethylene glycol)-siRNA conjugate through acid-labile beta-thiopropionate linkage to construct pH-sensitive polyion complex micelles achieving enhanced gene silencing in hepatoma cells. *J. Am. Chem. Soc.*, **127**(6), 1624–1625.
31. Harada-Shiba, M., Yamauchi, K., Harada, A., Takamisawa, I., Shimokado, K., et al. (2002). Polyion complex micelles as vectors in gene therapy-pharmacokinetics and *in vivo* gene transfer. *Gen. Ther.*, **9**(6), 407–414.

32. Elsabahy, M., Zhang, M., Gan, S. M., Waldron, K. C., Leroux, J. C. (2008). Synthesis and enzymatic stability of PEGylated oligonucleotide duplexes and their self-assemblies with polyamidoamine dendrimers. *Soft Matter*, **4**(2), 294–302.

33. Elsabahy, M., Wazen, N., Puxan, N., Deleavey, G., Servant, M., et al. (2009). Delivery of nucleic acids through the controlled disassembly of multifunctional nanocomplexes. *Adv. Funct. Mater.*, **19**(24), 3862–3867.

34. Li, S. D., Chono, S., Huang, L. (2008). Efficient gene silencing in metastatic tumor by siRNA formulated in surface-modified nanoparticles. *J. Control. Release*, **126**(1), 77–84.

35. Wettig, S. D., Badea, I., Donkuru, M., Verrall, R. E., Foldvari, M. (2007). Structural and transfection properties of amine-substituted gemini surfactant-based nanoparticles. *J. Gen. Med.*, **9**(8), 649–658.

36. Mok, H., Park, T. G. (2006). PEG-assisted DNA solubilization in organic solvents for preparing cytosol specifically degradable PEG/DNA nanogels. *Bioconjug.Chem.*, **17**(6), 1369–1372.

37. Alpar, H. O., Somavarapu, S., Atuah, K. N., Bramwell, V. W. (2005). Biodegradable mucoadhesive particulates for nasal and pulmonary antigen and DNA delivery. *Adv. Drug Deliv. Rev.*, **57**(3), 411–430.

38. Donkuru, M., Badea, I., Wettig, S., Verrall, R., Elsabahy, M., et al. (2010). Advancing nonviral gene delivery: Lipid- and surfactant-based nanoparticle design strategies. *Nanomedicine (Lond)*, **5**(7), 1103–1127.

39. Raghavachari, N., Fahl, W. E. (2002). Targeted gene delivery to skin cells *in vivo*: A comparative study of liposomes and polymers as delivery vehicles. *J. Pharm. Sci.*, **91**(3), 615–622.

40. Lee, E. H., Kim, A., Oh, Y. K., Kim, C. K. (2005). Effect of edge activators on the formation and transfection efficiency of ultradeformable liposomes. *Biomaterials*, **26**(2), 205–210.

41. Mahor, S., Rawat, A., Dubey, P. K., Gupta, P. N., Khatri, K., et al. (2007). Cationic transfersomes based topical genetic vaccine against hepatitis B. *Int. J. Pharm.*, **340**(1–2), 13–19.

42. Geusens, B., Lambert, J., De Smedt, S. C., Buyens, K., Sanders, N. N., et al. (2009). Ultradeformable cationic liposomes for delivery of small interfering RNA (siRNA) into human primary melanocytes. *J. Control. Release*, **133**(3), 214–220.

43. Li, J., Li, X., Zhang, Y., Zhou, X. K., Yang, H. S., et al. (2010). Gene therapy for psoriasis in the K14-VEGF transgenic mouse model by topical

transdermal delivery of interleukin-4 using ultradeformable cationic liposome. *J. Gen. Med.*, **12**(6), 481–490.

44. Vyas, S. P., Singh, R. P., Jain, S., Mishra, V., Mahor, S., et al. (2005). Non-ionic surfactant based vesicles (niosomes) for non-invasive topical genetic immunization against hepatitis B. *Int. J. Pharm.*, **296**(1–2), 80–86.
45. Manosroi, J., Khositsuntiwong, N., Manosroi, W., Gotz, F., Werner, R. G., et al. (2010). Enhancement of transdermal absorption, gene expression and stability of tyrosinase plasmid (pMEL34)-loaded elastic cationic niosomes: Potential application in vitiligo treatment. *J. Pharm. Sci.*, **99**(8), 3533–3541.
46. Wu, H., Ramachandran, C., Bielinska, A. U., Kingzett, K., Sun, R., et al. (2001). Topical transfection using plasmid DNA in a water-in-oil nanoemulsion. *Int. J. Pharm.*, **221**(1–2), 23–34.
47. Cui, Z., Fountain, W., Clark, M., Jay, M., Mumper, R. J. (2003). Novel ethanol-in-fluorocarbon microemulsions for topical genetic immunization. *Pharm. Res.*, **20**(1), 16–23.
48. Cui, Z., Sloat, B. R. (2006). Topical immunization onto mouse skin using a microemulsion incorporated with an anthrax protective antigen protein-encoding plasmid. *Int. J. Pharm.*, **317**(2), 187–191.
49. Foldvari, M., Kumar, P., King, M., Batta, R., Michel, D., et al. (2006). Gene delivery into human skin *in vitro* using biphasic lipid vesicles. *Curr. Drug Deliv.*, **3**(1), 89–93.
50. Babiuk, S., Baca-Estrada, M. E., Pontarollo, R., Foldvari, M. (2002). Topical delivery of plasmid DNA using biphasic lipid vesicles (Biphasix). *J. Pharm. Pharmacol.*, **54**(12), 1609–1614.
51. Badea, I., Verrall, R., Baca-Estrada, M., Tikoo, S., Rosenberg, A., et al. (2005). *In vivo* cutaneous interferon-gamma gene delivery using novel dicationic (gemini) surfactant-plasmid complexes. *J. Gen. Med.*, **7**(9), 1200–1214.
52. Badea, I., Wettig, S., Verrall, R., Foldvari, M. (2007). Topical non-invasive gene delivery using gemini nanoparticles in interferon-gamma-deficient mice. *Eur. J. Pharm. Biopharm.*, **65**(3), 414–422.
53. Yang, P., Singh, J., Wettig, S., Foldvari, M., Verrall, R. E., et al. (2010). Enhanced gene expression in epithelial cells transfected with amino acid-substituted gemini nanoparticles. *Eur. J. Pharm. Biopharm.*, **75**(3), 311–320.
54. Khalil, I. A., Kogure, K., Futaki, S., Hama, S., Akita, H., et al. (2007). Octaarginine-modified multifunctional envelope-type nanoparticles for gene delivery. *Gen. Ther.*, **14**(8), 682–689.

55. Tran, M. A., Gowda, R., Sharma, A., Park, E. J., Adair, J., et al. (2008). Targeting V600EB-Raf and Akt3 using nanoliposomal-small interfering RNA inhibits cutaneous melanocytic lesion development. *Cancer Res.*, **68**(18), 7638–7649.

56. Manosroi, A., Khositsuntiwong, N., Gotz, F., Werner, R. G., Manosroi, J. (2009). Transdermal enhancement through rat skin of luciferase plasmid DNA loaded in elastic nanovesicles. *J. Liposome Res.*, **19**(2), 91–98.

57. des Rieux, A., Shikanov, A., Shea, L. D. (2009). Fibrin hydrogels for non-viral vector delivery *in vitro*. *J. Control. Release*, **136**(2), 148–154.

58. Kulkarni, M., Breen, A., Greiser, U., O'Brien, T., Pandit, A. (2009). Fibrin-lipoplex system for controlled topical delivery of multiple genes. *Biomacromolecules*, **10**(6), 1650–1654.

59. Foldvari, M., Gesztes, A., Mezei, M. (1990). Dermal drug delivery by liposome encapsulation: Clinical and electron microscopic studies. *J. Microencapsul.*, **7**(4), 479–489.

60. Schaller, M., Korting, H. C. (1996). Interaction of liposomes with human skin: The role of the stratum corneum. *Adv. Drug Deliv. Rev.*, **18**(3), 303–309.

61. Betz, G., Imboden, R., Imanidis, G. (2001). Interaction of liposome formulations with human skin *in vitro*. *Int. J. Pharm.*, **229**(1–2), 117–129.

62. Elsayed, M. M., Abdallah, O. Y., Naggar, V. F., Khalafallah, N. M. (2007). Lipid vesicles for skin delivery of drugs: Reviewing three decades of research. *Int. J. Pharm.*, **332**(1–2), 1–16.

63. Cevc, G., Blume, G. (1992). Lipid vesicles penetrate into intact skin owing to the transdermal osmotic gradients and hydration force. *Biochim. Biophys. Acta*, **1104**(1), 226–232.

64. Honeywell-Nguyen, P. L., Bouwstra, J. A. (2003). The *in vitro* transport of pergolide from surfactant-based elastic vesicles through human skin: A suggested mechanism of action. *J. Control. Release*, **86**(1), 145–156.

65. Lin, A. J., Slack, N. L., Ahmad, A., George, C. X., Samuel, C. E., et al. (2003). Three-dimensional imaging of lipid gene-carriers: Membrane charge density controls universal transfection behavior in lamellar cationic liposome-DNA complexes. *Biophys. J.*, **84**(5), 3307–3316.

66. Dayan, N., Touitou, E. (2000). Carriers for skin delivery of trihexyphenidyl HCl: Ethosomes vs. liposomes. *Biomaterials*, **21**(18), 1879–1885.

67. Ainbinder, D., Touitou, E. (2005). Testosterone ethosomes for enhanced transdermal delivery. *Drug Deliv.*, **12**(5), 297–303.

68. Lopez-Pinto, J. M., Gonzalez-Rodriguez, M. L., Rabasco, A. M. (2005). Effect of cholesterol and ethanol on dermal delivery from DPPC liposomes. *Int. J. Pharm.*, **298**(1), 1–12.

69. van Kuijk-Meuwissen, M. E. M. J., Mougin, L., Junginger, H. E., Bouwstra, J. A. (1998). Application of vesicles to rat skin *in vivo*: A confocal laser scanning microscopy study. *J. Control. Release*, **56**(1–3), 189–196.

70. Paolino, D., Lucania, G., Mardente, D., Alhaique, F., Fresta, M. (2005). Ethosomes for skin delivery of ammonium glycyrrhizinate: *In vitro* percutaneous permeation through human skin and *in vivo* anti-inflammatory activity on human volunteers. *J. Control. Release*, **106**(1–2), 99–110.

71. Elsayed, M. M. A., Abdallah, O. Y., Naggar, V. F., Khalafallah, N. M. (2007). Deformable liposomes and ethosomes as carriers for skin delivery of ketotifen. *Pharmazie*, **62**(2), 133–137.

72. Touitou, E., Dayan, N., Bergelson, L., Godin, B., Eliaz, M. (2000). Ethosomes-novel vesicular carriers for enhanced delivery: Characterization and skin penetration properties. *J. Control. Release*, **65**(3), 403–418.

73. Thacharodi, D., Rao, K. P. (1994). Transdermal absorption of nifedipine from microemulsions of lipophilic skin penetration enhancers. *Int. J. Pharm.*, **111**(3), 235–240.

74. Williams, A. C., Barry, B. W. (2004). Penetration enhancers. *Adv. Drug Deliv. Rev.*, **56**(5), 603–618.

75. Kirjavainen, M., Monkkonen, J., Saukkosaari, M., Valjakka-Koskela, R., Kiesvaara, J., et al. (1999). Phospholipids affect stratum corneum lipid bilayer fluidity and drug partitioning into the bilayers. *J. Control. Release*, **58**(2), 207–214.

76. Lopez, A., Llinares, F., Cortell, C., Herraez, M. (2000). Comparative enhancer effects of Span 20 with Tween 20 and Azone on the *in vitro* percutaneous penetration of compounds with different lipophilicities. *Int. J. Pharm.*, **202**(1–2), 133–140.

77. Dalmora, M. E., Dalmora, S. L., Oliveira, A. G. (2001). Inclusion complex of piroxicam with beta-cyclodextrin and incorporation in cationic microemulsion. *In vitro* drug release and *in vivo* topical anti-inflammatory effect. *Int. J. Pharm.*, **222**(1), 45–55.

78. Kantaria, S., Rees, G. D., Lawrence, M. J. (1999). Gelatin-stabilised microemulsion-based organogels: Rheology and application in

iontophoretic transdermal drug delivery. *J. Control. Release*, **60**(2–3), 355–365.

79. King, M. J., Michel, D., Foldvari, M. (2003). Evidence for lymphatic transport of insulin by topically applied biphasic vesicles. *J. Pharm. Pharmacol.*, **55**(10), 1339–1344.
80. Baca-Estrada, M. E., Foldvari, M., Ewen, C., Badea, I., Babiuk, L. A. (2000). Effects of IL-12 on immune responses induced by transcutaneous immunization with antigens formulated in a novel lipid-based biphasic delivery system. *Vaccine*, **18**(17), 1847–1854.
81. Alcon, V. L., Baca-Estrada, M. E., Potter, A., Babiuk, L. A., Kumar, P., et al. (2006). Biphasic lipid vesicles as a subcutaneous delivery system for protein antigens and CpG oligonucleotides. *Curr. Drug Deliv.*, **3**(2), 129–135.
82. Babiuk, S., Baca-Estrada, M. E., Middleton, D. M., Hecker, R., Babiuk, L. A., et al. (2004). Biphasic lipid vesicles (Biphasix) enhance the adjuvanticity of CpG oligonucleotides following systemic and mucosal administration. *Curr. Drug Deliv.*, **1**(1), 9–15.
83. Foldvari, M., Badea, I., Kumar, P., Wettig, S., Batta, R., et al. (2011). Biphasic vesicles for topical delivery of interferon alpha in human volunteers and treatment of patients with human papillomavirus infections. *Curr. Drug Deliv.*, **8**(3), 307–319.
84. Foldvari, M., Badea, I., Wettig, S., Baboolal, D., Kumar, P., et al. (2010). Topical delivery of interferon alpha by biphasic vesicles: Evidence for a novel nanopathway across the stratum corneum. *Mol. Pharm.*, **7**(3), 751–762.
85. Menger, F. M., Keiper, J. S. (2000). Gemini surfactants. *Angew. Chem. Int. Ed.*, **39**(11), 1906–1920.
86. Zana, R. (2002). Dimeric (gemini) surfactants: Effect of the spacer group on the association behavior in aqueous solution. *J. Colloid Interface Sci.*, **248**(2), 203–220.
87. Rosenzweig, H. S., Rakhmanova, V. A., MacDonald, R. C. (2001). Diquaternary ammonium compounds as transfection agents. *Bioconjug. Chem.*, **12**(2), 258–263.
88. Wettig, S. D., Verrall, R. E., Foldvari, M. (2008). Gemini surfactants: A new family of building blocks for non-viral gene delivery systems. *Curr. Gen. Ther.*, **8**(1), 9–23.
89. Badea, I., Taylor, M., Rosenberg, A., Foldvari, M. (2009). Pathogenesis and therapeutic approaches for improved topical treatment in localized scleroderma and systemic sclerosis. *Rheumatology*, **48**(3), 213–221.

90. Holig, P., Bach, M., Volkel, T., Nahde, T., Hoffmann, S., et al. (2004). Novel RGD lipopeptides for the targeting of liposomes to integrin-expressing endothelial and melanoma cells. *Protein Eng. Des. Sel.*, **17**(5), 433–441.
91. Jaafari, M. R., Foldvari, M. (2002). Targeting of liposomes to melanoma cells with high levels of ICAM-1 expression through adhesive peptides from immunoglobulin domains. *J. Pharm. Sci.*, **91**(2), 396–404.
92. Jaafari, M. R., Foldvari, M. (1999). P0 protein mediated targeting of liposomes to melanoma cells with high level of ICAM-1 expression. *J. Drug Target.*, **7**(2), 101–112.

Chapter 32

Nanocarriers in the Therapy of Inflammatory Disease

Alf Lamprecht, PhD

Laboratory of Pharmaceutical Engineering,
Faculty of Medicine and Pharmacy,
University of Franche-Comté, Besamçon, France

Keywords: inflammation, arthritis, polymeric nanoparticles, liposomes, chitosan-DNA nanoparticles, dendrimers, inflammatory bowel disease, uveitis, colitis, polymeric micelles

32.1 Introduction

The use of nanoparticulate systems for the delivery of therapeutic agents in inflammatory diseases is receiving considerable attention for medical and pharmaceutical applications. This increasing interest results from the fact that these systems can target more or less selectively inflamed tissue, mainly on a cellular level. Among potential cellular targets by drug-loaded nanoparticles, liposomes, and others macrophages are considered because they play a central role in inflammation. The most

Handbook of Clinical Nanomedicine: Nanoparticles, Imaging, Therapy, and Clinical Applications
Edited by Raj Bawa, Gerald F. Audette, and Israel Rubinstein

ISBN 978-981-4669-20-7 (Hardcover), 978-981-4669-21-4 (eBook)
www.panstanford.com

common and potent drugs used in macrophage-mediated diseases treatment often induce unwanted side effects, when applied as a free form, due to the necessity of high doses to induce a satisfactory effect. This could result in their systemic spreading, a lack of bioavailability at the desired sites, and a short half-life. Therefore, the use of drug-loaded nanocarriers represents a good alternative to avoid, or at least decrease, side effects and increase efficacy. Here, an overview of the usefulness of nanocarriers for different therapeutic approaches in the treatment of inflammatory diseases is given.

In many cases nanocarrier-based therapy targets the immune related response, namely macrophages. Since the inflammatory reaction shows similarities in different disease forms the drug targeting strategies often resemble. Subsequently, the reader will see in this chapter various strategies for targeting those immune related cells and the related benefit in the several inflammatory diseases.

32.2 Rheumatoid Arthritis

First approaches in targeted arthritis therapy are rather old. In the beginning, anti-inflammatory drug were encapsulated into liposomes and administered locally to the inflammation site [1, 2]. First clinical results of this strategy showed that, intra-articular liposomal cortisol palmitate in a dose equivalent to 2 mg of cortisol produced a worthwhile therapeutic response in patients with rheumatoid arthritis.

Further studies on this strategy using other drugs also led to positive results [3]. Arthritis was induced in the right knee joint of Lewis rats. The rats were treated with a single intra-articular injection of different methotrexate formulations. Large multilamellar liposomal preparations of methotrexate were more effective than free drug and small unilamellar vesicles in suppressing inflammation. Their differential effects in treating the antigen-induced arthritis model were related to their retention within the joint space.

Very recently proposed was the amelioration of collagen-induced arthritis in rats by 13 nm gold particles [4]. Nanogold was administered intra-articularly to rats with collagen-induced

arthritis before the onset of arthritis. Nanogold bound to vascular endothelial growth factor in arthritis, resulting in inhibition of endothelial cell proliferation and migration. The histologic score (of synovial hyperplasia, cartilage erosion, and leukocyte infiltration), microvessel density, macrophage infiltration, and levels of TNF-alpha and IL-1beta were significantly reduced in the ankle joints of nanogold-treated rats. Nanogold exerted anti-angiogenic activities and subsequently reduced macrophage infiltration and inflammation, which resulted in attenuation of arthritis.

Polymeric drug nanoparticles have been evaluated for arthritis [5, 6]. Polyester nanoparticles were tested in order to investigate the tolerogenic effect of single administration of nanoparticles entrapping type II collagen on the development of collagen-induced arthritis. After single oral administration of nanoparticles, numerous particles approximately 300 nm in size were detectable in Peyer's patches 14 days after the original feeding. Nanoparticle formulations were also able to suppress arthritis after disease onset. Moreover, nanoparticle treated mice showed a higher level of TGF-beta mRNA expression in Peyer's patches, but a lower level of TNF-alpha mRNA expression in draining lymph nodes, compared with the other groups of mice. This approach may hold promise as a new treatment strategy in rheumatoid arthritis, but further in-depth studies were not reported on this therapeutic strategy.

Nanoparticles have also been proposed as an intra-articular delivery system for betamethasone in an ovalbumin-induced chronic synovitis model in the rabbit [6]. In the antigen-induced arthritic rabbit, the joint swelling decreased significantly by administering betamethasone-loaded nanospheres during a 21-day period after intra-articular challenge. Betamethasone-loaded nanospheres were phagocytosed by the synovial activated-cells and cartilage degradation was almost prevented.

A different approach was reported on the basis of chitosan-mediated gene delivery to rabbit knee joints [7]. This study first sought to confirm that foreign genes can be transferred to articular chondrocytes in primary culture. Next, chitosan-DNA nanoparticles containing IL-1Ra genes were injected directly into the knee joint cavities of osteoarthritis rabbits

to clarify the *in vivo* transfer availability of the vectors. Clear expression of IL-1Ra was detected in the knee joint synovial fluid of the chitosan IL-1Ra-injected group. A significant reduction was also noted in the severity of histologic cartilage lesions in the group that received the chitosan IL-1Ra-injection.

These locally administered nanocarriers all showed a significant therapeutic effect and would be promising as a therapeutic tool. However, their major drawback remains the need of a direct injection into the inflamed tissue, which can be delicate.

Another drug delivery approach is the selective accumulation of long-circulating liposomes at the inflammation site after intravenous administration. Several preclinical studies dealt with this strategy.

Liposomal prednisolone proved to be highly effective in the rat adjuvant-induced arthritis model [8]. A single injection of 10 mg/kg resulted in complete remission of the inflammatory response for almost a week. In contrast, the same dose of unencapsulated prednisolone did not reduce inflammation, and only a slight effect was observed after repeated daily injections. Evidence was found that preferential glucocorticoid delivery to the inflamed joint was the key factor explaining the observed strong therapeutic benefit obtained with the liposomal preparation, while other possible mechanisms, such as splenic accumulation or prolonged release of prednisolone in the circulation, were excluded.

In terms of mechanism of action a more detailed study showed the following [9]: Mice with collagen type II-induced arthritis treated with 10 mg/kg liposomal prednisolone resulted in a strong and lasting resolution of joint inflammation. 10 mg/kg free prednisolone only became slightly effective after repeated daily injections. Although joint inflammation recurred 1 week after treatment with liposomal prednisolone, knee joint sections prepared at this time indicated that the cartilage damage was still reduced. Localisation of gold labelled liposomes in the inflamed joints was seen in the proximity of blood vessels, in the cellular infiltrate, but mainly in the synovial lining. Unaffected joints did not take up liposomes.

Liposomal formulations of acylated superoxide dismutase and unmodified superoxide dismutase were prepared on the basis of two types of liposomes: conventional liposomes presenting an unmodified external surface and long circulating liposomes [10].

The "enzymosomes" are nanocarriers combining the advantages of expressing enzymatic activity in intact form and thus being able to exert therapeutic effect even before liposomes disruption, as well as acting as a sustained release of the enzyme.

In order to further increase the specificity of the drug targeting, dexamethasone-loaded long-circulating liposomes were modified exposing on their surface RGD peptides targeted to $\alpha_v\beta_3$ integrins expressed on angiogenic vascular endothelial cells and subsequently able to bind this cell type at inflammation sites [11]. RGD-liposomes were reported to bind and to be taken up by proliferating human VECs *in vitro*. *In vivo*, increased targeting to areas of lipopolysaccharide-induced inflammation in rats was observed. Specific association with the blood vessel wall at the site of inflammation was confirmed by intravital microscopy. One single intravenous injection of dexamethasone-loaded RGD-liposomes resulted in a strong and long-lasting antiarthritic effect in rats.

Another recent approach was based on the selective liposomal delivery of siRNA [12]. TNF-alpha is among the most prominent cytokines in rheumatoid arthritis and is secreted mainly by macrophages. A direct method for restoring the immunologic balance in arthritis is use of small interfering RNA (siRNA) for silencing the TNF-alpha transcript. The aim of this study was to determine the therapeutic effect of systemic administration of TNF-alpha siRNA in an experimental model of arthritis, optimizing its delivery using new liposome formulations. *In vivo,* complete cure of arthritis was observed when TNF-alpha siRNA was administered weekly, complexed with the liposome and combined with carrier DNA. Inhibition (50–70%) of articular and systemic TNF-alpha secretion was detected in the siRNA-injected groups, which correlated with a decrease in the levels of IL-6 and monocyte chemotactic protein 1.

When administering slightly different nanoparticles loaded with betamethasone by intravenous route a distinct therapeutic effect was also observed [13]. In adjuvant arthritis rats, a 30% decrease in paw inflammation was obtained in 1 day and maintained for 1 week with a single injection of 100 μg of nano-steroid. X-ray examination 7 days after this treatment showed decreased soft tissue swelling. In contrast, the same dose of free betamethasone after three administrations only moderately

reduced the severity of inflammation. In addition, a histological examination 7 days after the treatment showed a significant decrease of the inflammatory cells in the joints. The immune suppressive drug triptolide was entrapped into nanoparticles in order to increase its therapeutic index and to reduce adverse effects [14]. The results obtained in experiments indicated that nanoparticles significantly inhibited the adjuvant-induced arthritis, and had preferable anti-inflammatory effect with the long-time administration.

Also dendrimers have been applied for selective drug delivery to the inflammation site in arthritis. In this study indomethacin was linked to poly(amidoamine) dendrimers [15]. Intravenous administration of the drug-loaded dendrimer in rats showed a two-compartment pharmacokinetic profile. Enhanced effective indomethacin concentrations in the inflamed regions were obtained for the prolonged time period with the indomethacin-loaded dendrimer complex compared to the free drug in arthritic rats indicating its preferred accumulation. The targeting efficiency was 2.29 times higher compared to free drug. Moreover, inspite of lymphatic drainage, retention of dendrimers occurred at the inflammatory site.

32.3 Inflammatory Bowel Disease

Since anti-inflammatory, and more recently used immune suppressive drugs, are known for their distinct adverse effects, local drug delivery towards the site of inflammation is indispensable in the therapy of inflammatory bowel disease (IBD). The fact that ulcerative colitis and Crohn's disease affect limited areas of the distal intestine underlying distinct interindividual variability of the inflammation site turns drug therapy complicated. Although many efforts have been made in the development of specific drug delivery systems, classical drug delivery systems are still not completely successful. Beside incidences where the therapy fails due to insufficient drug concentrations at the site of action, adverse drug effects have been observed, which act as limiting factors for the respective therapy. These adverse effects are thought to be related to the lack of selective drug release as conventional colon delivery is triggered by factors widely independent from

physiological conditions of the inflammation and its location. Consequently, distinct drug loads are delivered unintentionally to areas with non-inflamed tissue during intestinal passage of the drug carrier. While drugs delivered towards the inflamed tissue mitigate the disease, healthy tissue surrounding the site of inflammation risk to absorb the drug, potentially provoking adverse reactions.

Several studies have indicated the strong involvement of macrophages and dendritic cells at the inflammation site of active IBD. A new therapeutic approach is proposed on the basis of this cellular immune response occurring in the inflamed regions, in general, an increased presence of neutrophils, natural killer cells, mast cells, and regulatory T cells [16, 17]. In consequence, it was hypothesized that particle uptake into those immunerelated cells or the disrupted intestinal barrier at ulcerated regions [18] could allow the selective accumulation of the particulate carrier system in the desired area (Fig. 32.1).

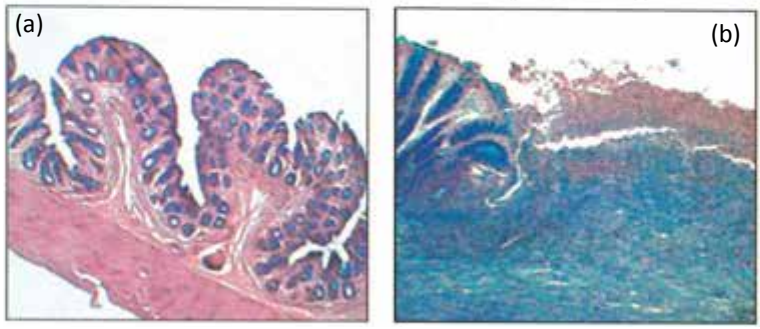

Figure 32.1 Examples for histologic colon sections of healthy (a), untreated TNBS colitis (b), in rats.

Subsequently, the size-dependent deposition of microparticles and nanoparticles after oral administration to rats using an experimental model colitis was examined with the aim of the development of a strategy of selective drug delivery [19]. In the inflamed tissue, an increased adherence of particles was observed at thicker mucus layers and in the ulcerated regions with a size dependency of the deposition compared with the control group. The ratio of colitis/control deposition increased with smaller particle sizes.

In the following studies, therapeutic efficiency of this approach was analysed [20, 21]. Nanoparticles were especially intended for targeted drug delivery to the inflammation site in severe cases of IBD where state-of-the-art delivery devices fail. The drug loaded nanoparticle formulations enabled the drug to accumulate in the inflamed tissue with higher efficiency than when given as solution. Further mechanistic studies showed that tacrolimus loaded nanoparticles allow an enhanced and selective drug penetration into the inflammation site as opposed to surrounding healthy tissue, presumably by protecting the encapsulated drug against influences from efflux systems and mucosal metabolism [21]. The relative drug penetration into the inflamed tissue is about 3-fold higher compared with healthy tissue when using nanoparticles as drug carriers.

In a comparative study between polyester nanopartices, similar to those administered above, and pH-sensitive nanoparticles therapeutic efficiency was not significantly different from both therapeutic approaches [22]. Free drug receiving groups (oral/subcutaneous) exhibited increased levels of adverse effects, whereas both nanoparticle types demonstrated their potential to reduce nephrotoxicity. The consequences from these observations are that the involved mechanisms are considered far more complex. Subsequently, it is impossible to estimate the efficiency of this therapeutic approach. In particular, clinical aspects need to be elucidated.

On the basis of cyclodextrines a promising approach was developed for the thrapy of ulcerative colitis [23]. Prednisolone-appended cyclodextrins were tested for their therapeutic efficiency after intracolonic administration in experimental colitis in rats. The local anti-inflammatory activity increased in the order of prednisolone alone = prednisolone alpha-cyclodextrin conjugate < prednisolone beta-cyclodextrin complex. As to systemic adverse effect, the prednisolone beta-cyclodextrin and prednisolone alone caused thymolysis at doses of 5–10 mg/kg while the prednisolone alpha-cyclodextrin conjugates showed no clear systemic adverse effect. The low adverse effect of the conjugate may be ascribed to the slow release of prednisolone in the colon, which keeps the local concentration in the colon at a low but constant level.

Recent approaches by different liposomal drug delivery approaches showed also distinct success. Based on adherence to intestinal mucosa, intralumenally administered liposomal formulations of 5-aminosalicylate and 6-mercaptopurine were studied for their potential to enhance local drug delivery to intestinal tissue for the treatment of IBD [24]. Liposomal adherence to intestinal tissue resulted in increased tissue levels for 5-aminosalicylate; however, 6-mercaptopurine local tissue levels were not improved compared to solution drug. While liposomal formulations show potential for local drug delivery to diseased bowel, drug physicochemical properties, absorption, and metabolic profiles dictate tissue-targeting potential.

Differences in liposome's surface charge were also exploited for a targeted drug delivery strategy in experimental colitis [25, 26]. Superoxide dismutase, 4-amino tempol, and catalase were encapsulated into negatively charged liposomes. The activity of the antioxidants in experimental colitis was tested in rats and compared to the anti-inflammatory activity of the native enzymes and free 4-amino tempol. In all cases, the liposomal preparations of the antioxidants were more effective than the free molecules in the treatment of the experimental colitis, probably due to the attachment of the negatively charged liposomes, and consequently a longer residence time and better uptake of the antioxidants to the inflamed mucosa.

Carnitine transporters have recently been implicated in susceptibility to IBD. Because carnitine is required for beta-oxidation, it was suggested that decreased carnitine transporters, and hence reduced carnitine uptake, could lead to impaired fatty acid oxidation in intestinal epithelial cells, and to cell injury. Treatment with carnitine-loaded liposomes corrected the butyrate metabolic alterations *in vitro* and reduced the severity of colitis *in vivo* [27]. These results suggest that carnitine depletion in colonocytes is associated with the inability of mitochondria to maintain normal butyrate beta-oxidation. It remains to confirm whether this approach may lead to a therapeutic development.

Intravenously administered liposomes showed an increased uptake in the inflamed colonic tissue owing the endothelium fenestration in the inflamed area and were able to visualize

colitic lesions [28]. First, liposomes were used to evaluate the extent and severity of abnormalities in IBD. Radiolabeled liposomes were given to animals suffering from a model colitis followed by scintigraphic evaluation. These liposomal formulations possess "adhesion" properties and therefore have attracted attention as drug delivery system for an endothelial delivery of drugs towards the inflammation site. In consequence, liposomes have been developed as drug targeting agents for the treatment of IBD [29]. Injected poly(ethylene glycocol)-liposomes preferentially accumulated in the inflamed tissue of colitis rats (around 13%), against 0.1% in the normal region of the control group.

It was shown recently that the up-regulation of endothelial cell adhesion molecules can be exploited to selectively target the inflamed endothelium which means a targeting approach from the "backside". Particles made from a biodegradable block copolymer of poly(lactic acid) and poly(ethylene glycocol), to which ligands to these adhesion molecules were conjugated, exhibit specific and augmented adhesion to inflamed endothelium relative to non-inflamed endothelium *in vitro* and *in vivo*. Also the specific targeting to vascular cell adhesion molecules-1 in a murine colitis model was demonstrated [30]. The prepared systems proved to significantly enhance particle adhesion to the inflamed endothelium whereas selectivity and ligand efficiency was dependent to the number of particles injected. However, it remains to be proven whether this approach is efficient enough to reach sufficiently high drug levels in the inflammation site and above all, is able to avoid adverse effects.

32.4 Uveitis

First, Ketorolac entrapped in polymeric micelles was proposed in ocular anti-inflammatory studies [31]. Polymeric micelles made of copolymer of *N*-isopropylacrylamide, vinyl pyrrolidone and acrylic acid having cross-linkage with *N*,*N*′-methylene bis-acrylamide were used as carrier in which up to 30% ketorolac (free acid) was entrapped. *In vitro* corneal permeation studies through excised rabbit cornea indicated two fold increase in ocular availability with no corneal damage compared to an aqueous suspension containing same amount of drug as in nanoparticles. The formulation showed significant inhibition of

lid closure up to 3 h and neutrophil migration up to 5 h compared to the suspension containing non-entrapped drug, which did not show any significant effect.

Others proposed an enhanced ocular anti-inflammatory activity by ibuprofen loaded Eudragit® RS100 nanoparticle suspension after topical administration [32]. The ibuprofen nanosuspension significantly reduced the primary signs of ocular inflammation as well as significantly reducing the protein level and the number of polymorphonuclear leukocytes in the aqueous humor compared with free ibuprofen. Furthermore, the aqueous humor drug concentration from the group treated with ibuprofen nanoparticles was significantly higher compared to the free drug group.

In a recent study, intraocular injection of tamoxifen-loaded nanoparticles were proposed as a new treatment of experimental autoimmune uveoretinitis [33]. To increase its bioavailability tamoxifen was incorporated into polyethylene glycolcoated nanoparticles. Some nanoparticles were distributed extracellularly throughout the ocular tissues, others were concentrated in resident ocular cells and in infiltrating macrophages. Whereas the injection of free tamoxifen did not alter the course of autoimmune uveoretinitis, injection of drug loaded nanoparticles performed before the onset of the disease resulted in significant inhibition. Low expression of TNF-alpha, IL-1beta, and RANTES mRNA were noted in eyes of nanoparticle-treated rats. Intravitreal injection of tamoxifen-loaded nanoparticles decreased S-Ag lymphocyte proliferation, IFN-gamma production by inguinal lymph node cells, and specific delayed-type hypersensitivity indicative of a reduced Th1-type response. It increased the anti-S-Ag IgG1 isotype indicating an antibody class switch to Th2 response.

Another study entrapped betamethasone in poly(lactic acid) nanoparticles [34]. The authors developed nanoparticles, which were capable of targeting a specific lesion and gradually releasing the agent at the site over a prolonged time period after a single intravenous administration for local delivery in experimental autoimmune uveoretinitis in rats. Intravenously injected nanoparticles accumulated in the retina and choroid of rats with autoimmune uveoretinitis within 3 hours and remained over the succeeding 7-day-period. Furthermore, systemically administered nanoparticles reduced the clinical scores of rats within 1 day,

which were maintained for 2 weeks and decreased the histological scores. In addition, the ocular infiltration of activated T-cells and macrophages were markedly reduced with this treatment. Systemically administered betamethasone loaded nanoparticles inhibited the development of autoimmune uveoretinitis due to the targeting and the sustained release of steroids *in situ*.

Considering all these different remarkable approaches in the therapy of inflammatory disease, the question arises for the reasons for the low number of clinical trials elucidating the efficiency of these approaches in humans.

Disclosures and Conflict of Interest

The opinions and perspectives here reflect the current views of the author. The author declares that he has no conflict of interest and has no affiliations or financial involvement with any organization or entity discussed in this chapter. No writing assistance was utilized in the production of this chapter and the author has received no payment for its preparation. This chapter is a reformatted version of the chapter published in 2009 in the book *Nanotherapeutics: Drug Delivery Concepts in Nanoscience*, Pan Stanford Publishing, Singapore.

Corresponding Author

Dr. Alf Lamprecht
Laboratory of Pharmaceutical Engineering
Faculty of Medicine and Pharmacy
University of Franche-Comté Besançon, France
Email: alf.lamprecht@univ-fcomte.fr

About the Author

Alf Lamprecht studied pharmacy at the Saarland University in Saarbrücken (Germany), where he received his PhD in 2001. After postdoctoral fellowships (2001–2002) at the University of Angers (France) and at the Gifu Pharmaceutical University (Japan), he was appointed assistant professor at the University of Nancy (France)

in 2003. He became professor of pharmaceutical engineering at the University of Franche-Comté in Besançon (France) in 2005. Prof. Lamprecht serves as a member of the editorial board of several pharmaceutical journals. Since 2007, he is external expert at the French Health Products Safety Agency. In 2007, he was appointed as Professor for Pharmaceutics at the University of Bonn (Germany), where he is the Head of School of Pharmacy since 2012. Alf has published more than 100 research articles and received several awards. He is an Alexander-von-Humboldt Fellow and was nominated as member of "Institut Universitaire de France" in 2007.

References

1. Dingle, J. T., Gordon, J. L., Hazelman, B. L., Knight, C. G., Page Thomas, D. P., et al. (1978). Novel treatment for joint inflammation. *Nature,* **271**, 372–373.
2. de Silva, M., Hazelman, B. L., Thomas, D. P., Wraight, P. (1979). Liposomes in arthritis, a new approach. *Lancet,* **1**, 1320–1322.
3. Williams, A. S., Camilleri, J. P., Goodfellow, R. M., and Williams, B.D. (1996). A single intra-articular injection of liposomally conjugated methotrexate suppresses join inflammation in rat antigen-induced arthritis. *Br. J. Rheumatol*., **35**, 719–724.
4. Tsai, C. Y., Shiau, A. L., Chen, S. Y., Chen, Y. H., Chang, M. Y., et al. (2007). Amelioration of collagen-induced arthritis in rats by nanogold. *Arthritis Rheum*., **56**, 544–554.
5. Kim, W. U., Le, W. K., Ryoo, J. W., Kim, S. H., Kim, J., et al. (2002). Suppression of collagen-induced arthritis by single administration of ploy(lactic-*co*-glycolic acid) nanoparticles entrapping type II collagen, a novel treatment strategy for induction of oral tolerance. *Arthritis Rheum*., **46**, 1109–1120.
6. Horisawa, E., Hirota, T., Kawazoe, S., Yamada, J., Yamamoto, H., Takeuchi, H., Kawashima, Y. (2002). Prolonged anti-inflammatory action of DL-lactide/glycolide copolymer nanospheres containing betamethasone sodium phosphate for an intra-articular delivery system in antigen-induced arthritic rabbit. *Pharm. Res*., **19**, 403–410.
7. Zhang, X., Yu, C., Xushi, Zhang, C., Tang, T., Dai, K. (2006). Direct chotsan-mediated gene delivery to the rabbit knee joints *in vitro* and *in vivo*. *Biochem. Biophys. Res. Commun*., **341**, 202–208.

8. Metselaar, J. M., Wauben, M. H., Wagenaar-Hilbers, J. P., Boerman, O. C., Sorm, G. (2003). Complete remission of experimental arthritis by joint targeting of glucorticoids with long-circulating liposomes. *Arthritis Rheum*., **48**, 2059–2066.
9. Metselaar, J. M., van den Berg, W. B., Holthuysen, A. E., Wauben, M. H., Storm, G., van Lent, P. L. (2004). Liposomal targeting of glucoritcoids to synovial lining cells stringly increases therapeutic benefit in collagen type II arthritis. *Ann. Rheum. Dis*., **63**, 348–353.
10. Gaspar, M. M., Boerman, O. C., Laverman, P., Corvo, M. L., Stonn, G., Cruz, M. E. (2007). Enzymosomes with surface-exposed superoxide dismutase, *in vivo* behaviour and therapeutic activity in a model of adjuvant arthritis. *J. Control. Rel.,* **117**, 186–195.
11. Koning, G. A., Schiffelers, R. M., Wauben, M. H., Kok, R. J., Mastrobattista, et al. (2006). Targeting of angiogenic endothelial cells at sites of inflammation by dexamethasone phosphate-containing RGD peptide liposomes inhibits experimental arthritis. *Arthritis Rheum.,* **54**, 1198–1208.
12. Khoury, M., Louis-Plence, P., Escriou, Y., Noel, D., Largeau, C., et al. (2006). Efficient new cationic liposome formulation for systemic delivery of small interfering RNA silencing tumor necrosis factor alpha in experimental arthritis. *Arthritis Rheum.,* **54**, 1867–1877.
13. Higaki, M., Ishihara, T., Izumo, N., Takatsu, M., Mizushima, Y. (2005). Treatment of experimental arthritis with poly(D,L-Iactic/glycolic acid) nanoparticles encapsulating betamethasone sodium phosphate. *Ann. Rheum. Dis.,* **64**, 1132–1136.
14. Liu, M., Dong, J., Yang, Y., Yang, X., Xu, H. (2005). Anti-inflammatory effects of triptolide loaded poly(D,L-lactic acid) nanoparticles on adjuvant-induced arthritis in rats. *J. Ethnopharmacol.,* **97**, 219–25.
15. Chauhan, A. S., Jain, N. K., Diwan, P. V., Khopade, A. J. (2004). Solubility enhancement of indomethacin with poly(arnidoamine) dendrimers and targeting to inflammatory regions of arthritic rats. *J. Drug Target.,* **12**, 575–583.
16. Allison, M. C., Coniwall, S., Poulter, L. W., Dhillon, A. P., Pounder, R. E. (1988). Macrophage heterogeneity in nonnal colonic mucosa and in inflammatory bowel disease. *Gut,* **29**, 1531–1538.
17. Seldenrijk, C. A., Drexhage, H. A., Meuwissen, S. G., Pals, S. T., Meijer, C. J. (1989). Dendritic cells and scavenger macrophages in chronic inflammatory bowel disease. *Gut,* **30**, 484–491.
18. Stein, J., Ries, J., Barrett, K. E. (1998). Disruption of intestinal barrier function associated with experimental colitis, possible role of mast cells. *Am. J. Physiol.,* **274**, G203–209.

19. Lamprecht, A., Schafer, U., Lehr, C. M. (2001). Size-dependent bioadhesion of micro- and nanoparticulate carriers to the inflamed colonic mucosa. *Pharm. Res.,* **18**, 788–793.
20. Lamprecht, A., Ubrich, N., Yamamoto, H., Schafer, U., Takeuchi, H., et al. (2001). Biodegradable nanoparticles for targeted drug delivery in treatment of inflammatory bowel disease. *J. Pharmacol. Exp. Ther.,* **299**, 775–781.
21. Lamprecht, A., Yamamoto, H., Takeuchi, H., Kawashima, Y. (2005). Nanoparticles enhance therapeutic efficiency by selectively increased local drug dose in experimental colitis in rats. *J. Pharmacol. Exp. Ther.* **315**, 196–202.
22. Meissner, Y., Pellequer, Y., Lamprecht, A. (2006). Nanoparticles in inflammatory bowel disease, particle targeting versus pH-sensitive delivery. *Int. J. Pharm.,* **316**, 138–143.
23. Yano, H., Hirayama, F., Arima, H., Uekama, K. (2001). Prednisolone-appended alpha-cyclodextrin, alleviation of systemic adverse effect of prednisolone after intracolonic administration in 2,4,6-trinitrobenzenesulfonic acid-induced colitis rats. *J. Pharm. Sci.,* **90,** 2103–2112.
24. Kesisoglou, F., Zhou, S. Y., Niemiec, S., Lee, J. W., Zimmermann, E. M., Fleisher, D. (2005). Liposomal formulations of inflammatory bowel disease drugs, local versus systemic drug delivery in a rat model. *Pharm. Res.,* **22**, 1320–1330.
25. Jubeh, T. T., Barenholz, Y., Rubinstein, A. (2004). Differential adhesion of normal and inflamed rat colonic mucosa by charged liposomes. *Pharm. Res.,* **21**, 447–453.
26. Jubeh, T. T., Nadler-Milbauer, M., Barenholz, Y., Rubinstein, A. (2006). Local treatment of experimental colitis in the rat by negatively charged liposomes of catalase. TMN and SOD. *J. Drug Target.,* **14**, 155–163.
27. D'Argenio, G., Calvani, M., Casamassirni, A., Petillo, O., Margarucci, S., et al. (2006). Experimental colitis, decreased Octn2 and AtbO+ expression in rat colonocytes induces carnitine depletion that is reversible by carnitine-loaded liposomes. *FASEB J.,* **20**, 2544–2546.
28. Oyen, W. J., Boerman, O. C., Dams, E. T., Storm, G., van Bloois, L., et al. (1997). Scintigraphic evaluation of experimental colitis in rabbits. *J. Nucl. Med.,* **38**, 1596–1600.
29. Awasthi, V. D., Goins, B., Klipper, R., Phillips, W. T. (2002). Accumulation of PEGliposomes in the inflamed colon of rats: Potential for therapeutic and diagnostic targeting of inflammatory bowel diseases. *J. Drug Target.,* **10**, 419–427.

30. Sakhalkar, H. S., Dalal, M. K., Salem, A. K., Ansari, R., Fu, J., et al. (2003). Leukocyte-inspired biodegradable particles that selectively and avidly adhere to inflamed endothelium *in vitro* and *in vivo*. *Proc. Natl. Acad. Sci.,* **100**, 15895–15900.

31. Gupta, A. K., Madan, S., Majumdar, D. K., Maitra, A. (2000). Ketorolac entrapped in polymeric micelles: Preparation, characterisation and ocular anti-inflammatory studies. *Int. J. Pharm.,* **209**, 1–14.

32. Bucolo, C., Maltese, A., Puglisi, G., Pignatello, R. (2002). Enhanced ocular anti-inflammatory activity of ibuprofen carried by an Eudragit RS100 nanoparticle suspension. *Ophthalmic. Res.,* **34**, 319–323.

33. de Kozak, Y., Andrieux, K., Villarroya, H., Klein, C., Thillaye-Goldenberg, B., et al. (2004). Intraocular injection of tamoxifen-loaded nanoparticles: A new treatment of experimental autoimmune uveoretinitis. *Eur. J. Immunol.,* **34**, 3702–3712.

34. Sakai, T., Kohno, H., Ishihara, T., Higaki, M., Saito, S. et al. (2006). Treatment of experimental autoimmune uveoretinitis with poly(lactic acid) nanoparticles encapsulating betamethasone phosphate. *Exp. Eye Res.,* **82**, 657–663.

Chapter 33

Advanced 3D Nano/Microfabrication Techniques for Tissue and Organ Regeneration

Benjamin Holmes, MSc,[a] Thomas J. Webster, PhD,[b] and Lijie Grace Zhang, PhD[a]

[a]*Department of Mechanical and Aerospace Engineering and Department of Medicine, The George Washington University, Washington, DC, USA*
[b]*Department of Chemical Engineering, Northeastern University, Boston, Massachusetts, USA*

Keywords: tissue engineering, biocompatible materials, biomimetic scaffolds, electrospinning, biodegradability, synthetic polymers, coatings, implants, poly-L-lactic acid, poly-caprolactone, polyaniline, polypyrrole, scaffold design, hydroxyapatite, extracellular matrix, bioactive, laminated object manufacturing, solvent casting, gas foaming, phase separation, laser assisted bioprinting, stereolithography, 3D printing, fused deposition modeling, nanotubes, nanofibers, hydrogel, electrospray, composite scaffolds, biomineralization, nanocomposites

33.1 Introduction

33.1.1 Introduction and Clinical Challenges

Modern medical treatment practice is beginning to favor customizable, patient specific options as technologies and their

Handbook of Clinical Nanomedicine: Nanoparticles, Imaging, Therapy, and Clinical Applications
Edited by Raj Bawa, Gerald F. Audette, and Israel Rubinstein

ISBN 978-981-4669-20-7 (Hardcover), 978-981-4669-21-4 (eBook)
www.panstanford.com

capabilities evolve. Nowhere is this more evident than in tissue repair and organ regeneration [3, 33]. Currently, the treatment of defects and injury to tissues with limited regenerative capacity, such as cartilage, vasculature, cardiac tissue, and nerves involve highly invasive and painful procedures, such as a total hip or knee replacement. In many of the cases listed, there are inadequate alternative treatment methods available other than traditional organ/tissue transplants, which contain their own inherent complications. In recent years, a great deal of research has focused on the treatment of traumatic and congenital injuries via stem cell therapy [25, 79, 97]. Despite the great promise stem cells hold in regenerative medicine, long-term clinical success has been limited when they are not used in conjunction with other treatment methods.

33.1.2 Tissue Engineering

Tissue engineering (TE) may hold the key to unlocking the potential of stem cell-based organ repair and tissue regeneration, and lead to better treatments which were previously only available at a great expense, if at all. Drs. Langer and Vacanti defined TE as "an interdisciplinary field that applies the principles of engineering and life sciences toward the development of biological substitutes that restore, maintain, or improve tissue function or a whole organ" [40, 82]. Over time, this discipline quickly developed to encompass a variety of cell types (e.g., stem cells, chondrocytes, osteoblasts, endothelial cells, fibroblasts, and smooth muscle cells), scaffolds (e.g., biodegradable, natural or synthetic materials, polymers, and nanocomposites), bioactive factors (e.g., various growth factors and cytokines), and physical stimuli (mechanical, electrical, etc.) to form biomimetic tissues and organs. Specifically, scaffolds play a critical role in providing a 3D environment to support cell growth, control cell differentiation, improve matrix deposition, and tissue/organ regeneration.

33.1.3 Scaffold-Based Approaches and Scaffold Roles

In scaffold-based TE, a micro/nanoscale biocompatible and biodegradable material is designed to mimic the nature biological microenvironment and enhance and direct stem cell behavior.

Stem cell behavior can be controlled not only by changing the physical dimensions of biomimetic scaffolds, but also by modulating the composition, surface chemistry, and mechanical properties [1, 14, 65].

An ideal scaffold should fulfill four key characteristics. It should provide (1) adequate structural support with a suitable degradation rate; (2) modulate the cellular microenvironment; (3) encourage cellular attachment, ingrowth and tissue formation; and (4) easily exchange nutrients and waste to and from cells within the construct [40, 82, 91]. Researchers in TE have been making great strides in designing and fabricating TE scaffolds to satisfy these design constraints via various nano- and microtechniques. This chapter will focus on two promising fabrication methods for micro- and nanofeatured TE scaffolds: electrospinning [101] and three–dimensional (3D) printing [12, 18]. Both methods offer a high degree of control over scaffold architecture and composition to include the incorporation of morphogenetic constituent materials. In addition to these two methods, several other scaffold fabrication techniques for the manufacture of TE scaffolds will be discussed.

33.2 Electrospinning

33.2.1 Introduction

Novel methodologies for TE scaffold fabrication have been explored and developed in order to solve and improve current medical problems. For many years, creating polymer scaffolds as a substrate for tissue growth has been one of the most popular and most promising approaches for various tissue regeneration applications [29]. A very common and well-established method for creating these scaffolds is a process known as electrospinning. Electrospinning has been considered favorable because of the ability of researchers to create fibrous porous polymer scaffolds with features ranging from the micro- to the nanoscale mimicking the extracellular matrix (ECM) of native tissue and creating an environment for improved cell behavior [74]. While the system parameters needed to obtain desired fiber dimensions have been thoroughly investigated, a great deal of research is currently focused on the means to fabricate polymeric scaffolds with modified physical and compositional

complexities. In order to elucidate the current state of electrospinning for TE and its future directions, the clinical challenges facing tissue engineers and an explanation of electrospinning and its application to TE will be discussed in the following sections.

33.2.2 Basic Principles, Materials and Practices

Electrospun polymer scaffolds may provide an advantageous new approach to organ/tissue defect treatment. Because of the ease by which one can create a scaffold of desired physical and mechanical dimensions with incorporated nano- and microcomposite materials, there is great potential to influence and promote cell differentiation and proliferation [27].

Electrospinning is a process for creating inherently porous materials composed of micro- and/or nanoscale polymer fibers. Briefly, a solid polymer is dissolved in an organic solvent to produce a viscous solution, which is then loaded into a syringe with a blunt point needle or capillary and syringe pump. The expelled mixture is subjected to a high voltage potential over a specific working distance used to charge the polymer chains drawing a long fiber to a grounded collector plate [55, 74, 91]. The solvent evaporates, due to either the voltage potential or natural evaporation in air, and a mesh of solid polymer fibers is created [49, 55, 80]. There are currently a number of different synthetic and natural polymers used in electrospinning. Synthetic polymers are chosen for their biodegradability and biocompatibility, as well as their ability to match characteristics of the target tissue [14, 27, 101]. Some popular polymers include poly-L-lactic acid (PLLA) and poly-caprolactone (PCL) for electrospinning in bone, cartilage and neural regeneration applications [15, 60, 66], while other materials such as polyaniline (PAN) and polypyrrole (PPy) are used for cardiac and other neural applications due to their inherent electrical conductivity [62]. In the case of natural polymers, materials such as collagen and chitosan are very often used [6, 7, 42, 60, 99] for various tissue regeneration constructs because of their biocompatibility properties. However, when electrospun, these materials are weak and require structural support, so they are often electrospun into coatings or in conjunction with a stronger, synthetic polymer [6, 27]. It is important to know that the number of polymers, both synthetic and natural, that are used for electrospinning are

numerous, and chosen based on whatever specific application the scaffold will be used for [62, 92, 101].

The variation of parameters in electrospinning, such as voltage, working distance, and polymer-solvent solution concentration, in correlation to scaffold characteristics have been well established and understood. This being the case, electrospinning has already been used in a wide variety of practical and experimental applications. One of the simplest applications is for surface coatings and membranes [62, 80]. Because of the ability of electrospinning to produce physical properties that mimic the ECM, it is often used to create coatings on implants and devices in order to promote cell adhesion [62]. Electrospinning can also be used to deposit natural polymers, proteins, and peptides onto surfaces, as well as onto electrospun polymer scaffolds for enhanced cell growth [15, 62, 80]. The same principles that make electrospun surface coatings on materials useful for promoting tissue regeneration also make electrospinning advantageous for scaffold design. Unlike coating an implant, where the goal is to induce existing cells and tissue to adhere on a biocompatible material, artificial tissue can be grown and incorporated into a target area in the body [29, 88, 91]. There are two different approaches to scaffold design: 2D and 3D scaffolds. An electrospun 2D scaffold is typically only several layers of fibers thick, and is intended to grow only one layer of cells [70]. While 2D scaffolds have been shown to promote cell growth, 3D scaffolds provide much better results, and are considered the most promising approach [6, 42].

An electrospun 3D scaffold is many fiber layers thick and is intended to fully mimic the ECM of the natural tissue. 3D scaffolds have been shown to promote much better cell adhesion and growth as compared to 2D scaffolds, and are potentially very powerful for their ability to grow larger amounts of bulk tissue at a time, as well as having the promise of being able to grow whole organs and systems [29, 40, 82].

As discussed, the ultimate goal of a scaffold is to provide a framework that provides structural support for growing cells, as well as promoting cell growth and directed cell differentiation. Cells are seeded onto a pre-fabricated, electrospun scaffold and are promoted to grow for an extended period of time, usually around one month in an experimental setting. Typically, cells in native tissues/organs are seeded into an electrospun scaffold for specific

tissue/organ regeneration such as chondrocytes for cartilage, osteoblasts for bone regeneration [46, 58, 68, 80]. In more recent years, research has been moving towards seeding electrospun scaffolds with various stem cells and attempting to direct their differentiation and proliferation to a desired tissue type [66, 68].

33.2.3 Modification of Scaffold Porosity

Enhancing porosity of TE scaffolds for tissue regeneration has been another important way to modify electrospun polymer scaffolds. In native tissue, the ECM forms naturally porous, nanostructured environments, which promote cell adhesion, proliferation, and differentiation [29, 88]. Therefore, it is important to construct a scaffold that mimics the scale and structure of the native ECM [60]. However, it is difficult to obtain purely electrospun polymers on the true nanoscale due to the inherent limitations of the technology as well as the loss of structural and mechanical integrity of a scaffold with small fiber dimensions. Because of these considerations, more and more research has sought to modify the surface characteristics of microscale and sub-micron scaffold fibers. One potential approach is to co-spin finer fibers onto thicker fibers in order to achieve nano-texturization of micro scale fibers [80]. This creates appropriate nanostructures on microscaled fibers, which have been shown to promote better cell adhesion, proliferation, and differentiation [80]. Another novel method for creating porous scaffolds is through a technique known as wet electrospinning. In wet electrospinning, fibers are collected in a coagulation bath of methanol or some other liquid, as opposed to on a collector plate in open air [73] yielding a highly porous structure that greatly improves cell adhesion. It was reported that cellular growth was four times greater than a control group after a 28-day growth period [35]. Yet another method for generating highly porous scaffolds is to fabricate a composite scaffold combining a chosen electrospun polymer as the matrix and an inherently porous material as a constituent. In one instance, a PCL scaffold was co-spun with mesoporous bioactive glass (MBG), which is a commonly used material in bone regeneration because of its high bioactivity [93]. This scaffold was then coated with hydroxyapatite (HA) and collagen to further enhance cell adhesion and tissue formation. The initial incorporation of MBG into the scaffold not only greatly enhanced osteoconductivity, biocompatibility, and cell affinity, but allowed

for a reduced coating time and a more effective HA and collagen coating [93].

33.2.4 Electrospun Composite Scaffolds

One of the most widely investigated methods to modify electrospun scaffolds for TE is the fabrication of composite scaffolds. Like other methods discussed, composite TE scaffolds contain constituent materials blended into a fibrous polymer matrix for enhanced structural and mechanical characteristics, modified surface chemistry, additional porosity and surface roughness or enhanced cellular properties. For osteogenic modification, for instance, one of the most frequently investigated materials for electrospun composite scaffolds is HA crystals [62]. Often, HA is simply blended with the polymer solution at a desired concentration and then electrospun into a scaffold per normal fabrication procedures [63]. HA is attractive because it fortifies and enhances several important scaffold parameters at once [17, 41, 63]. The incorporation of HA into a scaffold has been shown to stimulate the proliferation of osteoblasts and osteoblast-like cells and the differentiation and proliferation of bone marrow mesenchymal stem cells (MSCs) [54, 55, 60]. In several cases, MSCs have been seeded onto composite scaffolds containing nano-HA (nHA), and in all have shown improved results with regard to proliferation and osteogenic differentiation [56, 60]. Besides stimulated cellular growth, nHA also greatly enhances the surface roughness of electrospun fibers, specifically at the nanoscale [15, 41]. Cells preferentially adhere to rough surfaces with nanoscaled features and surface modifications provided by the addition of nHA greatly facilitates cellular adhesion and growth [17, 36, 60, 73]. Another important aspect for the inclusion of HA on electrospun scaffolds is an enhancement of mechanical properties [41, 54]. It has been shown that the inclusion of HA in a scaffold matrix increases scaffold yield strength, as well as Young's modulus, which not only creates a more robust and functional scaffold but also may help to direct the differentiation of stem cells [54].

In addition to HA, many other constituent materials have been used to enhance cell behavior for bone application. One such material is tricalcium phosphate (TCP). Tricalcium phosphate is a bioceramic found in both bone and in geological environments

[89]. It is commonly used for hard tissue regeneration due to its beneficial effect on improving cell activity, but it lacks toughness [15, 89]. Hence, its combination with an electrospun scaffold is advantageous because TCP scaffolds require structural support [89]. Another material with similar bioactive applications is collagen. Collagen is a natural polymer that is a critical component of the native ECM in a variety of native tissues [6, 10, 55].

As previously discussed, there are a wide variety of ways that collagen can be incorporated into a polymeric scaffold. Typically, collagen is used as a surface treatment to render a scaffold more cell-adherent as in the deposition of nanofibrous collagen on electrospun scaffolds [30, 42, 80]. However, collagen lacks significant structural and mechanical integrity and must be used with a robust polymer or other composite materials for functional TE scaffolds [89]. In lieu of these materials that naturally occur in human tissues, xeno-derived, natural, or synthetic materials have also been explored for bone tissue engineering applications. One common material is chitosan, a natural component found in the exoskeleton of crustaceans [6]. Chitosan has been shown to enhance cellular adhesion and growth, but needs to be structurally supported [6]. Other materials that have been investigated to increase porosity and surface roughness for bone regeneration include bioactive glass, gelatin, and the blending of different polymers [15, 17, 46, 56, 60]. One particularly interesting application of a blended polymer was the inclusion of a “sacrificial” PEO fibrous element to a PCL/collagen scaffold. In an aqueous and/or cellular active environment, the PEO fibers degraded much more rapidly, leaving a highly porous, complex PCL/collagen scaffold that greatly enhanced the osteogenesis of MSCs [60]. This is an especially important example because it highlights the novel application of materials to create dynamic scaffolds and systems.

33.2.5 Novel Methodology

As has been shown, there are many newly developed approaches to electrospin scaffolds for TE and regenerative medicine applications. Such new methods improve the functionality of scaffolds. This ranges from fiber dimensions to yield strength to directing the phenotypic expression of stem cells. While the direct correlation

of these modifications on cellular growth has yet to be fully understood, enough information has been accumulated that researchers are already looking at more novel ways to control the properties of electrospun tissue engineering scaffolds. These methods largely consist of creative new modifications and the manipulation of the electrospinning fabrication process, or the use of novel and highly experimental materials.

33.2.5.1 Co-spun scaffolds and co-deposited materials

One of the most heavily researched experimental methods for electrospun scaffolds has been co-electrospinning scaffolds. Co-spinning refers to the simultaneous deposition of two or more different materials onto a single collection agent in order to achieve a novel combination, distribution, or structure (see Fig. 33.1). As has already been discussed, this method has been applied to achieve a desired distribution of chemicals, constituents, and drugs, to create novel core-shell fiber structures for drug delivery, and to deposit materials in such a way as to create surface features of a desired size on larger, structural elements [64, 65, 80, 81, 90]. This method is also being investigated in relation to combining electrospinning and electrospraying, a process similar to electrospinning where the material is deposited in micro- or nano-sized beads, as opposed to fibers (see Fig. 33.2) [21, 58, 62]. This unique combination of electrospinning and electrospraying has just begun to be investigated by researchers, but has already been utilized in some creative ways [22, 58].

The combination of electrospinning/electrospraying has been used to create composite materials. For example, Francis *et al.* used the process to create composite scaffolds consisting of electrospun gelatin (gel) and electrosprayed nHA. Scaffolds were fabricated in a 4:1 and 2:1 Gel/nHA compositional ratio and were then evaluated for surface topography, material distribution and mechanical properties. The scaffolds were also analyzed for biocompatibility *in vitro* by seeding human fetal osteoblasts on the fabricated scaffolds. The studies showed that these composite scaffolds yielded better cell proliferation and enhanced biomineralization [21].

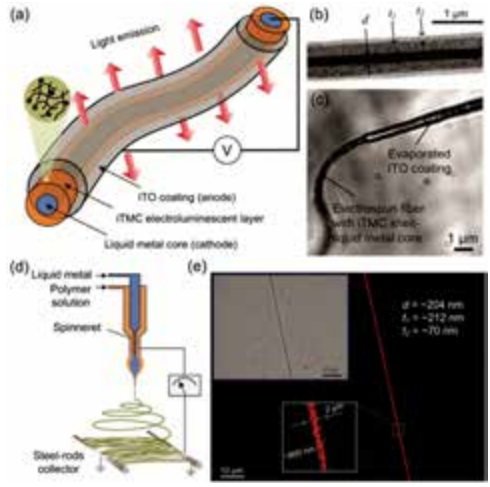

Figure 33.1 Diagram, TEM image and Raman spectroscopic image of novel core-sheath electrospun fibers for optical fabric [16].

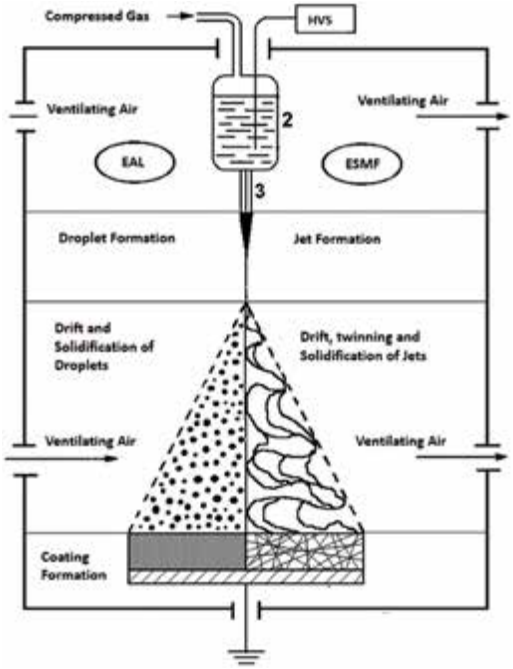

Figure 33.2 Diagram of electrospinning versus electrospraying [20].

The novel application of combining electrospinning/electrospraying has not been limited to composite scaffolding. For example, Paletta *et al.* published a recent study where osteoblasts suspended in medium were electrosprayed onto scaffolds composed of PLLA and PLLA/collagen. This method was not shown to inhibit cellular growth or scaffold degradation, and it was concluded by the researcher to be a suitable method for cell seeding of electrospun TE scaffolds [58].

33.2.5.2 Wet-electrospinning

Another example of novel modifications to the electrospinning process is that of "wet electrospinning." The process of wet electrospinning entails a standard electrospinning setup augmented with the collector plate submerged in a liquid bath (see Fig. 33.3). Shin *et al.* used wet electrospinning to create a 3D poly(trimethyle necarbonate-co-epsilon-caprolactone)-block-co-poly(p-dioxanone) scaffold for bone regeneration that was 90% porous and exhibited interconnected pores. This highly porous scaffold showed good cellular adhesion of osteoblasts at the center of the scaffold after only four days of *in vitro* cell seeding. The cells also proliferated 1.5 times faster than the control after seven days.

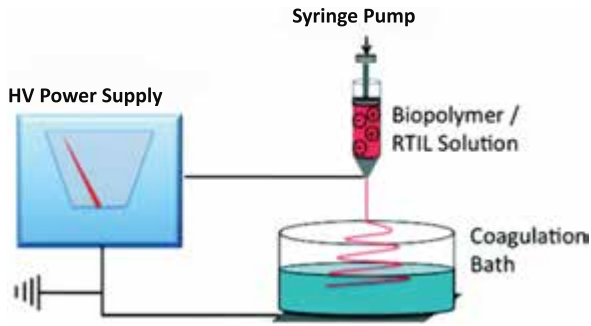

Figure 33.3 Diagram of wet electrospinning [50].

In addition, alkaline phosphate (a marker of bone formation) was four times higher than the control after 28 days [73]. These results showed that wet electrospun scaffolds can be a promising approach to creating scaffolds that are advantageous for bone growth.

33.2.5.3 Novel nanocomposites

With the amount of investigation into using natural materials native to bone and cartilage tissue, a novel area of research has been to incorporate non-natural or unconventional materials into scaffolds. One such material is octadecylamine-functionalized nanodiamonds (ND-OCT) [98]. Nanodiamonds (ND) are 5 nm diamond particles surrounded by amorphous and graphitic carbon, which has a large number of different functional groups on its surface. Because of this, NDs have chemically complex surfaces with the potential for combination with a variety of chemicals [53]. In a recent study, Zhang *et al.* created ND-OCT for use as a mechanically enhancing constituent for electrospun PLLA scaffolds. OCT was chosen as a functional group because it causes the NDs to be immiscible in water and hydrophilic organic solvents, but to have a high affinity toward hydrophobic solvents, making them ideal for uniform dispersion in a polymer while also being resilient in a biological environment [53, 98]. At 10 wt%, PLLA-ND-OCT scaffolds exhibited a 200% increase in Young's modulus and an 800% increase in hardness thus enhancing the mechanical properties of the ND-OCT-PLLA scaffold and rendering them very close to that of natural bone [98]. ND-OCTs also exhibited autofluorescence, giving off a very bright blue light when excited [53, 98]. However, unlike other fluorophores, ND-OCTs are non-toxic and very stable, which could make them a potentially powerful tool for *in vivo* analysis [53, 98].

Increasingly, nanotubes and nanotube/nanofibrous structures are being explored as a novel nanocomposite for electrospun scaffolds. Rosette nanotubes (RNTs) are an example of novel tubular structures currently being used. Rosette nanotubes are self-assembling tubes consisting of stacked disk shaped rings, or rosettes, made of the DNA base pairs guanine and cytosine [76]. Due to their unique biological and physiochemical properties, RNTs provide significant potential to enhance and promote cellular growth and development [9, 76, 96]. For example, Chen *et al.* used a novel electrospinning technique to fabricate hydrogel, rosette nanotube, and fibroblast-like cells into novel 3D scaffold for cartilage implantation. The results of their study showed that electrospun RNT/hydrogel composites improved both fibroblast and chondrocyte functions. RNT/hydrogel composites promoted

fibroblast cell chondrogenic differentiation in two-week culture experiments. Furthermore, studies demonstrated that RNTs enhanced the hydrogel adhesive strength to that of severed collagen. These results, thus, provided a nanostructured scaffold that enhanced fibroblast cell adhesion, viability, and chondrogenic differentiation [9].

In addition to RNTs, both single-walled and multiwalled carbon nanotubes (CNTs and MWCNTs) have been used to enhance the mechanical and physiochemical characteristics of electrospun scaffolds [51, 59]. CNTs and MWCNTs have a radius of around 10 to 20 nm and 50 to 60 nm, respectively, and are thus very biomimetic [95]. They are also electrically conductive, which can be conducive for certain types of tissue regeneration such as neural or cardiac applications, and they are also easily functionalized with biological molecules and/or proteins [83, 86, 95]. Pan *et al.* fabricated microcomposite fibers of regenerated silk fibroin (RSF) and MWCNTs by electrospinning. A quiescent blended solution and a three-dimensional Raman image of the composite fibers showed that functionalized MWCNTs (F-MWCNTs) were well dispersed in the solution and the RSF fibers, respectively. The mechanical properties of the RSF electrospun fibers were improved drastically by incorporating F-MWCNTs. Compared with the pure RSF electrospun fibers, a 2.8-fold increase in breaking strength, a 4.4-fold increase in Young's modulus, and a 2.1-fold increase in breaking energy was observed for the composite fibers with 1.0 wt% F-MWCNTs. Cytotoxicity tests preliminarily demonstrated that the electrospun fiber mats have good biocompatibility for tissue engineering scaffolds [59].

Sharma *et al.* used electrospinning to fabricate polyaniline-carbon nanotube/poly(N-isopropyl acrylamide-co-methacrylic acid) (PANI-CNT/PNIPAm-co-MAA) composite nanofibers and PNIPAm-co-MAA nanofibers as a three-dimensional conducting smart tissue scaffold. Cellular responses on the nanofibers were studied with mice L929 fibroblasts, and the PANI-CNT/PNIPAm-co-MAA composite nanofibers were shown to have the highest cell growth and cell viability as compared to PNIPAm-co-MAA nanofibers. Cell viability in the composite nanofibers was 98% higher, indicating that the composite nanofibers provided a better environment as a 3D scaffold for cell proliferation and attachment and are suitable for tissue engineering applications [69].

33.3 3D Printing

33.3.1 Introduction to 3D Printing and Medical Applications

While electrospinning has been established as one of the most widely and thoroughly investigated methods for scaffold fabrication, it still presents a number of limitations such as having weak or poor mechanical properties, having non-uniform pore distribution, random pore interconnectivity and void space, and limited control over the size, and distribution of fibers within the micro and nanoarchitecture of the scaffold [28, 62]. Recently, 3D printing and rapid prototyping processes have been used to create scaffolds that are 3D with user defined microstructures and microscaled architectures [12, 13]. This ensures that the scaffold is fully unoccluded with uniformly interconnected pores and has a more complex, controlled architecture.

Hard tissue is one of the most readily researched and treated defect and injury sites for TE scaffold-based solutions. One of the critical 3D scaffold design criteria for hard tissues is that they must have suitable mechanical properties. In addition, interconnected pores, specifically pore structures at the microscale, interconnected by smaller pores on a nano-scale are also indicative of the ECM of hard tissues, and are very important for hard tissue scaffold design [85, 89, 98]. This sort of complicated, hierarchical structure is one that is difficult to recapitulate, if at all, and then more difficult to control in even very advanced electrospinning setups and other common scaffold fabrication techniques. With the application of 3D printing, there is an allowance not only for the creation of delicate and intricate structures from the advanced working of strong and robust materials, but the potential to create highly ordered structures that could conceivably match any desired architecture [44]. This later advantage is one that also makes 3D printing attractive for other types of targeted tissue 3D scaffolds.

Theoretically, the versatility and precision of 3D printing could be used to print not only small scaffolds and patches for defect repair, but could eventually be used to print whole organs. Currently, 3D printing as applied to TE uses a layered manufacturing method of printing thin depositions of material in a given pattern on top of

previously printed and cured material [13, 44]. This could allow for large, macro-scale objects that have complex, user-defined internal features, mimicking the architecture a given organ. This could also allow for materials to be printed that encapsulate living cells into the artificial organ construct, creating a complex network of cells, advantageous architecture and structure conducive to organ function and cell/tissue growth [87]. Examples and discussion of this will be presented later in the chapter.

Moreover, one of the most important challenges facing 3D TE construct design is vascularization. Scaffolds seeded with cells that begin to mature and form tissue have problems with the transportation of nutrients and essential signaling chemicals and growth factors, as well as removal of waste products within the internal structure of the scaffold [11, 18, 60]. In the body, vascular networks accomplish this task, but new and under-formed vasculature presents a daunting limitation to scaffold-based tissue repairs. However, if a scaffold can be fabricated with designed transport channels and structures that mimic vascularized tissue, then it could be possible to alleviate this issue [84]. 3D printing presents a potential ability to accomplish this because, as stated previously, it is possible to create structures with predesigned complex, microscale internal architectures.

33.3.2 Methods

There are currently a number of methods for 3D printing and rapid prototyping that have been directly applied to the manufacture of 3D TE constructs. These methods provide fast and affordable design prototypes that have been applied in novel ways and modified to use and create unique materials and structures for TE purposes.

33.3.2.1 Fused deposition modeling

Fused deposition modeling (FDM) is one of the simplest forms of 3D fabrication. In FDM, a computer-aided design (CAD) drawing is used in conjunction with a 3D printer to create polymeric 3D structures. A FDM machine consists of a slightly heated printing bed, a printing head capable of 3D axial movement and a computer/controller. The printing head draws a solid polymeric filament

and forces it through a heated extruder head, which heats up the material and deposits it, in a molten form, on the printing surface in a thin layer. The machine then prints multiple thin layers on top of the previously deposited layer. In the end, one is left with a 3D construct of pre-determined design (see Fig. 33.4) [37, 67]. Fused deposition modeling is very rudimentary compared to other 3D fabrication methods, but it is important because it establishes an overarching methodology in all 3D fabrication techniques, where a fully 3D-designed structure is disassembled into very thin, successive slices and then physically recreated layer-by-layer. Fused deposition modeling itself has strong potential as a 3D fabrication method for 3D TE scaffolds because of its ability to employ a number of different polymers, but is not often utilized because it lacks a low enough resolution to create complex and biomimetic nano/microstructures [5].

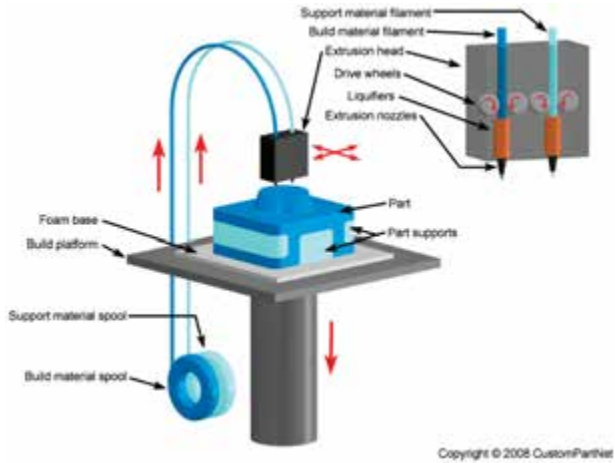

Figure 33.4 Diagram of Fused Deposition Modeling. Copyright 2008 CustomPartNet.

Shim *et al.* used a deposition system similar to FDM called solid freeform fabrication (see Fig. 33.5). A 3D scaffold was printed from a deposited, structurally sound polymer, while a cell-laden hydrogel was infused into the void spaces The printed hard scaffold served as a structural support while the printed soft hydrogel served to encapsulate cells and ensure their even distribution throughout the construct [72].

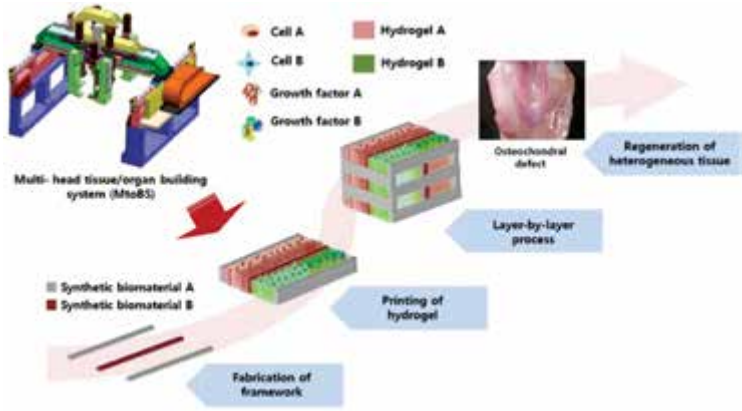

Figure 33.5 Fabrication diagram of a composite solid freeform fabrication of a hydrogel/polymer scaffold [71].

33.3.2.2 Selective laser sintering and stereolithography

Selective laser sintering (SLS) uses a construction method similar to FDM (see Fig. 33.6). In SLS, a printing surface on a movable piston is loaded with a material in powder form. A high-power pulsed laser is then used to cure a layer of the material in a defined pattern based on a user-designed CAD drawing. Once the layer is cured, the piston lowers the printing platform by one layer thickness. The powdered printing material is replenished and the laser cures the next layer of the structure [34, 35, 39]. Kolan *et al.* used SLS to fabricate porous constructs made of 13–93 bioactive glass, using stearic acid as a polymeric binder. The effect of particle size distribution, binder content, processing parameters, and sintering schedule on the microstructure and mechanical properties of porous constructs was investigated, and importantly improved mechanical properties were reported [39]. Lohfeld *et al.* created SLS scaffolds of PCL and PCL/TCP for bone tissue regeneration. Different scaffold designs were generated, and assessed for manufacturability, porosity, and mechanical performance. Furthermore, scaffolds were generated with increasing TCP content, and scaffold fabrication from PCL and PCL/TCP mixtures with up to a 50 mass% TCP was shown to be possible. With increasing macroporosity, the stiffness of the scaffolds dropped. However, the stiffness increased by minor geometrical changes, such as the addition of a cage around the scaffold [47].

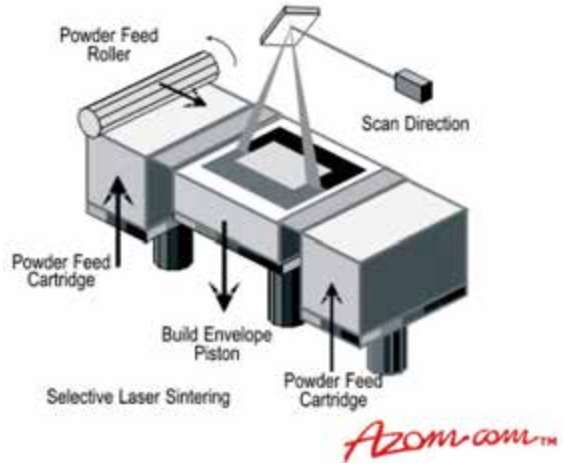

Figure 33.6 Diagram of selective laser sintering. Copyright azom.

Stereolithography (SL) is another laser-based printing method (see Fig. 33.7). SL also employs a moveable build platform and prints materials layer-by-layer. The platform and piston are immersed in a photocurable resin, which uses an ultraviolet wavelength laser to cure the polymer resin [32, 48, 94]. That is to say, that it is a liquid polymer that cross-links and forms a solid structure when exposed to certain wavelengths of light, as opposed to a polymer material that is sintered together at high energies as with SLS.

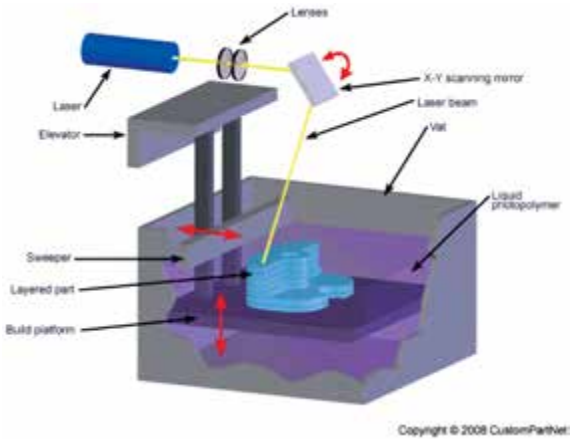

Figure 33.7 Diagram of traditional stereolithography. Copyright 2008 CustomPartNet.

Increasingly, modified SLS, SL and other laser-based printing methods have become very popular for the manufacturing of 3D TE constructs, due to the versatility of materials that can be printed and the high resolutions achievable. SL has also been especially popular due to the fact that there are a number of photocurable polymers that have ideal properties for biological applications and cell encapsulation. Catros *et al.* used a combination of a laser-based curing process called laser assisted bioprinting and electrospinning. Thin PCL membranes were spun and then patterned with a laser-cured bioink comprising MG63 cells and alginate in dispersion patterns. The finished 2D scaffold layers were then stacked to form a 3D construct. Circular patterns were maintained *in vitro* during the first week but they were no longer observable after 2 weeks, due to cell proliferation. The layer-by-layer printed construct provided an appropriate 3D environment for cell survival and enhanced cell proliferation *in vitro* and *in vivo* [4]. Koch *et al.* also used laser-assisted bioprinting to create 3D structured scaffolds for skin grafts. Fibroblasts and keratinocytes suspended in collagen were used as the print medium. It was demonstrated that the printed constructs incited cells to have enhanced adhesion and an affinity for the formation of gap junctions [38].

33.3.2.3 Laminated object manufacturing

Laminated object manufacturing (LOM) uses a large sheet of the printing material, coated with an adhesive, and a cutting tool or laser to cut out a given layer of a designed 3D shape and deposit it on top of the preexisting printed form (see Fig. 33.8). Laminated object manufacturing does not demonstrate the level of resolution of SLS or SL, but because of increased work into developing methods for 2D tissue engineering scaffolds and films, it could be a potential tool for processing such 2D constructs easily into a functional 3D scaffold [57]. Pirlo *et al.* created a series of formed and molded 2D biopapers, which were then stacked. 2D biopapers were created by pouring polymer dissolved in solvent into molds patterned with NaCl crystals. When hardened, the salt was washed off, leaving a robust pattered film.

Laser Assisted Bioprinting was then used to deposit human umbilical vein endothelial cells onto the bioapaper, which was then

stacked. The purpose was to create a pre-vascularized scaffold environment for future TE applications [61].

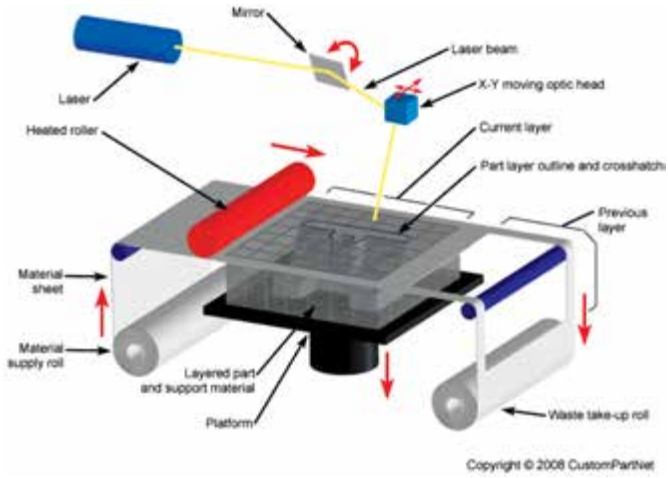

Figure 33.8 Diagram of laminated object manufacturing. Copyright 2008 CustomPartNet.

33.3.2.4 Inkjet 3D printing

Inkjet 3D Printing (3DP), like many other methods discussed, uses CAD or a computer generated drawing to create a 3D shape that is subsequently fabricated layer-by-layer (see Fig. 33.9). In 3DP, a printing head similar to that found in an inkjet printer moves across a bed of powdered printing material and selectively deposits a binding agent in the cross section of that layer. The construct is then coated in a new layer of powder and the process is continued. 3DP is popular because of the ease and cost effectiveness of the equipment and setup [12, 24]. Recently, it has become popular for 3D TE scaffold fabrication because it can use a wide variety of materials, and its inert fabrication method is not damaging to biological materials, growth factors, chemicals and even living cells that might be printed in a scaffold or construct.

Gaetani *et al.* utilized a deposition process similar to inkjet printing called tissue printing. Human cardiac-derived cardiomyocyte progenitor cells were printed into an alginate matrix where they experienced enhanced proliferation and cardiac differentiation.

The printed scaffold was also put into contact with and showed migration into a matrigel layer, which served as a simulation of targeted cell delivery into native tissue at the defect site [23].

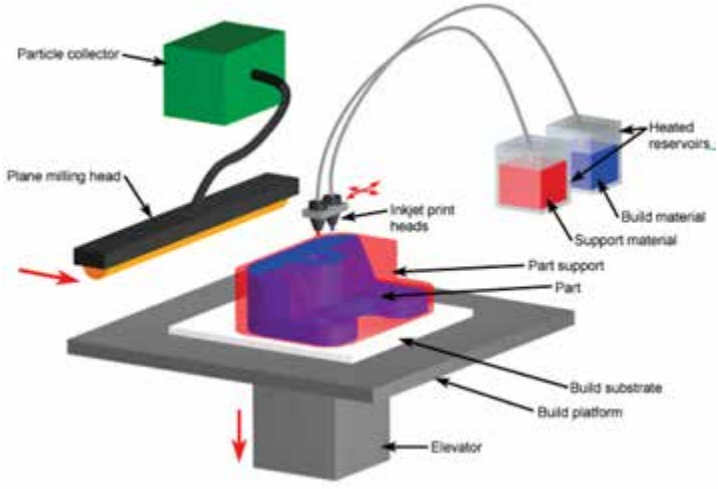

Figure 33.9 Diagram of inkjet 3D printing. Copyright 2008 CustomPartNet.

Xu *et al.* took a unique approach to 3D TE construct fabrication by fabricating a construct without the scaffold materials. Inkjet printing was utilized to print cells into a network of zigzagging tubes mimicking the size and shape of native tissue vascularization. The lack of a base scaffold material and the ability to achieve appropriately sized and shaped vasculature-like tubes made this a potential first step toward full organ printing [87].

33.3.2.5 Novel methodology and applications

In addition to the pre-established 3D printing fabrication methods discussed thus far, several unique fabrication methods for controlled, 3D TE scaffolds have been recently investigated. One such method that has been gaining popularity is 3D fiber deposition. 3D fiber deposition is similar to FDM, where a heated nozzle is used to deposit a melted polymer, but the outlet used is on the order of several hundred microns in diameter. The process yields micro-fiber arrays, with controllable fiber spacing and deposition angle. Fedorovich *et al.* used 3D Fiber Deposition to

create alginate hydrogel matrices containing chondrocytes and osteogenic progenitors, as well as separate printed layers for osteoblasts and osteoblast growth for osteochondral defects. Good cellular growth results were reported and a high degree of effect was demonstrated on the scaffold architecture by modulation of the above mentioned process parameters [19]. Sun *et al.* also used 3D fiber deposition to create and compare porous PCL scaffolds containing osteoblasts, which were fabricated at 45 degree and 90° deposition angles. The 3D printed scaffolds were compared to traditional salt-leeched scaffolds. The cell distribution on the 3D scaffolds was more homogeneous than the salt-leached scaffolds, demonstrating that 3D scaffolds are more effective for tissue engineering. The results also showed that it is possible to design and optimize the properties of amorphous polymer scaffolds by 3D fiber deposition [77].

Other novel demonstrations have been recently investigated that show the versatility and adaptability of 3D fabrication methods. Tarafder *et al.* recently used microwave sintering to create a 3D, porous TCP scaffold for bone tissue engineering. Tricalcium phosphate was printed into a microscale scaffold using 3D printing, but was then sintered in a microwave furnace. A significant increase in compressive strength, between 46% and 69% was achieved by this process, as compared to conventional sintering due to more efficient densification. *In vitro* cell studies exhibited an increase in cell density with a decrease in macropore size using human osteoblast cells. Histomorphological analysis also revealed that the presence of both micro- and macropores facilitated osteoid-like new bone formation [78].

Lu *et al.* also utilized projection printing, which works similarly to photolithography, in which a photo-mask is used to cure layers of photosensitive material in designed patterns when exposed to light. In projection printing, a UV light source is used in conjunction with a micro-mirror array, a digital masking device, imaging optics and a photocurable resin to photopolymerize the resin into complex, biomimetic shapes. Lu *et al.* was able to use this process to print precise closed channels and cavities that mimicked native vasculature [48].

33.4 Other Current Methodology

Electrospinning and 3D printing are currently the two most promising and most widely investigated methods for 3D scaffold fabrication. There are, however, a number of other preexisting methods that have been in use as 3D scaffold fabrication methods. Traditional methods do not offer the same level of control, biomimetic structure formation, or improved material, chemical and cellular incorporation into the construct, but there are several methodologies that are still being applied to TE scaffold fabrication in novel and relevant ways. In the following, we will briefly discuss several well-established methods.

33.4.1 Solvent Casting

Solvent casting is a process in which a polymer is dissolved in an organic solvent, after which particles of a specific or desired dimension are added to the solution. The solution is then added to a mold, where the solvent evaporates off, leaving a solid structure. The evaporation of the solvent in and of itself is not remarkable, but solvent-polymer solutions can be cast in molds of virtually any shape or size. This means that molds with complex micro-architectures can be fabricated and used to create highly ordered and biomimetic polymer scaffolds [2, 45, 92]. In some cases, the pre-cast solvent-polymer mixture is incorporated with some micro- or nano-sized porogen material. Once the solution is cast, the solid structure is put into a water bath, which dissolves the incorporated porogen leaving behind a rigid, porous structure. Yu *et al.* used a solvent casting method to create stackable poly(3-hydroxybutyrate-co-3-hydroxyhexanoate) films, which were then seeded with mesenchymal stem cells leading to enhanced adhesion, cellular aggregate formation, proliferation, and cellular migration within the scaffold [92]. Azami *et al.* devised a nanostructured scaffold for bone repair using hydroxyapatite and gelatin as its main components. The scaffold was prepared via layer solvent casting combined with freeze-drying and lamination techniques. Engineering analyses show that the scaffold possessed a three dimensional interconnected homogenous porous structure with a

porosity of about 82% and pore sizes ranging from 300 to 500 μm. The mechanical properties measured also matched those of spongy bone. The results obtained from biological assessment show that this scaffold did not negatively affect osteoblast proliferation rate and actually improved osteoblast function as shown by increasing the alkaline phosphate (ALP) activity and calcium deposition and formation of mineralized bone nodules. In addition, the scaffold promoted healing of critical sized calvarial bone defect in rats [2].

33.4.2 Gas Foaming

Gas foaming is a process for scaffold fabrication similar to solvent casting where a foam-forming agent, such as ammonium bicarbonate, is added to a polymer solvent solution. The polymer-solvent foam is then dried, and the solvent evaporates, leaving a rigid and porous structure. Gas foaming is very simple, in that one cannot create highly ordered or controllable porous materials. However, because of the inert nature of the pore formation process, a variety of materials and composite materials can be utilized to create tissue-engineered scaffolds. Ji *et al.* used gas foaming to create highly porous poly-DL-lactide and poly(ethylene glycol) co-polymer scaffolds foamed with CO_2 [31]. In addition to composite materials, gas foaming has the potential to create pre-seeded scaffolds, and to utilize material mixtures that have incorporated living cells and biological material into them. Chen *et al.* used a novel method to seed a calcium phosphate cement with human umbilical cord cells encapsulated in hydrogel spheres. The calcium phosphate/hydrogel sphere mixture was then foamed with a porogen to achieve high porosity and good cellular dispersion [7, 8]. Zhou *et al.* employed a new technique where "solid-state" foaming (SSF) was combined with immiscible polymer blends to achieve a variety of different pore sizes and distributions within the same structure. That is to say, highly interconnected micro- and nanopores were observed [100]. Gas foaming, due to the relative ease of preparation, also has great potential as a mass-production fabrication method for TE scaffolds and TE biomaterials. Henke *et al.* conducted a study into the effectiveness of oligo(poly(ethylene glycol)fumarate) (OPF) gas foamed hydrogel scaffolds for cell culture. Ready to use OPF-hydrogel scaffolds were prepared by gas

foaming, freeze drying, individual packing into bags and subsequent gamma-sterilization. The scaffolds could be stored and used "off-the-shelf" without any need for further processing prior to cell culture. Thus, the handling was simplified and the sterility of the cell carrier was assured [26].

33.4.3 Phase Separation

In phase separation, a polymer in liquid form is polymerized into a block co-polymer of different block morphologies that separate homogenously throughout the structure to form uniform, ordered, nanoscale structures. Chemical and molecular incompatibilities in the polymer blocks cause this phenomenon to occur, and the same principle can be applied to different materials as well. Zhao *et al.* used phase separation to create highly porous poly(propylene carbonate) scaffolds for bone regeneration with nanofibrous chitosan interconnecting the macropores. It was reported that these scaffolds were able to achieve as high as 91.9% porosity [99]. Sun *et al.* used a combination of injection molding and phase separation to create multi-channeled PLLA scaffolds intended for neuronal and tendon regeneration. These highly complex and porous scaffolds showed greatly enhanced protein adsorption and cellular adhesion [75]. Moawad *et al.* were able to employ sintered heat transfer to induce phase separation in glass–ceramic mixtures to form highly porous TE scaffolds with pores on the nanoscale [52]. Lee *et al.* was also able to employ a novel phase separation technique by using room-temperature ionic liquid to induce pore formation in poly(lactic acid) (PLA) scaffolds [43].

33.5 Summary

Today's clinical challenges provide great opportunity for the development of highly customizable methodologies for the treatment and repair of diseased, damaged, and injured tissue and organs. Stem cells provide a great deal of promise, but require chemical and physical cues for adequate differentiation and tissue formation. Scaffold-based TE approaches achieve this by using highly designed, biodegradable and biocompatible constructs with biomimetic micro/nano-featured architecture, modified surface chemistries and incorporated biological and chemical factors

for enhanced cellular adhesion, proliferation and differentiation. Electrospinning is one popular method for scaffold fabrication that creates micro and nano fibrous materials. It can be used with a variety of polymers, constituent materials, and can be augmented to work in tandem other fabrication processes, but it has begun to reach limitations. 3D printing does not have the ability to create biomimetic features as small as electrospinning, but it can create much more controlled and well-designed structures, and could potentially be used to rapidly produce constructs of complex micro and macro architecture. Several other popular methods exist, including solvent casting, gas foaming and phase separation that rely on more rudimentary chemical reactions and phenomena to create porous, biomimetic scaffolds. Still, they can be used with a variety of materials and continue to be applied in valid and novel ways.

Disclosures and Conflict of Interest

The authors declare that they have no conflict of interest and have no affiliations or financial involvement with any organization or entity discussed in this chapter. This includes employment, consultancies, honoraria, grants, stock ownership or options, expert testimony, patents (received or pending) or royalties. No writing assistance was utilized in the production of this chapter and the authors have received no payment for its preparation. This chapter originally appeared as "Nano/Microfabrication Techniques for Tissue and Organ Regeneration" in L. G. Zhang, A. Khademhosseini and T. J. Webster (eds.) (2014). *Tissue and Organ Regeneration: Advances in Micro- and Nanotechnology*, Pan Stanford Publishing, Singapore, and is reprinted here with edits by kind permission of the publisher.

Corresponding Author

Dr. Lijie Grace Zhang
Department of Mechanical and Aerospace Engineering
The George Washington University
800 22nd Street NW, 3590 Science and Engineering Hall
Washington, DC 20052, USA
Email: lgzhang@gwu.edu

About the Authors

Benjamin Holmes received a BS in mechanical and aerospace engineering from the University of Virginia, where he focused on material science, biomedical engineering and energy engineering. He is currently pursuing his PhD in mechanical and aerospace engineering with focus on tissue engineering, biomaterials and nanomedicine at George Washington University in Washington, DC, in Dr. Grace Zhang's laboratory. His work has focused on carbon nanomaterial polymer composites for cartilage repair, and 3D printing of thermoplastics, hydrogels and elastomers/other novel and composite polymers for bone, osteochondral, vascularized bone and cancer metastasis modeling, and has explored chemical functionalization and nanomaterials for surface modification, mechanical property modulation and drug delivery. He has also collaborated with other primary investigators at George Washington University and in the DC area, including on experimental hydrodynamic modeling of vascular bone structures and materials. In addition to research, he has demonstrated a strong interest in entrepreneurship, participating in the NSF I-Corps program, being a co-inventor, senior member and Vice President of the medical device startup, SonoStik, and endeavoring to start his own company for joint repair.

Thomas J. Webster's degrees are in chemical engineering from the University of Pittsburgh (BS, 1995) and in biomedical engineering from Rensselaer Polytechnic Institute (MS, 1997; PhD, 2000). He is currently The Arthur W. Zafiropoulo Chair and professor of chemical engineering at Northeastern University in Boston, USA. His research explores the use of nanotechnology in numerous applications. Specifically, his research addresses the design, synthesis, and evaluation of nanophase materials as more effective biomedical devices. He has completed extensive studies on the use of nanophase materials to regenerate tissues and has graduated/supervised over 109 visiting faculty, clinical fellows, post-doctoral students, and thesis completing BS, MS, and PhD students. To date, his lab group has generated over 9 textbooks, 48 book chapters,

over 300 invited presentations, over 400 peer-reviewed literature articles, at least 567 conference presentations, and 32 provisional or full patents. Some of these patents led to the formation of nine companies. His research on nanomedicine has received attention in media publications, including MSNBC (October 10, 2005), NBC Nightly News (May 14, 2007), PBS DragonFly TV (covered across the US during the winter, 2008), and the ABC Nightly News via the Ivanhoe Medical Breakthrough Segment (covered across the US during the winters of 2008 and a separate research segment in 2010 and 2011). His work has been on display at the London and Boston Science Museums. He is the founding editor-in-chief of the *International Journal of Nanomedicine* (the first international journal in nanomedicine), serves on the editorial board of 15 additional journals, has helped to organize 22 conferences emphasizing nanotechnology in medicine, and has organized over 53 symposia at numerous conferences emphasizing biological interactions with nanomaterials. He chaired the 2011 Annual Biomedical Engineering Society (BMES) conference and has organized numerous symposia for AIChE, IEEE, MRS, and ASME Annual Meetings. Dr. Webster has received numerous honors: 2002, Biomedical Engineering Society Rita Schaffer Young Investigator Award; 2003, Outstanding Young Investigator Award, Purdue University College of Engineering; 2005, American Association of Nanomedicine Young Investigator Award Finalist; 2005, Coulter Foundation Young Investigator Award; 2006, Fellow, American Association of Nanomedicine; 2010, Distinguished Lecturer in Nanomedicine, University of South Florida; 2011, Outstanding Leadership Award for the BMES; 2012, Fellow, AIMBE; and 2013 Fellow, BMES. He was recently appointed director of the Indo-U.S. Center for Biomaterials for Healthcare.

Lijie Grace Zhang's Bioengineering Laboratory for Nanomedicine and Tissue Engineering applies a range of interdisciplinary technologies and approaches in nanotechnology, stem cells, tissue engineering, biomaterials, and drug delivery for various biomedical applications. The main ongoing research projects include designing biologically inspired nanostructured scaffolds and developing 3D bioprinting techniques for bone, cartilage, osteochondral and

neural tissue regenerations; investigation of the influence of nano and chemical environments in directing stem cell differentiations for regenerative medicine; developing sustained drug formulations for long-term and controlled drug release at disease or cancer sites; and developing a novel 3D tunable bone model for breast cancer metastasis study.

References

1. Ahn, S. H., Lee, H. J., Kim, G. H. (2011). Polycaprolactone scaffolds fabricated with an advanced electrohydrodynamic direct-printing method for bone tissue regeneration, *Biomacromolecules*, **12**, 4256–4263.
2. Azami, M., Tavakol, S., Samadikuchaksaraei, A., et al. (2012). A porous hydroxyapatite/gelatin nanocomposite scaffold for bone tissue repair: in vitro and in vivo evaluation, *J. Biomater. Sci. Polym. Ed.*, **18**, 2353–2568.
3. Berthiaume, F., Maguire, T. J., Yarmush, M. L. (2011). Tissue engineering and regenerative medicine: History, progress, and challenges, *Annu. Rev. Chem. Biomol. Eng.*, **2**, 403–430.
4. Catros, S., Guillemot, F., Nandakumar, A., et al. (2012). Layer-by-layer tissue microfabrication supports cell proliferation in vitro and in vivo, *Tissue Eng. Part C Methods*, **18**, 62–70.
5. Centola, M., Rainer, A., Spadaccio, C., et al. (2010). Combining electrospinning and fused deposition modeling for the fabrication of a hybrid vascular graft, *Biofabrication*, **2**, 014102.
6. Chen, L., Zhu, C., Fan, D., et al. (2011). A human-like collagen/chitosan electrospun nanofibrous scaffold from aqueous solution: Electrospun mechanism and biocompatibility, *J. Biomed. Mater. Res. Part A*, **99A**, 395–409.
7. Chen, W., Zhou, H., Tang, M., et al. (2012). Gas-foaming calcium phosphate cement scaffold encapsulating human umbilical cord stem cells, *Tissue Eng. Part A*, **18**, 816–827.
8. Chen, W., Zhou, H., Weir, M. D., et al. (2012). Umbilical cord stem cells released from alginate-fibrin microbeads inside macroporous and biofunctionalized calcium phosphate cement for bone regeneration, *Acta Biomater.*, **8**, 2297–2306.
9. Chen, Y., Bilgen, B., Pareta, R. A., et al. (2010). Self-assembled rosette nanotube/hydrogel composites for cartilage tissue engineering, *Tissue Eng. Part C Methods*, **16**, 1233–1243.

10. Chen, Z. C., Ekaputra, A. K., Gauthaman, K., et al. (2008). In vitro and in vivo analysis of co-electrospun scaffolds made of medical grade poly(epsilon-caprolactone) and porcine collagen, *J. Biomater. Sci. Polym. Ed.*, **19**, 693–707.
11. Chung, E. J., Sugimoto, M., Koh, J. L., et al. (2012). Low-pressure foaming: A novel method for the fabrication of porous scaffolds for tissue engineering, *Tissue Eng. Part C Methods*, **18**, 113–121.
12. Cui, X., Boland, T., D'Lima, D. D., et al. (2012). Thermal inkjet printing in tissue engineering and regenerative medicine, *Recent Part. Drug Deliv. Formul.*, **6**, 149–155.
13. Cui, X., Breitenkamp, K., Finn, M. G., et al. (2012). Direct human cartilage repair using three-dimensional bioprinting technology, *Tissue Eng. Part A*, **18**, 1304–1312.
14. de Valence, S., Tille, J. C., Mugnai, D., et al. (2012). Long term performance of polycaprolactone vascular grafts in a rat abdominal aorta replacement model, *Biomaterials*, **33**, 38–47.
15. Dinarvand, P., Seyedjafari, E., Shafiee, A., et al. (2011). New approach to bone tissue engineering: Simultaneous application of hydroxyapatite and bioactive glass coated on a poly(L-lactic acid) scaffold, *ACS Appl. Mater. Interfaces*, **3**, 4518–4524.
16. Dong, L. (2012). Coaxial electrospinning produces a self-supporting micro/nanofiber electronic light source: SPIE Newsroom.
17. Fang, R., Zhang, E., Xu, L., et al. (2010). Electrospun PCL/PLA/HA based nanofibers as scaffold for osteoblast-like cells, *J. Nanosci. Nanotechnol.*, **10**, 7747–7751.
18. Fedorovich, N. E., Alblas, J., Hennink, W. E., et al. (2011). Organ printing: The future of bone regeneration? *Trends Biotechnol.*, **29**, 601–606.
19. Fedorovich, N. E., Schuurman, W., Wijnberg, H. M., et al. (2012). Biofabrication of osteochondral tissue equivalents by printing topologically defined, cell-laden hydrogel scaffolds, *Tissue Eng. Part C Methods*, **18**, 33–44.
20. Filatov, Y., Budyka, A., Kirichenko, V. (eds.) (2007). *Electrospinning of Micro- and Nanofibers: Fundamentals in Separation and Filtration Processes*, Begell House, Inc., Redding.
21. Francis, L., Venugopal, J., Prabhakaran, M. P., et al. (2010). Simultaneous electrospin-electrosprayed biocomposite nanofibrous scaffolds for bone tissue regeneration, *Acta Biomater.*, **6**, 4100–4109.
22. Francis, L., Venugopal, J., Prabhakaran, M. P., et al. (2010). Simultaneous electrospin-electrosprayed biocomposite nanofibrous scaffolds for bone tissue regeneration, *Acta Biomater.*, **6**, 4100–4109.

23. Gaetani, R., Doevendans, P. A., Metz, C. H., et al. (2012). Cardiac tissue engineering using tissue printing technology and human cardiac progenitor cells, *Biomaterials*, **33**, 1782–1790.

24. Godino, N., Gorkin, R., Bourke, K., et al. (2012). Fabricating electrodes for amperometric detection in hybrid paper/polymer lab-on-a-chip devices, *Lab Chip*, **12**, 3281–3284.

25. Gupta, P. K., Das, A. K., Chullikana, A., et al. (2012). Mesenchymal stem cells for cartilage repair in osteoarthritis, *Stem Cell Res. Ther.*, **3**, 25.

26. Henke, M., Baumer, J., Blunk, T., et al. (2014). Foamed oligo(poly(ethylene glycol)fumarate) hydrogels as versatile prefabricated scaffolds for tissue engineering, *J. Tissue Eng. Regen. Med.*, **8**(3), 248–52.

27. Holmes, B., Castro, N. J., Zhang, L. G., et al. (2012). Electrospun fibrous scaffolds for bone and cartilage tissue generation: Recent progress and future developments, *Tissue Eng. Part B Rev.*, **18**, 478–486.

28. Holzwarth, J. M., Ma, P. X. (2011). Biomimetic nanofibrous scaffolds for bone tissue engineering, *Biomaterials*, **32**, 9622–9629.

29. Hutmacher, D. W. (2000). Scaffolds in tissue engineering bone and cartilage, *Biomaterials*, **21**, 2529–2543.

30. Shabani, I., Haddai,V.-A., Soleimani, M., Seyedjafari, E., Babaeijandaghi, F., Ahmadbeigi, N. (2011). Enhanced infiltration and biomineralization of stem cells on collagen-grafted three-dimensional nanofibers, *Tissue Eng. Part A*, **17**, 1209–1218.

31. Ji, C., Annabi, N., Hosseinkhani, M., et al. (2012). Fabrication of poly-DL-lactide/polyethylene glycol scaffolds using the gas foaming technique, *Acta Biomater.*, **8**, 570–578.

32. Jolly, S. W., He, Z., McGuffey, C., et al. (2012). Stereolithography based method of creating custom gas density profile targets for high intensity laser-plasma experiments, *Rev. Sci. Instrum.*, **83**, 073503.

33. Jones, A. C., Arns, C. H., Sheppard, A. P., et al. (2007). Assessment of bone ingrowth into porous biomaterials using MICRO-CT, *Biomaterials*, **28**, 2491–2504.

34. Kang, H., Long, J. P., Urbiel Goldner, G. D., et al. (2012). A paradigm for the development and evaluation of novel implant topologies for bone fixation: Implant design and fabrication, *J. Biomech.*, **45**, 2241–2247.

35. Kettner, M., Schmidt, P., Potente, S., et al. (2011). Reverse engineering–rapid prototyping of the skull in forensic trauma analysis, *J. Forensic Sci.*, **56**, 1015–1017.

36. Ki, C. S., Park, S. Y., Kim, H. J., et al. (2008). Development of 3-D nanofibrous fibroin scaffold with high porosity by electrospinning: Implications for bone regeneration, *Biotechnol. Lett.*, **30**, 405–410.

37. Kim, J., McBride, S., Tellis, B., et al. (2012). Rapid-prototyped PLGA/beta-TCP/hydroxyapatite nanocomposite scaffolds in a rabbit femoral defect model, *Biofabrication*, **4**, 025003.

38. Koch, L., Deiwick, A., Schlie, S., et al. (2012). Skin tissue generation by laser cell printing, *Biotechnol. Bioeng.*, **109**, 1855–1863.

39. Kolan, K. C., Leu, M. C., Hilmas, G. E., et al. (2012). Effect of material, process parameters, and simulated body fluids on mechanical properties of 13–93 bioactive glass porous constructs made by selective laser sintering, *J. Mech. Behav. Biomed. Mater.*, **13C**, 14–24.

40. Langer, R., Vacanti, J. P. (1993). Tissue engineering, *Science*, **260**, 920–926.

41. Lao, L., Wang, Y., Zhu, Y., et al. (2011). Poly(lactide-co-glycolide)/hydroxyapatite nanofibrous scaffolds fabricated by electrospinning for bone tissue engineering, *J. Mater. Sci. Mater. Med.*, **22**, 1873–1884.

42. Lee, H., Yeo, M., Ahn, S., et al. (2011). Designed hybrid scaffolds consisting of polycaprolactone microstrands and electrospun collagen-nanofibers for bone tissue regeneration, *J. Biomed. Mater. Res. Part B: Appl. Biomater.*, **97B**, 263–270.

43. Lee, H. Y., Jin, G. Z., Shin, U. S., et al. (2012). Novel porous scaffolds of poly(lactic acid) produced by phase-separation using room temperature ionic liquid and the assessments of biocompatibility, *J. Mater. Sci. Mater. Med.*, **23**, 1271–1279.

44. Lee, M., Wu, B. M. (2012). Recent Advances in 3D printing of tissue engineering scaffolds, *Methods Mol. Biol.*, **868**, 257–267.

45. Li, X., Nan, K., Shi, S., et al. (2012). Preparation and characterization of nano-hydroxyapatite/chitosan cross-linking composite membrane intended for tissue engineering, *Int. J. Biol. Macromol.*, **50**, 43–49.

46. Linh, N. T., Lee, B. T. (2011). Electrospinning of polyvinyl alcohol/gelatin nanofiber composites and cross-linking for bone tissue engineering application, *J. Biomater. Appl.*, **27**, 255–266.

47. Lohfeld, S., Cahill, S., Barron, V., et al. (2012). Fabrication, mechanical and in vivo performance of polycaprolactone/tricalcium phosphate composite scaffolds, *Acta Biomater.*, **8**, 3446–3456.

48. Lu, Y., Chen, S. (2012). Projection printing of 3-dimensional tissue scaffolds, *Methods Mol. Biol.*, **868**, 289–302.

49. Ma, Z., Kotaki, M., Inai, R., et al. (2005). Potential of nanofiber matrix as tissue-engineering scaffolds, *Tissue Eng.*, **11**, 101–109.

50. Meli, L., Miao, J., Dordick, J. S., et al. (2010). Electrospinning from room temperature ionic liquids for biopolymer fiber formation *Green Chem.*, **12,** 1883–1892.

51. Miao, J., Miyauchi, M., Dordick, J. S., et al. (2012). Preparation and characterization of electrospun core sheath nanofibers from multi-walled carbon nanotubes and poly(vinyl pyrrolidone), *J. Nanosci. Nanotechnol.*, **12**, 2387–2393.

52. Moawad, H. M., Jain, H. (2012). Fabrication of nano-macroporous glass-ceramic bioscaffold with a water soluble pore former, *J. Mater. Sci. Mater. Med.*, **23**, 307–314.

53. Mochalin, V. N. (2010). *Nanodiamond*, AJ Drexel Nanotechnology Institute.

54. Mouthuy, P. A., Y. H., Triffitt, J., Oommen, G., Cui, Z. (2010). Physico-chemical characterization of functional electrospun scaffolds for bone and cartilage tissue engineering, *Proc. Inst. Mechan. Eng.*, **224**, 1401–1414.

55. Nair, L. S., Bhattacharyya, S., Laurencin, C. T. (2004). Development of novel tissue engineering scaffolds via electrospinning, *Expert Opin. Biol. Ther.*, **4**, 659–668.

56. Nandakumar, A., Fernandes, H., de Boer, J., et al. (2010). Fabrication of bioactive composite scaffolds by electrospinning for bone regeneration, *Macromol. Biosci.*, **10**, 1365–1373.

57. Nie, W., Zhang, J., Wang, Z., et al. (2008). Rapid-prototyping manufacture of human scoliosis based on laminated object technology, *J. Biomed. Eng.,* **25**, 1260–1263.

58. Paletta, J. R., Mack, F., Schenderlein, H., et al. (2011). Incorporation of osteoblasts (MG63) into 3D nanofibre matrices by simultaneous electrospinning and spraying in bone tissue engineering, *Eur. Cell. Mater.*, **21**, 384–395.

59. Pan, H., Zhang, Y., Hang, Y., et al. (2012). Significantly reinforced composite fibers electrospun from silk fibroin/carbon nanotube aqueous solutions, *Biomacromolecules*, **13**, 2859–2867.

60. Phipps, M. C., Clem, W. C., Grunda, J. M., et al. (2012). Increasing the pore sizes of bone-mimetic electrospun scaffolds comprised of polycaprolactone, collagen I and hydroxyapatite to enhance cell infiltration, *Biomaterials*, **33**, 524–534.

61. Pirlo, R. K., Wu, P., Liu, J., et al. (2012). PLGA/hydrogel biopapers as a stackable substrate for printing HUVEC networks via BioLP, *Biotechnol. Bioeng.*, **109**, 262–273.

62. Prabhakaran, M. P., Ghasemi-Mobarakeh, L., Ramakrishna, S. (2011). Electrospun Composite Nanofibers for Tissue Regeneration, *J. Nanosci. Nanotechnol.*, **11**, 3039–3057.

63. Rainer, A., Spadaccio, C., Sedati, P., et al. (2011). Electrospun hydroxyapatite-functionalized PLLA scaffold: Potential applications in sternal bone healing, *Ann. Biomed. Eng.*, **39**, 1882–1890.

64. Samavedi, S., Olsen Horton, C., Guelcher, S. A., et al. (2011). Fabrication of a model continuously graded co-electrospun mesh for regeneration of the ligament–bone interface, *Acta Biomater.*, **7**, 4131–4138.

65. Samer Srouji, D. B.-D., Rona Lotan, Erella Livne, Ron Avrahami, Eyal Zussman. (2011). Slow-release human recombinant bone morphogenetic protein-2 embedded within electrospun scaffolds for regeneration of bone defect: in vitro and in vivo evaluation, *Tissue Eng. Part A*, **17**, 269–277.

66. Schofer, M. D., Roessler, P. P., Schaefer, J., et al. (2011). Electrospun PLLA nanofiber scaffolds and their use in combination with BMP-2 for reconstruction of bone defects, *PLoS ONE*, **6**, e25462.

67. Schumann, D., Ekaputra, A. K., Lam, C. X., et al. (2007). Biomaterials/scaffolds. Design of bioactive, multiphasic PCL/collagen type I and type II-PCL-TCP/collagen composite scaffolds for functional tissue engineering of osteochondral repair tissue by using electrospinning and FDM techniques, *Methods Mol. Med.*, **140**, 101–124.

68. Shafiee, A., Soleimani, M., Chamheidari, G. A., et al. (2011). Electrospun nanofiber-based regeneration of cartilage enhanced by mesenchymal stem cells, *J. Biomed. Mater. Res. Part A*, **99A**, 467–478.

69. Sharma, Y., Tiwari, A., Hattori, S., et al. (2012). Fabrication of conducting electrospun nanofibers scaffold for three-dimensional cells culture, *Int. J. Biol. Macromol.*, **51**, 627–631.

70. Shim, I. K., Jung, M. R., Kim, K. H., et al. (2010). Novel three-dimensional scaffolds of poly(L-lactic acid) microfibers using electrospinning and mechanical expansion: Fabrication and bone regeneration, *J. Biomed. Mater. Res. Part B: Appl. Biomater.*, **95B**, 150–160.

71. Shim, J.-H., Lee, J.-S., Kim, J. Y., et al. (2012). Bioprinting of a mechanically enhanced three-dimensional dual cell-laden construct for osteochondral tissue engineering using a multi-head tissue/organ building system. *J. Micromechan. Microeng.*, **22**, 085014.

72. Shim, J. H., Kim, J. Y., Park, M., et al. (2011). Development of a hybrid scaffold with synthetic biomaterials and hydrogel using solid freeform fabrication technology, *Biofabrication*, **3**, 034102.

73. Shin, T. J., Park, S. Y., Kim, H. J., et al. (2010). Development of 3-D p oly(trimethylenecarbonate-co-epsilon-caprolactone)-block-poly (p-dioxanone) scaffold for bone regeneration with high porosity using a wet electrospinning method, *Biotechnol. Lett.*, **32**, 877–882.

74. Smith, L. A., Ma, P. X. (2004). Nano-fibrous scaffolds for tissue engineering, *Colloids Surf. B Biointerf.*, **39**, 125–131.

75. Sun, C., Jin, X., Holzwarth, J. M., et al. (2012). Development of channeled nanofibrous scaffolds for oriented tissue engineering, *Macromol. Biosci.*, **12**, 761–769.

76. Sun, L., Zhang, L., Hemraz, U. D., et al. (2012). Bioactive rosette nanotube-hydroxyapatite nanocomposites improve osteoblast functions, *Tissue Eng. Part A*, **18**, 1741–1750.

77. Sun, Y., Finne-Wistrand, A., Albertsson, A. C., et al. (2012). Degradable amorphous scaffolds with enhanced mechanical properties and homogeneous cell distribution produced by a three-dimensional fiber deposition method, *J. Biomed. Mater. Res. A*, **100**, 2739–2749.

78. Tarafder, S., Balla, V. K., Davies, N. M., et al. (2012). Microwave-sintered 3D printed tricalcium phosphate scaffolds for bone tissue engineering, *J. Tissue Eng. Regen. Med.*, **7**, 631–641.

79. Tel-Vered, R., Yehezkeli, O., Willner, I. (2012). Biomolecule/nanomaterial hybrid systems for nanobiotechnology, *Adv. Exp. Med. Biol.*, **733**, 1–16.

80. Thorvaldsson, A., Stenhamre, H., Gatenholm, P., et al. (2008). Electrospinning of highly porous scaffolds for cartilage regeneration, *Biomacromolecules*, **9**, 1044–1049.

81. Toyokawa, N., Fujioka, H., Kokubu, T., et al. (2010). Electrospun synthetic polymer scaffold for cartilage repair without cultured cells in an animal model, arthroscopy: *J. Arthroscopic. Amp. Relat. Surg.*, **26**, 375–383.

82. Vacanti, J. P., Langer, R. (1999). Tissue engineering: The design and fabrication of living replacement devices for surgical reconstruction and transplantation, *Lancet*, **354**, Suppl. 1, SI32–34.

83. van der Zande, M., Walboomers, X. F., Olalde, B., et al. (2011). Effect of nanotubes and apatite on growth factor release from PLLA scaffolds, *J. Tissue Eng. Regen. Med.*, **5**, 476–482.

84. Visconti, R. P., Kasyanov, V., Gentile, C., et al. (2010). Towards organ printing: Engineering an intra-organ branched vascular tree, *Expert Opin. Biol. Ther.*, **10**, 409–420.

85. Wang, Q., McGoron, A. J., Pinchuk, L., et al. (2010). A novel small animal model for biocompatibility assessment of polymeric materials for use in prosthetic heart valves, *J. Biomed. Mater. Res. A*, **93**, 442–453.

86. Xie, F., Weiss, P., Chauvet, O., et al. (2010). Kinetic studies of a composite carbon nanotube-hydrogel for tissue engineering by rheological methods, *J. Mater. Sci. Mater. Med.*, **21**, 1163–1168.

87. Xu, C., Chai, W., Huang, Y., et al. (2012). Scaffold-free inkjet printing of three-dimensional zigzag cellular tubes, *Biotechnol. Bioeng.*, **109**, 3152–3160.

88. Yaszemski, M. J., Payne, R. G., Hayes, W. C., et al. (1995). The ingrowth of new bone tissue and initial mechanical properties of a degrading polymeric composite scaffold, *Tissue Eng.*, **1**, 41–52.

89. Yeo, M., Lee, H., Kim, G. (2010). Three-dimensional hierarchical composite scaffolds consisting of polycaprolactone, β-tricalcium phosphate, and collagen nanofibers: Fabrication, physical properties, and in vitro cell activity for bone tissue regeneration, *Biomacromolecules*, **12**, 502–510.

90. Yoon, H., Kim, G. (2011). A three-dimensional polycaprolactone scaffold combined with a drug delivery system consisting of electrospun nanofibers, *J. Pharm. Sci.-US*, **100**, 424–430.

91. Yoshimoto, H., Shin, Y. M., Terai, H., et al. (2003). A biodegradable nanofiber scaffold by electrospinning and its potential for bone tissue engineering, *Biomaterials*, **24**, 2077–2082.

92. Yu, B. Y., Chen, P. Y., Sun, Y. M., et al. (2012). Response of human mesenchymal stem cells (hMSCs) to the topographic variation of poly(3-hydroxybutyrate-co-3-hydroxyhexanoate) (PHBHHx) films, *J. Biomater. Sci. Polym. Ed.*, **23**, 1–26.

93. Yun H. S., K. S., Khang D. W., Choi J. I., Kim H. H., Kang M. J. (2011). Biomimetic component coating on 3D scaffolds using high bioactivity of mesoporous bioactive ceramics *Intl. J. Nanomed.*, **6**, 2521–2531.

94. Zhang, A. P., Qu, X., Soman, P., et al. (2012). Rapid fabrication of complex 3D extracellular microenvironments by dynamic optical projection stereolithography, *Adv. Mater.*, **24**, 4266–4270.

95. Zhang, K., Choi, H. J., Kim, J. H. (2011). Preparation and characteristics of electrospun multiwalled carbon nanotube/polyvinylpyrrolidone nanocomposite nanofiber, *J. Nanosci. Nanotechnol.*, **11**, 5446–5449.

96. Zhang, L., Hemraz, U. D., Fenniri, H., et al. (2010). Tuning cell adhesion on titanium with osteogenic rosette nanotubes, *J. Biomed. Mater. Res. A*, **95**, 550–563.

97. Zhang, L., Zhou, Y., Zhu, J., et al. (2012). An updated view on stem cell differentiation into smooth muscle cells, *Vascul. Pharmacol.*, **56**, 280–287.

98. Zhang, Q., Mochalin, V. N., Neitzel, I., et al. (2011). Fluorescent PLLA-nanodiamond composites for bone tissue engineering, *Biomaterials*, **32**, 87–94.

99. Zhao, J., Han, W., Chen, H., et al. (2012). Fabrication and in vivo osteogenesis of biomimetic poly(propylene carbonate) scaffold with nanofibrous chitosan network in macropores for bone tissue engineering, *J. Mater. Sci. Mater. Med.*, **23**, 517–525.

100. Zhou, C., Ma, L., Li, W., et al. (2011). Fabrication of tissue engineering scaffolds through solid-state foaming of immiscible polymer blends, *Biofabrication*, **3**, 045003.

101. Zhou, H., Lawrence, J. G., Bhaduri, S. B. (2012). Fabrication aspects of PLA-CaP/PLGA-CaP composites for orthopedic applications: A review, *Acta Biomater.*, **8**, 1999–2016.

Chapter 34

Nanomedicine for Acute Lung Injury/Acute Respiratory Distress Syndrome: A Shifting Paradigm?

Ruxana T. Sadikot, MD,[a] and Israel Rubinstein, MD[b,c]

[a]*Emory University, Atlanta Georgia, USA*
[b]*Jesse Brown VA Medical Center, Chicago, Illinois, USA*
[c]*University of Illinois at Chicago College of Medicine, Section of Pulmonary, Critical Care, Sleep and Allergy, Chicago, Illinois, USA*

Keywords: nanomedicine, acute lung injury, acute respiratory distress syndrome, TREM-1, triggering receptor expressed on myeloid cells GLP-1, glucagon-like peptide-1(7–36) amide 17-AAG, SSM, sterically stabilized phospholipid micelles

34.1 Introduction

This chapter discusses the opportunities that nanomedicine offers to develop targeted therapies in diseases such as acute lung injury (ALI) and acute respiratory distress syndrome (ARDS), which have an abysmal prognosis. The mortality rate from ARDS remains unacceptably high, ranging from 34 to 64%. Hence, there is a

Handbook of Clinical Nanomedicine: Nanoparticles, Imaging, Therapy, and Clinical Applications
Edited by Raj Bawa, Gerald F. Audette, and Israel Rubinstein

ISBN 978-981-4669-20-7 (Hardcover), 978-981-4669-21-4 (eBook)
www.panstanford.com

need for effective pharmacotherapies to treat ARDS. Although several promising therapies are currently being identified for the treatment of ARDS, the delivery of these potential targets, particularly peptides and proteins, to the lung is also an ongoing challenge. Nanoscience and nanotechnology are the basis of innovative techniques that offer great potential of delivery of drugs targeted to the site of inflamed lungs. Nanoscale drug delivery systems have the ability to improve the pharmacokinetics and increase the biodistribution of therapeutic agents to target organs which results in improved efficacy while reducing the drug toxicity. These systems are exploited for therapeutic purpose to carry the drug in the body in a controlled manner from the site of administration to the therapeutic target. To this end, we have identified several potential targets and proposed the delivery of these agents using nanomicelles to improve the drug delivery.

In recent years, nanomedicine has become an attractive concept for the targeted delivery of therapeutic and diagnostic compounds to the lung [1–11]. Nanoscale drug delivery systems improve the pharmacokinetics, biodistribution and bioactivity of loaded drugs by prolonging circulation time, reducing the dose administered, and passively targeting to inflamed and injured organs through hyperpermeable ("leaky") microcirculation.

Among various drug delivery systems considered for pulmonary application, the use of biocompatible and biodegradable lipid-based and polymeric nanoparticles represents several advantages for the treatment of respiratory diseases. A number of different strategies have been proposed for modification of nanoparticle characteristics to control their behavior within biological environments, like cell-specific targeted drug delivery or modified biological distribution of drugs, both at the cellular and organ level. Thus, this method of targeted drug delivery to the lung is particularly attractive for inflammatory conditions such ALI and ARDS [4, 12–15].

Despite recent advances in diagnostic and therapeutic modalities, acute lung injury (ALI) and acute respiratory distress syndrome (ARDS) still represents an unmet medical need because it is associated with appreciable morbidity and mortality (30–40%) and substantial medical expenditure [16–18]. Hence, there is an urgent need to develop and test new drugs to treat this devastating disorder [19]. Unfortunately, contemporary drug development

approaches to address this challenge that center on mono-metabolic pathway inhibitors are hindered by diverse mechanisms underlying ALI and ARDS pathogenesis and by non-selective drug effects that could predispose to serious adverse events [20].

To overcome both barriers, we emulated the clinical success of combination therapy in cancer and HIV by devising an innovative nanopharmacotherapeutic strategy consisting of combination of 3 long-acting and safe nanomedicines that selectively target and inhibit three distinct key intracellular pro-inflammatory signaling cascades activated in ALI and ARDS [20]. Accordingly, we have harnessed unique attributes of three novel, long-acting, biocompatible, and biodegradable anti-inflammatory nanomedicines. They consist of two amphipathic peptide drugs, human glucagon-like peptide-1(7–36) amide (GLP-1) and triggering receptor expressed on myeloid cells (TREM-1) peptide, and 17-allylamino-17-demethoxygeldanamycin (17-AAG), a water-insoluble cytotoxic drug. This innovative approach consists of self-assembly of each drug with generally regarded as safe (GRAS) distearoylphosphatidylethanolamine covalently linked to polyethylene glycol of molecular weight 2000 (DSPE-PEG_{2000}), a component of FDA-approved Doxil®, that forms long-acting, biocompatible and biodegradable sterically stabilized phospholipid micelles in aqueous milieu (SSM; size ~15 nm) [20].

34.2 ALI and ARDS

ALI and ARDS arise from direct and indirect injury to the lungs and result in a life-threatening form of respiratory failure with diffuse, bilateral lung injury and severe hypoxemia caused by non-cardiogenic pulmonary edema, which affects approximately 1 million people worldwide annually [18]. As with other inflammatory processes, lung inflammation is accompanied by many cellular and biochemical processes; some of them are specific to the syndrome and include injury to both the pulmonary capillary endothelium and the alveolar epithelium [21, 22]. The importance of ALI and ARDS has been highlighted by the emergence of SARS (severe acute respiratory syndrome). ALI and ARDS are a leading cause of morbidity and mortality in the USA [16–18]. The major reason underlying the lag in improvement in outcome is the lack

of novel and specific therapies for ALI and ARDS. Thus, both ALI and ARDS represent an unmet medical need, and there is an urgent need to develop novel therapies for this condition.

The molecular pathobiology of ALI and ARDS is being extensively defined and the role of several molecules, including pattern recognition receptors present on the immune cells such as Toll-like receptors and downstream signaling molecules such as NF-κB and effector molecules such as TNF-α and IL-1β, are being investigated in the pathogenesis and treatment of acute lung injury and ARDS [22]. Targeting central molecules such as NF-κB attenuates lung inflammation but has major limitations because the inhibition of NF-κB is immunosuppressive and compromises host defense [22]. However, because of the complex nature of the disease, targeting single cytokine or chemokine has also failed to attenuate lung inflammation as these are not sufficient singly to attenuate lung inflammation in ALI and ARDS [17].

Thus, we propose innovative approaches that involve (1) targeting multiple upstream molecules (triggering receptor expressed on myeloid cells (TREM-1), reactive oxygen species and Hsp90 that lead to activation of NF-κB ultimately leading to ALI and ARDS with poor outcomes in many cases; (2) developing a novel approach to deliver inhibitors of these molecules *in vivo*. We have previously shown that these individual nanoformulations are effective at attenuating lung inflammation; and (3) using combination therapeutic approach, which involves three distinct intracellular metabolic pathways likely to be successful as it is in patients with cancer [20].

34.3 Nanomedicine for ALI and ARDS

34.3.1 Nanoparticles and Nanoscale Drug Delivery

Nanoparticles have potential application in medical field, including diagnostics and therapeutics. Nanoscale drug delivery systems have the ability to improve the pharmacokinetics and increase the biodistribution of therapeutic agents to target organs, which results in improved efficacy and reduces drug toxicity [7, 23–25]. Nanocarriers are particularly designed to target inflammation and cancer, which have permeable vasculature. Additionally, several nanocarriers have the desirable advantage of improving solubility

of hydrophobic compounds in the aqueous media to render them suitable for parenteral administration. In particular, delivery systems have shown to increase the stability of a wide variety of therapeutic agents such as hydrophobic molecules, peptides, and oligonucleotides [20, 23, 24].

These systems are exploited for diagnostic and therapeutic purposes to carry the drug in the body in a controlled manner from the site of administration to the therapeutic target [2, 9, 11, 12, 15]. This implies the trafficking of drug molecules and drug delivery system across numerous physiological barriers, which represents the most challenging goal in drug targeting. Nanoparticles can be constructed by various methodologies so that effect can be targeted at the desired site [8, 15, 20, 23, 24, 25].

34.3.2 How Do We Apply Nanomedicine to ALI and ARDS

To begin to address the role of nanomedicine in treating ALI and ARDS, we developed novel long-acting biocompatible and biodegradable phospholipid micelles (hydrodynamic size, ~15 nm) to modulate key signaling molecules that are critical to the inflammatory response in ALI and ARDS [21, 23–25]. We selected molecules that initiate and propagate inflammatory response by distinct mechanisms so that multiple pathways can be targeted either singly or by a combinatorial approach. Among these, triggering receptor expressed on myeloid cells (TREM-1), reactive oxygen species and Hsp90 were initially selected to modulate the inflammatory response in the lung [20].

Realizing short half-life of peptide drugs (minutes) hampers their clinical use, we invented micellar TREM-1 peptide and human glucagon-like peptide-1(7–36) amide (GLP-1), a 29-amino acid pleiotropic immunomodulator, where each peptide drug is stabilized in its active form (α-helix) and its bioactivity is prolonged for hours *in vivo*. Likewise, water-insolubility of 17-allylamino-17-demethoxygeldanamycin (17-AAG), a selective Hps90 inhibitor, constrains its use in humans. Accordingly, self-association of 17-AAG with these micelles overcomes this limitation while at the same time increasing its stability and bioavailability. These long-acting micellar drugs provide significant advancement in the treatment of experimental of ALI, which could then be extended

to critically ill patients. Nanoparticles can be introduced by systemic administration, such as oral, dermal and intravenous, or directly introduced into the lung through inhalation, intranasal, or oropharyngeal aspiration.

In a recent study, we tested the efficacy of GLP-1 nanomicelles in a rat model of lipopolysaccharide (LPS)-induced lung injury [24]. *In vivo* administration of GLP1-SSM to LPS-induced ALI rats resulted in significant downregulation of lung inflammation, with dose-dependent anti-inflammatory activity observed. Similar therapeutic activity was not detected for GLP- 1 in saline, indicating that these nanocarriers played a critical role in protecting the enzyme-labile GLP-1 and delivering it to inflamed tissues *in vivo*. This study showed that a lipid-based nanoformulation of GLP-1 is effective at attenuating inflammation in ALI and ARDS [23]. We have also tested the efficacy of TREM-1 nanomicellar peptide in a model of LPS-induced sepsis and lung injury and shown that TREM-1 nanomicelles are more efficacious than the naked peptide at abrogating inflammation [20]. Studies with other nanomicellar preparations such as 17 AAG for treatment of ALI and ARDS are currently ongoing in our laboratory [20]. Together, our studies demonstrate the feasibility of translating the use of these nanomicellar preparations for translational human studies to the clinics to treat this devastating disease. We posit that combinatorial administration of nanomicelles that modulate distinct signaling pathways will prove to be more potent but will need further studies to optimize the administration of the nanopreparations.

34.4 Nanomedicine for Drug Delivery to the Lung

34.4.1 Nanomedicine Targeted to Lung

We have used nanomicellar preparations for targeted delivery of drugs to the lung using systemic administration. Micelles are self-assemblies of amphiphiles that form supramolecular core–shell structures in the aqueous environment. Hydrophobic interactions are the predominant driving force in the assembly of the amphiphiles in the aqueous medium when their concentrations

exceed the critical micellar concentration. Sterically stabilized phospholipid micelles (SSM) are a novel, long-acting, biocompatible, and biodegradable phospholipid-based drug delivery platform that was developed and patented in our laboratory as versatile carrier for peptide and water-insoluble drugs [20, 23–25].

Our approach entails self-assembly of distearoylphosphatidyl-ethanolamine covalently linked to polyethylene glycol of molecular weight 2000 (DSPE-PEG_{2000}) with drugs such as GLP-1 to form long-acting sterically stabilized phospholipid micelles in aqueous milieu (hydrodynamic size ~15 nm) [20, 23–25]. These micelles are composed of hydrophilic corona that houses amphipathic peptide drugs, such as TREM-1 peptide and GLP-1, and hydrophobic core that accommodates water-insoluble drugs, such as 17-AAG. They are simple to prepare and, unlike liposomes, can be stored in lyophilized form without lyo- or cryo-protectants for extended period of time. Lipid-based nanomicelles stabilize TREM-1 peptide and GLP-1 in active biological form (α-helix), which is preferred for ligand–receptor interactions, and prevents rapid peptide degradation *in vivo* thereby prolonging bioactivity. In addition, SSM solubilize high concentrations of 17-AAG [20].

Unlike surfactant micelles, low critical micellar concentration (~1 μM) of these nanoparticles prevents their disintegration upon dilution in biological fluids. Importantly, the PEG_{2000} moiety of SSM confers steric hindrance in the circulation while their nanosize mitigates renal clearance and extravasation from intact microvessels. This, in turn, prolongs circulation time of drug-loaded micelles and promotes preferential extravasation from hyperpermeable lung microcirculation, the hallmark of ALI and ARDS, into injured lung [23–25].

34.4.2 Drug Delivery of Nanoparticles

Systemic delivery of these agents is based on the principle of passive targeting. Passive targeting occurs due to extravasation of the nanoparticles at the diseased site where the microvasculature is leaky [6]. Examples of diseases where passive targeting of nanocarriers can be achieved are tumor and inflamed tissues. Microvascular leakiness in ALI and ARDS is the result of increased permeability and the presence of cytokines and other vasoactive factors that enhance permeability [21]. Thus, drugs used for

treatment of ALI and ARDS can be administered systemically and will localize to the lungs by passive targeting. We propose that this innovative passively targeted therapeutic strategy amplifies drug delivery to lung thereby maximizing efficacy and enhancing resolution of inflammation while reducing collateral damage to innocent bystander organs as occurs in patients with ALI and ARDS.

Controlled drug delivery systems have also become increasingly attractive options for inhalation therapies [1, 2, 4, 7, 11–15]. The large surface area of the lungs and the minimal barriers impeding access to the lung periphery make this organ a suitable portal for a variety of therapeutic interventions. The blood barrier between the alveolar space and the pulmonary capillaries is very thin to allow for rapid gas exchange. Alveoli are small and there are approximately 300 million of them in each lung. Although alveoli are tiny structures, they have a very large surface area in total (~100 m^2) for performing efficient gas exchange making it an attractive organ for direct drug delivery [6, 17, 21]. Among various drug delivery systems considered for pulmonary application, nanoparticles demonstrate several advantages for the treatment of respiratory diseases, like prolonged drug release, cell specific targeted drug delivery or modified biological distribution of drugs, both at the cellular and organ level [1, 6, 10, 11, 15]. Nanoparticles composed of biodegradable lipid-based nanomicelles and polymers fulfill many requirements placed on these delivery systems, such as ability to be transferred into an aerosol, stability against forces generated during aerosolization, biocompatibility, targeting of specific sites or cell populations in the lung, release of the drug in a predetermined manner, and degradation within an acceptable period of time [8, 15, 23, 24]. Clearly, further studies are warranted to establish the role of aerosolized nanopreparations for inhalational therapy.

34.5 Conclusions

Nanomedicine, the medical application of nanobiotechnology, holds great promise in treatment of serious lung disorders that still represent unmet medical needs, such as ALI and ARDS. To this end, multifunctional engineered lipid- and polymer-based

nanoparticles are particularly advantageous because they could deliver simultaneously several drugs that selectively target distinct metabolic pathways that modulate ALI and ARDS without undue systemic toxicity. Undoubtedly, recent progress witnessed in this nascent field of biomedical research should be translated into clinical practice in the near future.

Disclosures and Conflict of Interest

The authors declare that they have no conflict of interest and have no affiliations or financial involvement with any organization or entity discussed in this chapter. This includes employment, consultancies, honoraria, grants, stock ownership or options, expert testimony, patents (received or pending) or royalties. No writing assistance was utilized in the production of this chapter and the authors have received no payment for its preparation.

Corresponding Author

Dr. Ruxana T. Sadikot
Emory University School of Medicine
Section of Pulmonary and Critical Care Medicine
201 Dowman Drive, Atlanta, GA 30322, USA
Email: ruxana.sadikot@emory.edu

About the Authors

Ruxana T. Sadikot is a professor of medicine at Emory University and is the chief of section of pulmonary and critical care medicine at the Atlanta VAMC. She received her medical training from the University of Bombay, India, and from Royal College of Physicians, London, UK. She received her Pulmonary and Critical Care training at Vanderbilt University in Nashville, TN, USA. Dr. Sadikot is funded by the US Department of Veterans Affairs and her research focuses on understanding the mechanisms of lung injury and immune response.

Israel Rubinstein is professor at the University of Illinois at Chicago College of Medicine in Chicago, Illinois, USA. He is also Director, Respiratory Therapy, Jesse Brown VA Medical Center in Chicago. He obtained an MD from the Hebrew University-Hadassah School of Medicine in Jerusalem, Israel. His clinical and research interests include nanomedicine, targeted drug delivery, and bioimaging.

References

1. Azarmi, S., Roa, W. H., Loebenberg, R. (2008). Targeted delivery of nanoparticles for the treatment of lung diseases. *Adv. Drug Deliv. Rev.,* **60**, 863–875.
2. Buxton, D. B. (2009).Nanomedicine for the management of lung and blood diseases. *Nanomedicine* (Lond.), **3**, 331–339.
3. Bur, M., Henning, A., Hein, S., Schneider, M., Lehr, C. M. (2009). Inhalative nanomedicine: Opportunities and challenges. *Inhal. Toxicol.,* **21,** 137–143.
4. Dames, P., Gleich, B., Flemmer, A., Hajek, K., Seidl, N., Wiekhorst, F., Eberbeck, D., Bittmann, I., Bergemann, C., Weyh, T., Trahms, L., Rosenecker, J., Rudolph, C. (2007). Targeted delivery of magnetic aerosol droplets to the lung. *Nat. Nanotechnol.,* **2**, 495–499.
5. Mansour, H. M., Rhee, Y. S., Wu, X. (2009). Nanomedicine in pulmonary delivery. *Int. J. Nanomed.* (Lond.), **4**, 299–319.
6. Pison, U., Welte, T., Giersig, M., Groneberg, D. A. (2006). Nanomedicine for respiratory diseases. *Eur. J. Pharmacol.,* **533**, 341–350.
7. Rudolph, C., Gleich, B., Flemmer, A. W. (2010). Magnetic aerosol targeting of nanoparticles to cancer: Nanomagnetosols. *Methods Mol. Biol.,* **624**, 267–280.
8. Rytting, E., Nguyen, J., Wang, X., Kissel, T. (2008). Biodegradable polymeric nanocarriers for pulmonary drug delivery. *Expert Opin. Drug Deliv.,* **5**, 629–639.
9. Smola, M., Vandamme, T., Sokolowski, A. (2008). Nanocarriers as pulmonary drug delivery systems to treat and to diagnose respiratory and non respiratory diseases. *Int. J. Nanomed.,* **3**, 1–19.
10. Sung, J. C., Pulliam, B. L., Edwards, D. A. (2007). Nanoparticles for drug delivery to the lungs. *Trends Biotechnol.,* **25**, 563–570.
11. Yang, W., Peters, J. I., Williams, III, R. O. (2008). Inhaled nanoparticles—a current review. *Int. J. Pharm.,* **356**, 239–247.

12. Bailey, M. M., Berkland, C. J. (2009). Nanoparticle formulations in pulmonary drug delivery. *Med. Res. Rev.,* **29**, 196–212.
13. Beck-Broichsitter, M., Gauss, J., Gessler, T., Seeger, W., Kissel, T., Schmehl, T. (2010). Pulmonary targeting with biodegradable salbutamol-loaded nanoparticles. *J. Aerosol Med. Pulm. Drug Deliv.,* **23**, 47–57.
14. Roy, I., Vij, N. (2010). Nanodelivery in airway diseases: Challenges and therapeutic applications. *Nanomedicine* (*Lond.*), **6**, 237–244.
15. Yacobi, N. R., Demaio, L., Xie, J., Hamm-Alvarez, S. F., Borok, Z., Kim, K. J., Crandall, E. D. (2008). Polystyrene nanoparticle trafficking across alveolar epithelium. *Nanomedicine (Lond.),* **4**, 139–145.
16. Girard, T. D., Bernard, G. B. (2007). Mechanical ventilation in ARDS: A state-of-the-art review. *Chest,* **131**, 921–929.
17. Matthay M. A. (2008). Treatment of acute lung injury: Clinical and experimental studies. *Proc. Am. Thorac. Soc.,* **5**, 297–299.
18. Rubenfeld, G. D., Herridge, M. S. (2007). Epidemiology and outcomes of acute lung injury. *Chest,* **131**, 554–562.
19. Sadikot, R. T., Christman, J. W., Blackwell, T. S. (2004). Molecular targets for modulating lung inflammation and injury. *Curr. Drug Targets,* **5**, 581–588.
20. Sadikot, R. T., Rubinstein, I. (2009). Long-acting, multi-targeted nanomedicine: Addressing unmet medical need in acute lung injury. *J. Biomed. Nanotechnol.,* **5**, 614–619.
21. Matthay, M. A., Ware, L. B. (2000). The acute respiratory distress syndrome. *N. Engl. J. Med.,* **342**, 1334–1349.
22. Sadikot, R. T., Zeng, H., Joo, M., Everhart, M. B., Sherrill, T. P., Li, B., Cheng, D. S., Yull, F. E., Christman, J. W., Blackwell, T. S. (2006). Targeted immunomodulation of the NF-kappaB pathway in airway epithelium impacts host defense against Pseudomonas aeruginosa. *J. Immunol.,* **176**, 4923–4930.
23. Koo, O. M., Rubinstein, I., Önyüksel, H. (2005). Role of nanotechnology in targeted drug delivery and imaging: A concise review. *Nanomedicine (Lond.),* **1**, 193–212.
24. Lim, S. B., Rubinstein, I., Sadikot, R. T., Artwohl, J. E., Onyüksel, H. (2011). A novel peptide nanomedicine against acute lung injury: GLP-1 in phospholipid micelles. *Pharm. Res.,* **28**, 662–672.
25. Rubinstein, I., Önyüksel, H. (2007). Biocompatible, biodegradable and sterically stabilized phospholipid nanomicelles improve cryopreservation of oral keratinocytes: A preliminary investigation. *Int. J. Pharm.,* **338**, 333–335.

Chapter 35

Nanoviricides: Targeted Anti-Viral Nanomaterials

Randall W. Barton, PhD, Jayant G. Tatake, PhD, and Anil R. Diwan, PhD

NanoViricides, Inc., West Haven, Connecticut, USA

Keywords: polymeric micelles, anti-viral agents, virus-specific targeting, polyethylene glycol, nanoviricide, virus neutralization, influenza virus, receptor-based interaction, cooperative binding, biomimicry

35.1 Introduction

Polymeric micelles have been exploited as nanomedicines because of several properties [1]. They can be composed of biocompatible amphiphilic block polymers with the capability of self-assembly in sizes ranging from 10 to 200 nm. Because of their unique core–shell structure, polymeric micelles have the capacity to solubilize hydrophobic drugs resulting in dose ranges that are clinically relevant. Also, polymeric micelles can be modified with molecules that specifically target the receptors expressed on the surface of cells, tissues, viruses, or bacteria.

Handbook of Clinical Nanomedicine: Nanoparticles, Imaging, Therapy, and Clinical Applications
Edited by Raj Bawa, Gerald F. Audette, and Israel Rubinstein

ISBN 978-981-4669-20-7 (Hardcover), 978-981-4669-21-4 (eBook)
www.panstanford.com

A micelle consists of a corona formed by the hydrophilic blocks extending into the aqueous solution and a core formed by the hydrophobic segments. In order to achieve biocompatibility and ability to evade host defense mechanisms, the hydrophilic block is generally a derivative of polyethylene glycol (PEG). The composition of the hydrophobic block varies enormously, which can be tailored to encapsulate drug molecules with a variety of structures, lipophilicity, and charges, contributing to the versatility of polymeric micelles as drug carriers [1–8].

35.2 Nanoviricides Polymeric Micelle Technology

NanoViricides, Inc., exploits its family of patented and proprietary polymeric micelle structures to develop its unique nanomedicines. This uniform (not random) polymer is made of a monomer that is composed of (a) an amphiphilic PEG chain, and (b) a multi-functional connector. The connector has covalently attached multiple lipid chains per monomer, thus resembling a biological lipid. In addition, the connector has multiple functional groups that enable attachment of specific targeting moieties that facilitate receptor-based interaction with a cell, virus, bacterium, or another assembly. Multiple chains come together to form micelles of 15–20 nm and larger sizes. These micelles enable the encapsulation of lipidic, amphiphilic, and aromatic guest molecules. These micelles exhibit the receptor ligand interactions, thus resembling microsomes or biological structures. Upon binding to its target via multipoint interactions, the micelle is capable of lipid–lipid fusion with the biological membrane of the target and thereby enables the transport of the encapsulated cargo, if present, into the target cell, virus particle, or bacterium. Immediately upon injection into the bloodstream, the solution undergoes infinite dilution, and yet the assembly remains intact because even the smallest structure remains micellar with this unique polymeric micelle chemistry. This is unlike liposomes, which fall apart upon injection, resulting in injection site reactions as well as significant “dumping” of the payload active pharmaceutical ingredient (API) long before reaching its target. This is described graphically in Figs. 35.1 and 35.2.

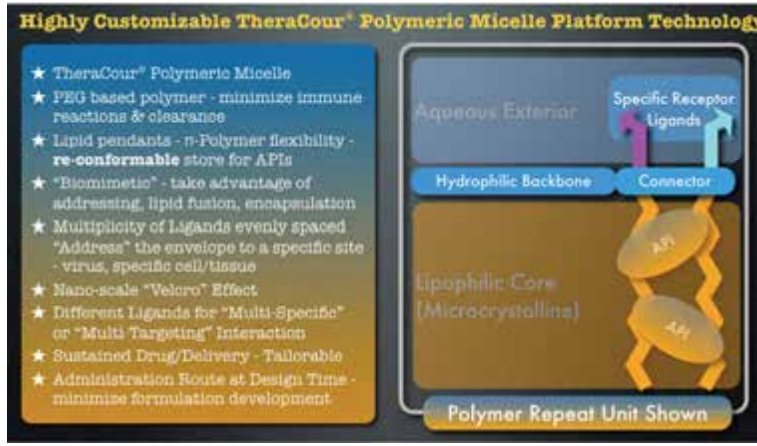

Figure 35.1 Description of the TheraCour polymeric micelle technology.

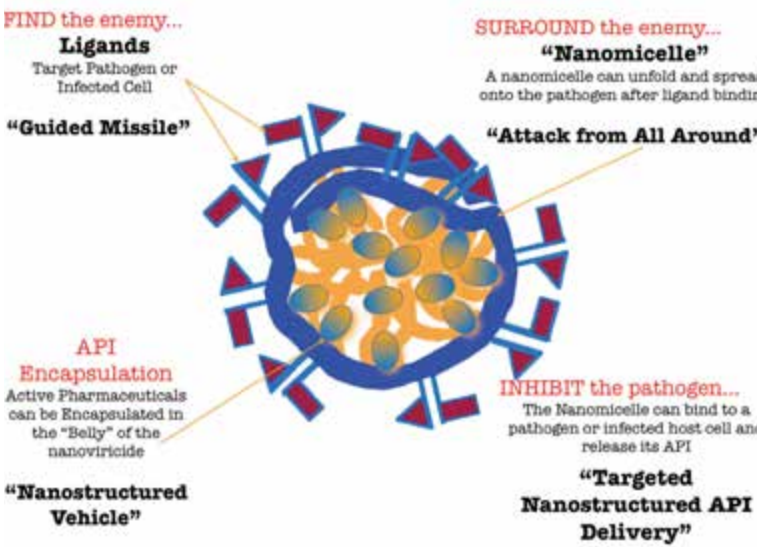

Figure 35.2 The properties of the polymeric micelle technology that can be individually tailored for specific mechanisms of action of the drug.

This biomimetic, yet chemically well-defined structure provides several additional advantages over other technologies. The chemistry creates inherently safe polymers, as demonstrated

by our antiviral drug developments. Several properties of the drug can be individually tailored by alterations in specific segments. The PEG chain length (m) is varied to obtain desired amphiphilicity (hydrophilic/hydrophobic balance) and solubility properties for the entire targeted, API-encapsulating nanostructured micelle. The fatty acid chain length (k) and type can be varied at will, to tailor the lipophilicity as well as to introduce biologically important lipids such as arachidonic acid, cholesterol derivatives, or other functional groups that may provide specific advantages. The overall polymer size (degree of polymerization, n; and overall polymer chemistry) can be tailored to enable (a) oral uptake and activity, and/or (b) a very long circulating lifetime with $t_{1/2}$ that may be of the order of 14 days or longer, based on anti-viral efficacy data in animals. The polymer can be designed with distinct, covalently attached, ligands that home onto different receptors.

Such multi-specific targeting may enable greater discrimination of the target than a single ligand may afford. At each monomer-connector site, we have been able to engineer multiple copies of a given ligand. This large ligand density is what enables the critical biomimicry necessary for successfully targeting certain cell types or viruses. The nanoviricide polymeric micelles provide a number of optimizable features that can be varied component-wise prior to synthesis to achieve desired design goals. The PEG chain length used as monomer (m); the size and nature of the lipid pendant used to introduce a hydrophobic core in aqueous media (p); the "connector" site chemistry at each repeat unit (C); the number of ligands attached per repeat unit (l); and their specific nature (L); the number of anionic charge groups on the surface (a); and their specific nature (A—e.g., sulfonate, carboxylate, other); the number of cationic groups attached per repeat unit (k) and their nature (B—e.g., substituted amines, imidazoles, guanidines, pyridines, etc.); and finally, the chain length of the overall polymer (and chain length distribution) (n) can all be varied over very large ranges of possible values using off the shelf available chemicals. There are thus six "numerical" degrees of freedom (m, p, l, a, k and n). In addition, there are at least four "categorical" degrees of freedom (C, L, A, and B).

Liposomes also provide a substantially large dimensional space. However, the composition ranges of stability of liposomes

tend to be very limited, and also highly temperature, as well as solvent (or fluid bulk) dependent. Liposomally encapsulated drugs are known to cause injection site reactions due to local deposition of the API. Liposomes are also in dynamic equilibrium, i.e., individual lipid molecules constantly dissociate and reassociate with individual liposomes. When injected into the bloodstream, a liposomal preparation undergoes infinite dilution and therefore the equilibrium is driven toward dissociation.

In contrast to liposomal systems, in our polymeric systems a single chain itself forms a micelle because of the pendant lipid chains coming together as a core and the PEG decorating them as the corona facing aqueous fluids, hence the phrase "polymeric micelles." The actual micelles in solution are much larger than that of a single micelle, usually encompassing multiple polymer chains, depending upon concentration, pH, and composition of the bulk fluid. In solution, the nanoviricide polymers exhibit a multi-modal distribution that changes with concentration while the particle sizes remain the same, indicating a phase-like equilibrium between different sizes of the population.

35.3 The Nanoviricide Antiviral Technology

NanoViricides, Inc., has employed its polymeric micelle technology to develop anti-viral agents that possess potent efficacy by targeting the mechanisms of cell attachment or cell binding of viruses. Unlike other polymeric micelle approaches that are dependent on the API encapsulation capability of the micelles, NanoViricides, Inc., utilizes its virus-targeted polymeric micelles to directly blunt viruses without the need for API encapsulation. When virus-specific ligands are chemically attached to a proprietary flexible polymer structure that mimics a biological cell membrane, a "nanoviricide®" is created. Our proprietary flexible polymer backbone is comprised of PEG and alkyl pendants. PEG forms the hydrophilic shell and imparts non-immunogenicity. The alkyl chains float together to make a flexible core, like an immobilized oil droplet. The resulting materials are polymeric surfactants that form stable micelles rather than liposomes, which form dynamic micelles. Thus, these nanoviricide micelles are freely soluble and conformationally flexible in bodily fluids.

Nanoviricide anti-viral agents are polymeric materials synthesized from subunits, so that the resulting polymer is a soluble, flexible material that is non-particulate, non-metallic, and non-accumulating in the body. An individual polymer chain would exist as a polymeric micelle in aqueous solutions by virtue of self-assembly driven by the lipid pendants incorporated in the monomer. The molecular size of an individual polymer chain is within the range of a medium to large size chemical drug substance that does not qualify as a nanomaterial under the "FDA Draft Guidance on Nanomedicines" [9]. (For a more exhaustive discussion on the definitional issues pertaining to nanomedicines and the FDA regulation of nanomedicines, refer to [10, 11].) Multiple polymer chains are capable of self-assembly in solution to form nanometer-scale micelles similar to liposomes, but less lipidic and more hydrophilic in nature than liposomes.

Chemical groups uniformly distributed along the polymer chain allow attachment of virus-specific ligands such as chemical moieties, peptides, antibody fragments or other proteins. On first contact with a virus particle, a nanoviricide micelle may bind to a virus particle because of specific interaction between a ligand attached to the nanoviricide and the glycoproteins on the virus surface. This may cause the flexible nanoviricide to reach very close to the virus surface, leading to additional ligands binding to additional viral coat proteins, in a mode called "cooperative binding." The attachment of multiple ligands to a single polymer chain coupled with the fact that multiple polymer chains make up a single micelle may lead to a very high avidity for the resulting micelle binding to the virus. This is analogous to the "Velcro" effect that results from cooperative interactions. This property enables the use of ligands that individually may have low affinity but the polyvalency can result in very high avidity. This concept has been shown quite convincingly with polymeric versus monomeric inhibitors in the scientific literature [12–14]. The company considers the nanoviricide construct a platform technology to target a spectrum of pathogenic virus species. Different virus-specific ligands can be conjugated to this PEG-based polymer backbone to produce different individual drug substances that specifically target different viral pathogens.

Viruses bind to specific cell surface ligands in order to attach to cells and internalize, e.g. sialic acid. These steps are primarily

where a neutralization strategy such as nanoviricides can be useful. A nanoviricide is designed to act like a decoy of a human cell. When the virus sees the appropriate ligand displayed on a nanoviricide micelle, the virus is believed to bind to it. As described graphically in Fig. 35.3, the nanoviricide, being flexible, could allow the maximization of binding by spreading onto the virus particle, and potentially leading to fusion with the lipid-coated virus surface by a phase-inversion, wherein the fatty core of the nanoviricide could merge with the viral lipid coat and the hydrophilic shell of the nanoviricide could become the exterior of the particle, thus potentially engulfing the virus. In the process, the coat proteins that the virus uses for binding to cells would be expected to become unavailable. This highly targeted surfactant attack may lead to loss of the coat proteins and the nanoviricide may further dismantle the engulfed virus capsid. The loss of virus particle integrity could render the virus non-infectious.

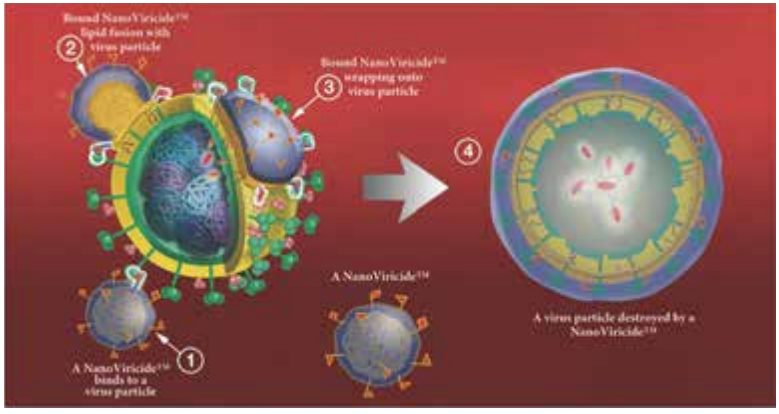

Figure 35.3 Graphic depiction of the putative mechanism of nanoviricide binding to and inactivation of viruses. The following steps are involved: (1) binding to a virus particle; (2) fusion with the viral lipid coat; (3) bound nanoviricide spreading onto viral particle; and (4) viral particle being engulfed by the nanoviricide.

Support for this mechanism is shown in Fig. 35.4 on the next page in the photomicrographs of murine cytomegalovirus (CMV) that has been incubated with a nanoviricide. As can be seen, the binding of the nanoviricide to the CMV results in loss of the viral envelope; the resulting CMV naked capsids are non-infectious. The

vehicle-treated, control MCMV remained intact. Thus, nanoviricide binding not only renders the CMV inactive but appears to result in the disruption of capsid organization. *In vivo* disrupted capsids would likely be rapidly cleared by host defense mechanisms.

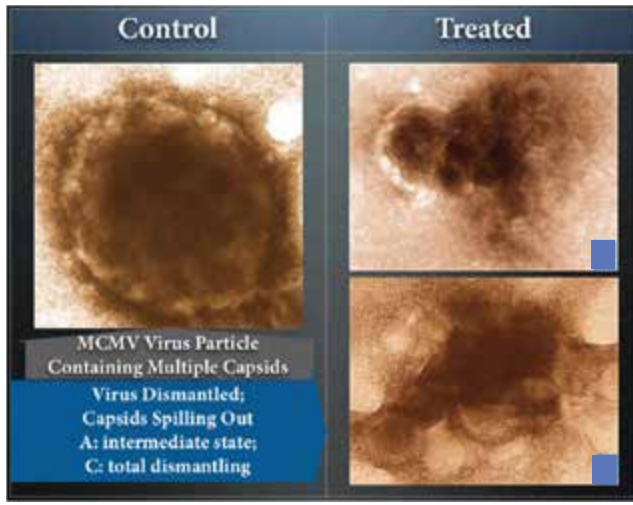

Figure 35.4 Electron photomicrographs of murine CMV. Control Panel: Untreated CMV; Treated Panel A & C: CMV incubated with a specific nanoviricide.

35.4 Nanoviricides Antiviral Effects

Influenza is a highly communicable acute respiratory disease that is considered to be one of the major infectious disease threats to the human population. During seasonal epidemics, 5–15% of the world population is typically infected, resulting in 36,000 to 5 million cases of severe illness affecting all age groups. Historically, each year in the United States, 5% to 20% of the population acquire influenza, more than 200,000 people are hospitalized from influenza-related complications, and approximately 36,000 people die from influenza-related causes [13]. The greatest risk to public health, however, is the emergence of influenza A viruses with HA antigens distinct from those formerly circulating, and for which immunity in the general population is lacking. Such novel viruses can spread rapidly and can result in a pandemic causing high levels of morbidity and mortality globally [16, 17].

Current inactivated seasonal influenza vaccines in the United States consist of trivalent preparations containing the hemagglutinin protein from two influenza A virus subtypes (H1N1 and H3N2) and the hemagglutinin protein from one influenza B virus strain. These vaccines elicit potent neutralizing antibody response to the influenza strains represented in the vaccine and to closely related isolates but only rarely extend to more diverged strains within a subtype and, especially, to other subtypes [15]. Therefore, the availability of potent antiviral agents for the prevention and/or treatment of both seasonal and pandemic influenza remains a clinical and public health priority. NanoViricides, Inc., has developed novel antiviral therapeutics that are believed to have potent activity against both influenza A and B viruses.

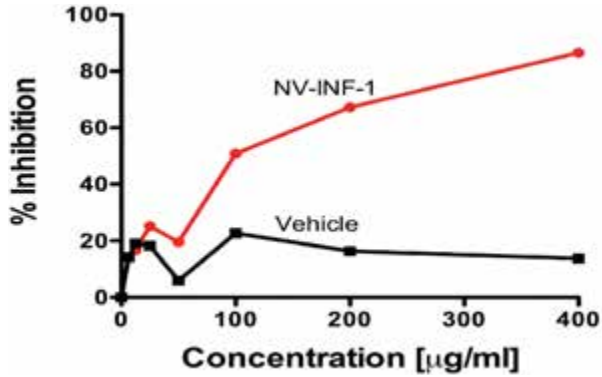

Figure 35.5 Effect of varying concentrations of an anti-influenza nanoviricide, NV-INF-1, on the infectivity of influenza A virus strain, A/W/S (H1N1) on MDCK cells.

NanoViricides, Inc., has conducted structure–activity relationship studies employing molecular modeling focused on sialic acid as the ligand for the cell surface receptor that is required for cell infection by the influenza virus. One of the chemical synthetic products of those studies, NV-INF-1, was tested in a virus infection assay in which the influenza A virus strain A/W/S (H1N1) was pre-incubated for 1 h with varying concentrations of NV-INF-1, then added to MDCK cells, and incubated overnight. The extent of virus infection was measured using anti-influenza A nucleoprotein (NP) antibodies in a cellular ELISA format. As shown in Fig. 35.5,

concentrations of NV-INF-1 greater than 50 μg/mL in the virus-infected cell cultures markedly reduced influenza virus strain A/W/S infection as compared to vehicle control.

NV-INF-1 has also been evaluated in a mouse model of influenza virus infection in which 10,000 viral particles of influenza A virus strain A/W/S/ (H1N1) were administered to the animals as a nasal spray at time 0 and at 23 h after the initial viral infection. The survival and body weight results of one study are described. Groups of mice were given 100 μL of NV-INF-1 (30 mg/kg), vehicle, or saline on days 1, 3, 5, 7, 9, 10, 12, 14, 16, 18, and 20 after the first virus inoculation. One group of mice was treated with Oseltamivir, 20 mg/kg p.o., 2× daily for the duration of the study, beginning 24 h after the first virus inoculation. An additional group of infected mice were left untreated. As shown in Fig. 35.6, the infected, untreated mice, the saline-treated mice, and the vehicle-treated mice all died with a mean survival of slightly longer than 5 days, 5.2, 5.3, and 5.1 days, respectively. At the dose of virus inoculated, the Oseltamivir-treated mice had a mean survival of 8.1 days, whereas the mice treated with NV-INF-1 had a markedly longer mean survival of 20.9 days.

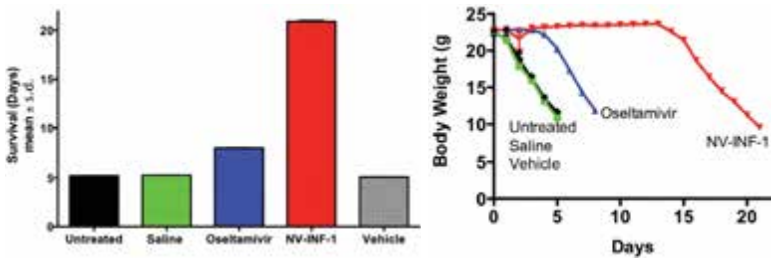

Figure 35.6 Effect of treatment with the anti-influenza nanoviricide, NV-INF-1, in mice infected with the influenza A virus strain A/W/S (H1N1).

As shown in Fig. 35.6, body weight began to decline by 2–3 days in the infected, untreated mice, the saline-treated mice and in the vehicle-treated mice and continued to decline until death. The Oseltamivir-treated mice maintained body weight through day 5 and then declined until death. Similar to the survival results, the mice treated with NV-INF-1 maintained their body weight

substantially longer through day 14 and then declined from day 15 thereafter until death.

The lungs of mice from each surviving group were evaluated for viral titers, weight, and histology. At day 4, the reduction in titers of influenza virus in the lungs of mice treated with NV-INF-1 in different experiments ranged from 20- to 1,000-fold compared with the virus titers measured in the infected, untreated mice and in the saline- and vehicle-treated mice. Following influenza virus infection, the infected mouse lungs showed a substantial increase in mass and histologically reveal substantial evidence of lesions caused by virus infection. Similar to the virus titers, the lungs from mice on day 4 that were treated with NV-INF-1 showed a substantially lower lung weight and displayed a markedly reduced presence of virus-induced lesions as compared to all control groups, untreated, saline-treated, and vehicle-treated.

Preliminary safety assessment as part of animal efficacy studies has not shown any overt adverse effects of treatment. Post-mortem investigation of animals after euthanasia under a dissection microscope revealed no lesions were found in the internal organs such as brain, liver, heart, diaphragm, and viscera. Visual observations of treated animals to assess neurological, respiratory problems, activity levels, and physical appearance revealed no observable adverse side effects.

In summary, NanoViricides has developed a polymeric micelle platform technology that has enabled the synthesis of potent anti-viral agents, specifically anti-influenza agents. These anti-influenza compounds compounds have been evaluated in mouse models of both H1N1 and H3N2 infections and they achieved substantially prolonged survival in these models of lethal infection. This prolonged survival was associated with marked reduction in both the virus-induced lung lesions and the titer of infectious virus recovered from the lungs. In contrast, Oseltamivir treatment in these same studies has resulted in substantially less protection in terms of survival, lung viral titers, and lung tissue damage.

Disclosures and Conflict of Interest

This work was supported by NanoViricides, Inc. Nanoviricide is a registered trademark of NanoViricides, Inc. The authors of this

chapter are employees of NanoViricides, Inc. No writing assistance was utilized in the production of this chapter and the authors have received no payment for its preparation.

Corresponding Author

Dr. Randall Barton
NanoViricides, Inc.
One Controls Drive
Shelton, CT 06484, USA
Email: rwbbarton@nanoviricides.com

About the Authors

Randall W. Barton is the chief scientific officer at NanoViricides, Inc., Shelton, CT, USA. Dr. Barton has over 25 years experience in drug discovery and development of both small molecule and biological therapeutics in virology, immunology, inflammation, oncology, and cardiovascular diseases in the pharmaceutical and biotech industry. He retired at the director level after 20 years at Boehringer Ingelheim Pharmaceuticals. Prior to joining Boehringer Ingelheim, Dr. Barton was on the faculty of the University of Connecticut School of Medicine. He has a PhD in biochemistry from the University of Tennessee at Oak Ridge National Laboratory and has authored over 80 scientific publications.

Jayant G. Tatake is vice-president of chemistry at NanoViricides, Inc., Shelton, CT, USA. He has over 25 years of experience in medicinal chemistry, synthetic organic chemistry, and analytical chemistry derived from both academic and industrial environments. He is co-inventor of the TheraCour polymeric micelle technology that is the backbone of the nanoviricide anti-viral agents. Dr. Tatake has led synthetic chemistry projects from concept to bench synthesis to production, encompassing chemical process development and analysis with successful transfer to pilot scale. He has a PhD in organic chemistry from Bombay University, India.

Anil R. Diwan is president and a founder of NanoViricides, Inc., Shelton, CT, USA. He is a co-inventor of the TheraCour polymeric micelle technologies that are the foundation of the nanoviricide anti-viral agents. He has over 25 years of bio-pharmaceutical R&D experience with over 20 years as an entrepreneur focused on the application of the platform technology upon which the nanoviricides technology is based. Dr. Diwan earned a BS in chemical engineering from the Indian Institute of Technology and a PhD in biochemical engineering from Rice University.

References

1. Gong, J., Chen, M., Zheng, Y., Wang, S., Wang, Y. (2012). Polymeric micelles drug delivery system in oncology. *J. Control. Release,* **159**, 312–323.
2. Xu, S., Olenyuk, B. Z., Okamoto, C. T., Hamm-Alvarez, S. F. (2013). Targeting receptor-mediated endocytotic pathways with nanoparticles: Rationale and advances. *Adv. Drug Deliv. Rev.,* **65,** 121–138.
3. Blanco, E., Kessinger, C. W., Sumer, B. D., Gao, J. (2009). Multifunctional micellar nanomedicine for cancer therapy. *Exp. Biol. Med.,* **234,** 123–131.
4. Kwon, G. S., Kataoka, K. (2012). Block copolymer micelles as long-circulating drug vehicles. *Adv. Drug Deliv. Rev.,* **64,** 237–245.
5. Torchilin, V. P. (2012). Multifunctional nanocarriers. *Adv. Drug Deliv. Rev.,* **64**, 302–315.
6. Tan, C., Wang, Y., Fan, W. (2013). Exploring polymeric micelles for improved delivery of anticancer agents: Recent developments in preclinical studies. *Pharmaceutics,* **5,** 201–219.
7. Aliabadi, H. M., Lavasanifar, A. (2006). Polymeric micelles for drug delivery. *Expert Opin. Drug Deliv.,* **3**, 139–162.
8. Uchegbu, I. F. (2006). Pharmaceutical nanotechnology: Polymeric vesicles for drug and gene delivery. *Expert Opin. Drug Deliv.,* **3**, 629–640.
9. Guidance for Industry, Considering whether an FDA-regulated product involves the application of nanotechnology. U.S., FDA. Available at: http://www.fda.gov/RegulatoryInformation/Guidances/ucm257698.htm (accessed on January 17, 2015).

10. Bawa, R. (2015). What's in a name? Defining "nano" in the context of drug delivery. *In*: Bawa, R., Audette, G. and Rubinstein, I. (Editors): *Handbook of Clinical Nanomedicine: Nanoparticles, Imaging, Therapy, and Clinical Applications*, Chapter 6, Pan Stanford Publishing, Singapore (in press).
11. Bawa, R. (2013). FDA and nanotech: Baby steps lead to regulatory uncertainty. *In*: D. Bagchi, et al. (editors). Bionanotechnology: A revolution in biomedical sciences and human health. Wiley Blackwell, UK, pp. 720–732.
12. Johansson, S. M. C., Arnberg, N., Elofsson, M., Wadell, G., Kihlberg, J. (2005). Multivalent HSA conjugates of 3′-sialyllactose are potent inhibitors of adenoviral cell attachment and infection. *ChemBioChem,* **6**, 358–364.
13. Johansson, S. M. C., Nilsson, E. C., Elofsson, M., Ahlskog, N., Kihlberg, J., Arnberg, N. (2007). Multivalent sialic acid conjugates inhibit adenovirus type 37 from binding to and infecting human corneal epithelial cells. *Antivir. Res.*, **73**, 92–100.
14. Honda, T., Yoshida, S., Arai, M., Masuda, T., Yamashita, M. (2002). Synthesis and anti-Influenza evaluation of polyvalent sialidase inhibitors bearing 4-guanidino-Neu5Ac2en derivatives. *Bioorg. Med. Chem. Lett.,* **12**, 1929–1932.
15. Centers for Disease Control and Prevention (CDC). (2010). Prevention and Control of Seasonal Influenza with Vaccines Recommendations of the Advisory Committee on Immunization Practices (ACIP). *Morb. Mortal. Weekly Rep.*, **59**, RR-8.
16. Centers for Disease Control and Prevention (CDC) (2014). H1N1 Flu (Swine Flu) Weekly Update. Available at: http://www.cdc.gov/h1n1flu/whatsnew.htm (accessed on January 15, 2015).
17. World Health Organization (WHO). Global Influenza Programme. Available at: http://www.who.int/influenza/en/ (accessed on December 3, 2014).

Chapter 36

Nanotechnology in Tissue Engineering for Orthopaedics

Lesley M. Hamming, PhD, JD,[a] and Mark G. Hamming, MD[b]

[a]*Winston & Strawn LLP, Chicago, Illinois, USA*
[b]*Department of Orthopedic Surgery,*
Duke University School of Medicine, Durham, North Carolina, USA

Keywords: orthopedic surgery, patient outcomes, tissue regeneration, tissue scaffolds, biocompatibility, tissue engineering, osteoblast adhesion, electrospun nanofibers, tendon regeneration, cartilage regeneration, nanoscale surface roughness

36.1 Introduction

Orthopedic surgeons are often considered the carpenters of the medical profession because of their use of saws, drills and permanent fixation devices. Innovation in orthopedic surgery, however, is poised to move from the macroscopic realm to the nanoscopic realm as the field embraces the possibilities of nanotechnology. These possibilities include improving implant compatibility at the cellular level as well as stimulating the regeneration of bone and cartilage via nanometer-structured scaffolds with novel properties.

This chapter is reprinted with kind permission of *Nanotechnology Law & Business* (Pasadena, California, USA) and originally appeared in *Nanotechnology Law and Business*, **7**, 318–328 (2010).

Handbook of Clinical Nanomedicine: Nanoparticles, Imaging, Therapy, and Clinical Applications
Edited by Raj Bawa, Gerald F. Audette, and Israel Rubinstein

ISBN 978-981-4669-20-7 (Hardcover), 978-981-4669-21-4 (eBook)
www.panstanford.com

Similar to the way Dr. Kuntscher's introduction of intramedullary fixation devices revolutionized fracture care during World War II, nanotechnology has the potential to create a new wave of innovation that may ultimately change the standard of care for patients [1].

As life expectancies increase, the prevalence of age- or sport-related joint pain and fractures will increase as well [2]. Advances in orthopedic surgery in the last sixty years have greatly improved the outcome of fractures, but these surgeries do not eliminate all adverse consequences. More than 600,000 joint replacements are performed in the US each year with risks of poor binding to native tissue and concomitant risks of infection, aseptic loosening and periprosthetic fractures [3].

Approximately 150,000 hip replacements are performed each year in the United States including approximately 37,000 hip revisions [4]. Hip fractures can have devastating outcomes in part due to the disrupted vascular supply to the femoral head causing a vascular necrosis. One-third of patients presenting with hip fracture will need nursing home care and 24% of patients over age fifty will die within a year after fracture [5]. While these statistics likely reflect the fragility of health of the people who are prone to hip fractures, they also highlight how debilitating these injuries are for the elderly. There are risks for younger patients as well. Younger patients will likely need to undergo at least two invasive procedures in their lifetime since current hip implants only last a mean of twenty years [6].

Along with increased life expectancy, rates of osteoporosis and obesity are similarly increasing. The number of people with osteoporosis is expected to increase from 10.1 million in 2002 to 13.9 million by 2020 [7]. The National Osteoporosis Foundation estimates that 50% of women and 25% of men over age fifty are at risk of breaking a bone due to osteoporosis [8]. Likewise, obesity rates are increasing at alarming rates in industrialized countries. In the US, thirty-three states now have obesity rates greater than 25% of their population up from zero states just ten years ago [9]. Bourne et al. compared orthopaedics patients to the general population in Canada and found a strong correlation between the risk for total hip arthroplasty and total knee arthroplasty and obesity because of the extra weight placed on the joints [10]. It is clear from these statistics that the number of fractures,

musculoskeletal injuries and joint replacements will continue to increase. Thus, there is substantial need for techniques with improved interfacial compatibility that stimulate the regeneration of host tissue in order to increase the longevity of implants as well as the efficacy of tissue scaffolds.

One strategy to improve orthopedic techniques is to develop tissue scaffolds *in vitro* and *in vivo* aimed at replacing, regenerating or repairing damaged bone and cartilage for improved patient outcomes [11]. The scaffolds play several roles such as recruiting and containing the cells of interest (osteoblasts and chondroblasts), providing support for adhering cells, and distributing bioactive substances such as growth factors [12].

Table 36.1 Ideal properties for scaffolds

• Biocompatible–integrates well with natural tissue
• Permeable
• Structural optimization
• Structural integrity
• Porosity for cell ingrowth
• Nanometer–structured topography for enhanced cell attachment and proliferation
• 3D lattice to orient regenerating tissue
• Customizable to fill heterogeneous defects
• Bioactive to promote cell proliferation and adhesion
• Biodegradable
• Easy fixation into native tissue bed
• Minimally invasive
• Uniform production
• Readily-available
• Affordable

Table 36.1 lists properties for an ideal tissue scaffold. Biocompatibility is important because foreign bodies like scaffolds and implants may induce an inflammatory response, increase rates of infection, prove cytotoxic, or yield poor surface interaction with native tissue. Some of these responses may be minimized with naturally-derived polymers, use of host tissue and host stem cells, or inclusion of infection-fighting agents. The scaffold

should be permeable to facilitate distribution of bioactive agents and cells throughout the scaffold. The scaffold should also have structural integrity appropriate for the location and should guide the regenerating tissue into a 3-dimensional orientation similar to the complex orientation of native tissue. As one example, articular cartilage generally has an asymmetric distribution of chondrocytes [13]. In addition, lesions vary in size and shape so a tissue scaffold must be malleable to meet the unique needs of each patient. The scaffold would ideally promote the proliferation of cells through the time-regulated release of bioactive agents and biodegrade at the same rate it can be replaced by regenerating tissue. Researchers should also consider the practical aspects of the tissue scaffold such as uniform reproduction, availability, affordability and ease of use.

36.2 Benefits of Nanometer-Scale Features

Bone, cartilage and extracellular matrix (ECM) are composed of nanometer-scale constituents (hydroxyapatite, collagen, calcium phosphate) with properties determined by both their size and chemistry. Mesenchymal stem cells (MSCs) are the precursors for the tissues in the musculoskeletal system and are thus attractive to researchers in the field of tissue regeneration. As researchers gain more understanding about the behavior of these nanometer-scale components, they can better design scaffolds for optimal control of tissue regeneration.

Arguably, the most important property for a scaffold is biocompatibility as this will determine its longevity. Some researchers argue that the protein adsorptions that occur within a few seconds after implantation of a scaffold determine its ultimate efficacy [14]. The quality of protein adsorption depends on nanometer-scale surface roughness, charge, chemistry and wettability [15]. Some researchers have evidence that these natural materials interact best with other nanometer-scale features and surfaces [16].

Palin et al. designed experiments to determine whether nanometer-scale surface roughness alone could account for increased calcium deposition by osteoblasts on nanometer-structured titania compared to conventional titania [17].

The researchers examined osteoblast activity on samples of synthetic polymer modified to have the same surface roughness as conventional and nanometer-structured titania in order to isolate the surface roughness effects. Their experiments showed greater osteoblast adhesion and proliferation on the synthetic polymer with nanometer-scale surface roughness that mimicked the surface roughness of natural bone. The results indicated that nanometer-scale features play a significant role in inciting osteoblast activity independently of the chemical composition of the substrate. Some researchers hypothesize that nanometer-scale features provide more binding sites for the cell membrane receptors and therefore encourage more protein adsorption [18].

Since the main constituents in bone and cartilage are nanometer-sized, researchers could in theory design synthetic nanometer structures with tailored surface chemistry to emulate the behavior of natural bone. This strategy would thereby improve the biocompatibility of synthetic implants. A second approach is to harness exogenous or autologous stem cells for proliferation in implanted tissue scaffolds. This method may be enhanced by attracting natural biomarkers, such as growth factors, to nanometer-structured scaffolds that can then act as mechanical guides for the regeneration of tissues with the same orientation as natural bone and cartilage.

Researchers envision ideally biocompatible implants and scaffolds as well as minimally-invasive techniques such as injecting a self-assembling gel that incites osteogenesis and biodegrades as it is replaced with regenerated bone and cartilage. The guided regeneration of bone and cartilage will significantly improve the quality of life of our aging and increasingly active population. Potential areas of orthopaedics with foreseeable need of nanometer-structured tissue scaffolds include healing of large bone defects, significant focal or widespread cartilage damage, prevention of infections, and improvement of implant-bone interface osseointegration.

36.3 Commercialization

In 2009, the global market for orthopedic products was $33 billion with its largest segment for spine, knee and hip replacements at

$18.2 billion [19]. While tissue engineering made up only 7.5% of the global market in 2009, it is currently the fastest growing and least competitive segment. A report by Medtech Insight in 2003 predicted a potential US market for tissue engineering orthopaedics products of $39 billion by 2013 [20].

Several external factors are currently negatively impacting profits for orthopaedics companies. These pressures include the expiration of basic patents leading to commoditization of traditional implants, increasing regulatory requirements, the Physician Payments Sunshine Act, the medical device excise tax beginning in 2013, postponement of procedures by patients during the economic downturn, and increasing pressure from bulk healthcare consumers to lower prices [21]. Since established orthopaedics companies will seek to minimize research and development costs in light of strained profits, much of the innovation in tissue engineering for orthopaedics may come from small companies spun off from research universities or research institutions.

In the last fifteen years, many universities have established centers for nanotechnology research. Despite the vast potential to create improved implants, few of these centers are specifically targeting orthopedic applications. The Methodist Hospital in Houston established the nation's first program dedicated solely to advancing nanotechnology in orthopaedics in January 2010. The program's leading research endeavor is BioNanoScaffolds aimed at replacing traditional invasive fixation methods with less invasive fracture putty. The objective of the fracture putty is to provide instantaneous load-bearing support, promote healing of bone by releasing growth factors and infection-fighting agents, and exhibit gradual degradation as the bone regenerates. The following is a non-exhaustive list of companies developing nanometer-structured materials for orthopedic applications spun off from various research institutions.

Audax Medical, Inc. (Littleton, Massachusetts) is developing an injectable material for healing vertebrae and osteoporosis. The osteobiological material includes self-assembling nanorings that mimic collagen. The size and shape of the nanorings allows for better integration with bone. Dr. Thomas Webster developed this technology at Brown University.

Indiana Nanotech, LLC (Indianapolis, Indiana) is developing nanometer- and mesostructured niobium oxide implants that

stimulate cell differentiation, promote osteoblast activity and induce mineralization because of a lattice-match mechanism.

NanoInk, Inc. (Skokie, Illinois) is developing its NanoStem Cell division to create nanopatterns on solid substrates with Dip-pen Nanolithography. The nanopatterns facilitate the homogeneous growth and differentiation of stem cells. By altering the nanopatterns, NanoInk's technique controls whether adult mesenchymal stem cells differentiate into chondrocytes (cartilage cells), osteoblasts (bone cells) or adipocytes (fat cells). Dr. Chad Mirkin started NanoInk based on his research at Northwestern University.

Nano Interface Technology, Inc. (Ocala, Florida) engineers nanometer-scale biomaterial coatings for orthopedic and dental implants. The implants are coated with nanometer-scale hydroxyapatite (HA) to decrease failure rates and improve biocompatibility.

NanoMech (Springdale, Arizona) utilizes nanospray electrostatic deposition to cover implants with nanometer-structured hydroxyapatite coatings. The nanometer-structured coatings improve the mechanical properties and biological performance of the implants. The coating is biofunctional and porous allowing for osseointegration.

Nanotope (Skokie, Illinois) developed a self-assembling nanofiber gel that promotes the growth of new cartilage by stimulating an animal's own stem cells. Tests demonstrate improved results compared to using microfracture alone for regeneration. The technique works without the addition of expensive growth factors and the self-assembled gel biodegrades as it is replaced with natural cartilage. Nanotope recently entered into a partnership with Smith & Nephew to further optimize the technology. Dr. Samuel Stupp started Nanotope based on his research at Northwestern University.

Orthovita (Malvern, Pennsylvania) has nanoparticle-structured technology in its patent portfolio.

Pioneer Surgical (Marquette, Michigan) engineered nanOss (TM) Bioactive, an osteoconductive bone graft that mimics the structure and biocompatibility of bone with nanocrystalline hydroxyapatite for enhanced bioactivity. NanOss Bioactive aids in bone formation in defects resulting from trauma or surgery in the posterolateral spine, extremities, and pelvis. A product introduced in 2008, FortrOss (TM), combines osteoconduction with promotion of bone repair and uses nanOss hydroxyapatite.

Tigenix (Belgium) acquired a design for an osteochondral scaffold, ChondroCelect, for regenerating both bone and cartilage simultaneously. The nanocomposite scaffold consists of two layers: a mineralized type I collagen-GAG scaffold to stimulate bone growth and a non-mineralized type II collagen-GAG scaffold to stimulate cartilage. The porous scaffold is approved for use in Europe. Dr. Lorna Gibson developed this technology at MIT.

36.4 Tissue Engineering for Bone

Due to the prevalence of orthopedic trauma and bone disease, bone defects are a frequently encountered clinical dilemma. Bone has the ability to regenerate and remodel, but does so only when osteoconductive, osteoinductive, and osteogenic potentials are optimized. Osteoconductive means a substance that can serve as a scaffold for new bone growth. Osteoinductive refers to growth factors that can stimulate bone growth. Osteogenic potential refers to the bone producing cells such as osteoblasts. Clinically, these potentials are optimized when a fracture has blood supply, mechanical stability, soft tissue coverage, and is free of infection. When one or more of these issues is compromised, bone healing is suboptimal and can result in nonunions or malunions.

Bone is a naturally occurring composite nanometer structure consisting of organic and inorganic phases. The two principle components of bone are hydroxyapatite crystals (20 to 80 nm long and 2 to 5 nm thick) and Type 1 collagen fibrils with triple helix diameters less than 500 nm [22]. This unique hierarchical substructure of bone lends one to conjecture a compatibility of bone with other nanometer-sized particulates. Nanotechnology has the potential to rewrite the way the orthopedic surgical field is practiced by optimizing the interactions between the scaffold or implant and native tissue.

Optimization may occur by matching the mechanical properties of bone and implants and scaffolds and by optimizing the interaction of natural tissue with the implants or scaffolds. Mechanically, the organic phase of bone is composed of collagen fibrils to enhance toughness while the inorganic phase composed of hydroxyapatite crystals lends mechanical stiffness and compressive strength. Researchers have mimicked the structure of bone with

composites of hydroxyapatite and synthetic polymer to achieve mechanical properties that approximate values of natural bone [23]. These composites reduce stress shielding between implants and natural bone that is seen in traditional metal implants.

Bone ingrowth into a prosthetic device is an area of research that has recently yielded promising results. Popat et al. demonstrated increased amounts of cell adhesion, cell proliferation and bone matrix deposition on anodized nanotubular titanium compared with titanium surfaces with micrometer surface roughness [24]. Changing the nanotopography of a material has the potential for significant property-altering characteristics of that material because of the increased number of active sites available for interaction with proteins. Nanometer-structured surface topography drastically increased the surface area of an implant in contact with bone for enhanced protein and osteoblast interaction in several studies [25].

Elias et al. found that the basic cells responsible for the production of bone, osteoblasts have increased proliferation on carbon nanofibers with diameters less than 100 nm compared to larger diameter fibers [26]. The researchers hypothesized that these nanofibers produce enhanced osteoblast activity because they closely resemble the physical size of hydroxyapatite crystals of bone [25]. This finding highlights the potential for enhanced bone healing or osseointegration of a nano-sized tissue scaffold.

Osteoblasts also have better adhesion on other nanometer-structured surfaces. In several studies, researchers observed increased protein (vitronectin and fibronection) adsorption as well as increased osteoblast attachment on nanometer-structured surfaces [28]. Woo et al. demonstrated more than 1.7 times the amount of osteoblast attachment on nanofibrous poly(L-lactic acid) scaffolds created by a phase separation technique compared to solid wall controls [29]. Fortunately, fibroblasts do not appear to have a similar affinity to nanometer-structured surfaces [30]. Fibroblasts are the cells responsible for soft tissue scarring that could inhibit osseointigration and adequate fixation of prostheses. Vance et al. showed a reduction in fibroblasts proliferation on nanometer-structured surfaces compared to micrometer-structured surfaces with similar surface chemistry and wettability [31]. It remains to be elucidated exactly why some cells show enhanced activity on nanometer-structured surface while others do not.

Capitalizing on the use of nanostructures for tissue scaffolds, Zhang et al. demonstrated increased osteoblast adhesion and hydroxyapatite nucleation and mineralization with a self-assembling nanoparticle hydrogel compared to a control hydrogel [32]. The nanoparticles self-assembled *in vitro* into helical rosette nanotubes that emulate the structure of collagen in bone.

Significantly, the addition of nanometer-sized hydroxyapatite into the system further increased osteoblast adhesion by more then 200 percent.

Nanotechnology also has the potential to affect the osteoinductive environment for bone. Liao et al. have demonstrated that bone morphogenic protein, a potent growth factor for bone, can be released from a composite nanofiber matrix made of collagen/polylactic acid and nanometer-sized hydroxyapatite [33]. This local leaching of growth factor near the scaffold could significantly improve rates of healing.

Another criterion for optimal bone healing is an environment that is free of infection. Nanophase ZnO and TiO_2 ceramics have shown decreased cell adhesion of Staphylococcus epidermidis without compromising the improvement of cell adhesion and function of osteoblasts [34]. The S. epidermidis cell density was decreased by 25% for nanophase ZnO and 40% for nanophase TiO_2. These results could be clinically significant due to the high prevalence of S. epidermidis as the offending bacteria in implant infections. Future tissue scaffolds may also include silver nanoparticles to eliminate infection. When compared directly to silver sulfadizine (a commonly used drug to prevent infection in wound therapy), wounds with nanometer-sized silver particles had lower bacterial growth and higher healing rates in a mouse model [35].

The tendon-bone interface is an area with unique structural properties. When a tendon ruptures directly off bone, surgical fixation of the tendon back to bone often does not regenerate the native transitional zone [36]. Tendon fibroblasts cultured on an electrospun nanofiber scaffold have recreated the complex native transition zone between the tendon and bone [37]. A clinical incorporation of such a scaffold in a tendon repair could help to eliminate tendon re-rupture and potentially hasten healing intervals.

Several methods exist to fabricate traditional tissue scaffolds and scaffolds with nanometer-structures (Table 36.2). Electrospinning and self-assembly techniques can create a nanofibrous scaffold suitable for clinical application [38]. Researchers demonstrated that electrospinning can be used to fabricate oriented nanostructure with high surface area, high aspect ratios, high porosity and low density to enhance protein adsorption [39]. These nanofibers can have diameters as small as a few nanometers in a 3-dimensional arrangement [40]. Self-assembly occurs when molecules spontaneously interact with other molecules via non-covalent interactions to create 3-dimensional nanometer-scale scaffolds [41]. Possible triggers for the spontaneous assembling include changes in pH, temperature, growth medium or concentration of molecules.

Table 36.2 Fabrication of tissue scaffolds

Traditional scaffolds [42]:
• Solvent casting and particulate leaching
• Gas foaming
• Emulsion free drying
• Thermally induced phase separation
• Gravity and microsphere sintering
• Solid freeform fabrication
Nanometer-structured scaffolds:
• Electrospinning [43]
• Phase separation [44]
• Self-assembling scaffolds [45]

36.5 Tissue Engineering for Cartilage

Cartilage regeneration has the potential to restore a damaged joint that would otherwise be doomed to prosthetic implantation. Cartilage damage can stem from a variety of etiologies that can include trauma, inflammatory arthropathy, septic arthritis and osteoarthritis. Regardless of the cause, the clinical outcome is

a reduced quality of life. The notion of the recapitulation to a healthy joint has been but a siren's song up to this point. Future endeavors involving nanotechnology could hold the key to regenerating not only healthy and functional cartilage, but also transforming the lives of millions of potential patients.

Like bone, cartilage is composed of nanometer-scale elements such as Type II collagen. Unlike bone, however, damaged articular cartilage has little inherent ability to repair itself because its poor vascularity as well as a paucity of actively replicating cells. Surgical techniques such as autologous chondrocyte implantation, microfracture and osteochondral autologous transfer provide some answers for cartilage defects but do not come without potential drawbacks. Complications that result from these procedures include need for further surgery, insufficient graft incorporation, cartilage overgrowth, insufficient cartilage growth, expense, time and infection.

Microfracture is a common technique for repairing focal cartilage defects but long-term studies have demonstrated deterioration in clinical outcomes after eighteen months [46]. In light of these clinical challenges, researchers are working toward procedures that are less invasive, promote enhanced integration with surrounding cartilage, and exhibit improved cell reproduction [47].

Current scaffolds for collagen defects in use include fibrin glue and collagen gels [48]. While fibrin glue is reported to maintain cell viability and cell-matrix interactions, some have reported it as insufficiently robust to effectively serve as a scaffold. Stronger scaffold materials such as polyglycolic acid have been proposed because of their uniformity and modifiable properties [49].

As an alternative, researchers at Northwestern University developed a novel scaffold for regenerating cartilage that is minimally invasive [50]. The scaffold is injected as a liquid containing bioactive peptide amphiphiles (PA) that self-assemble into supramolecular nanofibers inside the body. During self-assembly, the biosignaling peptides concentrate along the length of the nanofibers. This arrangement promotes chondrogenic differentiation of mesenchymal stem cells along the length of the nanofibers for localized regeneration of articular cartilage.

To promote osteoconductive cartilage regeneration, Shah et al. used a biosignaling peptide sequence in the self-assembling

scaffold that has an affinity for naturally occurring transforming growth factor beta 1 (TGF). After injection *in vivo*, the self-assembling scaffold with TGF-binding epitope demonstrated complete cartilage regeneration at twelve weeks in full-thickness lesions in rabbits without the need for injection of extra growth factor. The regeneration observed after injecting the self-assembling scaffold significantly out-performed the regeneration demonstrated by injection of only growth factor into the defect site in several commonly used measures to evaluate the quality of regeneration [51].

While promising work has been done to develop *in vivo* cartilage regeneration, challenges remain in the quest to find an ideal scaffold that is clinically efficacious. For example, the process of electrospinning can structurally produce only some features of native cartilage's extracellular matrix. Unfortunately for researchers hoping to mimic it, native articular cartilage is remarkably engineered with varying orientations of collagen fibrils depending on the depth into the cartilage. This unique configuration allows cartilage to resist tensile, shear and compressive forces [52]. It remains to be determined what level of sophistication will be required for clinical efficacy.

36.6 Conclusion

As researchers gain a better understanding of the processes that occur at the nanometer scale in living tissue, new opportunities will arise for improving patient outcomes in orthopaedics. Nanometer-structured tissue scaffolds and implants represent one promising avenue for development and commercialization. Although the nanometer-scale structures of cartilage and bone are intricately designed by nature, scientists have already made great strides in emulating the mechanical properties, improving biointeraction with grafts and implants through nanometer-scale features, and facilitating stem cell differentiation and tissue regeneration.

Further progress in this field depends on the coordinated efforts of experts in chemistry, cell and molecular biology, materials science and clinical medicine [52]. Together, these researchers

must not only focus on guiding and improving regeneration of tissue, but also on alleviating immunobiological problems such as rejection of the implant or scaffold, allergic reactions and infections. It also remains to be determined why some cells show enhanced adhesion near certain nanoscale features while other cells do not. With any advance in technology, the potential societal and ethical implications must be considered. In the case of tissue engineering, some segments of the public may have ethical concerns over using stem cells as well as concerns over the safety of the technology, environmental repercussions, and the ability of athletes to furtively enhance their performance [54]. The keys to minimizing concerns include employing targeted research in these areas as well as effectively educating the public about the technology.

Disclosures and Conflict of Interest

The authors declare that they have no conflict of interest and have no affiliations or financial involvement with any organization or entity discussed in this chapter. This includes employment, consultancies, honoraria, grants, stock ownership or options, expert testimony, patents (received or pending) or royalties. No writing assistance was utilized in the production of this chapter and the authors have received no payment for its preparation. The findings and conclusions here reflect the current views of the authors. They should not be attributed, in whole or in part, to the organizations with which they are affiliated, nor should they be considered as expressing an opinion with regard to the merits of any particular company or product discussed herein. Nothing contained herein is to be considered as the rendering of legal advice.

Corresponding Author

Dr. Lesley M. Hamming
Winston & Strawn LLP
35 W. Wacker Drive, Chicago, IL 60601-9703, USA
Email: LHamming@winston.com

About the Authors

Lesley Hamming is an attorney at Winston & Strawn LLP who focuses her practice on intellectual property and patent matters. She has special expertise in litigating pharmaceutical patent cases. She is registered to practice before the United States Patent and Trademark Office and is an inventor for a U.S. patent relating to bio-inspired adhesive polymer coatings. Dr. Hamming received her PhD in materials science and engineering and her BS in mechanical engineering from Northwestern University, where she conducted research in nanotechnology and biomaterials. In recognition of her research, she received a National Science Foundation Graduate Research Fellowship. She received her JD from Duke University School of Law, where she was named a University Scholar and a Mordecai Scholar. Dr. Hamming is a former member of the U.S. National Team in triathlon.

Mark Hamming is an orthopedic surgeon with Illinois Bone & Joint Institute in Chicago, Illinois, specializing in sports medicine. Prior to joining Illinois Bone & Joint Institute, Dr. Hamming worked closely with world experts in hip arthroscopy and multi-ligament knee repair at the Steadman Clinic in Vail, Colorado. He was a team physician for the U.S. Ski Team leading into the 2014 Sochi Winter Olympics. Dr. Hamming completed his orthopedic surgery training at Duke University, where he served as a team physician for Duke University's basketball, football, and lacrosse teams. He obtained his medical degree at Rush Medical College and graduated from Northwestern University with a BS in biology and a minor in Spanish. While at Northwestern, he was named MVP and captain of the swim team, received All-American honors, and competed at the U.S. Olympic Trials.

References

1. Harrold, A. J. (1982). Kuntscher's nails for femoral fractures. *BMJ*, **285,** 1446, 1446. Available at: http://www.ncbi.nlm.nih.gov/pmc/articles/PMC1500600/ (accessed on January 27, 2015).

2. Palin, E., Liu, H., Webster, T. J. (2005). Mimicking the nanofeatures of bone increases bone-forming cell adhesion and proliferation. *Nanotechnology*, **16**, 1828–1835.
3. Christenson, E. M., et al. (2007). Nanobiomaterial applications in orthopaedics. *J. Orthop. Res.*, **25**, 11–22.
4. Palin, *supra* note 2.
5. id.
6. Karlinsey, R. L., Mackey, A. C., Frederick, K. E. (2009). Structured niobium oxide: Morphology, bioactivity, and oxide-metal adhesion properties. In: Karlinsey, R. L., ed. *Recent Developments in Advanced Medical and Dental Materials Using Electrochemical Methodologies*, p. 41.
7. Palin, *supra* note 2.
8. Nat'l Osteoporosis Found., Bone health basics: Why bone health is important. Available at: http://nof.org/learn/basics (accessed on January 8, 2011).
9. Centers for Disease Control & Prevention, U.S. obesity trends: Trends by state 1985–2009. Available at: http://www.cdc.gov/mmwr/preview/mmwrhtml/mm5930a4.htm (accessed on January 8, 2011).
10. Bourne, R., et al. (2007). Role of obesity on the risk for total hip of knee arthroplasty. *Clin. Orthop. Related Res.*, **465**, 185–188.
11. Musgrave, D. S., Fu, F. H., Huard, J. (2002). Gene therapy and tissue engineering in orthopaedic surgery. *J. Am. Acad. Orthop. Surg.*, **10**, 6–15.
12. id.
13. Woodfield, T. B., et al. (2005). Polymer scaffolds fabricated with pore-size gradients as a model for studying the zonal organization within tissue-engineered cartilage constructs. *Tissue Eng.*, **11**, 1297–1311.
14. Liao, S., Chan, C. K., Ramakrishna, S. (2008). Nanostructures for musculoskeletal tissue engineering. In: *Nanotechnology and Tissue Engineering: The Scaffold*, p. 329.
15. Wilson, C. J., et al. (2005). Mediation of biomaterial–cell interactions by adsorbed proteins: A review. *Tissue Eng.*, **11**, 1.
16. Liao, Chan, Ramakrishna, *supra* note 14; Webster, T. J., et al. (2000). Enhanced functions of osteoblasts on nanophase ceramics. *Biomaterials*, **21**, 1803; Li, W.-J., Jiang, Y. J., Tuan, R. S. (2006). Chondrocytes phenotype in engineered fibrous matrix is regulated by fiber size. *Tissue Eng*., **12**, 1775.
17. Palin, *supra* note 2.

18. Stevens, M. M., George, J. H. (2005). Exploring and engineering the cell surface interface. *SCI*, **310**, 1135–1138.
19. Research and Markets (August 2010). Business Insights Report: The Top 10 Orthopedic Device Companies: Financial Performance, Research Activities, and Growth Strategies (Available at: http://www.research-store.com/technologynetworks/Browse/?N=355+361&page=9&Ns=title&Nso=1).
20. Liao, Chan, Ramakrishna, *supra* note 14.
21. Research and Markets, *supra* note 19.
22. Nair, L. S., Laurencin, C. T. (2008). Nanofibers and nanoparticles for orthopaedic surgery applications. *J. Bone Joint Sci*., **90**, 128–131.
23. Kokubo, T., Kim, H.-M., Kawashita, M. (2003). Novel bioactive materials with different mechanical properties. *Biomaterials*, **24**, 2161–2175.
24. Popat, K. C., et al. (2007). Influence of engineered titania nanotubular surfaces on bone cells. *Biomaterials*, **28**, 3188–3197.
25. Palin, *supra* note 2; Christenson, et al., *supra* note 3; Liao, Chan, Ramakrishna, *supra* note 14.
26. Palin, *supra* note 2; Christenson, et al., *supra* note 3; Elias, K. L., Price, R. L., Webster, T. J. (2002). Enhanced functions of osteoblasts on nanometer diameter carbon fibers. *Biomaterials*, **23**, 3279.
27. Palin, *supra* note 2; Christenson, et al., *supra* note 3; Elias, Price, Webster, *supra* note 26.
28. Liu, H., Webster, T. J. (2007). Nanomedicine for implants: A review of studies and necessary experimental tools. *Biomaterials*, **28**, 354–369.
29. Woo, K. M., Chen, V. J., Ma, P. X. (2003). Nano-fibrous scaffolding architecture selectively enhances protein adsorption contributing to cell attachment. *J. Biomed. Materials Res. A*, **67**, 531–537 (Available at: http://deepblue.lib.umich.edu/bitstream/2027.42/34430/1/10098_ftp.pdf).
30. Palin, *supra* note 2; Vance, R. J., et al. (2004). Decreased fibroblast cell density on chemically degraded poly-lactic-co-glycolic acid, polyurethane, and polycaprolactone. *Biomaterials*, **25**, 2095–2103.
31. Vance, et al., *supra* note 30.
32. Zhang, L., et al. (2009). Biologically inspired rosette nanotubes and nanocrystalline hydroxyapatite hydrogel nanocomposites as improved bone substitutes. *Nanotechnology*, **20**, 175101.
33. Liao, S. S., et al. (2004). Hierarchically biomimetic bone scaffold materials: Nano-HA/collagen/PLA composite. *J. Biomed. Materials Res. B*, **69**, 158.

34. Colon, G., Ward, B. C., Webster, T. J. (2006). Increased osteoblast and decreased staphylococcus epidermidis functions on nanophase ZnO and TiO_2. *J. Biomed. Materials Res. A*, **78**, 595.

35. Tian, J., et al. (2007). Topical delivery of silver nanoparticles promotes wound healing. *Chem. Med. Chem*., **2**, 129–136 (Available at: http://onlinelibrary.wiley.com/doi/10.1002/cmdc.200600171/abstract).

36. Galatz, L. M., et al. (2004). The outcome and repair integrity of completely and arthroscopically repaired large and massive rotator cuffs. *J. Bone Joint Surg.*, **86**, 219.

37. Xie, J., et al., "Aligned to random" nanofiber scaffolds for mimicking the structure of the tendon-to-bone insertion site. *Nanoscale*, **2**, 923–926 (2010) (Available at: http://www.ncbi.nlm.nih.gov/pmc/articles/PMC3609028/).

38. Nair, Laurencin, *supra* note 22.

39. id.

40. Liao, Chan, Ramakrishna, *supra* note 14.

41. id.

42. id; Nair, Laurencin, *supra* note 22.

43. Liao, Chan, Ramakrishna, *supra* note 14; Nair, Laurencin, *supra* note 42.

44. Liao, Chan, Ramakrishna, *supra* note 14; Woo, Chen, Ma, *supra* note 29; Smith, L. A., Ma, P. X., Nano-fibrous scaffolds for tissue engineering. *Colloids Surfaces B*, 39, 125 (2004).

45. Zhang, et al., *supra* note 32; Shah, R. N., et al. (2010). Supramolecular design of self-assembling nanofibers for cartilage regeneration. *Proceedings Nat'l Acad. Sci*., **107**, 3293 (Available at: http://www.pnas.org/content/107/8/3293.abstract); Stupp, S. I. (2010). Self-assembly and biomaterials. *Nano Lett.*, **10**, 4783.

46. Kreuz, P. C., et al. (2006). Results after microfracture of full-thickness chondral defects in different compartments in the knee. *Osteoarthr. Cartilage*, **14**, 1119.

47. Safron, M. R., Kim, H., Zaffagnini, S. (2008). The use of scaffolds in the management of articular cartilage injury. *J. Am. Acad. Orthop. Surg.*, 16, 306.

48. Gates, C. B., et al. (2008). Regenerative medicine for the musculoskeletal system based on muscle-derived stem cells. *J. Am. Acad. Orthop. Surg*., **16**, 68.

49. id.

50. Shah, et al., *supra* note 45.
51. id.
52. Nisbet, D. R., et al. (2009). Review paper: A review of the cellular response on electrospun nanofibers for tissue engineering. *J. Biomater. Appl.*, **24**, 7.
53. Liao, Chan, Ramakrishna, *supra* note 14.
54. Lea, R. D. (2009). Ethical considerations of biotechnologies used for performance enhancement. *J. Bone Joint Surg.*, **91**, 2048.

Chapter 37

Applications of Nanomaterials in Dentistry

Karolina Jurczyk, DDS, PhD,[a] and Mieczyslaw Jurczyk, PhD, DSc[b]

[a]*University of Medical Sciences, Conservative Dentistry and Periodontology Department, Poznan, Poland*
[b]*Poznan University of Technology, Institute of Materials Science and Engineering, Poznan, Poland*

Keywords: nanoimplant, nanosurface, scaffold, dental, dentistry, corrosion, roughness, cell viability, cell proliferation, MTT test, titanium, magnesium, hydroxyapatite, 45S5 Bioglass, silica, nanocomposite, mechanical properties, *in vitro* biocompatibility, osteoblast cells, fibroblast cells

There is a high demand for biomaterials to assist the replacement of organs and their functions. For this reason, researchers search for new biomaterials with advanced mechanical and biological properties and develop new technologies for the enhancement of those properties. Over the past, nanoscale materials become very popular in medical application [38, 78–80]. These nanostructured materials can exhibit enhanced mechanical, biological, chemical properties compared with their conventional counterparts [50].

Titanium and titanium alloys are preferred materials in the production of implants [14, 53]. These materials possess favorable

Handbook of Clinical Nanomedicine: Nanoparticles, Imaging, Therapy, and Clinical Applications
Edited by Raj Bawa, Gerald F. Audette, and Israel Rubinstein

ISBN 978-981-4669-20-7 (Hardcover), 978-981-4669-21-4 (eBook)
www.panstanford.com

properties, such as relatively low modulus, low density, and high strength. Titanium materials are resistant to corrosion because of the stable passivity of the surface oxide film [43]. Apart from that, titanium and titanium alloys are generally regarded to have good biocompatibility, although there are reports that show the accumulation of titanium in tissues adjacent to the implant, signifying metal release and corrosion *in vivo* [11, 12]. In addition, these metal implants may lose and even separate from the surrounding tissues during implantation [13–15]. Titanium and titanium-based alloys have relatively poor tribological properties because of their low hardness [16].

Current research focuses on improving the mechanical performance and biocompatibility of Ti-based systems through variations in alloy composition, microstructure and surface treatment [22, 23, 28, 33, 49, 60, 73, 82]. In the case of titanium, significant efforts go into enhancing the strength characteristics of commercial purity grades in order to avoid potential biotoxicity of alloying elements, especially in dental implants [2, 4, 6, 20, 55, 60].

To enhance the physicochemical and mechanical performance of implant materials through microstructure control, the top-down approaches known as severe plastic deformation (SPD) and mechanical alloying (MA) techniques were applied [38,68,74]. Recent studies clearly proved that nanostructuring of titanium can considerably improve not only the mechanical properties but also the biocompatibility [20, 32, 33, 60, 64, 74, 76–80, 84]. On the other hand, this approach also has the benefit of enhancing the biological response of the cp titanium surface [32, 33, 64, 79].

37.1 Bulk Nanostructured Titanium

Until now, a number of SPD methods for producing bulk ultra fine grain metals/alloys have been developed [74–80]. Valiev and co-workers apply a process known as equal channel angular pressing (ECAP), which is a viable processing route to grain refinement and property improvement [79]. Their study reports nanostructured titanium (n-Ti)—produced as long-sized rods with superior mechanical and biomedical properties—and demonstrates its applicability for dental implants. It turns out that the extreme grain

refinement of the bulk of the metal down to nanoscale transpires to surface morphology that turns out to be conducive for enhanced adhesion and growth of living cells.

Commercially pure titanium (Grade 4) of the following composition was used: 0.052% C, 0.34% O_2, 0.3% Fe, 0.015% N, base material Ti (wt.%). In the as-received condition, billets produced by hot rolling had a diameter of 40 mm with an average grain size of 25 μm. Nanostructuring was performed using SPD by equal-channel angular pressing with subsequent thermomechanical processing (TMP), which made it possible to manufacture rod semiproducts with a length of 3 m and a diameter of 7 mm [74–80].

This processing resulted in a large reduction in grain size, from the 25 μm equiaxed grain structure of the initial titanium rods to 150 nm after combined SPD and TMT processing, as shown in Fig. 37.1. The selected-area electron diffraction pattern (Fig. 37.1c) further suggests that the ultra fine grains contained predominantly high-angle non-equilibrium grain boundaries with increased grain-to-grain internal stresses. It is important to note, that a similar structure for cp Ti can be produced in small discs using other SPD methods, such as high-pressure torsion (HPT) [75].

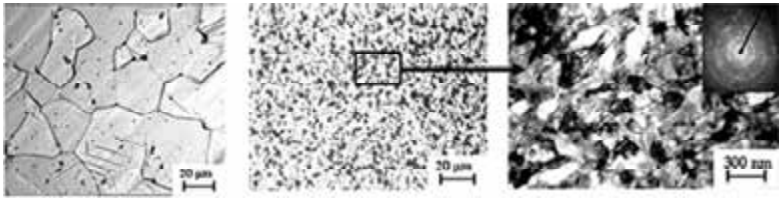

(a) (b) (c)

Figure 37.1 Microstructure of Grade 4 cp Ti: (a) the initial coarse-grained rod; (b, c) after ECAP + TMT (optical and electron photomicrographs) [79].

Mechanical properties of conventionally processed and nanostructured cp Grade 4 titanium is presented in Table 37.1. The strength of the nanostructured titanium is nearly twice that of conventional cp titanium. Additionally, it has been shown, that the fatigue strength of nanostructured cp titanium at 10^6 cycles is almost two times higher than for conventional cp titanium and exceeds that of the Ti–6Al–4V alloy.

Table 37.1 Mechanical properties of conventionally processed and nanostructured cp Grade 4 titanium [79]

Processing/ treatment conditions	UTS (MPa)	YS (MPa)	Elongation (%)	Reduction area (%)	Fatigue strength at 10^6 cycles
Conventional Ti (as received)	700	530	25	52	340
nTi ECAP + TMT	1240	1200	12	42	620
Ti–6Al–4V ELI annealed	940	840	16	45	530

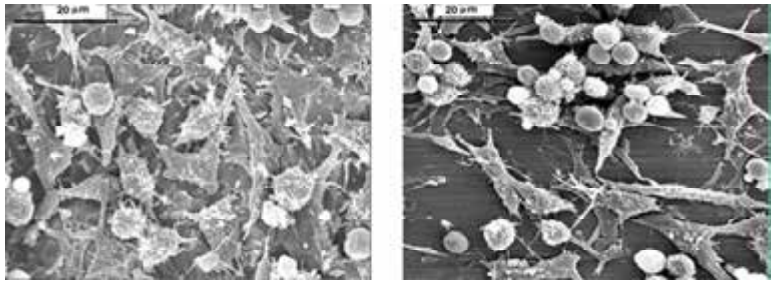

Figure 37.2 Occupation of the mice fibroblast cells L929 after 24 h; Nanostructured (left) and conventional (right) cp Grade 4 titanium [79].

(a) (b)

Figure 37.3 2.4 mm diameter Nanoimplant® (a) and 3.5 mm diameter Timplant® (b) [79].

Cytocompatibility tests utilizing fibroblast mice cells L929 were carried out. After nanostructuring, fibroblast colonization of the cp Grade 4 titanium surface dramatically increases (Fig. 37.2). For example, the surface cell occupation for conventional cp Ti was 53.0% after 72 h in contrast to 87.2% for nanostructured cp Grade 4 (Table 37.2). Compared to conventional titanium, high osteointegration rate should be expected with nanostructured cp Grade 4 titanium. Nanostructured (Nanoimplants®) implants have been successfully designed and fabricated (Fig. 37.3).

Table 37.2 Surface cell occupation for conventional and nanostructured cp Grade 4 titanium [79]

Material	Surface treatment	Occupied surface (pct.) after 72 h
cp Gr. 4 Ti	Machining, followed by hydrofluoric acid etching	53.0
Nanostructured Gr. 4 Ti		87.2

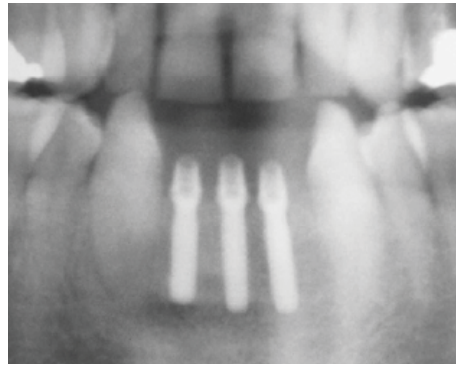

Figure 37.4 Implanted nanoimplants® [65].

The certified system of Timplant® manufactured according to standard EN ISO 13485:2003 was used during the development of the Nanoimplant® implant. The intraosseal nanoimplant of 2.4 mm diameter 2.4 mm has the strength equivalent to the conventional of 3.5 mm diameter implant. A number of over 250 Nanoimplants® have been implanted [65]. For example, a 55-year-old male with edentulous mandible and maxilla was treated by insertion of

conical implants laterally and Nanoimplants® in the narrow anterior part (Fig. 37.4). Primary retention of all implants was very good. Nanostructuring of titanium by SPD processing has made the material with significantly superior mechanical performance when compared to conventional cp Grade 4 titanium and Ti–6Al–4V alloy (Figs. 37.5 and 37.6).

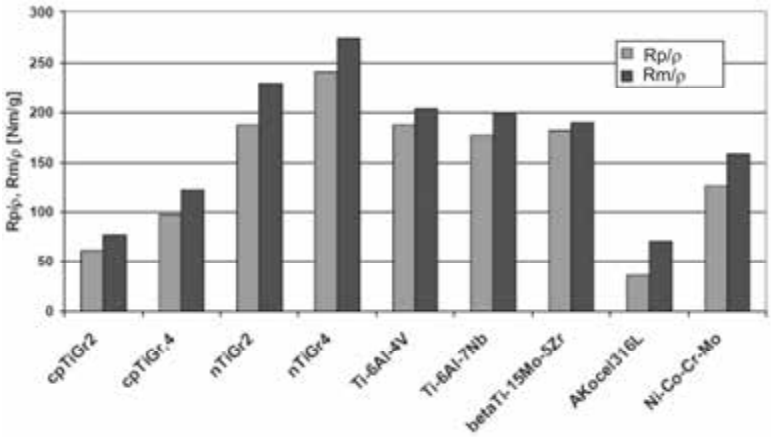

Figure 37.5 Selected mechanical properties of some implant alloys in comparison with nTiGr2 and nTiGr4 [65].

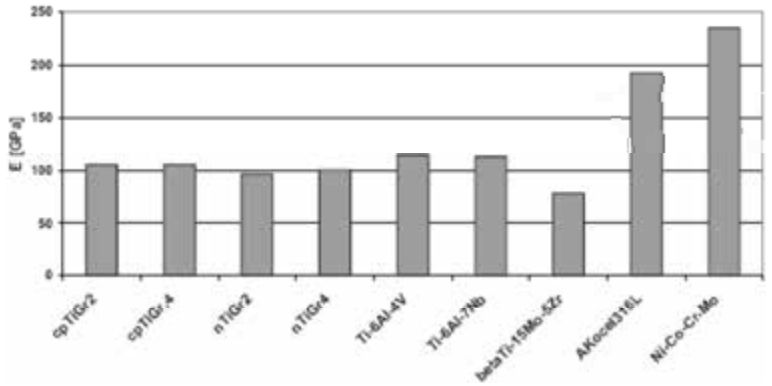

Figure 37.6 Young's modulus of different implant materials in comparison with nTiGr2 and nTiGr4 [65].

Currently, titanium and its alloys are used for dentistry devices such as implants, crowns, bridges, overdentures, and dental implant

prosthesis components (screw and abutment). There are currently four cp Ti grades and one titanium alloy specially made for dental implant applications. These metals are specified according to ASTM as grades 1 to 5. Grades 1 to 4 are unalloyed, while grade 5, with 6% aluminum and 4% vanadium, is the strongest. However, for permanent implant applications, the Ti–6Al–4V alloy has a possible toxic effect resulting from released vanadium and aluminum [4, 6]. For this reason, vanadium- and aluminum-free alloys have been introduced for implant applications. These new alloys include Ti–6Al–7Nb (ASTM F1295), Ti–13Nb–13Zr (ASTM F1713), and Ti–12Mo–6Zr (ASTM F1813) [14].

37.2 Bulk Titanium–Bioceramic Nanocomposites

One method that allows the change of mechanical, chemical and biological properties of Ti and Ti-based alloys is to produce a composite that will exhibit the favorable mechanical properties of titanium and excellent biocompatibility and bioactivity of ceramics [38]. The main ceramics used in medicine are hydroxyapatite (HA, $Ca_{10}(PO_4)_6(OH)_2$), silica (SiO_2) or 45S5 Bioglass [7, 30]. Hydroxyapatite shows good biocompatibility because of its chemical and crystallographic structure being similar to that of living bone. Besides, HA has the ability to form strong chemical bonds with natural bone. Unfortunately, the HA cannot be used for load bearing applications, due to its poor mechanical properties regarding to natural bone [13]. The ceramic coating on the titanium improves the surface bioactivity, but often flakes off as a result of poor ceramic/metal interface bonding, which may cause the surgery to fail [18, 19]. For this reason, the nanocomposite materials containing titanium and bioceramic as a reinforced phase are promising alternatives to conventional materials, because they can potentially be designed to match the properties of bone tissue in order to enhance patients' quality of life [20, 21].

Earlier, microcrystalline Ti–20 vol.% HA composite with a relative density of 97.86% was fabricated by a hot pressing technique [63]. The phase constitution of Ti–20 vol.% HA composite is similar to that of HA-based composite with Ti and HA as the predominant phases. Elastic modulus and Vickers hardness of

Ti–20 vol.% HA composite are 102.6 and 3.41 GPa, respectively. Additionally, the osteointegration ability of the composite is better than that of pure titanium, especially in the early stage after the implantation, which may be due to the presence of HA ceramic in the Ti-matrix composite [63].

Recently, the Vickers hardness and corrosion properties of Ti–HA (3, 10, 20 vol.%) nanocomposites, prepared by MA and powder metallurgical process were investigated [60]. Microhardness test showed that the obtained material exhibits Vickers microhardness as high as 1030 and 1500 $HV_{0.2}$, which is more than 4–6 times higher than that of conventional microcrystalline titanium. Titanium nanocomposite with 10 vol.% of HA was more corrosion resistant ($i_c = 1.19 \times 10^{-7}$ Acm^{-2}, $E_c = -0.41$ V vs. SCE) than microcrystalline titanium (Table 37.3).

Table 37.3 Mean values of Vickers hardness, corrosion current densities, corrosion potentials and corrosion rate of studied Ti–HA nanocomposites, microcrystalline titanium, and hydroxyapatite [60]

Sample	$HV_{0.2}$	i_c = (A/cm^2)	E_c = vs. SCE (V)	C_R (mm/a)
Ti-3 vol.% HA	480	9.06×10^{-8}	–0.34	0.003
Ti-10 vol.% HA	1500	1.19×10^{-7}	–0.41	0.004
Ti-20 vol.% HA	1030	8.5×10^{-8}	–0.55	0.003
Ti (microcrystalline)	250	1.31×10^{-5}	–0.36	0.363
HA (microcrystalline)	480	—	—	—

Mechanical alloying and powder metallurgy process for the fabrication of titanium-45S5 Bioglass nanocomposites with a unique microstructure, higher hardness and better corrosion resistance were developed, too [36, 37]. Microhardness test showed that the obtained material exhibits Vickers microhardness as high as 770 $HV_{0.2}$ for Ti-20 wt.% 45S5 Bioglass, which is more than three times higher than that of conventional microcrystalline titanium. Additionally, titanium-10 wt.% of 45S5 Bioglass nanocomposites ($i_c = 1.20 \times 10^{-7}$ A/cm^2, $E_c = -0.42$ V vs. SCE) were more corrosion resistant than microcrystalline titanium. *In vitro* biocompatibility of these materials was evaluated and compared with conventional microcrystalline titanium, where normal human osteoblast (NHOst) cells from Cambrex (CC-2538) were cultured

on the disks of the materials and cell growth was examined. The morphology of the cell cultures obtained on Ti-10 wt.% 45S5 Bioglass nanocomposite was similar to those obtained on the microcrystalline titanium.

Young's modulus of the sintered Ti-10 wt.% 45S5 Bioglass composite was found to be 110 GPa. The measured value of Young's modulus for microcrystalline titanium is about 150 GPa. From the point of view of future application for hard tissue replacement implants, a biomaterial with low elastic modulus is anticipated because the elastic modulus of natural bone is low (7–25 GPa) [14]. Implants with high elastic modulus can lead to severe stress concentration, namely load shielding from a natural bone, therefore destroying the implant/bone surface as well as the bone [6, 59].

Nanograined materials due to very high number of atoms on the surface possess large surface energy. Thus, they exhibit entirely different behavior compared to the micron-sized grains. The bone forming cells generally attach themselves to the surface whose roughness is of nanometer range. It has been shown, that composition, roughness and surface energy affect the initial adhesion and spreading of cells [83, 84].

Table 37.4 Microhardness, mean values of corrosion current densities and corrosion potentials of studied Ti-10 wt.% 45S5 Bioglass nanocomposite scaffolds with different porosities in comparison to bulk Ti-10 wt.% 45S5 Bioglass nanocomposite and microcrystalline titanium [39]

Sample	$HV_{0.2}$	i_c (A cm^{-2})	E_c vs. SCE (V)
Ti-10 wt.% 45S5 with porosity of 48%	—	3.63×10^{-6}	–0.51
Ti-10 wt.% 45S5 with porosity of 67%	—	4.23×10^{-6}	–0.49
Ti-10 wt.% 45S5 with porosity of 72%	—	4.71×10^{-6}	–0.56
bulk Ti-10 wt.% 45S5 Bioglass	620	1.20×10^{-7}	–0.42
Ti (microcrystalline, grade 2)	225	2.27×10^{-6}	–0.36

Titanium-10 wt.% 45S5 Bioglass scaffold nanocomposites were also synthesized (Table 37.4) [39]. *In vitro* biocompatibility of these materials was evaluated (Fig. 37.7). The morphology of the cell cultures obtained on Ti-10 wt.% 45S5 Bioglass nanocomposite was similar to those obtained on the microcrystalline titanium. On the other hand, on porous scaffold, the cells adhered with their

whole surface to the insert penetrating the porous structure, while on the polished surface, more spherical cells were observed with a smaller surface of adhesion. The present study has demonstrated that titanium-10 wt.% 45S5 Bioglass scaffold nanocomposite is a promising biomaterial for bone tissue engineering.

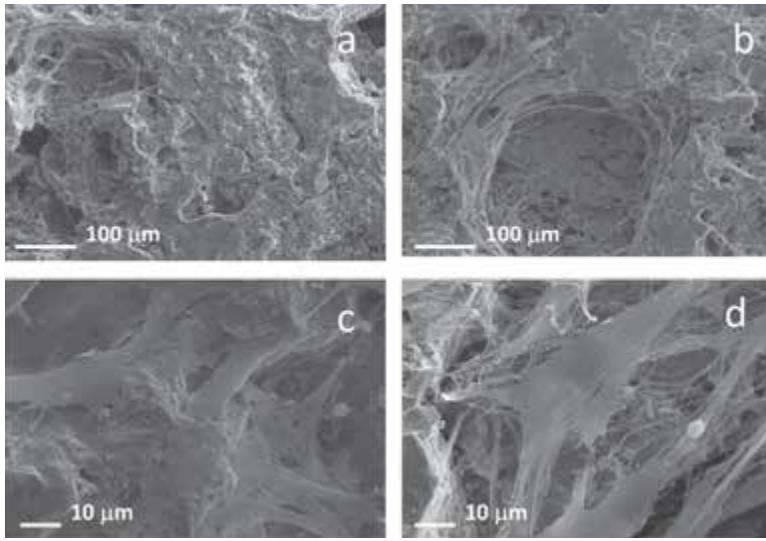

Figure 37.7 Scanning electron micrographs of osteoblasts cultured on Ti-10 wt.% 45S5 Bioglass scaffolds with 67% porosity after 1 day (a) and 5 days (b); Higher magnification micrograph are presented in c (1 day) and d (5 days) [39].

There are numerous reports that demonstrate that the surface roughness of titanium implants affects the rate of osseointegration and biomechanical fixation [32]. Surface roughness can be divided into three levels depending on the scale of the features: macro–, micro- and nano-sized topologies. The macro level is defined for topographical features as being in the range of millimeters to tens of microns. The microtopographic profile of dental implants is defined for surface roughness as being in the range of 1–10 µm. This range of roughness maximizes the interlocking between mineralized bone and the surface of the implant [83]. Surface profiles in the nanometer range play an important role in the adsorption of proteins, adhesion of osteoblastic cells and thus the rate of osseointegration [23, 83].

The commercial Ti dental implant produced by mechanical cutting has a surface roughness R_a ranging from about 0.08 to 1.3 mm [83]. Recent studies demonstrate that surface roughness affects cell spreading and proliferation, but not cell attachment, of human osteoblast-like cells [83, 85, 86]. These findings indicate that modification of surface roughness might provide a more suitable microenvironment for early osteoblast response to implant materials [45]. Cultures of human osteoblast-like cells revealed no significant difference in initial cell attachment among the various surfaces with surface roughness (R_a = 0.0374, 0.0911, and 0.2435 μm); however, cell spread was greater on rough surfaces than on glass slides and smoother surfaces. In addition, cell proliferation and Ki-67 expression were increased when cells were cultured on rough surfaces. These results suggest that a greater Ti–6Al–7Nb surface roughness supports the initial spread and proliferation of human osteoblast-like cells. Thus, modification of the surface roughness of dental implants might hasten osseointegration.

The process of osseointegration takes place *in vitro* as well as *in vivo* in four stages [46–48]. In the first stage, stem cells and osteoblast precursor cells migrate to the implant and adhere to it by the formation of foot-like protoplasmic processes. In the second stage, the cells begin to be anchored onto the substrate wall with the help of matrix proteins and produce a dense network of matrix proteins at the implant. The mineralization of the extracellular matrix occurs in stage 3 and is dependent on differentiation of osteoblasts. In the last stage, the network of extracellular matrix proteins and osteoblasts reorganizes and forms lamellar bone [46].

The surface roughness of the different Ti-based substrates was shown in Fig. 37.8 and the values of R_a, R_t, and R_z are reported in Table 37.5 [39]. The microcrystalline titanium presented a smooth surface with very low values of R_a, R_t, and R_z. The bulk Ti-10 wt.% 45S5 Bioglass nanocomposite had R_a, R_t, and R_z values of around 0.91, 12.99 and 10.21 μm, respectively. The Ti–10 wt.% 45S5 Bioglass scaffold with 67% porosity had average surface roughness, with R_a, R_t, and R_z in the 54–405 μm range. It has been documented that the optimal pore size for the cell attachment, differentiation and ingrowth osteoblasts, and vascularization is approximately 200–500 μm [26].

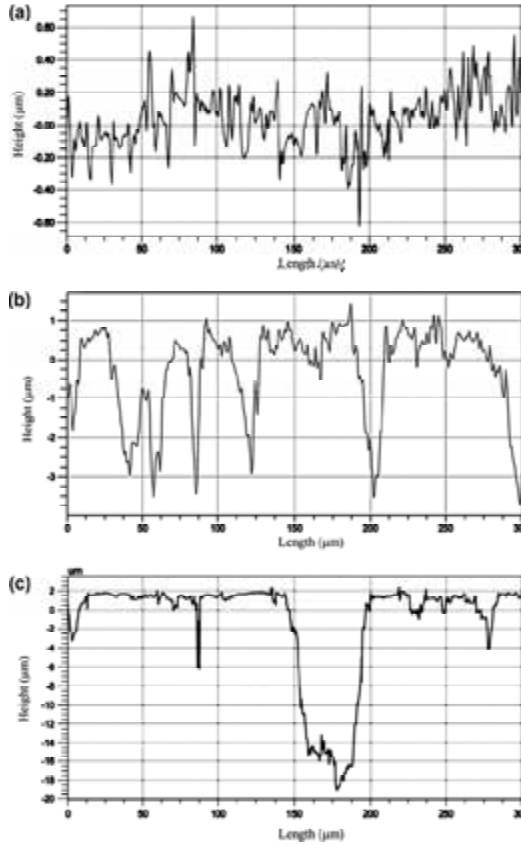

Figure 37.8 Roughness profiles of microcrystalline titanium (a), bulk Ti-10 wt.% 45S5 Bioglass nanocomposite (b) and Ti-10 wt.% 45S5 Bioglass scaffold with 67% porosity (c) [39].

Table 37.5 Roughness values R_a, R_t, and R_z (DIN) of the three surfaces used for culturing NHOst cells (the values are mean ± SD) [39]

	R_a (μm)	R_t (μm)	R_z (DIN) (μm)
microcrystalline Ti (grade 2)*	0.21 ± 0.06	4.92 ± 0.61	3.61 ± 0.29
bulk Ti-10 wt.% 45S5*	0.91 ± 0.09	12.99 ± 0.75	10.21 ± 0.63
Ti-10 wt.% 45S5 with porosity of 67%	54 ± 5	405 ± 25	392 ± 20

*Polished surface; arithmetic mean roughness—R_a; maximum height of the profile—R_t; 10-point mean roughness—R_z.

Surface characteristics of materials, such as their topography, chemistry or surface energy, play an essential part in osteoblast adhesion to biomaterials [22, 48]. Studies have demonstrated that nanostructured materials with cell favorable surface properties may promote greater amounts of specific protein interactions to stimulate more efficiently new bone growth compared to conventional materials [42, 48]. This may be one of the underlying reasons why nanomaterials are superior to conventional materials for tissue growth.

Silica (SiO_2) is a bioactive material that has high corrosion resistance. Silica bioceramics are used as prosthetic bone and dental implants because they promote the formation of apatite at their surfaces when immersed in simulated body fluid (SBF) [7, 47]. A biological basis for the role of silica in bone formation was established by Carlilse in a study of the role of silicon in bone calcification [8]. SiO_2 improves materials' bioactivity by leading to the formation of Si–OH groups on the material surface.

However, SiO_2 cannot be used for load-bearing applications because of its poor mechanical properties compared to natural bone. The ceramic coatings often flake off as a result of poor ceramic/metal interfacial bonding [17]. The above-mentioned problems may be overcome by fabricating titanium/bioceramic nanocomposites [40].

Ti-10 wt.% SiO_2 nanocomposites and their scaffolds were synthesized (Fig. 37.9) [40]. The Vickers hardness of the Ti-10 wt.% SiO_2 nanocomposites reached 670 $HV_{0.2}$. The *in vitro* cytocompatibility of these materials was evaluated. The intensity of cell growth on the surface depends on the surface structure of the sample. The osteoblasts that grew on the inserts exhibited adhesion to the material surface after one day and covered the majority of the surface after five days. The collected data reveals a significant difference in the morphological characteristics of the cells on the porous and polished materials even after one day of cell culturing. On the porous surface, cells adhered with their entire surface to the insert that penetrates the porous structure, whereas on the polished surface, more spherical cells were observed with a smaller surface of adhesion but with more filapodia. The ability to adhere and grow on a porous material is a specific characteristic of osteoblasts. Porous Ti-10 wt.% SiO_2

scaffolds have been developed in order to promote bone ingrowth and to induce prosthesis stabilization.

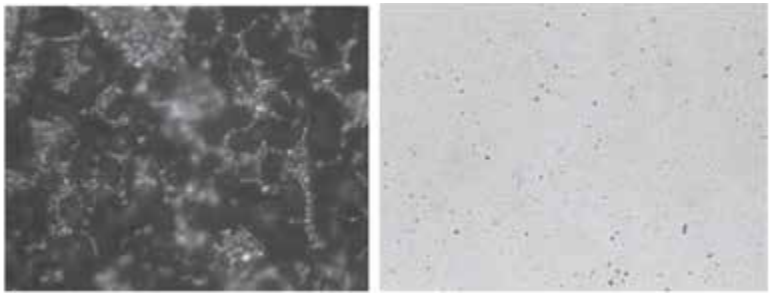

Figure 37.9 Optical micrographs of the Ti-10 wt.% SiO_2 nanocomposite scaffold with a 48% porosity after sintering under a vacuum of 10^{-4} Torr in two steps: at 175°C for 2 h and at 1150°C for 10 h (left) and the sintered bulk Ti-10 wt.% SiO_2 nanocomposite (MA 20 h, heat treatment 1150°C/2 h) (right) [40].

The bioactivity of silica is attributed to the formation of a hydroxycarbonated apatite (HCA) layer on its surface, which is considerably similar to the mineral component of bone [8]. The rate of tissue bonding appears to depend on the rate of HCA formation, which follows a sequence of reactions between the implanted material and the surrounding tissues and physiologic fluids [71]. Precipitation of the calcium and phosphate ions released from the glass together with those from the solution form a calcium–phosphate-rich layer (CaP) on the surface [72].

Recently, the *in vitro* cytocompatibility of Ti-45S5 Bioglass nanocomposites was evaluated (Figs. 37.10 and 37.11) [42]. During the studies, established cell line of human fibroblasts CCD-39Lu was cultured in the presence of tested materials and its survival rate, and proliferation activity were examined. Furthermore, the influence of the Ti–45S5 Bioglass nanocomposites and microcrystalline titanium was tested on the growth of Candida albicans yeast. Biocompatibility tests carried out indicate that the nanocomposite Ti-10 wt.% 45S5 Bioglass scaffolds could be a possible candidate for dental implants and other medicinal applications.

The cytocompatibility of synthesized bulk Ti-10 wt.% 45S5 Bioglass nanocomposites and their scaffolds was also investigated.

There was no cytotoxic properties of the tested materials against cells from CCD-39Lu cell line. Evaluation of survival rate demonstrated that growth of CCD-39Lu fibroblasts cultured in the presence of both nano- and microcrystalline materials depends on the quantity of suspended material. The viability of cells in culture decreased simultaneously with the increase of the tested material in the culture. Fibroblasts survival rate at 24 and 48 h of culture was more intensively inhibited in the presence of a microcrystalline Ti compared to the nanocrystalline Ti-10 wt.% 45S5 Bioglass powder. CCD-39Lu fibroblasts cultured in the presence of Ti-45S5 Bioglass nanocomposite in an amount of 0.005 mg/mL showed a higher survival rate as compared to the control population (Fig. 37.10).

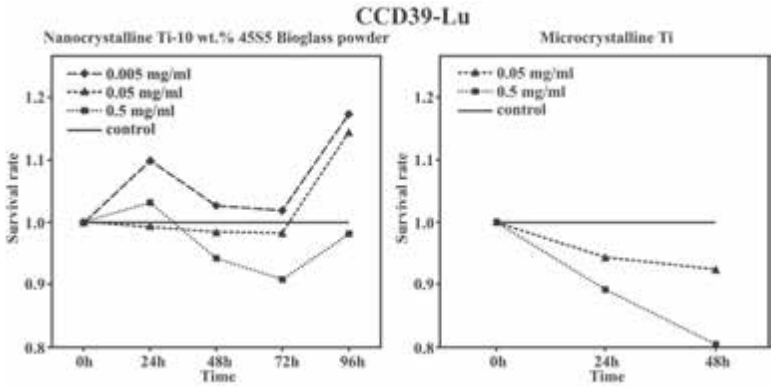

Figure 37.10 MTT test results. Survival rate of CCD39-Lu cell line cultured in the presence of Ti–10 wt.% 45S5 Bioglass nanocomposite and microcrystalline Ti, both in powder form [42].

The study indicated that nanocrystalline Ti-10 wt.% 45S5 Bioglass scaffold showing the porous structure potentiated the survival rate of CCD-39Lu fibroblasts. Nanocrystalline scaffold material (sample B) in the form of a disc affects the survival rate of treated cells in a similar manner as in the powder form, i.e., intensified survival rate of CCD-39Lu fibroblasts (Fig. 37.11).

In vitro biocompatibility studies showed that regardless of the type of material tested (nano- or microcrystalline) Ti-10 wt.% 45S5 Bioglass samples did not show cytotoxic properties against cultured cells. Despite this, the intensity of cell growth on the

surface is dependent on the surface structure of the sample. Obtained results suggest that nanocrystalline sample displays good cytocompatibility compared to microcrystalline titanium. Survival rate of CCD-39Lu fibroblasts was higher in the presence of the nanocrystalline material as compared with microcrystalline material in the same concentrations of the same intervals. On the other hand, the survival rate of CCD-39Lu fibroblasts was increased proportionally to the decrease of the amount of nanocrystalline material in powder form in sample. Most likely, the quantity of the powdered tested material presented in the sample can be crucial to the process of cell adhesion to the background. The barrier formed from tested material and the lack of physical contact of cells with the surface, limits their ability to start subdivision processes. The proliferative activity of CCD-39Lu fibroblasts cultured in the presence of a nanocrystalline material correlates with viability of these cells in the culture and is depended on the quantity of associated material. The percentage of replicating cells is increased simultaneously with decreasing amount of tested material in culture. However, keep in note that lack of cytotoxicity is not yet cell integrity.

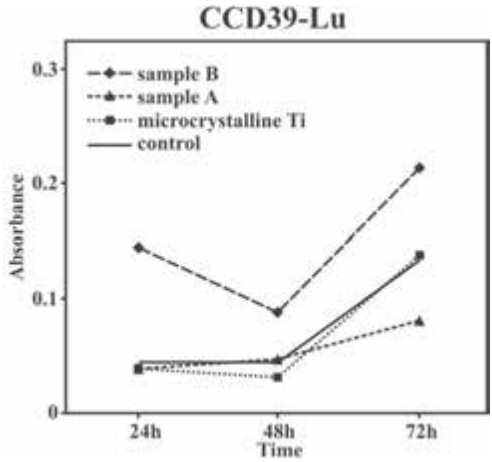

Figure 37.11 MTT test results. Survival rate of CCD39-Lu cell line cultured in the presence of Ti-10 wt.% 45S5 Bioglass nanocomposite (sample A) and their scaffold (sample B), and microcrystalline Ti, both in the form of a disk [42].

Independent study showed, that nanocrystalline Ti-10 wt.% 45S5 Bioglass materials (scaffold and bulk) regardless to the form (powder or disc) do not affect the viability of *Candida albicans* and do not inhibit the growth of yeast in the direct or indirect contact [42]. Despite the fact that tested nanomaterials do not have negative influence against yeast, their structure and/or surface limits the growth of tested *Candida* yeast. Knowledge of the interaction of fungal cells and materials from which dental implants are produced is still poor and requires further detailed studies at the molecular level.

The best surface of implant, from the viewpoint of cell biology, provides adequate adhesion and initiation of the cell subdivision process. However, these processes should be performed without excessive growth rate that could lead to escape of cells from the surveillance agents and exceeding of barriers carcinogenesis. It still seems very important to develop such materials or composites for the production of dental implants, which will demonstrate a reduced susceptibility to colonization, and implantation within the oral cavity they will not cause pathogenic effects. Because the shape of the surface is often critical to tissue function, it seems that the nanocrystalline Ti-10 wt.% 45S5 Bioglass scaffold may be an important step towards the production of such a structure, which can support the process of adaptation of the implant by the host organism. Scaffold Ti-10 wt.% 45S5 Bioglass nanocomposite would offer new structural and functional properties for innovative products in dental applications. Performed *in vitro* biocompatibility evaluation demonstrated that Ti-10 wt.% 45S5 Bioglass nanocomposites displays better cytocompatibility compared to that of microcrystalline titanium.

37.3 Dental Implants with Nanosurface

Nanoscale modification can alter the chemistry and/or topography of the implant surface [56]. There are many different methods to impart nanoscale features to the implant surface (Table 37.6). Several of these methods have already been used to modify implants available commercially [61, 62, 69]. Such changes alter the implant surface interaction with ions, biomolecules, and cells.

These interactions can favorably influence molecular and cellular activities and alter the process of osseointegration.

Table 37.6 Methods for creating nanofeatures on cp Titanium implants [56]

Methods	Characteristics
Self-assembly of monolayers	
	The exposed functional end group could be a molecule with different functions (an osteoinductive or cell adhesive molecule)
Physical approaches	
Compaction of nanoparticles	Conserves the chemistry of the surface among different topographies; Not readily applied over implant surfaces
Ion beam deposition	Can impart nanofeatures to the surface based on the material used
Chemical methods	
Acid etching	Combined with other methods (sandblasting and/or peroxidation) can impart nanofeatures to the surface and remove contaminants
Peroxidation	Produces a titania gel layer; both chemical and topography changes are imparted
Alkali treatment (NaOH)	Produces a sodium titanate gel layer allowing hydroxyapatite deposition; both chemical and topography changes are imparted
Anodization	Can impart nanofeatures to the surface creating a new oxide layer (based on the material used)
Nanoparticle deposition	
Sol–gel (colloidal particle adsorption)	Creates a thin-film of controlled chemical characteristics; atomic-scale interactions display strong physical interactions
Discrete crystalline deposition	Superimposes a nanoscale surface topographical complexity on the surface
Lithography and contact printing technique	
	Many different shapes and materials can be applied over the surface; approaches are labor intensive and require considerable development prior to clinical translation and application on implant surface

Until now, a few nanoscale surface topography modifications have been used to enhance bone responses at clinical dental implants. For example, the Osseo-Speed surface (Astra Tech AB, Molndal, Sweden) possesses nanostructured features created by TiO_2 blasting followed by a proprietary hydrofluoric acid treatment [1, 10, 16]. Greater osteoblastic gene expression (Runx2, Osterix, Alkaline Phosphatase, and Bone Sialoprotein) was measured in cells adherent to the nanoscale HF-treated surface compared to the micron-scale surface [27]. This nanotopography is associated with the elevated levels of gene expression that indicate rapid osteoblastic differentiation. Other studies have demonstrated an increased bone formation, torque removal value [15]. In the rabbit tibia model of osseointegration, histomorphometric evaluations demonstrated higher bone-to-implant contact for the nanoscale OsseoSpeed implants compared to the micron-scale TiOblast™ implants (Astra Tech AB, Mölndal, Sweden) at 1 month (35 ± 14% vs. 26 ± 8%) and 3 months (39 ± 11% vs. 31 ± 6%) after placement [67].

The Astra Tech TiOblast™ is the precursor of the OsseoSpeed™ surface [29]. This surface was grit blasted with titanium dioxide particles to achieve an isotropic, moderately roughened surface. The TiOblast surface shows excellent outcomes when compared with machined titanium surfaces in theoretical models, in terms of *in vitro* cell biocompatibility evaluations and *in vivo* studies [11, 19, 24, 25, 59].

On the other hand, OsseoSpeed™ was launched in the fall 2004 and was a further development of the moderately roughened (grit blasted with titanium dioxide particles) titanium surface TiOblast™ [67]. OsseoSpeed gains its additional surface characteristics via a chemical (fluoride) treatment and a slight topographic modification of the TiOblast surface. Incorporation of small amounts of fluoride ions in the oxide layer, a slight increase on the micrometer scale in surface roughness, and the appearance of a nanoscale topography have been reported for the OsseoSpeed surface. *In vitro* and animal experiments indicate that the OsseoSpeed surface leads to increased bone formation and stronger bone-to-implant bonding at shorter healing times than TiOblast or machined titanium surfaces. Enhanced osteoblast differentiation, platelet activation, and thrombogenic properties of the fluoride-treated surface have been reported [3, 16, 70].

Published data shows that the OsseoSpeed implant can be safely used with a range reported for survival rate from 94.5% to 100%, including the use of immediate loading protocol [13] even in the atrophic edentulous maxilla [72], in sinus lifted maxillary posterior jaw sites [71], immediate installation in extraction sockets [54], and implants placed in atrophied mandibles close to the nerve [66].

Another nanoscale surface implant presently available in the clinical marketplace involves a CaP nanoparticle modification of a minimally rough titanium alloy implant (see Figs. 37.12 and 37.13) [12]. The NanoTite™ implant starts with the industry-proven OSSEOTITE® Surface at the core. Next, discrete nanometer scale crystals of calcium phosphate (CaP) are deposited onto the OSSEOTITE Surface substrate. These crystals are bonded to the substrate, occupying approximately 50% of the surface, thereby being differentiated from the traditional plasma-sprayed CaP coatings that have been in commercial use for more than 20 years. The nanoscale topography and potential biologic benefits associated with the CaP crystals may play a key role in enhanced site response, potentially improving clinical predictability and outcomes. Preclinical studies demonstrate a substantial improvement on the rate and extent of osseointegration for the NanoTite implant versus the Osseotite implant.

The nanoscale CaP surface created by DCD (Nanotite, 3i) was evaluated [39]. The histologic evaluation of clinical implants revealed bone-to-implant contact of 19 ± 14.2% and 32.2 ± 18.5% for the Osseotite (3i) control and the Nanotite (3i) experimental implants, respectively. Additionally, greater bone formation at 4 and 8 weeks was observed [19].

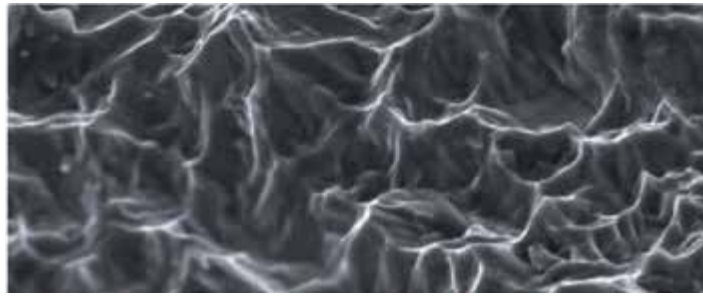

Figure 37.12 OSSEOTITE® Surface at 20,000× (http://biomet3i.com).

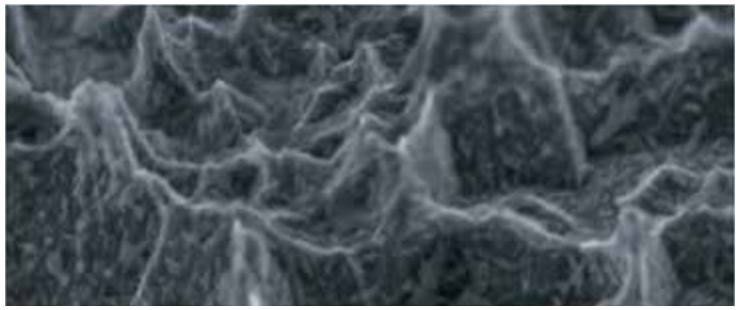

Figure 37.13 NanoTite™ Surface at 20,000× (http://biomet3i.com).

Recently, ion-beam assisted deposition (IBAD) process, which provides increased integration with the implant surface, known as high-energy sputter deposition, has been used to create a commercially available dental implant surface [6]. In the NanoTite™ process, a high-energy ion beam source aims a beam of ions at the surface of a target treated with HA. These high-energy ions eject the basic chemical elements of the HA from the target/substrate and create a molecular cloud whose molecules bond with the surface of the bicon integra-Ti™ implant. The bone formation was higher in the experimental group than in the control group (sandblasted/acid-etched) after 2 (13.56% vs. 24.04%) and 4 weeks (14.22% vs. 27.39%) [9].

Current studies are focused on synthesis of β-type titanium nanocrystalline alloys [34]. The Ti–6Zr–4Nb alloy surface improvement was achieved by electrochemical treatment, which composed of two stages: anodic oxidation and Ca–P deposition. The porous surface was produced by anodic oxidation in 1 M H_3PO_4 + 2%HF electrolyte at 10 V for 30 min. Next the calcium–phosphate (Ca–P) layer was deposited, onto the formed porous surface, using cathodic potential –5 V kept for 60 min in 0.042 M $Ca(NO_3)_2$ + 0.025 M $(NH_4)_2HPO_4$ + 0.1 M HCl electrolyte. The deposited Ca–P layer anchored in the pores. *In vitro* tests culture of normal human osteoblast (NHOst) cells showed very good cells proliferation, colonization and multilayering. It has been shown that surface with appropriate chemical composition and topography, after combined electrochemical anodic and cathodic surface treatment, supports osteoblast adhesion and proliferation (Fig. 37.14) [34, 51, 52, 87].

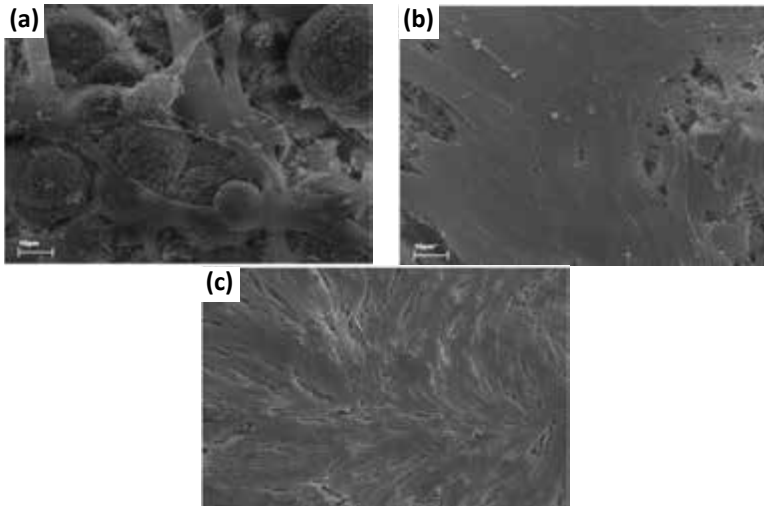

Figure 37.14 Osteoblast culture on the surface of the nano-Ti–6Zr–4Nb after anodic oxidation and additional Ca–P deposition after 1st (a) and 5th day (b, c; different magnifications) [34].

In order to improve the surface properties of titanium and expand its clinical application, boride microplasma surface alloying has been applied to modify its surface, too [5, 57, 58]. Plasma surface alloying gives a wide range of layer thickness, which is controlled by the amount of the placed powder and process parameters. Formation of TiB phase precipitation was confirmed. The Vickers microhardness was significantly improved from 180 HV for original titanium substrate to 900 HV in obtained composite layer structure, with a smooth hardness reduction in the cross section profile. Strong heat penetration from microplasma melt-in technique led to substrate dissolution with formation of stable TiB phase dispersed in α-Ti matrix. The electrochemical treatment in phosphoric acid electrolyte resulted in developed surface formation, attractive for tissue fixing and growth. The results of the *in vitro* test suggest that TiB phase dispersed in α-Ti matrix displays good cytocompatibility, compared to that of microcrystalline titanium. Additionally, the SEM observation reveals a significant difference in morphological characteristics of the cells on developed and polished material, just after 1 day of cell culture. It can be concluded that, plasma alloying is an effective method to produce TiB phase dispersed in α-Ti matrix with high hardness,

good cytocompatibility, which makes them potential candidates for biomedical applications.

37.4 Nanostructured Materials for Permanent and Bioresorbable Medical Implants

Development of metallic implant materials is driven by the biocompatibility requirements and also by the need for improved mechanical performance of biomedical implants. Additionally, the implants should strongly bond with the bone for the unfailing and long-term exploitation. For that reason, beside good mechanical and corrosion properties, the implant surface should be sufficiently rough for tissue growth and bone bonding [32, 33]. Different paradigms govern this development for permanent and temporary implants. While materials for permanent implants, e.g., for bone or tooth replacement, obviously need to be as inert in bodily fluids as possible, those for temporary implants must degrade at a rate suitable for the targeted application.

Recently, two alloy systems based on titanium and magnesium are investigated [18, 31, 81]. Indeed, Ti forms a protective surface layer of titania and is considered to be bio-inert, while Mg is extremely reactive and biodegradable. It is known, that the mechanical performance of implant materials is possible to enhance through microstructure control. An equal channel angular pressing is a viable processing route to grain refinement and property improvement. It turns out that the extreme grain refinement of the bulk of the metal down to nanoscale transpires to surface morphology that turns out to be conducive for enhanced adhesion and growth of living cells (Fig. 37.15). Indeed, proliferation of the preosteoblast cells on the surface of nanostructured Ti processed by ECAP was shown to be hugely enhanced, by a factor of about 20. Improved adhesion and accelerated rate of proliferation following ECAP processing of titanium was recently reported for osteoblast cells [40].

Bioactivity of titanium can be enhanced further by a combination of coating techniques, such as micro-arc oxidation (MAO), anodizing, and coating with hydroxyapatite (Fig. 37.16) [46, 48]. When HA was deposited on a MAO-treated surface, bioactivity was higher than in the case when only surface treatment was performed.

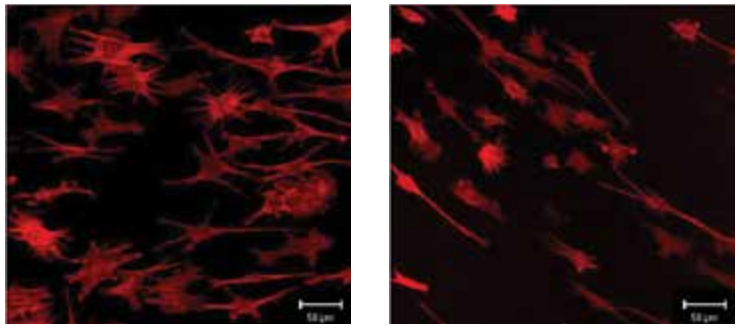

Figure 37.15 Enhanced growth of preosteoblast cells on nanostructured titanium (left) as compared to coarse-grained one (right) [20].

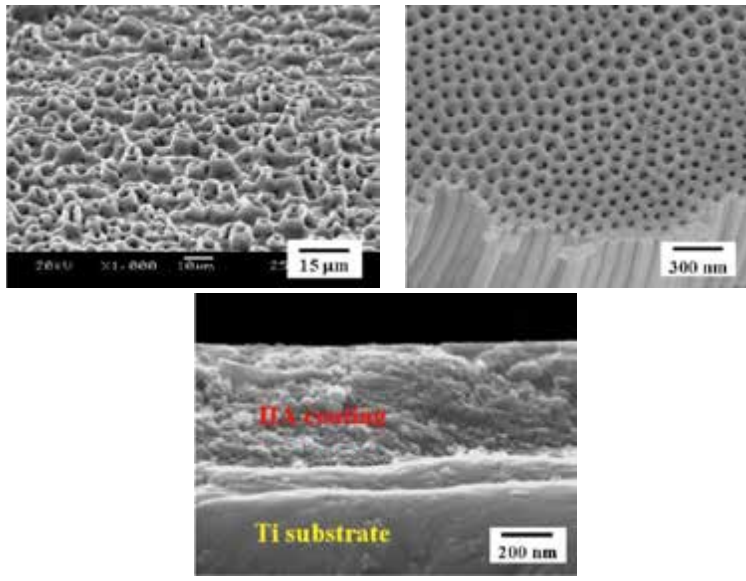

Figure 37.16 SEM micrographs of surface-modified titanium implants: Morphology of MAO-treated surface (left top), anodized surface (right top) and cross-sectional view of HA coating on Ti substrate (left bottom) [46].

The potential for using Mg alloys in bioresorbable vascular stents or bone implants has recently attracted a huge interest of researchers [18, 31, 41, 45, 88]. Reducing the danger of inflammations and avoiding the need for repeat surgery by using temporary, biodegradable metallic implants and at the same time capitalizing

on their good mechanical strength is, indeed, a very attractive possibility. Many groups worldwide have rapidly moved into this area. Despite some problems with biotoxicity of certain alloying elements, structural Mg alloys have been used in biocompatibility tests, both *in vitro* and *in vivo*. Clinical tests have demonstrated the viability of Mg alloys as stent implant materials. Recent results supported by the published work suggest, however, that *in vivo* tests are indispensable already at this stage, as biocompatibility of Mg alloys *in vitro* does not fully represent what happens *in vivo* [18, 88].

Recent work has demonstrated that bulk grain refinement techniques, such as equal-channel angular pressing, are potent tools to improve the fatigue strength and the bio-corrosion resistance of common structural Mg alloys [81]. We are exploring the ways to further improve the properties of Mg based alloys and make them fit for applications in bioresorbable implants.

However, bulk grain refinement may be insufficient to bring the bio-corrosion rate down to the levels required by the clinical needs. A natural way to contain corrosion of Mg and achieve controllable corrosion rates is by surface modification, particularly through smart coating design. For example, corrosion of Mg alloys is retarded markedly when a thin MgF_2 layer is formed on the surface in a fluoridation process. Furthermore, when a bioactive material, such as hydroxyapatite, is deposited on top of the MgF_2 layer, both the corrosion resistance and biocompatibility are enhanced significantly (Fig. 37.17).

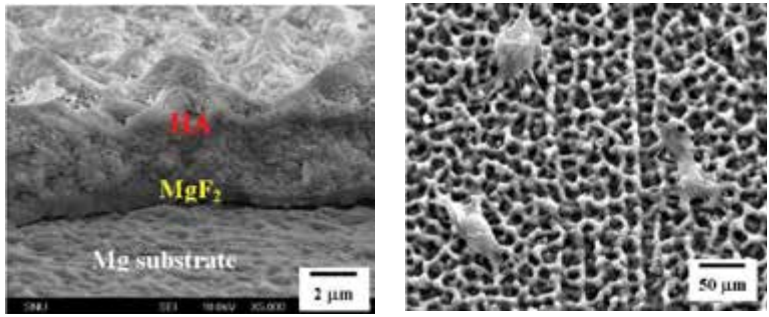

Figure 37.17 Coating layers of MgF_2 and hydroxyapatite (HA) on Mg (left) and osteoblast cells attached on the surface of Mg coated with MgF_2 and HA (right) [81].

37.5 Nanostructured Dental Composite Restorative Materials

In recent years, materials used for dental restorations have comprised principally acrylate or methacrylate polymers. However, acrylic materials exhibit high coefficients of thermal expansion relative to the coefficient of thermal expansion for the tooth structure, therefore these substances by themselves proved to be less than satisfactory. The disparity in thermal expansion, coupled with high shrinkage upon polymerization, resulted in poor marginal adaptability and ultimately led to secondary decay. Furthermore, the wear and abrasion characteristics and the overall physical, mechanical, and optical properties of these unfilled acrylic resinous materials were quite poor. Composite dental restorative materials containing methacrylate resins and fillers were thus developed.

The nanotechnology and nanoscience aim in designing and developing new dental composite materials with superior properties [35]. The filler composition comprises at least bound, nanostructured silica. The silica is in the form of nano-sized particles, preferably spherical particles. The individual particles have the largest dimension or diameter in the range from about 10 to about 100 nm and preferably from about 10 to about 50 nm. The silica particles are furthermore bound to each other so as to result in chains having lengths in the range from about 50 nm to about 400 nm. In order to improve bonding with the resin matrix, the bound colloidal silica filler particles may optionally be treated with a silane. These filled compositions are useful for a variety of dental treatments and restorative functions including crown and bridge materials, fillings, adhesives, sealants, luting agents or cements, denture base materials, orthodontic materials and sealants, and other dental restorative materials.

In addition to the bound, nanostructured silica, the filler composition may further comprise one or more of the inorganic fillers currently used in dental restorative materials. Preferred additional fillers include those that are capable of being covalently bonded to the resin matrix itself or to a coupling agent, which is covalently bonded to both. Examples of suitable filling materials include, but are not limited to, silica, silicate glass, quartz,

barium silicate, strontium silicate, barium borosilicate, strontium borosilicate, borosilicate, lithium silicate, lithium alumina silicate, amorphous silica, ammoniated or deammoniated calcium phosphate and alumina, zirconia, tin oxide, and titania. Suitable fillers have a particle size in the range from about 0.1–5.0 μm and may further comprise unbound silicate colloids of about 0.001 to about 0.07 μm. These additional fillers may also be silanized.

The amount of total filler composition in the dental composite can vary widely, in the range from about 1% to about 90% by weight (wt.%) of the total composition. The amount used is determined by the requirements of the particular application. Thus, for example, crown and bridge materials generally comprise from about 60 wt.% to about 90 wt.% filler, luting cements comprise from about 20 wt% to about 80 wt.% filler, sealants generally comprise from about 1 wt.% to about 20 wt.% filler, adhesives generally comprise from about 1 to about 30 wt.% filler and restorative materials comprise from about 50% to about 90% filler, with the remainder in all cases being the resin composition.

The expected outcomes are new formulations for dental composites with improved adhesive bonding to dentin and enamel surfaces, improved durability, esthetics, and biocompatibility. Nanostructured dental composites can have superior mechanical properties (e.g., increased elastic modulus, strength, or resistance to fatigue fracture) that can easily be tuned by small modifications of their building blocks.

Abbreviations

CaP: Calcium-phosphate
cp Ti: Commercial purity titanium
ECAP: Equal channel angular pressing
HA: Hydroxyapatite ($Ca_{10}(PO_4)_6(OH)_2$)
HCA: Hydroxycarbonated apatite
HPT: High-pressure torsion
MAO: Micro-arc oxidation
NHOst: Normal human osteoblast cell
R_a: Arithmetic mean roughness
R_t: Maximum height of the profile

R_z: Ten-point mean roughness
SBF: Simulated body fluid
SPD: Severe plastic deformation
TMP: Thermomechanical pressing
45S5 Bioglass: (45% SiO_2, 24.5% Na_2O, 24.5 CaO, 6% P_2O_5)

Disclosures and Conflict of Interest

This work was supported by grants from National Science Centre of Poland. The authors declare that they have no conflict of interest and have no affiliations or financial involvement with any organization or entity discussed in this chapter. This includes employment, consultancies, honoraria, grants, stock ownership or options, expert testimony, patents (received or pending) or royalties. No writing assistance was utilized in the production of this chapter and the authors have received no payment for its preparation.

Corresponding Author

Dr. Karolina Jurczyk
University of Medical Sciences
Conservative Dentistry and Periodontology Department
Bukowska 70 Str., 60-812 Poznan, Poland
Email: karolajur@gmail.com

About the Authors

Karolina Jurczyk is an adjunct professor in the Department of Conservative Dentistry and Periodontology at Poznan University of Medical Sciences in Poland, where she received her PhD in medical sciences in 2011. Her research focuses on the structural, chemical, and biological characterization of nanostructured biomaterials. Her recent research has focused on nanomaterials, cell survival rate, and proliferation activity. Since September 2014, Dr. Jurczyk has been an ITI scholar in the Department of Reconstructive Dentistry and Gerodontology at Bern University, Switzerland.

Mieczyslaw Jurczyk directs the Institute of Materials Science and Engineering at Poznan University of Technology, Poland and Functional Nanomaterials Division, which designs, synthesizes, and evaluates nanomaterials for various biomedical and engineering applications. Bio-nanomaterials investigated recently include nanostructured titanium and magnesium based biocomposites and scaffolds. Mieczyslaw Jurczyk's degrees are in condensed matter physics and materials science and engineering from the Polish Academy of Sciences (PhD, 1981 and DSc, 1996). In 2002, he was promoted to professor of materials science and engineering. Prof. Jurczyk's lab group has generated 7 books, 10 book chapters, 40 invited presentations, more than 250 literature articles and more than 80 conference presentations.

References

1. Abron, A., Hopfensperger, M., Thompson, J., Cooper L. F. (2001). Evaluation of a predictive model for implant surface topography effects on early osseointegration in the rat tibia model. *J. Prosthet. Dent*., **85**, 40–46.
2. Adamek, G., Jakubowicz, J. (2010). Mechanoelectrochemical synthesis and properties of porous nano Ti-6Al-4V alloy with hydroxyapatite layer for biomedical applications. *Electrochem. Commun*., **12**, 653–656.
3. Berglundh, T., Abrahamsson, I., Albouy, J. P., Lindhe, J. (2007). Bone healing at implants with a fluoride-modified surface: An experimental study in dogs. *Clin. Oral Implants Res.*, **18**, 147–152.
4. Boyer, R., Welsch, G., Collings, E. (1994). *Materials Properties Handbook: Titanium Alloys*, ASM International, Materials Park, OH.
5. Brossa, F., Cigada, A., Chiesa, R., Paracchini, L., Consonni, C. (1994). Post-deposition treatment effects on hydroxyapatite vacuum plasma spray coatings. *J. Mater. Sci. Mater. Med.,* **5**, 855–857.
6. Brunette, D. M., Tengvall, P., Textor, M., Thomsen, P. (2003). *Titanium in Medicine,* Springer-Verlag Berlin, Heidelberg.
7. Cao, W. P., Hench, L. (1966). Bioactive materials. *Ceramics Int.,* **22**, 493–507.
8. Carlisle, E. M. (1970). Silicon: A possible factor in bone calcification. *Science,* **167**, 279–280.

9. Coelho, P. G., Suzuki, M. (2005). Evaluation of an IBAD thin-film process as an alternative method for surface incorporation of bioceramics on dental implants. *J. Appl. Oral*., **13**, 87–92.
10. Cooper, L. F., Zhou, Y., Takebe, J., Guo, J., Abron, A., Holmen, A., Ellingsen, J. E. (2006). Fluoride modification effects on osteoblast behavior and bone formation at TiO_2 grit blasted c.p. titanium endosseous implants. *Biomaterials,* **27**, 926–936.
11. Cooper, L. F., Masuda, T., Whitson, S. W., Yliheikkila, P., Felton, D. A. (1999). Formation of mineralizing osteoblast cultures on machined, titanium oxide grit-blasted, and plasma-sprayed titanium surfaces. *Int. J. Oral Maxillofac Implants*, **14**, 37–47.
12. Davarpanah, M., Martinez, H., Etienne, D., Zabalegui, I., Mattout, P., Chiche, F., Michel, J. (2002). A prospective multicenter evaluation of 1,538 BIOMET 3i implants: One to five year data. *Int. J. Oral Maxillofac Implants*, **17**, 820–828.
13. Donati, M., La Scala, V., Billi, M., Di Dino, B., Torrisi, P., Berglundh, T. (2008). Immediate functional loading of implants in single tooth replacement: A prospective clinical multicenter study. *Clin. Oral Implants Res*., **19**, 740–748.
14. Elias, C. N., Lima, J. H. C., Valiev, R., Meyers, M. A. (2008). Biomedical applications of titanium and its alloys. *JOM J. Minerals Metals Mater. Soc.*, **60**, 46–49.
15. Ellingsen, J. E., Johansson, C. B., Wennerberg, A., Holmen, A. (2004). Improved retention and bone-to-implant contact with fluoride-modified titanium implants. *Int. J. Oral Maxillofac Implants*, **9**, 659–566.
16. Ellingsen, J. E. (2005). Pre-treatment of titanium implants with fluoride improves their retention in bone. *J. Mater. Sci. Mater. Med*., **6**, 749–753.
17. Ellingsen, J. E., Thomsen, P., Lyngstadaas, S. P. (2006). Advances in dental implant materials and tissue regeneration. *Periodontology 2000*, **41**, 136–156.
18. Erbel, R., Di Mario, C., Bartunek, J., Bonnier, J., de Bruyne, B., Eberli, F. R., Erne, P., Haude, M., et al. (2007). Temporary scaffolding of coronorary arteries with bioabsorbable magnesium stents: A prospective, non-randomized multo-centre trial. *Lancet,* **369**, 1869–1875.
19. Ericsson, I., Johansson, C. B., Bystedt, H., Norton, M. R. (1994). A histomorphometric evaluation of bone-to-implant contact on machine-prepared and roughened titanium dental implants. A pilot study in the dog. *Clin. Oral Implants Res.*, **5**, 202–206.

20. Estrin, Y., Kasper, C., Diederichs, S., Lapovok, R. (2008). Accelerated growth of preosteoblastic cells on ultrafine grained titanium. *J. Biomed. Nater. Res.* A, **90**, 1239–1242.

21. Fandridis, J., Papadopoulos, T. (2008). Surface characterization of three titanium dental implants. *Implant Dent.*, **17**, 91–99.

22. Goene, R. J., Testori, T., Trisi, P. (2007). Influence of a nanometer-scale surface enhancement on de novo bone formation on titanium implants: A histomorphometric study in human maxillae. *Int. J. Periodontics Restorative Dent.*, **27**, 211–219.

23. Godarzi, R., Rasmusson, L., Dasmah, A., Albrektsson, T. (2008). Effects of implant design and surface on osseointegration. An experimental study in the dog mandible. *Appl. Osseointegration Res.*, **7**, 58–60.

24. Gotfredsen, K., Nimb, L., Hjorting-Hansen, E., Jensen, J. S., Holmen, A. (1992). Histomorphometric and removal torque analysis for TiO_2-blasted titanium implants. An experimental study on dogs. *Clin. Oral Implants Res.*, **3**, 77–84.

25. Gotfredsen, K., Wennerberg, A., Johansson, C., Skovgaard, L. T. Hjorting-Hansen, E. (1995). Anchorage of TiO_2-blasted, HA-coated, and machined implants: An experimental study with rabbits. *J. Biomed. Mater. Res.*, **29**, 1223–1231.

26. Guo, J., Padilla, R. J., Ambrose, W., De Kok, I. J., Cooper, L. F. (2007). Modification of TiO_2 grit blasted titanium implants by hydrofluoric acid treatment alters adherent osteoblast gene expression *in vitro* and *in vivo*. *Biomaterials*, **28**, 5418–5425.

27. Guehennec, L., Souedan, A., Layrolle, P., Amouriq, Y. (2007). Surface treatments of titanium dental implants for rapid osseointegration. *Dent. Mater.,* **23**, 844–854.

28. Han, C. H., Johansson, C. B., Wennerberg, A., Albrektsson, T. (1998). Quantitative and qualitative investigations of surface enlarged titanium and titanium alloy implants. *Clin. Oral Implant. Res.*, **9**, 1–10.

29. Hansson, S. (2000). Surface roughness parameters as predictors of anchorage strength in bone: A critical analysis. *J. Biomech.*, **33**, 1297–1303.

30. Hench, L. L. (1991). Bioceramics: From concept to clinic. *J. Am. Ceram. Soc.,* **74**, 1487–1510.

31. Hoog, C., Birbilis, N., Zhang, M. X., Estrin, Y. (2008). Surface grain size effects on the corrosion of magnesium. *Key Eng. Mater.*, **384**, 229–240.

32. Jakubowicz, J., Jurczyk, K., Niespodziana, K., Jurczyk, M. (2009). Mechanoelectrochemical synthesis of porous Ti-based nanocomposite biomaterial. *Electrochem. Commun.,* **11**, 461–465.

33. Jakubowicz, J., Adamek, G. (2009). Preparation and properties of mechanically alloyed and electrochemically etched porous Ti–6Al–4V. *Electrochem. Commun*., **11**, 1772–1775.

34. Jakubowicz, J., Adamek, G., Jurczyk, M. U., Jurczyk, M. (2012). 3D topography study of the biofunctionalized nanocrystalline Ti–6Zr–4Nb/Ca-P. *Mater. Charact.*, **70**, 55-62.

35. Jia, W. T., Jin, S. H. (2002). Dental composite materials, US Patent 6417246.

36. Jurczyk, K., Niespodziana, K., Jurczyk, M. U., Jurczyk, M. (2011). Synthesis and characterization of titanium-45S5 Bioglass nanocomposites. *Mater. Des.,* **32**, 2554–2560.

37. Jurczyk, K., Niespodziana, K., Jurczyk, U. U., Jakubowicz, J., Jurczyk, M. (2011). Titanium-10 wt% 45S5 Bioglass nanocomposite for biomedical applications. *Mater. Chem. Phys*., **131**, 540–546.

38. Jurczyk, M. (ed.) (2012). *Bionanomaterials for Dental Applications*, Pan Stanford Publishing, Singapore.

39. Jurczyk, M. U., Jurczyk, K., Miklaszewski, A., Jurczyk, M. (2011). Nanostructured titanium-45S5 Bioglass scaffold composites for medical applications. *Mater. Des.,* **32**, 4882–4889.

40. Jurczyk, M. U., Jurczyk, K., Niespodziana, K., Miklaszewski, A., Jurczyk, M. (2013). Titanium-SiO_2 nanocomposites and their scaffolds for dental applications. *Mater. Charact.,* **77**, 99–108.

41. Kaese, V., Pinkvos, A., Haferkamp, H., Niemeyer, M., Bach, F. W. (2005). Process for producing bioresorbable implants, US Patent 6854172.

42. Kaczmarek, M., Jurczyk, M. U., Rubis, B., Banaszak, A., Kolecka, A., Paszel, A., Jurczyk, K., Murias, M., Sikora, J., Jurczyk, M. (2014). *In vitro* biocompatibility of Ti-45S5 Bioglass nanocomposites and their scaffolds. *J. Biomed. Mater. Res. A*., **102**, 1316–1324.

43. Khan, M. M., Williams, R. L. Williams, D. F. (1999). The corrosion behaviour of Ti–6Al–4V, Ti–6Al–7Nb and Ti-13Nb-13Zr in protein solutions. *Biomaterials*, **20**, 765–772.

44. Klein, C. P. A. T., Li, P., de Blieck-Hogervorst, J. M. A., de Groot, K. (1995). Effect of sintering temperature on silica gels and their bone bonding ability. *Biomaterials,* **16**, 715–719.

45. Krivoruchko, M., Allen, J., Birdsall, M. (2010). Bioresorbable stent, United States Patent 7651527.

46. Lee, S. H., Kim, H. E., Kim, H. W. (2007). Nano-sized hydroxyapatite coatings on Ti substrate with TiO_2 buffer layer by e-beam deposition. *J. Am. Ceram. Soc*., **90**, 50–56.
47. Lefebvre, L., Chevalier, J., Gremillard, L., Zenati, R., Thollet, G., Bernache-Assolant D., Govin, A. (2007). Structural transformations of bioactive glass 45S5 with thermal treatments. *Acta Mater*., **55**, 3305–3313.
48. Li, L. H., Kong, Y. M., Kim, H. W., Kim, Y. W., Kim, H. E., Heo, S. J., Koak, J. Y. (2004). Improved biological performance of Ti implants due to surface modification by micro-arc oxidation. *Biomaterials*, **25**, 2867–2875.
49. Lindhe, J., Karring, T., Lang, N. P. (2003). *Clinical Periodontology and Implant Dentistry*, *4th edition*, Blackwell Publishing Ltd, Oxford, UK.
50. Liu, H. N., Webster, T. J. (2007). Nanomedicine for implants: A review of studies and necessary experimental tools. *Biomaterials,* **28**, 354–369.
51. Liu, H., Yazici, H., Ergun, C., Webster, T. J., Bermek, H. (2008). An *in vitro* evaluation of the Ca/P ratio for the cytocompatibility of nano-to-micron particulate calcium phosphates for bone regeneration. *Acta Biomater.,* **4**, 1472–1479.
52. Liu, X., Chu, P. K., Ding, C. (2004). Surface modification of titanium, titanium alloys, and related materials for biomedical applications. *Mater. Sci. Eng*. *R,* **47**, 49–121.
53. Long, M., Rack, H. J. (1998). Titanium alloys in total joint replacement—A materials science perspective*. Biomaterials,* **19**, 1621–1638.
54. Lops, D., Chiapasco, M., Rossi, A., Bressan, E., Romeo, E. (2008). Incidence of inter-proximal papilla between a tooth and an adjacent immediate implant placed into a fresh extraction socket: 1-year prospective study. *Clin. Oral Implants Res*., **19**, 1135–1140.
55. Matusiewicz, H. (2014). Potential release of *in vivo* trace metals from metallic medical implants in the human body: From ions to nanoparticles—A systematic analytical review. *Acta Biomater.,* **10**, 2379–2403.
56. Mendonça, G., Mendonça, D. B. S., Aragaõ, F. J. L., Cooper L. F. (2008). Advancing dental implant surface technology—From micron to nanotopography—review. *Biomaterials,* **29**, 3822–3835.
57. Miklaszewski, A., Jurczyk, M. U., Jurczyk, K., Jurczyk, M. (2011). Plasma surface modification of titanium by TiB precipitation for biomedical applications. *Surface Coatings Technol.,* **206**, 330–337.
58. Miklaszewski, A., Jurczyk, M. U., Jurczyk, M. (2013). Microstructural development of Ti-B alloyed layer for hard tissue applications. *J. Mater. Sci. Technol.,* **29**, 565–572.

59. Mustafa, K., Silva Lopez, B., Hultenby, K., Wennerberg, A., Arvidson, K. (1998). Attachment and proliferation of human oral fibroblasts to titanium surfaces blasted with TiO_2 particles. A scanning electron microscopic and histomorphometric analysis. *Clin. Oral Implants Res*., **9**, 195–207.

60. Niespodziana, K., Jurczyk, K., Jakubowicz, J., Jurczyk, M. (2010). Fabrication and properties of titanium-hydroxyapatite nano-composites. *Mater. Chem. Phys*., **123**, 160–165.

61. Ning, C. Q., Zhou, Y. (2002). *In vitro* bioactivity of a biocomposite fabricated from HA and Ti powders by powder metallurgy method. *Biomaterials,* **23**, 2909–2915.

62. Orsini, G., Piattelli, M., Scarano, A., Petrone, G., Kenealy, J., Piattelli, A., Caputi, S. (2007). Randomized, controlled histologic and histomorphometric evaluation of implants with nanometer-scale calcium phosphate added to the dual acid-etched surface in the human posterior maxilla. *J. Periodontol*., **78**, 209–218.

63. Papargyri, S. A., Tsipas, D., Stergioudis, G., Chlopek, J. (2005). Production of titanium and hydroxyapatite composite biomaterial for use as biomedical implant by mechanical alloying process. *Eng. Biomater.*, **46**, 27–34.

64. Park, J. W., Kim, Y. J., Park, C. H., Lee, D. H., Ko, Y. G., Jang, J. H., Lee, C. S. (2009). Enhanced osteoblast response to an equal channel angular pressing-processed pure titanium substrate with microrough surface topography. *Acta Biomater*., **5**, 3272–3280,

65. Petruzelka, J., Dluhos, L., Hrusak, D., Sochova, J. (2006). Nanostructured titanium. Application in dental implants, *Sbornik Vedeckych Praci Vysoke Skoly Banske* (Technicke University Ostrava), **1**, 177–185.

66. Pinholt, E. M. (2006). Surface engineered dental implant insertion in conjunction with bilateral inferior mandibular nerve transposition-s case report. *Appl. Osseointegration Res.*, **5**, 59–61.

67. Rocci, M., Rocci, A., Martignoni, M., Albrektsson, T. (2008). A comparative study of TiOblast and OsseoSpeed implants retrieved from humans. *Appl. Osseointegration Res*., **7**, 26–30.

68. Suryanarayna, C. (2001). Mechanical alloying and milling. *Progr. Mater. Sci*., **46**, 1–184.

69. Stanford, C. M. (2008). Surface modifications of dental implants. *Aust. Dent. J.*, **53**, 26–33.

70. Takeshita, F., Ayukawa, Y., Iyama, S., Murai, K., Suetsugu, T. (1997). Long-term evaluation of bone-titanium interface in rat tibiae using light

microscopy, transmission electron microscopy, and image processing. *J. Biomed. Mater. Res.,* **37**, 235–242.

71. Thor, A. (2008). TiOblast and OsseoSpeed implant in sinus lift surgery. *Appl. Osseointegration Res*, **7**, 17–25.
72. Toljanic, J., Thor, A., Baer, R., Ekstrand, K. (2008). Immediate fixed restoration of implants in the atrophic edentulous maxilla. *Dent. Today*, **27**, 56–63.
73. Tulinski, M., Jurczyk, M. (2012). Nanostructured nickel-free austenitic stainless steel composites with different content of hydroxyapatite. *Appl. Surf. Sci.*, **260**, 80–83.
74. Valiev, R. Z., Islamgaliev, R. K., Alexandrov, I. V. (2000). Bulk nanostructured materials from severe plastic deformation. *Prog. Mater. Sci*., **45**, 103–189.
75. Valiev, R. Z., Sergueeva, A. V., Mukherjee, A. K. (2003). The effect of annealing on tensile deformation behavior of nanostructured SPD titanium. *Scripta Mater.,* **49**, 669–674.
76. Valiev, R. Z., Estrin, Y., Horita, Z., Langdon, T. G., Zehetbauer, M. J., Zhu, Y. T., (2006). Producing bulk ultrafine-grained materials by severe plastic deformation. JOM, **58**, 33–39.
77. Valiev, R. Z., Zehetbauer, M. J., Estrin, Y., Höppel, H. W., Ivanisenko, Y., Hahn, H., Wilde, G., Roven, H. J., Sauvage, X., Langdon, T. G. (2007). The innovation potential of bulk nanostructured materials. *Adv. Eng. Mater*., **9**, 527–533.
78. Valiev, R. Z., Semenova, I. P., Latysh, V. V., Shcherbakov, A. V., Yakushina, E. B. (2008). Nanostructured titanium for biomedical applications: New developments and challenges for **c**ommercialization. *Nanotechnol. Russia*, **3**, 593–601.
79. Valiev, R. Z., Semenova, I. P., Latysh, V. V., Rack, H., Lowe, T. C., Petruzelka, J., Dluhos, L., Hrusak, D., Sochova, J. (2008). Nanostructured titanium for biomedical applications. *Adv. Eng. Mater.*, **10**, 1–3.
80. Valiev, R. Z., Semenova, I. P., Latysh, V. V., Rack, H., Lowe, T. C., Petruzelka, J., Dluhos, L., Hrusak, D., Sochova, J. (2009). Nanostructured titanium for biomedical applications. *Adv. Eng. Mater*., **10**, B15–B17.
81. Wang, H., Estrin, Y., Zuberova, Z. (2008). Bio-corrosion of a magnesium alloy with different processing histories. *Mater. Lett*., **62**, 2476–2479.
82. Wang, K. (1996). The use of titanium for medical applications in the USA. *Mater. Sci. Eng. A*, **213**, 134–137.
83. Webster, T. J., Siegel, R. W., Bizios, R. (2001). Nanoceramic surface roughness enhances osteoblast and osteoclast functions for improved orthopaedic/dental implant efficacy. *Scripta Mater.,* **44**, 1639–1642.

84. Webster, T. J., Ejiofor, J. U. (2004). Increased osteoblast adhesion on nanophase metals: Ti, Ti6Al4V, and CoCrMo. *Biomaterials,* **25**, 4731–4739.

85. Wennerberg, A., Albrektsson, T. (2006). Implant surfaces beyond micron roughness. Experimental and clinical knowledge of surface topography and surface chemistry. *Appl. Osseointegration Res.*, **5**, 40–44.

86. Williams, D. F. (1987). Review: Tissue-biomaterial interactions. *J. Mater. Sci*., **22**, 3421–3445.

87. Yang, C. Y., Wang, B. C., Chang, E., Wu, B. C. (1995). Bone degradation at the plasma-sprayed HA coating/Ti–6Al–4V alloy interface: An *in vitro* study. *J. Mater. Sci. Mater. Med.*, **6**, 258–265.

88. Zhang, S. X., Zhang, X. N., Zhao, C. L., Li, J. A., Song, Y., Xie, C., Tao, H., Zhang, Y., He, Y., Jiang, Y., Bian, Y. (2010). Research on an Mg–Zn alloy as a degradable biomaterial. *Acta Biomater.*, **6**, 626–640.

Chapter 38

Biomimetic Applications in Regenerative Medicine: Scaffolds, Transplantation Modules, Tissue Homing Devices, and Stem Cells

David W. Green, PhD, and Besim Ben-Nissan, PhD

[a]*Department of Oral Biosciences, Faculty of Dentistry, University of Hong Kong, Hong Kong*
[b]*University of Technology, Faculty of Science, Sydney, Australia*

Keywords: biomimetics, tissue engineering, biomaterial scaffolds, mineralized polysaccahrides, self-adjusting scaffolds, biocargo modules, tissue building and homing

38.1 Introduction

Biomimetic approaches to the fabrication of advanced biomaterials and biostructures are used to address the shortcomings of existing scaffold designs that are traditionally biologically unresponsive throughout the regeneration process *in situ* and lack necessary versatility. Increasing focus is now being placed upon adaptating these advanced biomimetic scaffolds for human stem cells.

Handbook of Clinical Nanomedicine: Nanoparticles, Imaging, Therapy, and Clinical Applications
Edited by Raj Bawa, Gerald F. Audette, and Israel Rubinstein

ISBN 978-981-4669-20-7 (Hardcover), 978-981-4669-21-4 (eBook)
www.panstanford.com

In this chapter we describe new biomaterial led approaches to immobilization, maintenance, programming and promotion of desirable stem cell responses while regenerating clinically acceptable human tissues. We also describe efforts to enhance survivability of human cell transplantation inside protective devices. Biostructures are being designed into functional scaffolds that can adapt (evolve) to changing *in situ* environment during regeneration, regulate cell responses at nanostructured surfaces, as modules for self-assembling by the patient's own cells and as smart devices that possess tissue specific homing capabilities.

One of the major shortcomings of current synthetic implants is their inability to adapt to the local tissue environment [3]. Therefore new advanced bioactive materials are needed which can elicit regenerative responses. A major key approach towards driving tissue regeneration is the use of biochemical factors to trigger cell proliferation and differentiation. Bone Morphogenic Proteins (BMP's) are widely used in musculoskeletal tissue engineering to promote bone tissue formation and gene expression [3]. Increased understanding of growth factor function and the interplay during regeneration has increased development of pharmaceutical grade growth factors for use in the clinic. Alternative biological factors with unique cellular functions and activities are sought to establish more precise control of the regenerative response and simulate the sequential temporal and spatial secretion of secretory factors (proliferative, differentiation and growth). There is a clear and pertinent need for better tissue engineering scaffolds that possess more natural bio-responsive environments conducive to guiding the natural processes of regeneration which can be highly intricate and dynamic in space and time. Thus scaffolds must have intelligent designs to meet this biological challenge. We are convinced that there needs to be a step change to scaffold environments that are responsive to bone and extracellular tissue to implant nano-interactions and adaptability to applied functional loadings.

In biologic environment the synthesized biomatrix evolves in real-time to meet the demands and optimisations of adaptive growth and regeneration of human tissues.

As cells proliferate and differentiate they alter their environment. Future advanced biomimetic scaffolds must be able to adapt to these changes and meet the ever-changing needs of developing

tissues. We anticipate synthesizing biomaterial scaffolds with functional cross-links and pendant side groups that interact with surrounding integrated cell populations at three levels: at the surface, at the architectural and at a functional (e.g., mechanical enhancement).

Development of modular self-assembling biomaterials is an attempt to harness the cell as the master-builder of its own extracellular matrix using tailored synthetic components [5]. Biomaterial structures that are designed and built by human cells and their cellular components is only just being realized and is an important aim for future biomaterials for clinical applications.

38.2 Biomimetic Stem-Cell Scaffolds

Use of stem cells in regenerative medicine has increased the potential to restore a greater range of tissues in a more sustainable manner and for longer than with conventional tissue-specific differentiated cells. There is increasing awareness that the composition of scaffolds is important to control stem cell activities as they are so reliant on the extracellular surroundings to survive and generate tissues [1, 13]. Technologies that harness and modulate stem cell activities therefore offer exciting new prospects for tissue engineering of self-renewing tissues and organs [2]. They are pivotal for permanent reparation of self-renewing tissues such as skin and bone. Protocols that enhance the accession, processing, function and transplantation of conditioned cells to the patient are imperative.

Naturally derived polysaccharide hydrogels are ideal templates for organising cells in 3-dimensional configurations, directing tissue responses and delivering soluble factors to both embedded and co-cultured human cell populations [17]. Chitosan and alginate are biodegradable, non-toxic materials that elicit minimal immunoreactivity and break down into chemical constituents that can be completely metabolized and excreted (glucosamine and mannose/glucoronic acids respectively). Mineralized polysaccharide constructs have the advantage of being more mechanically stable than unmineralized ones [20]. Adjustments in capsule formation chemistry provide a programmable mechanism for controlling

the diffusion of soluble biological factors across the capsule wall. Mineral-polysaccharide capsules synthesized at a macroscopic scale have been investigated for their role in tissue regeneration, gene transfection and growth factor delivery [15].

Our original hypothesis was to use self-assembled mineralized polysaccharide capsules with readily specifiable properties to encapsulate enriched mesenchymal cell populations in biomimetic microenvironments for the generation of a range of tissue types. We have been able to successfully demonstrate the ability to modulate capsule composition and the physico-chemical properties of polysaccharide capsules for enhancement of cartilage, bone and adipogenic tissue formation and augmentation of the capsule environment tailored for specific tissue types. We also demonstrated a wide range of other significant biological and physical functions that show clinical potential including gene delivery, growth factor delivery and spatial and temporal segregation of cell populations in nested capsules.

Mineralized polysaccharide capsules are specially designed bioconstructs for tissue engineering applications [25].

The production of polysaccharide capsules involves a unique one step self-assembling process carried out at room temperature and in aqueous media thus avoiding toxic chemicals and harsh physical treatments. The shell and core properties, such as shell thickness and core cellularity, diffusion potential and mineralization can be modulated through simple adjustments to the chemistry of the forming solutions (Fig. 38.1).

It was found that the shell thickness and cell loading determined the potential to rupture and burst releasing the contents from the core. For example capsules with populations of cells between 500,000 and 800,000 dispersed encapsulated cells into the surrounding environment at 7 days due to rupturing of the shell (Fig. 38.2). Capsules with low mineralization burst. Modifications can also be made to generate capsules with different 3D shapes (rods, plates and spheres) and sizes ranging from 100 nm to 5 mm in diameter.

We have harnessed recent innovations in mineralized alginate-chitosan technology for a range of therapeutic applications using primary human stem cells. Microcapsules, nanocapsules

have been newly developed that enable more effective targeted delivery of functional biological factors, lead to mature tissue formation and generate bio-responsive native extracellular matrix environments. This addresses existing limitations of using stem cells in therapies for tissue replacement and augmentation, namely sourcing and obtaining enough stem cells from each sample, impaired differentiation potential and poor growth. We contend that such tailored polysaccharide microenvironments will directly address many of these issues, for example, by improving survival, initiating differentiation and enhancing proliferation.

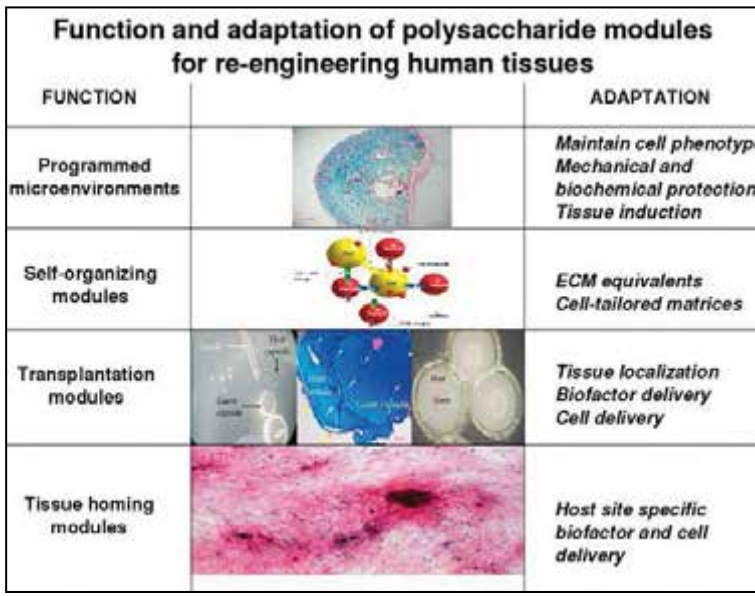

Figure 38.1 Development of polysaccharide (alginate, chitosan, chitin, hyaluronate) based modules (microscale and nanoscale) for strategies in tissue regeneration. (a) Polysaccharide capsules provide programmed microenvironments that translate enclosed stem cell populations into a specific tissue type. (b) Polysaccharide capsules with surfaces engineered to enable cell-mediated self organization into extracellular matrix equivalents. (c) Polyssaccharide capsules exist as injectable modules packed with stem cells and biocargo. (d) Polysaccharide capsules with decorated surfaces that encourage tissue homing capabilities.

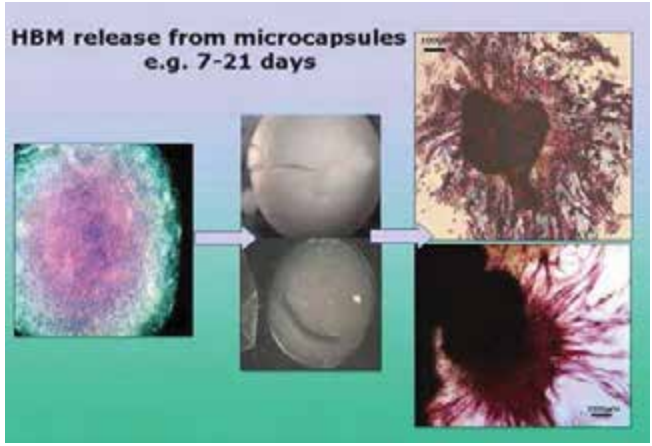

Figure 38.2 Demonstrated polysaccharide capsule busting to release core contents such as primary hBMSC shown here at 7–21 days.

Capsules provide viable enclaves for human cell proliferation, growth and differentiation. All skeletal cell populations remain viable at 91% (+/− 6%) within capsules at differing concentrations of calcium (5–25 mM) and phosphate ions (50–300 mM) used to vary shell thickness and hence diffusive and mechanical properties of the capsule. From histological observations proliferation is initially slow up until 21 days. Embedded cells remain rounded-up but retain their phenotype. Cell-cell interactions stimulate the formation of cell contacts and reshaping of cell morphology.

38.2.1 Bone Forming Osteogenic Polysaccharide Templates

The existence of an amorphous calcium phosphate mineral coating and the high calcium ion content inside polysaccharide capsules means they are particularly important as 3D templates for hard tissue (bone) tissue formation. A mineralized environment is conducive to osteogenesis, however to drive and accelerate the regenerative process further a growth factor, particularly BMP-2 are required for stimulation of progenitor cells. Within polysaccharide capsules BMP-2 is needed to generate significant quantities of osteoid *in vivo* within a clinically acceptable 4–6 week time frame for cultured tissue, as shown in Fig. 38.3.

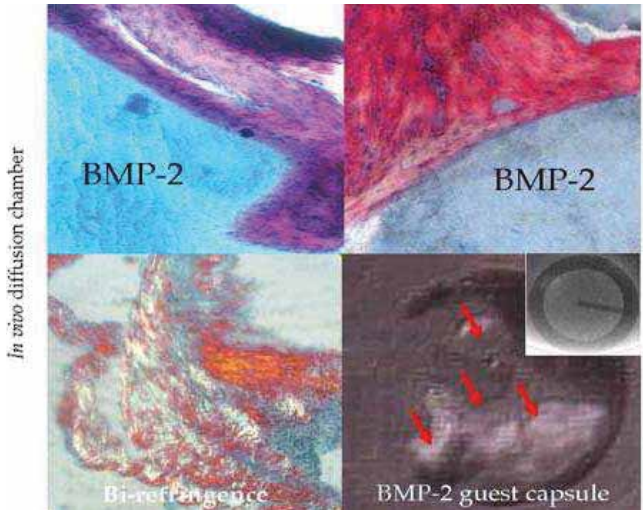

Figure 38.3 *In vivo* osteoid (mineralized) bone formation within capsules and nested capsules containing a physiologically relevant concentration of BBMP-2 (200 ng/mL) and primary hBMSC inside a diffusion chamber. Capsules are loaded in triplicate inside a diffusion chamber which prevents ingress of host cells into the capsules. Thus, all tissue generated comes from seeded primary hBMSC.

It is at this point collagen mineralization is expected to occur. At 6 weeks we observe hierarchical organization somewhat indicative of immature woven bone tissue. Furthermore, faxitron X-ray imagery shows significant mineralization exclusive to BMP-2 loaded "guest" capsules embedded in a "host" containing hBMSC covering a quarter of single capsules. X-ray imaging of a capsule without BMP-2 at the same time point does not show the opaque areas indicative of mineralization.

38.2.2 Chondrogenic Polysaccharide Templates

Mineralized polysaccharide capsules have demonstrable efficacy as programmablemicro-environments for initiating the tissue regeneration process from embedded musculoskeletal progenitor cell populations. We can demonstrate that augmenting the alginate core environment with specific native extracellular matrix molecules promotes osteogenesis and chondrogenesis from starting popula-

tions of hBMSC, hAC and human foetal cells depending on the matrix molecules used.

To illustrate the potential to grow cartilage tissue native Aggrecan blended into the alginate core induced chondrogenic responses from co-cultured human articular chondrocytes as validated by positive histological staining using antibodies targeted to specific cartilage matrix components such as cartilage type II and Sox-9. Matrix synthesis occured throughout each capsule (n = 4) with formation of cartilage architecture associated with native hyaline cartilage (Fig. 38.4). Chondrogenic biomaterials can be significantly improved by combining cartilage matrix components such as chondroitin sulphate, keratan sulphate and Aggrecan. Alginate alone does not provide sufficient cues to drive such differentiation. Chondroitin sulphate is an auxillary glycosaminoglycan molecule that decorates Aggrecan. Chondroitin sulphate was added to the alginate core of mineralized chitosan coated microcapsules to determine whether such a disarticulated native matrix component with a molecular size that facilitates direct, accessible associations with embedded chondrocyte cells can promote chondrogenesis. Chondroitin sulphate (extracted from basking shark cartilage) was blended into alginate at 2 separate functional concentrations of 0.25 mg/mL and 0.5 mg/mL of alginate. Capsules were maintained in basic chondrogenic media for 28 days *in vitro* and in rotating bioreactors to enhamce nutritient and gaseous exchange into the capsule core. Chondroitin sulphate blended capsules elicited unique, unique patterns of new matrix synthesized by embedded chondrocytes.

Matrix components also have an accessory effect on the structure of the alginate core by associating electrostatically with alginate polymer chains and modulating water binding affinities. Chitin nanofibrils co-associated with alginate increase nutritional support for cells by restructuring the alginate matrix into functional domains [16].

Dynamic mechanical compression testing has demonstrated increased stiffness in capsules bearing chondroitin sulphate compared to capsules tested without chondroitin sulphate. Thus, the original function of a matrix component, in this example providing high compressive stiffness, can be resurrected in an engineered matrix. Recreation of the native stem cell environment where stem cells normally reside (such as bone marrow, perios-

teum, endosteum etc.), are protected, stabilised as self-renewing undifferentiated cells and given instruction on regulation of progenitor and successor cell production is an active research area [6, 7].

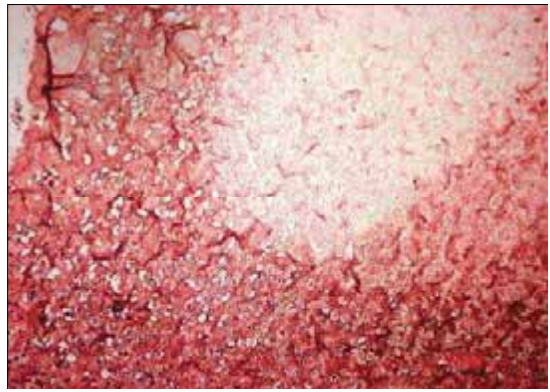

Figure 38.4 Immuno-staining for cartilage specific collagen type II molecules within matrix synthesized by embedded cultured human articular chondrocyte cells (500,000 cells per capsule). Staining of new matrix is strong throughout each sampled capsule. Individual cells are located in well-defined lacuane at a high density. New matrix is not formed in capsules containing primary hBMSC.

According to Cool and Nurcombe the glycosaminoglycan heparin sulphate is master in dynamically controlling almost all stem cell functions. Further investigations are underway therefore, to harness heparan sulphate and chito-oligomers and so control, regulate and differentiate polysaccharide embedded stem cell populations. Chito-oligomers for example, induce cartilage and bone formation in the bone environment only (along an endochondral ossification pathway) by up-regulating Sox-9 transcription factor expression and modulate the activity of YKL-40 cell signalling glycoprotein on progenitors located in the bone marrow, periosteum and endosteum [28]. These exemplars are part of a strategy to increase stem cell survival and direct differentiation.

38.2.3 Soft Tissue (fat) Polysaccharide Templates

Soft tissue reconstruction is a significant clinical aim. Previous studies have shown that polysaccharide capsules provide highly condu-

cive microenvironments for adipocyte differentiation, proliferation and growth. Templates are urgently needed for adipogenic tissue transplantation, augmentation and replacement of host adipogenic tissues.

Polysaccharide capsules were found to be conducive for the culture and expansion of human adipocytes from progenitor populations as shown in Fig. 38.5. Proliferation was more rapid over 14 days (as determined by increase in cell density) and was not localized to any specific region of the capsule when compared to other cell types (such as osteoprogenitors). The level of cell expansion and metabolic activity associated with that led to capsule rupture and release of cell populations onto the underlying tissue culture plastic surface within 10–14 days of culture *in vitro*. Adipogenesis fully occured inside capsules populated with progenitor fetal derived cells while cultured in specific adipogenic media conditions (complete media) within 21 days *in vitro*. Fat droplets stained red with oil red-O were seen throughout the capsule at high density (35–40%; $n = 4$).

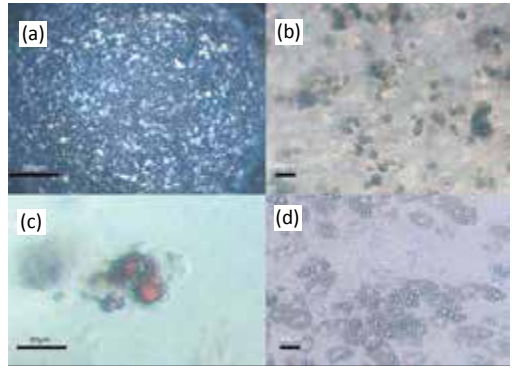

Figure 38.5 Human pre-adipocyte (derived from fresh human bone marrow) culture inside mineralized chitosan-coated alginate capsules ($n = 12$). (a) A single whole capsule containing 450,000 pre-adipocytes at 24 hours. Pre-adipocyte cells are metabolically very active and exapnd in numbers rapidly after encapsulation. (b) Embedded pre-adipocytes produce rounded colonies containing dense oil droplet formations in complete (+single insulin dose) media at day 38. (c) Oil droplets stained with oil red-O to indicate presence of fat inside observed droplets at day 12. (d) Oil-droplet formation from same population of cells grown in 2D mono-layer culture at day 38.

Adipogenic differentiation can be switched on/controlled using gene silencing techniques. This was demonstrated within 3D *in vivo* polysaccharide templates. SiRNA modulated fetal mesenchymal cells were encapsulated and implanted for 28 days *in vivo* and the results are highlighted in Fig. 38.6 using 3 different staining regimes. The manipulation of gene transcription in mouse derived muscle cells, this time using RUNX-2-fundamental to cellular differentiation into bone-led to equivalent control of cell differentiation (Fig. 38.7). Gene silencing suppressed the expression of bone specific alkaline phosphatase expression.

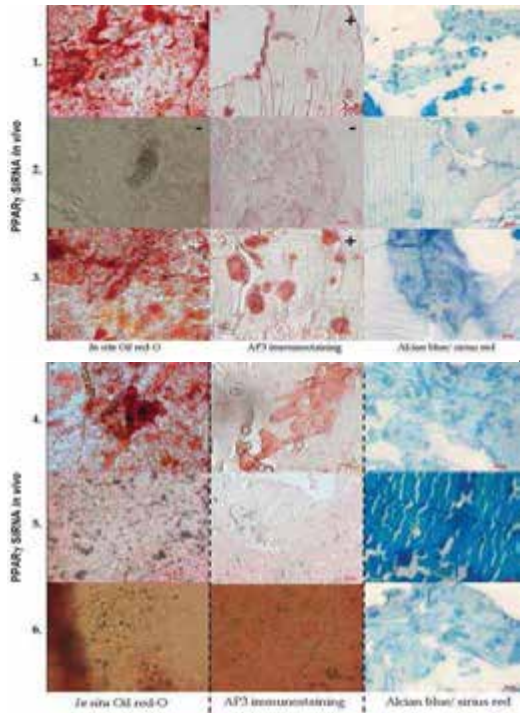

Figure 38.6 PPARgamma gene silenced (SiRNA) fetal derived mesenchymal cells embedded within polysaccharide capsules and implanted subcutaneously for 28 days. Capsule are sectioned and stained for presence of oil droplets using Oil red-O, AP3 antibodies and alcian blue and sirius red. Rows 2, 5, and 6 are thin sections of capsules in which embedded adipogenic progenitor cells have been silenced for expression of a transcription factor that regulates cellular differentiation and development typically found within adipose tissues. (1×10^6/mL alginate).

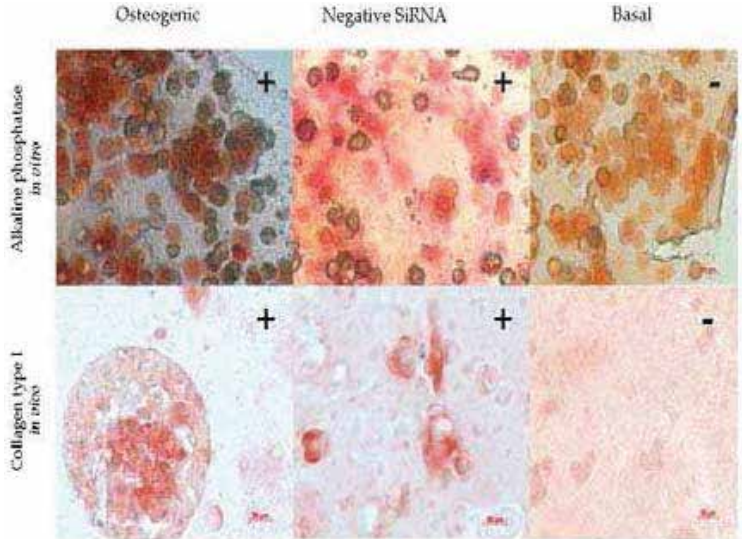

Figure 38.7 Modulation of RUNX-2 gene transcription in mouse derived muscle cells to induce bone cell differentiation. Gene silencing suppressed the expression of bone specific alkaline phosphatase expression in osteogenic conditions which would normally induce osteogenic cell differentiation. The panel of images show positive staining for alkaline phosphatase (upper level) in osteogenic and negative siRNA treatment. The bone lineage determination of cells is confirmed by positive collagen type I staining of these two groups in the lower level images. SiRNA modulated cells do not stain for alkaline phosphatase or collagen type I indicating that they remain as muscle cells and have not been redifferentiated.

38.2.4 Peptide Conjugated Alginate to Enhance Cell-to-Matrix and Tissue Responses Inside Polysaccharide Capsules

The alginate and chitosan components are amenable to chemical conjugation with pendant polypeptides, proteins and to chemical cross-linkages to create interpenetrating polymer networks. In doing this we can generate ordered bi-functional and tri-functional polymer hybrids such as carageenan/alginate IPN's [23]. Alginate matrices augmented with cell responsive peptides represent the first step in a process to generate the ideal bio-responsive polysaccharide capsule. Carbodiimide chemistry was used to

chemically couple biologically relevant adhesion peptides: RGD tripeptide and GRGD tetrapeptide onto and along the alginate polymer chain [22]. This cell binding sequence is Alginate hydrolysates were analysed to a degree that no other research group working to conjuagate alginates has done so far. GC (gas chromatography) and Mass spectrophotometry confirmed that RGD was integrated within chemically modified alginates. The amount of RGD bound is still not clear however. In order to test the potentially enhanced biofunctionality of modified alginates 2D membranes were prepared and seeded with hBMSC at different densities. The number of adherent cells on each membrane was counted at 24 hours and 7 days to determine RGD mediated enhancement of cell proliferation. We show that RGD alginate membranes increase cell adherence at 24 hours and increase cell proliferation at 7 days than non RGD alginate membranes. The G:M ratio has no effect on cell responses. Polysaccahride capsules (50:100 mM) could be stably synthesized using chemically modified alginates. Capsules loaded at low cell densities were generated to delineate the effect of RGD upon embedded human cell populations (matrix-cell interactions) from the effects of cell-cell interactions

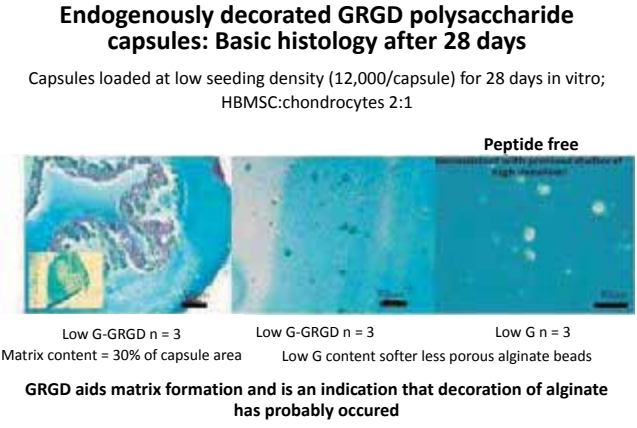

Figure 38.8 Primary hBMSC:chondrocyte (2:1 seeding ratio) responses inside chitosan-coated alginate capsules with chemically linked GRGD peptide at 28 days. The panel of images are thin sections of capsules that have been stained with alcian blue and Sirius red to indicate presence of collagen and proteoglycan extracellular matrix. GRGD induces a tissue formation response.

that come into play at high loading densities (above 400,000 cells/capsule). We show a small up-regulated response from RGD alginates compared to non-functionalised alginates as determined by histological observations of capsules. RGD combined with a glycine spacer group improved cellular responses (at the same cell densities (120,000 cells/capsule) as previously stated) probably due to enhanced presentation within the alginate polymer network (Fig. 38.8).

Such responses (cell proliferation and matrix synthesis) were stronger with low G:M ratio alginates where sparse osteoid nodules are observed. *In vitro* GRGD polysaccharide capsules (Low G; 50:100 mM) loaded at much higher densities of 400,000 cells per capsule (0.075 mL) show extensive proliferation and enhanced cell-matrix and cell-cell interactions. Thin sections of capsules with a significantly greater cell density compared to 2 week capsules prepared with identical seeding densities. At 28 days collagenous extracellular matrix is synthesized but is confined to cell aggregates. Similar capsules (50:300 mM LVG) chemically modified with a scrambled peptide sequence show fewer cells and no matrix production. The osteogenic nature of these encapsulated cell populations is confirmed by a significant increase in alkaline phosphatase expression within GRGD capsules compared to both RGE and non-RGD controls (Fig. 38.9).

Capsules dip coated using GRGD modified alginates were used to provide bulk surface for cell attachment and expansion. GRGD alginate coated capsules showed an increase in DNA content (represented as cell number) and ALP expression compared to alginate and scrambled peptide conjugated alginate capsule controls. The chitosan shell serves as a platform for the molecular attachment and elaboration of functional proteins (not just peptides) that associate with surrounding cells and tissues. The chemistry for attachment of a protein to chitosan is *facile* with few reaction steps, using tyrosinase to convert accessible protein residues into reactive o-quinones that can react with amines moieties on chitosan polymer chains, according to the method of [14, 19]. This chemistry is employed to sclerotize insect cuticles. Other accessible sites for entrapping useful functional biomolecules include at the interface between the chitosan shell and the alginate core. The utility of polysaccharides for applications in regenera-

tive medicine can be extended using nanofibre and nanocapsule technologies.

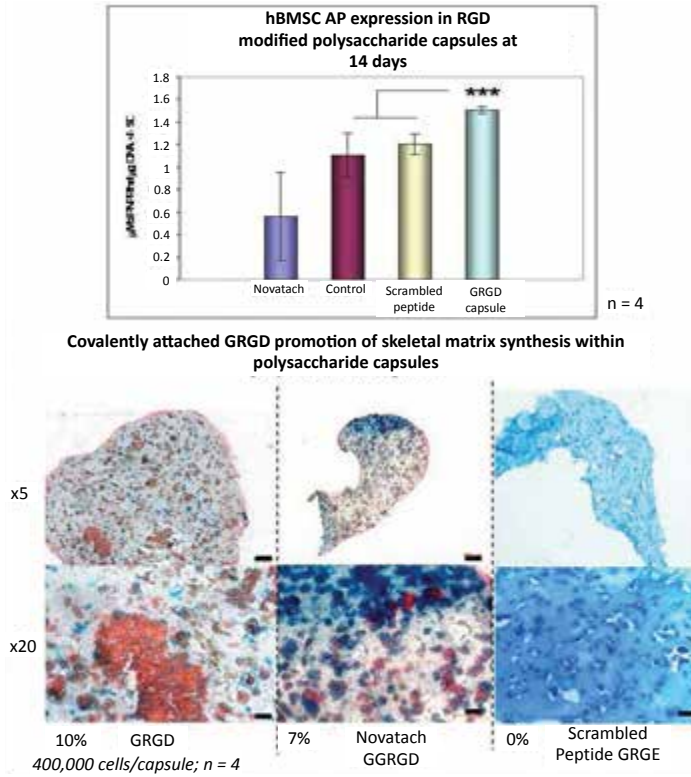

Figure 38.9 Primary hBMSC response to GRGD modified alginate-coated capsules at 14 days. Alkaline phosphatase expression is significantly increased in GRGD modified capsules compared to unmodified capsules and a proprietary peptide modified alginate. Histological examination of these same capsules reveal concentrated areas of organised collagen extracellular matrix ($n = 4$).

38.3 Electrospun Polysaccharide Core-Shell Fibres

Electrospinning is a *facile* method for making precision nanofibres and microfibres that can be used to replicate native extracellular matrix (ECM) fibrils.

Timely recent developments in melt electrospinning make it possible to potentially fabricate fibrous webs and networks with precise fibre diameters and patterning and thus provide fibrous architectures for cell integration and reassembly into organized tissue [11, 29]. Our innovative approach is to use polysaccharides in the fibre composition to deliver useful encapsulates and form better biological associations than currently used polymers. We therefore propose to use melt electrospun polysaccharide "core-shell" fibres for creating bio-responsive scaffolds augmented with growth factors and human cells for musculoskeletal tissue engineering. Such biologically tailored fibre compositions will optimize biological recognition and better simulate ECM niches giving rise to superior quality tissue. Electrospinning is being increasingly exploited to fabricate fibrous webs and networks for tissue engineering. The fibre dimensions that can be synthesized make ideal equivalents of extracellular matrix fibrils. However, no one has yet been able to fabricate organized layered hierarchical 3D constructs in the exact manner natural biomaterials are formed. Another shortcoming of existing conventional scaffolds is the suboptimal architectural design that can hinder tissue integration, nutritional support, vascular support and scaffold molecular associations. A research effort is underway to use computer-aided microfabrication techniques to print and pattern scaffolds with precisely defined and enacted fibre dimensions, fibre orientations, pore/channels sizes and interconnections. Techniques in development include 3D printing, soft lithography, laser sintering, extrusion/direct writing, inkjet and organ printing, stereolithography [7, 18]. Melt electrospinning is a new and promising technique. The greatest challenge of this approach is to deposit fibres in discrete areas and regions. Parameters governing melt electrospinning include flow rate, collector type, voltage and collector distance and these must be optimized fully for each substrate and application. Mimicking structural biomaterials that support and organize native tissues is an ideal approach. It is important to synthesize nanofibres into fibrous assemblies that simulate the extracellular matrix with the advantages of a high surface-volume ratio, high porosity and more precise control of mechanical properties. Small fibres and native protein compositions are optimal for cell interaction and tissue growth. Nanofibres can be fabricated with high productivity and efficiency using melt electrospinning. Melt

electrospinning is more desirable for biomedical applications than conventional solution electrospinning processes that use harmful solvents and lack high output (90% of material evaporates during electrospinning) needed to generate layered constructs necessary for the production of a functional tissue engineered construct.

The morphology and function can be controlled with precision. Directly applying the fibres to cells provides many opportunities for generating and investigating novel and complex tissue-engineered constructs [8, 9]. 3D constructs can be fabricated into macroscales using preformed templates. We propose to develop core-shell fibres from a formulation of polymer/alginate (core) and chitosan (shell with calcium phosphate) using more environment friendly solvent-free melt electrospinning. This will require controlled formulation (probably requiring use of a syringe pump) of alginate and chitosan and determination of the strict parameters governing electrospinning for these biomaterials. Previous experiments demonstrate the importance of being able to modulate the substrate compositions to prevent spontaneous gelling of the alginate. A number of variables (e.g., G:M ratio, polymer and cation concentrations) can be altered to retard this process and enable fibres to form uniformally and spontaneously mineralize at the fibre surface. Internal gelation technique can also be implemented involving slow delivery of calcium ions to cause gelation. Use of alginate/chitosan biomaterials will give capacity to encapsulate and release functional growth factors from fabricated fibres. Once this has been achieved fibrous layered assemblies (2D) will be constructed with mixtures of fabricated fibre diameters, compositions and preferred multilayered (hierarchical) organisations governed by computer controlled stage orientation and movement during electrospinning. There is also potential to harness model architectures from natural fibrous constructs.

38.4 Self-Adjusting Bioscaffolds

Nested capsules can be potentially used to spatially separate co-reactants in a single localized host environment and release them over time to generate a desired reaction. In the simplest construct

the reactant is encapsulated within a host bead. As time progresses the reactant gradually diffuses across the semi-permeable shell of the guest capsule (as demonstrated by growth factor and enzyme release studies) into the host and similarly in the alternate direction. As proof of this concept with significance to musculoskeletal tissue engineering we suggest integrating latent TGF-β into the host and to embed a guest bead with a higher pH.

Hydrogen ions from the guest would gradually diffuse into the host and so raise the pH leading to a chemical transformation of latent TGF-β into its functional form in the altered chemical environment. We have been able to synthesize capsules with an alginate core having a significantly lower pH than normal (from pH 6.5 to pH 4) to produce stable capsules by increasing the alginate concentration from 2% to 4%. We have also had success pulsing the release of an enzyme (2 mg Tyrosinase 25 KU/mg/mL sodium alginate) from guest capsules that modify the chemistry of the chitosan shell enabling chemical conjugation of proteins residing inside the host or exogenously. The potential to enclose one co-reactant within the same location as another and programme the timing for reactant mixing opens up new possibilities to engineer capsules that spontanesously produce emergent biofactors and modulate the matrix environment to compliment or respond to changes in the host enviroment.

38.5 Transplantation and Biocargo Modules

Our ability to generate “nested” capsules gives us the potential to spatially and temporally separate encapsulated populations of cells and growth factors. Such a function is highly significant since it is a way of in part simulating the kalaedoscopic sequential processes and cycling of biofactors (cytokines, growth factors, oligosaccharides, glycosaminoglycans etc.) that are involved in native repair and regeneration. Compartmentalization and layering by cells and phospholipids for example are predominant and vital features in biological systems. Defined layering of cell types associate in certain ways to guide regeneration [12].

Compartmentalization of growth factors within nested capsules with differing diffusion characteristics and load concentrations can establish concentration gradients between guest and host. Growth

factor gradients are important conditions during embryogenesis, tissue repair, remodelling and regeneration. Such sophistication requires.

Microfluidic devices are sufficiently well developed as effective biosensors and cell sorting devices. We have designed a potential microfluidic device to enable high-throughput and regularized nested capsules to be generated.

The blueprint printed below in Fig. 38.10 is very closely based on existing designs and technology [24]. In brief alginate is flowed into a junction through which chitosan solution flows.

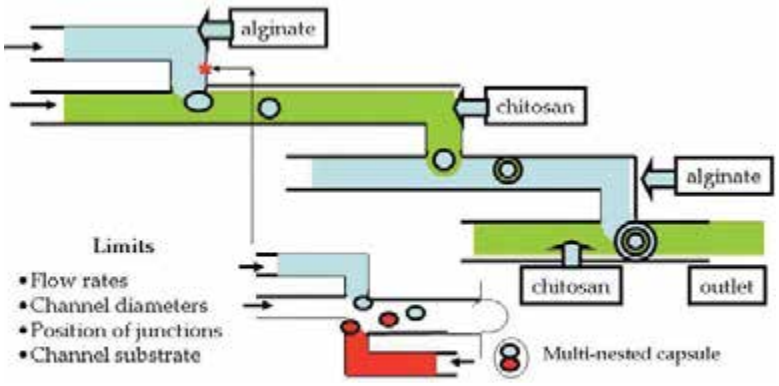

Figure 38.10 Microfluidic "lab on chip" design for the high throughput generation of multiple nested polysaccharide microcapsules based on the design published by [24]. Modifications are made to enable adequate flow of alginate and chitosan solutions through the channels. Determination of channel diameters, the position of junctions and channel substrate will need to be optimized.

The alginate flow disrupts and separates into a string of beads which are carried in the flow of chitosan, as they gel, towards the next junction where alginate is flowed through the next channel. At the second junction the alginate core is double coated in chitosan and alginate.

A further elaboration of the channel construction will enable guest capsules to be incorporated into developing host capsules at each junction. Further tests will need to be carried out to refine the operation of this device. Effective flow rates need to be determined for chitosan and alginate, channel diameters, positioning of

junctions to enable effective bead to bead encapsulation and the channel substrates all need to be configured to allow multi-nested capsules to be generated with high fidelity. The technology exists to incorporate this device into and injectable syringe enabling capsules to be fabricated remotely on-demand immediately prior to injection into the host.

There is a clear and present need for better tissue engineering scaffolds with increased natural bio-responsive molecular associations that guide the natural processes of regeneration. These processes can be highly intricate and dynamic in space and time. Polysaccharide constructs bristled with functional biomolecules involved in cell-cell and cell-matrix interactions can generate bioadhesive building blocks or modules for cell-mediated extra-cellular matrix reassembly instructed and guided by the cells themselves (Fig. 38.11). These modules are engineered to release soluble proliferation and differentiation factors to facilitate tissue formation within the newly cell-assembled polysaccharide matrices.

The use of modular self-assembling biomaterials for making equivalent structures to natural archetypes is a new approach. It simulates more accurately the way in which natural structures are constructed. In this proposal tailored modular elements are designed to be recognized by progenitor cells as matrix building blocks enabling them to be self-assembled by co-cultured cells into a cell-instructed matrix environment either *ex situ* or *in situ*. This is the first time that a scaffold can be fabricated through organized biomimetic assembly by cell associations, and genetic instruction. The modules are also augmented/integrated with inductive secretory factors that accelerate and promote tissue regeneration. Bio-responsive materials of this kind will have the capacity to gradually evolve within am ever changing environment.

Allowing human progenitor cells to reassemble their matrix environment using tailored synthetic biomaterial “building blocks” (multi-component segments) is a new concept. The approach promises a new class of biomaterials designed and constructed by biology. It allows biomaterials to be finely and precisely tailored with optimized properties [5]. Tissue engineer’s are presently developing prefabricated scaffolds with built in biorecognition elements (ligands) that are modulated by the naturally occuring activities and responses of progenitor cells that proceed during

regeneration. It is an attempt to simulate the complex time-dependant interactions between cells and matrix. For example, scaffolds possessing MMP-3 actuated cross-linkages and ligands have been synthesized such that their structure changes as metallo-proteinases are secreted by local cells [26]. The change is styled to give rise to matrix event that benefits regeneration.

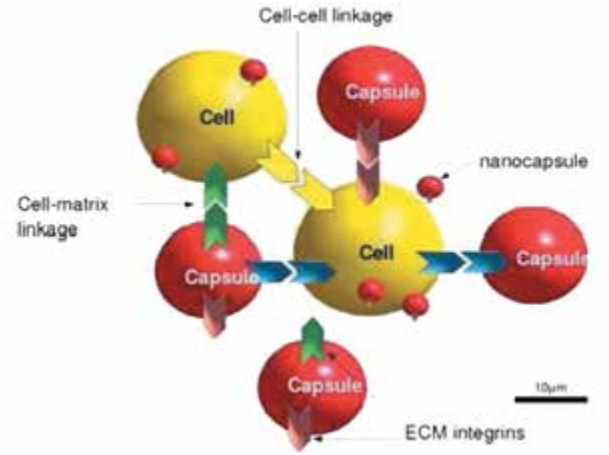

Figure 38.11 Schematic demonstrating the proposed function of peptide decorated microcapsules for cell driven, ordered self-assembly of capsules and promotion of cell activities intended for tissue repair and regeneration. Red spheres represent capsules decorated with extracellular matrix (ECM) integrins and/or carbohydrate moieties attached to the chitosan shell. Biolinkages can spontaneously form between capsules and with cells bearing complementary surface markers in a cordinated manner. Yellow spheres represent human progenitors. The purpose is to promote optimal cell-cell and cell matrix linkages.

While other researchers are developing cell-independent self-assembling biomaterial structures which better simulate their natural counter-parts. The promise of both approaches is to maximise biological responses and in turn increase native tissue regeneration.

In previous experiments calcium carbonate microsponges at or below the dimension of a single cell were manipulated (by individual cells) and preferentially arranged into aggregates by co-cultured human bone marrow stromal cells in mono-layer

culture at a range of cell densities [Green, unpublished data]. We have previously shown how it is possible to bristle the external shell with GGGRGD peptides to enable preferential cell attachment. We also envisage developing cellular assembly mimics. These are polysaccharide/human cell biocomposites that replicate the natural organisation of mature bone cells into discrete mineralized nodules which represent precursors to bone reconstruction [21]. We therefore propose to develop the capabilities of polysaccharide modules as (a) cell-recognized matrix elements for reassembly into macromolecular scale cellular niches and (b) to fabricate cellular assembly mimics-precursors to bone construction.

38.6 Polysaccharide Chitosan Coated Alginate Nanocapsules

Mineralized polysaccharide capsules have been shown to provide microenvironments that promote tissue formation and function as delivery vehicles for growth factors and genes. We have been able to extend the utility of our polysaccharide beads for intracellular activation and endogenous delivery of bioactive factors by synthesizing beads at the nanoscale (250–900 nm) using the method of Douglas et al. [5] (Fig. 38.12a). Polysaccharide beads will function as intracellular vehicles that deliver genes or proteins into the cell cytoplasm or nuclear envelope.

In brief alginate at concentrations of >0.005% are added to chitosan at a ratio of 1:2 and mixed vigorously to generate a stable nano-emulsion whereby ionic complexes of alginate are spontaneously formed within the chitosan solution. In proof-of-concept studies nanocapsules of mineralized polysaccharides can be produced using this *facile* method (Fig. 38.12). Surface decoration with important biological molecules using conventional carbodiimide chemistry will significantly enhance cellular responses and more rapidly promote the generation of human tissues [27]. Similar to there macroscopic counterparts these nanotemplates consist of an alginate core coated with a chitosan-CaP shell as confirmed by morphological appearance under TEM and EDAX elemental analysis for presence of calcium phosphate (Figs. 38.12a,b). Work will be carried out to reduce the wide dispersion of capsule sizes currently

obtained using a less than optimized synthesis. Nanocapsules have also been shown to retain encapsulates within the alginate core as shown in Fig. 38.12a. In cell culture nanoparticles have been demonstrated to readily co-associate with hBMSC within *in vitro* cell suspensions as shown in Fig. 38.13a. These nanoparticles possess a potential capacity to function as intracellular vehicles that can deliver genes or proteins into the cell cytoplasm or nuclear envelope respectively. TEM images show microcapsule localisation at the cell membrane and internalisation into the cell cytoplasm (Fig. 38.13b). Nanocapsule chemistry and size will be optimized to maximise cell internalization, release responses in vacuoles and the functional effects of encapsulates on targeted stem cells. An understanding of the mechanism (i.e., receptor-mediated?) by which these particles are endocytosed and assimilated within the cell will be met by deploying inhibitors of proteins (clathrin, adaptin and epsin) involved with phagocytosis and endocytosis such as cytochalasin B. Fluorescent dyes and confocal microscopy will be used to track these particles during their progress through the cell cytoplasm, alongside antibody marking of Stat-2 and AP-2 or presence of endocyte vesicles. Biochemical ELISA protein assays will be used to determine capsule induced over-expression of cytoplasmic and matrix proteins significant to musculoskeletal tissue regeneration such as osteonectin and osteocalcin. Imaging at a subcellular level will be carried out using TEM using coated gold nanoparticles.

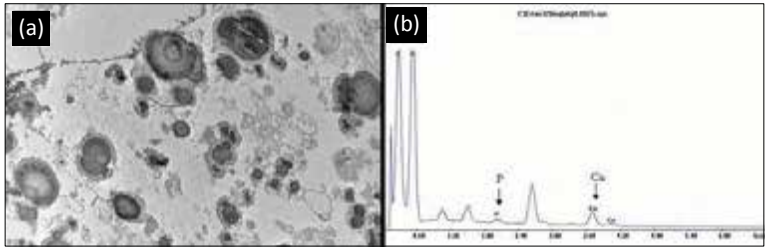

Figure 38.12 Mineralized polysaccharide (alginate-chitosan) nanocapsules; (a) TEM of nanocapsules with alginate stained black/dark grey surrounded by a lighter grey chitosan outer shell; (b) XRD analysis of a representative nanocapsule shows that calcium and phosphate ions are concentrated on capsules and therefore indicates the formation of a calcium phosphate outer shell. This provides evidence that alginate-chitosan capsules have been formed.

38.7 Native Extracellular Matrix Equivalents

Decorating the surfaces with important biological molecules will significantly enhance cellular responses and more rapidly promote the formation of human tissues. There is a current need for clinically relevant tissue engineering scaffolds with broad applicability and versatility that can be more specifically tailored to initiate cell responses and fashioned to mimic native ECM thus promote tissue formation that better match with the patient's own tissues. Our biologically enhanced constructs directly meet this significant need. In this task of the proposal we will prepare cell adhesion peptides/ proprietary functional ligands that stimulate stem cell activities and conjugate them to chitosan (Ca^{2+} ions 50 mM). Capsules will be synthesized to a range of micron length scales.

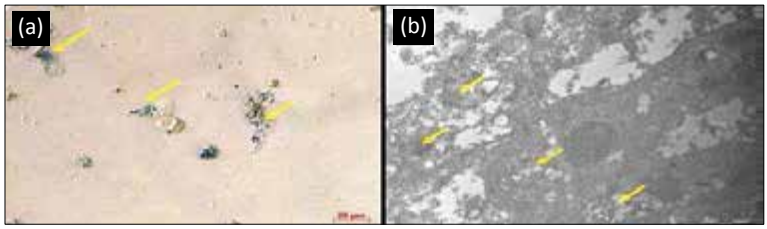

Figure 38.13 (a) High power microscope image showing that polysaccharide nanoparticles selectively associate with primary human bone marrow stromal cells in a 3D cell suspensions (n = 12). The alginate nanocapsule core is stained with a fluorescent dye (Cell Tracker Red) which in white transmitted light is blue. (b) TEM image showing presence of nanocapsules (i) at the surface of a primary hBMSC cell membrane and (ii) internalized within vacuoles. The yellow arrows denote position of nanocapsules.

Capsules of this kind were immersed in a primary hBMSC cell suspension to test the potential of peptide decorated capsules to attach cells to the external surface. It was found that within 7 days metabolically active/viable primary hBMSC preferentially adhered to chitosan-GGRGD complexed capsules (Figs. 38.14b,d). In capsules without chitosan conjugated GGRGD ligands only a few cells were seen to be attached (Figs. 38.14a,c).

This demonstrated the effectiveness of the RGD coupling to chitosan and the effectiveness of RGD presentation to cells in contact at the surface of the chitosan-CaP shell. This adaptation will

be used for (a) extra-cellular activation using a range of other bio-functional peptide sequences and (b) the potential for exogenous "stem cell-guided" ordered assembly of individual capsules into extra-cellular matrix mimics. Polysaccharide beads can therefore be surface decorated with covalently attached bioactive molecules (ligands) to enhance cell-to-bead interactions and promote cellular responses that instigate native regeneration processes.

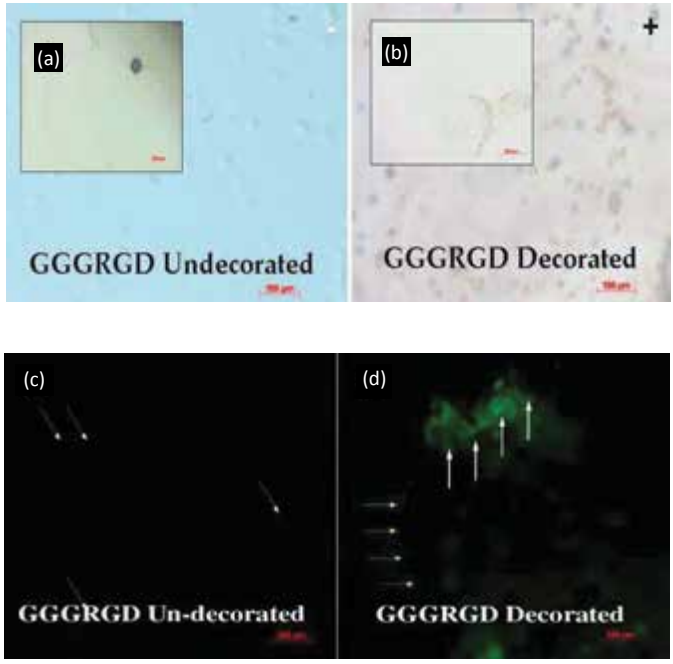

Figure 38.14 Preferential primary human bone marrow stromal cell (2.5×10^4/capsule) attachment to the surface of GGGRGD decorated chitosan coated alginate microcapsules (n = 4). (a) Bright-field microscope image of chitosan coated alginate capsule without primary hBMSC. (b) Bright-field microscope image of chitosan coated alginate capsule covered with primary hBMSC. (c) Fluorescence microscope image of chitosan coated alginate capsule *in situ* showing absence of primary hBMSC. (d) Fluorescence microscope image of chitosan coated alginate capsule outer surface showing attachment of primary hBMSC fluorescing positively with the cytoplasmic stain, Cell Tracker Green. Thus attached cells are alive and metabolically active. Yellow arrows denote edge of capsule, white arrows denote primary hBMSC.

38.8 Tissue Homing Devices

Protocols that enhance the accession, processing, function and transplantation of conditioned cells to the patient are imperative. Carrier materials and matrices have been developed extensively to safely and stably transplant sufficiently large numbers of stem cells and cell types required, into patients and more significantly directly to the site of need. Developments are occuring where transplantation modules are being engineered with homing functions directed to exact tissue sites or regions. A promising example of this technology is described in the invention by Caplan [4]. Protein/lipid compositions were formulated to coat living cells.

The lipid component formed strong associations with the cell membrane and by using specific biochemical targeting moieties conjugated with homing peptides (e.g., PWERSL, ASSLNIA, YSGKWGW), antibody fragments and carbohydrates, such treated cells possessed a mobile affinity for specific tissue types what has been termed selective direction to the target tissue [4]. Two approaches have been taken. The first is to coat selected progenitor cells with a linker followed by binding of a targeting moiety for a tissue type/character with the linker and administering these treated cells to a safe place where homing can effectively begin.

A second approach involves coating the progenitor cell with the linker, targeting moeity in one distinct complex. This may be at the site intended for repair or regeneration or at a distant site where treated cells can be passively transported to the designated location. The invention promises more effective, efficient use of cells and biofactors while reducing invasiveness and use of bulk biomaterials associated with more traditional strategies. We envisage developing polysaccharide modules and patented polysaccharide technology to target specific tissues using highly specific protein, peptide and antibody associations that are positioned on the outer surfaces of these new homing modules.

38.9 Summary

Biomimesis is a concept with growing relevance and importanceto a diverserange of sciences (biology, materials, chemistry and

physics), technologies (robotics, nanotechnology), clinical edicine and professions (architecture). Learning lessons from nature is pivotal to developing smart materials, structures and processes with self assembling, self-actuating and self stabilizing properties. Tissue engineers are faced with the problem of developing scaffolds with multifarious (often conflicting with each other) functions that must be bio-responsive and evolve in real time to a dynamic host environment. The principles of a bioinspired approach to tissue engineering scaffold design and synthesis have been described and augmented using BioTriz methodology. Further methods focus on nanoscale technologies and building structures and materials using nanoparticles. A number of worked examples show how biomimesis can generate innovative functional tissue engineering constructs with complex, intricate structures and morphologies unachievable using conventional methods such as vaterite microspheres that mimic plankton shell constructions. We provide an example of a self assembling organic scaffold around which spontaneous mineralization of calcium phosphate can be induced—a process analogous to template mediated mineralization in nature (e.g., mineralization of eggshell). The internal microenvironments for embedded cells can be modulated to recreate elements of a native extracellular matrix adding a further biomimetic element to this unique system.

Bioevaluation provided convincing evidence that these scaffolds may provide clinical success, as novel self-assembling scaffolds or gene/biofactor delivery vehicles for the engineering of mineralized and soft human tissues.

38.10 Conclusions

Regenerative medicine is confronted with a paucity of clinically relevant scaffold designs and biological factors that promote the natural cycle of regeneration. Understanding hierarchical design in nature and harnessing the chemical properties of natural structures at all length scales will be instrumental in re-assembling functional analogues of natural skeletal design. Designing and engineering smart biomaterials and modules with the ability to evolve with and adjust to the local host environment during

regeneration is a key aim of ours. We believe in using bio-inspired and nanoscale materials chemistry to do this. Such knowledge will enable tissue engineers to synthesize new advanced biostructures and materials that measure up to the functional demands of regenerating native human tissues that are truly patient ready.

Disclosures and Conflict of Interest

The authors would like to sincerely thank Professor Richard O. C. Oreffo and Professor Stephen Mann for their contribution to the genesis of biomimetics approach and their inspiration, guidance and support given to Dr. D. W. Green while carrying out part of this research at the University of Southampton. They acknowledge the contribution of Dr. Janos Kanclzer, Dr. Xuebin Yang and Dr. Xunhe Xu for provision of fetal derived mesenchymal stem cells and for carrying out *in vivo* trials and thank Dr. Paul Dalton for stimulating discussions on electrospinning for tissue engineering applications. Furthermore, the author gratefully acknowledge the financial support of the Australian Research Grant Commission (ARC Discovery), EPSRC (GR/N29860/01) and the Royal Society of UK travel grants. The authors declare that they have no conflict of interest and have no affiliations or financial involvement with any organization or entity discussed in this chapter. Neither any writing assistance was utilized in the production of this chapter nor was there any payment received for its preparation. This is a revised version of the authors' chapter that appeared in *Handbook of Materials for Nanomedicine*, 2010 (edited by V. Torchilin and M. M. Amiji), Pan Stanford Publishing Pte. Ltd., Singapore.

Corresponding Author

Dr. D. W. Green
Department of Oral Biosciences, Faculty of Dentistry
University of Hong Kong
The Prince Philip Dental Hospital, 34 Hospital Road
Sai Ying Pun, Hong Kong
Email: dwgreen@hku.hk

About the Authors

David W. Green received his PhD from Aston University. He is currently a research assistant professor in the Department of Oral Biosciences, Faculty of Dentistry, University of Hong Kong. His research interests focus on regenerative medicine, bioinspired engineering, and biomimetics materials chemistry.

Besim Ben-Nissan received his PhD from the University of New South Wales in Mechanical and Industrial Engineering/Biomedical Engineering. He is a visiting professor in the Faculty of Science at the University of Technology in Sydney, Australia. His areas of research expertise include nanocoatings, biomaterials, biomimetics, biomechanics, calcium phosphates, implant design, finite element modeling, marine structures, and slow drug delivery. Over the last three decades together with a large numbers of PhD students he has worked on production and analysis of various biomedical implants, hydroxyapatite ceramics, advanced ceramics (alumina, zirconia, silicon nitrides), sol-gel developed nanocoatings for enhanced bioactivity, corrosion and abrasion protections, optical and electronic ceramics. He also has contributed in the areas of mechanical properties of sol-gel developed nanocoatings.

References

1. Arinzeh, T. L., Peter, S. J., Archambault, M. P., Van Den, B. C., Gordon, S., Kraus, K., Smith, A., Kadiyala, S. (2003). Allogeneic mesenchymal stem cells regenerate bone in a critical-sized canine segmental defect. *J. Bone Joint Surg. Am.*, 85-A, **10**, 1927.
2. Bianco P., Robey, P. G. (2001). Stem cells in tissue engineering. *Nature*, **414**, 118–121.
3. Bielby, R. C., Polak, J. M. (2004). Stem cells and bioactive materials. In: Reis, R. L., Weiner, S., eds. *Learning from Nature How to Design New Implantable Biomaterials: From Biomineralization Fundamentals*

to Biomimetic Materials and Processing Routes, Kluwer Academic Publications.

4. Caplan, I. (2006). Cell Targeting methods and compositions. US2006/0263336 A1. United States Patent Application Publication.
5. Collier, J. H. (2008). Modular self-assembling biomaterials for directing cellular responses. *Soft Matter,* **4**, 2310–2315.
6. Cool, S. M., Nurcombe, V. (2006). Heparan sulfate regulation of stem cell fate. *J. Cell Biochem.*, **99**(4), 1040–1051.
7. Dombrowski, C., Song, S. J., Chuan, P., Lim, X. H., Susanto, E., Sawyer, A. A., Woodruff, M. A., Hutmacher, D.W., Nurcombeand, V., Cool, S. M. (2009). Heparan sulfate mediates the proliferation and differentiation of rat mesenchymal stem cells. *Stem Cells Dev. Aug*., **18**(4), 661–670.
8. Dalton, P., Joergensen, N. T., Groll, J., Moeller, M. (2008). Patterned melt electrospun substrates for tissue engineering. *Biomed. Mater.*, **3**, 034109.
9. Dalton, P. D., Kristina Klinkhammer, K., Salber, J., Klee, D., Möller, M. (2006). Direct *in vitro* electrospinning with polymer melts. *Biomacromolecules*, **7**(3), 686–690.
10. Douglas, K. L., Tabrizian, M. (2005). Effect of experimental parameters on the formation of alginate-chitosan particles used as nanoscale non-viral DNA carriers. *J. Biomat. Sci. Polym. Ed.*, **16**, 43–56.
11. Ekaputra, A. K., Prestwich, G. D., Cool, S. M., Hutmacher, D.W. (2008). Combining electrospun scaffolds with electrosprayed hydrogels leads to three-dimensional cellularization of hybrid constructs. *Biomacromolecules*, **9**(8), 2097–2103.
12. Eliesseeff, J. (2008). Hydrogel starts to gel. *Nat. Mater.*, **7**, 271–272.
13. Evans, N. D., Gentleman, E., Polak, J. (2006). Scaffolds for stem cells. *Mater. Today*, **9**(12), 26–33.
14. Freddi, G., Anghileri, A., Sampaio, S., Buchert, J., Monti, P., Taddei, P. (2006). Tyrosinase-catalyzed modification of Bombyx mori silk fibroin: Grafting of chitosan under heterogeneous reaction conditions. *Biotechnology*, **125**, 281–294.
15. Green, D. W., Mann, S., Oreffo, R. O. C. (2006). Mineralized polysaccharide capsules as biomimetic microenvironments for cell, gene and growth factor delivery in tissue engineering. *Soft Matter (Highlight)*, **2**, 732–737.
16. Green, D. (2008). Tissue bionics: Examples in biomimetic tissue engineering. *Biomed. Mat.*, **3**(3), 030410.

17. Green, D. W., Leveque, I., Walsh, D., Howard, D., Yang, X., Partridge, K., Mann, S., Oreffo, R. O. C. (2005). Biomineralized polysaccharide capsules for encapsulation, organization and delivery of human cell types and growth factors. *Adv. Funct. Mater.*, **15**(6), 917–923.

18. Hollister, S. J. (2005). Porous scaffold design for tissue engineering. *Nat. Mater.*, **4**, 518–524.

19. Kang, K. D., Lee, K. H., Ki, C. S., Nahm, J. H., Park, Y. H. (2004). Silk fibroin/chitosan conjugate cross-linked by tyrosinase. *Macromol. Res.*, **12**(5), 534–539.

20. Leveque, I., Rhodes, K. H., Mann, S., (2002). Biomineral-inspired fabrication of semi-permeable calcium-phosphate-polysaccharide microcapsules. *J. Mat. Chem.*, **12**, 2178–2180.

21. Mann, S. (2005). *Biomineralization: Principles and Concepts in Bioinorganic Materials Chemistry*, Oxford University Press, Oxford, 2001.

22. Mazuka, T., Iwasaki, N., Yamane, S., Funakoshi, T., Majima, T., Minami, A., Ohsuga, N., Ohta, T., Nishimura, S.-I. (2005). Chitosan-RGDSGGC conjugate as a scaffold material for musculoskeletal tissue engineering. *Biomaterials*, **26**(26), 5339–5347.

23. Mohamadnia, Z., Zohuriaan-Mehr, M. J., Kabiri, K., Jamshidi, A., Mobedi, H. (2007). pH-Sensitive IPN hydrogel beads of carrageenan-alginate for controlled drug delivery. *J. Bioact. Compat. Polym.*, **22**, 342–356.

24. Nisisako, T., Okushima, S., Torii, T. (2005). Controlled formulation of monodisperse double emulsions in a multi-phase microfluidic system. *Soft Matter*, **1**, 23–27.

25. Pound, J. C., Green, D. W., Roach, H. I., Mannand S., Oreffo, R. O. C. (2007). An *ex vivo* model for chondrogenesis and osteogenesis. *Biomaterials*, **28**(18), 2839–2849.

26. Raeber, G. P., Lutolf, M. P., Hubbell, J. A. (2005). Molecularly engineered PEG hydrogels: A novel model system for proteolytically mediated cell migration. *Biophys. J.*, **89**, 1374–1388.

27. Rowley, J. A., Mooney, D. J. (2002). Alginate type and RGD density control myoblast phenotype. *J. Biomed. Mater. Res.*, **60**(2), 217–223.

28. Silberman, M., Gislason, J., Einarsson, J. M., Martin, P. (2006). Use of chitosan for stimulating bone healing and bone formation. WO/2006/057011. International Patent Application.

29. Wnek, G. E., Carr, M. E., Simpson, D. G., Bowlin, G. L. (2003). Electrospinning of nanofiber fibrinogen structures. *Nano Lett.*, **3**, 213–216.

Chapter 39

Potential Applications of Nanotechnology in the Nutraceutical Sector

Shu Wang, MD, PhD, and Jia Zhang, MS

Department of Nutritional Sciences, Texas Tech University, Lubbock, Texas, USA

Keywords: biocompatible and biodegradable nanocarriers, phytochemicals, green tea catechins, (-)-epigallocatechin gallate, quercetin, resveratrol, curcumin, bioavailability, bioactivities, cancer, atherosclerosis, stability, sustained release, nanoliposomes, emulsions, micelles, lipid nanoparticles, PLGA nanoparticles

39.1 Introduction

The application of nanotechnology in improving bioavailability and bioactivities of nutrients and phytochemicals is a promising and innovative research area. Many natural phytochemicals show promise to remedy diseases, but their low level of solubility, stability, bioavailability and target specificity and the high level of metabolism in the body make administering them in therapeutic doses unrealistic. Green tea catechins and quercetin are well-studied phytochemicals and have beneficial potentials to human

Handbook of Clinical Nanomedicine: Nanoparticles, Imaging, Therapy, and Clinical Applications
Edited by Raj Bawa, Gerald F. Audette, and Israel Rubinstein

ISBN 978-981-4669-20-7 (Hardcover), 978-981-4669-21-4 (eBook)
www.panstanford.com

health. There is a critical need for using nanoparticles to enhance their stability, solubility, absorption, bioavailability, target specificity and bioactivities, protect them from premature degradation in the liver and other tissues, and lower their toxicity to normal tissues.

39.2 Nanoparticles

Although no official universally accepted definition for nanoparticles has been established, most experts consider them to be particles that are in the range of 10–1000 nm. Nanoliposomes, emulsions, micelles, lipid nanocarriers, and poly(lactic-co-glycolic acid) (PLGA) nanoparticles are commonly used biocompatible and biodegradable nanoparticles [1].

39.2.1 Nanoliposomes

Phospholipids and cholesterol are commonly used to synthesize nanoliposomes. The extruder and sonicator are common equipment to make nanoliposomes. After dissolving and drying phosphatidylcholine and cholesterol, saline or aqueous solutions can be added into the dry lipids. After vortexing, the suspension can either pass through the extruder with different sizes of filters or be sonicated to form nanoliposomes. Nanoliposomes are spherical and have lipid bilayered membrane structures. Multilamellar vesicles (MLVs), small unilamellar vesicles (SUVs) and large unilamellar vesicle (LUVs) are major types of nanoliposomes. Hydrophilic phytochemicals can be encapsulated into the central aqueous compartment of nanoliposomes, and the hydrophobic phytochemicals can be embedded into their lipid bilayers [2]. Since all components of nanoliposomes are biocompatible and biodegradable, nanoliposomes have been widely used as delivery carriers in pharmaceuticals and nutraceuticals [2–5].

39.2.2 Emulsions

Emulsions consist of two immiscible liquids. Oil-in-water (O/W) emulsions are made by adding oil into an aqueous phase, and water-in-oil (W/O) emulsions are made by adding an aqueous solution into an oil phase. In order to reduce the interfacial tension, surfactants or co-surfactants are needed. More surfactants or co-

surfactants are required to make the smaller size of emulsions. Since our physiological environment is aqueous, O/W emulsions are the common emulsion type. The first FDA approved intravenous fat emulsion was Intralipid®, which was composed of soybean oil, egg phospholipids, and glycerin. Intralipid® can deliver essential fatty acids via intravenous injection to the patients who cannot absorb those nutrients through diet [6]. Many phytochemicals, especially resveratrol, quercetin, and curcumin, are hydrophobic. O/W emulsions can increase their aqueous solubility, stability, bioavailability, and bioactivities.

39.2.3 Micelles

Micelles are composed of many amphiphilic monomers, such as phospholipids and some synthetic polymers. When reaction temperatures reach the critical micellization temperature and amphiphilic monomers concentrations reach the critical micelle concentration (CMC), micelles are formed [7, 8]. Micelles found in human intestines are made by phospholipids and bile acids. Hydrophilic (polar) phospholipid heads form the outer surface of micelles, while hydrophobic (nonpolar) phospholipid fatty acid tails form a hydrophobic core, which can accommodate dietary lipids, lipid-soluble vitamins, phytochemicals, and other hydrophobic compounds. Polymeric micelles are composed of block-copolymers that are made of hydrophobic (nonpolar) and hydrophilic (polar) monomer units in different arrangements [9]. The commonly used core-forming blocks are poly(caprolactone), poly(propylene oxide), poly(D,L-lactic acid) and poly(L-aspartic acid), and polyethylene glycol (PEG) is the widely used hydrophilic monomer [9, 10]. Many hydrophobic compounds can be encapsulated or incorporated into micelles and be used for oral, parenteral, nasal, ocular, and topical administration [9]. Micelles are excellent carriers for phytochemicals.

39.2.4 PLGA Nanoparticles

PLGA is a FDA approved and widely used biocompatible and biodegradable polymer [11]. PLGA is composed of lactic acid and glycolic acid. PLGA can have different numbers of lactic acid and glycolic acid that give PLGA different molecular weights and properties.

Many studies have used PLGA nanoparticles as carriers for phytochemicals, including quercetin and curcumin [12–14]. Those phytochemical can be incorporated into PLGA nanoparticles via encapsulation or adsorption on the surface of PLGA nanoparticle [15]. After PLGA nanoparticles deliver those phytochemicals into the animal body, they can be hydrolyzed into lactic acid and glycolic acid, which have minimal toxicity and side effects to human bodies.

39.2.5 Lipid Nanocarriers

Lipid nanocarriers are made of lipids, surfactants, co-surfactants and water [16]. Solid lipid nanoparticles (SLNs) were developed in the early 1990s [17]. The structure of SLNs is similar to lipoproteins, which have a hydrophilic shell and a hydrophobic solid lipid core, which may consist of saturated fatty acids, triglycerides, waxes, or a mixture of the above lipids [16, 18]. SLNs are excellent carriers for hydrophobic compounds, because they can be easily encapsulated into the hydrophobic lipid core. However, low loading capacity is the major limitation of SLNs [18]. The new generation of lipid nanocarriers are called nanostructured lipid carriers (NLCs), whose lipid core is composed of more complex lipid mixtures such as fatty acids with different chain lengths. Such lipid crystal structures are less perfect but they can accommodate more hydrophobic phytochemicals, nutrients, or other compounds, enhancing loading capacity [19–22]. Phase inversion, solvent evaporation/emulsification, cold homogenization, high pressure homogenization, hot homogenization /ultrasonication are common methods to synthesize SLNs or NLCs [22]. Many studies have used NLCs or SLNs as phytochemical carriers to improve their solubility, stability, bioavailability, and bioactivities.

39.3 Phytochemicals

39.3.1 (-)- Epigallocatechin Gallate (EGCG) Nanoparticles

Green tea (*Camellia sinensis*) is a popular beverage worldwide, especially in Asia. Green tea catechins constitute about 10–30% of total dry tea weight [23]. EGCG is the most abundant and bioactive

catechin, and accounts for 20–50% of total catechins. Therefore, one tea bag (2 g) contains about 60–300 mg of EGCG [24]. EGCG has anti-inflammatory, anti-oxidant, anti-angiogenic, and anti-tumorigenic properties [25]. EGCG is not stable in blood and physiological body fluids (neutral pH), but it is stable in an acidic solution (pH < 5.0) [26, 27].

Our group has synthesized EGCG encapsulated nanoliposomes (LIPO-EGCG) and chitosan-coated LIPO-EGCG (CSLIPO-EGCG) using a sonication method [28]. The mean diameter of LIPO-EGCG is 56 nm, and the mean diameter of CSLIPO-EGCG is 85 nm. EGCG encapsulation efficiency was more than 90%. As compared to native EGCG, LIPO-EGCG and CSLIPO-EGCG had significantly increased EGCG stability, decreased the viability (50%) of MCF7 breast cancer cells, and induced their apoptosis (27%).

Our group has also synthesized EGCG encapsulated NLCs (NLC-EGCG) and chitosan-coated NLC-EGCG (CSNLC-EGCG) using a novel phase inversion method. NLC-EGCG was composed of soy lecithin, glyceryl tripalmitate, glyceryl tridecanoate, polyoxyethylated 12-hydroxystearic acid, a nonionic surfactant, EGCG, NaCl, and deionized water. The mean diameter of NLC-EGCG is 46 nm, and the mean diameter of CSNLC-EGCG is 54 nm. EGCG encapsulation efficiency was about 99%. Compared to native EGCG and NLC-EGCG, CSNLC-EGCG increased EGCG stability, increased macrophage cellular EGCG content, decreased macrophage cholesteryl ester accumulation, decreased macrophage mRNA and protein levels of monocyte chemoattractant protein-1 (MCP-1), which indicate their anti-atherogenic potential.

The absorption rate of EGCG is extremely low in humans and research animals [29–31]. Many scientists have used rats to conduct pharmacokinetic and bioavailability studies of green tea catechins [32]. They found that the oral bioavailability was about 0.1% [32]. After men and women drinking tea containing 400 mg catechins throughout the day, the EGCG bioavailability is 0.14% and peak plasma EGCG concentrations are less than 2 μM [30, 31]. Many studies have demonstrated that nanoparticles, especially chitosan nanoparticles, significantly increased oral EGCG bioavailability through enhanced transcellular transport process [33, 34]. We summarize the properties and bioactivities of EGCG nanoparticles in Table 39.1.

Table 39.1 The characteristics, findings, and application of EGCG nanoparticles

NP type size	Experiment model/ dose/route	Findings and potential application	Year [ref.]
NLCs 53 nm	THP-1 derived macrophages were treated with 10 μM of free EGCG or nano-EGCG for 16 h.	↑EGCG stability ↑ Sustained release ↑Cellular uptake ↓ Inflammation ↓ Cellular cholesteryl ester content Application in anti-atherosclerosis	2013 [27]
Nanoliposome 85 nm	MCF7 breast cancer cells were treated with 0–10 μM of free EGCG or nano-EGCG.	↑EGCG stability ↑ Sustained release ↑Cellular uptake ↓ Cancer cell viability ↑ Cancer cell apoptosis Application in cancer chemoprevention	2013 [28]
PLGA 127.2 nm	7,12-Dimethy-lbenzanthracene (DMBA)-induced DNA damage in mouse skin	↑ Sustained release ↑ DNA damage Application in cancer chemoprevention	2013 [35]
PLGA-PEG 80 nm	PSMA positive prostate cancer (LNCaP) cells were treated with 30 μM of free EGCG or nano-EGCG for 48 and 72 h.	↑ Sustained release ↑ viability of LNCaP cells No effect on viability of normal cells Application in cancer chemoprevention	2011 [36]
Chitosan NPs 440 nm	Excised jejunum from male, Swiss outbred mice.	↑EGCG stability ↑EGCG intestinal absorption Application in Enhancing EGCG bioavailability	2010 [34]
NLCs 260 nm	N/A	↑EGCG stability	2009 [37]

NP type size	Experiment model/ dose/route	Findings and potential application	Year [ref.]
Polylactic acid–polyethylene glycol (PLA-PEG) NPs 285 nm	Prostate cancer (PC3) cells were treated with 1–80 μM of free or nano-EGCG for 24 and 48 h. Tumor xenograft mice were given 1 mg and 100 μg of free or nano-EGCG, respectively, via intraperitoneal injection three times per week.	↑ Apoptosis ↓ Cell viability ↓ Colony formation ↓ Tumor size ↓ Angiogenesis Nano-EGCG exhibits > 10-fold dose advantage over free EGCG Prostate cancer Application in cancer Chemoprevention and treatment	2009 [38]

N/A: not applicable; NP: Nanoparticle; PSMA: Prostate-specific membrane antigen; ↑, increase; ↓, decrease. Reprinted with kind permission of *Journal of Nutritional Biochemistry*.

39.3.2 Quercetin Nanoparticles

Quercetin (3,3′,4′,5′-7-pentahydroxy flavone) is abundant in berries, caper, buckwheat, tea leaves, onion, apple, broccoli, and other leafy green vegetables [39]. Quercetin has many beneficial effects to human health including anti-oxidant, anti-inflammatory, anti-viral and anti-tumorigenic properties [40–42]. Quercetin is a hydrophobic compound and has extremely low aqueous solubility. Quercetin is quickly metabolized in the human body, which results in low circulation time and concentrations [43].

We have successfully synthesized quercetin (Q) encapsulated NLCs (Q-NLCs) and chitosan-coated Q-NLCs (Q-CSNLCs) in our laboratory [44]. The encapsulation efficiency was 95% and the loading capacity of Q-NLCs was 11%. NLCs enhanced aqueous solubility of Q more than 1000 times. Q-NLCs decreased the viability of MCF7 and MDA-MB-231 breast cancer cells in a dose-dependent manner (0–50 μM). Q-NLCs had more than two-fold dose advantage than free Q in decreasing the viability of those breast cancer cells. This is partially due to enhanced cellular uptake of Q by Q-NLCs. We also conducted pharmacokinetic studies using male Sprague-Dawley rats. After 1-week acclimation, rats were fasted overnight, weighed and randomly grouped, and received

the following three treatments via oral gavage or intravenous injection: free Q, Q-NLCs and Q-CSNLCs dissolved in normal saline. Both Q-NLCs and Q-CSNLCs had significantly higher bioavailability than free Q. Q-NLCs and Q-CSNLCs also had significantly higher stability than free Q in blood and gastro-intestinal solutions. As shown in Table 39.2, other published studies also demonstrated that nanoencapsulated Q can increase the solubility, stability, bioavailability and bioactivities of Q, especially anti-cancer activities [45–48].

Table 39.2 The characteristics, findings, and application of quercetin nanoparticles

NP type size	Experiment model/ dose/route	Findings and potential application	Year [ref.]
NLCs 32 nm	MCF-7 and MDA-MB-231 breast cancer cells were treated with 0–50 μM of free quercetin or nano-quercetin for 24 and 48 h.	↑ Aqueous solubility of quercetin ↑ Cellular uptake ↑ Sustained release ↑ Apoptosis of cancer cells ↓ Viability of cancer cells Application in the breast cancer chemoprevention and treatment	2014 [44]
NLCs 126.6 nm	C57BL/6J mice were given 25 mg/kg body weight of free quercetin or nano-quercetin via oral administration.	↑ Sustained release ↑ Bioavailability Application in oral delivery of quercetin	2014 [49]
PLGA 50 nm	Swiss Albino rats having ischemia-reperfusion-induced neuronal damage were given 2.7 mg/kg body weight of free quercetin or nano-quercetin via oral gavage for 3 days.	↑ Anti-oxidant status ↓Inducible nitric oxide synthase (iNOS) and caspase-3 activities ↑ Neuronal count in the hippocampal subfields Application in the protection of ischemic neuronal damage	2013 [50]

NP type size	Experiment model/ dose/route	Findings and potential application	Year [ref.]
SLNs & NLCs 282 nm	*In vitro* permeation study using full thickness human skin	↑ Stability ↑ Sustained release ↑ Quercetin concentrations in skin Application in topical delivery	2012 [51]
NLCs 215.2 nm	*In vitro* skin permeation studies: Franz diffusion cells were treated with 1 mg/mL free quercetin or nano-quercetin for 1, 3, 6, 9 and 12 h. *In vivo* permeation study: male Kunming mice were given 1.0 mg/mL of free quercetin or nano-quercetin via topical application for 3, 6, 9 and 12 h.	↑ Quercetin concentrations in epidermis and dermis ↑ Anti-oxidant and anti-inflammation Application in topical delivery	2012 [52]
Nanomicelles 16 nm	Lung tumor mice were given 30 mg/kg body weight of free quercetin or nano-quercetin via oral gavage three times per week for three weeks.	↑ Stability ↓ Viability of cancer cells ↓ Tumor size Application in the lung cancer chemoprevention and treatment	2012 [46]
Nanoliposomes 62.3–191.5 nm	C6 glioma cells were treated with 0, 50, 100, 200 and 400 μM of free quercetin or nano-quercetin for 12, 24, 36, and 48 h.	↓ Viability of C6 glioma cells ↑ Necrotic cell death Application in the brain cancer chemoprevention and treatment	2012 [47]
PLGA 15 nm	Male Sprague-Dawley rats having gastric ulcer were given 2.5 and 50 mg/kg	↓ Inflammation ↓ Oxidative stress Application in preventing gastric ulcer formation	2012 [13]

(*Continued*)

Table 39.2 (*Continued*)

NP type size	Experiment model/ dose/route	Findings and potential application	Year [ref.]
	body weight of free quercetin or nano-quercetin via oral gavage.		
SLNs <200 nm	Male Wistar rats were given aluminum chloride (100 mg/kg) in combination with either free or nano- quercetin (equivalent to 4.41 mg/kg body weight of quercetin) via oral administration for 8 weeks.	↑ Brain anti-oxidant capacity ↑ Memory retention ↓ Aluminum-induced neurotoxicity Application in prevention of Alzheimer's disease	2011 [53]
Liposomes and PLA NPs 100 to 200 nm	Adult male Swiss Albino rats were given NaAsO2 (13 mg/kg body weight) through oral administration in combination with either free or nano-quercetin (2.7 mg/kg body weight) through intravenous injection.	↑ Liver quercetin concentrations ↑ Liver anti-oxidant capacity ↑ Arsenic-induced liver fibrosis Application in reducing arsenic-induced acute liver toxicity	2010 [54]
SLNs 155.3 nm	Male Waster rats were given 50 mg/kg body weight free quercetin or nano-quercetin via intragastric administration.	↑ Sustained release ↑ Blood quercetin concentrations Application in improving bioavailability	2009 [45]

N/A: not applicable; NP: nanoparticle; NLCs: nanostructured lipid carriers; PLA: poly (D,L-lactide); PLGA: poly (D,L-lactide-co-glycolide); SLNs: Solid lipid nanoparticle; ↑, increase; ↓, decrease. Reprinted with kind permission of *Journal of Nutritional Biochemistry*.

39.3.3 Resveratrol Nanoparticles

Resveratrol (3,5,4′-trihydroxy-*trans*-stilbene), a phytoalexin, is a naturally occurring polyphenolic compound. The solubility of resveratrol in water is very low, less than 0.05 mg/mL; its solubility is high in ethanol (50 mg/mL). Due to the low aqueous solubility, its bioactivities have been limited. Resveratrol has two isomeric forms: *cis*- and *trans*-resveratrol. *cis*-Resveratrol is not commonly found in foods and is unstable; hence, *trans*-resveratrol has been better studied. *Trans*-resveratrol is naturally found in grape, mainly in the skin but not in flesh; it is also present in the leaf epidermis of the grape vine [55]. Other than grapes, *trans*-resveratrol is also found in 72 other plant species and in foods like mulberry, peanuts and in small amounts in cocoa [56, 57]. Resveratrol has anti-inflammatory, anti-oxidant, and anti-tumorigenic activities [58–60]. However, it also has some problems, such as low levels of solubility, stability, bioavailability and target specificity. Biocompatible and biodegradable nanoparticles can overcome those problems, increase its bioactivities and lower its toxicity and side effects. We summarize the properties and bioactivities of resveratrol nanoparticles in Table 39.3.

Table 39.3 The characteristics, findings, and application of resveratrol nanoparticles (NPs)

NP type size	Experiment model/ dose/route	Findings and potential application	Year [ref.]
Nanoemulsions 128–235 nm	Caco-2 cells were treated with free or nano-resveratrol for 0–12 h.	↑ Stability ↑ Sustained release ↑ Transport through Caco-2 cell monolayer Application in improving bioavailability	2014 [61]
PLGA 154 nm	Prostate cancer (PCa) cell lines DU-145, PC-3, and LNCaP were treated with 0–40 μM of free or nano-resveratrol for 72 h.	↑ Sustained release ↑ Cellular uptake ↓ Cancer cell viability Application in prostate cancer chemoprevention	2013 [62]

(*Continued*)

Table 39.3 (*Continued*)

NP type size	Experiment model/ dose/route	Findings and potential application	Year [ref.]
SLNs and NLCs 150–250 nm	*In vitro* release and stability study	↑ Stability ↑ Sustained release Application in improving oral bioavailability	2013 [63]
SLNs and NLCs 110–280 nm	Normal Human Dermal Fibroblasts (NHDF) from juvenile foreskins and rat abdominal skin were treated with 10, 25, 50, 100, 250, and 500 μM of free or nano-resveratrol.	↓ Reactive oxygen species production ↑ Resveratrol concentrations in dermis Application in dermal delivery	2012 [64]
SLNs 180 nm	Human keratinocyte cell line NCTC2544 was treated with 100 μM of free or nano-resveratrol for 24 h.	↑ Cellular uptake ↓ Keratinocyte proliferation Application in skin cancer prevention and treatment	2010 [65]
PCL–PEG polymeric micelles 100 nm	PC12 cells were treated with 0–10 uM of free or nano-resveratrol for 48 h.	↑ Sustained release ↓ Reactive oxygen species accumulation ↑ Improve Aβ-induced PC12 cell viability Application in the prevention of Alzheimer's disease	2009 [66]

NP: nanoparticle; NLCs: nanostructured lipid carriers; PCL: poly-caprolactone; PEG: polyethylene glycol; SLNs: solid lipid nanoparticle; ↑, increase; ↓, decrease. Reprinted with kind permission of the *Journal of Nutritional Biochemistry*.

39.3.4 Curcumin Nanoparticles

Curcumin, a hydrophobic polyphenol, is extracted from the herb *Curcuma longa* [67]. Curcumin accounts for 2–8% of turmeric [68]. Due to its anti-angiogenic, anti-inflammatory, and anti-tumorigenic

bioactivities, it can be used to prevent or treat some chronic diseases including cancer, cardiovascular disease and diabetes [67]. Curcumin's application has been limited because of its poor aqueous solubility, low bioavailability and fast metabolism by hepatic enzymes in humans and research animals [69]. We summarize some studies using biocompatible and biodegradable nanoparticles to overcome these limitations and to improve its bioactivities in Table 39.4.

Table 39.4 The characteristics, findings, and application of curcumin nanoparticles

NP type size	Experiment model/dose/ route	Findings and potential application	Year [Ref.]
SLNs 148 nm	Wistar rats with Huntington's disease were given 40 mg/ kg body weight of nano-curcumin per day for 7 days.	↑ Anti-oxidant enzyme activities ↑ Activity of mitochondrial complexes and cytochrome levels ↓ Mitochondria dysfunction ↑ Neuromotor coordination Application in intervention of Huntington's disease	2014 [70]
NLCs 123–133 nm	HepG2 cells were incubated with 0–50 μg/mL of free curcumin and nano-curcumin for 24, 48 and 72 h.	↑ Cellular uptake ↑ Cytotoxicity Application in liver cancer chemoprevention and treatment	2014 [71]
PLGA 86–90 nm	HT29 cells were treated with 4 and 8 μg/mL of free curcumin and nano-curcumin for 2 h. Male SD rats were given 4 mg/kg body weight of nano-curcumin via intravenous administration.	↑ Cellular uptake ↓ Cancer cell viability ↑ Bioavailability Application in colon cancer chemoprevention and treatment	2014 [72]

(*Continued*)

Table 39.4 (*Continued*)

NP type size	Experiment model/dose/ route	Findings and potential application	Year [Ref.]
PLGA	XB-2 keratinocytes were treated with 100 μg of free curcumin and 20 μg of nano-curcumin for 90 min.	↑ Stability ↑Aqueous solubility ↑ Sustained release ↑Anti-inflammatory potential	2013 [73]
	RjHan:NMRI mice having wounds were treated with 0.5 mg of free curcumin and 0.15 mg of nano-curcumin on wounds.	↑ Sustained release ↑ Re-epithelialization Application in wound healing	
SLNs	Lung cancer cells NCL-H460 and A549 were treated with 0–200 μM of free curcumin and nano-curcumin for 24 h. Balb/c mice and nude mice bearing A549 xenografts were given 200 mg/kg of free or nano-curcumin via intraperitoneal or oral administration.	↑ Stability ↓ Cancer cell viability ↑ Bioavailability ↓ Tumor size Application in lung cancer chemoprevention and treatment	2013 [74]
PLGA PLGA-PEG 152 nm	Male adult Wistar rats were given 50 mg/kg of free or nano-curcumin via oral administration.	↑ Oral bioavailability Application in improving bioavailability	2013 [14]
SLNs 190 nm	Balb/c mice were given 400 mg/kg of free or nano-curcumin via intraperitoneal injection.	↑ Curcumin concentrations in lungs ↑ Inflammatory response in lung Application in asthma therapy	2012 [75]
Emulsions 218 nm	Caco-2 cells were treated with 20 μg/mL of free or nano-curcumin to measure the transportation of curcumin Female CD-1 mice were given 240 mg/kg of freeor nano-curcumin via oral gavage.	↑ Permeation rate across Caco-2 cells ↑ Oral bioavailability Application in improving bioavailability	2012 [76]

NP type size	Experiment model/dose/ route	Findings and potential application	Year [Ref.]
PLGA 80–100 nm	Human neuroblastoma SK-N-SH cells were treated with 0.035 to 0.1 μM of free or nano-curcumin.	↓ Reactive oxygen species accumulation ↑ Neurons against oxidative damage Application in the prevention of Alzheimer's disease	2012 [77]
PLGA <200 nm	Male Sprague-Dawley rats were given 10 mg/kg body weight of free or nano-curcumin by intravenous injection or 100 mg/kg body of weight free or nano-curcumin by oral administration.	↑ Stability ↑ Sustained release ↑ Oral bioavailability Application in improving bioavailability	2011 [78]
SLNs 135 nm	Male Wistar rats were given 1–50 mg /kg body weight of nano-curcumin, or 50 mg/kg body weight of free curcumin via oral administration.	↑ Stability ↑ Sustained release ↑ Oral bioavailability Application in improving bioavailability	2011 [79]
Nano-emulsions 192 nm	Cancer cells (PANC-1, MIA PaCa-2, K562, MCF 7, A549, and HCT-116) were treated with 0–40 μM of free or nano-curcumin. BALB/c mice were given 30 mg/kg body weight of free or nano-curcumin via tail vein injection.	↑Aqueous solubility ↑ Cellular uptake ↓ Viability of cancer cells ↑ Intravenous bioavailability Application in cancer chemoprevention and treatment	2010 [80]
PLGA 264 nm	Male Sprague-Dawley rats were given 250 mg/kg body weight of free curcumin, or 100 mg/kg body weight of nano-curcumin via oral gavage.	↑ Sustained release ↑ Oral bioavailability Application in improving bioavailability	2009 [81]

NP: nanoparticle; PEG: polyethylene glycol; PLGA: poly(D, L-lactide-co-glycolide); SLNs: Solid lipid nanoparticles; ↑, increase; ↓, decrease. Reprinted with kind permission of the *Journal of Nutritional Biochemistry*.

39.4 Conclusions and Future Prospects

Many phytochemicals have a potential to improve human health. However, their low levels of aqueous solubility, stability, and bioavailability limit their application. Biocompatible and biodegradable nanoparticles can overcome those problems. Many studies have demonstrated that nanoparticles can dramatically increase the solubility of phytochemicals in physiological solutions, and further increase their bioavailability and bioactivities. The release of free phytochemicals is in a burst pattern, but nanoencapsulated phytochemicals have a sustained release pattern, which in combination with increased stability can attain longer bioactive effects than free phytochemicals. Many nanoparticles are modified by PEG, which ensures the long circulation time in the body. Therefore, nanoparticles not only overcome many limitations of free phytochemicals, but also improve their physiological characteristics, functions, and bioactivities.

Most of biocompatible and biodegradable nanoparticles have a low level of short-term toxicity and side effects. However, their long-term toxicity has not been measured. The long-term toxicity should include broad and detailed tests, such as liver toxicity, kidney toxicity, and immune-system activation. Synthesizing nanoparticles is not simple and cheap. Researchers can engineer nanoparticles with exquisitely fine structural detail, which can have different functions in response to different physiological environments. The components and engineering processes are expensive. Even though application of nanotechnology in nutraceuticals is promising and has a bright future, cost-effectiveness and long-term safety of nanoparticles are required to address and investigate.

Abbreviations

1 X PBS: 1X phosphate buffered saline
CSLIPO-EGCG: Chitosan-coated EGCG encapsulated nanoliposomes
CSNLC-EGCG: Chitosan-coated EGCG encapsulated nanostructured lipid carriers
EGCG: (-)-Epigallocatechin gallate
LIPO-EGCG: EGCG encapsulated nanoliposomes

LUV: Large unilamellar vesicle
MCP-1: Monocyte chemoattractant protein-1
MLV: Multilamellar vesicle
N/A: not applicable
NLC-EGCG: EGCG encapsulated nanostructured lipid carriers
NLCs: Nanostructured lipid carriers
NP: nanoparticle
PCL: poly-caprolactone
PEG: polyethylene glycol
PLGA: Poly (lactic-co-glycolic acid)
Q: Quercetin
Q-NLCs: Q encapsulated nanostructured lipid carriers
Q-CSNLCs: Chitosan-coated Q encapsulated nanostructured lipid carriers
SLNs: Solid lipid nanoparticles
SUV: Small unilamellar vesicle

Disclosures and Conflict of Interest

This work was supported by Grant Number R15AT007013 from the National Center for Complementary & Alternative Medicine, National Institutes of Health (NIH), Bethesda, Maryland, and The Burleson's Family Foundation, Lubbock, Texas. The content of this chapter is solely the responsibility of the authors and does not necessarily represent the official views of National Center for Complementary & Alternative Medicine or NIH.

Furthermore, the authors declare that they have no conflict of interest. The authors declare that no writing assistance was utilized in the production of this chapter and they have received no payment for its preparation.

Corresponding Author

Dr. Shu Wang
Department of Nutritional Sciences
Texas Tech University
1301 Akron Avenue, Lubbock, TX 79409-1270, USA
Email: shu.wang@ttu.edu

About the Authors

Shu Wang is a tenured associate professor of nutritional sciences at Texas Tech University. She has more than 10 years of research experience in the area of atherosclerosis and nutrition. Following medical training, her PhD study in Human Nutrition and Metabolism from Tufts University provided additional and specific training in nutritional impact on atherosclerosis development. After joining Texas Tech University in 2008, her research has focused on nanocarrier-based studies. Dr. Wang's group focuses on targeted delivery of natural polyphenols and drugs to disease tissues or cells using biodegradable and biocompatible nanoparticles as carriers, which can increase their solubility, stability, payload, and cellular bioavailability, lower their toxicity, prolong their circulation time, and target them to specific cells or tissues for disease prevention, diagnosis and treatment.

Jia Zhang received her BS in food science and MS in nutrition and food sciences from Nanchang University, China. Currently, she is a PhD candidate at the Department of Nutritional Sciences at Texas Tech University. Her research focuses on the use of nanoencapsulated EGCG to prevent atherosclerotic lesion development.

References

1. Wang, S., Su, R., Nie, S., Sun, M., Zhang, J., Wu, D., Moustaid-Moussa, N. (2014). Application of nanotechnology in improving bioavailability and bioactivity of diet-derived phytochemicals. *J. Nutrit. Biochem.,* **25**(4), 363–376.
2. Langer, R. (1990). New methods of drug delivery. *Science,* **249**(4976), 1527–1533.
3. Mozafari, M. R., Johnson, C., Hatziantoniou, S., Demetzos, C. (2008). Nanoliposomes and their applications in food nanotechnology. *J. Liposome Res.,* **18**(4), 309–327.
4. Newman, G. C., Huang, C. (1975). Structural studies on phophatidyl-choline-cholesterol mixed vesicles. *Biochemistry*, **14**(15), 3363–3370.

5. Lasic, D. D. (1998). Novel applications of liposomes. *Trends Biotechnol.,* **16**(7), 307–321.
6. McNiff, B. L. (1977). Clinical use of 10% soybean oil emulsion. *Am. J. Hosp. Pharm.,* **34**(10), 1080–1086.
7. Torchilin, V. P. (2007). Micellar nanocarriers: Pharmaceutical perspectives. *Pharm. Res.,* **24**(1), 1–16.
8. Lim, S. B., Banerjee, A., Onyuksel, H. (2012). Improvement of drug safety by the use of lipid-based nanocarriers. *J. Control. Release.,* **163**(1), 34–45.
9. Torchilin, V. P. (2001). Structure and design of polymeric surfactant-based drug delivery systems. *J. Control. Release.,* **73**(2–3), 137–172.
10. Gong, J., Chen, M., Zheng, Y., Wang, S., Wang, Y. (2012). Polymeric micelles drug delivery system in oncology. *J. Control. Release.,* **159**(3), 312–323.
11. Mahapatro, A., Singh, D. K. (2011). Biodegradable nanoparticles are excellent vehicle for site directed in-vivo delivery of drugs and vaccines. *J. Nanobiotechnol.,* **9**, 55.
12. Bennet, D., Marimuthu, M., Kim, S., An, J. (2012). Dual drug-loaded nanoparticles on self-integrated scaffold for controlled delivery. *Int. J. Nanomed.,* **7**, 3399–3419.
13. Chakraborty, S., Stalin, S., Das, N., Choudhury, S. T., Ghosh, S., Swarnakar, S. (2012). The use of nano-quercetin to arrest mitochondrial damage and MMP-9 upregulation during prevention of gastric inflammation induced by ethanol in rat. *Biomaterials*, **33**(10), 2991–3001.
14. Khalil, N. M., do Nascimento, T. C., Casa, D. M., Dalmolin, L. F., de Mattos, A. C., et al. (2013). Pharmacokinetics of curcumin-loaded PLGA and PLGA-PEG blend nanoparticles after oral administration in rats. *Colloids Surf. B Biointerfaces*, **101**, 353–360.
15. Danhier, F., Ansorena, E., Silva, J. M., Coco, R., Le Breton, A., et al. (2012). PLGA-based nanoparticles: An overview of biomedical applications. *J. Control. Release.,* **161**(2), 505–522.
16. Mehnert, W., Mader, K. (2001). Solid lipid nanoparticles: Production, characterization and applications. *Adv. Drug Deliv. Rev.,* **47**(2–3), 165–196.
17. Muller, R. H., Maassen, S., Weyhers, H., Mehnert, W. (1996). Phagocytic uptake and cytotoxicity of solid lipid nanoparticles (SLNs) sterically stabilized with poloxamine 908 and poloxamer, 407. *J. Drug Target.,* **4**(3), 161–170.
18. Uner, M. (2006). Preparation, characterization and physico-chemical properties of solid lipid nanoparticles (SLNs) and nanostructured

lipid carriers (NLCs): Their benefits as colloidal drug carrier systems. *Pharmazie,* **61**(5), 375–386.

19. Puri, A., Loomis, K., Smith, B., Lee, J. H., Yavlovich, A., Heldman, E. (2009). Blumenthal R: Lipid-based nanoparticles as pharmaceutical drug carriers: From concepts to clinic. *Crit. Rev. Ther. Drug Carrier Syst.,* **26**(6), 523–580.
20. Teeranachaideekul, V., Muller, R. H., Junyaprasert, V. B. (2007). Encapsulation of ascorbyl palmitate in nanostructured lipid carriers (NLCs)-effects of formulation parameters on physicochemical stability. *Int. J. Pharm.,* **340**(1–2), 198–206.
21. Sanad, R. A., Abdelmalak, N. S., Elbayoomy, T. S., Badawi, A. A. (2010). Formulation of a novel oxybenzone-loaded nanostructured lipid carriers (NLCs). *Am. Assoc. Pharm. Sci. PharmSciTech*, **11**(4), 1684–1694.
22. Das, S., Chaudhury, A. (2011). Recent advances in lipid nanoparticle formulations with solid matrix for oral drug delivery. *Am. Assoc. Pharm. Sci. PharmSciTech,* **12**(1), 62–76.
23. Wang, S., Noh, S. K., Koo, S. I. (2006). Green tea catechins inhibit pancreatic phospholipase A(2) and intestinal absorption of lipids in ovariectomized rats. *J. Nutrit. Biochem.,* **17**(7), 492–498.
24. Basu, A., Lucas, E. A. (2007). Mechanisms and effects of green tea on cardiovascular health. *Nutrit. Rev.,* **65**(8 Pt 1), 361–375.
25. Chyu, K. Y., Babbidge, S. M., Zhao, X., Dandillaya, R., Rietveld, A. G., et al. (2004). Differential effects of green tea-derived catechin on developing versus established atherosclerosis in apolipoprotein E-null mice. *Circulation,* **109**(20), 2448–2453.
26. Proniuk, S., Liederer, B. M., Blanchard, J. (2002). Preformulation study of epigallocatechin gallate, a promising antioxidant for topical skin cancer prevention. *Eur. J. Pharm. Sci.,* **91**(1), 111–116.
27. Zhang, J., Nie, S., Wang, S. (2013). Nanoencapsulation enhances epigallocatechin-3-gallate stability and its antiatherogenic bioactivities in macrophages. *J. Agric. Food Chem.,* **61**(38), 9200–9209.
28. de Pace, R. C., Liu, X., Sun, M., Nie, S., Zhang, J., et al. (2013). Anticancer activities of (-)-epigallocatechin-3-gallate encapsulated nanoliposomes in MCF7 breast cancer cells. *J. Liposome Res.,* **23**(3), 187–196.
29. Chen, L., Lee, M. J., Li, H., Yang, C. S. (1997). Absorption, distribution, elimination of tea polyphenols in rats. *Drug Metab. Dispos.,* **25**(9), 1045–1050.

30. Warden, B. A., Smith, L. S., Beecher, G. R., Balentine, D. A., Clevidence, B. A. (2001). Catechins are bioavailable in men and women drinking black tea throughout the day. *J. Nutrit.,* **131**(6), 1731–1737.
31. Lee, M. J., Maliakal, P., Chen, L., Meng, X., Bondoc, F. Y., et al. (2002). Pharmacokinetics of tea catechins after ingestion of green tea and (-)-epigallocatechin-3-gallate by humans: Formation of different metabolites and individual variability. *Cancer Epidemiol. Biomarkers Prev.,* **11**(10 Pt 1), 1025–1032.
32. Lambert, J. D., Yang, C. S. (2003). Mechanisms of cancer prevention by tea constituents. *J. Nutrit.,* **133**(10), 3262S–3267S.
33. Hu, B., Ting, Y., Yang, X., Tang, W., Zeng, X., Huang, Q. (2012). Nanochemoprevention by encapsulation of (-)-epigallocatechin-3-gallate with bioactive peptides/chitosan nanoparticles for enhancement of its bioavailability. *Chem. Commun. (Camb).,* **48**(18), 2421–2423.
34. Dube, A., Nicolazzo, J. A., Larson, I. (2010). Chitosan nanoparticles enhance the intestinal absorption of the green tea catechins (+)-catechin and (-)-epigallocatechin gallate. *Eur. J. Pharm. Sci.,* **41**(2), 219–225.
35. Srivastava, A. K., Bhatnagar, P., Singh, M., Mishra, S., Kumar, P., Shukla, Y., Gupta, K. C. (2013). Synthesis of PLGA nanoparticles of tea polyphenols and their strong *in vivo* protective effect against chemically induced DNA damage. *Int. J. Nanomed.,* **8**, 1451–1462.
36. Sanna, V., Pintus, G., Roggio, A. M., Punzoni, S., Posadino, A. M., Arca, A., et al. (2011). Targeted biocompatible nanoparticles for the delivery of (-)-epigallocatechin 3-gallate to prostate cancer cells. *J. Med. Pharm. Chem.,* **54**(5), 1321–1332.
37. Barras, A., Mezzetti, A., Richard, A., Lazzaroni, S., Roux, S., et al. (2009). Formulation and characterization of polyphenol-loaded lipid nanocapsules. *Int. J. Pharm.,* **379**(2), 270–277.
38. Siddiqui, I. A., Adhami, V. M., Bharali, D. J., Hafeez, B. B., Asim, M., Khwaja, S. I., et al. (2009). Introducing nanochemoprevention as a novel approach for cancer control: Proof of principle with green tea polyphenol epigallocatechin-3-gallate. *Cancer Res.,* **69**(5), 1712–1716.
39. Bischoff, S. C. (2008). Quercetin: Potentials in the prevention and therapy of disease. *Curr. Opin. Clin. Nutrit. Metab. Care,* **11**(6), 733–740.
40. Kumari, A., Yadav, S. K., Pakade, Y. B., Singh, B., Yadav, S. C. (2010). Development of biodegradable nanoparticles for delivery of quercetin. *Colloid Surface B,* **80**(2), 184–192.

41. Yu, Y. B., Miyashiro, H., Nakamura, N., Hattori, M., Park, J. C. (2007). Effects of triterpenoids and flavonoids isolated from Alnus firma on HIV-1 viral enzymes. *Arch. Pharm. Res.,* **30**(7), 820–826.

42. Stewart, L. K., Soileau, J. L., Ribnicky, D., Wang, Z. Q., Raskin, I., et al. (2008). Quercetin transiently increases energy expenditure but persistently decreases circulating markers of inflammation in C57BL/6J mice fed a high-fat diet. *Metabolism,* **57**(7 Suppl 1), S39–S46.

43. Kumari, A., Kumar, V., Yadav, S. K. (2012). Plant extract synthesized PLA nanoparticles for controlled and sustained release of quercetin: A green approach. *Public Library Sci. One,* **7**(7), e41230.

44. Sun, M., Nie, S., Pan, X., Zhang, R., Fan, Z., Wang, S. (2014). Quercetin-nanostructured lipid carriers: Characteristics and anti-breast cancer activities *in vitro*. *Colloids Surfaces. B*, *Biointerfaces,* **113**, 15–24.

45. Li, H., Zhao, X., Ma, Y., Zhai, G., Li, L., Lou, H. (2009). Enhancement of gastrointestinal absorption of quercetin by solid lipid nanoparticles. *J. Control. Release*, **133**(3), 238–244.

46. Tan, B. J., Liu, Y., Chang, K. L., Lim, B. K., Chiu, G. N. (2012). Perorally active nanomicellar formulation of quercetin in the treatment of lung cancer. *Int. J. Nanomed.,* **7**, 651–661.

47. Wang, G., Wang, J. J., Yang, G. Y., Du, S. M., Zeng, N., et al. (2012). Effects of quercetin nanoliposomes on C6 glioma cells through induction of type III programmed cell death. *Int. J. Nanomed.,* **7**, 271–280.

48. Li, W., Yi, S., Wang, Z., Chen, S., Xin, S., et al. (2011). Self-nanoemulsifying drug delivery system of persimmon leaf extract: Optimization and bioavailability studies. *Int. J. Pharm.,* **420**(1), 161–171.

49. Liu, L., Tang, Y., Gao, C., Li, Y., Chen, S., et al. (2014). Characterization and biodistribution *in vivo* of quercetin-loaded cationic nanostructured lipid carriers. *Colloids Surfaces. B*, *Biointerfaces,* **115**, 125–131.

50. Ghosh, A., Sarkar, S., Mandal, A. K., Das, N. (2013). Neuroprotective role of nanoencapsulated quercetin in combating ischemia-reperfusion induced neuronal damage in young and aged rats. *Public Library Sci. One,* **8**(4), e57735.

51. Bose, S., Michniak-Kohn, B. (2012). Preparation and characterization of lipid based nanosystems for topical delivery of quercetin. *Eur. J. Pharm. Sci.,* **48**(3), 442–452.

52. Chen-yu, G., Chun-fen, Y., Qi-lu, L., Qi, T., Yan-wei, X., et al. (2012). Development of a quercetin-loaded nanostructured lipid carrier formulation for topical delivery. *Int. J. Pharm.,* **430**(1–2), 292–298.

53. Dhawan, S., Kapil, R., Singh, B. (2011). Formulation development and systematic optimization of solid lipid nanoparticles of quercetin for improved brain delivery. *J. Pharm. Pharmacol.,* **63**(3), 342–351.

54. Ghosh, D., Ghosh, S., Sarkar, S., Ghosh, A., Das, N., et al. (2010). Quercetin in vesicular delivery systems: Evaluation in combating arsenic-induced acute liver toxicity associated gene expression in rat model. *Chem. Biol. Interact.,* **186**(1), 61–71.

55. Fremont, L. (2000). Biological effects of resveratrol. *Life Sci.,* **66**(8), 663–673.

56. Burns, J., Yokota, T., Ashihara, H., Lean, M. E., Crozier, A. (2002). Plant foods and herbal sources of resveratrol. *Journal of Agricultural and Food Chemistry,* **50**(11), 3337–3340.

57. Hurst, W. J., Glinski, J. A., Miller, K. B., Apgar, J., Davey, M. H., et al. (2008). Survey of the trans-resveratrol and trans-piceid content of cocoa-containing and chocolate products. *J. Agric. Food Chem.,* **56**(18), 8374–8378.

58. Baur, J. A., Pearson, K. J., Price, N. L., Jamieson, H. A., Lerin, C., et al. (2006). Resveratrol improves health and survival of mice on a high-calorie diet. *Nature,* **444**(7117), 337–342.

59. Baur, J. A., Sinclair, D. A. (2006). Therapeutic potential of resveratrol: The *in vivo* evidence. *Nat. Rev. Drug Discov.,* **5**(6), 493–506.

60. Jang, M., Cai, L., Udeani, G. O., Slowing, K. V., Thomas, C. F., et al. (1997). Cancer chemopreventive activity of resveratrol, a natural product derived from grapes. *Science,* **275**(5297), 218–220.

61. Sessa, M., Balestrieri, M. L., Ferrari, G., Servillo, L., Castaldo, D., et al. (2014). Bioavailability of encapsulated resveratrol into nanoemulsion-based delivery systems. *Food Chem.,* **147**, 42–50.

62. Sanna, V., Siddiqui, I. A., Sechi, M., Mukhtar, H. (2013). Resveratrol-loaded nanoparticles based on poly(epsilon-caprolactone) and poly(D,L-lactic-co-glycolic acid)-poly(ethylene glycol) blend for prostate cancer treatment. *Mol. Pharm.,* **10**(10), 3871–3881.

63. Neves, A. R., Lúcio, M., Martins, S., Lima, J. L., Reis, S. (2013). Novel resveratrol nanodelivery systems based on lipid nanoparticles to enhance its oral bioavailability. *Int. J. Nanomed.,* **8**, 177–187.

64. Gokce, E. H., Korkmaz, E., Dellera, E., Sandri, G., Bonferoni, M. C., Ozer, O. (2012). Resveratrol-loaded solid lipid nanoparticles versus nanostructured lipid carriers: Evaluation of antioxidant potential for dermal applications. *Int. J. Nanomed.,* **7**, 1841–1850.

65. Teskac, K., Kristl, J. (2010). The evidence for solid lipid nanoparticles mediated cell uptake of resveratrol. *Int. J. Pharm.,* **390**(1), 61–69.

66. Lu, X., Ji, C., Xu, H., Li, X., Ding, H., Ye, M., et al. (2009). Resveratrol-loaded polymeric micelles protect cells from Abeta-induced oxidative stress. *Int. J. Pharm.,* **375**(1–2), 89–96.

67. Anand, P., Thomas, S. G., Kunnumakkara, A. B., Sundaram, C., Harikumar, K. B., et al. (2008). Biological activities of curcumin and its analogues (Congeners) made by man and Mother Nature. *Biochem. Pharmacol.,* **76**(11), 1590–1611.

68. Alappat, L., Awad, A. B. (2010). Curcumin and obesity: Evidence and mechanisms. *Nutrit. Rev.,* **68**(12), 729–738.

69. Bansal, S. S., Goel, M., Aqil, F., Vadhanam, M. V., Gupta, R. C. (2011). Advanced drug delivery systems of curcumin for cancer chemoprevention. *Cancer Prev. Res. (Philadelphia*, *Pa.)* **4**(8), 1158–1171.

70. Sandhir, R., Yadav, A., Mehrotra, A., Sunkaria, A., Singh, A., et al. (2014). Curcumin nanoparticles attenuate neurochemical and neurobehavioral deficits in experimental model of Huntington's disease. *Neuromol. Med.,* **16**(1), 106–118.

71. Chu, Y., Li, D., Luo, Y. F., He, X. J., Jiang, M. Y. (2014). Preparation and *in vitro* evaluation of glycyrrhetinic acid-modified curcumin-loaded nanostructured lipid carriers. *Molecules,* **19**(2), 2445–2457.

72. Li, L., Xiang, D., Shigdar, S., Yang, W., Li, Q., et al. (2014). Epithelial cell adhesion molecule aptamer functionalized PLGA-lecithin-curcumin-PEG nanoparticles for targeted drug delivery to human colorectal adenocarcinoma cells. *Int. J. Nanomed.,* **9**, 1083–1096.

73. Chereddy, K. K., Coco, R., Memvanga, P. B., Ucakar, B., des Rieux, A., et al. (2013). Combined effect of PLGA and curcumin on wound healing activity. *J. Control. Release,* **171**(2), 208–215.

74. Wang, P., Zhang, L., Peng, H., Li, Y., Xiong, J., et al. (2013). The formulation and delivery of curcumin with solid lipid nanoparticles for the treatment of on non-small cell lung cancer both *in vitro* and *in vivo*. *Mater. Sci. Eng. C, Mater. Biol. Appl.,* **33**(8), 4802–4808.

75. Wang, W., Zhu, R., Xie, Q., Li, A., Xiao, Y., et al. (2012). Enhanced bioavailability and efficiency of curcumin for the treatment of asthma by its formulation in solid lipid nanoparticles. *Int. J. Nanomed.,* **7**, 3667–3677.

76. Yu, H., Huang, Q. (2012). Improving the oral bioavailability of curcumin using novel organogel-based nanoemulsions. *J. Agric. Food Chem.,* **60**(21), 5373–5379.

77. Doggui, S., Sahni, J. K., Arseneault, M., Dao, L., Ramassamy, C. (2012). Neuronal uptake and neuroprotective effect of curcumin-loaded PLGA nanoparticles on the human SK-N-SH cell line. *J. Alzheimers Dis.,* **30**(2), 377–392.

78. Xie, X., Tao, Q., Zou, Y., Zhang, F., Guo, M., et al. (2011). PLGA nanoparticles improve the oral bioavailability of curcumin in rats: Characterizations and mechanisms. *J. Agric. Food Chem.,* **59**(17), 9280–9289.

79. Kakkar, V., Singh, S., Singla, D., Kaur, I. P. (2011). Exploring solid lipid nanoparticles to enhance the oral bioavailability of curcumin. *Mol. Nutrit. Food Res.,* **55**(3), 495–503.

80. Mohanty, C., Sahoo, S. K. (2010). The *in vitro* stability and *in vivo* pharmacokinetics of curcumin prepared as an aqueous nanoparticulate formulation. *Biomaterials,* **31**(25), 6597–6611.

81. Shaikh, J., Ankola, D. D., Beniwal, V., Singh, D., Kumar, M. N. (2009). Nanoparticle encapsulation improves oral bioavailability of curcumin by at least 9-fold when compared to curcumin administered with piperine as absorption enhancer. *Eur. J. Pharm. Sci.,* **37**(3–4), 223–230.

Chapter 40

Designing Nanocarriers for the Effective Treatment of Cardiovascular Diseases

Bhuvaneshwar Vaidya, MPharm, PhD,[a] and Suresh P. Vyas, MPharm, PhD[b]

[a]*Nanomedicine Research Centre, ISF College of Pharmacy, Moga, Punjab, India*
[b]*Department of Pharmaceutical Sciences, Dr. H. S. Gour University, Sagar, India*

Keywords: nanocarriers, cardiovascular diseases, myocardial infarction, thrombosis, restenosis, liposomes, thrombolytic agents, ATP, streptokinase, PEGylation, Targeting, RGD peptide, anticoagulant

40.1 Introduction

For decades, cardiovascular diseases (CVDs) have been the leading cause of death in developed nations. The diseases are disorders related to heart and blood vasculature [1]. Despite significant advances in pharmacological, interventional, and surgical therapy, CVDs account for about 36% of deaths in the United States and Europe, especially due to myocardial infarction and heart failure [2, 3].

Handbook of Clinical Nanomedicine: Nanoparticles, Imaging, Therapy, and Clinical Applications
Edited by Raj Bawa, Gerald F. Audette, and Israel Rubinstein

ISBN 978-981-4669-20-7 (Hardcover), 978-981-4669-21-4 (eBook)
www.panstanford.com

Three main categories of cardiovascular pathologies have been identified: (i) atherosclerotic heart disease (myocardial infarction); (ii) cerebrovascular disease (stroke); and (iii) venous thromboembolism (VTE) (deep vein thrombosis [DVT] and pulmonary embolism [PE]). Although the primary cause of myocardial or cerebral infarction is essentially the atherosclerotic degeneration of the vessel wall. However, thrombotic occlusion of critically situated blood vessels is the key event that triggers the clinical symptoms as syndrome [4].

A thrombus developed in the circulatory system can cause blockage of vascular blood flow leading to serious consequences such as myocardial infarction, ischemic stroke, peripheral arterial thrombosis, deep venous thrombosis, and pulmonary embolism. These are common and potentially life-threatening vascular diseases. To treat such thrombotic diseases, several plasminogen activators have been investigated. However, at present, no single agent has been approved by the United States Food and Drug Administration (US FDA) to be labeled for every indication. Therefore, for better control of these events, new delivery options and dosing regimens are being explored and under investigation [5].

40.2 Nanocarriers for the Treatment of Myocardial Infarction

Acute myocardial infarction (AMI), an irreversible damage of myocardial tissue caused due to persistent ischemia and hypoxia, is the leading cause of mortality in the western world. MI refers to a common clinical condition that leads to necrosis of myocardial tissue. The initiating event of many myocardial infarctions (heart attacks) is rupture of an atherosclerotic plaque. Such rupture may result in the formation of a thrombus or blood clot in the coronary artery that supplies the infarct zone. The damaged tissue is initially comprised of a necrotic core surrounded by a marginal (or border) zone that can either recover normal function or may become irreversibly damaged.

A major therapeutic goal of modern cardiology is to design therapeutic strategies aimed at minimizing myocardial necrosis and optimizing cardiac repair following myocardial infarction.

Under ischemic conditions, adenosine triphosphate (ATP) levels in the cardiomyocytes can drop to 20% of their initial value after approximately 15 min [6]. During ischemia, however, the ATP is provided by breakdown of the myocardial glycogen to glucose with subsequent glycolysis to produce a temporary, transient supply of ATP. In the continuing absence of an oxygen supply, these ATP sources become exhausted and ATP-dependent ion pumps in the outer membranes of myocytes cease to function, with resultant loss of ion balance. The ionic imbalance results in the cell swelling leading to cell burst [7].

The key factor responsible for eliciting an imbalance (e.g., decrease) in the ATP supply/demand ratio during myocardial ischemia is the lack of ATP [8]. Thus, the application of exogenous ATP might help in the restoration of its normal cellular level. Adenosine has been studied extensively as a cardioprotective agent [9]. In addition, adenosine has been shown to participate in myocardial ischemic preconditioning, which may be particularly important because MI in humans is generally caused by dynamic coronary occlusion with intermittent periods of blood flow [10, 11]. In animal models of reperfusion injury, adenosine has consistently reduced the infarct size and improved left ventricular function as well as coronary blood flow [12–16]. However, ATP, like other hydrophilic and strongly charged anions, cannot enter cells through the plasma membrane by simple diffusion process. Additionally, ATP very quickly degrades *in vivo* resulting in a short half-life in blood (Fig. 40.1). Therefore, these limitations do not allow for using exogenous ATP as an efficient therapeutically significant bio-energetic substrate or source.

Moreover, novel carriers have been widely studied for the delivery of such therapeutic molecules. Studies reported that liposomes protect ATP from the enzymatic degradation and can deliver ATP to the cytoplasm of myocytes followed by plugging and sealing [17, 18]. Thus, above-discussed limitations of ATP delivery may be addressed by the use of liposomes as carriers. It has earlier been reported that liposomes, especially the cationic liposomes, accumulated in the region of myocardial infarction [19]. Later, it was demonstrated that accumulation of liposomes to the ischemic area is a general phenomenon and might be because of impaired filtration in these areas, resulting in the trapping of liposomes within the ischemic zone [20–22]. This, in

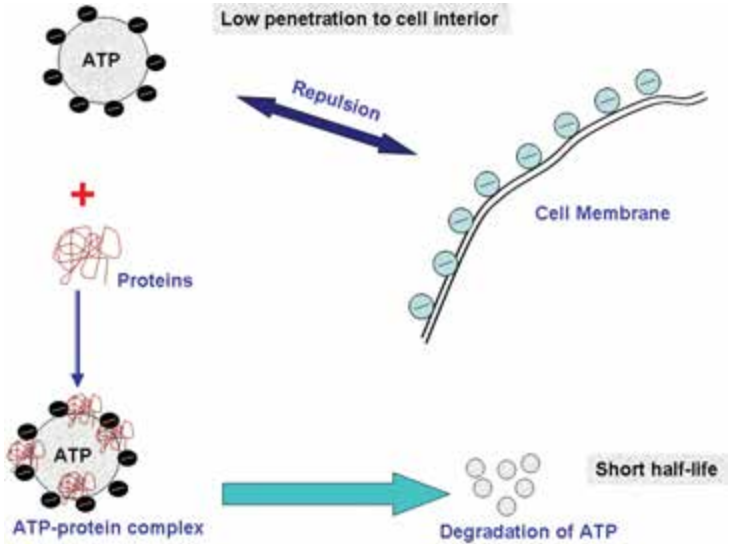

Figure 40.1 Limitations of ATP using as exogenous substrate.

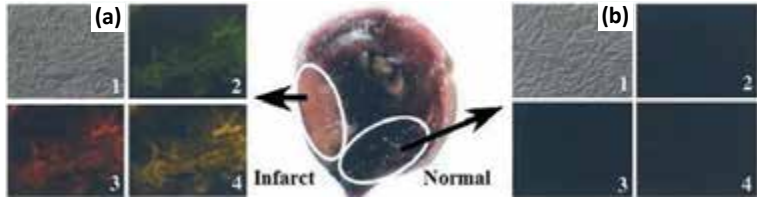

Figure 40.2 Microscopy of 7 μm thick heart cryosections with 4% formaldehyde, washed with PBS, and mounted with Flour mounting media (Trevigen). (a) Extensive association of Rh-PE and FITC fluorescence with infarcted (pink, NBT-negative) tissue; (b) Lack of fluorescence associated with normal (dark, NBT-positive) tissue. (1) Transmission microscopy, (2) fluorescence microscopy with FITC filter, (3) fluorescence microscopy with rhodamine filter, (4) superposition of (2) and (3). From ref. [17] with permission.

particular, could be considered a case of "enhanced permeability and retention" (EPR) effect [23, 24]. Furthermore, improvement in the passive delivery of ATP to the ischemic area can be achieved by increasing the circulation time of the liposomes in the blood, thus providing an increased opportunity to extravasate and

accumulate in the infarct zone. One of the most promising approaches to increase the half-life of liposomes is the coating of liposomes with polyethylene glycol (PEG) [22, 25]. PEG, a hydrophilic polymer, reportedly reduces the sequestering of liposomes by the macrophages and decreases their recognition by liver cells, which in turn increases the circulation half-life of the liposomes in the blood. In an *in vitro* experiment conducted on global ischemic isolated heart model using Langendorff apparatus, it was observed that liposomes accumulate in the infarct zone more efficiently than normal zone [17] (Fig. 40.2).

In a different experiment employing the rat model, it was observed via electron microscopy that liposomes specifically accumulate in ischemic/reperfused myocardium [26] (Fig. 40.3). It was also observed that an intravenous infusion of PEGylated liposomal adenosine (450 μg/kg/min) for 10 min, from 5 min prior to the onset of reperfusion, significantly reduced MI size (29.5 ± 6.5%) compared with an infusion of normal saline (53.2 ± 3.5%, $p < 0.05$) [26]. Verma et al. [27] also observed a protection effect of liposomal adenosine in the rabbit model. They assessed if the infusion of ATP-loaded liposomes (ATP-L) can limit the irreversibly damaged myocardium in rabbits with an experimental myocardial infarction. Unisperse Blue dye was used to demarcate the net size of the occlusion-induced ischemic zone (area at risk) and nitroblue tetrazolium staining was used to detect the final fraction of the irreversibly damaged myocardium within the total area at risk (Fig. 40.4). It was found that finally measured damage in ATP-L-treated animals was only 30% of the total area at risk as compared with 60% recorded in the group treated with EL ($p < 0.009$) and 70% in the KH buffer treated group ($p < 0.003$). The study concluded that ATP-L might serve as an effective exogenous source of the ATP *in vivo* and protect ischemically damaged cells.

Furthermore, to improve the delivery of ATP specifically into the ischemic myocardium, attempts have been made using antibody mediated targeting of liposomes to the myocardium [28]. The approaches used were based on the fact that myocardial cell death occurs as a result of ischemia, hence an antibody against intracellular antigen may be able to differentiate and discriminate viable cells from intact membranes and necrotic cells with disrupted

membranes. Cardiac myosin, which is not washed away following cell disintegration, has been chosen as the target molecular antigen, a typical characteristic of infracted myocardium [29–31]. Therefore, anti-myosin antibody has been explored as an agent for the active targeting of plain and long-circulating liposomes to the infracted myocardium [32–34]. The study demonstrated that these modified liposomes revealed long circulation half-half and accumulated selectively in the infarcted area as compared to normal myocardium (Table 40.1).

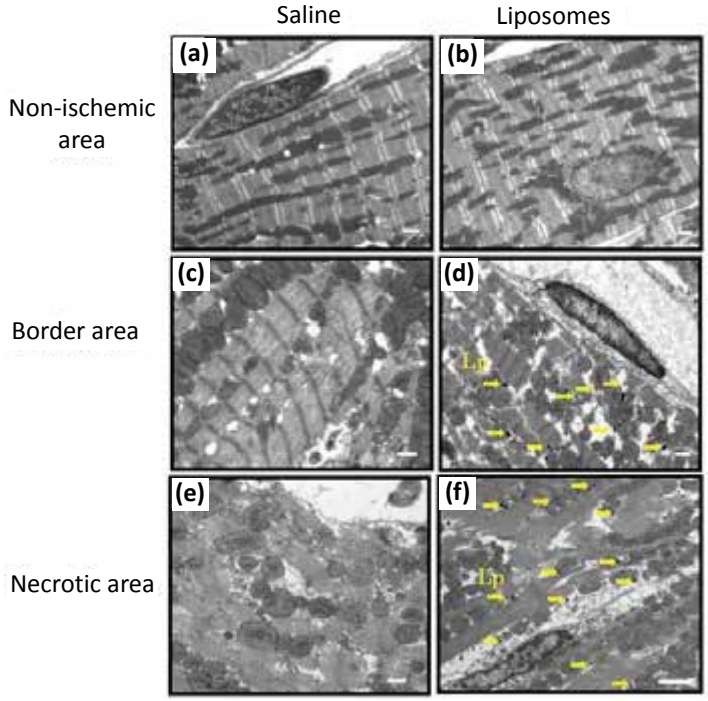

Figure 40.3 Liposomes in ischemic/reperfused myocardium. (a, b) Representative electron micrographs of the nonischemic area in rats that received saline (a) or liposomes (Lp) (b). (c, d) Representative electron micrographs of border area at 3 h after myocardial infarction (MI). Many dark dots accumulated in this area in the rat that received liposomes but not saline. (e, f) Representative electron micrographs of infarcted areas at 3 h after MI. Numerous dark dots accumulated in this area in the rat that received liposomes but not saline. Scale bars represent 1 μm. From ref. [26] with permission.

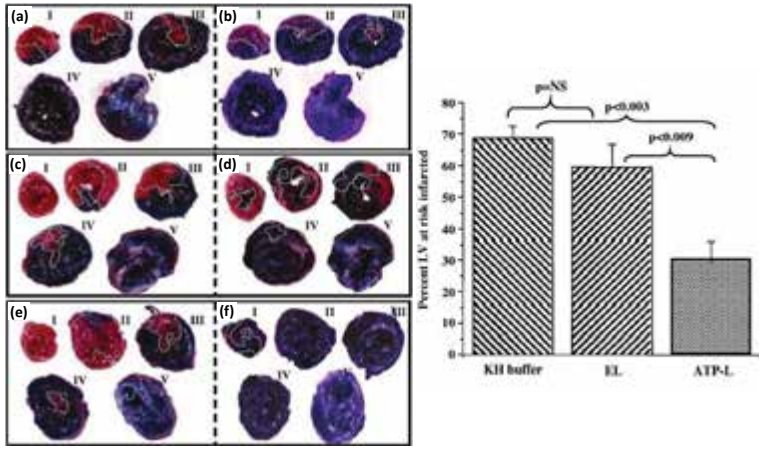

Figure 40.4 (i) USB- and NTB-stained sections of infarcted myocardium. Cardioprotective effect of ATP-L after 30 min of coronary occlusion and following 3 h of reperfusion in rabbits with an acute experimental myocardial infarction (a, b) Control KH buffer-treated animal; (c, d) EL-treated animal; (e, f) ATP-L-treated animal. (a, c, and e) Area at risk (USB-unstained red tissue) developed as a result of occlusion; (b, d, and f) infarcted area at the end of occlusion/reperfusion experiment (NBT-unstained tissue); heart slices I to V represent base to apex. (ii) Summary graph showing the fraction of infarcted area as a percentage of the total area at risk in the KH buffer-treated control group, EL-, and ATP-L-treated group; (mean ± SD), *n* = 4–10. From ref. [27] with permission.

Table 40.1 Characteristics of different liposomes and their accumulation ratio

Types of liposomes	Half-life	Accumulation ratio (infarct to normal tissue)
Plain Lip	10–15 min	5.17 ± 2.35
PEG-plain Lip	>1000 min	8.05 ± 5.03
AM-Lip	15–20 min	22.70 ± 2.38
PEG-AM-Lip	>600 min	14.70 ± 7.15*

*The lower target to non-target ratio of PEG-antimyosin immunoliposomes, relative to anti-myosin-immunoliposomes in the infarct, is due to the higher blood activity of the former at 5 h post intravenous administration of liposome preparation.

Verma et al. [18] have selectively delivered ATP to the ischemic myocardium to protect the myocardial viability. Antimyosin

antibody (2G4 antibody) was appended at the surface of liposomes as site directing receptor specific ligand. The study was performed in the isolated rat heart model. Results of the study showed that the use of ATP loaded immunoliposomes (ATP-IL) resulted in an effective protection to the myocardium under the ischemia/reperfusion allowing for the substantial normalization of left ventricle developed pressure (LVDP) as well as left ventricle end diastolic pressure (LVEDP). The lowest LVDP recorded in the case of KH buffer control indicated that the myocardial function was severely compromised in the case of global ischemia. ATP-L also demonstrated significant recovery of both systolic as well as diastolic functions as compared to IL and KH perfusion buffer studies.

40.3 Novel Carriers for the Treatment of Thromboembotic Diseases

Site-targeted drug delivery holds promise in the treatment of vascular injury-associated thrombotic and occlusive events due to CVDs (e.g., atherosclerosis) or interventional procedure (e.g., angioplasty and stenting). On the contrary, conventional techniques are expensive and also they require experienced personnel [35].

Among various drug delivery systems, liposomes have been explored by various research groups for delivery of thrombolytic drugs [36, 37]. Liposomal encapsulation of plasminogen activators might increase efficacy, improve selectivity, possibly reduce or eliminate antigenic complications, retard systemic deactivation and effectively prolong the circulation half-lives of the agents [38]. In an *in vitro* experiment, Nguyen et al. [36] demonstrated the ability of liposomes to protect streptokinase in plasma without significant loss of activity. Plasminogen activators entrapped in liposomes have shown substantial decrease in the time required to obtain reperfusion and an increased digestion of thrombus as compared to free plasminogen activators perfusion. One of the theories proposed to increase the effectiveness of the liposomal plasminogen activators is the obstruction of channeling by the liposomes that results in a pressure at the leading edge of the thrombus. To prove this theory, Heeremans et al. [39] compared the thrombolytic activity of free t-PA to free t-PA + empty liposomes

in a jugular vein model in rabbit. Moreover, the clot lysis activity of free t-PA recorded was nearly equal to that of t-PA + empty liposomes with an equivalent dose. Thus, based on these studies, it was concluded that increased thrombolytic activity of the liposomal plasminogen activator was not due to the pressure created following the blockage of the channels in the thrombus. Moreover, it was suggested that liposomal encapsulation reduces the premature inactivation and prevents degradation of plasminogen activator in the plasma vis-a-vis releases it at the site of thrombus under shear stress.

Erdogan et al. [40] developed three types of vesicular systems, (i.e., liposomes, niosomes, and sphingosomes) and evaluated their biodistribution using radiolabeled streptokinase and compared with intravenous injection of free streptokinase. Results demonstrated detectable amounts of streptokinase in the thrombi in all three types of vesicles, with higher amount at 4 h than 1 h.

Recently, Baek et al. [41] developed streptokinase (SK) bearing liposomes for the subconjunctival delivery of thrombolytic agents in order to increase the local concentration of drug while decreasing the systemic absorption and/or side effect of the drug. Results of the study demonstrated lower ocular absorption of liposomal SK as compared to non-liposomal SK. Additionally, no detectable systemic and ocular side effects were observed in animals study. Liposomal formulations also enhanced the rate of subconjunctival hemorrhage (SH) absorption.

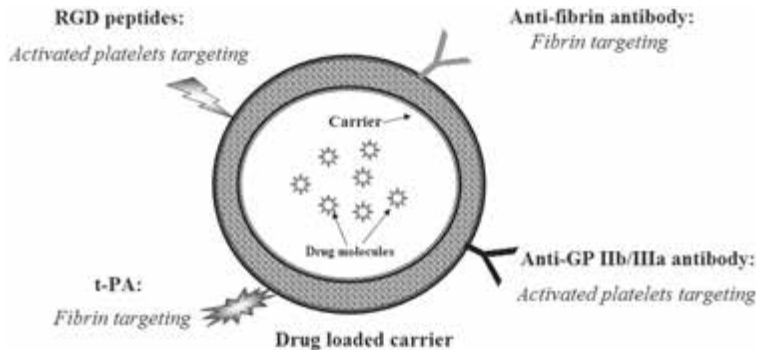

Figure 40.5 Schematic thrombus targeted drug delivery system.

For optimal drug delivery, the drug should be localized at the site of thrombus. It should avoid its non-specific uptake by or

delivery to normal non-target tissues. Therefore, a well designed drug delivery system, surface modified with a targeting moiety for targeted delivery of thrombolytic agents may provide an effective alternate (Fig. 40.5). Based on these principles, specific ligand-receptor based approaches have been studied by various research groups [42].

In a recent review [5], we have discussed the role of integrin receptors in the targeted delivery of thrombolytic agents. To target GP IIb/IIIa integrin receptors on the activated platelets, Arg-Gly-Asp (RGD) peptides have been explored by various groups as homing devices [43]. Lestini et al. [44] developed RGD-modified liposomes for the targeting of activated platelets. It was found that RGD-liposomes interact more efficiently with the activated platelets as compared to resting platelets. Thus, it was concluded that RGD-liposomes might be useful for the delivery of thrombolytic agents to the platelets embedded in the thrombus. Wang et al. [45] developed RGD peptide conjugated liposomes for the targeted delivery of urokinase to the site of thrombus and observed an increased thrombolytic efficacy. In this study, RGDS conjugated DSPE-PEG_{3500}-COOH was incorporated in to the liposomal bilayer. The hydrophilic PEG imparts long circulation whereas RGD provides selectivity to the carrier system toward activated platelets. It was observed that developed systems could significantly improve the thrombolytic efficacy as compared to plain urokinase liposomes. Suggested mechanism for the improved thrombolysis is the selective release of urokinase at the site of thrombus thereby converting plasminogen in to plasmin and simultaneously reducing the bleeding complications. Later, conformationally constrained cyclic RGD peptide conjugated liposomes were synthesized for improved selectivity towards GP IIb/IIIa integrin receptors expressed on the activated platelets [35]. In a recent study, we have developed cyclic RGD [CNPRGDY(OEt)RC] peptide conjugated long-circulatory liposomes for the delivery of SK to the site of occlusion [46]. *In vivo* biodistribution study confirmed higher accumulation of modified liposomes to the thrombus area as compared to non-liposomal formulations. RGD-liposomes accumulated 2- and 5-fold higher as compared to non-targeted liposomes and non-liposomal formulation, respectively. In addition, *in vivo* thrombolysis study revealed higher clot dissolving capacity of RGD-liposomes as compared to plain SK solution. Results showed

that 60 min after treatment RGD-liposomes dissolved 34% of initial clot weight whereas non-liposomal SK formulation dissolves only 22% of the clot.

Moreover, for the treatment of AMI, a rapid clot lysis is required so that tissue damage can be reduced. For increased and instant clot lysis, drug concentration should be high in the microenvironment of thrombus. Nevertheless, to achieve such concentration, a higher amount of drug is required to be administered, which may cause other circulatory side effects. Based on the hypothesis, target sensitive (TS) liposomes have been developed for the delivery of SK [47]. TS liposomes were prepared using dioleoylphosphatidyl ethanolamine (DOPE) and acylated cyclic RGD peptide. It was found that these liposomes not only specifically target the blood clot but also release drug instantly after interaction with activated platelets embedded in the clot. An *in vitro* clot dissolving study revealed that RGD conjugated TS liposomes could reduce the clot lysis time and also could increase the total clot dissolution (Fig. 40.6).

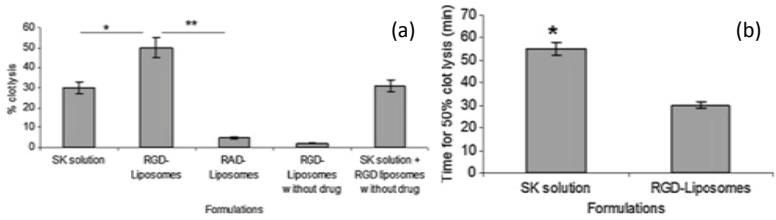

Figure 40.6 (a) Graphs showing percentage clot lysis with various SK formulations. % clot lysis for RGD liposomes are significantly higher (*$p < 0.01$, $n = 3$) than that of SK solution. Percentage clot lysis for RAD liposomes are significantly lower than that of SK solution ($p < 0.001$, $n = 3$) and RGD liposomes (**$p < 0.001$, $n = 3$). (b) Graphs showing clot lysis time ($t50$), time to dissolve 50% of clot wt., with various SK formulations. Clot lysis time for RGD liposomes are significantly shorter (*$p < 0.01$, $n = 3$) than that of SK solution. From ref. [47] with permission.

Although liposomal incorporation has proven to be an effective method for the delivery of thrombolytic drugs, however such delivery systems suffer a stability problem. To improve the stability, PEGylated (PEG coated) vesicles or polymeric carrier(s) have now being developed and studied for the delivery of various therapeutic

proteins. Encapsulation in polymeric carriers avoids protein deactivation during systemic circulation and increases circulation in to an acceptable half-life. Leach et al. [48] developed both types of formulations [liposomal (LESK) and polymeric microcapsules (MESK)] and evaluated for various thrombolytic parameters. It was found that both the formulations could reduce reperfusion times, residual clot mass and improved return of flow compared to conventional dosages of free streptokinase in a thrombosed rabbit carotid. The MESK showed comparatively better results.

In another experiment, the mechanism for increased thrombolysis by MESK was suggested; MESK resists adsorption to the leading edge of the thrombus, a common limitation for the permeation of free plasminogen activators. Thus, higher thrombolytic activity is due to improved penetration of the MESK to the interior of the clot [49].

Polymeric carriers for the delivery of thrombolytic agents should possess the following properties: (i) They should be small enough to circulate without the risk of vascular occlusion; (ii) they should possess anti-opsonizing properties; (iii) they should be tailored to accumulate at the site of thrombus; and (iv) they must release thrombolytic agents in sufficient concentration to induce and affect clot lysis. To confer these properties, Chiellini et al. [50] synthesized a polymeric material for the preparation of nanoparticles for targeting as well as long circulatory property. Developed carriers could releases the fibrinolytic agents in a controlled manner to fibrin clots [51]. The polymer was synthesized by covalent binding of poly(ethylene glycol) moieties and monoclonal antibody anti-fibrin Fab fragment to the polymer chain, Poly[(maleic anhydride)-alt-(butylvinyl ether)]s.

Moreover, size of the particles remains a major concern in their systemic administration and thereby drug delivery. Thus, polymeric nanoparticles were developed for the effective delivery of thrombolytic agents to the site of occlusion and subsequently to the interior of the clot. In the case of microparticles, it was hypothesized that the permeation/penetration of particles into the clot was due to pressure created at the clot. However, in the absence of hydrodynamic pressure, the pores of fibrin clots remain resistant to the permeation of carriers with a size of 1 μm or larger. Therefore, systems should be developed that permeate through the fibrin network into the interior of the clot for intra-clot lysis

even in the absence of pressure drop. Surface of the particles should also be modified to increase the interaction of particles with the components of the clot and thus favoring the permeation in to the interior of the clot as well.

Chung et al. [52] developed t-PA loaded PLGA nanoparticles coated with chitosan (CS) and CS-GRGD for electrostatic interaction between the positive charge of chitosan and the negative charge of fibrin as well as for ligand-receptor interaction between RGD peptide and GP IIb/IIIa receptors expressed on the activated platelets. A thrombolysis study in a blood clot-occluded tube model revealed that PLGA/CS nanoparticles showed the shortest clot lysis time whereas PLGA/CS-GRGD nanoparticles showed the highest weight percentage of digested clots. The permeation results of the NPs in the blood clots demonstrated that PLGA/CS-GRGD NPs were more adhered to the clot front and aggregated in the interior of the clots compared to other nanoparticles evaluated.

40.4 Nanocarriers for the Treatment of Restenosis

Restenosis may be defined as the process of re-obstruction of an artery following interventional procedures such as angioplasty, atherectomy, or stenting. Restenosis is a complex process that is thought to be possibly triggered by blood vessel wall injury that occurs during an intervention to relieve an arterial obstruction (Fig. 40.7) [53]. Mechanisms contributing to restenosis include elastic recoil, smooth muscle cell migration and proliferation, enhanced extracellular matrix synthesis, vessel wall remodeling, and thrombus formation [54]. A variety of different classes of drugs have been tested for the prevention and treatment of restenosis (Table 40.2).

Restenosis may be prevented by delivering drugs in high concentrations for a prolonged period of time. Local drug delivery is the most favorable treatment option for restenosis because it increases localized drug concentration to and above therapeutic levels in the immediate vicinity of vascular injury with minimal or the absence of systemic side effects [55]. However, studies revealed that direct infusion of drug solutions into the arterial wall using infusion catheters fail to offer and maintain adequate therapeutic levels into the arterial wall over time. Most of the drug from the

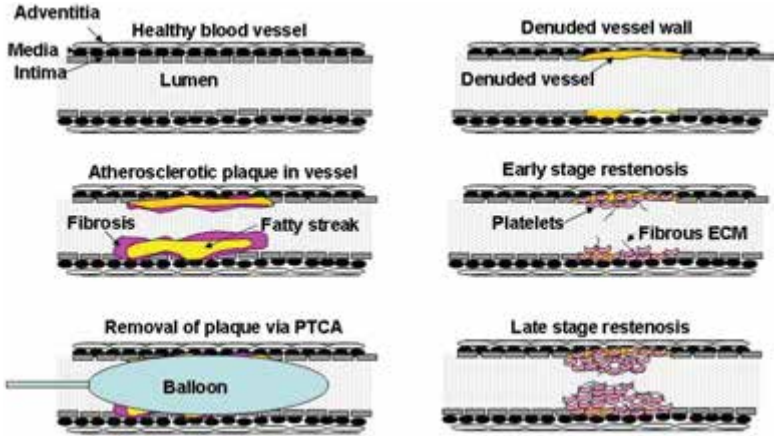

Figure 40.7 Schematic illustration of the processes leading to restenotic lesion development. The figures show a healthy blood vessel (**A**), formation of atherosclerotic plaque within the blood vessel showing a fatty streak and macrophages encapsulated within a fibrotic tissue (**B**), insertion of a balloon angioplasty catheter to remove the plaque (**C**), damage due to stripping of the endothelial cells of the vessel wall after removal of the balloon (**D**), platelet accumulation and activation as well as rapid growth of smooth muscle cells and fibrous extracellular matrix forming the scaffolding (**E**), and the late stage restenosis showing neointima protruding into the lumen causing occlusion within the vessel (**F**).

Table 40.2 Examples of drugs for prevention and treatment of restenosis

Drug action	Examples
Smooth muscle cell growth inhibition	Cytarabine, Doxorubicin, Vincristine, Cyclosporine A, Paclitaxel
Inflammatory response inhibition	Clodronate, Alendronate, Pamidronate, ISA
PDGF-receptor specific	AG-1295, AGL-2043
Antiplatelet	Cilostazol, Abciximab, Eptifibatide, Argatroban, Clopidogrel, Ticlopidin
Immunosuppressant	Methyl prednisolone, Dexamethasone, Sirolimus, Everolimus, Tacrolimus, Mycophenolic acid
Anticoagulant	Heparin, Hirudin, Iloprost

infusion site is washed out within an initial period of 20–30 min with a very small residual amount lasting for a maximum period of 48 h [56, 57]. Thus, colloidal drug carriers including liposomes and nanoparticles have been developed to provide local drug release and sustained retention of drug in the arterial wall [58]. These carriers offer a potentially improved delivery system, since they incorporate the advantages of local drug delivery and, in addition, enable drug targeting to the specific cells [59].

Particle size has been considered to be an important determinant for the effective arterial uptake. It was found that small particles (100 nm) exhibit 3-fold higher accumulation into the artery as compared to larger particles (266 nm). In a different study, it was also observed that small particles penetrate deep in the arterial wall; however, large particles accumulate at the luminal surface of arterial wall. Further, residence time of the particles also depends on the size. The smaller particles (90 nm) showed better ingress into the arterial tissue than the large particles (160 nm), as indicated by a 3.4-fold higher initial drug concentration in the tissue, whereby more than eight-fold higher amount of nanoparticles remained associated with the artery following the rapid washout phase and higher local drug levels were attained as well as maintained over 14 days following administration [60].

It is also well established that the surface charge of the particles influences the accumulation into the arterial wall. For example, it was observed that nanoparticles surface-modified with a cationic compound didodecyldimethylammonium bromide (DMAB), demonstrated 7- to 10-fold greater U-86 arterial levels in comparison to unmodified nanoparticles in different *ex vivo* and *in vivo* studies [61].

Balloon-injured coronary arteries also exhibit enhanced permeability analogous to a tumor and it was suggested that the enhanced permeability effect may also be a suitable means for the delivery of antirestenotic drugs to the injured arterial wall. Based on this hypothesis, Uwatoke et al. [62] developed nanoparticles of PEG-based block copolymer (polymeric micelles) for the encapsulation of doxorubicin (NK911). The NK911 accumulated in the vascular lesion; the tissue concentrations of doxorubicin were up to four-fold higher three hours following intravenous injection of NK911 in comparison to free doxorubicin. Low drug levels were recorded in the normal contralateral arteries. The

intravenous injected NK911 administered immediately, three and six days after the balloon injury, but not doxorubicin alone, significantly inhibited restenosis in the rat carotid artery as recorded at four weeks after injury in both single and double injury models. It was demonstrated by immunostaining that the antirestenotic efficacy of doxorubicin nanoparticles was achieved by the inhibition of SMCs proliferation, rather than due to enhancement of apoptosis or inhibition of inflammatory cell recruitment.

Systemic therapy may another approach for the effective treatment of restenosis. Numerous studies revealed the effective use of nanocarriers for the systemic therapy of restenosis [63–65]. Systemic delivery of antirestenotic drugs may be achieved by two methods; passive targeting of the arterial wall and/or active targeting of the carriers to the affected surface. The former might be achieved by controlling the properties of the carriers; however, for the latter approach, the surface of the particles should be appropriately modified using a tissue specific ligand.

A systemic approach, however failed to produce satisfactory results for the treatment of restenosis that may be ascribed to the low levels of drug in the injured artery [59]. Recently, better understanding of the involvement of innate immunity in the progression of restenosis evolved a new strategy for the systemic treatment of restenosis [66]. Monocytes/macrophages play a key role in the inflammation cascade and thus the progression of restenosis and comprise up to 60% of neointimal cells after stent-induced arterial injury in various animal models as well as in human autopsy specimens [67]. Following a stimulus, such as inflammation, the amount of circulating monocytes and their migration to the site of inflammation significantly increases [68]. Therefore, systemic inactivation of monocytes and macrophages may lead to the attenuation of neointimal formation. Various nanocarriers including liposomes and polymeric nanoparticles have been used for the targeted delivery of bisphosphonates to the macrophages. Studies demonstrated that systemically administered carriers reduced the level of systemic monocytes and tissue macrophages leading to the low accumulation in the arterial wall. Therefore, SMCs migration and proliferation were reduced as a result. Various nanocarriers used for the delivery of antirestenotic drugs, either locally or systemically, are summarized in Table 40.3.

Table 40.3 Examples of nanocarriers used for the delivery of anti-restenotic drugs

Carriers used	Drugs encapsulated/ loaded	Results of the study	Refs.
Liposomes	Bisphosphonates (clodronate, pamidronate, alendronate)	10 times more potent inhibitor of cytokine secretion from RAW 264 as compared to free drug Significant attenuation of intimal hyperplasia and luminal stenosis in balloon injured rabbit model	[69–71, 66]
	Estradiol benzoate (ESB)	*In vivo* studies in the balloon-injured rat carotid arteries revealed the potential of ESB-loaded liposomes as efficient local and controlled drug delivery systems to reduce restenosis	[72]
	Sirolimus	Local delivery of liposomal sirolimus showed a significant reduction in the neointimal formation, the neointimal area to media area ration and the percentage of stenosis as compared to controls	[73]
PLGA NPs	Alendronate	Inhibited macrophage build up, reducing restenosis in balloon injured hypercholesteremic rabbit carotid artery model	[74]
	Aminobisphosphonate (ISA)	Significant attenuation of intimal hyperplasia and stenosis in rat carotid injury model	[75]

(*Continued*)

Table 40.3 (*Continued*)

Carriers used	Drugs encapsulated/ loaded	Results of the study	Refs.
	Dexamethasone	Significant decrease in the intima/media ratio in rat carotid artery model	[76, 77]
	U-86 2-aminochromone	Significant reduction in neointimal hyperplasia development in balloon injured porcine coronary artery	[78]
PLA NPs	Tyrphostins (AG-1295, AGL-2043)	Significant antirestenotic effect was observed in pig model NP of AGL-2043 exhibited higher antirestenotic efficacy compared to AG-1295 NP	[60, 79]
	Sirolimus	Results of the study exhibited the potential of sirolimus loaded PLA NPs on promising local and sustained delivery systems administered intraluminary to reduce in-stent restenosis after stent implantation	[80]
PVA-g-PLGA	Paclitaxel	50% reduction in neointimal area in vessel segments of balloon injured rabbit iliac artery	[57]
Albumin NPs	Paclitaxel	Reduced neointimal growth in NZ white rabbit model	[81]
Polymeric micelles	Doxorubicin	Significant inhibition of SMCs proliferation in balloon injured rat carotid artery model	[62]

40.5 Concluding Remarks

Nanocarriers have been widely investigated and commercialized for the delivery of various therapeutic agents for the effective treatment of various disease states. Currently, numerous approved nanoparticle-based therapeutics are in clinical use, validating their ability to improve the therapeutic index of drugs [82–86]. Use of these carriers for the treatment of CVDs is an emerging area of biomedicine. Nanocarriers (e.g., liposomes, polymeric nanoparticles and micelles) have been extensively tested in various preclinical studies with promising results. Thus, based on results of these studies it can be concluded that nanocarrier-based therapeutic delivery could provide significant advantages over conventional approaches for the treatment of CVDs. As discussed in this chapter, various properties of nanocarriers and specific characters of a disease state are used for the designing of a system for delivery of drugs to that diseased area. Thus, in future, the designing of novel nanocarriers with respect to their size, shape and surface properties should offer useful approaches in the clinic for the effective treatment of various CVDs, including myocardial infarction, restenosis, and thromboembolism.

Abbreviations

CVDs: Cardiovascular diseases
VTE: Venous thromboembolism
DVT: Deep vein thrombosis
PE: Pulmonary embolism
US FDA: United States Food and Drug Administration
AMI: Acute myocardial infarction
ATP: Adenosine triphosphate
EPR: Enhanced permeability and retention
PEG: Polyethylene glycol
LVDP: Left ventricle developed pressure
LVEDP: Left ventricle end diastolic pressure
t-PA: Tissue plasminogen activator
SK: Streptokinase
RGD: Arg-Gly-Asp
DOPE: Dioleoylphosphatidyl ethanolamine
PLGA: Poly (lactide-co-glycolide)

Disclosures and Conflict of Interest

The authors declare that they have no conflict of interest and have no affiliations or financial involvement with any organization or entity discussed in this chapter. This includes employment, consultancies, honoraria, grants, stock ownership or options, expert testimony, patents (received or pending) or royalties. No writing assistance was utilized in the production of this chapter and the authors have received no payment for its preparation. The findings and conclusions here reflect the current views of the authors. They should not be attributed, in whole or in part, to the organizations with which they are affiliated, nor should they be considered as expressing an opinion with regard to the merits of any particular company or product discussed herein.

Corresponding Author

Prof. Suresh P. Vyas
Drug Delivery Research Laboratory
Department of Pharmaceutical Sciences
Dr. H. S. Gour University, Sagar, MP 470003, India
Email: vyas_sp@rediffmail.com

About the Authors

Bhuvaneshwar Vaidya is an associate professor in the Department of Pharmaceutics, ISF College of Pharmacy, Moga, Punjab, India. He obtained his BPharm, MPharm, and PhD from the Department of Pharmaceutical Sciences, Dr. H. S. Gour University, Sagar, India. He has previously worked as a research scientist in the Research and Development division of a pharmaceutical company. He has over 7 years of research and teaching experience. He has published more than 30 papers and has presented research papers at both national and international conferences. Dr. Vaidya has also contributed seven chapters in various books. His current area of research is controlled and targeted delivery of therapeutics for the treatment of diseases, including cardiovascular diseases, cancer, and infectious diseases.

Suresh P. Vyas is a professor of pharmaceutical biotechnology in the Department of Pharmaceutical Sciences, Dr. H. S. Gour University, Sagar, India. He has contributed substantially to research on novel drug delivery systems, drug targeting and nano-biotechnology involving colloidal drug carriers customized for targeted drug and vaccine delivery. He has over 33 years of teaching and research experience in the field of pharmaceutical sciences. His current focus is on the non-invasive, non-conventional delivery of bioactives for targeted therapy of diseases. Prof. Vyas has published over 310 papers, supervised 51 PhD students and 125 MPharm students, authored 16 books and contributed numerous book chapters. He is a Commonwealth Postdoctoral Fellowship awardee and has worked under fellowship at the School of Pharmacy University of London (UK). Prof. Vyas is a recipient of Pandit Lajja Shankar Jha award in the area of science and technology for the excellence in research from Government of Madhya Pradesh, India. In 2001, he received the Best Pharmacy Teacher of the Year award by the Association of Pharmaceutical Teachers of India. He currently serves on the editorial boards of *International Journal of Pharmaceutics* (Elsevier), *Recent Patents on Drug Delivery and Formulation* (Bentham), *Therapeutic Delivery* (Future Science), *Journal of Drug Delivery* (Hindawi), and *Journal of Nanoscience Letters* (Simplex publishers).

References

1. Godin, B., Sakamoto, J. H., Serda, R. E., Grattoni, A., Bouamrani, A., et al. (2010). Emerging applications of nanomedicine for the diagnosis and treatment of cardiovascular diseases. *Trends Pharmacol. Sci.*, **31**, 199–205.
2. Rosamond, W., Flegal, K., Friday, G., Furie, K., Go, A., et al. (2007). Heart disease and stroke statistics-2007 update: A report from the American heart association statistics committee and stroke statistics subcommittee. *Circulation*, **115**, e69–e171.
3. Mayer, C. R., Bekeredjian, R. (2008). Ultrasonic gene and drug delivery to the cardiovascular system. *Adv. Drug Deliv. Rev.*, **60**, 1177–1192.
4. Fuster, V., Badimon, L., Badimon, J. J., Chesebro, J. H. (1992). The pathogenesis of coronary artery disease and the acute coronary syndromes (2). *New England J. Med.*, **326**, 310–318.

5. Vyas, S. P., Vaidya, B. (2009). Targeted delivery of thrombolytic agents: Role of integrin receptors. *Expert Opin. Drug Deliv.*, **6**, 499–508.
6. Kingsley, P. B., Sako, E. Y., Yang, M. Q., Zimmer, S. D., Ugurbil, K., et al. (1991). Ischemic contracture begins when anaerobic glycolysis stops: A 31P-NMR study of isolated rat hearts. *Am. J. Physiol.*, **261**, H469–H478.
7. Leist, M., Single, B., Castoldi, A. F., Kuhnle, S., Nicotera, P. (1997). Intracellular adenosine triphosphate (ATP) concentration: A switch in the decision between apoptosis and necrosis. *J. Exp. Med.*, **185**, 1481–1486.
8. Gordon, J. L. (1986). Extracellular ATP: Effects, sources and fate. *Biochem. J.*, **233**, 309–319.
9. Mahaffey, K. W., Puma, J. A., Barbagelata, N. A., DiCarli, M. F., Leesar, M. A., et al. (1999). Adenosine as an adjunct to thrombolytic therapy for acute myocardial infarction. *J. Am. Coll. Cardiol.*, **34**, 1711–1720.
10. Liu, G. S., Thornton, J. D., Van Winkle, D. M., Stanley, A. W., Olsson, R. A., et al. (1991). Protection against infarction afforded by preconditioning is mediated by A_1 adenosine receptors in rabbit heart. *Circulation*, **84**, s350–s356.
11. Auchampach, J. A., Gross, G. J. (1993). Adenosine A_1 receptors, K_{ATP} channels and ischemic preconditioning in dogs. *Am. J. Physiol.*, **264**, H1327–H1336.
12. Olafsson, B., Forman, M. B., Puett, D. W., Pou, A., Cates, C. U., et al. (1987). Reduction of reperfusion injury in the canine preparation by intracoronary adenosine: Importance of the endothelium and the no-reflow phenomenon. *Circulation*, **76**, 1135–1145.
13. Babbitt, D. G., Virmani, R., Forman, M. B. (1989). Intracoronary adenosine administered after reperfusion limits vascular injury after prolonged ischemia in the canine model. *Circulation*, **80**, 1388–1399.
14. Babbitt, D. G., Virmani, R., Vildibill, H. D., Norton, E. D., Forman, M. B. (1990). Intracoronary adenosine administration during reperfusion following 3 hours of ischemia: Effects on infarct size, ventricular function and regional myocardial blood flow. *Am. Heart. J.*, **120**, 808–818.
15. Pitarys, C. J., Virmani, R., Vildibill, H. D., Jackson, E. K., Forman, M. B. (1991). Reduction of myocardial reperfusion injury by intravenous adenosine administered during the early reperfusion period. *Circulation*, **83**, 237–247.

16. Todd, J., Zhao, Z. Q., Williams, M. W., Sato, H., Van Wylen, D. G., et al. (1996). Intravascular adenosine at reperfusion reduces infarct size and neutrophil adherence. *Ann. Thorac. Surg.*, **62**, 1364–1372.
17. Verma, D. D., Levchenko, T. S., Bernstein, E. A., Torchilin, V. P. (2005). ATP-loaded liposomes effectively protect mechanical functions of the myocardium from global ischemia in an isolated rat heart model. *J. Control. Rel.*, **108**, 460–471.
18. Verma, D. D., Levchenko, T. S., Bernstein, E. A., Mongayt, D., Torchilin, V. P. (2006). ATP-loaded immunoliposomes specific for cardiac myosin provide improved protection of the mechanical functions of myocardium from global ischemia in an isolated rat heart model. *J. Drug Target.*, **14(5)**, 273–280.
19. Caride, V. J., Zaret, B. L. (1977). Liposome accumulation in regions of experimental myocardial infarction. *Science*, **198**, 735–738.
20. Palmer, T. N., Caride, V. J., Caldecourt, M. A., Twickler, J., Abdullah, V. (1984). The mechanism of liposome accumulation in infarction. *Biochim. Biophys. Acta*., **797**, 363–368.
21. Mueller, T. M., Marcus, M. L., Mayer, H. E., Williams, J. K., Hermsmeyer, K. (1981). Liposome concentration in canine ischemic myocardium and depolarized myocardial cells. *Circ. Res.*, **49**, 405–415.
22. Lukyanov, A. N., Hartner, W. C., Torchilin, V. P. (2004). Increased accumulation of PEG-PE micelles in the area of experimental myocardial infarction in rabbits. *J. Control. Rel.,* **94**, 187–193.
23. Maeda, H., Wu, J., Sawa, T., Matsumura, Y., Hori, K. (2000). Tumor vascular permeability and the EPR effect in macromolecular therapeutics: A review. *J. Control. Rel.,* **65**, 271–284.
24. Maeda, H. (2001). The enhanced permeability and retention (EPR) effect in tumor vasculature: The key role of tumor-selective macromolecular drug targeting. *Adv. Enzyme Regul.*, **41**, 189–207.
25. Klibanov, A. L., Maruyama, K., Torchilin, V. P., Huang, L. (1990). Amphipathic polyethyleneglycols effectively prolong the circulation time of liposomes. *FEBS Lett.*, **268**, 235–237.
26. Takahama, H., Minamino, T., Asanuma, H., Fujita, M., Asai, T., et al. (2009). Prolonged targeting of ischemic/reperfused myocardium by liposomal adenosine augments cardioprotection in rats. *J. Am. Coll. Cardiol.*, **53**, 709–717.
27. Verma, D. D., Hartner, W. C., Levchenko, T. S., Bernstein, E. A., Torchilin, V. P. (2005). ATP-loaded liposomes effectively protect the myocardium

in rabbits with an acute experimental myocardial infarction. *Pharm. Res.*, **22**, 2115–2120.

28. Khaw, B. A. (1994). Antimyosin antibody for the diagnosis of acute myocardial infarction: Experimental validation. In: Khaw, B. A., Narula, J., Strauss, H. W., eds. *Monoclonal Antibodies in Cardiovascular Diseases*, Lea and Febiger, Malvern, pp. 15–29.
29. Khaw, B. A., Beller, G. A., Haber, E., Smith, T. W. (1976). Localization of cardiac myosin-specific antibody in myocardial infarction. *J. Clin. Invest.*, **58**, 439–446.
30. Khaw, B. A., Fallon, J. T., Beller, G. A., Haber, E. (1979). Specificity of localization of myosin specific antibody fragments in experimental myocardial infarction: Histologic, histochemical, autoradiographic and scintigraphic studies. *Circulation*, **60**, 1527–1531.
31. Khaw, B. A., Scott, J., Fallon, J. T., Haber, E., Homcy, C. (1982). Myocardial injury: Quantitation by cell sorting initiated with antimyosin fluorescent spheres. *Science*, **217**, 1050–1053.
32. Torchilin, V. P. (1997). Targeting of liposomes within cardiovascular system. *J. Liposome Res.*, **7**, 433–454.
33. Torchilin, V. P., Narula, J., Halpern, E., Khaw, B. A. (1996). Poly(ethylene glycol)-coated anti-cardiac myosin immunoliposomes: Factors influencing targeted accumulation in the infarcted myocardium. *Biochim. Biophys. Acta*, **1279**, 75–83.
34. Liang, W., Levchenko, T., Khaw, B. A., Torchilin, V. P. (2004). ATP-Containing Immunoliposomes Specific for Cardiac Myosin. *Curr. Drug Deliv.*, **1**, 1–7.
35. Huang, G., Zhou, Z., Srinivasan, R., Penn, M. S., Kottke-Marchant, K., et al. (2008). Affinity manipulation of surface-conjugated RGD peptide to modulate binding of liposomes to activated platelets. *Biomaterials*, **29**, 1676–1685.
36. Nguyen, P. D., O'Rear, E. A., Johnson, A. E., Patterson, E., Whitsett, T. L., et al. (1990). Accelerated thrombolysis and reperfusion in a canine model of myocardial infarction by liposomal encapsulation of streptokinase. *Circ. Res.*, **66**, 875–878.
37. Holt, B., Gupta, A. S. (2012). Streptokinase loading in liposomes for vascular targeted nanomedicine applications: Encapsulation efficiency and effects of processing. *J. Biomater. Appl.*, **26**, 509–527.
38. Elbayoumi, T. A., Torchilin, V. P. (2008). Liposomes for targeted delivery of antithrombotic drugs. *Exp. Opin. Drug. Deliv.*, **5**, 1185–1198.

39. Heeremans, J. L., Prevost, R., Bekkers, M. E., Los, P., Emeis, J. J., et al. (1995). Thrombolytic treatment with tissue-type plasminogen activator (t-PA) containing liposomes in rabbits: A comparison with free t-PA. *Thromb. Haemost.*, **73**, 488–494.

40. Erdogan, S., Özer, A. Y., Volkan, B., Caner, B., Bilgili, H. (2006). Thrombus localization by using streptokinase containing vesicular systems. *Drug Deliv.*, **13**, 303–309.

41. Baek, S. H., Park, S. J., Jin, S. E., Kim, J. K., Kim, C. K., et al. (2009). Subconjunctivally injected, liposome-encapsulated streptokinase enhances the absorption rate of subconjunctival hemorrhages in rabbits. *Eur. J. Pharm. Biopharm.*, **72**, 546–551.

42. Vaidya, B., Agrawal, G. P., Vyas, S. P. (2012). Functionalized carriers for the improved delivery of plasminogen activators. *Int. J. Pharm*., **424**, 1–11.

43. Gupta, A. S., Huang, G., Lestini, B. J., Sagnella, S., Kottke-Marchant, K., et al. (2005). RGD-modified liposomes targeted to activated platelets as a potential vascular drug delivery system. *Thromb. Haemost.*, **93**, 106–114.

44. Lestini, B. J., Sagnella, S. M., Xu, Z., Shive, M. S., Richter, N. J., et al. (2002). Surface modification of liposomes for selective cell targeting in cardiovascular drug delivery. *J. Control. Rel.,* **78**, 235–247.

45. Wang, X. T., Li, S., Zhang, X. B., Hou, X. P. (2003). Preparation of thrombus-targeted urokinase liposomes and its thrombolytic effect in model rats. *Yao Xue Xue Bao*, **38**, 231–235.

46. Vaidya, B., Agrawal, G. P., and Vyas, S. P. (2011). Platelets directed liposomes for the delivery of streptokinase: Development and characterization. *Eur. J. Pharm. Sci*., **44**, 589–594.

47. Vaidya, B., Nayak, M. K., Dash, D., Agrawal, G. P., Vyas, S. P. (2011). Development and characterization of site specific target sensitive liposomes for the delivery of thrombolytic agents. *Int. J. Pharm.*, **203**, 254–261.

48. Leach, J. K., O'Rear, E. A., Patterson, E., Miao, Y., Johnson, A. E. (2003). Accelerated thrombolysis in a rabbit model of carotid artery thrombosis with liposome-encapsulated and microencapsulated streptokinase. *Thromb. Haemost.*, **90**, 64–70.

49. Leach, J. K., Patterson, E., O'Rear, E. A. (2004). Distributed intraclot thrombolysis: Mechanism of accelerated thrombolysis with encapsulated plasminogen activators. *J. Thromb. Haemost.*, **2**, 1548–1555.

50. Chiellini, F., Piras, A. M., Gazzarri, M., Bartoli, C., Ferri, M., et al. (2008). Bioactive polymeric materials for targeted administration of active agents: Synthesis and evaluation. *Macromol. Biosci.*, **8**, 516–525.
51. Piras, A. M., Chiellini, F., Fiumi, C., Bartoli, C., Chiellini, E., et al. (2008). A new biocompatible nanoparticle delivery system for the release of fibrinolytic drugs. *Int. J. Pharm.*, **357**, 260–271.
52. Chung, T. W., Wang, S. S., Tsai, W. J. (2008). Accelerating thrombolysis with chitosan-coated plasminogen activators encapsulated in poly-(lactide-co-glycolide) (PLGA) nanoparticles. *Biomaterials*, **29**, 228–237.
53. Brito, L., Amiji, M. (2007). Nanoparticulate carriers for the treatment of coronary restenosis. *Int. J. Nanomed.*, **2**, 143–161.
54. Labhasetwar, V., Song, C., Levy, R. J. (1997). Nanoparticle drug delivery system for restenosis. *Adv. Drug Deliv. Rev.*, **24**, 63–85.
55. Ettenson, D. S., Edelman, E. R. (2000). Local drug delivery: An emerging approach in the treatment of restenosis. *Vasc. Med.*, **5**, 97–102.
56. Mitchel, J. F., Fram, D. B., Palme, D., Foster, R., Hirst, J. A., et al. (1995). Enhanced intracoronary thrombolysis with urokinase using a novel, local drug delivery system. *In vitro*, *in vivo*, and clinical studies. *Circulation*, **91**, 785–793.
57. Song, C., Labhasetwar, V., Cui, X., Underwood, T., Levy, R. J. (1998). Arterial uptake of biodegradable nanoparticles for intravascular local drug delivery: Results with an acute dog model. *J. Control. Rel.,* **54**, 201–211.
58. Westedt, U., Kalinowski, M., Wittmar, M., Merdan, T., Unger, F., et al. (2007). Poly(vinyl alcohol)-graft-poly(lactide-co-glycolide) nanoparticles for local delivery of paclitaxel for restenosis treatment. *J. Control. Rel.,* **119**, 41–51.
59. Cohen-Sela E., Elazar V., Epstein-Barash H., and Golomb G. (2007). Nano-carriers of drugs and genes for the treatment of restenosis. In: Thassu, D., Deleers, M., Pathak, Y., eds. *Nanoparticulate Drug Delivery Systems*, Informa Healthcare USA, New York, pp. 235–269.
60. Fishbein, I., Chorny, M., Banai, S., Levitzki, A., Danenberg, H. D., et al. (2001). Formulation and delivery mode affect disposition and activity of tyrphostin-loaded nanoparticles in the rat carotid model. *Arterioscler. Thromb. Vasc. Biol.*, **21**, 1434–1439.
61. Labhasetwar, V., Song, C., Humphrey, W., Shebuski, R., Levy, R. J. (1998). Arterial uptake of biodegradable nanoparticles: Effect of surface modifications. *J. Pharm. Sci.*, **87**, 1229–1234.

62. Uwatoku, T., Shimokawa, H., Abe, K., Matsumoto, Y., Hattori, T., et al. (2003). Application of nanoparticle technology for the prevention of restenosis after balloon injury in rats. *Circ. Res.*, **92**, e62–e69.

63. Asrani, S., D'Anna, S., Alkan-Onyuksel, H., Wang, W., Goodman, D., et al. (1995). Systemic toxicology and laser safety of laser targeted angiography with heat sensitive liposomes. *J. Ocul. Pharmacol. Ther.*, **11**, 575–584.

64. Qi, X. R., Maitani, Y., Nagai, T. (1995). Rates of systemic degradation and reticuloendothelial system uptake of calcein in the dipalmitoyl-phosphatidylcholine liposomes with soybeanderived sterols in mice. *Pharm. Res.*, **12**, 49–52.

65. Michaelis, M., Zimmer, A., Handjou, N., Cinatl, J., Cinatl, J., Jr. (2005). Increased systemic efficacy of aphidicolin encapsulated in liposomes. *Oncol. Rep.*, **13**, 157–160.

66. Danenberg, H. D., Fishbein, I., Gao, J., Mönkkönen, J., Reich, R., et al. (2002). Macrophage depletion by clodronate-containing liposomes reduces neointimal formation after balloon injury in rats and rabbits. *Circulation*, **106**, 599–605.

67. Welt, F., Tso, C., Edelman, E., Kjelsberg, M. A., Paolini, J. F., et al. (2003). Leukocyte recruitment and expression of chemokines following different forms of vascular injury. *Vasc. Med*., **8**, 1–7.

68. Van Furth, R. (1988). Phagocytic cells: Development and distribution of mononuclear phagocytes in normal steady state and inflammation. *In*: Snyder, R. (ed.). *Inflammation: Basic Principles and Clinical Correlates*. Raven Press, Ltd., New York, pp. 281–295.

69. Monkkonen, J., Pennanen, N., Lapinjoki, S., Urtti, A. (1994). Clodronate (Dichloromethylene Bisphosphonate) inhibits LPS-stimulated Il-6 and TNF production by Raw-264 cells. *Life Sci.*, **54**, Pl229–Pl234.

70. Danenberg, H. D., Fishbein, I., Epstein, H., Waltenberger, J., Moerman, E., et al. (2003). Systemic depletion of macrophages by liposomal bisphosphonates reduces neointimal formation following balloon-injury in the rat carotid artery. *J. Cardiovasc. Pharmacol.*, **42**, 671–679.

71. Epstein-Barash, H., Gutman, D., Markovsky, E., Mishan-Eisenberg, G., Koroukhov, N., et al. (2010). Physicochemical parameters affecting liposomal bisphosphonates bioactivity for restenosis therapy: Internalization, cell inhibition, activation of cytokines and complement, and mechanism of cell death. *J. Control. Rel.,* **146**, 182–195.

72. Haeri,A., Sadeghian,S., Rabbani,S., Anvari,M.S., Erfan,M., Dadashzadeh, S. (2012). PEGylated estradiol benzoate liposomes as a potential local

vascular delivery system for treatment of restenosis. *J. Microencapsul.*, **29**, 83–94.

73. Haeri, A., Sadeghian, S., Rabbani, S., Anvari, M. S., Boroumand M. A., et al. (2011). Use of remote film loading methodology to entrap sirolimus into liposomes: Preparation, characterization and *in vivo* efficacy for treatment of restenosis. *Int. J. Pharm.*, **414**, 16–27.
74. Cohen-Sela, E., Rosenzweig, O., Gao, J., Epstein, H., Gati, I., et al. (2006). Alendronate-loaded nanoparticles deplete monocytes and attenuate restenosis. *J. Control. Rel.,* **113**, 23–30.
75. Zambaux, M. F., Bonneaux, F., Gref, R., Maincent, P., Dellacherie, E., et al. (1998). Influence of experimental parameters on the characteristics of poly(lactic acid) nanoparticles prepared by a double emulsion method. *J. Control. Rel.,* **50**, 31–40.
76. Guzman, L. A., Labhasetwar, V., Song, C., Jang, Y., Lincoff, A. M., et al. (1995). Single intraluminal infusion of biodegradable polymeric nanoparticles matrixed with dexamethasone decreases neointimal formation after vascular injury. *Circulation*, **92**, 1394–1394.
77. Guzman, L. A., Labhasetwar, V., Song, C. X., Jang, Y., Lincoff, A. M., et al. (1996). Local intraluminal infusion of biodegradable polymeric nanoparticles-A novel approach for prolonged drug delivery after balloon angioplasty. *Circulation*, **94**, 1441–1448.
78. Humphrey, W. R., Erickson, L. A., Simmons, C. A., Jennifer, L. N., Donn, G. W., et al. (1997). The effect of intramural delivery of polymeric nanoparticles loaded with the antiproliferative 2-aminochromone U-86983 on neointimal hyperplasia development in balloon-injured porcine coronary arteries. *Adv. Drug Deliv. Rev.***, 24**, 87–108.
79. Banai, S., Chorny, M., Gertz, S. D., Fishbein, I., Gao, J., et al. (2005). Locally delivered nanoencapsulated tyrphostin (AGL-2043) reduces neointima formation in balloon-injured rat carotid and stented porcine coronary arteries. *Biomaterials*, **26**, 451–461.
80. Luderer, F., Löbler, M., Rohm, H. W., Ocke, C., unna, K., et al. (2011). Biodegradable sirolimus-loaded poly(lactide) nanoparticles as drug delivery system for the prevention of in-stent restenosis in coronary stent application. *J. Biomater. Appl.*, **25**, 851–875.
81. Kolodgie, F. D., John, M., Khurana, C., Farb, A., Wilson, P. S., et al. (2002). Sustained reduction of in-stent neointimal growth with the use of a novel systemic nanoparticles paclitaxel. *Circulation*, **106**, 1195–1198.
82. Mansour, H. M., Park, C.-W., Bawa, R. (2015). Design and development of approved nanopharmaceutical products. In: Bawa, R., Audette, G.,

Rubinstein, I., eds. *Handbook of Clinical Nanomedicine: Nanoparticles, Imaging, Therapy, and Clinical Applications,* Chapter 9, Pan Stanford Publishing, Singapore (2015).

83. Bawa, R. (2008). Nanoparticle-based therapeutics in humans: A survey. *Nanotechnol. Law Bus.*, **5**(2), 135–155.
84. Bawa, R. (2013). FDA and nanotech: Baby steps lead to regulatory uncertainty. In: Bagchi, D., et al., eds. *Bionanotechnology: A Revolution in Biomedical Sciences and Human Health*. Wiley Blackwell, UK, pp. 720–732.
85. Etheridge, M. L., Campbell, S. A., Erdman, A. G., Haynes, C. L., Wolf, S. M., McCullough, J. (2013). The big picture on nanomedicine: The state of investigational and approved nanomedicine products. *Nanomed. Nanotechnol. Biol. Med.*, **9**(1), 1–14.
86. Cheng, Z., Zaki, A., Hui, J. Z., Muzykantov, V. R., Tsourkas, A. (2012). Targeting and imaging capabilities of multifunctional nanoparticles: Cost versus benefit of adding targeting and imaging capabilities. *Science*, **338**, 903–910.

Chapter 41

Carbon Nanotubes as Substrates for Neuronal Growth

Cécilia Ménard-Moyon, PhD

CNRS, Institut de Biologie Moléculaire et Cellulaire,
Laboratoire d'Immunopathologie et Chimie Thérapeutique (UPR 3572), France

Keywords: adhesion, carbon nanotubes, differentiation, electrical stimulation, electrodes, functionalization, growth, neurites, neurons, substrate

41.1 Introduction

Neurons are essential for the processing and transmission of cellular signals. A neuron consists of a central part known as the soma (or cell body) and long processes called neurites, constituted of axons and dendrites, extending over long distances (Fig. 41.1). The soma contains the nucleus of the cell. The growth of neurites and the formation of synapses are controlled by a highly motile structural specialisation at the tips of the neurites called the growth cones. Each neuron has multiple dendrites that carry signals into the soma and a single axon that carries signals away from the soma towards the next neuronal cell. The movement of

Handbook of Clinical Nanomedicine: Nanoparticles, Imaging, Therapy, and Clinical Applications
Edited by Raj Bawa, Gerald F. Audette, and Israel Rubinstein

ISBN 978-981-4669-20-7 (Hardcover), 978-981-4669-21-4 (eBook)
www.panstanford.com

ions across the ion channels found on the soma and the axon is driven by electrochemical gradients. It generates electrical signals called action potentials, which normally travel along the axon in one direction, away from the soma and towards the next neuron [1].

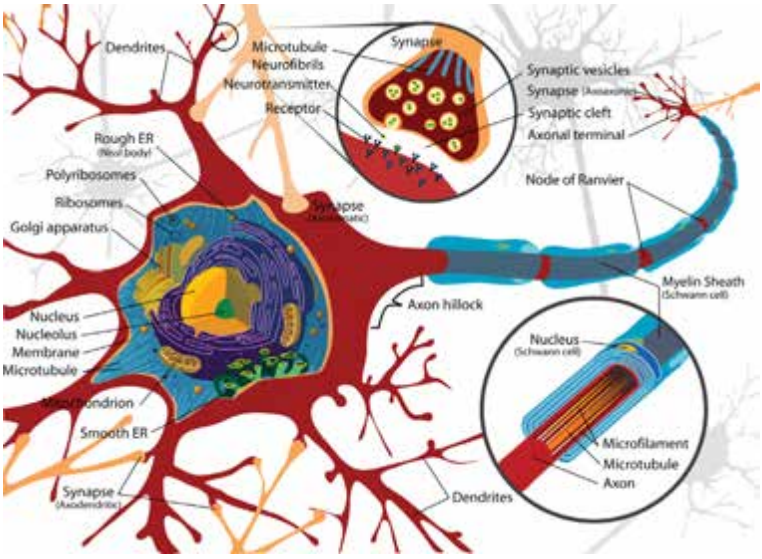

Figure 41.1 Structure of a typical myelinated vertebrate motoneuron.

Because of the lack of effective self-repair mechanisms in adults, central nervous system damage results in functional deficits that are often irreversible. The difficult challenge is to find means to cure the disabilities arising from injuries and disorders of nervous systems by stimulating inactive neurons and regulating their growth in a proper way. In order for neural prostheses to augment or restore damaged or lost functions of the nervous system, they need to be able to perform two main functions: stimulate the nervous system and record its activity. For this purpose, nanotechnology offers new perspectives by providing possibilities of repair [2]. Many crucial steps are necessary for a neuron to rebuild a functional network: (i) survival to the injury, (ii) regrowth of neurites (axons and dendrites) and (iii) reconstruction of active synapses that connect neurons [3a]. Therefore, any therapeutic strategy should promote each of these

steps. Nanotechnology and nanomaterials offer exciting promises in neuroscience [3b, 3c]. In particular, the unique combination of physical, chemical, mechanical and electronic properties of carbon nanotubes (CNTs) makes them very attractive in basic and applied neuroscience research because of their small size, electrical conductivity, high flexibility, mechanical strength, inertness, non-biodegradability and biocompatibility brought about by surface functionalisation [4]. Nevertheless, methods for manipulating the neuronal growth environment at the nanometer scale are still lacking.

CNTs have been found to be promising substrates for neuroscience applications. Single-walled carbon nanotube (SWNT) bundles and multi-walled carbon nanotubes (MWNTs) possess diameters that can mimic neuronal processes. In particular, the aspect ratio is similar to that of small nerve fibres, growth cone filopodia and synaptic contacts. Moreover, the high electrical conductivity of CNTs should enable the detection of neuronal electrical activity and allow delivering electrical stimulation to neuronal cells in contact with them.

In this chapter, we will present the use of CNTs as substrates for neuronal growth, favouring adhesion of neurons and their survival, growth and differentiation in neurites. We will also detail the use of CNTs to electrically stimulate neuronal cells as well as the influence of CNTs in promoting spontaneous synaptic activity in neuronal networks and in increasing the efficacy of neural transmission. We will then close this chapter by reporting the studies that investigated the mechanisms of the electrical interactions between CNTs and neurons.

41.2 Effects of Carbon Nanotubes on Neuronal Cells' Adhesion, Growth, Morphology and Differentiation

As it will be described in this part, numerous studies have revealed that CNTs can support and control the growth of neuronal cells as well as their morphology. SWNTs and MWNTs have been found to be permissive substrates for neuronal growth characterised by the presence of growth cones, neurite outgrowth and branching.

The first use of CNTs as substrates for nerve cell growth was reported by Mattson and coworkers [5]. In this study, embryonic rat hippocampal neurons were grown on MWNTs dispersed on glass coverslips coated with polyethyleneimine (PEI), which is a common substrate for neuronal growth [6]. Neurons require highly permissive substrates for cell attachment and neurite growth, which include positive-charge modification of glass and plastic culture substrates (e.g., polylysine or polyornithine [PLO]) [7] for optimum growth and neurite extension.

Two types of MWNTs were utilised to investigate neuronal growth: pristine MWNTs and MWNTs coated with 4-hydroxynonenal (4-HNE), a molecule that effects neurite growth. 4-HNE is known for its ability to regulate neurite outgrowth in cultured embryonic hippocampal neurons [8] via modulation of intracellular Ca^{2+} levels in cultured hippocampal neurons [9]. Physisorption of 4-HNE on the MWNT surface was achieved by sonicating MWNTs in an acidic solution of 4-HNE. Mattson et al. observed that neurons grown on MWNTs survived and continued to grow for at least eight days in culture, indicating that MWNTs support long-term neuronal survival and provide a permissive substrate for neurite outgrowth. It was observed that the direction of growth was not influenced by MWNTs. Scanning electron microscopy (SEM) was used to identify the morphological changes of the neurons grown on the MWNT substrate. Neurons were seen to be attached to the pristine MWNTs while extending one or two neurites. Interestingly, when neurites grew across the MWNTs and then on the glass coverslips coated with PEI, the neurites formed branches on the coverslips but not on the MWNTs. Therefore, the pristine MWNTs did not promote neurite branching, indicating a relatively weak adhesion of growth cones to the surface of non-functionalised nanotubes. This observation suggested that pristine MWNTs were not a suitable support for branch formation. Nevertheless, MWNTs coated with 4-HNE had more and longer neurites (Fig. 41.2). Both neurite outgrowth and branching were enhanced in this case.

The authors pointed out that the enhanced adhesion of growth cones to the MWNTs could be favoured by the presence of 4-HNE that could possibly induce changes in intracellular Ca^{2+} levels. Indeed, Ca^{2+} influx can regulate growth cone motility and neurite elongation [10].

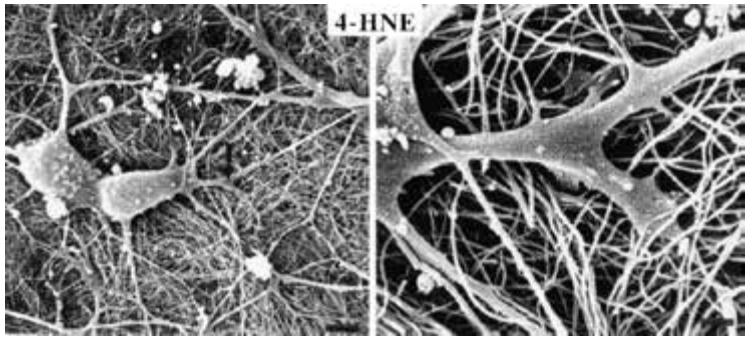

Figure 41.2 SEM images of neurons grown for three days on CNTs coated with 4-HNE. The right image is a high magnification of the neurite designated by the black arrow in the left image. Scale bars: left image, 5 μm; right image, 100 nm. Reproduced from Mattson et al. [5] with permission.

Further studies were conducted by Haddon et al., and they used MWNTs functionalised with molecules bearing different electrostatic charges to study neuronal growth [11]. The results showed that the neurite outgrowth was controlled by the surface charge of MWNTs.

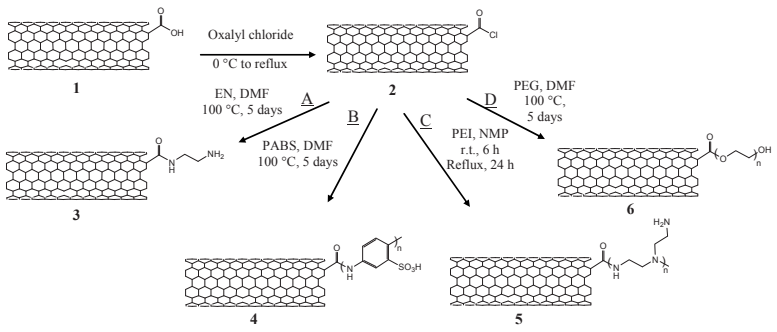

Scheme 41.1 Functionalisation of CNTs with EN, PABS, PEI and PEG.

Three types of functionalised MWNTs were designed to carry negative, neutral or positive charges at physiological pH. The approach relied on covalent functionalisation of MWNTs rather than on physisorption (used in the previous study) [5] to allow transient retention of grafted molecules on the nanotube surface. MWNTs were first oxidised using nitric acid, and the resulting

COOH functions introduced on the nanotube ends were then activated and coupled with either ethylenediamine (EN) or poly-*m*-aminobenzene sulphonic acid (PABS) [12], as illustrated in Scheme 41.1 (paths A and B).

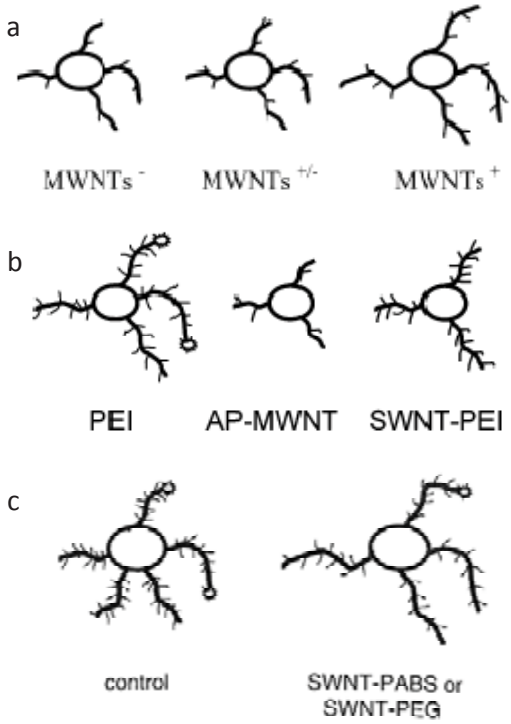

Scheme 41.2 The effects of pristine and functionalised CNTs on neurite outgrowth and number of growth cones in comparison with PEI. Reproduced with permission from Hu et al. [11] (a), Hu et al. [14] (b), and Ni et al. [15] (c) with permission.

At physiological pH used to grow neurons, the MWNTs exhibited different surface charges, from negatively charged MWNT-COOH (**1**), neutral/zwitterionic MWNT-PABS (**4**), to positively charged MWNT-EN (**3**). Finally, MWNT films were deposited on glass coverslips coated with PEI, and hippocampal neuronal cells were cultured on these substrates. In addition to SEM analysis, the morphological features of live (rather than fixed) neurons, which directly reflect their potential capability in synaptic

transmission, were characterised by fluorescence spectroscopy. The neurons were labelled with calcein, which is a fluorescent dye that stains only live cells. All neurons that grew on PEI and on MWNT substrates accumulated calcein, which is indicative of their viability. The number of neurites per neuron remained the same for the three substrates (Scheme 41.2a) [11, 15]. However, the average length of neurites was longer on the positively charged MWNT-EN (**3**), while the number of growth cones was higher on neurons cultured on zwitterionic MWNT-PABS (**4**) or on positive MWNT-EN (**3**). Furthermore, the branching of neurites increased as the substrate became more positive. Thus, by varying the surface charge of CNTs it was possible to control the number of growth cones, neurite outgrowth and branching.

The use of SWNT composite as scaffold for neuronal growth was also reported by Haddon and coworkers [13]. On the basis of the observations from the previous study showing that neurite outgrowth was enhanced by using positively charged MWNTs [11], a composite constituted of SWNTs functionalised with PEI polymer was prepared. PEI is commonly used as permissive substrate for neuronal growth, and it is positively charged at physiological pH [6]. The precoating of glass coverslips with PEI in the previous studies was necessary because the adhesion of MWNT films on non-coated glass coverslips was low when the films were exposed to aqueous culture medium [5, 11]. Functionalisation of CNTs with PEI should increase their ability to support neurite outgrowth, whereas the precoating of coverslips with PEI could be eliminated.

SWNTs were functionalised using a methodology that was comparable to the previous study [11]. PEI (branched PEI, $n \approx 20$) was covalently grafted on SWNT-COOH by amidation via oxalyl chloride activation of the carboxylic acid functions (Scheme 41.1, path C). Then, SWNT-PEI films were deposited on glass coverslips, and neuronal growth of hippocampal cells was monitored. The neuronal growth was visualised by SEM, and viability was determined using calcein staining. Neurons were shown to grow on the SWNT-PEI films with neurite outgrowth and branching that are intermediate to those observed for neuronal growth on PEI and as-produced MWNTs (AP-MWNTs). Indeed, the neurite branching on SWNT-PEI was enhanced by comparison with AP-

MWNTs, while it was comparable to PEI. The number of neurites and growth cones was similar to that of AP-MWNTs, and the neurite lengths were intermediate to those of neurons grown on pristine MWNTs and PEI (Scheme 41.2b). Hence, the growth parameters were found to be sensitive to the nature of the substrate, in particular the surface charge, since the effects of the SWNT-PEI composite on neuronal growth characteristics are intermediate to those observed when using pristine MWNTs and PEI. This behaviour can be explained by the reduced positive charge of PEI, which is proportional to the percentage of SWNTs in the composite. It should be noted that the results obtained in this study with SWNT-PEI were compared with those obtained with pristine MWNTs, not with unmodified SWNTs. Hence, the authors pointed out that the structural parameters of CNTs, in particular the diameter, could also contribute to the observed effects, in addition to the contribution of PEI.

In summary, neurite outgrowth and branching could be controlled by varying the ratio of SWNTs and PEI in the graft copolymer. This composite could be implemented in building scaffolds for the formation of neuronal circuits to develop neural prostheses.

Haddon et al. also investigated the possibility of using water-soluble SWNTs as substrate for neuronal growth [14]. The SWNTs soluble in water were found to induce an increase of neurite length, while a decrease of the number of neurites and growth cones was observed.

SWNTs were functionalised with either PABS [11] or polyethylene glycol (PEG, $n \approx 13$) [15] to form the corresponding graft copolymers (Scheme 41.1, paths B and D). Each polymer imparted water solubility to the SWNTs. The methodology used for the functionalisation was based on amidation of the COOH functions located at the nanotube ends. Hippocampal neuronal cells were cultured on the water-soluble SWNT substrates. The neurons accumulated the vital stain calcein, which is indicative of cell viability and of the biocompatibility of the functionalised SWNTs. The copolymers were found to modulate neurite outgrowth by increasing their length, while reducing the number of neurites and growth cones (Scheme 41.2c). Hence, the neurons treated with the water-soluble SWNTs exhibited sparser, but longer neurites.

The authors suggested that water-soluble SWNTs may modulate intracellular Ca^{2+} homeostasis as Ca^{2+} influx is known to regulate neurite elongation. Indeed, Ca^{2+} channel blockers can cause at low concentrations a simultaneous reduction of growth cone filopodia and an increased elongation of neurite [8a]. The same modifications were induced in this study by the water-soluble SWNTs. To confirm this hypothesis, the intracellular Ca^{2+} levels in cultured individual neurons were monitored. The experiments involved depolarisation of neurons via HiK^{+}-induced intracellular Ca^{2+} accumulation in neurons. PEG-functionalised SWNTs were found to provoke a reduction of the intracellular Ca^{2+} accumulation in a dose-dependent manner. Therefore, the SWNT-PEG copolymer could act as blocker of Ca^{2+} channels by inhibiting the depolarisation-dependent influx of Ca^{2+}. Evidence that CNTs can affect the function of ion channels, such as potassium channels, has already been reported [16].

The influence of the electrical conductivity of CNT films on the neuronal growth characteristics was recently studied by Haddon and coworkers [17]. The CNT films were prepared by spraying an aqueous dispersion of SWNT-PEG with an airbrush onto glass coverslips heated at 160°C. The electrical conductivity was controlled by varying the thickness of the nanotube film. Hippocampal rat neurons were then cultured on these substrates. The positive calcein labelling of cells was indicative of cell viability. By comparison with PEI-coated coverslips used as control, the total outgrowth of each neuron (i.e., summed length of all processes and their branches) was superior in neurons grown on the 10 nm thick SWNT-PEG films. However, other parameters of neuronal growth such as the total number of processes and neurites originating from the cell body were unchanged for each neuron. In addition, by increasing the nanotube film thickness to 30 and 60 nm, thus allowing for higher conductivity, these effects disappeared since the neurite outgrowth was unaffected.

In summary, Haddon et al. [17] demonstrated that SWNT-based substrates, having a narrow range of electrical conductivity, supported neurite outgrowth, with a decrease in the number of growth cones but an increase in cell body area.

Other research groups also reported the use of CNTs as substrate for neuronal growth. Shimizu et al. functionalised MWNTs

with neurotrophins (a family of proteins that induce survival, development and functions of neurons), in particular with a nerve growth factor (NGF) or brain-derived neurotrophic factor (BDNF) [18]. The aim of this study was to regulate the differentiation and survival of neurons.

Neurotrophins are key proteins for the differential function of neurons. They are endogenous soluble proteins regulating the survival [19], growth and function [20] of neurons. Neurotrophins belong to a class of growth factors, secreted proteins, which are capable of signalling particular cells to survive, differentiate or grow [21]. They may stimulate the synthesis of proteins in either axonal or dendritic compartments, thus allowing synapses to exert local control over the complement of proteins expressed at individual synaptic sites [22].

MWNTs were first oxidised using a mixture of sulphuric acid and nitric acid. Diaminoalkyl compounds were then introduced on the resulting MWNT-COOH via amidation. Neurotrophin was covalently bound to the resulting amino-modified MWNTs using a carbodiimide reagent. The influence of neurotrophin-functionalised MWNTs on the neurite outgrowth of embryonic chick dorsal root ganglion neurons was then examined. These MWNTs were found to promote the neurite outgrowth of dissociated neurons, in a similar manner to soluble NGF and BDNF, while the amino-terminated MWNTs did not promote neurite outgrowth.

Romero and coworkers reported the preparation of strong and highly electrically conducting semi-transparent sheets and yarns from pristine MWNTs [23].

The CNT sheets were fabricated by drawing the CNTs from a sidewall of an MWNT forest produced by chemical vapour deposition (CVD). The thickness of the CNT sheet was approximately 50 nm. The CNT yarn was then prepared by spinning the sheet [24]. The authors demonstrated that the CNT sheets were permissive substrates for primary central and peripheral neuronal culture. Indeed, the results indicated that the CNT substrates were able to promote cell attachment and differentiation of a variety of cell types, including cerebellar and sensory dorsal root ganglion neurons, and to support their long-term growth at a similar level to that achieved on PLO-coated glass substrates used in this study for comparison. The neuronal phenotype was demonstrated by

immunofluorescence using β-tubulin [25], which is a specific neuronal marker. In addition, the extension of neuronal axon growth cones was enhanced. Neurons from murine cerebellum and cerebral cortex, which are usually more sensitive to the substrate and the environment for survival and growth, were used too. Also in this case, the neurons were able to dissociate and extend their neurites onto the CNT sheets, as they did similarly onto PLO-coated glass substrates [26]. Thus, contrary to previous studies reporting that axonal growth is limited on pristine CNTs [5, 11], neurons were shown here to grow on pristine CNT sheets and to extend their neurites with similar characteristics (number and length) than those grown on PLO-treated glass substrates.

Furthermore, the authors demonstrated that the neuronal growth could be directed by CNT yarns. Neonatal dorsal root ganglion neuron explants were prepared by wrapping a single CNT yarn around the ganglia, where the free end suspended in culture media. The sensory neurons adhered and extended along the CNT yarn by intimately following the surface topography of the CNT substrate.

In summary, directionally oriented pristine CNTs configured as sheets or yarns were demonstrated to be viable substrates for neuronal growth.

Lu et al. recently reported that thin-film scaffolds constituted of a biocompatible polymer grafted on CNTs can promote neuron differentiation from human embryonic stem cells (hESCs) [27].

The CNT-based composite was prepared by *in situ* polymerisation of acrylic acid onto oxidised CNTs. The neuron differentiation efficiency on poly(acrylic acid)-grafted CNT (PAA-g-CNT) thin films was compared with that of thin films composed of poly(acrylic acid) (PAA) or PLO. The PAA-g-CNT thin films showed enhanced neuron differentiation while maintaining cell viability, as assessed by measuring the metabolic activity of dehydrogenases. SEM images showed that the differentiated neurons on PAA-g-CNT surfaces have more branches, suggesting that they are more mature. In addition, the CNT-based surface exhibited a higher cell adhesion and protein (laminin) adsorption. Laminin is a glycoprotein found in the extracellular matrix, the sheets of protein that form the substrate of all internal organs (i.e., basement membrane). Laminin has been reported to favour neuronal growth

[28]. Indeed, laminin is a substrate along which nerve axons can grow both in vivo and *in vitro*.

Thus, this work shows for the first time that CNT-based polymer thin films promote the differentiation of hESCs towards neuronal lineage.

The growth of somatosensory neurons on functionalised CNT mats was recently reported by Xie et al. [29] MWNTs were functionalised by oxidation using a mixture of sulphuric acid and nitric acid. The CNT mat was then deposited on a track-etch membrane. The CNT substrate was found to be a permissive substrate for the growth of somatosensory neurons from a dorsal root ganglion. Neurite outgrowth and branching were observed by SEM, as well as intertwinement between the neurites and the underlying functionalised CNTs, indicating a strong interaction between both entities at the nanoscale. No obvious neurite growth was observed on neurons plated on a blank polycarbonate membrane. The authors suggested that functional groups on the nanotube surface could act as anchoring seeds which may enhance the adhesion of neurites on the CNT-based substrate. This is consistent with previous studies, such as those reported by Haddon and coworkers, that emphasise the positive impact of the functionalisation of CNTs on permissivity for neuronal attachment and neurite outgrowth [11, 14, 15]. Neurons adhere to substrates via extracellular proteins such as laminin, whose size is about 70 nm [30]. The authors pointed out that the analogous dimension of CNTs and the roughness of the nanotube surface favour contact with neurites by promoting better adhesion.

Wick et al. recently investigated the effects of SWNTs with different degrees of agglomeration on primary cells of the nervous system (mixed neuroglial cultures derived from the chicken embryonic spinal cord [SPC] of the central nervous system or dorsal root ganglia [DRG] of the peripheral nervous system) [31]. The cells were exposed to SWNT agglomerates of submicrometre sizes (SWNT-a) and to SWNT bundles (SWNT-b) composed of 10 to 20 tubes. Suspensions of SWNTs-a and SWNTs-b affect glial cells from both tissue types. The level of toxicity was found to be dependent on the agglomeration state of the CNTs. Treatment of mixed neuroglial cultures with up to 30 μg/mL SWNTs significantly decreased the overall DNA content. This effect was more pronounced when

cells were exposed to highly agglomerated SWNTs-a compared with better-dispersed SWNTs-b. Indeed, higher concentrations of SWNTs-a were more toxic than the same amount of SWNTs-b. This result is in agreement with previous studies from Wick et al. in which the aggregation state of SWNTs might be a crucial factor in terms of toxic effects [32]. Additionally, SWNTs reduced the amount of glial cells in both derived cultures as measured by ELISA. The authors observed that neurons were only affected in DRG-derived cultures with regard to their ionic conductance (diminished inward conductivity) and resting membrane potential (more positive) according to whole-cell patch recordings. On the contrary, the neurite outgrowth and the electrophysiological properties of neurons derived from SPC cultures were not affected.

41.3 Electrical Stimulation of Neuronal Cells Grown on Carbon Nanotube-Based Substrates

Electrical stimulation of neuronal cells is widely employed in basic neuroscience research, in neural prostheses [33] and in clinical therapy (e.g., treatment of Parkinson's disease, dystonia and chronic pain) [34]. These applications require an implanted microelectrode array (MEA) with the capacity to stimulate neurons. Neuroprosthetic devices currently face various issues, including (i) long-term inflammatory response of the neuronal tissues, resulting in neuron depletion around the electrodes and their replacement with reactive astrocytes that prevent signal transduction; (ii) delamination and degradation of thin metal electrodes; (iii) miniaturisation of the electrodes and (iv) mechanical compliance with neuronal tissues for long-term performance. Currently, semiconductor devices can only partially solve some of these problems. Nevertheless, CNTs are excellent candidates for MEA applications because of their unique set of properties which offer the possibility of constructing small electrodes with high current density.

As will be detailed in this part, microelectrodes coated with CNTs have low impedance and high charge transfer characteristics and provide a rough surface that favours excellent cell–electrode

coupling, while remaining chemically inert and biocompatible. Different systems have been utilised to guide neuronal cell growth and have been tested for their function in cultured neuronal networks, such as metal electrodes coated with CNTs, patterned CNT surfaces and CNT-polymer composite thin films.

For instance, Ozkan et al. demonstrated the formation of directed neurite growth on patterned, vertically aligned MWNTs [35]. Different substrate geometries and nanotube heights were investigated for their ability to induce guided neuronal growth. Vertical MWNT arrays were functionalised with growth adherents that promote neuron adhesion and viability. In particular, the MWNTs were coated with a growth adherent, poly-L-lysine (PLL), which is known to enhance adhesion of neurons by altering surface charges on the culture substrate [36]. Hippocampal rat cells were cultured on patterns of short (500 nm high) and long (10 μm high) vertical MWNTs. Preferential directed growth of neurons was observed over the long MWNT array, but not over the short MWNT array. Indeed, in the latter case, neurons were seen to grow both on the short MWNT pattern and on the silicon chip, with no selection of one of the two types of substrate. On the contrary, in the former case, neurons showed preferential growth along the MWNT array, although the substrate was covered with PLL. The authors pointed out that the difference observed in terms of scaffolding capability between the short and long MWNT arrays could stem from the flexibility of the CNTs, which depends on the nanotube length. Indeed, to allow proliferation of neurites, the long MWNTs were found to undergo deformation, as observed by SEM. This deformation resulted from the extending neurite that interacted with the edges of the MWNT patterns. The neuronal cell networks were found to be viable after they were stained with Fluo-3 calcium. This fluorescent dye binds to the intracellular free calcium ions, which in principle are in high concentration in the cytoplasm of viable neuronal cells. The results of this study highlight the potential applications of long MWNT array substrates for the development of three-dimensional scaffolds suitable for implants.

Hanein and coworkers published a review on the development of CNT-based MEAs for neuronal interfacing and network engineering applications [37]. They also described the use of CNT patterns as substrate for neuronal growth [38]. The CNT templates

on which neurons adhered and assembled were fabricated by photolithography and microcontact printing. The deposition of iron nanoparticles on hydrophilic silicon dioxide or quartz substrates was controlled to allow the growth of regular arrays of CNT islands using CVD. During this process, long CNTs (on the order of 100 μm) can thermally fluctuate and may bind to other nanotubes to form a three-dimensional, entangled network. Neurons and glial cells were then deposited on the patterned quartz substrates. After four days' incubation, neurons were seen to adhere to and grow on the region of the substrate containing CNTs. Interconnections between neighbouring islands were also observed because of the formation of axons and dendrites. The electrical viability of the neuronal networks was then tested and the action potential, generated by electrical stimulations, displayed a normal shape. Thus, this study allowed for the formation of neuronal networks having a normal functionality with pre-defined geometry due to growth on substrates patterned with CNT islands.

An original method to pattern cultured neuronal networks was reported by Hanein et al. and was based on the anchoring of neuronal cell clusters constituted of tens of cells [39]. The anchors aimed at stabilising the neuronal cell clusters were CNTs or the strong adhesive substrate poly-D-lysine. The dynamics of the real-time network formation was monitored by placing cultures in an environmental chamber under a microscope. The cell clusters were seen to self-organise by moving away from each other and bridging gaps with concomitant formation of a neurite bundle between neighbouring clusters.

Hanein et al. also fabricated CNT-based electrodes by synthesising high-density CNT islands using CVD on a lithographically defined substrate [40]. A mixture of cortical neuron and glial cells from rats were plated and cultured on the surface of the CNT electrode chip. The CNT islands acted as adhesion agents because of the substrate's roughness, thus favouring the migration and adhesion of cells onto the electrode surface. High-fidelity extracellular recordings from cultured neuronal cells were then performed. A typical extracellular signal was obtained with a shape that reflected the first derivative of the intracellular action potential signal. The signal-to-noise ratio was high compared with that of a conventional TiN electrode.

It should be noted that one advantage of the CNT electrodes developed by Hanein et al. over standard microelectrodes is the cell-adhesive nature of the nanotubes. Neuronal proliferation can thus be induced without the need for additional adhesion, thereby promoting coating spread between the electrodes.

Electrical stimulation of primary neurons was reported by Wang and coworkers, who used vertically aligned MWNTs as microelectrodes [41]. Lithographic patterning of the catalyst allowed the control of the size and location of the MWNT pillars. The MWNT-based microelectrode was constituted of individual MWNTs having a diameter in the 30–50 nm range and separated by a distance of the order of tens of nanometres. The CNT electrode was 40 μm tall and was made more hydrophilic by coating with an amphiphilic PEG–lipid conjugate. Non-covalent binding of the PEG–lipid conjugate allowed for the preservation of the electronic properties of the CNTs. The MWNT MEA was coated with poly-D-lysine to favour cell adhesion to the nanotube substrates. Embryonic rat hippocampal neurons were deposited on the MWNT microelectrode and were shown to grow and differentiate. The viability and neurite outgrowth were comparable to those of cultures on plastic Petri dish controls. The neurons were then electrically stimulated by the MWNT electrode. The calcium indicator Fluo-4 allowed for the detection of action potentials by observation of intracellular Ca^{2+} level change. Fluo-4 can be loaded into cells and exhibits a large increase in fluorescence intensity on binding free Ca^{2+}. It was also demonstrated that the neurons could be stimulated repeatedly with the MWNT electrode, thus highlighting the long-term endurance of the MWNT electrode.

Recently, Hanein and coworkers investigated the neurite-CNT interactions at the nanoscale and elucidated the nature of the interface between neurons and CNTs [42]. Process entanglement was explained as a neuronal anchorage mechanism to CNT-based surfaces.

In this study, isolated islands of pristine CNTs were fabricated and plated with cells (mammalian cortex neurons from rats and insect ganglion cells from locusts). The arrangement of neurons and glial cells on CNT-based surfaces was characterised by high-resolution scanning electron microscopy (HRSEM), immunostaining and confocal microscopy. The neurons and cells were found to

preferentially adhere to CNT islands and extend towards their periphery. This is in agreement with previous reports that have demonstrated preferential adhesion to rough surfaces [39–41]. The processes at the periphery of the CNT islands were curled and entangled, thus leading to enhanced interactions with the CNT surface that facilitated their anchorage. However, the processes that appeared too thick to interact with CNTs had the tendency to intertwine. Therefore, Hanein et al. pointed out that the roughness of the surface must match the diameter of the neuronal processes to help them anchor. The authors also suggested that adhesion of neuronal cells was in part achieved through an entanglement process. This mechanical effect may thus contribute to the mechanism by which neurons adhere to rough surfaces.

Recently, Hanein et al. also investigated the use of CNT MEAs as an interface material for retinal recording and stimulation applications [43].

Electrodes were coated via CVD of CNTs, and electrical stimulation of retinal cells was achieved. The signals obtained with the CNT-based electrodes showed a remarkably high signal-to-noise ratio during recordings in comparison with commercial TiN electrodes. This would be particularly interesting for long-term *in vivo* implantation of electrodes. In addition, the authors observed an increase of the signal amplitude over several hours of recording. These results were indicative of an improved electrode–tissue coupling of CNT-based electrodes compared with conventional commercial electrodes. This is consistent with previous studies reported by Wang and coworkers, who validated the effectiveness of CNT electrodes for stimulation applications [42].

In summary, this work showed that CNT MEAs provide exceptional electrochemical and adhesive properties. This demonstrates the great potential of CNT-based electrodes for retinal implant applications.

The first example of CNT-coated electrodes implanted into different brain areas in rats or monkeys was reported by Keefer et al. [44]. These electrodes showed the ability to enhance the detection of neuronal signals and to stimulate neurons. Indeed, the results indicated that the CNT-coated electrodes improved the electrochemical and functional properties of cultured neurons. CNT coating enhanced both recording and electrical stimulation of

neurons in culture, rats and monkeys by decreasing the electrode impedance and increasing charge transfer. Electrical stimulation experiments were performed with cultured neuronal networks grown on CNT-based electrodes to determine if the CNT coating could alter the capacity to activate neurons. The CNT coating was found to be permissive for neuronal growth and function. Moreover, the performances of the CNT-coated electrodes were much higher than those of gold-coated control electrodes in evoking neuronal responses. This result highlights the potential of CNTs for the development of electrical brain interfaces.

The unique physical, mechanical, chemical and electronic properties of CNTs can be, in part, transferred into CNT composites to combine high electrical conductivity, chemical stability and physical strength with structural flexibility. CNT composite constituted of thin films were prepared by layer-by-layer (LBL) assembly by Kotov and coworkers, as will be detailed later. They demonstrated that CNT composite films were suitable substrates to support growth, proliferation and differentiation, as well as to electrically stimulate neuronal cells.

Applications of CNT substrates in medical implementations, such as implanted scaffolding, would require free-standing structure instead of CNTs attached to supporting glass or plastic. For this purpose, Kotov et al. reported the fabrication of free-standing SWNT-polymer thin-film membranes that are biologically compatible with neuronal cell cultures [45]. The membranes constituted of SWNT-polymer composite were prepared by the LBL assembly process. This technique allows for the construction of multilayered composite coatings and free-standing films of SWNTs with versatile architectures, which can be engineered at the nanoscale to attain desirable mechanical, structural, biological and electrical properties. It is based on alternating layers of CNTs and polymers. Coatings made by LBL are generally very mechanically robust [46]. SWNTs were dispersed in an aqueous solution of the amphiphilic poly(*N*-cetyl-4-vinylpyridinium bromide-*co*-*N*-ethyl-4-vinylpyridinium bromide-*co*-4-vinylpyridine). This polymer bears positively charged groups that favour cell adhesion. The biocompatibility of the SWNT composite thin films towards NG108-15 neuroblastoma × glioma hybrid culture cells was assessed using confocal microscopy and calcein. NG108-15 cells are used as neuronal model system since they

exhibit, after differentiation, many characteristics of mammalian nerve cells. After long-term incubation (up to 10 days) the cells grew and proliferated on the surface of the SWNT films. The neuronal cells were viable, as illustrated by their continuous intracellular esterase activity, which is determined by the enzymatic conversion of the non-fluorescent cell-permeant calcein dye. The neuronal outgrowth of the NG108-15 cells on the surface of the SWNT films was compared with that of the cells on a control culture dish. Neurons were observed by SEM, and their morphology was assessed by cell labelling with the neuronal lipophilic tracer dialkylcarbocyanine. This dye has the capacity to diffuse through the membrane of cells and to trace along their neurites in order to monitor the surface morphology and growth of neurons. On the substrate comprising SWNTs, many elongated neuronal processes were observed with extension of neurites. Many secondary neurites and elaborated branches were grown from these neurites. Interestingly, many processes were seen to start from the neurites and to terminate at the surface of the SWNT film.

Free-standing SWNT membranes were then prepared in order to be used as scaffold for neuronal growth and differentiation. The preparation involved the etching of an SWNT film from the surface of a glass substrate using HF and the subsequent rolling into a small elongated thread-like sample. The free-standing films showed a tensile strength that was sufficient for soft neural implants. It is noteworthy that the ionic conductivity of these free-standing films is brought about by its polyelectrolyte nature. This is essential for the interaction with ionic fluxes through neuron membrane. Adhesion and differentiation of NG108-15 cells were seen to be similar to those of SWNT films on solid supports. The neurite extension closely followed the morphological shape and curvature of the surface of the free-standing films.

In summary, SWNT composite thin films prepared by LBL and resulting free-standing films can support growth, viability and differentiation of NG108-15 neuroblastoma/glioma hybrid cells. The free-standing SWNT/polymer composite thin film membranes were found to guide the outgrowth of neurites. The combination of different properties, including flexibility, inertness, non-biodegradability and durability, allows us to envisage some applications. For instance, the free-standing films could potentially

be integrated into extracellular implants for cell stimulation and pain control and into neuroprosthetic devices for neuronal injuries.

Kotov and coworkers also reported the stimulation of the neurophysiological activity of NG108-15 cells grown on LBL-assembled SWNT-polymer composite films [47]. The LBL SWNT conductive films were prepared from positively charged SWNTs coated with a copolymer, poly(acrylic acid), and were made of 30 multilayers. The NG108-15 cells differentiated and extended long neurites on the surface of the SWNT films. The neurites developed into many secondary processes, branching in many directions on the surface. The SWNT films exhibited a sufficiently high electrical conductivity to electrically stimulate significant ion conductance in excitable neuronal cells that were electrically coupled to the SWNTs. The direction of the electrophysiological response suggested that cells were stimulated by the influx of cations in the cells.

Kotov et al. described that mouse cortical neural stem cells (NSCs) can differentiate to neurons, astrocytes and oligodendrocytes with formation of neurites on SWNT-based composite thin films [48]. Note that NSCs are well known for their sensitivity to the environment.

The SWNT-polymer composite thin films were prepared by LBL assembly of six bilayers of SWNT-PEI [$(PEI/SWNT)_6$]. SWNTs were first dispersed in a 1 wt% poly(sodium 4-styrene-sulphonate) solution and then assembled using LBL technique with PEI as polyelectrolyte. Mouse embryonic 14-day neurospheres (i.e., spherical clonal structures of NSCs) from the cortex were seen to attach to the SWNT-polyelectrolyte film substrates and to differentiate, in a similar manner to poly-L-ornithine (PLO)-coated substrates used as control. PLO is a standard substrate widely used for NSC cultures as it is known to alter the surface charge, thus providing a more suitable substrate for the negatively charged neurons [27]. The viability of neurospheres determined using the MTT assay was found to be similar on $(PEI/SWNT)_6$- and PLO-coated substrates. In addition, both types of substrates supported differentiation of neurospheres into the three primary neural cell types: neurons, astrocytes and oligodendrocytes, according to immunostaining experiments. Indeed, to analyse the differentiated phenotypes, neurospheres were immunostained with antinestin-,

antimicrotubule-associated protein 2 (anti-MAP2), antiglial fibrillary acidic protein (anti-GFAP) and anti-oligodendrocyte marker O4 (anti-O4). Thus, NSCs grown on LBL-assembled SWNT-polyelectrolyte composite films behaved similarly to NSCs cultured on PLO substrates in terms of biocompatility, neurite outgrowth and expression of neuronal markers.

In summary, this study is the first demonstration of the differentiation of environment-sensitive NSCs on a CNT-composite thin film. The results are promising for further development of CNTs for neural interfaces as the CNT-based substrate is able to promote cell viability and to induce the development of neuronal processes, as well as the appearance and progression of neural markers.

Further studies were conducted by Kotov and coworkers on the electrical stimulation of NSCs by the SWNT composite constituted of laminin [49].

LBL films (up to 30 bilayers) were prepared from SWNTs wrapped with poly(styrene-4-sulphonate) and laminin, a glycoprotein which is an important protein in the basement membrane. Laminin is commonly used to coat substrates to promote cell adhesion and neurite outgrowth [50]. The SWNT-laminin films were heat-treated to increase their electrical conductivity by enhancing the cross-linking of CNTs among the different layers of the films prepared by LBL. Cell adhesion was clearly seen to depend strongly on the composition of the final layer of the LBL films. Indeed, the film containing SWNTs as top layer was the most suitable for cell adhesion and attachment. Differentiation of NSCs was observed, as indicated by extensive formation of functional neuronal network showing the presence of synaptic connections. By comparison with laminin-coated substrates, longer neuronal outgrowth occurred on the SWNT-laminin substrates that were found to be biocompatible, as indicated by satisfactory cell viability assays. The functionality of the neuronal networks was assessed by immunostaining for the presence of synapsin protein with the above-mentioned neuronal markers. Synapsin was present between the differentiated cells. This indicated that neuronal network was functional. The electrical stimulation of NSCs by the SWNT-laminin films was then investigated. Cell response to chemical and electrical stimuli typically results in a change in the membrane voltage of the cells, referred to as action potential.

Detection of action potentials can be achieved via the invasive patch-clamp method [51]. The generation of action potentials upon the application of a lateral current through the SWNT film was deduced from the imaging of the NSCs with a Ca^{2+}-dependent dye and was found to be dependent on the status of the surrounding cells. Once one neuronal cell was excited, the excitation sequentially spread from one cell to another.

In summary, the combination of different properties of the SWNT/laminin thin film makes them a promising candidate for incorporation in neural electrodes. On the one hand, the films were suitable for NSCs' growth and proliferation. On the other, as SWNTs exhibit high electrical conductivity, they were able to electrically stimulate NSCs.

Chen et al. have been the first to explore the interface between neurons and CNT probes, both extracellularly and intracellularly (i.e., inside the neural membrane) [52]. CNT probes were used to monitor the neuronal activity elicited not only extracellularly but also intracellularly. This work is particularly interesting as it opens the way for intracellular neural probes that minimise damage to the neuron.

In this study, two types of CNT probes were fabricated. MWNT bundles were connected to a silver wire. In one case, CNTs were coated with insulating epoxy, while in the other, CNTs were inserted into a sharp glass pipette, whose tip was used to penetrate the neural membrane. Only the tips of the probes were made of CNTs, contrary to the CNT-coated microelectrodes that were also involved in interfacing neurons [41, 42, 53]. The CNT probes were examined with the escape neural circuit of crayfish (*Procambarus clarkia*) and were found to have comparable performances to conventional Ag/AgCl electrodes. The CNT probes, with the tip pressed against an axon, were able to detect an action potential extracellularly and some small spikes (i.e., potential waveforms) associated with other neurons in the nerve cord. The results obtained from these extracellular experiments were in agreement with those demonstrated with microelectrodes coated with CNTs [41, 42, 54].

The intracellular recording and stimulation with CNT probes has been investigated for the first time. The conduction mechanism was investigated on the basis of impedance

measurements and cyclic voltammetry. CNT probes were shown to transmit electrical signals through not only capacitive coupling but also resistive conduction to a comparable extent, contrary to the suggestion that capacitive impedance is the main mechanism to record and stimulate neural activity [41, 42, 54]. The resistive conduction helps record postsynaptic potentials and equilibrium membrane potentials intracellularly. It also facilitates the delivery of direct-current stimulation. The authors pointed out that the recording capability of the CNTs did not degrade and even improved after delivering direct-current stimuli for a long period of time. This highlights that the CNT probes are suitable for long-term use with a longer endurance compared with conventional Ag/AgCl electrodes, as the latter are inefficient once the silver chloride is reduced to silver. Thus, this work supports the potential use of CNT probes as a promising new neurophysiological tool.

Ballerini and coworkers reported that CNT substrates can boost neuronal electrical signalling under chronic growth conditions [54]. They demonstrated that the growth of primary hippocampal neurons on MWNTs increased the frequency of spontaneous postsynaptic currents, but did not affect the general electrophysiological characteristics of the neurons.

The substrates coated with CNTs were prepared by deposition of a homogeneous dispersion of pure MWNTs obtained by functionalisation using the 1,3-dipolar cycloaddition of azomethine ylides. Defunctionalisation of the resulting pyrrolidine-MWNTs was then induced at 350°C under nitrogen atmosphere to eliminate the organic functional groups introduced on the nanotube surface. This treatment provided purified non-functionalised MWNTs layered on the glass substrate. Previous attempts to prepare glass coverslips coated with as-produced MWNTs were not satisfactory because of poor reproducibility in terms of neurite growth and elongation. Hippocampal neurons were then seeded on glass coverslips. Attachment and growth of neurons were observed on the substrates covered with purified MWNTs, along with neurite extension. Hence, purified MWNTs layered on glass substrate were found to be permissive substrates to support neuron adhesion, survival and dendrite elongation.

Neural network activity was investigated using single-cell patch-clamp recordings. The frequency of spontaneous postsynaptic

currents (PSCs) of neurons deposited on the glass coverslips covered with MWNTs displayed a sixfold increase in comparison with the control substrate constituted of hippocampal neurons seeded directly on glass coverslips. The generation of PSCs was indicative of functional synapse formation. However, the height and half-width of action potentials of the neurons grown on both substrates were not significantly different. In addition, other electrophysiological characteristics of the neurons grown on the MWNT-coated substrates were nearly similar to those grown on the control substrate, in particular the resting membrane potential, input resistance and capacitance values. In summary, purified MWNTs obtained via a functionalisation/defunctionalisation sequence were demonstrated to be suitable growth surfaces for neurons. They boosted neuronal electrical signalling by promoting an increase in the efficacy of neuronal signal transmission. The authors pointed out that this effect was not attributable to differences in neuronal survival, morphology or passive membrane properties, but that it possibly represented a consequence of the properties of the SWNT substrates.

Pappas et al. also examined the use of functionalised SWNTs as substrate for neuronal attachment and growth [55]. They demonstrated that neurons were electrically coupled to SWNTs. Using the diazonium salt approach [56] SWNTs were functionalised to introduce 4-benzoic acid or 4-*tert*-butylphenyl functional groups on the nanotube surface. Transparent, conductive SWNT-polyethylene terephthalate (PET) films were prepared via pre-dispersion of the SWNTs in water by using 1% SDS. As already reported [46], neuroblastoma × glioma NG108 was used as model of neuronal cell. The highest cell growth and neurite extension of NG108 occurred on unmodified SWNT substrates, with decreasing growth on 4-*tert*-butylphenyl SWNT and 4-benzoic acid SWNT substrates. The neuronal cells were viable according to the vital dye calcein test. On the basis of acute attachment assays, SWNT substrates were found to display a more dramatic effect on cell attachment than on cell proliferation. It should be noted that cell adhesion is critical for cell survival. In fact, functional groups on the nanotube surface inhibited cell attachment. These results support those obtained by Haddon and coworkers on the influence of the surface charge of CNTs on neurite outgrowth where negatively charged functional groups at physiological pH or pristine MWNTs

induced a reduction of the neurite outgrowth, in comparison with positively charged substrates [11]. The neuronal cells were then electrically stimulated through the SWNT-PET substrates. NG108 and rat primary peripheral neurons showed robust voltage-activated currents. These results suggested that CNTs can be a physiologically compatible substrate to be incorporated into devices for electrical stimulation of neurons.

Gabriel et al. reported an alternative and simple method to fabricate CNT-based MEAs [57]. A suspension of purified SWNTs produced by arc discharge was deposited onto platinum electrodes [58]. This method has the advantage to be a post-process procedure that can be used with almost any MEA. The electrical properties of the CNT-based MEAs were found to be superior to those of metal electrodes, as shown by *in vitro* impedance and electrochemical characterisation. To investigate the biocompatibility of the CNT-based electrodes, *in vitro* cytotoxicity tests were carried out with different cell types from the nervous system: neurons (PC12 cells), glial cells (42MG-BA cells), fibroblasts (3T3 cells) and endothelial HEK cells (293T cells). The cell activity, estimated by the MTT assay, was not affected by the presence of CNTs, and no significant decrease in proliferation was detected. In addition, the SWNTs did not display any toxicity and remained attached to the surface of the electrode. Extracellular ganglion cell recordings in isolated superfused rabbit retinas were performed to evaluate the capacity of the CNT-based MEAs. It was the first time that CNTs were used to record electrophysiological activity in cultured retinal explants. The results indicated that the SWNT MEA arrays were more efficient in recording the action potential generated by a population of ganglion cells than Pt electrodes.

The effect of MWNTs functionalised with cell-adhesion peptides on neuronal functionality was recently investigated by Bianco et al. [59].

In this study, MWNTs were functionalised via 1,3-dipolar cycloaddition of azomethine ylides, and the resulting pyrrolidine ring was derivatised with two peptides, one including the cell-binding domain RGD sequence (GRGDSP) and the other comprising a domain of the laminin protein (IKVAV), as illustrated in Scheme 41.3. GRGDSP is a fibronectin-derived peptide capable of promoting cell adhesion and neurite outgrowth. RGD-containing

peptides are also involved in the mechanism of integrin regulation of neuronal gene expression [60]. Besides, peptides from different domains of laminin were used to stimulate neuronal growth and axon regeneration [61].

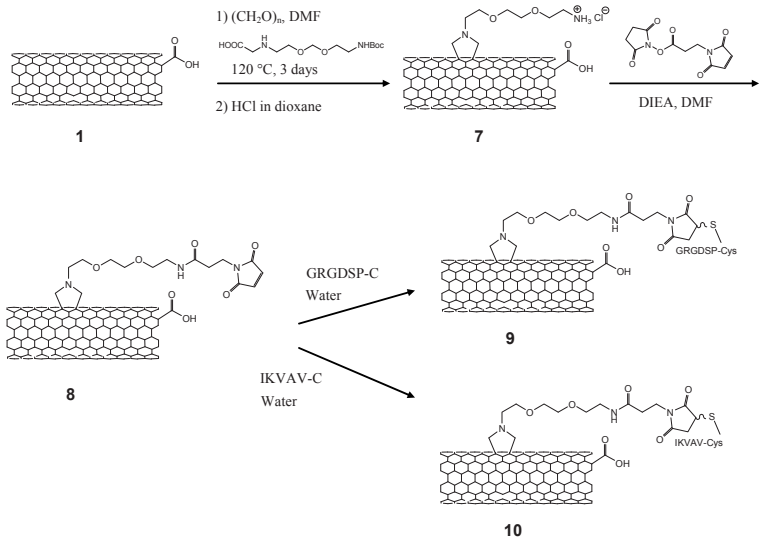

Scheme 41.3 Synthesis of peptide–CNT conjugates.

The activity of the two peptide–nanotube conjugates on different types of cells, including tumour cells (Jurkat), primary splenocytes and neurons, was examined. Upon incubation of Jurkat cells with increasing doses of the peptide–nanotube conjugates (up to 100 μg/mL), flow cytometry showed no significant loss of cell viability. Similarly, no cytotoxic effect of the peptide–nanotube conjugates on splenocytes isolated from healthy BALB/c mice was observed, thus highlighting the biocompatibility of the functionalised MWNTs. Furthermore, doubly functionalised peptide–nanotube conjugates containing FITC were prepared and found to be internalised into the neuronal cells.

The electrophysiological responses of rat dissociated hippocampal neurons in culture incubated with the two peptide–nanotube conjugates were then studied. The spontaneous activity of single neurons in voltage clamp configuration was recorded. The neuronal activity was detected as inward currents, corresponding

to synaptic events, of variable amplitude. These events represent a mixed population of inhibitory and excitatory spontaneous postsynaptic currents. Some neuronal passive properties were then examined and measured under voltage clamp. They are indicative of neuronal function such as membrane capacitance and input resistance. By quantifying peak amplitude of inward and outward currents to the membrane capacitance value of each recorded cell, inward and outward current densities were obtained. The values were found to be similar in the case of the RGD-containing peptide conjugated to MWNTs when compared with the peptide alone. Thus, the incubation of neurons in the presence of MWNTs functionalised with peptides did not modify neuronal spontaneous activity.

In summary, these data showed that peptide–nanotube conjugates incubated with neuronal cells did not alter the neuronal morphology, viability and basic functions of the neurons. These results are different from those obtained by Haddon and coworkers in which PEG-SWNTs were found to inhibit membrane endocytosis in stimulated neurons, which should lead to a progressive decrease of frequency in spontaneous PSCs, as will be detailed later [62]. Bianco et al. pointed out that this difference may be explained by the different types of treatment carried out on the CNTs (i.e., purification and functionalisation with different chemical groups). Thus, these data indicated that differently functionalised CNTs can have different impacts on neuronal activity, thereby highlighting the importance of determining the influence of the functionalisation of CNTs.

41.4 Investigation of the Mechanisms of the Electrical Interactions Between CNTs and Neurons

Numerous studies have demonstrated that CNTs can sustain and promote neuronal electrical activity in networks of cultured neuronal cells. But the mechanisms by which they affect cellular function are still poorly understood. Little is known about the details of the interactions between CNTs and neurons. A few studies investigating possible hypotheses have been recently reported.

In vitro models have been developed to investigate the electrophysiological properties of synapses, neurons and networks coupled to CNTs, and to study the electrical interactions between CNTs and membranes. Ballerini and coworkers reviewed various existing experimental *in vitro*, *in vivo* and in silico models of neuronal network and compared them by listing their advantages and disadvantages [3a]. The effects of CNT substrates on the electrical behavior of brain networks *in vitro* were reported for the first time.

Studies on the interface between neurons and SWNTs were performed recently by Ballerini and coworkers. They focused on the electrical signal transfer and the synaptic stimulation in cultured brain circuits [63]. Computer simulations were included in the study to model the electrical interactions between neurons connected via SWNTs. The results, strengthened by the modelling of the CNT–neuron junction, showed that SWNTs can directly stimulate brain circuit activity.

In this study, rat hippocampal cells were grown on a film of purified SWNTs, via deposition of functionalised SWNTs and subsequent defunctionalisation. Patch-clamp experiments were then performed to determine the neuronal responses to voltage steps delivered via conductive SWNT glass coverslips. The morphology of the neuronal network was determined by SEM and quantified by immunocytochemistry analysis. SEM confirmed the adhesion and growth of hippocampal neurons on SWNT substrates, accompanied by variable degree of neurite extension. The attachment and proliferation processes were similar to those observed for neuronal growth on control glass surfaces. At high magnification, tight interactions between cell membranes and SWNTs could be visualised. The distributed electrical stimulation of cultured hippocampal neurons was then investigated. Hippocampal neurons grown on SWNTs or on control glass substrates exhibited spontaneous electrical activity. In particular, a significant increase in action potentials and frequency of PSCs was observed for neurons grown on SWNT films when compared with control substrates.

To assess whether SWNTs could perform local network stimulations, short voltage pulses were delivered to SWNTs to induce the appearance of Na^+ fast inward current in the recorded

neuron. These stimulations should also induce action potentials in neighbouring neurons that should generate monosynaptic responses to the connected neurons. Indeed, brief SWNT voltage steps effectively delivered PSCs, in 65% of the recorded neurons. To elucidate the electrical interactions occurring in SWNT-neuron networks, the modelling of the neuron-SWNT junction was achieved. It was suggested that the coupling between neurons and SWNTs might be partly resistive. But the authors led to the conclusion that because of the non-idealities of the single electrode voltage clamp, eliciting Na^+ currents through SWNT stimulation did not conclusively prove a resistive coupling between SWNTs and neurons. Moreover, the authors pointed out that whole-cell patch-clamp recordings might yield deceiving results as any resistive coupling between biomembranes and SWNTs is qualitatively undistinguishable from a coupling between SWNTs and the patch pipette.

Ballerini and coworkers further investigated the influence of CNTs on the electrical properties of isolated neurons. In particular, the presence of after-depolarisation events in the cell soma was examined [64]. The aim of this study was to determine if the higher efficiency of the signal transmission of neurons grown on conductive nanotube substrates was linked to the interactions between CNTs and neurons at the nanoscale.

Purified SWNTs were deposited on glass substrates via the previously described process based on functionalisation and subsequent defunctionalisation. Rat hippocampal cells were cultured on the thin film of purified SWNTs. Electrogenesis was studied in single neurons. The authors injected a brief current pulse into the soma to force the neurons to fire a regular train of six action potentials and measured the presence of membrane depolarisation in the soma at the end of the last action potential. Neurons propagate electrical signals, i.e., action potentials, down an axon. Backpropagation of the action potentials to dendrites can occur occasionally. In this case, the propagation of the electrical signals takes place in the direction opposite to that of the flow. It has been shown that rat hippocampal neurons grown on SWNT substrates exhibited a significantly larger after-potential depolarisation (ADP) by comparison with neurons grown on control glass substrates. ADP was found to be dependent on the degree of

dendritic branching. Indeed, neurons with minimal dendritic branching grown on the CNT substrate did not display ADP. The backpropagating current induces a voltage change that increases the concentration of Ca^{2+} in the dendrites and can be measured through the presence of a slow membrane depolarisation following repetitive action potentials. Therefore, the interactions between CNTs and membranes of neurons can affect single-cell activity. These experiments were also conducted on two other types of substrates: indium tin oxide substrate, displaying high conductivity, and a non-conductive nanostructured substrate containing peptides that self-assemble into nanofibres. In both cases, no significant enhancement of ADP was observed, indicating that the ADP enhancement effect is specific to CNT substrate.

The authors suggested the electrotonic hypothesis to explain the physical neuron-SWNT interactions and elucidate the mechanisms by which SWNTs might affect the electrical activity of neuronal networks. Electrotonic potential is a non-propagated local potential induced by a local change in ionic conductance. It represents changes to the neuron membrane potential that do not lead to the generation of new current by action potentials. Electrotonic potential is conducted faster than action potential, but it attenuates rapidly and is therefore unsuitable for long-distance signalling.

The authors also examined if an electrotonic shortcut could occur between the soma and the dendrite. The results showed the absence of changes brought about by SWNTs in the dendritic passive time constants. Other hypotheses were drawn to tentatively explain the increased effects of ADP, such as (i) potentiation of Ca^{2+}-mediated currents occurring in neurons grown on SWNT thin films and (ii) channels clustering, induced by mechanical interactions between SWNT bundles and the cell cytoskeleton. The presence of the ADPs, their dependence on trains of action potentials, and the detected sensitivity to calcium channel blockers are indicative of the generation of dendritic Ca^{2+} currents. The discontinuous and tight contacts between CNTs and neuronal membranes were observed by transmission electron microscopy (TEM). The SWNTs were able to modulate the physiology of the neurons. The intimate interactions of the SWNTs with a small area of the neuritic membranes favoured electrical shortcuts between

the proximal and distal compartments of the neurons, thus supporting the electrotonic hypothesis. A mathematical model was proposed to simulate how ADP enhancement induced by SWNTs might affect the neuronal activity. More precisely, the aim was to model the membrane voltage input–output relationship between the soma and dendrites. The results indicated that SWNTs may be effectively short-circuiting the dendrites and soma. This shortcut would lead to diverting the electrical activity through the nanotubes, explaining the enhanced ADP effect.

In summary, this study reported that SWNTs might affect neuronal information processing. Indeed, the action potential backpropagation was substantially enhanced in neurons grown on SWNT substrates. However, the exact mechanisms at the origin of this effect are not totally clear. One hypothesis relies on the discontinuous and tight interactions between SWNTs and neuronal membranes.

Finally, following their study on neuronal growth on CNT substrates, Haddon and coworkers investigated the mechanism by which CNTs induce extension of neurite length [63]. They demonstrated that water-soluble SWNTs are able to inhibit stimulated membrane endocytosis in neurons. Following the observation that water-soluble SWNTs modified Ca^{2+} dynamics in neurons, thus leading to a decrease of the depolarisation-dependent influx of Ca^{2+} during cell stimulation, the authors investigated the effect of water-soluble SWNTs on membrane recycling. Indeed, the plasma membrane/vesicular recycling influences the extension of neurites [65] and is regulated by an influx of Ca^{2+} from the extracellular space induced by the depolarisation of neurons.

In this study, hippocampal neuronal cultures were treated with SWNT-PEG. The neurons were exposed to FM1-43 [*N*-(3-triethylammoniumpropyl)-4-(4-(dibutylamino)styryl)pyridinium dibromide] [66], a fluorescent dye that can monitor membrane recycling and that is internalised into cells by endocytosis as it does not passively diffuse across cell membranes. With regard to the constitutive vesicular recycling, taking place in unstimulated cells, the water-soluble graft copolymer SWNT-PEG had no effect on the endocytosis of FM1-43. However, in stimulated neurons (using HIK^{+}), the pegylated SWNTs reduced the endocytotic loading of FM1-43 in a dose-dependent way.

In summary, the mechanism responsible for the effects of water-soluble SWNTs on enhancement of selected neurite outgrowth was elucidated. The pegylated SWNTs inhibited regulated/stimulated plasma membrane/vesicular recycling, while the constitutive phenomenon was unaffected.

41.5 Conclusions and Perspectives

CNTs have been demonstrated as a biocompatible substrate that promotes neuronal growth, boosts neural activity and transmits electrical stimulation effectively. Indeed, many studies reported the use of CNTs as substrate to promote neuronal cell adhesion and to induce growth and differentiation of neurons. Functionalisation of CNTs can modulate some processes, such as the outgrowth and branching of neurites. In particular, the surface charge was found to have a strong effect on neuronal growth. Because of their electrical properties, CNTs have also been used as electrodes to stimulate neurons. CNTs were seen to form tight contacts with neuron cell membrane that might favour electrical shortcuts between the proximal and distal compartments of the neurons, thus altering their electrophysiological responses. Therefore, understanding the mechanisms at the origin of the effects of CNTs on neuronal cells is essential for designing functional neuronal circuits.

With regard to other materials or devices used for applications in neuroscience, CNTs show great potential as they possess a unique set of physical, chemical, mechanical and electronic properties [67]. A promising substrate candidate suitable for neuronal growth requires several characteristics, such as light weight, tight binding with neurons, controllable branching of neurites and directed neuron network formation. It should also ensure long-term cell viability. Besides, the combination of high electrical conductivity, corrosion resistance, nanoscale size, strength and flexibility is essential for neuroprosthetic devices for electrical recording and stimulation. CNTs can meet these requirements because of their dimension, high electrical conductivity and biocompatibility. Furthermore, CNTs have the exceptional characteristic to be highly flexible, while being very strong. The properties of CNTs can be, in part, transferred into CNT composites.

CNTs are relatively chemically inert, but the possibility of functionalising the nanotube surface offers opportunities to tune their properties. Compared with other devices or materials, CNTs have led to very promising results. Indeed, it has been demonstrated that CNT-based substrates can serve as an extracellular scaffold with a higher capability of directing neurite outgrowth and regulating neurite branching than other types of substrates such as PLL, PEI or PLO, as explained in part 41.2. In terms of recording and stimulating neuronal activity, CNT-based electrodes exhibited better performances because of higher signal-to-noise ratio, longer lifetime and higher tissue–electrode interface in comparison with conventional commercial electrodes.

In terms of future potential applications, CNTs are promising candidates for neural prostheses for restoring the function of damaged neuronal circuits. CNTs could serve as an extracellular scaffold to guide neurite outgrowth governed by their tips and growth cones, and also to regulate neurite branching. These processes would lead to the re-establishment of intricate connections between neurons forming synapses. CNTs could be used to selectively enhance neurite elongation directly at the site of nerve injury to aid in nerve regeneration, thus increasing the chance of connecting the injured sites to sustain functional recovery. Several neurological disorders and injuries, such as Parkinson's disease, epilepsy and stroke, require an implantable device to generate electrical activity in the damaged or diseased tissue.

Disclosures and Conflict of Interest

The author declares that she has no conflict of interest and has no affiliations or financial involvement with any organization or entity discussed in this chapter. No writing assistance was utilized in the production of this chapter and the author has received no payment for its preparation. This is a reformatted version of the authors' chapter that appeared in *Carbon Nanotubes: From Bench Chemistry to Promising Biomedical Applicaons*, 2011 (edited by Giorgia Pastorin), Pan Stanford Publishing Pte. Ltd., Singapore.

Corresponding Author

Dr. Cécilia Ménard-Moyon
CNRS, Institut de Biologie Moléculaire et Cellulaire
Laboratoire d'Immunopathologie et Chimie Thérapeutique (UPR 3572)
15 Rue René Descartes, 67084 Strasbourg, Cedex, France
E-mail: c.menard@ibmc-cnrs.unistra.fr

About the Author

Cécilia Ménard-Moyon obtained her PhD in 2005 at CEA/Saclay in France on carbon nanotubes, their applications for optical limitation, nanoelectronics, and on the development of novel methods of functionalization. She worked for 1 year as a post-doc fellow at the University of York (U.K.) on the total synthesis of a natural product. Then, she joined the R&D Department of Nanocyl company in Belgium for 18 months to work on the synthesis and functionalization of carbon nanotubes. Since 2008, she has been a researcher at CNRS in the group of Alberto Bianco in Strasbourg. Her research interests focus on the functionalization of carbon-based nanomaterials, mainly carbon nanotubes and graphene, for applications in therapy, imaging, and diagnosis.

References

1. (a) De Robertis, E. D. P., Bennett, H. S. (1955). Some features of the submicroscopic morphology of synapses in frog and earthworm. *J. Biophys. Biochem. Cytol.*, **1**, 47.

   (b) Bullock, T. H. (1959). Neuron doctrine and electrophysiology: A quiet revolution has been taking place in our concepts of how the nerve cells act alone and in concert. *Science*, **129**, 997.

   (c) Llinás, R. R. (1988). The intrinsic electrophysiological properties of mammalian neurons: A new insight into CNS function. *Science*, **242**, 1654.

   (d) Pereda, A. E., Rash, J. E., Nagi, J. I., Bennett, M. V. L. (2004). Dynamics of electrical transmission at club endings on the Mauthner cells. *Brain Res. Brain Res. Rev.*, **47**, 227.

(e) Bullock, T. H., Bennett, M. V. L., Johnston, D., Josephson, R., Marder, E., Fields, R. D. (2005). The neuron doctrine. redux, *Science*, **310**, 791.

2. Brösamle, C., Huber, A. B. (2006). Cracking the black box—and putting it back together again: Animal models of spinal cord injury. *Drug Discov. Today Dis. Models*, **3**, 341.
3. (a) Giugliano, M., Prato, M., Ballerini, L. (2008). Nanomaterial/neuronal hybrid system for functional recovery of the CNS. *Drug Discov. Today Dis. Models*, **5**, 37.

   (b) Silva, G. A. (2006). Neuroscience nanotechnology: Progress, opportunities and challenges. *Nature Rev. Neurosci.*, **7**, 65.

   (c) Zhang, L., Webster, T. J. (2009). Nanotechnology and nanomaterials: Promises for improved tissue regeneration. *Nano Today*, **4**, 66.
4. Prato, M., Kostarelos, K., Bianco, A. (2008). Functionalized carbon nanotubes in drug design and discovery. *Acc. Chem. Res.*, **41**, 60.
5. Mattson, M. P., Haddon, R. C., Rao, A. M. (2000). Molecular functionalization of carbon nanotubes and use as substrates for neuronal growth. *J. Mol. Neurosci.*, **14**, 175.
6. Rüegg, U. T., Hefti, F. (1984). Growth of dissociated neurons in culture dishes coated with synthetic polymeric amines. *Neurosci. Lett.*, **49**, 319.
7. Benson, M. D., Romero, M. I., Lush, M. E., Lu, Q. R., Henkemeyer, M., Parada, L. F. (2005). Ephrin-B3 is a myelin-based inhibitor of neurite outgrowth. *Proc. Natl. Acad. Sci. U. S. A.,* **102**, 10694.
8. (a) Mattson, M. P., Kater, S. B. (1987). Calcium regulation of neurite elongation and growth cone motility. *J. Neurosci.*, **7**, 4034.

   (b) Waeg, G., Dimsity, G., Esterbauer, H. (1996). Monoclonal antibodies for detection of 4-hydroxynonenal modified proteins. *Free Radic. Res.*, **25**, 149.
9. Mark, R. J., Lovell, M. A., Markesbery, W. R., Uchida, K., Mattson, M. P. (1997). A role for 4-hydroxynonenal, an aldehyde product of lipid peroxidation, in disruption of ion homeostasis and neuronal death induced by amyloid beta-peptide. *J. Neurochem.*, **68**, 255.
10. Kater, S. B., Mattson, M. P., Cohan, C., Connor, J. (1988). Calcium regulation of the neuronal growth cone. *Trends Neurosci.*, **11**, 315.
11. Hu, H., Ni, Y., Montana, V., Haddon, R. C., Parpura, V. (2004). Chemically functionalized carbon nanotubes as substrates for neuronal growth. *Nano Lett.*, **4**, 507.

12. (a) Chen, S. A., Hwang, G. W. (1995). Water-soluble self-acid-doped conducting polyaniline: Structure and properties. *J. Am. Chem. Soc.*, **117**, 10055.

(b) Roy, B. C., Gupta, M. D., Bhowmik, L., Ray, J. K. (1999). Studies on water soluble conducting polymer: Aniline initiated polymerization of *m*-aminobenzene sulfonic acid. *Synth. Met.*, **100**, 233.

(c) Zhao, B., Hu, H., Haddon, R. C. (2004). Synthesis and properties of a water-soluble single-walled carbon nanotube-poly(*m*-aminobenzene sulfonic acid) graft copolymer. *Adv. Funct. Mater.*, **14**, 71.

13. Hu, H., Ni, Y., Mandal, S. K., Montana, V., Zhao, B., Haddon, R. C., Parpura, V. (2005). Polyethyleneimine functionalized single-walled carbon nanotubes as a substrate for neuronal growth. *J. Phys. Chem. B*, **109**, 4285.

14. Ni, Y., Hu, H., Malarkey, E. B., Zhao, B., Montana, V., Haddon, R. C., Parpura, V. (2005). Chemically functionalized water soluble single-walled carbon nanotubes modulate neurite outgrowth. *J. Nanosci. Nanotechnol.*, **5**, 1707.

15. Zhao, B., Hu, H., Yu, A., Perea, D., Haddon, R. C. (2005). Synthesis and characterization of water soluble single-walled carbon nanotube graft copolymers. *J. Am. Chem. Soc.*, **127**, 8197.

16. (a) Park, K. H., Chhowalla, M., Iqbal, Z., Sesti, F. (2003). Single-walled carbon nanotubes are a new class of ion channel blockers. *J. Biol. Chem.*, **278**, 50212.

(b) Chhowalla, M., Unalan, H. E., Wang, Y., Iqbal, Z., Park, K., Sesti, F. (2005). Irreversible blocking of ion channels using functionalized single-walled carbon nanotubes. *Nanotechnology*, **16**, 2982.

17. Malarkey, E. B., Fisher, K. A., Bekyarova, E., Liu, W., Haddon, R. C., Parpura, V. (2009). Conductive single-walled carbon nanotube substrates modulate neuronal growth. *Nano Lett.*, **9**, 264.

18. Matsumoto, K., Sato, C., Naka, Y., Kitazawa, A., Whitby, R. L. D., Shimizu, N. (2007). Neurite outgrowths of neurons with neurotrophin-coated carbon nanotubes. *J. Biosci. Bioeng.*, **103**, 216.

19. Hempstead, B. L. (2006). Dissecting the diverse actions of pro- and mature neurotrophins. *Curr. Alzheimer Res.*, **3**, 19.

20. Reichardt, L. F. (2006). Neurotrophin-regulated signalling pathways. *Philos. Trans. R. Soc. Lond., Ser. B*, **361**, 1545.

21. Allen, S. J., Dawbarn, D. (2006). Clinical relevance of the neurotrophins and their receptors. *Clin. Sci. (Lond.)*, **110**, 175.

22. Kang, H., Schuman, E. M. (1996). A requirement for local protein synthesis in neurotrophin-induced hippocampal synaptic plasticity. *Science*, **273**, 1402.

23. Galvan-Garcia, P., Keefer, E. W., Yang, F., Zhang, M., Fang, S., Zakhidov, A. A., Baughman, R. H., Romero, M. I. (2007). Robust cell migration and neuronal growth on pristine carbon nanotube sheets and yarns. *J. Biomater. Sci. Polym. Ed.*, **18**, 1245.

24. (a) Zhang, M., Fang, S., Zakhidov, A. A., Lee, S. B., Aliev, A. E., Williams, C. D., Atkinson, K. R., Baughman, R. H. (2005). Strong, transparent, multifunctional, carbon nanotube sheets, *Science*, **309**, 1215.

    (b) Zhang, M., Atkinson, K. R., Baughman, R. H. (2004). Multifunctional carbon nanotube yarns by downsizing an ancient technology. *Science*, **306**, 1358.

25. (a) Baas, P. W., Joshi, H. C. (1992). Gamma-tubulin distribution in the neuron: Implications for the origins of neuritic microtubules. *J. Cell. Biol.*, **119**, 171.

    (b) Moody, S. A., Miller, V., Spanos, A., Frankfurter, A. (1996). Developmental expression of a neuron-specific beta-tubulin in frog (Xenopus laevis): A marker for growing axons during the embryonic period. *J. Comp. Neurol.*, **364**, 219.

26. (a) Letourneau, P. C. (1975). Cell-to-substratum adhesion and guidance of axonal elongation, *Dev. Biol.*, **44**, 92.

    (b) Letourneau, P. C. (1975). Possible roles for cell-to-substratum adhesion in neuronal morphogenesis, *Dev. Biol.*, **44**, 77.

    (c) Corey, J. M., Feldman, E. L. (2003). Substrate patterning: An emerging technology for the study of neuronal behavior. *Exp. Neurol.*, **184**, S89.

27. Chao, T.-I., Xiang, S., Chen, C.-S., Chin, W.-C., Nelson, A. J., Wang, C., Lu, J. (2009). Carbon nanotubes promote neuron differentiation from human embryonic stem cells. *Biochem. Biophys. Res. Commun.*, **384**, 426.

28. (a) Freire, E., Gomes, F. C., Linden, R., Neto, V. M., Coelho-Sampaio, T. (2002). Structure of laminin substrate modulates cellular signaling for neuritogenesis. *J. Cell Sci.*, **115**, 4867.

    (b) Kleinman, H. K., Cannon, F. B., Laurie, G. W., Hassell, J. R., Aumailley, M., Terranova, V. P., Martin, G. R., DuBois-Dalcq, M. (1985). Biological activities of laminin. *J. Cell. Biochem.*, **27**, 317.

    (c) Luckenbill-Edds, L. (1997). Laminin and the mechanism of neuronal outgrowth. *Brain Res. Brain Res. Rev.*, **23**, 1.

(d) He, W., Bellamkonda, R. V. (2005). Nanoscale neuro-integrative coatings for neural implants. *Biomaterials*, **26**, 2983.

(e) Sephel, G. C., Burrous, B. A., Kleinman, H. K. (1989). Laminin neural activity and binding proteins. *Dev. Neurosci.*, **11**, 313.

29. Xie, J., Chen, L., Aatre, K. R., Srivatsan, M., Varadan, V. K. (2006). Somatosensory neurons grown on functionalized carbon nanotube mats. *Smart Mater. Struct.*, **15**, N85.
30. Ayad, L. (1994). *The Extracellular Matrix Factsbook*, Plenum, New York.
31. Belyanskaya, L., Weigel, S., Hirsch, C., Tobler, U., Krug, H. F., Wick, P. (2009). Effects of carbon nanotubes on primary neurons and glial cells. *Neurotoxicology*, **30**, 702.
32. Wick, P., Manser, P., Limbach, L. K., Dettlaff-Weglikowska, U., Krumeich, F., Roth, S., Stark, W. J., Bruinink, A. (2007). The degree and kind of agglomeration affect carbon nanotube cytotoxicity. *Toxicol. Lett.*, **168**, 121.
33. (a) Wilson, B. S., Lawson, D. T., Muller, J. M., Tyler, R. S., Kiefer, J. (2003). Cochlear implants: Some likely next steps. *Annu. Rev. Biomed. Eng.*, **5**, 207.

    (b) Weiland, J. D., Liu, W., Humayun, M. S. (2005). Retinal prosthesis. *Annu. Rev. Biomed. Eng.*, **7**, 361.

    (c) Navarro, X., Krueger, T. B., Lago, N., Micera, S., Stieglitz, T., Dario, P. (2005). A critical review of interfaces with the peripheral nervous system for the control of neuroprostheses and hybrid bionic systems. *J. Peripher. Nerv. Syst.*, **10**, 229.
34. Benabid, A. L. (2003). Deep brain stimulation for Parkinson's disease. *Curr. Opin. Neurobiol.*, **13**, 696.
35. Zhang, X., Prasad, S., Niyogi, S., Morgan, A., Ozkan, M., Ozkan, C. S. (2005). Guided neurite growth on patterned carbon nanotubes. *Sens. Actuators B Chem.*, **106**, 843.
36. (a) Qian, L., Saltzman, W. M. (2004). Improving the expansion and neuronal differentiation of mesenchymal stem cells through culture surface modification. *Biomaterials*, **25**, 1331.

    (b) Yavin, E., Yavin, Z. (1974). Attachment and culture of dissociated cells from rat embryo cerebral hemispheres on polylysine-coated surface. *J. Cell Biol.*, **62**, 540.
37. Ben-Jacob, E., Hanein, Y. (2008). Carbon nanotube micro-electrodes for neuronal interfacing. *J. Mater. Chem.*, **18**, 5181.

38. Gabay, T., Jakobs, E., Ben-Jacob, E., Hanein, Y. (2005). Engineered self-organization of neural networks using carbon nanotube clusters. *Physica A*, **350**, 611.
39. Sorkin, R., Gabay, T., Blinder, P., Baranes, D., Ben-Jacob, E., Hanein, Y. (2006). Compact self-wiring in cultured neural networks. *J. Neural Eng.*, **3**, 95.
40. Gabay, T., Ben-David, M., Kalifa, I., Sorkin, R., Abrams, Z. R., Ben-Jacob, E., Hanein, Y. (2007). Electro-chemical and biological properties of carbon nanotube based multi-electrode arrays. *Nanotechnology*, **18**, 035201.
41. Wang, K., Fishman, H. A., Dai, H., Harris, J. S. (2006). Neural stimulation with a carbon nanotube microelectrode array. *Nano Lett.*, **6**, 2043.
42. Sorkin, R., Greenbaum, A., David-Pur, M., Anava, S., Ayali, A., Ben-Jacob, E., Hanein, Y. (2009). Process entanglement as a neuronal anchorage mechanism to rough surfaces. *Nanotechnology*, **20,** 015101.
43. Shoval, A., Adams, C., David-Pur, M., Shein, M., Hanein, Y., Sernagor, E. (2009). Carbon nanotube electrodes for effective interfacing with retinal tissue. *Front. Neuroengineering*, **2**, 4.
44. Keefer, E. W., Botterman, B. R., Romero, M. I., Rossi, A. F., Gross, G. W. (2008). Carbon nanotube coating improves neuronal recordings. *Nat. Nanotechnol.*, **3**, 434.
45. Gheith, M. K., Sinani, V. A., Wicksted, J. P., Matts, R. L., Kotov, N. A. (2005). Single-walled carbon nanotubes polyelectrolyte multilayers and freestanding films as a biocompatible platform for neuroprosthetic implants. *Adv. Mater.*, **17**, 2663.
46. Mamedov, A. A., Kotov, N. A., Prato, M., Guldi, D. M., Wicksted, J. P., Hirsch, A. (2002). Molecular design of strong SWNT/polyelectrolyte multilayers composites. *Nature Mater.*, **1**, 190.
47. Gheith, M. K., Pappas, T. C., Liopo, A. V., Sinani, V. A., Shim, B. S., Motamedi, M., Wicksted, J. P., Kotov, N. A. (2006). Stimulation of neural cells by lateral currents in conductive layer-by-layer films of single-walled carbon nanotubes. *Adv. Mater.*, **18**, 2975.
48. Jan, E., Kotov, N. A. (2007). Successful differentiation of mouse neural stem cells on layer-by-layer assembled single-walled carbon nanotube composite. *Nano Lett.*, **7**, 1123.
49. Kam, N. W. S., Jan, E., Kotov, N. A. (2009). Electrical stimulation of neural stem cells mediated by humanized carbon nanotube composite made with extracellular matrix protein. *Nano Lett.*, **9**, 273.

50. Freire, E., Gomes, F. C. A., Linden, R., Neto, V. M., Coelho-Sampaio, T. (2002). Structure of laminin substrate modulates cellular signaling for neuritogenesis. *J. Cell Sci.*, **115**, 4867.
51. Stuart, G. J., Sakmann, B. (1994). Active propagation of somatic action potentials into neocortical pyramidal cell dendrites. *Nature*, **367**, 69.
52. Yeh, S.-R., Chen, Y.-C., Su, H.-C., Yew, T.-R., Kao, H.-H., Lee, Y.-T., Liu, T.-A., Chen, H., Chang, Y.-C., Chang, P., Chen, H. (2009). Interfacing neurons both extracellularly and intracellularly using carbon-nanotube probes with long-term endurance. *Langmuir*, **25**, 7718.
53. Nguyen-Vu, T. D. B., Chen, H., Cassell, A. M., Andrews, R., Meyyappan, M., Li, J. (2006). Vertically aligned carbon nanofiber arrays: An advance toward electrical-neural interfaces. *Small*, **2**, 89.
54. Lovat, V., Pantarotto, D., Lagostena, L., Cacciari, B., Grandolfo, M., Righi, M., Spalluto, G., Prato, M., Ballerini, L. (2005). Carbon nanotube substrates boost neuronal electrical signaling. *Nano Lett.*, **5**, 1107.
55. Liopo, A. V., Stewart, M. P., Hudson, J., Tour, J. M., Pappas, T. C. (2006). Biocompatibility of native and functionalized single-walled carbon nanotubes for neuronal interface. *J. Nanosci. Nanotechnol.*, **6**, 1365.
56. Bahr, J. L., Tour, J. M. (2001). Highly functionalized carbon nanotubes using *in situ* generated diazonium compounds. *Chem. Mater.*, **13**, 3823.
57. Gabriel, G., Gómez, R., Bongard, M., Benito, N., Fernández, E., Villa, R. (2009). Easily made single-walled carbon nanotube surface microelectrodes for neuronal applications. *Biosens. Bioelectron.*, **24**, 1942.
58. Gabriel, G., Gómez-Martínez, R., Villa, R. (2008). Single-walled carbon nanotubes deposited on surface electrodes to improve interface impedance. *Physiol. Meas.*, **29**, S203.
59. Gaillard, C., Cellot, G., Li, S., Toma, F. M., Dumortier, H., Spalluto, G., Cacciari, B., Prato, M., Ballerini, L., Bianco, A. (2009). Carbon nanotubes carrying cell-adhesion peptides do not interfere with neuronal functionality. *Adv. Mater*, **21**, 2903.
60. Gall, C. M., Pinkstaff, J. K., Lauterborn, J. C., Xie, Y., Lynch, G. (2003). Integrins regulate neuronal neurotrophin gene expression through effects on voltage-sensitive calcium channels. *Neuroscience*, **118**, 925.
61. Anderson, D. G., Burdick, J. A., Langer, R. (2004). Smart biomaterials. *Science*, **305**, 1923.
62. Malarkey, E. B., Reyes, R. C., Zhao, B., Haddon, R. C., Parpura, V. (2008). Water soluble single-walled carbon nanotubes inhibit stimulated endocytosis in neurons. *Nano Lett.*, **8**, 3538.

63. Mazzatenta, A., Giugliano, M., Campidelli, S., Gambazzi, L., Businaro, L., Markram, H., Prato, M., Ballerini, L. (2007). Interfacing neurons with carbon nanotubes: Electrical signal transfer and synaptic stimulation in cultured brain circuits. *J. Neurosci.*, **27**, 6931.

64. (a) Cellot, G., Cilia, E., Cipollone, S., Rancic, V., Sucapane, A., Giordani, S., Gambazzi, L., Markram, H., Grandolfo, M., Scaini, D., Gelain, F., Casalis, L., Prato, M., Giugliano, M., Ballerini, L. (2009). Carbon nanotubes might improve neuronal performance by favouring electrical shortcuts, *Nat. Nanotechnol.*, **4**, 126. (b) Silva, G. A. (2009). Shorting neurons with nanotubes. *Nat. Nanotechnol.*, **4**, 82.

65. Zakharenko, S., Popov, S. (2000). Plasma membrane recycling and flow in growing neuritis. *Neuroscience*, **97**, 185.

66. Betz, W. J., Bewick, G. S. (1992). Optical analysis of synaptic vesicle recycling at the frog neuromuscular junction. *Science*, **255**, 200.

67. (a) Haddon, R. C. (2002). Carbon nanotubes. *Acc. Chem. Res.*, **35**, 997.

    (b) Ouyang, M., Huang, J. L., Lieber, C. M. (2002). Fundamental electronic properties and applications of single-walled carbon nanotubes. *Acc. Chem. Res.*, **35**, 1018.

    (c) Dai, H. (2002). Carbon nanotubes: Synthesis, integration, and properties. *Acc. Chem. Res.*, **35**, 1035.

    (d) Zhou, O., Shimoda, H., Gao, B., Oh, S., Fleming, L., Yue, G. (2002). Materials science of carbon nanotubes: Fabrication, integration, and properties of macroscopic structures of carbon nanotubes. *Acc. Chem. Res.*, **35**, 1045.

    (e) Niyogi, S., Hamon, M. A., Hu, H., Zhao, B., Bhowmik, P., Sen, R., Itkis, M. E., Haddon, R. C. (2002). Chemistry of single-walled carbon nanotubes. *Acc. Chem. Res.*, **35**, 1105.

Chapter 42

Polymeric Nanoparticles for Cancer Therapeutics

Mohit S. Verma, Joshua E. Rosen, Ameena Meerasa, Serge Yoffe, MEng, and Frank X. Gu, PhD

Department of Chemical Engineering and Waterloo Institute for Nanotechnology, University of Waterloo, Canada

Keywords: polymer, drug release, cancer, targeting, biodistribution, therapeutics, immune interaction, drug delivery, nanoprecipitation, copolymer, biocompatibility, micelles, dendrimers

42.1 Introduction

In recent years, the explosion of progress in science and engineering at the nanoscale has paved the way for a new category of healthcare technologies broadly termed nanomedicine. At its core, nanomedicine involves manipulating, engineering, and exploiting different material properties at the nanometer level to design products that can overcome many of the disadvantages found in currently available healthcare technologies. Nanotechnology has been used in a variety of applications: from improved cancer therapeutics with reduced side effects, to more sensitive imaging and diagnostic techniques, to improvements in implantable devices that allow for prolonged device lifetime and superior function;

Handbook of Clinical Nanomedicine: Nanoparticles, Imaging, Therapy, and Clinical Applications
Edited by Raj Bawa, Gerald F. Audette, and Israel Rubinstein

ISBN 978-981-4669-20-7 (Hardcover), 978-981-4669-21-4 (eBook)
www.panstanford.com

nanomedicine is clearly at the forefront of a new era of medical technology.

One of the main themes employed in nanomedicine is the concept of enhanced control and specificity. While traditional therapeutic agents have allowed for very little control in terms of where they are distributed in the body and how fast they are cleared, engineering at the nanoscale has allowed for significant advances in optimizing the biocompatibility, biodistribution, and pharmacokinetics of various medical technologies. For example, devices can be created that release drugs and other therapeutic agents in a controlled manner, resulting in prolonged and enhanced therapeutic effects. In addition, nanoscale manipulations allow for the development of therapeutic products that target and localize to the area of a particular disease, increasing both the safety and effectiveness of the therapeutic agent, while at the same time minimizing unpleasant side effects.

One prominent example of controlled delivery and release is the use of polymeric nanoparticles containing chemotherapeutic agents for the treatment of cancer (Fig. 42.1). In contrast to larger particles, nanoparticles have longer retention times in the body and can penetrate tumors more effectively [1, 2]. Nanoscale drug carriers have shown a remarkable ability to maintain an optimal drug release profile while localizing at the tumor site, minimizing deleterious effects on healthy tissues. Other nanoparticulate structures, such as liposomes, micelles, dendrimers, and metal nanoparticles, have also been evaluated for enhanced drug delivery applications.

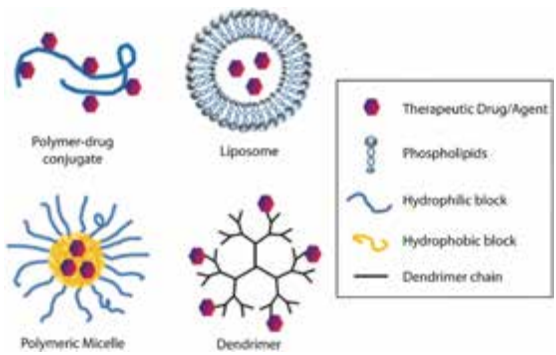

Figure 42.1 Commonly used drug delivery platforms for therapeutics in nanomedicine.

While nanomedical technology has many potential benefits, there are also some significant challenges that must be overcome before these technologies can be put widely to use. One of the major barriers to injecting nanoparticles into the bloodstream is the tendency of these particles to be recognized rapidly by the body's immune system as foreign entities. This results in their subsequent clearance from the bloodstream and accumulation in the liver and spleen before they have had a chance to exert their therapeutic or diagnostic effects. An equally important challenge is the potentially toxic nature of many types of nanoparticles, which can be a potential barrier towards their implementation in a clinical setting. This chapter serves to provide a general overview of important parameters in nanomedicine, such as biocompatibility and pharmacokinetics, and describes a variety of areas in which nanotechnology is being put to use to design polymer systems capable of delivering therapeutic payloads to tumors.

42.2 Biological Interactions of Nanomaterials

In order to gain an appreciation for the various properties and features of the many polymeric systems that will be discussed in this chapter, it is essential to have a basic understanding of the interactions that occur between nanomaterials and the living body. When designing nanotherapeutic systems, one must remember that the body treats any object administered to it as foreign and attempts to clear it as rapidly as possible. The interactions and physiological mechanisms discussed in this section are the basis of some of the most critical design challenges in the field of nanomedicine as they dictate important parameters such as blood circulation half-life, tissue biodistribution, and excretion pathways. The initial interactions that any nanoparticle encounters are typically dictated by its route of entry into the body; for example, interactions with blood plasma proteins for intravenous administration, the skin for dermal administration, or the upper GI tract for oral administration [3]. However, in all cases, a portion of the particles eventually reach the bloodstream and then accumulate in the liver [3]. This section focuses on the interactions nanoparticles undergo once they are in the bloodstream, as these interactions are generally applicable to a wide range of nanoparticle systems. For detailed reviews of nanoparticle interactions, see [4–10].

42.2.1 Immune System Response

The interaction of nanoparticles with the mononuclear phagocytic system (MPS), also known as the reticuloendothelial system (RES), can result in their degradation or sequestration and removal from circulation. The MPS consists of macrophages and monocytes that have the ability to remove altered cells, senescent cells and foreign particulates [8] including colloidal drug delivery systems, from circulation via non-specific or specific receptor mediated endocytosis. It has been established that the physicochemical properties of nanoparticles, such as particle size, surface charge, hydrophilicity, and polymer conformation, affect immune response and biocompatibility (Table 42.1).

Table 42.1 Optimal physicochemical properties of nanoparticles for biocompatibility

Physicochemical property	Desired parameter	Effect	Target site
Particle size	<100 nm	Biocompatibility; prolonged circulation	Bloodstream
	100–200 nm	Hepatic accumulation	Liver
	>200 nm	Splenic accumulation	Spleen
Surface charge	Neutral	Reduced opsonization; prolonged circulation	Bloodstream
Hydrophilicity	Hydrophilic surface polymers, e.g. PEG	Reduced opsonization; prolonged circulation	Bloodstream
Chain density	High	Reduced opsonization; prolonged circulation	Bloodstream
Conformation	Brush or mushroom-brush (e.g. 5000 MW PEG)	Steric hindrance; reduced opsonization; prolonged circulation	Bloodstream

42.2.2 Opsonization

Opsonization is a term used to describe the adsorption or binding of proteins to the surface of a nanoparticle. The specific proteins bound by a given nanoparticle depend on its composition,

although it has been shown that all particles tend to bind albumin, fibrinogen, IgG, and apolipoproteins [4]. 2D PAGE electrophoresis and Western blot analysis are two methods that are generally used to investigate the constitution of plasma protein adsorption onto a particle surface [4, 7].

Opsonins are defined as blood plasma proteins, such as complement proteins, immunoglobulins, fibronectin, and apolipoproteins, which coat foreign materials and make them more susceptible to phagocytic removal [4, 5, 9, 11]. Opsonization alters the physicochemical properties of the particle, resulting in an increase in particle size or a change in the surface conformation or charge that eventually leads to their recognition by macrophages [9, 10]. The accumulation of proteins on a particle's surface usually leads to rapid removal of the particle from circulation by cells such as the hepatic Kupffer cells found in the liver, macrophages in the spleen and bone marrow, or dendritic cells [9]. The degree of opsonization experienced by a nanoparticle system is a key parameter in determining its circulation half-life and biodistribution. Nanoparticles that are capable of avoiding opsonization and subsequent clearance are often referred to as "stealthy."

42.2.3 Complement Activation

The complement system is a component of the innate immune system; it comprises an ensemble of plasma proteins that participate in a biochemical cascade, which is activated upon exposure to foreign antigens. The protein-cleavage products produced throughout the cascade serve to activate the next stage of the cascade, induce an inflammatory response, and act as opsonins to facilitate the recognition of foreign particles by the immune system. The ultimate product of the complement cascade is the formation of a membrane attack complex (MAC), which acts to lyse any invading bacterial species [11]. Since liposomal particles are similar in composition to cell membranes, complement activation can lead to their destruction and the premature release of any payload compounds [10].

The complement system can be activated through three different pathways: classical, alternate, and lectin. The classical pathway is triggered by the binding of IgG and IgM antibodies onto the pathogen surface, which then bind and activate the first protein in the complement cascade. The alternative pathway is

constantly active at low levels due to the spontaneous cleavage of an intermediate complement protein; however, this activity is amplified by the presence of amine or hydroxyl groups on the surface of a foreign particle leading to full activation of the complement cascade. The lectin pathway is initiated by the binding of mannose-binding lectin to mannose or fructose groups on a pathogen surface, which leads to activation of the complement cascade [6, 10, 11]. Regardless of the mode of activation, the end result of all three pathways is the same: opsonization, inflammation, and MAC formation.

42.2.4 Biocompatibility

In order to be considered biocompatible, a nanoparticle should not elicit an immune or toxic response after administration to the body. Efforts to increase the biocompatibility of nanoparticles typically focus on reducing their susceptibility to opsonization or their ability to activate the complement system. Thus, responses such as macrophage uptake and lysis are reduced and the nanoparticles' circulation lifetime can be increased, allowing for sustained drug release and improved efficacy. In addition, biocompatible particles also reduce the effective dosage, which reduces possible side effects and toxicity to healthy cells [6].

In order for nanoparticles to be considered non-toxic, they must be both biodegradable and not illicit toxic reactions in the body. Nanoparticle biodegradability can be achieved by choosing biodegradable polymers or materials when synthesizing the particles, while toxic responses need to be evaluated post synthesis. One example of measuring the inherent toxicity of nanoparticles is to assess their hematocompatibility—the ability of nanoparticles to interact with erythrocytes in the bloodstream without causing hemolysis or thrombosis (blood clot formation), conditions that can cause life-threatening pathological conditions such as anemia and jaundice [5]. A percent hemolysis of less than 5% has been established to be acceptable for the use of biomaterials [12].

42.2.5 Effect of Particle Size

Particle size is a key parameter that influences the *in vivo* interactions of nanoparticles and is thus a major determinant of their pharmacokinetics and biodistribution profiles. Two of the

primary immune organs involved in nanoparticle clearance, the liver and spleen, have been shown to interact with nanoparticles in a size-dependent manner. Studies have shown that particles around 100 to 150 nm seem to be the most desirable for achieving both biocompatibility and prolonged circulation lifetime [8, 13]. In addition to their ability to avoid size-dependent filtration by both the liver and the spleen, smaller particles have a more rounded surface, which does not allow for strong protein–particle interactions, making opsonization and subsequent immune activation difficult [10]. In comparison, larger particles have increased surface area and a less curved surface, which produces areas of relative flatness that allows for increased complement activity. In addition to its influence upon clearance behavior, size is also a key determinant of a nanoparticle's ability to extravasate (leave the vasculature) and enter the tissue of organs or tumors to deliver a therapeutic payload.

42.2.6 Importance of Surface Properties

In addition to a nanoparticle's size, its surface properties are a second major factor in determining the degree of its interactions with various biological systems. It has been shown that hydrophobic and charged surfaces tend to show high degrees of protein binding, while neutral and hydrophilic surfaces show low amounts of opsonization [2, 9].

Studies have shown that the chain density and conformation of a hydrophilic polymer coating both play an important role in immune response. For effective evasion, nanoparticles require a high surface density of hydrophilic polymer chains, thus reducing the ability of proteins to see into the inner hydrophobic core of the particles [14]. In addition, it has been shown that depending on their surface density, polymer chains take on either a mushroom or brush conformation [7]. At lower surface densities, the polymers take on a mushroom-like conformation with flexible chains spread out in solution; at higher surface densities, they extend further from the surface and assume a brush-like conformation. Brush or intermediate mushroom-brush conformations have shown to decrease opsonization the most, as the rigid chains prevent the penetration of proteins into the hydrophobic core and also provide steric repulsive effects [7]. In addition to the general

physio-chemical properties of a surface, interactions can be further influenced by the presence of specific biomolecules or targeting ligands. As we will discuss now, this effect can be used to great advantage in order to deliver therapeutic materials to specific sites in the body.

42.3 Nanoparticle Targeting

One of the central trends in nanotechnology-based cancer therapeutics and diagnostics is the push to create agents that can distinguish between cancerous and healthy tissues. From a therapeutics standpoint, this is desirable because it will cause drugs and other therapeutic agents to affect cancer cells while reducing the drug's impact on healthy cells. This will lead to greater therapeutic efficacy, as well as the mitigation of many unpleasant side effects that patients currently face while undergoing chemotherapeutic treatment.

Targeting methods can be grouped into two categories that differ in the way in which they distinguish between cancerous and healthy tissues. Passive targeting methods rely on physiological abnormalities in cancer tissues (Table 42.2) such as leaky vasculature and malformed lymphatic drainage systems (collectively known as the enhanced permeability and retention, or EPR, effect) [15–18]. Active targeting methods require that a ligand be attached to the surface of the diagnostic or therapeutic agent, which will then bind to surface markers and receptors that are overexpressed on cancer cells [18]. Table 42.3 lists various surface markers that can be used for active targeting. It should be noted that all active targeting techniques are still subject to the inherent physiological differences between cancerous and normal tissues (Table 42.2), but they have increased specificity compared to purely passive techniques due to the presence of surface ligands.

A common problem that arises when employing active targeting ligands is developing a method to conjugate the ligand to the surface of the therapeutic agent without decreasing its affinity for the desired target. The conjugation method that is chosen must take into account both the functional groups available on the particles surface as well as the chemical structure of the ligand. Ligands can be conjugated either directly to the surface (e.g., using a disulfide or peptide bond) if the surface chemistry of the

particle allows for it or by using linker molecules such as NHS or PEG [48]. An interesting strategy that is sometimes used in active targeting is to use avidin–biotin binding to separate the targeting molecule from the nanoparticle. The targeting molecule (coupled to biotin) is administered first and then avidin-functionalized nanoparticles are administered. The particles will then bind to the biotin- tagged cells through the formation of the avidin–biotin complex [49, 50]. This targeting method offers some advantages as it can help reduce the overall size of the particle, which enhances both the particle's stealth characteristics and its ability to extravasate.

Table 42.2 Physiological abnormalities that can be utilized for passive targeting methods

Abnormality	Area of body	Result	Types of cancer that display this	Ref.
Leaky tumor vasculature	Many	Macromolecules such as polymer encapsulated drugs and diagnostic agents diffuse out of the vasculature and into the tumor interstitium where they can accumulate	Solid tumors	[15–18]
Poor lymphatic drainage system	Many	Once macromole–cules enter the tumor interstitium, they are not cleared out leading to the accumulation of therapeutic and diagnostic agents in clinically relevant levels	Solid tumors	[15–18]
Loss of phagocytosis	Liver and spleen	Tumor tissues in the liver and spleen cannot phagocytose macromolecules,	Hepatocellular carcinoma, Liver metastasis,	[19–22]

(*Contiued*)

Table 42.2 (*Contiued*)

Abnormality	Area of body	Result	Types of cancer that display this	Ref.
		while healthy liver and spleen tissues can. As a result, diagnostic agents can accumulate in healthy tissues providing added contrast against the cancer tissues.	Splenic metastasis	
Integrin expression	Activated and proliferating endothelial cells	Integrins such as $alpha_v beta_3$ are expressed on growing vasculature. Tumors have a need to recruit and form large amounts of vasculature in order to supply nutrients to their rapidly growing cell mass. As a result, the vasculature in a tumor tends to express high numbers of integrin receptors, which can be targeted by various peptide agents.	Solid tumors	[23–25]
Over-expression of surface receptors for nutrients needed for cell proliferation	Many	Due to their rapidly proliferating nature, cancer cells tend to overexpress surface receptors for molecules such as folate and transferrin, which are required for cell proliferation. These receptors can be targeted with various molecules.	Many types of cancers	[26–30]

Table 42.3 Active targeting ligands and surface receptors that are overexpressed on cancer cells

Targeting ligand	Surface receptor	References
Folic acid	Folate receptor	[26–30]
Transferrin	Transferrin receptor	[29, 30]
RGD peptides	$Alpha_v beta_3$ integrin	[23–25]
Monoclonal antibodies	Many	[31–34]
Nanobodies	Many	[35–37]
Affibodies	Many	[32, 38–41]
Aptamers	Many	[42–47]

Another advantage of active targeting is that once the agents bind to cell surface receptors, the particles are often internalized via receptor-mediated endocytosis [23, 48]. This allows the therapeutic agent to accumulate in the cytoplasm at clinically relevant levels. Since many receptor-mediated internalization pathways are fairly well characterized, it becomes possible to design "smart" agents that respond to changes in their external environment such as pH or salinity changes. These smart particles can be tailored to only release drugs once inside a cell; for example, a change in pH inside a lysosome can cause the particles to swell and release the drugs they contain.

42.4 Classes of Polymeric Nanosystems for Cancer Therapy

In chemotherapy, high concentrations of therapeutic agents are often required to achieve the desired anticancer effects. Unfortunately, when administered freely, these drugs tend to harm healthy cells in addition to cancerous tissue. Furthermore, many of the promising chemotherapeutic agents are hydrophobic compounds, making it challenging to administer them via intravenous routes in the hydrophilic internal environment of the body. The application of nanotechnology to drug delivery has allowed researchers to begin to address some of these drawbacks. Nanoscale drug delivery technologies allow for smaller doses of drug to be used for treatment, reduced toxicity to the patient, a higher localized build-up of the drug in the affected area and greater temporal stability

of drug concentrations in the tumor environment. These benefits can be realized by incorporating a desired chemotherapeutic agent in a nanoparticle delivery system. The drug–carrier complex can then be administered into the body where, with the aid of passive and active targeting methods, it will accumulate at the tumor site and begin to release the therapeutic agent while causing minimal damage to healthy tissue. The controlled release of the drug is dependent on the type of nanocarrier used, the materials it is constructed from, the procedures used to encapsulate the drug, and local environmental factors at the drug delivery site.

While each type of nanoparticle delivery system has its own advantages and disadvantages, direct comparisons between them are often not feasible or even possible. This is due to the wide variation in study conditions used to evaluate nanoparticles, which are rarely consistent. Consequently, the various classes of therapeutic carriers will be discussed with regard to their individual advantages and drawbacks, and any recent clinical implementations will be emphasized.

42.4.1 Liposomes

Liposomes are spherical vesicles composed of self-assembling amphiphilic phospholipids that can associate themselves into bilayers surrounding an aqueous core. While not strictly a polymer-based system, we have included a discussion of liposomes due to their prominence in the field of nanomedicine. Liposomes have achieved a considerable degree of clinical success as drug carriers [51] due to their versatility, ability to encapsulate a wide variety of drugs, low-toxicity, and biocompatibility, especially following surface modification with a hydrophilic polymer [52]. Drug loading into the liposomal core can be done through various methods, including performing the synthesis in drug-saturated aqueous solution and pH gradient methods [53]. Controlled drug release to the target site can be achieved by two methods. Targeted drug release involves outfitting a liposome with a ligand that upon reaching the target site will be endocytosed by the cell; following endocytosis, the increased acidity experienced by the liposome will result in the loss of its structural integrity and release of the drug. Alternatively, triggered drug release can be based upon the incorporation of materials into the liposome structure that

can respond to changes in temperature, pH, ionic strength, or irradiation in order to promote drug release [54].

Due to their aqueous core, liposomes are well suited for the containment of water-soluble molecules. FDA-approved Doxil®, which is a PEG-modified liposome product containing the water-soluble drug doxorubicin, has been used to demonstrate anti-tumor efficacy in numerous works [55], including a recent study with a doxorubicin-resistant colon cancer mouse model [56]. Poorly water-soluble drugs can also be incorporated into the lipid bilayer of the liposome, but the loading capacity may be insufficient for this purpose [57–59]. Nonetheless, a paclitaxel-carrying liposome (known by the trade name Lipusu®) has recently been approved for clinical use in China [60]. Studies on paclitaxel-containing liposomes have shown a significant increase in the tolerated dose of paclitaxel, as well as higher blood circulation times and improved anticancer efficacy for drug-resistant tumor models, when compared to free drug administration [60].

The active targeting of "stealth" liposomes that can evade the MPS and stay in the bloodstream for increased periods of time has been a focal point in modern liposome research. Polymers incorporated into the liposome bilayer, such as polyethylene glycol (PEG) and polyvinyl alcohol (PVA), increase blood circulation time but can hinder tumor interaction due to steric effects [53]. To alleviate this problem, targeting ligands such as transferrin have been conjugated to liposomes. Li et al. [53] have recently studied the biodistribution and pharmacokinetics of transferrin-targeted PEG-liposomes *in vivo.* It was found that the targeted liposomes increased drug uptake by transferrin receptor expressing cancer cells compared to non-targeted liposomes.

Despite their clinical success, the efficacy of liposomes as drug-carrying entities has been challenged due to problems arising *in vivo* with respect to their stability and controlled drug release [58, 61, 62]. Blood circulation times also remain limited as even targeted liposomes accumulate most readily in the liver and spleen [51, 53]. In addition, problems with batch-to-batch reproducibility, effective scale-up and sterilization have been brought to light [54].

In recent years, novel liposome-based nanocarriers have been developed. For instance, hybrid liposome-block copolymer nanocarrier platforms consisting of a hydrophobic core, a hydrophilic

shell and a lipid monolayer at the interface have been explored [52]. Additionally, lipid nanocapsules, which are composed of a triglyceride core and a shell made from polymers and surfactants, may have several important advantages over liposomes such as improved stability and a higher capacity for drug encapsulation [58].

42.4.2 Polymer–Drug Conjugates

Drugs can be conjugated to the backbones of water-soluble polymers to increase their blood circulation time and prolong their therapeutic effects. The most commonly used polymer for drug conjugation is N-(2-hydroxypropyl) methacrylamide (HPMA) [63]; it has a long history of clinical success [57]. Other polymers such as PEG, polyglutamate, cyclodextrin, dextran, and carboxymethyldextran have been conjugated with drugs such as doxorubicin, camptothecin, and paclitaxel [64]. Many of these conjugates, which are in various stages of clinical or pre-clinical trials [63, 65], have shown improved therapeutic efficacy over free drug administration. For instance, a PEG-camptothecin conjugate has been shown to improve the *in vivo* stability of the drug, and enhance cell uptake and apoptosis in a nude mouse model of human colon cancer xenografts when compared to the free-acting drug [66]. Drug release rates of polymer–drug conjugates can also be controlled in various ways, such as the use of spacer groups that respond to certain changes in pH or temperature by undergoing hydrolytic degradation [67]. Recently, the potential to use polymer–drug conjugates for combination drug therapy (multiple drugs conjugated to each polymer chain) has been reviewed [68].

Biodegradable polymeric nanoparticles can also be used to encapsulate drugs without covalent bonding. Drug release in this case is typically achieved by controlling diffusion through the polymer matrix or the surface, or by bulk erosion of the nanoparticle [32, 64]. The most common polymers used for this purpose are PEG, poly(lactic acid) (PLA), poly(glycolic acid) (PGA), poly(lactic-co-glycolic) acid (PLGA) and carbohydrates such as chitosan and dextran [64, 69, 70]. Some of the current challenges of polymer–drug conjugate development include molecular weight heterogeneity, difficulties in site-specific conjugation and low drug loading [63].

42.4.3 Polymeric Micelles

Polymeric micelles are core–shell particles in the nanoscale size range formed from amphiphilic block copolymers. They have been investigated extensively for drug delivery applications [59, 64, 70–72]. Polymeric micelles are a very promising technology and have achieved a degree of clinical success. While their small size can provide many advantages, it is also somewhat of a disadvantage because it constrains the amount of drug that can be incorporated into the core and can lead to difficulties with controlling drug release [59]. This example is typical of a design trade-off encountered in nanoparticle formulation, as small size enhances the biodistribution and pharmacokinetic properties while limiting the amount of therapeutic agent that can be encapsulated.

The core of a typical polymeric micelle consists of a hydrophobic polymer, such as PLA, PLGA, poly(ε-caprolactone) (PCL) or poly(L-aspartic acid) (PLAA), which allows for the incorporation of poorly water-soluble drugs. Drugs are typically loaded into the core via physical entrapment [73], although covalent bonding of drug to polymer can also be done in this context [74]. The core significantly increases the water solubility of hydrophobic drugs while protecting them from enzymatic degradation [59]. The outside layer of the micelle is hydrophilic, most often made from PEG or poly(N-vinyl-2-pyrrolidone) (PVP), and its main role is to improve the micelle's biocompatibility and bioavailability. Despite the various polymer and drug combinations that have been explored for their potential as polymeric micelle carriers, relatively few are undergoing clinical trials [71, 75]. Two of these, NK911 and NK105, are doxorubicin and paclitaxel carriers respectively, and are composed of PEG-PLAA with strong antitumor activities compared to the free drug [76, 77]. Another formulation of Paclitaxel with mPEG-poly(D,L-lactide) micelles has recently completed Phase II clinical trials and has shown tolerance at doses of 300 mg/m^2 over 3 weeks [78]. In addition, a PEG-Poly(glutamic acid) block copolymer has been used for forming Cisplatin complexes (NC 6004) and for encapsulating SN-38 (7-ethyl-10-hydroxy-camptothecin) (NK012), both of which have completed Phase I clinical trials [79].

Poloxamers (known by the trade name Pluronics®) are triblock copolymers composed of polyethylene oxide (PEO) and

propylene oxide (PPO). In this configuration, the hydrophobic PPO is sandwiched between two units of the hydrophilic PEO in the sequence PEO-PPO-PEO. Poloxamers have been used to form polymeric micelles for anticancer drug delivery [80]. Interestingly, poloxamers have been shown to have bioactive capabilities independent of the drug used, including the preferential targeting of cancer cells and suppression of surface proteins that cause cancer drug resistance [81].

42.4.4 Dendrimers

The class of synthetic, highly branched, spherical macromolecules known as dendrimers has gained prominence as an effective type of drug nanocarrier. Typically 1.5–14.5 nm in size, dendrimer molecules contain a central core surrounded by repeating units of highly branched layers with active terminal groups (Fig. 42.1) [32]. The most commonly used dendrimer backbone is polyamidoamine (PAMAM) [82], largely because it is biocompatible with a well-defined structure and can be easily conjugated with other molecules including drugs, targeting ligands and fluorophores for visualization. PAMAM dendrimers are also very small (<5 nm), which allows for them to be cleared from the body very quickly via the kidneys [61]. This fact lessens their potential toxicity but also can present challenges with respect to achieving sufficient accumulation at the target site [62].

Dendrimers have been shown to increase drug efficacy. Paclitaxel conjugated to a PAMAM dendrimer showed a tenfold increase in anticancer activity over the free-acting drug during an *in vitro* cytotoxicity assessment on A2780 human ovarian carcinoma cells [83]. In addition, the way that dendrimers are synthesized provides for a high degree of control over their biodistribution, pharmacokinetic properties, structural monodispersity, chemical homogeneity, and degradation kinetics [82, 84]. Perhaps the biggest advantage of dendrimers is their multivalent nature, which allows for high drug-loading and ligand attachment capacity, as well as the ability for combined conjugation of several types of drugs and targeting ligands to each dendrimer molecule. Dendrimers' lack of clinical success stems in part from their complex, multi-step synthesis, high cost of production and the high degree of process control that is required to maintain the heterogeneous properties of the product [82].

42.5 Synthesis Methods

As discussed previously, there is an array of nanoparticle systems for enhancing the therapeutic efficacy of a variety of drugs. A number of synthesis methods have been developed over the years in order to create nanoparticle systems with the desired set of physio-chemical characteristics. The choice of synthesis method is a key design decision that should take into consideration the types of materials that are being used, the chemical nature of the encapsulated therapeutic agent, and the desired physiological application. This section presents an outline of various synthesis methods for some common nanoparticle systems and aims to give the reader a general idea of some of the techniques, strategies, and important considerations involved in their use.

42.5.1 Polymer Synthesis

Polymers can be divided into two categories: linear and branched. Both of these polymer types have unique properties and take advantage of different qualities of the polymers. In nanomedicine, typically two or more polymers are combined to extract all of their strengths while overcoming the individual weaknesses of each polymer. A variety of polymers have been synthesized and studied for drug-delivery applications including polyesters, polyamides, and polyamines. Copolymers are synthesized to utilize the properties of multiple different polymers in one system. These copolymers can either be block copolymers, graft copolymers, dendritic copolymers or a combination of these three. One of the uses of copolymers is to improve the solubility of hydrophobic drugs and the biocompatibility of the nanocarrier. Typically, this is achieved by creating a hydrophobic core and a hydrophilic corona, which can also be utilized for surface functionalization. The corona is typically chosen so as to impart biocompatibility and can be modified with ligands for targeting purposes.

42.5.1.1 Block copolymers

Block copolymers are linear polymers with two or more polymer chains attached to each other from end-to-end. Such copolymers can be synthesized in a few different ways. One of the methods is ring-opening polymerization, where a catalyst such as stannous

(II) octoate is used for the polymerization of the monomers onto an initiator that is linked to the other block (Fig. 42.2).

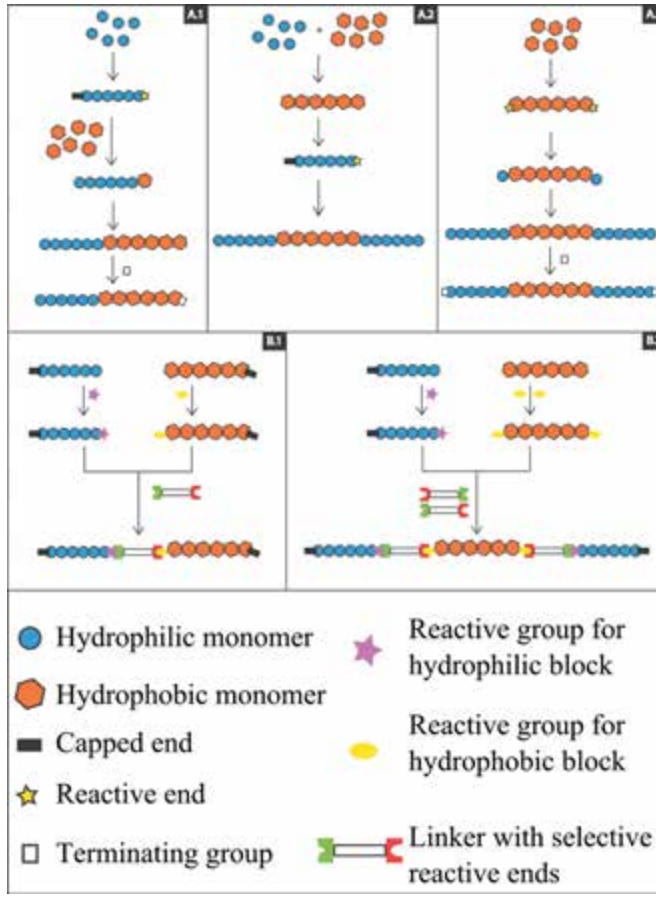

Figure 42.2 Strategies employed for the synthesis of block copolymers: (A) Synthesis of amphiphilic block copolymers starting from monomers by either (1) growing each block in a sequential manner to make a diblock copolymer, (2) sequential growth of each block starting from monomers and conjugation by reactive ends to make a triblock copolymer, or (3) synthesizing a triblock copolymer by the use of reactive ends on one block as initiator for the other two blocks; and (B) Starting from synthesized polymers and utilizing a bifunctional cross-linker to make (1) a diblock copolymer, or (2) a triblock copolymer.

Polymerization is stopped by using a terminator such as H^+. The length of the polymer is determined by the molar ratio of the initiator and the monomer added to the reaction. The diblock copolymers can then also be cross-linked to form triblock copolymers. Examples of this approach are illustrated in the synthesis of poly(DL-lactic acid)-*block*-poly(ethylene oxide) [85, 86], poly(DL-lactic acid)-*block*-poly(ethylene oxide)-*block*-poly(DL-lactic acid) [87], and poly(ethylene oxide)-*block*-poly(aspartic acid-Adriamycin) [88].

Another approach for the synthesis of block copolymers involves the use of a linker possessing multiple functional groups that can react specifically to the ends of each block. This requires the polymer blocks to be either protected or reactive at the ends depending on the desired result and application. Such an approach is illustrated in Fig. 42.2 and demonstrated in the synthesis of poly(DL-lactic-co-glycolic acid)-*block*-mono methoxy poly(ethyleneglycol) [89, 90].

Once block copolymers are synthesized and purified, they can be used for drug entrapment and/or undergo surface modification to include targeting ligands. Drug entrapment can be performed chemically or physically. The chemical method requires the conjugation of the drug to one of the blocks, whereas the physical approach involves the entrapment of the drug by hydrophobic interactions and is discussed in further detail in Section 42.5.2.

42.5.1.2 Graft copolymers

Branched copolymers are also used for drug delivery purposes. Graft copolymers are a subset of branched polymers, which comprise one backbone onto which several polymer segments are implanted or grafted. One of the methods of synthesizing graft copolymers is to use the polymer to be grafted on as a macromonomer and then creating the backbone by the respective monomers. Such an example can be seen in the synthesis of poly(N-isopropylacrylamide-co-methacrylic acid)-graft-poly(D,L-lactide) [91]. An alternate method is to synthesize each of the polymers first and then use specific functional groups on the backbone to add the other polymer. An example of this method of synthesis is seen in poly(ethyleneglycol)-g-poly(L-lysine) [92, 93]. Both these methods are illustrated in Fig. 42.3.

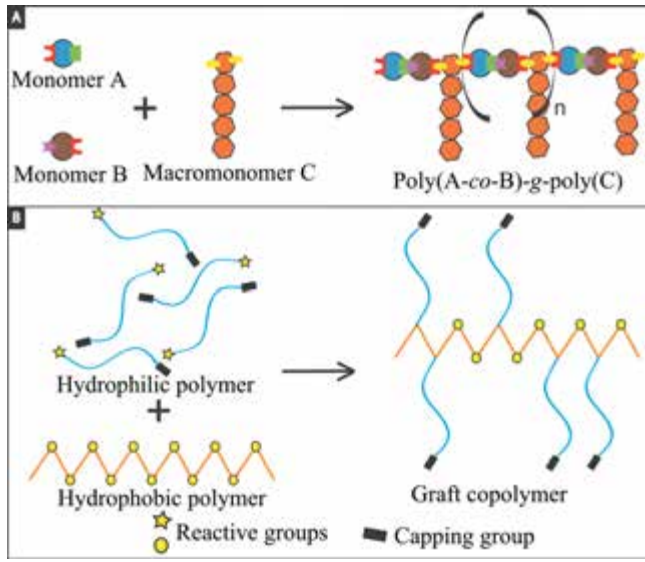

Figure 42.3 Strategies employed for the synthesis of graft copolymers: (A) monomers used as initiators, or (B) cross-linking of polymers.

42.5.1.3 Dendrimers

Dendrimers are well known for their highly controllable, multi-step synthesis. Each completed step is termed a generation; it is the buildup of these generations that determines the number of layers or shells and hence the size of the dendrimer [84]. Synthesis starts with an initiator, which is then reacted with monomers in an appropriate molar ratio. Repeating cycles of initiators and monomers are added to build up the dendrimer branches. Throughout this process the molar ratios of different monomers, as well as initiators and monomers, need to be controlled to end up with the desired number of reactive terminals [94].

42.5.2 Nanoparticle Formulations

42.5.2.1 Nanoprecipitation

A commonly used method of preparing nanoparticles from amphiphilic polymers is “nanoprecipitation” [95]. The first step in this process is to dissolve the polymer in an organic phase capable

of solubilizing both blocks of the polymer. The solvent used for this step must be miscible with water and is typically volatile for easy removal by evaporation. The organic phase with the dissolved polymer is then added slowly to water under magnetic stirring. Upon mixing with the water phase, the polymers will self-assemble into micelles with their hydrophobic blocks on the interior of the particles in order to remove them from contact with the water phase. The organic solvent is then removed by evaporation to form stable nanoparticles. Further purification can be done by ultracentrifugation or lyophilization, which will also remove water. In order to encapsulate drugs, the drug is dissolved in the same solvent as the amphiphilic polymer before adding it to water. The choice of solvent has been shown to affect particle size; solvents that are more water miscible seem to result in smaller nanoparticles [90]. Some examples of polymers and particle sizes observed from the nanoprecipitation method are summarized in Table 42.4.

Table 42.4 Copolymer types used to form nanoparticles via the nanoprecipitation method

Polymer	Solvent	Particle size range	Ref.
Poly[aminopoly(ethylene glycol) cyanoacrylate-co-hexadecyl cyanoacrylate]	Acetone	96 ± 9 nm	[96]
Poly(DL-lactic-co-glycolic acid)-*block*-mono methoxy poly(ethyleneglycol)	Acetone	61.5 ± 7.2 nm	[97]
Blends of poly(DL-lactic acid) and poly(DL-lactic acid)-mono methoxy poly(ethyleneglycol)	Acetone	74.8–230.6 nm	[98]
Poly(DL-lactic-co-glycolic acid)-*block*-mono methoxy poly(ethyleneglycol)	Acetonitrile	77.0–111.2 nm	[98]

42.5.2.2 Double emulsion

When the encapsulation of hydrophilic drugs is required, the nanoprecipitation method must be modified with an additional step involving a water/oil/water emulsion. The hydrophilic drug

is dissolved in water and then emulsified in an organic solution of the polymer by using an ultrasonicator. This emulsion is then added to an aqueous solution to form nanoparticles. This procedure was exemplified in the encapsulation of cisplatin in monomethoxy poly(ethylene glycol)-poly(lactic-co-glycolic acid) [99], which formed nanoparticles of sizes ranging from 112.0 to 152.3 nm. Thus, both hydrophilic and hydrophobic drugs can be encapsulated in nanoparticles formed by amphiphilic polymers.

42.5.2.3 Layer by layer assembly

Layer by layer assembly is a method that utilizes the interactions between different polymer species such as electrostatic interactions or interactions between hydrophobic and hydrophilic domains. A substrate (or drug) is first coated with one of the polymer species through some type of interaction (e.g., cationic drug and anionic polymer). Then the second species is added into solution where it will interact with the first species to form a layer. The different species can be successively added to the solution to build up many alternating layers around the payload agent. This method and its applications have been explored in detail in a review by Tang et al. [100].

42.6 Conclusions

Nanoparticle systems have an amazing potential to greatly enhance the treatment of a variety of diseases including cancer. In this chapter, we have summarized a number of different technologies currently being investigated for this purpose. One of the most important considerations in nanomedicine is how nanomaterials interact with the various body systems once they have been administered. The engineering of parameters such as particle size, surface charge, hydrophilicity, surface coating, and polymer conformation is crucial for achieving a desired pharmacokinetic profile and maintaining biocompatibility. One of the great promises of nanotechnology-based therapeutics is their ability to target and segregate to specific sites in the body. As new research continues to improve our understanding of the physiological abnormalities in cancerous tissue and their unique protein expression profiles, our ability to target them will continue to develop.

Anti-cancer drug delivery with nanoparticle systems, such as liposomes, polymer–drug conjugates, polymeric micelles, and dendrimers, is a vast research field that aims to deliver and release drugs in a controlled manner to the target site while minimizing the side effects present in traditional drug therapy. So far, only liposomes, polymer–drug conjugates and polymeric micelles have undergone extensive clinical trials, though challenges remain in various aspects of their implementation. The huge wave of interest in nanotechnology and biomedicine has given researchers the tools to create new and promising methods for diagnosis and treatment. Some of these are already commercialized while others are still at the experimental stage [101, 102]. With input from federal agencies such as the Food and Drug Administration [103] and the Patent and Trademark Office [104], as ongoing research continues in this field, it is apparent that more and more of these methods will come to fruition. As we enter the age of nanotheranostics [105], it is likely that nanomedicine will become the premier tool for dealing with terminal illnesses such as cancer.

Disclosures and Conflict of Interest

The Laboratory of Advanced Targeted Delivery Systems at the University of Waterloo, Canada, is funded by the Natural Sciences and Engineering Research Council of Canada (NSERC). Mohit S. Verma is funded by NSERC Canada Vanier Graduate Scholarship.

The authors declare that they have no conflict of interest and have no affiliations or financial involvement with any organization or entity discussed in this chapter. This includes employment, consultancies, honoraria, grants, stock ownership or options, expert testimony, patents (received or pending) or royalties. No writing assistance was utilized in the production of this chapter and the authors have received no payment for its preparation. The findings and conclusions here reflect the current views of the authors. They should not be attributed, in whole or in part, to the organizations with which they are affiliated, nor should they be considered as expressing an opinion with regard to the merits of any particular company or product discussed herein. Nothing contained herein is to be considered as the rendering of legal advice.

Corresponding Author

Dr. Frank X. Gu
Department of Chemical Engineering, University of Waterloo
200 University Avenue West, Waterloo, Ontario, N2L 3G1, Canada
Email: frank.gu@uwaterloo.ca

About the Authors

Mohit Verma is a PhD candidate in Prof. Frank Gu's laboratory at the University of Waterloo, Canada. He received his BASc in Nanotechnology Engineering from the University of Waterloo. He is the recipient of Vanier Canada Graduate Scholarship and three Undergraduate Student Research Awards from Natural Sciences and Engineering Research Council of Canada as well as President's Research Awards from University of Waterloo (2008–2010). His research interests are the development of nanotechnology for biomedical, environmental, and electronic applications.

Joshua Rosen is a medical student at Yale University, New Haven, USA. He received his BASc in Nanotechnology Engineering from the University of Waterloo while working in Prof. Frank Gu's research laboratory as a research assistant. He has received three Undergraduate Student Research Awards from the Natural Sciences and Engineering Research Council of Canada as well as the Dean's Undergraduate Award from the University of Waterloo. His research interests center on the development of nanotechnologies to enhance both the treatment and diagnosis of disease.

Ameena Meerasa is currently a medical student at the University of Toronto, Canada. She received her BASc in Nanotechnology Engineering from the University of Waterloo in 2012, at which time she worked in Prof. Frank Gu's Research group as a research assistant in the development of an assay for the assessment of material biocompatibility

and toxicity in nanomedicine. In 2010, she was awarded the Undergraduate Student Research Award from the Natural Sciences and Engineering Research Council of Canada (NSERC).

Serge Yoffe received his MEng from the University of Waterloo, Canada. He was a graduate student in Prof. Frank Gu's laboratory (2009–2010) with a research focus on nanomaterials for biomedical applications. He was the recipient of the Best Presentation prize at the University of Waterloo Graduate Student Conference in 2009.

Dr. Frank Gu received his BSc from Trent University and PhD from Queen's University, Canada, where he majored in chemical engineering. In 2006, he was awarded a NSERC Postdoctoral Fellowship to purse his research at the Massachusetts Institute of Technology and Harvard Medical School. Dr. Gu joined Department of Chemical Engineering at the University of Waterloo as an assistant professor in 2008. He currently holds a Canada Research Chair in Advanced Targeted Delivery Systems. His current research interests include the development of biomaterials for nanomedicine and biopharmaceutics applications and improvement of the therapeutic index of currently available drugs by optimizing their efficacy and toxicity. His research on the formulation of disease-targeted nanoparticles has generated over 40 scientific publications and 15 pending patent applications, some of which have been licensed to biotechnology companies as their core technologies for manufacturing clinical grade targeted nanoparticles.

References

1. Li, S., Huang, L. (2008). Pharmacokinetics and biodistribution of nanoparticles. *Mol. Pharm.,* **5**(4), 496–504.
2. Alexis, F., Farokhzad, O. C., Pridgen, E., Molnar, L. K. (2008). Factors affecting the clearance and biodistribution of polymeric nanoparticles. *Mol. Pharm.,* **5**(4), 505–515.
3. Marquis, B. J., Love, S. A., Braun, K. L., Haynes, C. L. (2009). Analytical methods to assess nanoparticle toxicity. *Analyst,* **134**(3), 425–439.

4. Aggarwal, P., Hall, J. B., McLeland, C. B., Dobrovolskaia, M. A., McNeil, S. E. (2009). Nanoparticle interaction with plasma proteins as it relates to particle biodistribution, biocompatibility and therapeutic efficacy. *Adv. Drug Deliv. Rev.,* **61**(6), 428–437.
5. Dobrovolskaia, M. A., Aggarwal, P., Hall, J. B., McNeil, S. E. (2008). Preclinical studies to understand nanoparticle interaction with the immune system and its potential effects on nanoparticle biodistribution. *Mol. Pharm.,* **5**(4), 487–495.
6. Jiskoot, W., Schie, R., Carstens, M., Schellekens, H. (2009). Immunological risk of injectable drug delivery systems. *Pharm. Res.,* **26**(6), 1303–1314.
7. Moghimi, S. M., Szebeni, J. (2003). Stealth liposomes and long circulating nanoparticles: Critical issues in pharmacokinetics, opsonization and protein-binding properties. *Prog. Lipid Res.,* **42**(6), 463–478.
8. Moghimi, S. M., Hunter, A. C., Murray, J. C. (2001). Long-circulating and target-specific nanoparticles: Theory to practice. *Pharm. Rev.,* **53**(2), 283–318.
9. Owens, D. E., Peppas, N. A. (2006). Opsonization, biodistribution, and pharmacokinetics of polymeric nanoparticles. *Int. J. Pharm.,* **307**(1), 93–102.
10. Vonarbourg, A., Passirani, C., Saulnier, P., Benoit, J.-P. (2006). Parameters influencing the stealthiness of colloidal drug delivery systems. *Biomaterials,* **27**(24), 4356–4373.
11. Meerasa, A., Huang, J. G., Gu, F. X. (2011). CH(50): A revisited hemolytic complement consumption assay for evaluation of nanoparticles and blood plasma protein interaction. *Curr. Drug Deliv.,* **8**(3), 290–298.
12. Qu, X., Wu, Q., Chen, G. (2006). *In vitro* study on hemocompatibility and cytocompatibility of poly(3-hydroxybutyrate-co-3-hydroxyhexanoate). *J. Biomater. Sci.-Polym. Ed.,* **17**(10), 1107–1121.
13. Chithrani, B. D., Ghazani, A. A., Chan, W. C. W. (2006). Determining the size and shape dependence of gold nanoparticle uptake into mammalian cells. *Nano Lett.,* **6**(4), 662–668.
14. Yague, C., Moros, M., Grazu, V., Arruebo, M., Santamaria, J. (2008). Synthesis and stealthing study of bare and PEGylated silica micro- and nanoparticles as potential drug-delivery vectors. *Chem. Eng. J.,* **137**(1), 45–53.
15. Noguchi, Y., Wu, J., Duncan, R., Strohalm, J., Ulbrich, K., et al. (1998). Early phase tumor accumulation of macromolecules: A great difference

in clearance rate between tumor and normal tissues. *Japanese J. Cancer Res.,* **89**(3), 307–314.

16. Brannon-Peppas, L., Blanchette, J. O. (2004). Nanoparticle and targeted systems for cancer therapy. *Adv. Drug Deliv. Rev.,* **56**(11), 1649–1659.
17. Iyer, A. K., Khaled, G., Fang, J., Maeda, H. (2006). Exploiting the enhanced permeability and retention effect for tumor targeting. *Drug Discov. Today,* **11**(17–18), 812–818.
18. Rosen, J. E., Chan, L., Shieh, D. B., Gu, F. X. (2012). Iron oxide nanoparticles for targeted cancer imaging and diagnostics. *Nanomed. Nanotechnol. Biol. Med.,* **8**(3), 275–290.
19. Weissleder, R., Hahn, P. F., Stark, D. D., Elizondo, G., Saini, S., et al. (1988). Superparamagnetic iron-oxide–enhanced detection of focal splenic tumors with MR imaging. *Radiology,* **169**(2), 399–403.
20. Imai, Y., Murakami, T., Yoshida, S., Nishikawa, M., Ohsawa, M., et al. (2000). Superparamagnetic iron oxide-enhanced magnetic resonance images of hepatocellular carcinoma: Correlation with histological grading. *Hepatology,* **32**(2), 205–212.
21. Saini, S., Stark, D. D., Hahn, P. F., Bousquet, J. C., Introcasso, J., et al. (1987). Ferrite particles: A superparamagnetic MR contrast agent for enhanced detection of liver-carcinoma. *Radiology,* **162**(1), 217–222.
22. Stark, D. D., Weissleder, R., Elizondo, G., Hahn, P. F., Saini, S., et al. (1988). Superparamagnetic iron-oxide: Clinical application as a contrast agent for MR imaging of the liver. *Radiology,* **168**(2), 297–301.
23. Zhang, C., Jugold, M., Woenne, E. C., Lammers, T., Morgenstern, B., et al. (2007). Specific targeting of tumor angiogenesis by RGD-conjugated ultrasmall superparamagnetic iron oxide particles using a clinical 1.5-T magnetic resonance scanner. *Cancer Res.,* **67**(4), 1555–1562.
24. Brooks, P. C., Clark, R. A. F., Cheresh, D. A. (1994). Requirement of vascular integrin alpha(v)beta(3) for angiogenesis. *Science,* **264** (5158), 569–571.
25. Cai, W., Rao, J., Gambhir, S. S., Chen, X. (2006). How molecular imaging is speeding up antiangiogenic drug development. *Mol. Cancer Ther.,* **5**(11), 2624–2633.
26. Weitman, S. D., Lark, R. H., Coney, L. R., Fort, D. W., Frasca, V., et al. (1992). Distribution of the folate receptor Gp38 in normal and malignant-cell lines and tissues. *Cancer Res.,* **52**(12), 3396–3401.
27. Ross, J. F., Chaudhuri, P. K., Ratnam, M. (1994). Differential regulation of folate receptor isoforms in normal and malignant tissues *in vivo*

and in established cell-lines: Physiological and clinical implications. *Cancer,* **73**(9), 2432–2443.

28. Sun, C., Sze, R., Zhang, M. (2006). Folic acid-PEG conjugated superparamagnetic nanoparticles for targeted cellular uptake and detection by MRI. *J. Biomed. Mater. Res. Part A,* **78A**(3), 550–557.
29. Wagner, E., Curiel, D., Cotten, M. (1994). Delivery of drugs, proteins and genes into cells using transferrin as a ligand for receptor-mediated endocytosis. *Adv. Drug Deliv. Rev.,* **14**(1), 113–135.
30. Daniels, T. R., Delgado, T., Rodriguez, J. A., Helguera, G., Penichet, M. L. (2006). The transferrin receptor part I: Biology and targeting with cytotoxic antibodies for the treatment of cancer. *Clin. Immunol.,* **121**(2), 144–158.
31. Allen, T. M. (2002). Ligand-targeted therapeutics in anticancer therapy. *Nat. Rev. Cancer,* **2**(10), 750–763.
32. Gu, F. X., Karnik, R., Wang, A. Z., Alexis, F., Levy-Nissenbaum, E., et al. (2007). Targeted nanoparticles for cancer therapy. *Nano Today,* **2**(3), 14–21.
33. Weissleder, R., Lee, A. S., Khaw, B. A., Shen, T., Brady, T. J. (1992). Antimyosin-labeled monocrystalline iron-oxide allows detection of myocardial infarct: MR antibody imaging. *Radiology,* **182**(2), 381–385.
34. Toma, A., Otsuji, E., Kuriu, Y., Okamoto, K., Ichikawa, D., et al. (2005). Monoclonal antibody A7-superparamagnetic iron oxide as contrast agent of MR imaging of rectal carcinoma. *Br. J. Cancer,* **93**(1), 131–136.
35. Wesolowski, J., Alzogaray, V., Reyelt, J., Unger, M., Juarez, K., et al. (2009). Single domain antibodies: Promising experimental and therapeutic tools in infection and immunity. *Med. Microbiol. Immunol.,* **198**(3), 157–174.
36. Willuda, J., Honegger, A., Waibel, R., Schubiger, P. A., Stahel, R., et al. (1999). High thermal stability is essential for tumor targeting of antibody fragments: Engineering of a humanized anti-epithelial glycoprotein-2 (epithelial cell adhesion molecule) single-chain fv fragment. *Cancer Res.,* **59**(22), 5758–5767.
37. Cortez-Retamozo, V., Backmann, N., Senter, P. D., Wernery, U., De Baetselier, P., et al. (2004). Efficient cancer therapy with a nanobody-based conjugate. *Cancer Res.,* **64**(8), 2853–2857.
38. Nord, K., Gunneriusson, E., Ringdahl, J., Stahl, S., Uhlen, M., et al. (1997). Binding proteins selected from combinatorial libraries of an alpha-helical bacterial receptor domain. *Nat. Biotechnol.,* **15**(8), 772–777.

39. Ronnmark, J., Gronlund, H., Uhlen, M., Nygren, P. A. (2002). Human immunoglobulin A (IgA)-specific ligands from combinatorial engineering of protein A. *Eur. J. Biochem.,* **269**(11), 2647–2655.

40. Alexis, F., Basto, P., Levy-Nissenbaum, E., Radovic-Moreno, A. F., Zhang, L., et al. (2008). HER-2-targeted nanoparticle-affibody bioconjugates for cancer therapy. *ChemMedChem,* **3**(12), 1839–1843.

41. Wikman, M., Steffen, A. C., Gunneriusson, E., Tolmachev, V., Adams, G. P., et al. (2004). Selection and characterization of HER2/neu-binding affibody ligands. *Protein Eng. Des. Sel.,* **17**(5), 455–462.

42. Dhar, S., Gu, F. X., Langer, R., Farokhzad, O. C., Lippard, S. J. (2008). Targeted delivery of cisplatin to prostate cancer cells by aptamer functionalized pt(IV) prodrug-PLGA-PEG nanoparticles. *Proc. Natl. Acad. Sci. U. S. A.,* **105**(45), 17356–17361.

43. Barbas, A. S., White, R. R. (2009). The development and testing of aptamers for cancer. *Curr. Opin. Invest. Drugs,* **10**(6), 572–578.

44. Chen, X. S. (2011). Introducing theranostics journal: From the editor-in-chief. *Theranostics,* **1**(1), 1–2.

45. Ellington, A. D., Szostak, J. W. (1990). *In vitro* selection of RNA molecules that bind specific ligands. *Nature,* **346**(6287), 818–822.

46. Gold, L. (1995). Oligonucleotides as research, diagnostic, and therapeutic agents. *J. Biol. Chem.,* **270**(23), 13581–13584.

47. Shangguan, D., Meng, L., Cao, Z. C., Xiao, Z., Fang, X., et al. (2008). Identification of liver cancer-specific aptamers using whole live cells. *Trends Anal. Chem.,* **80**(3), 721–728.

48. Sonvico, F., Mornet, S., Vasseur, S., Dubernet, C., Jaillard, D., et al. (2005). Folate-conjugated iron oxide nanoparticles for solid tumor targeting as potential specific magnetic hyperthermia mediators: Synthesis, physicochemical characterization, and *in vitro* experiments. *Bioconjug. Chem.,* **16**(5), 1181–1188.

49. Hainsworth, J. E. S., Harrison, P., Mather, S. J. (2006). Novel preparation and characterization of a trastuzumab-streptavidin conjugate for pretargeted radionuclide therapy. *Nucl. Med. Commun.,* **27**(5), 461–471.

50. Yu, A., Choi, J., Ohno, K., Levin, B., Rom, W. N., et al. (2000). Specific cell targeting for delivery of toxins into small-cell lung cancer using a streptavidin fusion protein complex. *DNA Cell Biol.,* **19**(7), 383–388.

51. Torchilin, V. P. (2005). Recent advances with liposomes as pharmaceutical carriers. *Nat. Rev. Drug Discov.,* **4**(2), 145–160.

52. Zhang, L., Gu, F. X., Wang, A. Z., Radovic-Moreno, A. F., Alexis, F., et al. (2008). Self-assembled Lipid–Polymer hybrid nanoparticles: A robust drug delivery platform. *ACS Nano,* **2**(8), 1696–1702.

53. Li, X., Ding, L., Xu, Y., Wang, Y., Ping, Q. (2009). Targeted delivery of doxorubicin using stealth liposomes modified with transferrin. *Int. J. Pharm.,* **373**(1–2), 116–123.

54. Gomez-Hens, A., Fernandez-Romero, J. M. (2006). Analytical methods for the control of liposomal delivery systems. *Trends Anal. Chem.,* **25**(2), 167–178.

55. O'Brien, M. E. R., Wigler, N., Inbar, M., Rosso, R., Grischke, E., et al. (2004). Reduced cardiotoxicity and comparable efficacy in a phase III trial of pegylated liposomal doxorubicin HCl (CAELYX™/Doxil®) versus conventional doxorubicin for first-line treatment of metastatic breast cancer. *Ann. Oncol.,* **15**(3), 440–449.

56. Ogawara, K., Un, K., Tanaka, K., Higaki, K., Kimura, T. (2009). *In vivo* anti-tumor effect of PEG liposomal doxorubicin (DOX) in DOX-resistant tumor-bearing mice: Involvement of cytotoxic effect on vascular endothelial cells. *J. Control. Release,* **133**(1), 4–10.

57. Khemtong, C., Kessinger, C. W., Gao, J. (2009). Polymeric nanomedicine for cancer MR imaging and drug delivery. *Chem. Commun.,* **28**(24), 3497–3510.

58. Huynh, N. T., Passirani, C., Saulnier, P., Benoit, J. P. (2009). Lipid nanocapsules: A new platform for nanomedicine. *Int. J. Pharm.,* **379**(2), 201–209.

59. Blanco, E., Kessinger, C. W., Sumer, B. D., Gao J. (2009). Multifunctional micellar nanomedicine for cancer therapy. *Exp. Biol. Med.,* **234**(2), 123–131.

60. Zhang, Q., Huang, X., Gao, L. (2009). A clinical study on the premedication of paclitaxel liposome in the treatment of solid tumors. *Biomed. Pharm.,* **63**(8), 603–607.

61. Peer, D., Karp, J. M., Hong, S., Farokhzad, O. C., Margalit, R., et al. (2007). Nanocarriers as an emerging platform for cancer therapy. *Nat. Nanotechnol.,* **2**(12), 751–760.

62. Arruebo, M., Fernandez-Pacheco, R., Ibarra, M. R., Santamaria, J. (2007). Magnetic nanoparticles for drug delivery. *Nano Today,* **2**(3), 22–32.

63. Li, C., Wallace, S. (2008). Polymer–drug conjugates: Recent development in clinical oncology. *Adv. Drug Deliv. Rev.,* **60**(8), 886–898.

64. Verma, M. S., Liu, S., Chen, Y. Y., Meerasa, A., Gu, F. X. (2012). Size-tunable nanoparticles composed of dextran-b-poly(D,L-lactide) for drug delivery applications. *Nano Res.,* **5**(1), 49–61.

65. Duncan, R. (2003). The dawning era of polymer therapeutics. *Nat. Rev. Drug Discov.,* **2**(5), 347–360.
66. Yu, D., Peng, P., Dharap, S. S., Wang, Y., Mehlig, M., et al. (2005). Antitumor activity of poly(ethylene glycol)-camptothecin conjugate: The inhibition of tumor growth *in vivo*. *J. Control. Release,* **110**(1), 90–102.
67. Park, J. H., Lee, S., Kim, J. -H., Park, K., Kim, K., et al. (2008). Polymeric nanomedicine for cancer therapy. *Prog. Polym. Sci.,* **33**(1), 113–137.
68. Greco, F., Vicent, M. J. (2009). Combination therapy: Opportunities and challenges for polymer–drug conjugates as anticancer nanomedicines. *Adv. Drug Deliv. Rev.,* **61**(13), 1203–1213.
69. Malam, Y., Loizidou, M., Seifalian, A. M. (2009). Liposomes and nanoparticles: Nanosized vehicles for drug delivery in cancer. *Trends Pharm. Sci.,* **30**(11), 592–599.
70. Verma, M. S., Gu, F. X. (2012). Microwave-enhanced reductive amination via Schiff's base formation for block copolymer synthesis. *Carbohydr. Polym.,* **87**(4), 2740–2744.
71. Torchilin, V. P. (2007). Micellar nanocarriers: Pharmaceutical perspectives. *Pharm. Res.,* **24**(1), 1–16.
72. Kim, S., Shi, Y., Kim, J. Y., Park, K., Cheng, J. (2010). Overcoming the barriers in micellar drug delivery: Loading efficiency, *in vivo* stability, and micelle–cell interaction. *Expert Opin. Drug Deliv.,* **7**(1), 49–62.
73. Kim, J. O., Kabanov, A. V., Bronich, T. K. (2009). Polymer micelles with cross-linked polyanion core for delivery of a cationic drug doxorubicin. *J. Control. Release,* **138**(3), 197–204.
74. Yokoyama, M., Okano, T., Sakurai, Y., Ekimoto, H., Shibazaki, C., et al. (1991). Toxicity and antitumor activity against solid tumors of micelle-forming polymeric anticancer drug and its extremely long circulation in blood. *Cancer Res.* **51**(12), 3229–3236.
75. Yokoyama, M. (2010). Polymeric micelles as a new drug carrier system and their required considerations for clinical trials. *Expert Opin. Drug Deliv.,* **7**(2), 145–158.
76. Nakanishi, T., Fukushima, S., Okamoto, K., Suzuki, M., Matsumura, Y., et al. (2001). Development of the polymer micelle carrier system for doxorubicin. *J. Control. Release,* **74**(1–3), 295–302.
77. Hamaguchi, T., Matsumura, Y., Suzuki, M., Shimizu, K., Goda, R., et al. (2005). NK105, a paclitaxel-incorporating micellar nanoparticle formulation, can extend *in vivo* antitumour activity and reduce the neurotoxicity of paclitaxel. *Br. J. Cancer,* **92**(7), 1240–1246.
78. Saif, M. W., Podoltsev, N. A., Rubin, M. S., Figueroa, J. A., Lee, M. Y., et al. (2010). Phase II clinical trial of paclitaxel loaded polymeric

micelle in patients with advanced pancreatic cancer. *Cancer Invest.,* **28**(2), 186–194.

79. Matsumura, Y., Kataoka, K. (2009). Preclinical and clinical studies of anticancer agent-incorporating polymer micelles. *Cancer Sci.,* **100**(4), 572–579.
80. Wang, Y., Yu, L., Han, L., Sha, X., Fang, X. (2007). Difunctional pluronic copolymer micelles for paclitaxel delivery: Synergistic effect of folate-mediated targeting and pluronic-mediated overcoming multidrug resistance in tumor cell lines. *Int. J. Pharm.,* **337**(1–2), 63–73.
81. Batrakova, E. V., Kabanov, A. V. (2008). Pluronic block copolymers: Evolution of drug delivery concept from inert nanocarriers to biological response modifiers. *J. Control. Release,* **130**(2), 98–106.
82. Lee, C. C., MacKay, J. A., Frechet, J. M. J., Szoka, F. C. (2005). Designing dendrimers for biological applications. *Nat. Biotechnol.,* **23**(12), 1517–1526.
83. Khandare, J. J., Jayant, S., Singh, A., Chna, P., Wang, Y., et al. (2006). Dendrimer versus linear conjugate: Influence of polymeric architecture on the delivery and anticancer effect of paclitaxel. *Bioconjug. Chem.* **17**(6), 1464–1472.
84. Tomalia, D. A., Reyna, L. A., Svenson, S. (2007). Dendrimers as multi-purpose nanodevices for oncology drug delivery and diagnostic imaging. *Biochem. Soc. Trans.,* **35**(Pt 1), 61–67.
85. Xichen, Z., Jackson, J. K., Burt, H. M. (1996). Development of amphiphilic diblock copolymers as micellar carriers of taxol. *Int. J. Pharm.,* **132**(1–2), 195–206.
86. Farokhzad, O. C., Jon, S. Y., Khademhosseini, A., Tran, T. N. T., LaVan, D. A., et al. (2004). Nanopartide-aptamer bioconjugates: A new approach for targeting prostate cancer cells. *Cancer Res.,* **64**(21), 7668–7672.
87. Zhu, K. J., Xiangzhou, L., Shilin, Y. (1990). Preparation, characterization, and properties of polylactide (PLA)–poly(ethylene glycol) (PEG) copolymers: A potential drug carrier. *J. Appl. Polym. Sci.,* **39**(1), 1–9.
88. Bae, Y., Nishiyama, N., Fukushima, S., Koyama, H., Yasuhiro, M., et al. (2005). Preparation and biological characterization of polymeric micelle drug carriers with intracellular pH-triggered drug release property: Tumor permeability, controlled subcellular drug distribution, and enhanced *in vivo* antitumor efficacy. *Bioconjug. Chem.,* **16**(1), 122–130.

89. Farokhzad, O. C., Cheng, J. J., Teply, B. A., Sherifi, I., Jon, S., et al. (2006). Targeted nanoparticle-aptamer bioconjugates for cancer chemotherapy *in vivo*. *Proc. Natl. Acad. Sci. U. S. A.,* **103**(16), 6315–6320.
90. Cheng, J., Teply, B. A., Sherifi, I., Sung, J., Luther, G., et al. (2007). Formulation of functionalized PLGA-PEG nanoparticles for *in vivo* targeted drug delivery. *Biomaterials,* **28**(5), 869–876.
91. Lo, C. L., Huang, C. K., Lin, K. M., Hsiue, G. H. (2007). Mixed micelles formed from graft and diblock copolymers for application in intracellular drug delivery. *Biomaterials,* **28**(6), 1225–1235.
92. Bogdanov, A., Wright, S. C., Marecos, E. M., Bogdanova, A., Martin, C., et al. (1997). A long-circulating co-polymer in "passive targeting" to solid tumors. *J. Drug Target.,* **4**(5), 321–330.
93. Weissleder, R., Tung, C., Mahmood, U., Bogdanov, A. (1999). *In vivo* imaging of tumors with protease-activated near-infrared fluorescent probes. *Nat. Biotechnol.,* **17**(4), 375–378.
94. Bhadra, D., Bhadra, S., Jain, S., Jain, N. K. (2003). A PEGylated dendritic nanoparticulate carrier of fluorouracil. *Int. J. Pharm.,* **257**(1–2), 111–124.
95. Fessi, C., Devissaguet, J., Puisieux, F., Thies, C. (1992). Process for the preparation of dispersible colloidal systems of a substance in the form of nanoparticles. (US Patent No. 5118528).
96. Stella, B., Arpicco, S., Peracchia, M. T., Desmaële, D., Hoebeke, J., et al. (2000). Design of folic acid-conjugated nanoparticles for drug targeting. *J. Pharm. Sci.,* **89**(11), 1452–1464.
97. Yoo, H. S., Park, T. G. (2001). Biodegradable polymeric micelles composed of doxorubicin conjugated PLGA–PEG block copolymer. *J. Control. Release,* **70**(1–2), 63–70.
98. Dong, Y., Feng, S. (2004). Methoxy poly(ethylene glycol)-poly(lactide) (MPEG-PLA) nanoparticles for controlled delivery of anticancer drugs. *Biomaterials,* **25**(14), 2843–2849.
99. Avgoustakis, K., Beletsi, A., Panagi, Z., Klepetsanis, P., Karydas, A. G., et al. (2002). PLGA–mPEG nanoparticles of cisplatin: *In vitro* nanoparticle degradation, *in vitro* drug release and *in vivo* drug residence in blood properties. *J. Control. Release,* **79**(1–3), 123–135.
100. Tang, Z., Wang, Y., Podsiadlo, P., Kotov, N. (2006). Biomedical applications of layer-by-layer assembly: From biomimetics to tissue engineering. *Adv. Mater.,* **18**(24), 3203–3224.
101. Bawa, R. (2010). Nanopharmaceuticals. *Eur. J. Nanomed.,* **3**(1), 34–39.

102. Mansour, H. M., Park, C.-W., Bawa, R. (2015). Design and development of approved nanopharmaceutical products. In: Bawa, R., Audette, G., Rubinstein, I., eds. *Handbook of Clinical Nanomedicine: Nanoparticles, Imaging, Therapy, and Clinical Applications,* Chapter 9, Pan Stanford Publishing, Singapore.
103. Bawa, R. (2013). FDA and nanotech: Baby steps lead to regulatory uncertainty. In: Bagchi, D., et al., eds. *Bionanotechnology: A Revolution in Biomedical Sciences and Human Health,* Wiley Blackwell, UK, pp. 720–732.
104. Bawa, R. (2007). Special Report: Patents and nanomedicine. *Nanomedicine,* **2**(3), 351–374.
105. Kievit, F. M., Zhang, M. (2011). Cancer nanotheranostics: Improving imaging and therapy by targeted delivery across biological barriers. *Adv. Mater.,* **2011**(23), H217–H247.

Chapter 43

Nanotechnology for Radiation Oncology

Srinivas Sridhar, PhD,[a,b] Ross Berbeco, PhD,[b]
Robert A. Cormack, PhD,[b] and G. M. Makrigiorgos, PhD[b]

[a]*Electronic Materials Research Institute and Department of Physics, Northeastern University, Boston, Massachusetts, USA*
[b]*Department of Radiation Oncology, Dana-Farber Cancer Institute, Brigham and Women's Hospital, Harvard Medical School, Boston, Massachusetts, USA*

Keywords: nanotechnology, radiation oncology, nanotubes, nanoparticles, image guided radio therapy, gold, DNA, X-ray, radiosensitizer, nano-coated, implant, drug release profile, radiation therapy, dose enhancement, nanotechnology, image guided, energy deposition, tumor, chemoradiation therapy

The unique interaction of X-rays with nanostructured materials offers many new opportunities for enhancement of the efficacy of the use of X-radiation. Materials with high atom and electron density lead to enhanced scattering or absorbance of X-rays acting thus as radiosensitizers and causing increased localized and targeted damage to cancer cells. Nanotechnology approaches can enable implants currently used for radiation therapy guidance to also deliver drugs to the tumor. High-*Z* NPs can be used as computed tomography (CT) contrast agents. Nanostructured materials offer new ways to develop micro-sources of X-ray beams.

Here we review some of the key areas where important developments have occurred recently in the use of X-rays and

Handbook of Clinical Nanomedicine: Nanoparticles, Imaging, Therapy, and Clinical Applications
Edited by Raj Bawa, Gerald F. Audette, and Israel Rubinstein

ISBN 978-981-4669-20-7 (Hardcover), 978-981-4669-21-4 (eBook)
www.panstanford.com

nanostructured materials for radiation oncology. The various applications discussed are as follows:

(1) gold NPs for enhanced radiation therapy
(2) nanoparticles as delivery agents for radiation sensitizers
(3) nano-coated drug-loaded implants for biologically *in situ* enhanced, image-guided radio therapy (BIS-IGRT)
(4) nanoparticles as imaging agents for radiation therapy; and
(5) nanotechnology for radiation sources.

X-rays have been used extensively in medicine for diagnosis and therapy since their discovery. In radiation oncology, X-rays act directly by altering or damaging biomolecules such as DNA, and also indirectly by the generation of free radicals that can destroy malignant cells. X-rays are attractive in oncology because they penetrate much deeper than optical electromagnetic waves, thus offering access to deep tumors. Today more than 60% of tumors are treated with radiation, usually as an adjuvant to chemotherapy and resection.

The unique interaction of X-rays with nanostructured materials offers many new opportunities for enhancement of the efficacy of radiation therapy using nanomaterials. Materials with high atom and electron density lead to enhanced scattering or absorbance of X-rays acting thus as radiosensitizers and causing increased localized and targeted damage to cancer cells. High-Z NPs can be used as computed tomography (CT) contrast agents. Nanostructured materials offer new ways to develop micro-sources of X-ray beams. Here we review some of the key areas where important developments have occurred recently in the use of X-rays and nanostructured materials for diagnosis and therapy.

43.1 Gold Nanoparticles for Radiation Therapy

Clinical radiation therapy of cancer is generally performed by either externally produced high-energy (MeV) photons or electrons, or internally placed radioactive isotopes emitting low-energy (keV) photons. For both treatment modalities, the therapeutic benefit is defined as the radiation dose to the cancer cells divided by the radiation dose to the normal tissue. The goal of radiation oncology treatment planning is the maximization of this ratio. At a certain point, particularly for external beam radiation therapy, increases

in radiation dose to the target volume are limited by toxicity to the normal tissue. For many disease sites, the maximum tolerable dose falls short of that which would provide the best therapeutic response.

Gold NPs have been investigated as platforms to carry drugs or radiosensitizing agents to tumors due to the biocompatibility of gold and relative ease of conjugation with therapeutic and targeting moieties. Recently, there has been interest in exploiting the physical properties of gold, specifically the high atomic number, to enhance radiation therapy. Localized X-ray absorption and localized energy deposition at the nanoscale can be achieved from low-energy electrons released from nanostructures interacting with hard X-ray radiation in aqueous solution through three key mechanisms: (1) localized absorption of X-rays by nanostructures, (2) effective release of low-energy electrons from small nanostructures (Fig. 43.1), and (3) efficient deposition of energy in water in the form of radicals and electrons. [1]

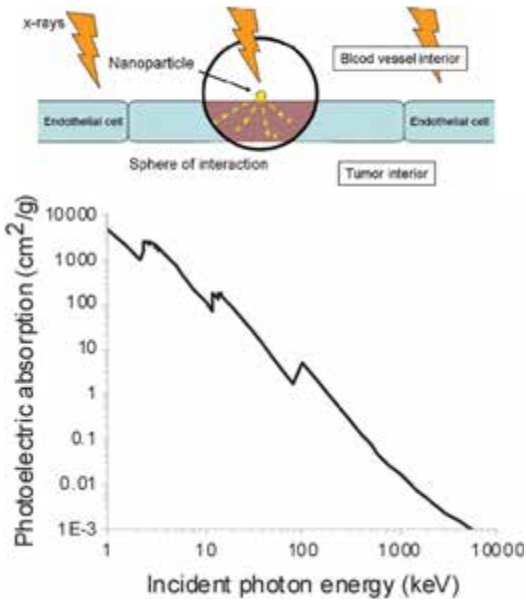

Figure 43.1 (Up) Schematic of interaction of X-rays with gold nanoparticles and resulting damage to endothelial cells for radiation therapy. From ref. [7]. (Down) Photoelectric absorption cross section shown as a function of incident photon energy for gold. From ref. [2] with permission.

In a photoelectric interaction, an incoming photon of energy E is absorbed by an atom, kicking off an electron with kinetic energy $E - E_b$, where E_b was the binding energy of the electron. The cross section for photoelectric interaction is proportional to Z^3/E^3, where Z is the atomic number of the atom under consideration and E is the energy of the incident photon. Therefore, the effect will be largest for low-energy photons interacting with high-Z atoms. Figure 43.1 shows the photoelectric interaction cross section as a function of photon energy for gold atoms [2]. The jumps in the curve represent the thresholds for successive atomic energy shells (M, L, and K). Further interactions within the atom can result in the ejection of multiple low-energy Auger electrons, which will only travel a short distance before absorption in the surrounding medium. The theoretically predicted nanoscale energy deposition distribution has been confirmed by observing enhanced damage to a 5600-bp DNA molecule from approximately 10 chemically conjugated small gold NPs under X-ray radiation [1].

Several research groups have performed theoretical calculations of the radiation dose enhancement from gold NPs using Monte Carlo simulations or analytic calculations. These studies can be divided into macroscopic and microscopic groups in terms of the spatial resolution of the results. In macroscopic studies, NPs are modeled as homogeneously distributed throughout a tumor at some depth in tissue. Due to the physical process of the photoelectric effect, the dose enhancement from low-energy X-ray brachytherapy or orthovoltage sources far exceeds that from megavoltage X-ray sources [3, 4].

Microscopic studies of the dose enhancement from gold NPs predict a substantial dose increase as a function of proximity for all X-ray energies investigated. However, the range will depend on the incident energy of the photon: lower energy X-ray sources will produce shorter range photo-electrons and higher-energy X-ray sources will produce longer range photo-electrons. Monte Carlo simulations of the photo-electron range and associated absorbed dose indicate that the majority of the dose will be deposited within a short distance, with a rapid falloff (Table 43.1) [3, 5]. As in the macroscopic studies, these studies also indicate that lower energy sources will produce the largest dose enhancement effect.

Table 43.1 The distance at which the relative dose is 50% and 10% of the maximum ($D_{50\%}$ and $D_{10\%}$) is shown for the results of Leung et al. (2011)

	Incident			
	Photon		Source	
	50 kVp	250 kVp	Co-60	6 MV @ 1 mm
$D_{50\%}$	5 μm	30 μm	1 mm	1 mm
$D_{10\%}$	10 μm	110 μm	4 mm	5 mm

Note: The values shown correspond to 100 nm nanoparticles.

Microscopic analytic calculations have been performed to estimate the absorbed dose to a tumor endothelial cell [6, 7], from gold NPs targeted to the tumor vasculature [8, 9]. These studies anticipate that gold NPs, used as vascular disruptive agents, will induce tumor endothelial cell death, hastening large scale cell death throughout the tumor [9]. The results indicate that the endothelial dose enhancement factor can be roughly 5.0 (500%) for low-energy sources and 1.5 (50%) for a clinical 6 MV photon beam (depending on the local nanoparticle concentration and low-energy X-ray source) [6, 7].

In vitro studies have been performed to quantify the dose enhancement experimentally [11–13]. These experimental configurations do not exactly match the theoretical models above as the NPs are continuously undergoing endocytosis and exocytosis. However, the experimental results are consistent with the theoretical modeling in that lower energy sources produce the highest effects. Most interestingly, the dose enhancement from megavoltage irradiation is much larger than expected (greater than 25%), due in part to the proximity of the NPs to the cell nuclei as well as the increasing proportion of low-energy photons at larger depths in water. It has also been found that clinical delivery conditions that increase the proportion of low-energy photons will cause more DNA damage [13].

Preliminary *in vivo* experiments have demonstrated the powerful anti-tumor effect of gold NPs aided radiotherapy. Hainfeld et al. [14] have reported an increase in overall survival from 20% to 86% for gold NPs plus radiation versus radiation alone in a

subcutaneous mammary carcinoma mouse model, 2.7 g/kg IV injection of 1.9 nm gold NPs and 250 kVp X-rays [14]. These results are summarized in Fig. 43.2. No *in vivo* studies have yet been performed with orthotopic tumors, targeted gold NPs, or high energy X-rays.

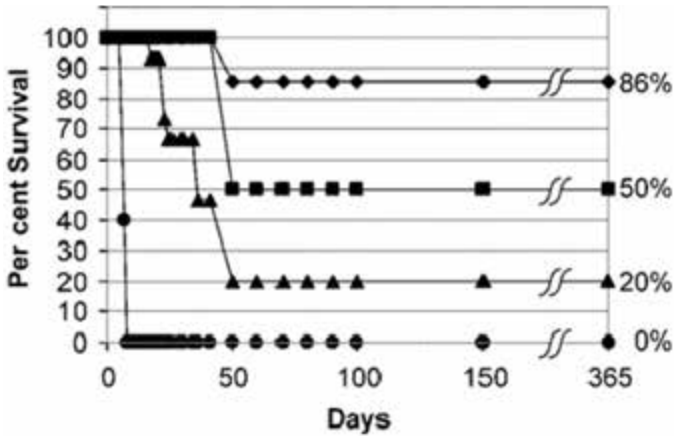

Figure 43.2 >1-year survival of mice after treatment of subcutaneous EMT-6 tumors. Circles: no treatment (n = 17), and gold only (n = 4), indistinguishable; triangles: irradiation only (26 Gy, 250 kVp) (n = 15); squares: irradiation plus 1.35 g Au/kg AuNP (n = 4); diamonds: irradiation plus 2.7 g Au/kg AuNP (n = 7). From Hainfeld et al. (2004) ref. 14 with permission.

The results of the early theoretical and experimental studies have shown great potential for gold nanoparticle aided radiation therapy to substantially improve cancer treatments. The use of gold NPs to enhance radiation therapy can be broken up into two steps. The first is the preferential targeting of the NPs to the appropriate biological components. The targeting is dependent on conjugation efficiency, molecular affinities, and the biophysical kinetics (extravasation, diffusion, endocytosis, etc.) of delivering the nanoparticle to the correct locations. Individual cells, stem cells, and tumor vasculature have all been proposed as potential targets, each with its own benefits and limitations. The second step is the irradiation either by internal or external radiation sources. In order to ensure safe coverage of the disease, the application of gold nanoparticle radiation therapy must be competitive with

conventional therapeutic irradiation. To this end, employing gold NPs as an adjuvant to accepted safe irradiation procedures is particularly attractive [7].

43.2 Nanoparticles as Delivery Agents for Radiation Sensitizers

Radiation therapy is often delivered in combination with other modalities, such as chemotherapy or hyperthermia. Several anti-cancer agents have been shown to act as radiosensitizers, enhancing the efficacy of RT when they are accumulated at the tumor site. A variety of nanoparticle formulations have been shown to be highly useful as delivery agents of radiation sensitizers. NK105, a micellar-formulation delivering paclitaxel (PTX) to tumors, has been shown to have superior radiosensitizing activity in Lewis-lung carcinoma bearing mice, attributable to the more severe cell cycle arrest at the G2/M phase induced by NK105 as compared to that induced by free PTX [15].

The potential of radiation for improving gene delivery by a virus-mimicking nanoparticle, transferrin (Tf)-cationic liposome-DNA complex (Tf-lipoplex), has been explored. Radiation (10–20 Gy) markedly induced transgene (LacZ) expression in Lewis Lung Carcinoma xenografts, correlating with increased plasmid content and TfR expression in irradiated tumors. The results show that radiation improves Tf-lipoplex gene delivery selectively to tumor cells both *in vitro* and *in vivo* [16].

It has been proposed that quantum dots (QDs) can be used to excite conjugated photosensitizers and produce cytotoxic singlet oxygen. The photon emission efficiency of CdSe/ZnS QDs on excitation by 6-MV X-rays was measured using dose rates of 100–600 cGy/min. A QD-Photofrin conjugate was synthesized by formation of an amide bond. The number of visible photons generated from QDs excited by 6-MV X-rays was linearly proportional to the radiation dose rate. The Förster resonance energy transfer efficiency approached 100% as the number of Photofrin molecules conjugated to the QDs increased. The combination of the conjugate with radiation resulted in significantly lower H460 cell survival in clonogenic assays compared with radiation alone. The novel QD-

Photofrin conjugate shows promise as a mediator for enhanced cell killing through a linear and highly efficient energy transfer from X-rays to Photofrin [17].

43.3 Nano-Coated Drug-Loaded Implants for Biologically *in situ* Enhanced, Image-Guided Radio Therapy

Radiation therapy is delivered either using a LINAC to focus beams of radiation on a target (external beam radiation therapy), or by placing radioactive material in the target to irradiate the target with radiation from the nuclear decay process (brachytherapy). Normal cells have a greater repair capability than cancerous cells so radiation generally kills a greater fraction of cancerous cells than normal cells. The radiation that can be delivered to the target is limited by complications that are associated with radiation damage to normal tissues in the vicinity of the high-dose region. Attempts to increase the therapeutic ratio have focused on decreasing the dose to surrounding normal tissues in order to decrease the normal tissue complication probability. Image-guided radiation therapy (IGRT) uses imaging during radiation therapy procedures to localize the target. Improved target localization allows the use of more conformal dose distributions, which irradiate less normal tissue and lead to fewer toxicities associated with treatments.

Two IGRT techniques implant small objects in the tumor as an essential part of the therapy. One to three radio-opaque gold markers, or fiducials, may be implanted in the target to make it visible with X-rays. X-ray imaging mounted on the treatment LINAC can then be used to localize the target immediately before treatment allowing the use of smaller radiation fields by reducing the uncertainty in target position. Permanent 125I prostate brachytherapy uses imaging [18, 19] to guide the insertion of 30 to 100 radioactive sources within the prostate gland. In addition to the radioactive sources, inert spacers are used to maintain a planned geometry between sources. In both these instances, implanted objects essential to reducing normal tissue irradiation offer an opportunity to further increase the therapeutic ratio by providing localized radiosensitization.

The therapeutic efficiency of IGRT can be further enhanced by biological *in situ* dose painting (BIS-IGRT) of radiosensitizers through localized delivery within the tumor using gold fiducial markers that have been coated with NPs and nanoporous polymer matrices. Although use of NPs for drug delivery is widely studied, the use of implantable nanoparticle eluters in radiation therapy is a nascent field. Studies of nanoparticle biodistribution involve analysis of nanoparticle accumulation after intravenous delivery. Given the large variety of nanoparticle properties, simulating the biologic effect of NPs offers insight on the particle diffusion and residency properties that are necessary for effective radiosensitization. Computational studies build upon calculations of radiation dose distributions and the biologic effect of radiation. Radiation dose distributions can be calculated by treatment planning systems following the guidelines of the American Association of Physicists in Medicine. Biologic effect can be calculated from the linear quadratic model that is used to describe the results of cell irradiation experiments in terms of the surviving cell fraction $\mathrm{SF}(d) \propto \exp(-\alpha d - \beta d^2)$, where d is dose, and the parameters α and β are related to the sensitivity of cells to radiation damage. Radiosensitizers enable a given survival fraction to be achieved with less dose, and the sensitization is expressed as $s = d_{\mathrm{sens}}/d_{\mathrm{ref}}$, where d_{sens} is the dose required for a given SF of sensitized cells and d_{ref} is the dose needed to achieve the same SF for unsensitized cells. The biologic effect of a localized distribution of radiosensitizing NPs can be calculated from the resulting sensitization distribution combined with the underlying radiation dose distribution as shown in Fig. 43.3. The concept of the equivalent uniform dose (EUD) [20], derived from the average survival fraction of a region of interest, is a useful construct to provide relative figure of merit to compare the effect of different distributions of radiation dose or nanoparticle sensitization.

Simulations of the distribution of particles in the vicinity of implanted eluters can guide the development of the physical characteristics of the eluters and drug carriers. Analytic solutions to the diffusion equation offer a means of understanding how potential radiosensitization depends on both eluter size and the diffusion elimination modulus ϕ_{b}. Cormack et al. [21] have shown that four implanted objects, releasing drug carriers with a low ϕ_{b}, could sensitize a substantial portion of a tumor of the size typical

of early stage lung cancer often treated with stereotactic body radiation therapy (SBRT). In prostate brachytherapy, avoiding the sensitization of nearby radiosensitive structures adds a competing advantage for higher values of ϕ_b.

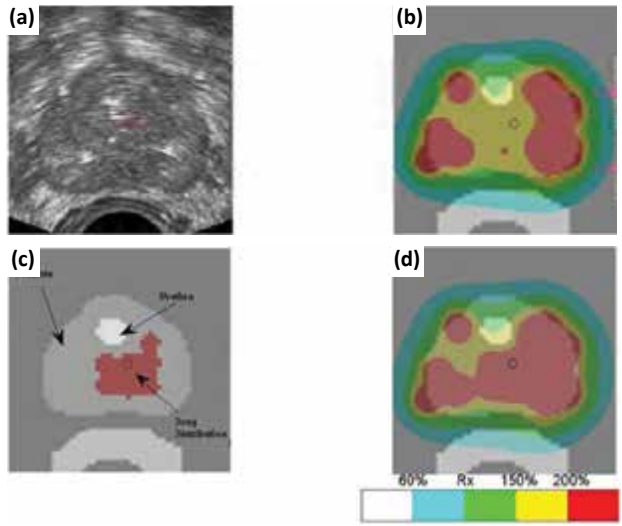

Figure 43.3 An example of the effect of *in situ* release of radiation sensitizer within a permanent 125I implant. (a) An axial ultrasound image of the prostate used for treatment planning and image guidance of the implant. (b) The planned radiation dose distribution. (c) A sensitized region achieved by a distribution of implanted radiosensitizer eluters on a 5 mm grid around a point of interest while avoiding the urethra. (d) The biologic effective dose arising from the radiation dose and the planned sensitization.

Radiation therapy may be delivered in a single treatment, many treatments over the course of an extended period of time or with dose being delivered continuously. Implants deliver radiation continuously with the variation of dose with time determined by the half-life of the implanted isotope. The temporal release of NPs from an implanted eluter can be controlled by the chemical composition of the eluter, and the release schedule of radiosensitizers will affect the biologic effect. Integrating the effect of radiation cell kill over the course of a permanent implant shows that the optimal release schedule depends on the concentration

of intracellular radiosensitizer that can be sustained by the distribution configuration of implanted eluters.

Accurate radiation dose calculations have been pursued throughout the history of radiation oncology. Modeling of *in vivo* distributions of radiation sensitizers has provided guidance to develop the concept of biologic *in situ* IGRT. Researchers in radiation oncology are investigating the use of biologic effect as a metric to optimize the radiation fields used in intensity modulated radiation therapy (IMRT) [22]. BIS-IGRT offers an additional level of complexity in the treatment planning process by allowing both radiation and drug distributions to be planned and using the biologic effect as a means to optimize the composite effect of both distributions.

43.3.1 Development of Nano-Coated Implants and Sensitizer Release Strategies

The feasibility of nano-coated implants for radiation therapy has been exploited by development of prototype radiosensitizer eluting nano-coated implants. Two approaches have been studied, a free drug release system and a dual-drug release system. The free drug release system comprised Doxorubicin (Dox), a hydrophilic drug, from a non-degradable polymer Poly(methyl methacrylate) (PMMA) coating. In the experiments, an initial release within the first few hours was followed by a sustained release over the course of next 3 months [23].

The dual-release system comprises Poly(D,L-lactic-co-glycolic acid) (PLGA) NPs loaded with fluorescent Coumarin-6, serving as a model for a hydrophobic drug, in a biodegradable chitosan matrix. In this platform, release of NPs and free drug were controlled by degradation rate of chitosan matrix and PLGA. Temporal release kinetics measurements in buffer were carried out using fluorescence spectroscopy. Considering the stability of chitosan film containing PLGA NPs on gold surfaces, this work demonstrates the use of this platform as a coating agent for gold implants. Furthermore, chitosan films could be loaded with hydrophilic model drug (Carboxyfluorescein) and FPTX-loaded PLGA NPs. The release profile of CF and PLGA from chitosan film as well as the release of FPTX from PLGA NPs demonstrated the promising

application of this platform for localized dual-drug release [22]. The results from these experiments (see Fig. 43.4) show that dosage and rate of release of these radiosensitizers coated on gold fiducials for IGRT can be precisely tailored to achieve the desired release profile for radiation therapy of cancer [24].

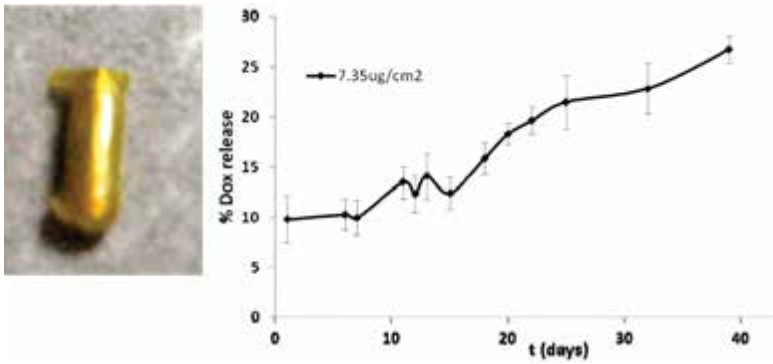

Figure 43.4 (Left) Coated fiducial. (Right) Release profile of Doxorubicin from a coated fiducial. From Nagesha, et al. (2010) ref. 24 with permission.

43.4 Nanoparticles as Imaging Agents for Radiation Therapy

Nanoplatforms containing NPs and other functional moieties find many applications as image-enhancing agents using a variety of imaging modalities that are relevant to radiation therapy. Aydogan et al. have studied the feasibility of using 2-deoxy-D-glucose (2-DG)-labeled gold nanoparticle (AuNP-DG) as a computed tomography (CT) contrast agent with tumor targeting capability through *in vitro* experiments [25, 26]. Significant contrast enhancement in the cell samples incubated with the AuNP-DG with respect to the cell samples incubated with the unlabeled AuNP was observed in multiple CT slices. Cinnamon-coated AuNP have been shown to be non-toxic and serve as excellent CT/ photoacoustic contrast enhancement agents [27]. Polymer-coated Bi(2)S(3) NPs have been shown to be attractive platforms for enhanced *in vivo* imaging of the vasculature, the liver, and lymph nodes in mice. These NPs and their bioconjugates show promise as an important adjunct to

in vivo imaging of molecular targets and pathological conditions [28].

A long circulating liposomal, nanoscale blood pool agent encapsulating traditional iodinated contrast agent has been used for micro-computed tomography (CT) imaging of rats implanted with R3230AC mammary carcinoma. Three-dimensional vascular architecture of tumors was imaged at 100-micron isotropic resolution [29]. Radio-opaque iodinated polymeric NPs in rats and mice (including those with a liver cancer model) CT-imaging have revealed a significant enhanced visibility of the blood pool for 30 min after injection, followed later by lymph nodes, liver and spleen due to strongly enhanced nanoparticle uptake by the reticuloendothelial system [30].

A novel X-ray luminescence computed tomography (XLCT) has been proposed as a new dual molecular/anatomical imaging modality. XLCT is based on the selective excitation and optical detection of X-ray-excitable NPs. As a proof of concept, a prototype XLCT system and imaged near-IR-emitting Gd(2)O(2)S:Eu phosphors was constructed and imaged in various phantoms. The linear response of the reconstructed images suggests that XLCT is capable of quantitative imaging [31].

Ultra-small paramagnetic iron oxide NPs have been shown to have greater accuracy as compared with conventional techniques and have been instrumental in delineating the lymphatic drainage of the prostate gland [32]. These NPs provide better target definition and delineation for fractionated radiation therapy. The use of multi-modal nanoparticle imaging agents, particularly in integrated clinical environments, such as the AMIGO suite at Brigham and Women's Hospital, will enable more precise definition of tumor margins and enable more accurate treatment planning for radiation therapy.

43.5 Nanotechnology for Radiation Sources

The ability to control nanostructures surfaces has led to several approaches for use as X-ray emission sources. Electrochemically grown nanotubes on TiO_2 surfaces have been explored as X-ray radiation sources [33]. Carbon nanotubes assembled in the TiO_2 nanotubes [34] are expected to enhance the emission properties

potentially leading to a new generation of controllable, portable sources. A prototype cellular irradiator utilizing a carbon nanotube (CNT)–based field emission electron source has been developed for microscopic image-guided cellular region irradiation. The CNT cellular irradiation system has shown great potential to be a high temporal and spatial resolution research tool to enable researchers to gain a better understanding of the intricate cellular and intercellular processes occurring following radiation deposition, which is critical to improving radiotherapy cancer treatment outcomes [35].

43.6 Conclusions

Several novel applications of nanotechnology and nanomedicines to radiation oncology have emerged in recent years. Radiation therapy is frequently used in conjunction with chemotherapy as multi-pronged therapies are needed to treat most cancers. The drug-releasing implants described above can be designed to utilize tailored-release profiles of biologics that are synchronous with the radiation treatment schedule. This chemo radiation therapeutic approach can utilize a wide variety of biologics such as chemotherapeutics like docetaxel, doxorubicin, and others, PARP inhibitors and siRNA, with the advantages of minimum systemic toxicity and high local drug concentrations. These nanoplatforms will provide oncologists with new weapons in the fight against a variety of cancers, including prostate, breast, lung, cervical and other carcinomas, and also sarcomas. Further development of these initial concepts over the next few years is being pursued to achieve successful clinical implementation.

Disclosures and Conflict of Interest

We thank D. Nagesha for helpful comments pertaining to this chapter. This work was supported by the Nanomedicine Science and Technology Center under NSF-DGE-096843 and the Electronic Materials Research Institute at Northeastern University, and by the Division of Medical Physics and Biophysics, Department of Radiation Oncology, Brigham and Women's Hospital.

The authors declare that they have no conflict of interest and have no affiliations or financial involvement with any organization or entity discussed in this chapter. This includes employment, consultancies, honoraria, grants, stock ownership or options, expert testimony, patents (received or pending) or royalties. No writing assistance was utilized in the production of this chapter and the authors received no payment for its preparation. The findings and conclusions here reflect the current views of the authors. They should not be attributed, in whole or in part, to the organizations with which they are affiliated, nor should they be considered as expressing an opinion with regard to the merits of any particular company or product discussed herein.

Corresponding Author

Prof. Srinivas Sridhar
Department of Physics, Northeastern University
435 Egan Research Center, 120 Forsyth Street, Boston, MA 02115, USA
Email: s.sridhar@neu.edu

About the Authors

Srinivas Sridhar is Arts and Sciences Distinguished Professor of Physics, Biomedical Engineering and Chemical Engineering at Northeastern University, and Lecturer on Radiation Oncology at Harvard Medical School. He is the Director and Principal Investigator of Nanomedicine Science and Technology, an IGERT (Integrative Graduate Education and Research Training) program funded by the National Cancer Institute and the National Science Foundation, and the Director of CaNCURE. He is the founding director of the Electronic Materials Research Institute, an interdisciplinary center with research and education thrusts in nanomedicine, nanomaterials and neurotechnology. From 2004 to 2008, he served as Vice Provost for Research at Northeastern University, overseeing the University's research portfolio. An elected Fellow of the American Physical Society, Sridhar's current areas of research are nanomedicine and neurotechnology. His paper in *Nature* in 2003 was listed among "Breakthroughs of 2003" by the journal *Science*.

He has published more than 190 articles on his work in nanomedicine, neurotechnology, nanophotonics, metamaterials, quantum chaos, superconductivity and collective excitations in materials.

Ross Berbeco is a board-certified medical physicist at the Dana-Farber Cancer Institute and Brigham and Women's Hospital and associate professor of radiation oncology at Harvard Medical School. Dr. Berbeco received undergraduate degrees in Physics and Astrophysics, with a minor in Philosophy, from the University of California-Berkeley. He earned his doctorate from the University of Michigan, based on high-energy experimental particle physics research performed at CERN in Geneva, Switzerland. His postdoctoral training in radiation oncology physics was completed at the Massachusetts General Hospital and Harvard Medical School. Dr. Berbeco's pre-clinical research is focused mainly on gold-nanoparticle aided radiotherapy. He has published numerous peer-reviewed articles and received federal and private funding to conduct this research.

Robert Cormack is a physicist at the Dana-Farber Cancer Institute and Brigham and Women's Hospital, and an associate professor of radiation oncology at Harvard Medical School. Dr. Cormack received a BA in Physics from Harvard College where he was first exposed to the field of medical physics at the Harvard Cyclotron Laboratory. He received his doctorate from Boston University for research in high-energy particle physics performed under the Gran Sasso at the INFN physics laboratory in L'Aquila, Italy. He completed his postdoctoral training at the Joint Center for Radiation Therapy and the Harvard Medical School. Dr. Cormack mentors students, fellows and residents in the Harvard Medical Physics Residency Program. His research interests include image-guided medical interventions, nano-therapeutics to increase the biologic effectiveness of radiation and adaptive radiation therapy.

G. M. Makrigiorgos is a professor of radiation oncology and director of the Medical Physics & Biophysics division at Dana-Farber Cancer Institute and Brigham and Women's Hospitals, Harvard Medical School. He also directs the DNA technology laboratory and the radiation pre-clinical facility. His research interests include dosimetry of radiation at the microscopic (molecular) level; the development of DNA technologies for molecular diagnostics in oncology and radio-sensitization of tissues using nanotechnology. He has developed molecular probes for detecting radiation at the molecular level (Coumarin), and PCR-based techniques for molecular diagnostics and mutation detection, including COLD-PCR. He is a member of the editorial board of Clinical Chemistry and has published over 120 articles, reviews and book chapters.

References

1. Carter, J. D., Cheng, N. N., Qu, Y., Suarez, G. D., Guo, T. (2007). Nanoscale energy deposition by X-ray absorbing nanostructures. *J. Phys. Chem. B,* **111**(40), 11622–11625.
2. NIST Database. Available at: http://www.nist.gov/srd/physics.htm (accessed on July 23, 2012).
3. Jones, B. L., Krishnan, S., Cho, S. H. (2010). Estimation of microscopic dose enhancement factor around gold nanoparticles by Monte Carlo calculations. *J. Med. Phys.,* **37**, 3809–3816.
4. Roeske, J. C., Nunez, L., Hoggarth, M., Labay, E., Weichselbaum, R. R. (2007). Characterization of the theorectical radiation dose enhancement from nanoparticles. *Technol. Cancer Res. Treat.,* **6**, 395–401.
5. Leung, M. K. K., Chow, J. C. L., Chithrani, D. B., Lee, M. J. G., Oms, B., et al. (2011). Irradiation of gold nanoparticles by x-rays: Monte Carlo simulation of dose enhancements and the spatial properties of the secondary electrons production. *J. Med. Phys.,* **38**, 624–631.
6. Ngwa, W., Makrigiorgos, G. M., Berbeco, R. I. (2010). Applying gold nanoparticles as tumor-vascular disrupting agents during brachytherapy: Estimation of endothelial dose enhancement. *Phys. Med. Biol.,* **55**, 6533–6548.

7. Berbeco, R. I., Ngwa, W., Makrigiorgos, G. M. (2011). Localized dose enhancement to tumor blood vessel endothelial cells via targeted gold nanoparticles: New potential for external Beam radiotherapy. *Int. J. Radiat. Oncol.,* **81**(1), 270–276.
8. Perrault, S. D., Walkey, C., Jennings, T., Fischer, H. C., Chen, W. C. W. (2009). Mediating tumor targeting efficiency of nanoparticles through design. *Nano Lett.,* **9**, 1909–1915.
9. Murphy, E. A., Majeti, B. K., Barnes, L. A., Makale, M., Weis, S. M., et al. (2008). Nanoparticle-mediated drug delivery to tumor vasculature suppresses metastasis. *Proc. Natl. Acad. Sci. U. S. A.,* **105**, 9343–9348.
10. Garcia-Barros, M., Paris, F., Cordon-Cardo, C., Fuks, Z., Kolesnick, R., et al. (2003). Tumor response to radiotherapy regulated by endothelial cell apoptosis. *Science,* **300**, 1155–1159.
11. Herold, D. M., Das, I. J., Stobbe, C. C., Iyer, R. V., Chapman, J. D. (2000). Gold microspheres: A selective technique for producing biologically effective dose enhancement. *Int. J. Radiat. Biol.,* **76**, 1357–1364.
12. Chithrani, D. B., Dunne, M., Stewart, J., Allen, C., Jaffray, D. A. (2010). Cellular uptake and transport of gold nanoparticles incorporated in a liposomal carrier. *Nanomedicine,* **6**, 161–169.
13. Berbeco, R. I., Korideck, H., Ngwa, W., Johnson, S., Makrigiorgos, G. M., et al. (2011). An *in vitro* study of dose enhancement from gold nanoparticles with a flattening filter free delivery. *Int. J. Radiat. Oncol. Biol. Phys.,* **81**, S150–S151.
14. Hainfeld, J. F., Slatkin, D. N., Smilowitz, H. M. (2004). The use of gold nanoparticles to enhance radiotherapy in mice. *Phys. Med. Biol.,* **49**, N309–N315.
15. Negishi, T., Koizumi, F., Uchino, H., Kuroda, J., Naito, S., Matsumura, Y., et al. (2006). NK105, a paclitaxel-incorporating micellar nanoparticle, is a more potent radiosensitising agent compared to free paclitaxel. *Br. J. Cancer* **95**(5), 601–606.
16. Abela, R. A., Qian, J., Xu, L., Lawrence, T. S., Zhang, M. (2008). Radiation improves gene delivery by a novel transferrin-lipoplex nanoparticle selectively in cancer cells. *Cancer Gene Ther.,* **15**, 496–507.
17. Yang, W., Read, P. W., Mi, J., Helmke, B. P., Sheng, K., et al. (2008). Semiconductor nanoparticles as energy mediators for photosensitizer-enhanced radiotherapy. *Int. J. Radiat. Oncol. Biol. Phys.,* **72**, 633–635.
18. Blasko, J. C., Radge, H., Schumacher, D. (1987). Transperineal percutaneous iodine-125 implantation of prostatic carcinoma

using transrectal ultrasound and template guidance. *Endocuriether Hypertherm. Oncol.,* **3**, 131–139.

19. D'Amico, A. V., Cormack, R., Tempany, C. M., Kooy, H. M., Coleman, C. N., et al. (1998). Real-time magnetic resonance image-guided interstitial brachytherapy in the treatment of select patients with clinically localized prostate cancer. *Int. J. Radiat. Oncol. Biol. Phys.,* **42**, 507–515.
20. Niemierko, A. (1998). Radiobiological models of tissue response to radiation treatment planning systems. *Tumori* **82**, 140–3.
21. Cormack, R. A., Sridhar, S., Suh, W. W., D'Amico, A. V., Makrigiorgos, G. M. (2010). Biological in-situ dose painting for image-guided radiation therapy using drug-loaded implantable devices, *Int. J. Radiat. Oncol. Biol. Phys.,* **76**, 615–623.
22. Ling, C. C., Humm, J., Larson, S., Leibel, S., Koutcher, J. A., et al. (2000). Towards multidimensional radiotherapy (MD-CRT): Biological imaging and biological conformality. *Int. J. Radiat. Oncol. Biol. Phys.,* **47**, 551–560.
23. Tada, D. B., Singh, S., Nagesha, D., Makrigiorgos, G. M., Sridhar, S., et al. (2010). Chitosan film containing poly(D,L-lactic-co-glycolic acid) nanoparticles: A platform for localized dual-drug release. *Pharm. Res.* **27**, 1738–1745.
24. Nagesha, D. K., Tada, D. B., Cormack, R., Makrigiorgos, G. M., Sridhar, S., et al. (2010). Radiosensitizer-eluting nanocoatings on gold fiducials for biological in-situ image-guided radio therapy (BIS-IGRT). *Phys. Med. Biol.,* **55**, 6039–6052.
25. Aydogan, B., Li, J., Wietholt, C., Kurtoglu, M., Redmond, P., et al. (2010). AuNP-DG: Deoxyglucose-labeled gold nanoparticles as X-ray computed tomography contrast agents for cancer imaging. *Mol. Imaging Biol.,* **12**(5), 463–467.
26. Li, J., Chaudhary, A., Wietholt, C., Kurtoglu, M., Aydogan, B., et al. (2010). A novel functional CT contrast agent for molecular imaging of cancer. *Phys. Med. Biol.,* **55**, 4389–4397.
27. Chanda, N., Shukla, R., Zambre, A., Mekapothula, S., Katti, K. V., et al. (2011). An effective strategy for the synthesis of biocompatible gold nanoparticles using cinnamon phytochemicals for phantom CT imaging and photoacoustic detection of cancerous cells. *Pharm. Res.,* **28**(2), 279–291.
28. Rabin, O., Manuel, Perez, J., Grimm, J., Wojtkiewicz, G., Weissleder, R. (2006). An X-ray computed tomography imaging agent based on long-circulating bismuth sulphide nanoparticles. *Nat. Mater.,* **5**(2), 118–122.

29. Samei, E., Saunders, R. S., Badea, C. T., Bentley, R. C., Mukundan, S. Jr., et al. (2009). Micro-CT imaging of breast tumors in rodents using a liposomal, nanoparticle contrast agent. *Int. J. Nanomed.,* **4**, 277–282.

30. Aviv, H., Bartling, S., Kieslling, F., Margel, S. (2009). Radiopaque iodinated copolymeric nanoparticles for X-ray imaging applications. *Biomaterials,* **30**, 5610–5616.

31. Pratx, G., Carpenter, C. M., Sun, C., Rao, R. P., Xing, L. (2010). Tomographic molecular imaging of x-ray-excitable nanoparticles. *Opt. Lett.,* **35**, 3345–3347.

32. John, S. S., Zietman, A. L., Shipley, W. U., Harisinghani, M. G. (2008). Newer imaging modalities to assist with target localization in the radiation treatment of prostate cancer and possible lymph node metastases. *Int. J. Radiat. Oncol. Biol. Phys.,* **71**(1 Suppl), S43–S47.

33. Alivov, Y., Klopfer, M., Molloi, S. (2010). Effect of TiO_2 nanotube parameters on field emission properties. *Nanotechnology,* **21**, 505706.

34. Gultepe, E., Nagesha, D. K., Selvarasah, S., Busnaina, A., Sridhar, S. (2008). Large scale 3D vertical assembly of single-wall carbon nanotubes at ambient temperatures. *Nanotechnology,* **19**, 455309.

35. Bordelon, D. E., Zhang, J., Graboski, S., Zhou, O. Z., Chang, S., et al. (2008). A nanotube based electron microbeam cellular irradiator for radiobiology research. *Rev. Sci. Instrum.,* **79**, 125102.

Chapter 44

Gold Nanoparticles against Cancer

Joan Comenge, PhD,[a] Francisco Romero, PhD,[b] Aurora Conill, MS,[c] and Víctor F. Puntes, PhD[a]

[a]*Inorganic Nanoparticles Group, Catalan Institute of Nanotechnology, Barcelona, Spain*
[b]*Molecular Science Institute, University of Valencia, Valencia, Spain*
[c]*Nanotargeting SL, Barcelona, Spain*

Keywords: nanotechnology, nanopharmaceutical, nanomedicine, targeting, gold, nanoparticles, cancer, drug delivery, enhanced permeability and retention effect, surface plasmon resonance, nanoparticle biodistribution, radiosensitizer, radiotherapy, photothermal therapy

Many of the conventional therapies can be improved using drug delivery systems (DDS). They are designed mainly to modify the pharmacokinetics and biodistribution of small molecular drugs. This is of special importance in the case of anticancer therapies in which a widespread distribution of small molecular chemotherapeutic drugs is often limiting treatments. In this context, nanotechnology emerges as a disruptive technology to design carriers that improve the delivery of drugs to their target organs. The composition of these nanocarriers comprises a wide range of materials such as polymeric nanocapsules, lipidic liposomes, or metallic nanoparticles. Gold nanoparticles (Au NPs) are of special interest due to its demonstrated biocompatibility, their tunable surface chemistry, and their special optical and electronic

Handbook of Clinical Nanomedicine: Nanoparticles, Imaging, Therapy, and Clinical Applications
Edited by Raj Bawa, Gerald F. Audette, and Israel Rubinstein

ISBN 978-981-4669-20-7 (Hardcover), 978-981-4669-21-4 (eBook)
www.panstanford.com

properties that allow its use not only as carriers but also as effectors. Hence, Au NPs are perfect candidates to be used for treatment of cancer in the clinics thanks to the capacity to be used as scaffolds to attach drugs or targeting molecules, as imaging agents, and as effectors themselves.

44.1 Historical Perspective on the Medical Use of Gold

Gold in different forms has been used for health in humans since ancient times. The synthesis of Au NPs has been in the spotlight since Faraday discovered in 1857 the mechanism of formation of pure gold colloids. This synthesis has been the keystone of a large amount of chemical routes to obtain Au NPs with controlled size, shape, and surface chemistry. Today, scientists have a wide catalog of Au NPs available, which can be used as excellent model systems to investigate the nano–bio interface. In the 1950s, the first use as contrast agents for radiotherapy was reported. Since the 1970s, Au NPs have been used in combination with antibodies (Abs) or other proteins to visualize specific cellular compartments, proteins, and receptors. Another well-known application of Au NPs is their use as probes of biomarkers in the pregnancy test (e.g., First Response®, marketed in the 1990s). This test is based on the specific recognition of human chorionic gonadotropin (hCG), a hormone produced during pregnancy, by Au NPs conjugated with an antihCG Ab. Nowadays, advanced NP bioconjugate chemistries allow scientists to tailor NPs for much higher sophisticated purposes, such as orchestrating chemical reactions inside cells and manipulating cell response. The successful development of these challenging tasks relies on intelligent surface structure design and the ability to synthesize NP bioconjugates with the desired architecture, which is also paramount in obtaining a well-defined and reproducible behavior.

44.2 Gold in the ERA of Nanotechnology: New Properties for a Known Material

Personalized health care, rational drug design, and targeted drug delivery are some of the proposed benefits of a nanomedicine-

based approach to therapy. The progress of the drug development is nowadays limited since most of the delivery methods are based mainly on oral or injection delivery routes, which strongly determines the formulation of the drugs. Precise drug release into highly specified targets involves miniaturizing the delivery systems to become much smaller than their targets. Nanoparticle DDS, due to their small size, can penetrate across the barriers through capillaries into individual cells to allow efficient accumulation at the targeted locations in the body. A wide variety of engineered NPs has been extensively used or is currently under investigation for drug delivery, imaging, biomedical diagnostics, and therapeutic applications. Among those, Au appears as one of the most use and most promising medical nanoparticles for diagnosis, therapy, and theranostics. The employment of NPs for the delivery of pharmaceuticals can result in higher concentrations than possible with other drug delivery methods, which could enhance the drug bioavailability or dosing at the targeted site as well as the overall efficiency of the used drug. For example, the involvement of stable conjugates of Au NPs coated with antibiotic molecules for therapy increases the efficiency of drug delivery to target cells in some studied cases.

Au is a biocompatible inert material that can be produced with extreme size control and monodispersity; its functionalization and derivatization are very well developed; and it has a very high electron density, which can be exploited as contrast agents for X-ray imaging or X-ray radiotherapy, or as contrast agents for imaging in the near infrared (a much weaker highly penetrating photon wavelength) and as photoablation (hyperthermia) agents.

44.3 Synthesis of Gold Nanoparticles

When using Au NPs for biological applications, special care has to be taken in the synthesis step since the size and size distribution play an important role in some biological responses such as biodistribution, tumor accumulation, and penetration, time of circulation, and immune response among others. Moreover, the nanoparticles surface should be ready for further chemical modifications in order to link the drug of interest.

The synthesis of colloidal gold was introduced by Michael Faraday in the 1850s [1], but it was not until 1951 when the most

usual synthetic methodology to obtain gold nanoparticles was exhaustively described by Turkevich [2]. This approach, based on the reduction of a gold salt by citrate, results in the production of 20 nm Au NPs with a relatively narrow size distribution. This methodology, as well as subsequent modifications [3], is based on supersaturation of the monomer in solution that induces homogenous nucleation followed by growth of these nuclei without additional nucleation events. This "burst nucleation" is a necessary condition to obtain highly uniform nanoparticles [4]. Nevertheless, the range of Au NP sizes available to obtain using these methods is small and goes from 7 to 25 nm. Frens proposed to decrease the citrate/$HAuCl_4$ ratio in order to increase the nanoparticle size up to 150 nm [5]. However, it has been recently demonstrated that this approach do not follow the "burst nucleation" mechanism and consequently monodispersity becomes poor, and also the spherical shape of the Au NPs is partially lost [6]. To overcome these limitations, a great number of synthetic protocols to achieve better control over the size and shape of nanoparticles have been developed during the past years [4]. Among them, the seeding-mediated strategies based on the temporal separation of nucleation and growth processes are considered very efficient methods to obtain monodisperse NPs [7–9]. In this strategy, small particles are synthesized first and later used as seeds (nucleation centers) to grow larger NPs. For example, Murphy and coworkers proposed the use of a weak reducing agent (ascorbic acid), which reduces Au^{3+} to Au^{+} and prevented the total reduction to Au^{0} unless seeds are present [10]. By using this methodology, additional nucleation that would lead to polydispersity is avoided. However, the use of CTAB as capping agent restricts the possibilities of further functionalization since their replacement by thiols is difficult to achieve [11]. This condition is especially important in nanomedicine, where the ability to render a biological functionality to inorganic nanostructures is one of the cornerstones of this emerging field [12]. In this context, citrate-stabilized Au NPs appear as unique candidates since the loosely bound capping layer provided by the sodium citrate can easily be exchanged by thiolated molecules that pseudo-covalently bind (~45 kcal/mol) to the gold surface [13]. However, the control of the size is complicated since the energy needed to form Au nuclei is not much higher than the needed to grow the NPs and therefore to separate nucleation

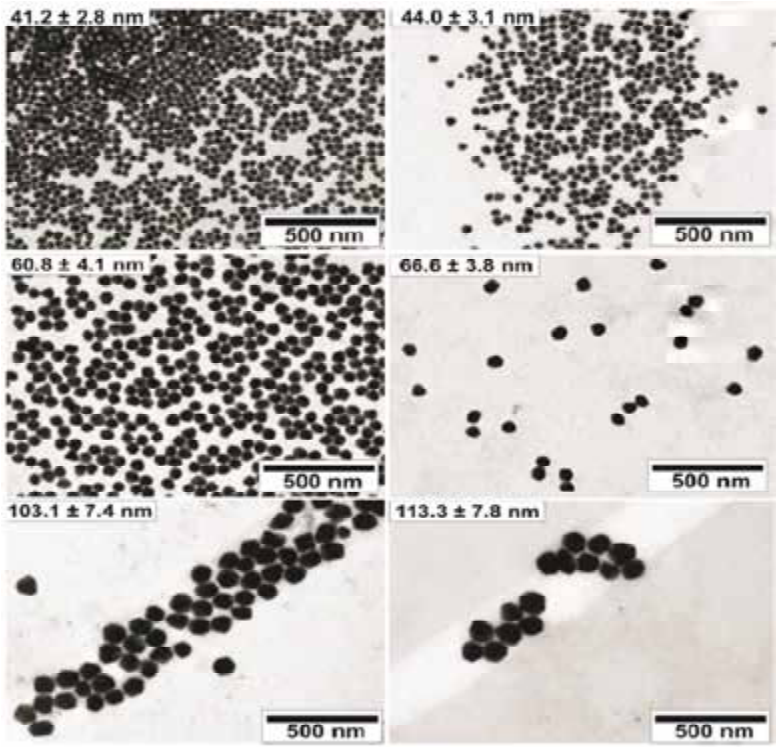

Figure 44.1 Representative TEM images of Au NPs after every growth step in the kinetically seeded growth approach. Monodispersity and absence of secondary populations are maintained all over the process. The morphology of the Au NPs is quasi-spherical in all cases avoiding the formation of elongated Au NPs.

from growth is not trivial. Obviously, the formation of new nuclei during growing stages would lead to a broadening of the size distribution and should be avoided in any seed growth approach. Recently, our group proposed a kinetically controlled seeded growth approach that allows obtaining citrate-capped Au NPs with a perfect control of the size from 8 to 200 nm [8]. This methodology, which avoids the use of any surfactants, is based on the reduction of $HaAuCl_4$ by sodium citrate (as in the classic synthesis of Au NPs). Here, the separation of nucleation and growth stages is achieved by manipulating the reaction conditions: pH, temperature, and ratio seed/monomer are key factors to avoid

secondary nucleation that would have led to a broadening of size distribution (Fig. 44.1).

Although spherical Au NPs are the most used in biomedical applications, nanoparticle synthesis is an extremely active field of research. In recent years, protocols allowing the synthesis of Au NPs of exotic shapes have been described. The special physico-chemical properties of anisotropic Au NPs, hollow structures or core–shell Au NPs make them appealing to be used in biomedicine as contrast agents, for cell labeling or as effectors for photothermal therapy. Anisotropic gold nanorods (Au NRs) can be synthesized following also a seeding growth approach proposed by El Sayed's and Murphy's groups [14, 15]. Au seeds (4 nm) are synthesized with a strong reducing agent ($NaBH_4$) in the presence of cetyltrimethylammonium bromide (CTAB). They are immediately used as nucleation centers for growing Au NRs. It is in this growth stage that the control of the size, and therefore the tuning of the Au NRs aspect ratio, is possible. The growth stage is based on the use of a weak reducing agent (ascorbic acid) to avoid secondary nucleations, and the presence of a micelle-forming surfactant (CTAB and/or benzyldimethylhexadecylammonium chloride, BDAC) and Ag ions to allow the growth in only one direction.

44.4 Gold Nanoparticles to Target Cancer

In cancer, the rapid growth of tumor results in leaky vessels. Macromolecules and NPs are able to permeate through the fenestrations in tumor vessels. In addition, they are retained due to the lack of a functional lymphatic system. This effect (Enhanced Permeability and Retention effect, EPR) is widely reported in the literature [16, 17] and has been exploited to passively accumulate nanocarriers in tumors [18]. This passive accumulation of NPs into the tumor may be even further improved if a ligand that is recognized by a receptor overexpressed in tumors is also attached to the NP. Examples include epidermal growth factor (EGF) [19], folate [20], and transferrin [21]. However, this point is still controversial and it is not clear if the addition of a ligand may change the final biodistribution of the NPs. It has been proposed that NPs with tumor-specific ligands are more rapidly taken up

by tumoral cells rather than affect the biodistribution which is mainly influenced by the physicochemical properties of the NP (size and surface charge) and composition (e.g., presence of stealthing agents) [22]. Long-time circulating NPs maximize the EPR effect since the changes to permeate through the tumor vessels are greater. Related to this, the size of NPs plays an important role in determine tumor accumulation and distribution: 60 nm Au NPs showed a greater accumulation than 20 nm Au NPs likely due to a slower clearance. However, larger Au NPs are accumulated in the perivascular region of the tumor failing to penetrate deeper, while 20 nm Au NPs were still found significantly at 50 μm from the blood vessel [23].

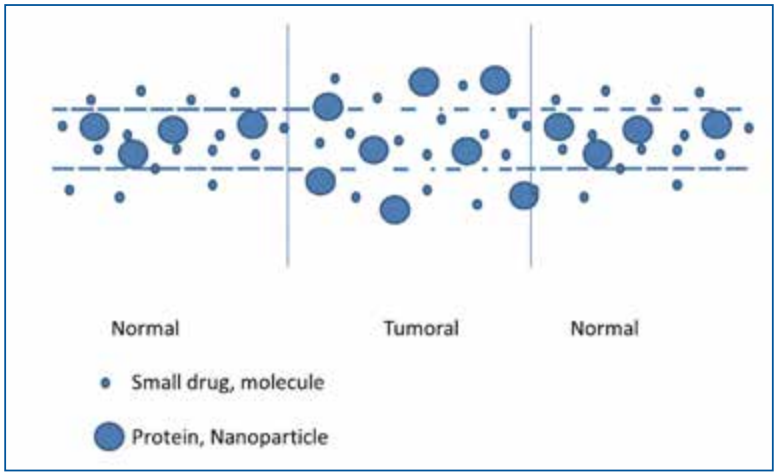

Figure 44.2 Diagram representing EPR effect.

Once the NPs are localized in the tumor, different strategies have been used to release the drug. Normally, the strategies are based on the different physicochemical properties found in the cytoplasm compared to the extracellular environment (e.g., blood). For example, NPs are known to be internalized via endocytic pathways, in which a pH drop is produced [24]. Thus, a pH-sensitive link between drug and NPs ensures non-specific release of drug during the circulation through the body [25]. A controlled release can be also achieved by the reduction of an oxidized inactive prodrug in the cytoplasm, releasing the drug in its active form

[26]. Also, one can take advantage of specific enzymes to cleave the link between NP and drug [27].

Thus, the use of Au NPs as carriers might provide several advantages, including the following:

- Increased blood half-life of the small drug. Renal filtration is avoided if the NP is larger than 6 nm.
- Accumulation in the tumor via the EPR effect.
- Reduced toxicity in normal tissue. The drug attached to Au NPs is not able to permeate through the continuous capillaries that irrigate the most part of organs.
- Controlled release of the drug, delivering high payloads directly to the site of action.
- Possibility of multiple functionalization, which allows combined therapy and/or tuning blood half-life, immune responses toward the vehicle, tumor uptake, etc.
- Increase in the solubility of poorly soluble drugs in plasma.
- Protection of the drug from immune system. Addition of stealthing agents (e.g., polyethylene glycol) may help to protect the drug from the immune system.
- Protection from agents present in the plasma that might deactivate the drug. Active site of the drug or the entire drug can be hindered during the journey through the organism until the moment of action.
- Promotion of a double effect by acting as carriers and as effectors by themselves. Physicochemical properties of Au NPs make possible their role as agents of photothermal therapy or as antennas to sensitize cells to radiotherapy.

44.5 Challenges of Using Gold Nanoparticles in Therapy

The use of Au NPs as new therapeutic tools open up a world of potential applications in the biomedical field, and specifically in cancer treatment. However, the use of any new technology needs to be seriously evaluated to minimize risks. Therefore, the use of Au NPs is concurrent to the appearance of challenges that should be considered.

Classical syntheses of Au NPs render concentrations of Au NPs in the range of 10^{12}–10^{13} NP/mL [28]; thus, Au NPs are typically synthesized at the nanomolar scale. Even though high densities of loading have been achieved [29, 30], concentrations of drugs onto NPs as synthesized will rarely be higher than 10 micromolar. Taking into account that there is a limitation of volume that can be injected into the body (e.g., 10 mL/Kg for intravenous injection in mice), the therapeutic dose might not be reached unless NPs had been previously concentrated. This concentration step is not always straightforward because concentration of Au NPs could lead to aggregation if special care is not taken (e.g., concentration of Au NPs without any surfactant increase the chances of aggregation). Note that colloids are intrinsically out of equilibrium and they tend to minimize surface energy when possible via either functionalization or aggregation. The need of concentration of Au NPs to reach therapeutic doses implies that a single lab-scale synthesis might not be enough to achieve the amount of NPs needed to perform *in vivo* experiments. Thus, not only monodispersity but also reproducibility batch to batch should be guaranteed to control size effects. In addition, robust synthesis protocols will also facilitate the scale-up of the production, which is essential for the transference of the technology to the industry [31] (Fig. 44.3).

Obviously, the special properties of Au NPs are lost if they aggregate. In too many cases, the loss of colloidal stability is behind the lack of (or unexpected) biological behaviors [32]. Therefore, one has to ensure the maintenance of colloidal stability along the process (synthesis–storage–exposure/treatment). It is common to assay the stability of Au NPs in the storage conditions (e.g., in aqueous media) even if they are different from the working conditions. However, biological fluids such as cell culture media or blood are complex mixtures of salts, proteins, sugars, etc., that may promote destabilization of Au NPs, and therefore stability should be assayed in this media. The same consideration is valid for the stability of the link with the drug. For example, cisplatin adsorbed on Au NPs is not released in aqueous media, while it is unspecifically and quickly released in cell culture media. On the other hand, cisplatin linked via coordination bond is stable in both media and only released after a pH drop [29].

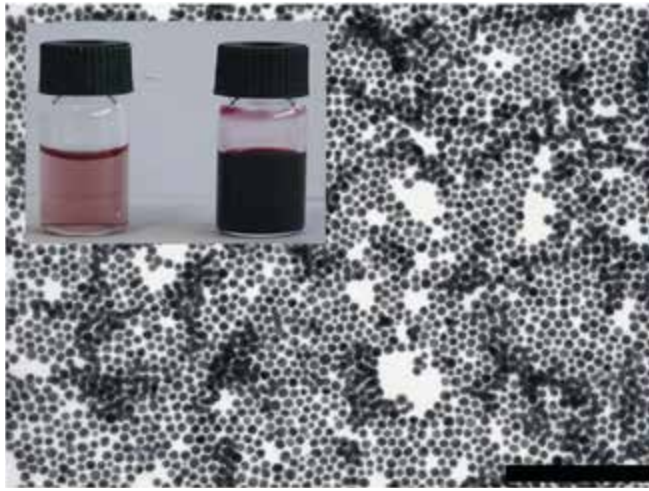

Figure 44.3 Example of classical synthesis of Au NPs (inset left) and concentrated Au NPs to reach therapeutic doses (inset right). The monodispersity of the concentrated solution is clearly observed in the TEM image. Scale bar is 200 nm.

The interactions of Au NPs and their environment need also to be evaluated. It is well known that proteins present in biological media interact with Au NPs forming a corona [33]. This corona can influence processes such as cell uptake or immune recognition [34]. Interestingly, the composition of the corona depends on the surfaces properties. Hydrophilic surfaces will likely induce protein corona in which albumin is the main component (note that albumin is the most abundant protein in blood) [33], while more hydrophobic surfaces will induce an increase of proteins such as fibrinogen, or lipoproteins [35]. It is worth noting also that protein corona formation is a dynamic process in which an initial protein corona is progressively hardened: Proteins interact strongly with NPs making the corona less labile. Indeed, the composition of the corona is modified with time from a corona formed by the most abundant proteins in serum to a progressively increase in the proteins that show more affinity to the surface [36].

The choice of appropriate models to determine the potential therapeutic benefits is also not trivial, especially for new technologies in which the amount of literature is limited. *In vitro* simple tests such as those assessed in monolayer cell cultures do not consider

important factors such as tumor vascularity, penetration and other differential properties given by the tumor microenvironment [37]. Consequently, *in vitro* results do not necessarily reflect the behavior of the assayed DDS in a real case. In this context, 3D cell cultures have been proposed as models to study the behavior of drugs in the particular environment of solid tumors due to the possibility to have an extracellular matrix and different regions of tumor (e.g., hypoxic cells in the intern areas). Since the advantages of using DDS are achieved mainly by modification on the pharmacokinetic properties of the drug, *in vivo* models are preferred. However, there is a great variety of tumor models including xenografted, orthotopic, and spontaneously and induced autochthonous tumor models [38]. This models show variations between them such as different size of porous in vessels or different immunological responses that may result in different efficiency of the same DDS depending on the model that has been used.

Finally, treatments with Au NPs are still very few and not beyond clinical trials. Thus, there is a lack of knowledge about regulatory aspects. Possible adverse effects of NPs such as acute toxicity and longtime accumulation should not be underestimated and should be studied case by case. There is a controversy regarding the *in vivo* toxicity of NPs and the parameters that play a role in the NPs-induced toxicity [39]. Some works have found no toxic signals after Au NP administration [40] or small alterations in the biochemical markers due to metabolization of the Au NPs or indicating a temporal inflammation [41]. On the other hand, it is believed that the dysfunction of major organs can be related to the presence of NPs at the site of abnormalities. For that reason, there are many studies regarding toxicity in spleen and liver, which are generally accepted to be the organs with the highest accumulation of NPs. The liver toxicity, when found, seems to be associated to a hyperplasia of Kupffer cells that induces an acute inflammation with neutrophils influx [42]. This acute inflammation is a transient response due to the insult of Au NPs; however, apoptosis and necrosis of hepatocytes as well as accumulation of Au NPs could be related to toxic effects [43]. Regarding the spleen, macrophages of the periphery seem to be involved in the uptake of NPs by this organ, thus leading to a temporal inflammation of the spleen. However, in other cases, a loss of weight has been observed after

intravenous administration [44]. White pulp aberration has been also observed [45]. Any general trend cannot be extracted from the current literature, but it is clear that there are some parameters that have to be taken into account before using Au NPs as a vehicle for medical applications: (i) size of the vehicle, since it will determine the clearance rate and the biodistribution [45]; (ii) surface composition; it has been seen that by changing the surface composition of Au NPs the toxicological profile might be different [46]; (iii) dose and administration route, since they will obviously play a role in the potential toxicity. Therefore, for every Au NP conjugate, a toxicology study must be done to prove their usability in medical applications.

44.6 Examples of Gold Nanoparticles in Cancer Therapy

44.6.1 Drug Delivery

The use of Au NPs as drug delivery agents has been largely reported and is attracting many efforts of both academia and industry. The control over the synthesis, the possibility of doing surface chemistry and consequently attach the molecules of interest (ligands and/or drugs), and the demonstrated biocompatibility of Au NPs are behind the interest of using them as platforms for drug delivery. The rational of using a drug delivery system is to increase the concentration of the drug of interest on the site of action respect the concentration of the drug on healthy organs. This implies that the total dose can be lower. In addition, the drug can be diverted away from organs in which a drug-associated damage is described (e.g., kidneys for cisplatin). Thus, systemic toxicity and/or specific side effects are generally minimized (Fig. 44.4).

Paciotti and coworkers demonstrated that TNF attached to 26 nm pegylated Au NPs showed a greater accumulation in tumors than free TNF [47]. Consequently, tumor volume was lower when mice received the Au NPs treatment than the free TNF. Interestingly, TNF plays here a double effect as targeting ligand and therapeutic agent. The therapeutic benefit was even greater when a second anticancer agent (paclitaxel) was added.

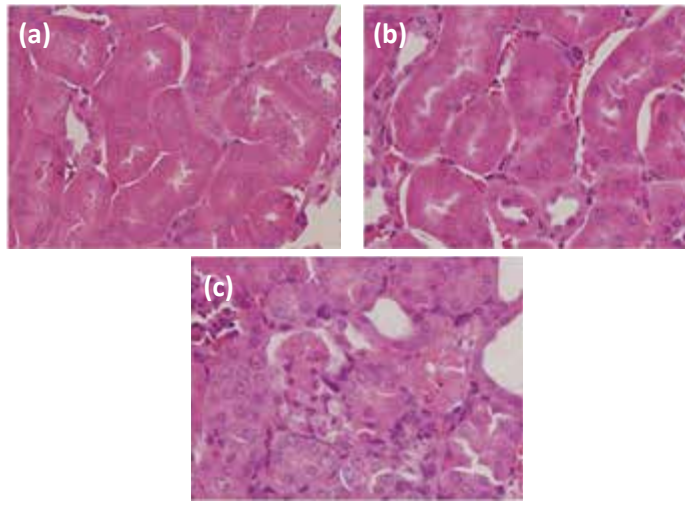

Figure 44.4 Toxicity of cisplatin in the kidneys. The appearance of histopathological changes in the proximal tubuli is evidence of nephrotoxicity. (a) Normal appearance of kidney section of control animals and (b) mice treated with Au NP-cisplatin. (c) Proximal tubular degeneration of animals taking high-dose free cisplatin. (Adapted from ref. 25).

In another example, Au NPs were used as a platform to minimize the side effects of one of the most used chemotherapeutic agents, cisplatin. This drug is associated to systemic toxicity and other side effects including nausea, renal toxicity, gastrointestinal toxicity, and peripheral neuropathy among others. Such side effects, especially nephrotoxicity, make it impossible to achieve the full benefit of the treatment in a large number of patients [48]. It is demonstrated in this work that by conjugating cisplatin to Au NPs via a pH-sensitive link, the drug is diverted away from organs irrigated by continuous capillaries such as those found in the kidneys, brain, and lungs in which cisplatin is known to induce toxicity. This is translated to a much lower levels of Pt in those organs. On the contrary, Au NP-cisplatin is accumulated in tumors and phagocytic organs like liver and spleen. Thus, while the toxicity is clearly reduced, the therapeutic benefits of the drug are maintained.

The field of drug delivery with Au NPs is very active and many examples can be found in reviews of the topic elsewhere [49, 50].

44.6.2 Radiosensitizers

Radiotherapy is a major modality to treat cancer. Its aim is to deliver a therapeutic radiation dose to the tumor while sparing the damage to the surrounding tissue [51]. However, radiotherapy is still limited by tumor cells that are radioresistant, under irradiated or outside the target region [52]. Moreover, tumor and surrounding tissue normally present similar X-ray absorption characteristics leading to side effects. To overcome these limitations, beam delivery methods are in constant improvement. The use of heavy elements that can be accumulated on the tumors has been also proposed due to their higher mass and energy absorption coefficients [53]. Among these elements, Au NPs are of special interest due to their strong photoelectric absorption coefficient and the ability to be differentially accumulated into tumors due to EPR effect. Therefore, the contrast between tumors and normal tissue would be improved if Au NPs accumulated into the tumor.

At KeV energies, X-ray primarily interacts with gold through the photoelectric effect, finally leading to a cascade of Auger electrons. The Auger electrons are weakly bound electrons released as result of electronic shell rearrangements. These electrons have low energies (<10 keV, with many <1 keV). In bulk gold, this effect is not important since these electrons have low energies and short ranges (<200 nm) and therefore they are stopped by the bulk gold. However, in the case of Au NPs, due to its high surface–volume ratio, the Auger electrons can escape the NP and deposit their energy in the surrounding environment. For a given type of ray or particle, the lower the energy is, the higher the Linear Energy Transfer (LET). Thus, Auger electrons have high LET, and consequently they deposit high doses of energy near an ionizing event in the Au NPs. This effect would also explain the experimental results observed at MeV energies since a large number of lower energy secondary electrons are produced after irradiation at high energies.

Radiation causes simple and complex lesions in the DNA. Simple lesions such as single strand break (SSB) are normally very efficiently repaired by the base excision repair mechanism (BER) since they are the same lesions as those extensively produced by endogenous oxidation. Consequently, they do not have any

biological effect. On the other hand, complex lesions such as double strand breaks (DSB) and other multiply damaged sites may fail to be repaired and are the responsible of the radiation-induced biological damage in cells with normal repairing mechanisms. Interestingly, hot spots produced due to dose inhomogeneity after irradiating Au NPs may lead to clusters of ionizations of a few nanometers [54]. Thus, there is a higher probability of having a complex, non-repairable lesion after an ionizing event on the Au NPs. For example, a DSB can be produced by a localized attack of two or more $^{\cdot}OH$ radicals.

44.6.3 Photothermal Therapy

The special optical properties of some Au NPs such as nanorods or nanocages that have a strong absorption in the near-infrared region of the spectra (therapeutic window) allow its use as photothermal therapy agents. In this case, irradiation works together with NP accumulation in tumor to achieve spatio-temporal control. Here, Au NPs act as antennas that absorb electromagnetic waves and locally deliver toxic amounts of heat. It is worth pointing out that it has been recently proposed that release of free radicals after irradiation may play an important role as well. It is necessary a light source such as lasers with spectral range of 650–900 nm for deep tissue penetration.

44.7 Conclusions

Despite the enormous advances in understanding cancer, today, the survival rates are still similar to those from 50 years ago. It is in this context that nanotechnology emerges as a “disruptive technology” with a great potential to contribute to improve cancer treatment by generating new diagnostic and therapeutic products. Thus, functionalized nanoparticles could deliver multiple therapeutic agents to tumor sites in order to simultaneously attack multiple points in the pathways involved in cancer. Therefore, more particles for drug delivery, diagnosis, and imaging are reaching the clinical trials, and it is expected that in the following decade, they will become a common tool for clinicians to treat cancer.

Disclosures and Conflict of Interest

The authors declare that they have no conflict of interest and have no affiliations or financial involvement with any organization or entity discussed in this chapter. This includes employment, consultancies, honoraria, grants, stock ownership or options, expert testimony, patents (received or pending) or royalties. No writing assistance was utilized in the production of this chapter and the authors have received no payment for its preparation.

Corresponding Author

Prof. Víctor F. Puntes
Inorganic Nanoparticles Group
Catalan Institute of Nanotechnology (ICN-2)
08193 Bellaterra, Barcelona, Spain
Email: victor.puntes.icn@gmail.com

About the Authors

Víctor F. Puntes' research spans in the field of nanoparticles: synthesis and conjugation of inorganic nanoparticles, their properties, nanotoxicology and nanosafety, and a variety of applications, including medicine and environment. In 1998, he obtained his PhD in physics from Universitat de Barcelona, Spain, working with Profs. Xavier Batlle and Amilcar Labarta in giant magnetoresistance in granular alloys. He had previously done his undergraduate studies in chemical engineering and materials science at the Université Louis Pasteur Strasbourg, France, and at Universitat Autònoma de Barcelona, Spain. After his PhD, he spent more than 3 years at the University of California—Berkeley and the Lawrence Berkeley National Laboratory, USA, in the groups of Profs. Paul Alivisatos and Kannan Krishnan, working on the synthesis and control of nano-structures. In 2003, he returned to Catalonia with a Ramón y Cajal research position at UB and in 2005 obtained an ICREA Professorship at the then Catalan Institute of Nanotechnology in Barcelona, Spain, to create the Inorganic Nanoparticles Group, which he leads today.

Francisco M. Romero, professor of inorganic chemistry at the University of Valencia, Spain, is a synthetic chemist who graduated in chemical engineering at European Higher Institute of Chemistry of Strasbourg (France) and received his PhD from the Université Louis Pasteur (Strasbourg I) under the supervision of Drs. Marc Drillon and Raymond Ziessel. Then he joined the group of Prof. Decurtins (Department für Chemie und Biochemie, University of Berne, Switzerland) as a post-doctoral researcher. Since 1999, he has been working as a researcher at the Institute for Molecular Science (ICMol, University of Valencia, Spain). His research interests cover different aspects at the interface of molecular chemistry and nanoscience, with a particular emphasis in nanomagnetism and in the development of diagnostic and therapeutic tools in biomedicine.

Joan Comenge studied chemistry and biochemistry at Universitat de Barcelona, Spain. He later obtained his MSc in nanoscience and nanotechnology from Universitat Autònoma de Barcelona, Spain. He spent 5 years working in the Inorganic Nanoparticles lab led by Prof. Víctor F. Puntes at the Catalan Institute of Nanotechnology, where he obtained his PhD in biomedicine. The research carried out during his PhD focused on the use of gold nanoparticles as drug delivery agents. He also performed a part of his research in the Radiation Biology group led by Prof. Kevin Prise at the Centre for Cancer Research and Cell Biology (Belfast, UK). Currently, he holds a position as a postdoctoral research associate at the Institute of Integrative Biology (University of Liverpool, UK) where he is developing nanoprobes for photoacoustic cell tracking.

Aurora Conill studied Biochemistry at Universitat Autónoma de Barcelona, Spain. In 1998, she obtained her MS in drug research and development at the Universidad de Navarra, Spain. From 1999 to 2007, she worked as clinical research project manager in R&D sections at Bayer and Novartis. Afterward, in 2007, she joined the Project Managing Department at the R&S Centre of Grupo Ferrer S.A., where she

focused on preclinical research managing. Since 2012, she has been project manager of Nanotargeting S.L., a startup company focused on the development of biomedical nanotechnological applications.

References

1. Faraday, M. (1857). The bakerian lecture: Experimental relations of gold (and other metals) to light. *Philos. Trans. R. Soc. Lond.,* **147**, 145–181.
2. Turkevich, J., Garton, G., Stevenson, P. C. (1954). The color of colloidal gold. *J. Colloid Sci.,* **9**, S26-S35.
3. Kimling, J., et al. (2006). Turkevich method for gold nanoparticle synthesis revisited. *J. Phys. Chem. B,* **110**, 15700–15707.
4. Park, J., Joo, J., Kwon, S. G., Jang, Y., Hyeon, T. (2007). Synthesis of monodisperse spherical nanocrystals. *Angew. Chem. Int. Ed.,* **46**, 4630–4660.
5. Frens, G. (1973). Controlled nucleation for regulation of particle-size in monodisperse gold suspensions. *Nat. Phys. Sci.,* **241**, 20–22.
6. Ji, X. H., et al. (2007). Size control of gold nanocrystals in citrate reduction: The third role of citrate. *J. Am. Chem. Soc.,* **129**, 13939–13948.
7. Jana, N. R., Gearheart, L., Murphy, C. J. (2001). Seeding growth for size control of 5–40 nm diameter gold nanoparticles. *Langmuir,* **17**, 6782–6786.
8. Bastús, N. G., Comenge, J., Puntes, V. C. (2011). Kinetically controlled seeded growth synthesis of citrate-stabilized gold nanoparticles of up to 200 nm: Size focusing versus Ostwald ripening. *Langmuir,* **27**, 11098–11105.
9. Niu, J. L., Zhu, T., Liu, Z. F. (2007). One-step seed-mediated growth of 30–150 nm quasispherical gold nanoparticles with 2-mercaptosuccinic acid as a new reducing agent. *Nanotechnology,* **18**, 325607.
10. Jana, N. R., Gearheart, L., Murphy, C. J. (2001). Evidence for seed-mediated nucleation in the chemical reduction of gold salts to gold nanoparticles. *Chem. Mater.,* **13**, 2313–2322.
11. Leonov, A. P., et al. (2008). Detoxification of gold nanorods by treatment with polystyrenesulfonate. *Acs Nano,* **2**, 2481–2488.
12. Eugenii, K., Itamar, W. (2004). Integrated nanoparticle-biomolecule hybrid systems: Synthesis, properties, and applications. *Angew. Chem. Int. Ed.,* **43**, 6042–6108.

13. Sellers, H., Ulman, A., Shnidman, Y., Eilers, J. E. (1993). Structure and binding of alkanethiolates on gold and silver surfaces: Implications for self-assembled monolayers. *J. Am. Chem. Soc.,* **115**, 9389–9401.
14. Nikoobakht, B., El-Sayed, M. A. (2003). Preparation and growth mechanism of gold nanorods (NRs) using seed-mediated growth method. *Chem. Mater.,* **15**, 1957–1962.
15. Jana, N. R., Gearheart, L., Murphy, C. J. (2001). Seed-mediated growth approach for shape-controlled synthesis of spheroidal and rod-like gold nanoparticles using a surfactant template. *Adv. Mater.,* **13**, 1389–1393.
16. Dreher, M. R., et al. (2006). Tumor vascular permeability, accumulation, and penetration of macromolecular drug carriers. *J. Natl. Cancer Inst.,* **98**, 335–344.
17. Maeda, H., Wu, J., Sawa, T., Matsumura, Y., Hori, K. (2000). Tumor vascular permeability and the EPR effect in macromolecular therapeutics: a review. *J. Control. Release,* **65**, 271–284.
18. Farokhzad, O. C., Langer, R. (2009). Impact of nanotechnology on drug delivery. *ACS Nano,* **3**, 16–20.
19. Tseng, C.-L., Su, W.-Y., Yen, K.-C., Yang, K.-C., Lin, F.-H. (2009). The use of biotinylated-EGF-modified gelatin nanoparticle carrier to enhance cisplatin accumulation in cancerous lungs via inhalation. *Biomaterials,* **30**, 3476–3485.
20. Hilgenbrink, A. R., Low, P. S. (2005). Folate receptor-mediated drug targeting: From therapeutics to diagnostics. *J. Pharm. Sci.,* **94**, 2135–2146.
21. Choi, C. H. J., Alabi, C. A., Webster, P. Davis, M. E. (2009). Mechanism of active targeting in solid tumors with transferrin-containing gold nanoparticles. *Proc. Natl. Acad. Sci.,* **107**, 1235–1240.
22. Pirollo, K. F., Chang, E. H. (2008). Does a targeting ligand influence nanoparticle tumor localization or uptake? *Trends Biotechnol.,* **26**, 552–558.
23. Perrault, S. D., Walkey, C., Jennings, T., Fischer, H. C., Chan, W. C. W. (2009). Mediating tumor targeting efficiency of nanoparticles through design. *Nano Lett.,* **9**, 1909–1915.
24. Nel, A. E., et al. (2009). Understanding biophysicochemical interactions at the nano-bio interface. *Nat. Mater.,* **8**, 543–557.
25. Comenge, J., et al. (2012). Detoxifying antitumoral drugs via nanoconjugation: The case of gold nanoparticles and cisplatin. *PLoS ONE*, **7**, e47562.

26. Dhar, S., Gu, F. X., Langer, R., Farokhzad, O. C., Lippard, S. J. (2008). Targeted delivery of cisplatin to prostate cancer cells by aptamer functionalized Pt(IV) prodrug-PLGA-PEG nanoparticles. *Proc. Natl. Acad. Sci.,* **105**, 17356–17361.
27. de la Rica, R., Aili, D., Stevens, M. M. (2012). Enzyme-responsive nanoparticles for drug release and diagnostics. *Adv. Drug Deliv. Rev.,* **64**, 967–978.
28. Daniel, M. C., Astruc, D. (2004). Gold nanoparticles: Assembly, supramolecular chemistry, quantum-size-related properties, and applications toward biology, catalysis, and nanotechnology. *Chem. Rev.,* **104**, 293–346.
29. Comenge, J., Romero, F. M., Sotelo, C., Dominguez, F., Puntes, V. (2010). Exploring the binding of Pt drugs to gold nanoparticles for controlled passive release of cisplatin. *J. Control. Release,* **148**, e31–e32.
30. Craig, G. E., Brown, S. D., Lamprou, D. A., Graham, D., Wheate, N. J. (2012). Cisplatin-tethered gold nanoparticles that exhibit enhanced reproducibility, drug loading, and stability: A step closer to pharmaceutical approval? *Inorg. Chem.,* **51**, 3490–3497.
31. Wheate, N. J. (2012). Nanoparticles: the future for platinum drugs or a research red herring? *Nanomedicine,* **7**, 1285–1287.
32. Ruenraroengsak, P., Cook, J. M., Florence, A. T. (2010). Nanosystem drug targeting: Facing up to complex realities. *J. Control. Release,* **141**, 265–276.
33. Casals, E., Pfaller, T., Duschl, A., Oostingh, G. J., Puntes, V. (2010). Time evolution of the nanoparticle protein corona. *ACS Nano,* **4**, 3623–3632.
34. Zhu, Z.-J., et al. (2012). The interplay of monolayer structure and serum protein interactions on the cellular uptake of gold nanoparticles. *Small,* **8**, 2659–2663.
35. Dell'Orco, D., Lundqvist, M., Oslakovic, C., Cedervall, T., Linse, S. (2010). Modeling the time evolution of the nanoparticle-protein corona in a body fluid. *PLoS ONE*, **5**, e10949.
36. Casals, E., Puntes, V. F. (2012). Inorganic nanoparticle biomolecular corona: formation, evolution and biological impact. *Nanomedicine,* **7**, 1917–1930, doi:10.2217/nnm.12.169.
37. Tredan, O., Galmarini, C. M., Patel, K., Tannock, I. F. (2007). Drug Resistance and the Solid Tumor Microenvironment. *J. Natl. Cancer Inst.,* **99**, 1441–1454.

38. Talmadge, J. E., Singh, R. K., Fidler, I. J., Raz, A. (2007). Murine models to evaluate novel and conventional therapeutic strategies for cancer. *Am. J. Pathol.,* **170**, 793–804.

39. Khlebtsov, N., Dykman, L. Biodistribution and toxicity of engineered gold nanoparticles: a review of *in vitro* and *in vivo* studies. *Chem. Soc. Rev.,* **40**, 1647–1671.

40. Lasagna-Reeves, C., et al. (2010). Bioaccumulation and toxicity of gold nanoparticles after repeated administration in mice. *Biochem. Biophys. Res. Commun.,* **393**, 649–655.

41. Zhang, X.-D., Wu, D., Shen, X., Liu, P.-X., Yang, N. Zhao, B., Zhang, H., Sun, Y.-M., Zhang, L.-A., Fan, F.-Y. (2011). Size-dependent in vivo toxicity of PEG-coated gold nanoparticles. *J. Int. J. Nanomed.,* **6**(1), 2071–2081

42. Cho, W.-S., et al. (2009). Acute toxicity and pharmacokinetics of 13 nm-sized PEG-coated gold nanoparticles. *Toxicol. Appl. Pharmacol.,* **236**, 16–24.

43. Abdelhalim, M., Jarrar, B. (2011). Gold nanoparticles administration induced prominent inflammatory, central vein intima disruption, fatty change and Kupffer cells hyperplasia. *Lipids Health Dis.,* **10**, 133.

44. Zhang, X.-D., et al. (2010). Toxicologic effects of gold nanoparticles *in vivo* by different administration routes. *Int. J. Nanomed.,* **5**, 771–781.

45. Chen, Y.-S., Hung, Y.-C., Liau, I., Huang, G. (2009). Assessment of the *in vivo* toxicity of gold nanoparticles. *Nanoscale Res. Lett.,* **4**, 858–864.

46. Simpson, C. A., Huffman, B. J., Gerdon, A. E., Cliffel, D. E. (2010). Unexpected toxicity of monolayer protected gold clusters eliminated by PEG-thiol place exchange reactions. *Chem. Res. Toxicol.,* **23**, 1608–1616.

47. Paciotti, G. F., et al. (2004). Colloidal gold: A novel nanoparticle vector for tumor directed drug delivery. *Drug Deliv.,* **11**, 169–183.

48. Oliver, T. G., et al. (2010). Chronic cisplatin treatment promotes enhanced damage repair and tumor progression in a mouse model of lung cancer. *Genes Dev.,* **24**, 837–852.

49. Ghosh, P., Han, G., De, M., Kim, C. K., Rotello, V. M. (2008). Gold nanoparticles in delivery applications. *Adv. Drug Deliv. Rev.,* **60**, 1307–1315.

50. Ojea-Jimenez, I., et al. (2013). Engineered inorganic nanoparticles for drug delivery applications. *Curr. Drug Metab*., **14**, 518–530.

51. Butterworth, K. T., McMahon, S. J., Currell, F. J., Prise, K. M. (2012). Physical basis and biological mechanisms of gold nanoparticle radiosensitization. *Nanoscale,* **4**, 4830–4838.

52. Hainfeld, J. F., Dilmanian, F. A., Slatkin, D. N., Smilowitz, H. M. (2008). Radiotherapy enhancement with gold nanoparticles.*J. Pharm. Pharm.,* **60**, 977–985.

53. McMahon, S. J., et al. (2011). Biological consequences of nanoscale energy deposition near irradiated heavy atom nanoparticles. *Sci. Rep.,* **1**(18), 19.

54. Lehnert, S. (2008). *Biomolecular Action of Ionizing Radiation*, CRC Press, Taylor & Francis Group, Boca Raton, FL.

Chapter 45

Solid Lipid Nanoparticles and Nanostructured Lipid Carriers for Cancer Therapy

Melike Üner, PhD

Istanbul University, Faculty of Pharmacy,
Department of Pharmaceutical Technology, Istanbul, Turkey

Keywords: solid lipid nanoparticles (SLN), nanostructured lipid carriers (NLC), nanopharmaceutical, targeting, stealth nanoparticles, particle size, particle charge, surface modification, cancer treatment, gene therapy, anti-cancer drugs, genes, non-steroidal anti-inflammatory drugs (NSAIDs), polyethylene glycol (PEG), pegylation, chitosan

45.1 Introduction

Solid lipid nanoparticles (SLN) are colloidal drug carrier systems, similar to nanoemulsions but differing in lipid nature. The liquid lipid used in emulsions is replaced by a solid lipid, including high-melting-point glycerides or waxes, to produce SLN [1, 2]. This makes SLN capable for the prolonged delivery of actives by reservoir action. Nanostructured lipid carriers (NLC), the second generation of SLN, can be produced by using spatially incompatible lipids together [3, 4]. Controlled drug delivery, enhancement of bioavailability

Handbook of Clinical Nanomedicine: Nanoparticles, Imaging, Therapy, and Clinical Applications
Edited by Raj Bawa, Gerald F. Audette, and Israel Rubinstein

ISBN 978-981-4669-20-7 (Hardcover), 978-981-4669-21-4 (eBook)
www.panstanford.com

of entrapped actives by improving their tissue distribution, and targeting of drugs are provided by employing SLN and NLC in various administration routes such as parenteral [5], ophthalmic [6], nasal [7], pulmonary [8], transdermal [4], and oral [9].

At the site of action with low systemic level and selective uptake of the drug by the target organ are great achievements in order to obtain ideal drug delivery by systemic application such as parenteral. Various research groups have focused on the targeting of lipid nanoparticles for primarily delivery of antineoplastic agents and biotechnological materials in the last decade, since the site delivery of those actives provides great benefits in the treatment of cancer and illness caused by genetic disorders [10, 11]. SLN and NLC are sophisticated systems for actives at cellular level. Thus, the incorporation of genetic materials such as deoxyribonucleic acid (DNA), ribonucleic acid (RNA) and oligonucleotides into lipid nanoparticles introduces a pathway for gene transfer to cells. This makes solid lipid-based drug carrier systems one of the most attractive systems for site-specific targeting primarily via parenteral application.

The safety of drug carrier systems is another important subject for researchers in addition to the great challenge for formulating sophisticated drug carrier systems. Nanoparticle-based synthetic and/or semisynthetic polymers, or contained residuals from organic solvents, often result in toxic or immunological side effects. However, lipids and surfactants used as components of SLN and NLC have been approved as "Generally Recognized as Safe" (GRAS status) due to their low toxicity. They have been using as excipients in pharmaceuticals and cosmetics for years [12]. SLN and NLC are 10–100-fold less cytotoxic than their polymeric counterparts since they do not contain residues typical for polymeric carriers like cytotoxic monomers, polymerization accelerators, etc. [13]. They are also safe and compatible with the environment. One can avoid the use of organic solvents, and surface-active agents at high concentrations by high-pressure homogenization, membrane contactor method, liquid flow-focusing using microchannels or microtubes, and supercritical fluid technology. In addition, excellent reproducibility with these cost-effective techniques, which are suitable for scaling-up, has been reported [14, 15]. Various drug incorporation methods have also been reported for years (e.g., preparation via O/W microemulsion and double (W/O/W)

emulsion, solvent emulsification-evaporation or -diffusion, and high shear homogenization and/or ultrasonication) [16].

Successfully formulated SLN and NLC can be stable for up to three years, which is of great importance with respect to colloidal drug carrier systems [13, 17]. They can be produced in desired size ranges, whereas liposomes are very often difficult to produce in a specific size range and with a sufficient drug payload. They have relatively low transfection rates to cells. Fast release of hydrophobic drugs and their instability are also emerging difficulties of liposomes [18].

In this chapter, targeting of SLN and NLC for delivery of anti-cancer drugs and biotechnological materials for the treatment of cancer is taken into consideration after a brief introduction of basic principles of the solid lipid nanotechnology. Methods that are used for protecting lipid nanoparticles from the phagocytic uptake, subsequently prolonging their existence in the systemic circulation after injection are mainly discussed. Incorporation of non-steroidal anti-inflammatory drugs (NSAIDs) into SLN and NLC as an adjuvant to cancer therapy is also presented in this chapter. Studies from past to present time, new approaches, and expectations for cancer treatment are discussed.

45.2 Principles of Drug Incorporation into SLN and NLC, and Drug Release

Solubility of drugs in the lipophilic phase, types of ingredients and their concentrations, and production methods have a great influence on types of SLN [4, 14]. Types of SLN and drug incorporation models define the drug release pattern and controlled drug delivery in general. Drug incorporation models of SLN have been characterized as follows (Fig. 45.1) [4]:

- *Solid solution model*: The drug is molecularly dispersed in the lipid matrix and strongly pronounced interactions with the lipid.
- *Drug-enriched shell model*: A solid lipid core forms when the recrystallization temperature of the lipid is reached. The drug concentrates on the surface of nanoparticles.
- *Drug-enriched core model*: The drug precipitates prior to the lipid crystallization during the cooling process of

the nanoemulsion after hot homogenization. Thus, further cooling finally leads to the recrystallization of the lipid surrounding the drug as a membrane.

Figure 45.1 Drug incorporation models of SLN.

NLC, the second-generation SLN, has been introduced by incorporation of liquid lipids into the solid structure to overcome various limitations related to classical SLN. Thus, better drug accommodation in order to increase the drug payload and to prevent drug expulsion during the storage can be possible with NLC.

Imperfect, amorphous, and multiple types of NLC have been described in the literature (Fig. 45.2) [4, 16]:

- *Imperfect type*: Accommodation of the drug is provided in large distances between fatty acid chains and amorphous clusters in the solid matrix (i.e., in the solid matrix containing imperfections in the crystal order).
- *Amorphous type*: A structureless solid amorphous matrix occurs by mixing solid lipids with liquid lipids. Nanoparticles are solid in an amorphous but not crystalline state in this case. Thus, drug expulsion can be prevented by the process of crystallization to β forms during the storage.
- *Multiple type*: This type is described as a multiple oil-in-fat-in-water (O/F/W) carrier since oil nanocompartments occur in lipid nanoparticles by addition of higher amounts of liquid lipids. Oil nanocompartments introduce a more appropriate medium for lipophilic drugs.

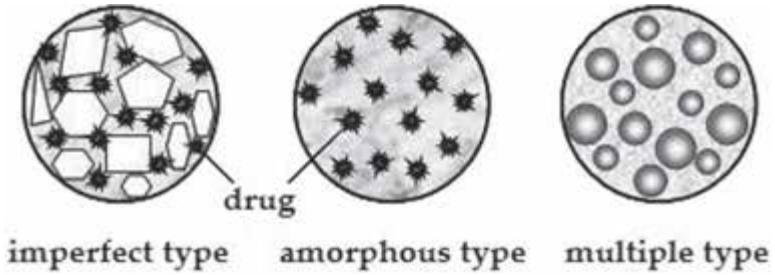

Figure 45.2 Types of NLCs.

Basic principles related in drug incorporation models of SLN and NLC help scientists to design lipid nanoparticles that have desired release profiles. The general principles of drug release from SLN and NLC have been described as follows [19–21]:

- Drug release rate decreases when the drug is homogeneously dispersed in the lipid matrix. Thus, a solid solution model of SLN can contribute sustained drug delivery.
- Drug release can be prolonged over several weeks by limiting mobility of the drug molecules in SLN. Slow crystallization behavior of the lipid carrier and high drug mobility lead to a faster drug release. There is an inverse relationship between crystallization degree and drug mobility.
- Release rate increases when the partition coefficient of a drug decreases.
- The burst effect, or fast initial drug release, usually occurs in the drug-enriched shell model of SLN due to the large surface area of drug deposition on the particle surface. About 100% of the drug is released within 5 min, particularly if surfactants are used at high concentrations.
- Drug release is usually governed by the Fick law of diffusion in the case of the drug-enriched core model of SLN since drug release is membrane controlled.
- Imperfect and amorphous types of NLC provide the desired prolonged release as compared to the multiple type of NLC.
- Drug release increases with an increase in the surface area of nanoparticles, i.e., drug release rate increases when particle size of nanoparticles decreases.

45.3 Targeting of SLN and NLC in the Treatment of Cancer

Great attention has been paid on nanotechnology in detecting and imaging tumors and their metastases, and for pre- and post-operative cancer treatment. Selective delivery of actives to the vasculature of tumors is the main goal in the cancer treatment [22, 23]. This can be possible by passive and active targeting of nanoparticles.

Active targeting is employed by specific modifications of drug carrier systems in the nanometer size range with several agents that have selective affinity for recognizing and interacting with a specific cell, tissue or organ. Active targeting is based on various mechanisms [24]:

- biochemical targeting to organs, cells, cell organelles, and intracellular cavity
- physical/external stimuli by ultrasound and magnetic field
- pretargeting/sandwich targeting
- promoter/transcriptional targeting

The inherent capability of nanoparticles and/or their appropriate modifications is required for site-specific delivery of drugs in passive targeting, whereas passive targeting of nanoparticles is based on various approaches:

- catheterization/direct injection of nanoparticle dispersion into the vessel opening to tumor vasculature/to target organ
- intravenous (i.v.) injection of nanoparticles after providing desired surface charge, particle size and/or modification with hydrophilic substances or polymers

Many studies have focused on i.v. injection of nanoparticles. On the other hand, exploiting the accessible targets on vascular endothelium can be possible by using catheters in the case of the first approach of passive targeting. Because, a tumor vasculature that has a defective and leaky structure is generally characterized by abnormalities such as unproportional and high amount of proliferation of endothelial cells, increased tortuosity and porosity, and irregular basement membrane formation due to the poorly regulated nature of tumor angiogenesis. Rapid vascularization is the result of fast-growing tumors and metastases to provide higher amounts of oxygen and nutrients than those needed by

normal healthy tissues (Fig. 45.3). In the meantime, lymphatic drainage decreases. In this case, carrier systems are expected to accumulate and permeate to tumors referring "Enhanced permeability and retention (EPR) effect" [25]. Thus, drugs or genes can be delivered with maximal efficacy and potency, and minimal side effects by targeting. Moreover, biodistribution of lipid nanoparticles can be manipulated by modifying surface characteristics for targeting.

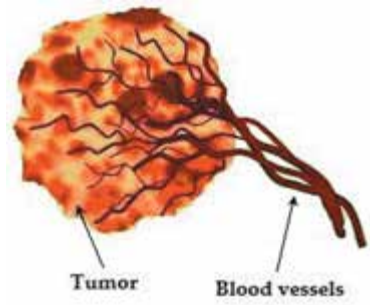

Figure 45.3 Tumor vasculature.

Modifying surface characteristic is inevitable in parenteral applications of nanoparticles. One must consider that there are various limitations for site-specific drug delivery caused by anatomical barriers and reticuloendothelial system (RES). Anatomical barriers limit and govern the distribution of drugs when macrophages remove them from systemic circulation by phagocytic uptake. Those limitations can be overcome by the chemical modification of drugs or loading them into the sophisticated drug carrier systems in the nanometer size range in order to provide site-specific drug delivery [26]. Sophisticated colloidal drug carrier systems, which are protected from phagocytic uptake by surface modification, can be transferred to organs or special tissues by both passive and active targeting. Therefore, colloidal drug carrier systems are expected to protect drugs or genetic materials from degradation, to bind to target cells, to be taken up and to deliver their contents in the required organelles or sites of cells.

Surface modification of SLN and NLC is also required for their parenteral application, as well. SLN and NLC can easily expose to phagocytic uptake due to their physicochemical properties such as

particle size, surface charge and surface hydrophobicity [27, 28]. Uptake by phagocytic cells is mediated by blood components that are called opsonins and specific cell receptors on macrophages that operate independently. Major opsonins are immunoglobulins (e.g., IgG and IgM), complement C_3b, and fibronectin, which are composed of proteins. Adsorption of opsonins onto nanoparticle surfaces results in immediate internalization of nanoparticles by macrophages of the mononuclear phagocytic system [29]. The surface characteristics of a particle determine whether or not opsonization will take place and which component will be involved. As a consequence, the mechanism of particle–cell interaction will also depend on the nature of the opsonic component and the relevant receptor-mediated process [30]. Also, plasma proteins may strongly affect biodistribution of drug carrier system in the systemic blood circulation.

45.3.1 Particle Size and Surface Charge of SLN and NLC

Nanoparticles should be produced in an optimum size range for their accumulation in a tumor and internalization by tumor cells. Studies indicated that the cutoff size of pores in tumor vessels as large as 200–1.2 mm. Decrease in size of nanoparticles results in easier uptake and leads to a significant increase in the rate of cellular uptake [31]. Therefore, particle size higher than 300 nm provides sustained drug delivery when the 50–300 nm size range displays rapid action. In a recent study, cellular uptake of nanoparticles that have sizes of about 200, 300, 400, 500 and 800 nm were investigated and compared with each other. It was found that the cellular uptake percentage of particles with a 200 nm diameter was about 1.5-fold higher than that of particles with an 800 nm diameter after a certain incubation time (12 h) [31].

Surface charge of nanoparticles that is resulted by nature of lipids, surface actives and coating materials, considerably affects their systemic half-life and biodistribution [28, 32]:

- Negatively charged nanoparticles usually have longer half-life compared to positively charged nanoparticles.
- Strong negative and strong positive charges usually lead to phagocytic uptake of nanoparticles more rapidly than weak-medium negative charge.

It should be considered that PEGylation usually suppresses the charge of nanoparticles and the zeta potential becomes to a less negative. This phenomena is attributed to an extension of the plane of shear the nanoparticles [33, 34].

45.3.2 Surface Modification of SLN and NLC with Polyethylene Glycol and Chitosan Polysaccharides

Surface modification of nanoparticles is a consistent and accurate approach for avoiding recognition of them by RES. Modification of lipid nanoparticles can be achieved using various techniques, including surface coating with polyethylene glycol (PEG) polymers and chitosan.

The history of the modification of actives and drug carrier systems with PEG is older than that of chitosan. Liu and Parsons found that each ethylene oxide residue of PEG binds three water molecules, which significantly altered the hydrodynamic properties of albumin when PEG attached to an albumin molecule [35]. Attachment of PEG to amino groups resulted in substantial changes in the physical and chemical properties of albumin. Abuchowski and his friends decreased immunological properties of bovine serum albumin by using PEG by taking this into consideration [36]. In the following years, this technique started to be used for decreasing the immunogenicity of proteins including enzymes such as superoxide dismutase [37], arginase [38], and asparaginase [39]. A decrease was observed in recognition of PEG-modified proteins by macrophages in those studies.

The same mechanism has been thought to be used for colloidal particles in an increase of their biodistribution. When colloidal particles are coated with PEG, which is an amphiphilic and flexible polymer, PEG can favorably modify the surface hydrophobicity of particles and sterically stabilize them, and thus, suppress the binding of serum proteins (e.g., apoproteins) and other opsonic factors [27].

Benefits and advantages of surface modification of colloidal particles can be briefly summarized as follows [40–42]:

(i) avoiding phagocytic uptake to modulate biodistribution parameters of drugs and improving presence of colloids in the blood circulation for systemic use

(ii) increasing stability of colloids in body fluids
(iii) acceleration of colloid transport across the epithelium
(iv) modulation of interaction of colloids with mucosa for specific delivery requirements and drug targeting
(v) minimizing side effects of drugs (this a great benefit especially for anti-neoplastic drugs), thus, increasing patient compliance to the treatment
(vi) increasing biocompatibility and decreasing thrombogenicity of drug carriers
(vii) providing reservoir function to colloid particles carrying hydrophobic drugs due to hydrophilic coating around the particles
(viii) providing good physical stability and dispersability of colloids
(ix) providing a cost-effective treatment by decreasing dose of actives

The passive targeting of nano-sized drug carrier systems to tumors was achieved with PEGylated liposomes through the EPR effect. Doxorubicin loaded liposomes had the FDA approval as Doxil® in 2003. Doxil® has been released to the market particularly for the treatment of ovarian carcinoma, acquired immunodeficiency syndrome (AIDS)-related Kaposi's sarcoma, and multiple myeloma. The liposome that obtained by modification with PEG, has been referred to as the "stealth liposome" since then [25]. Thereafter, PEGylated albumin nanoparticles that had FDA approval as Abraxane® in 2005 contains paclitaxel, a Taxol conjugate for the treatment of metastatic breast cancer.

The first attempt to produce vaccine formulations (recombinant malaria protein) using SLN was occurred in the early 1990s [43]. Almeida and colleagues described the first study on the incorporation of lysozymes, as a model peptide, in SLN [44]. SLN were produced under consideration of chemical and physical stabilization of the formulations in those studies. The first research on avoidance of phagocytic uptake was performed with the steric stabilization of nanoparticles with Poloxamine® 908 and Poloxamer® 407 and then Poloxamer® 188 [29, 45]. PEGylation of lipid nanoparticles was introduced at the end of the 1990s as PEGylation was one of the most popular and successful coating methods of nanoparticle based polymers and liposomes at that

time [46, 47]. Sterically stabilized SLN have also been called stealth SLN, but conversely non-stealth SLN by various research groups (Fig. 45.4) [46, 48]. Research on PEGylation of lipid nanoparticles accelerated particularly in the last decade. Although PEGylated SLN or NLC formulations have not been released commercially, lipid nanoparticles have a great potential for the targeting of actives due to the advantages regarded.

PEG derivatives at various molecular weights are used for PEGylation process. Those molecules are composed of block copolymers chemically containing hydrophilic and lipophilic residues that define their amphiphilic characteristics. Soluble hydrophilic residue of PEG turns to water and insoluble lipophilic residue is oriented on the lipophilic SLN by formation of a shell around the particle (Fig. 45.4). Lower molecular weight of PEG is more easily attached to the carrier system [28]. PEGylation of lipid nanoparticles can be easily achieved using all production methods reported for SLN and NLC (Table 45.1). This can be possible by incorporation of PEG or PEG-modified lipids into the lipid melt while production of nanoparticles.

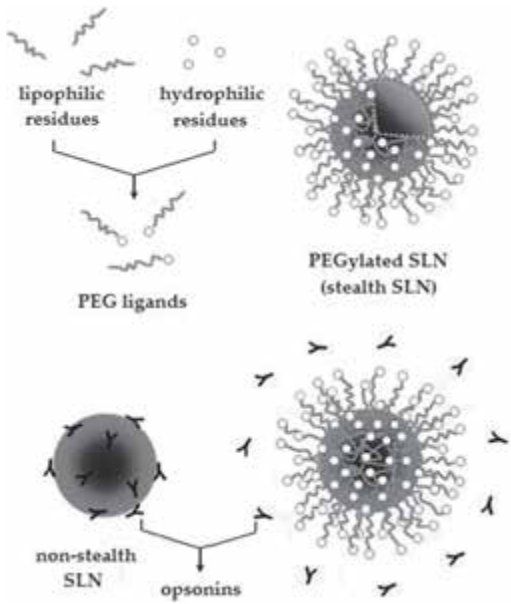

Figure 45.4 Illustrations of PEGylated SLN and non-stealth SLN in case of opsonization.

Factors affecting phagocytic uptake by RES and cellular uptake of PEGylated lipid nanoparticles [28, 49]:

(i) Increase in particle size decreases cellular uptake in general. Increase in PEG concentration results in significant increase in particle size. This can result in sustained drug delivery.
(ii) Increase in molecular weight of PEG, consequential decrease in the amount of hydrophilic residues may result in decrease in particle protection potential of PEG derivative from opsonization.
(iii) Increase of PEG density on particle surface improves the hydrophilicity of nanoparticles and consequently, complicates phagocytosis by RES more.
(iv) Lower melting point of PEG (lower molecular weight) leads to easier internalization by cell membrane and cellular uptake.
(v) Lipids with lower melting points contribute easier internalization by cell membrane and cellular uptake. Thus, NLC containing liquid lipids can meet this reality.

Indeed, mechanism of cellular uptake of PEGylated nanoparticles is not clear. While an inverse relationship between concentration and cellular uptake was observed [46], converse results were obtained in different studies [31]. Studies imply that interaction alters between PEG in various formulations and carriers with the cell membrane.

Several studies showed that PEGylation hindered intracellular trafficking of nanoparticles entrapped nucleic acids such as plasmid DNA (pDNA) and small interfering RNA (siRNA) [50]. Nucleic acids must be transferred to intracellular organelles for a successful function (e.g., cytosol for siRNA and nucleus for pDNA). Subsequent endosomal escape after cellular uptake is spoiled by PEGylation leading to significant loss in activity. Surface modification of nanoparticles by chitosan has been introduced as another approach to overcome limitations due to "PEG dilemma."

Chitosan is a biodegradable cationic polymer obtained by partial deacetylation of chitin [51]. It is commercially available in several types that vary in molecular weight ranging 10,000–1,000,000. It has a great potential for pharmaceutical applications due to its biocompatibility, non-toxicity, and mucoadhesive property. In recent years, chitosan has been one of the most

attractive water-soluble polymers for the targeting of drugs. For instance, surface modification by chitosan provides a long systemic circulation time when intracellular delivery of nucleic acids are successfully achieved. The same approach has been used for the targeting of colloidal drug carrier systems to tumor in the treatment of various types of cancer. The most advantageous property of chitosan is at the cellular level. It improves the internalization process and controls intracellular trafficking after providing stabilization of the carrier system in the systemic circulation.

For adsorption of chitosan onto a surface, the surface should display a negative charge (Fig. 45.5). Thus, interaction between positively charged chitosan and the negatively charged nanoparticle surface provides a coating process due to molecular attractive forces. Incorporation of chitosan into the aqueous phase is required in the production process.

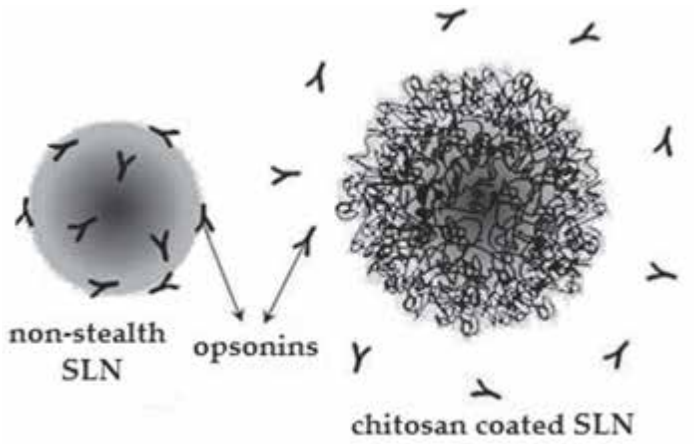

Figure 45.5 Illustrations of chitosan-coated SLN against opsonization.

Cross-linking agents such as glutaraldehyde can be used for improving the mechanical strength of chitosan layer [52]. The degree of cross-linking strongly affects the drug release rate. The drug release rate also decreases with a decrease in the molecular weight of chitosan. This can be attributed to the stronger folding ability of chitosan with low molecular weight that leads to the tight binding between chitosan and lipid nanoparticles. Drug diffuses through the chitosan coating with loose structure and reaches a relative fast drug release. Coating with other polysaccharides such

as mannose is another approach for site-specific delivery of lipid nanoparticles [53].

45.4 Incorporation of Anti-Neoplastic Drugs and Genes into SLN and NLC for Cancer Treatment

45.4.1 Anti-Neoplastic Drugs

Targeting of drugs also introduces several benefits particularly in the treatment of cancer since chemotherapy with anti-neoplastic agents lasts along with serious side effects that significantly disrupt the actual life and welfare of the patient. Hypersensitivity reactions, infections, neurotoxicity and painful conditions, nephrotoxicity, cardiotoxicity, anemia, coagulation disorders, hair loss, nausea and vomiting, exhaustion and various disorders are undesirable, grueling cases in the conventional chemotherapy with most of anti-neoplastic agents. In addition to difficulties in defining dosing schedule due to pharmacokinetic circumstances, various obstacles are reported at non-cellular and cellular levels with chemotherapy. Cancer cells display several defense mechanisms to diminish the toxicity of the chemotherapeutic agents to which they are exposed.

In addition, anti-neoplastic drug resistance occurs at the onset of therapy or during the advancing period by a tumor cell population over time due to a combination of spontaneous genetic mutations and selection by cytotoxic chemotherapy [54]. The mechanism of drug resistance has been categorized as pharmacokinetic and pharmacodynamic at non-cellular and cellular levels with altered response and angiogenesis. Permutations of various factors affect and define drug resistance mechanisms: sub-optimal dosing schedule, poor drug penetration due to high interstitial pressures, resistance to apoptosis, instability of drugs in body fluids, deficiency or alteration of drug mobility at cellular level, etc. [30]. As a consequence, drug resistance may be responsible for therapeutic failures. This phenomenon can be overcome by drug targeting.

Incorporation of anti-neoplastic drugs into SLN and NLC has been studied mostly in the last decade. Studies have indicated

that they have a great potential for localization on tumors and delivery of anti-neoplastics into tumor cells. Table 45.1 introduces anti-neoplastic drugs incorporated into SLN/NLC, coating materials, preparation techniques and types of cancer intended to be used for passive targeting via parenteral application.

45.4.2 Gene Therapy with SLN and NLC

Great advances have been made on the targeting of genetic materials in the prevention and treatment of diseases including cancer [78]. Incorporation of genetic materials into SLN and NLC such as DNA and RNA is intensively studied for many different types of cancer by various research groups (Table 45.2). Introduction of genetic materials into diseased cells and modification of their genes are called "gene therapy." Gene therapy is a very powerful technique for the treatment of various life-threatening illness caused by genetic disorders. Various precautions must be taken during the therapy and it must be precisely followed since it is relatively new and it may cause very harmful side effects if applied unwisely. Hereby, a proposed gene therapy can usually be employed in a clinic after permission of an authoritative commission according to juridical regulations [79].

There are several approaches to managing cancer with gene therapy [80, 81]:

(i) replacing missing or modified genes (e.g., p53) influencing cancer with healthy genes
(ii) improving immune response of the body to cancer
(iii) introducing healthy genes into cancer cells to provide higher sensitivity to chemo- and/or radiotherapy
(iv) activation of administered pro-drug in cancer cells with inserted suicide genes
(v) improving angiogenesis by developing new blood vessels

Improving the immune response to cancer can be employed by transfer a protein, T-cell receptor into T lymphocytes, white blood cells. Thus, T lymphocytes produce T-cell receptors that recognize and attach to the tumor cells. Thus, T lymphocytes attack and kill the tumor cells.

Table 45.1 Anti-neoplastic drugs incorporated into SLN and/or NLC

Drug		Coating material	Preparation technique	Type of cancer	Ref.
Alkylating agents	Carmustine	Cationic surfactants	Microemulsion	Malignant glioblastoma	[55]
	Chlorambucil	PEG	Probe sonication	Colon carcinoma	[56]
	Cisplatin	Anionic surfactants	Ultrasonication	Hepatocarcinoma	[57]
	Temozolomide	Anionic lipids	Emulsification and low-temperature solidification	—	[58]
Plant alkaloids	Bufadienolides	Anionic surfactants	Melt-emulsification and ultrasonication	Sarcoma	[59]
	Docetaxel	Anionic surfactants Folic acid	High shear homogenization, Modified film ultrasonication, Solvent emulsification-evaporation	Liver, ovarian and lung carcinomas, brain tumors	[60–62]
	Etoposide	Anionic surfactants, Cationic lipids	High-pressure homogenization	Lymphoma tumor, Brain malignancy	[63, 64]
	Paclitaxel	PEG Cationic lipids	Solvent emulsification-diffusion and high-pressure homogenization, Microemulsion, Emulsification-solidification	Lung, ovarian and breast adenocarcinomas, epithelial carcinoma	[65–68]

Drug		Coating material	Preparation technique	Type of cancer	Ref.
	Taspine	Polioxyethylene-stearyl ether galactoside	Film evaporation-extrusion	Hepatocarcinoma	[69]
	Vinorelbine bitartrate	Steric stabilization, PEG	High-pressure homogenization	Breast adenocarcinoma	[31, 70]
Antibiotics	Doxorubicin	Chitosan, PEG, Mannose, Cross-linked octadecylamine, Anionic lipids	Solvent diffusion, Solvent emulsification-diffusion, Solvent injection	Breast, lung and ovarian carcinomas	[52, 53, 71–73]
	Mitoxantrone	Steric stabilization	Ultrasonication	Breast carcinoma	[74]
Others	Edelfosine	Steric stabilization, Anionic lipids	Solvent emulsification-evaporation	—	[75]
	5-fluorouracil	Anionic surfactants	Solvent emulsification-evaporation	Colorectal carcinoma	[76]
	Tocotrienol	Steric stabilization	Microemulsion	Breast carcinoma	[77]
	Topotecan	Anionic surfactants	Microemulsion	Myelogenous leukemia	[10]

Table 45.2 Genetic materials incorporated into SLN and NLC for the treatment of cancer

Drug	Coating material	Preparation technique	Type of cancer	Ref.
DNA	Cationic excipients	Solvent emulsification-evaporation	—	[83]
DNA and streptavidin	Cationic lipids	Microemulsion	Lung cancer	[11]
Nonviral gene	Cetylated polyethylenimine	Solvent emulsification-evaporation	Lung adenocarcinoma	[82]
p53	Cationic lipids	High-pressure homogenization	Lung carcinoma	[84]
siRNA	PEG, Cationic lipids	Modified film ultrasonication, Emulsification-solidification	Fibrosarcoma, epithelial carcinoma	[50, 68]
Placebo	L-arginine Anionic surfactants	Microemulsion	Brain cancer	[5]

Introduction of genetic materials into cancer cells is possible using a special carrier known "vector" [11]. The most commonly used vectors are viruses (e.g. retroviruses and adenoviruses), which have agility to recognize tumor cells and to introduce genes into them for transferring to nucleus. Thus, genes are transferred to cell DNA and cell DNA is modified both temporarily and permanently. The use of nanoparticles instead of vectors attracts the attention of many researchers [82]. Suitable modification of nanoparticles associates the targeting of genetic material to certain cells, letting in and reaching to nucleus. Nanoparticles introduce several advantages over viruses in case of this gene therapy approach since viruses may infect healthy cells as well as tumor cells. Thus, viruses may modify and damage the DNA of healthy cells. Moreover, transferred genes may be overexpressed since they are produced with missed protein segments. This usually results in immune reactions and inflammation. If germ cells that are reproductive cells (i.e., human eggs and sperms) sustain damage at the genetic level, spoiled genes can pass on to future generations. However, well-formulated nanoparticles are capable to deliver genes only to tumor cells and to specific organelles of tumor cells.

Several studies on gene delivery with SLN and NLC have been employed with the aim of passive targeting (Table 45.2).

45.5 NSAIDs as Adjuvant to Cancer Chemotherapy

Prostaglandins act in a variety of pathophysiological processes such as stimulation of angiogenesis and inhibition of apoptosis [85, 86]. NSAIDs perform by inhibiting cyclooxygenase enzymes (COX), COX-1 and COX-2. They inhibit the conversion of arachidonic acid to thromboxane and prostaglandins (Fig. 45.6) COX-1, the first COX isoform is responsible for the regulation of platelet aggregation and the maintenance of gastric mucosa. COX-2, the second isoform, is involved in inflammation and tumorigenesis. Tumor progression and metastasis are strongly affected by inflammation [57]. Inhibition of inflammation is demonstrated to diminish pathological circumstances of cancer. In recent years, NSAIDs have been reported to suppress nuclear transcription factor, NF-κB, which controls the expression of genes such as COX-2 and cyclin D1 [87]. The expression of most genes that are involved in inflammation (e.g., COX-2) or in cellular proliferation (e.g., cyclin D1) are regulated by NF-κB. Both antiproliferative and anti-inflammatory effects of NSAIDs are shown to suppress NF-κB. Thus, this makes it one of the targets. NF-κB is commonly overexpressed in cancer cells. In particular, COX-2 expression results in a considerable proportion of various types of pre-invasive and invasive cancers indicating decrease in the risk of metastasis and large tumor size.

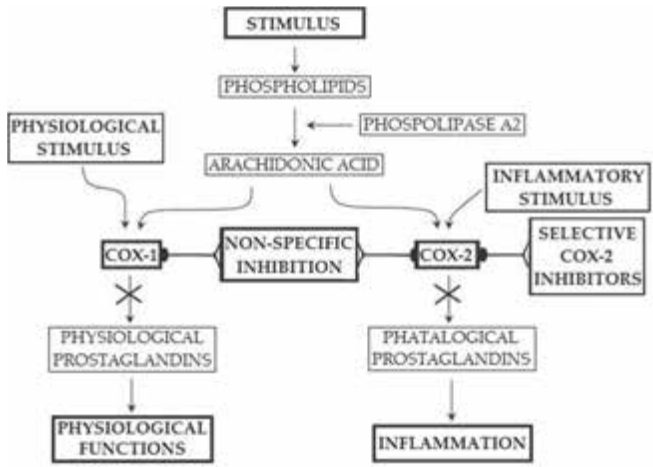

Figure 45.6 Function of COX-1 and COX-2, and mechanism of NSAIDs.

Nevertheless, suppressive effect of all types of NSAIDs on cancer has not been fully understood. In some cases such as aspirin, its inhibition effect on human colon cancer cells is through COX-independent mechanisms [88]. It displays its anti-cancer effects by expressing DNA mismatch repair proteins. Several researchers are studying the treatment of various types of cancer with selective COX-2 inhibitors. Their effect based on COX-2 inhibition has demonstrated their high potential for prevention of breast, colon, lung, prostate and bladder cancers. Therefore, their use as adjuvants has a growing interest for the cancer treatment.

Non-selective NSAIDs and selective COX-2 inhibitors have been researched for various types of cancer [89–95]. Their incorporation into sophisticated drug delivery systems is quite new for nanotechnology for the treatment of cancer. In the last decade, NSAIDs have been incorporated into SLN and NLC in order to use in the treatment of inflammation and rheumatoid disorders and formulation parameters have been intensively evaluated in each study. Nimesulid [96], indomethacin [97], celecoxib [3], valdecoxib [98], and flurbiprofen [6, 99] were successfully introduced into SLN and NLC for several purposes. Thus, their application in lipid nanoparticles via targeting to tumors may introduce a new approach for supportive therapy. As adjuvants, NSAID-loaded lipid nanoparticles will contribute advantages of targeting and controlled drug delivery in order to provide efficient therapy.

45.6 Conclusions

Both chemotherapy with anti-neoplastic drugs and radiotherapy are usually employed for traditional cancer treatments that introduce various difficulties for clinicians and patients. Because, side effects particularly caused by anti-neoplastic agents disrupt the actual life and welfare of the patient. Moreover, anti-neoplastic drug resistance usually occurs at the onset or the further steps of therapy. Those factors make the selective delivery of anti-neoplastic drugs to tumors is the main goal in the cancer treatment. Selective delivery also provides different approaches to manage cancer with gene therapy and supportive therapy. Selective delivery

can be possible by formulating drugs and genetic materials in sophisticated colloidal carrier systems. Colloidal drug carrier systems should be designed to protect drugs or genetic materials from degradation in the systemic circulation, to be taken up by target cells and to deliver their contents in the required organelles or sites of cells. Thus, drugs or genes can be delivered with maximal efficacy and potency, and minimal side effects.

SLN and NLC are colloidal drug carrier systems that have unique properties and a lot of advantages over their colloidal counterparts. Various research groups and pharmaceutical companies have focused on them. Their surface modification for selective drug delivery has been increasingly investigated in the past decade. Successful results indicate that SLN and NLC are promising colloidal drug carrier systems for the selective delivery of actives in cancer therapy.

Abbreviations

AIDS: Acquired immunodeficiency syndrome
COX: Cyclooxygenase
DNA: Deoxyribonucleic acid
EPR: Enhanced permeability and retention
FDA: Food and Drug Administration
GRAS: Generally recognized as safe
IgG: Immunoglobulin G
IgM: Immunoglobulin M
i.v.: Intravenous
NF-κB: Nuclear factor kappa B
NLC: Nanostructured lipid carriers
NSAID: Non-steroidal anti-inflammatory drug
O/F/W: Oil-in-fat-in-water
O/W: Oil-in-water
PEG: Polyethylene glycol
pDNA: Plasmid DNA
RES: Reticuloendothelial system
RNA: Ribonucleic acid
siRNA: Small interfering RNA
SLN: Solid lipid nanoparticles
W/O/W: Water-in-oil-in-water

Disclosures and Conflict of Interest

The author declares that she has no conflict of interest and has no affiliation or financial involvement with any organization or entity discussed in this chapter. This includes employment, consultancies, honoraria, grants, stock ownership or options, expert testimony, patents (received or pending) or royalties. No writing assistance was utilized in the production of this chapter and the author has received no payment for its preparation. The findings and conclusions here reflect the current view of the author and should not be attributed, in whole or in part, to the organizations with which she is affiliated, nor should she be considered as expressing an opinion with regard to the merits of any particular company or product discussed herein. Nothing contained herein is to be considered as the rendering of legal advice.

Corresponding Author

Dr. Melike Üner
Istanbul University, Faculty of Pharmacy
Department of Pharmaceutical Technology
Beyazit 34116, Istanbul, Turkey
Email: unerm@istanbul.edu.tr

About the Author

Melike Üner is an associate professor of pharmaceutical technology at the Faculty of Pharmacy, Istanbul University, Istanbul, Turkey. She received her undergraduate degree from the Faculty of Pharmacy, Istanbul University, in 1988 and MSc and PhD in pharmaceutical technology from the same Faculty in 1995 and 2001, respectively. Dr. Üner worked as a research assistant until 2006. She was an assistant professor from 2006 to 2008 in the same department. Her postdoctoral studies have focused on controlled drug delivery and nanotechnology. She has more than 50 publications, including 23 manuscripts and 27 proceedings/abstracts.

References

1. Mehnert, W., Mäder, C. (2001). Solid lipid nanoparticles. Production, characterization and applications. *Adv. Drug Deliv. Rev.,* **47**(2–3), 165–196.
2. Müller, R. H., Mehnert, W., Lucks, J. S., Schwarz, C., Zur Mühlen, A., et al. (1995). Solid lipid nanoparticles (SLN)-An alternative colloidal carrier system for controlled drug delivery. *Eur. J. Pharm. Biopharm.,* **41**(1), 62–69.
3. Joshi, M., Patravale, V. (2008). Nanostructured lipid carriers (NLC) based gel of celecoxib. *Int. J. Pharm.,* **346**(1–3), 124–132.
4. Müller, R. H., Radtke, M., Wissing, S. A. (2002). Solid lipid nanoparticles (SLN) and nanostructured lipid carriers (NLC) in cosmetic and dermatological preparations. *Adv. Drug Deliv. Rev.,* **54**(Suppl. 1), S131–S155.
5. Kuo, Y.-C., Lin, C.-W. (2009). Impact of arginine-modified solid lipid nanoparticles on the membrane charge of human brain-microvascular endothelial cells. *Colloids Surf. B Biointerfaces,* **72**(2), 201–207.
6. Gonzalez-Mira, E., Egea, M. A., Garcia, M. L., Souto, E. B. (2010). Design and ocular tolerance of flurbiprofen loaded ultrasound-engineered NLC. *Colloids Surf. B Biointerfaces,* **81**(2), 412–421.
7. Eskandari, S., Varshoaz, J., Minaiyan, M., Tabbakhian, M. (2011). Brain delivery of valproic acid via intranasal administration of nanostructured lipid carriers: *In vivo* pharmacodynamic studies using rat electroschock model. *Int. J. Nanomed.,* **6**, 363–371.
8. Hu, L. D., Jia, Y., Ding, W. (2010). Preparation and characterization of solid lipid nanoparticles loaded with epirubicin for pulmonary delivery. *Pharmazie,* **65**(8), 585–587.
9. Chakraborty, S., Shukla, D., Vuddanda P. R., Mishra, B., Singh, S. (2010). Utilization of adsorption technique in the development of oral delivery system of lipid based nanoparticles. *Colloids Surf. B Biointerfaces,* **81**(2), 563–569.
10. Souza, L. G., Silva, E. J., Martins, A. L. L., Mota, M. F., Braga, R. C., et al. (2011). Development of topotecan loaded lipid nanoparticles for chemical stabilization and prolonged release. *Eur. J. Pharm. Biopharm.,* **79**(1), 189–196.
11. Pedersen, N., Hansen, S., Heydenreich, A. V., Kristensen, H. G., Poulsen, H. S. (2006). Solid lipid nanoparticles can effectively bind DNA,

streptavidin and biotinylated ligands. *Eur. J. Pharm. Biopharm.,* **62**(2), 155–162.

12. U. S. Food and Drug Administration. (2007). Title 21, Code of Federal Regulations, Part 182, 184, 186. Office of the Federal Register, National Archives and Records Administration, Washington D.C.
13. Wissing, S. A., Kayser, O., Müller, R. H. (2004). Solid lipid nanoparticles for parenteral drug delivery. *Adv. Drug Deliv. Rev.,* **56**(9), 1257–1272.
14. Müller, R. H., Mäder, K., Gohla, S. (2000). Solid lipid nanoparticles (SLN) for controlled drug delivery-a review of the state of the art. *Eur. J. Pharm. Biopharm.,* **50**(1), 161–177.
15. Yun, J., Zhang, S., Shen, S., Chen, Z., Yao, K., et al. (2009). Continuous production of solid lipid nanoparticles by liquid flow-focusing and gas displacing method in microchannels. *Chem. Eng. Sci.,* **64**(19), 4115–4122.
16. Üner, M. (2006). Preparation, characterization and physico-chemical properties of solid lipid nanoparticles (SLN) and nanostructured lipid carriers (NLC): Their benefits as colloidal drug carrier systems. *Pharmazie,* **61**(5), 375–386.
17. Pandita, D., Ahuja, A., Velpandian, T., Lather, V., Dutta, T., et al. (2009). Characterization and *in vitro* assessment of paclitaxel loaded solid lipid nanoparticles formulated using modified solvent injection technique. *Pharmazie,* **64**(5), 301–310.
18. Rai, S., Paliwal, R., Gupta, P. N., Khatri, K., Goval, A. K., et al. (2008). Solid lipid nanoparticles (SLNs) as a rising tool in drug delivery science: One step up in nanotechnology, *Curr. Nanosci.,* **4**(1), 30–44.
19. Müller, R. H., Runge, S. A., Ravelli, V., Thünemann A. F., Mehnert, W., et al. (2008). Cyclosporine-loaded solid lipid nanoparticles (SLN®): Drug-lipid physicochemical interactions and characterization of drug incorporation. *Eur. J. Pharm. Biopharm.,* **68**(3), 535–544.
20. Westesen, K., Bunjes, H., Koch, M. H. J. (1997). Physicochemical characterization of lipid nanoparticles and evaluation of their drug loading capacity and sustained release potential. *J. Control. Release,* **48**(2–3), 223–236.
21. Zur Mühlen, A., Schwarz, C., Mehnert, W. (1998). Solid lipid nanoparticles (SLN) for controlled drug delivery—Drug release and release mechanism. *Eur. J. Pharm. Biopharm.,* **45**(2), 149–155.
22. Banerjee, D., Harfouche, R., Sengupta, S. (2011). Nanotechnology-mediated targeting of tumor angiogenesis. *Vasc. Cell,* **3**(1), 3.

23. Kelland, L. R. (2005). Targeting established tumor vasculature: A novel approach to cancer treatment. *Curr. Cancer Ther. Rev.,* **1**(1), 1–9.

24. Vasir, J. K., Reddy, M. K., Labhasetwar, V. D. (2005). Nanosystems in drug targeting: Opportunities and challenges. *Curr. Nanosci.,* **1**, 47–64.

25. Matsamura, Y., Maeda, H. (1986). A new concept for macromolecular therapeutics in cancer chemotherapy: Mechanism of tumoritropic accumulation of proteins and the antitumor agent smancs. *Cancer Res.,* **46**, 6387–6392.

26. Torchilin, V. P. (2010). Passive and active drug targeting: Drug delivery to tumors as an example. In: Schäfer-Korting, M., ed. *Drug Delivery. Handbook of Experimental Pharmacology,* Part I. Springer-Verlag, Berlin Heidelberg, Germany; pp. 3–53.

27. Zhang, X., Gan, Y., Gan, L., Nie, S., Pan, W. (2008). PEGylated nanostructured lipid carriers loaded with 10-hydroxycamptothecin: An efficient carrier with enhanced anti-tumor effects against lung cancer. *J. Pharm. Pharmacol.,* **60**(8), 1077–1087.

28. Üner, M., Yener, G. (2007). Importance of solid lipid nanoparticles (SLN) in various administration routes and future perspectives. *Int. J. Nanomed.,* **2**(3), 289–300.

29. Müller, R. H., Maassen, S., Schwarz, C., Mehnert, W. (1997). Solid lipid nanoparticles (SLN) as potential carrier for human use: Interaction with human granulocytes. *J. Control. Release,* **47**(3), 261–269.

30. Wong, H. L., Bendayan, R., Rauth, A. M., Li, Y., Wu, X. Y. (2007). Chemotherapy with anticancer drugs encapsulated in solid lipid nanoparticles. *Adv. Drug Deliv. Rev.,* **59**(6), 491–504.

31. Wan, F., You, J., Sun, Y., Zhang, X.-G., Cui, F.-D., et al. (2008). Studies on PEG-modified SLNs loading vinorelbine bitartrate (I): Preparation and evaluation *in vitro*. *Int. J. Pharm.,* **359**(1–2), 104–110.

32. Stossel, T. P., Mason, R. J., Hartwig, J., Waughan, M. (1972). Quantitative studies of phagocytosis by polymononuclear leukocytes: Use of emulsion to measure the initial rate of phagocytosis. *J. Clin. Invest.,* **51**(3), 615–624.

33. Gref, R., Lück, M., Quellec, P., Marchand, M., Dellacherie Harnisch, S., et al. (2000). "Stealth" corona-core nanoparticle surface modified by polyethylene glycol (PEG): Influence of the corona (PEG chain length and surface density) and of the core composition on phagocytic uptake and plasma protein adsorption. *Colloids Surf. B Biointerfaces,* **18**(3–4), 301–313.

34. Tröster, S. D., Wallis, K. H., Müller, R. H. (1992). Correlation of surface hydrophobicity of ^{14}C-poly(methyl methacrylate) nanoparticles to the body distribution. *J. Control. Release,* **20**(3), 247–253.

35. Liu, K.-J., Parsons, J. L. (1969). Solvent effects on the preferred conformation of poly(ethylene glycols). *Macromolecules,* **2**(5), 529–533.

36. Abuchowski, A., Van Es, T., Palczuk, N. C., Davis, F. F. (1977). Alteration of immunological properties of bovine serum albumin by covalent attachment of polyethylene glycol. *J. Biol. Chem.,* **252**(11), 3578–3581.

37. Gray, B. H., Stull, R. W. (1983). Radioprotection by polyethylene glycol-protein complexes in mice. *Radiat. Res.,* **93**(3), 581–587.

38. Savoca, K. V., Davis, F. F., Van Es, T., McCoy, J. R., Palczuk, N. C. (1984). Cancer therapy with chemically modified enzymes. II. The therapeutic effectiveness of arginase, and arginase modified by the covalent attachment of polyethylene glycol, on the taper liver tumor and the L517Y murine leukemia. *Cancer Biochem. Biophys.,* **7**(3), 261–268.

39. Abuchowski, A., Kazo, G. M., Verhoest, C. R., Van Es T., Kafkewitz, et al. (1984). Cancer therapy with chemically modified enzymes. I. Antitumor properties of polyethylene glycol asparaginase conjugates. *Cancer Biochem. Biophys.,* **7**(2), 175–186.

40. Otsuka, H., Nagasaki, Y., Kataoka, K. (2003). PEGylated nanoparticles for biological and pharmaceutical applications. *Adv. Drug Deliv. Rev.,* **55**(3), 403–419.

41. Oyewumi, M. O., Yokel, R. A., Jay, M., Coakley, T., Mumper, R. J. (2004). Comparison of cell uptake, biodistribution and tumor-bearing mice. *J. Control. Release,* **95**(3), 613–626.

42. Zhang, Y., Zhang, J. (2005). Surface modification of monodisperse magnetite nanoparticles for improved intracellular uptake to breast cancer cells. *J. Colloid Interf. Sci.,* **283**(2), 352–357.

43. Amselem, S., Domb, A. J., Alving, C. R. (1992). Lipospheres as a vaccine carrier system: Effects of size, charge, and phospholipid composition. *Vaccine Res.,* **1**(4), 383–395.

44. Almeida, A. J., Runge, S., Müller, R. H. (1997). Peptide-loaded solid lipid nanoparticles (SLN): Influence of production parameters. *Int. J. Pharm.,* **149**(2), 255–265.

45. Müller, R. H., Maassen, S., Weyhers, H., Mehnert, W. (1996). Phagocytic uptake and cytotoxicity of solid lipid nanoparticles (SLN) sterically stabilized with poloxamine 908 and poloxamer 407. *J. Drug Target.,* **4**(3), 161–170.

46. Bocca, C., Caputo, O., Cavalli, R., Gabriel, L., Miglietta, A., et al. (1998). Phagocytic uptake of fluorescent stealth and non-stealth solid lipid nanoparticles. *Int. J. Pharm.,* **175**(2), 185–193.

47. Zara, G. P., Cavalli, R., Fundaro, A., Bargoni, A., Caputo, O., et al. (1999). Pharmacokinetics of doxorubicin incorporated solid lipid nanospheres (SLN). *Pharm. Res.,* **40**(3), 281–286.

48. Fundaro, A., Cavalli, R., Bargoni., A., Vighetto, D., Zara, G. P., et al. (2000). Non-stealth and stealth solid lipid nanoparticles (SLN) carrying doxorubicin: Pharmacokinetics and tissue distribution after i.v. administration rats. *Pharm. Res.,* **42**(4), 337–343.

49. Cavalli, R., Caputo, O., Gasco, M. R. (2000). Preparation and characterization of solid lipid nanospheres containing paclitaxel. *Eur. J. Pharm. Sci.,* **10**(4), 305–309.

50. Hatakeyama, H., Akita, H., Ito, E., Hayashi, Y., Oishi, M., et al. (2011). Systemic delivery of siRNA to tumors using a lipid nanoparticle containing a tumor-specific cleavable PEG-lipid. *Biomaterials,* **32**(18), 4306–4316.

51. Rowe, R. C., Sheskey, P. J., Owen, S. C. (2006). *Handbook of pharmaceutical excipients*, 5th ed., Pharmaceutical Press, London, Chicago; pp. 159–162.

52. Ying X.-Y., Cui, D., Yu, L., Du, Y.-Z. (2011). Solid lipid nanoparticles modified with chitosan oligosaccharides for the controlled release of doxorubicin. *Carbohydr. Polym.,* **84**(4), 1357–1364.

53. Jain, A., Agarwal, A., Majumder, S., Lariya, N., Khaya, A., et al. (2010). Mannosylated solid lipid nanoparticles as vectors for site-specific delivery of an anti-cancer drug. *J. Control. Release,* **148**(3), 359–367.

54. Kroll, D. J. (1995). Circumventing antineoplastic drug resistance: When tumor cells just say “no” to drugs. *Am. J. Pharm. Educ.,* **59**(2), 184–191.

55. Kuo, Y.-C., Liang, C.-T. (2011). Inhibition of human brain malignant glioblastoma cells using carmustine-loaded catanionic solid lipid nanoparticles with surface anti-epithelial growth factor receptor. *Biomaterials,* **32**(12), 3340–3350.

56. Sharma, P., Ganta, S., Denny, W. A., Garg, S. (2009). Formulation and pharmacokinetics of lipid nanoparticles of a chemically sensitive nitrogen mustard derivative: Chlorambucil. *Int. J. Pharm.,* **367**(1–2), 187–194.

57. Tian, J., Pang, X., Yu, K., Liu, L., Zhou, J. (2008). Preparation, characterization and *in vivo* distribution of solid lipid nanoparticles loaded with cisplatin. *Pharmazie,* **63**(8), 593–597.

58. Huang, G., Zhang, N., Bi, X., Dou, M. (2008). Solid lipid nanoparticles of temozolomide: Potential reduction of cardial and nephric toxicity. *Int. J. Pharm.,* **355**(1–2), 314–320.

59. Li, F., Weng, Y., Wang, L., He, H., Yang, J., et al. (2010). The efficacy and safety of bufadienolides-loaded nanostructured lipid carriers. *Int. J. Pharm.,* **393**(1–2), 204–212.

60. Liu, D., Liu, Z., Wang, L., Zhang, C., Zhang, N. (2011). Nanostructured lipid carriers as novel carrier for parenteral of docetaxel. *Colloids Surf. B Biointerfaces,* **85**(2), 262–269.

61. Xu, Z., Chen, L., Gu, W., Gao, Y., Lin, L., et al. (2009). The performance of docetaxel-loaded solid lipid nanoparticles targeted to hepatocellular carcinoma. *Biomaterials,* **30**(2), 226–232.

62. Venishetty, V. K., Komuravelli, R., Kuncha, M., Sistla, R., Diwan, P. V. (2013). Increased brain uptake of docetaxel and ketoconazole loaded folate-grafted solid lipid nanoparticles. *Nanomedicine,* **9**(1), 111–121.

63. Reddy, L., Sharma, R., Chuttani, K., Mishra, A., Murthy, R. (2004). Etoposide-incorporated tripalmitin nanoparticles with different surface charge: Formulation, characterization, radiolabeling, and biodistribution studies. *AAPS J.,* **6**(3), 55–64.

64. Reddy, L. H., Sharma, R. K., Chuttani, K., Mishra, A. K., Murthy, R. S. R. (2005). Influence of administration route on tumor uptake and biodistribution of etoposide loaded solid lipid nanoparticles in Dalton's lymphoma tumor bearing mice. *J. Control. Release,* **105**(3), 185–198.

65. Dong, X., Mattingly, C. A., Tseng, M., Cho, M., Adams, V. R., et al. (2009). Development of new lipid-based paclitaxel nanoparticles using sequential simplex optimization. *Eur. J. Pharm. Biopharm.,* **72**(1), 9–17.

66. Lee, M.-K., Lim, S.-J., Kim, C.-K. (2007). Preparation, characterization and *in vitro* cytotoxicity of paclitaxel-loaded sterically stabilized solid lipid nanoparticles. *Biomaterials,* **28**(12), 2137–2146.

67. Yuan, H., Miao, J., Du, Y.-Z., You, J., Hu, F.-Q., et al. (2008). Cellular uptake of solid lipid nanoparticles and cytotoxicity of encapsulated paclitaxel in A549 cancer cells. *Int. J. Pharm.,* **348**(1–2), 137–145.

68. Yu, Y. H., Kim, E., Park, D. E., Shim, G., Lee, S., et al. (2012). Cationic solid lipid nanoparticles for co-delivery of paclitaxel and siRNA. *Eur. J. Pharm. Biopharm.,* **80**(2), 268–273.

69. Lu, W., He, L. C., Wang, C. H., Li, Y. H., Zhang, S. Q. (2008). The use of solid lipid nanoparticles to target a lipophilic molecule to the liver

after intravenous administration to mice. *Int. J. Biol. Macromol.,* **43**(3), 320–324.

70. You, J., Wan, F., de Cui, F., Sun., Y., D., Y.-Z., Hu, F. G. (2007). Preparation and characteristic of vinorelbine bitartrate-loaded solid lipid nanoparticles. *Int. J. Pharm.,* **343**(1), 270–276.
71. Subedi, R. K., Kang, K. W., Choi, H.-K. (2009). Preparation and characterization of solid lipid nanoparticles loaded with doxorubicin. *Eur. J. Pharm. Sci.,* **37**(3–4), 508–513.
72. Ying, X.-Y., Du, Y.-Z., Chen, W.-W., Yuan, H., Hu, F.-Q. (2008). Preparation and characterization of modified lipid nanoparticles for doxorubicin controlled release. *Pharmazie,* **63**(12), 878–882.
73. Zhang, X.-G., Miao, J., Dai, Y.-Q., Du, Y.-Z., Yuan, H., et al. (2008). Reversal activity of nanostructured lipid carriers loading cytotoxic drug in multi-drug resistant cancer cells. *Int. J. Pharm.,* **361**(1), 239–244.
74. Lu, B., Xiong, S.-B., Yang, H., Yin, X.-D., Chao, R.-B. (2006). Solid lipid nanoparticles of mitoxantrone for local injection against breast cancer and its lymph node metastases. *Eur. J. Pharm. Sci.,* **28**(1–2), 86–95.
75. De Mendoza, A., E.-H., Rayo, M., Mollinedo, F., Blanco-Prieto, M. J. (2008). Lipid nanoparticles for alkyl lysophospholipid edelfosine encapsulation: Development and *in vitro* characterization. *Eur. J. Pharm. Biopharm.,* **68**(2), 207–213.
76. Yassin, A. E. B., Anwer, M. K., Mowafy, H. A., El-Bagory, I. M., Bayomi, M. A., et al. (2010). Optimization of 5-fluorouracil solid lipid nanoparticles: A preliminary study to treat colon cancer. *Int. J. Med. Sci.,* **7**(6), 398–408.
77. Ali, H., Shirode, A. B., Sylvester, P. W., Nazzal, S. (2010). Preparation, characterization, and anticancer effects of simvastatin-tocotrienol lipid nanoparticles. *Int. J. Pharm.,* **389**(1–2), 223–231.
78. Wysocki, P. J., Mackiewicz-Wysocka, M., Mackiewicz, A. (2002). Cancer gene therapy-state-of-the-art. *Rep. Pract. Oncol. Radiother.,* **7**(4), 149–155.
79. Van der Linden, R. R. M., Haagmans, B. L., Mongiat-Artus, P., van Doornum, G. J., Kraaij, R., et al. (2005). Virus specific immune responses after human neoadjuvant adenovirus-mediated suicide gene therapy for prostate cancer. *Eur. Urol.* **48**(1), 153–161.
80. Fogar, P., Greco, E., Basso, D., Habeler, W., Navaglia, F., et al. (2003). Suicide gene therapy with HSV-TK in pancreatic cancer has no effect *in vivo* in a mouse model. *Eur. J. Surg. Oncol.,* **29**(9), 721–730.

81. Wang, Y., Canine, B. F., Hatefi, A. (2011). HSV-TK/GCV cancer suicide gene therapy by a designed recombinant multifunctional vector. *Nanomed. Nanotechnol. Biol. Med.,* **7**(2), 193–200.

82. Zhang, Z., Sha, X., Shen, A., Wang, Y., Sun, Z., et al. (2008). Polycation nanostructured lipid carrier, a novel nonviral vector constructed with triolein for efficient gene delivery. *Biochem. Biophys. Res. Commun.,* **370**(3), 478–482.

83. Del Pozo-Rodriquez, A., Delgado, D., Solinis, M. A., Pedraz, J. L., Echevarria, E., et al. (2010). Solid lipid nanoparticles as potential tools for gene therapy: *In vivo* protein expression after intravenous administration. *Int. J. Pharm.,* **385**(1), 157–162.

84. Choi, S. H., Jin, S.-E., Lee, M.-K., Lim, S. J., Park, J.-S., et al. (2008). Novel cationic solid lipid nanoparticles enhanced p53 gene transfer to lung cancer cells. *Eur. J. Pharm. Biopharm.,* **68**(3), 545–554.

85. Kapadia, G. J., Azuine, M. A., Shigeta, Y., Suzuki, N., Tokuda, H. (2010). Chemopreventive activities of etodolac and oxyphenbutazone against mouse skin carcinogenesis. *Bioorg. Med. Chem. Lett.,* **20**(8), 2546–2548.

86. Zhao Küchler, S., Wolf, N. B., Heilmann, S., Weindl, G., Helfmann, J., et al. (2010). 3D-Wound healing model: Influence of morphine and solid lipid nanoparticles. *J. Biotechnol.,* **148**(1), 24–30.

87. Takada, Y., Bhardwaj, A., Potdar, P., Aggarwal, B. B. (2004). Nonsteroidal anti-inflammatory agents differ in their ability to suppress NF-κB activation, inhibition of expression of cyclooxygenase-2 and cyclin D1, and abrogation of tumor cell proliferation. *Oncogene,* **23**(57), 9247–9258.

88. Fuchs, C. S. (2011). The role of aspirin in prevention and management of colorectal cancer. *Clin. Adv. Hematol. Oncol.,* **9**(4), 330–332.

89. Vaish, V., Sanyal, S. N. (2012). Role of sulindac and celecoxib in chemoprevention of colorectal cancer via intrinsic pathway of apoptosis: Exploring NHE-1, intracellular calcium homeostasis and Calpain 9. *Biomed. Pharmacother.,* **66**(2), 116–130.

90. Hojka-Osinska, A., Ziolo, E., Rapak, A. (2012). Combined treatment with fenretinide and indomethacine induces AIF-mediated, non-classical cell death in human acute T-cell leukemia Jurkat cells. *Biochem. Biophys. Res. Commun.,* **419**(3), 590–595.

91. Chow, L. W. C., Cheng, C. W. L., Wong, J. L. N., Toi, M. (2005). Serum lipid profiles in patients receiving endocrine treatment for breast cancer—the results from the celecoxib anti-aromatase neoadjuvant (CAAN) trial. *Biomed. Pharmacother.,* **59**(Suppl), S302–S305.

92. D'Arca, D., LeNoir, J., Wildemore, B., Gottardo, F., Braganyini, E., et al. (2010). Prevention of urinary bladder cancer in the FIGHT knock-out mouse with rofecoxib, a Cox-2 inhibitor. *Urol. Oncol. Semin. Orig. invest.,* **28**(2), 189–194.

93. Patti, R., Gumired, K., Reddanna, P., Sutton, L. N., Phillips, P. C., Reddy, C. D. (2002). Overexpression of cyclooxygenase-2 (COX-2) in human primitive neuroectodermal tumors: Effect of celecoxib and rofecoxib. *Cancer Lett.,* **180**(1), 13–21.

94. Thakur, P., Sanyal, S. N. (2010). Induction of pulmonary carcinogenesis in Wistar rats by a single dose of 9,10-dimethylbenz(a)anthrace ne (DMBA) and the chemopreventive role of diclofenac. *Exp. Mol. Pathol.,* **88**(3), 394–400.

95. Okamoto, A., Shirakawa, T., Bito, T., Shigemura, K., Hamada, K., et al. (2008). Etodolac, a selective cyclooxygenase-2 inhibitor, induces upregulation of E-cadhedrin and has antitumor effect on human bladder cancer cells *in vitro* and *in vivo*. *Urology*, **71**(1), 156–160.

96. Bondi, M. L., Azzolina, A., Craparo, E. F., Capuano, G., Lampiasi, N., et al. (2009). Solid lipid nanoparticles containing nimesulide: Preparation, characterization and cytotoxicity studies. *Curr. Nanosci.,* **5**(1), 39–44.

97. Castelli, F., Puglia, C., Sarpietro, M. G., Rizza, L., Bonina, F. (2005). Characterization of indomethacin-loaded lipid nanoparticles by differential scanning calorimetry. *Int. J. Pharm.,* **304**(1–2), 231–238.

98. Joshi, M., Patravale, V. (2006). Formulation and evaluation of nanostructured lipid carrier (NLC)-based gel of valdecoxib. *Drug Dev. Ind. Pharm.,* **32**(8), 911–918.

99. Araujo, J., Gonzalez, E., Egea, M. A., Garcia, M. L., Souto, E. B. (2009). Nanomedicines for ocular NSAIDs: Safety on drug delivery. *Nanomed. Nanotechnol. Biol. Med.,* **5**(4), 394–401.

Chapter 46

Nanomedicines Targeted to Aberrant Cancer Signaling and Epigenetics

Archana Retnakumari, MTech, Parwathy Chandran, MTech, Ranjith Ramachandran, MSc, Giridharan L. Malarvizhi, MTech, Shantikumar Nair, PhD, and Manzoor Koyakutty, PhD

Amrita Centre for Nanosciences and Molecular Medicine, Amrita Institute of Medical Sciences and Research Centre, Kochi, India

Keywords: cancer, nanomedicines, nanoparticles, core–shell, protein kinases, leukemia, breast cancer, glioma, hepatocellular carcinoma, drug resistance, kinome, genome, epigenome, chemotherapy, albumin, aberrant kinase signaling, small molecule inhibitors, metastasis, epigenetics, polymer, protein, core–shell nanoparticles, wafers, targeted drug delivery

46.1 Introduction

Cancer nanomedicine is an emerging area of specialization where the concept of nanomedicine extends beyond the typical issues of "drug-delivery" and rather addresses more challenging issues associated with the molecular mechanisms of cancer. Several studies indicated that cancer is an extremely complex disease involving dynamic changes not only in the genome but also in the proteome and epigenome [1–3]. It is well established that

Handbook of Clinical Nanomedicine: Nanoparticles, Imaging, Therapy, and Clinical Applications
Edited by Raj Bawa, Gerald F. Audette, and Israel Rubinstein

ISBN 978-981-4669-20-7 (Hardcover), 978-981-4669-21-4 (eBook)
www.panstanford.com

deregulated protein kinase signaling plays a key role in cancer progression, metastasis, and drug resistance [4]. The past few decades witnessed an unprecedented emergence, success, and unfortunate failures of many small-molecule kinase inhibitors (SMI) targeting aberrantly activated protein kinase signaling in cancer [5, 6]. More than the pharmacological limitations, the failures associated with conventional drugs are related to the inability of these drugs to target multiple pathways activated in cancer cells. It is very clear that, successful management of cancer requires targeting of more than one key mechanistic pathway, almost simultaneously [7]. Most of the current work on cancer nanomedicine has focused on improving the efficacy of conventional chemotherapy drugs by encapsulating them in polymeric, protein, or liposomal carriers. Although this approach could greatly improve the potency of several chemodrugs such as Doxorubicin (Doxil®), Paclitaxel® (Abraxane®), and Daunorubicin (Daunoxome®), most of the complications of cancer remain unaddressed, mainly because none of these systems addresses molecular mechanisms of the disease [8–10]. It is believed that combinatorial therapy using multi-drug combinations against genomics, epigenomics, and aberrant proteomics may deliver a lethal blow to highly aggressive cancers. Under these circumstances, a single nanoconstruct carrying single drug may not be effective. A wide array of biocompatible polymers, proteins, or liposomes offer the versatility to create novel nano-architectures capable of carrying multiple drugs in a target specific fashion [11]. In this chapter, we review some of the recent developments in the area of multi-drug-loaded protein/polymer nanomedicines that can almost simultaneously target more than one key mechanistic pathway involved in cancer.

46.2 Protein Nanomedicine Targeted to Aberrant Kinome Involved in Refractory Cancer

Proteins are non-toxic drug delivery platforms intended for safe use in humans [12, 13]. A typical example of protein nanomedicine that revolutionized cancer therapy is Abraxane (paclitaxel-loaded albumin) [20]. Albumin encapsulation could significantly improve the circulation kinetics of paclitaxel and also reduce its toxic side-

effects [14]. Celgene Inc, NJ, has developed *nab*-rapamycin having a mean particle size of ~100 nm, which is a saline dispersible nanoformulation intended for intravenous administration. *nab*-rapamycin has shown excellent efficacy and safety profile in initial clinical trials in patients with unresectable advanced non-hematologic malignancies [15]. The availability of hydrophilic functional groups in the protein nanocarriers also enable them to be conjugated with ligands suitable for cell-specific targeting [16]. In most of the cases, nanomedicines were intended only to increase the circulation of drugs or reduce the toxic side effects by better targeting them in to diseased cells. However, nanomedicines have great potential in addressing critical issues in cancer such as metastasis and drug resistance, which are currently not much intervened.

Drug resistance is a critical issue impeding cancer treatment [17]. The mode of evasion of cancer cells from the inhibitory effects of drugs can be attributed to pharmacokinetic, cytokinetic, cellular, and molecular mechanisms. Certain tumor cells may be inherently refractory to the inhibitory effects of cytotoxic chemodrugs and kinase inhibitors, owing to the presence of drug efflux proteins, highly active DNA repair mechanisms, presence of cancer stem cells etc. [18, 19]. Interestingly, certain cancers develop drug resistance owing to the activation of one or more alternative cell survival pathways other than the primary oncogenic pathway as in the case of chronic myeloid leukemia (CML) [20]. CML is a hematological malignancy attributed to the constitutive tyrosine kinase activity of BCR-ABL fusion protein. A small-molecule inhibitor, imatinib, had shown significant BCR-ABL kinase inhibition *in vivo* and has been the first-line therapy for newly diagnosed CML for the past few decades [21]. Although the drug is active in the early stages of the disease, a certain population of patients shows resistance to imatinib due to multitude of mechanisms such as point mutations in the BCR-ABL kinase domain and amplification of BCR-ABL oncogene [22]. Interestingly, apart from the above said mechanisms, preferential activation of certain protein kinases has also shown to play critical roles in drug resistant CML [23]. Among the preferentially activated survival kinases, STAT5 was over-expressed several folds in refractory cells compared to drug-sensitive cells [24, 25]. STAT5 is capable of transcriptionally regulating the expression of several other genes involved in cell cycle progression, anti-apoptotic

response, etc. Interestingly, in STAT5 active refractory cells over-expression of transferrin cell surface receptor (TfR1) was also found. Compared to normal cells or drug-sensitive cells, the expression of TfR1 was found to be several folds higher in refractory cells [24].

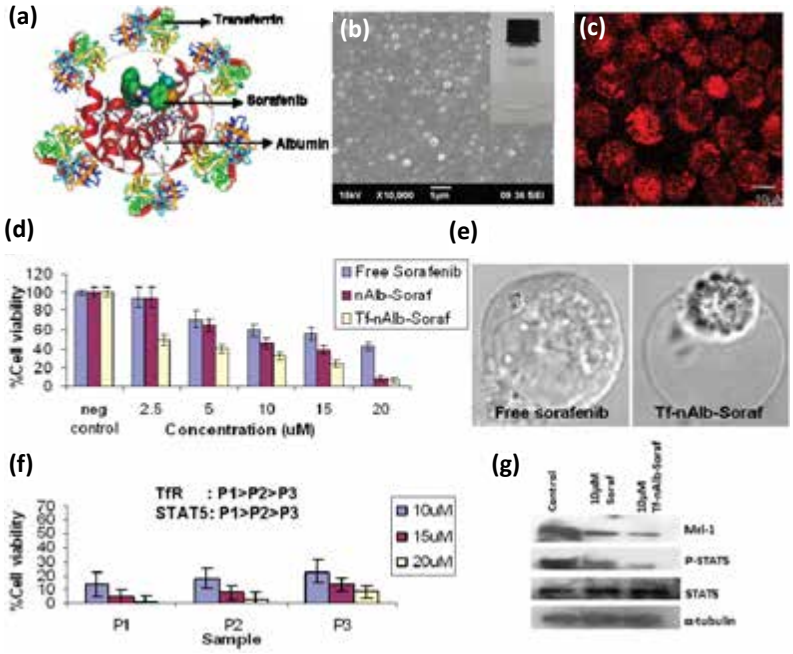

Figure 46.1 (a) Schematic of Tf-conjugated albumin bound sorafenib (Tf-nAlb-Soraf) nanomedicine, (b) SEM image of Tf-nAlb-Soraf nanoparticles showing size ~150 nm, Inset: Photograph of colloidal Tf-nAlb-Soraf nanomedicine, (c) flow cytogram showing differential uptake of 500 μg/ml of Tf-nAlb-Soraf in TfR over expressing CML cells, (d) cell viability analysis of K562R cells treated with free sorafenib, nAlb-Soraf and Tf-nAlb-Soraf, (e) confocal microscopic images showing morphological changes in K562R cells treated with 10 μM free sorafenib versus Tf-nAlb-Soraf, (f) cell viability of patient derived leukemic cells treated with different concentrations of Tf-nAlb-Soraf nanomedicine showing toxicity in all patient samples in the order of P1 > P2 > P3, (g) immunoblot analysis of MCL-1, pSTAT5, STAT5 with α-tubulin as loading control in nanomedicine treated sample. Adapted with permission from Retnakumari et al. (2012). *Mol. Pharm.,* **9**(11), 3062–3078 [24].

TfR1 was already utilized as a receptor suitable for targeted drug delivery of drugs and nanomedicines in to malignant cells [25]. However, studies done by Retnakumari et al. showed an interesting link between aberrantly active STAT5 and the correlative over-expression of TfR1 in refractory patients, although transcriptional regulation of TfR1 by STAT5 was earlier shown by Zhu et al. [24, 27]. This was utilized as a window of opportunity to induce cytotoxicity to highly refractory CML cells by TfR1-mediated delivery of STAT5 inhibitors. The multi-kinase inhibitor sorafenib loaded in albumin nanoparticles conjugated to transferrin ligand showed STAT5 inhibitory activity in highly refractory CML cells (Fig. 46.1). The strong binding affinity of sorafenib to the hydrophobic pockets of albumin enabled good encapsulation of sorafenib. Further, conjugation of transferrin to albumin sorafenib nanoparticles (Tf-nAlb-Soraf) enabled the targeted uptake in TfR1 over-expressing refractory CML cells. Tf-nAlb-Soraf induced enhanced cytotoxicity in refractory cells by the down-regulation of target proteins such as pSTAT5, Mcl-1, and TfR1 [24].

46.3 Protein–Protein Core–Shell Nanomedicine Targeted to Multiple Kinases in Refractory Cancer

The above-referred work showed potential of single kinase–targeted approach. However, recent studies indicate preferential activation of more than one kinase in the progression of several aggressive cancers [28]. In the case of refractory CML, there are two critically aberrant kinases that are constitutively active: STAT5 and BCR-ABL. Hence, it is important to target both BCR-ABL and STAT5 for achieving a complete leukemic cell kill. Retnakumari et al. developed core–shell nanoparticles using endogenous proteins albumin and transferrin for loading two different drugs (against BCR-ABL and STAT5) (unpublished data). BCR-ABL inhibitor imatinib/dasatinib was loaded in the albumin nano-core and STAT5 inhibitor sorafenib was loaded in the transferrin nano-shell. This protein–protein core–shell system showed enhanced cytotoxicity in refractory CML cells compared to the individual agents alone. Apart from delivering BCR-ABL inhibitor, transferrin nano-shell also facilitated TfR1-mediated targeted delivery of core–shell

nanoparticles in to refractory CML cells that over-expressed TfR1 in a correlative manner with drug resistance/STAT5 expression.

Other than cytotoxic chemodrugs and small-molecule inhibitors, RNA interference–mediated gene silencing is a well-established technique to induce inhibition of gene expression at the post-transcriptional level [29]. siRNAs have shown great promise in silencing oncogenes even at picomolar concentration ranges [30]. Studies using BCR-ABL siRNA have shown down-regulation of BCR-ABL expression in CML progenitors as well as $CD34^{+ve}$ CML cells, besides sensitizing the CML cells to BCR-ABL kinase inhibitors [31, 32]. Moreover, siRNAs also induced cytotoxicity in refractory CML cells bearing BCR-ABL oncogene with point mutations [33]. Thus, RNAi provided a wider approach for targeted destruction of CML quiescent cells/stem cells as well as mature fraction of leukemic population. However, the instability of siRNAs in the presence of serum nucleases, anionic nature preventing spontaneous intracellular uptake, and short half-life prevent the translation of this technique in to the clinics [34]. Past few decades have seen amazing advances in nanoparticle-mediated siRNA delivery for silencing critically aberrant oncogenes. Nanoparticles using proteins, polymers, lipids, etc., can effectively encapsulate siRNAs and protect them from degradation by serum nucleases [35]. In an imatinib-resistant patient, lipid nanoparticle-mediated delivery of BCR-ABL siRNA showed good response [36]. Moreover, siRNA loaded in nanoparticles can enhance the cellular uptake by conjugating the nanocarriers with cell-specific targeting ligands. Further, co-loading of contrast agents also enables optical imaging (fluorophores, luminescent metallic nanoclusters), magnetic imaging (magnetic nanoparticles), or nuclear imaging (radiolabeling of the nanoparticles) [37–39].

SiRNAs against drug efflux protein P-gp along with the cytotoxic chemodrug doxorubicin in micellar nanoparticles have shown anti-tumor effect in multidrug-resistant MDA-MB-435 human tumor models [40]. Similarly, Patil et al. showed that simultaneous administration of MDR siRNA and paclitaxel was able to overcome drug resistance in mice bearing spontaneous mammary adenocarcinoma [41]. However, because of co-administration, drug interactions can affect the endosomal escape and recognition of siRNA by the silencing machinery, which may also limit the translation of this potential technique into the clinics [42]. This demands rational design of

nanoparticles that can accommodate more than one inhibitory molecule without affecting the individual molecular activity. Core–shell architecture of nanoparticles enables the loading of siRNAs and small-molecule inhibitors together inthe same construct without much cross talk. Interestingly, protein–protein core–shell nanoparticles comprising protamine nano-core loaded with siRNA and transferrin nano-shell loaded with sorafenib (PS-siRNA)-(Tf-Soraf) could simultaneously inhibit both BCR-ABL and STAT5 irrespective of BCR-ABL point mutations or amplification in refractory CML (Unpublished data). Protamine being a low-molecular-weight

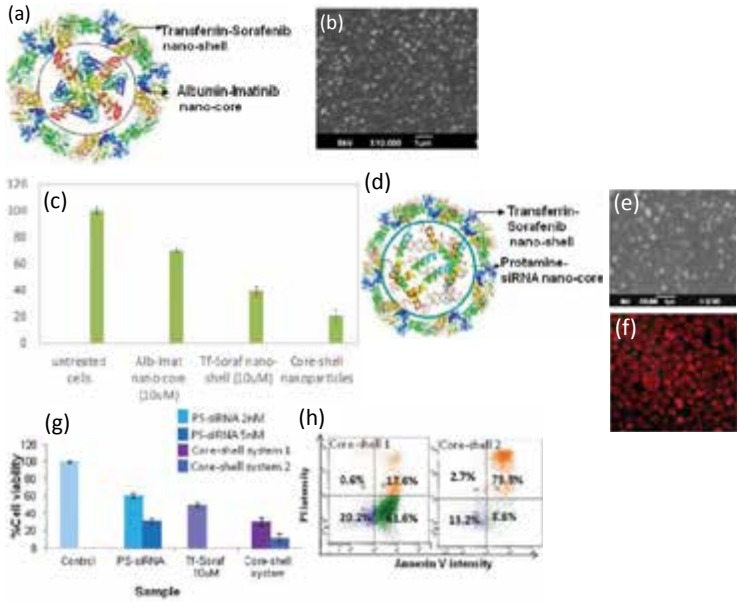

Figure 46.2 (a) Schematic representation of (Alb-Imat)-(Tf-Soraf) core–shell nanoparticles, (b) SEM image of (Alb-Imat)-(Tf-Soraf) core–shell nanoparticles, (c) cytotoxicity of (Alb-Imat)-(Tf-Soraf) core–shell nanoparticles in K562R refractory CML cells, (d) schematic representation of (PS-siRNA)-(Tf-Soraf) core–shell nanoparticles, (e) SEM image of (PS-siRNA)-(Tf-Soraf) core–shell nanoparticles, (f) TfR1-targeted uptake of (PS-siRNA)-(Tf-Soraf) core–shell nanoparticles in refractory CML cells over-expressing TfR1, (g) cytotoxicity of (PS-siRNA)-(Tf-Soraf) core–shell nanoparticles in K562R refractory CML cells, (h) flow cytogram showing apoptosis induced by (PS-siRNA)-(Tf-Soraf) core–shell nanoparticles in K562R refractory CML cells. Unpublished data, Retnakumari et al. (2014).

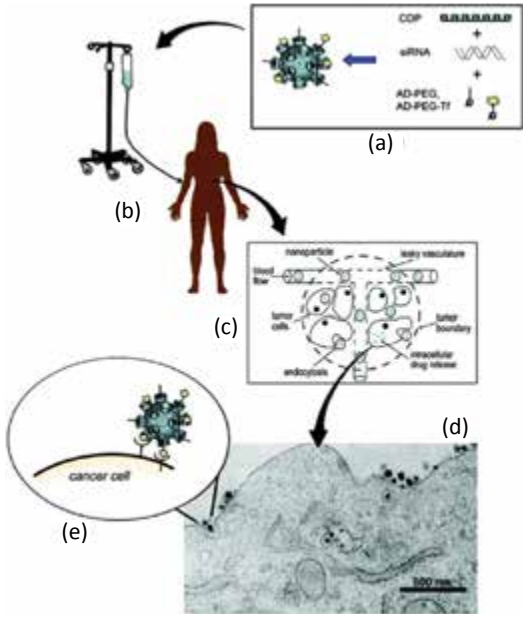

Figure 46.3 Schematic of how the targeted nanoparticles function. (a) Nanoparticles are assembled from the four components (see Fig. 46.2). (b) Aqueous solutions of nanoparticles are infused into patients. (c) The nanoparticles circulate in the blood of the patient and escape via the "leaking" blood vessels in tumors. (d) Nanoparticles penetrate though the tumor and enter into cells by receptor-mediated endocytosis (transmission electron micrograph of 50 nm nanoparticles entering a cancer cell). Note that the nanoparticles enter and are initially located in vesicles within the cell and must escape and disassemble to deliver their payload. (e) Targeted nanoparticles can have numerous interactions (e.g., Tf with its receptor) on the surface of the cancer cell that then stimulate entrance into the cell. Adapted with permission from Davis, M. E., et al. (2009). *Mol. Pharm*., **6**, 659–668 [45].

protein and cationic in nature enabled the strong complexation of negatively charged siRNA. Thus, protamine provided siRNA stability and protected siRNAs from the degradation caused by serum nucleases. In this case, too, Transferrin-Sorafenib nano-shell enabled the targeted delivery of core–shell nanoparticles to TfR1 over-expressing refractory cells. The simultaneous inhibition of the two aberrant kinases resulted in inducing synergistic toxicity to highly refractory CML cells irrespective of their sensitivity

to the standard drugs imatinib or dasatinib (Fig. 46.2). Similar studies conducted by Castillo et al. using multifunctional silica-PEI core–shell nanoparticles have shown enhanced cytotoxicity in HeLa cells [43]. Layer-by-layer assembly of nanoparticles carrying drugs and siRNA have also shown enhanced cytotoxic effects in several aggressive tumors [44]. Within the past few years, siRNA-based nanomedicines entered clinical trials (Fig. 46.3). Cyclodextrin loaded with siRNAs against RRM2 has shown promising effects in humans [45]. After this success, several clinical trials are going on in the area of nanoparticle-based siRNA delivery for cancer therapy.

46.4 Polymer–Protein Nanomedicine Targeting Aberrant Kinome in Acute Myeloid Leukemia

Similar to proteins, polymers have also played integral roles in the development of nanomedicines. Polymers offer several advantages as drug carriers such as controlled release of therapeutic agents in constant doses over long periods, tunable release of both hydrophilic and hydrophobic drugs, etc. [46]. Chandran et al. investigated the prospective of a kinome-targeted approach using polymer–protein core–shell nanoparticles in clinical management of hematological malignancies, taking acute myeloid leukemia (AML) as the test model [47]. Current perception about molecular mechanisms that drive leukemogenesis in AML implicates involvement of numerous derailed pathways including phosphatidylinositol 3-kinase/protein kinase B/mammalian target of rapamycin (PI3K/Akt/mTOR), Raf, mitogen-activated protein kinase (MAPK), and signal transducer and activator of transcription 5 (STAT5) cascades [48]. This genetic complexity of AML suggests that ablation of a single pathway is unlikely to produce sustained growth inhibition. Thus, therapeutic interference of multiple, inter-related kinases has been assumed necessary to achieve successful clinical outcome. However, a major challenge is the availability of a single molecule to target all these pathways simultaneously. Of the many molecules designed for targeting mTOR and MAPK pathways, everolimus and sorafenib have shown promising results in Phase II AML clinical trials [15, 49–51]. Moreover, sorafenib is now actively pursued as a potent inhibitor of STAT5 cascade

[51]. However, both these drugs suffer from poor aqueous solubility resulting in difficulty for the development of parenteral formulations. However, although aberrant in leukemia, these pathways are critical for regular functioning of healthy blood cells, which demands cell targeted delivery of kinase inhibitors to therapeutic antigen targets selectively expressed on malignant cells. CD33 is one of the myeloid markers that by virtue of its overexpression in AML blasts and absence in hematopoietic stem cells (HSC) have been identified as a potential candidate for targeted delivery of drugs to AML cells [52].

Considering these critical inputs, the authors developed a novel, polymer–protein core–shell nanomedicine and demonstrated its ability to inhibit critically aberrant pro-survival kinases (mTOR, MAPK and STAT5) in primitive (CD34+/CD38–) AML cells [47] (Fig. 46.4). Compared to currently used "single carrier-single drug" nanomedicines, the core–shell nanoconstruct was designed to simultaneously deliver two kinase inhibitors in a targeted fashion, while preserving the chemical stability and molecular activity of the individual agents. The nanocarrier components of the construct (Poly (lactic-co-glycolate) (PLGA) and albumin) of the construct were chosen particularly to ensure better loading for both the drugs. PLGA exhibits high encapsulation efficiency for hydrophobic molecules, including everolimus. However, because of its highly hydrophobic nature, PLGA undergoes opsonization by the reticulo-endothelial system (RES). Reports suggest that coating hydrophobic nanoparticles with human serum albumin may reduce their recognition by RES and extend circulation time [53]. In addition, since the plasma protein binding efficiency of sorafenib is ~99.5%, we designed our core–shell nanoconstruct such that everolimus is encapsulated in PLGA nano-core, encapsulating everolimus and human serum albumin nano-shell embedding sorafenib. The whole construct was surface conjugated with monoclonal antibody against CD33 receptor overexpressed in AML. Electron microscopy confirmed the formation of core–shell nanostructure (~290 nm) with distinct interphase and flow cytometry and confocal studies showed enhanced cellular uptake of the targeted nanomedicine. Simultaneous inhibition of critical kinases causing synergistic lethality against leukemic cells, without affecting healthy blood cells, was demonstrated using immunoblotting, cytotoxicity, and apoptosis assays. This cell receptor plus multi-kinase-targeted core–shell nanomedicine

showed better specificity compared to current clinical regime of cytarabine and daunorubicin.

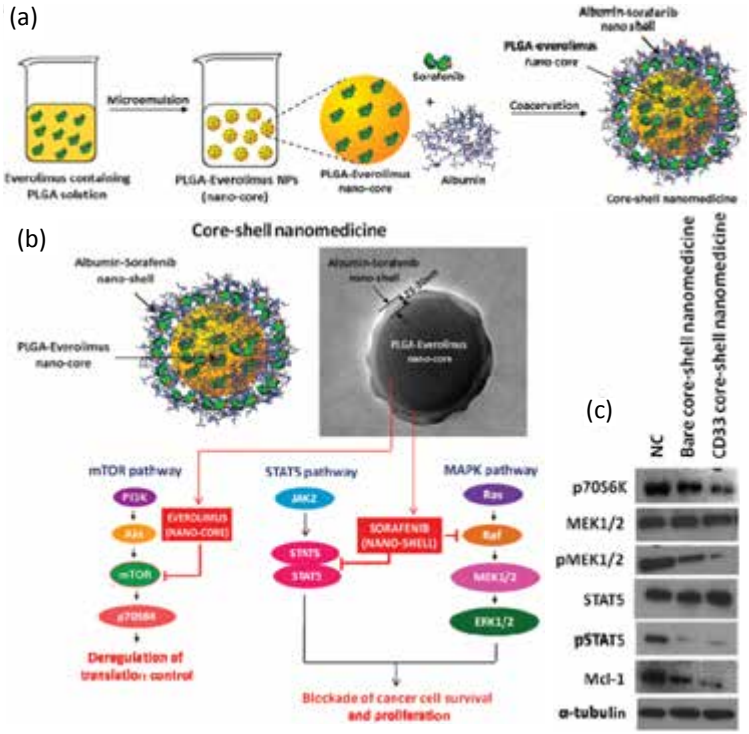

Figure 46.4 (a) Schematic representation of steps involved in the synthesis of core–shell nanomedicine. (b) Schematic overview of molecular targets of core–shell nanomedicine loaded with sorafenib and everolimus. (c) Immunoblot analysis of KG1a cells treated with bare nanomedicine and CD33-nanomedicine for 72 h. Adapted with permission from Chandran et al. (2014). *Nanomedicine,* **9**(8), 1317–1327 [47].

46.5 Polymer–Protein Core–Shell Nanomedicine Targeted to Cancer Metastasis

Metastasis, the dissemination of cancer cells from its original location to various organs, accounts for ~90% of cancer-associated death [54]. The underlying pathophysiology of metastasis is quite

complex, that many single-agent therapies miserably fail to produce desired therapeutic outcome [55]. Multiple signal transducing and cell adhesion molecules interplay and conduce to cancer migration and metastasis, among which the role of hyperactive Src kinase is pivotal [56]. Under normal physiological conditions, regulated levels of Src ensure stringent control over E-cadherin, integrins, and focal adhesion kinases (FAK), etc., and cell homeostasis is maintained [57]. However, during metastasis, Src gets hyperactivated. This aberrant phosphorylation in turn internalizes E-cadherin, hyperphosphorylates integrins and FAK, and extensively polymerizes invadopodia [58]. This leads to the loss of cell–cell contacts, initiates migration, and provides aggressive invasiveness to the metastatic cells [59]. Therefore, inhibiting hyperactive Src kinase would be a promising strategy to impair cancer cell migration by re-stabilizing E-cadherin, down-regulating FAK and integrins, and inhibiting the polymerization of invadopodia. Few studies have reported carrier-mediated combination drug delivery using liposomes, dendrimers, and polymeric and protein nanoparticles for treating metastatic cancers [60]. Recently, polymeric nanoparticles have gained attention for the combinatorial delivery of kinase inhibitor and cytotoxic chemodrugs against various cancers. Milane et al. reported that nanoparticles formed by self-assembly of amphiphilic block co-polymers, PEG/PLGA form core–shell micelles that can co-deliver mitochondrially bound hexokinase inhibitor, lonidamine, and paclitaxel specifically against EGFR overexpressing MDR breast cancer cells [61]. Similarly, Bae et al. demonstrated micellar polymer–lipid core–shell nanoparticles formed by the self-assembly of PEG-block-PHSA can effectively deliver cytotoxic Doxorubicin and PI3Kinase inhibitor, Wortmannin, toward breast cancer cells [62]. However, the major issue of metastasis, i.e., stopping the cell migration, has not been addressed in a nanocarrier-mediated combination chemotherapeutic setting. Further, since migration is a transient phenomenon, the control of cell motility must be substantiated with the cytotoxic killing of the metastatic cells. This means that the combination chemostrategy should first stop the cell migration by inhibiting the underlying molecular mechanisms and simultaneously impart cytotoxic stress to kill the metastatic cells. We have realized this idea by developing a multifunctional core–shell nanomedicine that can inhibit aberrant Src signaling kinase

together with exerting cytotoxic stress. The core-shell nanomedicine contained dasatinib (an anti-migratory drug) in albumin shell. This impaired the motility of the metastatic cancer cells due to P-Src inhibition. Thereafter, when the nanomedicine was irradiated with laser, mTHPC (ROS releasing drug) loaded in PLGA core exerted lethal dose of ROS to the motility-impaired metastatic cells. Studies performed in metastatic breast cancer cells, MDA-MB-231 demonstrated effective disruption of Src kinase by the nano-shell and generation of cytotoxic stress by the photoactivated mTHPC-PLGA nano-core. This unique combinatorial photo-chemo nanotherapy resulted synergistic cytotoxicity in ~99% of the motility-impaired metastatic cells. Furthermore, compared to the respective free drug counterpart, the core–shell nanomedicine showed improved aqueous solubility of the encapsulated drugs and demonstrated its enhanced *in vitro* cytotoxicity [63].

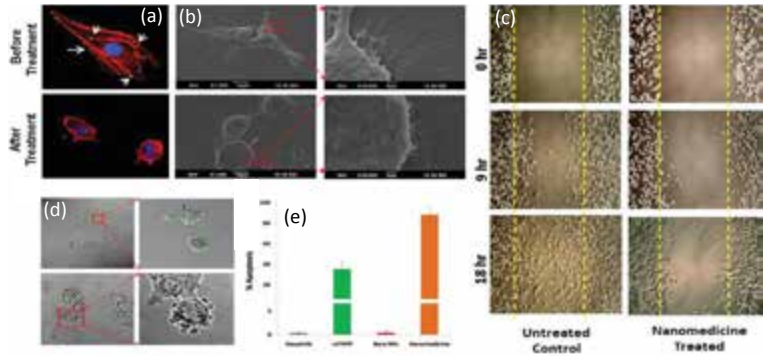

Figure 46.5 Nanomedicine-mediated combination therapy exploiting cancer cell migration inhibition followed by cytotoxic stress showing enhanced cytotoxicity to U87MG glioma cells. (a) Confocal images showing reduction focal adhesion points (arrowheads) by the anti-migratory agent, dasatinib released from the nanomedicine. (b) SEM images showing the loss of filopodia and cell morphology. (c) Scratch assay showing cell migration inhibition. (d) DIC-confocal image and (e) graph showing extend of apoptosis following laser triggering of photosensitizer in the nanomedicine. Adapted with permission from Ramachandran et al. (2014). *J. Biomed. Nanotechnol.,* **10**, 1401–1415 [65].

The above concept was further exploited to exert an enhanced anti-cancer effect in glioma. Gliomas are most aggressive kind of

brain tumors with marked tissue invasion and diffusive morphology. Glioma recurrence is very common after surgical resection, and mostly occur 2–3 cm away from the primary tumor margins. This is due to the local invasiveness leading to migration of individual cancer cells, due to activation of certain critical signaling pathways [64]. Recent study on glioma has exploited the concept of inhibiting focal adhesion point formation to prevent the local invasiveness and migration of individual cancer cells by a polymer–protein combination nanomedicine [65]. The migration inhibitor dasatinib released from the nanomedicine effectively down-regulated the phospho-Src, leading to reduced focal adhesion point formations resulted in substantial impaired the cell migration (Fig. 46.5). Enhanced cytotoxicity was achieved on these migration-impaired cells through laser-assisted PDT action on photosensitizer loaded in the nanomedicine and resulted in apoptosis-mediated cell death.

The efficacy of polymer–protein core–shell nanoparticles was also evaluated in metastatic cancer model hepatocellular carcinoma (HCC), which is the primary neoplasm of liver with worldwide incidence of ~1 million cases every year, and almost equal death rate [66]. Surgical resection and liver transplantation are the curative options; however, the recurrence rate is high [67]. The multikinase inhibitor Sorafenib is routinely used in clinics because the drug reduces cell proliferation by blocking C-RAF and B-RAF through the inhibition of RAF/MEK/ERK signaling [68]. However, most often HCC develops extensive signaling crosstalk and activates several other compensatory oncogenic pathways and the cancer cells easily evade the antiproliferative stress. Furthermore, after inhibiting RAF kinase using sorafenib, the cancer cells regain the cellular proliferation due to the activation ERK and AKT kinases through EGFR signaling pathway [69]. Owing to these reasons, systemic therapy using sorafenib offers only cytostatic effect with overall survival of ~6 months alone [70]. Another drug administered in the form of chemo-embolizing microparticles (DC beads®) is the cytotoxic Doxorubicin (Dox) [71]. Even though Dox is a potent DNA intercalator and topoisomerase inhibitor with effective reactive oxygen species (ROS) releasing capability, it renders only limited single-agent activity against HCC [72]. Chemoembolization using Doxorubicin eluting PVA microparticles (DC Beads), ethiodized oil (Lipiodol), and radioembolization using Yttrium-90 are used to manage the neoplasm, but only for tumor volume ~5 cm [73, 74].

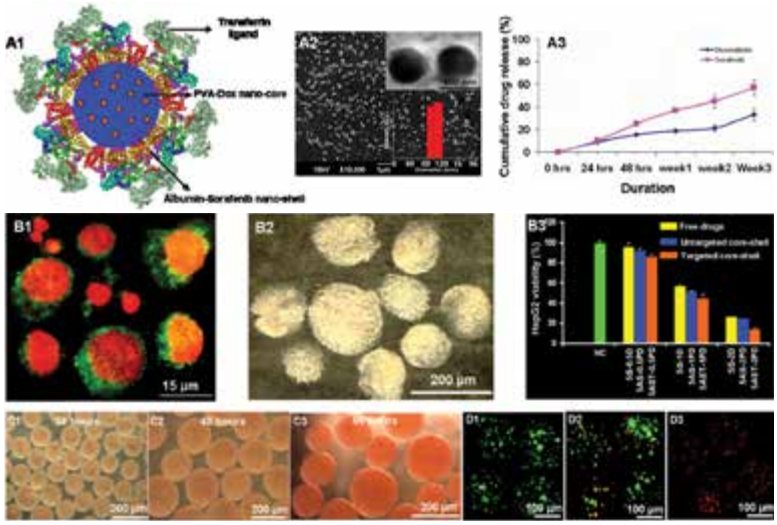

Figure 46.6 (A1) In silico model of PVA-Doxorubicin/albumin-sorafenib core–shell nanomedicine. (A2) SEM image shows the morphology of the nanomedicine. Inset: TEM image shows distinct core–shell interface (top), and DLS shows the narrow particle size distribution of the nanomedicine (bottom). (A3) Controlled release of Doxorubicin and Sorafenib from the core–shell particles. (B1) The nanomedicine treated cells display apoptotic (green) and damaged nucleus (red) as determined by annexin/PI apoptosis assay. (B2) Stereomicroscope image shows the morphology of HCC 3D spheroids. (B3) Alamar blue cytotoxicity assay shows synergistic cytotoxicity in the 3D spheroids. (C1–C3) Stereomicroscope image shows uniform uptake of core–shell nanomedicine throughout the spheroids in a time-dependent manner. Confocal image shows the shows the viability of 3D spheroids: (D1) before treatment, (D2) after treatment with core–shell nanomedicine containing 0.5 µM Dox and 5 µM sorafenib, and (D3) treatment after modulating the Dox concentration in the nanomedicine (2 µM Dox and 5 µM sorafenib). The viability was assessed using Live-dead assay; Green color indicates live cells, and red indicates dead cells, after core–shell treatment. (S-sorafenib, D-Doxorubicin, AS-PD: untargeted Albumin-Sorafenib/PVA-Dox core–shell, AST-PD: Transferrin-conjugated Albumin-Sorafenib/PVA-Dox core–shell). Adapted with permission from Malarvizhi et al. (2014) *Nanomed. Nanotechnol. Biol. Med.*, **10**(3), 579–587 [63].

Recently, Song et al. showed that PLGA nanoparticles can deliver both Vincristine and Verapamil toward HCC cells with slightly better antitumor activity compared to that of the free drug combinations [75]. Nevertheless, it is well appreciated that cytotoxic therapy should be combined with kinase inhibition to treat HCC effectively. This fact has also been realized in Phase-II trials conducted using sorafenib-Dox combination, which clearly revealed that combining multikinase inhibitor, sorafenib with cytotoxic drug, Doxorubicin, can significantly improve the overall survival of HCC patients up to ~13.7 months [76]. However, delivering both these drugs intracellularly toward HCC cells is a challenge. Considering the simultaneous delivery of more than one drug, and the significance of inhibiting signaling kinase together with targeting the DNA, we have reported a HCC-targeted core–shell nanomedicine for the combinatorial delivery of both Doxorubicin (Dox) and sorafenib [77]. This unified nanoconstruct was found to effectively impart DNA intercalation together with inhibiting RAF/MEK/ERK signaling kinases. The chemodrugs loaded in FDA-approved materials, PVA and albumin, showed excellent cellular uptake and exerted synergistic cytotoxicity in ~92% of the treated cells, studied in both 2D and 3D cultures of HCC. The antitumor efficacy of Dox and sorafenib was also significantly enhanced compared to that of the respective free drug combination in the treated cells (Fig. 46.6).

46.6 Protein Nanomedicine Targeted to Aberrant Epigenome

Another interesting work on protein nanomedicines is the formulation that targets aberrant epigenome. Epigenetic mechanisms, including genomic DNA methylation, histone modifications, nucleosomal remodeling, and microRNA regulation, contribute to defining heritable changes in gene expression, independent of changes in the primary DNA sequence [78]. These mechanisms are essential for the normal development and maintenance of tissue-specific gene expression patterns in mammals. Deregulation of epigenetic processes has been lately considered significant as genetic mutation in driving cancer initiation and progression. Cancer epigenome is characterized by global changes in DNA methylation and his-

tone modification patterns as well as altered expression profiles of chromatin-modifying enzymes [79]. Epi-modifications can lead to tumor suppressor gene silencing independently and in conjunction with deleterious genetic mutations, thus serving as the second hit required for cancer initiation according to the "two-hit" model proposed by Knudson [80]. The reversible nature of epigenetic aberrations has led to the emergence of the promising field of epigenetic therapy aimed at the restoration of a "normal epigenome." Chemical compounds acting on epigenetic control of gene expression mainly fall under two broad categories: inhibitors of DNA methyl-transferases (DNMTi) and inhibitors of histone deacetylase (HDACi).

Emerging data support the notion that recruitment of aberrant HDAC activity by oncogenic fusion proteins, resulting from chromosomal translocations, contributes to the silencing of vital genes in hematopoiesis and promotion of AML [81]. Vorinostat, a histone deacetylase (HDAC) inhibitor, has shown remarkable anti-leukemic activity against AML in clinical trials with acceptable safety and tolerability profiles [82]. However, the drug faces challenges of low aqueous solubility and cell permeability hindering development of its intravenous formulations [83]. Numerous nanoformulations, including poly(ethylene glycol)-b-poly(DL-lactic acid) (PEG-b-PLA) micelles and solid lipid nanoparticles of vorinostat, have been evaluated in pre-clinical settings [84, 85].

Chandran et al. have reported the development of a novel, human serum albumin-bound vorinostat nanomedicine exhibiting superior anti-leukemic activity against heterogeneous population of AML patient samples (n = 9), including refractory and relapsed cases, and three representative cell lines expressing CD34+/CD38– stem cell phenotype (KG-1a), promyelocytic phenotype (HL-60) and FLT3-ITD mutation (MV4-11) [86]. Nano-vorinostat having size of ~100 nm and encapsulation efficiency of ~73% exhibited enhanced cellular uptake, significantly lowering IC50 in cell lines and patient samples. Nano-vorinostat displayed excellent inhibition of HDAC activity and induced high levels of intracellular ROS, growth arrest, and apoptosis in cell lines as well as patient samples, irrespective of their French-American-British (FAB) classes, including refractory and relapsed cases. Selective toxicity of nanomedicine toward clonogenic growth potential of bone marrow–derived leukemic and healthy progenitors was studied

using colony–forming unit (CFU) assay. Interestingly, nano-vorinostat demonstrated excellent and differential, single-agent activity against the clonogenic proliferative capacity of leukemic bone marrow progenitors from a heterogeneous set of patient samples, sparing healthy bone marrow progenitors, suggestive of its chances of striking the AML primitive cell compartment (Fig. 46.7).

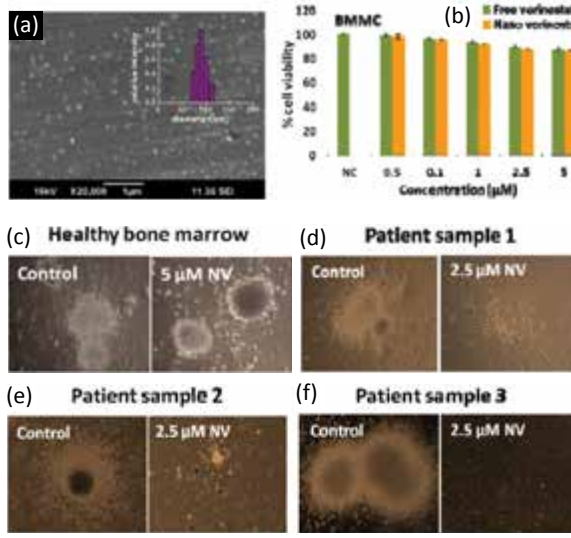

Figure 46.7 (a) Scanning electron micrograph showing spherical particles of ~100 nm. Inset: DLS data showing hydrodynamic diameter of ~94 ± 8 nm. (b) Nano-vorinostat sensitivity toward healthy BMMC. Colony-forming assay clonogenic growth pattern of nano-vorinostat-treated, (c) healthy BMMC, (d) patient sample 1, (e) patient sample 2, and (f) patient sample 3. Adapted with permission from Chandran et al. (2014). *Nanomedicine,* **10**, 721–732 [86].

Collectively, aberrant histone deacetylation–targeted protein-nanomedicine, nano-vorinostat, appears to be a promising therapeutic option against various FAB classes as well as poor prognosis cases of AML. Considering the toxicity challenges associated with clinically used DNA intercalating agents and anthracyclins, we believe that an epigenetic-targeted nanoformulation showing selective, single agent activity in patient-derived cells, sparing healthy bone marrow cells, holds great potential for clinical translation.

46.7 Conclusions and Future Prospects

The successful emergence of translational nanomedicines can make radical changes in the way we treat cancer. Nanotechnology can offer amazing "materials science" opportunities for the nanomedicine researchers to deal with complex biological challenges posed by cancer. Although earlier approaches focused primarily on improving the pharmacokinetics and bio-distribution of cytotoxic drugs such as paclitaxel, doxorubicin, daunorubicin, etc., the current strategy centers around molecular diagnosis–assisted design of nanomedicines that are capable of hitting at the specific multi-kinases, aberrant epigenetic factors, tumor micro-environment and cancer stem cells that drives drug/radiation resistance, metastasis, and recurrence. It is evident from the current understanding that a multi-targeted approach involving inhibition or silencing of more than one key pathway, together with imparting cytotoxic stress, may be required for managing cancer better. This demands novel drug delivery systems that can carry not only single drug but also multiple drug payloads with target specificity and sustained release. Optimization, validation, and translation of such nano-polypharmaceutics are a major challenge that need to be addressed by the nanomedicine research community as well as the pharmaceutical industry. The future prospects of such systems rely heavily on efficacy versus nanotoxicity profile of such multi-targeted approach and timely evolution of regulatory framework for testing and approving such relatively complex multi-functional nanomedicine.

Abbreviations

ABL: Abelson
AKT: Alpha serine/threonine protein kinase
AML: Acute myeloid leukemia
AS-PD: Unconjugated Albumin-Sorafenib/PVA-Doxorubicin
AST-PD: Transferrin-conjugated Albumin-Sorafenib/PVA-Doxorubicin
BMMC: Bone marrow mononuclear cells
BCR: Breakpoint cluster region
CFU: Colony–forming unit
CML: Chronic myeloid leukemia

DIC: Differential interference contrast
DLS: Dynamic light scattering
DNA: Deoxy ribo nucleic acid
DNMTi: DNA methyltransferase inhibitors
Dox: Doxorubicin
EGFR: Epidermal growth factor receptor
ERK: Extracellular signal regulated kinase
FAB: French-American-British
FAK: Focal adhesion kinase
FDA: Food and Drug Administration
HCC: Hepatocellular carcinoma
HDACi: Histone deacetylase inhibitors
HDAC: Histone deacetylase
HSC: Hematopoietic stem cell
IC50: Half-maximal inhibitory concentration
MAPK: Mitogen-activated protein kinase
Mcl-1: Myeloid cell leukemia-1
MDR: Multi-drug resistance
MEK: MAP kinase kinase
mTOR: Mammalian target of rapamycin
mTHPC: m-(Tetra hydroxyl phenyl chlorin)
PDT: Photodynamic therapy
PEG: Poly(ethylene glycol)
PEI: Polyethylenimine
PLGA: Poly (lactic-co-glycolate)
PHSA: Poly(N-(6-hexyl stearate)-L-aspartamide)
PI: Propidium iodide
PI3K: Phosphoinositide 3-kinase
pSTAT: Phosphorylated signal transducer and activator of transcription
PS: Protamine sulfate
PVA: Poly(vinyl alcohol)
RAF: Ras activation factor
RES: Reticuloendothelial system
RNA: Ribonucleic acid
RNAi: RNA interference
ROS: Reactive oxygen species
RRM2: Ribonucleoside-diphosphate reductase subunit M2
SEM: Scanning electron microscope

SMI: Small-molecule inhibitor
siRNA: Small interfering RNA
Soraf: Sorafenib
Src: Rous sarcoma virus proto-oncogene
STAT: Signal transducer and activator of transcription
TEM: Transmission electron microscope
TfR: Transferrin receptor
Tf: Transferrin

Disclosures and Conflict of Interest

This work was supported by the Department of Biotechnology, Government of India, under the RNAi program (BT/PR10716/AGR/36/603/2008) and in silico design, development, nanotoxicology and preclinical evaluation of theragnostic cancer nanomedicine (BT/PR14920/NNT/28/503/2010); Department of Science and Technology, Government of India, under theragnostics, regenerative medicine and stem cell research using cell-targeted nanomaterials (SP/NM/NS-99/2009); Marie Curie International Incoming Fellowship (Return Phase) by the European Commission (FP-7 program); senior research fellowship for Archana Retnakumari, Parwathy Chandran and Giridharan L. Malarvizhi from CSIR, Government of India; and senior research fellowship from ICMR, Government of India, for Ranjith Ramachandran Amrita Vishwa Vidyapeetham University provided core infrastructure facilities.

The authors declare that they have no conflict of interest or financial involvement with any organization or entity discussed in this chapter. No writing assistance was utilized in the production of this chapter and the authors have received no payment for its preparation.

Corresponding Author

Prof. Dr. Manzoor Koyakutty
Amrita Centre for Nanosciences and Molecular Medicine
Amrita Institute of Medical Sciences and Research Centre
Amrita Vishwa Vidyapeetham University
Ponekkara PO, Kochi, Kerala 682041, India
Email: manzoork@aims.amrita.edu

About the Authors

Archana Retnakumari is a PhD scholar working in cancer nanomedicine at the Amrita Centre for Nanosciences and Molecular Medicine. She received her BTech in biotechnology and biochemical engineering in 2007 and MTech in nanomedical sciences in 2009. She is the recipient of senior research fellowship from the Council of Science and Industrial Research (CSIR) Govt. of India (2011) and prestigious Malhotra Weikfield Young Scientist Award (2012). Her current research focuses on developing protein-based nanomedicines against refractory CML based on molecular diagnosis of patients.

Parwathy Chandran is a PhD scholar working in the field of cancer nanomedicine at the Amrita Centre for Nanosciences and Molecular Medicine, Amrita Vishwa Vidyapeetham. She received her MSc in biotechnology in 2007 and MTech in nanomedical sciences in 2009. She is the recipient of senior research fellowship from the CSIR (2011). Her research focuses on the development and functional characterization of polymer/protein-based nanopoly-pharmaceuticals against AML.

Ranjith Ramachandran joined the Cancer Nanomedicine Group at Amrita Centre for Nanosciences and Molecular medicine for his PhD after receiving his research fellowship from the Indian Council of Medical Research in 2009. Prior to joining Amrita, he completed his MSc in biotechnology from Mahatma Gandhi University, Kerala, in 2009. His work primarily focused on the design, development, and translation of multi-drug-loaded nanomedicine and local drug delivery devices for chemotherapeutic agents for brain cancer treatment.

Giridharan L. Malarvizhi is a PhD candidate at Amrita Centre for Nanosciences and Molecular Medicine in the campus of the Amrita Institute of Medical Sciences and Research Centre, India. He received his MTech in nanomedical sciences (2010), and MSc in bioinformatics (2008). His current research interests focus on the in silico design and development of multifunctional nanomedicine targeted against hepatocellular carcinoma. He is a recipient of various merit fellowships from the Government of India, including the CSIR Senior Research Fellowship (2012–2016), Department of Science and Technology award (2008–2010), and Jawaharlal Nehru Memorial trust award for academic excellence (2008).

Shantikumar Nair is the dean of research, Amrita Vishwa Vidyapeetham, and director of the Amrita Centre for Nanosciences and Molecular Medicine. He is a former IIT Bombay graduate in metallurgical engineering. Dr. Nair received his PhD from Columbia University, New York, in 1983. In 1986, he received the prestigious Presidential Young Investigator Award for research in composite materials. Prior to joining the Amrita Centre for Nanosciences and Molecular Medicine, he was a tenured professor at the University of Massachusetts, USA, for nearly two decades. Dr. Nair has several books and over 100 publications in international journals to his credit.

Manzoor Koyakutty is a professor at the Amrita Centre for Nanoscience and Molecular Medicine, Cochin, India, and specializes in the area of cancer nanomedicine. He joined the center in June 2007. Prior to his current position, he served as a staff-scientist at the Defence Research and Development Organization (DRDO), Government of India, in the area of nanotechnology application in defense. He is recipient of the Marie-Curie International Incoming fellowship, DRDO Scientist of the Year 2003, DRDO

Young Scientist Award 2004, and DRDO Technology Development Award 2006. He has 44 international publications in the area of nanomedicine and 12 patents filed. He is a member of the European Society of Nanomedicine and the European Foundation of Clinical Nanomedicine. He also serves on the editorial board of *Nanomedicine: Nanotechnology, Biology and Medicine*.

References

1. Negrini, S., Gorgoulis, V. G., Halazonetis, T. D. (2010). Genomic instability-an evolving hallmark of cancer. *Nat. Rev. Mol. Cell Biol.,* **11**(3), 220–228.
2. Unwin, R. D., Craven, R. A., Harnden, P., Hanrahan, S., Totty, N., et al. (2003). Proteomic changes in renal cancer and co-ordinate demonstration of both the glycolytic and mitochondrial aspects of the Warburg effect. *Proteomics*, **3**(8), 1620–1632.
3. Grønbaek, K., Hother, C., Jones, P. A. (2007). Epigenetic changes in cancer. *Acta Pathol. Microbiol. Immunol. Scand.,* **115**(10), 1039–1059.
4. Paul, M. K., Mukhopadhyay, A. K. (2004). Tyrosine kinase—Role and significance in Cancer. *Int. J. Med. Sci.,* **1**(2), 101–115.
5. Kantarjian, H. M., Talpaz, M. (2001). Imatinib mesylate: Clinical results in Philadelphia chromosome-positive leukemias. *Semin. Oncol.,* **28**(5 Suppl 17), 9–18.
6. Jabbour, E., Cortes, J. E., Kantarjian, H. M. (2009). Suboptimal response to or failure of imatinib treatment for chronic myeloid leukemia: What is the optimal strategy? *Mayo Clin. Proc.,* **84**(2), 161–169.
7. Petrelli, A., Giordano, S. (2008). From single- to multi-target drugs in cancer therapy: When aspecificity becomes an advantage. *Curr. Med. Chem.,***15**(5), 422–432.
8. Harries, M., Ellis, P., Harper, P. (2005). Nanoparticle albumin-bound paclitaxel for metastatic breast cancer. *J. Clin. Oncol.,* **23**(31), 7768–7771.
9. Drummond, D. C., Meyer, O., Hong, K., Kirpotin, D. B., Papahadjopoulos, D. (1999). Optimizing liposomes for delivery of chemotherapeutic agents to solid tumors. *Pharmacol. Rev.*, **51**(4), 691–743.
10. Liu, F. T., Kelsey, S. M., Newland, A. C., Jia, L. (2002). Liposomal encapsulation diminishes daunorubicin-induced generation of reactive oxygen species, depletion of ATP and necrotic cell death in human leukaemic cells. *Br. J. Haematol.*, **117**(2), 333–342.

11. Peer, D., Karp, J. M., Hong, S., Farokhzad, O. C., Margalit, R., Langer, R. (2007). Nanocarriers as an emerging platform for cancer therapy. *Nat. Nanotechnol.,* **2**(12), 751–760.
12. Elzoghby, A. O., Samy, W. M., Elgindy, N. (2012). Protein-based nanocarriers as promising drug and gene delivery systems. *J. Control. Release,* **161**(1), 38–49.
13. Kratz, F. (2008). Albumin as a drug carrier: Design of prodrugs, drug conjugates and nanoparticles. *J. Control. Release,* **132**(3), 171–183.
14. Montana, M., Ducros, C., Verhaeghe, P., Terme, T., Vanelle, P., et al. (2011). Albumin-bound paclitaxel: The benefit of this new formulation in the treatment of various cancers. *J. Chemother.,* **23**(2), 59–66.
15. Gonzalez-Angulo, A. M., Meric-Bernstam, F., Chawla, S., Falchook, G., Hong, D., et al. (2013). Weekly nab-Rapamycin in patients with advanced nonhematologic malignancies: Final results of a phase I trial. *Clin. Cancer Res.,* **19**(19), 5474–5484.
16. Retnakumari, A., Setua, S., Menon, D., Ravindran, P., Muhammed, H., et al. (2010). Molecular-receptor-specific, non-toxic, near-infrared-emitting Au cluster-protein nanoconjugates for targeted cancer imaging. *Nanotechnology,* **21**(5), 055103.
17. van der Kuip, H., Wohlbold, L., Oetzel, C., Schwab, M., Aulitzky, W. E. (2005). Mechanisms of clinical resistance to small molecule tyrosine kinase inhibitors targeting oncogenic tyrosine kinases. *Am. J. Pharmacogenomics,* **5**(2), 101–112.
18. Gillet, J. P., Gottesman, M. M. (2010) Mechanisms of multidrug resistance in cancer. *Methods Mol. Biol.,* **596**, 47–76.
19. Nambaru, P. K., Hübner, T., Köck, K., Mews, S., Grube, M., et al. (2011). Drug efflux transporter multidrug resistance-associated protein 5 affects sensitivity of pancreatic cancer cell lines to the nucleoside anticancer drug 5-fluorouracil. *Drug Metab. Dispos.,* **39**(1), 132–139.
20. Sierra, J. R., Cepero, V., Giordano, S. (2010). Molecular mechanisms of acquired resistance to tyrosine kinase targeted therapy. *Mol. Cancer,* **9**, 75.
21. Druker, B. J., Talpaz, M., Resta, D. J., Peng, B., Buchdunger, E., et al. (2001). Efficacy and safety of a specific inhibitor of the BCR-ABL tyrosine kinase in chronic myeloid leukemia. *N. Engl. J. Med.,* **344**(14), 1031–1037.
22. Gorre, M. E., Mohammed, M., Ellwood, K., Hsu, N., Paquette, R., et al. (2001). Clinical resistance to STI-571 cancer therapy caused by BCR-ABL gene mutation or amplification. *Science,* **293**(5531), 876–880.

23. Zhou, P., Qian, L., Kozopas, K. M., Craig, R. W. (1997). Mcl-1, a Bcl-2 family member, delays the death of hematopoietic cells under a variety of apoptosis-inducing conditions. *Blood,* **89**(2), 630–643.
24. Retnakumari, A. P., Hanumanthu, P. L., Malarvizhi, G. L., Prabhu, R., Sidharthan, N., et al. (2012). Rationally designed aberrant kinase-targeted endogenous protein nanomedicine against oncogene mutated/amplified refractory chronic myeloid leukemia. *Mol. Pharm.,* **9**(11), 3062–3078.
25. Warsch, W., Kollmann, K., Eckelhart, E., Fajmann, S., Cerny-Reiterer, S., et al. (2011). High STAT5 levels mediate imatinib resistance and indicate disease progression in chronic myeloid leukemia. *Blood,* **117**(12), 3409–3420.
26. Camp, E. R., Wang, C., Little, E. C., Watson, P. M., Pirollo, K. F., et al. (2013). Transferrin receptor targeting nanomedicine delivering wild-type p53 gene sensitizes pancreatic cancer to gemcitabine therapy. *Cancer Gene Ther.,* **20**(4), 222–228.
27. Zhu, B. M., McLaughlin, S. K., Na, R., Liu, J., Cui, Y., et al. (2008). Hematopoietic-specific Stat5-null mice display microcytic hypochromic anemia associated with reduced transferrin receptor gene expression. *Blood,* **112**(5), 2071–2080.
28. Giroux, V., Iovanna, J., Dagorn, J. C. (2006). Probing the human kinome for kinases involved in pancreatic cancer cell survival and gemcitabine resistance. *Federation Am. Soc. Exp. Biol. J.,* **20**(12), 1982–1991.
29. Fire, A., Xu, S., Montgomery, M. K., Kostas, S. A., Driver, S. E., et al. (1998). Potent and specific genetic interference by double-stranded RNA in *Caenorhabditis elegans*. *Nature,* **391**(6669), 806–811.
30. Dominska M., Dykxhoorn, D. M. (2010). Breaking down the barriers: siRNA delivery and endosome escape. *J. Cell Sci.,* **123**(Pt 8), 1183–1189.
31. Withey, J. M., Marley, S. B., Kaeda, J., Harvey, A. J., Crompton, M. R., et al. (2005). Targeting primary human leukaemia cells with RNA interference: Bcr-Abl targeting inhibits myeloid progenitor self-renewal in chronic myeloid leukaemia cells. *Br. J. Haematol.,* **129**(3), 377–380.
32. Wohlbold, L., van der Kuip, H., Miething, C., Vornlocher, H. P., Knabbe, C., et al. (2003). Inhibition of bcr-abl gene expression by small interfering RNA sensitizes for imatinib mesylate (STI571). *Blood,* **102**(6), 2236–2239.
33. Koldehoff, M., Kordelas, L., Beelen, D. W., Elmaagacli, A. H. (2010). Small interfering RNA against BCR-ABL transcripts sensitize mutated T315I cells to nilotinib. *Haematologica,* **95**(3), 388–397.

34. Aagaard, L., Rossi, J. J. (2007). RNAi therapeutics: Principles, prospects and challenges. *Adv. Drug Deliv. Rev.,* **59**(2–3), 75–86.

35. Reischl, D., Zimmer, A. (2009). Drug delivery of siRNA therapeutics: Potentials and limits of nanosystems. *Nanomedicine,* **5**(1), 8–20.

36. Koldehoff, M., Elmaagacli, A. H. (2009). Therapeutic targeting of gene expression by siRNAs directed against BCR-ABL transcripts in a patient with imatinib-resistant chronic myeloid leukemia. *Methods Mol. Biol.,* **487**, 451–466.

37. Sajja, H. K., East, M. P., Mao, H., Wang, Y. A, Nie, S., et al. (2009) Development of multifunctional nanoparticles for targeted drug delivery and noninvasive imaging of therapeutic effect. *Curr. Drug Discov. Technol.,* **6**(1), 43–51.

38. Bhaskar, S., Tian, F., Stoeger, T., Kreyling, W., de la Fuente, J. M., et al. (2010). Multifunctional Nanocarriers for diagnostics, drug delivery and targeted treatment across blood-brain barrier: Perspectives on tracking and neuroimaging. *Part. Fibre. Toxicol.,* **7**, 3.

39. Sajja, H. K., East, M. P., Mao, H., Wang, Y. A., Nie, S., and Yang, L. (2009). Development of multifunctional nanoparticles for targeted drug delivery and noninvasive imaging of therapeutic effect. *Curr. Drug Discov. Technol.,* **6**(1), 43–51.

40. Xiong, X. B., Lavasanifar, A. (2011). Traceable multifunctional micellar nanocarriers for cancer-targeted co-delivery of MDR-1 siRNA and doxorubicin. *ACS Nano,* **5**(6), 5202–5213.

41. Patil, Y. B., Swaminathan, S. K., Sadhukha, T., Ma, L., Panyam, J. (2010). The use of nanoparticle-mediated targeted gene silencing and drug delivery to overcome tumor drug resistance. *Biomaterials,* **31**(2), 358–365.

42. Lee, J. M., Yoon, T. J., Cho, Y. S. (2013). Recent developments in nanoparticle-based siRNA delivery for cancer therapy. *BioMed Res. Int.,* **17**(2013), 782041.

43. Castillo, B., Bromberg, L., López, X., Badillo, V., González Feliciano, J. A., et al. (2012). Intracellular delivery of siRNA by polycationic superparamagnetic nanoparticles. *J. Drug Deliv.,* **2012**, 218940.

44. Deng, Z. J., Morton, S. W., Ben-Akiva, E., Dreaden, E. C., Shopsowitz, K. E., et al. (2013). Layer-by-layer nanoparticles for systemic codelivery of an anticancer drug and siRNA for potential triple-negative breast cancer treatment. *ACS Nano,* **7**(11), 9571–9584.

45. Davis, M. E. (2009). The first targeted delivery of siRNA in humans via a self-assembling, cyclodextrin polymer-based nanoparticle: From concept to clinic. *Mol. Pharmacol.,* **6**(3), 659–668.

46. Kim, S., Kim, J. H., Jeon, O., Kwon, I. C., Park, K. (2009). Engineered polymers for advanced drug delivery. *Eur. J. Pharm. Biopharm.,* **71**(3), 420–430.

47. Chandran, P., Gupta, N., Retnakumari, A. P., Malarvizhi, G. L., Keechilat, P., et al. (2013). Simultaneous inhibition of aberrant cancer kinome using rationally designed polymer–protein core–shell nanomedicine. *Nanomedicine,* **9**(8), 1317–1327.

48. Steelman, L. S., Abrams, S. L., Whelan, J., Bertrand, F. E., Ludwig, D. E., et al. (2008). Contributions of the Raf/MEK/ERK, PI3K/PTEN/Akt/mTOR and Jak/STAT pathways to leukemia. *Leukemia,* **22**(4), 686–707.

49. Yee, K. W., Zeng, Z., Konopleva, M., Verstovsek, S., Ravandi, F., et. al. (2006). Phase I/II study of the mammalian target of rapamycin inhibitor everolimus (RAD001) in patients with relapsed or refractory hematologic malignancies. *Clin. Cancer Res.,* **12**(17), 5165–5173.

50. Ravandi, F., Cortes, J. E., Jones, D., Faderl, S., Garcia-Manero, G., et al. (2010). Phase I/II study of combination therapy with sorafenib, idarubicin, and cytarabine in younger patients with acute myeloid leukemia. *J. Clin. Oncol.,* **28**(11), 1856–1862.

51. Rahmani, M., Nguyen, T. K., Dent, P., Grant, S. (2007). The multikinase inhibitor sorafenib induces apoptosis in highly imatinib mesylate-resistant bcr/abl+ human leukemia cells in association with signal transducer and activator of transcription 5 inhibition and myeloid cell leukemia-1 down-regulation. *Mol. Pharmacol.,* **72**(3), 788–795.

52. Walter, R. B., Appelbaum, F. R., Estey, E. H., Bernstein, I. D. (2012). Acute myeloid leukemia stem cells and CD33-targeted immunotherapy. *Blood,* **119**(26), 6198–6208.

53. Manoocheheri, S., Darvishi, B., Kamalinia, G., Amini, M., Fallah, M., et al. (2013). Surface modification of PLGA nanoparticles via human serum albumin conjugation for controlled delivery of docetaxel. *Daru.,* **21**(1), 58.

54. Gupta, G. P., Massagué, J. (2006). Cancer metastasis: Building a framework. *Cell,* **127**(4), 679–695.

55. Miles, D., von Minckwitz, G., Seidman, A. D. (2002). Combination versus sequential single-agent therapy in metastatic breast cancer. *Oncologist,* **7**(Supplement 6), 13–19.

56. Yeatman, T. J. (2004). A renaissance for SRC. *Nat. Rev. Cancer,* **4**(6), 470–480.

57. Brunton, V. G., Frame, M. C. (2008). Src and focal adhesion kinase as therapeutic targets in cancer. *Curr. Opin. Pharmacol.,* **8**(4), 427–432.

58. Palacios, F., Tushir, J. S., Fujita, Y., D'Souza-Schorey, C. (2005). Lysosomal targeting of E-cadherin: A unique mechanism for the down-regulation of cell–cell adhesion during epithelial to mesenchymal transitions. *Mol. Cell. Biol.,* **25**(1), 389–402.

59. Bacac, M., Stamenkovic, I. (2008). Metastatic cancer cell. *Ann. Rev. Pathol. Mechan. Dis., **3***, 221–247.

60. Lee, J. H., Nan, A. (2012). Combination drug delivery approaches in metastatic breast cancer. *J. Drug Deliv.,* **2012**, 515375.

61. Milane, L., Duan, Z. F., Amiji, M. (2011). Pharmacokinetics and biodistribution of lonidamine/paclitaxel loaded, EGFR-targeted nanoparticles in an orthotopic animal model of multi-drug resistant breast cancer. *Nanomedicine.,* ***7***(4), 435–444.

62. Bae, Y., Diezi, T. A., Zhao, A., Kwon, G. S. (2007). Mixed polymeric micelles for combination cancer chemotherapy through the concurrent delivery of multiple chemotherapeutic agents. *J. Control. Release.,* **122**(3), 324–330.

63. Malarvizhi, G. L., Chandran, P., Retnakumari, A. P., Ramachandran, R., Gupta, N., Nair, S., Koyakutty, M. (2014). A rationally designed photo-chemo core–shell nanomedicine for inhibiting the migration of metastatic breast cancer cells followed by photodynamic killing. *Nanomedicine.,* **10**(3), 579–587.

64. Salhia, B., Tran, N. L., Symons, M., Winkles, J. A., Rutka, J. T., Berens, M. E. (2006). Molecular pathways triggering glioma cell invasion. *Expert Rev. Mol. Diagn.,* **6**, 613–626.

65. Ramachandran, R., Malarvizhi, G. L., Chandran, P., Gupta, N., Menon, D., Panikar, D., Nair, S., Koyakutty (2014). A polymer–protein core–shell nanomedicine for inhibiting cancer migration followed by photo-triggered killing. *J. Biomed. Nanotechnol.,* **10**, 1401–1415.

66. Ferlay, J., Shin, H. R., Bray, F., Forman, D., Mathers, C., Parkin, D. M. (2010). Estimates of worldwide burden of cancer in 2008: GLOBOCAN 2008. *Int. J. Cancer,* **127**(12), 2893–2917.

67. Liu, J. H., Chen, P. W., Asch, S. M., Busuttil, R. W., Ko, C. Y. (2004). Surgery for hepatocellular carcinoma: Does it improve survival? *Ann. Surg. Oncol.,* **11**(3), 298–303.

68. Wilhelm, S., Carter, C., Lynch, M., Lowinger, T., Dumas, J., Smith, R. A., et al. (2006). Discovery and development of sorafenib: A multikinase inhibitor for treating cancer. *Nat. Rev. Drug Discov.*, **5**(10), 835–844.

69. Zhai, B., Sun, X. Y. (2013). Mechanisms of resistance to sorafenib and the corresponding strategies in hepatocellular carcinoma. *World J. Hepatol.,* **5**(7), 345.

70. Cheng, A. L., Kang, Y. K., Chen, Z., Tsao, C. J., Qin, S., Kim, J. S., et al. (2009). Efficacy and safety of sorafenib in patients in the Asia-Pacific region with advanced hepatocellular carcinoma: A phase III randomised, double-blind, placebo-controlled trial. *Lancet Oncol.,* **10**(1), 25–34.

71. Malagari, K., Chatzimichael, K., Alexopoulou, E., Kelekis, A., Hall, B., Dourakis, S., et al. (2008). Transarterial chemoembolization of unresectable hepatocellular carcinoma with drug eluting beads: Results of an open-label study of 62 patients. *Cardiovasc. Int. Radiol.,* **31**(2), 269–280.

72. Yeo, W., Mok, T. S., Zee, B., Leung, T. W., Lai, P. B., Lau, W. Y., et al. (2005). A randomized phase III study of doxorubicin versus cisplatin/interferon α-2b/doxorubicin/fluorouracil (PIAF) combination chemotherapy for unresectable hepatocellular carcinoma. *J. Natl. Cancer Inst.,* **97**(20), 1532–1538.

73. Risse, J. H., Grünwald, F., Kersjes, W., Strunk, H., Caselmann, W. H., Palmedo, H., et al. (2000). Intraarterial HCC therapy with I-131-Lipiodol. *Cancer Biother. Radiopharm.,* **15**(1), 65–70.

74. Sangro, B., Bilbao, J. I., Boan, J., Martinez-Cuesta, A., Benito, A., Rodriguez, J., et al. (2006). Radioembolization using 90Y-resin microspheres for patients with advanced hepatocellular carcinoma. *Int. J. Radiat. Oncol. Biol. Phys.,* **66**(3), 792–800.

75. Song, X. R., Zheng, Y., He, G., Yang, L., Luo, Y. F., He, Z. Y., et al. (2010). Development of PLGA nanoparticles simultaneously loaded with vincristine and verapamil for treatment of hepatocellular carcinoma. *J. Pharm. Sci.,* **99**(12), 4874–4879.

76. Abou Alfa, G. K., Johnson, P., Knox, J., Lacava, J., Leung, T., Mori, A., et al. (2007). Preliminary results from a phase II, randomized, double-blind study of sorafenib plus doxorubicin versus placebo plus doxorubicin in patients with advanced hepatocellular carcinoma. *EJC Suppl.,* **5**(4), 259–259.

77. Malarvizhi, G. L., Retnakumari, A. P., Nair, S., & Koyakutty, M. (2014). Transferrin targeted core-shell nanomedicine for combinatorial delivery of Doxorubicin and Sorafenib against Hepatocellular carcinoma. *Nanomedicine.*, **10**(8), 1649–1659.

78. Sharma, S., Kelly, T. K., Jones, P. A. (2010). Epigenetics in cancer. *Carcinogenesis,* **31**(1), 27–36.

79. Choi, J. D., Lee, J. S. (2013). Interplay between epigenetics and genetics in cancer. *Genomics Informatics,* **11**(4), 164–173.

80. Kuska, B. (1997). Alfred knudson: Two hits times 25 years. *J. Natil. Cancer Inst.,* **89**(7), 470–473.

81. Minucci, S., Pelicci, P. G. (2006) Histone deacetylase inhibitors and the promise of epigenetic (and more) treatments for cancer. *Nat. Rev. Cancer.,* **6**(1), 38–51.

82. Garcia-Manero, G., Yang, H., Bueso-Ramos, C., Ferrajoli, A., Cortes, J., et al. (2008). Phase 1 study of the histone deacetylase inhibitor vorinostat (suberoylanilide hydroxamic acid [SAHA]) in patients with advanced leukemias and myelodysplastic syndromes. *Blood,* **111**(3), 1060–1066.

83. Sandhu, P., Andrews, P. A., Baker, M. P., Koeplinger, K. A., Soli, E. D., et al. (2007) Disposition of vorinostat, a novel histone deacetylase inhibitor and anticancer agent, in preclinical species. *Drug Metab. Lett.,* **1**(2), 153–161.

84. Mohamed, E. A., Zhao,Y., Meshali, M. M.,Remsberg, C.M., Borg, T.M., et al. Vorinostat with sustained exposure and high solubility in poly(ethylene glycol)-b-poly(DL-lactic acid) micelle nanocarriers: Characterization and effects on pharmacokinetics in rat serum and urine. *J. Pharm. Sci.,* **101**(10), 3787–3798.

85. Tran, T. H., Ramasamy, T., Truong, D. H., Shin, B. S., Choi, H. G., et al. (2014). Development of vorinostat-loaded solid lipid nanoparticles to enhance pharmacokinetics and efficacy against multidrug-resistant cancer cells. *Pharm. Res.*, **31**(8), 1978–88.

86. Chandran, P., Kavalakatt, A., Malarvizhi, G. L., Vasanthakumari, D. R., Retnakumari, A. P., et al. (2014). Epigenetics targeted protein-vorinostat nanomedicine inducing apoptosis in heterogeneous population of primary acute myeloid leukemia cells including refractory and relapsed cases. *Nanomedicine.,* **10**(4), 721–732.

Chapter 47

Biodegradable Nanoparticle-Based Antiretroviral Therapy across the Blood-Brain Barrier

Supriya D. Mahajan, PhD,[a] Yun Yu, PhD,[b] Ravikumar Aalinkeel, PhD,[a] Jessica L. Reynolds, PhD,[a] Bindukumar B. Nair, PhD,[a] Manoj J. Mammen, MD,[a] Tracey A. Ignatowski, PhD,[c] Chong Cheng, PhD,[b] and Stanley A. Schwartz, PhD, MD[a]

[a]*Department of Medicine, Division of Allergy, Immunology, and Rheumatology, State University of New York at Buffalo, Buffalo, New York, USA*
[b]*Department of Chemical and Biological Engineering, State University of New York, Buffalo, New York, USA*
[c]*Department of Pathology and Anatomical Sciences, State University of New York at Buffalo, New York, USA*

Keywords: HIV-1, blood–brain barrier, antiretroviral, Atazanavir, biodegradable, biopolymers, PLGA, biocompatible, nanoformulation, nanotechnology, nanocarriers, neuro-AIDS, central nervous system, THP-1 monocytic cell line, targeted drug delivery, drug release, latent HIV reservoirs, central nervous system, viral sequestration, brain targeting, transmigration, HIV-associated neurological disorders

47.1 Introduction

HIV sequestration in the central nervous system (CNS) and the failure of antiretroviral drugs to penetrate through blood–brain barrier

Handbook of Clinical Nanomedicine: Nanoparticles, Imaging, Therapy, and Clinical Applications
Edited by Raj Bawa, Gerald F. Audette, and Israel Rubinstein

ISBN 978-981-4669-20-7 (Hardcover), 978-981-4669-21-4 (eBook)
www.panstanford.com

(BBB) to eliminate latent CNS reservoir continues to be a major roadblock in AIDS therapy [1–3]. Nanotechnology can revolutionize the field of HIV medicine by improving delivery of antiretroviral drugs to targeted regions in the body and by significantly enhancing the efficacy of the currently available antiretroviral medication [1–15]. Nanotechnology-based delivery systems are being developed to target the virus within different tissue compartments and are being evaluated for safety and efficacy [11, 13, 14, 16–18]. Development of biocompatible nanoformulations that can target HIV-1 in sequestered sites requires the use of functionalized nanoparticles (NPs) that are engineered to deliver drugs to specific sites in the body where the virus is sequestered such as the brain [4, 5, 15, 19, 20]. Highly active anti-retroviral therapy (HAART) has significantly improved the prognosis for HIV infected patients, however, adverse side effects and adherence associated with prolonged HAART therapy remain major challenges in HIV therapy [21]. Transporters such as P-glycoprotein (P-gp) and multidrug resistance-associated proteins (MRPs), which are present on the BBB and on many circulating cells such as lymphocytes, monocytes, and macrophages, are involved in the extrusion of HIV protease inhibitors from cells [22].

A nanoformulation of an antiretroviral (ARV) drug would facilitate its transport across the BBB and allow sustained release of the drug thereby increasing its bioavailability would therefore have tremendous clinical translational value. ARV drug can be transported across the BBB if it can be efficiently bound to the nanoparticles that can transverse the BBB and can be released within the brain in a therapeutically relevant concentration and over a sustained period. An antiretroviral nanoformulation would provide a means to overcome the cellular and anatomical barrier such as the BBB to drug delivery, thereby targeting HIV that is sequestered in the brain, and is the underlying cause of various HIV-associated neurological disorders (HAND) and shows great promise as a neurotherapeutic. Optimization of an NP-based delivery system requires an understanding of the different mechanisms of biological interactions that may occur when a nanoformulation is given systemically. Advanced particle engineering is required to ensure that drug characteristics remain unaltered and yet its versatile formulation should allow specific

targeting to the site of viral sequestration and its sustained release within the microenvironment. Nanotechnology-based delivery systems are being developed to target the virus within different tissue compartments and are being evaluated for safety and efficacy [22–26]. Nanoparticles offer greater stability to encapsulated drugs in biological fluids and also protect the encapsulated drugs against enzymatic degradation. Further, nanomaterials can provide improved drug delivery, by virtue of their robustness, safety, and multimodality or multi-functionality [19, 20, 26, 27]. Thus, nanotechnology can revolutionize the field of HIV medicine by improving the delivery of antiretroviral drugs to targeted regions in the brain where the virus is sequestered and by significantly enhancing the efficacy of the currently available antiretroviral medication.

Efficient internalization within CNS cells and selective targeting are the major aims of such a HIV nanotherapeutic formulation. Ideally, it should also have the characteristics of (i) long circulation time in blood, (ii) self-regulation of drug release, (iii) low toxicity, and (iv) minimal side effects. Such a nanoformulation would increase solubility and enhance the stability of most poorly water-soluble therapeutic agents such as antiretroviral drugs and protect them from interacting with non-specific sites, thereby reducing toxicity. Targeted drug delivery of antiretroviral drugs to HIV-1 infected cells in the CNS would improve efficacy, reduce toxicity, reduce HIV resistance frequency, and decrease viral production. An advantage of an antiretroviral nanoformulation includes its ability to bypass the multidrug-resistant transporters that may efflux drugs entering freely through the plasma membrane. Thus, an antiretroviral nanoformulation would provide a means to overcome the cellular and anatomical barrier such as the BBB to drug delivery.

Several nanocarriers, including inorganic/organic nanoparticles, metal-based nanoparticles, polymeric nanoparticles, solid lipid nanoparticles, liposomes, micelles, dendrimers, nanogels, nanoemulsions, and nanosuspensions, have been studied for the delivery of CNS therapeutics [12, 22, 23, 28–30]. However if the materials used in nanocarrier fabrication are both biodegradable and biocompatible, they have increased clinical utility. Typically, polymeric nanoparticles made of the biodegradable polymers, like poly(lactide-co-glycolide) (PLGA) have been used for biomedical

applications. Among the commonly used protease inhibitors, Atazanavir has limited passage across the BBB [31]. Therefore, the goal of the current study was to use a nanoplatform that will enable Atazanavir to effectively cross the BBB and target specific HIV-1 infected cells in the brain and due to the fact that biodegradable PLGA NPs offer enhanced biocompatibility and superior drug encapsulation and have sustained release properties, we used biodegradable PLGA-based NPs in this study. The transcytosis efficacy of the PLGA NPs was investigated using the *in vitro* BBB model that was validated in our laboratory. Further, the anti-HIV efficacy of these nanoparticles was evaluated in HIV-1 infected THP-1 cells which is a monocytic cell line, which are cultured on the bottom of the lower chamber (basolateral end or CNS end) of the *in vitro* BBB model.

47.2 Methods

47.2.1 Study Design

Following the synthesis and characterization of the PLGA nanoformulations, we did cell viability studies using an MTT assay to determine cellular toxicity of the nanoformulation. We then evaluated the transversing ability of the nanoplexes (which were added to the apical end or systemic end) across the BBB using a well validated *in vitro* BBB model and tested their antiviral efficacy on HIV-1 infected THP-1 monocytic cells, which were cultured in the bottom chamber (basolateral end or CNS end) of our *in vitro* BBB model. The p24 antigen levels were measured, which indicated antiviral effects of the nanoformulation (Fig. 47.1).

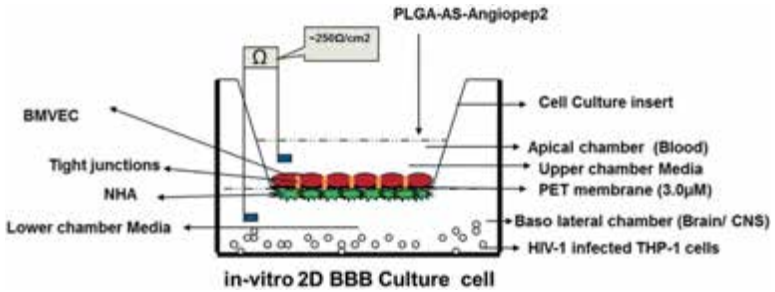

Figure 47.1 Study design: Evaluating the traversing potential and efficacy of PLGA-Atazanavir (AS)-Angiopep-2 nanoformulation.

47.2.2 Nanoparticle Synthesis

Well-defined multifunctional NPs with PLGA-based cores were synthesized and Atazanavir (AS) and a fluorescent dye (Nile Red) were encapsulated within this nanoformulation. The NPs possess a PEGylated corona, which enhances its circulation time, reduces toxicity and immunogenicity. The ω-terminals of PEG chains are functionalized with Angiopep-2, to facilitate the penetration of NPs across the BBB and cellular membranes. The Angiopep-2 peptide, binds to low-density lipoprotein receptor-related protein-1 (LRP-1), a receptor expressed on the endothelial cells that constitute the BBB [32]. The hydrodynamic size of these NPs is ~100 nm, which helps avoid fast systemic clearance. NPs are prepared by nanoprecipitation, followed by peptide conjugation (Fig. 47.2). Briefly, the hydrophobic components of NPs, including AS, Nile Red, and PLGA, are dissolved in a water-miscible organic solvent. The resulting solution is added drop wise using a syringe pump into 4% ethanol–water solution of 1,2-distearoyl-sn-glycero-3-phosphoethanolamine-N-[maleimide PEG-2000], i.e., DSPE-PEG-MAL, under continuous stirring. The dispersion formed is washed three times with water using Amicon Ultra centrifugal filter with a molecular weight cutoff of 10 kDa and then re-suspended in water or lyophilized into dry powder. The preparation of NPs is optimized by altering organic solvent, concentrations and feed ratios of hydrophobic components and surfactant, the composition of PLGA, as well as the nanoprecipitation conditions.

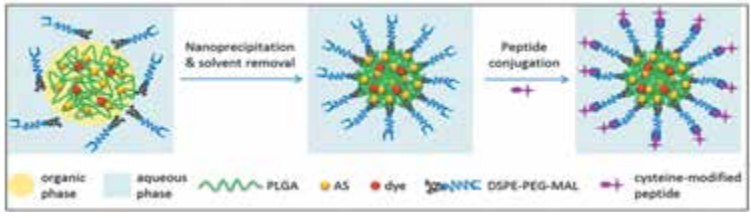

Figure 47.2 Schematic of synthesis of multifunctional NPs with PLGA-based cores and the Atazanavir (AS) and a fluorescent dye (Nile Red) encapsulated within this nanoformulation.

47.2.3 Nanoparticle Characterization

The NPs are characterized by ^{1}H NMR and UV-vis spectroscopies to determine the compositions of NPs and the loading wt% of AS

and dye, by dynamic light scattering (DLS) to analyze their zeta potential, hydrodynamic sizes and size distribution, and by transmission electron microscopy (TEM) to determine their sizes in dry state on TEM grids (Fig. 47.3). Loading efficiencies of AS and fluorescent dye are calculated based on the comparison of the experimental wt% of AS and dye with their initial feed wt%. The peptide (Angiopep-2) conjugation of NPs is done using sequential Michael addition reactions of the cysteine-modified peptide with the MAL groups of NPs in phosphate buffer 7.4 at room temperature for 12 h. The peptide-conjugated NPs are characterized systematically and the loading wt% of AS and fluorescent dye is determined to ensure that there is not a significant release of the cargo during the peptide conjugation process. The aqueous dispersion of the nanoparticles was drop cast on a TEM copper grid and visualized using a JEOL JEM 2020 (Electron Microscopy Sciences, Inc., Hatfield, PA), which is a high-resolution electron microscope with an accelerating voltage of 200 KV, and a point resolution of 0.19 nm. DLS measurements were carried out using a Brookhaven 90Plus particle size analyzer (Brookhaven Instruments Corporation, Holtsville, New York) with a scattering angle of 90°. UV-Vis absorption spectra were recorded using a Shimadzu UV-3101 PC spectrophotometer, using a quartz cuvette with 1 cm path length. Fluorescence spectra were recorded on a Fluorolog-3 (Jobin Yvon, Longjumeau, France) spectrofluorometer. ^{1}H NMR spectra were obtained on a Varian INOVA NMR spectrometer operating at 500 MHz at r.t., and the samples were dissolved in $CDCl_3$ (99.8 atom% D) containing 1.0 vol% tetramethylsilane (TMS) or methyl sulfoxide-d_6 (DMSO-d_6, >99.5 atom% D).

47.2.4 *In vitro* BBB Model

The *in vitro* BBB model [33–35] uses primary cultures of both BMVECs (Cat# ACBRI-376) and normal human astrocytes (NHAs, Cat# ACBRI-371), which were obtained from Applied Cell Biology Research Institute (ACBRI, Kirkland, WA). Characterization of BMVECs demonstrated that >95% cells were positive for cytoplasmic von Willibrand's factor/Factor VIII. BMVECs were cultured in CS-C complete serum-free medium (ABCRI, Cat # SF-4Z0-

500) with attachment factors (ABCRI, Cat # 4Z0-210) and Passage Reagent Group™ (ABCRI, Cat # 4Z0-800). NHAs were cultured in the CS-C medium, supplemented with 10 μg/mL human epidermal growth factor, 10 mg/mL insulin, 25 μg/mL progesterone, 50 mg/mL transferrin, 50 mg/mL gentamicin, 50 μg/mL amphotericin-B, and 10% FBS. NHAs were characterized on the basis of >99% of these cells being positive for glial fibrillary acidic protein (GFAP). Both BMVECs and NHAs were obtained at passage 2 for each experiment and were used for all experiments between 2–8 passages—within the 6 to 27 cumulative population doublings. The BBB model used consists of two-compartment wells in a six-well culture plate, with the upper compartment separated from the lower by a 3 μM polyethylene terephthalate (PET) insert (surface area = 4.67 cm^2). The BMVECs were grown to confluency on the upper side of the insert, while a confluent layer of NHAs were grown on the underside. The formation of a functional and intact BBB takes a minimum of 5 days, which can be confirmed by determining the transendothelial electrical resistance (TEER) value, as described below [35, 36]. Using the *in vitro* BBB model, we examined BBB permeability and the efficacy of drug delivery of the nanoformulations.

47.2.5 Measurement of TEER

TEER across the *in vitro* BBB was measured using an Ohm meter Millicell ERS system (Millipore, Bedford, MA, Cat # MERS 000-01). Electrodes were sterilized using 95% alcohol and rinsed in distilled water prior to measurement. A constant distance of 0.6 cm was maintained between the electrodes at all times during TEER measurement.

47.2.6 HIV-1 Infection of THP-1

Monocytic THP-1 cells (American Type Culture Collection [ATCC], Manassas, VA); were maintained at 37°C, under 5% CO_2 in RPMI 1640 medium supplemented with 10% (v/v) heat-inactivated fetal bovine serum (FBS) (Sigma, St. Louis, MO), penicillin (100 units/mL), streptomycin (100 mg/mL), and L-glutamine (2 mM). THP-1 cells are cultured as a single-cell suspension cultures and were split

at a ratio of 1:4 once a week. Undifferentiated THP-1 cells are susceptible to infection by T-tropic human immunodeficiency virus type 1 (HIV-1) isolates that use the co-receptor CXCR4 (X4 strains). Undifferentiated THP-1 (1×10^6 cells/mL) were infected for 3 h with HIV-1_{IIIB}(NIH AIDS Research and Reference Reagent Program) at a concentration of $10^{3.0}TCID_{50}$/mL cells, equivalent to 10 ng viral isolate/mL of culture media. Following that, the infected cells were washed with Hanks buffered saline, reconstituted in RPMI media (fortified with 10% FBS) and incubated at 37°C/5% CO_2 for 7 days. Levels of p24 in the culture supernatants were measured using a commercially available p24 ELISA kit (Zeptometrix, Buffalo, NY) 7 days post-infection. These infected THP-1 cells were then washed and reconstituted in fresh culture medium and used for evaluating the anti HIV-1 efficacy of the nanoplexes.

47.2.7 p24 ELISA

HIV-1 infection was monitored by the viral p24 level in harvested cell culture supernatants, using enzyme-linked immunosorbent assay (ELISA) plates obtained from a commercial vendor (Zeptometrix Buffalo, NY). The results are expressed in pg/mL as the mean and standard deviation (SD) of duplicate determinations from two wells.

47.2.8 Cell Viability Measurement Using an MTT Assay

The MTT assay is a quantitative, sensitive detection of cell proliferation. Cell viability was tested in BMVEC, NHA and THP-1 cells before and after treatment with the nanoplexes. Typically, 10,000 cells suspended in 100 µL of media were incubated for 24 h with various concentration of nanoformulation in a 96-well plate. At the end of the incubation period, 10 µL of MTT reagent (Cat # 30 –1010 K; ATCC) was added to the cells followed by incubation for approximately 3 h, which was followed by addition of a detergent solution to lyse the cells and solubilize the colored crystals. The amount of color produced was directly proportional to the number of viable cells. Colorimetric detection was done at a wavelength of 570 nm. MTT cell proliferation assay measures the reduction

of a tetrazolium component (MTT-3-(4,5-Dimethylthiazol-2-yl)-2,5-diphenyltetrazolium bromide, a tetrazole) into an insoluble formazan product by the mitochondria of viable cells.

47.2.9 Evaluation of the Ability of the Nanoformulation to Transverse the BBB and Antiviral Efficacy of the PLGA-AS-Angiopep-2 Nanoformulation

A hundred thousand HIV-1 infected THP-1 cells that were suspended in 1 mL of RPMI complete media were plated in the lower chamber (basolateral end) of the *in vitro* BBB model. The following formulations (Atazavanir alone, PLGA alone, PLGA-AS alone, PLGA-AS-Angiopep-2) were reconstituted in 500 μL of media and added separate to chambers (apical end) of the *in vitro* BBB and incubated at 37°C and 5% CO_2 for a period of 24–48 h. At the end of this incubation, the THP-1 cells were harvested from the lower chamber, washed, and then analyzed for antiviral efficacy of the nanoformulation by measuring p24 antigen levels using a p24 ELISA assay. Triplicate wells were used for each condition tested.

47.2.10 Statistical Analysis

The primary analysis consists of evaluating the transversing ability of the PLGA-AS-Angiopep-2 nanoformulation, additionally the efficacy of the PLGA-AS-Angiopep-2 nanoformulation is evaluated based on its ability to decrease viral replication as determined by HIV p24 measurements in the HIV-1 infected monocytes/macrophages harvested from the basolateral end, 48 h post-treatment of the BBB with the nanoformulation. Statistical analysis was done between PLGA-AS-Angiopep-2 treated BBB and other controls namely Atazavanir alone, PLGA alone, PLGA-AS alone, respectively. All experiments are done in triplicate, including the BBB experiments where each condition was done in triplicate. Data was analyzed using ANOVA. A p value of less than 0.05 was considered significant. Analyses were performed using the Prism (Graph Pad Software, Inc., San Diego, CA) software.

47.3 Results

47.3.1 Characterization of the Nanoplexes

The physical properties of the nanoparticle formulations are established using the following techniques: (a) DLS to estimate the hydrodynamic diameter and surface charge of the aqueous dispersed nanoparticles, (b) Transmission Electron Microscopy (TEM) to determine particle size and size distribution, (c) ^{1}H NMR and (d) evaluation of the spectral properties of the fluorescent nanomaterials using simple spectrophotometry and spectrofluorometry. Figure 47.3 shows the correlation of the hydrodynamic diameters with the concentrations and feed ratios of polymer to surfactant. Nile Red–loaded NPs allowed tracking intracellular uptake of the NPs. We synthesized Atazanavir or Nile Red–loaded NPs by the addition of an acetonitrile solution of PLGA and AS or Nile Red into the 4% ethanol–water solution of DSPE-PEG-MAL, followed by removal of organic solvents by using centrifugal filter. Our results showed considerable drug loading

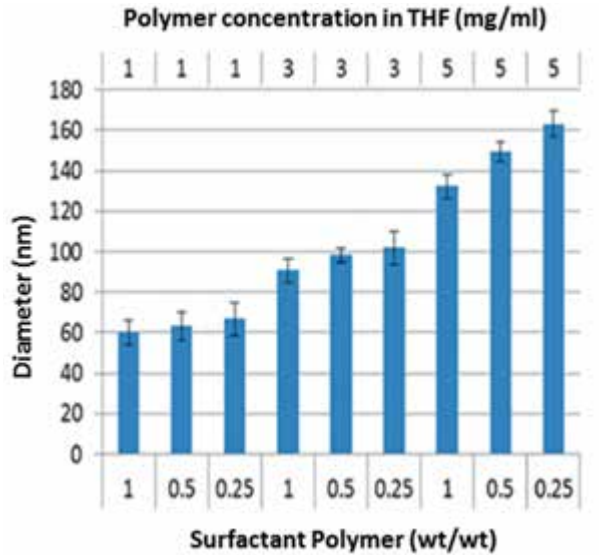

Figure 47.3 Correlation between the hydrodynamic diameters with the concentration and feed ratios of polymer to surfactant.

(2–5 wt% relative to PLGA) and effective Nile Red loading (~1 wt%) (For NP uptake tracking) could be obtained (Fig. 47.4). Because of the presence of MAL group at the PEG terminal of the surfactant, the Angiopep-2 peptide was readily conjugated with NPs by using a cysteine-modified Angiopep-2 to react with MAL group via Michael addition mechanism. The optimal concentration of PLGA used in the nanoformulation was 3 mg/mL and that of Atazanavir was 75 μM, respectively. The conjugation efficiency of Angiopep-2 to the PLGA was ~70% as measured by ^{1}H NMR analysis.

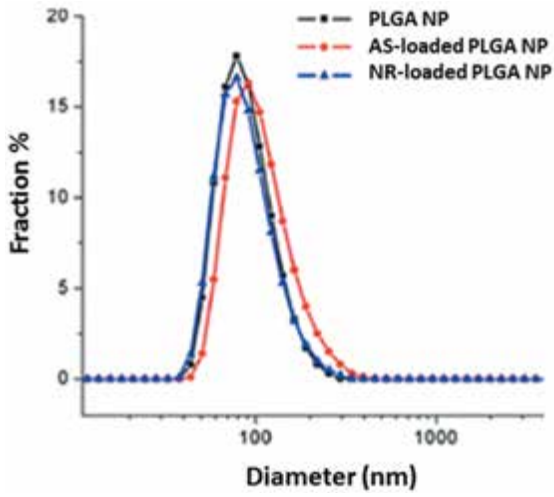

Figure 47.4 Drug loading capacity and size of the nanoformulation. Our nanoformulation had a 2–5 wt% Atazanavir loading capacity relative to PLGA and a ~1 wt% Nile Red loading capacity relative to PLGA.

47.3.2 Effect of the Nanoformulations on Cell Viability

Cell viability was tested in BMVEC, NHA and THP-1 cells before and after treatment with the nanoformulations. Our results (Fig. 47.5) indicate greater than 90% cell viability in all three cell lines tested confirming that the nanoformulation are non-toxic. The Atazanavir and PLGA concentrations in the nanoformulation are 75 μM and 3 mg/mL, respectively.

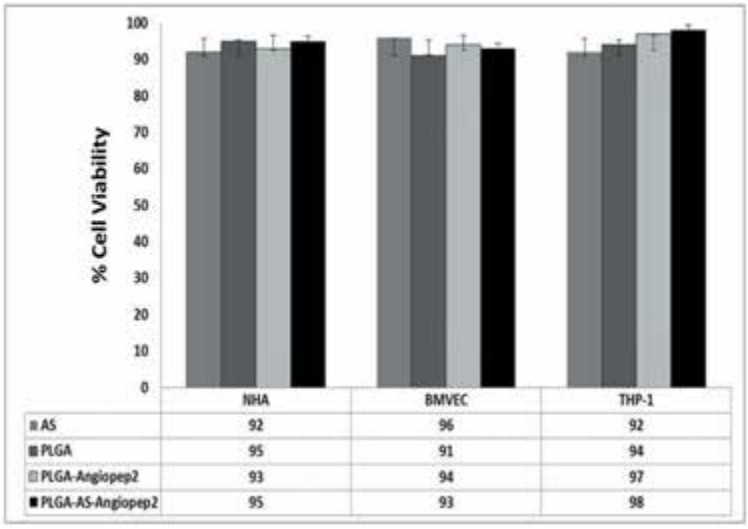

	NHA	BMVEC	THP-1
AS	92	96	92
PLGA	95	91	94
PLGA-Angiopep2	93	94	97
PLGA-AS-Angiopep2	95	93	98

Figure 47.5 Cell toxicity studies using the PLGA-AS-Angiopep-2 nanoformulation.

47.3.3 Determination of the Integrity of *in vitro* BBB during Transversing of the Nanoplex across the BBB

Our *in vitro* BBB model is a well-validated co-culture model and reflects several characteristics of the *in vivo* BBB. We have validated the BBB model of Persidsky et al. [36], which is composed of a co-culture of primary BMVEC and astrocytes, the astrocytic end-feet are in close apposition to the abluminal surface of the brain endothelium and allow formation of a tight BBB. Formation of an intact BBB was measured by determining TEER using Millicell-ERS microelectrodes (Millipore, Bedford, MA). A mean TEER value of ~250 Ohm/cm^2 is consistent with the formation of the BBB. No significant change was observed in the TEER values of the BBB, before and after treatment with the nanoformulations for 24 h (Table 47.1) indicating that the integrity of the BBB is maintained, and that the nanoformulations PLGA alone, Atazanavir-loaded PLGA, PLGA-Angiopep-2 and PLGA-Atazanivir-Angiopep-2 did not cause any damage to the BBB while traversing through this barrier.

Table 47.1 Measurement of transendothelial electrical resistance across the BBB pre- and post-treatment with the nanoformulations

Nanoformulation	Pre-treatment	Post-treatment	p value
PLGA	267.3 ± 13.5	279.6 ± 15.9	NS
PLGA-AS	255.8 ± 16.1	258.7 ± 10.2	NS
PLGA-Angiopep-2	262.2 ± 14.7	270.14 ± 16.7	NS
PLGA-AS-Angiopep-2	277.4 ± 11.3	282.9 ± 13.8	NS

47.3.4 Testing the Efficacy of the Nanoformulation Using the *in vitro* BBB Model

HIV-1 infected THP-1 cells (1×10^5 cells per mL) were added to the lower chamber (Basolateral or CNS end) of the *in vitro* BBB model. Five hundred microliters of the following solutions were added to the upper chamber (apical end) of the *in vitro* BBB followed by a 48 h incubation period: Atazavanir alone, PLGA alone, PLGA-AS alone, and PLGA-AS-Angiopep-2. We then harvested 500 μL of the media (i.e., volume of media equivalent to the formulations added in the apical chamber) from the lower basolateral chamber and measured the HIV-1 p24 antigen levels in the media using a commercially available p24 ELISA kit. Our results (n = 3) show a >90% decrease in HIV-1 p24 levels in the HIV-1 infected

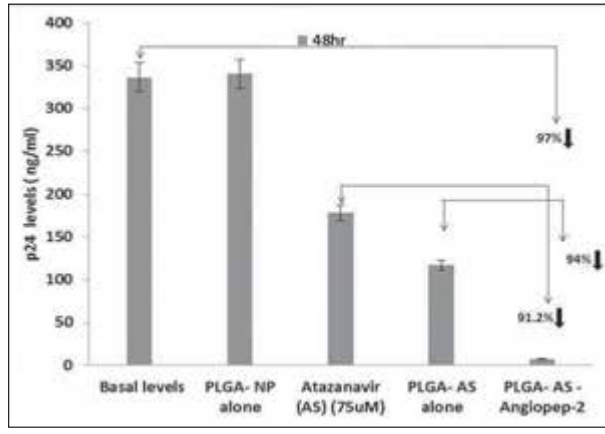

Figure 47.6 PLGA-AS-Angiopep-2 nanoformulation significantly decreased HIV-1 viral replication as evident from the decreased HIV p24 levels in HIV-1 infected THP-1 cells.

THP-1 cells treated with PLGA-AS-Angiopep-2 as compared to Atazavanir alone (91.2% decrease; $p < 0.001$) or PLGA-AS alone (94% decrease; $p < 0.001$) (Fig. 47.6). Comparison of HIV-1 p24 levels between PLGA-AS-Angiopep-2 and basal levels such as media alone or PLGA-NP alone showed a >97% decrease ($p < 0.001$).

47.4 Discussion

Nanocarriers provide a means to overcome cellular and anatomical barriers to drug delivery. Nanocarrier-mediated ARV delivery may allow modulation of drug delivery profiles thereby allowing sustained release of the drug at a specific site where the virus is sequestered such as the brain. The therapeutic efficacy and safety of drugs can be significantly improved by targeted delivery using nanocarriers. Nanocarriers enable ARV transport by passive or active transport mechanisms. It is their size that allows them to penetrate through cells and deliver drugs intracellularly without risking extracellular degradation. Biopolymers have attracted great attention for nanotechnology-based drug delivery due to their stability and sustained drug release characteristics and also their reproducibility during synthesis [23, 24]. The important determinants of the type of biopolymers to be used for nanoformulation depends on (1) drug loading capacity needed (2) the requisite drug release pattern and (3) the biodegradability of core polymers, all of which are key issues for a nanoformulation that will be used *in vivo*. Most antiretroviral drugs are ineffective in reducing the HIV viral load in the brain due to the poor transport of many antiretroviral drugs, particularly the protease inhibitors, across the BBB [16–18]. In the current study we used PLGA, which is been approved by the Food and Drug Administration (FDA). The advantage of using the PLGA biopolymer is that a wide range of drugs of different hydrophilicity or hydrophobicity can be incorporated into these polymers, and their release characteristics can modified by controlling the molecular weight or copolymer composition which influences properties such as degradation rate, thermal sensitivity, and pH sensitivity. These polymers have the capability to sustain drug release for several weeks. Further PLGA undergoes hydrolysis in the body to produce biodegradable metabolite monomers such as lactic acid and glycolic acid that are typically found

in the body and therefore, it is an ideal nanocarrier for the drug delivery applications because of minimal systemic toxicity associated with it. We used the PLGA biopolymer as a nanocarrier for an HIV antiretroviral drug called Atazanavir. The rationale for choosing Atazanavir was that this HIV protease inhibitor has limited passage across the BBB, due to its interaction with efflux P-gp and MRPs, which prevent its passage across the BBB and thus its entry into the CNS [31]. A nanoformulation of PLGA and Atazanavir would facilitate the entry of this ARV drug into the brain. In addition to evaluating the transcytosis efficacy of the PLGA nanoformulation using the an *in vitro* BBB model we tested the anti-HIV efficacy of this nanoformulation in HIV-1 infected THP-1 cells cultured on the bottom of the lower chamber (basolateral end or CNS end) of the *in vitro* BBB model. This study forms the basis for development of a biocompatible nanoformulation that can target HIV-1 in sequestered site such as the brain and can potentially be used as a neurotherapeutic in Neuro-AIDS.

Our PLGA-based nanoformulation (Fig. 47.2) is prepared via the nanoprecipitation technique followed by peptide conjugation [37], which avoids tedious synthesis procedure and results in biodegradable NPs with minimal long-term toxicity. TEM imaging was utilized to visualize the morphology and uniformity of these NPs and they showed uniform spherical morphology with average diameter of around 100 nm. Nanoprecipitation readily allows the formation of drug-encapsulated polymer-based NPs via the assembly process of water-insoluble polymers in drug-containing solutions. Using this technique, we were able to prepare a nanoformulation of Atazanavir-PLGA and were able to effectively control its size through modulation of the concentrations and feed ratios of polymer to the PEG-based surfactants (Fig. 47.3). DLS analysis shows the effects of biopolymer drug conjugate and the surfactant concentrations on the size and size distribution of PLGA-AS-Angiopep-2 NPs. The biopolymer drug conjugate concentrations in THF were 1, 3, and 5 mg/mL and the mass concentration ratio of surfactant to biopolymer drug conjugate was 1, 0.5, and 0.25. Figure 47.3 shows that under these experimental conditions the volume-average hydrodynamic diameter (D_h) of the NPs, as measured by TEM ranged from 60–163 nm, and significantly increased with polymer concentration. Besides size of NPs, size

distribution of NPs is also an important criterion to assess the quality of formulation. Our optimal PLGA nanoformulation that we used in the study used NPs that had a hydrodynamic diameter (D_h) of 100 nm as measured by TEM and a polydispersity index (PDI) of 0.19, which had an optimal PLGA concentration of 3 mg/mL and a surfactant to biopolymer drug conjugate mass ratio of 0.5. The ~100 nm hydrodynamic size of these NPs helps avoid fast systemic clearance.

In addition to size and homogeneity, colloidal stability of PLGA NPs is also crucial in drug delivery. The presence of charged surfactant molecules on surface, allows these PLGA NPs to be readily suspended in water and culture media without noticeable aggregation and they maintain their colloidal stability over extended time periods. A suspension of the PLGA NPs in deionized water (pH = 7.0) was monitored by DLS and showed that the hydrodynamic diameter (Dh) and scattering intensity of the NPs were essentially consistent during 60 days at room temperature, indicating relatively slow degradation of the PLA-based polymer backbones and significant colloidal stability of the NPs. PEGylation also helps avoid recognition by the reticulo-endothelial system. Presence of a MAL group at the ω-terminals of PEG chains allowed functionalization with Angiopep-2, which facilitate the penetration of NPs across the BBB. Angiopep-2 was readily conjugated with NPs by using cysteine-modified Angiopep-2 to react with MAL via Michael addition mechanism. The Angiopep-2 peptide, binds to low-density lipoprotein receptor-related protein-1 (LRP-1), a receptor expressed on the endothelial cells that constitute the BBB. Figure 47.4 showed considerable Atazanavir loading (2–5 wt% relative to PLGA) and Nile Red loading (~1 wt%) could be obtained and that the size of the biopolymer drug conjugate was ~100 nm.

Figure 47.5 shows that our nanoformulation is nontoxic, and greater than 90% cell viability was observed for all the three cell lines (BMVEC, NHA and THP-1) tested, indicating that it will be safe to use this nanoformulation *in vivo* studies.

We observed no appreciable change in the TEER measurements (Table 47.1) when the BBB was treated with PLGA-AS-Angiopep-2, PLGA alone, PLGA-AS and PLGA-Angiopep-2, indicating the absence of any functional damage to the BBB and therefore indicates that

this PLGA-based nanoformulation may be extremely effective in carrying therapeutic payload across the BBB.

The efficacy of this nanoformulation was determined by evaluating the level of HIV-1 p24 released from THP-1 monocytic cells cultured at the basolateral end of the BBB model. We observed a significant decrease (>90%) in HIV-1 p24 production from the HIV-1 infected THP-1, harvested from the lower chamber of the *in vitro* BBB model (Figs. 47.6). Our results suggest that our PLGA nanoformulation is a great nanocarrier for the antiretroviral drug Atazanavir and significantly enhances the antiviral efficacy of Atazanavir and this may be attributed to the presence of the Angiopep-2 peptide, which binds to low-density lipoprotein receptor-related protein-1 (LRP-1), receptor expressed on the endothelial cells that constitute the BBB [32]. The mechanism of the PLGA-AS-Angiopep-2-based antiretroviral drug transport across the BBB appears to be receptor-mediated endocytosis followed by transcytosis into the brain. Modification of the PLGA surface with covalently attached targeting ligands or by coating with certain surfactants such as PEG is necessary for this receptor-mediated uptake.

47.5 Conclusions and Future Prospects

In conclusion, we have demonstrated the ability to synthesize a biodegradable biopolymeric nanoformulation that contains an antiretroviral drug and a cell-penetrating peptide on its surface that is able transverse the BBB and significantly inhibit HIV-1 replication in the infected monocytic cells, demonstrating the anti-HIV-1 efficacy of this nanoformulation and its applicability as a neurotherapeutic. Our data encourage further *in vivo* investigation of these PLGA NPs for nanotherapy within the CNS as the biomedical functions of these PLGA NPs can be further enhanced by multifunctionalization via conjugation with specific targeting ligands and various other diagnostic moieties providing an effective nanotherapeutic strategy in treating Neuro-AIDS and other neurological disorders.

The latent HIV reservoir in the CNS serves as a major depot for HIV persistence, and therefore, effective nanotechnology-based approaches to eradicate HIV could provide valuable steps toward

HIV eradication. Majority of small and large pharmaceutical drugs are unable to cross the BBB, and drug delivery to directly access the brain via either the nasal cavity or inhibition of P-gp transporters to deliver ARV drugs across BBB has had limited success. Therefore, a nanotherapeutic approach that would (1) allow sustained ARV drug delivery, (2) allow accumulation of higher concentration of drug in the CNS, and (3) specifically target CNS cells that harbor the virus can potentially eliminate the virus effectively from the CNS. The important aspect of using PLGA-based nanoformulation is that PLGA has been approved by the United States Food and Drug Administration for human use; therefore, a potentially efficacious PLGA-based antiretroviral formulation could be quickly transitioned from the laboratory to the clinic. The PLGA-based drugs illicit minimal immune response and are biodegradable and are degraded into glycolic acid and lactic acid, via the tricarboxylic acid (TCA) cycle into bi-products like water and CO_2 and eliminated from the body. Furthermore, the PLGA nanoparticles allow encapsulation of both hydrophilic and hydrophobic drugs and permit surface modifications that not only allow it to escape immune surveillance but also allow the attachment of various molecules such as antibodies that provide targeting specificity and covalent binding to chemically modified ligands that permit tracking of the nanoparticle within the CNS, thus making it a theranostic (molecules that has both a therapeutic and diagnostic ability). The non-HIV drugs that have used modified PLGA as a delivery system include the 28-amino-acid polypeptide, vasoactive intestinal peptide (VIP), the naturally occurring antioxidant enzyme, superoxide dismutase (SOD) and the glucocorticoid dexamethasone [38–40]. Recent studies by Destache et al. showed that three antiretroviral drugs, namely ritonavir, lopinavir, and efavirenz, could be conjugated to PLGA (cART-NPs) and that sustained release of these antiretrovirals was observed from PLGA NP for 28 days without any noticeable toxicity [41]. The same group demonstrated that in HIV-1-infected H9 monocytic cells treated with cART NPs subcellular fractionation studies demonstrated that these cells contained significantly higher nuclear, cytoskeleton, and membrane antiretroviral drug levels compared to cells treated with ARV drug alone. cART-NPs efficiently inhibited HIV-1 infection and transduction thus demonstrating

the efficacy of the PLGA NPs formulation in inhibiting HIV-1 replication [42]. Chaowanachan et al. showed that antiretroviral drugs with different physicochemical properties such as Saquinavir, Efavirenz, and Tenofovir can be encapsulated individually into PLGA nanoparticles to potently inhibit HIV [43]. Kuo et al. demonstrated that a nanoparticles synthesized using a combination of three biodegradable components and the antiretroviral drug saquinavir (SQV) is encapsulated within the particle core which composed of PLGA to form SQV-PLGA NPs, and the surface of SQV-PLGA NPs was grafted successively with hydrophilic polyethyleneimine (PEI), poly-(γ-glutamic acid) (γ-PGA). They showed that this nanoparticulate carrier system proved efficacious in delivering antiretroviral drug across the BBB [44].

Based on our studies and data from other investigators, although antiretroviral drug-based nanotherapeutics show a promise for clinical translation, due to their ability to prolong systemic circulation, cross the BBB, provide specific cell targeting, enhance intracellular drug levels in the CNS and reduce the inherent toxicity of many antiretroviral drugs, no successful clinical trials that use nanoformulations of antiretroviral drugs for CNS delivery have been reported. Issues related to HIV latency, long-term accumulation of nanoparticles and antiretroviral drugs in the CNS thereby contributing to neurotoxicity have hindered their clinical utility. Extensive pharmacokinetic studies of these ARV-nanoformulations, their CNS biodistribution, and their toxicity need to be done. With the advent of innovations in personalized medicine, materials science, biomedical engineering, and interdisciplinary research collaborations between clinicians, chemists, and basic scientists, there is no doubt that nanotherapy will become mainstream clinical care within the next couple of decades.

Abbreviations

AIDS: Acquired immunodeficiency syndrome
ARV: Antiretroviral
AS: Atazanavir
BBB: Blood–brain barrier
BMVEC: Brain microvascular endothelial cells
CNS: Central nervous system
DLS: Dynamic light scattering

DSPE-PEG-MAL: 1,2-Distearoyl-sn-glycero-3 phosphoethanolamine-N-[maleimide PEG-2000]
GFAP: Glial fibrillary acidic protein
HAART: Highly active anti-retroviral therapy
HAND: HIV-associated neurological disorders
HIV: Human immunodeficiency virus
LRP-1: Lipoprotein receptor-related protein-1
MAL: Maleimide
MRPs: Multidrug resistance-associated proteins
MTT: 3-(4,5-Dimethylthiazol-2-yl)-2,5-diphenyl tetrazolium bromide
Neuro-AIDS: Neuro-Acquired immune deficiency syndrome
NHA: Normal human astrocytes NMR: Nuclear magnetic resonance
NPs: Nanoparticles
NR: Nile Red
PEG: Polyethylene glycol
P-gp: P-glycoprotein
PLGA: Poly(lactide-co-glycolide)
PET: Polyethylene terephthalate
PEI: Polyethyleneimine
γ-PGA: Poly-γ-glutamic acid
SOD: Superoxide dismutase
TCA: Tricarboxylic acid cycle
TEER: Transendothelial electrical resistance
TEM: Transmission electron microscopy
VIP: Vasoactive intestinal peptide

Disclosures and Conflict of Interest

The authors declare that they have no conflict of interest and have no affiliations or financial involvement with any organization cited in this manuscript. No writing assistance was utilized in the production of this chapter and the authors have received no payment for its preparation.

Atazanavir was obtained through the AIDS Research and Reference Reagent Program, Division of AIDS, NIAID, NIH, Bethesda, Maryland, USA. This study was supported by the following grants from the National Institutes of Health: 1R21DA030108-01 (S. Mahajan), K01DA024577 (J. Reynolds), and Kaleida Health Foundations, Buffalo, New York, USA.

Corresponding Author

Dr. Supriya Mahajan
Department of Medicine
Division of Allergy, Immunology, and Rheumatology
State University of New York at Buffalo
6074 UB's Clinical and Translational Research Center
875 Ellicott St, Buffalo, NY 14203, USA
Email: smahajan@buffalo.edu

About the Authors

Supriya D. Mahajan is an associate professor in the Department of Medicine, State University of New York at Buffalo. Her research interest is in the area of NeuroAIDS in the context of drug abuse and the current focus of her research work is nanotherapeutics for NeuroAIDS and other neurological diseases. Prof. Mahajan has developed and validated an *in vitro* blood–brain barrier (BBB) model and has used it to evaluate transendothelial transport of several drugs across the BBB.

Yun Yu recently graduated from the Department of Chemical and Biological Engineering, State University of New York at Buffalo. She has expertise in the synthesis of biopolymeric nanoparticles and was involved in the preparation of the PLGA nanoparticles used in this study.

Ravikumar Aalinkeel is a research assistant professor in the Department of Medicine, State University of New York at Buffalo. He has expertise in drug delivery systems in various disease states using nanotechnology and has done extensive work in delivery of siRNA therapeutics in the context of cancer biology and neuro-AIDS.

Jessica L. Reynolds is an assistant professor in the Department of Medicine, State University of New York at Buffalo. She has expertise in drug delivery using exosomes and has encapsulated antiretroviral (ARV) drugs within exosomes, which are then targeted to HIV-1-infected, CNS macrophage/microglial cells. Exosome-mediated delivery of ARV across the BBB provides increased concentrations of ARV within the CNS and elimination of viral reservoirs.

Bindukumar B. Nair is a research assistant professor in the Department of Medicine, State University of New York at Buffalo. He has expertise in cell transfections using various nanomaterials.

Manoj J. Mammen is a clinical assistant professor in the Division of Pulmonology in the Department of Medicine, State University of New York at Buffalo. His research focus is nanotherapy in asthma and COPD, and he has experience with intranasal nanodrug delivery systems.

Tracey A. Ignatowski is a research associate professor in the Department of Pathology and Anatomical Sciences at the State University of New York at Buffalo and is actively engaged in research investigating mechanisms involved in cytokine (TNF, IL-1β) regulation of neurotransmitter release in the brain, determining cytokine localization in the brain, and demonstrating brain-associated TNF regulation of peripheral macrophage function. She is involved in investigating biomedical application of nanoparticle formulations, specifically in the field of targeted RNA/DNA/therapeutic agent delivery.

Chong Cheng is a associate professor in the Department of Chemical and Biological Engineering, State University of New York at Buffalo. His research work focuses on the development of general methodologies for the preparation of well-defined biodegradable functional polymers and nanostructures, which can further serve as scaffolds for biomedical and bioengineering applications, especially drug and gene delivery.

Stanley A. Schwartz is a distinguished professor of medicine, pediatrics, and microbiology and Chief of the Division of Allergy, Immunology, and Rheumatology in the Department of Medicine at the State University of New York at Buffalo. He is director of the Nanomedicine center at UB's Clinical and Translational Research Center.

References

1. Rao, K. S., Ghorpade, A., Labhasetwar, V. (2009). Targeting anti-HIV drugs to the CNS. *Expert Opin. Drug Deliv.,* **6**, 771–784.
2. Destache, C. J. (2009). Brain as an HIV sequestered site: Use of nanoparticles as a therapeutic option. *Prog. Brain Res.,* **180**, 225–233.
3. Mahajan, S. D., Aalinkeel, R., Law, W. C., Reynolds, J. L., Nair, B. B., et al. (2012). Anti-HIV-1 nanotherapeutics: Promises and challenges for the future. *Int. J. Nanomed.,* **7**, 5301–5314.
4. Mahajan, S. D., Law, W. C., Aalinkeel, R., Reynolds, J. L., Nair, B. B., et al. (2012). Nanoparticle-mediated targeted delivery of antiretrovirals to the brain. *Methods Enzymol.,* **509**, 41–60.
5. Wong, H. L., Wu, X. Y., Bendayan, R. (2012). Nanotechnological advances for the delivery of CNS therapeutics. *Adv. Drug Deliv. Rev.,* **64**, 686–700.
6. Mahajan, S. D., Roy, I., Xu, G., Yong, K. T., Ding, H., et al. (2010). Enhancing the delivery of anti-retroviral drug "Saquinavir" across the blood brain barrier using nanoparticles. *Curr. HIV Res.,* **8**, 396–404.
6. Rao, K. S., Reddy, M. K., Horning, J. L., Labhasetwar, V. (2008). TAT-conjugated nanoparticles for the CNS delivery of anti-HIV drugs. *Biomaterials,* **29**, 4429–4438.

7. Wong, H. L., Chattopadhyay, N., Wu, X. Y., Bendayan, R. (2010). Nanotechnology applications for improved delivery of antiretroviral drugs to the brain. *Adv. Drug Deliv. Rev.,* **62**, 503–517.
8. Hwang, S. R., Kim, K. (2014). Nano-enabled delivery systems across the blood–brain barrier. *Arch. Pharm. Res.,* **37**, 24–30.
9. Wohlfart, S., Gelperina, S., Kreuter, J. (2012). Transport of drugs across the blood–brain barrier by nanoparticles. *J. Control. Release,* **161**, 264–273.
10. Olivier, J. C. (2005). Drug transport to brain with targeted nanoparticles. *NeuroRx.*, **2**, 108–119.
11. Armstead, A. L., Li, B. (2011). Nanomedicine as an emerging approach against intracellular pathogens. *Int. J. Nanomed.,* **6**, 3281–3293.
12. Biddlestone-Thorpe, L., Marchi, N., Guo, K., Ghosh, C., Janigro, D., et al. (2012). Nanomaterial-mediated CNS delivery of diagnostic and therapeutic agents. *Adv. Drug Deliv. Rev.,* **64**, 605–613.
13. Kim, P. S., Read, S. W. (2010). Nanotechnology and HIV: Potential applications for treatment and prevention. *Wiley Interdisciplinary Rev. Nanomed. Nanobiotechnol.,* **2**, 693–702.
14. Mamo, T., Moseman, E. A., Kolishetti, N., Salvador-Morales, C., Shi, J., et al. (2010). Emerging nanotechnology approaches for HIV/AIDS treatment and prevention. *Nanomedicine* (*London, England*), **5**, 269–285.
15. Nowacek, A., Gendelman, H. E. (2009). NanoART, NeuroAIDS and CNS drug delivery. *Nanomedicine (London, England),* **4**, 557–574.
16. Parboosing, R., Maguire, G. E., Govender, P., Kruger,H. G. (2012). Nanotechnology and the treatment of HIV infection. *Viruses,* **4**, 488–520.
17. Mallipeddi, R., Rohan, L. C. (2010). Progress in antiretroviral drug delivery using nanotechnology. *Int. J. Nanomed.,* **5**, 533–547.
18. Sharma, P., Garg, S. (2010). Pure drug and polymer based nanotechnologies for the improved solubility, stability, bioavailability and targeting of anti-HIV drugs. *Adv. Drug Deliv. Rev.,* **62**, 491–502.
19. Lee, D. E., Koo, H., Sun, I. C., Ryu, J. H., Kim, K., et al. (2012). Multifunctional nanoparticles for multimodal imaging and theranostics. *Chem. Soc. Rev.,* **41**, 2656–2672.
20. Lammers, T., Aime, S., Hennink, W. E., Storm, G., Kiessling, F. (2011). Theranostic nanomedicine. *Acc. Chem. Res.,* **44**, 1029–1038.
21. Patel, M. M., Goyal, B. R., Bhadada, S. V., Bhatt, J. S., Amin, A. F. (2009). Getting into the brain: Approaches to enhance brain drug delivery. *CNS Drugs,* **23**, 35–58.

22. Löscher, W., Potschka, H. (2005). Role of drug efflux transporters in the brain for drug disposition and treatment of brain diseases. *NeuroRX*, **76,** 22–76.

23. Kreuter, J. (2013). Drug delivery to the central nervous system by polymeric nanoparticles: What do we know? *Adv. Drug Deliv. Rev.,* pii: **S0169-409X**, 00191–9.

24. Tosi, G., Bortot, B., Ruozi, B., Dolcetta, D., Vandelli, M. A., et al. (2013). Potential use of polymeric nanoparticles for drug delivery across the blood–brain barrier. *Curr. Med. Chem.,* **20**, 2212–2225.

25. Costantino, L., Gandolfi, F., Tosi, G., Rivasi, F., Vandelli, M. A., et al. (2005). Peptide-derivatized biodegradable nanoparticles able to cross the blood–brain barrier. *J. Control. Release,* **108**, 84–96.

26. Destache, C. J., Belgum, T., Christensen, K., Shibata, A., Sharma, A., et al. (2009). Combination antiretroviral drugs in PLGA nanoparticle for HIV-1. *BMC Infect. Dis.,* **9**, 198.

27. Shibata, A., McMullen, E., Pham, A., Belshan, M., Sanford, B., et al. (2013). Polymeric nanoparticles containing combination antiretroviral drugs for HIV type 1 treatment. *AIDS Res. Hum. Retroviruses,* **29**, 746–754.

28. Kanmogne, G. D., Singh, S., Roy, U., Liu, X., McMillan, J., et al. (2012). Mononuclear phagocyte intercellular crosstalk facilitates transmission of cell-targeted nanoformulated antiretroviral drugs to human brain endothelial cells. *Int. J. Nanomed.,* **7**, 2373–2388.

29. Kuo, Y. C., Lee, C. L. (2012). Methylmethacrylate-sulfopropylmeth-acrylate nanoparticles with surface RMP-7 for targeting delivery of antiretroviral drugs across the blood–brain barrier. *Colloids Surf. B Biointerfaces,* **90**, 75–82.

30. Kuo, Y. C., Chung, C. Y. (2012). Transcytosis of CRM197-grafted polybutylcyanoacrylate nanoparticles for delivering zidovudine across human brain-microvascular endothelial cells. *Colloids Surf. B Biointerfaces,* **91**, 242–249.

31. Bousquet, L., Roucairol, C., Hembury, A., Nevers, M. C., Creminon, C., et al. (2008). Comparison of ABC transporter modulation by atazanavir in lymphocytes and human brain endothelial cells: ABC transporters are involved in the atazsanavir-limited passage across an *in vitro* human model of the blood–brain barrier. *AIDS Res. Hum. Retroviruses,* **24**, 1147–1154.

32. Bu, G., Maksymovitch, E. A., Nerbonne, J. M., Schwartz, A. L. (1994). Expression and function of the low density lipoprotein receptor-related protein (LRP) in mammalian central neurons. *J. Biol. Chem.,* **269**, 18521–18528.

33. Cucullo, L., Aumayr, B., Rapp, E., Janigro, D. (2005). Drug delivery and *in-vitro* models of the blood–brain barrier. *Curr. Opin. Drug Discov. Dev.,* **8**, 89–99.

34. Mahajan, S. D., Aalinkeel, R., Sykes, D. E., Reynolds, J. L., Nair, B. B., et al. (2008) Methamphetamine alters Blood brain barrier permeability via the modulation of tight junction expression: Implication for HIV-1 Neuropathogenesis in the context of drug abuse. *Brain Res.,* **1203**, 133–148.

35. Mahajan, S. D., Aalinkeel, R., Sykes, D. E., Reynolds, J. L., Nair, B. B., et al. (2008)**.** Tight junction regulation by Morphine and HIV-1 tat modulates blood brain barrier permeability. *J. Clin. Immunol.,* **28**, 528–5541.

36. Persidsky, Y., Ramirez, S. H., Haorah, J., Kanmogne, G. D. (2006). Blood–brain barrier: Structural components and function under physiologic and pathologic conditions. *J. Neuroimmune Pharmacol.,* **1**, 223–236.

37. Yun, Y., Chen, C. K., Law, W. C., Weinheimer, E., Sengupta, S., et al. (2014). Polylactide-graft-doxorubicin nanoparticles with precisely controlled drug loading for pH-triggered drug delivery. *Biomacromolecule*s, **15**, 524–532.

38. Onoue, S., Matsui, T., Kuriyama, K., Ogawa, K., Kojo, Y., et al. (2012). Inhalable sustained-release formulation of long-acting vasoactive intestinal peptide derivative alleviates acute airway inflammation. *Peptides*, **35**, 182–189.

39. Kim, D. H., Martin, D. C. (2006). Sustained release of dexamethasone from hydrophilic matrices using PLGA nanoparticles for neural drug delivery. *Biomaterials,* **27**, 3031–3037.

40. Reddy, M. K., Labhasetwar, V. (2009). Nanoparticle-mediated delivery of superoxide dismutase to the brain: An effective strategy to reduce ischemia-reperfusion injury. *FASEB J.,* **23**, 1384–1395.

41. Destache, C. J., Belgum, T., Christensen, K., Shibata, A., Sharma, A., et al. (2009). Combination antiretroviral drugs in PLGA nanoparticle for HIV-1. *BMC Infect. Dis.,* **9**, 198.

42. Shibata, A., McMullen, E., Pham, A., Belshan, M., Sanford, B., et al. (2013). Polymeric nanoparticles containing combination antiretroviral drugs for HIV type 1 treatment. *AIDS Res. Hum. Retroviruses,* **29**, 746–754.

43. Chaowanachan, T., Krogstad, E., Ball, C., Woodrow, K. A. (2013). Drug synergy of tenofovir and nanoparticle-based antiretrovirals for HIV prophylaxis. *PLOS ONE,* **8**, e61416.

44. Kuo, Y. C., Yu, H. W. (2011). Transport of saquinavir across human brain-microvascular endothelial cells by poly(lactide-co-glycolide) nanoparticles with surface poly-(γ-glutamic acid). *Int. J. Pharm.,* **416**, 365–375.

Chapter 48

HIV-Specific Immunotherapy with Synthetic Pathogen-Like Nanoparticles

Orsolya Lorincz, PhD, and Julianna Lisziewicz, PhD
eMMUNITY Inc., Bethesda, Maryland, USA

Keywords: DNA-nanomedicine vaccine, immunotherapy, Langerhans cell-targeted DNA delivery, HIV eradication, polyethylenimine (PEI), DermaVir, therapeutic vaccine, plasmid DNA, intracellular trafficking, gene delivery, polyplex

48.1 Introduction

HIV/AIDS is the leading infectious killer that affects more than 33 million people worldwide [1]. HIV/AIDS is treated with the combination of three or more antiretroviral drugs (ARVs) (highly active antiretroviral therapy, HAART), because using any single drug has not been efficient in controlling infection due to the development of resistant strains of the virus. Currently available HAART is potent in suppressing HIV replication and effective in decreasing HIV RNA levels below the limit of detection (50 copies/mL) with only minimum side effects. Long-term HAART decreased morbidity and mortality associated with HIV infection [2]. However, even optimal HAART, characterized by suppression of viral

Handbook of Clinical Nanomedicine: Nanoparticles, Imaging, Therapy, and Clinical Applications
Edited by Raj Bawa, Gerald F. Audette, and Israel Rubinstein

ISBN 978-981-4669-20-7 (Hardcover), 978-981-4669-21-4 (eBook)
www.panstanford.com

load to undetectable levels for years, has not provided a cure to the disease. Patients on optimal HAART have 12 years shorter life expectancy than HIV-negative people [3–4]. In addition, increased AIDS-related and non-AIDS-related morbidity and mortality has been described in a significant proportion of individuals on optimal HAART due to the lack of normalization of their $CD4^+$ T cell counts [5]. Optimal HAART also failed to decrease the viral reservoirs, especially in the gut mucosa, where the residual low-level viral replication may be the cause of persistent immune activation that facilitates the progression to AIDS and death [6]. One barrier of cure is the stable latent reservoirs of HIV-infected resting memory T cells that are able to produce HIV after cellular activation. HIV producing cells in the reservoirs that are not eliminated by ARVs would be susceptible to immune clearance, but long-term optimal HAART diminishes HIV-specific T cell responses [7]. Therefore, the immune system of successfully treated HIV-infected people is unprepared to kill infected cells, decrease viral reservoirs, and control the virus replication.

Immunotherapy improves the reactivity of the immune system to guard the body from internal and external intruders as infections (e.g., HIV), allergens, and malignancies. The innate arm, composed of the phagocytic cells, circulating macrophages and the complement system, is responsible for the immediate defense. Later, the adaptive arm responds in a highly specific manner against molecular determinants of the intruders. Nanoparticles (NPs) made from different types of materials, having various sizes, shapes and surface charges activate the innate and adaptive immune system [8–10]. Therefore, nanotechnology is suitable for improving efficacy and increasing specificity of products indicated as vaccine and immunotherapy. The immunotherapeutic efficacy of NPs is achieved by specific activation (e.g., cancer, infectious diseases) or suppression (e.g., allergy, autoimmune diseases) of the immune system. Efficacy of immune responses is improved by targeted delivery of antigens to professional immune cells specialized for either stimulation or suppression of immune reactivity. This is achieved by using NPs as antigen (virus-like particles; VLPs), NP formulation of soluble antigens (DNA, peptides, proteins) and new administration routes (transdermal, nasal, intratracheal). Increasing the specificity of immunotherapy is achieved by personalization of the antigens in the NP taking into account the

diversity of the disease (e.g., tumor cells) and genomic background of the individual (e.g., HLA type).

More than 30 ARVs and drug combinations are currently available to achieve long-term suppression of HIV RNA to <50 copies/mL and control HIV disease. The failure to develop a vaccine for HIV has recently changed the treatment strategy from the long-term suppression of viral load to the cure of the disease. Approaches for HAART intensification with additional potent drugs also failed to provide a cure or any additional treatment benefits [4, 11–15]. Consequently, it became evident that alternatives to vaccines and to ARVs are required to eradicate HIV disease. The first HIV cure approach is eradication of the virus. Eradication was demonstrated in one HIV^+ patient after bone marrow transplantation with donor cells resistant to HIV infection [16]. Alternative approach for HIV cure is the induction of a long-term remission, similarly to the cure of Hepatitis C infection. We have previously described the remission of an HIV^+ patient (Berlin patient, 1999) whose immune system was activated to kill infected cells by short interruptions of HAART [17]. This work has led to the identification of "elite controllers" representing a model for remission. Elite controllers have large numbers of cells containing replication competent HIV and their viral load is suppressed by the cellular arm of the immune system [18–19]. Recently, Siliciano and his team have demonstrated that boosting of HIV-specific T cell responses (CTL) prior to reactivating latent HIV will be essential for eradication of the virus [20]. These results suggest that HIV-specific immunotherapy is essential for both remission and eradication of HIV, consequently for the cure of HIV.

Here we review the molecular characteristics of the first pathogen-like nanomedicine, DermaVir, and its targeted delivery to Langerhans cells. We provide detailed description of the novel mechanism of action; discuss the available clinical results, and the potential contributions of DermaVir to the cure of HIV/AIDS.

48.2 Nanomedicines for Immunotherapy

Immunotherapeutic nanomedicines are new, complex, multi-modular, targeted products that provide superior therapeutic effects compared to all previous vaccine approaches. Their physical

size is usually over 50 nm, which is the approximate threshold of immune recognition [21]. Soluble antigens that are less than 50 nm in size are generally not recognized by the immune system and are consequently poorly immunogenic. In fact, the size range of immunotherapeutic nanomedicines corresponds to the size range of viruses. Nature developed an effective and specific immune surveillance against viruses. Accordingly, triggering the immune system with nanomedicines provides exceptional immunogenicity since our body considers NPs as harmful viruses that need to be eliminated [22]. The best examples for the superior immune recognition of nanomedicines are the human papilloma virus (HPV) vaccines, Gardasil and Cervarix. These vaccines are composed from one surface protein (L1) of the HPV that self-assemble to VLPs. These VLPs, morphologically similar to the wild-type HPV, induce potent immune responses in the absence of adjuvants. In contrast, the L1 protein purified from bacteria remains a soluble protein, does not assemble to VLPs, and does not induce immune responses [23]. These VLP vaccines are safe and protect young uninfected people from cancer. However, none of these vaccines prevents the development of cancer in HPV-infected people, since they are not able to induce therapeutically beneficial T cell responses [24].

Creating "particulate vaccines" has recently been recognized in the HIV field to improve the immunogenicity of small soluble antigens. This approach involves an increase in the physical size of the antigen to the size of pathogens. There are so-called "natural" particulate vaccines, based on VLPs that induce both humoral and cellular immune responses against HIV [25, 26]. HIV VLPs are essentially non-infective viruses consisting of self-assembled viral envelope proteins without the accompanying genetic material. A different approach is to use an adjuvant that increases the size of the antigen. One of the several proposed mechanisms of aluminum salts, the adjuvant approved in the US and EU, is attributed to their particulate nature; however, recently concerns are raised regarding their safety [26].

A new approach in vaccine development is the use of a plasmid DNA (pDNA) that can express one or more protein antigens in the body. pDNA is attractive for immunotherapeutic nanomedicine development because (i) it has excellent safety profile, (ii) intracellularly expressed antigens are processed and presented

on the host MHC molecules, and (iii) recently improved large-scale manufacturing capabilities provide cost effective production. Unfortunately, promising animal studies demonstrating the induction of immune responses with naked DNA-injected intramuscularly or intradermally could not be reproduced in human subjects. The possible reasons for the weak immunogenicity are that the naked DNA poorly enters into the cells and does not reach the nucleus, and the expressed soluble protein antigens are not recognized by the immune system, similarly to the previously described soluble L1 protein of the HPV.

Various biodegradable and non-biodegradable polymeric and liposomal delivery systems have been explored for transforming HIV-antigens to synthetic NPs in order to increase their immunogenicity and to protect them against extra- and intracellular degradation [27, 28]. Targeting dendritic cells (DCs) that are essential for initiating immune responses can be achieved by different nanomedicine size; > 100 nm nanomedicines target the peripheral immature DCs, and the smaller size ~50 nm nanomedicines drain to the lymph node resident DCs [29]. Modification of the surface of the nanomedicine with DC-specific receptor ligands has been shown to increase the targeting specificity [30]. However, several challenges including crossing physical barriers like the cell and nuclear membranes or adhesion to non-target tissues still need to be overcome during the development of a synthetic delivery system.

48.3 Pathogen-Like DNA-Nanomedicines for Immunotherapy

DermaVir is the first synthetic pathogen-like nanomedicine that has been developed for HIV-specific immunotherapy. A condensed pDNA constitutes the core and a mannobiosylated polymer, polyethylenimine-mannose (PEIm) represents the envelop of this synthetic virus [31, 32]. We have shown that nanomedicine not only looks like a virus but also functions as a replication defective virus: enters cells via receptor-mediated endocytosis, escapes from endosome, and delivers the pDNA to the nucleus. The pDNA expresses proteins that self-assemble to “complex virus-like particles” (VLP^+). The huge advantage of this synthetic pathogen-

like nanomedicine compared to biologic nanomedicines (VLPs, virus vectors, exosomes) is the reproducible and scalable manufacturing method that is independent of the antigens since these are encoded in the pDNA. Therefore, such pDNA-based pathogen-like nanomedicines are not only highly immunogenic but also cost effective to make and therefore suitable for the development of personalized HIV-specific immunotherapy.

48.3.1 Nanomedicine Formulation of Plasmid DNA for Vaccine Delivery

The immunologic objective of a pathogen-like pDNA/PEIm nanomedicine formulation is to target antigen-presenting cells (APCs) and efficiently express the antigens encoded in the pDNA. Targeted delivery is a complex challenge involving binding, nanomedicine uptake, pDNA expression, processing and antigen presentation to naïve T cells [33, 34].

The objectives of the pDNA-based antigen design are efficacy and safety. pDNA does not duplicate in human cells, it expresses protein antigens to induce specific immune responses. Efficacy is achieved by preserving the structure and the epitope content of the disease-causing virus, and safety is achieved by molecular modifications. The first pathogen-like NP, DermaVir, contains a single pDNA (Fig. 48.1a) driving the expression of fifteen HIV proteins. These proteins self-assemble to replication-, reverse transcription–, and integration-defective VLP^+. The pDNA is inherently safe because irreversible molecular modifications were introduced into essential viral proteins to prevent the replication and integration of the VLP^+. The expressed VLP^+ is structurally authentic to the wild-type HIV (Fig. 48.1b). The expression of fifteen HIV proteins from the single pDNA supports the presentation of the highest number of HLA-restricted HIV epitopes and the induction of HIV-specific T cell responses with the broadest specificity. DermaVir-induced T cell responses can kill HIV-infected cells.

Beyond inducing T cell responses, this antigen might be suitable for inducing neutralizing antibodies against viral and cellular antigens naturally occurring on the surface of HIV or structures present only during budding or entry [36]. Such a multi-faceted immune response is a unique feature of pDNA vaccines expressing an authentic-looking HIV [35].

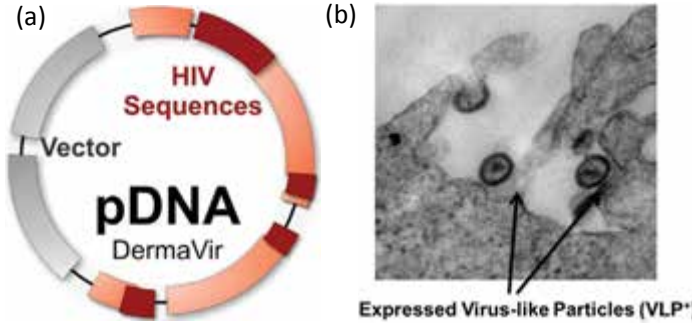

Figure 48.1 Key features of DermaVir nanomedicine developed for HIV-specific immunotherapy. (a) One single pDNA encoding 15 HIV antigens serves as the active pharmaceutical ingredient (API) [35]. Red: HIV sequences expressing the antigens in human cells. Gray: Bacterial sequences required for plasmid manufacturing in *E. coli*. (b) Expression of complex virus-like particles (VLP^+) visualized by transmission electron microscopy.

Table 48.1 Pathogen-like features of DermaVir nanomedicine compared to a DNA virus

DermaVir	Features	pDNA/PEIm nanomedicine	DNA virus
Pathogen look	Surface	Sugar residues	Glycoproteins
	Size, shape	70–300 nm, spherical NPs	50–500 nm, mostly spherical NPs
Pathogen features	Structure	PEIm envelop, condensed pDNA core	Glycoprotein envelop, condensed DNA core
	Delivery of DNA	PEIm-mediated endosomal escape and cytoplasmic trafficking	Viral protein-mediated endosomal escape and cytoplasmic trafficking
	Antigen expression	HIV VLP^+	HIV

PEIm component of DermaVir is responsible to form a athogen-like nanomedicine with the pDNA (Fig. 48.2a). The pathogen-like features are essential for binding and cellular uptake, and later for the pDNA processing and antigen expression (Table 48.1) [32]. Targeting of the APC population is ensured by the mannobiosylation of the polymer. We modified a transfection agent, the linear polyethylenimine, with mannobiose residues resulting in a mannobiosylated polyethylenimine (PEIm) having grafted sugar

molecules to resemble pathogens that usually bear similar residues (glycoproteins) on their surface [37–40]. This modified polymer spontaneously forms 70–300 nm NPs with pDNA, the optimal size range for receptor-mediated entry, as this is the size range of viruses [41, 42]. The formed NPs have positive surface charge, indicating that the polymer is on the outside covering the condensed pDNA in the core.

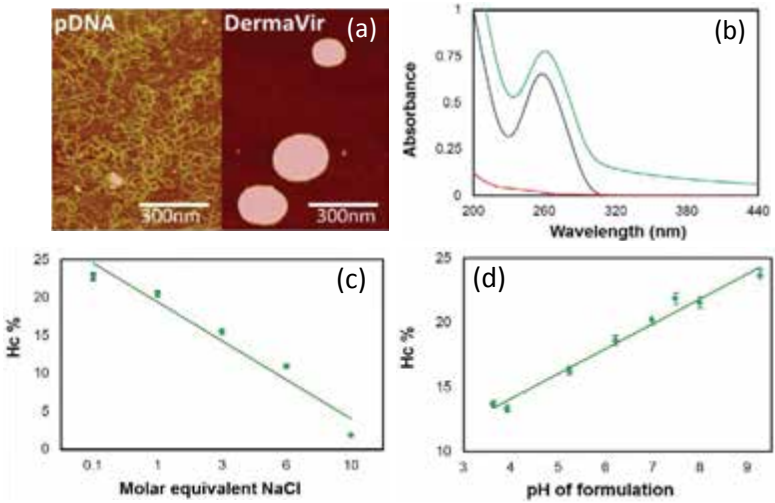

Figure 48.2 Biophysical characterization of DermaVir nanomedicine. (a) Atomic force microscopic image of naked pDNA and DermaVir pDNA/PEIm NPs. (b) Absorbance spectra of DermaVir nanomedicine (green) and its components; pDNA (blue) and PEIm (red). The shift of the nanomedicine is called hyperchromicity and is attributed to the forming interactions between the pDNA and the PEIm. (c) Inverse correlation between the NaCl concentration of the pDNA solution and the measured Hc%. Hc% is the increase of absorbance measured at 260 nm for DermaVir compared to the sum absorbance at 260 nm of its components expressed in percentage. Molar equivalent on the *x*-axis stands for molar equivalents calculated on the phosphate concentration of the pDNA ($y = -5.14x + 29.8$; $r^2 = .95$) (d) Linear correlation between the pH of the formulation and the Hc% ($y = 1.94x + 6.3$; $r^2 = .98$). Adapted from *Nanomed. Nanotechnol. Biol. Med.*, **8**, Lorincz, O., Toke, E. R., Somogyi, E., Horkay, F., Chandran, P. L., et al., Structure and biological activity of pathogen-like synthetic nanomedicines, 497–506, Copyright (2012), with permission from Elsevier.

Once the pathogen-like nanoparticles are taken up by endocytosis the nanomedicine continues its role and function as a pathogen through the intracellular processing. The NPs translocate to a cellular compartment, called endosomes. The polymer envelop buffers the low pH of the endosome that would otherwise degrade the pDNA [43]. The proton-sponge effect of the PEIm supports the buffering of the endosome mimicking the features of viruses that evolved to survive this environment and deliver their genetic material to the host cell's nucleus. When the NPs reach the cytosol the polymer envelop is loosened enough to release the pDNA at the nucleus. This way the pDNA can translocate to the nucleus where the pDNA-encoded antigens are transcribed. DermaVir's pDNA expresses a VLP^+, and these antigens stimulate the naïve T cells to become HIV-specific memory and effector T cells capable to kill infected cells.

The unique pathogen-like feature of the pDNA/PEIm DermaVir nanomedicine is its DNA delivery attributes. As the targeting and cellular uptake of the NPs are controlled by the surface and the size of the NPs, the NPs processing inside the cell is controlled by the PEIm that ensures that the pDNA reaches the nucleus [32, 44]. No other synthetic DNA delivery agents have similar properties, because the DNA either remains in the endosome and is degraded or cannot reach the nucleus where gene expression occurs [38]. The release dynamics of a pDNA-NP inside the cell is a process characterized with a very sensitive equilibrium. This balance is determined by the ionic properties and environment of the components. Since both pDNA and PEIm are polyionic macromolecules and their interaction is driven by electrostatic forces we explored the effect of ionic strength and pH on their biological activity and also on their fine structure. We found that the condensation of the pDNA by PEIm could be followed by UV spectrophotometry, because the structural changes occurring during complexation cause a shift in the UV-spectrum of DermaVir compared to its components (Figs. 48.2a,b). We called this shift hyperchromicity (Hc) and connected it to the forming interactions of the components during NP formation [32]. Our results showed that this phenomenon can be influenced by changing the ionic properties of the components; both ionic strength and pH of the nanomedicine formulation have high impact on Hc. By increasing the ionic strength of the pDNA solution, Hc decreases, and by increasing the pH of the formulation, Hc increases (Figs. 48.2c,d).

We also found that Hc was associated with the biological activity (Fig. 48.3). The differences in Hc and in biological activity are explained with the fine structure of the NPs. A DermaVir formulation with low Hc and low biological activity shows a loose NP structure where the pDNA protrudes from the polymer envelop [32]. The DermaVir formulation with optimal Hc and high biological activity has a smooth NP surface, where the pDNA is fully protected by a coherent polymer envelop (Fig. 48.2a).

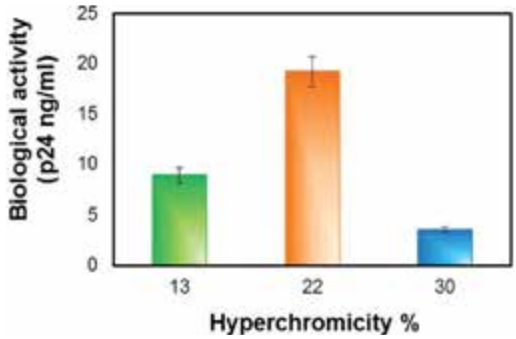

Figure 48.3 Structure and activity relationship of DermaVir nanomedicine. Biological activity of low, optimal, and high hyperchromicity (Hc%) DermaVir formulations.

The equilibrium of pDNA release dynamics inside the cells is controlled by the "compactness." Compactness is the degree of association between the components of the synthetic NPs that can be controlled by changing the ionic properties of the components. Very high ionic strength causes aggregation of the NPs [45]. When the ionic strength is slightly high or the pH is low, the pDNA and the PEIm will form fewer bonds because the pDNA will have less unprotonated phosphate groups. Low biophysical compactness represents a loose structure. The biological consequence of a loose structure is that the NPs do not survive the endosome and the pDNA is degraded (Fig. 48.4a). When the ionic strength of the pDNA solution is low or the pH is high, more bonds will be formed between the pDNA and the PEIm because the DNA will have many anionic phosphate groups. High compactness represents a tight structure; consequently the NPs reach the proximity of the nucleus but do not release the pDNA (Fig. 48.4b). Optimal NP that survives the endosome and releases the pDNA at the nucleus can be characterized by optimal compactness representing optimal ionic

strength of the pDNA solution and the optimal pH (6–7.5) of the formulation (Fig. 48.4c). DermaVir is one of the first clinically used nanomedicines in which the structure and biophysical activity have correlated to its biological activity.

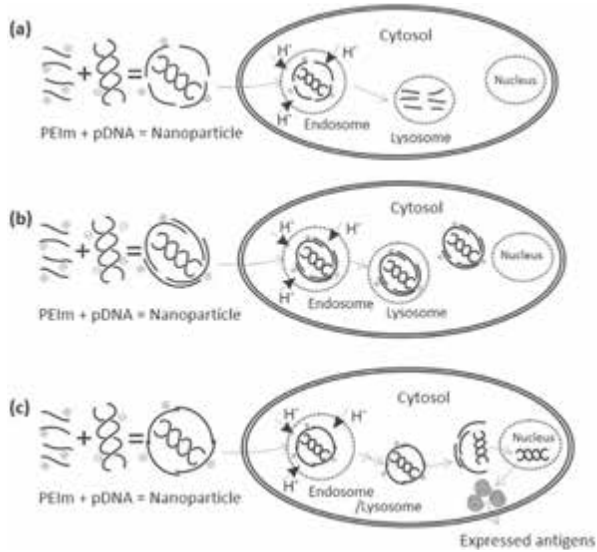

Figure 48.4 Compactness is a biophysical property of the pDNA/PEIm NP that determines the release dynamics of the pDNA inside the cell. (a) At low compactness, the NP disintegrates in the endosome. (b) At high compactness, the NP survives the endosome but cannot release the DNA in the cytosol. (c) At optimal compactness, the NP escapes from endosomal degradation, the pDNA is released in the cytosol and reaches the nucleus, where the DNA-encoded antigens are expressed.

48.3.2 Topical Administration of the Langerhans Cell–Targeted Nanomedicine Vaccines

Since Pasteur, the needle injection is the state of art for the administration of antigens. However, injection of soluble antigens (peptides, proteins) does not mimic the natural entry of pathogens in the body creating a challenge to induce potent immune responses. To improve potency, antigens are formulated with different adjuvants, and alternative needle injection techniques are introduced in the form of microneedles and electroporation. Virus vectors and pathogen-like NPs are very potent to deliver the

DNA into DCs if they are placed in an environment of activated DCs ready to pick up pathogens. Such environment is not created after needle injection for at least two reasons: (i) Injection is not activating DCs to pick up antigens and migrate to lymph nodes and (ii) injection is targeting dermis or muscle, organs that are not prepared for pathogen entry and therefore do not contain many DCs. We developed DermaPrep, the first Langerhans-cell (LC)-targeting administration device for pathogen-like nanomedicines. DermaPrep employs a skin preparation method that interrupts the stratum corneum facilitating nanomedicine penetration and providing the essential "danger" signal to the LCs residing just below this protective layer [46, 47]. Once activated, LCs are naturally looking for pathogens and capturing the pathogen-like DermaVir nanomedicine applied to the prepared skin surface under a semi-occlusive patch. The main advantage of DermaPrep is the natural targeting of a large number of LCs (8 million) that form a horizontal 900 to 1800 cells/mm^2 network under the skin surface [48].

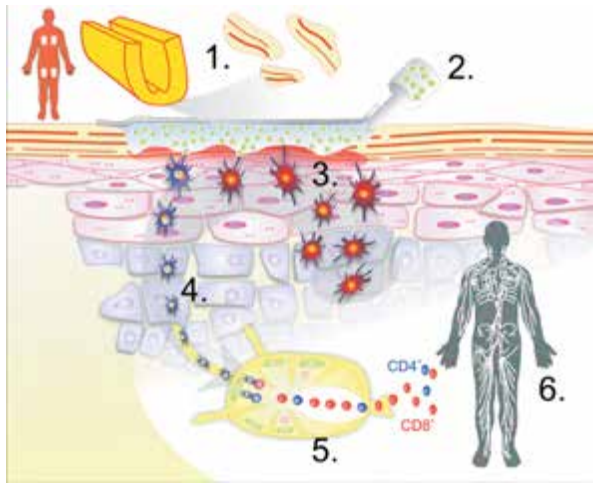

Figure 48.5 Langerhans cell-targeted delivery of DermaVir NPs after administration with DermaPrep. (1) Skin preparation using body sponge to generate "danger signal." (2) Nanomedicine application under the patch. (3) Uptake of the NPs by LCs. (4) Migration of LCs to the draining lymph nodes. (5) Antigen presentation in the lymph nodes and priming of naïve CD4$^+$ and CD8$^+$ T cells. (6) HIV-specific central memory T cells with high proliferative capacity circulating in the body [50, 51].

After DermaVir has been captured, activated LCs migrate to the local lymph nodes [49]. Here DCs express pDNA-encoded antigens and present most HIV epitopes to the passing naïve T cells. HIV-specific precursor/memory T cells primed by DCs further differentiate into HIV-specific effector T cells circulating out of the lymph node to seek virus-infected targets. Each killer effector cell can destroy several HIV-infected cells (Fig. 48.5).

During DermaPrep administration one million NPs could be picked up by each LC, because there are 8×10^{12} DermaVir NPs in 0.8 mL solution that is applied under each patch. In contrast, other popular vaccine administration systems such as electroporation and microneedles are needle in a haystack by means of targeting compared to DermaPrep; electroporation delivers naked pDNA usually to muscle and can potentially target APCs only at the site of injection, which usually does not reach the 1 mm^3 (which is only 900–1,800 LCs in the epidermal layer) [50–52]. In addition, the intra- and extracellular degradation of the pDNA after electroporation further decreases the success of antigen uptake and expression in the APC.

Table 48.2 Comparison of different vaccine delivery devices

	DermaPrep	**Electroporation**	**Microneedles**
Mechanism of action	Th1 memory T cells	Mainly antibodies	Antibodies and T cells
Targeting	Epidermal Langerhans cells	No	No
Number of targeted LCs	~8 million	1–2 thousand	A few thousand
DNA expression	Lymph node DCs	Skin or muscle cells	Skin
Potential indications	Therapeutic vaccines	Prophylactic & therapeutic vaccines	Prophylactic and therapeutic vaccines
Formulation	NPs	Naked DNA	Several formulations are being tested
Developmental status	CE marked	Safety testing in human ongoing	Testing in human ongoing

Microneedles that deliver the vaccines into the epidermis are more promising than electroporation, but their small size (few mm^2) allows the antigens to target only a few thousand DCs [53]. Regarding the immune responses electroporation is mainly capable

of inducing Th2-type while DermaPrep elicits Th1-type T cell-mediated immunity, microneedles are described to do everything [54, 55]. NP formulations can be administered to specifically target APCs using DermaPrep, electroporation uses naked pDNA with or without adjuvants. All formulations are applicable with microneedles; naked antigens or formulated molecules, coated devices and separate products [56–58]. Table 48.2 summarizes the main features of the pDNA delivery devices compared to DermaPrep.

48.4 DermaVir Immunotherapy for the Cure of HIV/AIDS

DermaVir is the most advanced nanomedicine developed for HIV-specific immunotherapy (therapeutic vaccine). It is the best-characterized nanomedicine and has successfully completed Phase II clinical development. Here we summarize the results of the main preclinical and clinical studies.

Preclinical studies in chronically infected macaques demonstrated that DermaVir immunotherapy improves the median survival time from 18 to 38 weeks compared to no treatment [50]. In other macaque trial, DermaVir in combination with HAART suppressed virus replication after HAART interruption. DermaVir treatment benefits were associated with the boosting of memory T cell responses. These primate experiments provided the rationale to investigate DermaVir immunotherapy in HIV-infected subjects both as monotherapy and in combination with HAART.

The Phase I dose escalation study conducted in Hungary was designed to evaluate the safety and immunogenicity of a single DermaVir immunization in HIV-infected subjects on fully suppressive HAART [51]. Increasing DermaVir doses up to 0.8 mg pDNA were administered by DermaPrep simultaneously on two, four and eight skin sites. DermaVir-associated side effects were limited to the skin, mild, transient and not dose-dependent. Boosting of HIV-specific effector $CD4^+$ and $CD8^+$ T cells expressing IFN-gamma and IL2 was detected against several HIV antigens in every subject of the medium dose cohort. The striking result was the dose-dependent expansion of HIV-specific central memory T cells with high proliferation capacity [59–60]. These findings demonstrated the first time that an immunotherapy (therapeutic

vaccine) is capable to induce potent antigen-specific memory T cell responses in infected subjects. We found that the frequency of DermaVir-boosted memory T cells decreases within a year suggesting that repeated DermaVir immunizations are required for durable high immune reactivity.

A Phase I/II clinical trial conducted in several USA clinical centers was designed to investigate repeated administrations of escalating DermaVir doses or placebo on HIV-infected adults receiving fully suppressive HAART. The incidence of adverse events was similar across groups suggesting that DermaVir was as safe as placebo [61, 62]. Immunogenicity data demonstrated the boosting of HIV-specific central memory T cells with high proliferative capacity. The highest frequency of HIV-specific memory T cells was induced in the 0.4 mg DNA dose group. The results of this trial were consistent with the macaque and Phase I studies and confirmed the excellent safety and immunogenicity features of DermaVir immunizations in patients on HAART [61].

The Phase II randomized, placebo controlled multicenter clinical trial conducted in Germany was designed to evaluate the safety and preliminary efficacy of repeated DermaVir immunizations in the absence of HAART. Thirty-six HIV-infected, treatment naïve adults were randomized to receive one of three different DermaVir doses or placebo at Study Weeks 0, 6, 12, and 18. The primary endpoint was safety at Week 24 and secondary endpoints were HIV RNA [63]. The Phase II trial confirmed the safety and the immunogenicity features of DermaVir. Consistently with previous trials, the 0.4 mg DermaVir dose was superior to the others. In this dose group the medium HIV RNA significantly decreased by 70% compared to placebo suggesting the killing of HIV infected cells. Viral load suppression occurred slowly, as predicted by DermaVir mechanism of action, similarly to cancer vaccines [64]. These results were consistent with the macaque and previous clinical studies and confirmed the safety and immunogenicity and antiviral activity of repeated DermaVir immunizations.

DermaVir immunotherapy might overcome the following limitations of present ARVs (Table 48.3): (i) reconstitution of HIV-specific immune responses that decreased during optimal HAART (ii) depletion of HIV-infected cells in contrast to current ARVs that inhibit only one step in HIV life cycle. Compared to HAART the antiviral activity of DermaVir is delayed, slow, and less potent,

because recognizing and killing of millions of infected cells with CTL in the presence of millions of new infections take more time to decrease viral load than blocking HIV replication with drugs. The effectiveness of killing infected cells is revealed by their capacity to manage the infection for ca. 15 years in the absence of any treatment. Therefore, 0.5 log reduction of HIV RNA in 24 weeks, demonstrated with DermaVir, should be sufficient to decrease the amount of HIV-infected cells that are not eliminated by HAART.

Table 48.3 Features of DermaVir nanomedicine developed toward the cure of HIV compared with the current state–of-the-art treatment of HIV/AIDS

Features/approach	DermaVir	HAART
Therapeutic target	HIV-expressing cells	HIV life cycle
Time needed for effectiveness	Slow and durable	Rapid and transient
Adverse events	Transient, skin	Cumulative, systemic
Administration schedule	Yearly	Daily
Viral load	Slow decrease	Rapid decrease
HIV immunity	Boosting	Decreasing
HIV-infected cells	Eliminated	No effect
Cure	Remission	No

48.5 Conclusions

HAART successfully suppresses HIV replication but cannot cure the disease because infected cells remain in the reservoirs. These resting latently infected cells will not be efficiently killed even after HIV reactivation; thus, boosting of T cell responses through HIV-specific immunotherapy will be essential for the cure of HIV [20]. DermaVir is the first synthetic pathogen-like nanomedicine developed to treat HIV. In the clinic, DermaVir is administered topically with DermaPrep targeting ~8 million LCs with ~10^{13} NPs containing 0.1 mg pDNA. One single dose and two repeated dose randomized, placebo controlled studies demonstrated that DermaVir induce potent and broadly directed HIV-specific central memory T cells in HIV-infected subjects. Such responses have been correlated with low viremia in untreated individuals, protection

in non-human primates and containment of viremia in elite controllers [19, 59, 65].

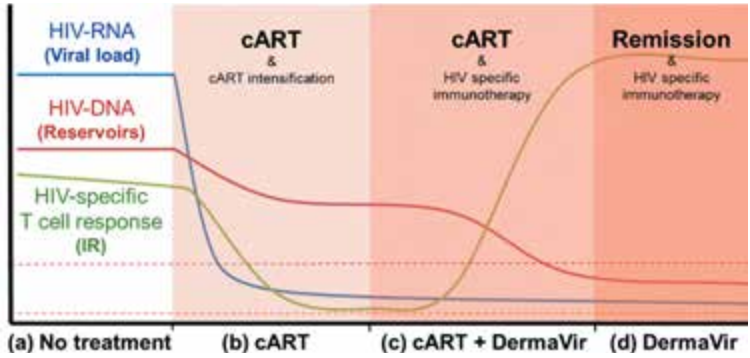

Figure 48.6 Nanomedicine applications toward the cure of HIV/AIDS: (a) untreated HIV infection: high viral load, high amount of HIV-infected cells in the reservoirs and the disease is partially controlled by the immune system alone for ca. 15 years. (b) HAART is effective in potent and durable suppression of HIV RNA to <50 copies/mL that is required to avoid the development of drug resistant mutants. However, HAART does not eliminate latently infected HIV-infected cells. In addition, HIV-specific T cell responses diminish in patients treated optimally with fully suppressive HAART. Consequently, HIV rebounds even after short interruption of therapy. (c) DermaVir HIV-specific immunotherapy in patients treated with optimal HAART demonstrated the maintenance of undetectable load and induction of long-lasting HIV-specific T cell responses [51]. These T cell responses, prior to reactivation of the latently infected cells, are essential for the clearance of latent HIV from the reservoirs and eradication of HIV [20]. (d) At one point, at least theoretically, HAART could be safely interrupted because the HIV-specific T cells are fully reconstituted. At this stage of the disease, the immune system alone will control the virus (remission) similarly to the Berlin patient and the elite controllers [17, 18]. Eradication of the virus cannot be achieved in the absence of reactivation of latent HIV, because the immune system cannot recognize the latently infected cells where the integrated provirus is transcriptionally silent.

Remission of HIV infected patient is characterized by the absence of HIV rebound after HAART interruption (Fig. 48.6). The different mechanism of action of HAART and DermaVir are complementary, suitable to achieve remission: the rapid and

potent viral load reduction with HAART is essential to block HIV replication and reach undetectable viral load. After that, DermaVir immunotherapy could address what drug intensification could not achieve: kill HIV-infected cells that remained in reservoirs and boost HIV-specific T cells to reconstitute immune responses. Since the immune system is slow to kill infected cells, it will take time to substantially decrease the infected cells from the reservoirs and fully reconstitute HIV-specific immune responses. We envision that repeated DermaVir immune intensification could eliminate significant amount of infected cells from the reservoirs. Consequently, patients could decrease drug exposure and their immune system could maintain a low or undetectable HIV RNA level. During remission, demonstrated by undetectable HIV RNA after interruption of HAART, maintenance of high-level T cell responses requires the repeated administration of DermaVir immunotherapy (e.g., four times yearly).

DermaVir in combination with HAART could kill infected cells in the reservoirs that might lead to cure of HIV (remission). Compared to competing products in development, the advantages of DermaVir nanomedicine include its excellent safety, repeated administration, high specificity and longevity of the immune responses, cost-effective scalable manufacturing methods. However, despite decades of research, no therapeutic HIV vaccine has reached the market. Challenges include (i) repeated failures of prophylactic vaccines, (ii) immune escape from T cell recognition based on the high genetic diversity of the virus and the HLA diversity of the host; (iii) the shortage of funding compared to vaccine and drug development. Any treatments that can eradicate HIV from infected patients or cure the disease have a huge commercial opportunity. Nanotechnology offers opportunities to develop new treatment approaches and to convert progressors to controllers. We envision that HIV-specific immunotherapy with synthetic pathogen-like nanomedicines might have the safety, efficacy, and cost features to contribute to the cure of HIV/AIDS and significantly improve public health.

Abbreviations

HIV: Human immunodeficiency virus
AIDS: Acquired immunodeficiency syndrome

HAART: Highly active antiretroviral therapy
ARV: Antiretroviral drug
NPs: Nanoparticles
VLP: Virus-like particle
HPV: Human papilloma virus
pDNA: Plasmid DNA
DC: Dendritic cell
PEIm: Polyethylenimine-mannose
VLP^+: Complex virus-like particle
API: Active pharmaceutical ingredient
APC: Antigen-presenting cell
LC: Langerhans cell

Disclosures and Conflict of Interest

Dr. Lisziewicz and Dr. Lorincz hold shares in Genetic Immunity (PWRV). This work was supported by grants HIKC05 and DVCLIN01 of the National Office for Research and Technology (NKTH) in Hungary.

No writing assistance was utilized in the production of this chapter and the authors have received no payment for its preparation. The findings and conclusions here reflect the current views of the authors.

Corresponding Author

Dr. Julianna Lisziewicz
eMMUNITY Inc.
4400 East West Hwy, Bethesda, MD 20814, USA
Email: julianna.lisziewicz@emmunityinc.com

About the Authors

Orsolya Lorincz is a co-founder of eMMUNITY, where she presently designs personalized cancer vaccines and heads the quality control team of the company. Between 2010 and 2013, she was the head of the Quality Control laboratory of Genetic Immunity. Dr. Lorincz has specialized in the development of nanomedicine formulation,

manufacturing technology, and analytical assays. She received her PhD in biotechnology from the University of Szeged, Hungary.

In 2013, **Julianna Lisziewicz** co-founded eMMUNITY, a biotech company focusing on the personalization of immunotherapy against cancer, where she is presently the president and chief scientific officer. From 1998 to 2013, Dr. Lisziewicz was the president and chief executive officer of Genetic Immunity, where she directed the translational research program on nanomedicine-based HIV-specific immunotherapy from discovery to successful phase II clinical trials. In 1994, she co-founded the non-profit Research Institute for Genetic and Human Therapy (RIGHT) and co-directed the research, clinical, and business affairs in the USA and Italy. RIGHT focused on the treatment of HIV/AIDS from multiple perspectives: virology, molecular biology, immunology, and medicine. From 1990 to 1995, she was head of the Antiviral Unit in the Laboratory of Tumor Cell Biology at the NCI, NIH in Bethesda, Maryland, USA. While at NIH, she discovered and developed antisense oligonucleotide therapy and gene therapy for HIV/AIDS. In 2005, she was awarded by the EU the Marie Curie Chair. She received her PhD in molecular biology from the Max-Planck Institute, Gottingen.

References

1. 2012 UNAIDS World AIDS Day Report, UNAIDS, Switzerland. Available at: http://www.unaids.org/en/media/unaids/contentassets/documents/epidemiology/2012/gr2012/JC2434_WorldAIDSday_results_en.pdf (accessed on December 3, 2014).
2. Palella, F. J., Delaney, K. M., Moorman, A. C., Loveless, M. O., Fuhrer, J., et al. (1998). Declining morbidity and mortality among patients with advanced Human Immunodeficiency Virus infection. *N. Engl. J. Med.*, **338**(13), 853–860.
3. Holtgrave, D. R. (2005). Causes of the decline in AIDS deaths, United States, 1995–2002: Prevention, treatment or both? *Int. J. STD AIDS*, **16**(12), 777–781.
4. Losina, E., Schackman, B. R., Sadownik, S. N., Gebo, K. A., Walensky, R. P., et al. (2009). Racial and sex disparities in life expectancy losses

among HIV-infected persons in the United States: Impact of risk behavior, late initiation, and early discontinuation of antiretroviral therapy. *Clin*. *Infect*. *Dis*., **49**, 1570–1578.

5. Baker, J. V., Peng, G., Rapkin, J., Abrams, D. I., Silverberg, M. J., et al. (2008). CD4+ count and risk of non-AIDS diseases following initial treatment for HIV infection. *AIDS*, **22**(7), 841–848.
6. Mavigner, M., Delobel, P., Cazabat, M., Dubois, M., L'faqihi-Olive, F. E., et al. (2009). HIV-1 residual viremia correlates with persisitent T-cell activation in poor immunological responders to combination antiretroviral therapy. *PLoS ONE*, **4**(10), e7658.
7. Casazza, J. P., Betts, M. R., Picker, L. J., Koup, R. A. (2001). Decay kinetics of human immunodeficiency virus-specific CD8+ T cells in peripheral blood after initiation of highly active antiretroviral therapy. *J*. *Virol*., **75**, 6508–6516.
8. Goldsmith, M., Mizrahy, S., Peer, D. (2011). Grand challenges in modulating the immune response with RNAi nanomedicines. *Nanomedicine*, **6** (10), 1771–1785.
9. Dobrovolskaia, M. A., McNeil, S. E. (2007). Immunological properties of engineered Nanomaterials. *Nat*. *Nanotechnol*., **2** (8), 469–478.
10. Zolnik, B. S., González-Fernández, A., Sadrieh, N., Dobrovolskaia, M. A., et al. (2010). Nanoparticles and the immune system. *Endocrinology*, **151**(2), 458–465.
11. Haase, A. T. (2005). Perils at mucosal front lines for HIV and SIV and their hosts. *Nat*. *Rev*. *Immunol*., **5**, 783–792.
12. Shen, L., Siliciano, R. F. (2008). Viral reservoirs, residual viremia, and the potential of highly active antiretroviral therapy to eradicate HIV infection. *J*. *Allergy Clin*. *Immunol*., **122**, 22–28.
13. Dinosoa, J. B., Kima, S. Y., Wiegandc, A. M., Palmerc, S. E., Ganged, S. J., et al. (2009). Treatment intensification does not reduce residual HIV-1 viremia in patients on highly active antiretroviral therapy. *Proc*. *Natl*. *Acad*. *Sci*. *U*. *S*. *A*., **106**, 9403–9408.
14. Gandhi, R. T., Zheng, L., Bosch, R. Z., Chan, E. S., Margolis, D. M., et al. (2011). The effect of Raltegravir intensification on low-level residual viremia in HIV-infected patients on antiretroviral therapy: A randomized controlled trial. *PLoS Med*., **7**, 1–11.
15. McMahon, D., Jones, J., Wiegand, A., Gange, S. J., Kearney, M., et al. (2010). Short-course Raltegravir intensification does not reduce persistent low-level viremia in patients with HIV-1 suppression during receipt of combination antiretroviral therapy. *Clin*. *Infect*. *Dis*., **50**, 912–919.

16. Allers, K., Hütter, G., Hofmann, J., Loddenkemper, C., Rieger, K., et al. (2011). Evidence for the cure of HIV infection by CCR5D32/D32 stem cell transplantation. *Blood*, **117**, 2791–2799.
17. Lisziewicz, J., Rosenberg, E., Lieberman, J., Jessen, H., Lopalco, L., et al. (1999). Control of HIV despite the discontinuation of antiretroviral therapy. *N*. *Engl*. *J*. *Med*., **340**(21), 1683–1684.
18. Deeks, S. G., Walker, B. D. (2007). Human immunodeficiency virus controllers: Mechanisms of durable virus control in the absence of antiretroviral therapy. *Immunity*, **27**, 406–416.
19. Ndhlovu, Z. M., Proudfoot, J., Cesa, K., Alvino, D. M., McMullen, A., et al. (2012). Elite controllers with low to absent effector CD8+ T cell responses maintain highly functional, broadly directed central memory responses. *J*. *Virol*., **86**(12), 6959–6969.
20. Shan, L., Dend, K., Shroff, N. S., Durand, C. M., Alireza, S., et al. (2012). Stimulation of HIV-1-specific cytolytic T lymphocytes facilitates elimination of latent viral reservoir after virus reactivation. *Immunity*, **36**, 1–11.
21. Xiang, S. D., Scholzen, A., Minigo, A., David, C., Apostolopoulos, V., et al. (2006). Pathogen recognition and development of particulate vaccines: Does size matter? *Methods*, **40**, 1–9.
22. Lisziewicz, J., Szebeni, J. (2010). The Janus face of immune stimulation by nanomedicines: Examples for the good and the bad. *Eur*. *J*. *Nanomed*., **3**, 13–18.
23. Christensen, N. D., Höpfl, R., DiAngelo, S. L., Cladel, N. M., Patrick, S. D., et al. (1994). Assembled baculovirus-expressed human papillomavirus type 11 L1 capsid protein virus-like particles are recognized by neutralizing monoclonal antibodies and induce high titres of neutralizing antibodies. *J*. *Gen*. *Virol*., **75**(9), 2271–2276.
24. Hildesheim, A., Herrero, R., Wacholder, S., Rodriguez, A. C., Solomon, D., et al. (2007). Effect of human papillomavirus 16/18 L1 viruslike particle vaccine among young women with preexisting infection-A randomized trial. *J*. *Am*. *Med*. *Assoc*., **298**(7), 743–753.
25. Martin, S. J., Vyakarnam, A., Cheingsong-Popov, R., Callow, D., Jones, K. L., et al. (1993). Immunization of human HIV-seronegative volunteers with recombinant p17/p24:Ty virus-like particles elicits HIV-1 p24-specific cellular and humoral immune responses. *AIDS*, **7**, 1315–1323.
26. Peek, L. J., Middaugh, C. R., Berkland, C. (2008). Nanotechnology in vaccine delivery. *Adv*. *Drug Deliv*. *Rev*., **60**, 915–928.

27. Lamalle-Bernard, D., Munier, S., Compagnon, C., Charles, M. H., Kalyanaraman, V. S., Delair, T., Verrier, B., Ataman-Onal, Y. (2006). Coadsorption of HIV-1 p24 and gp120 proteins to surfactant-free anionic PLA nanoparticles preserves antigenicity and immunogenicity. *J*. *Control*. *Release*, **115**(1), 57–67.
28. Fairman, J., Moore, J., Lemieux, M., Van Rompay, K., Geng, Y., Warner, J., Abel, K. (2009). Enhanced *in vivo* immunogenicity of SIV vaccine candidates with cationic liposome-DNA complexes in a rhesus macaque pilot study. *Hum*. *Vaccines*, **5**(3), 141–150.
29. Reddy, S. T., Rehor, A., Schmoekel, H. G., Hubbell, J. A., Swartz, M. A. (2006). *In vivo* targeting of dendritic cells in lymph nodes with poly(propylene sulfide) nanoparticles. *J*. *Control*. *Release*, **112**, 26–34.
30. Diebold, S. S., Kursa, M., Wagner, E., Cotton, M., Zenke, M. (1999). Mannose polyethylenimine conjugates for targeted DNA delivery into dendritic cell. *J*. *Biol*. *Chem*., **274**(27), 19087–19094.
31. Toke, E. R., Lorincz, O., Somogyi, E., Lisziewicz, J. (2010). Rational development of a stable liquid formulation for nanomedicine products. *Int*. *J*. *Pharm*., **392**(1–2), 261–267.
32. Lorincz, O., Toke, E. R., Somogyi, E., Horkay, F., Chandran, P. L., et al. (2012). Structure and biological activity of pathogen-like synthetic nanomedicines. *Nanomed*. *Nanotechnol*. *Biol*. *Med*., **8**, 497–506.
33. Reddy, S. T., Swartz, M. A., Hubbell, J. A. (2006). Targeting dendritic cells with biomaterials: Developing the next generation of vaccines. *Trends Immunol*., **27**(12), 573–579.
34. Suh, J., Wirtz, D., Hanes, J. (2003). Efficient active transport of gene nanocarriers to the nucleus. *Proc*. *Natl*. *Acad*. *Sci*. *U*. *S*. *A*., **100**, 3878–3882.
35. Somogyi, E., Xu, J., Gudics, A., Tóth, J., Kovács, A. L., Lori, F., Lisziewicz, J. (2011). A plasmid DNA immunogen expressing fifteen protein antigens and complex virus-like particles (VLP+) mimicking naturally occurring HIV. *Vaccine*, **29**(4), 744–753.
36. Mouquet, H., Scheid, J. F., Zoller, M. J., Krogsgaard, M., Ott, R. G., et al. (2010). Polyreactivity increases the apparent affinity of anti-HIV antibodies by heteroligation. *Nature*, **467**(7315), 591–595.
37. Shim, M. S., Kwon, Y. J. (2009). Controlled cytoplasmic and nuclear localization of plasmid DNA and siRNA by differentially tailored polyethylenimine. *J*. *Control*. *Release*, **133**(3), 206–213.
38. Ogay, I. D., Lihoradova, O. A., Azimova, S. S., Abdukarimov, A. A., Slack, J. M., Lynn, D. E. (2006). Transfection of insect cell lines using polyethylenimine. *Cytotechnology*, **51**(2), 89–98.

39. Salehi, N., Peng, C. A. (2012). Gene transfection of Toxoplasma gondii using PEI/DNA polyplexes. *J. Microbiol. Methods*, **91**(1), 133–137.
40. Han, X., Fang, Q., Yao, F., Wang, X., Wang, J. (2009). The heterogeneous nature of polyethylenimine-DNA complex formation affects transient gene expression. *Cytotechnology*, **60**(1–3), 63–75.
41. Bruewer, M., Utech, M., Ivanov, A. I., Hopkins, A. M., Parkos, C. A., Nusrat, A. (2005). Interferon-gamma induces internalization of epithelial tight junction proteins via a macropinocytosis-like process. *Federation Am. Soc. Exp. Biol.*, **19**, 923–933.
42. Racoosin, E. L., Swanson, J. A. (1992). M-CSF-induced macropinocytosis increases solute endocytosis but not receptor-mediated endocytosis in mouse macrophages. *J. Cell Sci.*, **102**, 867–880.
43. Boussif, O., Lezoualc'h, F., Zanta, M. A., Mergny, M. D., Scherman, D., Demeneix, B., Behr, J. P. *(*1995). A versatile vector for gene and oligonucleotide transfer into cells in culture and *in vivo*: Polyethylenimine. *Proc. Natl. Acad. Sci. U. S. A.*, **92**(16), 7297–7301.
44. Schaffer, D. V., Fidelman, N. A., Dan, N., Lauffenburger, D. A. (2000). Vector unpacking as a potential barrier for receptor-mediated polyplex gene delivery. *Biotechnol. Bioeng.*, **67**, 598–606.
45. Srinivasachari, S., Liu, Y., Prevette, E. L., Reineke, T. M. (2006). Trehalose click polymers inhibit nanoparticle aggregation and promote DNA delivery in serum. *J. Am. Chem. Soc.*, **128**, 8172–8184.
46. Matzinger, P. (2002). The danger model: A renewed sense of self. *Science*, **296**(5566), 301–305.
47. Nicolas, J. F., Guy, B. (2008). Intradermal, epidermal and transcutaneous vaccination: From immunology to clinical practice. *Expert Rev. Vaccines*, **7**(8), 1201–1214.
48. Bauer, J., Bahmer, F. A., Worl, J., Neuhuber, W., Schuler, G., et al. (2001). A strikingly constant ratio exists between Langerhans cells and other epidermal cells in human skin. A stereologic study using the optical disector method and the confocal laser scanning microscope. *J. Invest. Dermatol.*, **116**(2), 313–318.
49. Lisziewicz, J., Gabrilovich, D. I., Varga, G., Xu, J., Greenberg, P. D., et al. (2001). Induction of potent human immunodeficiency virus type 1-specific T-cell-restricted immunity by genetically modified dendritic cells. *J. Virol.*, **75**(16), 7621–7628.
50. Lisziewicz, J., Trocio, J., Xu, J., Whitman, L., Ryder, A., et al. (2005). Control of viral rebound through therapeutic immunization with DermaVir. *AIDS*, **19**(1), 35–43.

51. Lisziewicz, J., Bakare, N., Calarota, S. A., Bánhegyi, D., Szlávik, J., et al. (2012). Single DermaVir immunization: Dose-dependent expansion of precursor/memory T cells against all HIV antigens in HIV-1 infected individuals. *PLoS ONE*, **7**(5), e35416.

52. Elisabeth, T. T., Dietmar, R., Christian, O., Iacob, M., Rune, K. (2008). Taking electroporation-based delivery of DNA vaccination into humans: A generic clinical protocol. *Methods Mol*. *Biol*., **423**, 497–507.

53. Lee, J. W., Park, J. H., Prausnitz, M. R. (2008). Dissolving microneedles for transdermal drug delivery. *Biomaterials*, **29**(13), 2113–2124.

54. Albrecht, M. T., Livingston, B. D., Pesce, J. T., Bell, M. G., Hannaman, D., Keane-Myers, A. M. (2012). Electroporation of a multivalent DNA vaccine cocktail elicits a protective immune response against anthrax and plague. *Vaccine*, **30**(32), 4872–4883.

55. Kumar, A., Wonganan, P., Sandoval, M. A., Li, X., Zhu, S., Cui, Z. (2012). Microneedle-mediated transcutaneous immunization with plasmid DNA coated on cationic PLGA nanoparticles. *J*. *Control*. *Release*, **28**(163), 230–239.

56. Tenbusch, M., Ignatius, R., Nchinda, G., Trumpfheller, C., Salazar, A. M., Töpfer, K., Sauermann, U., Wagner, R., Hannaman, D., Tenner-Racz, K., Racz, P., Stahl-Hennig, C., Uberla, K. (2012). Immunogenicity of DNA vaccines encoding simian immunodeficiency virus antigen targeted to dendritic cells in rhesus macaques. *PLoS ONE*, **7**(6), e39038.

57. Andrianov, A. K., Mutwiri, G. (2012). Intradermal immunization using coated microneedles containing an immunoadjuvant. *Vaccine*, **30**(29), 4355–4360.

58. Kim, Y. C., Park, J. H., Prausnitz, M. R. (2012). Microneedles for drug and vaccine delivery. *Adv*. *Drug Deliv*. *Rev*., **64**(14), 1547–1568.

59. Calarota, S. A., Foli, A., Maserati, R., Baldanti, F., Paolucci, S., Young, M. A., Tsoukas, C. M., Lisziewicz, J., Lori, F. (2008). HIV-1-specific T cell precursors with high proliferative capacity correlate with low viremia and high CD4 counts in untreated individuals. *J*. *Immunol*., **180**(9), 5907–5915.

60. Lisziewicz, J., Calarota, S., Banhegyi, D., Lisziewicz, Z. S., Ujhelyi, E., Lori, F. (2008). Single DermaVir Patch treatment of HIV+ individuals induces long-lasting, high-magnitude, and broad HIV-specific T cell responses. Paper presented at the 15th Conference on Retroviruses and Opportunistic Infections, Boston, MA, USA, Poster #715.

61. Rodriguez, B., Asmuth, D., Matining, R., Spritzler, J., Li, X., et al. (2010). Repeated-dose transdermal administration of DermaVir, a candidate

plasmid DNA-based therapeutic HIV vaccine, is safe and well-tolerated: A 61-week analysis of ACTG Study 5176, paper presented at XVIIIth International AIDS Conference, Vienna, Austria, Abstract # A-240-0111-10145.

62. U.S. National Institutes of Health. Available at: http://www.clinicaltrials.gov/ct2/results?term=dermavir (accessed on December 3, 2014).
63. van Lunzen, J., et al. (2010). DermaVir for initial treatment of HIV-infected subjects demonstrates preliminary safety, immunogenicity and HIV-RNA reduction versus placebo immunization. Paper presented at the XVIIIth International AIDS Conference, Vienna, Austria, Abstract #A-240-0111-12561.
64. Kantoff, P. W., Higano, C. S., Shore, N. D., Berger, E. R., Small, E. J., et al. (2010). Sipuleucel-T immunotherapy for castration-resistant prostate cancer. *N. Engl. J. Med.*, **363**(5), 411–422.
65. Vaccari, M., Trindade, C. J., Venzon, D., Zanetti, M., Franchini, G. (2005). Vaccine-induced CD8+ central memory T cells in protection from simian AIDS. *J. Immunolol.*, **175**(6), 3502–3507.

Chapter 49

Biomedical Engineering and Nanoneurosurgery: From the Laboratory to the Operating Room

Mario Ganau, MD, PhD,[a,b,c] Roberto I. Foroni, PhD,[b] Andrea Soddu, PhD,[c] and Rossano Ambu, MD[a]

[a]*Department of Surgical Science & Graduate School of Biomedical Engineering, University of Cagliari, Italy*
[b]*Minimally Invasive Robotic Surgery Lab, Department of Neurosurgery, Verona, Italy*
[c]*Brain and Mind Institute & Physics and Astronomy Department, University of Western Ontario, Canada*

Keywords: nanoneurosurgery, neuroscience, biomedical engineering, surgical instruments, neuroimaging, nanodrugs, nanorobotics, neural interfaces, tissue repair, blood brain barrier, MRI, epilepsy, functional surgery, gold nanorods, chromophore-loaded nanoshells, lab-on-a-chip platform, carbon nanotubes

49.1 Neurosurgery at the Crossroads of Nanotechnology, Biomedical Engineering and Neuroscience

Recent neurosciences discoveries have progressively deepened the understanding of many vexing diseases affecting the central and

Handbook of Clinical Nanomedicine: Nanoparticles, Imaging, Therapy, and Clinical Applications
Edited by Raj Bawa, Gerald F. Audette, and Israel Rubinstein

ISBN 978-981-4669-20-7 (Hardcover), 978-981-4669-21-4 (eBook)
www.panstanford.com

peripheral nervous systems (CNS or PNS). This trend, paralleled by exponential advances in nanotechnology and biomedical engineering allowed for new translational projects, theorized and implemented by enlightened multidisciplinary research teams. As a result, the forefront of neurosurgery is now heading toward diagnosis and treatment at the nanoscale [1, 2]. In some cases, this paradigmatic change has already occurred but for the vast majority it will become more evident in the coming years (Table 49.1) when nanoneurosurgery is expected to nudge changes in every aspect revolving around our patients, from the design of hospital wards and operating rooms to the functions and potentialities of new drugs and scalpels. In this chapter, we will explore the applications of nanotechnology in the various neurosurgical subspecialties, and will finally focus on the forthcoming developments in the field of nanoneurosurgery.

Table 49.1 Current Applications and Future Trends in Nanoneurosurgery

Present	*Near-Term*	*Mid to Long-Term*
Drug-eluting stents for endovascular treatment	Ion-beam functionalization of bioactive endovascular stents	Nanorobots for screening of intracranial aneurysms
Coated-shunt catheters for CSF diversion	NEMS-functionalized microelectrode recording	Nanowires for brain-computer interfaces
Liposomal drugs for chemotherapy	Nanoshells and drug-delivery systems for chemotherapy	Nanorobots for detection and selective killing of cancer cells
Nanoparticles-coated spinal implants	NEMS-functionalized spinal implants	Nanoscaffolds for nerve regeneration in spinal cord injury
Nanoparticles with platelet-like functions	Super-paramagnetic oxide contrast agents for MRI	Quantum dots labeling of intracranial and spinal tumors

Vascular, Pediatric, Functional, Oncological, and Spinal Surgery; Haemostatic, and Contrast Agents

49.2 Applications in Neurovascular Surgery

A few decades ago, neurosurgeons could have hardly imagined that the treatment of neurovascular pathologies in the intracranial, extracranial and spinal compartments was deemed to become less surgical and to include radiosurgical and endovascular techniques [3]. The continuous evolution of vascular neurosurgery is best represented by the concept of endovascular remodeling, so that nowadays reconstructing cerebral arteries diseased with aneurysms is becoming more appealing than clipping or coiling the aneurismal dome itself. Nonetheless, stents are continually evolving and soon they will serve as more than just scaffolds [4].

Their nanofunctionalization, in fact, could offer surgical opportunities that were out of reach at the microsurgical level: Specifically, the production of biodegradable and bioactive-coated stents. On one hand, a biodegradable dual-drug-eluting stent could offer a sequential and sustained release of anti-platelet (i.e., acetylsalicylic acid) and anti-smooth muscle cell drug (i.e., paclitaxelin) to prevent thrombosis or lumen occlusion, the main long-term complication of any endovascular treatment. On the other hand, bioactive coatings restoring an antithrombotic surface could provide alternatives to systemic anticoagulation, or attract magnetized cells to repair the blood vessel [5, 6]. By modifying the stent coatings (i.e., using ion beams to create biomimetic surface textures), it would be possible to promote endothelial cell proliferation, activate resident stem cells from the arterial walls, and induce faster vessel repair [6].

Another area of significant innovation is represented by the introduction of laser tissue soldering (LTS) of biological tissues where the innovative functionalization of current energy absorbers is offering a substantial breakthrough for vascular anastomosis (i.e., intra-extracranial bypasses). Various studies on near-infrared absorbing gold nanorods or chromophore-loaded nanoshells, have demonstrated that with optimally chosen settings of irradiation time, and carefully selected coating and scaffold properties of energy-absorbing immunoneutral nanoparticles, improved LTS procedures can become easier to perform, while preserving in the long-term the vessels' mechanical properties and patency [7, 8].

49.3 Applications in Pediatric Neurosurgery

The advent of nanotechnology is affecting pediatric neurosurgery in two main areas: (1) the functionalization of shunt catheters for cerebrospinal fluid diversion used in the treatment of acute and chronic hydrocephalus; and (2) the management of pediatric brain tumors. Whereas the first area is considered in this section, the second will be further expanded in the following section on neuro-oncology.

The efficacy of polypropylene-grafted polyethylene glycol (PP-g-PEG) copolymer and silver nanoparticle-embedded PP-g-PEG (Ag-PP-g-PEG) polymer-coated ventricular catheters in preventing

catheter-related infection and reducing inflammatory reaction in the periventricular parenchyma has been largely demonstrated *in vitro*, in animal models, in the neonatal and the pediatric population [9]. Though evidence from randomized clinical trials is still missing, this is the rationale behind the BASICS trial currently recruiting 1,200 patients in 17 regional neurosurgical units in the UK and Ireland [10].

49.4 Applications in Neuro-Oncology

The availability of sophisticated technological aids to surgical removal of gliomas, the most aggressive primary brain tumors, have led over the last few years to the identification of better prognostic/predictive biomolecular factors, and the development of novel drugs meant to profoundly impact the outcome of those patients [2, 11]. Nanoneurosurgery is pervasing each one of those innovative strategies: Lab-on-a-chip platforms for proteomic analysis demonstrate a remarkable accuracy, providing a platform for single cell analysis (down to a few μl) of the stem cells considered responsible for tumor recurrence following initial

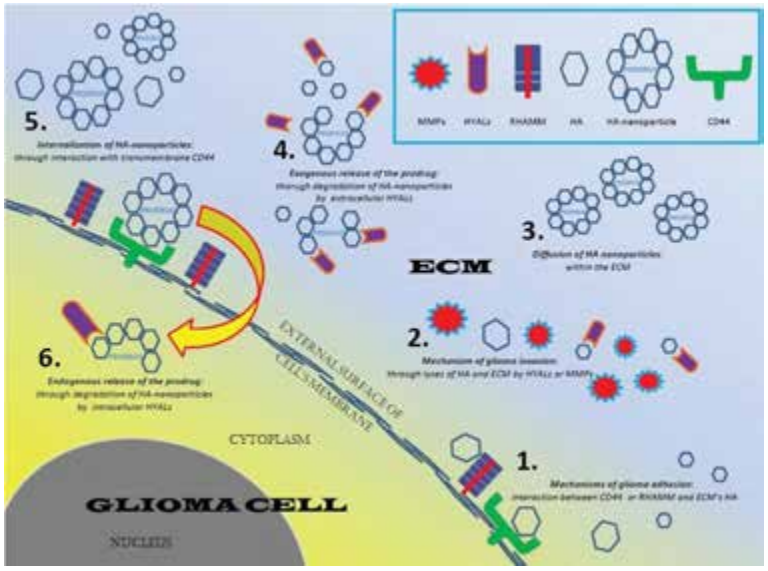

Figure 49.1 Nanoshells of HA and their mechanism of action. Adapted, with permission, from Ganau *et al.*, *Clin. Transl. Med.*, 2014 [13].

chemo-/radiotherapy [12]. Nanocomposites have also attracted much attention due to their applicability in neuroimaging and drug delivery systems. One elegant example is the encapsulation of prodrugs within nanoshells of hyaluronic acid (HA). The natural immunoneutrality of HA enables the passive diffusion of HA-nanoshells through the leaky blood brain barrier (BBB), and the overexpression of CD44 and RHAMM in tumoral cells represents the basis for their selective targeting and subsequent exogenous and endogenous release of the carried prodrug (Fig. 49.1) [13]. The role of HA-nanoshells as Trojan horses is now expected to offer better stability and biodistribution of contrast agents for conventional or high-Tesla MRI, radiotracers for nuclear medicine investigations, and radiosensitizers for adjuvant stereotactic radiosurgery [14–16].

49.5 Applications in Epilepsy and Functional Surgery

Despite the large number of available drugs, epilepsy is still one of the most clinically burdening neurological disorders due to the high percentage of patients (35–40%) resistant to pharmacotherapy [17]. Proven therapeutic strategies to control pharmacoresistant epilepsy include epilepsy surgery and neuromodulation. Unfortunately, not all patients are candidates for these therapies, however nanotechnology-based approaches are now attempting to widen their applicability. Beyond drug delivery strategies that share biological properties similar to those used in neuro-oncology or in neuro-HIV to bypass the BBB and interact with firing epileptic foci, another appealing area of research is the development of implantable neural interfaces based on semiconducting nanowires [18, 19]. Used as interface material in contact with neurons they allow both the delivery of electrical stimulation and detection of neuronal electrical activity. Such approaches are therefore opening new areas of research, including the optimization of the spatial accuracy of neurophysiological intraoperative recording, enhanced microelectrode arrays for deep brain stimulation (DBS), and brain-machine interfaces for neural prostheses inducing artificial synapses in neuromorphic circuits based on nanoscale memory devices [19].

49.6 Applications in Spinal Surgery

Spinal surgery is witnessing a fast-paced evolution due to the collaboration of neurologists with material scientists. This is becoming particularly evident in the definition of novel strategies for biomechanically efficient spinal stabilization and spinal cord injury repair. Several biomaterials (including nanoscaffolds, demineralized bone matrix, and ceramics) with propensity to incorporate mesenchymal stem cells, recombinant human bone morphogenetic protein, and endogenous/exogenous growth factors are already showing ideal characteristics to achieve enhanced arthrodesis following spinal fixation. The next steps include the ongoing incorporation of micro- and nanoelectromechanical systems (MEMS and NEMS) into current implants for dynamic stabilization. Indeed, successful studies conducted in animal models to assess the quality of arthrodesis, are now being translated in clinical practice with the aim to reduce the risk of pullout, osteolysis, and revision surgery [20].

In the area of spinal cord injury, where cell- and biomolecule-based delivery strategies, as well as scaffold-based therapeutic strategies, have failed when used alone, a combinatorial approach has, at least preliminary, shown to be effective in laboratory models. As such, translation from the lab to bedside is limited by the fact that many biomaterials investigated so far have been plagued by a wide range of adverse effects (especially in early stages of research), or by issues of widespread off-label use.

49.7 Hemostasis in Brain and Spine Surgery

In any surgical procedure achieving a satisfactory hemostasis can represent a challenging moment even for experienced neurosurgeons, either in case of accidental damage to large vessels' wall (i.e., dural sinuses) or in case of diffuse oozing from the surgical cavity (i.e., vascular tumors) [21, 22]. To address this problem, nanoparticles that exhibit platelet-like functions (PLNs) have been developed. PLNs mimic key mechanical and biochemical attributes of platelets, including vascular injury site-directed margination, site-specific adhesion, and amplification of injury site-specific

aggregation. *In vivo* studies using mouse models demonstrated that PLNs accumulate at the wound site and induce ~65% reduction in bleeding time, and are being proposed as injectable synthetic hemostats for vascularly targeted payload delivery in both cranial and spinal surgery [23].

49.8 New Horizons in Nanoneurosurgery

In the last decade, the interest toward strategies for tissue repair in neurodegenerative and inflammatory diseases (i.e., Amyotrophic Lateral Sclerosis, Alzheimer's and Parkinson's disease) and traumatic injuries (i.e., axonotemesis and neurotemesis following peripheral nerve and spinal cord injuries) has increased. In the future, should such approaches prove to be safe and effective, they will likely replace treatments like DBS or nerve grafts from autologous donor roots.

Due to the complexity of the CNS and PNS, conventional repair approaches used in other body compartments are usually pointless. In this framework, technologies based on covalent and non-covalent modification of carbon nanotubes (CNT) and graphene, have emerged as innovative tools due to their outstanding physical properties and the documented ability to interface synapses. Novel functionalized single-walled and multi-walled CNT nanoscaffolds have overcome toxicity limitations due to oxidative stress and reduced cell viability, typical of non-functionalized CNTs, and proved to deliver safely neural stem cells to injured sites of the CNS in animal models [19].

Finally, achievements in miniaturizing chip technology, along with progress in optics and micro mechanics, have led to the development of micro- and nanosized robots designed to navigate human biological systems. For instance, some prototypes using embedded nanoelectronic chemical sensors have been programmed for the proteomic detection of intravascular levels of nitric oxide synthase (NOS), their interpretation as pattern signals of the early stages of intracranial aneurysm development, and the communication of this information to the treating physician through radiofrequency wireless communication (allowed by the nanorobot's antenna) [24]. The rationale of this proposed

screening would be to monitor patients with a medical or family history of previous aneurismal subarachnoid hemorrhage, replacing the need for serial follow up with angioCT.

Similarly, others are working on swarms of nanorobots propelled into the bloodstream and able to recognize glioma cells, destroy them, and then forward information about the presence of cancer formation to other nanorobots, through acoustic signals in a distributed and decentralized fashion [25]. Given the striking pace of advancement of those technologies, the translation of such prototypes from laboratory settings to clinical trials is hopefully not far away.

49.9 Conclusion

As demonstrated by all the progresses highlighted in this chapter for every single neurosurgical subspecialty, nanoneurosurgery has proved not only to be potentially game-changing, but also has the potential to evolve into a ubiquitous revolution in the art of neurosurgery. In this chapter we have pinpointed why this revolution has what it takes to push forward the boundaries of clinical practice; as such, we will probably witness a revolution in our clinical and surgical careers where what is deemed untreatable today has realistic chances to become treatable if not curable in the coming decades.

Disclosures and Conflict of Interest

The opinions and perspectives here reflect the current views of the authors. The authors declare that they have no conflict of interest and have no affiliations or financial involvement with any organization or entity discussed in this chapter. No writing assistance was utilized in the production of this chapter and the authors have received no payment for its preparation. This chapter was written at the Brain and Mind Institute, University of Western Ontario, Canada, in the framework of the first author's PhD studies in biomedical engineering at the University of Cagliari, Italy. The authors express their deepest thanks to Prof. Giacomo Cao.

Corresponding Author

Dr. Mario Ganau
Department of Surgical Science
Asse Didattico di Medicina, Cittadella Universitaria
S.S. 554. 09042 Monserrato (CA), Italy
Email: mario.ganau@singularityu.org

About the Authors

Mario Ganau is a neurosurgeon and scientist with a wide breadth of knowledge regarding the application of innovation technology in clinical practice. He is the recipient of the Canada-Italy Innovation Award 2015; in this framework, he is conducting joint projects in the priority area of nanotechnology with the University of Western Ontario. Dr. Ganau holds a PhD in nanotechnology and is a PhD candidate in biomedical engineering.

Roberto I. Foroni is a cofounder of the Minimally Invasive Neurosurgery Unit and Director of the Robotic Surgery Lab at the Department of Neurosurgery of Verona, Italy. He is Principal Investigator in several international research consortia for projects on intraoperative monitoring, vascular connectivity reconstruction, microrobots and nanopharmacology. Dr. Foroni holds a PhD in theoretical nuclear physics.

Andrea Soddu is assistant professor of physics at the University of Western Ontario, Canada, where he is also member of the Brain and Mind Institute. His research focuses on the extraction from neuroimaging protocols (mostly functional MRI) of relevant biopatterns able to increase the specificity of this imaging modality as a reliable diagnostic tool in patients with disorders of consciousness. Dr. Soddu holds a PhD in particle physics from University of Virginia, USA and switched to neuroscience while at the Weizmann Institute, Israel.

Rossano Ambu is professor of pathology at the University of Cagliari, Italy, where he has forged a strong expertise in advanced diagnostics deepening the understanding of both the genetic and transcriptional bases of cancer, and improving the phenotype classification of degenerative diseases and their neoplastic transformation. He currently sits in the Board-of-Experts of the PhD program in biomedical engineering at the University of Cagliari.

References

1. Ganau, L., *et al.* (2015). Management of Gliomas: Overview of the latest technological advancements and related behavioral drawbacks. *Behav. Neurol.*, 2015, 862634.
2. Sboarina, A., *et al.* (2010). Software for hepatic vessel classification: Feasibility study for virtual surgery. *Int. J. Comput. Assist. Radiol. Surg.*, **5**(1), 39–48.
3. Graziano, F. (2014). Vertebro-basilar junction aneurysms: A single centre experience and meta-analysis of endovascular treatments. *Neuroradiol. J.*, **27**(6), 732–741.
4. Salmasi, S., Seifalian, A. M. (2014). Intracranial aneurysms; in need of early diagnostic and treatment using bio- and nanotechnology. *Curr. Med. Chem.*, **21**(37), 4300–4310.
5. Lee, C. H., *et al.* (2014). Promoting endothelial recovery and reducing neointimal hyperplasia using sequential-like release of acetylsalicylic acid and paclitaxel-loaded biodegradable stents. *Int. J. Nanomedicine*, **9**, 4117–4133.
6. Allain, J. C., Tigno, T., Armonda, R. (2013). In: Katek, B., and Heiss, J. D., eds. *The Textbook of Nanoneuroscience and Nanoneurosurgery*, CRC press, Boca Raton, FL, pp. 259–282.
7. Esposito, G., *et al.* (2012). Nanotechnology and vascular neurosurgery: An *in vivo* experimental study on microvessels repair using laser photoactivation of a nanostructured hyaluronan solder. *J. Biol. Regul. Homeost. Agents*, **26**(3), 447–456.
8. Schöni, D. S., *et al.* (2011). Nanoshell assisted laser soldering of vascular tissue. *Lasers Surg. Med.*, **43**(10), 975–983.
9. Thomas, R., *et al.* (2012). Antibiotic-impregnated catheters for the prevention of CSF shunt infections: A systematic review and meta-analysis. *Br. J. Neurosurg.*, **26**(2), 175–184.

10. Jenkinson, M. D., *et al.* (2014). The British antibiotic and silver-impregnated catheters for ventriculoperitoneal shunts multi-centre randomised controlled trial (the BASICS trial): Study protocol. *Trials*, **15**, 4.
11. Talacchi, A., *et al.* (2010). Surgical treatment of high-grade gliomas in motor areas. The impact of different supportive technologies: A 171-patient series. *J. Neurooncol.*, **100**(3), 417–426.
12. Ganau, M., *et al.* (2015). A DNA-based nano-immunoassay for the label-free detection of glial fibrillary acidic protein in multicell lysates. *Nanomedicine*, **11**(2), 293–300.
13. Ganau M. (2014). Tackling gliomas with nanoformulated antineoplastic drugs: Suitability of hyaluronic acid nanoparticles. *Clin. Transl. Oncol.*, **16**(2), 220–223.
14. Ganau, M., *et al.* (2012). Postoperative granulomas versus tumor recurrence: PET and SPET scans as strategic adjuvant tools to conventional neuroradiology. *Hell. J. Nucl. Med.*, **15**(3), 184–187.
15. Ganau, M., *et al.* (2015). Radiosurgical options in neuro-oncology: A review on current tenets and future opportunities. Part II: Adjuvant radiobiological tools. *Tumori*, **101**(1), 57–63.
16. Ganau, M., *et al.* (2014). Radiosurgical options in neuro-oncology: A review on current tenets and future opportunities. Part I: Therapeutic strategies. *Tumori*, **100**(4), 459–465.
17. Rosillo-de la Torre, A., *et al.* (2014). Pharmacoresistant epilepsy and nanotechnology. *Front. Biosci.*, **6**, 329–340.
18. Ganau, M., *et al.* (2012). Challenging New Targets for CNS-HIV Infection. *Front. Neurol.*, **3**, 43.
19. Vidu, R., *et al.* (2014). Nanostructures: A platform for brain repair and augmentation. *Front. Syst. Neurosci.*, **8**, 91.
20. Benzel, E., *et al.* (2004). Micromachines in spine surgery. *Spine*, **29**(6), 601–606.
21. Ganau, M., Nicassio, N., Tacconi, L. (2012). Postoperative aseptic intracranial granuloma: The possible influence of fluid hemostatics. *Case Rep. Surg.*, 2012, 614321.
22. Graziano, F., *et al.* (2015). Autologous fibrin sealant (Vivostat®) in the neurosurgical practice: Part I: Intracranial surgical procedure. *Surg. Neurol. Int.*, **6**, 77.
23. Anselmo, A. C., *et al.* (2014). Platelet-like nanoparticles: Mimicking shape, flexibility, and surface biology of platelets to target vascular injuries. *ACS Nano*, **8**(11), 11243–11253.

24. Cavalvanti, A., *et al.* (2009). Nanorobot for brain aneurysm. *Int. J. Robot. Res.*, **28**(4), 558–570.
25. Loscri, V., Vegni, A. M. (2015). An Acoustic Communication Technique of Nanorobot Swarms for Nanomedicine Applications. *IEEE Trans. Nanobioscience*, **14**(6), 598–607.

Chapter 50

Nanotechnology-Based Systems for Microbicide Development

Rute Nunes,[a,b,c] Carole Sousa,[b] Bruno Sarmento, PhD,[a,b,c] and José das Neves, PhD[a,b,c]

[a]*CESPU, Instituto de Investigação e Formação Avançada em Ciências e Tecnologias da Saúde, Gandra, Portugal*
[b]*INEB–Instituto de Engenharia Biomédica, Universidade do Porto, Porto, Portugal*
[c]*Instituto de Investigação e Inovação em Saúde, Universidade do Porto, Porto, Portugal*

Keywords: HIV/AIDS, pre-exposure prophylaxis, vaginal drug delivery, dendrimers, polymeric nanocarriers, mucoadhesion, rectal microbicides

50.1 Introduction

The development and application of nanotechnology to the diagnosis, treatment, and prevention of disease, commonly referred to as nanomedicine, gained substantial support over the past few decades and has shown the potential to affect global healthcare and contribute to personalized medicine [1–3]. While the majority of microbicide compounds previously and currently under pre-clinical/clinical investigation have been "simply" incorporated in conventional dosage forms (e.g., gels, tablets, suppositories, films, and intravaginal rings [IVRs]) [4–6], different reports support the idea that the use of nanotechnology-based systems may be

Handbook of Clinical Nanomedicine: Nanoparticles, Imaging, Therapy, and Clinical Applications
Edited by Raj Bawa, Gerald F. Audette, and Israel Rubinstein

ISBN 978-981-4669-20-7 (Hardcover), 978-981-4669-21-4 (eBook)
www.panstanford.com

beneficial [7–11]. These last may possess intrinsic antiviral activity or act as active agents carriers. For example, the dendrimer-based vaginal gel VivaGel® (Holdings (SPL7013 or astodrimer sodium) from Starpharma Holdings Ltd., Melbourne, Australia) showed promising results both *in vitro* and *in vivo* and is at present in an advanced stage of the development pipeline [12]. Even so, most of the research is now focusing on nanotechnology-based antiretroviral (ARV) drug carriers, in particular polymeric nanoparticles (NPs), rather than on nanosystems possessing intrinsic antiviral activity, such as the case of the SPL7013 dendrimer included in VivaGel®. Possible benefits of polymeric NPs for the vaginal delivery of ARV agents have been shown to include the enhancement of epithelial penetration, possibility of drug targeting, modulation of adhesion/diffusion through cervicovaginal mucus, and effective distribution throughout the genital tract [13–17]. Even if the potential of nanotechnology is valid for both vaginal and rectal microbicides, most research has been conducted toward the development of the first. Nonetheless, rectal transmission is well recognized as an important route for human immunodeficiency virus (HIV) dissemination in both male and female populations engaged in receptive anal intercourse (RAI), thus justifying the concurrent development of rectal nanotechnology-based microbicides. This chapter provides an overview of the possibilities and achievements in the field of nanotechnology-based microbicides for the prevention of sexual HIV transmission and, potentially, other pathogens (e.g., herpes simplex virus [HSV]). Parts of this chapter have been previously published by our group in different review articles [18–20].

50.2 Limitations of Microbicide Products Currently under Development

Different limitations have been pointed out to microbicide formulations currently used in clinical studies. One of the main issues of tested products seems to be their poor ability to provide an effective, continuous, and durable drug barrier along the epithelial lining that covers the cervicovaginal or rectal mucosae [21, 22]. In the particular case of solid dosage forms, this seems to be even more problematic since their ability to disaggregate

and/or dissolve in the limited amount of fluid present in the vagina/rectum can jeopardize the efficacy of microbicide compounds. The continuum of the rectum toward the colon raises even more challenging issues about the spreading of rectally administered products: too little can compromise effectiveness, while too much may lead to safety issues. Nonetheless, higher quantities of a product are expected to be necessary than for vaginal microbicides in order to outdistance and outlast the virus. Another factor to be taken into account is rectal drug absorption, which is generally lower but in line with what happens with oral administration [23, 24]. Thus, systemic exposure and even toxicity may be significant when delivering molecules that are well absorbed.

The inefficiency of microbicide formulations to provide sustained drug release (except for IVRs), and deliver active molecules to their targets (e.g., HIV-susceptible cells) are other limiting issues. Prolonged drug release (and mucosal residence) may help achieving coitally independent products and provide wider time frames of protection. For instance, a recent study in macaques showed that the enduring presence of MIV-150, a non-nucleoside reverse transcriptase inhibitor (NNRTI), after vaginal challenge with simian-human immunodeficiency virus (SHIV) was essential for protection [25]. Drug targeting seems highly desirable particularly for those agents exerting pharmacological activity at specific cell populations (e.g., immune cells) but the ability of products under development to do so is absent or limited. Once a microbicide compound is released from a dosage form/delivery system in the vaginal/rectal milieus, its fate is mostly determined by inherent physicochemical properties. Another important limitation is related with the poor solubility of many microbicide drug candidates, which may limit optimal activity and provides significant challenges during formulation stages. Different strategies such as micronization [26] or the use of cyclodextrins [27, 28] have been proposed but this may not be always feasible in terms of large-scale production or, such as in the particular case of cyclodextrins, toxicity issues may arise [29]. Moreover, poor drug stability, particularly of labile molecules such as proteins and genetic material, is common and requires dosage forms or delivery systems that protect payloads. Even so, degradation or inactivation may still occur after drug release in vaginal/rectal lumina. Loss of activity of microbicide compounds

in fluids present at the vagina or rectum, either permanently or transiently (e.g., semen), has also been described [30–33].

50.3 Why Nanotechnology-Based Microbicides? Potential and Perils

Nano-sized materials are characterized by a high surface-area-to-volume ratio, which considerably affects their physicochemical properties and, consequently, their biological behavior [1]. For example, simple issues such as poor solubility of many microbicide drug candidates may be resolved by reducing particle size to dimensions at the nanoscale [34, 35] or by their association with nanocarriers. More important, current investigation and opinion suggest that nanotechnology-based systems can substantially improve the local pharmacokinetics (PK) of microbicide compounds [8, 18]. Drug nanocarriers may possess interesting features such as the ability to modulate the release of active agents [36]; once-daily application microbicides may be feasible without common problems such as transient drug concentration peaks observed for immediate release dosage forms (e.g., gels or films), or high local drug levels achieved in the vicinities of sustained release devices, namely IVRs [37]. Enhanced distribution and retention at the vaginal/rectal lumina (e.g., by increasing mucoadhesion), penetration of epithelial cell linings, and enhanced tissue retention are other potentialities of nanosystems which may favor their use in the field of microbicides [17, 38–40]. Also, their possible use for targeted and intracellular drug delivery, namely to HIV-susceptible cells [41, 42], and potential capability to protect ARV agents from *in vivo* degradation [43] are interesting characteristics. Furthermore, nanosystems may allow obtaining combination microbicides that can potentially decrease the opportunity for resistance development and the obtention of antiviral synergism [44, 45]. Nanosystems can also possess intrinsic activity against pathogens, namely HIV, which make these interesting approaches toward the development of new microbicides [46]. Finally, nanocarriers administered in the vagina may provide an efficient way to deliver drugs to regional lymph nodes, where HIV amplification occurs before systemic infection is established [47, 48].

Despite all mentioned potential advantages of nanotechnology-based microbicides, some concerns remain, particularly related with toxicity and adverse effects. The overall knowledge of the harmful effects of therapeutic nanosystems is still relatively limited, particularly on their long-term effects [49–51]. Distribution of vaginally administered nanosystems to the upper genital tract and the impact of such phenomenon are of significance. For instance, polymeric NPs based on either poly(D,L-lactide-*co*-glycolide) (PLGA; 100–300 nm) [16] or poly(L-lactic acid) (PLLA; 75 nm) [52] have been shown able to migrate from the vagina to the uterine horns in mice. In the particular case of PLLA NPs [52], the expression of pro-inflammatory cytokines such as the regulated on activation, normal T cell expressed and secreted (RANTES) and tumor necrosis factor (TNF) was induced at the uterine level. The impact of these findings on HIV transmission is unknown, but authors foresee that this may interfere with the ability of women to get pregnant. However, contraception may not be detrimental; in fact, this may be desirable as a dual-approach strategy. For instance, perfluorocarbon-based NPs containing a bee-venom peptide component, melittin, were shown able to impair HIV and spermatozoids [53, 54]. Also, the surface of these NPs was functionalized with anti-spermatozoa antibodies, and ligands for gp120 and gp41, which allow active targeting to male gametes and HIV, respectively.

Contrasting with the previous reports in animals, one study in women showed that 100 nm technetium-99m (^{99m}Tc)-sulfur particles (used as a HIV surrogates) were able to be detected in the vaginal pericervical area but not in the uterus, as assessed by single photon emission computed tomography with computed tomography (SPECT/CT) and magnetic resonance imaging (MRI) [55]. NPs dispersed in semen simulant (3% HEC) were deposited in the vagina using a phallus in order to simulate vaginal intercourse. As for rectal administration, one similar pilot study conducted by the same research group showed that ^{99m}Tc-sulfur NPs could migrate as far as the splenic flexure after simulated rectal ejaculation in men engaging RAI [56]. However, in most cases (75%), the distribution was confined to the rectosigmoid colon. A further study confirmed that distribution of these particles was mostly limited to this last region [57]. Moreover, they used radio-

labeled lymphocytes in the semen simulant as cell-associated HIV surrogates and observed that the distribution of these cells was also limited to the rectosigmoid colon up to 24 h. Although these results should be analyzed with caution, they provide valuable insights to both the possible boundaries for viral infection as well as the possible distribution of nanotechnology-based microbicides.

Paralleling with multiple reports of different nanotechnology-based strategies for delivering ARV agents for HIV/acquired immunodeficiency syndrome (AIDS) therapy (reviewed elsewhere, see [58–63]), the use of nanotechnology for the development of microbicides has been investigated, in particular over the last few years. Nanosystems may be divided into two categories as proposed in this manuscript: (1) those presenting intrinsic activity against HIV or competing with the virus for host targets owing to surface chemical functionalization and (2) those acting as carriers for microbicide agents.

50.4 Nanosystems Presenting Intrinsic Activity against HIV/Competing with the Virus for Host Targets

In one of the earliest reports endorsing the possible use of nanotechnology-based microbicides, the groups of Baba and Akashi [64] described polystyrene (PS) nanospheres (400 nm) bearing a lectin, concanavalin-A, on their surface and demonstrated their ability to capture HIV-1 virions *in vitro* [64]. This effect was presumably due to the high affinity between concanavalin-A and viral gp120. Nanospheres were originally developed as mucosal vaccine adjuvants but their capacity to reduce HIV-1 infectivity led these investigators to suggest the study of nanosystems for microbicide development. An advantageous feature of PS nanospheres was their high surface area, which allowed increasing the amount of available concanavalin-A molecules for interacting with virions [65]. No further studies toward this goal have been conducted using concanavalin-A-bearing nanospheres but proof-of-concept was established and the potential of nanotechnology-based microbicides firstly recognized.

Without any doubt, the most successful nanotechnology-based microbicide has been so far VivaGel®, an antiviral dendrimer[1] (SPL7013) formulated as a carbomer gel, which is in an advanced stage in the development pipeline [66]. SPL7013 (Fig. 50.1) is a fourth-generation dendrimer comprising polylysine molecules attached to a central core of benzhydrylamine amide. Polylysine branches are terminally derivatized with naphthalene disulfonate groups, conferring an outer polyanionic surface that is allegedly responsible for its activity [12, 67, 68]. Unlike other dendrimers intended for therapeutic purposes, which act essentially as drug carriers, SPL7013 is the active substance; the dendrimer surface groups bind to gp120 and block viral attachment to CD4 receptors. This dendrimer also possesses high activity against HSV but a specific viral target was not described. Half-maximal effective concentration (EC_{50}) values for different HIV type 1 (HIV-1) and HIV type 2 (HIV-2) strains varied between 0.05–0.26 μM [67]. As for HSV (both type 1 and 2), values of EC_{50} were in the range of 0.03–0.12 μM and 0.23–0.37 μM for free and cell-associated virus, respectively [69]. Pre-clinical *in vivo* safety and efficacy data were considered promising [70–72] and VivaGel® is currently undergoing Phase 1/2 clinical testing for its ability to prevent the vaginal transmission of HIV-1 and HSV-2. The already available clinical results seem promising [73–75], even if a recent trial showed moderate but reversible increase in inflammatory markers after twice-daily administration of Vivagel®, thus raising some concerns about its safety [76]. In another clinical study, the incidence of low-grade related genital adverse events was higher for both Vivagel® and its placebo when compared to the "universal placebo" gel [77].

[1]The classification of dendrimers as nanosystems/nanocarriers is not universally agreed upon. For example, some experts (R. Duncan et al., *Adv. Drug Deliv. Rev.,* 2005, **57**, 2215–2237) suggest the use of the phrase "polymer therapeutics" as a more appropriate terminology. However, due to their importance and being of nanoscale size, dendrimers are usually considered as an integrant part of the field of nanomedicine (D. Peer et al. *Nature Nanotech.,* 2007, **2**, 751–760) However, note that widely used terms such as nanomedicines, nanotechnology, nanoparticles and nanotherapeutics also do not have a universally accepted nomenclature (R. Bawa (2015). What's in a Name? Defining "Nano" in the Context of Drug Delivery. In: Bawa, R., Audette, G. and Rubinstein, I. (Editors): *Handbook of Clinical Nanomedicine–Nanoparticles, Imaging, Therapy, and Clinical Applications*, Pan Stanford Publishing, Singapore)

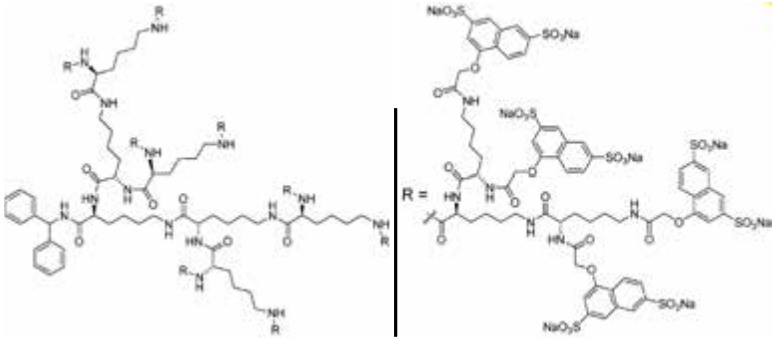

Figure 50.1 Chemical structure of SPL7013. Reprinted with permission from reference [12]. Copyright (2005) American Chemical Society.

In the meanwhile, other dendrimers are being actively developed as potential microbicides [78–82]. As an example, Chonco et al. [83] recently reported on the antiviral activity of a second-generation anionic sulfonate-91 terminated carbosilane dendrimer (2G-S16). This dendrimer (around 8 nm in diameter) presented *in vitro* antiviral activity in the micromolar range and partially blocked viral passage through monolayers of cervicovaginal cell lines. The mechanism behind antiviral activity, as determined by computational modeling, was mainly related with the interactions of the dendrimer with viral gp120. Also, 2G-S16 did not induce significant inflammatory responses both in cell-based assays and in a rabbit model, thus providing additional evidence of the potential of this dendrimer as a microbicide candidate [83].

Another type of nanoparticulate system was recently proposed by the group of Penadés [84–86], who developed oligomannose-coated gold NPs (1–2 nm in diameter) for interfering with the dendritic cell-specific intercellular adhesion molecule-3-grabbing non-integrin (DC-SIGN)-mediated binding between HIV and dendritic cells (DCs). *In vitro* results obtained by surface plasmon resonance indicated that α-1,2-mannose disaccharide-coated gold NPs were able to completely inhibit DC-SIGN/gp120 binding at levels of 10 nM, contrasting with 500 μM for α-1,2-mannose disaccharide alone. The mechanism behind this inhibition seems to be the direct competition with the virus for DC-SIGN binding

and internalization due to the ability of oligomannose-coated gold NPs to mimic *N*-linked high-mannose glycan clusters of gp120 [87]. Further, significantly higher *in vitro* inhibition of HIV-1 binding to DC-SIGN expressing cells and *trans*-infection of T cells by α-1,2-mannose disaccharide-coated gold NPs was observed as compared to the free disaccharide (100% inhibition was achieved at 115 nM and 2.2 mM, respectively) [85]. Besides other variations in oligomannose residues [86, 87], the same group also found interesting results for gold NPs bearing sulfate-ended ligands at their surface [88]. In this case, HIV inhibition resulted from direct interaction of sulfate groups with viral gp120, which was higher for NPs than for the free sulfate-ended ligands. Another nanosystem sharing the same mechanism of action, polyvinylpyrrolidone (PVP)-coated silver NPs (30–50 nm), was proposed by Lara et al. [89]. These NPs were able to provide protection against both cell-free and cell-associated HIV in human cervical mucosae explants. NPs seemed to be able to further inhibit other stages of the virus life cycle after cell entry, namely by reducing reverse transcription, proviral transcription and/or interacting with other viral proteins [90]. In a subsequent study by the same group, PVP-coated silver NPs significantly increased the *in vitro* potency of different anti-HIV neutralizing antibodies against cell-associated HIV-1 infection [91]. Taken together, the above examples seem to illustrate well that the high surface area provided by NPs is able to maximize the number of available molecules to interact with targets, namely DC-SIGN or gp120. However, further investigation is required (e.g., safety studies) in order to fully evaluate the potential of these nanosystems as microbicides.

50.5 Nanosystems Acting as Carriers for Microbicide Agents

Alongside nanosystems presenting surface moieties responsible for intrinsic activity against HIV or competing with this last for host targets, nanocarriers for microbicide agents have seen substantial development over the last years. In particular, polymeric-based systems have been preferred but others, such as those based in lipids, have also been proposed.

50.5.1 Polymeric-Based Nanocarriers

Polymeric-based NPs have been the most commonly used nanocarriers for microbicide development. In particular, those based in PLGA have been preferred owing to the well-known properties of this polymer, namely its biodegradability and biocompatibility [92]. However, other polymers have also been found useful, particularly those conferring interesting properties such as mucoadhesion or stimuli-sensitiveness. For instance, Meng et al. [93] developed tenofovir (TFV)-loaded chitosan NPs prepared by ionotropic gelation. The mucoadhesive properties of chitosan make it an interesting natural polymer in order to allow prolonged residence in the vaginal canal. Drug-loaded chitosan NPs ranging from 200–900 nm were obtained, presenting low *in vitro* toxicity to vaginal epithelial cells and *Lactobacillus crispatus*. However, relatively low values of drug association efficiency (no more than 20%) and drug loading (equal or less than 1.1%) were obtained, even when the aqueous phase was replaced by a mixture of water and ethanol in equal parts. Indeed, TFV is highly water soluble (log P = −1.6), making it a tough drug to incorporate into NPs with sufficient percentages of association efficiency when using water-based techniques. Besides allowing a mild increase in drug association efficiency, the use of ethanol also yielded larger particles (900 nm), which presented decreased mucoadhesive potential than smaller ones (200–270 nm) [93]. In the same line of work, Belletti et al. [94] proposed blends of chitosan and PLGA for increasing the association efficiency of TFV but results were not significantly better. Also, one point of concern of using chitosan in microbicide formulations is related to its well-recognized ability to open tight junctions and increase permeability [95]; the impact of this effect on the transmission of HIV and other pathogens is unknown but should be taken in consideration before regarding chitosan as a component of microbicides.

Another interesting nanocarrier system for TFV was proposed by Zhang et al. [96] and comprised the use of both PLGA (25%) and methacrylic acid/methyl methacrylate copolymer (Eudragit®S 100; 75%). NPs (300–400 nm) were prepared by an emulsion/solvent diffusion method. Since the solubility of Eudragit® S 100 is dependent on pH (the copolymer is only soluble in aqueous media at pH values above 7), its presence allowed obtaining

pH-sensitive NPs. These were able to release around four times more TFV in the presence of a simulated semen fluid (pH 7.6) than in simulated vaginal fluid (SVF; pH 4.2). This may potentially allow increasing drug levels upon ejaculation, which is responsible for the major amount of virus deposited in the vagina during sex. NPs were also able to be taken up by vaginal epithelial and endocervical cell lines as assessed by confocal fluorescence microscopy, suggesting that increased intracellular TFV levels could be obtained. Still, low association efficiency for TFV (around 10%) was obtained. The substitution of TFV by its disoproxil fumarate salt (TDF) resulted in increased association efficiency (around 24%) and drug loading (1.2%), presumably due to the higher hydrophobicity of the last (log P = 1.25). In another study, Yoo et al. [97] further explored the use of Eudragit® S 100 for obtaining pH-sensitive NPs. They used the copolymer as the sole matrix-forming material of NPs and found that the pH-dependent release of two associated model compounds, sodium fluorescein (hydrophilic) or nile red (hydrophobic), were in line with what happened in the previous example for TFV. Another potentially interesting stimuli-sensitive matrix-forming polymer for developing microbicide drug-loaded NPs is hyaluronic acid (HA). For example, Agrahari and Youan [98] developed TFV-loaded HA-based NPs and showed that the *in vitro* release of the drug could be significantly increased in the presence of hyaluronidase, a component of human semen [99], at pH 7.1 (80% at 48 h versus 40% in the absence of the enzyme). However, the actual drug release performance of developed NPs in the presence of the biological fluid was not demonstrated [98].

Our research group has been engaged in the development of different poly(ε-caprolactone) (PCL)-based NPs for the delivery of dapivirine, a potent NNRTI and one of the most promising microbicide drugs in the development pipeline [100]. NPs were prepared by a solvent displacement method using poloxamer 338 [a triblock copolymer of poly(ethylene oxide) (PEO) and poly(propylene oxide) (PPO) (PEO-PPO-PEO)], sodium laurylsulfate (SLS) or cetyltrimethylammonium bromide (CTAB) as surface modifiers [101]. NPs exhibited diameters around 180–200 nm and zeta potential dependent on the charge of used surface modifiers. In the case of PEO-modified NPs (PEO-PCL NPs) zeta potential was still negative owing to the contribution of PCL. Association

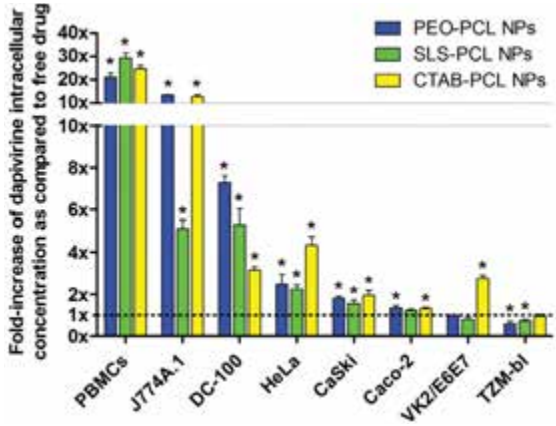

Figure 50.2 Levels of intracellular/cell associated dapivirine in different cell types as mediated by PCL-based NPs. Dotted line (1× level) indicates normalized results for free dapivirine used as a dispersion in media and was included for comparison purposes. (*) Indicates statistically significant differences when compared to the free drug for the same cell type ($p < 0.05$). PBMC, peripheral blood mononuclear cells; J774A.1, mouse macrophage cell line; DC-100, human dendritic cells; HeLa and CaSki, cervical-origin epithelial cell lines; Caco-2, colorectal-origin epithelial cell line; VK2/E6E7, vaginal-origin epithelial cell line; TZM-bl, $CD4^+/CCR5^+$ HeLa-derived cell line. Data derived from references [101, 104].

efficiency was very high (97% or higher) at a drug loading of nearly 13% (w/w) owing to the highly hydrophobic nature of dapivirine (log P = 5.3). Negatively charged systems (PEO-PCL and SLS-PCL NPs) were shown stable up to at least one year when stored at different temperatures (5–40°C) in aqueous dispersion; conversely, CTAB-PCL NPs (positively charged) showed colloidal instability that was dependent on storage temperature [102]. All NPs were shown to present sub-diffusive transport in a SVF containing 1.5% (w/v) mucin, as assessed by high-resolution fluorescence microscopy multiple particle tracking (MPT), but the degree of diffusion impairment was dependent on pH [103]. For instance, negatively charged NPs were around twice more mobile at pH values of 7.0 than at pH 4.2. In the case of CTAB-PCL NPs, entrapment in SVF was significantly higher and increased with pH. We also observed that NPs interacted differently with diverse cell types, allowing for differentiated

delivery of the drug to these last. In general, NPs allowed for enhanced *in vitro* intracellular/cell-associated levels of dapivirine in different immune cells, while there was a trend for similar outcome in cells of epithelial origin when compared to results for the free drug (Fig. 50.2) [101, 104]. The observed passive targeted delivery to immune cells was probably associated with the phagocytic nature of these last. In the case of CTAB-PCL NPs, electrostatic interactions of positively charged particles with negatively charged cell membranes may justify the generally higher drug levels obtained for epithelial cells as compared to PEO-PCL and SLS-PCL NPs.

Further, the *in vitro* ARV activity of dapivirine was maintained or moderately enhanced when the drug was included in NPs [101]. More important, the selectivity index values for drug-loaded, negatively charged NPs were increased as compared to dapivirine alone (approximately 10–50-fold) owing to their generally more favorable cytotoxicity profile. Presumably, sustained release from NPs was able to provide enough intracellular concentrations of free drug for inhibiting viral reverse transcription, while preventing peak levels thus causing reduced toxicity. In the case of CTAB-PCL NPs, unacceptable toxicity of the system limited its usefulness as a nanocarrier for dapivirine. In all cases, NPs did not induce pro-inflammatory response as assessed by the amounts of interleukin (IL)-1β, IL-6, IL-8 released by CaSki, VK2/E6E7 and Caco-2 cells incubated with NPs [104]. NPs were able to penetrate vaginal and rectal pig mucosae *in vitro* (Fig. 50.3) and modulate differently the permeability of dapivirine either in cell monolayer models and pig mucosae: in general, CTAB-PCL NPs enhanced, PEO-PCL NPs reduced and SLS-PCL did not affect drug permeability [104]. High and moderate toxicity for CTAB-PCL and SLS-PCL NPs, respectively, was confirmed by histological, viability and lactate dehydrogenase release analysis from pig mucosae. No *in vitro* toxicity issues were identified for PEO-PCL NPs. Because of the overall potential properties of dapivirine-loaded PEO-PCL NPs, we proceeded with PK and safety studies in a mouse model [105]. It was found that this particular nanocarrier was able to distribute throughout the lower genital tract of mice and penetrate vaginal and uterine mucosaee upon vaginal delivery of NPs dispersed in phosphate buffered saline (PBS). Also, increased drug levels at the lower genital tract and moderate reduction of the systemic

exposure of dapivirine were observed as compared to dapivirine in PBS suspension. PEO-PCL NPs were shown safe upon 14 days of daily vaginal administration [105]. Overall, adequate surface engineering of NPs may dramatically determine their activity, toxicity and biological fate, and aid in the selection of potentially useful nanocarriers for promising microbicide drugs, in this particular case, dapivirine.

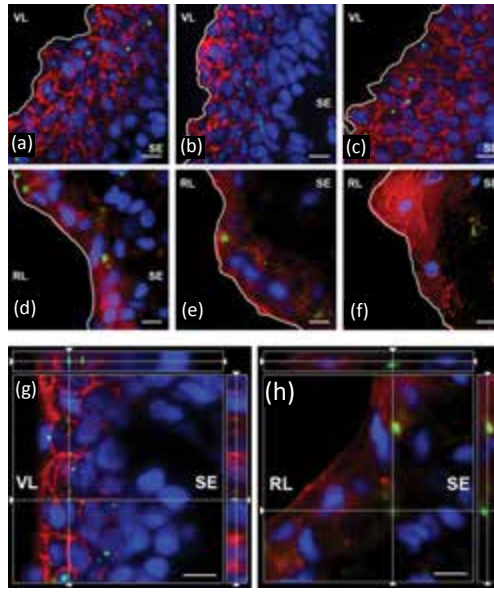

Figure 50.3 Evidence of the penetration of fluorescent rhodamine-123-labeled PCL (rhod-123-PCL) NPs in pig vaginal and rectal mucosae. Fluorescent microscopy images of pig (a–c) vaginal and (d–f) rectal mucosae after 2 h incubation with (a and d) PEO-rhod-123-PCL NPs, (b and e) SLS-rhod-123-PCL NPs, and (c and f) CTAB-rhod-123-PCL NPs. Detail fluorescent confocal microscopy images of pig (g) vaginal and (h) rectal mucosae after 2 h incubation with PEO-rhod-123-PCL NPs. In all cases, green, blue and red signals are from rhod-123-PCL (NPs), Hoechst 33342 (DNA) and WGA-Alexa Fluor® 594 conjugate (sialic acid/*N*-acetylglucosaminyl residues at cell membranes/mucin), respectively. White lining in a–f depicts the mucosal tissue surface. Scale bar = 10 μm. The *z*-axis range is 6 μm and 16 μm for (g) vaginal and (h) rectal mucosa, respectively. Legend: VL, vaginal lumen; RL, rectal lumen; SE, sub-epithelium. Reprinted with permission from [104]. Copyright (2013) American Chemical Society.

Contrasting with the previous reports in which a single drug was incorporated into NPs, Date et al. [106] developed a single PLGA-based nanocarrier for raltegravir and efavirenz. Developed system presented diameter of roughly 80 nm and association efficiencies of around 56% for raltegravir and 98% for efavirenz. When tested for activity in a TZM-bl cell setting, NPs presented 90% effective concentration (EC_{90}) values slightly lower than those for the drugs in solution (90 and 144 ng/mL, respectively). Moreover, intracellular levels in HeLa cells (cervical origin) were kept above the EC_{90} during 4 days and 14 days for raltegravir and efavirenz, respectively, with no significant cytotoxicity being observed. Further, NPs were incorporated in poloxamer-based thermosensitive gels; *in vitro* experiments demonstrated that nanosystems were able to be released from gels and taken up by an underlying HeLa cell lining, which simulated the cervicovaginal epithelium, within 30 min.

Different biopharmaceuticals have been proposed as microbicide compounds but their activity may be substantially reduced in the vaginal environment owing to enzymatic cleavage and physicochemical instability. Moreover, poor penetration of epithelial tissues may limit the usefulness of these bioactive molecules. Incorporation into nanocarriers may help minimize these issues. For instance, Ham et al. [15] studied the feasibility of PLGA NPs to encapsulate a RANTES analogue, PSC-RANTES (≈8 kDa). This protein is able to inhibit R5-tropic HIV-1 infection of Langerhans cells and T cells by blockage and sequestration (internalization) of the CCR5 co-receptor [107, 108]. Despite showing potent *in vitro* activity, *in vivo* experiments in rhesus macaques (*Macaca mulatta*) demonstrated that the required dose of PSC-RANTES for protection against SHIV was much higher than in cell models [109]. The strategy adopted by Ham et al. [15] envisioned the abbreviation of poor vaginal epithelial penetration of this protein, while allowing targeting CCR5-expressing cells, thus resolving poor distribution and retention issues. Obtained results showed that NPs (around 260 nm) loaded with biotinylated PSC-RANTES (used in substitution of PSC-RANTES to allow tissue localization by streptavidin-FITC staining) were able to penetrate human ectocervical tissues *in vitro*. Moreover, NPs seemed to mediate drug transfer to the deeper layers of the epithelium, immediately above the lamina propria where $CCR5^+$ cells are predominantly

located. Indeed, ectocervical/vaginal basal epithelia may be an optimal target site for NPs containing ARV agents as this site is not submitted to coital shearing felt in the vaginal lumen, which promotes leakage of microbicide products. Moreover, the basal epithelial layer is not located too deeply in the mucosa, which may allow drug diffusion to the nearby ectocervical/vaginal epithelia but probably not to the nearest blood vessels of the lamina propria in considerable amounts. The same group further observed that mucosal uptake of PSC-RANTES associated with NPs was nearly fivefold higher when compared to unformulated PSC-RANTES [15]. Also, association to nanosystems did not reduce the antiviral activity of PSC-RANTES as assessed by a TZM-bl cell-based assay. Despite these promising data, further *in vivo* testing is required in order to attest the real value of this nanocarrier.

Recent achievements and potential of RNA interference as a strategy for medical intervention raised interest in the field of microbicides [110, 111] and a few examples of nano-sized systems for delivering small interfering RNA (siRNA) have been described. For instance, Eszterhas et al. [112] studied the feasibility of a commercially available cationic polymeric transfection agent (INTERFERin®) for intravaginal delivery of siRNA targeting the expression of CD4 and CCR5. The obtained polyplexes (45–60 nm) provided effective silencing in human endometrium, endocervix and ectocervix explants and partially prevented the infection by HIV-1. Polyplexes also induced the release of interferon alpha (INF-α) which may potentially contribute to viral inactivation and reduce the risk of vaginal HIV-1 transmission [113]. Even if no particular mechanism was advance for the upregulation of IFN-α expression, results seem to indicate that the use of INTERFERin® is involved [112]. Moreover, gene silencing was also observed in the genital tract of mice after intrauterine instillation of a polyplex containing murine-specific CD4-siRNA. Overall, this combined approach seems to be interesting but further data is required, in particular related with the safety of polyplexes.

Indeed, one of the main issues related with the delivery of genetic material is the toxicity of most of the currently used delivery agents required for efficient cell transfection. An investigation by the group of W. Mark Saltzman [16] highlighted the favorable behavior that PLGA NPs have *in vivo* with the aim of developing

siRNA-based microbicides. These researchers developed 100–300 nm PLGA NPs containing siRNA targeted either against *mapk1* (encoding for mitogen-activated protein kinase 1, MAPK1) or *egfp* (encoding for enhanced green fluorescence protein, EGFP). NPs were prepared by a double-emulsion/solvent evaporation method, using poly(vinyl alcohol) (PVA) as stabilizer. Spermidine was also included in order to pre-complex siRNA thus increasing the amount of NP-associated genetic material. Of particular notice, the complex spermidine-siRNA was not able to be taken up *in vitro* by different cell lines (HepG2 hepatocytes and HeLa cervical cells), requiring association with PLGA-NPs to be delivered to the cell interior and lead to gene silencing. *In vitro* testing showed that optimized NPs were able to release siRNA in a sustained fashion for at least 30 days at pH 5.0 and 7.4, which seemed to correlate well with prolonged *mapk1* silencing in HepG2 cell cultures (over 14 days). *In vivo* studies in mice using multiphoton microscopy showed that coumarine-6-loaded PLGA NPs were able to distribute throughout the genital tract (vagina, cervix, and uterine horns), penetrate deeply the epithelium, and retain in the tissue for at least 7 days. Moreover, studies in a transgenic GFP mouse model showed complete gene knockdown in the genital tract up to around 2 weeks after vaginal instillation of NPs containing siRNA against *egfp*. Also, owing to the biocompatible nature of PLGA, NPs were not irritating or inflammatory contrasting with siRNA lipoplexes obtained using a mixture of commercially available cationic lipids (Lipofectamine™) [16].

In a subsequent study by this last group [114], genital protection from HSV-2 challenge was achieved after vaginal instillation of siRNA-loaded PLGA NPs in mice. Gene silencing focused on nectin-1, a host cell protein involved in viral cell binding and subsequent spreading. NPs (160–190 nm) were obtained in a similar manner to the previous study. Various spermidine:siRNA ratios were tested, and 3:1 was found optimal in terms of association and *in vitro* sustained release. Survival of mice challenged with a lethal dose of HSV-2 was increase from approximately 0% at 9 days in untreated animals to 60% at 30 days in those receiving NPs in three applications (one day and 3 h before, and 4 h after viral challenge). Results for NPs were related to gene expression knockdown *in vivo* and found comparable to those of siRNA lipoplexes and cholesterol conjugates. However, NPs were shown safe, contrasting

with lipoplexes and cholesterol conjugates which induced mild inflammatory responses. The results from Saltzman and colleagues [16, 114] combined seem to substantiate that PLGA NPs may confer prolonged action to incorporated siRNA and potentially other labile molecules owing to sustained drug-release and intracellular delivery. PLGA nanocarriers also seem to be safer for vaginal delivery than lipoplexes or polyplexes obtained using commercially available products [115].

Recently, polymeric nanofibers (200–700 nm) and microfibers (1.5–3.4 μm) have been proposed by Ball et al. [116] as a dual approach for preventing vaginal HIV-1/HSV-2 transmission and pregnancy. Drug-eluting fibers were obtaining by electrospinning PLLA/PEO or PLLA/poly(D,L-lactide) (PDLA) mixtures, or PCL with different active compounds such as anti-HIV (maraviroc and zidovudine), anti-HSV (acyclovir) and contraceptive [methyl-β-cyclodextrin, glycerol monolaureate, and iron(II) D-gluconate] agents. Upon collection in tampon-shaped molds, fiber meshes presented a microporous structure (mesh size down to 10 μm). This pore size was found able to physically entrap spermatozoids *in vitro* thus providing a potential additional mechanism of contraception. Fiber meshes were also shown able to sustain drug release in a SVF (pH 4.2) for several days even if burst effect could not be completely avoided. Nanofibers were shown safe *in vitro* and, when tested in mice, provided complete coating of the vaginal epithelium after 30 min from administration. Also Huang, Soenen et al. [117] developed nanofibers based on cellulose acetate phthalate (CAP) for the delivery of etravirine and TDF. Nanofibers were obtained by electrospinning and presented diameters of 500–800 nm. Interestingly, nanofibers were pH-sensitive, being insoluble in SVF. However, nanofibers dissolved rapidly when human semen was mixed with SVF because of the increase in pH. This behavior resulted in the fast release of incorporated drugs, which can potentially become available at higher concentrations upon ejaculation. The incorporation of other drug classes, namely spermicides, was not tested but it seems clear that the pH-responsiveness of CAP nanofibers may allow the use of this platform for contraceptive purposes. Moreover, plain nanofibers presented antiviral activity (EC_{50} = 0.05 mg/mL) and low cytotoxicity to TZM-bl and vaginal VK2/E6E7 cells. Overall, nanofiber-based approaches may provide interesting platforms for obtaining

multipurpose prevention (and potentially treatment) products for vaginal administration.

50.5.2 Lipid-Based Nanocarriers

Besides polymer-based nanocarriers, the usefulness of a few other nanosystems has been explored for delivering microbicide agents. Liposomes have been widely developed for vaginal delivery of different molecules [118–124], thus making these immediate potential carrier candidates for microbicide compounds. For example, Kish-Catalone et al. [125, 126] developed a new synthetic analogue of RANTES, termed −2 RANTES, and tested the ability of commercially available 200–700 nm paucilamellar non-phospholipidic liposomes (Novasome®) to incorporate this peptide drug. Loaded systems were able to release −2 RANTES *in vitro* in a dose-dependent manner over a time frame of 30–120 min, while retaining its antiviral activity [125]. Also, local safety studies performed in two rodent models (murine and rabbit) showed no evidence of cervicovaginal toxicity as assessed by histological analysis. This group further evaluated the efficacy of −2 RANTES-loaded liposomes in preventing infection of cynomolgus macaques (*Macaca fascicularis*) by R5-tropic SHIV [126]. A dispersion of liposomes in PBS was administered intravaginally at 30–45 min before viral challenge. Surprisingly, both blank and drug-loaded liposomes, exhibited considerable prophylactic effect against infection, contrasting with the poor results of −2 RANTES in PBS. Although unclear, the authors of this study suggest that a possible explanation for protection resides in the physicochemical properties of used nanosystems (e.g., surfactant properties of its components), which can provide a physical barrier above the epithelium lining that interacts and inactivates virions. Indeed, studies by others sustain that liposomes may be able to bind HIV-1 and modulate infectiveness depending on composition [127, 128].

A series of papers by different groups integrating an international consortium reported on hydrogenated lecithin/cholesterol-based liposomes for delivering the NNRTI drug MC1220 [129–131]. This formulation strategy was justified with the low aqueous solubility of the drug (log P = 2.76). Gels containing 0.1% MC1220 associated to liposomes (smaller than 1 μm) were found safe for vaginal administration in a rabbit model, and

provided faster and increased permeability when compared to a microemulsion [130]. Further, partial protection against SHIV was achieved in *Macaca mulatta* when liposomes were delivered in a gel formulation (0.5% and 1.5% MC1220 concentrations), with no apparent signs of toxicity [129–131]. Similarly, Wang et al. [132] explored the ability of octylglycerol-containing, phosphatidyl choline-based liposomes incorporated in gel formulations to be used as microbicide products. They showed that liposomes containing octylglycerol, an antimicrobial monoglyceride, were able to inhibit different sexually transmitted pathogens (*Neisseria gonorrhoeae*, HSV-2, and HIV-1) at lower concentrations than octylglycerol dispersed in gels. Additionally, liposome-containing gels were proved safe in human vaginal explants and in a macaque model, therefore showing potential for further development.

Ramanathan et al. [133] have recently proposed nanolipogels (around 200 nm), comprising liposomes with a hydrogel core, for the delivery of hydrophilic ARV compounds. Nanosystems were obtained by rehydration of a lipid film with an aqueous solution of hydrogel monomers, cross-linker, photo-initiator, and a model drug (zidovudine). Upon vesicle formation and extrusion, core gelation was induced by UV light. Of particular interest, these systems seem to provide increased drug release of zidovudine as compared to liposomes with similar size and composition (except for the hydrogel core). Also, drug release could be modulated and drug association increased by varying the extension of core cross-linking. Nanolipogels were readily taken up *in vitro* by bone marrow-derived DCs and showed comparable anti-HIV-1 activity to unformulated zidovudine in a TZM-bl cell assay. Even if these preliminary data seem promising, more information is required in order to assess the real potential of nanolipogels.

Solid lipid nanoparticles (SLNs) have shown great potential as carriers for many active molecules [134] and their use for the incorporation of TFV in the context of microbicide development was recently explored [135]. SLNs were prepared by a phase-inversion process and optimized for size using a Box-Behnken experimental design. Poly(acrylic acid) and bovine serum albumin were used as surface stabilizers and additional layers of polylysine and heparin were successively added by a layer-by-layer process and taking advantage of the electrostatic interaction between

components. The inclusion of polylysine and heparin in SLNs was hypothesized as enhancing the ability of nanocarriers to be taken up by epithelial cells. However, no experimental evidence was provided in order to support this claim. Hydrodynamic diameter of optimized SLNs was 154 nm but TFV association efficiency was poor (around 8%). SLNs were not cytotoxic to VK2/E6E7 vaginal epithelial cells up to concentrations of 900 μg/mL. Overall, the utility of these SLNs is not clear and extensive work is still required.

50.6 Mucoadhesive or Mucus-Penetrating Microbicide Nanosystems?

Knowledge on the potential interactions between nanosystems and mucus/mucosal fluids seems to be essential when discussing the use of nanotechnology-based microbicides. Traditionally, mucoadhesion is regarded as a valuable characteristic when considering mucosal drug delivery. Main advocated advantages are: (i) the possibility of prolonged in loco residence and intimate contact with mucosae, which invariably allows for enhanced delivery of drugs to the underlying tissues, (ii) the opportunity for sustained/prolonged drug release, and (iii) the protection of labile drugs. Mucoadhesive delivery platforms lead to increased drug concentrations at adhesion sites thus contributing for local targeted drug delivery [136]. Study of mucoadhesion phenomena at the nanoscale has deserved the attention of different investigators [137] and the basic principles by which mucoadhesive molecular interactions of nanoparticulates occur are the same as for conventional drug dosage forms (e.g., gels or tablets). Upon intimate contact between the surface of nanosystems and mucin chains composing mucus or the epithelial glycocalyx, interfacial forces contribute to the establishment of multiple adhesive bonds (mainly hydrogen bonding, electrostatic attraction, hydrophobic interaction and physical entanglement) [138, 139]. Therefore, the use of materials that promote adhesive bonding has been the main strategy for increasing mucoadhesion of nanosystems [140, 141]. When colloid systems are involved, counteracting repulsive forces are thought to be less prevalent in strength and number than

adhesive ones, thus resulting in long-lasting adhesive bonding after initial consolidation of adhesion [142].

The combination of size and surface properties has been shown to substantially influence the interactions between nanosystems and mucus (Fig. 50.4). Surface chemistry of nanosystems determines attraction/repulsion with mucin fibers, while size controls their ability to "fit" within the pores of the mucin mesh. Although not fully understood, the general mucus structure can be understood as a heterogeneous and complex system of differently sized intercommunicating channels delimited by mucin fibers and filled with aqueous fluid [143, 144]. In cases where particles fail to fit in the submicron range, they will tend to adhere only at the top layers and not in the bulk of mucus owing to steric hindrance related to limited channel diameters as created by the mucin mesh [145]. As a consequence, this failure to cross the mucus barrier will largely impair the ability of microparticles to directly deliver their payload to epithelial surfaces.

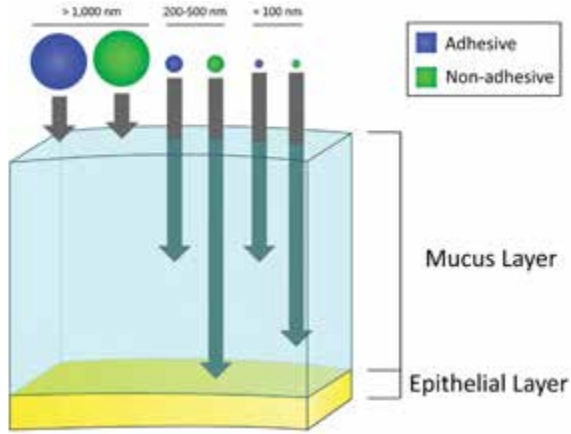

Figure 50.4 Schematic representation of the relative ability of particles to diffuse through mucus, considering their size and surface properties (i.e., engineered to interact or not with mucin). Reprinted from [19] with permission from John Wiley & Sons (Copyright 2011).

In the specific case of cervicovaginal fluids, studies using MPT indicate that NPs as large as 500 nm are able to fit the mucus mesh [13]. The diffusion rate of NPs is then governed by

adhesive bonding with mucin fibers and their different size ranges. It seems logical to assume that the stronger and the larger the number of adhesive bonds established between mucin and the surface of nanosystems, the greater the impairment to diffusion will be. Alongside, nanosystems with larger diameters will present limited ability to diffuse freely since these may only move through larger diameter channels. This has been recently confirmed experimentally by Wang et al. [146] by tracking the transport of adherent and non-adherent polymeric NPs through human cervicovaginal fluid. However, the same group also observed that smaller non-adherent NPs (around 100 nm) present higher hindrance than larger ones (200–500 nm) [13]. This fact may be attributed to the heterogeneous structure of mucus; smaller NPs are able to diffuse through smaller caliber channels, which often results in tortuous and dead-end paths, while larger NPs may only diffuse through wider and otherwise unhindered canals. Therefore, retention of nanoparticulates may not be exclusively or even directly related with the establishment of adhesive interactions, rather resulting from physical entrapment within the mucus channel network.

Despite its importance, interactions with mucosal fluids have been frequently neglected in the particular case of nanotechnology-based microbicides. When considering such issue, several questions arise: How do microbicide nanosystems interact with the mucus layer? Can physiological changes in the vaginal/rectal milieu influence these interactions? Do we require mucoadhesive or mucus-inert (also commonly referred to as mucus-penetrating) nanotechnology-based microbicides? There seems to be no straight answers as these questions should be analyzed on a case-by-case basis and enlightened in view of multiple factors. Even so, mucoadhesive nanosystems might prolong in loco residence and provide higher resistance to leakage during sexual intercourse, while allowing for sustained tissue concentrations of ARV drugs in the case where nanocarriers are considered. Conversely, adhesive systems may disturb the mucus barrier, limit distribution throughout the vaginal/rectal tracts after administration, increase systemic drug exposure, and restrain the amount of surface moieties available for interaction with the virus or cell membranes. Considering the mechanism of action of microbicides,

nanosystems with intrinsic anti-HIV activity may find in mucoadhesion a double-edged sword. On one hand, retention in the vaginal/rectal lumen increases with mucoadhesion, while possible tissue uptake and possible systemic exposure is diminished owing to a barrier effect; on the other hand, interactions with mucin may decrease the ability of nanosystems to interact with pathogens, since surface groups responsible for activity are not completely available, thus potentially reducing efficacy. However, the influence of mucin interactions on the efficacy of this type of nanosystems has been often disregarded in available studies but the possibility has not been completely discarded [147]. Also, evenly distribution through the vagina and rectum may be diminished for mucoadhesive nanosystems owing to their decreased ability to diffuse, thus depending on fluid dynamics of mucus to spread.

As for microbicide drug nanocarriers, there seems to be evidence that non-mucoadhesive or, at least, partially mucus diffusive systems are beneficial [103, 148, 149]. Mucus-penetrating nanocarriers might provide interesting platforms for suitable drug distribution throughout the mucosa, allow for direct contact with the underlying epithelium, and enhance interactions with cells and uptake or intracellular delivery of incorporated drugs. For example, short-chain poly(ethylene glycol) (PEG)-modified liposomes (200–350 nm) have been tested as mucus-penetrating carriers for siRNA to be delivered intravaginally [150]. In particular, PEG-liposomes were complexed with a model siRNA targeting lamin A/C protein expression. Obtained lipoplexes were further incorporated into alginate scaffolds, allowing for sustained and enhanced gene silencing in mice as compared to siRNA complexes with non-PEGylated dioleoyl trimethylammonium propane (DOTAP)-based liposomes. Enhanced diffusion of PEG-modified liposomes through mucus was presumably responsible for improved performance. In another study, Ensign et al. [151] demonstrated the enhanced performance of acyclovir monophosphate-loaded, PEG-modified NPs in protecting mice from HSV-2 infection after vaginal administration, when compared to the drug in solution (53% versus 16% of mice protected). A hydroxyethylcellulose (HEC)-based gel was used as a dosage form for NPs. Results were correlated with enhanced distribution and drug coverage over the vaginal and

ectocervical epithelium of PEG-modified NPs when compared to non-PEGylated ones. PEG-modification led to increased retention of mucus-penetrating particles owing to their rapid diffusion through vaginal fluid into mucosal folds. The same group also observed in a subsequent study that the use of liquid vehicles of decreasing tonicity for delivering PEG-modified NPs improved the vaginal distribution and retention of nanosystems in a mouse model [152]. For example, around 80% of 100 nm mucus-penetrating NPs were recovered from the vagina 10 min post-administration when delivered in water, contrasting with values of only near 20% when PBS was used. In both cases, animals were conscious and under no restrictive measures throughout experiments. Also, fluorescence imaging of vaginal cryosections indicated that NPs quickly diffused toward the mucosal surface (within a few minutes) and had a homogeneous distribution throughout the vagina, including *rugae*, when administered in water; in contrast, a heterogeneous distribution of NPs with poor vaginal fold penetration was apparent in the case of PBS use (Fig. 50.5). These observations are presumably associated with enhanced trafficking of NPs owing to osmotically induced advection toward the mucosae as verified by using a hypotonic vehicle.

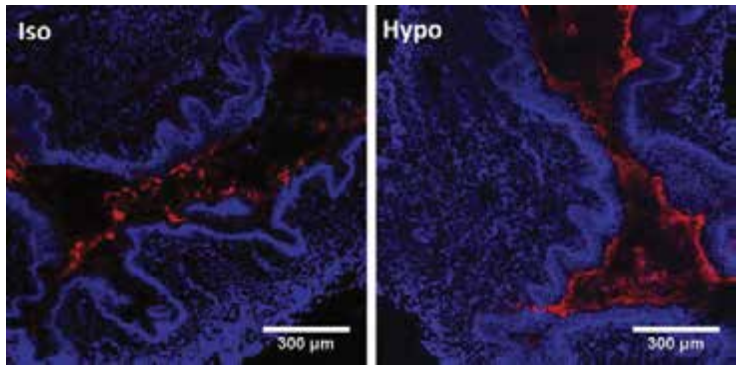

Figure 50.5 Vaginal distribution of 100 nm fluorescent mucus-penetrating NPs (red) administered in isotonic (Iso; PBS) or hypotonic (Hypo; water) aqueous fluids. Mouse tissues were collected and frozen immediately after administration of NPs and cryosections obtained. Cell nuclei were stained blue with DAPI. Reprinted from [152], Copyright (2013), with permission from Elsevier.

Most information regarding the adhesion of nanosystems have been so far obtained by using native human cervicovaginal mucus or model fluids mimicking a non-sexual scenario. The influence of the chain of events resulting from sexual stimulation and vaginal penetration/ejaculation on the mucoadhesive behavior of nanosystems is not clear. However, these environmental changes may well provide a window of opportunity for fine tuning "intelligent" microbicide nanosystems that can present variable mucoadhesive behavior. For instance, the variation of the vaginal pH from acidic to neutral or mildly alkaline upon ejaculation may be used for shifting the adhesive behavior of nanoparticulate systems by using pH-sensitive polymers as surface modifiers. Indeed, this type of pH-dependent adhesion/diffusion behavior in cervicovaginal fluids is thought to influence the infectivity of HIV [153]. However, further work is required to explore this possibility.

Overall, choosing between mucoadhesive or non-mucoadhesive nanotechnology-based systems for developing microbicides is not an easy task and requires thorough judgment of what is required for each specific drug nanocarrier or active nanosystem. A case-by-case analysis is advised. Golden rule may well be to modulate mucoadhesion as though required while maintaining or minimizing interference with the mucus fluid barrier. In fact, interference with the barrier properties of mucus fluids should be limited as these last constitute an important defense against different pathogens, namely HIV-1 or HSV-2 [154, 155]. When mucoadhesive interactions are established, rearrangements of the mucus structure are possible and have been demonstrated for positively charged NPs [156] or when fairly high amounts of PS NPs are used [157], thus recommending caution when mucoadhesion is a goal. In case interferences cannot be avoided (or eventually deemed advantageous), care should be taken in assuring that increased risk of infection is not observed. Finally, different strategies may be used in order to tailor the mucoadhesive behavior of nanosystems. Figure 50.6 provides a summary of the main approaches for modulating mucoadhesion based on size and surface chemistry. Their detailed discussion is out of the scope of this chapter; however, previous reviews by our group provide

thorough information on the subject, as well as on techniques used for determining the mucoadhesive potential of nanosystems [19, 137].

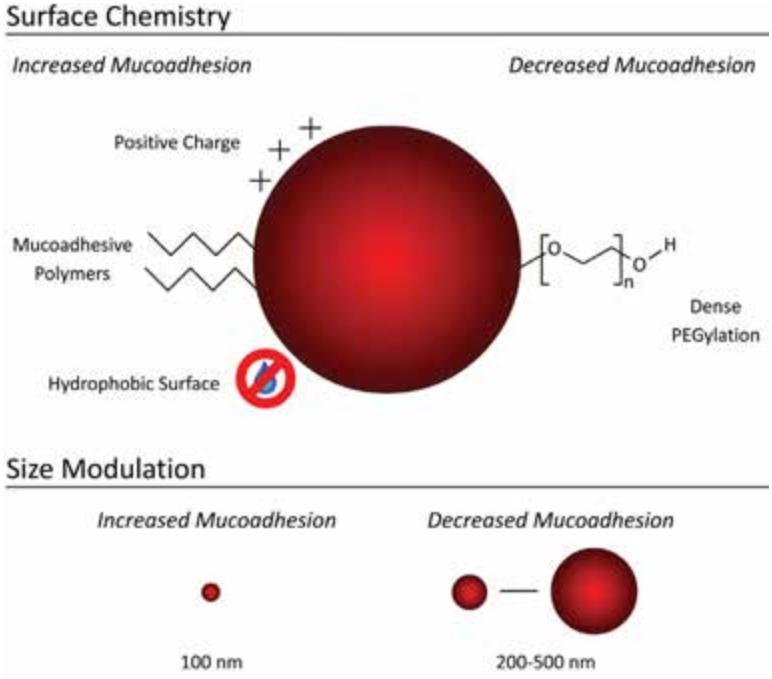

Figure 50.6 Summary of strategies used for engineering the mucoadhesive behavior of nanosystems based on surface chemistry and size modulation. Reprinted from [19] with permission from John Wiley & Sons (Copyright 2011).

50.7 Nanotechnology-Based Rectal Microbicides

As mentioned previously, efforts toward the development of specific rectal nanotechnology-based microbicides have been nearly non-existing [20]. Even if the studies conducted with VivaGel® focused mostly on its vaginal use, some data has also been generated for potential rectal use. *In vitro* studies using a 5% SPL7013 gel showed that the formulation presented reduced toxicity to the

Caco-2 colorectal cell line [158]. Observed cytotoxicity was mainly associated to the excipients of the gel rather than SPL7013 itself. Moreover, the integrity of Caco-2 cell monolayers was not compromised by the dendrimer-containing gel; the formulation was further able to prevent the transfer of HIV-1 across monolayers and the infection of peripheral blood mononuclear cells (PBMCs). A subsequent study [159] showed that the 5% SPL7013 gel induced epithelial shedding in human colorectal explants but without damaging the lamina propria. Even if these observations raise some concern, the formulation was able to reduce over 85% the viral infection of explants. In an *in vivo* animal study, the safety of a 3% SPL7013 gel was evaluated in pigtailed macaques (*Macaca nemestrina*) upon trice daily rectal application for four days [72]. The choice for testing a reduced concentration gel was based on previous observations of toxicity at 5% concentration upon vaginal administration in the same model. During the study no significant differences in terms of pH, normal microbiota, and epithelial shedding were observed as compared to the placebo gel. Overall, the dendrimer-containing gel was well tolerated even if long-term safety studies are required in order to confirm these results.

In the particular case of nanocarriers, our group proceeded with preliminary studies on the potential use of dapivirine-loaded PCL NPs (described above) for rectal delivery [101, 104]. In particular, PEO-PCL NPs were shown safer than the free drug when tested *in vitro* with the Caco-2 colorectal cell line. At the same time, permeability of dapivirine through Caco-2 cell monolayers and pig rectal mucosal tissue *ex vivo* was moderately reduced as compared to dapivirine in suspension. For example, the apparent permeability coefficient (P_{app}) of dapivirine was less than half when PEO-PCL NPs were used (0.9×10^{-6} cm $\cdot$ s^{-1} versus 2.2×10^{-6} cm $\cdot$ s^{-1} for free dapivirine); also, tissue accumulation of dapivirine was enhanced for NPs (around 10 times). Combined, these results suggested that the incorporation of dapivirine in PEO-PCL NPs may provide an interesting strategy for increasing drug levels at the rectal mucosae while reducing its systemic exposure. Even if promising, these preliminary results require further work in order to assess the real value of this dapivirine nanocarrier in protecting from rectal transmission of HIV.

50.8 Conclusions and Future Perspectives

Nanotechnology is progressively offering a wider range of solutions for some of the most challenging needs in the biomedical field. This may well be the case of microbicides and different efforts have been undertaken over recent years. So far, generated data are promising, but we still seem to be far away from a tangible nanotechnology-based microbicide product. Despite the promising results of VivaGel®, its development for the prevention of HIV and HSV transmission appears to be on hold. Nanocarriers for potent ARV compounds, particularly those polymeric in nature, are the new trend in the field. Mucus-penetrating nanocarriers may be particularly advantageous. However, definitive animal efficacy studies are required in order to categorically establish nanotechnology-based anti-HIV systems as forefront solutions toward the achievement of an effective microbicide product. Also, "smart" nanosystems that can specifically recognize HIV-target cells and/or the virus itself, modulate its action on a stimuli-sensitive fashion, and promote enhanced mucosal residence may prove to be interesting approaches.

Despite all the work done so far, there are several questions that need to be answered. For example, nanosystems require vehicles such as gels, films, or even IVRs in order to be conveniently administered in the vagina and/or rectum; but which are the most suitable and how will this additional formulation step affect the performance of nanosystems? After vaginal delivery, what is the fate of nanosystems and which long-term effects, if any, are we facing? This last question seems to be of particular importance because of potential toxicity concerns related with the use of microbicides. Also, production and affordability of nanotechnology-based microbicides may be a problematic issue. Scale-up of nanomedicines presents substantial challenges but recent successful marketing of biomedical nanotechnology-based products provides encouraging signals about feasibility [160]. Commonly advocated prices of US $1 or less for each microbicide application [161] may not be realistic for nanotechnology-based microbicides. However, potentially enhanced effectiveness, safety, and acceptability features such as those discussed above may

still justify development and use at higher prices. Public and non-governmental financial support will be essential.

Disclosures and Conflict of Interest

Dr. José das Neves acknowledges Fundação para a Ciência e a Tecnologia (FCT), Portugal, for financial support (grant SFRH/BPD/92934/2013). This work was supported by a grant from FCT (VIH/SAU/0021/2011). This chapter is a revised version of the author's chapter that appeared in *Drug Delivery and Development of Anti-HIV Microbicides*, José das Neves and Bruno Sarmento (editors), 2015, Pan Stanford Publishing, Singapore. Parts of this chapter are from review articles published by the authors' research group. Contents are re-used with kind permission from copyright owners, namely Elsevier, John Wiley & Sons, Pan Stanford Publishing Pte. Ltd., and Future Science Ltd. The authors declare that they have no conflict of interest and have no financial involvement with any organization or entity discussed in this chapter. No writing assistance was utilized in the production of this chapter and the authors have received no payment for its preparation.

Corresponding Author

Dr. José das Neves
INEB-Instituto de Engenharia Biomédica
University of Porto, Rua do Campo Alegre
823, 4150-180, Porto, Portugal
Email: j.dasneves@ineb.up.pt

About the Authors

Rute Nunes received an MSc in pharmaceutical sciences in 2013 from Instituto Superior de Ciências da Saúde-Norte, CESPU, Gandra, Portugal. She is currently a PhD student at INEB—Instituto de Engenharia Biomédica, University of Porto, Porto, Portugal, where she is conducting research work for the development of nanotechnology-based

systems for the delivery of antiretroviral drugs intended to be used as rectal anti-HIV microbicides. Her scientific interests span the fields of nanomedicine, nanotechnology-based strategies for the delivery of antiretroviral drugs, HIV/AIDS, microbicides, and rectal drug delivery.

Carole Sousa received a BSc in applied biology in 2007 and an MSc in molecular genetics in 2009, both from the University of Minho, Braga, Portugal. She has been a research fellow at the Life and Health Science Research Institute, Braga, Portugal, from 2008 to 2011 and at the Institute for Molecular and Cell Biology, Porto, Portugal, from 2011 to 2013. She is currently a PhD student at the University of Luxembourg, Luxembourg.

Bruno Sarmento received a BSc in pharmaceutical sciences in 2002 and a PhD in pharmaceutical technology in 2007, both from the University of Porto, Porto, Portugal. He is an affiliated researcher at INEB—Instituto de Engenharia Biomédica, University of Porto, and assistant professor of pharmaceutical and biopharmaceutical technology at Instituto Superior de Ciências da Saúde-Norte, CESPU, Gandra, Portugal. His current research is focused on the study of nanomedicines, namely polymer-based nanoparticles, solid lipid nanoparticles and polymeric micelles, and their application in the pharmaceutical and biomedical fields, as well as on the use of *in vitro* cell models as a tool to correlate the transport of biopharmaceuticals and nanoparticles across human intestinal mucosa. Dr. Sarmento is internationally recognized as an expert on oral delivery of biopharmaceuticals using nanomedicines. He is the author of several publications in this field, some of which are key references in the area, being a pioneer of polymeric and solid lipid nanoparticles for intestinal delivery of insulin. His work has been successfully acknowledged, with over 100 publications in less than eight years (more than 2500 citations according to Google Scholar), 3 edited books in the fields of pharmaceutical technology and nanomedicine, 26 book chapters, and more than

150 conference proceedings/abstracts. He also served as editorial board member of several international journals and evaluator of research projects from international agencies. Further, he worked as a research scientist in various scientific projects and is supervisor of PhD (more than 15) and MSc (more than 15) students, and postdoctoral investigators (3). He is also an active member of several international associations (AAPS, CRS, EUFEPS, EFSD, FIP, BRG) and collaborates in postgraduate programs at national and international levels on the fields of biotechnology and health. He has a strong list of national and international collaborations in the areas of controlled drug delivery, nanomedicine, and tissue engineering.

José das Neves received a BSc in pharmaceutical sciences in 2003, an MSc in pharmaceutical technology in 2007, and a PhD in pharmaceutical sciences in 2013, all from the University of Porto, Porto, Portugal. He was teaching assistant at the Faculty of Pharmacy, University of Porto (2005–2006), invited lecturer at the MSc course in molecular therapy at Instituto Superior de Ciências da Saúde-Norte, CESPU, Gandra, Portugal (2011 and 2012), and invited lecturer at the integrated MSc course in pharmaceutical sciences at the Faculty of Health Sciences, University of Beira Interior, Covilhã, Portugal (2012). He was also a visiting research scientist at Northeastern University, Boston, USA, in 2009–2010 and at the Institute of Tropical Medicine, Antwerp, Belgium, in 2010. His past research activities have been based at the Faculty of Pharmacy, University of Porto, and mainly on vaginal drug delivery, nanotechnology-based drug carriers, and biomaterials. Dr. das Neves joined INEB—Instituto de Engenharia Biomédica, University of Porto in 2014, where he is currently postdoctoral investigator. He is also a researcher at CESPU, Instituto de Investigação e Formação Avançada em Ciências e Tecnologias da Saúde, Gandra, Portugal. His research focuses specifically on the development of nanocarrier systems for the vaginal and rectal delivery of antiretroviral drugs to be used in the development of anti-HIV microbicides. He is the author of over 30 peer-reviewed articles, book chapters, and co-editor of three scientific books.

References

1. Farokhzad, O. C., Langer, R. (2009). Impact of nanotechnology on drug delivery. *ACS Nano*, **3**, 16–20.
2. Riehemann, K., Schneider, S. W., Luger, T. A., Godin, B., Ferrari, M., Fuchs, H. (2009). Nanomedicine—challenge and perspectives. *Angew. Chem. Int. Ed. Engl.*, **48**, 872–897.
3. Kim, B. Y., Rutka, J. T., Chan, W. C. (2010). Nanomedicine. *N. Engl. J. Med.*, **363**, 2434–2443.
4. Garg, S., Tambwekar, K. R., Vermani, K., Kandarapu, R., Garg, A., Waller, D. P., Zaneveld, L. J. (2003). Development pharmaceutics of microbicide formulations. Part II: Formulation, evaluation, and challenges. *AIDS Patient Care STDS*, **17**, 377–399.
5. Turpin, J. A. (2011). Topical microbicides to prevent the transmission of HIV: Formulation gaps and challenges. *Drug Deliv. Trans. Res.*, **1**, 194–200.
6. Agashe, H., Hu, M., Rohan, L. (2012). Formulation and delivery of microbicides. *Curr. HIV Res.*, **10**, 88–96.
7. Kim, P. S., Read, S. W. (2010). Nanotechnology and HIV: Potential applications for treatment and prevention. *Wiley Interdiscip. Rev. Nanomed. Nanobiotechnol.*, **2**, 693–702.
8. Mallipeddi, R., Rohan, L. C. (2010). Nanoparticle-based vaginal drug delivery systems for HIV prevention. *Expert Opin. Drug Deliv.*, **7**, 37–48.
9. Mamo, T., Moseman, E. A., Kolishetti, N., Salvador-Morales, C., Shi, J., Kuritzkes, D. R., Langer, R., von Andrian, U., Farokhzad, O. C. (2010). Emerging nanotechnology approaches for HIV/AIDS treatment and prevention. *Nanomedicine (Lond.)*, **5**, 269–285.
10. Khalil, N. M., Carraro, E., Cótica, L. F., Mainardes, R. M. (2011). Potential of polymeric nanoparticles in AIDS treatment and prevention. *Expert Opin. Drug Deliv.*, **8**, 95–112.
11. Boyapalle, S., Mohapatra, S. (2012). Nanotechnology applications to HIV vaccines and microbicides. *J. Glob. Infect. Dis.*, **4**, 62–68.
12. McCarthy, T. D., Karellas, P., Henderson, S. A., Giannis, M., O'Keefe, D. F., Heery, G., Paull, J. R., Matthews, B. R., Holan, G. (2005). Dendrimers as drugs: Discovery and preclinical and clinical development of dendrimer-based microbicides for HIV and STI prevention. *Mol. Pharm.*, **2**, 312–318.
13. Lai, S. K., O'Hanlon, D. E., Harrold, S., Man, S. T., Wang, Y. Y., Cone, R., Hanes, J. (2007). Rapid transport of large polymeric nanoparticles

in fresh undiluted human mucus. *Proc. Natl. Acad. Sci. U. S. A.*, **104**, 1482–1487.

14. Cu, Y., Saltzman, W. M. (2009). Controlled surface modification with poly(ethylene)glycol enhances diffusion of PLGA nanoparticles in human cervical mucus. *Mol. Pharm.*, **6**, 173–181.
15. Ham, A. S., Cost, M. R., Sassi, A. B., Dezzutti, C. S., Rohan, L. C. (2009). Targeted delivery of PSC-RANTES for HIV-1 prevention using biodegradable nanoparticles. *Pharm. Res.*, **26**, 502–511.
16. Woodrow, K. A., Cu, Y., Booth, C. J., Saucier-Sawyer, J. K., Wood, M. J., Saltzman, W. M. (2009). Intravaginal gene silencing using biodegradable polymer nanoparticles densely loaded with small-interfering RNA. *Nat. Mater.*, **8**, 526–533.
17. Cu, Y., Booth, C. J., Saltzman, W. M. (2011). *In vivo* distribution of surface-modified PLGA nanoparticles following intravaginal delivery. *J. Control. Release*, **156**, 258–264.
18. das Neves, J., Amiji, M. M., Bahia, M. F., Sarmento, B. (2010). Nanotechnology-based systems for the treatment and prevention of HIV/AIDS. *Adv. Drug Deliv. Rev.*, **62**, 458–477.
19. das Neves, J., Amiji, M., Sarmento, B. (2011). Mucoadhesive nanosystems for vaginal microbicide development: Friend or foe?. *Wiley Interdiscip. Rev. Nanomed. Nanobiotechnol.*, **3**, 389–399.
20. Sarmento, B., das Neves, J. (2012). Nanosystem formulations for rectal microbicides: A call for more research. *Ther. Deliv.*, **3**, 1–4.
21. Henderson, M. H., Couchman, G. M., Walmer, D. K., Peters, J. J., Owen, D. H., Brown, M. A., Lavine, M. L., Katz, D. F. (2007). Optical imaging and analysis of human vaginal coating by drug delivery gels. *Contraception*, **75**, 142–151.
22. Tasoglu, S., Katz, D. F., Szeri, A. J. (2012). Transient spreading and swelling behavior of a gel deploying an anti-HIV topical microbicide. *J. Nonnewton Fluid Mech.*, **187–188**, 36–42.
23. van Hoogdalem, E., de Boer, A. G., Breimer, D. D. (1991). Pharmacokinetics of rectal drug administration, part I. General considerations and clinical applications of centrally acting drugs. *Clin. Pharmacokinet.*, **21**, 11–26.
24. van Hoogdalem, E. J., de Boer, A. G., Breimer, D. D. (1991). Pharmacokinetics of rectal drug administration, part II. Clinical applications of peripherally acting drugs, and conclusions. *Clin. Pharmacokinet.*, **21**, 110–128.
25. Singer, R., Mawson, P., Derby, N., Rodriguez, A., Kizima, L., Menon, R., Goldman, D., Kenney, J., Aravantinou, M., Seidor, S., Gettie, A., Blanchard,

J., Piatak, M., Jr., Lifson, J. D., Fernandez-Romero, J. A., Robbiani, M., Zydowsky, T. M. (2012). An intravaginal ring that releases the NNRTI MIV-150 reduces SHIV transmission in macaques. *Sci. Trans. Med.*, **4**, 150ra123.

26. Neurath, A. R., Strick, N., Li, Y. Y. (2003). Water dispersible microbicidal cellulose acetate phthalate film. *BMC Infect. Dis.*, **3**, 27.
27. Yang, H., Parniak, M. A., Isaacs, C. E., Hillier, S. L., Rohan, L. C. (2008). Characterization of cyclodextrin inclusion complexes of the anti-HIV non-nucleoside reverse transcriptase inhibitor UC781. *AAPS J.*, **10**, 606–613.
28. Yang, H., Parniak, M. A., Hillier, S. L., Rohan, L. C. (2012). A thermodynamic study of the cyclodextrin-UC781 inclusion complex using a HPLC method. *J. Incl. Phenom. Macrocycl. Chem.*, **72**, 459–465.
29. Gali, Y., Delezay, O., Brouwers, J., Addad, N., Augustijns, P., Bourlet, T., Hamzeh-Cognasse, H., Ariën, K. K., Pozzetto, B., Vanham, G. (2010). *In vitro* evaluation of viability, integrity and inflammation in genital epithelia upon exposure to pharmaceutical excipients and candidate microbicides. *Antimicrob. Agents Chemother.*, **54**, 5105–5114.
30. Neurath, A. R., Strick, N., Li, Y. Y. (2006). Role of seminal plasma in the anti-HIV-1 activity of candidate microbicides. *BMC Infect. Dis.*, **6**, 150.
31. Patel, S., Hazrati, E., Cheshenko, N., Galen, B., Yang, H., Guzman, E., Wang, R., Herold, B. C., Keller, M. J. (2007). Seminal plasma reduces the effectiveness of topical polyanionic microbicides. *J. Infect. Dis.*, **196**, 1394–1402.
32. Keller, M. J., Mesquita, P. M., Torres, N. M., Cho, S., Shust, G., Madan, R. P., Cohen, H. W., Petrie, J., Ford, T., Soto-Torres, L., Profy, A. T., Herold, B. C. (2010). Postcoital bioavailability and antiviral activity of 0.5% PRO 2000 gel: Implications for future microbicide clinical trials. *PLoS One*, **5**, e8781.
33. Sassi, A. B., Bunge, K. E., Hood, B. L., Conrads, T. P., Cole, A. M., Gupta, P., Rohan, L. C. (2011). Preformulation and stability in biological fluids of the retrocyclin RC-101, a potential anti-HIV topical microbicide, *AIDS Res. Ther.*, **8**, 27.
34. Garg, S. (2009). Improving solubility of dapivirine by using nanotechnology. *Advancing Prevention Technologies for Sexual and Reproductive Health: A Strategy Symposium*, Berkeley, CA, USA.
35. Gupta, J., Sharma, P., Romano, J., Garg, S. (2009). Application of nanotechnology to enhance the solubility of poorly water soluble drug dapivirine. *ISPE Australasia Conference 2009*, Sydney, Australia.

36. Von Briesen, H., Ramge, P., Kreuter, J. (2000). Controlled release of antiretroviral drugs. *AIDS Rev.*, **2**, 31–38.

37. Whaley, K. J., Hanes, J., Shattock, R., Cone, R. A., Friend, D. R. (2010). Novel approaches to vaginal delivery and safety of microbicides: Biopharmaceuticals, nanoparticles, and vaccines. *Antiviral Res.*, **88 Suppl 1**, S55–S66.

38. Song, Y., Wang, Y., Thakur, R., Meidan, V. M., Michniak, B. (2004). Mucosal drug delivery: Membranes, methodologies, and applications. *Crit. Rev. Ther. Drug Carrier Syst.*, **21**, 195–256.

39. Yang, M., Yu, T., Wang, Y. Y., Lai, S. K., Zeng, Q., Miao, B., Tang, B. C., Simons, B. W., Ensign, L. M., Liu, G., Chan, K. W., Juang, C. Y., Mert, O., Wood, J., Fu, J., McMahon, M. T., Wu, T. C., Hung, C. F., Hanes, J. (2014). Vaginal delivery of paclitaxel via nanoparticles with non-mucoadhesive surfaces suppresses cervical tumor growth. *Adv. Healthc. Mater.*, **3**, 1044–1052.

40. Blum, J. S., Weller, C. E., Booth, C. J., Babar, I. A., Liang, X., Slack, F. J., Saltzman, W. M. (2011). Prevention of k-ras- and pten-mediated intravaginal tumors by treatment with camptothecin-loaded PLGA nanoparticles. *Drug Deliv. Trans. Res.*, **1**, 383–394.

41. Gunaseelan, S., Gunaseelan, K., Deshmukh, M., Zhang, X., Sinko, P. J. (2010). Surface modifications of nanocarriers for effective intracellular delivery of anti-HIV drugs. *Adv. Drug Deliv. Rev.*, **62**, 518–531.

42. Yang, S., Chen, Y., Gu, K., Dash, A., Sayre, C. L., Davies, N. M., Ho, E. A. (2013). Novel intravaginal nanomedicine for the targeted delivery of saquinavir to CD4(+) immune cells. *Int. J. Nanomed.*, **8**, 2847–2858.

43. Sharma, P., Garg, S. (2010). Pure drug and polymer based nanotechnologies for the improved solubility, stability, bioavailability and targeting of anti-HIV drugs. *Adv. Drug Deliv. Rev.*, **62**, 491–502.

44. Destache, C. J., Belgum, T., Christensen, K., Shibata, A., Sharma, A., Dash, A. (2009). Combination antiretroviral drugs in PLGA nanoparticle for HIV-1. *BMC Infect. Dis.*, **9**, 198.

45. Destache, C. J., Belgum, T., Goede, M., Shibata, A., Belshan, M. A. (2010). Antiretroviral release from poly(DL-lactide-co-glycolide) nanoparticles in mice. *J. Antimicrob. Chemother.*, **65**, 2183–2187.

46. Pillay, V., Mashingaidze, F., Choonara, Y. E., Du Toit, L. C., Buchmann, E., Maharaj, V., Ndesendo, V. M., Kumar, P. (2012). Qualitative and quantitative intravaginal targeting: Key to anti-HIV-1 microbicide delivery from test tube to *in vivo* success. *J. Pharm. Sci.*, **101**, 1950–1968.

47. Ballou, B., Andreko, S. K., Osuna-Highley, E., McRaven, M., Catalone, T., Bruchez, M. P., Hope, T. J., Labib, M. E. (2012). Nanoparticle transport from mouse vagina to adjacent lymph nodes. *PLoS One*, **7**, e51995.

48. Dukhin, S. S., Labib, M. E. (2013). Convective diffusion of nanoparticles from the epithelial barrier toward regional lymph nodes. *Adv. Colloid Interface Sci.*, **199–200**, 23–43.

49. Austin, R. H., Lim, S. F. (2008). The Sackler Colloquium on promises and perils in nanotechnology for medicine. *Proc. Natl. Acad. Sci. U. S. A.*, **105**, 17217–17221.

50. Maurer-Jones, M. A., Bantz, K. C., Love, S. A., Marquis, B. J., Haynes, C. L. (2009). Toxicity of therapeutic nanoparticles. *Nanomedicine (Lond.)*, **4**, 219–241.

51. Oberdörster, G. (2010). Safety assessment for nanotechnology and nanomedicine: Concepts of nanotoxicology. *J. Intern. Med.*, **267**, 89–105.

52. Malik, R., Maikhuri, J. P., Gupta, G., Misra, A. (2011). Biodegradable nanoparticles in the murine vagina: Trans-cervical retrograde transport and induction of proinflammatory cytokines. *J. Biomed. Nanotechnol.*, **7**, 5–46.

53. Wickline, S. A., Lanza, G., Hood, J., inventors. Washington University, assignee. (2011). Nanoparticulate compositions which employ membrane-integrating peptides to effect contraception and/or protection against infection by sexually transmitted virus are described. U.S. Patent 20120100186 A1.

54. Hood, J. L., Jallouk, A. P., Campbell, N., Ratner, L., Wickline, S. A. (2013). Cytolytic nanoparticles attenuate HIV-1 infectivity. *Antivir. Ther.*, **18**, 95–103.

55. Louissaint, N. A., Fuchs, E. J., Bakshi, R. P., Nimmagadda, S., Du, Y., Macura, K. J., King, K. E., Wahl, R., Goldsmith, A. J., Caffo, B., Cao, Y. J., Anderson, J., Hendrix, C. W. (2012). Distribution of cell-free and cell-associated HIV surrogates in the female genital tract after simulated vaginal intercourse. *J. Infect. Dis.*, **205**, 725–732.

56. Hendrix, C. W., Fuchs, E. J., Macura, K. J., Lee, L. A., Parsons, T. L., Bakshi, R. P., Khan, W. A., Guidos, A., Leal, J. P., Wahl, R. (2008). Quantitative imaging and sigmoidoscopy to assess distribution of rectal microbicide surrogates. *Clin. Pharmacol. Ther.*, **83**, 97–105.

57. Louissaint, N. A., Nimmagadda, S., Fuchs, E. J., Bakshi, R. P., Cao, Y., Lee, L. A., Goldsmith, J., Caffo, B. S., Du, Y., King, K. E., Menendez, F. A., Torbenson, M. S., Hendrix, C. W. (2011). Distribution of cell-free and cell-associated HIV surrogates in the colon following simulated

receptive anal intercourse in men who have sex with men. *J. Acquir. Immune Defic. Syndr.*, **49**, 10–17.

58. Vyas, T. K., Shah, L., Amiji, M. M. (2006). Nanoparticulate drug carriers for delivery of HIV/AIDS therapy to viral reservoir sites. *Expert Opin. Drug Deliv.*, **3**, 613–628.
59. Shahiwala, A., Amiji, M. M. (2007). Nanotechnology-based delivery systems in HIV/AIDS therapy. *Future HIV Ther.*, **1**, 49–59.
60. Mallipeddi, R., Rohan, L. C. (2010). Progress in antiretroviral drug delivery using nanotechnology. *Int. J. Nanomed.*, **5**, 533–547.
61. Wong, H. L., Chattopadhyay, N., Wu, X. Y., Bendayan, R. (2010). Nanotechnology applications for improved delivery of antiretroviral drugs to the brain. *Adv. Drug Deliv. Rev.*, **62**, 503–517.
62. Mahajan, S. D., Aalinkeel, R., Law, W. C., Reynolds, J. L., Nair, B. B., Sykes, D. E., Yong, K. T., Roy, I., Prasad, P. N., Schwartz, S. A. (2012). Anti-HIV-1 nanotherapeutics: Promises and challenges for the future. *Int. J. Nanomed.*, **7**, 5301–5314.
63. Parboosing, R., Maguire, G. E., Govender, P., Kruger, H. G. (2012). Nanotechnology and the treatment of HIV infection. *Viruses*, **4**, 488–520.
64. Hayakawa, T., Kawamura, M., Okamoto, M., Baba, M., Niikawa, T., Takehara, S., Serizawa, T., Akashi, M. (1998). Concanavalin A-immobilized polystyrene nanospheres capture HIV-1 virions and gp120: Potential approach towards prevention of viral transmission. *J. Med. Virol.*, **56**, 327–331.
65. Wang, X., Akagi, T., Akashi, M., Baba, M. (2007). Development of core-corona type polymeric nanoparticles as an anti-HIV-1 vaccine. *Mini-Rev. Org. Chem.*, **4**, 51–59.
66. Rupp, R., Rosenthal, S. L., Stanberry, L. R. (2007). VivaGel (SPL7013 gel): A candidate dendrimer-microbicide for the prevention of HIV and HSV infection. *Int. J. Nanomed.*, **2**, 561–566.
67. Tyssen, D., Henderson, S. A., Johnson, A., Sterjovski, J., Moore, K., La, J., Zanin, M., Sonza, S., Karellas, P., Giannis, M. P., Krippner, G., Wesselingh, S., McCarthy, T., Gorry, P. R., Ramsland, P. A., Cone, R., Paull, J. R., Lewis, G. R., Tachedjian, G. (2010). Structure activity relationship of dendrimer microbicides with dual action antiviral activity. *PLoS One*, **5**, e12309.
68. Telwatte, S., Moore, K., Johnson, A., Tyssen, D., Sterjovski, J., Aldunate, M., Gorry, P. R., Ramsland, P. A., Lewis, G. R., Paull, J. R., Sonza, S., Tachedjian, G. (2011). Virucidal activity of the dendrimer microbicide SPL7013 against HIV-1, *Antiviral Res.*, **90**, 195–199.

69. Gong, E., Matthews, B., McCarthy, T., Chu, J., Holan, G., Raff, J., Sacks, S. (2005). Evaluation of dendrimer SPL7013, a lead microbicide candidate against herpes simplex viruses. *Antiviral Res.*, **68**, 139–146.

70. Bernstein, D. I., Stanberry, L. R., Sacks, S., Ayisi, N. K., Gong, Y. H., Ireland, J., Mumper, R. J., Holan, G., Matthews, B., McCarthy, T., Bourne, N. (2003). Evaluations of unformulated and formulated dendrimer-based microbicide candidates in mouse and guinea pig models of genital herpes. *Antimicrob. Agents Chemother.*, **47**, 3784–3788.

71. Jiang, Y. H., Emau, P., Cairns, J. S., Flanary, L., Morton, W. R., McCarthy, T. D., Tsai, C. C. (2005). SPL7013 gel as a topical microbicide for prevention of vaginal transmission of SHIV89.6p in macaques. *AIDS Res. Hum. Retroviruses*, **21**, 207–213.

72. Patton, D. L., Cosgrove Sweeney, Y. T., McCarthy, T. D., Hillier, S. L. (2006). Preclinical safety and efficacy assessments of dendrimer-based (SPL7013) microbicide gel formulations in a nonhuman primate model. *Antimicrob. Agents Chemother.*, **50**, 1696–1700.

73. Chen, M. Y., Millwood, I. Y., Wand, H., Poynten, M., Law, M., Kaldor, J. M., Wesselingh, S., Price, C. F., Clark, L. J., Paull, J. R., Fairley, C. K. (2009). A randomized controlled trial of the safety of candidate microbicide SPL7013 gel when applied to the penis. *J. Acquir. Immune Defic. Syndr.*, **50**, 375–380.

74. O'Loughlin, J., Millwood, I. Y., McDonald, H. M., Price, C. F., Kaldor, J. M., Paull, J. R. (2010). Safety, tolerability, and pharmacokinetics of SPL7013 gel (VivaGel): A dose ranging, phase I study. *Sex. Transm. Dis.*, **37**, 100–104.

75. Price, C. F., Tyssen, D., Sonza, S., Davie, A., Evans, S., Lewis, G. R., Xia, S., Spelman, T., Hodsman, P., Moench, T. R., Humberstone, A., Paull, J. R., Tachedjian, G. (2011). SPL7013 gel (VivaGel®) retains potent HIV-1 and HSV-2 inhibitory activity following vaginal administration in humans. *PLoS One*, **6**, e24095.

76. Moscicki, A. B., Kaul, R., Ma, Y., Scott, M. E., Daud, II, Bukusi, E. A., Shiboski, S., Rebbapragada, A., Huibner, S., Cohen, C. R. (2012). Measurement of mucosal biomarkers in a phase 1 trial of intravaginal 3% StarPharma LTD 7013 gel (VivaGel) to assess expanded safety. *J. Acquir. Immune Defic. Syndr.*, **59**, 134–140.

77. McGowan, I., Gomez, K., Bruder, K., Febo, I., Chen, B. A., Richardson, B. A., Husnik, M., Livant, E., Price, C., Jacobson, C. (2011). Phase 1 randomized trial of the vaginal safety and acceptability of SPL7013 gel (VivaGel) in sexually active young women (MTN-004). *AIDS*, **25**, 1057–1064.

78. Kensinger, R. D., Catalone, B. J., Krebs, F. C., Wigdahl, B., Schengrund, C. L. (2004). Novel polysulfated galactose-derivatized dendrimers as

binding antagonists of human immunodeficiency virus type 1 infection. *Antimicrob. Agents Chemother.*, **48**, 1614–1623.

79. Pérez-Anes, A., Stefaniu, C., Moog, C., Majoral, J. P., Blanzat, M., Turrin, C. O., Caminade, A. M., Rico-Lattes, I. (2010). Multivalent catanionic galcer analogs derived from first generation dendrimeric phosphonic acids. *Bioorg. Med. Chem.*, **18**, 242–248.
80. Clayton, R., Hardman, J., LaBranche, C. C., McReynolds, K. D. (2011). Evaluation of the synthesis of sialic acid-pamam glycodendrimers without the use of sugar protecting groups, and the anti-HIV-1 properties of these compounds. *Bioconjug. Chem.*, **22**, 2186–2197.
81. Jiménez, J. L., Pion, M., de la Mata, F. J., Gomez, R., Muñoz, E., Leal, M., Muñoz-Fernandez, M. A. (2012). Dendrimers as topical microbicides with activity against HIV. *New J. Chem.*, **36**, 299–309.
82. Garcia-Vallejo, J. J., Koning, N., Ambrosini, M., Kalay, H., Vuist, I., Sarrami-Forooshani, R., Geijtenbeek, T. B., van Kooyk, Y. (2013). Glycodendrimers prevent HIV transmission via DC-SIGN on dendritic cells. *Int. Immunol.*, **25**, 221–233.
83. Chonco, L., Pion, M., Vacas, E., Rasines, B., Maly, M., Serramía, M. J., López-Fernández, L., De la Mata, J., Alvarez, S., Gómez, R., Muñoz-Fernández, M. A. (2012). Carbosilane dendrimer nanotechnology outlines of the broad HIV blocker profile. *J. Control. Release*, **161**, 949–958.
84. Martinez-Ávila, O., Bedoya, L. M., Marradi, M., Clavel, C., Alcamí, J., Penadés, S. (2009). Multivalent manno-glyconanoparticles inhibit DC-SIGN-mediated HIV-1 *trans*-infection of human T cells. *Chembiochem*, **10**, 1806–1809.
85. Martinez-Ávila, O., Hijazi, K., Marradi, M., Clavel, C., Campion, C., Kelly, C., Penadés, S. (2009). Gold manno-glyconanoparticles: Multivalent systems to block HIV-1 gp120 binding to the lectin DC-SIGN. *Chemistry*, **15**, 9874–9888.
86. Di Gianvincenzo, P., Chiodo, F., Marradi, M., Penadés, S. (2012). Gold manno-glyconanoparticles for intervening in HIV gp120 carbohydrate-mediated processes. *Methods Enzymol.*, **509**, 21–40.
87. Arnaiz, B., Martinez-Avila, O., Falcon-Perez, J. M., Penadés, S. (2012). Cellular uptake of gold nanoparticles bearing HIV gp120 oligomannosides. *Bioconjug. Chem.*, **23**, 814–825.
88. Di Gianvincenzo, P., Marradi, M., Martínez-Avila, O. M., Bedoya, L. M., Alcamí, J., Penadés, S. (2010). Gold nanoparticles capped with sulfate-ended ligands as anti-HIV agents. *Bioorg. Med. Chem. Lett.*, **20**, 2718–2721.
89. Lara, H. H., Ixtepan-Turrent, L., Garza-Treviño, E. N., Rodriguez-Padilla, C. (2010). PVP-coated silver nanoparticles block the transmission

of cell-free and cell-associated HIV-1 in human cervical culture. *J. Nanobiotechnol.*, **8**, 15.

90. Lara, H. H., Ayala-Nuñez, N. V., Ixtepan-Turrent, L., Rodriguez-Padilla, C. (2010). Mode of antiviral action of silver nanoparticles against HIV-1. *J. Nanobiotechnol.*, **8**, 1.
91. Lara, H. H., Ixtepan-Turrent, L., Garza Treviño, E. N., Singh, D. K. (2011). Use of silver nanoparticles increased inhibition of cell-associated HIV-1 infection by neutralizing antibodies developed against HIV-1 envelope proteins. *J. Nanobiotechnol.*, **9**, 38.
92. Shive, M. S., Anderson, J. M. (1997). Biodegradation and biocompatibility of PLA and PLGA microspheres. *Adv. Drug Deliv. Rev.*, **28**, 5–24.
93. Meng, J., Sturgis, T. F., Youan, B. B. (2011). Engineering tenofovir loaded chitosan nanoparticles to maximize microbicide mucoadhesion. *Eur. J. Pharm. Sci.*, **44**, 57–67.
94. Belletti, D., Tosi, G., Forni, F., Gamberini, M. C., Baraldi, C., Vandelli, M. A., Ruozi, B. (2012). Chemico-physical investigation of tenofovir loaded polymeric nanoparticles. *Int. J. Pharm.*, **436**, 753–763.
95. Thanou, M., Verhoef, J. C., Junginger, H. E. (2001). Chitosan and its derivatives as intestinal absorption enhancers. *Adv. Drug Deliv. Rev.*, **50 Suppl 1**, S91–S101.
96. Zhang, T., Sturgis, T. F., Youan, B. B. (2011). pH-responsive nanoparticles releasing tenofovir intended for the prevention of HIV transmission. *Eur. J. Pharm. Biopharm.*, **79**, 526–536.
97. Yoo, J. W., Giri, N., Lee, C. H. (2011). pH-sensitive Eudragit nanoparticles for mucosal drug delivery. *Int. J. Pharm.*, **403**, 262–267.
98. Agrahari, V., Youan, B. B. (2012). Sensitive and rapid HPLC quantification of tenofovir from hyaluronic acid-based nanomedicine. *AAPS PharmSciTech*, **13**, 202–210.
99. Swyer, G. (1947). The hyaluronidase content of semen. *Biochem. J.*, **41**, 409–413.
100. Lewi, P., Heeres, J., Arien, K., Venkatraj, M., Joossens, J., Van der Veken, P., Augustyns, K., Vanham, G. (2012). Reverse transcriptase inhibitors as microbicides. *Curr. HIV Res.*, **10**, 27–35.
101. das Neves, J., Michiels, J., Arien, K. K., Vanham, G., Amiji, M., Bahia, M. F., Sarmento, B. (2012). Polymeric nanoparticles affect the intracellular delivery, antiretroviral activity and cytotoxicity of the microbicide drug candidate dapivirine. *Pharm. Res.*, **29**, 1468–1484.
102. das Neves, J., Amiji, M., Bahia, M. F., Sarmento, B. (2013). Assessing the physical-chemical properties and stability of dapivirine-loaded polymeric nanoparticles. *Int. J. Pharm.*, **456**, 307–314.

103. das Neves, J., Rocha, C. M., Gonçalves, M. P., Carrier, R. L., Amiji, M., Bahia, M. F., Sarmento, B. (2012). Interactions of microbicide nanoparticles with a simulated vaginal fluid. *Mol. Pharm.*, **9**, 3347–3356.

104. das Neves, J., Araújo, F., Andrade, F., Michiels, J., Ariën, K. K., Vanham, G., Amiji, M., Bahia, M. F., Sarmento, B. (2013). *In vitro* and *ex vivo* evaluation of polymeric nanoparticles for vaginal and rectal delivery of the anti-HIV drug dapivirine. *Mol. Pharm.*, **10**, 2793–2807.

105. das Neves, J., Araújo, F., Andrade, F., Amiji, M., Bahia, M. F., Sarmento, B. (2014). Biodistribution and pharmacokinetics of dapivirine-loaded nanoparticles after vaginal delivery in mice. *Pharm. Res.*, **31**, 1834–1845.

106. Date, A. A., Shibata, A., Goede, M., Sanford, B., La Bruzzo, K., Belshan, M., Destache, C. J. (2012). Development and evaluation of a thermosensitive vaginal gel containing raltegravir + efavirenz loaded nanoparticles for HIV prophylaxis. *Antiviral Res.*, **96**, 430–436.

107. Pastore, C., Picchio, G. R., Galimi, F., Fish, R., Hartley, O., Offord, R. E., Mosier, D. E. (2003). Two mechanisms for human immunodeficiency virus type 1 inhibition by N-terminal modifications of RANTES. *Antimicrob. Agents Chemother.*, **47**, 509–517.

108. Kawamura, T., Bruse, S. E., Abraha, A., Sugaya, M., Hartley, O., Offord, R. E., Arts, E. J., Zimmerman, P. A., Blauvelt, A. (2004). PSC-RANTES blocks R5 human immunodeficiency virus infection of Langerhans cells isolated from individuals with a variety of CCR5 diplotypes. *J. Virol.*, **78**, 7602–7609.

109. Lederman, M. M., Veazey, R. S., Offord, R., Mosier, D. E., Dufour, J., Mefford, M., Piatak, M., Jr., Lifson, J. D., Salkowitz, J. R., Rodriguez, B., Blauvelt, A., Hartley, O. (2004). Prevention of vaginal SHIV transmission in rhesus macaques through inhibition of CCR5. *Science*, **306**, 485–487.

110. Palliser, D., Chowdhury, D., Wang, Q. Y., Lee, S. J., Bronson, R. T., Knipe, D. M., Lieberman, J. (2006). An siRNA-based microbicide protects mice from lethal herpes simplex virus 2 infection. *Nature*, **439**, 89–94.

111. Katakowski, J. A., Palliser, D. (2010). siRNA-based topical microbicides targeting sexually transmitted infections. *Curr. Opin. Mol. Ther.*, **12**, 192–202.

112. Eszterhas, S. K., Ilonzo, N. O., Crozier, J. E., Celaj, S., Howell, A. L. (2011). Nanoparticles containing siRNA to silence CD4 and CCR5 reduce expression of these receptors and inhibit HIV-1 infection in human female reproductive tract tissue explants. *Infect. Dis. Rep.*, **3**, e11.

113. Hirbod, T., Nilsson, J., Andersson, S., Uberti-Foppa, C., Ferrari, D., Manghi, M., Andersson, J., Lopalco, L., Broliden, K. (2006). Upregulation

of interferon-alpha and RANTES in the cervix of HIV-1-seronegative women with high-risk behavior. *J. Acquir. Immune Defic. Syndr.*, **43**, 137–143.

114. Steinbach, J. M., Weller, C. E., Booth, C. J., Saltzman, W. M. (2012). Polymer nanoparticles encapsulating siRNA for treatment of HSV-2 genital infection. *J. Control. Release*, **162**, 102–110.
115. Wu, Y., Navarro, F., Lal, A., Basar, E., Pandey, R. K., Manoharan, M., Feng, Y., Lee, S. J., Lieberman, J., Palliser, D. (2009). Durable protection from herpes simplex virus-2 transmission following intravaginal application of siRNAs targeting both a viral and host gene. *Cell Host Microbe*, **5**, 84–94.
116. Ball, C., Krogstad, E., Chaowanachan, T., Woodrow, K. A. (2012). Drug-eluting fibers for HIV-1 inhibition and contraception. *PLoS One*, **7**, e49792.
117. Huang, C., Soenen, S. J., van Gulck, E., Vanham, G., Rejman, J., Van Calenbergh, S., Vervaet, C., Coenye, T., Verstraelen, H., Temmerman, M., Demeester, J., De Smedt, S. C. (2012). Electrospun cellulose acetate phthalate fibers for semen induced anti-HIV vaginal drug delivery. *Biomaterials*, **33**, 962–969.
118. Jain, S. K., Singh, R., Sahu, B. (1997). Development of a liposome based contraceptive system for intravaginal administration of progesterone. *Drug Dev. Ind. Pharm.*, **23**, 827–830.
119. Ahmad, N., Alam, M. K., Shehbaz, A., Khan, A., Mannan, A., Hakim, S. R., Bisht, D., Owais, M. (2005). Antimicrobial activity of clove oil and its potential in the treatment of vaginal candidiasis. *J. Drug Target.*, **13**, 555–561.
120. Ning, M., Guo, Y., Pan, H., Chen, X., Gu, Z. (2005). Preparation, *in vitro* and *in vivo* evaluation of liposomal/niosomal gel delivery systems for clotrimazole. *Drug Dev. Ind. Pharm.*, **31**, 375–383.
121. Pavelić, Ž., Škalko-Basnet, N., Filipović-Grcić, J., Martinac, A., Jalsenjak, I. (2005). Development and *in vitro* evaluation of a liposomal vaginal delivery system for acyclovir. *J. Control. Release*, **106**, 34–43.
122. Kang, J. W., Davaa, E., Kim, Y. T., Park, J. S. (2010). A new vaginal delivery system of amphotericin B: A dispersion of cationic liposomes in a thermosensitive gel. *J. Drug Target.*, **18**, 637–644.
123. Gupta, P. N., Pattani, A., Curran, R. M., Kett, V. L., Andrews, G. P., Morrow, R. J., Woolfson, A. D., Malcolm, R. K. (2012). Development of liposome gel based formulations for intravaginal delivery of the recombinant HIV-1 envelope protein CN54gp140. *Eur. J. Pharm. Sci.*, **46**, 315–322.

124. Li, W. Z., Zhao, N., Zhou, Y. Q., Yang, L. B., Xiao-Ning, W., Bao-Hua, H., Peng, K., Chun-Feng, Z. (2012). Post-expansile hydrogel foam aerosol of PG-liposomes: A novel delivery system for vaginal drug delivery applications. *Eur. J. Pharm. Sci.*, **47**, 162–169.

125. Kish-Catalone, T. M., Lu, W., Gallo, R. C., DeVico, A. L. (2006). Preclinical evaluation of synthetic –2 RANTES as a candidate vaginal microbicide to target CCR5. *Antimicrob. Agents Chemother.*, **50**, 1497–1509.

126. Kish-Catalone, T., Pal, R., Parrish, J., Rose, N., Hocker, L., Hudacik, L., Reitz, M., Gallo, R., Devico, A. (2007). Evaluation of –2 RANTES vaginal microbicide formulations in a nonhuman primate simian/human immunodeficiency virus (SHIV) challenge model. *AIDS Res. Hum. Retroviruses*, **23**, 33–42.

127. Konopka, K., Davis, B. R., Larsen, C. E., Alford, D. R., Debs, R. J., Düzgüneş, N. (1990). Liposomes modulate human immunodeficiency virus infectivity. *J. Gen. Virol.*, **71 (Pt 12)**, 2899–2907.

128. Malavia, N. K., Zurakowski, D., Schroeder, A., Princiotto, A. M., Laury, A. R., Barash, H. E., Sodroski, J., Langer, R., Madani, N., Kohane, D. S. (2011). Liposomes for HIV prophylaxis. *Biomaterials*, **32**, 8663–8668.

129. Caron, M., Besson, G., Etenna, S. L., Mintsa-Ndong, A., Mourtas, S., Radaelli, A., Morghen Cde, G., Loddo, R., La Colla, P., Antimisiaris, S. G., Kazanji, M. (2010). Protective properties of non-nucleoside reverse transcriptase inhibitor (MC1220) incorporated into liposome against intravaginal challenge of rhesus macaques with RT-SHIV. *Virology*, **405**, 225–233.

130. Mourtas, S., Mao, J., Parsy, C. C., Storer, R., Klepetsanis, P., Antimisiaris, S. G. (2010). Liposomal gels for vaginal delivery of the microbicide MC-1220: Preparation and *in vivo* vaginal toxicity and pharmacokinetics. *Nano LIFE*, **1**, 195–206.

131. Stolte-Leeb, N., Loddo, R., Antimisiaris, S., Schultheiss, T., Sauermann, U., Franz, M., Mourtas, S., Parsy, C., Storer, R., La Colla, P., Stahl-Hennig, C. (2011). Topical nonnucleoside reverse transcriptase inhibitor MC 1220 partially prevents vaginal RT-SHIV infection of macaques. *AIDS Res. Hum. Retroviruses*, **27**, 933–943.

132. Wang, L., Sassi, A. B., Patton, D., Isaacs, C., Moncla, B. J., Gupta, P., Rohan, L. C. (2012). Development of a liposome microbicide formulation for vaginal delivery of octylglycerol for HIV prevention. *Drug Dev. Ind. Pharm.*, **38**, 995–1007.

133. Ramanathan, R., Mahadevan, R., Iadanza, M., Chaowanachan, T., Woodrow, K. A. (2012). Biophysical characterization of hydrogel-

core, lipid-shell nanolipogels for HIV chemoprohylaxis, 2012 *International Microbicides Conference*, Sydney, Australia.

134. Mehnert, W., Mader, K. (2001). Solid lipid nanoparticles: Production, characterization and applications. *Adv. Drug Deliv. Rev.*, **47**, 165–196.
135. Alukda, D., Sturgis, T., Youan, B. B. (2011). Formulation of tenofovir-loaded functionalized solid lipid nanoparticles intended for HIV prevention. *J. Pharm. Sci.*, **100**, 3345–3356.
136. Smart, J. D. (2005). The basics and underlying mechanisms of mucoadhesion. *Adv. Drug Deliv. Rev.*, **57**, 1556–1568.
137. das Neves, J., Bahia, M. F., Amiji, M. M., Sarmento, B. (2011). Mucoadhesive nanomedicines: Characterization and modulation of mucoadhesion at the nanoscale. *Expert Opin. Drug Deliv.*, **8**, 1085–1104.
138. Peppas, N. A., Huang, Y. (2004). Nanoscale technology of mucoadhesive interactions. *Adv. Drug Deliv. Rev.*, **56**, 1675–1687.
139. Serra, L., Domenech, J., Peppas, N. A. (2009). Engineering design and molecular dynamics of mucoadhesive drug delivery systems as targeting agents. *Eur. J. Pharm. Biopharm.*, **71**, 519–528.
140. Bernkop-Schnürch, A., Weithaler, A., Albrecht, K., Greimel, A. (2006). Thiomers: Preparation and *in vitro* evaluation of a mucoadhesive nanoparticulate drug delivery system. *Int. J. Pharm.*, **317**, 76–81.
141. Henning, A., Schneider, M., Nafee, N., Muijs, L., Rytting, E., Wang, X., Kissel, T., Grafahrend, D., Klee, D., Lehr, C. M. (2010). Influence of particle size and material properties on mucociliary clearance from the airways. *J. Aerosol. Med. Pulm. Drug Deliv.*, **23**, 233–241.
142. Durrer, C., Irache, J. M., Puisieux, F., Duchêne, D., Ponchel, G. (1994). Mucoadhesion of latexes. II. Adsorption isotherms and desorption studies. *Pharm. Res.*, **11**, 680–683.
143. Ceric, F., Silva, D., Vigil, P. (2005). Ultrastructure of the human periovulatory cervical mucus. *J. Electron Microsc. (Tokyo)*, **54**, 479–484.
144. Cone, R. A. (2009). Barrier properties of mucus. *Adv. Drug Deliv. Rev.*, **61**, 75–85.
145. Ponchel, G., Montisci, M. J., Dembri, A., Durrer, C., Duchêne, D. (1997). Mucoadhesion of colloidal particulate systems in the gastro-intestinal tract. *Eur. J. Pharm. Biopharm.*, **44**, 25–31.
146. Wang, Y. Y., Lai, S. K., Suk, J. S., Pace, A., Cone, R., Hanes, J. (2008). Addressing the PEG mucoadhesivity paradox to engineer nanoparticles that "slip" through the human mucus barrier. *Angew. Chem. Int. Ed. Engl.*, **47**, 9726–9729.
147. Lackman-Smith, C., Osterling, C., Luckenbaugh, K., Mankowski, M., Snyder, B., Lewis, G., Paull, J., Profy, A., Ptak, R. G., Buckheit, R. W.,

Jr., Watson, K. M., Cummins, J. E., Jr., Sanders-Beer, B. E. (2008). Development of a comprehensive human immunodeficiency virus type 1 screening algorithm for discovery and preclinical testing of topical microbicides. *Antimicrob. Agents Chemother.*, **52**, 1768–1781.

148. Tang, B. C., Dawson, M., Lai, S. K., Wang, Y. Y., Suk, J. S., Yang, M., Zeitlin, P., Boyle, M. P., Fu, J., Hanes, J. (2009). Biodegradable polymer nanoparticles that rapidly penetrate the human mucus barrier. *Proc. Natl. Acad. Sci. U. S. A.*, **106**, 19268–19273.
149. Yang, M., Lai, S. K., Wang, Y. Y., Zhong, W., Happe, C., Zhang, M., Fu, J., Hanes, J. (2011). Biodegradable nanoparticles composed entirely of safe materials that rapidly penetrate human mucus. *Angew. Chem. Int. Ed. Engl.*, **50**, 2597–2600.
150. Wu, S. Y., Chang, H. I., Burgess, M., McMillan, N. A. (2011). Vaginal delivery of siRNA using a novel PEGylated lipoplex-entrapped alginate scaffold system. *J. Control. Release*, **155**, 418–426.
151. Ensign, L. M., Tang, B. C., Wang, Y. Y., Tse, T. A., Hoen, T., Cone, R., Hanes, J. (2012). Mucus-penetrating nanoparticles for vaginal drug delivery protect against herpes simplex virus. *Sci. Trans. Med.*, **4**, 138ra179.
152. Ensign, L. M., Hoen, T. E., Maisel, K., Cone, R. A., Hanes, J. S. (2013). Enhanced vaginal drug delivery through the use of hypotonic formulations that induce fluid uptake. *Biomaterials*, **34**, 6922–6929.
153. Lai, S. K., Hida, K., Shukair, S., Wang, Y. Y., Figueiredo, A., Cone, R., Hope, T. J., Hanes, J. (2009). Human immunodeficiency virus type 1 is trapped by acidic but not by neutralized human cervicovaginal mucus. *J. Virol.*, **83**, 11196–11200.
154. Boukari, H., Brichacek, B., Stratton, P., Mahoney, S. F., Lifson, J. D., Margolis, L., Nossal, R. (2009). Movements of HIV-virions in human cervical mucus. *Biomacromolecules*, **10**, 2482–2488.
155. Lai, S. K., Wang, Y. Y., Hida, K., Cone, R., Hanes, J. (2010). Nanoparticles reveal that human cervicovaginal mucus is riddled with pores larger than viruses. *Proc. Natl. Acad. Sci. U. S. A.*, **107**, 598–603.
156. Chen, E. Y., Wang, Y. C., Chen, C. S., Chin, W. C. (2010). Functionalized positive nanoparticles reduce mucin swelling and dispersion. *PLoS One*, **5**, e15434.
157. McGill, S., Smyth, H. (2010). Disruption of the mucus barrier by topically applied exogenous particles. *Mol. Pharm.*, **7**, 2280–2288.
158. Dezzutti, C. S., James, V. N., Ramos, A., Sullivan, S. T., Siddig, A., Bush, T. J., Grohskopf, L. A., Paxton, L., Subbarao, S., Hart, C. E. (2004). *In vitro* comparison of topical microbicides for prevention of human

immunodeficiency virus type 1 transmission. *Antimicrob. Agents Chemother.*, **48**, 3834–3844.

159. Abner, S. R., Guenthner, P. C., Guarner, J., Hancock, K. A., Cummins, J. E., Jr., Fink, A., Gilmore, G. T., Staley, C., Ward, A., Ali, O., Binderow, S., Cohen, S., Grohskopf, L. A., Paxton, L., Hart, C. E., Dezzutti, C. S. (2005). A human colorectal explant culture to evaluate topical microbicides for the prevention of HIV infection. *J. Infect. Dis.*, **192**, 1545–1556.
160. Muthu, M. S., Wilson, B. (2012). Challenges posed by the scale-up of nanomedicines. *Nanomedicine (Lond.)*, **7**, 307–309.
161. Klasse, P. J., Shattock, R. J., Moore, J. P. (2006). Which topical microbicides for blocking HIV-1 transmission will work in the real world?. *PLOS Med.*, **3**, e351.

Chapter 51

Nanotechnology-Based Solutions to Combat the Emerging Threat of Superbugs: Current Scenario and Future Prospects

Nisha C. Kalarickal, PhD, and Yashwant R. Mahajan, PhD

Centre for Knowledge Management of Nanoscience and Technology, Tarnaka, Secunderabad, Telangana, India

Keywords: nanotechnology, nanomaterials, superbugs, antibiotic resistance, antibacterial, nanomedicine, nano-enabled antibiotics, silver nanoparticle, NO-releasing nanoparticles, nano-coatings, nano drug delivery systems, nano biosensors

51.1 Introduction

The recent report by the World Health Organization (WHO) revealed antibiotic resistance as a serious, worldwide threat to public health [1]. The first report by WHO on antimicrobial resistance provides the most comprehensive picture of antibiotic resistance to date, with data from 114 countries. "A post-antibiotic era—in which common infections and minor injuries can kill—far from being

Handbook of Clinical Nanomedicine: Nanoparticles, Imaging, Therapy, and Clinical Applications
Edited by Raj Bawa, Gerald F. Audette, and Israel Rubinstein

ISBN 978-981-4669-20-7 (Hardcover), 978-981-4669-21-4 (eBook)
www.panstanford.com

an apocalyptic fantasy, is instead a very real possibility for the 21st century," Keiji Fukuda, WHO's assistant director-general for Health Security, pointed out in a forward to the report. The alarming situation concerning antibiotic resistance and the so-called "superbugs" is sending shock waves through the medical community and public across the globe. Superbugs is a term coined to describe newly evolved species of bacteria that are resistant to multiple antibiotics. Excessive (overuse) use and misuse (wrong diagnosis or self-medication) of conventional antibiotics have given rise to the grave problem of antimicrobial resistance worldwide.

51.2 The Discovery and Consequent Development of Antibiotic Resistance

It seems appropriate to take a brief look back at the history of antibiotics discovery and consequent development of antibiotic resistance. An antibiotic is a compound or substance that kills or slows down the growth of bacteria by different mechanisms such as (1) inhibiting the cell wall synthesis, (2) blocking DNA/RNA expression, (3) stopping the folic acid synthesis, (4) disrupting cell membrane permeability and arresting the central dogma of bacteria (DNA, RNA and protein synthesis), and (5) inhibiting the protein synthesis [2]. "Antibiotic resistance" is the resistance of microorganism against a drug's action, which allows them to survive in drugged environment. "Superbugs" embody the group of bacteria that contains several resistance genes that when expressed lead to the development of antibiotic resistance by different mechanisms such as (1) coding for some specific enzymes that devastate antibiotics, (2) modifying the efflux pump, which causes trans-shipment of antibiotic out of the bacterial cell, and (3) inability of antibiotics to attach to target sites [3]. Figure 51.1 depicts the year of deployment of various antibiotics and consequent emergence of antibiotic resistance.

In the past 70 years, antibiotics have been critical in the fight against infectious diseases caused by bacteria and other microbes. Antimicrobial chemotherapy has been a leading cause for the dramatic rise of average life expectancy in the twentieth century. The most important development in medicine in this century was perhaps the discovery of penicillin by Alexander Fleming in 1928, a naturally occurring antibiotic that inhibits cell wall synthesis in

many pathogenic bacteria. In 1940, E. B. Chain and H. W. Florey were able to produce stable commercial formulations of this antibiotic. However, in 1947, just four years after drug companies began mass-producing penicillin, microbes began appearing that could resist it; the first bug to battle penicillin was *Staphylococcus aureus* [4]. *S. aureus* is often a harmless passenger in the human body, but it can cause illness such as pneumonia or toxic shock syndrome, when it overgrows or produces a toxin. In 1967, another type of penicillin-resistant pneumonia, caused by *Streptococcus pneumonia* and called pneumococcus, surfaced in a remote village in Papua, New Guinea. In 1983, a hospital acquired intestinal infection caused by the bacterium *Enterococcus faecium* joined the list of bugs that outwit penicillin. In the past half century, from penicillin to methicillin to vancomycin and daptomycin, a large number of multiple classes of antibiotics have been discovered that inhibit cell-wall synthesis.

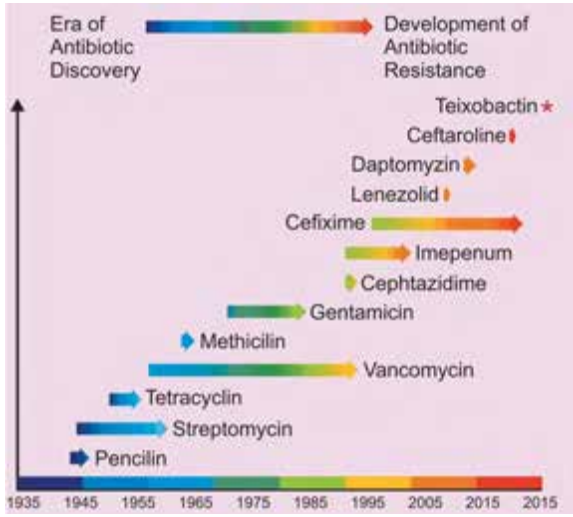

Figure 51.1 Timeline of antibiotics discovery and the evolution of antibiotic resistance.

In 1945, Fleming could foresee and had predicted that improper use and overuse of the new drug would lead to the development of resistant microorganisms [5]. Penicillin resistance soon materialized; however, the discovery of new antibiotics lessened the impact of the resistance problem. Streptomycin and other aminoglycosides,

chloramphenicol, tetracyclines, cephalosporins, quinolones, semi-synthetic penicillins like ampicillin and methicillin, and super-potent drugs like vancomycin enriched the antimicrobial arsenal. Over the years, however, more and more microorganisms, exposed to more and more antibiotics, have adapted to these compounds. Resistance to antimicrobial drugs has now become a worldwide problem. The emergence of methicillin-resistant *Staphylococcus aureus* (MRSA) in the 1970's was a major setback in antibiotic therapy [6]. The prospect of vancomycin-resistant *S. aureus* looms on the horizon. Multiple-drug-resistant strains of *Mycobacterium tuberculosis* have resulted from improper or incomplete therapy. Outbreaks of tuberculosis are now common among indigent populations in cities throughout India, China, Russia, Africa, and U.S. Since resistance is appearing to even the most potent antibiotics such as vancomycin and carbapenem, the development of new approaches in antimicrobial therapy is imperative.

With the approval of the three more recent antibacterial agents, linezolid in 2000, daptomycinin in 2004 and telithromycin in 2002–2004, three new classes of agents have been introduced into the market. However, resistance has already been reported for all these three agents, thus providing an opportunity to identify additional agents in these classes that can overcome the associated resistance. In addition, new targets should be explored to avoid these resistance already reported in the existing classes of antibiotics.

As the use of antibiotics increases for medical, veterinary, and agricultural purposes, the increasing emergence of antibiotic-resistant strains of pathogenic bacteria is an unwelcome consequence. The incidence of the multidrug resistance (MDR) of bacteria, which cause infections in hospitals/intensive care units is increasing, and finding microorganisms insensitive to more than 10 different antibiotics is not unusual. Examples of such resistant bacteria include methicillin/vancomycin-resistant *Staphylococcus aureus*; vancomycin-resistant enterococci, such as *Enterococcus faecalis* and *Enterococcus faecium*; penicillin-resistant *Streptococcus pneumoniae*; and cephalosporin and quinolone-resistant Gram-negative rods (coliforms), such as *E. coli, Salmonella* species, *Klebsiella pneumoniae, Pseudomonas* species, and *Enterobacter* species. More recently, pan-antibiotic-resistant Gram-negative and Gram-positive bacilli have also emerged. Figure 51.2 shows a few examples of antibiotic-resistant bacteria.

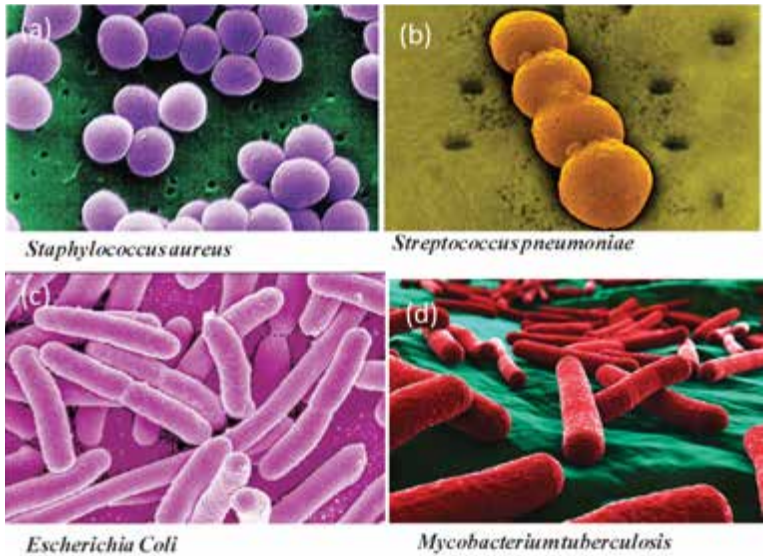

Figure 51.2 Color-enhanced SEM micrographs of a few of bacteria species that have developed antimicrobial-resistant over the years. Image credit: (a) and (c) to the Centers for Disease Control and Prevention's Public Health Image Library and Rocky Mountain Laboratories, NIAID, NIH respectively.

Indeed, people now die of certain bacterial infections that previously could have been easily treated with existing antibiotics. Such infections include, for instance, *Staphylococcus pneumoniae,* causing meningitis; Enterobacter sp., causing pneumonia; Enterococcus sp., causing endocarditis; and *Mycobacterium tuberculosis,* causing tuberculosis.

The most striking example is tuberculosis (TB), which is one of the most deadly diseases in the world. The bacteria causing multidrug-resistant TB (MDR-TB) are resistant to the most potent anti-TB drugs like isoniazid and rifampicin. Extensively drug-resistant TB (XDR-TB) is even more deadly and resistant to any of the second-line anti-TB injectable drugs. The statistics on trends in morbidity and mortality attributed to MDR-TB as reported by WHO is quite scary. According to them, every year about 440,000 MDR-TB cases are estimated to have appeared globally, out of which about 150,000 patients die [7]. India has the highest MDR-TB burden in the world. It is estimated that about 73,000 MDR-TB cases are emerging every year. Moreover, the average cost of

treating a patient with MDR-TB is quite prohibitive and is estimated to be about US $5000 as compared to $20 for drug-sensitive TB [8]. Hospital-acquired MRSA is estimated to cause ~19,000 deaths per year in the United States [9]. Apart from their high mortality rate, MRSA infections lead to an estimated $3 billion to $4 billion of additional health care costs per year.

NDM-1 gene is one of the newfangled perils since 2008 and is epidemic in India and Pakistan. According to one survey done by a UK team in 2010, the true cases of NDM-1 reported were 44 in Chennai, 26 in Haryana, 37 in the UK, and 73 in other sites of India and Pakistan [10] and it is now extending its boundary to countries such as USA, UK, Canada, and Australia. In a real sense, its nature is changing from epidemic to pandemic. NDM-1 (New Delhi metallo-beta-lactamase-1), is a gene carried by bacteria, which is responsible for producing an enzyme, carbapenemase, within the bacteria making them resistant to almost all of the present antibiotics. The spread of this gene is abetted by unhygienic conditions related to food or water. The fret with this DNA is that it can transfer from one bacterium to another via horizontal gene transfer. If this gene is transferred to bacterium that already has antibiotic resistance, altogether it can cause more lethal infections, which might be incurable [10, 11].

New strategies are being explored to target antibiotic resistance. In a new collaborative study, involving a group of researchers from various institutes in Germany and USA as well as pharmaceutical companies discovered a new antibiotic named Teixobactin [12]. It is the first member of a new class of lipid II binding antibiotics, which is structurally distinct from glycopeptides, lantibiotics, and defensins. In their study, they have reported that teixobactin works differently from other antibiotics by targeting not only the bacteria's proteins but also the cell walls. These properties of teixobactin are anticipated to minimize resistance development by target microorganisms.

51.3 Nanotechnology-Based Solutions against Superbugs

The emergence of superbugs has made it imperative to search for novel methods, which can combat the microbial resistance. Thus,

application of nanotechnology in pharmaceuticals and microbiology is gaining importance to prevent the catastrophic consequences of antibiotic resistance. Nanotechnology-based approaches are advantageous to improve various preventive measures such as coatings and filtration. Similarly, diagnosis using efficient nanosensors or probes can speed up the treatment process at an early stage of disease. Nano-based drug carriers for existing antibiotics enhance their bioavailability and make them more target-specific. In addition, the combination of nanoparticles (NPs) along with antibiotics makes them more lethal for microorganisms. The major areas where nanotechnology can offer significant improvement in terms of prevention, diagnosis, and treatment of superbugs are shown in Fig. 51.3.

Figure 51.3 Role of nanotechnology in the prevention, diagnosis, and treatment of superbugs.

Various mechanisms have been proposed for different nanoparticles for their antimicrobial activity [13, 14]. Most of these studies have been based on the morphological and structural changes occurring in the bacterial cells because of interaction with nanomaterials. Nanoparticles have the ability to anchor to the bacterial cell wall and subsequently cause structural changes in the cell membrane permeability leading to cell death. Large surface area of nanoparticles enables better contact with microorganisms

and enhances interaction with bacterial cell membrane. The affinity of metal nanoparticles to bind with sulfur- or phosphorus-containing biomaterials such as DNA, proteins, and enzymes; the tendency to produce free radicals; generation of reactive oxygen species because of disruption of respiratory chain; and inhibition of signal transduction are other pathways by which nanoparticles cause bacterial cell death (Fig. 51.4).

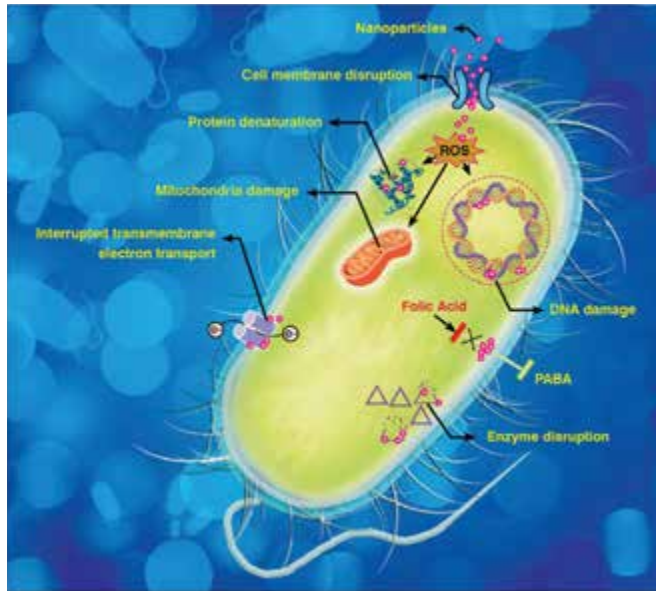

Figure 51.4 Probable mechanisms of antibacterial activity exerted by nanomaterials. Image credit: Centre for Knowledge Management of Nanoscience and Technology, Hyderabad, India, reprinted with permission.

51.3.1 Nanotechnology-Based Approaches for Diagnosing Superbugs

Although several conventional techniques with high sensitivity and reproducibility are available to detect MDR infections, they are cumbersome and time consuming. Nanoscience can offer various accurate, economical, and less time-consuming methods, which will help to avert microbial spread and its consequences. Figure 51.5 highlights some of these approaches, which are discussed below.

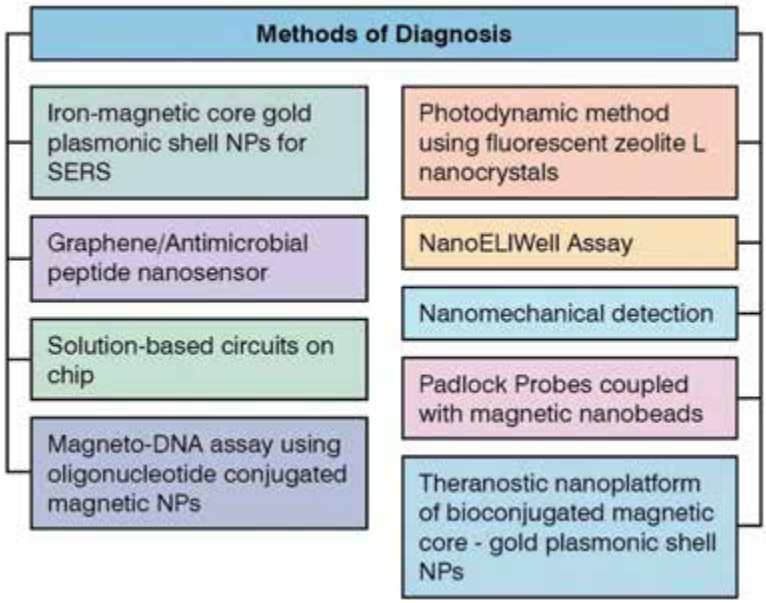

Figure 51.5 Nanotechnology-based approaches for diagnosing superbugs.

A team of researchers from Jackson State University, USA, has developed a new popcorn-shaped iron-magnetic core gold plasmonic shell nanoparticles for surface-enhanced Raman spectroscopy (SERS) detection and photothermal destruction of MDR Salmonella bacteria [15]. They have also reported that the same core–shell nanoparticle can be used in combination with near infrared (NIR) light to form light-directed nanoheaters for hyperthermic destruction of MDR [15]. In another approach, the solution-based circuit chip (SCC) for simultaneous identification of resistant and non-resistant *E. coli* causing urinary tract infections has been developed. These SCCs were fabricated by using a series of lithographic steps followed by electro-chemical deposition that create 3D nanoscopic morphology on microsensors. Further, these patterned microsensors were functionalized with peptide nucleic acid (PNA) probes to target specific region of pathogens. This multiplexed technique is also capable of distinguishing different bacterial strains like *S. aureus* and *E. coli* present in the same sample [16]. Similarly, Nguyen and the team from The Methodist Hospital Research Institute in Houston, USA, have invented a novel

NanoELIwell device for MDR-TB diagnosis. The technique is a combination of mycobacteria antigen immunoassay and microwell technologies. This device is able to perform fast identification and detection of antigens released by drug-susceptible and -resistant mycobacteria [17].

A different diagnostic approach was developed by using padlock probes (a type of linear oligonucleotide) coupled with magnetic nanobeads to detect rifampicin antibiotic-resistant TB bacteria. These padlock probes were used to target the mutated genes present in rifampicin-resistant bacteria [18]. A research team from Princeton University, USA, has developed a graphene based nanosensor to detect pathogenic bacteria at the surface of biomaterials like tooth enamel. The specificity of biorecognition was achieved by attaching odorranain-HP (an antimicrobial peptide derived from skin secretions of the diskless odorous frog, *Odorrana graham*) on graphene monolayers, which has a broad-spectrum activity towards pathogenic bacteria like MRSA [19]. Similarly, amino-functionalized zeolite-L-nanocrystals conjugated with a green fluorescent dye and a photosensitizer has shown potential for the detection of antibiotic-resistant bacteria. These crystals when adhere to the surface of bacteria impart green fluorescence and make them visible. The nanocrystals also have a bactericidal action, which is based on the "photodynamic principle" (when exposed to light starts the process of killing bacteria) [20]. In another research, Longo and colleagues from EPFL, University Hospital of Lausanne and the University of Lausanne have proposed the nanomechanical detection by using low-frequency fluctuations of cantilevers when coated with antibiotic-resistant bacteria. This nanomechanical approach, which is correlated to the cell metabolism of microorganism in presence of antibiotic, is useful in identifying resistant bacteria within minutes [21].

A generic diagnostic platform based on oligonucleotide conjugated magnetic nanoparticles was developed for the rapid detection and phenotyping of clinical pathogens by a group of researchers from Harvard Medical School, USA [22]. The 16S ribosomal RNA (16S rRNA) was selected as the target marker for universal and species-specific detection of pathogens and by further extending it to the detection of mRNA, different phenotypes (e.g., drug resistance) within closely related species can also be identified. The magneto-DNA assay is robust, fast (<2 h), and

sensitive (detection down to single bacteria and accurate, which is promising for implementing in the clinic as well as at other point-of-care settings.

In a recent study, a multifunctional theranostic nanoplatform has been designed using bioconjugated magnetic core–gold plasmonic shell nanoparticles for the early detection and noninvasive treatment of MRSA in whole blood samples [23]. APT^{SEB1} aptamer, which is specific for *S. aureus* was modified with photodynamic therapy drug, methylene blue, and attached to the theranostic nanoplatform for selective separation, imaging, and killing of MRSA from blood samples.

51.3.2 Nanotechnology-Based Preventive Measures against Superbugs

Recent advances in nanotechnology hold immense potential to modify surface properties, which can be exploited for targeting biofilms to control bacterial spread. EcoActive Surfaces Inc., USA, has developed a new mineral-based photocatalyst nanocoating of Zn/titanium dioxide named as OxiTitan. This sol-type coating can be easily applied to textiles and surfaces, which is cost effective, durable, and eco-friendly with proven action against *Clostridium difficile* spores and other antibiotic-resistant bacteria. According to the evaluation studies, it can reduce the infection of *C. difficile* up to 10 times in 24 hrs [24]. Similarly, a research team from Rensselaer Polytechnic Institute, USA, has developed a nanoscale coating for surgical equipments to target MRSA [25]. This nanocoating is made up of carbon nanotubes (CNTs) combined with enzyme lysostaphin (a natural enzyme, which attacks the bacterial cell wall causing its slicing). It is eco-friendly, as it does not leach out into environment with time. It is highly toxic to MRSA and has a dry shelf life of around six months. In another approach, scientists have developed nanoporous magnetic-like antimicrobial coating to trap and kill superbugs like *S. aureus* and *P. aeruginosa*. This coating is made up of positively charged dimethyldecylammonium chitosan methacrylate. The interaction with the negative charge present on bacterial cell wall results in the disintegration of cell wall, which causes cell death. This nanocoating can be widely applied on biomedical objects like catheters, implants and contact lenses [26].

Another commonly prevalent problem where the greater chances of infections are present is associated with the development of biofilms (Fig. 51.6). Bacteria, especially MRSA, stick to the surface of implants and form biofilm matrices, where they multiply and spread the infections. Nanotechnology can be used as an alternative approach against the accumulation of biofilms on the prosthesis and implanted devices. Several nanomaterials such as AgNPs [27], ZnO [28, 29], and AuNPs coated with vancomycin [30] have already shown good potential against antibiotic-resistant *E. coli*, *S. aureus* and vancomycin-resistant *S. aureus*. NPs were found to be effective as a coating for glass to prevent the formation of biofilms on its surface [31]. A layer-by-layer (LbL) coating that delivers antibiotics in a highly efficient, bioresponsive, and controlled-release mode has been developed using spin coating. Tannic acid (TA) with one of several cationic antibiotics (tobromycin, gentamicin, and polymyxin B) was used in this LbL coating that triggers an antibiotic burst release in response to a decrease in pH caused by typical bacterial pathogens such as *S. epidermidis*, *S. aureus*, and *E. coli*, which are known to cause infections associated with many implantable biomedical devices [32].

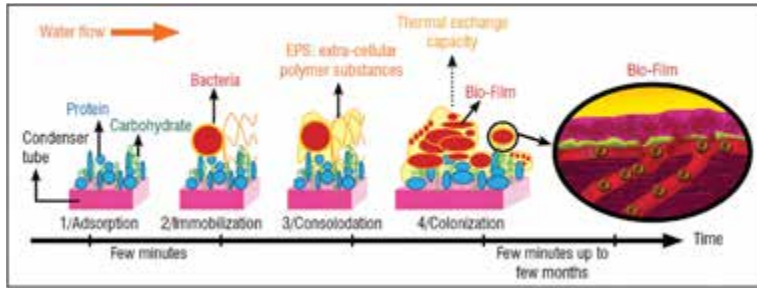

Figure 51.6 Formation of biofilm on the surface of medical devices.

51.3.3 Nano-Based Therapy to Combat Superbugs

General treatment of antibiotic-resistant bacteria requires multiple drugs regimen, which can cause many side effects. In addition, the treatment is costly and time consuming. Nanoscience and technology can pave way for new treatment methods at much accelerated rate as compared to developing new antibiotics, which probably takes 10–12 years at an estimated cost of approximately $4 billion. Nanomaterials that are emerging as effective against

antibiotic resistance and various approaches to combat superbugs are described in Fig. 51.7.

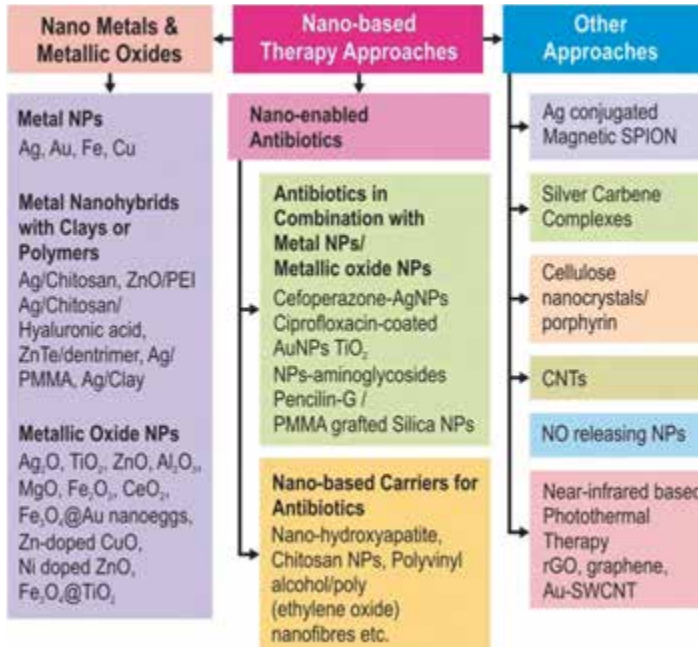

Figure 51.7 Nanotechnology-based therapeutic approaches to treat antibiotic resistance and superbugs.

Metal and Metallic Oxide NPs: Metal NPs are potential candidates to deal with emergent MDR strains. Among metal NPs, silver NPs have shown maximum potential in different studies and proven to be effective against a broad spectrum of antibiotic-resistant bacteria like MRSA, MRSE, erythromycin-resistant *Str. pyogenes*, ampicillin-resistant *E. coli*, and multidrug-resistant *P. aeruginosa* [33]. Su and his coworkers from National Chung Hsing University, Taiwan, have developed nanohybrids of AgNPs by adhering them with 1nm-thick inorganic silicate clay platelets. This modification improved the surface properties of AgNPs, reversed agglomeration and showed potent action on silver-resistant *E. coli* and MRSA [34]. Studies also supported the use of poly-methyl-methacrylate (PMMA) to load silver nanoparticles for reducing its toxicity on mammalian cells [35]. Combination of AgNPs and polymer chitosan acetate has shown potential against MRSA when used in

burn dressings [36]. Scientists have also used gold nanoclusters as potential antimicrobial agent against antibiotic-resistant bacteria. They have prepared functional gold nanoclusters (Au NCs) by using lysozyme as sequestering and reducing agent. These lysozyme–Au NCs were effectively inhibiting the growth of notorious antibiotic-resistant bacteria, like pan-drug-resistant *Acinetobacter baumannii* and vancomycin-resistant *Enterococcus faecalis* [37].

Lara et al. from Winston-Salem State University, USA, have reported the use of silver oxide nanoparticles (Ag_2O NPs) as good antibacterial agent against multidrug-resistant bacteria like erythromycin-resistant *Str. pyogenes*, ampicillin-resistant *E. coli*, MRSA and MRSE [38, 39]. In research studies performed at JNTU University, India, TiO_2 nanoparticles (TiO_2 NPs) were found to be effective against antibiotic-resistant *E. coli* [40]. TiO_2 NPs were also able to enhance the activity of various antibiotics like beta-lactams, cephalosporins, aminoglycosides, and macrolides against MRSA [41]. ZnO nanoparticles (ZnO NPs) were also found to possess good antibacterial action against MDR via targeting the bacterial cell membrane resulting in increased permeability leading to cell death. Further, polyvinyl alcohol-coated ZnO NPs also induced oxidative stress along with cell membrane targeting [42].

Nano-enabled Antibiotics: Researchers have also explored various nanosized carriers as drug delivery systems (DDS) for antibiotics, which have shown proven effectiveness against antibiotic-resistant bacteria. Nanosized drug delivery systems, owing to their unique physicochemical properties including small size and high surface-to-volume ratio enhance interaction with microorganisms. They are adaptable to various environments by structural and functional modifications, which also improve targeted delivery at infection sites and sustained drug release to decrease frequency of administration [43]. It is also envisaged that developing resistance to such systems are more unlikely as that would require multiple simultaneous gene mutations in the same microbial cell [44].

A research group at Fudan University, China, has prepared nano-hydroxyapatite (nHA) pellets as carrier for vancomycin and investigated its effectiveness against MRSA-induced chronic osteomyelitis and other bone defects. It was found that nHA pellets acted as a good bone graft material to reconstruct bone defects and to control bacterial infection [45]. Another study reported

the synergistic effect of chitosan NPs with sulfamethoxazole against resistant *P. aeruginosa* [46]. El-Newehy and group from King Saud University, Saudi Arabia, have used a novel technique of encapsulating antibiotic inside nanofibers made up of polyvinyl alcohol and polyethylene oxide, which actually boost up the power of antibiotics. The encapsulation controls the drug release thereby makes them effective for longer duration of time [47]. Combining antibiotics with metallic nanoparticles can also be a promising approach to overcome resistance in bacteria. Fayaz and co-workers from the University of Madras, India, have reported that antibacterial effect of cefoperazone against MRSA was increased when combined with AgNPs [48]. Similar effects were reported for vancomycin-capped AuNPs against VRE [49], ciprofloxacin-coated AuNPs [50] and penicillin-G complexed with PMMA grafted silica NPs [51]. Multifunctional vancomycin immobilized Fe_3O_4Au nanoeggs (egg-shaped Fe_3O_4-gold core–shell nanoparticles) as photothermal agents were also effective in killing antibiotic-resistant bacteria [52]. In another study, tetracycline encapsulated nanoporous silica nanoparticles were found to be efficient against susceptible and even doubly resistant bacteria without any significant mammalian cell cytotoxicity [53].

Other Approaches: Schoenfisch and team at the University of North Carolina, USA, have demonstrated that nitric oxide (NO) releasing silica nanoparticles are effective against antibiotic-resistant *P. aeruginosa* [54]. Similar results were obtained in another study where NO releasing nanoparticles had shown broad-spectrum antibacterial effect on antibiotic-resistant *K. pneumonia, E. faecalis, Str. pyogenes, E. coli*, and *P. aeruginosa*. These NPs actually targeted the bacterial cell membrane and altered its structure. Besides this, they also release reactive nitrogen species (RNS), which modifies the essential protein in bacteria causing cell death [55].

Scientists have also combined the unique properties of silver with superparamagnetic iron oxide nanoparticle (SPION) and targeted it against MRSA-biofilms. They reported for the first time that silver-conjugated SPION could be used as an effective antibacterial agent to target the site of infection as well as to eradicate MRSA biofilms in the presence of magnetic fields [56].

Several other nanomaterial combinations were also explored by various research groups to fight against superbugs. Antimicrobial photodynamic therapy has been investigated as an alternative

approach for treating microbial infections using cellulose nanocrystals modified with porphyrin-derived photosensitizer. These crystals were capable of inducing photodynamic inactivation of multidrug resistant *Acinetobacter baumannii* (MDRAB) and MRSA [57]. Silver carbine complexes (SCCs) encapsulated in poly (ethylene glycol)-poly(lactic acid) (PEG-PLA) nanoparticle complexes act as controlled release systems and were found to be active against various antibiotic resistant forms of bacteria such as MRSA, *P. aeruginosa*, *B. cepacia,* and *K. pneumonia* [58]. Various carbon nanostructures have been identified as effective photothermal therapy agents due to their unique optical properties that enable these materials to absorb light irradiation. They are also referred to as "optical nano heaters." CNT clusters have been explored for antimicrobial photothermal therapy by delivering CNT nanoclusters to the infected site followed by bacterial adsorption and selective destruction of antibiotic resistant bacteria by near IR irradiation [59]. Reduced graphene oxide functionalized with glutaraldehyde was studied as capturing agent for the effective killing of both Gram-positive (*S. aureus*) and Gram-negative (*E. coli*) bacteria upon near-infrared (NIR) laser irradiation. Further, the utilization of a microfluidic chip system provides a biocompatible platform for online photothermal sterilization [60].

Improved photothermal efficiency was observed with antibody-conjugated gold/CNT nanohybrid system to selectively detect and eradicate multiple drug resistant *Salmonella* (*MDRS*) *typhimurium DT104* bacteria. Anti-*Salmonella typhi* antibody AC04 conjugated to GNPs enables selective targeting and enhancement in the Raman spectral detection signal intensity by 5 orders of magnitude resulting in irreparable damage to more than 99% *Salmonella DT104* at the concentration of 10^5 CFU mL^{-1} [61].

Graphene quantum dots (GQD), a carbon-based honeycomb structure having similar physico-chemical properties of graphene have been explored as potential candidates for photodynamic therapy. GQD in suspension are able to generate reactive oxygen species (ROS) upon photoexcitation, which can be effectively used to eliminate microbial pathogens, including bacteria. However, due to the low tissue penetration of blue light and low absorbance of GQD at the higher wavelengths, GQD-based photodynamic therapy is more appropriate for skin and mucosal infections, or water and surface disinfection [62].

51.4 Conclusions and Future Perspectives

Antibiotics have long been considered the foundation of modern medicine because success of most of the current medical procedures, including surgery, organ transplantation, and cancer chemotherapy, heavily depend on them. Antibiotics have been saving an enormous number of lives from many infectious diseases for more than half a century. However, the emergence of resistance to antibiotics acquired by microbial variants is a serious, worldwide threat to public health. It has been realized that antibiotics solely can never be a solution for superbugs and thus, scientific community is exploring various alternative therapeutic approaches to address this looming challenge.

Nanotechnology-based multi-pronged approaches can be an effective alternative strategy to deal with the increasing antimicrobial resistance. Multifunctional nanomaterial-based theranostic platforms, metal nanoparticle-conventional antibiotic synergistic cocktails, nano-enabled drug carrier systems, etc., are some of the candidate strategies that can potentially be effective in the fight against superbugs. The unique physicochemical properties along with high surface area to volume ratio not only make metallic nanoparticles as effective antimicrobial agents but also show potential for developing synergistic combinations that increase the antibacterial effect of existing antibiotics. Nanomaterials exert antimicrobial activity by multiple mechanisms and hence are an ideal approach to combat superbugs. The use of nanosized drug carrier systems for delivering conventional antibiotics is also an effective approach to overcome drug resistance as well as to improve efficacy.

Although nanotechnology-based approaches promise significant benefits in addressing the key hurdles in dealing with antibiotic resistance, the immediate challenge in translating this technology to clinical use is the perceived toxicity of nanomaterials. At present, there are very little data on the toxicity of nano-enabled antibiotics and nanosized antibiotics carrier systems. Further work is still required in order to elucidate the entire mechanism of action of nanoparticles as bactericidal agent, their effects on human cells, tissues, and organs as well as the appropriate routes for their administration to obtain the desired therapeutic results.

Disclosures and Conflict of Interest

The authors declare that they have no conflict of interest and have no affiliations or financial involvement with any organization or entity discussed in this chapter. This includes employment, consultancies, honoraria, grants, stock ownership or options, expert testimony, patents (received or pending) or royalties. No writing assistance was utilized in the production of this chapter and the authors have received no payment for its preparation. The authors would like to thank Dr. S. V. Joshi, Additional Director, ARCI for his support, encouragement and valuable suggestions during the preparation of this chapter. They would also like to thank Dr. G. Sundararajan, Director, ARCI, for permitting to publish this book chapter.

Corresponding Author

Dr. Yashwant R. Mahajan
Centre for Knowledge Management of Nanoscience and Technology
12-5-32/8, Vijaypuri Colony, Tarnaka
Secunderabad 500017, Telangana, India
Email: mahajanyrm@gmail.com

About the Authors

Nisha C. Kalarickal received her PhD in 2004 from the Indian Institute of Chemical Technology, Council of Scientific and Industrial Research, Hyderabad, India. Subsequently, she took up postdoctoral positions at the Faculty of Pharmacy, University of Montreal, Canada and at Department of Materials Science and Engineering, University of California, Berkeley, USA. She returned to India as a research scientist at the Centre for DNA Fingerprinting and Diagnostics, Hyderabad. At present, she works at the Centre for Knowledge Management of Nanoscience and Technology (CKMNT), Hyderabad, India, as a senior knowledge officer and serves as editor of *Nanotech Insights*, a quarterly publication by the CKMNT. Her scientific and research interests include polymer self-assemblies and nanostructured materials for biomedical applications.

Yashwant R. Mahajan obtained his PhD in physical metallurgy in 1978 from the Polytechnic Institute of Brooklyn, New York. He carried out his postdoctoral research in the areas of titanium base alloys, powder metallurgy, and high temperature dispersion strengthened aluminum base alloys at the Air Force Materials Laboratory, WPAFB, Ohio, for four years. He has worked in various capacities, namely, scientist/associate director at the Defence Metallurgical Research Laboratory, ARC International, Defence Research and Development Laboratory, Hyderabad, India. He made major contributions in the areas of metal matrix composites (MMCs), advanced ceramics, and ceramic matrix composites (CMCs). Under his leadership, a number of ceramic-based technologies were developed and transferred to industry. He has published more than 130 technical papers in peer-reviewed journals and conference proceedings and holds 13 patents (including 2 US patents). He is a recipient of NRC Associateship of the National Academy of Sciences, USA, the Best Metallurgist of the year award (IIM), MRSI Medal, MRSI-IISC superconductivity award, and VASVIK Medal. He is a professional member of ASM International, TMS, MRS-USA, SPIE-USA, Institute of Materials-UK, American Ceramic Society, MRSI and IIM. Dr. Mahajan has been working as a technical advisor at the CKMNT since April 2009. He is a founding editor of *Nanotech Insights* newsletter published by the CKMNT. He has published several articles pertaining to nanotechnology applications in the areas of global warming, oil spill remediation, CNT-based body armor, nanostructured steels, mass production of graphene, nanoengineered steels for structural applications, etc. Recently he has edited a special issue of *Nanotech Insights* on "Defence, Aerospace and National Security." He has been also involved in bringing out techno-commercial multi-client as well as customized reports related to nanotechnology.

References

1. Antimicrobial Resistance: Global Report on Surveillance (2014). World Health Organization (WHO), Switzerland. Available at: http://apps.who.int/iris/bitstream/10665/112642/1/9789241564748_eng.pdf (accessed on January 9, 2015).

2. Jones, L. S., Howe, R. A. (2014). Microbial resistance and superbugs. In: Percival, S. L., Williams, D., Cooper, T., Randle, J., (eds.). *Biofilms in Infection Prevention and Control: A Healthcare Handbook*. Academic Press, USA.
3. Hawkey, P. M. (1998). The origins and molecular basis of antibiotic resistance. *BMJ*, **317**(7159), 657–660.
4. McDonald, L. C. (2006). Trends in antimicrobial resistance in health care-associated pathogens and effect on treatment. *Clin. Infect. Dis.*, **42**(Suppl. 2), S65–S71.
5. Fleming A. (1945). Sir Alexander Fleming—Nobel Lecture: Penicillin. Available at: http://www.nobelprize.org/nobel_prizes/medicine/laureates/1945/fleming-lecture.pdf (accessed on January 10, 2015).
6. Gould, I. M. (2009). Antibiotic resistance: The perfect storm. *Int. J. Antimicrob. Agents*, **34**, S2–S5.
7. Progress Report (2011). Towards Universal Access to Diagnosis and Treatment of Multidrug-resistant and Extensively Drug-resistant Tuberculosis by 2015. World Health Organization (WHO), Switzerland. Available at: http://whqlibdoc.who.int/publications/2011/9789241501330_eng.pdf?ua=1 (accessed on January 14, 2015).
8. Drug-resistant tuberculosis now at record levels (2010). Available at: http://www.who.int/mediacentre/news/releases/2010/drug_resistant_tb_20100318/en/ (accessed on January 14, 2015).
9. Klevens, R. M., Morrison, M. A., Nadle, J., et al. (2007). Invasive methicillin-resistant *Staphylococcus aureus* infections in the United States. *JAMA*, **298**(15), 1763–1771.
10. Kumarasamy, K. K., Toleman, M. A., Walsh, T. R., et al. (2010). Emergence of a new antibiotic resistance mechanism in India, Pakistan, and the UK: A molecular, biological, and epidemiological study. *Lancet Inf. Dis.*, **10**(9), 597–602.
11. Johnson, A. P., Woodford, N. (2013). Global spread of antibiotic resistance: the example of New Delhi metallo-β-lactamase (NDM)-mediated carbapenem resistance. *J. Med. Microbiol.,* **62**, 499–513.
12. Ling, L. L., Schneider, T., Peoples, A. J., et al. (2015). A new antibiotic kills pathogens without detectable resistance. *Nature*, **517**, 455–459.
13. Huh, A. J., Kwon, Y. J. (2011). Nanoantibiotics: A new paradigm for treating infectious diseases using nanomaterials in the antibiotics resistant era. *J. Control. Release,* **156**, 128–145.
14. Singh, R., Smitha, M. S., Singh, S. P. (2014). The role of nanotechnology in combating multi-drug resistant bacteria. *J. Nanosci. Nanotechnol.,* **14**, 4745–4756.

15. Fan, Z., Senapati, D., Khan, S. A., et al. (2013). Popcorn-shaped magnetic core–plasmonic shell multifunctional nanoparticles for the targeted magnetic separation and enrichment, label-free SERS imaging, and photothermal destruction of multidrug-resistant bacteria. *Chem. Eur. J.*, **19**(8), 2839–2847.
16. Lam, B., Das, J., Holmes, R. D. (2013). Solution-based circuits enable rapid and multiplexed pathogen detection. *Nat. Commun.*, **4**, article number 2001.
17. Nguyen, Y. H., Ma, X., Qin, L. (2012). Rapid identification and drug susceptibility screening of ESAT-6 secreting Mycobacteria by a NanoELIwell assay. *Sci. Rep.*, **2**, article number 635.
18. Engstrom, A., de la Torre, T. Z. G., Stromme, M., et al. (2013). Detection of rifampicin resistance in *Mycobacterium tuberculosis* by padlock probes and magnetic nanobead-based readout. *PLOS One*, **8**(4), article number e62015.
19. Mannoor, M. S., Tao, H., McAlpine, M. C., et al. (2012). Graphene-based wireless bacteria detection on tooth enamel. *Nat. Commun.*, **3**, article number 763.
20. Strassert, C. A., Otter, M., Albuquerque, R. Q., et al. (2009). Photoactive hybrid nanomaterial for targeting, labeling, and killing antibiotic-resistant bacteria. *Angew. Chem. Int. Ed.*, **48**(42), 7928–7931.
21. Longo, G., Alonso-Sarduy, L., Rio, L. M., et al. (2013). Rapid detection of bacterial resistance to antibiotics using AFM cantilevers as nanomechanical sensors. *Nat. Nanotechnol.*, **8**, 522–526.
22. Chung, H. J., Castro, C. M., Im, H., et al. (2013). A magneto-DNA nanoparticle system for rapid detection and phenotyping of bacteria. *Nat. Nanotechnol.*, **8**, 369–375.
23. Fan, Z., Khan, S. A., Dai, X., et al. (2014). Theranostic nanoplatforms for MRSA detection and destruction from whole blood. *Part. Part. Syst. Charact.*, **31**, 357–364.
24. SpecialChem. Available at: http://coatings.specialchem.com/news/product-news/ecoactive-surfaces-introduces-oxititan-vlr-new-light-powered-antimicrobial-coating-effective-aga-11976 (accessed on November 19, 2015).
25. Pangule, R. C., Brooks, S. J., Dinu, C. Z., et al. (2010). Antistaphylococcal nanocomposite films based on enzyme–nanotube conjugates. *ACS Nano*, **4**(7), 3993–4000.
26. Taylor, E., Webster, T. J. (2011). Reducing infections through nanotechnology and nanoparticles. *Int. J. Nanomed.*, **6**, 1463–1473.

27. Knetsch, M. L. W., Koole, L. H. (2011). New strategies in the development of antimicrobial coatings: The example of increasing usage of silver and silver nanoparticles. *Polymers*, **3**(1), 340–366.

28. Seil, J. T., Webster, T. J. (2011). Reduced *Staphylococcus aureus* proliferation and biofilm formation on zinc oxide nanoparticle PVC composite surfaces. *Acta Biomater.*, **7**(6), 2579–2584.

29. Applerot, G., Lellouche, J., Perkas, N. (2012). ZnO nanoparticle-coated surfaces inhibit bacterial biofilm formation and increase antibiotic susceptibility. *RSC Adv*., **2**, 2314–2321.

30. Mohammed, F. A., Girilal, M., Mahdy, S. A., et al. (2011). Vancomycin bound biogenic gold nanoparticles: A different perspective for development of anti VRSA agents. *Proc. Biochem.*, **46**(3), 636–641.

31. Lellouche, J., Kahana, E., Elias, S., et al. (2009). Antibiofilm activity of nanosized magnesium fluoride. *Biomaterials*, **30**, 5969–5978.

32. Zhuk, I., Jariwala, F., Attygalle, A. B., et al. (2014). Self-defensive layer-by-layer films with bacteria-triggered antibiotic release. *ACS Nano*, **8**(8), 7733–7745.

33. Rai, M. K., Deshmukh, S. D., Ingle, A. P., et al. (2012). Silver nanoparticles: The powerful nanoweapon against multidrug-resistant bacteria. *J Appl. Micro.*, **112**, 841–852.

34. Su, H. L., Lin, S. H., Wei, J. C., et al. (2011). Novel nanohybrids of silver particles on clay platelets for inhibiting silver-resistant bacteria. *PLOS One*, **6**(6), article number e21125.

35. Alt, V., Bechert, T., Steinrucke, P., et al. (2004). An *in vitro* assessment of the antibacterial properties and cytotoxicity of nanoparticulate silver bone cement. *Biomaterials*, **25**(18), 4383–4391.

36. Huang, L., Dai, T., Xuan, Y., et al. (2011). Synergistic combination of chitosan acetate with nanoparticle silver as a topical antimicrobial: efficacy against bacterial burn infections. *Antimicro. Agents Chemother.*, **55**(7), 3432–3438.

37. Chen, W. Y., Lin, J. Y., Chen, W. J., et al. (2010). Functional gold nano-clusters as antimicrobial agents for antibiotic-resistant bacteria. *Nanomedicine*, **5**(5), 755–764.

38. Lara, H. H., Ayala-Nunez, N. V., Ixtepan-Turrent, L., et al. (2010). Bactericidal effect of silver nanoparticles against multidrug-resistant bacteria. *World J. Microbiol. Biotechnol.*, **26**, 615–621.

39. Nanda, A., Saravanan, M. (2009). Biosynthesis of silver nanoparticles from *Staphylococcus aureus* and its antimicrobial activity against MRSA and MRSE *Nanomedicine: Nanotechnol. Biol. Med.*, **5**, 452–457.

40. Haghi, M., Hekmatafshar, M., Janipou, M. B., et al. (2012). Antibacterial effect of TiO_2 nanoparticles on pathogenic strain of *E. Coli. Int. J. Adv. Biotech. Res.*, **3**(3), 621–624.
41. Roy, A. S., Praveen, A., Koppalkar, A. R., et al. (2010). Effect of nano-titanium dioxide with different antibiotics against methicillin-resistant *Staphylococcus aureus. J. Biomater. Nanobiotechnol.*, **1**, 37–41.
42. Huang, Z., Zheng, X., Yan, D., et al. (2008). Toxicological effect of ZnO nanoparticles based on bacteria. *Langmuir*, **24**, 4140–4144.
43. Nunes, R., Sousa, C., Sarmento, B., das Neves, J. (2015). Nanotechnology-based systems for microbicide development. In: Bawa, R., Audette, G., Rubinstein, I., eds. *Handbook of Clinical Nanomedicine: Nanoparticles, Imaging, Therapy, and Clinical Applications*, Chapter 50, Pan Stanford Publishing, Singapore.
44. Pelgrift, R. Y., Pelgrift, A. J., Friedman, A. J. (2013). Nanotechnology as a therapeutic tool to combat microbial resistance. *Adv. Drug Deliv. Rev.*, **65**, 1803–1815.
45. Jiang, L. L., Li, Y. F., Fang, T. L., et al. (2012). Vancomycin-loaded nano-hydroxyapatite pellets to treat MRSA-induced chronic osteomyelitis with bone defect in rabbits. *Inflamm. Res*., **61**, 207–215.
46. Tin, S., Sakharkar, K. R., Lim, C. S., et al. (2009). Activity of chitosans in combination with antibiotics in *Pseudomonas aeruginosa*. *Int. J. Bio. Sci.*, **5**(2), 153–160.
47. Antibiotics wrapped in nanofibers turn resistant disease-producing bacteria into ghosts (2011). Available at: http://www.acs.org/content/acs/en/pressroom/newsreleases/2011/march/antibiotics-wrapped-in-nanofibers-turn-resistant-disease-producing-bacteria-into-ghosts.html (accessed on January 2, 2015).
48. Fayaz, A. M., Balaji, K., Girilal, M., et al. (2010). Biogenic synthesis of silver nanoparticles and their synergistic effect with antibiotics: A study against Gram-positive and Gram-negative bacteria. *Nanomedicine: Nanotechnol. Biol. Med.*, **6**, 103–109.
49. Gu, H., Ho, P. L., Tong, E., et al. (2003). Presenting vancomycin on nanoparticles to enhance antimicrobial activities. *Nano Lett.*, **3**, 1261–1263.
50. Tom, R. T., Suryanarayanan, V., Reddy, P. G., et al. (2004). Ciprofloxacin-protected gold nanoparticles. *Langmuir*, **20**(5), 1909–1914.
51. Wang, L., Chen, Y. P., Miller, K. P., et al. (2014). Functionalised nanoparticles complexed with antibiotic efficiently kill MRSA and other bacteria. *Chem. Commun.*, **50**, 12030–12033.

52. Huang, W. C., Tsai, P. J., Chen, Y. C. (2009). Multifunctional Fe_3O_4@Au nanoeggs as photothermal agents for selective killing of nosocomial and antibiotic-resistant bacteria. *Small*, **5**(1), 51–56.

53. Capeletti, L. B., França de Oliveira, L., Gonçalves, K. A., et al. (2014). Tailored silica–antibiotic nanoparticles: Overcoming bacterial resistance with low cytotoxicity. *Langmuir*, **30**(25), 7456–7464.

54. Hetrick, E. M., Shin, J. H., Stasko, N. A., et al. (2008). Bactericidal efficacy of nitric oxide-releasing silica nanoparticles. *ACS Nano*, **2**(2), 235–246.

55. Friedman, A. J., Blecher, K., Schairer, D., et al. (2011). Susceptibility of Gram-positive and -negative bacteria to novel nitric oxide-releasing nanoparticle technology. *Virulence*, **2**, 217–221.

56. Durmus, N. G., Webster, T. J. (2013). Eradicating antibiotic-resistant biofilms with silver-conjugated superparamagnetic iron oxide nanoparticles. *Adv. Healthcare Mater.*, **2**, 165–171.

57. Carpenter, B. L., Feese, E., Ghiladi, R. A., et al. (2012). Porphyrin-cellulose nanocrystals: A photobactericidal material that exhibits broad spectrum antimicrobial activity. *Photochem. Photobiol.*, **88**, 527–536.

58. Leid, J. G., Ditto, A. J., Knapp, A., et al. (2011). *In vitro* antimicrobial studies of silver carbene complexes: Activity of free and nanoparticle carbene formulations against clinical isolates of pathogenic bacteria. *J. Antimicrob. Chemother*., 138–148.

59. Maisch, T. (2009). A new strategy to destroy antibiotic resistant microorganisms: Antimicrobial photodynamic treatment. *Mini Rev. Med. Chem.,* **9**(8), 974–983.

60. Wu, M. C., Deokar, A. R., Liao, J. H., et al. (2013). Graphene-based photothermal agent for rapid and effective killing of bacteria. *ACS Nano*, **7**(2), 1281–1290.

61. Lin, Y., Hamme II, A. T. (2014). Targeted highly sensitive detection/eradication of multi-drug resistant Salmonella DT104 through gold nanoparticle–SWCNT bioconjugated nanohybrids. *Analyst*, **139**, 3702–3705.

62. Ristic, B. Z., Milenkovic, M. M., Dakic, I. R., et al. (2014). Photodynamic antibacterial effect of graphene quantum dots. *Biomaterials*, **35**(15), 4428–4435.

Chapter 52

Nanolithography and Biochips' Role in Viral Detection

Inbal Tsarfati-BarAd and Levi A. Gheber, PhD

Department of Biotechnology Engineering,
Ben-Gurion University of the Negev, Beer-Sheva, Israel

Keywords: viral detection, diagnostics, biosensors, biochips, nano-biolithography, miniaturization, nanografting, dip-pen nanolithography, nano-fountain pens, scanning probe microscopy

52.1 The Need for Portable Biochips for Viral Detection

A viral outbreak may cause heavy repercussions to human life as well as the economy and the environment. For this reason health services rely on fast diagnosis and disease surveillance to minimize consequences of such outbreaks [1]. Whether the epidemic is due to natural causes or a bioterrorism act, a main issue in controlling viral outbreaks is the ability to detect and identify the virus as early as possible. Only after the type and location of the virus is known, proper measures can be taken in order to contain the

Handbook of Clinical Nanomedicine: Nanoparticles, Imaging, Therapy, and Clinical Applications
Edited by Raj Bawa, Gerald F. Audette, and Israel Rubinstein

ISBN 978-981-4669-20-7 (Hardcover), 978-981-4669-21-4 (eBook)
www.panstanford.com

outbreak [2]. However, detection methods are currently expensive and time consuming and require complex laboratory equipment, for example, polymerase chain reaction (PCR) and enzyme-linked immunosorbent assay (ELISA). There is therefore a pressing need for deployable, on-site detection devices able to simultaneously screen a number of candidates and quickly identify and quantify the threat. Various degrees of deployment are conceivable, such as handled, point-of-care devices, monitoring devices for high-exposure institutions such as hospitals, or on a battlefield [3]. One of the most appealing approaches to high-throughput parallel screening is the arrayed biosensor, or *biochip.* The current microarray technology, however, produces large biochips which require heavy and expensive separate readout systems (scanners) and thus are used predominantly in large facilities such as research institutes and hospitals. Miniaturization of current microarrays by orders of magnitude is the first step in achieving portable, deployable, arrayed biosensors.

52.2 Arrayed Biosensors: Biochips

A biosensor array (biochip) is a device enabling the detection of target molecules in a sample. The target molecules may be of a biological nature, and/or the detection method is based on a biological capture molecule. It consists of an array of biological test sites, immobilized to a solid support. The test sites are dots of various biological molecules (termed "spots"), such as DNA, protein, and antibodies. These molecules serve as selective capture agents. Upon application of a solution on the surface, the target molecule will bind to the capture molecule if it is present in the solution.

In a direct assay, the target molecule itself is (nonspecifically) labeled. In an indirect assay, a secondary labeled specific detection molecule is subsequently applied. In both cases, the binding of the target protein to a certain spot is indicated by the appearance of a signal (typically a fluorescent signal). Spots consisting of various molecules on the same surface enable multiple tests simultaneously, thereby improving throughput and specificity [4]. This technology has launched a considerable advancement in the field of both proteomics and genomics research, as well as medical diagnostics [5].

52.3 The Need for Miniaturization

Current microarray technology produces spots ~100 μm in diameter, with a spacing of 300–400 μm. Reading of the assay results are based mostly on fluorescence; thus detection is done using a microscope objective with a typical viewfield ~1.5 mm in diameter. The spot size and spacing lead to imaging of only ~9 spots simultaneously in one such viewfield; therefore, the microarray is rasterscanned in front of the objective to allow collection of the whole array image. Scanning is performed over several centimeters in the horizontal directions. However, the Z (vertical) direction must be controlled with micrometer precision in order to avoid defocusing of the sample. To achieve this precision, large and complex machines—scanners—are employed, which use high precision robotic components. This fact makes scanners heavy, large, and expensive and thus not portable. Miniaturization of the active spots by two or three orders of magnitude would allow the observation of an array consisting of hundreds of spots in one view field, thus avoiding the need for large scanning machines. This alone can reduce considerably the biochip's basic investment and constitutes a big step toward portable chips.

Nanoarrays will furthermore reduce the amount of biomaterials used as capture molecules (which constitute a disproportionately large component of a biochip's cost) and thus reduce the biochip's production price. Moreover, since the reactions take place in small volumes, mass (and heat) transfer durations are dramatically reduced, leading to shortening of the incubation. This will lead to more rapid diagnostics [4].

Due to these considerations, there is a search for the most practical way to fabricate nanostructures of biological molecules, using several nanolithography techniques explained later.

52.4 Nanolithography

Lithography can be classified in a number of ways:

(1) **Positive/negative**: Positive lithography involves deposition of materials that accumulate on the surface. Negative lithography is the removal of material or the creating of depressions in the surface.

(2) **Direct/indirect**: Indirect lithography is a multistep procedure, in which patterns are first inscribed on the surface and the structures are fabricated after a number of subsequent steps, according to the "blueprint" previously inscribed. With direct lithography, the features are directly fabricated on to the surface in the desired locations.

Nanolithography is the application of these approaches, resulting in structures with typical dimensions of nanometers. All combinations between (1) and (2) are possible, and the choice depends on the type of desired structures, their composition, size, and precision of fabrication and the ultimate ease of production and cost.

These techniques can be used either to chemically modify the chip's surface in preparation for the molecules' immobilization (indirect) or to print the capture molecules themselves (direct). They can be used to fabricate libraries of different viruses and viruses' constituents or capture molecules recognizing these. These libraries will constitute a major source of knowledge and can promote a big step in biomedical research [5].

One example is the use of biologically active virus particles that can be used in the monitoring of single cell infectivity, for example, how the number of virus particles, their orientation, and their chemical immobilization and presentation affect cellular infectivity for single and small collections of virus particles [6]. Another is directly detecting viral particles by specific capture molecules such as antibodies against specific viral proteins. Obviously the reverse approach is possible: immobilization of viral constituents as capture molecules for detection of antibodies in patient samples.

52.5 SPM-Based Nanolithography Methods

The majority of classical lithography methods, borrowed from microelectronics, are unsuitable for biological materials. Most of them demand vacuum, etching with strong acids, or irradiation with UV light, all of which can be harmful to biomaterials such as DNA and proteins. Thus, nanobiolithography must use a method that operates under biological conditions: atmospheric pressure, room temperature, and moderate pH [7].

To create nanostructures an accurate and high-resolution device is required. The device must be able to operate in ambient

conditions and in liquid, thus making the scanning probe microscope (SPM) an excellent candidate. During the last decade a number of SPM-based nanolithography methods were developed. They use various modifications of the atomic force microscope (AFM), to create nanostructures of biological material on a substrate, with nanometer precision (nanobiolithography). The principal variations are listed later.

52.5.1 Nanografting

A thin molecular layer is formed on the surface, typically a self-assembled monolayer (SAM), which serves as the "resist" thus preventing the spontaneous adsorption of the biomolecules on the surface. In the next step, an AFM probe is used to "shave" molecules from the protective layer, revealing the substrate only in precisely controlled positions. The patterned surface is then incubated with a solution containing the desired molecules, which are adsorbed on the exposed parts of the substrate (see Fig. 52.1a) [8]. According to the earlier classification, this is an indirect method. Using this technique, cowpea mosaic virus (CPMV) particles were organized on a surface using nanografting, where a gold substrate was initially coated with athiol protein resist The AFM tip was used to shave lines that were subsequently functionalized with thiol linkers. These lines determined the location for the initial virus cluster formation [6].

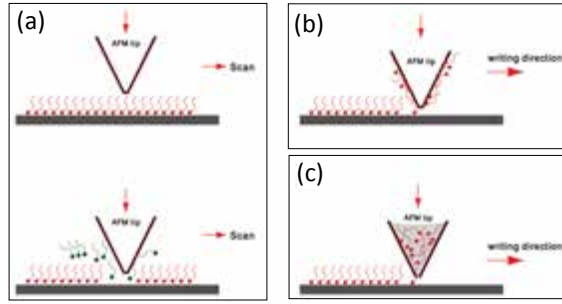

Figure 52.1 Three SPM-based lithography methods: (a) Nanographting: The shaving of a SAM from the sample's surface using an AFM tip. (b) DPN: The AFM probe tip is dipped into a solution, and intermolecular forces cause the adhesion of the solution on the tip. (c) NFP: A glass or quartz capillary in the shape of a sharp tip forms a nanopipette.

52.5.2 Dip-Pen Nanolithography

Similar to the dip pen, which is dipped in ink and subsequently used to write on paper, in dip-pen nanolithography (DPN) an AFM probe tip is dipped into a solution containing the molecules to be printed, and subsequently contacted with the substrate in desired positions, where the molecules are deposited (see Fig. 52.1b). The molecules can then react with the surface either instantly (direct method) or after a number of additional chemical steps [9]. For example, DPN and coordination chemistry (16-mercaptohexadecanoic acid [MHA] and zinc ions) were used to immobilize individual particles of tobacco mosaic virus (TMV) in a large array. This method, which enables control over particle position and orientation, can be generalized for many different viruses with a proper protein coating [5].

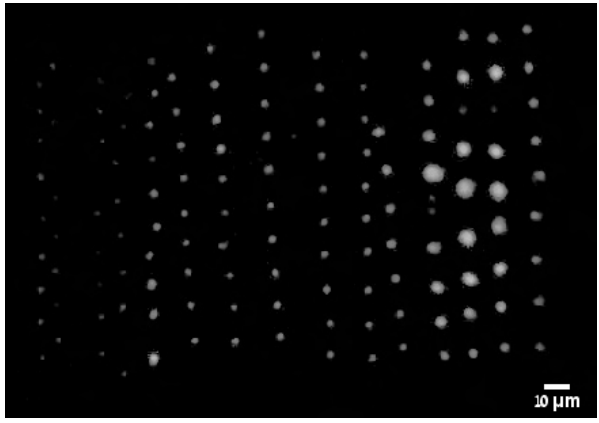

Figure 52.2 Direct immunoassay with spots as small as 200 nm [17].

The same chemical method was used for the immobilization of antibodies and fabrication of functional antibody arrays [10]. In a different case, DPN was used to manufacture nanoscale patterns of antibodies on a gold surface. These antibody spots, spaced less than 100 nm, were able to identify human immunodeficiency virus (HIV1) p24 antigen. The detection was demonstrated by applying a solution containing gold-labeled secondary antibody. The presence of the threelayer complex (capture molecule, HIV1 p24 antigen, and secondary gold-labeled antibody) was indicated by a small height increase. This method appeared to be both

more sensitive and more selective than the commonly used ELISA by more than a 1000-fold [11].

52.5.3 Nano-Fountain Pen

The nano-fountain pen (NFP) uses a glass or quartz capillary tapered to a sharp tip to form a nanopipette. The tip is then filled with a solution and mounted on an AFM [12].

Surface tension prevents the liquid from spilling until there is a contact with the surface (see Fig. 52.1c) [13]. Similar to the fountain pen, the NFP allows continuous writing, without a need for repeated dipping in ink. For example, the NFP was used to fabricate nanostructures of various proteins [14] or depressions, by delivering proteolytic enzymes to a proteincoated surface [15, 16]. Currently the development of a direct immunoassay with a spot radius as small as 200 nm is under development (see Fig. 52.2) [17].

The NFP can also be combined with other fabrication methods. In one example, a focused ion beam (FIB) was used to create depressions in a thin gold film that was later chemically modified with mercaptopropionic acid (MPA). The nanopipette was positioned directly over the depressions and functionalized IgG solution was then delivered. The functional antibodies were detected by confocal fluorescence microscopy [18].

52.6 Problems Associated with Miniaturization

While miniaturizing of biochips holds many advantages, a number of problems delay their deployment and wide use.

As the spots' diameter is reduced, the amount of fluorescence emitted decreases proportionally to the area of the spot (i.e., the square of the diameter). A more detailed analysis shows that the decrease in signal emission is stronger than quadratic in the diameter, due to limited binding site density of the immobilization surface. For example, low amounts and uneven distribution of capture agents might lead to the binding of a small number of labeled target molecules. This can cause a poor fluorescence signal relative to the noise created by the surface, making detection of binding impossible. Surfaces that are appropriately designed for nanobiolithography must be developed to overcome this

problem. Signal enhancement can be achieved either by increasing the surface density of binding sites or by using surfaces that produce lower fluorescence noise. Tsarfati et al. introduced a model enabling the characterization of binding site density at the nanoscale and a comparison between substrates for nanoarray fabrication. This model can be useful in the development of surfaces and selection for manufacturing of nanobiochips [17].

Another problem is the challenge of scaling up the patterning process. All of the methods above rely on an SPM for control on pattern size and location. The SPM is a slow scanning (serial) technique, which is not expected to reach fast fabrication speeds. Moreover the equipment used in nanolithography, and the need for different probes for different molecules, significantly increases the biochip's price. For mass production of nanobiochips, there is a need for a parallel writing technique, for example, "multipen" writing with "multi-ink" capabilities. A number of attempts have been reported in this direction. For example a nanoscale array of aminereactive dots was prepared using 26-pen DPN. The amine ends were bound to the protein A/G, which can subsequently bind antibodies [19].

In another case a multi-ink parallel NFP array was created. A pattern of two different inks was delivered in the liquid phase and written using a device with two onchip reservoirs feeding the NFP array with two different inks [20].

52.7 Conclusions

Although biochip miniaturization has not matured just yet, this approach is a promising precursor for the realization of the lab-on-a-chip concept. The continuing diversion of resources to the development of nanochips can result in various solutions to each of the challenges mentioned earlier. The ability to mass-produce multispot nanoarrays, with the subsequent development of nanofluidics, and miniaturization of the chip's transducers, will hasten the progression toward the portable biosensor vision. There is still much ground work to be done. However, as these lithography techniques become increasingly available to laboratories around the world, we will soon witness an expansion and hopefully an explosion of advancement in this field of research. Biochip fabrication will become more efficient and cost effective and will

provide a widespread platform for medical diagnosis as well as viral research.

Disclosures and Conflicts of Interest

The opinions and perspectives here reflect the current views of the authors. The authors declare that they have no conflict of interest and have no affiliations or financial involvement with any organization or entity discussed in this chapter. No writing assistance was utilized in the production of this chapter and the authors have received no payment for its preparation. This is a revised version of the authors' chapter that appeared in *Viral Diagnostics: Advances and Applications*, 2015 (edited by Robert S. Marks, Leslie Lobel, and Amadou Alpha Sall), Pan Stanford Publishing Pte. Ltd., Singapore.

Corresponding Author

Dr. Levi A. Gheber
Department of Biotechnology Engineering
Ben-Gurion University of the Negev
PO Box 653, Beer-Sheva 84105, Israel
Email: glevi@bgu.ac.il

About the Authors

Inbal Tsarfati-BarAd is a PhD candidate in the laboratory of Dr. L. Gheber at Ben Gurion University of the Negev, Israel. Her fields of expertise include optical microscopy, atomic force microscopy, nanobiolithography, and surface chemistry. Her research focuses on the development of strategies for fabrication and signal enhancement of miniaturized microarrays.

Levi A. Gheber is an associate professor in the Department of Biotechnology Engineering at Ben-Gurion University of the Negev in Israel. Research in Dr. Gheber's lab focuses on the molecular patterning of surfaces, biochemical nanolithography, membrane protein clustering and

the direct growth and differentiation of mesenchymal stem cells by micro patterning of the substrate and characterization of the early stages of biomineralization.

References

1. Pejcic, B., De Marco, R., Parkinson, G. (2006). The role of biosensors in the detection of emerging infectious diseases. *Analyst*, **131**(10), 1079.
2. Baril, L. (2007). Need for biosensors in infectious disease epidemiology. In: Robert S. Marks, Ed., *Handbook of Biosensors and Biochips*, John Wiley, Chichester, 1077.
3. Rosi, N. L., Mirkin, C. A. (2005). Nanostructures in biodiagnostics. *Chem. Rev.*, **105**(4), 1547.
4. Gheber, L. A. (2007). Nanobiolithography of biochips. In: Marks, R. S., Cullen, D. C., Karube, I., Lowe, C. R., Weetall, H. H., eds. *Handbook of Biosensors and Biochips*, John Wiley & Sons, Chichester, UK, vol. 2, 771–783.
5. Vega, R. A., Maspoch, D., Salaita, K., Mirkin, C. A. (2005). Nanoarrays of single virus particles. *Angew. Chem. Int. Ed. Eng.*, **44** (37), 6013.
6. Cheung, C. L., Chung, S. W., Chatterji, A., Lin, T., Johnson, J. E., Hok, S., Perkins, J., De Yoreo, J. J. (2006). Physical controls on directed virus assembly at nanoscale chemical templates. *J. Am. Chem. Soc.*, **128**(33), 10801.
7. Gheber, L. A. (2008). Nano fountain pen: Toward integrated, portable, lab-on-chip devices. In: Frank, A. G., ed. *Biological Applications of Microfluidics*, John Wiley & Sons, Chichester, UK, p. 369.
8. Wadu-Mesthrige, K., Xu, S., Amro, N. A., Liu, G. Y. (1999). Fabrication and imaging of nanometer-sized protein patterns. *Langmuir*, **15** (25), 8580.
9. Piner, R. D., Zhu, J., Xu, F., Hong, S., Mirkin, C. A. (1999). "Dip-pen" nanolithography. *Science*, **283**(5402), 661.
10. Vega, R. A., Maspoch, D., Shen, C. K. F., Kakkassery, J. J., Chen, B. J., Lamb, R. A., Mirkin, C. A. (2006). Functional antibody arrays through metal ion-affinity templates. *Chembiochem*, **7**(11), 1653.
11. Lee, K. B., Kim, E. Y., Mirkin, C. A., Wolinsky, S. M. (2004). The use of nanoarrays for highly sensitive and selective detection of human immunodeficiency virus type 1 in plasma. *Nano. Lett.*, **4**(10), 1869.

12. Hong, M. H., Kim, K. H., Bae, J., Jhe, W. (2000). Scanning nanolithography using a material-filled nanopipette. *Appl. Phys. Lett.*, **77**(16), 2604.
13. Lewis, A., Kheifetz, Y., Shambrodt, E., Radko, A., Khatchatryan, E., Sukenik, C. (1999). Fountain pen nanochemistry: Atomic force control of chrome etching. *Appl. Phys. Lett.*, **75**, 2689.
14. Taha, H., Marks, R. S., Gheber, L. A., Rousso, I., Newman, J., Sukenik, C., Lewis, A. (2003). Protein printing with an atomic force sensing nanofountain-pen. *Appl. Phys. Lett.*, **83**(5), 1041.
15. Ionescu, R. E., Marks, R. S., Gheber, L. A. (2003). Nanolithography using protease etching of protein surfaces. *Nano. Lett.*, **3**(12), 1639.
16. Ionescu, R. E., Marks, R. S., Gheber, L. A. (2005). Manufacturing of nanochannels with controlled dimensions using protease nanolithography. *Nano. Lett.*, **5**(5), 821.
17. Tsarfati-BarAd, I., Sauer, U., Preininger, C., Gheber L. A. (2011) Miniaturized protein arrays: Model and experiment. *Biosens. Bioelectron*., **26**(9), 3774–3781.
18. Bruckbauer, A., Zhou, D., Kang, D. J., Korchev, Y. E., Abell, C., Klenerman, D. (2004). An addressable antibody nanoarray produced on a nanostructured surface. *J. Am. Chem. Soc.*, **126** (21), 6508.
19. Lee, S. W., Oh, B. K., Sanedrin, R. G., Salaita, K., Fujigaya, T., Mirkin, C. A. (2006). Biologically active protein nanoarrays generated using parallel dip-pen nanolithography. *Adv. Mater.*, **18** (9), 1133.
20. Moldovan, N., Kim, K. H., Espinosa, H. D. (2006). A multiink linear array of nanofountain probes. *J. Micromechan. Microeng.*, **16**(10), 1935.

Chapter 53

Lectins as Nano-Tools in Drug Delivery

Anita Gupta, MSc (Hons), PhD,[a] and G. S. Gupta, MSc, PhD[b]

[a]*Department of Applied Science,*
Rayat and Bahra University, Mohali, Punjab, India
[b]*Department of Biophysics,*
Panjab University, Chandigarh, India

Keywords: lectins, drug carriers, nanotechnology, lectins as receptors, receptor-mediated targeting, lectins as drug carriers, carbohydrate–lectin interactions, active targeting, passive targeting, nanocarriers in drug delivery, polymeric nanoparticles (polymer–drug conjugates), lipid-based drug carriers, direct targeting, reverse lectin targeting, proteins in drug targeting, lectin-grafted prodrug, lectin-grafted carrier systems, lectins in drug targeting, carbohydrate-directed targeting, nanosystems, mannosylated poly(L-lysine), poly-(L-lysine citramide imide), Man-poly-ethyleneimine/poly-propyleneimine conjugates, PLGA, poly (lactic acid) (PLA), nanoparticles, mannans, mannose binding lectins, mannosylated NPs as gene carriers, mannose capped silicon nanoparticles, mannosylated liposomes, mannosylated cationic liposomes, mannosylated-emulsions, Man-cationic liposomes

53.1 Introduction

In recent years, the use of nanotechnology has been the emerging application in delivering therapeutic drugs effectively to diseased sites. Furthermore, most nanomaterial surfaces can be decorated

Handbook of Clinical Nanomedicine: Nanoparticles, Imaging, Therapy, and Clinical Applications
Edited by Raj Bawa, Gerald F. Audette, and Israel Rubinstein

ISBN 978-981-4669-20-7 (Hardcover), 978-981-4669-21-4 (eBook)
www.panstanford.com

with targeting ligands, enhancing their ability to home to diseased tissues through multivalent interactions with tissue-specific receptors. Thus, targeted therapy provides a means to circumvent the toxicities and lack of treatment response of conventional systemic chemotherapy. The advancement in nanoparticle drug delivery is expected to change the landscape of the pharmaceutical industry in the foreseeable future in terms of disease diagnosis, treatment, and prevention. Nanotechnologies, based on nanoparticles, can facilitate drug delivery to tumors, optimize the effects of drugs, reduce the toxic side effects, and overcome the lack of specificity of conventional chemotherapeutic agents [1]. Nanoparticles have been designed for optimal size and surface characteristics to increase their biological half-life in the bloodstream. They are able to carry the active drugs to cancer cells by selecting the unique pathology of tumors, such as their enhanced permeability and the tumor microenvironment. In addition to passive targeting, active targeting strategies amplify the specificity of therapeutic nanoparticles. Drug resistance, the obstacle that impedes the efficacy of conventional chemotherapeutic agents, is reduced, using nanoparticles. Nanoparticles are solid colloidal matrix-like particles made of polymers or lipids. They have been developed for the targeted delivery of therapeutic or imaging agents. Nanoparticles have the ability to accumulate in cells without being recognized by P-glycoprotein, one of the main mediators of multidrug resistance, resulting in the increased intracellular concentration of drugs. Multifunctional and multiplex nanoparticles are the next generation of nanoparticles, facilitating personalized and tailored cancer treatment [2]. The majority of studies on nanoparticles have dealt microparticles created from poly(D,L lactide), poly(lactic acid) (PLA), poly(D,L glycolide) (PLG), poly(lactide-co-glycolide) (PLGA), and poly-cyanoacrylate (PCA) [3]. These nanoparticles have been designed with therapeutic efficacy and vividly described in recent years.

53.2 Lectins

Lectins, a heterogeneous group of carbohydrate-binding proteins, which can agglutinate cells and/or precipitate glycoconjugates without affecting their covalent linkages, act as mediators of cell recognition in biological systems [4, 5]. First lectin was discovered

by Peter Hermann Stillmark while working with castor bean extracts 100 years ago. However, their presence has been confirmed in most living organisms. Therefore, lectins are ubiquitous in nature and found in plants, insects, animals, humans and microorganisms [6–8]. Lectins display specificity for sugar moieties by binding different kinds of carbohydrates. Some plant animal lectins are hardy proteins; they are resistant to stomach acid and digestive enzymes. Moreover, they can bind to gut wall, damage the epithelial cells, change gut permeability, pass through the gut into general circulation with other non-lectin proteins, and cause allergic reactions [9]. Thus, some plant and animal lectins are severely toxic to humans.

Lectins possess functionally diverse group of protein domains that can bind specific carbohydrate recognition domains (CRDs)/ oligosaccharide structures present on cell surfaces, extracellular matrix, and secreted glycoproteins. Lectin activities specific for different monosaccharides or glycans (fucose, galactose, mannose, *N*-acetylglucosamine, *N*-acetylgalactosamine, *N*-acetylneuraminic acid, and heparin) have been identified. Most of them show a cellular specificity and developmental regulation. However, some of them seem to be involved in signaling events both intracellularly or at the cell surface by autocrine and paracrine mechanisms. Of the 14 well-established animal lectin superfamilies [10], 4 contain lectins that are predominantly intracellular and four contain lectins that generally function outside the cell. In animals, many endogenous lectins have been implicated in a variety of immunological functions, including first-line of defense against pathogens, cell trafficking, and immune regulation. Among cell surface receptors, lectins are of peculiar interest because glycolipids, glycoproteins, and proteoglycans have been shown to interact with lectins on the surface of animal cells. These molecules are of great interest to immunologists mainly because of their ability to interact with lymphocytes and to induce blast cell transformation. As bioadhesin, lectins offer a recognized method of enhancing the absorption of drugs and vaccines at mucosal surfaces [9–11].

Carbohydrates acting as structural components of animal cells are widely distributed in tissues, especially on the cell surface, and are involved in diverse biological processes such as cell

adhesion, inflammation, cell activation, and immune responses [7, 8] through interaction of lectins. Diseases where carbohydrate-based drugs are making an impact include cancer, diabetes, AIDS, influenza, bacterial infections, and rheumatoid arthritis. Lectins can be incorporated into nanoparticles as targeting moieties that are directed to cell-surface carbohydrates (direct lectin targeting) and carbohydrates moieties can be coupled to nanoparticles to target lectins (reverse lectin targeting). The use of lectins and neoglyco-conjugates for direct or reverse targeting strategies is a usual approach of colon drug targeting. This review outlines applications, mainly of galactose and mannose binding lectins, mannose receptors in drug targeting, and their future scope in development of targeted delivery systems [9, 12].

53.2.1 Animal Lectins as Receptors for Receptor-Mediated Targeting

Mannose-binding lectins play a role in recognition of high-mannose type glycans of foreign micro-organisms or plant predators. Serum MBP, also known as mannan-binding lectin (MBL) from liver and serum of rabbits, humans, and rodents [13], DC-SIGN and structurally related receptors (DC-SIGNR), asialoglycoprotein receptor and macrophage mannose receptor belong to family of animal lectins classified as mannose-binding lectins [11, 12].

Asialoglycoprotein receptor: Asialoglycoprotein receptor (ASGP-R), also called hepatic lectin, is another lectin that is predominantly expressed on the sinusoidal surface of mammalian hepatocytes and is responsible for clearance of glycoproteins with desialylated galactose or acetylgalactosamine residues from circulation by receptor-mediated endocytosis [14]. Specificity of the receptor for D-galactose or D-mannose is accomplished by specific hydrogen bonding of 3- and 4-hydroxyl groups with carboxylate and amide side-chains. Therefore, mutation of the amino acid sequence in the CRD results in a conversion of its specificity [15]. Mannose-labeling shifted the ratio to more non-parenchymal cell incorporation (majority to Kupffer cells). Therefore, alternative approaches are needed to target liposomes to hepatocytes via ASGP-R [16, 17]. Studies on animal lectins have been reviewed in recent years [11].

Lectins on Antigen-presenting cells: To initiate immune responses against infection, antigen-presenting cells (APCs) must recognize and react to pathogens. Recognition is achieved by interaction of particular surface receptors on APCs with corresponding surface molecules on infectious agents. The three types of professional APCs are: (i) mature dendritic cells (DC), derived from immature tissue dendritic cells that interact with many distinct types of pathogens, (ii) macrophages, specialized to internalize extracellular pathogens and to present their antigens, and (iii) B cells, which have antigen-specific receptors that enable them to internalize large amounts of specific antigen, process it, and present it to a naïve T cell for activation. By contrast, pattern recognition receptors recognize and interact with pathogens directly. In addition to scavenger receptors and toll-like receptors, PRRs include C-type lectin-like receptors (CLR) that bind carbohydrate moieties of many pathogens [18, 19]. CLRs include (i) mannose receptors for mannose or its polymers [20]; (ii) mannose-binding lectins for encapsulated group B or *C meningococci*; (iii) DC-SIGN and structurally related receptors (DC-SIGNR) for mannose on HIV, *Leishmania*, and *Mycobacteria* [19, 21] and (iv) dectin-1 and dectin-2 for β-glucan on yeasts and fungi [22].

Mannose receptor (ManR): ManR is a type I transmembrane protein that contains three extracellular regions: an NH_2-terminal cysteine-rich domain, a domain containing fibronectin type II (FNII) repeats, and eight tandem C-type lectin CRDs. Primary structure of ManR reflects its diverse carbohydrate specificity. Size and shape parameters indicate that receptor is a monomeric, elongated, and asymmetric molecule. Domain organization of CRD-4 monomer in ManR represents two possible conformations: extended and U-shaped. *N*-terminal cysteine-rich domain and fibronectin type II repeat appear to increase the rigidity of the molecule. The rigid, extended conformation of the receptor places domains with different functions at distinct positions with respect to membrane [23]. An *N*-terminal cysteine-rich domain mediates recognition of sulfated *N*-acetylgalactosamine, which is terminal sugar of unusual oligosaccharides present on pituitary hormones. Extracellular domains of ManR are linked to a transmembrane region and a small cytoplasmic domain. Of the eight C-type CRDs,

CRD 4-8 are required for binding and endocytosis of mannose/GlcNAc/fucose-terminated ligands, but only CRD-4 has demonstrable sugar binding activity in isolation (Figure 53.1a) [23].

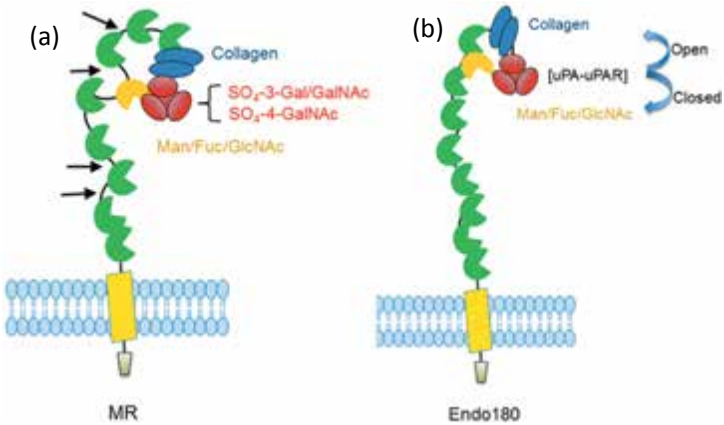

Figure 53.1 (a) The structural organization of mannose receptor (ManR) and (b) The structural organization of Endo 180. Globular conformation of the mannose receptor family members (ManR and Endo180) where the CysR domain (*red*) interacts with the physiologically active CTLD (*yellow*) and corresponding to CTLD4 in the ManR (a) and CTLD2 in Endo180 (b). The FNII domain has been colored *blue*, while the non-functional CTLDs are shown in *green*. This conformation can interact with several substrates, which are indicated with the corresponding color beside the domain responsible for the interaction. Proteolytic cleavage sites in ManR have been identified [23] and highlighted with *black arrows*. In an acidic environment, it is predicted that Endo180 switches to a more conformation (Adapted with permission from Boskovic et al. (2006). *J. Biol. Chem.,* **281**, 8780–8787 [24]).

ManR of macrophages, epithelial, and endothelial cells acts as a molecular scavenger by binding to and internalizing a variety of pathogenic microorganisms and harmful glycoproteins. Macrophage mannose receptor (MMR; 180 kDa) is a prototype member of a family of multi-lectin receptors that recognize carbohydrates on cell walls of infectious organisms [18, 24, 23] (Figure 53.1b). Role of ManR in innate immune response is well documented, with several clinically important pathogens, including

Mycobacterium tuberculosis and *Pneumocystis carinii*, subject to opsonin-independent phagocytosis by the receptor. Carbohydrate recognition by ManR facilitates macrophage uptake of bacteria, yeast, and parasites, thereby contributing to innate immunity toward variety of pathogens. Once internalized, ligands are released from the receptor following endosomal or phagosomal acidification, after which receptor recycles to the cell surface [23, 25–27].

Lectins of dendritic cells: Members of dendritic cell (DC) family are distributed to virtually all the organs (except brain), where they serve as tissue resident APCs, playing critical roles in presenting environmental, microbial, and tumor-associated antigens to immune system. Several cell-surface C-type lectin receptors, such as DC-SIGN (Figure 53.2a, (B), L-SIGN, ManR, macrophage galactose binding lectin, and other lectins, such as soluble collectins and galectin-3, recognize particular glycan antigens (Ags) of schistosomes and allergens, which may contribute to orchestrate Th2 associated adaptive responses. DC-SIGN receptor on DC binds with high affinity to both synthetic mannose- and fucose-containing glycoconjugates. These carbohydrate structures are abundantly expressed by pathogens as demonstrated by affinity of DC-SIGN for natural surface glycans of human pathogens [19, 21, 28–30) (*M. tuberculosis, H. pylori, Leishmania mexicana, Schistosoma mansoni, and HIV-1*) [25, 27, 31].

DEC-205, another mannose specific receptor, present on DC, internalizes antigens and present their fragments to naïve T lymphocytes for development of T cell dependent immunity. DEC-205, a type I membrane-integrated glycoprotein, contains 10 distinct CRD motifs in extracellular region. Both DEC-205 and MMR mediate uptake of glycosylated antigens by DC [25, 27, 31–34]. Unlike DEC-205 and MMR, which contain multiple CRD motifs in NH_2-terminal ends, second group of C-type lectins consists of polypeptides that contain a single CRD in their COOH termini. Members of this group include hepatic lectin (or asialoglycoprotein receptor), macrophage galactose/*N*-acetylgalactosamine-specific lectin (MGL), CD23, and various receptors encoded in the natural killer gene complex (CD69, CD94, Ly-49, and NKG2). Thus, DCs express both type I surface lectins (DEC-205 and MMR) and type II surface lectins (CD23, CD69, DCIR, dectin-1 and dectin-2) [35].

53.3 Carbohydrate–Lectin Interactions

The process of bioadhesion in drug delivery has been in use for 35 years, using mucoadhesive polymers. Many of these polymers were already used as excipients in pharmaceutical formulations. This facilitated the development of the bioadhesive drug products, which are now commercially available. A major disadvantage of the hitherto known mucoadhesives, however, is their non-specificity with respect to the substrate. Rather than only acting as a platform for controlled release systems, the concept of lectin-mediated bioadhesion therefore bears the potential for the controlled delivery of macromolecular biopharmaceuticals at relevant biological barriers, such as the epithelia of the intestinal or respiratory tract [36]. Carbohydrates exhibit properties of potential interest when developing drug delivery mechanisms, such as specificity in their interaction with their receptors and the nature of potentially targetable receptors available [10]. Considerable efforts have been made to develop carbohydrate-based therapeutics [37] targeting specific disease cells via carbohydrate–lectin interactions; and carbohydrate-based anti-thrombotic agents. In addition, many human pathogens possess surface proteins that complex with specific membrane-bound oligosaccharides on human cells [38, 39]. Variety of carbohydrate structures that occur on diseased cells gives rise to highly complex carbohydrate–lectin interactions and signaling processes. Emerging roles of carbohydrates and glycomimetics in anticancer drug design are being recognized [39, 40].

Carrying carbohydrate-tag, drug delivery system can be recognized by cells and internalized by endogenous lectins at cell surface [41, 42]. Mammalian mannose/galactose specific cell surface receptors, expressed on macrophages and other APCs such as DCs in skin and M-cells in intestine mediate the internalization of a wide range of molecules or microorganisms in a pattern recognition manner. Therefore, it represents an attractive entry for specific drug, gene, or antigen delivery to macrophages and DCs. Particles coated with carbohydrate ligands offer potential future. Based on this principle, delivery systems containing asialofetuin, galactose, mannose, or *N*-acetyl-galactosamine were developed and tested for endocytosis by macrophages, DCs, and liver cells.

Use of carbohydrate-modified HPMA or liposomes gave improved results [43, 44]. Liver or colon macrophages and mouse brain have been shown to be targeted by mannosylated liposomes (Man-liposome) [16]. Several APC surface C-type lectin receptors, such as DC-SIGN, L-SIGN, ManR, macrophage galactose binding lectin, and other lectins, such as collectins and galectin-3, recognizing specific glycans, offer future potential for targeting antigens for enhanced humoral and cellular immune responses [23, 28, 30].

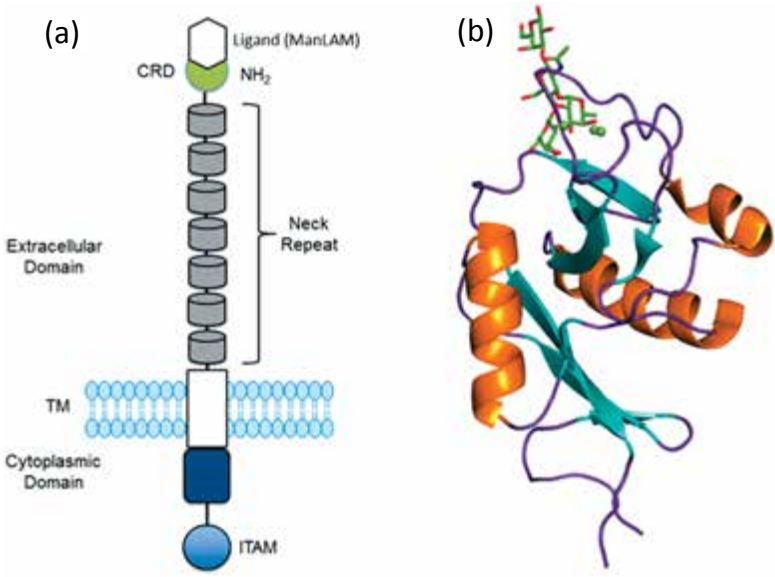

Figure 53.2 (a) Structure of DC-SIGN. Cytoplasmic domain, transmembrane region (TM) and extracellular domain are the three parts of DC-SIGN. The extracellular domain contains carbohydrate recognition domain (CRD) and neck domain. Cytoplasmic domain contains LL (di-leucine), EEE (tri-acidic clusters) and other internalization motifs and is connected to an incomplete ITAM. CRD recognizes certain carbohydrate-contained antigens like ManLAM and $Lewis^X$ by four amino acids (Glu347, Asn349, Glu354 and Asn365) and one Ca^{2+}-binding site [29]. (b) Ribbon diagram of DC-SIGN carbohydrate recognition domain (CRD) complexed with LNFP III (Dextra L504) PDB ID: 1sl5 [30]. The DC-SIGN CRD with the bound oligosaccharide is shown in a ball-and-stick representation.

53.4 Nanotechnology and Drug Targeting Strategies

Over the past two decades, glycosylated nanoparticles (i.e., glyconanoparticles having sugar residues on the surface) received much attention for biomedical applications such as bioassays and targeted drug delivery. Three aspects—(i) glycosylated gold nanoparticles, (ii) glycosylated quantum dots, and (iii) glyconanoparticles self-assembled from amphiphilic glycopolymers—have been reviewed [40, 45]. The synthetic methods and the multivalent interactions between glyconanoparticles and lectins have been illustrated. Two basic requirements should be realized while designing nanocarriers to achieve effective drug delivery. First, drugs should be able to reach the desired tumor sites after administration with minimal loss to their volume and activity in blood circulation. Second, drugs should only kill tumor cells without harmful effects to healthy tissue [2, 40]. These requirements may be enabled using two strategies: passive and active targeting of drugs and have been vividly described [45].

53.5 Nanocarriers Used in Drug Delivery Systems

The field of nanotechnology has exploded in recent years with diverse arrays of applications. Cancer therapeutics have benefited from nanotechnology with the approval of some nanoscale drug delivery systems. Nanoparticles applied as drug delivery systems are submicron-sized particles (2–200 nm), devices, or systems that employ a variety of materials, including polymers (polymeric nanoparticles, micelles, or dendrimers, etc.), lipids (liposomes), viruses (viral nanoparticles), and even organometallic compounds (nanotubes). A diversity of delivery systems are under investigation and an array of newly developed, customized particles have reached clinical application [46]. The recent explosion in engineering and technology has led to (i) development of many new nanoscale platforms, such as quantum dots, nanoshells, gold nanoparticles, paramagnetic nanoparticles, and carbon nanotubes, and (ii) improvements in traditional, lipid-based nanoscale platforms. The advantages of nanoparticles delivery system

include the following: (1) Particle size and surface characteristics of nanoparticles can be easily manipulated to achieve both passive and active drug targeting after parenteral administration. (2) They control sustained release of the drug during the transportation and at the site of localization, altering organ distribution of the drug and subsequent clearance of the drug with increased drug therapeutic efficacy and less side effects. (3) Controlled release and particle degradation characteristics can be readily modulated by the choice of matrix constituents. Drug loading is relatively high and drugs can be incorporated into the systems without any chemical reaction, an important factor for preserving the drug activity. (4) Site-specific targeting can be achieved by attaching targeting ligands to surface of particles or use of magnetic guidance. (5) The system can be used for various routes of administration, including oral, nasal, parenteral, intra-ocular, etc. In spite of these advantages, nanoparticles do have limitations. For example, their small size and large surface area can lead to particle–particle aggregation, making physical handling of nanoparticles difficult in liquid and dry forms. In addition, small particles size and large surface area readily result in limited drug loading and burst release. These practical problems have to be overcome before nanoparticles can be used clinically or made commercially available. The present review details the latest development of nanoparticulate drug delivery systems, surface modification issues, drug loading strategies, release control, and potential applications of nanoparticles [47].

Nanoparticles offer an important strategy to deliver conventional drugs, recombinant proteins, vaccines, and nucleotides. Nanoparticles modify kinetics, body distribution, and drug release of bound drug. Other advantages include tissue or cell specific targeting of drugs and reduction of unwanted side effects due to controlled release. Therefore, nanoparticles in pharmaceutical biotechnology provide solutions for future delivery problems for new drugs, including recombinant proteins and oligonucleotides. When linked with biotargeting ligands, such as monoclonal antibodies, peptides, or small molecules, these nanoparticles are used to target malignant tumors with high affinity and specificity. Long-lived quantum dots are replacing classical fluorescent dyes in staining and bioimaging. Polyethyleneglycol (PEG) coated quantum dots and mannosylated PEG (Man-

PEG) quantum dots, prepared for labeling macrophage exhibit extremely low cytotoxicity and are safe to macrophages [48]. The fate of injected nanoparticles can be controlled by adjusting their size and surface characteristics. The nanoparticles should be of appropriate size preferably up to 100 nm to reach specific tissue by passing through vascular structures. Nanoparticles should ideally have a hydrophilic surface to escape macrophage capture [49, 50]. Emerging implications of nanocarriers of drugs in cancer diagnosis and therapies form the basis of many reviews [2, 9, 12, 40, 49–51].

53.5.1 Polymeric Nanoparticles (Polymer–Drug Conjugates)

Depending on the method, the drug is either physically entrapped in or bound to the polymer matrix [50]. The resulting compounds may have the structure of capsules (polymeric nanoparticles), amphiphilic core/shell (polymeric micelles), or hyper-branched macromolecules (dendrimers). Polymers used as drug carriers can be natural or synthetic. Among natural polymers, albumin, lectins, chitosan, and heparin have been the material of choice for the delivery of oligonucleotides, DNA, and protein, as well as drugs. A nanoparticle formulation of paclitaxel, in which serum albumin is included as a carrier (albumin-bound paclitaxel (Abraxane), has been used in metastatic breast cancer [50, 51] and many other cancers, including non–small-cell lung cancer. Synthetic polymers being used are: *N*-(2-hydroxypropyl)-methacrylamide copolymer (HPMA), polystyrene-maleic anhydride copolymer, polyethylene glycol (PEG), and poly-L-glutamic acid (PGA) and poly-(lactic-co-glycolic acid) (PLGA). PGA was the first polymer used for conjugate synthesis [50, 51] and tested *in vitro* and *in vivo* with encouraging results. HPMA, PLGA, and PEG are the most widely used nonbiodegradable synthetic polymers [50–52].

PLGA nanoparticles for drug delivery to tumors: Cancer is the leading cause of death in economically developed countries and the second leading cause of death in developing countries [53, 54]. Many forms of cancer are treatable via current therapies, such as surgical procedure, chemotherapy, radiation therapy, and immunotherapy [55, 56]. The main weakness of most

chemotherapeutic approaches to cancer treatment is that most of them are nonspecific [50, 51] and result into well-known side effects. The rationale of using nanoparticles for tumor targeting is based on (1) NP's capability to deliver the requisite dose load of drug in the area of the tumor because of the enhanced permeability and retention effect or active targeting by ligands on the surface of NPs and (2) NP's ability to diminish the drug exposure to healthy tissues by limiting drug distribution to the target organ [57]. The properties of nanoparticles as precursor of good nanomedicine are nanoparticle size, size distribution, surface morphology, surface chemistry, surface charge, surface adhesion, surface erosion, inner porosity, drug diffusivity and encapsulation efficiency, drug stability, drug release kinetics, and hemodynamic [58]. A successful NP system may be the one, which has a high loading capacity to decrease the number of the carrier required for administration. Drug loading into the NPs is achieved by two methods: first, by incorporating the drug at the time of NP production or, secondly, by adsorbing the drug after the formation of NPs by incubating them in the drug solution. It is so obvious that a large amount of drug can be entrapped by the incorporation method when compared to the adsorption [50, 51].

Poly-(lactic-co-glycolic acid), the copolymer approved by the US Food and Drug Administration (FDA) as a therapeutic device, is a commonly used. PLGA is degraded by hydrolysis in the body and produces the original monomers, lactic acid and glycolic acid, which are by-products of various metabolic pathways. Because of its minimal toxicity and ability of controlled release of the drug, PLGA is suitable for drug delivery [59]. PLGA nanoparticles are versatile because of their biocompatibility for drug targeting at the cellular level [60]. The PLGA is being widely explored as nanocarriers for the controlled delivery of therapeutic drugs, proteins, peptides, oligonucleotides, and genes for their successful delivery *in vivo* [58]. Surface functionalization of PLGA nanoparticles has paved the way to a variety of engineered PLGA-based nanocarriers, which, depending on reticular requirements, can demonstrate a wide variety of combined properties and functions such as prolonged residence time in blood circulation, enhanced oral bioavailability, site-specific drug delivery, and tailored release characteristics [50, 51]. In PLGA nanoparticles,

drug like L-DOPA is encapsulated within the polymer matrix and released upon degradation [61]. In addition, to further improve the delivery efficacy of L-DOPA, a targeted drug system is designed by conjugating PLGA with the lectin: wheat germ agglutinin (WGA).

Among the diverse forms of PLGA-based drug delivery systems, microspheres or microparticles are the most common [62]. Other types consist of nanoparticles [63], films [64], cylinders [65], *in situ* forming implants or microparticles [66], scaffolds [67] and foams [62, 69]. Protocols have been optimized for PLGA nanoparticles synthesis and many cancer related drugs have been incorporated in PLGA [58]. These loaded nanoparticles protect poorly soluble and unstable payloads from the biological milieu and are tiny enough for capillary penetrations, internalization, and endosomal escape. In addition, their surface is modified for targeted delivery of molecules to tumor or other tissues [57]. They may have controlled-release properties owing to their biodegradability, pH, ions, and/or temperature sensitivity. Main anticancer drugs that have been investigated in PLGA nanoparticle preparations are *Paclitaxel* (Taxol), *Cisplatin* [54], *Hypericin* [68], *Vincristine sulfate* (VCR), *Etoposide* [70, 71], *9-Nitrocamptothecin* [58, 72], *Doxorubicin*, [70, 73–75], and *curcumin* [54]. A nanoparticle-based formulation of curcumin shows high adjuvant therapy in prostate tumor [54, 76]. Xanthones have strong inhibitory action on human cancer cell lines and Xanthone-loaded PLGA nanospheres have been prepared by solvent displacement techniques [58, 77]. Triptorelin is an analog of luteinizing releasing hormone (LRH) used for the treatment of sex hormone dependent tumors. Triptorelin-loaded PLGA nanospheres have been prepared via double emulsion solvent evaporation technique with encapsulation efficiency varying from 4% to 83% [50, 58]. Treatment of central nervous system diseases remains limited due to low transport of drugs across the blood–brain barrier (BBB). A number of drug carriers have been developed to improve brain delivery of drugs. The recent developments on PLGA or poly-(lactic acid) (PLA) nanoparticles designed for neural delivery, with emphasis on nanoparticle cytotoxicity, therapeutic efficacy of the entrapped drug, and brain uptake of PLGA and PLA nanoparticles as a function of their properties have been highlighted [73].

53.5.2 Lipid-Based Drug Carriers

Liposomes: Carbohydrate-mediated functions in biological systems have generated considerable interest in recent years. Carbohydrate moieties of cellular glycocalyx play an important role in biological recognition during pathologic conditions, such as inflammation and cancer. Lectin-modified liposomes have potential for site-specific drug delivery during the therapy of such diseases. Plain (unmodified) liposomes exhibit only unspecific adhesion to glycolipid membranes and have a tendency to coalesce; the degree of membrane interaction was significantly increased when plain liposomes were modified with the ConA. However, vesicle fusion also markedly increased as a result of lectin modification. Additional PEGylation of liposomes reduced unspecific adhesion phenomena, as well as coalescence [78].

Liposomes are self-assembling closed colloidal structures composed of lipid bilayers and have a spherical shape in which an outer lipid bilayer surrounds a central aqueous space. Several kinds of cancer drugs have been applied to this lipid-based system using a variety of methods. Among them, liposomal formulations of anthracyclines doxorubicin (Doxil, Myocet) and daunorubicin (DaunoXome) are approved for the treatment of metastatic breast cancer and AIDS-related Kaposi's sarcoma [79–81]. Besides these agents, many liposomal chemotherapeutics are under investigation [81–83]. The next generation of liposomal drugs may be immunoliposomes, which selectively deliver the drug to the desired sites of action [84]. Liposomes have long been considered promising pharmaceutical carriers *in vivo* and have already found their way into a real clinical practice. It was believed that the use of targeted liposomes, i.e., liposomes with a specific affinity for the affected organ or tissue, should increase the efficacy of the liposomal pharmaceutical agents.

Lectin-bearing polymerized liposomes: To target liposomal pharmaceuticals to organs other than the liver and spleen, liposomes have been modified with specific targeting moieties (antibodies). However, similar to "plain" liposomes, immune-liposomes also do not exhibit prolonged circulation and fail to accumulate sufficiently in targets with diminished blood supply and/or low antigen concentration. The problem of how

to achieve long circulation was solved with the development of polymer-coated liposomes with decreased opsonization rate and sharply increased circulation times (sterically protected liposomes, "stealth" liposomes, long-circulating liposomes). Alternatively, it was shown that small liposomes also possess an increased longevity compared to liposomes of a larger size [16–19]. However, since the entrapment capacity of liposomes for drugs strongly diminishes with decrease of liposome size, larger polymer-coated liposomes were considered more promising pharmaceutical carriers. The usual preparation method of such liposomes includes liposome coating with PEG [20–22], though some other polymers can also be successfully used [23–27].

The procedure for coupling various ligands to liposome-grafted PEG chains and to make it applicable for binding of a large variety of a primary amino group–containing substances, including proteins and small molecules are known. Torchilin et al. [85] have introduced a new amphiphilic PEG derivative, *p*-nitrophenylcarbonyl-PEG-1,2-dioleoyl-*sn*-glycero-3-phosphoethanolamine (pNP-PEG-DOPE). The pNP-PEG-DOPE readily incorporates into liposomes via its PE residue, and easily binds primary amino group-containing ligands via its water-exposed pNP groups, forming stable and non-toxic urethane (carbamate) bonds. Torchilin et al. [85] coupled several proteins, including ConA, WGA to PEG-liposomes via terminal pNP. All bound proteins fully preserved their specific activity whereas lectin-liposomes retained agglutination activity for appropriate substrates (mannan for ConA-liposomes and glycophorin for WGA-liposomes). In addition, the pNP-PEG-DOPE-liposomes, with or without attached ligands, showed increased stability in mouse serum [85, 86]. Delivery efficiencies of lectin-bearing liposomes in mice established that lectin-bearing liposomes can promote binding to Peyer's patches, which gave improved efficiency for Peyer's patch targeted delivery. All these point to the potential for these lectin-modified liposomes as novel vehicles for oral vaccination [86].

Polymeric micelles (amphiphilic block copolymers)*:* Block-copolymer micelles are spherical super-molecular assemblies of amphiphilic copolymer. The core of micelles can accommodate hydrophobic drugs, and the shell is a hydrophilic brush-like corona that makes the micelle water soluble, thereby allowing delivery of the poorly soluble contents. The functional properties of micelles

are based on amphiphilic block copolymers, which assemble to form a nanosized core/shell structure in aqueous media. The hydrophobic core serves as a reservoir for hydrophobic drugs, whereas the hydrophilic shell region stabilizes the hydrophobic core and renders the polymers water-soluble, making the particle an appropriate candidate for intravenous (i.v.) administration [2, 87]. The drug can be loaded into a polymeric micelle in two ways: physical encapsulation or chemical covalent attachment [88]. The first polymeric micelle formulation of paclitaxel, Genexol-PM (PEG-poly(D,L-lactide)-paclitaxel), is a chromophore-free polymeric micelle-formulated paclitaxel. Multifunctional polymeric micelles containing targeting ligands and imaging and therapeutic agents are being actively developed [89] and will become the mainstream among several models of the micellar formulation in the near future [2].

53.5.3 Dendrimers

A dendrimer is a synthetic polymeric macromolecule of nanometer dimensions, composed of multiple highly branched monomers that emerge radially from the central core. Properties associated with these dendrimers make them attractive for drug delivery [90]. Polyamidoamine dendrimer has been widely used as a scaffold, conjugated with cisplatin. In early studies, dendrimer-based drug delivery systems focused on encapsulating drugs. The recent developments have provided a new class of molecules called dendronized polymers, which are linear polymers that bear dendrons at each repeat unit. Their behavior differs from linear polymers and provides drug delivery advantages because of their enhanced circulation time. DOX was conjugated to a biodegradable dendrimer with optimized blood circulation time through the careful design of size and molecular architecture [79]. DOX-dendrimers were found 10 times less toxic than free DOX toward colon carcinoma cells and tumor uptake of DOX-dendrimers was nine-fold higher than free DOX; tumor regressed completely and mice survived 100% after 60 days. Bogdan et al. [91] developed up converting lanthanide (Ln^{3+})-doped NPs conjugated with glycodendrimers capable of recognizing lectins based on luminescence resonance energy transfer (LRET). The resulting water dispersible and

biocompatible mannose-coated PAMAM-LnNPs recognized ConA conjugated with tetramethylrhodamine (RITC-Con (A) *via* LRET from the up converting mannose-coated PAMAM-LnNPs, which act as energy donors to the RITC-labeled lectin molecules serving as energy acceptors [91]. A sensing device, constructed by using cyanuric chloride as an amine-linker between an amino residue of a polyamidoamine (PAMAM) dendrimer-coated colloidal gold surface and the amino residue of a 12-aminododecyl glycoside was able to detect carbohydrate-binding molecules by LSPR spectroscopy. LSPR-based sensing device provides a low-cost detection method for laboratory research or in medical glycan arrays [92].

53.5.4 Nanoshells

Nanoshells are mainly metal-based nanoparticles. Nanoshells have a core of silica with a top layer of gold. By changing the thickness of gold layer, it is possible to alter the optical absorption properties of these nanoshells when radiated with near-IR laser. The illumination of the tissue by the light generated by IR laser and absorbed by nanoshells generates intense heat. Thus, nanoshells destroy only tumors thermally without damaging the surrounding healthy cells [93]. Antibodies and/or therapeutic anticancer agents can be attached to their surfaces, enabling those nanoshells to target cancerous cells or tumors [89]. The gold nanoshell antibody complex can be used to ablate breast cancer cells. Gold nanoshells have been used in fast immunoassays, without any sample preparation [94].

53.5.5 Carbon Nanotubes

Carbon nanotubes have been applied in biology as sensors for detecting DNA and protein, diagnostic devices for the discrimination of different proteins from serum samples, and carriers to deliver vaccine or protein. Being insoluble in all solvents, they generate some health concerns and toxicity problems. However, carbon nanotubes can be rendered water soluble and can be linked to a wide variety of active molecules such as peptides, proteins, nucleic acids, and therapeutic agents [95–97]. Tumor-targeting single-walled carbon

nanotubes (SWCNTs) have been synthesized by covalently attaching multiple copies of tumor-specific monoclonal antibodies (mAbs), radiation ion chelates and fluorescent probes [98].

53.5.6 Other Nanoparticles

Polymersomes, hollow shell nanoparticles, have unique properties that allow delivery of distinct drugs. Polymersomes have been used to encapsulate paclitaxel and DOX for passive delivery to tumor-bearing mice [99]. The polymersome allows paclitaxel to embed within the shell. Recent studies have shown that cocktails of paclitaxel and DOX lead to better tumor regression than the either drug alone. XPclad nanoparticles use planetary ball milling to generate particles of uniform size, 100% loading efficiency of hydrophobic or hydrophilic drugs, subsequent coating for targeted delivery, and control of LogP for systemic, cutaneous, or oral administration of cancer drugs, vaccines, or therapeutic proteins [100]. A variety of viruses, including cowpea mosaic virus, cowpea chlorotic mottle virus, canine parvovirus, and bacteriophages, have been developed for biomedical and nanotechnology applications that include tissue targeting and drug delivery. In such attempts, several ligands or antibodies, including transferrin, folic acid, and single-chain antibodies, have been conjugated to viruses for specific tumor targeting *in vivo* [101]. Other nanotechnologies, mostly based on nanoparticles, that can facilitate delivering anticancer and imaging agents and kill cancerous cells and cancer diagnosis are quantum dots (QDs), gold nanoparticles, nanowires, and magnetic nanoparticles.

53.6 Lectins as Drug Carriers

Cell surface carbohydrates affect tumor cell interactions with normal cells or with the extracellular matrix during metastatic spread and growth. The family of the discovered endogenous lectins in animals is rapidly expanding [11]. Some lectins recognize the “foreign” patterns of cell surface carbohydrates on tumor cells and play a role in innate and adaptive immunity. It has been shown that lectins affect tumor cell survival, adhesion to

the endothelium, or extracellular matrix, as well as tumor vascularization and other processes that are crucial for metastatic spread and growth [102]. Two approaches to drug carrier formulation are basically pursued (Fig. 53.3). The first approach is preparation of prodrugs consisting of lectin as glycotargeting moiety, drug as active ingredient, and spacer as a link (Fig. 53.3b) (reverse lectin targeting in which lectins are incorporated into nanoparticles that are directed to cell surface carbohydrates). The second approach is development of lectin-grafted carrier systems (Figure 53.3a). A reservoir such as nanoparticles or liposomes contains the drug and lectins are immobilized at outer surface of the reservoir (i.e., development of nanoparticles containing carbohydrate moieties that are directed to certain lectins (direct lectin targeting). The lectin should help to guide the drug container to the site of absorption getting closer to the sight of expected. It was realized that both cell types, enterocytes and M-cells, are involved in transcytosis of particulate matter. Thus far, drug delivery systems that have been developed based on this novel interaction between carbohydrates and lectins are directed to whole organs, and could thus be harmful to normal tissues [103]. Despite these problems, lectins are continuing to be studied for the development of "smart carrier" molecules for drug delivery since their unique affinity for sugar moieties on the surface of tumor tissue seems to be an attractive tool for further enhancement of nanodrug delivery.

53.7 Reverse Lectin Targeting

53.7.1 Lectin-Grafted Prodrug

In use of lectins toward glycotargeting, drug delivery system is decorated with lectins of certain carbohydrate specificity so that it can interact with glycosylated surfaces. In prodrug design, drug (doxorubicin) was coupled to WGA by a *cis*-aconityl spacer. Targeting effect of colon cancer–directed prodrug derives from both high WGA-binding capacity of colon cancer cells and release of cytostatic agent not until reaching acidic lysosomal milieu of target cell. To get evidence if lectin-mediated cytoadhesion and cytoinvasion can facilitate absorption of proteins, fluorescent

labeled BSA was coupled to WGA via stable amide bonds (Fig. 53.3a). Results illustrated that WGA could mediate cellular uptake of even high molecular weight proteins. However, cut-off for uptake of proteins was still higher since IgG was also transported into cells by active transport mechanisms after conjugation to WGA. This shows that membrane barrier can be surmounted with the help of lectins. Diverse strategies like incorporation of

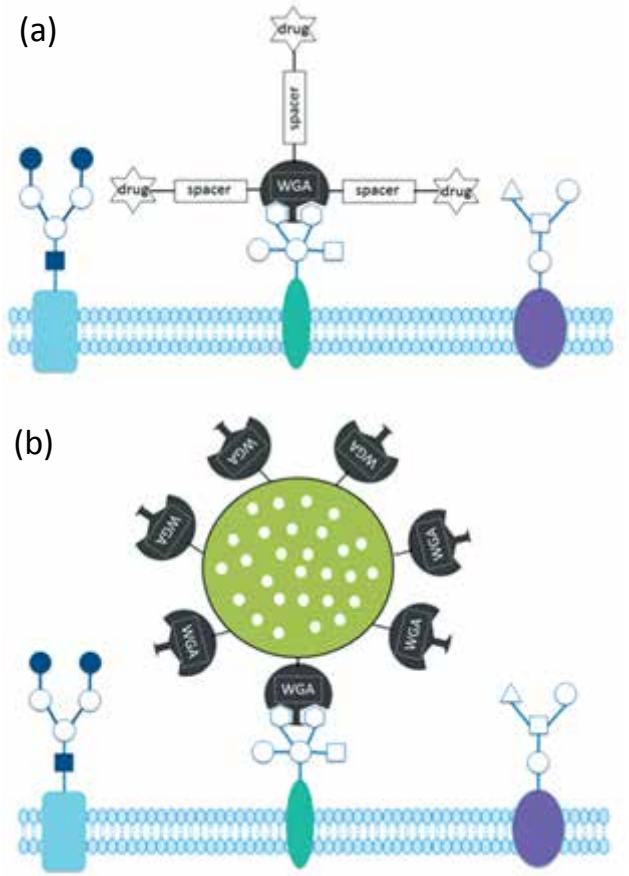

Figure 53.3 Lectin-grafted formulations: (a) Lectin-grafted pro-drug, (b). Lectin-grafted carrier system. Symbols: ⬡, ○, ●, □, ■, △ denote extracellular carbohydrate moieties. Symbol ⬡ denotes galactose, which recognizes WGA, a galactose specific lectin. Adapted with permission from Gupta et al. (2009). *J. Sci. Ind. Res.*, **68** 465–483 [9].

enzyme inhibitors or shielding by matrix systems are expected to solve the problem [103]. In terms of drug delivery, carbohydrate-mediated biorecognition of lectins, resulting in mucoadhesion, cytoadhesion, and/or cytoinvasion, might be advantageous for drug delivery to small intestine [104, 105]. Nonpathogenic strains of some bacteria can also be utilized through this approach. In addition to plant lectins recognizing glycans and mannans in particular, trimannoside-recognizing peptide sequences have been identified in T7 phage. These phage sequences PSVGLFTH [8-mer] and SVGLGLGFSTVNCF (14-mer) need to be examined for development of inhibitors or drug delivery systems targeting polysaccharides [106].

The concept of bioadhesion via lectins may be applied not only for GI tract but also for other biological barriers like nasal mucosa, lung, buccal cavity, eye, and BBB. Entering vesicular pathway by receptor-mediated endocytosis part of conjugated drug is accumulated within lysosomes. Additionally, part of the drug is supposed to be transported across the epithelium. As exemplified by lectin-grafted prodrug and carrier systems, this strategy is expected to improve absorption and probably bioavailability of poorly absorbable drugs, peptides and proteins as well as therapeutic DNA [100/103]. Conjugation of WGA onto PLGA nanoparticles effectively improved intestinal absorption of TP5 due to specific bioadhesion on GI cell membrane [107].

53.7.2 Lectin-Grafted Carrier Systems

Contrary to prodrugs, it is possible to achieve therapeutic levels of drugs by administration of microparticles, nanoparticles or liposomes (Fig. 53.3b). Matrix of drug carrier systems, which is preferably biocompatible and biodegradable, renders controlled release of drugs possible. Incorporation in appropriate carrier systems not only protects drugs against enzymatic and acidic degradation in intestine but also affords an increase in payload. Decoration of drug carrier system with lectins will enrich drug on glycosylated surfaces of gastrointestine (GI). Tomato lectin is useful for drug delivery as well as for oral vaccination. Moreover, tomato lectin exhibit adjuvant activity by priming systemic and mucosal immune responses [103, 104]. In such an approach, coupling of lectins to nanoparticles led to higher transcytosis than

that of free lectins. Moreover, rate of transcytosis increased with lectin density on surface of nanoparticles. Altogether, this points to the fact that nanoparticles open a trafficking route different to that of free lectin. It was suggested that immobilization of lectins on colloidal formulations induces enhanced receptor clustering which results in increased transcytosis of carrier. Characterization of interaction between the colloidal carriers and the cells is most important for *in vitro* evaluation of lectinized nanospheres. Cytoassociation rate strongly depends on orientation of device and agitation of suspension [103].

At first sight, plant lectins specific for complex glycosyl side chains such as *Phaseolus vulgaris* agglutinin from red kidney beans and lectin from *Robinia pseudoacacia* seemed to be superior for intestinal targeting. They strongly and reversibly bound to villous and crypt epithelia as well as M-cells followed by high rates of endocytosis and transcytosis [108]. In comparison to *Phaseolus vulgaris* agglutinin and lectin from *Robinia pseudoacacia*, lectin from snowdrops and other mannose-specific lectins exhibited only slight binding to jejunal epithelial cells and moderate binding to M-cells [109]. It appears that multivalency enhancement/cluster effect plays a significant role in binding events. Binding of glycodendrimers to fluorescently labeled ConA was small, in agreement with its widely spaced binding sites, whereas it was large for GNA, with its 12 much more closely spaced binding sites. The dendrimer-fitted chip represents a valuable screening tool for multivalency effects [110].

Lectinized liposomes are known to bind alveolar type II epithelial cells [111] for epithelial drug delivery. Amphiphiles, which carry many mannose residues as side chains, incorporated in liposomes were recognized by ConA and the interaction between sugar residues on liposome and the lectin was largely affected by degree of polymerization and surface density of amphiphile in liposomes. Positive entropy change for binding of ConA to mannose residues on liposome surface indicated that the recognition in liposome system is largely promoted by release of water molecules from both sugar residues on liposome surface and binding site of Con A. In search of non-viral vectors for gene therapy of cystic fibrosis, lectins were screened for binding and uptake into living human airway epithelium [112]. Whereas ConA was internalized within 1 h, lectins from *Erythrina cristagalli* and

Glycine max, peanut lectin, and jacalin were taken up into epithelium within 4 h.

Insulin delivery systems: An implantable ConA-based glucose-responsive insulin delivery system, which can be used for long-term diabetes treatment, has been described [113]. *In vitro* release experiments with ConA conjugate and glycosyl-poly-(ethylene glycol) (G-PEG)-insulin complex enclosed in membrane device indicated a pulsative, reversible release pattern for G-PEG-insulin in response to glucose challenges, demonstrating the feasibility of release system for chronic *in vivo* studies with diabetic-pancreatectomized dogs. Lectin-modified solid lipid nanoparticles (SLNs), containing insulin after oral administration of peptide and protein drugs, indicated that SLNs and WGA-modified SLNs promote the oral absorption of insulin. Perhaps, nanoparticle type and delivery site are important factors with respect to increasing bioavailability of insulin following oral administration.

ConA-polystyrene-HIV-1 nanospheres in immunization: Polystyrene derivatives contain mannose moieties that interact with ManR-carrying cell lines (DCs, macrophages) or mannan binding proteins. ConA, coupled to polystyrene nanoparticles via a poly-(ethyleneoxide) linker, protects protein conformation and activity. ConA-coated particles bind selectively to a series of different glycoproteins, and ConA-immobilized polystyrene nanospheres (ConA-NS) efficiently capture HIV-1. Intranasal immunization with inactivated HIV-1-capturing nanospheres (HIV-NS) produces vaginal anti-HIV-1 IgA antibody in mice. Intranasal immunization of macaques with ConA-NS or inactivated simian/HIV-KU-2-capturing nanospheres (SHIV-NS) and then intravaginally challenged with SHIV KU-2 exhibited partial protection [114, 115].

Bipartite drug delivery system: The ability to carry one or more therapeutic agents (biomolecular targeting) through one or more conjugated antibodies or other recognition agents (multifunctional nanoparticle) has been investigated. These nanoparticles are capable of detecting malignant cells (active targeting moiety), visualizing their location in the body (*in vivo* imaging), killing the cancer cells without side effects by saving normal cells (active targeting and controlled drug released system or photothermal ablation), and monitoring the treatment effect in real time. Robinson et al. [116] described a bipartite drug

delivery system that exploits (i) endogenous carbohydrate–lectin binding to localize glycosylated enzyme conjugates to specific, predetermined cell types followed by (ii) administration of a prodrug activated by that predelivered enzyme at the desired site. Combined *in vivo* and *in vitro* techniques demonstrated successful activation of α-L-rhamnopyranoside prodrug. Competition experiments revealed enhanced, specific and a strongly carbohydrate-dependent, 60-fold increase in selectivity toward target cell hepatocytes that generated >30-fold increase in protein delivered. Therapeutic effectiveness of lectin-directed enzyme-activated prodrug therapy was shown through construction of prodrug of doxorubicin, Rha-DOX, and its application to reduce tumor burden in a hepato-carcinoma mode [116].

53.7.3 Lectins in Drug Targeting

Various lectins, including tomato lectin, peanut agglutinin, WGA and MBLs [116–118], have been used as components of oral drug delivery systems. WGA from *Triticum vulgaris* shows a special affinity to *N*-acetyl-glucosamine (GlcNAc) and sialic acid, which are the major glycoproteins on the surface of most cells. WGA is regarded as a promising carrier for oral drugs because of its biochemical characteristics and non-toxic property. In solution, WGA exists as a heterodimer with a molecular weight of approximately 38 kDa, normally cationic under physiological conditions. β1-6 branching GlcNAc is abundantly expressed in various metastatic cancers. *Phaseolus vulgaris* agglutinin-L_4 isolectin (L_4-PHA) and WGA which interact with β1-6 GlcNAc, have been used for *in situ* cancer diagnosis. Bionanocapsules (BNCs), hollow particles (~80 nm), composed of hepatitis B surface antigen (HBsAg) and a lipid bilayer have been developed as human liver-specific nanocapsules for *in vivo* drug delivery system. PHA-BNCs systemically targeted mouse xenograft, which could accumulate in β1-6 GlcNAc-expressing malignant tumors. The PHA-BNCs were able to deliver DNA to malignant cancer cells. These studies open the usefulness of lectins as a targeting agent in drug delivery systems, and of nanodevices for tumor-specific bioimaging [118].

Lectins can be conjugated with drugs to enhance drug absorption in the gastrointestinal tract or to target drug to

a certain kind of cells, including intestine cells, cancer cells, and brain endothelial cells across the BBB [7]. In treatment of inflammatory bowel disease such as experimental colitis lectin-decorated drug-loaded NPs are used for active targeting. Peanut (PNA) and WGA lectins bound to surface of NP have shown their stability and degree of bioadhesion in murine colitis models. Lectin-conjugated NP exhibit a much higher binding and selectivity to inflamed tissue compared to plain NP. Hence, targeted NPs bound to lectins as PNA appear to be a promising tool in treatment of inflammatory bowel disease [119, 120]. WGA-conjugated PLGA nanoparticles enhanced intracellular delivery of paclitaxel to colon cancer cells. Gao et al. developed an enhanced delivery of vasoactive intestinal peptide with NPs conjugated with WGA [117]. Carvedilol is used in cardiovascular diseases. It has systemic bioavailability of 25–35%. Lectin-modified poly-(ethylene-co-vinyl acetate) was tested as mucoadhesive NP for bioavailability of carvedilol. Results showed that drug release rate was the most effective variable [121].

Applications of galactose and their conjugated polysaccharides, mannose and mannan conjugates, and their specific interacting proteins such as WGA, mannose receptors in macrophages and dendritic cells in drug targeting, have been described. Many therapeutic agents such as hydrophilic and macromolecular drugs cannot overcome the BBB. Wen et al conjugated odorranalectin (OL) to PEG-PLGA nanoparticles to improve nose-to-brain drug delivery in the treatment of central neuron system disorders [122]. The use of polymeric NPs such as PLGA NPs is promising solution as drug carrier. Significant breakthroughs have been made in developing suitable poly-(lactic-co-glycolic acid) (PGA) and poly-(lactic acid) (PLA) nanoparticles for drug delivery across the BBB. Several reports suggest that cellular uptake and therapeutic efficacy of drugs delivered with modified PLGA/PLA NPs were enhanced compared to free drugs or drugs delivered by unmodified PLGA NPs; no significant *in vitro* cytotoxicity was observed for PLGA NPs and PLA NPs. Surface modification of PLGA/PLA NPs by coating with surfactants/polymers or covalently conjugated with targeting ligands has been confirmed to enhance drug delivery across the BBB. WGA, conjugated to PLGA nanoparticles,

improved dopaminergic (DAergic) neuron delivery. Enhanced targeted delivery of PLGA-tWGA NPs to neurons compared with tWGA and PLGA-t NPs confirmed that PLGA-tWGA NPs had the potential to act as targeted neural delivery systems for the treatment of Parkinson's disease [123]. Lectin-conjugated gliadin nanoparticles are potential candidates for targeted drug delivery and are anticipated to be useful in treatment of *H. pylori* [124]. *Ulex europaeus* Agglutinin I (UEA-I) and ConA lectins, bound to gliadin nanoparticles (GNP) bearing acetohydroxamic acid (AHA) have been found effective in inhibiting *H. pylori* binding. In addition, antimicrobial activity of UEA-GNP and Con A-GNP was two-fold higher compared to GNP. This suggests that these nanomedicines have the potential to treat a number of diseases, including cancer, and improve the quality of life of patients.

Nanoparticles that satisfy the size and surface characteristics requirements should have the ability to circulate for longer times in the bloodstream and a greater chance of reaching the targeted tumor tissues. The pathophysiologic characteristics of tumor vessels enable macromolecules, including nanoparticles, to selectively accumulate in tumor tissues [125]. Fast-growing cancer cells demand the recruitment of new vessels (neovascularization) or rerouting of existing vessels near the tumor mass to supply them with oxygen and nutrients [126]. The resulting imbalance of angiogenic regulators such as growth factors and matrix metallo-proteinases makes tumor vessels highly disorganized and dilated with numerous pores showing enlarged gap junctions between endothelial cells and compromised lymphatic drainage [126]. These features, called the enhanced permeability and retention (EPR) effect, can selectively accumulate in the tumor interstitium through NPs. Many recently developed active targeting drug conjugates use a ternary structure composed of a ligand or antibody as a targeting moiety, a polymer or lipid as a carrier, and an active chemotherapeutic drug. The ternary structure nanoparticles create more efficient delivery systems such as specificity of tumor targets [127]. However, targeted conjugates can be internalized after binding to target cells should be an important criterion in the selection of proper targeting ligands [128].

53.8 Carbohydrate-Directed Targeting

Synthetic glycopolymers have been used as carriers of covalently conjugated drugs, bearing carbohydrate ligands that provide delivery specificity. However, these systems commonly rely on endogenous mechanisms (lysosomal degradation) for release of active drug, and so unwanted release of drug at sites other than desired site of action is possible. Glycotargeting is being followed through relying on use of oligosaccharide moiety or using lectin as a component of drug delivery system [73, 129, 130]. A general overview of published reports indicates the effectiveness of mannosylation strategies, although the optimization and full exploitation of mannose-targeted systems would require a deeper understanding of the structure-activity relationship [129]. Treatment of glioblastoma multiforme (GBM), a primary malignant tumor of brain, is one of the most challenging problems, as currently available treatments are not curative. Surgery remains basic treatment in which bulk of the tumor is removed and peripheral infiltrating part is target of supplementary treatments. Many of the nanotechnology-based devices can be applied in improvement of drug delivery to GBM [49, 131]. Mannan-methotrexate conjugate showed significantly improved anti-tumor activity compared to free methotrexate in mouse model of leukemia disseminated in peritoneal cavity treated with i.v. injected chemotherapy [132].

53.8.1 Mannosylated Particles as Cell-Specific Carriers

Mannosylated poly(L-lysine): A drug targeting system that utilizes ManR-mediated endocytosis to enhance cellular uptake of oligonucleotides (ONs) in alveolar macrophages (AMs) employs a molecular complex consisting of partially substituted mannosylated poly(L-lysine) (ManPL), linked to ON. Upon recognition by macrophage ManRs, ManPL was internalized by receptor-mediated pathway, co-transporting ON. AMs treated with ManPL:ON complex exhibited a significant increase in ON uptake over free ON-treated controls. Unmodified polylysine was less effective in promoting ON uptake. Following cellular internalization, ON largely accumulated in endocytic vesicles [133].

Poly-(L-lysine citramide imide): Commercially available quinic and shikimic acids appear as stable mannose bioisosteres,

which should prove valuable tools for specific cell delivery [134]. Internalization of norfloxacin antibiotic, which is active against some intracellular bacteria, was coupled to a polymeric carrier, (poly-(L-lysine citramide imide)), derived from two metabolites, citric acid and L-lysine, is known to be biocompatible and slowly degradable under slight acidic conditions. It was proposed that prodrug macromolecules compete effectively with glucose oxidase and thus should be able to bring drug up to mannosyl receptor-bearing membranes of macrophages infected by intracellular bacteria [135].

Cyclodextrin conjugates: Dendritic β-cyclodextrin (βCD) derivatives bearing multivalent mannosyl ligands were assessed for binding efficiency toward ConA and mammalian mannose/fucose specific cell surface receptor from macrophages. This type of βCD-dendrimer construct showed high drug solubilization capability. A subtle change in the structure of the conjugate shows important consequences on receptor affinity [136]. McNicholas et al. [108] synthesized amphiphilic β-cyclodextrins bearing hexylthio, dodecylthio, and hexadecylthio chains at 6-positions and glycosylthiocarbamoyl-oligo(ethylene glycol) units at 2-positions. Glycosyl residues (α-D-mannosyl) were intended for cell-targeting. These amphiphilic glycosylated cyclodextrins form vesicles in water. Hexylthio assemblies exhibited selective binding to *Lens culinaris* lectin. A bioeliminable amphiphilic poly(ethylene oxide)-b-poly(ε-caprolactone) diblock copolymer end-capped by a mannose residues showed that these colloidal systems have great potential for drug targeting and vaccine delivery systems [137].

Man-poly-ethyleneimine (ManPEI)/poly-propyleneimine (ManPPI) conjugates: Several ManPEI conjugates have been used for formation of ManPEI/DNA transfection complexes. DCs transfected with ManPEI/DNA complexes containing adenovirus particles are effective in activating T cells of T cell receptor transgenic mice in an antigen-specific fashion [138]. Evaluation study of anti-HIV activity of lamivudine (3TC)-loaded poly(propyleneimine) (PPI) and ManPPI dendrimers revealed that 3TC-loaded PPI and ManPPI formulations had higher anti-HIV activity, at a dose as low as 0.019 nM/mL as compared to free drug. The cellular uptake of 3TC loaded on ManPPI was 21 and 8.3 times higher than that of free drug and PPI respectively. Thus, ManPPI carrier holds higher potential with reduced toxicity of antiretroviral therapy [139].

Polysaccharides as carrier of drugs: A colon targeted tablet formulation, using chitosan and guar gum as carriers and diltiazem hydrochloride as model drug revealed that polysaccharides as carriers and inulin and shellac as coating materials can be used effectively for colon targeting for treating local as well as systemic disorders [140]. Konjac glucomannan (KGM), a water-soluble non-ionic polysaccharide hydrogels have a potential use for advanced controlled release [9, 141]. Water-soluble galactomannan made up of D-galactose and D-mannose, present in seed endosperm of *Cassia pleurocarpa*, can be exploited in areas such as drug delivery and tissue engineering [142]. The repeating unit of heteropolysaccharide shows a backbone of β(1-4) linked D-mannopyranosyl units to which D-galactopyranosyl units are linked as side chains through α(1-6) linkages.

53.8.2 Mannosylated NPs as Gene Carriers

Poly(*N*-p-Vinylbenzyl-O-β-Mannopyranosyl-(1-4)-D-Glucoamide) (PV-Mannose): PV-mannose contains mannose moieties and interacts with ManR-carrying cell line. PV-mannose strongly binds to macrophage cells, probably due to a specific interaction mediated by ManRs on cell membrane. Using a PV-mannose glycopolymer, receptor-mediated gene transfer via ManR is another method for targeted gene delivery into macrophages [143]. Polymeric nanospheres (NS) with a polystyrene core and a glucosyloxyethyl methacrylate (GEMA) oligomer corona nanosphere proved to be a useful material for studying sugar-biomolecule recognition and offered a potential for using a multi-lectin nanoparticle array in glycoprotein mapping [144, 145]. Poly(*N*-p-vinylbenzyl-O-D-glucopyranosyl-(1-4)-D-glucoamide) (PV-maltose) and PV-mannose, which contain glucose and mannose moieties, respectively, have specific binding ability with murine hematopoietic cells. Both PV-mannose and PV-maltose have been suggested for gene and drug delivery for hematopoietic cells and in therapeutic settings, respectively [146].

Mannose-capped silicon nanoparticles: Silicon nanoparticles (SiNPs) hold prominent interest in various aspects of biomedical applications. The surface functionalization of NPs is essential to stabilize them, target them to specific disease area, and allow them

to selectively bind to the cells. Stable D-mannose (Man) capped SiNPs have been synthesized from amine terminated SiNPs and D-mannopyranoside acid. Man functionalized SiNPs, treated with ConA, formed cross-linked aggregates suggesting that Man functionalized SiNPs can target cancerous cells [147]. Mesoporous silica NP (MSN) coupled with mannosylated polyethylenimine (ManPEI) were examined to transfect plasmid DNA *in vitro* [148]. Although MSN is biocompatible and has low cytotoxicity, it is not easily transfected into a variety of cell types. To overcome this barrier, ManPEI was coupled to MSN (abbreviated as MPS) to target macrophage cells with ManR. MPS/DNA complexes showed enhanced transfection efficiency through receptor-mediated endocytosis via ManR. MPS can be employed in future as a potential gene carrier to antigen-presenting cells.

Mannosylated liposomes: Direct respiratory delivery via inhalation of mannose modified liposomal carriers to alveolar macrophages is of great interest. However, clustering of mannose residues on liposomal surfaces or mannose density of Man-liposomes was important in determining binding affinity of Man-liposomes to MBP [149]. Mannosylated liposomes intercalated-benzyl derivative of an antibiotic MT81 (Bz2MT81) could eliminate intracellular amastigotes of *Leishmania donovani* within splenic macrophages more efficiently than liposome intercalated Bz2MT81 or free Bz2MT81. Liver and kidney function tests showed that toxicity of Bz2MT81 was reduced up to normal level when mannose-grafted liposomal Bz2MT81 were administered [150]. Using ConA as a model system for *in vitro* ligand-binding capacity, Man-liposomes showed potential applications for site-specific and ligand-directed delivery systems with better pharmacological activity [151]. In order to enhance localization to lymphatics, specifically to lymph node and spleen, surface engineered-mannosylated-liposomes showed biphasic response of zidovudine (ZDV) release. Man-liposomes appeared to be promising vesicular system for enhanced targeting of ZDV to lymphatics in AIDS chemotherapy [152].

Complexes of polylysine linked to ligands such as mannose [153] with DNA have been reported to enhance gene expression in macrophages. However, transfection efficiency of many of these vectors is handicapped due to endosomal or lysosomal degradation. Introduction of ligands for cell-surface receptors into liposomes

has improved transfection efficiency in macrophages. In most cases, liposomes were coated with macromolecular ligands such as transferrin, immunoglobulins, and asialoglycoproteins [152]. Various kinds of cationic lipids have been synthesized and shown to be able to deliver genes into cells. DC-Chol liposomes have been used in gene therapy applications in clinical settings. A galactosylated cholesterol derivative in combination with dioleoylphosphatidylethanolamine (DOPE) efficiently transferred a plasmid DNA into human hepatoma (HepG2) cells via an asialoglycoprotein receptor-mediated mechanism. However, these cationic liposomes did not exhibit any cell specificity *in vivo*.

Kawakami et al. [153] developed a low-molecular weight lipidic ligand, a mannosylated cholesterol derivative, cholesten-5-yloxy-*N*-(4-(1-imino-2-β-D-thiomannosylethyl) amino) butyl-formamide (Man-C4-Chol), for gene delivery to hepatocytes and compared with liposomes prepared with various molar ratios of Man-C4-Chol and particle size in transfection assays [154]. Gene expression with Man-C4-Chol/DOPE [6:4] liposome/DNA complexes in liver non-parenchymal cells was significantly reduced by predosing with Man-BSA. Higher gene expression in liver following intraportal injection suggested that plasmid DNA complexed with Man-liposomes exhibited high transfection activity due to recognition by ManR both *in vitro* and *in vivo*. Intravenous injection of DNA/cationic liposome complexes resulted in gene expression in many tissues, including heart, lung, liver, kidney, and spleen, and supported the participation of ManR in uptake of Man-liposome/DNA complexes and in liver Kupffer and/or endothelial cells. Like galactosylated protein, directly relating to surface density of galactose residues, Man-liposomes follow similar strategy in liver cells. Chemical structure and physicochemical characteristics of Man-C4-Chol seemed to satisfy the conditions for transfection in macrophages by offering a cationic charge and being recognized by mannose structure on liposomal surface. Wijagkanalan et al. [149] demonstrated efficient targeting to alveolar macrophages by intratracheally administered Man-liposomes via ManR-mediated endocytosis in rats. Study, testing Man-liposomes, with various ratio of mannosylated cholesterol derivatives, cholesten-5-yloxy-*N*-(4-((1-imino-2-D-thiomannosylethyl)-amino]alkyl)-formamide (Man-C4-Chol), suggested *in vitro* uptake of Man-liposomes in a concentration-dependent manner. Through

intratracheal route of administration of Man-7.5 and Man-5.0-liposomes, internalization was enhanced and selective to alveolar macrophages. However, serum MBP inhibits mannosylated liposome-mediated transfection to macrophages. Although Man-C4-Chol is a novel mannosylated cholesterol derivative, which exhibits a higher transfection activity than DC-Chol liposomes in mouse peritoneal macrophages based on a receptor-mediated mechanism, the role of serum proteins has to be examined. Since this compound itself has a positive charge, a high density of mannose residues can be deposited on liposome surface without adversely affecting binding ability of cationic liposomes to DNA. These characteristics of liposomes with Man-C4-Chol are reflected in their superior *in vivo* gene transfection [154].

Carbohydrate-grafted emulsions are one of the most promising cell-specific targeting systems for lipophilic drugs. *In vitro* study showed increased internalization of Man-5.0- and Man-7.5-emulsions and significant inhibition of uptake in the presence of mannan. Mannose density of Man-emulsions plays an important role in both cellular recognition and internalization via a ManR-mediated mechanism [154]. A mannosylated cationic liposomes/immunostimulatory CpG DNA complex (Man/CpG DNA lipoplex) is an effective inhibitor for peritoneal dissemination in mice. Intraperitoneal administration of Man/CpG DNA inhibited the proliferation of tumor cells more efficiently than Bare/CpG DNA lipoplex and Gal/CpG DNA lipoplex. Therefore, Man/CpG DNA lipoplex can be used for efficient immunotherapy to combat peritoneal dissemination [155].

53.9 Conclusions

Lectin–carbohydrate interactions are involved in a vast array of biological processes. The increased interest in lectin receptors has brought about a number of opportunities for developing therapies such as targeting cells for drugs and genes, and development of vaccines through endocytic cells. Lectins as new receptors have started to play a pivotal role in many drug delivery devices owing to their exquisite specificity for their cognate carbohydrates. To fully exploit these opportunities, it is essential to develop efficient methods to tag lectins with nanoparticles.

Nanoparticles are promising carriers of both small drug molecules as well as macromolecules such as genes and proteins. Nanoparticle-based targeted delivery systems such as liposomes, polymeric micelles, nanosystems, nanoshells, carbon nanotubes, dendrimers, quantum dots, etc., hold great potential to increase the cure rate of patients, particularly cancer patients, while minimizing toxicity of drugs. The views presented in this chapter will provide both new ideas in a single reference work for both the beginner and experienced scientists who work on lectins and glycopolymers as drug carriers.

Disclosures and Conflict of Interest

The authors declare that they have no conflict of interest with any organization or entity discussed in this chapter. The authors have not received any assistance or payment for preparation of this chapter from any source. The chapter has been written for academic purposes.

Corresponding Author

Dr. G. S. Gupta
Department of Biophysics, Panjab University
Chandigarh 160014, India
Email: drgsgupta53@rediffmail.com

About the Authors

Anita Gupta received MSc (Hons) in biophysics (1984) from Panjab University, Chandigarh, and PhD (1995) from the Department of Molecular Biology and Biochemistry, Guru Nanak Dev University, Amritsar. Since 1995, she has been engaged in teaching and research in biotechnology and biomedical engineering at prestigious institutes such as PIGMER, Chandigarh, UIET, Panjab University Chandigarh and RIEBT, Kharar (Mohali). Until recently, she was associate professor and chair of the Department of Biomedical Engineering and the Department of Applied Science at RIEBT.

Dr. Gupta has special research interest in lectinology and has coauthored the book *Animal Lectins: Form, Function and Clinical Applications* (Springer-Wien). She has published more than 40 articles in peer-reviewed journals and books in the field of health sciences.

G. S. Gupta is a former professor and chair of the Department of Biophysics, Panjab University, Chandigarh. His primary interest in research includes enzymology/protein chemistry of testis and associated organs, reproductive immunology, radiation-molecular biology, and lectinology. He has worked with Prof. E. Goldberg at Northwestern University, Evanston, (USA) in 1976–1977, with Dr. G. A. Voisin and Dr. R. G. Kinsky at INSERM, Paris (1982–1983 and 1987–1988) and the Centre of Cytogenetics and Immunogenetics, INSERM, Villejuif (France) (1989 and 1991). He has made significant research contribution and published more than 200 research articles and reviews in books and peer-reviewed journals with high impact factor. Dr. Gupta has authored *Proteomics of Spermatogenesis* (2005), published by Springer (New York, USA), in which he contributed 34 reviews on the subject. In November 2012, as principal author, he published *Animal Lectins: Form, Function and Clinical Applications*, in two volumes (Springer-Wien), in which he published 34 reviews on animal lectins. He is recipient of several awards and fellowships, including a WHO fellowship, the INSERM French Government fellowship, and the fellowships under Indo-French Exchange program. ICMR has honored him by conferring Swaran Kanta Dingley Oration Award (1993) for his contribution in male reproduction. He has been honored as emeritus scientist by CSIR (1997) and DST (2000), as emeritus professor by UGC (2001), and as emeritus medical scientist by ICMR (1997). The Indian Society for Study of Reproduction and Fertility has conferred to Dr. Gupta the Lifetime Achievement Award (2013) in recognition for his outstanding research contribution in Reproductive Health.

References

1. Ross, J. S., Schenkein, D. P., Pietrusko, R., et al. (2004). Targeted therapies for cancer. *Am. J. Clin. Pathol.*, **122**, 598–609.

2. Cho, K., Wang, X., Nie, S., Chen, Z., Dong, M. S. (2008). Therapeutic nanoparticles for drug delivery in cancer. *Clin. Cancer Res.*, **14**, 1310–1316.
3. Pitt. C. G., Gratzl, M., Kimmel, G. L., Surles, J., Schindler, A. (1981). Aliphatic polyesters II. The degradation of poly(DL-lactide), poly (epsilon-caprolactone), and their copolymers in vivo. *Biomaterials*, **2**, 215–220.
4. Gupta, A., Sandhu, R. S. (1997). A new high molecular weight agglutinin from garlic (Allium sativum). *Mol. Cell Biochem*., **166**, 1–9.
5. Gupta, A. (2005). Mannose specific lectins from edible garlic. *Panjab Univ. Res. J*., **56**, 205–214.
6. Miyake, K., Tanaka, T., McNeil, P. L. (2007). Lectin-based food poisoning: A new mechanism of protein toxicity. *PLoS ONE*, **2**, e687.
7. Wei, X., Chen, X., Ying, M., Lu, W. (2014). Brain tumor-targeted drug delivery strategies. *Acta Pharm. Sin. B*, **4**, 193–201.
8. Sharon, N., Lis, H. (2004). History of lectins: From hemagglutinins to biological recognition molecules. *Glycobiology*, **14**, 53R–62R.
9. Gupta, A., Gupta, R. K., Gupta, G. S. (2009). Targeting cells for drug and gene delivery: Emerging applications of mannans and mannan binding lectins. *J. Sci. Ind. Res.,* **68**, 465–483.
10. Silva. A. T., Chung, M. C., Castro, L. F., Guido, R. V., Ferreira, E. I. (2005). Advances in prodrug design. *Mini Rev. Med. Chem*., **5**, 893–914.
11. Gupta, G. S., ed. (2012). *Animal Lectins: Form, Function and Clinical Applications*, Springer-Wien.
12. Varki, A., Cummings, R., Esko, J., Freeze, H., Hart, G., Marth, J. (1999). *Essentials of Glycobiology*, Cold Spring Harbor Laboratory Press, USA.
13. Gupta, A. (2012). Collectins: Mannan-binding protein as a model lectin. In: Gupta, G. S., ed., *Animal Lectins: Form, Function and Clinical Applications*, Springer-Wien, pp. 483–499.
14. Gupta, A. (2012). Asialoglycoprotein receptor and the macrophage galactose-type lectin. In: Gupta, G. S., ed., *Animal Lectins: Form, Function and Clinical Applications*, Springer-Wien, 2012c, pp. 709–724.
15. Meier, M., Bider, M. D., Malashkevich, V. N., Spiess, M., Burkhard, P. (2000). Crystal structure of the carbohydrate recognition domain of the H1 subunit of the asialoglycoprotein receptor. *J. Mol. Biol.*, **300**, 857–865.
16. Wu, J., Nantz, M. H., Zern, M. A. (2002). Targeting hepatocytes for drug and gene delivery: Emerging novel approaches and applications. *Front Biosci.*, **7**, 717–7725.

17. Yamazaki, N., Kojima, S., Bovin, N. V., Andre, S., Gabius, S., Gabius, H. J. (2000). Endogenous lectins as targets for drug delivery. *Adv. Drug Del. Rev*., **43**, 225–244.
18. Weis, W. I., Taylor, M. E., Drickamer, K. (1998). The C-type lectin superfamily in the immune system. *Immunol. Rev.*, **163**, 19–34.
19. Torrelles, J. B., Azad, A. K., Henning, L. N., Carlson, T. K., Schlesinger, L. S. (2008). Role of C-type lectins in mycobacterial infections. *Curr. Drug Targets*, **9**, 102–112.
20. Gupta, R. K., Gupta, G. S. (2012). Mannose receptor family: R-type lectins. In: Gupta, G. S., ed. *Animal Lectins: Form, Function and Clinical Applications*, Springer-Wien, pp. 331–347.
21. Colmenares, M., Corbi, A. L., Turco, S. J., Rivas, L. (2004). The dendritic cell receptor DC-SIGN discriminates among species and life cycle forms of Leishmania. *J. Immunol*., **172**, 1186–1190.
22. Sato, K., Yang, X.-L., Yudate, T., Chung, J.-S., Wu, J., Luby-Phelps, K., et al. (2006). Dectin-2 is a pattern recognition receptor for fungi that couples with the fc receptor γ chain to induce innate immune responses. *J. Biol. Chem.*, **281**, 38854–38866.
23. Napper, C. E., Dyson, M. H., Taylor, M. E. (2001). An extended conformation of the macrophage mannose receptor. *J. Biol. Chem.*, **276**, 14759–14766.
24. Boskovic, J., Arnold, J. N., Stilion, R., et al. (2006). Structural model for the mannose receptor family uncovered by electron microscopy of Endo180 and the mannose receptor. *J. Biol. Chem.,* **281**, 8780–8787.
25. Gupta, R. K., Gupta, G. S. (2012). Dendritic cell lectin receptors (dectin-2 receptors family) In: Gupta, G. S., ed., *Animal Lectins: Form, Function and Clinical Applications*, Springer-Wien, pp. 749–771.
26. Drickamer, K., Taylor, M. E. (1993). Biology of animal lectins, *Ann. Rev. Cell Biol.*, **9**, 237–264.
27. Gupta, R. K., Gupta, G. S. (2012). Dectin-1 receptor family. In: Gupta, G. S., ed., *Animal Lectins: Form, Function and Clinical Applications*, Springer-Wien, pp. 725–747.
28. Appelmelk, B. J., van Die, I., van Vliet, S. J., et al. (2003). Cutting edge: Carbohydrate profiling identifies new pathogens that interact with dendritic cell-specific ICAM-3-grabbing nonintegrin on dendritic cells. *J. Immunol.*, **170**, 1635–1639.
29. Zhou, T., Chen, Y., Hao, L., Zhang, Y. (2006). DC-SIGN and immunoregulation. *Cell Mol. Immunol*., **3**, 279–283.
30. Feinberg, H., Mitchell, D. A., Drickamer, K., et al. (2001). Structural basis for selective recognition of oligosaccharides by DC-SIGN and DC-SIGNR. *Science*, **294**, 2163–2166.

31. Gupta, R. K., Gupta, G. S. (2012). DC-SIGN family of receptors. In: Gupta, G. S., ed., *Animal Lectins: Form, Function and Clinical Applications*, Springer-Wien, pp. 773–798.
32. Gupta, R. K., Gupta, A. (2012). Endogenous lectins as drug targets. In: Gupta, G. S., ed., *Animal Lectins: Form, Function and Clinical Applications*, Springer-Wien, pp. 1039–1057.
33. Jiang, W. P., Swiggard, W. J., Heufler, C., Peng, M., Mirza, A., Steinman, R. M., Nussenzweig, M. C. (1995). The receptor DEC-205 expressed by dendritic cells and thymic epithelial cells is involved in antigen processing. *Nature*, **375**, 151–155.
34. Sallusto, F., Cella, M., Danieli, C., Lanzavecchia, A. (1995). Dendritic cells use macropinocytosis and the mannose receptor to concentrate macromolecules in the major histocompatibility complex class II compartment: Downregulation by cytokines and bacterial products. *J. Exp. Med.*, **182**, 389–400.
35. Dennehy, K. M., Brown, G. D. (2007). The role of the β-glucan receptor Dectin-1 in control of fungal infection. *J. Leuko. Biol.*, **82**, 253–258.
36. Haas, J., Lehr, C. M. (2002). Developments in the area of bioadhesive drug delivery systems. *Expert Opin. Biol. Ther.*, **2**, 287–298.
37. Helen, M., Osborn, I., Evans, P. G., Gemmell, N., Sadie, D., Osborne, S. D. (2004). Carbohydrate-based therapeutics. *J. Pharm. Pharmacol.*, **56**, 691–702.
38. Takahashi, Y., Yajima, A., Cisar, J. O., Konishi, K. (2004). Functional analysis of the Streptococcus gordonii DL1 sialic acid-binding adhesin and its essential role in bacterial binding to platelets. *Infect. Immun.,* **72**, 3876–3882.
39. Pelley, R. P., Strickland, F. M. (2000). Plants polysaccharides, and the treatment and prevention of neoplasia. *Crit. Rev. Oncol.*, **11**, 189–225.
40. Bamrungsap, S., Zhao, Z., Chen, T., Wang, L., Li, C., Fu, T., Tan, W. (2012). A Focus on nanoparticles as a drug delivery system. *Nanomedicine,* **7**, 1253–1271.
41. Nag, A., Ghosh, R. C. (1999). Assessment of targeting potential of galactosylated and mannosylated sterically stabilized liposomes to different cell types of mouse liver. *J. Drug Target.*, **6**, 427–438.
42. Wadhwa, M. S., Rice, K. G. (1995). Receptor mediated glycotargeting. *J. Drug Target.*, **3**, 111–127.
43. Dasi, F., Benet, M., Crespo, J., Alino, S. F. (2001). Asialofetuin liposome-mediated human alpha1-antitrypsin gene transfer in vivo results in stationary long-term gene expression. *J. Mol. Med.*, **79**, 205– 212.

44. Fiume, L., Cerenzia, M. R. T., Bonino, F., Busi, C., Mattioli, A., Brunetto, M. R., Chiaberge, E., Verne, G. (1994). Inhibition of hepatitis B. virus replication by vidarabine monophosphate conjugated with lactosaminated serum albumin. *Lancet*, **2**, 13–15.
45. Sinha, R., Kim, G. J., Nie, S., Shin, D. M. (2006). Nanotechnology in cancer therapeutics: Bioconjugated nanoparticles for drug delivery. *Mol. Cancer Ther.*, **5**, 1909–1917.
46. Jones, T., Saba, N. (2011). Nanotechnology and drug delivery: An update in oncology. *Pharmaceutics*, **3**, 171–185.
47. Mohanraj, V. J., Chen, Y. (2006). Nanoparticles—A review. *Trop. J. Pharm. Res.*, **5**, 561–573.
48. Higuchi, Y., Oka, M., Kawakami, S., Hashida, M. (2008). Mannosylated semiconductor quantum dots for the labeling of macrophages. *J. Control. Release*, **125**, 131–136.
49. Jain, K. K. (2007). Use of nanoparticles for drug delivery in glioblastoma multiforme. *Expert Rev. Neurother.*, **7**, 363–372.
50. Jain, A. K., Das, M., Swarnakar, N. K., Jain, S. (2011). Engineered PLGA nanoparticles: An emerging delivery tool in cancer therapeutics. *Crit. Rev. Ther. Drug Carrier Syst.*, **28**, 1–45.
51. Mirakabad, F. S. T., Nejati-Koshki, K., Akbarzadeh, A., Yamchi, M. R., Milani, M., et al. (2014). PLGA-based nanoparticles as cancer drug delivery systems. *Asian Pac. J. Cancer Prev.*, **15**, 517–535.
52. Duncan, R. (2003). The dawning era of polymer therapeutics. *Nat. Rev. Drug Discov.*, **2**, 347–360.
53. Jemal, A., Bray, F., Center, M. M., et al. (2011). Global cancer statistics. *CA Cancer J. Clin.*, **61**, 69–90.
54. Dinarvand, R., Sepehri, N., Manoochehri, S., Rouhani, H., Atyabi, F. (2011). (Polylactide-co-glycolide nanoparticles for controlled delivery of anticancer agents. *Int. J. Nanomed.*, **6**, 877.
55. Liu, Y., Miyoshi, H., Nakamura, M. (2007). Nanomedicine for drug delivery and imaging: A promising avenue for cancer therapy and diagnosis using targeted functional nanoparticles. *Int. J. Cancer*, **120**, 2527–2537.
56. Lü, J. M., Wang, X., Marin-Muller, C., et al. (2009). Current advances in research and clinical applications of PLGA-based nanotechnology. *Expert Rev. Mol. Diagn.*, **9**, 325–341.
57. Mahapatro, A., Singh, D. K. (2011). Biodegradable nanoparticles are excellent vehicle for site directed in-vivo delivery of drugs and vaccines. *J. Nanobiotechnol.*, **9**, 55.

58. Kumari, A., Yadav, S. K., Yadav, S. C. (2010). Biodegradable polymeric nanoparticles based drug delivery systems. *Colloids Surf. B: Biointerfaces*, **75**, 1–18.

59. Astete, C. E., Sabliov, C. M. (2006). Synthesis and characterization of PLGA nanoparticles. *J. Biomater. Sci.*, **17**, 247–289.

60. Mohamed, F., van der Walle, C. F. (2008). Engineering biodegradable polyester particles with specific drug targeting and drug release properties. *J. Pharm. Sci*., **97**, 71–87.

61. Pillay, S., Pillay, V., Choonara, Y. E., Naidoo, D., Khan, R. A., Toit, L. C., et al. (2009). Design, biometric simulation and optimization of a nano-enabled scaffold device for enhanced delivery of dopamine to the brain. *Int. J. Pharm.*, **382**, 277–290.

62. Fredenberg, S., Wahlgren, M., Reslow, M., Axelsson, A. (2011). The mechanisms of drug release in poly(lactic-co-glycolic acid).-based drug delivery systems-A review. *Int. J. Pharm.*, **415**, 34–52.

63. Sharma, G., Italia, J. L., Sonaje, K., et al. (2007). Biodegradable in situ gelling system for subcutaneous administration of ellagic acid and ellagic acid loaded nanoparticles: Evaluation of their antioxidant potential against cyclosporine induced nephrotoxicity in rats. *J. Control. Release*, **118**, 27–37.

64. Klose, D., Siepmann, F., Elkharraz, K., Siepmann, J. (2008). PLGA-based drug delivery systems: Importance of the type of drug and device geometry. *Int. J. Pharm.*, **354**, 95–103.

65. Desai, K. G. H., Olsen, K. F., Mallery, S. R., Stoner, G. D., Schwendeman, S. P. (2010). Formulation and in vitro-in vivo evaluation of black raspberry extract-loaded PLGA/PLA injectable millicylindrical implants for sustained delivery of chemopreventive anthocyanins. *Pharm. Res.*, **27**, 628–643.

66. Dong, W. Y., Körber, M., López Esguerra, V., Bodmeier, R. (2006). Stability of poly(D,L-lactide-co-glycolide) and leuprolide acetate in *in-situ* forming drug delivery systems. *J. Control. Release*, **115**, 158–167.

67. Xiong, Y., Zeng, Y. S., Zeng, C. G., et al. (2009). Synaptic transmission of neural stem cells seeded in 3-dimensional PLGA scaffolds. *Biomaterials*, **30**, 3711–3722.

68. Zeisser-Labouèbe, M., Lange, N., Gurny, R., Delie, F. (2006). Hypericin-loaded nanoparticles for the photodynamic treatment of ovarian cancer. *Int. J. Pharm.,* **326**, 174–181.

69. Ong, B., Ranganath, S. H., Lee, L. Y., et al. (2009). Paclitaxel delivery from PLGA foams for controlled release in post-surgical chemotherapy against glioblastoma multiforme. *Biomaterials*, **30**, 3189–3196.

70. Acharya, S., Sahoo, S. K. (2011). PLGA nanoparticles containing various anticancer agents and tumour delivery by EPR effect. *Adv. Drug Deliv. Rev*., **63**, 170–183.
71. Reddy, L. H., Sharma, R. K., Chuttani, K., Mishra, A. K., Murthy, R. R. (2004). Etoposide-incorporated tripalmitin nanoparticles with different surface charge: Formulation, characterization, radiolabeling, and biodistribution studies. *AAPS J.*, **6**, 55–64.
72. Derakhshandeh, K., Erfan, M., Dadashzadeh, S. (2007). Encapsulation of 9-nitrocamptothecin, a novel anticancer drug, in biodegradable nanoparticles: Factorial design, characterization and release kinetics. *Eur. J. Pharm. Biopharm.*, **66**, 34–41.
73. Chen, Y., Liu, L. (2012). Modern methods for delivery of drugs across the blood-brain barrier. *Adv. Drug Deliv. Rev.*, **64**, 640–665.
74. Misra, R., Sahoo, S. K. (2010). Intracellular trafficking of nuclear localization signal conjugated nanoparticles for cancer therapy. *Eur. J. Pharm. Sci*., **39**, 152–163.
75. Park, H., Yang, J., Lee, J., et al. (2009). Multifunctional nanoparticles for combined doxorubicin and photothermal treatments. *ACS Nano*, **3**, 2919–2926.
76. Mukerjee, A., Vishwanatha, J. K. (2009). Formulation, characterization and evaluation of curcumin-loaded PLGA nanospheres for cancer therapy. *Anticancer Res*., **29**, 3867–3875.
77. Teixeira, M., Alonso, M. J., Pinto, M. M. M., Barbosa, C. M. (2005). Development and characterization of PLGA nanospheres and nanocapsules containing xanthone and 3-methoxyxanthone. *Eur. J. Pharm. Biopharm.*, **59**, 491–500.
78. Bakowsky, H., Richter, T., Kneuer, C., Hoekstra, D. et al. (2008). Adhesion characteristics and stability assessment of lectin-modified liposomes for site-specific drug delivery. *Biochim. Biophys. Acta*, **1778**, 242–249.
79. Lee, C., Gillies, E. R., Fox, M. E., Guillaudeu, S. J., Fréchet, J. M., Dy, E. E., Szoka, F. C. (2006). A single dose of doxorubicin-functionalized bow-tie dendrimer cures mice bearing C-26 colon carcinomas. *Proc. Natl. Acad. Sci. USA*, **103**, 16649–16654.
80. Markman, M. (2006). Pegylated liposomal doxorubicin in the treatment of cancers of the breast and ovary. *Expert Opin. Pharmacother*., **7**, 1469–1474.
81. Uckun, F. M., Qazi, S., Cely, I., Sahin, K., Shahidzadeh, A., Ozercan, I., Yin, Q., Gaynon, P., Termuhlen, A., Cheng, J., Seang Yiv, S. (2013).

Nanoscale liposomal formulation of a SYK P-site inhibitor against B-precursor leukemia. *Blood*, **121**, 4348–4354.

82. Hofheinz, R. D., Gnad-Vogt, S. U., Beyer, U., Hochhaus, A. (2005). Liposomal encapsulated anti-cancer drugs. *Anticancer Drugs*, **16**, 691–707.
83. Uckun, F. M., Qazi, S., Cely, I., Sahin, K., Shahidzadeh, A., Ozercan, I., Yin, Q., Gaynon, P., et al. (2013). Nanoscale liposomal formulation of a SYK P-site inhibitor against B-precursor leukemia. *Blood*, **121**, 4348–4354.
84. Wu, J., Liu, Q., Lee, R. J. (2006). A folate receptor-targeted liposomal formulation for paclitaxel. *Int. J. Pharm.*, **316**, 148–153.
85. Torchilin, V. P., Levchenko, T. S., Lukyanov, A. N., et al. (2001). *p*-Nitrophenylcarbonyl-PEG-PE-liposomes: Fast and simple attachment of specific ligands, including monoclonal antibodies, to distal ends of PEG chains via *p*-nitrophenylcarbonyl groups. *Biochim. Biophys. Acta*, **1511**, 397–411.
86. Chen, H., Torchilin, V., Langer, R. (1996). Lectin-bearing polymerized liposomes as potential oral vaccine carriers. *Pharm. Res*., **13**, 1378–1383.
87. Adams, M. L., Lavasanifar, A., Kwon, G. S. (2003). Amphiphilic block copolymers for drug delivery. *J. Pharm. Sci.*, **92**, 1343–1355.
88. Nakanishi, T., Fukushima, S., Okamoto, K., Suzuki, M., Matsumura, Y., Yokoyama, M., Okano, T., Sakurai, Y., Kataoka, K. (2001). Development of the polymer micelle carrier system for doxorubicin. *J. Control. Release*, **74**, 295–302.
89. Nasongkla, N., Bey, E., Ren, J., Ai, H., Khemtong, C., Guthi, J. S. (2006). Multifunctional polymeric micelles as cancer-targeted, MRI-ultrasensitive drug delivery systems. *Nano Lett*., **6**, 2427–2430.
90. Svenson, S., Tomalia, D. A. (2005). Dendrimers in biomedical applications—reflections on the field. *Adv. Drug Deliv. Rev*., **57**, 2106–29.
91. Bogdan, N., Vetrone, F., Roy, R., Capobianco, J. A. (2010). Carbohydrate-coated lanthanide-doped up converting nanoparticles for lectin recognition. *J. Mater. Chem.*, **20**, 7543–7550.
92. Ogiso, M., Kobayashi, J., Tomoko Imai, T., et al. (2013). Carbohydrate immobilized on a dendrimer-coated colloidal gold surface for fabrication of a lectin-sensing device based on localized surface plasmon resonance spectroscopy. *Biosen. Bioelec.*, **41**, 465–470.
93. West, J. L., Halas, N. J. (2003). Engineered nanomaterials for biophotonics applications: Improving sensing, Imaging, and therapeutics. *Ann. Rev. Biomed. Eng.*, **5**, 285–292.

94. Kewal, K., Jain, T., Jain, K. K. (2005). Review nanotechnology in clinical laboratory diagnostics. *Clin. Chim. Acta*, **358**, 37–54.

95. Bianco, A., Kostarelos, K., Prato, M. (2005). Applications of carbon nanotubes in drug delivery. *Curr. Opin. Chem. Biol*., **9**, 674–679.

96. Wu, W., Wieckowski, S., Pastorin, G., Benincasa, M., Klumpp, C., Briand, J. P., Gennaro, R., Prato, M., Bianco, A. (2005). Targeted delivery of amphotericin B to cells by using functionalized carbon nanotubes. *Angew. Chem. Int. Ed. Engl*., **44**, 6358–6362.

97. Pastorin, G., Wu, W., Wieckowski, S., Briand, J. P., Kostarelos, K., Prato, M., Bianco, A. (2006). Double functionalisation of carbon nanotubes for multimodal drug delivery. *Chem. Commun*., **11**, 1182–1184.

98. McDevitt, M. R., Chattopadhyay, D., Kappel, B. J., Jaggi, J. S., Schiffman, S. R., Antczak, C., Njardarson, J. T., Brentjens, R., Scheinberg, D. A. (2007). Tumor targeting with antibody-functionalized, radiolabeled carbon nanotubes. *J. Nucl. Med.*, **48**, 1180–1189.

99. Ahmed, F., Pakunlu, R. I., Srinivas, G., Brannan, A., Bates, F., Klein, M. L., Minko, T., Discher, D. E. (2006). Shrinkage of a rapidly growing tumor by drug-loaded polymersomes: pH-triggered release through copolymer degradation. *Mol. Pharm.*, **3**, 340–350.

100. Singh, R., Lillard, J. W., Jr. (2009). Nanoparticle-based targeted drug delivery. *Exp. Mol. Pathol.*, **86**, 215–223.

101. Manchester, M., Singh, P. (2005). Virus-based nanoparticles (Vnanoparticles): Platform technologies for diagnostic imaging. *Adv. Drug Deliv. Rev.*, **58**, 505–522.

102. Gorelik, E., Galili, U., Raz, A. (2001). On the role of cell surface carbohydrates and their binding proteins (lectins) in tumor metastasis. *Cancer Metastasis Rev*., **20**, 245–277.

103. Gabor, F., Bogner, E., Weissenboeck, A., Wirth, M. (2004). The lectin-cell interaction and its implications to intestinal lectin-mediated drug delivery. *Adv. Drug Deliv. Rev.*, **56**, 459–480.

104. Yewale, C., Baradia, D., Vhora, I., Misra, A. (2013). Proteins: Emerging carrier for delivery of cancer therapeutics. *Expert Opin. Drug Deliv.*, **10**, 1429–1448.

105. Bies, C., Lehr, C. M., Woodley, J. F. (2004). Lectin-mediated drug targeting: History and applications, *Adv. Drug Deliv. Rev.*, **56**, 425–435.

106. Nishiyama, K., Takakusagi, Y., Kusayanagi, T., Matsumoto, Y., Habu, S., et al. (2009). Identification of trimannoside-recognizing peptide sequences from a T7 phage display screen using a QCM device. *Bioorg. Med. Chem*., **17**, 195–202.

107. Yin, Y., Chen, D., Qiao, M., Lu, Z., Hu, H. (2006). Preparation and evaluation of lectin-conjugated PLGA nanoparticles for oral delivery of thymopentin. *J. Control. Release*, **116**, 337–345.

108. McNicholas, S., Rencurosi, A., Lay, L., Mazzaglia, A., Sturiale, L., Perez, M., Darcy, R. (2007). Amphiphilic *N*-glycosyl-thiocarbamoyl cyclodextrins: Synthesis, self-assembly, and fluorimetry of recognition by Lens culinaris lectin. *Biomacromolecules,* **8**, 1851–1857.

109. Pusztai, A., Grant, G., Spencer, R. J., Diguid, T. J., Brown, D. S., Ewen, S W B., Peumans, W. J., et al. (1993). Kidney bean lectin-induced Escherichia coli overgrowth in the small intestine is blocked by GNA, a mannose-specific lectin. *J. Appl. Bacteriol.*, **75**, 360–368.

110. Branderhorst, H. M., Ruijtenbeek, R., Liskamp, R. M., Pieters, R. J. (2008). Multivalent carbohydrate recognition on a glycodendrimer-functionalized flow-through chip, *Chembiochem*, **9**, 1836–1844.

111. Brück, A., Abu-Dahab, R., Borchard, G., Schäfer, U. F., Lehr, C. M. (2001). Lectin-functionalized liposomes for pulmonary drug delivery: Interaction with human alveolar epithelial cells. *J. Drug Target.*, **9**, 241–251.

112. Yi, S. M., Harson, R. E., Zabner, J. Welsh, M. J. (2001). Lectin binding and endocytosis at the apical membrane of human airway epithelia. *Gene Ther*., **8**, 1826–1832.

113. Zhang, N., Ping, Q. N., Huang, G. H., Xu, W. F. (2005). Investigation of lectin-modified insulin liposomes as carriers for oral administration. *Int. J. Pharm*., **295**, 247–259.

114. Akashi, M., Niikawa, T., Serizawa, T., Hayakawa, T., Baba, M. (1998). Capture of HIV-1 gp120 and virions by lectin-immobilized polystyrene nanospheres. *Bioconjug. Chem*., **9**, 50–53.

115. Miyake, A., Akagi, T., Enose, Y., Ueno, M., Kawamura, M., Horiuchi, R., et al. (2004). Induction of HIV-specific antibody response and protection against vaginal transmission by intranasal immunization with inactivated-capturing nanospheres in macaques. *J. Med. Virol.*, **73**, 368–377.

116. Robinson, M. A., Charlton, S. T., Garnier, P., Wang, X. T., Davis, S. S., et al. (2004). LEAPT: Lectin-directed enzyme-activated prodrug therapy. *Proc. Natl. Acad. Sci. USA*, **101**, 14527–14532.

117. Gao, X., Chen, J., Tao, W., Zhu, J., Zhang, Q., Chen, H., Jiang, X. (2007). UEA I-bearing nanoparticles for brain delivery following intranasal administration. *Int. J. Pharm*., **340**, 207–215.

118. Kasuya, T., Jung, J., Kadoya, H., et al. (2008). In vivo delivery of bionanocapsules displaying Phaseolus vulgaris agglutinin-L4

isolectin to malignant tumors overexpressing *N*-acetylglucosaminyl transferase V. *Hum. Gene Ther.*, **19**, 887–895.

119. Moulari, B., Béduneau, A., Pellequer, Y., Lamprecht, A. (2014). Lectin-decorated nanoparticles enhance binding to the inflamed tissue in experimental colitis. *Control. Release,* **188**, 9–17.
120. Ulbrich, W., Lamprecht, A. (2010). Targeted drug-delivery approaches by nanoparticulate carriers in the therapy of inflammatory diseases. *J. R. Soc. Interface*, **7**, S55–S66.
121. Varshosaz, J., Moazen, E. (2014). Novel lectin-modified poly(ethylene-co-vinyl acetate) mucoadhesive nanoparticles of carvedilol: Preparation and in vitro optimization using a two-level factorial design. *Pharm. Dev. Technol.*, **19**, 605–617.
122. Wen, X., Wang, T., Wang, Z., Li, L., Zhao, C. (2008). Preparation of konjac glucomannan hydrogels as DNA-controlled release matrix. *Int. J. Biol. Macromol.*, **42**, 256–263.
123. Sah, H., Thoma, L. A., Desu, H. R., Sah, E., Wood, G. C. (2013). Concepts and practices used to develop functional PLGA-based nanoparticulate systems. *Int. J. Nanomed*., **8**, 747–765.
124. Umamaheshwari, R. B., Jain, N. K. (2003). Receptor mediated targeting of lectin conjugated gliadin nanoparticles in the treatment of Helicobacter pylori. *J. Drug Target.*, **11**, 415–423.
125. Maeda, H. (2001). The enhanced permeability and retention (EPR) effect in tumor vasculature: The key role of tumor-selective macromolecular drug targeting. *Adv. Enzyme Regul.*, **41**, 189–207.
126. Carmeliet, P., Jain, R. K. (2000). Angiogenesis in cancer and other diseases. *Nature*, **407**, 249–257.
127. Allen, T. M. (2002). Ligand-targeted therapeutics in anticancer therapy. *Nat. Rev. Cancer*, **2**, 750–763.
128. Leamon, C. P., Reddy, J. A. (2004). Folate-targeted chemotherapy. *Adv. Drug Deliv. Rev.*, **56**, 1127–1141.
129. Irache, J. M., Salman, H. H., Gamazo, C., Espuelas, S. (2008). Mannose-targeted systems for the delivery of therapeutic. *Expert Opin. Drug Deliv.*, **5**, 703–724.
130. Smart, J. D. (2004). Lectin-mediated drug delivery in the oral cavity. *Adv. Drug Deliv. Rev*., **56**, 481–489.
131. Cuenca, A. G., Jiang, H., Hochwald, S. N., Delano, M., Cance, W. G., Grobmyer, S. R. (2006). Emerging implications of nanotechnology on cancer diagnostics and therapeutics. *Cancer*, **107**, 459–466.

132. Budzynska, R., Nevozhay, D., Kanska, U., Jagiello, M., Opolski, A., Wietrzyk, J., Boratynski, J. (2007). Antitumor activity of mannan-methotrexate conjugate in vitro and in vivo. *Oncol. Res.*, **16**, 415–421.

133. Liang, W. W., Shi, X., Deshpande, D., Malanga, C. J., Rojanasakul, Y. (1996). Oligonucleotide targeting to alveolar macrophages by mannose receptor-mediated endocytosis. *Biochim. Biophys. Acta*, **1279**, 227–234.

134. Grandjean, C., Angyalosi, G., Loing, E., Adriaenssens, E., Melnyk, O., et al. (2001). Novel hyperbranched glycomimetics recognized by the human mannose receptor: Quinic or shikimic acid derivatives as mannose bioisosteres. *Chembiochem*, **2**, 747–757.

135. Gac, S., Coudane, J., Boustta, M., Domurado, M., Vert, M. (2000). Synthesis, characterisation and in vivo behaviour of a norfloxacin-poly(L-lysine citramide imide) conjugate bearing mannosyl residues. *J. Drug Target*, **7**, 393–406.

136. Benito, J. M., Gomez-Garcia, M., Ortiz Mellet, C., Baussanne, I., et al. (2004). Optimizing saccharide-directed molecular delivery to biological receptors: Design, synthesis, and biological evaluation of glycodendrimer-cyclodextrin conjugates. *J. Am. Chem. Soc*., **126**, 10355–10363.

137. Rieger, J., Stoffelbach, F., Cui, D., Imberty, A., Lameignere, E., et al. (2007). Mannosylated poly(ethylene oxide)-b-poly(epsilon-caprolactone) diblock copolymers: Synthesis, characterization, and interaction with a bacterial lectin. *Biomacromolecules*, **8**, 2717–2725.

138. Diebold, S. S., Kursa, M., Wagner, E., Cotten, M., Zenke, M. (1999). Mannose polyethylenimine conjugates for targeted DNA delivery into dendritic cells. *J. Biol. Chem.*, **274**, 19087–19094.

139. Dutta, T., Jain, N. K. (2007). Targeting potential and anti-HIV activity of lamivudine loaded mannosylated poly(propyleneimine) dendrimer. *Biochim. Biophys. Acta*, **1770**, 681–686.

140. Ravi, V., Siddaramaiah, Pramod Kumar, T. M. (2008). Influence of natural polymer coating on novel colon targeting drug delivery system. *J. Mater. Sci. Mater. Med.*, **19**, 2131–2136.

141. Alvarez-Manceñido, F., Landin, M., Martínez-Pacheco, R. (2008). Konjac glucomannan/xanthan gum enzyme sensitive binary mixtures for colonic drug delivery. *Eur. J. Pharm. Biopharm*., **69**, 573–581.

142. Singh, V., Sethi, R., Tiwari, A. (2009). Structure elucidation and properties of a non-ionic galactomannan derived from the Cassia pleurocarpa seeds. *Int. J. Biol. Macromo.,* **44**, 9–13.

143. Park, K. H., Sung, W. J., Kim, S., Kim, D. H., Akaike, T., Chung, H. M. (2005). Specific interaction of mannosylated glycopolymers with macrophage cells mediated by mannose receptor. *J. Biosci. Bioeng.*, **99**, 285–289.

144. Fromell, K., Andersson, M., Elihn, K., Caldwell, K. D. (2005). Nanoparticle decorated surfaces with potential use in glycosylation analysis. *Colloids Surf. B Biointerfaces*, **46**, 84–91.

145. Serizawa, T., Yasunaga, S., Akashi, M. (2001). Summer). Synthesis and lectin recognition of polystyrene core-glycopolymer corona nanospheres, *Biomacromolecules*, **2**, 469–475.

146. Lee, Y. S., Park, K. H., Kim, T. S., Kim, J. M., Sohn, I. S., Park, J. K., Chang, W. K.., Kim, D. K. (2008). Interaction of glycopolymers with human hematopoietic cells from cord blood and peripheral blood. *J. Biomed. Mater. Res. A*, **86**, 1069–1076.

147. Ahire, J. H., Chambrier, I., Mueller, A., Bao, Y., Chao, Y. (2013). Synthesis of D-mannose capped silicon nanoparticles and their interactions with MCF-7 human breast cancerous cells. *ACS Appl. Mater. Interfaces,* **5**, 7384–7391.

148. Park, I. Y., Kim, I. Y., Yoo, M. K., Choi, Y. J., Cho, C. S. (2008). Mannosylated polyethylenimine coupled mesoporous silica nanoparticles for receptor-mediated gene delivery. *Int. J. Pharm.*, **359**, 280–287.

149. Wijagkanalan, W., Kawakami, S., Takenaga, M., Igarashi, R., Yamashita, F., Hashida, M. (2008). Efficient targeting to alveolar macrophages by intratracheal administration of mannosylated liposomes in rats. *J. Control. Release*, **125**, 121–130.

150. Mitra, M., Mandal, A. K., Chatterjee, T. K., Das, N. (2005). Targeting of mannosylated liposome incorporated benzyl derivative of Penicillium nigricans derived compound MT81 to reticuloendothelial systems for the treatment of visceral leishmaniasis. *J. Drug Target*, **13**, 285–293.

151. Garg, M., Asthana, A., Agashe, H. B., Agrawal, G. P., Jain, N. K. (2006). Stavudine-loaded mannosylated liposomes: In-vitro anti-HIV-I activity, tissue distribution and pharmacokinetics. *J. Pharm. Pharmacol.,* **58**, 605–616.

152. Kawakami, S., Sato, A., Nishikawa, M., Yamashita, F., Hashida, M. (2000). Mannose receptor-mediated gene transfer into macrophages using novel mannosylated cationic liposomes. *Gene Ther.*, **7**, 292–299.

153. Kawakami, S., Hattori, Y., Lu, Y. Y., Yamashita, F., Hashida, M. (2004). Effect of cationic charge on receptor-mediated transfection using

mannosylated cationic liposome/plasmid DNA complexes following the intravenous administration in mice. *Pharmazie*, **59**, 405–408.

154. Yeeprae, W., Kawakami, S., Yamashita, F., Hashida, M. (2006). Effect of mannose density on mannose receptor-mediated cellular uptake of mannosylated O/W emulsions by macrophages. *J. Control. Release*, **114**, 193–201.

155. Kuramoto, Y., Kawakami, S., Zhou, S., Fukuda, K., Yamashita, F., Hashida, M. (2008). Use of mannosylated cationic liposomes/immunostimulatory CpG DNA complex for effective inhibition of peritoneal dissemination in mice. *J. Gene Med.*, **10**, 392–399.

Chapter 54

Diagnostics of Ebola Hemorrhagic Fever Virus

Ariel Sobarzo, PhD,[a] Robert S. Marks, PhD,[b,c] and Leslie Lobel, MD, PhD[a]

[a]*Department of Microbiology, Immunology and Genetics, Faculty of Health Sciences, Ben-Gurion University of the Negev, Beer-Sheva, Israel*
[b]*Department of Biotechnology Engineering, Ben-Gurion University of the Negev, Beer-Sheva, Israel*
[c]*The National Institute of Biotechnology in the Negev, Ben-Gurion University of the Negev, Beer-Sheva, Israel*

Keywords: Ebola virus, Ebola Hemorrhagic Fever, diagnostics, viral transmission, RNA virus, reemerging pathogens, public health, WHO, CDC, biosensors, enzyme-linked immunosorbent assay, clinical assessment, biosafety level 4, viral culture assay, real-time PCR, recombinant protein antigens, quantum dots, gold nanoparticles, carbon nanotubes, electrochemical detection

54.1 Ebola Virus

The Ebola virus is a member of the family *Filoviridae*, which is the cause for Ebola hemorrhagic fever (EHF). The single-stranded, negative-sense RNA virus, which can produce high-mortality disease in humans and nonhuman primates, has caused sporadic outbreaks in Central Africa throughout the last 40 years. Public

Handbook of Clinical Nanomedicine: Nanoparticles, Imaging, Therapy, and Clinical Applications
Edited by Raj Bawa, Gerald F. Audette, and Israel Rubinstein

ISBN 978-981-4669-20-7 (Hardcover), 978-981-4669-21-4 (eBook)
www.panstanford.com

health concerns about Ebola have increased in recent years due to large natural outbreaks and its potential use as a bioweapon agent. Despite the capabilities of laboratory diagnostics, the initial diagnosis of Ebola infection is based on clinical assessment. Today, laboratories located in high-risk areas are still not equipped to diagnose Ebola infections; thus specimens must be sent to reference laboratories around the world for viral confirmation. This chapter reviews current diagnostic methods and further aspects involved in the identification of the Ebola virus. The important features of each method are discussed and compared, along with an introduction to novel advanced biosensors and future technological tools for viral detection.

54.2 Etiology and Epidemiology

Filoviruses are taxonomically classified within the order *Mononegavirales,* a large group of enveloped viruses whose genomes are composed of a nonsegmented, negative-strand (NNS) RNA molecule [1]. The unique and distinctive members of the family include the Marburg and Ebola viruses, the latter having five different subtypes: Zaire, Sudan, Reston, the Ivory Coast, and Bondibugyo [2–9]. The NNS RNA genomes of the Ebola virus show the gene arrangement 3′-NP-VP35-VP40-GP-VP30-VP24-L-5′, with a total molecular length of approximately 19 kb. The virion morphology appears either as a long, filamentous form, sometimes branched (shaped as a short U, a figure 6, or a mace) or in circular configurations [6, 10].

The first recognition of the Ebola virus happened in 1976, when two parallel epidemics occurred in Zaire near the Ebola River and in Sudan. More than 550 cases with 430 associated deaths were recorded during those outbreaks [9, 11, 12]. Since then, more than 17 outbreaks have occurred in periodic cycles, responsible for more than 2,000 cases, 1,400 deaths [13–15], and a case fatality rate that ranges from 30–90%. Despite a few isolated cases in different regions of Africa, Ebola has mainly emerged and reemerged in Central Africa in the regions of Sudan, the Democratic Republic of the Congo, the Ivory Coast, Gabon, and Uganda [16].

54.3 Disease Transmission and Clinical Behavior

Until this day, the routes of viral transmissions of the Ebola virus are unknown, although several outbreaks over the years were clearly linked to animal carcasses [13]. Studies indicate that during outbreaks, the virus appears primarily transmitted by close and physical contact with infected persons, their clothing, bodily fluids, blood, vomit, stool, saliva, and, possibly, sweat [13]. In addition, further studies suggest that transmission may also occur through sexual and aerosol contacts [4, 17–19].

In general, the onset of infection is insidious, beginning with symptoms that resemble a cold or influenza virus infection, rapidly deteriorating into hemorrhaging from every orifice, and usually ending in death [19]. The incubation period ranges from several days to three weeks. The majority of cases become symptomatic within 5 to 12 days, and death ensues after 7 to 14 days following the onset of symptoms [4, 18–20].

Despite much research in recent years, the key elements of recovery from Ebola infection have yet to be established in either human or animal models. Studies of fatal cases of Ebola infection show high viremia and no evidence of an immune response; however, the reasons remain a mystery.

54.4 Therapy

Despite limited successes in animal models [14, 21–36], it seems that the challenges imposed by Ebola virus infection mechanisms have hampered development of an effective and safe vaccine for humans. A recently developed DNA/adenovirus prime-boost vaccine is undergoing safety testing on human volunteers [37]. Several other products have been tested or are currently in late-stage development [34, 38]. Antibodies acting as prophylactics have yet to provide conclusive efficacy, demonstrating little or no effect at all [34, 38–41]. Thus, no specific treatment for Ebola hemorrhagic fever is yet available, and treatment is mainly symptomatic, focused on providing adequate hydration and nutritional support.

54.5 The Fear of Ebola

Epidemics and pandemics have had a great impact on the course of human history. The emergence and reemergence of high-risk diseases to the individual and/or the community are specific interests and concerns to public health systems, be they in developed or in developing countries [16]. Ebola viruses represent a prime example of such reemerging pathogens. Although rare, Ebola outbreaks are unpredictable, with a high severity and fatality rate. These facts, together with their high infectivity and lack of vaccines and chemotherapy, elucidate why Ebola viruses have been classified as biosafety level (BSL)-4 pathogens and are regarded as potential bioweapon agents by the World Health Organization (WHO) and the Centers for Disease Control (CDC) [35, 42].

In comparison to other viruses affecting millions of people every year, Ebola stands out, from all other diseases, revealing an alarming gap in our immune system's ability to defend itself against it. Ebola is still a threat, although outbreaks have been relatively infrequent, largely confined to remote areas and effectively quarantined [20]. Unstable political situations worldwide and the potential threat of Ebola used as a bioweapon have dramatically changed world perspective and emphasizes why our future security against emerging pathogens such as this requires much research and further resources.

54.6 Current Methods in Ebola Diagnostics (Table 54.1)

First attempts to develop fast and efficient diagnostic tests for Ebola were unsatisfying, some demonstrating more success than others. Early methods, such as the indirect fluorescent antibody test, were used for acute diagnosis and sero-epidemiology; however, their limitations were quickly recognized [43]. Further confirmatory tests, including neutralization, also showed unsuccessful results. The important clinical finding that acutely ill patients were intensely viremic enabled the construction of an enzyme-linked immunosorbent assay (ELISA) assay, which provided a sensitive and specific method for quickly screening large numbers of samples.

However, safety and specificity were still concerns, and many Ebola-infected patients still assayed negative in these tests.

Table 54.1 Current methods of Ebola diagnostics

Method	Objective	Target protein	Strain	Reference
Culture	Virus isolation	—	All	59–61
EM	Virus	NP/VP40	All	56
ELISA	Antigen	NP/VP40/GP	Zaire	50
Capture ELISA	Antibody	VP40/NP	Zaire	48, 49, 63, 66
IFA	Antigen	—	All	75–78
IHC	Antigen	—	All	43
T-PCR		NP/GP/L	Sudan/Zaire	45, 46, 84, 87, 153
Real-time PCR	Antigen	NP/GP	Sudan/Zaire	44, 51, 52
Mass Tag PCR	VHF	All Virus	Sudan/Zaire	80, 85
ELISA	Antibody	rNP/rGP/ rVP35	Zaire	57, 65, 90, 91
IFA	Antibody	rNP	Zaire	91

Abbreviations: EM, electron microscopy; IFA, immunofluorescence assay; IHC, immunohisto-chemistry; RT, reverse transcriptase; PCR, polymerase chain reaction; VHF, viral hemorrhagic fever; NP, nuclear protein; VP, virus protein; L, RNA-dependent RNA polymerase; GP, glycoprotein; r, recombinant.

Regardless of the wide range of methods and capabilities of laboratory diagnostics, the initial Ebola diagnosis is typically based first on clinical assessment and known Ebola contact. Identification may be difficult due to a wide variety of infectious diseases bearing similar clinical symptoms. Ebola is detected by identification of either the host's specific immune response or viral particles in an infected individual. Confirmation is typically obtained by virus isolation, electron microscopy, histological techniques, specific detection of nucleic acid, immunofluorescence, and immunoassays of both antigen and antibodies [44–53]. Although constant improvements, new reagents, and equipment have drastically reduced the detection and confirmation time of Ebola and enhanced sensitivity, they are still not used routinely and are

not well established. Results can be obtained within 24 to 48 hours, depending on the method being used, once samples are received at the appropriate laboratories. Risk of transmission increases when contact has been made with a patient in the later stages of illness [54]. Early diagnosis is key for curtailing spread of the disease and providing more time for effective intervention as therapeutics are developed.

Although five different subtypes (i.e., Zaire, Sudan, Ivory Coast, Reston, and Bondibugyo) of Ebola have been defined and characterized, most diagnostic attempts have focused specifically on the Ebola Zaire strain due to its high fatality rate, which can reach 90% [4].

However, today there is focus on new, improved assays for the detection of both Zaire and Sudan strains, which are considered the most dangerous and deadly to humans. In addition, risks from rapidly sporadic infectious outbreak locations and biothreat contaminants have encouraged researchers to develop fast, easy-to-use, sensitive, specific, and available detection systems, which could provide a useful tool for both individuals and populations at risk.

54.6.1 Culture Virus Isolation

Culture and other related methods remain the most sensitive and widely used for viral identification. As a result, basic culture, staining, and microscopy can be found throughout public health laboratory systems [55, 56].

Since Ebola is relatively easy to isolate and propagates well in various cell cultures [57], virus isolation is a basic, simple, and sensitive method for diagnosis. The rate of growth in tissue culture varies, between 5 and 14 days, depending on the strain. This approach requires specimens be sent to BSL-4 laboratories, located mostly in developed countries, far from the outbreak. Confirmation and adequate response measures are therefore delayed. Further issues include the need for proper shipment, preparation of specimens for virus isolation, requirements of considerable expertise, and, often, further characterization by molecular techniques for confirmation [58]. Nonetheless, cell culture is still performed routinely during suspicious outbreaks and as part of virus identification in BSL-4 laboratories around the world.

54.6.2 Electron Microscopy

Transmission electron microscopy was applied for diagnosis and studies of filoviruses since the first outbreak during the late sixties [59] and is still in use today. The technique has enabled investigators to identify filoviruses during outbreaks and help understand their mechanism of infection [60]. Owning, in part, to the relatively high viremia during Ebola infection in humans, electron microscopy has been useful for diagnosis over the years [5, 59, 61, 62]. Virus particles that are present in sera and cell culture fluids can be directly visualized by negative staining and detected easily in thin sections of infected tissues. Electron microscopy has provided rapid results, but it is usually available only in well-equipped research facilities. Thus identification or conclusive confirmation is usually achieved with other techniques [62]. Further disadvantages, such as work safety issues and the high level of expertise required for this technique, resulted in it mainly being used for research purposes and less as a tool for viral diagnostics.

54.6.3 Serological Assays

Serological assays are now regularly used to confirm the clinical diagnosis of Ebola [63]. They are used reliably for screening large numbers of small-volume test samples in the simplest of laboratory environments, with relatively high sensitivity and specificity, as compared to culture and gene amplification approaches. The course of Ebola virus infection is such that patients usually die before there is a significant antibody response. This suggests that serological diagnostics are suitable for infected patients likely to survive but not for those who succumb. High viremic titers are present in the blood and tissues of patients during the early stages of the illness, during a narrow window of time, indicating that detection of virus antigens is suitable for diagnosis of EHF. Assays such as these, directly intended for the detection of Ebola virus antigens, were developed and tested in clinical settings, including virus outbreaks in the Congo, 1995; Gabon, 1996; and Uganda, 2000, and were confirmed as efficacious tools for diagnosis [46, 49–51].

Most commonly used assays for antibody detection in the later stages of the disease are the direct IgG and IgM ELISAs and IgM capture ELISA [49, 50, 64–67].

These systems have been developed by several groups [68–73] using the *NP, VP40,* and *GP* genes as target proteins directed toward the detection of anti-Ebola virus, Zaire, Sudan, and Reston antibodies [69]. The important key element in all immunological assays remains the antibodies. Their affinities and specificities are limiting factors, and those selected must be carefully evaluated. Even so, without any manipulation prior to analysis, many of these immunoassays have a sensitivity threshold of 100- to 1000-fold above the estimated titer, potentially limiting their utility [74, 75]. Furthermore the necessary specificity to be useful for detection, let alone definitive identification, may be lacking. In addition to the ELISAs, Ebola diagnosis includes immunoblot, indirect immunofluorescence (IF), and immunohistochemistry (IHC), which were used for confirmation, surveillance, and screening, [44, 67, 76–79] each demonstrating specific advantages over the other. In the last decade, the detection of Ebola antigens or antibodies by enhanced serological assays has proven to be a useful and efficient diagnostic tool, both for the early and late stages of the disease. As such, the ELISA test, with all its varieties, is now considered the most accurate, rapid, and sensitive one for the diagnosis of EHF.

54.7 Nucleic Acid-Based Techniques

By definition, any self-replicating biological entity can be discriminated on the basis of its own unique nucleic acid sequences. Newly developed hemorrhagic fever assays [80, 81] and the emergence of mobile diagnostic capabilities [46, 82], incorporating nucleic acid-based identification techniques, have become tools with enormous potential for outbreak management of Ebola infection around the world. New assays have shown a huge potential in the detection and identification of pathogenic agents like Ebola because of their specificity, sensitivity, and speed in which results can be obtained without the necessity for BSL-4 facilities [83]. The use of these systems for viral identification has increased

rapidly during the last decade, under routine use in many large clinical laboratories and reference centers around the world [84].

A majority of diagnostic PCR systems are designed to be highly specific for detection of the selected target virus. Molecular diagnostic methods for EHF [85], including nested and RT-PCR techniques, were developed and performed well in epidemic settings during outbreaks in the Congo, 1995; Gabon, 1996; and Uganda, 2000 [46, 47, 86]. Recent assays also include real-time quantitative RT-PCR and mass tag PCR [45, 46, 52, 53, 81, 87]. Overall, these molecular diagnostic techniques for EHF detection have been proven sensitive, specific, and efficacious during Ebola outbreaks. They have demonstrated the potential for wide adoption in the near future, coming within the scope of several selected reference laboratories [81].

Although RT-PCR assays, especially nested RT-PCR and real-time quantitative RT-PCR, have proven useful, false-positive and false-negative results must always be excluded.

Index case diagnoses of either outbreaks or imported cases should not be solely based on RT-PCR methods. The sensitivities of the RT-PCR systems in different laboratories worldwide show significant variation [88]. Despite some disadvantages of nucleic acid-based techniques, they are still considered one of the most powerful tools for detection, as described above, especially under field conditions. Current RT-PCR techniques [46, 47, 53, 89], along with antigen detection ELISA [50, 64, 69–72, 90], are considered the primary assays for the diagnosis of an acute infection of Ebola virus. While nucleic acid-based detection systems are more specific and sensitive than immunological-based detection assays, the latter are faster and more robust.

54.8 Engineered Recombinant Proteins

Technological improvements and the fear of unpredictable outbreaks have stimulated the developments of rapid advances in diagnostics. Monoclonal antibodies have shown to be more commercially reliable than polyclonal antibodies, and in the foreseeable future these will themselves be replaced by engineered recombinant antibodies. Although the construction and development of recombinant products for viral detection has focused

primarily on antigen reagents, production of fully human full-sized antibodies poses promise of some benefit from a diagnostics point of view.

Considering several factors, for example, sporadic rise of Ebola outbreaks, increase in world travel, bioterrorism, and the risk of using authentic antigens from infectious viruses for diagnostics, it is clear why the development of systems using engineered proteins for Ebola detection is specifically essential in countries where BSL-4 laboratories are not available. To overcome these difficulties and to provide a suitable solution, several groups have recently developed various recombinant antigen protein-based diagnostic systems for EHF detection [66, 91, 92]. These systems include the use of recombinant proteins, for example, the nucleoprotein (rNP), glycoprotein (rGP), and recombinant VP35 of Zaire Ebola virus, for the detection of IgG and IgM antibodies. These assays have demonstrated the potential to detect IgG antibodies, not only for one strain, but also for other Ebola virus species, while some showed specific strain recognition, depending on the recombinant protein used. An alternative method for detecting specific antibodies for the Ebola virus, an immunofluorescence technique, was also developed using rNP and was confirmed to be highly sensitive and specific [93].

In contrast to the recent development of recombinant antigens for diagnostics use, efforts to produce antibodies for the same objective have been carried out to a lesser extent. Cloning and expression of whole antibodies, or antibody fragments, has so far not had a great impact on immunoassay technology for Ebola detection—but the possibilities of antibody engineering are tremendous and will have an effect on the development for immunoassays. Recently a study included the creation of single-chain antibody fragments (scFv) against the Ebola virus using a phage display method [94]. The antibodies produced demonstrated a highly specific interaction with viral NP and coat proteins VP40 and VP24 of the Ebola virus, indicating their potential use as diagnostic tools.

Recombinant proteins were confirmed to be useful as antigens for detecting specific antibodies in IgG- and IgM-ELISAs systems and demonstrated high sensitivity and specificity, not only for the detection of one virus strain, but also for the detection of several others simultaneously [91]. Today, it is clear that the ability to

produce recombinant proteins for diagnostics use will ensure the safety of future detection systems with low background and high specificity, allowing for easy scale-up in the commercial manufacture of kits with high-quality assurance and accessibility [95], certain to have a huge impact on viral detection and therapeutics.

54.9 New Trends in Ebola Diagnostics

At present, the most commonly used techniques for diagnostics of an acute Ebola infection are based mainly on RT-PCR technology and antigen capture ELISA, supplemented with antibody detection assays [82, 96]. During the last decade, these assays were developed and established in national and international reference laboratories worldwide and have shown variable success with a good measure of sensitive and specific detection for all of the Ebola virus strains from previous outbreaks [49, 51, 97]. Although the use of these conventional virological methods for analyses has been successful and well adapted, they may not fully contend with the variety of challenges required for detection and outbreak prevention. There is still a continuous need worldwide for development of new and improved detection systems that will provide fast, accurate, direct, low-cost, and field operability for Ebola diagnostics (see Fig. 54.1).

Progress in technological devices has led to the development of several prototype biosensors enabling the production of simple, sensitive, specific, and safe detection systems. The new systems include the use of biosensor technologies, for example, surface plasmon resonance (SPR), quartz crystal microbalance (QCM) sensors, optical fiber immunosensor (OFIS), and a reverse genetics (RG) system. These new assays have shown the potential ability to provide rapid and specific disease diagnosis on-site so that clinicians can quickly determine whether treatment is needed [98]. Recently, there has been considerable development of label-free piezoelectric biosensors based on the use of QCM. QCM is an extremely sensitive mass-measuring device, which allows dynamic monitoring of hybridization events, using an oscillating crystal with a probe immobilized on its surface. The increased mass, associated with the hybridization reaction, results in a decrease of the oscillating frequency. Applications of this technology include

detection and characterization of viruses, including Ebola [81, 99, 100]. These systems not only eliminate the need for labels, but also offer the potential advantage of rapid, real-time monitoring of specific hybridization, as well as high sensitivity and specificity. They have previously shown high promise in sensor research and gained momentum in detection of viral samples, with a limitation around the subnanogram region. The development of such a sensor for Ebola antigen detection [98] has produced binding results and sensitivity comparable to ELISA. Its significant promise is a result of its rapid detection, ease of use, low cost of operation, and deployment ability to outbreak areas [98, 99, 101].

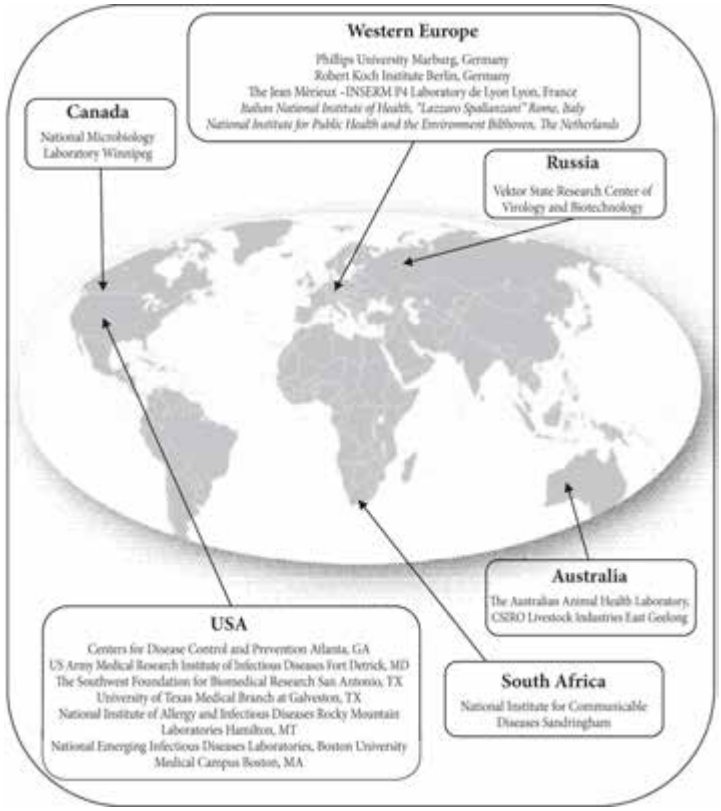

Figure 54.1 Select BSL-4 facilities around the world. *Note*: The map is not intended to serve as a definitive source on the status of BSL-4 facilities around the world. The list of facilities was taken from a review done by Feldmann et al. (2007).

In a recent study [102], a newly developed OFIS for the detection of antibodies to Ebola virus strains Zaire and Sudan was presented. This new device showed high sensitivity and specificity compared to a standard-luminescence ELISA. The results of the study suggested that the detection of Ebola virus antibodies using this technique would contribute significantly to serological and epidemiological studies. With some modification, an easy-to-use procedure for Ebola virus antibody or antigen detection will be available in the future as a field operable clinical tool [102].

Although not defined as a biosensor or detection device per se, RG technology has shown the potential to be used as such, combined with an appropriate detection system. Use of RG has been rapidly increasing, and systems using this technology have been developed for many of the negative-stranded RNA viruses [103, 104], including the Ebola virus [105–107]. This technique has enabled the generation of artificial replication systems and recombinant mutant viruses that were used mainly to study different aspects of virus biology but could also have an important role in viral detection. Recently two groups [106, 108] have developed RG systems that demonstrate a new EboZ-eGFP virus that was useful for detecting horizontal and vertical transmission following experimental infections of candidate reservoir species, with a fluorescence signal that was more robust than that observed by standard IHC.

Despite the search of new breakthrough devices for future Ebola diagnosis, improvements of existing methodologies are continually being developed. New protocols and methods in nucleic acid detection and sera assays are being introduced and tested under field conditions in order to provide a simple and rapid solution. A recent example of an assay such as this has been seen in a swift and somewhat less sophisticated method developed by Lunchet [90]. The assay based on a new immuno-filtration technique for the detection of Ebola virus antigen has provided a novel tool for a future field response to outbreaks of EHF. Being less sensitive than other tests but with a rapidity far less prone to technical complications [90], the assay demonstrated for the first time the applicability of the immuno-filtration system to detect viral antigen and its usefulness under field conditions with a sensitivity similar to that of the widely used antigen detection ELISA [50, 51].

54.10 Future Diagnostics

There has been increased interest in developing rapid and reliable methods of detection for microorganisms, which naturally pose a very high risk for human and animal populations and have the potential to be used as bioterrorism agents. Application of the new diversity of assays for viral detection includes a variety of techniques and devices only recently developed especially for diagnostic properties. Although not intended specifically for Ebola detection diagnostics, these devices may well be adapted in the near future. It should be pointed out that this review does not intend to reflect the full scope of methods and systems that have been or are undergoing development but rather presents a glimpse of future diagnostics, as summarized in Table 54.2.

New advances in technology, biosensor devices, and molecular biological systems are constantly influencing the field of viral detection. Label-free optical biosensors are among the most desirable for bioassays because they utilize light as their detection mechanism [109, 110]. Assays using this method are fast, in real time, and with high sensitivity to surface modifications. A study done by Huang et al. [111] demonstrated a compact, label-free, optoelectronic biosensor system utilizing a photonic crystal as the sensor surface and a tunable VCSEL-based detection platform of human antidengue antibodies from serum samples. The sensor proved highly sensitive to surface modifications, with the ability to detect biomolecular interactions of human antibodies and potentially a versatile tool for clinical diagnostics in resource-poor environments, where infectious disease monitoring is most critical. The results obtained indicated comparable detection sensitivity as the predominant technologies, such as ELISA, with sufficient signal differentiation for diagnosis but with shorter and simpler assay preparation [111].

One of the most highlighted and fast-moving interfaces of nanotechnology is the application of QDs in biology. The unparalleled advantages of the size-tunable fluorescent emission and the simultaneous excitation at a single wavelength make QDs a great possibility for use in optical encoding detection. A new development of QD-based biosensors has consisted of mixtures of green- and orange-QD-labeled chromatophores for the detection of different kinds of viruses. This sensor could be used as the convenient, cheap,

reversible, and effective fluorescent probe for dual, simultaneous, and independent detection of viruses based on antibody-antigen reactions [112].

Table 54.2 Future technological tools for viral diagnostics

Technology	Target	Developer	Category	Ref.
SPR & QCM	Ebola	Yu et al.	Biosensor	97
OFIS	Ebola	Petrosova et al.	Biosensor	100
VCSEL	Dengue	Huang et al.	Biosensor	109
QDs	Influenza	Deng et al.	Biosensor	110
Electrochemical using conductive polypyrole polymers	HIV, HBV	Bouchet et al.	Biosensor	112
CNTs	FMDV	Jithesh et al.	Biosensor/ nanoarray	114
SAW	Sin Nombre virus	Bisoffi et al.	Biosensor	118
Electrochemical	HBV	Ding et al.	Biosensor	119
Phage display on gold surface	—	Gervais et al.	Biosensor	120
Phage display on optical fiber	WNV	Herrman et al.	Biosensor	121
DPN	Influenza	Liu et al.	Biosensor/ nanoarray	122
PDA microarray gold nanoparticles	Papilloma virus	Baek et al.	Biochip	141
ICS	Influenza	Oh et al.	Biosensor	123
Functional polymers (PDA-polydiacetylene)	Influenza	Amano et al.	Biosensor	96
Nanowire	Influenza	Patolsky et al.	Biosensor	132
Fluorescent micro beads	FMDV	Perkins et al.	Microarray	154
Nanometer-sized gold particles using microfluidic immunoassay	HBV	Liang et al.	Lab on chip	155
Magnetic bead with metal oxide semiconductor	Dengue virus	Aytur et al.	Lab on chip	135
DNA hybridization using paramagnetic nanoparticles	HCV	Fuentes et al.	Lab on chip	156
Bioluminescence reporter gene	Anthrax	Rider et al.	Biosensor	142

Abbreviations: VCSEL vertical-cavity surface emitting laser; DPN, dip-pen nanolithography; PDA, photodiode array; QD, quantum dot; CNT, carbon nanotube; SAW, surface acoustic wave; ICS, ion channel switch; HIV, human immunodeficiency virus; HBV, hepatitis B virus; FMDV, foot-and-mouth disease virus; HCV, hepatitis C virus.

Electrochemical detection has emerged as a challenging and well-adapted technique for the realization of cheap, single-use, and portable diagnoses systems [113].

A promising strategy based on the use of conducting polymers has presented a new, real-time, multidetection biosensor for biological samples using the electrochemical properties of cylinder shaped conducting polypyrrole, grown on miniaturized electrodes. The new developed technique could easily be generalized for the elaboration of peptide or protein microarrays and thus be adapted for miniaturization and integration for lab-on-chip systems, including viral detection [114].

There has been significant interest in biological applications of novel inorganic nanomaterials, such as nanotubes, with the motivation to create new types of analytical tools for life sciences and biotechnology. The electrical conductance of nanotube components is highly sensitive to its environment and varies significantly with changes in electrostatic charges and surface adsorption [115]. Consequently, nanotube-based biosensors were developed with the capability for selective detection of proteins, such as antibodies in solution. Recent work has demonstrated the ability of CNTs to act as a platform for immunosensor devices [116]. Using label and nonlabel antibodies that are attached to the CNTs, the immunosensor can then be visualized by microscopy techniques, for example, atomic force, electron scanning (scanning electron microscopy [SEM]), and confocal. CNT technology provides a miniaturized, multiplexed, immunosensor assay for point-of-care testing that could be of use for viral detection.

A new biosensor based on a shear, horizontal surface acoustic wave (SH-SAW) device was developed and recently presented. This sensor enabled label-free, sensitive, and cost-effective realtime detection of bacterial and viral DNA [117–119]. Bisoffi et al. [120] have shown the ability to use SAW technology based on a protein interaction device to detect category A viral agents, such as the Sin Nombre virus. The assay demonstrated high sensitivity and selectivity of the detector that was not compromised by the presence of other viruses, indicating its usefulness for specific detection in complex solutions. The platform allowed detection of viral bioagents without preprocessing of the analyte and with the potential to be applied in portable field conditions. Further developments of diagnostics devices have a label-free biosensor for the detection

of hepatitis B virus [121], a sensor based on the phage display technique designed for highly sensitive and specific platforms for detection and identification of a pathogenic agent [122, 123], and a nanopattern the F0F1-ATPase biosensor for viral detection [124].

With a somewhat different approach, a new rapid point-of-care test using a novel ion channel switch biosensor (ICSB) for viral detection of influenza A was recently presented [125]. This sensor uses a simple electrical reader for objective measurement, without the required time-consuming steps of specimen extraction. The assay demonstrated the ability to achieve high sensitivity and specificity for the detection of a virus such as influenza as compared to the traditional method, such as ELISA, with the possibility for multiple analyses in a single test [125].

The use of colorimetric sensors employing functional polymers has allowed direct analysis of target analytes through a color change without requiring additional instruments [98]. Theses sensors based on smart materials with physical, optical, or electrical properties have shown an ability to respond to specific environmental stimulation. Photodiode array (PDA)-conjugated polymer sensors, which can undergo significant optical property changes in response to fluctuations in environmental conditions, [126–128] have been used for viral detection with promising results [129–131].

In a recent publication [132], several immunosensing assays for viral detection were reviewed. The study describes current development and future potential technologies, including the use of nanowires, microbeads, microarrays, and a whole-cell-based immunoassay-sensing system. Nanowire technology, based on a metallic multistriped nanowire platform, enabled rapid fabrication of addressable barcodes. This multistriped system could be coated with anti-Ebola specific antibodies, allowing simultaneously an efficient and accurate multiplex detection assay for several biowarfare agents [133]. Further improvements have expanded the use of this technique for viral detection [134–136] using nanowires configured as field effect transistors that can detect slight variations on the nanowire surface that cause a change in conductivity. Micrometer-sized beads have proven their utility in bio- and viral sensing applications over the years [10, 137]. The great advantages of these devices are their ability to be engineered by diverse surface chemistry, and they are easily manipulated by either magnetic

forces or electrical fields. Combined with a flow cytometry device, the system would be able to detect multiplexed antigen binding and be used for efficient pathogen detection. Further work presented an improved biobarcode system, which included reporter beads, decorated with specific coding DNA sequences. Although DNA-based microarray chip technology is used in diagnostics, new developments have included antibody [138] and aptamer [139–141] microarrays, which when combined with technologies such as SPR [142] and PDA biochip using gold nanoparticles could enable better sensitivities [143].

Finally, a promising and unusual pathogen detection system, using a whole-cell immunoassay sensor (CANARY) was recently presented [144]. Engineered B lymphocyte cells with pathogen-sensing membrane-bound antibodies and an associated light-emitting reporting system were conveniently expressed in vivo. The system expressed a calcium-sensitive bioluminescent protein named Aquaria. When exposed to targeted biowarfare pathogenic compounds, an increase in photons was observed within the B lymphocyte cells that later could easily be detected using an inexpensive optical system. In addition, several other groups extended the potential of the methodology by further developing whole-virus particles or a bacteriophage-sensing system for diagnostics use [145–147]. Overall, technological progress has made a significant impact on traditional and new developments of pathogen and viral diagnostics during the past few years. The ability to miniaturize and adapt current assays and protocols to fully automated devices will be certain to hold tremendous promise for new multiplex, efficient, cost-effective, and accurate viral detection systems for pathogens such as Ebola.

54.11 The Effort Continues

Historically, the Ebola virus has affected populations primarily throughout Central Africa. Although it has only affected a limited geographic region, its effects have reverberated worldwide due to its extremely high mortality rate and the lack of reservoir identification. Today it is clear that Ebola has evoked much fear in populations living outside Central Africa and has become a biodefense concern [17, 34, 88, 148]. The early identification and diagnosis of emerging diseases, such as Ebola, are of great importance

with respect to treatment, containment, and public health control. The importance of early detection lies not only with clinicians and public health experts but also with veterinarians, animal scientists, and wildlife ecologists [149, 150] who require effective communication and collaboration for the etiological identification and epidemiological assessment of the virus.

Since its discovery 40 years ago, several methodologies and protocols were developed and adapted for diagnostics of the Ebola virus. Today, detection is done traditionally by laboratory diagnosis, which is defined by common methods used to confirm the clinical observations of a physician by evaluation of standard clinical specimens, for example, blood, serum, exudates, saliva, stool, and tissues [34]. Despite the success of methods such as RT-PCR and ELISA for viral detection, standardization and evaluation of diagnostic procedures are still difficult because of the restricted availability of virologic and clinical material. In addition, outbreaks of the virus usually occur in remote areas where sophisticated medical support systems are limited and timely diagnostic services are extremely difficult to provide, constituting major problems. When considering the various issues during a virus outbreak and its huge impact on both an individual and his or her surroundings, it is clear why further research for development of diagnostic tools must continue.

The production of recombinant engineered reagents, along with the development of innovative devices and instruments, enables investigators to use the Ebola virus outside BSL-4 lab facilities in developing countries and under field conditions. The rapid growth of improvements in existing methods, along with the development of revolutionary technologies, will be certain to have a great impact on Ebola detection. Fast and portable tools for Ebola diagnostics will eventually lead to a more rapid control of the epidemic. In addition, early detection of the virus using portable and sensitive assays will allow scientists to quickly identify the index case(s) and as a result to detect the potential reservoir. The early detection and diagnostics of Ebola is an essential step if intervention is to occur at a point where the prognosis can still be influenced and selection of optimum therapeutic strategies can still be relevant.

The threat of the Ebola virus as a potential bioterrorism agent has been previously established and discussed [35, 42, 88].

Although new technologies mainly for detecting the release of specific biothreat agents have been widely introduced, further improvements and development are needed. The recent outbreaks of the virus in Central Africa, including the one in 2007 [18, 151–154], have clearly emphasized the virus's importance not only as a biothreat agent but also as a natural cause of death to humans. Due to its ability to develop new lethal strains, such as the recent one, 2007–2008 [152], or to distinguish engineered strains from other pathogens that may produce similar symptoms, continuous efforts toward developing new, advanced assays, which will be quick and reliable with minimum sample handling and laboratory skill requirement, are a necessity [98]. Today, traditional detection systems, such as virus culture, electron microscopy, and IF, are still considered key elements in the confirmation and detection of Ebola and will continue to be so despite their risk to lab workers, the requirement for special facilities, and the high cost in time and labor intensity. It is clear that future diagnostics of viruses, such as Ebola, will evolve depending on new developments of cutting-edge technologies, as well as a greater understanding of Ebola immunology [155, 156] which will produce detection systems able to cope with and overcome difficulties existing today and in the future.

Disclosures and Conflict of Interest

The authors declare that they have no conflict of interest and have no affiliations or financial involvement with any organization or entity discussed in this chapter. No writing assistance was utilized in the production of this chapter and the authors have received no payment for its preparation. This chapter is a revised version of the chapter that originally appeared in *Viral Diagnostics: Advances and Applications,* edited by Robert S. Marks, Leslie Lobel, and Amadou Alpha Sall, 2015, Pan Stanford Publishing Pte. Ltd.

Corresponding Author

Dr. Ariel Sobarzo
Department of Microbiology, Immunology and Genetics
Faculty of Health Sciences
Ben-Gurion University of the Negev
POB 653, Beer-Sheva 84105, Israel
Email: tautau.ariel@gmail.com

About the Authors

Ariel Sobarzo received his BMed LSc in 2005 and MSc in 2007 with excellence from the department of Virology, Faculty of Health Science, Ben-Gurion University of the Negev, Beer-Sheva, Israel. He completed his PhD in the departments of Virology and Biotechnology Engineering at Ben-Gurion University of the Negev. Dr. Sobarzo's research involves an international collaboration for a sera-screening study to detect conserved epitopes of the Ebola Sudan virus that are recognized by the immune response, with an aim for the future development of diagnostic and prophylactics tools. He is currently a research assistant in the laboratory Dr. Lobel, studying the humoral immune signatures of infectious diseases in collaboration with of Prof. Marks for the development of advanced biosensors.

Robert Marks is a professor in the department of Biotechnology Engineering at Ben-Gurion University of the Negev. He is also co-founder of Polyrizon Ltd., a health care seed-stage company that develops novel biological-gels based on its novel C&C (capture and contain) platform technology. The C&C technology, with its unique specificity capabilities, can be readily adapted for a wide range of applications to protect human body from pathogens such as pollen, viruses, bacterium and more.

Leslie Lobel is an American-born Israeli virologist and physician at Ben-Gurion University, where he is a senior lecturer and leading researcher attempting to develop a vaccine and cure for infectious diseases, in particular Ebola.

References

1. Feldmann, H., et al. (2004). Ebola virus ecology: A continuing mystery. *Trends Microbiol*., **12**(10), 433–437.
2. Pringle, C. R. (1991). The Bunyaviridae and their genetics: An overview. *Curr. Top. Microbiol. Immunol*., **169**, 1–25.
3. Feldmann, H., Klenk, H. D. (1996). Marburg and Ebola viruses. *Adv. Virus Res*., **47**, 1–52.
4. Colebunders, R., Borchert, M. (2000). Ebola haemorrhagic fever: A review. *J. Infect*., **401**, 16–20.

5. Murphy, F. A., van der Groen, G., Whitfield, S. G., Lange, J. V. (1978). Ebola and Marburg virus morphology and taxonomy. In: Pattyn, S. R., ed. *Ebola Virus Haemorrhagic Fever*, Elsevier, Amsterdam, pp. 61–84.
6. Kiley, M. P., et al. (1982). Filoviridae: A taxonomic home for Marburg and Ebola viruses? *Intervirology*, **181**(2), 24–32.
7. Cox, N. J., et al. (1983). Evidence for two subtypes of Ebola virus based on oligonucleotide mapping of RNA. *J. Infect. Dis*., **147**(2), 272–275.
8. Buchmeier, M. J., et al. (1983). Comparative analysis of the structural polypeptides of Ebola viruses from Sudan and Zaire. *J. Infect. Dis.*, **147**(2), 276–281.
9. Bowen, E. T., et al. (1980). A comparative study of strains of Ebola virus isolated from southern Sudan and northern Zaire in 1976. *J. Med. Virol*., **6**(2), 129–138.
10. Aytur, T., et al. (2006). A novel magnetic bead bioassay platform using a microchip-based sensor for infectious disease diagnosis. *J. Immunol. Methods*., **3141**(2), 21–29.
11. Johnson, K. M. (1979). Ebola virus and hemorrhagic fever: Andromeda strain or localized pathogen? *Annu. Intern. Med*., **91**(1), 117–119.
12. Heymann, D. L., et al. (1980). Ebola hemorrhagic fever: Tandala, Zaire, 1977–1978. *J. Infect. Dis.*, **142**(3), 372–376.
13. Pourrut, X., et al. (2005). The natural history of Ebola virus in Africa. *Microbes Infect*., **77**(8), 1005–1014.
14. Feldmann, H., et al. (2007). Effective post-exposure treatment of Ebola infection. *PLoS Pathog*., **3**(1), e2.
15. Feldmann, H., Geisbert, T., Kawaoka, Y. (2007). Filoviruses: Recent advances and future challenges. *J. Infect. Dis.*, **196**(Suppl 2), S129–S130.
16. Feldmann, H., et al. (2002). Emerging and re-emerging infectious diseases. *Med. Microbiol. Immunol*., **191**(2), 63–74.
17. Peters, C. J., LeDuc, J. W. (1999). An introduction to Ebola: The virus and the disease. *J. Infect. Dis.*, **179**(Suppl 1), ix–xvi.
18. Okware, S. I., et al. (2002). An outbreak of Ebola in Uganda. *Trop. Med. Int. Health*, **71**(2), 1068–1075.
19. Bruce, J., Brysiewicz, P. (2002). Ebola fever: The African emergency. *Int. J. Trauma Nurs*., **8**(2), 36–41.
20. Geisbert, T. W., Jahrling, P. B. (2004). Exotic emerging viral diseases: Progress and challenges. *Nat. Med*., **10**(12), S110–S121.
21. Xu, L., et al. (1998). Immunization for Ebola virus infection. *Nat. Med*., **4**(1), 37–42.

22. Wilson, J. A., et al. (2001). Vaccine potential of Ebola virus VP24, VP30, VP35, and VP40 proteins. *Virology*, **286**(2), 384–390.

23. Wilson, J. A., Bosio, C. M., Hart, M. K. (2001). Ebola virus: The search for vaccines and treatments. *Cell Mol. Life Sci*., **5812**(13), 1826–1841.

24. Wang, D., et al. (2006). Development of a cAdVax-based bivalent Ebola virus vaccine that induces immune responses against both the Sudan and Zaire species of Ebola virus. *J. Virol*., **80**(6), 2738–2746.

25. Vanderzanden, L., et al. (1998). DNA vaccines expressing either the GP or NP genes of Ebola virus protect mice from lethal challenge. *Virology*, **246**(1), 134–144.

26. Sullivan, N. J., et al. (2000). Development of a preventive vaccine for Ebola virus infection in primates. *Nature*, **408**(6812), 605–609.

27. Sullivan, N., Yang, Z. Y., Nabel, G. J. (2003). Ebola virus pathogenesis: Implications for vaccines and therapies. *J. Virol*., **77**(18), 9733–9737.

28. Reed, D. S., Mohamadzadeh, M. (2007). Status and challenges of filovirus vaccines. *Vaccine*, **25**(11), 1923–1934.

29. Pushko, P., et al. (2000). Recombinant RNA replicons derived from attenuated Venezuelan equine encephalitis virus protect guinea pigs and mice from Ebola hemorrhagic fever virus. *Vaccine*, **19**(1), 142–153.

30. Leroy, E. M., et al. (2002). Sequence analysis of the GP, NP, VP40 and VP24 genes of Ebola virus isolated from deceased, surviving and asymptomatically infected individuals during the 1996 outbreak in Gabon: Comparative studies and phylogenetic characterization. *J. Gen. Virol*., **83**(Pt 1), 67–73.

31. Jones, S. M., et al. (2007). Assessment of a vesicular stomatitis virus-based vaccine by use of the mouse model of Ebola virus hemorrhagic fever. *J. Infect. Dis.*, **196**(Suppl 2), S404–S412.

32. Geisbert, T. W., et al. (2002). Evaluation in nonhuman primates of vaccines against Ebola virus. *Emerg. Infect. Dis*., **8**(5), 503–507.

33. Feldmann, H., et al. (2003). Ebola virus: From discovery to vaccine. *Nat. Rev. Immunol*., **3**(8), 677–685.

34. Burnett, J. C., et al. (2005). The evolving field of biodefence: Therapeutic developments and diagnostics. *Nat. Rev. Drug Discov*., **4**(4), 281–297.

35. Borio, L., et al. (2002). Hemorrhagic fever viruses as biological weapons: Medical and public health management. *JAMA*, **287**(18), 2391–2405.

36. Riemenschneider, J., et al. (2003). Comparison of individual and combination DNA vaccines for B. anthracis, Ebola virus, Marburg

virus and Venezuelan equine encephalitis virus. *Vaccine*, **2125**(26), 4071–4080.

37. Martin, J. E., et al. (2006). A DNA vaccine for Ebola virus is safe and immunogenic in a phase I clinical trial. *Clin. Vaccine Immunol*., **13**(11), 1267–1277.
38. Fox, J. L. (2007). Antivirals become a broader enterprise. *Nat. Biotechnol*., **25**(12), 1395–1402.
39. Oswald, W. B., et al. (2007). Neutralizing antibody fails to impact the course of Ebola virus infection in monkeys. *PLoS Pathog*., **3**(1), e9.
40. Mupapa, K., et al. (1999). Treatment of Ebola hemorrhagic fever with blood transfusions from convalescent patients. International Scientific and Technical Committee. *J. Infect. Dis.*, **179**(Suppl 1), S18– S23.
41. Jahrling, P. B., et al. (2007). Ebola hemorrhagic fever: Evaluation of passive immunotherapy in nonhuman primates. *J. Infect. Dis.*, **196**(Suppl 2), S400–S403.
42. Niiler, E. (2002). Bioterrorism: Biotechnology to the rescue? *Nat. Biotechnol.*, **20**, 21–25.
43. Van der Groen, G., Pattyn, S. R. (1979). Measurement of antibodies to Ebola virus in human sera from N. W. Zaire. *Annu. Soc. Belg. Med. Trop*., **59**(1), 87–92.
44. Zaki, S. R., et al. (1999). A novel immunohistochemical assay for the detection of Ebola virus in skin: Implications for diagnosis, spread, and surveillance of Ebola hemorrhagic fever. Commission de Lutte contre les Epidemies a Kikwit. *J. Infect. Dis.*, **179**(Suppl 1), S36–S47.
45. Weidmann, M., Muhlberger, E., Hufert, F. T. (2004). Rapid detection protocol for filoviruses. *J. Clin. Virol*., **30**(1), 94–99.
46. Towner, J. S., et al. (2004). Rapid diagnosis of Ebola hemorrhagic fever by reverse transcription-PCR in an outbreak setting and assessment of patient viral load as a predictor of outcome. *J. Virol*., **78**(8), 4330–4341.
47. Sanchez, A., et al. (1999). Detection and molecular characterization of Ebola viruses causing disease in human and nonhuman primates. *J. Infect. Dis.*, **179**(Suppl 1), S164–S169.
48. Leroy, E. M., et al. (2000). Human asymptomatic Ebola infection and strong inflammatory response. *Lancet*, **355**(9222), 2210–2215.
49. Ksiazek, T. G., et al. (1999). ELISA for the detection of antibodies to Ebola viruses. *J. Infect. Dis.*, **179**(Suppl 1), S192–S198.
50. Ksiazek, T. G., et al. (1999). Clinical virology of Ebola hemorrhagic fever (EHF): Virus, virus antigen, and IgG and IgM antibody findings

among EHF patients in Kikwit, Democratic Republic of the Congo, 1995. *J. Infect. Dis*., **179**(Suppl 1), S177–S187.

51. Ksiazek, T. G., et al. (1992). Enzyme immunosorbent assay for Ebola virus antigens in tissues of infected primates. *J. Clin. Microbiol.*, **30**(4), 947–950.
52. Gibb, T. R., et al. (2001). Development and evaluation of a fluorogenic 5' nuclease assay to detect and differentiate between Ebola virus subtypes Zaire and Sudan. *J. Clin. Microbiol.*, **39**(11), 4125–4130.
53. Drosten, C., et al. (2002). Rapid detection and quantification of RNA of Ebola and Marburg viruses, Lassa virus, Crimean-Congo hemorrhagic fever virus, Rift Valley fever virus, dengue virus, and yellow fever virus by real-time reverse transcription-PCR. *J. Clin. Microbiol*., **40**(7), 2323–2330.
54. Dowell, S. F., et al. (1999). Transmission of Ebola hemorrhagic fever: A study of risk factors in family members, Kikwit, Democratic Republic of the Congo, 1995. Commission de Lutte contre les Epidemies a Kikwit. *J. Infect. Dis.*, **179**(Suppl 1), S87–S91.
55. Henchal, E. A., Teska, J. D., Ezzell, J. W. (2000). Responding to biological terrorism: A role for the clinical laboratory. *Clin. Lab. News*, **26**, 14–18.
56. Gilchrist, M. J. (2000). A national laboratory network for bioterrorism: Evolution from a prototype network of laboratories performing routine surveillance. *Mil. Med*., **1657**(Suppl 2), 28–31.
57. Guimard, Y., et al. (1999). Organization of patient care during the Ebola hemorrhagic fever epidemic in Kikwit, Democratic Republic of the Congo, 1995. *J. Infect. Dis*., **179**(Suppl 1), S268–S273.
58. Saijo, M., et al. (2006). Laboratory diagnostic systems for Ebola and Marburg hemorrhagic fevers developed with recombinant proteins. *Clin. Vaccine Immunol*., **13**(4), 444–451.
59. Siegert, R., et al. (1967). On the etiology of an unknown human infection originating from monkeys. *Dtsch. Med. Wochenschr*., **92**(51), 2341–2343.
60. Geisbert, T. W., Jahrling, P. B. (1990). Use of immunoelectron microscopy to show Ebola virus during the 1989 United States epizootic. *J. Clin. Pathol*., **43**(10), 813–816.
61. Geisbert, T. W., Rhoderick, J. B., Jahrling, P. B. (1991). Rapid identification of Ebola virus and related filoviruses in fluid specimens using indirect immunoelectron microscopy. *J. Clin. Pathol*., **44**(6), 521–522.

62. Geisbert, T. W., Jahrling, P. B. (1995). Differentiation of filoviruses by electron microscopy. *Virus Res*., **392**(3), 129–150.

63. Murray, P. R. (2003). *Manual of Clinical Microbiology*, ASM Press, Washington, DC.

64. Ksiazek, T. G. (1991). Laboratory diagnosis of filovirus infections in nonhuman primates. *Lab. Anim*., **20**, 34–46.

65. Ikegami, T., et al. (2003). Immunoglobulin G enzyme-linked immunosorbent assay using truncated nucleoproteins of Reston Ebola virus. *Epidemiol. Infect*., **130**(3), 533–539.

66. Groen, J., et al. (2003). Serological reactivity of baculovirus-expressed Ebola virus VP35 and nucleoproteins. *Microbes Infect*., **5**(5), 379–385.

67. Becker, S., et al. (1992). Evidence for occurrence of filovirus antibodies in humans and imported monkeys: Do sub-clinical filovirus infections occur worldwide? *Med Microbiol. Immunol*., **181**(1), 43–55.

68. Saijo, M., et al. (2005). Characterization of monoclonal antibodies to Marburg virus nucleoprotein (NP) that can be used for NP-capture enzyme-linked immunosorbent assay. *J. Med. Virol*., **76**(1), 111–118.

69. Niikura, M., et al. (2001). Detection of Ebola viral antigen by enzyme-linked immunosorbent assay using a novel monoclonal antibody to nucleoprotein. *J. Clin. Microbiol.*, **39**(9), 3267–3671.

70. Lucht, A., et al. (2004). Production of monoclonal antibodies and development of an antigen capture ELISA directed against the envelope glycoprotein GP of Ebola virus. *Med. Microbiol. Immunol*., **193**(4), 181–187.

71. Lucht, A., et al. (2003). Development, characterization and use of monoclonal VP40-antibodies for the detection of Ebola virus. *J. Virol. Methods*, **111**(1), 21–28.

72. Ikegami, T., et al. (2003). Antigen capture enzyme-linked immunosorbent assay for specific detection of Reston Ebola virus nucleoprotein. *Clin. Diagn. Lab. Immunol*., **10**(4), 552–557.

73. Shahhosseini, S., et al. (2007). Production and characterization of monoclonal antibodies against different epitopes of Ebola virus antigens. *J. Virol. Methods*, **143**(1), 29–37.

74. Franz, D. R., et al. (2001). Clinical recognition and management of patients exposed to biological warfare agents. *Clin. Lab. Med*., **21**(3), 435–473.

75. Franz, D. R., et al. (1997). Clinical recognition and management of patients exposed to biological warfare agents. *JAMA*, **278**(5), 399–411.

76. Zaki, S. R., Goldsmith, C. D. (1999). Pathologic features of filovirus infections in humans. *Curr. Top. Microbiol. Immunol*., **235**, 97–116.

77. Lloyd, E. S., et al. (1999). Long-term disease surveillance in Bandundu region, Democratic Republic of the Congo: A model for early detection and prevention of Ebola hemorrhagic fever. *J. Infect. Dis.*, **179**(Suppl 1), S274–S280.

78. Elliott, L. H., Kiley, M. P., McCormick, J. B. (1985). Descriptive analysis of Ebola virus proteins. *Virology*, **147**(1), 169–176.

79. Elliott, L. H., et al. (1993). Improved specificity of testing methods for filovirus antibodies. *J. Virol. Methods*, **43**(1), 85–89.

80. Zhai, J., et al. (2007). Rapid molecular strategy for filovirus detection and characterization. *J. Clin. Microbiol*., **45**(1), 224–226.

81. Palacios, G., et al. (2006). MassTag polymerase chain reaction for differential diagnosis of viral hemorrhagic fever. *Emerg. Infect. Dis*., **12**(4), 692–695.

82. Grolla, A., et al. (2005). Laboratory diagnosis of Ebola and Marburg hemorrhagic fever. *Bull. Soc. Pathol. Exot*., **98**(3), 205–209.

83. Garcia-de-Lomas, J., Navarro, D. (1997). New directions in diagnostics. *Pediatr. Infect. Dis. J*., **163**(Suppl 3), S43–S48.

84. Whelen, A. C., Persing, D. H. (1996). The role of nucleic acid amplification and detection in the clinical microbiology laboratory. *Annu. Rev. Microbiol*., **50**, 349–373.

85. Sobarzo, A., Perelman, E., Groseth, A., Dolnik, O., Becker, S., Lutwama, J. J., Dye, J., Yavelsky, V., Lobel, L., Marks, R. S. (2013). Profiling the native specific human humoral immune response to Sudan ebolavirus (Gulu) by chemiluminescense ELISA. *Clin. Vaccine Immunol*., **19**(11), 1844–1852.

86. Leroy, E. M., et al. (2000). Diagnosis of Ebola haemorrhagic fever by RT-PCR in an epidemic setting. *J. Med. Virol*., **60**(4), 463–467.

87. Panning, M., et al. (2007). Diagnostic reverse-transcription polymerase chain reaction kit for filoviruses based on the strain collections of all European biosafety level 4 laboratories. *J. Infect. Dis.*, **196**(Suppl 2), S199–S204.

88. Niedrig, M., et al. (2004). First international quality assurance study on the rapid detection of viral agents of bioterrorism. *J. Clin. Microbiol.*, **42**(4), 1753–1755.

89. Sanchez, A. F. H. (1995). Detection of Marburg and Ebola virus infections by polymerase chain reaction assays, in *Protocols for Diagnosis of Human and Animal Virus Diseases*, pp. 411–419.

90. Lucht, A., et al. (2007). Development of an immunofiltration-based antigen-detection assay for rapid diagnosis of Ebola virus infection. *J. Infect. Dis.*, **196**(Suppl 2), S184–S192.

91. Saijo, M., et al. (2001). Enzyme-linked immunosorbent assays for detection of antibodies to Ebola and Marburg viruses using recombinant nucleoproteins. *J. Clin. Microbiol.*, **39**(1), 1–7.

92. Prehaud, C., et al. (1998). Recombinant Ebola virus nucleoprotein and glycoprotein (Gabon 94 strain) provide new tools for the detection of human infections. *J. Gen. Virol.*, **79**(Pt 11), 2565–2572.

93. Saijo, M., et al. (2001). Immunofluorescence method for detection of Ebola virus immunoglobulin G, using HeLa cells which express recombinant nucleoprotein. *J. Clin. Microbiol.*, **39**(2), 776–778.

94. Nissim, A., et al. (1994). Antibody fragments from a "single pot" phage display library as immunochemical reagents. *EMBO J.*, **13**(3), 692–698.

95. Chen, H., et al. (2003). Evaluation of a nucleoprotein-based enzyme-linked immunosorbent assay for the detection of antibodies against infectious bronchitis virus. *Avian Pathol.*, **32**(5), 519–526.

96. Strong J. E., Jahrling, P. B., Feldmann, H. (2006). Filoviruses and arenaviruses. In: *Manual of Molecular and Clinical Laboratory Immunology*, pp. 774–790.

97. Rowe, A. K., et al. (1999). Clinical, virologic, and immunologic follow-up of convalescent Ebola hemorrhagic fever patients and their household contacts, Kikwit, Democratic Republic of the Congo. Commission de Lutte contre les Epidemies a Kikwit. *J. Infect. Dis.*, **179**(Suppl 1), S28–S35.

98. Amano, Y., Cheng, Q. (2005). Detection of influenza virus: Traditional approaches and development of biosensors. *Anal. Bioanal. Chem.*, **381**(1), 156–164.

99. Yu, J. S., et al. (2006). Detection of Ebola virus envelope using monoclonal and polyclonal antibodies in ELISA, surface plasmon resonance and a quartz crystal microbalance immunosensor. *J. Virol. Methods*, **137**(2), 219–228.

100. Dell'Atti, D., et al. (2007). Development of combined DNA-based piezoelectric biosensors for the simultaneous detection and genotyping of high risk Human Papilloma Virus strains. *Clin. Chim. Acta*, **383**(1–2), 140–146.

101. Gerdon, A. E., Wright, D. W., Cliffel, D. E. (2005). Quartz crystal microbalance detection of glutathione-protected nanoclusters using antibody recognition. *Anal. Chem.*, **77**(1), 304–310.

102. Petrosova, A., Konry, T., Cosnier, S., Trakht, I., Lutwama, J., Rwaguma, E., Chepurnov, A., Mühlberger, E., Lobel, L., and Marks, R. S. (2007). Development of a highly sensitive, field operable biosensor for serological studies of Ebola virus in central Africa. *Sens. Actuators, B,* **122**, 578–586.

103. Ebihara, H., Groseth, A., Neumann, G., Kawaoka, Y., Feldmann, H. (2005). The role of reverse genetics systems in studying viral hemorrhagic fevers. *Thromb. Haemost.*, **94**(2), 240–253.

104. Neumann, G., Kawaoka, Y. (2004). Reverse genetics systems for the generation of segmented negative-sense RNA viruses entirely from cloned cDNA. *Curr. Top. Microbiol. Immunol*., **283**, 43–60.

105. Volchkov, V. E., et al. (2001). Recovery of infectious Ebola virus from complementary DNA: RNA editing of the GP gene and viral cytotoxicity. *Science*, **291**(5510), 1965–1969.

106. Towner, J. S., et al. (2005). Generation of eGFP expressing recombinant Zaire Ebola virus for analysis of early pathogenesis events and high-throughput antiviral drug screening. *Virology*, **332**(1), 20–27.

107. Neumann, G., et al. (2002). Reverse genetics demonstrates that proteolytic processing of the Ebola virus glycoprotein is not essential for replication in cell culture. *J. Virol*., **76**(1), 406–410.

108. Ebihara, H., et al. (2007). In vitro and in vivo characterization of recombinant Ebola viruses expressing enhanced green fluorescent protein. *J. Infect. Dis.*, **196**(Suppl 2), S313–S322.

109. Ramsden, J. J. (1997). Optical biosensors. *J. Mol. Recognit.*, **10**(3), 109–120.

110. Cooper, M. A. (2002). Optical biosensors in drug discovery. *Nat. Rev. Drug Discov*., **1**(7), 515–528.

111. Huang, M. C. Y., Jonathan, C. F. R. M., Foley, E., Beatty, R., Cunningham, B. T., Chang-Hasnain, C. J. (2008). VCSEL optoelectronic biosensor for detection of infectious diseases. *IEEE Photonics Technol. Lett.*, **20**, 443–445.

112. Deng, Z., et al. (2007). Green and orange CdTe quantum dots as effective pH-sensitive fluorescent probes for dual simultaneous and independent detection of viruses. *J. Phys. Chem. B.*, **111**(41), 12024–12031.

113. Drummond, T. G., Hill, M. G., Barton, J. K. (2003). Electrochemical DNA sensors. *Nat. Biotechnol.*, **21**(10), 1192–1199.

114. Bouchet, A., et al. (2007). Cylinder-shaped conducting polypyrrole for labelless electrochemical multidetection of DNA. *Biosens. Bioelectron.*, **23**(5), 735–740.

115. Chen, R. J., et al. (2003). Noncovalent functionalization of carbon nanotubes for highly specific electronic biosensors. *Proc. Natl. Acad. Sci. U S A*, **100**(9), 4984–4989.

116. Veetil, J. V., Ye, K. (2007). Development of immunosensors using carbon nanotubes. *Am. Chem. Soc. Am. Inst. Chem. Eng.*, **23**, 517–531.

117. Berkenpas, E., Millard, P., Pereira da Cunha, M. (2006). Detection of *Escherichia coli* O157:H7 with langasite pure shear horizontal surface acoustic wave sensors. *Biosens. Bioelectron*., **21**(12), 2255–2262.

118. Moll, N., et al. (2007). A. Love wave immunosensor for whole E. coli bacteria detection using an innovative two-step immobilisation approach. *Biosens. Bioelectron.*, **229**(10), 2145–2150.

119. Branch, D. W., Brozik, S. M. (2004). Low-level detection of a bacillus anthracis simulant using Love-wave biosensors on 36 degrees YX $LiTaO_3$. *Biosens. Bioelectron.*, **19**(8), 849–859.

120. Bisoffi, M., et al. (2008). Detection of viral bioagents using a shear horizontal surface acoustic wave biosensor. *Biosens. Bioelectron.*, **23**(9), 1397–1403.

121. Ding, C., et al. (2008). Hybridization biosensor using 2,9-dimethyl-1,10-phenantroline cobalt as electrochemical indicator for detection of hepatitis B virus DNA. *Bioelectrochemistry*, **72**(1), 28–33.

122. Gervais, L., Gel, M., Allain, B., Tolba, M., Brovko, L., Zourob, M., Mandeville, R., Griffiths, M., Evoy, S. (2007). Immobilization of biotinylated bacteriophage on biosensor surfaces. *Sens. Actuators B*, **125**, 615–621.

123. Herrmann, S., et al. (2007). T7 phage display of Ep15 peptide for the detection of WNV IgG. *J. Virol. Methods*, **141**(2), 133–140.

124. Liu, X., Yue, J., Zhang, Z. (2008). WITHDRAWN: Generation of F0F1-ATPase nanoarray by Dip-Pen Nanolithography and its application as biosensors. *Arch. Biochem. Biophys.* in press.

125. Oh, S. Y., et al. (2008). Rapid detection of influenza A virus in clinical samples using an ion channel switch biosensor. *Biosens. Bioelectron.*, **23**(7), 1161–1165.

126. Leclerc, M. (1999). Optical and electrochemical transducers based on functionalized conjugated polymers. *Adv. Mater*. **11**, 1491–1498.

127. Jung, Y. K., Park, H. G., Kim, J. M. (2006). Polydiacetylene (PDA)-based colorimetric detection of biotinstreptavidin interactions. *Biosens. Bioelectron.*, **21**(8), 1536–1544.

128. Charych, D., et al. (1996). A "litmus test" for molecular recognition using artificial membranes. *Chem. Biol*., **3**(2), 113–120.

129. Dore, K., et al. (2004). Fluorescent polymeric transducer for the rapid, simple, and specific detection of nucleic acids at the zeptomole level. *J. Am. Chem. Soc*., **126**(13), 4240–4244.

130. Charych, D. H., et al. (1993). Direct colorimetric detection of a receptor-ligand interaction by a polymerized bilayer assembly. *Science*, **261**(5121), 585–588.

131. Reichert, A., Nagy, J. O., Spevak, W., Charych, D. (1995). Polydiacetylene liposomes functionalized with sialic acid bind and colorimetrically detect influenza virus. *J. Am. Chem. Soc.*, **117**, 829–830.

132. Fischer, N. O., Tarasow, T. M., Tok, J. B. (2007). Heightened sense for sensing: Recent advances in pathogen immunoassay sensing platforms. *Analyst*, **132**(3), 187–191.

133. Tok, J. B., et al. (2006). Metallic striped nanowires as multiplexed immunoassay platforms for pathogen detection. *Angew. Chem., Int. Ed. Engl*., **45**(41), 6900–6904.

134. Wang, W. U., et al. (2005). Label-free detection of small-molecule-protein interactions by using nanowire nanosensors. *Proc. Natl. Acad. Sci. U S A*, **102**(9), 3208–3212.

135. Patolsky, F., Zheng, G., Lieber, C. M. (2006). Nanowire sensors for medicine and the life sciences. *Nanomedicine*, **1**(1), 51–65.

136. Patolsky, F., et al. (2004). Electrical detection of single viruses. *Proc. Natl. Acad. Sci. U S A*, **101**(39), 14017–14022.

137. Wilson, R., Cossins, A. R., Spiller, D. G. (2006). Encoded microcarriers for high-throughput multiplexed detection. *Angew. Chem., Int. Ed. Engl*., **45**(37), 6104–6117.

138. Gehring, A. G., et al. (2006). Antibody microarray detection of *Escherichia coli* O157:H7: Quantification, assay limitations, and capture efficiency. *Anal. Chem*., **78**(18), 6601–6607.

139. Lubin, A. A., et al. (2006). Sequence-specific, electronic detection of oligonucleotides in blood, soil, and foodstuffs with the reagentless, reusable E-DNA sensor. *Anal. Chem*., **78**(16), 5671–5677.

140. Baker, B. R., et al. (2006). An electronic, aptamer-based small-molecule sensor for the rapid, label-free detection of cocaine in adulterated samples and biological fluids. *J. Am. Chem. Soc.*, **128**(10), 3138–3139.

141. Lee, S., et al. (2007). Chip-based detection of hepatitis C virus using RNA aptamers that specifically bind to HCV core antigen. *Biochem. Biophys. Res. Commun.*, **358**(1), 47–52.

142. Endo, T., et al. (2006). Multiple label-free detection of antigen-antibody reaction using localized surface plasmon resonance-based

core-shell structured nanoparticle layer nanochip. *Anal. Chem.*, **78**(18), 6465–6475.

143. Baek, T. J., et al. (2008). Development of a photodiode array biochip using a bipolar semiconductor and its application to detection of human papilloma virus. *Anal. Bioanal. Chem.*, **390**(5), 1373–1378.
144. Rider, T. H., et al. (2003). A B cell-based sensor for rapid identification of pathogens. *Science*, **301**(5630), 213–215.
145. Williams, D. D., Benedek, O., Turnbough, C. L., Jr. (2003). Species-specific peptide ligands for the detection of Bacillus anthracis spores. *Appl. Environ. Microbiol.*, **69**(10), 6288–6293.
146. Sapsford, K. E., et al. (2006). A cowpea mosaic virus nanoscaffold for multiplexed antibody conjugation: Application as an immunoassay tracer. *Biosens. Bioelectron.*, **21**(8), 1668–1673.
147. Martin, B. D., et al. (2006). An engineered virus as a bright fluorescent tag and scaffold for cargo proteins: Capture and transport by gliding microtubules. *J. Nanosci. Nanotechnol.*, **6**(8), 2451–2460.
148. Cunha, B. A. (2002). Anthrax, tularemia, plague, Ebola or smallpox as agents of bioterrorism: Recognition in the emergency room. *Clin. Microbiol. Infect.*, **8**(8), 489–503.
149. Murphy, F. A. (1998). Emerging zoonoses. *Emerg. Infect. Dis.*, **4**, 429–435.
150. Chomel, B. B. (2003). Control and prevention of emerging zoonoses. *J. Vet. Med. Educ.*, **30**(2), 145–147.
151. Onyango, C. O., et al. (2007). Laboratory diagnosis of Ebola hemorrhagic fever during an outbreak in Yambio, Sudan, 2004. *J. Infect. Dis.*, **196**(Suppl 2), S193–S198.
152. Outbreak news (2008). Ebola haemorrhagic fever, Uganda: End of the outbreak. *Wkly. Epidemiol. Rec.*, **83**(10), 89–90.
153. Outbreak news (2007). Ebola virus haemorrhagic fever, Democratic Republic of the Congo. *Wkly. Epidemiol. Rec.*, **82**(38), 329.
154. Outbreak of Ebola haemorrhagic fever, Uganda, August 2000–January 2001. 2001. *Wkly. Epidemiol. Rec.*, **76**(6), 41–46.
155. Sobarzo, A., Ochayon, D. E., Lutwama, J. J., Balinandi, S., Guttmn, O., Marks, R. S., Kuehne, A. I., Dye, J. M., Yavelsky, V., Lewis, E. C., Lobel, L. (2013). Persistent immune responses after Ebola virus infection. *N. Engl. J. Med*., **369**(5), 492–493.
156. Sobarzo, A., Groseth, A., Dolnik, O., Becker, S., Lutwama, J. J., Perelman, E., Yavelsky, V., Muhammad, M., Kuene, A. I., Marks, R. S., Dye, J. M., Lobel, L. (2013). Profile and persistence of the virus-specific

neutralizing humoral immune response in human survivors of Sudan ebolavirus (Gulu). *J. Infect. Dis.*, **208**(2), 299–309.

Chapter 55

Nanomedicine as a Strategy to Fight Thrombotic Diseases

Mariana Varna, PhD,[a,b,*] Maya Juenet, MSc,[a,b,*]
Richard Bayles, PhD,[a] Mikael Mazighi, MD, PhD,[a,c]
Cédric Chauvierre, PhD,[a,b] and Didier Letourneur, PhD[a,b]

[a]*INSERM U1148, LVTS, Cardiovascular Bio-Engineering, X. Bichat Hospital, Paris, France*
[b]*Institut Galilée, Université Paris 13, Villetaneuse, France*
[c]*AP-HP, Lariboisière Hospital, Paris, France*

Keywords: preclinical models, drug delivery, ischemic heart, microbubbles, nanocarriers, stroke, thrombolytic, lipid nanoparticles, polymer nanoparticles, inorganic nanoparticles, clinical trials, nanotherapy, ultrasound, atherosclerosis

Overview

This review highlights the preclinical and clinical research based on the use of nano- and microcarriers in thrombolytic drug delivery. Ischemic heart and stroke caused by thrombosis are the main causes of death in the world. Because of their inactivation in the blood, high doses of thrombolytics are administered to patients, increasing the risk of intracranial hemorrhage. Preclinical research conducted with lipid, polymer or magnetic nanoparticles loaded with thrombolytic drugs showed an enhancement of thrombolysis and a reduction of undesirable side effects. Targeted nanocarriers

*Authors contributed equally.

Handbook of Clinical Nanomedicine: Nanoparticles, Imaging, Therapy, and Clinical Applications
Edited by Raj Bawa, Gerald F. Audette, and Israel Rubinstein

ISBN 978-981-4669-20-7 (Hardcover), 978-981-4669-21-4 (eBook)
www.panstanford.com

exhibited an increased accumulation into clot. Clinical trials were already conducted with lipid-based microbubbles combined with ultrasound and thrombolytic drug and showed thrombolysis improvement. Future validation of nanosystems is awaited in clinic. This research opens new strategies for the management of thrombotic diseases.

To degrade a thrombus, thrombolytic drugs are administered, but they are rapidly inactivated in the blood. High amounts are thus injected to patients with the risk to develop intracranial hemorrhages. Nanocarriers and microbubbles have been tested in preclinical models to deliver thrombolytic drugs. These systems show the advantage to protect the drug from degradation. In clinical trials, galactose and lipid-based microbubbles associated with ultrasound and thrombolytic drugs showed an enhancement of thrombolysis. Other systems are also under development with new drugs combined or not with endovascular intervention to treat ischemic heart or stroke.

55.1 Introduction

Atherosclerosis is a multifactorial and slowly progressing pathophysiological disease. It is responsible for 17.3 million deaths per year. Among cardiovascular diseases related to atherosclerosis, myocardial infarction and ischemic stroke are, and will remain the principal cause of death in the world [1]. Development of atherosclerosis is linked to some risk factors, including diabetes, hypertension, smoking, high total cholesterol, high BMI and physical inactivity [1].

The stages of this disease are now understood in detail. Atherosclerotic lesions begin as fatty streaks in lesion-prone areas in aortic bifurcations. These regions exposed to a disturbed flow may develop an activated endothelium. Low-density lipoprotein (LDL)-derived cholesterol extravasates through the defective endothelium into the subendothelial space. There, LDLs are oxidized (oxLDLs) by enzymes such as myelo-peroxidase, 15-lipoxygenase or nitric oxide synthase. The recruitment of monocytes is stimulated in part by oxLDLs and is regulated by adhesion molecules expressed on the surface of endothelial cells (VCAM-1, ICAM-1). Monocytes are subsequently differentiated into macrophages (Fig. 55.1A). The macrophages express scavenger receptors (SR-A and CD36)

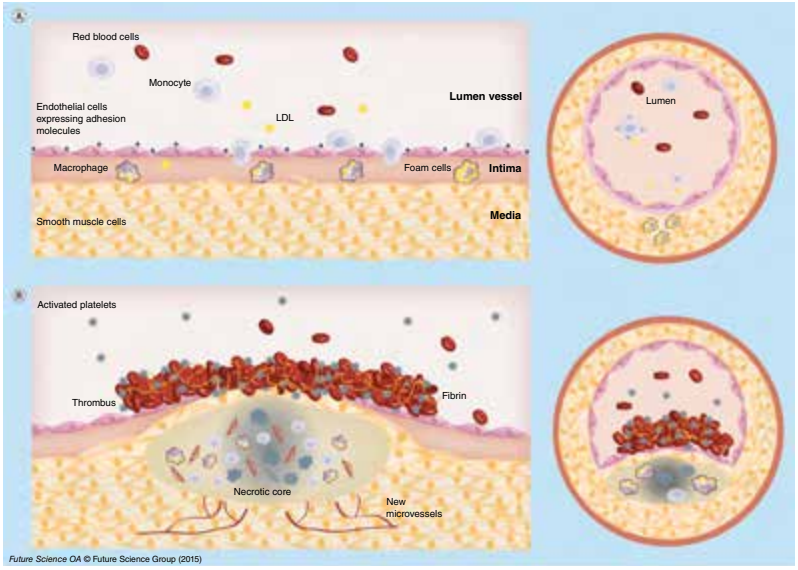

Figure 55.1 Atherosclerotic plaque development. (A) Cholesterol derived low-density lipoproteins extravasate in the intima where they are oxidized. Endothelial cells are activated and express specific adhesion molecules. These phenomena drive the recruitment of monocytes, which differentiate into macrophages expressing scavenger receptors, and the uptake of oxidized low-density lipoproteins. Smooth muscle cells migrate into the intima, proliferate and contribute to foam cell formation. (B) In advanced stages, a fibrous cap made of smooth muscle cells and collagen fibers is formed. Apoptotic events and necrotic zones appear in a hypoxic environment inducing new microvessel development. With plaque rupture, thrombogenic substances are released into the circulation and promote platelet activation and adhesion to endothelium and thrombus formation.

which recognize oxLDLs. In an advanced lesion, smooth muscle cells (SMCs) present in media, proliferate, express scavenger receptors and can also take up oxLDLs contributing to foam cell formation. SMCs also synthesize extracellular matrix proteins leading to fibrous cap development. During the progression of atherosclerosis, endothelial cells, macrophages and smooth muscle cells die by apoptosis or necrosis contributing to necrotic core formation within the plaque [2, 3]. Focal calcifications, neovascularization and intraplaque hemorrhages characterize high-risk plaques

with a thin fibrous cap [4]. The development of atherosclerosis begins in childhood. Later in life, growing plaques may become suddenly complicated and could break inducing a luminal thrombosis (Fig. 55.1B). Some factors have been identified to cause plaque rupture. The key role of the thickness of the fibrous cap and intraplaque hemorrhages induced by neovascularization is now recognized. Plaque rupture exposes thrombogenic substances of the plaque to the circulating blood, promoting platelet activation and adhesion to endothelium and thrombus formation [5]. The thrombus development is initiated by tissue factor and culminates with the circulating platelet recruitment and concomitant generation of thrombin and fibrin [6]. The thrombus is composed of fibrin monomers cross-linked through lysine side chains [5].

Atherosclerosis alone is rarely fatal, but the complications induced by thrombosis, myocardial ischemia and stroke, are the most common causes of death in Western societies [3]. Arterial thrombosis differs from venous thrombosis and is therefore treated in a different way. The arterial thrombi formed after plaque rupture are rich in activated platelets, while thrombi formed in veins are rather rich in fibrin and trapped red blood cells [7]. Arterial thrombosis is thus treated with drugs targeting platelets, whereas venous thrombosis is treated with antithrombotic drugs.

55.1.1 Therapeutic Drugs and Side Effects

Thrombolytic agents are able to induce thrombus lysis by the degradation of fibrin contained in clots [8]. Clot dissolution (fibrinolysis or thrombolysis) is enzymatically driven by a serine protease named plasmin, which is obtained from plasminogen. The conversion of plasminogen into plasmin is made by tissue plasminogen activators (tPAs). There are two groups of thrombolytic drugs: those which are able to bind both free circulating and clot bound plasminogen and those which bind only clot bound plasminogen (Fig. 55.2). Few plasminogen activators [5, 9, 10] have been approved by the US FDA for clinical applications: urokinase (UK), streptokinase (SK), alteplase (tPA), tenecteplase (TNKtPA) and reteplase (rPA) (Table 55.1). Natural inhibitors of plasminogen activators have been described such as α-2-antiplasmine, α-2-macroglobuline, anti-C1 esterase, α-1 antitrypsin

and PAI-1 [11, 12]. Because of their relatively short half-life, high quantities of thrombolytic drugs need to be administered into patients. After being administered to patients, the drugs undergo cell metabolism and are distributed throughout the body. In order to obtain a therapeutic effect, high doses have to be injected, which may lead to undesirable risk of hemorrhagic transformation after thrombolytic therapy [8]. On one hand, degradation of the components of neurovascular unit (endothelial cells, basal membrane, perivascular astrocytes and neurons) induced by ischemia leads to the passage of fluids from intravascular space into the brain, with formation of edema and intracranial hemorrhages. In these conditions, tPA can also pass the blood–brain barrier and through interaction with the NMDA-type-glutamate receptor can potentially amplify excitotoxic calcium currents. On the other hand, indirect upregulation by tPA of MMP9 activity, which degrades extracellular matrix integrity, increases the risk of neurovascular cell death and blood–brain barrier disruption [13].

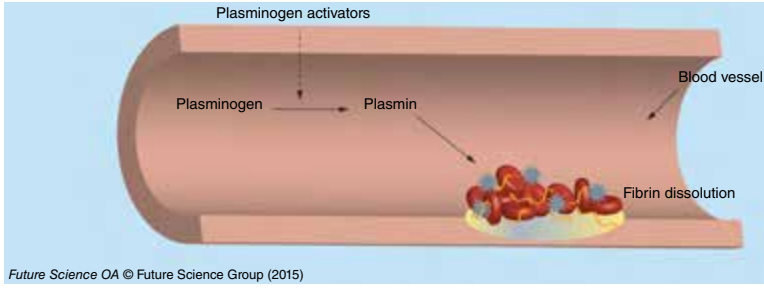

Figure 55.2 Schematic representation of fibrin clot thrombolysis induced by thrombolytic agents in blood vessels.

The development of new formulations of these drugs gains more and more interest. A promising strategy consists in the use of nano- and microcarriers [14, 15]. The most important advantages of these platforms are the prevention of the degradation of the drugs by enzymes in the blood and the possibility to target a thrombus using specific ligands leading to an increase of the drug amount into the clot. In the next section we detail the different categories of nano- and microcarriers used to deliver thrombolytic drugs.

Table 55.1 Examples of clinically used thrombolytic drugs.

Thrombolytic agent	Abbreviation	Molecular weight (kDa)	Indication	US FDA status	Structure (domains)	Half-life (min)	Fibrino selective	Elimination
Urokinase (Abbokinase®, Abbot Laboratories, TX, USA)	UK	2 polypeptides chains (32/54)	AMI, PE	Approved	P/K/ EGF	15–20	No	Kidney
Streptokinase (Streptase)	SK	47	AMI, PE, DVT, PAO	Approved	α, β, γ	10–16	No	Kidney
Alteplase (Activase®, Genentech, CA, USA; Actilyse®, Boehringer Ingelheim, Germany)	tPA, rtPA	68	AMI, PE, IS	Approved	F/EGF/K1/K2/S	4–6	Yes	Liver
Tenecteplase (TNKase®, Genentech, USA; Metalyse®, Boehringer Ingelheim, Germany)	TNK-tPA	70	AMI	Approved	F/EGF/K1	20	Yes	Kidney
Reteplase (Retavase®, Chiesi Farmaceutici S.p.A, Italy; Rapilysin®, Actavis, NJ, USA)	rPA	40	AMI, DVT, PAO	Phase II	K2/SP	18	Yes	Kidney
Staphylokinase	SAK	16.5	AMI	Phase II	2 chains: a, b	6	Yes	Liver
Lanoteplase	nPA	53.5	AMI	Phase II	F/K1/K2/SP	37	Yes	Liver
Desmoteplase	batPA	52	IS	Phase III	F/EGF/K1/SP	240	Yes	Liver

AMI: Acute myocardial infarction; DVT: Deep-vein thrombosis; EGF: EGF domain; F: Finger domain; IS: Ischemic stroke; K1: Kringle 1 domain; K2: Kringle 2 domain; PAO: Peripheral arterial occlusion; PE: Pulmonary embolism; SP: Serine protease domain.

55.2 Composition of Nano- and Microcarriers Used in Thrombolytic Therapy

Several types of materials, polymer, lipid or metal based, can be employed to deliver thrombolytic drugs (Fig. 55.3). These materials are well tolerated *in vivo*, possess low toxicity, and are easy to biofunctionalize. Depending on their composition, hydrophobic or hydrophilic drugs can be incorporated or attached. The formulations of nano- and microcarriers include spheres, capsules and vesicles.

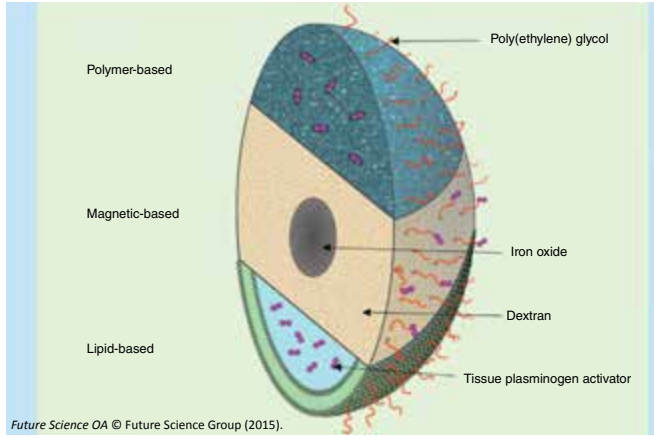

Figure 55.3 Schematic representation of polymer-, magnetic- and lipid-based stealth nanocarriers loaded with thrombolytic drugs.

Some factors, such as the size, surface charge and the presence or not of a polymer coating, affect the clearance and the biodistribution of nano- and microcarriers. The size can be modulated during the synthesis of nanoparticles. The charge and the composition of the surface determine the clearance by the monocyte macrophage system (MPS). Following intravenous administration, the naked nano- and microcarriers are cleared by the MPS and recognition is induced by the attachment on the surface of the carriers of plasma proteins named opsonins (C3b, iC3, IgG, IgM) [16]. To avoid this and to prolong the circulation time in the body, poly(ethylene glycol) (PEG), a hydrophilic biocompatible and biodegradable polymer, has been commonly

used in the coating. PEG is approved by the FDA for clinical use. PEG, either adsorbed or covalently attached to the surface of nano- and microcarriers, induces steric inhibition of opsonins and thus their attachment at the surface of the carrier [17]. Moreover PEG is easy to functionalize. Another advantage provided by the coating of nano- and microcarriers with PEG is the possibility to attach different ligands on the surface of the carriers, in order to target a tissue or cells of interest [18, 19].

55.2.1 Lipid-Based Nanocarriers

Among the lipid-based, only liposomes and some types of microbubbles have been used in thrombo-therapy. Described 50 years ago by Bangham, liposomes represent the most used carriers to deliver active drugs. Liposomes are defined as bilayer phospholipid vesicles, mimicking the cellular membrane, enclosing an aqueous core. Since their discovery the preparation methods were diversified [20]. The choice of the method and subsequent processing steps are important because it determines the loading efficacy as well as the size. The lack of toxicity of liposomes and their biodegradation represent a significant advantage in their use as carriers to deliver thrombolytic drugs [21]. However, one of the limitations of liposomes is their poor stability in the blood flow.

55.2.2 Polymer-Based Nano- and Microcarriers

Synthetic and natural polymers are used in the design of nano- and microcarriers charged with thrombolytic drugs. Polymers have the advantage of being more resistant to mechanical constraints than lipid-based systems. In addition to their biocompatibility and biodegradability, polymer carriers can be tuned in terms of size, porosity and hydrophobicity. Polymers are either functionalized with reactive groups, such as primary amines, for reaction with the drug further to the nanoparticle synthesis or are designed to directly interact with the therapeutic agent during the nanoparticle formulation. The first strategy leads to systems where the drug is charged at the surface of the particle. It has especially been applied to magnetic particles coated with a polymer shell (Fig. 55.3). The most common is dextran, which is a polysaccharide

composed of α-d-glycose units that bind to each other through glycosidic bonds. Because of its affinity for iron, dextran is largely used in the coating of iron oxide nanoparticles [22]. With this strategy, the drug covalent binding is often achieved via a functionalized PEG spacer. The second method results in drug encapsulation and has been set up with different polymer types. For example, polyvinyl alcohol (PVA), a biodegradable synthetic polymer, has been formulated into a porous material to encapsulate the drug. Poly(lactic-*co*-glycolic acid) (PLGA), an FDA and EMA-approved polymer, is another promising candidate for drug encapsulation. It is largely used in medical research because of its good biodegradability and biocompatibility.

Another mechanism of nanoparticle formation is the ionic gelation process. Chitosan nanoparticles are obtained by this method allowing for drug entrapment during the assembly process. Chitosan is a natural water-soluble polysaccharide. It possesses cationic and hydrophilic properties as well as good biodegradability and biocompatibility, low toxicity and low immunogenicity [23]. In some cases drug retention is enhanced by ionic interaction between the drug and the polymer chains. Gelatin, a natural polymer that shows the advantage to be biodegradable and easily tunable, has been modified for an enhanced interaction [24].

55.2.3 Inorganic Nanocarriers

Inorganic nanocarriers used in the delivery of thrombolytic drugs are principally represented by magnetic nanoparticles. They are composed of a paramagnetic iron oxide core, made of magnetite (Fe_3O_4) or maghemite (γ-Fe_2O_3) or a mixture of both, surrounded by a shell made of polymers, to improve colloidal stability (Fig. 55.3). Depending on the size, magnetic nanoparticles are divided into two categories: ultrasmall superparamagnetic iron oxides (USPIO), with a hydrodynamic size less than 50 nm and superparamagnetic iron oxides (SPIO) particles, with hydrodynamic size between 50 and a few hundred nanometers. Magnetic nanoparticles are biodegradable, participating in the iron homeostasis in the body [22].

One important aspect of the use of magnetic nanoparticles in the delivery of drugs is linked to their magnetic capabilities. Under the local application of a magnet generating a strong

magnetic field, magnetic nanoparticles tend to accumulate into a specific site. This property was evaluated in regenerative medicine for cardiovascular applications [25–27].

In the next section, we describe the preclinical uses of nanosystems in the delivery of thrombolytic drugs.

55.3 Thrombolytic Therapy Using Nanocarriers and Microbubbles in Preclinical Development

The use of nano- and microcarriers to deliver thrombolytic drugs shows several advantages such as protection from inhibitors present in the blood and concentration of drugs at the thrombus. The nanocarriers have a size between a few nanometers to a few hundred of nanometers. Microbubbles have a size between 2 and 8 μm and are composed of a shell made of phospholipid, polymer or albumin, and a core loaded with air or high-molecular-weight gas [28]. Only three thrombolytic drugs have been loaded into nano- and microcarriers and tested *in vivo*. These aspects will be detailed in this section dedicated to preclinical development.

55.3.1 Streptokinase

The history of thrombolytic therapy began in 1933, with the discovery, by Tillett and Garner, that certain strains of Streptococcus were able to dissolve fibrin clots [10, 29]. SK is a single chain protein produced by different strains of streptococcal bacteria [30]. This protein has a molecular weight of 47 kDa and contains 414 amino acids. SK indirectly catalyzes the activation of plasminogen [31] by binding with free circulating plasminogen and thus forming a complex that converts plasminogen to plasmin [9]. SK activates not only fibrin-bound plasminogen but also the free plasminogen inducing serious bleeding complications [30]. This protein shows a biphasic half-life, a first one rapid (16 min) and a second one longer (90 min). The first initial half-life is linked to the complexation of anti-SK antibodies while the second half-life is due to biological elimination of the protein. SK is inexpensive but shows an immunogenic effect and its activity is affected by the presence of antibodies [9, 10].

55.3.2 Nanocarriers Loaded with SK

In order to reduce side effects induced by SK (Streptase®) treatment, Leach *et al.* encapsulated the enzyme into naked liposomes and into a water-soluble double emulsion polymer (PEG and PVA). The authors noted some difficulties with the stability of the liposomes. Only 30% of the initial SK was entrapped within liposomes. The SK yield into polymeric porous particles was 82%. When injected into rabbits with autologous carotid artery thrombosis, the time necessary for reperfusion was significantly reduced: on average 7.3 min were necessary for SK loaded into polymers, 19.3 min for SK-liposome and 74.5 min for free SK [32]. Later, the same team tested these polymer-based nanoparticles in dogs with autologous coronary thrombus. The polymer-based nanoparticles showed a greater reduction in the time required to achieve reperfusion than free SK. In parallel, a reduction of infarct size and less hemorrhage were observed. These results were probably due to the enhanced transport of the encapsulated drug into the core of the thrombus. This accumulation was associated with the polymer dissolution and the release of protected SK [33, 34].

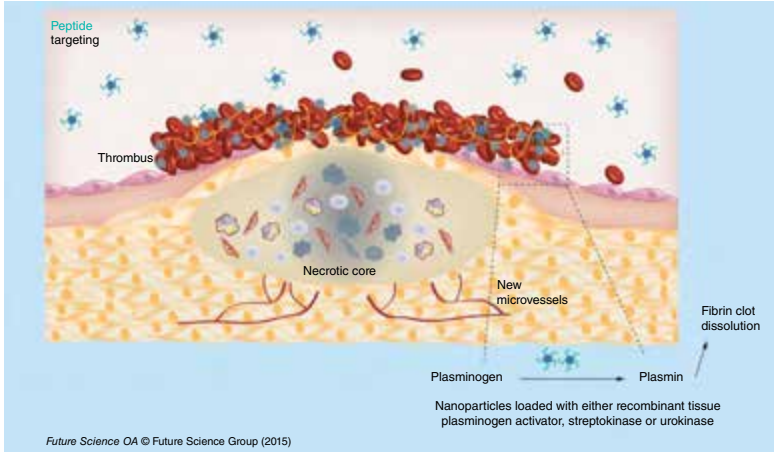

Figure 55.4 Targeting modality by peptides. Nanocarriers loaded with thrombolytic drugs and decorated with RGD peptides that recognize GPIIb/IIIa receptor at the surface of activated platelets, show an accumulation in the thrombus and lead to an enhancement of thrombus lysis.

Vaidya *et al.* obtained 18% of SK entrapment efficacy into liposomes. The SK was loaded into liposomes during hydration of the lipid film. The liposomes were moreover loaded with RGD (arginine-glycine-aspartic acid) peptide in order to target GPIIb/IIIa receptor expressed at the surface of the activated platelets in thrombi (Fig. 55.4). The liposomes were injected into rats with carotid thrombosis generated by a human clot. Thirty minutes after treatment, a better thrombolytic activity was observed in rats receiving liposomes encapsulating SK compared with SK alone (28% vs. 17%, respectively). This thrombolytic effect was explained by the protection of the SK simultaneous to the accumulation of targeted liposomes into clot [35].

Taken together these preclinical results show that loading the SK into nanocarriers protects it from premature inactivation in the blood and improves its accumulation into the clot leading to an enhanced thrombolysis.

55.3.3 Urokinase

UK is a serine protease that activates plasminogen into plasmin thus degrading fibrin clots [36]. It is a protein with two polypeptide chains of 32 and 54 kDa, respectively. Originally obtained from human urine, UK is now produced from human renal cell lines. Into whole blood, UK has a half-life of 15 to 20 min. High amounts are necessary to obtain a significant thrombolytic effect, inducing undesirable side effects such as hemorrhages [9]. Like SK, UK activates both the circulating and the fibrin-bound plasminogen [10].

55.3.4 Nanocarriers Loaded with UK

Jin *et al.* prepared UK-loaded in water-soluble chitosan nanocarriers using an ionic cross-linking method. The final size was 236 nm with a drug encapsulation efficiency of 95%. They injected these nanocarriers into rabbits with jugular thrombosis obtained after administration of thrombin. An increased capacity of clot lysis was observed when compared with free UK. *In vivo*, free UK was metabolized rapidly with a half-life <20 min, while the UK loaded inside the NPs showed a slow release rate [37].

Dextran-coated magnetic nanoparticles were used for covalent bioconjugation with UK via primary amine. The nanoparticles with an average 116 nm size were injected into rats with autologous carotid artery and left jugular vein thrombosis. When applying permanent magnets in the thrombus area, the nanoparticles were concentrated into the thrombotic site, showing a fivefold higher thrombolytic activity than free UK [38].

In an interesting approach, Marsh *et al.* developed perfluorocarbon (PFC) nanoparticles covalently coupled with UK. In order to target femoral thrombi generated in dogs, they coupled antifibrin antibody on the surface of the nanoparticles. When injected into the animals, the thrombus degradation was higher in animals receiving PFC-UK loaded and antifibrin functionalized nanoparticles than in control animals receiving irrelevant IgG targeted UK PFC nanoparticles [39]. This thrombus specificity was achieved by fibrin monoclonal antibodies allowing an enhanced delivery of UK.

Mu *et al.* successfully loaded UK and RGD to the surface of a microbubble-based ultrasound contrast agent. They observed an aggregation at the surface of femoral arterial thrombi in rabbits. However, the authors did not quantify the *in vivo* thrombolytic activity [40]. In rabbits with middle cerebral artery occlusion receiving UK and sulfur hexafluoride microbubbles, the addition of transcranial Doppler ultrasound (2 MHz) showed an enhancement of the recanalization rate compared with animals receiving only UK [41].

55.3.5 Tissue Plasminogen Activator and Its Recombinant Forms (tPA, rtPA)

tPA is encoded in humans by a gene on chromosome 8 and is produced by endothelial cells. tPA has two inhibitors, PAI-1 and PAI-2, which belong to the serpin superfamily. The tPA residues 296–304 are critical for the interaction with PAI-1. It shows a limited half-life of about 4–6 min [9]. Recombinant tPA (rtPA, Alteplase) is a serine protease with a molecular weight of 68 kDa. This recombinant form is produced by Chinese hamster ovary (CHO) cell lines by cDNA technology. This enzyme cleaves the Arg–Val bond, inducing the plasminogen conversion into plasmin [10].

55.3.6 Nanocarriers Loaded with rtPA

Uesugi *et al.* loaded rtPA (Cleactor®) on cationizated gelatin and PEG-grafted nanocarriers. When injected into rabbits with balloon injury of right femoral artery, the half-life of rtPA was three times enhanced due to its complexation with gelatin. In order to induce thrombolysis they applied ultrasound (1 MHz, 0.75 W/cm^2) for up for 60 min [24]. A complete recanalization was observed, which was probably linked to the dissociation of rtPA from gelatin and maybe to the effects of ultrasound on thrombus. Similar results were obtained on swine with acute myocardial infarction with a thrombotic occlusion of left coronary artery. A high recanalization rate was observed in 9 out of 10 swines when receiving nanocarriers, whereas only 1 out of 10 showed complete recanalization in a group with rtPA alone [42].

Zhou *et al.* developed PLGA nanocarriers loaded with rtPA (Alteplase). In order to enhance the accumulation in a rat model of abdominal aortic thrombi induced using ferric chloride, they covered the nanocarriers with a chitosan shell and targeted it with cyclic RGD peptide via a carbodiimide bond. The rtPA loaded into the nanocarriers showed a prolonged half-life. The authors reported some limitations such as the encapsulation efficacy of the rtPA (between 54% and 64%) simultaneously to a partial loss of rtPA activity [43].

Magnetic nanoparticles coated with polyacrylic acid (PAA) were covalently coupled with an amine group of rtPA (Alteplase). Magnetic nanoparticles show the advantage of being made of a magnetite (Fe_3O_4) core that responds to an external magnetic field with superparamagnetic properties. The nanoparticles were concentrated into a thrombus under external magnetic guidance after injection into rats with iliac artery embolisms (Fig. 55.5). Blood flow restoration was observed 75 min later with an equivalent of 0.2 mg/kg of rtPA coupled with magnetic nanoparticles. With a dose of 1 mg/kg, blood flow restoration was obtained within only 30 min [44]. The same team later developed magnetic nanoparticles coated with a shell of poly (aniline-co-N-[1-one-butyric acid] aniline) and loaded with rtPA. With this strategy the amount of rtPA loaded was 50% higher than the amount loaded previously into PAA-coated nanoparticles. After injection into rats with iliac embolisms, the nanoparticles

were guided towards the clots using an external magnetic field [45]. rtPA (Alteplase) was covalently immobilized on chitosan-coated magnetic nanoparticles and injected into rats with iliac artery embolisms. The administration of rtPA loaded on chitosan magnetic nanoparticles associated with a magnetic guidance resulted in 70–80% blood flow recovery with a fivefold lower dosage, 0.2 mg/kg compared with 1 mg/kg required for thrombolysis with free rtPA [23].

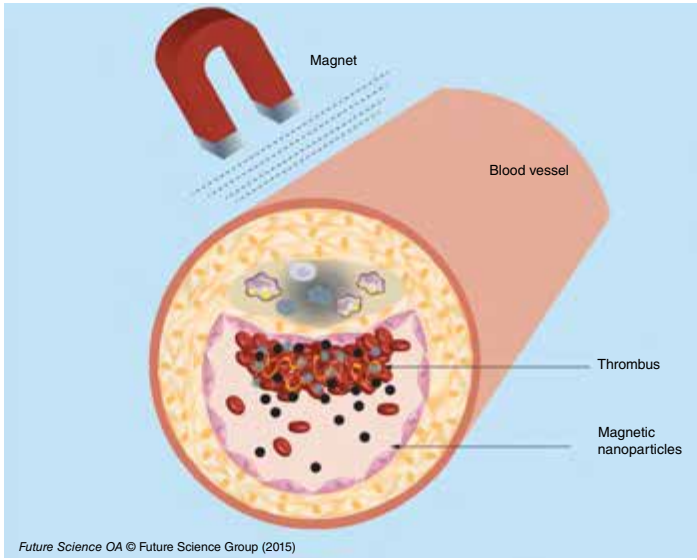

Figure 55.5 Targeting modality by magnet. Ultrasmall paramagnetic iron oxide nanocarriers loaded with thrombolytic drugs are concentrated by an external magnet in the thrombus to enhance its lysis.

These nanocarriers reduce the effective dose of active principle injected but also increase the local concentration and prevent side effects. A limitation of this method could be linked to the fact that the external magnetic field decreases with the tissue depth, and thus makes it difficult to target a site deeper in the body. Kempe *et al.* implanted ferromagnetic stents for the treatment of in-stent thrombosis. In their approach, they used PEGylated magnetic nanoparticles loaded with rtPA (Alteplase). The nanoparticles were injected in pigs with ferromagnetic stents in their coronary artery. The restoration of blood flow with rtPA-

loaded nanoparticles was reached with a lower amount of drug compared with free rtPA [46].

The McCarthy team coupled rtPA (Alteplase) to cross-linked dextran-coated iron oxide nanoparticles (CLIO). In order to increase the distance between the fibrinolytic drug and the particles and to minimize steric interactions, they added a PEG spacer moiety. The nanoparticles were moreover functionalized by covalent grafting of activated factor XIII (FXIIIa) via peptide affinity ligands. They injected these targeted nanoparticles (CLIO-FXIII-PEG-rtPA) into mice with pulmonary embolisms obtained with human clots. This choice was based on the facts that the murine plasminogen system is tenfold less sensitive than human tPA. The authors concluded that the targeted nanoagent displayed similar thrombolytic potential as free tPA [47]. These studies showed that magnetic nanoparticles have a potential for local delivery of thrombolytic drugs either by an external magnetic field or with peptides.

The loading of rtPA (Alteplase) into liposomes obtained using the freeze-thawing preparation method, did not alter the fibrinolytic activity of the drug. The rtPA loaded into PEGylated liposomes showed 21-fold prolonged circulation time compared with free rtPA [17]. Absar *et al.* developed liposomes, either coated with PEG or not, and decorated with a peptide sequence of fibrinogen gamma-chain targeting GPIIb/IIIa. Entrapment efficacy of rtPA (Alteplase) varied from 12% to 26% for non-PEGylated liposomes and from 36% to 52% for PEGylated liposomes. These nanoparticles were injected into rats with inferior vena cava thrombosis induced with a $FeCl_3$ solution. An enhancement of 35% of thrombolytic activity was observed for rtPA-loaded into targeted liposomes when compared with native rtPA. Tested *ex vivo* on human clot, liposomal rtPA showed a slightly lower activity compared with native rtPA, this being probably linked to the incomplete release of the drug from liposomes [48].

An interesting approach to enhance the thrombolysis is the use of ultrasound as adjuvant therapy. This strategy was developed with echogenic liposomes as well as with microbubbles. Echogenic liposomes (ELIP) are composed of a phospholipid bilayer enclosing both gas and liquid. The advantage of this system is the follow-up by echography of thrombus evolution before, during

and after thrombolysis. Moreover, ELIP are not only ultrasound contrast agents but also potential vectors for thrombolysis. Laing *et al.* developed ELIP loaded with rtPA (Alteplase) in the core (15%) or associated with the phospholipid bilayer (35%). The rtPA solution was loaded into liposomes during the hydration of lipid film. ELIP loaded with rtPA were injected into rabbits with abdominal aortic thrombi exposed to ultrasound (pulsed ultrasound 5.7 MHz for 2 min). The degree of recanalization determined by Doppler flow measurements, showed that ELIP charged with rtPA had similar efficacy to free rtPA for thrombus dissolution *in vivo*. Injection of saline (control), empty ELIP, or empty ELIP associated with ultrasound did not show any thrombolytic effect [49]. The recanalization rate was variable in the absence of ultrasound, showing that ultrasound therapy enhances thrombolytic effect [50]. This enhancement could be explained by acoustic cavitation, thermal effects or microstreaming (Fig. 55.6) [51–53].

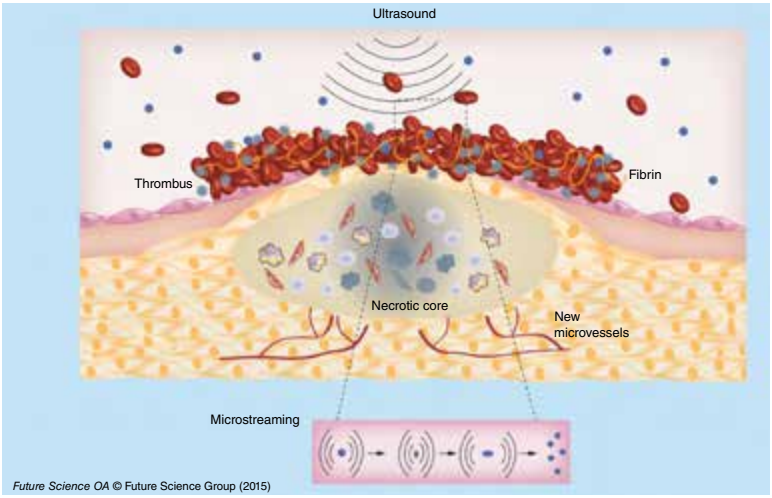

Figure 55.6 Schematic representation of thrombus dissolution by ultrasound.

In order to enhance accumulation into thrombus, Hagisawa *et al.* developed perfluorocarbon-based echogenic liposomes targeted with a RGD peptide loaded or not with rt-PA (Monteplase). They injected them intravenously into rabbits with thrombus in

ilio-femoral arteries and they applied ultrasound. A higher recanalization rate (9 out of 10 rabbits) was observed when ultrasound was applied, compared with that of animals receiving nontargeted liposomes (2 out of 10 rabbits) or rtPA monotherapy (4 out of 10 rabbits) [54].

Microbubbles with a size from 2 to 8 μm represent another class of lipid-based carriers used in thrombolytic strategies. They are composed of a shell made of phospholipids, polymers or albumin, and a core of air or high-molecular-weight gas [28]. The effect of sulfur hexafluoride lipid-based microbubbles associated with ultrasound was compared with intravenous administration of rtPA (10 mg/kg) into rats with acute cerebral ischemia obtained after autologous thrombus injection into carotid artery. The two modalities of treatment showed equivalent result in the restoration of blood flow [55].

Nedelmann *et al.* showed on rats with filament occlusion of the right middle cerebral artery that the association of rtPA (Alteplase) with microbubbles and ultrasound completely restored the blood flow, while rtPA alone partially improved hemispheric perfusion [56]. In a rabbit model of embolic stroke obtained with a clot from a donor rabbit, the combination of microbubbles with rtPA and pulsed ultrasound (1 MHz) showed a good recanalization rate [57]. These studies demonstrated that ultrasound could be associated with microbubbles and/ or thrombolytic drugs to enhance the recanalization effect.

55.4 Microbubbles Associated with Thrombolytic Drugs and/or Ultrasound for Clinical Applications

Microbubbles are the only platform tested in the clinic for thrombolytic therapy. In clinical trials, they were associated or not with ultrasound and showed encouraging results. Molina *et al.* included 111 patients with middle cerebral artery occlusions. The 38 patients who received galactose-based microbubbles, rtPA and 2 MHz ultrasound pulse showed a better recanalization rate than the other 73 patients who received either rtPA and ultrasound or rtPA only [58, 59]. Later, they associated in another clinical trial perflutren lipid (MRX-801) microbubbles with rtPA and

ultrasound and obtained 67% of recanalization rate compared with 46% for the group receiving only rtPA [60]. Alexandrov *et al.* showed that half of patients receiving rtPA, 2 MHz continuous TCD monitoring and perflutren-lipid-based microbubbles demonstrated a complete recanalization rate (6 patients out of 12) while none of the patients receiving only rtPA reached a complete recanalization [61]. Microbubbles based on phospholipids encapsulating sulfur hexafluoride combined with transcranial ultrasound and rtPA showed a better recanalization rate compared with patients receiving rtPA and ultrasound [62].

Another clinical trial was made by Pagola *et al.* in patients with stroke with basilar artery occlusion. All the 20 patients received intravenous rtPA, ultrasound and galactose-based microbubbles. At 24 h, only 50% of patients showed a progressive recanalization while the other 50% did not show any recanalization [63].

Rubiera *et al.* showed that the recanalization was similar in patients receiving either galactose-based microbubbles or phospholipid-based microbubbles encapsulating sulfur-hexafluoride, and rtPA associated with 2 MHz transcranial Doppler [64].

One possible explanation of thrombolysis enhancement when microbubbles and ultrasound are associated with rtPA is the mechanical damage induced by the streaming of microbubbles at the surface of the thrombus allowing a higher diffusion of rtPA. This opens new perspectives for clinical thrombolytic therapy with the aim to reduce the dose and, therefore, hemorrhagic side effects.

55.5 Discussion and Conclusion

Nano- and microcarriers are able to replace the systemic therapy of whole body with a local therapy reducing significantly undesirable side effects. Although ischemic heart and stroke caused by thrombosis are the main causes of death in the world, there is no existing nanocarrier loaded with thrombolytic drug in clinic. Currently, only galactose or lipid-based microbubbles associated to ultrasound with or without rtPA systemic injection have been evaluated in clinical trials and showed an enhancement of thrombolytic effect. In other pathologies such as cancer or infectious diseases, different therapeutic drugs loaded to nanocarriers have already reached the market. This gap could

be partly explained by the distinctive features of thrombosis and of the thrombolytic drugs.

In the case of heart ischemia or stroke, it is necessary to act rapidly within the first minutes or hours (<4.30 h) after the appearance of the symptoms. Thrombolytic drugs administered by systemic way are quickly inactivated by inhibitors in blood. Nanocarriers have the advantage to protect the drug, enhancing its half-life in the blood. Encouraging results were thus obtained on preclinical models with lipid or polymer systems loaded with thrombolytic drugs.

The drugs loaded into nanocarriers must keep their therapeutic capacities. The therapeutic drugs are either charged on the surface of the nanoparticles, as for magnetic nanoparticles, or loaded inside nanocarriers, which is the case of polymer or lipid-based systems. Another critical point is linked to the amount of drug loaded into nanocarriers. The loading capacity must be maximal in order to reduce the injected quantity of carriers. The preclinical results obtained with liposomes showed a low entrapment efficacy, while a better efficacy was usually obtained with polymer-based nanoparticles.

An interesting aspect linked to the use of nanocarriers loaded with therapeutic drugs is the capacity to achieve an active targeting of the thrombus, improving the therapeutic efficacy. This was for instance possible by using targeting peptides on the surface of nanocarriers. Another modality of targeting tested on preclinical models was based on the use of magnetic nanoparticles. Although encouraging results were obtained in small animals, this method seems difficult to apply in patients because of the deep localization of the thrombus. Maybe, the use of large and ultrastrong magnets would be a possibility to overcome this limitation in the near future.

For all systems, a common limitation is linked to the difficulty to obtain a controlled release. The use of ultrasound can partially control the release into thrombus of therapeutics loaded into echogenic liposomes. However, the ultrasound has a limited penetration into the body, and the use of high frequencies could induce blood vessel lesions. Again, improvements of ultrasound equipment may increase its efficacy.

Another important aspect is linked to the thrombus itself in preclinical studies. Some preclinical models are made on animals with an autologous thrombus. However, the affinity of

thrombolytics used in clinics for the animal clot is not similar to the affinity for the human one. The use of animal models obtained with a human clot would thus be more relevant. The aging of the used thrombus is also relevant.

In conclusion, more in-depth preclinical research and developments are necessary to improve the targeted delivery of thrombolytic drugs before their translation into clinical practice.

55.6 Future Perspective

Nanomedicine offers an opportunity and a challenge in the management of a targeted thrombolytic therapy. There are some specific features to take into account for thrombus therapy using nanocarriers. The nanocarrier should load a maximum amount of drug while keeping the thrombolytic efficacy, protect the drug from enzymatic degradation and ensure a rapid release in the thrombus. A balance between all these aspects is mandatory for a better patient care. The development of new materials for nanocarriers and the discovery of new thrombolytic drugs are also considered in the development of nanothrombolysis.

Executive Summary

- Heart ischemia and stroke are the main causes of death in the world.
- Tissue plasminogen activator but also urokinase and streptokinase are the thrombolytic drugs used in clinic. These drugs are inactivated by circulating inhibitors. Therefore, high amounts are injected to patients in order to obtain a therapeutic effect but with a risk of undesirable side effects such as intracranial hemorrhages.
- Polymer-, lipid- or magnetic-based nano- and microcarriers are able to deliver thrombolytic drugs according to their size and structure.
- In preclinical studies, nanoparticles loaded with urokinase, streptokinase or recombinant tissue plasminogen activator (rtPA) have been evaluated. As compared with free drug, a lower amount of drug loaded into nanoparticles was necessary to induce a thrombolytic effect. In parallel, a reduction of intracranial hemorrhages was observed.

- In clinical trials, only galactose and lipid-based microbubbles were evaluated. They were associated to ultrasound and /or rtPA. Enhancement of thrombolytic efficacy was observed with microbubbles associated to ultrasound and rtPA. However, further validation is necessary before a daily clinical use.
- In conclusion, loading thrombolytic drugs into nanocarriers opens new perspectives for thrombotic diseases therapy.

Disclosures and Conflict of Interest

This chapter is reprinted from *Future Science OA,* an open-access journal distributed under the terms of the Creative Commons Attribution 4.0 License. Permission to reprint it as a chapter was obtained from the publisher, Future Science Group. The original article was published as: Varna, M., Juenet, M., Bayles, R., Mazighi, M., Chauvierre, C., Letourneur, D. (2015). Nanomedicine as a strategy to fight thrombotic diseases. *Future Science OA*, pp. 1–14; posted online on July 3, 2015 (doi:10.4155/fso.15.46). This work was supported by Lefoulon-Delalande scholarships (to M. Varna and R. Bayles), EU project NanoAthero FP7-NMP2012-LARGE-6–309820, IMOVA project (FUI/OSEO, CG93), and ANR-13-LAB1–0005–01 'FucoChem,' University Paris 13 and INSERM. The authors have no other relevant affiliations or financial involvement with any organization or entity with a financial interest in or financial conflict with the subject matter or materials discussed in the manuscript apart from those disclosed. No writing assistance was utilized in the production of this manuscript.

Corresponding Author

Didier Letourneur
INSERM U1148, LVTS, Cardiovascular Bio-Engineering
X. Bichat Hospital, Paris, France
Email: didier.letourneur@inserm.fr

References

1. Go, A. S., Mozaffarian, D., Roger, V. L., et al. (2013). Heart disease and stroke statistics—2013 update: A report from the American heart association. *Circulation*, **127**(1), e6–e245.

2. Hilgendorf, I., Swirski, F. K., Robbins, C. S. (2015). Monocyte fate in atherosclerosis. *Arterioscler. Thromb. Vasc. Biol.*, **35**(2), 272–279.
3. Falk, E. (2006). Pathogenesis of atherosclerosis. *J. Am. Coll. Cardiol.*, **47**(8 Suppl.), C7–C12.
4. Fuster, V., Fayad, Z. A., Moreno, P. R., Poon, M., Corti, R., Badimon, J. J. (2005). Atherothrombosis and high-risk plaque: Part II: Approaches by noninvasive computed tomographic/magnetic resonance imaging. *J. Am. Coll. Cardiol.*, **46**(7), 1209–1218.
5. Bivard, A., Lin, L., Parsonsb, M. W. (2013). Review of stroke thrombolytics. *J. Stroke*, **15**(2), 90–98.
6. Furie, B., Furie, B. C. (2008). Mechanisms of thrombus formation. *N. Engl. J. Med.*, **359**(9), 938–949.
7. Mackman, N. (2008). Triggers, targets and treatments for thrombosis. *Nature*, **451**(7181), 914–918.
8. Mazighi, M., Serfaty, J. M., Labreuche, J., et al. (2009). Comparison of intravenous alteplase with a combined intravenous- endovascular approach in patients with stroke and confirmed arterial occlusion (recanalise study): A prospective cohort study. *Lancet Neurol.*, **8**(9), 802–809.
9. Baruah, D. B., Dash, R. N., Chaudhari, M. R., Kadam, S. S. (2006). Plasminogen activators: A comparison. *Vascul. Pharmacol.*, **44**(1), 1–9.
10. Kotb, E. (2014). The biotechnological potential of fibrinolytic enzymes in the dissolution of endogenous blood thrombi. *Biotechnol. Prog*. **30**(3), 656–672.
11. Van De Craen, B., Declerck, P. J., Gils, A. (2012). The biochemistry, physiology and pathological roles of pai-1 and the requirements for pai-1 inhibition *in vivo*. *Thromb. Res.*, **130**(4), 576–585.
12. Fortenberry, Y. M. (2013). Plasminogen activator inhibitor-1 inhibitors: A patent review (2006–present). *Expert Opin. Ther. Pat.*, **23**(7), 801–815.
13. Copin, J. C., Bengualid, D. J., Da Silva, R. F., Kargiotis, O., Schaller, K., Gasche, Y. (2011). Recombinant tissue plasminogen activator induces blood–brain barrier breakdown by a matrix metalloproteinase-9-independent pathway after transient focal cerebral ischemia in mouse. *Eur. J. Neurosci.*, **34**(7), 1085–1092.
14. Klink, A., Hyafil, F., Rudd, J., et al. (2011). Diagnostic and therapeutic strategies for small abdominal aortic aneurysms. *Nat. Rev. Cardiol.*, **8**(6), 338–347.
15. Silva, A. K., Letourneur, D., Chauvierre, C. (2014). Polysaccharide nanosystems for future progress in cardiovascular pathologies. *Theranostics*, **4**(6), 579–591.

16. Ricklin, D., Hajishengallis, G., Yang, K., Lambris, J. D. (2010). Complement: A key system for immune surveillance and homeostasis. *Nat. Immunol.*, **11**(9), 785–797.
17. Kim, J. Y., Kim, J. K., Park, J. S., Byun, Y., Kim, C. K. (2009). The use of pegylated liposomes to prolong circulation lifetimes of tissue plasminogen activator. *Biomaterials*, **30**(29), 5751–5756.
18. Koshkaryev, A., Sawant, R., Deshpande, M., Torchilin, V. (2013). Immunoconjugates and long circulating systems: Origins, current state of the art and future directions. *Adv. Drug. Deliv. Rev.*, **65**(1), 24–35.
19. Rabanel, J. M., Hildgen, P., Banquy, X. (2014). Assessment of peg on polymeric particles surface, a key step in drug carrier translation. *J. Control. Release*, **185**, 71–87.
20. Bowey, K., Tanguay, J. F., Tabrizian, M. (2012). Liposome technology for cardiovascular disease treatment and diagnosis. *Expert Opin. Drug Deliv.*, **9**(2), 249–265.
21. Ruiz-Esparza, G. U., Flores-Arredondo, J. H., Segura-Ibarra, V., et al. (2013). The physiology of cardiovascular disease and innovative liposomal platforms for therapy. *Int. J. Nanomed.,* **8**, 629–640.
22. Tassa, C., Shaw, S. Y., Weissleder, R. (2011). Dextran-coated iron oxide nanoparticles: A versatile platform for targeted molecular imaging, molecular diagnostics, and therapy. *Acc. Chem. Res.*, **44**(10), 842–852.
23. Chen, J. P., Yang, P. C., Ma, Y. H., Wu, T. (2011). Characterization of chitosan magnetic nanoparticles for *in situ* delivery of tissue plasminogen activator. *Carbohydr. Polym.,* **84**(1), 364–372.
24. Uesugi, Y., Kawata, H., Jo, J., Saito, Y., Tabata, Y. (2010). An ultrasound-responsive nano delivery system of tissue-type plasminogen activator for thrombolytic therapy. *J. Control. Release*, **147**(2), 269–277.
25. Robert, D., Fayol, D., Le Visage, C., et al. (2010). Magnetic micro-manipulations to probe the local physical properties of porous scaffolds and to confine stem cells. *Biomaterials*, **31**(7), 1586–1595.
26. Cheng, K., Li, T. S., Malliaras, K., Davis, D. R., Zhang, Y., Marban, E. (2010). Magnetic targeting enhances engraftment and functional benefit of iron-labeled cardiosphere-derived cells in myocardial infarction. *Circ. Res.*, **106**(10), 1570–1581.
27. Silva, A. K., Luciani, N., Gazeau, F., et al. (2015). Combining magnetic nanoparticles with cell derived microvesicles for drug loading and targeting. *Nanomedicine*, **11**(3), 645–655.

28. De Saint Victor, M., Crake, C., Coussios, C. C., Stride, E. (2014). Properties, characteristics and applications of microbubbles for sonothrombolysis. *Expert Opin. Drug Deliv.*, **11**(2), 187–209.
29. Collen, D., Lijnen, H. R. (2005). Thrombolytic agents. *Thromb. Haemost.*, **93**(4), 627–630.
30. Butcher, K., Shuaib, A., Saver, J., et al. (2013). Thrombolysis in the developing world: Is there a role for streptokinase ? *Int. J. Stroke*, **8**(7), 560–565.
31. Kunamneni, A., Abdelghani, T. T., Ellaiah, P. (2007). Streptokinase–the drug of choice for thrombolytic therapy. *J. Thromb. Thrombolysis*, **23**(1), 9–23.
32. Leach, J. K., O'Rear, E. A., Patterson, E., Miao, Y., Johnson, A. E. (2003). Accelerated thrombolysis in a rabbit model of carotid artery thrombosis with liposome-encapsulated and microencapsulated streptokinase. *Thromb. Haemost.*, **90**(1), 64–70.
33. Leach, J. K., Patterson, E., O'Rear, E. A. (2004). Encapsulation of a plasminogen activator speeds reperfusion, lessens infarct and reduces blood loss in a canine model of coronary artery thrombosis. *Thromb. Haemost.*, **91**(6), 1213–1218.
34. Leach, J. K., Patterson, E., O'Rear, E. A. (2004). Distributed intraclot thrombolysis: Mechanism of accelerated thrombolysis with encapsulated plasminogen activators. *J. Thromb. Haemost.*, **2**(9), 1548–1555.
35. Vaidya, B., Agrawal, G. P., Vyas, S. P. (2011). Platelets directed liposomes for the delivery of streptokinase: Development and characterization. *Eur. J. Pharm. Sci.*, **44**(5), 589–594.
36. Kunamneni, A., Ravuri, B. D., Saisha, V., Ellaiah, P., Prabhakhar, T. (2008). Urokinase–a very popular cardiovascular agent. *Recent Pat. Cardiovasc. Drug Discov.*, **3**(1),45–58.
37. Jin, H. J., Zhang, H., Sun, M. L., Zhang, B. G., Zhang, J. W. (2013). Urokinase-coated chitosan nanoparticles for thrombolytic therapy: Preparation and pharmacodynamics *in vivo*. *J. Thromb. Thrombolysis,* **36**(4), 458–468.
38. Bi, F., Zhang, J., Su, Y., Tang, Y.C., Liu, J. N. (2009). Chemical conjugation of urokinase to magnetic nanoparticles for targeted thrombolysis. *Biomaterials*, **30**(28), 5125–5130.
39. Marsh, J. N., Hu, G., Scott, M. J., et al. (2011). A fibrin-specific thrombolytic nanomedicine approach to acute ischemic stroke. *Nanomedicine (Lond.)*, **6**(4), 605–615.
40. Mu, Y., Li, L., Ayoufu, G. (2009). Experimental study of the preparation of targeted microbubble contrast agents carrying urokinase and rgds. *Ultrasonics*, **49**(8), 676–681.

41. Liu, W. S., Huang, Z. Z., Wang, X. W., Zhou, J. (2012). Effects of microbubbles on transcranial doppler ultrasound-assisted intracranial urokinase thrombolysis. *Thromb. Res.*, **130**(3), 547–551.
42. Kawata, H., Uesugi, Y., Soeda, T., et al. (2012). A new drug delivery system for intravenous coronary thrombolysis with thrombus targeting and stealth activity recoverable by ultrasound. *J. Am. Coll. Cardiol.*, **60**(24), 2550–2557.
43. Zhou, J., Guo, D., Zhang, Y., Wu, W., Ran, H., Wang, Z. (2014). Construction and evaluation of Fe3O4-based PLGA nanoparticles carrying rtPA used in the detection of thrombosis and in targeted thrombolysis. *ACS. Appl. Mater. Interfaces*, **6**(8), 5566–5576.
44. Ma, Y. H., Wu, S. Y., Wu, T., Chang, Y. J., Hua, M. Y., Chen, J. P. (2009). Magnetically targeted thrombolysis with recombinant tissue plasminogen activator bound to polyacrylic acid-coated nanoparticles. *Biomaterials*, **30**(19), 3343–3351.
45. Yang, H. W., Hua, M. Y., Lin, K. J., et al. (2012). Bioconjugation of recombinant tissue plasminogen activator to magnetic nanocarriers for targeted thrombolysis. *Int. J. Nanomed.,* **7**, 5159–5173.
46. Kempe, M., Kempe, H., Snowball, I., et al. (2010). The use of magnetite nanoparticles for implant-assisted magnetic drug targeting in thrombolytic therapy. *Biomaterials*, **31**(36), 9499–9510.
47. Mccarthy, J. R., Sazonova, I. Y., Erdem, S. S., et al. (2012). Multifunctional nanoagent for thrombus-targeted fibrinolytic therapy. *Nanomedicine (Lond.)*, **7**(7), 1017–1028.
48. Absar, S., Nahar, K., Kwon, Y. M., Ahsan, F. (2013). Thrombus-targeted nanocarrier attenuates bleeding complications associated with conventional thrombolytic therapy. *Pharm. Res.*, **30**(6), 1663–1676.
49. Laing, S. T., Moody, M., Smulevitz, B., et al. (2011). Ultrasound-enhanced thrombolytic effect of tissue plasminogen activator-loaded echogenic liposomes in an *in vivo* rabbit aorta thrombus model–brief report. *Arterioscler. Thromb. Vasc. Biol.*, **31**(6), 1357–1359.
50. Laing, S. T., Moody, M. R., Kim, H., et al. (2012). Thrombolytic efficacy of tissue plasminogen activator-loaded echogenic liposomes in a rabbit thrombus model. *Thromb. Res.*, **130**(4), 629–635.
51. Brujan, E. A. (2009). Cardiovascular cavitation. *Med. Eng. Phys.*, **31**(7), 742–751.
52. Unger, E., Porter, T., Lindner, J., Grayburn, P. (2014). Cardiovascular drug delivery with ultrasound and microbubbles. *Adv. Drug Deliv. Rev.*, **72**, 110–126.

53. Chen, X., Leeman, J. E., Wang, J., Pacella, J. J., Villanueva, F. S. (2014). New insights into mechanisms of sonothrombolysis using ultra-high-speed imaging. *Ultrasound Med. Biol.*, **40**(1), 258–262.
54. Hagisawa, K., Nishioka, T., Suzuki, R., et al. (2013). Thrombus–targeted perfluorocarbon-containing liposomal bubbles for enhancement of ultrasonic thrombolysis: *in vitro* and *in vivo* study. *J. Thromb. Haemost.*, **11**(8), 1565–1573.
55. Moumouh, A., Barentin, L., Tranquart, F., Serrierre, S., Bonnaud, I., Tasu, J. P. (2010). Fibrinolytic effects of transparietal ultrasound associated with intravenous infusion of an ultrasound contrast agent: Study of a rat model of acute cerebral stroke. *Ultrasound Med. Biol.*, **36**(1), 51–57.
56. Nedelmann, M., Ritschel, N., Doenges, S., et al. (2010). Combined contrast-enhanced ultrasound and rt-pa treatment is safe and improves impaired microcirculation after reperfusion of middle cerebral artery occlusion. *J. Cereb. Blood Flow Metab.*, **30**(10), 1712–1720.
57. Brown, A. T., Flores, R., Hamilton, E., Roberson, P. K., Borrelli, M. J., Culp, W. C. (2011). Microbubbles improve sonothrombolysis *in vitro* and decrease hemorrhage *in vivo* in a rabbit stroke model. *Invest. Radiol.*, **46**(3), 202–207.
58. Tsivgoulis, G., Culp, W. C., Alexandrov, A. V. (2008). Ultrasound enhanced thrombolysis in acute arterial ischemia. *Ultrasonics*, **48**(4), 303–311.
59. Molina, C. A., Ribo, M., Rubiera, M., et al. (2006). Microbubble administration accelerates clot lysis during continuous 2-MHz ultrasound monitoring in stroke patients treated with intravenous tissue plasminogen activator. *Stroke*, **37**(2), 425–429.
60. Molina, C. A., Barreto, A. D., Tsivgoulis, G., et al. (2009). Transcranial ultrasound in clinical sonothrombolysis (tucson) trial. *Ann. Neurol.*, **66**(1), 28–38.
61. Alexandrov, A. V., Mikulik, R., Ribo, M., et al. (2008). A pilot randomized clinical safety study of sonothrombolysis augmentation with ultrasound-activated perflutren–lipid microspheres for acute ischemic stroke. *Stroke*, **39**(5), 1464–1469.
62. Perren, F., Loulidi, J., Poglia, D., Landis, T., Sztajzel, R. (2008). Microbubble potentiated transcranial duplex ultrasound enhances iv thrombolysis in acute stroke. *J. Thromb. Thrombolysis*, **25**(2), 219–223.
63. Pagola, J., Ribo, M., Alvarez-Sabin, J., Lange, M., Rubiera, M., Molina, C. A. (2007). Timing of recanalization after microbubble-enhanced

intravenous thrombolysis in basilar artery occlusion. *Stroke*, **38**(11), 2931–2934.

64. Rubiera, M., Ribo, M., Delgado-Mederos, R., et al. (2008). Do bubble characteristics affect recanalization in stroke patients treated with microbubble-enhanced sonothrombolysis? *Ultrasound Med. Biol.*, **34**(10), 1573–1577.

Index

"*Dr. Bawa and his team have meticulously gathered the distilled experience of world-class researchers, clinicians and business leaders addressing the most salient issues confronted in product concept development and translation. Knowledge is power, particularly in nanomedicine translation, and this handbook is an essential guide that illustrates and clarifies our way to commercial success.*"

Gregory Lanza, MD, PhD
Professor of Medicine and Oliver M. Langenberg Distinguished Professor
Washington University Medical School, USA

"*This is an outstanding, comprehensive volume that crosscuts disciplines and topics fitting individuals from a variety of fields looking to become knowledgeable in medical nanotech research and its translation from the bench to the bedside.*"

Shaker A. Mousa, PhD, MBA
Vice Provost and Professor of Pharmacology
Albany College of Pharmacy and Health Sciences, USA

"*Masterful! This handbook will have a welcome place in the hands of students, educators, clinicians and experienced scientists alike. In a rapidly evolving arena, the authors have harnessed the field and its future by highlighting both current and future needs in diagnosis and therapies. Bravo!*"

Howard E. Gendelman, MD
Margaret R. Larson Professor and Chair
University of Nebraska Medical Center, USA

"*It is refreshing to see a handbook that does not merely focus on preclinical aspects or exaggerated projections of nanomedicine. Unlike other books, this handbook not only highlights current advances in diagnostics and therapies but also addresses critical issues like terminology, regulatory aspects and personalized medicine.*"

Gert Storm, PhD
Professor of Pharmaceutics
Utrecht University, The Netherlands

This handbook provides a comprehensive roadmap of basic research in nanomedicine as well as clinical applications. However, unlike other texts in nanomedicine, it not only highlights current advances in diagnostics and therapeutics but also explores related issues like nomenclature, historical developments, regulatory aspects, nanosimilars and 3D nanofabrication. While bridging the gap between basic biomedical research, engineering, medicine and law, the handbook provides a thorough understanding of nano's potential to address (i) medical problems from both the patient and health provider's perspective and (ii) current applications and their potential in a healthcare setting.

About the Series Editor

Dr. Raj Bawa is president of Bawa Biotech LLC, a biotech/pharma consultancy and patent law firm based in Ashburn, VA, USA. He is an entrepreneur, professor, researcher, inventor, and registered patent agent licensed to practice before the U.S. Patent and Trademark Office. Trained as a biochemist and microbiologist, he is currently an adjunct professor of biological sciences at Rensselaer Polytechnic Institute in Troy, NY, as well as a scientific advisor to Teva Pharmaceutical Industries, Israel. He has authored over 100 publications, coedited 4 texts and serves on the editorial board of 17 journals.

V486
ISBN 978-981-4669-20-7
9 789814 669207

PAN STANFORD PUBLISHING
www.panstanford.com